ISSN 1007-9327 (print)
ISSN 2219-2840 (online)

World Journal of *Gastroenterology*

World J Gastroenterol 2022 May 7; 28(17): 1725-1874



Published by Baishideng Publishing Group Inc

World Journal of Gastroenterology

Contents

Weekly Volume 28 Number 17 May 7, 2022

REVIEW

1725 Gut homeostasis, injury, and healing: New therapeutic targets

Oncel S, Basson MD

1751 New insights in diagnosis and treatment of gastroenteropancreatic neuroendocrine neoplasms

Yin F, Wu ZH, Lai JP

MINIREVIEWS

1768 Current status and future of targeted peptide receptor radionuclide positron emission tomography imaging and therapy of gastroenteropancreatic-neuroendocrine tumors

Grey N, Silosky M, Lieu CH, Chin BB

ORIGINAL ARTICLE

Basic Study

1781 Forkhead Box q1 promotes invasion and metastasis in colorectal cancer by activating the epidermal growth factor receptor pathway

Zhang JJ, Cao CX, Wan LL, Zhang W, Liu ZJ, Wang JL, Guo Q, Tang H

1798 Sirtuin1 attenuates acute liver failure by reducing reactive oxygen species *via* hypoxia inducible factor 1α

Cao P, Chen Q, Shi CX, Wang LW, Gong ZJ

1814 Peroxisome proliferator-activated receptor-alpha activation and dipeptidyl peptidase-4 inhibition target dysbiosis to treat fatty liver in obese mice

Silva-Veiga FM, Miranda CS, Vasques-Monteiro IML, Souza-Tavares H, Martins FF, Daleprane JB, Souza-Mello V

Retrospective Cohort Study

1830 Epidemiological characteristics of Asian children with inflammatory bowel disease at diagnosis: Insights from an Asian-Pacific multi-centre registry network

Huang JG, Wong YKY, Chew KS, Tanpowpong P, Calixto Mercado KS, Reodica A, Rajindrajith S, Chang KC, Ni YH, Treepongkaruna S, Lee WS, Aw MM

Retrospective Study

1845 Clinical outcomes of endoscopic papillectomy of ampullary adenoma: A multi-center study

Choi SJ, Lee HS, Kim J, Choe JW, Lee JM, Hyun JJ, Yoon JH, Kim HJ, Kim JS, Choi HS

1860 Biliary metal stents should be placed near the hilar duct in distal malignant biliary stricture patients

Sugimoto M, Takagi T, Suzuki R, Konno N, Asama H, Sato Y, Irie H, Okubo Y, Nakamura J, Takasumi M, Hashimoto M, Kato T, Kobashi R, Yanagita T, Hikichi T, Ohira H

LETTER TO THE EDITOR

1871 Could microbiome analysis be a new diagnostic tool in gastric carcinogenesis for high risk, *Helicobacter pylori* negative patients?

Turshudzhyan A, Rezaizadeh H

ABOUT COVER

Associate Editor of *World Journal of Gastroenterology*, Marc D Basson, MD, PhD, MBA, FACS, Senior Associate Dean for Medicine and Research, School of Medicine and Health Sciences, University of North Dakota, 1301 N Columbia Road, Grand Forks, ND 58201, United States. marc.basson@und.edu

AIMS AND SCOPE

The primary aim of *World Journal of Gastroenterology* (*WJG*, *World J Gastroenterol*) is to provide scholars and readers from various fields of gastroenterology and hepatology with a platform to publish high-quality basic and clinical research articles and communicate their research findings online. *WJG* mainly publishes articles reporting research results and findings obtained in the field of gastroenterology and hepatology and covering a wide range of topics including gastroenterology, hepatology, gastrointestinal endoscopy, gastrointestinal surgery, gastrointestinal oncology, and pediatric gastroenterology.

INDEXING/ABSTRACTING

The *WJG* is now indexed in Current Contents®/Clinical Medicine, Science Citation Index Expanded (also known as SciSearch®), Journal Citation Reports®, Index Medicus, MEDLINE, PubMed, PubMed Central, and Scopus. The 2021 edition of Journal Citation Report® cites the 2020 impact factor (IF) for *WJG* as 5.742; Journal Citation Indicator: 0.79; IF without journal self cites: 5.590; 5-year IF: 5.044; Ranking: 28 among 92 journals in gastroenterology and hepatology; and Quartile category: Q2. The *WJG*'s CiteScore for 2020 is 6.9 and Scopus CiteScore rank 2020: Gastroenterology is 19/136.

RESPONSIBLE EDITORS FOR THIS ISSUE

Production Editor: *Ying-Yi Yuan*; **Production Department Director:** *Xiang Li*; **Editorial Office Director:** *Ze-Mao Gong*.

NAME OF JOURNAL
World Journal of Gastroenterology

ISSN
ISSN 1007-9327 (print) ISSN 2219-2840 (online)

LAUNCH DATE
October 1, 1995

FREQUENCY
Weekly

EDITORS-IN-CHIEF
Andrzej S Tarnawski

EDITORIAL BOARD MEMBERS
http://www.wjgnet.com/1007-9327/editorialboard.htm

PUBLICATION DATE
May 7, 2022

COPYRIGHT
© 2022 Baishideng Publishing Group Inc

INSTRUCTIONS TO AUTHORS
https://www.wjgnet.com/bpg/gerinfo/204

GUIDELINES FOR ETHICS DOCUMENTS
https://www.wjgnet.com/bpg/GerInfo/287

GUIDELINES FOR NON-NATIVE SPEAKERS OF ENGLISH
https://www.wjgnet.com/bpg/gerinfo/240

PUBLICATION ETHICS
https://www.wjgnet.com/bpg/GerInfo/288

PUBLICATION MISCONDUCT
https://www.wjgnet.com/bpg/gerinfo/208

ARTICLE PROCESSING CHARGE
https://www.wjgnet.com/bpg/gerinfo/242

STEPS FOR SUBMITTING MANUSCRIPTS
https://www.wjgnet.com/bpg/GerInfo/239

ONLINE SUBMISSION
https://www.f6publishing.com

© 2022 Baishideng Publishing Group Inc. All rights reserved. 7041 Koll Center Parkway, Suite 160, Pleasanton, CA 94566, USA
E-mail: bpgoffice@wjgnet.com https://www.wjgnet.com

World Journal of Gastroenterology

Submit a Manuscript: https://www.f6publishing.com

World J Gastroenterol 2022 May 7; 28(17): 1725-1750

DOI: 10.3748/wjg.v28.i17.1725

ISSN 1007-9327 (print) ISSN 2219-2840 (online)

REVIEW

Gut homeostasis, injury, and healing: New therapeutic targets

Sema Oncel, Marc D Basson

Specialty type: Gastroenterology and hepatology

Provenance and peer review: Invited article; Externally peer reviewed.

Peer-review model: Single blind

Peer-review report's scientific quality classification

Grade A (Excellent): 0
Grade B (Very good): B
Grade C (Good): C, C
Grade D (Fair): 0
Grade E (Poor): 0

P-Reviewer: Barisani D, Italy; Dbar S, Russia; Gassler N, Germany

Received: October 4, 2021
Peer-review started: October 4, 2021
First decision: December 4, 2021
Revised: December 12, 2021
Accepted: March 25, 2022
Article in press: March 25, 2022
Published online: May 7, 2022

Sema Oncel, Marc D Basson, Department of Biomedical Sciences, University of North Dakota School of Medicine and Health Sciences, Grand Forks, ND 58202, United States

Marc D Basson, Department of Surgery, University of North Dakota School of Medicine and Health Sciences, Grand Forks, ND 58202, United States

Marc D Basson, Department of Pathology, University of North Dakota School of Medicine and Health Sciences, Grand Forks, ND 58202, United States

Corresponding author: Marc D Basson, MD, PhD, Professor, Department of Biomedical Sciences, University of North Dakota School of Medicine and Health Sciences, 1301 North Columbia Road, Grand Forks, ND 58202, United States. marc.basson@und.edu

Abstract

The integrity of the gastrointestinal mucosa plays a crucial role in gut homeostasis, which depends upon the balance between mucosal injury by destructive factors and healing *via* protective factors. The persistence of noxious agents such as acid, pepsin, nonsteroidal anti-inflammatory drugs, or *Helicobacter pylori* breaks down the mucosal barrier and injury occurs. Depending upon the size and site of the wound, it is healed by complex and overlapping processes involving membrane resealing, cell spreading, purse-string contraction, restitution, differentiation, angiogenesis, and vasculogenesis, each modulated by extracellular regulators. Unfortunately, the gut does not always heal, leading to such pathology as peptic ulcers or inflammatory bowel disease. Currently available therapeutics such as proton pump inhibitors, histamine-2 receptor antagonists, sucralfate, 5-aminosalicylate, antibiotics, corticosteroids, and immunosuppressants all attempt to minimize or reduce injury to the gastrointestinal tract. More recent studies have focused on improving mucosal defense or directly promoting mucosal repair. Many investigations have sought to enhance mucosal defense by stimulating mucus secretion, mucosal blood flow, or tight junction function. Conversely, new attempts to directly promote mucosal repair target proteins that modulate cytoskeleton dynamics such as tubulin, talin, Ehm^2, filamin-a, gelsolin, and flightless I or that proteins regulate focal adhesions dynamics such as focal adhesion kinase. This article summarizes the pathobiology of gastrointestinal mucosal healing and reviews potential new therapeutic targets.

Key Words: Intestine; Mucosa; Repair; Restitution; Sheet migration; Stomach ulcer

©The Author(s) 2022. Published by Baishideng Publishing Group Inc. All rights reserved.

Core Tip: The integrity of the gastrointestinal mucosa is crucial in gut homeostasis, which depends upon the balance between mucosal injury by destructive factors and healing *via* protective factors. An excess of destructive agents breaks down the mucosal barrier. Upon injury, under physiological conditions, gastrointestinal mucosa heals itself by complex processes. However, the gut may not heal under pathological conditions. Currently available drugs attempt to minimize or reduce injury to the gastrointestinal tract. Recent studies have focused on improving mucosal defense or directly promoting mucosal repair. This article summarizes the pathobiology of gastrointestinal mucosal healing and reviews potential new therapeutic targets.

Citation: Oncel S, Basson MD. Gut homeostasis, injury, and healing: New therapeutic targets. *World J Gastroenterol* 2022; 28(17): 1725-1750
URL: https://www.wjgnet.com/1007-9327/full/v28/i17/1725.htm
DOI: https://dx.doi.org/10.3748/wjg.v28.i17.1725

INTRODUCTION

Upon injury, gastrointestinal (GI) epithelial tissue is capable of renewing itself within hours to months by replacing damaged or dead cells, depending on the site and size of the wound. In order to appreciate potential new therapeutic targets, this review will first summarize the current understanding of the processes of mucosal healing and defense and describe their major extracellular regulators. Then, the importance of the quality of ulcer healing and novel approaches to promote such healing will be reviewed. This review focuses on mucosal injury and repair. Deeper injuries such as a deep ulcer, trauma, fistula, or surgical transection and anastomotic healing all require a complex interaction among endothelial cells, fibroblasts, and other cell types to reconstitute the submucosal and muscular layers of the bowel wall. This is beyond the scope of the current review but has been previously reviewed[1-5]. Angiogenesis is critical to these efforts, and requires a complex interaction between endothelial cells, the extracellular matrix, growth factors and cytokines, and other cell types[6,7].

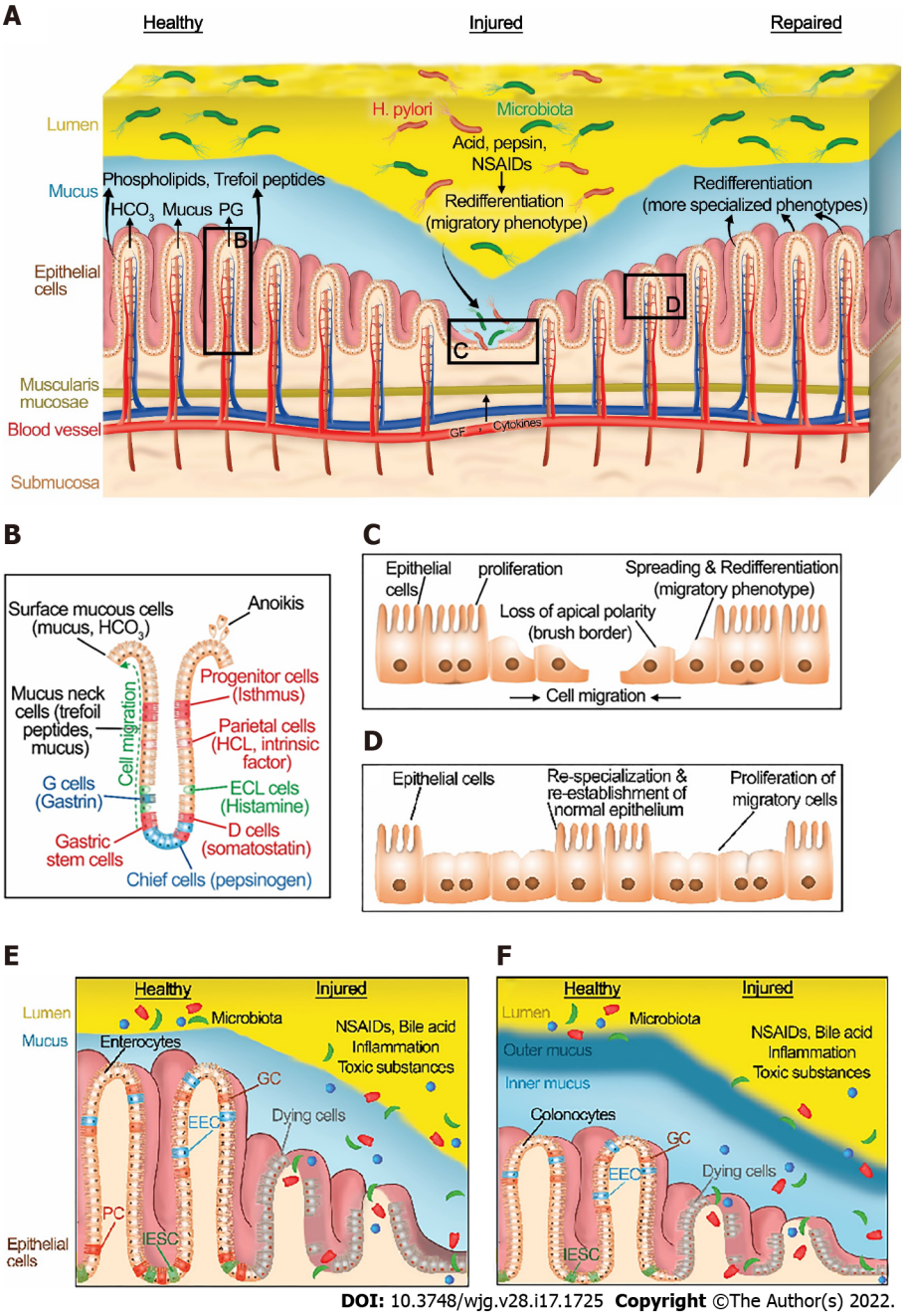
PHYSIOLOGY OF MUCOSAL HEALING

The integrity of the gastrointestinal mucosa is crucial for gut homeostasis. The gut lining is continuously injured during normal gut function[8] by a variety of noxious luminal substances and abrasive interactions with luminal contents (Figure 1A). However, there is normally an equilibrium between gut injury, mucosal healing, and diverse factors that protect the mucosa[5]. This equilibrium favors healing in a healthy state. Under normal physiological conditions, GI epithelial cells migrate from the base of the crypt to the villi, where their interaction with each other and the extracellular matrix (ECM) is disrupted leading to epithelial cell shedding (anoikis)[9] (Figure 1B).

PROTECTIVE FACTORS FOR THE GASTROINTESTINAL MUCOSA

The gastrointestinal mucosa is protected at three levels: pre-epithelial, epithelial, and sub-epithelial defenses. Pre-epithelial protection, the first line of mucosal defense, is provided by the secretion of mucus, bicarbonate, phospholipids, prostaglandins, and trefoil peptides (Figure 1A and B). These factors not only neutralize the acid but also inactivate pepsin at the gastric mucosal surface. In addition, phospholipids secreted into mucus contribute to the hydrophobicity of mucus and prevent back-diffusion of hydrogen ions[10]. Prostaglandins are abundant in gastric juice. They inhibit acid secretion and stimulate mucus and bicarbonate secretion[11]. Bicarbonate-rich mucus is secreted throughout the GI tract, by mucoid cells in the stomach and goblet cells in the intestines, creating a near-neutral pH at the epithelial surfaces in the GI tract, thereby protecting the GI mucosa against autodigestion by the gastric juice and other noxious agents in the lumen[12,13].

Intestinal epithelial cells consist of four important cell types (Figure 1E and F). Enterocytes and colonocytes are most common in the surface epithelium. They are critical for the digestion and absorption of nutrients. Paneth cells are highly specialized cells located in small intestinal crypts. Paneth cells are essential for the secretion of antimicrobial peptides (AMP) such as defensins. These AMPs modulate the composition of the small intestinal microbiota. Goblet cells produce various types of mucin and are found throughout the GI tract. Similarly, enteroendocrine cells are scattered along with the epithelial cells of the GI tract. They produce and secrete more than 20 different hormones in response to nutrients in the lumen that regulate hunger, appetite, and satiety[14]. Intestinal epithelial



DOI: 10.3748/wjg.v28.i17.1725 **Copyright** ©The Author(s) 2022.

Figure 1 Normal gastrointestinal homeostasis, injury, and healing. A: Structure of gastric epithelium in healthy, injured, and repaired states. A healthy gastric barrier is essential to maintain gastric homeostasis. In a healthy state, there is an equilibrium between gastric injury and mucosal healing. An excess of destructive factors such as acid, pepsin, nonsteroidal anti-inflammatory drugs (NSAIDs), and *H. pylori* leads to gastric barrier disruption. These noxious agents then diffuse deeper into the mucosa and create wounds. Epithelial cells at the edge of the injury redifferentiate to a migratory phenotype and collectively migrate as a sheet to close the wound. After successful restitution, the migrated cells redifferentiate to more specialized phenotypes. B: A diagram depicting the structure and cell types of gastric epithelium. C: In the injured state, epithelial cells at the edge of the wound spread and redifferentiate to a migratory phenotype, losing their classical apical brush border and assuming a more squamous morphology. Then, they migrate as a sheet to cover the injured area, with cells at the front of the migrating sheet transmitting traction forces to cells farther back *via* cell-cell contacts. Epithelial cells behind these migrating cells subsequently proliferate to provide more cells to fully cover larger wounds. D: Cells that have migrated across the defect may themselves then proliferate once the barrier has been reformed. In addition, following migration and proliferation, the migrated cells redifferentiate back to more specialized phenotypes. E: Structure of small intestinal epithelium in healthy and injured states. F: Structure of large intestinal epithelium in healthy and injured states. A healthy intestinal barrier is essential to maintain intestinal homeostasis. In the healthy state, there is an equilibrium between intestinal injury and mucosal healing. An excess of destructive factors such as NSAIDs, inflammation, bile acid, and toxic luminal substances leads to intestinal barrier disruption. These noxious agents then diffuse deeper into the mucosa and create wounds. Epithelial cells at the edge of the injury follow the processes described in the figure legends for in Figure 1C and D. IESC: Intestinal epithelial stem cells; EEC: Enteroendocrine cells; GC: Goblet cells; NSAIDs: Nonsteroidal anti-inflammatory drugs; *H. pylori*: *Helicobacter pylori*; PG: Prostaglandins; ECL cells: Enterochromaffin-like cells; PC: Paneth cells; IESC: Intestinal epithelial stem cells.

stem cells (IESCs) are crucial to maintaining intestinal epithelial function and homeostasis in both the small intestine and large intestine. IESCs divide for self-renewal and generate progenitor cells that undergo differentiation into enterocytes, colonocytes, Paneth cells, goblets cells, and enteroendocrine cells[15].

Epithelial protection represents the second line of defense. GI epithelial cells are connected to each other *via* tight junctions and act as a physical barrier against acid or toxic luminal agents. In addition to stimulating mucus and bicarbonate secretion, prostaglandins reduce the permeability of the epithelium by closing the apical spaces between the epithelial cells, and thus decreasing the exposure of deeper layers along the GI tract to noxious agents by modulating these tight junctions[16]. Tight junction proteins are either transmembrane proteins such as occludin, claudins, and junction adhesion molecule proteins or cytoplasmic plaque proteins such as the zonula occludens proteins. The dysregulation of these proteins *via* toxin exposure or autoimmune diseases such as celiac disease may lead to disruption of gastrointestinal barrier function[17]. For example, ulcerative colitis may alter the intestinal barrier function *via* changing the phosphorylation of colonic claudins[18]. The architecture and function of tight junctions are slightly divergent between the different regions of the GI tract and also between different epithelial cells. For example, disruption of occludin alters intestinal barrier function whereas occludin disruption does not cause barrier dysfunction in the stomach[19]. Moreover, the expression of tight junction proteins varies even among the different epithelial cells. For instance, IESCs and Paneth cells have high occludin levels whereas claudin-1, -2, and -7 expression is elevated in Paneth cells, IESCs, and enterocytes, respectively[20].

The final mucosal defense is sub-epithelial protection through augmentation of mucosal blood flow. Vascular flow not only removes acid rather than allowing it to diffuse deeper into the mucosa but also supplies necessary nutrients and oxygen to the epithelial cells for energy-consuming processes such as ion transport and secretion. Gut epithelial cells undergo continuous dynamic self-renewal in response to the damage caused by destructive factors under normal physiological conditions[21,22].

DRIVERS OF MUCOSAL INJURY

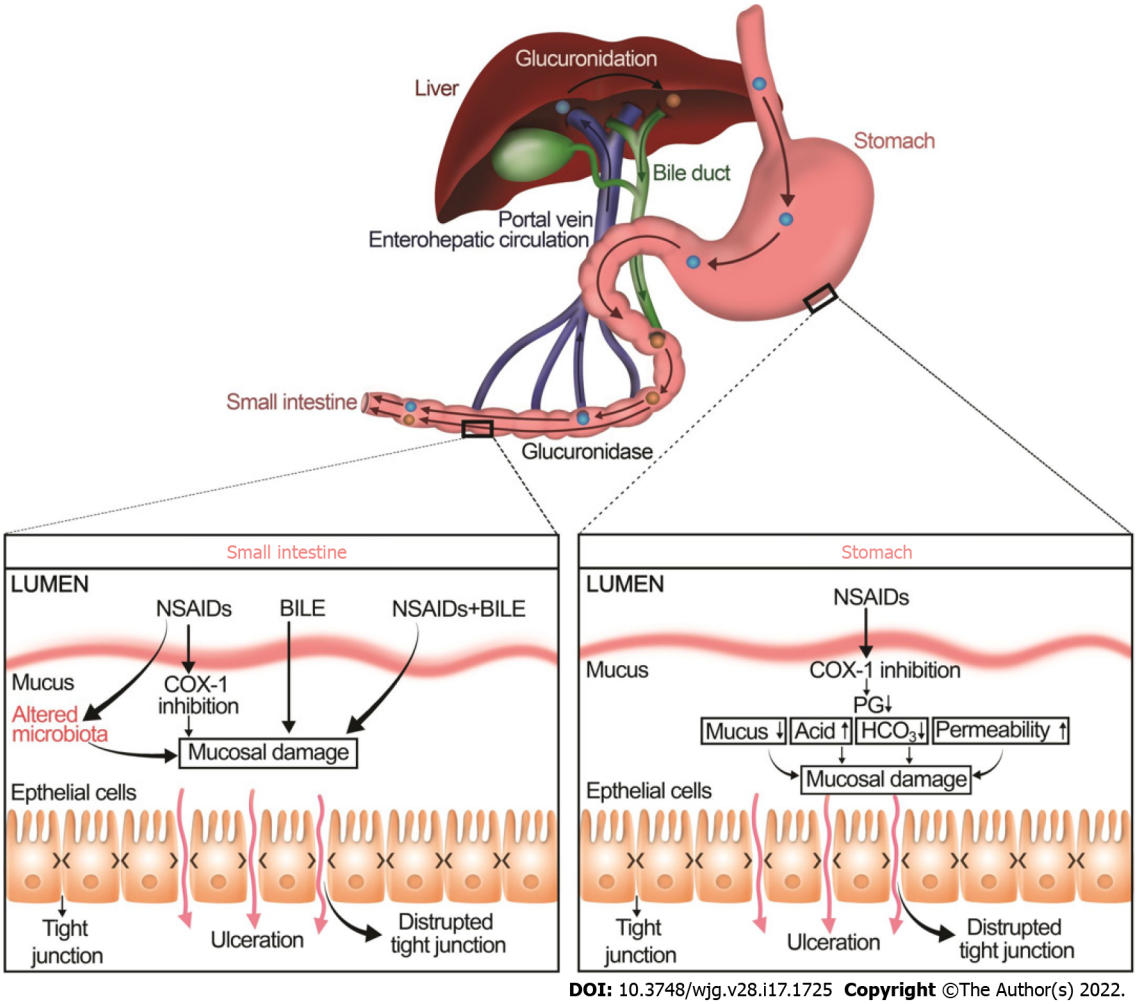
Although the gut epithelium can maintain normal homeostasis in the presence of modest or transient exposure to injurious stimuli, high level or extensive interactions with noxious factors such as excessive secretion of gastric acid and pepsinogen, the substantial inflammation caused by inflammatory bowel disease, or toxic luminal contents including ethanol or medication such as non-steroidal anti-inflammatory drugs (NSAIDs) can unbalance the equilibrium between mucosal injury and healing (Figure 1A).

Gastric juice includes mucus, hydrochloric acid (HCl), bicarbonate, pepsin, and intrinsic factor secreted by mucoid cells, parietal (oxyntic) cells, and chief (zymogenic) cells in the stomach (Figure 1B). *Helicobacter pylori (H. pylori)* infection, a gram-negative bacterium responsible for 90% of duodenal and gastric ulcers, impairs the bicarbonate secretion and promotes gastric acidity as well[23]. Such hyperacidity may injure the mucosa, causing gastritis, duodenitis, peptic ulcer disease (PUD), or gastroesophageal reflux disease (GERD)[24].

The gastrointestinal mucosa is subjected to numerous physical forces such as strain and pressure during both normal gut function and illness. For instance, luminal chyme, peristalsis contractions, rhythmic villous motility, and some pathological conditions such as inflammatory bowel disease (IBD) may adversely impact GI mucosal healing by increasing luminal pressure[25-29]. Such pressure increases have been shown to inhibit mucosal healing, at least in mice, despite increased mucosal proliferation, and appear to act by inhibiting the cell motility required for restitution[28].

The balance between mucosal injury and healing may also be shifted by drugs such as NSAIDs, corticosteroids, bisphosphonates, potassium chloride, steroids, and fluorouracil[23,30,31]. In particular, many studies have documented that NSAIDs decrease mucus hydrophobicity as measured by contact angle goniometry whereas prostaglandins, gastroprotective compounds, increase the contact angle of gastric mucosa[32,33]. NSAIDs, the most commonly prescribed medications, increase the development of ulcers in the upper and lower GI tract by two distinct mechanisms (Figure 2)[34-37].

NSAIDs injure the upper GI mucosa mainly by cyclooxygenase (COX)-1 inhibition, resulting in a decrease in prostaglandins, mucus, and bicarbonate secretion. Moreover, NSAIDs also alter another important component of mucosal defense, the gastric microcirculatory system. Upon irritation, the gastric mucosa normally increases blood flow to remove any toxins, bacterial products, or back-diffusing acid. Impairment of this hyperemic reaction increases the vulnerability of gastric mucosa to damage[38]. Inhibition of prostaglandins, potent vasodilators, by NSAIDs leads to an increase in vascular tone and thus reduces gastric mucosal blood flow[39], consequently, increases ischemic tissue damage and exacerbating the mucosal injury[40]. NSAIDs may also induce local gastric mucosal injury independent of prostaglandin deficiency[41]. NSAIDs may lyse phospholipids from mucosal epithelial cells and may increase mucosal permeability, which then allows mucosal exposure to luminal aggressive factors such as bacteria and gastric acid[42].



DOI: 10.3748/wjg.v28.i17.1725 **Copyright** ©The Author(s) 2022.

Figure 2 Non-steroidal anti-inflammatory drugs induce mucosal injury in the upper and lower gastrointestinal tract by two distinct mechanisms. In addition to principal luminal aggressors such as acid, pepsin, *Helicobacter pylori* in the stomach and acid, bile, and pathogens in the small intestine, nonsteroidal anti-inflammatory drugs (NSAIDs) increase mucosal damage in both upper and lower GI by two different mechanisms. In the stomach, the inhibition of COX-1 by NSAIDs reduces prostaglandin secretion which in turn reduces mucus and bicarbonate secretion and increases acid secretion, resulting in increased permeability and eventually mucosal damage. In the small intestine, NSAIDs bind to bile in the enterohepatic circulation. This potentiates the mucosal damage caused by bile. NSAIDs also increase mucosal damage in the small intestine by altering the gut microbiota. The NSAID-associated increase in enteric gram-negative bacteria appears to contribute to intestinal lesions by increasing inflammation. NSAIDs: Nonsteroidal anti-inflammatory drugs.

The molecular and cellular mechanisms of NSAID-induced lower GI mucosal injury are clearly distinct from NSAID-induced upper GI injury[42,43]. As in the stomach, NSAIDs may inhibit COX-1 and contribute to mucosal damage. However, unlike gastric injury, the bile acid and intestinal microbiota play a crucial role in the pathophysiology of NSAID-induced intestinal injury[42,44]. NSAIDs and gut microbiota have complex and dynamic interactions. The gut microbiota can alter the efficacy and toxicity of NSAIDs either directly by biotransforming them into metabolites or indirectly by altering the host metabolism (*e.g.*, interfering with hepatic function)[45]. On the other hand, NSAIDs themselves can directly change the composition and function of the gut microbiota or indirectly by altering the physiological functions of the host[45]. For instance, NSAIDs alter the intestinal microbiome by increasing the total number of bacteria and the proportion of gram-negative bacteria, which seems to be linked to the activation of toll-like receptor (TLR) 4 that increases inflammation and contributes to an intestinal injury[46-48].

NSAIDs make complexes with bile acids by glucuronidation in the liver. This interaction alters the stability and structure of bile acids and potentiates bile acid toxicity in the lower GI tract[42]. These NSAID-bile acid complexes are secreted into the duodenum and subsequently reabsorbed back in the ileum *via* the enterohepatic circulation. Within the intestinal lumen, particularly, in the colon, conjugated primary bile acids are deconjugated into more toxic secondary bile acids, mainly by the gram-positive bacteria[49]. There is crosstalk between the microbiome and the bile acids because bile acids can control the composition of the intestinal microbiome, which in turn regulates the composition and size of the bile acid pool[50,51]. Alteration in the colonic microbiota may cause a shift towards to generation of more toxic secondary bile acids, which eventually increase intestinal permeability, particularly in the colon, bacterial translocation, and mucosal inflammation[52-54].

NSAID-induced ulcers are traditionally treated with proton pump inhibitors (PPIs) or histamine-2 receptor antagonists (H2-antagonists)[55,56], which permit ulcer healing by reducing gastric acid secretion without directly affecting mucosal restitution[5,57,58]. Although PPIs have historically been co-prescribed with NSAIDs to ameliorate gastroduodenal injury and are used to treat NSAID injury, such use may increase the risk of a different problem. There is no evidence that gastric acid plays a key role in the pathogenesis of NSAID-induced lower GI[42,59]. PPIs may worsen NSAID-induced enteropathy by increasing gastric pH and thus changing the enteric microbiome by increasing the number of gram-negative bacteria[35,42,60-62]. Thus, even though PPIs are still recommended to treat upper GI ulcers, their prophylactic use with NSAIDs to prevent upper GI injury is no longer recommended unless the patient has a moderate to high risk of peptic ulcer disease[62,63]. Similar concerns are likely to exist for H-2 blockers.

Inflammatory bowel disease is a broad term to describe disorders including Crohn's disease (CD) and ulcerative colitis (UC) that are characterized by excessive activation of the mucosal immune system to normal microflora. This causes chronic inflammation and damages the gut mucosa[64,65]. Since the etiology of IBD is still unclear, the primary goal of treatment is centered on the elimination of inflammation with medical therapies such as 5-aminosalicylate, antibiotics, corticosteroids, immunosuppressants, and biological therapy[66-68]. Management of IBD with targeted therapies has been discussed in detail in a recent review[68]. However, none of these therapies is perfect, and even if patients achieve symptomatic remission, maintaining that remission can be challenging[69]. Recent evidence highlights the importance of mucosal healing over and above symptomatic remission in the quality of life and long-term prognosis of IBD patients[70-72].

MUCOSAL HEALING PROCESSES

Once an injury has occurred, diverse processes such as redifferentiation to a migratory phenotype[73-75], migration, proliferation, and eventual redifferentiation back to more specialized cells after healing are all regulated by various factors including growth factors, cytokines, physical forces, and the extracellular matrix itself. These coordinate healing of the injury (Figure 1). At the subcellular level, wounding of the apical plasma membrane is common in the epithelial cells of the intact, normal functioning stomach and intestines *in vivo* after mechanical and chemical stressors[8,76,77]. Since maintenance of plasma membrane integrity is essential for cell viability, the wounded cell rapidly repairs the injury to restore internal homeostasis and prevent cell death. Plasma repair processes such as tension reduction, budding, patch, endocytosis, and exocytosis may be triggered by the toxic level of Ca^{2+} influx through the plasma membrane wound to then reseal the injured plasma membrane[78,79].

Relatively small or superficial multicellular mucosal injury undergoes complex wound healing processes that quickly reconstitute the mucosal barrier, depending on the size and depth of the injury. Small wounds, less than eight cells in size, may close by the spreading of neighboring cells and formation of new cell-cell contacts[80,81] or by purse-string wound closure, which involves the formation of a multicellular actin cable purse string around the wound, with actin cables that parallel the wound edge. This then contracts, pulling the adjacent cells together[5,82].

Mucosal injury involving more than eight cells is generally too large for purse-string wound closure. This then requires restitutive epithelial sheet migration to close the injury. Depending on the size and depth of these larger wounds, wound closure will require a longer healing time and may require one or more complex overlapping processes such as differentiation, proliferation, and angiogenesis for wound healing[5,83,84].

Restitution requires a phenotypic redifferentiation. Although some authors describe the initial steps of this process as dedifferentiation, it is the firm opinion of the senior author that this should rather be considered a redifferentiation toward a migratory phenotype. The gut epithelium normally consists of a monostratified layer of differentiated epithelial cells. At the edge of a mucosal wound, epithelial cells change their phenotype from differentiated columnar enterocytes or gastric cells to a migratory phenotype. They lose their typical morphology and (for enterocytes and parietal cells) their microvilli [85], disassemble their apical specialized membrane components[86], flatten out and extend lamellipodia toward the defect. Such migrating cells adopt a squamous morphology with altered integrin[87-89] and cytoskeletal organization[73,85] and specialized cell signaling pathways[90-93] that adapt these cells toward motility (Figure 1C)[73,85,94-96] Moreover, it is worth noting that these signaling events are not only regulated by the activation of signaling proteins but also by the distribution and the amount of the signaling proteins within the migrating cells. For instance, both the actual amount of total focal adhesion kinase (FAK) and the amount of active FAK decrease while the ratio of activated to total FAK increases both in vitro[94] and in vivo[92] as the epithelial cells shift to the migratory phenotype[73]. Similarly, both paxillin protein and tyrosine-phosphorylated paxillin decrease in migrating cells compare to static cells[94]. (Paxillin is an adapter protein critical to focal adhesion complex assembly and disassembly in response to various stimuli.)[97-100]. Total p38, ERK1, and ERK2 proteins do not show differences between migrating and static cells[94]. However, phosphorylated p38 increases, and phosphorylated ERK1 and ERK2 decreases in motile cells compared with nonmigrating

cells[94].

Furthermore, the distribution of these signaling proteins also changes in migratory phenotype. In confluent cells, FAK localizes mainly in a perinuclear pattern while FAK appears explicitly at the cell borders contacting other cells in motile cells, with FAK immunoreactivity decreasing toward the migrating lamellipodia that face the wound edge[94]. In contrast to FAK, paxillin is localized at the lamellipodial edges in migrating cells[94]. The difference is more than semantic because considering these migratory cells as a specialized phenotype opens up the possibility for therapy to modulate that phenotype and thereby promote mucosal healing.

The transverse actin cables that drive purse-string closure for smaller wounds line up parallel to the wound edge at the migrating front, connected by cell-cell contacts, and unite the migrating front, so that these redifferentiated cells collectively migrate as a sheet, a.k.a., restitution, to close the wound (Figure 1C)[101-103]. Slightly deeper wounds that injure the basement membrane expose the cells to the interstitial extracellular matrix. While the basement membrane is predominantly laminin and type IV collagen, the deeper interstitial matrix is rich in type I collagen, across which the cells may migrate more rapidly[104,105].

After the closure of the wound by successful restitution, the migrating cells must redifferentiate back to the more specialized phenotypes required for the normal biology of the mucosa (Figure 1D)[102]. Tarnawski *et al*[106] have demonstrated the critical relationship between defective redifferentiation of these migratory cells and subsequent ulcer recurrence. This will be considered in more detail below.

If the wound surface area is extensive, restitution will likely be insufficient to seal the wound. In this situation, epithelial cell proliferation increases behind the migrating cells to create a larger pool of epithelial cells that can then migrate across and cover the defect (Figure 1C)[107]. However, if the wound extends into deeper layers such as the submucosa and muscularis, these must also be reconstructed for healing by processes beyond the scope of this review. In particular, the reconstitution of nutrient vessels in the submucosa is critical for mucosal wound healing because these provide oxygen and nutrients to the mucosa and remove waste products from the wound site[108,109]. This neovascularization can occur by two distinct processes called angiogenesis and vasculogenesis[110-114]. Angiogenesis refers to the process where new blood vessels are formed from preexisting blood vessels from the wound's adjacent vasculature by sprouting and forming tube-like structures and networks. Vasculogenesis is the *de novo* formation of new blood vessels from the differentiation of bone marrow-derived progenitor stem cells.

RESTITUTION AND QUALITY OF ULCER HEALING AS THE SINE QUA NON FOR WOUND HALING

GI ulcers have traditionally been assessed in clinical settings by a superficial visual endoscopic examination that cannot assess the histological and ultrastructural characteristics of the mucosa or deeper layers. Ulcer recurrence is, unfortunately, common, with rates exceeding 60% if the underlying problem has not been successfully addressed[23]. Recurrence of GI ulcers may be related to many factors including gastric acid secretion, *H. pylori*, NSAIDs, hormonal complications, size and depth of ulcers, anti-ulcer treatment, age, gender, comorbidity, alcohol consumption, and smoking[115-118]. In 1991, Tarnawski *et al*[119] drew attention to the relationship between recurrence of ulcers and ultrastructural abnormalities of deeper layers such as poor `redifferentiation, dilation of glands, reduced mucosal height, and disorganized microvascular network after ulcer healing and proposed the concept of the quality of ulcer healing (QOUH)[119-121]. QOUH is defined as ideal ulcer healing, demonstrating flat ulcer scar, high functional restoration, and histological maturity of the regenerated tissue[115,122]. Many patients treated with PPIs for GI ulcers still suffered from a recurrence of ulcers despite continuous anti-ulcer therapy[115,122-124]. It appears that acid inhibition by PPIs or H_2-antagonists may be insufficient for successful high-quality gastroduodenal ulcer healing because low levels of prostaglandins and high levels of oxygen free radicals entail poor QOUH and thus potentiate ulcer recurrence[122,125,126].

Overall, cumulative data highlight the necessity of QOUH for successful and permanent ulcer healing and point out that contemporary treatments such as PPIs and H_2-antagonists do not always provide such high-quality healing. Therefore, to improve QOUH and decrease the rate of recurrence of GI ulcers, new antiulcer drugs need to be developed to address this. Investigation of the endogenous biologic regulation of mucosal healing, suggests new therapeutic targets, both extracellular and intracellular.

REGULATORS OF MUCOSAL HEALING AND POTENTIAL NEW THERAPEUTIC TARGETS

Supplementing available therapeutic modalities that attempt to minimize or reduce injury, investigators have more recently focused on enhancing mucosal defense or promoting mucosal repair. Both mucosal defense and mucosal healing processes such as restitution, proliferation, angiogenesis, and vasculogenesis can be influenced by acid secretagogues, growth factors, trefoil peptides, cytokines, angiogenic factors, luminal nutrients, and the gastrointestinal microbiota[5,25,127]. In addition, physical forces like strain and pressure, engendered by peristalsis, villous motility, and interaction with luminal contents can influence intestinal epithelial migration and proliferation in a complex manner influenced by the deposition of fibronectin at the site of injury[25,128,129].

Acid secretagogues

Under physiological conditions, the stomach protects itself against various forms of endogenous and exogenous injury, primarily by gastric acid. Gastroprotective mechanisms could be triggered by acid secretagogues such as gastrin, histamine, and thyrotropin-releasing hormone (TRH)[130-132]. Pentagastrin, synthetic gastrin, stimulates gastroprotection in acidified aspirin-induced gastric injury in rats, likely through the activation of histamine-2 receptors, since this is abolished by ranitidine[133]. However, exogenous gastrin protects the rat gastric mucosa against ethanol-induced lesions but not against aspirin-induced gastric damage in rats[134]. Several studies have shown that exogenous histamine-stimulated acid secretion also exerts a protective effect on the gastric mucosa against erosions induced by exogenous HCl in rabbits and frogs by stimulating a greater alkaline tide[135,136]. The central vagal activation by intracisternal injection of the thyrotropin-releasing hormone analog RX77368 enhances mucosal resistance as well by stimulating mucosal blood flow *via* prostaglandin-independent manner which eventually results in the removal of diffused acid from the subepithelial interstitial space [137]. In addition, RX77368 increases the thickness of the mucus gel *via* prostaglandin-dependent manner which slows down the acidification of surface cells[137]. The potential therapeutic adaptation of molecules like RX77368 and other acid secretagogues awaits the further exploration of the disparities between results depending on how the ulcers are induced, as well as challenges with their pharmacologic delivery.

Growth factors, trefoil peptides, and cytokines

Growth factors have diverse pathophysiologic effects, including cytoprotection against destructive agents, epithelial wound healing in response to injury[102,138-140], and angiogenesis[141-144]. Epidermal growth factor (EGF) and transforming growth factor TGF-α are structurally related but different polypeptide growth factors[145]. They both bind to the same cell-surface EGF/TGF-α -receptor and induce generally similar effects[145].

EGF may act in a cytoprotective fashion against mucosal injury by increasing secretion of mucus and bicarbonate[146-148], enhancing blood flow[149-151], or releasing other cytoprotective agents such as prostaglandins[152]. Pretreatment of the stomach[153,154], small intestine[146,155], and colon[149,150] tissues, both *in vivo* and *in vitro*, with EGF decreases mucosal damage by various noxious agents. TGF-α is similarly cytoprotective against gastric injury by ethanol, acetic acid, or aspirin[156,157]. Pretreatment of Caco-2 cells with EGF prevents deoxycholate-induced cellular damage, at least in part, by changes in intracellular calcium content[158], suggesting that EGF exerts direct cytoprotective effects on the epithelium in addition to its effects on blood flow and mucus secretion. Furthermore, because this EGF-induced cytoprotection was observed following only 30 minutes of pretreatment (insufficient for proliferation), these results also suggest that this protection is independent of the mitogenic effects of EGF [158]. Consistent with this idea, adding EGF to the basal surface of rabbit primary gastric epithelial cell monolayers cultured on collagen-coated inserts enhances cytoprotection against apical surface acid by opening the plasma membrane calcium channels and increasing intracellular calcium[159].

In addition to their cytoprotective effects, EGF and TGF-α also promote mucosal healing after injury, stimulating both cell motility and cell proliferation[104,140,154]. Indeed, part of the epithelial mucosal shift to a phenotype adapted to wound healing may be an increase in sensitivity to these growth factors. A recent study demonstrated a 75-fold increase in the number of cells expressing detectable EGF-receptors at the ulcer margin after gastric ulcer induction in rats[160]. Either parenteral or local submucosal intra-ulcer injection of EGF caused a comparable acceleration in the healing of acetic-acid-induced rat gastric ulcers, at least in part by increasing gastric blood flow, decreasing gastric acid secretion, and upregulating COX-2 expression[161]. This is in agreement with previous reports suggesting that COX-2 -influences mucosal healing by regulating both the hyperemic response and epithelial cell proliferation[162,163].

The trefoil peptides may also offer new opportunities for therapy because they are important both for mucosal defense[164-166] (by increasing the viscoelasticity of mucus[167,168]) and mucosal repair[169-171] (by influencing reepithelization[171] and inflammation[172]). The trefoil factor (TFF) family includes TFF1 (also called pS2) expressed in gastric surface mucous cells, TFF2 (also called a spasmolytic polypeptide or SP) produced by mucus-producing gastric mucous neck cells, antral gland cells, and duodenal Brunner's glands, and TFF3 (also called intestinal trefoil factor or ITF), predominantly

produced by goblet cells of the small and large intestine and found abundantly within the mucus. A trefoil domain consists of three loops created by disulfide bonds and all TFFs are comprised of two trefoil domains[173]. Trefoil peptides have been detected in different forms including monomers, dimers, and complexes with other molecules. This influences the strength of their association with mucin[173]. In particular, TFF dimers tightly interact with mucin, increasing the viscosity and elasticity of mucus in comparison to the effect of TFF monomers[167,174].

The TFFs are mostly distributed to the basolateral domain of gastric neck cells and parietal cells in the stomach, the Paneth cells in the small intestine, and the crypt cells in the colon[175]. TFF interactions and specific functions have been discussed in detail in a recent review[176]. A specific TFF receptor has not yet been described. However, some binding and functional studies propose potential TFF receptors that may influence epithelial restitution. TFFs have been reported to bind to transmembrane proteins such as the β1 integrin subunit, CRP-ductin, CXC chemokine receptor (CXCR) 4, CXCR7, proteinase-activated receptor (PAR) 2, PAR4, leucine-rich repeat and Immunoglobin-like domain-containing protein (LINGO) 2, LINGO3, and EGFR[177-181]. TFF3 enhances wound healing by activating EGFR and inducing MAPK[182] and PI3K/Akt signaling pathways *in vitro*[183] whereas TFF2 directly activates CXCR4 and enhances the phosphorylation of ERK1/2 and Akt in gastric epithelial cells[184]. Indeed, the CXCR4 antagonist AMD3100 blocks TFF2-dependent gastric epithelial repair[170]. TFFs, specifically TFF2 and TFF3, regulate epithelial motility *via* integrin-binding and activating focal adhesion kinase as well[175]. TFF2 also promotes cell migration *via* PAR4[185], while TFF3 activates PAR2[186]. Furthermore, TFF2 peptide may be required for optimum activity of EGFR and/or EGF signaling in the stomach because heparin-binding EGF and TGF-α do not induce EGFR activation in the stomachs of *Tff2* KO mice[177].

Oral administration of trefoil peptides, recombinant human SP, or rat ITF protects the gastric mucosa against ethanol or indomethacin-induced injury in a prostaglandin-independent manner[164]. Similarly, a more recent study has also shown that both parentally and topically applied trefoil peptides reduce ethanol-induced gastric damage, assessed by measurement of gastric mucosal Na^+ leakage and area of macroscopic injury in rats[187]. Complementing these results, transgenic mice that overexpress human TFF1 display increased resistance to indomethacin-induced small intestinal damage[188] whereas ITF-deficient mice are more prone to ulceration and hemorrhage after oral administration of dextran sulfate sodium (DSS)[189], suggesting that trefoil peptides play an important role in GI mucosal protection. There are likely to be several mechanisms by which the trefoil peptides promote mucosal healing. For instance, exogenous recombinant TFF2 increases epithelial wound healing by decreasing inflammation by negatively regulating IL-12 production from macrophages and dendritic cells[172] whereas exogenous TFF3 activates epithelial wound healing *via* the Na/H exchanger-2[171] and accelerates gastric repair *via* a mechanism that does not require cyclooxygenase activation[170].

TGF-β expression increases in affected mucosa from patients with IBD[190], and at the edge of human gastric and colonic ulcers[92]. Intravenous administration of recombinant bone morphogenetic protein (BMP)-7, a subfamily of TGF-β superfamily, for five days significantly accelerates the healing of trinitrobenzene sulfonic acid (TNBS)-induced colitis in rats by decreasing the expression of pro-inflammatory cytokines (IL-6, TNF-b, ICAM-1)[191]. It should be noted that all of these growth factors and cytokines mentioned in this section interact in a complex fashion, and TGF-β potentiates many of them [127,192,193]. TGF-β also stimulates the synthesis of FAK, a key intracellular signal protein for cell motility and proliferation[92].

Basic fibroblast growth factor (bFGF) and hepatocyte growth factor (HGF) stimulate the healing of acetic acid-induced gastric lesions in rats similarly when administered intraperitoneally or by local submucosal injection at the ulcer site, suggesting that these growth factors also accelerate mucosal repair[161]. The healing of gastric ulcers by bFGF and HGF may involve enhancement of gastric blood blow around the ulcer, suppression of gastric acid secretion, and upregulation of COX-2 expression [161].

When the mucus barrier fails due to overexposure to the noxious agents, acid-back diffusion occurs. In healthy mucosa, increased blood flow response rapidly increases the circulation of pH neutral or slightly alkaline blood through the mucosa to neutralize the diffused acid[103]. Moreover, new vasculature is needed to perfuse and support the newly forming tissue. Therefore, wounds deeper than the epithelial layer also require the formation of new blood vessels in granulation tissue for mucosal healing. Like restitution and proliferation, neovascularization is also modulated by growth factors. Vascular endothelial growth factor (VEGF), platelet-derived growth factor (PDGF), nerve growth factor (NGF), fibroblast growth factor (FGF), and angiopoietin-1(Ang1) are essential for blood vessel regeneration *via* angiogenesis and vasculogenesis following mucosal damage[141-144] and can therefore facilitate deep wound healing[112,193-195]. VEGF, the most potent angiogenic factor, is an indispensable regulator of angiogenesis, making it potentially an ideal candidate to induce angiogenesis/vasculogenesis in mucosal healing. Since VEGF is digested in the lumen by proteolytic enzymes, Jones *et al*[141] used a single injection of a nonviral naked DNA plasmid encoding VEGF and Ang1 directly into the injured area to reduce such deleterious effects. They demonstrated that local gene therapy with a combination of VEGF and Ang1 cDNAs increases gastric ulcer healing and generates more mature vessels and a more complete epithelial structure in acetic acid-induced gastric injury in rats, suggesting that a combination of growth factors may have better therapeutic potency than the use

of any individual factor[141]. Similarly, local gene therapy with serum response factor (SRF) accelerates ulcer healing as well as muscle restoration in acetic acid-induced gastric ulcers in rats[196]. A recent study indicated that angiogenesis and vasculogenesis go hand in hand while forming new vessels in granulation tissue[197]. Delivering such naked genes to a damaged site at endoscopy may be a promising tool to treat such ulcers by increasing the bioavailability of essential GFs.

Cytokines are also involved in the regulation of mucosal barrier function at multiple levels including mucosal homeostasis and inflammation[198]. Proinflammatory cytokines such as tumor necrosis factor (TNF) and IL-13 are upregulated in the inflamed mucosa of IBD patients. Anti-TNF therapy promotes mucosal healing in many patients, but not all patients respond to anti-TNF therapy. Many investigators have therefore focused on other cytokines to improve mucosal barrier function. Unfortunately, many of these attempts have ended disappointingly. For instance, experimental colitis in mice is controlled by using ROR-gamma null Th17 cells, which cannot produce IL17A/F and not induce colitis[199]. However, an anti-IL17A monoclonal antibody not only failed to improve CD in clinical trials but actually aggravated adverse symptoms[200]. IL-13 has seemed similarly promising in pre-clinical studies[201-204], but a trial of IL-13 blockade in UC failed[205]. Such failures of blockade of pro-inflammatory cytokines have recently prompted attempts to use anti-inflammatory IL-10 family cytokines to promote colonic mucosal healing. IL-10 is a major anti-inflammatory cytokine that targets hematopoietic cells in various autoimmune diseases[206]. Gene therapy with a single intravenous injection of an adenoviral vector encoding IL-10 (AdvmuIL-10) diminishes TNBS-induced colitis in mice, decreasing histological injury scores, weight loss, stool markers of inflammation (IL-1β and TNFR-II), and serum amyloid protein in comparison to empty cassette virus (Adv0) or PBS treated mice in TNBS-induced colitis model[207]. Gelatin microspheres containing IL-10 have been developed to increase local bioavailability as a sustained release preparation[208]. Gelatin-microsphere-IL-10 treatment remarkably decreases colonic inflammation in IL-10(-/-) mice compared to treatment with IL-10 alone treatment, at least in part by decreasing IL-12 mRNA expression and down-regulating CD40 expression in macrophage-1 positive cells[208]. However, recombinant IL-10 did not improve clinical symptoms in Crohn's disease[209]. Such disappointing results raise the possibility that manipulating a single cytokine may have unpredictable results because of its effects on the web of compensatory pro-inflammatory and anti-inflammatory cytokine pathways in the inflamed mucosa[198].

One cytokine that may be promising is IL-22. Even though it belongs to the IL-10 family of cytokines, IL-22 is unlike IL-10 in that it targets non-hematopoietic epithelial cells. IL-22 is produced by, apart from the adaptive T cell, innate cells including innate lymphoid cells (ILCs), specifically ILC3 cells in the GI tract. IL-22 has dual roles in inflammation. It can act as a protective (anti-inflammatory) cytokine or a pathological (pro-inflammatory) cytokine[210]. IL-22 influences various tissue epithelial functions such as inflammation[211,212], barrier integrity, regeneration, wound healing[213-215], and host defense against pathogens[216,217]. Beneficial effects of IL-22 have been demonstrated in various murine colitis models[210,218]. However, IL-22 actually appears to worsen the anti-CD40-induced colitis model, in that neutralization of IL-22 reduces the weight loss and colitis scores caused by the anti-CD40 injection and administration of IL-22 then recreates the colitis[219]. Thus, although most animal studies raise the possibility that recombinant human (rh) IL-22 might be a promising therapy for IBD, it remains unclear which effect will be seen in human disease. However, as for other cytokines, the short half-life of rhIL-22 (less than 2 h) limits its clinical applications. Several groups have sought to overcome this obstacle by engineering recombinant fusion proteins with a half-life of 1-2 wk to improve the cytokine's pharmacokinetic properties. Currently, seven IL-22 clinical trials have been investigated for different indications. UTTR1147A is a human IL-22 fusion protein that links the human IL-22 with the Fc portion of human immunoglobulin (Ig) G4, which is prepared for IBD studies[220]. Extensive *in vitro* and *in vivo* studies suggest that UTTR1147A decreases histologic colitis severity by a pathway involving STAT3 activation[220]. These pre-clinical studies demonstrate that UTTR1147A is well tolerated and is not associated with increased inflammatory cytokines in mouse, rat, and monkey studies[220]. A randomized phase-I healthy volunteer study of UTTR1147A demonstrated satisfactory safety and pharmacokinetic profile[221]. A phase-II open-label extension study to evaluate the long-term safety and tolerability of UTTR1147A in patients with moderate to severe UC and CD continues with an estimated completion date in 2025[222].

Therapeutic use of growth factors (except BMP-7) may be limited by their low protein stability[144]. In addition, despite their beneficial effects on the GI tract, long-term or systemic use of any growth factors, trefoil peptides, or cytokines that stimulate cell proliferation, either for cytoprotection or for mucosal healing, may raise concerns about inducing hyperproliferative or dysplastic lesions and potential tumorigenesis. This remains an open issue for such mitogens.

Luminal nutrients and GI microbiota

Luminal nutrients and microbiota are also crucial for the maintenance and repair of the gut mucosa. Short-chain fatty acids (SCFAs) are produced by commensal microbiota, mostly by gram-positive anaerobic bacteria, and are essential for perpetuating intestinal health[223,224]. These SCFAs, especially butyrate, are a major energy source for enterocytes and support gut homeostasis[225-227]. SCFAs may stimulate the differentiation of epithelial cells and their proliferation in vivo[228-230], whereas they promote only differentiation in cell culture models but inhibit proliferation and migration[231-235].

Long known as an energy supply for colonocytes and enterocytes, SCFAs have attracted may also enhance gut barrier function. SCFAs decrease acid-back diffusion by dilating arterial walls and increasing blood flow in gut mucosa[236,237]. In addition, several studies have documented improved intestinal barrier function after SCFA supplementation[238-240]. The SCFAs activate 5′ adenosine monophosphate (AMP) kinase and therefore promote tight junction assembly, which in turn enhances intestinal barrier function[241,242]. However, a recent clinical study found no evidence that butyrate monotherapy or a combination of three SCFAs offered any advantage over placebo in improving the disease activity index in ulcerative colitis patients receiving maintenance oral anti-inflammatory medication[243].

Amino acids such as arginine, histidine, and glutamine promote enterocyte proliferation and decrease mucosal permeability by regulating tight junction proteins[244-247]. A recent study proposed that histidine and arginine play an important role in stimulating intestinal restitution, probably stimulating FAK *via* the TGF-β/Smad2 signaling pathway[248]. Glutamine modulates the phenotype of gut epithelial cells by stimulating proliferation and decreasing differentiation *in vitro*[249]. Similarly, many studies have been shown that glutamine also promotes cell proliferation of intestinal epithelial cells in weanling mice[250] and weaning piglets[251], prevents mucosal injury, and regulates enterocyte restitution following acetic acid-induced intestinal injury in rats[252].

Biologically active phospholipids in milk, phosphatidylcholine (PC) and phosphatidic acid (PA), and their metabolites such as lysophosphatidic acid (LPA), all act to increase the barrier function of GI mucosa by increasing the hydrophobicity of the mucus[253]. This makes the tissue non-wettable[10] and provides mucosal protection against aspirin-induced gastric injury in mice[253]. Dietary essential omega-6 fatty acids can enhance the biosynthesis of prostaglandins and increase the GI mucosal barrier [254]. Milk fat globule-epidermal growth factor 8 (MFG-E8), a glycoprotein found in mammary epithelial cells but also produced by lamina propria macrophages, also plays a vital role in modulating enterocyte migration along the crypt-villus axis[255].

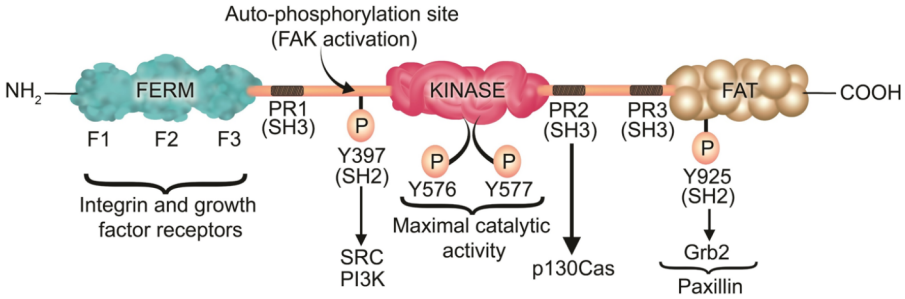
Extracellular matrix

Epithelial sheet migration during gut-healing requires crosstalk between focal adhesion (FA) complexes in the lamellipodium and the ECM. The extracellular matrix is an extremely dynamic meshwork comprised of proteins, glycosaminoglycans, and glycoconjugates. Its composition and organization differ between tissue types and with physiological and pathological conditions[256,257]. Besides its structural support, the ECM has a direct role in gastrointestinal wound healing by inducing extensive signaling cascades[258-260]. Plasma and tissue fibronectin accumulating in deeper wounds also help to shift the cells to a phenotype that responds to repetitive deformation by increased motility rather than by classical differentiation[129,261]. ECM remodeling is performed by matrix proteinases such as matrix metalloproteinases (MMPs), lysyl oxidases, and heparanases[262]. The gelatinases, a subgroup of MMPs, consist of two proteinases gelatinase A (MMP-2) and gelatinase B (MMP-9). In particular, MMP-9 is upregulated in the inflamed intestinal mucosa of IBD patients[263-267]. Furthermore, anti-gelatinase neutralizing antibodies have been reported effective in murine DSS-induced colitis[268]. However, a phase II, randomized, placebo-controlled study found that the MMP-9 inhibitor andecaliximab did not induce a significant symptomatic or endoscopic response in patients with active Crohn's disease[269]. This lack of efficacy in Crohn's disease prompted the termination of another clinical trial of the same agent in active ulcerative colitis[270]. Thus, while modulation of matrix metalloproteinases remains an attractive target in IBD, further exploration of the science involved and the reasons for the failure of the clinical trial are needed.

Regulation of cytoskeleton

Epithelial restitution begins at the edge of the wound with the redifferentiation of epithelial cells. Reorganization of the actin cytoskeleton is controlled by the Rho family of GTPases including RhoA, Rac1, and Cdc42 (Figure 1C)[93,271-273]. Epithelial cells then form protrusions called lamellipodia with new focal adhesions (FAs) at the leading edge of the motile cells. The migrating cell increases its contractile forces and disassembles focal adhesions at the rear edge allowing the entire cell to move forward[274-276]. Cell-cell linkages[276] transmit this force to other cells behind the migrating front and stretch the epithelial layer across the wound as a sheet. This sheet migration is characteristic of epithelial cells and differs from the individual cell motility displayed by other cell types.

The cytoskeleton, a complex and dynamic network of actin filaments, microtubules, and intermediate filaments, is also an important factor in wound healing[277]. Epithelial restitution relies on the coordination of forward protrusions and retraction forces at the rear edge, which is orchestrated by the actin and microtubule cytoskeleton[278]. In the lamellipodium, the elongating actin filaments produce the driving forces for the protrusion while microtubules form a polarized network that permits organelle and protein transport throughout the cell during cell migration[279,280]. Intermediate filaments, however, are generally considered for the maintenance of the overall cell shape[280]. Alternatively, or in combination with therapy to reduce ongoing injury by improving mucus barrier function and promoting angiogenesis, one could consider attempting to directly stimulate restitution in order to accelerate barrier reconstitution. Thus, proteins that modulate cytoskeleton dynamics might be targeted for optimal wound repair. Fidgetin-like 2 (FL2), a microtubule-severing enzyme, regulates the



DOI: 10.3748/wjg.v28.i17.1725 **Copyright** ©The Author(s) 2022.

Figure 3 Focal adhesion kinase structure, phosphorylation sites, and its associated proteins. Focal adhesion kinase (FAK) contains an N-terminal band 4.1-ezrin-radixin-moesin (FERM) domain comprised of three lobes (F1, F2, and F3), a central kinase domain, a C-terminal FAT domain, and two linker domains with three PR regions that bind SH3 domain containing protein such as p130Cas. Y397 is the site of the FAK autophosphorylation, crucial for FAK activation, which interacts with proteins containing the SH2 domain such as Src and PI3K. Subsequently to the SH2 binding, Src binds to the PR1 SH3 domain (PXXP) and further phosphorylates the Y576/577 sites on FAK, which are crucial for the maximal catalytic activity of FAK. Further FAK phosphorylation at Y925 creates a binding site for Grb2. The phosphorylation of FAK-Y-925 and subsequent Grb2 binding disassociates paxillin from FAK, which results in FAK release from FAs, thus stimulating FA disassembly. The FERM domain regulates the interactions of FAK with growth factor receptors and integrins. The FAT domain recruits FAK to FAs by associating with paxillin. FERM: Band 4.1-ezrin-radixin-moesin; FAT: Focal adhesion targeting; PR: Proline-rich region; SH: Src homology; P: Phosphorylation.

organization of the microtubule cytoskeleton for faster and successful repair of murine wounds[281]. Actin remodeling proteins such as talin[282], Ehm^2[283], filamin-a[284], gelsolin[285], and flightless I (Flii)[286] have also been identified as potential new targets for improved wound healing. Unlike other members of the gelsolin family, Flii inhibits actin polymerization and FA turnover, thus decreasing migration[286,287]. Flii neutralizing antibodies (FnAb) decreased wound area with a quicker rate of healing in porcine and murine models of wound healing, respectively[288,289].

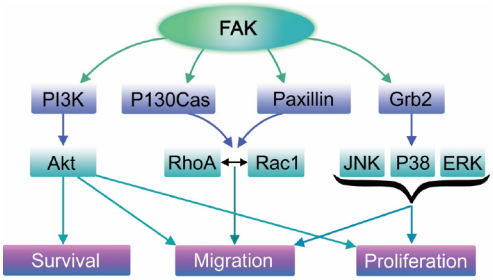
Regulation of FAs

Cell migration, and consequently wound healing, depend critically on the dynamics of assembly and disassembly of FAs. The subunit composition of integrin receptors and the downstream signaling pathways may vary in different scenarios[290-293]. Nevertheless, integrin binding to ECM triggers focal adhesion formation by recruiting many structural and signaling proteins including FAK, a non-receptor tyrosine kinase[294-298]. FAK regulates FA dynamics both by recruiting other FA proteins such as Src to FA sites and by phosphorylating other signaling and adapter FA proteins such as paxillin and p130Cas [299-301]. FAK also influences the cytoskeletal remodeling essential for cell migration by regulating the Rho family of small GTPases such as Cdc42, Rac1, and RhoA[302-305]. Inhibition of FAK inhibits cell migration[94,298].

Although FAK appears to activate cell motility and promote restitution, and FAK is indeed activated during cell motility, levels of both activated FAK and total FAK protein (including both active and inactive FAK) actually decrease in migrating GI epithelial cells *in vitro* and at the edge of human gastric and colonic ulcers *in vivo* even though the proportion of activated FAK increases (at least *in vitro*)[92, 94]. This reflects decreased FAK synthesis in cells that have adopted the migratory phenotype[306]. This apparently paradoxical reduction in this important protein makes FAK an attractive target for possible therapeutic intervention to promote mucosal healing.

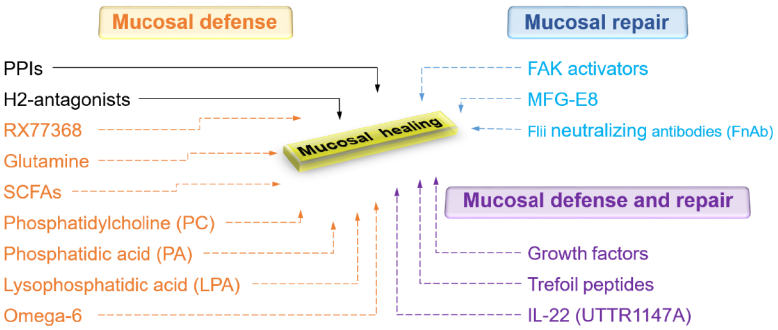
FAK is a 125 kDa protein comprised of an N-terminal FERM (band 4.1-ezrin-radixin-moesin) domain, a central kinase domain, three proline-rich regions that are binding sites for Src homology 3 (SH3) domain-containing proteins, and a C-terminal focal adhesion targeting (FAT) domain (Figure 3).

The FAT domain consists of a four-helix bundle[307] and is critical for targeting FAK to FAs *via* binding to paxillin[308]. In an inactive (autoinhibited) state there is an interaction between the FERM and kinase domains which prevents FAK autophosphorylation at Y397[309]. Upon competitive binding of candidate activating proteins such as the cytoplasmic regions of β-integrins or growth factor receptors on the F2 domain of FERM, the autoinhibited conformation of FAK is disassembled[310]. This conformational change allows Y397 phosphorylation, a key event in FAK activation[311]. In a subsequent step, Src is recruited and activated *via* SH2 binding to pY397 and SH3 binding to the PxxP sequence in the linker region, an essential step in promoting cell migration[311]. Then, Src phosphorylates the activation loop residues Y576 and Y577 of FAK and it acquires full catalytic activity after phosphorylation of the activation loop[312]. Phosphorylation of FAK at tyrosine 925 residue creates an SH2 binding site for the growth factor receptor-bound protein 2 (Grb2), adaptor protein[313]. The Grb2 binding site at FAK-Y-925 overlaps with one of the paxillin binding sites in the FAT domain of FAK[313]. The binding of Grb2 disassociates paxillin from FAK and potentiates the release of FAK from FAs[313]. On the other hand, paxillin acts as a scaffold protein for ERK signaling[305]. Subsequently, ERK may modulate FA turnover by further phosphorylating paxillin[305]. Therefore, Paxillin and Grb2 are critical FA proteins that interact with FAK and play an important role in FA turnover[97,313].



DOI: 10.3748/wjg.v28.i17.1725 **Copyright** ©The Author(s) 2022.

Figure 4 Focal adhesion kinase plays a crucial role in several signaling pathways that promote migration, proliferation, and survival. Upon its activation, focal adhesion kinase (FAK) directly binds PI3K, leading to the activation of Akt. Activated Akt then stimulates numerous cellular functions including cell survival, proliferation, and migration *via* various signaling cascades depending on the cell type and species. In addition, FAK may recruit Grb2 and subsequently activate the Ras/Raf/MAPK pathway, enhancing cell proliferation and motility. Finally, FAK may directly bind to paxillin and p130Cas, promoting lamellipodium formation, and thus migration *via* Rac GTPase activation.



DOI: 10.3748/wjg.v28.i17.1725 **Copyright** ©The Author(s) 2022.

Figure 5 Current and promising new therapeutic approaches to gastrointestinal mucosal healing. Green represents currently available drugs. Red represents promising new therapeutic approaches that increase mucosal defense. Blue represents promising new therapeutic approaches that promote mucosal repair. Purple represents promising new therapeutic approaches that stimulate both mucosal defense and repair. PPIs: Proton pump inhibitors; H2-antagonists: Histamine-2 receptor antagonists; RX77368: The thyrotropin-releasing hormone analog; SCFAs: Short-chain fatty acids; FAK: Focal adhesion kinase; MFG-E8: Milk fat globule-epidermal growth factor 8; Flii: Flightless I.

FAK has both a structural role as a scaffold for protein-protein interactions and a kinase function that phosphorylates many substrates in diverse signaling events[314,315]. Its non-kinase scaffolding function allows several different proteins to bind its N-terminal FERM domain and C-terminal FAT domain, tethering them into complexes (Figure 3). For instance, FAK may regulate cell migration serving as a scaffold for Src phosphorylation of p130Cas[316] in FAs. Similarly, nuclear FAK may promote cell survival functioning as a scaffold to stabilize p53-Mdm^2 complexes, promoting p53 ubiquitination and proteasomal degradation[317]. On the other hand, in its kinase signaling capacity, FAK triggers many downstream signals including the Ras/Raf/MAPK[97,296,318-320], p130Cas-Crk[321-324], and phosphatidylinositol 3-kinase (PI3K)-Akt pathways[317], which in turn coordinate to regulate cell proliferation, migration, and survival (Figure 4)[313,325].

Recent evidence suggests that direct modulation of FAK activity is possible, practical, and effective *via* small molecule FAK activators[326]. A novel small molecule with drug-like properties, ZINC40099027 (ZN27), that mimics the FERM domain of FAK has been identified from the ZINC database and activates FAK in human intestinal epithelial cells without activating Pyk2, the closest paralogue of FAK, or Src, another canonical nonreceptor tyrosine kinase within focal adhesions[327]. Indeed, ZN27 directly activates both full-length 125 kDa and its 35 kDa kinase domain, increasing the maximal activity (V_{max}) of FAK, suggesting that ZN27 is a highly potent and selective activator acting allosterically on the 35 kDa FAK kinase domain[328]. ZN27 not only activates FAK but also stimulates intestinal epithelial migration *in vitro* and mucosal healing in mice after ischemic injury or injury by indomethacin[327]. ZN27 also activates FAK in gastric epithelial cells and promotes gastric mucosal healing in mice subjected to chronic ongoing injury by aspirin[58]. Structure-activity-relationship studies have developed a library of novel FAK activators based on ZN27, that have drug-like properties, activate FAK, and stimulate epithelial sheet migration in vitro[329]. At least one such molecule (dubbed compound 3) demonstrates reasonable drug-like properties based on *in vitro*, *in vivo*, and *in silico* results with no obvious toxicity[329]. Further development of this lead molecule may offer the potential for a new therapeutic approach to actually stimulate mucosal healing by activating FAK.

CONCLUSION

Given the enormous impact of GI mucosal healing on human health, there is certainly a need to expand therapeutic options in this regard. A new understanding of the biology of mucosal healing suggests several different possibilities (Figure 5). These include FAK activators, UTTR1147A, endoscopic gene therapy for angiogenic growth factors, mucus barrier enhancement *via* the thyrotropin-releasing hormone analog RX77368 or trefoil peptides, enhanced energy for the mucosa with butyrate, and attempts to increase the regenerative ability of the epithelium with growth factors, cytokines, or trefoil peptides. Future work will determine which of these potentially promising avenues will prove successful and will need to balance their effects against potential risks and issues, including bioavailability, mitogenicity, and tumorigenesis.

FOOTNOTES

Author contributions: Oncel S and Basson MD equally contributed to this manuscript with regards to the conception and structure of the manuscript in addition to the literature review; The final draft of the manuscript was read and approved by all the authors.

Conflict-of-interest statement: The senior author (Basson MD) is co-inventor on patents applied for by the University of North Dakota describing the use of small molecule FAK activators to promote mucosal healing. The authors have no other conflicts of interest.

Open-Access: This article is an open-access article that was selected by an in-house editor and fully peer-reviewed by external reviewers. It is distributed in accordance with the Creative Commons Attribution NonCommercial (CC BY-NC 4.0) license, which permits others to distribute, remix, adapt, build upon this work non-commercially, and license their derivative works on different terms, provided the original work is properly cited and the use is non-commercial. See: https://creativecommons.org/Licenses/by-nc/4.0/

Country/Territory of origin: United States

ORCID number: Sema Oncel 0000-0001-5551-2271; Marc D Basson 0000-0001-9696-2789.

S-Editor: Gong ZM
L-Editor: A
P-Editor: Gong ZM

REFERENCES

1 **Li C**, Kuemmerle JF. Mechanisms that mediate the development of fibrosis in patients with Crohn's disease. *Inflamm Bowel Dis* 2014; **20**: 1250-1258 [PMID: 24831560 DOI: 10.1097/MIB.0000000000000043]
2 **Aviello G**, Knaus UG. ROS in gastrointestinal inflammation: Rescue Or Sabotage? *Br J Pharmacol* 2017; **174**: 1704-1718 [PMID: 26758851 DOI: 10.1111/bph.13428]
3 **Lam A**, Fleischer B, Alverdy J. The Biology of Anastomotic Healing-the Unknown Overwhelms the Known. *J Gastrointest Surg* 2020; **24**: 2160-2166 [PMID: 32524361 DOI: 10.1007/s11605-020-04680-w]
4 **Mortensen JH**, Lindholm M, Langholm LL, Kjeldsen J, Bay-Jensen AC, Karsdal MA, Manon-Jensen T. The intestinal tissue homeostasis - the role of extracellular matrix remodeling in inflammatory bowel disease. *Expert Rev Gastroenterol Hepatol* 2019; **13**: 977-993 [PMID: 31587588 DOI: 10.1080/17474124.2019.1673729]
5 **Basson MD**. Hierarchies of healing in gut mucosal injury. *J Physiol Pharmacol* 2017; **68**: 789-795 [PMID: 29550790]
6 **Powell RJ**, Bhargava J, Basson MD, Sumpio BE. Coculture conditions alter endothelial modulation of TGF-beta 1 activation and smooth muscle growth morphology. *Am J Physiol* 1998; **274**: H642-H649 [PMID: 9486269 DOI: 10.1152/ajpheart.1998.274.2.H642]
7 **Ahluwalia A**, Patel K, Hoa N, Brzozowska I, Jones MK, Tarnawski AS. Melatonin ameliorates aging-related impaired angiogenesis in gastric endothelial cells *via* local actions on mitochondria and VEGF-survivin signaling. *Am J Physiol Gastrointest Liver Physiol* 2021; **321**: G682-G689 [PMID: 34668398 DOI: 10.1152/ajpgi.00101.2021]
8 **McNeil PL**, Ito S. Gastrointestinal cell plasma membrane wounding and resealing in vivo. *Gastroenterology* 1989; **96**: 1238-1248 [PMID: 2703112 DOI: 10.1016/S0016-5085(89)80010-1]
9 **Liu X**, Xiao L, Wang JY. Posttranscriptional control of intestinal epithelium homeostasis by RNA-binding protein HuR. *Sheng Li Xue Bao* 2020; **72**: 325-335 [PMID: 32572430 DOI: 10.13294/j.aps.2020.0034]
10 **Lichtenberger LM**. The hydrophobic barrier properties of gastrointestinal mucus. *Annu Rev Physiol* 1995; **57**: 565-583 [PMID: 7778878 DOI: 10.1146/ANNUREV.PH.57.030195.003025]
11 **Wallace JL**. Prostaglandins, NSAIDs, and gastric mucosal protection: why doesn't the stomach digest itself? *Physiol Rev* 2008; **88**: 1547-1565 [PMID: 18923189 DOI: 10.1152/physrev.00004.2008]
12 **Matúz J**. Role of mucus in mucosal protection through ethanol and pepsin damage models. *Acta Physiol Hung* 1992; **80**: 189-194 [PMID: 1345186]

13 **Atuma C**, Strugala V, Allen A, Holm L. The adherent gastrointestinal mucus gel layer: thickness and physical state in vivo. *Am J Physiol Gastrointest Liver Physiol* 2001; **280**: G922-G929 [PMID: 11292601 DOI: 10.1152/AJPGI.2001.280.5.G922]

14 **Gribble FM**, Reimann F. Function and mechanisms of enteroendocrine cells and gut hormones in metabolism. *Nat Rev Endocrinol* 2019; **15**: 226-237 [PMID: 30760847 DOI: 10.1038/s41574-019-0168-8]

15 **Moorefield EC**, Andres SF, Blue RE, Van Landeghem L, Mah AT, Santoro MA, Ding S. Aging effects on intestinal homeostasis associated with expansion and dysfunction of intestinal epithelial stem cells. *Aging (Albany NY)* 2017; **9**: 1898-1915 [PMID: 28854151 DOI: 10.18632/aging.101279]

16 **Takezono Y**, Joh T, Oshima T, Suzuki H, Seno K, Yokoyama Y, Alexander JS, Itoh M. Role of prostaglandins in maintaining gastric mucus-cell permeability against acid exposure. *J Lab Clin Med* 2004; **143**: 52-58 [PMID: 14749685 DOI: 10.1016/J.LAB.2003.09.004]

17 **Slifer ZM**, Blikslager AT. The Integral Role of Tight Junction Proteins in the Repair of Injured Intestinal Epithelium. *Int J Mol Sci* 2020; **21** [PMID: 32024112 DOI: 10.3390/IJMS21030972]

18 **Li J**, Li YX, Chen MH, Li J, Du J, Shen B, Xia XM. Changes in the phosphorylation of claudins during the course of experimental colitis. *Int J Clin Exp Pathol* 2015; **8**: 12225-12233 [PMID: 26722407]

19 **Saitou M**, Furuse M, Sasaki H, Schulzke JD, Fromm M, Takano H, Noda T, Tsukita S. Complex phenotype of mice lacking occludin, a component of tight junction strands. *Mol Biol Cell* 2000; **11**: 4131-4142 [PMID: 11102513 DOI: 10.1091/MBC.11.12.4131]

20 **Pearce SC**, Al-Jawadi A, Kishida K, Yu S, Hu M, Fritzky LF, Edelblum KL, Gao N, Ferraris RP. Marked differences in tight junction composition and macromolecular permeability among different intestinal cell types. *BMC Biol* 2018; **16**: 19 [PMID: 29391007 DOI: 10.1186/s12915-018-0481-z]

21 **Liu Y**, Chen YG. Intestinal epithelial plasticity and regeneration *via* cell dedifferentiation. *Cell Regen* 2020; **9**: 14 [PMID: 32869114 DOI: 10.1186/s13619-020-00053-5]

22 **Xiao S**, Zhou L. Gastric Stem Cells: Physiological and Pathological Perspectives. *Front Cell Dev Biol* 2020; **8**: 571536 [PMID: 33043003 DOI: 10.3389/fcell.2020.571536]

23 **Malik TF**, Gnanapandithan K, Singh K. Peptic Ulcer Disease. In: StatPearls [Internet]. Treasure Island (FL): StatPearls Publishing; 2021: 170-179

24 **Osefo N**, Ito T, Jensen RT. Gastric acid hypersecretory states: recent insights and advances. *Curr Gastroenterol Rep* 2009; **11**: 433-441 [PMID: 19903418 DOI: 10.1007/S11894-009-0067-6]

25 **Basson MD**. Paradigms for mechanical signal transduction in the intestinal epithelium. Category: molecular, cell, and developmental biology. *Digestion* 2003; **68**: 217-225 [PMID: 14739529 DOI: 10.1159/000076385]

26 **Gayer CP**, Basson MD. The effects of mechanical forces on intestinal physiology and pathology. *Cell Signal* 2009; **21**: 1237-1244 [PMID: 19249356 DOI: 10.1016/j.cellsig.2009.02.011]

27 **Kellow JE**, Phillips SF. Altered small bowel motility in irritable bowel syndrome is correlated with symptoms. *Gastroenterology* 1987; **92**: 1885-1893 [PMID: 3569764 DOI: 10.1016/0016-5085(87)90620-2]

28 **Flanigan TL**, Owen CR, Gayer C, Basson MD. Supraphysiologic extracellular pressure inhibits intestinal epithelial wound healing independently of luminal nutrient flow. *Am J Surg* 2008; **196**: 683-689 [PMID: 18954600 DOI: 10.1016/j.amjsurg.2008.07.016]

29 **Andersson P**, Olaison G, Hallböök O, Boeryd B, Sjödahl R. Increased anal resting pressure and rectal sensitivity in Crohn's disease. *Dis Colon Rectum* 2003; **46**: 1685-1689 [PMID: 14668596 DOI: 10.1007/BF02660776]

30 **Yamamoto K**, Kishino M, Nakamura S, Tokushige K. Symptoms and Upper Gastrointestinal Mucosal Injury Associated with Bisphosphonate Therapy. *Intern Med* 2019; **58**: 1049-1056 [PMID: 30626809 DOI: 10.2169/internalmedicine.1271-18]

31 **Scarpignato C**, Bjarnason I. Drug-Induced Small Bowel Injury: a Challenging and Often Forgotten Clinical Condition. *Curr Gastroenterol Rep* 2019; **21**: 55 [PMID: 31720893 DOI: 10.1007/s11894-019-0726-1]

32 **Lugea A**, Antolín M, Mourelle M, Guarner F, Malagelada JR. Deranged hydrophobic barrier of the rat gastroduodenal mucosa after parenteral nonsteroidal anti-inflammatory drugs. *Gastroenterology* 1997; **112**: 1931-1939 [PMID: 9178685 DOI: 10.1053/GAST.1997.V112.PM9178685]

33 **Kaunitz JD**. Barrier function of gastric mucus. *Keio J Med* 1999; **48**: 63-68 [PMID: 10405521 DOI: 10.2302/KJM.48.63]

34 **Davis JS**, Lee HY, Kim J, Advani SM, Peng HL, Banfield E, Hawk ET, Chang S, Frazier-Wood AC. Use of non-steroidal anti-inflammatory drugs in US adults: changes over time and by demographic. *Open Heart* 2017; **4**: e000550 [PMID: 28674622 DOI: 10.1136/openhrt-2016-000550]

35 **Gwee KA**, Goh V, Lima G, Setia S. Coprescribing proton-pump inhibitors with nonsteroidal anti-inflammatory drugs: risks versus benefits. *J Pain Res* 2018; **11**: 361-374 [PMID: 29491719 DOI: 10.2147/JPR.S156938]

36 **Higuchi K**, Umegaki E, Watanabe T, Yoda Y, Morita E, Murano M, Tokioka S, Arakawa T. Present status and strategy of NSAIDs-induced small bowel injury. *J Gastroenterol* 2009; **44**: 879-888 [PMID: 19568687 DOI: 10.1007/s00535-009-0102-2]

37 **Yamagata M**, Hiraishi H. [Prevalence and incidence of NSAID-induced gastrointestinal ulcers and bleeding]. *Nihon Rinsho* 2007; **65**: 1749-1753 [PMID: 17926519]

38 **Holzer P**, Livingston EH, Guth PH. Sensory neurons signal for an increase in rat gastric mucosal blood flow in the face of pending acid injury. *Gastroenterology* 1991; **101**: 416-423 [PMID: 2065919 DOI: 10.1016/0016-5085(91)90020-L]

39 **Wallace JL**. Pathogenesis of NSAID-induced gastroduodenal mucosal injury. *Best Pract Res Clin Gastroenterol* 2001; **15**: 691-703 [PMID: 11566035 DOI: 10.1053/BEGA.2001.0229]

40 **Maricic N**, Ehrlich K, Gretzer B, Schuligoi R, Respondek M, Peskar BM. Selective cyclo-oxygenase-2 inhibitors aggravate ischaemia-reperfusion injury in the rat stomach. *Br J Pharmacol* 1999; **128**: 1659-1666 [PMID: 10588920 DOI: 10.1038/SJ.BJP.0702966]

41 **Matsui H**, Shimokawa O, Kaneko T, Nagano Y, Rai K, Hyodo I. The pathophysiology of non-steroidal anti-inflammatory drug (NSAID)-induced mucosal injuries in stomach and small intestine. *J Clin Biochem Nutr* 2011; **48**: 107-111 [PMID: 21373261 DOI: 10.3164/jcbn.10-79]

42 **Wallace JL**. NSAID gastropathy and enteropathy: distinct pathogenesis likely necessitates distinct prevention strategies. *Br J Pharmacol* 2012; **165**: 67-74 [PMID: 21627632 DOI: 10.1111/j.1476-5381.2011.01509.x]

43 **Whittle BJ**. Mechanisms underlying intestinal injury induced by anti-inflammatory COX inhibitors. *Eur J Pharmacol* 2004; **500**: 427-439 [PMID: 15464050 DOI: 10.1016/J.EJPHAR.2004.07.042]

44 **Otani K**, Tanigawa T, Watanabe T, Shimada S, Nadatani Y, Nagami Y, Tanaka F, Kamata N, Yamagami H, Shiba M, Tominaga K, Fujiwara Y, Arakawa T. Microbiota Plays a Key Role in Non-Steroidal Anti-Inflammatory Drug-Induced Small Intestinal Damage. *Digestion* 2017; **95**: 22-28 [PMID: 28052268 DOI: 10.1159/000452356]

45 **Maseda D**, Ricciotti E. NSAID-Gut Microbiota Interactions. *Front Pharmacol* 2020; **11**: 1153 [PMID: 32848762 DOI: 10.3389/fphar.2020.01153]

46 **Tai FWD**, McAlindon ME. NSAIDs and the small bowel. *Curr Opin Gastroenterol* 2018; **34**: 175-182 [PMID: 29438118 DOI: 10.1097/MOG.0000000000000427]

47 **Zhou Y**, Dial EJ, Doyen R, Lichtenberger LM. Effect of indomethacin on bile acid-phospholipid interactions: implication for small intestinal injury induced by nonsteroidal anti-inflammatory drugs. *Am J Physiol Gastrointest Liver Physiol* 2010; **298**: G722-G731 [PMID: 20203063 DOI: 10.1152/ajpgi.00387.2009]

48 **Watanabe T**, Higuchi K, Kobata A, Nishio H, Tanigawa T, Shiba M, Tominaga K, Fujiwara Y, Oshitani N, Asahara T, Nomoto K, Takeuchi K, Arakawa T. Non-steroidal anti-inflammatory drug-induced small intestinal damage is Toll-like receptor 4 dependent. *Gut* 2008; **57**: 181-187 [PMID: 17639086 DOI: 10.1136/gut.2007.125963]

49 **Hegyi P**, Maléth J, Walters JR, Hofmann AF, Keely SJ. Guts and Gall: Bile Acids in Regulation of Intestinal Epithelial Function in Health and Disease. *Physiol Rev* 2018; **98**: 1983-2023 [PMID: 30067158 DOI: 10.1152/physrev.00054.2017]

50 **Ticho AL**, Malhotra P, Dudeja PK, Gill RK, Alrefai WA. Intestinal Absorption of Bile Acids in Health and Disease. *Compr Physiol* 2019; **10**: 21-56 [PMID: 31853951 DOI: 10.1002/cphy.c190007]

51 **Urdaneta V**, Casadesús J. Interactions between Bacteria and Bile Salts in the Gastrointestinal and Hepatobiliary Tracts. *Front Med (Lausanne)* 2017; **4**: 163 [PMID: 29043249 DOI: 10.3389/fmed.2017.00163]

52 **Murakami Y**, Tanabe S, Suzuki T. High-fat Diet-induced Intestinal Hyperpermeability is Associated with Increased Bile Acids in the Large Intestine of Mice. *J Food Sci* 2016; **81**: H216-H222 [PMID: 26595891 DOI: 10.1111/1750-3841.13166]

53 **Higashimura Y**, Naito Y, Takagi T, Uchiyama K, Mizushima K, Ushiroda C, Ohnogi H, Kudo Y, Yasui M, Inui S, Hisada T, Honda A, Matsuzaki Y, Yoshikawa T. Protective effect of agaro-oligosaccharides on gut dysbiosis and colon tumorigenesis in high-fat diet-fed mice. *Am J Physiol Gastrointest Liver Physiol* 2016; **310**: G367-G375 [PMID: 26767984 DOI: 10.1152/ajpgi.00324.2015]

54 **Ajouz H**, Mukherji D, Shamseddine A. Secondary bile acids: an underrecognized cause of colon cancer. *World J Surg Oncol* 2014; **12**: 164 [PMID: 24884764 DOI: 10.1186/1477-7819-12-164]

55 **Tuskey A**, Peura D. The use of H2 antagonists in treating and preventing NSAID-induced mucosal damage. *Arthritis Res Ther* 2013; **15** Suppl 3: S6 [PMID: 24267478 DOI: 10.1186/ar4178]

56 **Sturkenboom MC**, Burke TA, Tangelder MJ, Dieleman JP, Walton S, Goldstein JL. Adherence to proton pump inhibitors or H2-receptor antagonists during the use of non-steroidal anti-inflammatory drugs. *Aliment Pharmacol Ther* 2003; **18**: 1137-1147 [PMID: 14653834 DOI: 10.1046/J.1365-2036.2003.01795.X]

57 **Vanderhoff BT**, Tahboub RM. Proton pump inhibitors: an update. *Am Fam Physician* 2002; **66**: 273-280 [PMID: 12152963]

58 **Oncel S**, Gupta R, Wang Q, Basson MD. ZINC40099027 Promotes Gastric Mucosal Repair in Ongoing Aspirin-Associated Gastric Injury by Activating Focal Adhesion Kinase. *Cells* 2021; **10** [PMID: 33920786 DOI: 10.3390/cells10040908]

59 **Hunt RH**, Lanas A, Stichtenoth DO, Scarpignato C. Myths and facts in the use of anti-inflammatory drugs. *Ann Med* 2009; **41**: 423-437 [PMID: 19430988 DOI: 10.1080/07853890902887295]

60 **Mahmoud YI**, Abd El-Ghffar EA. Spirulina ameliorates aspirin-induced gastric ulcer in albino mice by alleviating oxidative stress and inflammation. *Biomed Pharmacother* 2019; **109**: 314-321 [PMID: 30396089 DOI: 10.1016/j.biopha.2018.10.118]

61 **Handa O**, Naito Y, Fukui A, Omatsu T, Yoshikawa T. The impact of non-steroidal anti-inflammatory drugs on the small intestinal epithelium. *J Clin Biochem Nutr* 2014; **54**: 2-6 [PMID: 24426183 DOI: 10.3164/jcbn.13-84]

62 **Marlicz W**, Loniewski I, Grimes DS, Quigley EM. Nonsteroidal anti-inflammatory drugs, proton pump inhibitors, and gastrointestinal injury: contrasting interactions in the stomach and small intestine. *Mayo Clin Proc* 2014; **89**: 1699-1709 [PMID: 25440891 DOI: 10.1016/j.mayocp.2014.07.015]

63 **Szeto CC**, Sugano K, Wang JG, Fujimoto K, Whittle S, Modi GK, Chen CH, Park JB, Tam LS, Vareesangthip K, Tsoi KKF, Chan FKL. Non-steroidal anti-inflammatory drug (NSAID) therapy in patients with hypertension, cardiovascular, renal or gastrointestinal comorbidities: joint APAGE/APLAR/APSDE/APSH/APSN/PoA recommendations. *Gut* 2020; **69**: 617-629 [PMID: 31937550 DOI: 10.1136/gutjnl-2019-319300]

64 **Kaser A**, Zeissig S, Blumberg RS. Inflammatory bowel disease. *Annu Rev Immunol* 2010; **28**: 573-621 [PMID: 20192811 DOI: 10.1146/annurev-immunol-030409-101225]

65 **Danese S**, Fiocchi C. Ulcerative colitis. *N Engl J Med* 2011; **365**: 1713-1725 [PMID: 22047562 DOI: 10.1056/NEJMra1102942]

66 **Klenske E**, Bojarski C, Waldner M, Rath T, Neurath MF, Atreya R. Targeting mucosal healing in Crohn's disease: what the clinician needs to know. *Therap Adv Gastroenterol* 2019; **12**: 1756284819856865 [PMID: 31236140 DOI: 10.1177/1756284819856865]

67 **Strober W**, Fuss I, Mannon P. The fundamental basis of inflammatory bowel disease. *J Clin Invest* 2007; **117**: 514-521 [PMID: 17332878 DOI: 10.1172/JCI30587]

68 **Baumgart DC**, Le Berre C. Newer Biologic and Small-Molecule Therapies for Inflammatory Bowel Disease. *N Engl J Med* 2021; **385**: 1302-1315 [PMID: 34587387 DOI: 10.1056/nejmra1907607]

69 **Matsuoka K**, Kobayashi T, Ueno F, Matsui T, Hirai F, Inoue N, Kato J, Kobayashi K, Koganei K, Kunisaki R, Motoya S, Nagahori M, Nakase H, Omata F, Saruta M, Watanabe T, Tanaka T, Kanai T, Noguchi Y, Takahashi KI, Watanabe K,

Hibi T, Suzuki Y, Watanabe M, Sugano K, Shimosegawa T. Evidence-based clinical practice guidelines for inflammatory bowel disease. *J Gastroenterol* 2018; **53**: 305-353 [PMID: 29429045 DOI: 10.1007/s00535-018-1439-1]

70 **Atreya R**, Neurath MF. Current and Future Targets for Mucosal Healing in Inflammatory Bowel Disease. *Visc Med* 2017; **33**: 82-88 [PMID: 28612022 DOI: 10.1159/000458006]

71 **Pineton de Chambrun G**, Peyrin-Biroulet L, Lémann M, Colombel JF. Clinical implications of mucosal healing for the management of IBD. *Nat Rev Gastroenterol Hepatol* 2010; **7**: 15-29 [PMID: 19949430 DOI: 10.1038/nrgastro.2009.203]

72 **Lichtenstein GR**, Rutgeerts P. Importance of mucosal healing in ulcerative colitis. *Inflamm Bowel Dis* 2010; **16**: 338-346 [PMID: 19637362 DOI: 10.1002/ibd.20997]

73 **Basson MD**, Rashid Z, Turowski GA, West AB, Emenaker NJ, Sgambati SA, Hong F, Perdikis DM, Datta S, Madri JA. Restitution at the cellular level: regulation of the migrating phenotype. *Yale J Biol Med* 1996; **69**: 119-129 [PMID: 9112743]

74 **Modlin IM**, Basson MD, Soroka CJ, Wright N, Poulsom R, Chinnery R, Hanby A, Patel K, Rogers L, Alison M. Ulcer-induced alterations in cell phenotype and growth factor expression. *Eur J Gastroenterol* 1993; **93**: S59-S67

75 **Basson MD**, Modlin IM, Turowski G, Madri JA. Enterocyte-matrix interactions in the healing of mucosal injury. *Eur J Gastroenterol* 1993; **5**: S21-S28

76 **McNeil PL**, Terasaki M. Coping with the inevitable: how cells repair a torn surface membrane. *Nat Cell Biol* 2001; **3**: E124-E129 [PMID: 11331898 DOI: 10.1038/35074652]

77 **Cooper ST**, McNeil PL. Membrane Repair: Mechanisms and Pathophysiology. *Physiol Rev* 2015; **95**: 1205-1240 [PMID: 26336031 DOI: 10.1152/physrev.00037.2014]

78 **Andrews NW**, Corrotte M. Plasma membrane repair. *Curr Biol* 2018; **28**: R392-R397 [PMID: 29689221 DOI: 10.1016/j.cub.2017.12.034]

79 **Blazek AD**, Paleo BJ, Weisleder N. Plasma Membrane Repair: A Central Process for Maintaining Cellular Homeostasis. *Physiology (Bethesda)* 2015; **30**: 438-448 [PMID: 26525343 DOI: 10.1152/physiol.00019.2015]

80 **Walsh MF**, Thamilselvan V, Grotelueschen R, Farhana L, Basson M. Absence of adhesion triggers differential FAK and SAPKp38 signals in SW620 human colon cancer cells that may inhibit adhesiveness and lead to cell death. *Cell Physiol Biochem* 2003; **13**: 135-146 [PMID: 12876384 DOI: 10.1159/000071864]

81 **Williams JM**, Duckworth CA, Burkitt MD, Watson AJ, Campbell BJ, Pritchard DM. Epithelial cell shedding and barrier function: a matter of life and death at the small intestinal villus tip. *Vet Pathol* 2015; **52**: 445-455 [PMID: 25428410 DOI: 10.1177/0300985814559404]

82 **Bement WM**, Forscher P, Mooseker MS. A novel cytoskeletal structure involved in purse string wound closure and cell polarity maintenance. *J Cell Biol* 1993; **121**: 565-578 [PMID: 8486737 DOI: 10.1083/jcb.121.3.565]

83 **Landén NX**, Li D, Ståhle M. Transition from inflammation to proliferation: a critical step during wound healing. *Cell Mol Life Sci* 2016; **73**: 3861-3885 [PMID: 27180275 DOI: 10.1007/s00018-016-2268-0]

84 **Zundler S**, Tauschek V, Neurath MF. Immune Cell Circuits in Mucosal Wound Healing: Clinical Implications. *Visc Med* 2020; **36**: 129-136 [PMID: 32355670 DOI: 10.1159/000506846]

85 **Ubelmann F**, Chamaillard M, El-Marjou F, Simon A, Netter J, Vignjevic D, Nichols BL, Quezada-Calvillo R, Grandjean T, Louvard D, Revenu C, Robine S. Enterocyte loss of polarity and gut wound healing rely upon the F-actin-severing function of villin. *Proc Natl Acad Sci U S A* 2013; **110**: E1380-E1389 [PMID: 23520048 DOI: 10.1073/pnas.1218446110]

86 **Albers TM**, Lomakina I, Moore RP. Fate of polarized membrane components and evidence for microvillus disassembly on migrating enterocytes during repair of native intestinal epithelium. *Lab Invest* 1995; **73**: 139-148 [PMID: 7603035]

87 **Goggins BJ**, Chaney C, Radford-Smith GL, Horvat JC, Keely S. Hypoxia and Integrin-Mediated Epithelial Restitution during Mucosal Inflammation. *Front Immunol* 2013; **4**: 272 [PMID: 24062740 DOI: 10.3389/fimmu.2013.00272]

88 **Keely S**, Glover LE, MacManus CF, Campbell EL, Scully MM, Furuta GT, Colgan SP. Selective induction of integrin beta1 by hypoxia-inducible factor: implications for wound healing. *FASEB J* 2009; **23**: 1338-1346 [PMID: 19103643 DOI: 10.1096/fj.08-125344]

89 **Lotz MM**, Rabinovitz I, Mercurio AM. Intestinal restitution: progression of actin cytoskeleton rearrangements and integrin function in a model of epithelial wound healing. *Am J Pathol* 2000; **156**: 985-996 [PMID: 10702414 DOI: 10.1016/S0002-9440(10)64966-8]

90 **Tétreault MP**, Chailler P, Beaulieu JF, Rivard N, Ménard D. Specific signaling cascades involved in cell spreading during healing of micro-wounded gastric epithelial monolayers. *J Cell Biochem* 2008; **105**: 1240-1249 [PMID: 18802922 DOI: 10.1002/jcb.21924]

91 **Sanders MA**, Basson MD. Collagen IV regulates Caco-2 migration and ERK activation *via* alpha1beta1- and alpha2beta1-integrin-dependent Src kinase activation. *Am J Physiol Gastrointest Liver Physiol* 2004; **286**: G547-G557 [PMID: 14604860 DOI: 10.1152/ajpgi.00262.2003]

92 **Walsh MF**, Ampasala DR, Hatfield J, Vander Heide R, Suer S, Rishi AK, Basson MD. Transforming growth factor-beta stimulates intestinal epithelial focal adhesion kinase synthesis *via* Smad- and p38-dependent mechanisms. *Am J Pathol* 2008; **173**: 385-399 [PMID: 18583311 DOI: 10.2353/ajpath.2008.070729]

93 **Sanders MA**, Ampasala D, Basson MD. DOCK5 and DOCK1 regulate Caco-2 intestinal epithelial cell spreading and migration on collagen IV. *J Biol Chem* 2009; **284**: 27-35 [PMID: 19004829 DOI: 10.1074/jbc.M808010200]

94 **Yu CF**, Sanders MA, Basson MD. Human caco-2 motility redistributes FAK and paxillin and activates p38 MAPK in a matrix-dependent manner. *Am J Physiol Gastrointest Liver Physiol* 2000; **278**: G952-G966 [PMID: 10859226 DOI: 10.1152/ajpgi.2000.278.6.g952]

95 **Olson AD**. Contraction of collagen gels by intestinal epithelial cells depends on microfilament function. *Dig Dis Sci* 1993; **38**: 388-395 [PMID: 8444067 DOI: 10.1007/BF01316489]

96 **Yu CF**, Basson MD. Matrix-specific FAK and MAPK reorganization during Caco-2 cell motility. *Microsc Res Tech* 2000; **51**: 191-203 [PMID: 11054869 DOI: 10.1002/1097-0029(20001015)51:2<191::AID-JEMT10>3.0.CO;2-1]

97 **López-Colomé AM**, Lee-Rivera I, Benavides-Hidalgo R, López E. Paxillin: a crossroad in pathological cell migration. *J Hematol Oncol* 2017; **10**: 50 [PMID: 28214467 DOI: 10.1186/s13045-017-0418-y]

98 **Conway WC**, Van der Voort van Zyp J, Thamilselvan V, Walsh MF, Crowe DL, Basson MD. Paxillin modulates squamous cancer cell adhesion and is important in pressure-augmented adhesion. *J Cell Biochem* 2006; **98**: 1507-1516 [PMID: 16552730 DOI: 10.1002/JCB.20819]

99 **Ibata N**, Terentjev EM. Development of Nascent Focal Adhesions in Spreading Cells. *Biophys J* 2020; **119**: 2063-2073 [PMID: 33068539 DOI: 10.1016/j.bpj.2020.09.037]

100 **Legerstee K**, Houtsmuller AB. A Layered View on Focal Adhesions. *Biology (Basel)* 2021; **10** [PMID: 34827182 DOI: 10.3390/BIOLOGY10111189]

101 **Blikslager AT**, Moeser AJ, Gookin JL, Jones SL, Odle J. Restoration of barrier function in injured intestinal mucosa. *Physiol Rev* 2007; **87**: 545-564 [PMID: 17429041 DOI: 10.1152/physrev.00012.2006]

102 **Sturm A**, Dignass AU. Epithelial restitution and wound healing in inflammatory bowel disease. *World J Gastroenterol* 2008; **14**: 348-353 [PMID: 18200658 DOI: 10.3748/wjg.14.348]

103 **Laine L**, Takeuchi K, Tarnawski A. Gastric mucosal defense and cytoprotection: bench to bedside. *Gastroenterology* 2008; **135**: 41-60 [PMID: 18549814 DOI: 10.1053/j.gastro.2008.05.030]

104 **Basson MD**, Modlin IM, Madri JA. Human enterocyte (Caco-2) migration is modulated in vitro by extracellular matrix composition and epidermal growth factor. *J Clin Invest* 1992; **90**: 15-23 [PMID: 1634605 DOI: 10.1172/JCI115828]

105 **Basson MD**, Modlin IM, Flynn SD, Jena BP, Madri JA. Independent modulation of enterocyte migration and proliferation by growth factors, matrix proteins, and pharmacologic agents in an in vitro model of mucosal healing. *Surgery* 1992; **112**: 299-307; discussion 307 [PMID: 1353641]

106 **Tarnawski A**, Tanoue K, Santos AM, Sarfeh IJ. Cellular and molecular mechanisms of gastric ulcer healing. Is the quality of mucosal scar affected by treatment? *Scand J Gastroenterol Suppl* 1995; **210**: 9-14 [PMID: 8578218 DOI: 10.3109/00365529509090261]

107 **Gao JH**, Guo LJ, Huang ZY, Rao JN, Tang CW. Roles of cellular polyamines in mucosal healing in the gastrointestinal tract. *J Physiol Pharmacol* 2013; **64**: 681-693 [PMID: 24388882]

108 **Basson MD**. Gut mucosal healing: is the science relevant? *Am J Pathol* 2002; **161**: 1101-1105 [PMID: 12368182 DOI: 10.1016/S0002-9440(10)64385-4]

109 **Baatar D**, Jones MK, Tsugawa K, Pai R, Moon WS, Koh GY, Kim I, Kitano S, Tarnawski AS. Esophageal ulceration triggers expression of hypoxia-inducible factor-1 alpha and activates vascular endothelial growth factor gene: implications for angiogenesis and ulcer healing. *Am J Pathol* 2002; **161**: 1449-1457 [PMID: 12368217 DOI: 10.1016/S0002-9440(10)64420-3]

110 **Dudar GK**, D'Andrea LD, Di Stasi R, Pedone C, Wallace JL. A vascular endothelial growth factor mimetic accelerates gastric ulcer healing in an iNOS-dependent manner. *Am J Physiol Gastrointest Liver Physiol* 2008; **295**: G374-G381 [PMID: 18583458 DOI: 10.1152/ajpgi.90325.2008]

111 **Bauer SM**, Bauer RJ, Velazquez OC. Angiogenesis, vasculogenesis, and induction of healing in chronic wounds. *Vasc Endovascular Surg* 2005; **39**: 293-306 [PMID: 16079938 DOI: 10.1177/153857440503900401]

112 **Tarnawski AS**, Ahluwalia A, Jones MK. Angiogenesis in gastric mucosa: an important component of gastric erosion and ulcer healing and its impairment in aging. *J Gastroenterol Hepatol* 2014; **29** Suppl 4: 112-123 [PMID: 25521743 DOI: 10.1111/jgh.12734]

113 **Sen S**, McDonald SP, Coates PT, Bonder CS. Endothelial progenitor cells: novel biomarker and promising cell therapy for cardiovascular disease. *Clin Sci (Lond)* 2011; **120**: 263-283 [PMID: 21143202 DOI: 10.1042/CS20100429]

114 **Sato T**, Amano H, Ito Y, Eshima K, Minamino T, Ae T, Katada C, Ohno T, Hosono K, Suzuki T, Shibuya M, Koizumi W, Majima M. Vascular endothelial growth factor receptor 1 signaling facilitates gastric ulcer healing and angiogenesis through the upregulation of epidermal growth factor expression on VEGFR1+CXCR4 + cells recruited from bone marrow. *J Gastroenterol* 2014; **49**: 455-469 [PMID: 23982810 DOI: 10.1007/s00535-013-0869-z]

115 **Arakawa T**, Kobayashi K. Quality of ulcer healing--a new concept to rank healed peptic ulcers. *Gastroenterol Jpn* 1993; **28** Suppl 5: 158-162 [PMID: 8103020 DOI: 10.1007/BF02989227]

116 **Seo JH**, Hong SJ, Kim JH, Kim BW, Jee SR, Chung WC, Shim KN, Baik GH, Kim SS, Kim SG, Kim JI. Long-Term Recurrence Rates of Peptic Ulcers without Helicobacter pylori. *Gut Liver* 2016; **10**: 719-725 [PMID: 27114412 DOI: 10.5009/gnl15262]

117 **Pantea M**, Negovan A, Banescu C, Bataga S, Neagoe R, Mocan S, Iancu M. Factors Associated with Recurrent Ulcers in Patients with Gastric Surgery after More Than 15 Years: A Cross-Sectional Single-Center Study. *Gastroenterol Res Pract* 2018; **2018**: 8319481 [PMID: 30524477 DOI: 10.1155/2018/8319481]

118 **Ramakrishnan K**, Salinas RC. Peptic ulcer disease. *Am Fam Physician* 2007; **76**: 1005-1012 [PMID: 17956071]

119 **Tarnawski A**, Douglass TG, Stachura J, Krause WJ. Quality of gastric ulcer healing: histological and ultrastructural assessment. *Aliment Pharmacol Ther* 1991; **5** Suppl 1: 79-90 [PMID: 1888836 DOI: 10.1111/J.1365-2036.1991.TB00751.X]

120 **Tarnawski A**, Stachura J, Krause WJ, Douglass TG, Gergely H. Quality of gastric ulcer healing: a new, emerging concept. *J Clin Gastroenterol* 1991; **13** Suppl 1: S42-S47 [PMID: 1719066 DOI: 10.1097/00004836-199112001-00007]

121 **Arakawa T**, Watanabe T, Tanigawa T, Tominaga K, Fujiwara Y, Morimoto K. Quality of ulcer healing in gastrointestinal tract: its pathophysiology and clinical relevance. *World J Gastroenterol* 2012; **18**: 4811-4822 [PMID: 23002355 DOI: 10.3748/WJG.V18.I35.4811]

122 **Young Oh T**, Ok Ahn B, Jung Jang E, Sang Park J, Jong Park S, Wook Baik H, Hahm KB. Accelerated Ulcer Healing and Resistance to Ulcer Recurrence with Gastroprotectants in Rat Model of Acetic Acid-induced Gastric Ulcer. *J Clin Biochem Nutr* 2008; **42**: 204-214 [PMID: 18545642 DOI: 10.3164/jcbn.2008030]

123 **Kangwan N**, Park JM, Kim EH, Hahm KB. Quality of healing of gastric ulcers: Natural products beyond acid suppression. *World J Gastrointest Pathophysiol* 2014; **5**: 40-47 [PMID: 24891974 DOI: 10.4291/wjgp.v5.i1.40]

124 **Nebiki H**, Arakawa T, Higuchi K, Kobayashi K. Quality of ulcer healing influences the relapse of gastric ulcers in humans. *J Gastroenterol Hepatol* 1997; **12**: 109-114 [PMID: 9083911 DOI: 10.1111/J.1440-1746.1997.TB00393.X]

125 **Niv Y**. H pylori recurrence after successful eradication. *World J Gastroenterol* 2008; **14**: 1477-1478 [PMID: 18330934 DOI: 10.3748/WJG.14.1477]

126 **Tarnawski A**, Hollander D, Krause WJ, Dabros W, Stachura J, Gergely H. "Healed" experimental gastric ulcers remain histologically and ultrastructurally abnormal. *J Clin Gastroenterol* 1990; **12** Suppl 1: S139-S147 [PMID: 2212540 DOI: 10.1097/00004836-199001001-00024]

127 **Iizuka M**, Konno S. Wound healing of intestinal epithelial cells. *World J Gastroenterol* 2011; **17**: 2161-2171 [PMID: 21633524 DOI: 10.3748/wjg.v17.i17.2161]

128 **Kovalenko PL**, Flanigan TL, Chaturvedi L, Basson MD. Influence of defunctionalization and mechanical forces on intestinal epithelial wound healing. *Am J Physiol Gastrointest Liver Physiol* 2012; **303**: G1134-G1143 [PMID: 22997197 DOI: 10.1152/ajpgi.00321.2012]

129 **Zhang J**, Owen CR, Sanders MA, Turner JR, Basson MD. The motogenic effects of cyclic mechanical strain on intestinal epithelial monolayer wound closure are matrix dependent. *Gastroenterology* 2006; **131**: 1179-1189 [PMID: 17030187 DOI: 10.1053/j.gastro.2006.08.007]

130 **Komuro Y**, Ishihara K, Ohara S, Saigenji K, Hotta K. Effects of tetragastrin on mucus glycoprotein in rat gastric mucosal protection. *Gastroenterol Jpn* 1992; **27**: 597-603 [PMID: 1385248 DOI: 10.1007/BF02774973]

131 **Yoneda M**, Taché Y. Central thyrotropin-releasing factor analog prevents ethanol-induced gastric damage through prostaglandins in rats. *Gastroenterology* 1992; **102**: 1568-1574 [PMID: 1568566 DOI: 10.1016/0016-5085(92)91715-G]

132 **Takeuchi K**, Nishiwaki H, Okada M, Okabe S. Mucosal protective action of histamine against gastric lesions induced by HCl in rats: importance of antigastric motor activity mediated by H2-receptors. *J Pharmacol Exp Ther* 1988; **245**: 632-638 [PMID: 2966857]

133 **Tanaka S**, Akiba Y, Kaunitz JD. Pentagastrin gastroprotection against acid is related to H2 receptor activation but not acid secretion. *Gut* 1998; **43**: 334-341 [PMID: 9863477 DOI: 10.1136/GUT.43.3.334]

134 **Konturek SJ**, Brzozowski T, Bielanski W, Schally AV. Role of endogenous gastrin in gastroprotection. *Eur J Pharmacol* 1995; **278**: 203-212 [PMID: 7589156 DOI: 10.1016/0014-2999(95)00120-A]

135 **Kivilaakso E**, Fromm D, Silen W. Effect of the acid secretory state on intramural pH of rabbit gastric mucosa. *Gastroenterology* 1978; **75**: 641-648 [PMID: 30670 DOI: 10.1016/S0016-5085(19)31673-7]

136 **Smith P**, O'Brien P, Fromm D, Silen W. Secretory state of gastric mucosa and resistance to injury by exogenous acid. *Am J Surg* 1977; **133**: 81-85 [PMID: 13668 DOI: 10.1016/0002-9610(77)90198-2]

137 **Tanaka S**, Taché Y, Kaneko H, Guth PH, Kaunitz JD. Central vagal activation increases mucus gel thickness and surface cell intracellular pH in rat stomach. *Gastroenterology* 1997; **112**: 409-417 [PMID: 9024294 DOI: 10.1053/GAST.1997.V112.PM9024294]

138 **Ciacci C**, Lind SE, Podolsky DK. Transforming growth factor beta regulation of migration in wounded rat intestinal epithelial monolayers. *Gastroenterology* 1993; **105**: 93-101 [PMID: 8514065 DOI: 10.1016/0016-5085(93)90014-4]

139 **Dignass AU**, Podolsky DK. Interleukin 2 modulates intestinal epithelial cell function in vitro. *Exp Cell Res* 1996; **225**: 422-429 [PMID: 8660931 DOI: 10.1006/EXCR.1996.0193]

140 **Dise RS**, Frey MR, Whitehead RH, Polk DB. Epidermal growth factor stimulates Rac activation through Src and phosphatidylinositol 3-kinase to promote colonic epithelial cell migration. *Am J Physiol Gastrointest Liver Physiol* 2008; **294**: G276-G285 [PMID: 17991704 DOI: 10.1152/AJPGI.00340.2007]

141 **Jones MK**, Kawanaka H, Baatar D, Szabó IL, Tsugawa K, Pai R, Koh GY, Kim I, Sarfeh IJ, Tarnawski AS. Gene therapy for gastric ulcers with single local injection of naked DNA encoding VEGF and angiopoietin-1. *Gastroenterology* 2001; **121**: 1040-1047 [PMID: 11677194 DOI: 10.1053/GAST.2001.29308]

142 **Ferrara N**. The role of VEGF in the regulation of physiological and pathological angiogenesis. *EXS* 2005; 209-231 [PMID: 15617481 DOI: 10.1007/3-7643-7311-3_15]

143 **Szabo S**, Folkman J, Vattay P, Morales RE, Pinkus GS, Kato K. Accelerated healing of duodenal ulcers by oral administration of a mutein of basic fibroblast growth factor in rats. *Gastroenterology* 1994; **106**: 1106-1111 [PMID: 8143978 DOI: 10.1016/0016-5085(94)90773-0]

144 **Tarnawski AS**, Ahluwalia A. The Critical Role of Growth Factors in Gastric Ulcer Healing: The Cellular and Molecular Mechanisms and Potential Clinical Implications. *Cells* 2021; **10** [PMID: 34440733 DOI: 10.3390/CELLS10081964]

145 **Ebner R**, Derynck R. Epidermal growth factor and transforming growth factor-alpha: differential intracellular routing and processing of ligand-receptor complexes. *Cell Regul* 1991; **2**: 599-612 [PMID: 1777504 DOI: 10.1091/MBC.2.8.599]

146 **Ishikawa S**, Cepinskas G, Specian RD, Itoh M, Kvietys PR. Epidermal growth factor attenuates jejunal mucosal injury induced by oleic acid: role of mucus. *Am J Physiol* 1994; **267**: G1067-G1077 [PMID: 7810653 DOI: 10.1152/AJPGI.1994.267.6.G1067]

147 **Sarosiek J**, Bilski J, Murty VL, Slomiany A, Slomiany BL. Role of salivary epidermal growth factor in the maintenance of physicochemical characteristics of oral and gastric mucosal mucus coat. *Biochem Biophys Res Commun* 1988; **152**: 1421-1427 [PMID: 3259876 DOI: 10.1016/S0006-291X(88)80444-3]

148 **Kelly SM**, Hunter JO. Epidermal growth factor stimulates synthesis and secretion of mucus glycoproteins in human gastric mucosa. *Clin Sci (Lond)* 1990; **79**: 425-427 [PMID: 2174308 DOI: 10.1042/CS0790425]

149 **Procaccino F**, Reinshagen M, Hoffmann P, Zeeh JM, Lakshmanan J, McRoberts JA, Patel A, French S, Eysselein VE. Protective effect of epidermal growth factor in an experimental model of colitis in rats. *Gastroenterology* 1994; **107**: 12-17 [PMID: 8020654 DOI: 10.1016/0016-5085(94)90055-8]

150 **Riegler M**, Sedivy R, Sogukoglu T, Castagliuolo I, Pothoulakis C, Cosentini E, Bischof G, Hamilton G, Teleky B, Feil W, Lamont JT, Wenzl E. Epidermal growth factor attenuates Clostridium difficile toxin A- and B-induced damage of human colonic mucosa. *Am J Physiol* 1997; **273**: G1014-G1022 [PMID: 9374697 DOI: 10.1152/ajpgi.1997.273.5.G1014]

151 **Hui WM**, Chen BW, Kung AW, Cho CH, Luk CT, Lam SK. Effect of epidermal growth factor on gastric blood flow in rats: possible role in mucosal protection. *Gastroenterology* 1993; **104**: 1605-1610 [PMID: 8500716 DOI: 10.1016/0016-5085(93)90635-P]

152 **Konturek PK**, Brzozowski T, Konturek SJ, Dembiński A. Role of epidermal growth factor, prostaglandin, and sulfhydryls in stress-induced gastric lesions. *Gastroenterology* 1990; **99**: 1607-1615 [PMID: 2227276 DOI: 10.1016/0016-5085(90)90464-C]

153 **Sakamoto T**, Swierczek JS, Ogden WD, Thompson JC. Cytoprotective effect of pentagastrin and epidermal growth factor

on stress ulcer formation. Possible role of somatostatin. *Ann Surg* 1985; **201**: 290-295 [PMID: 2858183 DOI: 10.1097/00000658-198503000-00005]

154 **Tarnawski AS**, Jones MK. The role of epidermal growth factor (EGF) and its receptor in mucosal protection, adaptation to injury, and ulcer healing: involvement of EGF-R signal transduction pathways. *J Clin Gastroenterol* 1998; **27** Suppl 1: S12-S20 [PMID: 9872493 DOI: 10.1097/00004836-199800001-00004]

155 **Kirkegaard P**, Olsen PS, Poulsen SS, Nexø E. Epidermal growth factor inhibits cysteamine-induced duodenal ulcers. *Gastroenterology* 1983; **85**: 1277-1283 [PMID: 6605273 DOI: 10.1016/S0016-5085(83)80007-9]

156 **Kosone T**, Takagi H, Kakizaki S, Sohara N, Horiguchi N, Sato K, Yoneda M, Takeuchi T, Mori M. Integrative roles of transforming growth factor-alpha in the cytoprotection mechanisms of gastric mucosal injury. *BMC Gastroenterol* 2006; **6**: 22 [PMID: 16879752 DOI: 10.1186/1471-230X-6-22]

157 **Konturek SJ**, Brzozowski T, Majka J, Dembinski A, Slomiany A, Slomiany BL. Transforming growth factor alpha and epidermal growth factor in protection and healing of gastric mucosal injury. *Scand J Gastroenterol* 1992; **27**: 649-655 [PMID: 1439546 DOI: 10.3109/00365529209000134]

158 **Kokoska ER**, Wolff AB, Smith GS, Miller TA. Epidermal growth factor-induced cytoprotection in human intestinal cells involves intracellular calcium signaling. *J Surg Res* 2000; **88**: 97-103 [PMID: 10644473 DOI: 10.1006/JSRE.1999.5740]

159 **Nylander-Koski O**, Mustonen H, Puolakkainen P, Kiviluoto T, Kivilaakso E. Epidermal growth factor enhances intracellular pH regulation *via* calcium signaling in acid-exposed primary cultured rabbit gastric epithelial cells. *Dig Dis Sci* 2006; **51**: 1322-1330 [PMID: 16832619 DOI: 10.1007/S10620-006-9075-7]

160 **Tarnawski AS**, Jones MK, Ahluwalia A. Dedifferentiation and reprogramming of epithelial cells during gastric ulcer healing is triggered by hypoxia and a well-coordinated, sequential activation of EGFR signaling: cross talk with IGF1 and COX2. *Gastroenterology* 2021; **160**: 77-78 [DOI: 10.1016/S0016-5085(21)00932-X]

161 **Brzozowski T**, Konturek PC, Konturek SJ, Schuppan D, Drozdowicz D, Kwiecień S, Majka J, Nakamura T, Hahn E. Effect of local application of growth factors on gastric ulcer healing and mucosal expression of cyclooxygenase-1 and -2. *Digestion* 2001; **64**: 15-29 [PMID: 11549833 DOI: 10.1159/000048835]

162 **Eberhart CE**, Dubois RN. Eicosanoids and the gastrointestinal tract. *Gastroenterology* 1995; **109**: 285-301 [PMID: 7797026 DOI: 10.1016/0016-5085(95)90296-1]

163 **Jones MK**, Sasaki E, Halter F, Pai R, Nakamura T, Arakawa T, Kuroki T, Tarnawski AS. HGF triggers activation of the COX-2 gene in rat gastric epithelial cells: action mediated through the ERK2 signaling pathway. *FASEB J* 1999; **13**: 2186-2194 [PMID: 10593866 DOI: 10.1096/FASEBJ.13.15.2186]

164 **Babyatsky MW**, deBeaumont M, Thim L, Podolsky DK. Oral trefoil peptides protect against ethanol- and indomethacin-induced gastric injury in rats. *Gastroenterology* 1996; **110**: 489-497 [PMID: 8566596 DOI: 10.1053/GAST.1996.V110.PM8566596]

165 **FitzGerald AJ**, Pu M, Marchbank T, Westley BR, May FE, Boyle J, Yadollahi-Farsani M, Ghosh S, Playford RJ. Synergistic effects of systemic trefoil factor family 1 (TFF1) peptide and epidermal growth factor in a rat model of colitis. *Peptides* 2004; **25**: 793-801 [PMID: 15177874 DOI: 10.1016/J.PEPTIDES.2003.12.022]

166 **Vandenbroucke K**, Hans W, Van Huysse J, Neirynck S, Demetter P, Remaut E, Rottiers P, Steidler L. Active delivery of trefoil factors by genetically modified Lactococcus lactis prevents and heals acute colitis in mice. *Gastroenterology* 2004; **127**: 502-513 [PMID: 15300583 DOI: 10.1053/J.GASTRO.2004.05.020]

167 **Thim L**, Madsen F, Poulsen SS. Effect of trefoil factors on the viscoelastic properties of mucus gels. *Eur J Clin Invest* 2002; **32**: 519-527 [PMID: 12153553 DOI: 10.1046/J.1365-2362.2002.01014.X]

168 **Bastholm SK**, Samson MH, Becher N, Hansen LK, Stubbe PR, Chronakis IS, Nexo E, Uldbjerg N. Trefoil factor peptide 3 is positively correlated with the viscoelastic properties of the cervical mucus plug. *Acta Obstet Gynecol Scand* 2017; **96**: 47-52 [PMID: 27731893 DOI: 10.1111/aogs.13038]

169 **Wong WM**, Poulsom R, Wright NA. Trefoil peptides. *Gut* 1999; **44**: 890-895 [PMID: 10323896 DOI: 10.1136/GUT.44.6.890]

170 **Xue L**, Aihara E, Podolsky DK, Wang TC, Montrose MH. In vivo action of trefoil factor 2 (TFF2) to speed gastric repair is independent of cyclooxygenase. *Gut* 2010; **59**: 1184-1191 [PMID: 20587547 DOI: 10.1136/gut.2009.205625]

171 **Xue L**, Aihara E, Wang TC, Montrose MH. Trefoil factor 2 requires Na/H exchanger 2 activity to enhance mouse gastric epithelial repair. *J Biol Chem* 2011; **286**: 38375-38382 [PMID: 21900251 DOI: 10.1074/jbc.M111.268219]

172 **McBerry C**, Egan CE, Rani R, Yang Y, Wu D, Boespflug N, Boon L, Butcher B, Mirpuri J, Hogan SP, Denkers EY, Aliberti J, Herbert DR. Trefoil factor 2 negatively regulates type 1 immunity against Toxoplasma gondii. *J Immunol* 2012; **189**: 3078-3084 [PMID: 22896633 DOI: 10.4049/jimmunol.1103374]

173 **Järvå MA**, Lingford JP, John A, Soler NM, Scott NE, Goddard-Borger ED. Trefoil factors share a lectin activity that defines their role in mucus. *Nat Commun* 2020; **11**: 2265 [PMID: 32404934 DOI: 10.1038/s41467-020-16223-7]

174 **Newton JL**, Allen A, Westley BR, May FE. The human trefoil peptide, TFF1, is present in different molecular forms that are intimately associated with mucus in normal stomach. *Gut* 2000; **46**: 312-320 [PMID: 10673290 DOI: 10.1136/GUT.46.3.312]

175 **Aihara E**, Engevik KA, Montrose MH. Trefoil Factor Peptides and Gastrointestinal Function. *Annu Rev Physiol* 2017; **79**: 357-380 [PMID: 27992733 DOI: 10.1146/annurev-physiol-021115-105447]

176 **Braga Emidio N**, Brierley SM, Schroeder CI, Muttenthaler M. Structure, Function, and Therapeutic Potential of the Trefoil Factor Family in the Gastrointestinal Tract. *ACS Pharmacol Transl Sci* 2020; **3**: 583-597 [PMID: 32832864 DOI: 10.1021/acsptsci.0c00023]

177 **Farrell JJ**, Taupin D, Koh TJ, Chen D, Zhao CM, Podolsky DK, Wang TC. TFF2/SP-deficient mice show decreased gastric proliferation, increased acid secretion, and increased susceptibility to NSAID injury. *J Clin Invest* 2002; **109**: 193-204 [PMID: 11805131 DOI: 10.1172/JCI12529]

178 **Belle NM**, Ji Y, Herbine K, Wei Y, Park J, Zullo K, Hung LY, Srivatsa S, Young T, Oniskey T, Pastore C, Nieves W, Somsouk M, Herbert DR. TFF3 interacts with LINGO2 to regulate EGFR activation for protection against colitis and gastrointestinal helminths. *Nat Commun* 2019; **10**: 4408 [PMID: 31562318 DOI: 10.1038/s41467-019-12315-1]

179 **Hoffmann W**. Trefoil Factor Family (TFF) Peptides and Their Links to Inflammation: A Re-evaluation and New Medical

Perspectives. *Int J Mol Sci* 2021; **22** [PMID: 34066339 DOI: 10.3390/IJMS22094909]

180 **Dieckow J**, Brandt W, Hattermann K, Schob S, Schulze U, Mentlein R, Ackermann P, Sel S, Paulsen FP. CXCR4 and CXCR7 Mediate TFF3-Induced Cell Migration Independently From the ERK1/2 Signaling Pathway. *Invest Ophthalmol Vis Sci* 2016; **57**: 56-65 [PMID: 26780310 DOI: 10.1167/iovs.15-18129]

181 **Orime K**, Shirakawa J, Togashi Y, Tajima K, Inoue H, Ito Y, Sato K, Nakamura A, Aoki K, Goshima Y, Terauchi Y. Trefoil factor 2 promotes cell proliferation in pancreatic β-cells through CXCR-4-mediated ERK1/2 phosphorylation. *Endocrinology* 2013; **154**: 54-64 [PMID: 23183167 DOI: 10.1210/en.2012-1814]

182 **Taupin D**, Wu DC, Jeon WK, Devaney K, Wang TC, Podolsky DK. The trefoil gene family are coordinately expressed immediate-early genes: EGF receptor- and MAP kinase-dependent interregulation. *J Clin Invest* 1999; **103**: R31-R38 [PMID: 10225980 DOI: 10.1172/JCI3304]

183 **Sun Z**, Liu H, Yang Z, Shao D, Zhang W, Ren Y, Sun B, Lin J, Xu M, Nie S. Intestinal trefoil factor activates the PI3K/Akt signaling pathway to protect gastric mucosal epithelium from damage. *Int J Oncol* 2014; **45**: 1123-1132 [PMID: 24990304 DOI: 10.3892/ijo.2014.2527]

184 **Dubeykovskaya Z**, Dubeykovskiy A, Solal-Cohen J, Wang TC. Secreted trefoil factor 2 activates the CXCR4 receptor in epithelial and lymphocytic cancer cell lines. *J Biol Chem* 2009; **284**: 3650-3662 [PMID: 19064997 DOI: 10.1074/jbc.M804935200]

185 **Zhang Y**, Yu G, Wang Y, Xiang Y, Gao Q, Jiang P, Zhang J, Lee W, Zhang Y. Activation of protease-activated receptor (PAR) 1 by frog trefoil factor (TFF) 2 and PAR4 by human TFF2. *Cell Mol Life Sci* 2011; **68**: 3771-3780 [PMID: 21461878 DOI: 10.1007/s00018-011-0678-6]

186 **Barrera GJ**, Tortolero GS. Trefoil factor 3 (TFF3) from human breast milk activates PAR-2 receptors, of the intestinal epithelial cells HT-29, regulating cytokines and defensins. *Bratisl Lek Listy* 2016; **117**: 332-339 [PMID: 27546365 DOI: 10.4149/BLL_2016_066]

187 **McKenzie C**, Thim L, Parsons ME. Topical and intravenous administration of trefoil factors protect the gastric mucosa from ethanol-induced injury in the rat. *Aliment Pharmacol Ther* 2000; **14**: 1033-1040 [PMID: 10930897 DOI: 10.1046/J.1365-2036.2000.00796.X]

188 **Playford RJ**, Marchbank T, Goodlad RA, Chinery RA, Poulsom R, Hanby AM. Transgenic mice that overexpress the human trefoil peptide pS2 have an increased resistance to intestinal damage. *Proc Natl Acad Sci USA* 1996; **93**: 2137-2142 [PMID: 8700898 DOI: 10.1073/PNAS.93.5.2137]

189 **Mashimo H**, Wu DC, Podolsky DK, Fishman MC. Impaired defense of intestinal mucosa in mice lacking intestinal trefoil factor. *Science* 1996; **274**: 262-265 [PMID: 8824194 DOI: 10.1126/SCIENCE.274.5285.262]

190 **Babyatsky MW**, Rossiter G, Podolsky DK. Expression of transforming growth factors alpha and beta in colonic mucosa in inflammatory bowel disease. *Gastroenterology* 1996; **110**: 975-984 [PMID: 8613031 DOI: 10.1053/GAST.1996.V110.PM8613031]

191 **Maric I**, Poljak L, Zoricic S, Bobinac D, Bosukonda D, Sampath KT, Vukicevic S. Bone morphogenetic protein-7 reduces the severity of colon tissue damage and accelerates the healing of inflammatory bowel disease in rats. *J Cell Physiol* 2003; **196**: 258-264 [PMID: 12811818 DOI: 10.1002/JCP.10275]

192 **Sommer K**, Wiendl M, Müller TM, Heidbreder K, Voskens C, Neurath MF, Zundler S. Intestinal Mucosal Wound Healing and Barrier Integrity in IBD-Crosstalk and Trafficking of Cellular Players. *Front Med (Lausanne)* 2021; **8**: 643973 [PMID: 33834033 DOI: 10.3389/fmed.2021.643973]

193 **Bulut K**, Pennartz C, Felderbauer P, Ansorge N, Banasch M, Schmitz F, Schmidt WE, Hoffmann P. Vascular endothelial growth factor (VEGF164) ameliorates intestinal epithelial injury in vitro in IEC-18 and Caco-2 monolayers *via* induction of TGF-beta release from epithelial cells. *Scand J Gastroenterol* 2006; **41**: 687-692 [PMID: 16716967 DOI: 10.1080/00365520500408634]

194 **Ahluwalia A**, Jones MK, Brzozowski T, Tarnawski AS. Nerve growth factor is critical requirement for in vitro angiogenesis in gastric endothelial cells. *Am J Physiol Gastrointest Liver Physiol* 2016; **311**: G981-G987 [PMID: 27742705 DOI: 10.1152/ajpgi.00334.2016]

195 **Velazquez OC**. Angiogenesis and vasculogenesis: inducing the growth of new blood vessels and wound healing by stimulation of bone marrow-derived progenitor cell mobilization and homing. *J Vasc Surg* 2007; **45** Suppl A: A39-A47 [PMID: 17544023 DOI: 10.1016/J.JVS.2007.02.068]

196 **Chai J**, Baatar D, Tarnawski A. Serum response factor promotes re-epithelialization and muscular structure restoration during gastric ulcer healing. *Gastroenterology* 2004; **126**: 1809-1818 [PMID: 15188176 DOI: 10.1053/J.GASTRO.2004.03.021]

197 **Ahluwalia A**, Jones MK, Brzozowska I, Tarnawski AS. In vitro model of vasculo-angiogenesis: demonstration that bone marrow derived endothelial progenitor cells form new hybrid capillary blood vessels jointly with gastric endothelial cells. *J Physiol Pharmacol* 2017; **68**: 841-846 [PMID: 29550796]

198 **Neurath MF**. Cytokines in inflammatory bowel disease. *Nat Rev Immunol* 2014; **14**: 329-342 [PMID: 24751956 DOI: 10.1038/nri3661]

199 **Leppkes M**, Becker C, Ivanov II, Hirth S, Wirtz S, Neufert C, Pouly S, Murphy AJ, Valenzuela DM, Yancopoulos GD, Becher B, Littman DR, Neurath MF. RORgamma-expressing Th17 cells induce murine chronic intestinal inflammation *via* redundant effects of IL-17A and IL-17F. *Gastroenterology* 2009; **136**: 257-267 [PMID: 18992745 DOI: 10.1053/j.gastro.2008.10.018]

200 **Hueber W**, Sands BE, Lewitzky S, Vandemeulebroecke M, Reinisch W, Higgins PD, Wehkamp J, Feagan BG, Yao MD, Karczewski M, Karczewski J, Pezous N, Bek S, Bruin G, Mellgard B, Berger C, Londei M, Bertolino AP, Tougas G, Travis SP; Secukinumab in Crohn's Disease Study Group. Secukinumab, a human anti-IL-17A monoclonal antibody, for moderate to severe Crohn's disease: unexpected results of a randomised, double-blind placebo-controlled trial. *Gut* 2012; **61**: 1693-1700 [PMID: 22595313 DOI: 10.1136/gutjnl-2011-301668]

201 **Rosen MJ**, Frey MR, Washington MK, Chaturvedi R, Kuhnhein LA, Matta P, Revetta FL, Wilson KT, Polk DB. STAT6 activation in ulcerative colitis: a new target for prevention of IL-13-induced colon epithelial cell dysfunction. *Inflamm Bowel Dis* 2011; **17**: 2224-2234 [PMID: 21308881 DOI: 10.1002/ibd.21628]

202 **Heller F**, Fuss IJ, Nieuwenhuis EE, Blumberg RS, Strober W. Oxazolone colitis, a Th2 colitis model resembling ulcerative colitis, is mediated by IL-13-producing NK-T cells. *Immunity* 2002; **17**: 629-638 [PMID: 12433369 DOI: 10.1016/S1074-7613(02)00453-3]

203 **Weigmann B**, Lehr HA, Yancopoulos G, Valenzuela D, Murphy A, Stevens S, Schmidt J, Galle PR, Rose-John S, Neurath MF. The transcription factor NFATc2 controls IL-6-dependent T cell activation in experimental colitis. *J Exp Med* 2008; **205**: 2099-2110 [PMID: 18710929 DOI: 10.1084/jem.20072484]

204 **Hoving JC**. Targeting IL-13 as a Host-Directed Therapy Against Ulcerative Colitis. *Front Cell Infect Microbiol* 2018; **8**: 395 [PMID: 30460209 DOI: 10.3389/fcimb.2018.00395]

205 **Tilg H**, Kaser A. Failure of interleukin 13 blockade in ulcerative colitis. *Gut* 2015; **64**: 857-858 [PMID: 25804632 DOI: 10.1136/gutjnl-2015-309464]

206 **Ouyang W**, Rutz S, Crellin NK, Valdez PA, Hymowitz SG. Regulation and functions of the IL-10 family of cytokines in inflammation and disease. *Annu Rev Immunol* 2011; **29**: 71-109 [PMID: 21166540 DOI: 10.1146/annurev-immunol-031210-101312]

207 **Lindsay J**, Van Montfrans C, Brennan F, Van Deventer S, Drillenburg P, Hodgson H, Te Velde A, Sol Rodriguez Pena M. IL-10 gene therapy prevents TNBS-induced colitis. *Gene Ther* 2002; **9**: 1715-1721 [PMID: 12457286 DOI: 10.1038/sj.gt.3301841]

208 **Li MC**, He SH. IL-10 and its related cytokines for treatment of inflammatory bowel disease. *World J Gastroenterol* 2004; **10**: 620-625 [PMID: 14991925 DOI: 10.3748/WJG.V10.I5.620]

209 **Fedorak RN**, Gangl A, Elson CO, Rutgeerts P, Schreiber S, Wild G, Hanauer SB, Kilian A, Cohard M, LeBeaut A, Feagan B. Recombinant human interleukin 10 in the treatment of patients with mild to moderately active Crohn's disease. The Interleukin 10 Inflammatory Bowel Disease Cooperative Study Group. *Gastroenterology* 2000; **119**: 1473-1482 [PMID: 11113068 DOI: 10.1053/GAST.2000.20229]

210 **Wei HX**, Wang B, Li B. IL-10 and IL-22 in Mucosal Immunity: Driving Protection and Pathology. *Front Immunol* 2020; **11**: 1315 [PMID: 32670290 DOI: 10.3389/fimmu.2020.01315]

211 **Zheng Y**, Danilenko DM, Valdez P, Kasman I, Eastham-Anderson J, Wu J, Ouyang W. Interleukin-22, a T(H)17 cytokine, mediates IL-23-induced dermal inflammation and acanthosis. *Nature* 2007; **445**: 648-651 [PMID: 17187052 DOI: 10.1038/NATURE05505]

212 **Wolk K**, Witte E, Hoffmann U, Doecke WD, Endesfelder S, Asadullah K, Sterry W, Volk HD, Wittig BM, Sabat R. IL-22 induces lipopolysaccharide-binding protein in hepatocytes: a potential systemic role of IL-22 in Crohn's disease. *J Immunol* 2007; **178**: 5973-5981 [PMID: 17442982 DOI: 10.4049/JIMMUNOL.178.9.5973]

213 **Pickert G**, Neufert C, Leppkes M, Zheng Y, Wittkopf N, Warntjen M, Lehr HA, Hirth S, Weigmann B, Wirtz S, Ouyang W, Neurath MF, Becker C. STAT3 links IL-22 signaling in intestinal epithelial cells to mucosal wound healing. *J Exp Med* 2009; **206**: 1465-1472 [PMID: 19564350 DOI: 10.1084/jem.20082683]

214 **Gao B**, Xiang X. Interleukin-22 from bench to bedside: a promising drug for epithelial repair. *Cell Mol Immunol* 2019; **16**: 666-667 [PMID: 29921965 DOI: 10.1038/s41423-018-0055-6]

215 **Lee DW**, Zhong S, Pai R, Rae J, Sukumaran S, Stefanich EG, Lutman J, Doudement E, Wang X, Harder B, Lekkerkerker A, Herman A, Ouyang W, Danilenko DM. Nonclinical safety assessment of a human interleukin-22FC IG fusion protein demonstrates in vitro to in vivo and cross-species translatability. *Pharmacol Res Perspect* 2018; **6**: e00434 [PMID: 30464842 DOI: 10.1002/prp2.434]

216 **Zheng Y**, Valdez PA, Danilenko DM, Hu Y, Sa SM, Gong Q, Abbas AR, Modrusan Z, Ghilardi N, de Sauvage FJ, Ouyang W. Interleukin-22 mediates early host defense against attaching and effacing bacterial pathogens. *Nat Med* 2008; **14**: 282-289 [PMID: 18264109 DOI: 10.1038/nm1720]

217 **Aujla SJ**, Chan YR, Zheng M, Fei M, Askew DJ, Pociask DA, Reinhart TA, McAllister F, Edeal J, Gaus K, Husain S, Kreindler JL, Dubin PJ, Pilewski JM, Myerburg MM, Mason CA, Iwakura Y, Kolls JK. IL-22 mediates mucosal host defense against Gram-negative bacterial pneumonia. *Nat Med* 2008; **14**: 275-281 [PMID: 18264110 DOI: 10.1038/nm1710]

218 **Sugimoto K**, Ogawa A, Mizoguchi E, Shimomura Y, Andoh A, Bhan AK, Blumberg RS, Xavier RJ, Mizoguchi A. IL-22 ameliorates intestinal inflammation in a mouse model of ulcerative colitis. *J Clin Invest* 2008; **118**: 534-544 [PMID: 18172556 DOI: 10.1172/JCI33194]

219 **Eken A**, Singh AK, Treuting PM, Oukka M. IL-23R+ innate lymphoid cells induce colitis *via* interleukin-22-dependent mechanism. *Mucosal Immunol* 2014; **7**: 143-154 [PMID: 23715173 DOI: 10.1038/mi.2013.33]

220 **Stefanich EG**, Rae J, Sukumaran S, Lutman J, Lekkerkerker A, Ouyang W, Wang X, Lee D, Danilenko DM, Diehl L, Loyet KM, Herman A. Pre-clinical and translational pharmacology of a human interleukin-22 IgG fusion protein for potential treatment of infectious or inflammatory diseases. *Biochem Pharmacol* 2018; **152**: 224-235 [PMID: 29608910 DOI: 10.1016/j.bcp.2018.03.031]

221 **Rothenberg ME**, Wang Y, Lekkerkerker A, Danilenko DM, Maciuca R, Erickson R, Herman A, Stefanich E, Lu TT. Randomized Phase I Healthy Volunteer Study of UTTR1147A (IL-22Fc): A Potential Therapy for Epithelial Injury. *Clin Pharmacol Ther* 2019; **105**: 177-189 [PMID: 29952004 DOI: 10.1002/cpt.1164]

222 **Genentech**, Inc. An Extension Study to Evaluate the Long-Term Safety and Tolerability of UTTR1147A in Participants With Moderate to Severe Ulcerative Colitis or Crohn's Disease. ClinicalTrials.gov Identifier: NCT03650413 Available from: https://clinicaltrials.gov/ct2/show/NCT03650413

223 **Canani RB**, Costanzo MD, Leone L, Pedata M, Meli R, Calignano A. Potential beneficial effects of butyrate in intestinal and extraintestinal diseases. *World J Gastroenterol* 2011; **17**: 1519-1528 [PMID: 21472114 DOI: 10.3748/wjg.v17.i12.1519]

224 **Rao JN**, Wang JY. Regulation of Gastrointestinal Mucosal Growth. In: Integrated Systems Physiology: from Molecule to Function to Disease. San Rafael (CA): Morgan & Claypool Life Sciences; 2010 [PMID: 21634069 DOI: 10.4199/C00028ED1V01Y201103ISP015]

225 **Hamer HM**, Jonkers D, Venema K, Vanhoutvin S, Troost FJ, Brummer RJ. Review article: the role of butyrate on colonic function. *Aliment Pharmacol Ther* 2008; **27**: 104-119 [PMID: 17973645 DOI: 10.1111/J.1365-2036.2007.03562.X]

226 **Bedford A**, Gong J. Implications of butyrate and its derivatives for gut health and animal production. *Anim Nutr* 2018; **4**: 151-159 [PMID: 30140754 DOI: 10.1016/j.aninu.2017.08.010]

227 **Okumura R**, Takeda K. Roles of intestinal epithelial cells in the maintenance of gut homeostasis. *Exp Mol Med* 2017; **49**: e338 [PMID: 28546564 DOI: 10.1038/emm.2017.20]

228 **Park JH**, Kotani T, Konno T, Setiawan J, Kitamura Y, Imada S, Usui Y, Hatano N, Shinohara M, Saito Y, Murata Y, Matozaki T. Promotion of Intestinal Epithelial Cell Turnover by Commensal Bacteria: Role of Short-Chain Fatty Acids. *PLoS One* 2016; **11**: e0156334 [PMID: 27232601 DOI: 10.1371/journal.pone.0156334]

229 **Parada Venegas D**, De la Fuente MK, Landskron G, González MJ, Quera R, Dijkstra G, Harmsen HJM, Faber KN, Hermoso MA. Short Chain Fatty Acids (SCFAs)-Mediated Gut Epithelial and Immune Regulation and Its Relevance for Inflammatory Bowel Diseases. *Front Immunol* 2019; **10**: 277 [PMID: 30915065 DOI: 10.3389/fimmu.2019.00277]

230 **Bilotta AJ**, Ma C, Yang W, Yu Y, Zhao X, Zhou Z, Yao S, Dann SM, Cong Y. Propionate Enhances Cell Speed and Persistence to Promote Intestinal Epithelial Turnover and Repair. *Cell Mol Gastroenterol Hepatol* 2021; **11**: 1023-1044 [PMID: 33238220 DOI: 10.1016/j.jcmgh.2020.11.011]

231 **Basson MD**, Liu YW, Hanly AM, Emenaker NJ, Shenoy SG, Gould Rothberg BE. Identification and comparative analysis of human colonocyte short-chain fatty acid response genes. *J Gastrointest Surg* 2000; **4**: 501-512 [PMID: 11077326 DOI: 10.1016/S1091-255X(00)80093-1]

232 **Basson MD**, Turowski GA, Rashid Z, Hong F, Madri JA. Regulation of human colonic cell line proliferation and phenotype by sodium butyrate. *Dig Dis Sci* 1996; **41**: 1989-1993 [PMID: 8888712 DOI: 10.1007/BF02093601]

233 **Basson MD**, Emenaker NJ, Hong F. Differential modulation of human (Caco-2) colon cancer cell line phenotype by short chain fatty acids. *Proc Soc Exp Biol Med* 1998; **217**: 476-483 [PMID: 9521097 DOI: 10.3181/00379727-217-44261]

234 **Gamet L**, Daviaud D, Denis-Pouxviel C, Remesy C, Murat JC. Effects of short-chain fatty acids on growth and differentiation of the human colon-cancer cell line HT29. *Int J Cancer* 1992; **52**: 286-289 [PMID: 1521915 DOI: 10.1002/IJC.2910520222]

235 **Dyson JE**, Daniel J, Surrey CR. The effect of sodium butyrate on the growth characteristics of human cervix tumour cells. *Br J Cancer* 1992; **65**: 803-808 [PMID: 1377482 DOI: 10.1038/BJC.1992.172]

236 **Mortensen FV**, Nielsen H, Mulvany MJ, Hessov I. Short chain fatty acids dilate isolated human colonic resistance arteries. *Gut* 1990; **31**: 1391-1394 [PMID: 2265780 DOI: 10.1136/GUT.31.12.1391]

237 **Mortensen FV**, Hessov I, Birke H, Korsgaard N, Nielsen H. Microcirculatory and trophic effects of short chain fatty acids in the human rectum after Hartmann's procedure. *Br J Surg* 1991; **78**: 1208-1211 [PMID: 1958986 DOI: 10.1002/BJS.1800781019]

238 **Peng L**, He Z, Chen W, Holzman IR, Lin J. Effects of butyrate on intestinal barrier function in a Caco-2 cell monolayer model of intestinal barrier. *Pediatr Res* 2007; **61**: 37-41 [PMID: 17211138 DOI: 10.1203/01.pdr.0000250014.92242.f3]

239 **Suzuki T**, Yoshida S, Hara H. Physiological concentrations of short-chain fatty acids immediately suppress colonic epithelial permeability. *Br J Nutr* 2008; **100**: 297-305 [PMID: 18346306 DOI: 10.1017/S0007114508888733]

240 **Terzi C**, Sevinç AI, Koçdor H, Oktay G, Alanyali H, Küpelioğlu A, Ergör G, Füzün M. Improvement of colonic healing by preoperative rectal irrigation with short-chain fatty acids in rats given radiotherapy. *Dis Colon Rectum* 2004; **47**: 2184-2194 [PMID: 15657672 DOI: 10.1007/S10350-004-0724-7]

241 **Elamin EE**, Masclee AA, Dekker J, Pieters HJ, Jonkers DM. Short-chain fatty acids activate AMP-activated protein kinase and ameliorate ethanol-induced intestinal barrier dysfunction in Caco-2 cell monolayers. *J Nutr* 2013; **143**: 1872-1881 [PMID: 24132573 DOI: 10.3945/jn.113.179549]

242 **Peng L**, Li ZR, Green RS, Holzman IR, Lin J. Butyrate enhances the intestinal barrier by facilitating tight junction assembly *via* activation of AMP-activated protein kinase in Caco-2 cell monolayers. *J Nutr* 2009; **139**: 1619-1625 [PMID: 19625695 DOI: 10.3945/jn.109.104638]

243 **Scheppach W**. Treatment of distal ulcerative colitis with short-chain fatty acid enemas. A placebo-controlled trial. German-Austrian SCFA Study Group. *Dig Dis Sci* 1996; **41**: 2254-2259 [PMID: 8943981 DOI: 10.1007/BF02071409]

244 **Duggan C**, Gannon J, Walker WA. Protective nutrients and functional foods for the gastrointestinal tract. *Am J Clin Nutr* 2002; **75**: 789-808 [PMID: 11976152 DOI: 10.1093/AJCN/75.5.789]

245 **Robinson EK**, Kelly DP, Mercer DW, Kozar RA. Differential effects of luminal arginine and glutamine on metalloproteinase production in the postischemic gut. *JPEN J Parenter Enteral Nutr* 2008; **32**: 433-438 [PMID: 18596315 DOI: 10.1177/0148607108319806]

246 **Kim MH**, Kim H. The Roles of Glutamine in the Intestine and Its Implication in Intestinal Diseases. *Int J Mol Sci* 2017; **18** [PMID: 28498331 DOI: 10.3390/ijms18051051]

247 **Fritz JH**. Arginine cools the inflamed gut. *Infect Immun* 2013; **81**: 3500-3502 [PMID: 23897606 DOI: 10.1128/IAI.00789-13]

248 **Matsui T**, Ichikawa H, Fujita T, Takemura S, Takagi T, Osada-Oka M, Minamiyama Y. Histidine and arginine modulate intestinal cell restitution *via* transforming growth factor-β_1. *Eur J Pharmacol* 2019; **850**: 35-42 [PMID: 30753862 DOI: 10.1016/j.ejphar.2019.02.006]

249 **Turowski GA**, Rashid Z, Hong F, Madri JA, Basson MD. Glutamine modulates phenotype and stimulates proliferation in human colon cancer cell lines. *Cancer Res* 1994; **54**: 5974-5980 [PMID: 7954430]

250 **Chen S**, Xia Y, Zhu G, Yan J, Tan C, Deng B, Deng J, Yin Y, Ren W. Glutamine supplementation improves intestinal cell proliferation and stem cell differentiation in weanling mice. *Food Nutr Res* 2018; **62** [PMID: 30083086 DOI: 10.29219/fnr.v62.1439]

251 **Ji FJ**, Wang LX, Yang HS, Hu A, Yin YL. Review: The roles and functions of glutamine on intestinal health and performance of weaning pigs. *Animal* 2019; **13**: 2727-2735 [PMID: 31407650 DOI: 10.1017/S1751731119001800]

252 **Swaid F**, Sukhotnik I, Matter I, Berkowitz D, Hadjittofi C, Pollak Y, Lavy A. Dietary glutamine supplementation prevents mucosal injury and modulates intestinal epithelial restitution following acetic acid induced intestinal injury in rats. *Nutr Metab (Lond)* 2013; **10**: 53 [PMID: 23919638 DOI: 10.1186/1743-7075-10-53]

253 **Tanaka T**, Morito K, Kinoshita M, Ohmoto M, Urikura M, Satouchi K, Tokumura A. Orally administered phosphatidic acids and lysophosphatidic acids ameliorate aspirin-induced stomach mucosal injury in mice. *Dig Dis Sci* 2013; **58**: 950-

958 [PMID: 23161268 DOI: 10.1007/s10620-012-2475-y]
254 **Hollander D**, Tarnawski A. Is there a role for dietary essential fatty acids in gastroduodenal mucosal protection? *J Clin Gastroenterol* 1991; **13** Suppl 1: S72-S74 [PMID: 1940200 DOI: 10.1097/00004836-199112001-00012]
255 **Bu HF**, Zuo XL, Wang X, Ensslin MA, Koti V, Hsueh W, Raymond AS, Shur BD, Tan XD. Milk fat globule-EGF factor 8/lactadherin plays a crucial role in maintenance and repair of murine intestinal epithelium. *J Clin Invest* 2007; **117**: 3673-3683 [PMID: 18008006 DOI: 10.1172/JCI31841]
256 **Hussey GS**, Keane TJ, Badylak SF. The extracellular matrix of the gastrointestinal tract: a regenerative medicine platform. *Nat Rev Gastroenterol Hepatol* 2017; **14**: 540-552 [PMID: 28698662 DOI: 10.1038/nrgastro.2017.76]
257 **Sonbol HS**. Extracellular Matrix Remodeling in Human Disease. *J Microsc Ultrastruct* 2018; **6**: 123-128 [PMID: 30221137 DOI: 10.4103/JMAU.JMAU_4_18]
258 **Olson AD**, Pysher T, Bienkowski RS. Organization of intestinal epithelial cells into multicellular structures requires laminin and functional actin microfilaments. *Exp Cell Res* 1991; **192**: 543-549 [PMID: 1988292 DOI: 10.1016/0014-4827(91)90074-5]
259 **Vachon PH**, Beaulieu JF. Extracellular heterotrimeric laminin promotes differentiation in human enterocytes. *Am J Physiol* 1995; **268**: G857-G867 [PMID: 7539221 DOI: 10.1152/AJPGI.1995.268.5.G857]
260 **Göke M**, Zuk A, Podolsky DK. Regulation and function of extracellular matrix intestinal epithelial restitution in vitro. *Am J Physiol* 1996; **271**: G729-G740 [PMID: 8944685 DOI: 10.1152/AJPGI.1996.271.5.G729]
261 **Zhang J**, Li W, Sanders MA, Sumpio BE, Panja A, Basson MD. Regulation of the intestinal epithelial response to cyclic strain by extracellular matrix proteins. *FASEB J* 2003; **17**: 926-928 [PMID: 12626437 DOI: 10.1096/FJ.02-0663FJE]
262 **Shimshoni E**, Yablecovitch D, Baram L, Dotan I, Sagi I. ECM remodelling in IBD: innocent bystander or partner in crime? *Gut* 2015; **64**: 367-372 [PMID: 25416065 DOI: 10.1136/gutjnl-2014-308048]
263 **Baugh MD**, Perry MJ, Hollander AP, Davies DR, Cross SS, Lobo AJ, Taylor CJ, Evans GS. Matrix metalloproteinase levels are elevated in inflammatory bowel disease. *Gastroenterology* 1999; **117**: 814-822 [PMID: 10500063 DOI: 10.1016/S0016-5085(99)70339-2]
264 **Kirkegaard T**, Hansen A, Bruun E, Brynskov J. Expression and localisation of matrix metalloproteinases and their natural inhibitors in fistulae of patients with Crohn's disease. *Gut* 2004; **53**: 701-709 [PMID: 15082589 DOI: 10.1136/GUT.2003.017442]
265 **Efsen E**, Saermark T, Hansen A, Bruun E, Brynskov J. Ramiprilate inhibits functional matrix metalloproteinase activity in Crohn's disease fistulas. *Basic Clin Pharmacol Toxicol* 2011; **109**: 208-216 [PMID: 21535409 DOI: 10.1111/j.1742-7843.2011.00713.x]
266 **Kofla-Dlubacz A**, Matusiewicz M, Krzystek-Korpacka M, Iwanczak B. Correlation of MMP-3 and MMP-9 with Crohn's disease activity in children. *Dig Dis Sci* 2012; **57**: 706-712 [PMID: 21997756 DOI: 10.1007/s10620-011-1936-z]
267 **Faubion WA Jr**, Fletcher JG, O'Byrne S, Feagan BG, de Villiers WJ, Salzberg B, Plevy S, Proctor DD, Valentine JF, Higgins PD, Harris JM, Diehl L, Wright L, Tew GW, Luca D, Basu K, Keir ME. EMerging BiomARKers in Inflammatory Bowel Disease (EMBARK) study identifies fecal calprotectin, serum MMP9, and serum IL-22 as a novel combination of biomarkers for Crohn's disease activity: role of cross-sectional imaging. *Am J Gastroenterol* 2013; **108**: 1891-1900 [PMID: 24126633 DOI: 10.1038/ajg.2013.354]
268 **Sela-Passwell N**, Kikkeri R, Dym O, Rozenberg H, Margalit R, Arad-Yellin R, Eisenstein M, Brenner O, Shoham T, Danon T, Shanzer A, Sagi I. Antibodies targeting the catalytic zinc complex of activated matrix metalloproteinases show therapeutic potential. *Nat Med* 2011; **18**: 143-147 [PMID: 22198278 DOI: 10.1038/nm.2582]
269 **Schreiber S**, Siegel CA, Friedenberg KA, Younes ZH, Seidler U, Bhandari BR, Wang K, Wendt E, McKevitt M, Zhao S, Sundy JS, Lee SD, Loftus EV. A Phase 2, Randomized, Placebo-Controlled Study Evaluating Matrix Metalloproteinase-9 Inhibitor, Andecaliximab, in Patients With Moderately to Severely Active Crohn's Disease. *J Crohns Colitis* 2018; **12**: 1014-1020 [PMID: 29846530 DOI: 10.1093/ecco-jcc/jjy070]
270 **Schreiber S**. Lack of Efficacy in Crohn's Disease Prompts Unplanned Interim Analysis and Termination of Study in Ulcerative Colitis. *J Crohns Colitis* 2020; **14**: 282 [PMID: 32037454 DOI: 10.1093/ecco-jcc/jjz142]
271 **Spiering D**, Hodgson L. Dynamics of the Rho-family small GTPases in actin regulation and motility. *Cell Adh Migr* 2011; **5**: 170-180 [PMID: 21178402 DOI: 10.4161/CAM.5.2.14403]
272 **Abreu-Blanco MT**, Watts JJ, Verboon JM, Parkhurst SM. Cytoskeleton responses in wound repair. *Cell Mol Life Sci* 2012; **69**: 2469-2483 [PMID: 22349211 DOI: 10.1007/s00018-012-0928-2]
273 **Chaturvedi LS**, Marsh HM, Basson MD. Role of RhoA and its effectors ROCK and mDia1 in the modulation of deformation-induced FAK, ERK, p38, and MLC motogenic signals in human Caco-2 intestinal epithelial cells. *Am J Physiol Cell Physiol* 2011; **301**: C1224-C1238 [PMID: 21849669 DOI: 10.1152/ajpcell.00518.2010]
274 **Kopecki Z**, Cowin AJ. The Role of Actin Remodelling Proteins in Wound Healing and Tissue Regeneration. In: Wound Healing - New insights into Ancient Challenges. Intech Open, 2016 [DOI: 10.5772/64673]
275 **Heath JP**. Epithelial cell migration in the intestine. *Cell Biol Int* 1996; **20**: 139-146 [PMID: 8935158 DOI: 10.1006/CBIR.1996.0018]
276 **Tang DD**, Gerlach BD. The roles and regulation of the actin cytoskeleton, intermediate filaments and microtubules in smooth muscle cell migration. *Respir Res* 2017; **18**: 54 [PMID: 28390425 DOI: 10.1186/s12931-017-0544-7]
277 **Hohmann T**, Dehghani F. The Cytoskeleton-A Complex Interacting Meshwork. *Cells* 2019; **8** [PMID: 31003495 DOI: 10.3390/CELLS8040362]
278 **Etienne-Manneville S**. Actin and microtubules in cell motility: which one is in control? *Traffic* 2004; **5**: 470-477 [PMID: 15180824 DOI: 10.1111/J.1600-0854.2004.00196.X]
279 **Rottner K**, Schaks M. Assembling actin filaments for protrusion. *Curr Opin Cell Biol* 2019; **56**: 53-63 [PMID: 30278304 DOI: 10.1016/j.ceb.2018.09.004]
280 **Garcin C**, Straube A. Microtubules in cell migration. *Essays Biochem* 2019; **63**: 509-520 [PMID: 31358621 DOI: 10.1042/EBC20190016]
281 **Charafeddine RA**, Nosanchuk JD, Sharp DJ. Targeting Microtubules for Wound Repair. *Adv Wound Care (New Rochelle)* 2016; **5**: 444-454 [PMID: 27785378 DOI: 10.1089/WOUND.2015.0658]

282 **Campbell ID**, Ginsberg MH. The talin-tail interaction places integrin activation on FERM ground. *Trends Biochem Sci* 2004; **29**: 429-435 [PMID: 15362227 DOI: 10.1016/J.TIBS.2004.06.005]

283 **Bosanquet DC**, Ye L, Harding KG, Jiang WG. FERM family proteins and their importance in cellular movements and wound healing (review). *Int J Mol Med* 2014; **34**: 3-12 [PMID: 24820650 DOI: 10.3892/ijmm.2014.1775]

284 **Gurtner GC**, Wong VW. Filamin A Mediates Wound Closure by Promoting Elastic Deformation and Maintenance of Tension in the Collagen Matrix. *J Invest Dermatol* 2015; **135**: 2569-2571 [PMID: 26548489 DOI: 10.1038/jid.2015.327]

285 **Sun HQ**, Yamamoto M, Mejillano M, Yin HL. Gelsolin, a multifunctional actin regulatory protein. *J Biol Chem* 1999; **274**: 33179-33182 [PMID: 10559185 DOI: 10.1074/JBC.274.47.33179]

286 **Kopecki Z**, O'Neill GM, Arkell RM, Cowin AJ. Regulation of focal adhesions by flightless i involves inhibition of paxillin phosphorylation *via* a Rac1-dependent pathway. *J Invest Dermatol* 2011; **131**: 1450-1459 [PMID: 21430700 DOI: 10.1038/jid.2011.69]

287 **Mohammad I**, Arora PD, Naghibzadeh Y, Wang Y, Li J, Mascarenhas W, Janmey PA, Dawson JF, McCulloch CA. Flightless I is a focal adhesion-associated actin-capping protein that regulates cell migration. *FASEB J* 2012; **26**: 3260-3272 [PMID: 22581781 DOI: 10.1096/fj.11-202051]

288 **Jackson JE**, Kopecki Z, Adams DH, Cowin AJ. Flii neutralizing antibodies improve wound healing in porcine preclinical studies. *Wound Repair Regen* 2012; **20**: 523-536 [PMID: 22672080 DOI: 10.1111/j.1524-475X.2012.00802.x]

289 **Kopecki Z**, Ruzehaji N, Turner C, Iwata H, Ludwig RJ, Zillikens D, Murrell DF, Cowin AJ. Topically applied flightless I neutralizing antibodies improve healing of blistered skin in a murine model of epidermolysis bullosa acquisita. *J Invest Dermatol* 2013; **133**: 1008-1016 [PMID: 23223144 DOI: 10.1038/jid.2012.457]

290 **Danen EH**, Sonneveld P, Brakebusch C, Fassler R, Sonnenberg A. The fibronectin-binding integrins alpha5beta1 and alphavbeta3 differentially modulate RhoA-GTP loading, organization of cell matrix adhesions, and fibronectin fibrillogenesis. *J Cell Biol* 2002; **159**: 1071-1086 [PMID: 12486108 DOI: 10.1083/jcb.200205014]

291 **Ballestrem C**, Hinz B, Imhof BA, Wehrle-Haller B. Marching at the front and dragging behind: differential alphaVbeta3-integrin turnover regulates focal adhesion behavior. *J Cell Biol* 2001; **155**: 1319-1332 [PMID: 11756480 DOI: 10.1083/JCB.200107107]

292 **Laukaitis CM**, Webb DJ, Donais K, Horwitz AF. Differential dynamics of alpha 5 integrin, paxillin, and alpha-actinin during formation and disassembly of adhesions in migrating cells. *J Cell Biol* 2001; **153**: 1427-1440 [PMID: 11425873 DOI: 10.1083/JCB.153.7.1427]

293 **Zaidel-Bar R**, Ballestrem C, Kam Z, Geiger B. Early molecular events in the assembly of matrix adhesions at the leading edge of migrating cells. *J Cell Sci* 2003; **116**: 4605-4613 [PMID: 14576354 DOI: 10.1242/JCS.00792]

294 **Gardel ML**, Schneider IC, Aratyn-Schaus Y, Waterman CM. Mechanical integration of actin and adhesion dynamics in cell migration. *Annu Rev Cell Dev Biol* 2010; **26**: 315-333 [PMID: 19575647 DOI: 10.1146/annurev.cellbio.011209.122036]

295 **Alam A**, Neish A. Role of gut microbiota in intestinal wound healing and barrier function. *Tissue Barriers* 2018; **6**: 1539595 [PMID: 30404570 DOI: 10.1080/21688370.2018.1539595]

296 **Owen KA**, Abshire MY, Tilghman RW, Casanova JE, Bouton AH. FAK regulates intestinal epithelial cell survival and proliferation during mucosal wound healing. *PLoS One* 2011; **6**: e23123 [PMID: 21887232 DOI: 10.1371/journal.pone.0023123]

297 **Burridge K**. Focal adhesions: a personal perspective on a half century of progress. *FEBS J* 2017; **284**: 3355-3361 [PMID: 28796323 DOI: 10.1111/febs.14195]

298 **Gilmore AP**, Romer LH. Inhibition of focal adhesion kinase (FAK) signaling in focal adhesions decreases cell motility and proliferation. *Mol Biol Cell* 1996; **7**: 1209-1224 [PMID: 8856665 DOI: 10.1091/mbc.7.8.1209]

299 **Parsons JT**. Focal adhesion kinase: the first ten years. *J Cell Sci* 2003; **116**: 1409-1416 [PMID: 12640026 DOI: 10.1242/jcs.00373]

300 **Schlaepfer DD**, Mitra SK. Multiple connections link FAK to cell motility and invasion. *Curr Opin Genet Dev* 2004; **14**: 92-101 [PMID: 15108811 DOI: 10.1016/j.gde.2003.12.002]

301 **Thomas JW**, Cooley MA, Broome JM, Salgia R, Griffin JD, Lombardo CR, Schaller MD. The role of focal adhesion kinase binding in the regulation of tyrosine phosphorylation of paxillin. *J Biol Chem* 1999; **274**: 36684-36692 [PMID: 10593973 DOI: 10.1074/JBC.274.51.36684]

302 **Hu YL**, Lu S, Szeto KW, Sun J, Wang Y, Lasheras JC, Chien S. FAK and paxillin dynamics at focal adhesions in the protrusions of migrating cells. *Sci Rep* 2014; **4**: 6024 [PMID: 25113375 DOI: 10.1038/srep06024]

303 **Webb DJ**, Donais K, Whitmore LA, Thomas SM, Turner CE, Parsons JT, Horwitz AF. FAK-Src signalling through paxillin, ERK and MLCK regulates adhesion disassembly. *Nat Cell Biol* 2004; **6**: 154-161 [PMID: 14743221 DOI: 10.1038/ncb1094]

304 **Klemke RL**, Cai S, Giannini AL, Gallagher PJ, de Lanerolle P, Cheresh DA. Regulation of cell motility by mitogen-activated protein kinase. *J Cell Biol* 1997; **137**: 481-492 [PMID: 9128257 DOI: 10.1083/JCB.137.2.481]

305 **Ishibe S**, Joly D, Liu ZX, Cantley LG. Paxillin serves as an ERK-regulated scaffold for coordinating FAK and Rac activation in epithelial morphogenesis. *Mol Cell* 2004; **16**: 257-267 [PMID: 15494312 DOI: 10.1016/j.molcel.2004.10.006]

306 **Basson MD**, Sanders MA, Gomez R, Hatfield J, Vanderheide R, Thamilselvan V, Zhang J, Walsh MF. Focal adhesion kinase protein levels in gut epithelial motility. *Am J Physiol Gastrointest Liver Physiol* 2006; **291**: G491-G499 [PMID: 16899713 DOI: 10.1152/ajpgi.00292.2005]

307 **Arold ST**, Hoellerer MK, Noble ME. The structural basis of localization and signaling by the focal adhesion targeting domain. *Structure* 2002; **10**: 319-327 [PMID: 12005431 DOI: 10.1016/S0969-2126(02)00717-7]

308 **Deramaudt TB**, Dujardin D, Noulet F, Martin S, Vauchelles R, Takeda K, Rondé P. Altering FAK-paxillin interactions reduces adhesion, migration and invasion processes. *PLoS One* 2014; **9**: e92059 [PMID: 24642576 DOI: 10.1371/journal.pone.0092059]

309 **Lietha D**, Cai X, Ceccarelli DF, Li Y, Schaller MD, Eck MJ. Structural basis for the autoinhibition of focal adhesion kinase. *Cell* 2007; **129**: 1177-1187 [PMID: 17574028 DOI: 10.1016/j.cell.2007.05.041]

310 **Mousson A**, Sick E, Carl P, Dujardin D, De Mey J, Rondé P. Targeting Focal Adhesion Kinase Using Inhibitors of Protein-Protein Interactions. *Cancers (Basel)* 2018; **10** [PMID: 30134553 DOI: 10.3390/cancers10090278]

311 **Cary LA**, Chang JF, Guan JL. Stimulation of cell migration by overexpression of focal adhesion kinase and its association with Src and Fyn. *J Cell Sci* 1996; **109** (Pt 7): 1787-1794 [PMID: 8832401 DOI: 10.1242/jcs.109.7.1787]

312 **Lawson C**, Schlaepfer DD. pHocal adhesion kinase regulation is on a FERM foundation. *J Cell Biol* 2013; **202**: 833-836 [PMID: 24043698 DOI: 10.1083/jcb.201308034]

313 **Mitra SK**, Hanson DA, Schlaepfer DD. Focal adhesion kinase: in command and control of cell motility. *Nat Rev Mol Cell Biol* 2005; **6**: 56-68 [PMID: 15688067 DOI: 10.1038/nrm1549]

314 **Fan H**, Zhao X, Sun S, Luo M, Guan JL. Function of focal adhesion kinase scaffolding to mediate endophilin A2 phosphorylation promotes epithelial-mesenchymal transition and mammary cancer stem cell activities in vivo. *J Biol Chem* 2013; **288**: 3322-3333 [PMID: 23255596 DOI: 10.1074/jbc.M112.420497]

315 **McLean GW**, Carragher NO, Avizienyte E, Evans J, Brunton VG, Frame MC. The role of focal-adhesion kinase in cancer - a new therapeutic opportunity. *Nat Rev Cancer* 2005; **5**: 505-515 [PMID: 16069815 DOI: 10.1038/nrc1647]

316 **Zhao X**, Guan JL. Focal adhesion kinase and its signaling pathways in cell migration and angiogenesis. *Adv Drug Deliv Rev* 2011; **63**: 610-615 [PMID: 21118706 DOI: 10.1016/j.addr.2010.11.001]

317 **Lim ST**, Chen XL, Lim Y, Hanson DA, Vo TT, Howerton K, Larocque N, Fisher SJ, Schlaepfer DD, Ilic D. Nuclear FAK promotes cell proliferation and survival through FERM-enhanced p53 degradation. *Mol Cell* 2008; **29**: 9-22 [PMID: 18206965 DOI: 10.1016/j.molcel.2007.11.031]

318 **Teranishi S**, Kimura K, Nishida T. Role of formation of an ERK-FAK-paxillin complex in migration of human corneal epithelial cells during wound closure in vitro. *Invest Ophthalmol Vis Sci* 2009; **50**: 5646-5652 [PMID: 19494198 DOI: 10.1167/iovs.08-2534]

319 **Tanimura S**, Takeda K. ERK signalling as a regulator of cell motility. *J Biochem* 2017; **162**: 145-154 [PMID: 28903547 DOI: 10.1093/jb/mvx048]

320 **Wang Y**, Zheng J, Han Y, Zhang Y, Su L, Hu D, Fu X. JAM-A knockdown accelerates the proliferation and migration of human keratinocytes, and improves wound healing in rats *via* FAK/Erk signaling. *Cell Death Dis* 2018; **9**: 848 [PMID: 30154481 DOI: 10.1038/s41419-018-0941-y]

321 **Chodniewicz D**, Klemke RL. Regulation of integrin-mediated cellular responses through assembly of a CAS/Crk scaffold. *Biochim Biophys Acta* 2004; **1692**: 63-76 [PMID: 15246680 DOI: 10.1016/J.BBAMCR.2004.03.006]

322 **Sanders MA**, Basson MD. p130cas but not paxillin is essential for Caco-2 intestinal epithelial cell spreading and migration on collagen IV. *J Biol Chem* 2005; **280**: 23516-23522 [PMID: 15817476 DOI: 10.1074/jbc.M413165200]

323 **Sharma A**, Mayer BJ. Phosphorylation of p130Cas initiates Rac activation and membrane ruffling. *BMC Cell Biol* 2008; **9**: 50 [PMID: 18793427 DOI: 10.1186/1471-2121-9-50]

324 **Geiger B**. A role for p130Cas in mechanotransduction. *Cell* 2006; **127**: 879-881 [PMID: 17129774 DOI: 10.1016/J.CELL.2006.11.020]

325 **Cox BD**, Natarajan M, Stettner MR, Gladson CL. New concepts regarding focal adhesion kinase promotion of cell migration and proliferation. *J Cell Biochem* 2006; **99**: 35-52 [PMID: 16823799 DOI: 10.1002/JCB.20956]

326 **Raschka S**, More SK, Devadoss D, Zeng B, Kuhn LA, Basson MD. Identification of potential small-molecule protein-protein inhibitors of cancer metastasis by 3D epitope-based computational screening. *J Physiol Pharmacol* 2018; **69** [PMID: 29980145 DOI: 10.26402/jpp.2018.2.11]

327 **Wang Q**, More SK, Vomhof-DeKrey EE, Golovko MY, Basson MD. Small molecule FAK activator promotes human intestinal epithelial monolayer wound closure and mouse ulcer healing. *Sci Rep* 2019; **9**: 14669 [PMID: 31604999 DOI: 10.1038/s41598-019-51183-z]

328 **Rashmi**, More SK, Wang Q, Vomhof-DeKrey EE, Porter JE, Basson MD. ZINC40099027 activates human focal adhesion kinase by accelerating the enzymatic activity of the FAK kinase domain. *Pharmacol Res Perspect* 2021; **9**: e00737 [PMID: 33715263 DOI: 10.1002/prp2.737]

329 **Wang Q**, Gallardo-Macias R, Rashmi, Golovko MY, Elsayed AAR, More SK, Oncel S, Gurvich VJ, Basson MD. Discovery of Novel Small-Molecule FAK Activators Promoting Mucosal Healing. *ACS Med Chem Lett* 2021; **12**: 356-364 [PMID: 33738062 DOI: 10.1021/acsmedchemlett.0c00311]

World Journal of Gastroenterology

Submit a Manuscript: https://www.f6publishing.com

World J Gastroenterol 2022 May 7; 28(17): 1751-1767

DOI: 10.3748/wjg.v28.i17.1751

ISSN 1007-9327 (print) ISSN 2219-2840 (online)

REVIEW

New insights in diagnosis and treatment of gastroenteropancreatic neuroendocrine neoplasms

Feng Yin, Zi-Hao Wu, Jin-Ping Lai

Specialty type: Gastroenterology and hepatology

Provenance and peer review: Invited article; Externally peer reviewed.

Peer-review model: Single blind

Peer-review report's scientific quality classification
Grade A (Excellent): 0
Grade B (Very good): B
Grade C (Good): 0
Grade D (Fair): D
Grade E (Poor): 0

P-Reviewer: Massironi S, Italy; Skrlec I, Croatia

Received: October 21, 2021
Peer-review started: October 21, 2021
First decision: December 27, 2021
Revised: January 6, 2022
Accepted: April 4, 2022
Article in press: April 4, 2022
Published online: May 7, 2022

Feng Yin, Department of Pathology and Anatomical Sciences, University of Missouri, Columbia, MO 65212, United States

Zi-Hao Wu, Department of Surgery, University of Missouri, Columbia, MO 65212, United States

Jin-Ping Lai, Department of Pathology, Kaiser Permanente Sacramento Medical Center, Sacramento, CA 95825, United States

Corresponding author: Jin-Ping Lai, MD, PhD, Associate Professor, Doctor, Department of Pathology, Kaiser Permanente Sacramento Medical Center, 2025 Morse Ave, Sacramento, CA 95825, United States. jinping.x.lai@kp.org

Abstract

Gastroenteropancreatic neuroendocrine neoplasms (GEP-NENs) are rare epithelial neoplasms derived from pluripotent endocrine cells along the gastrointestinal tract and pancreas. GEP-NENs are classified into well-differentiated neuroendocrine tumors and poorly differentiated neuroendocrine carcinomas. Despite overlapping morphological features, GEP-NENs vary in molecular biology, epigenetic, clinical behavior, treatment response, and prognosis features and remain an unmet clinical challenge. In this review, we introduce recent updates on the histopathologic classification, including the tumor grading and staging system, molecular genetics, and systemic evaluation of the diagnosis and treatment of GEP-NENs at different anatomic sites, together with some insights into the diagnosis of challenging and unusual cases. We also discuss the application of novel therapeutic approaches for GEP-NENs, including peptide receptor radionuclide therapy, targeted therapy, and immunotherapy with immune checkpoint inhibitors. These findings will help improve patient care with precise diagnosis and individualized treatment of patients with GEP-NENs.

Key Words: Gastroenteropancreatic neuroendocrine neoplasms; Neuroendocrine tumours; Neuroendocrine carcinoma; World Health Organization classification; Diagnosis; Treatment

©The Author(s) 2022. Published by Baishideng Publishing Group Inc. All rights reserved.

Core Tip: Gastroenteropancreatic neuroendocrine neoplasms (GEP-NENs) are rare tumors, but their incidence rates have been steadily increasing over the past 3 decades. GEP-NENs consist of a genetically heterogeneous group of tumors ranging from slow-growing well-differentiated neuroendocrine tumor to aggressive, poorly differentiated neuroendocrine carcinoma. Surgery is the cornerstone for the clinical management of localized tumors. However, GEP-NENs have frequently been diagnosed at a later stage and, therefore, remain an unmet clinical challenge. In this review, we discuss recent updates on the histopathologic classification, molecular genetics, and systemic evaluation of diagnosis and treatment of GEP-NENs at different anatomic sites.

Citation: Yin F, Wu ZH, Lai JP. New insights in diagnosis and treatment of gastroenteropancreatic neuroendocrine neoplasms. *World J Gastroenterol* 2022; 28(17): 1751-1767
URL: https://www.wjgnet.com/1007-9327/full/v28/i17/1751.htm
DOI: https://dx.doi.org/10.3748/wjg.v28.i17.1751

INTRODUCTION

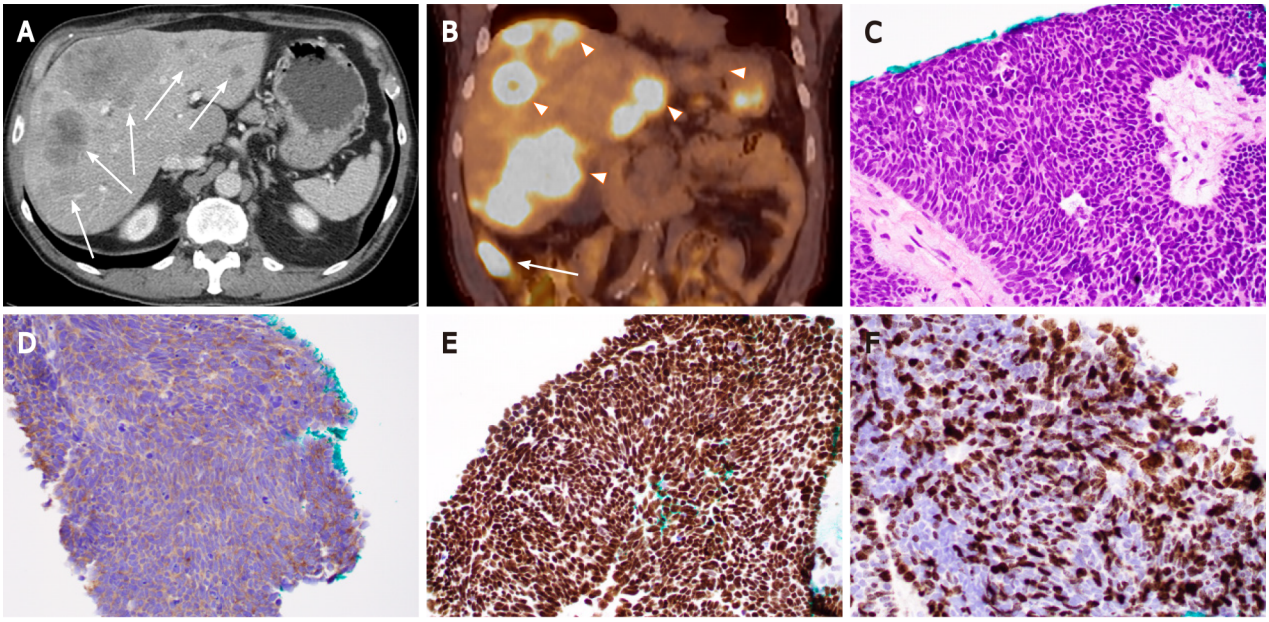
Gastroenteropancreatic neuroendocrine neoplasms (GEP-NENs) are epithelial neoplasms with neuroendocrine differentiation that occur inside the gastrointestinal (GI) tract and the pancreas[1]. They are a group of tumors with significant heterogeneity and complex clinical behavior, ranging from slowly growing well-differentiated gastroenteropancreatic neuroendocrine tumors (GEP-NETs) to highly aggressive, poorly differentiated gastroenteropancreatic neuroendocrine carcinomas (GEP-NECs)[1-3]. The traditional term for a NET is carcinoid, which has been largely discouraged in the updated disease classification published by the World Health Organization (WHO)[1].

GEN-NENs are relatively rare (1.0%-1.5% of all GEP neoplasms, 6.98 and 0.4 new cases *per* year *per* 100000 individuals in the United States for GEP-NETs and GEP-NECs, respectively)[4-7], although their incidence has significantly increased in the past 3 decades, largely due to the improved awareness and detection rate. The majority (> 95%) of GEP-NENs are sporadic, although some (approximately 5%) could be part of syndromic presentations, including multiple endocrine neoplasm type 1 (MEN1), neurofibromatosis type 1 (NF1), and von Hippel–Lindau syndrome (VHL)[1-4].

Based on the embryological development of the GI tract, GEP-NENs can be divided into foregut (the esophagus to the proximal duodenum and pancreas), midgut (the distal duodenum to proximal two thirds of the transverse colon), and hindgut NENs (distal third of the transverse colon to the rectum)[5, 6], with the midgut (especially the small intestine) being the most common site for GEP-NENs. For example, Figure 1 shows the case of a 71-year-old Caucasian man who was initially identified to have multiple liver masses on computed tomography (CT) scans. CT-guided percutaneous liver needle core biopsy showed poorly differentiated neuroendocrine carcinoma and a small cell type, and the tumor cells were positive for neuroendocrine markers and GI tumor markers. A positron emission tomography (PET)/CT scan revealed the primary lesion in the ileum (Figure 1). In addition, compared with their foregut and hindgut counterparts, midgut NENs are more commonly associated with carcinoid syndrome[7]. In this review, we will discuss anatomic origin and pathologic feature-based classification systems for GEP-NETs as well as the diagnosis and current update of therapy. Based on our practice, we will also share some experience in the work-up of some unusual and challenging cases with diagnostic pitfalls.

HISTOPATHOLOGIC CLASSIFICATION

Tumor differentiation is closely associated with the clinical behavior of GEP-NENs and refers to how much the tumor tissue looks like the normal tissue that it was derived from. Based on tumor differentiation and histopathologic features, GEP-NENs can be classified into three major categories: Well-differentiated NETs, poorly differentiated NECs, and mixed neuroendocrine-nonneuroendocrine neoplasms (MiNENs)[8]. Well-differentiated GEP-NETs commonly present with a uniform population of tumor cells with round nuclei and finely stippled "salt-and-pepper" chromatin[9]. Their common growth patterns include nests, trabeculae, acini, and ribbons. On the other hand, poorly differentiated GEP-NECs could be further classified into small-cell NECs and large-cell NECs based on their cytological features and commonly grow in sheets or nests with frequent tumor necrosis[10]. Small-cell NECs have features that include blue cells with scant cytoplasm, finely dispersed chromatin, nuclear molding, smudging, no distinct nucleoli, high mitotic rate, and patterns of rosettes and/or peripheral palisading (Figure 1). Large-cell NECs also have a neuroendocrine architecture and features of large cells with abundant cytoplasm, round and vesicular nuclei, and prominent nucleoli. Some NECs have a concurrent adenocarcinoma component and are categorized as MiNENs[11,12].



DOI: 10.3748/wjg.v28.i17.1751 **Copyright** ©The Author(s) 2022.

Figure 1 Ileal small cell neuroendocrine carcinoma with liver metastases in a 71-year-old man. A: Computed tomography (CT) image (axial) showing ileal and multifocal liver lesions (arrow); B: Positron emission tomography-CT image showing ileal (arrow) and liver lesions (arrowheads) with hypermetabolic activity; C: Histopathologic features of small cell neuroendocrine carcinoma. Note the tumor cells with peripheral palisading, rosetting, scant cytoplasm, nuclear molding, finely granular chromatin, and lack of prominent nucleoli; D-F: Tumor cells with positive immunoreactivity for synaptophysin (D) and CDX2 (E) as well as a high Ki-67 proliferation index (70%) (F). (C-F: 400 ×).

Tumor grade is another important factor closely correlated with the clinical behavior of GEP-NENs. It refers to how abnormal the tumor cells look under a microscope, and in the case of GEP-NENs, the tumor grade is usually determined by the proliferation rate of the tumor cells that could be reported by the mitotic rate (number of mitoses *per* 2 mm^2) and/or the Ki-67 proliferation index (average nuclear immunolabeling based on at least 500 tumor cells) (Table 1). The current guidelines use a 3-tier tumor grading system: Low-grade (grade 1, G1) tumors with a mitotic rate up to 2 *per* 2 mm^2 or a Ki-67 proliferation index up to 3%, intermediate-grade (grade 2, G2) tumors with a mitotic rate from 2 to 20 *per* 2 mm^2 or a Ki-67 proliferation index from 3% to 20%, and high-grade (grade 3, G3) tumors with a mitotic rate greater than 20 *per* 2 mm^2 or a Ki-67 proliferation index greater than 20%[13]. A suggestion has been made to use a Ki-67 proliferation index of 5% as the cutoff level, instead of 3% according to current guidelines, for better risk stratification in patients with G1 to G2 tumors[14], although additional large-scale studies are needed to validate this proposed cutoff value. Due to the heterogeneity among tumor tissues, a routine practice is to perform measurements in the most mitotically active tumor area. In cases with discrepancies between the mitotic rate and Ki-67 proliferation index, the tumor will be placed into the highest-grade category. A higher Ki-67 proliferation index is associated with a poorer prognosis[15]. In fact, the Ki-67 proliferation index appears to be a better prognostic marker than the mitotic rate for metastatic pancreatic and midgut NENs[16]. Of note, all NECs were high-grade carcinomas with a poorly differentiated morphology and a high Ki-67 proliferation index (> 20%, more than 50% in the majority of the cases) (Figure 1) and high mitotic count (> 20 *per* 2 mm^2). Historically, all G3 GEP-NENs were conceptually equal to NECs before 2017. However, recent studies have clearly demonstrated that G3 GEP-NETs and GEP-NECs are genetically different entities[17]. In general, G3 GEP-NETs are morphologically well differentiated and clinically less aggressive than GEP-NECs and have a poorer response to platinum-based chemotherapy[18].

All GEP-NENs are characterized by the expression of neuroendocrine markers, with or without secretion of biologically active substances. Immunohistochemical staining is often necessary, not only to confirm the diagnosis and to assign the tumor grade category but also to investigate the tumor origin in cases of metastasis. GEN-NENs are derived from the neuroendocrine epithelium and therefore normally express cytokeratin (CK), with CK8 and CK18 being the most common[19]. The expression of CK could separate GEP-NENs from their great mimics pheochromocytoma/paraganglioma. General neuroendocrine markers are also frequently used in routine practice to establish the diagnosis. Well-differentiated NETs usually express somatostatin receptors. In fact, the expression of somatostatin receptor subtype 2A (SSTR2A) is the basis of functional imaging (such as gallium Ga 68 dotatate) and somatostatin analog (SSA) therapy, including octreotide acetate and peptide receptor radionuclide therapy (PRRT) (such as lutetium Lu 177 dotatate)[20]. Some commonly used neuroendocrine immunohistochemical markers include chromograin A (CgA), synaptophysin (SYN), and CD56. Recent studies have demonstrated INSM1 (insulinoma-associated protein 1) as a novel and more specific marker of

Table 1 World Health Organization classification for gastroenteropancreatic neuroendocrine neoplasms[1]

	Differentiation	Mitotic rate (%)	Ki-67 proliferation index (%)
G1 NET	Well-differentiated	< 2	< 3
G2 NET	Well-differentiated	2-20	3-20
G3 NET	Well-differentiated	> 20	> 20
SCNEC	Poorly-differentiated	> 20	> 20
LCNEC	Poorly-differentiated	> 20	> 20
MiNEN	Well- or poorly-differentiated	Variable	Variable

NET: Neuroendocrine tumor; SCNEC: Small cell neuroendocrine carcinoma; LCNEC: Large cell neuroendocrine carcinoma; MiNEN: Mixed neuroendocrine-non-neuroendocrine neoplasm.
[1]Data derived from Klimstra *et al*[1].

neuroendocrine differentiation. In the case of poorly differentiated NECs, INSM1 appears much more sensitive (95%) than CgA (83%) and SYN (82%)[21]. Immunohistochemical staining could also be helpful to identify unknown primary tumors in cases of metastasis. Up to 20% of NETs originally present as liver or bone metastasis from unknown primary tumors, and identification of the primary tumor has significant therapeutic and prognostic implications. The jejunum, ileum, and pancreas appear to be the most common primary sites for patients with NET liver metastases of occult origin[22,23]. CDX2 immunoreactivity is present in the majority of jejuno-ileal NETs, and up to 24% of metastases are primarily pancreatic NETs[24]. The novel marker SATB2 (special AT-rich sequence-binding protein 2) is frequently and strongly expressed in NETs of the lower GI tract and has shown value in assigning NEC sites of origin[25]. For metastatic GEP-NENs, additional immunohistochemical panels include PDX-1 (pancreatic and duodenal homeobox 1), PAX6 (paired Box 6), PAX8 (paired Box 8), ISL1 (islet 1), NESP55 (neuroendocrine secretory protein 55), PR (progesterone receptor), and PrAP (prostate acid phosphatase)[26,27]. We performed PAX6 and PAX8 immunohistochemical staining on 178 NETs, including 110 primary NETs (26 pancreatic, 10 gastric, 12 duodenal, 22 jejuno-ileal, 10 rectal, and 30 pulmonary) and 68 NETs metastatic to the liver (24 pancreatic, 1 duodenal, 37 jejuno-ileal, 1 rectal, and 5 pulmonary). Among primary GEP-NETs, PAX6 and PAX8 were positive in 65% (17/26) and 73% (19/26) of pancreatic, 0% (0/10) and 10% (1/10) of gastric, 92% (11/12) and 92% (11/12) of duodenal, 0% (0/22) and 0% (0/22) of jejuno-ileal, and 90% (9/10) and 80% (8/10) of rectal NETs, respectively. PAX6 and PAX8 positivity was seen in 46% (11/24) and 50% (12/24) of metastatic pancreatic NETs to the liver, respectively. None of the nonpancreatic NETs metastatic to the liver were immunoreactive for either PAX6 or PAX8[27].

MOLECULAR GENETICS

GEP-NENs consist of a biologically distinct group of tumors with great genetic heterogeneity. Largely driven by high-throughput technologies and next-generation sequencing, significant progress has been made in recent years in understanding the key molecular drivers of tumorigenesis and progression, especially pancreatic and small bowel NENs[28-30]. Approximately 10%-20% of pancreatic NETs (P-NETs) are associated with hereditary genetic syndromes, including MEN-1, NF1, VHL, and tuberous sclerosis[31]. In cases with sporadic P-NETs, three types of major molecular alterations have been detected, including somatic mutations in *MEN1* (44%), *DAXX* (death-domain associated protein)/*ATRX* (alpha thalassaemia/mental retardation syndrome X-linked mutations) (43%), and mammalian target of rapamycin (mTOR) pathway genes such as *PTEN*, *TSC2*, and *PIK3CA* (14%)[32]. Identification of mTOR pathway gene alterations has clinical relevance due to the available targeted therapy. Germline mutations in DNA repair genes, including *MUTYH*, *CHEK2*, and *BRCA2*, have been reported in sporadic P-NETs[33]. Chromosome 18 deletion is detected in 60%-90% of small intestinal NETs (SI-NETs), although its significance is still unclear at this time[34]. Chromosome 14 gain is also frequently detected in advanced and metastatic disease[35]. Approximately 8% of SI-NETs have somatic mutations in *CDKN1B*[36,37]. A recent study demonstrated that, as epigenetically dysregulated tumors, SI-NETs could be divided into three subgroups: (1) Chromosome 18 deletion with *CDKN1B* mutations and CpG island methylator phenotype (CIMP) negativity, the largest subgroup (55%) with the most favorable prognosis; (2) The absence of arm-level copy-number variation (CNV) with a high level of CIMP positivity, the subgroup (19%) with intermediate prognosis; and (3) The presence of multiple CNVs, the subgroup (26%) with a young age at onset and the worst prognosis[38]. In addition to P-NETs and SI-NETs, more studies are needed to understand the molecular genetics of GEP-NETs in other anatomic

sites.

From a molecular genetics point of view, pancreatic NECs (P-NECs) are entirely biologically different entities from P-NETs. The most common molecular alterations in P-NECs are somatic mutations in *TP53*, *RB1*, *CDKN2A*, and *KRAS*[39]. Notably, mutations in the *TP53* and *RB1* genes appear to be recurrent molecular events in GEP-NECs from different anatomic sites, including the stomach and colorectum [40]. *KRAS* mutations have also been detected in gastric and colorectal NECs, although *BRAF* mutations have only been reported in colorectal NECs[30]. Interestingly, somatic mutations in *DAXX*, *ATRX*, and *MEN1* are almost exclusively detected in well-differentiated NETs but not poorly differentiated NECs [41].

The pathological diagnosis of grade-3 well-differentiated NETs and poorly differentiated NECs could be challenging in some cases because of the high mitotic rate (> 20 *per* 2 mm^2) and high Ki-67 proliferation index (> 20%), particularly for the limited sample made from endoscopic ultrasound-guided fine-needle aspiration (EUS-FNA). The distinct molecular profile could help to separate these two entities. In practice, immunohistochemistry using antibodies against DAXX, ATXR, p53, and RB1 could be performed to surrogate for genetic status[42]. Poorly differentiated NECs frequently have absent RB1 and aberrant p53 protein expression, together with normal expression of DAXX and ATRX. On the other hand, normal RB1 and p53 protein expression is normally found in well-differentiated NETs.

CLINICAL PRESENTATION, DIAGNOSIS, AND TREATMENT

Gastric NENs

Gastric NENs (G-NENs) originate from different neuroendocrine cell types in the gastric mucosa, including enterochromaffin (EC) cells (serotonin producing), enterochromaffin-like (ECL) cells (histamine producing), D-cells (somatostatin producing), and G-cells (gastrin producing)[43]. The diagnosis of G-NENs is usually performed incidentally during upper GI endoscopy due to the lack of specific symptoms, although rare cases could be seen in systemic syndromes, especially Zollinger-Ellison syndrome. Gastric NETs (G-NETs) are commonly subclassified into three distinct types that are mostly derived from ECL cells (Table 2). NETs derived from D cells, G cells, and EC cells are extremely rare.

Type 1 G-NETs are the most common NETs (80%-90%) in the stomach and associated with advanced autoimmune metaplastic atrophic gastritis. It is more commonly seen in females that frequently have additional autoimmune disorders, such as type 1 diabetes mellites and Hashimoto's thyroiditis. The presence of autoimmune antibodies, including anti-parietal cell antibodies and anti-intrinsic factor antibodies, leads to the destruction of parietal cells and achlorhydria[44]. Laboratory testing shows elevated serum gastrin, decreased vitamin B12, and high gastric pH (> 7). Gastrin induces ECL cell hyperplasia (< 0.5 mm) and ultimately G-NETs when the lesions measure 0.5 mm or larger.

Type 1 G-NETs are usually diagnosed under upper GI endoscopy with biopsy. It usually presents with multiple small (< 1 cm) reddish polyps or nodules of the gastric body (Figure 2A) and fundus. Histologically, type 1 G-NETs show tumor cells with abundant eosinophilic cytoplasm, monotonous round nuclei, and characteristic chromatin arranged in trabecular or nested patterns (Figure 2B and C). Necrosis is not a feature for this type of tumor. The background gastric mucosa shows atrophic gastritis with frequent intestinal metaplasia (Figure 2B and C inset). In addition, the spindle cell morphology of type 1 G-NETs has been reported by us with histological features mimicking spindle cell gastrointestinal stromal tumors (GISTs) (Figure 2D)[45] and therefore represents a potential diagnostic pitfall.

Most type 1 G-NETs are small G1 tumors and are limited to the mucosa and rarely the submucosa. Imaging study is usually unnecessary. However, EUS is likely warranted if the tumor is greater than 1-2 cm due to a higher risk for lymph node metastasis (2%-9%), muscularis propria invasion, and angioinvasion[46]. The management of type 1 G-NET is generally conservative with endoscopic surveillance due to its favorable prognosis. Endoscopic resection could be performed on cases with larger lesions (> 5 mm) (Figure 3). Gastrectomy is only reserved for rare high-risk cases.

Type 2 G-NETs are rare and account for 5%-6% of G-NETs. They occur in Zollinger-Ellison syndrome in the setting of MEN-1 syndrome, and patients are younger. Type 2 G-NETs are usually caused by duodenal gastrinoma[47]. The common clinical presentation includes abdominal pain and watery diarrhea. Laboratory testing shows elevated serum gastrin and low gastric pH (< 2). Additional genetic testing is recommended to confirm MEN-1 syndrome in suspicious cases. Endoscopically, type 2 G-NENs present with multiple gastric polyps or nodules. Multiple gastric peptic ulcers are common findings. These polypoid lesions are usually larger but typically less than 2 cm. The microscopic features of type 2 G-NENs are similar to those of type 1 G-NENs, presenting as low-grade tumors (G1 tumors being the most common) in a background of ECL hyperplasia. However, background gastric mucosa in type 2 G-NETS demonstrates parietal cell hypertrophy/hyperplasia. Type 2 G-NETs are mostly limited to the mucosa and submucosa. It has a higher risk of lymph node metastases (up to 30%) and therefore a slightly worse prognosis than type 1 G-NETs.

The clinical management of type 2 G-NETs also includes endoscopic surveillance, endoscopic resection, and rarely surgery. It is of clinical importance to locate and resect the primary gastrinoma.

Table 2 Clinicopathologic characteristics of gastric neuroendocrine tumor

	Type 1	Type 2	Type 3
Relative frequency (%)	70-80	5-6	10-15
Gender	F > M	F = M	M > F
Cell of origin	ECL	ECL	ECL, EC, *etc.*
Associated disease	AMAG; Pernicious anemia	MEN1; ZES	None (Sporadic)
Site of tumors	Fundus and corpus	Fundus and corpus, occasionally antrum	Anywhere
Size of tumors	< 1 cm	< 2 cm	2-5 cm
Number of tumors	Multiple	Multiple	Single
Plasma gastrin level	High	High	Normal
Gastric acid output	Low or absent	High	Normal
Metastatic rate (%)	2-5	10-30	50-100
Tumor related death (%)	Approximately 0	< 10	25-30

ECL: Enterochromaffin-like cell; EC: Enterochromaffin cell; F: Female; M: Male; AMAG: Autoimmune metaplastic atrophic gastritis; MEN1: Multiple endocrine neoplasm type 1; ZES: Zollinger-Ellison syndrome.

SSAs have been proposed in the treatment of type 2 G-NETs, although large-scale cohort studies are necessary for their validation.

Type 3 G-NETs are sporadic tumors and account for 10%-15% of all G-NETs. Laboratory testing showed normal serum gastrin and gastric pH. The clinical presentations are nonspecific, including abdominal pain, melena, and weight loss. Carcinoid syndrome could be seen in patients with liver metastases. Endoscopically, the tumor is usually a single large lesion (> 2 cm) arising in the normal background mucosa. These tumors commonly have aggressive clinical behavior, characterized by higher tumor grade, higher tumor stage, and frequent lymph node and distant metastases. The diagnosis involves upper GI endoscopy and biopsy. EUS is required to measure the depth of invasion and to evaluate lymph node status. Additional imaging studies, including computed tomography (CT), magnetic resonance imaging (MRI), and somatostatin receptor scintigraphy (SRS), are recommended for perioperative tumor staging.

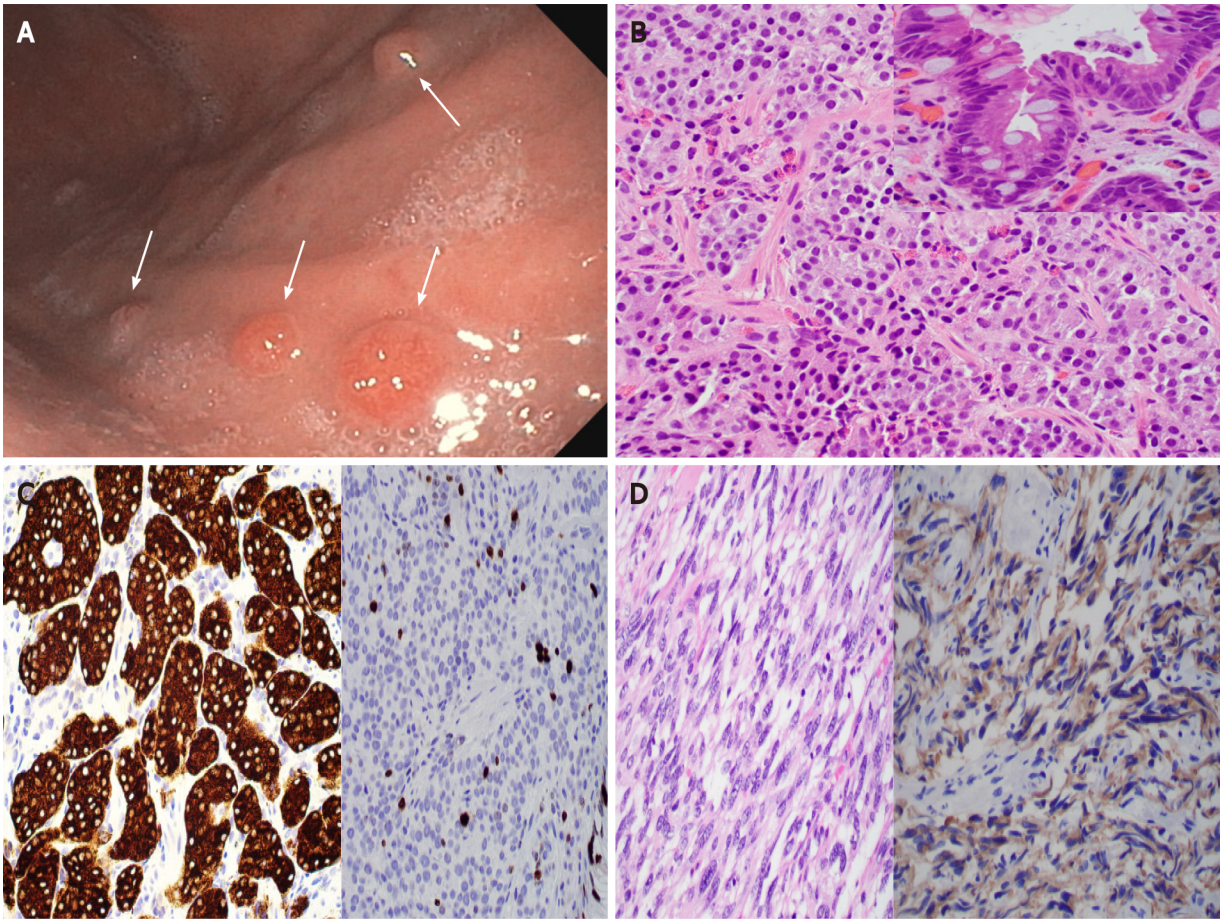
Compared with the favorable prognosis in types 1 and 2 G-NETs, type 3 G-NETs frequently present as high-grade and deeply invasive tumors. Lymph node metastases are found in up to 71% of type 3 G-NETs measuring 2 cm or larger[48]. Although endoscopic resection could be applied for small and superficial lesions, radical surgical resection (total or subtotal gastrectomy) with lymphadenectomy is often the treatment of choice for type 3 G-NETs.

Gastric NECs (G-NECs) are poorly differentiated carcinomas with high mitotic counts and frequent necrosis. They have been further subclassified into small cell NECs (SCNECs) and large cell NECs (LCNECs)[49]. Histologically, SCNECs are similar to their counterparts in the lung, featuring small neoplastic cells with scant cytoplasm and hyperchromatic nuclei. Prominent nucleolus is uncommon. In contrast, LCNECs have large neoplastic cells with abundant eosinophilic cytoplasm, vesicular nuclei, and prominent nucleoli. G-NECs are high-grade neoplasms by definition, with a high Ki-67 proliferation index (> 20%, often more than 60%-70%) and a high mitotic rate (> 20 *per* 2 mm^2). For G-NECs, surgical resection is often required, and postoperative chemotherapy is advised in cases with metastatic disease[50].

Small intestinal NENs

The incidence of small intestinal NENs (SI-NENs) has been increasing steadily over the past 3 decades to 1.05 new cases *per* 100000 individuals *per* year[51,52], and they are the most common GEP-NENs (29.5%) in the United States, followed by the rectum (29.2%) and pancreas (13.5%)[52]. The clinical presentations include nonspecific abdominal pain, mass effects (small bowel obstruction), and symptoms related to excess hormone secretion. Ampullary NENs could cause jaundice and acute or chronic pancreatitis. Duodenal gastrinoma is a cause of Zollinger-Ellison syndrome. Despite relatively slow growth, the small intestine is the most common primary NET site for metastatic disease along the GI tract[53].

CT scans are the most common imaging modalities for the diagnosis of SI-NENs. Other imaging studies include ultrasound, MRI, and SRS. Endoscopy with biopsy is the gold standard for the diagnosis of SI-NENs. Endoscopic examination of SI-NENs includes capsule endoscopy, colonoscopy, and double-balloon enteroscopy. Duodenal and periampullary NETs are usually single small (< 2 cm) polypoid or nodular lesions limited to the mucosa and submucosa. NETs at the jejunum and ileum are usually large



DOI: 10.3748/wjg.v28.i17.1751 **Copyright** ©The Author(s) 2022.

Figure 2 Type 1 gastric neuroendocrine tumor with usual and unusual histology. A: Endoscopic photo showing four nodules (arrows) in the gastric body of a 56-year-old woman with a history of autoimmune chronic atrophic gastritis (ACAG); B and C: Biopsy of the nodules showing well-differentiated neuroendocrine tumor (B, H&E stain, 400 ×) with intestinal metaplasia on the overlying mucosa (B inset), positivity for synaptophysin (C, left), and a 7% Ki67 index (C, right); D: Gastric biopsy in an 83-year-old woman with ACAG showing a neuroendocrine tumor with unusual spindle cell morphology mimicking gastrointestinal stromal tumor (GIST) (left, H&E stain), which is positive for synaptophysin (right) and negative for GIST markers.

(> 2 cm) and multifocal, with frequent deep invasion and lymph node metastases[54].

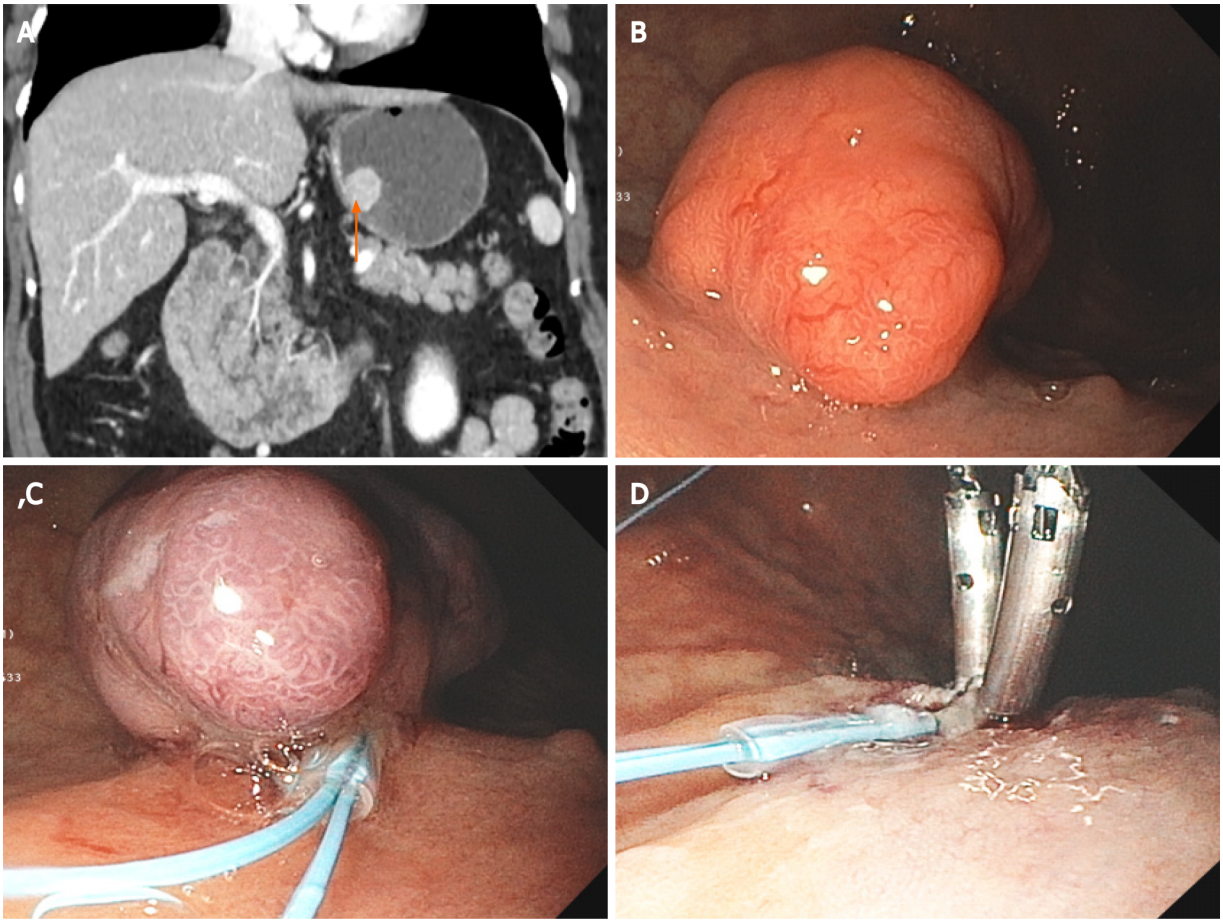
SI-NENs are morphologically similar to NENs at other sites. A few relatively specific histological features include psammoma bodies in somatostatin-producing D-cell NETs and nested growth patterns with peripheral palisading in serotonin-producing EC-cell NETs. Gangliocytic paraganglioma is a rare NET that is typically encountered in the second part of the duodenum and is characterized by the presence of three distinct components: A neuroendocrine epithelioid component, a Schwannian spindle cell component, and a ganglion cell-like component[55].

For localized SI-NETs, the standard of care is complete surgical resection of the primary tumor, regional lymph nodes, and mesenteric fibrotic tissue. A consensus has not been reached with routine administration of octreotide preoperatively or intraoperatively[56]. For metastatic disease, treatment options are surgical resection, liver-directed therapy (in cases predominantly with liver metastasis), and systemic therapy including SSA, PRRT, everolimus (mTOR inhibitor), and cytotoxic chemotherapy.

Appendiceal NENs

The appendix is a frequent primary site for GEP-NENs, with an incidence rate of approximately 0.15-0.6 new cases *per* 100000 individuals *per* year in the United States[52,57,58]. They frequently occur in children and young adults with a slight female predominance[59]. Appendiceal NENs (A-NENs) have the most favorable prognosis among all subgroups of GEP-NENs[52].

The common clinical presentations of A-NENs are similar to those of acute appendicitis. Carcinoid syndrome is extremely rare in A-NENs and is mostly associated with metastatic disease. Histopathologic evaluation is crucial to establish the diagnosis of A-NENs. The application of imaging studies, including CT and MRI, has limited value for the detection of small primary A-NENs. However, colonoscopy is recommended given that up to 18% of patients with A-NENs have concurrent GI neoplasms[60].



DOI: 10.3748/wjg.v28.i17.1751 **Copyright** ©The Author(s) 2022.

Figure 3 Large gastric neuroendocrine tumor. A: Computed tomography image showing a 2.3 cm mass (arrow) at the posterior wall of the body of a 74-year-old woman with a history of autoimmune chronic atrophic gastritis; B: Endoscopic image showing the large polypoid lesion in the gastric body; C and D: Endoscopic mucosal resection of the polypoid type 1 neuroendocrine tumor.

The majority (80%) of A-NENs are small and only incidentally found in appendectomy specimens [52]. Most A-NENs (60%-75%) are located at the appendiceal tip; therefore, the appendiceal tip should be examined carefully on all appendectomy specimens. The histological features of A-NENs are similar to those of NENs of other primary sites, with the exception of tubular NETs. Tubular NETs are rare benign neoplasms with a predominant tubular growth pattern, so it is important not to misdiagnose them as adenocarcinomas[61]. Of note, goblet cell adenocarcinoma (formerly goblet cell carcinoid) is no longer considered an A-NEN[62]. Currently, we believe that this is an unusual type of adenocarcinoma with neuroendocrine differentiation.

The management of A-NENs depends on the stage of the disease determined by the tumor size, location, and tumor extension. Simple appendectomy is considered adequate for tumors less than 10 mm. Right hemicolectomy is indicated for tumors larger than 20 mm. The implication of right hemicolectomy in A-NETs with a size of 10-20 mm is still controversial, likely depending on the presence of high-risk features (positive margin after appendectomy, base location, Ki-67 index of 3% or higher, > 3 mm mesoappendiceal invasion, angioinvasion, and perineural invasion)[63,64]. For patients with more advanced disease (stages III and IV), the treatment usually includes curative surgery and systemic therapy.

Colorectal NENs

The incidence rates of colonic and rectal NENs are 0.2 and 1.2 new cases *per* 100000 individuals *per* year in the United States, respectively[52]. The mean age for colonic NENs is 65 years, which is significantly older than that for rectal NENs (56 years) due to late detection. The presentation of colorectal NENs is similar to that of colorectal adenocarcinoma with nonspecific mass-related effects, abdominal pain, and bleeding. Classic carcinoid symptoms could be seen in some cases, often with liver metastases.

The majority (70%) of colonic NETs (C-NETs) are located on the right side of the colon, especially the cecum[65]. C-NETs are usually larger, with an average size of 4.9 cm[66]. Approximately 30%-40% of C-NETs have local or distant metastasis at the time of presentation. Colonoscopy with biopsy is commonly performed to establish the diagnosis. C-NETs are usually derived from EC cells or Kulchitsky cells

within the crypts of Lieburkuhn. Therefore, C-NETs typically show EC cell features, including insular growth patterns and CDX2 immunoreactivity. Necrosis is usually absent. The preferred treatment is colectomy with lymphadenectomy.

Rectal NETs (R-NETs) are relatively smaller (< 1 cm), smooth, round polypoid lesions and generally have a better prognosis than their counterparts in the colon. R-NETs are subgrouped into the L-cell (glucagon-like peptide and pancreatic polypeptide producing) type and non-L-cell type according to their origin[67], with the L-cell type being the dominant type. L-cell R-NETs typically present with trabecular or tubular growth patterns. Of note, non-L-cell-type rectal NETs usually present as larger masses and have an increased risk of lymphovascular invasion and worse prognosis[68].

For the purpose of tumor staging, it is recommended to use EUS and MRI of the pelvis to determine the depth of invasion and lymph node status and to use SRS-based scans to determine distant metastases. Endoscopic mucosal resection and endoscopic submucosal dissection are indicated for small (1 cm or smaller) and superficial R-NETs if there is no evidence of muscularis propria invasion or lymph node metastases[69]. For R-NETs larger than 2 cm in size, low anterior resection or abdominal resection is recommended.

Pancreatic NENs

As rare neoplasms, the incidence rate for pancreatic NENs (P-NENs) is 1.0 new cases *per* 100000 individuals *per* year in the United States[70] and accounts for 2%-4% of all pancreatic neoplasms[71]. All P-NETs are considered to have malignant potential. These tumors are derived from pancreatic islet cells and could be subclassified into functioning and nonfunctioning subgroups. Functioning P-NETs, including insulinoma, gastrinoma, VIPoma, and glucogonoma, cause clinical hormone hypersecretion syndromes. The clinical presentations of functioning P-NETs are mostly related to hormone effects, such as hyperglycemia in insulinoma and large-volume secretory diarrhea in VIPoma. In contrast, nonfunctioning P-NETs are usually incidental findings on imaging studies for other causes or mass effects at late stages. With the increased use of imaging studies, nonfunctioning P-NENs have become more common, accounting for more than 60% of all P-NENs[72].

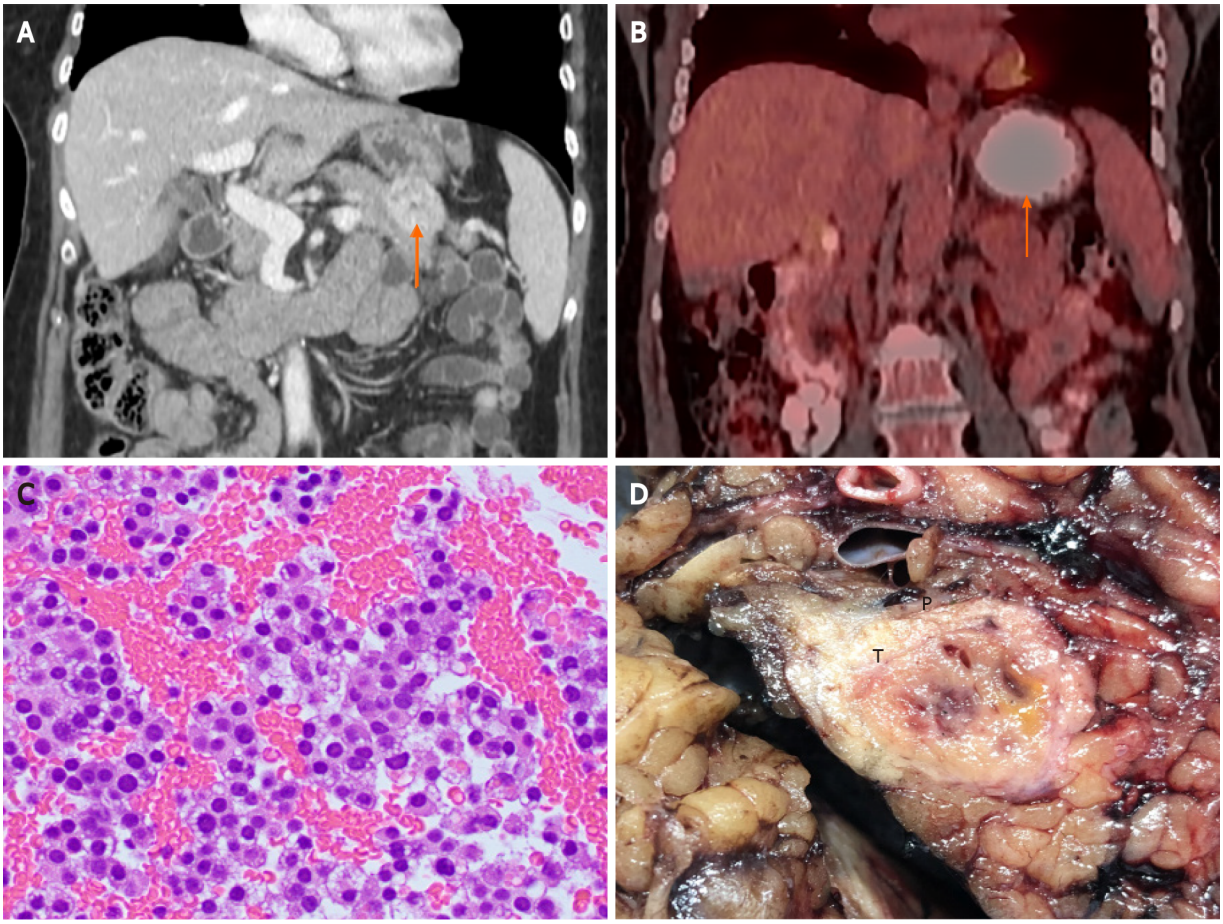
Insulinoma and gastrinoma are the two most common functioning P-NETs. In suspected cases of insulinoma, 72-h fasting tests for blood glucose, insulin, C-peptide, and proinsulin levels should be performed together with drug tests for sulfonylurea. In suspected cases of gastrinoma, laboratory testing includes fasting gastrin level and gastric pH. Laboratory testing for serum glucagon and VIP levels would be helpful for the diagnosis of glucagonoma and VIPoma. The circulating CgA level is also a sensitive and specific diagnostic marker for P-NETs, with the exception of insulinoma[73], and it has no added value for the diagnosis of nonfunctioning P-NETs.

The most common imaging studies for P-NENs include EUS, CT, MRI, and 68Ga-dotatate PET. Radiolabeled glucagon-like peptide-1 receptor (GLP-1R) scintigraphy is another sensitive tool to detect small insulinomas[74]. Based on our experience, P-NETs could appear as thin-walled cystic lesions with no communication with the pancreatic duct (Figure 4) that clinically and radiologically may mimic mucinous cystic neoplasms. Clinicians and pathologists should be aware of this unusual presentation to avoid misdiagnosis.

Microscopically, P-NETs are well-differentiated neoplasms that do not differ from NETs from other primary sites (Figure 5). One or more neuroendocrine markers (CgA, SYN, CD56, and neuron-specific enolase) and one epithelial marker (cytokeratin AE1/AE3 and CAM5.2) are indicated for the diagnosis of P-NENs. Ki-67 immunoreactivity is warranted to assign tumor grade. Insulin immunoreactivity is necessary in the diagnosis of insulinoma in cases of multifocal tumors or insulinomatosis. In the cases of metastatic disease, some markers (Pax 6, Pax8, ISL-1, PDX-1, and CDX2) could be helpful to determine pancreatic origin[75].

Surgical resection is the preferred and only curative therapy for P-NENs. Conservative management was suggested for small (< 2 cm) low-grade nonfunctioning P-NETs due to their excellent prognosis[76, 77]. However, even for small-sized nonfunctioning P-NETs, surgical resection is indicated in cases with high-risk features (55 years or older, grade 3 tumor, and distant metastases)[78]. Local resection or enucleation could be applied in localized and easily accessible disease to maximally reserve pancreatic tissue[79], especially if the tumor is located more than 2-3 mm from the pancreatic duct. Depending on the tumor location, surgical resection procedures for P-NENs include partial pancreaticoduodenectomy and distal pancreatectomy. Regional lymphadenectomy is recommended for surgical resection of P-NENs.

P-NENs commonly present with liver metastases. Surgical resection should be considered in metastatic disease for both nonfunctioning and functioning P-NENs. The presence of liver metastases is not a counterindication to surgical management for P-NEN patients[80]. Efforts should be made if surgical removal is feasible for both primary pancreatic tumors and metastatic liver lesions. However, it is still under debate whether to resect the primary tumor in cases of unresectable metastatic liver lesions. Surgical resection of metastatic liver lesions should be avoided in cases with unresectable primary P-NENs[81].



DOI: 10.3748/wjg.v28.i17.1751 **Copyright** ©The Author(s) 2022.

Figure 4 Pancreatic neuroendocrine tumor. A: Computed tomography (CT) image showing a 3.5 cm distal pancreatic mass (arrow); B: Positron emission tomography-CT image showing a pancreatic mass with hypermetabolic activity (SUVmax = 4.3) (arrow); C: Endoscopic ultrasound-guided fine-needle aspiration showing clusters of neuroendocrine tumor cells with round nuclei and fine stippled "salt-and-pepper" chromatin (H&E stain, 400 ×); D: Distal pancreatectomy showing the gross cut surface of a firm fibrotic pancreatic neuroendocrine tumor (T) with focal hemorrhage.

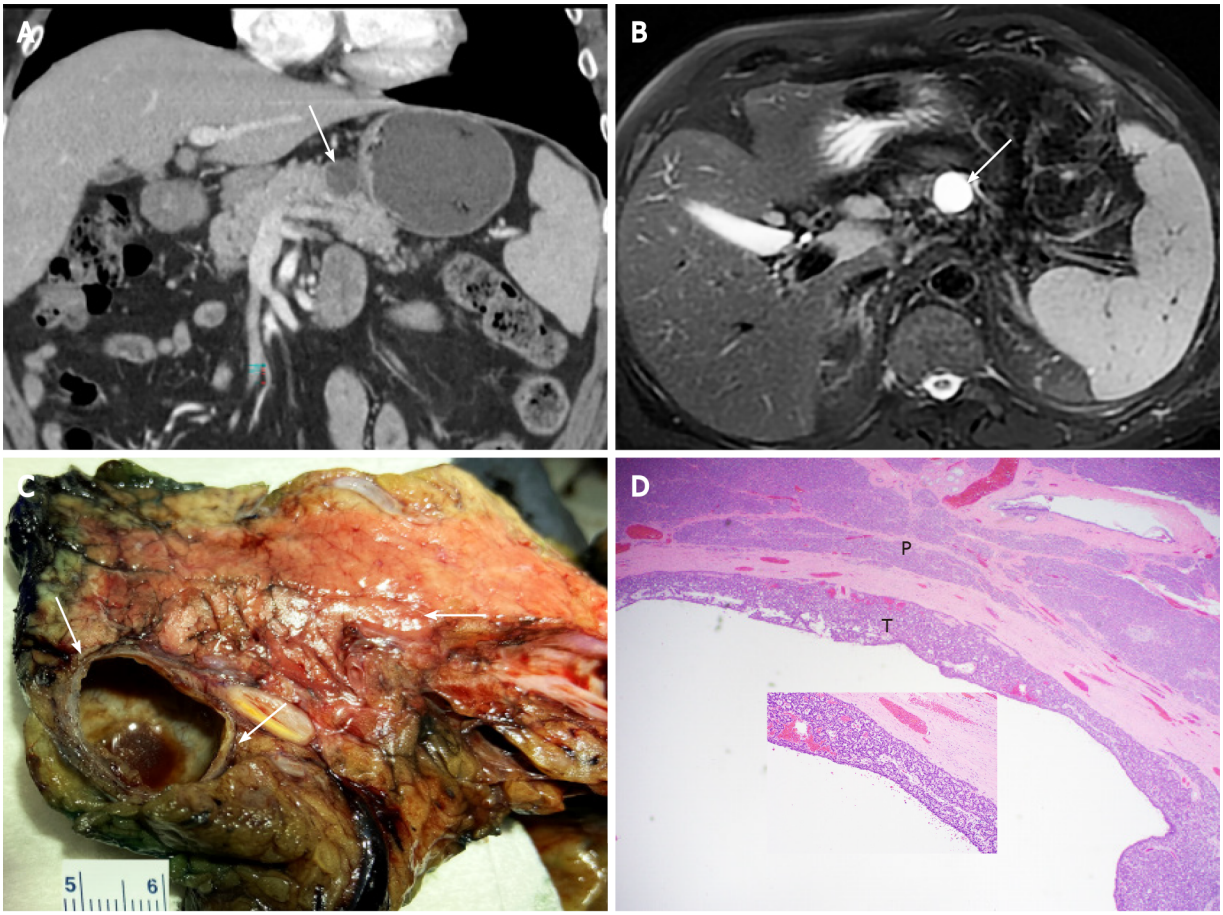
NOVEL THERAPEUTIC APPROACHES

The treatment options for advanced and metastatic GEP-NENs have significantly expanded during the past two decades[82,83]. Some important clinical studies, including the PROMID[84] and CLARINET [85] trials, have demonstrated a significant efficacy of SSA in the control of tumor growth in patients with metastatic GEP-NETs. A recent CLARINET FORTE phase 2 clinical trial further supports the clinical benefit of the SSA lanreotide autogel (LAN), which led to significantly improved progression-free survival (PFS) and disease control rate in patients with GEN-NETs, especially in cases with a Ki67 index ≤ 10%[86]. In addition to SSA[87], novel therapeutic approaches, including PRRT, targeted therapy, and immunotherapy, have demonstrated promising clinical benefits[88-90].

PRRT is a type of systemic radiotherapy specifically targeting tumor cells expressing SSTR[91]. In the phase 3 NETTER-1 trial, for patients with metastatic well-differentiated midgut NETs, treatment with ^{177}Lu-dotatate led to a significantly improved PFS (median PFS not reached *vs* 8.4 mo in the control group with high-dose octreotide alone) and an improved radiographic response rate (18% *vs* 3% in the control group)[92]. The most common adverse effects for ^{177}Lu-dotatate are nausea and vomiting. Based on this trial, PRRT with ^{177}Lu-dotatate has been approved for patients with advanced GEP-NETs and SSTR expression on imaging.

Due to the hypervascularity in GEP-NETs, multiple clinical trials have investigated the therapeutic effects of targeted therapy against vascular endothelial growth factor (VEGF) receptors. In a phase 3 trial, patients with low- to intermediate-grade P-NETs received placebo *vs* sunitinib, a tyrosine kinase inhibitor targeting multiple receptors, including VEGF receptors-1, 2, and 3. Sunitinib led to a significantly longer median PFS [11.4 mo *vs* 5.5 mo in the control group; hazard ratio (HR) for progression or death, 0.42; $P < 0.001$][93]. Sunitinib has been approved for patients with advanced P-NETs.

mTOR is a multifunctional serine/threonine kinase related to NET growth. mTOR pathway genes, including *PTEN*, *TSC2*, and *PIK3CA*, are also frequently mutated in NETs. Multiple clinical trials have been conducted to test the treatment effect of the mTOR inhibitor everolimus in GEP-NETs. In the



DOI: 10.3748/wjg.v28.i17.1751 **Copyright** ©The Author(s) 2022.

Figure 5 Pancreatic cystic neuroendocrine tumor mimicking mucinous cystic neoplasm. A: Computed tomography image (axial) showing a 2.2 cm cystic lesion (arrow) in the pancreatic body of a 68-year-old man; B: Magnetic resonance imaging (T2, axial) showing the cystic mass (arrow); C: Partial pancreatectomy specimen showing cut surface of the thin-walled cystic pancreatic neuroendocrine tumor mimicking mucinous cystic neoplasm with no communication with the pancreatic duct (arrows); D: Histopathologic features of cystic pancreatic neuroendocrine tumor with acinar and trabecular architecture (T) and surrounding pancreatic parenchyma (P) (H&E stain, 40 ×, inset 200 ×).

RADIANT-3 trial, for patients with advanced P-NETs, everolimus treatment led to a significantly longer median PFS (11 mo *vs* 4.6 mo in the control group; HR: 0.35)[94]. In the RADIANT-4 trial, patients with advanced nonfunctioning GI and lung NETs had a longer median PFS in the everolimus arm (11 mo *vs* 3.9 mo in the control group; HR: 0.48)[95]. Everolimus is approved for patients with advanced P-NETs and nonfunctioning GI NETs.

Immune checkpoint inhibitors and antibodies targeting programmed cell death protein-1 (PD-1), programmed cell death protein ligand-1 (PD-L1), or cytotoxic T lymphocyte-associated antigen 4 (CTLA-4), have demonstrated promising therapeutic responses in various types of cancers[96]. Based on the durable antitumor efficacy and favorable safety profile in patients with advanced metastatic Merkel-cell carcinoma, a high-grade cutaneous NEC[97], immunotherapy has been proposed to be potentially effective for advanced NENs with microsatellite instability, high tumor burden, and/or mutational load [98]. Multiple clinical trials have been conducted to test the efficacy of immunotherapy in GEP-NENs. Currently, these studies only showed very limited therapeutic effects for GEP-NENs[99-101]. Interestingly, in a phase 1b trial on toripalimab (an anti-PD-1 antibody) for patients with high-grade NENs, patients with PD-L1 expression greater than 10% and/or high tumor mutational burden (TMB) had a better objective response rate (ORR) than low PD-L1 (< 10%) (50.0% *vs* 10.7%, $P = 0.019$) and low TMB patients (75.0% *vs* 16.1%, $P = 0.03$)[100]. Therefore, PD-L1 expression is a potential therapeutic and prognostic biomarker for GEP-NENs.

CONCLUSION

GEP-NENs are relatively rare tumors, although the incidence rates have been steadily increasing over the past three decades. GEP-NENs consist of a genetically heterogeneous group of tumors ranging from slow-growing, well-differentiated NETs to aggressive, poorly differentiated NECs. Great progress has

been made toward understanding their unique molecular genetics and combating advanced disease through improved diagnostic tools and effective therapeutic regimens. A multidisciplinary and personalized treatment approach would be crucial to achieve optimal clinical outcomes for patients with GEP-NENs.

FOOTNOTES

Author contributions: Yin F wrote and finalized the manuscript; Wu ZH critically reviewed the manuscript; Lai JP collected and analyzed the data, made the figures, and finalized the manuscript; all authors have approved the final manuscript.

Conflict-of-interest statement: The authors declare that they have no competing interests in this study.

Open-Access: This article is an open-access article that was selected by an in-house editor and fully peer-reviewed by external reviewers. It is distributed in accordance with the Creative Commons Attribution NonCommercial (CC BY-NC 4.0) license, which permits others to distribute, remix, adapt, build upon this work non-commercially, and license their derivative works on different terms, provided the original work is properly cited and the use is non-commercial. See: https://creativecommons.org/Licenses/by-nc/4.0/

Country/Territory of origin: United States

ORCID number: Feng Yin 0000-0002-8444-1123; Zi-Hao Wu 0000-0003-4188-3527; Jin-Ping Lai 0000-0001-5365-2481.

S-Editor: Fan JR
L-Editor: Wang TQ
P-Editor: Fan JR

REFERENCES

1 **Klimstra DSKG**, La Rosa S, Rindi G. Classification of neuroendocrine neoplasms of the digestive system. WHO Classification of Tumours Editorial Board, editor. WHO classification of tumours: Digestive system tumours. Lyon: IARC Press; 2019
2 **Jensen RT**, Berna MJ, Bingham DB, Norton JA. Inherited pancreatic endocrine tumor syndromes: advances in molecular pathogenesis, diagnosis, management, and controversies. *Cancer* 2008; **113**: 1807-1843 [PMID: 18798544 DOI: 10.1002/cncr.23648]
3 **Kidd M**, Modlin IM, Bodei L, Drozdov I. Decoding the Molecular and Mutational Ambiguities of Gastroenteropancreatic Neuroendocrine Neoplasm Pathobiology. *Cell Mol Gastroenterol Hepatol* 2015; **1**: 131-153 [PMID: 28210673 DOI: 10.1016/j.jcmgh.2014.12.008]
4 **Ito T**, Masui T, Komoto I, Doi R, Osamura RY, Sakurai A, Ikeda M, Takano K, Igarashi H, Shimatsu A, Nakamura K, Nakamoto Y, Hijioka S, Morita K, Ishikawa Y, Ohike N, Kasajima A, Kushima R, Kojima M, Sasano H, Hirano S, Mizuno N, Aoki T, Ohtsuka T, Okumura T, Kimura Y, Kudo A, Konishi T, Matsumoto I, Kobayashi N, Fujimori N, Honma Y, Morizane C, Uchino S, Horiuchi K, Yamasaki M, Matsubayashi J, Sato Y, Sekiguchi M, Abe S, Okusaka T, Kida M, Kimura W, Tanaka M, Majima Y, Jensen RT, Hirata K, Imamura M, Uemoto S. JNETS clinical practice guidelines for gastroenteropancreatic neuroendocrine neoplasms: diagnosis, treatment, and follow-up: a synopsis. *J Gastroenterol* 2021; **56**: 1033-1044 [PMID: 34586495 DOI: 10.1007/s00535-021-01827-7]
5 **Williams ED**, Sandler M. The classification of carcinoid tum ours. *Lancet* 1963; **1**: 238-239 [PMID: 14000847 DOI: 10.1016/s0140-6736(63)90951-6]
6 **Capelli P**, Fassan M, Scarpa A. Pathology - grading and staging of GEP-NETs. *Best Pract Res Clin Gastroenterol* 2012; **26**: 705-717 [PMID: 23582914 DOI: 10.1016/j.bpg.2013.01.003]
7 **Cheung VTF**, Khan MS. A guide to midgut neuroendocrine tumours (NETs) and carcinoid syndrome. *Frontline Gastroenterol* 2015; **6**: 264-269 [PMID: 28839822 DOI: 10.1136/flgastro-2014-100483]
8 **Rindi G**, Klimstra DS, Abedi-Ardekani B, Asa SL, Bosman FT, Brambilla E, Busam KJ, de Krijger RR, Dietel M, El-Naggar AK, Fernandez-Cuesta L, Klöppel G, McCluggage WG, Moch H, Ohgaki H, Rakha EA, Reed NS, Rous BA, Sasano H, Scarpa A, Scoazec JY, Travis WD, Tallini G, Trouillas J, van Krieken JH, Cree IA. A common classification framework for neuroendocrine neoplasms: an International Agency for Research on Cancer (IARC) and World Health Organization (WHO) expert consensus proposal. *Mod Pathol* 2018; **31**: 1770-1786 [PMID: 30140036 DOI: 10.1038/s41379-018-0110-y]
9 **Anlauf M**. Neuroendocrine neoplasms of the gastroenteropancreatic system: pathology and classification. *Horm Metab Res* 2011; **43**: 825-831 [PMID: 22105474 DOI: 10.1055/s-0031-1291307]
10 **Ilett EE**, Langer SW, Olsen IH, Federspiel B, Kjær A, Knigge U. Neuroendocrine Carcinomas of the Gastroenteropancreatic System: A Comprehensive Review. *Diagnostics (Basel)* 2015; **5**: 119-176 [PMID: 26854147 DOI: 10.3390/diagnostics5020119]
11 **La Rosa S**, Marando A, Sessa F, Capella C. Mixed Adenoneuroendocrine Carcinomas (MANECs) of the Gastrointestinal Tract: An Update. *Cancers (Basel)* 2012; **4**: 11-30 [PMID: 24213223 DOI: 10.3390/cancers4010011]
12 **de Mestier L**, Cros J. Digestive system mixed neuroendocrine-non-neuroendocrine neoplasms (MiNEN). *Ann Endocrinol*

(Paris) 2019; **80**: 172-173 [PMID: 31064662 DOI: 10.1016/j.ando.2019.04.006]
13 **Inzani F**, Petrone G, Rindi G. The New World Health Organization Classification for Pancreatic Neuroendocrine Neoplasia. *Endocrinol Metab Clin North Am* 2018; **47**: 463-470 [PMID: 30098710 DOI: 10.1016/j.ecl.2018.04.008]
14 **Scarpa A**, Mantovani W, Capelli P, Beghelli S, Boninsegna L, Bettini R, Panzuto F, Pederzoli P, delle Fave G, Falconi M. Pancreatic endocrine tumors: improved TNM staging and histopathological grading permit a clinically efficient prognostic stratification of patients. *Mod Pathol* 2010; **23**: 824-833 [PMID: 20305616 DOI: 10.1038/modpathol.2010.58]
15 **Singh S**, Hallet J, Rowsell C, Law CH. Variability of Ki67 labeling index in multiple neuroendocrine tumors specimens over the course of the disease. *Eur J Surg Oncol* 2014; **40**: 1517-1522 [PMID: 25088936 DOI: 10.1016/j.ejso.2014.06.016]
16 **Khan MS**, Luong TV, Watkins J, Toumpanakis C, Caplin ME, Meyer T. A comparison of Ki-67 and mitotic count as prognostic markers for metastatic pancreatic and midgut neuroendocrine neoplasms. *Br J Cancer* 2013; **108**: 1838-1845 [PMID: 23579216 DOI: 10.1038/bjc.2013.156]
17 **Busico A**, Maisonneuve P, Prinzi N, Pusceddu S, Centonze G, Garzone G, Pellegrinelli A, Giacomelli L, Mangogna A, Paolino C, Belfiore A, Kankava K, Perrone F, Tamborini E, Pruneri G, Fazio N, Milione M. Gastroenteropancreatic High-Grade Neuroendocrine Neoplasms: Histology and Molecular Analysis, Two Sides of the Same Coin. *Neuroendocrinology* 2020; **110**: 616-629 [PMID: 31557757 DOI: 10.1159/000503722]
18 **Rinke A**, Gress TM. Neuroendocrine Cancer, Therapeutic Strategies in G3 Cancers. *Digestion* 2017; **95**: 109-114 [PMID: 28161703 DOI: 10.1159/000454761]
19 **Ordóñez NG**. Broad-spectrum immunohistochemical epithelial markers: a review. *Hum Pathol* 2013; **44**: 1195-1215 [PMID: 23427873 DOI: 10.1016/j.humpath.2012.11.016]
20 **John M**, Meyerhof W, Richter D, Waser B, Schaer JC, Scherübl H, Boese-Landgraf J, Neuhaus P, Ziske C, Mölling K, Riecken EO, Reubi JC, Wiedenmann B. Positive somatostatin receptor scintigraphy correlates with the presence of somatostatin receptor subtype 2. *Gut* 1996; **38**: 33-39 [PMID: 8566856 DOI: 10.1136/gut.38.1.33]
21 **Bellizzi AM**. Immunohistochemistry in the diagnosis and classification of neuroendocrine neoplasms: what can brown do for you? *Hum Pathol* 2020; **96**: 8-33 [PMID: 31857137 DOI: 10.1016/j.humpath.2019.12.002]
22 **Wang SC**, Parekh JR, Zuraek MB, Venook AP, Bergsland EK, Warren RS, Nakakura EK. Identification of unknown primary tumors in patients with neuroendocrine liver metastases. *Arch Surg* 2010; **145**: 276-280 [PMID: 20231629 DOI: 10.1001/archsurg.2010.10]
23 **Mayo SC**, de Jong MC, Pulitano C, Clary BM, Reddy SK, Gamblin TC, Celinksi SA, Kooby DA, Staley CA, Stokes JB, Chu CK, Ferrero A, Schulick RD, Choti MA, Mentha G, Strub J, Bauer TW, Adams RB, Aldrighetti L, Capussotti L, Pawlik TM. Surgical management of hepatic neuroendocrine tumor metastasis: results from an international multi-institutional analysis. *Ann Surg Oncol* 2010; **17**: 3129-3136 [PMID: 20585879 DOI: 10.1245/s10434-010-1154-5]
24 **Zimmermann N**, Lazar-Karsten P, Keck T, Billmann F, Schmid S, Brabant G, Thorns C. Expression Pattern of CDX2, Estrogen and Progesterone Receptors in Primary Gastroenteropancreatic Neuroendocrine Tumors and Metastases. *Anticancer Res* 2016; **36**: 921-924 [PMID: 26976979]
25 **Bellizzi AM**. SATB2 in neuroendocrine neoplasms: strong expression is restricted to well-differentiated tumours of lower gastrointestinal tract origin and is most frequent in Merkel cell carcinoma among poorly differentiated carcinomas. *Histopathology* 2020; **76**: 251-264 [PMID: 31233624 DOI: 10.1111/his.13943]
26 **Maguire A**, Brogi E. Sentinel lymph nodes for breast carcinoma: an update on current practice. *Histopathology* 2016; **68**: 152-167 [PMID: 26768036 DOI: 10.1111/his.12853]
27 **Lai JP**, Mertens RB, Mirocha J, Koo J, Venturina M, Chung F, Mendez AB, Kahn M, Dhall D. Comparison of PAX6 and PAX8 as immunohistochemical markers for pancreatic neuroendocrine tumors. *Endocr Pathol* 2015; **26**: 54-62 [PMID: 25433656 DOI: 10.1007/s12022-014-9346-3]
28 **Asa SL**, La Rosa S, Basturk O, Adsay V, Minnetti M, Grossman AB. Molecular Pathology of Well-Differentiated Gastro-entero-pancreatic Neuroendocrine Tumors. *Endocr Pathol* 2021; **32**: 169-191 [PMID: 33459926 DOI: 10.1007/s12022-021-09662-5]
29 **Mapelli P**, Aboagye EO, Stebbing J, Sharma R. Epigenetic changes in gastroenteropancreatic neuroendocrine tumours. *Oncogene* 2015; **34**: 4439-4447 [PMID: 25435371 DOI: 10.1038/onc.2014.379]
30 **Mafficini A**, Scarpa A. Genetics and Epigenetics of Gastroenteropancreatic Neuroendocrine Neoplasms. *Endocr Rev* 2019; **40**: 506-536 [PMID: 30657883 DOI: 10.1210/er.2018-00160]
31 **Esposito I**, Segler A, Steiger K, Klöppel G. Pathology, genetics and precursors of human and experimental pancreatic neoplasms: An update. *Pancreatology* 2015; **15**: 598-610 [PMID: 26365060 DOI: 10.1016/j.pan.2015.08.007]
32 **Jiao Y**, Shi C, Edil BH, de Wilde RF, Klimstra DS, Maitra A, Schulick RD, Tang LH, Wolfgang CL, Choti MA, Velculescu VE, Diaz LA Jr, Vogelstein B, Kinzler KW, Hruban RH, Papadopoulos N. DAXX/ATRX, MEN1, and mTOR pathway genes are frequently altered in pancreatic neuroendocrine tumors. *Science* 2011; **331**: 1199-1203 [PMID: 21252315 DOI: 10.1126/science.1200609]
33 **Scarpa A**, Chang DK, Nones K, Corbo V, Patch AM, Bailey P, Lawlor RT, Johns AL, Miller DK, Mafficini A, Rusev B, Scardoni M, Antonello D, Barbi S, Sikora KO, Cingarlini S, Vicentini C, McKay S, Quinn MC, Bruxner TJ, Christ AN, Harliwong I, Idrisoglu S, McLean S, Nourse C, Nourbakhsh E, Wilson PJ, Anderson MJ, Fink JL, Newell F, Waddell N, Holmes O, Kazakoff SH, Leonard C, Wood S, Xu Q, Nagaraj SH, Amato E, Dalai I, Bersani S, Cataldo I, Dei Tos AP, Capelli P, Davì MV, Landoni L, Malpaga A, Miotto M, Whitehall VL, Leggett BA, Harris JL, Harris J, Jones MD, Humphris J, Chantrill LA, Chin V, Nagrial AM, Pajic M, Scarlett CJ, Pinho A, Rooman I, Toon C, Wu J, Pinese M, Cowley M, Barbour A, Mawson A, Humphrey ES, Colvin EK, Chou A, Lovell JA, Jamieson NB, Duthie F, Gingras MC, Fisher WE, Dagg RA, Lau LM, Lee M, Pickett HA, Reddel RR, Samra JS, Kench JG, Merrett ND, Epari K, Nguyen NQ, Zeps N, Falconi M, Simbolo M, Butturini G, Van Buren G, Partelli S, Fassan M; Australian Pancreatic Cancer Genome Initiative, Khanna KK, Gill AJ, Wheeler DA, Gibbs RA, Musgrove EA, Bassi C, Tortora G, Pederzoli P, Pearson JV, Waddell N, Biankin AV, Grimmond SM. Whole-genome landscape of pancreatic neuroendocrine tumours. *Nature* 2017; **543**: 65-71 [PMID: 28199314 DOI: 10.1038/nature21063]
34 **Kytölä S**, Höög A, Nord B, Cedermark B, Frisk T, Larsson C, Kjellman M. Comparative genomic hybridization identifies

loss of 18q22-qter as an early and specific event in tumorigenesis of midgut carcinoids. *Am J Pathol* 2001; **158**: 1803-1808 [PMID: 11337378 DOI: 10.1016/S0002-9440(10)64136-3]

35 **Andersson E**, Swärd C, Stenman G, Ahlman H, Nilsson O. High-resolution genomic profiling reveals gain of chromosome 14 as a predictor of poor outcome in ileal carcinoids. *Endocr Relat Cancer* 2009; **16**: 953-966 [PMID: 19458023 DOI: 10.1677/ERC-09-0052]

36 **Crona J**, Gustavsson T, Norlén O, Edfeldt K, Åkerström T, Westin G, Hellman P, Björklund P, Stålberg P. Somatic Mutations and Genetic Heterogeneity at the CDKN1B Locus in Small Intestinal Neuroendocrine Tumors. *Ann Surg Oncol* 2015; **22** Suppl 3: S1428-S1435 [PMID: 25586243 DOI: 10.1245/s10434-014-4351-9]

37 **Francis JM**, Kiezun A, Ramos AH, Serra S, Pedamallu CS, Qian ZR, Banck MS, Kanwar R, Kulkarni AA, Karpathakis A, Manzo V, Contractor T, Philips J, Nickerson E, Pho N, Hooshmand SM, Brais LK, Lawrence MS, Pugh T, McKenna A, Sivachenko A, Cibulskis K, Carter SL, Ojesina AI, Freeman S, Jones RT, Voet D, Saksena G, Auclair D, Onofrio R, Shefler E, Sougnez C, Grimsby J, Green L, Lennon N, Meyer T, Caplin M, Chung DC, Beutler AS, Ogino S, Thirlwell C, Shivdasani R, Asa SL, Harris CR, Getz G, Kulke M, Meyerson M. Somatic mutation of CDKN1B in small intestine neuroendocrine tumors. *Nat Genet* 2013; **45**: 1483-1486 [PMID: 24185511 DOI: 10.1038/ng.2821]

38 **Karpathakis A**, Dibra H, Pipinikas C, Feber A, Morris T, Francis J, Oukrif D, Mandair D, Pericleous M, Mohmaduvesh M, Serra S, Ogunbiyi O, Novelli M, Luong T, Asa SL, Kulke M, Toumpanakis C, Meyer T, Caplin M, Meyerson M, Beck S, Thirlwell C. Prognostic Impact of Novel Molecular Subtypes of Small Intestinal Neuroendocrine Tumor. *Clin Cancer Res* 2016; **22**: 250-258 [PMID: 26169971 DOI: 10.1158/1078-0432.CCR-15-0373]

39 **Yachida S**, Vakiani E, White CM, Zhong Y, Saunders T, Morgan R, de Wilde RF, Maitra A, Hicks J, Demarzo AM, Shi C, Sharma R, Laheru D, Edil BH, Wolfgang CL, Schulick RD, Hruban RH, Tang LH, Klimstra DS, Iacobuzio-Donahue CA. Small cell and large cell neuroendocrine carcinomas of the pancreas are genetically similar and distinct from well-differentiated pancreatic neuroendocrine tumors. *Am J Surg Pathol* 2012; **36**: 173-184 [PMID: 22251937 DOI: 10.1097/PAS.0b013e3182417d36]

40 **Makuuchi R**, Terashima M, Kusuhara M, Nakajima T, Serizawa M, Hatakeyama K, Ohshima K, Urakami K, Yamaguchi K. Comprehensive analysis of gene mutation and expression profiles in neuroendocrine carcinomas of the stomach. *Biomed Res* 2017; **38**: 19-27 [PMID: 28239029 DOI: 10.2220/biomedres.38.19]

41 **Konukiewitz B**, Jesinghaus M, Steiger K, Schlitter AM, Kasajima A, Sipos B, Zamboni G, Weichert W, Pfarr N, Klöppel G. Pancreatic neuroendocrine carcinomas reveal a closer relationship to ductal adenocarcinomas than to neuroendocrine tumors G3. *Hum Pathol* 2018; **77**: 70-79 [PMID: 29596894 DOI: 10.1016/j.humpath.2018.03.018]

42 **Tang LH**, Basturk O, Sue JJ, Klimstra DS. A Practical Approach to the Classification of WHO Grade 3 (G3) Well-differentiated Neuroendocrine Tumor (WD-NET) and Poorly Differentiated Neuroendocrine Carcinoma (PD-NEC) of the Pancreas. *Am J Surg Pathol* 2016; **40**: 1192-1202 [PMID: 27259015 DOI: 10.1097/PAS.0000000000000662]

43 **La Rosa S**, Vanoli A. Gastric neuroendocrine neoplasms and related precursor lesions. *J Clin Pathol* 2014; **67**: 938-948 [PMID: 25053544 DOI: 10.1136/jclinpath-2014-202515]

44 **Rindi G**, Bordi C, Rappel S, La Rosa S, Stolte M, Solcia E. Gastric carcinoids and neuroendocrine carcinomas: pathogenesis, pathology, and behavior. *World J Surg* 1996; **20**: 168-172 [PMID: 8661813 DOI: 10.1007/s002689900026]

45 **Lee AA**, Poddar N, Hammami MB, Veerapong J, Cao D, Lai JP. Gastric Spindle Cell Neuroendocrine Tumor Mimicking Gastrointestinal Stromal Tumor: Unique Morphology and Diagnostic Pitfall. *Anticancer Res* 2017; **37**: 5893-5897 [PMID: 28982917 DOI: 10.21873/anticanres.12035]

46 **Scherübl H**, Cadiot G, Jensen RT, Rösch T, Stölzel U, Klöppel G. Neuroendocrine tumors of the stomach (gastric carcinoids) are on the rise: small tumors, small problems? *Endoscopy* 2010; **42**: 664-671 [PMID: 20669078 DOI: 10.1055/s-0030-1255564]

47 **Chin JL**, O'Toole D. Diagnosis and Management of Upper Gastrointestinal Neuroendocrine Tumors. *Clin Endosc* 2017; **50**: 520-529 [PMID: 29207862 DOI: 10.5946/ce.2017.181]

48 **Rorstad O**. Prognostic indicators for carcinoid neuroendocrine tumors of the gastrointestinal tract. *J Surg Oncol* 2005; **89**: 151-160 [PMID: 15719376 DOI: 10.1002/jso.20179]

49 **Gonzalez RS**. Diagnosis and Management of Gastrointestinal Neuroendocrine Neoplasms. *Surg Pathol Clin* 2020; **13**: 377-397 [PMID: 32773190 DOI: 10.1016/j.path.2020.04.002]

50 **Liu DJ**, Fu XL, Liu W, Zheng LY, Zhang JF, Huo YM, Li J, Hua R, Liu Q, Sun YW. Clinicopathological, treatment, and prognosis study of 43 gastric neuroendocrine carcinomas. *World J Gastroenterol* 2017; **23**: 516-524 [PMID: 28210088 DOI: 10.3748/wjg.v23.i3.516]

51 **Yao JC**, Hassan M, Phan A, Dagohoy C, Leary C, Mares JE, Abdalla EK, Fleming JB, Vauthey JN, Rashid A, Evans DB. One hundred years after "carcinoid": epidemiology of and prognostic factors for neuroendocrine tumors in 35,825 cases in the United States. *J Clin Oncol* 2008; **26**: 3063-3072 [PMID: 18565894 DOI: 10.1200/JCO.2007.15.4377]

52 **Dasari A**, Shen C, Halperin D, Zhao B, Zhou S, Xu Y, Shih T, Yao JC. Trends in the Incidence, Prevalence, and Survival Outcomes in Patients With Neuroendocrine Tumors in the United States. *JAMA Oncol* 2017; **3**: 1335-1342 [PMID: 28448665 DOI: 10.1001/jamaoncol.2017.0589]

53 **Hallet J**, Law CH, Cukier M, Saskin R, Liu N, Singh S. Exploring the rising incidence of neuroendocrine tumors: a population-based analysis of epidemiology, metastatic presentation, and outcomes. *Cancer* 2015; **121**: 589-597 [PMID: 25312765 DOI: 10.1002/cncr.29099]

54 **Klöppel G**, Perren A, Heitz PU. The gastroenteropancreatic neuroendocrine cell system and its tumors: the WHO classification. *Ann N Y Acad Sci* 2004; **1014**: 13-27 [PMID: 15153416 DOI: 10.1196/annals.1294.002]

55 **Witkiewicz A**, Galler A, Yeo CJ, Gross SD. Gangliocytic paraganglioma: case report and review of the literature. *J Gastrointest Surg* 2007; **11**: 1351-1354 [PMID: 17653595 DOI: 10.1007/s11605-007-0217-9]

56 **Howe JR**, Cardona K, Fraker DL, Kebebew E, Untch BR, Wang YZ, Law CH, Liu EH, Kim MK, Menda Y, Morse BG, Bergsland EK, Strosberg JR, Nakakura EK, Pommier RF. The Surgical Management of Small Bowel Neuroendocrine Tumors: Consensus Guidelines of the North American Neuroendocrine Tumor Society. *Pancreas* 2017; **46**: 715-731 [PMID: 28609357 DOI: 10.1097/MPA.0000000000000846]

57 **Mehrvarz Sarshekeh A**, Advani S, Halperin DM, Conrad C, Shen C, Yao JC, Dasari A. Regional lymph node involvement and outcomes in appendiceal neuroendocrine tumors: a SEER database analysis. *Oncotarget* 2017; **8**: 99541-99551 [PMID: 29245922 DOI: 10.18632/oncotarget.20362]

58 **Moris D**, Tsilimigras DI, Vagios S, Ntanasis-Stathopoulos I, Karachaliou GS, Papalampros A, Alexandrou A, Blazer DG 3RD, Felekouras E. Neuroendocrine Neoplasms of the Appendix: A Review of the Literature. *Anticancer Res* 2018; **38**: 601-611 [PMID: 29374682 DOI: 10.21873/anticanres.12264]

59 **Shaib W**, Krishna K, Kim S, Goodman M, Rock J, Chen Z, Brutcher E, Staley CI, Maithel SK, Abdel-Missih S, El-Rayes BF, Bekaii-Saab T. Appendiceal Neuroendocrine, Goblet and Signet-Ring Cell Tumors: A Spectrum of Diseases with Different Patterns of Presentation and Outcome. *Cancer Res Treat* 2016; **48**: 596-604 [PMID: 26044156 DOI: 10.4143/crt.2015.029]

60 **Boudreaux JP**, Klimstra DS, Hassan MM, Woltering EA, Jensen RT, Goldsmith SJ, Nutting C, Bushnell DL, Caplin ME, Yao JC; North American Neuroendocrine Tumor Society (NANETS). The NANETS consensus guideline for the diagnosis and management of neuroendocrine tumors: well-differentiated neuroendocrine tumors of the Jejunum, Ileum, Appendix, and Cecum. *Pancreas* 2010; **39**: 753-766 [PMID: 20664473 DOI: 10.1097/MPA.0b013e3181ebb2a5]

61 **Volante M**, Grillo F, Massa F, Maletta F, Mastracci L, Campora M, Ferro J, Vanoli A, Papotti M. Neuroendocrine neoplasms of the appendix, colon and rectum. *Pathologica* 2021; **113**: 19-27 [PMID: 33686307 DOI: 10.32074/1591-951X-230]

62 **Popa O**, Taban SM, Pantea S, Plopeanu AD, Barna RA, Cornianu M, Pascu AA, Dema ALC. The new WHO classification of gastrointestinal neuroendocrine tumors and immunohistochemical expression of somatostatin receptor 2 and 5. *Exp Ther Med* 2021; **22**: 1179 [PMID: 34475969 DOI: 10.3892/etm.2021.10613]

63 **Pawa N**, Clift AK, Osmani H, Drymousis P, Cichocki A, Flora R, Goldin R, Patsouras D, Baird A, Malczewska A, Kinross J, Faiz O, Antoniou A, Wasan H, Kaltsas GA, Darzi A, Cwikla JB, Frilling A. Surgical Management of Patients with Neuroendocrine Neoplasms of the Appendix: Appendectomy or More. *Neuroendocrinology* 2018; **106**: 242-251 [PMID: 28641291 DOI: 10.1159/000478742]

64 **Liu E**, Telem DA, Hwang J, Warner RR, Dikman A, Divino CM. The clinical utility of Ki-67 in assessing tumor biology and aggressiveness in patients with appendiceal carcinoids. *J Surg Oncol* 2010; **102**: 338-341 [PMID: 20607756 DOI: 10.1002/jso.21634]

65 **Anthony LB**, Strosberg JR, Klimstra DS, Maples WJ, O'Dorisio TM, Warner RR, Wiseman GA, Benson AB 3rd, Pommier RF; North American Neuroendocrine Tumor Society (NANETS). The NANETS consensus guidelines for the diagnosis and management of gastrointestinal neuroendocrine tumors (nets): well-differentiated nets of the distal colon and rectum. *Pancreas* 2010; **39**: 767-774 [PMID: 20664474 DOI: 10.1097/MPA.0b013e3181ec1261]

66 **Berardi RS**. Carcinoid tumors of the colon (exclusive of the rectum): review of the literature. *Dis Colon Rectum* 1972; **15**: 383-391 [PMID: 4561188 DOI: 10.1007/BF02587418]

67 **Lee SH**, Kim BC, Chang HJ, Sohn DK, Han KS, Hong CW, Lee EJ, Lee JB, Lee DS, Lee IT, Youk EG. Rectal neuroendocrine and L-cell tumors: diagnostic dilemma and therapeutic strategy. *Am J Surg Pathol* 2013; **37**: 1044-1052 [PMID: 23648459 DOI: 10.1097/PAS.0b013e3182819f0f]

68 **Sugimoto S**, Hotta K, Shimoda T, Imai K, Yamaguchi Y, Nakajima T, Oishi T, Mori K, Takizawa K, Kakushima N, Tanaka M, Kawata N, Matsubayashi H, Ono H. The Ki-67 labeling index and lymphatic/venous permeation predict the metastatic potential of rectal neuroendocrine tumors. *Surg Endosc* 2016; **30**: 4239-4248 [PMID: 26718357 DOI: 10.1007/s00464-015-4735-3]

69 **de Mestier L**, Brixi H, Gincul R, Ponchon T, Cadiot G. Updating the management of patients with rectal neuroendocrine tumors. *Endoscopy* 2013; **45**: 1039-1046 [PMID: 24163193 DOI: 10.1055/s-0033-1344794]

70 **Milan SA**, Yeo CJ. Neuroendocrine tumors of the pancreas. *Curr Opin Oncol* 2012; **24**: 46-55 [PMID: 22080942 DOI: 10.1097/CCO.0b013e32834c554d]

71 **D'Haese JG**, Tosolini C, Ceyhan GO, Kong B, Esposito I, Michalski CW, Kleeff J. Update on surgical treatment of pancreatic neuroendocrine neoplasms. *World J Gastroenterol* 2014; **20**: 13893-13898 [PMID: 25320524 DOI: 10.3748/wjg.v20.i38.13893]

72 **Falconi M**, Eriksson B, Kaltsas G, Bartsch DK, Capdevila J, Caplin M, Kos-Kudla B, Kwekkeboom D, Rindi G, Klöppel G, Reed N, Kianmanesh R, Jensen RT; Vienna Consensus Conference participants. ENETS Consensus Guidelines Update for the Management of Patients with Functional Pancreatic Neuroendocrine Tumors and Non-Functional Pancreatic Neuroendocrine Tumors. *Neuroendocrinology* 2016; **103**: 153-171 [PMID: 26742109 DOI: 10.1159/000443171]

73 **Qiao XW**, Qiu L, Chen YJ, Meng CT, Sun Z, Bai CM, Zhao DC, Zhang TP, Zhao YP, Song YL, Wang YH, Chen J, Lu CM. Chromogranin A is a reliable serum diagnostic biomarker for pancreatic neuroendocrine tumors but not for insulinomas. *BMC Endocr Disord* 2014; **14**: 64 [PMID: 25099181 DOI: 10.1186/1472-6823-14-64]

74 **Christ E**, Wild D, Forrer F, Brändle M, Sahli R, Clerici T, Gloor B, Martius F, Maecke H, Reubi JC. Glucagon-like peptide-1 receptor imaging for localization of insulinomas. *J Clin Endocrinol Metab* 2009; **94**: 4398-4405 [PMID: 19820010 DOI: 10.1210/jc.2009-1082]

75 **Koo J**, Mertens RB, Mirocha JM, Wang HL, Dhall D. Value of Islet 1 and PAX8 in identifying metastatic neuroendocrine tumors of pancreatic origin. *Mod Pathol* 2012; **25**: 893-901 [PMID: 22388755 DOI: 10.1038/modpathol.2012.34]

76 **Bettini R**, Partelli S, Boninsegna L, Capelli P, Crippa S, Pederzoli P, Scarpa A, Falconi M. Tumor size correlates with malignancy in nonfunctioning pancreatic endocrine tumor. *Surgery* 2011; **150**: 75-82 [PMID: 21683859 DOI: 10.1016/j.surg.2011.02.022]

77 **Lee LC**, Grant CS, Salomao DR, Fletcher JG, Takahashi N, Fidler JL, Levy MJ, Huebner M. Small, nonfunctioning, asymptomatic pancreatic neuroendocrine tumors (PNETs): role for nonoperative management. *Surgery* 2012; **152**: 965-974 [PMID: 23102679 DOI: 10.1016/j.surg.2012.08.038]

78 **Cherenfant J**, Stocker SJ, Gage MK, Du H, Thurow TA, Odeleye M, Schimpke SW, Kaul KL, Hall CR, Lamzabi I, Gattuso P, Winchester DJ, Marsh RW, Roggin KK, Bentrem DJ, Baker MS, Prinz RA, Talamonti MS. Predicting aggressive behavior in nonfunctioning pancreatic neuroendocrine tumors. *Surgery* 2013; **154**: 785-91; discussion 791 [PMID: 24074416 DOI: 10.1016/j.surg.2013.07.004]

79 **Cauley CE**, Pitt HA, Ziegler KM, Nakeeb A, Schmidt CM, Zyromski NJ, House MG, Lillemoe KD. Pancreatic enucleation: improved outcomes compared to resection. *J Gastrointest Surg* 2012; **16**: 1347-1353 [PMID: 22528577 DOI: 10.1007/s11605-012-1893-7]

80 **Sarmiento JM**, Heywood G, Rubin J, Ilstrup DM, Nagorney DM, Que FG. Surgical treatment of neuroendocrine metastases to the liver: a plea for resection to increase survival. *J Am Coll Surg* 2003; **197**: 29-37 [PMID: 12831921 DOI: 10.1016/S1072-7515(03)00230-8]

81 **Jin K**, Xu J, Chen J, Chen M, Chen R, Chen Y, Chen Z, Cheng B, Chi Y, Feng ST, Fu D, Hou B, Huang D, Huang H, Huang Q, Li J, Li Y, Liang H, Lin R, Liu A, Liu J, Liu X, Lu M, Luo J, Mai G, Ni Q, Qiu M, Shao C, Shen B, Sheng W, Sun J, Tan C, Tan H, Tang Q, Tang Y, Tian X, Tong D, Wang X, Wang J, Wang W, Wang Y, Wu Z, Xue L, Yan Q, Yang N, Yang Y, Yang Z, Yin X, Yuan C, Zeng S, Zhang R, Yu X. Surgical management for non-functional pancreatic neuroendocrine neoplasms with synchronous liver metastasis: A consensus from the Chinese Study Group for Neuroendocrine Tumors (CSNET). *Int J Oncol* 2016; **49**: 1991-2000 [PMID: 27826620 DOI: 10.3892/ijo.2016.3711]

82 **Pavel M**, Öberg K, Falconi M, Krenning EP, Sundin A, Perren A, Berruti A; ESMO Guidelines Committee. Gastroenteropancreatic neuroendocrine neoplasms: ESMO Clinical Practice Guidelines for diagnosis, treatment and follow-up. *Ann Oncol* 2020; **31**: 844-860 [PMID: 32272208 DOI: 10.1016/j.annonc.2020.03.304]

83 **Dawod M**, Gordoa TA, Cives M, De Mestier L, Crona J, Spada F, Oberg K, Pavel M, Lamarca A. Antiproliferative Systemic Therapies for Metastatic Small Bowel Neuroendocrine Tumours. *Curr Treat Options Oncol* 2021; **22**: 73 [PMID: 34185197 DOI: 10.1007/s11864-021-00863-y]

84 **Rinke A**, Müller HH, Schade-Brittinger C, Klose KJ, Barth P, Wied M, Mayer C, Aminossadati B, Pape UF, Bläker M, Harder J, Arnold C, Gress T, Arnold R; PROMID Study Group. Placebo-controlled, double-blind, prospective, randomized study on the effect of octreotide LAR in the control of tumor growth in patients with metastatic neuroendocrine midgut tumors: a report from the PROMID Study Group. *J Clin Oncol* 2009; **27**: 4656-4663 [PMID: 19704057 DOI: 10.1200/JCO.2009.22.8510]

85 **Caplin ME**, Pavel M, Ćwikła JB, Phan AT, Raderer M, Sedláčková E, Cadiot G, Wolin EM, Capdevila J, Wall L, Rindi G, Langley A, Martinez S, Blumberg J, Ruszniewski P; CLARINET Investigators. Lanreotide in metastatic enteropancreatic neuroendocrine tumors. *N Engl J Med* 2014; **371**: 224-233 [PMID: 25014687 DOI: 10.1056/NEJMoa1316158]

86 **Pavel M**, Ćwikła JB, Lombard-Bohas C, Borbath I, Shah T, Pape UF, Capdevila J, Panzuto F, Truong Thanh XM, Houchard A, Ruszniewski P. Efficacy and safety of high-dose lanreotide autogel in patients with progressive pancreatic or midgut neuroendocrine tumours: CLARINET FORTE phase 2 study results. *Eur J Cancer* 2021; **157**: 403-414 [PMID: 34597974 DOI: 10.1016/j.ejca.2021.06.056]

87 **Massironi S**, Conte D, Rossi RE. Somatostatin analogues in functioning gastroenteropancreatic neuroendocrine tumours: literature review, clinical recommendations and schedules. *Scand J Gastroenterol* 2016; **51**: 513-523 [PMID: 26605828 DOI: 10.3109/00365521.2015.1115117]

88 **Borga C**, Businello G, Murgioni S, Bergamo F, Martini C, De Carlo E, Trevellin E, Vettor R, Fassan M. Treatment personalization in gastrointestinal neuroendocrine tumors. *Curr Treat Options Oncol* 2021; **22**: 29 [PMID: 33641005 DOI: 10.1007/s11864-021-00825-4]

89 **Cidon EU**. New therapeutic approaches to metastatic gastroenteropancreatic neuroendocrine tumors: A glimpse into the future. *World J Gastrointest Oncol* 2017; **9**: 4-20 [PMID: 28144395 DOI: 10.4251/wjgo.v9.i1.4]

90 **Cives M**, Pelle' E, Strosberg J. Emerging Treatment Options for Gastroenteropancreatic Neuroendocrine Tumors. *J Clin Med* 2020; **9** [PMID: 33202931 DOI: 10.3390/jcm9113655]

91 **Hirmas N**, Jadaan R, Al-Ibraheem A. Peptide Receptor Radionuclide Therapy and the Treatment of Gastroentero-pancreatic Neuroendocrine Tumors: Current Findings and Future Perspectives. *Nucl Med Mol Imaging* 2018; **52**: 190-199 [PMID: 29942397 DOI: 10.1007/s13139-018-0517-x]

92 **Strosberg J**, El-Haddad G, Wolin E, Hendifar A, Yao J, Chasen B, Mittra E, Kunz PL, Kulke MH, Jacene H, Bushnell D, O'Dorisio TM, Baum RP, Kulkarni HR, Caplin M, Lebtahi R, Hobday T, Delpassand E, Van Cutsem E, Benson A, Srirajaskanthan R, Pavel M, Mora J, Berlin J, Grande E, Reed N, Seregni E, Öberg K, Lopera Sierra M, Santoro P, Thevenet T, Erion JL, Ruszniewski P, Kwekkeboom D, Krenning E; NETTER-1 Trial Investigators. Phase 3 Trial of ^{177}Lu-Dotatate for Midgut Neuroendocrine Tumors. *N Engl J Med* 2017; **376**: 125-135 [PMID: 28076709 DOI: 10.1056/NEJMoa1607427]

93 **Fazio N**, Kulke M, Rosbrook B, Fernandez K, Raymond E. Updated Efficacy and Safety Outcomes for Patients with Well-Differentiated Pancreatic Neuroendocrine Tumors Treated with Sunitinib. *Target Oncol* 2021; **16**: 27-35 [PMID: 33411058 DOI: 10.1007/s11523-020-00784-0]

94 **Yao JC**, Shah MH, Ito T, Bohas CL, Wolin EM, Van Cutsem E, Hobday TJ, Okusaka T, Capdevila J, de Vries EG, Tomassetti P, Pavel ME, Hoosen S, Haas T, Lincy J, Lebwohl D, Öberg K; RAD001 in Advanced Neuroendocrine Tumors, Third Trial (RADIANT-3) Study Group. Everolimus for advanced pancreatic neuroendocrine tumors. *N Engl J Med* 2011; **364**: 514-523 [PMID: 21306238 DOI: 10.1056/NEJMoa1009290]

95 **Yao JC**, Fazio N, Singh S, Buzzoni R, Carnaghi C, Wolin E, Tomasek J, Raderer M, Lahner H, Voi M, Pacaud LB, Rouyrre N, Sachs C, Valle JW, Fave GD, Van Cutsem E, Tesselaar M, Shimada Y, Oh DY, Strosberg J, Kulke MH, Pavel ME; RAD001 in Advanced Neuroendocrine Tumours, Fourth Trial (RADIANT-4) Study Group. Everolimus for the treatment of advanced, non-functional neuroendocrine tumours of the lung or gastrointestinal tract (RADIANT-4): a randomised, placebo-controlled, phase 3 study. *Lancet* 2016; **387**: 968-977 [PMID: 26703889 DOI: 10.1016/S0140-6736(15)00817-X]

96 **Bagchi S**, Yuan R, Engleman EG. Immune Checkpoint Inhibitors for the Treatment of Cancer: Clinical Impact and Mechanisms of Response and Resistance. *Annu Rev Pathol* 2021; **16**: 223-249 [PMID: 33197221 DOI: 10.1146/annurev-pathol-042020-042741]

97 **Kaufman HL**, Russell J, Hamid O, Bhatia S, Terheyden P, D'Angelo SP, Shih KC, Lebbé C, Linette GP, Milella M, Brownell I, Lewis KD, Lorch JH, Chin K, Mahnke L, von Heydebreck A, Cuillerot JM, Nghiem P. Avelumab in patients with chemotherapy-refractory metastatic Merkel cell carcinoma: a multicentre, single-group, open-label, phase 2 trial.

Lancet Oncol 2016; **17**: 1374-1385 [PMID: 27592805 DOI: 10.1016/S1470-2045(16)30364-3]

98 **Weber MM**, Fottner C. Immune Checkpoint Inhibitors in the Treatment of Patients with Neuroendocrine Neoplasia. *Oncol Res Treat* 2018; **41**: 306-312 [PMID: 29742518 DOI: 10.1159/000488996]

99 **Mehnert JM**, Bergsland E, O'Neil BH, Santoro A, Schellens JHM, Cohen RB, Doi T, Ott PA, Pishvaian MJ, Puzanov I, Aung KL, Hsu C, Le Tourneau C, Hollebecque A, Élez E, Tamura K, Gould M, Yang P, Stein K, Piha-Paul SA. Pembrolizumab for the treatment of programmed death-ligand 1-positive advanced carcinoid or pancreatic neuroendocrine tumors: Results from the KEYNOTE-028 study. *Cancer* 2020; **126**: 3021-3030 [PMID: 32320048 DOI: 10.1002/cncr.32883]

100 **Strosberg J**, Mizuno N, Doi T, Grande E, Delord JP, Shapira-Frommer R, Bergsland E, Shah M, Fakih M, Takahashi S, Piha-Paul SA, O'Neil B, Thomas S, Lolkema MP, Chen M, Ibrahim N, Norwood K, Hadoux J. Efficacy and Safety of Pembrolizumab in Previously Treated Advanced Neuroendocrine Tumors: Results From the Phase II KEYNOTE-158 Study. *Clin Cancer Res* 2020; **26**: 2124-2130 [PMID: 31980466 DOI: 10.1158/1078-0432.CCR-19-3014]

101 **Vijayvergia N**, Dasari A, Deng M, Litwin S, Al-Toubah T, Alpaugh RK, Dotan E, Hall MJ, Ross NM, Runyen MM, Denlinger CS, Halperin DM, Cohen SJ, Engstrom PF, Strosberg JR. Pembrolizumab monotherapy in patients with previously treated metastatic high-grade neuroendocrine neoplasms: joint analysis of two prospective, non-randomised trials. *Br J Cancer* 2020; **122**: 1309-1314 [PMID: 32152503 DOI: 10.1038/s41416-020-0775-0]

World Journal of Gastroenterology

Submit a Manuscript: https://www.f6publishing.com

World J Gastroenterol 2022 May 7; 28(17): 1768-1780

DOI: 10.3748/wjg.v28.i17.1768

ISSN 1007-9327 (print) ISSN 2219-2840 (online)

MINIREVIEWS

Current status and future of targeted peptide receptor radionuclide positron emission tomography imaging and therapy of gastroenteropancreatic-neuroendocrine tumors

Neil Grey, Michael Silosky, Christopher H Lieu, Bennett B Chin

Specialty type: Gastroenterology and hepatology

Provenance and peer review: Invited article; Externally peer reviewed.

Peer-review model: Single blind

Peer-review report's scientific quality classification
Grade A (Excellent): 0
Grade B (Very good): B, B
Grade C (Good): 0
Grade D (Fair): 0
Grade E (Poor): 0

P-Reviewer: Bergsma H, Netherlands; Yang X, China

Received: October 19, 2021
Peer-review started: October 19, 2021
First decision: December 3, 2021
Revised: January 7, 2022
Accepted: March 25, 2022
Article in press: March 25, 2022
Published online: May 7, 2022

Neil Grey, Radiology-Nuclear Medicine, University of Colorado School of Medicine, Anschutz Medical Campus, Aurora, CO 80045, United States

Michael Silosky, Bennett B Chin, Department of Radiology, University of Colorado School of Medicine, Anschutz Medical Campus, Aurora, CO 80045, United States

Christopher H Lieu, Medical Oncology, University of Colorado School of Medicine, Anschutz Medical Campus, Aurora, CO 80045, United States

Corresponding author: Bennett B Chin, MD, Professor, Department of Radiology, University of Colorado School of Medicine, Anschutz Medical Campus, 12401 East 17th Avenue, Mail Stop L954A, Aurora, CO 80045, United States. bennett.chin@cuanschutz.edu

Abstract

Theranostics is the highly targeted molecular imaging and therapy of tumors. Targeted peptide receptor radionuclide therapy has taken the lead in demonstrating the safety and effectiveness of this molecular approach to treating cancers. Metastatic, well-differentiated gastroenteropancreatic neuroendocrine tumors may be most effectively imaged and treated with DOTATATE ligands. We review the current practice, safety, advantages, and limitations of DOTATATE based theranostics. Finally, we briefly describe the exciting new areas of development and future directions of gastroenteropancreatic neuroendocrine tumor theranostics.

Key Words: DOTATATE; Theranostics; Gastroenteropancreatic neuroendocrine tumors; ^{68}Ga DOTATATE; ^{177}Lu DOTATATE; Review

©The Author(s) 2022. Published by Baishideng Publishing Group Inc. All rights reserved.

Core Tip: ^{68}Ga and ^{64}Cu DOTATATE positron emission tomography imaging is the most sensitive and accurate method to identify well-differentiated gastroenteropancreatic neuroendocrine tumors (GEP-NETs). The paired therapeutic radiotracer, ^{177}Lu DOTATATE, delivers targeted radiation which can prolong progression free survival. This is now established as the therapeutic best standard of care for patients with progressive, metastatic, or unresectable well-differentiated somatostatin receptors positive GEP-NETs. Ongoing investigations continue to expand the potential indications for DOTATATE theranostics. Additional novel ligands are also currently being developed for targeted imaging and therapy of GEP-NETs.

Citation: Grey N, Silosky M, Lieu CH, Chin BB. Current status and future of targeted peptide receptor radionuclide positron emission tomography imaging and therapy of gastroenteropancreatic-neuroendocrine tumors. *World J Gastroenterol* 2022; 28(17): 1768-1780
URL: https://www.wjgnet.com/1007-9327/full/v28/i17/1768.htm
DOI: https://dx.doi.org/10.3748/wjg.v28.i17.1768

INTRODUCTION

Neuroendocrine tumors (NETs) are a relatively rare and heterogeneous group of tumors arising from neuroendocrine cells throughout the body, which can cause a variety of symptoms based on the location and cell type. Midgut NETs are the most common, with the small bowel being the most frequent site of the primary lesion[1,2]. Although the incidence is relatively low, the majority are slow-growing, well-differentiated tumors which effectively contributes to a high prevalence. Improved clinical, laboratory, and imaging detection also likely contribute to an apparent increasing prevalence. NETs are often detected incidentally or after they metastasize and cause clinical symptoms either from their hormonal release and/or from mass effect.

Gastroenteropancreatic neuroendocrine tumors (GEP-NETs) comprise the majority of NETs (over 75%), with lung NETs comprising an additional approximately 15%[1]. GEP-NETs are characterized according to the WHO 2010 classification system based on the Ki-67 index, a widely used marker of cell proliferation. In this classification, GEP-NETs are scored as G1 (Ki-67 ≤ 2%), G2 (Ki-76 = 3%-20%), or G3 (Ki-67 > 20%), with G1 and G2 classified as well-differentiated tumors, and G3 tumors classified as poorly differentiated/de-differentiated carcinomas. Further stratification of G3 tumors can be assigned into well-differentiated (Ki-67 20%-50%) and poorly differentiated carcinomas (Ki-67 > 50%). This classification system, as well as the proposed subdivision of G3 tumors, has prognostic utility and helps direct appropriate diagnostic imaging and therapy.

The majority of well differentiated GEP-NETs (> 90%) express the G-coupled protein somatostatin receptors (SSTR)[3-5]. The WHO classification typically correlates with SSTR expression with well-differentiated tumors (G1 and G2) highly expressing SSTRs, and poorly differentiated tumors (G3) having lower SSTR expression. Diagnostic imaging and targeted radionuclide therapy take advantage of tumor SSTR expression by utilizing radiopharmaceuticals that bind to the same ligand. This elegant duality is emblematic of the expanding field of "theranostics", a portmanteau of therapy and diagnostics.

In this paper, we review the current approaches to the diagnosis and treatment of GEP-NETs. We focus primarily on DOTATATE (^{68}Ga DOTATATE and ^{64}Cu DOTATATE) positron emission tomography (PET)/computed tomography (CT) imaging and ^{177}Lu DOTATATE peptide receptor radionuclide therapy (PRRT), and conclude with future directions of GEP-NET theranostics.

DOTATATE PET IMAGING

Somatostatin is an endogenously produced peptide hormone that binds to various SSTRs. In humans, there are 5 subtypes[6], with GEP-NETs predominantly expressing SSTR-2 both in the primary tumor and in their metastases[7].

The currently approved nuclear medicine DOTATATE PET imaging agents used to bind SSTR-2 are composed of three functional parts: (1) The radioactive PET imaging component (^{68}Ga or ^{64}Cu); (2) The PET radiometal chelator and linker, DOTA (tetraazacyclododecanetetraacetic acid); and (3) The peptide binding part, TATE (tyrosine-3-octreotate)[8]. The earlier imaging agents used to visualize GEP-NETs was a single photon octreotide-based agent, [^{123}I-Tyr^3]octreotide[4], followed by ^{111}In pentetreotide (Octreoscan, Mallinkcrodt)[9]. ^{111}In pentetreotide remained the mainstay of GEP-NET imaging until the approval of the PET imaging agents. Both ^{68}Ga DOTATATE and the closely related ^{68}Ga DOTATOC have received approvals in Europe and the United States[10,11], as has the more recently approved ^{64}Cu

DOTATATE. Because of the extremely high binding affinity of ^{68}Ga DOTATATE to SSTR-2 (approximately 100 times greater than ^{111}In-pentetreotide)[12], the superior imaging characteristics of PET compared to SPECT, and the lower radiation delivered, DOTATATE PET imaging is now recommended in all cases over ^{111}In-pentetreotide[13], including use in both adults and children[14].

Indications

The appropriate use criteria for SSTR imaging in cases of known or suspected well-differentiated NETs with ^{68}Ga- and ^{64}Cu DOTATATE PET/CT imaging and ^{177}Lu DOTATATE peptide receptor radionuclide have been recently summarized[13]. These include the following nine indications: (1) Initial staging after the histologic diagnosis of NET; (2) Evaluation of an unknown primary; (3) Evaluation of a mass suggestive of NET not amenable to endoscopic or percutaneous biopsy; (4) Staging of NET before planned surgery; (5) Monitoring of NET seen predominantly on SSTR PET; (6) Evaluation of patients with biochemical evidence and symptoms of a NET; (7) Evaluation of patients with biochemical evidence of a NET without evidence on conventional imaging or a prior histologic diagnosis; (8) Restaging at time of clinical or laboratory progression without progression on conventional imaging; and (9) New indeterminate lesion on conventional imaging with unclear progression[13].

In addition to its primary use in GEP-NETs, ^{68}Ga DOTATATE PET has been used to image other SSTR positive tumors such as paragangliomas, pheochromocytomas, neuroblastomas, meningiomas, medullary thyroid cancers, Merkel cell carcinomas, small cell carcinomas, esthesioneuroblastomas, and tumor-induced oncogenic osteomalacia[8].

Technique

^{68}Ga DOTATATE is readily compounded from generator eluted ^{68}Ga and a sterile vial kit[15]. Before intravenous administration, there is little patient preparation except for good hydration and frequent voiding to minimize radiation dose to the kidneys. An uptake phase between radiotracer administration and PET imaging is typically approximately 60 min, similar to ^{18}F fluorodeoxyglucose (FDG) PET. This allows time for tumor uptake and for background washout clearance *via* the kidneys, which is analogous to the procedure used in FDG PET. Patients are typically imaged from the mid-thigh to the skull. In cases where tumor is known or suspected outside of this field of view, or in cases of unknown primary, longer imaging times may be needed to include the extremities. Intravenous contrast is not essential for accurate interpretation in most cases, but it can be helpful in some clinical settings. Additional procedural details are listed in the European Association of Nuclear Medicine guidelines [14].

Many patients with GEP-NETs will be on short- or long-acting somatostatin analogue (SSA) therapy which could interfere with ^{68}Ga DOTATATE PET uptake due to competitive binding. Temporary discontinuation of short-acting SSAs is recommended for 24-48 h, and long-acting SSAs should be avoided for approximately 4-6 wk[8,16]. Long-acting release (LAR) SSAs are administered on 4 wk cycles, allowing ^{68}Ga DOTATATE imaging to be scheduled for the end of the monthly cycle prior to redosing. Regardless of the specific approach, subsequent ^{68}Ga DOTATATE scans are preferably performed with the exact timing between SSA injections.

Normal biodistribution

The normal biodistribution of ^{68}Ga DOTATATE differs in several aspects compared to the most commonly used radiotracer, ^{18}F FDG. For both ^{68}Ga DOTATATE and ^{18}F FDG, the genitourinary tract is the normal route of excretion for unbound radiotracer, and thus high radiotracer activity can be seen in the kidneys, ureters, and bladder. In ^{68}Ga DOTATATE, the spleen has the highest normal activity, followed by the adrenal glands[17]. Unlike FDG, the pituitary is the only part of the central nervous system with high physiologic uptake. Salivary glands and the thyroid can have moderate uptake. Activity in the pancreas is variable and occasionally focal in the head and uncinate process[18]. Variable but typically lower-level diffuse uptake is seen in the small and large bowel[8]. Physiologic uptake in the liver can be quite variable[19], and uptake can be low in the spleen and liver if total body tumor burden is high ("sink effect")[20]. ^{68}Ga DOTATATE uptake is otherwise low throughout the muscles, adipose tissue, and bone.

Dosimetry

The recommended dose for ^{68}Ga DOTATATE is 2 MBq/kg of body weight (0.054 mCi/kg) up to 200 MBq (5.4 mCi). The organ with the highest dose delivered is the spleen due to its high uptake. The whole body radiation effective dose equivalent (EDE) from ^{68}Ga DOTATATE PET is 2-3 mSv[21,22], which is approximately only 10% of the 26 mSv received from a typical dose (222 MBq or 6 mCi) of ^{111}In pentetreotide. Despite the addition of an EDE of 1-9 mSv from the CT component, which is needed for attenuation correction and anatomic localization, the total dose of ^{68}Ga DOTATATE PET/CT (3-12 mSv) remains significantly lower than that of ^{111}In pentetreotide.

Imaging performance

Due to the very high affinity of ^{68}Ga DOTATATE for SSTR-2, target lesions typically show extremely

high uptake. With deficient (*i.e.*, very low) background radiotracer uptake throughout most of the body including the thorax, head and neck, bone marrow, muscle, and brain (except the pituitary), the tumor to background ratio can be exceptionally high. In a large prospective study of GEP-NETs comparing accuracy of ^{68}Ga DOTATATE, conventional imaging [CT and magnetic resonance imaging (MRI)], and ^{111}In pentetreotide, ^{68}Ga DOTATATE showed clear superiority in lesion detectability with mean tumor SUVmax values of over 65[23]. Figure 1 shows an example of normal intense uptake in the spleen and adrenals and moderate ^{68}Ga DOTATATE uptake in the liver. Small liver lesions can also be visualized despite relatively high liver background activity. Extremely high radiotracer activity can be seen in larger lesions, as shown in Figure 2.

False positives are uncommon and do not typically present a diagnostic dilemma. The most common causes of false positives are inflammation or infection due to leukocytes and macrophages expressing SSTR-2[24]. For example, inflammatory prostatitis is relatively common and can show intense focal uptake within the prostate[25]. Other potential causes of false positive can arise from osteoblastic activity[26], such as in degenerative changes, fractures, fibrous dysplasia, vertebral hemangiomas, and epiphyses in pediatric patients[27,28].

False negative results may be due to loss of receptor expression. GEP-NETs that dedifferentiate and subsequently lose SSTR-expression may show lower ^{68}Ga DOTATATE avidity. Another cause of false negatives, as seen in PET imaging, may arise from small lesions below PET resolution. In our experience, however, the highly avid ^{68}Ga DOTATATE uptake in well differentiated GEP-NETs is commonly adequate to overcome the limitations of partial volume effect. If tumor uptake is sufficiently high, it can also overcome the detrimental effects of a relatively low administered dose and other physical limitations of ^{68}Ga compared to ^{18}F[29-32]. Small lesions can be readily visualized in phantom and patient clinical studies if the background activity is low. The non-contrast portion of the CT frequently does not reveal hepatic lesions; however, hepatic GEP-NETs as small 5 mm may be visualized despite high normal background liver activity[30].

Role in evaluation and value in management

^{68}Ga DOTATATE PET is an excellent study for evaluating GEP-NETs and demonstrates very high sensitivity and specificity of 93% and 95%, respectively[33]. Its superior performance in detecting GEP-NETs compared to ^{111}In pentetreotide and CT or MRI is well established[23]. This can result in a significant change in clinical management in up to a third of patients even when compared to ^{111}In pentetreotide[34-36]. ^{68}Ga DOTATATE has also shown increasing utility in detecting lesions not seen on other modalities. It can confirm suspicion of GEP-NET found on other modalities, determine the true extent of tumor, stage disease, identify otherwise occult tumors such as thoracic ACTH-secreting carcinoids, and guide treatment options. It may be used to confirm a clinical or biochemical suspicion of GEP-NET, identify the primary lesion in known metastatic disease, determine resectability, exclude greater extent of disease prior to resection, and importantly, identify candidates for hormonal therapy or PRRT[8].

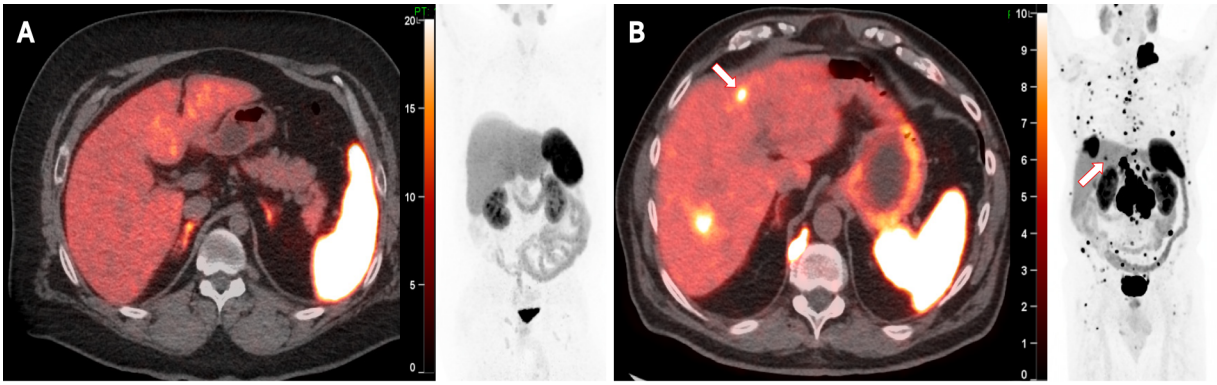
^{64}Cu DOTATATE

The primary practical advantage of ^{64}Cu DOTATATE is its longer physical half-life (^{64}Cu t½ = 12.7 h). This allows for more flexibility in production, shipment to distant locations, and flexibility in the timing of PET imaging. ^{68}Ga DOTATATE (^{68}Ga t½ = 68 minutes) is typically produced at a site close to the PET imaging center due to the short physical half-life. ^{64}Cu DOTATATE allows flexibility for delayed imaging three hours after injection with no significant difference in lesion detectability[37]. Compared to the DOTATOC ligand, the ^{64}Cu DOTATATE showed slightly higher lesion detectability than ^{68}Ga DOTATOC[38]. Other differences between ^{64}Cu compared to ^{68}Ga do not appear to have a large clinical impact on lesion detectability. ^{64}Cu compared to ^{68}Ga has a disadvantage in a lower percentage of positrons emitted *per* decay (17.5% *vs* 88.9%). However, ^{64}Cu has the physical advantage of shorter mean positron range prior to annihilation (0.7 mm *vs* 3.5 mm) which can improve spatial resolution[39]. Data are emerging to support quantitative imaging of ^{64}Cu DOTATATE which correlates with prognosis[40, 41]. Finally, pre-clinical studies of new investigational agents, such as ^{55}Co DOTATATE, show the potential for further improvements in tumor uptake and image contrast when compared to currently approved agents[42].

Role of FDG-PET

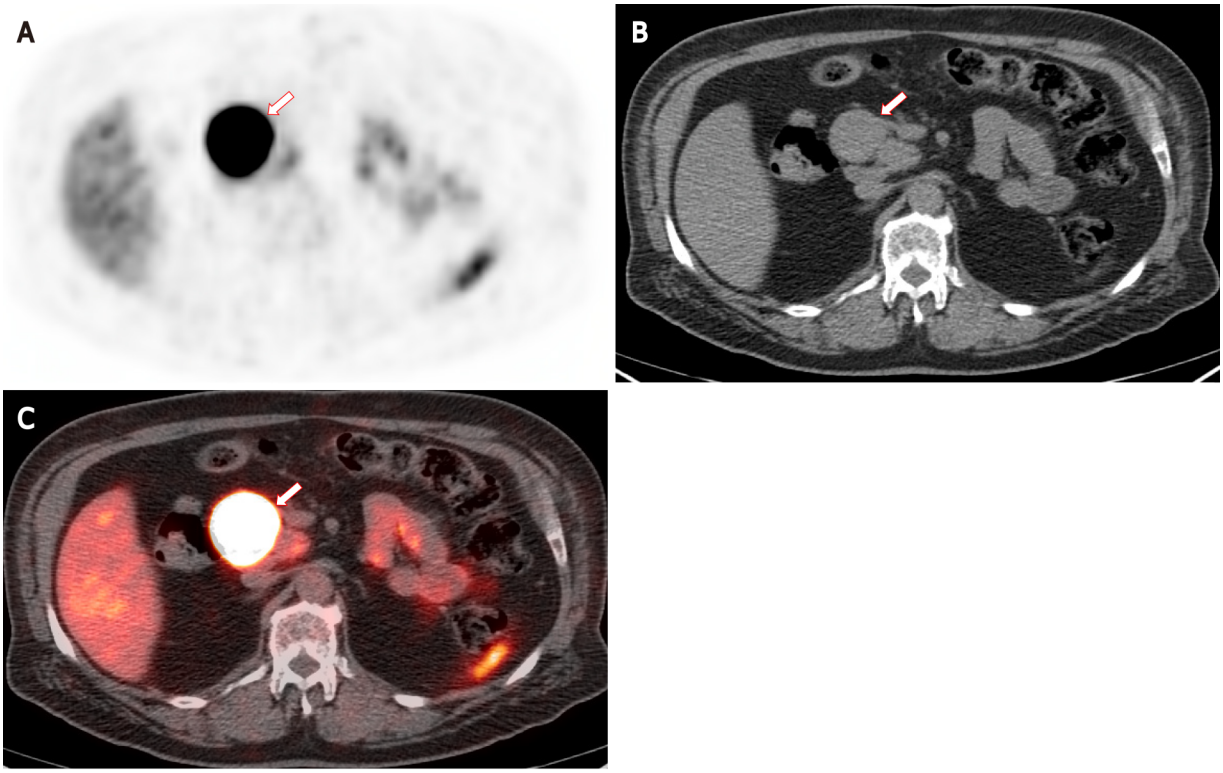
FDG is a glucose analogue that enters cells through glucose transporters, undergoes phosphorylation, and then remains trapped within the cell as FDG-6-phosphate. This imaging metric of glycolysis is frequently upregulated in many cancers and generally associated with more aggressive, rapidly growing malignancies.

Well differentiated GEP-NETs, however, are typically slower growing, have lower mitotic rates, and have lower rates of proliferation including lower Ki-67 indices. The WHO classification of GEP-NETs relies on the Ki-67 index which reflects cellular proliferation. As GEP-NETs become more dedifferentiated, they tend to lose SSTRs expression and decrease in ^{68}Ga DOTATATE avidity. These often exhibit a more aggressive and faster growing phenotype with increasing proliferation (Ki-67) and increasing



DOI: 10.3748/wjg.v28.i17.1768 **Copyright** ©The Author(s) 2022.

Figure 1 ^{68}Ga DOTATATE positron emission tomography/computed tomography transaxial fusion and whole body projection positron emission tomography. A: A normal patient; B: A different patient with well-differentiated pancreatic neuroendocrine tumor with nodal, bone, and liver metastases. Small liver metastases can be seen SUVmax = 10.4 (arrow).

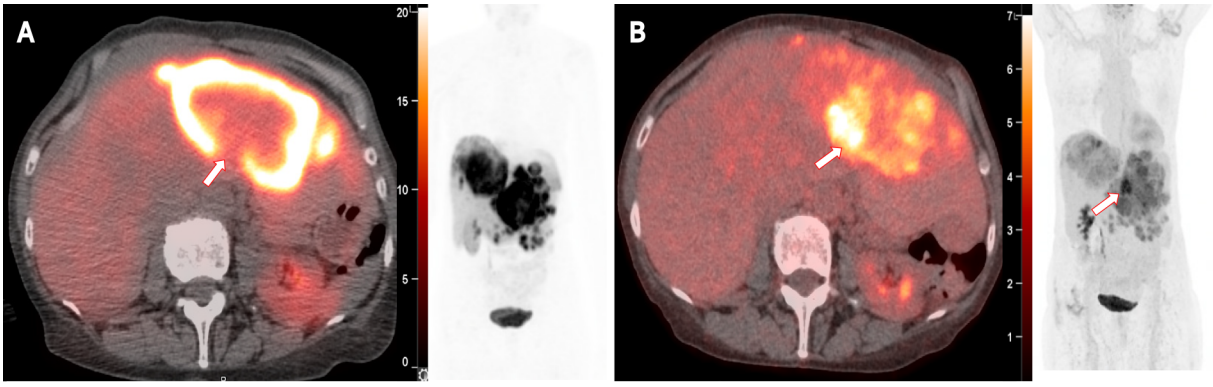


DOI: 10.3748/wjg.v28.i17.1768 **Copyright** ©The Author(s) 2022.

Figure 2 70 year old female with abdominal mass (arrow) showing intense ^{68}Ga DOTATATE uptake. Pancreaticoduodenectomy showed a 4 cm well-differentiated (Ki-67 = 5%) pancreatic neuroendocrine tumor. A: ^{68}Ga DOTATATE positron emission tomography (PET) lesion SUVmax = 118; B: Computed tomography (CT); C: PET/CT fusion.

glycolytic activity. Clinically, when a known GEP-NET tumor increases in size, yet decreases in ^{68}Ga DOTATATE avidity, an FDG-PET can be useful in identifying tumor which may be exhibiting this dedifferentiating phenotype ("flip-flop" effect), and warrant consideration of a change in therapy. Patients with NETs demonstrating FDG avid disease are at a 10 fold increased risk of death[43]. Other studies have shown similar findings[44,45].

FDG PET may also be useful in identifying heterogeneity of tumors by directing biopsy of tumors suspicious for a more aggressive or higher-grade histology. When both ^{68}Ga DOTATATE PET-CT and FDG PET-CT are performed, the differential imaging features may assist in prognosis and guide therapy options. FDG PET can therefore be complementary and aid in management decisions in which tumor dedifferentiation is suspected. An example of an FDG positive hepatic metastasis is shown in Figure 3.



DOI: 10.3748/wjg.v28.i17.1768 **Copyright** ©The Author(s) 2022.

Figure 3 73 year old female with well-differentiated neuroendocrine tumor (Ki-67 = 6%) and liver metastases with an unknown primary. A: ^{68}Ga DOTATATE positron emission tomography (PET)/computed tomography (CT) fusion and whole-body PET projection confirms multifocal hepatic metastases SUVmax 34.4 with an area of focal decreased DOTATATE avidity (arrow); B: Fluorodeoxyglucose (FDG) PET/CT fusion and whole-body PET shows mismatched focal intense increased FDG uptake SUVmax 9.1 (arrow), suggestive of heterogeneous tumor phenotype with areas of dedifferentiation.

THERAPY

Treatment options

Partial or complete surgical resection of GEP-NET is the preferred approach when possible[46]. Hormone therapy is another mainstay of GEP-NET treatment. Short- or long-acting SSAs bind to SSRTs and inhibit or slow tumor growth while simultaneously helping with hormone secretion related symptoms. Additional treatment options may include mTOR inhibitors, VEGF inhibitors, chemotherapy, radiation, and liver metastases directed embolization therapies[47]. More recently, ^{177}Lu DOTATATE PRRT has been established as a safe and effective treatment of metastatic GEP-NETs.

PRRT

PRRT is the logical extension of SSTR imaging into the treatment realm and comprises the therapy component of theranostics. The imaging radionuclide (^{68}Ga or ^{64}Cu) is replaced with a beta emitter, ^{177}Lu, which deposits lethal radiation precisely to the SSTR-2 positive cells, providing targeted radiotherapy to tumors. The resultant ^{177}Lu DOTATATE radionuclide delivers local radiation specifically to tumor visualized on ^{68}Ga DOTATATE imaging. ^{177}Lu is primarily a beta emitter with a mean range of 2 mm in tissue, and a small fraction is gamma radiation (6.6% at 113-keV and 11% at 208-keV). This results in a relatively low exposure to individuals surrounding the patient, allowing therapies to be performed as an outpatient. The relatively long half-life of 6.7 d (160 h) delivers sustained radiotherapy for a prolonged period; however, this requires extended precautions to avoid exposure from urinary contamination. ^{177}Lu DOTATATE (Lutathera) was approved by the EMA in 2017 and by the FDA in January 2018[47].

Patient selection

^{177}Lu DOTATATE was approved specifically for treatment of SSTR-positive GEP-NETs that have progressed on SSA therapy[47]. The most appropriate patients for therapy are based upon guidelines developed by the NETTER-1 trial[48]. There are multiple considerations for patient selection for PRRT; however, patients with progressive metastatic low and intermediate grade GEP-NETs typically have highly positive SSTR scans and are most likely to benefit.

Technique

The standard protocol for ^{177}Lu DOTATATE therapy is based upon the NETTER-1 trial[48]. Patients are prescribed four doses of 7.4 GBq (200 mCi) eight weeks apart for a cumulative dose of 29.6 GBq (800 mCi). At least 30 min prior to therapy administration, an amino acid infusion is started for renal protection and lasts four hours. The two amino acids required for renal protection are arginine and lysine. Although other formulations of different amino acids exist, they do not provide any additional benefit and can cause significant nausea and vomiting.

Based on the typical dose of 7.4 GBq of ^{177}Lu DOTATATE, the exposure rate at 1 m is 2 mR/h and decreases by 50% within 24 h[47]. If the patient is able to abide by standard radiation safety precautions, this can be performed as an outpatient. Precautions include bathroom hygiene, similar to radioiodine treatments, and appropriate distancing from others, specifically children and pregnant women, for approximately 3 d after therapy. Individualized safety instructions may be prepared by a radiation safety officer or radiation physicist, depending on the institution, and reviewed with the patient during the consent process.

Efficacy

^{177}Lu DOTATATE therapy in GEP-NETs has demonstrated efficacy in many studies over several years. The most notable large prospective randomized trial is the NETTER-1 trial[48]. This prospective randomized trial in adults with biopsy-proven low- and intermediate grade (G1 or G2, *i.e.*, Ki-67 level ≤ 20%) GEP-NETs evaluated subjects treated with ^{177}Lu DOTATATE and SSA compared to a control group on high dose SSA alone. Inclusion criteria were metastatic disease or locally advanced and inoperable disease which was progressing on SSA[48].

The primary endpoint of the study was progression free survival (PFS) with secondary endpoints of objective response rate (ORR), overall survival (OS), safety, and the side-effect profile. Patients were judged to have failed treatment if there was tumor progression based on follow up imaging by CT or MRI according to RECIST 1.1 criteria[49].

Patients in the treatment arm experienced significantly better PFS at 20 mo of 65.2% (95%CI: 50.0-76.8) compared to 10.8% (95%CI: 3.5-23.0) in the control group. In other words, in the treatment group there was a 79% lower risk of disease progression or death and a 60% lower risk of death alone. The secondary endpoint of ORR was 18% in the treatment group and 3% in the control group. As noted in the NETTER-1 study, multiple large randomized trials with other systemic therapies, such as SSAs alone or in combination with other non-radionuclides, showed response rates of only 5% or less[50-53]. Median overall survival could not be calculated yet at the conclusion of NETTER-1, but there was a trend towards longer overall survival in the treatment group. An example of a patient with partial response to ^{177}Lu DOTATATE is shown in Figure 4.

Adverse side effects and overall safety

In NETTER-1, transient WHO grade 3 and 4 hematologic toxicity (thrombocytopenia 2%; lymphopenia 9%; neutropenia 1%) and no renal toxicity were reported after 14 mo of follow up[48]. Rare but serious side effects including acute leukemia and myelodysplastic syndrome have been reported, occurring in < 1% and < 1%-2% of patients, respectively[47,48,54]. Other studies have similarly shown limited side effects with ^{177}Lu DOTATATE therapy[54,55].

Common mild side effects (Grade 1 or 2) include nausea (59%) and vomiting (47%)[48]; however, this has been primarily attributed to the specific amino acid infusion. Use of the simpler arginine and lysine infusion appears to have much lower incidence and severity of side effects. Fatigue (40%), decreased appetite (18%), headache (16%), and alopecia (11%) were significantly higher in the ^{177}Lu DOTATATE treatment group[48]. Although relatively frequent, abdominal pain (26%), and diarrhea (29%) were not statistically different compared to the control group. An uncommon side effect of treatment is hormone crisis, which in one study of 504 patients happened in only 6 (or 1.2%) and can be adequately managed in a brief hospital stay with complete recovery[54].

FUTURE DIRECTIONS

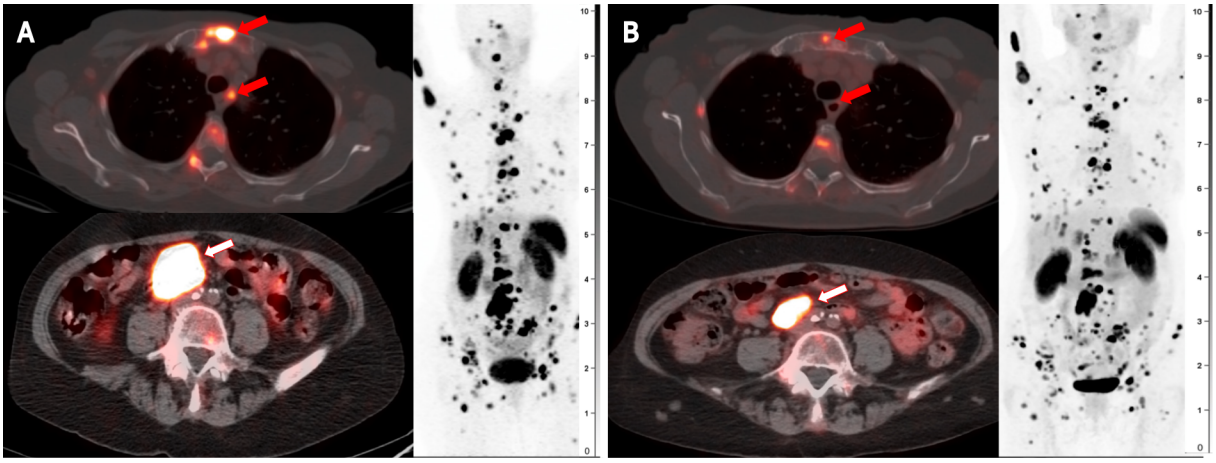
While ^{68}Ga- and ^{177}Lu DOTATATE have shown remarkable efficacy in imaging and treatment of GEP-NETs, many additional imaging and treatment options are currently under investigation. A comprehensive review is not possible in the context of the rapidly evolving landscape of theranostics. A few representative clinical trials are briefly mentioned to provide a perspective of the breadth of ongoing investigations.

Current clinical trials

Extending PRRT into higher grade GEP-NETs is an active area of investigation. The COMPOSE trial compares well-differentiated higher grade (G2 or G3, Ki-67 index between 10%-55%) GEP-NETs treated with ^{177}Lu Edotreotide (DOTATOC) compared to best standard of care chemotherapy regimens[56]. The COMPETE trial similarly evaluates advanced GEP-NETs for safety and efficacy of ^{177}Lu DOTATOC compared to Everolimus[57]. The NETTER-2 trial investigates higher proliferation index tumors (G2 or G3) as first line therapy with ^{177}Lu DOTATATE therapy and SSA compared to high dose SSR therapy alone[58].

^{177}Lu DOTATATE retreatment

While ^{177}Lu DOTATATE is now given as a four dose regimen, additional doses have been administered on an investigational basis. If a patient shows continued improvement in tumor burden and symptoms throughout the ^{177}Lu DOTATATE treatment course established by NETTER-1, (four cycles, 8 wk apart), they may benefit from continued treatment with additional doses of ^{177}Lu DOTATATE. A meta-analysis suggests that ^{177}Lu DOTATATE re-treatment in patients with advanced GEP-NETs is well tolerated with a safety profile similar to initial PRRT[59]. This provides an additional treatment strategy potentially to improve PFS, OS, and disease related survival.



DOI: 10.3748/wjg.v28.i17.1768 **Copyright** ©The Author(s) 2022.

Figure 4 79 year old female with well-differentiated neuroendocrine tumors, unknown primary, treated with a complete ^{177}Lu-DOTATATE regimen showing mild response. ^{177}Ga-DOTATATE positron emission tomography (PET) computed tomography transaxial fusion and whole body projection PET pre-therapy and post-therapy. A: Pre-therapy; B: Post-therapy. (A; top) Sternal osseous metastases are partially improved (red arrow; B top), and a mediastinal node is resolving (red arrow; paratracheal). (Bottom row) Dominant pelvic nodal mass (A; white arrow) has decreased (B; white arrow) in size 3.3 × 2.1 (previously 3.7 × 2.6), and uptake SUVmax 39.6 (previously 46.8).

Alternative PRRT agents

Either systemic or arterially-delivered PRRT with ^{90}Y DOTATATE or -DOTATOC is an approach that is under further investigation. ^{90}Y is beta emitter with a higher energy and longer mean free path in soft tissue than ^{177}Lu. This theoretically favors treatment of larger tumors where high intratumor pressure limits blood flow and radiotracer delivery. However, a variety of factors mediate tumor killing including bystander effect[60]. A major limiting drawback of ^{90}Y is its greater toxic effects to surrounding tissues and bone marrow[61]. Renal dose is also higher than ^{177}Lu which poses a higher risk of nephrotoxicity[62]. Arterially-administered ^{90}Y DOTATATE is more focally directed but is operator intensive and requires a prolonged procedure typically performed in the interventional radiology suite.

Novel imaging and treatment agents

Antagonists: In contrast to the established SSTR agonists (*e.g.*, DOTATATE), somatostatin antagonists are currently being investigated for imaging and therapy of GEP-NETs. Agonist-ligand complexes are internalized into the cell and entrapped, which is believed to generate higher contrast imaging and prolonged tumor targeted therapy. Antagonists were developed to evaluate the functions of receptors [63] and are typically not internalized, but this may be overcome by binding to a higher number of receptor sites than agonists[64]. The SSTR-2 antagonist JR11 has shown uptake in renal cell cancers, most breast cancers, non-Hodgkin lymphomas, and medullary thyroid cancers with binding comparable to NET targeting with SSTR-2 agonists[65]. This study also showed that peritumoral vessels, lymphocytes, nerves, mucosa, and stroma were more strongly labeled with the antagonist than with the agonist. Antagonists, therefore, may show higher binding leading to improved detection and more avid tumor binding in targeted radiotherapy. ^{68}Ga NODAGA-LM3, ^{68}Ga DOTA-LM3, and ^{68}Ga NODAGA-JR11 (OPS202) are three of the agents showing early promise[66-68] with clinical trials underway[69]. Similar to DOTATATE, therapeutic radionuclides can be attached to these antagonists for PRRT[70,71].

Alpha emitters: PRRT for GEP-NETs is currently performed primarily by beta emitters (^{177}Lu and ^{90}Y), but targeted alpha therapy (TAT) is potentially much more effective[72,73]. Alpha particles travel a much shorter distance in tissue, typically on the order of only a few cell diameters, and deliver a dramatically higher damaging radiation effect to cells compared to beta emitters. In contrast to beta emission, which results primarily in single breaks in DNA, highly energetic alpha particles result in clusters of double stranded DNA breaks which are irreparable and highly lethal[72]. Alpha particles also generate more ionization events and an immunogenic cell death which could generate an immunostimulatory environment and promote an abscopal effect[73]. The dual effect of higher tumor cell death and limited radiation to non-target tissues increases the lethality to tumor cells and decreases the off-target adverse side effects.

The primary systemic alpha emitter under investigation is ^{225}Ac which can be stably bound to DOTATATE or DOTATOC[73]. Early studies have shown promising results[74,75] with avoidance of severe renal and hematologic toxicity[76]. In the future, this could be given as an initial treatment strategy, in sequence with ^{177}Lu DOTATATE, or as a salvage therapy for patients progressing on ^{177}Lu PRRT.

Additional therapies or combination therapies

Beyond radionuclides, there are other drugs and regimens being developed for treatment of GEP-NETs. These therapies may provide additional benefits to PRRT, particularly if they can be used to sensitize tumors to PRRT or be sequenced in such a way to deliver synergistic lethality. Alternative methods of administration may also allow higher local dose PRRT *via* intra-arterial rather than systemic delivery[77, 78]. PRRT could also be used in a neoadjuvant fashion prior to surgery to make some patients operative candidates and increase the chances of curative resection[54]. The sorting out of the milieu of therapies, their timing, and indications will require ongoing research.

CONCLUSION

Currently, the most sensitive and accurate established method to image well-differentiated GEP-NETs is with DOTATATE PET imaging. Due to the favorable uptake properties and biodistribution, targeted PRRT with ^{177}Lu DOTATATE has been established as best standard of care for patients with progressive, metastatic, or unresectable well-differentiated SSTR positive GEP-NETs. ^{177}Lu DOTATATE is well tolerated with a very mild toxicity profile and rare serious adverse events. Ongoing investigations are continuing to expand in both imaging and therapy applications for DOTATATE and novel ligand theranostics for GEP-NETs.

FOOTNOTES

Author contributions: Grey N, Silosky M, Lieu CH, and Chin BB all contributed to the writing and editing of the manuscript; all authors have read and approve the final manuscript.

Conflict-of-interest statement: All authors declare no conflict of interest in the content of this review article.

Open-Access: This article is an open-access article that was selected by an in-house editor and fully peer-reviewed by external reviewers. It is distributed in accordance with the Creative Commons Attribution NonCommercial (CC BY-NC 4.0) license, which permits others to distribute, remix, adapt, build upon this work non-commercially, and license their derivative works on different terms, provided the original work is properly cited and the use is non-commercial. See: https://creativecommons.org/Licenses/by-nc/4.0/

Country/Territory of origin: United States

ORCID number: Neil Grey 0000-0002-9707-5695; Michael Silosky 0000-0003-3675-5387; Christopher H Lieu 0000-0002-4852-4642; Bennett B Chin 0000-0002-2907-5968.

Corresponding Author's Membership in Professional Societies: Society of Nuclear Medicine, No. 134373.

S-Editor: Fan JR
L-Editor: A
P-Editor: Fan JR

REFERENCES

1 **Riihimäki M**, Hemminki A, Sundquist K, Sundquist J, Hemminki K. The epidemiology of metastases in neuroendocrine tumors. *Int J Cancer* 2016; **139**: 2679-2686 [PMID: 27553864 DOI: 10.1002/ijc.30400]
2 **Yao JC**, Hassan M, Phan A, Dagohoy C, Leary C, Mares JE, Abdalla EK, Fleming JB, Vauthey JN, Rashid A, Evans DB. One hundred years after "carcinoid": epidemiology of and prognostic factors for neuroendocrine tumors in 35,825 cases in the United States. *J Clin Oncol* 2008; **26**: 3063-3072 [PMID: 18565894 DOI: 10.1200/JCO.2007.15.4377]
3 **de Herder WW**, Hofland LJ, van der Lely AJ, Lamberts SW. Somatostatin receptors in gastroentero-pancreatic neuroendocrine tumours. *Endocr Relat Cancer* 2003; **10**: 451-458 [PMID: 14713257 DOI: 10.1677/erc.0.0100451]
4 **Krenning EP**, Bakker WH, Breeman WA, Koper JW, Kooij PP, Ausema L, Lameris JS, Reubi JC, Lamberts SW. Localisation of endocrine-related tumours with radioiodinated analogue of somatostatin. *Lancet* 1989; **1**: 242-244 [PMID: 2563413 DOI: 10.1016/s0140-6736(89)91258-0]
5 **Papotti M**, Bongiovanni M, Volante M, Allìa E, Landolfi S, Helboe L, Schindler M, Cole SL, Bussolati G. Expression of somatostatin receptor types 1-5 in 81 cases of gastrointestinal and pancreatic endocrine tumors. A correlative immunohistochemical and reverse-transcriptase polymerase chain reaction analysis. *Virchows Arch* 2002; **440**: 461-475 [PMID: 12021920 DOI: 10.1007/s00428-002-0609-x]
6 **Reubi JC**. Neuropeptide receptors in health and disease: the molecular basis for *in vivo* imaging. *J Nucl Med* 1995; **36**: 1825-1835 [PMID: 7562050]
7 **Reubi JC**. Peptide receptor expression in GEP-NET. *Virchows Arch* 2007; **451** Suppl 1: S47-S50 [PMID: 17684767 DOI:

10.1007/s00428-007-0443-2]
8 **Hofman MS**, Lau WF, Hicks RJ. Somatostatin receptor imaging with 68Ga DOTATATE PET/CT: clinical utility, normal patterns, pearls, and pitfalls in interpretation. *Radiographics* 2015; **35**: 500-516 [PMID: 25763733 DOI: 10.1148/rg.352140164]
9 **Hicks RJ**. Use of molecular targeted agents for the diagnosis, staging and therapy of neuroendocrine malignancy. *Cancer Imaging* 2010; **10** Spec no A: S83-S91 [PMID: 20880795 DOI: 10.1102/1470-7330.2010.9007]
10 **Wangerin KA**, Muzi M, Peterson LM, Linden HM, Novakova A, Mankoff DA, Kinahan PE. A virtual clinical trial comparing static *vs* dynamic PET imaging in measuring response to breast cancer therapy. *Phys Med Biol* 2017; **62**: 3639-3655 [PMID: 28191877 DOI: 10.1088/1361-6560/aa6023]
11 **Hennrich U**, Benešová M. [^{68}Ga]Ga-DOTA-TOC: The First FDA-Approved ^{68}Ga-Radiopharmaceutical for PET Imaging. *Pharmaceuticals (Basel)* 2020; **13** [PMID: 32138377 DOI: 10.3390/ph13030038]
12 **Reubi JC**, Schär JC, Waser B, Wenger S, Heppeler A, Schmitt JS, Mäcke HR. Affinity profiles for human somatostatin receptor subtypes SST1-SST5 of somatostatin radiotracers selected for scintigraphic and radiotherapeutic use. *Eur J Nucl Med* 2000; **27**: 273-282 [PMID: 10774879 DOI: 10.1007/s002590050034]
13 **Hope TA**, Bergsland EK, Bozkurt MF, Graham M, Heaney AP, Herrmann K, Howe JR, Kulke MH, Kunz PL, Mailman J, May L, Metz DC, Millo C, O'Dorisio S, Reidy-Lagunes DL, Soulen MC, Strosberg JR. Appropriate Use Criteria for Somatostatin Receptor PET Imaging in Neuroendocrine Tumors. *J Nucl Med* 2018; **59**: 66-74 [PMID: 29025982 DOI: 10.2967/jnumed.117.202275]
14 **Virgolini I**, Ambrosini V, Bomanji JB, Baum RP, Fanti S, Gabriel M, Papathanasiou ND, Pepe G, Oyen W, De Cristoforo C, Chiti A. Procedure guidelines for PET/CT tumour imaging with 68Ga-DOTA-conjugated peptides: 68Ga-DOTA-TOC, 68Ga-DOTA-NOC, 68Ga-DOTA-TATE. *Eur J Nucl Med Mol Imaging* 2010; **37**: 2004-2010 [PMID: 20596866 DOI: 10.1007/s00259-010-1512-3]
15 **Byrd DW**, Doot RK, Allberg KC, MacDonald LR, McDougald WA, Elston BF, Linden HM, Kinahan PE. Evaluation of Cross-Calibrated ^{68}Ge/^{68}Ga Phantoms for Assessing PET/CT Measurement Bias in Oncology Imaging for Single- and Multicenter Trials. *Tomography* 2016; **2**: 353-360 [PMID: 28066807 DOI: 10.18383/j.tom.2016.00205]
16 **Bodei L**, Ambrosini V, Herrmann K, Modlin I. Current Concepts in ^{68}Ga-DOTATATE Imaging of Neuroendocrine Neoplasms: Interpretation, Biodistribution, Dosimetry, and Molecular Strategies. *J Nucl Med* 2017; **58**: 1718-1726 [PMID: 28818983 DOI: 10.2967/jnumed.116.186361]
17 **Kuyumcu S**, Özkan ZG, Sanli Y, Yilmaz E, Mudun A, Adalet I, Unal S. Physiological and tumoral uptake of (68)Ga-DOTATATE: standardized uptake values and challenges in interpretation. *Ann Nucl Med* 2013; **27**: 538-545 [PMID: 23543506 DOI: 10.1007/s12149-013-0718-4]
18 **Al-Ibraheem A**, Bundschuh RA, Notni J, Buck A, Winter A, Wester HJ, Schwaiger M, Scheidhauer K. Focal uptake of 68Ga-DOTATOC in the pancreas: pathological or physiological correlate in patients with neuroendocrine tumours? *Eur J Nucl Med Mol Imaging* 2011; **38**: 2005-2013 [PMID: 21792572 DOI: 10.1007/s00259-011-1875-0]
19 **Anderson J**, Silosky M, Karki R, Morgan R, Chin B. Normal biodistribution and tumor uptake of 68Ga DOTATATE PET / CT in the clinical setting: normal background activity, and organ specific tumor characterization of metastatic lesions. *J Nucl Med* 2019; **60(supplement** 1): 3031 [DOI: 10.1097/rlu.0000000000001499]
20 **Beauregard JM**, Hofman MS, Kong G, Hicks RJ. The tumour sink effect on the biodistribution of 68Ga-DOTA-octreotate: implications for peptide receptor radionuclide therapy. *Eur J Nucl Med Mol Imaging* 2012; **39**: 50-56 [PMID: 21932117 DOI: 10.1007/s00259-011-1937-3]
21 **Deppen SA**, Blume J, Bobbey AJ, Shah C, Graham MM, Lee P, Delbeke D, Walker RC. 68Ga-DOTATATE Compared with 111In-DTPA-Octreotide and Conventional Imaging for Pulmonary and Gastroenteropancreatic Neuroendocrine Tumors: A Systematic Review and Meta-Analysis. *J Nucl Med* 2016; **57**: 872-878 [PMID: 26769864 DOI: 10.2967/jnumed.115.165803]
22 **Sandström M**, Velikyan I, Garske-Román U, Sörensen J, Eriksson B, Granberg D, Lundqvist H, Sundin A, Lubberink M. Comparative biodistribution and radiation dosimetry of 68Ga-DOTATOC and 68Ga-DOTATATE in patients with neuroendocrine tumors. *J Nucl Med* 2013; **54**: 1755-1759 [PMID: 23929824 DOI: 10.2967/jnumed.113.120600]
23 **Sadowski SM**, Neychev V, Millo C, Shih J, Nilubol N, Herscovitch P, Pacak K, Marx SJ, Kebebew E. Prospective Study of 68Ga-DOTATATE Positron Emission Tomography/Computed Tomography for Detecting Gastro-Entero-Pancreatic Neuroendocrine Tumors and Unknown Primary Sites. *J Clin Oncol* 2016; **34**: 588-596 [PMID: 26712231 DOI: 10.1200/JCO.2015.64.0987]
24 **Li X**, Samnick S, Lapa C, Israel I, Buck AK, Kreissl MC, Bauer W. 68Ga-DOTATATE PET/CT for the detection of inflammation of large arteries: correlation with18F-FDG, calcium burden and risk factors. *EJNMMI Res* 2012; **2**: 52 [PMID: 23016793 DOI: 10.1186/2191-219X-2-52]
25 **Schmidt MQ**, Trenbeath Z, Chin BB. Neuroendocrine prostate cancer or prostatitis? *World J Nucl Med* 2019; **18**: 304-306 [PMID: 31516377 DOI: 10.4103/wjnm.WJNM_11_19]
26 **Mackie EJ**, Trechsel U, Bruns C. Somatostatin receptors are restricted to a subpopulation of osteoblast-like cells during endochondral bone formation. *Development* 1990; **110**: 1233-1239 [PMID: 1712702 DOI: 10.1242/dev.110.4.1233]
27 **Brogsitter C**, Hofmockel T, Kotzerke J. ^{68}Ga DOTATATE uptake in vertebral hemangioma. *Clin Nucl Med* 2014; **39**: 462-463 [PMID: 24152639 DOI: 10.1097/RLU.0000000000000282]
28 **Klinaki I**, Al-Nahhas A, Soneji N, Win Z. 68Ga DOTATATE PET/CT uptake in spinal lesions and MRI correlation on a patient with neuroendocrine tumor: potential pitfalls. *Clin Nucl Med* 2013; **38**: e449-e453 [PMID: 23531732 DOI: 10.1097/RLU.0b013e31827a2325]
29 **Silosky MS**, Patten L, Chin BB. Target activity repeatability in a clinically relevant phantom: ^{18}F *vs* ^{68}Ga. *J Nucl Med* 2021; **62(Suppl** 1): 1442 [DOI: 10.1186/s13550-021-00839-x]
30 **Silosky MS**, Karki R, Morgan R, Anderson J, Chin BB. Physical characteristics of ^{68}Ga DOTATATE PET/CT affecting small lesion detectability. *Am J Nucl Med Mol Imaging* 2021; **11**: 27-39 [PMID: 33688453]
31 **Chin BB**, Silosky M, Morgan R, Karki R, Anderson J. ^{68}Ga DOTATATE organ specific tumor signal to noise (S/N) ratios: Comparison of lesion detectability from phantom studies to lesion detectability in clinical practice. *J Nucl Med* 2019;

60(supplement 1): 478 [DOI: 10.21203/rs.3.rs-740940/v1]

32 **Silosky M**, Karki R, Chin BB. ^{68}Ga and ^{18}F quantification, and detectability of hot spots using an ACR Phantom: Contributions of radionuclide physical differences to hot spot detectability. *J Nucl Med* 2019; **60** (supplement 1): 1200

33 **Geijer H**, Breimer LH. Somatostatin receptor PET/CT in neuroendocrine tumours: update on systematic review and meta-analysis. *Eur J Nucl Med Mol Imaging* 2013; **40**: 1770-1780 [PMID: 23873003 DOI: 10.1007/s00259-013-2482-z]

34 **Hofman MS**, Kong G, Neels OC, Eu P, Hong E, Hicks RJ. High management impact of Ga-68 DOTATATE (GaTate) PET/CT for imaging neuroendocrine and other somatostatin expressing tumours. *J Med Imaging Radiat Oncol* 2012; **56**: 40-47 [PMID: 22339744 DOI: 10.1111/j.1754-9485.2011.02327.x]

35 **Deppen SA**, Liu E, Blume JD, Clanton J, Shi C, Jones-Jackson LB, Lakhani V, Baum RP, Berlin J, Smith GT, Graham M, Sandler MP, Delbeke D, Walker RC. Safety and Efficacy of 68Ga-DOTATATE PET/CT for Diagnosis, Staging, and Treatment Management of Neuroendocrine Tumors. *J Nucl Med* 2016; **57**: 708-714 [PMID: 26769865 DOI: 10.2967/jnumed.115.163865]

36 **Barrio M**, Czernin J, Fanti S, Ambrosini V, Binse I, Du L, Eiber M, Herrmann K, Fendler WP. The Impact of Somatostatin Receptor-Directed PET/CT on the Management of Patients with Neuroendocrine Tumor: A Systematic Review and Meta-Analysis. *J Nucl Med* 2017; **58**: 756-761 [PMID: 28082438 DOI: 10.2967/jnumed.116.185587]

37 **Loft M**, Carlsen EA, Johnbeck CB, Johannesen HH, Binderup T, Pfeifer A, Mortensen J, Oturai P, Loft A, Berthelsen AK, Langer SW, Knigge U, Kjaer A. ^{64}Cu-DOTATATE PET in Patients with Neuroendocrine Neoplasms: Prospective, Head-to-Head Comparison of Imaging at 1 Hour and 3 Hours After Injection. *J Nucl Med* 2021; **62**: 73-80 [PMID: 32444370 DOI: 10.2967/jnumed.120.244509]

38 **Johnbeck CB**, Knigge U, Loft A, Berthelsen AK, Mortensen J, Oturai P, Langer SW, Elema DR, Kjaer A. Head-to-Head Comparison of ^{64}Cu-DOTATATE and ^{68}Ga-DOTATOC PET/CT: A Prospective Study of 59 Patients with Neuroendocrine Tumors. *J Nucl Med* 2017; **58**: 451-457 [PMID: 27660147 DOI: 10.2967/jnumed.116.180430]

39 **Anderson CJ**, Ferdani R. Copper-64 radiopharmaceuticals for PET imaging of cancer: advances in preclinical and clinical research. *Cancer Biother Radiopharm* 2009; **24**: 379-393 [PMID: 19694573 DOI: 10.1089/cbr.2009.0674]

40 **Carlsen EA**, Johnbeck CB, Loft M, Pfeifer A, Oturai P, Langer SW, Knigge U, Ladefoged CN, Kjaer A. Semiautomatic Tumor Delineation for Evaluation of ^{64}Cu-DOTATATE PET/CT in Patients with Neuroendocrine Neoplasms: Prognostication Based on Lowest Lesion Uptake and Total Tumor Volume. *J Nucl Med* 2021; **62**: 1564-1570 [PMID: 33637589 DOI: 10.2967/jnumed.120.258392]

41 **Carlsen EA**, Johnbeck CB, Binderup T, Loft M, Pfeifer A, Mortensen J, Oturai P, Loft A, Berthelsen AK, Langer SW, Knigge U, Kjaer A. ^{64}Cu-DOTATATE PET/CT and Prediction of Overall and Progression-Free Survival in Patients with Neuroendocrine Neoplasms. *J Nucl Med* 2020; **61**: 1491-1497 [PMID: 32111685 DOI: 10.2967/jnumed.119.240143]

42 **Andersen TL**, Baun C, Olsen BB, Dam JH, Thisgaard H. Improving Contrast and Detectability: Imaging with [^{55}Co]Co-DOTATATE in Comparison with [^{64}Cu]Cu-DOTATATE and [^{68}Ga]Ga-DOTATATE. *J Nucl Med* 2020; **61**: 228-233 [PMID: 31519803 DOI: 10.2967/jnumed.119.233015]

43 **Binderup T**, Knigge U, Loft A, Federspiel B, Kjaer A. 18F-fluorodeoxyglucose positron emission tomography predicts survival of patients with neuroendocrine tumors. *Clin Cancer Res* 2010; **16**: 978-985 [PMID: 20103666 DOI: 10.1158/1078-0432.CCR-09-1759]

44 **Karfis I**, Marin G, Levillain H, Drisis S, Muteganya R, Critchi G, Taraji-Schiltz L, Guix CA, Shaza L, Elbachiri M, Mans L, Machiels G, Hendlisz A, Flamen P. Prognostic value of a three-scale grading system based on combining molecular imaging with ^{68}Ga-DOTATATE and ^{18}F-FDG PET/CT in patients with metastatic gastroenteropancreatic neuroendocrine neoplasias. *Oncotarget* 2020; **11**: 589-599 [PMID: 32110279 DOI: 10.18632/oncotarget.27460]

45 **Han S**, Lee HS, Woo S, Kim TH, Yoo C, Ryoo BY, Ryu JS. Prognostic Value of 18F-FDG PET in Neuroendocrine Neoplasm: A Systematic Review and Meta-analysis. *Clin Nucl Med* 2021; **46**: 723-731 [PMID: 34028406 DOI: 10.1097/RLU.0000000000003682]

46 **Ramage JK**, Ahmed A, Ardill J, Bax N, Breen DJ, Caplin ME, Corrie P, Davar J, Davies AH, Lewington V, Meyer T, Newell-Price J, Poston G, Reed N, Rockall A, Steward W, Thakker RV, Toubanakis C, Valle J, Verbeke C, Grossman AB; UK and Ireland Neuroendocrine Tumour Society. Guidelines for the management of gastroenteropancreatic neuroendocrine (including carcinoid) tumours (NETs). *Gut* 2012; **61**: 6-32 [PMID: 22052063 DOI: 10.1136/gutjnl-2011-300831]

47 **Mittra ES**. Neuroendocrine Tumor Therapy: ^{177}Lu-DOTATATE. *AJR Am J Roentgenol* 2018; **211**: 278-285 [PMID: 29949416 DOI: 10.2214/AJR.18.19953]

48 **Strosberg J**, El-Haddad G, Wolin E, Hendifar A, Yao J, Chasen B, Mittra E, Kunz PL, Kulke MH, Jacene H, Bushnell D, O'Dorisio TM, Baum RP, Kulkarni HR, Caplin M, Lebtahi R, Hobday T, Delpassand E, Van Cutsem E, Benson A, Srirajaskanthan R, Pavel M, Mora J, Berlin J, Grande E, Reed N, Seregni E, Öberg K, Lopera Sierra M, Santoro P, Thevenet T, Erion JL, Ruszniewski P, Kwekkeboom D, Krenning E; NETTER-1 Trial Investigators. Phase 3 Trial of ^{177}Lu-Dotatate for Midgut Neuroendocrine Tumors. *N Engl J Med* 2017; **376**: 125-135 [PMID: 28076709 DOI: 10.1056/NEJMoa1607427]

49 **Therasse P**, Arbuck SG, Eisenhauer EA, Wanders J, Kaplan RS, Rubinstein L, Verweij J, Van Glabbeke M, van Oosterom AT, Christian MC, Gwyther SG. New guidelines to evaluate the response to treatment in solid tumors. European Organization for Research and Treatment of Cancer, National Cancer Institute of the United States, National Cancer Institute of Canada. *J Natl Cancer Inst* 2000; **92**: 205-216 [PMID: 10655437 DOI: 10.1093/jnci/92.3.205]

50 **Janson ET**, Oberg K. Long-term management of the carcinoid syndrome. Treatment with octreotide alone and in combination with alpha-interferon. *Acta Oncol* 1993; **32**: 225-229 [PMID: 7686765 DOI: 10.3109/02841869309083916]

51 **Ducreux M**, Ruszniewski P, Chayvialle JA, Blumberg J, Cloarec D, Michel H, Raymond JM, Dupas JL, Gouerou H, Jian R, Genestin E, Hammel P, Rougier P. The antitumoral effect of the long-acting somatostatin analog lanreotide in neuroendocrine tumors. *Am J Gastroenterol* 2000; **95**: 3276-3281 [PMID: 11095353 DOI: 10.1111/j.1572-0241.2000.03210.x]

52 **Pavel M**, O'Toole D, Costa F, Capdevila J, Gross D, Kianmanesh R, Krenning E, Knigge U, Salazar R, Pape UF, Öberg K; Vienna Consensus Conference participants. ENETS Consensus Guidelines Update for the Management of Distant Metastatic Disease of Intestinal, Pancreatic, Bronchial Neuroendocrine Neoplasms (NEN) and NEN of Unknown Primary

Site. *Neuroendocrinology* 2016; **103**: 172-185 [PMID: 26731013 DOI: 10.1159/000443167]

53 **Pavel ME**, Hainsworth JD, Baudin E, Peeters M, Hörsch D, Winkler RE, Klimovsky J, Lebwohl D, Jehl V, Wolin EM, Öberg K, Van Cutsem E, Yao JC; RADIANT-2 Study Group. Everolimus plus octreotide long-acting repeatable for the treatment of advanced neuroendocrine tumours associated with carcinoid syndrome (RADIANT-2): a randomised, placebo-controlled, phase 3 study. *Lancet* 2011; **378**: 2005-2012 [PMID: 22119496 DOI: 10.1016/S0140-6736(11)61742-X]

54 **Kwekkeboom DJ**, de Herder WW, Kam BL, van Eijck CH, van Essen M, Kooij PP, Feelders RA, van Aken MO, Krenning EP. Treatment with the radiolabeled somatostatin analog [177 Lu-DOTA 0,Tyr3]octreotate: toxicity, efficacy, and survival. *J Clin Oncol* 2008; **26**: 2124-2130 [PMID: 18445841 DOI: 10.1200/JCO.2007.15.2553]

55 **Yordanova A**, Eppard E, Kürpig S, Bundschuh RA, Schönberger S, Gonzalez-Carmona M, Feldmann G, Ahmadzadehfar H, Essler M. Theranostics in nuclear medicine practice. *Onco Targets Ther* 2017; **10**: 4821-4828 [PMID: 29042793 DOI: 10.2147/OTT.S140671]

56 **ClinicalTrials.gov**. Lutetium 177Lu-Edotreotide Versus Best Standard of Care in Well-differentiated Aggressive Grade-2 and Grade-3 GastroEnteroPancreatic NeuroEndocrine Tumors (GEP-NETs)-COMPOSE (COMPOSE) [website]. 2021. [cited 15 August 2021]. Available from: https://clinicaltrials.gov/ct2/show/NCT04919226

57 **ClinicalTrials.gov**. Efficacy and Safety of 177Lu-edotreotide PRRT in GEP-NET Patients (COMPETE) 2017. [cited 15 August 2021]. Available from: https://clinicaltrials.gov/ct2/show/NCT03049189

58 **ClinicalTrials.gov**. Study to Evaluate the Efficacy and Safety of Lutathera in Patients With Grade 2 and Grade 3 Advanced GEP-NET (NETTER-2) 2019. [cited 15 August 2021]. Available from: https://clinicaltrials.gov/ct2/show/NCT03972488

59 **Strosberg J**, Leeuwenkamp O, Siddiqui MK. Peptide receptor radiotherapy re-treatment in patients with progressive neuroendocrine tumors: A systematic review and meta-analysis. *Cancer Treat Rev* 2021; **93**: 102141 [PMID: 33418096 DOI: 10.1016/j.ctrv.2020.102141]

60 **Wang R**, Zhou T, Liu W, Zuo L. Molecular mechanism of bystander effects and related abscopal/cohort effects in cancer therapy. *Oncotarget* 2018; **9**: 18637-18647 [PMID: 29719632 DOI: 10.18632/oncotarget.24746]

61 **Kunikowska J**, Królicki L, Hubalewska-Dydejczyk A, Mikołajczak R, Sowa-Staszczak A, Pawlak D. Clinical results of radionuclide therapy of neuroendocrine tumours with 90Y-DOTATATE and tandem 90Y/177Lu-DOTATATE: which is a better therapy option? *Eur J Nucl Med Mol Imaging* 2011; **38**: 1788-1797 [PMID: 21553086 DOI: 10.1007/s00259-011-1833-x]

62 **Konijnenberg M**, Melis M, Valkema R, Krenning E, de Jong M. Radiation dose distribution in human kidneys by octreotides in peptide receptor radionuclide therapy. *J Nucl Med* 2007; **48**: 134-142 [PMID: 17204710]

63 **Bass RT**, Buckwalter BL, Patel BP, Pausch MH, Price LA, Strnad J, Hadcock JR. Identification and characterization of novel somatostatin antagonists. *Mol Pharmacol* 1996; **50**: 709-715 [PMID: 8863814]

64 **Ginj M**, Zhang H, Waser B, Cescato R, Wild D, Wang X, Erchegyi J, Rivier J, Mäcke HR, Reubi JC. Radiolabeled somatostatin receptor antagonists are preferable to agonists for *in vivo* peptide receptor targeting of tumors. *Proc Natl Acad Sci U S A* 2006; **103**: 16436-16441 [PMID: 17056720 DOI: 10.1073/pnas.0607761103]

65 **Reubi JC**, Waser B, Mäcke H, Rivier J. Highly Increased 125I-JR11 Antagonist Binding In Vitro Reveals Novel Indications for sst2 Targeting in Human Cancers. *J Nucl Med* 2017; **58**: 300-306 [PMID: 27561878 DOI: 10.2967/jnumed.116.177733]

66 **Nicolas GP**, Schreiter N, Kaul F, Uiters J, Bouterfa H, Kaufmann J, Erlanger TE, Cathomas R, Christ E, Fani M, Wild D. Sensitivity Comparison of ^{68}Ga-OPS202 and ^{68}Ga-DOTATOC PET/CT in Patients with Gastroenteropancreatic Neuroendocrine Tumors: A Prospective Phase II Imaging Study. *J Nucl Med* 2018; **59**: 915-921 [PMID: 29191855 DOI: 10.2967/jnumed.117.199760]

67 **Nicolas GP**, Beykan S, Bouterfa H, Kaufmann J, Bauman A, Lassmann M, Reubi JC, Rivier JEF, Maecke HR, Fani M, Wild D. Safety, Biodistribution, and Radiation Dosimetry of ^{68}Ga-OPS202 in Patients with Gastroenteropancreatic Neuroendocrine Tumors: A Prospective Phase I Imaging Study. *J Nucl Med* 2018; **59**: 909-914 [PMID: 29025985 DOI: 10.2967/jnumed.117.199737]

68 **Zhu W**, Cheng Y, Jia R, Zhao H, Bai C, Xu J, Yao S, Huo L. A Prospective, Randomized, Double-Blind Study to Evaluate the Safety, Biodistribution, and Dosimetry of 68Ga-NODAGA-LM3 and 68Ga-DOTA-LM3 in Patients with Well-Differentiated Neuroendocrine Tumors. *J Nucl Med* 2021; **62**: 1398-1405 [PMID: 33579804 DOI: 10.2967/jnumed.120.253096]

69 **Zhu W**, Jia R, Yang Q, Cheng Y, Zhao H, Bai C, Xu J, Yao S, Huo L. A prospective randomized, double-blind study to evaluate the diagnostic efficacy of ^{68}Ga-NODAGA-LM3 and ^{68}Ga-DOTA-LM3 in patients with well-differentiated neuroendocrine tumors: compared with ^{68}Ga-DOTATATE. *Eur J Nucl Med Mol Imaging* 2021 [PMID: 34874478 DOI: 10.1007/s00259-021-05512-y]

70 **Baum RP**, Zhang J, Schuchardt C, Mueller D, Maecke H. First-in-human study of novel SSTR antagonist 177Lu-DOTA-LM3 for peptide receptor radionuclide therapy in patients with metastatic neuroendocrine neoplasms: Dosimetry, safety and efficacy. *J Nucl Med* 2021; **62**: 1571-1581 [PMID: 33674401 DOI: 10.2967/jnumed.120.258889]

71 **Dalm SU**, Nonnekens J, Doeswijk GN, de Blois E, van Gent DC, Konijnenberg MW, de Jong M. Comparison of the Therapeutic Response to Treatment with a 177Lu-Labeled Somatostatin Receptor Agonist and Antagonist in Preclinical Models. *J Nucl Med* 2016; **57**: 260-265 [PMID: 26514177 DOI: 10.2967/jnumed.115.167007]

72 **Targeted Alpha Therapy Working Group**, Parker C, Lewington V, Shore N, Kratochwil C, Levy M, Lindén O, Noordzij W, Park J, Saad F. Targeted Alpha Therapy, an Emerging Class of Cancer Agents: A Review. *JAMA Oncol* 2018; **4**: 1765-1772 [PMID: 30326033 DOI: 10.1001/jamaoncol.2018.4044]

73 **Nelson BJB**, Andersson JD, Wuest F. Targeted Alpha Therapy: Progress in Radionuclide Production, Radiochemistry, and Applications. *Pharmaceutics* 2020; **13** [PMID: 33396374 DOI: 10.3390/pharmaceutics13010049]

74 **Ballal S**, Yadav MP, Bal C, Sahoo RK, Tripathi M. Broadening horizons with ^{225}Ac-DOTATATE targeted alpha therapy for gastroenteropancreatic neuroendocrine tumour patients stable or refractory to ^{177}Lu-DOTATATE PRRT: first clinical experience on the efficacy and safety. *Eur J Nucl Med Mol Imaging* 2020; **47**: 934-946 [PMID: 31707430 DOI: 10.1007/s00259-019-04567-2]

75 **Zhang J**, Kulkarni HR, Baum RP. Peptide Receptor Radionuclide Therapy Using 225Ac-DOTATOC Achieves Partial Remission in a Patient With Progressive Neuroendocrine Liver Metastases After Repeated β-Emitter Peptide Receptor Radionuclide Therapy. *Clin Nucl Med* 2020; **45**: 241-243 [PMID: 31977472 DOI: 10.1097/RLU.0000000000002915]

76 **Kratochwil C**, Apostolidis L, Rathke H, Apostolidis C, Bicu F, Bruchertseifer F, Choyke PL, Haberkorn U, Giesel FL, Morgenstern A. Dosing ^{225}Ac-DOTATOC in patients with somatostatin-receptor-positive solid tumors: 5-year follow-up of hematological and renal toxicity. *Eur J Nucl Med Mol Imaging* 2021; **49**: 54-63 [PMID: 34448031 DOI: 10.1007/s00259-021-05474-1]

77 **Kratochwil C**, López-Benítez R, Mier W, Haufe S, Isermann B, Kauczor HU, Choyke PL, Haberkorn U, Giesel FL. Hepatic arterial infusion enhances DOTATOC radiopeptide therapy in patients with neuroendocrine liver metastases. *Endocr Relat Cancer* 2011; **18**: 595-602 [PMID: 21791571 DOI: 10.1530/ERC-11-0144]

78 **Zhang J**, Kulkarni HR, Singh A, Baum RP. Successful Intra-arterial Peptide Receptor Radionuclide Therapy of DOTATOC-Negative High-Grade Liver Metastases of a Pancreatic Neuroendocrine Neoplasm Using ^{177}Lu-DOTA-LM3: A Somatostatin Receptor Antagonist. *Clin Nucl Med* 2020; **45**: e165-e168 [PMID: 31977464 DOI: 10.1097/RLU.0000000000002906]

World Journal of Gastroenterology

Submit a Manuscript: https://www.f6publishing.com

World J Gastroenterol 2022 May 7; 28(17): 1781-1797

DOI: 10.3748/wjg.v28.i17.1781

ISSN 1007-9327 (print) ISSN 2219-2840 (online)

ORIGINAL ARTICLE

Basic Study

Forkhead Box q1 promotes invasion and metastasis in colorectal cancer by activating the epidermal growth factor receptor pathway

Jin-Jin Zhang, Chang-Xiong Cao, Li-Lan Wan, Wen Zhang, Zhong-Jiang Liu, Jin-Li Wang, Qiang Guo, Hui Tang

Specialty type: Gastroenterology and hepatology

Provenance and peer review: Invited article; Externally peer reviewed.

Peer-review model: Single blind

Peer-review report's scientific quality classification

Grade A (Excellent): A, A
Grade B (Very good): B, B
Grade C (Good): 0
Grade D (Fair): 0
Grade E (Poor): 0

P-Reviewer: Emran TB, Bangladesh; Herold Z, Hungary; Martin MJ, Argentina

Received: October 18, 2021
Peer-review started: October 18, 2021
First decision: December 12, 2021
Revised: December 31, 2021
Accepted: March 27, 2022
Article in press: March 27, 2022
Published online: May 7, 2022

Jin-Jin Zhang, Chang-Xiong Cao, Li-Lan Wan, Wen Zhang, Zhong-Jiang Liu, Jin-Li Wang, Qiang Guo, Hui Tang, Yunnan Digestive Endoscopy Clinical Medical Center, Department of Gastroenterology, the First People's Hospital of Yunnan Province, the Affiliated Hospital of Kunming University of Science and Technology, Kunming 650032, Yunnan Province, China

Jin-Jin Zhang, Chang-Xiong Cao, Li-Lan Wan, Wen Zhang, Zhong-Jiang Liu, Jin-Li Wang, Qiang Guo, Hui Tang, Department of Medical Faculty, Kunming University of Science and Technology, Kunming 650504, Yunnan Province, China

Jin-Jin Zhang, State Key Laboratory of Genetic Resources and Evolution, Kunming Institute of Zoology, Chinese Academy of Sciences, Kunming 650223, Yunnan Province, China

Corresponding author: Hui Tang, PhD, Professor, Yunnan Digestive Endoscopy Clinical Medical Center, Department of Gastroenterology, the First People's Hospital of Yunnan Province, the Affiliated Hospital of Kunming University of Science and Technology, No. 157 Jinbi Road, Xishan District, Kunming 650032, Yunnan Province, China.
htang1122@aliyun.com

Abstract

BACKGROUND

Colorectal cancer (CRC) is an extremely malignant tumor with a high mortality rate. Little is known about the mechanism by which forkhead Box q1 (FOXQ1) causes CRC invasion and metastasis through the epidermal growth factor receptor (EGFR) pathway.

AIM

To illuminate the mechanism by which FOXQ1 promotes the invasion and metastasis of CRC by activating the heparin binding epidermal growth factor (HB-EGF)/EGFR pathway.

METHODS

We investigated the differential expression and prognosis of FOXQ1 and HB-EGF in CRC using the Gene Expression Profiling Interactive Analysis (GEPIA) website (http://gepia.cancer-pku.cn/index.html). Quantitative real-time polymerase chain reaction (qRT-PCR) and Western blotting were used to detect the expression of FOXQ1 and HB-EGF in cell lines and tissues, and we constructed a stable low-expressing FOXQ1 cell line and verified it with the above method. The expression

changes of membrane-bound HB-EGF (proHB-EGF) and soluble HB-EGF (sHB-EGF) in the low-expressing FOXQ1 cell line were detected by flow cytometry and ELISA. Western blotting was used to detect changes in the expression levels of HB-EGF and EGFR pathway-related downstream genes when exogenous recombinant human HB-EGF was added to FOXQ1 knockdown cells. Proliferation experiments, transwell migration experiments, and scratch experiments were carried out to determine the mechanism by which FOXQ1 activates the EGFR signaling pathway through HB-EGF, and then to evaluate the clinical relevance of FOXQ1 and HB-EGF.

RESULTS

GEPIA showed that the expression of FOXQ1 in CRC tissues was relatively high and was related to a lower overall survival rate. PCR array results showed that FOXQ1 is related to the HB-EGF and EGFR pathways. Knockdown of FOXQ1 suppressed the expression of HB-EGF, and led to a decrease in EGFR and its downstream genes *AKT*, *RAF*, *KRAS* expression levels. After knockdown of FOXQ1 in CRC cell lines, cell proliferation, migration and invasion were attenuated. Adding HB-EGF restored the migration and invasion ability of CRC, but not the cell proliferation ability. Kaplan–Meier survival analysis results showed that the combination of FOXQ1 and HB-EGF may serve to predict CRC survival.

CONCLUSION

Based on these collective data, we propose that FOXQ1 promotes the invasion and metastasis of CRC *via* the HB-EGF/EGFR pathway.

Key Words: Colorectal cancer; Forkhead Box Q1; Heparin binding epidermal growth factor; Epidermal growth factor receptor pathway; Migration; Invasion

©The Author(s) 2022. Published by Baishideng Publishing Group Inc. All rights reserved.

Core Tip: Invasion and metastasis play important roles in tumorigenesis, resulting in the death of most colorectal cancer (CRC) patients. Forkhead Box q1 (FOXQ1) is a well-established oncogene in multiple tumors, including CRC. Our previous study suggested that FOXQ1 positively regulates the expression of heparin-binding epidermal growth factor (HB-EGF) and triggers the activation of the epidermal growth factor receptor (EGFR) pathway in CRC. However, the role and mechanism of how FOXQ1 promotes tumorigenesis in CRC by activating the HB-EGF/EGFR pathway remain unexplored. In the present study, our findings demonstrated that the essential role of FOXQ1-induced invasion and metastasis in CRC was related to activation of the HB-EGF/EGFR pathway.

Citation: Zhang JJ, Cao CX, Wan LL, Zhang W, Liu ZJ, Wang JL, Guo Q, Tang H. Forkhead Box q1 promotes invasion and metastasis in colorectal cancer by activating the epidermal growth factor receptor pathway. *World J Gastroenterol* 2022; 28(17): 1781-1797

URL: https://www.wjgnet.com/1007-9327/full/v28/i17/1781.htm

DOI: https://dx.doi.org/10.3748/wjg.v28.i17.1781

INTRODUCTION

Colorectal cancer (CRC) is the third most common cancer in the world and the fourth most common cause of cancer death in the world[1]. Among all cancerous processes involved, local invasion and metastasis are the main factors related to cancer. The metastatic dissemination of primary tumors is directly related to the survival rate of patients, accounting for approximately 90% of all colon cancer deaths[2]. The median survival of metastatic CRC is less than 2 years[3]. Therefore, clarifying the mechanism of invasion and metastasis is the key to improving the survival rate of patients with CRC.

Forkhead Box q1 (FOXQ1) is a member of the forkhead transcription factor family[4], and it promotes tumorigenesis by activating cell proliferation, invasion and apoptosis[5]. Kaneda *et al*[6] found that compared to adjacent tissues, *FOXQ1* is overexpressed in CRC. Overexpression of *FOXQ1* reduces cell proliferation but increases cell tumorigenicity and tumor growth, and it inhibits apoptosis and promotes angiogenesis, thereby promoting CRC tumorigenesis. Liu *et al*[7] also demonstrated that the expression of *FOXQ1* in either CRC tissue samples or cancer cell lines is higher than that in normal colorectal tissues and cell lines, and they reported that FOXQ1 promotes cancer metastasis by regulating PI3K/AKT signaling. Weng *et al*[8] verified that FOXQ1 can be used as an independent indicator of the prognosis of CRC patients.

The epidermal growth factor receptor (EGFR) signaling pathway plays an important role in physiological processes, such as cell growth, proliferation, and differentiation. The expression level of *EGFR* gradually increases from normal mucosa, adenomas with low-grade dysplasia, and adenomas with high-grade dysplasia to CRC, confirming that EGFR plays an important role in CRC[9]. Heparin-binding epidermal growth factor (HB-EGF) is one of the seven major ligands of EGFR. HB-EGF was originally identified as a secreted product from human macrophage U937 cells, and it induces cell proliferation and differentiation[10,11]. Soluble HB-EGF (sHB-EGF) is the main stimulator of cell proliferation. The affinity of sHB-EGF binding to target cells to promote proliferation of the target cells and activation of EGFR tyrosine kinase activity is 20-40 times higher than that of EGF. Thus, sHB-EGF is the most effective EGFR signaling pathway activator[12,13]. Membrane-bound HB-EGF (proHB-EGF) is affected by a variety of proteins, and it can be shed into active sHB-EGF to promote cell proliferation[14-16].

There is evidence that poor prognosis and low survival rates for CRC are associated with abnormally activated signaling pathways, including the EGFR signaling pathway[17]. In advanced CRC the most commonly used targeted therapies are the monoclonal antibodies cetuximab and panitumab, which block EGFR activation[18]. Activation of EGFR signaling leads to resistance to chemotherapy in CRC cells and promotes cell survival, while inhibition of EGFR signaling significantly reduces proliferation in CRC cells[19]. In nasopharyngeal carcinoma, Luo *et al*[20] reported that FOXQ1 induces vasculogenic mimicry through the EGFR signaling pathway, thereby promoting the metastasis of nasopharyngeal carcinoma cells. Our previous study suggested that FOXQ1 positively regulates the expression of HB-EGF and triggers the activation of the EGFR pathway in CRC[21]. However, the role and mechanism of how FOXQ1 promotes tumorigenesis in CRC by activating the HB-EGF/EGFR pathway remain largely unknown. Therefore, we analyzed the correlation between FOXQ1 and the HB-EGF/EGFR pathway by constructing *FOXQ1* knockdown cells and using tissue microarrays, cell function experiments, quantitative real-time polymerase chain reaction (qRT-PCR), and western blotting. Our findings elucidated the critical role of the FOXQ1 and HB-EGF/EGFR pathways in CRC, providing theoretical support for the clinical application of targeted FOXQ1 in the treatment of CRC.

MATERIALS AND METHODS

Cell cultures

The human CRC cell lines, DLD1 and SW480, as well as the human embryonic kidney 293 (HEK293) cell line were purchased and authenticated from the Cell Bank of the Chinese Academy of Science in Shanghai, China. DLD1 cells were cultured in RPMI 1640. SW480 and HEK293 cells were cultured in DMEM. All media were supplemented with 10% heat-inactivated fetal bovine serum (Life Technologies BRL), and the cells were maintained in a 5% CO_2-humidified atmosphere at 37 °C.

Plasmid construction and transfection

Three siRNAs targeting the human FOXQ1 sequence (NM_033260.3) were designed using siRNA Target Finder (InvivoGen, San Diego, CA, United States), and one scrambled siRNA was designed as a negative control, refer to our previous research[21]. The pSPAX2 packaging system from Addgene was used to construct a lentiviral PLKO.1 vector (PLKO.1-puro-shFOXQ1). After each group of recombinant plasmids was confirmed by sequencing, lentiviral vectors and packing vectors (pRSV-rev, pMDlg-pRRE and pCMV-VSV-G) were cotransfected into HEK293 cells using Lipofectamine® 2000 transfection reagent (Life Technologies). Lentivirus was collected to infect DLD1 and SW480 cells. Stable cells were generated after selection with puromycin (Solarbio, Beijing, China) (0.4 ng/μL for DLD1 cells and 0.1 ng/μL for SW480 cells) for 7-14 d after infection. The most effective knockdown cells were designated DLD1-shFOXQ1 and SW480-shFOXQ1, and the corresponding controls were named DLD1-shControl and SW480-shControl, respectively.

Flow cytometry

Cell surface HB-EGF was detected using APC-conjugated anti-human HB-EGF (eBioscience, San Diego, CA, United States). APC-conjugated mouse IgG2ak isotype was used as a control (eBioscience, San Diego, CA, United States) according to the manufacturer's directions. Briefly, CRC cells were harvested and blocked with blocking buffer (PBS containing 2% BSA) for 10 min at 4 °C and then stained with 5 μL of monoclonal HB-EGF antibody (eBioscience, San Diego, CA, United States) for 30 min at 4 °C. After two washes, cells were resuspended in 100 μL of PBS. Samples were analyzed using a MoFlo flow cytometer (Beckman Coulter) and FlowJo software (Becton, Dickinson and Company).

Western blotting

Protein extracts were isolated from 10^6 treated cells using mammalian cell lysis reagent containing protease inhibitor cocktail (Sigma–Aldrich, St. Louis, MO, United States) and phosphatase inhibitors (Roche, United States) following the manufacturer's directions. Equal amounts of protein (30 μg) were resolved on a 10% sodium dodecyl sulfate (SDS)-precast polyacrylamide gel (Bio–Rad Laboratories) and

Table 1 Oligonucleotide sequences used for real-time polymerase chain reaction

Gene name	Forward (5'→3')	Reverse (5'→3')
FOXQ1	TGACTTCAACAGCGACACCCA	CACCCTGTTGCTGTAGCCAAA
EGFR	AGACGCAGATAGTCGCCCAAAG	TCCATCAGGGCACGGTAGAAG
HB-EGF	CCATGTCTTCGGAAATACAAGGA	CCAGGATGGTTGTGTGGTCA
Akt	AGACGCAGATAGTCGCCCAAAG	TCCATCAGGGCACGGTAGAAG
RAF1	AGACGCAGATAGTCGCCCAAAG	TCCATCAGGGCACGGTAGAAG
KRAS	GTGGACGAATATGATCCAACAATAG	TGCTGTGTCGAGAATATCCAAGAG
GAPDH	GGCAACGGGCTACAGCTTTA	GGCACCCCACATACATAATCAA

transferred to an Immobilon-polyvinylidene difluoride membrane (Millipore, Billerica, MA, United States). The membranes were blocked and incubated with the following primary antibodies: FOXQ1 (Abcam, Cambridge, MA, United States), HB-EGF (Abcam, Cambridge, MA, United States), phosphor-PI3K (Cell Signaling Technology, Cold Spring Harbor, NY, United States), PI3K (Proteintech, Wuhan, China), Akt (Proteintech, Wuhan, China), phosphor-Akt (Proteintech, Wuhan, China), phosphor-MAPK (Cell Signaling Technology, Cold Spring Harbor, NY, United States), MAPK (Proteintech, Wuhan, China), EGFR (Proteintech, Wuhan, China), KRAS (Proteintech, Wuhan, China), RAF (Proteintech, Wuhan, China), E-cadherin, N-cadherin, vimentin and β-actin (Proteintech, Wuhan, China). Blots were then incubated with the appropriate peroxidase-conjugated secondary antibody as follows: HRP-Rb-anti-goat (Cell Signaling Technology, Cold Spring Harbor, NY, United States) or HRP-goat-anti-mouse (Proteintech, Wuhan, China), respectively. The proteins were detected using an ECL system (Millipore, Braunschweig, Germany) and visualized with a ChemiDoc XRS system (Bio–Rad, Hercules, CA, United States).

RNA isolation and qRT–PCR

Total RNA was isolated using TRIzol (Invitrogen, Carlsbad, CA, United States) according to the manufacturer's protocol. Total RNA (1 μg) was reverse transcribed into cDNA using PrimeScript RT reagent (TakaraBio, Japan), and qRT–PCR was performed using a LightCycler 480 (Roche, United States) with SYBR Premix Ex Taq (Takara, China). Each sample was analyzed in triplicate, and Glyceraldehyde-3-phosphate dehydrogenase(GAPDH) was used as the reference. Quantitative results were calculated using the $2^{-\Delta\Delta CT}$ method. Primers used for qRT–PCR were designed and synthesized by Takara (Dalian, China) (Table 1).

Epidermal growth factor/platelet-derived growth factor pathway cDNA array assay

The human epidermal growth factor (EGF)/platelet-derived growth factor (PDGF) Signaling RT² Profiler™ PCR Array (SABiosciences), which profiles the expression of 84 genes related to EGF/PDGF-mediated signal transduction, five housekeeping genes and three controls, was used to analyze the effect of FOXQ1 on EGF/PDGF signaling-related gene expression (Table 2). Total RNA was extracted with TRIzol reagent according to the manufacturer's manual. DNase treatment was performed by amplification grade I DNase I (Sigma–Aldrich, St. Louis, MO, United States) according to the manufacturer's instructions. Each total RNA preparation (5 μg) was digested with 1 μL of DNase I (1 unit/μL) and 1 μL of 10 reaction buffer in a volume of 10 μL. After incubation and addition of Stop Solution, DNase I was denatured by incubation at 70 °C for 10 min. The RNA samples were kept on ice for another 5 min and then converted into cDNA with the RT² PCR Array First Strand Kit (SuperArray) according to the manufacturer's protocol. cDNA (20 ng) was combined with RT² SYBR Green/Fluorescein PCR master mix (SuperArray), and equal amounts of this mixture (25 μL) were added to each well of the RT² Profiler PCR plate containing the predispensed gene-specific primer sets. PCR cycles were performed according to the manufacturer's instructions. The relative level of mRNA expression for each gene in each sample was first normalized to the expression of GAPDH in that sample and then normalized to the level of mRNA expression in the DLD1-shControl.

ELISA

Exogenous recombinant HB-EGF protein at a final concentration of 50 ng/mL was added to the cell culture medium when the cell density reached 80%, and the culture medium was changed after incubation for 24 h[22]. The supernatant was collected after the cells were cultured for another 24 h. The protein concentrations of soluble HB-EGF, ADAM9, ADAM10, ADAM12 and MMP-7 in the cell culture medium were determined by ELISA detection kits against human HB-EGF, ADAM9, ADAM10, ADAM12 and MMP-7, respectively (R&D Systems, Minneapolis, United States).

Table 2 List of up- and down-regulated genes between DLDL-shFOXQ1 and DLD1-shControl with a fold-change ≥ 2.0 or ≤ -2.0 by using epidermal growth factor/platelet-derived growth factor SuperArray

Symbol	Gene information	Fold change (shFOXQ1/shControl)	*P* value	FOXQ1 binding sites (TSS: -2k_+1k)
PLAT	Plasminogen activator, tissue	-8.01	0.0375	3
COL1A1	Collagen, type I, alpha 1	-5.72	0.0138	1
ELK1	ELK1, member of ETS oncogene family	-5.45	0.0228	1
BCAR1	Breast cancer anti-estrogen resistance 1	-3.97	0.0479	2
PIK3R2	Phosphoinositide-3-kinase, regulatory subunit 2	-3.63	0.0197	3
NCK2	NCK adaptor protein 2	-3.51	0.0237	6
JUN	Jun proto-oncogene v-jun	-3.43	0.0077	12
EGR1	Early growth response 1	-3.36	0.0166	11
LTA	Lymphotoxin alpha (TNF superfamily, member 1)	-3.18	0.0796	3
PDGFB	Platelet-derived growth factor beta	-2.91	0.1896	5
STAT3	Signal transducer and activator of transcription 3 (acute-phase response factor)	-2.49	0.0038	6
HB-EGF	Heparin-binding EGF-like growth factor	-2.19	0.0278	3
FN1	Fibronectin 1	-2.10	0.0005	6
FASLG	Fas ligand (TNF superfamily, member 6)	-2.08	0.2026	17
HRAS	V-Ha-ras Harvey rat sarcoma viral oncogene homolog	-2.06	0.0058	2
MAP2K1	Mitogen-activated protein kinase kinase 1	-2.02	0.0243	5
AKT3	V-akt murine thymoma viral oncogene homolog 3	-2.02	0.1440	11
FOS	FBJ murine osteosarcoma viral oncogene homolog	-2.01	0.0470	5

Cell proliferation

DLD1-shFOXQ1 and SW480-shFOXQ1 cells (2,000 cells/well in a 96-well plate) were incubated with medium containing 10% FBS at 37 °C for 24, 48, 72 and 96 h. At the end of incubation, 10 μL of Cell Counting Kit-8 (CCK-8) solution (Beyotime Biotech, Shanghai, China) was added to each well with 100 μL of medium and incubated for another 4 h at 37 °C, and the OD at 450 nm was measured by a microplate reader (BioTek, Winooski, VT, United States). The effect of siRNA FOXQ1 on CRC cell viability was assessed as the percent of cell viability compared to vehicle-treated control cells, which were arbitrarily assigned as 100% viability.

Cell migration and wound-healing assay

Cell migration was analyzed using Transwell inserts with 8.0 μm membrane pores (BD, San Jose, CA, United States) according to the manufacturer's protocol. Migration was additionally evaluated with the wound-healing assay. Briefly, DLD1-shFOXQ1/SW480-shFOXQ1 and DLD1-shControl/SW480-shControl cells were seeded in 6-well plates at a density that enabled a confluency of 80% to be attained 24 h after plating. A 10 μL filter tip was used to gently scratch the cell monolayer across the center of the well. Cells were then gently washed twice with PBS to remove the dislodged cells, and fresh medium was added. The first images of the scratch area were then acquired. Cells were cultured in serum-free medium for another 48 h, and a second set of images was then acquired to determine the extent of wound closure.

CRC tissue microarray

Tissue microarrays containing a total of 90 pairs of colorectal tumor tissues and matched adjacent normal tissues, together with pathological staging data in accordance with TNM classification of the American Joint Committee on Cancer (2010) and follow-up survival time after surgery, were obtained from Shanghai Biochip Co. Ltd., Shanghai, China (HCol-Ade180Sur-06). FOXQ1 (ab51340) and HB-EGF (ab192545) antibodies were purchased from Abcam (Cambridge, MA, United States). Tissue microarray analysis was performed using a standard immunohistochemistry (IHC) protocol. The median value of the immunoreactivity score (IRS) was selected as the cutoff for high and low protein expression levels based on a measure of heterogeneity according to the log-rank test with respect to disease-specific survival (DSS) as described previously. Cutoff values for the scoring system were assigned as follows:

Table 3 Correlation between heparin binding epidermal growth factor expression and clinicopathological characteristics of colorectal cancers in cohort of human colorectal cancer tissues

Clinicopathological variables		Cohort tumor HB-EGF expression		*P* value
		Negative (*n* = 26)	Positive (*n* = 39)	
Age (yr)		65.72 (10.37)	69.43 (7.98)	
Gender	Female	11	23	> 0.05
	Male	14	16	
Size of tumor (mm)	≤ 10	5	7	> 0.05
	> 10	21	32	
Lymphatic metastasis	Absent	19	19	> 0.05
	Present	7	20	
Tumor differentiation	I-II	12	24	> 0.05
	III-IV	14	15	
TNM stage	I-II	11	8	> 0.05
	III-IV	15	31	
AJCC clinical stage according to 7th issue	1 and 2A	17	24	> 0.05
	3 and 3B	9	15	

HB-EGF: Heparin binding epidermal growth factor; AJCC: American Journal of Critical Care.

Table 4 Correlation analysis of forkhead Box q1 and heparin binding epidermal growth factor expression in cohort (*n* = 65) colorectal cancer tissues

		FOXQ1, negative (*n* = 31)	FOXQ1, positive (*n* = 34)	χ^2	*P* value
HB-EGF	Negative (*n* = 26)	20	6	4.116	< 0.05
	Positive (*n* = 39)	11	28		

FOXQ1: Forkhead Box q1; HB-EGF: Heparin binding epidermal growth factor.

High expression of FOXQ1 and HB-EGF were defined as an IRS of ≥ 4 (4, 6, 8, 9 and 12); and low expression was defined as an IRS of < 4 (0, 1, 2 and 3)[23]. Immunostained sections were scanned using a microscope (Axiovert 200, Carl Zeiss, Gttingen, Germany). Data for 25 patients were excluded because the dots were off the chips during the experiment. In total, data for 65 patients with CRC were included in the final analysis (Tables 3 and 4).

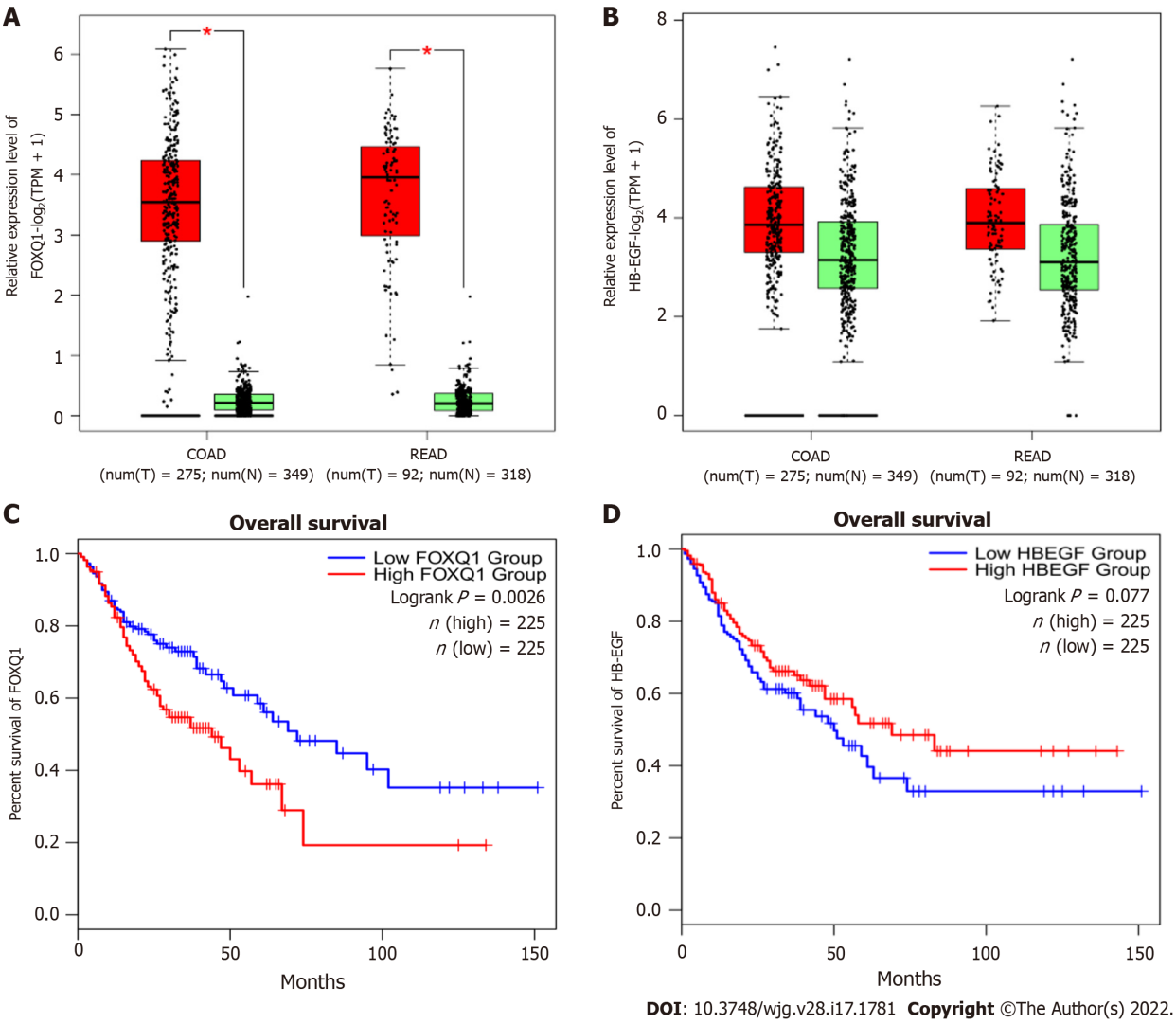
Statistical analysis

Statistical analyses were performed using GraphPad Prism 8 and SPSS v.19. An unpaired two-tailed Student's *t*-test was performed for two-group comparisons, and one-way analysis of variance (ANOVA) was performed for multiple group comparisons. Survival curves were calculated using the Kaplan–Meier algorithm and log-rank test. $P < 0.05$ was considered to indicate a statistically significant difference.

RESULTS

Expression and prognosis of FOXQ1 and HB-EGF in CRC and normal colorectal tissues

To determine the expression levels of FOXQ1 and HB-EGF in CRC, we investigated the expression and prognosis of FOXQ1 and HB-EGF in CRC in the Gene Expression Profiling Interactive Analysis (GEPIA) online database (Figure 1). The results showed that FOXQ1 was upregulated in CRC compared to normal samples according to GEPIA (Figure 1A). Increased expression of FOXQ1 was also associated with worse overall survival (Figure 1C). The expression of HB-EGF in CRC was not significantly different from that in normal colorectal tissues (Figure 1B), and its expression had no significant effect



DOI: 10.3748/wjg.v28.i17.1781 **Copyright** ©The Author(s) 2022.

Figure 1 Expression and prognosis of forkhead Box q1 and heparin binding epidermal growth factor in colorectal cancer and normal colorectal tissues. A and B: Forkhead Box q1 (FOXQ1) (left) and heparin binding epidermal growth factor (HB-EGF) (right) expression was analyzed in human colorectal cancer (CRC) tissues and normal tissues using the Gene Expression Profiling Interactive Analysis online database. $^{a}P < 0.05$; C and D: Overall survival rate of FOXQ1 (left) and HB-EGF (right) in CRC patients. FOXQ1: Forkhead Box q1; HB-EGF: Heparin binding epidermal growth factor; GEPIA: Gene Expression Profiling Interactive Analysis.

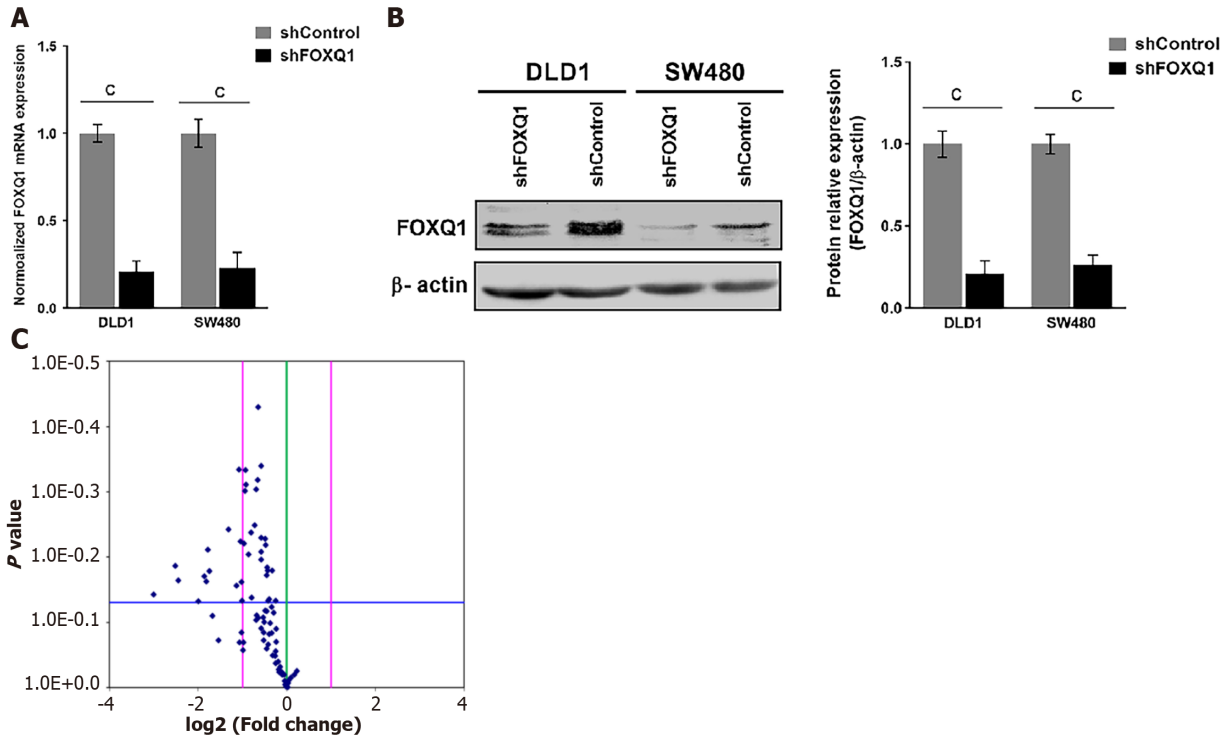
on the overall survival of patients with CRC (Figure 1D).

Construction of FOXQ1 knockdown CRC cell lines

To elucidate the functional roles of FOXQ1 in CRC, we generated CRC lines with stable FOXQ1 knockdown. Among the CRC lines we tested, DLD1 and SW480 cells had relatively high endogenous FOXQ1 expression as described previously[21]. Because the high expression of FOXQ1 in these two cells lines has also been confirmed in several other independent studies[3,4,8,9,24], we selected these two cell lines for knockdown studies. qRT–PCR assays verified significant FOXQ1 knockdown in DLD1-shFOXQ1 and SW480-shFOXQ1 cells. FOXQ1 mRNA expression in DLD1-shFOXQ1 and SW480-shFOXQ1 cells was significantly reduced compared to that in the control DLD1-shControl and SW480-shControl cells (Figure 2A). Western blot analysis also verified that the expression of FOXQ1 was significantly downregulated (Figure 2B).

Knockdown of FOXQ1 suppresses the expression of HB-EGF and blocks the EGF/PDGF signaling pathway in vitro

A panel of PCR arrays consisting of 84 representative genes related to the EGF/PDGF signaling pathways was used to detect the transcriptional signatures of DLD1-shFOXQ1 and DLD1-shControl cells. Differentially expressed genes with statistical significance were identified by volcano plot filtering. The results showed that 18 genes had expression changes with a fold-change ≥ 2.0 ($P < 0.05$)(Figure 2C). Among these 18 genes, 12 genes were associated with EGFR signaling pathways, including HB-EGF (FC = -2.19), and there were several novel genes of the three main EGF/PDGF downstream signaling



DOI: 10.3748/wjg.v28.i17.1781 **Copyright** ©The Author(s) 2022.

Figure 2 Forkhead Box q1 knockdown induces heparin binding epidermal growth factor suppression and epidermal growth factor/platelet-derived growth factor signaling pathway blockade *in vitro* according to transcriptional analysis of the generated forkhead Box q1 knockdown cell line. A: Quantitative real-time polymerase chain reaction was performed to evaluate mRNA expression in the knockdown of forkhead Box q1 in DLD1 cells (DLD1-shFOXQ1) and SW480-shFOXQ1 cells (two-tailed, unpaired Student's *t* test). Bars represent the mean ± SE of three independent experiments; B: Western blotting was performed to evaluate FOXQ1 protein expression in DLD1-shFOXQ1 and SW480-shFOXQ1 cells; C: Volcano plot illustrating differentially expressed genes using the epidermal growth factor (EGF)/platelet-derived growth factor (PDGF) array to compare DLD1-shFOXQ1 and DLD1-shControl cells. The vertical blue points in the plot represent 84 genes related to the EGF/PDGF signaling pathways. The vertical green line indicates a fold-change in gene expression of 1. The vertical pink lines indicate the threshold for fold-change (≥ 2.0 and ≤ -2.0). The horizontal blue line indicates the threshold for the *P* value of the *t* test. $^{a}P < 0.05$; $^{b}P < 0.01$; $^{c}P < 0.001$. DLD1-shFOXQ1: The knockdown of forkhead Box q1 in DLD1 cells; SW480-shFOXQ1: The knockdown of forkhead Box q1 in SW480 cells.

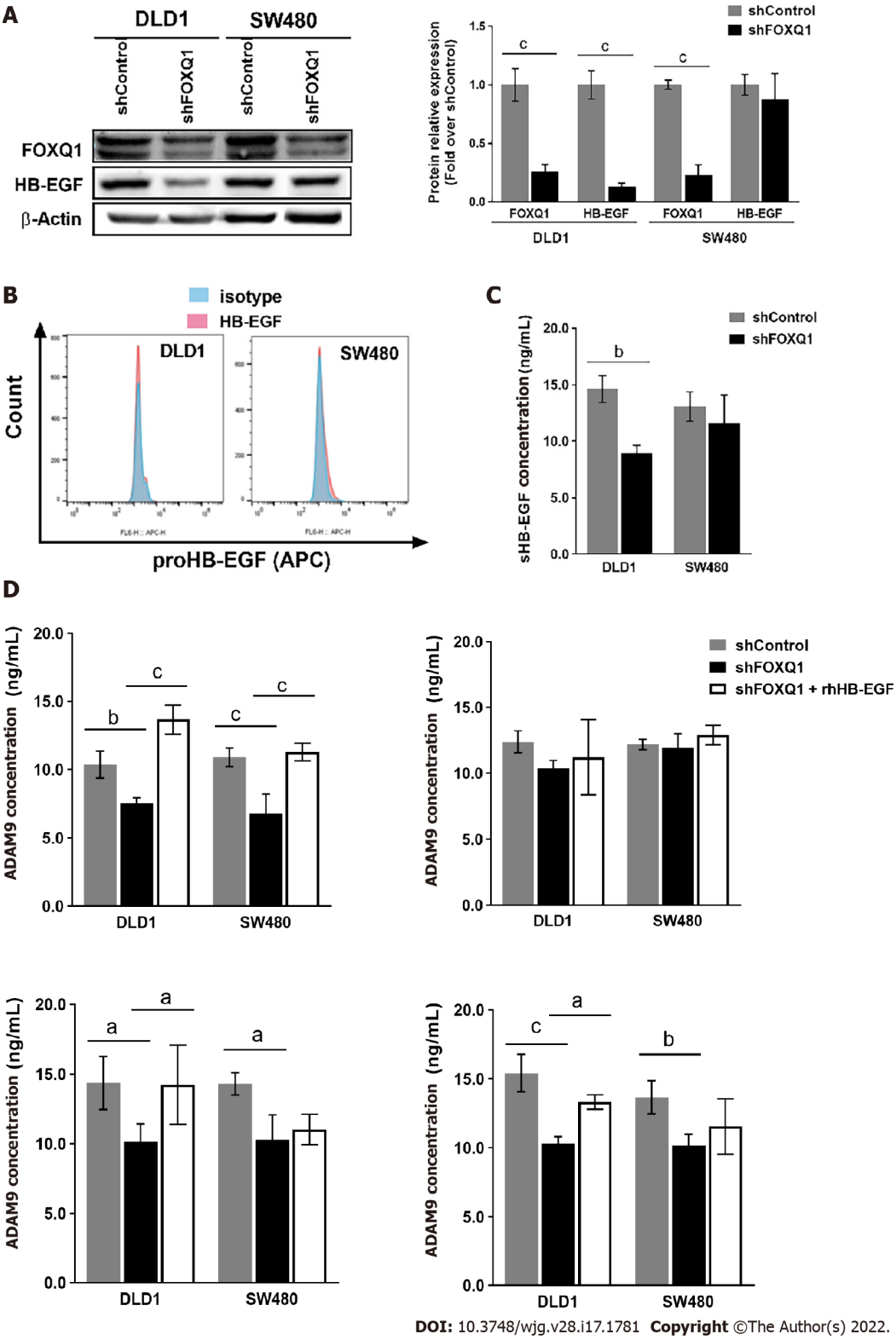
pathways (MAPK/ERK1/2, PI3K/AKT and JAK/STAT3). These novel genes included RAS, PI3K and STAT3 as well as several intracellular transcription factors activated by these signaling pathways, such as c-JUN and c-FOS (Table 2).

Effect of FOXQ1 expression on HB-EGF expression and extracellular release ability in CRC cells

Western blot analysis confirmed that knockdown of FOXQ1 in CRC cells resulted in a significant decrease in the expression of HB-EGF in DLD1 cells (Figure 3A), but no significant changes in HB-EGF were observed in SW480 cells (Figure 3A). Flow cytometry analysis confirmed that knockdown of FOXQ1 expression in CRC cells did not affect the expression level of proHB-EGF (Figure 3B). ELISA results indicated that knockdown of FOXQ1 significantly reduced the shedding of soluble HB-EGF (sHB-EGF) in DLD1 cells but did not affect the shedding of HB-EGF in SW480 cells (Figure 3C). Among the four proteins that affect the release of the extracellular domain of proHB-EGF, three (ADAM9, ADAM12 and ADAM7) were decreased significantly in both DLD1-shFOXQ1 and SW480-shFOXQ1 cells, while ADAM10 was not changed. The feedback regulation of ADAM9, ADAM12 and MMP7 secretion by HB-EGF from CRC cells was studied by adding exogenous recombinant human HB-EGF (rhHB-EGF). The results showed that rhHB-EGF reversed the decline in the expression of ADAM9, ADAM12 and MMP7 in DLD-shFOXQ1 cells. However, only the decreased expression of ADAM9 was reversed by rhHB-EGF in SW480-shFOXQ1 cells (Figure 3D).

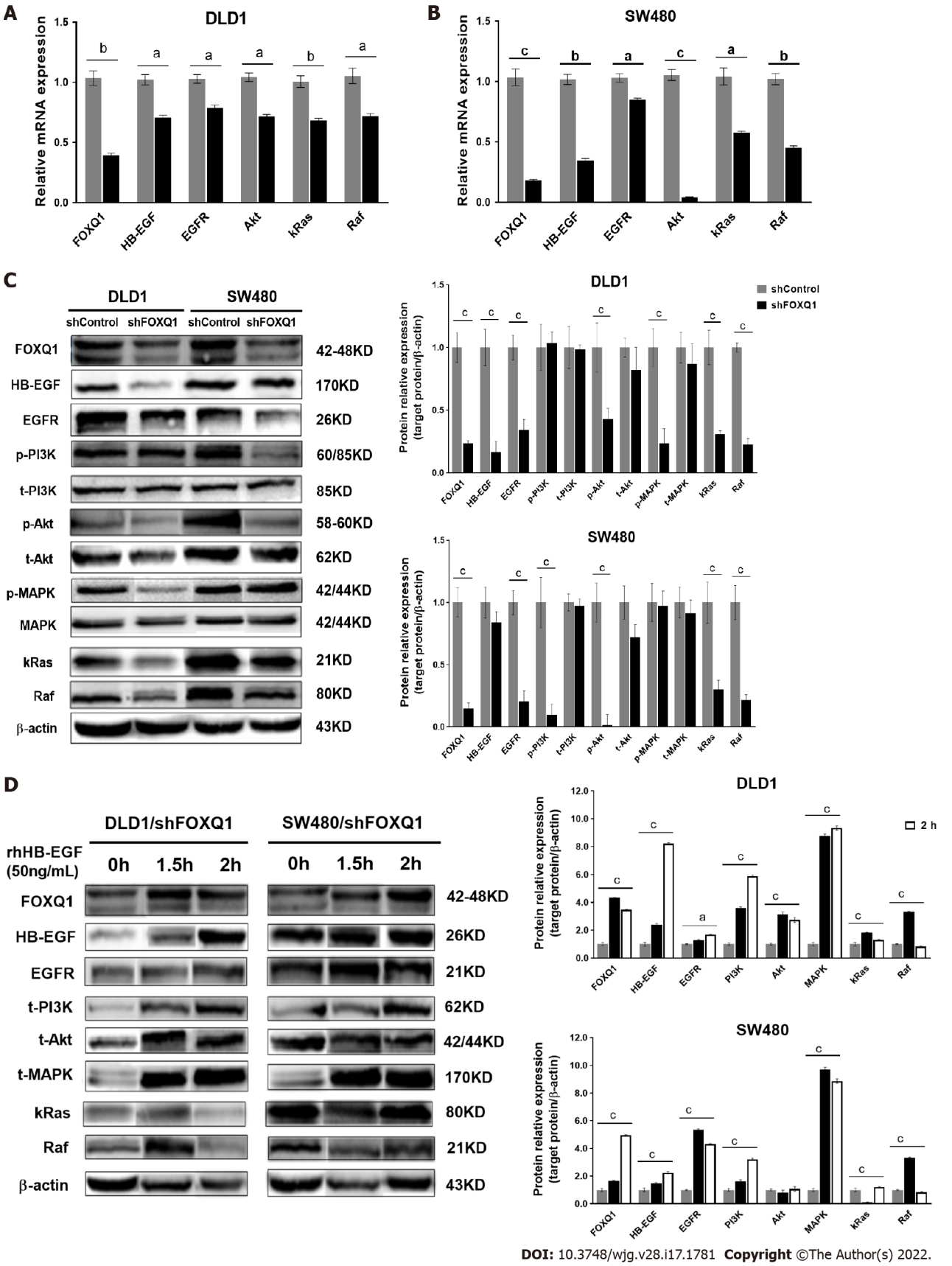
FOXQ1 regulates EGFR and downstream signaling pathways by regulating HB-EGF

To verify the role of FOXQ1 in activating the HB-EGF/EGFR signaling pathway, we performed qRT–PCR analysis in DLD1-shFOXQ1 and SW480-shFOXQ1 cells. The results confirmed that FOXQ1 knockdown resulted in a significant decrease in the mRNA expression of HB-EGF, EGFR and downstream genes (AKT, RAF and KRAS) in DLD1-shFOXQ1 and SW480-shFOXQ1 cells (Figure 4A and B). In addition, the Western blot analysis showed that knockdown of FOXQ1 resulted in a significant decrease in HB-EGF and EGFR expression as well as decreased AKT and MAPK



DOI: 10.3748/wjg.v28.i17.1781 **Copyright** ©The Author(s) 2022.

Figure 3 Effect of forkhead Box q1 expression on heparin binding epidermal growth factor expression and extracellular release ability in colorectal cancer cells. A: Quantitative analysis of western blots was performed to detect the expression of heparin binding epidermal growth factor (HB-EGF) with forkhead Box q1 (FOXQ1) inhibition; B: Flow cytometry was performed to detect the effect of changes in FOXQ1 expression on the expression of proHB-EGF in DLD1 and SW480 cells; C: ELISA verified the effect of FOXQ1 knockdown on sHB-EGF expression in DLD1 and SW480 cells; D: ELISA confirmed the effect of FOXQ1 on the expression of proHB-EGF extracellular release proteins (ADAM9, ADAM10, ADAM12 and MMP-7) in DLD1 and SW480 cells. $^{a}P < 0.05$; $^{b}P < 0.01$; $^{c}P < 0.001$. FOXQ1: Forkhead Box q1; HB-EGF: Heparin binding epidermal growth factor; ProHB-EGF: Membrane-bound HB-EGF; SHB-EGF: Souble HB-EGF; ADAM9: A disintegrin and a metalloprotease 9; ADAM10: A disintegrin and a metalloprotease 10; ADAM12: A disintegrin and a metalloprotease 12; MMP7: Matrix metallopeptidase 7.



DOI: 10.3748/wjg.v28.i17.1781 **Copyright** ©The Author(s) 2022.

Figure 4 Forkhead Box q1 regulates epidermal growth factor receptor and downstream signaling pathways by regulating heparin binding epidermal growth factor. A: Quantitative real-time polymerase chain reaction (qRT–PCR) was performed to analyze the levels of forkhead Box q1 (FOXQ1), heparin binding epidermal growth factor (HB-EGF), epidermal growth factor receptor (EGFR), Akt, kRas and Raf in DLD1-shFOXQ1 and DLD1-shControl cells; B: qRT–PCR was performed to analyze the levels of FOXQ1, HB-EGF, EGFR, AKT, RAF and KRAS in SW480-shFOXQ1 and SW480-shControl cells; C: Western blot analyses were performed to analyze the protein levels of FOXQ1, HB-EGF, EGFR, RAF and KRAS as well as the phosphorylation levels of PI3K, Akt, and MAPK in

DLD1-shFOXQ1, SW480-shFOXQ1, DLD1-shControl and SW480-shControl cells. β-actin was used as the loading control; D: Exogenous rhHB-EGF (50 ng/mL) was added to the culture media of DLD1-shFOXQ1 and SW480-shFOXQ1 cells for 1.5 h and 2 h, respectively. Western blotting was performed to detect the expression of proteins in the HB-EGF/EGFR signaling pathway. $^{a}P < 0.05$; $^{b}P < 0.01$; $^{c}P < 0.001$ indicate significant differences compared to the control group (two-tailed, unpaired Student's *t* test). Bars represent the mean ± S.E. of three independent experiments. rhHB-EGF: Recombinant human HB-EGF; FOXQ1: Forkhead Box q1; HB-EGF: Heparin binding epidermal growth factor.

phosphorylation in DLD1-shFOXQ1 cells compared to DLD1-shControl cells. In SW480-shFOXQ1 cells, EGFR and HB-EGF expression was significantly decreased, and AKT and PI3K phosphorylation was inhibited compared to that in SW480-shControl cells (Figure 4C). Furthermore, Western blot analysis confirmed that the decreased expression of important downstream genes was rescued by rhHB-EGF protein in either DLD1-shFOXQ or SW480-shFOXQ1 cells (Figure 4D).

rhHB-EGF reverses the FOXQ1 knockdown-induced suppression of CRC cell proliferation and migration in vitro

CCK-8 results confirmed that FOXQ1 knockdown significantly inhibited the proliferation of DLD1-shFOXQ1 and SW480-shFOXQ1 cells, and the inhibitory effect was partially reversed by exogenous rhHB-EGF (Figure 5A). The results of the Transwell migration assay confirmed that FOXQ1 knockdown also reduced the migration of DLD1 and SW480 cells, and the inhibitory effect was also reversed to a large extent by rhHB-EGF (Figure 5B and C). Scratch experiment results confirmed that FOXQ1 knockdown reduced the wound-healing ability of DLD1 and SW480 cells, which was also reversed to a large extent by rhHB-EGF (Figure 5D and E). We next analyzed the protein expression during cell invasion and metastasis (Ecadherin, N-cadherin, Vimentin and Snail), Western blot analysis indicated that FOXQ1 knockdown reduced the expression in DLD1-shFOXQ1 and SW480-shFOXQ1 cells (Figure 5F).

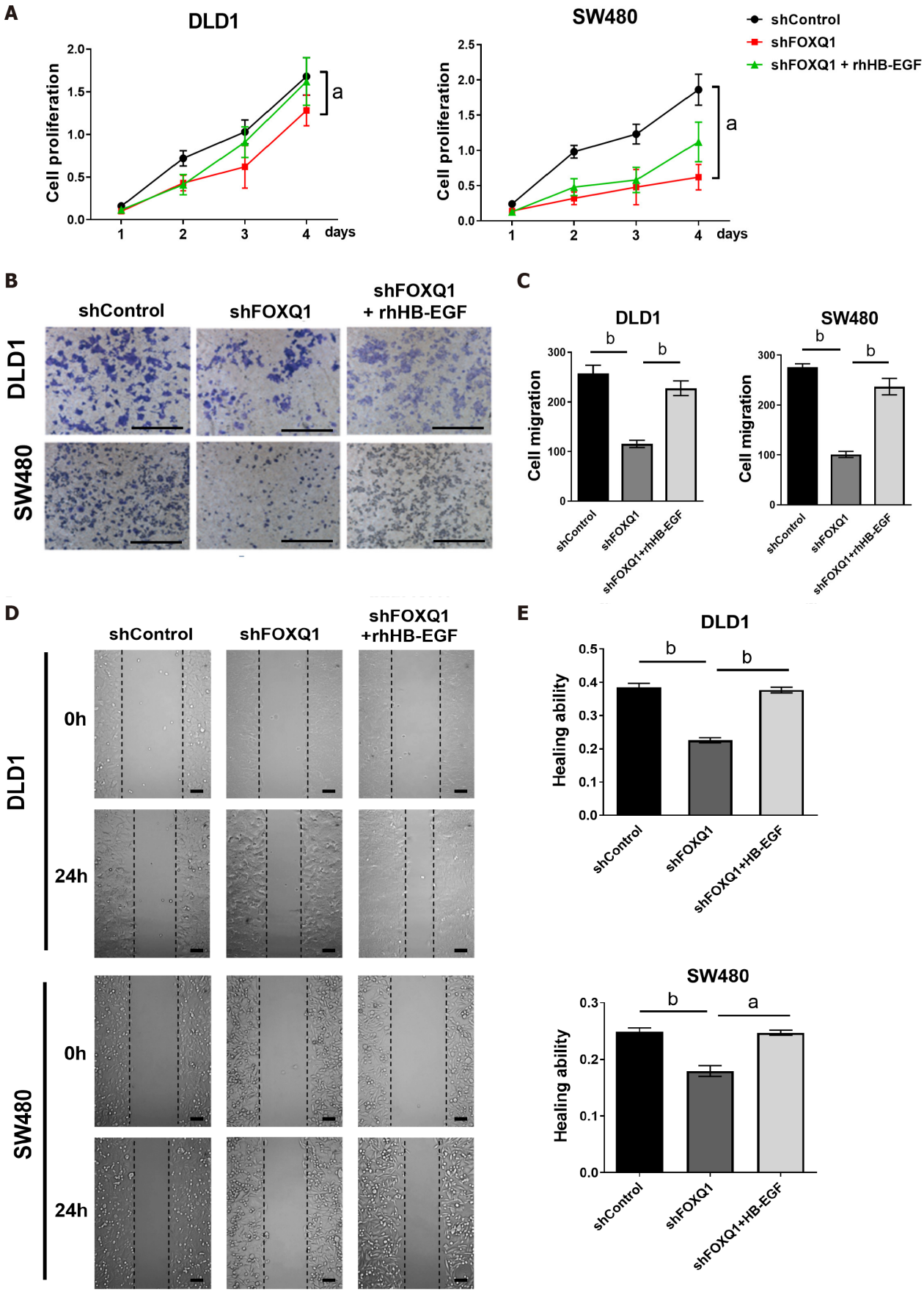
Prognostic value of the combination of FOXQ1 and HB-EGF

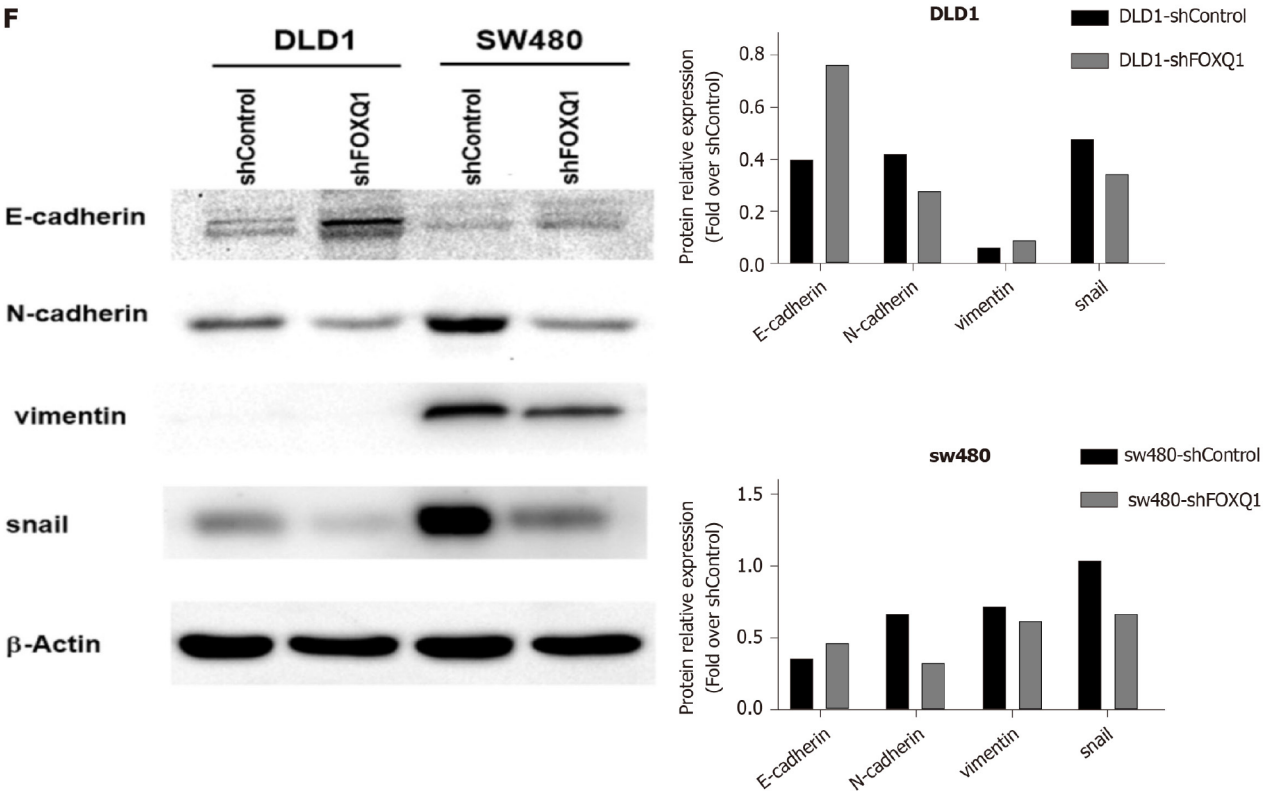
To verify the clinical relevance of our findings, we evaluated the expression of FOXQ1 and HB-EGF in human CRC tissue biopsies (cohort, $n = 65$) (Tables 3 and 4). IHC analysis showed that FOXQ1 was significantly upregulated in CRC tissues compared to adjacent nontumorous tissues and that HB-EGF was moderately upregulated (Figure 6A). Although the overexpression of HB-EGF had no significant correlation with any clinicopathological characteristics of CRCs (Table 3), further analysis verified the positive correlation between FOXQ1 and HB-EGF (Table 4). In a cohort of 65 CRC patients, Kaplan–Meier survival analysis results showed that CRC patients with positive expression of FOXQ1 had shorter overall survival than those with negative expression of FOXQ1. Furthermore, Kaplan–Meier survival analysis of CRC patients with positive coexpression of FOXQ1 and HB-EGF had the shortest overall survival times compared to the corresponding single-negative or double-negative groups in the cohort of 65 CRC patients (Figure 6B).

DISCUSSION

Studies have indicated that *FOXQ1* is an oncogene in multiple tumors, including CRC[24], breast cancer [25], lung cancer[26], gastric cancer[27], liver cancer[28], pancreatic cancer[29], ovarian cancer[30], and neuroglioma[31]. In CRC, FOXQ1 promotes tumor invasion and metastasis through the Wnt signaling pathway, and it affects the prognosis of patients[24]. EGFR is overexpressed in a variety of cancers, including CRC. EGFR overexpression and activation have a positive effect on the cell growth and metastasis of a variety of solid tumors, including CRC[17]. Metastasis is a multistep process in which tumor cells spread from the primary site to distant sites and form secondary tumors[32], and is the leading cause of death in CRC patients. Many downstream targets of HB-EGF and EGFR include MAPK, p-MAPK, RAS, RAF, PI3K, p-PI3K, AKT, p-AKT, and AKT protein kinases, leading to many processes related to tumor progression, including cell growth[33], epithelial-mesenchymal transition (EMT)[34], metastasis[35], and angiogenesis[36]. FOXQ1 can regulate FAK, PI3K, AKT, and many other key proteins in the PI3K/AKT signaling pathway and promotes the phosphorylation of the above proteins to maintain the activation of PI3K/AKT signaling[37]. FOXQ1 can also combine with VEGFR2 and VE-cadherin to promote angiogenesis and endothelial cell migration and rearrangement[24].

In our previous studies, we found that the mRNA and protein expression levels of FOXQ1 gradually increase with the pathological development of colorectal adenoma to colorectal adenocarcinoma, and the increased expression of FOXQ is not only involved in the process of colorectal adenoma carcinogenesis, but is also closely related to invasion and metastasis of CRC[38]. The differential expression of genes that are involved in the process of colorectal adenoma carcinogenesis screened by the gene chip has been analyzed by signal pathway analysis, suggesting that the abnormally high expression of FOXQ1 is closely related to the activation of the EGFR signaling pathway[39]. Studies have shown that the abnormal activation of the EGFR pathway plays an important role in malignant growth, invasion,


A
DLD1
SW480
shControl
shFOXQ1
shFOXQ1 + rhHB-EGF
Cell proliferation
days
a
B
shControl
shFOXQ1
shFOXQ1 + rhHB-EGF
DLD1
SW480
C
DLD1
SW480
Cell migration
b
shControl
shFOXQ1
shFOXQ1+rhHB-EGF
D
shControl
shFOXQ1
shFOXQ1 +rhHB-EGF
DLD1
SW480
0h
24h
E
DLD1
SW480
Healing ability
b
a
shControl
shFOXQ1
shFOXQ1+HB-EGF



DOI: 10.3748/wjg.v28.i17.1781 **Copyright** ©The Author(s) 2022.

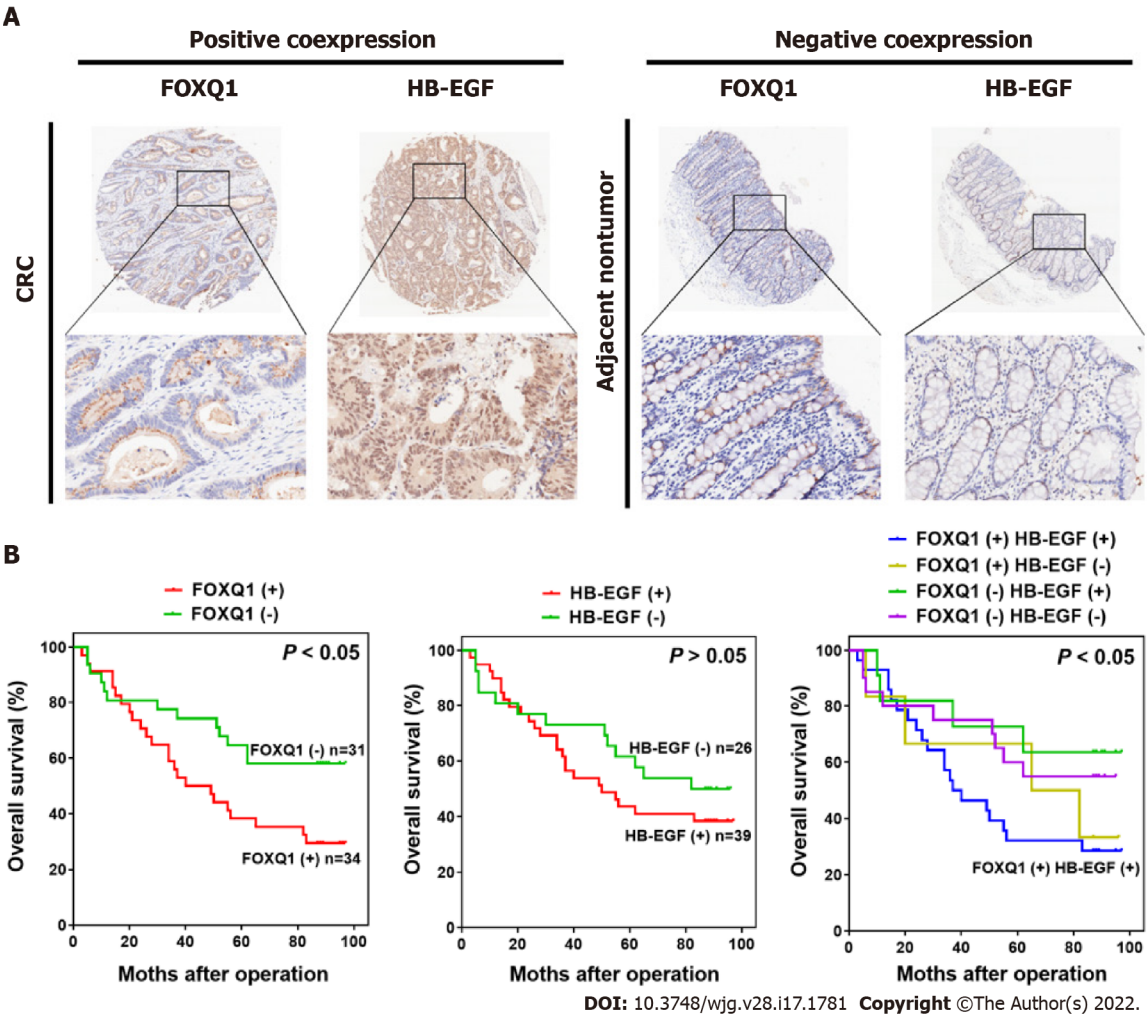
Figure 5 Recombinant human heparin binding epidermal growth factor reverses the forkhead Box q1-induced suppression of colorectal cancer cell proliferation and migration *in vitro*. A: A cell counting Kit-8 (CCK-8) assay was performed to detect the effects of recombinant human heparin binding epidermal growth factor (rhHB-EGF) on the proliferation of forkhead Box q1 (FOXQ1)-deficient DLD1 and SW480 cells; B: The Transwell migration assay was performed to evaluate the migration ability after knocking out FOXQ1 and after adding rhHB-EGF; C: A statistical analysis of the results of the Transwell migration assay was performed. $^{b}P < 0.01$; D: After 0 h and 24 h, the scratch experiment evaluated the migration ability of DLD1 and SW480 cells with downregulated FOXQ1 and rhHB-EGF; E: Statistical analysis of the above scratch experiment results. $^{a}P < 0.05$; $^{b}P < 0.01$; $^{c}P < 0.001$; F: Quantitative analysis of Western blot to detect the expression of E-cadherin, N-cadherin, vimentin and Snail protein levels in DLD-shFOXQ1 and SW480-shFOXQ1 cells compared to DLD1-shControl and SW480-shControl cells. β-actin was used as the loading control. CCK-8: Cell Counting Kit-8.

and metastasis of colorectal tumors. When sHB-EGF binds to EGFR, the tyrosine kinase activity of EGFR is activated, mainly by activating the MAPK/ERK1/2, PI3K/AKT, and JAK/STAT3 signaling pathways, leading to the proliferation, invasion, metastasis, and apoptosis of tumor cells[40]. The results of this study also proved that knockout of *FOXQ1* caused a decrease in gene expression in these three signaling pathways.

Combined with the analysis in Figure 3B-D, these results suggested that FOXQ1 may regulate the EGFR pathway by promoting the separation of ProHB-EGF into sHB-EGF. AMAD7, AMAD9, and AMAD12 are also factors that affect the separation of ProHB-EGF[41]. In this study, decreased expression levels of AMAD7, AMAD9, and AMAD12 were also observed in DLD1-shFOXQ1 and SW480-shFOXQ1 cells, but this indirect regulation should be further verified in other CRC cell lines.

In this study, FOXQ1 was determined to be upregulated in CRC cell lines. The results showed that *FOXQ1* knockdown inhibited the proliferation, migration and repair capabilities of CRC, which was consistent with our previous results[21,42]. When rhHB-EGF protein was added, the proliferation ability of the cells was not completely restored, but the migration and repair ability of CRC cells was partially restored. These results indicated that the effect of FOXQ1 in promoting the proliferation of CRC cells is not directly mediated by HB-EGF; however, the regulation of the invasion and metastasis of CRC cells by FOXQ1 is partly mediated by HB-EGF. HB-EGF is related to the abnormal proliferation of skin and mucosal cells, and high expression of HB-EGF is closely related to the occurrence and development of a variety of tumors; the expression of the *HB-EGF* gene is significantly increased in various human cancers and cancer-derived cell lines, indicating that HB-EGF plays an important role in tumor invasion and metastasis[43-46].

Studies have shown that FOXQ1 is related to the poor prognosis of CRC[47]. In this study, we conducted pathological and survival analyses on 65 CRC patients. These findings suggested that the expression of FOXQ1 and its coregulatory protein HB-EGF may have a prognostic correlation with CRC. Thus, FOXQ1 may serve as a therapeutic target for CRC treatment by blocking the HB-EGF/EGFR pathway. Our research suggests that FOXQ1 activates the EGFR signaling pathway by regulating the expression of HB-EGF, thereby affecting the invasion and metastasis of CRC. Regarding the limitations



DOI: 10.3748/wjg.v28.i17.1781 **Copyright** ©The Author(s) 2022.

Figure 6 Prognostic value of the combination of forkhead Box q1 and heparin binding epidermal growth factor. A: Representative immunohistochemical images of forkhead Box q1 (FOXQ1) and heparin binding epidermal growth factor (HB-EGF) positive coexpression and negative coexpression in human colorectal cancer tissues and adjacent nontumorous tissues. Scale bars represent 200 μm; B: Kaplan-Meier survival analysis was used to evaluate the overall survival rate in the following patients: FOXQ1-positive and FOXQ1-negative patients; HB-EGF-positive and HB-EGF-negative patients; and FOXQ1-positive and FOXQ1-negative coexpressing HB-EGF-positive and HBEGF-negative patients. $^{a}P < 0.05$; $^{b}P < 0.01$; $^{c}P < 0.001$ indicate a significant difference between the indicated groups (log-rank test). FOXQ1: Forkhead Box q1; HB-EGF: Heparin binding epidermal growth factor.

of this study, it is necessary to construct a FOXQ1 high-expressing cell line and combine it with the dual luciferase reporter gene system to further verify whether FOXQ1 is directly involved in the transcriptional regulation of HB-EGF. Next, we will further explore the regulation of FOXQ1 on EGFR and its downstream signaling pathways through *in vivo* and *in vitro* studies. We will conduct a more comprehensive study on the role of HB-EGF in the invasion and metastasis of CRC to provide more possibilities for the treatment of CRC.

CONCLUSION

In conclusion, we have demonstrated that decreased FOXQ1 expression was also associated with a lower ability to invade and metastasize in CRC. FOXQ1 promotes the invasion and metastasis of CRC by activating the HB-EGF/EGFR pathway. These data indicated that FOXQ1 and HB-EGF may be potential biomarkers to improve the accuracy of CRC diagnosis and treatment.

ARTICLE HIGHLIGHTS

Research background

Invasion and metastasis play important roles in tumorigenesis, resulting in the death of most colorectal cancer (CRC) patients. Forkhead Box q1 (FOXQ1) is a well-established oncogene in multiple tumors,

including CRC. However, the role and mechanism of how FOXQ1 promotes tumorigenesis in CRC by activating the heparin-binding epidermal growth factor (HB-EGF)/epidermal growth factor receptor (EGFR) pathway remain largely unknown.

Research motivation
Our study aims to elucidate the critical role of FOXQ1 and HB-EGF/EGFR pathways in CRC, and to provide theoretical support for the clinical application of targeted FOXQ1 in the treatment of CRC.

Research objectives
To determine the role of FOXQ1-induced invasion and metastasis, which are related to activating the HB-EGF/EGFR pathway, and to explore the mechanism by which FOXQ1 promotes tumorigenesis by activating the HB-EGF/EGFR pathway in CRC.

Research methods
We analyzed the correlation between FOXQ1 and the HB-EGF/EGFR pathway by constructing *FOXQ1* knockdown cells, tissue microarray, cell function experiments, quantitative real-time polymerase chain reaction (qRT–PCR), flow cytometry, ELISA, western blot, and the Gene Expression Profiling Interactive Analysis (GEPIA) website.

Research results
GEPIA showed that the expression of FOXQ1 in CRC tissues was relatively high and was related to a lower overall survival rate. PCR array results showed that *FOXQ1* is related to the HB-EGF and EGFR pathways. Knockdown of *FOXQ1* suppressed the expression of HB-EGF and led to a decrease in EGFR and its downstream genes *AKT*, *RAF*, *KRAS* expression levels. After knockdown of *FOXQ1* in CRC cell lines, cell proliferation, migration, and invasion were attenuated. Adding HB-EGF restored the migration and invasion ability of CRC, but the cell proliferation ability was not restored. Kaplan–Meier survival analysis results showed that the combination of FOXQ1 and HB-EGF may serve to predict CRC survival.

Research conclusions
FOXQ1 promotes the invasion and metastasis of CRC by activating the HB-EGF/EGFR pathway.

Research perspectives
In this study, our results indicated that FOXQ1 and HB-EGF may be potential biomarkers to improve the accuracy of CRC diagnosis and treatment.

FOOTNOTES

Author contributions: Zhang JJ and Cao CX contributed equally to this work; Tang H and Guo Q designed the project; Cao CX and Zhang JJ analyzed data and wrote the manuscript; Zhang JJ and Wan LL performed qRT-PCR, Elisa, and Western blotting; Zhang W and Wang JL carried out migration assay; Liu ZJ and Tang H analyzed colorectal tissue microarray and survival data; all authors participated in critical revision of the manuscript and approved the final manuscript.

Supported by National Natural Science Foundation of China, No. 81502556; and Yunnan Digestive Endoscopy Clinical Medical Center Foundation for Health Commission of Yunnan Province, No. 2X2019-01-02.

Institutional review board statement: Our research does not involve humans and animals.

Conflict-of-interest statement: The authors declare no competing interests.

Data sharing statement: No additional data are available.

Open-Access: This article is an open-access article that was selected by an in-house editor and fully peer-reviewed by external reviewers. It is distributed in accordance with the Creative Commons Attribution NonCommercial (CC BY-NC 4.0) license, which permits others to distribute, remix, adapt, build upon this work non-commercially, and license their derivative works on different terms, provided the original work is properly cited and the use is non-commercial. See: https://creativecommons.org/Licenses/by-nc/4.0/

Country/Territory of origin: China

ORCID number: Jin-Jin Zhang 0000-0001-9261-6571; Chang-Xiong Cao 0000-0002-2806-5370; Li-Lan Wan 0000-0002-3489-436X; Wen Zhang 0000-0002-0825-1440; Zhong-Jiang Liu 0000-0003-4945-6642; Jin-Li Wang 0000-0002-2371-0799; Qiang Guo 0000-0003-0636-5548; Hui Tang 0000-0002-8146-7184.

S-Editor: Fan JR
L-Editor: A
P-Editor: Guo X

REFERENCES

1 **Gu MJ**, Huang QC, Bao CZ, Li YJ, Li XQ, Ye D, Ye ZH, Chen K, Wang JB. Attributable causes of colorectal cancer in China. *BMC Cancer* 2018; **18**: 38 [PMID: 29304763 DOI: 10.1186/s12885-017-3968-z]
2 **Christofori G**. New signals from the invasive front. *Nature* 2006; **441**: 444-450 [PMID: 16724056 DOI: 10.1038/nature04872]
3 **Arlt F**, Stein U. Colon cancer metastasis: MACC1 and Met as metastatic pacemakers. *Int J Biochem Cell Biol* 2009; **41**: 2356-2359 [PMID: 19666136 DOI: 10.1016/j.biocel.2009.08.001]
4 **Lai E**, Prezioso VR, Smith E, Litvin O, Costa RH, Darnell JE Jr. HNF-3A, a hepatocyte-enriched transcription factor of novel structure is regulated transcriptionally. *Genes Dev* 1990; **4**: 1427-1436 [PMID: 2227418 DOI: 10.1101/gad.4.8.1427]
5 **Gao M**, Shih IeM, Wang TL. The role of forkhead box Q1 transcription factor in ovarian epithelial carcinomas. *Int J Mol Sci* 2012; **13**: 13881-13893 [PMID: 23203039 DOI: 10.3390/ijms131113881]
6 **Kaneda H**, Arao T, Tanaka K, Tamura D, Aomatsu K, Kudo K, Sakai K, De Velasco MA, Matsumoto K, Fujita Y, Yamada Y, Tsurutani J, Okamoto I, Nakagawa K, Nishio K. FOXQ1 is overexpressed in colorectal cancer and enhances tumorigenicity and tumor growth. *Cancer Res* 2010; **70**: 2053-2063 [PMID: 20145154 DOI: 10.1158/0008-5472.CAN-09-2161]
7 **Liu JY**, Wu XY, Wu GN, Liu FK, Yao XQ. FOXQ1 promotes cancer metastasis by PI3K/AKT signaling regulation in colorectal carcinoma. *Am J Transl Res* 2017; **9**: 2207-2218 [PMID: 28559972]
8 **Weng W**, Okugawa Y, Toden S, Toiyama Y, Kusunoki M, Goel A. FOXM1 and FOXQ1 Are Promising Prognostic Biomarkers and Novel Targets of Tumor-Suppressive miR-342 in Human Colorectal Cancer. *Clin Cancer Res* 2016; **22**: 4947-4957 [PMID: 27162244 DOI: 10.1158/1078-0432.CCR-16-0360]
9 **Fujii H**, Iihara H, Suzuki A, Kobayashi R, Matsuhashi N, Takahashi T, Yoshida K, Itoh Y. Hypomagnesemia is a reliable predictor for efficacy of anti-EGFR monoclonal antibody used in combination with first-line chemotherapy for metastatic colorectal cancer. *Cancer Chemother Pharmacol* 2016; **77**: 1209-1215 [PMID: 27106835 DOI: 10.1007/s00280-016-3039-1]
10 **Higashiyama S**, Abraham JA, Miller J, Fiddes JC, Klagsbrun M. A heparin-binding growth factor secreted by macrophage-like cells that is related to EGF. *Science* 1991; **251**: 936-939 [PMID: 1840698 DOI: 10.1126/science.1840698]
11 **Taylor SR**, Markesbery MG, Harding PA. Heparin-binding epidermal growth factor-like growth factor (HB-EGF) and proteolytic processing by a disintegrin and metalloproteinases (ADAM): a regulator of several pathways. *Semin Cell Dev Biol* 2014; **28**: 22-30 [PMID: 24680771 DOI: 10.1016/j.semcdb.2014.03.004]
12 **Zhou Z**, Harding PA. Amino-terminal deletion of heparin-binding epidermal growth factor-like growth factor4-127 stimulates cell proliferation but lacks insulin-like activity. *Cell Prolif* 2007; **40**: 213-230 [PMID: 17472728 DOI: 10.1111/j.1365-2184.2007.00425.x]
13 **Nanba D**, Mammoto A, Hashimoto K, Higashiyama S. Proteolytic release of the carboxy-terminal fragment of proHB-EGF causes nuclear export of PLZF. *J Cell Biol* 2003; **163**: 489-502 [PMID: 14597771 DOI: 10.1083/jcb.200303017]
14 **Suzuki M**, Raab G, Moses MA, Fernandez CA, Klagsbrun M. Matrix metalloproteinase-3 releases active heparin-binding EGF-like growth factor by cleavage at a specific juxtamembrane site. *J Biol Chem* 1997; **272**: 31730-31737 [PMID: 9395517 DOI: 10.1074/jbc.272.50.31730]
15 **Yan Y**, Shirakabe K, Werb Z. The metalloprotease Kuzbanian (ADAM10) mediates the transactivation of EGF receptor by G protein-coupled receptors. *J Cell Biol* 2002; **158**: 221-226 [PMID: 12119356 DOI: 10.1083/jcb.200112026]
16 **Sunnarborg SW**, Hinkle CL, Stevenson M, Russell WE, Raska CS, Peschon JJ, Castner BJ, Gerhart MJ, Paxton RJ, Black RA, Lee DC. Tumor necrosis factor-alpha converting enzyme (TACE) regulates epidermal growth factor receptor ligand availability. *J Biol Chem* 2002; **277**: 12838-12845 [PMID: 11823465 DOI: 10.1074/jbc.M112050200]
17 **Shi YH**, Zhao DM, Wang YF, Li X, Ji MR, Jiang DN, Xu BP, Zhou L, Lu CZ, Wang B. The association of three promoter polymorphisms in interleukin-10 gene with the risk for colorectal cancer and hepatocellular carcinoma: A meta-analysis. *Sci Rep* 2016; **6**: 30809 [PMID: 27489033 DOI: 10.1038/srep30809]
18 **Wang J**, Chen Y, Dai C, Shang Y, Xie J. Ginsenoside Rh2 alleviates tumor-associated depression in a mouse model of colorectal carcinoma. *Am J Transl Res* 2016; **8**: 2189-2195 [PMID: 27347326]
19 **Wu L**, Shi B, Huang K, Fan G. MicroRNA-128 suppresses cell growth and metastasis in colorectal carcinoma by targeting IRS1. *Oncol Rep* 2015; **34**: 2797-2805 [PMID: 26352220 DOI: 10.3892/or.2015.4251]
20 **Luo Y**, Wang J, Wang F, Liu X, Lu J, Yu X, Ma X, Peng X, Li X. Foxq1 promotes metastasis of nasopharyngeal carcinoma by inducing vasculogenic mimicry *via* the EGFR signaling pathway. *Cell Death Dis* 2021; **12**: 411 [PMID: 33875643 DOI: 10.1038/s41419-021-03674-z]
21 **Tang H**, Zheng J, Bai X, Yue KL, Liang JH, Li DY, Wang LP, Wang JL, Guo Q. Forkhead Box Q1 Is Critical to Angiogenesis and Macrophage Recruitment of Colorectal Cancer. *Front Oncol* 2020; **10**: 564298 [PMID: 33330033 DOI: 10.3389/fonc.2020.564298]
22 **Princz MA**, Sheardown H. Heparin-modified dendrimer crosslinked collagen matrices for the delivery of heparin-binding epidermal growth factor. *J Biomed Mater Res A* 2012; **100**: 1929-1937 [PMID: 22492552 DOI: 10.1002/jbm.a.34128]
23 **Lee JH**, Lee JH, Ahn BK, Paik SS, Kim H, Lee KH. Loss of ASXL1 expression is associated with lymph node metastasis in colorectal cancer. *Indian J Pathol Microbiol* 2020; **63**: 221-225 [PMID: 32317519 DOI: 10.4103/IJPM.IJPM_822_19]
24 **Peng X**, Luo Z, Kang Q, Deng D, Wang Q, Peng H, Wang S, Wei Z. FOXQ1 mediates the crosstalk between TGF-β and Wnt signaling pathways in the progression of colorectal cancer. *Cancer Biol Ther* 2015; **16**: 1099-1109 [PMID: 25955104

DOI: 10.1080/15384047.2015.1047568]
25 **Han X**, Guo X, Zhang W, Cong Q. MicroRNA-937 inhibits the malignant phenotypes of breast cancer by directly targeting and downregulating forkhead box Q1. *Onco Targets Ther* 2019; **12**: 4813-4824 [PMID: 31417280 DOI: 10.2147/OTT.S207593]
26 **Feng J**, Xu L, Ni S, Gu J, Zhu H, Wang H, Zhang S, Zhang W, Huang J. Involvement of FoxQ1 in NSCLC through regulating EMT and increasing chemosensitivity. *Oncotarget* 2014; **5**: 9689-9702 [PMID: 25356753 DOI: 10.18632/oncotarget.2103]
27 **Xiang XJ**, Deng J, Liu YW, Wan LY, Feng M, Chen J, Xiong JP. MiR-1271 Inhibits Cell Proliferation, Invasion and EMT in Gastric Cancer by Targeting FOXQ1. *Cell Physiol Biochem* 2015; **36**: 1382-1394 [PMID: 26159618 DOI: 10.1159/000430304]
28 **Han S**, Shi Y, Sun L, Liu Z, Song T, Liu Q. MiR-4319 induced an inhibition of epithelial-mesenchymal transition and prevented cancer stemness of HCC through targeting FOXQ1. *Int J Biol Sci* 2019; **15**: 2936-2947 [PMID: 31853229 DOI: 10.7150/ijbs.38000]
29 **Christensen J**, Bentz S, Sengstag T, Shastri VP, Anderle P. FOXQ1, a novel target of the Wnt pathway and a new marker for activation of Wnt signaling in solid tumors. *PLoS One* 2013; **8**: e60051 [PMID: 23555880 DOI: 10.1371/journal.pone.0060051]
30 **Wang C**, Zhang W, Xing S, Wang Z, Wang J, Qu J. MiR-342-3p inhibits cell migration and invasion through suppressing forkhead box protein Q1 in ovarian carcinoma. *Anticancer Drugs* 2019; **30**: 917-924 [PMID: 31517731 DOI: 10.1097/CAD.0000000000000801]
31 **Sun HT**, Cheng SX, Tu Y, Li XH, Zhang S. FoxQ1 promotes glioma cells proliferation and migration by regulating NRXN3 expression. *PLoS One* 2013; **8**: e55693 [PMID: 23383267 DOI: 10.1371/journal.pone.0055693]
32 **Yang B**, Tan Z, Song Y. Study on the molecular regulatory mechanism of MicroRNA-195 in the invasion and metastasis of colorectal carcinoma. *Int J Clin Exp Med* 2015; **8**: 3793-3800 [PMID: 26064276]
33 **Morato A**, Martignani E, Miretti S, Baratta M, Accornero P. External and internal EGFR-activating signals drive mammary epithelial cells proliferation and viability. *Mol Cell Endocrinol* 2021; **520**: 111081 [PMID: 33181234 DOI: 10.1016/j.mce.2020.111081]
34 **Tulchinsky E**, Demidov O, Kriajevska M, Barlev NA, Imyanitov E. EMT: A mechanism for escape from EGFR-targeted therapy in lung cancer. *Biochim Biophys Acta Rev Cancer* 2019; **1871**: 29-39 [PMID: 30419315 DOI: 10.1016/j.bbcan.2018.10.003]
35 **Shen H**, He M, Lin R, Zhan M, Xu S, Huang X, Xu C, Chen W, Yao Y, Mohan M, Wang J. PLEK2 promotes gallbladder cancer invasion and metastasis through EGFR/CCL2 pathway. *J Exp Clin Cancer Res* 2019; **38**: 247 [PMID: 31182136 DOI: 10.1186/s13046-019-1250-8]
36 **Yu X**, Li W, Deng Q, You S, Liu H, Peng S, Liu X, Lu J, Luo X, Yang L, Tang M, Weng X, Yi W, Liu W, Wu S, Ding Z, Feng T, Zhou J, Fan J, Bode AM, Dong Z, Liu J, Cao Y. Neoalbaconol inhibits angiogenesis and tumor growth by suppressing EGFR-mediated VEGF production. *Mol Carcinog* 2017; **56**: 1414-1426 [PMID: 27996164 DOI: 10.1002/mc.22602]
37 **Song Y**, Zhao Y, Ding X, Wang X. microRNA-532 suppresses the PI3K/Akt signaling pathway to inhibit colorectal cancer progression by directly targeting IGF-1R. *Am J Cancer Res* 2018; **8**: 435-449 [PMID: 29636999]
38 **Tang H**, Guo Q, Zhang C, Zhu J, Yang H, Zou YL, Yan Y, Hong D, Sou T, Yan XM. Identification of an intermediate signature that marks the initial phases of the colorectal adenoma-carcinoma transition. *Int J Mol Med* 2010; **26**: 631-641 [PMID: 20878084 DOI: 10.3892/ijmm_00000508]
39 **Zhang Y**, Wang X, Wang Z, Tang H, Fan H, Guo Q. miR-182 promotes cell growth and invasion by targeting forkhead box F2 transcription factor in colorectal cancer. *Oncol Rep* 2015; **33**: 2592-2598 [PMID: 25738520 DOI: 10.3892/or.2015.3833]
40 **Normanno N**, De Luca A, Bianco C, Strizzi L, Mancino M, Maiello MR, Carotenuto A, De Feo G, Caponigro F, Salomon DS. Epidermal growth factor receptor (EGFR) signaling in cancer. *Gene* 2006; **366**: 2-16 [PMID: 16377102 DOI: 10.1016/j.gene.2005.10.018]
41 **Cissé MA**, Sunyach C, Lefranc-Jullien S, Postina R, Vincent B, Checler F. The disintegrin ADAM9 indirectly contributes to the physiological processing of cellular prion by modulating ADAM10 activity. *J Biol Chem* 2005; **280**: 40624-40631 [PMID: 16236709 DOI: 10.1074/jbc.M506069200]
42 **Qiao Y**, Jiang X, Lee ST, Karuturi RK, Hooi SC, Yu Q. FOXQ1 regulates epithelial-mesenchymal transition in human cancers. *Cancer Res* 2011; **71**: 3076-3086 [PMID: 21346143 DOI: 10.1158/0008-5472.CAN-10-2787]
43 **Ota I**, Higashiyama S, Masui T, Yane K, Hosoi H, Matsuura N. Heparin-binding EGF-like growth factor enhances the activity of invasion and metastasis in thyroid cancer cells. *Oncol Rep* 2013; **30**: 1593-1600 [PMID: 23917679 DOI: 10.3892/or.2013.2659]
44 **Zhou ZN**, Sharma VP, Beaty BT, Roh-Johnson M, Peterson EA, Van Rooijen N, Kenny PA, Wiley HS, Condeelis JS, Segall JE. Autocrine HBEGF expression promotes breast cancer intravasation, metastasis and macrophage-independent invasion in vivo. *Oncogene* 2014; **33**: 3784-3793 [PMID: 24013225 DOI: 10.1038/onc.2013.363]
45 **Nabeshima A**, Matsumoto Y, Fukushi J, Iura K, Matsunobu T, Endo M, Fujiwara T, Iida K, Fujiwara Y, Hatano M, Yokoyama N, Fukushima S, Oda Y, Iwamoto Y. Tumour-associated macrophages correlate with poor prognosis in myxoid liposarcoma and promote cell motility and invasion *via* the HB-EGF-EGFR-PI3K/Akt pathways. *Br J Cancer* 2015; **112**: 547-555 [PMID: 25562433 DOI: 10.1038/bjc.2014.637]
46 **Zhang L**, Shimizu D, Killeen JL, Honda SA, Lu D, Stanoyevitch A, Lin F, Wang B, Monuki ES, Carbone M. Serous carcinomatous component championed by heparin-binding EGF-like growth factor (HB-EGF) predisposing to metastasis and recurrence in stage I uterine malignant mixed mullerian tumor. *Hum Pathol* 2016; **53**: 159-167 [PMID: 26980026 DOI: 10.1016/j.humpath.2016.02.014]
47 **Liang SH**, Yan XZ, Wang BL, Jin HF, Yao LP, Li YN, Chen M, Nie YZ, Wang X, Guo XG, Wu KC, Ding J, Fan DM. Increased expression of FOXQ1 is a prognostic marker for patients with gastric cancer. *Tumour Biol* 2013; **34**: 2605-2609 [PMID: 23609035 DOI: 10.1007/s13277-013-0808-x]

World Journal of Gastroenterology

Submit a Manuscript: https://www.f6publishing.com

World J Gastroenterol 2022 May 7; 28(17): 1798-1813

DOI: 10.3748/wjg.v28.i17.1798

ISSN 1007-9327 (print) ISSN 2219-2840 (online)

ORIGINAL ARTICLE

Basic Study

Sirtuin1 attenuates acute liver failure by reducing reactive oxygen species *via* hypoxia inducible factor 1α

Pan Cao, Qian Chen, Chun-Xia Shi, Lu-Wen Wang, Zuo-Jiong Gong

Specialty type: Gastroenterology and hepatology

Provenance and peer review: Unsolicited article; Externally peer reviewed.

Peer-review model: Single blind

Peer-review report's scientific quality classification

Grade A (Excellent): 0
Grade B (Very good): B, B
Grade C (Good): 0
Grade D (Fair): D
Grade E (Poor): 0

P-Reviewer: Cao L, China; Shamseldeen AA, Egypt; Subramaniyan V, Malaysia

Received: October 28, 2021
Peer-review started: October 28, 2021
First decision: December 12, 2021
Revised: December 21, 2021
Accepted: March 25, 2022
Article in press: March 25, 2022
Published online: May 7, 2022

Pan Cao, Qian Chen, Chun-Xia Shi, Lu-Wen Wang, Zuo-Jiong Gong, Department of Infectious Diseases, Renmin Hospital of Wuhan University, Wuhan 430060, Hubei Province, China

Corresponding author: Zuo-Jiong Gong, PhD, Full Professor, Department of Infectious Diseases, Renmin Hospital of Wuhan University, No. 238 Jiefang Road, Wuhan 430060, Hubei Province, China. zjgong@163.com

Abstract

BACKGROUND

The occurrence and development of acute liver failure (ALF) is closely related to a series of inflammatory reactions, such as the production of reactive oxygen species (ROS). Hypoxia inducible factor 1α (HIF-1α) is a key factor that regulates oxygen homeostasis and redox, and the stability of HIF-1α is related to the ROS level regulated by Sirtuin (Sirt) family. The activation of Sirt1 will lead to a powerful antioxidant defense system and therapeutic effects in liver disease. However, little is known about the relationship between HIF-1α and Sirt1 in the process of ALF and the molecular mechanism.

AIM

To investigate whether HIF-1α may be a target of Sirt1 deacetylation and what the effects on ALF are.

METHODS

Mice were administrated lipopolysaccharide (LPS)/D-gal and exposed to hypoxic conditions as animal model, and resveratrol was used as an activator of Sirt1. The cellular model was established with L02 cells stimulated by LPS. N-acetyl-L-cysteine was used to remove ROS, and the expression of Sirt1 was inhibited by nicotinamide. Western blotting was used to detect Sirt1 and HIF-1α activity and related protein expression. The possible signaling pathways involved were analyzed by immunofluorescent staining, co-immunoprecipitation, dihydro-ethidium staining, and Western blotting.

RESULTS

Compared with mice stimulated with LPS alone, the expression of Sirt1 decreased, the level of HIF-1α acetylation increased in hypoxic mice, and the levels of carbonic anhydrase 9 and Bcl-2-adenovirus E1B interacting protein 3 increased significantly, which was regulated by HIF-1α, indicating an increase of HIF-1α activity. Under hypoxia, the down-regulation of Sirt1 activated and

acetylated HIF-1α in L02 cells. The inhibition of Sirt1 significantly aggravated this effect and the massive production of ROS. The regulation of ROS was partly through peroxisome proliferator-activated receptor alpha or AMP-activated protein kinase. Resveratrol, a Sirt1 activator, effectively relieved ALF aggravated by hypoxia, the production of ROS, and cell apoptosis. It also induced the deacetylation of HIF-1α and inhibited the activity of HIF-1α.

CONCLUSION
Sirt1 may have a protective effect on ALF by inducing HIF-1α deacetylation to reduce ROS.

Key Words: Acute liver failure; Deacetylation; Hypoxia inducible factor 1α; Reactive oxygen species; Sirtuin1

©The Author(s) 2022. Published by Baishideng Publishing Group Inc. All rights reserved.

Core Tip: Hypoxia inducible factor 1α (HIF-1α) is a transcription factor that regulates oxygen homeostasis. Under hypoxic conditions, HIF-1α translocates to the nucleus and binds to β-subunits, resulting in transcription of target genes. In acute liver failure, HIF-1α contributes to early liver cell necrosis. The activation of Sirtuin1 (Sirt1) will result in a powerful antioxidant defense system. This study examined the influence of Sirt1-mediated pathways on HIF-1α expression *in vivo* and *in vitro*, explored the relationship between Sirt1 and HIF-1α, and further explored its potential mechanism.

Citation: Cao P, Chen Q, Shi CX, Wang LW, Gong ZJ. Sirtuin1 attenuates acute liver failure by reducing reactive oxygen species *via* hypoxia inducible factor 1α. *World J Gastroenterol* 2022; 28(17): 1798-1813
URL: https://www.wjgnet.com/1007-9327/full/v28/i17/1798.htm
DOI: https://dx.doi.org/10.3748/wjg.v28.i17.1798

INTRODUCTION

Acute liver failure (ALF) refers to a large number of necrosis of liver cells or severe liver damage caused by various reasons[1]. ALF is often accompanied by coagulation dysfunction and progressive multiple organ failure due to liver metabolism disorders and decreased immune function[2]. The occurrence and development of ALF is closely related to a series of inflammatory reactions, such as the release of inflammatory cytokines and the production of reactive oxygen species (ROS)[3].

Hypoxia-inducible factor (HIF)-1 consists of an oxygen-regulated subunit HIF-1α and a constitutive expression subunit HIF-1β. The activity and stability of the alpha subunit of HIF are regulated by its post-translational modifications such as acetylation[4]. Under hypoxic conditions, HIF-1α acts as a primary transcription factor to regulate hypoxia-related anti-inflammatory responses[5]. HIF-1α is a key factor that regulates oxygen homeostasis and redox and promotes effective adaptation to hypoxia[6]. During the development of liver diseases such as liver cancer, hypoxia is a common finding. Hypoxia promotes the stabilization of HIF-1α. HIF signal in innate immune cells and liver cancer cells is beneficial to the recruitment and maintenance of primordial tumorigenic immune cells and promotes immune evasion[7].

The monitoring of HIF-1α activity by members of the Sirtuin (Sirt) family has been a topic of interest in recent years[8-10]. According to reports, HIF-1α has been confirmed to be related to Sirt1, Sirt2, and Sirt3 in the Sirt family, and the stability of HIF-1α is related to the ROS level regulated by Sirt3 and the oxygen level regulated by Sirt6[11-14]. Sirt2 causes protein hydroxylation and ubiquitination by increasing the binding of HIF-1α to propylamine hydroxylase[8]. However, the regulation mechanism of Sirt1 on HIF-1α activity has always been a controversial topic.

Sirt1 in the sirtuin family is a nicotinamide adenine dinucleotide-dependent protein lysine deacetylase with diverse physiological functions such as anti-inflammation, neuronal signaling, DNA repair, and stress response. Sirt1 has been shown to be an important target for the treatment of various diseases[15,16], and its activation will lead to a powerful antioxidant defense system and therapeutic effects in liver ischemia reperfusion[17]. Studies have shown that Sirt1 regulates HIF-1α through the formation of physical complexes between proteins, and Sirt1 may have a negative regulatory effect on HIF-1α[18]. Sirt1 has also been reported to regulate HIF-1α actively by stabilizing the protein[19]. Whether Sirt1 is used as a negative regulator or a positive regulator of HIF-1α or depends on the experimental conditions or experimental models remains to be further studied.

In this study, we examined the regulation of Sirt1 on HIF-1α activity in ALF and explored its possible molecular mechanisms.

MATERIALS AND METHODS

Mice

Male C57BL/6J wild-type mice aged 5-6 wk were purchased from Wuhan Biomedical Research Institute of Wuhan University. All mice were raised in the specific pathogen free animal facility of Renmin Hospital of Wuhan University with conditions of light-controlled, room temperature 25 °C, and humidity 55 ± 5%, and they were free to eat and drink. All animal operations were approved by the Animal Care and Use Committee of Renmin Hospital of Wuhan University, China (Approval No. WDRY2021-K016).

Animal models

The mice were randomly divided into six groups with 6 mice in each group: Saline control group; Hypoxia group; Lipopolysaccharide (LPS) group; Hypoxia + LPS group; Resveratrol group; and LPS + Hypoxia + Resveratrol group. Hypoxia group and Hypoxia + LPS group were cultured in COY Vinyl Anaerobic Chambers (COY, Grass Lake, MI, United States). To avoid pulmonary and cerebral edema caused by a rapid drop in oxygenation, the fraction of inspired oxygen (FiO_2) (1%/d) was gradually decreased from 21% normoxia (room-air oxygen) to 8% oxygen (severe hypoxia) over the course of 2 wk, followed by continual exposure to 8% oxygen for an additional 2 wk. On the 14th d after being exposed to 8% oxygen, Resveratrol (10 mg/kg; Sigma–Aldrich, St. Louis, MI, United States)[20] was given intragastrically in Resveratrol group and LPS + Hypoxia + Resveratrol group while LPS (100 μg/kg; Sigma–Aldrich) was administrated by intraperitoneal injection combined with D-Gal (400 mg/kg) in LPS group and LPS + Hypoxia + Resveratrol group[21]. Twenty-four hours after LPS administration, animals were quickly euthanized with inhaled CO_2, followed by the collection of blood samples and liver tissues[21].

Cell culture

Human embryonic liver cell line L02 was purchased from China Center for Type Culture Collection (Wuhan, China). N-acetyl-L-cysteine (NAC) (Beyotime, Shanghai, China) (5 mmol/L)[22], nicotinamide (NAM) (Beyotime) (5 mmol/L)[23], GW6471 (Sigma-Aldrich) (3 μM)[24] or Compound C (Sigma-Aldrich) (10 μM)[25], which were dissolved in dimethyl sulfoxide (Sigma-Aldrich), were used to pretreat L02 cells for 1 h, followed by LPS (5 μg/mL)[26] treatment. Hypoxic conditions (1% O_2) were obtained using humidified variable aerobic workstation InVivo2 400 (Ruskinn, Pencoed, United Kingdom)[27]. For transient transfection, cells were transfected with 2 μg plasmid of pECE-flag-Sirt1 (Addgene, Cambridge, MA, United States) and pECE empty vector (Addgene).

Biochemical analyses

Blood samples were collected after mice were anesthetized. The level of malondialdehyde (Cat. No. GM1134), superoxide dismutase (Cat. No. GM1133), and glutathione peroxidase (Cat. No. GM1135) were determined with commercial kits (Servicebio, Wuhan, China), respectively, according to the manufacturer's instructions.

Histopathological examination

The liver tissues were sliced completely and stained with hematoxylin-eosin. The pathological changes of liver tissue were observed and evaluated by light microscope (Olympus, Tokyo, Japan). The degree of liver damage in the ALF models were assessed by the liver histology score.

Immunofluorescent staining

Liver tissue sections were intact, and L02 cell suspensions were fixed on glass slides. Sections were fixed with 4% paraformaldehyde for 30 min, and 50-100 μL membrane rupture working solution and 3 % hydrogen peroxide solution were added in sequence according to the manufacturer's instructions. Primary antibody against acetyl-lysine or HIF-1α (Santa Cruz Biotechnologies, Dallas, TX, United States) diluted 1:100 with 5% bovine serum albumin was added on the slides and tissue sections, and the slides were incubated overnight at 4 °C in a wet box. Then, slides were incubated with secondary antibody (1:50 dilution, Beyotime), and they were imaged using a fluorescent microscope (Olympus).

Immunoprecipitation

Approximately 1 mg of total protein was incubated with anti-Sirt1 antibody (Servicebio) or anti-HIF-1α antibody (Servicebio) overnight at 4 °C followed by precipitation with 20 μl of protein A/G-Plus-Agarose (Servicebio) for 4 h at 4 °C. The precipitated complex was immunoblotted with anti-Sirt1, anti-HIF-1α, or anti-acetyl-lysine.

Detection of ROS production

L02 cell suspensions were fixed on glass slides. Cell culture fluid (2 mL) was added and the culture was continued for about 6 h. Dihydroethidium (1 mL) (Cat. No. GDP1018), which was dissolved in dimethyl

sulfoxide at a ratio of 1:1000, was added to each well, and the samples were incubated in the dark. An appropriate amount of DAPI solution was added to the wells and stained. Then, a drop of anti-fluorescence quenching medium was added into the hole; the slides were imaged under a fluorescent microscope.

Western blotting

Proteins were extracted from cells and tissues as directed by the radioimmunoprecipitation assay kit (Sigma-Aldrich). An appropriate amount of concentrated sodium dodecyl sulfate polyacrylamide gel electrophoresis protein loading buffer was added to the collected protein samples, and then 5-10 μL of the sample was loaded in the sodium dodecyl sulfate polyacrylamide gel electrophoresis gel sample holes. Low voltage constant pressure electrophoresis for the upper gel and high voltage constant voltage electrophoresis were applied, when bromophenol blue entered the lower gel. After electrophoresis, the proteins were transferred to polyvinylidene fluoride membranes. The following primary antibodies were used: Sirt1 (Cat. No. 9475, Cell Signaling Technology, Danvers, MA, United States), peroxisome proliferator-activated receptor alpha (PPARα, Cat. No. 23398R, Bioss, Woburn, MA, United States), HIF-1α (Cat. No. 20398R, Bioss), AMP-activated protein kinase (AMPK, Cat. No. 32047, Abcam, Cambridge, United Kingdom), p-AMPK (Cat. No. 131357, Abcam), Bnip3 (Cat. No. 109414, Abcam), and glyceraldehyde-3-phosphate dehydrogenase (Cat. No. 8245, Abcam). Image Lab statistical software (Bio-Rad, Hercules, CA, United States) was used to evaluate band intensities on Western blots.

Statistical analyses

Statistical analysis was performed using GraphPad Prism software version 8.0 (San Diego, CA, United States). The Y axis was labeled as fold of control mean. Data were expressed as the means ± standard deviations. Differences among multiple groups were evaluated using conventional Student's *t* test or analysis of variance. Statistical significance was considered at $P < 0.05$.

RESULTS

Hypoxia aggravated ALF and increased the expression and acetylation of HIF-1α

The liver structure of each group was shown by histopathological examination. Compared with the control group, large-scale hepatocyte necrosis in the LPS and Hypoxia groups and the number of infiltrating inflammatory cells were significantly increased, while the inflammatory response was significantly more severe in the LPS + Hypoxia group (Figure 1A). Next, we tested the expression of some key proteins in ALF. As shown in Figure 1B, compared with the control group, the expression of Sirt1 in the LPS group was significantly reduced, and hypoxia aggravated this effect. The expression of Bcl-2 adenovirus E1B-interacting protein 3 (Bnip3) in the LPS + hypoxia group was significantly increased, as was carbonic anhydrase 9 (CA9), both of which are regulated by HIF-1α, suggesting that hypoxia significantly increased the activity of HIF-1α in the LPS group. Of note, the expression of HIF-1α in the LPS + Hypoxia group was significantly increased in the form of acetylation. LPS significantly increased HIF-1α acetylation induced by hypoxia (Figure 1C).

Hypoxia reduced the expression of Sirt1, causing the activation and acetylation of HIF-1α

To detect changes in the expression of Sirt1 in L02 cells during hypoxia, we measured the expression levels of Sirt1, HIF-1α, and Bnip3 using Western blotting. Compared to the control group, hypoxia reduced Sirt1 expression and upregulated HIF-1α and Bnip3 expression in a time-dependent manner (Figure 2A-D). Through immunofluorescence experiments, we found that as the duration of hypoxia increased, the expression of HIF-1α increased significantly in the form of acetylation (Figure 2E). We then analyzed the interaction between Sirt1 and HIF-1α. After hypoxia induced endogenous HIF-1α, Sirt1-HIF-1α binding was observed (Figure 2F). We next examined whether Sirt1 deacetylates HIF-1α. Immunoblotting with anti-acetyl-lysine in HIF-1α immunoprecipitates was used to detect the lysine acetylation level of HIF-1α. As shown in Figure 2G, Sirt1 overexpression significantly decreased HIF-1α acetylation, suggesting that Sirt1 regulated lysyl acetylation of HIF-1α. These results suggested that hypoxia-induced enhancement of HIF-1α activity and lysine acetylation were related to the down-regulation of Sirt1.

The inhibition of Sirt1 induced activation of HIF-1α and subsequently increased the production of ROS induced by hypoxia

Next, we explored the possible molecular mechanisms of the interaction between Sirt1 and HIF-1α. As shown in the Figure 3A, LPS increased the expression of HIF-1α, and the expression of Sirt1 was further reduced after HIF-1α was increased by hypoxia in L02 cells. At the same time, the use of a specific Sirt1 inhibitor NAM to inhibit Sirt1 further aggravated this effect. Sirt1 appear to interact with HIF-1α in L02 cells. Studies have found that excessive production of ROS is considered harmful and related to hypoxia [28]. Oxidative stress has been shown to promote inflammation during ALF[29]. How oxidative stress is

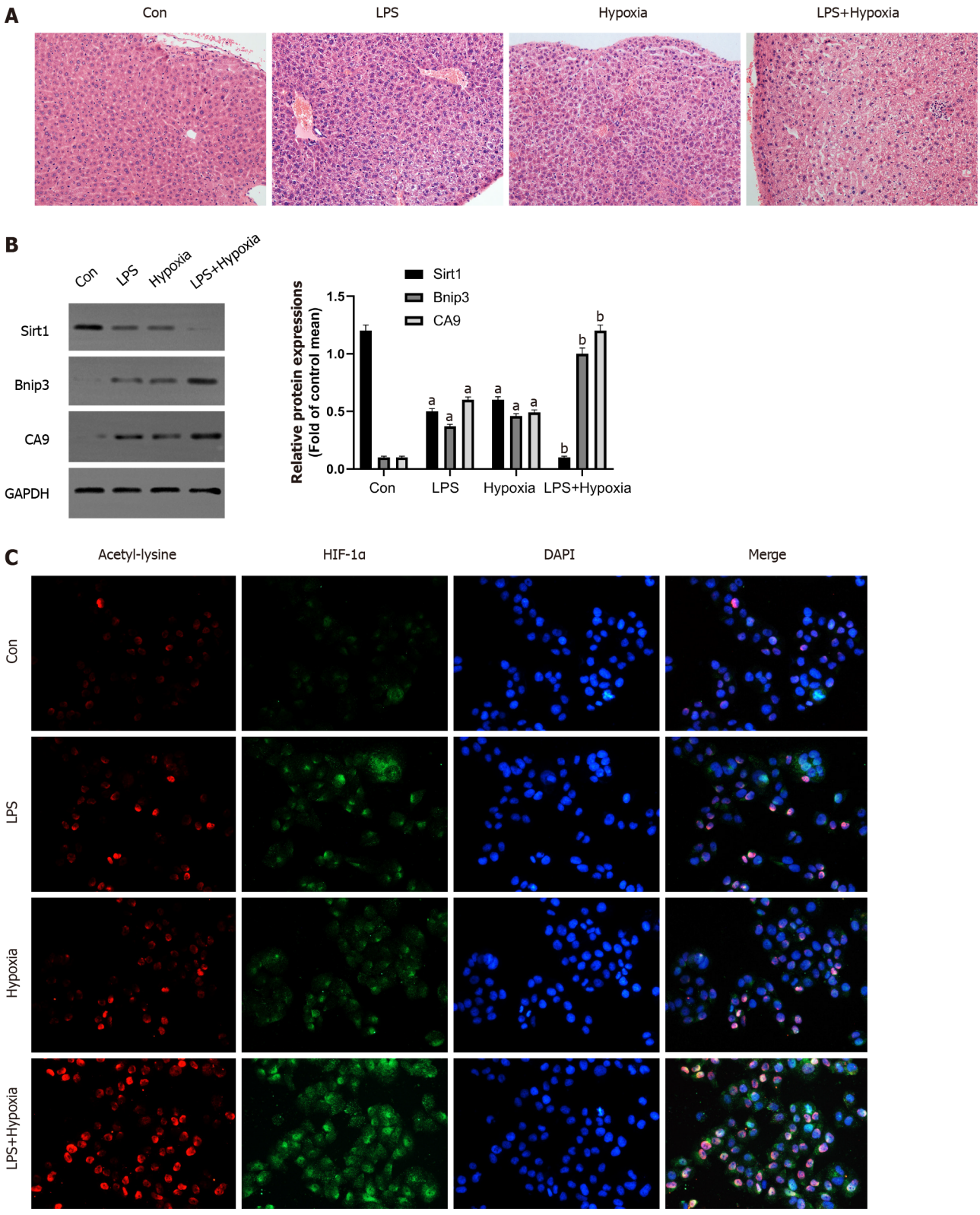


Figure 1 Hypoxia aggravated acute liver failure and increased the expression of hypoxia inducible factor-1α and its acetylation. A: The representative images of hematoxylin and eosin staining of liver in each group; B: Western blotting was performed to measure the levels of Sirtuin1 (Sirt1), Bcl-2 adenovirus E1B-interacting protein 3 (Bnip3) and carbonic anhydrase 9 (CA9) in liver tissues; C: The representative images of immunofluorescence staining for Acetyl-lysine and hypoxia inducible factor (HIF)-1α. Data shown are means ± standard deviation of three separate experiments. $^{a}P < 0.05$ *vs* Control group; $^{b}P < 0.05$ *vs* Lipopolysaccharide (LPS)-treated group; one-way analysis of variance combined with Bonferroni's *post hoc* test; the error bars indicate the standard deviations. GAPDH: Glyceraldehyde-3-phosphate dehydrogenase.

involved in inflammation during ALF remains unclear. Therefore, we examined the antioxidant effect of Sirt1 during hypoxia. DHE staining showed that the level of ROS stimulated by LPS was significantly increased by hypoxia, and this effect was enhanced when NAM was used to inhibit the Sirt1 signaling

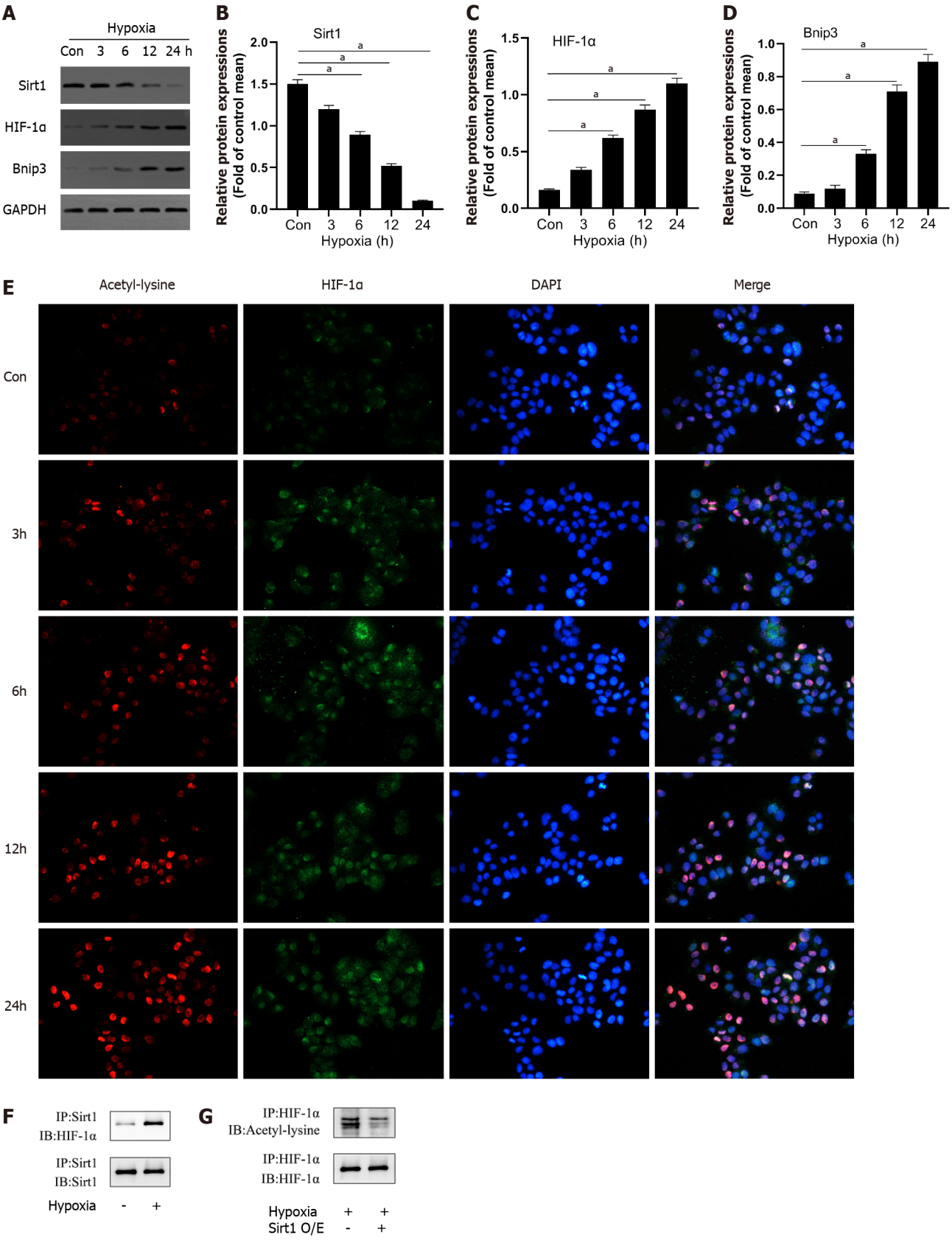


Figure 2 Hypoxia decreased Sirtuin1 expression leading to the acetylation and activation of hypoxia inducible factor-1α. A-D: Western blotting was performed to measure the levels of Sirtuin1 (Sirt1), Bcl-2 adenovirus E1B-interacting protein 3 (Bnip3), and hypoxia inducible factor (HIF)-1α in L02 cells; E: The representative images of immunofluorescence staining for Acetyl-lysine and HIF-1α; F and G: Equal amounts of protein were subjected to immunoprecipitation with Sirt1 antibody or HIF-1α antibody followed by immunoblotting with antibody against Sirt1, HIF-1α, or acetyl-lysine and effect of Sirt1 overexpression (O/E) was shown. Data shown are means ± standard deviations (SDs) of three separate experiments. $^{a}P < 0.05$ *vs* Control group; one-way analysis of variance combined with Bonferroni's *post hoc* test; the error bars indicate the SDs.

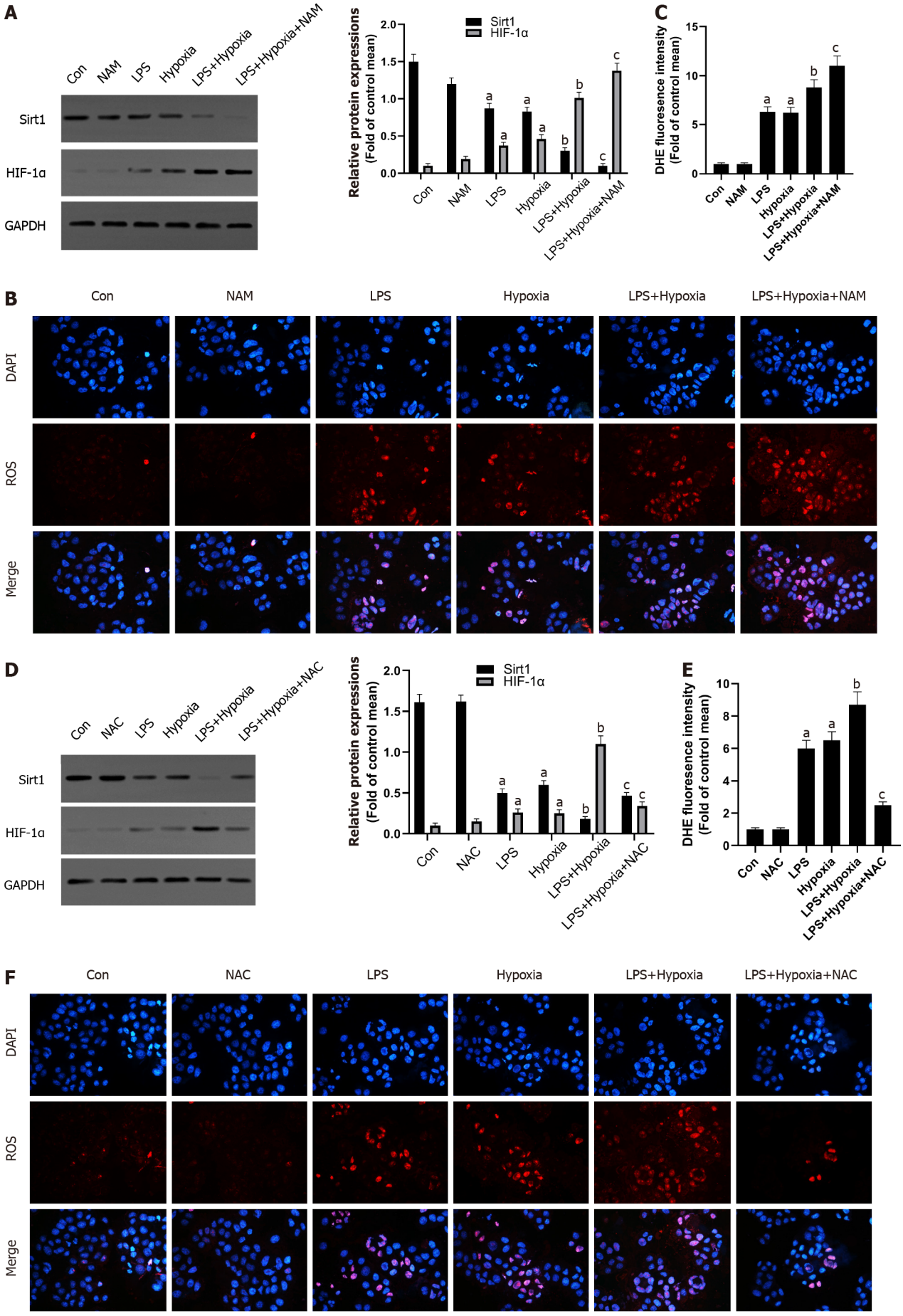


Figure 3 The inhibition of Sirtuin1 induced activation of hypoxia inducible factor-1α and subsequently increased hypoxia-induced

reactive oxygen species production. A: Western blotting was performed to measure the levels of Sirtuin1 (Sirt1) and hypoxia inducible factor (HIF)-1α in L02 cells; B: Reactive oxygen species (ROS) productions were detected by dihydroethidium (DHE) staining. Representative images of the DHE staining in different groups; C: ROS productions were evaluated by quantification of mean fluorescence intensity in DHE staining; D: Western blotting was performed to measure the levels of Sirt1 and HIF-1α in L02 cells; E and F: ROS productions were detected by DHE staining. Data shown are means ± standard deviations (SDs) of three separate experiments. [a]*P* < 0.05 *vs* Control group; [b]*P* < 0.05 *vs* Lipopolysaccharide (LPS)-treated group; [c]*P* < 0.05 *vs* LPS + Hypoxia-treated group; one-way analysis of variance with Bonferroni's *post hoc* test; the error bars indicate the SDs.

pathway (Figure 3B and C). Next, we found that the expression of Sirt1 was increased and HIF-1α was opposite when NAC was used, which is an effective ROS scavenger (Figure 3D). At the same time, LPS-induced levels of ROS were significantly reversed by NAC (Figure 3E and F).

The inhibition of Sirt1/PPARα signaling pathway increased hypoxia-induced ROS production in vitro

Some studies have shown that liver PPARα expression is lower in patients with hepatitis C and advanced nonalcoholic fatty liver disease, perhaps due to the inhibitory effect of multiple cytokines[30]. This also shows that increasing PPARα may help reduce liver inflammation. In our study, as shown in Figure 4A, in the L02 cells stimulated by LPS, PPARα expression was decreased and aggravated after hypoxia intervention, and its effect was further aggravated when NAM was used to inhibit the Sirt1 signaling pathway, suggesting that hypoxia-induced PPARα inhibition was closely related to Sirt1. In addition, Sirt1 expression was further reduced by the PPARα inhibitor GW6471, while HIF-1α was opposite (Figure 4B) and the levels of ROS were also improved (Figure 4C), suggesting that the inhibition of Sirt1/PPARα signaling pathway might increase hypoxia-induced ROS production in L02 cells.

The inhibition of Sirt1/AMPK signaling pathway increased hypoxia-induced ROS production in vitro

AMPK acts as a regulator of cellular energy metabolism and redox homeostasis. More and more evidence shows that AMPK plays a protective role by regulating the redox system[31]. Next, we further studied whether Sirt1 can regulate AMPK and its role in cell hypoxia in L02 cells. As shown in Figure 5A, the phosphorylation level of AMPK in L02 cells induced by LPS after hypoxia treatment was significantly reduced, while NAM pretreatment aggravated this effect, indicating AMPK could be modulated by hypoxia *via* Sirt1. In addition, AMPK inhibitor Compound C further reduced the expression of Sirt1, the expression of HIF-1α was further increased (Figure 5B), and the levels of ROS were also improved (Figure 5C). Therefore, these results suggested that Sirt1/AMPK signaling pathway might be involved in modulating ROS in LPS-stimulated L02 cells during hypoxia.

The activation of Sirt1 induced the inactivation and deacetylation of HIF-1α and subsequently rescued the progressive aggravation of ALF induced by hypoxia in vivo

Finally, to determine further whether Sirt1 attenuated the progressive aggravation of ALF induced by hypoxia through the Sirt1/AMPK or the Sirt1/PPARα pathway, LPS-stimulated mice were exposed to hypoxia with or without resveratrol treatment, which is a Sirt1 activator. Compared with the LPS group, activation of Sirt1 by resveratrol alleviated the more sever liver tissue damage in the LPS + Hypoxia group (Figure 6A and B). LPS + Hypoxia group mice showed lower activity of superoxide dismutase and glutathione peroxidase, while malondialdehyde levels were increased, indicating that hypoxia led to decreased antioxidant activity. However, resveratrol treatment could significantly improve the activity (Figure 6C). As shown in Figure 6D, resveratrol dramatically alleviated hypoxia-induced reduction levels of PPARα protein and the phosphorylation of AMPK in LPS-stimulated mice, suggesting that Sirt1 was a key regulator on the activation of PPARα and the phosphorylation of AMPK during hypoxia in ALF. Finally, we demonstrated with animals whether Sirt1 has a regulatory effect on hypoxia-induced HIF-1α lysine acetylation and HIF-1α activity. As shown in Figure 6E, with the intervention of resveratrol, the expression of HIF-1α and the level of acetylation decreased significantly. These findings indicate that the activation of Sirt1 induced HIF-1α inactivation and deacetylation, thereby alleviating the progressive aggravation of ALF induced by hypoxia.

DISCUSSION

Recently, more and more studies have confirmed the effect of Sirt1 in liver disease. Sirt1 has been confirmed to have a protective effect in a variety of disease models, including liver fibrosis[32], drug-induced liver injury[33], non-alcoholic fatty liver disease[34], and fatty liver[35]. As well known, HIF-1α is a transcription factor that can promote the adaptive response of cells to hypoxia. Some reports have mentioned the connection between Sirt1 and HIF protein, but there are still many controversies about the results. According to reports, in hypoxic Hep3B or HEK293 cells, Sirt1 targeted HIF-2α and increased the transcriptional activity of HIF-2α but not HIF-1α[36]. On the contrary, another group of studies

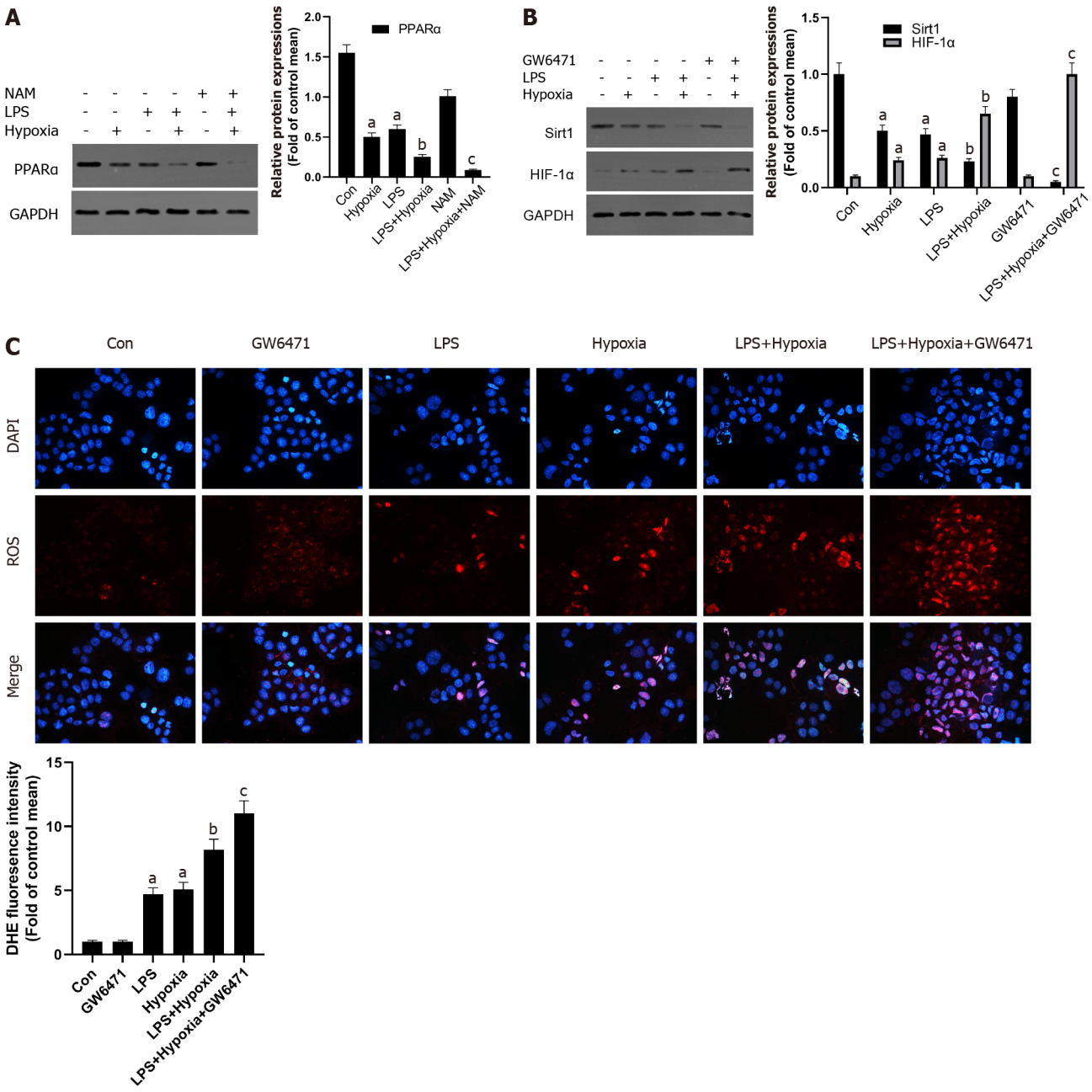


Figure 4 The inhibition of Sirtuin1/peroxisome proliferator-activated receptor alpha signaling pathway increased hypoxia-induced reactive oxygen species production. A: Western blotting was performed to measure the levels of peroxisome proliferator-activated receptor alpha (PPARα) in L02 cells; B: The levels of Sirtuin1 (Sirt1) and hypoxia inducible factor (HIF)-1α in L02 cells; C: Reactive oxygen species productions were detected by dihydroethidium (DHE) staining and evaluated by quantification of mean fluorescence intensity in DHE staining. Data shown are means ± standard deviations (SDs) of three separate experiments. $^{a}P < 0.05$ *vs* Control group; $^{b}P < 0.05$ *vs* Lipopolysaccharide (LPS)-treated group; $^{c}P < 0.05$ *vs* LPS + Hypoxia-treated group; one-way analysis of variance with Bonferroni's *post hoc* test; the error bars indicate the SDs.

showed that Sirt1 interacted with HIF-1α, causing HIF-1α deacetylation to promote its activity in Hep3B and Huh7 cells[19]. Therefore, the regulation of Sirt1 on the activity of HIF-1α and its expression seems to be cell-type-specific, which is currently unclear. It has not been reported that the beneficial effect of Sirt1 activation is related to its HIF-1α deacetylation against ALF.

In our research, we found that the activity of HIF-1α increased after acetylation and promoted hepatocyte apoptosis in ALF models and hypoxia models *in vitro*. In addition, we demonstrated that the expression of Sirt1 in L02 cells decreased in a time-dependent manner due to hypoxia, which was closely related to the activation and acetylation of HIF-1α. During hypoxia, with the decrease of the level of nicotinamide adenine dinucleotide, the activity of Sirt1 decreased and HIF-1α transcription activity further increased[18,19]. Therefore, the insufficient expression of Sirt1 in the liver or the acetylation of HIF-1α might be the key mediators of ALF.

Next, we carefully evaluated Sirt1's regulatory effect on HIF-1α activity in ALF and explored its possible molecular mechanisms. ROS are by-products of normal metabolism in living cells, but

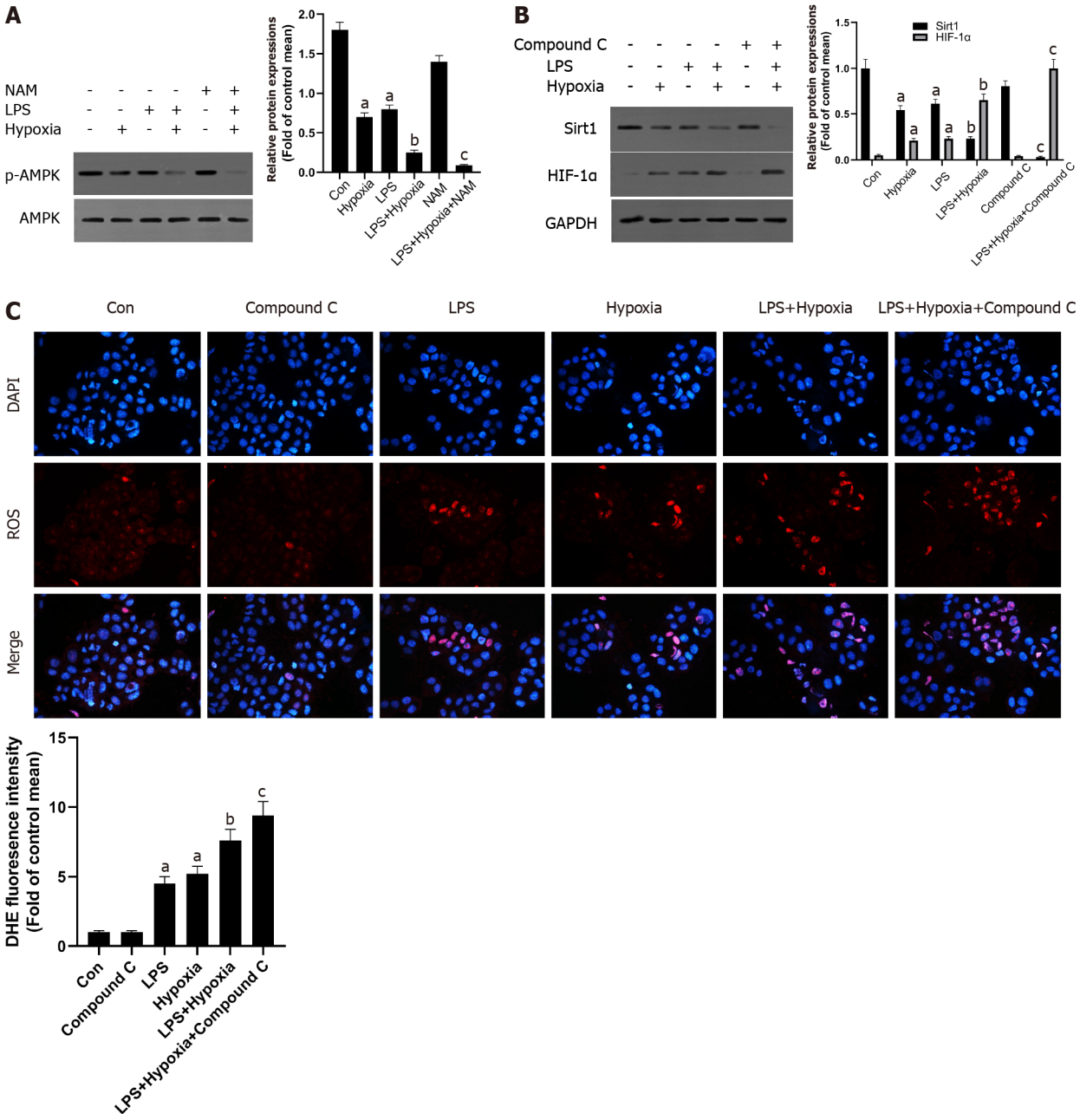
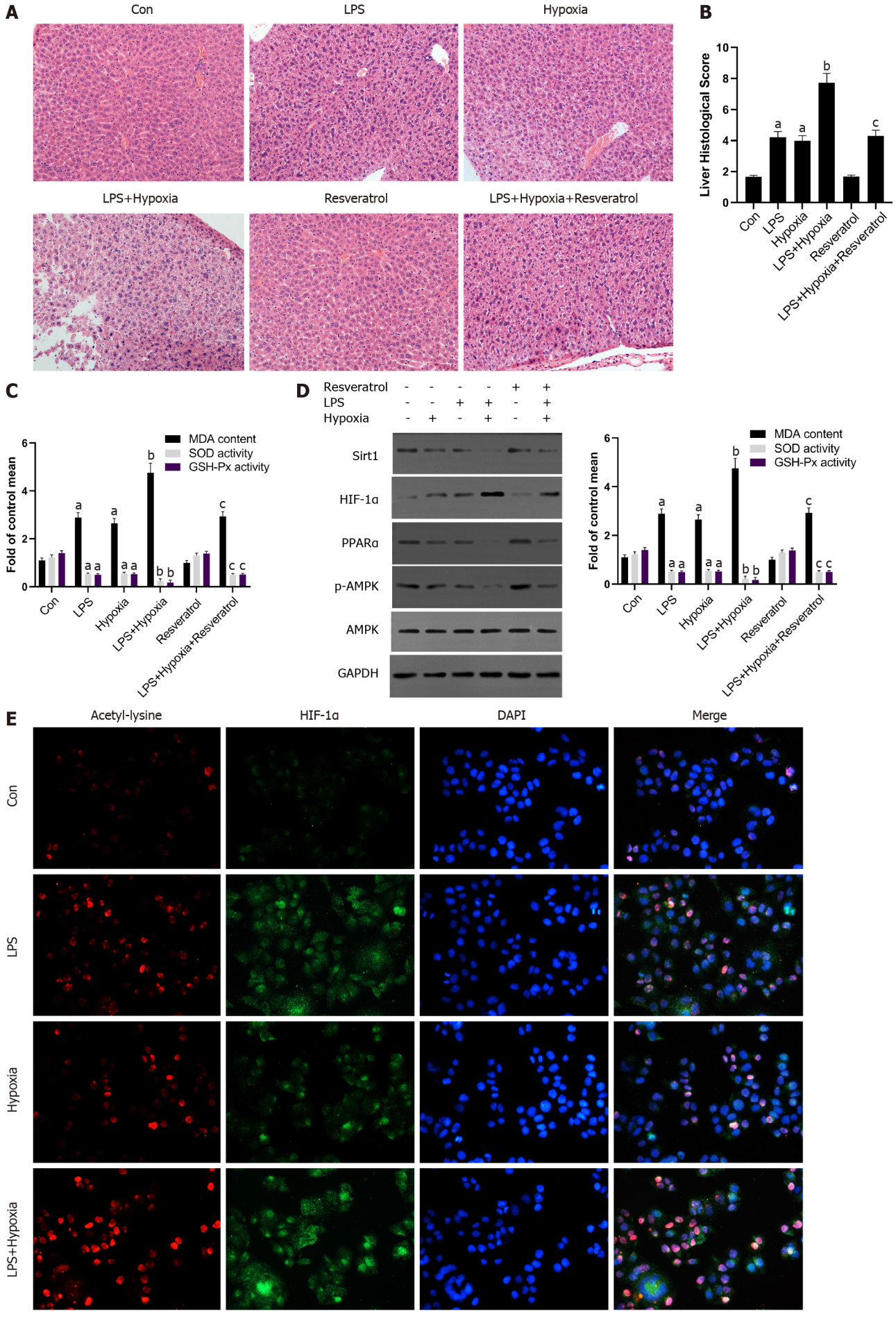


Figure 5 The inhibition of Sirtuin1/AMP-activated protein kinase signaling pathway increased hypoxia-induced reactive oxygen species production. A: Western blotting was performed to measure the levels of AMP-activated protein kinase (AMPK) and p-AMPK in L02 cells; B: The levels of Sirtuin1 (Sirt1) and hypoxia inducible factor (HIF)-1α in L02 cells; C: Reactive oxygen species (ROS) productions were detected by dihydroethidium (DHE) staining and evaluated by quantification of mean fluorescence intensity in DHE staining. Data shown are means ± standard deviations (SDs) of three separate experiments. $^{a}P < 0.05$ *vs* Control group; $^{b}P < 0.05$ *vs* Lipopolysaccharide (LPS)-treated group; $^{c}P < 0.05$ *vs* LPS + Hypoxia-treated group; one-way analysis of variance combined with Bonferroni's post hoc test; the error bars indicate the SDs.

excessive ROS accumulation can damage organelles, leading to increased oxidative stress[37,38]. ALF produces excessive amounts of ROS due to insufficient detoxification of toxic substances in the liver [39]. Sirt1 has been reported to play an important role in anti-inflammatory and antioxidant processes [40]. Here, we demonstrated that HIF-1α was over-activated in hypoxia due to increased level of ROS in the absence of Sirt1, and the effect was inhibited by the antioxidant NAC, indicating that ROS was involved in this activation.

In particular, PPARα is reported to be a potent inhibitor of NF-κB signaling pathway and inflammation[41]. The positive effect of Sirt1 on the inflammatory pathway may be related to PPARα[42], and the interference of PPAR transcriptional activity may disturb estrogen/androgen receptor expression and impair steroidogenesis and ROS metabolism[43]. In addition, PPARα contributes to the protection of redox homeostasis[44]. Previous studies have confirmed that Sirt1 can regulate AMPK, which is an important energy sensor[45]. AMPK acts as a regulator of cellular energy metabolism and redox homeostasis. More and more evidence shows that AMPK plays a cardiovascular protective role by


A
Con
LPS
Hypoxia
LPS+Hypoxia
Resveratrol
LPS+Hypoxia+Resveratrol
B
Liver Histological Score
Con
LPS
Hypoxia
LPS+Hypoxia
Resveratrol
LPS+Hypoxia+Resveratrol
C
MDA content
SOD activity
GSH-Px activity
Fold of control mean
D
Resveratrol
LPS
Hypoxia
Sirt1
HIF-1α
PPARα
p-AMPK
AMPK
GAPDH
E
Acetyl-lysine
HIF-1α
DAPI
Merge
Con
LPS
Hypoxia
LPS+Hypoxia

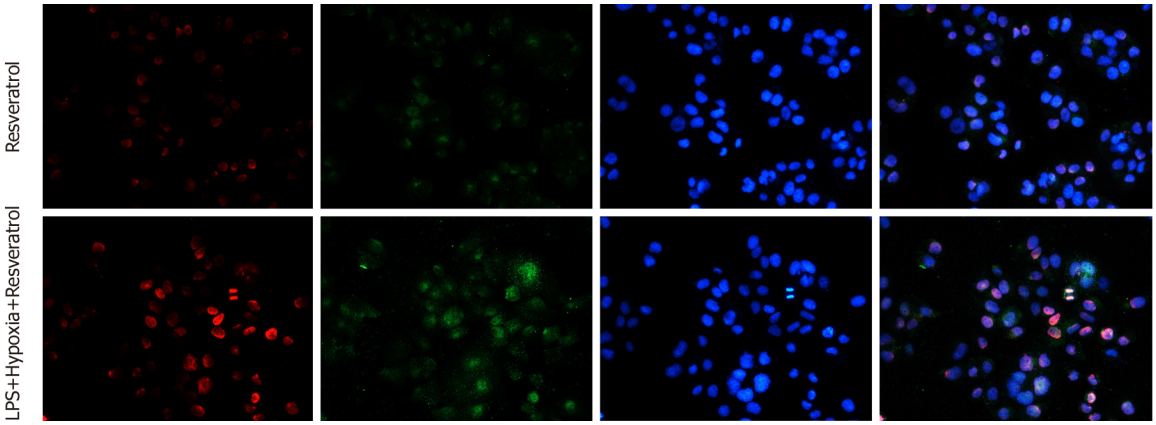


Figure 6 The activation of Sirtuin1 induced the deacetylation and inactivation of hypoxia inducible factor-1α, and subsequently rescued the progressive aggravation of acute liver failure induced by hypoxia. A: Mice were pretreated with resveratrol or exposed to hypoxia and then stimulated with lipopolysaccharide (LPS). The representative images of hematoxylin and eosin staining of liver in each group; B: The liver histological score of liver in each group; C: The levels of malondialdehyde (MDA), superoxide dismutase (SOD), and glutathione peroxidase (GSH-Px) of mice in each group; D: Western blotting was performed to measure the levels of Sirtuin1 (Sirt1), hypoxia inducible factor (HIF)-1α, peroxisome proliferator-activated receptor alpha (PPARα) and p-AMP-activated protein kinase (AMPK) in liver tissues and the protein expression were quantified; E: The representative images of immunofluorescence staining for Acetyl-lysine and HIF-1α. Data shown are means ± standard deviations (SDs) of three separate experiments. $^{a}P < 0.05$ *vs* Control group; $^{b}P < 0.05$ *vs* LPS-treated group; $^{c}P < 0.05$ *vs* LPS + Hypoxia-treated group; one-way analysis of variance combined with Bonferroni's *post hoc* test; the error bars indicate the SDs.

regulating the redox system[46]. In diabetes, the activation of AMPK increases the expression of mitochondrial antioxidant enzymes and leads to a decrease in the production of mitochondrial ROS in endothelial cell[47].

Our experiments revealed that the inhibition of PPARα and the phosphorylation of AMPK induced by hypoxia were closely related to Sirt1, and the inhibition of Sirt1/PPARα or Sirt1/AMPK signaling pathway might increase hypoxia-induced ROS production in L02 cells. In order to determine whether the activation of Sirt1 induced inactivation of HIF-1α, the progressive aggravation of ALF induced by hypoxia *in vivo* was rescued in mice treated with resveratrol. As expected, the activation of Sirt1 significantly alleviated the degree of liver damage in ALF and enhanced antioxidant activity. Resveratrol dramatically alleviated the hypoxia-induced reduction level of PPARα protein and the phosphorylation of AMPK in LPS-stimulated mice. In addition, the activation of Sirt1 induced the deacetylation of HIF-1α compared to LPS-stimulated mice exposed to hypoxia; the expression of HIF-1α and the level of acetylation decreased significantly.

One limitation of our study is that we did not use HIF-1α overexpressing mice *in vivo* to test whether the increase of Sirt1 activity can rescue ALF. We need to conduct further experiments to solve this problem.

CONCLUSION

In summary, we have demonstrated that Sirt1 reduced oxidative stress in ALF by regulating the activity and acetylation of HIF-1α, achieved by normalizing the Sirt1/PPARα and Sirt1/AMPK pathway. Our research showed that the deacetylation and inactivation of HIF-1α induced by the activation of Sirt1 might have therapeutic benefits in reducing liver damage during ALF.

ARTICLE HIGHLIGHTS

Research background

Acute liver failure (ALF) is a life-threatening disease that can rapidly develop into multiple organ failure. The mortality rate is high. If effective treatment measures are not taken, various complications will occur, including cerebral edema, sepsis, renal failure, gastrointestinal bleeding, and respiratory failure. Hypoxia inducible factor 1α (HIF-1α) is a transcription factor that regulates oxygen homeostasis. In ALF, HIF-1α contributes to early liver cell necrosis. Sirtuin1 (Sirt1) plays a key role in health by deacetylating target proteins in many tissues, including the liver. The activation of Sirt1 will result in a powerful antioxidant defense system. However, the role of Sirt1 in ALF and the relationship between Sirt1 and HIF-1α remain unclear and require further investigation.

Research motivation

The results of this study might provide a basis for the application of Sirt1 in the treatment of ALF and further understanding of the mechanism of Sirt1 and HIF-1α in the process of ALF.

Research objectives

This study detected the changes in the expression of Sirt1 and HIF-1α in liver tissues and hepatocytes under hypoxia during the ALF process as well as the differences in the expression levels of key enzymes. In addition, this study further explored the relationship and mechanism of Sirt1 signaling pathway and HIF-1α expression.

Research methods

Western blotting was used to detect the expression levels of Sirt1 and HIF-1α related proteins in mouse liver tissues, and immunofluorescence staining was used to observe the acetylation level of HIF-1α. Detection of HIF-1α and reactive oxygen species (ROS) levels and the correlation analysis between Sirt1 and HIF-1α were performed. Finally, Sirt1 was activated to observe the influence of the Sirt1 signaling pathway and HIF-1α on ALF, and changes in the expression levels of related markers were detected.

Research results

The expression of Sirt1 decreased and the level of HIF-1α acetylation increased in hypoxic mice, and the levels of carbonic anhydrase 9 and Bcl-2-adenovirus E1B interacting protein 3 increased significantly, which was regulated by HIF-1α, indicating an increase of HIF-1α activity. Under hypoxia, the down-regulation of Sirt1 activated and acetylated HIF-1α in L02 cells. The inhibition of Sirt1 significantly aggravated this effect and the massive production of ROS. The regulation of ROS was partly through peroxisome proliferator-activated receptor alpha or AMP-activated protein kinase (AMPK). The activation of Sirt1 effectively relieved ALF aggravated by hypoxia, the production of ROS, and cell apoptosis. It also induced the deacetylation of HIF-1α and inhibited the activity of HIF-1α.

Research conclusions

The inhibition of peroxisome proliferator-activated receptor alpha and the phosphorylation of AMPK induced by hypoxia were closely related to Sirt1, and the inhibition of Sirt1/PPARα or Sirt1/AMPK signaling pathway might increase hypoxia-induced ROS production. The activation of Sirt1 reduced oxidative stress in ALF by regulating the activity and acetylation of HIF-1α.

Research perspectives

The results of this study showed that the deacetylation and inactivation of HIF-1α induced by the activation of Sirt1 might have therapeutic benefits in reducing liver damage during ALF. This study preliminarily clarified the role of Sirt1 and HIF-1α in ALF, so as to deepen the understanding of the mechanism of ALF, and provided guidance for the selection of ALF treatment targets. The results of this study indicate that Sirt1 activator may have a certain prospective application as a therapeutic drug for ALF.

ACKNOWLEDGEMENTS

The authors would like to thank the central laboratory at Renmin Hospital of Wuhan University (Wuhan, Hubei Province, China) for their support of our study.

FOOTNOTES

Author contributions: Cao P and Gong ZJ designed the study; Cao P, Chen Q and Shi CX performed most of the experiments and wrote the article; Wang LW analyzed the data; All authors approved the final version of the article.

Supported by National Natural Science Foundation of China, No. 82070609.

Institutional review board statement: This study was approved by the Institutional Review Board of Renmin Hospital of Wuhan University.

Institutional animal care and use committee statement: All animal operations were reviewed and approved by the Institutional Animal Care and Use Committee of Renmin Hospital of Wuhan University (Approval No. WDRY2021-K016), and were conducted in accordance with the established International Guiding Principles for Animal Research.

Conflict-of-interest statement: The authors declare no conflict of interest.

Data sharing statement: No additional data are available.

ARRIVE guidelines statement: The authors have read the ARRIVE Guidelines, and the manuscript was prepared and revised according to the ARRIVE Guidelines.

Open-Access: This article is an open-access article that was selected by an in-house editor and fully peer-reviewed by external reviewers. It is distributed in accordance with the Creative Commons Attribution NonCommercial (CC BY-NC 4.0) license, which permits others to distribute, remix, adapt, build upon this work non-commercially, and license their derivative works on different terms, provided the original work is properly cited and the use is non-commercial. See: https://creativecommons.org/Licenses/by-nc/4.0/

Country/Territory of origin: China

ORCID number: Pan Cao 0000-0001-6216-6901; Qian Chen 0000-0002-2411-2838; Chun-Xia Shi 0000-0001-8977-2784; Lu-Wen Wang 0000-0002-0654-1196; Zuo-Jiong Gong 0000-0002-4676-5856.

Corresponding Author's Membership in Professional Societies: Renmin Hospital of Wuhan University, Renmin Hospital of Wuhan University.

S-Editor: Wu YXJ
L-Editor: Filipodia
P-Editor: Yuan YY

REFERENCES

1 **Dong V**, Nanchal R, Karvellas CJ. Pathophysiology of Acute Liver Failure. *Nutr Clin Pract* 2020; **35**: 24-29 [PMID: 31840297 DOI: 10.1002/ncp.10459]
2 **Larson-Nath C**, Vitola BE. Neonatal Acute Liver Failure. *Clin Perinatol* 2020; **47**: 25-39 [PMID: 32000927 DOI: 10.1016/j.clp.2019.10.006]
3 **Manakkat Vijay GK**, Ryan JM, Abeles RD, Ramage S, Patel V, Bernsmeier C, Riva A, McPhail MJ, Tranah TH, Markwick LJ, Taylor NJ, Bernal W, Auzinger G, Willars C, Chokshi S, Wendon JA, Ma Y, Shawcross DL. Neutrophil Toll-Like Receptor 9 Expression and the Systemic Inflammatory Response in Acetaminophen-Induced Acute Liver Failure. *Crit Care Med* 2016; **44**: 43-53 [PMID: 26457748 DOI: 10.1097/CCM.0000000000001309]
4 **Baumeister J**, Chatain N, Hubrich A, Maié T, Costa IG, Denecke B, Han L, Küstermann C, Sontag S, Seré K, Strathmann K, Zenke M, Schuppert A, Brümmendorf TH, Kranc KR, Koschmieder S, Gezer D. Hypoxia-inducible factor 1 (HIF-1) is a new therapeutic target in JAK2V617F-positive myeloproliferative neoplasms. *Leukemia* 2020; **34**: 1062-1074 [PMID: 31728053 DOI: 10.1038/s41375-019-0629-z]
5 **Tak E**, Jung DH, Kim SH, Park GC, Jun DY, Lee J, Jung BH, Kirchner VA, Hwang S, Song GW, Lee SG. Protective role of hypoxia-inducible factor-1α-dependent CD39 and CD73 in fulminant acute liver failure. *Toxicol Appl Pharmacol* 2017; **314**: 72-81 [PMID: 27899277 DOI: 10.1016/j.taap.2016.11.016]
6 **Xu E**, Ji Z, Jiang H, Lin T, Ma J, Zhou X. Hypoxia-Inducible Factor 1A Upregulates HMGN5 by Increasing the Expression of GATA1 and Plays a Role in Osteosarcoma Metastasis. *Biomed Res Int* 2019; **2019**: 5630124 [PMID: 31930127 DOI: 10.1155/2019/5630124]
7 **Yuen VW**, Wong CC. Hypoxia-inducible factors and innate immunity in liver cancer. *J Clin Invest* 2020; **130**: 5052-5062 [PMID: 32750043 DOI: 10.1172/JCI137553]
8 **Seo KS**, Park JH, Heo JY, Jing K, Han J, Min KN, Kim C, Koh GY, Lim K, Kang GY, Uee Lee J, Yim YH, Shong M, Kwak TH, Kweon GR. SIRT2 regulates tumour hypoxia response by promoting HIF-1α hydroxylation. *Oncogene* 2015; **34**: 1354-1362 [PMID: 24681946 DOI: 10.1038/onc.2014.76]
9 **De Matteis S**, Scarpi E, Granato AM, Vespasiani-Gentilucci U, La Barba G, Foschi FG, Bandini E, Ghetti M, Marisi G, Cravero P, Gramantieri L, Cucchetti A, Ercolani G, Santini D, Frassineti GL, Faloppi L, Scartozzi M, Cascinu S, Casadei-Gardini A. Role of SIRT-3, p-mTOR and HIF-1α in Hepatocellular Carcinoma Patients Affected by Metabolic Dysfunctions and in Chronic Treatment with Metformin. *Int J Mol Sci* 2019; **20** [PMID: 30917505 DOI: 10.3390/ijms20061503]
10 **Hu Q**, Qin Y, Ji S, Xu W, Liu W, Sun Q, Zhang Z, Liu M, Ni Q, Yu X, Xu X. UHRF1 promotes aerobic glycolysis and proliferation *via* suppression of SIRT4 in pancreatic cancer. *Cancer Lett* 2019; **452**: 226-236 [PMID: 30905812 DOI: 10.1016/j.canlet.2019.03.024]
11 **Li A**, Peng R, Sun Y, Liu H, Peng H, Zhang Z. LincRNA 1700020I14Rik alleviates cell proliferation and fibrosis in diabetic nephropathy *via* miR-34a-5p/Sirt1/HIF-1α signaling. *Cell Death Dis* 2018; **9**: 461 [PMID: 29700282 DOI: 10.1038/s41419-018-0527-8]
12 **Lee SD**, Kim W, Jeong JW, Park JW, Kim JE. AK-1, a SIRT2 inhibitor, destabilizes HIF-1α and diminishes its transcriptional activity during hypoxia. *Cancer Lett* 2016; **373**: 138-145 [PMID: 26808575 DOI: 10.1016/j.canlet.2016.01.031]
13 **Wang X**, Shen K, Wang J, Liu K, Wu G, Li Y, Luo L, Zheng Z, Hu D. Hypoxic preconditioning combined with curcumin promotes cell survival and mitochondrial quality of bone marrow mesenchymal stem cells, and accelerates cutaneous wound healing *via* PGC-1α/SIRT3/HIF-1α signaling. *Free Radic Biol Med* 2020; **159**: 164-176 [PMID: 32745765 DOI: 10.1016/j.freeradbiomed.2020.07.023]

14 **Yang Z**, Yu W, Huang R, Ye M, Min Z. SIRT6/HIF-1α axis promotes papillary thyroid cancer progression by inducing epithelial-mesenchymal transition. *Cancer Cell Int* 2019; **19**: 17 [PMID: 30675128 DOI: 10.1186/s12935-019-0730-4]

15 **Alves-Fernandes DK**, Jasiulionis MG. The Role of SIRT1 on DNA Damage Response and Epigenetic Alterations in Cancer. *Int J Mol Sci* 2019; **20** [PMID: 31261609 DOI: 10.3390/ijms20133153]

16 **Imperatore F**, Maurizio J, Vargas Aguilar S, Busch CJ, Favret J, Kowenz-Leutz E, Cathou W, Gentek R, Perrin P, Leutz A, Berruyer C, Sieweke MH. SIRT1 regulates macrophage self-renewal. *EMBO J* 2017; **36**: 2353-2372 [PMID: 28701484 DOI: 10.15252/embj.201695737]

17 **Mahmoud AR**, Ali FEM, Abd-Elhamid TH, Hassanein EHM. Coenzyme Q_{10} protects hepatocytes from ischemia reperfusion-induced apoptosis and oxidative stress *via* regulation of Bax/Bcl-2/PUMA and Nrf-2/FOXO-3/Sirt-1 signaling pathways. *Tissue Cell* 2019; **60**: 1-13 [PMID: 31582012 DOI: 10.1016/j.tice.2019.07.007]

18 **Lim JH**, Lee YM, Chun YS, Chen J, Kim JE, Park JW. Sirtuin 1 modulates cellular responses to hypoxia by deacetylating hypoxia-inducible factor 1alpha. *Mol Cell* 2010; **38**: 864-878 [PMID: 20620956 DOI: 10.1016/j.molcel.2010.05.023]

19 **Laemmle A**, Lechleiter A, Roh V, Schwarz C, Portmann S, Furer C, Keogh A, Tschan MP, Candinas D, Vorburger SA, Stroka D. Inhibition of SIRT1 impairs the accumulation and transcriptional activity of HIF-1α protein under hypoxic conditions. *PLoS One* 2012; **7**: e33433 [PMID: 22479397 DOI: 10.1371/journal.pone.0033433]

20 **Wang G**, Xie X, Yuan L, Qiu J, Duan W, Xu B, Chen X. Resveratrol ameliorates rheumatoid arthritis *via* activation of SIRT1-Nrf2 signaling pathway. *Biofactors* 2020; **46**: 441-453 [PMID: 31883358 DOI: 10.1002/biof.1599]

21 **Wang Y**, Yang F, Jiao FZ, Chen Q, Zhang WB, Wang LW, Gong ZJ. Modulations of Histone Deacetylase 2 Offer a Protective Effect through the Mitochondrial Apoptosis Pathway in Acute Liver Failure. *Oxid Med Cell Longev* 2019; **2019**: 8173016 [PMID: 31183000 DOI: 10.1155/2019/8173016]

22 **Oh SI**, Park JK, Park SK. Lifespan extension and increased resistance to environmental stressors by N-acetyl-L-cysteine in Caenorhabditis elegans. *Clinics (Sao Paulo)* 2015; **70**: 380-386 [PMID: 26039957 DOI: 10.6061/clinics/2015(05)13]

23 **Gazanion E**, Vergnes B, Seveno M, Garcia D, Oury B, Ait-Oudhia K, Ouaissi A, Sereno D. In vitro activity of nicotinamide/antileishmanial drug combinations. *Parasitol Int* 2011; **60**: 19-24 [PMID: 20884376 DOI: 10.1016/j.parint.2010.09.005]

24 **Luo D**, Zhang Y, Yuan X, Pan Y, Yang L, Zhao Y, Zhuo R, Chen C, Peng L, Li W, Jin X, Zhou Y. Oleoylethanolamide inhibits glial activation *via* moudulating PPARα and promotes motor function recovery after brain ischemia. *Pharmacol Res* 2019; **141**: 530-540 [PMID: 30660821 DOI: 10.1016/j.phrs.2019.01.027]

25 **Yu PB**, Hong CC, Sachidanandan C, Babitt JL, Deng DY, Hoyng SA, Lin HY, Bloch KD, Peterson RT. Dorsomorphin inhibits BMP signals required for embryogenesis and iron metabolism. *Nat Chem Biol* 2008; **4**: 33-41 [PMID: 18026094 DOI: 10.1038/nchembio.2007.54]

26 **Chen J**, Wang B, Lai J, Braunstein Z, He M, Ruan G, Yin Z, Wang J, Cianflone K, Ning Q, Chen C, Wang DW. Trimetazidine Attenuates Cardiac Dysfunction in Endotoxemia and Sepsis by Promoting Neutrophil Migration. *Front Immunol* 2018; **9**: 2015 [PMID: 30233596 DOI: 10.3389/fimmu.2018.02015]

27 **Bell EL**, Emerling BM, Ricoult SJ, Guarente L. SirT3 suppresses hypoxia inducible factor 1α and tumor growth by inhibiting mitochondrial ROS production. *Oncogene* 2011; **30**: 2986-2996 [PMID: 21358671 DOI: 10.1038/onc.2011.37]

28 **Yu LM**, Zhang WH, Han XX, Li YY, Lu Y, Pan J, Mao JQ, Zhu LY, Deng JJ, Huang W, Liu YH. Hypoxia-Induced ROS Contribute to Myoblast Pyroptosis during Obstructive Sleep Apnea *via* the NF-κB/HIF-1α Signaling Pathway. *Oxid Med Cell Longev* 2019; **2019**: 4596368 [PMID: 31885794 DOI: 10.1155/2019/4596368]

29 **Tian Z**, Chen Y, Yao N, Hu C, Wu Y, Guo D, Liu J, Yang Y, Chen T, Zhao Y, He Y. Role of mitophagy regulation by ROS in hepatic stellate cells during acute liver failure. *Am J Physiol Gastrointest Liver Physiol* 2018; **315**: G374-G384 [PMID: 29648877 DOI: 10.1152/ajpgi.00032.2018]

30 **Kersten S**, Stienstra R. The role and regulation of the peroxisome proliferator activated receptor alpha in human liver. *Biochimie* 2017; **136**: 75-84 [PMID: 28077274 DOI: 10.1016/j.biochi.2016.12.019]

31 **Chang C**, Su H, Zhang D, Wang Y, Shen Q, Liu B, Huang R, Zhou T, Peng C, Wong CC, Shen HM, Lippincott-Schwartz J, Liu W. AMPK-Dependent Phosphorylation of GAPDH Triggers Sirt1 Activation and Is Necessary for Autophagy upon Glucose Starvation. *Mol Cell* 2015; **60**: 930-940 [PMID: 26626483 DOI: 10.1016/j.molcel.2015.10.037]

32 **Song L**, Chen TY, Zhao XJ, Xu Q, Jiao RQ, Li JM, Kong LD. Pterostilbene prevents hepatocyte epithelial-mesenchymal transition in fructose-induced liver fibrosis through suppressing miR-34a/Sirt1/p53 and TGF-β1/Smads signalling. *Br J Pharmacol* 2019; **176**: 1619-1634 [PMID: 30632134 DOI: 10.1111/bph.14573]

33 **Nagappan A**, Kim JH, Jung DY, Jung MH. Cryptotanshinone from the *Salvia miltiorrhiza* Bunge Attenuates Ethanol-Induced Liver Injury by Activation of AMPK/SIRT1 and Nrf2 Signaling Pathways. *Int J Mol Sci* 2019; **21** [PMID: 31906014 DOI: 10.3390/ijms21010265]

34 **Li CX**, Gao JG, Wan XY, Chen Y, Xu CF, Feng ZM, Zeng H, Lin YM, Ma H, Xu P, Yu CH, Li YM. Allyl isothiocyanate ameliorates lipid accumulation and inflammation in nonalcoholic fatty liver disease *via* the Sirt1/AMPK and NF-κB signaling pathways. *World J Gastroenterol* 2019; **25**: 5120-5133 [PMID: 31558861 DOI: 10.3748/wjg.v25.i34.5120]

35 **Ding RB**, Bao J, Deng CX. Emerging roles of SIRT1 in fatty liver diseases. *Int J Biol Sci* 2017; **13**: 852-867 [PMID: 28808418 DOI: 10.7150/ijbs.19370]

36 **Dioum EM**, Chen R, Alexander MS, Zhang Q, Hogg RT, Gerard RD, Garcia JA. Regulation of hypoxia-inducible factor 2alpha signaling by the stress-responsive deacetylase sirtuin 1. *Science* 2009; **324**: 1289-1293 [PMID: 19498162 DOI: 10.1126/science.1169956]

37 **Roux C**, Jafari SM, Shinde R, Duncan G, Cescon DW, Silvester J, Chu MF, Hodgson K, Berger T, Wakeham A, Palomero L, Garcia-Valero M, Pujana MA, Mak TW, McGaha TL, Cappello P, Gorrini C. Reactive oxygen species modulate macrophage immunosuppressive phenotype through the up-regulation of PD-L1. *Proc Natl Acad Sci U S A* 2019; **116**: 4326-4335 [PMID: 30770442 DOI: 10.1073/pnas.1819473116]

38 **He L**, He T, Farrar S, Ji L, Liu T, Ma X. Antioxidants Maintain Cellular Redox Homeostasis by Elimination of Reactive Oxygen Species. *Cell Physiol Biochem* 2017; **44**: 532-553 [PMID: 29145191 DOI: 10.1159/000485089]

39 **Hwang Y**, Kim JC, Tae G. Significantly enhanced recovery of acute liver failure by liver targeted delivery of stem cells *via*

heparin functionalization. *Biomaterials* 2019; **209**: 67-78 [PMID: 31026612 DOI: 10.1016/j.biomaterials.2019.04.019]

40 **Liu TF**, Vachharajani V, Millet P, Bharadwaj MS, Molina AJ, McCall CE. Sequential actions of SIRT1-RELB-SIRT3 coordinate nuclear-mitochondrial communication during immunometabolic adaptation to acute inflammation and sepsis. *J Biol Chem* 2015; **290**: 396-408 [PMID: 25404738 DOI: 10.1074/jbc.M114.566349]

41 **Shavva VS**, Mogilenko DA, Nekrasova EV, Trulioff AS, Kudriavtsev IV, Larionova EE, Babina AV, Dizhe EB, Missyul BV, Orlov SV. Tumor necrosis factor α stimulates endogenous apolipoprotein A-I expression and secretion by human monocytes and macrophages: role of MAP-kinases, NF-κB, and nuclear receptors PPARα and LXRs. *Mol Cell Biochem* 2018; **448**: 211-223 [PMID: 29442267 DOI: 10.1007/s11010-018-3327-7]

42 **Planavila A**, Iglesias R, Giralt M, Villarroya F. Sirt1 acts in association with PPARα to protect the heart from hypertrophy, metabolic dysregulation, and inflammation. *Cardiovasc Res* 2011; **90**: 276-284 [PMID: 21115502 DOI: 10.1093/cvr/cvq376]

43 **Wang G**, Cheng S, Zhang S, Zhu Y, Xiao Y, Ju L. LPS impairs steroidogenesis and ROS metabolism and induces PPAR transcriptional activity to disturb estrogen/androgen receptor expression in testicular cells. *Mol Biol Rep* 2020; **47**: 1045-1056 [PMID: 31741264 DOI: 10.1007/s11033-019-05196-6]

44 **Huang Y**, Lang H, Chen K, Zhang Y, Gao Y, Ran L, Yi L, Mi M, Zhang Q. Resveratrol protects against nonalcoholic fatty liver disease by improving lipid metabolism and redox homeostasis *via* the PPARα pathway. *Appl Physiol Nutr Metab* 2020; **45**: 227-239 [PMID: 31173696 DOI: 10.1139/apnm-2019-0057]

45 **Lan F**, Cacicedo JM, Ruderman N, Ido Y. SIRT1 modulation of the acetylation status, cytosolic localization, and activity of LKB1. Possible role in AMP-activated protein kinase activation. *J Biol Chem* 2008; **283**: 27628-27635 [PMID: 18687677 DOI: 10.1074/jbc.M805711200]

46 **Song P**, Zou MH. Regulation of NAD(P)H oxidases by AMPK in cardiovascular systems. *Free Radic Biol Med* 2012; **52**: 1607-1619 [PMID: 22357101 DOI: 10.1016/j.freeradbiomed.2012.01.025]

47 **Cai Y**, Martens GA, Hinke SA, Heimberg H, Pipeleers D, Van de Casteele M. Increased oxygen radical formation and mitochondrial dysfunction mediate beta cell apoptosis under conditions of AMP-activated protein kinase stimulation. *Free Radic Biol Med* 2007; **42**: 64-78 [PMID: 17157194 DOI: 10.1016/j.freeradbiomed.2006.09.018]

World Journal of Gastroenterology

Submit a Manuscript: https://www.f6publishing.com

World J Gastroenterol 2022 May 7; 28(17): 1814-1829

DOI: 10.3748/wjg.v28.i17.1814

ISSN 1007-9327 (print) ISSN 2219-2840 (online)

ORIGINAL ARTICLE

Basic Study

Peroxisome proliferator-activated receptor-alpha activation and dipeptidyl peptidase-4 inhibition target dysbiosis to treat fatty liver in obese mice

Flavia Maria Silva-Veiga, Carolline Santos Miranda, Isabela Macedo Lopes Vasques-Monteiro, Henrique Souza-Tavares, Fabiane Ferreira Martins, Julio Beltrame Daleprane, Vanessa Souza-Mello

Specialty type: Gastroenterology and hepatology

Provenance and peer review: Invited article; Externally peer reviewed.

Peer-review model: Single blind

Peer-review report's scientific quality classification

Grade A (Excellent): 0
Grade B (Very good): B, B
Grade C (Good): 0
Grade D (Fair): 0
Grade E (Poor): 0

P-Reviewer: Dziegielewska-Gesiak S, Poland; Li YL, China

Received: December 30, 2021
Peer-review started: December 30, 2021
First decision: January 27, 2022
Revised: February 4, 2022
Accepted: March 26, 2022
Article in press: March 26, 2022
Published online: May 7, 2022

Flavia Maria Silva-Veiga, Carolline Santos Miranda, Isabela Macedo Lopes Vasques-Monteiro, Henrique Souza-Tavares, Fabiane Ferreira Martins, Vanessa Souza-Mello, Department of Anatomy, Institute of Biology, State University of Rio de Janeiro, Laboratory of Morphometry, Metabolism and Cardiovascular Diseases, Rio de Janeiro 20551-030, Brazil

Julio Beltrame Daleprane, Department of Clinical and Toxicology Analysis, State University of Rio de Janeiro, Nutrition Institute, State University of Rio de Janeiro, Nutrition Institute, University of Sao Paulo, Rio de Janeiro 20551-030, Brazil

Corresponding author: Vanessa Souza-Mello, PhD, Associate Professor, Department of Anatomy, Institute of Biology, State University of Rio de Janeiro, Laboratory of Morphometry, Metabolism and Cardiovascular Diseases, Blvd. 28 de Setembro 87, Fundos, Vila Isabel, Rio de Janeiro 20551-030, Brazil. souzamello.uerj@gmail.com

Abstract

BACKGROUND

Obesity and comorbidities onset encompass gut dysbiosis, altered intestinal permeability, and endotoxemia. Treatments that target gut dysbiosis can cope with obesity and nonalcoholic fatty liver disease (NAFLD) management. Peroxisome proliferator-activated receptor (PPAR)-alpha activation and dipeptidyl-peptidase-4 (DPP-4) inhibition alleviate NAFLD, but the mechanism may involve gut microbiota modulation and merits further investigation.

AIM

To address the effects of PPAR-alpha activation and DPP-4 inhibition (isolated or combined) upon the gut-liver axis, emphasizing inflammatory pathways in NAFLD management in high-fat-fed C57BL/6J mice.

METHODS

Male C57BL/6J mice were fed a control diet (C, 10% of energy as lipids) or a high-fat diet (HFD, 50% of energy as lipids) for 12 wk, when treatments started, forming the groups: C, HF, HFA (HFD + PPAR-alpha agonist WY14643, 2.5 mg/kg body mass), HFL (HFD + DPP-4 inhibitor linagliptin, 15 mg/kg body mass), and HFC (HFD + the combination of WY14643 and linagliptin).

RESULTS

The HFD was obesogenic compared to the C diet. All treatments elicited significant body mass loss, and the HFC group showed similar body mass to the C group. All treatments tackled oral glucose intolerance and raised plasma glucagon-like peptide-1 concentrations. These metabolic benefits restored *Bacteroidetes*/*Firmicutes* ratio, resulting in increased goblet cells *per* area of the large intestine and reduced lipopolysaccharides concentrations in treated groups. At the gene level, treated groups showed higher intestinal *Mucin 2*, *Occludin*, and *Zo-1* expression than the HFD group. The reduced endotoxemia suppressed inflammasome and macrophage gene expression in the liver of treated animals. These observations complied with the mitigation of liver steatosis and reduced hepatic triacylglycerol, reassuring the role of the proposed treatments on NAFLD mitigation.

CONCLUSION

PPAR alpha activation and DPP-4 inhibition (isolated or combined) tackled NAFLD in diet-induced obese mice by restoration of gut-liver axis. The reestablishment of the intestinal barrier and the rescued phylogenetic gut bacteria distribution mitigated liver steatosis through anti-inflammatory signals. These results can cope with NAFLD management by providing pre-clinical evidence that drugs used to treat obesity comorbidities can help to alleviate this silent and harmful liver disease.

Key Words: Nonalcoholic fatty liver disease; High-fat diet; Peroxisome proliferator-activated receptor-alpha; Dipeptidyl-peptidase-4-inhibitor; Dysbiosis; Inflammation

©The Author(s) 2022. Published by Baishideng Publishing Group Inc. All rights reserved.

Core Tip: Chronic high-fat diet (HF) intake alters the phylogenetic microbiota composition, sending harmful proinflammatory signals to the liver that elicit nonalcoholic fatty liver disease in mice. Here, we treated HF diet-induced obese mice with a peroxisome proliferator-activated receptor-alpha agonist (WY14643), a dipeptidyl-peptidase-4 inhibitor (linagliptin), or their combination, focusing on gut–liver axis modulation. The treatments rescued gut dysbiosis and endotoxemia due to increased tight junction gene expression, mucin production, and numerical density of goblet cells in the intestinal crypts. Treated mice benefited from downregulated *Tlr4*, *Cd206*, and *Nlrp3*, alleviating fatty liver through anti-inflammatory signals such as increased *IL-10* and *IL-13*.

Citation: Silva-Veiga FM, Miranda CS, Vasques-Monteiro IML, Souza-Tavares H, Martins FF, Daleprane JB, Souza-Mello V. Peroxisome proliferator-activated receptor-alpha activation and dipeptidyl peptidase-4 inhibition target dysbiosis to treat fatty liver in obese mice. *World J Gastroenterol* 2022; 28(17): 1814-1829
URL: https://www.wjgnet.com/1007-9327/full/v28/i17/1814.htm
DOI: https://dx.doi.org/10.3748/wjg.v28.i17.1814

INTRODUCTION

The prevalence of obesity worldwide has tripled during recent decades, necessitating large budgets for public health systems due to associated comorbidities[1,2]. Excessive dietary saturated fat intake triggers insulin resistance, white adipocyte hypertrophy, low-grade inflammation (metainflammation), brown adipose tissue dysfunction (whitening), fatty liver, and, as more recently described, alteration in the composition of the gut microbiota (dysbiosis)[3,4].

The digestive tract is populated by several microorganisms, predominantly including bacteria from the *Firmicutes* and *Bacteroidetes* phyla, and this population is influenced by the quality of the diet[5]. Excessive saturated fat in the diet increases the proportion of gram-negative bacteria with lipopolysaccharides (LPS) in the composition of their outer wall[6]. LPS is an endotoxin that compromises the integrity of the intestinal mucosa through alterations in the structural proteins of tight junctions (TJs), resulting in increased intestinal permeability and the migration of LPS to other tissues[5,7].

The gut–liver axis comprises the anatomical communication between these two organs *via* the portal vein[8]. A recent study by our group has demonstrated phylogenetic changes in the gut microbiota of mice after seventeen weeks of high-fructose diet feeding, with a significant increase in liver steatosis and inflammation, indicating the progression of nonalcoholic fatty liver disease (NAFLD) (fatty liver disease associated with metabolic dysfunction) to more harmful forms of liver diseases[9]. Given this scenario, the identification of metabolic pathways that rescue gut dysbiosis and mitigate the liver changes arising

from a dietary excess of saturated fat is pertinent, considering the high prevalence of obesity, its deleterious health effects, and the fact that there is, thus far, no treatment directed exclusively toward NAFLD[10].

Peroxisome proliferator-activated receptors (PPARs) are transcription factors involved in several metabolic pathways. The pharmacological activation of the PPAR-alpha isoform promotes reduced body mass, increased insulin sensitivity, the formation of beige adipocytes[11], and a significant reduction in NAFLD by increasing mitochondrial beta-oxidation[9]. Recently, PPAR-alpha deletion promoted intestinal dysbiosis and inflammation in mice[12]. The dipeptidyl-peptidase-4 (DPP-4) inhibitor linagliptin extends the glucagon-like peptide-1 (GLP1) time of action through beneficial brown and white adipocyte remodeling, browning induction, and M2 macrophage polarization, in addition to enhancing liver vascularization, supressing *de novo* lipogenesis, and alleviating endoplasmic reticulum stress[13,14].

This study aimed to address the effects of PPAR-alpha activation and DPP-4 inhibition (isolated or combined) on the gut–liver axis, emphasizing inflammatory pathways in NAFLD management in high-fat-fed C57BL/6J mice.

MATERIALS AND METHODS

Animals and diet

Adult male C57BL/6J mice were group-housed (n = 5 *per* cage) and maintained under controlled temperature (21 ± 2 °C) and humidity (60 ± 10%) with free access to water and feed in a ventilated rack containing cages for the mice (NexGen mouse 500, Allentown, PA, United States). The environment comprised a 12/12 h light–dark period and air renewal cycles (15 min/h). The procedures followed the recommendations of the National Institutes of Health Guide for the Care and Use of Laboratory Animals (NIH publication No. 85-23, revised 1996) and were approved by our local Ethics Committee (Institute of Biology, CEUA number 041/2018).

Experimental protocol

Fifty adult male C57BL/6J mice (3 month old) from the Central Biotery of the Federal Minas Gerais University were used in this study. Initially, the animals were randomly assigned to two nutritionally different groups: (1) Control group (C) – animals that received a control diet (14% of energy as protein, 10% as fat, and 76% as carbohydrates; total energy 15 KJ/g, n = 10); and (2) High-fat group (HF) – animals that received a high-fat diet (14% of energy as protein, 50% as fat and 36% as carbohydrates; total energy 21 KJ/g, n = 40).

After twelve weeks, the C group and ten animals from the HF group continued the same food scheme for an additional five weeks, whereas the remaining animals from the HF group were randomly subdivided according to the treatment into the following groups: (1) HFA received the PPAR-alpha agonist (WY14643, Sigma–Aldrich, 3.5 mg/kg body mass) incorporated into the HF diet (n = 10) for five weeks; (2) HFL received the DPP-4 inhibitor (linagliptin, Boehringer Ingelheim, 15 mg/kg body mass) incorporated into the HF diet (n = 10) for five weeks; and (3) HFC received the combination of a PPAR-alpha agonist with a DPP-4 inhibitor (at the same doses used in the groups receiving monotherapy) incorporated into the HF diet (n = 10) for five weeks.

The entire experimental protocol lasted for 17 wk (12 wk of obesity induction + 5 wk of treatment). The doses of WY-14643 and linagliptin were based on previous experiments conducted by our group[4,9]. PragSoluções (Jaú, São Paulo, Brazil) produced the experimental diets according to the recommendations of the American Institute of Nutrition (AIN 93M)[15]. All groups were treated following the order in which the groups were described.

Food/energy intake and body mass

Food intake was measured daily by subtracting the remainder of the diet verified on the following day from the amount of diet offered on the previous day. Energy intake comprised the product of the food consumption and the energy contained in 1 g of each diet (in kJ). Animal body masses were assessed on a digital scale once a week (BL-3200H, precision 0.01 g).

Metabolic analysis

One week before sacrifice, the animals were subjected to the oral glucose tolerance test (OGTT). Under a 6-h fast (time 0) and after 15, 30, 60, and 120 minutes of the orogastric gavage of a glucose solution (2 g/kg body mass), blood samples were obtained from the caudal vein. A manual glucometer (Accu-Chek, Roche, São Paulo, SP, Brazil) was used to measure the blood glucose levels at different times. The area under the curve (AUC) indicated the oral glucose tolerance (GraphPad Prism, version 8.3 for Windows, GraphPad Software, La Jolla, CA, United States).

Sacrifice and ELISA

Mice were fasted for 6 h. Under intraperitoneal anesthesia with ketamine (240 mg/kg) and xylazine (30 mg/kg), blood samples obtained by cardiac puncture were separated by centrifugation (712 ×*g*) to obtain plasma samples to perform biochemical analyses. The liver, large intestine (cecum), and small intestine (jejunum and ileum) were carefully dissected, weighed, and analyzed following the protocols for different techniques.

An ELISA was performed to measure plasma GLP1 (multispecies GLP1 ELISA Kit Cat. #EZGLP1T-36K, Millipore, Missouri, United States), and LPS (multispecies LPS ELISA Kit Cat. #SEB526Ge-96T, Cloud-Clone Corp., Katy, United States). A semiautomatic spectrophotometer and a commercial kit (K117, Bioclin, Quibasa, Belo Horizonte, MG, Brazil) were used to measure hepatic triacylglycerol (TAG) as previously described[16].

Histology

Liver and cecum fragments fixed in Millonig-buffered formalin (pH 7.2-7.4) were subsequently dehydrated, diaphanized, embedded in Paraplast Plus (Sigma–Aldrich, St. Louis, MO, United States) and sectioned (5 µm thick) with a microtome. Slides stained with hematoxylin and eosin (liver) or Alcian Blue (Sigma Chemical Company-pH 2.5) plus Periodic Acid-Schiff (PAS, intestine-Sigma Chemical Company) were photographed using a Leica DMRBE microscope (Wetzlar, Germany) and an Infinity Lumenera digital camera (Ottawa, ON, Canada). The images were analyzed in a blinded manner with STEPanizer (www.stepanizer.com) as described below:

Hepatic stereology: Five animals *per* group and ten images *per* animal were analyzed. The volume density of liver steatosis [Vv (liver, st)] was estimated by the point-counting technique, following the formula: Vv (liver, st) = Pp (liver, st)/PT (Pp is the number of points that reached fat droplets, and PT is the total test points). The images were analyzed with STEPanizer using a 36-point test system[17].

Gut stereology: The number of goblet cells *per* area [Q_A(goblet)] was estimated using STEPanizer. All goblet cells within the test area were counted, except those touching the forbidden lines. The result was divided by the test area measured in mm^2.

16S rDNA polymerase chain reaction amplification

The feces found in the mouse cecum were used to extract microbial DNA using the QIAamp Fast DNA Stool Mini Kit (Qiagen, Düsseldorf, Germany) according to the manufacturer's instructions. The DNA quantity, purity, and concentration were determined using Qubit (Life Technologies, Carlsbad, California, United States) and horizontal electrophoresis (1% agarose gel). Real-time quantitative polymerase chain reaction (PCR) assays were used for the relative quantification of specific phyla of microorganisms (*Bacteroidetes, Firmicutes, Actinobacteria, Proteobacteria*) in fecal microbiota from the mouse guts by detecting 16S rRNA genes. For relative quantification, the abundances of different phyla were normalized by the $^{\Delta\Delta}$Ct method relative to the total bacterial amount in the samples[18]. The indicators used are described in Table 1.

Real-time reverse transcriptase–PCR

Total RNA was extracted from 50 mg of the liver and 70 mg of the small intestine (jejunum and ileum) using TRIzol reagent (Invitrogen, CA, United States). Afterward, the addition of 200 µL of chloroform was followed by centrifugation (1200 *g* for 10 min at 4 °C for liver samples and 12000 *g* for 15 min at 4 °C for intestine samples). The RNA extract portion was separated, and 500 µL of isopropanol was added and allowed to stand for 10 min (liver samples) or 15 min (intestine samples) to precipitate the RNA. Then, the samples were centrifuged (1200 *g* for 10 min at 4 °C for liver samples and 12000 *g* for 10 min at 4 °C for intestine samples). The isopropanol was removed, and the formed pellet was resuspended in 500 µL of 75% ethanol for liver samples or 70% ethanol (ice-cold) for intestine samples and then centrifuged (1200 *g* for 5 min at 4 °C for liver samples and 10000 *g* for 5 min at 4 °C for intestine samples).

The ethanol was removed, and the pellet was resuspended in 20 µL (liver)/50 µL (intestine) of deionized water (Milli-Q). The samples were subjected to a dry bath (50 °C for 5 min) and quantified by using Nanovue equipment (GE Life Sciences). For RNA transcription into complementary DNA (cDNA), 1.0 µg RNA was treated with DNAse I (Invitrogen, CA, United States). First-strand cDNA synthesis was performed using Oligo (dT) primers for reverse transcriptase mRNA and Superscript III (both from Invitrogen). qPCR was performed using a CFX96 recycler (Bio–Rad, Hercules, CA, United States) and SYBR Green mix (Invitrogen, Carlsbad, CA, United States). *Beta-actin* was used to correct the expression of the target genes in liver samples, and *Gapdh* was used for intestine samples. The primer sequences used are shown in Table 2 (liver) and Table 3 (intestine). All gene symbols are italicized (the first letter capitalized), and protein symbols are italicized in uppercase[19].

Data analysis

Sample size calculation considered that, in metabolic and molecular biology analyses, if a factor

Table 1 Initiators of the phylum or class of microorganisms of gut microbiota

Phylum or class	Forward initiator	Reverse initiator
Eubacteria (All Bacteria)	[5′-ACTCCTACGGGAGGCAGAGT-3′]	[5′-ATTACCGCGGCTGCTGGC-3′]
Bacteroidetes	[5′-CRAACAGGATTAGATACCCT-3′]	[5′-GGTAAGGTTCCTCGCGTAT-3′]
Firmicutes	[5′-TGAAACTYAAAGGAATTGACG-3′]	[5′-ACCATGCACCACCTGTC-3′]
Actinobacteria	[5′-TACGGCCGCAAGGCTA-3′]	[5′-TCRTCCCCACCTTCCTCCG-3′]
Class-γ-Proteobacteria	[5′-TCGTCAGCTCGTGTYGTGA -3′]	[5′-CGTAAGGGCCATGATG-3′]

Table 2 Forward and reverse sequences of real-time reverse transcriptase–polymerase chain reaction primers–liver

Gene	5’-3’ Left	3’-5’ Right
Lbp	GGTGGCTGCTGAATCTCTTC	TCTGCTGTGACTGGCAGAGT
Tlr4	GCCGGAAGGTTATTGTGGTA	GAAACTGCCATGTTTGAGCA
Nlrp3	ATGCTGCTTCGACATCTCCT	GTTTCTGGAGGTTGCAGAGC
Cd206	CAAGGAAGGTTGGCATTTGT	CCTTTCAGTCCTTTGCAAGC
IL-10	GCCTTATCGGAAATGATCCA	TCCTGAGGGTCTTCAGCTTC
IL-13	CTGGATTCCCTGACCAACAT	GGTTACAGAGGCCATGCAAT
Beta-actin	TGTTACCAACTGGGACGACA	GGGGTGTTGAAGGTCTCAAA

Table 3 Forward and reverse sequences of real-time reverse transcriptase–polymerase chain reaction primers–intestine

Gene	5’-3’ Left	3’-5’ Right
Mucin2	GTAGTTTCCGTTGGAACAGTGAA	ATGCCCACCTCCTCAAAGAC
Occludin	CCTTCTGCTTCATCGCTTCC	AGCGCTGACTATGATCACGA
Zo-1	TCAGAGCCCTCCGATCATTC	GCTTTGGGTGGATGATCGTC
Tlr4	GCCGGAAGGTTATTGTGGTA	GAAACTGCCATGTTTGAGCA
Gapdh	CATCACTGCCACCCAGAAGACTG	ATGCCAGTGAGCTTCCCGTTCAG

increases or decreases in five replicates, the probability of occurrence is $P = (1/2)^5 = 0.05$. Therefore, a minimum of 5 replicates was adopted for the analyses[20]. The data are shown as the mean and SD. During the first 12 wk, statistical analysis comprised Student’s t test and Welch's correction. At the treatment phase, data were analyzed using Brown–Forsythe and Welch one-way ANOVA with the Dunnett T3 post hoc test[21]. A $P < 0.05$ was considered significant (GraphPad Prism version 8.3 for Windows, GraphPad Software, La Jolla, CA, United States).

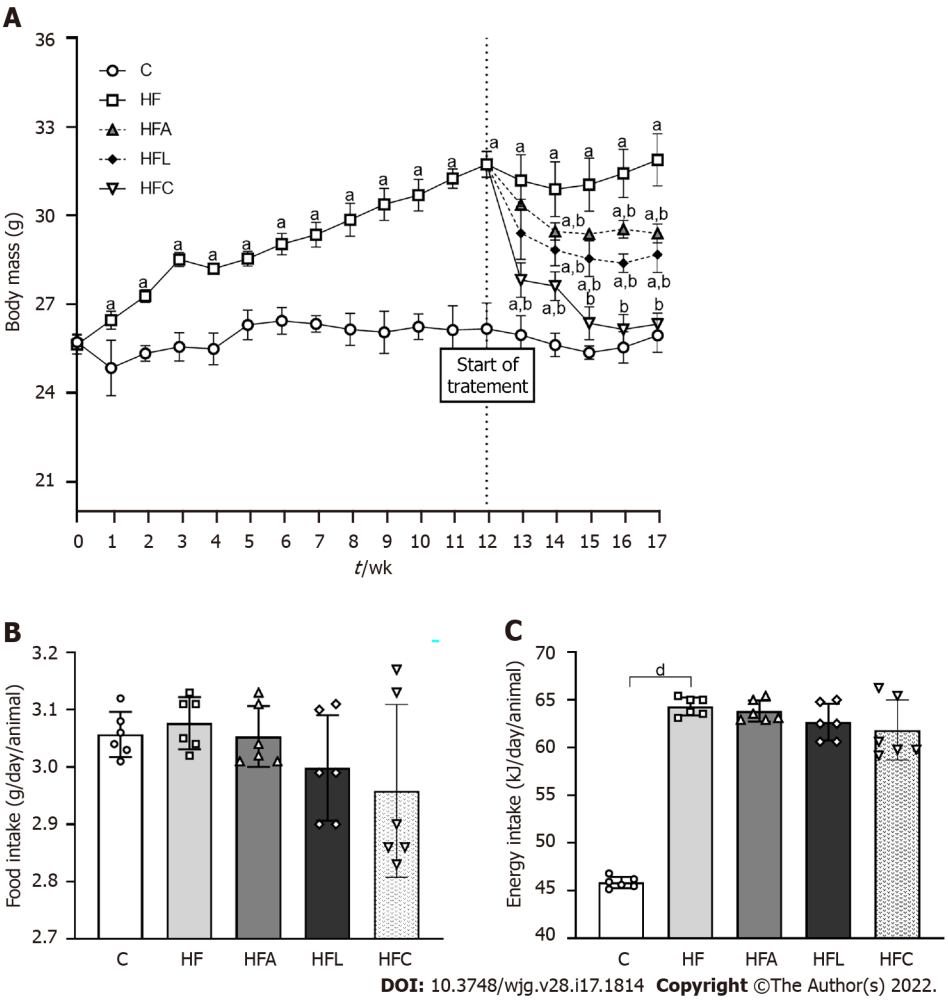
RESULTS

Treatment reduced body mass without altering energy intake

The animals in the C and HF groups had equal body mass (BM) at baseline. All animals tolerated the diets and treatments well. The protocol was maintained as previously stated. In the 13th week, the HF group was overweight compared to the C group (+30%), and this characteristic persisted until the end of the experiment. Figure 1A depicts these results. Although food intake did not differ between the groups (Figure 1B), the energy intake in the HF-fed groups was higher than that in the C group (Figure 1C).

All proposed treatments rescued glucose tolerance and increased GLP1 concentrations

Figure 2A shows the OGTT curve, in which the HF group showed a significant increase in fasting glucose (T0) compared to the C group. This difference remained until the end of the test (T120). The C group and the treated groups exhibited rescued baseline blood glucose levels at the other evaluation times (T30, T60, and T120). On the other hand, the HF group did not reach baseline glucose levels,



DOI: 10.3748/wjg.v28.i17.1814 **Copyright** ©The Author(s) 2022.

Figure 1 Body mass and food behavior. A: Body mass evolution; B: Food intake; C: Energy intake. Brown-Forsythe and Welch one-way ANOVA and Dunnett T3 *post hoc* test (mean ± SD, $n = 6$). Significant differences are indicated as follows: $^{a}P < 0.05$; $^{b}P < 0.01$; $^{d}P < 0.0001$. C: Control diet; HF: High-fat diet; HFA: High-fat diet plus PPAR-alpha agonist (WY14643); HFL: High-fat diet plus DPP-4 inhibitor (linagliptin); HFC: High-fat diet plus the combination of WY14643 with linagliptin.

indicating a delay after glucose overload and implying oral glucose intolerance, as confirmed by the higher AUC for OGTT in the HF group than in the C group (+23%, Figure 2B). In contrast, all treated groups showed lower AUCs than the HF group, indicating oral glucose intolerance alleviation.

Plasma GLP1 concentrations diminished in the HF group compared to the C group (Figure 2C). As expected, treatment with linagliptin enhanced GLP1 concentrations in the HFL group (+13%), which also occurred in the HFC group and after the single treatment with the PPAR-alpha agonist in the HFA group compared to the HF group (Figure 2C).

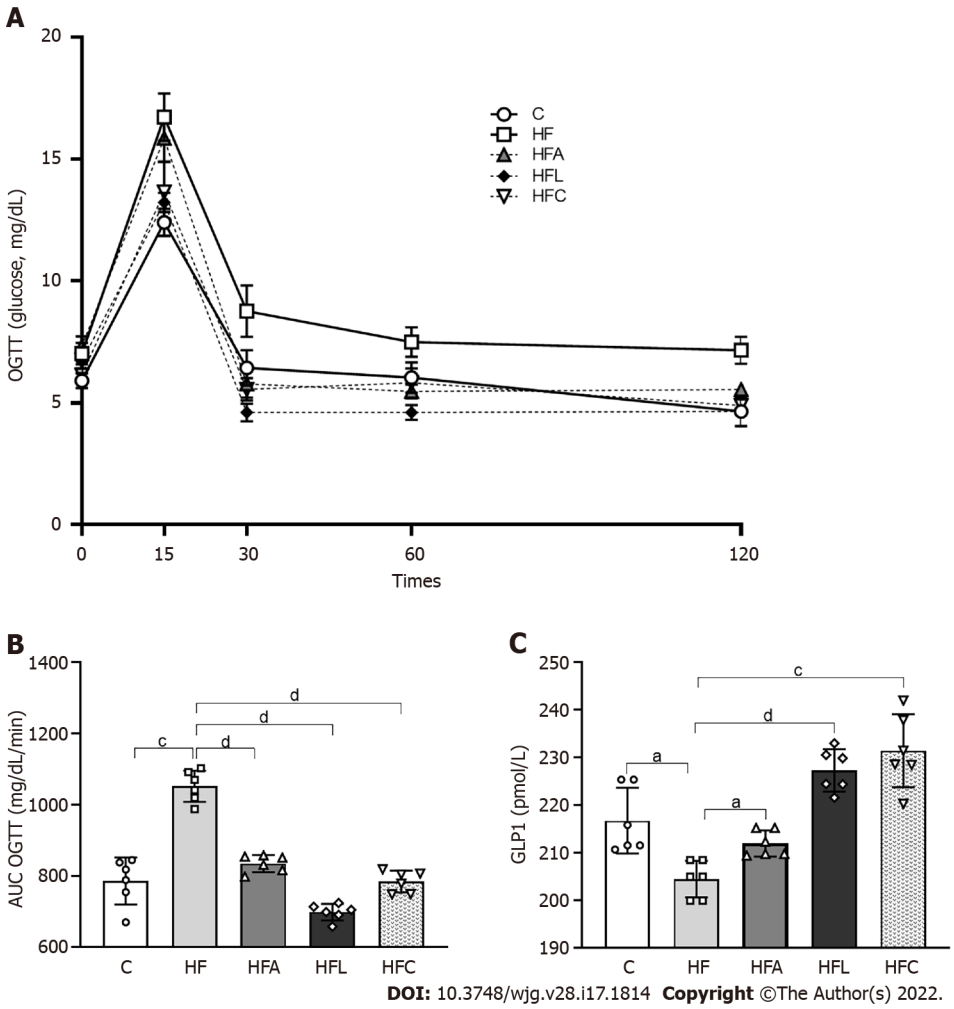
Treatments recovered the microbiota composition and reversed endotoxemia in HF-fed mice

The amplified 16S rRNA genes of cecal gut bacteria were measured at the end of the experiment to evaluate the microbiota composition. The HF group showed a *Firmicutes* phylum increase coupled with decreases in the *Proteobacteria* and *Bacteroidetes* phyla compared to the C group, as shown in Figure 3A. However, all treatments reversed these phylogenetic alterations in the treated groups. The treatments restored the amount of *Bacteroidetes* to resemble that in the C group and caused a significant decrease in *Proteobacteria*, which can play a decisive role in the beneficial effects observed due to the proposed treatments. Changes in the microbiota composition in the HF group triggered increased LPS concentrations (+10%, Figure 3B), while the HFL and HFC groups showed significantly reduced plasma LPS concentrations (-11% for HFL *vs* HF and -12% for HFC *vs* HF).

The hepatic mRNA expression of both *Lbp* (Figure 3C) and *Tlr4* (Figure 3D) genes increased in the HF group compared to the C group, while the treated groups showed significantly reduced expression.

DPP-4 inhibitor and PPAR-alpha agonist improved the intestinal barrier structure and protection

The HF group showed an 80% decrease in intestinal *Mucin2* gene expression compared with the C group. Conversely, the HFA, HFL, and HFC groups showed significant increases in *Mucin2* expression (+439% for HFA *vs* HF, +345% for HFL *vs* HF, and +670% for HFC *vs* HF; Figure 4A).



DOI: 10.3748/wjg.v28.i17.1814 **Copyright** ©The Author(s) 2022.

Figure 2 Carbohydrate metabolism. A: Oral glucose tolerance test; B: Area under the curve for oral glucose tolerance test; C: Plasma glucagon-like peptide 1 concentrations. Brown-Forsythe and Welch one-way ANOVA and Dunnett T3 *post hoc* test (mean ± SD, $n = 6$). Significant differences are indicated as follows: $^{a}P < 0.05$; $^{c}P < 0.001$; $^{d}P < 0.0001$. C: Control diet; HF: High-fat diet; HFA: High-fat diet plus PPAR-alpha agonist (WY14643); HFL: High-fat diet plus DPP-4 inhibitor (linagliptin); HFC: High-fat diet plus the combination of WY14643 with linagliptin; AUC: Area under the curve; OGTT: Oral glucose tolerance test; GLP1: Glucagon-like peptide 1.

In agreement with the previous result, the HF group also had reduced intestinal *Zo-1* (-38%, Figure 4B) and *Occludin* (-78%, Figure 4C) expression compared to the C group. On the other hand, the HFA group showed a 238% increase in *Occludin* expression, whereas the HFL and HFC groups had > 500% increases in the expression of this gene (Figure 4C). Regarding *Zo-1* gene expression, all treated groups had a significant increase (+166% for HFA *vs* HF, +397% for HFL *vs* HF, and +102% for HFC *vs* HF; Figure 4B).

The high intake of saturated fat altered the histochemical pattern of the intestinal mucosal cells, as revealed by the reaction with Alcian Blue and PAS. Figure 4D shows decreased mucus in the HF group, while the treatments elicited an increase in mucus production in the apical region of the crypts, followed by an increased presence of goblet cells (mucus-producing cells). Gut stereology confirmed these observations with the results of Q_A (goblet), which showed a reduction in the HF group compared to the C group (-44%), while the HFA (+68%), HFL (+47%), and HFC (+56%) groups showed an increase in the number of goblet cells *per* tissue area (Figure 4E).

DPP-4 inhibitor and PPAR-alpha activation mitigated liver steatosis

HF-fed mice exhibited noticeable microvesicular liver steatosis, while mice in all treated groups showed liver steatosis mitigation, with the liver parenchyma resembling that in the C group (Figure 5A).

In accordance with these histological findings, Vv (liver, st) in the HF group was higher than that in the C group (+38%, Figure 5B). All treated groups showed drastic reductions in liver steatosis (-72% for HFA *vs* HF, -50% for HFL *vs* HF, and -77% for HFC *vs* HF).

Consistent with the stereological findings, hepatic TAG levels increased in the HF group (+38%). Conversely, the treated groups showed lower hepatic TAG concentrations than that in the HF group (-11% for HFA, -16% for HFL, and -13% for HFC; Figure 5C).

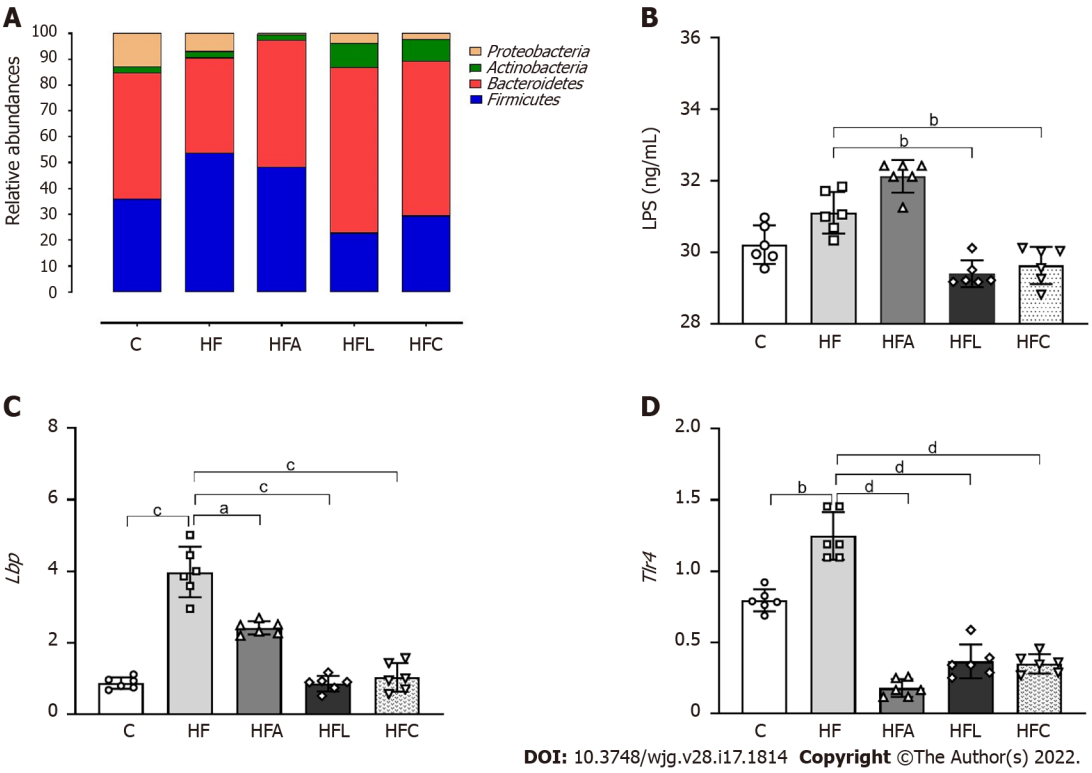


Figure 3 Gut-liver axis. A: Phylogenetic microbiota composition; B: Plasma lipopolysaccharide concentrations; C: Hepatic *Lbp* gene expression; D: Hepatic *Tlr4* gene expression. Brown-Forsythe and Welch one-way ANOVA and Dunnett T3 *post hoc* test (mean ± SD, $n = 6$). Significant differences are indicated as follows: $^{a}P < 0.05$; $^{b}P < 0.01$; $^{c}P < 0.001$; $^{d}P < 0.0001$. C: Control diet; HF: High-fat diet; HFA: High-fat diet plus PPAR-alpha agonist (WY14643); HFL: High-fat diet plus DPP-4 inhibitor (linagliptin); HFC: High-fat diet plus the combination of WY14643 with linagliptin; LPS: Lipopolysaccharide.

DPP-4 inhibition and PPAR-alpha activation attenuated macrophage activation and reduced liver inflammation in HF-fed mice

The HF group showed higher expression of *Cd206*, which is a specific marker of macrophages, than the C group (+103%, Figure 6A). In contrast, the treated groups showed reduced *Cd206* expression (-67% for HFA *vs* HF, -65% for HFL *vs* HF, and -74% for HFC *vs* HF).

In addition to the *Cd206* results, the HF diet significantly reduced *IL-10* expression compared to the C group (-54%), whereas the combined treatment yielded an 80% decrease in HFC *IL-10* expression compared to HF (Figure 6B). *Nlrp3* showed similar results to those of the *Cd206* gene, with higher expression in the HF group than in the C group (+128%) and reduced expression in the HFA (-72%), HFL (-88%), and HFC (-85%) groups compared to the HF group (Figure 6C).

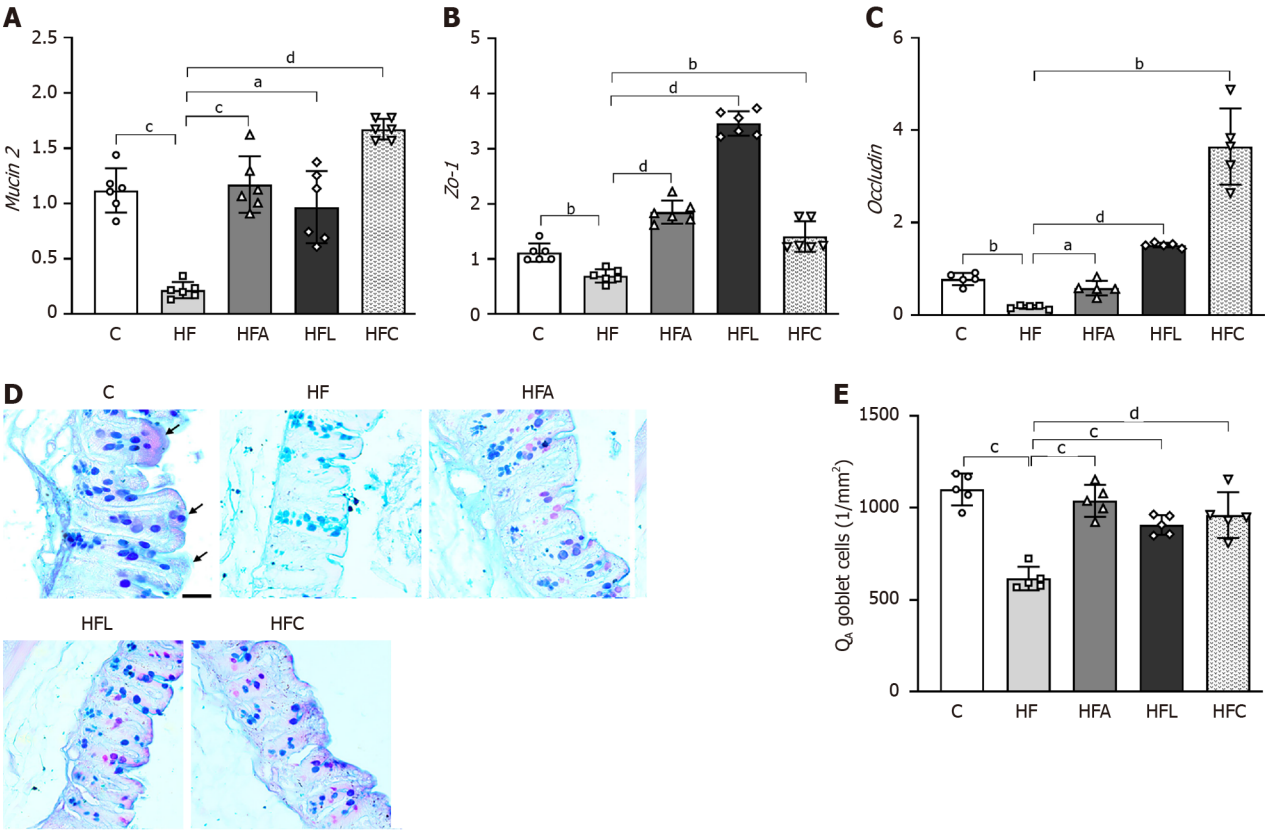
Regarding the *IL-13* cytokine, the HF group exhibited a significant increase compared to the C group (+290%). Only the HFA and HFC treatments were able to reduce the expression of this cytokine in comparison with the HF group (-39% and -67%) (Figure 6D).

DISCUSSION

Excessive saturated fat intake causes overweightness, oral glucose intolerance, gut dysbiosis, and morphological and functional intestinal barrier alterations. Hence, HF animals had endotoxemia with proinflammatory signals directed toward the liver, causing substantial NAFLD. Single treatment with the PPAR-alpha agonist or DPP-4 inhibitor and the combined treatment yielded beneficial results, rescuing body mass, oral glucose tolerance, gut goblet cell numerical density *per* area, *TJ* gene expression, phylogenetic microbiota distribution, and LPS concentrations. Thus, treated animals showed liver steatosis and inflammation mitigation due to gut dysbiosis and endotoxemia control.

The chronic ingestion of a diet with a high content of saturated fats increases body mass and impairs glucose and lipid metabolism[22]. Accordingly, HF-fed mice were overweight and showed oral glucose intolerance, along with difficulty in rescuing glycemic levels during the OGTT compared to the C group. These metabolic alterations were paralleled by gut dysbiosis in the HF group, confirming that dietary patterns interfere with the gut–liver axis, favoring NAFLD pathogenesis and progression.

The integrity of the intestinal barrier structure and function relates to the gut microbiota composition. The gut microbiota comprises a great diversity of symbiotic bacteria, whereas the intestinal barrier relies on junctional proteins that make this epithelium less permeable to pathogens and toxins. In this way,



DOI: 10.3748/wjg.v28.i17.1814 **Copyright** ©The Author(s) 2022.

Figure 4 Gut gene expression, histology, and stereology. A: Gut *Mucin2*; B: *Zo-1*; C: *Occludin* gene expression; D: Large intestine stained with Alcian Blue and Periodic Acid-Schiff (PAS); E: Numerical density of goblet cells *per* area. Alcian blue and PAS stain glycoproteins produced by goblet cells (scale bar = 40 μm), which were markedly reduced by the high-fat diet and rescued by the treatments according to stereology (Q_A goblet). Brown-Forsythe and Welch one-way ANOVA and Dunnett T3 *post hoc* test (mean ± SD, n = 6 for real-time reverse transcriptase–polymerase chain reaction and n = 5 for stereology). Significant differences are indicated as follows: $^aP < 0.05$; $^bP < 0.01$; $^cP < 0.001$; $^dP < 0.0001$. C: Control diet; HF: High-fat diet; HFA: High-fat diet plus PPAR-alpha agonist (WY14643); HFL: High-fat diet plus DPP-4 inhibitor (linagliptin); HFC: High-fat diet plus the combination of WY14643 with linagliptin; PAS: Periodic Acid-Schiff; Q_A: Numerical density *per* area.

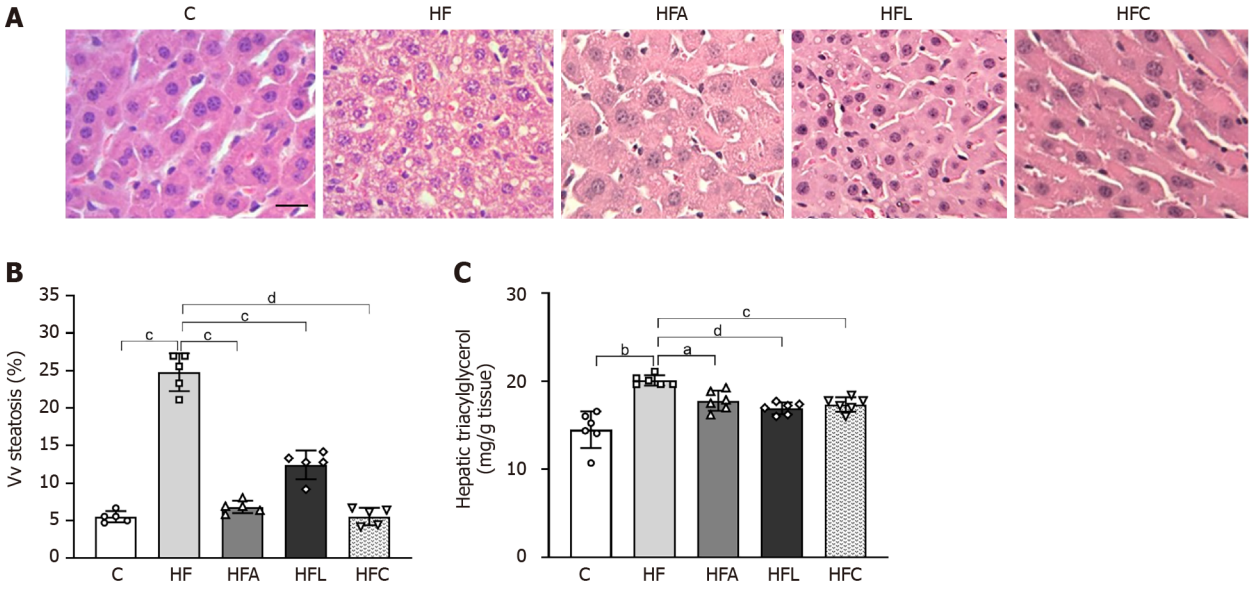
both mechanisms prevent metabolic dysregulation and contribute to maintaining gut homeostasis[23-25].

Dysbiosis caused by the chronic consumption of fats is usually characterized by an increase in *Firmicutes* relative to *Bacteroidetes*, as shown by the HF group. These two phyla constitute more than 90% of the phylogenetic category currently known and characterized in the intestine of experimental models [26]. Conversely, all treated groups showed a reduction in the quantitative percentage of *Firmicutes*, especially the groups treated with the DPP-4 inhibitor and the combined therapy.

The rescuing of gut dysbiosis in the treated groups resulted in marked improvements in TJ gene expression. An HF diet also impairs the junctional components present in the intestinal epithelium, making it more permeable and consequently more susceptible to the translocation of microorganisms and toxins into systemic circulation. The increase in intestinal permeability is known as a leaky gut[25, 27].

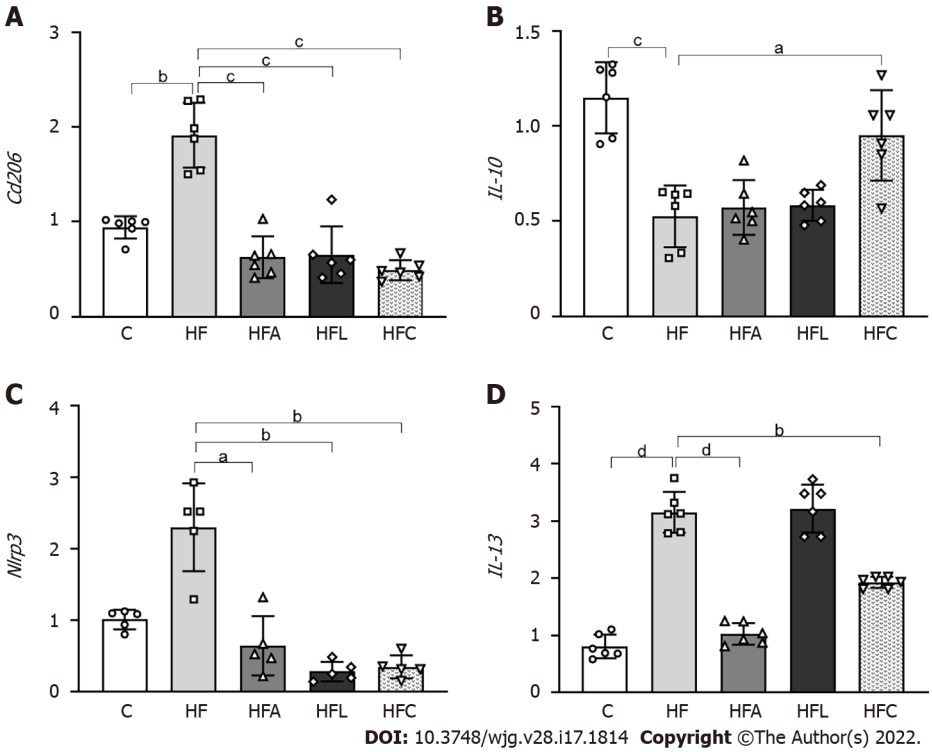
The leaky gut was rescued through enhanced expression of TJ genes in all treated groups. MUCIN2 knockout mice exhibit alterations in TJ structural proteins, in addition to mitochondrial damage and inflammation, which agrees with a leaky gut[28]. The treatments significantly augmented *Mucin2*, which is the major goblet cell gene responsible for mucin secretion, in addition to the gene expression of the TJs *Occludin* and *Zo-1*[29]. PPAR-alpha has recently been described as essential for lipid droplet formation and crypt expansion in the intestine during chronic HF diet intake[30]. Sitagliptin, as a DPP-4 inhibitor, exerted protective effects on the intestinal barrier (high *occludin* and *Zo-1* levels) by GLP-2 induction in experimental colitis[31]. Herein, the combination of these drugs resulted in the highest intestinal expression of *Mucin2* and *Occludin*, indicating that adequate function of goblet cells and well-preserved TJs may underlie the mechanisms involved in the beneficial results obtained in the HFC group.

HF diet intake also impairs the epithelium lining the intestinal mucosa. The goblet cells found in the intestinal villi and crypts are mucin producers that play a crucial role in protecting and lubricating the intestinal mucosa. The number of goblet cells indirectly reflects the ability to secrete mucus[25]. Herein, the HF diet caused a reduced number of goblet cells *per* area of the gut crypt, while all treatments



DOI: 10.3748/wjg.v28.i17.1814 **Copyright** ©The Author(s) 2022.

Figure 5 Liver histology, stereology, and biochemistry. A: Hematoxylin-eosin liver sections; B: Volume density (Vv) (liver steatosis); C: Hepatic triacylglycerol. Liver sections show widespread hepatic steatosis after chronic HF diet intake and expressive reduction in all treated groups (scale bar = 50 µm. Both stereology (Vv steatosis) and biochemical analyses (hepatic triacylglycerol) confirm these observations. Brown-Forsythe and Welch one-way ANOVA and Dunnett T3 *post hoc* test (mean ± SD, $n = 6$ for biochemistry and $n = 5$ for stereology). Significant differences are indicated as follows: $^{a}P < 0.05$; $^{b}P < 0.01$; $^{c}P < 0.001$; $^{d}P < 0.0001$. C: Control diet; HF: High-fat diet; HFA: High-fat diet plus PPAR-alpha agonist (WY14643); HFL: High-fat diet plus DPP-4 inhibitor (linagliptin); HFC: High-fat diet plus the combination of WY14643 with linagliptin; Vv: Volume density.



DOI: 10.3748/wjg.v28.i17.1814 **Copyright** ©The Author(s) 2022.

Figure 6 Liver gene expression. A: *Cd206*; B: *IL-10*; C: *Nlrp3*; D: *IL-13*. Brown-Forsythe and Welch one-way ANOVA and Dunnett T3 *post hoc* test (mean ± SD, $n = 5$ or 6). Significant differences are indicated as follows: $^{a}P < 0.05$; $^{b}P < 0.01$; $^{c}P < 0.001$; $^{d}P < 0.0001$. C: Control diet; HF: High-fat diet; HFA: High-fat diet plus PPAR-alpha agonist (WY14643); HFL: High-fat diet plus DPP-4 inhibitor (linagliptin); HFC: High-fat diet plus the combination of WY14643 with linagliptin.

reversed this alteration with the normalization of the numerical density of goblet cells and *Mucin2* gene expression. Hence, the treatments supported intestinal barrier integrity and reduced the translocation of endotoxins, such as LPS, into systemic circulation, rescuing the mice from a condition called metabolic endotoxemia[32].

The high translocation of endotoxins derived from the gut microbiota induces Toll-like receptor (TLR) activation. LPS is the most common pathogen-associated molecular pattern (PAMP), and its binding to TLR4 is catalyzed by lipopolysaccharide-binding protein (LBP), which is mainly expressed in the liver and adipose tissue[32].

LPS stems from the destruction of the bacterial cell wall. An increase in LPS in systemic circulation triggers the release of proinflammatory cytokines and an inadequate amplification of the immune response, causing tissue damage[26]. An increase in plasma LPS levels was observed in the HF group, characterizing the involvement of the epithelium with a consequent increase in intestinal permeability, making the epithelium more permeable to the entry of microorganisms. Additionally, we showed that hepatic *Lbp* and *Tlr4* gene expression increased in the HF group, inducing the translocation of cytokines associated with inflammation and changing hepatic lipid metabolism, reconfiguring this metabolism to become a potent inducer of fatty liver, and contributing to the pathogenesis of NAFLD.

In contrast, the treatments normalized *Lbp* and *Tlr4* expression, with both emerging as targets for NAFLD treatment. The DPP-4 inhibitor alogliptin suppressed TLR4 *via* ERK activation, resulting in decreased matrix metalloproteinases and proinflammatory cytokines in U937 histiocytes[33]. Sitagliptin was previously shown to attenuate NAFLD by suppressing inflammation and insulin resistance due to TLR4/NF-kB pathway downregulation in diabetic rats[34]. PPAR-alpha activation by WY-14643 mitigated liver steatosis in high-fructose-fed mice by reducing LPS concentrations, improving the intestinal barrier ultrastructure, upregulating hepatic beta-oxidation, and suppressing lipogenesis in mice[9].

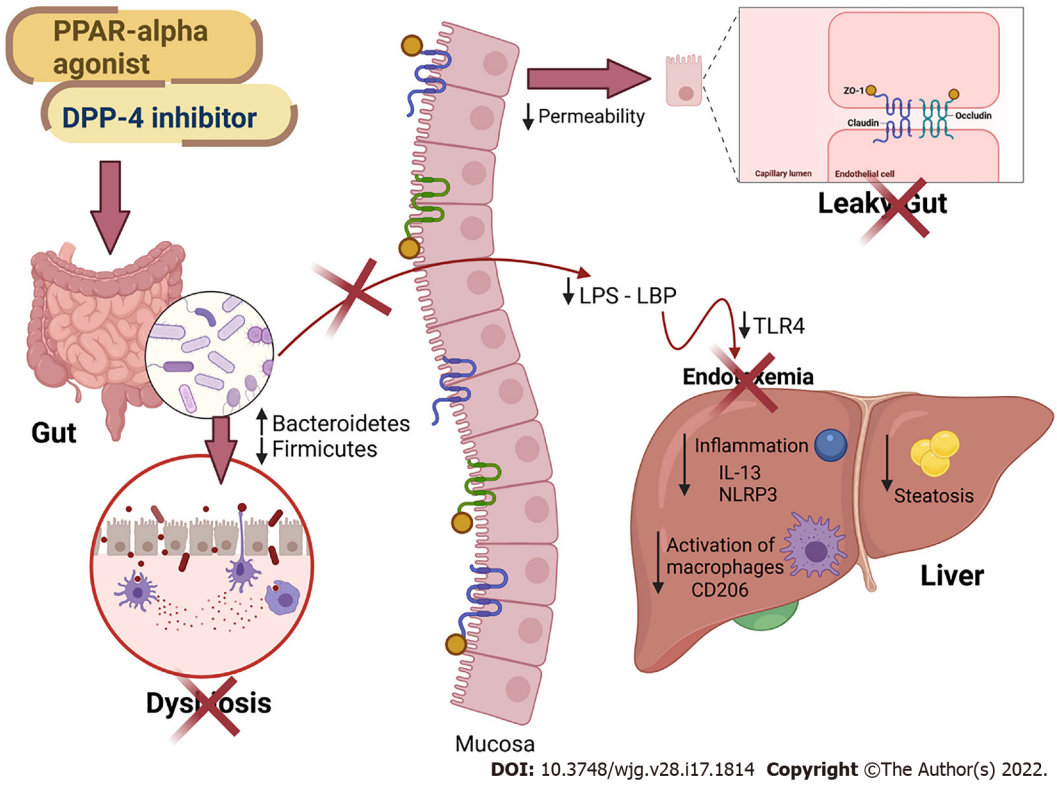
A recent study showed that systemic LBP blockade or decreased LBP levels in the liver normalized glucose homeostasis, mainly by reducing fasting glucose levels, without changing adiposity or liver steatosis[35]. In this study, the group treated with the PPAR-alpha agonist as monotherapy did not show reduced LPS concentrations. However, the treatment reduced *Lbp* expression, producing anti-inflammatory and anti-steatotic effects similar to those of the other treatments.

In this context, macrophages play roles in acute and chronic inflammatory liver diseases. Macrophages have receptors, such as CD163 and CD206, which participate in the phagocytosis of harmful substances. Due to its high affinity for macrophages, CD206 is a potential biomarker of hepatic macrophage (Kupffer cells) activation, which indicates inflammation and fibrosis in chronic liver diseases[36]. In response to LPS and other stimuli, the metabolic profile of macrophages and dendritic cells stimulates the glycolytic pathway, resulting in the metabolic accumulation of citrate and succinate, which, in turn, regulate the gene expression of cytokines such as interleukin 10 (IL-10)[37]. Recent evidence shows that IL-10 may play a dual role in some contexts by stimulating the immune response rather than suppressing it. However, the cytokine IL-10 has emerged as an anti-inflammatory mediator determining the protection of its host in response to pathogens[38].

Our results showed that *Cd206* macrophages were activated in the HF group, reinforcing the idea that the chronic consumption of this type of diet activates inflammatory pathways that contribute to the development of liver disease. In contrast, the groups treated with the PPAR-alpha activator and DPP-4 inhibitor showed reduced expression of *Cd206* macrophages, conferring a protective effect against the activation of inflammatory pathways. Recent evidence showed that highly fibrous livers had a higher density of *Cd206* macrophages[36]. *IL-10* gene expression was reduced in the HF group. However, only the combined treatment increased *IL-10* expression, implying that the isolated treatments might have acted through another anti-inflammatory pathway. IL-13 overexpression in HF diet-fed mice is a pathway related to fatty liver and insulin resistance onset. Combined treatment and PPAR-alpha activation alone markedly reduced hepatic *IL-13* expression, which combined with reduced macrophage activation and glycemic homeostasis to alleviate fatty liver[39].

Concerning inflammasomes, NLRP3 is present mainly in immune and inflammatory cells, such as macrophages, monocytes, dendritic cells, and neutrophils, after activation by inflammatory stimuli. NLRP3 is activated by numerous PAMPs, such as hyperglycemia, fatty acids, bacterial toxins, and bacterial and viral nucleic acids[40]. Studies in macrophages and animal models have shown that oxidized low-density lipoproteins and cholesterol crystals trigger NLRP3 activation. In macrophage and type 2 diabetes animal models, glucose and free fatty acids trigger inflammasome activation, damaging glucose metabolism and favoring insulin resistance[41]. Thus, NLRP3 may contribute to the appearance and progression of several diseases related to metabolic syndrome.

In this study, we showed that treatment with the PPAR-alpha agonist and DPP-4 inhibitor produced a potent anti-inflammatory effect in the liver, as they demonstrated reduced gene expression of *Nlrp3* and *Cd206*. The blockade of NLRP3 has recently improved NAFLD and mitigated liver fibrosis in two models of steatohepatitis[42], highlighting the proposed treatments as viable tools to control fatty liver. Two DPP-4 inhibitors were previously shown to suppress NLRP3 in human macrophages by downregulating the TLR4-IL-1beta pathway[43]. Sitagliptin alleviated liver injury caused by thioacetamide in mice by decreasing NLRP3 and exerting anti-apoptotic effects[44]. Regarding PPAR-alpha activation, oleoylethanolamide protected against LPS-induced liver injury in mice by suppressing NLRP3[45]. However, the present study is the first to report the effects of both drugs and their combination on the gut–liver axis in HF-fed mice. Figure 7 summarizes our main findings.



DOI: 10.3748/wjg.v28.i17.1814 **Copyright** ©The Author(s) 2022.

Figure 7 Main findings of the study. All treatments alleviated fatty liver by countering gut dysbiosis and rescuing the intestinal barrier integrity. The reduced lipopolysaccharide (LPS) influx to the liver caused reduced inflammasome and CD206 macrophage activation. Peroxisome proliferator-activated receptor-alpha activation and DPP-4 inhibition can be regarded as viable tools to treat leaky gut and prevent LPS-driven hepatic steatosis. PPAR: Peroxisome proliferator-activated receptor; DPP-4: Dipeptidyl peptidase-4; LPS: Lipopolysaccharide; LBP: Lipopolysaccharide-binding protein; TLR4: Toll-Like receptor 4; ZO-1: Zonula occludens 1; NLRP3: NLR family pyrin domain containing 3; CD206: Cluster of differentiation 206; IL: Interleukin. Created with Biorender: www.biorender.com.

Some limitations of the present study comprise the absence of female mice evaluations to determine possible sexual dimorphism, the lack of plasma glucose concentration measurements, and the inability to determine LBP concentrations, although its gene expression was evaluated. Future research should also include the evaluation of genera and families in the *Proteobacteria* phylum, as it seems to be involved in the harmful evolution of NAFLD.

CONCLUSION

In conclusion, HF-fed mice showed impairment of the intestinal barrier and alteration in the phylogenetic diversity of the gut microbiota, leading to dysbiosis, and contributing to the influx of LPS into the liver. An impaired gut–liver axis favors liver damage, making the liver more susceptible to NAFLD through proinflammatory signals (*Tlr4* and *Nlrp3* upregulation). Treatment with the PPAR-alpha agonist and the DPP-4 inhibitor modulated the gut microbiota and rescued intestinal barrier gene expression and goblet cell numerical density, reducing endotoxemia and liver steatosis through anti-inflammatory signaling. Given the beneficial effects of the treatments found, these treatments have become possible therapeutic strategies for the NAFLD spectrum of diseases.

ARTICLE HIGHLIGHTS

Research background

Gut microbiota can be modified by the dietary composition and play a role in fatty liver pathogenesis through endotoxemia. Peroxisome proliferator-activated receptor (PPAR)-alpha activation has previously rescued the gut–liver axis with anti-steatotic effects in high-fructose-fed mice, whereas a high-dose dipeptidyl peptidase-4 (DPP-4) inhibitor (linagliptin) inhibited hepatic lipogenesis in high-fat-fed mice. The combination of these drugs could restore the gut–liver axis in obese mice.

Research motivation

Nonalcoholic fatty liver disease (NAFLD) is highly prevalent among obese individuals and can evolve into harmful liver diseases. Currently, there is no treatment directly prescribed to counter NAFLD. Herein, we propose a drug combination (PPAR-alpha agonist plus DPP-4 inhibitor) that can alleviate fatty liver by modulating the gut–liver axis with anti-inflammatory properties.

Research objectives

To evaluate the effects of monotherapy with a PPAR-alpha agonist (WY14643) or a DPP-4 inhibitor (linagliptin) and their combined treatment on the gut–liver axis, highlighting the intestinal barrier, endotoxemia, and inflammatory pathways in the livers of high-fat-fed mice. These preclinical insights can help establish new strategies for the treatment of NAFLD.

Research methods

Mice were fed a control diet (C, 10% of energy as lipids) or a high-fat diet (HF, 50% of energy as lipids) for 12 wk. Then, the HF group was randomly divided into four groups: HF, HF-A (treated with the PPAR-alpha agonist), HFL (treated with the DPP-4 inhibitor), and HFC (treated with the combination of both drugs). The treatments lasted for five weeks. The gut–liver axis was assessed by histological, biochemical, stereological, and molecular techniques.

Research results

The HF diet yielded overweightness and oral glucose intolerance, altered gut microbiota composition, and decreased the numerical density of goblet cells and tight junction gene expression, with increased plasma lipopolysaccharide (LPS) concentrations and increased fatty liver. The combined treatment rescued all of these metabolic alterations by restoring the gut microbiota and intestinal barrier markers, resulting in decreased LPS concentrations and fatty liver through anti-inflammatory signals. Further studies may focus on the *Proteobacteria* phylum, whose alteration can trigger harmful signaling to the liver.

Research conclusions

The combination of PPAR-alpha activation with DPP-4 inhibition yielded marked anti-steatotic effects by modulating the gut–liver axis, with reduced endotoxemia and amelioration of the intestinal barrier histology and gene expression. In turn, the livers of obese mice treated with the drug combination benefited from downregulation of the *Tlr4* and *Nlrp3* pathways and exhibited a hepatic parenchyma similar to that in the C group. Of note, we used stereology to estimate the numerical density of goblet cells in cecum slides stained with Alcian Blue and Periodic Acid-Schiff. This technique can be used to assess the effects of different interventions on the intestinal barrier and leaky gut in further studies.

Research perspectives

This study brings novelty to the treatment of NAFLD, which is a challenge to the scientific community. Our results confirm the importance of the gut–liver axis in the pathogenesis of fatty liver and propose a combined treatment that targets the gut microbiota composition, endotoxemia, and intestinal barrier alterations to alleviate fatty liver through local anti-inflammatory effects in HF-fed mice.

ACKNOWLEDGEMENTS

The authors would like to thank Aline Penna for her technical assistance.

FOOTNOTES

Author contributions: Silva-Veiga FM, Martins FF, Daleprane JB, and Souza-Mello V designed and coordinated the study; Silva-Veiga FM, Miranda CS, Vasques-Monteiro IML, Souza-Tavares H, Martins FF, Daleprane JB, and Souza-Mello V performed the experiments, acquired and analyzed data; Silva-Veiga FM, Miranda CS, Vasques-Monteiro IML, Martins FF, Daleprane JB, and Souza-Mello V interpreted the data; Silva-Veiga FM and Souza-Mello V wrote the manuscript; all authors approved the final version of the article.

Supported by Coordenação de Aperfeiçoamento de Pessoal de Nível Superior–Brasil, No. CAPES–Finance Code 001; Fundação Carlos Chagas Filho de Amparo à Pesquisa do Rio de Janeiro (FAPERJ) to Souza-Mello V, No. E-26/202.657/2018 and No. E-26/010.002136/2019; The corresponding author is supported by Conselho Nacional de Desenvolvimento Científico e Tecnológico (CNPq), No. 303785/2020-9.

Institutional review board statement: The study was reviewed and approved by the CEUA of State University of Rio de Janeiro Institutional Review Board, No. 041/2018.

Conflict-of-interest statement: The authors have no conflict of interest to declare.

Data sharing statement: Technical appendix, statistical code, and dataset available from the corresponding author at souzamello.uerj@gmail.com.

ARRIVE guidelines statement: The authors have read the ARRIVE Guidelines, and the manuscript was prepared and revised according to the ARRIVE Guidelines.

Open-Access: This article is an open-access article that was selected by an in-house editor and fully peer-reviewed by external reviewers. It is distributed in accordance with the Creative Commons Attribution NonCommercial (CC BY-NC 4.0) license, which permits others to distribute, remix, adapt, build upon this work non-commercially, and license their derivative works on different terms, provided the original work is properly cited and the use is non-commercial. See: https://creativecommons.org/Licenses/by-nc/4.0/

Country/Territory of origin: Brazil

ORCID number: Flavia Maria Silva-Veiga 0000-0002-3320-5825; Carolline Santos Miranda 0000-0001-5488-0179; Isabela Macedo Lopes Vasques-Monteiro 0000-0003-1729-3201; Henrique Souza-Tavares 0000-0001-79314384; Fabiane Ferreira Martins 0000-0002-3831-6604; Julio Beltrame Daleprane 0000-0002-3493-1386; Vanessa Souza-Mello 0000-0002-2510-9569.

S-Editor: Fan JR
L-Editor: A
P-Editor: Li X

REFERENCES

1 **GBD 2017 Diet Collaborators**. Health effects of dietary risks in 195 countries, 1990-2017: a systematic analysis for the Global Burden of Disease Study 2017. *Lancet* 2019; **393**: 1958-1972 [PMID: 30954305 DOI: 10.1016/S0140-6736(19)30041-8]
2 **Hruby A**, Hu FB. The Epidemiology of Obesity: A Big Picture. *Pharmacoeconomics* 2015; **33**: 673-689 [PMID: 25471927 DOI: 10.1007/s40273-014-0243-x]
3 **Volynets V**, Louis S, Pretz D, Lang L, Ostaff MJ, Wehkamp J, Bischoff SC. Intestinal Barrier Function and the Gut Microbiome Are Differentially Affected in Mice Fed a Western-Style Diet or Drinking Water Supplemented with Fructose. *J Nutr* 2017; **147**: 770-780 [PMID: 28356436 DOI: 10.3945/jn.116.242859]
4 **Miranda CS**, Silva-Veiga F, Martins FF, Rachid TL, Mandarim-De-Lacerda CA, Souza-Mello V. PPAR-α activation counters brown adipose tissue whitening: a comparative study between high-fat- and high-fructose-fed mice. *Nutrition* 2020; **78**: 110791 [PMID: 32682271 DOI: 10.1016/j.nut.2020.110791]
5 **Matsushita N**, Osaka T, Haruta I, Ueshiba H, Yanagisawa N, Omori-Miyake M, Hashimoto E, Shibata N, Tokushige K, Saito K, Tsuneda S, Yagi J. Effect of Lipopolysaccharide on the Progression of Non-Alcoholic Fatty Liver Disease in High Caloric Diet-Fed Mice. *Scand J Immunol* 2016; **83**: 109-118 [PMID: 26524607 DOI: 10.1111/sji.12397]
6 **Leung C**, Rivera L, Furness JB, Angus PW. The role of the gut microbiota in NAFLD. *Nat Rev Gastroenterol Hepatol* 2016; **13**: 412-425 [PMID: 27273168 DOI: 10.1038/nrgastro.2016.85]
7 **Zhou X**, Han D, Xu R, Li S, Wu H, Qu C, Wang F, Wang X, Zhao Y. A model of metabolic syndrome and related diseases with intestinal endotoxemia in rats fed a high fat and high sucrose diet. *PLoS One* 2014; **9**: e115148 [PMID: 25502558 DOI: 10.1371/journal.pone.0115148]
8 **Gray H**. Gray Anatomia Charles Mayo Goss. Rio de Janeiro: Guanabara Koogan; 1988
9 **Silva-Veiga FM**, Miranda CS, Martins FF, Daleprane JB, Mandarim-de-Lacerda CA, Souza-Mello V. Gut-liver axis modulation in fructose-fed mice: a role for PPAR-alpha and linagliptin. *J Endocrinol* 2020; **247**: 11-24 [PMID: 32698143 DOI: 10.1530/JOE-20-0139]
10 **Younossi ZM**, Koenig AB, Abdelatif D, Fazel Y, Henry L, Wymer M. Global epidemiology of nonalcoholic fatty liver disease-Meta-analytic assessment of prevalence, incidence, and outcomes. *Hepatology* 2016; **64**: 73-84 [PMID: 26707365 DOI: 10.1002/hep.28431]
11 **Rachid TL**, Silva-Veiga FM, Graus-Nunes F, Bringhenti I, Mandarim-de-Lacerda CA, Souza-Mello V. Differential actions of PPAR-α and PPAR-β/δ on beige adipocyte formation: A study in the subcutaneous white adipose tissue of obese male mice. *PLoS One* 2018; **13**: e0191365 [PMID: 29351550 DOI: 10.1371/journal.pone.0191365]
12 **Manoharan I**, Suryawanshi A, Hong Y, Ranganathan P, Shanmugam A, Ahmad S, Swafford D, Manicassamy B, Ramesh G, Koni PA, Thangaraju M, Manicassamy S. Homeostatic PPARα Signaling Limits Inflammatory Responses to Commensal Microbiota in the Intestine. *J Immunol* 2016; **196**: 4739-4749 [PMID: 27183583 DOI: 10.4049/jimmunol.1501489]
13 **Santana-Oliveira DA**, Fernandes-da-Silva A, Miranda CS, Martins FF, Mandarim-de-Lacerda CA, Souza-Mello V. A PPAR-alpha agonist and DPP-4 inhibitor mitigate adipocyte dysfunction in obese mice. *J Mol Endocrinol* 2022 [PMID: 35302950 DOI: 10.1530/JME-21-0084]
14 **Sakai Y**, Chen G, Ni Y, Zhuge F, Xu L, Nagata N, Kaneko S, Ota T, Nagashimada M. DPP-4 Inhibition with Anagliptin Reduces Lipotoxicity-Induced Insulin Resistance and Steatohepatitis in Male Mice. *Endocrinology* 2020; **161** [PMID: 32790863 DOI: 10.1210/endocr/bqaa139]

15 **Reeves PG**, Nielsen FH, Fahey GC Jr. AIN-93 purified diets for laboratory rodents: final report of the American Institute of Nutrition ad hoc writing committee on the reformulation of the AIN-76A rodent diet. *J Nutr* 1993; **123**: 1939-1951 [PMID: 8229312 DOI: 10.1093/jn/123.11.1939]

16 **Catta-Preta M**, Mendonca LS, Fraulob-Aquino J, Aguila MB, Mandarim-de-Lacerda CA. A critical analysis of three quantitative methods of assessment of hepatic steatosis in liver biopsies. *Virchows Arch* 2011; **459**: 477-485 [PMID: 21901430 DOI: 10.1007/s00428-011-1147-1]

17 **Tschanz SA**, Burri PH, Weibel ER. A simple tool for stereological assessment of digital images: the STEPanizer. *J Microsc* 2011; **243**: 47-59 [PMID: 21375529 DOI: 10.1111/j.1365-2818.2010.03481.x]

18 **Livak KJ**, Schmittgen TD. Analysis of relative gene expression data using real-time quantitative PCR and the 2(-Delta Delta C(T)) Method. *Methods* 2001; **25**: 402-408 [PMID: 11846609 DOI: 10.1006/meth.2001.1262]

19 **Davisson MT**. Rules and guidelines for nomenclature of mouse genes. International Committee on Standardized Genetic Nomenclature for Mice. *Gene* 1994; **147**: 157-160 [PMID: 7926794 DOI: 10.1016/0378-1119(94)90060-4]

20 **Cruz-Orive LM**, Weibel ER. Recent stereological methods for cell biology: a brief survey. *Am J Physiol* 1990; **258**: L148-L156 [PMID: 2185653 DOI: 10.1152/ajplung.1990.258.4.L148]

21 **Dunnett CW**. Pairwise multiple comparisons in the unequal variance case. *J Am Stat Assoc* 1980; **75**: 796-800 [DOI: 10.1080/01621459.1980.10477552]

22 **De Lorenzo A**, Gratteri S, Gualtieri P, Cammarano A, Bertucci P, Di Renzo L. Why primary obesity is a disease? *J Transl Med* 2019; **17**: 169 [PMID: 31118060 DOI: 10.1186/s12967-019-1919-y]

23 **Cremonini E**, Daveri E, Mastaloudis A, Adamo AM, Mills D, Kalanetra K, Hester SN, Wood SM, Fraga CG, Oteiza PI. Anthocyanins protect the gastrointestinal tract from high fat diet-induced alterations in redox signaling, barrier integrity and dysbiosis. *Redox Biol* 2019; **26**: 101269 [PMID: 31330482 DOI: 10.1016/j.redox.2019.101269]

24 **Blüher M**. Obesity: global epidemiology and pathogenesis. *Nat Rev Endocrinol* 2019; **15**: 288-298 [PMID: 30814686 DOI: 10.1038/s41574-019-0176-8]

25 **Odenwald MA**, Turner JR. The intestinal epithelial barrier: a therapeutic target? *Nat Rev Gastroenterol Hepatol* 2017; **14**: 9-21 [PMID: 27848962 DOI: 10.1038/nrgastro.2016.169]

26 **Schoeler M**, Caesar R. Dietary lipids, gut microbiota and lipid metabolism. *Rev Endocr Metab Disord* 2019; **20**: 461-472 [PMID: 31707624 DOI: 10.1007/s11154-019-09512-0]

27 **Ortigão R**, Pimentel-Nunes P, Dinis-Ribeiro M, Libânio D. Gastrointestinal Microbiome - What We Need to Know in Clinical Practice. *GE Port J Gastroenterol* 2020; **27**: 336-351 [PMID: 32999906 DOI: 10.1159/000505036]

28 **Borisova MA**, Achasova KM, Morozova KN, Andreyeva EN, Litvinova EA, Ogienko AA, Morozova MV, Berkaeva MB, Kiseleva E, Kozhevnikova EN. Mucin-2 knockout is a model of intercellular junction defects, mitochondrial damage and ATP depletion in the intestinal epithelium. *Sci Rep* 2020; **10**: 21135 [PMID: 33273633 DOI: 10.1038/s41598-020-78141-4]

29 **Meyer R**. Comment on Guenette, S.A., Beaudry, F., Marier, J.F., and Vachon, P. (2006). Pharmacokinetics and anesthetic activity of eugenol in male Sprague-Dawley rats. J. Vet. Pharmacol. Ther. 29, 265-270. *J Vet Pharmacol Ther* 2007; **30**: 91; author reply 92 [PMID: 17217408 DOI: 10.1111/j.1365-2885.2007.00814.x]

30 **Stojanović O**, Altirriba J, Rigo D, Spiljar M, Evrard E, Roska B, Fabbiano S, Zamboni N, Maechler P, Rohner-Jeanrenaud F, Trajkovski M. Dietary excess regulates absorption and surface of gut epithelium through intestinal PPARα. *Nat Commun* 2021; **12**: 7031 [PMID: 34857752 DOI: 10.1038/s41467-021-27133-7]

31 **Ning MM**, Yang WJ, Guan WB, Gu YP, Feng Y, Leng Y. Dipeptidyl peptidase 4 inhibitor sitagliptin protected against dextran sulfate sodium-induced experimental colitis by potentiating the action of GLP-2. *Acta Pharmacol Sin* 2020; **41**: 1446-1456 [PMID: 32398684 DOI: 10.1038/s41401-020-0413-7]

32 **Do MH**, Lee E, Oh MJ, Kim Y, Park HY. High-Glucose or -Fructose Diet Cause Changes of the Gut Microbiota and Metabolic Disorders in Mice without Body Weight Change. *Nutrients* 2018; **10** [PMID: 29899272 DOI: 10.3390/nu10060761]

33 **Ta NN**, Li Y, Schuyler CA, Lopes-Virella MF, Huang Y. DPP-4 (CD26) inhibitor alogliptin inhibits TLR4-mediated ERK activation and ERK-dependent MMP-1 expression by U937 histiocytes. *Atherosclerosis* 2010; **213**: 429-435 [PMID: 20843518 DOI: 10.1016/j.atherosclerosis.2010.08.064]

34 **Allam MM**, Ibrahim RM, El Gazzar WB, Said MA. Dipeptedyl peptidase-4 (DPP-4) inhibitor downregulates HMGB1/TLR4/NF-κB signaling pathway in a diabetic rat model of non-alcoholic fatty liver disease. *Arch Physiol Biochem* 2021; 1-9 [PMID: 34543583 DOI: 10.1080/13813455.2021.1975758]

35 **Molinaro E**, Andrikou K, Casadei-Gardini A, Rovesti G. BRCA in Gastrointestinal Cancers: Current Treatments and Future Perspectives. *Cancers (Basel)* 2020; **12** [PMID: 33198203 DOI: 10.3390/cancers12113346]

36 **Nielsen MC**, Hvidbjerg Gantzel R, Clària J, Trebicka J, Møller HJ, Grønbæk H. Macrophage Activation Markers, CD163 and CD206, in Acute-on-Chronic Liver Failure. *Cells* 2020; **9** [PMID: 32397365 DOI: 10.3390/cells9051175]

37 **Kelly B**, O'Neill LA. Metabolic reprogramming in macrophages and dendritic cells in innate immunity. *Cell Res* 2015; **25**: 771-784 [PMID: 26045163 DOI: 10.1038/cr.2015.68]

38 **Saraiva M**, Vieira P, O'Garra A. Biology and therapeutic potential of interleukin-10. *J Exp Med* 2020; **217** [PMID: 31611251 DOI: 10.1084/jem.20190418]

39 **Darkhal P**, Gao M, Ma Y, Liu D. Blocking high-fat diet-induced obesity, insulin resistance and fatty liver by overexpression of Il-13 gene in mice. *Int J Obes (Lond)* 2015; **39**: 1292-1299 [PMID: 25869601 DOI: 10.1038/ijo.2015.52]

40 **Groslambert M**, Py BF. Spotlight on the NLRP3 inflammasome pathway. *J Inflamm Res* 2018; **11**: 359-374 [PMID: 30288079 DOI: 10.2147/JIR.S141220]

41 **Duewell P**, Kono H, Rayner KJ, Sirois CM, Vladimer G, Bauernfeind FG, Abela GS, Franchi L, Nuñez G, Schnurr M, Espevik T, Lien E, Fitzgerald KA, Rock KL, Moore KJ, Wright SD, Hornung V, Latz E. NLRP3 inflammasomes are required for atherogenesis and activated by cholesterol crystals. *Nature* 2010; **464**: 1357-1361 [PMID: 20428172 DOI: 10.1038/nature08938]

42 **Mridha AR**, Wree A, Robertson AAB, Yeh MM, Johnson CD, Van Rooyen DM, Haczeyni F, Teoh NC, Savard C, Ioannou GN, Masters SL, Schroder K, Cooper MA, Feldstein AE, Farrell GC. NLRP3 inflammasome blockade reduces

liver inflammation and fibrosis in experimental NASH in mice. *J Hepatol* 2017; **66**: 1037-1046 [PMID: 28167322 DOI: 10.1016/j.jhep.2017.01.022]

43 **Dai Y**, Dai D, Wang X, Ding Z, Mehta JL. DPP-4 inhibitors repress NLRP3 inflammasome and interleukin-1beta *via* GLP-1 receptor in macrophages through protein kinase C pathway. *Cardiovasc Drugs Ther* 2014; **28**: 425-432 [PMID: 25022544 DOI: 10.1007/s10557-014-6539-4]

44 **El-Kashef DH**, Serrya MS. Sitagliptin ameliorates thioacetamide-induced acute liver injury *via* modulating TLR4/NF-KB signaling pathway in mice. *Life Sci* 2019; **228**: 266-273 [PMID: 31077717 DOI: 10.1016/j.lfs.2019.05.019]

45 **Hu J**, Zhu Z, Ying H, Yao J, Ma H, Li L, Zhao Y. Oleoylethanolamide Protects Against Acute Liver Injury by Regulating Nrf-2/HO-1 and NLRP3 Pathways in Mice. *Front Pharmacol* 2020; **11**: 605065 [PMID: 33536915 DOI: 10.3389/fphar.2020.605065]

World Journal of Gastroenterology

Submit a Manuscript: https://www.f6publishing.com

World J Gastroenterol 2022 May 7; 28(17): 1830-1844

DOI: 10.3748/wjg.v28.i17.1830

ISSN 1007-9327 (print) ISSN 2219-2840 (online)

ORIGINAL ARTICLE

Retrospective Cohort Study

Epidemiological characteristics of Asian children with inflammatory bowel disease at diagnosis: Insights from an Asian-Pacific multi-centre registry network

James Guoxian Huang, Yoko Kin Yoke Wong, Kee Seang Chew, Pornthep Tanpowpong, Karen Sophia Calixto Mercado, Almida Reodica, Shaman Rajindrajith, Kai-Chi Chang, Yen-Hsuan Ni, Suporn Treepongkaruna, Way-Seah Lee, Marion Margaret Aw

Specialty type: Gastroenterology and hepatology

Provenance and peer review: Invited article; Externally peer reviewed.

Peer-review model: Single blind

Peer-review report's scientific quality classification

Grade A (Excellent): 0
Grade B (Very good): B, B, B
Grade C (Good): C
Grade D (Fair): 0
Grade E (Poor): 0

P-Reviewer: Naftali T, Israel; Poddighe D, Kazakhstan; Sugimoto M, Japan

Received: November 3, 2021
Peer-review started: November 3, 2021
First decision: December 26, 2021
Revised: January 3, 2022
Accepted: March 25, 2022
Article in press: March 25, 2022
Published online: May 7, 2022

James Guoxian Huang, Marion Margaret Aw, Khoo Teck Puat-National University Children's Medical Institute, National University Health System, Singapore 119228, Singapore

James Guoxian Huang, Marion Margaret Aw, Department of Pediatrics, Yong Loo Lin School of Medicine, National University of Singapore, Singapore 119228, Singapore

Yoko Kin Yoke Wong, Epidemiology, Singapore Clinical Research Institute, Singapore 138669, Singapore

Kee Seang Chew, Way-Seah Lee, Department of Paediatrics, Faculty of Medicine, University Malaya, Kuala Lumpur 50603, Malaysia

Pornthep Tanpowpong, Suporn Treepongkaruna, Department of Pediatrics, Faculty of Medicine Ramathibodi Hospital, Mahidol University, Bangkok 10400, Thailand

Karen Sophia Calixto Mercado, Department of Pediatrics, Makati Medical Centre, Manila 1229, Philippines

Almida Reodica, Department of Pediatrics, The Medical City, Manila 0900, Philippines

Shaman Rajindrajith, Department of Pediatrics, Faculty of Medicine, University of Colombo, Colombo 00800, Sri Lanka

Kai-Chi Chang, Yen-Hsuan Ni, Department of Pediatrics, National Taiwan University Hospital, Taipei 100229, Taiwan

Corresponding author: James Guoxian Huang, MBBS, Assistant Professor, Doctor, Staff Physician, Khoo Teck Puat-National University Children's Medical Institute, National University Health System, NUHS Tower Block Level 12, 1E Kent Ridge Road, Singapore 119228, Singapore. james_huang@nuhs.edu.sg

Abstract

BACKGROUND

There remains a dearth of Asian epidemiological literature for paediatric inflam-

matory bowel disease (PIBD).

AIM

To describe the presenting features of PIBD from 7 Asia-Pacific pediatric gastroenterology centers *via* a central standardised electronic data platform.

METHODS

Clinical, endoscopic and radiologic data at diagnosis from the registry were extracted between 1st January 1995 to 31st December 2019. Disease phenotypic characteristics were classified as per the Paris classification system.

RESULTS

There was a distinct rise in new PIBD cases: Nearly half (48.6%) of the cohort was diagnosed in the most recent 5 years (2015-2019). The ratio of Crohn's disease (CD):Ulcerative colitis (UC):IBD-Unclassified was 55.9%:38.3%:5.8%. The mean age was 9.07 years with a high proportion of very early onset IBD (VEO-IBD) (29.3%) and EO-IBD (52.7%). An over-representation of the Indian/South Asian ethnic group was observed which accounted for 37.0% of the overall Singapore/Malaysia subcohort (6.8%-9.0% Indians in census). Indian/South Asian CD patients were also most likely to present with symptomatic perianal disease (P = 0.003). CD patients presented with significantly more constitutional symptoms (fever, anorexia, malaise/fatigue and muscle-wasting) than UC and higher inflammatory indices (higher C-reactive protein and lower albumin levels).

CONCLUSION

We observed a high incidence of VEO-IBD and an over-representation of the Indian ethnicity. South Asian CD patients were more likely to have symptomatic perianal disease.

Key Words: Asia; Inflammatory bowel disease; Paediatrics; Crohn's disease; Ulcerative colitis; Registry

©The Author(s) 2022. Published by Baishideng Publishing Group Inc. All rights reserved.

Core Tip: We describe the presenting features of paediatric inflammatory bowel disease (IBD) in 7 paediatric gastroenterology centers across six Asia-Pacific regions *via* a centrally-hosted electronic data capture platform. Clinical, endoscopic and radiologic data of 311 paediatric patients diagnosed with IBD between 1995 and 2019 were extracted. The ratio of Crohn's (CD):Ulcerative colitis:IBD-Unclassified was 55.9%:38.3%:5.8%. The mean age was 9.07 years with a high proportion of very early onset IBD (VEO-IBD) and EO-IBD. An over-representation of the Indian/South Asian ethnic group was observed in the multiethnic subpopulations of Singapore and Malaysia. Patients of Indian/South Asian ethnicity were also most likely to present with symptomatic perianal CD.

Citation: Huang JG, Wong YKY, Chew KS, Tanpowpong P, Calixto Mercado KS, Reodica A, Rajindrajith S, Chang KC, Ni YH, Treepongkaruna S, Lee WS, Aw MM. Epidemiological characteristics of Asian children with inflammatory bowel disease at diagnosis: Insights from an Asian-Pacific multi-centre registry network. *World J Gastroenterol* 2022; 28(17): 1830-1844

URL: https://www.wjgnet.com/1007-9327/full/v28/i17/1830.htm

DOI: https://dx.doi.org/10.3748/wjg.v28.i17.1830

INTRODUCTION

The epidemiology of inflammatory bowel disease (IBD) is a dynamic and rapidly evolving landscape. Recent publications over the past decade document the rise in IBD incidence in traditionally low-prevalence regions (Asia, Africa, South America) while the incidence is somewhat stabilising in high-prevalence western nations[1]. In particular, there is an increased impetus to focus on paediatric IBD (PIBD) epidemiology as the rising incidence of childhood-onset disease appears to be driving this overall trend in certain regions[2]. Very-early onset IBD (VEO-IBD), generally defined as disease onset prior to the age of 6 years, was once considered rare but now represents the fastest growing age bracket of IBD incidence in certain countries[3]. Yet in spite of these global trends, there remains a dearth of epidemiological literature for PIBD in Asia, in particular the regions of Central, South and Southeast Asia. This begets the question whether these countries are truly 'low prevalence' in the absence of national IBD registries such as those established in Japan[4] and South Korea[5]. Apart from studies

published out of these East Asian cohorts, current literature is mostly limited to single centre publications[6-8] from countries in the Asia-Pacific region. Epidemiological data from these publications would only represent 'the tip of the iceberg' of the true burden of IBD and may not necessarily encapsulate recent regional epidemiological trends in disease incidence and behaviour.

There are numerous challenges in establishing a robust disease registry within Asia, especially with chronic diseases of emerging importance such as PIBD. For one, there is significant heterogeneity in disease awareness, diagnostic evaluation processes and therapeutic strategies across the vast Asian continent. This inevitably results in variations in case definitions with consequent epidemiological data inconsistencies. The aim of the present study was to describe the presenting features of PIBD managed in 7 paediatric gastroenterology centers across six Asia-Pacific countries and regions *via* a centrally-hosted electronic data capture platform using international standardised definitions.

MATERIALS AND METHODS

Establishing a multi-centre Asian PIBD registry network

The concept and goal of establishing a standardised disease data capture platform across Asian paediatric gastroenterology centres were first discussed amongst paediatric gastroenterologists practising across 7 tertiary centres in 6 Asian countries (Malaysia, Philippines, Singapore, Sri Lanka, Taiwan R.O.C., Thailand) in 2017. A consensus was established amongst the network committee members with regards to the standardisation of disease data collected both retrospectively and prospectively. Anonymised clinical data was to be collected on patient demographics, diagnostic evaluation and disease characteristics based on clinical examination, laboratory, endoscopy and radiology investigations. The diagnosis and classification of IBD into one of three disease subtypes [Crohn's disease (CD), Ulcerative colitis (UC) and IBD-unclassified (IBD-U)] was determined by each participating centre based on the revised Porto criteria[9] as agreed within the network. The Paris Classification[10] (paediatric modification of the Montreal classification for IBD) system was then utilised to describe disease behaviour and phenotype. Electronic case report forms were thereafter loaded on a secure REDCAP data-capture platform centrally hosted by the Singapore Clinical Research Institute.

Ethics approval

Ethics approval for the storage of anonymised clinical data on a multi-centre central data registry hosted by the Singapore Clinical Research Institute was granted by the National Healthcare Group (NHG) Domain Specific Review Board (Approval letter for study code NUH/2019-00060 dated 23rd January 2020), followed by a separate ethics approval for data extraction and analysis (Approval letter for study code 2019/00751 dated 20th October 2021 to 19th October 2022).

Data extraction and analysis

For the purposes of analysis of clinical features at diagnosis, data from the registry was extracted for patients diagnosed with IBD between 1st January 1995 to 31st December 2019. The patient's inclusion criteria were: (1) Gastroenterologist-confirmed diagnosis of IBD at the participating site; (2) Age below 18 years at the point of diagnosis; and (3) Resident (citizens, permanent residents or long-term visitors) of the country of the participating site. Medical tourists (non-resident patients visiting the country solely for the purpose for medical assessment/treatment) were excluded. We stratified the cohort (1995-2019) into five equal time-intervals, each of 5-year duration, for the intent of analysing change in IBD incidence and evolution of diagnostic practices with time.

VEO-IBD was defined by an age of onset less than 6 years and EO-IBD, by an age of onset less than 10 years. Symptomatic perianal disease was defined as perianal pain or discharge due to a fistula or abscess/collection. A 'perianal manifestation' of CD, symptomatic or otherwise, was defined broadly as large inflamed perianal tags, poorly healing perianal fissures ascribed to CD or perianal fistula/abscess or collection evident clinically or *via* imaging. South Asians were defined as people of Indian, Bangladeshi, Pakistani, Sri Lankan (Sinhalese/Tamil) or Maldivian origin. Anthropometric Z-scores for children of age 0-5 years were measured based on the World Health Organization (WHO) Child Growth Standards, while those for children aged 5-19 years were measured on the WHO Reference 2007. Linear growth failure was defined as a height Z-score of -2 and lower.

Disease severity was defined based on the patients' respective Paediatric Crohn's Disease Activity Index (PCDAI) (Inactive: ≤ 10, mild: 11-30, moderate-severe: > 30)[11] and Paediatric Ulcerative Colitis Activity Index (Inactive: < 10, mild: 10-34, moderate: 35-64, severe ≥ 65)[12] scores.

The date of IBD diagnosis was taken as the date of diagnostic endoscopy. For the purposes of this publication discussing solely the presenting clinical features at diagnosis, we only included clinical data occurring within 3-mo prior or after the date of diagnosis and before any therapeutic intervention.

Statistical analysis was done through SPSS Version 27 whereby we compared presenting symptoms, biochemical indices and growth indices between the key phenotypic subgroups (CD and UC); the overall effect of ethnicity on IBD phenotype and behaviour. Continuous variables (laboratory invest-

igation values, anthropometric indices) were compared through the student's *t*-test while most of the other outcomes (clinical findings, disease phenotype and behaviour) were classified as categorical variables/dichotomous outcomes and these were compared through the chi-square test. A *P* value of less than 0.05 was deemed as a significant difference in outcomes, otherwise stated as 'NS' (non-significant). Whereby multivariate analysis was required in determining the effect of South Asian ethnicity on the incidence of perianal disease in CD adjusting for inter-ethnic variability in disease phenotype, logistic regression was used to calculate an adjusted odds ratio.

RESULTS

Three hundred and eleven children were recruited from seven participating tertiary centres across six countries within the Asia-Pacific region. There was a distinct rise in the number of new PIBD cases recorded across the network, with nearly half (48.6%, 151/311) of the entire cohort being diagnosed in the most recent 5 years (2015-2019) of recruitment (Figure 1). Table 1 illustrates the overall distribution of CD *vs* UC *vs* IBD-U, in which the CD:UC ratio was approximately 1.5:1 while the proportion of IBD-U was 5.8%. While there were more males in the overall cohort (58.2% male), we did not observe any significant gender predilection across the three disease subtypes: Male CD 58.0% *vs* male UC 57.0% *vs* male IBD-U 66.7% ($P = 0.75$).

High incidence of VEO and EO disease

The mean age of disease presentation was 9.07 years for the entire IBD cohort which is within the age definition of EO disease. UC patients presented at a significantly younger age than CD patients (7.73 years *vs* 10.18 years, $P < 0.001$), with the mean age of IBD-U patients (7.34 years) similar to that of UC. When stratifying age of onset into VEO disease and EO disease, 29.3% of the entire cohort was classified as VEO-IBD and more than half (52.7%) was early-onset. There was a significantly higher proportion of VEO-IBD and EO-IBD presenting as a UC phenotype as compared to CD (Table 1). Across a period of 20 years, the proportions of VEO-IBD and EO-IBD remained relatively stable, approximately at 30% and 50% of the cohort per time interval respectively (Figure 2).

Over-representation of the Indian/South Asian ethnicity

For a meaningful interpretation of ethnic predilection amongst Asian IBD patients, the multi-racial sub cohorts from Singapore and Malaysia were chosen as the other participating sites were relatively more homogeneous in ethnic group distribution. The three main ethnic groups in these two countries are Chinese, Indian/South Asian and Malay as listed in Table 2[13,14]. A distinct over-representation of the Indian/South Asian ethnic group was observed, with Indians/South Asians accounting for 37.0% of the overall Singapore/Malaysia IBD cohort relative to a minority representation of 6.8%-9.0% in both the countries' respective population census. There was a significantly higher proportion of UC patients relative to CD amongst the Malay ethnic group (CD:UC ratio 0.7, $P = 0.037$).

Increased constitutional symptoms, extraintestinal manifestations and higher inflammatory indices in CD

Abdominal pain ($P = 0.004$) and clinically evident abdominal tenderness ($P = 0.003$), fever ($P < 0.001$), loss of appetite ($P = 0.001$) and malaise/fatigue ($P = 0.016$) were significantly more common amongst CD patients relative to UC. While there was a non-significant higher proportion of CD patients presenting with weight loss (46.6% CD *vs* 37.0% UC), clinically evident muscle wasting was significantly more common in CD (14.4% CD *vs* 5.9% UC, $P = 0.022$).

Although CD patients had numerically lower mean weight Z-scores [(-1.4) *vs* (-1.0)] and height Z-scores [(-0.8) *vs* (-0.6)] than UC, only the mean body-mass index Z-score of CD patients was significantly lower [(-1.5) *vs* (-0.9), $P = 0.013$]. There were approximately similar rates of linear growth failure across the three disease subtypes: 18.4% CD *vs* 16.1% UC *vs* 17.6% IBD-U (Table 3). There was a non-significant higher proportion of patients with joint pains (7.5% CD *vs* 5% UC) and clinically evident arthritis (6.9% CD *vs* 2.5% UC) in CD patients. Other extraintestinal manifestations (EIMs) such as oral ulcers (20.7% CD *vs* 0.8% UC, $P < 0.001$) and erythema nodosum (4.6% CD *vs* 0.0% UC, $P = 0.018$) were more common in CD than UC. Hepatic involvement (hepatomegaly and elevated transaminases) was however more commonly observed in UC than CD, consistent with a significantly higher association of autoimmune liver disease/primary sclerosing cholangitis with UC than CD (17.6% UC *vs* 1.1% CD, $P < 0.001$).

CD patients also presented with significantly higher C-reactive protein (CRP) levels (mean 54.6 CD *vs* 20.1 UC, $P < 0.001$) and lower albumin levels relative to UC. However, there was no significant difference in mean haemoglobin and proportion of severe anaemia (defined as ≤ 7.0g/dL: 4.0% CD *vs* 5.0% UC, $P = 0.601$) at presentation between CD and UC.

Faecal calprotectin testing

16.1% of the cohort had a faecal calprotectin (50/211) assayed at baseline. There was no significant

Table 1 Demographic features of 311 children with inflammatory bowel disease in 6 Asia-Pacific regions

	IBD subtypes				*P* value (CD *vs* UC)
	ALL IBD, *n* = 311	CD, *n* = 174 (55.9%)	UC, *n* = 119 (38.3%)	IBD-U, *n* = 18 (5.8%)	
Country (*n*, row %)					
Malaysia	95	39 (41.1)	47 (49.5)	9 (9.5)	
Philippines	29	24 (82.8)	1 (3.4)	4 (13.8)	
Singapore	108	59 (54.6)	49 (45.4)	0 (0.0)	-
Sri Lanka	19	10 (52.6)	7 (36.8)	2 (10.5)	
Taiwan R.O.C.	19	19 (100.0)	0 (0.0)	-	
Thailand	41	23 (56.1)	15 (36.6)	3 (7.3)	
Mean age at diagnosis, yr (SD)	9.07 (4.56)	10.18 (4.34)	7.73 (4.39)	7.34 (5.1)	< 0.001
Age groups (*n*, column %)					
Very early onset < 6 yr	91 (29.3)	30 (17.2)	51 (42.9)	10 (55.6)	< 0.001
Early onset < 10 yr	164 (52.7)	75 (43.1)	78 (65.5)	11 (61.1)	0.001
Sex (*n*, column %)					
Male	181 (58.2)	101 (58.0)	68 (57.1)	12 (66.7)	NS
Female	130 (41.8)	73 (42.0)	51 (42.9)	6 (33.3)	

CD: Crohn's disease; IBD-U: Inflammatory bowel disease- Unclassified; UC: Ulcerative colitis.

Table 2 Ethnic distribution of inflammatory bowel disease *vs* population census in countries with multiracial populations (Singapore and Malaysia)

	Total, *n* = 203	Singapore population census 2020[1]	Malaysian population census 2020[2]	CD, *n* = 92	UC, *n* = 91	IBD-U, *n* = 9	CD:UC ratio	*P* value
Ethnic group (*n*, column %)								
Chinese	70/203 (36.5)	74.3	22.6	38 (41.3)	31 (34.1)	1 (11.1)	1.2	NS
Indian/South Asian	71/203 (37.0)	9.0	6.8	35 (38.0)	33 (36.3)	3 (33.3)	1.0	NS
Malay	51/203 (26.6)	13.5	69.6	19 (20.7)	27 (29.7)	5 (55.6)	0.7	0.037

CD: Crohn's disease; IBD-U: Inflammatory bowel disease-Unclassified; UC: Ulcerative colitis.

difference between the mean values in CD and UC (Table 3). Amongst children with CD, faecal calprotectin values were lower in patients with isolated ileal disease (L1) compared to ileocolonic (L3) disease (468.7 in L1 *vs* 749.2 μg/g in L3, $P = 0.05$). No discernible difference in mean faecal calprotectin values was noted amongst children with UC; left sided disease (E1/E2: 547.0 μg/g) *vs* more extensive disease (E3/E4: 555.6 μg/g).

Small bowel imaging and endoscopy

There was a progressive decline in the use of small bowel follow through studies across the cohort. Since 2010, there has been increasing use of either MR enterography or intestinal ultrasound although approximately 60% of the cohort have not had any form of small bowel imaging (Figure 3). Complete endoscopy as per Porto guidelines (upper and lower endoscopy) was performed in 79.1% of the cohort.

Disease behaviour and phenotype of CD patients

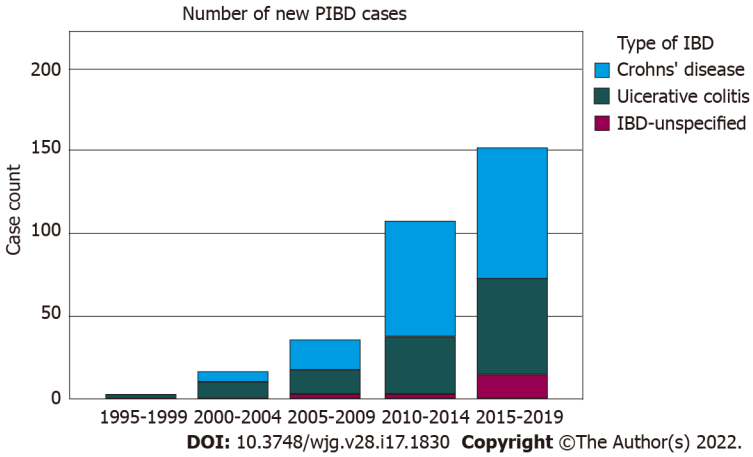
The ileocolonic location was the most common disease location in the entire cohort of CD patients, with pure inflammatory disease being most common (90.7%) followed by luminal penetrating disease (5.3%) and stricturing disease (3.3%). Isolated L4 disease (absence of terminal ileal or colonic disease) was relatively uncommon at 4.0% of the CD cohort. Over half of the CD patients had at least moderate

Table 3 Clinical features in different subtypes of PIBD in the Asia-Pacific region

	IBD subtypes			*P* value (CD *vs* UC)
	CD, *n* = 174 (55.9%)	UC, *n* = 119 (38.3%)	IBD-U, *n* = 18 (5.8%)	
Symptoms at diagnosis (*n*, column %)				
Abdominal pain	107 (61.5)	53 (44.5)	7 (38.9)	0.004
Chronic diarrhoea	104 (59.8)	69 (58.0)	10 (55.6)	0.760
Bloody diarrhoea	60 (34.5)	89 (74.8)	11 (61.1)	< 0.001
Weight loss	81 (46.6)	44 (37.0)	9 (50.0)	0.104
Fever	66 (37.9)	21 (17.6)	2 (11.1)	< 0.001
Loss of appetite	57 (32.8)	19 (16.0)	6 (33.3)	0.001
Malaise/fatigue	28 (16.1)	8 (6.7)	1 (5.6)	0.016
Oral ulcers	36 (20.7)	1 (0.8)	0 (0.0)	< 0.001
Perianal symptoms (pain/discharge)	23 (13.2)	3 (2.5)	1 (5.6)	0.002
Joint pains	13 (7.5)	6 (5.0)	0 (0.0)	0.407
Physical signs at diagnosis (*n*, column %)				
Pallor	68 (39.1)	32 (26.9)	5 (27.8)	0.031
Hepatomegaly	8 (4.6)	12 (10.1)	2 (11.1)	0.067
Abdominal tenderness	47 (27.0)	15 (12.6)	2 (11.1)	0.003
Asymptomatic perianal tags	25 (14.4)	3 (2.5)	1 (5.6)	0.001
Perianal fissure	20 (11.5)	2 (1.7)	1 (5.6)	0.002
Muscle wasting	25 (14.4)	7 (5.9)	1 (5.6)	0.022
Arthritis	12 (6.9)	3 (2.5)	0 (0.0)	0.095
Erythema nodosum	8 (4.6)	0 (0.0)	0 (0.0)	0.018
Anthropometric parameters (SD)				
Mean weight Z-score	-1.4 (1.7)	-1.0 (1.7)	-0.7 (2.2)	0.110
Mean height Z-score	-0.8 (1.5)	-0.6 (1.6)	-0.6 (2.4)	0.583
Growth failure (Height Z-score less than -2) (%)	18.4	16.1	17.6	0.907
Mean BMI Z-score	-1.5 (1.8)	-0.9 (1.7)	-0.6 (1.8)	0.013
Laboratory investigations at diagnosis (SD)				
Mean haemoglobin, g/dL	10.6 (1.9)	11.0 (2.5)	10.9 (1.5)	0.221
Mean ESR, mm/hr	50.8 (30.5)	42.6 (34.4)	34.9 (32.2)	0.063
Mean C-reactive protein, mg/L	54.6 (55.0)	20.1 (24.3)	7.1 (9.1)	< 0.001
Mean albumin, g/dL	33.0 (8.7)	35.4 (8.4)	37.2 (7.1)	0.040
Mean ALT, U/L	18.5 (20.5)	72.7 (162.0)	20.4 (13.4)	< 0.001
Mean AST, U/L	27.0 (32.9)	84.2 (170.7)	30.5 (10.5)	0.001
Mean GGT, U/L	38.3 (79.8)	126.7 (160.8)	30.8 (40.0)	< 0.001
Mean faecal calprotectin, μg/g	783 (1009.0)	583.4 (353.1)	593.5 (300.5)	0.447

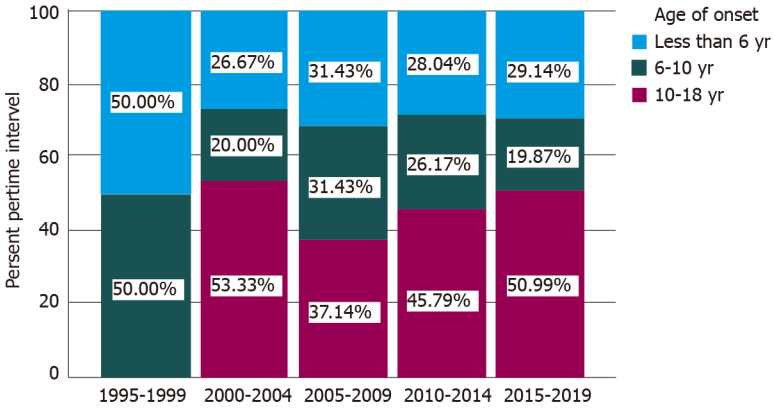
ALT: Alanine transaminase; AST: Aspartate transaminase; BMI: Body mass index; CD: Crohn's disease; ESR: Erythrocyte sedimentation rate; GGT: Gamma-glutamyl transferase; IBD-U: Inflammatory bowel disease-Unclassified; UC: Ulcerative colitis.

disease severity at presentation (54.3%), with no differences in mean PCDAI scores noted with the South Asian subgroup. Upper gastrointestinal involvement was seen in 49.0% of the entire CD cohort. Symptomatic perianal disease was seen in 13.2% of the CD cohort and up to 30.5% of the CD cohort had some form of perianal manifestation as earlier defined.



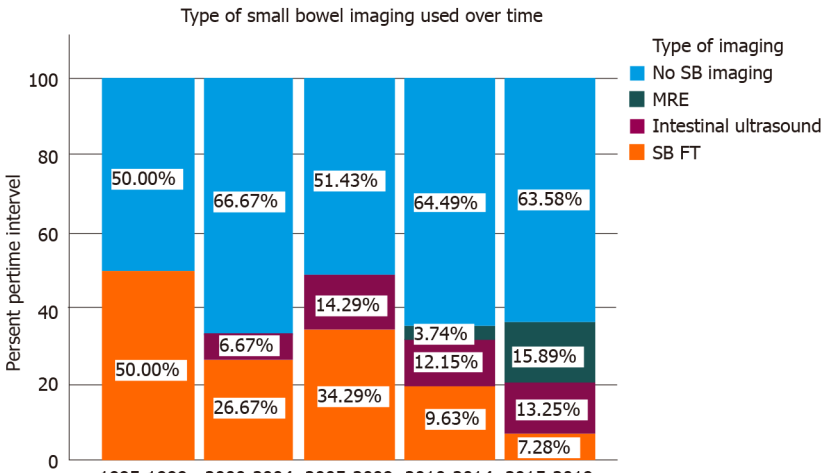
DOI: 10.3748/wjg.v28.i17.1830 **Copyright** ©The Author(s) 2022.

Figure 1 Rising trend of newly diagnosed paediatric inflammatory bowel disease in six Asian Pacific regions, 1995-2019. PIBD: Paediatric inflammatory bowel disease; IBD: Inflammatory bowel disease.



DOI: 10.3748/wjg.v28.i17.1830 **Copyright** ©The Author(s) 2022.

Figure 2 Age distribution of paediatric inflammatory bowel disease (1995-2019).



DOI: 10.3748/wjg.v28.i17.1830 **Copyright** ©The Author(s) 2022.

Figure 3 Type of small bowel imaging used over time (1995-2019). MRE: MR enterography; FT: Follow through; SB: Small bowel.

South Asian CD patients were strongly associated with perianal symptoms at presentation (P = 0.003), the physical finding of asymptomatic perianal tags (15.5% South Asian *vs* 7.5%, P = 0.042), as well as any form of perianal manifestation (symptomatic and asymptomatic, detected on either clinical examination or perianal imaging; P = 0.003). Adjusting for inter-ethnic differences in CD incidence, the

South Asian ethnicity remained strongly associated with symptomatic perianal disease at presentation (B co-efficient 1.264, $P = 0.001$). Sri Lanka was the only participating South Asian site in this study, and only 1 out of 19 Sri Lankan IBD patients had presented with symptomatic perianal disease. All the South Asian CD patients in this subgroup analysis (Table 4) were either first- or second-generation immigrants within Singapore or Malaysia.

Disease behaviour and phenotype of UC patients

Overall, pan colonic involvement was the most common location in UC (72.6%) and almost half (48.8%) of UC patients had at least moderate disease severity at presentation. South Asian UC patients had slightly less cases of isolated proctitis than the non-South Asian UC sub cohort (6.9% proctitis South Asian *vs* 7.8% non-South Asian).

DISCUSSION

This first publication from the Asian PIBD registry gives valuable insights into the distinct epidemiological patterns of a rapidly emerging chronic disease in the Asia-Pacific region. Existing literature from published adult cohorts documents the distinct rapid rise in overall IBD incidence across the Asia-Pacific region[15] ascribed to increased urbanisation and industrialisation of developing areas with a consequent change in lifestyle and environmental factors. Our pooled data across major paediatric gastroenterology centres in the Asia-Pacific region verifies the rise in PIBD incidence, particularly in the last decade of data collection (2010-2019). This is also consistent with rising trends observed in other Asian paediatric cohorts in Saudi Arabia[16], Bahrain[17], Japan[18], South Korea[19] and China[20]. There still remains a knowledge gap on the epidemiological trends of PIBD in many parts of Asia, particularly Central and South Asian regions, although recently published studies out of Kazakhstan [21], India[22] and Nepal[23] reaffirm IBD as an emerging health issue.

Several other factors have been proposed as reasons for the observed rise in IBD incidence within the Asia-Pacific region, namely increased disease awareness amongst healthcare professionals, improved access to healthcare resources and better diagnostic modalities in rapidly industrialising areas. While such factors may account for part of the initial observed rise in incidence in the earlier decades, they do not sufficiently explain the sustained year-on-year rise in PIBD incidence seen in developed regions of our network[6,24] as well as other highly industrialised regions in Japan and South Korea.

The key strength of a multi-centre registry in this ethnically and culturally diverse region would be to allow epidemiological comparisons amongst multi-racial Asian populations (*e.g.*, Singapore/Malaysia) and ethnically homogeneous populations (*e.g.*, Philippines/Sri Lanka/Thailand). In Singapore and Malaysia where the Chinese and Malay populations form the majority ethnic group respectively and the Indians are an ethnic minority, we affirm earlier findings from adult Southeast Asian cohorts[25,26] that there is an ethnic predisposition to IBD incidence with an over-representation of the Indian/South Asian subgroup (37% IBD *vs* 6%-9% general population). This is similar to observations in the United Kingdom and Canada where IBD is seen with greater frequency amongst both South Asians born in the United Kingdom[27] and South Asian migrants to the United Kingdom[28], as well as the paediatric South Asian community in British Columbia, Canada[29]. Similarly, in a study of 30812 IBD subjects diagnosed in the United States, Malhotra *et al*[30] found that residents of Indian ancestry carried the highest risk for all types of IBD, compared to residents of Jewish, East Asian or Hispanic ancestries.

With combined Singaporean and Malaysian data, we were able to discern unique characteristics of each ethnic group. The CD:UC ratio varied distinctly across the three ethnic groups (Chinese 1.2; Indian/South Asian 1.0 and Malay 0.7) and this is likely attributed to inter-ethnic differences in environmental factors, such as diet, diversity in gut microbiome[31] including *Helicobacter pylori* (*H. pylori*)[32] as well as socio-economic status[33]. This inter-ethnic variation in IBD incidence has been observed between African Americans and white Americans previously[34]; white Americans were reported to have a CD:UC ratio > 1.0 with Hispanic Americans having an inverse ratio[35], paralleling what is observed between Chinese and Malays in our cohort. A similar variegation of CD:UC ratio was seen in a Latin American systematic review by Kotze *et al*[36], in which only certain states in Brazil reported a CD:UC ratio > 1 whereas most of the other Latin American countries had a CD:UC ratio < 1. The authors concluded similarly that regions within Latin America that experienced higher degrees of economic development and 'Westernisation' had a higher proportion of CD cases.

We also observed a strongly significant association between the South Asian ethnicity and symptomatic perianal disease (pain or perianal discharge) at presentation, only in the South Asian populations of Singapore and Malaysia. Interestingly, despite less South Asians having the CD phenotype than Chinese, the South Asian ethnicity was significantly associated with asymptomatic perianal tags. The latter physical finding may be a prelude to developing symptomatic perianal Crohn's later in the clinical course, as seen in this study by Singer *et al*[37] showing a higher rate of perianal fistulisation in patients initially presenting with non-penetrating perianal lesions. The observation of increased rates of symptomatic perianal disease was not appreciated in the native South Asian population of Sri Lanka within the limits of small patient numbers recruited in this sub cohort. A

Table 4 Disease characteristics of Crohn's disease and ulcerative colitis

Disease characteristics	*N*	SA	*P* value (SA *vs* non-SA)
CD	*n* = 174	*n* = 35 (20.1)	
Disease severity based on PCDAI score (*n*, column %)[1]			
Inactive (≤ 10)	17 (12.3)	4 (14.3)	NS
Mild (11-30)	46 (33.3)	9 (32.1)	
Moderate-severe (> 30)	75 (54.3)	15 (53.6)	
Disease location (*n*, column %)			
L1 (distal 1/3 ileum +/- limited caecal disease)	28 (18.7)	4 (12.5)	0.505 (SA)
L2 (colonic)	54 (36.0)	10 (31.3)	
L3 (ileocolonic)	62 (41.3)	16 (50.0)	
Isolated L4 disease	6 (4.0)	2 (6.3)	
L4a	59 (40.7)	13 (39.4)	0.973 (SA)
L4b	12 (8.3)	3 (9.1)	
No L4 disease	74 (51.0)	17 (51.3)	
Disease behaviour (*n*, %)			
B1 (inflammatory)	136 (90.7)	31 (93.9)	0.858 (SA)
B2 (stricturing)	5 (3.3)	1 (3.0)	
B3 (penetrating)	8 (5.3)	1 (3.0)	
B2/B3	1 (0.7)	0 (0.0)	
Perianal involvement (*n*, %)			
Perianal symptoms at presentation	23 (13.2)	10 (28.6)	0.003 (SA)
Any form of perianal manifestation (clinical exam or imaging)	53 (30.5)	18 (51.4)	0.003 (SA)
UC	*n* = 119	*n* = 33 (27.7)	
Disease severity based on PUCAI score (*n*, column %)[2]			
Inactive (< 10)	7 (8.3)	0 (0.0)	0.353 (SA)
Mild (10-34)	36 (42.9)	11 (47.8)	
Moderate (35-64)	28 (33.3)	9 (39.1)	
Severe (≥ 65)	13 (15.5)	3 (13.0)	
Disease location (*n*, column %)			
E1 (proctitis)	8 (7.5)	2 (6.9)	0.353 (SA)
E2 (left sided)	16 (15.1)	5 (17.2)	
E3 (extensive)	5 (4.7)	5 (17.2)	
E4 (pancolitis)	77 (72.6)	17 (58.6)	
Disease severity (*n*, column %)			
S0 (never severe)	79 (78.2)	20 (74.1)	0.542 (SA)
S1 (ever severe)	22 (21.8)	7 (25.9)	

[1]Disease activity scores available only for 138/174 Crohn's disease patients.
[2]Disease severity scores available for 84/119 Ulcerative colitis patients.
CD: Crohn's disease; PCDAI: Pediatric Crohn's Disease Activity Index; PUCAI: Pediatric Ulcerative Colitis Activity Index; SA: South Asian; UC: Ulcerative colitis.

previous questionnaire survey conducted in India estimated the incidence of perianal disease at presentation in Indian paediatric CD patients at 18.0%, which is not strikingly higher than paediatric cohorts in Israel (13.3%)[38] and Canada (16.0%)[39]. More recent Indian studies, which included

perianal disease developed both at diagnosis and subsequent follow-up, however, have found even lower rates than other Asian cohorts. Banerjee *et al*[40] reported 7.4% perianal involvement amongst CD patients and a multicentre paediatric study in India reported 10.9% of CD patients with perianal disease(fistula or abscess). These findings suggest South Asian CD patients in their native countries do not experience disproportionately high rates of perianal disease.

On the contrary, countries with a high South Asian immigrant population report findings congruent with our cohort's. A previous paediatric study in San Francisco likewise demonstrated similar findings in our cohort, where South Asians tended to have more perianal fistulising disease at presentation than their Caucasian counterparts[41]. A recent adult cohort study published by Jangi *et al*[42] also showed South Asian CD patients in the United States were more likely to experience symptomatic perianal disease than white patients. Current findings from our study and the above-mentioned cohorts may suggest these phenotypic trends may be unique only to South Asians who have migrated from their native countries to relatively more developed and urbanised regions. A possible explanation is that South Asians may carry an intrinsic genetic predisposition for IBD, which results in a distinct disease phenotype in the setting of specific environmental exposures after migration[43]. A review by Foster and Jacobson[44] discusses these hypothetical gene-environmental interactions in South Asian immigrants, postulating the role of dietary changes from a traditionally high carbohydrate/low saturated fat diet to one which is highly processed. Other possible factors discussed include an increased exposure to urban pollutants and a reduced exposure to potentially protective factors such as vitamin D, *H. pylori* and helminths.

Overall, we do report a moderately high rate of perianal involvement in our CD patients at presentation (13.2% with symptomatic perianal disease and up to 30.5% with some form of perianal manifestation of CD either clinically detected or *via* imaging. An earlier Singaporean paediatric cohort reported a 21.6% incidence of perianal disease amongst CD patients at diagnosis[6] with mainland Chinese and South Korean paediatric CD cohorts reporting even higher rates of perianal involvement 42.4% Shanghai[45] , 47.1% [(perianal fistulising disease) only South Korean[46]]. Some variability in the reported rates of perianal involvement across CD cohorts could be accounted by differences in disease definitions as well as the extent of perianal imaging performed, which may detect indolent perianal fistulising disease in otherwise asymptomatic patients. A large IBD cohort of 5223 white Americans, 35 United States-born Asians and 81 Asian immigrants also reported Asians having a significantly higher rate of perianal disease (at presentation and follow-up) than whites (33% *vs* 18%)[47]. Further prospective follow-up of our cohort is required to ascertain if an even greater proportion of CD patients will evolve to develop perianal disease beyond the point of diagnosis.

Interestingly, we also found a very high proportion of VEO-IBD (29.3%) in our cohort, which appears to be stably high across a 20-year period of analysis. In comparison, data from the EPIMAD registry in France (n = 1412) reported a VEO-IBD rate of 3.0% based on a similar age definition for VEO-IBD[48]. Other Asian cohorts have similarly reported comparatively high rates of VEO-IBD, albeit using varying ages for definition. A single centre study in Beijing, Mainland China (n = 184) reported 41.8% of hospitalised children with IBD were VEO[49]; a cohort in Saudi Arabia reported 15.9% of patients were younger than 4 years at time of onset[16] and a recent Indian multicentre paediatric study had reported 19.1% of patients being VEO[22]. It is not certain if this epidemiologic trend is unique to regions where IBD is of emerging importance, as a Canadian study across 5 provinces reported VEO-IBD as the subgroup with the most rapid increase in incidence relative to the other age groups[2].

Aside from the South Asian predisposition and younger age of onset, the clinical presentation and extra-intestinal manifestations of CD and UC were similar to other Asian and Western paediatric and adult cohorts[50]. Abdominal pain and constitutional symptoms (fever, loss of appetite, oral ulcers, malaise) were more common presenting features in CD than UC; bloody diarrhoea and associated liver disease/primary sclerosing cholangitis were more common in UC at presentation, the latter being a well-established association. EIMs such as arthritis and erythema nodosum were more common in CD than UC, as also seen in a Mainland Chinese cohort[20]. We also reaffirm the finding of significant heterogeneity of CRP response between CD and UC, as discussed extensively in published literature[51, 52]. Within the limits of a small sample size, we noted that faecal calprotectin values vary with disease location in CD but not in UC. Previous correlation studies have also similarly observed lower values of faecal calprotectin in CD patients with pure ileal disease[53].

While CD patients had numerically lower weight Z-scores and height Z-scores than UC patients, these comparisons were not statistically significant. This is due to a relatively high rate of linear growth failure (16.1%) reported in UC patients in our cohort, which is higher than the typical prevalence of 3%-10% previously described[54]. It is uncertain if this truly reflects a unique UC phenotype or whether some of these UC patients will be re-classified as CD with evolution of disease and/or further diagnostic modalities performed. As approximately 60% of our cohort did not undergo any form of small bowel imaging and 20% did not undergo an upper gastrointestinal endoscopy, we could expect changes in these initial diagnostic labels had more complete evaluation been performed.

There are a few limitations to our study; firstly, as most of the data was collected retrospectively, we were not able to compute patient disease activity indices in all patients because of incomplete clinical, biochemical, imaging or endoscopy records. Secondly, a lack of access and/or consistency in performing small bowel imaging and upper gastrointestinal endoscopy could have resulted in inaccurate disease

classification. However, as almost half of our cohort was diagnosed in the recent 5 years, we are confident that the disease phenotype has been more accurately assessed and documented in these later years.

Another limitation was the predominance of Southeast Asian participating centres in our network, with the lack of East and West Asian representation. However, we were able to mitigate this as there already exists a substantial amount of published literature from established Japanese, South Korean and mainland Chinese cohorts as previously cited. Hence, we were able to compare certain epidemiological features such as age of onset and the proportion of perianal disease as discussed above.

Lastly, the number of patients captured within our network may only represent 'the tip of an iceberg'. We acknowledge that access to healthcare services may be very limited in rural regions of the participating countries, and there may be an inevitable selection bias in recruiting patients living in the proximity of major Asian city centres (Singapore, Kuala Lumpur, Bangkok, Manila, Colombo, Chinese Taipei) where our participating sites are located. Hence, there could be a number of children with IBD who do not present to centres equipped with adequate disease knowledge and diagnostic capability, and thus remain undiagnosed. At the same time, there could be a number of adolescent IBD patients who are managed by adult gastroenterologists. The general lack of national chronic disease registries for PIBD in the respective countries of this network further adds to the challenges in obtaining complete epidemiologic data. These factors discussed suggest the true burden of PIBD in the Asia-Pacific region is very likely under-estimated.

CONCLUSION

Our study presents epidemiological data from the largest multi-centre Asian-Pacific paediatric cohort to date, and reaffirms the rising trend of PIBD across our registry, particularly in the past decade (2010-2019). We also report a substantially higher incidence of VEO-IBD than European cohorts and this is similarly observed in other Asian cohorts in mainland China and the Middle East. The unique multi-ethnic demographic composition of our cohort allows for distinct phenotypic differences to be seen between ethnicities, chiefly the over-representation of the Indian/South Asian ethnicity and its strong association with symptomatic perianal CD. Prospective follow-up data from this registry would also ascertain if any of these observed epidemiologic trends within this publication have implications on medium to longer term disease outcomes.

This inaugural publication from our registry likely under-estimates the true burden of IBD in Asia, and the way forward to address these identified knowledge gaps, would be to encourage more tertiary centres from diverse parts of Asia to partake in the Asian PIBD registry. This will improve the representativeness of our cohort and enhance the ability to make both intra- and inter-regional comparisons in disease behaviour and phenotypic trends.

ARTICLE HIGHLIGHTS

Research background

There remains a dearth of epidemiological literature on paediatric inflammatory bowel disease (IBD) in most parts of Asia. While there have been several published cohort studies out of East Asia, little is known on the actual disease burden beyond isolated case series and single-centre studies in the rest of the Asia-Pacific region. This would represent the first cohort study from a multi-centre Asian-Pacific PIBD registry first initiated in 2017.

Research motivation

The main issue was a lack of a standardised data platform in Asian-Pacific paediatric gastroenterology centres. A standardised data platform is vital to allow an accurate and validated way of reporting the disease behaviour and phenotype of PIBD across different healthcare systems in the heterogeneous Asia-Pacific region. This facilitates meaningful epidemiological comparisons with other established PIBD cohorts from North America and Western Europe.

Research objectives

This cohort study describes the epidemiological characteristics of all PIBD patients at the point of initial presentation, whom are managed at one of seven paediatric gastroenterology centres in the Asian-Pacific region (Singapore, Sri Lanka, Malaysia, Thailand, Philippines, Taiwan R.O.C). The objectives were to establish if there were unique disease characteristics of PIBD in the Asia-Pacific region in contrast to East Asian and Caucasian cohorts, as well as inter-ethnic disease phenotypic differences in the multi-ethnic populations of Asia-Pacific.

Research methods

Standardised disease data collection forms using existing validated disease activity indices and disease classification systems for PIBD were stored electronically on a centrally-hosted secure REDCAP platform. Participating Asian-Pacific sites were invited to enrol patients with an established diagnosis of IBD from the point of initial presentation.

Research results

Epidemiological data from our registry demonstrates a rapid rise in PIBD incidence, particularly in the last 5 years. The unique disease characteristics of our Asian-Pacific cohort include a large proportion of very-early onset (VEO)-IBD (29.3%) similar to the high proportions of VEO disease reported from mainland China, Saudi Arabia and India. There is also a relative over-representation of the Indian/South Asian ethnicity in the multi-ethnic countries of Singapore and Malaysia. Patients of Indian ethnicity with Crohn's disease (CD) were also most likely to present with symptomatic perianal disease.

Research conclusions

The rise in PIBD incidence across the Asian-Pacific region is consistent with the observed rise in incidence in many other global cohorts. The high proportion of very early onset IBD in the Asia-Pacific region may represent a shift in epidemiological trends in PIBD, as other established IBD cohorts similarly report the fastest growth in IBD incidence amongst very young children. The higher incidence of symptomatic perianal CD amongst Indian patients in Singapore/Malaysia suggests inter-ethnic genetic differences may cause variability in disease behaviour.

Research perspectives

Future research should be targeted at establishing national disease data registries to fully encapsulate the true burden of IBD in the Asia-Pacific region, and prospective follow-up data from this multi-centre registry is essential to determine if any of the observed epidemiological trends at diagnosis have implications on longer term outcomes.

ACKNOWLEDGEMENTS

We thank Dr Dimple Rajgor for helping with editing, formatting, and submission of the manuscript for publication.

FOOTNOTES

Author contributions: Huang JG, Wong YKY, Chew KS, Tanpowpong P, Calixto Mercado KS, Reodica A, Rajindrajith S, Chang KC, Ni YH, Treepongkaruna S, Lee WS, and Aw MM were involved in the conception of the work and data collection; Wong YKY was involved in the data interpretation; Huang JG, Wong YKY, Treepongkaruna S, Lee WS, and Aw MM contributed to the article drafting; Huang JG, Treepongkaruna S, Lee WS, and Aw MM were involved in the critical revision of the article; and all authors were involved in final approval of the published version.

Institutional review board statement: The study was reviewed and approved for publication by our Institutional Reviewer. Ethics approval for the storage of anonymised clinical data on a multi-centre central data registry hosted by the Singapore Clinical Research Institute was granted by the National Healthcare Group (NHG) Domain Specific Review Board (Approval letter for study code NUH/2019-00060 dated 23rd January 2020), followed by a separate ethics approval for data extraction and analysis (Approval letter for study code 2019/00751 dated 20th October 2021 to 19th October 2022).

Informed consent statement: All study participants or their legal guardian provided informed written consent about personal and medical data collection prior to study enrolment.

Conflict-of-interest statement: All the Authors have no conflict of interest related to the manuscript.

Data sharing statement: The original anonymous dataset is available on request from the corresponding author at james_huang@nuhs.edu.sg on reasonable request.

STROBE statement: The authors have read the STROBE Statement-checklist of items, and the manuscript was prepared and revised according to the STROBE Statement-checklist of items.

Open-Access: This article is an open-access article that was selected by an in-house editor and fully peer-reviewed by external reviewers. It is distributed in accordance with the Creative Commons Attribution NonCommercial (CC BY-NC 4.0) license, which permits others to distribute, remix, adapt, build upon this work non-commercially, and license their derivative works on different terms, provided the original work is properly cited and the use is non-

commercial. See: https://creativecommons.org/Licenses/by-nc/4.0/

Country/Territory of origin: Singapore

ORCID number: James Guoxian Huang 0000-0002-5869-4194; Yoko Kin Yoke Wong 0000-0002-1276-7060; Kee Seang Chew 0000-0002-9259-6993; Pornthep Tanpowpong 0000-0002-3246-8009; Karen Sophia Calixto Mercado 0000-0002-1587-1875; Almida Reodica 0000-0002-4622-1752; Shaman Rajindrajith 0000-0003-1379-5052; Kai-Chi Chang 0000-0002-9720-3810; Yen-Hsuan Ni 0000-0002-1158-5249; Suporn Treepongkaruna 0000-0002-6651-2282; Way-Seah Lee 0000-0001-9163-2828; Marion Margaret Aw 0000-0002-6668-4623.

S-Editor: Wang JJ
L-Editor: Filipodia
P-Editor: Wang JJ

REFERENCES

1 **Ng SC**, Shi HY, Hamidi N, Underwood FE, Tang W, Benchimol EI, Panaccione R, Ghosh S, Wu JCY, Chan FKL, Sung JJY, Kaplan GG. Worldwide incidence and prevalence of inflammatory bowel disease in the 21st century: a systematic review of population-based studies. *Lancet* 2017; **390**: 2769-2778 [PMID: 29050646 DOI: 10.1016/S0140-6736(17)32448-0]

2 **Benchimol EI**, Bernstein CN, Bitton A, Carroll MW, Singh H, Otley AR, Vutcovici M, El-Matary W, Nguyen GC, Griffiths AM, Mack DR, Jacobson K, Mojaverian N, Tanyingoh D, Cui Y, Nugent ZJ, Coulombe J, Targownik LE, Jones JL, Leddin D, Murthy SK, Kaplan GG. Trends in Epidemiology of Pediatric Inflammatory Bowel Disease in Canada: Distributed Network Analysis of Multiple Population-Based Provincial Health Administrative Databases. *Am J Gastroenterol* 2017; **112**: 1120-1134 [PMID: 28417994 DOI: 10.1038/ajg.2017.97]

3 **Benchimol EI**, Mack DR, Nguyen GC, Snapper SB, Li W, Mojaverian N, Quach P, Muise AM. Incidence, outcomes, and health services burden of very early onset inflammatory bowel disease. *Gastroenterology* 2014; **147**: 803-813.e7; quiz e14 [PMID: 24951840 DOI: 10.1053/j.gastro.2014.06.023]

4 **Morita N**, Toki S, Hirohashi T, Minoda T, Ogawa K, Kono S, Tamakoshi A, Ohno Y, Sawada T, Muto T. Incidence and prevalence of inflammatory bowel disease in Japan: nationwide epidemiological survey during the year 1991. *J Gastroenterol* 1995; **30** Suppl 8: 1-4 [PMID: 8563866]

5 **Yang SK**, Yun S, Kim JH, Park JY, Kim HY, Kim YH, Chang DK, Kim JS, Song IS, Park JB, Park ER, Kim KJ, Moon G, Yang SH. Epidemiology of inflammatory bowel disease in the Songpa-Kangdong district, Seoul, Korea, 1986-2005: a KASID study. *Inflamm Bowel Dis* 2008; **14**: 542-549 [PMID: 17941073 DOI: 10.1002/ibd.20310]

6 **Ong C**, Aw MM, Liwanag MJ, Quak SH, Phua KB. Rapid rise in the incidence and clinical characteristics of pediatric inflammatory bowel disease in a South-East Asian cohort in Singapore, 1994-2015. *J Dig Dis* 2018; **19**: 395-403 [PMID: 29927059 DOI: 10.1111/1751-2980.12641]

7 **Lee WS**, Ng RT, Chan KW, Lau YL. Variable outcome in infantile-onset inflammatory bowel disease in an Asian cohort. *World J Gastroenterol* 2016; **22**: 10653-10662 [PMID: 28082818 DOI: 10.3748/wjg.v22.i48.10653]

8 **Treepongkaruna S**, Pienvichit P, Sornmayura P, Pornkul R, Wisedopas N, Phuapradit P. Inflammatory bowel disease in Thai children: presentations and outcomes of treatment. *Asian Pac J Allergy Immunol* 2006; **24**: 73-79 [PMID: 16913191]

9 **Levine A**, Koletzko S, Turner D, Escher JC, Cucchiara S, de Ridder L, Kolho KL, Veres G, Russell RK, Paerregaard A, Buderus S, Greer ML, Dias JA, Veereman-Wauters G, Lionetti P, Sladek M, Martin de Carpi J, Staiano A, Ruemmele FM, Wilson DC; European Society of Pediatric Gastroenterology, Hepatology, and Nutrition. ESPGHAN revised porto criteria for the diagnosis of inflammatory bowel disease in children and adolescents. *J Pediatr Gastroenterol Nutr* 2014; **58**: 795-806 [PMID: 24231644 DOI: 10.1097/MPG.0000000000000239]

10 **Levine A**, Griffiths A, Markowitz J, Wilson DC, Turner D, Russell RK, Fell J, Ruemmele FM, Walters T, Sherlock M, Dubinsky M, Hyams JS. Pediatric modification of the Montreal classification for inflammatory bowel disease: the Paris classification. *Inflamm Bowel Dis* 2011; **17**: 1314-1321 [PMID: 21560194 DOI: 10.1002/ibd.21493]

11 **Hyams J**, Markowitz J, Otley A, Rosh J, Mack D, Bousvaros A, Kugathasan S, Pfefferkorn M, Tolia V, Evans J, Treem W, Wyllie R, Rothbaum R, del Rosario J, Katz A, Mezoff A, Oliva-Hemker M, Lerer T, Griffiths A; Pediatric Inflammatory Bowel Disease Collaborative Research Group. Evaluation of the pediatric crohn disease activity index: a prospective multicenter experience. *J Pediatr Gastroenterol Nutr* 2005; **41**: 416-421 [PMID: 16205508 DOI: 10.1097/01.mpg.0000183350.46795.42]

12 **Turner D**, Hyams J, Markowitz J, Lerer T, Mack DR, Evans J, Pfefferkorn M, Rosh J, Kay M, Crandall W, Keljo D, Otley AR, Kugathasan S, Carvalho R, Oliva-Hemker M, Langton C, Mamula P, Bousvaros A, LeLeiko N, Griffiths AM; Pediatric IBD Collaborative Research Group. Appraisal of the pediatric ulcerative colitis activity index (PUCAI). *Inflamm Bowel Dis* 2009; **15**: 1218-1223 [PMID: 19161178 DOI: 10.1002/ibd.20867]

13 **Department of Statistics Malaysia Official Portal**. Current Population Estimates, Malaysia 2020. [cited 3 October 2021]. Available from: https://www.dosm.gov.my/v1/index.php?r=column/cthemeByCat&cat=155&bul_id=OVByWjg5YkQ3MWFZRTN5bDJiaEVhZz09&menu_id=L0pheU43NWJwRWVSZklWdzQ4TlhUUT09

14 **Singapore Department of Statistics**. Singapore Census of Population 2020. [cited 3 October 2021]. Available from: https://www.singstat.gov.sg/publications/reference/cop2020/cop2020-sr1

15 **Mak WY**, Zhao M, Ng SC, Burisch J. The epidemiology of inflammatory bowel disease: East meets west. *J Gastroenterol Hepatol* 2020; **35**: 380-389 [PMID: 31596960 DOI: 10.1111/jgh.14872]

16 **El Mouzan MI**, Saadah O, Al-Saleem K, Al Edreesi M, Hasosah M, Alanazi A, Al Mofarreh M, Asery A, Al Qourain A,

Nouli K, Al Hussaini A, Telmesani A, AlReheili K, Alghamdi S, Alrobiaa N, Alzaben A, Mehmadi A, Al Hebbi H, Al Sarkhy A, Al Mehaidib A, Al Saleem B, Assiri A, Wali S. Incidence of pediatric inflammatory bowel disease in Saudi Arabia: a multicenter national study. *Inflamm Bowel Dis* 2014; **20**: 1085-1090 [PMID: 24788219 DOI: 10.1097/MIB.0000000000000048]

17 **Zayyani NR**, Malaty HM, Graham DY. Increasing Incidence of Crohn's Disease with Familial Clustering in the Kingdom of Bahrain: A 25-Year Population-based Study. *Inflamm Bowel Dis* 2017; **23**: 304-309 [PMID: 28092308 DOI: 10.1097/MIB.0000000000001016]

18 **Ishige T**, Tomomasa T, Hatori R, Tatsuki M, Igarashi Y, Sekine K, Arakawa H. Temporal Trend of Pediatric Inflammatory Bowel Disease: Analysis of National Registry Data 2004 to 2013 in Japan. *J Pediatr Gastroenterol Nutr* 2017; **65**: e80-e82 [PMID: 28207475 DOI: 10.1097/MPG.0000000000001547]

19 **Jung YS**, Han M, Kim WH, Park S, Cheon JH. Incidence and Clinical Outcomes of Inflammatory Bowel Disease in South Korea, 2011-2014: A Nationwide Population-Based Study. *Dig Dis Sci* 2017; **62**: 2102-2112 [PMID: 28593437 DOI: 10.1007/s10620-017-4640-9]

20 **Wang XQ**, Zhang Y, Xu CD, Jiang LR, Huang Y, Du HM, Wang XJ. Inflammatory bowel disease in Chinese children: a multicenter analysis over a decade from Shanghai. *Inflamm Bowel Dis* 2013; **19**: 423-428 [PMID: 23340680 DOI: 10.1097/MIB.0b013e318286f9f2]

21 **Poddighe D**, Telman A, Tuleutayev E, Ibrayeva A. Pediatric Ulcerative Colitis in Kazakhstan: First Case Series from Central Asia and Current Clinical Management. *Gastroenterol Insights* 2020; **11**: 27-35 [DOI: 10.3390/gastroent11020006]

22 **Srivastava A**, Sathiyasekharan M, Jagadisan B, Bolia R, Peethambaran M, Mammayil G, Acharya B, Malik R, Sankaranarayanan S, Biradar V, Malhotra S, Philip M, Poddar U, Yachha SK. Paediatric inflammatory bowel disease in India: a prospective multicentre study. *Eur J Gastroenterol Hepatol* 2020; **32**: 1305-1311 [PMID: 32796356 DOI: 10.1097/MEG.0000000000001859]

23 **Paudel MS**, Khanal A, Shrestha B, Purbey B, Paudel BN, Shrestha G, Thapa J, Dewan KR, Gurung R, Joshi N. Epidemiology of Inflammatory Bowel Diseases in Nepal. *Cureus* 2021; **13**: e16692 [PMID: 34466323 DOI: 10.7759/cureus.16692]

24 **Shen YM**, Wu JF, Chen HL, Hsu HY, Chang MH, Hsieh TK, Ni YH. Characteristics and incidences of pediatric Crohn's disease in the decades before and after 2000. *Pediatr Neonatol* 2011; **52**: 317-320 [PMID: 22192258 DOI: 10.1016/j.pedneo.2011.08.003]

25 **Lee YM**, Fock K, See SJ, Ng TM, Khor C, Teo EK. Racial differences in the prevalence of ulcerative colitis and Crohn's disease in Singapore. *J Gastroenterol Hepatol* 2000; **15**: 622-625 [PMID: 10921415 DOI: 10.1046/j.1440-1746.2000.02212.x]

26 **Hilmi I**, Jaya F, Chua A, Heng WC, Singh H, Goh KL. A first study on the incidence and prevalence of IBD in Malaysia--results from the Kinta Valley IBD Epidemiology Study. *J Crohns Colitis* 2015; **9**: 404-409 [PMID: 25744112 DOI: 10.1093/ecco-jcc/jjv039]

27 **Montgomery SM**, Morris DL, Pounder RE, Wakefield AJ. Asian ethnic origin and the risk of inflammatory bowel disease. *Eur J Gastroenterol Hepatol* 1999; **11**: 543-546 [PMID: 10755259 DOI: 10.1097/00042737-199905000-00013]

28 **Fellows IW**, Freeman JG, Holmes GK. Crohn's disease in the city of Derby, 1951-85. *Gut* 1990; **31**: 1262-1265 [PMID: 2253910 DOI: 10.1136/gut.31.11.1262]

29 **Pinsk V**, Lemberg DA, Grewal K, Barker CC, Schreiber RA, Jacobson K. Inflammatory bowel disease in the South Asian pediatric population of British Columbia. *Am J Gastroenterol* 2007; **102**: 1077-1083 [PMID: 17378907 DOI: 10.1111/j.1572-0241.2007.01124.x]

30 **Malhotra R**, Turner K, Sonnenberg A, Genta RM. High prevalence of inflammatory bowel disease in United States residents of Indian ancestry. *Clin Gastroenterol Hepatol* 2015; **13**: 683-689 [PMID: 25083563 DOI: 10.1016/j.cgh.2014.06.035]

31 **Brooks AW**, Priya S, Blekhman R, Bordenstein SR. Gut microbiota diversity across ethnicities in the United States. *PLoS Biol* 2018; **16**: e2006842 [PMID: 30513082 DOI: 10.1371/journal.pbio.2006842]

32 **Castaño-Rodríguez N**, Kaakoush NO, Lee WS, Mitchell HM. Dual role of Helicobacter and Campylobacter species in IBD: a systematic review and meta-analysis. *Gut* 2017; **66**: 235-249 [PMID: 26508508 DOI: 10.1136/gutjnl-2015-310545]

33 **Khalid MA**, Yang L. Income inequality and ethnic cleavages in Malaysia: Evidence from distributional national accounts (1984–2014). *J Asian Econ* 2021; **72**: 101252 [DOI: 10.1016/j.asieco.2020.101252]

34 **Loftus EV Jr**. Update on the Incidence and Prevalence of Inflammatory Bowel Disease in the United States. *Gastroenterol Hepatol (N Y)* 2016; **12**: 704-707 [PMID: 28035199]

35 **Wang YR**, Loftus EV Jr, Cangemi JR, Picco MF. Racial/Ethnic and regional differences in the prevalence of inflammatory bowel disease in the United States. *Digestion* 2013; **88**: 20-25 [PMID: 23797316 DOI: 10.1159/000350759]

36 **Kotze PG**, Underwood FE, Damião AOMC, Ferraz JGP, Saad-Hossne R, Toro M, Iade B, Bosques-Padilla F, Teixeira FV, Juliao-Banos F, Simian D, Ghosh S, Panaccione R, Ng SC, Kaplan GG. Progression of Inflammatory Bowel Diseases Throughout Latin America and the Caribbean: A Systematic Review. *Clin Gastroenterol Hepatol* 2020; **18**: 304-312 [PMID: 31252191 DOI: 10.1016/j.cgh.2019.06.030]

37 **Singer AAM**, Bloom DA, Adler J. Factors Associated With Development of Perianal Fistulas in Pediatric Patients With Crohn's Disease. *Clin Gastroenterol Hepatol* 2021; **19**: 1071-1073 [PMID: 32360805 DOI: 10.1016/j.cgh.2020.04.060]

38 **Assa A**, Rinawi F, Shamir R. The Long-Term Predictive Properties of the Paris Classification in Paediatric Inflammatory Bowel Disease Patients. *J Crohns Colitis* 2018; **12**: 39-47 [PMID: 28961726 DOI: 10.1093/ecco-jcc/jjx125]

39 **Dhaliwal J**, Walters TD, Mack DR, Huynh HQ, Jacobson K, Otley AR, Debruyn J, El-Matary W, Deslandres C, Sherlock ME, Critch JN, Bax K, Seidman E, Jantchou P, Ricciuto A, Rashid M, Muise AM, Wine E, Carroll M, Lawrence S, Van Limbergen J, Benchimol EI, Church P, Griffiths AM. Phenotypic Variation in Paediatric Inflammatory Bowel Disease by Age: A Multicentre Prospective Inception Cohort Study of the Canadian Children IBD Network. *J Crohns Colitis* 2020; **14**: 445-454 [PMID: 31136648 DOI: 10.1093/ecco-jcc/jjz106]

40 **Banerjee R**, Pal P, Nabi Z, Shava U, Ganesh G, Reddy DN. Very early onset inflammatory bowel disease in a South Asian country where inflammatory bowel disease is emerging: a distinct clinical phenotype from later onset disease. *Intest Res*

2021; **19**: 398-407 [PMID: 33207854 DOI: 10.5217/ir.2020.00107]

41 **Li BH**, Guan X, Vittinghoff E, Gupta N. Comparison of the presentation and course of pediatric inflammatory bowel disease in South Asians with Whites: a single center study in the United States. *J Pediatr* 2013; **163**: 1211-1213 [PMID: 23706360 DOI: 10.1016/j.jpeds.2013.04.017]

42 **Jangi S**, Ruan A, Korzenik J, de Silva P. South Asian Patients With Inflammatory Bowel Disease in the United States Demonstrate More Fistulizing and Perianal Crohn Phenotype. *Inflamm Bowel Dis* 2020; **26**: 1933-1942 [PMID: 32115633 DOI: 10.1093/ibd/izaa029]

43 **Ray G**. Inflammatory bowel disease in India - Past, present and future. *World J Gastroenterol* 2016; **22**: 8123-8136 [PMID: 27688654 DOI: 10.3748/wjg.v22.i36.8123]

44 **Foster A**, Jacobson K. Changing incidence of inflammatory bowel disease: environmental influences and lessons learnt from the South asian population. *Front Pediatr* 2013; **1**: 34 [PMID: 24400280 DOI: 10.3389/fped.2013.00034]

45 **Wang XQ**, Xiao Y, Xu X, Yu Y, Shan CY, Guo Y, Gong L, Zhou T, Gao SS, Yuan YZ, Wang XJ, Xu CD. Study of disease phenotype and its association with prognosis of paediatric inflammatory bowel disease in China. *BMC Pediatr* 2018; **18**: 229 [PMID: 30001197 DOI: 10.1186/s12887-018-1212-x]

46 **Kim HJ**, Oh SH, Kim DY, Lee HS, Park SH, Yang SK, Kim KM. Clinical Characteristics and Long-Term Outcomes of Paediatric Crohn's Disease: A Single-Centre Experience. *J Crohns Colitis* 2017; **11**: 157-164 [PMID: 27651220 DOI: 10.1093/ecco-jcc/jjw146]

47 **Kochar B**, Barnes EL, Herfarth HH, Martin CF, Ananthakrishnan AN, McGovern D, Long M, Sandler RS. Asians have more perianal Crohn disease and ocular manifestations compared with white Americans. *Inflamm Intest Dis* 2018; **2**: 147-153 [PMID: 29876356 DOI: 10.1159/000484347]

48 **Gower-Rousseau C**, Vasseur F, Fumery M, Savoye G, Salleron J, Dauchet L, Turck D, Cortot A, Peyrin-Biroulet L, Colombel JF. Epidemiology of inflammatory bowel diseases: new insights from a French population-based registry (EPIMAD). *Dig Liver Dis* 2013; **45**: 89-94 [PMID: 23107487 DOI: 10.1016/j.dld.2012.09.005]

49 **Guan DX**, Yu FH, Wang GL, Zhou J, Wang DY, Nie XL, Xu XW. [Single center retrospective study of 184 children with inflammatory bowel disease seen from 2000-2014]. *Zhonghua Er Ke Za Zhi* 2017; **55**: 493-498 [PMID: 28728256 DOI: 10.3760/cma.j.issn.0578-1310.2017.07.005]

50 **Sawczenko A**, Sandhu BK. Presenting features of inflammatory bowel disease in Great Britain and Ireland. *Arch Dis Child* 2003; **88**: 995-1000 [PMID: 14612366 DOI: 10.1136/adc.88.11.995]

51 **Saverymuttu SH**, Hodgson HJ, Chadwick VS, Pepys MB. Differing acute phase responses in Crohn's disease and ulcerative colitis. *Gut* 1986; **27**: 809-813 [PMID: 3732890 DOI: 10.1136/gut.27.7.809]

52 **Vermeire S**, Van Assche G, Rutgeerts P. Laboratory markers in IBD: useful, magic, or unnecessary toys? *Gut* 2006; **55**: 426-431 [PMID: 16474109 DOI: 10.1136/gut.2005.069476]

53 **D'Haens G**, Ferrante M, Vermeire S, Baert F, Noman M, Moortgat L, Geens P, Iwens D, Aerden I, Van Assche G, Van Olmen G, Rutgeerts P. Fecal calprotectin is a surrogate marker for endoscopic lesions in inflammatory bowel disease. *Inflamm Bowel Dis* 2012; **18**: 2218-2224 [PMID: 22344983 DOI: 10.1002/ibd.22917]

54 **Hildebrand H**, Karlberg J, Kristiansson B. Longitudinal growth in children and adolescents with inflammatory bowel disease. *J Pediatr Gastroenterol Nutr* 1994; **18**: 165-173 [PMID: 8014763 DOI: 10.1097/00005176-199402000-00008]

World Journal of Gastroenterology

Submit a Manuscript: https://www.f6publishing.com

World J Gastroenterol 2022 May 7; 28(17): 1845-1859

DOI: 10.3748/wjg.v28.i17.1845

ISSN 1007-9327 (print) ISSN 2219-2840 (online)

ORIGINAL ARTICLE

Retrospective Study

Clinical outcomes of endoscopic papillectomy of ampullary adenoma: A multi-center study

Seong Ji Choi, Hong Sik Lee, Jiyeong Kim, Jung Wan Choe, Jae Min Lee, Jong Jin Hyun, Jai Hoon Yoon, Hyo Jung Kim, Jae Seon Kim, Ho Soon Choi

Specialty type: Gastroenterology and hepatology

Provenance and peer review: Unsolicited article; Externally peer reviewed.

Peer-review model: Single blind

Peer-review report's scientific quality classification

Grade A (Excellent): A
Grade B (Very good): B, B
Grade C (Good): 0
Grade D (Fair): 0
Grade E (Poor): 0

P-Reviewer: Philipose J, United States; Sahin TT, Turkey; Tsuji Y, Japan

Received: September 25, 2021
Peer-review started: September 25, 2021
First decision: November 16, 2021
Revised: November 26, 2021
Accepted: March 25, 2022
Article in press: March 25, 2022
Published online: May 7, 2022

Seong Ji Choi, Jai Hoon Yoon, Ho Soon Choi, Department of Internal Medicine, Hanyang University College of Medicine, Seoul 04763, South Korea

Hong Sik Lee, Jung Wan Choe, Jae Min Lee, Jong Jin Hyun, Hyo Jung Kim, Jae Seon Kim, Division of Gastroenterology and Hepatology, Department of Internal Medicine, Korea University College of Medicine, Seoul 02841, South Korea

Jiyeong Kim, Lab of Biostatistical Consulting and Research, Medical Research Collaborating Center, Industry-University Cooperation Foundation, Hanyang University, Seoul 04763, South Korea

Corresponding author: Hong Sik Lee, MD, PhD, Professor, Division of Gastroenterology and Hepatology, Department of Internal Medicine, Korea University College of Medicine, 73 Goryeodae-ro, Seongbuk-gu, Seoul 02841, South Korea. hslee60@korea.ac.kr

Abstract

BACKGROUND

Ampullary adenoma is a rare premalignant lesion, but its incidence is increasing. Endoscopic papillectomy has become the first treatment of choice for ampullary adenomas due to its safety and effectiveness, thereby replacing surgical resection. However, recurrence rates and adverse events after endoscopic papillectomy were reported in up to 30% of cases.

AIM

To review the long-term outcomes of endoscopic papillectomy and investigate the factors that affect these outcomes.

METHODS

We retrospectively analyzed the data of patients who underwent endoscopic papillectomy for ampullary adenoma at five tertiary hospitals between 2013 and 2020. We evaluated clinical outcomes and their risk factors. The definitions of outcomes were as follow: (1) curative resection: complete endoscopic resection without recurrence; (2) endoscopic success: treatment of ampullary adenoma with endoscopy without surgical intervention; (3) early recurrence: reconfirmed adenoma at the first endoscopic surveillance; and (4) late recurrence: reconfirmed adenoma after the first endoscopic surveillance.

RESULTS

A total of 106 patients were included for analysis. Of the included patients, 81 (76.4%) underwent curative resection, 99 (93.4%) had endoscopic success, showing that most patients with non-curative resection were successfully managed with endoscopy. Sixteen patients (15.1%) had piecemeal resection, 22 patients (20.8%) had shown positive/uncertain resection margin, 11 patients (16.1%) had an early recurrence, 13 patients (10.4%) had a late recurrence, and 6 patients (5.7%) had a re-recurrence. In multivariate analysis, a positive/uncertain margin [Odds ratio (OR) = 4.023, P = 0.048] and piecemeal resection (OR = 6.610, P = 0.005) were significant risk factors for early and late recurrence, respectively. Piecemeal resection was also a significant risk factor for non-curative resection (OR = 5.424, P = 0.007). Twenty-six patients experienced adverse events (24.5%).

CONCLUSION

Endoscopic papillectomy is a safe and effective treatment for ampullary adenomas. Careful selection and follow-up of patients is mandatory, particularly in cases with positive/uncertain margin and piecemeal resection.

Key Words: Endoscopic papillectomy; Ampullary adenoma; Clinical outcome; Recurrence; Adverse event

©The Author(s) 2022. Published by Baishideng Publishing Group Inc. All rights reserved.

Core Tip: This is a multi-center study evaluating the clinical outcomes of 106 patients who underwent endoscopic papillectomy for ampullary adenoma. In our results, margin-positive/uncertain pathologic reports and piecemeal resection were significant factors for the curative resection and recurrences. Unexpectedly, many recurrences were observed in margin-negative resection, but in most cases, they were successfully managed with minimally invasive endoscopic therapies. Since there is no definite factor for predicting and preventing recurrence and re-recurrence, regular follow-up with endoscopy should be performed in every patient regardless of resection margin or resection type, especially in patients with margin-positive/uncertain and piecemeal resection.

Citation: Choi SJ, Lee HS, Kim J, Choe JW, Lee JM, Hyun JJ, Yoon JH, Kim HJ, Kim JS, Choi HS. Clinical outcomes of endoscopic papillectomy of ampullary adenoma: A multi-center study. *World J Gastroenterol* 2022; 28(17): 1845-1859

URL: https://www.wjgnet.com/1007-9327/full/v28/i17/1845.htm

DOI: https://dx.doi.org/10.3748/wjg.v28.i17.1845

INTRODUCTION

Ampullary adenomas (AAs) are rare lesions, with a prevalence of 0.04%-0.12% in autopsy, and account for 0.2%-5% of newly diagnosed intestinal neoplasms[1-3]. As the number of endoscopic surveillance or computed tomography (CT) scans has increased, the number of AAs detected has also increased. Patients with AA are often asymptomatic, and other complaints are related to biliary or pancreatic obstruction, such as jaundice, biliary colic, or pancreatitis. Even in asymptomatic patients, an AA needs to be removed because of its malignant potential[4]. Furthermore, complete excision of AAs is necessary because of poor diagnostic accuracy with false-negative rates of up to 30% and diagnostic discrepancy of pathologic results, reported as 25%-60%, with forceps biopsy[5,6].

Endoscopic papillectomy (EP) was first introduced for the treatment of AA by Suzuki *et al*[7] in 1983, and both endoscopic and surgical approaches have been considered for the treatment of AA. EP is now considered as the first treatment of choice for benign AA due to the high recurrence, mortality, and morbidity of surgery[8-11]. Nevertheless, there remain concerns regarding EP. The reported EP adverse event rate is over 20% and while most cases are not severe, this cannot be neglected[12]. The recurrence rate after EP is high at 58.3%, and re-recurrence or persistence of AA has often been reported, requiring patients to undergo additional procedures or surgery[13,14]. Despite recent guidelines, there is no consensus on outcome parameters, and there are no established indication for EP or guidelines for EP technique, and no guidelines for the management of recurrence and re-recurrence[12,15,16].

Here, we aimed to evaluate the clinical outcomes of patients who underwent EP and investigate the factors that affect recurrence and adverse events to assist in improving the outcomes of EP and establishing the guidelines for EP.

MATERIALS AND METHODS

Study design

We retrospectively reviewed the medical charts of patients who underwent EP for AA between January 2013 and December 2019 and their follow-up data until December 2020 at five tertiary hospitals: Korea University Anam Hospital, Korea University Guro Hospital, Korea University Ansan Hospital, Hanyang University Seoul Hospital, and Hanyang University Guri Hospital. We excluded patients who underwent EP or surgical ampullectomy prior to enrollment and those who were followed up for less than a year after EP. Patients with non-adenomatous lesions were also excluded.

Patient baseline characteristics including age, sex, body mass index, clinical presentations, and initial pathologic reports of the lesion were recorded. Patients were screened for familial adenomatous polyposis (FAP), and mean follow-up periods were calculated. Parameters for EP techniques were recorded using written reports of EP, endoscopic images, and fluoroscopic images. These parameters included endoscopic ultrasound (EUS), cholangiogram, pancreatogram, submucosal lifting, type of resection(*en-bloc*/piecemeal), thermal ablation after resection, complete endoscopic resection, bile duct stent insertion (BDS), and pancreatic duct stent insertion (PDS).

EP procedure

EP was performed at five tertiary hospitals with over 500 endoscopic retrograde cholangiography (ERCP) annual cases by seven experts with over five years of ERCP experience. Before EP, EUS was performed at the endoscopist's discretion. After adequate sedation, the ampulla of Vater was carefully inspected for its size, extent, and signs of malignancy (Figure 1A). Following the inspection, a cholangiogram and pancreatogram were obtained in cases requiring evaluation of a possible intraductal invasion. Then, snare polypectomy was performed (Figure 1B). Mucosal lifting using saline was performed if needed. With a standard polypectomy snare, the adenoma was tightly grasped, and the electrical current was applied until complete resection of the lesion was achieved.

En-bloc resection of AA was first attempted, and a piecemeal resection was performed if *en-bloc* resection was not possible. The resected specimen was removed and sent for pathologic evaluation (Figure 1C). The specimen was reviewed by a gastrointestinal pathologist and one or more residents in each hospital.

The EP site was observed for possible remnant lesions and immediate adverse events. Where remnant tissue was suspected, removal was performed with repeated biopsy, snaring, or thermal ablation with argon plasma coagulation (APC). In the event of immediate bleeding, epinephrine was sprayed with additional APC if bleeding persisted. In the event of duodenal perforation, endoscopic hemoclips were applied for the primary closure and surgery was subsequently performed. Sphinterotomies, BDS, and PDS were performed if needed (Figure 1D). The procedure was terminated if there was no more residual tissue or in the absence of immediate adverse events. Subsequently, the patient was observed on the ward with physical examination, monitoring of vital signs, laboratory tests, and X-rays for early adverse events. The details of each endoscopic procedure were determined by the endoscopist.

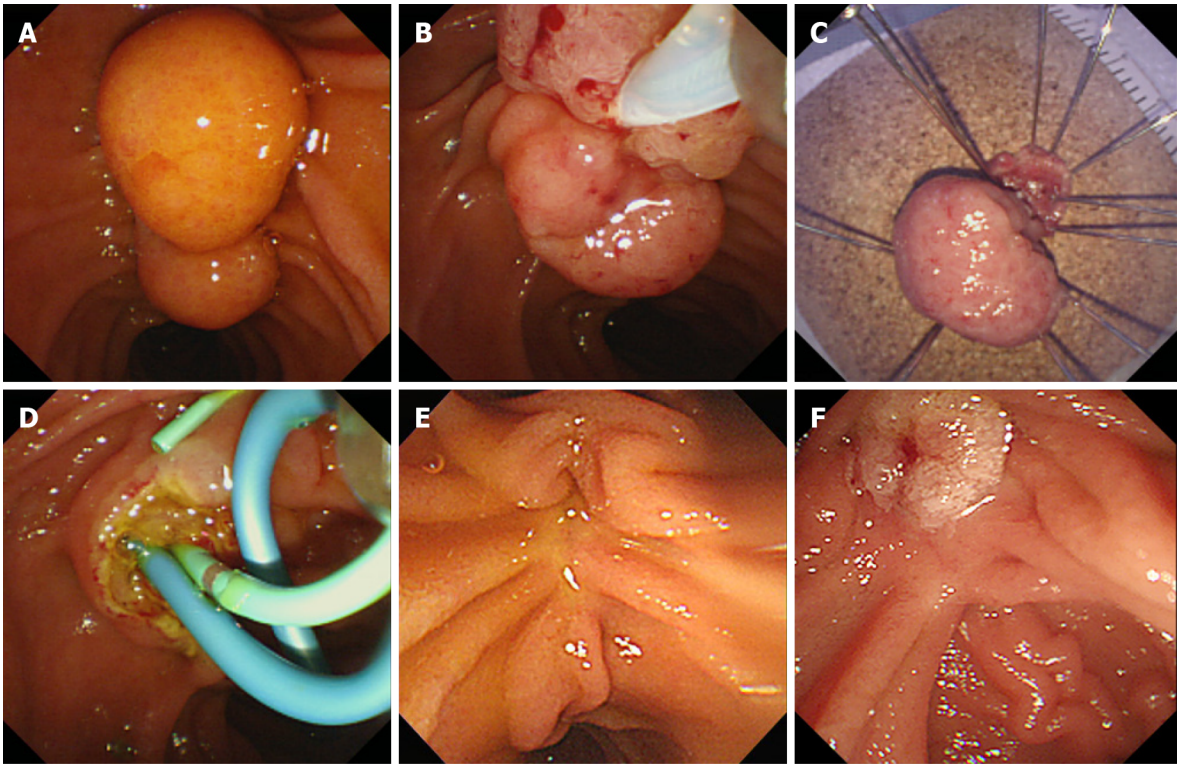
All patients underwent routine follow-up after EP. Within 3 mo of the procedure, patients underwent endoscopic surveillance for assessment of remnant tissue and recurrence, and stent removal (Figure 1E). Biopsy was performed if any remnant lesion was suspected. If the biopsy result showed remnants or early recurrence, additional therapeutic plans were decided by the endoscopist with the patient (Figure 1F). If no abnormal lesion was identified, the patient underwent further surveillance at six-monthly intervals for the first two years and annually thereafter.

Outcome measures

EP results included the resection specimen size, pathologic findings, accuracy of endoscopic biopsy, resection margin, curative resection, early and late recurrence, re-recurrence, endoscopic success, mean hospital stay, and mean adenoma-free period. EP outcomes were obtained from pathologic reports and medical charts.

Curative resection was defined as complete endoscopic resection without recurrence during follow-up. Early recurrence was defined as reconfirmed adenoma following biopsy at the first surveillance endoscopy. Late recurrence was defined as reconfirmed adenoma following biopsy after the first surveillance endoscopy. Re-recurrence was defined as recurrence of adenoma at the follow-up biopsy after the treatment of early or late recurrence. Endoscopic success was defined as treatment of AA with endoscopy, including cases with residual tissue, recurrence or complications, without surgical intervention. Resection margins were categorized into 3 groups, negative, positive, and uncertain, and they were analyzed as positive/uncertain group and negative group[17,18].

Adverse events of EP were categorized into early events (pancreatitis, delayed bleeding, cholangitis, and perforation) occurring within 30 d of the procedure and late events (papillary stenosis and death) occurring after 30 d following the procedure. Endoscopic adverse events and their severity were graded according to the American Society for Gastrointestinal Endoscopy criteria[19]. We set the minimum follow-up duration to one year to avoid underestimation of recurrence and adverse events. Univariate analysis and multivariate analysis were performed to evaluate the risk factors of early and late



DOI: 10.3748/wjg.v28.i17.1845 **Copyright** ©The Author(s) 2022.

Figure 1 Endoscopic papillectomy of ampullary adenoma. A: Careful inspection of the ampulla was required before the procedure; B: Endoscopic papillectomy was performed using a conventional polypectomy snare; C: The resected specimen was retrieved and pinned on a cork with nails for pathological evaluation; D: The resected area was carefully inspected, and an additional procedure including common bile duct stenting (blue stent) or pancreatic duct stenting (green stent) was performed; E: Endoscopic surveillance was mandatory; F: If recurrence was suspected, additional treatment was considered.

recurrence, non-curative resection, and adverse events.

Statistical analysis

Continuous variables were expressed as mean and standard deviation, and Categorical variables were expressed as a number and percentage. Univariate logistic regression analysis was performed to analyze the risk factors for early and late recurrences, non-curative resection, and adverse events. Variables that were significant in the univariate analysis were included in the multivariate logistic regression analysis. A P value < 0.05 was considered significant. The probability of adenoma-free after EP was analyzed using the Kaplan–Meier method. The statistical analyses were performed using the SPSS version 22.0 software (IBM Corp., Armonk, N.Y., USA).

RESULTS

We retrospectively collected the medical records of 119 patients and their follow-up data (Figure 2). We excluded seven patients who failed to meet the follow-up criteria or were lost to follow-up within a year of the procedure, and six patients because of non-adenomatous lesions. After the exclusion criteria were applied, 106 patients were finally included for analysis.

Patient baseline characteristics are shown in Table 1. Seventy-three patients (68.9%) were asymptomatic, and AA was diagnosed incidentally from screening endoscopy or CT scan. The most frequent symptoms associated with AA were jaundice in 16 patients (15.1%) and abdominal discomfort in 13 patients (12.3%). All patients underwent biopsy before the EP procedure, and their pathology reports were as follows: chronic inflammation in 2 patients (1.9%), atypical proliferative epithelium in 3 patients (2.8%), adenoma with low-grade dysplasia in 91 patients (85.8%), and adenoma with high-grade dysplasia in 10 patients (9.4%).

The EP techniques used for the patients are listed in Table 2. EUS was performed in 37 patients (34.9%), and a cholangiogram and pancreatogram were obtained in 70 patients (66.0%) and 87 patients (82.1%), respectively. Four patients (3.8%) underwent submucosal lifting with normal saline. *En-bloc* resection was performed in 90 patients (84.9%), and piecemeal resection was performed in 16 patients (15.1%). After the resection, thermal ablation was performed in 24 patients (22.6%) because of remnant tissue or immediate bleeding. Complete endoscopic resection was successfully performed in 105

Table 1 Baseline characteristics of patients

Characteristics	*n* (%)/mean ± SD (*n* = 106)
Age, yr	61.4 ± 12.8
≤ 65	57.5)
> 65	45 (42.5)
Sex	
Male	62 (58.5)
Female	44 (41.5)
Body mass index (kg/m^2)	23.3 ± 2.2
≤ 25	90 (84.9)
> 25	16 (15.1)
Clinical presentation	
Asymptomatic	73 (68.9)
Jaundice	16 (15.1)
Abdominal discomfort	13 (12.3)
Other	4 (3.8)
Familial adenomatous polyposis	3 (2.8)
Initial pathology	
Chronic inflammation	2 (1.9)
Atypical proliferative epithelium	3 (2.8)
Low-grade dysplasia	91 (85.8)
High-grade dysplasia	10 (9.4)
Mean follow-up, mo	36.2 ± 18.3

patients (99.1%), and in one patient the lesion could not be completely removed due to underlying fibrosis and a diagnosis of adenocarcinoma was finally made. BDS and PDS were performed in 25 patients (23.6%) and 78 patients (73.6%), respectively.

Table 2 also summarizes the results of the EP. The mean size of the resected specimen was 13.6 ± 5.5 mm, and the final pathologic results were as follows: chronic inflammation in 3 cases (2.8%), low-grade dysplasia in 81 cases (76.4%), high-grade dysplasia in 18 cases (17.0%), and adenocarcinoma in 4 cases (3.8%). Figure 2 shows the diagnostic discrepancies between the initial and final pathologies. Lesions that showed chronic inflammation or atypical proliferative epithelium on initial biopsy were all low-grade dysplasia on final diagnosis. Out of 91 cases of low-grade dysplasia on the initial biopsy, the final pathologic results were chronic inflammation in three cases (2.8%), low-grade dysplasia in 75 cases (82.4%), high-grade dysplasia in 9 cases (9.9%), and adenocarcinoma in four cases (3.8%). Out of 10 cases of high-grade dysplasia on the initial biopsy, the final pathologic results were low-grade dysplasia in one case and high-grade dysplasia in nine cases. Endoscopic biopsy was accurate in 84 patients (79.2%), with underestimation in 18 patients (17.0%) and overestimation in 4 patients (3.8%).

R0 resection was achieved in 84 patients (79.2%), and curative resection was achieved in 81 patients (76.4%). Early recurrence was found in 11 patients (10.4%), late recurrence was found in 13 patients (12.3%), and all recurrences were local lesions. Re-recurrence occurred in six patients (5.7%), and patient characteristics are summarized in Supplementary Table 1. Figure 2 also shows the number of early and late recurrences from final pathologic results, how these cases were managed, how many re-recurrences occurred after the initial management, and final management of re-recurrences.

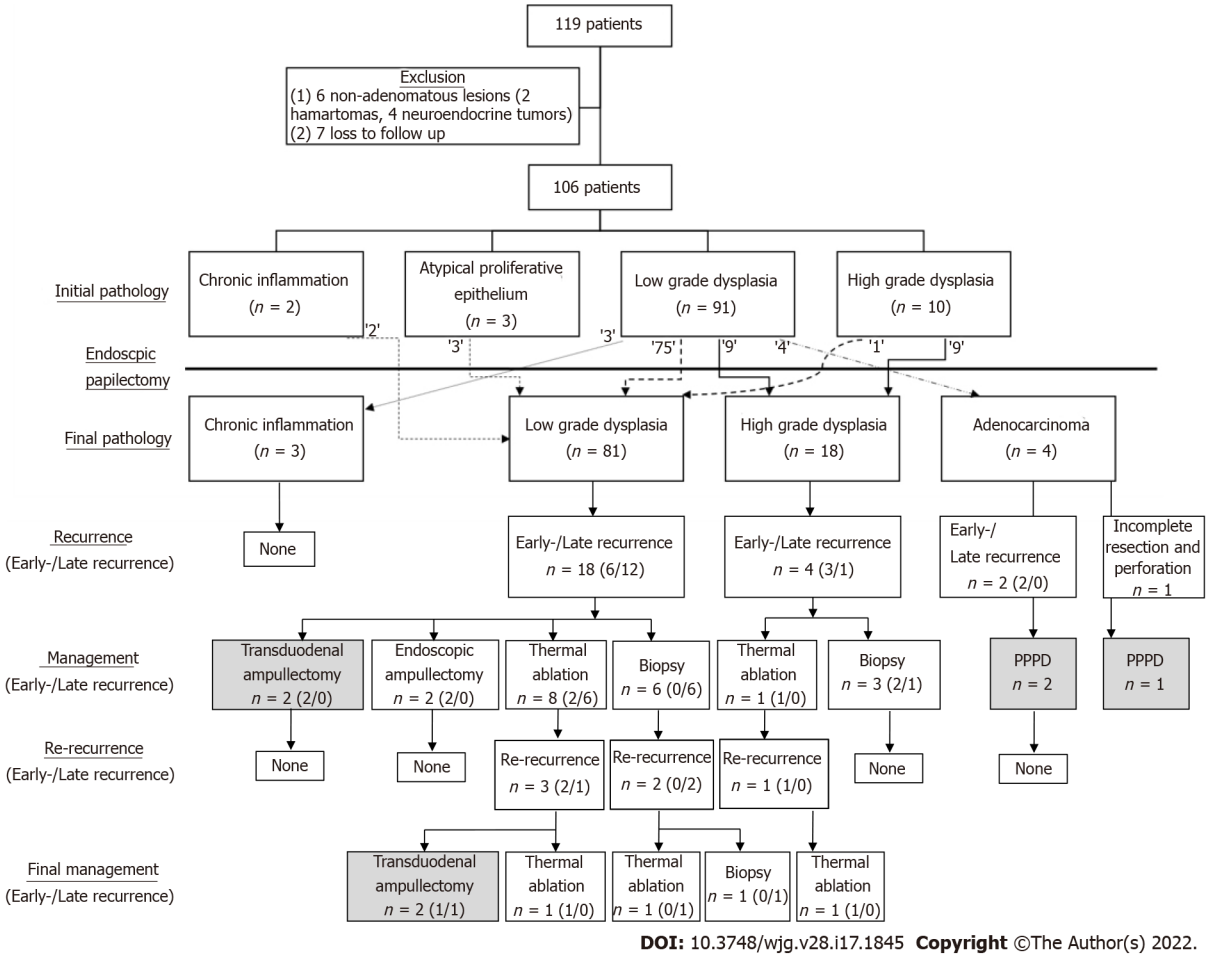
Initial management of the 11 patients with early recurrence involved endoscopic therapy in 7 cases (two EPs, two biopsies, and three thermal ablations) and surgery in four cases [two transduodenal ampullectomies (TA) and two pylorus-preserving pancreaticoduodenectomies (PPPD)]. Three patients with re-recurrence were managed with thermal ablation (two cases) and TA (one case). The 13 patients with late recurrence were initially managed endoscopically (six biopsies and seven ablations), and three patients with re-recurrence underwent thermal ablation, biopsy, and TA, respectively. Altogether, 99 patients (93.4%) were managed by endoscopy alone, and seven patients (6.6%) underwent additional surgical management: four patients due to a remnant lesion, two patients due to re-recurrence, and one patient due to incomplete resection and perforation (Figure 2). The mean adenoma-free period was 29.6

Table 2 Techniques and outcomes of endoscopic papillectomy

	n **(%)/mean ± SD (*n* = 106)**
EUS	37 (34.9)
ERCP	
Cholangiogram	70 (66.0)
Pancreatogram	87 (82.1)
Submucosal lifting	4 (3.8)
Type of resection	
En-bloc	90 (84.9)
Piecemeal	16 (15.1)
Thermal ablation after resection	24 (22.6)
Complete endoscopic resection	105 (99.1)
Stent implantation	
Bile duct	25 (23.6)
Pancreatic duct	78 (73.6)
Resection specimen size, mm	13.6 ± 5.5
≤ 15	77 (72.6)
> 15	29 (27.4)
Final pathology	
Chronic inflammation	3 (2.8)
Adenoma	
Low grade	81 (76.4)
High grade	18 (17.0)
Adenocarcinoma	4 (3.8)
Accuracy of endoscopic biopsy	
Underestimate	18 (17.0)
Overestimate	4 (3.8)
Resection margin	
Negative	84 (79.2)
Positive/Uncertain	22 (20.8)
Positive	19 (17.9)
Uncertain	3 (2.8)
Curative resection	81 (76.4)
Early recurrence	11 (10.4)
Late recurrence	13 (12.3)
Re-recurrence	6 (5.7)
Endoscopic success	99 (93.4)
Mean hospital stay, d	5.7 ± 3.0
Mean adenoma-free period, mo	29.6 ± 21.3

EUS: Endoscopic ultrasound; ERCP: Endoscopic retrograde cholangiography.

± 21.3 mo, and the adenoma-free survival is shown in Figure 3. Except for a patient who showed recurrence after 27 mo of the EP procedure, 12 patients (92.3%) experienced recurrence within a year of the EP procedure.



DOI: 10.3748/wjg.v28.i17.1845 **Copyright** ©The Author(s) 2022.

Figure 2 Flowchart of the study. After applying the exclusion criteria, 106 patients were enrolled, showing the correlation between the initial and final pathology. After the procedure, remnant and recurrent lesions were identified in follow-up surveillances. Most of these lesions were successfully managed with endoscopy. The gray-colored box indicates surgical management.

Table 3, Table 4, and Table 5 show the univariate and multivariate analysis of the risk factors for early recurrence, late recurrence and non-curative resection, respectively. Age over 65, EUS, size > 1.5 cm and positive/uncertain resection margin were statistically significant risk factors for early recurrence in univariate analysis, and positive/uncertain resection margin [Odds ratio (OR) = 4.023; 95%CI: 1.088-16.387; P = 0.048] was the significant factor for early recurrence in multivariate analysis. Presence of symptom (OR = 4.659; 95%CI: 1.292-16.797; P = 0.019) and piecemeal resection (OR = 7.114; 95%CI: 1.993-25.398; P = 0.003) were significant risk factors for late recurrence in univariate analysis, and piecemeal resection (OR = 6.610; 95%CI: 1.760-24.820; P = 0.005) was the only significant factor for late recurrence in multivariate analysis. Body mass index over 25, presence of symptom, and piecemeal resection were significant risk factors for non-curative resection, and multivariate analysis showed that piecemeal resection (OR = 5.424; 95%CI: 1.582-18.600; P = 0.007) was a significant risk factor for non-curative resection.

Altogether, adverse events occurred in 26 patients as shown in Table 6. Early adverse events were as follows: pancreatitis in 14 patients (13.2%), delayed bleeding in 11 patients (10.4%), cholangitis in six patients (5.7%), and perforation in one patient (0.9%). No late adverse events were reported. In most cases, the severity of adverse events was classified as either mild or moderate, except for one case with perforation. Table 7 shows the univariate and multivariate analysis of risk factors for adverse events, including pancreatitis and delayed bleeding. FAP, pancreatogram, thermal ablation and PDS were significant risk factors for pancreatitis in univariate analysis, and in multivariate analysis, thermal ablation (OR = 4.128; 95%CI: 1.005-17.128; P = 0.048) was a positive risk factor, while PDS (OR = 0.205; 95%CI: 0.044-0.945; P = 0.042) was a negative risk factor for pancreatitis. Cholangiogram, piecemeal resection, and BDS were significant risk factors for delayed bleeding in univariate analysis, and piecemeal resection (OR = 6.698; 95%CI: 1.1.599-28.057; P = 0.009) was the only significant risk factor in multivariate analysis. No significant risk factor for cholangitis or perforation was identified.

Table 3 Risk factors of early recurrence

	Simple logistic regression (Univariate analysis)		Multiple logistic regression (Multivariate analysis)	
	OR (95%CI)	*P* value	OR (95%CI)	*P* value
Age, > 65 yr	4.18 (1.042-16.774)	0.044	3.441 (0.807-14.672)	0.095
Sex, Male	1.8 (0.513-6.319)	0.359		
Body mass index > 25 kg/m^2	1.286 (0.251-6.587)	0.763		
Symptomatic	3.022 (0.851-10.738)	0.087		
EUS	3.792 (1.031-13.946)	0.045	1.622 (0.290-9.073)	0.582
Cholangiogram	1.125 (0.307-4.128)	0.859		
Pancreatogram	2.338(0.281-19.450)	0.432		
Submucosal lifting	3.067 (0.291-32.329)	0.351		
Piecemeal resection	1.286 (0.251-6.587)	0.763		
Thermal ablation	0.313 (0.038-2.578)	0.280		
BDS	1.244 (0.304-5.096)	0.761		
PDS	0.901 (0.221-3.675)	0.885		
Size, > 15 mm	3.757 (1.048-13.461)	0.042	1.811 (0.344-9.521)	0.483
Initial pathology				
Benign	Ref			
LGD	0.683 (0.074-6.272)	0.736		
HGD	2.333 (0.167-32.584)	0.529		
Positive/uncertain resection margin	5.925 (1.610-21.801)	0.007	4.023 (1.088-16.387)	0.048
Complication	2.937 (0.815-10.582)	0.100		

OR: Odds ratio; EUS: Endoscopic ultrasound; BDS: Bile duct stent insertion; PDS: Pancreatic duct stent insertion; LGD: Low grade dysplasia; HGD: High grade dysplasia.

DISCUSSION

Of the 106 patients, curative resection was performed in 81 patients (76.4%) with 26 cases of adverse events (24.5%), 11 early recurrences (10.4%), 13 Late recurrences (12.3%), and 6 re-recurrences (5.7%). Our results were consistent with those of previous studies showing curative resection rates of 73.0%-82.7%, adverse events rates of 15.0%-43.6%, early recurrence rates of 2.7%-19.0%, and late recurrence rates of 0-23.9%[14,20-23]. There are large variations in the reported outcomes, particularly among studies involving small numbers of cases because there is no consensus on which parameter best represents the performance of EP. The parameters used in previous studies are inconsistent, and inclusion criteria for EP vary.

Factors used for the evaluation of outcomes in previous studies include visual resection margin, histologic resection margin, recurrence, adverse events, need for surgery, and combinations of these factors. We suggest that curative resection (negative visual resection margin and no recurrence), adverse events, and endoscopic success (negative visual resection margin and no need for surgery) best represent the outcomes of EP. An ideal outcome for EP is the achievement of complete removal of the AA, without adverse events, and without recurrence, which is curative resection with no adverse event. Moreover, even in the event of recurrence, most of these patients can be and are managed endoscopically, representing cases of endoscopic success. We attempted to identify the factors that could predict and improve these outcomes.

In 84 patients (79.2%) the initial and final pathologic results were consistent, which is comparable to previously reported studies[20,23]. The initial biopsy result for the four patients with adenocarcinoma was reported as low-grade dysplasia. Biopsies of AA can occasionally be insufficient because the biopsy is often performed using a forward-viewing endoscope, making a targeted biopsy difficult. Therefore, even if the initial result is benign, it is important to remove the lesion completely with an adequate margin-free area in case of malignancy.

The ampullary lesions found after EP are often described as remnant/residual or recurrence in the literature[14,20,22-24]. Currently, these two categories are clinically distinguished according to the

Table 4 Risk factors of late recurrence

	Simple logistic regression (Univariate analysis)		Multiple logistic regression (Multivariate analysis)	
	OR (95%CI)	*P* value	OR (95%CI)	*P* value
Age, > 65 yr	0.564 (0.162-1.961)	0.368		
Sex, Male	0.865 (0.263-2.847)	0.812		
Body mass index > 25 kg/m^2	2.095 (0.645-6.810)	0.219		
Symptomatic	4.659 (1.292-16.797)	0.019	4.213 (0.091-16.728)	0.061
EUS	0.521 (0.134-2.023)	0.346		
Cholangiogram	1.250 (0.377-4.140)	0.715		
Pancreatogram	2.880 (0.351-23.609)	0.324		
Submucosal lifting	2.500 (0.240-26.004)	0.443		
Piecemeal resection	7.114 (1.993-25.398)	0.003	6.610 (1.760-24.820)	0.005
Thermal ablation	2.434 (0.715-8.293)	0.155		
BDS	1.524 (0.426-5.449)	0.517		
PDS	4.657 (0.576-37.636)	0.149		
Size, > 15 mm	0.444 (0.092-2.140)	0.312		
Positive/uncertain resection margin	0.286 (0.035-2.326)	0.242		
Complication	0.913 (0.231-3.606)	0.897		

OR: Odds ratio; EUS: Endoscopic ultrasound; BDS: Bile duct stent insertion; PDS: Pancreatic duct stent insertion.

timing of lesion discovery: most studies define remnant/residual as the part of the previous lesion found at the first or any surveillance endoscopy performed 3-6 mo after EP, and recurrence as the lesion found after the first surveillance endoscopy or 6 mo after EP. Both are confirmed histologically. There is a clear difference between these definitions as remnant/residual refers to the remaining part of the pathologic lesion, while recurrence refers to a pathologic lesion that is newly developed after the procedure[25]. However, it is often difficult to separate these cases clinically. Diagnosis of a remnant could be delayed and the lesion may be found after the first surveillance endoscopy for a number of reasons including small size of remnant tissues and tissue burn from the procedure, and the delay in diagnosis leads to underestimation of remnant/residual lesions and overestimation of recurrence cases [18]. Considering a newly identified lesion at the first surveillance endoscopy as a remnant/residual in R0 resection may also be controversial. Therefore, instead of labeling these two groups differently, it is preferable to refer to both lesions as recurrence and distinguish these cases according to the timing of diagnosis. The recent European Society of Gastrointestinal Endoscopy guideline states that up to two thirds of recurrences are early recurrences[15].

These two groups differ in terms of the timing of the diagnosis and clinical implications, and there may also be differences in patient management. Recurrences were managed at the endoscopist's discretion using various strategies, including endoscopic and surgical management. Except for early recurrence from adenocarcinoma that was managed with PPPD, it was difficult to identify which factors were considered for a particular treatment. However, early recurrences tend to be managed more aggressively than late recurrences, although the numbers were small for comparisons to be statistically significant (3 *vs* 1 TA and 2 *vs* 0 additional EP for early *vs* late recurrences). This tendency may be explained in that in cases of early recurrence, the initial removal of the lesion has been incomplete, so more invasive treatment may be required compared to the previous treatment method. Conversely, late recurrences are newly developed lesions that are typically small or are early lesions.

It is often difficult to establish which area of the adenoma is responsible for the recurrence because recurrences are typically small, but it can be presumed that they occur from the bile duct, pancreatic orifice, base of ampulla, or resection margin. Reported risk factors for recurrence include age, sex, FAP, intraductal involvement, incomplete resection, piecemeal resection, and final pathology, although the results of these studies are rather inconsistent[13,23,25-27]. Here, a positive/uncertain resection margin in the pathologic report was a significant risk factor for early recurrence, and piecemeal resection was a significant risk factor for late recurrence. This is the first study to analyze the risk factors for both early and late recurrence, considering the different definitions and characteristics of recurrence. A positive resection margin could increase the risk of remnants at the resection margin, but this association was not found to be significant in previous studies[25]. This may be because the positive margin following an EP

Table 5 Risk factors of non-curative resection

	Simple logistic regression (Univariate analysis)		Multiple logistic regression (Multivariate analysis)	
	OR (95% CI)	*P* value	OR (95% CI)	*P* value
Age, > 65 yr	1.485 (0.595-3.703)	0.397		
Sex, Male	1.256 (0.503-3.141)	0.625		
Body mass index > 25 kg/m^2	3.340 (1.090-10.235)	0.035	2.942 (0.855-10.117)	0.087
Symptomatic	2.905 (1.133-7.466)	0.026	3.509 (0.942-9.914)	0.058
EUS	1.455 (0.572-3.699)	0.431		
Cholangiogram	1.222 (0.475-3.148)	0.678		
Pancreatogram	2.877 (0.615-13.458)	0.179		
Submucosal lifting	3.636 (0.484-27.302)	0.209		
Piecemeal resection	4.625 (1.510-14.162)	0.007	5.424 (1.582-18.600)	0.007
Thermal ablation	1.185 (0.410-3.427)	0.754		
BDS	1.464 (0.526-4.076)	0.466		
PDS	1.949 (0.601-6.322)	0.266		
Size, > 15 mm	1.452 (0.543-3.881)	0.457		
Initial pathology				
Benign	Ref			
LGD	0.446 (0.098-2.036)	0.297		
HGD	0.556 (0.065-4.755)	0.592		
Positive/uncertain resection margin	1.839 (0.648-5.220)	0.252		
Complication	1.778 (0.656-4.817)	0.258		

OR: Odds ratio; EUS: Endoscopic ultrasound; BDS: Bile duct stent insertion; PDS: Pancreatic duct stent insertion; LGD: Low grade dysplasia; HGD: High grade dysplasia.

Table 6 Adverse events of endoscopic papillectomy

	n (%) (*n* = 106)
Early	
Pancreatitis	14 (13.2)
Delayed bleeding	11 (10.4)
Cholangitis	6 (5.7)
Perforation	1 (0.9)
Late	
Papillary stenosis	0 (0.0)
Mortality	0 (0.0)
Total	26 (24.5)

procedure is occasionally unreliable, as the resected lesions are often too small to be properly manipulated, and cauterization may mask a positive margin[17]. Also, many previous studies do not clearly state how they analyzed the lesion with uncertain margin. More studies are needed to understand the clinical implications of a positive/uncertain resection margin and develop further management strategies for margin-positive/uncertain lesions. Additionally, to reduce recurrence after EP, it is important to check the peripheral and deep margin of the lesion meticulously before the EP, including intraductal involvement, and secure the resection margin properly during the EP. This is because recurrence could be caused by the poor selection of patients or inability to secure the margin

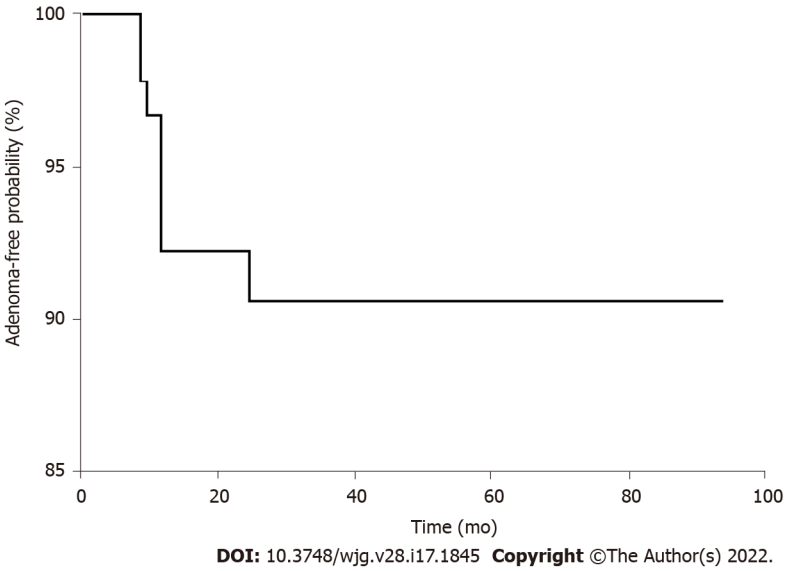
Table 7 Univariate and multivariate analysis of risk factors for pancreatitis and bleeding

	Pancreatitis				Bleeding			
	Univariate analysis		Multivariate analysis		Univariate analysis		Multivariate analysis	
	OR (95%CI)	*P* value	OR (95%CI)	*P* value	OR (95%CI)	*P* value	OR (95%CI)	*P* value
Age, > 65 yr	0.722 (0.225-2.323)	0.585			0.753 (0.206-2.745)	0.667		
Sex, Male	1.486 (0.481-4.590)	0.491			1.800 (0.513-6.319)	0.359		
Body mass index > 25 kg/m^2	0.412 (0.071-3.902)	0.635			0.533 (0.063-4.480)	0.563		
Symptomatic	0.144 (0.018-1.153)	0.068			1.994 (0.562-7.073)	0.285		
EUS	2.067 (0.664-6.428)	0.210			1.641 (0.465-5.788)	0.442		
FAP	15.167 (1.277-180.166)	0.031	9.363 (0.429-204.392)	0.155	4.650 (0.386-55.945)	0.226		
Cholangiogram	1.550 (0.493-4.870)	0.453			3.983 (1.081-14.669)	0.038	2.235 (0.323-15.460)	0.415
Pancreatogram	0.278 (0.087-0.885)	0.030	0.534 (0.106-2.678)	0.446	2.338 (0.281-19.450)	0.432		
Piecemeal resection	0.929 (0.187-4.606)	0.928			6.364 (1.661-24.375)	0.007	6.698 (1.599-28.057)	0.009
Thermal ablation	4.412 (1.366-14.250)	0.013	4.128 (1.005-17.128)	0.048	2.143 (0.570-8.052)	0.259		
BDS	0.868 (0.222-3.393)	0.838			4.800 (1.323-17.418)	0.017	2.647 (0.398-17.619)	0.314
PDS	0.102 (0.030-0.349)	0.000	0.205 (0.044-0.945)	0.042	1.607 (0.325-7.951)	0.561		
Size, > 15 mm	1.072 (0.308-3.731)	0.913			2.465 (0.690-8.812)	0.165		
Initial pathology								
Benign	Ref				Ref			
LGD	0.975 (0.109-8.693)	0.982			0.293 (0.050-1.697)	0.171		
HGD	2.333 (0.167-32.584)	0.529			0.429 (0.031-5.985)	0.529		
Positive/uncertain resection margin	3.562 (1.086-11.685)	0.036			0.833 (0.167-4.167)	0.824		

OR: Odds ratio; EUS: Endoscopic ultrasound; FAP: Familial adenomatous polyposis; BDS: Bile duct stent insertion; PDS: Pancreatic duct stent insertion; LGD: Low grade dysplasia; HGD: High grade dysplasia.

during the procedure, which is sometimes inevitable due to the characteristics of the lesion or the procedure itself. A more aggressive procedure could secure an adequate margin but may cause adverse events such as perforation, so proper selection of patients and careful approaches are mandatory. Similar considerations apply to the higher risk of late recurrence in piecemeal resection. In piecemeal resection, the resection margin may be unreliable, and a thorough evaluation and follow-up for recurrence is required. Piecemeal resection was a significant risk factor for non-curative resection, meaning *en-bloc* resection is a significant protective factor for curative resection, while a pathologic margin was not significant. A positive/uncertain margin and piecemeal resection are important factors for recurrence prediction, although their negative predictive values were 79.8% and 77.4%, respectively; thus, curative resection cannot be assumed in lesions with a negative margin or *en-bloc* resection.

Interestingly, our study was the first to compare the effects of factors including hospital setting and endoscopist experience on the outcome of EP (Supplementary Table 2), and these were not significant for remnant, recurrence, or adverse events. These findings suggest that there was no significant difference in EP results between hospitals with a certain volume of ERCP cases and endoscopists with a certain level of experience. Further studies with larger number of patients are needed to support our



DOI: 10.3748/wjg.v28.i17.1845 **Copyright** ©The Author(s) 2022.

Figure 3 Adenoma-free survival after endoscopic papillectomy. The vertical axis of the graph indicates the adenoma-free probability, and the horizontal axis shows time to remnant or recurrence after endoscopic papillectomy. The longest adenoma-free period before recurrence was 27 mo, and the longest adenoma-free period without recurrence was 94 mo.

suggestion.

Of the six patients with re-recurrence, two patients experienced re-recurrence even after a further session of endoscopic treatment and underwent surgery. Patients with persistent AA showed no specific features to guide the early prediction of the lesion characteristics and early transition to more invasive therapy. The finding that EUS was performed in both patients with re-recurrence suggests that EUS may not adequately predict recurrence or persistence. Moreover, it is unclear as to what extent a benign, although premalignant, AA lesion should be treated at recurrence, considering the adverse events associated with the available treatments. High-quality recommendations or guidelines are necessary.

Our results showed that most adverse events caused by EP showed mild- to moderate-grade severity. The role of thermal ablation in bleeding remains controversial and studies have shown that the risk of pancreatitis increased with the size of the lesion and when hemostasis was performed[22,23,28]. Here, thermal ablation was not significantly associated with bleeding or recurrence although it increased the risk of pancreatitis. The role of PDS is still under debate, but results of several studies, including ours, advocate the use of PDS for prophylaxis of pancreatitis[29-31]. Moreover, no pancreatic stenosis was observed, and this could be explained by our relatively high PDS rate at 73.6%. Hence, it is expected that PDS will help prevent pancreatitis and pancreatic stenosis, and we recommend routine pancreatic stenting, if possible. Also, our result showed that piecemeal resection was the only significant risk factor for delayed bleeding. Piecemeal resection was performed for lesions where *en-bloc* resection was impossible, therefore, the lesions with piecemeal resection tend to be larger[32]. A previous study did not show the correlation between piecemeal resection and bleeding, based on the small number of piecemeal resection cases, but colonic lesions with piecemeal resection show significant bleeding during endoscopic mucosal resection[32,33]. Further research is needed to support the role and adverse events of piecemeal resection in endoscopic papillectomy.

Our study has several limitations. As the indications for EP have not been established, selection bias could not be avoided. Moreover, due to the lack of guidelines on the optimal EP technique, several decisions made during the procedure were at the discretion of the endoscopist. Not all hospitals distinguished margin-positive cases as vertical or lateral involvement, therefore, we simplified the involvement of the margin as positive/uncertain or negative. Finally, the study design was retrospective, and factors regarding the procedure and follow-up could not be controlled.

CONCLUSION

EP is a feasible treatment option for AA with high technical success. However, diagnostic discrepancy, remnant lesions, recurrence, and adverse events cannot be neglected. Unlike gastric or colon adenoma resection, even in cases of complete resection, remnant lesions, recurrence, and re-recurrence were identified, emphasizing the importance of follow-up. For patients with a positive/uncertain resection margin in particular, close follow-up for early recurrence is required, and the possibility of late recurrence should be considered in patients with piecemeal resection. Especially in patients with a positive/uncertain resection margin or piecemeal resection, the possibility of recurrence should be

considered, and closer follow-up for recurrence is required.

ARTICLE HIGHLIGHTS

Research background

The incidence of ampullary adenoma (AA) is increasing, partly from increasing number of imaging studies and from true increase in incidence. Because of its malignant potential, AA has to be removed either surgically or endoscopically.

Research motivation

The role of endoscopic papillectomy (EP) in treatment of AA has been growing due to its relatively low invasiveness, but recurrences and side effects are reported in up to 30% of cases.

Research objectives

Our study aimed to evaluate the clinical outcomes of EP in patients with AA, performed at five tertiary hospitals.

Research methods

We collected the clinical data of patients with AA who underwent EP at five tertiary hospitals between 2013 and 2020 and analyzed the clinical outcomes and adverse events. Clinical outcomes were curative resection, defined as complete endoscopic resection without recurrence, endoscopic success, defined as treatment of ampullary adenoma with endoscopy alone, and recurrence, defined reconfirmed adenoma in endoscopy. Recurrence was divided into early and late, based on an interval of 6 mo.

Research results

Among 106 patients included, curative resection was achieved in 81 patients (76.4%), endoscopic success was achieved in 99 patients (93.4%), early recurrence was identified in 11 patients (16.1%), and late recurrence was identified in 13 patients, and re-recurrence was identified in 6 patients (12.3%). In multivariate analysis, the risk of early and late recurrences was significantly increased in a positive/uncertain margin and piecemeal resection, respectively. The risk of non-curative resection was significantly increased in piecemeal resection. Twenty-six patients experienced adverse events (24.5%): 14 pancreatitis, 11 delayed bleeding, 6 cholangitis, and 1 perforation.

Research conclusions

EP is a relatively safe procedure with high endoscopic success rate. Due to the diagnostic discrepancy, recurrence, re-recurrence and adverse events, careful selection and follow-up of patients are also needed.

Research perspectives

A positive/uncertain margin and piecemeal resection were significant risk factors for poor outcomes; therefore, every effort should be made to ensure adequate free margin and to perform *en-bloc* resection during EP.

FOOTNOTES

Author contributions: Choi SJ and Lee HS carried out the concept and design, drafting of the article, and critical revision; Choe JW, Lee JM, Hyun JJ, and Yoon JH collected the data; Kim J, Kim HJ, Kim JS, Choi HS carried out data analysis and interpretation; and all authors approved the final version of the article.

Supported by National Research Foundation of Korea grant funded by the Korean Government, No. NRF-2021M3E5D1A01015177; and National Research Foundation of Korea grant funded by the Ministry of Education, No. NRF-2018R1D1A1B07048202.

Institutional review board statement: The study protocol was consistent with the guidelines outlined in the Declaration of Helsinki and was approved by the institutional review boards of each participating institution.

Informed consent statement: Patients were not required to give informed consent to the study because the analysis used anonymous clinical data that were obtained after each patient agreed to treatment by written consent.

Conflict-of-interest statement: Authors declare no conflict of interest in this article.

Data sharing statement: No additional unpublished data are available.

Open-Access: This article is an open-access article that was selected by an in-house editor and fully peer-reviewed by external reviewers. It is distributed in accordance with the Creative Commons Attribution NonCommercial (CC BY-NC 4.0) license, which permits others to distribute, remix, adapt, build upon this work non-commercially, and license their derivative works on different terms, provided the original work is properly cited and the use is non-commercial. See: https://creativecommons.org/Licenses/by-nc/4.0/

Country/Territory of origin: South Korea

ORCID number: Seong Ji Choi 0000-0002-1969-516X; Hong Sik Lee 0000-0001-9726-5416; Jiyeong Kim 0000-0002-7969-1419; Jung Wan Choe 0000-0002-8371-9672; Jae Min Lee 0000-0001-9553-5101; Jong Jin Hyun 0000-0002-5632-7091; Jai Hoon Yoon 0000-0003-3194-5149; Hyo Jung Kim 0000-0003-3284-3793; Jae Seon Kim 0000-0002-2012-6781; Ho soon Choi 0000-0002-5257-3586.

S-Editor: Wang JL
L-Editor: A
P-Editor: Wang JL

REFERENCES

1 **Rosenberg J**, Welch JP, Pyrtek LJ, Walker M, Trowbridge P. Benign villous adenomas of the ampulla of Vater. *Cancer* 1986; **58**: 1563-1568 [PMID: 3742474 DOI: 10.1002/1097-0142(19861001)58:7<1563::aid-cncr2820580730>3.0.co;2-e]
2 **Scarpa A**, Capelli P, Zamboni G, Oda T, Mukai K, Bonetti F, Martignoni G, Iacono C, Serio G, Hirohashi S. Neoplasia of the ampulla of Vater. Ki-ras and p53 mutations. *Am J Pathol* 1993; **142**: 1163-1172 [PMID: 8475992]
3 **Ramai D**, Ofosu A, Singh J, John F, Reddy M, Adler DG. Demographics, tumor characteristics, treatment, and clinical outcomes of patients with ampullary cancer: a Surveillance, Epidemiology, and End Results (SEER) cohort study. *Minerva Gastroenterol Dietol* 2019; **65**: 85-90 [PMID: 30488680 DOI: 10.23736/S1121-421X.18.02543-6]
4 **Stolte M**, Pscherer C. Adenoma-carcinoma sequence in the papilla of Vater. *Scand J Gastroenterol* 1996; **31**: 376-382 [PMID: 8726307 DOI: 10.3109/00365529609006414]
5 **Jung S**, Kim MH, Seo DW, Lee SK. Endoscopic snare papillectomy of adenocarcinoma of the major duodenal papilla. *Gastrointest Endosc* 2001; **54**: 622 [PMID: 11677480 DOI: 10.1067/mge.2001.117765]
6 **Askew J**, Connor S. Review of the investigation and surgical management of resectable ampullary adenocarcinoma. *HPB (Oxford)* 2013; **15**: 829-838 [PMID: 23458317 DOI: 10.1111/hpb.12038]
7 **Suzuki K**. Two cases with ampullary cancer who underwent endoscopic excision. *Prog Dig Endosc* 1983; **23**: 236-239
8 **Hong S**, Song KB, Lee YJ, Park KM, Kim SC, Hwang DW, Lee JH, Shin SH, Kwon J, Ma CH, Hwang S, Park G, Park Y, Lee SJ, Kim YW. Transduodenal ampullectomy for ampullary tumors - single center experience of consecutive 26 patients. *Ann Surg Treat Res* 2018; **95**: 22-28 [PMID: 29963536 DOI: 10.4174/astr.2018.95.1.22]
9 **Lee R**, Huelsen A, Gupta S, Hourigan LF. Endoscopic ampullectomy for non-invasive ampullary lesions: a single-center 10-year retrospective cohort study. *Surg Endosc* 2021; **35**: 684-692 [PMID: 32215745 DOI: 10.1007/s00464-020-07433-7]
10 **Ceppa EP**, Burbridge RA, Rialon KL, Omotosho PA, Emick D, Jowell PS, Branch MS, Pappas TN. Endoscopic versus surgical ampullectomy: an algorithm to treat disease of the ampulla of Vater. *Ann Surg* 2013; **257**: 315-322 [PMID: 23059497 DOI: 10.1097/SLA.0b013e318269d010]
11 **Dubois M**, Labgaa I, Dorta G, Halkic N. Endoscopic and surgical ampullectomy for non-invasive ampullary tumors: Short-term outcomes. *Biosci Trends* 2017; **10**: 507-511 [PMID: 27990004 DOI: 10.5582/bst.2016.01193]
12 **Spadaccini M**, Fugazza A, Frazzoni L, Leo MD, Auriemma F, Carrara S, Maselli R, Galtieri PA, Chandrasekar VT, Fuccio L, Aljahdli E, Hassan C, Sharma P, Anderloni A, Repici A. Endoscopic papillectomy for neoplastic ampullary lesions: A systematic review with pooled analysis. *United European Gastroenterol J* 2020; **8**: 44-51 [PMID: 32213054 DOI: 10.1177/2050640619868367]
13 **Ma T**, Jang EJ, Zukerberg LR, Odze R, Gala MK, Kelsey PB, Forcione DG, Brugge WR, Casey BW, Syngal S, Chung DC. Recurrences are common after endoscopic ampullectomy for adenoma in the familial adenomatous polyposis (FAP) syndrome. *Surg Endosc* 2014; **28**: 2349-2356 [PMID: 24566750 DOI: 10.1007/s00464-014-3467-0]
14 **Napoleon B**, Gincul R, Ponchon T, Berthiller J, Escourrou J, Canard JM, Boyer J, Barthet M, Ponsot P, Laugier R, Helbert T, Coumaros D, Scoazec JY, Mion F, Saurin JC; Société Française d'Endoscopie Digestive (SFED, French Society of Digestive Endoscopy). Endoscopic papillectomy for early ampullary tumors: long-term results from a large multicenter prospective study. *Endoscopy* 2014; **46**: 127-134 [PMID: 24477368 DOI: 10.1055/s-0034-1364875]
15 **Vanbiervliet G**, Strijker M, Arvanitakis M, Aelvoet A, Arnelo U, Beyna T, Busch O, Deprez PH, Kunovsky L, Larghi A, Manes G, Moss A, Napoleon B, Nayar M, Pérez-Cuadrado-Robles E, Seewald S, Barthet M, van Hooft JE. Endoscopic management of ampullary tumors: European Society of Gastrointestinal Endoscopy (ESGE) Guideline. *Endoscopy* 2021; **53**: 429-448 [PMID: 33728632 DOI: 10.1055/a-1397-3198]
16 **Fritzsche JA**, Fockens P, Barthet M, Bruno MJ, Carr-Locke DL, Costamagna G, Coté GA, Deprez PH, Giovannini M, Haber GB, Hawes RH, Hyun JJ, Itoi T, Iwasaki E, Kylänpaä L, Neuhaus H, Park JY, Reddy DN, Sakai A, Bourke MJ, Voermans RP. Expert consensus on endoscopic papillectomy using a Delphi process. *Gastrointest Endosc* 2021; **94**: 760-773.e18 [PMID: 33887269 DOI: 10.1016/j.gie.2021.04.009]
17 **Sakai A**, Tsujimae M, Masuda A, Iemoto T, Ashina S, Yamakawa K, Tanaka T, Tanaka S, Yamada Y, Nakano R, Sato Y, Kurosawa M, Ikegawa T, Fujigaki S, Kobayashi T, Shiomi H, Arisaka Y, Itoh T, Kodama Y. Clinical outcomes of ampullary neoplasms in resected margin positive or uncertain cases after endoscopic papillectomy. *World J Gastroenterol*

2019; **25**: 1387-1397 [PMID: 30918431 DOI: 10.3748/wjg.v25.i11.1387]

18 **Yasuda I**, Kobayashi S, Takahashi K, Nanjo S, Mihara H, Kajiura S, Ando T, Tajiri K, Fujinami H. Management of Remnant or Recurrent Lesions after Endoscopic Papillectomy. *Clin Endosc* 2020; **53**: 659-662 [PMID: 31794653 DOI: 10.5946/ce.2019.171]

19 **Cotton PB**, Eisen GM, Aabakken L, Baron TH, Hutter MM, Jacobson BC, Mergener K, Nemcek A Jr, Petersen BT, Petrini JL, Pike IM, Rabeneck L, Romagnuolo J, Vargo JJ. A lexicon for endoscopic adverse events: report of an ASGE workshop. *Gastrointest Endosc* 2010; **71**: 446-454 [PMID: 20189503 DOI: 10.1016/j.gie.2009.10.027]

20 **Kang SH**, Kim KH, Kim TN, Jung MK, Cho CM, Cho KB, Han JM, Kim HG, Kim HS. Therapeutic outcomes of endoscopic papillectomy for ampullary neoplasms: retrospective analysis of a multicenter study. *BMC Gastroenterol* 2017; **17**: 69 [PMID: 28558658 DOI: 10.1186/s12876-017-0626-5]

21 **Bohnacker S**, Seitz U, Nguyen D, Thonke F, Seewald S, deWeerth A, Ponnudurai R, Omar S, Soehendra N. Endoscopic resection of benign tumors of the duodenal papilla without and with intraductal growth. *Gastrointest Endosc* 2005; **62**: 551-560 [PMID: 16185970 DOI: 10.1016/j.gie.2005.04.053]

22 **Nam K**, Song TJ, Kim RE, Cho DH, Cho MK, Oh D, Park DH, Lee SS, Seo DW, Lee SK, Kim MH, Baek S. Usefulness of argon plasma coagulation ablation subsequent to endoscopic snare papillectomy for ampullary adenoma. *Dig Endosc* 2018; **30**: 485-492 [PMID: 29288506 DOI: 10.1111/den.13008]

23 **Li S**, Wang Z, Cai F, Linghu E, Sun G, Wang X, Meng J, Du H, Yang Y, Li W. New experience of endoscopic papillectomy for ampullary neoplasms. *Surg Endosc* 2019; **33**: 612-619 [PMID: 30421083 DOI: 10.1007/s00464-018-6577-2]

24 **Sahar N**, Krishnamoorthi R, Kozarek RA, Gluck M, Larsen M, Ross AS, Irani S. Long-Term Outcomes of Endoscopic Papillectomy for Ampullary Adenomas. *Dig Dis Sci* 2020; **65**: 260-268 [PMID: 31463668 DOI: 10.1007/s10620-019-05812-2]

25 **Ridtitid W**, Tan D, Schmidt SE, Fogel EL, McHenry L, Watkins JL, Lehman GA, Sherman S, Coté GA. Endoscopic papillectomy: risk factors for incomplete resection and recurrence during long-term follow-up. *Gastrointest Endosc* 2014; **79**: 289-296 [PMID: 24094466 DOI: 10.1016/j.gie.2013.08.006]

26 **Catalano MF**, Linder JD, Chak A, Sivak MV Jr, Raijman I, Geenen JE, Howell DA. Endoscopic management of adenoma of the major duodenal papilla. *Gastrointest Endosc* 2004; **59**: 225-232 [PMID: 14745396 DOI: 10.1016/s0016-5107(03)02366-6]

27 **Klein A**, Qi Z, Bahin FF, Awadie H, Nayyar D, Ma M, Voermans RP, Williams SJ, Lee E, Bourke MJ. Outcomes after endoscopic resection of large laterally spreading lesions of the papilla and conventional ampullary adenomas are equivalent. *Endoscopy* 2018; **50**: 972-983 [PMID: 29768645 DOI: 10.1055/a-0587-5228]

28 **Yang JK**, Hyun JJ, Lee TH, Choi JH, Lee YN, Choe JW, Park JS, Kwon CI, Jeong S, Kim HJ, Moon JH, Park SH. Can prophylactic argon plasma coagulation reduce delayed post-papillectomy bleeding? *J Gastroenterol Hepatol* 2021; **36**: 467-473 [PMID: 32677716 DOI: 10.1111/jgh.15186]

29 **Harewood GC**, Pochron NL, Gostout CJ. Prospective, randomized, controlled trial of prophylactic pancreatic stent placement for endoscopic snare excision of the duodenal ampulla. *Gastrointest Endosc* 2005; **62**: 367-370 [PMID: 16111953 DOI: 10.1016/j.gie.2005.04.020]

30 **Menees SB**, Schoenfeld P, Kim HM, Elta GH. A survey of ampullectomy practices. *World J Gastroenterol* 2009; **15**: 3486-3492 [PMID: 19630102 DOI: 10.3748/wjg.15.3486]

31 **Singh P**, Das A, Isenberg G, Wong RC, Sivak MV Jr, Agrawal D, Chak A. Does prophylactic pancreatic stent placement reduce the risk of post-ERCP acute pancreatitis? *Gastrointest Endosc* 2004; **60**: 544-550 [PMID: 15472676 DOI: 10.1016/s0016-5107(04)02013-9]

32 **Yamamoto K**, Sofuni A, Tsuchiya T, Ishii K, Tsuji S, Tanaka R, Tonozuka R, Honjo M, Mukai S, Fujita M, Asai Y, Matsunami Y, Nagakawa Y, Yamaguchi H, Itoi T. Clinical Impact of Piecemeal Resection Concerning the Lateral Spread of Ampullary Adenomas. *Intern Med* 2019; **58**: 901-906 [PMID: 30568115 DOI: 10.2169/internalmedicine.1147-18]

33 **Kim HH**, Kim JH, Park SJ, Park MI, Moon W. Risk factors for incomplete resection and complications in endoscopic mucosal resection for lateral spreading tumors. *Dig Endosc* 2012; **24**: 259-266 [PMID: 22725112 DOI: 10.1111/j.1443-1661.2011.01232.x]

World Journal of Gastroenterology

Submit a Manuscript: https://www.f6publishing.com

World J Gastroenterol 2022 May 7; 28(17): 1860-1870

DOI: 10.3748/wjg.v28.i17.1860

ISSN 1007-9327 (print) ISSN 2219-2840 (online)

ORIGINAL ARTICLE

Retrospective Study

Biliary metal stents should be placed near the hilar duct in distal malignant biliary stricture patients

Mitsuru Sugimoto, Tadayuki Takagi, Rei Suzuki, Naoki Konno, Hiroyuki Asama, Yuki Sato, Hiroki Irie, Yoshinori Okubo, Jun Nakamura, Mika Takasumi, Minami Hashimoto, Tsunetaka Kato, Ryoichiro Kobashi, Takumi Yanagita, Takuto Hikichi, Hiromasa Ohira

Specialty type: Gastroenterology and hepatology

Provenance and peer review: Unsolicited article; Externally peer reviewed.

Peer-review model: Single blind

Peer-review report's scientific quality classification

Grade A (Excellent): 0
Grade B (Very good): B, B, B
Grade C (Good): 0
Grade D (Fair): 0
Grade E (Poor): 0

P-Reviewer: Kim JH, South Korea; Sun SY, China; Zeng YY, China

Received: September 17, 2021
Peer-review started: September 17, 2021
First decision: November 16, 2021
Revised: December 4, 2021
Accepted: March 25, 2022
Article in press: March 25, 2022
Published online: May 7, 2022

Mitsuru Sugimoto, Tadayuki Takagi, Rei Suzuki, Naoki Konno, Hiroyuki Asama, Yuki Sato, Hiroki Irie, Yoshinori Okubo, Jun Nakamura, Mika Takasumi, Minami Hashimoto, Tsunetaka Kato, Ryoichiro Kobashi, Takumi Yanagita, Hiromasa Ohira, Department of Gastroenterology, Fukushima Medical University, Fukushima 9601295, Japan

Yoshinori Okubo, Jun Nakamura, Minami Hashimoto, Tsunetaka Kato, Ryoichiro Kobashi, Takuto Hikichi, Department of Endoscopy, Fukushima Medical University Hospital, Fukushima 9601295, Japan

Corresponding author: Mitsuru Sugimoto, MD, PhD, Assistant Professor, Department of Gastroenterology, Fukushima Medical University, 1 Hikarigaoka, Fukushima 9601295, Japan. kitachuuou335@yahoo.co.jp

Abstract

BACKGROUND

Endoscopic biliary drainage using a self-expandable metallic stent (SEMS) has been widely performed to treat distal malignant biliary obstruction (DMBO). However, the optimal position of the stent remains unclear.

AIM

To determine the ideal position for SEMS placement.

METHODS

In total, 135 DMBO patients underwent SEMS (uncovered or covered) placement over a ten-year period. A total of 127 patients with biliary obstruction between the junction of the cystic duct and Vater's papilla were enrolled. An SEMS was placed through the upper common bile duct 2 cm from the biliary hilar duct in 83 patients (Hilar group) or near the top of the biliary obstruction in 44 patients (Lower group). Technical and functional success, adverse events, and risk factors for SEMS dysfunction were evaluated.

RESULTS

The stent patency period was significantly longer in the Hilar group than in the Lower group (P value < 0.01). In multivariate analysis, the only statistically significant risk factor for SEMS dysfunction was being in the Lower group

(hazard ratio: 9.94, 95% confidence interval: 2.25–44.0, $P < 0.01$).

CONCLUSION
A longer patency period was achieved by positioning the SEMS near the biliary hilar duct.

Key Words: Endoscopic biliary drainage; Malignant biliary obstruction; Uncovered self-expandable metallic stent; Covered self-expandable metallic stent; Biliary hilar duct; Patency period

©The Author(s) 2022. Published by Baishideng Publishing Group Inc. All rights reserved.

Core Tip: Endoscopic biliary drainage using a self-expandable metallic stent (SEMS) has been widely performed to treat distal malignant biliary obstruction (DMBO). However, the optimal position of the SEMS remains unclear. This study indicated that the stent patency period was significantly longer when the SEMS was placed near the biliary hilar duct. Furthermore, the placement of a longer SEMS from the biliary hilar duct was thought to overcome several factors of recurrent biliary obstruction in DMBO patients.

Citation: Sugimoto M, Takagi T, Suzuki R, Konno N, Asama H, Sato Y, Irie H, Okubo Y, Nakamura J, Takasumi M, Hashimoto M, Kato T, Kobashi R, Yanagita T, Hikichi T, Ohira H. Biliary metal stents should be placed near the hilar duct in distal malignant biliary stricture patients. *World J Gastroenterol* 2022; 28(17): 1860-1870
URL: https://www.wjgnet.com/1007-9327/full/v28/i17/1860.htm
DOI: https://dx.doi.org/10.3748/wjg.v28.i17.1860

INTRODUCTION

Stricture of the common bile duct (CBD) can occur in several severe diseases (for example, bile duct cancer, pancreatic cancer, or metastasis of other cancers). Since transpapillary biliary stent insertion was first reported by Sohendra and Reynders-Frederix[1], it has become the first choice for biliary drainage in patients with malignant biliary obstruction. At present, uncovered self-expandable metallic stents (USEMSs) and covered SEMSs (CSEMSs) have been reported to be more effective at preventing recurrent biliary obstruction (RBO) than plastic stents (PSs) in distal malignant biliary obstruction (DMBO) patients[2,3].

Whether a USEMS or CSEMS should be used remains a topic of debate. Three reports have asserted that the patency period of CSEMSs is superior to that of USEMSs[4-6]. However, others have found that the patency period is similar between CSEMSs and USEMSs[7-9]. Although CSEMS insertion has some disadvantages (such as cholecystitis, pancreatitis, and migration), the stent can be removed[7,10-13].

Based on the above findings, SEMS placement may help drain unresectable DMBOs. Determining which stent (USEMS or CSEMS) should be used has gained increasing attention. However, the optimal position of the inserted SEMS has rarely been discussed and remains unclear. Therefore, we aimed to determine the ideal position for SEMS placement.

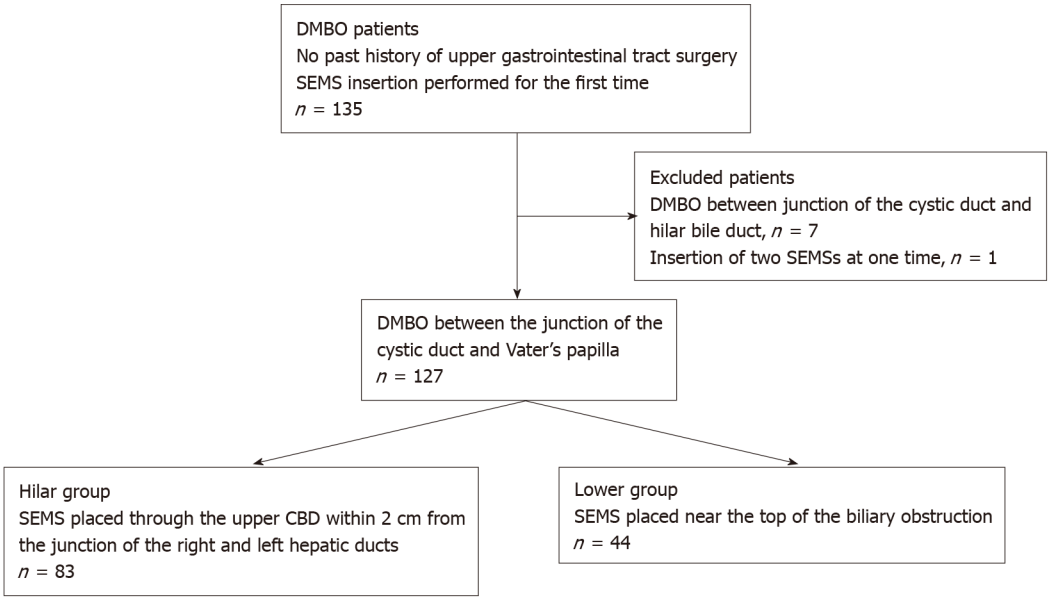
MATERIALS AND METHODS

Study design and ethics approval

This was a retrospective study. The patients were not required to provide informed consent because this study used anonymized clinical data obtained after each patient had provided written consent and agreed to undergo medical procedures. Additional details of this study are published on the home page of Fukushima Medical University (approval number 2453).

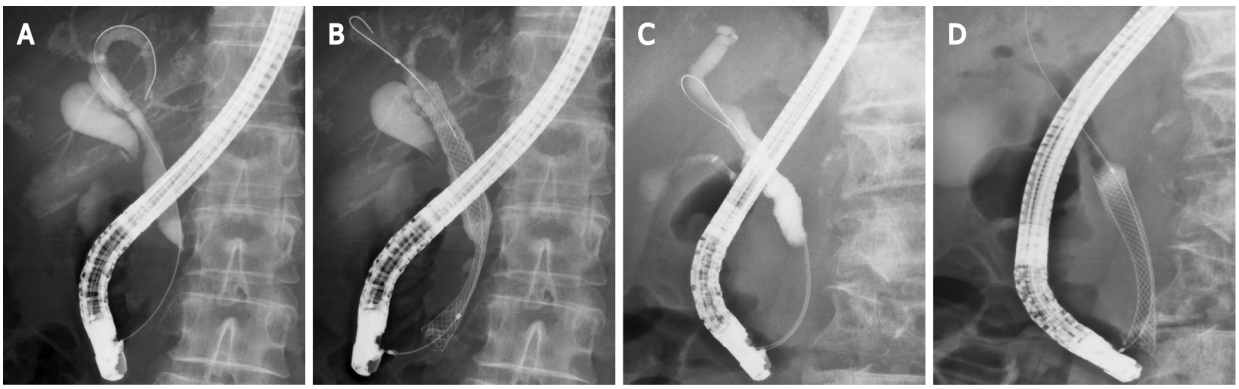
Patients

A total of 135 DMBO patients underwent SEMS placement between January 2011 and February 2021 (Figure 1). These patients did not undergo previous surgery of the upper gastrointestinal tract and were undergoing SEMS placement for the first time. Seven of these patients whose biliary obstruction was located between the junction of the cystic duct and hilar bile duct were excluded from this study. In addition, one patient who underwent double SEMS placement was excluded. Finally, 127 patients whose biliary obstruction was located between the junction of the cystic duct and Vater's papilla were enrolled. The SEMS was placed through the upper CBD within 2 cm from the junction of the right and left hepatic ducts in 83 patients (Hilar group) (Figure 2A and B). In the other 44 patients (Lower group),



DOI: 10.3748/wjg.v28.i17.1860 **Copyright** ©The Author(s) 2022.

Figure 1 Patient flowchart. DMBO: Distal malignant biliary obstruction; SEMS: Self-expandable metallic stent; CBD: Common bile duct.



DOI: 10.3748/wjg.v28.i17.1860 **Copyright** ©The Author(s) 2022.

Figure 2 Representative cases from each group. A and B: A patient with distal malignant biliary obstruction (DMBO) in the Hilar group who underwent self-expandable metallic stent (SEMS) placement near the biliary hilar duct; C and D: A patient with DMBO in the Lower group who underwent SEMS placement near the top of the biliary obstruction.

the SEMS was placed near the top of the biliary obstruction (Figure 2C and D).

Endoscopic biliary drainage

With the patient in a prone position, a duodenoscope was inserted after the patient was sufficiently sedated with midazolam. When the duodenoscope reached Vater's papilla, biliary cannulation was initiated. After the range of the DMBO was confirmed by cholangiography, an SEMS was inserted from the upper part of the obstruction to Vater's papilla. Endoscopic sphincterotomy (EST) was performed for first-time endoscopic biliary drainage with a PS or before SEMS insertion. The position and type of SEMS (USEMS or CSEMS) were randomly determined by each endoscopist. All the procedures were performed by pancreaticobiliary specialists or trainees under the guidance of specialists.

The USEMSs used in this study were as follows: BileRush, 8 mm × 6 cm, 10 mm × 6 or 8 cm (Piolax, Kanagawa, Japan); Bonastent, 10 mm × 8 cm (Standard Sci Tech, Seoul, Korea); HANARO, 10 mm × 7 cm (Boston Scientific, Tokyo, Japan); Niti-S Large cell, 10 mm × 5, 6, 8, or 10 cm (Taewoong Medical, Gyeoenggi-do, Korea); WallFlex, 10 mm × 6, 8, or 10 cm (Boston Scientific); X Suit NIR, 10 mm × 8 cm (Olympus Medical, Tokyo, Japan); and Zilver, 10 mm × 6 cm, and Zilver 635, 10 mm × 6, 8, or 10 cm (Cook Medical Japan, Tokyo, Japan). The CSEMSs used in this study were as follows: Bonastent, 10 mm × 7 cm (Standard Sci Tech); HANARO, 10 mm × 5, 6, or 8 cm (Boston Scientific); Niti-S Comvi, partially covered, 10 mm × 6, 7, or 8 cm (Taewoong Medical); WallFlex, fully covered, 10 mm × 6 cm, and partially covered, 10 mm × 6 or 8 cm (Boston Scientific); and X Suit NIR, 10 mm × 4, 6, or 8 cm (Olympus Medical).

Outcomes of interest

The primary outcome was the stent patency period. The secondary outcomes were the technical success rate, functional success rate, adverse events (pancreatitis, post-EST bleeding), severity of adverse events, and stent dysfunction rate. These outcomes were defined according to partially revised versions of the reported criteria[14]. The stent patency period was determined as the time from first SEMS insertion to SEMS dysfunction. SEMS dysfunction was defined as the recurrence of hepatic dysfunction, jaundice, or dilated bile tract on ultrasonography or computed tomography (CT), which required secondary SEMS placement. Technical success was defined as successful placement of an SEMS that reached from the upper part of the obstruction to Vater's papilla. Functional success was defined as the return of alanine transaminase (ALT) or total bilirubin (TB) levels to normal values (ALT < 27 U/L, TB < 1.2 mg/dL) or less than half of the pretreatment values. Adverse events and the severity of adverse events were defined according to Cotton's criteria[15]. Posttreatment pancreatitis was also confirmed by contrast-enhanced CT.

In addition, the patient characteristics (age, sex, serum ALT level, serum TB level, cause of stricture, chemotherapy, duodenal stricture, CBD diameter above the stricture, CBD stricture diameter, CBD stricture length), year of procedure (2011-2015, or 2016-2021), stent diameter, type of SEMS used (USEMS or CSEMS), SEMS shortening, and observational period were compared between the Hilar group and the Lower group. The maximum serum ALT and TB values recorded in the previous week up to endoscopic SEMS insertion were used. The cause of stricture was divided into pancreaticobiliary and metastatic. Duodenal stricture was defined as a stricture that was difficult for the upper gastrointestinal scope to pass through. The diameter and length of the CBD stricture were measured by endoscopic retrograde cholangiography. The year of the procedure was compared between the groups because the techniques and devices have advanced over the approximately ten-year study duration. SEMS shortening was determined as more than 1 cm of shortening evident on X-ray or CT imaging after SEMS placement.

Statistical analyses

Student's t test or Welch's t test was used to compare continuous variables. Fisher's exact test was used to compare nominal variables. To analyze the SEMS patency period, the log-rank test was used. To analyze the factors that influenced SEMS dysfunction, a Cox proportional hazard model was used. $P < 0.05$ was considered statistically significant. All statistical analyses were performed using EZR (Saitama Medical Centre, Jichi Medical University, Saitama, Japan).

RESULTS

The patient characteristics are shown in Table 1. There was no significant difference in age, sex, serum ALT level, serum TB level, stricture cause, chemotherapy, duodenal stricture, CBD diameter above the stricture, CBD stricture diameter, or CBD stricture length between the Hilar group and the Lower group.

The outcomes of SEMS placement are shown in Table 2. There was no difference in the procedure year, technical success rate, functional success rate, adverse events, or SEMS shortening between the two groups. The rate of CSEMS use and the SEMS diameter were also not significantly different between the two groups. Regarding the type of SEMS used, the covered WallFlex (Boston Scientific) stent was used significantly more frequently in the Hilar group than in the Lower group (28/83 (33.7%) *vs* 7/44 (15.9%), *P* value = 0.038), and the X Suit NIR stent was used significantly more frequently in the Lower group than in the Hilar group (6/44 (13.6%) *vs* 0/83 (0%), *P* value < 0.01). SEMS dysfunction was observed significantly more often in the Lower group than in the Hilar group [18/44 (41%) *vs* 2/83 (2.4%), *P* value < 0.01]. The causes of SEMS dysfunction were as follows: Ingrowth (1) and overgrowth (1) in the Hilar group, and ingrowth (3), overgrowth (2), ingrowth and overgrowth (8), top edge closed by the CBD wall (4), and dislocation (1) in the Lower group. In the cases in which the top edge was closed by the CBD wall, the SEMSs used were the Zilver 635 (Cook Medical), WallFlex (Boston Scientific), Niti-S large cell (Taewoong Medical), and HANARO (Boston Scientific) stents. A representative case in which the top edge of the SEMS was closed by the CBD wall is shown in Figure 3. The observational period was longer in the Lower group than in the Hilar group (9.12 ± 12.07 mo *vs* 4.16 ± 5.76 mo, *P* value = 0.012).

The results of the stent patency comparison are shown in Figure 4 and Supplementary Figure 1. The stent patency period was significantly longer in the Hilar group than in the Lower group (Figure 4A, *P* value < 0.01). The stent patency period was not significantly different between the groups when the patients were divided according to the use of a covered WallFlex stent, use of a covered X Suit NIR stent, observational period (Figure 4B-D), age, sex, serum ALT level, serum TB level, metastatic or pancreaticobiliary status, presence or absence of chemotherapy, presence or absence of duodenal stricture, CBD diameter above the stricture, CBD stricture diameter, CBD stricture length, year of procedure, USEMS or CSEMS, presence or absence of SEMS shortening (Supplementary Figure 1).

Table 1 Patient characteristics

	Hilar group (*n* = 83)	Lower group (*n* = 44)	*P* value
Age, yr	68.4 ± 11.8	71.2 ± 11.2	0.22
Sex			
Female	33 (39.8)	16 (36.4)	0.85
Male	50 (60.2)	28 (63.6)	
ALT, U/L	126.0 ± 116.3	174.8 ± 177.1	0.11
TB, mg/dL	5.9 ± 7.5	6.8 ± 6.8	0.47
Cause of stricture			0.77
Pancreaticobiliary tumor	73 (88.0)	40 (90.9)	
Pancreas	67	31	
Biliary tract	6	9	
Metastasis	10 (12.0)	4 (9.1)	
Lung	3	1	
Stomach	3		
Rhabdomyosarcoma	1		
Uterine	1		
Ovarian	1		
Esophagus		1	
Breast		1	
Colon		1	
Lymph node metastasis from gallbladder cancer	1		
Chemotherapy	35 (42.2)	23 (52.3)	0.35
Duodenal stricture	15 (18.1)	7 (15.9)	0.81
CBD diameter above stricture, mm	11.5 ± 4.3	12.2 ± 4.0	0.40
CBD stricture diameter, mm	0.61 ± 0.89	0.72 ± 0.8	0.50
CBD stricture length, cm	2.64 ± 1.35	2.34 ± 1.11	0.21

Values are presented as the mean ± SD or *n* (%).
ALT: Alanine transaminase; TB: Total bilirubin; CBD: Common bile duct.

The risk factors for SEMS dysfunction are shown in Table 3. Serum ALT level and lower placement were statistically significant factors in the univariate analysis [ALT: hazard ratio (HR): 1.003, 95% confidence interval (CI): 1.001–1.01, *P* value < 0.01; Lower group: HR: 11.42, 95%CI: 2.61–49.83, *P* value < 0.01]. However, the only statistically significant risk factor in the multivariate analysis was lower placement (HR: 9.94, 95%CI: 2.25–44.0, *P* < 0.01).

DISCUSSION

In this study, we investigated the ideal position for SEMS insertion in DMBO patients. The results demonstrated that the SEMS patency period was longer when the stent was placed near the hilar duct.

This finding suggests that this position overcomes several causes of SEMS dysfunction. As shown in Table 2, the main causes of SEMS dysfunction were tumor ingrowth and/or overgrowth and a top edge closed by the CBD wall; notably, overgrowth and a top edge closed by the CBD wall were prevented by using a longer SEMS. Longer SEMSs can delay stent dysfunction due to tumor overgrowth. In the four patients in the Lower group, the top edge of the SEMS was closed by the CBD wall, which may be caused by linearization of the SEMS. The axial force on the stent is thought to be related to the linearization and closing of the top edge by the CBD wall. However, in the four patients with SEMS dysfunction caused by closure of the top edge by the CBD wall, the SEMSs were not necessarily affected

Table 2 Outcome of biliary self-expandable metallic stent placement

Variable	Hilar group (*n* = 83)	Lower group (*n* = 44)	*P* value
Year of procedure			0.18
2011-2015	48 (57.8)	31 (70.5)	
2016-2021	35 (42.2)	13 (29.5)	
Diameter of SEMS			1.0
8 mm	1 (1.2)	0 (0)	
10 mm	82 (98.8)	44 (100)	
USEMS:CSEMS	35:48	20:24	0.85
USEMS used			
BileRush	2 (2.4)	1 (2.3)	1
Bonastent	1 (1.2)	0 (0)	1
HANARO	1 (1.2)	0 (0)	1
Niti-S Large cell	9 (10.8)	5 (11.4)	1
WallFlex	24 (28.9)	7 (15.9)	0.13
X Suit NIR	0 (0)	2 (4.5)	0.12
Zilver	0 (0)	1 (2.3)	0.35
Zilver 635	4 (4.8)	6 (13.6)	0.09
CSEMS used			
Bonastent	0 (0)	1 (2.3)	0.35
HANARO	3 (3.6)	1 (2.3)	1
Niti-S Comvi	11 (13.3)	7 (15.9)	0.79
WallFlex	28 (33.7)	7 (15.9)	0.038
X Suit NIR	0 (0)	6 (13.6)	< 0.01
Technical success	83 (100)	44 (100)	
Functional success	81 (97.6)	41 (93.2)	0.34
Adverse events	2 (2.4)	0 (0)	0.54
Pancreatitis	2	0	
Mild	2	0	
Post-EST bleeding	1	0	
Severe	1	0	
SEMS shortening[1]	1 (1.3)	2 (4.7)	0.28
SEMS dysfunction	2 (2.4)	18 (41)	< 0.01
Cause of SEMS dysfunction			
Ingrowth	1	3	
Overgrowth	1	2	
Ingrowth and overgrowth		8	
Top edge closed by CBD wall		4	
Dislocation		1	
Observational period, months	4.16 ± 5.76	9.12 ± 12.07	0.012

Values are presented as n, *n* (%), or mean ± SD.

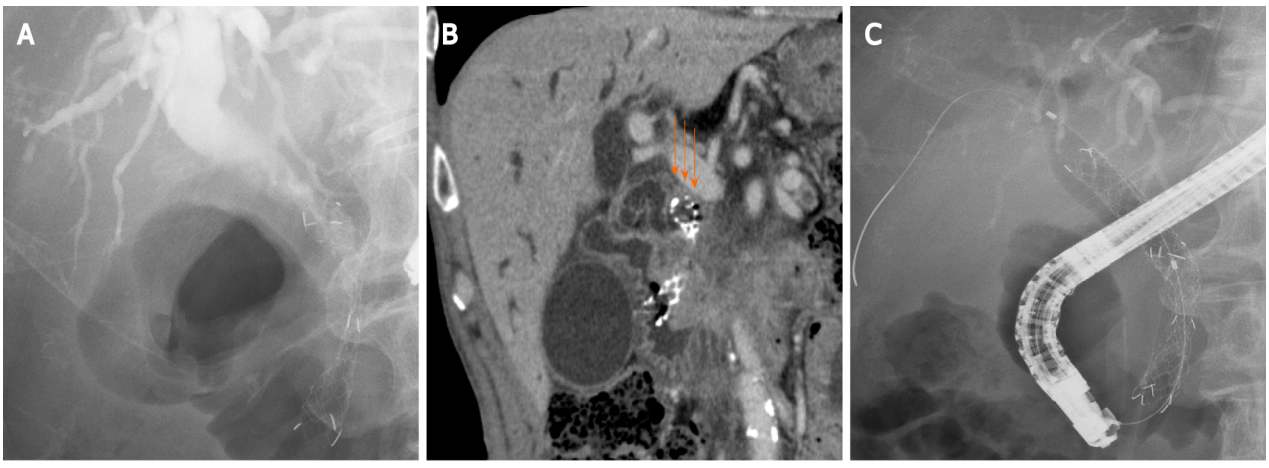
[1]The presence or absence of SEMS shortening was confirmed in 79 patients in the Hilar group and 43 patients in the Lower group.

SEMS: Self-expandable metallic stent; USEMS: Uncovered SEMS; CSEMS: Covered SEMS; EST: Endoscopic sphincterotomy; CBD: Common bile duct.

Table 3 Risk factors for self-expandable metallic stent dysfunction

	Univariate analysis			Multivariate analysis		
	Hazard ratio	95%CI	*P* value	Hazard ratio	95%CI	*P* value
Lower group	11.42	2.61–49.83	< 0.01	9.94	2.25–44.0	< 0.01
Age	1.04	0.997–1.09	0.07			
Sex, male	0.88	0.35–2.2	0.8			
ALT	1.003	1.001–1.01	< 0.01	1.002	1.0–1.004	0.07
TB	1.05	0.99–1.12	0.1			
Cause of stricture, pancreaticobiliary	0.41	0.09–1.9	0.26			
Chemotherapy	0.89	0.34–2.31	0.81			
Duodenal stricture	1.27	0.42–3.83	0.67			
CBD above diameter stricture	1.06	0.94–1.19	0.35			
CBD stricture diameter	1.004	0.56–1.79	0.99			
CBD stricture length	0.99	0.69–1.41	0.95			
Year (2011–2015)	1.35	0.55-3.32	0.52			
Use of CSEMS	0.67	0.28–1.62	0.37			
Use of covered WallFlex stent	0.4	0.12–1.36	0.14			
Use of covered X Suit NIR usage stent	3.20	0.92–11.14	0.07			
SEMS shortening	1.28	0.17–9.73	0.81			
Observational period	0.98	0.92–1.04	0.43			

SEMS: Self-expandable metallic stent; ALT: Alanine transaminase; TB: Total bilirubin; CBD: Common bile duct; CSEMS: Covered SEMS; CI: Confidence interval.

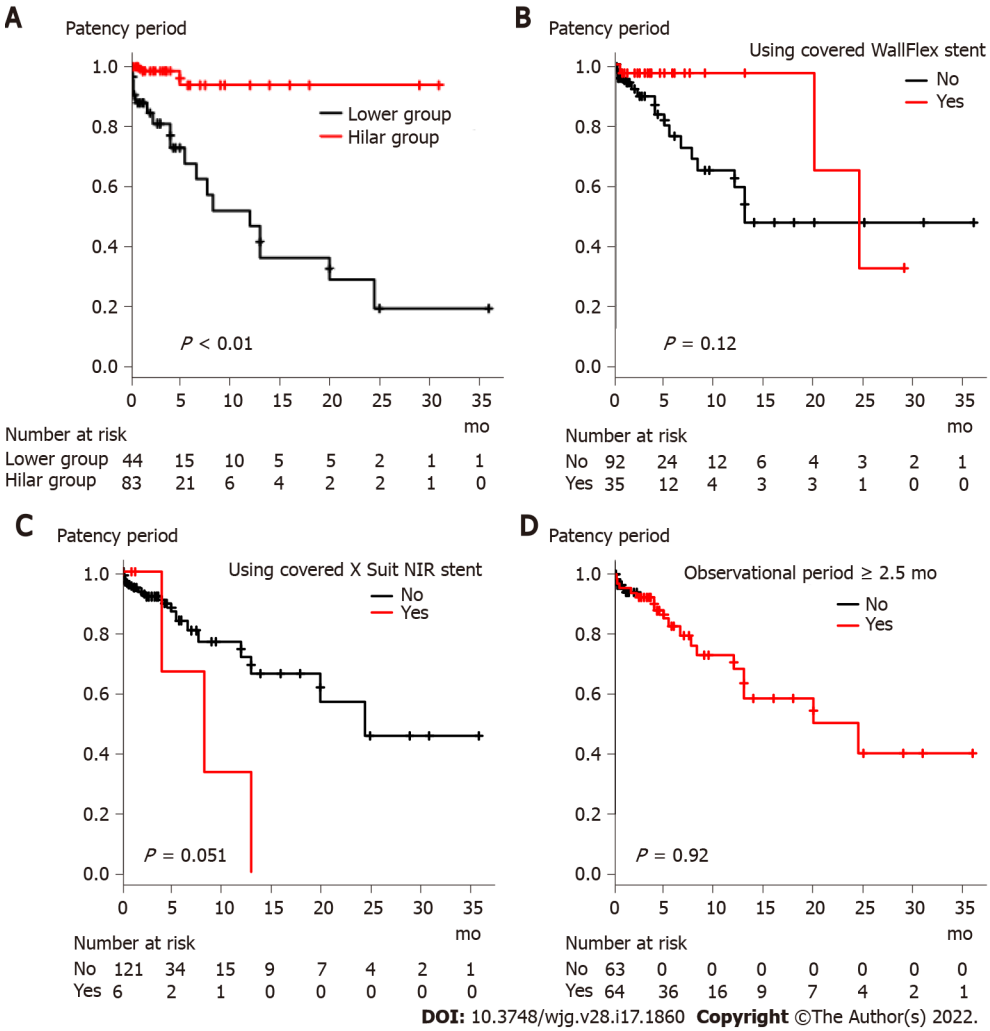


DOI: 10.3748/wjg.v28.i17.1860 **Copyright** ©The Author(s) 2022.

Figure 3 A patient with closure of the top edge of the self-expandable metallic stent by the common bile duct wall. A: A patient with distal malignant biliary obstruction who underwent uncovered self-expandable metallic stents (USEMS) placement near the top of the biliary obstruction; B: The top edge of the SEMS was closed by the common bile duct wall (arrows). Upper bile tract dilation was observed; C: An additional USEMS was placed near the biliary hilar duct.

by high axial force, except for the WallFlex (Boston Scientific) stent. When a short SEMS is placed near the top edge of the DMBO, the axial force might be enhanced by the biliary stricture. Using longer SEMSs overcomes this problem because the axial force decreases with increasing distance between the top edge of the SEMS and CBD stricture[16]. In fact, a biliary obstruction was relieved by placing a second SEMS near the biliary hilar duct (Figure 3C).

In past reports, time to adequate expansion, degree of CBD stricture[17], duodenal invasion[18], duodenal SEMS[19], and anticancer treatment[18,20] were reported as risk factors for RBO. The factors



DOI: 10.3748/wjg.v28.i17.1860 **Copyright** ©The Author(s) 2022.

Figure 4 Comparison of stent patency period based on factors that were significantly different between the Hilar group and Lower group.
A: Stent placement position (Hilar group *vs* Lower group); B: Use of the covered WallFlex stent; C: Use of the covered X Suit NIR stent; D: Observational period (< 2.5 mo *vs* ≥ 2.5 mo).

related to SEMS expansion and CBD stricture were not an issue in this study because functional success was achieved in almost all the patients. Anticancer treatment has been reported to cause RBO as follows. Although anticancer treatment reduces the tumor burden, it can dislocate the CSEMS or induce neutropenia and bacterial overgrowth and, ultimately, cholangitis or sludge formation in the bile duct [20]. However, anticancer treatment was not proposed as a risk factor for RBO in a study that involved patients with a USEMS[21]. This study involved both USEMSs and CSEMSs. Therefore, anticancer treatment may not be a risk factor for SEMS dysfunction. Duodenal invasion from tumors reduces peristalsis and causes food impaction in the biliary duct, and a duodenal SEMS prevents the outflow of bile juice[19]. In this study, any RBO requiring additional SEMS placement was defined as SEMS dysfunction so that SEMS occlusion caused by tumors could be properly evaluated and cases of SEMS occlusion by food impaction could be excluded. Therefore, SEMS placement near the biliary hilar duct was revealed as a new factor related to longer SEMS patency.

There were some limitations to this study. First, this was a retrospective observational study performed at a single institution. In the future, it is hoped that a prospective multicenter study will confirm our findings. Second, the type of SEMS was not unified. The axial force or shortening length varied among the SEMSs. Measurement of the axial force was difficult in this study; instead, different kinds of SEMSs were compared. As a result, the type of SEMS did not influence SEMS dysfunction. The WallFlex stent (Boston Scientific), which has a high axial force and a high shortening rate[22], was used significantly more often in the Hilar group. However, remarkable shortening was rarely observed (the presence or absence of shortening was confirmed in 23 patients 24 h after SEMS placement and in 99 patients more than 48 h after SEMS placement). This was likely due to the placement of an SEMS with a longer than established length because the SEMS could not fully expand in the area of the stricture. As described above, the axial force decreases with increasing SEMS length. Because of these factors, the difference in the type of SEMS did not influence the outcomes. Third, SEMS obstruction of sludge or food debris was not considered SEMS dysfunction. In past reports, sludge formation has been proposed

to be a cause of SEMS dysfunction[4,5,21]. This factor is surely important for comparisons of patency periods between USEMS and CSEMS. If SEMS obstruction of sludge or food debris was considered stent dysfunction, the patency period was also significantly longer in the Hilar group than in the Lower group (Supplementary Figure 2). Therefore, the obstruction of sludge or food debris did not influence the results of this study. As described above, the SEMS obstruction of sludge or food debris was excluded from SEMS dysfunction to properly evaluate the relationship between the positions of the SEMS and tumor in this study.

CONCLUSION

The results of our study revealed that placement of an SEMS near the biliary hilar duct could delay tumor overgrowth and prevent closure of the top edge of the SEMS by the CBD wall. Thus, in DMBO patients, the SEMS should be placed near the biliary hilar duct to achieve a longer patency period.

ARTICLE HIGHLIGHTS

Research background

Endoscopic biliary drainage using a self-expanding metallic stent (SEMS) has a longer patency period than endoscopic biliary drainage using a plastic stent. Therefore, endoscopic SEMS placement is desirable for the treatment of unresectable distant malignant biliary obstruction (DMBO).

Research motivation

The type of SEMS that should be used for DMBO is a point of active discussion. However, the appropriate position for SEMS insertion is unknown.

Research objectives

To clarify the appropriate SEMS insertion point for DMBO.

Research methods

Among 135 DMBO patients who underwent SEMS placement, 127 patients with biliary obstruction between the junction of the cystic duct and Vater's papilla were enrolled. In 83 patients (Hilar group), an SEMS was placed through the upper common bile duct within 2 cm from the biliary hilar duct. In the other 44 patients (Lower group), an SEMS was placed near the top of the biliary obstruction. The patency period was compared between the Hilar group and Lower group. The risk factors for SEMS dysfunction were also investigated.

Research results

The patency period of SEMS was significantly longer in the Hilar group patients. Multivariate analysis revealed that the Lower group classification was the only significant risk factor for SEMS dysfunction.

Research conclusions

SEMS placement near the biliary hilar duct extends the patency period in DMBO patients.

Research perspectives

SEMS placement near the biliary hilar duct might prevent obstructive jaundice and cholangitis and contribute to improved prognosis in DMBO patients.

ACKNOWLEDGEMENTS

We thank the entire staff at the Department of Gastroenterology of Fukushima Medical University, the Department of Endoscopy of Fukushima Medical University Hospital, and the gastroenterology ward of Fukushima Medical University Hospital.

FOOTNOTES

Author contributions: Sugimoto M wrote the paper and designed and performed the study; Takagi T and Ohira H designed and oversaw the study; Suzuki R, Konno N, HA, Hikichi T, Nakamura J, Takasumi M, Sato Y, Irie H, Okubo Y, Hashimoto M, Kato T, Kobashi R, and Yanagita T provided clinical advice; and all the authors read and

approved the final version of the manuscript.

Institutional review board statement: This study was approved by the Institutional Review Board of Fukushima Medical University, No. 2453.

Informed consent statement: The patients were not required to give informed consent because this study used anonymous clinical data obtained after each patient had agreed to medical activities by written consent. For full disclosure, the details of this study are published on the home page of Fukushima Medical University.

Conflict-of-interest statement: The authors declare that they have no competing interests.

Data sharing statement: The datasets analyzed during the current study are available from the corresponding author upon reasonable request.

Open-Access: This article is an open-access article that was selected by an in-house editor and fully peer-reviewed by external reviewers. It is distributed in accordance with the Creative Commons Attribution NonCommercial (CC BY-NC 4.0) license, which permits others to distribute, remix, adapt, build upon this work non-commercially, and license their derivative works on different terms, provided the original work is properly cited and the use is non-commercial. See: https://creativecommons.org/Licenses/by-nc/4.0/

Country/Territory of origin: Japan

ORCID number: Mitsuru Sugimoto 0000-0002-4223-613X; Tadayuki Takagi 0000-0003-0696-5973; Rei Suzuki 0000-0002-4049-0484; Naoki Konno 0000-0001-9830-4317; Hiroyuki Asama 0000-0002-0102-0404; Yuki Sato 0000-0001-8000-0972; Hiroki Irie 0000-0002-4805-6244; Yoshinori Okubo 0000-0003-0567-3805; Jun Nakamura 0000-0001-6006-1778; Mika Takasumi 0000-0002-6025-8084; Minami Hashimoto 0000-0002-5750-7182; Tsunetaka Kato 0000-0002-2529-2463; Ryoichiro Kobashi 0000-0003-0991-6042; Takumi Yanagita 0000-0002-1236-857X; Takuto Hikichi 0000-0002-9815-1557; Hiromasa Ohira 0000-0003-4331-0634.

S-Editor: Fan JR
L-Editor: A
P-Editor: Fan JR

REFERENCES

1 **Soehendra N**, Reynders-Frederix V. Palliative bile duct drainage - a new endoscopic method of introducing a transpapillary drain. *Endoscopy* 1980; **12**: 8-11 [PMID: 7353562 DOI: 10.1055/s-2007-1021702]
2 **Davids PH**, Groen AK, Rauws EA, Tytgat GN, Huibregtse K. Randomised trial of self-expanding metal stents *vs* polyethylene stents for distal malignant biliary obstruction. *Lancet* 1992; **340**: 1488-1492 [PMID: 1281903 DOI: 10.1016/0140-6736(92)92752-2]
3 **Isayama H**, Yasuda I, Ryozawa S, Maguchi H, Igarashi Y, Matsuyama Y, Katanuma A, Hasebe O, Irisawa A, Itoi T, Mukai H, Arisaka Y, Okushima K, Uno K, Kida M, Tamada K. Results of a Japanese multicenter, randomized trial of endoscopic stenting for non-resectable pancreatic head cancer (JM-test): Covered Wallstent *vs* DoubleLayer stent. *Dig Endosc* 2011; **23**: 310-315 [PMID: 21951091 DOI: 10.1111/j.1443-1661.2011.01124.x]
4 **Isayama H**, Komatsu Y, Tsujino T, Sasahira N, Hirano K, Toda N, Nakai Y, Yamamoto N, Tada M, Yoshida H, Shiratori Y, Kawabe T, Omata M. A prospective randomised study of "covered" *vs* "uncovered" diamond stents for the management of distal malignant biliary obstruction. *Gut* 2004; **53**: 729-734 [PMID: 15082593 DOI: 10.1136/gut.2003.018945]
5 **Krokidis M**, Fanelli F, Orgera G, Bezzi M, Passariello R, Hatzidakis A. Percutaneous treatment of malignant jaundice due to extrahepatic cholangiocarcinoma: covered Viabil stent *vs* uncovered Wallstents. *Cardiovasc Intervent Radiol* 2010; **33**: 97-106 [PMID: 19495871 DOI: 10.1007/s00270-009-9604-9]
6 **Krokidis M**, Fanelli F, Orgera G, Tsetis D, Mouzas I, Bezzi M, Kouroumalis E, Pasariello R, Hatzidakis A. Percutaneous palliation of pancreatic head cancer: randomized comparison of ePTFE/FEP-covered *vs* uncovered nitinol biliary stents. *Cardiovasc Intervent Radiol* 2011; **34**: 352-361 [PMID: 20467870 DOI: 10.1007/s00270-010-9880-4]
7 **Almadi MA**, Barkun AN, Martel M. No benefit of covered *vs* uncovered self-expandable metal stents in patients with malignant distal biliary obstruction: a meta-analysis. *Clin Gastroenterol Hepatol* 2013; **11**: 27-37.e1 [PMID: 23103324 DOI: 10.1016/j.cgh.2012.10.019]
8 **Shamah SP**, Chapman CG, Haider H, Liao C, Waxman I, Siddiqui UD. Partially Covered Versus Uncovered Self-Expandable Metal Stents: Coating Nor Diameter Affect Clinical Outcomes. *Dig Dis Sci* 2019; **64**: 2631-2637 [PMID: 31041643 DOI: 10.1007/s10620-019-05643-1]
9 **Elkilany A**, Alwarraky M, Geisel D, Maaly MA, Denecke T. Stent performance in palliative transhepatic treatment of malignant biliary obstruction: a randomized study comparing covered *vs* uncovered stents. *Acta Radiol* 2020; **61**: 1591-1599 [PMID: 32212829 DOI: 10.1177/0284185120911187]
10 **Gómez-Oliva C**, Guarner-Argente C, Concepción M, Jiménez FJ, Rodríguez S, Gonzalez-Huix F, Mugica F, Cabriada JL, Rodríguez C, Aguilar CG; Collaborating Group of the COBIWA Register. Partially covered self-expanding metal stent for unresectable malignant extrahepatic biliary obstruction: results of a large prospective series. *Surg Endosc* 2012; **26**: 222-229 [PMID: 21858574 DOI: 10.1007/s00464-011-1858-z]

11 **Shimizu S**, Naitoh I, Nakazawa T, Hayashi K, Miyabe K, Kondo H, Yoshida M, Yamashita H, Umemura S, Hori Y, Ohara H, Joh T. Predictive factors for pancreatitis and cholecystitis in endoscopic covered metal stenting for distal malignant biliary obstruction. *J Gastroenterol Hepatol* 2013; **28**: 68-72 [PMID: 23020651 DOI: 10.1111/j.1440-1746.2012.07283.x]

12 **Nakahara K**, Morita R, Michikawa Y, Suetani K, Morita N, Fujita A, Sato J, Igarashi Y, Ikeda H, Matsunaga K, Watanabe T, Kobayashi S, Otsubo T, Itoh F. Endoscopic Transpapillary Gallbladder Drainage for Acute Cholecystitis After Biliary Self-Expandable Metal Stent Placement. *Surg Laparosc Endosc Percutan Tech* 2020; **30**: 416-423 [PMID: 32398448 DOI: 10.1097/SLE.0000000000000802]

13 **Takinami M**, Murohisa G, Yoshizawa Y, Shimizu E, Nagasawa M. Risk factors for cholecystitis after stent placement in patients with distal malignant biliary obstruction. *J Hepatobiliary Pancreat Sci* 2020; **27**: 470-476 [PMID: 32462813 DOI: 10.1002/jhbp.767]

14 **Isayama H**, Hamada T, Yasuda I, Itoi T, Ryozawa S, Nakai Y, Kogure H, Koike K. TOKYO criteria 2014 for transpapillary biliary stenting. *Dig Endosc* 2015; **27**: 259-264 [PMID: 25209944 DOI: 10.1111/den.12379]

15 **Cotton PB**, Lehman G, Vennes J, Geenen JE, Russell RC, Meyers WC, Liguory C, Nickl N. Endoscopic sphincterotomy complications and their management: an attempt at consensus. *Gastrointest Endosc* 1991; **37**: 383-393 [PMID: 2070995 DOI: 10.1016/s0016-5107(91)70740-2]

16 **Isayama H**, Nakai Y, Toyokawa Y, Togawa O, Gon C, Ito Y, Yashima Y, Yagioka H, Kogure H, Sasaki T, Arizumi T, Matsubara S, Yamamoto N, Sasahira N, Hirano K, Tsujino T, Toda N, Tada M, Kawabe T, Omata M. Measurement of radial and axial forces of biliary self-expandable metallic stents. *Gastrointest Endosc* 2009; **70**: 37-44 [PMID: 19249766 DOI: 10.1016/j.gie.2008.09.032]

17 **Kim HS**, Lee DK, Kim HG, Park JJ, Park SH, Kim JH, Yoo BM, Roe IH, Moon YS, Myung SJ. Features of malignant biliary obstruction affecting the patency of metallic stents: a multicenter study. *Gastrointest Endosc* 2002; **55**: 359-365 [PMID: 11868009 DOI: 10.1067/mge.2002.121603]

18 **Nakai Y**, Isayama H, Kogure H, Hamada T, Togawa O, Ito Y, Matsubara S, Arizumi T, Yagioka H, Mizuno S, Sasaki T, Yamamoto N, Hirano K, Tada M, Koike K. Risk factors for covered metallic stent migration in patients with distal malignant biliary obstruction due to pancreatic cancer. *J Gastroenterol Hepatol* 2014; **29**: 1744-1749 [PMID: 24720610 DOI: 10.1111/jgh.12602]

19 **Hamada T**, Nakai Y, Isayama H, Sasaki T, Kogure H, Kawakubo K, Sasahira N, Yamamoto N, Togawa O, Mizuno S, Ito Y, Hirano K, Toda N, Tada M, Koike K. Duodenal metal stent placement is a risk factor for biliary metal stent dysfunction: an analysis using a time-dependent covariate. *Surg Endosc* 2013; **27**: 1243-1248 [PMID: 23073685 DOI: 10.1007/s00464-012-2585-9]

20 **Nakai Y**, Isayama H, Mukai T, Itoi T, Maetani I, Kawakami H, Yasuda I, Maguchi H, Ryozawa S, Hanada K, Hasebe O, Ito K, Kawamoto H, Mochizuki H, Igarashi Y, Irisawa A, Sasaki T, Togawa O, Hara T, Kamada H, Toda N, Hamada T, Kogure H. Impact of anticancer treatment on recurrent obstruction in covered metallic stents for malignant biliary obstruction. *J Gastroenterol* 2013; **48**: 1293-1299 [PMID: 23354624 DOI: 10.1007/s00535-013-0749-6]

21 **Kitano M**, Yamashita Y, Tanaka K, Konishi H, Yazumi S, Nakai Y, Nishiyama O, Uehara H, Mitoro A, Sanuki T, Takaoka M, Koshitani T, Arisaka Y, Shiba M, Hoki N, Sato H, Sasaki Y, Sato M, Hasegawa K, Kawabata H, Okabe Y, Mukai H. Covered self-expandable metal stents with an anti-migration system improve patency duration without increased complications compared with uncovered stents for distal biliary obstruction caused by pancreatic carcinoma: a randomized multicenter trial. *Am J Gastroenterol* 2013; **108**: 1713-1722 [PMID: 24042190 DOI: 10.1038/ajg.2013.305]

22 **Hori Y**, Hayashi K, Yoshida M, Naitoh I, Nakazawa T, Miyabe K, Shimizu S, Kondo H, Nishi Y, Umemura S, Kato A, Ohara H, Joh T. New concept of traction force applied to biliary self-expandable metallic stents. *Endoscopy* 2016; **48**: 472-476 [PMID: 26859555 DOI: 10.1055/s-0041-111566]

World Journal of Gastroenterology

Submit a Manuscript: https://www.f6publishing.com

World J Gastroenterol 2022 May 7; 28(17): 1871-1874

DOI: 10.3748/wjg.v28.i17.1871

ISSN 1007-9327 (print) ISSN 2219-2840 (online)

LETTER TO THE EDITOR

Could microbiome analysis be a new diagnostic tool in gastric carcinogenesis for high risk, *Helicobacter pylori* negative patients?

Alla Turshudzhyan, Houman Rezaizadeh

Specialty type: Gastroenterology and hepatology

Provenance and peer review: Invited article; Externally peer reviewed.

Peer-review model: Single blind

Peer-review report's scientific quality classification

Grade A (Excellent): 0
Grade B (Very good): 0
Grade C (Good): C
Grade D (Fair): 0
Grade E (Poor): E

P-Reviewer: Kawabata H, Japan; Poddighe D, Kazakhstan

Received: January 21, 2022
Peer-review started: January 21, 2022
First decision: February 24, 2022
Revised: February 28, 2022
Accepted: March 27, 2022
Article in press: March 27, 2022
Published online: May 7, 2022

Alla Turshudzhyan, Department of Medicine, University of Connecticut, Farmington, CT 06030, United States

Houman Rezaizadeh, Department of Gastroenterology and Hepatology, University of Connecticut, Farmington, CT 06030, United States

Corresponding author: Houman Rezaizadeh, MD, Assistant Professor, Department of Gastroenterology and Hepatology, University of Connecticut, 263 Farmington Ave, Farmington, CT 06030, United States. rezaizadeh@uchc.edu

Abstract

Helicobacter pylori (*H. pylori*) has long been believed to be the major colonizer of the stomach, but recent advances in genetic sequencing have allowed for further differentiation of the gastric microbiome and revealed the true complexity of the gastric microbiome. One of the few studies specifically evaluated the microbiome in the *H. pylori* negative patient population. They concluded that various stages of gastric carcinogenesis are associated with distinct bacterial taxa that could service both a predictive and diagnostic purpose. While the study has some limitations, the conclusions they make are intriguing and should prompt a larger prospective study to be done that spans multiple geographic regions.

Key Words: Gastric cancer; Gastric carcinogenesis; Microbiome; Dysplasia; Intestinal metaplasia

©The Author(s) 2022. Published by Baishideng Publishing Group Inc. All rights reserved.

Core Tip: Gastric tumorigenesis in *Helicobacter pylori* (*H. pylori*) negative patients remained a mystery for many years until genetic sequencing allowed for a closer look at the composition of the gastric microbiome. Primary colonizers of the stomach in *H. pylori* negative patients at various stages of gastric tumorigenesis and were able to conclude that there are distinct bacterial taxa associated with these stages. Their study is comprehensive but needs a larger prospective study to further support this hypothesis, particularly in other geographic areas with varying risk profiles.

Citation: Turshudzhyan A, Rezaizadeh H. Could microbiome analysis be a new diagnostic tool in gastric carcinogenesis for high risk, *Helicobacter pylori* negative patients? *World J Gastroenterol* 2022; 28(17): 1871-1874
URL: https://www.wjgnet.com/1007-9327/full/v28/i17/1871.htm
DOI: https://dx.doi.org/10.3748/wjg.v28.i17.1871

TO THE EDITOR

We read with great interest the case control study by Sun *et al*[1]. These authors performed a genetic analysis of gastric mucosa from 134 *Helicobacter pylori* (*H. pylori*) negative patients, which included a variety of gastric pathology: 56 cases of superficial gastritis, 9 cases of atrophic gastritis, 27 cases of intestinal metaplasia, 29 cases of dysplasia, and 13 cases of gastric cancer[1]. Additionally, gastric juice samples from 18 cases of superficial gastritis, intestinal metaplasia, and dysplasia were included and analyzed[1]. Genetic analysis was performed using a 16S rRNA[1]. The goal of the study was to understand whether there is a distinct pattern in the microbiome of various gastric disease types.

The study demonstrated that microbiota of the gastric mucosa varies across different stages of gastric carcinogenesis[1]. Specifically, Sun *et al*[1] found that as the stages of carcinogenesis progress, there is less microbiota variability within gastric mucosa[1]. Of note, their data established that different stages of gastric carcinogenesis had distinguishable microbiota taxa for both gastric mucosa and gastric juice [1]. For example, intestinal metaplasia and dysplasia had predominantly *Ralstonia* and *Rhodococcus* while *Streptococcacaeae* and *Lactobacillaceae* were more prominent in pre-cancerous lesions and gastric cancer [1]. Sun *et al*[1] concluded that their results may facilitate prediction of intestinal metaplasia and dysplasia progression to gastric cancer.

It was long believed that due to the highly acidic environment, *H. pylori* was the predominant colonizer of the stomach. In the recent years, however, genetic sequencing allowed further differentiation of the gastric microbiota[2]. Similar to the study by Sun *et al*[1], prior studies established that microbial diversity decreased significantly with gastric carcinogenesis[3,4]. There were a few studies, however, that were arguing that the opposite is true. The studies by Castaño-Rodríguez *et al*[5] and Eun *et al*[6] suggested that gastric cancer was associated with increased diversity of microbiome[5,6]. These results were supported by the more recent studies. A recently published study by Dai *et al*[7] analyzed gastric microbiome of 37 patients with gastric cancer using the same 16s rRNA gene sequencing[7]. They concluded that pre-cancerous and cancerous gastric lesions had an increased diversity in microbiome and specifically an abundance of *Lactobacillus*, *Streptococcus*, *Bacteroides*, and *Prevotella*[7]. While their conclusions on the increased microbial diversity in gastric cancer argues against conclusions set forth by Sun *et al*[1], they do agree on the distinguishable bacterial taxa associated with gastric cancer that could be used as a predictive marker of neoplastic conversion in pre-malignant lesions. Perhaps these observational disparities could be attributed to geographic, environmental, and patient population differences or even variability of the microbiome throughout various stages of gastric cancer itself.

Sun *et al*[1] concluded that there are certain bacteria that predispose patients to development of gastric cancer. With this, we wonder, if there are bacteria that would instead be protective against gastric cancer. Goldin and Gorbach[8] were one of the first to establish an association between probiotics and cancer prevention back in 1980[8]. Since then, multiple studies have attempted to investigate probiotics as a possible adjunct to cancer therapy. Lee *et al*[9] found that *Bacillus polyfermenticus* was able to reduce gastric adenocarcinoma cell proliferation by more than 90% *in vitro*[9]. Similarly, Han *et al*[10] found that *Lactococcus lactis* was able to reduce gastric adenocarcinoma cell proliferation by more than 80% *in vitro*[10]. While both studies were done *in vitro*, they proposed interesting conclusions that should be further investigated for efficacy *in vivo*. If proved to be successful and safe *in vivo*, targeted probiotics could be a new exciting adjunctive therapy for patients with gastric cancer.

The study conducted by Sun *et al*[1] was retrospective. The patients in the study had a known diagnosis of gastric cancer. Subsequently, it is important to consider a theory that the observed bacterial taxa were a result of neoplastic changes rather than bacteria being responsible for cancer development (*i.e.* reactive changes rather than causal association). This theory can be better investigated by a prospective study in which patients at high risk for developing gastric cancer are followed over time and changes in their microbiome are documented along with histopathological or endoscopic findings.

Sun *et al*[1] rightfully excluded patients who were on active antibiotic therapy, however, it is unclear how many of them had significant antibiotic exposure prior to the study. The association between antibiotic use and cancer remains unclear, however, there is literature reporting cases of antibiotic use and subsequent development of malignancy. Petrelli *et al*[11] conducted a systematic review with meta-analysis and concluded that antibiotics were an independent risk factor for cancer development (OR: 1.18, 95%CI: 1.12-1.24, $P < 0.001$)[11]. This is the reason we believe a thorough antibiotic use history should be collected on patients in studies investigating microbiome and its effects on cancer development.

Gastric cancer is a prominent malignancy affecting many people worldwide but has a notoriously higher incidence rate in Asia[12]. As a result, many of the studies on this topic originate from Asia. Sun *et al*[1] study, for example, was limited to Peking University Hospitals patient population in China, which may have introduced a geographic confounding variable. This may make their conclusions less applicable to the patients of other geographic areas. The study recruitment period was limited to September 2019 to October 2020. Lastly, gastric juice data was only collected for superficial gastritis, intestinal metaplasia, and dysplasia patients, and not for atrophic gastritis or gastric cancer patients. Despite some of the limitations, the study by Sun *et al*[1] had a comprehensive analysis and proposed very interesting conclusions that should be further replicated in larger studies.

In summary, the authors should be commended for their work. They investigated the microbiome in a large group of patients at different stages of gastric cancer tumorigenesis in an *H. pylori* negative patient population, which is generally understudied. Sun *et al*[1] study set comprehensive exclusion criteria limiting many confounding factors. They have demonstrated a well conducted analysis that showed there are distinct bacterial taxa associated with each of the stages of gastric carcinogenesis that could be of great clinical value and help triage gastric lesions. Going forward, large prospective randomized controlled trials that encompass multiple geographic areas could help solidify the conclusions set forth by Sun *et al*[1].

FOOTNOTES

Author contributions: Turshudzhyan A wrote the letter; Rezaizadeh H revised the letter.

Conflict-of-interest statement: Dr. Turshudzhyan and Dr. Rezaizadeh have no relevant conflicts of interest to disclose.

Open-Access: This article is an open-access article that was selected by an in-house editor and fully peer-reviewed by external reviewers. It is distributed in accordance with the Creative Commons Attribution NonCommercial (CC BY-NC 4.0) license, which permits others to distribute, remix, adapt, build upon this work non-commercially, and license their derivative works on different terms, provided the original work is properly cited and the use is non-commercial. See: https://creativecommons.org/Licenses/by-nc/4.0/

Country/Territory of origin: United States

ORCID number: Alla Turshudzhyan 0000-0001-6867-7569; Houman Rezaizadeh 0000-0002-1066-5394.

S-Editor: Fan JR
L-Editor: A
P-Editor: Fan JR

REFERENCES

1 **Sun QH**, Zhang J, Shi YY, Fu WW, Ding SG. Microbiome changes in the gastric mucosa and gastric juice in different histological stages of *Helicobacter pylori*-negative gastric cancers. *World J Gastroenterol* 2022; **28**: 365-380 [PMID: 35110955 DOI: 10.3748/wjg.v28.i3.365]
2 **Qin J**, Li R, Raes J, Arumugam M, Burgdorf KS, Manichanh C, Nielsen T, Pons N, Levenez F, Yamada T, Mende DR, Li J, Xu J, Li S, Li D, Cao J, Wang B, Liang H, Zheng H, Xie Y, Tap J, Lepage P, Bertalan M, Batto JM, Hansen T, Le Paslier D, Linneberg A, Nielsen HB, Pelletier E, Renault P, Sicheritz-Ponten T, Turner K, Zhu H, Yu C, Jian M, Zhou Y, Li Y, Zhang X, Qin N, Yang H, Wang J, Brunak S, Doré J, Guarner F, Kristiansen K, Pedersen O, Parkhill J, Weissenbach J; MetaHIT Consortium, Bork P, Ehrlich SD, Wang J. A human gut microbial gene catalogue established by metagenomic sequencing. *Nature* 2010; **464**: 59-65 [PMID: 20203603 DOI: 10.1038/nature08821]
3 **Coker OO**, Dai Z, Nie Y, Zhao G, Cao L, Nakatsu G, Wu WK, Wong SH, Chen Z, Sung JJY, Yu J. Mucosal microbiome dysbiosis in gastric carcinogenesis. *Gut* 2018; **67**: 1024-1032 [PMID: 28765474 DOI: 10.1136/gutjnl-2017-314281]
4 **Gantuya B**, El Serag HB, Matsumoto T, Ajami NJ, Uchida T, Oyuntsetseg K, Bolor D, Yamaoka Y. Gastric mucosal microbiota in a Mongolian population with gastric cancer and precursor conditions. *Aliment Pharmacol Ther* 2020; **51**: 770-780 [PMID: 32133670 DOI: 10.1111/apt.15675]
5 **Castaño-Rodríguez N**, Goh KL, Fock KM, Mitchell HM, Kaakoush NO. Dysbiosis of the microbiome in gastric carcinogenesis. *Sci Rep* 2017; **7**: 15957 [PMID: 29162924 DOI: 10.1038/s41598-017-16289-2]
6 **Eun CS**, Kim BK, Han DS, Kim SY, Kim KM, Choi BY, Song KS, Kim YS, Kim JF. Differences in gastric mucosal microbiota profiling in patients with chronic gastritis, intestinal metaplasia, and gastric cancer using pyrosequencing methods. *Helicobacter* 2014; **19**: 407-416 [PMID: 25052961 DOI: 10.1111/hel.12145]
7 **Dai D**, Yang Y, Yu J, Dang T, Qin W, Teng L, Ye J, Jiang H. Interactions between gastric microbiota and metabolites in gastric cancer. *Cell Death Dis* 2021; **12**: 1104 [PMID: 34819503 DOI: 10.1038/s41419-021-04396-y]
8 **Goldin BR**, Gorbach SL. Effect of Lactobacillus acidophilus dietary supplements on 1,2-dimethylhydrazine dihydrochloride-induced intestinal cancer in rats. *J Natl Cancer Inst* 1980; **64**: 263-265 [PMID: 6766509 DOI: 10.1093/jnci/64.2.263]

9 **Lee NK**, Son SH, Jeon EB, Jung GH, Lee JY, Paik HD. The prophylactic effect of probiotic Bacillus polyfermenticus KU3 against cancer cells. *J Funct Food* 2015; 513-518 [DOI: 10.1016/j.jff.2015.02.019]

10 **Han KJ**, Lee NK, Park H, Paik HD. Anticancer and Anti-Inflammatory Activity of Probiotic Lactococcus lactis NK34. *J Microbiol Biotechnol* 2015; **25**: 1697-1701 [PMID: 26165315 DOI: 10.4014/jmb.1503.03033]

11 **Petrelli F**, Ghidini M, Ghidini A, Perego G, Cabiddu M, Khakoo S, Oggionni E, Abeni C, Hahne JC, Tomasello G, Zaniboni A. Use of Antibiotics and Risk of Cancer: A Systematic Review and Meta-Analysis of Observational Studies. *Cancers (Basel)* 2019; **11** [PMID: 31416208 DOI: 10.3390/cancers11081174]

12 **Bray F**, Ferlay J, Soerjomataram I, Siegel RL, Torre LA, Jemal A. Global cancer statistics 2018: GLOBOCAN estimates of incidence and mortality worldwide for 36 cancers in 185 countries. *CA Cancer J Clin* 2018; **68**: 394-424 [PMID: 30207593 DOI: 10.3322/caac.21492]



Published by **Baishideng Publishing Group Inc**
7041 Koll Center Parkway, Suite 160, Pleasanton, CA 94566, USA
Telephone: +1-925-3991568
E-mail: bpgoffice@wjgnet.com
Help Desk: https://www.f6publishing.com/helpdesk
https://www.wjgnet.com



© 2022 Baishideng Publishing Group Inc. All rights reserved.

ISSN 1007-9327 (print)
ISSN 2219-2840 (online)

World Journal of *Gastroenterology*

World J Gastroenterol 2022 May 14; 28(18): 1875-2033



Published by Baishideng Publishing Group Inc

World Journal of Gastroenterology

Contents

Weekly Volume 28 Number 18 May 14, 2022

REVIEW

1875 Gut microbiota in various childhood disorders: Implication and indications

Saeed NK, Al-Beltagi M, Bediwy AS, El-Sawaf Y, Toema O

1902 Therapeutic strategies in Crohn's disease in an emergency surgical setting

Chiarello MM, Pepe G, Fico V, Bianchi V, Tropeano G, Altieri G, Brisinda G

MINIREVIEWS

1922 Novel drug delivery systems for inflammatory bowel disease

Yasmin F, Najeeb H, Shaikh S, Hasanain M, Naeem U, Moeed A, Koritala T, Hasan S, Surani S

1934 Targeting pancreatic cancer immune evasion by inhibiting histone deacetylases

Sim W, Lim WM, Hii LW, Leong CO, Mai CW

ORIGINAL ARTICLE

Basic Study

1946 Gut mucosal microbiota profiles linked to colorectal cancer recurrence

Huo RX, Wang YJ, Hou SB, Wang W, Zhang CZ, Wan XH

1965 Effect of ancient Khorasan wheat on gut microbiota, inflammation, and short-chain fatty acid production in patients with fibromyalgia

Baldi S, Pagliai G, Dinu M, Di Gloria L, Nannini G, Curini L, Pallecchi M, Russo E, Niccolai E, Danza G, Benedettelli S, Ballerini G, Colombini B, Bartolucci G, Ramazzotti M, Sofi F, Amedei A

1981 Fusobacterium nucleatum promotes colon cancer progression by changing the mucosal microbiota and colon transcriptome in a mouse model

Wu N, Feng YQ, Lyu N, Wang D, Yu WD, Hu YF

Retrospective Cohort Study

1996 Incidental gallbladder cancer diagnosis confers survival advantage irrespective of tumour stage and characteristics

Alarabiyat M, Raza SS, Isaac J, Mirza D, Marudanayagam R, Roberts K, Abradelo M, Bartlett DC, Dasari BV, Sutcliffe RP, Chatzizacharias NA

Retrospective Study

2008 Risk factors for major gastrointestinal bleeding in the general population in Finland

Vora P, Herrera R, Pietila A, Mansmann U, Brobert G, Peltonen M, Salomaa V

Observational Study

2021 Clinical utility of two-dimensional shear-wave elastography in monitoring disease course in autoimmune hepatitis-primary biliary cholangitis overlap syndrome

Yan YL, Xing X, Wang Y, Wang XZ, Wang Z, Yang L

World Journal of Gastroenterology

Weekly Volume 28 Number 18 May 14, 2022

Contents

ABOUT COVER

Editorial Board Member of *World Journal of Gastroenterology*, Vishal Sharma, MD, DM, Associate Professor, Department of Gastroenterology, Postgraduate Institute of Medical Education and Research, Chandigarh 160012, India. sharma.vishal@pgimer.edu.in

AIMS AND SCOPE

The primary aim of *World Journal of Gastroenterology* (*WJG*, *World J Gastroenterol*) is to provide scholars and readers from various fields of gastroenterology and hepatology with a platform to publish high-quality basic and clinical research articles and communicate their research findings online. *WJG* mainly publishes articles reporting research results and findings obtained in the field of gastroenterology and hepatology and covering a wide range of topics including gastroenterology, hepatology, gastrointestinal endoscopy, gastrointestinal surgery, gastrointestinal oncology, and pediatric gastroenterology.

INDEXING/ABSTRACTING

The *WJG* is now indexed in Current Contents®/Clinical Medicine, Science Citation Index Expanded (also known as SciSearch®), Journal Citation Reports®, Index Medicus, MEDLINE, PubMed, PubMed Central, and Scopus. The 2021 edition of Journal Citation Report® cites the 2020 impact factor (IF) for *WJG* as 5.742; Journal Citation Indicator: 0.79; IF without journal self cites: 5.590; 5-year IF: 5.044; Ranking: 28 among 92 journals in gastroenterology and hepatology; and Quartile category: Q2. The *WJG*'s CiteScore for 2020 is 6.9 and Scopus CiteScore rank 2020: Gastroenterology is 19/136.

RESPONSIBLE EDITORS FOR THIS ISSUE

Production Editor: *Hua-Ge Yu*; **Production Department Director:** *Xu Guo*; **Editorial Office Director:** *Ze-Mao Gong*.

NAME OF JOURNAL
World Journal of Gastroenterology

ISSN
ISSN 1007-9327 (print) ISSN 2219-2840 (online)

LAUNCH DATE
October 1, 1995

FREQUENCY
Weekly

EDITORS-IN-CHIEF
Andrzej S Tarnawski

EDITORIAL BOARD MEMBERS
http://www.wjgnet.com/1007-9327/editorialboard.htm

PUBLICATION DATE
May 14, 2022

COPYRIGHT
© 2022 Baishideng Publishing Group Inc

INSTRUCTIONS TO AUTHORS
https://www.wjgnet.com/bpg/gerinfo/204

GUIDELINES FOR ETHICS DOCUMENTS
https://www.wjgnet.com/bpg/GerInfo/287

GUIDELINES FOR NON-NATIVE SPEAKERS OF ENGLISH
https://www.wjgnet.com/bpg/gerinfo/240

PUBLICATION ETHICS
https://www.wjgnet.com/bpg/GerInfo/288

PUBLICATION MISCONDUCT
https://www.wjgnet.com/bpg/gerinfo/208

ARTICLE PROCESSING CHARGE
https://www.wjgnet.com/bpg/gerinfo/242

STEPS FOR SUBMITTING MANUSCRIPTS
https://www.wjgnet.com/bpg/GerInfo/239

ONLINE SUBMISSION
https://www.f6publishing.com

© 2022 Baishideng Publishing Group Inc. All rights reserved. 7041 Koll Center Parkway, Suite 160, Pleasanton, CA 94566, USA

E-mail: bpgoffice@wjgnet.com https://www.wjgnet.com

World Journal of Gastroenterology

Submit a Manuscript: https://www.f6publishing.com

World J Gastroenterol 2022 May 14; 28(18): 1875-1901

DOI: 10.3748/wjg.v28.i18.1875

ISSN 1007-9327 (print) ISSN 2219-2840 (online)

REVIEW

Gut microbiota in various childhood disorders: Implication and indications

Nermin Kamal Saeed, Mohammed Al-Beltagi, Adel Salah Bediwy, Yasser El-Sawaf, Osama Toema

Specialty type: Pediatrics

Provenance and peer review: Invited article; Externally peer reviewed.

Peer-review model: Single blind

Peer-review report's scientific quality classification
Grade A (Excellent): 0
Grade B (Very good): B
Grade C (Good): C
Grade D (Fair): 0
Grade E (Poor): 0

P-Reviewer: Liao JX, China; Liu Z, China

Received: January 19, 2022
Peer-review started: January 19, 2022
First decision: March 8, 2022
Revised: March 8, 2022
Accepted: March 27, 2022
Article in press: March 27, 2022
Published online: May 14, 2022

Nermin Kamal Saeed, Medical Microbiology Section, Department of Pathology, Salmaniya Medical Complex, Ministry of Health, Manama 12, Bahrain

Nermin Kamal Saeed, Microbiology Section, Department of Pathology, Irish Royal College of Surgeon, Busaiteen 15503, Bahrain

Mohammed Al-Beltagi, Department of Pediatrics, University Medical Center, Arabian Gulf University, Dr. Sulaiman Al Habib Medical Group, Manama 26671, Bahrain

Mohammed Al-Beltagi, Osama Toema, Department of Pediatrics, Faculty of Medicine, Tanta University, Tanta 31511, Egypt

Adel Salah Bediwy, Department of Chest Disease, Faculty of Medicine, Tanta University, Tanta 31527, Egypt

Adel Salah Bediwy, Department of Pulmonology, University Medical Center, Arabian Gulf University, Dr. Sulaiman Al Habib Medical Group, Manama 26671, Bahrain

Yasser El-Sawaf, Department of Tropical Medicine, Faculty of Medicine, Tanta University, Tanta 31527, Egypt

Yasser El-Sawaf, Department of Gastroenterology, University Medical Center, Arabian Gulf University, Dr. Sulaiman Al-Habib Medical Group, Manama 26671, Bahrain

Corresponding author: Mohammed Al-Beltagi, MBChB, MD, MSc, PhD, Chairman, Professor, Department of Pediatrics, University Medical Center, Arabian Gulf University, Dr. Sulaiman Al Habib Medical Group, King Abdulaziz Avenu, Block 328, BLd 61, Manama 26671, Bahrain. mbelrem@hotmail.com

Abstract

Gut microbiota has a significant role in gut development, maturation, and immune system differentiation. It exerts considerable effects on the child's physical and mental development. The gut microbiota composition and structure depend on many host and microbial factors. The host factors include age, genetic pool, general health, dietary factors, medication use, the intestine's pH, peristalsis, and transit time, mucus secretions, mucous immunoglobulin, and tissue oxidation-reduction potentials. The microbial factors include nutrient availability, bacterial cooperation or antagonism, and bacterial adhesion. Each part of the gut has its microbiota due to its specific characteristics. The gut microbiota interacts with different body parts, affecting the pathogenesis of many local and systemic

diseases. Dysbiosis is a common finding in many childhood disorders such as autism, failure to thrive, nutritional disorders, coeliac disease, Necrotizing Enterocolitis, helicobacter pylori infection, functional gastrointestinal disorders of childhood, inflammatory bowel diseases, and many other gastrointestinal disorders. Dysbiosis is also observed in allergic conditions like atopic dermatitis, allergic rhinitis, and asthma. Dysbiosis can also impact the development and the progression of immune disorders and cardiac disorders, including heart failure. Probiotic supplements could provide some help in managing these disorders. However, we are still in need of more studies. In this narrative review, we will shed some light on the role of microbiota in the development and management of common childhood disorders.

Key Words: Gut microbiota; Dysbiosis; Children; Gastrointestinal disorders; Immune disorders; Allergic disorders; Cardiac disorders

©The Author(s) 2022. Published by Baishideng Publishing Group Inc. All rights reserved.

Core Tip: Gut microbiota has an intimate relationship with the various health conditions of the human body. It interacts with different body parts, affecting the pathogenesis of many local and systemic diseases. Gut dysbiosis is observed in many childhood disorders, inside and outside the gastrointestinal tract. Probiotic supplements could provide some help in managing these disorders. However, we are still in need of more studies. In this narrative review, we will shed some light on the role of microbiota in the development and management of common childhood disorders.

Citation: Saeed NK, Al-Beltagi M, Bediwy AS, El-Sawaf Y, Toema O. Gut microbiota in various childhood disorders: Implication and indications. *World J Gastroenterol* 2022; 28(18): 1875-1901
URL: https://www.wjgnet.com/1007-9327/full/v28/i18/1875.htm
DOI: https://dx.doi.org/10.3748/wjg.v28.i18.1875

INTRODUCTION

The human has an intimate symbiotic relationship with microbes. The human body harbors about 10-100 trillion microbial cells. Most of these microbes are present mainly in the gut as it provides a warm, stable, and eutrophic environment. There is significant variability in microbial composition at different body sites, with a vast difference between health and disease. Although the term microbiota is sometimes interchangeably used with the term microbiome, microbiota refers to the organisms living in a specific environment, and microbiome refers to the microorganisms and their genome in a particular environment[1]. The microbial microbiome has a set of genes of approximately 3.3 million active genes compared to 22000 human genes. The gut microbiota is the organisms that inhabit the gut, forming about 60% of the dry faces; 99% are anaerobic bacteria. Though bacteria form the main bulk of the microbiome, viruses, archaea, and eukaryotes are present in fewer numbers, but we should not ignore their presence[2].

Microbial colonization with more than 1000 species plays an essential role in gut development and maturation. There is evidence that gut colonization started in utero, and bacteria were detected from the amniotic fluid meconium and placenta in healthy term babies[3]. After delivery, the microbiota of the vaginally delivered neonates resembles those of their mother's vagina, while those delivered by cesarean section resemble those of the mother's skin. Then the infant microbiota changes gradually with every change in the infant diet from the simple neonatal microbiota with a predominance of facultative anaerobic bacteria, such as *Enterobacteria, Enterococci*, and *Streptococci*, to the more complex adult-type by the first few years of life with greater diversity and ability to biosynthesize vitamins and digest polysaccharides[4]. However, the child's microbiota continues to develop throughout childhood and adolescence. Despite being like the adult regarding the number of the detected species, the gut microbiota of children and adolescents may differ in genera's relative abundances[5]. Their gut microbiota has more abundances of *Bifidobacterium spp.*, *Faecalibacterium spp.*, and members of the *Lachnospiraceae* than the adults' gut microbiota with more abundances of *Bacteroides spp.* The microbiome also is different in children with more genes involved in amino acid degradation, vitamin synthesis, triggering mucosal inflammation, and oxidative phosphorylation compared with that observed in the adults with more genes associated with inflammation and obesity. So, as expected, the gut microbiota and microbiome go through a continuous and persistent development throughout life[6].

FUNCTION OF GUT MICROBIOTA

Gut microbiota exerts some essential functions in the human body's immunological, metabolic, structural, and neurological landscapes. Gut microbiota also significantly influences an individual's physical and mental health[7]. Gut microbiota significantly impacts normal and physiological gut development and helps gut mucosa maturation and differentiation and its immune system. It restricts the growth of the pathogenic and the potential pathogenic microbes, competes with them, and inhibits their ability to invade and implement the ecosystem. Some microbiota strains can secrete bacteriocins antimicrobial substances to inhibit other bacterial proliferation.

Other microbiota strains can ferment and digest nondigestible carbohydrates, fibers, and endogenous intestinal mucus, producing gases and short-chain fatty acids (SCFAs) such as acetate (the most abundant), propionate, and butyrate. These SCFAs can modulate the various activities in the gastrointestinal tract, including cell proliferation and differentiation, water and electrolytes absorption, hormonal secretion, and immune system activation[8,9]. SCFAs can serve as a food substrate for colonocytes (butyrate) and regulate leukocyte function and immune system activation by producing different eicosanoids, cytokines (IL-2, IL-6, IL-10, and TNF-α), and chemokines production with inducing balance among pro-inflammatory and anti-inflammatory mechanisms. SCFAs may also affect leucocyte chemotaxis, affecting their ability to migrate to the focus of infection or inflammation to destroy the target microbes[10].

Lack of SCFA is one of the causes of leaky gut and local gut inflammation that enhance microbial invasion. Butyrate can also induce colon cancer cells apoptosis and activate intestinal gluconeogenesis to enhance energy balance. It is crucial for glucose homeostasis by regulating hepatic gluconeogenesis and stimulating satiety signaling. The metabolic effects of SCFAs are not limited to the intestine but have extra-intestinal effects. Acetate SCFAs play a crucial role in regulating cholesterol metabolism and lipogenesis[11]. Microbiota also has an essential metabolic function in the biosynthesis of vitamins (vitamin K, biotin, folic acid, vitamin B12, and pantothenic acid) and amino acids from urea or ammonia. It also plays a role in xenobiotics and drug metabolism[12].

Gut microbiota can affect the host's energy balance through different mechanisms. It extracts energy from nondigestible dietary components and impacts gut transit, energy intake, and energy expenditure [13]. It also can modify the available pool of bile acids, affecting their composition and abundance. Gut microbiota-derived enzymes can metabolize the bile acids produced by the liver, a critically crucial process to maintain a healthy gut microbiota, enhance lipid and carbohydrate metabolism, increase insulin sensitivity, and enhance innate immunity[14]. The gut microbiota connects with the brain through several various mechanisms. These mechanisms include neurotransmitters production or modulation of their catabolism, vagus nerve signaling, and the hypothalamus-pituitary axis activation [15]. Gut microbiota produces hundreds of neurochemical substances used by the brain to regulate its basic physiological processes and mental functions such as learning, memory, and mood[16].

FACTORS AFFECTING THE CHILDREN'S GUT MICROBIOTA

The type and the quantities of the gut microbiota show wide individual variability. Many host and bacterial-related factors affect bacterial colonization in the different parts of the human gut. The host factors include the host's age, genetic pool, general health, dietary factors, using medication, pH, peristalsis, and the transit time of the part of the intestine, mucus secretions containing immunoglobulin, and the tissue oxidation-reduction potentials. The microbial factors include nutrient availability, bacterial cooperation or antagonism, and bacterial adhesion[17,18]. Each part of the gut has its microbiota due to its specific characteristics. Table 1 shows the microbiota in the different parts of the gut.

The ability of the host genetics pool to modify the gut microbiome structure is still controversial. There is a strong association between the Lactase gene and the relative abundance of *Bifidobacterium*. However, this association could be related to lactose consumption[19]. The vitamin D receptor gene is associated with some variation in gut microbiota[20]. Other studies proved the association of some host genetic variations with the abundance of certain microbiota species. However, the origin of association is still uncertain[21]. The host diet is crucial in developing gut microbiota as carbohydrate fermentation is one of its core functions. The microbiota of the small intestine adapts quickly to varying nutrient availability in the lumen and can rapidly metabolize the simple carbohydrates. On the other hand, the colon microbiota can degrade complex carbohydrates. A high-fat diet stimulates the proliferation of *Clostridium* and suppresses the proliferation of *Bifidobacterium* and *Bacteroides*[22]. Dietary modification produces rapid alteration of the colonic microbiota within two days and long-term changes[23].

The type of delivery can early-life microbiome. However, this effect may differ upon intrapartum antibiotic exposure. The gut microbiota of vaginally delivered infants shows enrichment of *Bifidobacterium spp.* and reduction of *Enterococcus* and *Klebsiella spp.* Over the first year of life, the gut microbiota in infants born with caesarean section appears less stable with a predominance of pathogenic bacteria such as *Klebsiella* and *Enterococcus* and delayed acquisition of the beneficial *Bifidobacterium*[24]. Breast or

Table 1 The microbiota in the different parts of the gut

Site	pH	Predominant microbiota	Bacterial load (CFU/gram content)	Other factors
Mouth	6.5-7	Bacteria (esp *Fusobacterium nucleatum)*, fungi, viruses and protozoa	700 species	Ideal warm environment
Stomach	Strong acidic	*Lactobacilli, streptococci, Lactobacillus, Peptostreptococcus, Helicobacter pylori*, and yeasts	Low (10^2)	Gastric acidity, Acid suppressive therapy, *H. pylori* colonization, the reflux of bile, mucus thickness and gastric peristalsis
Duodenum	4-5	*Lactobacilli* and *Streptococci*	More than (10^2-10^4)	Age, diet, antibiotic, and proton pump inhibitor use
Jejunum-ileum	6-7.4	*Firmicutes* and *Proteobacteria*	More than duodenum (10^6-10^8)	Nutrient reach environment faster transit time, bile acids, and antimicrobial peptide exposure
Colon	Left colon 6.1-7.5; Cecum 5.7; Rectum 6.7	*Bacteriodetes* (especially the genera *Bacteroides* and *Prevotella*) and *Firmicutes* (especially members of the genus *Clostridium*). Methanogenic archaea and fungi; Cecum: Aerobic bacteria; Rectum: *Bacteroides* and *Prevotella*.	10^{10}-10^{12}	High diversity and density, no digestive secretions, nutrient-poor environment, & slow transit time (30 h)

H. pylori: *Helicobacter pylori*.

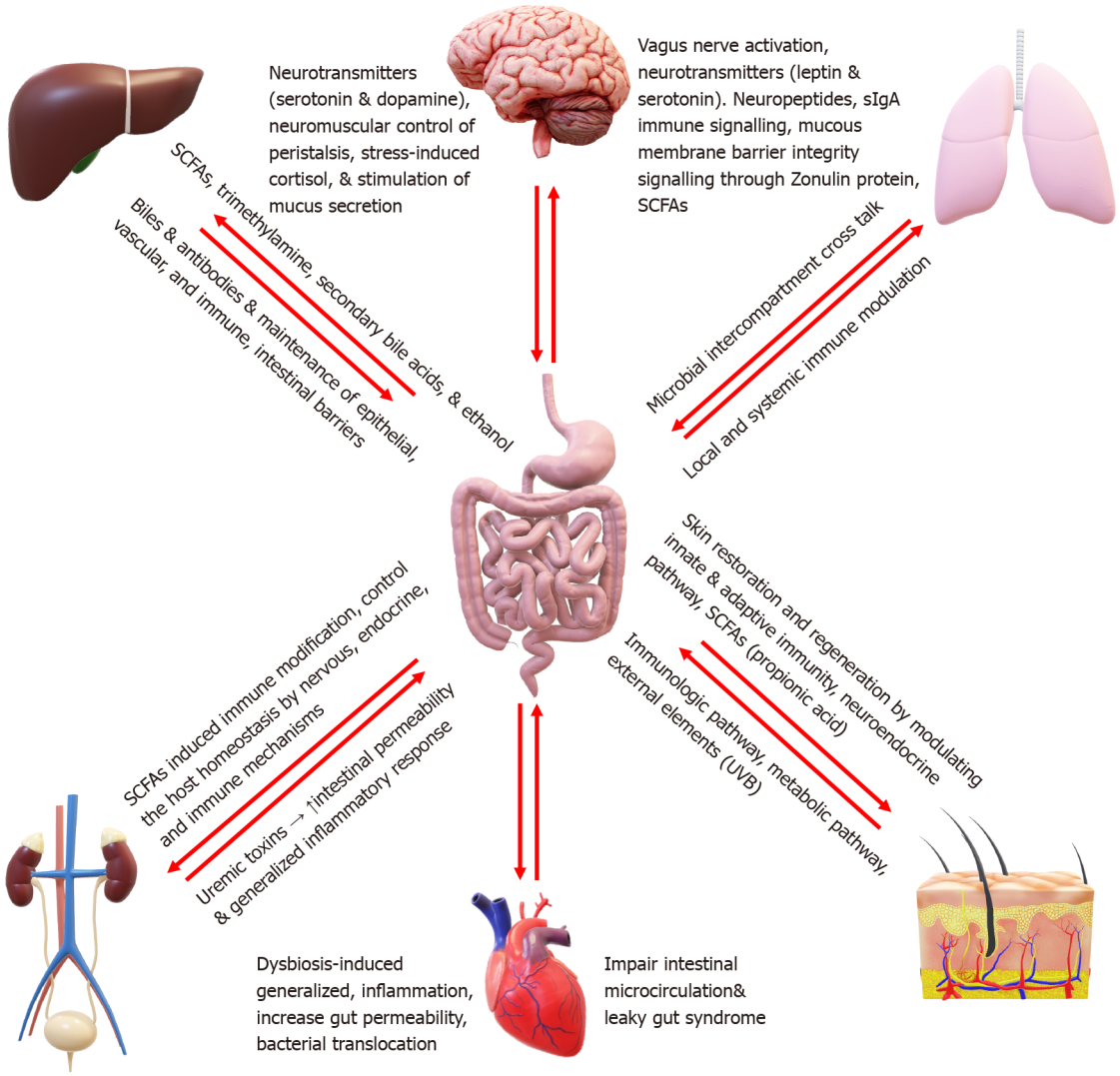
bottle feeding also significantly impacts the gut microbiota. Exclusively breastfed infants have lower microbial diversity with a predominance of infant-type *Bifidobacteria* than formula-fed babies whose gut microbiota is more diverse and like older children. The predominance of infant-type *Bifidobacteria* significantly impacts the immune system's maturation and development, which may help decrease the incidence of childhood infections[25].

The gut microbiota develops throughout human life in predictable patterns, with fast change from the neonatal pattern to the age of three, reaching the adult pattern. Then the microbiota goes into a stable phase until middle age, and then it goes into accelerated changes in late adulthood. These changes could be related to aging itself, underlying diseases, and the use of medications. At the same time, changes in the microbiota pattern can predict decreased longevity[26]. The use of the proton pump inhibitors is associated with decreased bacterial richness and predominance of an unhealthy gut microbiome which predisposes to *Clostridium difficile* enteric infections[27]. Antibiotics negatively impact the gut microbiota by reducing the species diversity, altering the metabolic activity, and favoring the predominance of antibiotic-resistant microbial strains, which sequentially can cause antibiotic-associated diarrhea and recurrent *Clostridium difficile* infections[28].

Microbial cooperation is a characteristic feature of microbial communities. An example of bacterial cooperation appears clearly in *Bacteroidales*, the predominant Gram-negative bacteria in the human gut. *Bacteroides ovatus* and *Bacteroides vulgatus* showed a mutual relation where *Bacteroides ovatus* can digest the dietary complex polysaccharide inulin producing energy and food source for other *Bacteroides*, including *Bacteroides vulgatus*. In return, *Bacteroides vulgatus* benefits *Bacteroides ovatus* by detoxifying inhibitory substances and the secretion of a depleted or growth-promoting factor. This bacterial cooperation is vital to stabilize the gut ecosystem[29]. Bacterial antagonism is common in microbial communities and contributes to specific bacterial strains' different compositions and relative abundance. It also helps for the long-term stability of the microbial community. This antagonism can occur by interference competition with the secretion of specific molecules such as antibacterial peptides and proteins that inhibit other strains. These antimicrobial toxins perform a significant role in microbiota-mediated colonization resistance by inhibiting the invasive pathogens[30]. Bacterial adhesion to gut epithelial surfaces affects their retention time and, therefore, considerably impacts interactions between the microbiota and their hosts. This adhesion ability of some bacteria could help their transient colonization in the gut and help to boost their immunomodulatory effects and enhance the gut barrier and metabolic functions[31].

GUT-MICROBIOTA AXES

The intestinal microbiota is considered an organ of the human body, with its features making it crucial in various body functioning. There is a mutual bidirectional relation of the gut, microbiota, and the other body systems, forming different systemic axes, *e.g.*, Brain-gut-microbiota axis, liver- gut-microbiota axis, skin- gut-microbiota axis, kidney- gut-microbiota axis, lung- gut-microbiota axis (Figure 1).



DOI: 10.3748/wjg.v28.i18.1875 **Copyright** ©The Author(s) 2022.

Figure 1 The different gut-microbiota-axes (brain-gut-microbiota axis, liver- gut-microbiota axis, skin- gut-microbiota axis, kidney- gut-microbiota axis, lung- gut-microbiota axis).

BRAIN-GUT-MICROBIOTA AXIS

The brain and the gut interact together through the central and the enteric nervous system. The brain interacts with the gut through several mechanisms, including neurocrine and endocrine pathways, which may be involved in gut microbiota-to-brain signaling, and the brain can, in turn, alter gut microbiota composition. The brain controls the gut and gut microbiota through neurotransmitters such as serotonin and dopamine, neuromuscular control of peristalsis, stress-induced cortisol, and stimulation of mucus secretion[32]. On the other hand, the gut affects the brain through vagus nerve activation, neuropeptides, and neurotransmitters such as leptin and serotonin, immune signaling through secretory IgA, mucous membrane barrier integrity signaling through Zonulin protein, and SCFAs such as butyrate[15,33]. Alternatively, the microbiota affects the brain through different mechanisms. Some strains of Lactobacillus and Bifidobacterium can produce gamma-aminobutyric acid (GABA), which is the dominant brain inhibitory neurotransmitter. Other bacterial species such as *Enterococcus* and *Escherichia* and some candida strains can produce serotonin. Some bacillus species can produce dopamine neurotransmitters. Bacteria can also affect the brain by making SCFAs (such as butyric acid, propionic acid, and acetic acid), stimulating the sympathetic nervous system, and inducing mucosal serotonin release sequentially, impacting the memory and learning process in the brain[34].

LIVER-GUT-MICROBIOTA AXIS

The liver-gut-microbiota axis is a bidirectional relationship between the liver and the gut and its

microbiota on the other side. The gut-derived products are transported directly to the liver through the portal veins, and the liver manufactures the bile and antibodies to be transported back to the intestine. The gut microbiota is essential for preserving the immune homeostasis of the liver-gut-microbiota axis. Microbe-derived metabolites, such as SCFAs, trimethylamine, secondary bile acids, and ethanol, may play a role in non-alcoholic fatty liver disease pathogenesis. On the other hand, liver cirrhosis induces intense changes in gut microbiota and impairment of the intestinal epithelial, vascular, and immune barriers[35]. A change in gut microbiota structure can activate the mucosal immune response triggering homeostasis imbalance. This imbalance results in bacterial transport and immune cells migrating to the liver, inducing inflammation-mediated liver injury and tumor progression[36,37].

HEART-GUT-MICROBIOTA AXIS

The heart-gut axis is relatively newly described based on intestinal microbiota's ability to affect the cardiovascular status and vice versa. Gut dysbiosis is linked to the state of generalized inflammation associated with increased risk of obesity and type II diabetes mellitus, which are important cardiovascular risk factors, especially for atherosclerosis and heart failure. At the same time, the diet that can cause dysbiosis, *e.g.*, a high fatty diet, can also cause metabolic syndrome. On the other side, Most cardiovascular disease (CVD) risk factors, such as aging, dietary patterns, obesity, and a sedentary lifestyle, can induce gut dysbiosis. Dysbiosis can also increase gut permeability, leaky gut syndrome, and bacterial translocation and are considered risk factors for CVD. Meanwhile, congestive heart failure will impair intestinal microcirculation aggravating the leaky gut syndrome and causing more bacterial translocation worsening the heart failure with a vicious cycle[38-40].

KIDNEY-GUT-MICROBIOTA AXIS

The gut microbiota has critical roles in various diseases involving hypertension and chronic kidney disease. The gut microbiota connects with the nervous, endocrine, and immune systems to control the host homeostasis, involving blood pressure and renal functions. The gut–kidney axis is conducted through metabolism-dependent mechanisms and immune pathways[41]. SCFAs produced by commensal gut microbiota can affect the kidneys through a wide range of mechanisms, including immune system modification and interactions with the renal cognate receptors and transporters[42]. On the other side, kidney injury causes uremic toxins accumulation in the intestine with increased intestinal permeability and generalized inflammatory response[43]. Uraemia increases bacterial translocation and impairs immunity by decreasing T and B cell responses from vaccination and decreasing the memory of T and B cells. Increased nitrogen waste products in uremia promote the overgrowth of proteolytic bacteria[44].

LUNG-GUT-MICROBIOTA AXIS

Despite the clear anatomical distinction between the gut and the lung, recent evidence showed that the gut and lung microbiota affect each other, significantly impacting respiratory diseases[45]. The lung microbiome is much lower than the gut microbiota. Its composition depends on the oropharynx and upper respiratory tract microbial colonization through salivary micro-inhalations, the host abilities for microbial elimination, primarily through cough and mucociliary clearance, the interactions with the host immune system, and on local conditions that control the microbial proliferation, such as oxygen concentration and local pH[46]. The lung microbiota composition is also strongly correlated with the gut microbiota composition. The gut microbiota enriches the lung bacteria, impacting the gut microbiota composition. For example, inhalation of gastroesophageal content (through gastroesophageal reflux) and sputum swallowing may explain this inter-organ connection. The lung-gut-microbiota axis may also involve indirect communications through the host immune modulation either by gut microbiota's local or systemic immune impact, especially on the pulmonary immune system[47].

SKIN-GUT-MICROBIOTA AXIS

Skin and gut play crucial immune and neuro-endocrine roles and are distinctively related in function. The gut microbiota affects the skin microbiome through the skin-gut-microbiota axis. SCFAs produced from fiber fermentation by gut microbiota have a significant role in skin microbiota composition and immune defense mechanisms[44]. Propionic acid has a powerful antimicrobial effect against the community-acquired methicillin-resistant Staphylococcus aureus[49]. Gut microbiota also helps skin

restoration and regeneration by modulating innate and adaptive immunity. It enhances the skin barrier through modulation of T cell differentiation in response to different immune stimuli[50]. Several environmental factors, *e.g.*, diet and psychological stress, can impact the gut microbiome, directly or indirectly influencing skin health.

GUT MICROBIOTA IN COMMON PEDIATRIC DISORDERS

Table 2 summarizes the disease-associated dysbiosis and the proposed probiotics.

GUT MICROBIOTA AND CHILD NEURODEVELOPMENT

Gut microbiota exerts a considerable effect on the child's physical and mental development. The human brain has a rapid growth rate throughout the perinatal period, matching the remarkable maternal and infant microbiota changes[51]. The microbiota plays an essential role during brain development through its effects on gamma-aminobutyric acid and serotonin synthesis from tryptophan and altered neurotransmitters such as noradrenaline and dopamine. Serotonin is crucial to brain development. Decreased brain serotonin impair synaptogenesis and the brain wiring, causing long-term neurodevelopmental impairment[52]. About 95% of the body's serotonin is formed by the gut microbiota, affecting mood and gastrointestinal activity. However, scientists found that serotonin cannot cross the blood-brain barrier. So, it works mainly on the peripheral enteric nervous system and works as a hormone affecting different tissues, including those regulating metabolic homeostasis[53]. However, the beneficial role of probiotics in alleviating the manifestation of many psychiatric disorders such as depression and anxiety could be related to their ability to secrete serotonin, a significant player in many psychiatric disorders[54]. Meanwhile, animal studies showed that probiotic use might cause rising plasma tryptophan levels, decreased serotonin concentrations in the frontal cortex, and decreased cortical dopamine metabolites, thus improving depressive symptoms[55].

SCFAs, a product from the fermenting effects of the colonic bacteria, regulate microglial homeostasis. The effects of SCFAs are markedly observed during the early phases of brain development during the early postnatal stage, while brain plasticity is still preserved[56]. Two interesting studies showed that gut microbiota is crucial to maintain healthy microglia functions, vital to preventing neurodevelopmental and neurodegenerative disorders[57,58]. Tamana *et al*[59] showed that boys who have a higher *Bacteroidetes* ratio in the gut microbiota at one year have higher cognitive functions and advanced linguistic skills after one year of follow-up. They also observed that girls have cognitive and linguistic scores than boys at the same age. They also noted a higher *Bacteroidetes* ratio in girls than boys. They related this increase in cognitive function due to the sphingolipid production by *Bacteroidetes*, which is an essential substrate for brain structures and functions. Factors that deplete *Bacteroidetes*, *e.g.*, caesarean section or flourish *Bacteroidetes* such as normal vaginal delivery, breastfeeding, high-fiber diet, exposure to pets, and outdoor nature with green spaces can negatively or positively impact child cognitive functions[60].

Investigating the underlying mechanisms of neural development and neuropsychiatric disorders proved that the intestinal microbiota could affect brain physiology and behavior through the humoral and neural pathways of gut-brain communication, suggesting that the gut microbiota has a vital role in many neuropsychiatric disorders[61]. Autism is a multifactorial disease in which the gut microbiota plays an important role. The gut microbiota in children with autism showed plenty of *Bacteroidetes* and a lesser amount of *Firmicutes* than controls with characteristic mucosal microbiota signatures. This dysbiosis observed in children with autism correlates with cytokine quantities and tryptophan homeostasis. However, we do not know whether the observed dysbiosis is a cause or a result of the associated behavior problem observed in children with autism[62,63]. The effect of the gut microbiota is not limited to the child's gut but is also related to the maternal gut microbiota. A study by Li *et al*[64] found significant differences in the gut microbiota composition between the mothers and children with autism spectrum disorder (ASD) compared to healthy children and their mothers. They found that mothers of children with ASD had more *Alphaproteobacteria, Proteobacteria, Acinetobacter, and Moraxellaceae* than mothers of healthy children. Children with late-onset (regressive) autism have more colony numbers of fecal clostridial species and non-spore-forming anaerobes and microaerophilic bacteria, which are absent in the typically developed children, which could be related to the frequent use of antibiotics, disrupting the microbiota with more colonization by these types of autism-promoting microbiota species[65]. According to this hypothesis, the use of minimally absorbed oral vancomycin can induce temporary improvement in autistic symptoms[66]. However, a metanalysis that included 28 studies done on children with autism by Bezawada *et al*[67] showed the inconsistency of the data due to heterogeneity of the included populations and the used methods. They suggested that despite several reasons to consider the role of gut microbiota and their product in the pathogenesis of autism, we need more studies to understand better and confirm their effects. The developing hypothesis of a microbiota-gut-brain axis proposes that gut microbiota modulation may be an amenable strategy to developing a

Table 2 The diseases-associated dysbiosis and the proposed probiotics

The disease	Encountered dysbiosis	The proposed probiotics
Autism[57,58]	Mother have abundance of *Alphaproteobacteria, Proteobacteria, Acinetobacter,* & *Moraxellaceae*. Children have more clostridial species, non-spore-forming anaerobes, and microaerophilic bacteria	No suggested type yet
Malnutrition[60]	Less Bifidobacteria. More pathogenic microbes (Escherichia coli, Fusobacterium mortiferum, & Streptococcus spp.)	The lack of strong evidence for specific types of probiotics
Obesity[75-78]	Less *bifidobacteria*. More *Bacteroides* & Staphylococcus spp.	Bifidobacterium lactis and Lactobacillus GG
Infant colic[85-87]	More abundance of *Proteobacteria*. Less abundance of the genera *Lactobacillus* & *Bifidobacterium*. Reduced gut bacterial diversity	Lactobacillus reuteri DSM17938 in breastfeeding infants
Functional abdominal pain[90,91]	More *Prevotella*, *Lactobacillus*, *Veillonella*, & *Parasporo* bacterium. Less *Verrucomicrobium* & *Bifidobacterium*	Sporobacter & Subdoligranulum
Functional constipation[94,95]	More Prevotella. More butyrate-producing bacteria as Roseburia, Coprococcus, & Faecalibacterium	Still investigational
Necrotizing entero-colitis[98,99]	More Citrobacter koseri and/or Klebsiella pneumoniae. Reduced diversity. Less Lactobacillus abundance	*Bifidobacteria* and *Lactobacillus*
Helicobacter pylori infection[102,106,107]	Prevotella, Clostridium, Proteobacteria, and Firmicutes. Less Bacteroides	Saccharomyces boulardii, L. acidophilus, L. casei DN-114001, L. gasseri, and Bifidobacterium infantis 2036 and Lactobacillus reuteri Gastrus
Coeliac disease[109, 114-116]	Reduced Gram-positive/Gram-negative bacteria ratio. Less *Bifidobacterium, Clostridium histolyticum, Clostridium. lituseburense* and *Faecalibacterium prausnitzii*. More *Bacteroides-Prevotella* group. Less IgA coating the *Bacteroides-Prevotella* group	*Lactobacillus rhamnosus, Bifidobactera breve* & *Longum,* and *Lactobacilli* strains (*L. ruminis, L. Johndoni, L. amylovorus, L. salivaris*)
Inflammatory bowel diseases[122,126-128]	Less abundance of the healthy commensal (such as Clostridium IXa and IV groups, Bacteroides, Bifidobacteria). More abundance of the pathogenic bacteria as sulphate-reducing Escherichia coli	Still controversial. Saccharomyces boulardi. Escherichia coli Nissle1917, Bifidobacterium breve, Bifidobacterium bifidum, Lactobacillus acidophilus
Cystic fibrosis[135-137]	Aberrant colonization of gut and respiratory microbiota due to altered intestinal & airway microenvironment	*Lactobacillus rhamnosus GG* & *Lactobacillus reuteri*
Allergic rhinitis[140, 142-144]	Decrease gut bacterial diversity	*Lactobacillus paracasei*. *Bifidobacteria* mixture
Bronchial asthma[147]	Relative abundance of the bacterial genera *Rothia*, *Veillonella*, *Lachnospira*, & *Faecalibacterium*. Low total & gut microbial diversity	Still controversial
Atopic dermatitis[154-157]	Reduced microbial diversity. More abundance of pathogenic Staphylococcus aureus and Malassezia. Presence of Clostridioides difficile. More Bifidobacteria abundance. Lower lactobacilli abundance	Topical Roseomonas mucosa
Psoriasis[160,161,163, 164]	More bacterial diversity & heterogeneity. More *Staphylococcus aureus*. Less Staphylococcus epidermidis & Propionibacterium acnes. Reduced microbiota stability. Variable topographic dysbiosis	Sill controversial. Oral Lactobacillus, one sachet thrice daily with biotin
Systemic lupus erythematosus[166, 168]	Less microbiota abundance and diversity	Animal studies showed *Lactobacillus fermentum* CECT5716 (LC40)
Juvenile idiopathic arthritis[172,174]	Less Faecalibacterium Prausnitzii abundance. More Bifidobacterium abundance, mostly B. adolescentis	Not conclusive. Trial with Lactobacillus acidophilus, Lactobacillus casei, Lactobacillus bulgaricus, Lactobacillus rhamnosus, Bifidobacterium breve, Streptococcus thermophile & Bifidobacterium longum
Dental caries[176,178, 179]	More abundance of Prevotella melaninogenica, Leptotrichia shahii, Leptotrichia HOT 498, Veillonella dispar, and Streptococcus mutans	Insufficient evidence. Lactobacillus rhamnosus may help
Chronic congestive heart failure[180,184, 187,189]	Decreased gut microbiota diversity. More pathogenic Microbes as *Campylobacter, Yersinia enterocolitica, Salmonella, Shigella* & *candida*. Low *Coriobacteriaceae*, *Erysipelotrichaceae* and *Ruminococcaceae*	*Bifidobacteria,* yeasts, and lactic acid-producing bacteria such as *Lactobacillus rhamnosus* GR-1. *Saccharomyces boulardii*

new therapeutic approach for complex central nervous system disorders[68].

Epilepsy is a common childhood disorder. There is a close relation between epilepsy and autoimmune diseases and between gut microbiota and autoimmune disease; a suggested association arises between epilepsy and gut microbiota. An exciting study by Huang *et al*[69] presented forty children who developed benign infantile convulsions after mild gastroenteritis, linking changing the gut microbiota and the epileptogenesis. Şafak *et al*[70] tried to elaborate on the relationship between gut microbiota and epileptogenesis. They studied the intestinal microbiota composition in patients with idiopathic focal epilepsy and compared them to a healthy volunteer group. They found an increased prevalence of *Fusobacteria species* in patients with epilepsy (10.6%) but not in the healthy volunteer

group. This significant taxonomic drift and variations in the intestinal microbiota and the resulting gut dysbiosis may be associated with certain forms of epilepsy.

Meanwhile, some anticonvulsants can be metabolized by the gut microbiota, affecting their efficacy. For example, the intestinal microbiota can metabolize Zonisamide to 2-sulfamoyl-acetyl-phenol, which is pharmacologically not active[71]. In addition, the anti-epileptic effects of the ketogenic diet used in drug-resistance epilepsy (although its exact mechanism of action is unclear) could be related to the ketogenic diet-induced changes in the gut microbiome composition and function of patients with epilepsy. The gut microbes modify the seizure vulnerability through mechanisms different from just alterations of beta-hydroxybutyrate levels (a measure of ketosis). The anti-seizure protective effects of diet and microbiota are associated with elevating hippocampal GABA relative to glutamate content[72]. The probiotics supplement could provide additional benefits to the anti-epileptics, especially in drug-resistant epilepsy. Gómez-Eguílaz *et al*[73] supplied patients with drug-resistant epilepsy with a probiotic mixture for four months. The patients showed a significant reduction in seizures frequency and improved quality of their life. Consequently, reformation of the gut microbiota through fecal microbiota transplantation, probiotic supplement, and the ketogenic diet has potential favorable impacts on drug-resistant epilepsy[74].

GUT MICROBIOTA AND CHILD PHYSICAL DEVELOPMENT AND NUTRITION

The gut microbiota typically develops hand in hand with the child's growth. The prenatal microbial communities affect fetal and postnatal development. Maternal microbiota is a crucial element for intrauterine growth. An exciting study by Sato *et al*[75] showed that the maternal gut microbiota correlates with the neonatal anthropometrics measures. In male neonates, the head circumference and weight are negatively correlated with genus *Eggerthella* and *Parabacteroides*. In female neonates, a high ratio of *Streptococcus* correlates with low anthropometric measures. Neonates with very low birth weight and restricted extrauterine growth had a predominance of *Proteobacteria* of their intestinal microbiota [76]. The gut microbiota affects growth by affecting growth hormone and insulin-like growth factor 1 production and regulation through its effects on the hypothalamic-pituitary–somatotropic axis. Delayed maturation and colonization of the gut microbiota may result from underlying food insecurity, malnutrition, and infections and could negatively impact the child's nutritional status[77]. The malnutrition-associated dysbiosis of the gut microbiota starts with depletion of the *Bifidobacteria* followed by the establishment of potentially pathogenic microbes (*Escherichia coli, Fusobacterium mortiferum*, and *Streptococcus spp*.), causing diarrhea and essential nutrients malabsorption[78]. Dysbiosis may result in a generalized inflammatory state and enteropathy that may precipitate growth faltering. The effects of these microbiota changes are significant in the first 1000 d. It provides a window of opportunity for modifying the gut microbiota through different interventions such as diet, antibiotic use, supplementary probiotics, prebiotics, symbiotics, postbiotics, or fecal microbiota transplantation to restore the proper growth and development[79].

Dysbiosis may explain why malnourished children may miss up the desired weight compared to their well-fed counterparts, despite gaining some weight and growing better with nutrient-rich supplements. Subramanian *et al*[80] showed significant differences in the proportions and species of gut microbiota in children up to two years of age with and without malnutrition. Children with malnutrition showed the immaturity of their gut microbiota, resembling their healthy counterparts but at a younger age. This malnutrition-induced microbiota imbalance fails to recover even after correcting the malnutrition. Oral probiotic supplements with beneficial gut bacteria and fecal transplantation from healthy children can restore the malnutrition-induced dysbiosis, and the malnourished children thrive. Probiotic supplements can improve a child's growth by preventing infections and micronutrient deficiency. They have been shown to improve the absorption of specific nutrients (vitamin B12, calcium, and zinc) and decrease the possibility of anemia[81]. However, there is no clear evidence to use them in the treatment of malnutrition. This lack of evidence is also augmented by the difficulty of modifying the gut microbiota. It resists long-term change and is affected by other factors such as diet and sleep pattern [82].

The cause of malnutrition also impacts the composition of gut microbiota. For example, moderate-to-severe diarrhea in children reduces bacterial diversity and changes gut microbiota composition[83]. Diarrhea can also affect weight, height, and the child's mental development, especially for diarrhea occurring below the age of 2 years[84]. The diarrhea-induced changes in gut microbiota increase the risk of persistent diarrhea, which causes stunted growth and decreases the affected children's mental abilities. Interventions to restore the gut microbiota as prebiotic and probiotic supplementation could help to combat the risk of diarrhea and the resulting malnutrition[85].

Meanwhile, subclinical changes in the gut microbiota may result in stunting even in the absence of clinically evident infections such as diarrhea. For example, poor hygiene may cause persistent exposure to environmental pathogens inducing subclinical alteration in the gut microbiota structure and function and consequently cause stunting[86]. For instance, poor sanitary conditions with chronic exposure to environmental pathogens resulting in subclinical alteration in the gut microbiota structure and function

initiate a condition known as environmental enteric dysfunction. This environmental enteric dysfunction induces a cell-mediated inflammation that ends in stunting[87].

CHILDHOOD OBESITY

The link between gut microbiota and obesity was evident in the adult population but not yet well documented in childhood. Obesity correlates with altered gut microbiota distinguished by raised *Firmicutes* and reduced *Bacteroidetes* abundance. This correlation is believed to be through the powerful effects of the gut microbiota on the human metabolic and immune status. Higher levels of SCFAs, a fermentation product by the gut microbiota, were found in children with obesity which tightened the relationship between the gut microbiota and the development of obesity[88]. The maturation patterns of gut microbiota in infancy can impact the relative chance of developing overweight and obesity in later childhood. Pregnant women with a high body mass index (BMI) have a higher load of *Bacteroides* than those with normal BMI[89].

Consequently, the maternal microbiota during pregnancy and breastfeeding significantly affects the newborn microbiota. The presence of *Bacteroides spp.* or their relatives and the relative lower abundances of *Bifidobacteria* in early infancy are related to developing childhood overweight and obesity. *Staphylococcus* spices may also serve as a predictive but inconsistent tool for childhood BMI[90]. Children with an average BMI at seven years have more *Bifidobacterium spp.* in their gut during their first year of life than children with high BMI[91]. Gut microbiota could modify obesity through its role in metabolic regulation, food availability, and digestion. Gut microbiota has extra-intestinal effects involving the brain, liver, and adipose tissue, possibly linked to obesity, insulin resistance, diabetes mellitus type-II, and related cardiovascular disorders. Gut microbiota might also impact food intake and satiation through gut peptide signaling[92].

Consequently, gut microbiota can modify energy regulation and systemic inflammation, two crucial pillars for obesity development. Early modification and restoration of gut microbiota may be an encouraging tool to counteract the increasing childhood metabolic disorders, including overweight and obesity, providing the specific anti-obesity microbiota[93]. Despite the evidence of the beneficial effects of probiotics on glucose tolerance, insulin sensitivity, and inflammatory markers, there is no substantial evidence to recommend the use of probiotics in obesity[94]. Antenatal supplement with *Bifidobacterium lactis and Lactobacillus GG* decreases the risk of gestational diabetes mellitus and consequently reduces the risk of macrosomia and large baby size at birth, an effect that could last up to six months after birth [95,96].

GUT MICROBIOTA AND FUNCTIONAL GASTROINTESTINAL DISORDERS IN INFANCY AND CHILDHOOD

Gut microbiota can modulate various types of chronic pain through direct modulation of neuronal excitability dorsal root ganglia and neuroinflammation regulation in the central and peripheral nervous systems[97]. Numerous studies reported a strong association between the human gut microbiota and the development of functional gastrointestinal disorders, especially for infant colic, functional constipation, and irritable bowel disease. Randomized controlled trials showed that probiotics could be helpful in a variety of functional gastrointestinal disorders, including infant colic and irritable bowel syndrome. Probiotics may induce gut microbiota diversity with strain-specific effects on colonization resistance, the integrity of the epithelial barrier, signal transduction modulation, with a significant impact on both innate and adaptive immune responses, and notable effects on visceral hyperalgesia[98,99].

Infant colic

About 20% of infants developed infant colic, with prolonged crying without apparent cause. The exact etiology of infant colic is unknown, but many factors are proposed to have a role, such as gastrointestinal, psychosocial, and neurodevelopmental factors[100]. Several studies addressed the role of the gut microbiota in developing infant colic. Gut dysbiosis was described in infant colic in the form of more abundance of *Proteobacteria* and less abundance of the genera *Lactobacillus* and *Bifidobacterium* with reduced gut bacterial diversity[101]. A metanalysis done by Sung *et al*[102] showed that *Lactobacillus reuteri* DSM17938 was an effective treatment for infant colic in breastfed infants. Still, they cannot generalize this recommendation to formula-fed infants with colic, which needs further research. The unique effect of *Lactobacillus reuteri* DSM17938 in the breastfed infant may be related to the distinctive structure of breast milk or probably the direct effects of *Lactobacillus reuteri* or human milk oligosaccharides in breast milk[103]. How probiotics improve infant colic is not yet determined but may be mediated *via* modifying the activity of the colonic intrinsic sensory neurons with improving the gut motility. In addition, they have positive impacts on function and visceral pain[104].

Functional abdominal pain

About one-third of the school-aged children suffer from abdominal pain weekly, which causes school absenteeism and limitation of their social activities in about 20% of them. In children, functional abdominal pain is defined as when it persists for two or more months without an evident organic cause [105]. Function abdominal pain is further subclassified into four conditions: irritable bowel syndrome (IBS), functional dyspepsia, abdominal migraine, and functional abdominal pain not otherwise specified [106]. Despite the high prevalence of dysfunctional abdominal pain, the exact pathogenesis is not well-defined. However, many risk factors increase the rate of dysfunctional abdominal pain, including the winter season, sleep, school stress, and diet. Many studies relate dysbiosis of the gut microbiota to dysfunctional abdominal pain such as irritable bowel syndrome. Rigsbee *et al*[107] showed that children with irritable bowel syndrome had more abundance of *Prevotella*, *Lactobacillus*, *Veillonella*, and *Parasporo* bacterium and less quantity of *Verrucomicrobium* and *Bifidobacterium*.

On the other hand, a low fermentable substrate diet decreased the abdominal pain frequency in children with irritable bowel syndrome by increasing the abundance of bacterial taxa belonging to the genera *Sporobacter* and *Subdoligranulum* and reduced the abundance of taxa belonging to *Bacteroides* [108]. Probiotic use might change the gut microbiota composition and decrease inflammation. It could also promote the physiology of the gut and improve functional symptoms. Some probiotics may impact colonic motility by increasing stool fluidity through modifying water and electrolytes secretion and absorption, smooth muscle cell contractions modification, increasing the production of lactate and SCFAs, and reducing intraluminal pH[109].

Functional constipation

Functional constipation is a common childhood disorder characterized by reduced gut movements and/or hard stools without organic causes. Functional constipation affects about 18% of infants and 3% of children and adolescents worldwide, with considerable influence on the child's and family's quality of life[110]. The pathophysiology of functional constipation is multifactorial, with a complex interaction between gastrointestinal dysmotility, psychological factors, and gut microbiota. Disturbances in gut microbiota may promote development and affect the outcome of functional constipation in children [111]. Zhu *et al*[112] showed that obese children suffering from constipation had a low-fiber diet and lower prevalence of gut *Prevotella* with an increased ratio of butyrate-producing bacteria such as *Roseburia*, *Coprococcus,* and *Faecalibacterium* than the control, which could be related to the low fiber intake. Probiotics can enhance intestinal transit time, stool frequency, and consistency[113]. Data about the efficacy of probiotic use to treat functional constipation are conflicting. A metanalysis by Gomes *et al* [114] showed that "despite the probiotics' positive effects on certain characteristics of the intestinal habitat, there is still no evidence to recommend it in the treatment of constipation in pediatrics". So, the use of probiotics to treat functional constipation is still investigational.

GUT MICROBIOTA AND GASTROINTESTINAL DISEASES IN INFANCY AND CHILDHOOD

Necrotizing enterocolitis

Necrotizing enterocolitis (NEC) is a significant danger to neonatal life, especially preterm neonates. Prematurity is associated with many risk factors that alter the infant microbiome. These factors include mode of delivery, maternal microbiome diversity, feeding pattern, antibiotic use, environmental exposure to pathogenic and commensal bacteria in the neonatal intensive care unit[115]. Dysbiosis, alterations in the gut microbiome, and low microbial diversity of the preterm neonate significantly correlate with a higher risk and raised rate of complication of necrotizing enterocolitis and, consequently, the development of late-onset sepsis. Low microbiota diversity may provoke pathogenic bacteria overgrowth, a significant risk factor that promotes NEC development[116]. Dobbler *et al*[117] found powerful domination of *Citrobacter koseri* and/or *Klebsiella pneumoniae*, reduced diversity, less *Lactobacillus* abundance, and an altered microbial-network structure during the first days of life, correlate with NEC risk in preterm infants.

Oral administration of probiotics shows a significant reduction of NEC incidence. However, their safety still needs to be proven as preterm babies have immature immune systems with possible vulnerability even to the commensal bacteria[115]. Probiotic supplementation allows restoration of the normal commensal bacteria with the transition to the beneficial bacteria through enhancement of mucosal barrier function competitive inhibition of the pathogenic bacteria. It induces an anti-inflammatory effect on mucosal signaling[118]. Probiotics upregulate the cytoprotective genes of the gut and down-regulate the pro-inflammatory gene expression. They also enhance butyrate and other SCFAs productions to nourish colonocytes. Some probiotics decrease the pH and lower the oxygen tension in the intestinal lumen, thus inhibiting the growth of pathogenic bacteria, especially *Enterobacteriaceae*. Other probiotics can support the maturation intestinal barrier and functions and regulate cellular immunity through balancing the Th1:Th2 ratio[119].

Helicobacter pylori infection

Helicobacter pylori (*H. pylori*) is a flagellated, spiral-shaped, Gram-negative bacillus that colonizes the human gastric mucosa causing gastric mucosa inflammatory response, gastric and/or duodenal ulcers, intestinal metaplasia, or even gastric cancer[120]. *H. pylori* infection in children differs from the adults in the prevalence, rate of complications, difficulties in diagnosis, and the higher rate of antibiotic resistance. The prevalence of *H. pylori* in children is higher in developing countries (20%) than in developed countries (0.5%)[121]. *H. pylori* infection in children increases the risk of gut colonization with *Prevotella, Clostridium, Proteobacteria, and Firmicutes* compared to children without infection who have more *Bacteroides*. These changes in the gut microbiota associated with *H. pylori* infection could be related to the development of chronic gastrointestinal diseases and drug resistance[122]. Eradication of *H. pylori* has a positive and negative impact on the host. It may restore the gut microbiota with decreased abundance of *Bacteroidetes* and increase *Firmicutes*, producing plenty of SCFAs with positive and negative effects[123]. While supplements with probiotic strain can improve infection conditions, it is not enough to eradicate *H. pylori* infection[124]. Adding probiotics to the traditional triple therapy to eliminate *H. pylori* increases the chance of successful treatment and decreases the therapy-related side effects compared to treatment without probiotics[125]. The addition of *Saccharomyces boulardii* to the standard treatment of *H. pylori* increases the eradication rate and reduces the therapy-related side effects [126]. Addition of *Lactobacillus*- and *Bifidobacterium*-containing probiotics such as *L. acidophilus*, *L. casei* DN-114001, *L. gasseri*, *Bifidobacterium infantis* 2036, and *Lactobacillus reuteri Gastrus h*ad the same beneficial effects during *H. pylori* therapy[127]. Various studies reported that certain probiotic strains could demonstrate an inhibitory activity against *H. pylori* bacteria. In contrast, other strains can ease the side effects of antibiotic therapy and subsequently improve the *H. pylori* eradication rate[128].

Coeliac disease

Coeliac disease (CD) is a life-long chronic autoimmune inflammatory systemic disorder but mainly affects the small intestine due to a deviated immune response to dietary gluten proteins (glutenins and gliadins) in genetically susceptible individuals. Several risk factors increase the risk of CD, including a family history of CD or dermatitis herpetiformis, delivery with caesarean section, type-1 diabetes mellitus, chromosomal abnormalities (Down syndrome or Turner syndrome), Addison's disease, and presence of other autoimmune disorders as autoimmune thyroiditis, or microscopic colitis[129]. As mucosal immune response *via* IgA secretion is among the first defense lines accountable for neutralizing harmful antigens and pathogens, patients with CD have significantly lower levels of IgA-coated fecal bacteria than in healthy controls. De Palma *et al*[130] found a significant reduction of the Gram-positive/Gram-negative bacteria ratio in patients with CD than in healthy controls. They also found less predominance of *Bifidobacterium, Clostridium histolyticum, Clostridium lituseburense and Faecalibacterium prausnitzii*, more abundance of *Bacteroides-Prevotella* group, and reduced IgA coating the *Bacteroides-Prevotella* group. Dysbiosis and predominance of the bacteria associated with the development of CD can be a risk factor for CD, either by its direct effects on the mucosal immune responses or by increasing the inflammatory reactions to gluten[131]. Fasano *et al*[132] found increased Zonulin expression in the intestinal tissues during flaring of celiac disease. Zonulin is a human protein like a toxin derived from *Vibrio cholera* called Zonula occludens toxin. Both Zonulin and Zonula occludens toxin increase intestinal permeability by decreasing the mucosal epithelium's tight intercellular junction.

Meanwhile, dysbiosis may result in a complication of the strict gluten-free diet, which reduces the beneficial bacteria, especially *Bifidobacterium* and *Lactobacillus*, and abundance of gram-negative bacteria such as *Bacteroides* and *Escherichia coli*[133]. The gluten-free diet-induced dysbiosis results from excluding crucial dietary carbohydrate resources, the primary resources for the energy required by the beneficial bacteria[134]. Despite being the only available treatment for CD, compliance with the gluten-free diet is complex. Consequently, there is a strong need for alternative therapy. Probiotics could supplement a gluten-free diet in patients refractory to the gluten-free diet. Probiotics can help to support the gluten-free diet through different mechanisms: improving the intestinal barrier function by *Lactobacillus rhamnosus* containing probiotics[135], anti-inflammatory modulation by *Bifidobacterium breve* and *Bifidobacterium longum*[136], and gluten degradation, lysing the proline/glutamine-rich gluten peptides, and reduction of the gluten concentration and toxicity by *Lactobacilli* strains (*L. ruminis, L. Johndoni, L. amylovorus, L. salivaris*)[137]. The use of probiotics enriched with *Lactobacilli* species may relieve the effects of accidental or contaminant gluten exposure by chopping up gluten proteins into smaller portions, not triggering an immune reaction or damaging the patients[138]. However, we need more studies and effort to evaluate probiotics in CD management.

Inflammatory bowel diseases

Inflammatory bowel diseases (IBD, Crohn's disease, ulcerative colitis, and unclassified) are a group of chronic, relapsing, and remitting inflammatory diseases of the gastrointestinal tract in a genetically predisposed person due to an aberrant immune response against gut microbiota, causing intestinal damage[139]. About 25% of the patients develop the disease before the age of 20 years, 18% before the age of 10 years, and 4% before the age of 5 years, and still on the rise[140]. Crohn's disease and ulcerative colitis affect the terminal ileum and colon, where there is heavy bacterial colonization. The

presence of IgG antibodies and hyperactive presentation of T-lymphocytes in the intestinal mucosa indicates a decrease in the local tolerance mechanisms[141]. In normal situations, the commensal bacteria cannot invade the intestinal mucosal barrier. Even when succussed to pass through it, it is rapidly phagocytosed and eliminated by the mucosal macrophage. Under unusual conditions, these commensal bacteria can cross the mucosal barrier and induce the inflammatory cascade[142]. Fava *et al* [143] found that patients with IBDs have different microbiota composition than that observed in the healthy controls, with decreased abundance of the healthy commensal (such as *Clostridium* IXa and IV groups, *Bacteroides*, *Bifidobacteria*) and increased the pathogenic bacteria as sulfate-reducing *Escherichia coli* reaching up to 40% of the dominant bacteria and consequently decreasing the microbiota diversity. The observed dysbiosis coupled with defective innate immunity and reduced bacterial killing ability due to impaired phagocytosis, decreased mucosal IgA and defensins, and over destructive adaptive immunity with ineffective regulatory T cells and antigen-presenting cells initiate the process of the pathogenesis of IBDs[144].

Treatment of pediatric IBDs is one of the fundamental challenges to pediatricians with frequent treatment failure and numerous therapy-associated side effects. Gut microbiota modification is one of the promising therapies for IBDs but is still controversial. Probiotics supplementation can restore the metabolic activity of the intestinal microbiota and modify their relative components by inhibiting the pathogenic bacterial overgrowth, decomposing their antigen, secreting antimicrobial substances, and increasing mucosal IgA. Probiotics also help to improve mucosal barrier function and preserve their integrity by tightening the epithelial junction and stabilizing the intestinal permeability. They also modulate intestinal epithelial and mucosal cells' immune response and induce T-cell apoptosis. Consequently, probiotics regulate the immune response and decrease the production of pro-inflammatory factors[145,146].

However, probiotic treatment for IBDs is still controversial. Vilela *et al*[147] showed that administering *Saccharomyces boulardii* helped maintain remission, improve intestinal permeability, and bowel sealing in patients with Crohn's disease. Kato *et al*[148] and Kruis *et al*[149] showed that *Escherichia coli* Nissle1917, *Bifidobacterium breve*, *Bifidobacterium bifidum*, and *Lactobacillus acidophilus* showed a promising effect on in maintaining the remission phase in patients with ulcerative colitis as effective as the standard mesalazine therapy but with high safety and tolerability profiles. However, Bousvaros *et al* [150] showed that the addition of probiotic *Lactobacillus rhamnosus* strain GG (LGG) to the standard therapy showed no significant differences compared to placebo in prolonging remission in children with Crohn's disease. Moreover, we need more randomized controlled studies to evaluate the effectiveness of *Lactobacillus GG* and other probiotic strains in children with IBDs.

GUT MICROBIOTA AND RESPIRATORY DISORDERS IN INFANCY AND CHILDHOOD

The gastrointestinal microbiota plays a crucial role in future lung development and future health status. Perinatal antibiotic use induces highly selective alterations on the resident gut microbiota, leading to precise modifications in susceptibility to TH2- or TH1-/TH17- determined lung inflammatory disorders [151].

The coronavirus disease 2019 infections in childhood

The coronavirus disease 2019 (COVID-19) is a real worldwide threat for all individuals of different ages, including children. Despite being mainly a respiratory disease, the gastrointestinal tract is a significant target, especially children. The virus can actively infect the gastrointestinal tract cells and replicate in the epithelium of the small and large intestine, stimulating an excessive immunological reaction in the host [152]. Angiotensin-converting enzyme-2 (ACE2) receptors are highly expressed in the upper esophagus and absorptive enterocytes from the ileum till the colon. The ACE2 receptor is an essential receptor for the virus entry to the cell membrane of host cells, with the interaction between the S protein of severe acute respiratory syndrome coronavirus-2 (SARS-CoV-2). This interaction induces a state of an inflammatory cascade that ends with dysbiosis and leaky gut syndrome. The degree of expression of ACE2 throughout the gut is an essential factor that aggravates or alleviates the resulting gut dysbiosis and gastrointestinal leakage[153]. Meanwhile, SARS-CoV-2 infection causes many plasma cells and lymphocytes infiltration. It possibly provokes interstitial edema and the deterioration of the intestinal-blood barrier, causing the spread of endotoxins, viruses, bacteria, and microbial metabolites into the systemic circulation, impairing the host's response to SARS-CoV-2 infection and causing multisystem dysfunction and even septic shock[154].

The resulting dysbiosis lasts for a long time after clearance of SARS-CoV-2 virus from the body, indicating the presence of a more long-long-term harmful effect on the gut microbiome, in the form of reduced beneficial bacteria such as *Lactobacillus*, *Bifidobacterium,* and *Faecalibacterium prausnitzii* and more abundance of *Clostridium hathewayi, Clostridium ramosum, Coprobacillus, Candida* and *Aspergillus.* The presence of comorbidities such as diabetes mellitus, hypertension, and old age, and antibiotics, antivirals, antifungal, and steroid use increase dysbiosis severity[155]. Diversity of the gut microbiota and the gut predominance of beneficial bacteria share in determining the course of COVID-19 infection.

Restoring the gut microbiota diversity could help improve the severity of the disease. Dietary supplements with specialized pre/probiotics such as fructooligosaccharide, galactooligosaccharide could improve gut dysbiosis, especially in patients presenting with gastrointestinal manifestations such as diarrhea and thus improving the overall immune response in these patients[156]. Probiotics can produce bioactive peptides capable of inhibiting the ACE receptors by blocking the active sites, preventing the entry of SARS-CoV-2 from attacking the enterocytes. We can use prebiotics, probiotics, or symbiotics to protect the high-risk groups, such as healthy contacts with a suspected case or the front-line caregivers[157]. However, microbiota modulation as a treatment method of patients with COVID-19 disease is based on indirect evidence and needs further studies.

Cystic fibrosis

Cystic fibrosis is an inherited systemic disease that produces severe injury to the lungs, digestive system, and other body organs and might lead to death. The relation between the microbiota and cystic fibrosis is bidirectional. Loss of the function of cystic fibrosis transmembrane conductance regulator results in aberrant colonization of gut and respiratory microbiota due to altered intestinal and airway microenvironment even in the absence of antibiotic use[158,159]. Homozygous cystic fibrosis is associated with more significant changes in the gut microbiome and the severity of the disease. The resulting changes in the gut microbiota associated with cystic fibrosis induce changes in the airway microbiota due to the dynamic interaction between gut and airway microbiota[160].

On the other hand, the gut microbiota could impact the disease severity and progression. Restoration of the gut microbiota in cystic fibrosis either by adding oral probiotics, prebiotics, or even postbiotics by adding certain bacterial strains, indigestible fibers, or SCFAs; namely, butyrate improves the gut and the systemic inflammation, energy intake, nutritional status, and the respiratory function of the patients [161]. Oral probiotic intake, especially with LGG and *Lactobacillus reuteri*, can reduce inflammation, improve body weight, reduce pulmonary exacerbations, and upper respiratory infections and improve the pulmonary functions in children with cystic fibrosis with mild-to-moderate lung disease. These effects are related to the probiotics' anti-inflammatory and immunomodulatory properties and their impact on the intestinal barrier[162-164]. However, a recent multicentre study by Bruzzese *et al*[165] showed that LGG supplementation had no significant effect on the respiratory and nutritional outcomes in a large group of children with cystic fibrosis. This study's failure to show a beneficial effect for LGG supplementation could be related to the lower dose of probiotics. They used 109 colony-forming units instead of 1010 in the previous two studies. Meanwhile, we remain in need of more studies to confirm these effects.

Allergic rhinitis

Allergic rhinitis in children has a significant impact on the child's health with many comorbidities, impaired quality of life, and poor educational performance. It may progress to asthma or complicate the control of existing asthma[166]. Many factors that cause decreased microbial diversity (*e.g.*, delivery by caesarean section) are associated with an increased risk of allergic rhinitis and other atopic diseases such as atopic dermatitis and asthma. Bisgaard *et al*[167] found that the bacterial diversity in the early gut microbiota at one and twelve months after birth was negatively associated with the increased risk of allergic sensitization, peripheral blood eosinophilia, and allergic rhinitis. As the gut microbiome shows significant development during the first year of life, it is highly susceptible to disruption during that time. Early antibiotic use has a significant adverse effect on the gut microbiota by modifying the relative abundance of the bacterial composition and initiating dysbiosis, with increasing the risk for childhood allergic diseases[168].

Oral Probiotic supplementation can alter the gut microbiota in children with notable positive immunomodulatory effects help prevention of allergic diseases, including allergic rhinitis. Lin *et al*[169] examined the effects of *Lactobacillus paracasei* supplementation on the treatment of perennial allergic rhinitis in children between 6-13 years. They found significant improvement in individual parameters in the rhino-conjunctivitis quality of life questionnaires, including sneezing, nasal itching, and swollen puffy eyes in the supplemented group, but without significant effects on total symptom score and the nasal total symptoms score. Miraglia Del Giudice *et al*[170] found that children supplemented with probiotic *Bifidobacteria* mixture for four weeks achieved a significant improvement of allergic rhinitis symptoms than the control without probiotic supplementation. A metanalysis by Güvenç *et al*[171] showed the evident beneficial immunologic and clinical effects of probiotics, especially for *Lactobacillus paracasei*-33 strains in managing patients with allergic rhinitis despite the high heterogeneity among the included studies. However, despite the beneficial effects of probiotics in improving allergic rhinitis symptoms and the patient quality of life, there is limited evidence for the primary preventive role of probiotics supplementations in children with a high risk of allergic rhinitis[172,173].

Bronchial asthma

Asthma is a prevalent childhood disease. More than 300 million children and adults are affected by asthma worldwide. The development of asthma is multifactorial and is affected by environmental and other exogenous factors and genetic predisposition. Shaping the lung microbiota, especially during birth

and very early life, plays a crucial role in asthma development. Arrieta *et al*[174] found a significant decrease in the relative abundance of the bacterial genera *Rothia*, *Veillonella*, *Lachnospira*, and *Faecalibacterium*, in children at risk of asthma. The noticed abundance of these bacteria decreases the fecal acetate levels and consequently induces dysregulation of enterohepatic metabolites. In the same context, Abrahamsson *et al*[175] showed that children who developed asthma at the age of 7 years had a reduced total and gut microbial diversity in the first month of life than healthy children.

On the other hand, more abundance of the good bacteria as *Bifidobacterium longum* and less quantity of *bacteroid fragilis* in the gut microbiota early in life reduces the risk of asthma[176]. The recent decrease in pediatric asthma incidence, noted in some parts of Europe and North America, could be related to judicious antibiotic use during early infancy and childhood that preserve the gut microbiota community [177]. The use of oral probiotics, prebiotics, or synbiotics (combination of pro and prebiotics) could modify the airway microbiota directly through microaspiration of the probiotic strain from the gastrointestinal tract to the airway or indirectly through their metabolic products[178]. Probiotics might generate local effects, such as reducing mucosal permeability and thus decreasing systemic antigens penetration, enhancing local IgA production, and tolerance induction. Their systemic anti-inflammatory effects are mediated through Toll-like receptors, stimulating Th1 response to allergens, enhancing tolerogenic dendritic cells, and the production of Treg[179]. Probiotic supplementation could restore the airway microbiota dysbiosis, promoting the healthy microbiota, which could modify the course of the pulmonary disorders. However, there are not enough studies concerned with the effects of probiotic supplementation on childhood asthma. A systemic review by Lin *et al*[180] failed to confirm the beneficial role of probiotic supplementation on the disease course in children with bronchial asthma.

GUT MICROBIOTA AND SKIN DISORDERS IN INFANCY AND CHILDHOOD

Atopic dermatitis

Atopic dermatitis (AD) is a common chronic, recurrent inflammatory skin disease in children, affecting about 20% worldwide and on the rise, especially in developed countries. Skin microbiota can reflect general human health. The quantitative and qualitative skin and gut microbiota composition alteration can trigger various diseases, including allergic dermatoses[181]. The skin microbiota of children with AD shows significant dysbiosis, with reduced microbial diversity and more abundance of pathogenic *Staphylococcus aureus* and *Malassezia*[182]. Melli *et al*[183] showed an association between the presence of *Clostridioides difficile*, more quantity of *Bifidobacteria*, and a lower abundance of lactobacilli in the gut microbiota of children with atopic dermatitis. Bacterial strains such as *Staphylococcus epidermidis*, *Staphylococcus cohnii*, Gram-negative *Roseomonas mucosa,* and *Cutibacterium* strains that inhibit *Staphylococcus aureus* can serve as potential probiotics in children with atopic dermatitis[184]. Myles *et al*[185] showed that the local application of *Roseomonas mucosa* to the skin of 10 adults and five children with atopic dermatitis was associated with significant improvement of atopic dermatitis severity, a decrease in topical steroid requirement, and *Staphylococcus aureus* burden with no adverse events or treatment complications. Probiotics can decrease the severity and progression of atopic dermatitis by reducing inflammation through modulating T-cell immune response and improving the Th1/Th2 ratio; inhibiting Th2 cell response, and decreasing cytokines production such as IL-4, IL-5, IL-6, IL-13, and INF, enhance phagocytosis, increase serum IgA is increased[186]. Probiotics also inhibit the differentiation of mature dendritic cells and naive T cells' transformation into Th2[158]. Probiotics also can regulate brain function involving stress response on the gut-brain axis[187].

Psoriasis

Psoriasis is a chronic, complex, immune-mediated, inflammatory disease characterized by keratinocytes hyperproliferation. Unlike atopic dermatitis, patients with psoriasis have more bacterial diversity and heterogeneity with increased *Staphylococcus aureus* and decreased *Staphylococcus epidermidis* and *Propionibacterium acnes* and reduced microbiota stability than in healthy controls. *Staphylococcus aureus* colonization of the skin triggers Th17-induced inflammation with impaired community stability and accumulation of pathogenic bacteria[188]. The bacterial dysbiosis in psoriasis shows topographic changes. An exciting study by Fahlén *et al*[189] showed a significant decrease in the ratio of *Staphylococci* and *Propionibacteria* in psoriasis limb skin and enriched *Proteobacteria* in the trunk skin in patients with psoriasis than in controls. Gut dysbiosis also plays a significant role in psoriasis. There is a decrease in gut *Bifidobacterium* and *Firmicutes* and an increase in *Bacteroidetes* in patients with psoriasis than in healthy children. This gut dysbiosis also correlates with the severity of the disease[190]. Probiotics use in the treatment of psoriasis is promising *via* immune modifying response through restoring the gut microbiome. Vijayashankar *et al*[191] described the successful use of oral *Lactobacillus* strain with biotin to treat pustular psoriasis. However, a systematic review and meta-analysis by Zeng *et al*[192] showed that prebiotics might positively impact relieving the clinical symptoms of psoriasis with a low incidence of side effects. The probiotics exert their effects through their immunomodulatory effect on the skin and repair the skin barrier by decreasing the bacterial load and restoring the skin microbiota.

GUT MICROBIOTA AND IMMUNE DISORDERS

The relation between adaptive immunity and gut microbiota is well documented. Systemic lupus erythematosus (SLE) is a chronic systemic severe autoimmune disease that affects connective tissues. Pathogenesis of SLE results from the interaction between genetic and environmental factors[193]. Gut microbiota dysbiosis with disturbed composition and activity plays a role in many autoimmune diseases, including SLE and rheumatoid arthritis. A study done by Ma *et al*[194] found that the fecal microbiota of SLE mice had lesser community abundance and diversity than healthy mice. They can also induce anti-double-stranded DNA (anti-dsDNA) antibodies production in germ-free mice, promote the inflammatory response resembling SLE inflammation, and modify the SLE susceptibility genes expression in these mice by fecal microbiota transplantation. Another interesting experimental study by Ma *et al*[195] performed fecal microbiota transplantation from healthy controls and patients with active untreated SLE to germ-free mice. The Germ-free mice developed a series of lupus-like phenotypic and laboratory features that confirm the contributing role of abnormal gut microbiota in promoting SLE development.

On the other hand, Toral *et al*[196] found that *Lactobacillus fermentum* CECT5716 (LC40) ameliorates disease activity and cardiovascular complications in female mice models by improving gut barrier integrity. At the same time, de la Visitación *et al*[197] showed that *Lactobacillus fermentum* CECT5716 (LC40) prevented renal damage in a female mouse model of SLE. Long-standing use of probiotics is supposed to counteract the imbalance in the gut microbiota that causes reduced antibody production and attenuated inflammatory response, resulting in reduced severity and improving the signs and the manifestation of SLE[198]. However, we need more human-based studies on patients with SLE, as most animal-based studies confirmed the potential beneficial role for oral probiotics intake, which can alter the gut microbiome's composition and prevent SLE progression.

Gut dysbiosis is also a potential pathogenic factor for developing juvenile idiopathic arthritis (JIA). Wu *et al*[199] were able to induce autoimmune arthritis in mice using segmented filamentous bacteria, which could elaborate the potential role of the microbiota and development of autoimmune arthritis. On the other hand, some degree of intestinal inflammation is observed in about two-thirds of children with spondyloarthritis arthritis which may indicate that gut microbiota in children with spondyloarthritis is both modified and unusually affected by the deviated immune system[200]. Meanwhile, Stoll *et al*[201] found less abundance of *Faecalibacterium Prausnitzii* and a more abundance of *Bifidobacterium*, mostly *B. adolescentis*, in children with enthesitis-related arthritis than in healthy control. However, Öman *et al* [202] found no significant variations in microbiota α-diversity or composition between children with JIA, their healthy siblings, or unrelated healthy controls. Trials to modify gut microbiota using probiotics, exclusive enteral nutrition, or other modalities have variable success. Esmaeili *et al*[203] found no significant differences in the improvement criteria of rheumatoid arthritis in patients supplemented with synbiotic (500 mg capsule containing a prebiotic (fructooligosaccharides) and probiotics including 10^9 CFU/mL of *Lactobacillus acidophilus, Lactobacillus casei, Lactobacillus bulgaricus, Lactobacillus rhamnosus, Bifidobacterium breve, Streptococcus thermophile, and Bifidobacterium longum*,) for three months and placebo groups. They suggested that lack of response is probably related to the short duration of the treatment, but we think that the dose also was suboptimal. However, we need more studies with different probiotic strains and concentrations.

GUT MICROBIOTA AND DENTAL DISORDERS

Dental caries is a common pediatric disorder, especially in children with special needs. Understanding the association between specific bacterial strains in dental biofilms and different health conditions is crucial to preventing and combating dental caries. Richard *et al*[204] found that the microbiomes of supragingival dental plaque vary considerably between tooth surfaces and in children with different caries activities. Qudeimat *et al*[205] found that children with active caries have a significantly higher abundance of *Prevotella melaninogenica, Leptotrichia shahii, Leptotrichia HOT 498, Veillonella dispar,* and *Streptococcus mutans*. In comparison, children without active caries had a significantly higher abundance of *Lautropia mirabilis, Corynebacterium durum, Corynebacterium matruchotii,* and *Neisseria elongata*. Kanasi *et al*[206] also confirmed the presence of diverse microbiota that varied in children with severe caries from caries-free children. Probiotics might be helpful to inhibit or treat dental caries, periodontitis, or gingivitis. Certain probiotic bacterial strains have variable effects on the gut microbiome. Each probiotic bacterial strain has specific abilities to inhibit the growth of particular strains, particularly cariogenic bacterial strains and yeast[207].

Probiotic dairy products have a naturally occurring buffer to acid. When combined with calcium and calcium lactate effects, it produces anti-cariogenic properties that benefit the oral cavity. In the short term, probiotic products can hamper the development of harmful strains, but the long-term effects have not been thoroughly studied. Lee *et al*[208] showed that *Lactobacillus* species strongly inhibited the growth of oral *streptococci*. They also showed that *Lactobacillus rhamnosus* might inhibit oral biofilm formation by decreasing the glucan production of *Streptococcus mutans*. Systematic review and meta-

analysis by Gruner *et al*[209] showed insufficient current evidence to recommend probiotics in managing dental caries but support using probiotics to manage gingivitis or periodontitis. Future studies are needed to confirm the role of probiotics in the management of dental caries.

GUT MICROBIOTA AND CARDIAC DISORDERS

Recent evidence revealed that modifications of the gut microbiota composition and function could accelerate the progression of CVDs. The gut microbiota has a crucial effect in inducing inflammatory and immune responses that could link the gut microflora to heart failure. The gut microbiota of patients with chronic heart failure has more pathogenic bacteria such as *Campylobacter* and *Shigella* and more candida than the healthy controls. The ratios of these pathogenic bacteria and candida positively correlated with the severity of heart failure[210]. Increased intestinal permeability is observed in a significant portion of patients with congestive or right-sided heart failure, which correlates with right atrial pressure[211]. This observation could explain the increased serum endotoxin levels in patients with chronic heart failure. Reduced cardiac output and systemic congestion observed in heart failure cause intestinal mucosal ischemia and/or edema, which increases the bacterial translocation and the circulating endotoxins that can promote the underlying inflammation observed in patients with heart failure[212]. These mucosal changes also cause enhanced bacterial growth, which is reflected by the increase in serum levels of immunoglobulin A-antilipopolysaccharide[213]. In heart failure, there is a decreased gut microbiota diversity with an increased ratio of the pathogenic bacteria such as *Shigella*, *Campylobacter*, *Yersinia enterocolitica*, *Salmonella*, and *Candida* species[214]. Luedde *et al*[215] also observed significant downregulation of key intestinal bacterial groups such as *Coriobacteriaceae*, *Erysipelotrichaceae*, and *Ruminococcaceae*.

Probiotics may have significant beneficial effects on cardiovascular health. The effects are strain-specific and target specific cardiovascular risk factors. For example, *Lactobacillus rhamosus* can significantly reduce body weight while *Lactobacillus acidophilus*, *Lactobacillus rhamnosus,* and *Bifidobacterium bifidum* can dramatically lower blood glucose levels by 38% in patients with DM type II. At the same time, *Lactobacillus acidophilus* and *Bifidobacterium lactis Bb12* significantly lower fasting blood glucose, hemoglobin A1c, and malondialdehyde and raise erythrocyte glutathione peroxidase and superoxide dismutase activities and improve total antioxidant states. Meanwhile, *Lactobacillus acidophilus, Lactobacillus reuteri,* and *Bifidobacterium longum* improve dyslipidemia, increase high-density lipoprotein (HDL) cholesterol level, and reduce low-density lipoprotein (LDL)/HDL cholesterol ratio. *Lactobacillus curvatus* and *Lactobacillus Plantarum* increase apolipoprotein AV and LDL particles size. *Streptococcus thermophiles* can significantly decrease systolic blood pressure[92,216-219].

Probiotics may have a role in managing heart failure, primarily those containing *Bifidobacteria*, yeasts, and lactic acid-producing bacteria, as they can reduce inflammation, repair, protect the intestinal mucosal barrier, and improve its function[220]. Gan *et al*[221] showed that six weeks of supplementation with *Lactobacillus rhamnosus* GR-1-containing probiotic could significantly improve left ventricular hypertrophy and increase its ejection fraction in rates with induced myocardial infarction due to coronary artery occlusion. Animal studies also showed that probiotics could decrease myocardial cell apoptosis and alleviate ventricular remodeling in rat models of spontaneous hypertension[222]. There are very few studies of the effects of probiotics in human patients with heart failure. Costanza *et al*[223] studied the impact of three months of supplementation with *S. boulardii* (1000 mg per day) on outpatients with heart failure with NYHA class II or III and left ventricular ejection fraction (LVEF) < 50%. The supplemented patients showed a significant reduction of left atrium diameter and improvement of LVEF compared to the patients supplemented with placebo. Children with heart failure may have underlying cardiac conditions that increase the risk of infective endocarditis. Probiotics in such patients are not entirely safe, and there is a risk of bacterial translocation with a possible occurrence of sepsis and infective endocarditis. Their safety in such vulnerable patients requires additional studies.

LIMITATIONS FOR PROBIOTIC USE

Despite probiotics being part of the body's good microbiota and are safe in most cases, there are some limitations to their use. The side effects of probiotics lie in four categories: excessive immune stimulation, adverse metabolic activities, generalized infections, and gene transfer[224]. They may occasionally trigger allergic reactions, especially with *Saccharomyces boulardii* in those with a history of yeast allergy, and should be used judiciously. Abdominal discomfort could happen in the first few days of therapy, occasionally with diarrhea and bloating. Probiotics are safe to be used by children, especially those containing *Bifidobacteria* or *Lactobacillus*, which can be used for up to one year without any safety issues[225]. Bacteriemia and infective endocarditis have been recorded in a few patients taking probiotics containing *Bifidobacteria* or *Lactobacillus* probiotics, especially among patients with central lines or impaired immunity, *e.g.*, who are suffering from tuberculosis or acquired immune deficiency

syndrome[226]. Probiotics containing *Lactobacilli* can cause mural and valvular infective endocarditis. Although this is extremely rare, patients with valvular heart disease may be more prone to this complication. Before dental or surgical procedures, patients with valvular or congenital heart disease with high-pressure shunt should discontinue probiotic use[227]. Some probiotics may transmit antibiotic resistance genes, such as enterococci. Other probiotic strains such as the Bacillus cereus group can produce enterotoxins and emetic toxins[228]. Another limitation is the lack of international regulatory measures that control probiotics production and prescription. Another limitation is the need to elucidate the mechanism of action of each probiotic, the ideal strain and its effect for each medical condition, and which health benefits can be gained[229]. We need to do more clinical and mechanistic studies to understand better the interaction between the microbes and host cells, including the mucus and immune defenses, and produce effective interventions.

CONCLUSION

There is an intimate relationship between the human and his body microbes. The gut is the primary residence for this microbiota, as it provides the bacteria with a convenient environment for thriving. The microbiota plays a significant role in gut development, maturation, and immune system differentiation. It exerts a considerable effect on the child's physical and mental development. Gut dysbiosis is also a potential pathogenic factor for developing various childhood disorders inside and outside the gastrointestinal tract. Probiotics may have a role in managing these disorders with variable degrees. Even though probiotics could help address these disorders, we need more studies to prove the efficacy, select the proper probiotic for each disease, the appropriate dose, and ensure its safety.

ACKNOWLEDGEMENTS

We thank the anonymous referees for their valuable suggestions.

FOOTNOTES

Author contributions: Nermin Kamal Saeed, Mohammed Al-Biltagi, Adel Salah Bediwy, Yasser El-Sawaf, and Osama Toema collected the data and wrote and revised the manuscript.

Conflict-of-interest statement: No conflict of interest.

Open-Access: This article is an open-access article that was selected by an in-house editor and fully peer-reviewed by external reviewers. It is distributed in accordance with the Creative Commons Attribution NonCommercial (CC BY-NC 4.0) license, which permits others to distribute, remix, adapt, build upon this work non-commercially, and license their derivative works on different terms, provided the original work is properly cited and the use is non-commercial. See: https://creativecommons.org/Licenses/by-nc/4.0/

Country/Territory of origin: Bahrain

ORCID number: Nermin Kamal Saeed 0000-0001-7875-8207; Mohammed Al-Beltagi 0000-0002-7761-9536; Adel Salah Bediwy 0000-0002-0281-0010; Yasser El-Sawaf 0000-0001-8083-3042; Osama Toema 0000-0003-2408-1573.

S-Editor: Zhang H
L-Editor: A
P-Editor: Zhang H

REFERENCES

1 **Thursby E**, Juge N. Introduction to the human gut microbiota. *Biochem J* 2017; **474**: 1823-1836 [PMID: 28512250 DOI: 10.1042/BCJ20160510]
2 **Ursell LK**, Metcalf JL, Parfrey LW, Knight R. Defining the human microbiome. *Nutr Rev* 2012; **70** Suppl 1: S38-S44 [PMID: 22861806 DOI: 10.1111/j.1753-4887.2012.00493.x]
3 **Collado MC**, Segata N. Initial exploration of in utero microbial colonization. *Nat Med* 2020; **26**: 469-470 [PMID: 32231297 DOI: 10.1038/s41591-020-0836-1]
4 **Silverstein RB**, Mysorekar IU. Group therapy on in utero colonization: seeking common truths and a way forward. *Microbiome* 2021; **9**: 7 [PMID: 33436100 DOI: 10.1186/s40168-020-00968-w]
5 **Ihekweazu FD**, Versalovic J. Development of the Pediatric Gut Microbiome: Impact on Health and Disease. *Am J Med*

Sci 2018; **356**: 413-423 [PMID: 30384950 DOI: 10.1016/j.amjms.2018.08.005]
6 **Agans R**, Rigsbee L, Kenche H, Michail S, Khamis HJ, Paliy O. Distal gut microbiota of adolescent children is different from that of adults. *FEMS Microbiol Ecol* 2011; **77**: 404-412 [PMID: 21539582 DOI: 10.1111/j.1574-6941.2011.01120.x]
7 **Adak A**, Khan MR. An insight into gut microbiota and its functionalities. *Cell Mol Life Sci* 2019; **76**: 473-493 [PMID: 30317530 DOI: 10.1007/s00018-018-2943-4]
8 **Engevik MA**, Versalovic J. Biochemical Features of Beneficial Microbes: Foundations for Therapeutic Microbiology. *Microbiol Spectr* 2017; **5** [PMID: 28984235 DOI: 10.1128/microbiolspec.BAD-0012-2016]
9 **den Besten G**, van Eunen K, Groen AK, Venema K, Reijngoud DJ, Bakker BM. The role of short-chain fatty acids in the interplay between diet, gut microbiota, and host energy metabolism. *J Lipid Res* 2013; **54**: 2325-2340 [PMID: 23821742 DOI: 10.1194/jlr.R036012]
10 **Russo E**, Giudici F, Fiorindi C, Ficari F, Scaringi S, Amedei A. Immunomodulating Activity and Therapeutic Effects of Short Chain Fatty Acids and Tryptophan Post-biotics in Inflammatory Bowel Disease. *Front Immunol* 2019; **10**: 2754 [PMID: 31824517 DOI: 10.3389/fimmu.2019.02754]
11 **Morrison DJ**, Preston T. Formation of short chain fatty acids by the gut microbiota and their impact on human metabolism. *Gut Microbes* 2016; **7**: 189-200 [PMID: 26963409 DOI: 10.1080/19490976.2015.1134082]
12 **Rowland I**, Gibson G, Heinken A, Scott K, Swann J, Thiele I, Tuohy K. Gut microbiota functions: metabolism of nutrients and other food components. *Eur J Nutr* 2018; **57**: 1-24 [PMID: 28393285 DOI: 10.1007/s00394-017-1445-8]
13 **Valdes AM**, Walter J, Segal E, Spector TD. Role of the gut microbiota in nutrition and health. *BMJ* 2018; **361**: k2179 [PMID: 29899036 DOI: 10.1136/bmj.k2179]
14 **Jia W**, Xie G, Jia W. Bile acid-microbiota crosstalk in gastrointestinal inflammation and carcinogenesis. *Nat Rev Gastroenterol Hepatol* 2018; **15**: 111-128 [PMID: 29018272 DOI: 10.1038/nrgastro.2017.119]
15 **Strandwitz P**. Neurotransmitter modulation by the gut microbiota. *Brain Res* 2018; **1693**: 128-133 [PMID: 29903615 DOI: 10.1016/j.brainres.2018.03.015]
16 **Carabotti M**, Scirocco A, Maselli MA, Severi C. The gut-brain axis: interactions between enteric microbiota, central and enteric nervous systems. *Ann Gastroenterol* 2015; **28**: 203-209 [PMID: 25830558 DOI: 10.2220/biomedres.41.199]
17 **Roberfroid M**, Gibson GR, Hoyles L, McCartney AL, Rastall R, Rowland I, Wolvers D, Watzl B, Szajewska H, Stahl B, Guarner F, Respondek F, Whelan K, Coxam V, Davicco MJ, Léotoing L, Wittrant Y, Delzenne NM, Cani PD, Neyrinck AM, Meheust A. Prebiotic effects: metabolic and health benefits. *Br J Nutr* 2010; **104** Suppl 2: S1-63 [PMID: 20920376 DOI: 10.1017/S0007114510003363]
18 **Salminen S**, Collado MC, Endo A, Hill C, Lebeer S, Quigley EMM, Sanders ME, Shamir R, Swann JR, Szajewska H, Vinderola G. The International Scientific Association of Probiotics and Prebiotics (ISAPP) consensus statement on the definition and scope of postbiotics. *Nat Rev Gastroenterol Hepatol* 2021; **18**: 649-667 [PMID: 33948025 DOI: 10.1038/s41575-021-00440-6]
19 **Kato K**, Ishida S, Tanaka M, Mitsuyama E, Xiao JZ, Odamaki T. Association between functional lactase variants and a high abundance of Bifidobacterium in the gut of healthy Japanese people. *PLoS One* 2018; **13**: e0206189 [PMID: 30339693 DOI: 10.1371/journal.pone.0206189]
20 **Wang J**, Thingholm LB, Skiecevičienė J, Rausch P, Kummen M, Hov JR, Degenhardt F, Heinsen FA, Rühlemann MC, Szymczak S, Holm K, Esko T, Sun J, Pricop-Jeckstadt M, Al-Dury S, Bohov P, Bethune J, Sommer F, Ellinghaus D, Berge RK, Hübenthal M, Koch M, Schwarz K, Rimbach G, Hübbe P, Pan WH, Sheibani-Tezerji R, Häsler R, Rosenstiel P, D'Amato M, Cloppenborg-Schmidt K, Künzel S, Laudes M, Marschall HU, Lieb W, Nöthlings U, Karlsen TH, Baines JF, Franke A. Genome-wide association analysis identifies variation in vitamin D receptor and other host factors influencing the gut microbiota. *Nat Genet* 2016; **48**: 1396-1406 [PMID: 27723756 DOI: 10.1038/ng.3695]
21 **Hughes DA**, Bacigalupe R, Wang J, Rühlemann MC, Tito RY, Falony G, Joossens M, Vieira-Silva S, Henckaerts L, Rymenans L, Verspecht C, Ring S, Franke A, Wade KH, Timpson NJ, Raes J. Genome-wide associations of human gut microbiome variation and implications for causal inference analyses. *Nat Microbiol* 2020; **5**: 1079-1087 [PMID: 32572223 DOI: 10.1038/s41564-020-0743-8]
22 **Martinez-Guryn K**, Hubert N, Frazier K, Urlass S, Musch MW, Ojeda P, Pierre JF, Miyoshi J, Sontag TJ, Cham CM, Reardon CA, Leone V, Chang EB. Small Intestine Microbiota Regulate Host Digestive and Absorptive Adaptive Responses to Dietary Lipids. *Cell Host Microbe* 2018; **23**: 458-469.e5 [PMID: 29649441 DOI: 10.1016/j.chom.2018.03.011]
23 **Kastl AJ Jr**, Terry NA, Wu GD, Albenberg LG. The Structure and Function of the Human Small Intestinal Microbiota: Current Understanding and Future Directions. *Cell Mol Gastroenterol Hepatol* 2020; **9**: 33-45 [PMID: 31344510 DOI: 10.1016/j.jcmgh.2019.07.006]
24 **Reyman M**, van Houten MA, van Baarle D, Bosch AATM, Man WH, Chu MLJN, Arp K, Watson RL, Sanders EAM, Fuentes S, Bogaert D. Impact of delivery mode-associated gut microbiota dynamics on health in the first year of life. *Nat Commun* 2019; **10**: 4997 [PMID: 31676793 DOI: 10.1038/s41467-019-13014-7]
25 **Ma J**, Li Z, Zhang W, Zhang C, Zhang Y, Mei H, Zhuo N, Wang H, Wang L, Wu D. Comparison of gut microbiota in exclusively breast-fed and formula-fed babies: a study of 91 term infants. *Sci Rep* 2020; **10**: 15792 [PMID: 32978424 DOI: 10.1038/s41598-020-72635-x]
26 **Wilmanski T**, Diener C, Rappaport N, Patwardhan S, Wiedrick J, Lapidus J, Earls JC, Zimmer A, Glusman G, Robinson M, Yurkovich JT, Kado DM, Cauley JA, Zmuda J, Lane NE, Magis AT, Lovejoy JC, Hood L, Gibbons SM, Orwoll ES, Price ND. Gut microbiome pattern reflects healthy ageing and predicts survival in humans. *Nat Metab* 2021; **3**: 274-286 [PMID: 33619379 DOI: 10.1038/s42255-021-00348-0]
27 **Imhann F**, Bonder MJ, Vich Vila A, Fu J, Mujagic Z, Vork L, Tigchelaar EF, Jankipersadsing SA, Cenit MC, Harmsen HJ, Dijkstra G, Franke L, Xavier RJ, Jonkers D, Wijmenga C, Weersma RK, Zhernakova A. Proton pump inhibitors affect the gut microbiome. *Gut* 2016; **65**: 740-748 [PMID: 26657899 DOI: 10.1136/gutjnl-2015-310376]
28 **Ramirez J**, Guarner F, Bustos Fernandez L, Maruy A, Sdepanian VL, Cohen H. Antibiotics as Major Disruptors of Gut Microbiota. *Front Cell Infect Microbiol* 2020; **10**: 572912 [PMID: 33330122 DOI: 10.3389/fcimb.2020.572912]
29 **Rakoff-Nahoum S**, Foster KR, Comstock LE. The evolution of cooperation within the gut microbiota. *Nature* 2016; **533**:

255-259 [PMID: 27111508 DOI: 10.1038/nature17626]
30 **García-Bayona L**, Comstock LE. Bacterial antagonism in host-associated microbial communities. *Science* 2018; **361** [PMID: 30237322 DOI: 10.1126/science.aat2456]
31 **de Wouters T**, Jans C, Niederberger T, Fischer P, Rühs PA. Adhesion Potential of Intestinal Microbes Predicted by Physico-Chemical Characterization Methods. *PLoS One* 2015; **10**: e0136437 [PMID: 26295945 DOI: 10.1371/journal.pone.0136437]
32 **Martin CR**, Osadchiy V, Kalani A, Mayer EA. The Brain-Gut-Microbiome Axis. *Cell Mol Gastroenterol Hepatol* 2018; **6**: 133-148 [PMID: 30023410 DOI: 10.1016/j.jcmgh.2018.04.003]
33 **Osadchiy V**, Martin CR, Mayer EA. The Gut-Brain Axis and the Microbiome: Mechanisms and Clinical Implications. *Clin Gastroenterol Hepatol* 2019; **17**: 322-332 [PMID: 30292888 DOI: 10.1016/j.cgh.2018.10.002]
34 **Mayer EA**, Tillisch K, Gupta A. Gut/brain axis and the microbiota. *J Clin Invest* 2015; **125**: 926-938 [PMID: 25689247 DOI: 10.1172/JCI76304]
35 **Albillos A**, de Gottardi A, Rescigno M. The gut-liver axis in liver disease: Pathophysiological basis for therapy. *J Hepatol* 2020; **72**: 558-577 [PMID: 31622696 DOI: 10.1016/j.jhep.2019.10.003]
36 **Yang X**, Lu D, Zhuo J, Lin Z, Yang M, Xu X. The Gut-liver Axis in Immune Remodeling: New insight into Liver Diseases. *Int J Biol Sci* 2020; **16**: 2357-2366 [PMID: 32760203 DOI: 10.7150/ijbs.46405]
37 **Wu X**, Tian Z. Gut-liver axis: gut microbiota in shaping hepatic innate immunity. *Sci China Life Sci* 2017; **60**: 1191-1196 [PMID: 28840534 DOI: 10.1007/s11427-017-9128-3]
38 **Forkosh E**, Ilan Y. The heart-gut axis: new target for atherosclerosis and congestive heart failure therapy. *Open Heart* 2019; **6**: e000993 [PMID: 31168383 DOI: 10.1136/openhrt-2018-000993]
39 **Sata Y**, Marques FZ, Kaye DM. The Emerging Role of Gut Dysbiosis in Cardio-metabolic Risk Factors for Heart Failure. *Curr Hypertens Rep* 2020; **22**: 38 [PMID: 32385705 DOI: 10.1007/s11906-020-01046-0]
40 **Ahmad AF**, Ward NC, Dwivedi G. The gut microbiome and heart failure. *Curr Opin Cardiol* 2019; **34**: 225-232 [PMID: 30575647 DOI: 10.1097/HCO.0000000000000598]
41 **Yang T**, Richards EM, Pepine CJ, Raizada MK. The gut microbiota and the brain-gut-kidney axis in hypertension and chronic kidney disease. *Nat Rev Nephrol* 2018; **14**: 442-456 [PMID: 29760448 DOI: 10.1038/s41581-018-0018-2]
42 **Foresto-Neto O**, Ghirotto B, Câmara NOS. Renal sensing of bacterial metabolites in the gut-kidney axis. *Kidney360* 2021; **2**: 1501-1509 [DOI: 10.34067/KID.0000292021]
43 **Sabatino A**, Regolisti G, Brusasco I, Cabassi A, Morabito S, Fiaccadori E. Alterations of intestinal barrier and microbiota in chronic kidney disease. *Nephrol Dial Transplant* 2015; **30**: 924-933 [PMID: 25190600 DOI: 10.1093/ndt/gfu287]
44 **Anders HJ**, Andersen K, Stecher B. The intestinal microbiota, a leaky gut, and abnormal immunity in kidney disease. *Kidney Int* 2013; **83**: 1010-1016 [PMID: 23325079 DOI: 10.1038/ki.2012.440]
45 **Enaud R**, Prevel R, Ciarlo E, Beaufils F, Wieërs G, Guery B, Delhaes L. The Gut-Lung Axis in Health and Respiratory Diseases: A Place for Inter-Organ and Inter-Kingdom Crosstalks. *Front Cell Infect Microbiol* 2020; **10**: 9 [PMID: 32140452 DOI: 10.3389/fcimb.2020.00009]
46 **Wilson MT**, Hamilos DL. The nasal and sinus microbiome in health and disease. *Curr Allergy Asthma Rep* 2014; **14**: 485 [PMID: 25342392 DOI: 10.1007/s11882-014-0485-x]
47 **Chiu L**, Bazin T, Truchetet ME, Schaeverbeke T, Delhaes L, Pradeu T. Protective Microbiota: From Localized to Long-Reaching Co-Immunity. *Front Immunol* 2017; **8**: 1678 [PMID: 29270167 DOI: 10.3389/fimmu.2017.01678]
48 **Salem I**, Ramser A, Isham N, Ghannoum MA. The Gut Microbiome as a Major Regulator of the Gut-Skin Axis. *Front Microbiol* 2018; **9**: 1459 [PMID: 30042740 DOI: 10.3389/fmicb.2018.01459]
49 **Jones CJ**, Brinton LA, Hamman RF, Stolley PD, Lehman HF, Levine RS, Mallin K. Risk factors for in situ cervical cancer: results from a case-control study. *Cancer Res* 1990; **50**: 3657-3662 [PMID: 2340514 DOI: 10.1371/journal.pone.0055380]
50 **Hacini-Rachinel F**, Gheit H, Le Luduec JB, Dif F, Nancey S, Kaiserlian D. Oral probiotic control skin inflammation by acting on both effector and regulatory T cells. *PLoS One* 2009; **4**: e4903 [PMID: 19300508 DOI: 10.1371/journal.pone.0004903]
51 **Harkness S**. A cultural model for the acquisition of language: implications for the innateness debate. *Dev Psychobiol* 1990; **23**: 727-740 [PMID: 2286300 DOI: 10.1016/j.cell.2012.07.008]
52 **Migliarini S**, Pacini G, Pelosi B, Lunardi G, Pasqualetti M. Lack of brain serotonin affects postnatal development and serotonergic neuronal circuitry formation. *Mol Psychiatry* 2013; **18**: 1106-1118 [PMID: 23007167 DOI: 10.1038/mp.2012.128]
53 **Gao K**, Mu CL, Farzi A, Zhu WY. Tryptophan Metabolism: A Link Between the Gut Microbiota and Brain. *Adv Nutr* 2020; **11**: 709-723 [PMID: 31825083 DOI: 10.1093/advances/nmz127]
54 **Evrensel A**, Ceylan ME. The Gut-Brain Axis: The Missing Link in Depression. *Clin Psychopharmacol Neurosci* 2015; **13**: 239-244 [PMID: 26598580 DOI: 10.9758/cpn.2015.13.3.239]
55 **Huang R**, Wang K, Hu J. Effect of Probiotics on Depression: A Systematic Review and Meta-Analysis of Randomized Controlled Trials. *Nutrients* 2016; **8**: 483 [PMID: 27509521 DOI: 10.3390/nu8080483]
56 **Erny D**, Hrabě de Angelis AL, Jaitin D, Wieghofer P, Staszewski O, David E, Keren-Shaul H, Mahlakoiv T, Jakobshagen K, Buch T, Schwierzeck V, Utermöhlen O, Chun E, Garrett WS, McCoy KD, Diefenbach A, Staeheli P, Stecher B, Amit I, Prinz M. Host microbiota constantly control maturation and function of microglia in the CNS. *Nat Neurosci* 2015; **18**: 965-977 [PMID: 26030851 DOI: 10.1038/nn.4030]
57 **Majnik AV**, Lane RH. The relationship between early-life environment, the epigenome and the microbiota. *Epigenomics* 2015; **7**: 1173-1184 [PMID: 26585860 DOI: 10.2217/epi.15.74]
58 **Harry GJ**. Microglia during development and aging. *Pharmacol Ther* 2013; **139**: 313-326 [PMID: 23644076 DOI: 10.1016/j.pharmthera.2013.04.013]
59 **Tamana SK**, Tun HM, Konya T, Chari RS, Field CJ, Guttman DS, Becker AB, Moraes TJ, Turvey SE, Subbarao P, Sears MR, Pei J, Scott JA, Mandhane PJ, Kozyrskyj AL. Bacteroides-dominant gut microbiome of late infancy is associated

with enhanced neurodevelopment. *Gut Microbes* 2021; **13**: 1-17 [PMID: 34132157 DOI: 10.1080/19490976.2021.1930875]

60 **Zhang S**, Qian Y, Li Q, Xu X, Li X, Wang C, Cai H, Zhu J, Yu Y. Metabolic and Neural Mechanisms Underlying the Associations Between Gut *Bacteroides* and Cognition: A Large-Scale Functional Network Connectivity Study. *Front Neurosci* 2021; **15**: 750704 [PMID: 34733135 DOI: 10.3389/fnins.2021.750704]

61 **Cryan JF**, Dinan TG. More than a gut feeling: the microbiota regulates neurodevelopment and behavior. *Neuropsychopharmacology* 2015; **40**: 241-242 [PMID: 25482171 DOI: 10.1038/npp.2014.224]

62 **Finegold SM**, Dowd SE, Gontcharova V, Liu C, Henley KE, Wolcott RD, Youn E, Summanen PH, Granpeesheh D, Dixon D, Liu M, Molitoris DR, Green JA 3rd. Pyrosequencing study of fecal microflora of autistic and control children. *Anaerobe* 2010; **16**: 444-453 [PMID: 20603222 DOI: 10.1016/j.anaerobe.2010.06.008]

63 **Luna RA**, Oezguen N, Balderas M, Venkatachalam A, Runge JK, Versalovic J, Veenstra-VanderWeele J, Anderson GM, Savidge T, Williams KC. Distinct Microbiome-Neuroimmune Signatures Correlate With Functional Abdominal Pain in Children With Autism Spectrum Disorder. *Cell Mol Gastroenterol Hepatol* 2017; **3**: 218-230 [PMID: 28275689 DOI: 10.1016/j.jcmgh.2016.11.008]

64 **Li N**, Yang J, Zhang J, Liang C, Wang Y, Chen B, Zhao C, Wang J, Zhang G, Zhao D, Liu Y, Zhang L, Li G, Gai Z, Zhao G. Correlation of Gut Microbiome Between ASD Children and Mothers and Potential Biomarkers for Risk Assessment. *Genomics Proteomics Bioinformatics* 2019; **17**: 26-38 [PMID: 31026579 DOI: 10.1016/j.gpb.2019.01.002]

65 **Finegold SM**, Molitoris D, Song Y, Liu C, Vaisanen ML, Bolte E, McTeague M, Sandler R, Wexler H, Marlowe EM, Collins MD, Lawson PA, Summanen P, Baysallar M, Tomzynski TJ, Read E, Johnson E, Rolfe R, Nasir P, Shah H, Haake DA, Manning P, Kaul A. Gastrointestinal microflora studies in late-onset autism. *Clin Infect Dis* 2002; **35**: S6-S16 [PMID: 12173102 DOI: 10.1086/341914]

66 **Sandler RH**, Finegold SM, Bolte ER, Buchanan CP, Maxwell AP, Väisänen ML, Nelson MN, Wexler HM. Short-term benefit from oral vancomycin treatment of regressive-onset autism. *J Child Neurol* 2000; **15**: 429-435 [PMID: 10921511 DOI: 10.1177/088307380001500701]

67 **Bezawada N**, Phang TH, Hold GL, Hansen R. Autism Spectrum Disorder and the Gut Microbiota in Children: A Systematic Review. *Ann Nutr Metab* 2020; **76**: 16-29 [PMID: 31982866 DOI: 10.1159/000505363]

68 **Al-Beltagi M**. Autism medical comorbidities. *World J Clin Pediatr* 2021; **10**: 15-28 [PMID: 33972922 DOI: 10.5409/wjcp.v10.i3.15]

69 **Huang TS**, Lu XG, Li B, Chen Y, Wen JL, Hu Y, Chen L, Xiao YH, Zhang J, Liao JX. [Benign infantile convulsions with mild gastroenteritis: clinical analysis of 40 cases]. *Zhongguo Dang Dai Er Ke Za Zhi* 2010; **12**: 533-535 [PMID: 20637150]

70 **Şafak B**, Altunan B, Topçu B, Eren Topkaya A. The gut microbiome in epilepsy. *Microb Pathog* 2020; **139**: 103853 [PMID: 31730997 DOI: 10.1016/j.micpath.2019.103853]

71 **Kitamura S**, Sugihara K, Kuwasako M, Tatsumi K. The role of mammalian intestinal bacteria in the reductive metabolism of zonisamide. *J Pharm Pharmacol* 1997; **49**: 253-256 [PMID: 9231340 DOI: 10.1111/j.2042-7158.1997.tb06790.x]

72 **Dahlin M**, Prast-Nielsen S. The gut microbiome and epilepsy. *EBioMedicine* 2019; **44**: 741-746 [PMID: 31160269 DOI: 10.1016/j.ebiom.2019.05.024]

73 **Gómez-Eguílaz M**, Ramón-Trapero JL, Pérez-Martínez L, Blanco JR. The beneficial effect of probiotics as a supplementary treatment in drug-resistant epilepsy: a pilot study. *Benef Microbes* 2018; **9**: 875-881 [PMID: 30198325 DOI: 10.3920/BM2018.0018]

74 **Yue Q**, Cai M, Xiao B, Zhan Q, Zeng C. The Microbiota-Gut-Brain Axis and Epilepsy. *Cell Mol Neurobiol* 2022; **42**: 439-453 [PMID: 34279746 DOI: 10.1007/s10571-021-01130-2]

75 **Sato Y**, Sakurai K, Tanabe H, Kato T, Nakanishi Y, Ohno H, Mori C. Maternal gut microbiota is associated with newborn anthropometrics in a sex-specific manner. *J Dev Orig Health Dis* 2019; **10**: 659-666 [PMID: 31106719 DOI: 10.1017/S2040174419000138]

76 **Robertson RC**, Manges AR, Finlay BB, Prendergast AJ. The Human Microbiome and Child Growth - First 1000 Days and Beyond. *Trends Microbiol* 2019; **27**: 131-147 [PMID: 30529020 DOI: 10.1016/j.tim.2018.09.008]

77 **Li H**, He Z, Gao D, Lv Y, Zhou Q, Xiao B, Huang W. Characteristics of the Intestinal Microbiota in Very Low Birth Weight Infants With Extrauterine Growth Restriction. *Front Pediatr* 2019; **7**: 99 [PMID: 30972313 DOI: 10.3389/fped.2019.00099]

78 **Becker-Dreps S**, Allali I, Monteagudo A, Vilchez S, Hudgens MG, Rogawski ET, Carroll IM, Zambrana LE, Espinoza F, Azcarate-Peril MA. Gut Microbiome Composition in Young Nicaraguan Children During Diarrhea Episodes and Recovery. *Am J Trop Med Hyg* 2015; **93**: 1187-1193 [PMID: 26350452 DOI: 10.4269/ajtmh.15-0322]

79 **Salvucci E**. The human-microbiome superorganism and its modulation to restore health. *Int J Food Sci Nutr* 2019; **70**: 781-795 [PMID: 30843443 DOI: 10.1080/09637486.2019.1580682]

80 **Subramanian S**, Huq S, Yatsunenko T, Haque R, Mahfuz M, Alam MA, Benezra A, DeStefano J, Meier MF, Muegge BD, Barratt MJ, VanArendonk LG, Zhang Q, Province MA, Petri WA Jr, Ahmed T, Gordon JI. Persistent gut microbiota immaturity in malnourished Bangladeshi children. *Nature* 2014; **510**: 417-421 [PMID: 24896187 DOI: 10.1038/nature13421]

81 **Onubi OJ**, Poobalan AS, Dineen B, Marais D, McNeill G. Effects of probiotics on child growth: a systematic review. *J Health Popul Nutr* 2015; **34**: 8 [PMID: 26825706 DOI: 10.1186/s41043-015-0010-4]

82 **Tidjani Alou M**, Million M, Traore SI, Mouelhi D, Khelaifia S, Bachar D, Caputo A, Delerce J, Brah S, Alhousseini D, Sokhna C, Robert C, Diallo BA, Diallo A, Parola P, Golden M, Lagier JC, Raoult D. Gut Bacteria Missing in Severe Acute Malnutrition, Can We Identify Potential Probiotics by Culturomics? *Front Microbiol* 2017; **8**: 899 [PMID: 28588566 DOI: 10.3389/fmicb.2017.00899]

83 **Pop M**, Walker AW, Paulson J, Lindsay B, Antonio M, Hossain MA, Oundo J, Tamboura B, Mai V, Astrovskaya I, Corrada Bravo H, Rance R, Stares M, Levine MM, Panchalingam S, Kotloff K, Ikumapayi UN, Ebruke C, Adeyemi M, Ahmed D, Ahmed F, Alam MT, Amin R, Siddiqui S, Ochieng JB, Ouma E, Juma J, Mailu E, Omore R, Morris JG,

Breiman RF, Saha D, Parkhill J, Nataro JP, Stine OC. Diarrhea in young children from low-income countries leads to large-scale alterations in intestinal microbiota composition. *Genome Biol* 2014; **15**: R76 [PMID: 24995464 DOI: 10.1186/gb-2014-15-6-r76]

84 **Guerrant RL**, DeBoer MD, Moore SR, Scharf RJ, Lima AA. The impoverished gut--a triple burden of diarrhoea, stunting and chronic disease. *Nat Rev Gastroenterol Hepatol* 2013; **10**: 220-229 [PMID: 23229327 DOI: 10.1038/nrgastro.2012.239]

85 **Bandsma RHJ**, Sadiq K, Bhutta ZA. Persistent diarrhoea: current knowledge and novel concepts. *Paediatr Int Child Health* 2019; **39**: 41-47 [PMID: 30079818 DOI: 10.1080/20469047.2018.1504412]

86 **Korpe PS**, Petri WA Jr. Environmental enteropathy: critical implications of a poorly understood condition. *Trends Mol Med* 2012; **18**: 328-336 [PMID: 22633998 DOI: 10.1016/j.molmed.2012.04.007]

87 **Campbell DI**, McPhail G, Lunn PG, Elia M, Jeffries DJ. Intestinal inflammation measured by fecal neopterin in Gambian children with enteropathy: association with growth failure, Giardia lamblia, and intestinal permeability. *J Pediatr Gastroenterol Nutr* 2004; **39**: 153-157 [PMID: 15269619 DOI: 10.1097/00005176-200408000-00005]

88 **Riva A**, Borgo F, Lassandro C, Verduci E, Morace G, Borghi E, Berry D. Pediatric obesity is associated with an altered gut microbiota and discordant shifts in Firmicutes populations. *Environ Microbiol* 2017; **19**: 95-105 [PMID: 27450202 DOI: 10.1111/1462-2920.13463]

89 **Collado MC**, Isolauri E, Laitinen K, Salminen S. Distinct composition of gut microbiota during pregnancy in overweight and normal-weight women. *Am J Clin Nutr* 2008; **88**: 894-899 [PMID: 18842773 DOI: 10.1093/ajcn/88.4.894]

90 **Jian C**, Carpén N, Helve O, de Vos WM, Korpela K, Salonen A. Early-life gut microbiota and its connection to metabolic health in children: Perspective on ecological drivers and need for quantitative approach. *EBioMedicine* 2021; **69**: 103475 [PMID: 34256346 DOI: 10.1016/j.ebiom.2021.103475]

91 **Angelakis E**, Armougom F, Million M, Raoult D. The relationship between gut microbiota and weight gain in humans. *Future Microbiol* 2012; **7**: 91-109 [PMID: 22191449 DOI: 10.2217/fmb.11.142]

92 **Sanchez M**, Panahi S, Tremblay A. Childhood obesity: a role for gut microbiota? *Int J Environ Res Public Health* 2014; **12**: 162-175 [PMID: 25546278 DOI: 10.3390/ijerph120100162]

93 **Korpela K**, Renko M, Vänni P, Paalanne N, Salo J, Tejesvi MV, Koivusaari P, Ojaniemi M, Pokka T, Kaukola T, Pirttilä AM, Tapiainen T. Microbiome of the first stool and overweight at age 3 years: A prospective cohort study. *Pediatr Obes* 2020; **15**: e12680 [PMID: 32638554 DOI: 10.1111/ijpo.12680]

94 **Musso G**, Gambino R, Cassader M. Obesity, diabetes, and gut microbiota: the hygiene hypothesis expanded? *Diabetes Care* 2010; **33**: 2277-2284 [PMID: 20876708 DOI: 10.2337/dc10-0556]

95 **Luoto R**, Kalliomäki M, Laitinen K, Isolauri E. The impact of perinatal probiotic intervention on the development of overweight and obesity: follow-up study from birth to 10 years. *Int J Obes (Lond)* 2010; **34**: 1531-1537 [PMID: 20231842 DOI: 10.1038/ijo.2010.50]

96 **Luoto R**, Laitinen K, Nermes M, Isolauri E. Impact of maternal probiotic-supplemented dietary counselling on pregnancy outcome and prenatal and postnatal growth: a double-blind, placebo-controlled study. *Br J Nutr* 2010; **103**: 1792-1799 [PMID: 20128938 DOI: 10.1017/S0007114509993898]

97 **Guo R**, Chen LH, Xing C, Liu T. Pain regulation by gut microbiota: molecular mechanisms and therapeutic potential. *Br J Anaesth* 2019; **123**: 637-654 [PMID: 31551115 DOI: 10.1016/j.bja.2019.07.026]

98 **Abrahamsson TR**, Wu RY, Sherman PM. Microbiota in Functional Gastrointestinal Disorders in Infancy: Implications for Management. *Nestle Nutr Inst Workshop Ser* 2017; **88**: 107-115 [PMID: 28346927 DOI: 10.1159/000455219]

99 **Hemarajata P**, Versalovic J. Effects of probiotics on gut microbiota: mechanisms of intestinal immunomodulation and neuromodulation. *Therap Adv Gastroenterol* 2013; **6**: 39-51 [PMID: 23320049 DOI: 10.1177/1756283X12459294]

100 **Mai T**, Fatheree NY, Gleason W, Liu Y, Rhoads JM. Infantile Colic: New Insights into an Old Problem. *Gastroenterol Clin North Am* 2018; **47**: 829-844 [PMID: 30337035 DOI: 10.1016/j.gtc.2018.07.008]

101 **Dubois NE**, Gregory KE. Characterizing the Intestinal Microbiome in Infantile Colic: Findings Based on an Integrative Review of the Literature. *Biol Res Nurs* 2016; **18**: 307-315 [PMID: 26721871 DOI: 10.1177/1099800415620840]

102 **Sung V**, D'Amico F, Cabana MD, Chau K, Koren G, Savino F, Szajewska H, Deshpande G, Dupont C, Indrio F, Mentula S, Partty A, Tancredi D. *Lactobacillus reuteri* to Treat Infant Colic: A Meta-analysis. *Pediatrics* 2018; **141** [PMID: 29279326 DOI: 10.1542/peds.2017-1811]

103 **Chichlowski M**, German JB, Lebrilla CB, Mills DA. The influence of milk oligosaccharides on microbiota of infants: opportunities for formulas. *Annu Rev Food Sci Technol* 2011; **2**: 331-351 [PMID: 22129386 DOI: 10.1146/annurev-food-022510-133743]

104 **Rasquin A**, Di Lorenzo C, Forbes D, Guiraldes E, Hyams JS, Staiano A, Walker LS. Childhood functional gastrointestinal disorders: child/adolescent. *Gastroenterology* 2006; **130**: 1527-1537 [PMID: 16678566 DOI: 10.1053/j.gastro.2005.08.063]

105 **Choung RS**, Locke GR 3rd. Epidemiology of IBS. *Gastroenterol Clin North Am* 2011; **40**: 1-10 [PMID: 21333897 DOI: 10.1016/j.gtc.2010.12.006]

106 **Thapar N**, Benninga MA, Crowell MD, Di Lorenzo C, Mack I, Nurko S, Saps M, Shulman RJ, Szajewska H, van Tilburg MAL, Enck P. Paediatric functional abdominal pain disorders. *Nat Rev Dis Primers* 2020; **6**: 89 [PMID: 33154368 DOI: 10.1038/s41572-020-00222-5]

107 **Rigsbee L**, Agans R, Shankar V, Kenche H, Khamis HJ, Michail S, Paliy O. Quantitative profiling of gut microbiota of children with diarrhea-predominant irritable bowel syndrome. *Am J Gastroenterol* 2012; **107**: 1740-1751 [PMID: 22986438 DOI: 10.1038/ajg.2012.287]

108 **Chumpitazi BP**, Hollister EB, Oezguen N, Tsai CM, McMeans AR, Luna RA, Savidge TC, Versalovic J, Shulman RJ. Gut microbiota influences low fermentable substrate diet efficacy in children with irritable bowel syndrome. *Gut Microbes* 2014; **5**: 165-175 [PMID: 24637601 DOI: 10.4161/gmic.27923]

109 **van den Berg MM**, Benninga MA, Di Lorenzo C. Epidemiology of childhood constipation: a systematic review. *Am J Gastroenterol* 2006; **101**: 2401-2409 [PMID: 17032205 DOI: 10.1111/j.1572-0241.2006.00771.x]

110 **Waller PA**, Gopal PK, Leyer GJ, Ouwehand AC, Reifer C, Stewart ME, Miller LE. Dose-response effect of

Bifidobacterium lactis HN019 on whole gut transit time and functional gastrointestinal symptoms in adults. *Scand J Gastroenterol* 2011; **46**: 1057-1064 [PMID: 21663486 DOI: 10.3109/00365521.2011.584895]

111 **Avelar Rodriguez D**, Popov J, Ratcliffe EM, Toro Monjaraz EM. Functional Constipation and the Gut Microbiome in Children: Preclinical and Clinical Evidence. *Front Pediatr* 2020; **8**: 595531 [PMID: 33553067 DOI: 10.3389/fped.2020.595531]

112 **Zhu L**, Liu W, Alkhouri R, Baker RD, Bard JE, Quigley EM, Baker SS. Structural changes in the gut microbiome of constipated patients. *Physiol Genomics* 2014; **46**: 679-686 [PMID: 25073603 DOI: 10.1152/physiolgenomics.00082.2014]

113 **Dimidi E**, Christodoulides S, Fragkos KC, Scott SM, Whelan K. The effect of probiotics on functional constipation in adults: a systematic review and meta-analysis of randomized controlled trials. *Am J Clin Nutr* 2014; **100**: 1075-1084 [PMID: 25099542 DOI: 10.3945/ajcn.114.089151]

114 **Gomes DOVS**, Morais MB. Gut microbiota and the use of probiotics in constipation in children and adolescents: systematic review. *Rev Paul Pediatr* 2020; **38**: e2018123 [PMID: 31778407 DOI: 10.1590/1984-0462/2020/38/2018123]

115 **Baranowski JR**, Claud EC. Necrotizing Enterocolitis and the Preterm Infant Microbiome. *Adv Exp Med Biol* 2019; **1125**: 25-36 [PMID: 30680646 DOI: 10.1007/5584_2018_313]

116 **Zhuang L**, Chen H, Zhang S, Zhuang J, Li Q, Feng Z. Intestinal Microbiota in Early Life and Its Implications on Childhood Health. *Genomics Proteomics Bioinformatics* 2019; **17**: 13-25 [PMID: 30986482 DOI: 10.1016/j.gpb.2018.10.002]

117 **Dobbler PT**, Procianoy RS, Mai V, Silveira RC, Corso AL, Rojas BS, Roesch LFW. Low Microbial Diversity and Abnormal Microbial Succession Is Associated with Necrotizing Enterocolitis in Preterm Infants. *Front Microbiol* 2017; **8**: 2243 [PMID: 29187842 DOI: 10.3389/fmicb.2017.02243]

118 **Patel RM**, Denning PW. Therapeutic use of prebiotics, probiotics, and postbiotics to prevent necrotizing enterocolitis: what is the current evidence? *Clin Perinatol* 2013; **40**: 11-25 [PMID: 23415261 DOI: 10.1016/j.clp.2012.12.002]

119 **Crowe SE**. *Helicobacter pylori* Infection. *N Engl J Med* 2019; **380**: 1158-1165 [PMID: 30893536 DOI: 10.1056/NEJMcp1710945]

120 **Patel RM**, Underwood MA. Probiotics and necrotizing enterocolitis. *Semin Pediatr Surg* 2018; **27**: 39-46 [PMID: 29275816 DOI: 10.1053/j.sempedsurg.2017.11.008]

121 **Kalach N**, Bontems P, Raymond J. Helicobacter pylori infection in children. *Helicobacter* 2017; **22** Suppl 1 [PMID: 28891139 DOI: 10.1111/hel.12414]

122 **Benavides-Ward A**, Vasquez-Achaya F, Silva-Caso W, Aguilar-Luis MA, Mazulis F, Urteaga N, Del Valle-Mendoza J. Helicobacter pylori and its relationship with variations of gut microbiota in asymptomatic children between 6 and 12 years. *BMC Res Notes* 2018; **11**: 468 [PMID: 30005690 DOI: 10.1186/s13104-018-3565-5]

123 **Yap TW**, Gan HM, Lee YP, Leow AH, Azmi AN, Francois F, Perez-Perez GI, Loke MF, Goh KL, Vadivelu J. Helicobacter pylori Eradication Causes Perturbation of the Human Gut Microbiome in Young Adults. *PLoS One* 2016; **11**: e0151893 [PMID: 26991500 DOI: 10.1371/journal.pone.0151893]

124 **Mourad-Baars P**, Hussey S, Jones NL. Helicobacter pylori infection and childhood. *Helicobacter* 2010; **15** Suppl 1: 53-59 [PMID: 21054654 DOI: 10.1111/j.1523-5378.2010.00776.x]

125 **Losurdo G**, Cubisino R, Barone M, Principi M, Leandro G, Ierardi E, Di Leo A. Probiotic monotherapy and *Helicobacter pylori* eradication: A systematic review with pooled-data analysis. *World J Gastroenterol* 2018; **24**: 139-149 [PMID: 29358890 DOI: 10.3748/wjg.v24.i1.139]

126 **Szajewska H**, Horvath A, Kołodziej M. Systematic review with meta-analysis: Saccharomyces boulardii supplementation and eradication of Helicobacter pylori infection. *Aliment Pharmacol Ther* 2015; **41**: 1237-1245 [PMID: 25898944 DOI: 10.1111/apt.13214]

127 **Emara MH**, Mohamed SY, Abdel-Aziz HR. Lactobacillus reuteri in management of Helicobacter pylori infection in dyspeptic patients: a double-blind placebo-controlled randomized clinical trial. *Therap Adv Gastroenterol* 2014; **7**: 4-13 [PMID: 24381643 DOI: 10.1177/1756283X13503514]

128 **Sharma N**, Bhatia S, Chunduri V, Kaur S, Sharma S, Kapoor P, Kumari A, Garg M. Pathogenesis of Celiac Disease and Other Gluten Related Disorders in Wheat and Strategies for Mitigating Them. *Front Nutr* 2020; **7**: 6 [PMID: 32118025 DOI: 10.3389/fnut.2020.00006]

129 **Homan M**, Orel R. Are probiotics useful in Helicobacter pylori eradication? *World J Gastroenterol* 2015; **21**: 10644-10653 [PMID: 26457024 DOI: 10.3748/wjg.v21.i37.10644]

130 **De Palma G**, Nadal I, Medina M, Donat E, Ribes-Koninckx C, Calabuig M, Sanz Y. Intestinal dysbiosis and reduced immunoglobulin-coated bacteria associated with coeliac disease in children. *BMC Microbiol* 2010; **10**: 63 [PMID: 20181275 DOI: 10.1186/1471-2180-10-63]

131 **Sjöberg V**, Sandström O, Hedberg M, Hammarström S, Hernell O, Hammarström ML. Intestinal T-cell responses in celiac disease - impact of celiac disease associated bacteria. *PLoS One* 2013; **8**: e53414 [PMID: 23326425 DOI: 10.1371/journal.pone.0053414]

132 **Fasano A**, Not T, Wang W, Uzzau S, Berti I, Tommasini A, Goldblum SE. Zonulin, a newly discovered modulator of intestinal permeability, and its expression in coeliac disease. *Lancet* 2000; **355**: 1518-1519 [PMID: 10801176 DOI: 10.1016/S0140-6736(00)02169-3]

133 **Nadal I**, Donant E, Ribes-Koninckx C, Calabuig M, Sanz Y. Imbalance in the composition of the duodenal microbiota of children with coeliac disease. *J Med Microbiol* 2007; **56**: 1669-1674 [PMID: 18033837 DOI: 10.1099/jmm.0.47410-0]

134 **Sánchez E**, De Palma G, Capilla A, Nova E, Pozo T, Castillejo G, Varea V, Marcos A, Garrote JA, Polanco I, López A, Ribes-Koninckx C, García-Novo MD, Calvo C, Ortigosa L, Palau F, Sanz Y. Influence of environmental and genetic factors linked to celiac disease risk on infant gut colonization by Bacteroides species. *Appl Environ Microbiol* 2011; **77**: 5316-5323 [PMID: 21642397 DOI: 10.1128/AEM.00365-11]

135 **De Angelis M**, Rizzello CG, Fasano A, Clemente MG, De Simone C, Silano M, De Vincenzi M, Losito I, Gobbetti M. VSL#3 probiotic preparation has the capacity to hydrolyze gliadin polypeptides responsible for Celiac Sprue. *Biochim Biophys Acta* 2006; **1762**: 80-93 [PMID: 16311022 DOI: 10.1016/j.bbadis.2005.09.008]

136 **Primec M**, Mičetić-Turk D, Langerholc T. Analysis of short-chain fatty acids in human feces: A scoping review. *Anal*

Biochem 2017; **526**: 9-21 [PMID: 28300535 DOI: 10.1016/j.ab.2017.03.007]
137 **Duar RM**, Clark KJ, Patil PB, Hernández C, Brüning S, Burkey TE, Madayiputhiya N, Taylor SL, Walter J. Identification and characterization of intestinal lactobacilli strains capable of degrading immunotoxic peptides present in gluten. *J Appl Microbiol* 2015; **118**: 515-527 [PMID: 25376327 DOI: 10.1111/jam.12687]
138 **Greco L**, Gobbetti M, Auricchio R, Di Mase R, Landolfo F, Paparo F, Di Cagno R, De Angelis M, Rizzello CG, Cassone A, Terrone G, Timpone L, D'Aniello M, Maglio M, Troncone R, Auricchio S. Safety for patients with celiac disease of baked goods made of wheat flour hydrolyzed during food processing. *Clin Gastroenterol Hepatol* 2011; **9**: 24-29 [PMID: 20951830 DOI: 10.1016/j.cgh.2010.09.025]
139 **Shanahan F**. Inflammatory bowel disease: immunodiagnostics, immunotherapeutics, and ecotherapeutics. *Gastroenterology* 2001; **120**: 622-635 [PMID: 11179240 DOI: 10.1053/gast.2001.22122]
140 **Rosen MJ**, Dhawan A, Saeed SA. Inflammatory Bowel Disease in Children and Adolescents. *JAMA Pediatr* 2015; **169**: 1053-1060 [PMID: 26414706 DOI: 10.1001/jamapediatrics.2015.1982]
141 **Kelsall BL**. Innate and adaptive mechanisms to control [corrected] pathological intestinal inflammation. *J Pathol* 2008; **214**: 242-259 [PMID: 18161750 DOI: 10.1002/path.2286]
142 **Macpherson AJ**, Gatto D, Sainsbury E, Harriman GR, Hengartner H, Zinkernagel RM. A primitive T cell-independent mechanism of intestinal mucosal IgA responses to commensal bacteria. *Science* 2000; **288**: 2222-2226 [PMID: 10864873 DOI: 10.1126/science.288.5474.2222]
143 **Fava F**, Danese S. Intestinal microbiota in inflammatory bowel disease: friend of foe? *World J Gastroenterol* 2011; **17**: 557-566 [PMID: 21350704 DOI: 10.3748/wjg.v17.i5.557]
144 **Niess JH**. Role of mucosal dendritic cells in inflammatory bowel disease. *World J Gastroenterol* 2008; **14**: 5138-5148 [PMID: 18777590 DOI: 10.3748/wjg.14.5138]
145 **Salminen S**, Benno Y, de Vos W. Intestinal colonisation, microbiota and future probiotics? *Asia Pac J Clin Nutr* 2006; **15**: 558-562 [PMID: 17077076]
146 **Morais MB**, Jacob CM. The role of probiotics and prebiotics in pediatric practice. *J Pediatr (Rio J)* 2006; **82**: S189-S197 [PMID: 17136295 DOI: 10.2223/JPED.1559]
147 **Garcia Vilela E**, De Lourdes De Abreu Ferrari M, Oswaldo Da Gama Torres H, Guerra Pinto A, Carolina Carneiro Aguirre A, Paiva Martins F, Marcos Andrade Goulart E, Sales Da Cunha A. Influence of Saccharomyces boulardii on the intestinal permeability of patients with Crohn's disease in remission. *Scand J Gastroenterol* 2008; **43**: 842-848 [PMID: 18584523 DOI: 10.1080/00365520801943354]
148 **Kato K**, Mizuno S, Umesaki Y, Ishii Y, Sugitani M, Imaoka A, Otsuka M, Hasunuma O, Kurihara R, Iwasaki A, Arakawa Y. Randomized placebo-controlled trial assessing the effect of bifidobacteria-fermented milk on active ulcerative colitis. *Aliment Pharmacol Ther* 2004; **20**: 1133-1141 [PMID: 15569116 DOI: 10.1111/j.1365-2036.2004.02268.x]
149 **Kruis W**, Fric P, Pokrotnieks J, Lukás M, Fixa B, Kascák M, Kamm MA, Weismueller J, Beglinger C, Stolte M, Wolff C, Schulze J. Maintaining remission of ulcerative colitis with the probiotic Escherichia coli Nissle 1917 is as effective as with standard mesalazine. *Gut* 2004; **53**: 1617-1623 [PMID: 15479682 DOI: 10.1136/gut.2003.037747]
150 **Bousvaros A**, Guandalini S, Baldassano RN, Botelho C, Evans J, Ferry GD, Goldin B, Hartigan L, Kugathasan S, Levy J, Murray KF, Oliva-Hemker M, Rosh JR, Tolia V, Zholudev A, Vanderhoof JA, Hibberd PL. A randomized, double-blind trial of Lactobacillus GG *vs* placebo in addition to standard maintenance therapy for children with Crohn's disease. *Inflamm Bowel Dis* 2005; **11**: 833-839 [PMID: 16116318 DOI: 10.1097/01.mib.0000175905.00212.2c]
151 **Russell SL**, Gold MJ, Reynolds LA, Willing BP, Dimitriu P, Thorson L, Redpath SA, Perona-Wright G, Blanchet MR, Mohn WW, Finlay BB, McNagny KM. Perinatal antibiotic-induced shifts in gut microbiota have differential effects on inflammatory lung diseases. *J Allergy Clin Immunol* 2015; **135**: 100-109 [PMID: 25145536 DOI: 10.1016/j.jaci.2014.06.027]
152 **McKone EF**, Emerson SS, Edwards KL, Aitken ML. Effect of genotype on phenotype and mortality in cystic fibrosis: a retrospective cohort study. *Lancet* 2003; **361**: 1671-1676 [PMID: 12767731 DOI: 10.1016/S0140-6736(03)13368-5]
153 **Ojetti V**, Saviano A, Covino M, Acampora N, Troiani E, Franceschi F; GEMELLI AGAINST COVID-19 group. COVID-19 and intestinal inflammation: Role of fecal calprotectin. *Dig Liver Dis* 2020; **52**: 1231-1233 [PMID: 33060042 DOI: 10.1016/j.dld.2020.09.015]
154 **Hashimoto T**, Perlot T, Rehman A, Trichereau J, Ishiguro H, Paolino M, Sigl V, Hanada T, Hanada R, Lipinski S, Wild B, Camargo SM, Singer D, Richter A, Kuba K, Fukamizu A, Schreiber S, Clevers H, Verrey F, Rosenstiel P, Penninger JM. ACE2 Links amino acid malnutrition to microbial ecology and intestinal inflammation. *Nature* 2012; **487**: 477-481 [PMID: 22837003 DOI: 10.1038/nature11228]
155 **Kim S**, Rigatto K, Gazzana MB, Knorst MM, Richards EM, Pepine CJ, Raizada MK. Altered Gut Microbiome Profile in Patients With Pulmonary Arterial Hypertension. *Hypertension* 2020; **75**: 1063-1071 [PMID: 32088998 DOI: 10.1161/HYPERTENSIONAHA.119.14294]
156 **Al-Beltagi M**, Saeed NK, Bediwy AS, El-Sawaf Y. Paediatric gastrointestinal disorders in SARS-CoV-2 infection: Epidemiological and clinical implications. *World J Gastroenterol* 2021; **27**: 1716-1727 [PMID: 33967552 DOI: 10.3748/wjg.v27.i16.1716]
157 **Dhar D**, Mohanty A. Gut microbiota and Covid-19- possible link and implications. *Virus Res* 2020; **285**: 198018 [PMID: 32430279 DOI: 10.1016/j.virusres.2020.198018]
158 **Olaimat AN**, Aolymat I, Al-Holy M, Ayyash M, Abu Ghoush M, Al-Nabulsi AA, Osaili T, Apostolopoulos V, Liu SQ, Shah NP. The potential application of probiotics and prebiotics for the prevention and treatment of COVID-19. *NPJ Sci Food* 2020; **4**: 17 [PMID: 33083549 DOI: 10.1038/s41538-020-00078-9]
159 **Cox MJ**, Allgaier M, Taylor B, Baek MS, Huang YJ, Daly RA, Karaoz U, Andersen GL, Brown R, Fujimura KE, Wu B, Tran D, Koff J, Kleinhenz ME, Nielson D, Brodie EL, Lynch SV. Airway microbiota and pathogen abundance in age-stratified cystic fibrosis patients. *PLoS One* 2010; **5**: e11044 [PMID: 20585638 DOI: 10.1371/journal.pone.0011044]
160 **Rogers GB**, Carroll MP, Hoffman LR, Walker AW, Fine DA, Bruce KD. Comparing the microbiota of the cystic fibrosis lung and human gut. *Gut Microbes* 2010; **1**: 85-93 [PMID: 21326915 DOI: 10.4161/gmic.1.2.11350]
161 **Li L**, Somerset S. The clinical significance of the gut microbiota in cystic fibrosis and the potential for dietary therapies.

Clin Nutr 2014; **33**: 571-580 [PMID: 24767984 DOI: 10.1016/j.clnu.2014.04.004]
162 **Bruzzese E**, Raia V, Spagnuolo MI, Volpicelli M, De Marco G, Maiuri L, Guarino A. Effect of Lactobacillus GG supplementation on pulmonary exacerbations in patients with cystic fibrosis: a pilot study. *Clin Nutr* 2007; **26**: 322-328 [PMID: 17360077 DOI: 10.1016/j.clnu.2007.01.004]
163 **Weiss B**, Bujanover Y, Yahav Y, Vilozni D, Fireman E, Efrati O. Probiotic supplementation affects pulmonary exacerbations in patients with cystic fibrosis: a pilot study. *Pediatr Pulmonol* 2010; **45**: 536-540 [PMID: 20503277 DOI: 10.1002/ppul.21138]
164 **Di Nardo G**, Oliva S, Menichella A, Pistelli R, De Biase RV, Patriarchi F, Cucchiara S, Stronati L. Lactobacillus reuteri ATCC55730 in cystic fibrosis. *J Pediatr Gastroenterol Nutr* 2014; **58**: 81-86 [PMID: 24121143 DOI: 10.1097/MPG.0000000000000187]
165 **Bruzzese E**, Raia V, Ruberto E, Scotto R, Giannattasio A, Bruzzese D, Cavicchi MC, Francalanci M, Colombo C, Faelli N, Daccò V, Magazzù G, Costa S, Lucidi V, Majo F, Guarino A. Lack of efficacy of Lactobacillus GG in reducing pulmonary exacerbations and hospital admissions in children with cystic fibrosis: A randomised placebo controlled trial. *J Cyst Fibros* 2018; **17**: 375-382 [PMID: 29128317 DOI: 10.1016/j.jcf.2017.10.014]
166 **Schuler Iv CF**, Montejo JM. Allergic Rhinitis in Children and Adolescents. *Pediatr Clin North Am* 2019; **66**: 981-993 [PMID: 31466686 DOI: 10.1016/j.pcl.2019.06.004]
167 **Bisgaard H**, Li N, Bonnelykke K, Chawes BL, Skov T, Paludan-Müller G, Stokholm J, Smith B, Krogfelt KA. Reduced diversity of the intestinal microbiota during infancy is associated with increased risk of allergic disease at school age. *J Allergy Clin Immunol* 2011; **128**: 646-52.e1 [PMID: 21782228 DOI: 10.1016/j.jaci.2011.04.060]
168 **Ni J**, Friedman H, Boyd BC, McGurn A, Babinski P, Markossian T, Dugas LR. Early antibiotic exposure and development of asthma and allergic rhinitis in childhood. *BMC Pediatr* 2019; **19**: 225 [PMID: 31277618 DOI: 10.1186/s12887-019-1594-4]
169 **Lin WY**, Fu LS, Lin HK, Shen CY, Chen YJ. Evaluation of the effect of Lactobacillus paracasei (HF.A00232) in children (6-13 years old) with perennial allergic rhinitis: a 12-week, double-blind, randomized, placebo-controlled study. *Pediatr Neonatol* 2014; **55**: 181-188 [PMID: 24269033 DOI: 10.1016/j.pedneo.2013.10.001]
170 **Miraglia Del Giudice M**, Indolfi C, Capasso M, Maiello N, Decimo F, Ciprandi G. Bifidobacterium mixture (B longum BB536, B infantis M-63, B breve M-16V) treatment in children with seasonal allergic rhinitis and intermittent asthma. *Ital J Pediatr* 2017; **43**: 25 [PMID: 28270216 DOI: 10.1186/s13052-017-0340-5]
171 **Güvenç IA**, Muluk NB, Mutlu FŞ, Eşki E, Altıntoprak N, Oktemer T, Cingi C. Do probiotics have a role in the treatment of allergic rhinitis? *Am J Rhinol Allergy* 2016; **30**: 157-175 [PMID: 27442711 DOI: 10.2500/ajra.2016.30.4354]
172 **Zajac AE**, Adams AS, Turner JH. A systematic review and meta-analysis of probiotics for the treatment of allergic rhinitis. *Int Forum Allergy Rhinol* 2015; **5**: 524-532 [PMID: 25899251 DOI: 10.1002/alr.21492]
173 **Peng Y**, Li A, Yu L, Qin G. The role of probiotics in prevention and treatment for patients with allergic rhinitis: A systematic review. *Am J Rhinol Allergy* 2015; **29**: 292-298 [PMID: 26163249 DOI: 10.2500/ajra.2015.29.4192]
174 **Arrieta MC**, Stiemsma LT, Dimitriu PA, Thorson L, Russell S, Yurist-Doutsch S, Kuzeljevic B, Gold MJ, Britton HM, Lefebvre DL, Subbarao P, Mandhane P, Becker A, McNagny KM, Sears MR, Kollmann T; CHILD Study Investigators, Mohn WW, Turvey SE, Finlay BB. Early infancy microbial and metabolic alterations affect risk of childhood asthma. *Sci Transl Med* 2015; **7**: 307ra152 [PMID: 26424567 DOI: 10.1126/scitranslmed.aab2271]
175 **Abrahamsson TR**, Jakobsson HE, Andersson AF, Björkstén B, Engstrand L, Jenmalm MC. Low gut microbiota diversity in early infancy precedes asthma at school age. *Clin Exp Allergy* 2014; **44**: 842-850 [PMID: 24330256 DOI: 10.1111/cea.12253]
176 **Vael C**, Nelen V, Verhulst SL, Goossens H, Desager KN. Early intestinal Bacteroides fragilis colonisation and development of asthma. *BMC Pulm Med* 2008; **8**: 19 [PMID: 18822123 DOI: 10.1186/1471-2466-8-19]
177 **Patrick DM**, Sbihi H, Dai DLY, Al Mamun A, Rasali D, Rose C, Marra F, Boutin RCT, Petersen C, Stiemsma LT, Winsor GL, Brinkman FSL, Kozyrskyj AL, Azad MB, Becker AB, Mandhane PJ, Moraes TJ, Sears MR, Subbarao P, Finlay BB, Turvey SE. Decreasing antibiotic use, the gut microbiota, and asthma incidence in children: evidence from population-based and prospective cohort studies. *Lancet Respir Med* 2020; **8**: 1094-1105 [PMID: 32220282 DOI: 10.1016/S2213-2600(20)30052-7]
178 **Forsythe P**. Probiotics and lung diseases. *Chest* 2011; **139**: 901-908 [PMID: 21467057 DOI: 10.1378/chest.10-1861]
179 **Sestito S**, D'Auria E, Baldassarre ME, Salvatore S, Tallarico V, Stefanelli E, Tarsitano F, Concolino D, Pensabene L. The Role of Prebiotics and Probiotics in Prevention of Allergic Diseases in Infants. *Front Pediatr* 2020; **8**: 583946 [PMID: 33415087 DOI: 10.3389/fped.2020.583946]
180 **Lin J**, Zhang Y, He C, Dai J. Probiotics supplementation in children with asthma: A systematic review and meta-analysis. *J Paediatr Child Health* 2018; **54**: 953-961 [PMID: 30051941 DOI: 10.1111/jpc.14126]
181 **Murzina E**, Kaliuzhna L, Bardova K, Yurchyk Y, Barynova M. Human Skin Microbiota in Various Phases of Atopic Dermatitis. *Acta Dermatovenerol Croat* 2019; **27**: 245-249 [PMID: 31969237]
182 **Koh LF**, Ong RY, Common JE. Skin microbiome of atopic dermatitis. *Allergol Int* 2022; **71**: 31-39 [PMID: 34838450 DOI: 10.1016/j.alit.2021.11.001]
183 **Melli LCFL**, Carmo-Rodrigues MSD, Araújo-Filho HB, Mello CS, Tahan S, Pignatari ACC, Solé D, Morais MB. Gut microbiota of children with atopic dermatitis: Controlled study in the metropolitan region of São Paulo, Brazil. *Allergol Immunopathol (Madr)* 2020; **48**: 107-115 [PMID: 32061427 DOI: 10.1016/j.aller.2019.08.004]
184 **Rusu E**, Enache G, Cursaru R, Alexescu A, Radu R, Onila O, Cavallioti T, Rusu F, Posea M, Jinga M, Radulian G. Prebiotics and probiotics in atopic dermatitis. *Exp Ther Med* 2019; **18**: 926-931 [PMID: 31384325 DOI: 10.3892/etm.2019.7678]
185 **Myles IA**, Earland NJ, Anderson ED, Moore IN, Kieh MD, Williams KW, Saleem A, Fontecilla NM, Welch PA, Darnell DA, Barnhart LA, Sun AA, Uzel G, Datta SK. First-in-human topical microbiome transplantation with Roseomonas mucosa for atopic dermatitis. *JCI Insight* 2018; **3** [PMID: 29720571 DOI: 10.1172/jci.insight.120608]
186 **Kim HJ**, Kim HY, Lee SY, Seo JH, Lee E, Hong SJ. Clinical efficacy and mechanism of probiotics in allergic diseases. *Korean J Pediatr* 2013; **56**: 369-376 [PMID: 24223597 DOI: 10.3345/kjp.2013.56.9.369]

187 **Messaoudi M**, Lalonde R, Violle N, Javelot H, Desor D, Nejdi A, Bisson JF, Rougeot C, Pichelin M, Cazaubiel M, Cazaubiel JM. Assessment of psychotropic-like properties of a probiotic formulation (Lactobacillus helveticus R0052 and Bifidobacterium longum R0175) in rats and human subjects. *Br J Nutr* 2011; **105**: 755-764 [PMID: 20974015 DOI: 10.1017/S0007114510004319]

188 **Chang HW**, Yan D, Singh R, Liu J, Lu X, Ucmak D, Lee K, Afifi L, Fadrosh D, Leech J, Vasquez KS, Lowe MM, Rosenblum MD, Scharschmidt TC, Lynch SV, Liao W. Alteration of the cutaneous microbiome in psoriasis and potential role in Th17 polarization. *Microbiome* 2018; **6**: 154 [PMID: 30185226 DOI: 10.1186/s40168-018-0533-1]

189 **Fahlén A**, Engstrand L, Baker BS, Powles A, Fry L. Comparison of bacterial microbiota in skin biopsies from normal and psoriatic skin. *Arch Dermatol Res* 2012; **304**: 15-22 [PMID: 22065152 DOI: 10.1007/s00403-011-1189-x]

190 **Huang L**, Gao R, Yu N, Zhu Y, Ding Y, Qin H. Dysbiosis of gut microbiota was closely associated with psoriasis. *Sci China Life Sci* 2019; **62**: 807-815 [PMID: 30264198 DOI: 10.1007/s11427-018-9376-6]

191 **Vijayashankar M**, Raghunath N. Pustular psoriasis responding to Probiotics – a new insight. *Our Dermatology Online* 2012; **3**: 326-328 [DOI: 10.7241/ourd.20124.71]

192 **Zeng L**, Yu G, Wu Y, Hao W, Chen H. The Effectiveness and Safety of Probiotic Supplements for Psoriasis: A Systematic Review and Meta-Analysis of Randomized Controlled Trials and Preclinical Trials. *J Immunol Res* 2021; **2021**: 7552546 [PMID: 34938815 DOI: 10.1155/2021/7552546]

193 **Picascia A**, Grimaldi V, Pignalosa O, De Pascale MR, Schiano C, Napoli C. Epigenetic control of autoimmune diseases: from bench to bedside. *Clin Immunol* 2015; **157**: 1-15 [PMID: 25576661 DOI: 10.1016/j.clim.2014.12.013]

194 **Ma Y**, Xu X, Li M, Cai J, Wei Q, Niu H. Gut microbiota promote the inflammatory response in the pathogenesis of systemic lupus erythematosus. *Mol Med* 2019; **25**: 35 [PMID: 31370803 DOI: 10.1186/s10020-019-0102-5]

195 **Ma Y**, Guo R, Sun Y, Li X, He L, Li Z, Silverman GJ, Chen G, Gao F, Yuan J, Wei Q, Li M, Lu L, Niu H. Lupus gut microbiota transplants cause autoimmunity and inflammation. *Clin Immunol* 2021; **233**: 108892 [PMID: 34813937 DOI: 10.1016/j.clim.2021.108892]

196 **Toral M**, Robles-Vera I, Romero M, de la Visitación N, Sánchez M, O'Valle F, Rodriguez-Nogales A, Gálvez J, Duarte J, Jiménez R. *Lactobacillus fermentum* CECT5716: a novel alternative for the prevention of vascular disorders in a mouse model of systemic lupus erythematosus. *FASEB J* 2019; **33**: 10005-10018 [PMID: 31173526 DOI: 10.1096/fj.201900545RR]

197 **de la Visitación N**, Robles-Vera I, Toral M, O'Valle F, Moleon J, Gómez-Guzmán M, Romero M, Duarte M, Sánchez M, Jiménez R, Duarte J. Lactobacillus fermentum CECT5716 prevents renal damage in the NZBWF1 mouse model of systemic lupus erythematosus. *Food Funct* 2020; **11**: 5266-5274 [PMID: 32458936 DOI: 10.1039/d0fo00578a]

198 **Wu HJ**, Ivanov II, Darce J, Hattori K, Shima T, Umesaki Y, Littman DR, Benoist C, Mathis D. Gut-residing segmented filamentous bacteria drive autoimmune arthritis *via* T helper 17 cells. *Immunity* 2010; **32**: 815-827 [PMID: 20620945 DOI: 10.1016/j.immuni.2010.06.001]

199 **Esmaeili SA**, Mahmoudi M, Momtazi AA, Sahebkar A, Doulabi H, Rastin M. Tolerogenic probiotics: potential immunoregulators in Systemic Lupus Erythematosus. *J Cell Physiol* 2017; **232**: 1994-2007 [PMID: 27996081 DOI: 10.1002/jcp.25748]

200 **Stoll ML**. Gut microbes, immunity, and spondyloarthritis. *Clin Immunol* 2015; **159**: 134-142 [PMID: 25967460 DOI: 10.1016/j.clim.2015.05.001]

201 **Stoll ML**, Kumar R, Morrow CD, Lefkowitz EJ, Cui X, Genin A, Cron RQ, Elson CO. Altered microbiota associated with abnormal humoral immune responses to commensal organisms in enthesitis-related arthritis. *Arthritis Res Ther* 2014; **16**: 486 [PMID: 25434931 DOI: 10.1186/s13075-014-0486-0]

202 **Öman A**, Dicksved J, Engstrand L, Berntson L. Fecal Microbiota in Untreated Children With Juvenile Idiopathic Arthritis: A Comparison With Healthy Children and Healthy Siblings. *J Rheumatol* 2021; **48**: 1589-1595 [PMID: 33262301 DOI: 10.3899/jrheum.200551]

203 **Esmaeili F**, Salesi M, Askari G, Esmaeilisharif A, Maracy M, Karimzadeh H, Shojaie B. Efficacy of synbiotic supplementation in improving rheumatoid arthritis. *Res Pharm Sci* 2020; **15**: 263-272 [PMID: 33088326 DOI: 10.4103/1735-5362.288432]

204 **Richards VP**, Alvarez AJ, Luce AR, Bedenbaugh M, Mitchell ML, Burne RA, Nascimento MM. Microbiomes of Site-Specific Dental Plaques from Children with Different Caries Status. *Infect Immun* 2017; **85** [PMID: 28507066 DOI: 10.1128/IAI.00106-17]

205 **Qudeimat MA**, Alyahya A, Karched M, Behbehani J, Salako NO. Dental plaque microbiota profiles of children with caries-free and caries-active dentition. *J Dent* 2021; **104**: 103539 [PMID: 33248211 DOI: 10.1016/j.jdent.2020.103539]

206 **Kanasi E**, Dewhirst FE, Chalmers NI, Kent R Jr, Moore A, Hughes CV, Pradhan N, Loo CY, Tanner AC. Clonal analysis of the microbiota of severe early childhood caries. *Caries Res* 2010; **44**: 485-497 [PMID: 20861633 DOI: 10.1159/000320158]

207 **Lee SH**, Kim YJ. A comparative study of the effect of probiotics on cariogenic biofilm model for preventing dental caries. *Arch Microbiol* 2014; **196**: 601-609 [PMID: 24919536 DOI: 10.1007/s00203-014-0998-7]

208 **Jindal G**, Pandey RK, Singh RK, Pandey N. Can early exposure to probiotics in children prevent dental caries? *J Oral Biol Craniofac Res* 2012; **2**: 110-115 [PMID: 25737845 DOI: 10.1016/j.jobcr.2012.05.001]

209 **Gruner D**, Paris S, Schwendicke F. Probiotics for managing caries and periodontitis: Systematic review and meta-analysis. *J Dent* 2016; **48**: 16-25 [PMID: 26965080 DOI: 10.1016/j.jdent.2016.03.002]

210 **Organ CL**, Otsuka H, Bhushan S, Wang Z, Bradley J, Trivedi R, Polhemus DJ, Tang WH, Wu Y, Hazen SL, Lefer DJ. Choline Diet and Its Gut Microbe-Derived Metabolite, Trimethylamine N-Oxide, Exacerbate Pressure Overload-Induced Heart Failure. *Circ Heart Fail* 2016; **9**: e002314 [PMID: 26699388 DOI: 10.1161/CIRCHEARTFAILURE.115.002314]

211 **Polsinelli VB**, Sinha A, Shah SJ. Visceral Congestion in Heart Failure: Right Ventricular Dysfunction, Splanchnic Hemodynamics, and the Intestinal Microenvironment. *Curr Heart Fail Rep* 2017; **14**: 519-528 [PMID: 29075956 DOI: 10.1007/s11897-017-0370-8]

212 **Sandek A**, Bjarnason I, Volk HD, Crane R, Meddings JB, Niebauer J, Kalra PR, Buhner S, Herrmann R, Springer J, Doehner W, von Haehling S, Anker SD, Rauchhaus M. Studies on bacterial endotoxin and intestinal absorption function

in patients with chronic heart failure. *Int J Cardiol* 2012; **157**: 80-85 [PMID: 21190739 DOI: 10.1016/j.ijcard.2010.12.016]

213 **Sandek A**, Swidsinski A, Schroedl W, Watson A, Valentova M, Herrmann R, Scherbakov N, Cramer L, Rauchhaus M, Grosse-Herrenthey A, Krueger M, von Haehling S, Doehner W, Anker SD, Bauditz J. Intestinal blood flow in patients with chronic heart failure: a link with bacterial growth, gastrointestinal symptoms, and cachexia. *J Am Coll Cardiol* 2014; **64**: 1092-1102 [PMID: 25212642 DOI: 10.1016/j.jacc.2014.06.1179]

214 **Pasini E**, Aquilani R, Testa C, Baiardi P, Angioletti S, Boschi F, Verri M, Dioguardi F. Pathogenic Gut Flora in Patients With Chronic Heart Failure. *JACC Heart Fail* 2016; **4**: 220-227 [PMID: 26682791 DOI: 10.1016/j.jchf.2015.10.009]

215 **Luedde M**, Winkler T, Heinsen FA, Rühlemann MC, Spehlmann ME, Bajrovic A, Lieb W, Franke A, Ott SJ, Frey N. Heart failure is associated with depletion of core intestinal microbiota. *ESC Heart Fail* 2017; **4**: 282-290 [PMID: 28772054 DOI: 10.1002/ehf2.12155]

216 **Jia Q**, Li H, Zhou H, Zhang X, Zhang A, Xie Y, Li Y, Lv S, Zhang J. Role and Effective Therapeutic Target of Gut Microbiota in Heart Failure. *Cardiovasc Ther* 2019; **2019**: 5164298 [PMID: 31819762 DOI: 10.1155/2019/5164298]

217 **Moroti C**, Souza Magri LF, de Rezende Costa M, Cavallini DC, Sivieri K. Effect of the consumption of a new symbiotic shake on glycemia and cholesterol levels in elderly people with type 2 diabetes mellitus. *Lipids Health Dis* 2012; **11**: 29 [PMID: 22356933 DOI: 10.1186/1476-511X-11-29]

218 **Kiessling G**, Schneider J, Jahreis G. Long-term consumption of fermented dairy products over 6 mo increases HDL cholesterol. *Eur J Clin Nutr* 2002; **56**: 843-849 [PMID: 12209372 DOI: 10.1038/sj.ejcn.1601399]

219 **Ahn HY**, Kim M, Chae JS, Ahn YT, Sim JH, Choi ID, Lee SH, Lee JH. Supplementation with two probiotic strains, Lactobacillus curvatus HY7601 and Lactobacillus plantarum KY1032, reduces fasting triglycerides and enhances apolipoprotein A-V levels in non-diabetic subjects with hypertriglyceridemia. *Atherosclerosis* 2015; **241**: 649-656 [PMID: 26117402 DOI: 10.1016/j.atherosclerosis.2015.06.030]

220 **Kawase M**, Hashimoto H, Hosoda M, Morita H, Hosono A. Effect of administration of fermented milk containing whey protein concentrate to rats and healthy men on serum lipids and blood pressure. *J Dairy Sci* 2000; **83**: 255-263 [PMID: 10714858 DOI: 10.3168/jds.S0022-0302(00)74872-7]

221 **Gan XT**, Ettinger G, Huang CX, Burton JP, Haist JV, Rajapurohitam V, Sidaway JE, Martin G, Gloor GB, Swann JR, Reid G, Karmazyn M. Probiotic administration attenuates myocardial hypertrophy and heart failure after myocardial infarction in the rat. *Circ Heart Fail* 2014; **7**: 491-499 [PMID: 24625365 DOI: 10.1161/CIRCHEARTFAILURE.113.000978]

222 **Lin PP**, Hsieh YM, Kuo WW, Lin YM, Yeh YL, Lin CC, Tsai FJ, Tsai CH, Huang CY, Tsai CC. Probiotic-fermented purple sweet potato yogurt activates compensatory IGFIR/PI3K/Akt survival pathways and attenuates cardiac apoptosis in the hearts of spontaneously hypertensive rats. *Int J Mol Med* 2013; **32**: 1319-1328 [PMID: 24127171 DOI: 10.3892/ijmm.2013.1524]

223 **Costanza AC**, Moscavitch SD, Faria Neto HC, Mesquita ET. Probiotic therapy with Saccharomyces boulardii for heart failure patients: a randomized, double-blind, placebo-controlled pilot trial. *Int J Cardiol* 2015; **179**: 348-350 [PMID: 25464484 DOI: 10.1016/j.ijcard.2014.11.034]

224 **Suez J**, Zmora N, Segal E, Elinav E. The pros, cons, and many unknowns of probiotics. *Nat Med* 2019; **25**: 716-729 [PMID: 31061539 DOI: 10.1038/s41591-019-0439-x]

225 **Kelesidis T**, Pothoulakis C. Efficacy and safety of the probiotic Saccharomyces boulardii for the prevention and therapy of gastrointestinal disorders. *Therap Adv Gastroenterol* 2012; **5**: 111-125 [PMID: 22423260 DOI: 10.1177/1756283X11428502]

226 **Boumis E**, Capone A, Galati V, Venditti C, Petrosillo N. Probiotics and infective endocarditis in patients with hereditary hemorrhagic telangiectasia: a clinical case and a review of the literature. *BMC Infect Dis* 2018; **18**: 65 [PMID: 29390976 DOI: 10.1186/s12879-018-2956-5]

227 **Banerjee S**. Recommendation and limitation of probiotics supplements. *Curr Trends Pharm Pharm Chem* 2021; **3**: 19-22 [DOI: 10.18231/j.ctppc.2021.006]

228 **Anadón A**, Martínez-Larrañaga MR, Aranzazu Martínez M. Probiotics for animal nutrition in the European Union. Regulation and safety assessment. *Regul Toxicol Pharmacol* 2006; **45**: 91-95 [PMID: 16563585 DOI: 10.1016/j.yrtph.2006.02.004]

229 **Ayichew T**, Belete A, Alebachew T, Tsehaye H, Berhanu H and Minwuyelet A. Bacterial Probiotics their Importances and Limitations: A Review. *J Nutr Health Sci* 2017; **4**: 1-8

World Journal of Gastroenterology

Submit a Manuscript: https://www.f6publishing.com

World J Gastroenterol 2022 May 14; 28(18): 1902-1921

DOI: 10.3748/wjg.v28.i18.1902

ISSN 1007-9327 (print) ISSN 2219-2840 (online)

REVIEW

Therapeutic strategies in Crohn's disease in an emergency surgical setting

Maria Michela Chiarello, Gilda Pepe, Valeria Fico, Valentina Bianchi, Giuseppe Tropeano, Gaia Altieri, Giuseppe Brisinda

Specialty type: Surgery, gastroenterology and hepatology

Provenance and peer review: Invited article; Externally peer reviewed.

Peer-review model: Single blind

Peer-review report's scientific quality classification

Grade A (Excellent): 0
Grade B (Very good): B
Grade C (Good): C
Grade D (Fair): 0
Grade E (Poor): 0

P-Reviewer: Keese D, Germany; Matsumoto S, Japan

Received: February 4, 2022
Peer-review started: February 4, 2022
First decision: February 24, 2022
Revised: February 28, 2022
Accepted: March 27, 2022
Article in press: March 27, 2022
Published online: May 14, 2022

Maria Michela Chiarello, Department of Surgery, San Giovanni in Fiore Hospital, Azienda Sanitaria Provinciale di Cosenza, Cosenza 87100, Italy

Gilda Pepe, Valeria Fico, Valentina Bianchi, Giuseppe Tropeano, Gaia Altieri, Emergency Surgery and Trauma Center, Fondazione Policlinico Universitario A Gemelli IRCCS, Rome 00168, Italy

Giuseppe Brisinda, Department of Surgery, Fondazione Policlinico Universitario A Gemelli IRCCS, Rome 00168, Italy

Giuseppe Brisinda, Medical and Surgical Science, Università Cattolica del Sacro Cuore, Rome 00168, Italy

Corresponding author: Giuseppe Brisinda, MD, Professor, Surgeon, Department of Surgery, Fondazione Policlinico Universitario A Gemelli IRCCS, Largo Agostino Gemelli 8, Rome 00168, Italy. gbrisin@tin.it

Abstract

Crohn's disease (CD) remains a chronic, incurable disorder that presents unique challenges to the surgeon. Multiple factors must be considered to allow development of an appropriate treatment plan. Medical therapy often precedes or complements the surgical management. The indications for operative management of CD include acute and chronic disease complications and failed medical therapy. Elective surgery comes into play when patients are refractory to medical treatment if they have an obstructive phenotype. Toxic colitis, acute obstruction, perforation, acute abscess, or massive hemorrhage represent indications for emergency surgery. These patients are generally in critical conditions and present with intra-abdominal sepsis and a preoperative status of immunosuppression and malnutrition that exposes them to a higher risk of complications and mortality. A multidisciplinary team including surgeons, gastroenterologists, radiologists, nutritional support services, and enterostomal therapists are required for optimal patient care and decision making. Management of each emergency should be individualized based on patient age, disease type and duration, and patient goals of care. Moreover, the recurrent nature of disease mandates that we continue searching for innovative medical therapies and operative techniques that reduce the need to repeat surgical operations. In this review, we aimed to discuss the acute complications of CD and their treatment.

Key Words: Crohn's disease; Intestinal obstruction; Free perforation; Intra-abdominal sepsis; Perineal sepsis; Acute bleeding

©The Author(s) 2022. Published by Baishideng Publishing Group Inc. All rights reserved.

Core Tip: Crohn's disease remains a chronic and incurable disorder. Multiple factors must be considered to allow the development of an appropriate treatment. The indications for operative management of Crohn's disease include acute and chronic disease complications and failed medical therapy. Progression into a complicated phenotype can be characterized by the formation of stenosis or abscesses/fistulas. Elective surgery comes into play when patients are refractory to medical treatment if they have an obstructive phenotype. Indications for emergency surgery include intestinal obstruction, abdominal and perineal sepsis, toxic colitis, or massive hemorrhage.

Citation: Chiarello MM, Pepe G, Fico V, Bianchi V, Tropeano G, Altieri G, Brisinda G. Therapeutic strategies in Crohn's disease in an emergency surgical setting. *World J Gastroenterol* 2022; 28(18): 1902-1921
URL: https://www.wjgnet.com/1007-9327/full/v28/i18/1902.htm
DOI: https://dx.doi.org/10.3748/wjg.v28.i18.1902

INTRODUCTION

Crohn's disease (CD) is a chronic and unremitting inflammatory disease that can involve all the gastrointestinal tract. It was first described by Crohn *et al*[1] in a case series presented at the American Medical Association annual meeting in 1932, at which time they noted a transmural inflammatory condition of the terminal ileum[1].

The incidence of CD has increased in recent years[2,3]; Ng *et al*[4] described that the higher prevalence was in Europe (322 *per* 100000 in Germany) and North America (319 *per* 100000 in Canada). In the last 30 years, a major increase has also been described in Asia, Africa, and South America[5,6].

There is no agreement between the various authors on the gender predominance[7]. Some case studies propose a female predominance in Western population and a male predominance in Eastern countries; in others there are no differences[8]. The age of presentation shows a bimodal trend with a first peak between 15-30 years (men manifest the disease earlier than women) and a second peak between 60 years and 70 years (mostly women)[9].

CD has a multifactorial etiology[10-12]. It has been described in the literature that patients who had an appendectomy for perforating appendix have a major risk to develop CD, while appendectomy for other causes is linked to a lower risk of CD[13].

The pathogenesis is unclear[5]. An excessive immune response against intraluminal bacteria occurs in the mucosa in susceptible patients and leads to a chronic inflammation that can involve all the gastrointestinal tract[7]. It is localized in the small intestine or proximal right colon with a preference of the terminal ileum in most cases[14]. The histologic findings that characterized the disease are non-caseating granulomas and discontinuous transmural lesions with inflammation penetrating to the muscolaris propria, resulting in structuring and fistulization[15].

Due to the high variability of localization and severity of inflammation, the disease can have different clinical manifestations that range from very mild to severe. Sometimes, the disease can present as an acute and severe form since from beginning[7,14,16,17].

A cure remains elusive, and efficient management of CD is essentially multidisciplinary[18,19]. Surgery is still required even if the number of operations has decreased in recent years mainly for the introduction of biological therapy[19,20].

Uncomplicated forms identified patients with a prevalent inflammatory phenotype[7,19]. On the other hand, patients affected by a form of CD with a progressive complicated phenotype present with stenosis (structuring phenotype) or abscesses/fistulas (penetrating phenotype). Elective surgery comes into play when patients are refractory to medical treatment if they have an obstructive phenotype. According to the existing literature, the risk of surgery at 1, 5, and 10 years after diagnosis of CD is 16.3%, 33.3%, and 46.6%, respectively[21]. It is still controversial whether medical treatment reduces the need for surgery[22] or not[23,24].

The indications for operative management of CD also include acute and chronic disease complications. Since CD is characterized by periods of exacerbation and remission, it is not uncommon that an acute presentation of complications that requires urgent/emergency surgery in 6%-16% of cases[24]. Patients requiring emergency surgery are generally in critical conditions and present with intra-abdominal sepsis and a preoperative status of immunosuppression and malnutrition that exposes them to a higher risk of complications and mortality. Although most acute complications of CD are managed

nonoperatively, it is important to recognize those that require a surgical approach. In this review, we aimed to discuss the acute complications of CD and their treatment, focusing on the recent results of surgical, endoscopic, and percutaneous treatments, as individual treatments and as integrated therapy.

DIAGNOSIS

Patients with CD, who present to the emergency department with symptoms of acute complications, must be properly framed to formulate an accurate diagnosis and decide what is the best possible treatment. First, a blood chemistry panel must be obtained. It must include full blood count, electrolytes, liver enzymes, renal function, and inflammatory biomarkers, such as C-reactive protein, serum albumin, and fecal calprotectin level. It is fundamental to rule out possible blood infections by carrying out blood and stool cultures and toxin test for *Clostridium difficile*[7,19].

Typically, the laboratory panel of a patient with acute CD complications is characterized by anemia, increased leukocytosis, thrombocytosis, altered liver and kidney function, and increased inflammatory markers. Neutrophil/lymphocyte ratio, obtained by dividing the absolute number of neutrophils by the absolute number of lymphocytes, is described by many authors as a good predictor of sepsis and in the case of CD as an index of acute disease complicated by the presence of abscesses. In this context, Khoury *et al*[25] developed a clinical score to predict the presence of intra-abdominal abscess (Table 1). For patients with a low score (≤ 7) the probability of an intra-abdominal abscess is very low, and therefore an urgent computerized tomography (CT) scan can be avoided. On the other hand, a high score (> 9) would warrant urgent imaging for the elevated risk of this intra-abdominal finding. In this scenario, the disease severity indices, such as Harvey-Bradshaw Index[26] (Table 2), Crohn's disease activity index (Table 3)[27-29], and Prognostic Nutrition Index[30], are also useful. This last index, calculated using the formula Prognostic Nutrition Index = 10 × albumin (g/dL) + 0.005 × total lymphocyte count/μL measured in peripheral blood with a reference value ≤ 40, is widely used to evaluate the nutritional status of the patient and to predict the risk of postoperative complications after gastrointestinal surgery [30,31]. A preoperative low nutritional prognostic index is a useful predictor of postoperative infectious complications in patients with CD-related bowel resection[31,32].

Abdominal CT scan with intravenous contrast is the first choice of examination for the diagnosis[33]. It allows the evaluation of the presence of complications such as bleeding, perforation, obstruction due to strictures, and the presence of abscesses. The procedure is essential to decide whether to proceed with a surgical treatment or opt for initial nonoperative management[34]. A frequent use of CT scan has been reported for all patients who were admitted to the emergency department for abdominal pain[35], but CD patients are irradiated more often for diagnostic purpose, with a higher exposure to X-rays[36]. Several studies evidenced that CD patients are exposed to CT scan radiation up to 2-3 times *per* year[36-39]. It is also described that children who are exposed early to CT scan have an increased risk of brain tumor and leukemia[40,41]. Craig *et al*[41] evaluated a low dose CT protocol, reaching radiation levels as low as a plain abdominal X-ray, which provided similar diagnostic efficacy even with low-quality images. The diagnostic accuracy of magnetic resonance imaging (MRI) enterography/enteroclysis is like CT scan and prevents exposure to ionizing radiations. It has a few detriments such as limited availability, high cost, and time consumption[27].

As recommended by recent guidelines for the management of CD in the emergency setting[7], point of care ultrasonography can have a role in showing free fluid, abscess, or intestinal distension, especially when CT scan is not available. Bettenworth *et al*[42] in their review showed that sensitivity of the ultrasonography for stricture diagnosis runs from 80% to 100% with specificity rates of 63%-75%. A systematic review by Panés *et al*[43] revealed that the sensitivity and specificity for ultrasound in the detection of complication are high and comparable to MRI[43].

INITIAL OPTIMIZATION

Since urgent surgery in patients with CD is burdened by a high rate of complications due to intra-abdominal sepsis, immunosuppression, and malnutrition, it is necessary to optimize their general conditions and nutritional status, delaying surgery` if feasible.

Preoperative corticosteroid use is associated with increased risk of postoperative complications[44,45]. Reduction of corticosteroid doses may decrease postoperative complications but should be carefully monitored to avoid increasing CD burden[19]. Meta-analyses of prospective and retrospective studies reported up to a doubling of surgical site infection for patients on steroids[46,47].

The application of biologic therapy before urgent surgery is still unclear. The PUCCINI trial showed no effect of anti-tumor necrosis factor α on postoperative complications[48]. Current evidence suggests that preoperative treatment with vedolizumab or ustekinumab does not increase the risk of postoperative complications in patients with CD having abdominal surgery, and cessation of these therapies prior to surgery is not mandatory[49-51].

Table 1 Variables independently associated with abscess in the clinical score of Khoury *et al*[25]

Parameters	Coefficient estimate	*P* value	Weight appointed for the score
Ileo-colonic location	0.32 ± 0.16	0.04	× 1
Perianal disease	1.17 ± 0.32	0.0002	× 3
Absence of current corticosteroids	0.62 ± 0.21	0.003	× 2
NLR > 11.75	1.15 ± 0.17	< 0.0001	× 3
CRP > 0.5 mg/dL	1.67 ± 0.21	0.03	× 5

Modified from Khoury *et al*[25]. NLR: Neutrophil/lymphocyte ratio; CRP: C-reactive protein.

Table 2 Harvey-Bradshaw index (simple index)

Variable No.	Variable description
1	General well-being (0 = Very well; 1 = Slightly below par; 2 = Poor; 3 = Very poor; 4 = Terrible)
2	Abdominal pain (0 = None; 1 = Mild; 2 = Moderate; 3 = Severe)
3	Number of liquid stools daily
4	Abdominal mass (0 = None; 1 = Dubious; 2 = Definite; 3 = Definite and tender)
5	Complications: arthralgia, uveitis, erythema nodosum, aphthous ulcer, pyoderma gangrenosum, anal fissure, new fistula, abscess (score 1 for item)

Modified from Harvey and Bradshaw[26].

Table 3 Crohn's disease activity index

Variable No.	Variable description	Multiplier
1	Number of liquid or soft stools (each day for 7 d)	× 2
2	Abdominal pain, sum of 7 daily ratings (0 = None, 1 = Mild, 2 = Moderate, 3 = Severe)	× 5
3	General well-being, sum of 7 daily ratings (0 = Generally well, 1 = Slightly under par, 2 = Poor, 3 = Very poor, 4 = Terrible)	× 7
4	Number of listed complications (arthritis or arthralgia, iritis or uveitis, erythema nodosum or pyoderma gangrenosum or aphthous stomatitis, anal fissure or fistula or abscess, other fistula, fever over 37.8 °C	× 20
5	Use of diphenoxylate or loperamide for diarrhea (0 = No, 1 = Yes)	× 30
6	Abdominal mass (0 = No, 2 = Questionable, 5 = Definite)	× 10
7	Hematocrit (males 47-Hct %, females 42-Hct %)	× 6
8	Body weight (1-weight/standard weight) × 100 (add or subtract according to sign)	× 1

Modified from Best *et al*[29]. Hct: Hematocrit.

Malnutrition is an independent risk factor for postoperative poor outcomes[52,53]. Preoperative nutritional assessment should be performed for all patients with CD who need surgery[19]. The European Society for Clinical Nutrition and Metabolism stated that serum albumin of < 3 g/dL, body mass index < 18.5 kg/m^2, and weight loss > 10%-15% within 6 mo are the best indicators of severe malnutrition in CD patients[54]. The nutrition of choice should be the enteral nutrition that can be replaced with the parenteral one only in those patients who cannot tolerate the first or have severe contraindications such as a high flow intestinal fistula, intestinal perforation, or intestinal ischemia[55,56]. Brennan *et al*[57] observed that patients who received preoperative nutritional support had a rate of postoperative complications of 20% compared with 61.3% in the group without nutritional support. Zhu *et al*[58] suggested that enteral nutrition is feasible in CD patients with non-radiologically-drainable abdominal abscess.

INDICATIONS TO EMERGENCY SURGERY

Acute bowel obstruction, intra-abdominal sepsis, hemorrhage, acute toxic colitis, and perianal sepsis are the indications for an emergency procedure in patients with CD. The incidence of acute complications of CD are shown in Table 4.

Acute surgical emergencies in patients with CD are associated with high morbidity and mortality. Postoperative mortality rates for nonelective surgeries in CD have decreased but remain significantly higher than the mortality rate following elective surgery (3.6% *vs* 0.6%)[59,60]. Although most acute complications of CD are managed nonoperatively, it is important to recognize those that require surgical management. Another issue is the prevention of recurrence, which is still much debated.

INTESTINAL OBSTRUCTION

Acute intestinal obstruction is the most frequent complication in patients with CD, especially in patients with ileo-colic localization (35%-54%), while in jejunal (22%-36%) or colic (5%-17%) localizations the frequency is lower[19,61-63]. Gastroduodenal obstruction is rare, occurring in 0.5% to 13% of patients [62,64]. Patients with gastroduodenal strictures present with postprandial fullness, early satiety, vomiting, and upper abdominal pain[65,66]. Patients with obstruction of the small intestine present with nausea, vomiting, dehydration, crampy abdominal pain, bloating, obstipation, and constipation. Patients with colonic obstruction may present without nausea and vomiting but with bloating, distension, and abdominal pain, in addition to constipation. Initial management of bowel obstruction includes bowel rest, intravenous hydration, and nasogastric decompression in the presence of vomiting [42].

Strictures complicating CD can be classified as inflammatory or fibrostenotic[67]. Patients with inflammatory disease deserve medical therapy, such as steroids for reducing inflammation. Patients who do not improve with medical therapy and in whom an occlusion due to fibrosis can be hypothesized need receive a CT scan or an MRI. In these patients, an interventional approach, endoscopic or surgical, is usually needed[7]. Deferred surgery is the preferred option in adult patients with small bowel obstruction without bowel ischemia or peritonitis. Endoscopic balloon dilatation (EBD) is a suitable treatment option for patients with short (< 5 cm) strictures[68]. For fibrotic strictures, EBD has a technical success rate of 89% to 92%, with 70% to 81% of patients presenting free of occlusive symptoms in the short term[69]. In contrast for the long term, 73.5% of patients require repeat dilatation and 43% a surgical intervention within 2 years[70]. Fully covered self-expandable metal stents (FCSEMS) have been used for endoscopic treatment of patients for whom EBD was unsuccessful. In a multicenter, open-label, randomized trial[71], 80 patients were randomly assigned to treatment: 39 (49%) patients to the FCSEMS group and 41 (51%) patients to the EBD group. Overall, 33 (80%) of 41 patients in the EBD group and 20 (51%) of 39 patients in the FCSEMS group could avoid a new therapeutic intervention in 1 year (odds ratio: 3.9; 95% confidence interval: 1.4–10.6; $P = 0.0061$). Two of 80 patients had perforations (1 patient in the EBD group and 1 patient in the FCSEMS group)[71]. EBD is more effective than FCSEMS for CD strictures, with a good safety profile for both the treatments.

Surgery is mandatory for intestinal obstruction with potential impending perforation, with long or multiple strictures, when the strictures are not endoscopically accessible, when medical or endoscopic treatment does not result in an adequate reduction of clinical symptoms, or when there is a suspicion of an underlying malignancy[7,72,73]. If emergency surgery is indicated, a laparoscopic approach is recommended when appropriate expertise exists[74,75].

The surgical treatment of choice is a segmental resection of the involved segment with primary anastomosis. In fact, the most important principle in the surgical management of CD is to resect only the segment of bowel affected by the complication to prevent short bowel syndrome. Even if adjacent areas of bowel are clearly diseased, that should be ignored[76]. Furthermore, when two intestinal segments are involved, but with a healthy segment in between, the resection of the healthy segment depends on its length, too[77]. If it is 10 cm or longer, it probably should be saved. If it is 5 cm or shorter it should be included. In the other cases, the surgical attitude will depend on previous resection, configuration of blood supply, and mobility of the mesentery. The anastomosis could be either hand-sewn or stapled, end-to-end or side-to-side[78]. The literature does not describe a superiority of one technique over another, and the final decision can be left to the surgeon preference[78-80]. If a stapled anastomosis is performed, some authors advise performing it with an isoperistaltic configuration to allow an easier subsequent endoscopic surveillance. If the bowel wall is edematous due to chronically inflammation, a hand-sewn anastomosis would be better[80]. The general conclusion favors stapled side-to-side anastomosis. The diameter of the anastomosis plays a role as well, with the assumption that a wider anastomosis will have a lower rate of clinical and surgical complications[81,82].

Other surgical options include stricturoplasty, intestinal bypass, and creation of ileostomy. Short fibrous strictures, multiple strictures, short bowel syndrome, rapid recurrence of obstruction due to CD, and duodenal CD are indications for stricturoplasty. Contraindications to stricturoplasty are multiple strictures in a short intestinal segment, a long stricture (> 20 cm), or stricture close to the resection site

Table 4 Incidence of acute complications in Crohn's disease

Complication	Incidence (%)	Ref.
Small bowel obstruction	35.0-59.0	[63]
Gastroduodenal obstruction	0.5-15.0	[64]
Colonic strictures	5.0-17.0	[73]
Intra-abdominal abscess	10.0-28.0	[85,156]
Free bowel perforation	1.0-6.5	[104,105]
Acute appendicitis	0.1-2.0	[113]
Bleeding	1.0-6.0	[126]
Perianal disease with left-sided colon or rectal involvement	17.0-43.0	[145]
Isolated perianal involvement	5.0	[146]

[83]. Bypass operations have largely been abandoned because of the subsistence of disease activity[83]. An ileostomy is required when it is not safe to perform an anastomosis, such as in case of severe patient instability, malnutrition, intra-abdominal sepsis, chronic immunosuppression, or when a small bowel resection is performed together with colonic or rectal resection[76,79].

INTRA-ABDOMINAL SEPSIS

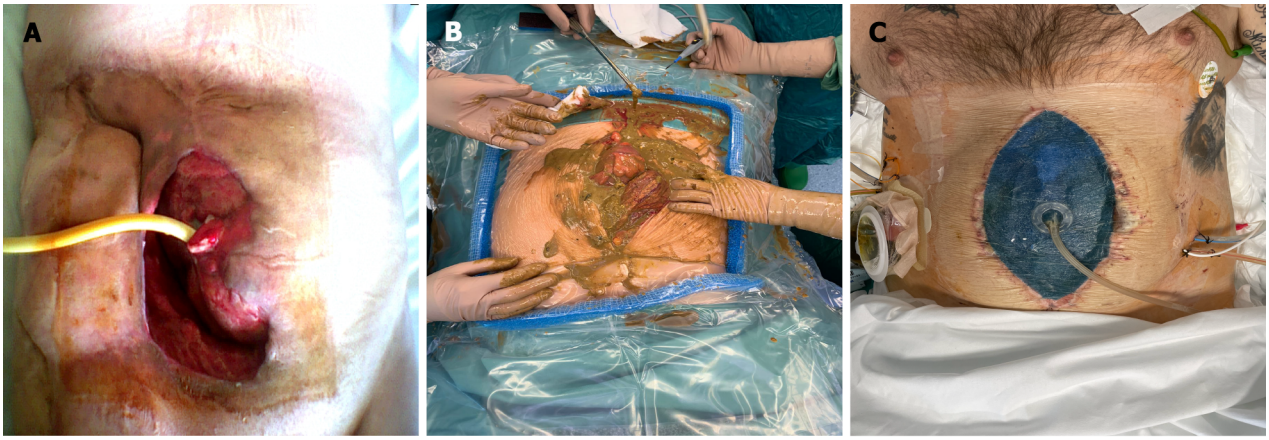
Abscess

The presence of an abscess occurs in up to 20% of CD patients[84-86]. It typically results from a penetrating disease phenotype with a distal stricture[80]. An abscess is categorized as active at Harvey-Bradshaw Index[26] and severe with a Crohn's disease activity index > 450[27-29]. Abscess is defined as an inflammatory mass consequent to bowel perforation promptly covered by fibrin that adheres to the loops surface causing adhesions among them. It can be associated with other CD complications such as fistulas (40%) and stenosis (51%)[14,85]. Usually, these patients present to the emergency department with fever associated with abdominal pain, palpable masses, and rebound tenderness. In 28% of cases they can have a generalized sepsis[84]. Therefore, it is crucial that they receive a proper clinical evaluation. If an abscess is suspected, cross-sectional imaging is recommended. CT scan is the gold standard for their detection in the emergency setting, and it also identifies concomitant fistulae or bleedings. MRI has a similar accuracy with a lower ionizing radiation exposure, but it is not always accessible in the emergency department. Point of care in the United States can have a role in the initial assessment, and it is extremely useful in rural hospitals where CT is not available[7,87,88]. Moreover, if there is an indication to the positioning of a percutaneous drainage, both ultrasonography and CT can be used as guides[86,89]. In selected cases, endoscopic ultrasound can be employed for draining the cavity by a transvaginal or transrectal approach[90,91].

When the abscess diagnosis is confirmed, the best patient tailored treatment must be defined. In stable patients with abscesses smaller than 3 cm, early empiric antimicrobial therapy is recommended with a close clinical and biochemical monitoring. If the abscess is > 3 cm, percutaneous drainage with antibiotics is endorsed[7,89]. The drainage approach depends on the abscess site. It can be transgluteal for pelvic abscesses but also transabdominal. The catheter, whose size must be chosen considering the viscosity of the fluid collected, is left in place, and the daily quantity and quality of the drain must be recorded carefully[84,92].

Percutaneous drainage is a validated procedure because it may avoid an immediate operation, delaying to elective surgery[93,94]. Inflammation will have enough time to resolve, making possible limited intestinal resections and reducing the need of a diverting stoma creation. In addition, the nutritional status could be optimized and steroids interrupted before surgery, reducing the risk of anastomotic leak[53,84]. According to some studies, percutaneous drainage is a bridge to definitive surgical treatment. On the other hand, more recent studies have demonstrated that most patients do well with only percutaneous drainage and do not need any other surgical treatment with success rates that vary from 50% to 95%. The risk of recurrence, more often within 3 years, must be considered[95-97]. Immediate surgery should be considered in cases of patients with septic shock or failure of percutaneous drainage due to multiple and multilocular abscesses and those associated with a fistula (Figure 1A)[84,98].

Another key factor in the conservative treatment in CD patients with abscess is antibiotic therapy. Therefore, it is important to collect a sample of drained fluid and send it for a microbiological test. The culture can reveal the type of microorganisms in the pus, allowing the optimization of the antimicrobial



DOI: 10.3748/wjg.v28.i18.1902 **Copyright** ©The Author(s) 2022.

Figure 1 Intra-abdominal sepsis. A: Abscess in the right iliac fossa, spontaneously draining to the skin, associated with high-flow enteric fistula. Foley catheter placed in the fistulized small intestine; B: Fecal contamination of the peritoneal cavity in a patient with Crohn's disease with perforation of the transverse colon; C: Open abdomen after treatment of intestinal perforation in Crohn's disease. Negative pressure intraperitoneal device placement.

therapy, increasing the chances of conservative treatment success. Reuken *et al*[99] found that the culture was positive in about 88% of patients and usually polimicrobic. The most common pathogens were *Escherichia coli*, *Streptococcus spp*., *Enterococci*, *Candida*, and anaerobes. The most used empirical first-line antibiotics were broad spectrum penicillins, followed by cephalosporins and quinolones[99]. These treatments were inadequate in patients on immunosuppression or with a prolonged hospitalization and that could be linked to a higher risk of failure[80]. The appropriate duration of antibiotic therapy is unclear. Also, anti-tumor necrosis factor therapy can have a role in the treatment of an abscess, but only if associated to antimicrobial treatment that must be continued for 3 mo[100].

After antimicrobial treatment and percutaneous drainage clinical improvement is expected in 3–5 d, with a gradual decrease in the drain output. According to the American Society of Colon and Rectal surgeons, after a successful resolution of an abscess with percutaneous drainage and antibiotics, a drain study to exclude a concomitant fistula could be beneficial[80]. If a patient's condition does not improve, a re-evaluation is mandatory[84], and if the abscess has not been adequately drained, repositioning of the drain or an operation must be considered.

When a surgical exploration must be performed for conservative treatment failure or for concomitant CD complications, some issues need to be considered. First, if the patient is unstable, an open approach is recommended, considering the damage control surgery principles. There is also room for open abdomen use. An operation with a bowel resection gives better results than an operative drainage alone, which determines a higher rate of reoperation and enterocutaneous fistula formation. In case of septic shock, it may be appropriate to perform bowel resection with stapled off bowel stumps, peritoneal lavage, and open abdomen with a planned second exploration in the next 24-48 h after the patient has been stabilized in the intensive care unit. At this point, surgeons must decide whether to create a stoma or anastomize the stumps[89,101]. In the case of a stable patient and technical skills available, laparoscopy is recommended to reduce hospital stay and morbidity. Both open and laparoscopic extensive resections must be avoided because they can lead to immediate or future short bowel syndrome in these patients[80].

Even after success of conservative treatment, patients with a concomitant stenosis, an enterocutaneous fistula, or refractory active disease are likely to require surgery[102]. It is believed that a window of 6 to 8 wk after the resolution of the acute clinical scenario could permit a good improvement of the clinical and nutritional status as well as a proper imaging and endoscopic work-up. This work-up aims to avoid unexpected findings during the elective operation[93]. Moreover, as already discussed, the surgical outcomes will be better and comparable to CD patients with non-penetrating disease, as it is also confirmed by recent research[103]. In their study on 592 patients, Collard *et al*[103] compared patients who underwent an ileocolonic resection after a conservative treatment for an abscess to CD patients without a penetrating disease who had the same operation[103]. In the first group, all the patients underwent a CT scan after the percutaneous drainage to demonstrate a complete resolution of the abscess. Nevertheless, the persistence of an abscess, defined by the presence of a pus-like or purulent collection in the site of the original abscess, was found in 25% of cases. There were no differences between the two groups for rate of primary anastomosis, need of additional intestinal resection, incidence of intraoperative and postoperative complications, and length of hospital stay.

Free perforation

Free peritoneal perforation in CD is a rare condition that occurs in 1%-3% of CD patients as a first manifestation or in the course of the disease[104,105]. It is one of the main indications for emergency

surgery with a high rate of morbidity and mortality in the case of delayed surgery[104]. Greenstein *et al* [106] reported that perforation can occur in the ileum or in the colon indifferently, without a preference for location. Instead, the Connect study of Doh *et al*[105] found that ileal perforation had a higher incidence (86.2%), while colonic perforation occurred in only 7.4% of the patients. Some authors described that steroid treatment increases the risk of free perforation[107-110]. The role of anti-tumor necrosis factor agents in the etiopathogenesis of free perforation is not clear yet[111]. The mechanism leading to free perforation is still unclear, but there are two most likely hypotheses. The first and more conceivable is that the increase of intraluminal pressure proximal to a stenosis causes a bowel distension that can perforate the thin layer overlying a deep ulcer, while the second suggests that the perforation is consequent to intestinal ischemia due to inflammation of the small vessels[105].

The intestinal segment affected by the perforation should be resected by either directly performing a primary anastomosis or proceeding with an enterostomy. According to our practice, in the case of severe abdominal contamination (Figure 1B), we recommend not to close the laparotomy but to perform a second look as already described by Liu *et al*[112], using the technique of open abdomen with negative pressure wound therapy (Figure 1C). In this way, it is possible to prevent intra-abdominal sepsis and during the second look, optimize the resection. In some selected cases, a primary anastomosis could be feasible as the vacuum system allows a good intra-abdominal clearance. We also recommend this technique in the setting of damage control surgery with a hemodynamically unstable patient, when the decision to perform an enterostomy will be postponed to the second look.

Acute appendicitis

Appendiceal CD is a rare condition, whose incidence varies from 0.1% to 2.0%[113]. After the first case described in 1953[114], there was an initial interest in the topic with most of the cases described in the late 1980s and early 1990s[115,116]. In 1990, Ruiz *et al*[117] identified 85 cases of CD limited to the appendix[117]. The disease was found most frequently in the second and third decades. The authors suggest that a prolonged preoperative history of symptoms should alert the surgeon to this possibility [117]. Lindhagen *et al*[118] identified 50 cases and added 12 of their own[118]. The indication for surgery in their patients were appendicitis in 8 patients, appendiceal abscess in 2 patients, suspected pyosalpinx in 1 patient, and ovarian cyst in 1 patient. All but 2 of the 8 appendicitis patients underwent appendectomy; the others underwent a more extensive resection. There were no postoperative complications. The authors concluded that when CD is confined to the appendix the prognosis is very favorable [118].

When considering acute appendicitis in CD patients, it is essential to differentiate between patients admitted to the emergency department with a possible appendicitis who already have been diagnosed with CD and patients who underwent an appendectomy. The histopathology reveals the disease. In a recent study, a group from Seoul analyzed 2179 appendectomies. Among these only 12 (0.55%) were compatible with CD at histology[113]. The 12 patients presented to the emergency department with right lower quadrant pain, abdominal pain, and diarrhea. The duration of symptoms varied from 2 to 5 mo[113]. They did not present systemic manifestations such as uveitis, arthralgia, and arthritis. The histological examination revealed transmural inflammation, lymphoid aggregates, and epithelioid granulomas as peculiar features present in all the cases, followed by appendiceal wall thickening and mucosal ulceration. When the diagnosis is made, the patient must be referred to a tertiary center for future gastroenterology follow-up.

Sometimes the appendix inflammation is consequent/reactive to terminal ileitis in patients affected by CD. Since the acute presentation is like common appendicitis, it is crucial to focus on symptoms like recurrent abdominal pain or diarrhea, lack of fever, weight loss, microcytic anemia, hypoalbuminemia, and hypoproteinemia. In fact, these symptoms are more typical of CD rather than appendicitis. If there is a suspicion of CD, the entire small and large bowel should be carefully examined to verify the presence of the disease and its extent.

In patients with known CD, medical treatment for ileocecal CD is recommended. In fact, if in the rare cases of CD localized only in the appendix, the appendectomy can be performed safely. The clinical scenario is completely different when there is active ileocecal disease. In this situation, there are some issues that need to be considered. The main goal is to avoid an ileocecal resection, when possible, for limiting the unnecessary excision of intestinal segments. An ileocecal resection is the operation of choice in the case of cecum involvement to reduce the risk of leak from the appendix stump and formation of enterocutaneous fistula. Furthermore, if the patient has experienced severe symptoms due to ileitis, an ileocecal resection is the treatment of choice, followed by biologic therapy. Otherwise, the patient will continue suffering CD symptoms with 38% requiring a resection within 1 year. Finally, it is not necessary to remove a macroscopically normal appendix during an exploration for suspected appendicitis if there are findings that raise doubts of CD[119].

ACUTE COLITIS

Toxic colitis represents a potentially fatal condition that may in occur in patients affected by inflam-

matory bowel disease. Studies have demonstrated that as many as 50% of all toxic colitis cases may be secondary to Crohn's colitis[72,120,121]. Diagnostic criteria include: Severe diarrhea (6 or more bloody bowel movements *per* day); temperature higher than 37.8 °C; heart rate > 90 beats/min; anemia (hemoglobin < 10.5 g/dL); an elevated erythrocyte sedimentation rate (< 30 mm/h); hypoalbuminemia (< 3.0 g/L); and leukocytosis (> 10.5 × 10^9 cells/L)[122]. Toxic megacolon is defined when radiographic imaging demonstrating dilation of the transverse colon to at least 6 cm is associated to the previously mentioned criteria[7,72]. Cytomegalovirus infection has been identified in 25% to 36% of patients with steroid-refractory acute colitis. Studies have demonstrated that *Clostridium difficile* infection in the setting of severe or toxic colitis is associated with increased morbidity and mortality.

When toxic colitis is diagnosed, intensive medical therapy should be promptly administered. Intravenous methylprednisolone, 60 mg *per* day, or hydrocortisone, 300 mg, are the medications of choice[123]. Treatment with higher doses of intravenous corticosteroids have not been demonstrated to reduce colectomy rate and should not be considered. In general, a response to steroid therapy includes improvement or resolution of the systemic inflammatory response syndrome and a decrease in stool frequency. In the case of overall clinical improvements over the course of the following 3 d, maintenance therapy could be considered. If there is no response to corticosteroid therapy, rescue therapy is used. Infliximab has now emerged as the most widely used rescue therapy due to its low toxicity, ease of administration, and consequently the possibility to be used for maintenance therapy. One recent literature review demonstrated immediate response rates to infliximab as a rescue therapy agent range between 50% and 83%, with long-term response rates slightly lower at 50% to 63%[124].

Contrarily, in the case of worsening clinical condition or failure to improve, a transition to either rescue therapy or an urgent colectomy should be taken into account. If a patient presents with peritonitis or evidence of free perforation on imaging, surgical exploration is mandatory. Perforation in patients with toxic megacolon is associated with a high mortality rate (27%–57%), regardless of whether the perforation is contained or free[7]. The transverse colon is the area of greatest concern in toxic megacolon. The surgical option of choice is subtotal colectomy with end ileostomy, which allows for future reconstructive options avoiding permanent stoma by ileorectal anastomosis (Figure 2). This could be suggested for patients without rectal or perianal involvement. A total proctocolectomy should be avoided even if total proctocolectomy with permanent stoma is the safest option to avoid further operation in high-risk patients[72] because it is associated with greater postoperative morbidity and mortality due to increased operative time, risk of blood loss, pelvic sepsis, and pelvic nerve damage. The patient typically improves over the ensuing few days. An ileoproctostomy can be recommended 6 mo later in selected patients who demonstrate minimal mucosal inflammation, adequate rectal compliance, absence of significant anoperineal disease, and sufficient sphincter strength[72].

BLEEDING

Gastrointestinal bleeding is a common complication in patients affected by CD. Inflammation/ulceration of the bowel are the basis of its onset. Usually, conservative treatment and endoscopy are sufficient to resolve this condition that rarely requires an emergency surgical procedure. Severe intestinal hemorrhage, on the other hand, is a rare occurrence in CD, with reported incidence between 0% and 6%[125,126]. The underlying pathophysiology of the hemorrhage most often is a result of focal erosion into an intestinal vessel. Due to the infrequency of significant bleeding in CD, as stated before, all common causes of upper and lower gastrointestinal bleeding should be assessed. Localization of the bleeding site is essential regardless of the planned therapy.

Management of gastrointestinal bleeding related to CD begins with hemodynamic assessment. In a stable patient the localization of the lesion could be identify by endoscopy or radiology. Nasogastric tube, in case of hematemesis, should be inserted to protect the airway and decompress the stomach. Gastroscopy could be required to rule out upper gastrointestinal bleeding. If a lower gastrointestinal source is suspected, a retrospective study[127] reported that the detection rate for vascular lesions was higher for colonoscopy following contrast-enhanced CT scan than for colonoscopy alone.

The role of angiography and of angioembolization must be still clarified. Most of the data suggest that angiography/angioembolization could be feasible in stable patients, but further studies are needed to better define outcomes in the emergency setting[7]. The major advantage is that it can control severe bleeding without bowel preparation. Disadvantages include the risk of bowel ischemia and the administration of intravenous contrast. In particular the rate of bowel ischemia following embolization was 1%–4% in recent studies[128].

In the case of hemodynamic instability, resuscitation by intravenous fluid/blood product administration is fundamental aiming to normalize blood pressure and heart rate prior to endoscopic evaluation/intervention. Packed red blood cells should be transfused to maintain the hemoglobin above 7 g/dL. A threshold of 9 g/dL should be considered in patients with massive bleeding, significant comorbidities (especially cardiovascular ischemia), or possible delay in receiving therapeutic interventions[7]. The decision to perform an urgent surgical procedure depends on the bleeding source itself, the hemodynamic condition of the patient, and on the availability/feasibility of less invasive



DOI: 10.3748/wjg.v28.i18.1902 **Copyright** ©The Author(s) 2022.

Figure 2 Surgical specimen of total intra-abdominal colectomy in patient with acute colitis.

therapeutic options (*i.e.* endoscopy or angiography). In the case of persistent hemodynamic instability, operative management is necessary. The most challenging situation is represented by patients who have a primary or recurrent hemorrhage without an identifiable source of bleeding. In these cases, the likelihood of successfully eradicating the source of hemorrhage through a "blind" intestinal resection must be weighed against the risk of recurrent bleeding and of creating short bowel syndrome in patients with extensive disease or multiple previous resections.

POSTOPERATIVE RECURRENCE

Postoperative recurrence is the appearance of new lesions after surgery for CD. After the first intestinal resection, 25%-45% of patients are likely to need further operations within 10 years[129]. One year after an initial resection, 60%-80% of patients possess endoscopic recurrence, 10%-20% experience clinical relapse, and 5% demonstrate operative recurrence[130]. Diagnosis of postoperative recurrence is primarily based on clinical symptoms and endoscopic findings. Rutgeerts *et al*[131] developed an endoscopic scoring system to assess endoscopic recurrence (Table 5).

Therefore, ileocolonoscopy is the gold standard to identify the presence and severity of CD recurrence, and it is recommended within the first year after surgery[20]. An emerging and less invasive method to identify postoperative recurrence is the small intestine contrast ultrasonography, which is comparable to ileocolonoscopy to detect lesions related to CD[132]. Fecal calprotectin is another noninvasive diagnostic and monitoring tool because a later correlation was found between endoscopic severity and calprotectin levels[133].

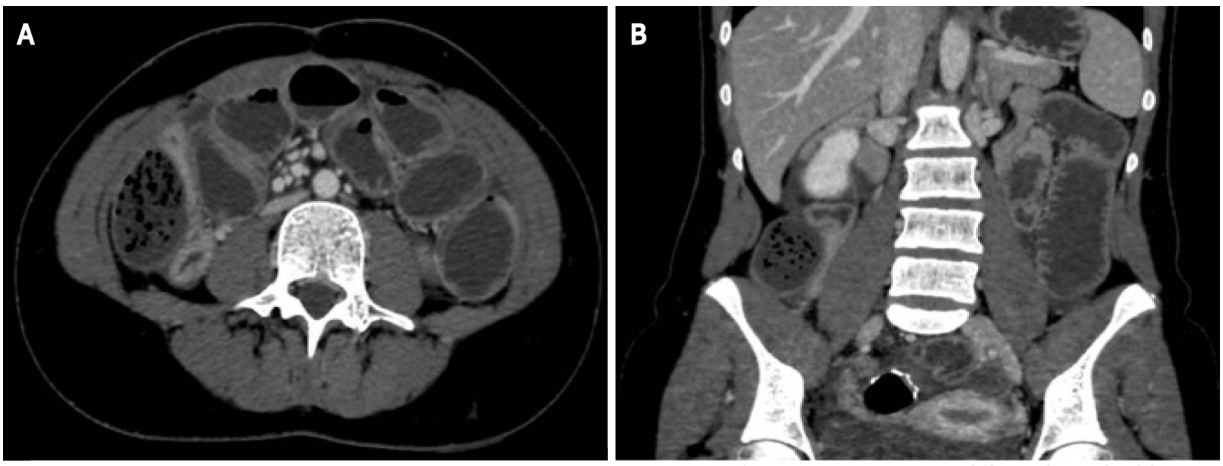
In the last few decades, the risk of major abdominal surgery within the first 5 years of diagnosis has declined, due to the advances in medical treatment of CD. However, there is still a great debate in the literature about risk factors for postoperative recurrence in Crohn's disease (Figure 3). According to the European Crohn's and Colitis Organization guidelines, smoking, prior intestinal surgery, penetrating disease, absence of prophylactic treatment, perianal location, presence of granulomas in the surgical specimen, and myenteric plexitis are considered predictors of early postoperative recurrence after ileocolonic resection[20]. Santiago *et al*[134] identified the presence of colic disease as an independent risk factor for postoperative recurrence and reoperation, while colectomy or proctocolectomy performed during the first surgery have a protective role against reoperation in patients with CD[134]. Liu *et al*[112] in 2020 published a series on the comparison between primary anastomosis and staged surgery in emergency treatment of complicated CD. The results of this study showed a lower surgical recurrence rate for staged surgery, probably linked to the reduction of inflammatory activity when a fecal diversion is performed[112]. A young age, less than 16 years, was identified as another risk factor for repeated abdominal surgery in CD patients by a multicenter study of the Korean Inflammatory Bowel Disease Study Group as well as the presence of stricturing disease behavior[135].

Other recent fields of investigation focus on the role of anastomotic technique in the pathogenesis of postoperative recurrence. In 2014 and 2018, two meta-analyses were performed to define the optimal surgical technique of anastomosis. The conclusions were that stapled isoperistaltic side-to-side anastomosis, because of its larger lumen, can significantly reduce the incidence of postoperative complications and recurrence[136,137]. In 2011, Kono *et al*[138] introduced a new anastomotic technique. The Kono-S is an antimesenteric functional end-to-end hand sewn anastomosis, with the two stumps sutured to create a "supporting column," which allows preservation of the diameter and prevents stenosis and distortion of the anastomosis[138]. The SuPREMe-CD Study, a randomized clinical trial

Table 5 Endoscopic scoring system for postoperative recurrence

Grade	Endoscopic findings
0	No endoscopic recurrence
1	≤ 5 aphthous lesions
2	> 5 aphthous lesions with normal mucosa between the lesions, or skip areas of larger lesions, or lesions confined to ileocolonic anastomosis
3	Diffuse aphthous ileitis with diffuse inflammation of the mucosa
4	Diffuse inflammation with larger ulcers, nodules, and/or narrowing

Modified from Rutgeerts *et al*[131].



DOI: 10.3748/wjg.v28.i18.1902 **Copyright** ©The Author(s) 2022.

Figure 3 Computed tomography scan. Coronal view and sagittal view showing postoperative recurrence of Crohn's disease with small bowel stenosis in patient previously treated by colectomy and ileo-anal anastomosis. A: Coronal view; B: Sagittal view.

that compared Kono-S anastomosis and stapled side-to-side anastomosis, confirmed the reduction of postoperative recurrence when the Kono-S anastomosis was performed[139].

Few studies in the literature analyzed the correlation between emergency surgery for CD and postoperative recurrence. However, emergency surgery would seem to be another independent risk factor for surgical recurrence[140]. Urgent surgery may be related to more aggressive disease, and greater variation in the anastomotic technique in urgent surgery may affect the risk of recurrence[81]. Furthermore, a recent paper highlights that an end-to-end anastomosis is associated with an increased risk of early postoperative recurrence in the subset of patients undergoing an emergency operation as well as smoking and the failure to commence early medical prophylaxis[141].

Another important topic about the risk of recurrence in CD is represented by the role of the mesentery. Patients with CD are characterized by a peculiar form of adipose tissue hypertrophy, known as "creeping fat"[142], which seems to be an independent predictor of early clinical recurrence of CD when there is an advanced mesenteric involvement in the surgical specimen[143]. An international, multicenter, randomized controlled trial by Li *et al*[144] is ongoing to compare conservative limited resection and surgery with mesenteric excision in CD, and its results may provide important insights about the most appropriate surgical technique. One of the most common components of CD that manifests itself after proctocolectomy is the recurrence of disease in the ileostomy or remaining small bowel.

PERIANAL SEPSIS

Perianal fistulas and abscesses are common in CD with an incidence up to 43% and are more frequent in patients with distant colonic or rectal disease[145,146]. They require a multidisciplinary (both medical and surgical) approach to achieve a complete fistula healing and reduce the negative effect on the patient's lifestyle[147,148].

Abscess is a consequence of cryptoglandular inflammation/infection as described by Eisenhammer [149] in 1956 and can be the first sign of CD. It may result in a fistula that is classified based on its

Table 6 Perianal Crohn's disease activity index

Categories affected by fistulas	Score
Discharge	
No discharge	0
Minimal mucous discharge	1
Moderate mucous or purulent discharge	2
Substantial discharge	3
Gross fecal soiling	4
Pain/restriction of activities	
No activity restriction	0
Mild discomfort, no restriction	1
Moderate discomfort, some limitation of activities	2
Marked discomfort, marked limitation	3
Severe pain, severe limitation	4
Restriction of sexual activity	
No restriction sexual activity	0
Slight restriction sexual activity	1
Moderate limitation sexual activity	2
Marked limitation sexual activity	3
Unable to engage in sexual activity	4
Type of perineal disease	
No perineal disease/skin tags	0
Anal fissure or mucosal tear	1
< 3 Perianal fistulae	2
≥ Perianal fistulae	3
Anal sphincter ulceration or fistulae with significant undermining of skin	4
Degree of induration	
No induration	0
Minimal induration	1
Moderate induration	2
Substantial induration	3
Gross fluctuance/abscess	4

Modified from Irvine[151].

location as described by Parks and Gordon[150], in up to 40% of cases. Both abscesses and fistulas are manifestations that can bring the patient to emergency physicians attention (Table 6)[151].

Most patients with a perianal abscess present with pain, swelling, and redness of the interested area. High abscesses also known as supraelevator abscesses do not extend to the more superficial perianal tissues and are not associated to visible and palpable inflammatory signs but more often to systemic signs like fever and malaise[7,149]. If a supraelevator source is suspected, a CT scan or MRI is useful because it gives more information about the abscess extension but also on eventual associated intrabdominal findings[7].

When approaching a patient with a perianal abscess or fistula, the initial goal must be the sepsis control. The early drainage is the only accepted treatment for this purpose, eventually associated to gram negative and anaerobic spectrum antibiotics in patients on immunosuppression and in those with septic shock[152,153]. It is recommended to leave a Petzer or a Malecot catheter in wide ischiorectal abscesses[147,153]. It is better to perform the drainage under general anesthesia, especially if the patient

is in pain, because this will allow a better exploration.

As a result of the inflammation, it could be challenging to find the underlying fistula, and unsuccessful attempts could cause tissue destruction and create an iatrogenic track. There is no evidence to support wound packing following the drainage. Nevertheless, it could have a hemostatic role in the case of bleeding. If the fistula track is evident, a loose draining seton should be inserted. There should be no attempt to lay the fistula open at the same time to preserve future anal function whose damage would negatively impact the patient's lifestyle[153].

In the emergency setting, there is no room for treatment such as fibrin glue, fistula plug, ligation of the intersphincteric fistula tract, advancement flap, and stem cells. These will be considered when the acute process is completely solved. At this point, the patient will be referred to a tertiary center, and a multidisciplinary team will decide the best treatment plan[154]. The work-up will also include a sigmoidoscopy to define if perianal sepsis was associated to an active proctitis[147].

A recent United Kingdom survey summarized the state of the art on acute management of perianal sepsis in CD; 32% of the responding surgeons (133/179) confirmed that they would drain sepsis, 31.1% would consider placement of a seton, and only 0.6% would consider excision of the fistula track. That is in accordance with the previous evidence. When further investigations are needed, MRI is the imaging procedure of choice (96.1%). Most respondents (42.2%) would start antimicrobial therapy preoperatively, and the antibiotic of choice is metronidazole (77.9%). In the case of recurrent sepsis, most respondents created a diverting stoma. In fact, as demonstrated in other studies, it may improve quality of life in patients with severe and recurrent perianal CD[155,156].

CONCLUSION

CD is a chronic and recurrent inflammatory disease that can present with acute complications. The patient's clinical status and assessment of the background disease location and severity must be considered to guide diagnosis and treatment of the acute complications. CD is unremitting and incurable. Therefore, treatment aims to induce a deep and prolonged remission, prevent and address complications of the disease, avoid extensive bowel resections, and improve quality of life. Acute surgical emergencies in patients with CD are associated with a high morbidity and mortality. Although most acute complications of CD are managed nonoperatively, it is important to recognize those that require surgical management.

ACKNOWLEDGEMENTS

The authors thank Dr Neill James Adams who supervised the writing of the manuscript and proofread the text for the appropriate use of the English language, grammar, punctuation and spelling.

FOOTNOTES

Author contributions: Chiarello MM and Pepe G equally contributed to the drafting of the manuscript and both should be considered first author; Brisinda G and Chiarello MM designed the research; Bianchi V, Pepe G, Fico V, and Altieri G performed the research; Bianchi V and Fico V analyzed the data; Pepe G, Chiarello MM, Tropeano G, Fico V, Bianchi V, and Brisinda G wrote the paper.

Conflict-of-interest statement: The authors declare that they have no conflict of interest.

Open-Access: This article is an open-access article that was selected by an in-house editor and fully peer-reviewed by external reviewers. It is distributed in accordance with the Creative Commons Attribution NonCommercial (CC BY-NC 4.0) license, which permits others to distribute, remix, adapt, build upon this work non-commercially, and license their derivative works on different terms, provided the original work is properly cited and the use is non-commercial. See: https://creativecommons.org/Licenses/by-nc/4.0/

Country/Territory of origin: Italy

ORCID number: Maria Michela Chiarello 0000-0003-3455-0062; Gilda Pepe 0000-0001-9852-6243; Valeria Fico 0000-0003-1619-4164; Valentina Bianchi 0000-0002-8817-3760; Giuseppe Tropeano 0000-0001-9006-5040; Gaia Altieri 0000-0002-0324-2430; Giuseppe Brisinda 0000-0001-8820-9471.

S-Editor: Fan JR
L-Editor: Filipodia
P-Editor: Fan JR

REFERENCES

1 **Crohn BB**, Ginzburg L, Oppenheimer GD. Landmark article Oct 15, 1932. Regional ileitis. A pathological and clinical entity. By Burril B. Crohn, Leon Ginzburg, and Gordon D. Oppenheimer. *JAMA* 1984; **251**: 73-79 [PMID: 6361290 DOI: 10.1001/jama.251.1.73]

2 **Armuzzi A**, Riegler G, Furfaro F, Baldoni M, Costa F, Fortuna M, Iaquinto G, Paese P, Papi C, Bossa F, Tontini GE, Di Fino S, Gualberti G, Merolla R, Rizzello F. Epidemiological features and disease-related concerns of a large cohort of Italian patients with active Crohn's disease. *Dig Liver Dis* 2019; **51**: 804-811 [PMID: 30685416 DOI: 10.1016/j.dld.2018.12.019]

3 **Terlizzi EP**, Dahlhamer JM, Xu F, Wheaton AG, Greenlund KJ. Health Care Utilization Among U.S. Adults With Inflammatory Bowel Disease, 2015-2016. *Natl Health Stat Report* 2021; 1-7 [PMID: 33663650]

4 **Ng SC**, Shi HY, Hamidi N, Underwood FE, Tang W, Benchimol EI, Panaccione R, Ghosh S, Wu JCY, Chan FKL, Sung JJY, Kaplan GG. Worldwide incidence and prevalence of inflammatory bowel disease in the 21st century: a systematic review of population-based studies. *Lancet* 2017; **390**: 2769-2778 [PMID: 29050646 DOI: 10.1016/S0140-6736(17)32448-0]

5 **Kaplan GG**, Windsor JW. The four epidemiological stages in the global evolution of inflammatory bowel disease. *Nat Rev Gastroenterol Hepatol* 2021; **18**: 56-66 [PMID: 33033392 DOI: 10.1038/s41575-020-00360-x]

6 **GBD 2017 Inflammatory Bowel Disease Collaborators**. The global, regional, and national burden of inflammatory bowel disease in 195 countries and territories, 1990-2017: a systematic analysis for the Global Burden of Disease Study 2017. *Lancet Gastroenterol Hepatol* 2020; **5**: 17-30 [PMID: 31648971 DOI: 10.1016/S2468-1253(19)30333-4]

7 **De Simone B**, Davies J, Chouillard E, Di Saverio S, Hoentjen F, Tarasconi A, Sartelli M, Biffl WL, Ansaloni L, Coccolini F, Chiarugi M, De'Angelis N, Moore EE, Kluger Y, Abu-Zidan F, Sakakushev B, Coimbra R, Celentano V, Wani I, Pintar T, Sganga G, Di Carlo I, Tartaglia D, Pikoulis M, Cardi M, De Moya MA, Leppaniemi A, Kirkpatrick A, Agnoletti V, Poggioli G, Carcoforo P, Baiocchi GL, Catena F. WSES-AAST guidelines: management of inflammatory bowel disease in the emergency setting. *World J Emerg Surg* 2021; **16**: 23 [PMID: 33971899 DOI: 10.1186/s13017-021-00362-3]

8 **Mak WY**, Zhao M, Ng SC, Burisch J. The epidemiology of inflammatory bowel disease: East meets west. *J Gastroenterol Hepatol* 2020; **35**: 380-389 [PMID: 31596960 DOI: 10.1111/jgh.14872]

9 **Molodecky NA**, Soon IS, Rabi DM, Ghali WA, Ferris M, Chernoff G, Benchimol EI, Panaccione R, Ghosh S, Barkema HW, Kaplan GG. Increasing incidence and prevalence of the inflammatory bowel diseases with time, based on systematic review. *Gastroenterology* 2012; **142**: 46-54.e42; quiz e30 [PMID: 22001864 DOI: 10.1053/j.gastro.2011.10.001]

10 **Ananthakrishnan AN**. Epidemiology and risk factors for IBD. *Nat Rev Gastroenterol Hepatol* 2015; **12**: 205-217 [PMID: 25732745 DOI: 10.1038/nrgastro.2015.34]

11 **Hashash JG**, Sigal R, Wein-Levy P, Szigethy EM, Merusi JJ, Regueiro MD. Inflammatory Bowel Disease (IBD) Connect: A Novel Volunteer Program for Hospitalized Patients with IBD and Their Families. *Inflamm Bowel Dis* 2016; **22**: 2748-2753 [PMID: 27755272 DOI: 10.1097/MIB.0000000000000952]

12 **Lightner AL**, Vogel JD, Carmichael JC, Keller DS, Shah SA, Mahadevan U, Kane SV, Paquette IM, Steele SR, Feingold DL. The American Society of Colon and Rectal Surgeons Clinical Practice Guidelines for the Surgical Management of Crohn's Disease. *Dis Colon Rectum* 2020; **63**: 1028-1052 [PMID: 32692069 DOI: 10.1097/DCR.0000000000001716]

13 **Andersson RE**, Olaison G, Tysk C, Ekbom A. Appendectomy is followed by increased risk of Crohn's disease. *Gastroenterology* 2003; **124**: 40-46 [PMID: 12512028 DOI: 10.1053/gast.2003.50021]

14 **Fontana T**, Falco N, Torchia M, Tutino R, Gulotta G. Bowel perforation in Crohn's Disease: correlation between CDAI and Clavien-Dindo scores. *G Chir* 2017; **38**: 303-312 [PMID: 29442063 DOI: 10.11138/gchir/2017.38.6.303]

15 **Podolsky DK**. Inflammatory bowel disease. *N Engl J Med* 2002; **347**: 417-429 [PMID: 12167685 DOI: 10.1056/NEJMra020831]

16 **Ballou S**, Hirsch W, Singh P, Rangan V, Nee J, Iturrino J, Sommers T, Zubiago J, Sengupta N, Bollom A, Jones M, Moss AC, Flier SN, Cheifetz AS, Lembo A. Emergency department utilisation for inflammatory bowel disease in the United States from 2006 to 2014. *Aliment Pharmacol Ther* 2018; **47**: 913-921 [PMID: 29411411 DOI: 10.1111/apt.14551]

17 **Goldstone RN**, Steinhagen RM. Abdominal Emergencies in Inflammatory Bowel Disease. *Surg Clin North Am* 2019; **99**: 1141-1150 [PMID: 31676053 DOI: 10.1016/j.suc.2019.08.007]

18 **Torres J**, Bonovas S, Doherty G, Kucharzik T, Gisbert JP, Raine T, Adamina M, Armuzzi A, Bachmann O, Bager P, Biancone L, Bokemeyer B, Bossuyt P, Burisch J, Collins P, El-Hussuna A, Ellul P, Frei-Lanter C, Furfaro F, Gingert C, Gionchetti P, Gomollon F, González-Lorenzo M, Gordon H, Hlavaty T, Juillerat P, Katsanos K, Kopylov U, Krustins E, Lytras T, Maaser C, Magro F, Marshall JK, Myrelid P, Pellino G, Rosa I, Sabino J, Savarino E, Spinelli A, Stassen L, Uzzan M, Vavricka S, Verstockt B, Warusavitarne J, Zmora O, Fiorino G. ECCO Guidelines on Therapeutics in Crohn's Disease: Medical Treatment. *J Crohns Colitis* 2020; **14**: 4-22 [PMID: 31711158 DOI: 10.1093/ecco-jcc/jjz180]

19 **Adamina M**, Bonovas S, Raine T, Spinelli A, Warusavitarne J, Armuzzi A, Bachmann O, Bager P, Biancone L, Bokemeyer B, Bossuyt P, Burisch J, Collins P, Doherty G, El-Hussuna A, Ellul P, Fiorino G, Frei-Lanter C, Furfaro F, Gingert C, Gionchetti P, Gisbert JP, Gomollon F, González Lorenzo M, Gordon H, Hlavaty T, Juillerat P, Katsanos K, Kopylov U, Krustins E, Kucharzik T, Lytras T, Maaser C, Magro F, Marshall JK, Myrelid P, Pellino G, Rosa I, Sabino J, Savarino E, Stassen L, Torres J, Uzzan M, Vavricka S, Verstockt B, Zmora O. ECCO Guidelines on Therapeutics in Crohn's Disease: Surgical Treatment. *J Crohns Colitis* 2020; **14**: 155-168 [PMID: 31742338 DOI: 10.1093/ecco-jcc/jjz187]

20 **Gionchetti P**, Dignass A, Danese S, Magro Dias FJ, Rogler G, Lakatos PL, Adamina M, Ardizzone S, Buskens CJ, Sebastian S, Laureti S, Sampietro GM, Vucelic B, van der Woude CJ, Barreiro-de Acosta M, Maaser C, Portela F, Vavricka SR, Gomollón F; ECCO. 3rd European Evidence-based Consensus on the Diagnosis and Management of Crohn's Disease 2016: Part 2: Surgical Management and Special Situations. *J Crohns Colitis* 2017; **11**: 135-149 [PMID: 27660342 DOI: 10.1093/ecco-jcc/jjw169]

21 **Frolkis AD**, Dykeman J, Negrón ME, Debruyn J, Jette N, Fiest KM, Frolkis T, Barkema HW, Rioux KP, Panaccione R, Ghosh S, Wiebe S, Kaplan GG. Risk of surgery for inflammatory bowel diseases has decreased over time: a systematic

review and meta-analysis of population-based studies. *Gastroenterology* 2013; **145**: 996-1006 [PMID: 23896172 DOI: 10.1053/j.gastro.2013.07.041]

22 **Schnitzler F**, Fidder H, Ferrante M, Noman M, Arijs I, Van Assche G, Hoffman I, Van Steen K, Vermeire S, Rutgeerts P. Long-term outcome of treatment with infliximab in 614 patients with Crohn's disease: results from a single-centre cohort. *Gut* 2009; **58**: 492-500 [PMID: 18832518 DOI: 10.1136/gut.2008.155812]

23 **Cosnes J**, Nion-Larmurier I, Beaugerie L, Afchain P, Tiret E, Gendre JP. Impact of the increasing use of immunosuppressants in Crohn's disease on the need for intestinal surgery. *Gut* 2005; **54**: 237-241 [PMID: 15647188 DOI: 10.1136/gut.2004.045294]

24 **Lazarev M**, Ullman T, Schraut WH, Kip KE, Saul M, Regueiro M. Small bowel resection rates in Crohn's disease and the indication for surgery over time: experience from a large tertiary care center. *Inflamm Bowel Dis* 2010; **16**: 830-835 [PMID: 19798731 DOI: 10.1002/ibd.21118]

25 **Khoury T**, Daher S, Massarwa M, Hakimian D, Benson AA, Viener E, Farah R, Mari A, Hazou W, Kadah A, Sbeit W, Mahamid M, Israeli E. A Validated Score Assessing the Risk of an Intra-Abdominal Abscess in Patients with Crohn's Disease Presenting at the Emergency Department. *J Crohns Colitis* 2019; **13**: 1131-1137 [PMID: 30768181 DOI: 10.1093/ecco-jcc/jjz043]

26 **Harvey RF**, Bradshaw JM. A simple index of Crohn's-disease activity. *Lancet* 1980; **1**: 514 [PMID: 6102236 DOI: 10.1016/s0140-6736(80)92767-1]

27 **Gajendran M**, Loganathan P, Catinella AP, Hashash JG. A comprehensive review and update on Crohn's disease. *Dis Mon* 2018; **64**: 20-57 [PMID: 28826742 DOI: 10.1016/j.disamonth.2017.07.001]

28 **Van Assche G**, Dignass A, Reinisch W, van der Woude CJ, Sturm A, De Vos M, Guslandi M, Oldenburg B, Dotan I, Marteau P, Ardizzone A, Baumgart DC, D'Haens G, Gionchetti P, Portela F, Vucelic B, Söderholm J, Escher J, Koletzko S, Kolho KL, Lukas M, Mottet C, Tilg H, Vermeire S, Carbonnel F, Cole A, Novacek G, Reinshagen M, Tsianos E, Herrlinger K, Bouhnik Y, Kiesslich R, Stange E, Travis S, Lindsay J; European Crohn's and Colitis Organisation (ECCO). The second European evidence-based Consensus on the diagnosis and management of Crohn's disease: Special situations. *J Crohns Colitis* 2010; **4**: 63-101 [PMID: 21122490 DOI: 10.1016/j.crohns.2009.09.009]

29 **Best WR**, Becktel JM, Singleton JW. Rederived values of the eight coefficients of the Crohn's Disease Activity Index (CDAI). *Gastroenterology* 1979; **77**: 843-846 [PMID: 467941]

30 **Onodera T**, Goseki N, Kosaki G. [Prognostic nutritional index in gastrointestinal surgery of malnourished cancer patients]. *Nihon Geka Gakkai Zasshi* 1984; **85**: 1001-1005 [PMID: 6438478]

31 **Zhou W**, Cao Q, Qi W, Xu Y, Liu W, Xiang J, Xia B. Prognostic Nutritional Index Predicts Short-Term Postoperative Outcomes After Bowel Resection for Crohn's Disease. *Nutr Clin Pract* 2017; **32**: 92-97 [PMID: 27566600 DOI: 10.1177/0884533616661844]

32 **Maeda K**, Nagahara H, Shibutani M, Otani H, Sakurai K, Toyokawa T, Tanaka H, Kubo N, Muguruma K, Kamata N, Yamagami H, Hirakawa K. A preoperative low nutritional prognostic index correlates with the incidence of incisional surgical site infections after bowel resection in patients with Crohn's disease. *Surg Today* 2015; **45**: 1366-1372 [PMID: 25319215 DOI: 10.1007/s00595-014-1044-8]

33 **Guglielmo FF**, Anupindi SA, Fletcher JG, Al-Hawary MM, Dillman JR, Grand DJ, Bruining DH, Chatterji M, Darge K, Fidler JL, Gandhi NS, Gee MS, Grajo JR, Huang C, Jaffe TA, Park SH, Rimola J, Soto JA, Taouli B, Taylor SA, Baker ME. Small Bowel Crohn Disease at CT and MR Enterography: Imaging Atlas and Glossary of Terms. *Radiographics* 2020; **40**: 354-375 [PMID: 31951512 DOI: 10.1148/rg.2020190091]

34 **Verdalle-Cazes M**, Charpentier C, Benard C, Joly LM, Dacher JN, Savoye G, Savoye-Collet C. Abdominopelvic CT-scan in emergency departments for patients with suspected complications of Crohn's disease: a single tertiary center experience. *BMC Emerg Med* 2021; **21**: 113 [PMID: 34620106 DOI: 10.1186/s12873-021-00512-5]

35 **Larson DB**, Johnson LW, Schnell BM, Salisbury SR, Forman HP. National trends in CT use in the emergency department: 1995-2007. *Radiology* 2011; **258**: 164-173 [PMID: 21115875 DOI: 10.1148/radiol.10100640]

36 **Chatu S**, Subramanian V, Pollok RC. Meta-analysis: diagnostic medical radiation exposure in inflammatory bowel disease. *Aliment Pharmacol Ther* 2012; **35**: 529-539 [PMID: 22239831 DOI: 10.1111/j.1365-2036.2011.04975.x]

37 **Desmond AN**, O'Regan K, Curran C, McWilliams S, Fitzgerald T, Maher MM, Shanahan F. Crohn's disease: factors associated with exposure to high levels of diagnostic radiation. *Gut* 2008; **57**: 1524-1529 [PMID: 18443021 DOI: 10.1136/gut.2008.151415]

38 **Palmer L**, Herfarth H, Porter CQ, Fordham LA, Sandler RS, Kappelman MD. Diagnostic ionizing radiation exposure in a population-based sample of children with inflammatory bowel diseases. *Am J Gastroenterol* 2009; **104**: 2816-2823 [PMID: 19690524 DOI: 10.1038/ajg.2009.480]

39 **Kroeker KI**, Lam S, Birchall I, Fedorak RN. Patients with IBD are exposed to high levels of ionizing radiation through CT scan diagnostic imaging: a five-year study. *J Clin Gastroenterol* 2011; **45**: 34-39 [PMID: 20679907 DOI: 10.1097/MCG.0b013e3181e5d1c5]

40 **Pearce MS**, Salotti JA, Little MP, McHugh K, Lee C, Kim KP, Howe NL, Ronckers CM, Rajaraman P, Sir Craft AW, Parker L, Berrington de González A. Radiation exposure from CT scans in childhood and subsequent risk of leukaemia and brain tumours: a retrospective cohort study. *Lancet* 2012; **380**: 499-505 [PMID: 22681860 DOI: 10.1016/S0140-6736(12)60815-0]

41 **Craig O**, O'Neill S, O'Neill F, McLaughlin P, McGarrigle A, McWilliams S, O'Connor O, Desmond A, Walsh EK, Ryan M, Maher M, Shanahan F. Diagnostic accuracy of computed tomography using lower doses of radiation for patients with Crohn's disease. *Clin Gastroenterol Hepatol* 2012; **10**: 886-892 [PMID: 22469992 DOI: 10.1016/j.cgh.2012.03.014]

42 **Bettenworth D**, Bokemeyer A, Baker M, Mao R, Parker CE, Nguyen T, Ma C, Panés J, Rimola J, Fletcher JG, Jairath V, Feagan BG, Rieder F; Stenosis Therapy and Anti-Fibrotic Research (STAR) Consortium. Assessment of Crohn's disease-associated small bowel strictures and fibrosis on cross-sectional imaging: a systematic review. *Gut* 2019; **68**: 1115-1126 [PMID: 30944110 DOI: 10.1136/gutjnl-2018-318081]

43 **Panés J**, Bouzas R, Chaparro M, García-Sánchez V, Gisbert JP, Martínez de Guereñu B, Mendoza JL, Paredes JM, Quiroga S, Ripollés T, Rimola J. Systematic review: the use of ultrasonography, computed tomography and magnetic

resonance imaging for the diagnosis, assessment of activity and abdominal complications of Crohn's disease. *Aliment Pharmacol Ther* 2011; **34**: 125-145 [PMID: 21615440 DOI: 10.1111/j.1365-2036.2011.04710.x]

44 **Aberra FN**, Lewis JD, Hass D, Rombeau JL, Osborne B, Lichtenstein GR. Corticosteroids and immunomodulators: postoperative infectious complication risk in inflammatory bowel disease patients. *Gastroenterology* 2003; **125**: 320-327 [PMID: 12891531 DOI: 10.1016/s0016-5085(03)00883-7]

45 **Nguyen GC**, Elnahas A, Jackson TD. The impact of preoperative steroid use on short-term outcomes following surgery for inflammatory bowel disease. *J Crohns Colitis* 2014; **8**: 1661-1667 [PMID: 25107847 DOI: 10.1016/j.crohns.2014.07.007]

46 **Huang W**, Tang Y, Nong L, Sun Y. Risk factors for postoperative intra-abdominal septic complications after surgery in Crohn's disease: A meta-analysis of observational studies. *J Crohns Colitis* 2015; **9**: 293-301 [PMID: 25572276 DOI: 10.1093/ecco-jcc/jju028]

47 **Subramanian V**, Saxena S, Kang JY, Pollok RC. Preoperative steroid use and risk of postoperative complications in patients with inflammatory bowel disease undergoing abdominal surgery. *Am J Gastroenterol* 2008; **103**: 2373-2381 [PMID: 18616660 DOI: 10.1111/j.1572-0241.2008.01942.x]

48 **Cohen BL**, Fleshner P, Kane SV, Herfarth HH, Palekar N, Farraye FA, Leighton JA, Katz J, Cohen RD, Gerich ME, Cross RK, Higgins PD, Tinsley A, Glover SC, Siegel CA, Bohl JL, Iskandar H, Raymond S, Huang R, Suarez-Farinas M, Sands BE. 415a – Anti-Tumor Necrosis Factor Therapy is Not Associated with Post-Operative Infection: Results from Prospective Cohort of Ulcerative Colitis and Crohn's Disease Patients Undergoing Surgery to Identify Risk Factors for Postoperative Infection I (Puccini). *Gastroenterology* 2019; **156(6,** Supplement 1): S80 [DOI: 10.1016/s0016-5085(19)36987-2]

49 **Amiot A**, Bouguen G, Bonnaud G, Bouhnik Y, Hagege H, Peyrin-Biroulet L; French National Consensus Clinical guidelines for the management of IBD study group. Clinical guidelines for the management of inflammatory bowel disease: Update of a French national consensus. *Dig Liver Dis* 2021; **53**: 35-43 [PMID: 33160886 DOI: 10.1016/j.dld.2020.10.018]

50 **Cohen RD**, Bhayat F, Blake A, Travis S. The Safety Profile of Vedolizumab in Ulcerative Colitis and Crohn's Disease: 4 Years of Global Post-marketing Data. *J Crohns Colitis* 2020; **14**: 192-204 [PMID: 31504340 DOI: 10.1093/ecco-jcc/jjz137]

51 **Armuzzi A**, Ardizzone S, Biancone L, Castiglione F, Danese S, Gionchetti P, Orlando A, Rizzello F, Scribano ML, Vecchi M, Daperno M. Ustekinumab in the management of Crohn's disease: Expert opinion. *Dig Liver Dis* 2018; **50**: 653-660 [PMID: 29610019 DOI: 10.1016/j.dld.2018.02.017]

52 **Mijac DD**, Janković GL, Jorga J, Krstić MN. Nutritional status in patients with active inflammatory bowel disease: prevalence of malnutrition and methods for routine nutritional assessment. *Eur J Intern Med* 2010; **21**: 315-319 [PMID: 20603043 DOI: 10.1016/j.ejim.2010.04.012]

53 **Chiarello MM**, Brisinda G. A commentary on: Preoperative hypoalbuminemia is an independent risk factor for postoperative complications in Crohn's disease patients with normal BMI: A cohort study. *Int J Surg* 2020; **81**: 100-101 [PMID: 32768447 DOI: 10.1016/j.ijsu.2020.07.020]

54 **Bischoff SC**, Escher J, Hébuterne X, Kłęk S, Krznaric Z, Schneider S, Shamir R, Stardelova K, Wierdsma N, Wiskin AE, Forbes A. ESPEN practical guideline: Clinical Nutrition in inflammatory bowel disease. *Clin Nutr* 2020; **39**: 632-653 [PMID: 32029281 DOI: 10.1016/j.clnu.2019.11.002]

55 **Schwartz E**. Perioperative Parenteral Nutrition in Adults With Inflammatory Bowel Disease: A Review of the Literature. *Nutr Clin Pract* 2016; **31**: 159-170 [PMID: 26245541 DOI: 10.1177/0884533615594011]

56 **Akobeng AK**, Zhang D, Gordon M, MacDonald JK. Enteral nutrition for maintenance of remission in Crohn's disease. *Cochrane Database Syst Rev* 2018; **8**: CD005984 [PMID: 30098021 DOI: 10.1002/14651858.CD005984.pub3]

57 **Brennan GT**, Ha I, Hogan C, Nguyen E, Jamal MM, Bechtold ML, Nguyen DL. Does preoperative enteral or parenteral nutrition reduce postoperative complications in Crohn's disease patients: a meta-analysis. *Eur J Gastroenterol Hepatol* 2018; **30**: 997-1002 [PMID: 29738326 DOI: 10.1097/MEG.0000000000001162]

58 **Zhu Y**, Xu L, Liu W, Qi W, Cao Q, Zhou W. Safety and Efficacy of Exclusive Enteral Nutrition for Percutaneously Undrainable Abdominal Abscesses in Crohn's Disease. *Gastroenterol Res Pract* 2017; **2017**: 6360319 [PMID: 28947899 DOI: 10.1155/2017/6360319]

59 **Justiniano CF**, Aquina CT, Becerra AZ, Xu Z, Boodry CI, Swanger AA, Monson JRT, Fleming FJ. Postoperative Mortality After Nonelective Surgery for Inflammatory Bowel Disease Patients in the Era of Biologics. *Ann Surg* 2019; **269**: 686-691 [PMID: 29232213 DOI: 10.1097/SLA.0000000000002628]

60 **Singh S**, Al-Darmaki A, Frolkis AD, Seow CH, Leung Y, Novak KL, Ghosh S, Eksteen B, Panaccione R, Kaplan GG. Postoperative Mortality Among Patients With Inflammatory Bowel Diseases: A Systematic Review and Meta-analysis of Population-Based Studies. *Gastroenterology* 2015; **149**: 928-937 [PMID: 26055136 DOI: 10.1053/j.gastro.2015.06.001]

61 **Hanauer SB**, Sandborn W; Practice Parameters Committee of the American College of Gastroenterology. Management of Crohn's disease in adults. *Am J Gastroenterol* 2001; **96**: 635-643 [PMID: 11280528 DOI: 10.1111/j.1572-0241.2001.3671_c.x]

62 **Lowenfeld L**, Michelassi F. Management of acute complications in patients with Crohn's Disease. In: Nigri G, Tsoulfa G, editors. Gastrointestinal surgical emergencies. 2021 ed. United States of America: American College of Surgeons, 2021: 180-193

63 **Toh JW**, Stewart P, Rickard MJ, Leong R, Wang N, Young CJ. Indications and surgical options for small bowel, large bowel and perianal Crohn's disease. *World J Gastroenterol* 2016; **22**: 8892-8904 [PMID: 27833380 DOI: 10.3748/wjg.v22.i40.8892]

64 **Annunziata ML**, Caviglia R, Papparella LG, Cicala M. Upper gastrointestinal involvement of Crohn's disease: a prospective study on the role of upper endoscopy in the diagnostic work-up. *Dig Dis Sci* 2012; **57**: 1618-1623 [PMID: 22350786 DOI: 10.1007/s10620-012-2072-0]

65 **Balendran K**, Udumalagala S, Nawaraththne NMM. Pyloric stenosis as a manifestation of isolated gastric Crohn's disease responding to intralesional steroid injection and balloon dilation: a case report. *J Med Case Rep* 2019; **13**: 331 [PMID:

31718712 DOI: 10.1186/s13256-019-2272-8]

66 **Guellouz S**, Pariente B, Benet C, Baudry C, Lourenco N, Kraemer A, Allez M, Gornet JM. Cephalic duodenopancreatectomy for hyperalgic duodenal Crohn's disease fistulized in the pancreatic gland. *Case Rep Gastroenterol* 2014; **8**: 72-76 [PMID: 24748861 DOI: 10.1159/000360844]

67 **Shivaji UN**, Evans M, Critchlow T, Gui X, Smith SCL, Pinkney T, Iacucci M, Cooney R, Ghosh S, Skordilis K. Chronic inflammation and other changes are significant components of clinically fibrotic strictures in Crohn's disease: a histological study of resected strictures clinically characterized as noninflamed. *Eur J Gastroenterol Hepatol* 2020; **32**: 1432-1439 [PMID: 32639416 DOI: 10.1097/MEG.0000000000001796]

68 **Shen B**, Kochhar G, Navaneethan U, Farraye FA, Schwartz DA, Iacucci M, Bernstein CN, Dryden G, Cross R, Bruining DH, Kobayashi T, Lukas M, Shergill A, Bortlik M, Lan N, Tang SJ, Kotze PG, Kiran RP, Dulai PS, El-Hachem S, Coelho-Prabhu N, Thakkar S, Mao R, Chen G, Zhang S, Suárez BG, Lama YG, Silverberg MS, Sandborn WJ. Practical guidelines on endoscopic treatment for Crohn's disease strictures: a consensus statement from the Global Interventional Inflammatory Bowel Disease Group. *Lancet Gastroenterol Hepatol* 2020; **5**: 393-405 [PMID: 31954438 DOI: 10.1016/S2468-1253(19)30366-8]

69 **Lamb CA**, Kennedy NA, Raine T, Hendy PA, Smith PJ, Limdi JK, Hayee B, Lomer MCE, Parkes GC, Selinger C, Barrett KJ, Davies RJ, Bennett C, Gittens S, Dunlop MG, Faiz O, Fraser A, Garrick V, Johnston PD, Parkes M, Sanderson J, Terry H; IBD guidelines eDelphi consensus group, Gaya DR, Iqbal TH, Taylor SA, Smith M, Brookes M, Hansen R, Hawthorne AB. British Society of Gastroenterology consensus guidelines on the management of inflammatory bowel disease in adults. *Gut* 2019; **68**: s1-s106 [PMID: 31562236 DOI: 10.1136/gutjnl-2019-318484]

70 **Lan N**, Shen B. Endoscopic Stricturotomy Versus Balloon Dilation in the Treatment of Anastomotic Strictures in Crohn's Disease. *Inflamm Bowel Dis* 2018; **24**: 897-907 [PMID: 29546384 DOI: 10.1093/ibd/izx085]

71 **Loras C**, Andújar X, Gornals JB, Sanchiz V, Brullet E, Sicilia B, Martín-Arranz MD, Naranjo A, Barrio J, Dueñas C, Foruny JR, Busquets D, Monfort D, Pineda JR, González-Huix F, Pérez-Roldán F, Pons V, González B, Reyes Moreno J, Sainz E, Guardiola J, Bosca-Watts MM, Fernández-Bañares F, Mayor V, Esteve M; Grupo Español de Trabajo de la Enfermedad de Crohn y Colitis Ulcerosa (GETECCU). Self-expandable metal stents versus endoscopic balloon dilation for the treatment of strictures in Crohn's disease (ProtDilat study): an open-label, multicentre, randomised trial. *Lancet Gastroenterol Hepatol* 2022; **7**: 332-341 [PMID: 35065738 DOI: 10.1016/S2468-1253(21)00386-1]

72 **Chiarello MM**, Cariati M, Brisinda G. Colonic Crohn's disease - decision is more important than incision: A surgical dilemma. *World J Gastrointest Surg* 2021; **13**: 1-6 [PMID: 33552390 DOI: 10.4240/wjgs.v13.i1.1]

73 **Freeman HJ**. Natural history and long-term clinical course of Crohn's disease. *World J Gastroenterol* 2014; **20**: 31-36 [PMID: 24415855 DOI: 10.3748/wjg.v20.i1.31]

74 **Lesperance K**, Martin MJ, Lehmann R, Brounts L, Steele SR. National trends and outcomes for the surgical therapy of ileocolonic Crohn's disease: a population-based analysis of laparoscopic vs. open approaches. *J Gastrointest Surg* 2009; **13**: 1251-1259 [PMID: 19301075 DOI: 10.1007/s11605-009-0853-3]

75 **McLeod RS**, Wolff BG, Ross S, Parkes R, McKenzie M; Investigators of the CAST Trial. Recurrence of Crohn's disease after ileocolic resection is not affected by anastomotic type: results of a multicenter, randomized, controlled trial. *Dis Colon Rectum* 2009; **52**: 919-927 [PMID: 19502857 DOI: 10.1007/DCR.0b013e3181a4fa58]

76 **Celentano V**, O'Leary DP, Caiazzo A, Flashman KG, Sagias F, Conti J, Senapati A, Khan J. Longer small bowel segments are resected in emergency surgery for ileocaecal Crohn's disease with a higher ileostomy and complication rate. *Tech Coloproctol* 2019; **23**: 1085-1091 [PMID: 31664551 DOI: 10.1007/s10151-019-02104-9]

77 **Kosmidis C**, Anthimidis G. Emergency and elective surgery for small bowel Crohn's disease. *Tech Coloproctol* 2011; **15** Suppl 1: S1-S4 [PMID: 21901520 DOI: 10.1007/s10151-011-0728-y]

78 **Guo Z**, Li Y, Zhu W, Gong J, Li N, Li J. Comparing outcomes between side-to-side anastomosis and other anastomotic configurations after intestinal resection for patients with Crohn's disease: a meta-analysis. *World J Surg* 2013; **37**: 893-901 [PMID: 23354925 DOI: 10.1007/s00268-013-1928-6]

79 **Celentano V**, Pellino G, Spinelli A, Selvaggi F; SICCR Current status of Crohn's disease surgery collaborative, Celentano V, Pellino G, Rottoli M, Poggioli G, Sica G, Giglio MC, Campanelli M, Coco C, Rizzo G, Sionne F, Colombo F, Sampietro G, Lamperti G, Foschi D, Ficari F, Vacca L, Cricchio M, Giudici F, Selvaggi L, Sciaudone G, Peltrini R, Manfreda A, Bucci L, Galleano R, Ghazouani O, Zorcolo L, Deidda S, Restivo A, Braini A, Di Candido F, Sacchi M, Carvello M, Martorana S, Bordignon G, Angriman I, Variola A, Di Ruscio M, Barugola G, Geccherle A, Tropeano FP, Luglio G, Tanzanu M, Sasia D, Migliore M, Giuffrida MC, Marrano E, Moretto G, Impellizzeri H, Gallo G, Vescio G, Sammarco G, Terrosu G, Calini G, Bondurri A, Maffioli A, Zaffaroni G, Resegotti A, Mistrangelo M, Allaix ME, Botti F, Prati M, Boni L, Perotti S, Mineccia M, Giuliani A, Romano L, Graziano GMP, Pugliese L, Pietrabissa A, Delaini G, Spinelli A, Selvaggi F; , on behalf of the Italian Society of Colorectal Surgery SICCR. Anastomosis configuration and technique following ileocaecal resection for Crohn's disease: a multicentre study. *Updates Surg* 2021; **73**: 149-156 [PMID: 33409848 DOI: 10.1007/s13304-020-00918-z]

80 **Strong S**, Steele SR, Boutrous M, Bordineau L, Chun J, Stewart DB, Vogel J, Rafferty JF; Clinical Practice Guidelines Committee of the American Society of Colon and Rectal Surgeons. Clinical Practice Guideline for the Surgical Management of Crohn's Disease. *Dis Colon Rectum* 2015; **58**: 1021-1036 [PMID: 26445174 DOI: 10.1097/DCR.0000000000000450]

81 **Aaltonen G**, Keränen I, Carpelan-Holmström M, Lepistö A. Risk factors for anastomotic recurrence after primary ileocaecal resection in Crohn's disease. *Eur J Gastroenterol Hepatol* 2018; **30**: 1143-1147 [PMID: 30024490 DOI: 10.1097/MEG.0000000000001206]

82 **Bertucci Zoccali M**, Fichera A. Anastomotic Techniques for Abdominal Crohn's Disease: Tricks and Tips. *J Laparoendosc Adv Surg Tech A* 2021; **31**: 861-866 [PMID: 34265213 DOI: 10.1089/lap.2020.1041]

83 **Gardiner KR**, Dasari BV. Operative management of small bowel Crohn's disease. *Surg Clin North Am* 2007; **87**: 587-610 [PMID: 17560414 DOI: 10.1016/j.suc.2007.03.011]

84 **Richards RJ**. Management of abdominal and pelvic abscess in Crohn's disease. *World J Gastrointest Endosc* 2011; **3**: 209-212 [PMID: 22110836 DOI: 10.4253/wjge.v3.i11.209]

85 **Yamaguchi A**, Matsui T, Sakurai T, Ueki T, Nakabayashi S, Yao T, Futami K, Arima S, Ono H. The clinical characteristics and outcome of intraabdominal abscess in Crohn's disease. *J Gastroenterol* 2004; **39**: 441-448 [PMID: 15175942 DOI: 10.1007/s00535-003-1317-2]

86 **Gervais DA**, Hahn PF, O'Neill MJ, Mueller PR. Percutaneous abscess drainage in Crohn disease: technical success and short- and long-term outcomes during 14 years. *Radiology* 2002; **222**: 645-651 [PMID: 11867780 DOI: 10.1148/radiol.2223010554]

87 **Yarur AJ**, Mandalia AB, Dauer RM, Czul F, Deshpande AR, Kerman DH, Abreu MT, Sussman DA. Predictive factors for clinically actionable computed tomography findings in inflammatory bowel disease patients seen in the emergency department with acute gastrointestinal symptoms. *J Crohns Colitis* 2014; **8**: 504-512 [PMID: 24275204 DOI: 10.1016/j.crohns.2013.11.003]

88 **Lowe SC**, Ream J, Hudesman D, Malter L, Bosworth B, Xia Y, Zhong H, Dane B, Megibow A, Chang S. A clinical and radiographic model to predict surgery for acute small bowel obstruction in Crohn's disease. *Abdom Radiol (NY)* 2020; **45**: 2663-2668 [PMID: 32296895 DOI: 10.1007/s00261-020-02514-6]

89 **Clancy C**, Boland T, Deasy J, McNamara D, Burke JP. A Meta-analysis of Percutaneous Drainage Versus Surgery as the Initial Treatment of Crohn's Disease-related Intra-abdominal Abscess. *J Crohns Colitis* 2016; **10**: 202-208 [PMID: 26512133 DOI: 10.1093/ecco-jcc/jjv198]

90 **Varadarajulu S**, Drelichman ER. Effectiveness of EUS in drainage of pelvic abscesses in 25 consecutive patients (with video). *Gastrointest Endosc* 2009; **70**: 1121-1127 [PMID: 19962502 DOI: 10.1016/j.gie.2009.08.034]

91 **Fernandez-Urien I**, Vila JJ, Jimenez FJ. Endoscopic ultrasound-guided drainage of pelvic collections and abscesses. *World J Gastrointest Endosc* 2010; **2**: 223-227 [PMID: 21160937 DOI: 10.4253/wjge.v2.i6.223]

92 **Golfieri R**, Cappelli A, Giampalma E, Rizzello F, Gionchetti P, Laureti S, Poggioli G, Campieri M. CT-guided percutaneous pelvic abscess drainage in Crohn's disease. *Tech Coloproctol* 2006; **10**: 99-105 [PMID: 16773292 DOI: 10.1007/s10151-006-0260-7]

93 **da Luz Moreira A**, Stocchi L, Tan E, Tekkis PP, Fazio VW. Outcomes of Crohn's disease presenting with abdominopelvic abscess. *Dis Colon Rectum* 2009; **52**: 906-912 [PMID: 19502855 DOI: 10.1007/DCR.0b013e31819f27c3]

94 **Alves A**, Panis Y, Bouhnik Y, Pocard M, Vicaut E, Valleur P. Risk factors for intra-abdominal septic complications after a first ileocecal resection for Crohn's disease: a multivariate analysis in 161 consecutive patients. *Dis Colon Rectum* 2007; **50**: 331-336 [PMID: 17252288 DOI: 10.1007/s10350-006-0782-0]

95 **Lobatón T**, Guardiola J, Rodriguez-Moranta F, Millán-Scheiding M, Peñalva M, De Oca J, Biondo S. Comparison of the long-term outcome of two therapeutic strategies for the management of abdominal abscess complicating Crohn's disease: percutaneous drainage or immediate surgical treatment. *Colorectal Dis* 2013; **15**: 1267-1272 [PMID: 24102970 DOI: 10.1111/codi.12419]

96 **Gutierrez A**, Lee H, Sands BE. Outcome of surgical versus percutaneous drainage of abdominal and pelvic abscesses in Crohn's disease. *Am J Gastroenterol* 2006; **101**: 2283-2289 [PMID: 17032194 DOI: 10.1111/j.1572-0241.2006.00757.x]

97 **Bermejo F**, Garrido E, Chaparro M, Gordillo J, Mañosa M, Algaba A, López-Sanromán A, Gisbert JP, García-Planella E, Guerra I, Domènech E. Efficacy of different therapeutic options for spontaneous abdominal abscesses in Crohn's disease: are antibiotics enough? *Inflamm Bowel Dis* 2012; **18**: 1509-1514 [PMID: 22674826 DOI: 10.1002/ibd.21865]

98 **Kumar RR**, Kim JT, Haukoos JS, Macias LH, Dixon MR, Stamos MJ, Konyalian VR. Factors affecting the successful management of intra-abdominal abscesses with antibiotics and the need for percutaneous drainage. *Dis Colon Rectum* 2006; **49**: 183-189 [PMID: 16322960 DOI: 10.1007/s10350-005-0274-7]

99 **Reuken PA**, Kruis W, Maaser C, Teich N, Büning J, Preiß JC, Schmelz R, Bruns T, Fichtner-Feigl S, Stallmach A; German IBD Study group [GISG]. Microbial Spectrum of Intra-Abdominal Abscesses in Perforating Crohn's Disease: Results from a Prospective German Registry. *J Crohns Colitis* 2018; **12**: 695-701 [PMID: 29415186 DOI: 10.1093/ecco-jcc/jjy017]

100 **Cullen G**, Vaughn B, Ahmed A, Peppercorn MA, Smith MP, Moss AC, Cheifetz AS. Abdominal phlegmons in Crohn's disease: outcomes following antitumor necrosis factor therapy. *Inflamm Bowel Dis* 2012; **18**: 691-696 [PMID: 21648022 DOI: 10.1002/ibd.21783]

101 **Udholm LS**, Rasmussen SL, Madsbøll TK, Omairi M, El-Hussuna A. A systemic review and metaanalysis of postoperative outcomes in urgent and elective bowel resection in patients with Crohn's disease. *Int J Colorectal Dis* 2021; **36**: 253-263 [PMID: 33048241 DOI: 10.1007/s00384-020-03786-6]

102 **de Groof EJ**, Carbonnel F, Buskens CJ, Bemelman WA. Abdominal abscess in Crohn's disease: multidisciplinary management. *Dig Dis* 2014; **32** Suppl 1: 103-109 [PMID: 25531361 DOI: 10.1159/000367859]

103 **Collard MK**, Benoist S, Maggiori L, Zerbib P, Lefevre JH, Denost Q, Germain A, Cotte E, Beyer-Berjot L, Corté H, Desfourneaux V, Rahili A, Duffas JP, Pautrat K, Denet C, Bridoux V, Meurette G, Faucheron JL, Loriau J, Souche R, Vicaut E, Panis Y, Brouquet A. A Reappraisal of Outcome of Elective Surgery After Successful Non-Operative Management of an Intra-Abdominal Abscess Complicating Ileocolonic Crohn's Disease: A Subgroup Analysis of a Nationwide Prospective Cohort. *J Crohns Colitis* 2021; **15**: 409-418 [PMID: 33090205 DOI: 10.1093/ecco-jcc/jjaa217]

104 **Werbin N**, Haddad R, Greenberg R, Karin E, Skornick Y. Free perforation in Crohn's disease. *Isr Med Assoc J* 2003; **5**: 175-177 [PMID: 12725136]

105 **Doh YS**, Kim YS, Bae SI, Im JP, Cheon JH, Ye BD, Kim JW, Park YS, Lee JH, Kim YH, Kim JS, Han DS, Kim WH. The clinical characteristics of patients with free perforation in Korean Crohn's disease: results from the CONNECT study. *BMC Gastroenterol* 2015; **15**: 31 [PMID: 25887913 DOI: 10.1186/s12876-015-0262-x]

106 **Greenstein AJ**, Sachar DB, Mann D, Lachman P, Heimann T, Aufses AH Jr. Spontaneous free perforation and perforated abscess in 30 patients with Crohn's disease. *Ann Surg* 1987; **205**: 72-76 [PMID: 3541802 DOI: 10.1097/00000658-198701000-00013]

107 **Steinberg DM**, Cooke WT, Alexander-Williams J. Free perforation in Crohn's disease. *Gut* 1973; **14**: 187-190 [PMID: 4700432 DOI: 10.1136/gut.14.3.187]

108 **Katz S**, Schulman N, Levin L. Free perforation in Crohn's disease: a report of 33 cases and review of literature. *Am J*

Gastroenterol 1986; **81**: 38-43 [PMID: 3510528]
109 **Cooke WT**, Fielding JF. Corticosteroid or corticotrophin therapy in Crohn's disease (regional enteritis). *Gut* 1970; **11**: 921-927 [PMID: 4321681 DOI: 10.1136/gut.11.11.921]
110 **Abascal J**, Diaz-Rojas F, Jorge J, Sanchez-Vegazo I, Escartin P, Abreu L, Chantar C. Free perforation of the small bowel in Crohn's disease. *World J Surg* 1982; **6**: 216-220 [PMID: 7090407 DOI: 10.1007/BF01654694]
111 **Ye BD**. Could early anti-tumor necrosis factor therapy change the prognosis of Crohn's disease? *Intest Res* 2014; **12**: 263-265 [PMID: 25374489 DOI: 10.5217/ir.2014.12.4.263]
112 **Liu RQ**, Guo D, Qiao SH, Yin Y, Guo Z, Gong JF, Li Y, Zhu WM. Comparison of primary anastomosis and staged surgery in emergency treatment of complicated Crohn's disease. *J Dig Dis* 2020; **21**: 724-734 [PMID: 33012107 DOI: 10.1111/1751-2980.12949]
113 **Han H**, Kim H, Rehman A, Jang SM, Paik SS. Appendiceal Crohn's disease clinically presenting as acute appendicitis. *World J Clin Cases* 2014; **2**: 888-892 [PMID: 25516865 DOI: 10.12998/wjcc.v2.i12.888]
114 **Meyerding EV**, Bertram HF. Nonspecific granulomatous inflammation (Crohn's disease) of the appendix; a case report. *Surgery* 1953; **34**: 891-894 [PMID: 13113513]
115 **Vanek VW**, Spirtos G, Awad M, Badjatia N, Bernat D. Isolated Crohn's disease of the appendix. Two case reports and a review of the literature. *Arch Surg* 1988; **123**: 85-87 [PMID: 3276297 DOI: 10.1001/archsurg.1988.01400250095017]
116 **Haddad M**, Azim F, Koren A, Stelman E, Mor C, Zelikovski A. Crohn's disease of the appendix. *Eur J Surg* 1993; **159**: 191-192 [PMID: 8102900]
117 **Ruiz V**, Unger SW, Morgan J, Wallack MK. Crohn's disease of the appendix. *Surgery* 1990; **107**: 113-117 [PMID: 2404347]
118 **Lindhagen T**, Ekelund G, Leandoer L, Hildell J, Lindström C, Wenckert A. Crohn's disease confined to the appendix. *Dis Colon Rectum* 1982; **25**: 805-808 [PMID: 6756829 DOI: 10.1007/BF02553319]
119 **Quaresma AB**, Miranda EF, Kotze PG. Management of ileocecal Crohn's disease during surgical treatment for acute appendicitis: A systematic review. *Arq Gastroenterol* 2021; **58**: 560-565 [PMID: 34909865 DOI: 10.1590/S0004-2803.202100000-98]
120 **Farmer RG**, Easley KA, Rankin GB. Clinical patterns, natural history, and progression of ulcerative colitis. A long-term follow-up of 1116 patients. *Dig Dis Sci* 1993; **38**: 1137-1146 [PMID: 8508710 DOI: 10.1007/BF01295733]
121 **Cima RR**. Timing and indications for colectomy in chronic ulcerative colitis: Surgical consideration. *Dig Dis* 2010; **28**: 501-507 [PMID: 20926879 DOI: 10.1159/000320409]
122 **Truelove SC**, Witts LJ. Cortisone in ulcerative colitis; final report on a therapeutic trial. *Br Med J* 1955; **2**: 1041-1048 [PMID: 13260656 DOI: 10.1136/bmj.2.4947.1041]
123 **Kornbluth A**, Sachar DB; Practice Parameters Committee of the American College of Gastroenterology. Ulcerative colitis practice guidelines in adults: American College Of Gastroenterology, Practice Parameters Committee. *Am J Gastroenterol* 2010; **105**: 501-23; quiz 524 [PMID: 20068560 DOI: 10.1038/ajg.2009.727]
124 **Gisbert JP**, Chaparro M. Acute severe ulcerative colitis: State of the art treatment. *Best Pract Res Clin Gastroenterol* 2018; **32-33**: 59-69 [PMID: 30060940 DOI: 10.1016/j.bpg.2018.05.007]
125 **Berg DF**, Bahadursingh AM, Kaminski DL, Longo WE. Acute surgical emergencies in inflammatory bowel disease. *Am J Surg* 2002; **184**: 45-51 [PMID: 12135718 DOI: 10.1016/s0002-9610(02)00879-6]
126 **Podugu A**, Tandon K, Castro FJ. Crohn's disease presenting as acute gastrointestinal hemorrhage. *World J Gastroenterol* 2016; **22**: 4073-4078 [PMID: 27122659 DOI: 10.3748/wjg.v22.i16.4073]
127 **Nagata N**, Niikura R, Aoki T, Moriyasu S, Sakurai T, Shimbo T, Shinozaki M, Sekine K, Okubo H, Watanabe K, Yokoi C, Yanase M, Akiyama J, Uemura N. Role of urgent contrast-enhanced multidetector computed tomography for acute lower gastrointestinal bleeding in patients undergoing early colonoscopy. *J Gastroenterol* 2015; **50**: 1162-1172 [PMID: 25812518 DOI: 10.1007/s00535-015-1069-9]
128 **Ali M**, Ul Haq T, Salam B, Beg M, Sayani R, Azeemuddin M. Treatment of nonvariceal gastrointestinal hemorrhage by transcatheter embolization. *Radiol Res Pract* 2013; **2013**: 604328 [PMID: 23844289 DOI: 10.1155/2013/604328]
129 **Heimann TM**, Greenstein AJ, Lewis B, Kaufman D, Heimann DM, Aufses AH Jr. Comparison of primary and reoperative surgery in patients with Crohns disease. *Ann Surg* 1998; **227**: 492-495 [PMID: 9563535 DOI: 10.1097/00000658-199804000-00007]
130 **Froehlich F**, Juillerat P, Felley C, Mottet C, Vader JP, Burnand B, Michetti P, Gonvers JJ. Treatment of postoperative Crohn's disease. *Digestion* 2005; **71**: 49-53 [PMID: 15711050 DOI: 10.1159/000083873]
131 **Rutgeerts P**, Geboes K, Vantrappen G, Beyls J, Kerremans R, Hiele M. Predictability of the postoperative course of Crohn's disease. *Gastroenterology* 1990; **99**: 956-963 [PMID: 2394349 DOI: 10.1016/0016-5085(90)90613-6]
132 **Rispo A**, Imperatore N, Testa A, Nardone OM, Luglio G, Caporaso N, Castiglione F. Diagnostic Accuracy of Ultrasonography in the Detection of Postsurgical Recurrence in Crohn's Disease: A Systematic Review with Meta-analysis. *Inflamm Bowel Dis* 2018; **24**: 977-988 [PMID: 29688470 DOI: 10.1093/ibd/izy012]
133 **Schoepfer AM**, Beglinger C, Straumann A, Trummler M, Vavricka SR, Bruegger LE, Seibold F. Fecal calprotectin correlates more closely with the Simple Endoscopic Score for Crohn's disease (SES-CD) than CRP, blood leukocytes, and the CDAI. *Am J Gastroenterol* 2010; **105**: 162-169 [PMID: 19755969 DOI: 10.1038/ajg.2009.545]
134 **Santiago M**, Magro F, Correia L, Portela F, Ministro P, Lago P, Trindade E, Dias CC. Inflammatory Bowel Disease Reoperation Rate Has Decreased Over Time If Corrected by Prevalence. *Clin Transl Gastroenterol* 2020; **11**: e00227 [PMID: 33094955 DOI: 10.14309/ctg.0000000000000227]
135 **Lee KY**, Yu CS, Lee KY, Cho YB, Park KJ, Choi GS, Yoon SN, Yoo H; IBD Study Group, Korean Society of Coloproctology. Risk factors for repeat abdominal surgery in korean patients with Crohn's disease: a multi-center study of a korean inflammatory bowel disease study group. *J Korean Soc Coloproctol* 2012; **28**: 188-194 [PMID: 22993704 DOI: 10.3393/jksc.2012.28.4.188]
136 **He X**, Chen Z, Huang J, Lian L, Rouniyar S, Wu X, Lan P. Stapled side-to-side anastomosis might be better than handsewn end-to-end anastomosis in ileocolic resection for Crohn's disease: a meta-analysis. *Dig Dis Sci* 2014; **59**: 1544-1551 [PMID: 24500450 DOI: 10.1007/s10620-014-3039-0]

137 **Feng JS**, Li JY, Yang Z, Chen XY, Mo JJ, Li SH. Stapled side-to-side anastomosis might be benefit in intestinal resection for Crohn's disease: A systematic review and network meta-analysis. *Medicine (Baltimore)* 2018; **97**: e0315 [PMID: 29642162 DOI: 10.1097/MD.0000000000010315]

138 **Kono T**, Ashida T, Ebisawa Y, Chisato N, Okamoto K, Katsuno H, Maeda K, Fujiya M, Kohgo Y, Furukawa H. A new antimesenteric functional end-to-end handsewn anastomosis: surgical prevention of anastomotic recurrence in Crohn's disease. *Dis Colon Rectum* 2011; **54**: 586-592 [PMID: 21471760 DOI: 10.1007/DCR.0b013e318208b90f]

139 **Luglio G**, Rispo A, Imperatore N, Giglio MC, Amendola A, Tropeano FP, Peltrini R, Castiglione F, De Palma GD, Bucci L. Surgical Prevention of Anastomotic Recurrence by Excluding Mesentery in Crohn's Disease: The SuPREMe-CD Study - A Randomized Clinical Trial. *Ann Surg* 2020; **272**: 210-217 [PMID: 32675483 DOI: 10.1097/SLA.0000000000003821]

140 **Yang KM**, Yu CS, Lee JL, Kim CW, Yoon YS, Park IJ, Lim SB, Park SH, Ye BD, Yang SK, Kim JC. Risk factors for postoperative recurrence after primary bowel resection in patients with Crohn's disease. *World J Gastroenterol* 2017; **23**: 7016-7024 [PMID: 29097874 DOI: 10.3748/wjg.v23.i38.7016]

141 **Thin LWY**, Picardo S, Sooben S, Murray K, Ryan J, Wallace MH. Ileocolonic End-to-End Anastomoses in Crohn's Disease Increase the Risk of Early Post-operative Endoscopic Recurrence in Those Undergoing an Emergency Resection. *J Gastrointest Surg* 2021; **25**: 241-251 [PMID: 32378095 DOI: 10.1007/s11605-020-04578-7]

142 **Sheehan AL**, Warren BF, Gear MW, Shepherd NA. Fat-wrapping in Crohn's disease: pathological basis and relevance to surgical practice. *Br J Surg* 1992; **79**: 955-958 [PMID: 1422768 DOI: 10.1002/bjs.1800790934]

143 **Petagna L**, Antonelli A, Ganini C, Bellato V, Campanelli M, Divizia A, Efrati C, Franceschilli M, Guida AM, Ingallinella S, Montagnese F, Sensi B, Siragusa L, Sica GS. Pathophysiology of Crohn's disease inflammation and recurrence. *Biol Direct* 2020; **15**: 23 [PMID: 33160400 DOI: 10.1186/s13062-020-00280-5]

144 **Li Y**, Mohan H, Lan N, Wu X, Zhou W, Gong J, Shen B, Stocchi L, Coffey JC, Zhu W. Mesenteric excision surgery or conservative limited resection in Crohn's disease: study protocol for an international, multicenter, randomized controlled trial. *Trials* 2020; **21**: 210 [PMID: 32085793 DOI: 10.1186/s13063-020-4105-x]

145 **Safar B**, Sands D. Perianal Crohn's disease. *Clin Colon Rectal Surg* 2007; **20**: 282-293 [PMID: 20011424 DOI: 10.1055/s-2007-991027]

146 **Hurst RD**, Molinari M, Chung TP, Rubin M, Michelassi F. Prospective study of the features, indications, and surgical treatment in 513 consecutive patients affected by Crohn's disease. *Surgery* 1997; **122**: 661-7; discussion 667 [PMID: 9347840 DOI: 10.1016/s0039-6060(97)90071-4]

147 **Spinelli A**, Armuzzi A, Ciccocioppo R, Danese S, Gionchetti P, Luglio G, Orlando A, Rispo A, Rizzello F, Sofo L, Solina G, Poggioli G. Management of patients with complex perianal fistulas in Crohn's disease: Optimal patient flow in the Italian clinical reality. *Dig Liver Dis* 2020; **52**: 506-515 [PMID: 31901310 DOI: 10.1016/j.dld.2019.11.016]

148 **Pogacnik JS**, Salgado G. Perianal Crohn's Disease. *Clin Colon Rectal Surg* 2019; **32**: 377-385 [PMID: 31507348 DOI: 10.1055/s-0039-1687834]

149 **Sneider EB**, Maykel JA. Anal abscess and fistula. *Gastroenterol Clin North Am* 2013; **42**: 773-784 [PMID: 24280399 DOI: 10.1016/j.gtc.2013.08.003]

150 **Jimenez M**, Mandava N. Anorectal Fistula. StatPearls. Treasure Island (FL), 2022

151 **Irvine EJ**. Usual therapy improves perianal Crohn's disease as measured by a new disease activity index. McMaster IBD Study Group. *J Clin Gastroenterol* 1995; **20**: 27-32 [PMID: 7884173]

152 **Steele SR**, Kumar R, Feingold DL, Rafferty JL, Buie WD; Standards Practice Task Force of the American Society of Colon and Rectal Surgeons. Practice parameters for the management of perianal abscess and fistula-in-ano. *Dis Colon Rectum* 2011; **54**: 1465-1474 [PMID: 22067173 DOI: 10.1097/DCR.0b013e31823122b3]

153 **Lee MJ**, Heywood N, Sagar PM, Brown SR, Fearnhead NS; pCD Collaborators. Surgical management of fistulating perianal Crohn's disease: a UK survey. *Colorectal Dis* 2017; **19**: 266-273 [PMID: 27423057 DOI: 10.1111/codi.13462]

154 **Kasparek MS**, Glatzle J, Temeltcheva T, Mueller MH, Koenigsrainer A, Kreis ME. Long-term quality of life in patients with Crohn's disease and perianal fistulas: influence of fecal diversion. *Dis Colon Rectum* 2007; **50**: 2067-2074 [PMID: 17680311 DOI: 10.1007/s10350-007-9006-5]

155 **Archampong D**, Borowski D, Wille-Jørgensen P, Iversen LH. Workload and surgeon's specialty for outcome after colorectal cancer surgery. *Cochrane Database Syst Rev* 2012; CD005391 [PMID: 22419309 DOI: 10.1002/14651858.CD005391.pub3]

156 **Nagler SM**, Poticha SM. Intraabdominal abscess in regional enteritis. *Am J Surg* 1979; **137**: 350-354 [PMID: 434328 DOI: 10.1016/0002-9610(79)90065-5]

World Journal of Gastroenterology

Submit a Manuscript: https://www.f6publishing.com

World J Gastroenterol 2022 May 14; 28(18): 1922-1933

DOI: 10.3748/wjg.v28.i18.1922

ISSN 1007-9327 (print) ISSN 2219-2840 (online)

MINIREVIEWS

Novel drug delivery systems for inflammatory bowel disease

Farah Yasmin, Hala Najeeb, Shehryar Shaikh, Muhammad Hasanain, Unaiza Naeem, Abdul Moeed, Thoyaja Koritala, Syedadeel Hasan, Salim Surani

Specialty type: Gastroenterology and hepatology

Provenance and peer review: Invited article; Externally peer reviewed.

Peer-review model: Single blind

Peer-review report's scientific quality classification

Grade A (Excellent): A
Grade B (Very good): 0
Grade C (Good): C
Grade D (Fair): 0
Grade E (Poor): 0

P-Reviewer: Zhang Y, China; Zhou Y, China;

Received: November 13, 2021
Peer-review started: November 13, 2021
First decision: January 9, 2022
Revised: January 22, 2022
Accepted: March 26, 2022
Article in press: March 26, 2022
Published online: May 14, 2022

Farah Yasmin, Hala Najeeb, Muhammad Hasanain, Unaiza Naeem, Abdul Moeed, Department of Medicine, Dow University of Health Science, Karachi 74200, Pakistan

Shehryar Shaikh, Department of Medicine, Dow OJha University Hospital, Karachi 74200, Pakistan

Thoyaja Koritala, Department of Medicine, Mayo Clinic Health System, Mankato, MN 56001, United States.

Syedadeel Hasan, Department of Medicine, University of Louisville, Louisville, KY 40292, United States

Salim Surani, Department of Medicine, Texas A&M University, College Station, TX 77843, United States

Salim Surani, Department of Anesthesiology, Mayo Clinic, Rochester, MN 55901, United States

Corresponding author: Salim Surani, FACP, FCCP, MD, MSc, Doctor, Professor, Department of Medicine, Texas A&M University, 400 Bizzell Street, College Station, TX 77843, United States. srsurani@hotmail.com

Abstract

Inflammatory bowel disease (IBD) is a chronic illness characterized by relapsing inflammation of the intestines. The disorder is stratified according to the severity and is marked by its two main phenotypical representations: Ulcerative colitis and Crohn's disease. Pathogenesis of the disease is ambiguous and is expected to have interactivity between genetic disposition, environmental factors such as bacterial agents, and dysregulated immune response. Treatment for IBD aims to reduce symptom extent and severity and halt disease progression. The mainstay drugs have been 5-aminosalicylates (5-ASAs), corticosteroids, and immunosuppressive agents. Parenteral, oral and rectal routes are the conventional methods of drug delivery, and among all, oral administration is most widely adopted. However, problems of systematic drug reactions and low specificity in delivering drugs to the inflamed sites have emerged with these regular routes of delivery. Novel drug delivery systems have been introduced to overcome several therapeutic obstacles and for localized drug delivery to target tissues. Enteric-coated microneedle pills, various nano-drug delivery techniques, prodrug systems, lipid-based vesicular systems, hybrid drug delivery systems, and biologic drug delivery systems constitute some of these novel methods. Microneedles are painless, they dislodge their content at the affected site, and their release can be prolonged. Recombinant

bacteria such as genetically engineered *Lactococcus Lactis* and eukaryotic cells, including GM immune cells and red blood cells as nanoparticle carriers, can be plausible delivery methods when evaluating biologic systems. Nano-particle drug delivery systems consisting of various techniques are also employed as nanoparticles can penetrate through inflamed regions and adhere to the thick mucus of the diseased site. Prodrug systems such as 5-ASAs formulations or their derivatives are effective in reducing colonic damage. Liposomes can be modified with both hydrophilic and lipophilic particles and act as lipid-based vesicular systems, while hybrid drug delivery systems containing an internal nanoparticle section for loading drugs are potential routes too. Leukosomes are also considered as possible carrier systems, and results from mouse models have revealed that they control anti- and pro-inflammatory molecules.

Key Words: Inflammation; Inflammatory bowel diseases; Colitis; Ulcerative; Crohn's disease; Drug delivery systems; Drug carrier

©The Author(s) 2022. Published by Baishideng Publishing Group Inc. All rights reserved.

Core Tip: Current literature on novel drug delivery systems is extensive. However, limited content is available that focuses on the novel drug delivery strategies, focally the enteric-coated microneedles pills and biological drug delivery systems. In our review, we discuss multiple novel approaches comprehensively, after outlining the disease course in inflammatory bowel diseases (IBD) and how the conventional routes of drug administrations are deficient in addressing some aspects of disease treatment. We specify that novel carrier systems can be considered for targeting inflamed sites in IBD and discuss the implications of choosing such routes.

Citation: Yasmin F, Najeeb H, Shaikh S, Hasanain M, Naeem U, Moeed A, Koritala T, Hasan S, Surani S. Novel drug delivery systems for inflammatory bowel disease. *World J Gastroenterol* 2022; 28(18): 1922-1933
URL: https://www.wjgnet.com/1007-9327/full/v28/i18/1922.htm
DOI: https://dx.doi.org/10.3748/wjg.v28.i18.1922

INTRODUCTION

Inflammatory bowel disease (IBD) is chronic, relapsing intestinal inflammation[1]. The disorder is most common in Western industrialized countries[2] and is mainly characterized by the two idiopathic phenotypes of IBD; Ulcerative colitis (UC) and Crohn's disease (CD)[3]. The illness can be classified as mild, moderate, or severe based on clinical, para clinical parameters and symptoms such as abdominal spasms, rectal bleeding[4]. Intestinal and extraintestinal complications also manifest in the disease[2], and IBD is known to significantly affect the quality of life of the patients[4].

The main aim of IBD treatment is to ameliorate patients' quality of life[5] by diminishing the extent and symptoms of intestinal inflammation[3], revitalizing nutrition lost, assisting psychosocially, and altering disease course in those undergoing severe forms[5]. Therapy is decided after determining the type of disease and site involved[3]. Routine treatment options for mild attacks include 5-aminosalicylates (5-ASA) such as mesalazine or olsalazine, while for moderate to severe IBD, corticosteroids are prescribed. Probiotics, antibiotics, chemically modified drugs, enzymatic, prodrug therapy, enteric-coated drugs can be used in the early stages, too[5]. For severe disease stages, immunosuppressive agents like azathioprine and anti-TNF-α-antibodies are specified[2]. Surgery is performed in the refractory or fulminate disease stages[2] and is reported to be required by 30%-40% UC and all CD patients at least once in a lifetime[3].

The IBD medication administration's modes are the conventional parenteral, peroral, and rectal routes[2], while the peroral route is most preferred, indicated for targeting the colon[3]. However, there is variable intestinal absorption *via* this route, and treating intermittent inflamed areas is challenging by oral drug delivery systems[2]. Systematic drug reactions by absorption of luminal released active agents through the healthy and inflamed mucosal wall into systematic circulation, inability to deliver to an affected gastrointestinal section only[2] and the reliance of the conventional delivery systems on unstable parameters such as intestinal motility, time, pH, and microbial and enzymatic degradation for optimal drug delivery[5] have rendered these standard methods unsatisfactory.

To balance therapeutic efficacy and risk of adverse side effects[2], novel drug delivery systems have been suggested that provide a more localized delivery and circumvent unnecessary drug exposure[6]. Inspired by the German physician Paul Ehrlich who first proposed drug targeting of active agents to pathogenic or cancerous cells while preventing side effects, the new synthetic/biologic drug delivery

systems known[2] incorporate liposomes, solid lipid nanoparticles, nanostructured lipid carriers, nano emulsions, hydrogel, and eukaryotic systems *via* resealed erythrocytes, macrophages, prokaryotic cells such as bacterial capsules[5]. These innovative approaches minimize drug loss, increase drug bioavailability[5], increase the local concentration of drugs at inflamed tissue and increase patient's compliance lowering the frequency of drug intake[2]. This review presents an overview of enteric-coated microneedle pills, nano-drug delivery systems, including size-mediated targeting, surface-charged targeting, redox-mediated targeting, and ligand-mediated targeting techniques. Furthermore, prodrug delivery systems, lipid-based vesicular delivery systems, hybrid drug delivery systems, and biologic drug delivery systems are also discussed. All that is being seen as a more disease-oriented[2] approach for restoring gut homeostasis in IBD.

PATHOLOGICAL MECHANISM OF IBD

In IBD, the intestinal barrier is disrupted, characterized by a reduced number of secretory cells, which lead to a decrease in antimicrobial secretion, and a loss of epithelium. A decrease in goblet cells at the inflamed site causes a reduction in mucus. Bacteria from the lumina side and immune-related cells infiltrate the mucosa and constitute the pathophysiological state in IBD[2]. The two main phenotypes of IBD are UC and CD, respectively. Inflammation in UC is superficial, limited to the colon. The disease starts in the rectum and extends continuously through the colon. The extent of colonic involvement defines disease distribution; proctitis to left-sided colitis or extensive colitis (pancolitis)[7]. In CD, the inflammation extends to the serosa. The disease is transmural and is found anywhere along the gastrointestinal length, mostly the ileum and colon. Endoscopy reveals mucosa's "sandpaper" appearance in UC, while in CD, the mucosa is cobblestone[8]. The etiology of IBD is unknown, and the interaction of genetic disposition with environmental factors in the microbiome leads to improper immune activation resulting in clinical presentation observed in IBD[9].

Rare genetic variants have been identified in early onset and severe IBD patients indicating a relation with pathways leading to intestinal inflammation. Genome-wide association studies have also identified 201 Loci implicated in IBD[9]. NOD2 is the first gene associated with IBD[9], and is related to CD susceptibility[3]. Environmental agents can trigger IBD in genetically susceptible individuals; medications can alter the intestinal microbiome, which is linked with an increased risk of developing IBD. An increase in bacteria with inflammatory potentialities and a decrease in anti-inflammatory bacteria are reported[9]. Mucolytic bacteria are also found to be increased in the intestine[9]. A dysregulation between anti and pro-inflammatory signals, causing migration of leukocytes to the intestinal mucosa exacerbated by an enhanced T-cell immune response, is noted in UC and CD[9]. Th-2 cell response is dominant in UC and antibodies recruitment. IL-5 is also elevated in UC. However, antigens eliciting the response are not known[3]. Moreover, a Th-1 inflammatory response is signified in CD, resulting in granulomatous inflammation with increased levels of proinflammatory cytokines such as IFN-γ, IL-2, and TNF-α. Suppressor cytokines produced by T regulatory cells are reduced[3].

ENTERIC-COATED MICRONEEDLE PILLS

Microneedle pills were first considered as a fix to deliver drugs through the transdermal system in 1998 [10]. Increasing the permeability of the human skin, a painless drug delivery system was formulated. However, the lack of stratum corneum in the GI tract established a strong case for microneedles in oral delivery. Coated microneedles provide extended controlled release reducing the required dosage frequency of many medications[11]. An ingestible microneedle pill for adalimumab, a tumor necrosis factor blocker, developed by Rani Therapeutics LLC[12] demonstrated a higher serum adalimumab concentration for the first eight hours to its administration as compared to the subcutaneous route.

Microneedles are either solid or hollow with the biologics contained in the reservoir, released upon breach of the mucosal lining of the GI tract. Microneedles are prepared using biodegradable polymers and coated by a pH-resistant coating to withstand the acidic range of pH of the gut[13]. Following ingestion, microneedles travel to the required location and spill their contents upon peristalsis and or penetrate the tissue and break off in hollow and solid microneedles, respectively[13].

The retention time of the microneedles was seven days at the minimum in a study[13], with no tissue damage reported. The safety profile and the extended retention warrants its potential use as a drug delivery system in IBD. However, patient-to-patient variation in intraluminal pressure presents a significant challenge along with the impact of food in the GI tract on the efficacy of the drug delivery system[14].

NANOPARTICLE DRUG DELIVERY SYSTEM

Size-mediated targeting

Size-dependent targeting is the most common mechanism for NPs drug delivery systems targeting the inflamed colon. During inflammation, enhanced permeability and retention (EPR) is observed, which increases penetration of nano-particles in the inflamed regions[15-18]. Furthermore, increased secretion of mucus leads to a thick mucus layer which increases the probability of adhesion of nanoparticles[19, 20]. The size of mucous fiber networks varies from 10-200 nm; hence modifying the particle size to nano-formulations assists in movement inside the fiber network[21-24]. It is reported that diarrhea affects particles > 200 μm, which are subsequently washed away[25] whereas, neutrophils, macrophages, M cells, and enterocytes rapidly internalize particles < 500 nm *via* the process of transcytosis[26]. Lamprecht *et al*[27] compared fluorescent polystyrene particles of sizes 10 mm, 1 mm, and 100 nm following oral gavage among healthy and trinitrobenzene sulfonic acid (TNBS)-induced colitic rats. The 100 nm formulation displayed the greatest bio adhesion to the inflamed colon compared to healthy rats. Another study done on oxazolone-induced colitis in mice reported that budesonide-filled poly lactic-co-glycolic acid (PLGA) NPs of size 200 nm accumulated at the inflamed colon[28]. Similarly, Nagasaki's group[29,30] developed a nanoparticle sized 40 nm (RNP O), which localized in the inflamed colonic mucosa, and reduced inflammation by consuming the excessive ROS. The increased epithelial enhanced permeability and retention (epEPR) during inflammation leads to increased uptake of NPs and prolongs the retention time[31]. This consequently leads to the accumulation of drugs and increased efficacy. Another study investigated the penetration of fluorescently labeled PLGA particles, sized 250 nm and 3 nm, into rectal mucosa in healthy and IBD human subjects. They reported that significantly more 3 nm particles were found accumulated in the mucosal surface, while most of the 250 nm particles had penetrated inside and translocated to the serosal surface[32]. The probability of systemic absorption increases with smaller particles and could lead to adverse side effects. This difference in the behavior of NPs accumulation in humans and rodent colitis models requires further studies to reach a definite conclusion.

Surface-charge targeting

The surface charge of the nanoparticles can be altered to control interaction with the colonic mucosa to increase the efficacy of the drug delivery system. The colonic mucosa comprises negatively charged carbohydrates molecules, sulfates, sialic acid, and colonic mucins, which enable the positively charged NPs to adhere to the mucosal surface due to electrostatic interaction. In a study, clodronate loaded nanoparticles based on cationic polymethacrylate (Eudragit RL) and free clodronate were administered in mice induced with 2,4,6-TNBS and oxazolone colitis. A significant reduction in myeloperoxidase activity was observed in colitis-induced mice models, whereas free clodronate failed to produce ameliorating effect[33]. In an *ex vivo* study, Lautenschlager demonstrated that cationic chitosan modified PLGA nanoparticles adhered to intestinal mucosa[34]. However, the cation became immobilized after attaching to the mucosa, which led to a premature release of the drug. This was due to the strong electrostatic attraction experienced by the negatively charged mucosa[34]. In comparison, negatively charged NPs precisely attach to specific positively charged proteins and show greater penetration into the intestinal mucosa. During the inflammatory process of colonic mucosa, the epithelium is damaged, and positively charged proteins such as transferrin and eosinophil cationic proteins accumulate[35,36]. This enables nanoparticles with the negative surface charge to adhere to the positively charged mucosal surface due to electrostatic interaction. Jubeh *et al*[37] studied the varied adhesion of anionic, neutral, and cationic liposomes in healthy and inflamed colon explants from rats inflicted with DNBS colitis. They reported that anionic liposomes were 2-times more likely to adhere to the inflamed mucosa than neutral or cationic liposomes. In healthy colonic mucosa, the cationic liposomes displayed preferential binding, which was 3-fold higher than neutral or anionic liposomes[38]. Similarly, Beloqui *et al*[39] reported that negatively charged NPs, comprised of budesonide, invaded deeper into mucosa in the colitis group while staying on the mucosal surface in a healthy cohort.

Redox-mediated targeting

Endogenous ROS are produced because of the physiological metabolism of oxygen. In patients suffering from IBD, increased production of ROS is observed, which is localized to the site of inflammation and correlated with disease progression[40,41]. This increase is due to the inflammatory cells present in the intestinal mucosa[42]. Subsequently, redox-dependent nanoparticle drug delivery systems have emerged[43,44]. Zhang *et al* developed oxidation-sensitive β-cyclodextrin material (OxβCD), which was loaded with Tpl. This drug delivery system could successfully consume ROS and mitigate symptoms in 3 mouse colitis models[45,46]. Sun *et al*[47] synthesized redox-sensitive NPs composed of carboxymethyl inulin. The NPs accumulate in the inflamed regions of the intestine. Vong *et al*[30] developed NPs composed of nitroxide radicals (RNPo), which exhaust the ROS in the inflamed gut regions and thereby reduce inflammation. The group of mice treated with oral RNPo for one week showed reduced disease activity compared with the group administered mesalamine[30]. Li *et al*[48] synthesized Ac2-26-encapsulated nano therapy using OxβCD. This drug delivery system is ROS-responsive and stimulates

the release of Ac2-26 in response to increased ROS concentration in GIT.

In conclusion, since a high concentration of ROS is found in the inflamed regions of GIT[42], redox-dependent targeting *via* NPs may produce beneficial results. However, volatility in low pH, high enzyme environment, and rapid drug release hinder the use of redox-mediated drug delivery systems.

Ligand-mediated targeting

Under inflammatory processes, ligand-dependent NPs have shown to be a precise method of drug localization, minimal side effects, and increased therapeutic efficacy[49]. Overexpression of inflammatory markers on cell surface provides molecular targets for anchoring NPs[50,51]. PLA NPs, which carry CD98 Fab antibodies, and chitosan/polyethyleneimine NPs modified with CD98 antibody were developed to treat mice with colitis. During inflammation, cells in colonic mucosa overexpress CD98 glycoprotein, which becomes the target of action for the ligand-modified NPs[52,53]. Similarly, mannose receptors are overexpressed on macrophages, which are targeted by mannosylated poly (amido amine)-modified NPs[54]. Moreover, increased expression of CD44 is observed in the macrophages and inflamed epithelial cells during colitis[55-57]. Hyaluronic acid can attach to CD44; hence, HA-modified NPs have been developed and tested successfully in mice with UC[58]. Increased expression of folate receptors has also been observed during inflammation[59-61]. Naserifar *et al*[62] successfully demonstrated the efficacy of oral administration of folic acid conjugated PLGA NPs loaded with resveratrol in TNBS rats.

Besides overexpression of ligands/receptors on colonic epithelial cells, endothelial adhesion molecules (ECAMs) are also upregulated. Vascular adhesion molecules-1 are ECAMs against which polylactic acid (PLA)-PEG particles modified with monoclonal antibodies have been developed. The drug delivery system showed increased adhesion to the endothelium in dextran sodium sulfate (DSS)-induced colitis[63]. In conclusion, ligand-modified NPs promise to be a potential alternative for targeted drug delivery in cases of IBD. However, concerns regarding IV administration, antibody precipitated immune reaction, ligand instability inside GIT hamper its utilization.

PRODRUG

In prodrug systems, a pharmacologically active agent is protected in a temporarily inactive form that gains bioactivity on exposure to enzymes overexpressed in inflammatory tissues. This allows drug delivery to specific sites[64]. Several 5-ASA formulations have been used as prodrugs for selective delivery to the colon, azo conjugates being the most common and effective[65]. Many 5-ASA derivates were also shown to be transportable substrates for Intestinal H+-coupled oligopeptide transporter 1, the expression of which is increased in chronic inflammatory conditions such as IBD[66]. Furthermore, a synthetic prodrug of 4-ASA, an isomer of 5-ASA, was prepared and shown to be suitable for the treatment of colon inflammatory diseases[67]. To reduce endoplasmic reticulum (ER) stress, an aggravating factor for IBD, Kim *et al*[68] synthesized prodrugs for 4-phenyl butyric acid, which effectively reduced the colonic damage and inflammation in a rat colitis model. Moreover, Shen *et al*[69] designed a novel pH/reactive oxygen species (ROS) dual-responsive prodrug micelle GC-B-Que. In his vivo experiments, he found that the GC-B-Que micelles tended to accumulate in sites of inflammation within the intestine and showed better therapeutic efficacy than free drugs[69]. Using a prodrug approach for management of IBD allows accumulation of drugs at sites of inflammation, avoiding unwanted side effects on healthy intestinal tissue.

LIPID-BASED VESICULAR DELIVERY SYSTEM

Liposomes are lipid bilayer vesicles that consist of an aqueous core. They can carry both hydrophilic and lipophilic drugs[70]. For use as a drug delivery system for IBD, liposomes can be modified with lactoferrin which can specifically bind to low-density lipoprotein receptor-related protein that is expressed on the inflammatory macrophages. Zhao *et al*[71] designed a lactoferrin-modified liposome (LF-lipo) for delivering patchouli alcohol to colonic macrophages for anti-inflammatory activity. The results showed decreased disease activity index and body weight loss in DSS salt -induced colitis mice. In another study, an oxymatrine loaded, nitric oxide releasing liposome, tested in DSS-induced ulcerative colitis mice, was shown to significantly alleviate inflammation. Moreover, the results also revealed that liposomes could accumulate in the inflammatory colon efficiently and can be maintained for more than 36 h[72]. Furthermore, in an *in vivo* experiment, curcumin-loaded liposomes (CUR-LPs) were shown to allow sustained release of CUR in the simulated gastrointestinal tract, attenuate the clinical symptoms of ulcerative colitis and prevent DSS-induced colon tissue damage and colon shortening[73]. Liposomes have also been loaded with heparin for intrarectal delivery in the form of enema, which has demonstrated dose-dependent anti-inflammatory activity *in vivo*[74]. Krill oil incorporation into liposomes has demonstrated a high capacity to entrap the IBD drug budesonide, and

results of an *in vitro* study indicate that using KO liposomes as an IBD drug carrier may yield increased drug accumulation in the inflamed intestinal region[75]. Keratinocyte growth factor (KGF), previously shown to be an effective drug for ulcerative colitis, faces several obstacles for clinical such as poor stability, short half-life, and easy degradation; therefore, liposomes were considered as a potential delivery system. KGF was encapsulated into liposomes (KGF-Lips), and neutrophil membrane vesicles were then inlaid in KGF-Lips to construct a neutrophile-like liposome (KGF-Neu) which was shown to significantly improve the chemical stability of KGF[76]. Anemia is frequently seen in patients with IBD, which is responsible for a significant loss of quality of life. Treatment with oral liposomal iron was shown to be effective in improving mild iron deficiency anemia and quality of life, as well as in decreasing fatigue in patients with inactive or mildly active IBD[77].

HYBRID DRUG DELIVERY SYSTEMS

Although difficult to prepare, hybrid drug delivery systems hold great promise as they integrate the advantages of several different carriers into one. An external compartment is used to protect drugs from gastric degradation and denaturation at low pH, and the internal section of NPs is developed for loading drugs[78]. Kotla *et al*[79] fabricated hyaluronan (HA) functionalized polymeric nano-drug delivery system (Cur-HA NPs) using curcumin as a model fluorescent drug. HA functionalization was shown to increase cellular interaction and uptake following the use of Cur-HA NPs on colon epithelial-like (HT-29) monolayers cell cultures indicating that this system is effective for oral delivery of drugs to treat local colonic disease[79]. Furthermore, encapsulation of curcumin with bovine b-lactoglobulin has been shown to increase its aqueous solubility, and encapsulation with succinylated- b-lactoglobulin prevented its release when subjected to gastric fluids[80]. In another study, Zhang *et al*[81] developed a phospholipid vesicle co-hybridized with HA and ethanol (HA-ES) for transdermal delivery of eugenol (EUG)/cinnamaldehyde (CAH). Results of the subsequent study showed that HA-ES as carriers effectively improved the percutaneous absorption of EUG and CAH in a rat ulcerative colitis model[81]. To improve the colon targeted oral delivery of Berberine, Zhang *et al*[82] designed a micro-and nano-encapsulated hybrid delivery system, which resulted in significant alleviation of acute colitis in a DSS induced colitis mice model. To overcome limitations faced by nanoparticle systems, Naeem *et al*[83] developed a "nanoparticles-in-enteric microparticles" (NPsinMPs) system. A (PLGA) polymer-based NP system was encapsulated in pH-sensitive Eudragit FS30D microparticles. NPisMPs provided complete protection of NPs in both gastric acid and intestinal-like pH. Moreover, NPs, after releasing from NPsinMPs, accumulated in the inflamed colon of mice after oral administration and significantly alleviated murine experimental colitis when compared to the bare nanoparticle[83].

BIOLOGICAL DRUG DELIVERY SYSTEMS

Apart from maintaining intestinal homeostasis and synthesizing bile acids[84], bacteria could also be used as a potential delivery system in IBD. Recently, scientists ventured to use bioengineered bacteria as a delivery system of therapeutics in various diseases[85]. *Lactococcus Lactis (L. Lactis)* was the front runner in the race of effective biological vectors. *L. Lactis* is present in abundance in plants in an inactive state, gaining the active status in the gut of ruminants[86].

In 2006, genetically engineered *L. Lactis* was graded safe as a drug delivery system[87]. Due to the immunomodulatory functions of *L. Lactis*, its use as a vector to transport cytokines has been reported in numerous studies. One of the first applications of genetically modified (GM) *L. Lactis* in mice to produce interleukin-10 (IL-10) for IBD treatment was reported in 2000[88]. In 2003, recombinant *L. Lactis* strain labeled Thy12 successfully produced IL-10 in pigs[89].

A phase I clinical trial aimed to treat CD patients with genetically engineered *L. Lactis*. The results backed up its safety profile and solidified the effectiveness of the containment strategy[90]. In another study, orally administered *L. Lactis* was seen to ameliorate inflammation of the colon in mice by delivering anti-murine TNF nanobodies to the inflamed site[91]. Similarly, a study of mice with induced colitis showed mitigation of the disease upon application of *L. Lactis* carrying the anti-TNF scFv expression vector[92]. In a 2020 study of a DSS induced colitis mouse model, inflammation was seen to be reduced by blocking the IL-1 signaling using genetically modified Lactic acid bacteria (gmLAB)[93].

These studies show the therapeutic nature of recombinant bacteria as a vector in the treatment of IBD. *L. Lactis* is demonstrated to be safe and potent in inducing anti-inflammatory effects. However, studies should investigate further into the risk of unintended transgene escape, and focus attempts must be made to develop various other anti-inflammatory substances by *L. Lactis*[89].

Apart from bacteria, eukaryotic cells can be utilized as a delivery system of therapeutics for IBD. GM immune and red blood cells (RBCs) are used as nanoparticle (NP) carriers *via* injection from these cells. Endothelial cells in blood vessels present as a barricade in the route of NPs to their target destination. In a study of a mouse model of acute inflammation, activated neutrophils took up intravenously administered NPs and crossed the barrier into the inflamed tissues[94]. This study highlighted the

ability to "hijack" neutrophils to transport NPs to the diseased site.

Another study by Corbo *et al*[95] implemented the mechanism of α4β7 integrins, which promote entry of T cells to intestinal sites[96]. The study employed this principle to investigate the effect of specialized leukosomes (SLKs) in alleviating inflammation in mice models of IBD. SLKs were associated with modulating both pro and anti-inflammatory molecules. Immune cells are presumably blocked by SLKs, as indicated by the reduction in CD45+ cells in the colon of mice treated with SLKs. However, further studies must be initiated examining the mechanism of functioning of SLKs in-depth. Furthermore, a risk-benefit analysis must be conducted to assess its safety.

Similarly, RBCs are increasingly being popular based on their high bioavailability in blood. Due to the rapid clearance of NPs in blood, a study successfully reported a novel method of adhering them to circulating RBCs to enhance their vascular circulation[97]. A clinical trial by Castro *et al*[98] assessed the impact of autologous RBCs loaded with dexamethasone 21-Phosphate (Dex 21-P) on children with steroid-dependent Crohn's disease. During treatment, the pediatric Crohn's Disease Activity Index was sufficiently reduced, and 78% of the patients stopped taking steroids. Overall, 44% showed remission, indicating the safe and efficacious nature of RBCs laden with Dex 21-P. Another study corroborated these findings as steroids were withdrawn entirely in all the patients and were in clinical remission after three infusions[99]. Further large-scale controlled studies should examine the safety and potency of this therapy in IBD patients. In future studies focus should be on the delivery of drugs directly to the inflamed sites and on the concentration of dexamethasone to increase the bioavailability.

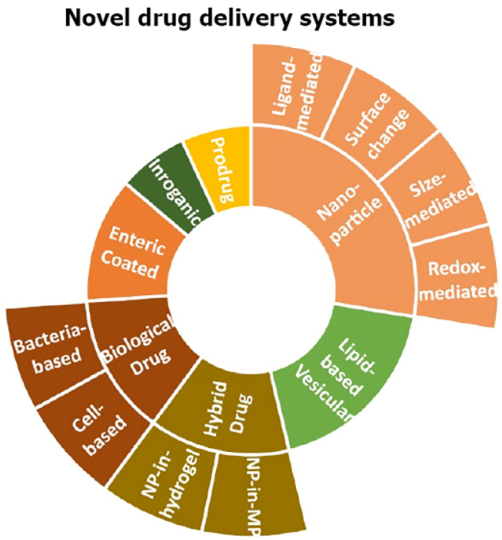
DISCUSSION

Various nanoparticle drug-delivery systems exist. Size-dependent is the most popular mechanism. During inflammation, increased permeability, and retention (EPR) and enhanced mucosal secretions lead to increased efficacy of size-dependent targeting. However, systemic absorption of nanoparticles could lead to adverse side effects, which require further investigation. In addition to size, the surface charge of nanoparticles can also be modified to increase effectiveness. Due to electrostatic attraction, positively charged nanoparticles can adhere to the negatively charged colonic mucosa.

Moreover, redox-dependent nanoparticles use the increased amounts of ROS produced by intestinal mucosal cells during inflammation. However, volatility in low pH and quick drug release limit their use. Lastly, ligand-dependent NPs precisely target colonic mucosa with increased efficacy. NPs attach to the inflammatory markers' ligands/receptors and ECAMs on the cell surface. A ligand-dependent deliveries system is a promising alternative; however, the concern of antibody precipitated immune reaction and instability inside GIT warrants further investigations. The existing targeted novel drug delivery systems are illustrated in Figure 1.

CONCLUSION

In our review, we divulged several drug delivery systems that have been under investigation in previous studies. These carrier systems were found to be potential options for drug delivery, with enteric-coated microneedles and recombinant bacteria termed safe upon use, while further analysis needs to be undertaken to assess the reliability of eukaryotic cells as delivery systems. Due to increased epithelial permeability and retention, Nanoparticles are well-absorbed in inflamed mucosa and have shown to be efficacious. However, accumulation of NPs might be observed that requires further study. Redox-dependent nanoparticle drug delivery systems have also emerged, such as NPs composed of nitroxide radicals (RNPo), which have successfully reduced inflammation by exhausting ROS, but their utilization might be limited due to factors such as rapid drug release. Ligand-depending NPs are efficient localized treatment, and HA-coated NPs and folic acid conjugated PLGA NPs loaded with resveratrol in TNBS have shown positive results in animal models. 5-ASA formulations, its isomers comprise some of the prodrug systems well in practice, and a novel pH/ROS dual-responsive prodrug micelle GC-B-Que has been found to display high therapeutic efficacy. Liposomes modified with lactoferrin, CUR-LPs, and heparin loaded liposomes are lipid based vesicular systems that have been anti-inflammatory. Importantly, oral liposomal iron is advantageous in alleviating anemia often observed in IBD patients. Hybrid methods of drug delivery have been proven to be effective in alleviating colitis across various studies. Leukosomes as carrier systems have also been found to be effective in mediating inflammatory response in IBD, but more clinical trials involving human subjects are warranted. Conventional drug delivery systems have certain caveats associated with their use, and novel drug delivery systems are being resorted to avoiding the adverse outcomes reported with the former routes; however, more research is needed to substantiate the efficacy of the novel carrier systems. Overall, given the challenge of delivering a drug to the inflamed site in IBD and the unique presentations of the disease in various patients, the new strategies can be instrumental in improving disorder symptoms and disease course.



DOI: 10.3748/wjg.v28.i18.1922 **Copyright** ©The Author(s) 2022.

Figure 1 The existing targeted novel drug delivery systems.

FOOTNOTES

Author contributions: Yasmin F primarily drafted the work, Yasmin F, Najeeb H, Shaikh S, Hasanain M, Naeem U, Moeed A and Surani S contributed to the conception of this study; Najeeb H, Shaikh S, Hasanain M, Naeem U and Moeed A did the drafting of the work; Surani S critically revised the manuscript; Koritala T and Hassan SA did the literature search and reviewed the manuscript; Najeeb H, Shaikh S, Hasanain M, Naeem U, Moeed A and Surani S did the final approval, and agreed to the accuracy of the work.

Conflict-of-interest statement: None.

Open-Access: This article is an open-access article that was selected by an in-house editor and fully peer-reviewed by external reviewers. It is distributed in accordance with the Creative Commons Attribution NonCommercial (CC BY-NC 4.0) license, which permits others to distribute, remix, adapt, build upon this work non-commercially, and license their derivative works on different terms, provided the original work is properly cited and the use is non-commercial. See: https://creativecommons.org/Licenses/by-nc/4.0/

Country/Territory of origin: United States

ORCID number: Farah Yasmin 0000-0002-5264-6140; Hala Najeeb 0000-0001-7075-4674; Shehryar Shaikh 0000-0003-2354-4994; Muhammad Hasanain 0000-0001-9214-7840; Unaiza Naeem 0000-0002-0455-7864; Abdul Moeed 0000-0003-4429-1391; Thoyaja Koritala 0000-0002-1020-9882; Syedadeel Hasan 0000-0002-8484-0319; Salim Surani 0000-0001-7105-4266.

Corresponding Author's Membership in Professional Societies: American College of Chest Physicians.

S-Editor: Wu YXJ
L-Editor: A
P-Editor: Wu YXJ

REFERENCES

1 **Matsuoka K**, Kanai T. The gut microbiota and inflammatory bowel disease. *Semin Immunopathol* 2015; **37**: 47-55 [PMID: 25420450 DOI: 10.1007/s00281-014-0454-4]
2 **Lautenschläger C**, Schmidt C, Fischer D, Stallmach A. Drug delivery strategies in the therapy of inflammatory bowel disease. *Adv Drug Deliv Rev* 2014; **71**: 58-76 [PMID: 24157534 DOI: 10.1016/j.addr.2013.10.001]
3 **Kesisoglou F**, Zimmermann EM. Novel drug delivery strategies for the treatment of inflammatory bowel disease. *Expert Opin Drug Deliv* 2005; **2**: 451-463 [PMID: 16296767 DOI: 10.1517/17425247.2.3.451]
4 **Talaei F**, Atyabi F, Azhdarzadeh M, Dinarvand R, Saadatzadeh A. Overcoming therapeutic obstacles in inflammatory bowel diseases: a comprehensive review on novel drug delivery strategies. *Eur J Pharm Sci* 2013; **49**: 712-722 [PMID: 23665411 DOI: 10.1016/j.ejps.2013.04.031]
5 **Singh D**, Srivastava S, Pradhan M, Kanwar JR, Singh MR. Inflammatory Bowel Disease: Pathogenesis, Causative Factors, Issues, Drug Treatment Strategies, and Delivery Approaches. *Crit Rev Ther Drug Carrier Syst* 2015; **32**: 181-214 [PMID: 26080808 DOI: 10.1615/critrevtherdrugcarriersyst.2015011095]

6 **Steidler L**. Microbiological and immunological strategies for treatment of inflammatory bowel disease. *Microbes Infect* 2001; **3**: 1157-1166 [PMID: 11709296 DOI: 10.1016/s1286-4579(01)01476-9]

7 **Ordaìs I**, Eckmann L, Talamini M, Baumgart DC, Sandborn WJ. Ulcerative colitis. In: The Lancet. Lancet; 2012. page 1606-19 [DOI: 10.1016/S0140-6736(12)60150-0]

8 **Yu YR**, Rodriguez JR. Clinical presentation of Crohn's, ulcerative colitis, and indeterminate colitis: Symptoms, extraintestinal manifestations, and disease phenotypes. *Semin Pediatr Surg* 2017; **26**: 349-355 [PMID: 29126502 DOI: 10.1053/j.sempedsurg.2017.10.003]

9 **Ramos GP**, Papadakis KA. Mechanisms of Disease: Inflammatory Bowel Diseases. *Mayo Clin Proc* 2019; **94**: 155-165 [PMID: 30611442 DOI: 10.1016/j.mayocp.2018.09.013]

10 **Henry S**, McAllister DV, Allen MG, Prausnitz MR. Microfabricated microneedles: a novel approach to transdermal drug delivery. *J Pharm Sci* 1998; **87**: 922-925 [PMID: 9687334 DOI: 10.1021/js980042+]

11 **Gill HS**, Prausnitz MR. Coating formulations for microneedles. *Pharm Res* 2007; **24**: 1369-1380 [PMID: 17385011 DOI: 10.1007/s11095-007-9286-4]

12 **Confidential Rani-1**. Available from: http://a.wethrive.com/ext/rani/docs/rani_pre-clinical_data_July_2014_1.pdf

13 **Traverso G**, Schoellhammer CM, Schroeder A, Maa R, Lauwers GY, Polat BE, Anderson DG, Blankschtein D, Langer R. Microneedles for drug delivery *via* the gastrointestinal tract. *J Pharm Sci* 2015; **104**: 362-367 [PMID: 25250829 DOI: 10.1002/jps.24182]

14 **Vllasaliu D**, Thanou M, Stolnik S, Fowler R. Recent advances in oral delivery of biologics: nanomedicine and physical modes of delivery. *Expert Opin Drug Deliv* 2018; **15**: 759-770 [PMID: 30033780 DOI: 10.1080/17425247.2018.1504017]

15 **Powell JJ**, Faria N, Thomas-McKay E, Pele LC. Origin and fate of dietary nanoparticles and microparticles in the gastrointestinal tract. *J Autoimmun* 2010; **34**: J226-J233 [PMID: 20096538 DOI: 10.1016/j.jaut.2009.11.006]

16 **Tolstanova G**, Deng X, French SW, Lungo W, Paunovic B, Khomenko T, Ahluwalia A, Kaplan T, Dacosta-Iyer M, Tarnawski A, Szabo S, Sandor Z. Early endothelial damage and increased colonic vascular permeability in the development of experimental ulcerative colitis in rats and mice. *Lab Invest* 2012; **92**: 9-21 [PMID: 21894149 DOI: 10.1038/labinvest.2011.122]

17 **Xiao B**, Merlin D. Oral colon-specific therapeutic approaches toward treatment of inflammatory bowel disease. *Expert Opin Drug Deliv* 2012; **9**: 1393-1407 [PMID: 23036075 DOI: 10.1517/17425247.2012.730517]

18 **Collnot EM**, Ali H, Lehr CM. Nano- and microparticulate drug carriers for targeting of the inflamed intestinal mucosa. *J Control Release* 2012; **161**: 235-246 [PMID: 22306429 DOI: 10.1016/j.jconrel.2012.01.028]

19 Erratum for the Report "Global distribution of earthworm diversity" by H. R. P. Phillips, C. A. Guerra, M. L. C. Bartz, M. J. I. Briones, G. Brown, T. W. Crowther, O. Ferlian, K. B. Gongalsky, J. van den Hoogen, J. Krebs, A. Orgiazzi, D. Routh, B. Schwarz, E. M. Bach, J. Bennett, U. Brose, T. Decaëns, B. König-Ries, M. Loreau, J. Mathieu, C. Mulder, W. H. van der Putten, K. S. Ramirez, M. C. Rillig, D. Russell, M. Rutgers, M. P. Thakur, F. T. de Vries, D. H. Wall, D. A. Wardle, M. Arai, F. O. Ayuke, G. H. Baker, R. Beauséjour, J. C. Bedano, K. Birkhofer, E. Blanchart, B. Blossey, T. Bolger, R. L. Bradley, M. A. Callaham, Y. Capowiez, M. E. Caulfield, A. Choi, F. V. Crotty, A. Dávalos, D. J. Diaz Cosin, A. Dominguez, A. E. Duhour, N. van Eekeren, C. Emmerling, L. B. Falco, R. Fernández, S. J. Fonte, C. Fragoso, A. L. C. Franco, M. Fugère, A. T. Fusilero, S. Gholami, M. J. Gundale, M. Gutiérrez López, D. K. Hackenberger, L. M. Hernández, T. Hishi, A. R. Holdsworth, M. Holmstrup, K. N. Hopfensperger, E. Huerta Lwanga, V. Huhta, T. T. Hurisso, B. V. Iannone III, M. Iordache, M. Joschko, N. Kaneko, R. Kanianska, A. M. Keith, C. A. Kelly, M. L. Kernecker, J. Klaminder, A. W. Koné, Y. Kooch, S. T. Kukkonen, H. Lalthanzara, D. R. Lammel, I. M. Lebedev, Y. Li, J. B. Jesus Lidon, N. K. Lincoln, S. R. Loss, R. Marichal, R. Matula, J. H. Moos, G. Moreno, A. Morón-Ríos, B. Muys, J. Neirynck, L. Norgrove, M. Novo, V. Nuutinen, V. Nuzzo, M. Rahman P, J. Pansu, S. Paudel, G. Pérès, L. Pérez-Camacho, R. Piñeiro, J.-F. Ponge, M. I. Rashid, S. Rebollo, J. Rodeiro-Iglesias, M. Á. Rodríguez, A. M. Roth, G. X. Rousseau, A. Rozen, E. Sayad, L. van Schaik, B. C. Scharenbroch, M. Schirrmann, O. Schmidt, B. Schröder, J. Seeber, M. P. Shashkov, J. Singh, S. M. Smith, M. Steinwandter, J. A. Talavera, D. Trigo, J. Tsukamoto, A. W. de Valença, S. J. Vanek, I. Virto, A. A. Wackett, M. W. Warren, N. H. Wehr, J. K. Whalen, M. B. Wironen, V. Wolters, I. V. Zenkova, W. Zhang, E. K. Cameron, N. Eisenhauer. *Science* 2020; **369** [PMID: 32732396 DOI: 10.1126/science.abd9834]

20 **Youshia J**, Lamprecht A. Size-dependent nanoparticulate drug delivery in inflammatory bowel diseases. *Expert Opin Drug Deliv* 2016; **13**: 281-294 [PMID: 26637060 DOI: 10.1517/17425247.2016.1114604]

21 **Lai SK**, Wang YY, Hanes J. Mucus-penetrating nanoparticles for drug and gene delivery to mucosal tissues. *Adv Drug Deliv Rev* 2009; **61**: 158-171 [PMID: 19133304 DOI: 10.1016/j.addr.2008.11.002]

22 **García-Díaz M**, Birch D, Wan F, Nielsen HM. The role of mucus as an invisible cloak to transepithelial drug delivery by nanoparticles. *Adv Drug Deliv Rev* 2018; **124**: 107-124 [PMID: 29117511 DOI: 10.1016/j.addr.2017.11.002]

23 **Murgia X**, Loretz B, Hartwig O, Hittinger M, Lehr CM. The role of mucus on drug transport and its potential to affect therapeutic outcomes. *Adv Drug Deliv Rev* 2018; **124**: 82-97 [PMID: 29106910 DOI: 10.1016/j.addr.2017.10.009]

24 **Lieleg O**, Ribbeck K. Biological hydrogels as selective diffusion barriers. *Trends Cell Biol* 2011; **21**: 543-551 [PMID: 21727007 DOI: 10.1016/j.tcb.2011.06.002]

25 **Viscido A**, Capannolo A, Latella G, Caprilli R, Frieri G. Nanotechnology in the treatment of inflammatory bowel diseases. *J Crohns Colitis* 2014; **8**: 903-918 [PMID: 24686095 DOI: 10.1016/j.crohns.2014.02.024]

26 **Meissner Y**, Pellequer Y, Lamprecht A. Nanoparticles in inflammatory bowel disease: particle targeting vs pH-sensitive delivery. Int J Pharm 2006; 316: 138-143 [PMID: 16675176 DOI: 10.1016/j.ijpharm.2006.01.032]

27 **Lamprecht A**, Schäfer U, Lehr CM. Size-dependent bioadhesion of micro- and nanoparticulate carriers to the inflamed colonic mucosa. *Pharm Res* 2001; **18**: 788-793 [PMID: 11474782 DOI: 10.1023/a:1011032328064]

28 **Ali H**, Weigmann B, Neurath MF, Collnot EM, Windbergs M, Lehr CM. Budesonide loaded nanoparticles with pH-sensitive coating for improved mucosal targeting in mouse models of inflammatory bowel diseases. *J Control Release* 2014; **183**: 167-177 [PMID: 24685705 DOI: 10.1016/j.jconrel.2014.03.039]

29 **Vong LB**, Mo J, Abrahamsson B, Nagasaki Y. Specific accumulation of orally administered redox nanotherapeutics in the inflamed colon reducing inflammation with dose-response efficacy. *J Control Release* 2015; **210**: 19-25 [PMID: 25998050 DOI: 10.1016/j.jconrel.2015.05.275]

30 **Vong LB**, Tomita T, Yoshitomi T, Matsui H, Nagasaki Y. An orally administered redox nanoparticle that accumulates in the colonic mucosa and reduces colitis in mice. *Gastroenterology* 2012; **143**: 1027-36.e3 [PMID: 22771506 DOI: 10.1053/j.gastro.2012.06.043]

31 **Lamprecht A**. IBD: selective nanoparticle adhesion can enhance colitis therapy. *Nat Rev Gastroenterol Hepatol* 2010; **7**: 311-312 [PMID: 20523352 DOI: 10.1038/nrgastro.2010.66]

32 **Schmidt C**, Lautenschlaeger C, Collnot EM, Schumann M, Bojarski C, Schulzke JD, Lehr CM, Stallmach A. Nano- and microscaled particles for drug targeting to inflamed intestinal mucosa: a first in vivo study in human patients. *J Control Release* 2013; **165**: 139-145 [PMID: 23127508 DOI: 10.1016/j.jconrel.2012.10.019]

33 **Niebel W**, Walkenbach K, Béduneau A, Pellequer Y, Lamprecht A. Nanoparticle-based clodronate delivery mitigates murine experimental colitis. *J Control Release* 2012; **160**: 659-665 [PMID: 22445727 DOI: 10.1016/j.jconrel.2012.03.004]

34 **Lautenschläger C**, Schmidt C, Lehr CM, Fischer D, Stallmach A. PEG-functionalized microparticles selectively target inflamed mucosa in inflammatory bowel disease. *Eur J Pharm Biopharm* 2013; **85**: 578-586 [PMID: 24084650 DOI: 10.1016/j.ejpb.2013.09.016]

35 **Antoni L**, Nuding S, Wehkamp J, Stange EF. Intestinal barrier in inflammatory bowel disease. *World J Gastroenterol* 2014; **20**: 1165-1179 [PMID: 24574793 DOI: 10.3748/wjg.v20.i5.1165]

36 **Larsson JM**, Karlsson H, Sjövall H, Hansson GC. A complex, but uniform O-glycosylation of the human MUC2 mucin from colonic biopsies analyzed by nanoLC/MSn. *Glycobiology* 2009; **19**: 756-766 [PMID: 19321523 DOI: 10.1093/glycob/cwp048]

37 **Jubeh TT**, Barenholz Y, Rubinstein A. Differential adhesion of normal and inflamed rat colonic mucosa by charged liposomes. *Pharm Res* 2004; **21**: 447-453 [PMID: 15070095 DOI: 10.1023/B:PHAM.0000019298.29561.cd]

38 **Jubeh TT**, Nadler-Milbauer M, Barenholz Y, Rubinstein A. Local treatment of experimental colitis in the rat by negatively charged liposomes of catalase, TMN and SOD. *J Drug Target* 2006; **14**: 155-163 [PMID: 16753829 DOI: 10.1080/10611860600648429]

39 **Beloqui A**, Coco R, Alhouayek M, Solinís MÁ, Rodríguez-Gascón A, Muccioli GG, Préat V. Budesonide-loaded nanostructured lipid carriers reduce inflammation in murine DSS-induced colitis. *Int J Pharm* 2013; **454**: 775-783 [PMID: 23694806 DOI: 10.1016/j.ijpharm.2013.05.017]

40 **Zhu H**, Li YR. Oxidative stress and redox signaling mechanisms of inflammatory bowel disease: updated experimental and clinical evidence. *Exp Biol Med (Maywood)* 2012; **237**: 474-480 [PMID: 22442342 DOI: 10.1258/ebm.2011.011358]

41 **Lih-Brody L**, Powell SR, Collier KP, Reddy GM, Cerchia R, Kahn E, Weissman GS, Katz S, Floyd RA, McKinley MJ, Fisher SE, Mullin GE. Increased oxidative stress and decreased antioxidant defenses in mucosa of inflammatory bowel disease. *Dig Dis Sci* 1996; **41**: 2078-2086 [PMID: 8888724 DOI: 10.1007/BF02093613]

42 **Mahida YR**, Wu KC, Jewell DP. Respiratory burst activity of intestinal macrophages in normal and inflammatory bowel disease. *Gut* 1989; **30**: 1362-1370 [PMID: 2511088 DOI: 10.1136/gut.30.10.1362]

43 **Bertoni S**, Machness A, Tiboni M, Bártolo R, Santos HA. Reactive oxygen species responsive nanoplatforms as smart drug delivery systems for gastrointestinal tract targeting. *Biopolymers* 2020; **111**: e23336 [PMID: 31724750 DOI: 10.1002/bip.23336]

44 **Wang X**, Yan J, Wang L, Pan D, Xu Y, Wang F, Sheng J, Li X, Yang M. Oral delivery of anti-TNF antibody shielded by natural polyphenol-mediated supramolecular assembly for inflammatory bowel disease therapy. *Theranostics* 2020; **10**: 10808-10822 [PMID: 32929381 DOI: 10.7150/thno.47601]

45 **Zhang Q**, Tao H, Lin Y, Hu Y, An H, Zhang D, Feng S, Hu H, Wang R, Li X, Zhang J. A superoxide dismutase/catalase mimetic nanomedicine for targeted therapy of inflammatory bowel disease. *Biomaterials* 2016; **105**: 206-221 [PMID: 27525680 DOI: 10.1016/j.biomaterials.2016.08.010]

46 **Zhang S**, Langer R, Traverso G. Nanoparticulate Drug Delivery Systems Targeting Inflammation for Treatment of Inflammatory Bowel Disease. *Nano Today* 2017; **16**: 82-96 [PMID: 31186671 DOI: 10.1016/j.nantod.2017.08.006]

47 **Sun Q**, Luan L, Arif M, Li J, Dong QJ, Gao Y, Chi Z, Liu CG. Redox-sensitive nanoparticles based on 4-aminothiophenol-carboxymethyl inulin conjugate for budesonide delivery in inflammatory bowel diseases. *Carbohydr Polym* 2018; **189**: 352-359 [PMID: 29580419 DOI: 10.1016/j.carbpol.2017.12.021]

48 **Li C**, Zhao Y, Cheng J, Guo J, Zhang Q, Zhang X, Ren J, Wang F, Huang J, Hu H, Wang R, Zhang J. A Proresolving Peptide Nanotherapy for Site-Specific Treatment of Inflammatory Bowel Disease by Regulating Proinflammatory Microenvironment and Gut Microbiota. *Adv Sci (Weinh)* 2019; **6**: 1900610 [PMID: 31559126 DOI: 10.1002/advs.201900610]

49 **Zhang X**, Wu W. Ligand-mediated active targeting for enhanced oral absorption. *Drug Discov Today* 2014; **19**: 898-904 [PMID: 24631680 DOI: 10.1016/j.drudis.2014.03.001]

50 **Cox D**, Brennan M, Moran N. Integrins as therapeutic targets: lessons and opportunities. *Nat Rev Drug Discov* 2010; **9**: 804-820 [PMID: 20885411 DOI: 10.1038/nrd3266]

51 **Kim E**, Schueller O, Sweetnam PM. Targeting the leukocyte activation cascade: getting to the site of inflammation using microfabricated assays. *Lab Chip* 2012; **12**: 2255-2264 [PMID: 22437145 DOI: 10.1039/c2lc21078a]

52 **Xiao B**, Yang Y, Viennois E, Zhang Y, Ayyadurai S, Baker M, Laroui H, Merlin D. Glycoprotein CD98 as a receptor for colitis-targeted delivery of nanoparticle. *J Mater Chem B* 2014; **2**: 1499-1508 [PMID: 24729869 DOI: 10.1039/c3tb21564d]

53 **Xiao B**, Laroui H, Viennois E, Ayyadurai S, Charania MA, Zhang Y, Zhang Z, Baker MT, Zhang B, Gewirtz AT, Merlin D. Nanoparticles with surface antibody against CD98 and carrying CD98 small interfering RNA reduce colitis in mice. *Gastroenterology* 2014; **146**: 1289-300.e1 [PMID: 24503126 DOI: 10.1053/j.gastro.2014.01.056]

54 **Xiao B**, Laroui H, Ayyadurai S, Viennois E, Charania MA, Zhang Y, Merlin D. Mannosylated bioreducible nanoparticle-mediated macrophage-specific TNF-α RNA interference for IBD therapy. *Biomaterials* 2013; **34**: 7471-7482 [PMID: 23820013 DOI: 10.1016/j.biomaterials.2013.06.008]

55 **Fromont Hankard G**, Cezard JP, Aigrain Y, Navarro J, Peuchmaur M. CD44 variant expression in inflammatory colonic mucosa is not disease specific but associated with increased crypt cell proliferation. *Histopathology* 1998; **32**: 317-321 [PMID: 9602327 DOI: 10.1046/j.1365-2559.1998.00404.x]

56 **Farkas S**, Hornung M, Sattler C, Anthuber M, Gunthert U, Herfarth H, Schlitt HJ, Geissler EK, Wittig BM. Short-term treatment with anti-CD44v7 antibody, but not CD44v4, restores the gut mucosa in established chronic dextran sulphate sodium (DSS)-induced colitis in mice. *Clin Exp Immunol* 2005; **142**: 260-267 [PMID: 16232212 DOI: 10.1111/j.1365-2249.2005.02911.x]

57 **Dreaden EC**, Morton SW, Shopsowitz KE, Choi JH, Deng ZJ, Cho NJ, Hammond PT. Bimodal tumor-targeting from microenvironment responsive hyaluronan layer-by-layer (LbL) nanoparticles. *ACS Nano* 2014; **8**: 8374-8382 [PMID: 25100313 DOI: 10.1021/nn502861t]

58 **Xiao B**, Xu Z, Viennois E, Zhang Y, Zhang Z, Zhang M, Han MK, Kang Y, Merlin D. Orally Targeted Delivery of Tripeptide KPV *via* Hyaluronic Acid-Functionalized Nanoparticles Efficiently Alleviates Ulcerative Colitis. *Mol Ther* 2017; **25**: 1628-1640 [PMID: 28143741 DOI: 10.1016/j.ymthe.2016.11.020]

59 **Chapkin RS**, Kamen BA, Callaway ES, Davidson LA, George NI, Wang N, Lupton JR, Finnell RH. Use of a novel genetic mouse model to investigate the role of folate in colitis-associated colon cancer. *J Nutr Biochem* 2009; **20**: 649-655 [PMID: 18926688 DOI: 10.1016/j.jnutbio.2008.07.001]

60 **Spencer SP**, Belkaid Y. Dietary and commensal derived nutrients: shaping mucosal and systemic immunity. *Curr Opin Immunol* 2012; **24**: 379-384 [PMID: 22857854 DOI: 10.1016/j.coi.2012.07.006]

61 **Zhang M**, Xu C, Liu D, Han MK, Wang L, Merlin D. Oral Delivery of Nanoparticles Loaded With Ginger Active Compound, 6-Shogaol, Attenuates Ulcerative Colitis and Promotes Wound Healing in a Murine Model of Ulcerative Colitis. *J Crohns Colitis* 2018; **12**: 217-229 [PMID: 28961808 DOI: 10.1093/ecco-jcc/jjx115]

62 **Naserifar M**, Hosseinzadeh H, Abnous K, Mohammadi M, Taghdisi SM, Ramezani M, Alibolandi M. Oral delivery of folate-targeted resveratrol-loaded nanoparticles for inflammatory bowel disease therapy in rats. *Life Sci* 2020; **262**: 118555 [PMID: 33035579 DOI: 10.1016/j.lfs.2020.118555]

63 **Sakhalkar HS**, Hanes J, Fu J, Benavides U, Malgor R, Borruso CL, Kohn LD, Kurjiaka DT, Goetz DJ. Enhanced adhesion of ligand-conjugated biodegradable particles to colitic venules. *FASEB J* 2005; **19**: 792-794 [PMID: 15764649 DOI: 10.1096/fj.04-2668fje]

64 **Manda JN**, Markovic M, Zimmermann EM, Ben-Shabat S, Dahan A, Aponick A. Phospholipid Cyclosporine Prodrugs Targeted at Inflammatory Bowel Disease (IBD) Treatment: Design, Synthesis, and in Vitro Validation. *ChemMedChem* 2020; **15**: 1639-1644 [PMID: 32618133 DOI: 10.1002/cmdc.202000317]

65 **Kotla NG**, Rana S, Sivaraman G, Sunnapu O, Vemula PK, Pandit A, Rochev Y. Bioresponsive drug delivery systems in intestinal inflammation: State-of-the-art and future perspectives. *Adv Drug Deliv Rev* 2019; **146**: 248-266 [PMID: 29966684 DOI: 10.1016/j.addr.2018.06.021]

66 **Yuri T**, Kono Y, Okada T, Terada T, Miyauchi S, Fujita T. Transport Characteristics of 5-Aminosalicylic Acid Derivatives Conjugated with Amino Acids *via* Human H^+-Coupled Oligopeptide Transporter PEPT1. *Biol Pharm Bull* 2020; **43**: 697-706 [PMID: 32238712 DOI: 10.1248/bpb.b19-01048]

67 **Sadeghi F**, Eidizade A, Saremnejad F, Hadizadeh F, Khodaverdi E, Akhgari A. Synthesis of a novel PEGylated colon-specific azo-based 4- aminosalicylic acid prodrug. *Iran J Basic Med Sci* 2020; **23**: 781-787 [PMID: 32695295 DOI: 10.22038/ijbms.2020.41152.9736]

68 **Kim S**, Lee S, Lee H, Ju S, Park S, Kwon D, Yoo JW, Yoon IS, Min DS, Jung YS, Jung Y. A Colon-Targeted Prodrug, 4-Phenylbutyric Acid-Glutamic Acid Conjugate, Ameliorates 2,4-Dinitrobenzenesulfonic Acid-Induced Colitis in Rats. *Pharmaceutics* 2020; **12** [PMID: 32899177 DOI: 10.3390/pharmaceutics12090843]

69 **Shen C**, Zhao L, Du X, Tian J, Yuan Y, Jia M, He Y, Zeng R, Qiao R, Li C. Smart Responsive Quercetin-Conjugated Glycol Chitosan Prodrug Micelles for Treatment of Inflammatory Bowel Diseases. *Mol Pharm* 2021; **18**: 1419-1430 [PMID: 33522827 DOI: 10.1021/acs.molpharmaceut.0c01245]

70 **Zhang JX**, Wang K, Mao ZF, Fan X, Jiang DL, Chen M, Cui L, Sun K, Dang SC. Application of liposomes in drug development--focus on gastroenterological targets. *Int J Nanomedicine* 2013; **8**: 1325-1334 [PMID: 23630417 DOI: 10.2147/IJN.S42153]

71 **Zhao Y**, Yang Y, Zhang J, Wang R, Cheng B, Kalambhe D, Wang Y, Gu Z, Chen D, Wang B, Huang Y. Lactoferrin-mediated macrophage targeting delivery and patchouli alcohol-based therapeutic strategy for inflammatory bowel diseases. *Acta Pharm Sin B* 2020; **10**: 1966-1976 [PMID: 33163347 DOI: 10.1016/j.apsb.2020.07.019]

72 **Tang Q**, Zhang W, Zhang C, Guan Y, Ding J, Yuan C, Tan C, Gao X, Tan S. Oxymatrine loaded nitric oxide-releasing liposomes for the treatment of ulcerative colitis. *Int J Pharm* 2020; **586**: 119617 [PMID: 32650111 DOI: 10.1016/j.ijpharm.2020.119617]

73 **Wang C**, Han Z, Wu Y, Lu X, Tang X, Xiao J, Li N. Enhancing stability and anti-inflammatory properties of curcumin in ulcerative colitis therapy using liposomes mediated colon-specific drug delivery system. *Food Chem Toxicol* 2021; **151**: 112123 [PMID: 33744379 DOI: 10.1016/j.fct.2021.112123]

74 **Ahmad A**, Vaghasiya K, Kumar A, Alam P, Raza SS, Verma RK, Khan R. Enema based therapy using liposomal formulation of low molecular weight heparin for treatment of active ulcerative colitis: New adjunct therapeutic opportunity. *Mater Sci Eng C Mater Biol Appl* 2021; **121**: 111851 [PMID: 33579485 DOI: 10.1016/j.msec.2020.111851]

75 **Kim JH**, Hong SS, Lee M, Lee EH, Rhee I, Chang SY, Lim SJ. Krill Oil-Incorporated Liposomes As An Effective Nanovehicle To Ameliorate The Inflammatory Responses Of DSS-Induced Colitis. *Int J Nanomedicine* 2019; **14**: 8305-8320 [PMID: 31806959 DOI: 10.2147/IJN.S220053]

76 **Zhao YZ**, ZhuGe DL, Tong MQ, Lin MT, Zheng YW, Jiang X, Yang WG, Yao Q, Xiang Q, Li XK, Xu HL. Ulcerative colitis-specific delivery of keratinocyte growth factor by neutrophils-simulated liposomes facilitates the morphologic and functional recovery of the damaged colon through alleviating the inflammation. *J Control Release* 2019; **299**: 90-106 [PMID: 30807805 DOI: 10.1016/j.jconrel.2019.02.034]

77 **de Alvarenga Antunes CV**, de Alvarenga Nascimento CR, Campanha da Rocha Ribeiro T, de Alvarenga Antunes P, de Andrade Chebli L, Martins Gonçalves Fava L, Malaguti C, Maria Fonseca Chebli J. Treatment of iron deficiency anemia with liposomal iron in inflammatory bowel disease: efficacy and impact on quality of life. *Int J Clin Pharm* 2020; **42**: 895-902 [PMID: 32367457 DOI: 10.1007/s11096-020-01044-x]

78 **Li X**, Lu C, Yang Y, Yu C, Rao Y. Site-specific targeted drug delivery systems for the treatment of inflammatory bowel

disease. *Biomed Pharmacother* 2020; **129**: 110486 [PMID: 32768972 DOI: 10.1016/j.biopha.2020.110486]
79 **Kotla NG**, Burke O, Pandit A, Rochev Y. An Orally Administrated Hyaluronan Functionalized Polymeric Hybrid Nanoparticle System for Colon-Specific Drug Delivery. *Nanomaterials (Basel)* 2019; **9** [PMID: 31480704 DOI: 10.3390/nano9091246]
80 **Pujara N**, Giri R, Wong KY, Qu Z, Rewatkar P, Moniruzzaman M, Begun J, Ross BP, McGuckin M, Popat A. pH - Responsive colloidal carriers assembled from β-lactoglobulin and Epsilon poly-L-lysine for oral drug delivery. *J Colloid Interface Sci* 2021; **589**: 45-55 [PMID: 33450459 DOI: 10.1016/j.jcis.2020.12.054]
81 **Zhang Y**, Zhang H, Zhang K, Li Z, Guo T, Wu T, Hou X, Feng N. Co-hybridized composite nanovesicles for enhanced transdermal eugenol and cinnamaldehyde delivery and their potential efficacy in ulcerative colitis. *Nanomedicine* 2020; **28**: 102212 [PMID: 32334099 DOI: 10.1016/j.nano.2020.102212]
82 **Zhang L**, Li M, Zhang G, Gao C, Wang S, Zhang T, Ma C, Wang L, Zhu Q. Micro- and Nanoencapsulated Hybrid Delivery System (MNEHDS): A Novel Approach for Colon-Targeted Oral Delivery of Berberine. *Mol Pharm* 2021; **18**: 1573-1581 [PMID: 33629860 DOI: 10.1021/acs.molpharmaceut.0c00970]
83 **Naeem M**, Lee J, Oshi MA, Cao J, Hlaing SP, Im E, Jung Y, Yoo JW. Colitis-targeted hybrid nanoparticles-in-microparticles system for the treatment of ulcerative colitis. *Acta Biomater* 2020; **116**: 368-382 [PMID: 32937207 DOI: 10.1016/j.actbio.2020.09.017]
84 **Weingarden AR**, Vaughn BP. Intestinal microbiota, fecal microbiota transplantation, and inflammatory bowel disease. *Gut Microbes* 2017; **8**: 238-252 [PMID: 28609251 DOI: 10.1080/19490976.2017.1290757]
85 **Wegmann U**, Carvalho AL, Stocks M, Carding SR. Use of genetically modified bacteria for drug delivery in humans: Revisiting the safety aspect. *Sci Rep* 2017; **7**: 2294 [PMID: 28536456 DOI: 10.1038/s41598-017-02591-6]
86 **Bolotin A**, Wincker P, Mauger S, Jaillon O, Malarme K, Weissenbach J, Ehrlich SD, Sorokin A. The complete genome sequence of the lactic acid bacterium Lactococcus lactis ssp. lactis IL1403. *Genome Res* 2001; **11**: 731-753 [PMID: 11337471 DOI: 10.1101/gr.gr-1697r]
87 **Steidler L**, Rottiers P. Therapeutic drug delivery by genetically modified Lactococcus lactis. *Ann N Y Acad Sci* 2006; **1072**: 176-186 [PMID: 17057198 DOI: 10.1196/annals.1326.031]
88 **Steidler L**, Hans W, Schotte L, Neirynck S, Obermeier F, Falk W, Fiers W, Remaut E. Treatment of murine colitis by Lactococcus lactis secreting interleukin-10. *Science* 2000; **289**: 1352-1355 [PMID: 10958782 DOI: 10.1126/science.289.5483.1352]
89 **Steidler L**, Neirynck S, Huyghebaert N, Snoeck V, Vermeire A, Goddeeris B, Cox E, Remon JP, Remaut E. Biological containment of genetically modified Lactococcus lactis for intestinal delivery of human interleukin 10. *Nat Biotechnol* 2003; **21**: 785-789 [PMID: 12808464 DOI: 10.1038/nbt840]
90 **Braat H**, Rottiers P, Hommes DW, Huyghebaert N, Remaut E, Remon JP, van Deventer SJ, Neirynck S, Peppelenbosch MP, Steidler L. A phase I trial with transgenic bacteria expressing interleukin-10 in Crohn's disease. *Clin Gastroenterol Hepatol* 2006; **4**: 754-759 [PMID: 16716759 DOI: 10.1016/j.cgh.2006.03.028]
91 **Vandenbroucke K**, de Haard H, Beirnaert E, Dreier T, Lauwereys M, Huyck L, Van Huysse J, Demetter P, Steidler L, Remaut E, Cuvelier C, Rottiers P. Orally administered L. lactis secreting an anti-TNF Nanobody demonstrate efficacy in chronic colitis. *Mucosal Immunol* 2010; **3**: 49-56 [PMID: 19794409 DOI: 10.1038/mi.2009.116]
92 **Chiabai MJ**, Almeida JF, de Azevedo MGD, Fernandes SS, Pereira VB, de Castro RJA, Jerônimo MS, Sousa IG, de Souza Vianna LM, Miyoshi A, Bocca AL, Maranhão AQ, Brigido MM. Mucosal delivery of Lactococcus lactis carrying an anti-TNF scFv expression vector ameliorates experimental colitis in mice. *BMC Biotechnol* 2019; **19**: 38 [PMID: 31238939 DOI: 10.1186/s12896-019-0518-6]
93 **Namai F**, Shigemori S, Ogita T, Sato T, Shimosato T. Microbial therapeutics for acute colitis based on genetically modified Lactococcus lactis hypersecreting IL-1Ra in mice. *Exp Mol Med* 2020; **52**: 1627-1636 [PMID: 32989233 DOI: 10.1038/s12276-020-00507-5]
94 **Chu D**, Gao J, Wang Z. Neutrophil-Mediated Delivery of Therapeutic Nanoparticles across Blood Vessel Barrier for Treatment of Inflammation and Infection. *ACS Nano* 2015; **9**: 11800-11811 [PMID: 26516654 DOI: 10.1021/acsnano.5b05583]
95 **Corbo C**, Cromer WE, Molinaro R, Toledano Furman NE, Hartman KA, De Rosa E, Boada C, Wang X, Zawieja DC, Agostini M, Salvatore F, Abraham BP, Tasciotti E. Engineered biomimetic nanovesicles show intrinsic anti-inflammatory properties for the treatment of inflammatory bowel diseases. *Nanoscale* 2017; **9**: 14581-14591 [PMID: 28932838 DOI: 10.1039/c7nr04734g]
96 **DeNucci CC**, Pagán AJ, Mitchell JS, Shimizu Y. Control of alpha4beta7 integrin expression and CD4 T cell homing by the beta1 integrin subunit. *J Immunol* 2010; **184**: 2458-2467 [PMID: 20118278 DOI: 10.4049/jimmunol.0902407]
97 **Chambers E**, Mitragotri S. Prolonged circulation of large polymeric nanoparticles by non-covalent adsorption on erythrocytes. *J Control Release* 2004; **100**: 111-119 [PMID: 15491815 DOI: 10.1016/j.jconrel.2004.08.005]
98 **Castro M**, Rossi L, Papadatou B, Bracci F, Knafelz D, Ambrosini MI, Calce A, Serafini S, Isacchi G, D'Orio F, Mambrini G, Magnani M. Long-term treatment with autologous red blood cells loaded with dexamethasone 21-phosphate in pediatric patients affected by steroid-dependent Crohn disease. *J Pediatr Gastroenterol Nutr* 2007; **44**: 423-426 [PMID: 17414137 DOI: 10.1097/MPG.0b013e3180320667]
99 **Annese V**, Latiano A, Rossi L, Lombardi G, Dallapiccola B, Serafini S, Damonte G, Andriulli A, Magnani M. Erythrocytes-mediated delivery of dexamethasone in steroid-dependent IBD patients-a pilot uncontrolled study. *Am J Gastroenterol* 2005; **100**: 1370-1375 [PMID: 15929772 DOI: 10.1111/j.1572-0241.2005.41412.x]

World Journal of Gastroenterology

Submit a Manuscript: https://www.f6publishing.com

World J Gastroenterol 2022 May 14; 28(18): 1934-1945

DOI: 10.3748/wjg.v28.i18.1934

ISSN 1007-9327 (print) ISSN 2219-2840 (online)

MINIREVIEWS

Targeting pancreatic cancer immune evasion by inhibiting histone deacetylases

Wynne Sim, Wei-Meng Lim, Ling-Wei Hii, Chee-Onn Leong, Chun-Wai Mai

Specialty type: Gastroenterology and hepatology

Provenance and peer review: Invited article; Externally peer reviewed.

Peer-review model: Single blind

Peer-review report's scientific quality classification

Grade A (Excellent): 0
Grade B (Very good): B, B
Grade C (Good): 0
Grade D (Fair): 0
Grade E (Poor): 0

P-Reviewer: Balcerczyk A, Poland; Isaji S, Japan

Received: January 7, 2022
Peer-review started: January 7, 2022
First decision: March 9, 2022
Revised: March 17, 2022
Accepted: April 4, 2022
Article in press: April 4, 2022
Published online: May 14, 2022

Wynne Sim, School of Medicine, International Medical University, Kuala Lumpur 57000, Malaysia

Wei-Meng Lim, Ling-Wei Hii, School of Pharmacy, International Medical University, Kuala Lumpur 57000, Malaysia

Wei-Meng Lim, Ling-Wei Hii, Chee-Onn Leong, Center for Cancer and Stem Cell Research, Institute for Research, Development, and Innovation, International Medical University, Kuala Lumpur 57000, Malaysia

Chee-Onn Leong, AGTC Genomics, Kuala Lumpur 57000, Malaysia

Chun-Wai Mai, State Key Laboratory of Oncogenes and Related Genes, Renji-Med X Clinical Stem Cell Research Center, Ren Ji Hospital, School of Medicine, Shanghai Jiao Tong University, Shanghai 200127, China

Chun-Wai Mai, Department of Pharmaceutical Chemistry, Faculty of Pharmaceutical Sciences, UCSI University, Kuala Lumpur 56000, Malaysia

Corresponding author: Chun-Wai Mai, BPharm, PhD, Postdoctoral Fellow, State Key Laboratory of Oncogenes and Related Genes, Renji-Med X Clinical Stem Cell Research Center, Ren Ji Hospital, School of Medicine, Shanghai Jiao Tong University, No. 160 Pujian Road, Building No. 17, Pudong New District, Shanghai 200127, China. mai.chunwai@outlook.com

Abstract

The immune system plays a vital role in maintaining the delicate balance between immune recognition and tumor development. Regardless, it is not uncommon that cancerous cells can intelligently acquire abilities to bypass the antitumor immune responses, thus allowing continuous tumor growth and development. Immune evasion has emerged as a significant factor contributing to the progression and immune resistance of pancreatic cancer. Compared with other cancers, pancreatic cancer has a tumor microenvironment that can resist most treatment modalities, including emerging immunotherapy. Sadly, the use of immunotherapy has yet to bring significant clinical breakthrough among pancreatic cancer patients, suggesting that pancreatic cancer has successfully evaded immunomodulation. In this review, we summarize the impact of genetic alteration and epigenetic modification (especially histone deacetylases, HDAC) on immune evasion in pancreatic cancer. HDAC overexpression significantly suppresses tumor suppressor genes, contributing to tumor growth and pro-

gression. We review the evidence on HDAC inhibitors in tumor eradication, improving T cells activation, restoring tumor immunogenicity, and modulating programmed death 1 interaction. We provide our perspective in targeting HDAC as a strategy to reverse immune evasion in pancreatic cancer.

Key Words: Histone acetylation; Histone deacetylases inhibitors; Immune evasion; Pancreatic cancers; Pancreatic ductal adenocarcinoma

©The Author(s) 2022. Published by Baishideng Publishing Group Inc. All rights reserved.

Core Tip: There are several broad reviews covering histone deacetylases (HDAC) in cancer but none on its role in modulating immune evasion in pancreatic cancer. This is the first review to discuss the role of HDAC in the context of immune-evading pancreatic cancer. We also summarize the evidence of HDAC inhibitors in targeting immune-evading pancreatic cancer. This mini review also covers our perspective in the strategies to target overexpression of HDAC in pancreatic cancer.

Citation: Sim W, Lim WM, Hii LW, Leong CO, Mai CW. Targeting pancreatic cancer immune evasion by inhibiting histone deacetylases. *World J Gastroenterol* 2022; 28(18): 1934-1945
URL: https://www.wjgnet.com/1007-9327/full/v28/i18/1934.htm
DOI: https://dx.doi.org/10.3748/wjg.v28.i18.1934

INTRODUCTION

Pancreatic cancer is the seventh most common cause of cancer-related deaths worldwide[1]. Pancreatic ductal adenocarcinoma (PDAC) is the most ubiquitous type of pancreatic cancer and remains incurable for 95% of patients. Pancreatic cancer is characterized by a devastating prognosis, with the lowest overall 5-year survival rate among all cancers[2]. The average survival time for pancreatic cancer is less than six months if left untreated[3]. Pancreatic cancer is thus estimated to be the second leading cause of death in the United States by 2030[3].

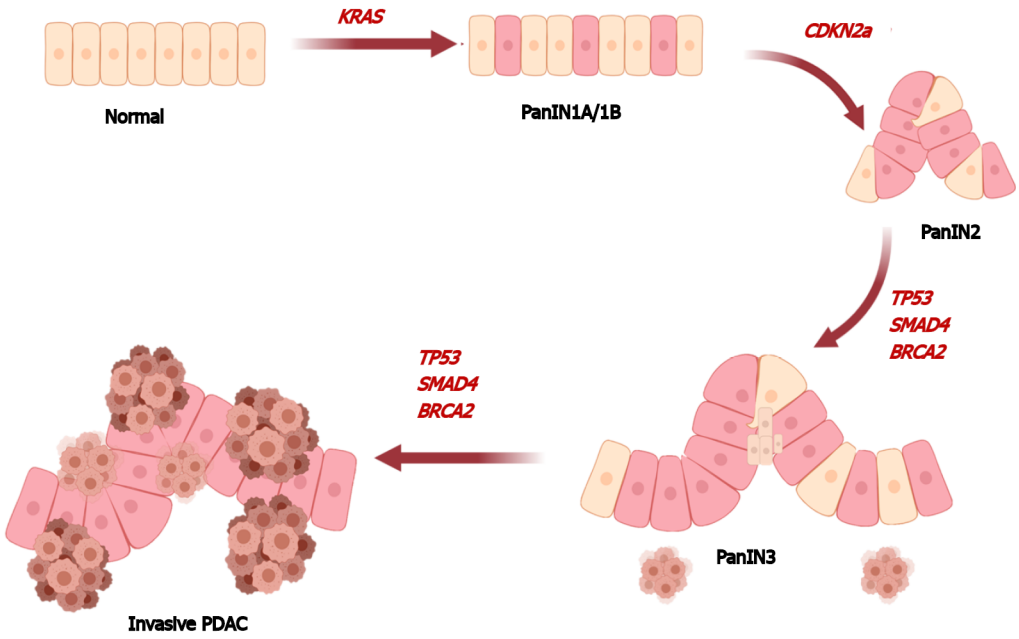
The dismal prognosis of PDAC is partly contributed by the lack of early clinical symptoms and poor sensitivity of PDAC diagnostic tests. Moreover, the treatment modalities available to date are generally ineffective for management of PDAC. Currently, the mainstay treatment for PDAC is surgery but only approximately 10% of PDAC patients qualify for surgical resection upon diagnosis[4]. Among the patients who undergo surgical resection, only < 25% could survive for more than five years. Besides, chemotherapeutic strategies have been exhausted in PDAC treatment, in which the use of chemotherapy has been limited by its well-established low efficacy, high toxicity and drastic decline in quality of life [5]. As a result, the search for an effective treatment regimen for PDAC remains a significant challenge.

Recently, immunotherapy has been hailed as a breakthrough in the realm of cancer therapy, which warrants further exploration for PDAC treatment. The use of immunotherapy in PDAC, however, is largely limited by its immune evasion barrier[6]. Thus, understanding the diverse mechanisms underlying the immune evasion in pancreatic cancer may empower the search for methods to tackle and prevent the bypass of immune surveillance[6,7].

GENETIC ALTERATION IN PDAC POTENTIATES ITS IMMUNE EVASION CAPABILITY

PDAC is an exocrine pancreatic cancer derived from pancreatic ductal cells. The progression to PDAC is characterized by its transition from normal pancreatic ductal cells to pancreatic intraepithelial neoplasia (PanIN) or its precursor lesions[8]. PanIN may be differentiated into three grades based on its histological or architectural changes[8]. PanIN1A and PanIN1B are characterized by the low-grade dysplasia while PanIN2 is characterized by the loss of polarity, nuclear crowding, enlargement of cell, and its typical papillary development. PanIN3 represents mature lesions with drastic nuclear aberrations, luminal necrosis, and show epithelial cell budding into the ductal lumen[8]. High-grade PanIN is almost uniquely found in invasive PDAC[8]. These precursor lesions develop into invasive PDAC following the accumulation of genetic mutations (Figure 1). Pertinent genetic alterations include *KRAS* oncogene mutation, the initiating genetic event in PDAC, followed by the loss of function in essential tumor suppressor genes such as *CDKN2a*, *TP53* and *SMAD4* (Figure 1).

KRAS oncogene mutation is found in nearly all PDACs[9]. High expression of the mutated *KRAS* is also associated with poor prognosis[9]. The *KRAS* GTPase switches between being bound to guanosine



DOI: 10.3748/wjg.v28.i18.1934 **Copyright** ©The Author(s) 2022.

Figure 1 Association of common genetic alterations and pancreatic ductal adenocarcinoma pathogenesis. The progression from the early to invasive stage of pancreatic ductal adenocarcinoma (PDAC) is supported by different genes alteration at different stages. *KRAS* mutation transforms the normal pancreatic ductal cells to pancreatic intraepithelial neoplasia (PanIN). The PanIN1A, PanIN1B and PanIN2 are low grade PanIN. Additional mutation such as *CDKN2A* is required to develop PanIN2. As the disease deteriorates, additional genes mutation such as *TP53*, *SMAD4* and *BRCA2* are involved to develop high grade PanIN3 and eventually invasive PDAC. PDAC: Pancreatic ductal adenocarcinoma. The figure in this review paper is created by using BioRender.com by the authors.

diphosphate, GDP (inactive state) and being bound to guanosine triphosphate, GTP (active state)[10]. In cancer development, missense mutations cause RAS to be persistently bound to GTP allowing an unlimited cellular proliferation. The alteration of *CDKN2a* results in unimpeded G1/S transformation and unrestrained cell division, facilitating tumor to evade host immunomodulation[11]. As expected, PDAC patients with *CDKN2a* inactivation are associated with poor overall survival and prognosis[11].

The metastasized tumors also exhibit several genetic alterations, namely *TP53*, *BRCA2* and *SMAD4*, indicating that these tumors have successfully evaded host immunosurveillance by leveraging on these genetic alterations[12-14]. *TP53* tumor suppressor gene on chromosome 17p is often mutated in cancer [15]. Up to 75% of PDACs present with loss or mutation of *TP53* expression[15]. The loss of *TP53* gene expression decreases cell cycle arrest and apoptosis, allowing for damaged DNA to replicate and aggregate genetic alterations. Accumulation of *TP53* mutants significantly increases the incidence of cancer metastasis[12]. Similarly, *BRCA2* is essential in restoring damages to double-stranded DNA. *BRCA2* mutations can cause alterations of *TP53* tumor suppressor genes, leading to pancreatic tumorigenesis[13]. Loss of *SMAD4* (an effector of the transforming growth factor β signaling pathway) promotes pancreatic cancer progression and increases rate of metastasis[14]. *SMAD4* inactivation in PDAC is also associated with poor prognosis and short overall survival[14].

Nevertheless, the genetic alterations in PDAC are still unable to explain the complex immune evasion in PDAC, indicating that other more pertinent underlying factors may be the driving force for immune-evading PDAC.

HISTONE DEACETYLASES IN CANCER

Epigenetic abnormalities are also crucial in carcinogenesis and the pathophysiology of cancer. Histone modification is one of the essential epigenetic processes involved in tumorigenesis and progression[16]. Histone acetylation is strictly controlled by a balance between histone acetyltransferase and histone deacetylases (HDAC) with opposing enzymatic activities. Histone acetylation is associated with an increased transcription level, while deacetylation is correlated with its repression. Histone deacetylation increases the ionic interactions between positively charged histones and negatively charged DNA, this limits the access to transcription machinery and represses gene transcription[17]. HDACs also remove acetyl groups and repress the transcription of essential genes such as tumor suppressor genes[18]. HDACs can also regulate the transcription of tumor suppressor gene *via* the formation of corepressor complexes or direct interaction with the transcription factors[19]. Notably, HDACs may also deacetylate

nonhistone proteins, resulting in dysregulation of cellular homeostasis including cell-cycle progression and apoptosis[18,19]. There are 18 potential HDACs grouped into four classes, based on their homology to yeast proteins. Class I (HDAC 1–3 and 8), Class II (HDAC 4–7, 9 and 10) and Class IV (HDAC 11) HDACs are zinc dependent while Class III HDACs are nicotinamide adenine dinucleotide (Figure 2). Class III HDACs are also referred to as sirtuins (SIRT 1–7) (Figure 2)[20].

The dysregulation of post-translational histone modification, especially histone acetylation, leads to gene transcription dysregulation. Overexpression of HDAC results in significant suppression of tumor suppressor genes, contributing to tumor growth and progression[17,20]. In PDAC, more than half of PDACs were stained positive for HDAC 1. The high expression of HDAC 1 has been correlated with a poorer distant metastasis-free survival[21]. Separately, another study also showed that overexpression of HDAC 1 was linked to a lower overall survival[22]. Treatment with HDAC 1 inhibitors decreased the invasion and metastasis ability of PDAC[21]. In addition, HDAC 2[23], HDAC 7 [24] and HDAC 8[24] overexpression is commonly found in PDAC.

Recently, HDAC has been highlighted for its contribution towards immune evasion. For example, HDAC 3 transcriptionally regulates programmed death ligand 1 (PD-L1) expression[25]. It is reported that higher expression of HDAC 3 is positively correlated with increased PD-L1 expression[25]. Such phenomena suppress immune cells that carry PD-L1 receptors, thus disputing immunosurveillance[25]. HDAC overexpression is also a common observation among other immune-evading solid tumors[17]. In particular, the high expression HDAC 1 is found in gastric and prostate cancers; while HDAC 2 overexpression is associated with gastric, cervical and breast cancers[17]. HDAC 1–3 are highly expressed in renal cell cancer and Hodgkin's lymphoma[17]. Overexpression of HDACs is linked to a significant decline in overall survival and prognosis[20]. It is believed that mutation or loss of HDAC expression is correlated with increased oncogene expression[17]. For instance, *Rb* tumor suppressor gene needs the concomitant action of HDAC to suppress transcription of other essential oncogenes. Loss of HDAC reduces the protective effect of *Rb* tumor suppressor gene[26]. Due to the roles and targetability of HDACs, targeting HDAC has garnered much attention as an effective anticancer therapeutic strategy.

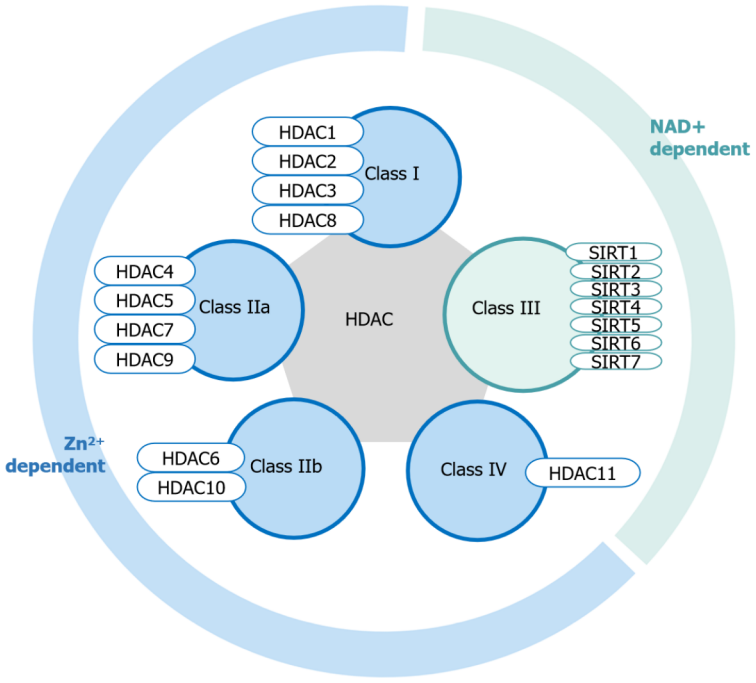
HDAC INHIBITORS AS CANCER THERAPY

HDAC inhibitors bind directly to the active sites on HDAC enzymes, and inhibit the deacetylation effect of HDAC. Each HDAC inhibitor contains a cap, connecting unit, linker and a zinc-binding group that chelates the cation in the target HDAC[27]. HDAC inhibitors can be classified based on their specificity towards HDACs, namely the pan-HDAC inhibitors, Class I or Class II specific inhibitors. HDAC inhibitors can change the acetylation status of both nonhistone proteins and chromatin, causing a viable gene expression alteration, induction of apoptosis and cell cycle arrest[27]. HDAC inhibitors can target not only the tumor cell itself, but also the tumor microenvironment and immune milieu, making the use of HDAC inhibitor a promising strategy to eradicate immune evaded PDAC[27].

The overexpression of HDACs in cancer allows cancer cells to have increased sensitivity to HDAC inhibitors, leading to the induction of growth arrest, differentiation inhibition and eventual tumor cell death without compromising the nontumor cells[27]. Given PDAC's therapeutic resistance to conventional therapy, it is not surprising that the use of HDAC inhibitor as an alternative treatment option has been studied. Ivaltinostat (CG200745), a pan-HDAC inhibitor, demonstrates inhibitory effects on PDAC tumor growth by upregulating proapoptotic proteins BAX and p21[28]. Treatment of PDAC cells with belinostat (PXD101), a Class I and II HDAC inhibitor, also induces cell cycle arrest and tumor regression [29]. A Phase I clinical study using escalating doses of dacinostat (LAQ824), another pan-HDAC inhibitor, showed that the drug was well tolerated by PDAC patients[30]. A significant accumulation of histone acetylation was reported among the patients treated with dacinostat[30]. However, most patients in this trial discontinued dacinostat treatment due to disease progression[30], indicating an unresolved limitation of prescribing HDAC inhibitor as monotherapy for pancreatic cancer.

In combination, HDAC inhibitors show a better effect with other chemotherapeutic agents. The combination of two Class I HDAC inhibitors, romidepsin and ricolinostat (ACY-1215), showed potent synergy with gemcitabine in a panel of PDAC cell lines[31]. Combination of entinostat (Class I HDAC inhibitor), vorinostat (Class I and II HDAC inhibitor) and cyclooxygenase (COX)-2 inhibitors showed complete stalling of PDAC cell growth[32]. In addition, the use of vorinostat and trichostatin A (Class I and II HDAC inhibitor), showed induction of apoptosis in caspase-independent pathways, even for antineoplastic drug-resistant PDAC cell lines[24]. Combination of trichostatin A and proteasome inhibitor PS-341 downregulated antiapoptotic factors and synergistically induced apoptosis[33]. In a separate study, trichostatin A together with silibinin demonstrated a synergistic growth inhibitory effect on PDAC cells by inducing G2/M cell cycle arrest and apoptosis[34].

Meanwhile, the combination of ivaltinostat, gemcitabine and erlotinib significantly reduced PDAC tumor size up to 50%[28]. Ivaltinostat enhanced gemcitabine sensitivity in gemcitabine-resistant pancreatic cancer cells[28]. The use of valproic acid (Class I HDAC inhibitor) confers a synergistic effect with gemcitabine on PDAC cells, lending support to the postulation that targeting HDAC may be a promising strategy to overcome therapeutic resistance and circumvent immune evasion strategies[35].



DOI: 10.3748/wjg.v28.i18.1934 **Copyright** ©The Author(s) 2022.

Figure 2 Histone deacetylases classification. Histone deacetylases (HDAC) can be divided into two major classes, namely Zn-dependent and NAD dependent. Class I (HDAC 1–3 and 8), Class IIa (HDAC 4, 5, 7 and 9), Class IIb (HDAC 6 and 10) and Class IV (HDAC 11) are Zn-dependent HDAC. Class III (SIRT1 to 7) is NAD^+ dependent HDAC. HDAC: Histone deacetylases. The figure in this review paper is created by using BioRender.com by the authors.

HDAC inhibitors demonstrated anti-angiogenic effects by regulating angiogenic related transcriptional factors such as von Hippel-Lindau (VHL), hypoxia inducible factor-1a (HIF-1a) and vascular endothelial growth factor (VEGF)[36]. Rosengren RJ team found novel HDAC inhibitors, Jazz90 and Jazz167, which had a superior potency and anti-angiogenic effects than conventional HDAC inhibitor suberoylanilide hydroxamic acid (SAHA) in prostate cancer cell lines[37]. Independently, Vyas A team synthesised novel SAHA analogues with greater anti-angiogenic effects using the chick chorioallantonic membrane assay[38]. Several clinical trials are ongoing to evaluate the clinical benefits of HDAC inhibitors in targeting angiogenesis in cancer, however, to the best of our knowledge, there is no solid evidence on its benefits among pancreatic cancer patients. More studies are needed to investigate the potential of HDAC inhibitors as anti-angiogenesis agents in PDAC.

In view of their promising combinatory therapeutic efficacy, there has been growing interest in the use of HDAC inhibitors with other therapeutic agents for pancreatic cancer patients (Table 1). However, the use of HDAC inhibitors has been studied in the treatment of lymphoma and other nonpancreatic tumors[39]. For example, HDAC inhibitor has been approved by the FDA for various cancer treatments. Romidepsin[40] and vorinostat[41] have been approved for refractory cutaneous T cell lymphoma while panobinostat[42] (Class I, II and IV HDAC inhibitor) has been approved for multiple myeloma. Likewise, belinostat[42] and tucidinostat[39] (Class I, II, and III inhibitor) have been approved for the treatment of peripheral T cell lymphoma.

HDAC INHIBITORS REVERSE IMMUNE EVASION IN CANCER

HDAC inhibitors enhance immune cell activation

The PDAC tumor microenvironment is composed of regulatory T cells, tumor-associated macrophages (TAMs) and myeloid-deprived suppressive cells (MDSCs) that inhibit ability of cytotoxic T cells (CTLs) in tumor recognition and clearance[6,43]. Cells in the tumor microenvironment can also produce immunosuppressive cytokines including interleukin (IL)-1, IL-6, IL-10, and tumor necrosis factor-α (TNF-α) to cause T cell anergy or tolerance, resulting in immune evasion[44]. Other important cells in the tumor microenvironment include the fibrotic matrix, pancreatic stellate cells and cancer associated fibroblasts (CAFs); all of which can adhere to infiltrating T lymphocytes and prevent their entry into cancer cells, resulting in T cell anergy[44]. In particular, the activated CAFs create a dense stroma that dominates in PDAC, mediating tumor growth and survival by the production of extracellular matrix proteins, growth factors and cytokines[6,45]. CAFs represent the majority type of cells in PDAC stroma and have been acknowledged to be one of the key contributing factors to the immune evasion of cancer cells[45]. CAFs can limit access of infiltrating immune cells to cancer cells through the release of dense

Table 1 Investigational histone deacetylases inhibitors in pancreatic cancer patients

HDAC[1] specificity	Intervention	Clinical trial phase	Study start date	Status	Clinical trial reference code
Pan-HDAC	Vorinostat + Marizomib	I	March 2008	Completed	NCT00667082
Pan-HDAC	Vorinostat + Capecitabine + Radiation Therapy	I	October 2009	Completed	NCT00983268
Pan-HDAC	Vorinostat + Gemcitabine + Sorafenib + Radiation Therapy	I	January 2015	Active	NCT02349867
Pan-HDAC	Vorinostat + Radiation Therapy	I and II	March 2009	Terminated	NCT00831493
Pan-HDAC	Vorinostat + 5-fluorouracil + Radiation Therapy	I and II	August 2009	Terminated	NCT00948688
Pan-HDAC	Panobinostat + Bortezomib	II	September 2010	Terminated	NCT01056601
Class I	Entinostat	I	March 2001	Completed	NCT00020579
Class I	Entinostat + Nivolumab	II	November 2017	Completed	NCT03250273
Class I	Entinostat + ZEN003694	I and II	March 2022	Not yet recruiting	NCT05053971
Class I	Entinostat + Molibresib	I	September 2020	Withdrawn	NCT03925428
Class I	Entinostat + FOLFOX[2]	I	January 2021	Withdrawn	NCT03760614
Class I	Tacedinaline + Gemcitabine	II	October 1999	Completed	NCT00004861

[1]HDAC: Histone deacetylases.
[2]FOLFOX regimen consists of folinic acid, 5-fluorouracil, and oxaliplatin.

collagen networks, resulting in a physical hurdle that disrupts T cell dispersal and inhibition of T cell migration in areas of increased collagen deposition, such as that of PDAC tumors[45]. CAFs have been demonstrated to upregulate immune checkpoints on Cluster of Differentiation (CD)4$^+$ T cells and CTLs, thus resulting in reduced immune function of T cells[45]. Within the immunosuppressive tumor microenvironment, PDACs can disrupt the immunogenic effects of CTLs, by which the CTLs that presented in PDACs may be poorly cytotoxic and nonfunctional[46]. Multiplex staining has demonstrated that proximity of T cells to PDACs is correlated with patient prognosis and survival[47]. As a result, exclusion of T cells from the tumor microenvironment correlates with the tumor initiation and progression.

HDAC inhibitors can modulate immune evasion by modulating immune cell functions[48]. HDAC inhibitors can also increase the expression of major histocompatibility complex (MHC) and its costimulatory molecules leading to T-cell activation[48]. For example, AR42 (a pan-HDAC inhibitor) enhances its adaptive immunity through improving the functions and capabilities of CTLs and natural killer (NK) cells in murine melanoma[49]. Meanwhile, trichostatin A suppresses CD4 T cells from undergoing apoptosis, leading to enhanced antitumor effect[50]. Entinostat increases CTL cytotoxic function and T cell signatures in ovarian tumors[51]. Entinostat also reverses CTL–T regulatory (Treg) cell ratios in the ovarian tumor microenvironment, thus facilitating CTL accumulation at the tumor site[51]. Therefore, HDAC inhibitors have a pivotal role in sustaining T-cell-mediated antitumor immunity. Further studies are required to understand their underlying mechanisms in reversing T cell resistance.

HDAC inhibitors enhance tumor immunogenicity

The intrinsic resistance of PDAC tumors to immune eradication is mainly due to its nonimmunogenic characteristic[6,7]. Tumors can further evade CTL-induced tumor lysis *via* immunoediting, or changes in immunogenicity of cancer cells[52]. Host immune system can alter the expression profile of tumors, in turn enabling them to evade immune detection[53]. The development of PDAC has been described to reflect the three Es of cancer immunoediting, which are elimination, equilibrium and escape[6,54]. The elimination phase occurs during cancer immunosurveillance, when immune effector cells are enlisted to the cancerous tissue to eliminate PDAC cancer cells. Immune effector cells, including CTLs can eliminate most of the vulnerable tumor cells, leaving the resistant tumor clones behind. These resistant tumor clones then expand and remain undetected by the immune system. During the equilibrium phase, a unique equilibrium between antitumor and protumor immune cells is sustained until tumor escape mechanisms are established. During the escape phase, an immunosuppressive microenvironment is formed with the presence of TAMs and MDSCs, creating an effective barrier against the effector immune cells such as CTLs[6,54]. Taken together, such immunoediting has allowed PDAC to bypass immune detection, whereby PDAC continues to grow, progress and metastasize.

HDAC inhibitors may reverse immune evasion in tumors by enhancing tumorigenicity. Trichostatin A induced suppression of tumor growth by improving the immunogenicity of the metastatic tumor cells in a murine study[21,55]. Trichostatin A also increased the MHC Class I expression that translated into enhanced susceptibility to being killed by cytotoxic T cells[55]. Entinostat altered the tumor microenvironment by increasing the MHC Class II expression and its transactivator[56]. Entinostat also re-expressed the natural killer cell receptor and ligand, leading to a decrease in the immunosuppressive effects by host immune cells[57]. Another study using vorinostat and entinostat revealed that breast and prostate carcinoma cells became more sensitive to T-cell-mediated lysis after treatment with HDAC inhibitors. Treatment with vorinostat increased CTL sensitivity, leading to tumor lysis, demonstrating the enhancement of antigen-specific CTL-mediated killing by HDAC inhibitors[58]. Entinostat can sensitize immune checkpoint inhibitors by ablating MDSC-mediated immunosuppressive effects in PDAC tumor-bearing mice[59]. Such exciting findings have rendered the researchers to launch their human clinical trial to investigate the combination of entinostat with nivolumab (a checkpoint inhibitor) in unresectable PDAC patients (Clinical Trial NCT03250273)[60]. Other studies showed that epigenetic modulators[61,62] (including HDAC) could improve tumor immunogenicity and could be a promising translational intervention in cancer.

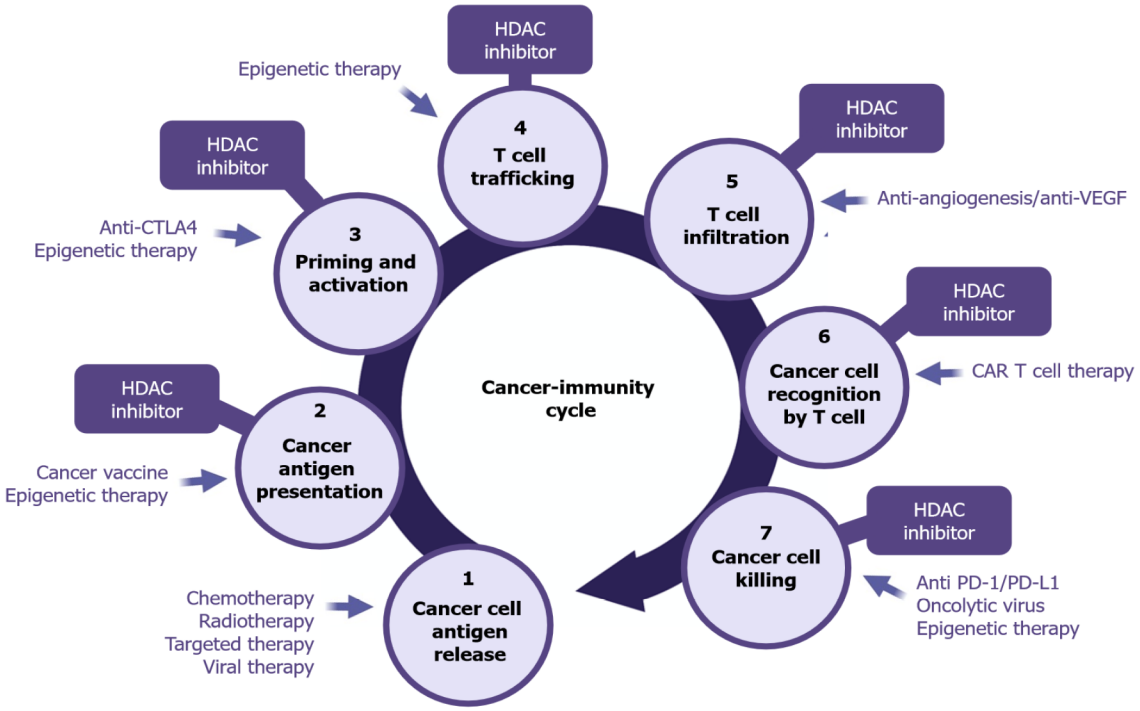
Given the high frequency of *KRAS* mutations in pancreatic cancer patients, mRNA vaccine that targets a specific mutant has gained attraction[63]. In theory, mRNA vaccine encodes KRAS mutant-specific antigens into the host's cytoplasm, leading to the eradication of tumor cells with KRAS mutation by host's immune system[63]. mRNA-5671/V941 is being investigated as monotherapy or in combination with immunotherapy for pancreatic cancer patients with *KRAS* mutation (NCT03948763). However, it remains uncertain whether cancer vaccine could be given along with HDAC inhibitors since HDAC inhibitors may also enhance tumor immunogenicity. Barouch DH group demonstrated that the combination of romidepsin, I-BET151 and cancer vaccine enhanced the CTL cell response in a mouse model, indicating the possible synergism between HDAC inhibitor and cancer vaccine[64]. Thus, further studies are warranted to explore the efficacy of cancer vaccine as a monotherapy or in combination with other therapeutic agents.

HDAC inhibitors counteract PD-L1 and PD-1 interaction

Tumor-infiltrating lymphocytes including CTLs produce a high level of programmed death (PD)-1 while PDAC cells counteract by overproducing the specific ligand of PD-1, which is PD-L1. The interaction between PD-1 and PD-L1 results in T-cell depletion[6,65]. Studies have shown that PD-1 and PD-L1 interaction impedes T-cell growth and that tumor-cell-borne PD-L1, and thus induce apoptosis of tumor-specific T-cell clones[66]. Such transformation turns CTLs into a dysfunctional state of exhaustion that characterized by the loss of CTL proliferation ability as well as the loss of CTL cytotoxic functions [67,68]. As a result, CTLs will be downregulated, and tumor cells can then escape the cytotoxic killing by CTLs.

PD-L1 is overexpressed in PDAC and the higher level of PD-L1 has been linked to a poorer prognosis for PDAC patients[52,67]. In addition, a higher HDAC 3 expression has been linked to the increased PD-L1 expression on PDAC cells[25]. HDAC 3 modulates PD-L1 expression *via* the signal transducer and activator of transcription 3 pathway[22]. HDAC 3 inhibitor (RGFP966) reduces PD-L1 mRNA and protein expression levels, thus enhancing immunosurveillance and aiding the reversal of immune evasion[25].

Another study reported that combination of CG-745 (HDAC Class I and IIb inhibitor) and anti-PD-1 antibody showed synergistic tumor eradication in two syngeneic cancer mouse models[69]. Further mechanistic studies indicated CG-745 increased T-cell activation and macrophage M1 polarization, helping the anti-PD-1 anticancer effect[69]. In addition, HDAC inhibition with entinostat improved the antitumor effect of PD-1 blockade in two syngeneic cancer mouse models[70]. The combination of entinostat and PD-1 inhibitor reduced the tumor burden and improved its survival[70]. Additional analyses indicated that entinostat upregulated PD-L1 in tumors, blocked the immunosuppressive function of MDSCs, and reduced *COX-2*, *inducible nitric oxide synthase* (*iNOS*) and *arginase-1* mRNA expression[70]. Romidepsin enhanced the PD-1 blockade in a murine tumor model, leading to tumor rejection[71]. Individual treatment with romidepsin or PD-1 blocker did not result in significant tumor suppression[71]. Further analyses indicated that romidepsin increased PD-L1 Levels in the tumor[71]. Romidepsin and PD-1 blocker synergized by unleashing the interferon-dependent response in T-cell recruitment to the upregulated PD-L1 tumor cells[71]. Unlike entinostat[70], romidepsin-treated tumor did not alter the MDSC population[71], indicating that HDAC inhibitors have varied impacts on PD-1 and PD-L1 interaction, which can be independent of MDSC modulation. Further study is warranted to explore how HDAC inhibitor affects PD-1 and PD-L1 interaction. Such findings support the notion that HDAC inhibitors can modulate PD-1 and PD-L1 interaction in tumors apart from their canonical role in inhibiting HDAC.



DOI: 10.3748/wjg.v28.i18.1934 **Copyright** ©The Author(s) 2022.

Figure 3 Role of histone deacetylases inhibitors in targeting cancer immune evasion. Cancer–immunity cycle is a continuously cyclical process to amplify the immune response leading to cancer eradication. The cancer–immunity cycle has seven steps: Step 1: Dying cancer cells release neoantigen (Step 2). These neoantigens are captured by antigen-presenting cells and present the antigens on the major histocompatibility complex to T cells (Step 3), allowing the T cells to be primed and activated. Once T cells are activated (Step 4), T cells are transported to the tumor site and (Step 5) infiltrate the tumor. Once inside the tumor (Step 6), T cells recognize the tumor cells, and (Step 7) kill the tumor cells. Histone deacetylases inhibitors will support Steps 2–7 of the cancer–immunity cycle. Such effects can be synergized with other therapeutic agents. CAR: Chimeric antigen receptor; CTLA4: Cytotoxic T-lymphocyte associated antigen 4; PD-1: Programmed death protein 1; PD-L1: Programmed death ligand 1; VEGF: Vascular endothelial growth factor; HDAC: Histone deacetylases. The figure in this review paper is created by using BioRender.com by the authors.

CONCLUSION

PDAC is often synonymous with a "death sentence". The high mortality and poor outcome of PDAC are mainly due to PDAC being refractory to most forms of contemporary therapeutic strategies. Given that the hallmark of PDAC is a highly dense stroma and immense microenvironment, immunotherapy stands out as a promising novel approach to PDAC treatment. Chen and Mellman proposed that cancer immunity is a series of ongoing cyclical events (Figure 3)[72]. Disruption in the major events in the cancer–immunity cycle leads to immune evasion in cancer[6].

HDAC inhibitors have grained traction in medical research as a promising approach to counteracting immune evasion strategies to strengthen Steps 2–7 of the cancer–immunity cycle (Figure 3). HDAC overexpression as a contributing factor to immune evasion and subsequent carcinogenesis have been increasingly recognized. The use of HDAC inhibitors to eliminate cancerous cells (Step 7 of the cancer–immunity cycle, Figure 3) is also gaining traction. Further research is warranted to investigate the effectiveness of HDAC inhibitors in cancer patients. HDAC inhibitor use may well be the key to a long-awaited treatment regimen for cancer patients. The direction for HDAC inhibitors in cancer treatment seems to lean towards combination therapy (Figure 3), with chemotherapy, radiotherapy or immunotherapy. HDAC inhibitors have been widely used with checkpoint inhibitor antibodies in preclinical models. Such combinations have demonstrated successful enhancement of antitumor efficacy and an increase in immune-cell activation.

Studies on HDAC inhibition to circumvent immune evasion are still limited. Current use of HDAC inhibitor to treat PDAC has had promising results, but studies are often still in the early preclinical stage, with much still unknown about the effect of HDAC inhibitors in PDAC patients. There remain much hope and scope in investigating HDAC inhibitors in clinical trials, which will help shed light on the effectiveness of HDAC inhibitors as an adjunct therapy in PDAC.

The ability of HDAC inhibitors to inhibit histone deacetylation may also have its limitations. HDAC inhibitors have poor physiochemical features and unfavorable pharmacokinetics[73]. HDAC inhibitors may also nonspecifically block angiogenesis, which may disrupt drug delivery through blood vessels to solid tumors[73]. In addition, the anti-inflammatory properties of HDAC inhibitors have been postulated to induce apoptosis among immune cells[73]. Current evidence supports the understanding

that HDAC inhibitors may counter immune-cell suppression and apoptosis by enhancing anti-PD1 blockade effects[25]. Moreover, there must be an intact immune function in the host as a prerequisite for HDAC inhibitors to modulate antitumor immune response[6]. Moreover, HDAC inhibitors have yet to utilize the current advanced drug delivery systems that offer site-specific drug delivery[74] with enhanced tumor targeting and reduced toxicity[73]. We believe that, by targeting HDAC in the immune evaded pancreatic cancer, the greatest therapeutic outcome will emerge.

FOOTNOTES

Author contributions: Sim W provided the first draft; Sim W, Lim WM and Hii LW prepared the figures and tables; Sim W, Lim WM, Hii LW, Leong CO, Mai CW wrote and finalized the manuscript; Lim WM and Mai CW designed the outline and coordinated the writing of the paper.

Supported by International Medical University to Sim W, Lim WM, and Leong CO, No. BMS I/2020(10); Shanghai Municipal Science and Technology Commission to Mai CW, No. 20WZ250460.

Conflict-of-interest statement: There is no conflict of interest with any authors contributed to this manuscript.

Open-Access: This article is an open-access article that was selected by an in-house editor and fully peer-reviewed by external reviewers. It is distributed in accordance with the Creative Commons Attribution NonCommercial (CC BY-NC 4.0) license, which permits others to distribute, remix, adapt, build upon this work non-commercially, and license their derivative works on different terms, provided the original work is properly cited and the use is non-commercial. See: https://creativecommons.org/Licenses/by-nc/4.0/

Country/Territory of origin: China

ORCID number: Wynne Sim 0000-0003-2608-9149; Wei-Meng Lim 0000-0002-5076-9390; Ling-Wei Hii 0000-0003-0537-3693; Chee-Onn Leong 0000-0002-6353-9703; Chun-Wai Mai 0000-0001-6532-184X.

Corresponding Author's Membership in Professional Societies: International Pharmaceutical Federation (FIP), No. 36982; European Association Cancer Research (EACR), No. EACR27345; Royal Society of Chemistry, No. 538435; Malaysian Pharmaceutical Society, No. 8141.

S-Editor: Fan JR
L-Editor: A
P-Editor: Fan JR

REFERENCES

1 **Sung H**, Ferlay J, Siegel RL, Laversanne M, Soerjomataram I, Jemal A, Bray F. Global Cancer Statistics 2020: GLOBOCAN Estimates of Incidence and Mortality Worldwide for 36 Cancers in 185 Countries. *CA Cancer J Clin* 2021; **71**: 209-249 [PMID: 33538338 DOI: 10.3322/caac.21660]

2 **Siegel RL**, Miller KD, Fuchs HE, Jemal A. Cancer Statistics, 2021. *CA Cancer J Clin* 2021; **71**: 7-33 [PMID: 33433946 DOI: 10.3322/caac.21654]

3 **Doleh Y**, Lal LS, Blauer-Petersen C, Antico G, Pishvaian M. Treatment patterns and outcomes in pancreatic cancer: Retrospective claims analysis. *Cancer Med* 2020; **9**: 3463-3476 [PMID: 32212262 DOI: 10.1002/cam4.3011]

4 **Strobel O**, Neoptolemos J, Jäger D, Büchler MW. Optimizing the outcomes of pancreatic cancer surgery. *Nat Rev Clin Oncol* 2019; **16**: 11-26 [PMID: 30341417 DOI: 10.1038/s41571-018-0112-1]

5 **Chin V**, Nagrial A, Sjoquist K, O'Connor CA, Chantrill L, Biankin AV, Scholten RJ, Yip D. Chemotherapy and radiotherapy for advanced pancreatic cancer. *Cochrane Database Syst Rev* 2018; **3**: CD011044 [PMID: 29557103 DOI: 10.1002/14651858.CD011044.pub2]

6 **Gan LL**, Hii LW, Wong SF, Leong CO, Mai CW. Molecular Mechanisms and Potential Therapeutic Reversal of Pancreatic Cancer-Induced Immune Evasion. *Cancers (Basel)* 2020; **12** [PMID: 32664564 DOI: 10.3390/cancers12071872]

7 **Looi CK**, Chung FF, Leong CO, Wong SF, Rosli R, Mai CW. Therapeutic challenges and current immunomodulatory strategies in targeting the immunosuppressive pancreatic tumor microenvironment. *J Exp Clin Cancer Res* 2019; **38**: 162 [PMID: 30987642 DOI: 10.1186/s13046-019-1153-8]

8 **Miyazaki T**, Ohishi Y, Miyasaka Y, Oda Y, Aishima S, Ozono K, Abe A, Nagai E, Nakamura M. Molecular Characteristics of Pancreatic Ductal Adenocarcinomas with High-Grade Pancreatic Intraepithelial Neoplasia (PanIN) Are Different from Those without High-Grade PanIN. *Pathobiology* 2017; **84**: 192-201 [PMID: 28291966 DOI: 10.1159/000455194]

9 **Buscail L**, Bournet B, Cordelier P. Role of oncogenic KRAS in the diagnosis, prognosis and treatment of pancreatic cancer. *Nat Rev Gastroenterol Hepatol* 2020; **17**: 153-168 [PMID: 32005945 DOI: 10.1038/s41575-019-0245-4]

10 **Pantsar T**. The current understanding of KRAS protein structure and dynamics. *Comput Struct Biotechnol J* 2020; **18**: 189-198 [PMID: 31988705 DOI: 10.1016/j.csbj.2019.12.004]

11 **Luo W**, Yang G, Qiu J, Luan J, Zhang Y, You L, Feng M, Zhao F, Liu Y, Cao Z, Zheng L, Zhang T, Zhao Y. Novel

discoveries targeting gemcitabine-based chemoresistance and new therapies in pancreatic cancer: How far are we from the destination? *Cancer Med* 2019; **8**: 6403-6413 [PMID: 31475468 DOI: 10.1002/cam4.2384]

12 **Voutsadakis IA**. Mutations of p53 associated with pancreatic cancer and therapeutic implications. *Ann Hepatobiliary Pancreat Surg* 2021; **25**: 315-327 [PMID: 34402431 DOI: 10.14701/ahbps.2021.25.3.315]

13 **Vietri MT**, D'Elia G, Caliendo G, Albanese L, Signoriello G, Napoli C, Molinari AM. Pancreatic Cancer with Mutation in BRCA1/2, MLH1, and APC Genes: Phenotype Correlation and Detection of a Novel Germline BRCA2 Mutation. *Genes (Basel)* 2022; **13** [PMID: 35205366 DOI: 10.3390/genes13020321]

14 **Ahmed S**, Bradshaw AD, Gera S, Dewan MZ, Xu R. The TGF-β/Smad4 Signaling Pathway in Pancreatic Carcinogenesis and Its Clinical Significance. *J Clin Med* 2017; **6** [PMID: 28067794 DOI: 10.3390/jcm6010005]

15 **Khan AA**, Liu X, Yan X, Tahir M, Ali S, Huang H. An overview of genetic mutations and epigenetic signatures in the course of pancreatic cancer progression. *Cancer Metastasis Rev* 2021; **40**: 245-272 [PMID: 33423164 DOI: 10.1007/s10555-020-09952-0]

16 **Yang G**, Yuan Y, Yuan H, Wang J, Yun H, Geng Y, Zhao M, Li L, Weng Y, Liu Z, Feng J, Bu Y, Liu L, Wang B, Zhang X. Histone acetyltransferase 1 is a succinyltransferase for histones and non-histones and promotes tumorigenesis. *EMBO Rep* 2021; **22**: e50967 [PMID: 33372411 DOI: 10.15252/embr.202050967]

17 **Wang X**, Zhao J. Targeted Cancer Therapy Based on Acetylation and Deacetylation of Key Proteins Involved in Double-Strand Break Repair. *Cancer Manag Res* 2022; **14**: 259-271 [PMID: 35115826 DOI: 10.2147/CMAR.S346052]

18 **Lee JH**, Bollschweiler D, Schäfer T, Huber R. Structural basis for the regulation of nucleosome recognition and HDAC activity by histone deacetylase assemblies. *Sci Adv* 2021; **7** [PMID: 33523989 DOI: 10.1126/sciadv.abd4413]

19 **Li Y**, Wang F, Chen X, Wang J, Zhao Y, Li Y, He B. Zinc-dependent Deacetylase (HDAC) Inhibitors with Different Zinc Binding Groups. *Curr Top Med Chem* 2019; **19**: 223-241 [PMID: 30674261 DOI: 10.2174/1568026619666190122144949]

20 **Milazzo G**, Mercatelli D, Di Muzio G, Triboli L, De Rosa P, Perini G, Giorgi FM. Histone Deacetylases (HDACs): Evolution, Specificity, Role in Transcriptional Complexes, and Pharmacological Actionability. *Genes (Basel)* 2020; **11** [PMID: 32429325 DOI: 10.3390/genes11050556]

21 **Shinke G**, Yamada D, Eguchi H, Iwagami Y, Asaoka T, Noda T, Wada H, Kawamoto K, Gotoh K, Kobayashi S, Takeda Y, Tanemura M, Mori M, Doki Y. Role of histone deacetylase 1 in distant metastasis of pancreatic ductal cancer. *Cancer Sci* 2018; **109**: 2520-2531 [PMID: 29917299 DOI: 10.1111/cas.13700]

22 **Huang R**, Zhang X, Sophia S, Min Z, Liu X. Clinicopathological features and prediction values of HDAC1, HDAC2, HDAC3, and HDAC11 in classical Hodgkin lymphoma. *Anticancer Drugs* 2018; **29**: 364-370 [PMID: 29481474 DOI: 10.1097/CAD.0000000000000610]

23 **Krauß L**, Urban BC, Hastreiter S, Schneider C, Wenzel P, Hassan Z, Wirth M, Lankes K, Terrasi A, Klement C, Cernilogar FM, Öllinger R, de Andrade Krätzig N, Engleitner T, Schmid RM, Steiger K, Rad R, Krämer OH, Reichert M, Schotta G, Saur D, Schneider G. HDAC2 Facilitates Pancreatic Cancer Metastasis. *Cancer Res* 2022; **82**: 695-707 [PMID: 34903606 DOI: 10.1158/0008-5472.CAN-20-3209]

24 **Cai MH**, Xu XG, Yan SL, Sun Z, Ying Y, Wang BK, Tu YX. Depletion of HDAC1, 7 and 8 by Histone Deacetylase Inhibition Confers Elimination of Pancreatic Cancer Stem Cells in Combination with Gemcitabine. *Sci Rep* 2018; **8**: 1621 [PMID: 29374219 DOI: 10.1038/s41598-018-20004-0]

25 **Hu G**, He N, Cai C, Cai F, Fan P, Zheng Z, Jin X. HDAC3 modulates cancer immunity *via* increasing PD-L1 expression in pancreatic cancer. *Pancreatology* 2019; **19**: 383-389 [PMID: 30670333 DOI: 10.1016/j.pan.2019.01.011]

26 **Zhou Y**, Jin X, Ma J, Ding D, Huang Z, Sheng H, Yan Y, Pan Y, Wei T, Wang L, Wu H, Huang H. HDAC5 Loss Impairs RB Repression of Pro-Oncogenic Genes and Confers CDK4/6 Inhibitor Resistance in Cancer. *Cancer Res* 2021; **81**: 1486-1499 [PMID: 33419772 DOI: 10.1158/0008-5472.CAN-20-2828]

27 **He X**, Hui Z, Xu L, Bai R, Gao Y, Wang Z, Xie T, Ye XY. Medicinal chemistry updates of novel HDACs inhibitors (2020 to present). *Eur J Med Chem* 2022; **227**: 113946 [PMID: 34775332 DOI: 10.1016/j.ejmech.2021.113946]

28 **Lee HS**, Park SB, Kim SA, Kwon SK, Cha H, Lee DY, Ro S, Cho JM, Song SY. A novel HDAC inhibitor, CG200745, inhibits pancreatic cancer cell growth and overcomes gemcitabine resistance. *Sci Rep* 2017; **7**: 41615 [PMID: 28134290 DOI: 10.1038/srep41615]

29 **Dovzhanskiy DI**, Arnold SM, Hackert T, Oehme I, Witt O, Felix K, Giese N, Werner J. Experimental in vivo and in vitro treatment with a new histone deacetylase inhibitor belinostat inhibits the growth of pancreatic cancer. *BMC Cancer* 2012; **12**: 226 [PMID: 22681698 DOI: 10.1186/1471-2407-12-226]

30 **Park S**, Park JA, Jeon JH, Lee Y. Traditional and Novel Mechanisms of Heat Shock Protein 90 (HSP90) Inhibition in Cancer Chemotherapy Including HSP90 Cleavage. *Biomol Ther (Seoul)* 2019; **27**: 423-434 [PMID: 31113013 DOI: 10.4062/biomolther.2019.051]

31 **Laschanzky RS**, Humphrey LE, Ma J, Smith LM, Enke TJ, Shukla SK, Dasgupta A, Singh PK, Howell GM, Brattain MG, Ly QP, Black AR, Black JD. Selective Inhibition of Histone Deacetylases 1/2/6 in Combination with Gemcitabine: A Promising Combination for Pancreatic Cancer Therapy. *Cancers (Basel)* 2019; **11** [PMID: 31500290 DOI: 10.3390/cancers11091327]

32 **Peulen O**, Gonzalez A, Peixoto P, Turtoi A, Mottet D, Delvenne P, Castronovo V. The anti-tumor effect of HDAC inhibition in a human pancreas cancer model is significantly improved by the simultaneous inhibition of cyclooxygenase 2. *PLoS One* 2013; **8**: e75102 [PMID: 24040391 DOI: 10.1371/journal.pone.0075102]

33 **Bai J**, Demirjian A, Sui J, Marasco W, Callery MP. Histone deacetylase inhibitor trichostatin A and proteasome inhibitor PS-341 synergistically induce apoptosis in pancreatic cancer cells. *Biochem Biophys Res Commun* 2006; **348**: 1245-1253 [PMID: 16904634 DOI: 10.1016/j.bbrc.2006.07.185]

34 **Feng W**, Cai D, Zhang B, Lou G, Zou X. Combination of HDAC inhibitor TSA and silibinin induces cell cycle arrest and apoptosis by targeting survivin and cyclinB1/Cdk1 in pancreatic cancer cells. *Biomed Pharmacother* 2015; **74**: 257-264 [PMID: 26349994 DOI: 10.1016/j.biopha.2015.08.017]

35 **Li H**, Zhang Z, Gao C, Wu S, Duan Q, Wu H, Wang C, Shen Q, Yin T. Combination chemotherapy of valproic acid (VPA) and gemcitabine regulates STAT3/Bmi1 pathway to differentially potentiate the motility of pancreatic cancer cells. *Cell Biosci* 2019; **9**: 50 [PMID: 31244991 DOI: 10.1186/s13578-019-0312-0]

36 **Karagiannis D**, Rampias T. HDAC Inhibitors: Dissecting Mechanisms of Action to Counter Tumor Heterogeneity. *Cancers (Basel)* 2021; **13** [PMID: 34298787 DOI: 10.3390/cancers13143575]

37 **Rana Z**, Diermeier S, Walsh FP, Hanif M, Hartinger CG, Rosengren RJ. Anti-Proliferative, Anti-Angiogenic and Safety Profiles of Novel HDAC Inhibitors for the Treatment of Metastatic Castration-Resistant Prostate Cancer. *Pharmaceuticals (Basel)* 2021; **14** [PMID: 34681244 DOI: 10.3390/ph14101020]

38 **Moku G**, Vangala S, Yakati V, Gali CC, Saha S, Madamsetty VS, Vyas A. Novel Suberoylanilide Hydroxamic Acid Analogs Inhibit Angiogenesis and Induce Apoptosis in Breast Cancer Cells. *Anticancer Agents Med Chem* 2022; **22**: 914-925 [PMID: 34488592 DOI: 10.2174/1871520621666210901102425]

39 **Bondarev AD**, Attwood MM, Jonsson J, Chubarev VN, Tarasov VV, Schiöth HB. Recent developments of HDAC inhibitors: Emerging indications and novel molecules. *Br J Clin Pharmacol* 2021; **87**: 4577-4597 [PMID: 33971031 DOI: 10.1111/bcp.14889]

40 **VanderMolen KM**, McCulloch W, Pearce CJ, Oberlies NH. Romidepsin (Istodax, NSC 630176, FR901228, FK228, depsipeptide): a natural product recently approved for cutaneous T-cell lymphoma. *J Antibiot (Tokyo)* 2011; **64**: 525-531 [PMID: 21587264 DOI: 10.1038/ja.2011.35]

41 **Mann BS**, Johnson JR, Cohen MH, Justice R, Pazdur R. FDA approval summary: vorinostat for treatment of advanced primary cutaneous T-cell lymphoma. *Oncologist* 2007; **12**: 1247-1252 [PMID: 17962618 DOI: 10.1634/theoncologist.12-10-1247]

42 **Fenichel MP**. FDA approves new agent for multiple myeloma. *J Natl Cancer Inst* 2015; **107**: djv165 [PMID: 26032612 DOI: 10.1093/jnci/djv165]

43 **Liu X**, Xu J, Zhang B, Liu J, Liang C, Meng Q, Hua J, Yu X, Shi S. The reciprocal regulation between host tissue and immune cells in pancreatic ductal adenocarcinoma: new insights and therapeutic implications. *Mol Cancer* 2019; **18**: 184 [PMID: 31831007 DOI: 10.1186/s12943-019-1117-9]

44 **Thomas D**, Radhakrishnan P. Tumor-stromal crosstalk in pancreatic cancer and tissue fibrosis. *Mol Cancer* 2019; **18**: 14 [PMID: 30665410 DOI: 10.1186/s12943-018-0927-5]

45 **Valkenburg KC**, de Groot AE, Pienta KJ. Targeting the tumour stroma to improve cancer therapy. *Nat Rev Clin Oncol* 2018; **15**: 366-381 [PMID: 29651130 DOI: 10.1038/s41571-018-0007-1]

46 **Farhood B**, Najafi M, Mortezaee K. $CD8^+$ cytotoxic T lymphocytes in cancer immunotherapy: A review. *J Cell Physiol* 2019; **234**: 8509-8521 [PMID: 30520029 DOI: 10.1002/jcp.27782]

47 **Gorchs L**, Fernández Moro C, Bankhead P, Kern KP, Sadeak I, Meng Q, Rangelova E, Kaipe H. Human Pancreatic Carcinoma-Associated Fibroblasts Promote Expression of Co-inhibitory Markers on $CD4^+$ and $CD8^+$ T-Cells. *Front Immunol* 2019; **10**: 847 [PMID: 31068935 DOI: 10.3389/fimmu.2019.00847]

48 **Banik D**, Moufarrij S, Villagra A. Immunoepigenetics Combination Therapies: An Overview of the Role of HDACs in Cancer Immunotherapy. *Int J Mol Sci* 2019; **20** [PMID: 31067680 DOI: 10.3390/ijms20092241]

49 **Booth L**, Roberts JL, Poklepovic A, Kirkwood J, Dent P. HDAC inhibitors enhance the immunotherapy response of melanoma cells. *Oncotarget* 2017; **8**: 83155-83170 [PMID: 29137331 DOI: 10.18632/oncotarget.17950]

50 **Cao K**, Wang G, Li W, Zhang L, Wang R, Huang Y, Du L, Jiang J, Wu C, He X, Roberts AI, Li F, Rabson AB, Wang Y, Shi Y. Histone deacetylase inhibitors prevent activation-induced cell death and promote anti-tumor immunity. *Oncogene* 2015; **34**: 5960-5970 [PMID: 25745993 DOI: 10.1038/onc.2015.46]

51 **McCaw TR**, Goel N, Brooke DJ, Katre AA, Londoño AI, Smith HJ, Randall TD, Arend RC. Class I histone deacetylase inhibition promotes CD8 T cell activation in ovarian cancer. *Cancer Med* 2021; **10**: 709-717 [PMID: 33369199 DOI: 10.1002/cam4.3337]

52 **Knudsen ES**, Vail P, Balaji U, Ngo H, Botros IW, Makarov V, Riaz N, Balachandran V, Leach S, Thompson DM, Chan TA, Witkiewicz AK. Stratification of Pancreatic Ductal Adenocarcinoma: Combinatorial Genetic, Stromal, and Immunologic Markers. *Clin Cancer Res* 2017; **23**: 4429-4440 [PMID: 28348045 DOI: 10.1158/1078-0432.CCR-17-0162]

53 **Balachandran VP**, Łuksza M, Zhao JN, Makarov V, Moral JA, Remark R, Herbst B, Askan G, Bhanot U, Senbabaoglu Y, Wells DK, Cary CIO, Grbovic-Huezo O, Attiyeh M, Medina B, Zhang J, Loo J, Saglimbeni J, Abu-Akeel M, Zappasodi R, Riaz N, Smoragiewicz M, Kelley ZL, Basturk O; Australian Pancreatic Cancer Genome Initiative; Garvan Institute of Medical Research; Prince of Wales Hospital; Royal North Shore Hospital; University of Glasgow; St Vincent's Hospital; QIMR Berghofer Medical Research Institute; University of Melbourne, Centre for Cancer Research; University of Queensland, Institute for Molecular Bioscience; Bankstown Hospital; Liverpool Hospital; Royal Prince Alfred Hospital, Chris O'Brien Lifehouse; Westmead Hospital; Fremantle Hospital; St John of God Healthcare; Royal Adelaide Hospital; Flinders Medical Centre; Envoi Pathology; Princess Alexandria Hospital; Austin Hospital; Johns Hopkins Medical Institutes; ARC-Net Centre for Applied Research on Cancer, Gönen M, Levine AJ, Allen PJ, Fearon DT, Merad M, Gnjatic S, Iacobuzio-Donahue CA, Wolchok JD, DeMatteo RP, Chan TA, Greenbaum BD, Merghoub T, Leach SD. Identification of unique neoantigen qualities in long-term survivors of pancreatic cancer. *Nature* 2017; **551**: 512-516 [PMID: 29132146 DOI: 10.1038/nature24462]

54 **Foucher ED**, Ghigo C, Chouaib S, Galon J, Iovanna J, Olive D. Pancreatic Ductal Adenocarcinoma: A Strong Imbalance of Good and Bad Immunological Cops in the Tumor Microenvironment. *Front Immunol* 2018; **9**: 1044 [PMID: 29868007 DOI: 10.3389/fimmu.2018.01044]

55 **Setiadi AF**, Omilusik K, David MD, Seipp RP, Hartikainen J, Gopaul R, Choi KB, Jefferies WA. Epigenetic enhancement of antigen processing and presentation promotes immune recognition of tumors. *Cancer Res* 2008; **68**: 9601-9607 [PMID: 19047136 DOI: 10.1158/0008-5472.CAN-07-5270]

56 **McCaw TR**, Li M, Starenki D, Liu M, Cooper SJ, Arend RC, Forero A, Buchsbaum DJ, Randall TD. Histone deacetylase inhibition promotes intratumoral $CD8^+$ T-cell responses, sensitizing murine breast tumors to anti-PD1. *Cancer Immunol Immunother* 2019; **68**: 2081-2094 [PMID: 31720815 DOI: 10.1007/s00262-019-02430-9]

57 **Ni L**, Wang L, Yao C, Ni Z, Liu F, Gong C, Zhu X, Yan X, Watowich SS, Lee DA, Zhu S. The histone deacetylase inhibitor valproic acid inhibits NKG2D expression in natural killer cells through suppression of STAT3 and HDAC3. *Sci Rep* 2017; **7**: 45266 [PMID: 28338101 DOI: 10.1038/srep45266]

58 **Krug LM**, Kindler HL, Calvert H, Manegold C, Tsao AS, Fennell D, Öhman R, Plummer R, Eberhardt WE, Fukuoka K,

Gaafar RM, Lafitte JJ, Hillerdal G, Chu Q, Buikhuisen WA, Lubiniecki GM, Sun X, Smith M, Baas P. Vorinostat in patients with advanced malignant pleural mesothelioma who have progressed on previous chemotherapy (VANTAGE-014): a phase 3, double-blind, randomised, placebo-controlled trial. *Lancet Oncol* 2015; **16**: 447-456 [PMID: 25800891 DOI: 10.1016/S1470-2045(15)70056-2]

59 **Christmas BJ**, Rafie CI, Hopkins AC, Scott BA, Ma HS, Cruz KA, Woolman S, Armstrong TD, Connolly RM, Azad NA, Jaffee EM, Roussos Torres ET. Entinostat Converts Immune-Resistant Breast and Pancreatic Cancers into Checkpoint-Responsive Tumors by Reprogramming Tumor-Infiltrating MDSCs. *Cancer Immunol Res* 2018; **6**: 1561-1577 [PMID: 30341213 DOI: 10.1158/2326-6066.CIR-18-0070]

60 **Baretti M**, Durham JN, Walker R, Mitcheltree A-L, Christmas B, Cope L, Jaffee EM, Azad NS. Entinostat in combination with nivolumab for patients with advanced cholangiocarcinoma and pancreatic adenocarcinoma. *J Clin Oncol* 2018; **36(15_suppl)**: TPS4151-TPS [DOI: 10.1200/jco.2018.36.15_suppl.tps4151]

61 **Cao J**, Yan Q. Cancer Epigenetics, Tumor Immunity, and Immunotherapy. *Trends Cancer* 2020; **6**: 580-592 [PMID: 32610068 DOI: 10.1016/j.trecan.2020.02.003]

62 **Villanueva L**, Álvarez-Errico D, Esteller M. The Contribution of Epigenetics to Cancer Immunotherapy. *Trends Immunol* 2020; **41**: 676-691 [PMID: 32622854 DOI: 10.1016/j.it.2020.06.002]

63 **Zhang Y**, Ma JA, Zhang HX, Jiang YN, Luo WH. Cancer vaccines: Targeting KRAS-driven cancers. *Expert Rev Vaccines* 2020; **19**: 163-173 [PMID: 32174221 DOI: 10.1080/14760584.2020.1733420]

64 **Badamchi-Zadeh A**, Moynihan KD, Larocca RA, Aid M, Provine NM, Iampietro MJ, Kinnear E, Penaloza-MacMaster P, Abbink P, Blass E, Tregoning JS, Irvine DJ, Barouch DH. Combined HDAC and BET Inhibition Enhances Melanoma Vaccine Immunogenicity and Efficacy. *J Immunol* 2018; **201**: 2744-2752 [PMID: 30249811 DOI: 10.4049/jimmunol.1800885]

65 **Kim S**, Kwon D, Koh J, Nam SJ, Kim YA, Kim TM, Kim CW, Jeon YK. Clinicopathological features of programmed cell death-1 and programmed cell death-ligand-1 expression in the tumor cells and tumor microenvironment of angioimmunoblastic T cell lymphoma and peripheral T cell lymphoma not otherwise specified. *Virchows Arch* 2020; **477**: 131-142 [PMID: 32170448 DOI: 10.1007/s00428-020-02790-z]

66 **Luo F**, Cao J, Lu F, Zeng K, Ma W, Huang Y, Zhang L, Zhao H. Lymphocyte activating gene 3 protein expression in nasopharyngeal carcinoma is correlated with programmed cell death-1 and programmed cell death ligand-1, tumor-infiltrating lymphocytes. *Cancer Cell Int* 2021; **21**: 458 [PMID: 34454491 DOI: 10.1186/s12935-021-02162-w]

67 **Zhang W**, Zhang K, Zhang P, Zheng J, Min C, Li X. Research Progress of Pancreas-Related Microorganisms and Pancreatic Cancer. *Front Oncol* 2020; **10**: 604531 [PMID: 33520714 DOI: 10.3389/fonc.2020.604531]

68 **Lu C**, Talukder A, Savage NM, Singh N, Liu K. JAK-STAT-mediated chronic inflammation impairs cytotoxic T lymphocyte activation to decrease anti-PD-1 immunotherapy efficacy in pancreatic cancer. *Oncoimmunology* 2017; **6**: e1291106 [PMID: 28405527 DOI: 10.1080/2162402X.2017.1291106]

69 **Kim YD**, Park SM, Ha HC, Lee AR, Won H, Cha H, Cho S, Cho JM. HDAC Inhibitor, CG-745, Enhances the Anti-Cancer Effect of Anti-PD-1 Immune Checkpoint Inhibitor by Modulation of the Immune Microenvironment. *J Cancer* 2020; **11**: 4059-4072 [PMID: 32368288 DOI: 10.7150/jca.44622]

70 **Orillion A**, Hashimoto A, Damayanti N, Shen L, Adelaiye-Ogala R, Arisa S, Chintala S, Ordentlich P, Kao C, Elzey B, Gabrilovich D, Pili R. Entinostat Neutralizes Myeloid-Derived Suppressor Cells and Enhances the Antitumor Effect of PD-1 Inhibition in Murine Models of Lung and Renal Cell Carcinoma. *Clin Cancer Res* 2017; **23**: 5187-5201 [PMID: 28698201 DOI: 10.1158/1078-0432.CCR-17-0741]

71 **Zheng H**, Zhao W, Yan C, Watson CC, Massengill M, Xie M, Massengill C, Noyes DR, Martinez GV, Afzal R, Chen Z, Ren X, Antonia SJ, Haura EB, Ruffell B, Beg AA. HDAC Inhibitors Enhance T-Cell Chemokine Expression and Augment Response to PD-1 Immunotherapy in Lung Adenocarcinoma. *Clin Cancer Res* 2016; **22**: 4119-4132 [PMID: 26964571 DOI: 10.1158/1078-0432.CCR-15-2584]

72 **Chen DS**, Mellman I. Oncology meets immunology: the cancer-immunity cycle. *Immunity* 2013; **39**: 1-10 [PMID: 23890059 DOI: 10.1016/j.immuni.2013.07.012]

73 **Hafez DA**, Hassanin IA, Teleb M, Khattab SN, Elkhodairy KA, Elzoghby AO. Recent advances in nanomedicine-based delivery of histone deacetylase inhibitors for cancer therapy. *Nanomedicine (Lond)* 2021; **16**: 2305-2325 [PMID: 34551585 DOI: 10.2217/nnm-2021-0196]

74 **Maniam G**, Mai CW, Zulkefeli M, Fu JY. Co-encapsulation of gemcitabine and tocotrienols in nanovesicles enhanced efficacy in pancreatic cancer. *Nanomedicine (Lond)* 2021; **16**: 373-389 [PMID: 33543651 DOI: 10.2217/nnm-2020-0374]

World Journal of Gastroenterology

Submit a Manuscript: https://www.f6publishing.com

World J Gastroenterol 2022 May 14; 28(18): 1946-1964

DOI: 10.3748/wjg.v28.i18.1946

ISSN 1007-9327 (print) ISSN 2219-2840 (online)

ORIGINAL ARTICLE

Basic Study

Gut mucosal microbiota profiles linked to colorectal cancer recurrence

Rui-Xue Huo, Yi-Jia Wang, Shao-Bin Hou, Wei Wang, Chun-Ze Zhang, Xue-Hua Wan

Specialty type: Microbiology

Provenance and peer review: Invited article; Externally peer reviewed.

Peer-review model: Single blind

Peer-review report's scientific quality classification

Grade A (Excellent): 0
Grade B (Very good): B
Grade C (Good): C
Grade D (Fair): 0
Grade E (Poor): 0

P-Reviewer: Amedei A, Italy; Moochhala S, Singapore

Received: December 7, 2021
Peer-review started: December 7, 2021
First decision: January 27, 2022
Revised: February 1, 2022
Accepted: March 25, 2022
Article in press: March 25, 2022
Published online: May 14, 2022

Rui-Xue Huo, Department of Oncology, Tianjin Union Medical Center, Nankai University, Tianjin 300121, China

Yi-Jia Wang, Laboratory of Oncologic Molecular Medicine, Tianjin Union Medical Center, Nankai University, Tianjin 300121, China

Shao-Bin Hou, Advanced Studies in Genomics, Proteomics and Bioinformatics, University of Hawaii at Manoa, Honolulu, HI 96822, United States

Wei Wang, Xue-Hua Wan, TEDA Institute of Biological Sciences and Biotechnology, Nankai University, Tianjin 300457, China

Chun-Ze Zhang, Department of Colorectal Surgery, Tianjin Union Medical Center, Nankai University, Tianjin 300121, China

Chun-Ze Zhang, Tianjin Institute of Coloproctology, Tianjin 300121, China

Corresponding author: Xue-Hua Wan, PhD, Assistant Professor, Senior Researcher, TEDA Institute of Biological Sciences and Biotechnology, Nankai University, No. 23 Hongda Street, Tianjin 300457, China. xuehua.wan@nankai.edu.cn

Abstract

BACKGROUND

Emerging evidence links gut microbiota to various human diseases including colorectal cancer (CRC) initiation and development. However, gut microbiota profiles associated with CRC recurrence and patient prognosis are not completely understood yet, especially in a Chinese cohort.

AIM

To investigate the relationship between gut mucosal microbiota profiles and CRC recurrence and patient prognosis.

METHODS

We obtained the composition and structure of gut microbiota collected from 75 patients diagnosed with CRC and 26 healthy controls. The patients were followed up by regular examination to determine whether tumors recurred. Triplet-paired samples from on-tumor, adjacent-tumor and off-tumor sites of patients diagnosed with/without CRC recurrence were analyzed to assess spatial-specific patterns of gut mucosal microbiota by 16S ribosomal RNA sequencing. Next, we carried out

bioinformatic analyses, Kaplan-Meier survival analyses and Cox regression analyses to determine the relationship between gut mucosal microbiota profiles and CRC recurrence and patient prognosis.

RESULTS

We observed spatial-specific patterns of gut mucosal microbiota profiles linked to CRC recurrence and patient prognosis. A total of 17 bacterial genera/families were identified as potential biomarkers for CRC recurrence and patient prognosis, including *Anaerotruncus*, *Bacteroidales*, *Coriobacteriaceae*, *Dialister*, *Eubacterium*, *Fusobacterium*, *Filifactor*, *Gemella*, *Haemophilus*, *Mogibacteriazeae*, *Pyramidobacter*, *Parvimonas*, *Porphyromonadaceae*, *Slackia*, *Schwartzia*, TG5 and *Treponema*.

CONCLUSION

Our work suggests that intestinal microbiota can serve as biomarkers to predict the risk of CRC recurrence and patient death.

Key Words: Gut microbiota; Colorectal cancer; Prognosis; Colorectal cancer recurrence; Biomarker; 16S rRNA sequencing analysis

©The Author(s) 2022. Published by Baishideng Publishing Group Inc. All rights reserved.

Core Tip: Emerging evidence indicates that besides genetic and epigenetic factors, the gut microbiota is capable of driving colorectal cancer (CRC) progression. Here, we analyzed the gut mucosal microbiota of 75 triplet-paired samples collected from on-tumor, adjacent-tumor and off-tumor sites of patients diagnosed with/without CRC recurrence and 26 healthy controls. After a long-term follow-up, we identified spatial-specific bacterial taxa whose abundances are associated with overall survival and disease-free survival. Our data reveal the profiles of gut mucosal microbiota that increase risk of CRC recurrence and affect patient prognosis, which may serve as potential new biomarkers for CRC diagnosis.

Citation: Huo RX, Wang YJ, Hou SB, Wang W, Zhang CZ, Wan XH. Gut mucosal microbiota profiles linked to colorectal cancer recurrence. *World J Gastroenterol* 2022; 28(18): 1946-1964
URL: https://www.wjgnet.com/1007-9327/full/v28/i18/1946.htm
DOI: https://dx.doi.org/10.3748/wjg.v28.i18.1946

INTRODUCTION

Colorectal cancer (CRC) is a major cause of cancer-related deaths with the third highest mortality and the fourth highest incidence worldwide, according to GLOBOCAN 2020 (global cancer statistics)[1], which indicates a public health issue. Although many new treatment options of CRC have doubled, survival prognosis for early-stage patients with non-metastasized disease is still better than that for advanced-stage patients[2]. Currently, treatment of CRC mainly depends upon tumor-node-metastasis (TNM) stage of disease, and the patient's physical fitness and intent. However, previous studies showed that disease recurrence was observed in 40% of treated patients with stage I-II CRC (lymph node negative postoperative) and 70% of those with stage III CRC[3], which is proposed to be related to rat sarcoma viral oncogene and microsatellite status[4]. Thus, treatment strategy merely depending on CRC TNM stage may cause over-treatment or under-treatment, leading to CRC recurrence. Moreover, the molecular mechanisms behind CRC recurrence are not yet completely understood. Therefore, we still need to explore more suitable biomarkers for assessing prognosis of CRC patients in order to achieve optimal personalized treatment.

In addition to hereditary and lifestyle factors, the human gut microbiota is considered as an important risk factor for CRC initiation as well as development. With the continuous development of high-throughput sequencing, the compositional structure of the human gut microbiota is revealed to be closely involved in CRC initiation, development and treatment[5]. Moreover, pathogenic bacteria have been identified from the human gut microbiota and their procarcinogenic properties have been demonstrated to play a role in causing gut microbial dysbiosis in the complex environment of the human intestinal tract. Certain bacterial species, including *Bacteroides fragilis* (*B. fragilis*), *Clostridium septicum*, *Enterococcus faecalis*, *Escherichia coli*, *Fusobacterium* spp., *Helicobacter pylori* and *Streptococcus bovis* have been identified to play a role in driving colorectal carcinogenesis[6]. The mechanisms behind these pathogenic bacteria involve bacterial-derived genotoxicity and other virulence factors that regulate host defense systems, metabolism, oxidative stress and antioxidative defense modulation[6].

Evidence has linked gut microbiota to prognosis of CRC. A pilot study has shown that high abundance of *Fusobacterium nucleatum* (*F. nucleatum*) and *B. fragilis* were independent indicators for poor patient survival, while high abundance of *Faecalibacterium prausnitzii* predicted improved survival rate [7]. In addition, most studies supported that increased relative abundance of *B. fragilis* and *F. nucleatum* were associated with short-term survival and late stage of CRC[8]. Enterotoxigenic *B. fragilis* (ETBF) and *Fusobacterium* spp. levels were significantly higher in late stage (III/IV) CRC than those in early stage (I/II) CRC, and high abundance of *Fusobacterium* was reported to be associated with high microsatellite instability (MSI)[9,10]. Compared to *F. nucleatum*-negative cases, multivariable hazard ratio for CRC-specific mortality in *F. nucleatum*-high cases was 1.58[9]. After neoadjuvant chemoradiotherapy, *F. nucleatum* persistence was associated with high relapse rates in locally advanced CRC[11]. CRC patients with low levels of *F. nucleatum* had significantly longer overall survival (OS) and disease-free survival (DFS) than patients with moderate and high levels of *F. nucleatum* that were obvious in late-stage CRC patients[12-15]. However, extensive bacterial taxa associated with prognosis of CRC are unclear, especially in a Chinese cohort.

To investigate the profiles of gut mucosal microbiota associated with CRC recurrence and survival of CRC patients, we collected gut mucosal microbiota from CRC patients when they received radical resection or palliative surgery in Tianjin Union Medical Center, China. For each patient, triplet-paired CRC samples were collected from on-tumor, adjacent-tumor and off-tumor sites. Additional samples were collected from 26 healthy controls. We performed 16S ribosomal RNA (rRNA) gene sequencing and analyses on these gut mucosal microbiota. Next, we carried out Kaplan-Meier survival curve analyses for OS and DFS. Our data suggest that a number of bacterial genera/families, including *Anaerotruncus*, *Bacteroidales*, *Coriobacteriaceae*, *Dialister*, *Eubacterium*, *Fusobacterium*, *Filifactor*, *Gemella*, *Haemophilus*, *Mogibacteriazeae*, *Pyramidobacter*, *Parvimonas*, *Porphyromonadaceae*, *Slackia*, *Schwartzia*, TG5 and *Treponema*, are associated with survival of CRC patients and CRC recurrence. We further performed the univariate and multivariate Cox regression analyses. Our data reveal that high abundance of *Anaerotruncus*, *Bacteroidales*, *Coriobacteriaceae*, *Dialister*, *Eubacterium*, *Filifactor*, *Haemophilus*, *Mogibacteriazeae*, *Pyramidobacter*, *Slackia*, *Treponema* and TG5 are associated with worse OS or DFS.

MATERIALS AND METHODS

Patients and sample collection procedures

This study analyzed 69 pathologically confirmed CRC patients, who received radical or palliative surgeries at Tianjin Union Medical Center, Tianjin, China from December 2016 to September 2017. These patients were followed up by regular examination or telephone survey. DFS was defined as the time period from the date of surgery to the time of tumor recurrence, and OS was defined as the time period from the date of surgery to the time of death. Our study was conducted in accordance with the Declaration of Helsinki. Every patient provided written informed consent for the collection of samples and subsequent analysis when required, and the study was approved by the Ethics Committee of Tianjin Union Medical Center. The TNM staging was determined according to the American Joint Committee on Cancer staging handbook (8th edition). Whether a patient received chemotherapy or not depended on his/her TNM stage, physical state score and intention. Imaging examination was arranged for every 2-6 mo or when a patient's condition changed to determine whether the disease recurrence occurred.

DNA library preparation and 16S rRNA sequencing

ZR Fungal/Bacterial DNA kit (Zymo Research, Irvine, CA, United States) was used to isolate bacterial DNA from intestinal microbiota samples according to the manufacturer's instructions. Quant-iT PicoGreen dsDNA assay kit (Thermo Fisher, Sunnyvale, CA, United States) was used to quantify the DNA amounts. The hypervariable regions of 16S rRNA gene amplicon libraries targeting the V3-V4 regions were prepared according to the Illumina manufacturer's manual. The amplification primers were used according to the Illumina manufacturer's manual. The forward and reverse primers were used as follows: 5'-TCGTCGGCAGCGTCAGATGTGTATAAGAGACAGCCTACGGGNGGCWGCAG and 5'-GTCTCGTGGGCTCGGAGATGTGTATAAGAGACAGGACTACHVGGGTATCTAATCC. The products of polymerase chain reaction were examined using agarose gel electrophoresis (1% concentration of agarose gel; 100 V; 40 min electrophoresis time). The AMPure XP beads (Beckman Coulter, Fullerton, CA, United States) were used to purify the amplified DNA libraries, and Quant-iT PicoGreen dsDNA assay kit (Thermo Fisher, Sunnyvale, CA, United States) was used to quantify the DNA library amounts. All the DNA samples were stored at -20 °C until used.

Quality control, operational taxonomic unit picking and diversity analyses of 16S rRNA amplicons

The 16S rRNA amplicon libraries were sequenced for 2 × 300 bp on Illumina MiSeq platform. The read information was listed in Supplementary Table 1. The FastQC program was used to perform quality control and filtering of raw paired-end reads (https://www.bioinformatics.babraham.ac.uk/projects/fastqc/, accessed on 5 June 2019). Next, PandaSeq v2.10 was used to assemble paired-end reads

with default parameters[16]. The QIIME pipeline v1.9.1 (http://qiime.org/home_static/dataFiles.html, accessed on June 5, 2019) and Greengenes database v13.8 were used for de novo operational taxonomic unit (OTU) picking and taxonomic assignment[17]. Briefly, we generated the mapping file that contains all the information about the sequencing samples including sample ID, barcode sequences and sample types. The python command, pick_otus.py, was used to pick OTUs based on sequence similarity (threshold of 97%) of the assembled reads, which is commonly used to define bacterial species. The python command, pick_rep_set.py, was used to pick the representative sequences for each OTU. USEARCH 6.1 was used for chimera detection and filtering. The python command, assign_taxonomy.py, was used to assign taxonomy to OTU representative sequences. The python command, make_rarefaction_plots.py and online MicrobiomeAnalyst (https://dev.microbiomeanalyst.ca/MicrobiomeAnalyst/home.xhtml, accessed on 28 August 2021) were used to calculate alpha diversities within the samples[18,19]. The 16S rRNA paired-end reads have been submitted to the Sequence Read Archive database at the National Center for Biotechnology Information website under accession number PRJNA606879.

Bioinformatic analyses of gut mucosal microbiota for CRC patients

The beta diversity of gut mucosal microbiota among the samples collected from CRC patients with and without recurrence was calculated using principal component analysis on MicrobiomeAnalyst website [18,19]. The linear discriminant analysis (LDA) effect size was analyzed using online MicrobiomeAnalyst[18,19].

Statistical analysis

Statistical analyses were performed using SPSS Version 23. The statistical significance of multiple sample comparisons were calculated using one-way analysis of variance with Kruskal-Wallis test. The Kaplan-Meier survival curves for OS and DFS and the optimal cutoff value of RiskScore were calculated using R software package maxstat (maximally selected rank statistics with several *P* value approximations version: 0.7-25)[20]. We set the minimum number of samples in the grouping to be greater than 25% and the maximum number of samples in the grouping to be less than 75% and finally obtained the optimal cutoff value of each bacterial taxa. Based on this cutoff threshold, the patients were divided into groups with high and low abundance of the bacterial taxa. Furthermore, the survivfit function of R software was used to analyze the prognostic differences between the two groups, and the significance of prognostic differences between the two groups was evaluated by logrank test. According to the cutoff value of each bacterial taxon, we divided the patients into groups with high and low abundance of the bacterial taxa and then conducted Cox regression analyses. The Cox regression analyses based on the proportional hazards model were carried out using SPSS v. 23 program.

RESULTS

Clinicopathological features of CRC patients

We summarized the patients' clinicopathological data in Table 1. The median age of 75 patients was 63.4 years, and 60% of them were males. The pathological type of all patients was categorized as adenocarcinoma, and most of the tumor cells were poorly differentiated. Most patients were diagnosed as microsatellite stable based on immunohistochemical evaluation of components of the mismatch repair machinery, including MLH1, MSH2, MSH6 and PMS2. All patients did not receive chemotherapy or other antitumor therapy before surgery. After surgery, 44 of 75 patients received chemotherapy based on FOLFOX (CapeOX) or FOLFIRI regimen, 4 of them received radiotherapy, and 6 of them received targeted therapy. The median follow-up duration for all cases after surgery was 51.2 mo (2.90-57.03 mo). There were 6 patients who failed to be followed up. Until August 23, 2021, a total of 17 patients diagnosed with I-III stages had relapsed and 20 patients had died.

Altered alpha-diversity of gut mucosal microbiota at adjacent-tumor sites for CRC recurrence

Although tumor tissues can be removed by surgery, the microbiota residing in the tumor surrounding tissues, *e.g.*, those at the adjacent-tumor sites as well as those in the remaining intestinal tissues where tumors are removed, may retain pathogenic bacteria that have the capabilities to drive CRC, leading to CRC recurrence. Therefore, we hypothesize that gut mucosal microbiota profiles at on-tumor or adjacent-tumor sites may be linked to CRC recurrence. To examine this, we assessed microbial alpha-diversities of biopsy samples collected from on-tumor, adjacent-tumor and off-tumor sites of patients with and without CRC recurrence. The 16S rRNA gene hypervariable V3-V4 regions were sequenced and analyzed for five α-diversity indices including Chao1, Fisher, Observed OTU, Shannon and Simpson (Figure 1). Analyses of species variations based on these five metrics consistently indicated that species diversities at on-tumor or off-tumor sites of patients with and without CRC recurrence showed no significant differences (Student *t*-test, $P < 0.05$) (Figure 1). Analyses of species variations based on Chao1 (Student *t*-test, $P = 0.0092$), Fisher (Student *t*-test, $P = 0.0092$) and observed OTU (Student *t*-test, *P*

Table 1 Summary of clinicopathological factors of colorectal cancer patients

Characteristics	*n*	%	Characteristics	*n*	%
Age, yr			Sex		
Mean	63.4 ± 11.0		Male	45	60.0
Range	29-82		Female	30	40.0
AJCC stage			T stage		
I-II	38	50.7	1-2	11	14.7
III-IV	37	49.3	3-4	64	85.3
Location			Lymph node metastasis		
Left colon	21	28.0	Present	36	48.0
Right colon	11	14.7	Absent	39	52.0
Rectum	43	57.3	Distant metastasis		
History of alcohol use			Present	11	14.7
Nondrinker	50	66.7	Absent	64	85.3
Drinker	25	33.3	Smoking history		
Differentiation			Nonsmoker	43	57.3
High	1	1.3	Smoker	32	42.7
High-moderately	3	4.0	Microsatellite status		
Moderately	38	50.7	Stability (MSS)	46	61.3
Low-moderately	21	28.0	Instability (MSI)	24	32.0
Low	12	16.0	Unclear	5	6.7

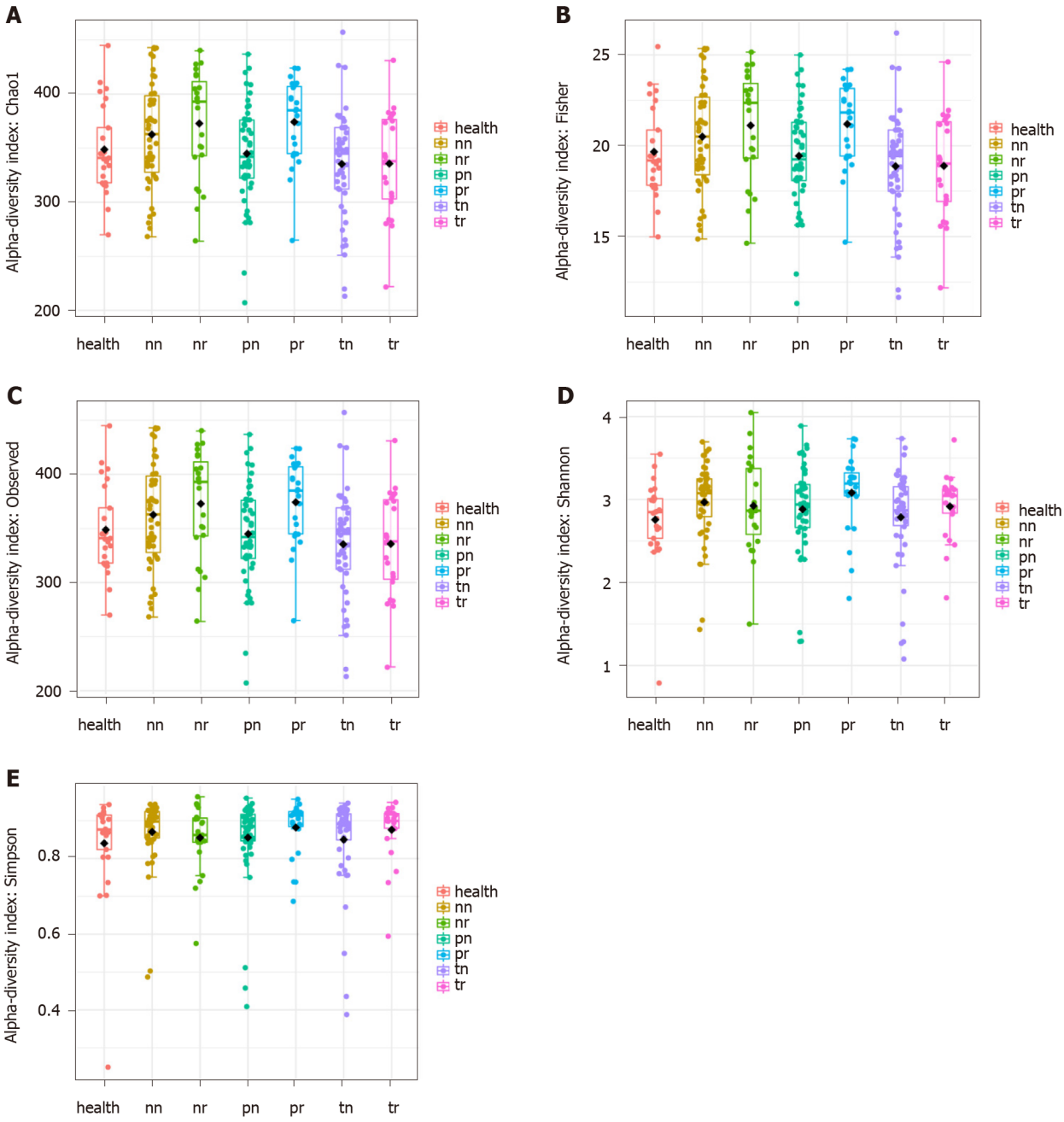
AJCC: American Joint Committee on Cancer; MSS: Microsatellite stable; MSI: Microsatellite instability.

= 0.0092), but not Shannon (Student *t*-test, $P = 0.1314$) and Simpson (Student *t*-test, $P = 0.2513$), showed significant differences at adjacent-tumor sites of patients with and without CRC recurrence (Figure 1). Although Shannon and Simpson metrics did not show statistical significance, analyses of the α-diversities based on the five metrics suggested that at adjacent-tumor sites, those from patients with CRC recurrence were higher than those from patients without recurrence (Figure 1). These data suggest that there is no significant difference of composition of gut mucosal species at on-tumor and off-tumor sites between patients with and without CRC recurrence. However, compositions of internal species showed differences at adjacent-tumor sites between patients with and without CRC recurrence.

Microbiota profiles linked to CRC recurrence

To assess whether the structure diversities (beta-diversity) of gut microbiota show differences between patients with and without CRC recurrence, we performed principal component analysis for abundance of genera identified at on-tumor, adjacent tumor and off-tumor sites of CRC patients diagnosed with and without disease recurrence. The microbiota structure diversities at on-tumor, adjacent tumor and off-tumor sites of CRC patients diagnosed with and without disease recurrence showed differences (Figure 2), suggesting that the structures of gut microbiota were different at these sites in patients with and without CRC recurrence.

We next compared the differential relative abundance of bacterial taxa at the phylum level between patients with and without CRC recurrence. Among all the samples, *Firmicutes*, *Proteobacteria*, *Bacteroidetes* and *Fusobacteria* showed the top relative abundance (Figure 3). *Firmicutes*, *Bacteroidetes* and *Fusobacteria* showed higher relative abundance at on-tumor sites of patients diagnosed with CRC recurrence than those at on-tumor sites of patients diagnosed without CRC recurrence (Figure 3). At adjacent-tumor sites, the relative abundance of *Fusobacteria* in patients with CRC recurrence were dramatically higher than those in patients without CRC recurrence (Figure 3). By contrast, the relative abundance of *Fusobacteria* at off-tumor sites showed no differences between patients with and without CRC recurrence (Figure 3). The relative abundance of *Firmicutes* and *Bacteroidetes* at off-tumor sites of patients with CRC recurrence were lower than those of patients without CRC recurrence (Figure 3). Collectively, these data suggest that species from *Fusobacteria*, *Bacteroidetes* and *Firmicutes* may play roles in worsening or improving the patient prognosis.

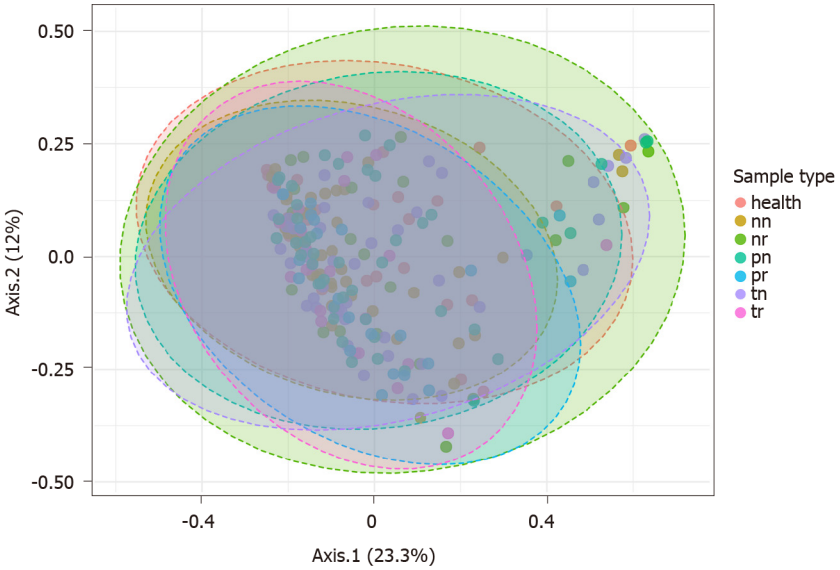


DOI: 10.3748/wjg.v28.i18.1946 **Copyright** ©The Author(s) 2022.

Figure 1 Microbial alpha-diversities showing significant differences at adjacent-tumor site. A: Alpha diversity evaluated using Chao1 index; B: Alpha diversity evaluated using Fisher index; C: Alpha diversity evaluated using observed operational taxonomic unit index; D: Alpha diversity evaluated using Shannon index; E: Alpha diversity evaluated using Simpson index. health: Healthy control; nn: Off-tumor site of patient without colorectal cancer (CRC) recurrence; nr: Off-tumor site of patient with CRC recurrence; pn: Adjacent-tumor site of patient without CRC recurrence; pr: Adjacent-tumor site of patient with CRC recurrence; tn: On-tumor site of patient without CRC recurrence; tr: On-tumor site of patient with CRC recurrence. Alpha-diversity differences were compared using student's *t*-test.

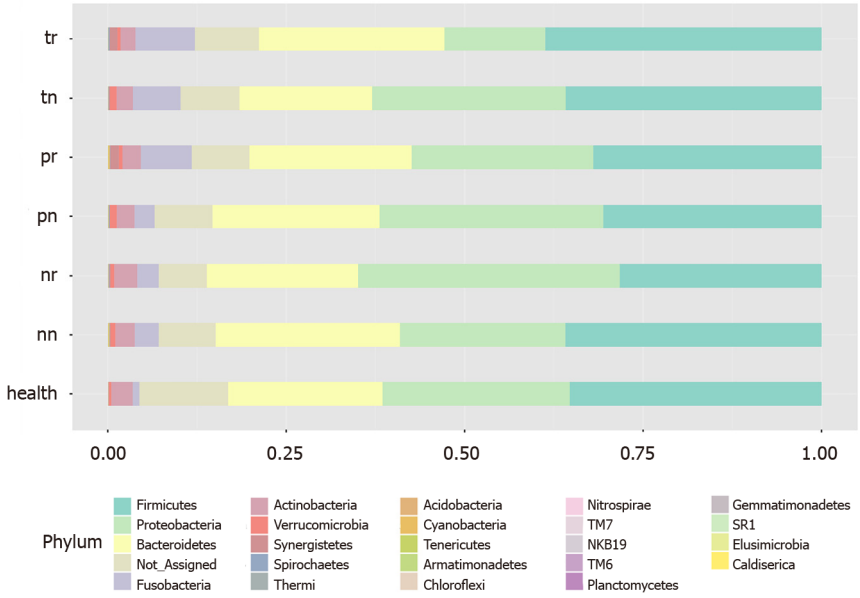
Altered gut mucosal microbiota signatures in CRC recurrence

We next carried out the linear discriminant analysis effect size to predict site-specific biomarkers that are associated with CRC recurrence. By setting LDA score > 3.0 [false discovery rate (FDR) adjusted *P* value < 0.1], a total of 100 genera were identified to show significant differences of relative abundance between patients with and without CRC recurrence (Figure 4, Supplementary Table 2). The top 10 genera/families with the highest LDA scores were *Fusobacterium* (LDAscore = 5.56, FDR adjusted *P* = 0.0026), *Faecalibacterium* (LDAscore = 5.29, FDR adjusted *P* = 0.0176), *Peptostreptococcus* (LDAscore = 5.13, FDR adjusted *P* = 0.0026), *Streptococcus* (LDAscore = 5.08, FDR adjusted *P* = 0.0639), *Parvimonas* (LDAscore = 5.04, FDR adjusted *P* = 0.0072), *Burkholderiales* (LDAscore = 5.03, FDR adjusted *P* = 0.0018), *Pseudomonas* (LDAscore = 4.82, FDR adjusted *P* = 0.0301), *Caulobacteraceae* (LDAscore = 4.77, FDR adjusted *P* = 0.0043), *Mitsuokelia* (LDAscore = 4.77, FDR adjusted *P* = 0.0011) and *Pseudomonadales*



DOI: 10.3748/wjg.v28.i18.1946 **Copyright** ©The Author(s) 2022.

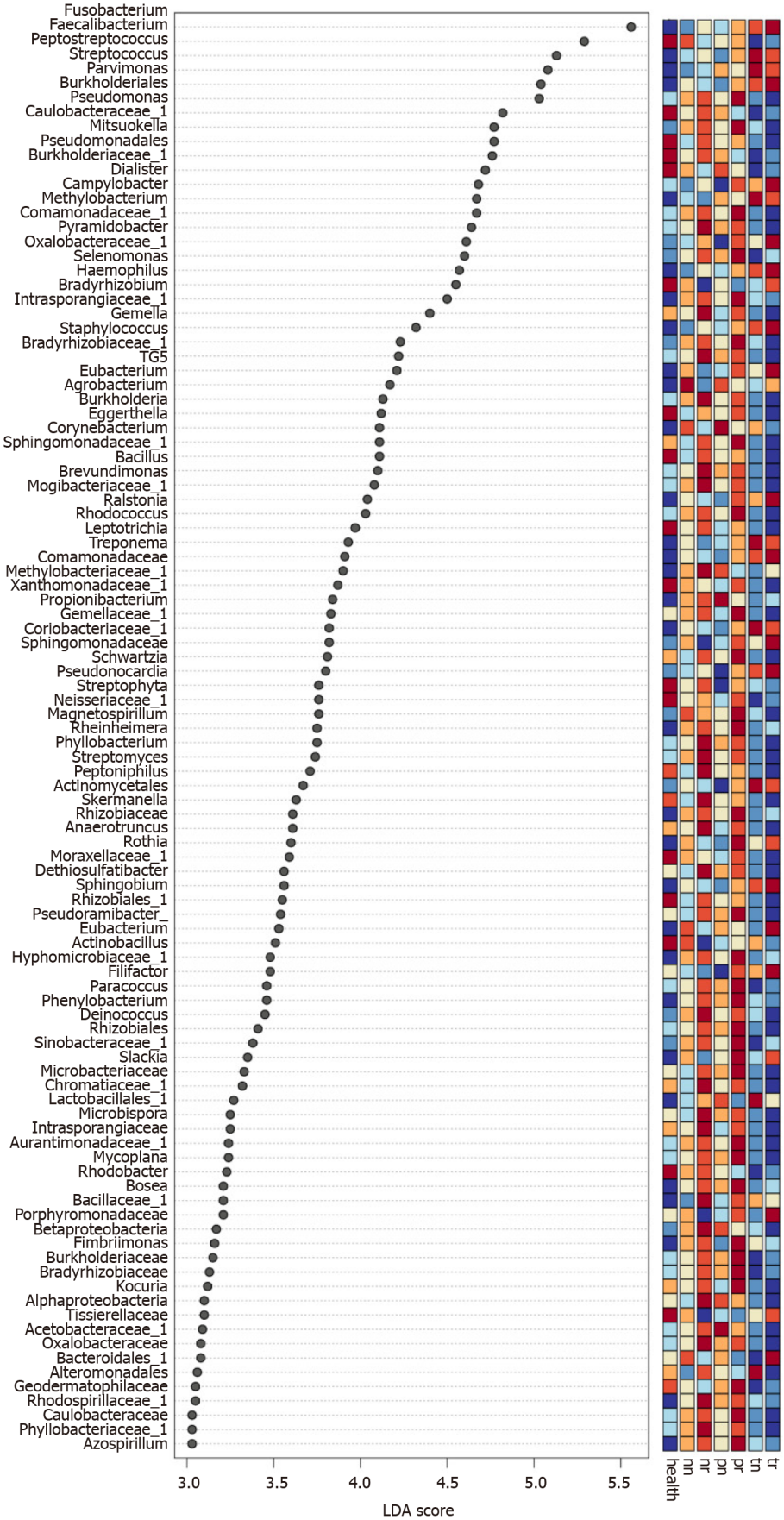
Figure 2 Principal component analysis showed spatial- and recurrence-specific patterns of microbiota profiles. health: Healthy control; nn: Off-tumor site of patient without colorectal cancer (CRC) recurrence; nr: Off-tumor site of patient with CRC recurrence; pn: Adjacent-tumor site of patient without CRC recurrence; pr: Adjacent-tumor site of patient with CRC recurrence; tn: On-tumor site of patient without CRC recurrence; tr: On-tumor site of patient with CRC recurrence.



DOI: 10.3748/wjg.v28.i18.1946 **Copyright** ©The Author(s) 2022.

Figure 3 Patterns of bacterial taxonomy at the phylum level collected from spatial-specific sites of patients with or without colorectal cancer recurrence. health: Healthy control; nn: Off-tumor site of patient without colorectal cancer (CRC) recurrence; nr: Off-tumor site of patient with CRC recurrence; pn: Adjacent-tumor site of patient without CRC recurrence; pr: Adjacent-tumor site of patient with CRC recurrence; tn: On-tumor site of patient without CRC recurrence; tr: On-tumor site of patient with CRC recurrence.

(LDAscore = 4.76, FDR adjusted P = 0.0106) (Supplementary Table 2). Seven genera/families, including *Fusobacterium*, *Pyramidobacter*, *Mogibacteriaceae*, *Coriobacteriaceae*, *Anaerotruncus*, *Slackia* and *Bacteroidales*, showed higher abundance at on-tumor and adjacent-tumor sites (but not off-tumor sites of patients with CRC recurrence than those without CRC recurrence and healthy controls (Supplementary Table 2). Four genera, including *Dialister*, *Selenomonas*, TG5 and *Schwartzia*, showed higher abundance at on-tumor, adjacent-tumor and off-tumor sites of patients with CRC recurrence than those without CRC recurrence and healthy controls (Supplementary Table 2). By contrast, some well-recognized CRC drivers, *e.g.*, *Peptostreptococcus* and *Streptococcus*, showed lower abundance at on-tumor sites of patients with CRC recurrence than those without CRC recurrence. These CRC-recurrence-associated genera may play roles



DOI: 10.3748/wjg.v28.i18.1946 **Copyright** ©The Author(s) 2022.

Figure 4 Linear discriminant analysis effect size analysis showed the genera or families with unknown genus with significant differential abundances at off-tumor, adjacent-tumor or on-tumor sites of patients with and without colorectal cancer recurrence. The colors in the

heatmap represent the abundance of genera/families with unknown genus. Red: High abundance; Blue: low abundance. health: Healthy control; nn: Off-tumor site of patient without colorectal cancer (CRC) recurrence; nr: Off-tumor site of patient with CRC recurrence; pn: Adjacent-tumor site of patient without CRC recurrence; pr: Adjacent-tumor site of patient with CRC recurrence; tn: On-tumor site of patient without CRC recurrence; tr: On-tumor site of patient with CRC recurrence; LDA: The linear discriminant analysis.

in interacting with host cells and worsening patient prognosis.

Gut mucosal microbiota profiles associated with prognosis and survival of CRC patients

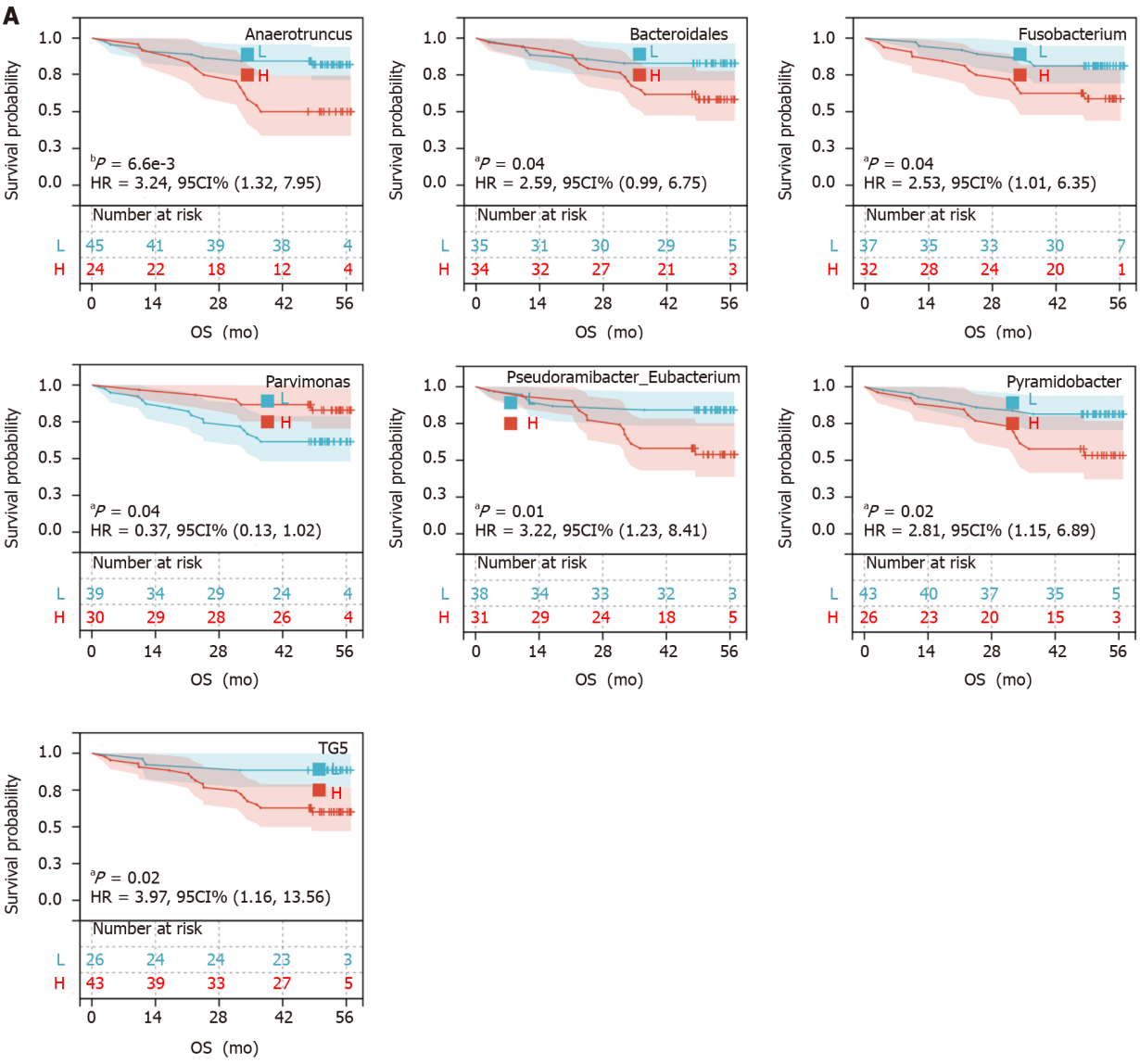
Next, we selected those genera/families that were significantly associated with CRC recurrence based on LDA effect size analysis and used their abundance to evaluate their effects on prognosis and patient survival. The Kaplan-Meier survival analysis curves showed that seven bacterial genera at on-tumor sites and nine bacterial genera at adjacent-tumor sites were capable of significantly predicting the OS of patients ($P < 0.05$) (Figure 5). High abundance of *Anaerotruncus*, *Bacteroidales*, *Fusobacterium*, *Pyramidobacter*, *Pseudoramibacter_Eubacterium* and TG5 at on-tumor sites predicted shorter OS, whereas high abundance of *Parvimonas* was associated with longer OS (Figure 5A). At adjacent-tumor sites, high abundance of *Anaerotruncus*, *Coriobacteriaceae*, *Dialister*, *Filifactor*, *Mogibacteriazeae*, *Pyramidobacter* and *Treponema* predicted shorter OS, whereas high abundance of *Haemophilus* and *Bacteroidales* indicated longer OS (Figure 5B). The cutoff values were shown in Supplementary Table 3.

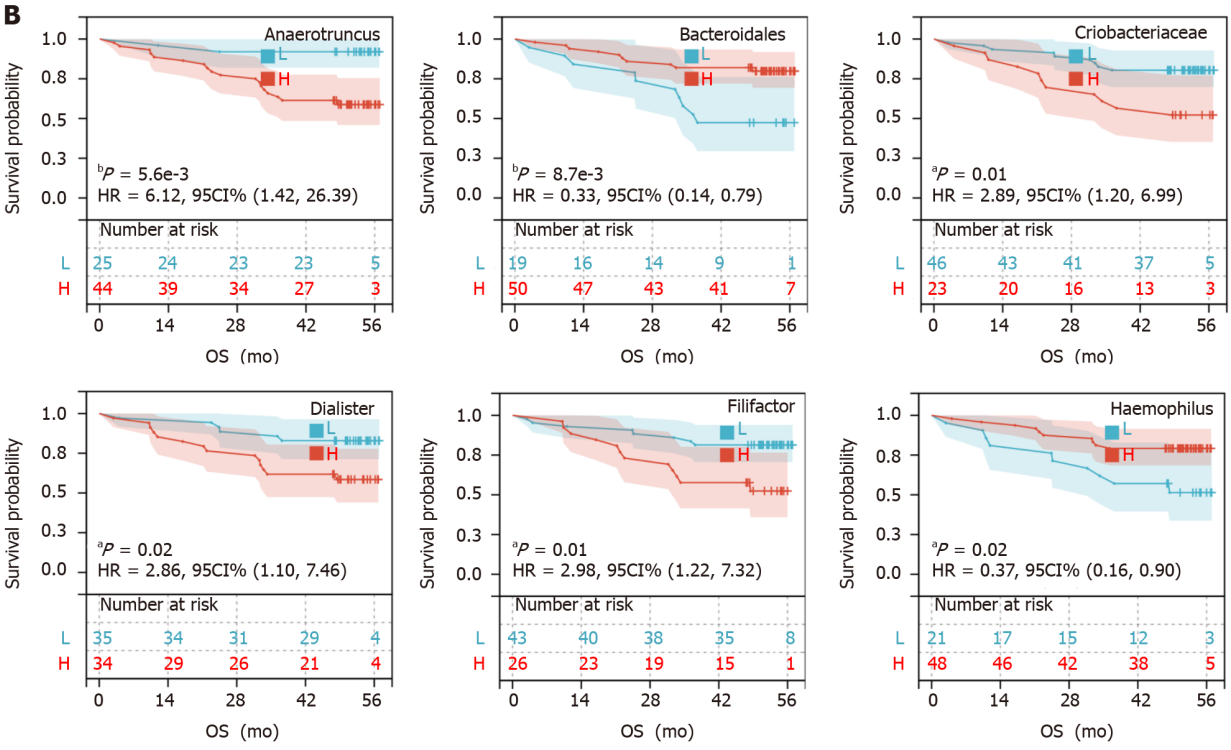
We next performed Kaplan-Meier survival analyses to analyze DFS between patients with high and low abundance of specific bacterial taxa. A total of eleven genera at on-tumor sites and eight genera at adjacent-tumor sites were capable of predicting DFS obviously ($P < 0.05$) (Figure 6). High abundance of *Anaerotruncus*, *Bacteroidales*, *Erysipelotrichaceae_Eubacterium*, *Filifactor*, *Mogibacteriazeae*, *Pyramidobacter*, *Pseudoramibacter_Eubacterium*, *Porphyromonadaceae*, *Slackia* and TG5 at on-tumor sites were associated with shorter DFS, whereas high abundance of *Gemella* was associated with longer DFS (Figure 6A). At the adjacent-tumor sites, high abundance of *Anaerotruncus*, *Coriobacteriaceae*, *Dialister*, *Filifactor*, *Pyramidobacter* and *Schwartzia* showed shorter DFS, while high abundance of *Haemophilus* and *Bacteroidales* were associated with longer DFS (Figure 6B).

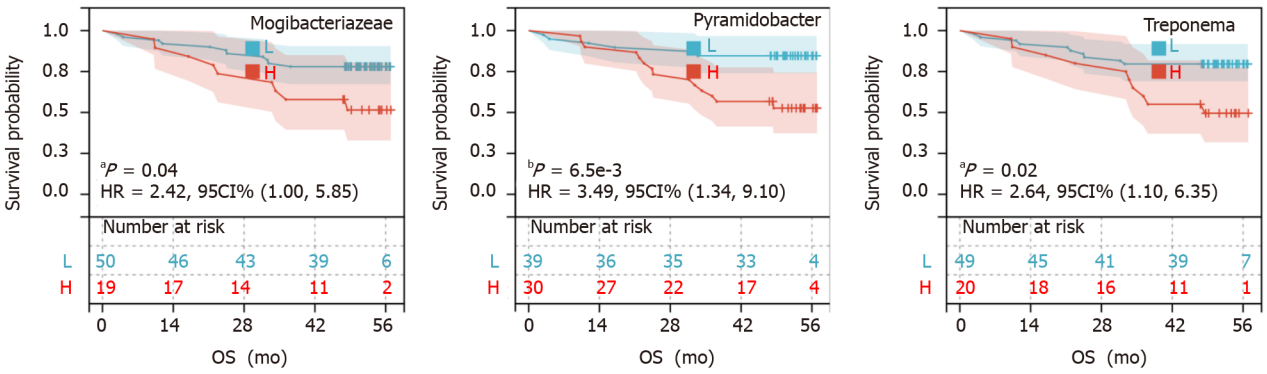
According to the abundance cutoff value of each genus calculated by Kaplan-Meier survival analyses (Supplementary Table 3), we divided the patients into two groups with high or low abundance of each genus. Then, we investigated the survival risk associated with the abundance of each genus/family and other clinicopathological features *via* univariate and multivariate COX regression analyses. According to the univariate Cox regression analysis results, we chose bacterium or clinicopathological feature with significance ($P < 0.1$) and additional bacterium with significance in Kaplan-Meier analysis ($P < 0.05$) to further perform multivariate Cox regression analysis.

Interestingly, although gender, age, differentiation, smoking and drinking histories showed no significance ($P > 0.05$) in univariate DFS or OS Cox regression analyses (Supplementary Tables 4 and 5), the TNM stage and location of tumor in intestine showed significant influences on patient survival based on multivariate OS Cox regression analysis ($P < 0.05$) (Supplementary Figures 1 and 2). CRC III/IV stage and CRC located in the right colon revealed shorter OS than CRC I/II stage and CRC located in the left colon or rectum, respectively. Moreover, only CRC III/IV stage showed shorter DFS than CRC I/II stage (Supplementary Figure 2). In addition, MSI was associated with improved DFS rates in all patients based on multivariate Cox regression analysis (Supplementary Figure 3). Univariate Cox regression OS analysis indicated patients with high abundance of *Anaerotruncus*, *Bacteroidales*, *Pyramidobacter*, *Pseudoramibacter_Eubacterium* and TG5 at on-tumor sites were associated with shorter OS rates (Supplementary Figure 1). However, no significant differences were found between these bacteria and OS in multivariate analysis (Supplementary Figure 1). At adjacent-tumor sites, univariate analysis showed high abundance of *Anaerotruncus*, *Coriobacteriaceae*, *Dialister*, *Filifactor*, *Mogibacteriazeae*, *Pyramidobacter* and *Treponema* and low abundance of *Bacteroidales* were associated with shorter OS rates. In multivariate analysis, high abundance of *Anaerotruncus* and low abundance of *Haemophilus* were associated with shorter OS rates (Supplementary Figure 2).

High abundance of *Anaerotruncus*, *Bacteroidales*, *Erysipelotrichaceae_Eubacterium*, *Mogibacteriazeae*, *Pyramidobacter* and *Pseudoramibacter_Eubacterium* at on-tumor sites predicted shorter DFS rates in univariate analysis, whereas high abundance of *Mogibacteriazeae* and *Slackia* were associated with shorter DFS rates in multivariate analysis (Supplementary Figure 3). In univariate analysis of bacterial taxa at adjacent-tumor sites, high abundance of *Anaerotruncus, Coriobacteriaceae*, *Dialister*, *Filifactor, Pyramidobacter* and *Schwartzia* indicated shorter DFS rates (Supplementary Figure 4). Meanwhile, low abundance of *Bacteroidales* was associated with shorter DFS rates (Supplementary Figure 4). In multivariate analysis, there was no correlation between these bacteria and DFS rates (Supplementary Figure 4).


A
Anaerotruncus
[b]P = 6.6e-3
HR = 3.24, 95CI% (1.32, 7.95)
Bacteroidales
[a]P = 0.04
HR = 2.59, 95CI% (0.99, 6.75)
Fusobacterium
[a]P = 0.04
HR = 2.53, 95CI% (1.01, 6.35)
Parvimonas
[a]P = 0.04
HR = 0.37, 95CI% (0.13, 1.02)
Pseudoramibacter_Eubacterium
[a]P = 0.01
HR = 3.22, 95CI% (1.23, 8.41)
Pyramidobacter
[a]P = 0.02
HR = 2.81, 95CI% (1.15, 6.89)
TG5
[a]P = 0.02
HR = 3.97, 95CI% (1.16, 13.56)
Survival probability
Number at risk
OS (mo)


B
Anaerotruncus
[b]P = 5.6e-3
HR = 6.12, 95CI% (1.42, 26.39)
Bacteroidales
[b]P = 8.7e-3
HR = 0.33, 95CI% (0.14, 0.79)
Criobacteriaceae
[a]P = 0.01
HR = 2.89, 95CI% (1.20, 6.99)
Dialister
[a]P = 0.02
HR = 2.86, 95CI% (1.10, 7.46)
Filifactor
[a]P = 0.01
HR = 2.98, 95CI% (1.22, 7.32)
Haemophilus
[a]P = 0.02
HR = 0.37, 95CI% (0.16, 0.90)
Survival probability
Number at risk
OS (mo)



DOI: 10.3748/wjg.v28.i18.1946 **Copyright** ©The Author(s) 2022.

Figure 5 The relationship between bacterial abundance and overall survival. A: Kaplan-Meier curves of bacteria at on-tumor site and overall survival (OS); B: Kaplan-Meier curves of bacteria at adjacent-tumor site and OS. [a]$P < 0.05$; [b]$P < 0.01$; [c]$P < 0.001$; [d]$P < 0.0001$. X-axis: OS (mo), Y-axis: Survival probability.

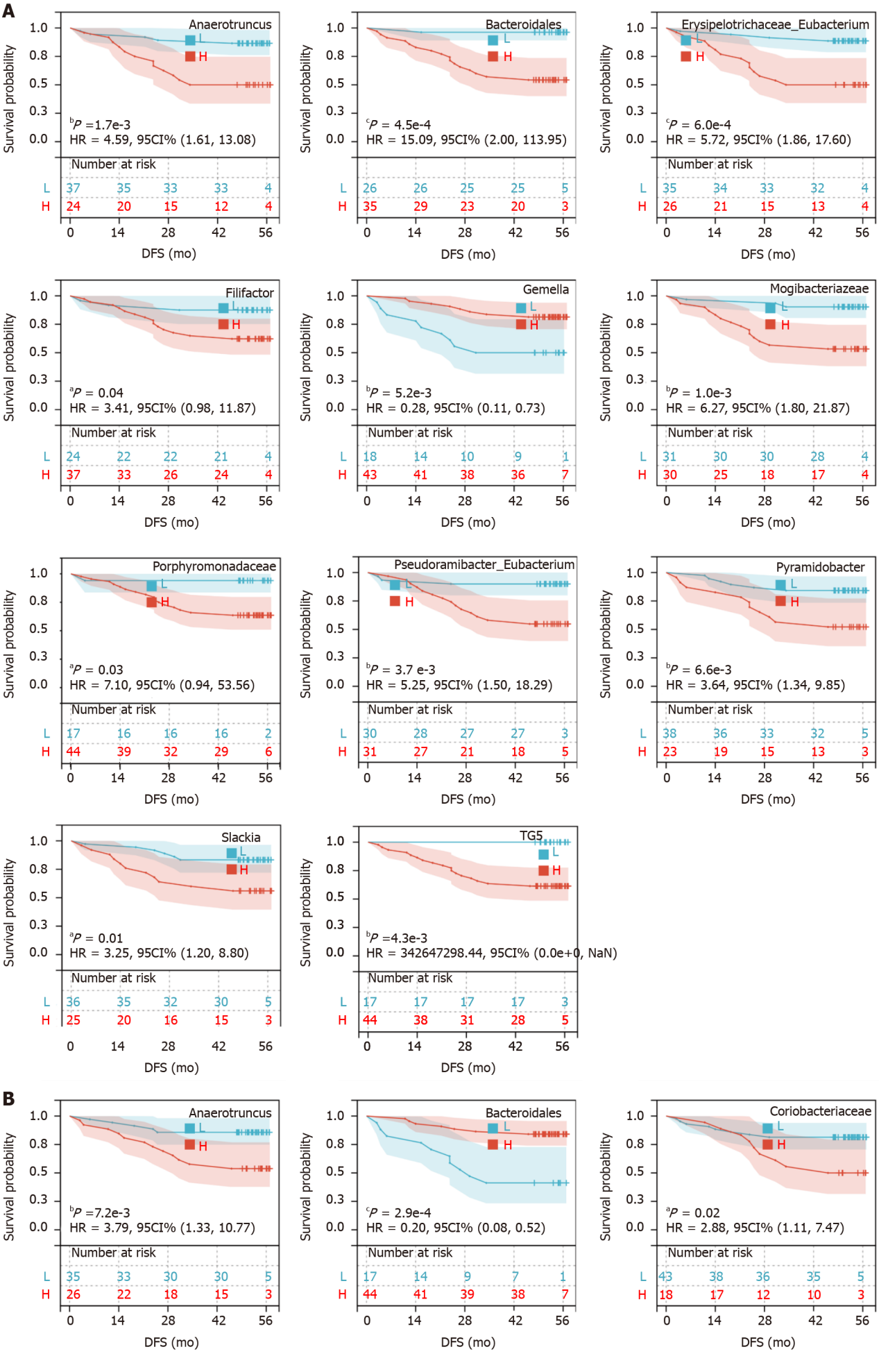
DISCUSSION

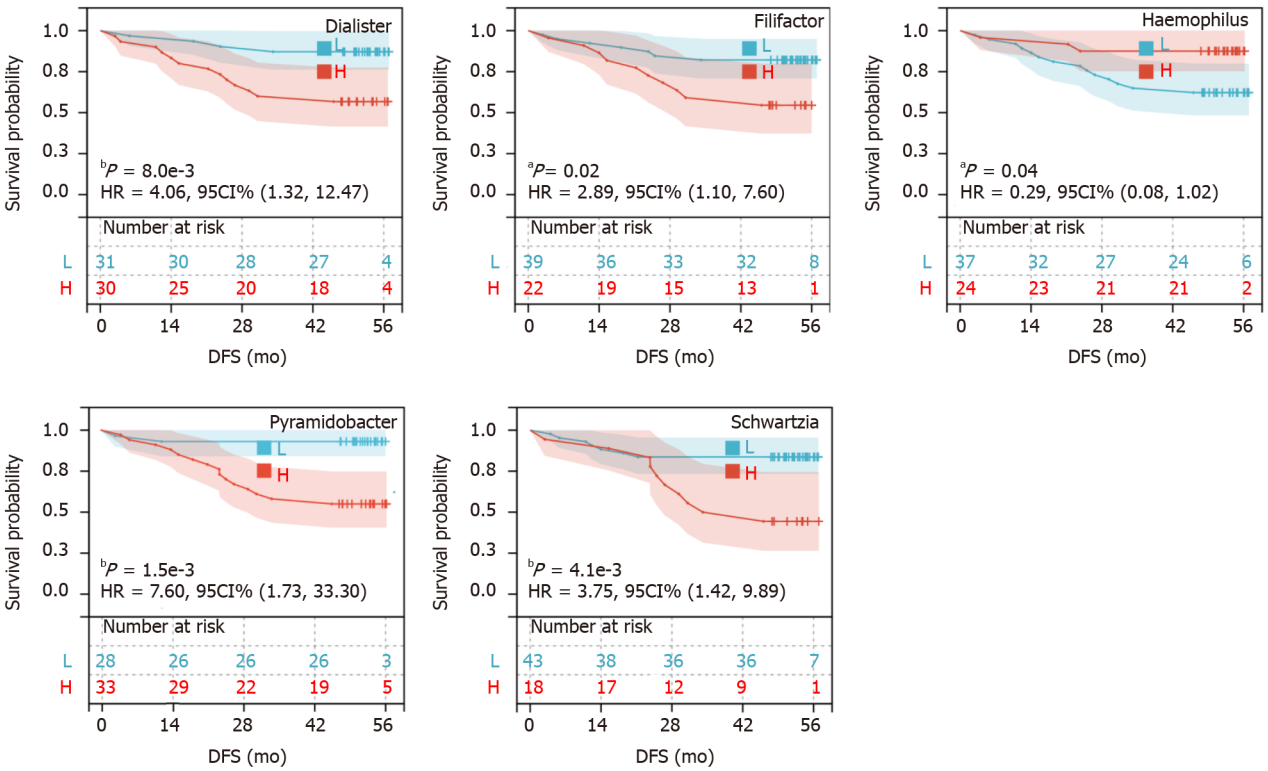
Emerging evidence indicates that the gut microbiota plays pivotal roles in CRC incidence and progression[21]. Most previous studies have focused on identifying gut microbiota profiles linked to CRC carcinogenesis and revealing the physiological roles of specific species, *e.g.*, *F. nucleatum*, *Peptostreptococcus anaerobius*, *B. fragilis* and *Eubacterium rectale*, in CRC tumorigenesis and development [22-25]. However, few reports have fully screened the gut microbiota profiles linked to prognosis and survival of CRC patients[7]. Up to date, only *F. nucleatum* and *B. fragilis* were evaluated for their impacts on patient prognosis[7,8,13,14]. Therefore, our understanding of bacterial taxa associated with clinical outcomes of CRC is incomplete. Profiling these bacterial taxa will pave a way for further understanding their functional roles in impairing clinical outcome of CRC and development of novel strategies for prevention of CRC recurrence. In this study, we explored large-scale screening of gut mucosal microbiota of triplet-paired biopsy samples collected from on-tumor, adjacent-tumor and off-tumor sites of CRC patients and identified critical bacterial taxa that were linked to prognosis and survival of CRC patients.

Our data revealed that a number of bacterial genera/families at on-tumor and adjacent-tumor sites are capable of influencing DFS and OS rates. High abundance of *Anaerotruncus* and *Pyramidobacter* indicated shorter DFS and OS rates in Kaplan-Meier survival analyses and increased the risk of CRC recurrence and patient death according to our Cox regression analyses ($P < 0.05$). High abundance of *Coriobacteriaceae*, *Dialister* and *Filifactor* at adjacent-tumor sites and high abundance of *Bacteroidales*, *Pseudoramibacter_Eubacterium* and TG5 at on-tumor sites indicated shorter DFS and OS rates and increased the risk of CRC recurrence and patient death ($P < 0.05$). Conversely, high abundance of *Parvimonas* at on-tumor sites showed longer OS rates. Meanwhile, high abundances of *Bacteroidales* and *Haemophilus* at adjacent-tumor sites indicated longer DFS and OS rates, but only *Haemophilus* decreased the risk of death in multivariate Cox regression analysis ($P < 0.05$). High abundances of *Fusobacterium* at on-tumor sites and *Treponema* at adjacent-tumor sites indicated shorter OS rates, but only *Treponema* increased the risk of death ($P < 0.05$). High abundance of *Erysipelotrichaceae_Eubacterium*, *Gemella*, *Porphyromonadaceae* and *Slackia* at on-tumor sites and *Coriobacteriaceae* at adjacent-tumor sites indicated shorter DFS rates, and *Erysipelotrichaceae_Eubacterium*, *Gemella*, *Slackia* and *Schwartzia* increased the risk of recurrence ($P < 0.05$). In multivariate regression analysis, *Haemophilus* showed a protective effect and *Anaerotruncus* showed a detrimental effect when referred to death ($P < 0.05$), and *Mogibacteriazeae* and *Slackia* showed obvious detrimental effects when referred to recurrence ($P < 0.05$).

As well-recognized oral pathogens, *F. nucleatum*, *Parvimonas micra* and *Gemella morbillorum* were significantly enriched in both right- and left-sided CRC tumors[26]. *F. nucleatum* in tumor samples was reported to be associated with worse outcomes in terms of OS, DFS or cancer-specific survival, with hazard ratios ranging from 1.58 to 19.96[27]. However, our data showed that the abundance of *F. nucleatum* only affected OS but not DFS rates. This observation is consistent with two previous studies. Wei *et al*[7] reported that high abundance of *F. nucleatum* or *B. fragilis* was associated with poor OS rates after surgery. A meta-analysis found that enrichment of *F. nucleatum* in tumor tissue was associated with worse OS among CRC patients ($n = 5$ studies, HR = 1.87; 95%CI: 1.12–3.11; $I^2 = 60.6\%$) but was not associated with DFS ($n = 3$ studies, HR = 1.48; 95%CI: 0.84–2.59; $I^2 = 88.5\%$)[28].

F. nucleatum may contribute to CRC progression in an established tumor microenvironment due to its highly adherent, invasive and proinflammatory nature that can take advantage of a compromised colonic epithelial cell layer. Moreover, *F. nucleatum* is an asaccharolytic bacterium that will not compete for glucose, a preferred substrate in tumor metabolism, and *F. nucleatum* can tolerate the hypoxic tumor environment[26,29]. In addition, *F. nucleatum* is capable of functioning as a bridge-forming bacterium to interact with other bacterial colonizers, leading to a complex biofilm formation in the human body[30,


A
Anaerotruncus
[b]P =1.7e-3
HR = 4.59, 95CI% (1.61, 13.08)
Bacteroidales
[c]P = 4.5e-4
HR = 15.09, 95CI% (2.00, 113.95)
Erysipelotrichaceae_Eubacterium
[c]P = 6.0e-4
HR = 5.72, 95CI% (1.86, 17.60)
Filifactor
[a]P = 0.04
HR = 3.41, 95CI% (0.98, 11.87)
Gemella
[b]P = 5.2e-3
HR = 0.28, 95CI% (0.11, 0.73)
Mogibacteriazeae
[b]P = 1.0e-3
HR = 6.27, 95CI% (1.80, 21.87)
Porphyromonadaceae
[a]P = 0.03
HR = 7.10, 95CI% (0.94, 53.56)
Pseudoramibacter_Eubacterium
[b]P = 3.7 e-3
HR = 5.25, 95CI% (1.50, 18.29)
Pyramidobacter
[b]P = 6.6e-3
HR = 3.64, 95CI% (1.34, 9.85)
Slackia
[a]P = 0.01
HR = 3.25, 95CI% (1.20, 8.80)
TG5
[b]P =4.3e-3
HR = 342647298.44, 95CI% (0.0e+0, NaN)
B
Anaerotruncus
[b]P =7.2e-3
HR = 3.79, 95CI% (1.33, 10.77)
Bacteroidales
[c]P = 2.9e-4
HR = 0.20, 95CI% (0.08, 0.52)
Coriobacteriaceae
[a]P = 0.02
HR = 2.88, 95CI% (1.11, 7.47)
Survival probability
DFS (mo)
Number at risk
L
H



DOI: 10.3748/wjg.v28.i18.1946 **Copyright** ©The Author(s) 2022.

Figure 6 The relationship between bacterial abundance and disease-free survival. A: Kaplan-Meier curves of bacteria at on-tumor site and disease-free survival (DFS); B: Kaplan-Meier curves of bacteria at adjacent-tumor site and DFS. [a]$P < 0.05$; [b]$P < 0.01$; [c]$P < 0.001$; [d]$P < 0.0001$.

31]. The increases in *F. nucleatum* abundance were observed in both biopsy site and saliva samples of CRC[32].

Flynn *et al*[33] proposed a polymicrobial synergy model that certain oral pathogens may cooperate to fight off the host immune system for survival and be able to establish a niche containing mixed species in the gut. The intestinal mucosa and epithelium are falling off and replaced constantly, which provide available nutrients and binding sites for adhesive bacteria. Intestinal and oral environments share similar pH, which is conducive for bacteria to form biofilm and persist in the host. Initiation or progression of tumorigenesis benefit these bacteria for proliferation because local inflammatory responses during tumorigenesis increase available nutrients in the niche[33]. Polymicrobial colonization at the tumor site by bacterial species that are phylogenetically related to those classified as oral pathogens (*e.g.*, *Fusobacterium*, *Anaerococcus* and *Parvimonas*) could promote tumorigenesis by modifying the tumor microenvironment and eliciting an elevated response of T helper 17 cells, which is linked to a poor prognosis of CRC patients[34].

The order *Bacteroidales* contains more than 35 species, including the best studied genus *Bacteroides*, which is highly abundant in gut microbiota of a healthy human[35-39]. Due to its high density, it is proposed that the species in this order may form mutualistic relationships with the host gut and play a role in stabilizing the compositional structure of the gut microbiota. However, certain species from this order are pathogenic and considered as potential driver bacteria for CRC. For example, ETBF secretes a zinc metalloprotease toxin, known as *B. fragilis* toxin, that is associated with inflammatory bowel disease and CRC[40]. ETBF can induce production of reactive oxygen species in host cells that cause oxidative DNA damage, induce inflammation and disrupt the integrity of the epithelial barrier. In addition, ETBF is able to activate the β-catenin nuclear signaling cascade and induce proliferation of host cells[41]. Although *B. fragilis* may enhance the efficiency of immune checkpoint inhibitor therapy[42], ETBF has been reported to decrease OS and DFS of CRC patients[27,42].

Unexpectedly, our data showed that *Bacteroides* at on-tumor and adjacent-tumor sites displayed distinguishable effects on OS and DFS (Figures 5 and 6). High abundance of *Bacteroides* at on-tumor sites manifested worse OS and DFS, whereas those at adjacent-tumor sites showed better OS and DFS. It was reported that high levels of defined chemokines (*e.g.*, CCL5 and CCL17) in CRC tissues may attract beneficial T cells [cytotoxic T lymphocytes, T-helper (Th) 1 cells, interleukin-17-producing Th cells and regulatory T cells] and lead to improved patient survival. Titers of *Bacteroidales* were positively correlated with expression levels of individual chemokines and the extent of T cell infiltration[43]. Loading *Bacteroidales* to tumor xenografts recruited T cells, indicating that *Bacteroidales* is capable of controlling the extent of tumor infiltration by beneficial immune cells[43]. However, CRC tissue was

infiltrated by more "not effector" T cells (Th2/Th0/regulatory T cells/Tnull) with regulatory or anergic properties, which are unable to kill CRC cells and may contribute to CRC promotion[44]. Therefore, *Bacteroidales* at off-tumor sites here may play a protective role in recruiting beneficial T cells (*e.g.*, Th1, Th17, *etc*), leading to improved prognosis of CRC patients. On the other hand, *Bacteroidales* at on-tumor sites may contribute to CRC recurrence as pathogens or thrive as passenger bacteria.

In our Kaplan-Meier survival analyses, high abundance of *Anaerotruncus* at either on-tumor sites or adjacent-tumor sites was associated with shorter OS and DFS, suggesting that the genus increases the risk of CRC recurrence and patient death. The genus *Anaerotruncus* contains only one validly published species, namely *Anaerotruncus colihominis*. *Anaerotruncus colihominis* was first identified as a Gram-positive, anaerobic bacillus that was isolated from the stool specimens of two children[45]. Moreover, this species was isolated from the blood culture of humans with nosocomial bacteremia[45]. Significant enrichment of *Anaerotruncus* was found in the endometrium of patients with endometrial cancer, suggesting that this bacterium promotes inflammation and tumorigenesis[46]. High fat diets are generally considered as a high risk factor for CRC. Abundance of *Anaerotruncus* is considered to be linked to consumption of saturated fatty acids in both men and women[47]. In mouse model experiments, high fat diets and high sucrose diets led to conditional pathogenic bacterial growth, such as *Anaerotruncus* and *Bacteroides*. These bacteria played a proinflammatory role in disrupting the integrity of epithelial barrier function[48-50].

Several genera, including *Pyramidobacter* and *Mogibacteriaceae*, are sulfidogenic and associated with CRC[51-55]. *Pyramidobacter* is mainly isolated from the human oral cavity, upper gastrointestinal tract and bile[56,57]. The genus *Pyramidobacter* contains anaerobic, Gram-negative bacilli that produce acetic, isovaleric acids and many other trace chemicals as metabolism products[51]. Abundance of *Pyramidobacter* was found to be higher in older adults and was positively correlated with proinflammatory cytokine interleukin-6 that promotes CRC development[58]. In addition, the family *Mogibacteriaceae* was reported to be associated with CRC and observed to co-occur with *F. nucleatum*[53,59]. Our previous study also reported that *Mogibacterium* from the family *Mogibacteriaceae* was associated with *Peptostreptococcus* in gut microbiota isolated from CRC patients[60].

Several genera identified in this study were reported to be associated with CRC previously. The role of *Eubacterium* in CRC initiation was underestimated for a long time. Recently, we identified *Eubacterium* as a potential driver bacteria contributing to CRC and experimentally showed that the lipopolysaccharide of *Eubacterium rectale* activates the transcription factor NF-κB, which regulates innate and adaptive immune responses in normal colon epithelial cells[22]. The genus *Dialister* was detected in the blood of patients with oral infections that cause bacteremia[61]. A meta-analysis based on 26 studies that used next-generation sequencing to analyze microbiota showed that the relative abundance of *Dialister* was significantly higher in cancer patients than those in control samples[62]. The metabolism end products of *Dialister* include acetate, lactate and propionate that may cause carcinogenesis[62]. *Treponema denticola* is an oral pathogen and associated with an increased risk of CRC[63]. The genus *Schwartzia* is linked to CRC carcinogenesis-related gene methylation[64]. The family *Coriobacteriacea*e is considered a commensal or probiotic bacteria residing in the human gut[65]. Their roles in driving CRC recurrence are unknown.

Unlike other critical genera analyzed in this study, low abundance of *Haemophilus* at adjacent-tumor sites indicated longer OS and DFS than those with high abundance in our Kaplan-Meier analyses. *Haemophilus* is a commensal microorganism, which belongs to the phylum *Proteobacteria*. It is an opportunistic pathogen that may lead to infections such as endocarditis and pneumonia. *Haemophilus* in stool samples showed significantly higher proportions in the CRC group than in the control group[66]. The proportions of *Haemophilus* decreased after tumor removal *via* surgery, indicating it is a carcinogenesis pathogen indirectly[67]. However, decreased abundance of *Haemophilus* was observed in stage I/II CRC compared to stage 0 (earliest) CRC, which may be due to overgrowth of other harmful bacteria that acted as competitors during the transition from precancerous lesions to late-stage CRC[68].

According to our COX regression analysis, location (right/left colon or rectum) is another risk factor for patient death. Compared to left colon or rectum, right colon obviously increased risk of death. Consistent with our results, a study showed that the 10-year OS of patients with CRC at the right-sided colon was shorter than that of patients with CRC at the left-sided colon[68]. There is a more abundant blood supply in the right-sided colon than other parts of colon, which benefits tumor growth and results in common clinical symptoms including anemia, emaciation, fever and dyscrasia. Tight-sided CRC exhibits more mucinous and advanced TNM stage[69]. Obviously different patterns of microbiota structures and abundances were found between left-sided and right-sided colons of CRC patients[69]. Moreover, invasive bacterial biofilms were found in 89% of right-sided CRC cases but in only 12% of left-sided CRC cases[69]. Therefore, right-sided CRC specific bacterial species with concomitant procarcinogenic epithelial responses may contribute to the development of right-sided CRC[70].

We further identified that TNM stage showed an obvious impact on survival of CRC patients. Patients with stage III/IV CRC had a higher risk of death and disease recurrence, which is consistent with previously reported results[71]. At the same time, microsatellite status was another factor that influenced patient survival in our study. MSI may decrease the risk of CRC recurrence compared to microsatellite stable patients. Moreover, it was reported that MSI shows stage-specific impacts on the prognosis of CRC patients[70]. In stages II and III CRC, high MSI tumors had superior prognosis

compared with high microsatellite stable tumors. In stage IV CRC, although 4% of tumors were identified as high MSI tumors, these tumors were recognized to be associated with inferior survival[70]. Sequencing paired colon tumor and normal-adjacent tissue and mucosa samples revealed significant enrichment of *B. fragilis* and *F. nucleatum* in deficient mismatch repair CRC but not in proficient mismatch repair CRC[72].

CONCLUSION

In this work, we identified critical bacterial taxa that are associated with prognosis and survival of CRC patients. Our work suggests that intestinal microbiota can serve as biomarkers to predict the risk of CRC recurrence and patient death. Unexpectedly, most of these identified genera have not been investigated for their physiological roles in interacting with host intestinal cells. On the other hand, some well-recognized CRC drivers, *e.g.*, *Peptostreptococcus* and *Streptococcus*, are not associated with CRC recurrence according to our observations. Thus, the mechanism behind bacteria-driving CRC recurrence may be different from those proposed for bacteria-driving CRC development. The activities of complex immune cells, *e.g.*, various types of T cells (*e.g.*, Th1, Th2 and Th17) and macrophages, in response to these bacterial activities may need to be considered. Further functional analyses of physiological roles of these bacteria in patient prognosis and CRC recurrence will shed light on developing novel strategies for CRC treatment and prevention.

ARTICLE HIGHLIGHTS

Research background

Colorectal cancer (CRC) is one of the most common malignant tumors. Gut mucosal microbiota is considered to be one of the key factors promoting CRC. There is evidence that certain gut bacteria are linked to the prognosis (recurrence, overall survival and disease-free survival) of CRC, but there is a lack of research on the relationship between large-scale intestinal microbiota profiles and CRC recurrence/patient prognosis.

Research motivation

Our study focused on the relationship between the abundance of intestinal microbiota at different positions and CRC recurrence/patient prognosis. This study provides novel potential biomarkers for patient prognosis in the future.

Research objectives

The main objective of this study was to evaluate whether the abundance of intestinal microbiota at on-tumor or adjacent-tumor sites can predict CRC recurrence and patient prognosis. Our study has preliminarily suggested that some gut bacteria may have predictive values for CRC recurrence and patient prognosis. These results can provide new biomarkers for prediction of CRC recurrence in the future.

Research methods

We collected intestinal bacteria from different locations of the intestinal mucosa of patients and healthy controls. The bacterial taxa and abundance were determined by high-throughput 16S ribosomal RNA sequencing. The relationship between gut mucosal microbiota profiles and CRC recurrence and patient prognosis was explored by bioinformatics analysis, Kaplan-Meier survival analysis and Cox regression analysis. These methods have been well established in the field.

Research results

Through analysis, gut mucosal microbiota profiles are associated with CRC recurrence and patient prognosis. Abundance of some bacterial genera/families, *e.g.*, *Anaerotruncus*, *Bacteroidales* and *Fusobacterium*, may have prognostic value for CRC recurrence and patient prognosis. The mechanism studies exploring the roles of gut mucosal microbiota in CRC recurrence and patient prognosis need to be carried out in the future.

Research conclusions

This study provides new potential biomarkers identified from gut mucosal microbiota for CRC recurrence and patient prognosis.

Research perspectives

In the future, it is necessary to explore the mechanism of how gut mucosal bacteria affect CRC recurrence and patient prognosis.

FOOTNOTES

Author contributions: Wan XH contributed to the conception of the study; Huo RX and Wang YJ contributed significantly to follow-up, analysis and manuscript preparation; Huo RX, Hou SB and Wan XH performed the data analyses and wrote the manuscript; Wang W and Zhang CZ helped perform the analysis with constructive discussions; Zhang CZ collected the samples; All authors have read and approve the final manuscript.

Supported by Tianjin Science and Technology Plan Project, No. 19YFZCSY00170; Tianjin Union Medical Center, No. 2019YJ007; Beijing Medical and Health Foundation, No. F1814B; Key R&D Projects in the Tianjin Science and Technology Pillar Program, No. 19YFZCSY00420; National Key R&D Program of China, No. 2017YFC1700606 and 2017YFC1700604.

Institutional review board statement: The study was reviewed and approved by the Tianjin Union Medical Center Institutional Review Board (Approval No. B31).

Conflict-of-interest statement: The authors declare that there is no conflict of interest.

Data sharing statement: Technical appendix, statistical code, and dataset available from the corresponding author at xuehua.wan@nankai.edu.cn.

Open-Access: This article is an open-access article that was selected by an in-house editor and fully peer-reviewed by external reviewers. It is distributed in accordance with the Creative Commons Attribution NonCommercial (CC BY-NC 4.0) license, which permits others to distribute, remix, adapt, build upon this work non-commercially, and license their derivative works on different terms, provided the original work is properly cited and the use is non-commercial. See: https://creativecommons.org/Licenses/by-nc/4.0/

Country/Territory of origin: China

ORCID number: Rui-Xue Huo 0000-0001-5755-4934; Yi-Jia Wang 0000-0002-4026-9245; Shao-Bin Hou 0000-0003-3467-8242; Wei Wang 0000-0002-6660-8540; Chun-Ze Zhang 0000-0002-2063-5631; Xue-Hua Wan 0000-0002-6367-848X.

S-Editor: Zhang H
L-Editor: Filipodia
P-Editor: Wu RR

REFERENCES

1 **Sung H**, Ferlay J, Siegel RL, Laversanne M, Soerjomataram I, Jemal A, Bray F. Global Cancer Statistics 2020: GLOBOCAN Estimates of Incidence and Mortality Worldwide for 36 Cancers in 185 Countries. *CA Cancer J Clin* 2021; **71**: 209-249 [PMID: 33538338 DOI: 10.3322/caac.21660]
2 **Dekker E**, Tanis PJ, Vleugels JLA, Kasi PM, Wallace MB. Colorectal cancer. *Lancet* 2019; **394**: 1467-1480 [PMID: 31631858 DOI: 10.1016/S0140-6736(19)32319-0]
3 **Chen SL**, Bilchik AJ. More extensive nodal dissection improves survival for stages I to III of colon cancer: a population-based study. *Ann Surg* 2006; **244**: 602-610 [PMID: 16998369 DOI: 10.1097/01.sla.0000237655.11717.50]
4 **Ogunwobi OO**, Mahmood F, Akingboye A. Biomarkers in Colorectal Cancer: Current Research and Future Prospects. *Int J Mol Sci* 2020; **21** [PMID: 32726923 DOI: 10.3390/ijms21155311]
5 **Yang Y**, Han Z, Li X, Huang A, Shi J, Gu J. Epidemiology and risk factors of colorectal cancer in China. *Chin J Cancer Res* 2020; **32**: 729-741 [PMID: 33446996 DOI: 10.21147/j.issn.1000-9604.2020.06.06]
6 **Gagnière J**, Raisch J, Veziant J, Barnich N, Bonnet R, Buc E, Bringer MA, Pezet D, Bonnet M. Gut microbiota imbalance and colorectal cancer. *World J Gastroenterol* 2016; **22**: 501-518 [PMID: 26811603 DOI: 10.3748/wjg.v22.i2.501]
7 **Wei Z**, Cao S, Liu S, Yao Z, Sun T, Li Y, Li J, Zhang D, Zhou Y. Could gut microbiota serve as prognostic biomarker associated with colorectal cancer patients' survival? *Oncotarget* 2016; **7**: 46158-46172 [PMID: 27323816 DOI: 10.18632/oncotarget.10064]
8 **Colov EP**, Degett TH, Raskov H, Gögenur I. The impact of the gut microbiota on prognosis after surgery for colorectal cancer - a systematic review and meta-analysis. *APMIS* 2020; **128**: 162-176 [PMID: 32017196 DOI: 10.1111/apm.13032]
9 **Mima K**, Nishihara R, Qian ZR, Cao Y, Sukawa Y, Nowak JA, Yang J, Dou R, Masugi Y, Song M, Kostic AD, Giannakis M, Bullman S, Milner DA, Baba H, Giovannucci EL, Garraway LA, Freeman GJ, Dranoff G, Garrett WS, Huttenhower C, Meyerson M, Meyerhardt JA, Chan AT, Fuchs CS, Ogino S. Fusobacterium nucleatum in colorectal carcinoma tissue and patient prognosis. *Gut* 2016; **65**: 1973-1980 [PMID: 26311717 DOI: 10.1136/gutjnl-2015-310101]
10 **Viljoen KS**, Dakshinamurthy A, Goldberg P, Blackburn JM. Quantitative profiling of colorectal cancer-associated bacteria reveals associations between fusobacterium spp., enterotoxigenic Bacteroides fragilis (ETBF) and clinicopathological features of colorectal cancer. *PLoS One* 2015; **10**: e0119462 [PMID: 25751261 DOI: 10.1371/journal.pone.0119462]
11 **Serna G**, Ruiz-Pace F, Hernando J, Alonso L, Fasani R, Landolfi S, Comas R, Jimenez J, Elez E, Bullman S, Tabernero J, Capdevila J, Dienstmann R, Nuciforo P. Fusobacterium nucleatum persistence and risk of recurrence after preoperative treatment in locally advanced rectal cancer. *Ann Oncol* 2020; **31**: 1366-1375 [PMID: 32569727 DOI: 10.1016/j.annonc.2020.06.003]

12 **Flanagan L**, Schmid J, Ebert M, Soucek P, Kunicka T, Liska V, Bruha J, Neary P, Dezeeuw N, Tommasino M, Jenab M, Prehn JH, Hughes DJ. Fusobacterium nucleatum associates with stages of colorectal neoplasia development, colorectal cancer and disease outcome. *Eur J Clin Microbiol Infect Dis* 2014; **33**: 1381-1390 [PMID: 24599709 DOI: 10.1007/s10096-014-2081-3]

13 **Liu Y**, Baba Y, Ishimoto T, Iwatsuki M, Hiyoshi Y, Miyamoto Y, Yoshida N, Wu R, Baba H. Progress in characterizing the linkage between Fusobacterium nucleatum and gastrointestinal cancer. *J Gastroenterol* 2019; **54**: 33-41 [PMID: 30244399 DOI: 10.1007/s00535-018-1512-9]

14 **Yamaoka Y**, Suehiro Y, Hashimoto S, Hoshida T, Fujimoto M, Watanabe M, Imanaga D, Sakai K, Matsumoto T, Nishioka M, Takami T, Suzuki N, Hazama S, Nagano H, Sakaida I, Yamasaki T. Fusobacterium nucleatum as a prognostic marker of colorectal cancer in a Japanese population. *J Gastroenterol* 2018; **53**: 517-524 [PMID: 28823057 DOI: 10.1007/s00535-017-1382-6]

15 **Yan X**, Liu L, Li H, Qin H, Sun Z. Clinical significance of *Fusobacterium nucleatum*, epithelial-mesenchymal transition, and cancer stem cell markers in stage III/IV colorectal cancer patients. *Onco Targets Ther* 2017; **10**: 5031-5046 [PMID: 29081665 DOI: 10.2147/OTT.S145949]

16 **Masella AP**, Bartram AK, Truszkowski JM, Brown DG, Neufeld JD. PANDAseq: paired-end assembler for illumina sequences. *BMC Bioinformatics* 2012; **13**: 31 [PMID: 22333067 DOI: 10.1186/1471-2105-13-31]

17 **Caporaso JG**, Kuczynski J, Stombaugh J, Bittinger K, Bushman FD, Costello EK, Fierer N, Peña AG, Goodrich JK, Gordon JI, Huttley GA, Kelley ST, Knights D, Koenig JE, Ley RE, Lozupone CA, McDonald D, Muegge BD, Pirrung M, Reeder J, Sevinsky JR, Turnbaugh PJ, Walters WA, Widmann J, Yatsunenko T, Zaneveld J, Knight R. QIIME allows analysis of high-throughput community sequencing data. *Nat Methods* 2010; **7**: 335-336 [PMID: 20383131 DOI: 10.1038/nmeth.f.303]

18 **Chong J**, Liu P, Zhou G, Xia J. Using MicrobiomeAnalyst for comprehensive statistical, functional, and meta-analysis of microbiome data. *Nat Protoc* 2020; **15**: 799-821 [PMID: 31942082 DOI: 10.1038/s41596-019-0264-1]

19 **Dhariwal A**, Chong J, Habib S, King IL, Agellon LB, Xia J. MicrobiomeAnalyst: a web-based tool for comprehensive statistical, visual and meta-analysis of microbiome data. *Nucleic Acids Res* 2017; **45**: W180-W188 [PMID: 28449106 DOI: 10.1093/nar/gkx295]

20 **Ogluszka M**, Orzechowska M, Jędroszka D, Witas P, Bednarek AK. Evaluate Cutpoints: Adaptable continuous data distribution system for determining survival in Kaplan-Meier estimator. *Comput Methods Programs Biomed* 2019; **177**: 133-139 [PMID: 31319941 DOI: 10.1016/j.cmpb.2019.05.023]

21 **Song M**, Chan AT. The Potential Role of Exercise and Nutrition in Harnessing the Immune System to Improve Colorectal Cancer Survival. *Gastroenterology* 2018; **155**: 596-600 [PMID: 30076837 DOI: 10.1053/j.gastro.2018.07.038]

22 **Wang Y**, Wan X, Wu X, Zhang C, Liu J, Hou S. Eubacterium rectale contributes to colorectal cancer initiation *via* promoting colitis. *Gut Pathog* 2021; **13**: 2 [PMID: 33436075 DOI: 10.1186/s13099-020-00396-z]

23 **Long X**, Wong CC, Tong L, Chu ESH, Ho Szeto C, Go MYY, Coker OO, Chan AWH, Chan FKL, Sung JJY, Yu J. Peptostreptococcus anaerobius promotes colorectal carcinogenesis and modulates tumour immunity. *Nat Microbiol* 2019; **4**: 2319-2330 [PMID: 31501538 DOI: 10.1038/s41564-019-0541-3]

24 **Zhang S**, Cai S, Ma Y. Association between *Fusobacterium nucleatum* and colorectal cancer: Progress and future directions. *J Cancer* 2018; **9**: 1652-1659 [PMID: 29760804 DOI: 10.7150/jca.24048]

25 **Rhee KJ**, Wu S, Wu X, Huso DL, Karim B, Franco AA, Rabizadeh S, Golub JE, Mathews LE, Shin J, Sartor RB, Golenbock D, Hamad AR, Gan CM, Housseau F, Sears CL. Induction of persistent colitis by a human commensal, enterotoxigenic Bacteroides fragilis, in wild-type C57BL/6 mice. *Infect Immun* 2009; **77**: 1708-1718 [PMID: 19188353 DOI: 10.1128/IAI.00814-08]

26 **Drewes JL**, White JR, Dejea CM, Fathi P, Iyadorai T, Vadivelu J, Roslani AC, Wick EC, Mongodin EF, Loke MF, Thulasi K, Gan HM, Goh KL, Chong HY, Kumar S, Wanyiri JW, Sears CL. High-resolution bacterial 16S rRNA gene profile meta-analysis and biofilm status reveal common colorectal cancer consortia. *NPJ Biofilms Microbiomes* 2017; **3**: 34 [PMID: 29214046 DOI: 10.1038/s41522-017-0040-3]

27 **Lauka L**, Reitano E, Carra MC, Gaiani F, Gavriilidis P, Brunetti F, de'Angelis GL, Sobhani I, de'Angelis N. Role of the intestinal microbiome in colorectal cancer surgery outcomes. *World J Surg Oncol* 2019; **17**: 204 [PMID: 31791356 DOI: 10.1186/s12957-019-1754-x]

28 **Gethings-Behncke C**, Coleman HG, Jordao HWT, Longley DB, Crawford N, Murray LJ, Kunzmann AT. *Fusobacterium nucleatum* in the Colorectum and Its Association with Cancer Risk and Survival: A Systematic Review and Meta-analysis. *Cancer Epidemiol Biomarkers Prev* 2020; **29**: 539-548 [PMID: 31915144 DOI: 10.1158/1055-9965.EPI-18-1295]

29 **Hurtado CG**, Wan F, Housseau F, Sears CL. Roles for Interleukin 17 and Adaptive Immunity in Pathogenesis of Colorectal Cancer. *Gastroenterology* 2018; **155**: 1706-1715 [PMID: 30218667 DOI: 10.1053/j.gastro.2018.08.056]

30 **Wu C**, Al Mamun AAM, Luong TT, Hu B, Gu J, Lee JH, D'Amore M, Das A, Ton-That H. Forward Genetic Dissection of Biofilm Development by Fusobacterium nucleatum: Novel Functions of Cell Division Proteins FtsX and EnvC. *mBio* 2018; **9** [PMID: 29691334 DOI: 10.1128/mBio.00360-18]

31 **Kolenbrander PE**, Palmer RJ Jr, Periasamy S, Jakubovics NS. Oral multispecies biofilm development and the key role of cell-cell distance. *Nat Rev Microbiol* 2010; **8**: 471-480 [PMID: 20514044 DOI: 10.1038/nrmicro2381]

32 **Russo E**, Bacci G, Chiellini C, Fagorzi C, Niccolai E, Taddei A, Ricci F, Ringressi MN, Borrelli R, Melli F, Miloeva M, Bechi P, Mengoni A, Fani R, Amedei A. Preliminary Comparison of Oral and Intestinal Human Microbiota in Patients with Colorectal Cancer: A Pilot Study. *Front Microbiol* 2017; **8**: 2699 [PMID: 29375539 DOI: 10.3389/fmicb.2017.02699]

33 **Flynn KJ**, Baxter NT, Schloss PD. Metabolic and Community Synergy of Oral Bacteria in Colorectal Cancer. *mSphere* 2016; **1** [PMID: 27303740 DOI: 10.1128/mSphere.00102-16]

34 **Flemer B**, Lynch DB, Brown JM, Jeffery IB, Ryan FJ, Claesson MJ, O'Riordain M, Shanahan F, O'Toole PW. Tumour-associated and non-tumour-associated microbiota in colorectal cancer. *Gut* 2017; **66**: 633-643 [PMID: 26992426 DOI: 10.1136/gutjnl-2015-309595]

35 **Coyne MJ**, Roelofs KG, Comstock LE. Type VI secretion systems of human gut Bacteroidales segregate into three genetic architectures, two of which are contained on mobile genetic elements. *BMC Genomics* 2016; **17**: 58 [PMID: 26768901

DOI: 10.1186/s12864-016-2377-z]
36 **Faith JJ**, Guruge JL, Charbonneau M, Subramanian S, Seedorf H, Goodman AL, Clemente JC, Knight R, Heath AC, Leibel RL, Rosenbaum M, Gordon JI. The long-term stability of the human gut microbiota. *Science* 2013; **341**: 1237439 [PMID: 23828941 DOI: 10.1126/science.1237439]
37 **Kurokawa K**, Itoh T, Kuwahara T, Oshima K, Toh H, Toyoda A, Takami H, Morita H, Sharma VK, Srivastava TP, Taylor TD, Noguchi H, Mori H, Ogura Y, Ehrlich DS, Itoh K, Takagi T, Sakaki Y, Hayashi T, Hattori M. Comparative metagenomics revealed commonly enriched gene sets in human gut microbiomes. *DNA Res* 2007; **14**: 169-181 [PMID: 17916580 DOI: 10.1093/dnares/dsm018]
38 **Eckburg PB**, Bik EM, Bernstein CN, Purdom E, Dethlefsen L, Sargent M, Gill SR, Nelson KE, Relman DA. Diversity of the human intestinal microbial flora. *Science* 2005; **308**: 1635-1638 [PMID: 15831718 DOI: 10.1126/science.1110591]
39 **Zitomersky NL**, Coyne MJ, Comstock LE. Longitudinal analysis of the prevalence, maintenance, and IgA response to species of the order Bacteroidales in the human gut. *Infect Immun* 2011; **79**: 2012-2020 [PMID: 21402766 DOI: 10.1128/IAI.01348-10]
40 **Zamani S**, Taslimi R, Sarabi A, Jasemi S, Sechi LA, Feizabadi MM. Enterotoxigenic *Bacteroides fragilis*: A Possible Etiological Candidate for Bacterially-Induced Colorectal Precancerous and Cancerous Lesions. *Front Cell Infect Microbiol* 2019; **9**: 449 [PMID: 32010637 DOI: 10.3389/fcimb.2019.00449]
41 **Saus E**, Iraola-Guzmán S, Willis JR, Brunet-Vega A, Gabaldón T. Microbiome and colorectal cancer: Roles in carcinogenesis and clinical potential. *Mol Aspects Med* 2019; **69**: 93-106 [PMID: 31082399 DOI: 10.1016/j.mam.2019.05.001]
42 **Kaźmierczak-Siedlecka K**, Daca A, Fic M, van de Wetering T, Folwarski M, Makarewicz W. Therapeutic methods of gut microbiota modification in colorectal cancer management - fecal microbiota transplantation, prebiotics, probiotics, and synbiotics. *Gut Microbes* 2020; **11**: 1518-1530 [PMID: 32453670 DOI: 10.1080/19490976.2020.1764309]
43 **Cremonesi E**, Governa V, Garzon JFG, Mele V, Amicarella F, Muraro MG, Trella E, Galati-Fournier V, Oertli D, Däster SR, Droeser RA, Weixler B, Bolli M, Rosso R, Nitsche U, Khanna N, Egli A, Keck S, Slotta-Huspenina J, Terracciano LM, Zajac P, Spagnoli GC, Eppenberger-Castori S, Janssen KP, Borsig L, Iezzi G. Gut microbiota modulate T cell trafficking into human colorectal cancer. *Gut* 2018; **67**: 1984-1994 [PMID: 29437871 DOI: 10.1136/gutjnl-2016-313498]
44 **Niccolai E**, Ricci F, Russo E, Nannini G, Emmi G, Taddei A, Ringressi MN, Melli F, Miloeva M, Cianchi F, Bechi P, Prisco D, Amedei A. The Different Functional Distribution of "Not Effector" T Cells (Treg/Tnull) in Colorectal Cancer. *Front Immunol* 2017; **8**: 1900 [PMID: 29375559 DOI: 10.3389/fimmu.2017.01900]
45 **Lau SK**, Woo PC, Woo GK, Fung AM, Ngan AH, Song Y, Liu C, Summanen P, Finegold SM, Yuen K. Bacteraemia caused by Anaerotruncus colihominis and emended description of the species. *J Clin Pathol* 2006; **59**: 748-752 [PMID: 16467163 DOI: 10.1136/jcp.2005.031773]
46 **Walther-António MR**, Chen J, Multinu F, Hokenstad A, Distad TJ, Cheek EH, Keeney GL, Creedon DJ, Nelson H, Mariani A, Chia N. Potential contribution of the uterine microbiome in the development of endometrial cancer. *Genome Med* 2016; **8**: 122 [PMID: 27884207 DOI: 10.1186/s13073-016-0368-y]
47 **Bailén M**, Bressa C, Martínez-López S, González-Soltero R, Montalvo Lominchar MG, San Juan C, Larrosa M. Microbiota Features Associated With a High-Fat/Low-Fiber Diet in Healthy Adults. *Front Nutr* 2020; **7**: 583608 [PMID: 33392236 DOI: 10.3389/fnut.2020.583608]
48 **Gao Z**, Wu H, Zhang K, Hossen I, Wang J, Wang C, Xu D, Xiao J, Cao Y. Protective effects of grape seed procyanidin extract on intestinal barrier dysfunction induced by a long-term high-fat diet. *J Funct Foods* 2020; **64**: 103663 [DOI: 10.1016/j.jff.2019.103663]
49 **Kong C**, Gao R, Yan X, Huang L, Qin H. Probiotics improve gut microbiota dysbiosis in obese mice fed a high-fat or high-sucrose diet. *Nutrition* 2019; **60**: 175-184 [PMID: 30611080 DOI: 10.1016/j.nut.2018.10.002]
50 **Zhang X**, Coker OO, Chu ES, Fu K, Lau HCH, Wang YX, Chan AWH, Wei H, Yang X, Sung JJY, Yu J. Dietary cholesterol drives fatty liver-associated liver cancer by modulating gut microbiota and metabolites. *Gut* 2021; **70**: 761-774 [PMID: 32694178 DOI: 10.1136/gutjnl-2019-319664]
51 **Downes J**, Vartoukian SR, Dewhirst FE, Izard J, Chen T, Yu WH, Sutcliffe IC, Wade WG. Pyramidobacter piscolens gen. nov., sp. nov., a member of the phylum 'Synergistetes' isolated from the human oral cavity. *Int J Syst Evol Microbiol* 2009; **59**: 972-980 [PMID: 19406777 DOI: 10.1099/ijs.0.000364-0]
52 **Gao Z**, Guo B, Gao R, Zhu Q, Qin H. Microbiota disbiosis is associated with colorectal cancer. *Front Microbiol* 2015; **6**: 20 [PMID: 25699023 DOI: 10.3389/fmicb.2015.00020]
53 **Yazici C**, Wolf PG, Kim H, Cross TL, Vermillion K, Carroll T, Augustus GJ, Mutlu E, Tussing-Humphreys L, Braunschweig C, Xicola RM, Jung B, Llor X, Ellis NA, Gaskins HR. Race-dependent association of sulfidogenic bacteria with colorectal cancer. *Gut* 2017; **66**: 1983-1994 [PMID: 28153960 DOI: 10.1136/gutjnl-2016-313321]
54 **Fang CY**, Chen JS, Hsu BM, Hussain B, Rathod J, Lee KH. Colorectal Cancer Stage-Specific Fecal Bacterial Community Fingerprinting of the Taiwanese Population and Underpinning of Potential Taxonomic Biomarkers. *Microorganisms* 2021; **9** [PMID: 34442626 DOI: 10.3390/microorganisms9081548]
55 **McCann SE**, Hullar MAJ, Tritchler DL, Cortes-Gomez E, Yao S, Davis W, O'Connor T, Erwin D, Thompson LU, Yan L, Lampe JW. Enterolignan Production in a Flaxseed Intervention Study in Postmenopausal US Women of African Ancestry and European Ancestry. *Nutrients* 2021; **13**: 919 [PMID: 33809130 DOI: 10.3390/nu13030919]
56 **Ye F**, Shen H, Li Z, Meng F, Li L, Yang J, Chen Y, Bo X, Zhang X, Ni M. Influence of the Biliary System on Biliary Bacteria Revealed by Bacterial Communities of the Human Biliary and Upper Digestive Tracts. *PLoS One* 2016; **11**: e0150519 [PMID: 26930491 DOI: 10.1371/journal.pone.0150519]
57 **Saab M**, Mestivier D, Sohrabi M, Rodriguez C, Khonsari MR, Faraji A, Sobhani I. Characterization of biliary microbiota dysbiosis in extrahepatic cholangiocarcinoma. *PLoS One* 2021; **16**: e0247798 [PMID: 33690612 DOI: 10.1371/journal.pone.0247798]
58 **Xu Y**, Wang Y, Li H, Dai Y, Chen D, Wang M, Jiang X, Huang Z, Yu H, Huang J, Xiong Z. Altered Fecal Microbiota Composition in Older Adults With Frailty. *Front Cell Infect Microbiol* 2021; **11**: 696186 [PMID: 34485176 DOI: 10.3389/fcimb.2021.696186]

59 **Nakazawa F**, Sato M, Poco SE, Hashimura T, Ikeda T, Kalfas S, Sundqvist G, Hoshino E. Description of Mogibacterium pumilum gen. nov., sp. nov. and Mogibacterium vescum gen. nov., sp. nov., and reclassification of Eubacterium timidum (Holdeman *et al* 1980) as Mogibacterium timidum gen. nov., comb. nov. *Int J Syst Evol Microbiol* 2000; **50** Pt 2: 679-688 [PMID: 10758875 DOI: 10.1099/00207713-50-2-679]

60 **Wang Y**, Zhang C, Hou S, Wu X, Liu J, Wan X. Analyses of Potential Driver and Passenger Bacteria in Human Colorectal Cancer. *Cancer Manag Res* 2020; **12**: 11553-11561 [PMID: 33209059 DOI: 10.2147/CMAR.S275316]

61 **Kogure M**, Suzuki H, Ishiguro S, Ueda A, Nakahara T, Tamai K, Notake S, Shiotani S, Umemoto T, Morishima I, Ueno E. Dialister pneumosintes bacteremia caused by dental caries and sinusitis. *Intern Med* 2015; **54**: 663-667 [PMID: 25786460 DOI: 10.2169/internalmedicine.54.2904]

62 **Sertkaya Z**. Re: Sancar S, Demirci H, Guzelsoy M, et. al. Fear of Circumcision in Boys Considerably Vanishes within Ten Days of Procedure. Urol J. 2016 Mar 5-2541:)1(13;5. *Urol J* 2016; **13**: 2735-2736 [PMID: 27351332]

63 **Yang Y**, Cai Q, Shu XO, Steinwandel MD, Blot WJ, Zheng W, Long J. Prospective study of oral microbiome and colorectal cancer risk in low-income and African American populations. *Int J Cancer* 2019; **144**: 2381-2389 [PMID: 30365870 DOI: 10.1002/ijc.31941]

64 **Rezasoltani S**, Asadzadeh-Aghdaei H, Nazemalhosseini-Mojarad E, Dabiri H, Ghanbari R, Zali MR. Gut microbiota, epigenetic modification and colorectal cancer. *Iran J Microbiol* 2017; **9**: 55-63 [PMID: 29213996]

65 **Tjalsma H**, Boleij A, Marchesi JR, Dutilh BE. A bacterial driver-passenger model for colorectal cancer: beyond the usual suspects. *Nat Rev Microbiol* 2012; **10**: 575-582 [PMID: 22728587 DOI: 10.1038/nrmicro2819]

66 **Kasai C**, Sugimoto K, Moritani I, Tanaka J, Oya Y, Inoue H, Tameda M, Shiraki K, Ito M, Takei Y, Takase K. Comparison of human gut microbiota in control subjects and patients with colorectal carcinoma in adenoma: Terminal restriction fragment length polymorphism and next-generation sequencing analyses. *Oncol Rep* 2016; **35**: 325-333 [PMID: 26549775 DOI: 10.3892/or.2015.4398]

67 **Park SS**, Kim B, Kim MJ, Roh SJ, Park SC, Kim BC, Han KS, Hong CW, Sohn DK, Oh JH. The effect of curative resection on fecal microbiota in patients with colorectal cancer: a prospective pilot study. *Ann Surg Treat Res* 2020; **99**: 44-51 [PMID: 32676481 DOI: 10.4174/astr.2020.99.1.44]

68 **Yang TW**, Lee WH, Tu SJ, Huang WC, Chen HM, Sun TH, Tsai MC, Wang CC, Chen HY, Huang CC, Shiu BH, Yang TL, Huang HT, Chou YP, Chou CH, Huang YR, Sun YR, Liang C, Lin FM, Ho SY, Chen WL, Yang SF, Ueng KC, Huang HD, Huang CN, Jong YJ, Lin CC. Enterotype-based Analysis of Gut Microbiota along the Conventional Adenoma-Carcinoma Colorectal Cancer Pathway. *Sci Rep* 2019; **9**: 10923 [PMID: 31358825 DOI: 10.1038/s41598-019-45588-z]

69 **Xi Y**, Yuefen P, Wei W, Quan Q, Jing Z, Jiamin X, Shuwen H. Analysis of prognosis, genome, microbiome, and microbial metabolome in different sites of colorectal cancer. *J Transl Med* 2019; **17**: 353 [PMID: 31665031 DOI: 10.1186/s12967-019-2102-1]

70 **Lee MS**, Menter DG, Kopetz S. Right Versus Left Colon Cancer Biology: Integrating the Consensus Molecular Subtypes. *J Natl Compr Canc Netw* 2017; **15**: 411-419 [PMID: 28275039 DOI: 10.6004/jnccn.2017.0038]

71 **Flemer B**, Herlihy M, O'Riordain M, Shanahan F, O'Toole PW. Tumour-associated and non-tumour-associated microbiota: Addendum. *Gut Microbes* 2018; **9**: 369-373 [PMID: 29420132 DOI: 10.1080/19490976.2018.1435246]

72 **Temraz S**, Nassar F, Nasr R, Charafeddine M, Mukherji D, Shamseddine A. Gut Microbiome: A Promising Biomarker for Immunotherapy in Colorectal Cancer. *Int J Mol Sci* 2019; **20** [PMID: 31450712 DOI: 10.3390/ijms20174155]

World Journal of Gastroenterology

Submit a Manuscript: https://www.f6publishing.com

World J Gastroenterol 2022 May 14; 28(18): 1965-1980

DOI: 10.3748/wjg.v28.i18.1965

ISSN 1007-9327 (print) ISSN 2219-2840 (online)

ORIGINAL ARTICLE

Basic Study

Effect of ancient Khorasan wheat on gut microbiota, inflammation, and short-chain fatty acid production in patients with fibromyalgia

Simone Baldi, Giuditta Pagliai, Monica Dinu, Leandro Di Gloria, Giulia Nannini, Lavinia Curini, Marco Pallecchi, Edda Russo, Elena Niccolai, Giovanna Danza, Stefano Benedettelli, Giovanna Ballerini, Barbara Colombini, Gianluca Bartolucci, Matteo Ramazzotti, Francesco Sofi, Amedeo Amedei

Specialty type: Nutrition and dietetics

Provenance and peer review: Invited article; Externally peer reviewed.

Peer-review model: Single blind

Peer-review report's scientific quality classification

Grade A (Excellent): 0
Grade B (Very good): B
Grade C (Good): C
Grade D (Fair): D
Grade E (Poor): 0

P-Reviewer: Almeida C, Portugal; Ren JY, China

Received: November 26, 2021
Peer-review started: November 26, 2021
First decision: January 8, 2022
Revised: January 19, 2022
Accepted: March 27, 2022
Article in press: March 27, 2022
Published online: May 14, 2022

Simone Baldi, Giuditta Pagliai, Monica Dinu, Leandro Di Gloria, Giulia Nannini, Lavinia Curini, Edda Russo, Elena Niccolai, Barbara Colombini, Francesco Sofi, Amedeo Amedei, Department of Experimental and Clinical Medicine, University of Florence, Florence 50134, Italy

Giuditta Pagliai, Monica Dinu, Francesco Sofi, Unit of Clinical Nutrition, Careggi University Hospital, Florence 50134, Italy

Marco Pallecchi, Gianluca Bartolucci, Department of Neurosciences, Psychology, Drug Research and Child Health, Section of Pharmaceutical and Nutraceutical Sciences, University of Florence, Sesto Fiorentino 50019, Italy

Giovanna Danza, Matteo Ramazzotti, Department of Biomedical, Experimental and Clinical Sciences "Mario Serio", University of Florence, Florence 50134, Italy

Stefano Benedettelli, Department of Agriculture, Food, Environment and Forestry, University of Florence, Florence 50144, Italy

Giovanna Ballerini, Multidisciplinary Center for Pain Therapy, Reference Center for Fibromyalgia, Piero Palagi Hospital, USL Toscana Centro, Florence 50122, Italy

Amedeo Amedei, SOD of Interdisciplinary Internal Medicine, Careggi University Hospital, Florence 50134, Italy

Corresponding author: Amedeo Amedei, BSc, Reader (Associate Professor), Department of Experimental and Clinical Medicine, University of Florence, Largo Brambilla 3, Florence 50134, Italy. aamedei@unifi.it

Abstract

BACKGROUND

Fibromyalgia (FM) syndrome is mainly characterized by widespread pain, sleeping disorders, fatigue, and cognitive dysfunction. In many cases, gastrointestinal distress is also reported, suggesting the potential pathogenic role of the gut microbiota (GM). The GM is deeply influenced by several environmental factors, especially the diet, and recent findings highlighted significant symptom improvement in FM patients following various nutritional interventions such as vegetarian diet, low-fermentable oligosaccharides, disaccharides,

monosaccharides, and polyols based diets, gluten-free diet, and especially an ancient grain supplementation. In particular, a recent study reported that a replacement diet with ancient Khorasan wheat led to an overall improvement in symptom severity of FM patients.

AIM

To examine the effects of ancient Khorasan wheat on the GM, inflammation, and short-chain fatty acid production in FM patients.

METHODS

After a 2-wk run-in period, 20 FM patients were enrolled in this randomized, double-blind crossover trial. In detail, they were assigned to consume either Khorasan or control wheat products for 8 wk and then, following an 8-wk washout period, crossed. Before and after treatments, GM characterization was performed by 16S rRNA sequencing while the fecal molecular inflammatory response and the short-chain fatty acids (SCFAs) were respectively determined with the Luminex MAGPIX detection system and a mass chromatography-mass spectrometry method.

RESULTS

The Khorasan wheat replacement diet, in comparison with the control wheat diet, had more positive effects on intestinal microbiota composition and on both the fecal immune and SCFAs profiles such as the significant increase of butyric acid levels (P = 0.054), candidatus *Saccharibacteria* (P = 9.95e-06) and *Actinobacteria*, and the reduction of *Enterococcaceae* (P = 4.97e-04). Moreover, the improvement of various FM symptoms along with the variation of some gut bacteria after the Khorasan wheat diet have been documented; in fact we reported positive correlations between *Actinobacteria* and both Tiredness Symptoms Scale (P < 0.001) and Functional Outcome of Sleep Questionnaire (P < 0.05) scores, between *Verrucomicrobiae* and both Widespread Pain Index (WPI) + Symptom Severity scale (SS) (P < 0.05) and WPI (P < 0.05) scores, between candidatus *Saccharibacteria* and SS score (P < 0.05), and between *Bacteroidales* and Sleep-Related and Safety Behaviour Questionnaire score (P < 0.05).

CONCLUSION

The replacement diet based on ancient Khorasan wheat results in beneficial GM compositional and functional modifications that positively correlate with an improvement of FM symptomatology.

Key Words: Fibromialgya; Gut microbiota; Khorasan wheat; Fibromialgya symptoms; Ancient wheat

©The Author(s) 2022. Published by Baishideng Publishing Group Inc. All rights reserved.

Core Tip: Fibromyalgia (FM) syndrome is mainly characterized by widespread pain but in many cases, gastrointestinal distress is also reported, suggesting the potential pathogenic role of the intestinal microbiota. Since gut microbiota is deeply influenced by diet, significant symptom improvement has been reported in FM patients following various nutritional interventions such as vegetarian diet, low-fermentable oligosaccharides, disaccharides, monosaccharides, and polyols based diets, gluten-free diet, and especially an ancient grain based diet. We reported that a replacement diet based on ancient Khorasan wheat, compared to a control wheat diet, resulted in beneficial gut microbiota compositional and functional modifications that positively correlated with an improvement of FM symptomatology.

Citation: Baldi S, Pagliai G, Dinu M, Di Gloria L, Nannini G, Curini L, Pallecchi M, Russo E, Niccolai E, Danza G, Benedettelli S, Ballerini G, Colombini B, Bartolucci G, Ramazzotti M, Sofi F, Amedei A. Effect of ancient Khorasan wheat on gut microbiota, inflammation, and short-chain fatty acid production in patients with fibromyalgia. *World J Gastroenterol* 2022; 28(18): 1965-1980
URL: https://www.wjgnet.com/1007-9327/full/v28/i18/1965.htm
DOI: https://dx.doi.org/10.3748/wjg.v28.i18.1965

INTRODUCTION

Fibromyalgia (FM) is a systemic syndrome of unclear etiology, characterized by widespread pain and tenderness, sleeping disorders, fatigue, and cognitive dysfunction[1]. It has been hypothesized that low-grade systemic inflammation, a preponderance of pro-oxidative state, and an insufficient antioxidant

capability – as demonstrated by the low levels of some minerals and vitamins in FM patients – could contribute to the disease development, by reducing the pain threshold and inducing fatigue and mood disorders[2]. In many cases, gastrointestinal distress is also reported, suggesting a potential involvement of the gut microbiota (GM), as demonstrated by the rather frequent dysbiosis found in FM subjects[3,4].

The GM is a complex ecosystem composed of hundreds of thousands of microorganisms involved in various useful functions that range from the host organism's defense to homeostasis maintenance and the metabolite production, such as short-chain fatty acids (SCFAs) that show anti-inflammatory properties[5]. The GM is deeply influenced by several environmental factors, especially the diet, which seems to be involved also in the FM syndrome. Recent evidence documented a significant symptom improvement in FM patients following various nutritional interventions such as vegetarian diet, low-fermentable oligosaccharides, disaccharides, monosaccharides, and polyols based diets or gluten-free diet[6].

In recent years, the potential health benefits of ancient grains have emerged and we have shown that the consumption of products made with *Triticum turgidum ssp. turanicum* (Khorasan) improves both the inflammatory profile and the gastrointestinal symptoms in different patient groups[7]. Furthermore, our recent study demonstrated that a replacement diet with ancient Khorasan grain led to an overall improvement in symptom severity and sleep pattern of FM patients[8]. However, as far as we know, no studies are available to evaluate the possible beneficial effects of ancient grain consumption on the GM of FM patients. Therefore, the aim of this present study was to examine whether a replacement diet with ancient Khorasan wheat could influence the GM composition, the fecal molecular immune profile, and SCFAs production in patients suffering of fibromyalgia syndrome.

MATERIALS AND METHODS

Study design and participants

Participants were considered eligible for inclusion in this randomized, double-blind crossover trial (Figure 1) if they were aged 18-70 years and had a documented diagnosis of FM. The exclusion criteria were as follows: celiac disease, gluten sensitivity (assessed on the basis of medical evaluation, taking into account both the negative results of blood tests for celiac disease and the absence of celiac symptoms during a diet containing gluten) or wheat allergy, any known organic disease or clinical alarm signs, pregnancy or breast-feeding, and use of probiotics or antibiotics in the past 2 mo.

The experimental wheat used in this study was organic Khorasan wheat (*Triticum turgidum subsp. Turanicum*), KAMUT brand, supplied by Kamut Enterprises of Europe. KAMUT®, a registered trademark of Kamut International, Ltd., and Kamut Enterprises of Europe, bv, guarantees that the wheat is pure ancient Khorasan wheat and is organically grown and processed. The organically cultivated modern variety named "palesio" was used as control wheat.

After a 2-wk run-in period, eligible participants were randomly assigned to consume either Khorasan or control wheat products (500 g/wk of pasta, 150 g/d of bread, 500 g/mo of crackers, and 1 kg/mo of biscuits) for 8 wk and then, following an 8-wk washout period, crossed.

During both intervention periods, all participants were encouraged to maintain their usual eating habits, but they were not allowed to eat other cereal-based products. Instead, during the washout period participants were allowed to eat all foods according to their usual eating habits. In the second intervention period, the group assigned to consume the control grain products in the first intervention period was assigned to consume the Khorasan products, and *vice versa*.

At the beginning and at the end of each intervention period, we collected stool samples, in order to perform GM characterization, SCFAs evaluation, and immunological analysis. The following validated self-administered questionnaires were used for evaluation: Widespread Pain Index (WPI), Symptom Severity scale (SS), FM severity scale (WPI + SS), FM Impact Questionnaire (FIQ), Fatigue Severity Scale (FSS), Tiredness Symptoms Scale (TSS), Sleep-Related and Safety Behaviour Questionnaire (SRSBQ), Restorative Sleep Questionnaire-Daily, and Functional Outcome of Sleep Questionnaire (FOSQ).

In general, as previously reported[8], both interventions resulted in an amelioration of all questionnaires scores; however, a statistically significant decrease in WPI + SS, FOSQ, and FIQ scores was observed only after the Khorasan diet.

The study was approved by the local Ethics Committee "Comitato Etico Regionale per la Sperimentazione Clinica della Regione Toscana, Sezione AREA VASTA CENTRO" (SPE 12.630), and adhered to the principles of the Declaration of Helsinki and the Data Protection Act.

Microbiota characterization

Total DNA was extracted using the DNeasy PowerLyzer PowerSoil Kit (Qiagen, Hilden, Germany) from frozen (-80 °C) stool samples, according to the manufacturer's instructions. Briefly, 0.25 g of stool samples were added to a bead beating tube and homogenized with TissueLyser II for 5 min at 30 Hz. Genomic DNA was captured on a silica membrane in a spin column format, washed, and subsequently eluted. The quality and quantity of extracted DNA were assessed with a Qubit Fluorometer (Thermo Fisher Scientific, Waltham, United States) and then frozen at -20 °C.

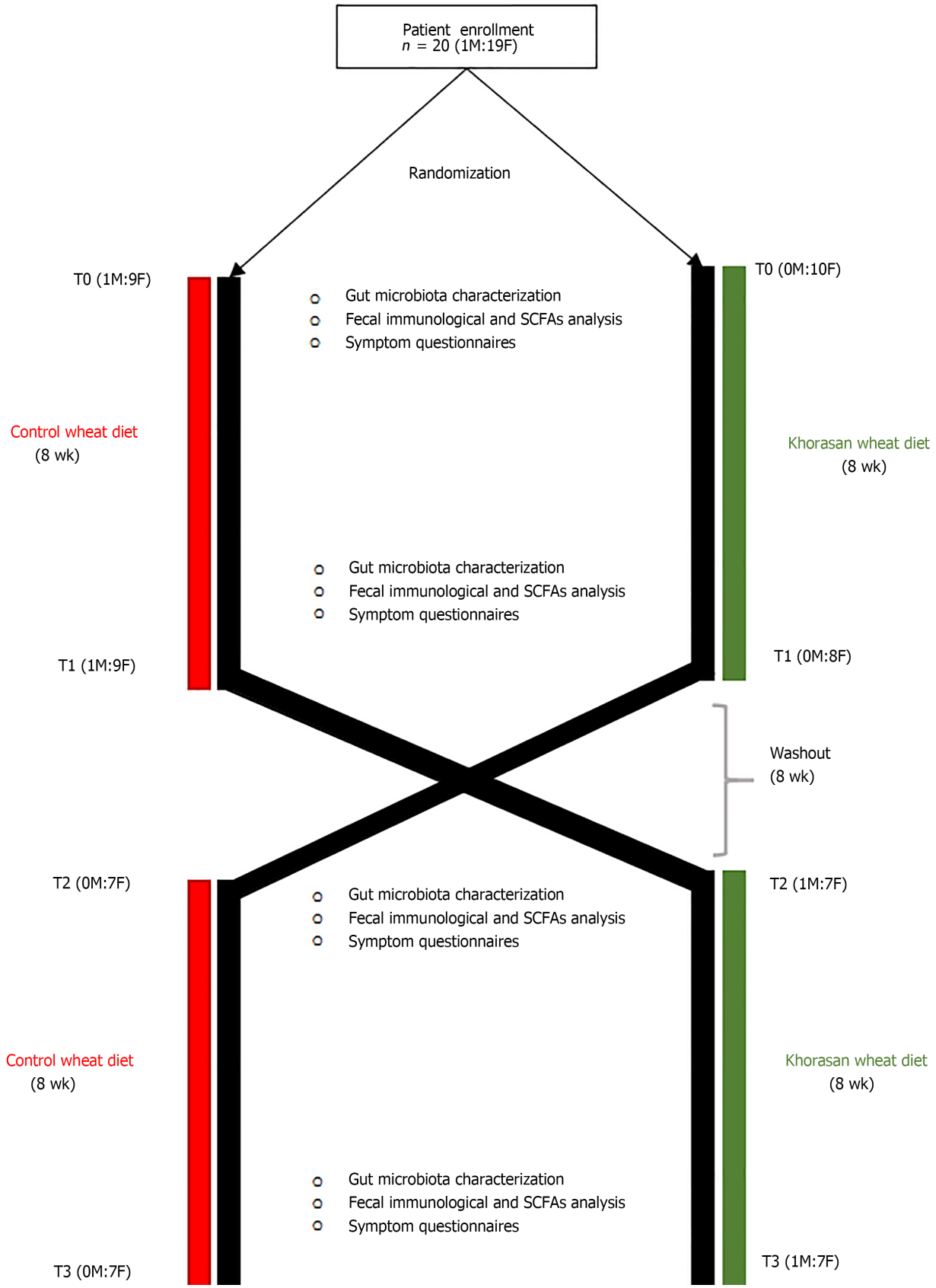


Figure 1 Workflow of the crossover intervention study.

Subsequently, DNA samples were sent to IGA Technology Services (Udine, Italy) where amplicons of the variable V3-V4 region of the bacterial 16S rRNA gene were sequenced by producing paired-end reads (2 × 300 cycles) on the Illumina MiSeq platform, according to the Illumina 16S Metagenomic Sequencing Library Preparation protocol.

Afterwards, the raw data were processed following the software pipeline MICCA (MICrobial Community Analysis) as we previously described[9].

Briefly, paired end reads were assembled, maintaining a minimum overlap of 20 bp and an edit distance in the maximum overlap of 2 bp. Next, the sequences were cut to remove the primers and all the reads having a length lower than 350 bp and with an error rate higher than or equal to 0.5 were removed. The cleaned reads were merged into a single file and transformed into a FASTA file. The operational taxonomic units (OTUs) were generated by setting a 97% identity threshold and performing an automatic removal of chimeras and so the longest sequence of each OTU was used for the taxonomic assignment, *i.e.*, using the Ribosomal Database Project classifier that is able to obtain classification and confidence for taxonomic ranks up to genus.

SCFA determination by gas chromatography-mass spectrometry analysis

The qualitative and quantitative evaluation of fecal SCFAs was performed using the Agilent gas chromatography-mass spectrometry (GC-MS) system composed of a 5971 single quadrupole mass spectrometer, a 5890 gas-chromatograph, and a 7673 autosampler, through our previously described GC-MS method[10].

Just before the analysis, fecal samples were thawed and combined with 10 mM sodium bicarbonate solution (1:1 w/v) in a 1.5 mL centrifuge tube. Then, the obtained suspension was sonicated for 5 min and centrifuged at 5000 rpm for 10 min, and then the supernatant was collected. Finally, SCFAs were extracted as follows: an aliquot of 100 μL of sample solution (corresponding to 0.1 mg of stool sample) was added to 50 μL of internal standards mixture, 1 mL of tert-butyl methyl ether, and 50 μL of 1.0 M HCl solution in a 1.5 mL centrifuge tube. Subsequently, each tube was shaken in a vortex apparatus for 2 min and centrifuged at 10000 rpm for 5 min, and finally the solvent layer was transferred to an autosampler vial and analyzed three times.

Evaluation of fecal molecular inflammatory response

Fecal samples were collected into 1.5 mL centrifuge tubes, added with phosphate-buffer saline w/o calcium w/o magnesium (1:2 w/v), stirred in a vortex apparatus for 2 min, sonicated for 5 min, and then centrifuged at 14000 rpm for 5 min. The supernatants were then transferred in 1.5 mL centrifuge tubes and stored at -20 °C.

The inflammatory response was evaluated through Milliplex custom kit Human Cytokines panel A for Luminex MAGPIX detection system (Affymetrix, eBioscience), following the manufacturers' instructions for supernatants.

In detail, the levels of interleukin (IL)-1α, IL-1β, IL-17A, IL-4, and interferon (IFN)-γ were assessed. Cytokine levels were estimated using a 5-parameter polynomial curve (ProcartaPlex Analyst 1.0) and values under the lower limit of quantitation were considered as 0 pg/mL.

Statistical analysis

Parametric variables are expressed as the mean ± SD whereas non parametric continuous variables are presented as the median and interquartile range. Statistical analyses on the bacterial communities were performed in R using the packages phyloseq 1.26.1, DESeq2 1.22.2, and other packages satisfying their dependencies, in particular, vegan 2.5-5. For the cluster analysis of the entire community, the OTU table was first normalized using the total OTU counts of each sample and then adjusted using square root transformation.

The differential analysis of abundance at the OTUs as well as at different taxonomic ranks (created using the tax_glom function in phyloseq) was performed with DESeq2 using the paired Wilcoxon signed-rank test to compare pre- and post- intervention data. Spearman correlations were performed in R with the package Hmisc 4.5.0, while heatmaps were prepared using the package ggplot2 3.3.5.

Furthermore, GraphPad Prism (v.5) was used for paired statistical analysis of both the fecal molecular inflammatory profile and the SCFA levels before and after each diet.

RESULTS

Characteristics of the study population

Twenty FM patients (1 male and 19 females) with a mean age of 48.9 ± 12.3 years and a mean BMI of 25.30 ± 4.67 kg/m^2 provided written informed consent and were enrolled in this randomized double-blind crossover trial.

As showed in Figure 1, after randomization, ten patients (1M:9F) with a mean age of 51.70 ± 12.93 years and a mean BMI of 25.66 ± 5.59 kg/m^2 were assigned to consume control wheat products while the other ten patients (0M:10F) with a mean age of 46.20 ± 11.52 years and a mean BMI of 24.95 ± 3.81 kg/m^2 were assigned to consume Khorasan wheat products. Subsequently, after the washout period, the intervention groups were crossed and, because of the retirement of five subjects, seven patients (0M:7F) consumed control wheat products and eight patients (1M:7F) consumed Khorasan wheat

products.

Effects of dietary interventions on gut microbiota composition

First of all, aiming to examine the impact of both a control wheat diet (CD) [pre- (CD_0) and post- (CD_1)] and Khorasan wheat diet (KD) [pre- (KD_0) and post- (KD_1)] on the GM composition, we performed the analysis of alpha diversity; however, no significant differences were reported for Shannon index, Chao1 index, or Evenness (data not shown).

Taxonomic analysis, detailed in Table 1, revealed the presence of 14 phyla (> 99% reads), 24 classes (> 99% reads), 35 orders (> 98% of reads), 60 families (> 94% reads), and 142 genera (> 84% reads).

Furthermore, the cluster analysis and the principal coordinate analysis computed using the Bray-Curtis dissimilarity metric did not highlight any clear separation between the pre- and post-CD groups or the pre- and post-KD groups at the phylum level (Figure 2), neither to other taxonomic ranks.

Subsequently, in order to evaluate the impact of both the dietary interventions on microbial abundances, we performed differential analysis at all taxonomic ranks.

In detail, among taxonomic levels, no significant changes were observed except for genus level; in particular, as shown in Figure 3, CD resulted in a significant increase in the abundance of Turicibacter spp. (shrinked FC = 0.969, P = 0.014).

Evaluation of fecal SCFAs profiles before and after dietary interventions

We analyzed the abundances of fecal SCFAs (acetic, propionic, butyric, isobutyric, isovaleric 2-methyl-butyric, and valeric acids) before and after both diets and no influence on their amounts was found after CD or KD (Table 2).

Since these analyses could be in part influenced by the total amount of each SCFA, we repeated the same comparisons on the SCFA percentage compositions and no statistically significant differences were found.

Analysis of fecal molecular inflammatory profile before and after dietary interventions

We evaluated the levels of fecal cytokines (IFN-γ, IL-1α, IL-1β, IL-4, and IL-17A) before and after both dietary interventions (Table 3) and we found that CD only resulted in a significant increase in IL-4 (P = 0.041) while no statistical differences were found after the KD (Figure 4).

Evaluation of impact of dietary interventions on gut microbiota excluding the washout period

Finally, in order to evaluate the impact of both dietary interventions on GM composition excluding eventual "carry-over effects", we focused on each single arm of both KD and CD.

In particular, at the end of the KD first arm (KDT_1), we found a significant increase in members of the phyla candidatus *Saccharibacteria* (log2FC = 2.679, P = 9.95e-06) and *Actinobacteria* (log2FC = 1.384, P = 9.63e-05) (Figure 5A), while at the end of the KD second arm (KDT_3), a reduction of *Enterococcaceae* (log2FC = -4.829, P = 4.97e-04) was reported (Figure 5B).

On the other hand, at the end of the CD first arm (CDT_1), we reported a significant reduction of *Bacteroidales* members (log2FC = -0.916, P = 0.002) (Figure 5C) while the CD second arm (CDT_3) resulted in significantly higher levels of the order *Erysipelotrichales* (log2FC = 1.342, P = 2.03e-5) and the class *Verrucomicrobiae* (log2FC = 1.975, P = 0.005) (Figure 5D).

Fecal SCFA assessment excluding the washout period

The analysis of the fecal SCFAs concentrations displayed an almost significant increase of butyric acid levels (P = 0.054) (Figure 6) at the end of the KDT_1, while no differences were reported after the KDT_3 and after both the CDT_1 and CDT_3.

Evaluation of fecal molecular inflammatory profile excluding the washout period

The assessment of the fecal cytokines concentration excluding eventual "carry-over effects" displayed that the CDT_3 resulted in a significant increase of IL-1β levels (P = 0.031), whereas no significant differences were found at the end of the CDT_1 or at the end of both the KDT_1 and KDT_3 (Figure 7).

Correlation between gut microbiota composition and questionnaire scores

To examine the association between statistically different taxa (post/pre-intervention) and the results of the questionnaire scores (post/pre-intervention), we conducted Spearman correlation for each diet (Figure 8).

In detail, a positive correlation between the phylum *Actinobacteria* and both TSS (P < 0.001) and FOSQ (P < 0.05) scores and between the class *Verrucomicrobiae* and both WPI + SS (P < 0.05) and WPI (P < 0.05) scores was reported in patients following KD. Moreover, a positive correlation between the phylum candidatus *Saccharibacteria* and SS score (P < 0.05) and between the order *Bacteroidales* and SRSBQ score (P < 0.05) was reported after KD. On the other hand, we documented a negative correlation between *Bacteroidales* and FSS score (P < 0.05) and between *Enteococcaceae* and WPI score (P < 0.05).

Table 1 Summary of taxonomic analysis of obtained operational taxonomic units

Rank	Count	Reads	Reads %	OTU	OTU %
Phylum	14	1842915	99.78942	946	94.97992
Class	24	1828920	99.03162	911	91.46586
Order	35	1826444	98.89755	903	90.66265
Family	60	1745260	94.50164	773	77.61044
Genus	142	1568830	84.94838	447	44.87952

OTU: Operational taxonomic unit.

Table 2 Short-chain fatty acid variations according to the provided diet

SCFAs (μmol/g)	CD_0	CD_1	*P* value	KD_0	KD_1	*P* value
Acetic acid	24.04 ± 19.34	27.21 ± 20.69	0.463	24.07 ± 19.75	26.77 ± 14.91	0.431
Propionic acid	6.81 ± 4.86	6.68 ± 5.16	0.939	6.02 ± 6.31	8.43 ± 5.73	0.891
Butyric acid	4.49 ± 9.51	6.15 ± 6.67	0.375	4.29 ± 6.61	5.43 ± 8.34	0.403
Isobutyric acid	0.91 ± 0.50	0.84 ± 0.91	0.82	0.87 ± 0.88	0.90 ± 0.51	0.547
2-Methylbutyric acid	0.62 ± 0.39	0.54 ± 0.65	0.899	0.41 ± 0.52	0.48 ± 0.34	0.174
Isovaleric acid	0.76 ± 0.32	0.69 ± 0.80	0.705	0.58 ± 0.61	0.57 ± 0.29	0.579
Valeric acid	0.94 ± 0.84	1.31 ± 1.07	0.82	0.52 ± 1.69	1.18 ± 1.49	0.352
Total	38.53 ± 33.26	44.35 ± 40.98	0.596	45.32 ± 29.69	44.62 ± 33.69	0.403

Data are presented as the median (interquartile range). *P* values were calculated using the Wilcoxon signed-rank test. CD_0: Pre-control wheat diet; CD_1: Post-control wheat diet; KD_0: Pre-Khorasan wheat diet; KD_1: Post-Khorasan wheat diet.

Table 3 Interleukins variations according to the provided diet

ILs (pg/mL)	CD_0	CD_1	*P* value	KD_0	KD_1	*P* value
IFN-γ	19.00 ± 28.35	22.67 ± 125.37	0.141	15.22 ± 10.43	15.76 ± 29.06	0.205
IL-1α	1958.84 ± 2650.46	2291.12 ± 3412.85	0.171	933.79 ± 1516.38	1683.52 ± 2538.99	0.187
IL-1β	136.84 ± 123.32	167.83 ± 157.13	0.171	127.99 ± 68.04	123.09 ± 100.29	0.485
IL-4	2.39 ± 5.31	2.64 ± 11.61	0.041	2.49 ± 1.76	2.04 ± 3.77	0.205
IL-17A	17.36 ± 20.39	29.67 ± 50.38	0.155	23.67 ± 12.83	26.03 ± 41.11	0.979

Data are showed as the median (interquartile range). *P* values were calculated using the Wilcoxon signed-rank test. IFN: Interferon; IL: Interleukin; CD_0: Pre-control wheat diet; CD_1: Post-control wheat diet; KD_0: Pre-Khorasan wheat diet; KD_1: Post-Khorasan wheat diet.

In addition, regarding the patients who underwent CD intervention, negative correlations were found between *Actinobacteria* and WPI + SS score ($P < 0.05$) and between *Erysipelothichales* and FSS score ($P < 0.05$).

DISCUSSION

Different nutritional interventions provide benefits in fibromyalgia management[11], and we recently demonstrated that the replacement diet with ancient Khorasan wheat led to an overall improvement in symptom severity and sleep pattern of FM patients[8].

Currently, the relationship between FM syndrome and irritable bowel disease has been confirmed but the link between gut dysbiosis and FM is still poorly understood[4]. Furthermore, it has been documented that the worsening causes for the distinctive musculoskeletal pain associated with FM have

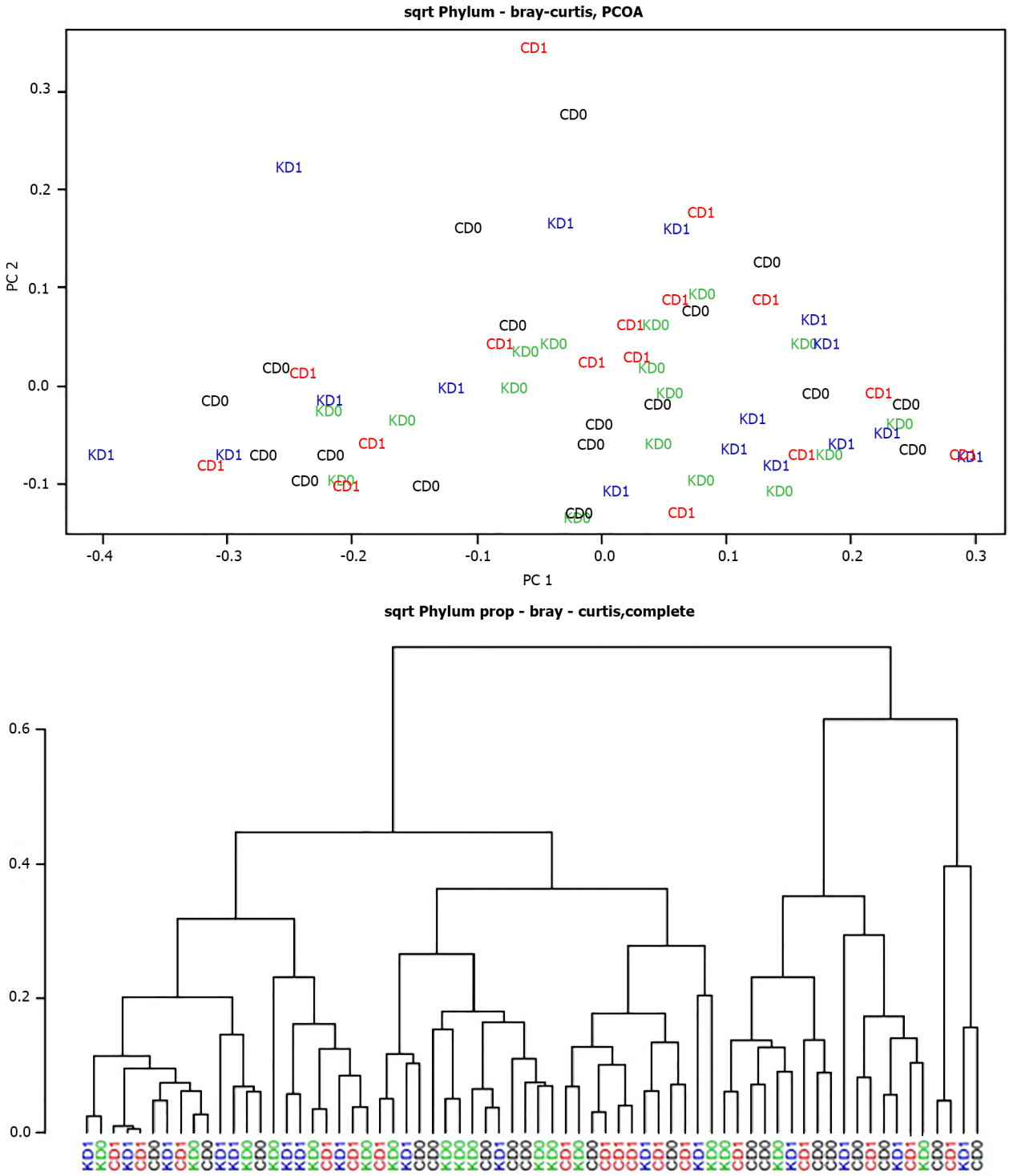


Figure 2 Cluster analysis and principal coordinate analysis of pre- and post-control-wheat-diet samples and pre- and post-Khorasan-wheat-diet samples. A: Cluster analysis; B: Principal coordinate analysis. CD_0: Pre-control wheat diet; CD_1: Post-control wheat diet; KD_0: Pre-Khorasan wheat diet; KD_1: Post-Khorasan wheat diet.

been related to obesity and unhealthy diet[12,13].

Since the whole Khorasan-based diet seems to favor an healthy microbiota[14], the goal of our study was to examine, for the first time, its effects in FM patients.

In detail, we performed a randomized, double blind crossover trial where enrolled FM patients consumed control wheat products or Khorasan wheat products for 8 wk and then crossed.

Then we analyzed the effects of the diets on GM composition, the fecal SCFAs levels, the intestinal inflammatory profile, and symptom improvement in FM patients.

First, concerning the fecal microbiota analysis of FM patients, we found that both 8-wk interventions did not significantly modify either the microbial composition and diversity or the SCFAs levels. Whereas, looking at the changes in microbial abundances produced by each dietary intervention, KD

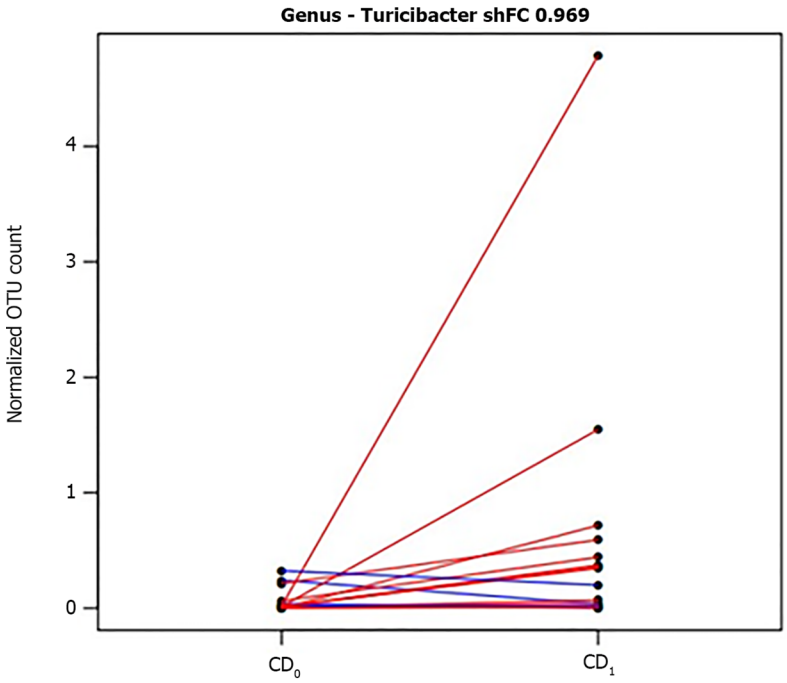


Figure 3 Segment plot showing significantly different taxa between pre- and post-control diet. Lines link paired samples and red or blue colors respectively highlight the increase or decrease of normalized abundance for the indicated rank. Plot title reports shrinked fold change (according to the DESeq2 function lfcShrink) between pre- and post-control-wheat-diet samples. CD_0: Pre-control wheat diet; CD_1: Post-control wheat diet.

did not result in modifications at any taxonomic level; instead, CD was associated with a significant increase of *Turicibacter spp*.

Previous studies documented that the abundance of the genus *Turicibacter* was markedly reduced in mice with high fat feeding[15,16] and recent findings reported its negative correlation with body fat[17, 18]. In addition, Zhong *et al*[19] found a positive correlation between *Turicibacter spp*. and butyric acid, an SCFA famous for its anti-inflammatory properties; hence, CD seems to exert a slight beneficial effect on FM patients.

In addition, the evaluation of the fecal molecular inflammatory profile showed that CD resulted in an increased level of the anti-inflammatory IL-4, while no significant differences were reported after KD.

In contrast, current evidence suggests that, compared to healthy controls, FM patients showed lower plasma levels of IL-4[20,21]. Nevertheless, given its demonstrated role in the transcription enhancement of opioid receptors, a lower IL-4 abundance could be associated with an increase in pain perception[22].

Anyway, in general, both 8-wk dietary interventions displayed modest effects on GM composition and metabolic function (SCFAs) and on the fecal cytokine profile of FM patients.

Nonetheless, our findings are consistent with other previous studies[23,24] which demonstrated the remarkable stability, resilience, and inter-individual variability of the GM in response to short-term dietary modifications.

Finally, although our cross-over study, as it usually is, typically contains a washout period to exclude the repercussion of the modifications (carry-over effect) of one intervention phase on subsequent[25], given that we did not have the possibility to supervise FM patients in the meantime, we repeated all of the analysis at the end of each intervention arm.

Interestingly, the subjects included in the first KD arm, before the unrestricted washout period diet, reported a significant increase of the phyla candidatus *Saccharibacteria* and *Actinobacteria* phyla and a significantly higher abundance of butyric acid.

As previously demonstrated, the *Saccharibacteria* members colonize the human oral cavity and are associated with oral mucosal infectious diseases[26]. However, most members of the *Saccharibacteria* phylum remain uncultivable and no in-depth metabolic analysis of these bacteria is yet available; hence, their potential role in the microbial community has not been fully elucidated[27].

On the other hand, *Actinobacteria*, which play a key role in the maintenance of gut homeostasis by producing SCFAs and modulating the immune response, were reduced in a cohort of FM patients[28, 29].

Concerning the increase of fecal butyric acid abundance after the first KD arm, a recent study reported that FM patients showed lower levels of butyrate-producing bacteria, such as many members of the *Lachnospiraceae* family, than healthy subjects[30]. In addition, comparing the effect of a Kamut-based diet *vs* a modern wheat-based diet in healthy subjects, Saa and colleagues reported that the concentration of butyrate and its esters in stool and urine samples were increased after the Kamut-diet [31].

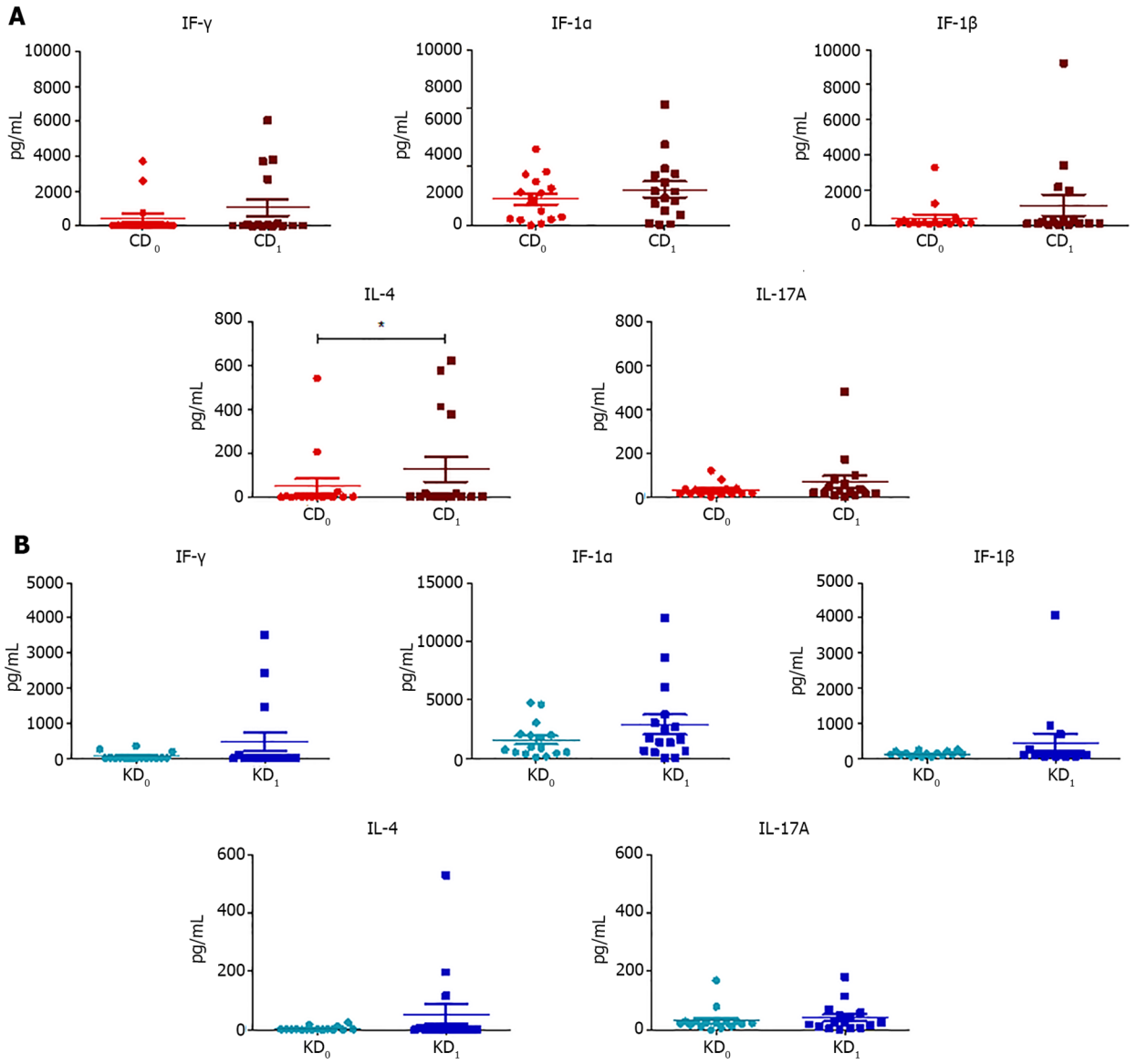


Figure 4 Scatter plots representing the fecal concentrations of interferon-γ, interleukin-1α, interleukin-1β, interleukin-4, and interleukin-17A evaluated before and after control wheat diet and before and after Khorasan wheat diet. A: Before and after control wheat diet; B: Before and after Khorasan wheat diet. Analyses were assessed using the paired Wilcoxon signed-rank test and *P* values less than 0.05 were considered statistically significant. [a] *P* < 0.05, [b]*P* < 0.01, [c]*P* < 0.001. CD_0: Pre-control wheat diet; CD_1: Post-control wheat diet; KD_0: Pre-Khorasan wheat diet; KD_1: Post-Khorasan wheat diet; IL: Interleukin.

Butyric acid, which is secreted by the GM and absorbed in the blood stream, exerts anti-inflammatory effects and induces naive T cell differentiation into regulatory T cells (Tregs)[30]. Furthermore, it acts as a potent histone deacetylase inhibitor, thus exerting analgesic and antidepressant effects[32,33]. In addition, reports suggest that butyric acid improves pain behaviors in models of nerve injury-induced pain and ameliorates neuropathic pain by acting directly on the peripheral nerve system[34,35].

The KDT_3 only resulted in a significant reduction of the *Enterococcaceae* family, whose members were instead over-represented in patients with chronic fatigue syndrome[36].

Given these different findings between the two arms of KD interventions, the possible carry-over effects of the washout period or of the CD intervention cannot be excluded.

In contrast, at the end of the CDT_1, we found a significant decrease of *Bacteroidales* members; a reduction of this order was strongly associated with different disorders, especially in Crohn's disease [37].

On the other hand, the CDT_2 was surprisingly associated with a significant increase of the order *Erysipelotrichales* and the class *Verrucomicrobiae*, which have been respectively associated with irritable bowel syndrome and chronic pain severity[38,39].

Moreover, the CDT_3 showed a significant increase of IL-1β, a potent pro-inflammatory cytokine that acts on nociceptors and results in an improvement in the transduction of pain through various ion channels. But, the IL-1β overexpression is also involved in many autoimmune disorders featuring pain such as inflammatory bowel disease, multiple sclerosis, and rheumatoid arthritis[40,41].

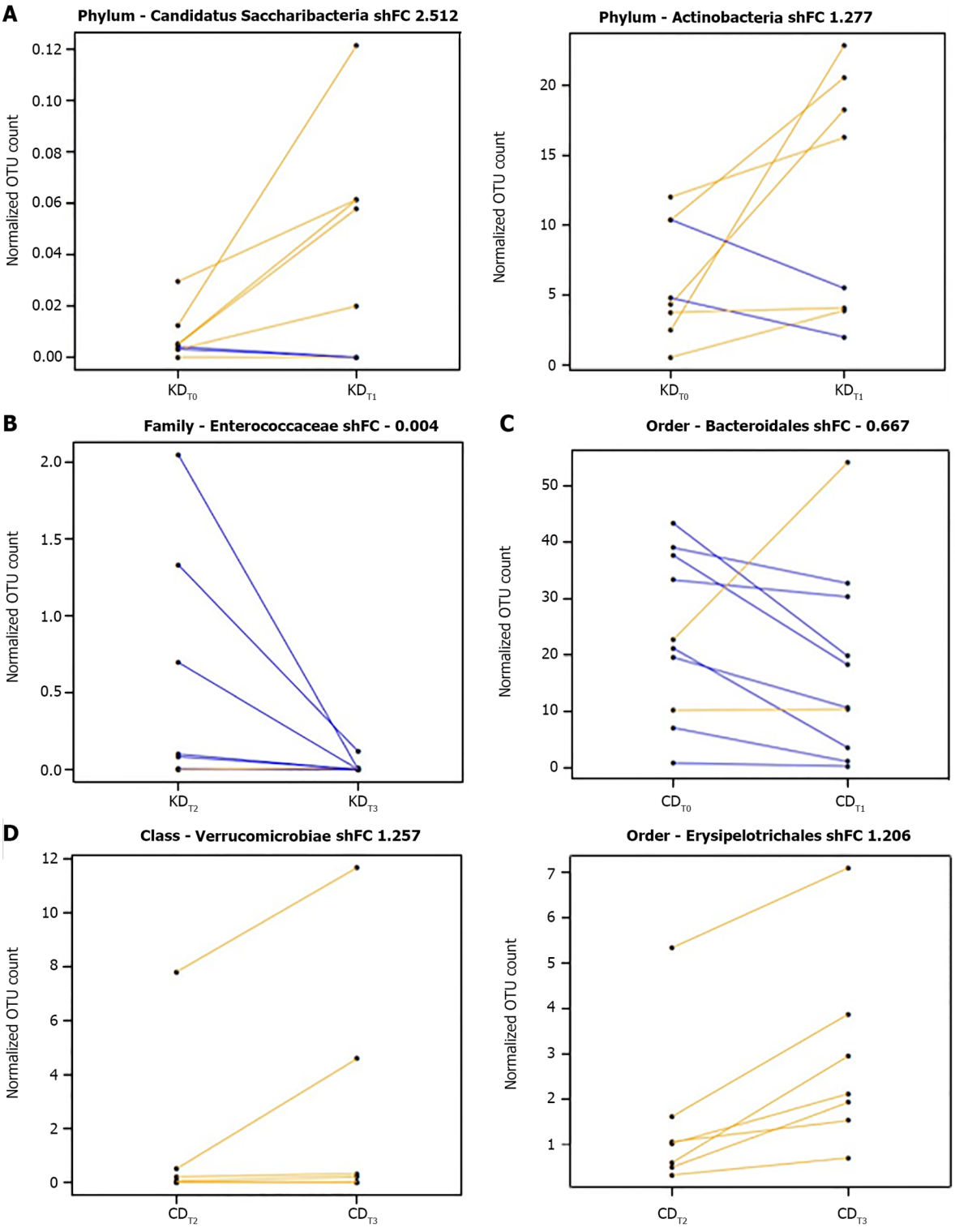


Figure 5 Segment plots showing significantly different taxa during the first arm or the second arm of the Khorasan wheat intervention and over the first arm or the second arm of the control wheat intervention. A: The first arm of the Khorasan wheat intervention; B: The second arm of the Khorasan wheat intervention; C: The first arm of the control wheat intervention; D: The second arm of the control wheat intervention. Lines link paired samples and yellow or blue colors respectively highlight the increase or decrease of normalized abundance for the indicated rank. Plot title reports Shrinked fold change (according to the DESeq2 function lfcShrink) between pre- and post-diet groups included in the two arms of either Khorasan wheat or control wheat interventions. CDT_0: Pre-control-wheat-diet first arm; CDT_1: Post-control-wheat-diet first arm; CDT_2: Pre-control-wheat-diet second arm; CDT_3: Post-control-wheat-diet second arm; KDT_0: Pre-Khorasan-wheat-diet first arm; KDT_1: Post-Khorasan-wheat-diet first arm; KDT_2: Pre-Khorasan-wheat-diet second arm; KDT_3: Post-Khorasan-wheat-diet second arm.

In addition, several studies have shown increased levels of IL-1β in FM patients compared to healthy controls, suggesting an association between IL-1β and some FM symptoms such as hyperalgesia, fatigue, sleep disorders, cognitive dysfunctions, and stress[42,43].

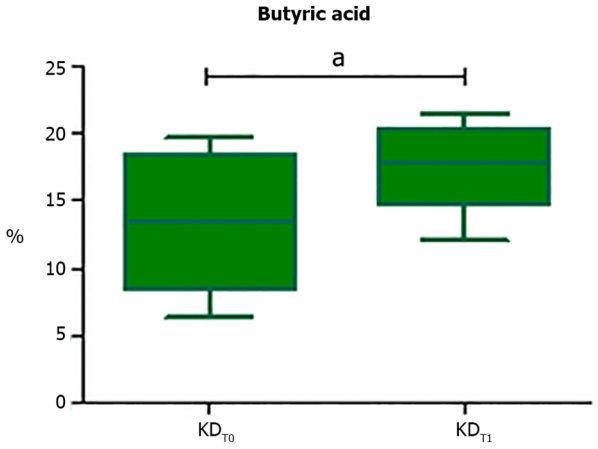


Figure 6 Box plot reporting statistically significant different butyric acid contents at the end of the Khorasan-wheat-diet first arm. Analyses were assessed using the paired Wilcoxon signed-rank test and *P* values less than 0.05 were considered statistically significant. $^{a}P < 0.05$, $^{b}P < 0.01$, $^{c}P < 0.001$. KDT$_0$: Pre-Khorasan-wheat-diet first arm; KDT$_1$: Post-Khorasan-wheat-diet first arm.

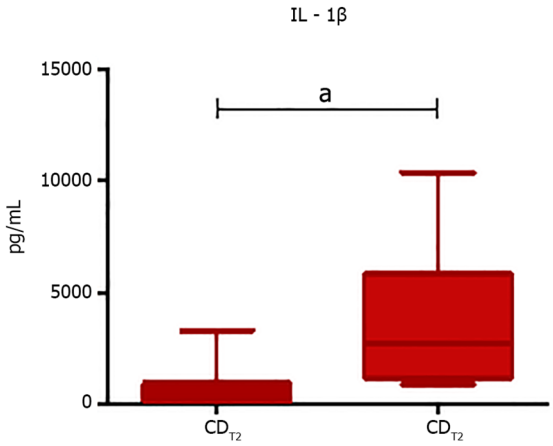


Figure 7 Box plot representing statistically significant different IL-1β levels at the end of the second control wheat diet arm. Analyses were assessed using the paired Wilcoxon signed-rank test and *P* values less than 0.05 were considered statistically significant. $^{a}P < 0.05$, $^{b}P < 0.01$, $^{c}P < 0.001$. IL: Interleukin; CDT$_2$: Pre-control-wheat-diet second arm; CDT$_3$: Post-control-wheat-diet second arm.

Finally, to evaluate the association between GM composition and FM symptoms, we performed Spearman correlations between the self-administered questionnaires and the differentially abundant taxa before and after both diets.

In detail, after KD, FM patients reported a positive association between an increasing abundance of *Actinobacteria* and the improvement of the TSS and FOSQ scores. In addition, we documented a positive correlation between the phylum candidatus *Saccharibacteria* and SS scores and a negative association between a reduced abundance of *Enterococcaceae* and an improved WPI score.

On the contrary, FM patients in the CD intervention reported a detrimental negative correlation between increasing *Erysipelothichales* and the amelioration of FSS score.

A significant relationship between the differential abundances of several gut bacteria and FM symptom indices such as pain intensity, WPI score, cognitive deficits, and fatigue was reported by Minerbi *et al*[44]. Moreover, Clos-Garcia *et al*[29] showed a correlation between some genera and FM pain indicators. Finally, several studies suggest that increased reactive oxygen species in FM patients, resulting in impaired mitochondrial function and reduced ATP in muscle and neural cells, might lead to chronic widespread pain in these patients[45]. Therefore, the improvement of various FM symptoms along with the variation of some gut bacteria after the KD intervention could be related to the reported antioxidant effects of the ancient Khorasan wheat[46].

Despite our present study having some limitations such as the limited number of enrolled patients, the low taxonomical resolution of 16S rRNA sequencing, the short period of dietary administrations, and the lack of patients' supervision during the washout period, our study suggest that a replacement diet with Khorasan wheat products improves the symptoms of patients with fibromyalgia.

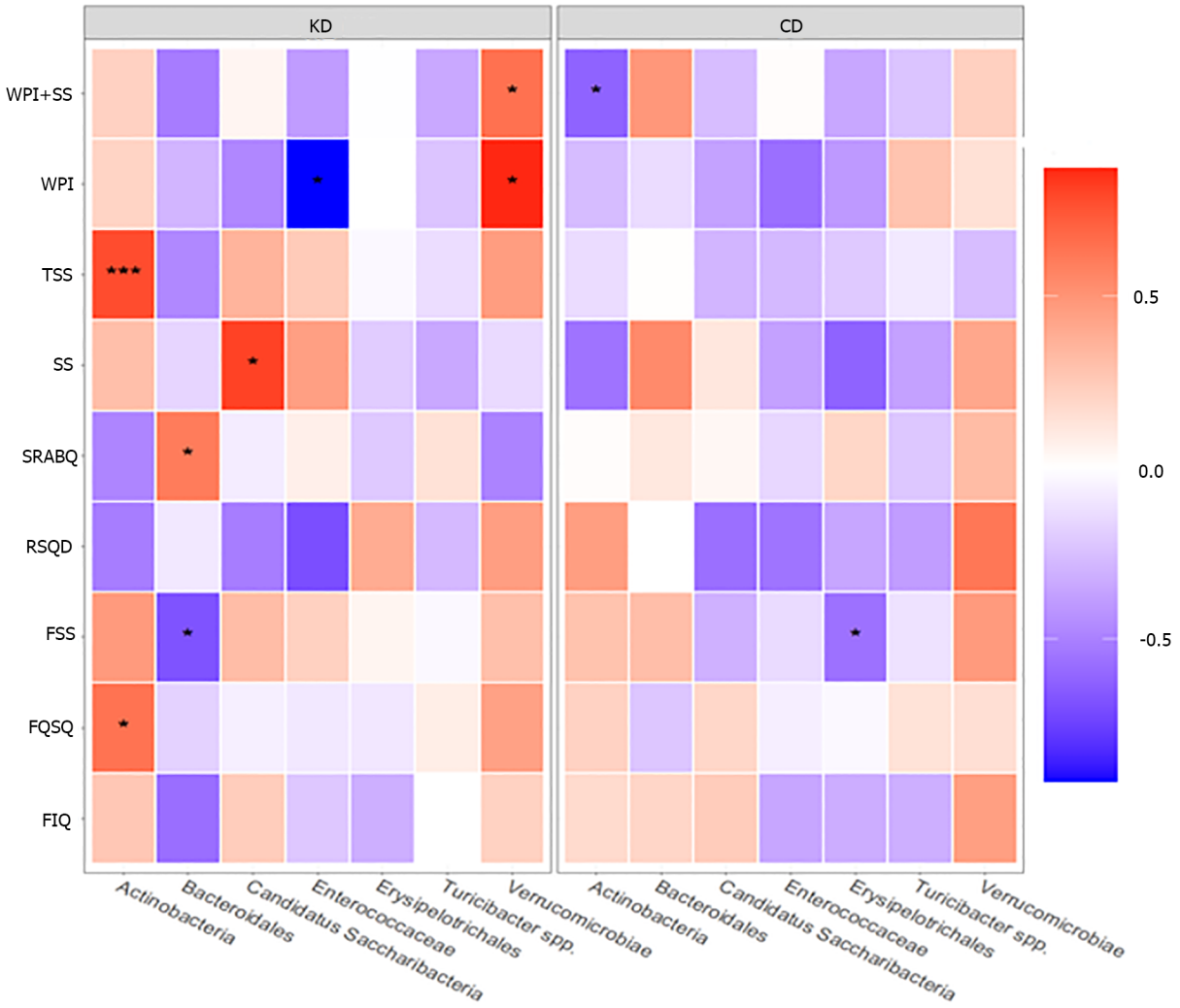


Figure 8 Heatmap of Spearman correlations between statistically significant different taxa (post-pre) and changes in questionnaire scores (post-pre), according to the Khorasan wheat diet or control wheat diet. Red shades indicate positive correlations, whereas blue shades indicate negative correlations; the intensity of colors represents the degree of association. *P* values less than 0.05 were considered statistically significant. [a]*P* < 0.05, [b]*P* < 0.01, [c]*P* < 0.001. KD: Khorasan wheat diet; CD: Control wheat diet.

CONCLUSION

In conclusion, although further studies with a long-term administration of Khorasan wheat products in high numbers of FM patients are necessary, we demonstrated for the first time that an ancient Khorasan wheat diet results in some beneficial GM compositional and functional modifications that positively correlate with an improvement of fibromyalgia symptomatology.

ARTICLE HIGHLIGHTS

Research background

Fibromyalgia (FM) is a syndrome characterized by widespread pain, sleeping disorders, fatigue, and cognitive dysfunction. Frequently, gastrointestinal distress is also reported, suggesting the potential pathogenic role of the gut microbiota (GM).

Research motivation

The GM is deeply influenced by several factors, including diet, and recent findings highlighted a significant symptom improvement in FM patients following various nutritional interventions such as vegetarian diet, low-fermentable oligosaccharides, disaccharides, monosaccharides, and polyols based diets, gluten-free diet, and an ancient grain supplementation. Therefore, a replacement diet with ancient Khorasan grain could improve FM symptomatology.

Research objectives

The main objective of our study was to examine the effects of ancient Khorasan wheat on GM composition, fecal molecular immune profile, and short-chain fatty acids (SCFAs) production in FM patients.

Research methods

In this randomized, double-blind crossover trial, 20 FM patients were randomly assigned to consume either Khorasan or control wheat products for 8 wk and then, after an 8-wk washout period, crossed. At the beginning and at the end of each intervention period, symptom questionnaires and stool samples were collected and GM characterization was performed by 16S rRNA sequencing, while the fecal molecular inflammatory response and the SCFAs were respectively determined with a Luminex MAGPIX detection system and a mass chromatography-mass spectrometry method.

Research results

The Khorasan wheat replacement diet exhibited positive effects on GM composition and on both the fecal immune and SCFAs profiles. Moreover, we documented the improvement of various FM symptoms along with the variation of some gut bacteria after the Khorasan wheat diet.

Research conclusions

An ancient Khorasan wheat diet represents a good strategy to result in positive GM compositional and functional modifications that positively correlate with an improvement of FM symptomatology.

Research perspectives

We demonstrated that a replacement diet based on ancient Khorasan wheat seems to represent a non-invasive successful strategy to ameliorate FM patient's symptomatology. We believe that our data will be a starting point for future studies on FM, especially with a long-term administration of Khorasan wheat products in high numbers of FM patients.

FOOTNOTES

Author contributions: Baldi S and Pagliai G contributed equally to writing the manuscript; Baldi S, Pagliai G, Dinu M, and Russo E contributed to paper conceptualization and design; Baldi S, Pagliai G, Dinu M, Ramazzotti M, Bartolucci G, Pallecchi M, Di Gloria L, Curini L, Nannini G, Niccolai E, and Russo E performed the research analysis; Amedei A, Sofi F, Ramazzotti M, Bartolucci G, Danza G, Ballerini G, Colombini B, and Benedettelli S critically revised the paper; Amedei A and Sofi F equally coordinated and supervised the research. All authors read and approved the final version of the manuscript.

Supported by a grant from Kamut Enterprises of Europe, Oudenaarde, Belgium.

Institutional review board statement: The study was approved by the local ethics committee "Comitato Etico Regionale per la Sperimentazione Clinica della Regione Toscana, Sezione AREA VASTA CENTRO" (SPE 12.630), and adhered to the principles of the Declaration of Helsinki and the Data Protection Act.

Informed consent statement: Informed written consent was obtained from the patients for publication of this report and any accompanying images.

Conflict-of-interest statement: The authors declare no competing interests for this article.

Data sharing statement: No additional data are available.

Open-Access: This article is an open-access article that was selected by an in-house editor and fully peer-reviewed by external reviewers. It is distributed in accordance with the Creative Commons Attribution NonCommercial (CC BY-NC 4.0) license, which permits others to distribute, remix, adapt, build upon this work non-commercially, and license their derivative works on different terms, provided the original work is properly cited and the use is non-commercial. See: https://creativecommons.org/Licenses/by-nc/4.0/

Country/Territory of origin: Italy

ORCID number: Simone Baldi 0000-0002-5151-2618; Giuditta Pagliai 0000-0002-2177-2857; Monica Dinu 0000-0003-1687-2527; Leandro Di Gloria 0000-0002-8630-8166; Giulia Nannini 0000-0002-6481-6864; Lavinia Curini 0000-0002-7437-7789; Marco Pallecchi 0000-0002-0057-6531; Edda Russo 0000-0003-3141-1091; Elena Niccolai 0000-0002-9205-8079; Giovanna Danza 0000-0002-0320-3167; Stefano Benedettelli 0000-0002-6035-1801; Giovanna Ballerini 0000-0003-0963-3018; Barbara Colombini 0000-0003-1397-9791; Gianluca Bartolucci 0000-0002-5631-8769; Matteo Ramazzotti 0000-0002-6862-9409; Francesco Sofi 0000-0001-7113-7424; Amedeo Amedei 0000-0002-6797-9343.

S-Editor: Zhang H
L-Editor: Wang TQ
P-Editor: Cai YX

REFERENCES

1 **Littlejohn G**, Guymer E. Key milestones contributing to the understanding of the mechanisms underlying fibromyalgia. *Biomedicines* 2020; **8** [PMID: 32709082 DOI: 10.3390/biomedicines8070223]
2 **Banfi G**, Diani M, Pigatto PD, Reali E. T cell subpopulations in the physiopathology of fibromyalgia: evidence and perspectives. *Int J Mol Sci* 2020; **21** [PMID: 32054062 DOI: 10.3390/ijms21041186]
3 **Malatji BG**, Mason S, Mienie LJ, Wevers RA, Meyer H, van Reenen M, Reinecke CJ. The GC-MS metabolomics signature in patients with fibromyalgia syndrome directs to dysbiosis as an aspect contributing factor of FMS pathophysiology. *Metabolomics* 2019; **15**: 54 [PMID: 30919098 DOI: 10.1007/s11306-019-1513-6]
4 **Erdrich S**, Hawrelak JA, Myers SP, Harnett JE. Determining the association between fibromyalgia, the gut microbiome and its biomarkers: a systematic review. *BMC Musculoskelet Disord* 2020; **21**: 181 [PMID: 32192466 DOI: 10.1186/s12891-020-03201-9]
5 **Thursby E**, Juge N. Introduction to the human gut microbiota. *Biochem J* 2017; **474**: 1823-1836 [PMID: 28512250 DOI: 10.1042/BCJ20160510]
6 **Silva AR**, Bernardo A, Costa J, Cardoso A, Santos P, de Mesquita MF, Vaz Patto J, Moreira P, Silva ML, Padrão P. Dietary interventions in fibromyalgia: a systematic review. *Ann Med* 2019; **51**: 2-14 [PMID: 30735059 DOI: 10.1080/07853890.2018.1564360]
7 **Sofi F**, Whittaker A, Gori AM, Cesari F, Surrenti E, Abbate R, Gensini GF, Benedettelli S, Casini A. Effect of Triticum turgidum subsp. turanicum wheat on irritable bowel syndrome: a double-blinded randomised dietary intervention trial. *Br J Nutr* 2014; **111**: 1992-1999 [PMID: 24521561 DOI: 10.1017/S000711451400018X]
8 **Pagliai G**, Colombini B, Dinu M, Whittaker A, Masoni A, Danza G, Amedei A, Ballerini G, Benedettelli S, Sofi F. Effectiveness of a Khorasan wheat-based replacement on pain symptoms and quality of life in patients with fibromyalgia. *Pain Med* 2020; **21**: 2366-2372 [PMID: 32488245 DOI: 10.1093/pm/pnaa134]
9 **Niccolai E**, Russo E, Baldi S, Ricci F, Nannini G, Pedone M, Stingo FC, Taddei A, Ringressi MN, Bechi P, Mengoni A, Fani R, Bacci G, Fagorzi C, Chiellini C, Prisco D, Ramazzotti M, Amedei A. Significant and conflicting correlation of IL-9 with Prevotella and Bacteroides in human colorectal cancer. *Front Immunol* 2020; **11**: 573158 [PMID: 33488574 DOI: 10.3389/fimmu.2020.573158]
10 **Niccolai E**, Baldi S, Ricci F, Russo E, Nannini G, Menicatti M, Poli G, Taddei A, Bartolucci G, Calabrò AS, Stingo FC, Amedei A. Evaluation and comparison of short chain fatty acids composition in gut diseases. *World J Gastroenterol* 2019; **25**: 5543-5558 [PMID: 31576099 DOI: 10.3748/wjg.v25.i36.5543]
11 **Lowry E**, Marley J, McVeigh JG, McSorley E, Allsopp P, Kerr D. Dietary interventions in the management of fibromyalgia: a systematic review and best-evidence synthesis. *Nutrients* 2020; **12** [PMID: 32878326 DOI: 10.3390/nu12092664]
12 **Malatji BG**, Meyer H, Mason S, Engelke UFH, Wevers RA, van Reenen M, Reinecke CJ. A diagnostic biomarker profile for fibromyalgia syndrome based on an NMR metabolomics study of selected patients and controls. *BMC Neurol* 2017; **17**: 88 [PMID: 28490352 DOI: 10.1186/s12883-017-0863-9]
13 **Kaleth AS**, Slaven JE, Ang DC. Obesity moderates the effects of motivational interviewing treatment outcomes in fibromyalgia. *Clin J Pain* 2018; **34**: 76-81 [PMID: 28272119 DOI: 10.1097/AJP.0000000000000500]
14 **Fassarella M**, Blaak EE, Penders J, Nauta A, Smidt H, Zoetendal EG. Gut microbiome stability and resilience: elucidating the response to perturbations in order to modulate gut health. *Gut* 2021; **70**: 595-605 [PMID: 33051190 DOI: 10.1136/gutjnl-2020-321747]
15 **Dimova LG**, Zlatkov N, Verkade HJ, Uhlin BE, Tietge UJF. High-cholesterol diet does not alter gut microbiota composition in mice. *Nutr Metab (Lond)* 2017; **14**: 15 [PMID: 28239402 DOI: 10.1186/s12986-017-0170-x]
16 **Zhang J**, Yi C, Han J, Ming T, Zhou J, Lu C, Li Y, Su X. Novel high-docosahexaenoic-acid tuna oil supplementation modulates gut microbiota and alleviates obesity in high-fat diet mice. *Food Sci Nutr* 2020; **8**: 6513-6527 [PMID: 33312536 DOI: 10.1002/fsn3.1941]
17 **Dhakal S**, McCormack L, Dey M. Association of the gut microbiota with weight-loss response within a retail weight-management program. *Microorganisms* 2020; **8** [PMID: 32824364 DOI: 10.3390/microorganisms8081246]
18 **Guo X**, Li J, Tang R, Zhang G, Zeng H, Wood RJ, Liu Z. High fat diet alters gut microbiota and the expression of Paneth cell-antimicrobial peptides preceding changes of circulating inflammatory cytokines. *Mediators Inflamm* 2017; **2017**: 9474896 [PMID: 28316379 DOI: 10.1155/2017/9474896]
19 **Zhong Y**, Nyman M, Fåk F. Modulation of gut microbiota in rats fed high-fat diets by processing whole-grain barley to barley malt. *Mol Nutr Food Res* 2015; **59**: 2066-2076 [PMID: 26184884 DOI: 10.1002/mnfr.201500187]
20 **Sturgill J**, McGee E, Menzies V. Unique cytokine signature in the plasma of patients with fibromyalgia. *J Immunol Res* 2014; **2014**: 938576 [PMID: 24741634 DOI: 10.1155/2014/938576]
21 **Uçeyler N**, Valenza R, Stock M, Schedel R, Sprotte G, Sommer C. Reduced levels of antiinflammatory cytokines in patients with chronic widespread pain. *Arthritis Rheum* 2006; **54**: 2656-2664 [PMID: 16871547 DOI: 10.1002/art.22026]
22 **Labuz D**, Celik MÖ, Seitz V, Machelska H. Interleukin-4 induces the release of opioid peptides from M1 macrophages in pathological pain. *J Neurosci* 2021; **41**: 2870-2882 [PMID: 33593854 DOI: 10.1523/JNEUROSCI.3040-20.2021]
23 **Zhang C**, Björkman A, Cai K, Liu G, Wang C, Li Y, Xia H, Sun L, Kristiansen K, Wang J, Han J, Hammarström L, Pan-Hammarström Q. Impact of a 3-months vegetarian diet on the gut microbiota and immune repertoire. *Front Immunol* 2018; **9**: 908 [PMID: 29755475 DOI: 10.3389/fimmu.2018.00908]

24 **Pagliai G**, Russo E, Niccolai E, Dinu M, Di Pilato V, Magrini A, Bartolucci G, Baldi S, Menicatti M, Giusti B, Marcucci R, Rossolini GM, Casini A, Sofi F, Amedei A. Influence of a 3-month low-calorie Mediterranean diet compared to the vegetarian diet on human gut microbiota and SCFA: the CARDIVEG Study. *Eur J Nutr* 2020; **59**: 2011-2024 [PMID: 31292752 DOI: 10.1007/s00394-019-02050-0]

25 **Evans SR**. Clinical trial structures. *J Exp Stroke Transl Med* 2010; **3**: 8-18 [PMID: 21423788 DOI: 10.6030/1939-067x-3.1.8]

26 **Bor B**, Bedree JK, Shi W, McLean JS, He X. Saccharibacteria (TM7) in the human oral microbiome. *J Dent Res* 2019; **98**: 500-509 [PMID: 30894042 DOI: 10.1177/0022034519831671]

27 **Figueroa-Gonzalez PA**, Bornemann TLV, Adam PS, Plewka J, Révész F, von Hagen CA, Táncsics A, Probst AJ. Saccharibacteria as organic carbon sinks in hydrocarbon-fueled communities. *Front Microbiol* 2020; **11**: 587782 [PMID: 33424787 DOI: 10.3389/fmicb.2020.587782]

28 **Binda C**, Lopetuso LR, Rizzatti G, Gibiino G, Cennamo V, Gasbarrini A. Actinobacteria: a relevant minority for the maintenance of gut homeostasis. *Dig Liver Dis* 2018; **50**: 421-428 [PMID: 29567414 DOI: 10.1016/j.dld.2018.02.012]

29 **Clos-Garcia M**, Andrés-Marin N, Fernández-Eulate G, Abecia L, Lavín JL, van Liempd S, Cabrera D, Royo F, Valero A, Errazquin N, Vega MCG, Govillard L, Tackett MR, Tejada G, Gónzalez E, Anguita J, Bujanda L, Orcasitas AMC, Aransay AM, Maíz O, López de Munain A, Falcón-Pérez JM. Gut microbiome and serum metabolome analyses identify molecular biomarkers and altered glutamate metabolism in fibromyalgia. *EBioMedicine* 2019; **46**: 499-511 [PMID: 31327695 DOI: 10.1016/j.ebiom.2019.07.031]

30 **Furusawa Y**, Obata Y, Fukuda S, Endo TA, Nakato G, Takahashi D, Nakanishi Y, Uetake C, Kato K, Kato T, Takahashi M, Fukuda NN, Murakami S, Miyauchi E, Hino S, Atarashi K, Onawa S, Fujimura Y, Lockett T, Clarke JM, Topping DL, Tomita M, Hori S, Ohara O, Morita T, Koseki H, Kikuchi J, Honda K, Hase K, Ohno H. Commensal microbe-derived butyrate induces the differentiation of colonic regulatory T cells. *Nature* 2013; **504**: 446-450 [PMID: 24226770 DOI: 10.1038/nature12721]

31 **Saa DT**, Turroni S, Serrazanetti DS, Rampelli S, Maccaferri S, Candela M, Severgnini M, Simonetti E, Brigidi P, Gianotti A. Impact of Kamut® Khorasan on gut microbiota and metabolome in healthy volunteers. *Food Res Int* 2014; **63**: 227-232 [DOI: 10.1016/j.foodres.2014.04.005]

32 **Qiao M**, Jiang QS, Liu YJ, Hu XY, Wang LJ, Zhou QX, Qiu HM. Antidepressant mechanisms of venlafaxine involving increasing histone acetylation and modulating tyrosine hydroxylase and tryptophan hydroxylase expression in hippocampus of depressive rats. *Neuroreport* 2019; **30**: 255-261 [PMID: 30640193 DOI: 10.1097/WNR.0000000000001191]

33 **Zammataro M**, Sortino MA, Parenti C, Gereau RW 4th, Chiechio S. HDAC and HAT inhibitors differently affect analgesia mediated by group II metabotropic glutamate receptors. *Mol Pain* 2014; **10**: 68 [PMID: 25406541 DOI: 10.1186/1744-8069-10-68]

34 **Kukkar A**, Singh N, Jaggi AS. Attenuation of neuropathic pain by sodium butyrate in an experimental model of chronic constriction injury in rats. *J Formos Med Assoc* 2014; **113**: 921-928 [PMID: 23870713 DOI: 10.1016/j.jfma.2013.05.013]

35 **Bonomo RR**, Cook TM, Gavini CK, White CR, Jones JR, Bovo E, Zima AV, Brown IA, Dugas LR, Zakharian E, Aubert G, Alonzo F 3rd, Calcutt NA, Mansuy-Aubert V. Fecal transplantation and butyrate improve neuropathic pain, modify immune cell profile, and gene expression in the PNS of obese mice. *Proc Natl Acad Sci U S A* 2020; **117**: 26482-26493 [PMID: 33020290 DOI: 10.1073/pnas.2006065117]

36 **Sheedy JR**, Wettenhall RE, Scanlon D, Gooley PR, Lewis DP, McGregor N, Stapleton DI, Butt HL, DE Meirleir KL. Increased d-lactic acid intestinal bacteria in patients with chronic fatigue syndrome. *In Vivo* 2009; **23**: 621-628 [PMID: 19567398]

37 **Cénit MC**, Matzaraki V, Tigchelaar EF, Zhernakova A. Rapidly expanding knowledge on the role of the gut microbiome in health and disease. *Biochim Biophys Acta* 2014; **1842**: 1981-1992 [PMID: 24882755 DOI: 10.1016/j.bbadis.2014.05.023]

38 **Li S**, Hua D, Wang Q, Yang L, Wang X, Luo A, Yang C. The role of bacteria and its derived metabolites in chronic pain and depression: recent findings and research progress. *Int J Neuropsychopharmacol* 2020; **23**: 26-41 [PMID: 31760425 DOI: 10.1093/ijnp/pyz061]

39 **Barandouzi ZA**, Lee J, Maas K, Starkweather AR, Cong XS. Altered gut microbiota in irritable bowel syndrome and its association with food components. *J Pers Med* 2021; **11** [PMID: 33429936 DOI: 10.3390/jpm11010035]

40 **Ji RR**, Chamessian A, Zhang YQ. Pain regulation by non-neuronal cells and inflammation. *Science* 2016; **354**: 572-577 [PMID: 27811267 DOI: 10.1126/science.aaf8924]

41 **Baral P**, Udit S, Chiu IM. Pain and immunity: implications for host defence. *Nat Rev Immunol* 2019; **19**: 433-447 [PMID: 30874629 DOI: 10.1038/s41577-019-0147-2]

42 **Rodriguez-Pintó I**, Agmon-Levin N, Howard A, Shoenfeld Y. Fibromyalgia and cytokines. *Immunol Lett* 2014; **161**: 200-203 [PMID: 24462815 DOI: 10.1016/j.imlet.2014.01.009]

43 **Peck MM**, Maram R, Mohamed A, Ochoa Crespo D, Kaur G, Ashraf I, Malik BH. The influence of pro-inflammatory cytokines and genetic variants in the development of fibromyalgia: a traditional review. *Cureus* 2020; **12**: e10276 [PMID: 33042712 DOI: 10.7759/cureus.10276]

44 **Minerbi A**, Gonzalez E, Brereton NJB, Anjarkouchian A, Dewar K, Fitzcharles MA, Chevalier S, Shir Y. Altered microbiome composition in individuals with fibromyalgia. *Pain* 2019; **160**: 2589-2602 [PMID: 31219947 DOI: 10.1097/j.pain.0000000000001640]

45 **Meeus M**, Nijs J, Hermans L, Goubert D, Calders P. The role of mitochondrial dysfunctions due to oxidative and nitrosative stress in the chronic pain or chronic fatigue syndromes and fibromyalgia patients: peripheral and central mechanisms as therapeutic targets? *Expert Opin Ther Targets* 2013; **17**: 1081-1089 [PMID: 23834645 DOI: 10.1517/14728222.2013.818657]

46 **Trozzi C**, Raffaelli F, Vignini A, Nanetti L, Gesuita R, Mazzanti L. Evaluation of antioxidative and diabetes-preventive properties of an ancient grain, KAMUT® khorasan wheat, in healthy volunteers. *Eur J Nutr* 2019; **58**: 151-161 [PMID: 29143934 DOI: 10.1007/s00394-017-1579-8]

World Journal of Gastroenterology

Submit a Manuscript: https://www.f6publishing.com

World J Gastroenterol 2022 May 14; 28(18): 1981-1995

DOI: 10.3748/wjg.v28.i18.1981

ISSN 1007-9327 (print) ISSN 2219-2840 (online)

ORIGINAL ARTICLE

Basic Study

Fusobacterium nucleatum promotes colon cancer progression by changing the mucosal microbiota and colon transcriptome in a mouse model

Na Wu, Yu-Qing Feng, Na Lyu, Di Wang, Wei-Dong Yu, Yong-Fei Hu

Specialty type: Gastroenterology and hepatology

Provenance and peer review: Unsolicited article; Externally peer reviewed.

Peer-review model: Single blind

Peer-review report's scientific quality classification

Grade A (Excellent): 0
Grade B (Very good): B
Grade C (Good): C
Grade D (Fair): 0
Grade E (Poor): 0

P-Reviewer: Batyrbekov K, Kazakhstan; Díez M, Germany

Received: January 30, 2022
Peer-review started: January 30, 2022
First decision: February 24, 2022
Revised: February 28, 2022
Accepted: March 26, 2022
Article in press: March 26, 2022
Published online: May 14, 2022

Na Wu, Di Wang, Wei-Dong Yu, Department of Central Laboratory & Institute of Clinical Molecular Biology, Peking University People's Hospital, Beijing 100044, China

Yu-Qing Feng, Yong-Fei Hu, State Key Laboratory of Animal Nutrition, College of Animal Science and Technology, China Agricultural University, Beijing 100193, China

Na Lyu, CAS Key Laboratory of Pathogenic Microbiology and Immunology, Institute of Microbiology, Chinese Academy of Sciences, Beijing 100101, China

Corresponding author: Yong-Fei Hu, PhD, Professor, State Key Laboratory of Animal Nutrition, College of Animal Science and Technology, China Agricultural University, No. 2 Yuanmingyuan West Road, Haidian District, Beijing 100193, China. huyongfei@cau.edu.cn

Abstract

BACKGROUND

Fusobacterium nucleatum (*F. nucleatum*) has long been known to cause opportunistic infections and has recently been implicated in colorectal cancer (CRC), which has attracted broad attention. However, the mechanism by which it is involved in CRC development is not fully understood.

AIM

To explore its potential causative role in CRC development, we evaluated the colon pathology, mucosa barrier, colon microbiota and host transcriptome profile after *F. nucleatum* infection in an azoxymethane/dextran sulfate sodium salt (AOM/DSS) mouse model.

METHODS

Three groups of mice were compared to reveal the differences, *i.e.*, the control, AOM/DSS-induced CRC and AOM/DSS-FUSO infection groups.

RESULTS

Both the AOM/DSS and AOM/DSS-FUSO groups exhibited a significantly reduced body weight and increased tumor numbers than the control group, and AOM/DSS mice with *F. nucleatum* infection showed the highest tumor formation ratio among the three groups. Moreover, the colon pathology was the most serious in the AOM/DSS-FUSO group. We found that the structure of the colon

microbiota changed considerably after *F. nucleatum* infection; striking differences in mucosal microbial population patterns were observed between the AOM/DSS-FUSO and AOM/DSS groups, and inflammation-inducing bacteria were enriched in the mucosal microbiota in the AOM/DSS-FUSO group. By comparing intestinal transcriptomics data from AOM *vs* AOM/DSS-FUSO mice, we showed that transcriptional activity was strongly affected by dysbiosis of the gut microbiota. The most microbiota-sensitive genes were oncogenes in the intestine, and the cyclic adenosine monophosphate signaling pathway, neuroactive ligand–receptor interaction, PPAR signaling pathway, retinol metabolism, mineral absorption and drug metabolism were highly enriched in the AOM/DSS-FUSO group. Additionally, we showed that microbial dysbiosis driven by *F. nucleatum* infection enriched eight taxa belonging to Proteobacteria, which correlates with increased expression of oncogenic genes.

CONCLUSION

Our study demonstrated that *F. nucleatum* infection altered the colon mucosal microbiota by enriching pathogens related to the development of CRC, providing new insights into the role of *F. nucleatum* in the oncogenic microbial environment of the colon.

Key Words: *Fusobacterium nucleatum*; Mucosal microbiota; Transcriptome; Colorectal cancer; Inflammation-inducing bacteria

©The Author(s) 2022. Published by Baishideng Publishing Group Inc. All rights reserved.

Core Tip: *Fusobacterium nucleatum* (*F. nucleatum*) has long been known to cause oppo-rtunistic infections and has recently been implicated in colorectal cancer (CRC). However, the mechanism by which it is involved in CRC development is not fully understood. Here, striking differences in mucosal microbial population patterns were observed and inflammation-inducing bacteria were enriched in the mucosal microbiota in the azoxymethane/dextran sulfate sodium salt-FUSO group. We showed that transcriptional activity was strongly affected by dysbiosis of the gut microbiota. Additionally, we showed that microbial dysbiosis driven by *F. nucleatum* infection enriched eight taxa belonging to Proteobacteria, which correlates with increased expression of oncogenic genes.

Citation: Wu N, Feng YQ, Lyu N, Wang D, Yu WD, Hu YF. Fusobacterium nucleatum promotes colon cancer progression by changing the mucosal microbiota and colon transcriptome in a mouse model. *World J Gastroenterol* 2022; 28(18): 1981-1995
URL: https://www.wjgnet.com/1007-9327/full/v28/i18/1981.htm
DOI: https://dx.doi.org/10.3748/wjg.v28.i18.1981

INTRODUCTION

Colorectal cancer (CRC) is the third most common cancer and the fourth leading cause of cancer death worldwide[1]. The incidence of CRC in China has increased dramatically during the past decade[2].

Fusobacterium nucleatum (*F. nucleatum*), a gram-negative anaerobe, was recently identified as an emerging pathogen that has been frequently found in CRC[3-5]. Importantly, overload of *F. nucleatum* was found to be associated with an advanced tumor stage and a poor prognosis in CRC[6]. Accumulating evidence has revealed that *F. nucleatum* influences different stages of CRC progression. *F. nucleatum* can promote the initiation and development of CRC by adhering to epithelial cells through its unique FadA protein[7], which can bind vascular endothelial cadherin and alters endothelial integrity [8]. The activation of oncogenic miR21 under *F. nucleatum* stimulation results in the overexpression of TLR-4/nuclear factor-kappaB, increasing the proliferation of CRC cells and promoting tumor development[9]. Once a colon tumor has developed, *F. nucleatum* can adhere to Gal-GalNAc-expressing tumor cells by binding to the Fap2 Lectin, leading to enrichment of *F. nucleatum*[10]. *F. nucleatum* infection was also proven to increase the expression levels of inflammatory genes, transcription factors, and oncogenes[8,11]. These studies enhance our knowledge of the mechanisms by which *F. nucleatum* shapes the tumor microenvironment.

Evidences have revealed that the local microbiota is also an important part of the tumor microenvironment. Gut microbiota dysbiosis can reshape the tumor microenvironment and make it favorable for tumor growth[12]. The mechanisms involved include increasing mutagenesis, regulation of oncogenic pathways, and modulation of host immune system[13]. These oncogenic functions of gut microbiota are probably due to the microbial products or metabolites they produce when the community structure

balance is disrupted and a resulting overgrowth of specific bacteria. For example, the overload of colibactin-producing *Escherichia coli* and other Enterobacteriaceae can induce DNA damage of host cells and exert tumorigenic effect[14]. These facts suggest a close relationship between gut microbiota, the tumor microenvironment, and CRC. However, the regulatory role of *F. nucleatum* in the "oncogenic microbial environment" of the colon remains mostly unknown. Revealing the effects of *F. nucleatum* infection on the changes of mucosal microbiota will help to provide further insight into the mechanisms of the tumorigenic effect of *F. nucleatum*.

In the present study, we explored the role of *F. nucleatum* in the development of CRC and in altering the mucosal microbial community structure and investigated the association between microbial dysbiosis and the expression of oncogenic signaling pathways. *F. nucleatum* strain ATCC 25586 was gavaged into azoxymethane/dextran sulfate sodium salt (AOM/DSS) mice to explore the role of *Fusobacterium* overload in the progression of intestinal adenoma against a background of environmental inflammatory factors. RNA-seq transcriptomic analysis was used to identify the differentially expressed gene (DEG) signatures driven by *F. nucleatum* infection, and integrated network analysis was conducted to reveal the relationship between microbial dysbiosis and the DEGs. Our study lays a foundation for understanding the regulatory role of *F. nucleatum* in the oncogenic microbial environment of the colon.

MATERIALS AND METHODS

Bacterial strain and culture conditions

The *F. nucleatum* strain ATCC 25586 was purchased from American Type Culture Collection (ATCC) and was cultured as described previously[3]. In brief, *F. nucleatum* was grown in Columbia blood agar supplemented with 5 mg/mL haemin, 5% defibrinated sheep blood, and 1 mg/mL Vitamin K1 in an anaerobic condition with 85% N_2, 10% H_2, and 5% CO_2 at 37 °C. And 10^9 colony-forming units *per* mL (CFU/mL) were prepared for *F. nucleatum* colonization.

Animal model

Thirty-six conventional C57BL/6J wild-type male mice (4 wk of age) were obtained from the Beijing Animal Study Centre and maintained in the Laboratory Animal Services Centre at the Chinese Center for Disease Control and Prevention. The Institutional Animal Care Committee of the Peking University People's Hospital approved all animal experimentation.

To create the mouse model of colon neoplasia induced by AOM/DSS-induced colon neoplasia[15], 24 mice at 6 wk of age were injected intraperitoneally with a single dose of 10 mg/kg AOM (Sigma), designated week 0. DSS (MP Biochemicals; 36000-50000 mw) was dissolved in filtered drinking water and administered to the mice for 7 d during the following weeks: Weeks 1 (1% DSS), 3 (1% DSS), and 5 (1% DSS). After 1 wk of AOM/DSS treatment, the 24 mice were divided into 2 groups, each with 12 mice. At week 7 they were orally gavaged daily with 10^9 CFU/mL (in 100 μL volume for each mouse) *F. nucleatum* (AOM/DSS-FUSO group) or phosphate-buffered saline (AOM/DSS group) for two weeks. The 12 mice in the control group were sibling littermates and received no treatment.

After 2 wk after *Fusobacterium* inoculation as previous study described[16], the mice were sacrificed, colon mucosal contents were collected for microbiota profiling, the colons were dissected, and the polyps were counted. For a subset of the samples, the distal portion of the colon was fixed in 4% paraformaldehyde, paraffin-embedded, and sectioned for hematoxylin and eosin staining. The remaining colon tissue was then prepared for RNA sequencing.

The body weight, colon length, colorectal tumor formation ratio, immune cell patterns, gut microbiota structure and intestine transcriptomics were assessed to explore the potential role of ATCC 25586 in the carcinogenesis/development of CRC.

Histological evaluation

The colon segments were submitted for histological processing. All slides were stained with hematoxylin and eosin. Dysplasia was assessed by the presence of hyperchromasia, nuclear pleomorphism, and increased nuclear-to-cytoplasmic ratios.

Immunohistochemical staining

The expression of E-cadherin and Ki-67 was determined by immunohistochemistry staining. Serial 3 mm sections of the formalin-fixed paraffin-embedded colon tissues on the slides were heated in a microwave with sodium citrate for antigen repair, followed by 2% goat serum for blocking. The slides were then treated with mouse anti-E-cadherin (BD Biosciences, catalog 610181) and anti-Ki-67 (Cell Signaling Technology, catalog 9192) overnight at 4 °C, visualized with diaminobenzidine, counter-stained with hematoxylin, dehydrated and mounted. Staining index of Ki-67 immunostaining was determined by percentage of positive cells having brown nuclear staining from three randomly selected fields at 400 × magnification.

Microbial DNA extraction and 16S rRNA gene sequencing

Microbiota DNA from the colon mucosal contents was extracted using the QIAamp DNA Stool Mini Kit (Qiagen, catalog 51604). For all samples, polymerase chain reaction (PCR) amplification of the 16S rRNA gene with the V3-V4 variable regions was performed using the primers 341F (5′-CCTAYGG-GRBGCASCAG-3′) and 806R (5′-GGACTACNNGGGTATCTAAT-3′)[17]. The pooled library was sequenced on the Ion S5™ XL System (Thermo Fisher Scientific). Single-end reads were assigned to the samples based on their unique barcodes and trimmed by removing the barcodes and primer sequences. Raw fastq files were quality-filtered using fastp[18]. Chimeric sequences were detected and removed by vsearch software[19]. Operational taxonomic units (OTUs) were clustered with 97% identity using UPARSE v7.0.1001[20]. The most frequent sequences were selected as the representative sequences for each OTU. Representative sequences for each OTU were annotated using Mothur software at Threshold: 0.8-1 against the SILVA V132 database (http://www.arb-silva.de/) at each taxonomic rank (kingdom, phylum, class, order, family, genus and species)[21]. OTU abundance information was normalized using a standard sequence number corresponding to the sample with the fewest sequences. To avoid biases, the normalized data were subjected to alpha diversity and beta diversity analyses. Alpha diversity indices (Chao1, ACE, Shannon index, Simpson) and UniFrac distance were calculated by QIIME v1.9.1[22,23]. Beta diversities were visualized by principal coordinate analysis (PCoA) and nonmetric multidimensional (NMDS) based on Bray–Curtis dissimilarity.

Quantitative real-time PCR for F. nucleatum

The Q-PCR assay was performed to determine the colonization of *F. nucleatum*. The 16S primers for *F. nucleatum* quantification were F-TGCGATAAGCCTAGATAAGTTGCA and R-CTTAATAGAT-TGCTCCATTCGGAAA. Primers for total bacterial DNA were F-ACTCCTACGGGAGGCAGCAGT and R-GTATTACCGCGGCTGCTGGCAC[16]. The level of *F. nucleatum* was evaluated by the following formula: The relative value (RV) of *F. nucleatum* was determined by the $2^{-\Delta ct}$ method using total bacterial level as a normalizer. The relative abundance (RA) of *F. nucleatum* was scaled to a reasonable range with the following equation: $RA = \log_2(RV \times 10000 + 1)$.

RNA extraction and RNA sequencing

Total RNA was isolated using TRIzol reagent (Invitrogen, Carlsbad, CA) according to the manufacturer's recommendations. A total of 3 μg RNA *per* sample was used as the input material for the RNA sample preparations. Sequencing libraries were generated using the NEBNext® UltraTM RNA Library Prep Kit for Illumina® (NEB, United States) following the manufacturer's recommendations. The library preparations were sequenced on an Illumina platform, and 150 bp paired-end reads were generated.

The raw reads were first processed through in-house Perl scripts. Adaptor sequences, duplicated sequences, poly-N reads containing more than 10% "N", and low-quality reads containing more than 50% bases with Q ≤ 5 were removed to obtain high-quality clean reads. Clean reads were aligned to the reference genome using Hisat2 v2.0.5[24]. FeatureCounts v1.5.0-p3 was used to count the read numbers mapped to each gene[25]. Then, the FPKM of each gene was calculated based on the length of the gene and the read count mapped to this gene. Prior to the differential gene expression analysis, for each sequenced library, the read counts were adjusted by the edgeR package. Differential gene expression analysis of the two conditions was performed using the edgeR package v3.18.1. The *P* values were adjusted using the Benjamini & Hochberg method[26]. A corrected *P* value of 0.05 and absolute fold change of 2 were set as the thresholds for significantly DEGs. Gene Ontology (GO) enrichment analysis of the DEGs was implemented by the clusterProfiler R package. GO terms with corrected *P* values less than 0.05 were considered significantly enriched by the DEGs. We used the clusterProfiler R package to test the statistical enrichment of the DEGs in the KEGG pathways[27].

Statistical analysis and visualization

The Kruskal–Wallis test was performed when comparing samples from more than two groups. The difference in ratio of diarrhea and bloody was assessed using Chi-square measure. Permutational multivariate analysis was applied with a parameter of 999 permutations in R[28]. Linear discriminant analysis effect size (LEfSe) was used to estimate which microbiome attributes differed significantly by treatments[29]. The relationship between the gut microbiota and DEGs was determined by calculating Spearman's correlations, and then network visualization was performed using Cytoscape v3.6.1[30]. Heatmaps were generated using the R package pheatmap (https://github.com/raivokolde/pheatmap). The relationship between the different gut microbiota and the pathways was determined by calculating Spearman's correlations. The R package ggplot2 was used for the other data visualization in the figures in the present study.

Ethics statement

All animal protocols were approved by the Animal Experimentation Ethics Committee of the Peking University People's Hospital in China. The experiments were conducted in accordance with the Animal Research: Reporting of in Vivo Experiments (ARRIVE) guidelines.

RESULTS

F. nucleatum infection promotes the development of CRC

A flow chart illustrating the *F. nucleatum* infection strategy combined with AOM/DSS treatment is shown in Figure 1A. The colonization of *F. nucleatum* was confirmed by 16S-sequencing and Q-PCR (Supplementary Figure 1). The body weight of the mice in each group increased slowly (Figure 1B), and it differed significantly between the control mice and the AOM/DSS models (two-way ANOVA, $P < 0.05$). After AOM/DSS treatment for six weeks, four mice in the AOM/DSS group and six mice in the AOM/DSS-FUSO group developed diarrhea and bloody stools (Chi-square, $P > 0.05$). No bloody stool was observed in the control group. Over the eight-week treatment, only three mice in the AOM/DSS group and five mice in the AOM/DSS-FUSO group survived.

The AOM/DSS-FUSO group had a trend but not significantly reduced colon length than the AOM/DSS group (Figure 1C), and AOM/DSS-FUSO had the highest tumor formation ratio among the three groups (Figure 1D). The AOM/DSS mice exhibited histological inflammation. In addition, the colon pathology was the most serious in the AOM/DSS-FUSO group, which was confirmed by hematoxylin-eosin (H&E) staining (Figure 1E). The presence of hyperchromasia and nuclear pleomorphism were observed in the AOM/DSS-FUSO group. We also found increased epithelial cell proliferation in the colons of AOM/DSS-FUSO mice, as indicated by a higher expression of Ki-67 than in the other two groups (Supplementary Figure 2). The abnormal expression of E-cadherin in the AOM/DSS-FUSO mice reflected the impaired function of the intestinal barrier.

Aberrant activation of epithelial-mesenchymal transition (EMT) is considered an important trigger of cancer invasion and metastasis[31]. The AOM/DSS-FUSO colon tissues showed morphological features of partial EMT, which was not observed in the AOM/DSS model (Figure 1E). In addition to the morphology-based analysis of colon tissue by H&E staining, the assessment of E-cadherin expression by immunohistochemistry can support the evaluation of partial EMT[31]. The expression of the barrier protein E-cadherin was modestly reduced in the AOM/DSS-FUSO group. Loss of the prototypical epithelial barrier protein E-cadherin is an additional sign of partial EMT[32]. The abnormal histology changes and the reduction of E-cadherin in AOM/DSS-FUSO mouse colons indicated that the AOM/DSS mice with *F. nucleatum* infection had undergone partial EMT, which is critical for CRC progression.

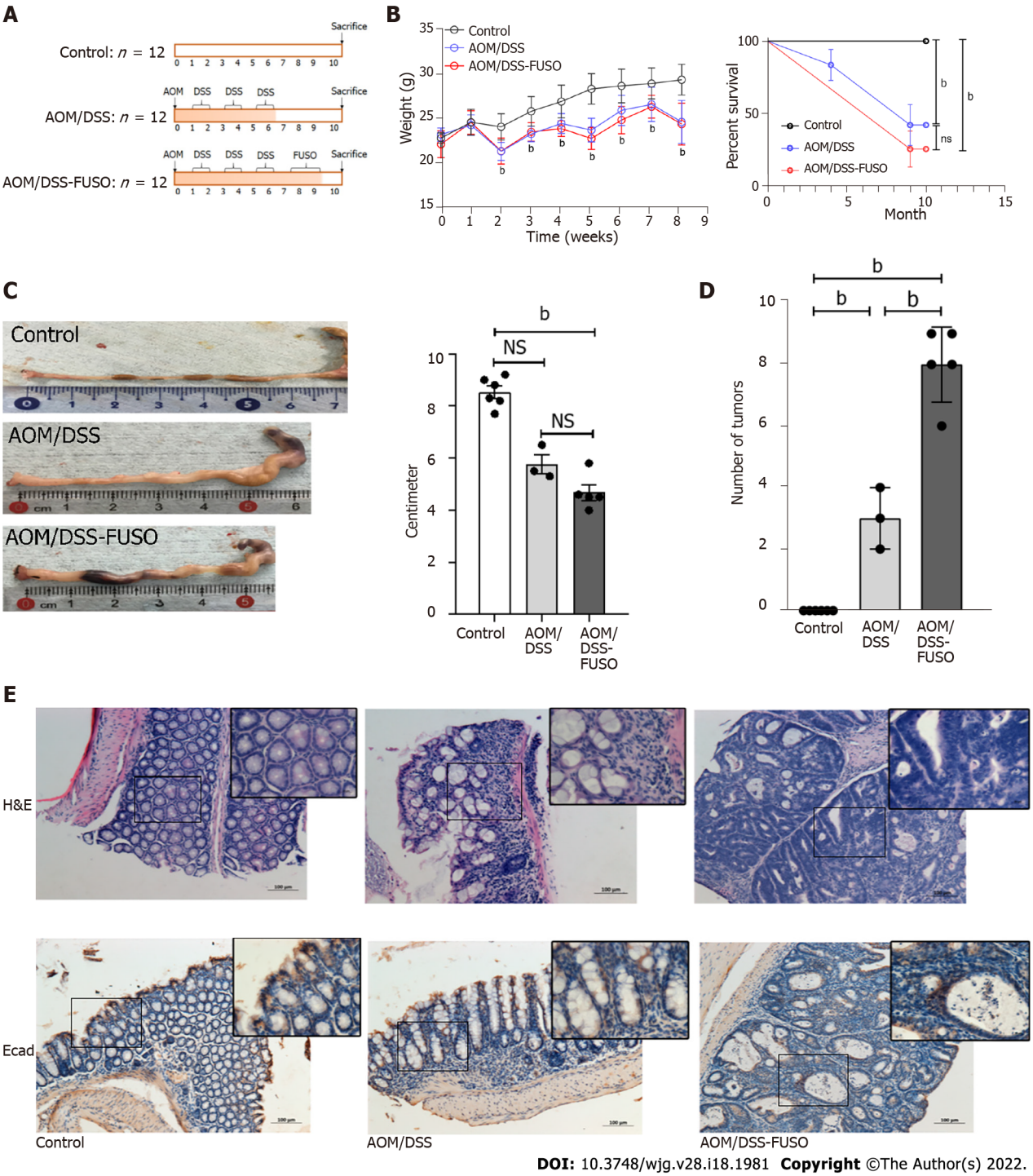
F. nucleatum infection changes the mucosal microbiota community structure

To investigate the effect of *F. nucleatum* infection on the mucosal microbiota, we compared the mucosal microbial composition of the three groups. The β diversity was very different among the three groups. The control group was clearly separated from the AOM/DSS-FUSO and AOM/DSS groups, as shown in the NMDS analysis (Figure 2A). This trend was also found in the PCoA analysis and was confirmed by the weighted UniFrac distance (Figure 2B and C). Around 12.8% of the bacterial composition variance could be explained by the addition of *F. nucleatum* (Permutation based analysis of variance). In AOM/DSS models, AOM/DSS-FUSO and AOM/DSS mice developed different mucosal microbiota with *F. nucleatum* infection as a significant factor in driving the differences. We then assessed the shared and unique OTUs in the AOM/DSS and AOM/DSS-FUSO groups to detect the effect of *F. nucleatum* infection. We observed that the AOM/DSS-FUSO group had more unique OTUs, approximately 44.9% (1117/2490), than the AOM/DSS group, 24.9% (456/1829), signifying that *F. nucleatum*-infected mice largely harbor unique inhabitant niches (Figure 2D). The Shannon, Simpson, observed species, and Chao1 indices for alpha diversity showed no significant differences among the three groups (Supplementary Figure 3).

Differentially abundant mucosal microbial taxa driven by *F. nucleatum* infection

We then explored the specific microbial members related to *F. nucleatum infection*. First, we compared the bacterial RA between groups at different taxa levels. We showed that the phylum Proteobacteria and eight other potential pathogens belonging to Proteobacteria (LEfSe, Figure 3A and B) were the dominant taxa in AOM/DSS-FUSO mice. Meanwhile, the phylum Bacteroides and the family Bacteroidaceae were enriched in AOM/DSS mice, which were evident CRC signature taxa[33]. The enrichment of potential pathogenic taxa and depletion of probiotic bacteria such as Lactobacillales were features of the mucosal microbiota caused by *F. nucleatum* infection (Figure 3C). Comparing the two CRC model groups, the mucosal microbiota in the control mice was dominated by the phylum Firmicutes and the probiotic taxa (Figure 3A and B).

We further compared the distribution of the top 50 most abundant taxa among the three groups. We found that the mucosal microbial population patterns were different in the three groups; the structure of the colon mucosal microbiota changed considerably after *F. nucleatum* infection in the AOM/DSS-FUSO mice (Figure 3D). Inflammation-inducing bacteria were significantly enriched in the mucosa microbiota of AOM/DSS-FUSO group compared with AOM/DSS group, such as *Denitratisom*, *Stenotrophomonas* and unidentified Enterobacteriaceae ($P = 0.036$, 0.018, and 0.048, respectively, wilcon rank-sum test, one-sided), while the potential probiotic genera were remarkably less abundant in AOM/DSS-FUSO group, such as unidentified Ruminococcaceae, unidentified Lachnospiraceae, and *Akkermansia* ($P = 0.036$, 0.036,



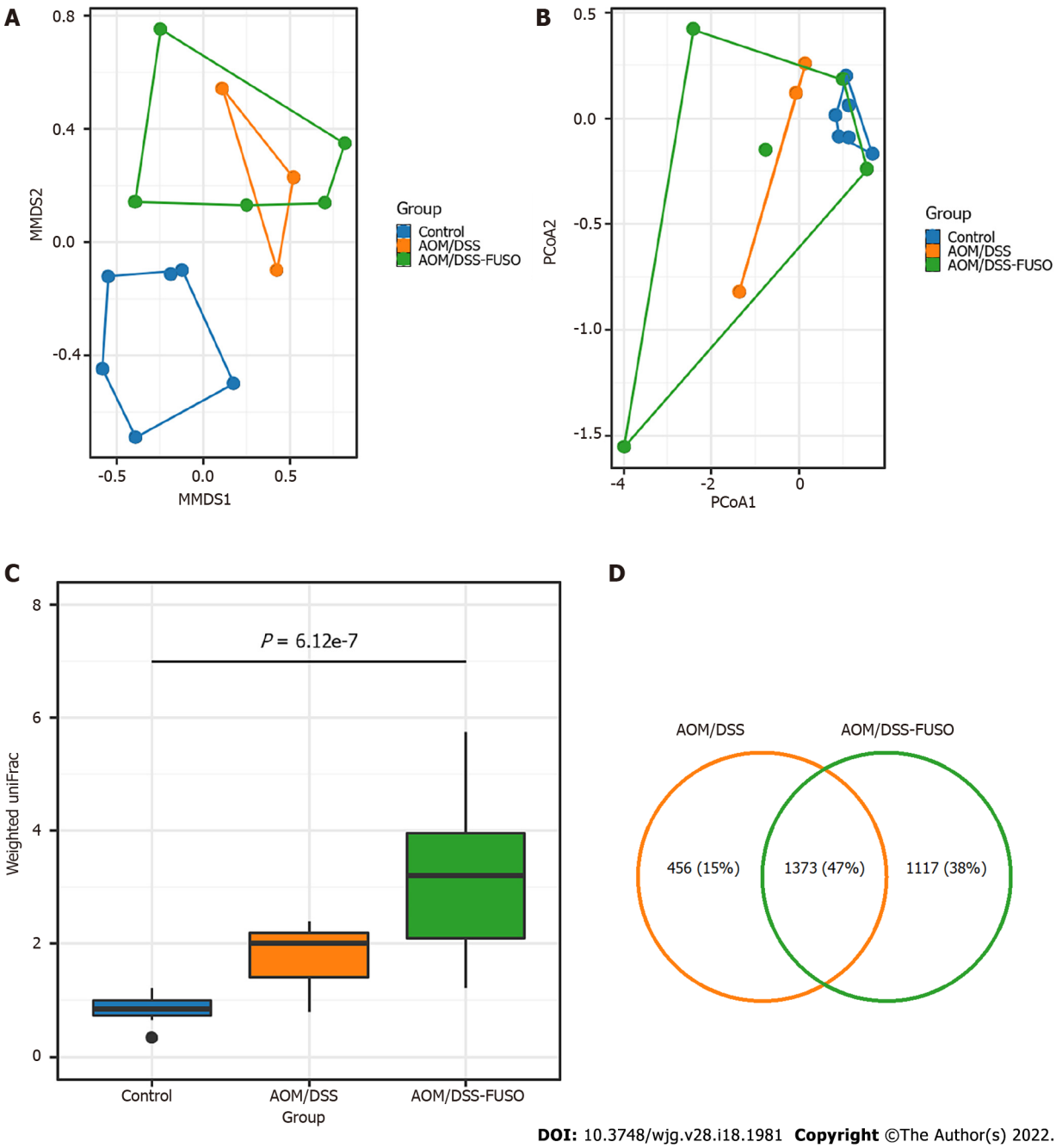
DOI: 10.3748/wjg.v28.i18.1981 **Copyright** ©The Author(s) 2022.

Figure 1 Effect of *F. nucleatum* infection on colon carcinogenesis in the azoxymethane/dextran sulfate sodium-induced model. A: Experimental design illustrating the *F. nucleatum* infection strategy combined with azoxymethane/dextran sulfate sodium salt treatment; B: The body weight and survival curve of the three groups during the experiment was evaluated with two-way ANOVA; C: The colon lengths of the three groups were compared using a t-test; D: The numbers of tumors in the colon of the three groups were compared using a t-test; E: Hematoxylin-eosin staining and immunohistochemistry of E-cadherin-positive cells in the colon of the three groups. $^{a}P < 0.05$; $^{b}P < 0.01$. NS: No signification; AOM: Azoxymethane; DSS: Dextran sulfate sodium salt.

and 0.071, respectively, wilcon rank-sum test, one-sided). Taken together, these results suggested that *F. nucleatum* infection further worsens the dysbiosis of the colon mucosal microbiota by increasing the abundance of pathogenic bacteria while reducing probiotics.

Altered host signaling pathways in colon tissue under F. nucleatum infection

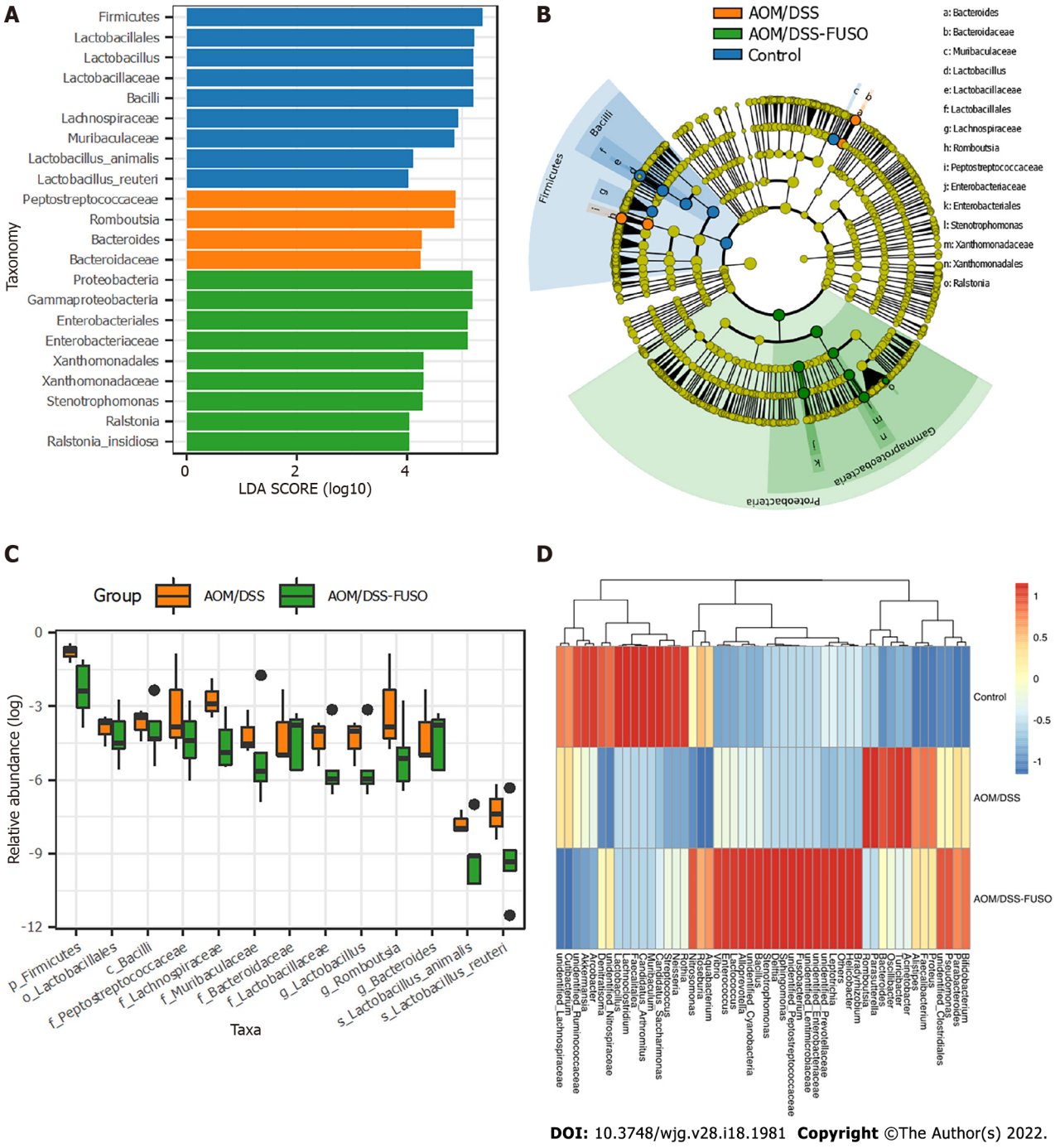
To gain insights into the molecular basis underlying the protumorigenic effect of *Fusobacterium* infection, RNA-seq was performed to reveal the transcriptomic changes driven by *F. nucleatum*. We observed different number of DEGs in the three comparions, *i.e.*, AOM/DSS *vs* Control, AOM/DSS-FUSO *vs* Control, and AOM/DSS-FUSO *vs* AOM/DSS (Figure 4A-C), and compared with the



DOI: 10.3748/wjg.v28.i18.1981 **Copyright** ©The Author(s) 2022.

Figure 2 Diversity and shared operational taxonomic units of the gut microbiota in different groups. A: Nonmetric multidimensional plot of the cecal microbiota from the 14 samples based on Bray-Curtis similarities; B: Principal coordinate analysis plot of the cecal microbiota from the 14 samples based on Bray-Curtis similarities; C: Weighted UniFrac distance of the samples from different groups. Kruskal-Wallis test: $P = 6.12 \times 10^{-7}$; D: Number of shared operational taxonomic units between the samples from the azoxymethane-dextran sulfate sodium salt (AOM/DSS)-FUSO group and the AOM/DSS group. AOM: Azoxymethane; DSS: Dextran sulfate sodium salt.

AOM/DSS mice, there were 231 upregulated genes and 92 downregulated genes in the AOM/DSS-FUSO mice (Figure 4C). The heatmap of DEGs showed the distinct gene expression profile between AOM/DSS-induced CRC models with or without overloaded *F. nucleatum* treatment (Figure 4D). These upregulated genes included FABP1 (fatty acid binding protein 1)[34], sucrase isomaltase, defensin, ATP-binding cassette[35], homeobox C6[36] and tolloid-like 2 (NETO2)[37], all of which were overexpressed more than 3-fold and were correlated with a poor prognosis of colorectal carcinoma in previous studies (Supplementary Table 1). KEGG pathway enrichment analysis suggested that the microbiota-transcriptome interaction significantly upregulated neuroactive ligand–receptor interaction, cyclic adenosine monophosphate (cAMP) signaling pathway, PPAR signaling pathway, steroid hormone biosynthesis, retinol metabolism, mineral absorption and drug metabolism in the AOM/DSS-FUSO group (Figure 5), and 36 DEGs were included in these KEGG pathways (Supplementary Figure 4). Among them, several CRC-related DEGs, PPARα[38], PCK1[39,40], GCG[41], VAV2[42], and ANGPTL4 [43] were also revealed to be correlated with the CRC prognosis in previous studies. These results



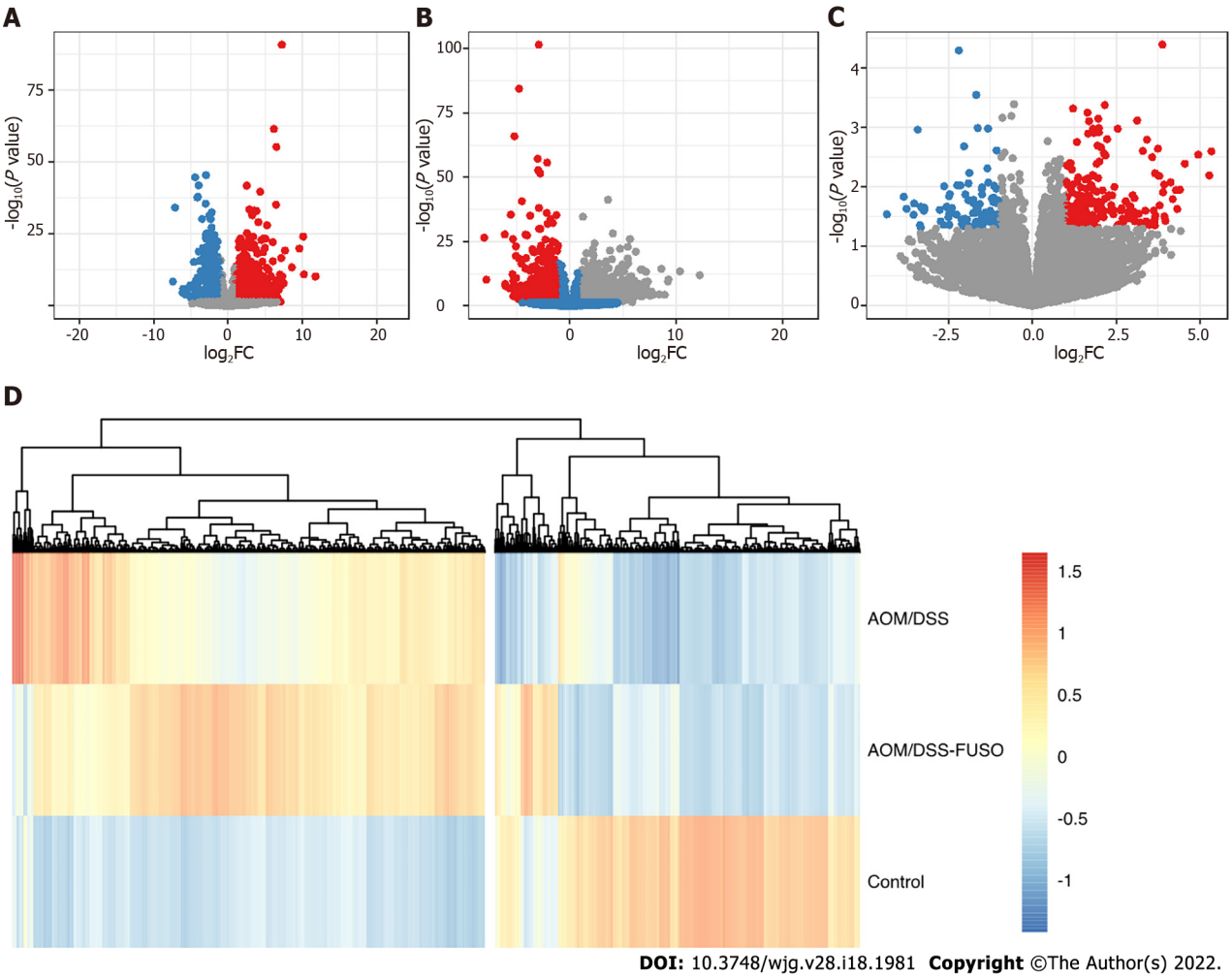
DOI: 10.3748/wjg.v28.i18.1981 **Copyright** ©The Author(s) 2022.

Figure 3 The differentially abundant taxa among the three groups. A: Histogram of the linear discriminant analysis scores computed for taxa that were differentially abundant among the three groups; B: Taxonomic representation of statistically and biologically consistent differences among the three groups. The differences are represented in the color of the most abundant class; C: Relative abundance of the taxa in azoxymethane/dextran sulfate sodium salt (AOM/DSS)-FUSO and AOM/DSS; D: Patterns of the abundance of the top 50 operational taxonomic units in all samples. The colors indicate the Z scores of the mean abundance in each group. AOM: Azoxymethane; DSS: Dextran sulfate sodium salt.

suggested that dramatic changes occurred in the host signaling pathways that are related to the tumorigenesis of CRC after *F. nucleatum* infection and the resulting disturbance of the mucosal microbiota.

Hub bacteria and key genes involved in the carcinogenesis/development of CRC

To further explore the hub bacteria and the hub DEGs, MCODE plugged in Cytoscape was used to explore the key modules involved in CRC development (Figure 6). The differential bacterial taxa identified by LEfSe analysis and the genes involved in the top seven significantly differential KEGG pathways were processed. The results showed that seven potentially harmful hub taxa were closely related to the overexpression of 12 hub genes. These taxa, *Stenotrophomonas*[44], Xanthomonadaceae, Xanthomonadales, Enterobacteriaceae, Enterobacteriales, Gammaproteobacteria, and Proteobacteria, have been shown to exhibit proinflammatory and procarcinogenic properties. This key module with the



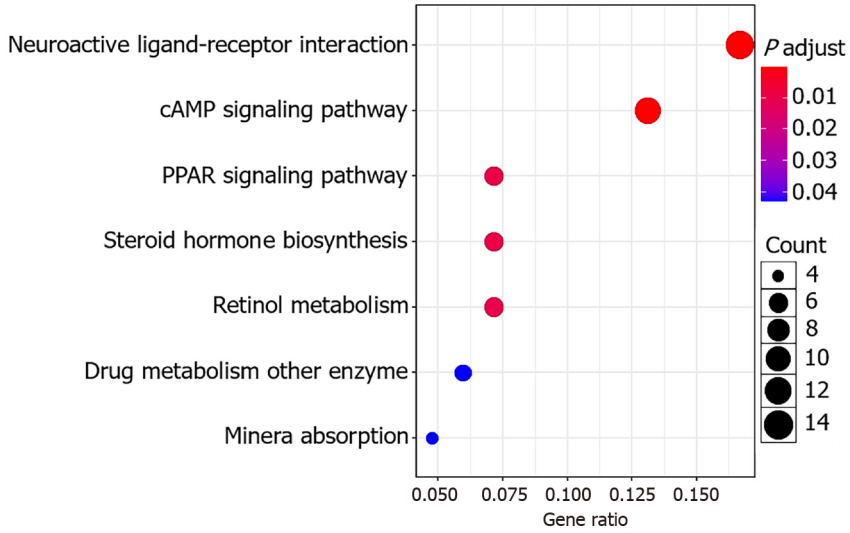
DOI: 10.3748/wjg.v28.i18.1981 **Copyright** ©The Author(s) 2022.

Figure 4 The differentially expressed genes of the mucosa. A: Volcano plot showing the differentially expressed genes between the azoxymethane/dextran sulfate sodium salt (AOM/DSS) group and the control group; B: Volcano plot showing the differentially expressed genes between the AOM/DSS-FUSO group and the control group; C: Volcano plot showing the differentially expressed genes between the AOM/DSS-FUSO group and the AOM/DSS group. Significantly upregulated genes are shown in red ($P < 0.05$ and $\log_2FC \geq 1$). Significantly downregulated genes are shown in blue ($P < 0.05$ and $\log_2FC \leq -1$). The numbers of significantly upregulated genes were 1374 for (A), 1939 for (B) and 231 for (C). The numbers of significantly downregulated genes were 1050 for (A), 1104 for (B) and 92 for (C); D: Patterns of the abundance of all of the differentially expressed genes in the upper panels. The colors indicate the Z scores of the mean abundance in each group. AOM: Azoxymethane; DSS: Dextran sulfate sodium salt.

seven hub microbial taxa and 12 hub genes may regulate the occurrence and development of CRC through CRC-related pathways such as the cAMP and PPAR signaling pathways. Enterobacteriaceae correlated with eight oncogenes, *i.e.*, *PCK1*, *GalR2*, *GCG*, *SLC6A19*, *CHRM1*, *ADRB1*, *UGT2B38*, and *GRID2*, and three taxa (Xanthomonadales, Xanthomonadaceae and *Stenotrophomonas*) were positively correlated with *VAV2*, *SCTR* and *ANGPTL4*. These results suggested that the dysbiosis of gut microbes driven by *F. nucleatum* infection may have the potential to affect the transcriptional activity of tumor-related metabolic pathways, especially those containing oncogenes.

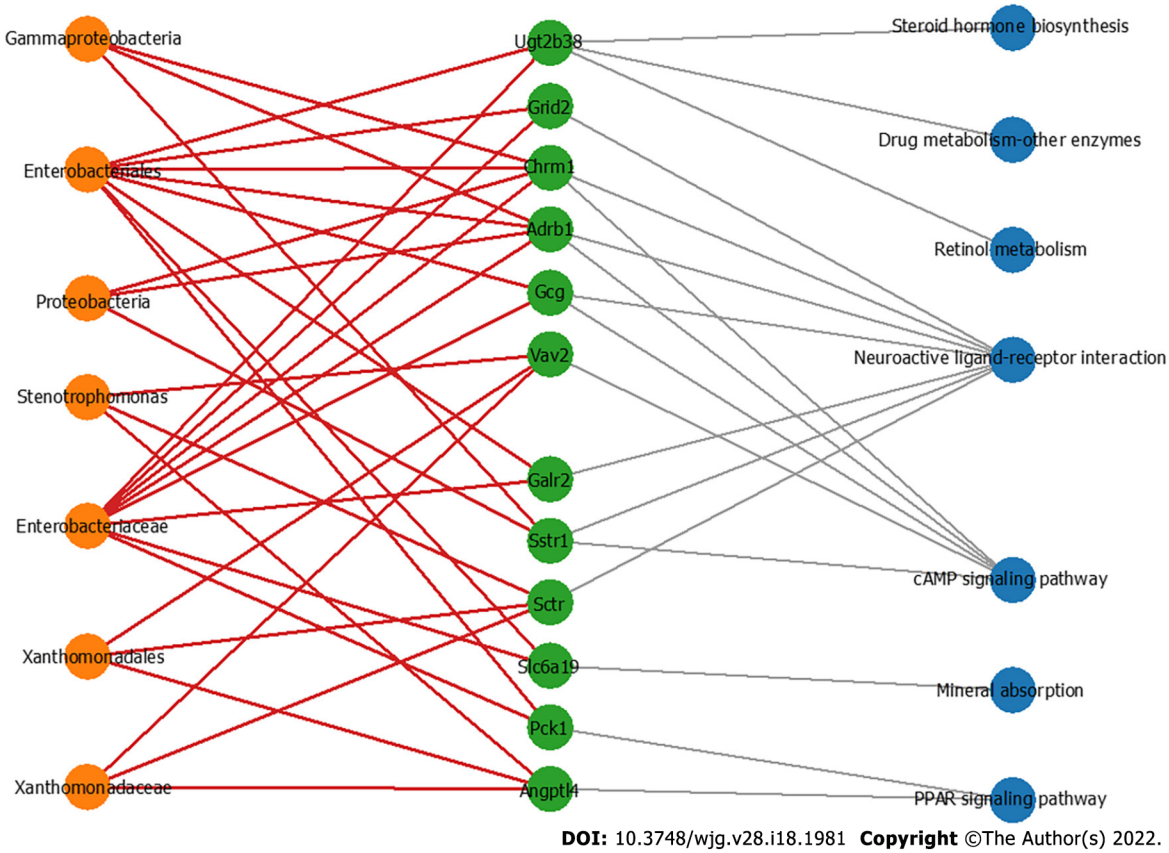
DISCUSSION

F. nucleatum has long been known to cause opportunistic infections and has recently been implicated in CRC, which has attracted broad attention. Previously, we found that the RA of *F. nucleatum* in the fecal microbiota was significantly increased in CRC patients[33]. However, the effect of *F. nucleatum* infection on the mucosal microbiota and the resulting relationship between gut microbiome alterations and CRC development are still open questions. AOM/DSS mice can spontaneously develop multiple intestinal adenomas and have been used extensively as a model of colorectal carcinogenesis inflammation-associated tumors[45]. We showed that AOM/DSS mice with *F. nucleatum* infection have a higher burden of intestinal adenoma and worse colon histology. At the same time, an impaired mucosal barrier as shown by E-cadherin expression and increased epithelial cell proliferation by Ki-67 in the AOM/DSS-FUSO group were observed.



DOI: 10.3748/wjg.v28.i18.1981 **Copyright** ©The Author(s) 2022.

Figure 5 Bubble plot of the KEGG pathways. The size of the bubble indicates the relative number of genes in the set. The color of the bubble indicates the adjusted *P* value.



DOI: 10.3748/wjg.v28.i18.1981 **Copyright** ©The Author(s) 2022.

Figure 6 The co-occurrence network shows the correlations of the colon mucosa microbiota with the differentially expressed genes. Edges: Correlations with *P* values < 0.01; red edges: Positive correlations; gray edges: Relationship between the genes and the pathways; green nodes: Genes involved in the top seven significantly differential KEGG pathways in the azoxymethane/dextran sulfate sodium salt (AOM/DSS)-FUSO group compared with the AOM/DSS group; orange nodes: The differential bacterial taxa identified by LEfSe analysis; blue nodes: Related pathways of defferentially expressed genes.

After the introduction of *F. nucleatum*, we propose that *F. nucleatum* needs to adapt to and change the symbiotic microbial environment, which could activate and promote the progression of colorectal carcinogenesis. In this study, three increased inflammation-inducing bacteria and three decreased probiotic genera in the top 50 differentially expressed genera were recognized as dysbiotic mucosal taxa after *F. nucleatum* stimulation. Furthermore, changes in the structure of the mucosal microbiota among the three groups were identified. Proteobacteria and eight other pathogenic bacterial taxa (Figure 3A)

were the dominant taxa in the AOM/DSS-FUSO mice compared with the AOM/DSS group. In agreement with previous studies, gut microbial comparisons of CRC patients and non-CRC subjects are characterized by a high prevalence of pro-inflammatory bacteria (mostly Proteobacteria) and a decrease in commensal beneficial bacteria (mostly Firmicutes)[33,46,47]. Notably, the transfer of two Enterobacteriaceae species (*Klebsiella pneumoniae* and *Proteus mirabilis*) was sufficient to provoke colitis in the recipient mice[48]. The overload of Proteobacteria promoted intestinal inflammation in a T-bet$^{-/-}$ Rag2$^{-/-}$ mouse model of colitis[48-50]. Similar to studies in mice, microbiota studies in humans have shown that the gut microbial structure of inflammatory bowel disease patients is characterized by an expansion of Proteobacteria, particularly Enterobacteriaceae. Consistent with previous studies, we observed that the RA of Enterobacteriaceae in the mucosal microbiota was positively correlated with the expression of key oncogenes. Moreover, three other taxa, *Stenotrophomonas*, Xanthomonadales, and Xanthomonadaceae, were positively correlated with ATGPTL4 (angiopoietin-like 4), the VAV2 oncogene, and SCTR (secretin receptor), as shown in Figure 6. *Stenotrophomonas* was proven to be significantly increased during the exacerbated phase of UC compared to the remission phase[51]. Based on the above evidence, we propose that abnormal expansion of Proteobacteria, especially Enterobacteriaceae and *Stenotrophomonas*, is the signature of microbial dysbiosis driven by *F. nucleatum*.

To further reveal the effects of *F. nucleatum* infection and microbial dysbiosis on the transcriptome of AOM/DSS mice, RNA-seq was performed, and 323 DEGs were identified that were influenced by the oncogenic microbial environment. Interestingly, we found that the *F. nucleatum*-driven DEGs were significantly enriched in cancer-related KEGG signaling pathways. The neuroactive ligand–receptor interaction, cAMP signaling pathway, and PPAR signaling pathway were significantly overexpressed in the AOM/DSS-FUSO group. Among them, ANGPTL4, VAV2, and PCK1 were significantly highly expressed in the AOM/DSS-FUSO groups and positively correlated with the Proteobacteria taxa. In CRC cell lines, Zheng *et al*[52] found that *F. nucleatum* infection provoked glucose uptake and subsequently promoted glycolysis activity of CRC cells *via* ATGPTL4, which could in turn facilitate its own colonization in CRC cells[52]. *F. nucleatum*-mediated glycolysis activation *via* ATGPTL4 plays important roles in the pathogenesis of CRC and subsequently provides a beneficial environment for the outgrowth of CRC-related taxa.

Consistent with our results, other recent studies have demonstrated that *F. nucleatum* provokes glycolysis by upregulating lncRNA ENO-1[53], and an increase in cellular metabolic activity provides ample cellular energy for EMT-mediated metastasis[54]. Another oncogene, *VAV2*, related to three Proteobacteria taxa, is a member of the VAV guanine nucleotide exchange factor family of oncogenes and is one of the five combined prognostic genes that was identified to form a prognostic mutation panel for predicting cancer recurrence in stage II and III CRC[55]. Loss of VAV2, VAV3 and TIAM1 is sufficient to strongly suppress the cancer phenotypes and tumorigenesis induced by APC loss[56].

It is important to note that the eight upregulated hub genes shown in the microbiota-transcriptome network were positively correlated with high levels of Enterobacteriaceae, *e.g.*, PCK1, GalR2, GCG, SLC6A19, CHRM1, ADRB1, UGT2B38, and GRID2. Among them, PCK1 enhanced liver metastatic growth by driving pyrimidine nucleotide biosynthesis under hypoxia[40]. G-protein-coupled receptor galanin receptor 1 (GalR1) was identified as a novel regulator of drug resistance[57]. Notably, silencing either GalR1 or its ligand, galanin, induced apoptosis in both drug-sensitive and drug-resistant cell lines and synergistically enhanced the effects of chemotherapy. Mechanistically, GalR1/galanin silencing resulted in downregulation of the endogenous caspase-8 inhibitor FLIP(L), resulting in induction of caspase-8-dependent apoptosis. *Galanin* mRNA was found to be overexpressed in colorectal tumors, and importantly, high galanin expression was correlated with poor disease-free survival of patients with early-stage CRC. In the future, additional studies need to be performed to explore the effect of *F. nucleatum* on Proteobacteria-related oncogenes to clarify the roles of *F. nucleatum* in CRC diseases.

Therefore, our data present the key microbial signature after *F. nucleatum* infection, which may provide new insights into the role of dysbiosis in the mucosal microbiota driven by *F. nucleatum* in promoting CRC. We provide direct evidence that Proteobacteria expansion, in particular Enterobacteriaceae and *Stenotrophomonas*, occurs during *F. nucleatum* infection, leading to the differential expression of oncogene transcriptomes in the AOM/DSS model. We provide evidence that *F. nucleatum* interacts with other species, how it remodels the microbiota, and how it alters the tumor microenvironment. Furthermore, we revealed the dysbiosis signature of the colon mucosa microbiota driven by *Fusobacterium* and the interaction between the hub microbial taxa and the host transcriptome. A deeper understanding of CRC etiology will also help identify new targets for prevention and treatment.

CONCLUSION

In conclusion, these data extend our previous work to provide evidence for microbial dysbiosis in CRC and suggest the existence of a defined set of microbiota whose composition is essential. Our study is also distinct in taking a holistic approach, given the observation of important bacterial-host networks and evidence for an oncogenic microbial environment of the colon promoting the formation of CRC. Our study is limited by: (1) The lack of time-course experiments to validate the effects of *F. nucleatum* on

the symbiotic microenvironment; and (2) The limited sample size due to the deaths of mice when establishing the disease model. Therefore, further studies using more mice to establish the disease model are required to confirm the findings here and to disentangle the defined role of the Proteobacteria-related oncogenes driven by *F. nucleatum* during the progression of colorectal adenomas.

ARTICLE HIGHLIGHTS

Research background

Fusobacterium nucleatum (*F. nucleatum*) has long been known to cause opportunistic infections and has recently been implicated in colorectal cancer (CRC), which has attracted broad attention. Exploring the roles and underlying mechanism of *F. nucleatum* has important theoretical and practical significance for diagnosis and targeted therapy of CRC.

Research motivation

The aim of this study is to reveal the effect of *F. nucleatum* infection on the changes of mucosal microbiota, and investigate the regulatory role of *F. nucleatum* in the CRC progression.

Research objectives

The azoxymethane/dextran sulfate sodium salt (AOM/DSS)-induced mice were used to investigate the role of *F. nucleatum* in the "oncogenic microbial environment" of the colon.

Research methods

The mucosal microbial composition and RNA-seq transcriptomic analysis were used to identify the differentially expressed gene (DEG) signatures driven by *F. nucleatum* infection, and integrated network analysis was conducted to reveal the relationship between microbial dysbiosis and the DEGs.

Research results

We provide direct evidence that *F. nucleatum* interacts with other species, remodels the microbiota, and alters the tumor microenvironment. In addition, we revealed the dysbiosis signature of the colon mucosa microbiota driven by *F. nucleatum* and the interaction between the hub microbial taxa and the host transcriptome.

Research conclusions

Dysbiosis in the mucosal microbiota driven by *F. nucleatum*, in particular Enterobacteriaceae and *Stenotrophomonas*, occurs during *F. nucleatum* infection, leading to the differential expression of oncogene transcriptomes in the AOM/DSS model.

Research perspectives

Our study provides a deeper insight into CRC etiology driven by *F. nucleatum* infection and the mechanisms of the tumorigenic effect of *F. nucleatum*. Targeting *F. nucleatum* infection is a potential treatment for CRC.

FOOTNOTES

Author contributions: Wu N and Feng YQ contributed equally to this work and performed the majority of experiments. Wu N, Yu WD, and Hu YF designed and coordinated the study; Wu N, Feng YQ, Lyu N, and Wang D performed the experiments; Wu N and Feng YQ analyzed and interpreted the data; Wu N, Feng YQ and Hu YF wrote the manuscript; all authors approved the final version of the article.

Supported by National Natural Science Foundation of China, No. 32070116; and Open Project Program of CAS Key Laboratory of Pathogenic Microbiology and Immunology, No. CASPMI202102.

Institutional animal care and use committee statement: The study was reviewed and approved by the Institutional Animal Care Committee of the Peking University People's Hospital. All animal experiments conformed to the internationally accepted principles for the care and use of laboratory animals.

Conflict-of-interest statement: The authors declare no competing interests.

Data sharing statement: The raw 16S amplicon sequencing and transcriptome data in this study have been deposited in the NCBI Sequence Read Archive (SRA) under BioProject number PRJNA767246.

ARRIVE guidelines statement: The authors have read the ARRIVE guidelines, and the manuscript was prepared and

revised according to the ARRIVE guidelines.

Open-Access: This article is an open-access article that was selected by an in-house editor and fully peer-reviewed by external reviewers. It is distributed in accordance with the Creative Commons Attribution NonCommercial (CC BY-NC 4.0) license, which permits others to distribute, remix, adapt, build upon this work non-commercially, and license their derivative works on different terms, provided the original work is properly cited and the use is non-commercial. See: https://creativecommons.org/Licenses/by-nc/4.0/

Country/Territory of origin: China

ORCID number: Na Wu 0000-0001-6803-8337; Yu-Qing Feng 0000-0002-7742-5272; Na Lyu 0000-0003-0603-6170; Di Wang 0000-0003-0553-7977; Wei-Dong Yu 0000-0002-7573-4979; Yong-Fei Hu 0000-0002-2158-6018.

S-Editor: Fan JR
L-Editor: A
P-Editor: Yu HG

REFERENCES

1 **Song M**, Garrett WS, Chan AT. Nutrients, foods, and colorectal cancer prevention. *Gastroenterology* 2015; **148**: 1244-60.e16 [PMID: 25575572 DOI: 10.1053/j.gastro.2014.12.035]
2 **Chen W**, Zheng R, Baade PD, Zhang S, Zeng H, Bray F, Jemal A, Yu XQ, He J. Cancer statistics in China, 2015. *CA Cancer J Clin* 2016; **66**: 115-132 [PMID: 26808342 DOI: 10.3322/caac.21338]
3 **Kostic AD**, Chun E, Robertson L, Glickman JN, Gallini CA, Michaud M, Clancy TE, Chung DC, Lochhead P, Hold GL, El-Omar EM, Brenner D, Fuchs CS, Meyerson M, Garrett WS. *Fusobacterium nucleatum* potentiates intestinal tumorigenesis and modulates the tumor-immune microenvironment. *Cell Host Microbe* 2013; **14**: 207-215 [PMID: 23954159 DOI: 10.1016/j.chom.2013.07.007]
4 **Castellarin M**, Warren RL, Freeman JD, Dreolini L, Krzywinski M, Strauss J, Barnes R, Watson P, Allen-Vercoe E, Moore RA, Holt RA. *Fusobacterium nucleatum* infection is prevalent in human colorectal carcinoma. *Genome Res* 2012; **22**: 299-306 [PMID: 22009989 DOI: 10.1101/gr.126516.111]
5 **Li YY**, Ge QX, Cao J, Zhou YJ, Du YL, Shen B, Wan YJ, Nie YQ. Association of *Fusobacterium nucleatum* infection with colorectal cancer in Chinese patients. *World J Gastroenterol* 2016; **22**: 3227-3233 [PMID: 27004000 DOI: 10.3748/wjg.v22.i11.3227]
6 **Mima K**, Nishihara R, Qian ZR, Cao Y, Sukawa Y, Nowak JA, Yang J, Dou R, Masugi Y, Song M, Kostic AD, Giannakis M, Bullman S, Milner DA, Baba H, Giovannucci EL, Garraway LA, Freeman GJ, Dranoff G, Garrett WS, Huttenhower C, Meyerson M, Meyerhardt JA, Chan AT, Fuchs CS, Ogino S. *Fusobacterium nucleatum* in colorectal carcinoma tissue and patient prognosis. *Gut* 2016; **65**: 1973-1980 [PMID: 26311717 DOI: 10.1136/gutjnl-2015-310101]
7 **Xu M**, Yamada M, Li M, Liu H, Chen SG, Han YW. FadA from *Fusobacterium nucleatum* utilizes both secreted and nonsecreted forms for functional oligomerization for attachment and invasion of host cells. *J Biol Chem* 2007; **282**: 25000-25009 [PMID: 17588948 DOI: 10.1074/jbc.M611567200]
8 **Fardini Y**, Wang X, Témoin S, Nithianantham S, Lee D, Shoham M, Han YW. *Fusobacterium nucleatum* adhesin FadA binds vascular endothelial cadherin and alters endothelial integrity. *Mol Microbiol* 2011; **82**: 1468-1480 [PMID: 22040113 DOI: 10.1111/j.1365-2958.2011.07905.x]
9 **Yang Y**, Weng W, Peng J, Hong L, Yang L, Toiyama Y, Gao R, Liu M, Yin M, Pan C, Li H, Guo B, Zhu Q, Wei Q, Moyer MP, Wang P, Cai S, Goel A, Qin H, Ma Y. *Fusobacterium nucleatum* increases proliferation of colorectal cancer cells and tumor development in mice by activating Toll-like receptor 4 signaling to nuclear factor-κB, and up-regulating expression of microRNA-21. *Gastroenterology* 2017; **152**: 851-866.e24 [PMID: 27876571 DOI: 10.1053/j.gastro.2016.11.018]
10 **Abed J**, Emgård JE, Zamir G, Faroja M, Almogy G, Grenov A, Sol A, Naor R, Pikarsky E, Atlan KA, Mellul A, Chaushu S, Manson AL, Earl AM, Ou N, Brennan CA, Garrett WS, Bachrach G. Fap2 mediates *Fusobacterium nucleatum* colorectal adenocarcinoma enrichment by binding to tumor-expressed Gal-GalNAc. *Cell Host Microbe* 2016; **20**: 215-225 [PMID: 27512904 DOI: 10.1016/j.chom.2016.07.006]
11 **Kang W**, Sun T, Tang D, Zhou J, Feng Q. Time-course transcriptome analysis of gingiva-derived mesenchymal stem cells reveals that *Fusobacterium nucleatum* triggers oncogene expression in the process of cell differentiation. *Front Cell Dev Biol* 2019; **7**: 359 [PMID: 31993418 DOI: 10.3389/fcell.2019.00359]
12 **Wang L**, Peng F, Peng C, Du JR. Gut microbiota in tumor microenvironment: A critical regulator in cancer initiation and development as potential targets for Chinese medicine. *Am J Chin Med* 2021; **49**: 609-626 [PMID: 33683187 DOI: 10.1142/S0192415X21500270]
13 **Wong-Rolle A**, Wei HK, Zhao C, Jin C. Unexpected guests in the tumor microenvironment: microbiome in cancer. *Protein Cell* 2021; **12**: 426-435 [PMID: 33296049 DOI: 10.1007/s13238-020-00813-8]
14 **Garrett WS**. Cancer and the microbiota. *Science* 2015; **348**: 80-86 [PMID: 25838377 DOI: 10.1126/science.aaa4972]
15 **Doulberis M**, Angelopoulou K, Kaldrymidou E, Tsingotjidou A, Abas Z, Erdman SE, Poutahidis T. Cholera-toxin suppresses carcinogenesis in a mouse model of inflammation-driven sporadic colon cancer. *Carcinogenesis* 2015; **36**: 280-290 [PMID: 25550315 DOI: 10.1093/carcin/bgu325]
16 **Liu L**, Liang L, Liang H, Wang M, Lu B, Xue M, Deng J, Chen Y. *Fusobacterium nucleatum* aggravates the progression of colitis by regulating M1 macrophage polarization *via* AKT2 pathway. *Front Immunol* 2019; **10**: 1324 [PMID: 31249571

DOI: 10.3389/fimmu.2019.01324]
17 **Yu Y**, Lee C, Kim J, Hwang S. Group-specific primer and probe sets to detect methanogenic communities using quantitative real-time polymerase chain reaction. *Biotechnol Bioeng* 2005; **89**: 670-679 [PMID: 15696537 DOI: 10.1002/bit.20347]
18 **Chen S**, Zhou Y, Chen Y, Gu J. fastp: An ultra-fast all-in-one FASTQ preprocessor. *Bioinformatics* 2018; **34**: i884-i890 [PMID: 30423086 DOI: 10.1093/bioinformatics/bty560]
19 **Rognes T**, Flouri T, Nichols B, Quince C, Mahé F. VSEARCH: A versatile open source tool for metagenomics. *PeerJ* 2016; **4**: e2584 [PMID: 27781170 DOI: 10.7717/peerj.2584]
20 **Edgar RC**. UPARSE: highly accurate OTU sequences from microbial amplicon reads. *Nat Methods* 2013; **10**: 996-998 [PMID: 23955772 DOI: 10.1038/nmeth.2604]
21 **Schloss PD**. A high-throughput DNA sequence aligner for microbial ecology studies. *PLoS One* 2009; **4**: e8230 [PMID: 20011594 DOI: 10.1371/journal.pone.0008230]
22 **Caporaso JG**, Kuczynski J, Stombaugh J, Bittinger K, Bushman FD, Costello EK, Fierer N, Peña AG, Goodrich JK, Gordon JI, Huttley GA, Kelley ST, Knights D, Koenig JE, Ley RE, Lozupone CA, McDonald D, Muegge BD, Pirrung M, Reeder J, Sevinsky JR, Turnbaugh PJ, Walters WA, Widmann J, Yatsunenko T, Zaneveld J, Knight R. QIIME allows analysis of high-throughput community sequencing data. *Nat Methods* 2010; **7**: 335-336 [PMID: 20383131 DOI: 10.1038/nmeth.f.303]
23 **Lozupone C**, Knight R. UniFrac: A new phylogenetic method for comparing microbial communities. *Appl Environ Microbiol* 2005; **71**: 8228-8235 [PMID: 16332807 DOI: 10.1128/AEM.71.12.8228-8235.2005]
24 **Kim D**, Langmead B, Salzberg SL. HISAT: A fast spliced aligner with low memory requirements. *Nat Methods* 2015; **12**: 357-360 [PMID: 25751142 DOI: 10.1038/nmeth.3317]
25 **Liao Y**, Smyth GK, Shi W. featureCounts: An efficient general purpose program for assigning sequence reads to genomic features. *Bioinformatics* 2014; **30**: 923-930 [PMID: 24227677 DOI: 10.1093/bioinformatics/btt656]
26 **Klipper-Aurbach Y**, Wasserman M, Braunspiegel-Weintrob N, Borstein D, Peleg S, Assa S, Karp M, Benjamini Y, Hochberg Y, Laron Z. Mathematical formulae for the prediction of the residual beta cell function during the first two years of disease in children and adolescents with insulin-dependent diabetes mellitus. *Med Hypotheses* 1995; **45**: 486-490 [PMID: 8748093 DOI: 10.1016/0306-9877(95)90228-7]
27 **Wu T**, Hu E, Xu S, Chen M, Guo P, Dai Z, Feng T, Zhou L, Tang W, Zhan L, Fu X, Liu S, Bo X, Yu G. clusterProfiler 4.0: A universal enrichment tool for interpreting omics data. *Innovation (N Y)* 2021; **2**: 100141 [PMID: 34557778 DOI: 10.1016/j.xinn.2021.100141]
28 **Zapala MA**, Schork NJ. Multivariate regression analysis of distance matrices for testing associations between gene expression patterns and related variables. *Proc Natl Acad Sci U S A* 2006; **103**: 19430-19435 [PMID: 17146048 DOI: 10.1073/pnas.0609333103]
29 **Segata N**, Izard J, Waldron L, Gevers D, Miropolsky L, Garrett WS, Huttenhower C. Metagenomic biomarker discovery and explanation. *Genome Biol* 2011; **12**: R60 [PMID: 21702898 DOI: 10.1186/gb-2011-12-6-r60]
30 **Shannon P**, Markiel A, Ozier O, Baliga NS, Wang JT, Ramage D, Amin N, Schwikowski B, Ideker T. Cytoscape: A software environment for integrated models of biomolecular interaction networks. *Genome Res* 2003; **13**: 2498-2504 [PMID: 14597658 DOI: 10.1101/gr.1239303]
31 **Neufert C**, Heichler C, Brabletz T, Scheibe K, Boonsanay V, Greten FR, Neurath MF. Inducible mouse models of colon cancer for the analysis of sporadic and inflammation-driven tumor progression and lymph node metastasis. *Nat Protoc* 2021; **16**: 61-85 [PMID: 33318692 DOI: 10.1038/s41596-020-00412-1]
32 **Stemmler MP**, Eccles RL, Brabletz S, Brabletz T. Non-redundant functions of EMT transcription factors. *Nat Cell Biol* 2019; **21**: 102-112 [PMID: 30602760 DOI: 10.1038/s41556-018-0196-y]
33 **Wu N**, Yang X, Zhang R, Li J, Xiao X, Hu Y, Chen Y, Yang F, Lu N, Wang Z, Luan C, Liu Y, Wang B, Xiang C, Wang Y, Zhao F, Gao GF, Wang S, Li L, Zhang H, Zhu B. Dysbiosis signature of fecal microbiota in colorectal cancer patients. *Microb Ecol* 2013; **66**: 462-470 [PMID: 23733170 DOI: 10.1007/s00248-013-0245-9]
34 **Zhang Y**, Zhang W, Xia M, Xie Z, An F, Zhan Q, Tian W, Zhu T. High expression of FABP4 in colorectal cancer and its clinical significance. *J Zhejiang Univ Sci B* 2021; **22**: 136-145 [PMID: 33615754 DOI: 10.1631/jzus.B2000366]
35 **Zhang Q**, Zhao H, Wu D, Cao D, Ma W. A comprehensive analysis of the microbiota composition and gene expression in colorectal cancer. *BMC Microbiol* 2020; **20**: 308 [PMID: 33050883 DOI: 10.1186/s12866-020-01938-w]
36 **Ji M**, Feng Q, He G, Yang L, Tang W, Lao X, Zhu D, Lin Q, Xu P, Wei Y, Xu J. Silencing homeobox C6 inhibits colorectal cancer cell proliferation. *Oncotarget* 2016; **7**: 29216-29227 [PMID: 27081081 DOI: 10.18632/oncotarget.8703]
37 **Hu L**, Chen HY, Cai J, Yang GZ, Feng D, Zhai YX, Gong H, Qi CY, Zhang Y, Fu H, Cai QP, Gao CF. Upregulation of NETO2 expression correlates with tumor progression and poor prognosis in colorectal carcinoma. *BMC Cancer* 2015; **15**: 1006 [PMID: 26699544 DOI: 10.1186/s12885-015-2018-y]
38 **Chang H**, Zhao F, Xie X, Liao Y, Song Y, Liu C, Wu Y, Wang Y, Liu D, Zou J, Qi Z. PPARα suppresses Th17 cell differentiation through IL-6/STAT3/RORγt pathway in experimental autoimmune myocarditis. *Exp Cell Res* 2019; **375**: 22-30 [PMID: 30557558 DOI: 10.1016/j.yexcr.2018.12.005]
39 **Yang J**, Gao S, Qiu M, Kan S. Integrated Analysis of Gene Expression and metabolite data reveals candidate molecular markers in colorectal carcinoma. *Cancer Biother Radiopharm* 2020 [PMID: 33259728 DOI: 10.1089/cbr.2020.3980]
40 **Yamaguchi N**, Weinberg EM, Nguyen A, Liberti MV, Goodarzi H, Janjigian YY, Paty PB, Saltz LB, Kingham TP, Loo JM, de Stanchina E, Tavazoie SF. PCK1 and DHODH drive colorectal cancer liver metastatic colonization and hypoxic growth by promoting nucleotide synthesis. *Elife* 2019; **8**: e52135 [PMID: 31841108 DOI: 10.7554/eLife.52135]
41 **Bian Q**, Chen J, Qiu W, Peng C, Song M, Sun X, Liu Y, Ding F, Zhang L. Four targeted genes for predicting the prognosis of colorectal cancer: A bioinformatics analysis case. *Oncol Lett* 2019; **18**: 5043-5054 [PMID: 31612015 DOI: 10.3892/ol.2019.10866]
42 **Hebeis B**, Vigorito E, Kovesdi D, Turner M. Vav proteins are required for B-lymphocyte responses to LPS. *Blood* 2005; **106**: 635-640 [PMID: 15811961 DOI: 10.1182/blood-2004-10-3919]
43 **Wen L**, Zhang Y, Yang B, Han F, Ebadi AG, Toughani M. Knockdown of Angiopoietin-like protein 4 suppresses the

development of colorectal cancer. *Cell Mol Biol (Noisy-le-grand)* 2020; **66**: 117-124 [PMID: 33040824 DOI: 10.3892/or.2018.6253]

44 **Merlo LMF**, DuHadaway JB, Montgomery JD, Peng WD, Murray PJ, Prendergast GC, Caton AJ, Muller AJ, Mandik-Nayak L. Differential roles of IDO1 and IDO2 in T and B cell inflammatory immune responses. *Front Immunol* 2020; **11**: 1861 [PMID: 32973768 DOI: 10.3389/fimmu.2020.01861]

45 **Neufert C**, Becker C, Neurath MF. An inducible mouse model of colon carcinogenesis for the analysis of sporadic and inflammation-driven tumor progression. *Nat Protoc* 2007; **2**: 1998-2004 [PMID: 17703211 DOI: 10.1038/nprot.2007.279]

46 **Chamorro N**, Montero DA, Gallardo P, Farfán M, Contreras M, De la Fuente M, Dubois K, Hermoso MA, Quera R, Pizarro-Guajardo M, Paredes-Sabja D, Ginard D, Rosselló-Móra R, Vidal R. Landscapes and bacterial signatures of mucosa-associated intestinal microbiota in Chilean and Spanish patients with inflammatory bowel disease. *Microb Cell* 2021; **8**: 223-238 [PMID: 34527721 DOI: 10.15698/mic2021.09.760]

47 **Wassenaar TM**. E. coli and colorectal cancer: A complex relationship that deserves a critical mindset. *Crit Rev Microbiol* 2018; **44**: 619-632 [PMID: 29909724 DOI: 10.1080/1040841X.2018.1481013]

48 **Garrett WS**, Gallini CA, Yatsunenko T, Michaud M, DuBois A, Delaney ML, Punit S, Karlsson M, Bry L, Glickman JN, Gordon JI, Onderdonk AB, Glimcher LH. Enterobacteriaceae act in concert with the gut microbiota to induce spontaneous and maternally transmitted colitis. *Cell Host Microbe* 2010; **8**: 292-300 [PMID: 20833380 DOI: 10.1016/j.chom.2010.08.004]

49 **Shin NR**, Whon TW, Bae JW. Proteobacteria: microbial signature of dysbiosis in gut microbiota. *Trends Biotechnol* 2015; **33**: 496-503 [PMID: 26210164 DOI: 10.1016/j.tibtech.2015.06.011]

50 **Rooks MG**, Veiga P, Wardwell-Scott LH, Tickle T, Segata N, Michaud M, Gallini CA, Beal C, van Hylckama-Vlieg JE, Ballal SA, Morgan XC, Glickman JN, Gevers D, Huttenhower C, Garrett WS. Gut microbiome composition and function in experimental colitis during active disease and treatment-induced remission. *ISME J* 2014; **8**: 1403-1417 [PMID: 24500617 DOI: 10.1038/ismej.2014.3]

51 **Walujkar SA**, Kumbhare SV, Marathe NP, Patangia DV, Lawate PS, Bharadwaj RS, Shouche YS. Molecular profiling of mucosal tissue associated microbiota in patients manifesting acute exacerbations and remission stage of ulcerative colitis. *World J Microbiol Biotechnol* 2018; **34**: 76 [PMID: 29796862 DOI: 10.1007/s11274-018-2449-0]

52 **Zheng X**, Liu R, Zhou C, Yu H, Luo W, Zhu J, Liu J, Zhang Z, Xie N, Peng X, Xu X, Cheng L, Yuan Q, Huang C, Zhou X. ANGPTL4-mediated promotion of glycolysis facilitates the colonization of *Fusobacterium nucleatum* in colorectal cancer. *Cancer Res* 2021; **81**: 6157-6170 [PMID: 34645607 DOI: 10.1158/0008-5472.CAN-21-2273]

53 **Hong J**, Guo F, Lu SY, Shen C, Ma D, Zhang X, Xie Y, Yan T, Yu T, Sun T, Qian Y, Zhong M, Chen J, Peng Y, Wang C, Zhou X, Liu J, Liu Q, Ma X, Chen YX, Chen H, Fang JY. *F. nucleatum* targets lncRNA ENO1-IT1 to promote glycolysis and oncogenesis in colorectal cancer. *Gut* 2021; **70**: 2123-2137 [PMID: 33318144 DOI: 10.1136/gutjnl-2020-322780]

54 **Teo Z**, Sng MK, Chan JSK, Lim MMK, Li Y, Li L, Phua T, Lee JYH, Tan ZW, Zhu P, Tan NS. Elevation of adenylate energy charge by angiopoietin-like 4 enhances epithelial-mesenchymal transition by inducing 14-3-3γ expression. *Oncogene* 2017; **36**: 6408-6419 [PMID: 28745316 DOI: 10.1038/onc.2017.244]

55 **Sho S**, Court CM, Winograd P, Russell MM, Tomlinson JS. A prognostic mutation panel for predicting cancer recurrence in stages II and III colorectal cancer. *J Surg Oncol* 2017; **116**: 996-1004 [PMID: 28767131 DOI: 10.1002/jso.24781]

56 **Pickering KA**, Gilroy K, Cassidy JW, Fey SK, Najumudeen AK, Zeiger LB, Vincent DF, Gay DM, Johansson J, Fordham RP, Miller B, Clark W, Hedley A, Unal EB, Kiel C, McGhee E, Machesky LM, Nixon C, Johnsson AE, Bain M, Strathdee D, van Hoof SR, Medema JP, Anderson KI, Brachmann SM, Stucke VM, Malliri A, Drysdale M, Turner M, Serrano L, Myant K, Campbell AD, Sansom OJ. A RAC-GEF network critical for early intestinal tumourigenesis. *Nat Commun* 2021; **12**: 56 [PMID: 33397922 DOI: 10.1038/s41467-020-20255-4]

57 **Stevenson L**, Allen WL, Turkington R, Jithesh PV, Proutski I, Stewart G, Lenz HJ, Van Schaeybroeck S, Longley DB, Johnston PG. Identification of galanin and its receptor GalR1 as novel determinants of resistance to chemotherapy and potential biomarkers in colorectal cancer. *Clin Cancer Res* 2012; **18**: 5412-5426 [PMID: 22859720 DOI: 10.1158/1078-0432.CCR-12-1780]

World Journal of Gastroenterology

Submit a Manuscript: https://www.f6publishing.com

World J Gastroenterol 2022 May 14; 28(18): 1996-2007

DOI: 10.3748/wjg.v28.i18.1996

ISSN 1007-9327 (print) ISSN 2219-2840 (online)

ORIGINAL ARTICLE

Retrospective Cohort Study

Incidental gallbladder cancer diagnosis confers survival advantage irrespective of tumour stage and characteristics

Moath Alarabiyat, Syed Soulat Raza, John Isaac, Darius Mirza, Ravi Marudanayagam, Keith Roberts, Manuel Abradelo, David C Bartlett, Bobby V Dasari, Robert P Sutcliffe, Nikolaos A Chatzizacharias

Specialty type: Surgery

Provenance and peer review: Unsolicited article; Externally peer reviewed.

Peer-review model: Single blind

Peer-review report's scientific quality classification

Grade A (Excellent): 0
Grade B (Very good): B, B
Grade C (Good): C, C
Grade D (Fair): 0
Grade E (Poor): 0

P-Reviewer: Aktas S, Turkey; Garg PK, India; Kai K, Japan; Yasukawa K, Japan

Received: November 13, 2021
Peer-review started: November 13, 2021
First decision: January 9, 2022
Revised: January 22, 2022
Accepted: March 26, 2022
Article in press: March 26, 2022
Published online: May 14, 2022

Moath Alarabiyat, Syed Soulat Raza, John Isaac, Darius Mirza, Ravi Marudanayagam, Keith Roberts, Manuel Abradelo, David C Bartlett, Bobby V Dasari, Robert P Sutcliffe, HPB and Liver Transplant Unit, Queen Elizabeth Hospital, Birmingham B15 2GW, United Kingdom

Nikolaos A Chatzizacharias, Department of HPB and Liver Transplantation, Queen Elizabeth Hospital, University Hospitals Birmingham, Birmingham B15 2TH, United Kingdom

Corresponding author: Nikolaos A Chatzizacharias, FACS, FRCS, MD, PhD, Surgeon, Department of HPB and Liver Transplantation, Queen Elizabeth Hospital, University Hospitals Birmingham, Third Floor, Nuffield House, Mindelsohn Way, Birmingham B15 2TH, United Kingdom. chatzizacharias@gmail.com

Abstract

BACKGROUND

Incidental gallbladder cancer (IGBC) represents 50%-60% of gallbladder cancer cases. Data are conflicting on the role of IGBC diagnosis in oncological outcomes. Some studies suggest that IGBC diagnosis does not affect outcomes, while others that overall survival (OS) is longer in these cases compared to non-incidental diagnosis (NIGBC). Furthermore, some studies reported early tumour stages and histopathologic characteristics as possible confounders, while others not.

AIM

To investigate the role of IGBC diagnosis on patients' overall survival, especially after surgical treatment with curative intent.

METHODS

Retrospective analysis of all patient referrals with gallbladder cancer between 2008 and 2020 in a tertiary hepatobiliary centre. Statistical comparison of patient and tumour characteristics between IGBC and NIGBC subgroups was performed. Survival analysis for the whole cohort, surgical and non-surgical subgroups was done with the Kaplan-Meier method and the use of log rank test. Risk analysis was performed with univariable and multivariable Cox regression analysis.

RESULTS

The cohort included 261 patients with gallbladder cancer. 65% of cases had NIGBC and 35% had IGBC. A total of 90 patients received surgical treatment (66% of IGBC cases and 19% of NIGBC cases). NIGBC patients had more advanced T

stage and required more extensive resections than IGBC ones. OS was longer in patients with IGBC in the whole cohort (29 *vs* 4 mo, $P < 0.001$), as well as in the non-surgical (14 *vs* 2 mo, $P < 0.001$) and surgical subgroups (29 *vs* 16.5 mo, $P = 0.001$). Disease free survival (DFS) after surgery was longer in patients with IGBC (21.5 mo *vs* 8.5 mo, $P = 0.007$). N stage and resection margin status were identified as independent predictors of OS and DFS. NIGBC diagnosis was identified as an independent predictor of OS.

CONCLUSION

IGBC diagnosis may confer a survival advantage independently of the pathological stage and tumour characteristics. Prospective studies are required to further investigate this, including detailed pathological analysis and molecular gene expression.

Key Words: Gallbladder cancer; Incidental gallbladder cancer; Non-incidental gallbladder cancer; Gallbladder cancer survival

©The Author(s) 2022. Published by Baishideng Publishing Group Inc. All rights reserved.

Core Tip: Data are conflicting on the role of incidental gallbladder cancer (IGBC) diagnosis in oncological outcomes. Some studies suggest that IGBC diagnosis does not affect outcomes, while others that overall survival (OS) is longer in these cases compared to non-incidental diagnosis (NIGBC). In our study, IGBC diagnosis conferred better OS in all patients with gallbladder cancer, as well as within the surgical and non-surgical groups. Similarly, disease free survival was significantly longer in patients with IGBC. NIGBC diagnosis was identified as an independent predictor of OS along with N stage and resection margin status.

Citation: Alarabiyat M, Raza SS, Isaac J, Mirza D, Marudanayagam R, Roberts K, Abradelo M, Bartlett DC, Dasari BV, Sutcliffe RP, Chatzizacharias NA. Incidental gallbladder cancer diagnosis confers survival advantage irrespective of tumour stage and characteristics. *World J Gastroenterol* 2022; 28(18): 1996-2007
URL: https://www.wjgnet.com/1007-9327/full/v28/i18/1996.htm
DOI: https://dx.doi.org/10.3748/wjg.v28.i18.1996

INTRODUCTION

Gallbladder cancer (GBC) is associated with poor prognosis even after treatment, with median overall survival (OS) ranging in the literature between 3 and 22 mo[1,2]. Incidental gallbladder cancer (IGBC) discovered on routine histological examination of gallbladder specimens after cholecystectomy is more common than non-incidental gallbladder cancer (NIGBC) and represents 50%-60% of all cases[3-5]. The prognostic implication of incidental or non-incidental diagnosis in oncological outcomes is still a matter of debate as is the effect of the timing of curative intent resection which is performed as a secondary operation in IGBC.

Published evidence are contradictory with some studies suggesting that incidental diagnosis does not affect survival[5-8], while others showed longer survival with IGBC[9-11]. Earlier tumour stages in the IGBC group have been suggested as a confounding factor for any potential survival benefit[5]. On the contrary, other studies identified a survival benefit in IGBC even after controlling for tumour stage and degree of differentiation[9,10].

The aim of this study was to investigate the role of IGBC diagnosis in patient OS and especially after surgical treatment with curative intent.

MATERIALS AND METHODS

This is a retrospective single tertiary centre cohort study between January 2008 and December 2020. The sample included all patients with a histological diagnosis of GBC obtained by surgery or biopsy. The management of all patients was discussed and agreed in the hepatobiliary multidisciplinary (MDT) meeting. IGBC diagnosis was established after histopathological examination of specimens following cholecystectomy for benign aetiology. This was followed by complete staging with a computerized tomography scan of the thorax, abdomen and pelvis (CT-TAP) with subsequent curative intent resection if appropriate. NIGBC diagnosis was made based on imaging and/or biopsy after MDT discussion of referred patients. All patients had staging with CT-TAP, followed by surgery if clinically appropriate. In

patients with locally advanced disease, neoadjuvant chemotherapy was administered and resection was contemplated after restaging. Liver magnetic resonance imaging and positron emission tomography scans were used selectively in both groups if liver metastases or extrahepatic disease was suspected on CT. Following surgical resection all patients were referred to oncology for assessment of adjuvant chemotherapy (AC).

Data were collected and recorded for patient's demographics, American society of anesthesiology (ASA) score, extent of surgical resection, histology, chemotherapy, recurrence and survival. The extent of surgery was defined as minor if radical cholecystectomy, gallbladder (GB) bed resection or liver segments IVb/V resection with or without bile duct resection was performed. It also included patients who only had bile duct resection. The resection was defined as major if a major hepatectomy (three or more liver segments) or multi-visceral resection was performed. Recurrence was defined as local/regional (GB bed, hilar lymph nodes), distant or both. The primary outcome of the study was difference in OS between IGBC and NIGBC and the secondary outcome was difference in disease-free survival (DFS).

T-test, Chi-Square, Fisher's Exact and Mann-Whitney U tests were used as appropriate to compare variables and outcomes between the two groups, with statistical significance set at $P < 0.05$. Survival analysis was performed with the Kaplan-Meier method and log rank test was used to compare survival curves between the study groups. Univariable and multivariable time to event analyses were performed using the Cox proportional hazard model to determine risk factors for OS and DFS. Variables were subjected to a univariable analysis first and those with $P < 0.2$ were introduced into a multivariable model. Hazard ratios (HR) and associated 95% confidence intervals (CI) were calculated. A two-tailed *P* value < 0.05 was considered statistically significant. All statistical analyses were performed using the software package SPSS Statistics for Windows (version 25.0; SPSS Inc., Chicago, IL, United States).

RESULTS

Cohort characteristics and management pathway

The study cohort comprised of 261 patients, with 35% presenting as IGBC and 65% had non incidental presentation (NIGBC) at the time of diagnosis (Figure 1). Median age was 69 years [interquartile range (IQR) 61-77] and male to female ratio was 1:3. Eighty-one percent of NIGBC and 34% of IGBC patients did not undergo resection. For the majority of these (82%) locally advanced or metastatic disease was the main reason. Other causes included patient's choice, poor medical status and pathological stage < 1b (where resection is not indicated) (Table 1). Reasons for not having AC after resection were patients' choice or comorbidities and early tumour stages (CIS, T1/T2, N0) with negative resection margins.

Patient and tumour characteristics of surgical patients

A total of 90 patients had curative intent resection. The type of resection depended on IGBC *vs* NIGBC diagnosis, pre-operative staging, intra-operative findings, cystic duct margin status and the T stage of IGBC patients. Hepatoduodenal (portal) lymphadenectomy was performed in all patients. For IGBC cases, the median time from the time of the index cholecystectomy to the curative resection was 13.5 wk (IQR: 11-16 wk).

Patient and tumour characteristics are shown on Table 2. Patients with NIGBC had more advanced T stage and underwent more extensive resections compared to those with IGBC. Similarly, N stage approached but did not reach significance. The types of procedures performed are shown on Table 3.

Survival analysis

For the whole cohort, median OS was longer in patients with IGBC diagnosis, (29 *vs* 4 mo, $P < 0.001$). OS of IGBC patients was significantly longer compared to NIGBC patients in the non-surgical group (14 *vs* 2 mo, $P < 0.001$), as well as the surgical group (29 *vs* 16.5 mo, $P = 0.001$). Similarly, DFS was significantly longer in patients with IGBC (21.5 mo *vs* 8.5 mo, $P = 0.007$) (Figure 2).

Risk analysis

Univariable Cox regression analysis (Table 4) identified that age, ASA, T stage, N stage, resection margin status and NIGBC diagnosis were significantly related to OS ($P < 0.05$). On multivariable analysis, N stage, resection margin status and NIGBC diagnosis were identified as independent predictors of survival, increasing the risk of mortality by 3, 5 and 2 times respectively (Table 4).

Similarly, T stage, N stage, resection margin status and NIGBC diagnosis were identified to be associated with worse DFS on univariable analysis, however only N stage and resection margin status were found to be independent predictors on multivariable analysis (Table 5).

In an effort to statistically investigate if NIGBC diagnosis acted as a confounding factor for the T stage of the disease despite the use of time-dependent regression analysis, models without this parameter were produced. Again, only N stage and margin status were identified as independent prognostic factors for OS and DFS, while T stage was not (Tables 4 and 5).

Table 1 Reasons for not proceeding with oncological resection, *n* (%)

Reason	IGBC (*n* = 33, 19%)	NIGBC (*n* = 138, 81%)	Total number (*n* = 171)[1]
Locally advanced inoperable disease	0	41 (30)	41 (24)
Metastatic disease	21 (64)	78 (56)	99 (58)
Patient declined surgery	5 (15)	3 (2)	8 (5)
Unfit for surgery	4 (12)	15 (11)	19 (11)
Surgery not required	3 (9)	0	3 (2)

[1]Data missing for one patient.

Table 2 Patient and tumour characteristics for the surgical group, *n* (%)

Variable	IGBC (*n* = 58)	NIGBC (*n* = 32)	*P* value
Median age (range)	63 yr (55.8-71.3)	66 yr (66.0-71.5)	0.302
Gender			0.08
Male	9 (16)	10 (32)	
Female	49 (84)	22 (68)	
Ethnicity			0.507
Caucasian	39 (67)	23 (72)	
Asian	15 (26)	5 (16)	
Black	3 (5)	2 (6)	
Missing	1 (2)	2 (6)	
Median BMI (range)	28.2 (24.3-32.1)	28.2 (24.2-30.7)	0.563
ASA score			0.829
1	4 (7)	2 (6)	
2	43 (74)	23 (72)	
3	10 (17)	6 (19)	
Missing	1 (2)	1 (3)	
Median CCI (range)	4 (3-5)	4 (4-6)	0.635
Extent of surgery			**< 0.001**
Minor resection	57 (98)	24 (75)	
Major resection	1 (2)	8 (25)	
T stage			**< 0.001**
CIS	1 (2)	1 (3)	
T1a	3 (5)	0	
T1b	4 (7)	1 (3)	
T2	42 (72)	12 (38)	
T3	7 (12)	15 (47)	
T4	1 (2)	3 (9)	
N status			0.051
N0	41 (71)	16 (50)	
N1/2	17 (29)	16 (50)	
Histologic type			0.746

CIS	1 (2)	1 (3)	
Adenocarcinoma	55 (94)	30 (94)	
Adeno-squamous	1 (2)	1 (3)	
Mixed	1 (2)	0	
Degree of differentiation (CIS excluded)			0.614
Well	7 (12)	4 (13)	
Moderate	30 (52)	20 (63)	
Poor	12 (21)	5 (16)	
Undifferentiated/unclassified	8 (14)	2 (6)	
Resection margin			0.169
Negative	53 (91)	26 (81)	
Positive	5 (9)	6 (19)	
Cystic duct margin on index cholecystectomy	6 (10)	N/A	N/A
Post-operative complications	15 (26)	11 (34)	0.394
Pattern of recurrence			0.628
Local/regional	5 (9)	5 (16)	
Distant	6 (10)	5 (16)	
Local and distant	2 (3)	1 (3)	
Adjuvant chemotherapy	12 (21)	8 (25)	0.502

ASA: American Society of Anesthesiology; CCI: Charlson Comorbidity Index; BMI: Body mass index.

DISCUSSION

GBC is a rare malignancy with unfavorable prognosis despite the advances in oncological treatments[1,2,12]. The timing of GBC diagnosis, whether incidental after cholecystectomy for benign causes or pre-operative on imaging and/or biopsy, has been previously under investigation for the potential effect in outcomes, however evidence is scarce. Violation of the anatomical planes around the tumour and incomplete clearance during the index laparoscopic cholecystectomy with residual disease in 35%-46% of the patients have been proposed as factors responsible for adverse oncological outcomes in IGBC patients[13-15]. Furthermore, inadvertent GB perforation during cholecystectomy has been reported in up to 22%[16,17], and this could theoretically lead to tumour seeding and metastatic disease. Interestingly, the site of invasion of local disease has also been shown to play an important role in T2 disease[15]. Nonetheless, some published evidence suggested that IGBC diagnosis confers favourable survival, regardless of the stage or degree of differentiation of the disease[9,11]. On the other hand, in other studies, NIGBC diagnosis did not adversely affect survival[5-8]. In a meta-analysis of 51 studies by Pyo *et al*[18], IGBC patients had favorable survival in comparison to NIGBC. However, not all studies included in this meta-analysis were able to show the same difference between both groups.

Sixty five percent of referred patients in our cohort had a preoperative radiological diagnosis of GBC. Sixty six percent of all patients did not proceed to an oncological resection (81% of NIGBC and 36% of IGBC patients), 16% of these due to locally advanced disease (all NIGBC patients) and 38% due to metastatic disease on staging imaging (23% of IGBC and 46% of NIGBC patients). Only 3% of IGBC were stage T1a or below and therefore, no further resection was indicated. Of note only 7% of patients were deemed unfit for surgical treatment. It is clear that the majority of the patients that did not proceed to management with curative intent were due to the late presentation of the disease, a fact that is well described for GBC[19]. The percentage of patients who had AC after curative intent surgery was low (22%). This is comparable with the published literature of around 24%[20]. The reasons for this may include patients' choice and comorbidities, however, may also be attributed to the change in recommended best practice over the years of the study. According to a previously published expert consensus statement, AC was considered only in patients with high risk pathologic features: T3-T4 stages, metastatic lymph nodes and positive resection margins[21]. However, after the BILCAP trial showing improved survival with capecitabine (36.4 mo to 51.1 mo; P = 0.028), it is currently recommended that all patients with resected biliary tract malignancy, including GB cancer, receive 6 mo of adjuvant capecitabine[22]. The results of the currently ongoing ACTICCA-1 trial are eagerly awaited and will provide further evidence if the combination chemotherapy of gemcitabine and cisplatin is

Table 3 Types of surgeries performed in surgically treated patients of the study group, *n* (%)

Type of surgery	IGBC (*n* = 58)	NIGBC (*n* = 32)	Total number (*n* = 90)
Radical cholecystectomy	0	18 (56)	18 (20)
Radical cholecystectomy +extrahepatic bile duct excision	0	6 (19)	6 (7)
Gallbladder bed resection	36 (62)	0	36 (40)
Gallbladder bed resection + extrahepatic bile duct excision	17 (30)	0	17 (19)
Segment IVb + V liver resection	2 (3)	0	2 (2)
Extrahepatic bile duct excision	2 (3)	0	2 (2)
Extended resections:			4 (4)
Central hepatectomy + caudate lobe resection + extrahepatic bile duct excision	0	1 (3)	1 (1)
Pancreaticoduodenectomy + Gallbladder bed resection + right hemicolectomy	0	1 (3)	
Pancreaticoduodenectomy + right hepatectomy	0	1 (3)	
Radical cholecystectomy + right hemicolectomy + partial gastrectomy	0	1 (3)	

Portal lymphadenectomy performed in all cases.

Table 4 Cox proportional hazard analysis for overall survival

Variable	*P* value	HR (95%CI)	*P* value	HR (95%CI)	*P* value	HR (95%CI)
	Univariable analysis		Multivariable analysis		Multivariable analysis (excluding timing of diagnosis variable)	
Age	**0.011**	1.04 (1.01-1.07)	0.453	1.02 (0.97-1.08)	0.153	1.04 (0.99-1.10)
Gender	0.96	1.01 (0.71-1.44)	-	-	-	-
Race	0.853	1.05 (0.61-1.81)	-	-	-	-
BMI	0.601	0.983 (0.92-1.05)	-	-	-	-
ASA score	**0.024**	1.96 (1.09-3.52)	0.121	2.26 (0.81-6.31)	0.061	2.53 (0.96-6.66)
CCI score	0.064	1.19 (0.99-1.42)	0.66	0.91 (0.58-1.41)	0.269	0.78 (0.50-1.21)
T stage	**< 0.001**	2.73 (1.72-4.34)	0.913	1.04 (0.56-1.90)	0.088	1.62 (0.93-2.81)
N stage	**< 0.001**	5.65 (2.84-11.25)	**< 0.001**	3.07 (1.72-5.46)	**0.001**	3.59 (1.72-7.49)
R status	**< 0.001**	7.35 (3.38-15.95)	**< 0.001**	5.26 (2.10-13.13)	**0.012**	3.00 (1.27-7.07)
Post-operative complications	0.885	1.05 (0.53-2.09)	-	-	-	-
Non-incidental diagnosis	**0.004**	2.41 (1.32-4.38)	**0.026**	2.25 (1.10-4.58)	**Not included in analysis**	**Not included in analysis**
Degree of differentiation	0.443	1.40 (0.61-3.21)	-	-	-	-
Adjuvant chemotherapy	0.87	1.07 (0.47-2.44)	-	-	-	-

ASA: American Society of Anesthesiology; CCI: Charlson Comorbidity Index; BMI: Body mass index.

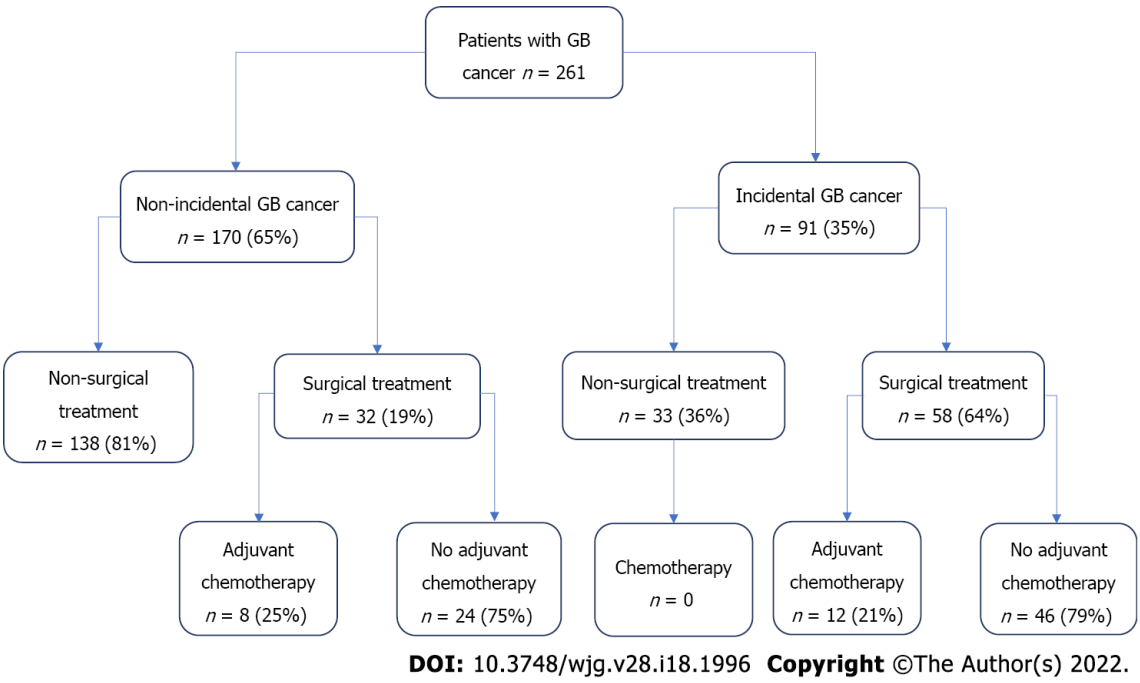
superior to capecitabine monotherapy in the adjuvant setting.

Our data suggests that NIGBC diagnosis adversely affected oncological outcomes. NIGBC patients were more likely to have higher stages of the disease (T3/4), consequently undergoing more extensive resections. The range of oncological procedures for selected cases included multi-visceral resections and major hepatectomies to achieve histologically clear resection margins. Routine performance of such procedures is not associated with survival benefit and has high morbidity rates; however, it is still indicated when the vascular inflow or resection margins are/may be compromised[23-25]. Positive lymph node status was more common in patients with NIGBC with the difference approaching statistical significance. OS of all patients with NIGBC diagnosis was substantially worse than those with IGBC and this was also noted in both surgical and non-surgical subgroups. Furthermore, in the surgical

Table 5 Cox proportional hazard analysis for disease free survival

Variable	*P* value	HR (95%CI)	*P* value	HR (95%CI)	*P* value	HR (95%CI)
	Univariable analysis		Multivariable analysis		Multivariable analysis (excluding timing of diagnosis variable)	
Age	0.275	1.02 (0.98-1.06)	-	-	-	-
Gender	0.732	0.85 (0.34-2.13)	-	-	-	-
Race	0.997	1.13 (0.15-8.51)	-	-	-	-
BMI	0.782	0.99 (0.91-1.07)	-	-	-	-
ASA score	0.817	0.91 (0.42-1.98)	-	-	-	-
CCI score	0.842	0.98 (0.76-1.26)	-	-	-	-
T stage	**0.021**	2.06 (1.12-3.82)	0.504	1.26 (0.64-2.47)	0.21	1.53 (0.79-2.97)
N stage	**0.001**	4.08 (1.83-9.08)	**0.006**	3.18 (1.39-7.26)	**0.008**	3.08 (1.35-7.06)
R status	**< 0.001**	11.05 (3.31-36.94)	**0.006**	5.76 (1.67-19.88)	**0.002**	6.95 (1.98-24.34)
Post-operative complications	0.404	0.63 (0.22-1.85)	-	-	-	-
Non-incidental diagnosis	**0.011**	2.78 (1.26-6.12)	0.09	2.13 (0.89-5.09)	**Not included in analysis**	**Not included in analysis**
Degree of differentiation	0.211	0.65 (0.33-1.28)	-	-	-	-
Adjuvant chemotherapy	0.457	1.42 (0.56-3.58)	-	-	-	-

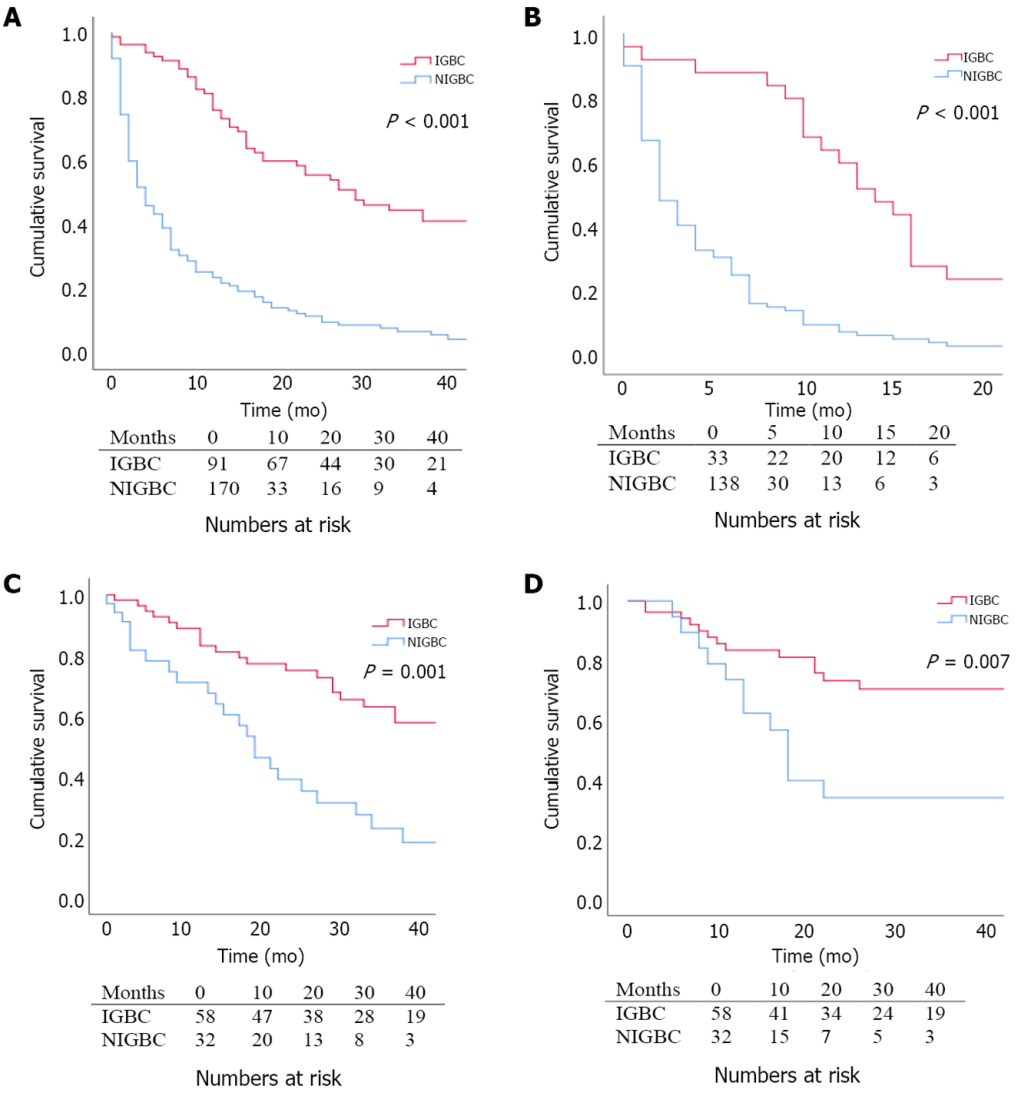
ASA: American Society of Anesthesiology; CCI: Charlson Comorbidity Index; BMI: Body mass index.



DOI: 10.3748/wjg.v28.i18.1996 **Copyright** ©The Author(s) 2022.

Figure 1 Management pathways of whole cohort.

subgroup, NIGBC diagnosis was identified as an independent predictor of OS; doubling the risk of mortality. Stronger predictors were pN stage and margin status, increasing the risk by 3 and 5 times respectively. These findings persisted when models computed that accounted for the possibility of NIGBC diagnosis acting as a confounding factor for T stage (by not including this parameter in the analysis), indicating that it is not true. This seemingly paradoxical observation may be explained by the presence of micro-metastases in early stages of GBC [26], which would affect and in the end dictate OS and DFS, rather than pT stage. Similar were the results for DFS, with N stage and margin status



DOI: 10.3748/wjg.v28.i18.1996 **Copyright** ©The Author(s) 2022.

Figure 2 Kaplan Meier survival curves for incidental gallbladder cancer *vs* non-incidental gallbladder cancer. A: Overall survival (OS) of all cohort; B: Overall survival (OS) of non-surgical treatment; C: OS for surgical treatment; D: Disease-free survival for surgical treatment. IGBC: Incidental gallbladder cancer; NIGBC: Non-incidental gallbladder cancer.

conferring higher relative risk of recurrence, while NIGBC diagnosis approached but did not reach significance.

Lymph node status is an important prognostic factor in GBC. Widmann *et al*[27] in a meta-analysis of 18 observational studies which included more than 27000 patients, has shown that lymph node involvement has significant effect on OS and DFS. Lymphadenectomy also was associated with better OS and DFS in patients with T1b, T2 and T3 disease. This was not clearly demonstrated with T4 disease due to the low number of cases undergoing curative resection in this stage. Lymph node micrometastases, defined as disease detected on immune-histochemical staining, have also been described to correlate with the pathologic N stage of the disease and disease prognosis[28]. Nonetheless, the significance of the extent of lymphadenectomy and lymph node yield is controversial in the published literature, with data from two studies suggesting that harvesting more than four lymph nodes during surgery is associated with improved survival[29,30], whilst a third study concluded that lymph node yield does not correlate with improved survival[31]. These differences may be explained by the differences in pathological reporting (higher lymph node yield may result in more accurate pN staging) and/or variations in the non-surgical part of the patients' management, such differences in the administration of neoadjuvant and adjuvant chemotherapy, regimens, duration *etc*.

Overall, our data suggest that the timing of diagnosis of GBC may play a significant role in the oncological outcomes. Due to the retrospective nature of the study and the long study period, data on the site of invasion (hepatic *vs* peritoneal) were not available, hence this could not be investigated as a possible explanation[32,33]. Another possibility is a difference in the genetic profile of the tumours which could account for different behavior, such as early micrometastases, that cannot be captured by the common radiological investigations and standard pathological parameters of stage and differen-

tiation [34]. However, this cannot be investigated by the current study and would require a prospective molecular study design.

The limitations of the study include its single centre retrospective methodology. The long study period also included differences and evolution in the surgical approach during the oncological resection, with more bile duct resections done during the early study period to achieve a negative margin and a greater lymph node yield. In the later years, bile duct resection was only performed in the presence of a positive cystic duct margin. Nonetheless, this is the first study to include all patients referred for GBC to a tertiary regional centre, rather than only the ones receiving surgical treatment, therefore providing outcome data in an intention to treat basis over the whole referral cohort including the patients that did not receive surgical treatment. It is also one of few studies to demonstrate the effect of non-incidental diagnosis on the oncological outcomes.

CONCLUSION

Conclusively, the presented data suggest that IGBC diagnosis may confer a survival advantage, including patients that received surgical treatment, independently of the pathological stage and tumour characteristics. Prospective studies are required to investigate the reasons behind this, including detailed pathological analysis and molecular gene expression.

ARTICLE HIGHLIGHTS

Research background

Incidental gallbladder cancer (IGBC) represents 50%-60% of gallbladder cancer cases. Data are conflicting on the role of IGBC diagnosis in oncological outcomes. Some studies suggest that IGBC diagnosis does not affect outcomes, while others that overall survival (OS) is longer in these cases compared to non-incidental diagnosis (NIGBC). Furthermore, some studies reported early tumour stages and histopathologic characteristics as possible confounders, while others not.

Research motivation

GB cancer is an uncommon malignancy with poor survival. Data suggest whether the diagnosis is incidental or not may play a role in the oncological outcomes. Confirmation of this observation may lead in further research aiming to better identify the reasons and refining the treatment strategy based on the presenting diagnosis.

Research objectives

This study aimed to investigate the role of IGBC diagnosis on patients' overall survival, especially after surgical treatment with curative intent.

Research methods

This is a retrospective analysis of all patient referrals with gallbladder cancer between 2008 and 2020 in a tertiary hepatobiliary centre. All patients had complete staging and were discussed in the multidisciplinary meeting prior to deciding on the treatment plan. Demographic, surgical and tumour variables were collected and compared between patients with IGBC and NIGBC using the appropriate statistical tests. Survival curves for OS and DFS were created using Kaplan-Meier method and compared with the log rank test. Risk analysis for independent predictors of OS and DFS was performed with univariable time to event analysis using the Cox proportional hazard model. Factors with a P value of < 0.200 were entered into a multivariable model and independent predictors (those with $P < 0.05$) were indentified. All statistical analysis was done using the software SPSS for Windows (Version 25.0, SPSS Inc., Chicago, IL, United States).

Research results

261 patients with GB cancer were included. Almost one-third pf patients had IGBC (91/261 patients) and two-thirds had NIGC. A total of 90/261 (34%) patients proceeded to have oncological resection. Metastatic disease was the most common reason for not having oncological resection. Patients with NIGBC were more likely to have advanced T stages of the disease and required more extensive resections than patients with IGBC. Survival analysis shows that patients with IGBC had better OS than patients with NIGBC in the whole cohort (29 *vs* 4 mo, $P < 0.001$), as well as in the non-surgical (14 *vs* 2 mo, $P < 0.001$) and surgical subgroups (29 *vs* 16.5 mo, $P = 0.001$). DFS was similarly better in patients with IGBC who underwent oncological resection (21.5 mo *vs* 8.5 mo, $P = 0.007$). After univariable and multivariable risk analysis, N stage, resection margin status and non-incidental diagnosis were identified as independent predictors of OS. N stage and resection margin status were also independent

predictors of DFS. Within the limitations of a retrospective single centre study, our data suggest that difference in the oncological outcomes between the two groups cannot be solely explained by differences in pathologic or tumour features.

Research conclusions

Our study suggests that IGBC diagnosis may confer a survival advantage, including patients that received surgical treatment, independently of the pathological stage and tumour characteristics. Prospective studies are required to investigate the reasons behind this, including detailed pathological analysis and molecular gene expression.

Research perspectives

Published evidence is still contradicting. The theory that IGBC and NIGBC are two distinct variants of the same disease remains to be proven by detailed pathologic assessment and research in cancer molecular genetics.

FOOTNOTES

Author contributions: Alarabiyat M and Raza SS are responsible for the data collection, statistical analysis, and wrote the manuscript; Alarabiyat M did the statistical analysis; Isaac J, Mirza DF, Marudanayagam R, Roberts K, Abradelo M, Bartlett DC, Dasari B, Sutcliffe BP are responsible for interpretation of data, manuscript revision and editing, approval of finalized version of the manuscript; Chatzizacharias N is responsible for developed research concept, writing, manuscript preparation, editing and review.

Institutional review board statement: The study was approved by the departmental ethics committee.

Informed consent statement: As this was an anonymised retrospective cohort study over a period of 12 years, individual consent forms were not required based on the policy of Queen Elizabeth Hospital and the UK on ethics and research.

Conflict-of-interest statement: The authors have no conflicts of interest to disclose.

Data sharing statement: The original dataset is anonymized and available upon request from the corresponding author at Nikolaos.chatzizacharias@uhb.nhs.net.

STROBE statement: The authors have read the STROBE Statement—checklist of items, and the manuscript was prepared and revised according to the STROBE Statement—checklist of items.

Open-Access: This article is an open-access article that was selected by an in-house editor and fully peer-reviewed by external reviewers. It is distributed in accordance with the Creative Commons Attribution NonCommercial (CC BY-NC 4.0) license, which permits others to distribute, remix, adapt, build upon this work non-commercially, and license their derivative works on different terms, provided the original work is properly cited and the use is non-commercial. See: https://creativecommons.org/Licenses/by-nc/4.0/

Country/Territory of origin: United Kingdom

ORCID number: Moath Alarabiyat 0000-0003-4757-053X; Syed Soulat Raza 0000-0003-3052-7527; John Isaac 0000-0002-7946-1277; Darius Mirza 0000-0002-7531-9089; Ravi Marudanayagam 0000-0002-0640-3535; Keith Roberts 0000-0003-1799-9829; Manuel Abradelo 0000-0003-1269-7936; David C Bartlett 0000-0001-8564-9420; Bobby V Dasari 0000-0003-2375-1141; Robert P Sutcliffe 0000-0002-1881-7655; Nikolaos A Chatzizacharias 0000-0002-4864-189X.

S-Editor: Wu YXJ
L-Editor: A
P-Editor: Wu YXJ

REFERENCES

1 **Jaruvongvanich V**, Yang JD, Peeraphatdit T, Roberts LR. The incidence rates and survival of gallbladder cancer in the USA. *Eur J Cancer Prev* 2019; **28**: 1-9 [PMID: 28683010 DOI: 10.1097/CEJ.0000000000000402]

2 **Chen C**, Geng Z, Shen H, Song H, Zhao Y, Zhang G, Li W, Ma L, Wang L. Long-Term Outcomes and Prognostic Factors in Advanced Gallbladder Cancer: Focus on the Advanced T Stage. *PLoS One* 2016; **11**: e0166361 [PMID: 27846279 DOI: 10.1371/journal.pone.0166361]

3 **Shih SP**, Schulick RD, Cameron JL, Lillemoe KD, Pitt HA, Choti MA, Campbell KA, Yeo CJ, Talamini MA. Gallbladder cancer: the role of laparoscopy and radical resection. *Ann Surg* 2007; **245**: 893-901 [PMID: 17522515 DOI: 10.1097/SLA.0b013e31806beec2]

4 **Duffy A**, Capanu M, Abou-Alfa GK, Huitzil D, Jarnagin W, Fong Y, D'Angelica M, Dematteo RP, Blumgart LH, O'Reilly EM. Gallbladder cancer (GBC): 10-year experience at Memorial Sloan-Kettering Cancer Centre (MSKCC). *J Surg Oncol* 2008; **98**: 485-489 [PMID: 18802958 DOI: 10.1002/jso.21141]

5 **Löhe F**, Meimarakis G, Schauer C, Angele M, Jauch KW, Schauer RJ. The time of diagnosis impacts surgical management but not the outcome of patients with gallbladder carcinoma. *Eur J Med Res* 2009; **14**: 345-351 [PMID: 19666394 DOI: 10.1186/2047-783x-14-8-345]

6 **Fong Y**, Jarnagin W, Blumgart LH. Gallbladder cancer: comparison of patients presenting initially for definitive operation with those presenting after prior noncurative intervention. *Ann Surg* 2000; **232**: 557-569 [PMID: 10998654 DOI: 10.1097/00000658-200010000-00011]

7 **Yip VS**, Gomez D, Brown S, Byrne C, White D, Fenwick SW, Poston GJ, Malik HZ. Management of incidental and suspicious gallbladder cancer: focus on early referral to a tertiary centre. *HPB (Oxford)* 2014; **16**: 641-647 [PMID: 24279377 DOI: 10.1111/hpb.12189]

8 **Cavallaro A**, Piccolo G, Di Vita M, Zanghì A, Cardì F, Di Mattia P, Barbera G, Borzì L, Panebianco V, Di Carlo I, Cavallaro M, Cappellani A. Managing the incidentally detected gallbladder cancer: algorithms and controversies. *Int J Surg* 2014; **12** Suppl 2: S108-S119 [DOI: 10.1016/j.ijsu.2014.08.367]

9 **Mazer LM**, Losada HF, Chaudhry RM, Velazquez-Ramirez GA, Donohue JH, Kooby DA, Nagorney DM, Adsay NV, Sarmiento JM. Tumour characteristics and survival analysis of incidental *vs* suspected gallbladder carcinoma. *J Gastrointest Surg* 2012; **16**: 1311-1317 [DOI: 10.1007/s11605-012-1901-y]

10 **Cha BH**, Bae JM. Comparison of clinical outcomes of incidental and non- incidental gallbladder cancers: a single-centre cross- sectional study. *Asian Pac J Cancer Prev* 2014; **15**: 1281-1283 [DOI: 10.7314/apjcp.2014.15.3.1281]

11 **Ethun CG**, Le N, Lopez-Aguiar AG, Pawlik TM, Poultsides G, Tran T, Idrees K, Isom CA, Fields RC, Krasnick BA, Weber SM, Salem A, Martin RCG, Scoggins CR, Shen P, Mogal HD, Schmidt C, Beal E, Hatzaras I, Shenoy R, Russell MC, Maithel SK. Pathologic and Prognostic Implications of Incidental *versus* Nonincidental Gallbladder Cancer: A 10-Institution Study from the United States Extrahepatic Biliary Malignancy Consortium. *Am Surg* 2017; **83**: 679-686 [PMID: 28738935 DOI: 10.1177/000313481708300721]

12 **Bacalbasa N**, Balescu I, Dima S and Popescu I. Surgical Advances in the Treatment of Gallbladder Carcinoma at Different Stages, Bile Duct Cancer, Luis Rodrigo, IntechOpen, 2019 [DOI: 10.5772/intechopen.84154]

13 **Pawlik TM**, Gleisner AL, Vigano L, Kooby DA, Bauer TW, Frilling A, Adams RB, Staley CA, Trindade EN, Schulick RD, Choti MA, Capussotti L. Incidence of finding residual disease for incidental gallbladder carcinoma: implications for re-resection. *J Gastrointest Surg* 2007; **11**: 1478-86; discussion 1486 [PMID: 17846848 DOI: 10.1007/s11605-007-0309-6]

14 **de Savornin Lohman EAJ**, van der Geest LG, de Bitter TJJ, Nagtegaal ID, van Laarhoven CJHM, van den Boezem P, van der Post CS, de Reuver PR. Re-resection in Incidental Gallbladder Cancer: Survival and the Incidence of Residual Disease. *Ann Surg Oncol* 2020; **27**: 1132-1142 [PMID: 31741109 DOI: 10.1245/s10434-019-08074-4]

15 **Vega EA**, Vinuela E, Okuno M, Joechle K, Sanhueza M, Diaz C, Jarufe N, Martinez J, Troncoso A, Diaz A, Chun YS, Tzeng CD, Lee JE, Vauthey JN, Conrad C. Incidental *vs* non-incidental gallbladder cancer: index cholecystectomy before oncologic re-resection negatively impacts survival in T2b tumors. *HPB (Oxford)* 2019; **21**: 1046-1056 [PMID: 30711243 DOI: 10.1016/j.hpb.2018.12.006]

16 **Goetze TO**, Paolucci V. Use of retrieval bags in incidental gallbladder cancer cases. *World J Surg* 2009; **33**: 2161-2165 [PMID: 19636610 DOI: 10.1007/s00268-009-0163-7]

17 **Lee HY**, Kim YH, Jung GJ, Roh YH, Park SY, Kang NU, Yoon SH, Cho JH, Roh MH, Han SY, Lee SW, Baek YH, Jeong JS. Prognostic factors for gallbladder cancer in the laparoscopy era. *J Korean Surg Soc* 2012; **83**: 227-236 [PMID: 23091795 DOI: 10.4174/jkss.2012.83.4.227]

18 **Pyo JS**, Son BK, Lee HY, Oh IW, Chung KH. Incidental Carcinoma after Cholecystectomy for Benign Disease of the Gallbladder: A Meta-Analysis. *J Clin Med* 2020; **9** [PMID: 32423156 DOI: 10.3390/jcm9051484]

19 **Andrén-Sandberg A**. Diagnosis and management of gallbladder cancer. *N Am J Med Sci* 2012; **4**: 293-299 [DOI: 10.4103/1947-2714.98586]

20 **Kemp Bohan PM**, Kirby DT, Chick RC, Bader JO, Clifton GT, Vreeland TJ, Nelson DW. Adjuvant Chemotherapy in Resectable Gallbladder Cancer is Underutilized Despite Benefits in Node-Positive Patients. *Ann Surg Oncol* 2021; **28**: 1466-1480 [PMID: 32749621 DOI: 10.1245/s10434-020-08973-x]

21 **Aloia TA**, Járufe N, Javle M, Maithel SK, Roa JC, Adsay V, Coimbra FJ, Jarnagin WR. Gallbladder cancer: expert consensus statement. *HPB (Oxford)* 2015; **17**: 681-690 [PMID: 26172135 DOI: 10.1111/hpb.12444]

22 **Shroff RT**, Kennedy EB, Bachini M, Bekaii-Saab T, Crane C, Edeline J, El-Khoueiry A, Feng M, Katz MHG, Primrose J, Soares HP, Valle J, Maithel SK. Adjuvant Therapy for Resected Biliary Tract Cancer: ASCO Clinical Practice Guideline. *J Clin Oncol* 2019; **37**: 1015-1027 [PMID: 30856044 DOI: 10.1200/JCO.18.02178]

23 **D'Angelica M**, Dalal KM, DeMatteo RP, Fong Y, Blumgart LH, Jarnagin WR. Analysis of the extent of resection for adenocarcinoma of the gallbladder. *Ann Surg Oncol* 2009; **16**: 806-816 [PMID: 18985272 DOI: 10.1245/s10434-008-0189-3]

24 **Araida T**, Higuchi R, Hamano M, Kodera Y, Takeshita N, Ota T, Yoshikawa T, Yamamoto M, Takasaki K. Hepatic resection in 485 R0 pT2 and pT3 cases of advanced carcinoma of the gallbladder: results of a Japanese Society of Biliary Surgery survey--a multicenter study. *J Hepatobiliary Pancreat Surg* 2009; **16**: 204-215 [PMID: 19219399 DOI: 10.1007/s00534-009-0044-3]

25 **D'Souza MA**, Valdimarsson VT, Campagnaro T, Cauchy F, Chatzizacharias NA, D'Hondt M, Dasari B, Ferrero A, Franken LC, Fusai G, Guglielmi A, Hagendoorn J, Hidalgo Salinas C, Hoogwater FJH, Jorba R, Karanjia N, Knoefel WT, Kron P, Lahiri R, Langella S, Le Roy B, Lehwald-Tywuschik N, Lesurtel M, Li J, Lodge JPA, Martinou E, Molenaar IQ, Nikov A, Poves I, Rassam F, Russolillo N, Soubrane O, Stättner S, van Dam RM, van Gulik TM, Serrablo A, Gallagher TM, Sturesson C; E-AHPBA scientific and research committee. Hepatopancreatoduodenectomy -a controversial treatment for bile duct and gallbladder cancer from a European perspective. *HPB (Oxford)* 2020; **22**: 1339-1348 [PMID: 31899044 DOI: 10.1016/j.hpb.2019.12.008]

26 **Endo I**, Shimada H, Takimoto A, Fujii Y, Miura Y, Sugita M, Morioka D, Masunari H, Tanaka K, Sekido H, Togo S.

Microscopic liver metastasis: prognostic factor for patients with pT2 gallbladder carcinoma. *World J Surg* 2004; **28**: 692-696 [PMID: 15175901 DOI: 10.1007/s00268-004-7289-4]

27 **Widmann B**, Warschkow R, Beutner U, Weitzendorfer M, Ukegjini K, Schmied BM, Tarantino I, Steffen T. Effect of lymphadenectomy in curative gallbladder cancer treatment: a systematic review and meta-analysis. *Langenbecks Arch Surg* 2020; **405**: 573-584 [PMID: 32458141 DOI: 10.1007/s00423-020-01878-z]

28 **Tanabe M**, Endo I, Masunari H, Sugita M, Morioka D, Ishikawa T, Ichikawa Y, Shimada H. Is lymph-node micrometastasis in gallbladder cancer a significant prognostic factor? *Hepatogastroenterology* 2012; **59**: 31-35 [PMID: 22251520 DOI: 10.5754/hge10010]

29 **Ito H**, Ito K, D'Angelica M, Gonen M, Klimstra D, Allen P, DeMatteo RP, Fong Y, Blumgart LH, Jarnagin WR. Accurate staging for gallbladder cancer: implications for surgical therapy and pathological assessment. *Ann Surg* 2011; **254**: 320-325 [PMID: 21617582 DOI: 10.1097/SLA.0b013e31822238d8]

30 **Tran TB**, Nissen NN. Surgery for gallbladder cancer in the US: a need for greater lymph node clearance. *J Gastrointest Oncol* 2015; **6**: 452-458 [PMID: 26487937 DOI: 10.3978/j.issn.2078-6891.2015.062]

31 **Ong SL**, Garcea G, Thomasset SC, Neal CP, Lloyd DM, Berry DP, Dennison AR. Ten-year experience in the management of gallbladder cancer from a single hepatobiliary and pancreatic centre with review of the literature. *HPB (Oxford)* 2008; **10**: 446-458 [PMID: 19088932 DOI: 10.1080/13651820802392346]

32 **Lee W**, Jeong CY, Jang JY, Kim YH, Roh YH, Kim KW, Kang SH, Yoon MH, Seo HI, Yun SP, Park JI, Jung BH, Shin DH, Choi YI, Moon HH, Chu CW, Ryu JH, Yang K, Park YM, Hong SC. Do hepatic-sided tumours require more extensive resection than peritoneal-sided tumours in patients with T2 gallbladder cancer? *Surgery* 2017; **162**: 515-524 [DOI: 10.1016/j.surg.2017.05.004]

33 **Lee H**, Choi DW, Park JY, Youn S, Kwon W, Heo JS, Choi SH, Jang KT. Surgical Strategy for T2 Gallbladder Cancer According to Tumor Location. *Ann Surg Oncol* 2015; **22**: 2779-2786 [PMID: 25519930 DOI: 10.1245/s10434-014-4300-7]

34 **Wardell CP**, Fujita M, Yamada T, Simbolo M, Fassan M, Karlic R, Polak P, Kim J, Hatanaka Y, Maejima K, Lawlor RT, Nakanishi Y, Mitsuhashi T, Fujimoto A, Furuta M, Ruzzenente A, Conci S, Oosawa A, Sasaki-Oku A, Nakano K, Tanaka H, Yamamoto Y, Michiaki K, Kawakami Y, Aikata H, Ueno M, Hayami S, Gotoh K, Ariizumi SI, Yamamoto M, Yamaue H, Chayama K, Miyano S, Getz G, Scarpa A, Hirano S, Nakamura T, Nakagawa H. Genomic characterization of biliary tract cancers identifies driver genes and predisposing mutations. *J Hepatol* 2018; **68**: 959-969 [PMID: 29360550 DOI: 10.1016/j.jhep.2018.01.009]

World Journal of Gastroenterology

Submit a Manuscript: https://www.f6publishing.com

World J Gastroenterol 2022 May 14; 28(18): 2008-2020

DOI: 10.3748/wjg.v28.i18.2008

ISSN 1007-9327 (print) ISSN 2219-2840 (online)

ORIGINAL ARTICLE

Retrospective Study

Risk factors for major gastrointestinal bleeding in the general population in Finland

Pareen Vora, Ronald Herrera, Arto Pietila, Ulrich Mansmann, Gunnar Brobert, Markku Peltonen, Veikko Salomaa

Specialty type: Gastroenterology and hepatology

Provenance and peer review: Unsolicited article; Externally peer reviewed.

Peer-review model: Single blind

Peer-review report's scientific quality classification

Grade A (Excellent): A
Grade B (Very good): B
Grade C (Good): 0
Grade D (Fair): 0
Grade E (Poor): 0

P-Reviewer: Gaman MA, Romania; Govindarajan KK, India

Received: November 14, 2021
Peer-review started: November 14, 2021
First decision: January 9, 2022
Revised: January 22, 2022
Accepted: March 26, 2022
Article in press: March 26, 2022
Published online: May 14, 2022

Pareen Vora, Ronald Herrera, Integrated Evidence Generation, Bayer AG, Berlin 13353, Germany

Pareen Vora, Ulrich Mansmann, Institute for Medical Information Processing, Biometry, and Epidemiology, Ludwig Maximilians Universität, Munich 81337, Germany

Pareen Vora, Ulrich Mansmann, Pettenkofer School of Public Health, Ludwig Maximilians Universität, Munich 81337, Germany

Arto Pietila, Markku Peltonen, Veikko Salomaa, Department of Public Health and Welfare, National Institute for Health and Welfare (THL), Helsinki FI-00271, Finland

Gunnar Brobert, Medical Affairs, Bayer AB, Solna 171 65, Sweden

Corresponding author: Pareen Vora, MSc, Director, Integrated Evidence Generation, Bayer AG, Muellerstrasse 178, Berlin 13353, Germany. pareen.vora@bayer.com

Abstract

BACKGROUND

Data on non-drug related risk-factors for gastrointestinal bleeding (GIB) in the general population are limited, especially for life-style factors, clinical measurements and laboratory parameters.

AIM

To identify and investigate non-drug risk factors for major GIB in the general population of Finland.

METHODS

We performed a retrospective cohort study using data from the FINRISK health examination surveys, which have been conducted every 5 years across Finland from 1987 to 2007. Participants were adults aged 25 years to 74 years, excluding those with a previous hospitalization for GIB. Follow-up from enrollment was performed through linkage to national electronic health registers and ended at an event of GIB that led to hospitalization/death, death due to any other cause, or after 10 years. Covariates included demographics, socioeconomic and lifestyle factors, clinical measurements, laboratory parameters and comorbidities. Variable selection was undertaken using Least Absolute Shrinkage and Selection Operator

(LASSO) and factors associated with GIB were identified using Cox regression.

RESULTS

Among 33,508 participants, 403 (1.2%) experienced GIB [256 men (63.5%); mean age, 56.0 years (standard deviation (SD) ± 12.1)] and 33105 who did not experience GIB [15768 men (47.6%); mean age, 46.8 (SD ± 13) years], within 10 years of follow-up. Factors associated with a significantly increased risk of GIB were baseline age [per 10-year increase; hazard ratio (HR) 1.62, 95% confidence interval (CI): 1.42-1.86], unemployment (HR: 1.70, 95%CI: 1.11-2.59), body mass index (BMI) (HR: 1.15, 95%CI: 1.01-1.32), gamma-glutamyl transferase (GGT) (HR: 1.05, 95%CI: 1.02-1.09), precursors of GIB (HR: 1.90, 95%CI: 1.37-2.63), cancer (HR: 1.47, 95%CI: 1.10-1.97), psychiatric disorders (HR: 1.32, 95%CI: 1.01-1.71), heart failure (HR: 1.46, 95%CI: 1.04-2.05), and liver disorders (HR: 3.20, 95%CI: 2.06-4.97). Factors associated with a significantly decreased risk of GIB were systolic blood pressure (SBP) (HR: 0.78, 95%CI: 0.64-0.96), 6-10 cups of coffee a day (HR: 0.67, 95%CI: 0.46-0.99), or > 10 cups (HR: 0.43, 95%CI: 0.23-0.81).

CONCLUSION

Our study confirms established risk-factors for GIB and identifies potential risk-factors not previously reported such as unemployment, BMI, GGT, SBP and coffee consumption.

Key Words: Risk factors; Gastrointestinal hemorrhage; General population; Finland; Life style; Population health

©The Author(s) 2022. Published by Baishideng Publishing Group Inc. All rights reserved.

Core Tip: This retrospective study of 33508 Finnish survey participants aimed to identify and investigate non-drug factors associated with the risk of major gastrointestinal bleeding (GIB) in the general population in Finland. Aside from established risk factors, our study identified unemployment, body mass index and gamma-glutamyl transferase enzyme were all associated with increased risk of major GIB. Systolic blood pressure and coffee consumption were associated with a decreased risk of major GIB.

Citation: Vora P, Herrera R, Pietila A, Mansmann U, Brobert G, Peltonen M, Salomaa V. Risk factors for major gastrointestinal bleeding in the general population in Finland. *World J Gastroenterol* 2022; 28(18): 2008-2020
URL: https://www.wjgnet.com/1007-9327/full/v28/i18/2008.htm
DOI: https://dx.doi.org/10.3748/wjg.v28.i18.2008

INTRODUCTION

Gastrointestinal bleeding (GIB) is one of the most frequent types of major bleeding events seen in clinical practice and it can be potentially life-threatening if not managed appropriately[1]. Although several studies have investigated risk factors of GIB, these have largely evaluated associations with medications[2-5] or have been conducted in specific population groups, such as those who were critically ill[6-8]. Only a few have investigated potential associations with lifestyle factors such as smoking, alcohol consumption, and physical activity or laboratory parameters[9-11]. Furthermore, several studies on this topic have lacked information on lifestyle factors, clinical measurements, and laboratory parameters as well as long longitudinal follow-up. To identify independent risk factors for GIB, it is important to understand the association of these additional parameters on the risk of GIB when taken in account together with demographic data and comorbidities in the general population. Establishing independent risk factors for GIB is important because it will help to identify patients at high risk of GIB and to better target preventative interventions. In addition, it would be particularly relevant for designing future studies on GIB. Using data from FINRISK surveys and national health registers, we aimed to identify and investigate risk factors for major GIB in the general population of Finland.

MATERIALS AND METHODS

Ethics statement

The National FINRISK Study surveys (started in 1972) followed the EHES (European Health Examination Survey)[12] and the MONICA (Monitoring of Trends and Determinants in Cardiovascular

Disease)[13] project protocols and were approved by the ethics committee of the Finnish Institute of Health and Welfare and the Coordinating Ethical Committee of Helsinki and Uusimaa Hospital District in Finland (THL/66/0.05.00/2015). All participants in the FINRISK surveys provided their informed consent at the time of enrollment and the study was conducted following the principles of the Declaration of Helsinki. Data from the participants was pseudonymized for this study and the secondary use of the survey data was approved by the Finnish Institute of Health and Welfare in 2017.

Study design, data source, and study population

This retrospective cohort study used data from the FINRISK health examination surveys - a series of large population-based, cross-sectional surveys (with 6000 to 8800 participants per survey) carried out every 5 years to determine the risk factors for chronic, noncommunicable diseases. Survey participants were randomly chosen using the population register of Finland to obtain a representative sample of individuals across several geographic regions of Finland; those who responded to the invitation were subsequently enrolled in the study as participants in the first quarter of each survey year. From each geographical area, the surveys enrolled at least 250 subjects of each sex and 10-year age group. From the 1972 survey to the 2007 survey, the participation rate gradually decreased from approximately 80% to 65%[14].

Using data from the 1987, 1992, 1997, 2002, 2007 FINRISK survey cohorts, we identified 33796 unique participants aged 25 years to 74 years. Of these, 288 were excluded due to having hospitalization for GIB before baseline, resulting in a final cohort of 33508 individuals. Using record linkage of FINRISK participants to nationwide electronic health care registers, including the hospital discharge register and causes of death register, we identified incident cases of major GIB. These national registers cover virtually all persons living in Finland. The possibility of linking demographics, lifestyle factors, clinical measurements and laboratory parameters collected in the FINRISK surveys with national health registers increased the granularity of the dataset. The follow-up period was from the date of enrollment in the FINRISK survey to the incidence of GIB that led to hospitalization/death, death from any cause, or a maximum of 10 years, whichever occurred first. The overall design of the study is presented in Supplementary Figure 1.

Study outcome

Major GIB was defined as GIB that led to hospitalization or GIB-specific death (see Supplementary Table 1 for codes), recorded as either the main or the top three contributing factors for the hospitalization, or the underlying, direct, or contributing cause of death. We followed participants from survey enrollment for a maximum of 10 years to allow equal follow-up time for all survey cohorts to observe GIB. In the previous analyses, we have shown that the overall age standardized incidence rate of GIB in the FINRISK cohorts to be 2.10 per 1000 person-years [men: 2.62 per 1000 person-years (95%CI: 2.40-2.86) and women: 1.62 per 1000 person-years (95%CI: 1.45-1.81)][15].

Covariates

Baseline data collected at enrollment into FINRISK surveys included demographic data (age, sex, year of enrollment and region); socioeconomic factors (marital status, occupation, education); lifestyle factors (smoking status, alcohol consumption, coffee consumption, body mass index [BMI], waist hip ratio [WHR], physical activity); blood pressure measurements (systolic [SBP] and diastolic blood pressure [DBP]); and laboratory parameters (total cholesterol, high density lipoprotein cholesterol [HDL], gamma-glutamyl transferase enzyme [GGT]).

Morbidities were identified in the participant's history any time before the GIB or any time before the end of follow-up for participants without GIB. These were obtained from the hospital discharge register, causes of death register, as well as from drug reimbursement register, and prescription register using drugs as proxies for chronic conditions. Conditions were identified using the International Classification of Diseases, Ninth Revision (ICD-9) or the International Statistical Classification of Diseases and Related Health Problems, Tenth Revision (ICD-10) codes as well as prescription codes identified using Anatomical Therapeutic Chemical (ATC) codes and database specific codes of the Finnish Social Insurance. Morbidities included any cancer diagnosis, any psychiatric illness, cardiovascular diseases (stroke, venous thromboembolism, ischemic heart disease, valvular heart disease, atrial fibrillation, peripheral artery disease, heart failure, high blood pressure), a composite of precursors of GIB without bleeding (including gastritis, intestinal diseases, esophageal varices, esophagitis, hemorrhoids, colitis and Crohn's disease), osteoarthritis, connective tissue disorders, diabetes, chronic obstructive pulmonary disease, asthma, liver disorders and anemia (see Supplementary Table 2 for codes).

Statistical analyses

Participants' characteristics were summarized using counts and percentages for categorical variables and means with standard deviation (SD) for continuous variables. We conducted univariate Cox regression using all covariates. We used the Least Absolute Shrinkage and Selection Operator (LASSO) method for variable selection, which provides a relevant and interpretable group of variables from a larger set of covariates including potentially multicollinear variables[16]. LASSO regression maximizes

the partial likelihood of the regression coefficients by imposing a constraint on the sum of the absolute value of all regression coefficients in the model producing coefficients that are exactly zero, thereby regulating the impact of a coefficient in the regression[16]. This effectively excludes some variables which are unnecessary/uninfluential without the need for formal statistical testing thereby reducing the likelihood of overfitting using cross validation. Moreover, the LASSO method is less variable than the stepwise approach and yields interpretable models. The Cox LASSO regression including all the available variables showed the best model could be fitted between 12 to 39 variables (see Supplementary Figure 2). Further, we fitted a Cox proportional hazards model using variables selected by LASSO, *i.e.*, we did not include variables whose coefficients shrank towards zero. Using this approach, we obtained hazard ratios (HRs) with 95% confidence intervals (CI) for the variables in the final model[17]. Using statistical tests and graphical diagnostics, we checked the proportional hazards assumption on the *scaled Schoenfeld residuals*. Continuous variables in the Cox model were standardized by subtracting the value of the variable from its mean and dividing by its SD. For interpretation, it provides a change in risk when the value of the variable changes by one SD. There were few participants with missing baseline data (< 3%); they were excluded from the analysis and no imputations were performed. All statistical analyses were done with R, version 3.6.1 using 'glmnet' package (R Foundation for Statistical Computing).

RESULTS

Characteristics

Of the total 33508 participants, 403 (1.2%) experienced at least one GIB within the maximum 10 years of follow-up. Baseline characteristics of the study cohort are summarized in Table 1. The mean age at enrollment was 56 years (SD ± 12.1) for participants with an incident of GIB and 46.8 years (SD ± 13.0) for those who did not experience GIB. Of the participants experiencing GIB compared to those who did not have GIB, the majority were male (63.5% *vs* 47.6%), from the western region (40.4% *vs* 38.0%), single (31.0% *vs* 26.0%), a current/ex-smoker (56.1% *vs* 46.2%), a heavy alcohol drinker (25.1% *vs* 20.8%), consumed 6-10 cups of coffee per day (21.3% *vs* 27.2%) and undertook moderate-to-heavy physical activity (12.9% *vs* 21.4%). Overall, participants with GIB had a higher prevalence of comorbidities than participants without GIB as seen in Table 2, except osteoarthritis (5.0% *vs* 6.2%) which was lower. Participants developing a GIB also had a higher mean BMI (28.3 kg/m^2, SD ± 5.19 *vs* 26.6 kg/m^2, SD ± 4.61), mean WHR (0.93, SD ± 0.1 *vs* 0.88, SD ± 0.1), and mean SBP (141 mmHg, SD ± 21.7 *vs* 136 mmHg, SD ± 19.8) than those who did not experience a GIB. Of the laboratory parameters, GGT appeared to be higher in participants with GIB (59.5 U/L, SD ± 141 *vs* 31.2 U/L SD ± 45). Participants with GIB had more precursors of GIB (11.9% *vs* 4.5%) compared to participants without GIB. The results of univariate analyses showing each variable's association with the risk of major GIB are presented in Table 3.

Risk factors for major GIB

The LASSO method identified the most important predictors from larger set of variables. Variables with negative coefficients exhibit decreased risk, positive coefficients exhibit increased risk, and coefficient with value zero are the least important predictor variables in the model to predict gastrointestinal bleeding and can be removed from the final model. The aim of LASSO method is model prediction by selecting the most important predictor variables and therefore statistical significance of regression coefficients is not computed here (see Supplementary Table 3). Using these results from LASSO, we excluded variables such as DBP, HDL, VTE and Inflammatory connective tissue diseases from the final Cox model. Categorical variables for which one of the strata had a zero coefficient were kept in the final model.

Increased risk of major GIB

In terms of socio-demographics and lifestyle factors, the Cox regression showed that baseline age (HR: 1.62, 95%CI: 1.42-1.86, per 10-year increase), unemployment (HR: 1.70, 95%CI: 1.11-2.59), and higher BMI (HR: 1.15, 95%CI: 1.01-1.32) were all associated with an increased risk of GIB (Table 3). Among clinical variables, higher GGT levels (HR: 1.05, 95%CI: 1.02-1.09), having ≥ 1 precursor of GIB (HR: 1.90, 95%CI: 1.37-2.63), previous cancer (HR: 1.47, 95%CI: 1.10-1.97), psychiatric disorders (HR: 1.32, 95%CI: 1.01-1.71), heart failure (HR: 1.46, 95%CI: 1.04-2.05), and liver disorders (HR: 3.20, 95%CI: 2.06-4.97) were all associated with an increased risk of GIB. There was no clear evidence that history of cardiovascular disease was associated with the risk of major GIB.

Decreased risk of major GIB

SBP (HR: 0.78, 95%CI: 0.64-0.96) as well as drinking 6-10 cups of coffee a day (HR: 0.67, 95%CI: 0.46-0.99) or more than 10 cups of coffee a day (HR: 0.43, 95%CI: 0.23-0.81), and history of osteoarthritis (HR: 0.39, 95%CI: 0.24-0.65) were all associated with a decreased risk of GIB.

Table 1 Baseline characteristics for participants with and without major gastrointestinal bleedings during follow-up

Baseline characteristics	GIB, *n* = 403	No GIB, *n* = 33105	Overall, *n* = 33508
Age at baseline, mean (SD)	56.0 (12.1)	46.8 (13.0)	46.9 (13.0)
Sex			
Male	256 (63.5)	15768 (47.6)	16024 (47.8)
Female	147 (36.5)	17337 (52.4)	17484 (52.2)
Yr of enrollment, Q1			
1987	45 (11.2)	5872 (17.7)	5917 (17.7)
1992	51 (12.7)	5371 (16.2)	5422 (16.2)
1997	126 (31.3)	7857 (23.7)	7983 (23.8)
2002	108 (26.8)	8155 (24.6)	8263 (24.7)
2007	73 (18.1)	5850 (17.7)	5923 (17.7)
Region[1]			
West	163 (40.4)	12570 (38.0)	12733 (38.0)
East	240 (59.6)	20535 (62.0)	20775 (62.0)
Marital status			
Married, cohabiting, or registered partnership	278 (69.0)	24391 (73.7)	24669 (73.6)
Single, separated, divorced, or widow	125 (31.0)	8623 (26.0)	8748 (26.1)
Missing	0 (0.0)	91 (0.3)	91 (0.3)
Occupation			
Non-manual (office/studying)	102 (25.3)	15889 (48.0)	15991 (47.7)
Manual (factory/construction/farming/forestry)	62 (15.4)	6692 (20.2)	6754 (20.2)
Family/housewife/pensioner	191 (47.4)	8033 (24.3)	8224 (24.5)
Unemployed	37 (9.2)	2006 (6.1)	2043 (6.1)
Missing	11 (2.7)	485 (1.5)	496 (1.5)
Education in tertiles[2]			
Low	128 (31.8)	10029 (30.3)	10157 (30.3)
Moderate	113 (28.0)	10735 (32.4)	10848 (32.4)
High	144 (35.7)	11619 (35.1)	11763 (35.1)
Missing	18 (4.5)	722 (2.2)	740 (2.2)
Smoking			
Never	168 (41.7)	17381 (52.5)	17549 (52.4)
Ex-smoker	121 (30.0)	7028 (21.2)	7149 (21.3)
Smoker	105 (26.1)	8273 (25.0)	8378 (25.0)
Missing	9 (2.2)	423 (1.3)	432 (1.3)
Alcohol consumption in grams per week			
Non-drinker	164 (40.7)	12548 (37.9)	12712 (37.9)
Mild (0.1 g to 36.9 g)	65 (16.1)	6835 (20.6)	6900 (20.6)
Moderate (37 g to 86.9 g)	54 (13.4)	5914 (17.9)	5968 (17.8)
Heavy (≥ 87g)	101 (25.1)	6879 (20.8)	6980 (20.8)
Missing	19 (4.7)	929 (2.8)	948 (2.8)
Coffee consumption per day, cups			
0	38 (9.4)	2858 (8.6)	2896 (8.6)

1–5	267 (66.3)	20294 (61.3)	20561 (61.4)
6–10	86 (21.3)	9008 (27.2)	9094 (27.1)
> 10	4 (1.0)	637 (1.9)	641 (1.9)
Missing	8 (2.0)	308 (0.9)	316 (0.9)
Physical activity			
Minimal to mild	335 (83.1)	25306 (76.4)	25641 (76.5)
Moderate to heavy	52 (12.9)	7095 (21.4)	7147 (21.3)
Missing	16 (4.0)	704 (2.1)	720 (2.1)
Body mass index in kg/m^2, mean (SD)	28.3 (5.2)	26.6 (4.6)	26.6 (4.6)
Missing	10 (2.5)	389 (1.2)	399 (1.2)
Waist-hip ratio, mean (SD)	0.93 (0.1)	0.88 (0.1)	0.88 (0.1)
Missing	5 (1.2)	404 (1.2)	409 (1.2)
Systolic blood pressure in mm Hg, mean (SD)	141.0 (22)	136.0 (20)	136.0 (20)
Missing	2 (0.5)	268 (0.8)	270 (0.8)
Diastolic blood pressure in mm Hg, mean (SD)	83.5 (12.7)	81.0 (11.7)	81.0 (11.7)
Missing	2 (0.5)	271 (0.8)	273 (0.8)
Total cholesterol in mmol/L, mean (SD)	5.69 (1.09)	5.58 (1.12)	5.58 (1.12)
Missing	5 (1.2)	347 (1.0)	352 (1.1)
High density lipoprotein in mmol/L, mean (SD)	1.39 (0.44)	1.44 (0.38)	1.44 (0.38)
Missing	5 (1.2)	347 (1.0)	352 (1.1)
Gamma-glutamyl transferase in U/L, mean (SD)	59.5 (141)	31.2 (45.0)	31.5 (47.4)
Missing	5 (1.2)	356 (1.1)	361 (1.1)

[1]West Finland includes Turku and Loimaa as well as Helsinki and Vantaa. East Finland includes North Karelia, North Savo, Oulu, and Lapland.
[2]Educational tertiles were calculated according to years of education and were specific to the birth cohorts.
Data are *n* (%), unless otherwise indicated. GIB: Gastrointestinal bleeding; SD: Standard deviation; IQR: Interquartile range.

DISCUSSION

Our large population-based study enabled the evaluation of a wide range of potential risk factors for GIB in the general population, including demographics, socioeconomic and lifestyle factors, comorbidities, clinical measurements and laboratory parameters. Aside from confirming previously known risk factors for major GIB, we also identified unemployment, higher BMI, and higher levels of GGT as associated with a significantly increased risk of GIB, whereas increased daily coffee consumption (> 5 cups) as well as higher SBP were associated with a significantly decreased risk of GIB.

While many studies have investigated the effect of coffee on GI tract including GI cancer prevention, we believe ours is the first to investigate its association with GIB, with 29% of our study population with daily coffee consumption of > 5 cups[18]. A recent review by Iriondo-DeHond *et al*[18], outlined potential mechanisms and summarized the current evidence on the effects of individual coffee components on GI tract concluding that support for a possible causal association is insufficient. Nonetheless, several meta-analyses have reported a protective effect of coffee consumption on colon cancer[19-24] which is a major cause of GIB. A few studies[25-28] have shown that low SBP is associated with an increased risk of GIB, which supports the protective effect of high SBP seen in our study. Our results indicated that approximately 22 units decrease in SBP would increase the risk of GIB by 15%. Therefore, apart from diagnosis of hypertension, SBP values should be considered and included in the analyses of GIBs whenever available. Level of education was not associated with an increased risk for major GIBs, in contrast to being unemployed which is in line with previous research consistently showing that unemployment is associated with poor health[29,30]. Increase in age has been consistently associated with increased risk of major GIBs in the literature as in our study[28,31]. In relation to anthropometric measures, higher BMI was associated with an increased risk of GIB but not WHR or low physical activity and we are unaware of any other studies that have evaluated these variables in this context. We found no association between alcohol consumption and the risk of major GIB, in contrast to previous studies on upper GIBs[32,33]. However, association with an increased risk of major GIB were seen with a history of liver disorders as well as high levels of GGT which can be caused by chronic

Table 2 Medical history in participants with and without gastrointestinal bleeding

Comorbidities	GIB, *n* = 403	No GIB, *n* = 33105	Overall, *n* = 33508
Precursors of GIBs[1]			
0	355 (88.1)	31621 (95.5)	31976 (95.4)
1	45 (11.2)	1399 (4.2)	1444 (4.3)
2	3 (0.7)	78.0 (0.2)	81.0 (0.2)
3	0 (0)	7.00 (0.0)	7.00 (0.0)
Any cancer	63 (15.6)	2421 (7.3)	2484 (7.4)
Any psychiatric disorders	104 (25.8)	4653 (14.1)	4757 (14.2)
Stroke including SAH	39 (9.7)	1239 (3.7)	1278 (3.8)
Venous thromboembolism	17 (4.2)	728 (2.2)	745 (2.2)
Ischemic heart disease	101 (25.1)	3433 (10.4)	3534 (10.5)
Valvular heart disease	23 (5.7)	689 (2.1)	712 (2.1)
Atrial fibrillation	55 (13.6)	1512 (4.6)	1567 (4.7)
Peripheral artery disease	23 (5.7)	553 (1.7)	576 (1.7)
Heart failure	76 (18.9)	1810 (5.5)	1886 (5.6)
High blood pressure	128 (31.8)	6572 (19.9)	6700 (20.0)
Osteoarthritis	20 (5.0)	2062 (6.2)	2082 (6.2)
Inflammatory connective tissue diseases	29 (7.2)	1458 (4.4)	1487 (4.4)
Diabetes[2]	52 (12.9)	2390 (7.2)	2442 (7.3)
COPD	24 (6.0)	638 (1.9)	662 (2.0)
Asthma	54 (13.4)	3828 (11.6)	3882 (11.6)
Liver disorder	29 (7.2)	389 (1.2)	418 (1.2)
Anemia	6 (1.5)	70 (0.2)	76 (0.2)

[1]Includes conditions without gastrointestinal bleeding such as gastritis, intestinal diseases, esophageal varices, esophagitis, hemorrhoids, colitis, Crohn's disease.
[2]Excluding gestational diabetes.
Data are *n* (%). GIB: Gastrointestinal bleeding; COPD: Chronic obstructive pulmonary disease; SAH: Sub-arachnoid hemorrhage.

heavy alcohol consumption and is in line with the components of some GIB-risk scores[28].

Very few studies mostly focusing on upper GIBs have shown increased risk associated with smoking [32,34], however our multivariate analyses showed no association between self-reported smoking (ex- or current) and major GIB. In terms of morbidities, consistent with previous studies[28,35], a history of heart failure was associated with an increased risk of GIB. This could be related to the treatments and to the fact that heart failure often coexists with atrial fibrillation which is treated with anticoagulants. As medications commonly used to treat osteoarthritis - non-steroidal anti-inflammatory drugs (NSAIDs) and corticosteroids - are thought to increase the risk of GIB[36,37], a number of possible explanations could account for our finding that osteoarthritis was associated with a decreased risk for GIB including that the patients with osteoarthritis were actively monitored, received better care and management of the disease, were prescribed PPI to prevent GIBs, or used other available treatments[38]. Although medications such as antiplatelet agents and anticoagulants, which are associated with an increased risk of GIBs[9] are often used to treat cardiovascular diseases, our study did not find an association between history of cardiovascular diseases and GIB. Our study suggests that the predictors of major GIBs in the general population might be slightly different than in critically ill populations or comorbid patients using multiple medications[3,4,6-8,11].

Strengths and limitations

Our study has several strengths. A key strength was the long follow-up (up to 10 years) of individuals from a large representative sample of the general population of Finland enabling identification of more than 400 incident cases of GIB. The loss to follow-up was minimal, and the data sources enabled us to incorporate a wide range of potential risk factors in our analyses. Missing data amongst the participants

Table 3 Multivariate analysis for the risk factors for major gastrointestinal bleeding

Variables	Univariate model, HR (95%CI)	Multivariate model, HR (95%CI)
Baseline age (10-yr increase)	1.83 (1.69–1.99)	1.62 (1.42–1.86)
Sex		
Male	1	1
Female	0.51 (0.42–0.63)	0.83 (0.59–1.17)
Yr of enrollment		
1987	1	1
1992	1.23 (0.83-1.84)	1.15 (0.74–1.79)
1997	2.10 (1.50–2.96)	1.36 (0.91–2.04)
2002	1.72 (1.21–2.43)	1.10 (0.72–1.68)
2007	1.66 (1.15–2.41)	0.90 (0.57–1.43)
Region[1]		
West Finland	1	1
East Finland	0.90 (0.74–1.10)	0.96 (0.77–1.20)
Marital status		
Married, cohabiting, or registered partnership	1	1
Single, separated, divorced, or widow	1.29 (1.04–1.59)	1.09 (0.86–1.38)
Occupation		
Non-manual (office/studying)	1	1
Manual (factory/ construction/ farming/ forestry)	1.45 (1.06–1.98)	1.25 (0.88–1.78)
Family/ housewife/ pensioner	3.90 (3.06–4.95)	1.26 (0.90–1.75)
Unemployed	2.92 (2.00–4.25)	1.70 (1.11–2.59)
Education[2]		
Low	1	1
Moderate	0.82 (0.64–1.06)	0.81 (0.62–1.06)
High	0.96 (0.76–1.22)	1.05 (0.80–1.38)
Smoking		
Never	1	1
Ex-smoker	1.80 (1.43–2.28)	1.18 (0.90–1.53)
Smoker	1.34 (1.05–1.71)	1.30 (0.97–1.74)
Alcohol consumption in grams per week		
Non-User	1	1
Mild (0.1 g to 36.9 g)	0.72 (0.54–0.96)	0.88 (0.66–1.19)
Moderate (37 g to 86.9 g)	0.69 (0.51–0.94)	0.76 (0.54–1.06)
Heavy (≥ 87 g)	1.13 (0.88–1.44)	1.02 (0.76–1.37)
Coffee consumption per day, cups		
0	1	1
1–5	1.00 (0.71–1.40)	0.72 (0.50–1.02)
6–10	0.72 (0.49–1.06)	0.67 (0.46–0.99)
> 10	0.48 (0.17–1.33)	0.43 (0.23–0.81)
Physical activity		
None to Mild	1	1

Moderate to Heavy	0.55 (0.41–0.73)	0.85 (0.62–1.16)
Body mass index standardized	1.38 (1.27–1.50)	1.15 (1.01–1.32)
Waist hip ratio standardized	1.70 (1.55–1.86)	1.18 (0.98–1.43)
Systolic blood pressure standardized	1.30 (1.19–1.42)	0.85 (0.76-0.96)
Diastolic blood pressure standardized	1.24 (1.13–1.37)	-
Total cholesterol standardized	1.10 (1.00–1.21)	0.94 (0.84–1.05)
High density lipoprotein standardized	0.86 (0.77–0.95)	-
Gamma-glutamyl transferase standardized	1.10 (1.08–1.12)	1.05 (1.02-1.09)
Precursors of GIB[3]		
0	1	1
≥ 1	9.44 (7.65–11.65)	1.90 (1.37–2.63)
Any cancer	2.66 (2.03–3.48)	1.47 (1.10–1.97)
Any psychiatric disorders	2.21 (1.77–2.77)	1.32 (1.01–1.71)
Stroke including SAH	2.98 (2.14–4.15)	1.31 (0.90–1.90)
Venous thromboembolism	2.04 (1.26–3.32)	-
Ischemic heart disease	3.14 (2.51–3.94)	1.16 (0.87-1.55)
Valvular heart disease	2.91 (1.91–4.44)	1.40 (0.88-2.25)
Atrial fibrillation	3.46 (2.60–4.60)	1.05 (0.73–1.51)
Peripheral artery disease	3.94 (2.59–6.00)	1.39 (0.87–2.23)
Heart failure	4.35 (3.39–5.58)	1.46 (1.04–2.05)
High blood pressure	1.92 (1.55–2.36)	0.90 (0.69–1.17)
Osteoarthritis	0.78 (0.50–1.23)	0.39 (0.24–0.65)
Connective tissue diseases	1.72 (1.18–2.51)	-
Diabetes[4]	1.97 (1.47–2.64)	0.76 (0.54–1.08)
Chronic obstructive pulmonary disease	3.57 (2.36–5.39)	1.26 (0.77–2.06)
Asthma	1.19 (0.89–1.58)	0.80 (0.58–1.11)
Liver disorder	6.95 (4.76–10.15)	3.20 (2.06–4.97)
Anemia	7.16 (3.20–16.04)	1.52 (0.48–4.83)

[1]West Finland includes Turku and Loimaa as well as Helsinki and Vantaa. East Finland includes North Karelia, North Savo, Oulu, and Lapland.
[2]Educational tertiles were calculated according to years of education and were specific to the birth cohorts.
[3]Includes conditions without gastrointestinal bleeding such as gastritis, intestinal diseases, esophageal varices, esophagitis, hemorrhoids, colitis, or Crohn's disease.
[4]Excluding gestational diabetes.
'-' indicates that the variable was not included in the final multivariate Cox model based on the results from LASSO.
CI: Confidence Interval; GIB: Gastrointestinal bleeding; HR: Hazard ratio; SAH: Subarachnoid hemorrhage.

was also minimal. Compared to stepwise selection of variables into the regression model, the LASSO method helped to address multicollinearity and to avoid overfitting. The LASSO approach also performed an internal validation by inbuilt cross-validation techniques, although an external validation of the newly proposed risk factors is still warranted. A small degree of misclassification of GIB is possible because the electronic health register data was collected for administrative purposes, however the magnitude is likely to be very small. We used hospital diagnoses as well as drug prescriptions to identify chronic conditions. Further, NSAIDs can be obtained over the counter and not recorded in the data sources, hence could not be included in our analyses. Also, due to the insufficient numbers of cases, factors such as hemophilia, thyroid disorders, pancreatitis and chronic kidney failure could not be investigated. Information on lifestyle factors such as smoking, and alcohol consumption are self-reported and might be under-reported. Lastly, the data on demographic, lifestyle, and laboratory parameters were only collected at baseline and no repeated measurements were conducted during the study period. Therefore, we could not account for lifestyle modifications on the risk of GI bleeding in our analyses.

Clinical implications and future research

In addition to previously established risk factors for GIB, we have identified additional potential independent risk factors for major GIB, further helping build the knowledge base on this topic. This will support in identifying patients at high risk of GIB. Further, this will support early interventions or counseling to prevent incident or recurrent GIBs as well as help in monitoring the prevalence of these risk factors. The results from our study are exploratory and future studies are required to establish causal associations and hopefully stimulate research of these factors in the general population which currently is scarce.

CONCLUSION

Our study showed that older age, unemployment, higher BMI, higher GGT levels, history of precursors of GIBs, cancer, psychiatric illness, heart failure and liver disorders were associated with an increased risk of major GIBs. Moreover, higher coffee consumption (> 5 cups per day) and higher SBP showed an inverse association with major GIB. These associations in the general population need to be confirmed by future research and other epidemiological studies.

ARTICLE HIGHLIGHTS

Research background

Limited information is available on the risk factors of gastrointestinal bleedings (GIB) in the general population. Previous research mainly focused on the population using specific medications such as antiplatelets, anticoagulants *etc.* or the critically ill population such as hospitalized patients or elderly. Therefore, we investigated the risk factors for major GIB using data representative of the general population having a high granularity of the data source and long-term follow-up of participants.

Research motivation

Many studies investigating risk factors of GIB lacked information on lifestyle factors, clinical measurements and laboratory parameters. We wanted to better understand the effect of these additional variables on GIB as well as how this affects established risk factors. Additionally, to better understand the factors that predict the risk of GIB in the presence of a multicollinear set of variables [*e.g.*, Body mass index (BMI), Waist-hip ratio (WHR) or physical activity].

Research objectives

The overall objective of the study was to identify and investigate new risk factors of major GIB in the general population of Finland considering established risk factors as well as demographics and morbidities. We were able to identify new risk factors of major GIB together with established risk factors which needs to be evaluated and confirmed by further research.

Research methods

We conducted a retrospective cohort study using record linkage of data from the FINRISK health examination surveys which are representative of the general population of Finland to the national electronic health registers with 10 years of follow-up. This linkage enabled us to include and investigate demographics, socioeconomic and lifestyle factors, clinical measurements, laboratory parameters, and comorbidities on the risk of major GIB. We further implemented Least Absolute Shrinkage and Selection Operator (LASSO) to select the most important predictor variables for model prediction and association of these predictor variables were evaluated using Cox regression. The novelty of using LASSO is that it helps in the variable selection and in excluding unnecessary/uninfluential variables from the model thus reducing the likelihood of overfitting a model. It also helps to address multicollinearity that can be problematic in the traditional forms of regression.

Research results

The main results of the study showed that baseline age, unemployment, and higher BMI, higher gamma-glutamyl transferase (GGT) levels, having ≥1 precursor of GIB, previous cancer, psychiatric disorders, heart failure and liver disorders were all associated with an increased risk of GIB. Systolic blood pressure, above average coffee consumption per day, and history of osteoarthritis were all associated with a decreased risk of GIB. This study adds to the scarce literature on risk factors on gastrointestinal bleeding in the general population. Additionally, results are hypothesis generating for the new risk factors identified in this study which must be confirmed by future mechanistic and epidemiological studies.

Research conclusions

This study identified new risk factors associated with major GIB which are unemployment, BMI, GGT, SBP and coffee consumption. Accounting for physical activity and waist-hip ratio, our study suggests that BMI is a better predictor of major GIB. Above average coffee consumption per day, which seems to be more common in Finland with the highest per capita coffee consumption in the world, was associated with a decreased risk of major GIB. Our study suggests that the risk factors of major GIBs might be slightly different in the general population than the at-risk population.

Research perspectives

Future mechanistic and epidemiological studies should evaluate these risk factors in different study populations or countries across the world to establish causal associations. This will further support in complementing and refining existing risk scores for major GIBs.

FOOTNOTES

Author contributions: Vora P, Brobert G and Salomaa V proposed the concept and design; Salomaa V and Pietila A supported in acquisition of the collected data; Vora P, Herrera R, Pietila A and Mansmann U performed the statistical analysis; Vora P drafted the manuscript; Vora P, Brobert G and Salomaa V obtained funding; Pietila A and Salomaa V provided the administrative, technical, and material support; Salomaa V, Mansmann U and Brobert G were responsible for supervision; All authors were involved in the interpretation of the results, critical revision of the manuscript and approved the final version of the article for publication.

Supported by Bayer AG.

Institutional review board statement: The National FINRISK Study surveys started in 1972 were approved by the ethics committee of the Finnish Institute of Health and Welfare and the Coordinating Ethical Committee of Helsinki and Uusimaa Hospital District in Finland (THL/66/0.05.00/2015). Data from the participants were pseudonymized for this study, and the secondary use of the survey data was approved by the Finnish Institute of Health and Welfare in 2017.

Informed consent statement: All participants provided their informed consents at enrollment in to the FINRISK surveys and it was conducted following the principles of the World Medical Association's Declaration of Helsinki.

Conflict-of-interest statement: Vora P and Herrera R are employees at Integrated Evidence Generation, Bayer AG, Berlin Germany. Vora P is affiliated to Institute for Medical Information Processing, Biometry, and Epidemiology - IBE, Ludwig Maximilians Universität Munich, Munich, Germany, and Pettenkofer School of Public Health, Munich, Germany. Brobert G was an employee at Medical Affairs, Bayer AB, Solna Sweden. Salomaa V reported being an employee of the Finnish Institute for Health and Welfare, which received a funding from Bayer AG during the conduct of the study, as well as receiving honorarium for consultation from Sanofi and grants from Finnish foundation for Cardiovascular research outside the submitted work. Pietila A reported being an employee of the Finnish Institute for Health and Welfare, which received a funding from Bayer AG during the conduct of the study. Peltonen M works for the Department of Public Health and Welfare, National Institute for Health and Welfare (THL), Helsinki, Finland. Mansmann U is the director of IBE - Institute for Medical Information Processing, Biometry, and Epidemiology, Ludwig Maximilians Universität Munich, Munich, Germany.

Data sharing statement: Salomaa V and Pietila A had full access to all the data in the study and take responsibility for the integrity of the data and the accuracy of the data analysis.

Open-Access: This article is an open-access article that was selected by an in-house editor and fully peer-reviewed by external reviewers. It is distributed in accordance with the Creative Commons Attribution NonCommercial (CC BY-NC 4.0) license, which permits others to distribute, remix, adapt, build upon this work non-commercially, and license their derivative works on different terms, provided the original work is properly cited and the use is non-commercial. See: https://creativecommons.org/Licenses/by-nc/4.0/

Country/Territory of origin: Finland

ORCID number: Pareen Vora 0000-0002-5822-2453; Ronald Herrera 0000-0002-3070-8312; Arto Pietila 0000-0002-9298-0012; Ulrich Mansmann 0000-0002-9955-8906; Gunnar Brobert 0000-0002-7446-9851; Markku Peltonen 0000-0002-3767-4223; Veikko Salomaa 0000-0001-7563-5324.

Corresponding Author's Membership in Professional Societies: International Society of Pharmacoepidemiology; European Respiratory Society.

S-Editor: Wu YXJ
L-Editor: Filipodia

P-Editor: Wu YXJ

REFERENCES

1 **Peery AF**, Dellon ES, Lund J, Crockett SD, McGowan CE, Bulsiewicz WJ, Gangarosa LM, Thiny MT, Stizenberg K, Morgan DR, Ringel Y, Kim HP, DiBonaventura MD, Carroll CF, Allen JK, Cook SF, Sandler RS, Kappelman MD, Shaheen NJ. Burden of gastrointestinal disease in the United States: 2012 update. *Gastroenterology* 2012; **143**: 1179-1187.e3 [PMID: 22885331 DOI: 10.1053/j.gastro.2012.08.002]

2 **Lin XH**, Young SH, Luo JC, Peng YL, Chen PH, Lin CC, Chen WM, Hou MC, Lee FY. Risk Factors for Upper Gastrointestinal Bleeding in Patients Taking Selective COX-2 Inhibitors: A Nationwide Population-Based Cohort Study. *Pain Med* 2018; **19**: 225-231 [PMID: 28460044 DOI: 10.1093/pm/pnx097]

3 **Valkhoff VE**, Sturkenboom MC, Kuipers EJ. Risk factors for gastrointestinal bleeding associated with low-dose aspirin. *Best Pract Res Clin Gastroenterol* 2012; **26**: 125-140 [PMID: 22542151 DOI: 10.1016/j.bpg.2012.01.011]

4 **Lin CC**, Hu HY, Luo JC, Peng YL, Hou MC, Lin HC, Lee FY. Risk factors of gastrointestinal bleeding in clopidogrel users: a nationwide population-based study. *Aliment Pharmacol Ther* 2013; **38**: 1119-1128 [PMID: 24099473 DOI: 10.1111/apt.12483]

5 **Beyan E**, Beyan C, Vaizoğlu SA. Risk factors in patients with gastrointestinal bleeding due to warfarin usage. *Int J Surg* 2010; **8**: 257-258 [PMID: 20060938 DOI: 10.1016/j.ijsu.2009.12.010]

6 **Lenti MV**, Pasina L, Cococcia S, Cortesi L, Miceli E, Caccia Dominioni C, Pisati M, Mengoli C, Perticone F, Nobili A, Di Sabatino A, Corazza GR; REPOSI Investigators. Mortality rate and risk factors for gastrointestinal bleeding in elderly patients. *Eur J Intern Med* 2019; **61**: 54-61 [PMID: 30522789 DOI: 10.1016/j.ejim.2018.11.003]

7 **Kumar S**, Ramos C, Garcia-Carrasquillo RJ, Green PH, Lebwohl B. Incidence and risk factors for gastrointestinal bleeding among patients admitted to medical intensive care units. *Frontline Gastroenterol* 2017; **8**: 167-173 [PMID: 28839905 DOI: 10.1136/flgastro-2016-100722]

8 **Terdiman JP**, Ostroff JW. Gastrointestinal bleeding in the hospitalized patient: a case-control study to assess risk factors, causes, and outcome. *Am J Med* 1998; **104**: 349-354 [PMID: 9576408 DOI: 10.1016/s0002-9343(98)00055-2]

9 **Tielleman T**, Bujanda D, Cryer B. Epidemiology and Risk Factors for Upper Gastrointestinal Bleeding. *Gastrointest Endosc Clin N Am* 2015; **25**: 415-428 [PMID: 26142028 DOI: 10.1016/j.giec.2015.02.010]

10 **Kim SH**, Yun JM, Chang CB, Piao H, Yu SJ, Shin DW. Prevalence of upper gastrointestinal bleeding risk factors among the general population and osteoarthritis patients. *World J Gastroenterol* 2016; **22**: 10643-10652 [PMID: 28082817 DOI: 10.3748/wjg.v22.i48.10643]

11 **Vonbach P**, Reich R, Möll F, Krähenbühl S, Ballmer PE, Meier CR. Risk factors for gastrointestinal bleeding: a hospital-based case-control study. *Swiss Med Wkly* 2007; **137**: 705-710 [PMID: 18197486 DOI: 10.4414/smw.2007.11912]

12 **Tolonen H**, Koponen P, Al-Kerwi A, Capkova N, Giampaoli S, Mindell J, Paalanen L, Ruiz-Castell M, Trichopoulou A, Kuulasmaa K; EHES Network. European health examination surveys - a tool for collecting objective information about the health of the population. *Arch Public Health* 2018; **76**: 38 [PMID: 29988297 DOI: 10.1186/s13690-018-0282-4]

13 **Tunstall-Pedoe H**, Kuulasmaa, Kari, Tolonen, Hanna, Davidson, Moira, Mendis, Shanthi. et al MONICA monograph and multimedia sourcebook : world's largest study of heart disease, stroke, risk factors, and population trends 1979-2002 / edited by Hugh Tunstall-Pedoe ; prepared by Hugh Tunstall-Pedoe ... [et al.] with 64 other contributors for the WHO MONICA Project. World Health Organization 2003.

14 **Borodulin K**, Tolonen H, Jousilahti P, Jula A, Juolevi A, Koskinen S, Kuulasmaa K, Laatikainen T, Männistö S, Peltonen M, Perola M, Puska P, Salomaa V, Sundvall J, Virtanen SM, Vartiainen E. Cohort Profile: The National FINRISK Study. *Int J Epidemiol* 2018; **47**: 696-696i [PMID: 29165699 DOI: 10.1093/ije/dyx239]

15 **Vora P**, Pietila A, Peltonen M, Brobert G, Salomaa V. Thirty-Year Incidence and Mortality Trends in Upper and Lower Gastrointestinal Bleeding in Finland. *JAMA Netw Open* 2020; **3**: e2020172 [PMID: 33034641 DOI: 10.1001/jamanetworkopen.2020.20172]

16 **Tibshirani R**. The lasso method for variable selection in the Cox model. *Stat Med* 1997; **16**: 385-395 [PMID: 9044528 DOI: 10.1002/(sici)1097-0258(19970228)16:4<385::aid-sim380>3.0.co;2-3]

17 **Cox DR**. Regression Models and Life-Tables. *J Royal Statistical Society Series B (Methodological)* 1972; **34**: 187-220 [DOI: 10.1111/j.2517-6161.1972.tb00899.x]

18 **Iriondo-DeHond A**, Uranga JA, Del Castillo MD, Abalo R. Effects of Coffee and Its Components on the Gastrointestinal Tract and the Brain-Gut Axis. *Nutrients* 2020; **13** [PMID: 33383958 DOI: 10.3390/nu13010088]

19 **Wang Y**, Chen J, Zhao R, Xia L, Cui YP, Rao ZY, Zhou Y, Wu XT. Dose-response meta-analysis of coffee consumption and risk of colorectal adenoma. *Eur J Clin Nutr* 2020; **74**: 297-306 [PMID: 31308476 DOI: 10.1038/s41430-019-0467-0]

20 **Sartini M**, Bragazzi NL, Spagnolo AM, Schinca E, Ottria G, Dupont C, Cristina ML. Coffee Consumption and Risk of Colorectal Cancer: A Systematic Review and Meta-Analysis of Prospective Studies. *Nutrients* 2019; **11** [PMID: 30909640 DOI: 10.3390/nu11030694]

21 **Micek A**, Gniadek A, Kawalec P, Brzostek T. Coffee consumption and colorectal cancer risk: a dose-response meta-analysis on prospective cohort studies. *Int J Food Sci Nutr* 2019; **70**: 986-1006 [PMID: 30922134 DOI: 10.1080/09637486.2019.1591352]

22 **Wang A**, Wang S, Zhu C, Huang H, Wu L, Wan X, Yang X, Zhang H, Miao R, He L, Sang X, Zhao H. Coffee and cancer risk: A meta-analysis of prospective observational studies. *Sci Rep* 2016; **6**: 33711 [PMID: 27665923 DOI: 10.1038/srep33711]

23 **Gan Y**, Wu J, Zhang S, Li L, Cao S, Mkandawire N, Ji K, Herath C, Gao C, Xu H, Zhou Y, Song X, Chen S, Chen Y, Yang T, Li J, Qiao Y, Hu S, Yin X, Lu Z. Association of coffee consumption with risk of colorectal cancer: a meta-analysis of prospective cohort studies. *Oncotarget* 2017; **8**: 18699-18711 [PMID: 27078843 DOI: 10.18632/oncotarget.8627]

24 **Li G**, Ma D, Zhang Y, Zheng W, Wang P. Coffee consumption and risk of colorectal cancer: a meta-analysis of observational studies. *Public Health Nutr* 2013; **16**: 346-357 [PMID: 22694939 DOI: 10.1017/S1368980012002601]

25 **Quach DT**, Nguyen NT, Vo UP, Le LT, Vo CH, Ho PT, Nguyen TN, Bo PK, Nguyen NH, Vu KT, Van Dang M, Dinh MC, Nguyen TQ, Van Nguyen X, Le ST, Tran CP. Development and Validation of a Scoring System to Predict Severe Acute Lower Gastrointestinal Bleeding in Vietnamese. *Dig Dis Sci* 2021; **66**: 823-831 [PMID: 32285322 DOI: 10.1007/s10620-020-06253-y]

26 **Zhang M**, Liu D, Wang Q, Geng X, Hou Q, Gu G, Xie R, Cui W. Gastrointestinal bleeding in patients admitted to cardiology: risk factors and a new risk score. *Hellenic J Cardiol* 2021; **62**: 291-296 [PMID: 32687882 DOI: 10.1016/j.hjc.2020.07.003]

27 **Bellido-Caparó Á**, Espinoza-Ríos J, Gómez Hinojosa P, Prochazka-Zarate R, Bravo Paredes E, León Rabanal CP, Tagle Arróspide M, Pinto Valdivia JL. [Independent risk factors for severity and mortality in lower gastrointestinal bleeding]. *Rev Gastroenterol Peru* 2019; **39**: 229-238 [PMID: 31688846]

28 **Kim MS**, Choi J, Shin WC. AIMS65 scoring system is comparable to Glasgow-Blatchford score or Rockall score for prediction of clinical outcomes for non-variceal upper gastrointestinal bleeding. *BMC Gastroenterol* 2019; **19**: 136 [PMID: 31349816 DOI: 10.1186/s12876-019-1051-8]

29 **Norström F**, Waenerlund AK, Lindholm L, Nygren R, Sahlén KG, Brydsten A. Does unemployment contribute to poorer health-related quality of life among Swedish adults? *BMC Public Health* 2019; **19**: 457 [PMID: 31035994 DOI: 10.1186/s12889-019-6825-y]

30 **Norström F**, Virtanen P, Hammarström A, Gustafsson PE, Janlert U. How does unemployment affect self-assessed health? *BMC Public Health* 2014; **14**: 1310 [PMID: 25535401 DOI: 10.1186/1471-2458-14-1310]

31 **Rodríguez-Hernández H**, Rodríguez-Morán M, González JL, Jáquez-Quintana JO, Rodríguez-Acosta ED, Sosa-Tinoco E, Guerrero-Romero F. [Risk factors associated with upper gastrointestinal bleeding and with mortality]. *Rev Med Inst Mex Seguro Soc* 2009; **47**: 179-184 [PMID: 19744387]

32 **Nagata N**, Niikura R, Sekine K, Sakurai T, Shimbo T, Kishida Y, Tanaka S, Aoki T, Okubo H, Watanabe K, Yokoi C, Akiyama J, Yanase M, Mizokami M, Uemura N. Risk of peptic ulcer bleeding associated with Helicobacter pylori infection, nonsteroidal anti-inflammatory drugs, low-dose aspirin, and antihypertensive drugs: a case-control study. *J Gastroenterol Hepatol* 2015; **30**: 292-298 [PMID: 25339607 DOI: 10.1111/jgh.12805]

33 **Kurata JH**, Nogawa AN. Meta-analysis of risk factors for peptic ulcer. Nonsteroidal antiinflammatory drugs, Helicobacter pylori, and smoking. *J Clin Gastroenterol* 1997; **24**: 2-17 [PMID: 9013343 DOI: 10.1097/00004836-199701000-00002]

34 **Jennings DL**, Truby LK, Littlefield AJ, Ciolek AM, Marshall D, Jain R, Topkara VK. Impact of heart failure drug therapy on rates of gastrointestinal bleeding in LVAD recipients: An INTERMACS analysis. *Int J Artif Organs* 2021; **44**: 965-971 [PMID: 33977770 DOI: 10.1177/03913988211013366]

35 **Narum S**, Westergren T, Klemp M. Corticosteroids and risk of gastrointestinal bleeding: a systematic review and meta-analysis. *BMJ Open* 2014; **4**: e004587 [PMID: 24833682 DOI: 10.1136/bmjopen-2013-004587]

36 **Sostres C**, Gargallo CJ, Lanas A. Nonsteroidal anti-inflammatory drugs and upper and lower gastrointestinal mucosal damage. *Arthritis Res Ther* 2013; **15** Suppl 3: S3 [PMID: 24267289 DOI: 10.1186/ar4175]

37 **Gwee KA**, Goh V, Lima G, Setia S. Coprescribing proton-pump inhibitors with nonsteroidal anti-inflammatory drugs: risks *vs* benefits. *J Pain Res* 2018; **11**: 361-374 [PMID: 29491719 DOI: 10.2147/JPR.S156938]

World Journal of Gastroenterology

Submit a Manuscript: https://www.f6publishing.com

World J Gastroenterol 2022 May 14; 28(18): 2021-2033

DOI: 10.3748/wjg.v28.i18.2021

ISSN 1007-9327 (print) ISSN 2219-2840 (online)

ORIGINAL ARTICLE

Observational Study

Clinical utility of two-dimensional shear-wave elastography in monitoring disease course in autoimmune hepatitis-primary biliary cholangitis overlap syndrome

Yu-Ling Yan, Xian Xing, Yi Wang, Xiao-Ze Wang, Zhi Wang, Li Yang

Specialty type: Gastroenterology and hepatology

Provenance and peer review: Invited article; Externally peer reviewed.

Peer-review model: Single blind

Peer-review report's scientific quality classification

Grade A (Excellent): 0
Grade B (Very good): B
Grade C (Good): C, C, C
Grade D (Fair): 0
Grade E (Poor): 0

P-Reviewer: Mohamed GA, Egypt; Morozov S, Russia; Zharikov YO, Russia

Received: October 13, 2021
Peer-review started: October 13, 2021
First decision: December 3, 2021
Revised: December 16, 2021
Accepted: April 2, 2022
Article in press: April 2, 2022
Published online: May 14, 2022

Yu-Ling Yan, Xian Xing, Yi Wang, Xiao-Ze Wang, Zhi Wang, Li Yang, Department of Gastroenterology and Hepatology, West China Hospital, Sichuan University, Chengdu 610041, Sichuan Province, China

Yu-Ling Yan, Xian Xing, Yi Wang, Xiao-Ze Wang, Zhi Wang, Li Yang, Sichuan University, University of Oxford Huaxi Joint for Gastrointestinal Cancer Centre, Chengdu 610207, Sichuan Province, China

Corresponding author: Li Yang, MD, Director, Doctor, Full Professor, Department of Gastroenterology and Hepatology, West China Hospital, Sichuan University, No. 37 Guoxue Lane, Chengdu 610041, Sichuan Province, China. yangli_hx@scu.edu.cn

Abstract

BACKGROUND

Autoimmune hepatitis-primary biliary cholangitis (AIH-PBC) overlap syndrome has a worse prognosis than AIH or PBC alone. Therefore, accurately staging liver fibrosis and dynamically monitoring disease progression are essential.

AIM

To investigate the performance of two-dimensional shear-wave elastography (2D-SWE) for noninvasively staging liver fibrosis and assessing the clinical utility of repeated 2D-SWE for monitoring treatment response in AIH-PBC overlap syndrome.

METHODS

A total of 148 patients diagnosed with AIH-PBC overlap syndrome were retrospectively enrolled. Among them, 82 patients had a 2D-SWE follow-up time of more than 1 year. The Scheuer scoring system was used to evaluate stages of hepatic inflammation and liver fibrosis. The performance of 2D-SWE for staging liver fibrosis was evaluated with the liver biopsy. Changes in liver stiffness (LS) measured by 2D-SWE in patients with or without complete biochemical remission were evaluated.

RESULTS

LS value was strongly correlated with liver fibrosis stage (Spearman $r = 0.84$, $P < 0.0001$). The areas under the receiver operating characteristic curves of LS for

diagnosing significant fibrosis (≥ S2), severe fibrosis (≥ S3), and cirrhosis (S4) were 0.91, 0.97, and 0.96, respectively. Patients with complete biochemical remission had a considerable decrease in LS values (P < 0.0001). More importantly, the declined LS in patients with S0-S2 was significantly lower than that in patients with S3-S4 (P = 0.0002). In contrast, patients who failed to achieve biochemical remission had a slight but not significant decrease in LS (P = 0.37).

CONCLUSION

LS measured by 2D-SWE is an accurate and reliable method in assessing liver fibrosis, especially for diagnosing severe fibrosis (≥ 3) and monitoring treatment response in patients with AIH-PBC overlap syndrome.

Key Words: Liver fibrosis; Liver biopsy; Diagnostic tests; Autoimmune hepatitis; Primary biliary cholangitis; Inflammation

©The Author(s) 2022. Published by Baishideng Publishing Group Inc. All rights reserved.

Core Tip: Two-dimensional shear-wave elastography is an accurate and reliable method in monitoring treatment response in patients with autoimmune hepatitis-primary biliary cholangitis overlap syndrome.

Citation: Yan YL, Xing X, Wang Y, Wang XZ, Wang Z, Yang L. Clinical utility of two-dimensional shear-wave elastography in monitoring disease course in autoimmune hepatitis-primary biliary cholangitis overlap syndrome. *World J Gastroenterol* 2022; 28(18): 2021-2033
URL: https://www.wjgnet.com/1007-9327/full/v28/i18/2021.htm
DOI: https://dx.doi.org/10.3748/wjg.v28.i18.2021

INTRODUCTION

Autoimmune hepatitis-primary biliary cholangitis (AIH-PBC) overlap syndrome is defined as presenting features of AIH and PBC simultaneously or sequentially. AIH is a progressive inflammatory liver disorder characterized histologically by interface hepatitis, serologically by high levels of transaminases and immunoglobulin G (IgG) and the presence of autoantibodies. PBC is progressive autoimmune liver disease with nonsuppurative destructive cholangitis and interlobular bile duct destruction[1]. AIH-PBC overlap syndrome has a worse prognosis than AIH or PBC alone[2]. Therefore, accurately assessing stage of liver disease and dynamically monitoring the progression of disease are essential for some AIH-PBC overlap syndromes with rapid disease progression.

Liver biopsy still remains the gold standard for establishing the diagnosis, assessing disease severity and determining treatment. According to the most recent guidelines, long-term treatment with immunosuppressants in combination with ursodeoxycholic acid is recommended when AIH-PBC overlap syndrome is established[3,4]. Frequent biochemical markers measurement during the follow-up was necessary to monitor the therapeutic response. However, they cannot monitor the histologically progression and reflect the severity of liver fibrosis. Furthermore, hepatic histological remission usually lagged behind biochemical remission by several months[5]. Therefore, detecting the severity of histology at the beginning of treatment and frequent monitoring during long-term follow-up are important for management of AIH-PBC overlap syndrome. Liver biopsy is still the gold standard for diagnosing AIH-PBC overlap syndrome and staging liver fibrosis, and can be accepted by most patients, but the second or repeated liver biopsy cannot be easily performed due to its costly and invasive procedure during the long-term follow-up.

During the past decades, several noninvasive markers are found to have high accuracy for detecting liver fibrosis and disease progression. 2D-SWE by using the supersonic shear imaging technique is an ultrasound-based real-time imaging method with the following advantages for assessing liver disease: (1) nontarget structure and elastic artifacts can be effectively avoided to improve reliability by integrating B-mode imaging and color-coded tissue stiffness maps in real time; (2) it is widely applied to measure liver stiffness in the whole world; and (3) there is no limitation in patients with ascites[6]. Our previous studies showed that 2D-SWE has a great performance for staging liver fibrosis in AIH[7] and PBC patients[8]. However, the utility of 2D-SWE in monitoring treatment response remains blank.

The aim of this study was to evaluate the clinical utility of 2D-SWE in evaluating liver fibrosis and to assess the usefulness of repeated 2D-SWE for monitoring treatment response in AIH-PBC overlap syndrome.

MATERIALS AND METHODS

Patients

This is a single-center retrospective study, which was approved by the ethics committee of our hospital, and due to the retrospective feature, the patients informed consent was waived. Patients was strictly diagnosed according to the Paris criteria[9,10]. The presence of at least two of the three accepted criteria was required for the diagnosis of AIH and PBC. The AIH criteria were as follows: (1) Alanine aminotransferase (ALT) levels at least five times higher than the upper limit of normal (ULN); (2) Serum IgG levels at least two times higher than the ULN or a positive test for anti-smooth muscle antibodies; and (3) Moderate or severe periportal or periseptal piecemeal lymphocytic necrosis in liver biopsy. PBC criteria were as follows: (1) Alkaline phosphatase (ALP) levels at least two times higher than the ULN or γ-glutamyltranspeptidase (GGT) levels at least five times higher than the ULN; (2) A positive test for anti-mitochondrial antibodies; and (3) Florid bile duct lesions in liver biopsy. Among them, moderate interfacial inflammation of the liver was necessary for diagnosis of AIH-PBC overlap syndrome. The patients between September, 2016 and April 2021 in West China hospital were enrolled. The inclusion criteria were as follows: (1) Patients met the diagnosis criteria of PBC-AIH overlap syndrome with liver biopsy; and (2) Age was adults with lower than 75 years old. The exclusion criteria were as follows: (1) Patients with overlapping etiologies of liver disease, such as virus, alcohol liver disease[11], non-alcoholic fatty liver disease[12], drug-induced liver disease[13], hereditary metabolic liver disease or other causes of liver damage; (2) Patients with primary hepatic carcinoma or other malignant tumors; (3) 2D-SWE measurement after liver biopsy for more than 1 mo and with treatment; (4) Patients without 2D-SWE results or serological data; (5) Patients with ascites, varices bleeding, esophageal variceal ligation (EVL) or splenectomy; and (6) Patients with severe systemic disease. Among them, the follow-up time with 2D-SWE greater than 1 year was subsequently analyzed to evaluate the changes of LS values after standard treatment. Complete biochemical remission was defined by normalization of serum AST, ALT, ALP and IgG levels[14].

2D-SWE measurement

2D-SWE measurements were obtained by using the Aixplorer system (SuperSonic Imagine, Aix-en-Provence) with a SC6-1 (frequency of 1-6 MHz) convex probe. Two experience radiologists independently performed the procedures according to the guidelines developed by the World Federation for Ultrasound in Medicine and Biology[15]. The 2D-SWE measurements were performed following our previous study[8], Briefly, the elasticity image box, approximately 4 cm × 3 cm, was placed 1-2 cm under the liver capsule in the parenchyma area of the right hepatic lobe. At least three valid measurements were obtained in each patient. The median LS value was recorded (in kPa)[16]. When less than two-thirds of the signal filled in the 2D SWE region of interest or the large vessels and biliary tracts were not avoided, measurements were considered failed or unqualified[17].

Liver biopsy and histologic stages

Ultrasound-guided liver biopsy was performed in the right liver lobe. Quality of the liver specimen was evaluated. All specimens were analyzed by one experienced pathologist. The Scheuer scoring system, a common scoring system in clinical practice, evaluates liver fibrosis and necroinflammatory activity. Liver fibrosis was scored as follows the previous studies[7]: the liver fibrosis was staged from stage 0 (S0) to stage 4 (S4) cirrhosis (S0-S4). Necroinflammative was also scored from grade 0 (G0), no portal or periportal and lobular necroinflammatory activity to grade 4 (G4), severe piecemeal portal or periportal necrosis and severe or diffuse hepatocellular damage inside the lobule (G0-G4). Significant fibrosis was liver fibrosis stage ≥ S2; severe fibrosis was liver fibrosis stage ≥ S3 and cirrhosis was liver fibrosis stage = S4. Mild liver necroinflammation was defined as necroinflammatory activity lower than G2 (G0–G2), and significant liver necroinflammation was defined as necroinflammatory activity higher than G2 (G3-G4).

Statistical analysis

Statistical analyses were performed in SPSS Statistics version 24.0 (IBM Corporation, Armonk, NY), MedCalc software version 19.1.0 (MedCalc Software, Mariakerke, Belgium). A P value lower than 0.05 was considered statistically significant. Descriptive statistics were summarized as the median and interquartile (25%-75%). One-way ANOVA analysis or the Mann-Whitney test was used to compare quantitative variables. Correlations between LS values and biochemical biomarkers and histological features were evaluated with the Spearman correlation test, and those with $P < 0.05$ were subsequently included in multiple regression analysis. The performance of noninvasive methods in the assessment of liver fibrosis stages was determined by using the area under the receiver operating characteristic curve (AUC). Optimal cutoff values to predict different fibrosis stages were identified with the highest Youden's index. The corresponding sensitivity, specificity, negative predictive value, positive predictive value and accuracy were calculated. The cutoff values of LS for ruling out and ruling in were defined with sensitivity > 95% and specificity > 95%, respectively. The AUCs of noninvasive biomarkers were compared with the DeLong test. The Z test was used to compare the AUCs of LS for predicting liver

fibrosis in the G0-G2 subgroups and G3-G4 subgroups. Two-way ANOVA was used to evaluate the changes in LS. Wilcoxon matched pairs test was used to compare the LS values before treatment and each follow-up.

RESULTS

Patients' characteristics

A total of 177 patients considered AIH-PBC patients were enrolled. Eight patients without 2D-SWE results or liver biopsy, 2 patients of with the 2D-SWE measurements after liver biopsy for more than 1 mo and with treatment, 15 patients with varices bleeding or EVL, 1 patient with splenectomy, 1 patient with portal venous thrombosis, 1 patient with age < 18 years old, and 1 patient with hepatic carcinoma were excluded. Finally, 148 patients were included to analyze the LS for staging liver fibrosis in this study (Figure 1). Among them, 82 patients had a 2D-SWE follow-up of more than 1 year, 36 patients had complete biochemical remission, and 46 patients had no biochemical remission. The characteristics of the patients are described in Table 1. The numbers of patients with S0–S1, S2, S3 and S4 were 25 (15.4%), 48 (30.2%), 13 (9.9%) and 62 (44.4%), respectively.

Correlation of liver stiffness and serum biomarkers, histological features

LS had a strong correlation with serum biomarkers and histological features (Table 2). PLT (Spearman r = -0.43, P < 0.0001), total bilirubin (Spearman r = 0.60, P < 0.0001), AST (Spearman r = 0.33, P < 0.0001), albumin (Spearman r = -0.67, P < 0.0001), and IgG (Spearman r = 0.38, P < 0.0001) had significant correlations with LS values. The necroinflammatory activity grades (Spearman r = 0.32, P < 0.0001) and fibrosis stages (Spearman r = 0.84, P < 0.0001) also had a significant correlation with LS. In multiple regression analysis, only total bilirubin (P = 0.005) and fibrosis stages (P < 0.0001) had strong correlations with LS values (Supplementary Table 1). In addition, LS values in patients were increased with fibrosis stage S0-S1 [7.2 (6.3-9.9) kPa], S2 [10.7 (8.6-12.2) kPa], S3 [13.8 (12.0-20.8)], S4 [21.1 (17.1-28.4) kPa] (P < 0.0001) (Figure 2).

Diagnostic utility of 2D-SWE for assessing liver fibrosis stages

The utility of LS measured by 2D-SWE for staging liver fibrosis is shown in Table 3. For diagnosing significant fibrosis (≥ S2), the AUC of LS was 0.91 (95%CI: 0.85-0.96). The optimal cutoff value of LS was 12.1 kPa with the highest combined sensitivity (67.5%) and specificity (96.0%). The cutoff values of LS for ruling out and ruling in significant fibrosis (≥ S2) were 7.9 kPa and 12.1 kPa, respectively. For assessing severe fibrosis (≥ S3), the AUC of LS was 0.97 (95%CI: 0.94-0.99). The optimal cutoff value of LS was 15.0 kPa with the highest combined sensitivity (85.3%) and specificity (95.9%). The cutoff values of LS for ruling out and ruling in severe fibrosis (≥ S3) were 11.9 kPa and 15.0 kPa, respectively. For diagnosing cirrhosis (S4), the AUC of 2D-SWE was 0.96 (95%CI: 0.92-0.99). The optimal cutoff value of 2D-SWE was 18.0 kPa with the highest combined sensitivity (90.3%) and specificity (91.9%). The cutoff values of LS for ruling out and ruling in liver cirrhosis were 13.9 kPa and 19.4 kPa, respectively.

Effects of different degree of necroinflammation on LS measured by 2D-SWE

The effects of necroinflammatory activity on LS measured by 2D-SWE were evaluated. LS values in the subgroup of patients with G0-G2 and the subgroup of patients with G3-G4 showed no significant difference for staging liver fibrosis S0-S1 (P = 0.57), S2 (P = 0.51), S3 (P = 0.62) and S4 (P = 0.77) (Supplementary Table 2). The effect of necroinflammatory activity on the accuracy of LS values for staging liver fibrosis is shown in Supplementary Table 3. The AUCs of LS for diagnosing significant fibrosis (≥ S2) (P = 0.57), severe fibrosis (≥ S3) (P = 0.89), and cirrhosis (S4) (P = 0.06) were not significantly different between subgroups of patients with G0-G2 and G3-G4 necroinflammatory activity.

Accuracy of liver stiffness for evaluating liver fibrosis

The cutoff values for ruling out significant fibrosis (≥ S2), severe fibrosis (≥ S3) and cirrhosis (S4) were 7.9 kPa, 11.9 kPa and 13.9 kPa, respectively. The accuracy of these cutoff values for predicting each stage of liver fibrosis is listed in Supplementary Table 4. In patients with S0–S1, S2, S3 and S4, 15/25 (60.0%), 26/48 (54.2%), 4/13 (30.8%) and 58/62 (93.5%) of them were correctly classified, respectively. The accuracy of 2D-SWE for predicting severe fibrosis (≥ S3) was 71/75 (94.7%).

Complete biochemical remission is associated with changes in LS values

Eighty-two patients with 2D-SWE follow-up time of more than 1 year were evaluated. The total median follow-up time of these patients was 3.3 (2.2-4.1) years. The median follow-up time of 2D-SWE in these patients was 2.5 (1.5-3.5) years. Among these patients, 36 patients had complete biochemical remission, and 46 patients had no biochemical remission. The baseline characteristics of patients with or without complete biochemical remission were shown in Table 4. Total bilirubin (P = 0.009), ALP (P = 0.0005) and

Table 1 Baseline characteristics of the patients

Characteristic	Value
Gender, female, *n* (%)	132 (90)
Age, yr	49 (44-55)
BMI (kg/m^2)	21.5 (19.6-22.9)
Total bilirubin, μmol/L	36.6 (19.3-72.7)
ALB, g/L	38.7 (34.1-43.7)
PLT, × 10^9/L	127 (79-185)
ALT, IU/L	100 (63-185)
AST, IU/L	114 (74-177)
ALP, IU/L	342 (194-518)
GGT, IU/L	298 (176-499)
IgG, g/L	20.5 (16.1-24.7)
IgM, g/L	3250 (2023-5095)
LKM, positive, *n* (%)	0
ANA, positive, *n* (%)	144/148 (97.3)
AMA, positive, *n* (%)	89/148 (60.1)
Fibrosis stage, *n* (%)	
S0-S1	25 (15.4)
S2	48 (30.2)
S3	13 (9.9)
S4	62 (44.4)
Activity grade, *n* (%)	
G0-G1	10 (6.8)
G2	53 (35.2)
G3	78 (53.1)
G4	7 (4.9)
LS, kPa	13.6 (9.8-20.6)

Data are presented as median and interquartile range, number (percentage). The reference laboratory parameter value: Total bilirubin: 5-28 μmol/L; alanine aminotransferase < 50 IU/L; aspartate aminotransferase < 40 IU/L; albumin: 40-55 g/L; platelet count: 100-300 × 10^9/L; alkaline phosphatase: 51-160 IU/L; gamma-glutamyl transpeptidase: < 60 IU/L; immunoglobulin G: 8-15.5 g/L; immunoglobulin M: 700-2200 mg/L. BMI: Body mass index; TB: Total bilirubin; ALB: Albumin; PLT: Platelet count; ALT: Alanine aminotransferase; AST: Aspartate aminotransferase; ALP: Alkaline phosphatase; GGT: Gamma-glutamyl transpeptidase; IgG: Immunoglobulin G; IgM: Immunoglobulin M; LKM: Liver-kidney microsomal antibody; AMA: Antimitochondrial antibodies; ANA: Antinuclear antibody; LS: Liver stiffness.

GGT (P = 0.005) in patients with biochemical remission were lower than those in patients without biochemical remission. The change of LS values in patients with biochemical remission was significantly more than that in patients without biochemical remission (P < 0.0001). LS values in patients with complete biochemical remission present a considerable decrease (P < 0.0001). The LS values in all follow-up time points were lower than control point (all P < 0.01). In contrast, LS values in patients who failed to achieve complete biochemical remission showed a slight but not significant decrease (P = 0.37) (Figure 3). In patients with complete biochemical remission, the changes in LS in patients with S0-S2 fibrosis stages were significantly lower than those in patients with S3-S4 fibrosis stages (P = 0.0002) (Figure 4A). However, there was no similar change in patients without biochemical remission (Figure 4B).

Table 2 Correlation of liver stiffness and serum biomarkers, histological features

	Spearman *r*	*P* value
Necro-inflammatory activity grades	0.32	0.0006
Fibrosis stages	0.84	< 0.0001
PLT, × 10^9/L	-0.43	< 0.0001
TB, μmol/L	0.60	< 0.0001
ALT, IU/L	-0.04	0.63
AST, IU/L	0.33	< 0.0001
ALB, g/L	-0.67	< 0.0001
ALP, IU/L	0.02	0.77
IgG, IU/L	0.38	< 0.0001

PLT: Platelet count; TB: Total bilirubin; ALB: Albumin; ALT: Alanine aminotransferase; AST: Aspartate aminotransferase; ALP: Alkaline phosphatase; GGT: Gamma-glutamyl transpeptidase; IgG: Immunoglobulin G.

Table 3 Diagnostic accuracy of two-dimensional shear-wave elastography for diagnosing liver fibrosis

	Cutoff	AUC (95%CI)	Sensitivity	Specificity	PPV	NPV	Accuracy
Significant fibrosis (≥ S2)							
LS, kPa	12.1	0.91 (0.85-0.96)	67.5%	96.0%	98.8%	37.5%	72.3%
Rule out	7.9		95.1%	60.0%	92.1%	71.3%	89.2%
Rule in	12.1		67.5%	96.0%	98.8%	37.5%	72.3%
Severe fibrosis (≥ S3)							
LS, kPa	15.0	0.97 (0.94-0.99)	85.3%	95.9%	95.5%	86.4%	90.5%
Rule out	11.9		94.7%	75.3%	79.8%	93.3%	85.1%
Rule in	15.0		85.3%	95.9%	95.5%	86.4%	90.5%
Cirrhosis (S4)							
LS, kPa	15.1	0.96 (0.92-0.99)	90.3%	91.9%	88.9%	92.9%	91.2%
Rule out	13.9		95.2%	84.9%	82.0%	96.1%	89.2%
Rule in	19.4		58.1%	95.3%	89.9%	75.9%	79.7%

AUC: Area under the receiver operating characteristic curve; LS: Liver stiffness; PPV: Positive predictive value; NPV: Negative predictive value.

DISCUSSION

AIH-PBC overlap syndrome is a special clinical subgroup of chronic liver disease with poor clinical prognosis and higher risk of liver related complications than AIH or PBC alone. Therefore, disease progression needs intensive follow-up and dynamic monitoring in a timely manner. Noninvasive methods for staging liver fibrosis and monitoring disease progression are worthy of more concern. In this study, we assessed the clinical utility of 2D-SWE for staging liver fibrosis and evaluated the usefulness of repeated 2D-SWE to monitor disease progression in patients with AIH-PBC overlap syndrome.

2D-SWE is equal or superior to TE in staging liver fibrosis[18-21]. A meta-analysis study reported 2D-SWE had an excellent performance for staging fibrosis in common causes of liver disease, such as hepatitis C, hepatitis B, and nonalcoholic fatty liver disease, the AUCs were ranged from 86% to 96%. Autoimmune liver disease (AILD) is a rare group of liver diseases in the whole world, especially AIH-PBC overlap syndrome. Few studies have assessed the performance of 2D-SWE to evaluate severity of AILD. Our studies reported that the AUCs of LS measured by 2D-SWE for staging liver fibrosis were ranged from 0.88-0.99 in patients with PBC and 0.84-0.94 in patients with AIH, respectively. Recently, Janik *et al*[22] showed that the AUC of 2D-SWE for diagnosing cirrhosis was 0.93 in patients with AIH. In addition, Wu *et al*[23] reported that the AUCs of LS measured by TE for diagnosing F ≥ 2, F ≥ 3, and

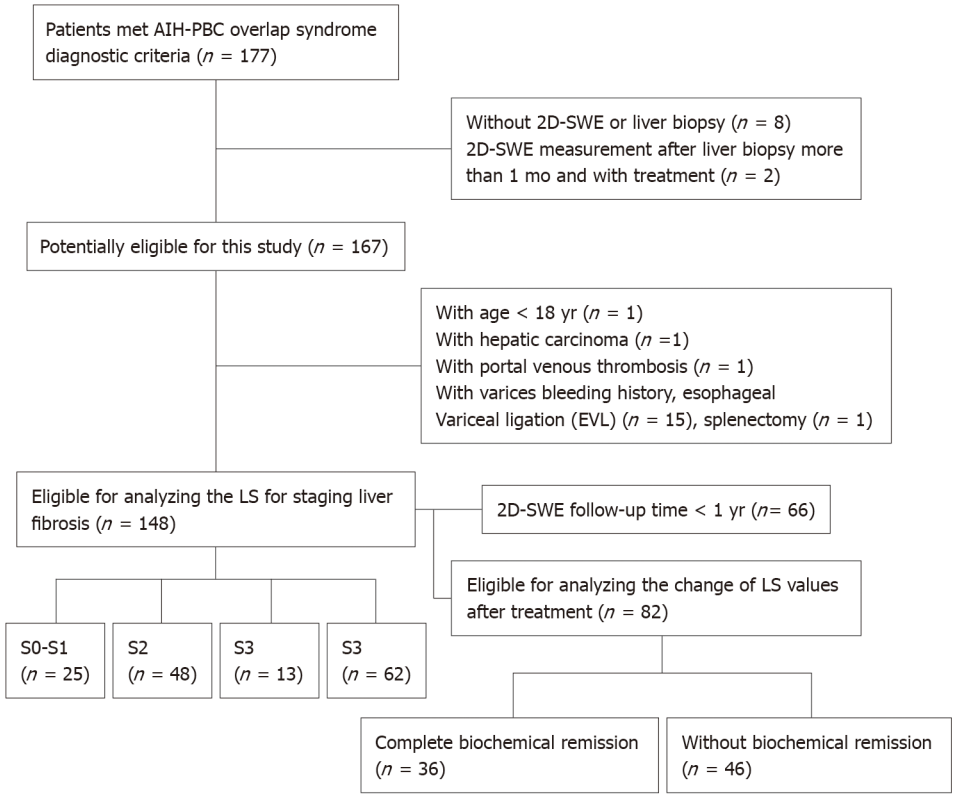
Table 4 Baseline characteristics of the patients between patients with complete biochemical remission and without biochemical remission

Characteristic	Without biochemical remission (*n* = 46)	Complete biochemical remission (*n* = 36)	*P* value
Sex, female, *n* (%)	39 (90)	35 (97.2)	0.07
Age, yr	50 (43-54)	49 (44-55)	0.99
BMI (kg/m^2)	21.1 (19.4-22.4)	21.9 (20.0-23.0)	0.27
TB, μmol/L	38.7 (27.4-61.2)	19.6 (15.5-43.6)	0.009
ALB, g/L	39.7 (34.8-45.3)	41 (35.5-44.8)	0.56
PLT, × 10^9/L	126 (90-170)	150 (85-215)	0.18
ALT, IU/L	98 (71-136)	146 (50-215.3)	0.17
AST, IU/L	111 (82-153)	126 (68-247)	0.63
ALP, IU/L	417 (297-533)	217 (143-412)	0.0005
GGT, IU/L	419 (269-558)	289 (111-451)	0.005
IgG, g/L	19.2 (15.3-22.3)	21.9 (16.5-26.2)	0.06
IgM, g/L	3500 (2400-4830)	3290 (2245-5925)	0.86
Fibrosis stage, *n*			0.19
S0-S1	4	9	
S2	19	14	
S3	6	2	
S4	17	11	
Activity grad, *n*			0.29
G0-G1	1	1	
G2	19	8	
G3	24	26	
G4	2	1	
LS, kPa	12.9 (10.0-17.0)	11.3 (7.7-15.4)	0.14

Data are presented as median and interquartile range, number (percentage). The reference laboratory parameter value: Total bilirubin: 5-28 μmol/L; alanine aminotransferase < 50 IU/L; aspartate aminotransferase < 40 IU/L; albumin: 40-55 g/L; platelet count: 100-300 × 10^9/L; alkaline phosphatase: 51-160 IU/L; gamma-glutamyl transpeptidase: < 60 IU/L; immunoglobulin G: 8-15.5 g/L; immunoglobulin M: 700-2200 mg/L. BMI: Body mass index; TB: Total bilirubin; ALB: Albumin; PLT: Platelet count; ALT: Alanine aminotransferase; AST: Aspartate aminotransferase; ALP: Alkaline phosphatase; GGT: Gamma-glutamyl transpeptidase; IgG: Immunoglobulin G; IgM: Immunoglobulin M; LS: Liver stiffness.

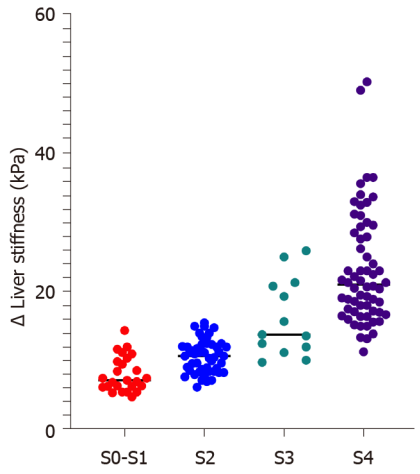
F4 were 0.84, 0.91, and 0.97, respectively, in patients with AIH-PBC overlap syndrome. In this study, the AUCs of LS measured by 2D-SWE in detecting significant fibrosis (S ≥ 2), severe fibrosis (S ≥ 3), and cirrhosis (S4) were 0.91, 0.97, and 0.96, respectively, which showed a broadly consistent accuracy with previous studies. 61/114 (53.5%) patients with AILD, 68/103 (66.02%) patients with AIH, 116/157 (73.9%) patients with PBC, respectively, can be correctly classified[7,8,24]. 105/148 (69.6%) patients with AIH-PBC overlap syndrome can be correctly classified in this study. These results suggest that LS measured by 2D-SWE is reliable method for staging liver fibrosis in patients with AIH-PBC over syndrome, even in patients with AILD.

The cutoff value of LS may vary among different etiologies and should be considered in diagnosing liver fibrosis[18,25,26]. The LS values ranged from 7.0 kPa to 8.3 kPa, 8.2 kPa to 9.2 kPa, and 9.9 kPa to 13.3 kPa for detecting significant fibrosis (S ≥ 2), severe fibrosis (S ≥ 3) and cirrhosis (S = 4), respectively. Patients with hepatitis B or C viruses have lower LS values for detecting corresponding fibrosis stages [25]. A study including 114 patients with AILD concluded that the optimal LS values for detecting significant fibrosis (S ≥ 2), severe fibrosis (S ≥ 3) and cirrhosis (S = 4) were 9.7 kPa, 13.2 kPa, and 16.3 kPa, respectively[24]. Our previous study showed that the optimal LS values for diagnosing significant fibrosis (S ≥ 2), severe fibrosis (S ≥ 3) and cirrhosis (S4) were 10.0 kPa, 15.8 kPa and 19.3 kPa, respectively in patients with AIH and 10.7 kPa, 12.2 kPa and 14.1 kPa, respectively in patients with PBC[7,8]. In this study, the optimal cutoff values of LS for staging significant fibrosis (S ≥ 2), severe fibrosis (S ≥ 3) and



DOI: 10.3748/wjg.v28.i18.2021 **Copyright** ©The Author(s) 2022.

Figure 1 Flowchart of patients' selection.

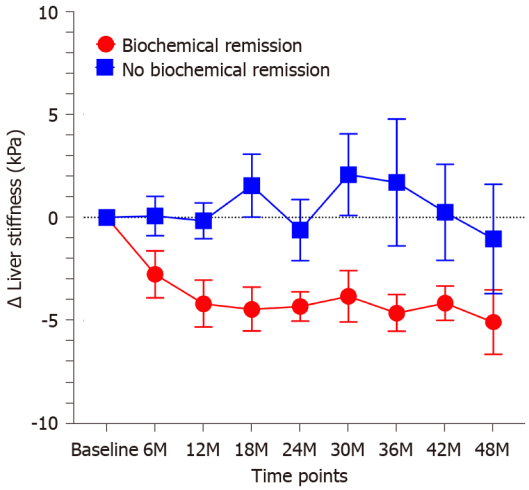


DOI: 10.3748/wjg.v28.i18.2021 **Copyright** ©The Author(s) 2022.

Figure 2 Liver stiffness values of different liver fibrosis stages in patients with autoimmune hepatitis-primary biliary cholangitis overlap syndrome.

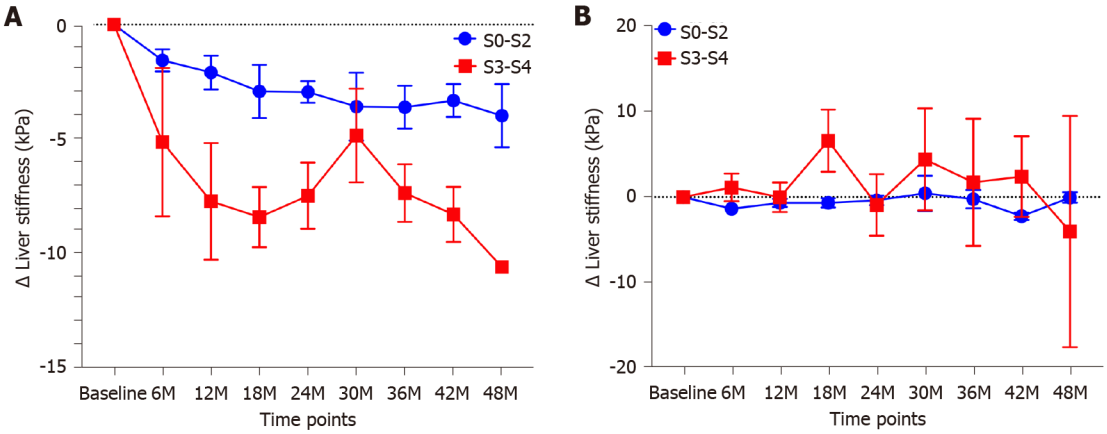
cirrhosis (S4) were 12.1 kPa, 15.0 kPa and 15.1 kPa, respectively in patients with AIH-PBC overlap syndrome. The cutoff values of LS for ruling out significant fibrosis (S ≥ 2), severe fibrosis (S ≥ 3) and cirrhosis (S4) were 7.9 kPa, 11.9 kPa and 13.9 kPa, respectively. According to these current studies, we try to draw a conclusion that the causes of liver disease might affect the LS values and that AIH-PBC over syndrome might have higher cutoff values than other causes of liver disease for diagnosing liver fibrosis.

As discussed in the current European Association for the Study of the Liver Clinical Practice Guidelines, the active liver inflammation may affect the LS values. The increased transaminase and total bilirubin might lead to overestimation of LS measurements[27,28]. In this study, LS showed a strong correlation with several serum biomarkers, such as PLT, total bilirubin, AST, albumin and IgG (P < 0.0001). However, in the multiple regression analysis, only liver fibrosis stages and total bilirubin were



DOI: 10.3748/wjg.v28.i18.2021 **Copyright** ©The Author(s) 2022.

Figure 3 The change of liver stiffness in patient with complete biochemical remission and without biochemical remission.



DOI: 10.3748/wjg.v28.i18.2021 **Copyright** ©The Author(s) 2022.

Figure 4 In patients with complete biochemical remission, the change of liver stiffness in patients with S0-S2 and S3-S4. A: Change of liver stiffness in patients with S0-S2; B: Change of liver stiffness in patients with S3-S4.

associated with the LS values. These findings were consistent with previous studies[28-31], and the LS values might be influenced by elevated total bilirubin. Therefore, considering the feature of AIH-PBC over syndrome, the cutoff values for diagnosing liver fibrosis could be higher than other causes of liver disease. The treatment history may affect the diagnostic accuracy of 2D-SWE for staging fibrosis. ALT could affect the LS values measured by TE, which are mainly reported in patients with chronic hepatitis B[32-34]. However, the ALT did not associate with LS in this study. Xu *et al*[35] also reported that in patients with AIH, ALT cannot affect the LS values measured by transient elastography. Therefore, whether the level of ALT can represent liver histological inflammatory activity needs more study to validate it.

Hartl *et al*[29] reported a significant decrease in LS measured by TE in AIH patients with complete biochemical remission, especially in subgroups of patients with S3-S4 fibrosis stages. The declines in LS measured by TE may reflect the remission of both liver inflammation and fibrosis[36,37]. In this study, the LS values were significantly decreased in patients with complete biochemical remission. In addition, the changes in LS values in patients with S3-S4 were more than those in patients with S0-S2. However, there was no significant change in LS values in patients without biochemical remission. These results demonstrate that LS measured by 2D-SWE can monitor the therapeutic effect. Due to the lack of liver biopsy after treatment, there was no definite correlation between the decline in LS values and remission of liver inflammation or fibrosis.

This study has some limitations that warrant discussion: (1) The patient cohort was small, which can be understood that the prevalence of AIH-PBC overlap syndrome also very low; (2) There is no detailed information on the failure rate of 2D-SWE; (3) In this cohort, we did not acquire the TE data, therefore, we cannot compare the performance of 2D-SWE with TE for diagnosing fibrosis and monitoring treatment due to the retrospective features of this study; and (4) There was no liver biopsy after

treatment with complete biochemical remission.

CONCLUSION

In conclusion, LS measured by 2D-SWE is a potential noninvasive method for staging liver fibrosis, especially for diagnosing severe fibrosis (≥ 3) in patients with AIH-PBC overlap syndrome. The diagnostic performance of 2D-SWE is superior to that of serum fibrosis models for staging liver fibrosis. More importantly, 2D-SWE can monitor the treatment response in patients with complete biochemical remission with a significant decline in LS values.

ARTICLE HIGHLIGHTS

Research background

Autoimmune hepatitis-primary biliary cholangitis (AIH-PBC) overlap syndrome has a worse prognosis than AIH or PBC alone. Therefore, accurately diagnosing liver fibrosis and dynamically monitoring disease progression are essential.

Research motivation

The evaluation of two-dimensional shear-wave elastography (2D-SWE) in detecting liver fibrosis and monitoring treatment response in patients with AIH-PBC overlap syndrome remains blank.

Research objectives

To evaluate the diagnostic utility of 2D-SWE in staging liver fibrosis and assess the usefulness of repeated 2D-SWE for monitoring treatment response in AIH-PBC overlap syndrome.

Research methods

Patients with biopsy-proven AIH-PBC overlap syndrome were retrospectively enrolled. The performances of 2D-SWE and serum indexes for staging liver fibrosis were evaluated. The Scheuer scoring system was used to evaluate hepatic inflammation and liver fibrosis. Changes in liver stiffness (LS) measured by 2D-SWE in patients with or without complete biochemical remission were measured.

Research results

LS was strongly correlated with liver fibrosis stage (Spearman $r = 0.84$, $P < 0.0001$). The areas under the receiver operating characteristic curves of LS for significant fibrosis, severe fibrosis, and cirrhosis were 0.91, 0.97, and 0.96, respectively. Patients with complete biochemical remission showed a considerable decrease in LS values ($P < 0.0001$). More importantly, the decline in LS in patients with S0-S2 was significantly lower than that in patients with S3-S4 ($P = 0.0002$). In contrast, patients who failed to achieve biochemical remission showed a slight but not significant decrease in LS ($P = 0.37$).

Research conclusions

2D-SWE is an accurate and reliable method in assessing liver fibrosis and monitoring treatment response in patients with AIH-PBC overlap syndrome.

Research perspectives

2D-SWE can monitor the treatment effect in patients with AIH-PBC overlap syndrome.

FOOTNOTES

Author contributions: Yan YL and Yang L designed the research study; Wang Z, Wang Y, Xing X and Yan YL performed the research; Wang XZ and Wang Y contributed new reagents and analytic tools; Yan YL and Xing X analyzed the data and wrote the manuscript; All authors have read and approve the final manuscript.

Supported by China Postdoctoral Science Foundation, No. 2020M673263.

Institutional review board statement: The study was reviewed and approved by the West China Hopsital Institutional Review Board (Approval No. 459).

Informed consent statement: The Informed consent was waived by the West China Hopsital Institutional Review Board.

Conflict-of-interest statement: There are no conflicts of interest to be declared.

Data sharing statement: No additional data are available.

STROBE statement: The authors have read the STROBE statement, and the manuscript was prepared and revised according to the STROBE statement.

Open-Access: This article is an open-access article that was selected by an in-house editor and fully peer-reviewed by external reviewers. It is distributed in accordance with the Creative Commons Attribution NonCommercial (CC BY-NC 4.0) license, which permits others to distribute, remix, adapt, build upon this work non-commercially, and license their derivative works on different terms, provided the original work is properly cited and the use is non-commercial. See: https://creativecommons.org/Licenses/by-nc/4.0/

Country/Territory of origin: China

ORCID number: Yu-Ling Yan 0000-0002-2765-8350; Xian Xing 0000-0001-9134-0673; Yi Wang 0000-0001-9011-9758; Xiao-Ze Wang 0100-0002-3992-5866; Zhi Wang 0000-0003-1148-7793; Li Yang 0000-0003-3821-9342.

S-Editor: Zhang H
L-Editor: A
P-Editor: Zhang H

REFERENCES

1 **Purohit T**, Cappell MS. Primary biliary cirrhosis: Pathophysiology, clinical presentation and therapy. *World J Hepatol* 2015; **7**: 926-941 [PMID: 25954476 DOI: 10.4254/wjh.v7.i7.926]
2 **Silveira MG**, Talwalkar JA, Angulo P, Lindor KD. Overlap of autoimmune hepatitis and primary biliary cirrhosis: long-term outcomes. *Am J Gastroenterol* 2007; **102**: 1244-1250 [PMID: 17319931 DOI: 10.1111/j.1572-0241.2007.01136.x]
3 **Bonder A**, Retana A, Winston DM, Leung J, Kaplan MM. Prevalence of primary biliary cirrhosis-autoimmune hepatitis overlap syndrome. *Clin Gastroenterol Hepatol* 2011; **9**: 609-612 [PMID: 21440668 DOI: 10.1016/j.cgh.2011.03.019]
4 **Mack CL**, Adams D, Assis DN, Kerkar N, Manns MP, Mayo MJ, Vierling JM, Alsawas M, Murad MH, Czaja AJ. Diagnosis and Management of Autoimmune Hepatitis in Adults and Children: 2019 Practice Guidance and Guidelines From the American Association for the Study of Liver Diseases. *Hepatology* 2020; **72**: 671-722 [PMID: 31863477 DOI: 10.1002/hep.31065]
5 **Hartl J**, Denzer U, Ehlken H, Zenouzi R, Peiseler M, Sebode M, Hübener S, Pannicke N, Weiler-Normann C, Quaas A, Lohse AW, Schramm C. Transient elastography in autoimmune hepatitis: Timing determines the impact of inflammation and fibrosis. *J Hepatol* 2016; **65**: 769-775 [PMID: 27238753 DOI: 10.1016/j.jhep.2016.05.023]
6 **Wang K**, Lu X, Zhou H, Gao Y, Zheng J, Tong M, Wu C, Liu C, Huang L, Jiang T, Meng F, Lu Y, Ai H, Xie XY, Yin LP, Liang P, Tian J, Zheng R. Deep learning Radiomics of shear wave elastography significantly improved diagnostic performance for assessing liver fibrosis in chronic hepatitis B: a prospective multicentre study. *Gut* 2019; **68**: 729-741 [PMID: 29730602 DOI: 10.1136/gutjnl-2018-316204]
7 **Xing X**, Yan Y, Shen Y, Xue M, Wang X, Luo X, Yang L. Liver fibrosis with two-dimensional shear-wave elastography in patients with autoimmune hepatitis. *Expert Rev Gastroenterol Hepatol* 2020; **14**: 631-638 [PMID: 32510248 DOI: 10.1080/17474124.2020.1779589]
8 **Yan Y**, Xing X, Lu Q, Wang X, Luo X, Yang L. Assessment of biopsy proven liver fibrosis by two-dimensional shear wave elastography in patients with primary biliary cholangitis. *Dig Liver Dis* 2020; **52**: 555-560 [PMID: 32111390 DOI: 10.1016/j.dld.2020.02.002]
9 **European Association for the Study of the Liver**. EASL Clinical Practice Guidelines: management of cholestatic liver diseases. *J Hepatol* 2009; **51**: 237-267 [PMID: 19501929 DOI: 10.1016/j.jhep.2009.04.009]
10 **Chazouillères O**, Wendum D, Serfaty L, Montembault S, Rosmorduc O, Poupon R. Primary biliary cirrhosis-autoimmune hepatitis overlap syndrome: clinical features and response to therapy. *Hepatology* 1998; **28**: 296-301 [PMID: 9695990 DOI: 10.1002/hep.510280203]
11 **Crabb DW**, Bataller R, Chalasani NP, Kamath PS, Lucey M, Mathurin P, McClain C, McCullough A, Mitchell MC, Morgan TR, Nagy L, Radaeva S, Sanyal A, Shah V, Szabo G; NIAAA Alcoholic Hepatitis Consortia. Standard Definitions and Common Data Elements for Clinical Trials in Patients With Alcoholic Hepatitis: Recommendation From the NIAAA Alcoholic Hepatitis Consortia. *Gastroenterology* 2016; **150**: 785-790 [PMID: 26921783 DOI: 10.1053/j.gastro.2016.02.042]
12 **Hashimoto E**, Taniai M, Tokushige K. Characteristics and diagnosis of NAFLD/NASH. *J Gastroenterol Hepatol* 2013; **28** Suppl 4: 64-70 [PMID: 24251707 DOI: 10.1111/jgh.12271]
13 **Yu YC**, Mao YM, Chen CW, Chen JJ, Chen J, Cong WM, Ding Y, Duan ZP, Fu QC, Guo XY, Hu P, Hu XQ, Jia JD, Lai RT, Li DL, Liu YX, Lu LG, Ma SW, Ma X, Nan YM, Ren H, Shen T, Wang H, Wang JY, Wang TL, Wang XJ, Wei L, Xie Q, Xie W, Yang CQ, Yang DL, Yu YY, Zeng MD, Zhang L, Zhao XY, Zhuang H; Drug-induced Liver Injury (DILI) Study Group; Chinese Society of Hepatology (CSH); Chinese Medical Association (CMA). CSH guidelines for the diagnosis and treatment of drug-induced liver injury. *Hepatol Int* 2017; **11**: 221-241 [PMID: 28405790 DOI: 10.1007/s12072-017-9793-2]
14 **European Association for the Study of the Liver**. EASL Clinical Practice Guidelines: Autoimmune hepatitis. *J Hepatol*

2015; **63**: 971-1004 [PMID: 26341719 DOI: 10.1016/j.jhep.2015.06.030]
15 **Ferraioli G**, Filice C, Castera L, Choi BI, Sporea I, Wilson SR, Cosgrove D, Dietrich CF, Amy D, Bamber JC, Barr R, Chou YH, Ding H, Farrokh A, Friedrich-Rust M, Hall TJ, Nakashima K, Nightingale KR, Palmeri ML, Schafer F, Shiina T, Suzuki S, Kudo M. WFUMB guidelines and recommendations for clinical use of ultrasound elastography: Part 3: liver. *Ultrasound Med Biol* 2015; **41**: 1161-1179 [PMID: 25800942 DOI: 10.1016/j.ultrasmedbio.2015.03.007]
16 **Paisant A**, Lemoine S, Cassinotto C, de Lédinghen V, Ronot M, Irlès-Depé M, Vilgrain V, Le Bail B, Paradis V, Canivet CM, Michalak S, Rousselet MC, Rautou PE, Lebigot J, Hunault G, Crouan A, Aubé C, Boursier J. Reliability Criteria of Two-Dimensional Shear Wave Elastography: Analysis of 4277 Measurements in 788 Patients. *Clin Gastroenterol Hepatol* 2020 [PMID: 33340779 DOI: 10.1016/j.cgh.2020.12.013]
17 **Gao Y**, Zheng J, Liang P, Tong M, Wang J, Wu C, He X, Liu C, Zhang S, Huang L, Jiang T, Cheng C, Meng F, Mu X, Lu Y, Li Y, Ai H, Qiao X, Xie XY, Wang W, Yin LP, Wu YY, Zheng R. Liver Fibrosis with Two-dimensional US Shear-Wave Elastography in Participants with Chronic Hepatitis B: A Prospective Multicenter Study. *Radiology* 2018; **289**: 407-415 [PMID: 30040048 DOI: 10.1148/radiol.2018172479]
18 **Furlan A**, Tublin ME, Yu L, Chopra KB, Lippello A, Behari J. Comparison of 2D Shear Wave Elastography, Transient Elastography, and MR Elastography for the Diagnosis of Fibrosis in Patients With Nonalcoholic Fatty Liver Disease. *AJR Am J Roentgenol* 2020; **214**: W20-W26 [PMID: 31714842 DOI: 10.2214/AJR.19.21267]
19 **Imajo K**, Honda Y, Kobayashi T, Nagai K, Ozaki A, Iwaki M, Kessoku T, Ogawa Y, Takahashi H, Saigusa Y, Yoneda M, Kirikoshi H, Utsunomiya D, Aishima S, Saito S, Nakajima A. Direct Comparison of US and MR Elastography for Staging Liver Fibrosis in Patients With Nonalcoholic Fatty Liver Disease. *Clin Gastroenterol Hepatol* 2020 [PMID: 33340780 DOI: 10.1016/j.cgh.2020.12.016]
20 **Cassinotto C**, Boursier J, Paisant A, Guiu B, Irles-Depe M, Canivet C, Aube C, de Ledinghen V. Transient Versus Two-Dimensional Shear-Wave Elastography in a Multistep Strategy to Detect Advanced Fibrosis in NAFLD. *Hepatology* 2021; **73**: 2196-2205 [PMID: 33236409 DOI: 10.1002/hep.31655]
21 **Cassinotto C**, Lapuyade B, Guiu B, Marraud des Grottes H, Piron L, Merrouche W, Irles-Depe M, Molinari N, De Ledinghen V. Agreement Between 2-Dimensional Shear Wave and Transient Elastography Values for Diagnosis of Advanced Chronic Liver Disease. *Clin Gastroenterol Hepatol* 2020; **18**: 2971-2979.e3 [PMID: 32348907 DOI: 10.1016/j.cgh.2020.04.034]
22 **Janik MK**, Kruk B, Szczepankiewicz B, Kostrzewa K, Raszeja-Wyszomirska J, Górnicka B, Lammert F, Milkiewicz P, Krawczyk M. Measurement of liver and spleen stiffness as complementary methods for assessment of liver fibrosis in autoimmune hepatitis. *Liver Int* 2021; **41**: 348-356 [PMID: 33159831 DOI: 10.1111/liv.14726]
23 **Wu HM**, Sheng L, Wang Q, Bao H, Miao Q, Xiao X, Guo CJ, Li H, Ma X, Qiu DK, Hua J. Performance of transient elastography in assessing liver fibrosis in patients with autoimmune hepatitis-primary biliary cholangitis overlap syndrome. *World J Gastroenterol* 2018; **24**: 737-743 [PMID: 29456412 DOI: 10.3748/wjg.v24.i6.737]
24 **Zeng J**, Huang ZP, Zheng J, Wu T, Zheng RQ. Non-invasive assessment of liver fibrosis using two-dimensional shear wave elastography in patients with autoimmune liver diseases. *World J Gastroenterol* 2017; **23**: 4839-4846 [PMID: 28765706 DOI: 10.3748/wjg.v23.i26.4839]
25 **Herrmann E**, de Lédinghen V, Cassinotto C, Chu WC, Leung VY, Ferraioli G, Filice C, Castera L, Vilgrain V, Ronot M, Dumortier J, Guibal A, Pol S, Trebicka J, Jansen C, Strassburg C, Zheng R, Zheng J, Francque S, Vanwolleghem T, Vonghia L, Manesis EK, Zoumpoulis P, Sporea I, Thiele M, Krag A, Cohen-Bacrie C, Criton A, Gay J, Deffieux T, Friedrich-Rust M. Assessment of biopsy-proven liver fibrosis by two-dimensional shear wave elastography: An individual patient data-based meta-analysis. *Hepatology* 2018; **67**: 260-272 [PMID: 28370257 DOI: 10.1002/hep.29179]
26 **Serra C**, Grasso V, Conti F, Felicani C, Mazzotta E, Lenzi M, Verucchi G, D'errico A, Andreone P. A New Two-Dimensional Shear Wave Elastography for Noninvasive Assessment of Liver Fibrosis in Healthy Subjects and in Patients with Chronic Liver Disease. *Ultraschall Med* 2018; **39**: 432-439 [PMID: 29458217 DOI: 10.1055/s-0043-119356]
27 **Liang XE**, Chen YP, Zhang Q, Dai L, Zhu YF, Hou JL. Dynamic evaluation of liver stiffness measurement to improve diagnostic accuracy of liver cirrhosis in patients with chronic hepatitis B acute exacerbation. *J Viral Hepat* 2011; **18**: 884-891 [PMID: 21062388 DOI: 10.1111/j.1365-2893.2010.01389.x]
28 **Kim SU**, Han KH, Park JY, Ahn SH, Chung MJ, Chon CY, Choi EH, Kim DY. Liver stiffness measurement using FibroScan is influenced by serum total bilirubin in acute hepatitis. *Liver Int* 2009; **29**: 810-815 [PMID: 19018979 DOI: 10.1111/j.1478-3231.2008.01894.x]
29 **Hartl J**, Ehlken H, Sebode M, Peiseler M, Krech T, Zenouzi R, von Felden J, Weiler-Normann C, Schramm C, Lohse AW. Usefulness of biochemical remission and transient elastography in monitoring disease course in autoimmune hepatitis. *J Hepatol* 2018; **68**: 754-763 [PMID: 29180000 DOI: 10.1016/j.jhep.2017.11.020]
30 **Seo YS**, Um SH, Jung ES, Yim HJ, Kim CD, Ryu HS. Serum alanine aminotransferase level alone may not accurately represent necro-inflammation in patients with acute hepatitis. *Hepatology* 2009; **49**: 1053-4; author reply 1054 [PMID: 19241482 DOI: 10.1002/hep.22805]
31 **Das K**, Sarkar R, Ahmed SM, Mridha AR, Mukherjee PS, Das K, Dhali GK, Santra A, Chowdhury A. "Normal" liver stiffness measure (LSM) values are higher in both lean and obese individuals: a population-based study from a developing country. *Hepatology* 2012; **55**: 584-593 [PMID: 21952989 DOI: 10.1002/hep.24694]
32 **Fung J**, Lai CL, Cheng C, Wu R, Wong DK, Yuen MF. Mild-to-moderate elevation of alanine aminotransferase increases liver stiffness measurement by transient elastography in patients with chronic hepatitis B. *Am J Gastroenterol* 2011; **106**: 492-496 [PMID: 21157442 DOI: 10.1038/ajg.2010.463]
33 **Jia J**, Hou J, Ding H, Chen G, Xie Q, Wang Y, Zeng M, Zhao J, Wang T, Hu X, Schuppan D. Transient elastography compared to serum markers to predict liver fibrosis in a cohort of Chinese patients with chronic hepatitis B. *J Gastroenterol Hepatol* 2015; **30**: 756-762 [PMID: 25353058 DOI: 10.1111/jgh.12840]
34 **Yang X**, Chang X, Wu S, Sun X, Zhu X, Wang L, Xu Y, Yao X, Rao S, Hu X, Xia M, Bian H, Yan H, Gao X. Performance of liver stiffness measurements obtained with FibroScan is affected by glucose metabolism in patients with nonalcoholic fatty liver disease. *Lipids Health Dis* 2021; **20**: 27 [PMID: 33757528 DOI: 10.1186/s12944-021-01453-5]
35 **Xu Q**, Sheng L, Bao H, Chen X, Guo C, Li H, Ma X, Qiu D, Hua J. Evaluation of transient elastography in assessing liver

fibrosis in patients with autoimmune hepatitis. *J Gastroenterol Hepatol* 2017; **32**: 639-644 [PMID: 27505153 DOI: 10.1111/jgh.13508]

36 **Liang X**, Xie Q, Tan D, Ning Q, Niu J, Bai X, Chen S, Cheng J, Yu Y, Wang H, Xu M, Shi G, Wan M, Chen X, Tang H, Sheng J, Dou X, Shi J, Ren H, Wang M, Zhang H, Gao Z, Chen C, Ma H, Chen Y, Fan R, Sun J, Jia J, Hou J. Interpretation of liver stiffness measurement-based approach for the monitoring of hepatitis B patients with antiviral therapy: A 2-year prospective study. *J Viral Hepat* 2018; **25**: 296-305 [PMID: 29080299 DOI: 10.1111/jvh.12814]

37 **Vinikoor MJ**, Sinkala E, Chilengi R, Mulenga LB, Chi BH, Zyambo Z, Hoffmann CJ, Saag MS, Davies MA, Egger M, Wandeler G; IeDEA- Southern Africa. Impact of Antiretroviral Therapy on Liver Fibrosis Among Human Immunodeficiency Virus-Infected Adults With and Without HBV Coinfection in Zambia. *Clin Infect Dis* 2017; **64**: 1343-1349 [PMID: 28158504 DOI: 10.1093/cid/cix122]



Published by **Baishideng Publishing Group Inc**
7041 Koll Center Parkway, Suite 160, Pleasanton, CA 94566, USA
Telephone: +1-925-3991568
E-mail: bpgoffice@wjgnet.com
Help Desk: https://www.f6publishing.com/helpdesk
https://www.wjgnet.com



© 2022 Baishideng Publishing Group Inc. All rights reserved.

ISSN 1007-9327 (print)
ISSN 2219-2840 (online)

World Journal of *Gastroenterology*

World J Gastroenterol 2022 May 21; 28(19): 2034-2151



Published by Baishideng Publishing Group Inc

World Journal of Gastroenterology

Contents

Weekly Volume 28 Number 19 May 21, 2022

REVIEW

2034 Review on acute pancreatitis attributed to COVID-19 infection

Onoyama T, Koda H, Hamamoto W, Kawahara S, Sakamoto Y, Yamashita T, Kurumi H, Kawata S, Takeda Y, Matsumoto K, Isomoto H

2057 Clinical significance of variant hepatic artery in pancreatic resection: A comprehensive review

Xu YC, Yang F, Fu DL

MINIREVIEWS

2076 Mixed neuroendocrine-non-neuroendocrine neoplasms of the digestive system: A mini-review

Toor D, Loree JM, Gao ZH, Wang G, Zhou C

2088 Mechanisms of ductular reaction in non-alcoholic steatohepatitis

Chen Y, Gao WK, Shu YY, Ye J

ORIGINAL ARTICLE

Basic Study

2100 Ultrastructural changes in porcine liver sinusoidal endothelial cells of machine perfused liver donated after cardiac death

Bochimoto H, Ishihara Y, Mohd Zin NK, Iwata H, Kondoh D, Obara H, Matsuno N

2112 Snare-assisted flexible endoscope in trans-gastric endoscopic gallbladder-preserving surgery: A pilot animal study

Guo XW, Liang YX, Huang PY, Liang LX, Zeng YQ, Ding Z

Retrospective Cohort Study

2123 Development and external validation of models to predict acute respiratory distress syndrome related to severe acute pancreatitis

Li YL, Zhang DD, Xiong YY, Wang RF, Gao XM, Gong H, Zheng SC, Wu D

Prospective Study

2137 Non-optical polyp-based resect and discard strategy: A prospective clinical study

Taghiakbari M, Hammar C, Frenn M, Djinbachian R, Pohl H, Deslandres E, Bouchard S, Bouin M, von Renteln D

LETTER TO THE EDITOR

2148 Effects of diabetes type 2 and metformin treatment in Swedish patients with colorectal cancer

Dimberg J, Shamoun L, Landerholm K, Wågsäter D

World Journal of Gastroenterology

Weekly Volume 28 Number 19 May 21, 2022

Contents

ABOUT COVER

Editorial Board Member of *World Journal of Gastroenterology*, Cheng-Fu Xu, MD, Chief Physician, Department of Gastroenterology, The First Affiliated Hospital, Zhejiang University School of Medicine, No. 79 Qingchun Road, Hangzhou, Zhejiang Province 310003, China. xiaofu@zju.edu.cn

AIMS AND SCOPE

The primary aim of *World Journal of Gastroenterology* (*WJG*, *World J Gastroenterol*) is to provide scholars and readers from various fields of gastroenterology and hepatology with a platform to publish high-quality basic and clinical research articles and communicate their research findings online. *WJG* mainly publishes articles reporting research results and findings obtained in the field of gastroenterology and hepatology and covering a wide range of topics including gastroenterology, hepatology, gastrointestinal endoscopy, gastrointestinal surgery, gastrointestinal oncology, and pediatric gastroenterology.

INDEXING/ABSTRACTING

The *WJG* is now indexed in Current Contents®/Clinical Medicine, Science Citation Index Expanded (also known as SciSearch®), Journal Citation Reports®, Index Medicus, MEDLINE, PubMed, PubMed Central, and Scopus. The 2021 edition of Journal Citation Report® cites the 2020 impact factor (IF) for *WJG* as 5.742; Journal Citation Indicator: 0.79; IF without journal self cites: 5.590; 5-year IF: 5.044; Ranking: 28 among 92 journals in gastroenterology and hepatology; and Quartile category: Q2. The *WJG*'s CiteScore for 2020 is 6.9 and Scopus CiteScore rank 2020: Gastroenterology is 19/136.

RESPONSIBLE EDITORS FOR THIS ISSUE

Production Editor: *Wen-Wen Qi*; **Production Department Director:** *Xiang Li*; **Editorial Office Director:** *Ze-Mao Gong*.

NAME OF JOURNAL

World Journal of Gastroenterology

ISSN

ISSN 1007-9327 (print) ISSN 2219-2840 (online)

LAUNCH DATE

October 1, 1995

FREQUENCY

Weekly

EDITORS-IN-CHIEF

Andrzej S Tarnawski

EDITORIAL BOARD MEMBERS

http://www.wjgnet.com/1007-9327/editorialboard.htm

PUBLICATION DATE

May 21, 2022

COPYRIGHT

© 2022 Baishideng Publishing Group Inc

INSTRUCTIONS TO AUTHORS

https://www.wjgnet.com/bpg/gerinfo/204

GUIDELINES FOR ETHICS DOCUMENTS

https://www.wjgnet.com/bpg/GerInfo/287

GUIDELINES FOR NON-NATIVE SPEAKERS OF ENGLISH

https://www.wjgnet.com/bpg/gerinfo/240

PUBLICATION ETHICS

https://www.wjgnet.com/bpg/GerInfo/288

PUBLICATION MISCONDUCT

https://www.wjgnet.com/bpg/gerinfo/208

ARTICLE PROCESSING CHARGE

https://www.wjgnet.com/bpg/gerinfo/242

STEPS FOR SUBMITTING MANUSCRIPTS

https://www.wjgnet.com/bpg/GerInfo/239

ONLINE SUBMISSION

https://www.f6publishing.com

© 2022 Baishideng Publishing Group Inc. All rights reserved. 7041 Koll Center Parkway, Suite 160, Pleasanton, CA 94566, USA

E-mail: bpgoffice@wjgnet.com https://www.wjgnet.com

World Journal of Gastroenterology

Submit a Manuscript: https://www.f6publishing.com

World J Gastroenterol 2022 May 21; 28(19): 2034-2056

DOI: 10.3748/wjg.v28.i19.2034

ISSN 1007-9327 (print) ISSN 2219-2840 (online)

REVIEW

Review on acute pancreatitis attributed to COVID-19 infection

Takumi Onoyama, Hiroki Koda, Wataru Hamamoto, Shiho Kawahara, Yuri Sakamoto, Taro Yamashita, Hiroki Kurumi, Soichiro Kawata, Yohei Takeda, Kazuya Matsumoto, Hajime Isomoto

Specialty type: Gastroenterology and hepatology

Provenance and peer review: Invited article; Externally peer reviewed.

Peer-review model: Single blind

Peer-review report's scientific quality classification

Grade A (Excellent): 0
Grade B (Very good): B, B
Grade C (Good): 0
Grade D (Fair): 0
Grade E (Poor): 0

P-Reviewer: Omar BJ, India; Sivanand N, India

Received: December 29, 2021
Peer-review started: January 4, 2022
First decision: March 10, 2022
Revised: March 20, 2022
Accepted: April 4, 2022
Article in press: April 4, 2022
Published online: May 21, 2022

Takumi Onoyama, Hiroki Koda, Wataru Hamamoto, Shiho Kawahara, Yuri Sakamoto, Taro Yamashita, Hiroki Kurumi, Soichiro Kawata, Yohei Takeda, Kazuya Matsumoto, Hajime Isomoto, Division of Gastroenterology and Nephrology, Department of Multidisciplinary Internal Medicine, Tottori University Faculty of Medicine, Yonago 683-8504, Tottori Prefecture, Japan

Kazuya Matsumoto, Department of Internal Medicine, Irisawa Medical Clinic, Matsue 690-0025, Shimane Prefecture, Japan

Corresponding author: Takumi Onoyama, MD, PhD, Doctor, Division of Gastroenterology and Nephrology, Department of Multidisciplinary Internal Medicine, Tottori University Faculty of Medicine, 36-1 Nishi-cho, Yonago 683-8504, Tottori Prefecture, Japan. golf4to@yahoo.co.jp

Abstract

The coronavirus disease 2019 (COVID-19) is known to cause gastrointestinal symptoms. Recent studies have revealed COVID-19-attributed acute pancreatitis (AP). However, clinical characteristics of COVID-19-attributed AP remain unclear. We performed a narrative review to elucidate relation between COVID-19 and AP using the PubMed database. Some basic and pathological reports revealed expression of angiotensin-converting enzyme 2 and transmembrane protease serine 2, key proteins that aid in the entry of severe acute respiratory syndrome coronavirus 2 (SARS-CoV-2) into the pancreas. The experimental and pathological evaluation suggested that SARS-CoV-2 infects human endocrine and exocrine pancreas cells, and thus, SARS-CoV-2 may have a direct involvement in pancreatic disorders. Additionally, systemic inflammation, especially in children, may cause AP. Levels of immune mediators associated with AP, including interleukin (IL)-1β, IL-10, interferon-γ, monocyte chemotactic protein 1, and tumor necrosis factor-α are higher in the plasma of patients with COVID-19, that suggests an indirect involvement of the pancreas. In real-world settings, some clinical features of AP complicate COVID-19, such as a high complication rate of pancreatic necrosis, severe AP, and high mortality. However, clinical features of COVID-19-attributed AP remain uncertain due to insufficient research on etiologies of AP. Therefore, high-quality clinical studies and case reports that specify methods for differential diagnoses of other etiologies of AP are needed.

Key Words: COVID-19; SARS-CoV-2; Pancreatitis; Revised atlanta classification; Prognosis; Etiology

©The Author(s) 2022. Published by Baishideng Publishing Group Inc. All rights reserved.

Core Tip: Several review articles have explored the relationship between coronavirus disease 2019 (COVID-19) and acute pancreatitis (AP). However, due to various etiologies associated with AP, COVID-19-attributed AP is controversially defined. Therefore, this narrative review attempted to reveal clinical features of COVID-19-attributed AP focused on surveillance of the other etiologies of AP. The clinical features of COVID-19-attributed AP remain uncertain due to insufficient data on etiologies of AP. Therefore, prospective cohort studies focused on patients with COVID-19 with idiopathic AP are required, especially to clearly exclude other etiologies of AP.

Citation: Onoyama T, Koda H, Hamamoto W, Kawahara S, Sakamoto Y, Yamashita T, Kurumi H, Kawata S, Takeda Y, Matsumoto K, Isomoto H. Review on acute pancreatitis attributed to COVID-19 infection. *World J Gastroenterol* 2022; 28(19): 2034-2056
URL: https://www.wjgnet.com/1007-9327/full/v28/i19/2034.htm
DOI: https://dx.doi.org/10.3748/wjg.v28.i19.2034

INTRODUCTION

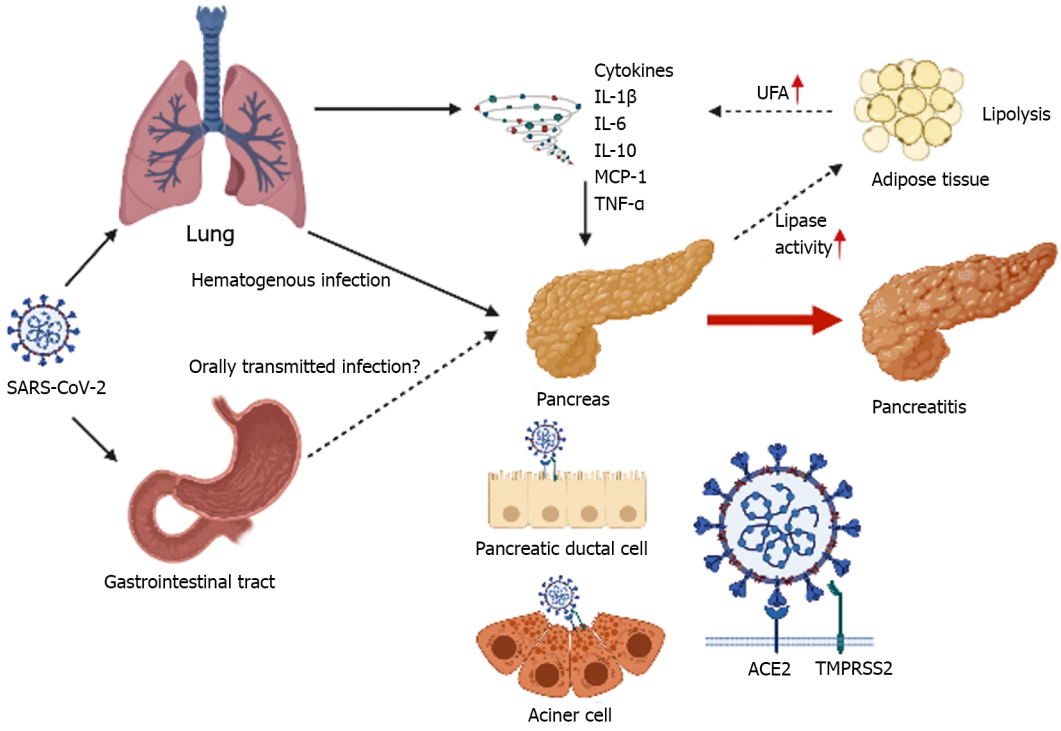
The novel coronavirus disease 2019 (COVID-19), caused by severe acute respiratory syndrome coronavirus-2 (SARS-CoV-2), was declared a pandemic by the World Health Organization (WHO) on March 11, 2020. COVID-19 causes respiratory symptoms, such as cough, fever, sputum production, and shortness of breath, and also leads to gastrointestinal symptoms, such as nausea, vomiting, and diarrhea [1,2]. Some studies revealed that SARS-CoV-2 RNA can be detected in the gastrointestinal tract[3,4]. SARS-CoV-2 binds to angiotensin-converting enzyme 2 (ACE2) protein that serves as an entry point for the virus into epithelial cells[5]. SARS-CoV-2 also invades the gastrointestinal tract *via* ACE2, allowing development of gastrointestinal symptoms[2,6-9]. Recent studies suggest that SARS-CoV-2 infection might induce pancreatic injury or acute pancreatitis (AP)[10,11]. Schepis *et al*[12] identified SARS-CoV-2 RNA in a pancreatic pseudocyst sample collected from a patient with COVID-19[12]. Moreover, ACE2 expressed in the pancreas is associated with pancreatic injury[13]. In experimental system, SARS-CoV-2 infects human endocrine and exocrine cells of the pancreas, *ex vivo* and *in vivo*[14]. However, clinical features of COVID-19-attributed AP remain uncertain. Some systematic reviews have reported COVID-19-attributed pancreatic injury[15,16], but it remains uncertain whether the pancreatic injury is truly caused by SARS-CoV-2 due to insufficient search for the etiology of AP. Gallstones and alcoholism are two common etiological factors of AP[17-19]. Certain medications (valproic acid, azathioprine, and sulfonamides), metabolic disturbances (hypercalcemia and hypertriglyceridemia), and infections are also rare etiologies[19,20]. Trauma, iatrogenic considerations [*e.g.*, endoscopic retrograde cholangiopancreatography (ERCP)], anatomy (*e.g.*, pancreatic tumor or pancreatic divisum), ischemia/reperfusion, and genetic mutation are also reported as etiologies of AP[19,21-23]. Many studies have reported that bacterial, mycobacterial, helminthic, protozoan, and fungal infections are etiologies of AP[24,25]. Furthermore, hepatotropic virus, Coxsackie virus, Echovirus, Cytomegalovirus, human immunodeficiency virus, Herpes simplex virus, mumps virus, measles virus, varicella-zoster virus, and other viruses may cause infectious AP[24-26]. Therefore, the COVID-19-attributed AP should be diagnosed by sufficient exclusion of other etiologies of AP. Additionally, the diagnostic criteria for COVID-19 is reverse transcription-polymerase chain reaction (RT-PCR) or serological test for SARS-CoV-2, and also clinical examinations, such as chest computed tomography (CT) and clinical history. Moreover, the diagnostic criteria for AP and severity of COVID-19 and AP are not unified across reports. Thus, it is required to sufficiently evaluate etiologies of AP, and clearly define diagnostic and severity criteria of COVID-19 and AP for reviewing COVID-19-attributed AP. A sufficient evaluation of etiologies of AP should be performed, especially in case studies.

This study aimed to perform a review of literature to reveal recent findings on the association between AP and SARS-CoV-2. The review also focusses on the real-world data of COVID-19-attributed AP, with surveillance for other etiologies of AP, and reveals some clinical features of COVID-19-attributed AP.

MECHANISMS OF AP WITH COVID-19

Direct association between the pancreas and SARS-CoV-2

Coronaviruses constantly circulate in human populations and usually cause mild respiratory symptoms. The gastrointestinal symptoms, although not as common as respiratory symptoms, have been observed in some patients with COVID-19[2]. The SARS-CoV-2 depends on ACE2, a protein that binds to viral spike (S) protein, to enter epithelial cells[5]. SARS-CoV-2 also invades the gastrointestinal tract *via* ACE2



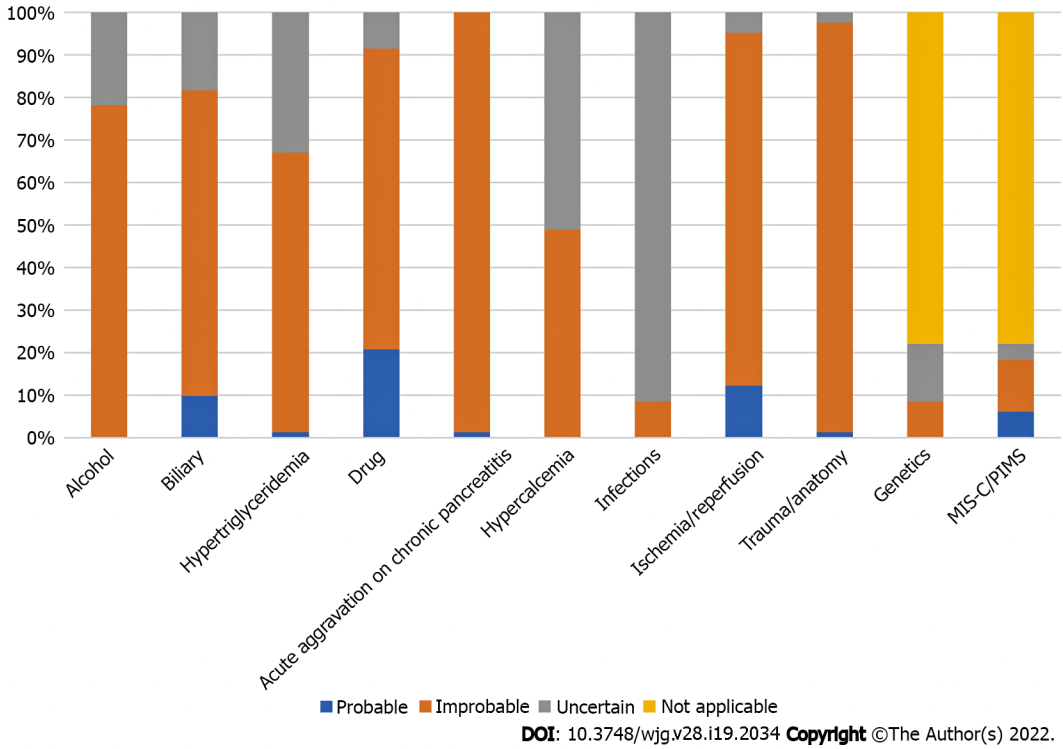
DOI: 10.3748/wjg.v28.i19.2034 **Copyright** ©The Author(s) 2022.

Figure 1 Direct and indirect pathways of pancreatic injury caused by severe acute respiratory syndrome coronavirus-2. Severe acute respiratory syndrome coronavirus-2 (SARS-CoV-2) disseminates through the bloodstream mainly to the pancreas. SARS-CoV-2 may be transported to the pancreas *via* the gastrointestinal tract. The pancreas expresses angiotensin converting enzyme-2 (ACE2) and the transmembrane protease serine 2 (TMPRSS2). SARS-CoV-2 binds to ACE2 after the viral spike (S) protein is primed by TMPRSS2 for cell entry. Therefore, SARS-CoV-2 may potentially cause direct pancreatic injury, including acute pancreatitis. However, indirect pancreatic injury may also be caused by systemic inflammatory responses from respiratory failure induced by SARS-CoV-2 infection. Levels of proinflammatory immune mediators associated with pancreatitis, including interleukin (IL)-1β, IL-6, IL-10, interferon-γ, monocyte chemotactic protein-1, and tumor necrosis factor-α are higher in the plasma of patients with coronavirus disease 2019. These mediators may indirectly cause pancreatic injury. An increase in lipase activity triggers lipolysis in the adipose tissues, and enhances levels of serum unsaturated fatty acids (UFA). UFA may cause an increase in levels of proinflammatory immune mediators that lead to systemic inflammation. SARS-CoV-2: Severe acute respiratory syndrome coronavirus-2; ACE2: Angiotensin converting enzyme-2; TMPRSS2: Transmembrane protease serine 2; IL: Interleukin, IFN-γ: Interferon-γ; MCP-1: Monocyte chemotactic protein-1; TNF-α: Tumor necrosis factor-α; UFA: Unsaturated fatty acids.

and leads to development of gastrointestinal symptoms[2,6-9]. The pancreas also expresses ACE2, with mRNA of ACE2 being expressed in the exocrine glands and islets (Figure 1)[13,27]. The transmembrane protease serine 2 (TMPRSS2), co-expressed with ACE2, is known to be required for virus entry[5,28]. TMPRSS2 is associated with proteolytic cleavage of the viral S protein, and mediates membrane insertion of S protein and viral membrane fusion. TMPRSS2 is also expressed in the pancreas, including the pancreatic ductal epithelial cells, acinar cells, and islet cells[29,30]. According to single cell analysis of human pluripotent stem cells, ACE2 and TMPRSS2 are co-expressed in the acinar cells, ductal cells, alpha cells, and beta cells[31]. Furthermore, ACE2 protein is expressed in the islet and exocrine tissue microvasculature and in a subset of pancreatic ducts, whereas TMPRSS2 is restricted to ductal cells[30]. In tissue sections derived from the pancreas of five healthy humans, the expression of ACE2 was detected in endothelial cells, a subpopulation of ductal cells, and endocrine cells, while TMPRSS2 was detected in beta cells. However, both ACE2 and TMPRSS2 were poorly expressed in acinar cells[14]. Pathological evaluation of patients deceased due to COVID-19 identified SARS-CoV-2 positivity in some ductal cells, a few acinar cells, and endocrine cells. Therefore, SARS-CoV-2 was confirmed to infect human endocrine and exocrine cells of the pancreas, *in vivo*[14]. Moreover, infection with SARS-CoV-2 increases expression of C-X-C motif chemokine ligand 12 (CXCL12), nuclear factor kappa β subunit 1 (NFKβ1), and signal transducer and activator of transcription 3 (STAT3) that are known to be associated with pancreatitis-related inflammation[32]. Therefore, SARS-CoV-2 may directly injure the pancreas. SARS-CoV-2 is considered to primarily disseminate *via* the bloodstream, but there are no data on how SARS-CoV-2 is transported to the pancreas[15]. Some patients with COVID-19 develop AP without any respiratory symptoms at onset[33]. However, it is uncertain whether SARS-CoV-2 is transported to the pancreas *via* the gastrointestinal tract, where SARS-CoV-2 is detected in patients with COVID-19[3].

Pancreatic injury caused by SARS-CoV-2-induced cytokine storm

Recent studies reported that the rate of pancreatic enzyme elevation ranged between 12.1% and 17.3% in patients with COVID-19[10,34,35]. Wang *et al*[10] reported the first case series of COVID-19-attributed



DOI: 10.3748/wjg.v28.i19.2034 **Copyright** ©The Author(s) 2022.

Figure 2 The probability of other etiologies of acute pancreatitis in cases with concurrent coronavirus disease 2019 and acute pancreatitis. The potential of other etiologies, including alcoholism, biliary, hypertriglyceridemia, hypercalcemia, drug-induced, acute aggravation on chronic pancreatitis, ischemia/reperfusion, and trauma/anatomy. In children, the potential of genetic and multisystemic inflammatory syndrome in children/pediatric inflammatory multisystem syndrome-induced acute pancreatitis (AP) are also evaluated. Moreover, these causes are regarded as inapplicable etiologies of AP in adults. The probability of AP is disregarded in cases with insufficient information on the etiologies of AP. Some etiologies of AP, such as alcohol, acute aggravation on chronic pancreatitis, and trauma/anatomy are well verified. Furthermore, the etiological workup for infections and hypercalcemia is insufficient. Moreover, some cases of AP may have been caused by drug and biliary disease as it may be difficult to exclude them from the etiology of AP. MIS-C: Multisystemic inflammatory syndrome in children; PIMS: Pediatrics inflammatory multisystem syndrome; AP: Acute pancreatitis.

pancreatic injury and suggested two pathophysiological theories of how pancreatic injury was caused by SARS-CoV-2[10]. First, viral infection causes direct pancreatic injury, as described above. Second, an indirect pancreatic injury is caused by systemic inflammatory responses to respiratory failure or by harmful systemic immune response induced by SARS-CoV-2 infection (Figure 1). Severe COVID-19, including acute respiratory distress syndrome (ARDS) and multiorgan failure is also known to be associated with cytokine storms in the host[36,37]. Levels of proinflammatory immune mediators associated with pancreatitis, including interleukin (IL)-1β, IL-6, IL-10, interferon-γ (IFN-γ), monocyte chemotactic protein-1 (MCP-1), and tumor necrosis factor-α (TNF-α) are higher in the plasma of patients with COVID-19 than those in healthy controls. Furthermore, in infected patients, levels of MCP-1 and TNF-α are significantly higher requiring admission to intensive care units (ICUs) than those in patients not being treated in ICUs[2,38,39]. Another study suggested that levels of IL-6, IL-10, and TNF-α were increased in patients with severe COVID-19 than in those with non-severe COVID-19[40]. Several points remain unclear in the relationship between proinflammatory immune mediators regulated by the viral effect and AP, but serum amylase and lipase elevation in patients with COVID-19 are associated with severity of COVID-19[41-44]. Additionally, AP is also more complicated in cases with severe COVID-19 than in patients with non-severe COVID-19[45]. These facts may support that cytokine storm caused by SARS-CoV-2 induces AP. In contrast, recent research suggests that the release of pancreatic lipase is associated with an increase in levels of unsaturated fatty acids[46]. It is hypothesized that the intestinal release of pancreatic lipase increases lipolysis and plasma levels of unsaturated fatty acids that may damage mitochondria and cause an increase in proinflammatory immune mediators[47]. This increase in cytokines can accelerate disease pathogenesis and lead to severe COVID-19[41,48]. Additional research and analyses are needed to validate this hypothesis, but it is uncertain whether severe COVID-19 causes AP or complicated AP is associated with increased severity of COVID-19 or both. Moreover, severe COVID-19 may complicate AP with other etiologies, including ischemia, hypercalcemia, and drugs[48]. Corticosteroid is known to induce pancreatitis; but, drug-induced AP is observed in < 5% of total AP cases, and corticosteroid accounts for only 2.8% of the drug-induced AP cases[19,49]. Tocilizumab, an antibody for IL-6 indicated for COVID-19, is also reported as an etiology for AP[50,51].

Further, multisystemic inflammatory syndrome in children (MIS-C)/pediatric inflammatory multisystem syndrome (PIMS), novel multisystem inflammatory conditions with some features similar to those of Kawasaki disease, and toxic shock syndrome leading to multiorgan failure and shock cause gastrointestinal symptoms in children[52-54]. Recent case studies also revealed that MIS-C/PIMS may complicate AP[55-58]. An international survey on children with co-occurrence of COVID-19 and AP showed that 2 of 22 patients had MIS-C/PIMS. The mechanisms of MIS-C/PIMS are unclear, but SARS-CoV-2 may cause AP *via* inflammatory immune mediators.

REAL-WORLD DATA ON COVID-19 AND AP

Cohort and case-control studies on COVID-19 and AP

In a prospective, cohort study in the Netherlands, Bulthuis *et al*[59] confirmed COVID-19 in 433 patients with RT-PCR and/or chest CT scores[59]. Eight of the 433 patients met the Revised Atlanta Classification of AP and all were teetotalers. Three of eight patients had other etiologies (two biliary and one post-ERCP); thus, five (1.2%) were suspected with COVID-19-attributed AP. The median age of the five cases was 60 (range, 47–71) years, and 80% were men. Necrotic changes were not observed in the pancreas of the five patients. All five had organ failures, and three (60%) succumbed to non-pancreatitis-related complications of COVID-19 although their AP was not severe. Vatansev *et al*[60] reported a retrospective cohort study comprising 150 patients, of which 29 had AP, and COVID-19 was confirmed with RT-PCR[60]. The mean age of 29 patients was 64.07 years, and 18 were men. In this study, AP was defined as abdominal pain, increased serum amylase and lipase levels (values not disclosed), and contrast-enhanced abdominal CT findings. Patients with some complications and history of habits, including gallstones, hypercalcemia, hypertriglyceridemia, alcohol consumption, and chronic pancreatitis were excluded from the study. All 29 patients had respiratory failures when diagnosed with AP. According to the Revised Atlanta Classification, the severity of AP was mild and moderate in 19 and 10 cases, respectively. The mortality was 8 of 29 patients (28%) died due to respiratory failure and multiple organ failure. These findings suggest a high mortality rate in patients with COVID-19-attributed AP. However, despite a strict investigation of etiologies of AP in the latter study, the number of patients suspected with COVID-19-attributed AP was higher, although a simple comparison was not possible due to differences in COVID-19 diagnostic criteria. Nevertheless, these studies failed to exclude other etiologies of AP, such as drugs, infections except SARS-CoV-2, and ischemia/reperfusion.

Akarsu *et al*[45] investigated the impact of AP on prognosis of COVID-19 in a prospective study[45]. They included 316 patients with COVID-19, of which 40 had complicated AP with various etiologies. AP was defined according to the Revised Atlanta Classification. The study showed a positive correlation between the severity of pneumonia and AP, and indicated that the frequency of AP increased with severity of pneumonia. Moreover, the mortality rate in patients with COVID-19-attributed AP was higher than that in patients with COVID-19 without AP (32.5% *vs* 7.97%, $P < 0.0001$). These studies showed that the incidence of COVID-19-attributed AP was rare, whereas comorbid COVID-19 was severe and had poor prognosis regardless of the severity of AP. This tendency was identified in suspected COVID-19-attributed AP and also AP with other etiologies. Furthermore, as described above, it is possible that severe conditions that needed treatment at ICU, induced AP in patients with COVID-19. Interestingly, Kumar *et al*[33] focused on the difference in the onset of AP in patients with COVID-19 in a retrospective study[33]. Lipase levels were measured and COVID-19 was confirmed with RT-PCR in 985 patients; of these, 17 cases were diagnosed with AP according to the Revised Atlanta Classification. Eight of these 17 presented with typical symptoms of AP on admission. The others developed AP after the onset of COVID-19 pneumonia and treatment with mechanical ventilation for ARDS. The number of patients were less, but the mortality rate in patients who were primarily admitted for AP was higher than that in patients who developed AP later (12.5% *vs* 33.3%). Several different clinical backgrounds should be considered as the reasons, etiologies of AP also seemed to be one of the causes, and it was not clear in the study. Ischemia/reperfusion and drugs were considered as etiologies of AP in patients who developed AP later, as they were treated with mechanical ventilation for ARDS.

There are several studies on AP and SARS-CoV-2 during the COVID-19 pandemic, and some of them focused on differences in the clinical course of AP, with or without comorbid COVID-19. Pandanaboyana *et al*[61] conducted a prospective, international, multicenter, large cohort study on patients with AP and coexistent SARS-CoV-2 infection[61]. The study, called the COVID PAN collaborative study, comprised 1777 patients with AP with various etiologies, of which 149 were SARS-CoV-2 positive. The study had some limitations, such as the diagnostic criteria of AP was uncertain, although the severity of AP was based on the Revised Atlanta Classification. The most important limitation was that the criteria for diagnosis of COVID-19 was RT-PCR for SARS-CoV-2 and also chest CT images and/or clinical course. The authors performed subgroup analysis to compare outcomes between patients negative for SARS-CoV-2 and those positive for SARS-CoV-2 confirmed by RT-PCR. After exclusion of patients from the subgroup analysis due to missing values, 82 of 909 patients with AP were positive for SARS-CoV-2. The 30-d mortality, rate of persistent organ failure, and acute pancreatic fluid collection were higher, and the length of hospital stay was longer in patients positive for SARS-CoV-2 than in those negative for

Table 1 Demographic characteristic of cases with suspected coronavirus disease 2019-attributed acute pancreatitis

Patient characteristics	Value
Age, median (range, yr)	42.0 (6-87)
Gender, male/female/NA	37/44/1
Comorbidities	
Hypertension	22
Diabetes	15
Dyslipidemia	4
Heart disease	3
Cerebrovascular	0
Respiratory disease	4
Renal dysfunction	5
Obesity	16
Pregnancy	2
Malignancy	2
History of abdominal surgery	13
Others	10
Alcohol consumption, none/low/heavy/NA	53/9/0/20
History of smoking, never/experience/current/NA	32/2/0/48
Severity of COVID-19	
Non-severe/severe/critical/NA	35/23/20/4
Symptoms	
Fever	49
Breath shortness	16
Cough	28
Dyspnea	18
Sore throat	18
Fatigue	9
Headache	7
Myalgia	10
Anorexia	13
Diarrhea	16
Abdominal pain	75
Nausea	39
Vomiting	48
Others	23
Blood test	
WBC, median (range, $\times 10^3/mm^3$)	13.10 (3.40-230.00)
PLT, median (range, $\times 10^3/mm^3$)	235.5 (52.0-502.0)
D-Dimer, median (range, μg/mL)	4.9 (0.3-17.7)
Amylase, median (range, U/L)	635 (47-4530)
Lipase, median (range, U/L)	895.5 (35.6-11920.0)
LDH, median (range, U/L)	366.0 (170-3553)

CRP, median (range, mg/dL)	8.5 (0.3-59.7)
Imaging findings (*n* = 75)	
Pancreatic enlargement	42
Peripancreatic fluid collection	33
Peripancreatic inflammatory change	48
Pancreatic ischemic change	12
No change of pancreas	6
Not visualized	2
Severity of acute pancreatitis	
Mild/moderate/severe/NA	28/20/28/6
Therapy for COVID-19	
Lopinavir/ritonavir	4
Favipiravir	4
Umifenovir	2
Remdesivir	8
Hydroxychloroquine	2
Tocilizumab	2
Corticosteroid (*n* = 53)	21
Oxygen therapy (*n* = 69)	42
Mechanical ventilation	19
Therapy for acute pancreatitis	
Conservative therapy/surgical drainage/NA	72/4/6
Period of hospitalization, median (range, day)	7.5 (2-76)
Prognosis	
Alive/death/NA	69/10/3

RT-PCR: Reverse transcription polymerase chain reaction; IgM: Immunoglobulin M; IgG: Immunoglobulin G; WBC: White blood cell; PLT: Platelet; LDH: Lactate dehydrogenase; CRP: C-reactive protein; NA: Not available; SARS-CoV-2: Severe acute respiratory syndrome coronavirus-2; COVID-19: Coronavirus disease 2019.

SARS-CoV-2. Three retrospective cohort studies also reported results similar to those of the COVID PAN collaborative study[62-64]. Thus, concurrent AP and SARS-CoV-2 infection may lead to worse clinical outcomes, such as prolonged hospital stay, requirement of mechanical ventilation, high incidence of multiple organ failure, and high mortality than that with AP-alone. In contrast, two of three studies also revealed that the incidence of idiopathic AP in patients positive for SARS-CoV-2 was higher than that in patients negative for SARS-CoV-2[62,63]. Interestingly, the COVID PAN collaborative study also revealed that[65] SARS-CoV-2 infection may cause AP similar to other infections. Miró *et al*[66] conducted a retrospective case-control study, called the Unusual Manifestations of COVID-19 (UMC-19) study, comprising emergency units in Spain[66]. The diagnostic criteria for AP were according to the Revised Atlanta Classification. The diagnosis of COVID-19 was based on RT-PCR or antigen detection test, and also on chest image findings and clinical conditions. In 62 emergency departments, of the 1463693 patients tested for COVID-19, 74814 cases tested positive, and 54 of them (0.072%) developed AP. Furthermore, the frequency of non-COVID-19 patients with AP was 0.161% (2231/13888879). To compare outcomes between AP and COVID-19 groups, patients were randomly distributed into two groups-162 patients with AP without COVID-19 and 162 patients without AP with COVID-19. Patients with AP with COVID-19 showed severe clinical courses with high mortality than patients without AP with COVID-19. Moreover, there were no differences in the etiologies of AP with or without concurrent SARS-CoV-2 infections. Additionally, the incidence of AP in patients with COVID-19 was lower than that in patients with AP without COVID-19, consistent with results discussed above (0.072% *vs* 0.161%). In contrast, there were no differences between patients with COVID-19 with AP and those with COVID-19 without AP, except for the length of hospitalization. These results suggest that COVID-19 affects the prognosis of patients with concurrent AP and COVID-19 than those with AP-alone. A recent meta-

Table 2 Baseline characteristics of cases with coronavirus disease 2019 and acute pancreatitis coexistent

Case No.	Ref.	Age	Gender	Diagnostic evidence for SARS-CoV-2	Severity of COVID-19	Abdominal pain	Amylase/lipase (IU/L)	Abdominal image findings	Modality of image	Severity of acute pancreatitis	Treatment for pancreatitis	Prognosis
1	Anand *et al*[70]	59	Female	RT-PCR	Non-severe	Presence	NA/NA	Diffuse pancreatic enlargement	CT	Mild	Conservative	Alive
2	Hadi *et al*[71]	47	Female	RT-PCR	Critical	Absence	1500/NA	Diffuse pancreatic enlargement	AUS	Severe	NA	NA
3	Hadi *et al*[71]	68	Female	RT-PCR	Critical	Presence	934/NA	NA	NA	Severe	NA	NA
4	Aloysius *et al*[72]	36	Female	RT-PCR	Critical	Presence	325/627	No change	CT	Severe	Conservative	Alive
5	Miao *et al*[73]	26	Female	RT-PCR	Non-severe	Presence	NA/430	Diffuse pancreatic enlargement	CT	NA	NA	Alive
6	Szatmary *et al*[74]	29	Male	RT-PCR	Non-severe	Presence	77/NA	Diffuse pancreatic enlargement, peripancreatic inflammatory change, fluid collection	CT	Moderate	Conservative	Alive
7	Szatmary *et al*[74]	47	Male	RT-PCR	Non-severe	Presence	211/NA	Diffuse pancreatic enlargement, peripancreatic inflammatory change, fluid collection	CT	Moderate	Conservative	Alive
8	Rabice *et al*[75]	36	Female	RT-PCR	Severe	Presence	88/875	Not visualized	AUS	Mild	Conservative	Alive
9	Alloway *et al*[76]	7	Female	RT-PCR	Non-severe	Presence	NA/1672	Diffuse pancreatic enlargement	AUS and CT	Mild	Conservative	Alive
10	Karimzadeh *et al* [77]	65	Female	RT-PCR	Severe	Presence	285/294	No change	CT	Mild	Conservative	Alive
11	Gonzalo-Voltas *et al*[78]	76	Male	RT-PCR	Non-severe	Presence	3568/NA	Diffuse pancreatic enlargement	CT	Moderate	Conservative	Alive
12	Bokhari *et al*[79]	32	Male	RT-PCR	Non-severe	Presence	672/721	Diffuse pancreatic enlargement, peripancreatic inflammatory change, fluid collection	CT	Mild	Conservative	Alive
13	Mazrouei *et al*[80]	24	Male	RT-PCR	Non-severe	Presence	391/578	Enlargement of pancreatic tail, peripancreatic fluid collection	CT	Mild	Conservative	Alive
14	Ahmed *et al*[81]	47	Male	RT-PCR	Severe	Presence	349/NA	Peripancreatic inflammatory change	CT	Severe	NA	Alive
15	Brikman *et al*[82]	61	Male	RT-PCR	Severe	Presence	142/203	Peripancreatic inflammatory change	CT	Mild	Conservative	Alive
16	Kataria *et al*[83]	49	Female	RT-PCR	Severe	Presence	501/1541	Diffuse pancreatic enlargement, peripancreatic fluid collection	CT	Mild	Conservative	Alive
17	Cerda-Contreras *et al*[84]	72	Female	RT-PCR	Severe	Absence	1789/1247	Diffuse pancreatic enlargement, peripancreatic inflammatory change, fluid collection	CT	Severe	Conservative	Dead

18	Cheung *et al*[85]	38	Male	RT-PCR	Non-severe	Presence	NA/338.7	Acute pancreatitis	CT	NA	Conservative	Alive
19	Kumaran *et al*[86]	67	Female	RT-PCR	Severe	Presence	1483/NA	Peripancreatic inflammatory change and fluid collection, non-enhancement of most of the head and proximal body	CT	Severe	Conservative	Alive
20	Purayil *et al*[87]	58	Male	RT-PCR	Non-severe	Presence	249/NA	Not visualized	AUS	Mild	Conservative	Alive
21	Dietrich *et al*[88]	72	Male	RT-PCR	Critical	Presence	NA/185	Normal pancreas	CT	Mild	NA	Alive
22	Patnaik *et al*[89]	29	Male	RT-PCR	Non-severe	Presence	2861/1650	Diffuse pancreatic enlargement, peripancreatic fluid collection	CT	Mild	Conservative	Alive
23	Wang *et al*[90]	42	Male	RT-PCR	Critical	Presence	132/382	Pancreatic enlargement, peripancreatic fluid collection	CT	Moderate	Conservative	Dead
24	Wang *et al*[90]	35	Male	RT-PCR	Non-severe	Presence	NA/1042	Pancreatic enlargement, peripancreatic fluid collection	CT	Moderate	Conservative	Alive
25	Alves *et al*[91]	56	Female	RT-PCR	Critical	Presence	544/2993	Dffuse pancreatic enlargement, peripancreatic inflammatory change	CT and MRI	Severe	Conservative	Alive
26	Kurihara *et al*[92]	55	Male	RT-PCR	Critical	Absence	252/263	Pancreatic enlargement, peripancreatic inflammatory change	CT	Severe	Conservative	Alive
27	Lakshmanan and Malik[93]	68	Male	RT-PCR	Non-severe	Absence	1030/2035	Peripancreatic inflammatory change	CT	Mild	Conservative	Alive
28	Samies *et al*[94]	15	Male	RT-PCR	Non-severe	Presence	NA/233	Peripancreatic inflammatory change	CT	Mild	Conservative	Alive
29	Samies *et al*[94]	11	Male	RT-PCR	Non-severe	Presence	215/953	No change	CT	Mild	Conservative	Alive
30	Samies *et al*[94]	16	Female	RT-PCR	Non-severe	Presence	NA/1909	Pancreatic enlargement	CT	Mild	Conservative	Alive
31	Fernandes *et al*[95]	36	Female	RT-PCR	NA	Presence	710/640	Pancreatic enlargement, peripancreatic fluid collection	CT	Moderate	Conservative	Alive
32	Stevens *et al*[55]	10	Female	Serological IgG	Severe	Presence	NA/1371	Peripancreatic inflammatory change	CT	Severe	Conservative	Alive
33	Shinohara *et al*[96]	58	Male	RT-PCR	Critical	Presence	795/NA	Diffuse pancreatic enlargement peripancreatic inflammatory change	CT	Moderate	Conservative	Alive
34	Meyers *et al*[97]	67	Male	RT-PCR	NA	Presence	NA/5295	Interstitial edematous pancreatitis peripancreatic inflammatory change	CT	Moderate	NA	NA
35	Ghosh *et al*[98]	63	Male	RT-PCR	Severe	Absence	58/412	Focal pancreatic enlargement, peripancreatic fluid collection	CT	NA	Conservative	Alive
36	Tollard *et al*[99]	32	Female	RT-PCR	Critical	Presence	NA/321	Diffuse pancreatic enlargement peripancreatic inflammatory change	CT	Severe	Conservative	Dead
37	Kandasamy *et al*[100]	45	Female	RT-PCR	Severe	Presence	364/293	Diffuse pancreatic enlargement, peripancreatic inflammatory change and fluid collection	CT	Moderate	Conservative	Alive

38	Hassani *et al*[101]	78	Female	RT-PCR	Critical	Presence	1200/1450	Pancreatic enlargement necrotizing pancreatitis	AUS and CT	Severe	Conservative	Dead
39	Suchman *et al*[56]	10	Female	RT-PCR	Non-severe	Presence	NA/365.7	NA	NA	Moderate	Conservative	Alive
40	Suchman *et al*[56]	16	Male	RT-PCR	Critical	Presence	NA/233.3	NA	NA	Severe	Conservative	Alive
41	Narang *et al*[102]	20	Female	RT-PCR	Severe	Presence	1168/916	Acute pancreatitis	MRI	Severe	Conservative	Alive
42	Acherjya *et al* [103]	57	Female	RT-PCR	Severe	Presence	80/8352	Diffuse pancreatic enlargement, peripancreatic inflammatory change	CT	Moderate	Conservative	Alive
43	Alwaeli *et al*[104]	30	Male	RT-PCR	Critical	Presence	151/1022	Diffuse pancreatic enlargement, peripancreatic inflammatory change	CT	Severe	Conservative	Alive
44	Simou *et al*[105]	67	NA	RT-PCR	Severe	Absence	NA/576	Diffuse pancreatic enlargement, peripancreatic inflammatory change	CT	Severe	Conservative	Dead
45	Jespersen Nizamic *et al*[106]	49	Female	RT-PCR	Non-severe	Presence	NA/2864	Peripancreatic inflammatory change, fluid collection	CT	Moderate	Conservative	Alive
46	Abraham *et al* [107]	61	Female	RT-PCR	Non-severe	Presence	NA/1018	NA	NA	Mild	Conservative	Alive
47	Abhinay *et al*[108]	13	Female	RT-PCR	NA	Presence	217/365	Peripancreatic inflammatory change, fluid collection	CT	Moderate	Conservative	Alive
48	Bouali *et al*[109]	60	Female	RT-PCR	Critical	Presence	NA/627	Peripancreatic fluid collection	CT	Severe	Drainage of abdominal cavity, total gasterectomy	Dead
49	Alharmi *et al*[110]	52	Female	RT-PCR	Non-severe	Presence	47/NA	Atrophic pancreas, peripancreatic inflammatory change, peripancreatic fluid collection	CT	Moderate	Conservative	Alive
50	Abbas *et al*[57]	13	Female	RT-PCR	Critical	Presence	217.8/NA	Fluid collection	CT	Severe	Conservative	Alive
51	Bineshfar *et al* [111]	14	Male	RT-PCR	Non-severe	Presence	1914/NA	Diffuse pancreatic enlargement, peripancreatic inflammatory change	CT	Mild	Conservative	Alive
52	Paz *et al*[112]	14	Male	RT-PCR	Non-severe	Presence	196/247	Peripancreatic inflammatory change, fluid collection	MRI	Mild	Conservative	Alive
53	Wifi *et al*[113]	72	Female	RT-PCR	Non-severe	Presence	1667/710	No change	CT	Mild	Conservative	Alive
54	Sandhu *et al*[114]	25	Female	RT-PCR	Critical	Presence	350/35.6	Diffuse pancreatic enlargement	CT	Severe	Conservative	Dead
55	Mohammadi Arbati *et al*[115]	28	Male	RT-PCR	Critical	Presence	1273/758	Peripancreatic inflammatory change, fluid collection, acute necrotic pancreatitis	CT	Severe	Conservative	Alive
56	Amé *et al*[116]	42	Female	RT-PCR	NA	Presence	2263/2799	Pancreatic enlargement, peripancreatic inflammatory change, fluid collection	CT	NA	Conservative	Alive
57	Gupta *et al*[117]	25	Female	RT-PCR	Severe	Presence	1814/11920	Diffuse pancreatic enlargement,	CT	Severe	Conservative	Alive

								peripancreatic inflammatory change, fluid collection				
58	Muhammad Abrar Jeelani *et al* [118]	24	Male	RT-PCR	Non-severe	Presence	NA/4174	Peripancreatic inflammatory change, fluid collection	CT	Moderate	Conservative	Alive
59	Maalouf *et al*[119]	62	Male	RT-PCR	Non-severe	Presence	NA/4361	Peripancreatic inflammatory change, necrotic collection	MRI	Moderate	Conservative	Alive
60	Sanchez *et al*[120]	16	Male	RT-PCR	Severe	Presence	NA/961	Peripancreatic inflammatory change, fluid collection	CT	Moderate	Conservative	Alive
61	Ehsan *et al*[121]	13	Female	RT-PCR	Severe	Presence	598/2331	Peripancreatic inflammatory change, fluid collection	CT	Moderate	Conservative	Alive
62	Hanif *et al*[122]	30	Female	RT-PCR	Severe	Presence	820/626	Diffuse pancreatic enlargement, peripancreatic inflammatory change	CT	Severe	Conservative	Alive
63	Chandra *et al* [123]	53	Male	RT-PCR	Critical	Presence	NA/1200	Peripancreatic inflammatory change	CT	Severe	Conservative	Alive
64	Alfishawy *et al* [124]	17	Male	RT-PCR	Severe	Absence	285/273	Pancreatic loculations	CT	Moderate	Conservative	Alive
65	Berrichi *et al*[125]	36	Female	RT-PCR	Critical	Presence	NA/2570	Diffuse pancreatic enlargement, peripancreatic inflammatory change	CT	Severe	Conservative	Dead
66	Berrichi *et al*[125]	51	Female	RT-PCR	Severe	Presence	NA/676	Diffuse pancreatic enlargement	CT	Mild	Conservative	Alive
67	Kripalani *et al* [126]	79	Female	RT-PCR	Critical	Presence	1075/6178	Diffuse pancreatic enlargement, peripancreatic inflammatory change, acute necrotic pancreatitis	CT	Severe	Cycto-jejunostomy	Alive
68	Narayan *et al* [127]	28	Male	RT-PCR	Critical	Presence	Elevated/elevated	Diffuse pancreatic enlargement, peripancreatic inflammatory change and acute necrotic pancreatitis	CT	Severe	Conservative	Dead
69	Narayan *et al* [127]	45	Female	RT-PCR	Severe	Presence	Elevated/elevated	Peripancreatic inflammatory change	CT	Mild	Conservative	Alive
70	Eldaly *et al*[128]	44	Male	RT-PCR	Non-severe	Presence	773/286	Diffuse pancreatic enlargement	CT	Mild	Conservative	Alive
71	Basukala *et al* [129]	49	Female	RT-PCR	Non-severe	Presence	1563/568	Diffuse pancreatic enlargement, peripancreatic inflammatory change, fluid collection, necrotic pancreatitis	CT	Severe	Gastrocolic ligament and followed by necrotic debridement, and drainage placement	Dead
72	Schembri Higgans *et al*[130]	63	Female	RT-PCR	Non-severe	Presence	1079/NA	After Whipple surgery	CT	Mild	Conservative	Alive
73	Schembri Higgans *et al*[130]	87	Female	RT-PCR	Non-severe	Presence	499/NA	Peripancreatic inflammatory change	CT	Mild	Conservative	Alive
74	Schembri	64	Female	RT-PCR	Non-severe	Presence	2141/NA	Peripancreatic inflammatory change	CT	Mild	Conservative	Alive

	Higgans *et al*[130]											
75	Kopiczko *et al* [131]	6	Female	RT-PCR	Non-severe	Presence	1124/4250	Diffuse pancreatic enlargement, peripancreatic inflammatory change, fluid collection	CT	Mild	Conservative	Alive
76	Kareva *et al*[58]	11	Male	Serological IgG	Non-severe	Presence	489/576	Edematous appendix no change of pancreas	AUS	NA	Conservative	Alive
77	da Costa Ferreira *et al*[132]	35	Male	RT-PCR	Severe	Presence	1669/NA	Diffuse pancreatic enlargement, peripancreatic inflammatory change, fluid collection normal gallbladder and biliary tract	CT	Severe	Conservative	Alive
78	Sánchez-Gollarte *et al*[133]	60	Male	Serological IgG	Severe	Presence	4530/2220	Diffuse pancreatic enlargement, peripancreatic inflammatory change, fluid collection, necrotic pancreatitis	CT	Severe	Drainage of abdominal cavity	Alive
79	Sudarsanam *et al* [134]	35	Male	RT-PCR	Non-severe	Presence	Normal/normal	Peripancreatic inflammatory change, fluid collection, necrotic pancreatitis of tail	CT	NA	Conservative	Alive
80	Faghih Dinevari *et al*[135]	18	Female	RT-PCR	Non-severe	Presence	1288/1541	Diffuse pancreatic enlargement, peripancreatic inflammatory change, fluid collection	CT	Mild	Conservative	Alive
81	Goldstein *et al* [136]	11	Male	Serological IgG	Severe	Presence	1607/2434	Peripancreatic inflammatory change, fluid collection, necrotic pancreatitis	MRI	Moderate	Conservative	Alive
82	Gadiparthi *et al* [137]	74	Female	RT-PCR	Non-severe	Presence	229/7550	Peripancreatic inflammatory change	CT	Mild	Conservative	Alive

RT-PCR: Reverse transcription polymerase chain reaction; IgG: Immunoglobulin G; SARS-CoV-2: Severe acute respiratory syndrome coronavirus-2; COVID-19: Coronavirus disease 2019; AUS: Abdominal ultrasonography; CT: Computed tomography; MRI: Magnetic resonance imaging; NA: Not available.

analysis suggested that patients with AP and COVID-19 were frequently men, had idiopathic etiology of AP, a high rate of pancreatic necrosis, higher severity of AP, and serious clinical courses, such as requirement of ICU admission and mechanical ventilation, and high mortality than patients with AP without COVID-19[67]. The prognoses in patients with COVID-19 with AP and those with COVID-19 without AP were different. It remains unclear whether SARS-CoV-2 infections increase AP, as the incidence of AP is rare, but its severity is high when concurrent with COVID-19. An online survey[68] including 22 children with AP and COVID-19 was reported. They were diagnosed as COVID-19 with RT-PCR or detection of SARS-CoV-2 IgG antibodies, while the diagnostic criteria for AP was unavailable. Children aged 10–14 years accounted for 54.5% of all participants in the study. Their clinical courses were serious-60% of them required treatment in the ICU, 45% had multi-organ involvement, 11% had complicated pancreatic necrosis, and 24% developed shock.

The association of AP with SARS-CoV-2 remains unclear, but patients with concurrent AP and COVID-19 show worse prognoses. The fact that some studies reported idiopathic AP during the COVID-19 pandemic indicates existence of COVID-19-attributed AP. Therefore, prospective cohort

studies focused on patients with COVID-19 with idiopathic AP, especially on how to exclude other etiologies of AP, are needed to clarify the COVID-19-attributed AP.

REVIEW OF CASE REPORTS CONTRIBUTED TO CONCURRENT COVID-19 AND AP

Literature search strategy

We identified relevant studies in the literature by searching the PubMed database. The review was restricted to articles published between December 2019 and October 2021, and selected case reports published in English. The search terms were as follows: COVID-19 pancreatitis AND "2019/01/01" (Date-Publication) to "2021/10/31" (Date-Publication) OR SARS-CoV-2 pancreatitis AND "2019/01/01" (Date-Publication) to "2021/10/31" (Date-Publication). We also screened reference lists of selected studies to manually identify relevant studies and include them in the narrative review.

Diagnosis and severity of AP

AP was defined according to diagnostic criteria of the Revised Atlanta Classification[17]. The presence of two out of three features, including abdominal pain consistent with AP, serum lipase activity (or amylase activity) at least three-times greater than the upper normal limit, and characteristic findings of AP on abdominal imaging, was required for the diagnosis of AP.

The severity (mild, moderately severe, and severe) of AP was also defined according to the Revised Atlanta Classification[17].

Diagnosis and severity of COVID-19

The diagnosis of COVID-19 was defined as a positive RT-PCR result or serological test for SARS-CoV-2. The other methods, such as medical history, or chest CT findings, were excluded.

The severity of COVID-19 (mild, moderate, severe, and critical), as classified by the WHO guidelines, was used to stratify patients in the study (https://www.who.int/publications/i/item/clinical-management-of-covid-19). Critical COVID-19 was defined based on the criteria for ARDS, sepsis, septic shock, or other conditions that would normally require life-sustaining therapies, such as mechanical ventilation (invasive or non-invasive) or vasopressor therapy. Severe COVID-19 was defined based on any of the following criteria: (1) Oxygen saturation < 90% on room air; (2) Respiratory rate > 30 breaths/min in adults and children aged > 5 years, ≥ 60 breaths/min in children aged < 2 mo, ≥ 50 in children aged 2–11 mo, and ≥ 40 in children aged 1–5 years; and (3) Signs of severe respiratory distress (accessory muscle use, inability to complete full sentences, and, in children, very severe chest-wall indrawing, grunting, central cyanosis, or presence of any other general danger signs). Non-severe COVID-19 was defined as the absence of any criteria for severe or critical COVID-19.

The data for some cases was insufficient to confirm the severity of COVID-19, but patients who received oxygen therapy were considered to have severe condition. Nevertheless, the indication for oxygen administration varied with institution. However, oxygen saturation < 90%, a criteria for severe COVID-19, was generally used as an indication for oxygen therapy. Additionally, patients who received oxygen therapy generally required hospitalization. Therefore, patients who received oxygen therapy were considered to have severe condition.

Reports included in the review

The literature search of the PubMed database identified 735 studies that met the criteria. We identified eight additional relevant articles in the references of these studies. We excluded 580 non-case study articles, a study in non-English language, three preprints, and an article that could not be reviewed. Of the remaining 158 case studies, 61 were without pancreatic injury or pancreatitis, and thus, were excluded. Moreover, 16 case reports on AP caused by other etiologies, such as biliary disease, alcohol, acute on chronic pancreatitis, hypertriglyceridemia, cytomegalovirus infection, methanol, lymphoma, and vaccination were excluded. In the remaining 81 case studies, six studies comprised eight cases that were not confirmed for AP based on the Revised Atlanta Classification. Two case studies did not include objective data for COVID-19 diagnosis. After removing these studies, 73 studies that included eight case series and 65 case reports were finally assessed in this review. In three of eight case series, one patient without pancreatitis (but with acute cholecystitis), two with negative RT-PCR test, and eight without RT-PCR test or serological IgG for SARS-CoV-2 were excluded. Eighty-two cases of suspected COVID-19-attributed AP were evaluated. Four of 82 cases were RT-PCR negative, but were serological IgG positive for SARS-CoV-2. However, these studies had a limitation that the etiological search for AP was insufficient in almost all cases. Therefore, we classified the potential of other etiologies for AP as-probable, improbable, and uncertain-for each case. The definition of "probable" for each etiology was as follows: Alcoholic AP, consuming ≥ 60 g of ethanol every day before AP onset; biliary AP, gallstones or biliary tract dilation on the abdominal image findings at AP onset (regarded as biliary AP when any serological hepatobiliary test results exceeded more than three-times the upper normal limit unless endoscopic ultrasonography or ERCP excluded any biliary diseases); hypertriglyceridemia, fasting

triglycerides > 1000 mg/dL (11.3 mmol/L) at AP onset[19]; hypercalcemia, serological calcium > 10.4 mg/dL (2.60 mmol/L) at AP onset; drug-induced AP, new medication within one month before AP onset; acute aggravation on chronic pancreatitis, chronic pancreatitis existed, such as pancreatic calcification, before AP onset; infections, positive serological diagnosis for pathogens at AP onset; ischemia/reperfusion, episodes of hypoxic or hypovolemic status, *i.e.*, cardiopulmonary arrest, shock, or mechanical ventilation, before pancreatitis onset; and trauma/anatomy, history of abdominal trauma or upper abdominal surgery with reconstruction of the gastrointestinal tract. In children, genetic AP was defined as existence of a family history of AP, *i.e.*, ≥ 2 first-degree relatives (or ≥ 3 s-degree relatives) to have unexplained recurrent acute or chronic pancreatitis in ≥ 2 generations[69]. Moreover, in cases aged 0–19 years, MIS-C/PIMS-induced AP was also evaluated. The MIS-C/PIMS was defined according to the WHO definition (https://www.who.int/news-room/commentaries/detail/multisystem-inflammatory-syndrome-in-children-and-adolescents-with-covid-19). In case of insufficient etiological information, the probability of AP was regarded as uncertain.

Reports results

The characteristics of patients with COVID-19-attributed AP are shown in Tables 1–3. The probability of other etiologies for AP in included cases were as follows-alcohol: 0 probable, 64 improbable, and 18 uncertain; biliary AP: 8, 59, and 15; hypertriglyceridemia: 1, 54, and 27; hypercalcemia: 0, 40, and 42; drug-induced AP: 17, 58, and 17; acute aggravation on chronic pancreatitis: 1, 81, and 0; infections: 0, 7, and 75; ischemia/reperfusion: 10, 68, and 4; trauma/anatomy: 1, 79, and 2; genetic AP: 0, 7, and 11; and MIS-C/PIMS: 5, 10, and 3, respectively (Table 3 and Figure 2).

The median age at onset of COVID-19-attributed AP was 42.0 (range, 6–87) years. The men-to-women ratio of COVID-19-attributed AP was 37:44. The patient comorbidities were: Hypertension (22 cases), diabetes (15 cases), heart disease (3 cases), respiratory disease (4 cases), obesity (16 cases), renal dysfunction (5 cases), dyslipidemia (4 cases), hyper/hypothyroidism (4 cases), gastroesophageal reflux disease (2 cases), thrombophilia (1 case), thrombosis (1 case), osteoporosis (1 case), anxiety (2 cases), and malignant disease (2 cases). There were 13 patients with histories of abdominal surgeries, including cholecystectomy, hysterectomy, cesarean section, appendectomy, Whipple procedure, small bowel resection, and renal transplantation. Two pregnant women were also included. Almost all patients had no history of alcohol and cigarette abuse. Abdominal pain was the most frequent symptom (91.5%, 75/82), followed by fever (59.8%, 49/78), vomiting (58.5%, 48/79), nausea (47.6%, 39/66), and cough (34.1%, 28/78). None of the patients had any symptoms. The median levels of white blood cells, platelets, D-Dimer, amylase, lipase, lactate dehydrogenase, and C-reactive protein were 13100/μL (range, 3400–230000), 235500/μL (range, 52000–502000), 4.9 μg/mL (range, 0.3–17.7), 635 U/L (range, 47–4530), 895.5 U/L (range, 35.6–11920.0), 366 U/L (range, 170–3553), and 8.5 mg/dL (range, 0.3–59.7), respectively.

The study included 43 patients (55.8%, 43/77) with severe or critical COVID-19. Oxygen therapy for COVID-19 was required in 42 patients (51.2%, 42/69); of those, 19 were treated with mechanical ventilation. Seventeen patients received antiviral therapy with lopinavir/ritonavir, favipiravir, umifenovir, or remdesivir. One of them was treated with both lopinavir/ritonavir and favipiravir. Moreover, two patients received hydroxychloroquine, an antimalarial drug, for treatment of COVID-19. Two cases were treated with tocilizumab, an anti-IL-6 monoclonal antibody, for COVID-19. Corticosteroids were also administered for the treatment of COVID-19 in 21 patients (39.6%, 21/53).

Abdominal images were evaluated in 75 patients, except in two patients as the pancreases could not be visualized *via* abdominal ultrasonography. Two other patients underwent abdominal CT or magnetic resonance imaging, and the findings were consistent with those of pancreatitis-alone, without details. Of the remaining 71 patients, 48 showed peripancreatic inflammatory changes and 33 had peripancreatic fluid collections. Pancreatic enlargement occurred in 42 patients. Pancreatic ischemic changes, such as decreased contrast enhancement in pancreatic parenchyma on abdominal computed tomography was observed in 12 patients (16.9%, 12/71). However, no change was observed in the abdominal image findings in six patients.

In this review, 28 patients were classified as having severe AP (36.8%, 28/76). Almost all patients with AP received conservative therapy, except for four cases. These four patients underwent invasive treatment; of which, one patient with AP and gastric necrosis underwent drainage of the peripancreatic necrotic collections and total gastrectomy, but failed to recover. The other patient received gastrocolic ligament, necrotic debridement, and drainage placement for acute hemorrhagic necrotizing pancreatitis, and died two days after surgery.

The median period of hospitalization for recovering from COVID-19-attributed AP was 8.0 d (range, 2–76). Ten patients (12.7%, 10/79) died due to critical COVID-19 (median hospitalization, 7.0 d; range, 2–22 d).

In summary, patients suspected with COVID-19-attributed AP were relatively young (median age, 42 years), 36.8% of them had severe conditions, and had a high mortality rate (12.7%) similar to that reported in cohort studies and meta-analyses. However, it cannot be ignored that many AP cases reported in these studies may have occurred due to etiologies other than SARS-CoV-2.

Table 3 The probability of other etiologies of acute pancreatitis in cases with coronavirus disease 2019 and acute pancreatitis coexistent

Case No.	Alcohol	Biliary	Hypertrig-lyceride-mia	Drug	Acute aggravati-on on chronic pancreati-tis	Hypercal-cemia	Infection-s	Ischemia/ reperfusi-on	Trauma/ anatomy	Genetics	MIS-C/PIMS
1	N	?	?	Y	N	?	?	N	N	-	-
2	N	N[1]	N	?	N	N	?	Y	N	-	-
3	?	?	N	?	N	N	?	Y	N	-	-
4	N	N	N	N	N	?	?	N	N	-	-
5	N	N	N	N	N	N	N[2]	N	N	-	-
6	N	N	N	N	N	?	?	?	N	-	-
7	N	N	N	N	N	?	?	?	N	-	-
8	N	N	N	N	N	?	?	N	N	-	-
9	N	?	?	N	N	?	?	N	N	?	N
10	?	N	N	N	N	N	?	N	N	-	-
11	N	N	?	Y	N	?	?	N	N	-	-
12	N	N	N	N	N	N	?	N	N	-	-
13	N	N	?	N	N	?	?	N	N	-	-
14	?	Y	?	Y	N	?	?	N	N	-	-
15	N	N	N	Y	N	N	?	N	N	-	-
16	N	N	N	Y	N	N	?	N	N	-	-
17	?	?	N	Y	N	N	?	Y	N	-	-
18	N	N	N	N	N	N	?	N	N	-	-
19	N	N	N	N	N	N	?	N	N	-	-
20	N	N	?	N	N	?	?	N	N	-	-
21	N	N	?	N	N	?	?	N	N	-	-
22	N	N	N	N	N	N	?	N	N	-	-
23	N	N	N	N	N	N	?	N	N	-	-
24	N	N	N	N	N	N	?	N	N	-	-
25	N	N	N	N	N	N	?	N	N	-	-
26	?	N	N	Y	N	N	?	Y	N	-	-
27	N	N	N	N	N	N	?	N	N	-	-
28	N	?	N	N	N	?	?	N	N	N	N
29	N	N	N	N	N	?	?	N	N	N	?
30	N	Y	N	N	Y	?	?	N	N	N	N
31	N	N[1]	?	N	N	?	?	N	N	-	-
32	N	Y	N	N	N	?	?	N	N	?	Y
33	N	N	N	Y	N	N	?	Y	N	-	-
34	N	N	N	N	N	?	?	N	N	-	-
35	N	?	?	?	N	?	?	N	N	-	-
36	N	Y	N	N	N	N	?	Y	N	-	-
37	N	N	?	N	N	?	?	N	N	-	-

38	N	N	N	N	N	N	?	N	N	-	-
39	N	?	?	?	N	?	?	?	?	?	Y
40	N	?	?	?	N	?	?	?	?	?	N
41	N	N	N	Y	N	?	?	Y	N	-	-
42	N	N	N	Y	N	N	?	N	N	-	-
43	N	N	N	N	N	N	N[2]	N	N	-	-
44	N	N	N	Y	N	N	N[2]	Y	N	-	-
45	N	?	?	N	N	?	?	N	N	-	-
46	?	?	?	N	N	N	?	N	N	-	-
47	?	?	?	N	N	?	?	N	N	?	N
48	?	?	?	N	N	?	?	N	N	-	-
49	N	N	N	Y	N	N	?	N	N	-	-
50	N	N	N	Y	N	?	N[2]	N	N	N	Y
51	N	N	?	N	N	?	?	N	N	?	N
52	?	N	N	N	N	?	?	N	N	N	N
53	?	N	N	N	N	N	?	N	N	-	-
54	N	Y	N	N	N	N	?	N	N	-	-
55	N	N	N	N	N	N	?	N	N	-	-
56	N	N	N	N	N	N	?	N	N	-	-
57	N	N	N	?	N	N	?	N	N	-	-
58	N	N	N	N	N	N	?	N	N	-	-
59	N	N	N	N	N	?	?	N	N	-	-
60	N	N	?	N	N	N	?	N	N	N	N
61	N	N	N	N	N	?	?	N	N	?	?
62	N	?	N	Y	N	N	N	Y	N	-	-
63	N	N	N	N	N	?	?	N	N	-	-
64	N	Y	Y	N	N	?	?	N	N	?	?
65	?	N	?	N	N	?	?	N	N	-	-
66	?	N	?	N	N	?	?	N	N	-	-
67	N	N	?	N	N	?	?	N	N	-	-
68	?	N	N	Y	N	?	?	N	N	-	-
69	?	?	?	Y	N	?	?	Y	N	-	-
70	N	N	N	N	N	?	?	N	N	-	-
71	N	N	N	N	N	N	?	N	N	-	-
72	N	N	?	N	N	?	?	N	Y	-	-
73	?	N	N	N	N	?	?	N	N	-	-
74	?	Y	?	N	N	?	?	N	N	-	-
75	N	N	N	N	N	N	N	N	N	?	N
76	N	N	?	N	N	N	?	N	N	?	Y
77	N	Y	N	N	N	N	?	N	N	-	-
78	?	N	?	?	N	N	?	N	N	-	-
79	N	N	N	N	N	N	?	N	N	-	-
80	N	N	N	N	N	N	?	N	N	N	N
81	?	?	?	Y	N	?	N[2]	N	N	?	Y

82	N	N	N	N	N	N	?	N	N	-	-

[1]Serological hepatobiliary test was not shown.
[2]Some infections were denied although others were not.
Y: Probable; N: Improbable; MIS-C: Multisystemic inflammatory syndrome in children; PIMS: Pediatrics inflammatory multisystem syndrome.

CONCLUSION

It remains controversial whether SARS-CoV-2 infections increase AP, but some basic and pathological approaches suggest mechanisms of direct and indirect involvement of the pancreas caused by SARS-CoV-2. Moreover, there are several clinical data to support existence of COVID-19-attributed AP. First, the incidence of idiopathic AP in patients positive for SARS-CoV-2 is higher than that in patients negative for SARS-CoV-2 in some cohorts with concurrent COVID-19 and AP. Second, SARS-CoV-2 infects pancreatic exocrine and endocrine cells as *per* the pathological evaluation of patients deceased due to COVID-19. Moreover, some clinical features of COVID-19-attributed AP, including various etiologies of AP, are revealed, such as a high rate of pancreatic necrosis, higher severity of AP, and serious clinical courses. However, clinical features of COVID-19-attributed AP remain uncertain. A sufficient investigation on etiologies of AP would improve understanding of the clinical features of COVID-19-attributed AP. High-quality clinical studies and case reports that specify the method for differential diagnoses of the other etiologies of AP, including alcohol, biliary, hypertriglyceridemia, hypercalcemia, drugs, ischemia/reperfusion, trauma, infections, and genetic associations need to be evaluated. The present review of case studies suggests criteria to classify the possibility of other etiologies for AP. The criteria may not be appropriate, but the review highlights the insufficient etiological workup of AP, especially for other infections and hypercalcemia. Moreover, in some cases, it is difficult to completely exclude drug-induced and biliary AP from the etiology of AP. These details may be informative for designing future clinical studies.

Several unsolved questions remain, such as the risk factors of AP in patients with COVID-19. It is also uncertain why some patients with COVID-19-attributed AP become severe while others do not. AP may be a rare complication of COVID-19, but some cases develop severe AP attributed to SARS-CoV-2 infection. Thus, the potential of COVID-19-attributed AP should be thoroughly investigated.

ACKNOWLEDGEMENTS

We thank our colleagues in the Division of Gastroenterology and Nephrology, Department of Multidisciplinary Internal Medicine, Faculty of Medicine, Tottori University (Tottori, Japan) for their support.

FOOTNOTES

Author contributions: Isomoto H and Onoyama T conceptualized and designed the review; all authors contributed to the conception and design of the study; Onoyama T, Koda H, Hamamoto W, Kawahara S, Sakamoto Y, Yamashita T, Kurumi H, Kawata S, Takeda Y, and Matsumoto K performed material preparation, data collection, and analysis; Onoyama T drafted the initial manuscript; all authors reviewed and approved the final manuscript as submitted.

Conflict-of-interest statement: The authors declare that they have no conflict of interest associated with the study.

Open-Access: This article is an open-access article that was selected by an in-house editor and fully peer-reviewed by external reviewers. It is distributed in accordance with the Creative Commons Attribution NonCommercial (CC BY-NC 4.0) license, which permits others to distribute, remix, adapt, build upon this work non-commercially, and license their derivative works on different terms, provided the original work is properly cited and the use is non-commercial. See: https://creativecommons.org/Licenses/by-nc/4.0/

Country/Territory of origin: Japan

ORCID number: Takumi Onoyama 0000-0003-0310-0720; Hiroki Koda 0000-0003-4000-6899; Wataru Hamamoto 0000-0003-2220-9916; Shiho Kawahara 0000-0001-8173-8207; Yuri Sakamoto 0000-0001-9682-6410; Taro Yamashita 0000-0003-2726-3356; Hiroki Kurumi 0000-0002-2372-1631; Soichiro Kawata 0000-0002-2194-0582; Yohei Takeda 0000-0003-1096-5909; Kazuya Matsumoto 0000-0002-5680-4791; Hajime Isomoto 0000-0001-8998-7865.

S-Editor: Fan JR
L-Editor: A
P-Editor: Fan JR

REFERENCES

1 **Guan WJ**, Ni ZY, Hu Y, Liang WH, Ou CQ, He JX, Liu L, Shan H, Lei CL, Hui DSC, Du B, Li LJ, Zeng G, Yuen KY, Chen RC, Tang CL, Wang T, Chen PY, Xiang J, Li SY, Wang JL, Liang ZJ, Peng YX, Wei L, Liu Y, Hu YH, Peng P, Wang JM, Liu JY, Chen Z, Li G, Zheng ZJ, Qiu SQ, Luo J, Ye CJ, Zhu SY, Zhong NS; China Medical Treatment Expert Group for Covid-19. Clinical Characteristics of Coronavirus Disease 2019 in China. *N Engl J Med* 2020; **382**: 1708-1720 [PMID: 32109013 DOI: 10.1056/NEJMoa2002032]

2 **Huang C**, Wang Y, Li X, Ren L, Zhao J, Hu Y, Zhang L, Fan G, Xu J, Gu X, Cheng Z, Yu T, Xia J, Wei Y, Wu W, Xie X, Yin W, Li H, Liu M, Xiao Y, Gao H, Guo L, Xie J, Wang G, Jiang R, Gao Z, Jin Q, Wang J, Cao B. Clinical features of patients infected with 2019 novel coronavirus in Wuhan, China. *Lancet* 2020; **395**: 497-506 [PMID: 31986264 DOI: 10.1016/S0140-6736(20)30183-5]

3 **Cheung KS**, Hung IFN, Chan PPY, Lung KC, Tso E, Liu R, Ng YY, Chu MY, Chung TWH, Tam AR, Yip CCY, Leung KH, Fung AY, Zhang RR, Lin Y, Cheng HM, Zhang AJX, To KKW, Chan KH, Yuen KY, Leung WK. Gastrointestinal Manifestations of SARS-CoV-2 Infection and Virus Load in Fecal Samples From a Hong Kong Cohort: Systematic Review and Meta-analysis. *Gastroenterology* 2020; **159**: 81-95 [PMID: 32251668 DOI: 10.1053/j.gastro.2020.03.065]

4 **Rokkas T**. Gastrointestinal involvement in COVID-19: a systematic review and meta-analysis. *Ann Gastroenterol* 2020; **33**: 355-365 [PMID: 32624655 DOI: 10.20524/aog.2020.0506]

5 **Hoffmann M**, Kleine-Weber H, Schroeder S, Krüger N, Herrler T, Erichsen S, Schiergens TS, Herrler G, Wu NH, Nitsche A, Müller MA, Drosten C, Pöhlmann S. SARS-CoV-2 Cell Entry Depends on ACE2 and TMPRSS2 and Is Blocked by a Clinically Proven Protease Inhibitor. *Cell* 2020; **181**: 271-280.e8 [PMID: 32142651 DOI: 10.1016/j.cell.2020.02.052]

6 **Wan Y**, Shang J, Graham R, Baric RS, Li F. Receptor Recognition by the Novel Coronavirus from Wuhan: an Analysis Based on Decade-Long Structural Studies of SARS Coronavirus. *J Virol* 2020; **94** [PMID: 31996437 DOI: 10.1128/JVI.00127-20]

7 **Xiao F**, Tang M, Zheng X, Liu Y, Li X, Shan H. Evidence for Gastrointestinal Infection of SARS-CoV-2. *Gastroenterology* 2020; **158**: 1831-1833.e3 [PMID: 32142773 DOI: 10.1053/j.gastro.2020.02.055]

8 **Parasa S**, Desai M, Thoguluva Chandrasekar V, Patel HK, Kennedy KF, Roesch T, Spadaccini M, Colombo M, Gabbiadini R, Artifon ELA, Repici A, Sharma P. Prevalence of Gastrointestinal Symptoms and Fecal Viral Shedding in Patients With Coronavirus Disease 2019: A Systematic Review and Meta-analysis. *JAMA Netw Open* 2020; **3**: e2011335 [PMID: 32525549 DOI: 10.1001/jamanetworkopen.2020.11335]

9 **Yan R**, Zhang Y, Li Y, Xia L, Guo Y, Zhou Q. Structural basis for the recognition of SARS-CoV-2 by full-length human ACE2. *Science* 2020; **367**: 1444-1448 [PMID: 32132184 DOI: 10.1126/science.abb2762]

10 **Wang F**, Wang H, Fan J, Zhang Y, Zhao Q. Pancreatic Injury Patterns in Patients With Coronavirus Disease 19 Pneumonia. *Gastroenterology* 2020; **159**: 367-370 [PMID: 32247022 DOI: 10.1053/j.gastro.2020.03.055]

11 **Bruno G**, Fabrizio C, Santoro CR, Buccoliero GB. Pancreatic injury in the course of coronavirus disease 2019: A not-so-rare occurrence. *J Med Virol* 2021; **93**: 74-75 [PMID: 32497298 DOI: 10.1002/jmv.26134]

12 **Schepis T**, Larghi A, Papa A, Miele L, Panzuto F, De Biase L, Annibale B, Cattani P, Rapaccini GL. SARS-CoV2 RNA detection in a pancreatic pseudocyst sample. *Pancreatology* 2020; **20**: 1011-1012 [PMID: 32498972 DOI: 10.1016/j.pan.2020.05.016]

13 **Liu F**, Long X, Zhang B, Zhang W, Chen X, Zhang Z. ACE2 Expression in Pancreas May Cause Pancreatic Damage After SARS-CoV-2 Infection. *Clin Gastroenterol Hepatol* 2020; **18**: 2128-2130.e2 [PMID: 32334082 DOI: 10.1016/j.cgh.2020.04.040]

14 **Müller JA**, Groß R, Conzelmann C, Krüger J, Merle U, Steinhart J, Weil T, Koepke L, Bozzo CP, Read C, Fois G, Eiseler T, Gehrmann J, van Vuuren J, Wessbecher IM, Frick M, Costa IG, Breunig M, Grüner B, Peters L, Schuster M, Liebau S, Seufferlein T, Stenger S, Stenzinger A, MacDonald PE, Kirchhoff F, Sparrer KMJ, Walther P, Lickert H, Barth TFE, Wagner M, Münch J, Heller S, Kleger A. SARS-CoV-2 infects and replicates in cells of the human endocrine and exocrine pancreas. *Nat Metab* 2021; **3**: 149-165 [PMID: 33536639 DOI: 10.1038/s42255-021-00347-1]

15 **Samanta J**, Gupta R, Singh MP, Patnaik I, Kumar A, Kochhar R. Coronavirus disease 2019 and the pancreas. *Pancreatology* 2020; **20**: 1567-1575 [PMID: 33250089 DOI: 10.1016/j.pan.2020.10.035]

16 **Pribadi RR**, Simadibrata M. Increased serum amylase and/or lipase in coronavirus disease 2019 (COVID-19) patients: Is it really pancreatic injury? *JGH Open* 2021; **5**: 190-192 [PMID: 33553654 DOI: 10.1002/jgh3.12436]

17 **Banks PA**, Bollen TL, Dervenis C, Gooszen HG, Johnson CD, Sarr MG, Tsiotos GG, Vege SS; Acute Pancreatitis Classification Working Group. Classification of acute pancreatitis--2012: revision of the Atlanta classification and definitions by international consensus. *Gut* 2013; **62**: 102-111 [PMID: 23100216 DOI: 10.1136/gutjnl-2012-302779]

18 **Boxhoorn L**, Voermans RP, Bouwense SA, Bruno MJ, Verdonk RC, Boermeester MA, van Santvoort HC, Besselink MG. Acute pancreatitis. *Lancet* 2020; **396**: 726-734 [PMID: 32891214 DOI: 10.1016/S0140-6736(20)31310-6]

19 **Forsmark CE**, Vege SS, Wilcox CM. Acute Pancreatitis. *N Engl J Med* 2016; **375**: 1972-1981 [PMID: 27959604 DOI: 10.1056/NEJMra1505202]

20 **Tenner S**, Baillie J, DeWitt J, Vege SS; American College of Gastroenterology. American College of Gastroenterology guideline: management of acute pancreatitis. *Am J Gastroenterol* 2013; **108**: 1400-15; 1416 [PMID: 23896955 DOI: 10.1038/ajg.2013.218]

21 **Lucidi V**, Alghisi F, Dall'Oglio L, D'Apice MR, Monti L, De Angelis P, Gambardella S, Angioni A, Novelli G. The etiology of acute recurrent pancreatitis in children: a challenge for pediatricians. *Pancreas* 2011; **40**: 517-521 [PMID: 21499205 DOI: 10.1097/MPA.0b013e318214fe42]

22 **Vue PM**, McFann K, Narkewicz MR. Genetic Mutations in Pediatric Pancreatitis. *Pancreas* 2016; **45**: 992-996 [PMID: 26692446 DOI: 10.1097/MPA.0000000000000589]

23 **Sakorafas GH**, Tsiotos GG, Sarr MG. Ischemia/Reperfusion-Induced pancreatitis. *Dig Surg* 2000; **17**: 3-14 [PMID: 10720825 DOI: 10.1159/000018793]

24 **Imam Z**, Simons-Linares CR, Chahal P. Infectious causes of acute pancreatitis: A systematic review. *Pancreatology*

2020; **20**: 1312-1322 [PMID: 32938554 DOI: 10.1016/j.pan.2020.08.018]
25 **Rawla P**, Bandaru SS, Vellipuram AR. Review of Infectious Etiology of Acute Pancreatitis. *Gastroenterology Res* 2017; **10**: 153-158 [PMID: 28725301 DOI: 10.14740/gr858w]
26 **Simons-Linares CR**, Imam Z, Chahal P. Viral-Attributed Acute Pancreatitis: A Systematic Review. *Dig Dis Sci* 2021; **66**: 2162-2172 [PMID: 32789532 DOI: 10.1007/s10620-020-06531-9]
27 **Dong M**, Zhang J, Ma X, Tan J, Chen L, Liu S, Xin Y, Zhuang L. ACE2, TMPRSS2 distribution and extrapulmonary organ injury in patients with COVID-19. *Biomed Pharmacother* 2020; **131**: 110678 [PMID: 32861070 DOI: 10.1016/j.biopha.2020.110678]
28 **Bourgonje AR**, Abdulle AE, Timens W, Hillebrands JL, Navis GJ, Gordijn SJ, Bolling MC, Dijkstra G, Voors AA, Osterhaus AD, van der Voort PH, Mulder DJ, van Goor H. Angiotensin-converting enzyme 2 (ACE2), SARS-CoV-2 and the pathophysiology of coronavirus disease 2019 (COVID-19). *J Pathol* 2020; **251**: 228-248 [PMID: 32418199 DOI: 10.1002/path.5471]
29 **Kerslake R**, Hall M, Randeva HS, Spandidos DA, Chatha K, Kyrou I, Karteris E. Coexpression of peripheral olfactory receptors with SARSCoV2 infection mediators: Potential implications beyond loss of smell as a COVID19 symptom. *Int J Mol Med* 2020; **46**: 949-956 [PMID: 32705281 DOI: 10.3892/ijmm.2020.4646]
30 **Coate KC**, Cha J, Shrestha S, Wang W, Gonçalves LM, Almaça J, Kapp ME, Fasolino M, Morgan A, Dai C, Saunders DC, Bottino R, Aramandla R, Jenkins R, Stein R, Kaestner KH, Vahedi G; HPAP Consortium, Brissova M, Powers AC. SARS-CoV-2 Cell Entry Factors ACE2 and TMPRSS2 Are Expressed in the Microvasculature and Ducts of Human Pancreas but Are Not Enriched in β Cells. *Cell Metab* 2020; **32**: 1028-1040.e4 [PMID: 33207245 DOI: 10.1016/j.cmet.2020.11.006]
31 **Yang L**, Han Y, Nilsson-Payant BE, Gupta V, Wang P, Duan X, Tang X, Zhu J, Zhao Z, Jaffré F, Zhang T, Kim TW, Harschnitz O, Redmond D, Houghton S, Liu C, Naji A, Ciceri G, Guttikonda S, Bram Y, Nguyen DT, Cioffi M, Chandar V, Hoagland DA, Huang Y, Xiang J, Wang H, Lyden D, Borczuk A, Chen HJ, Studer L, Pan FC, Ho DD, tenOever BR, Evans T, Schwartz RE, Chen S. A Human Pluripotent Stem Cell-based Platform to Study SARS-CoV-2 Tropism and Model Virus Infection in Human Cells and Organoids. *Cell Stem Cell* 2020; **27**: 125-136.e7 [PMID: 32579880 DOI: 10.1016/j.stem.2020.06.015]
32 **Shaharuddin SH**, Wang V, Santos RS, Gross A, Wang Y, Jawanda H, Zhang Y, Hasan W, Garcia G Jr, Arumugaswami V, Sareen D. Deleterious Effects of SARS-CoV-2 Infection on Human Pancreatic Cells. *Front Cell Infect Microbiol* 2021; **11**: 678482 [PMID: 34282405 DOI: 10.3389/fcimb.2021.678482]
33 **Kumar V**, Barkoudah E, Souza DAT, Jin DX, McNabb-Baltar J. Clinical course and outcome among patients with acute pancreatitis and COVID-19. *Eur J Gastroenterol Hepatol* 2021; **33**: 695-700 [PMID: 33787541 DOI: 10.1097/MEG.0000000000002160]
34 **Barlass U**, Wiliams B, Dhana K, Adnan D, Khan SR, Mahdavinia M, Bishehsari F. Marked Elevation of Lipase in COVID-19 Disease: A Cohort Study. *Clin Transl Gastroenterol* 2020; **11**: e00215 [PMID: 32764201 DOI: 10.14309/ctg.0000000000000215]
35 **McNabb-Baltar J**, Jin DX, Grover AS, Redd WD, Zhou JC, Hathorn KE, McCarty TR, Bazarbashi AN, Shen L, Chan WW. Lipase Elevation in Patients With COVID-19. *Am J Gastroenterol* 2020; **115**: 1286-1288 [PMID: 32496339 DOI: 10.14309/ajg.0000000000000732]
36 **Blanco-Melo D**, Nilsson-Payant BE, Liu WC, Uhl S, Hoagland D, Møller R, Jordan TX, Oishi K, Panis M, Sachs D, Wang TT, Schwartz RE, Lim JK, Albrecht RA, tenOever BR. Imbalanced Host Response to SARS-CoV-2 Drives Development of COVID-19. *Cell* 2020; **181**: 1036-1045.e9 [PMID: 32416070 DOI: 10.1016/j.cell.2020.04.026]
37 **Coperchini F**, Chiovato L, Croce L, Magri F, Rotondi M. The cytokine storm in COVID-19: An overview of the involvement of the chemokine/chemokine-receptor system. *Cytokine Growth Factor Rev* 2020; **53**: 25-32 [PMID: 32446778 DOI: 10.1016/j.cytogfr.2020.05.003]
38 **Watanabe T**, Kudo M, Strober W. Immunopathogenesis of pancreatitis. *Mucosal Immunol* 2017; **10**: 283-298 [PMID: 27848953 DOI: 10.1038/mi.2016.101]
39 **Ding L**, Yang Y, Li H, Wang H, Gao P. Circulating Lymphocyte Subsets Induce Secondary Infection in Acute Pancreatitis. *Front Cell Infect Microbiol* 2020; **10**: 128 [PMID: 32296650 DOI: 10.3389/fcimb.2020.00128]
40 **Chen G**, Wu D, Guo W, Cao Y, Huang D, Wang H, Wang T, Zhang X, Chen H, Yu H, Zhang M, Wu S, Song J, Chen T, Han M, Li S, Luo X, Zhao J, Ning Q. Clinical and immunological features of severe and moderate coronavirus disease 2019. *J Clin Invest* 2020; **130**: 2620-2629 [PMID: 32217835 DOI: 10.1172/JCI137244]
41 **Ramsey ML**, Elmunzer BJ, Krishna SG. Serum Lipase Elevations in COVID-19 Patients Reflect Critical Illness and not Acute Pancreatitis. *Clin Gastroenterol Hepatol* 2021; **19**: 1982-1987 [PMID: 33882344 DOI: 10.1016/j.cgh.2021.04.019]
42 **Li G**, Liu T, Jin G, Li T, Liang J, Chen Q, Chen L, Wang W, Wang Y, Song J, Liang H, Zhang C, Zhu P, Zhang W, Ding Z, Chen X, Zhang B. Multidisciplinary T. Serum amylase elevation is associated with adverse clinical outcomes in patients with coronavirus disease 2019. [cited 10 December 2021]. Available from: http://www.aging-us.com
43 **Ahmed A**, Fisher JC, Pochapin MB, Freedman SD, Kothari DJ, Shah PC, Sheth SG. Hyperlipasemia in absence of acute pancreatitis is associated with elevated D-dimer and adverse outcomes in COVID 19 disease. *Pancreatology* 2021; **21**: 698-703 [PMID: 33741267 DOI: 10.1016/j.pan.2021.02.021]
44 **Troncone E**, Salvatori S, Sena G, De Cristofaro E, Alfieri N, Marafini I, Paganelli C, Argirò R, Giannarelli D, Monteleone G, Del Vecchio Blanco G. Low Frequency of Acute Pancreatitis in Hospitalized COVID-19 Patients. *Pancreas* 2021; **50**: 393-398 [PMID: 33835971 DOI: 10.1097/MPA.0000000000001770]
45 **Akarsu C**, Karabulut M, Aydin H, Sahbaz NA, Dural AC, Yegul D, Peker KD, Ferahman S, Bulut S, Dönmez T, Asar S, Yasar KK, Adas GT. Association between Acute Pancreatitis and COVID-19: Could Pancreatitis Be the Missing Piece of the Puzzle about Increased Mortality Rates? *J Invest Surg* 2022; **35**: 119-125 [PMID: 33138658 DOI: 10.1080/08941939.2020.1833263]
46 **El-Kurdi B**, Khatua B, Rood C, Snozek C, Cartin-Ceba R, Singh VP; Lipotoxicity in COVID-19 Study Group. Mortality From Coronavirus Disease 2019 Increases With Unsaturated Fat and May Be Reduced by Early Calcium and Albumin Supplementation. *Gastroenterology* 2020; **159**: 1015-1018.e4 [PMID: 32470338 DOI: 10.1053/j.gastro.2020.05.057]

47 **Hegyi P**, Szakács Z, Sahin-Tóth M. Lipotoxicity and Cytokine Storm in Severe Acute Pancreatitis and COVID-19. *Gastroenterology* 2020; **159**: 824-827 [PMID: 32682765 DOI: 10.1053/j.gastro.2020.07.014]

48 **Muniraj T**, Dang S, Pitchumoni CS. PANCREATITIS OR NOT? *J Crit Care* 2015; **30**: 1370-1375 [PMID: 26411523 DOI: 10.1016/j.jcrc.2015.08.020]

49 **Meczker Á**, Hanák L, Párniczky A, Szentesi A, Erőss B, Hegyi P; Hungarian Pancreatic Study Group. Analysis of 1060 Cases of Drug-Induced Acute Pancreatitis. *Gastroenterology* 2020; **159**: 1958-1961.e8 [PMID: 32687926 DOI: 10.1053/j.gastro.2020.07.016]

50 **Salama C**, Han J, Yau L, Reiss WG, Kramer B, Neidhart JD, Criner GJ, Kaplan-Lewis E, Baden R, Pandit L, Cameron ML, Garcia-Diaz J, Chávez V, Mekebeb-Reuter M, Lima de Menezes F, Shah R, González-Lara MF, Assman B, Freedman J, Mohan SV. Tocilizumab in Patients Hospitalized with Covid-19 Pneumonia. *N Engl J Med* 2021; **384**: 20-30 [PMID: 33332779 DOI: 10.1056/NEJMoa2030340]

51 **Flaig T**, Douros A, Bronder E, Klimpel A, Kreutz R, Garbe E. Tocilizumab-induced pancreatitis: case report and review of data from the FDA Adverse Event Reporting System. *J Clin Pharm Ther* 2016; **41**: 718-721 [PMID: 27670839 DOI: 10.1111/jcpt.12456]

52 **Riphagen S**, Gomez X, Gonzalez-Martinez C, Wilkinson N, Theocharis P. Hyperinflammatory shock in children during COVID-19 pandemic. *Lancet* 2020; **395**: 1607-1608 [PMID: 32386565 DOI: 10.1016/S0140-6736(20)31094-1]

53 **DeBiasi RL**, Song X, Delaney M, Bell M, Smith K, Pershad J, Ansusinha E, Hahn A, Hamdy R, Harik N, Hanisch B, Jantausch B, Koay A, Steinhorn R, Newman K, Wessel D. Severe Coronavirus Disease-2019 in Children and Young Adults in the Washington, DC, Metropolitan Region. *J Pediatr* 2020; **223**: 199-203.e1 [PMID: 32405091 DOI: 10.1016/j.jpeds.2020.05.007]

54 **Whittaker E**, Bamford A, Kenny J, Kaforou M, Jones CE, Shah P, Ramnarayan P, Fraisse A, Miller O, Davies P, Kucera F, Brierley J, McDougall M, Carter M, Tremoulet A, Shimizu C, Herberg J, Burns JC, Lyall H, Levin M; PIMS-TS Study Group and EUCLIDS and PERFORM Consortia. Clinical Characteristics of 58 Children With a Pediatric Inflammatory Multisystem Syndrome Temporally Associated With SARS-CoV-2. *JAMA* 2020; **324**: 259-269 [PMID: 32511692 DOI: 10.1001/jama.2020.10369]

55 **Stevens JP**, Brownell JN, Freeman AJ, Bashaw H. COVID-19-associated Multisystem Inflammatory Syndrome in Children Presenting as Acute Pancreatitis. *J Pediatr Gastroenterol Nutr* 2020; **71**: 669-671 [PMID: 33093376 DOI: 10.1097/MPG.0000000000002860]

56 **Suchman K**, Raphael KL, Liu Y, Wee D, Trindade AJ; Northwell COVID-19 Research Consortium. Acute pancreatitis in children hospitalized with COVID-19. *Pancreatology* 2021; **21**: 31-33 [PMID: 33309015 DOI: 10.1016/j.pan.2020.12.005]

57 **Abbas M**, Törnhage CJ. Family Transmission of COVID-19 Including a Child with MIS-C and Acute Pancreatitis. *Int Med Case Rep J* 2021; **14**: 55-65 [PMID: 33574714 DOI: 10.2147/IMCRJ.S284480]

58 **Kareva L**, Stavrik K, Mironska K, Hasani A, Bojadzieva S, Shuntov NC. A Case of Multisystem Inflammatory Syndrome in Children Presenting as Acute Appendicitis and Pancreatitis. *Pril (Makedon Akad Nauk Umet Odd Med Nauki)* 2021; **42**: 95-101 [PMID: 34699709 DOI: 10.2478/prilozi-2021-0027]

59 **Bulthuis MC**, Boxhoorn L, Beudel M, Elbers PWG, Kop MPM, van Wanrooij RLJ, Besselink MG, Voermans RP. Acute pancreatitis in COVID-19 patients: true risk? *Scand J Gastroenterol* 2021; **56**: 585-587 [PMID: 33715577 DOI: 10.1080/00365521.2021.1896776]

60 **Vatansev H**, Yıldırım MA, Kuccukturk S, Karaselek MA, Kadiyoran C. Clinical Evaluation of Acute Pancreatitis Caused by SARS-CoV-2 Virus Infection. *Gastroenterol Res Pract* 2021; **2021**: 5579795 [PMID: 34035804 DOI: 10.1155/2021/5579795]

61 **Pandanaboyana S**, Moir J, Leeds JS, Oppong K, Kanwar A, Marzouk A, Belgaumkar A, Gupta A, Siriwardena AK, Haque AR, Awan A, Balakrishnan A, Rawashdeh A, Ivanov B, Parmar C, M Halloran C, Caruana C, Borg CM, Gomez D, Damaskos D, Karavias D, Finch G, Ebied H, K Pine J, R A Skipworth J, Milburn J, Latif J, Ratnam Apollos J, El Kafsi J, Windsor JA, Roberts K, Wang K, Ravi K, V Coats M, Hollyman M, Phillips M, Okocha M, Sj Wilson M, A Ameer N, Kumar N, Shah N, Lapolla P, Magee C, Al-Sarireh B, Lunevicius R, Benhmida R, Singhal R, Balachandra S, Demirli Atıcı S, Jaunoo S, Dwerryhouse S, Boyce T, Charalampakis V, Kanakala V, Abbas Z, Nayar M; COVID PAN collaborative group. SARS-CoV-2 infection in acute pancreatitis increases disease severity and 30-day mortality: COVID PAN collaborative study. *Gut* 2021; **70**: 1061-1069 [PMID: 33547182 DOI: 10.1136/gutjnl-2020-323364]

62 **Dirweesh A**, Li Y, Trikudanathan G, Mallery JS, Freeman ML, Amateau SK. Clinical Outcomes of Acute Pancreatitis in Patients With Coronavirus Disease 2019. *Gastroenterology* 2020; **159**: 1972-1974 [PMID: 32721439 DOI: 10.1053/j.gastro.2020.07.038]

63 **Inamdar S**, Benias PC, Liu Y, Sejpal DV, Satapathy SK, Trindade AJ; Northwell COVID-19 Research Consortium. Prevalence, Risk Factors, and Outcomes of Hospitalized Patients With Coronavirus Disease 2019 Presenting as Acute Pancreatitis. *Gastroenterology* 2020; **159**: 2226-2228.e2 [PMID: 32860787 DOI: 10.1053/j.gastro.2020.08.044]

64 **Karaali R**, Topal F. Evaluating the effect of SARS-Cov-2 infection on prognosis and mortality in patients with acute pancreatitis. *Am J Emerg Med* 2021; **49**: 378-384 [PMID: 34246968 DOI: 10.1016/j.ajem.2021.06.045]

65 **Nayar M**, Varghese C, Kanwar A, Siriwardena AK, Haque AR, Awan A, Balakrishnan A, Rawashdeh A, Ivanov B, Parmar C, Halloran CM, Caruana C, Borg CM, Gomez D, Damaskos D, Karavias D, Finch G, Ebied H, Pine JK, Skipworth JRA, Milburn J, Latif J, Apollos J, El Kafsi J, Windsor JA, Roberts K, Wang K, Ravi K, Coats MV, Hollyman M, Phillips M, Okocha M, Wilson MS, Ameer NA, Kumar N, Shah N, Lapolla P, Magee C, Al-Sarireh B, Lunevicius R, Benhmida R, Singhal R, Balachandra S, Demirli Atıcı S, Jaunoo S, Dwerryhouse S, Boyce T, Charalampakis V, Kanakala V, Abbas Z, Tewari N, Pandanaboyana S; COVIDPAN Collborative Group; COVID Pain Collborative Group. SARS-CoV-2 infection is associated with an increased risk of idiopathic acute pancreatitis but not pancreatic exocrine insufficiency or diabetes: long-term results of the COVIDPAN study. *Gut* 2021 [PMID: 34764192 DOI: 10.1136/gutjnl-2021-326218]

66 **Miró Ò**, Llorens P, Jiménez S, Piñera P, Burillo-Putze G, Martín A, Martín-Sánchez FJ, Lamberechts J, Alquézar-Arbé A, Jacob J, Noceda J, Cano Cano MJ, Fortuny Bayarri MJ, Marín Porrino JM, Meléndez N, Pérez García C, Brasó Aznar JV,

Ponce MC, Díaz Fernández E, Ejarque Martínez L, Peiró Gómez A, Tost J, Domínguez MJ, Teigell Muñoz FJ, González Del Castillo J; Spanish Investigators on Emergency Situations TeAm (SIESTA) network. A case-control emergency department-based analysis of acute pancreatitis in Covid-19: Results of the UMC-19-S_6. *J Hepatobiliary Pancreat Sci* 2021; **28**: 953-966 [PMID: 33259695 DOI: 10.1002/jhbp.873]

67 **Yang F**, Huang Y, Li T, Fu Y, Sun C, Xu Y, Windsor J, Fu D. Prevalence and outcomes of acute pancreatitis in COVID-19: a meta-analysis. *Gut* 2021 [PMID: 34670809 DOI: 10.1136/gutjnl-2021-325941]

68 **Slae M**, Wilschanski M, Sanjines E, Abu-El-Haija M, Sellers ZM. International Survey on Severe Acute Respiratory Syndrome Coronavirus 2 and Acute Pancreatitis Co-occurrence in Children. *Pancreas* 2021; **50**: 1305-1309 [PMID: 34860816 DOI: 10.1097/MPA.0000000000001923]

69 **Howes N**, Lerch MM, Greenhalf W, Stocken DD, Ellis I, Simon P, Truninger K, Ammann R, Cavallini G, Charnley RM, Uomo G, Delhaye M, Spicak J, Drumm B, Jansen J, Mountford R, Whitcomb DC, Neoptolemos JP; European Registry of Hereditary Pancreatitis and Pancreatic Cancer (EUROPAC). Clinical and genetic characteristics of hereditary pancreatitis in Europe. *Clin Gastroenterol Hepatol* 2004; **2**: 252-261 [PMID: 15017610 DOI: 10.1016/s1542-3565(04)00013-8]

70 **Anand ER**, Major C, Pickering O, Nelson M. Acute pancreatitis in a COVID-19 patient. *Br J Surg* 2020; **107**: e182 [PMID: 32339257 DOI: 10.1002/bjs.11657]

71 **Hadi A**, Werge M, Kristiansen KT, Pedersen UG, Karstensen JG, Novovic S, Gluud LL. Coronavirus Disease-19 (COVID-19) associated with severe acute pancreatitis: Case report on three family members. *Pancreatology* 2020; **20**: 665-667 [PMID: 32387082 DOI: 10.1016/j.pan.2020.04.021]

72 **Aloysius MM**, Thatti A, Gupta A, Sharma N, Bansal P, Goyal H. COVID-19 presenting as acute pancreatitis. *Pancreatology* 2020; **20**: 1026-1027 [PMID: 32444169 DOI: 10.1016/j.pan.2020.05.003]

73 **Miao Y**, Lidove O, Mauhin W. First case of acute pancreatitis related to SARS-CoV-2 infection. *Br J Surg* 2020; **107**: e270 [PMID: 32492174 DOI: 10.1002/bjs.11741]

74 **Szatmary P**, Arora A, Thomas Raraty MG, Joseph Dunne DF, Baron RD, Halloran CM. Emerging Phenotype of Severe Acute Respiratory Syndrome-Coronavirus 2-associated Pancreatitis. *Gastroenterology* 2020; **159**: 1551-1554 [PMID: 32497545 DOI: 10.1053/j.gastro.2020.05.069]

75 **Rabice SR**, Altshuler PC, Bovet C, Sullivan C, Gagnon AJ. COVID-19 infection presenting as pancreatitis in a pregnant woman: A case report. *Case Rep Womens Health* 2020; **27**: e00228 [PMID: 32537425 DOI: 10.1016/j.crwh.2020.e00228]

76 **Alloway BC**, Yaeger SK, Mazzaccaro RJ, Villalobos T, Hardy SG. Suspected case of COVID-19-associated pancreatitis in a child. *Radiol Case Rep* 2020; **15**: 1309-1312 [PMID: 32572339 DOI: 10.1016/j.radcr.2020.06.009]

77 **Karimzadeh S**, Manzuri A, Ebrahimi M, Huy NT. COVID-19 presenting as acute pancreatitis: Lessons from a patient in Iran. *Pancreatology* 2020; **20**: 1024-1025 [PMID: 32576441 DOI: 10.1016/j.pan.2020.06.003]

78 **Gonzalo-Voltas A**, Uxia Fernández-Pérez-Torres C, Baena-Díez JM. Acute pancreatitis in a patient with COVID-19 infection. *Med Clin (Engl Ed)* 2020; **155**: 183-184 [PMID: 32835111 DOI: 10.1016/j.medcle.2020.05.010]

79 **Bokhari SMMA**, Mahmood F. Case Report: Novel Coronavirus-A Potential Cause of Acute Pancreatitis? *Am J Trop Med Hyg* 2020; **103**: 1154-1155 [PMID: 32662399 DOI: 10.4269/ajtmh.20-0568]

80 **Mazrouei SSA**, Saeed GA, Al Helali AA. COVID-19-associated acute pancreatitis: a rare cause of acute abdomen. *Radiol Case Rep* 2020; **15**: 1601-1603 [PMID: 32685078 DOI: 10.1016/j.radcr.2020.06.019]

81 **Ahmed AOE**, Mohamed SF, Saleh AO, Al-Shokri SD, Ahmed K, Mohamed MFH. Acute abdomen -like-presentation associated with SARS-CoV-2 infection. *IDCases* 2020; **21**: e00895 [PMID: 32691004 DOI: 10.1016/j.idcr.2020.e00895]

82 **Brikman S**, Denysova V, Menzal H, Dori G. Acute pancreatitis in a 61-year-old man with COVID-19. *CMAJ* 2020; **192**: E858-E859 [PMID: 32719021 DOI: 10.1503/cmaj.201029]

83 **Kataria S**, Sharif A, Ur Rehman A, Ahmed Z, Hanan A. COVID-19 Induced Acute Pancreatitis: A Case Report and Literature Review. *Cureus* 2020; **12**: e9169 [PMID: 32802606 DOI: 10.7759/cureus.9169]

84 **Cerda-Contreras C**, Nuzzolo-Shihadeh L, Camacho-Ortiz A, Perez-Alba E. Baricitinib as Treatment for Coronavirus Disease 2019 (COVID-19): Friend or Foe of the Pancreas? *Clin Infect Dis* 2021; **73**: e3977-e3978 [PMID: 32797239 DOI: 10.1093/cid/ciaa1209]

85 **Cheung S**, Delgado Fuentes A, Fetterman AD. Recurrent Acute Pancreatitis in a Patient with COVID-19 Infection. *Am J Case Rep* 2020; **21**: e927076 [PMID: 32833954 DOI: 10.12659/AJCR.927076]

86 **Kumaran NK**, Karmakar BK, Taylor OM. Coronavirus disease-19 (COVID-19) associated with acute necrotising pancreatitis (ANP). *BMJ Case Rep* 2020; **13** [PMID: 32900752 DOI: 10.1136/bcr-2020-237903]

87 **Purayil N**, Sirajudeen J, Va N, Mathew J. COVID-19 Presenting as Acute Abdominal Pain: A Case Report. *Cureus* 2020; **12**: e9659 [PMID: 32923256 DOI: 10.7759/cureus.9659]

88 **Dietrich CG**, Hübner D, Marx G, Bickenbach J, Bootsveld A. Primary presentation of COVID-19 solely with gastrointestinal symptoms: a problem for the containment of the disease. *Eur J Gastroenterol Hepatol* 2020; **32**: 1475-1478 [PMID: 32925503 DOI: 10.1097/MEG.0000000000001922]

89 **Patnaik RNK**, Gogia A, Kakar A. Acute pancreatic injury induced by COVID-19. *IDCases* 2020; **22**: e00959 [PMID: 32934906 DOI: 10.1016/j.idcr.2020.e00959]

90 **Wang K**, Luo J, Tan F, Liu J, Ni Z, Liu D, Tian P, Li W. Acute Pancreatitis as the Initial Manifestation in 2 Cases of COVID-19 in Wuhan, China. *Open Forum Infect Dis* 2020; **7**: ofaa324 [PMID: 32959016 DOI: 10.1093/ofid/ofaa324]

91 **Alves AM**, Yvamoto EY, Marzinotto MAN, Teixeira ACS, Carrilho FJ. SARS-CoV-2 leading to acute pancreatitis: an unusual presentation. *Braz J Infect Dis* 2020; **24**: 561-564 [PMID: 32961108 DOI: 10.1016/j.bjid.2020.08.011]

92 **Kurihara Y**, Maruhashi T, Wada T, Osada M, Oi M, Yamaoka K, Asari Y. Pancreatitis in a Patient with Severe Coronavirus Disease Pneumonia Treated with Veno-venous Extracorporeal Membrane Oxygenation. *Intern Med* 2020; **59**: 2903-2906 [PMID: 32963170 DOI: 10.2169/internalmedicine.5912-20]

93 **Lakshmanan S**, Malik A. Acute Pancreatitis in Mild COVID-19 Infection. *Cureus* 2020; **12**: e9886 [PMID: 32968552 DOI: 10.7759/cureus.9886]

94 **Samies NL**, Yarbrough A, Boppana S. Pancreatitis in Pediatric Patients With COVID-19. *J Pediatric Infect Dis Soc* 2021; **10**: 57-59 [PMID: 33075134 DOI: 10.1093/jpids/piaa125]

95 **Fernandes DA**, Yumioka AS, Filho HRM. SARS-CoV-2 and acute pancreatitis: a new etiological agent? *Rev Esp Enferm Dig* 2020; **112**: 890 [PMID: 33054297 DOI: 10.17235/reed.2020.7481/2020]

96 **Shinohara T**, Otani A, Yamashita M, Wakimoto Y, Jubishi D, Okamoto K, Kanno Y, Ikeda M, Ishigaki K, Nakai Y, Harada S, Okugawa S, Koike K, Moriya K. Acute Pancreatitis During COVID-19 Pneumonia. *Pancreas* 2020; **49**: e106-e108 [PMID: 33122537 DOI: 10.1097/MPA.0000000000001695]

97 **Meyers MH**, Main MJ, Orr JK, Obstein KL. A Case of COVID-19-Induced Acute Pancreatitis. *Pancreas* 2020; **49**: e108-e109 [PMID: 33122538 DOI: 10.1097/MPA.0000000000001696]

98 **Ghosh A**, Gupta V, Misra A. COVID19 induced acute pancreatitis and pancreatic necrosis in a patient with type 2 diabetes. *Diabetes Metab Syndr* 2020; **14**: 2097-2098 [PMID: 33152555 DOI: 10.1016/j.dsx.2020.10.008]

99 **Tollard C**, Champenois V, Delemer B, Carsin-Vu A, Barraud S. An inaugural diabetic ketoacidosis with acute pancreatitis during COVID-19. *Acta Diabetol* 2021; **58**: 389-391 [PMID: 33184733 DOI: 10.1007/s00592-020-01624-3]

100 **Kandasamy S**. An unusual presentation of COVID-19: Acute pancreatitis. *Ann Hepatobiliary Pancreat Surg* 2020; **24**: 539-541 [PMID: 33234760 DOI: 10.14701/ahbps.2020.24.4.539]

101 **Hassani AH**, Beheshti A, Almasi F, Ketabi Moghaddam P, Azizi M, Shahrokh S. Unusual gastrointestinal manifestations of COVID-19: two case reports. *Gastroenterol Hepatol Bed Bench* 2020; **13**: 410-414 [PMID: 33244387 DOI: 10.22037/ghfbb.v13i4.2156]

102 **Narang K**, Szymanski LM, Kane SV, Rose CH. Acute Pancreatitis in a Pregnant Patient With Coronavirus Disease 2019 (COVID-19). *Obstet Gynecol* 2021; **137**: 431-433 [PMID: 33355431 DOI: 10.1097/AOG.0000000000004287]

103 **Acherjya GK**, Rahman MM, Islam MT, Alam AS, Tarafder K, Ali M, Deb SR. Acute pancreatitis in a COVID-19 patient: An unusual presentation. *Clin Case Rep* 2020; **8**: 3400-3407 [PMID: 33363941 DOI: 10.1002/ccr3.3412]

104 **Alwaeli H**, Shabbir M, Khamissi Sobi M, Alwaeli K. A Case of Severe Acute Pancreatitis Secondary to COVID-19 Infection in a 30-Year-Old Male Patient. *Cureus* 2020; **12**: e11718 [PMID: 33391949 DOI: 10.7759/cureus.11718]

105 **Simou EM**, Louardi M, Khaoury I, Abidi MA, Mansour A, Louadghiri AE, Fahmaoui K, Ezzouine H, Charra B. Coronavirus disease-19 (COVID-19) associated with acute pancreatitis: case report. *Pan Afr Med J* 2020; **37**: 150 [PMID: 33425183 DOI: 10.11604/pamj.2020.37.150.25873]

106 **Jespersen Nizamic T**, Huang Y, Alnimri M, Cheng M, Chen LX, Jen KY. COVID-19 Manifesting as Renal Allograft Dysfunction, Acute Pancreatitis, and Thrombotic Microangiopathy: A Case Report. *Transplant Proc* 2021; **53**: 1211-1214 [PMID: 33436168 DOI: 10.1016/j.transproceed.2020.10.048]

107 **Abraham G**, Rohit A, Mathew M, Parthasarathy R. Successful Automated Peritoneal Dialysis (APD) in a COVID-19 patient with acalculous pancreatitis with no detectable virus in the dialysate effluent. *Indian J Med Microbiol* 2021; **39**: 128-129 [PMID: 33610245 DOI: 10.1016/j.ijmmb.2020.10.010]

108 **Abhinay A**, Pradhap K, Singh A, Rao SK, Prasad R, Mishra OP. Corona Virus Disease-19 Presented with Acute Pancreatitis. *Indian J Pediatr* 2021; **88**: 482-483 [PMID: 33447927 DOI: 10.1007/s12098-020-03618-z]

109 **Bouali M**, Ouchane M, Elbakouri A, Bensardi F, Elhattabi K, Fadil A. Total gastric necrosis following acute pancreatitis in a patient with COVID -19: Case report and literature review. *Ann Med Surg (Lond)* 2021; **62**: 362-364 [PMID: 33520227 DOI: 10.1016/j.amsu.2021.01.061]

110 **AlHarmi RAR**, Fateel T, Sayed Adnan J, AlAwadhi K. Acute pancreatitis in a patient with COVID-19. *BMJ Case Rep* 2021; **14** [PMID: 33574045 DOI: 10.1136/bcr-2020-239656]

111 **Bineshfar N**, Mirahmadi A, Karbasian F, Pourbakhtyaran E, Karimi A, Sarafi M. Acute Pancreatitis as a Possible Unusual Manifestation of COVID-19 in Children. *Case Rep Pediatr* 2021; **2021**: 6616211 [PMID: 33575053 DOI: 10.1155/2021/6616211]

112 **Paz L**, Eslava E, Ribes M, Mayer EF. Acute Pancreatitis in a Teenager With SARS-CoV-2 Infection. *Pediatr Infect Dis J* 2021; **40**: e161-e162 [PMID: 33710983 DOI: 10.1097/INF.0000000000003046]

113 **Wifi MN**, Nabil A, Awad A, Eltatawy R. COVID-induced pancreatitis: case report. *Egypt J Intern Med* 2021; **33**: 10 [PMID: 33716498 DOI: 10.1186/s43162-021-00039-y]

114 **Sandhu H**, Mallik D, Lokavarapu MJ, Huda F, Basu S. Acute Recurrent Pancreatitis and COVID-19 Infection: A Case Report with Literature Review. *Cureus* 2021; **13**: e13490 [PMID: 33777577 DOI: 10.7759/cureus.13490]

115 **Mohammadi Arbati M**, Molseghi MH. COVID-19 Presenting as Acute Necrotizing Pancreatitis. *J Investig Med High Impact Case Rep* 2021; **9**: 23247096211009393 [PMID: 33847153 DOI: 10.1177/23247096211009393]

116 **Amé RM**, Balderramo D. Is necessary to rule out Severe Acute Respiratory Syndrome Coronavirus 2 infection in every patient admitted for acute pancreatitis? *Gastroenterol Hepatol* 2021 [PMID: 34023480 DOI: 10.1016/j.gastrohep.2021.02.021]

117 **Gupta A**, Bansal DP, Rijhwani P, Singh V. A Case Report on Acute Pancreatitis in a Patient With Coronavirus Disease 2019 (COVID-19) Pneumonia. *Cureus* 2021; **13**: e14628 [PMID: 34046267 DOI: 10.7759/cureus.14628]

118 **Muhammad Abrar Jeelani H**, Sheikh MM, Samuel SS, Omotosho YB, Sharko A, Albetar R. Acute Pancreatitis in a Patient With COVID-19 After the Resolution of Respiratory Symptoms. *J Investig Med High Impact Case Rep* 2021; **9**: 23247096211024773 [PMID: 34130536 DOI: 10.1177/23247096211024773]

119 **Maalouf RG**, Kozhaya K, El Zakhem A. SARS-CoV-2 induced necrotizing pancreatitis. *Med Clin (Barc)* 2021; **156**: 629-630 [PMID: 33618836 DOI: 10.1016/j.medcli.2021.01.005]

120 **Sanchez RE**, Flahive CB, Mezoff EA, Gariepy C, Hunt WG, Vaz KKH. Case Report: Acute Abdominal Pain as Presentation of Pneumonia and Acute Pancreatitis in a Pediatric Patient With COVID-19. *JPGN Rep* 2021; **2**: e011 [PMID: 34192290 DOI: 10.1097/PG9.0000000000000011]

121 **Ehsan P**, Haseeb M, Khan Z, Rehan A, Singh R. Coronavirus Disease 2019 Pneumonia and Acute Pancreatitis in a Young Girl. *Cureus* 2021; **13**: e15374 [PMID: 34249527 DOI: 10.7759/cureus.15374]

122 **Hanif M**, Khan AW, Ullah S, Sundas F, Khan SJ. Can COVID-19 Cause Pancreatitis? *J Coll Physicians Surg Pak* 2021; **31**: S120-S122 [PMID: 34271809 DOI: 10.29271/jcpsp.2021.Supp2.S120]

123 **Chandra R**, Lazar NJ, Goldman S, Imam Z, Mansour R. Novel Coronavirus (COVID-19) Infection-Attributed Acute Pancreatitis: A Case Report and Literature Review. *Cureus* 2021; **13**: e15725 [PMID: 34295577 DOI:

10.7759/cureus.15725]
124 **Alfishawy M**, Nassar M, Mohamed M, Fatthy M, Elmessiery RM. New-onset Type 1 Diabetes Mellitus with Diabetic Ketoacidosis and Pancreatitis in a Patient with COVID-19. *Sci Afr* 2021; **13**: e00915 [PMID: 34368517 DOI: 10.1016/j.sciaf.2021.e00915]
125 **Berrichi S**, Bouayed Z, Jebar K, Zaid I, Nasri S, Bkiyar H, Skiker I, Housni B. Acute pancreatitis as an atypical manifestation of COVID-19: A report of 2 cases. *Ann Med Surg (Lond)* 2021; **68**: 102693 [PMID: 34377453 DOI: 10.1016/j.amsu.2021.102693]
126 **Kripalani Y**, Houssein K, Shaikh A. Acute Necrotizing Pancreatitis with Cystic Lesion Concomitant with SARS-CoV-2. *Eur J Case Rep Intern Med* 2021; **8**: 002712 [PMID: 34377701 DOI: 10.12890/2021_002712]
127 **Narayan VSG**, Datley AY, Upadhyay R. Acute Pancreatitis in Severe COVID Pneumonia. *J Assoc Physicians India* 2021; **69**: 11-12 [PMID: 34431277]
128 **Eldaly AS**, Fath AR, Mashaly SM, Elhadi M. Acute pancreatitis associated with severe acute respiratory syndrome coronavirus-2 infection: a case report and review of the literature. *J Med Case Rep* 2021; **15**: 461 [PMID: 34503570 DOI: 10.1186/s13256-021-03026-7]
129 **Basukala S**, Shah KB, Karki B, Thapa N, Basukala B, Karki S, Pathak BD. Acute hemorrhagic necrotizing pancreatitis in patient with COVID-19: a case report and review of literature. *J Surg Case Rep* 2021; **2021**: rjab401 [PMID: 34567518 DOI: 10.1093/jscr/rjab401]
130 **Schembri Higgans J**, Bowman S, Abela JE. COVID-19 associated pancreatitis: A mini case-series. *Int J Surg Case Rep* 2021; **87**: 106429 [PMID: 34567954 DOI: 10.1016/j.ijscr.2021.106429]
131 **Kopiczko N**, Kwiatek-Średzińska K, Uścinowicz M, Kowalczuk-Krystoń M, Lebensztejn DM. SARS-CoV-2 Infection as a Cause of Acute Pancreatitis in a Child-A Case Report. *Pediatr Rep* 2021; **13**: 552-557 [PMID: 34698241 DOI: 10.3390/pediatric13040065]
132 **da Costa Ferreira CP**, Marques KR, de Mattos GHF, de Campos T. Acute pancreatitis in a COVID-19 patient in Brazil: a case report. *J Med Case Rep* 2021; **15**: 541 [PMID: 34702363 DOI: 10.1186/s13256-021-02911-5]
133 **Sánchez-Gollarte A**, Jiménez-Álvarez L, Pérez-González M, Vera-Mansilla C, Blázquez-Martín A, Díez-Alonso M. *Clostridium perfringens* necrotizing pancreatitis: an unusual pathogen in pancreatic necrosis infection. *Access Microbiol* 2021; **3**: 000261 [PMID: 34712906 DOI: 10.1099/acmi.0.000261]
134 **Sudarsanam H**, Ethiraj D, Govarthanan NK, Kalyanasundaram S, Chitra SA, Mohan S. COVID-19 Associated Acute Necrotizing Pancreatitis with Normal Serum Amylase and Lipase Levels: Report of an Unusual Finding. *Oman Med J* 2021; **36**: e304 [PMID: 34733550 DOI: 10.5001/omj.2021.129]
135 **Faghih Dinevari M**, Rasoolimanesh M, Tarverdizadeh M, Riazi A, Abbasian S, Zeinolabedini A, Hassannezhad S. Acute pancreatitis in a young woman with COVID-19 infection: A case-report. *Caspian J Intern Med* 2021; **12**: S474-S478 [PMID: 34760109 DOI: 10.22088/cjim.12.0.474]
136 **Goldstein R**, Kogan D, Fiorito TM, Glasser CL. Suspected Case of Multisystem Inflammatory Syndrome in Children Associated With SARS-CoV-2 Infection Presenting as Acute Pancreatitis in a Child With Leukemia. *Infect Dis Clin Pract (Baltim Md)* 2021; **29**: e465-e467 [PMID: 34803353 DOI: 10.1097/IPC.0000000000001013]
137 **Gadiparthi C**, Mohapatra S, Kanna S, Vykuntam V, Chen W. Acute pancreatitis in a patient with COVID-19: a case report. *Transl Gastroenterol Hepatol* 2021; **6**: 65 [PMID: 34805587 DOI: 10.21037/tgh-20-234]

World Journal of Gastroenterology

Submit a Manuscript: https://www.f6publishing.com

World J Gastroenterol 2022 May 21; 28(19): 2057-2075

DOI: 10.3748/wjg.v28.i19.2057

ISSN 1007-9327 (print) ISSN 2219-2840 (online)

REVIEW

Clinical significance of variant hepatic artery in pancreatic resection: A comprehensive review

Ye-Cheng Xu, Feng Yang, De-Liang Fu

Specialty type: Gastroenterology and hepatology

Provenance and peer review: Invited article; Externally peer reviewed.

Peer-review model: Single blind

Peer-review report's scientific quality classification

Grade A (Excellent): A
Grade B (Very good): B
Grade C (Good): 0
Grade D (Fair): 0
Grade E (Poor): 0

P-Reviewer: Dilek ON, Turkey; Nah YW, South Korea

Received: January 3, 2022
Peer-review started: January 3, 2022
First decision: March 10, 2022
Revised: March 16, 2022
Accepted: April 9, 2022
Article in press: April 9, 2022
Published online: May 21, 2022

Ye-Cheng Xu, Feng Yang, Department of Pancreatic Surgery, Huashan Hospital, Shanghai 200040, China

De-Liang Fu, Department of Pancreatic Surgery, Pancreatic Disease Institute, Huashan Hospital, Shanghai 200040, China

Corresponding author: Feng Yang, MD, PhD, Associate Chief Physician, Associate Professor, Department of Pancreatic Surgery, Huashan Hospital, No. 12 Central Urumqi Road, Shanghai 200040, China. yffudan98@126.com

Abstract

The anatomical structure of the pancreaticoduodenal region is complex and closely related to the surrounding vessels. A variant of the hepatic artery, which is not a rare finding during pancreatic surgery, is prone to intraoperative injury. Inadvertent injury to the hepatic artery may affect liver perfusion, resulting in necrosis, liver abscess, and even liver failure. The preoperative identification of hepatic artery variations, detailed planning of the surgical approach, careful intraoperative dissection, and proper management of the damaged artery are important for preventing hepatic hypoperfusion. Nevertheless, despite the potential risks, planned artery resection has become acceptable in carefully selected patients. Arterial reconstruction is sometimes essential to prevent postoperative ischemic complications and can be performed using various methods. The complexity of procedures such as pancreatectomy with en bloc celiac axis resection may be mitigated by the presence of an aberrant right hepatic artery or a common hepatic artery originating from the superior mesenteric artery. Here, we comprehensively reviewed the anatomical basis of hepatic artery variation, its incidence, and its effect on the surgical and oncological outcomes after pancreatic resection. In addition, we provide recommendations for the prevention and management of hepatic artery injury and liver hypoperfusion. Overall, the hepatic artery variant may not worsen surgical and oncological outcomes if it is accurately identified pre-operatively and appropriately managed intraoperatively.

Key Words: Hepatic artery; Pancreatectomy; Pancreaticoduodenectomy; Arterial reconstruction; Celiac axis resection; Outcome; Prognosis

©The Author(s) 2022. Published by Baishideng Publishing Group Inc. All rights reserved.

Core Tip: Variations in hepatic artery anatomy are not rare during pancreatic surgery and have a significant impact on planning and performance of the procedure. Inadvertent intraoperative injury to hepatic artery may affect liver perfusion and result in ischemic complications. Detailed knowledge and awareness of its anatomical variants are critical, and thorough pre- and intraoperative planning is important to prevent hepatic hypoperfusion. This article comprehensively reviews the hepatic artery anatomy and variations, highlights its impact on surgical and oncological outcomes after pancreatic resection, and discusses prevention and management of hepatic artery injury and liver hypoperfusion.

Citation: Xu YC, Yang F, Fu DL. Clinical significance of variant hepatic artery in pancreatic resection: A comprehensive review. *World J Gastroenterol* 2022; 28(19): 2057-2075
URL: https://www.wjgnet.com/1007-9327/full/v28/i19/2057.htm
DOI: https://dx.doi.org/10.3748/wjg.v28.i19.2057

INTRODUCTION

The mortality rate of pancreatectomy has decreased in recent years; however, several complex pancreatic resections such as the pancreaticoduodenectomy (PD), total pancreatectomy (TP), and modified Appleby procedure have high complication rates[1,2]. The anatomy of the pancreaticoduodenal region is complex and closely related to the surrounding blood vessels. Therefore, this region is vulnerable to injury during surgery. Moreover, the presence of vascular anatomical variants makes PD more challenging. Aberrant hepatic artery (AHA) is not rare in patients undergoing PD, with an incidence ranging from 15.1% to 24.8%[3-6]. This variant increases the risk of iatrogenic vascular injury and the incidence of postoperative hepatobiliary ischemic events, inducing complications such as bilioenteric anastomotic leakage and liver abscess[5,7,8]. Therefore, a thorough understanding of the anatomy of the hepatic artery is essential for safer pancreatic resection[9]. Herein, we provide a comprehensive review of the clinical significance of hepatic artery variants in pancreatic surgery.

LITERATURE SEARCH

A thorough search was performed in the PubMed database for relevant studies on hepatic artery variants and pancreatic resection. The search terms used were "aberrant" or "variant" or "anomaly" AND "hepatic artery" AND "pancreaticoduodenectomy" or "pancreatectomy". All available studies published in English or Chinese between January 2000 and November 2021 (131 articles) were screened.

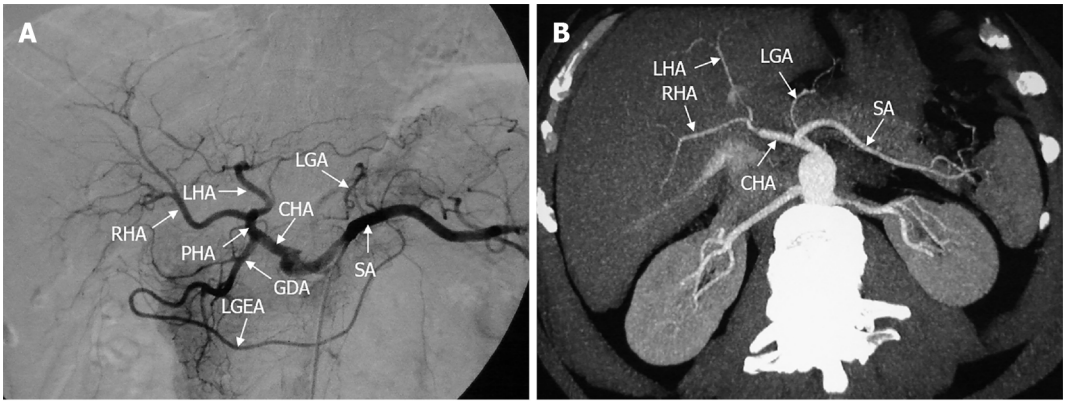
EMBRYOLOGY

It is important to understand the embryology of the hepatic artery to determine the origin of these variants. During embryogenesis, four visceral roots, known as ventral segmental arteries, originate from the dorsal aorta[10]. These ventral vessels are interconnected by longitudinal anastomoses[11,12]. The second and third roots and their connections, usually disappear during embryonic development. Thereafter, the celiac artery (CA) develops from the junction of the first three vessels and forms the left gastric artery (LGA), splenic artery, and common hepatic artery (CHA). The fourth trunk becomes the superior mesenteric artery (SMA). As the embryo grows, the channel between the roots of the CA and SMA fades away, resulting in anatomic division of the CA from the SMA[13]. This process can lead to several abnormalities in the CA and SMA. The associated changes are thought to depend on the degree of degeneration and longitudinal connectivity of primitive splanchnic vessels[10,11,13,14].

In addition, the hepatobiliary-pancreaticoduodenal region has the largest number of organs and the densest vascular branches. It is located at the junction of the foregut and midgut and is bound by the duodenal papilla. The vessels in this region frequently intersect between the CA and SMA, resulting in vascular variations. The three branches of the CA, from anterior to posterior are the LGA, splenic artery, and CHA. The CHA and its branches, which primarily maintain the blood supply between the foregut and midgut, are the most prone to variation.

ANATOMY

The normal anatomy of the hepatic artery refers to the CHA originating from the CA and crossing from



DOI: 10.3748/wjg.v28.i19.2057 **Copyright** ©The Author(s) 2022.

Figure 1 Classic hepatic arterial anatomy. A: Digital subtraction angiography showed normal anatomy of the hepatic arteries; B: Axial maximum intensity projection image showed normal anatomy of the hepatic arteries. CHA: Common hepatic artery; GDA: Gastroduodenal artery; LGA: Left gastric artery; LGEA: Left gastroepiploic artery; LHA: Left hepatic artery; PHA: Proper hepatic artery; RHA: Right hepatic artery; SA: Splenic artery.

the retroperitoneum toward the liver (Figure 1). This gives rise to a branch at the superior margin of the pancreatic head called the gastroduodenal artery (GDA). In this process, the CHA passes in front of the portal vein (PV), which is also known as the preportal route. Subsequently, it gives rise to the right gastric artery (RGA) and becomes the proper hepatic artery (PHA). Thereafter, it bifurcates into the left and right hepatic arteries (LHA/RHA). However, this so-called normal anatomy of the hepatic vessels is observed in only 55%-75.5% of individuals[15].

A series of terms are used to describe hepatic artery anomalies: “Aberrant”, “anomalous”, “accessory”, and “replaced”[16], and the definitions of these terms vary between studies. An aberrant or anomalous hepatic artery originates outside the typical route. It includes “accessory” and “replaced” hepatic arteries[17]. The term "replaced" RHA (rRHA) or LHA (rLHA) is used when the normal artery is absent, and a replaced artery arises from another artery and supplies blood to the corresponding hepatic lobe. The term "accessory" RHA (aRHA) or LHA (aLHA) is used when an additional artery originating from another source and a standard artery is present[16-18].

TYPES AND INCIDENCE

In terms of the anatomical classification of hepatic arteries, the Michels and Hiatt systems are well-established (Figure 2)[19,20]. The Michels system[20] is more extensive, classifying hepatic arteries into 10 types based on their origins. Hiatt *et al*[19] simplified the Michels system into six types. In addition, Garg *et al*[21] advocated a new classification that highlighted the distal branches of the hepatic arteries. However, despite these classifications of the hepatic arteries, several infrequent and unclassified hepatic artery variations have been detected in clinical practice. For example, an aberrant RHA may arise directly from the CA (Figure 3), which is an important anomaly to take note of during hepato-pancreato-biliary surgery because of the high risk of inadvertent injury[22]. More rarely, the origins of the CHA, splenic artery, and SMA mix seamlessly to form a hepato-spleno-mesenteric trunk (Figure 4), with a prevalence ranging from 0.67% to 0.90%[23,24]. The presence of a hepato-spleno-mesenteric trunk implies that only one trunk is responsible for the majority of the blood supply to abdominal organs, complicating operations around it[12].

AHAs can be categorized into three types based on their origin: Type I, an AHA originating from the SMA; type II, an AHA originating from the LGA; and type III, an AHA originating from other arteries such as the GDA, abdominal aorta, and right renal artery. Numerous studies[3,5,7,25] have reported that the most frequently encountered AHA type during PD is type I, with an aberrant RHA from the SMA accounting for most of the cases. This anomalous hepatic artery is of great concern because it can be close to or cross the pancreatic head, and lie posterior to the common bile duct[26]. Most frequently, the aberrant RHA runs from behind the pancreatic head to the posterior and lateral sides of the main PV, before reaching the liver. However, despite the extremely low frequency of intrapancreatic routes, PD becomes complicated when an aberrant RHA or CHA is found traversing the pancreatic parenchyma[27]. Therefore, variants involving the RHA or CHA should be assessed carefully when performing PD[3-5,7,9,17,25,26,28,29], although the incidence may not be high (Table 1)[30-34]. Unfortunately, the actual incidence of AHA may be underestimated because of the limited accuracy of the current preoperative diagnostic methods. Although a preoperative diagnosis of AHA may be negative, its presence should be suspected intraoperatively.

Table 1 Incidences of aberrant right and common hepatic artery during pancreaticoduodenectomy in the English literature (> 50 cases)

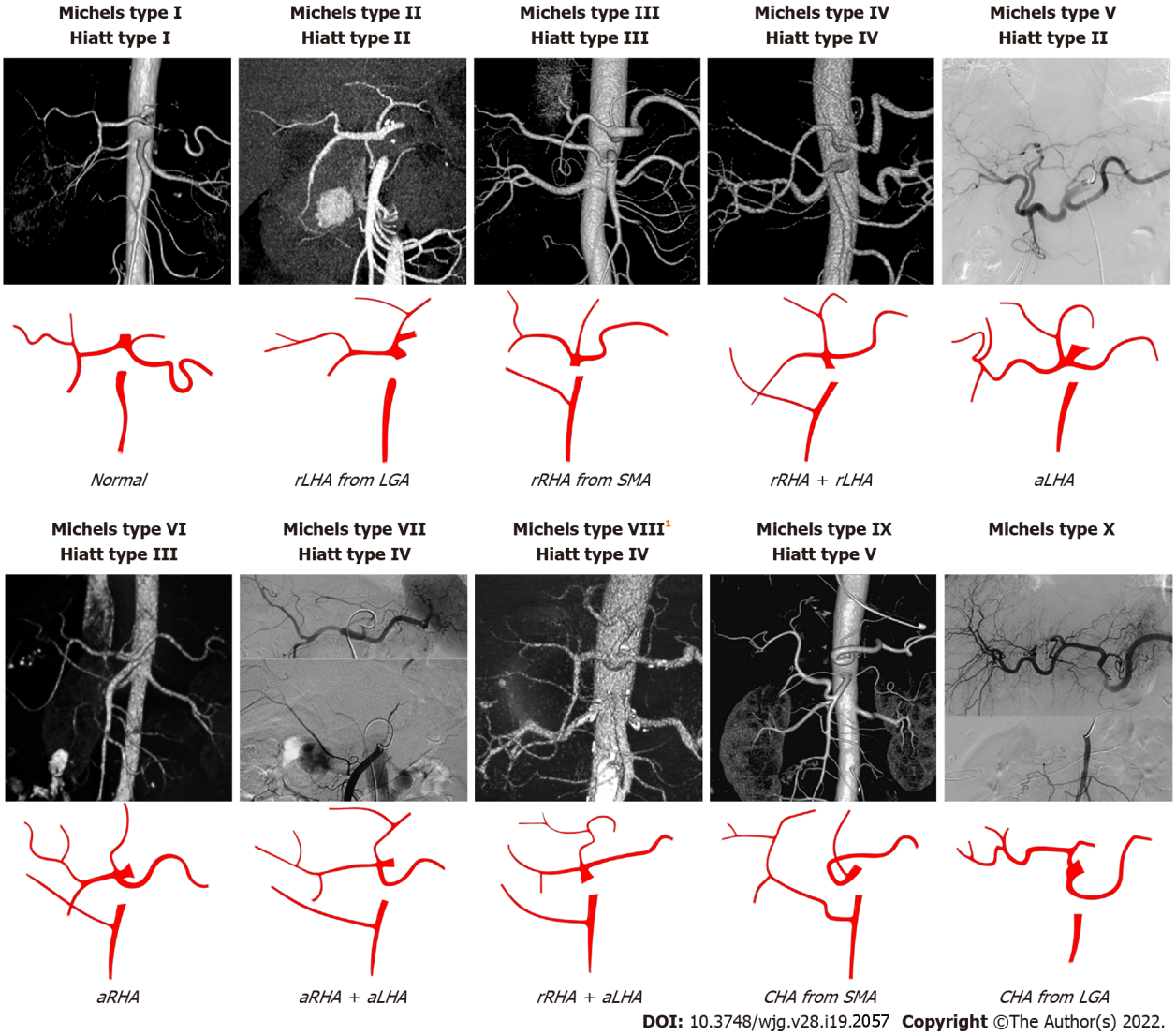
Ref.	Year	Total, *n*	Male, *n*	PDAC, *n*	a/rRHA, *n* (%)	aRHA[1], *n* (%)	rRHA[1], *n* (%)	rCHA, *n* (%)	Detecting methods
Wang *et al*[7]	2021	576	317	149	72 (12.5)	27 (4.7)	28 (4.9)	20 (3.5)	CTA
Mansour *et al*[5]	2021	202	NA	NA	37 (18.3)	3 (1.5)	29 (14.4)	0	Surgical finding
Giani *et al*[25]	2021	270	NA	NA	66 (24.4)	3 (1.1)	39 (14.4)	10 (3.7)	CT
Zhang *et al*[3]	2020	218	122	61	36 (16.5)	13 (6.0)	11 (5.1)	7 (3.2)	CTA
Crocetti *et al*[34]	2019	297	178	297	44 (14.8)	NA	NA	NA	CTA, surgical finding
Alexakis *et al*[4]	2019	232	NA	NA	32 (13.8)	19 (8.2)	13 (5.6)	1 (0.4)	Surgical finding
Balzan *et al*[9]	2019	200	93	NA	26 (13.0)	2 (1.0)	17 (8.5)	7 (3.5)	CT
Kim *et al*[33]	2016	73	35	24	15 (20.5)	4 (5.5)	11 (15.1)	NA	CT, surgical finding
Nguyen *et al*[31]	2015	142	76	57	16 (11.3)	0	14 (9.9)	9 (6.3)	CT, surgical finding
Yang *et al*[32]	2015	458	242	291	54 (11.8)	15 (3.3)	29 (6.3)	10 (2.2)	CT, DSA, surgical finding
Rammohan *et al*[17]	2014	225	167	31	42 (18.7)	10 (4.4)	31 (13.8)	1 (0.4)	CT, surgical finding
Kim *et al*[26]	2014	289	158	289	38 (13.1)	3 (1.0)	31 (10.7)	2 (0.7)	Surgical finding
Sulpice *et al*[30]	2013	213	NA	NA	29 (13.6)	NA	NA	NA	CT, surgical finding
Turrini *et al*[29]	2010	471	NA	471	47 (10.0)	2 (0.4)	44 (9.3)	NA	CT, surgical finding
Lee *et al*[28]	2009	103	73	0	15 (14.6)	0	12 (11.7)	0	MRA, surgical finding
Total		3969	1461	1670	540 (14.4)	101 (2.9)	309 (8.9)	67 (2.3)	

[1]These columns contain only variants of the right hepatic artery originating from the superior mesenteric artery.
a/rRHA: Accessory/replaced right hepatic artery; aRHA: Accessory right hepatic artery; CT: Computed tomography; CTA: Computed tomography angiography; CHA: Common hepatic artery; DSA: Digital subtraction angiography; NA: Not available; MRA: Magnetic resonance angiography; PDAC: Pancreatic ductal adenocarcinoma; rCHA: Replaced common hepatic artery; RHA: Right hepatic artery; rRHA: Replaced right hepatic artery.

COLLATERAL PATHWAYS

In general, the blood flow in the hepatic artery is predominantly from the CA. However, when the hepatic artery is involved in the tumor, retrograde flow from the SMA may develop (Figure 5). Similarly, celiac artery stenosis (CAS), which is not rare in patients undergoing PD (2%-11%)[35-37], may alter the hemodynamic profile of the hepatic artery. Retrograde blood flow in the CHA is a strong predictor of CAS[38,39]. In patients with CAS, the arterial blood supply to the upper abdominal organs is generally maintained by a steadily growing system of collaterals. Compensatory circulation between the CA and SMA is important in patients with hepatic artery stenosis or CAS because PD may disrupt these collaterals. Four possible collaterals have been reported: The pancreaticoduodenal arcade (key collateral supplying the liver and stomach), the dorsal pancreatic artery, the arc of Bühler, and the connection of the RHA and SMA[35,40-44], as shown in Figure 6. It is noteworthy that the pancreaticoduodenal and right gastroepiploic arcades are vital to the gastric and hepatic blood supply following pancreatectomy with en bloc celiac axis resection[45,46].

However, few studies have focused on collateral circulation in patients diagnosed with both CAS and hepatic artery variants. In patients with an aberrant RHA arising from the SMA, intrahepatic collaterals may develop between RHA and LHA. In cases of PHA or CHA originating from the SMA, the peribiliary vascular plexus in the hepatoduodenal ligament, which connects the central hepatic artery and GDA, is subsequently enlarged. These patients have a compensatory circulation that interconnects the LHA and LGA, and the RGA and LGA[40,43]. During PD, most of these collaterals are sacrificed, inducing an ischemic threat to the midgut viscera, especially to the liver and common bile duct. Thus, the presence of CAS is an important finding during PD, regardless of external compression, which may require preoperative endovascular stenting or intraoperative revascularization[35,36].



DOI: 10.3748/wjg.v28.i19.2057 **Copyright** ©The Author(s) 2022.

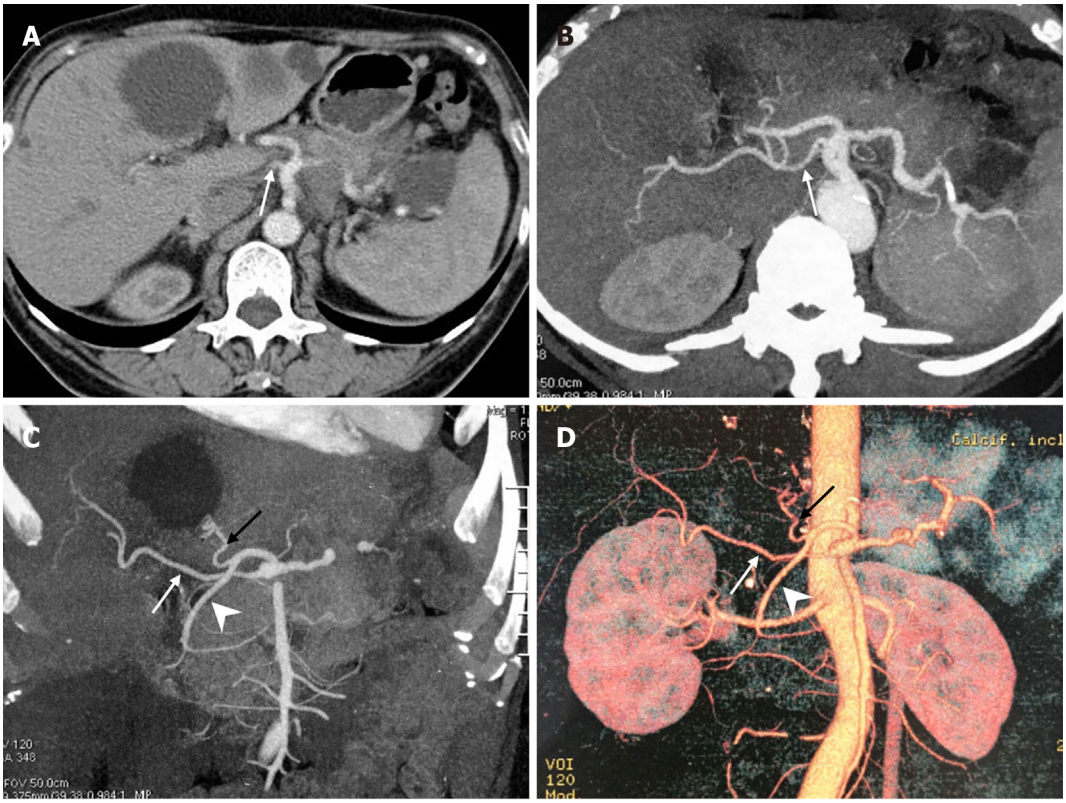
Figure 2 The Michels and Hiatt classifications of hepatic artery. [1]Michels type VIII includes replaced right hepatic artery (rRHA) + accessory left hepatic artery (aLHA) or replaced left hepatic artery (rLHA) + accessory right hepatic artery (aRHA). The common hepatic artery (CHA) from aorta is classified as Hiatt type VI. LGA: Left gastric artery; SMA: Superior mesenteric artery; rRHA: Replaced right hepatic artery; aLHA: Accessory left hepatic artery; rLHA: Replaced left hepatic artery; CHA: Common hepatic artery; aRHA: Accessory right hepatic artery.

PREOPERATIVE DIAGNOSIS

The importance of preoperative identification of AHA cannot be overemphasized. Although digital subtraction angiography (DSA) is considered the gold standard for the assessment of visceral anatomy and variation, its use is limited because of its invasive nature, minor but non-negligible risk of complications, and high cost[47]. Multidetector computed tomography angiography (MDCTA) is one of the most widely used modalities for diagnosis and identification of AHA and has been shown to reduce the incidence of iatrogenic injuries and postoperative complications[48-51]. Furthermore, magnetic resonance angiography (MRA) provides diagnostic image quality in 72% of the hepatic and visceral arteries and enables the delineation of hepatic arterial anatomical features with high accuracy[47]. Significant advances in computed tomography angiography (CTA) and MRA have led to the marginalization of DSA[52]. However, considering the relatively high human and financial resources required to visualize the vasculature, it is impossible to subject every patient to CTA or MRA. Yang *et al*[32] showed that multidetector computed tomography (MDCT) without arterial reconstruction aided in the evaluation of aberrant RHA for preoperative planning of pancreatic surgery. Therefore, conventional MDCT combined with meticulous analysis may be helpful for preoperative detection of AHA.

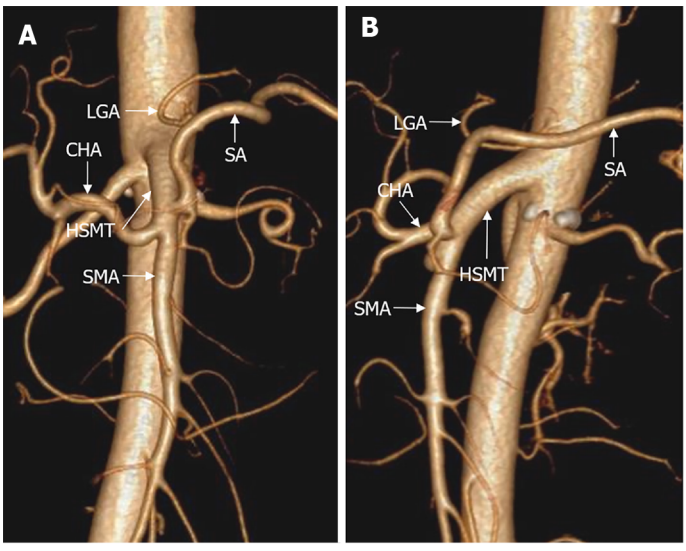
SURGICAL AND ONCOLOGICAL OUTCOMES

Studies examining the effect of AHA on the perioperative outcomes of either open PD (OPD) or



DOI: 10.3748/wjg.v28.i19.2057 **Copyright** ©The Author(s) 2022.

Figure 3 A peculiar replaced right hepatic artery arising directly from the celiac artery. A: Axial contrast enhanced computed tomography scan; B-D: Axial maximum intensity projection (MIP, B), coronal MIP (C) and 3D-volume rendering (D) images showed that the replaced right hepatic artery (white arrow) originated directly from the celiac artery, and the common hepatic artery divided into the left hepatic artery (black arrow) and gastroduodenal artery (arrowhead).



DOI: 10.3748/wjg.v28.i19.2057 **Copyright** ©The Author(s) 2022.

Figure 4 The hepato-spleno-mesenteric trunk. 3D-volume rendering computed tomography images showed that the hepato-spleno-mesenteric trunk was formed by the common hepatic artery, splenic artery and superior mesenteric artery, and the left gastric artery (LGA) originated from the aorta. A: Coronal view; B: Sagittal view. HSMT: Hepato-spleno-mesenteric trunk; CHA: Common hepatic artery; SA: Splenic artery; SMA: Superior mesenteric artery; LGA: Left gastric artery.

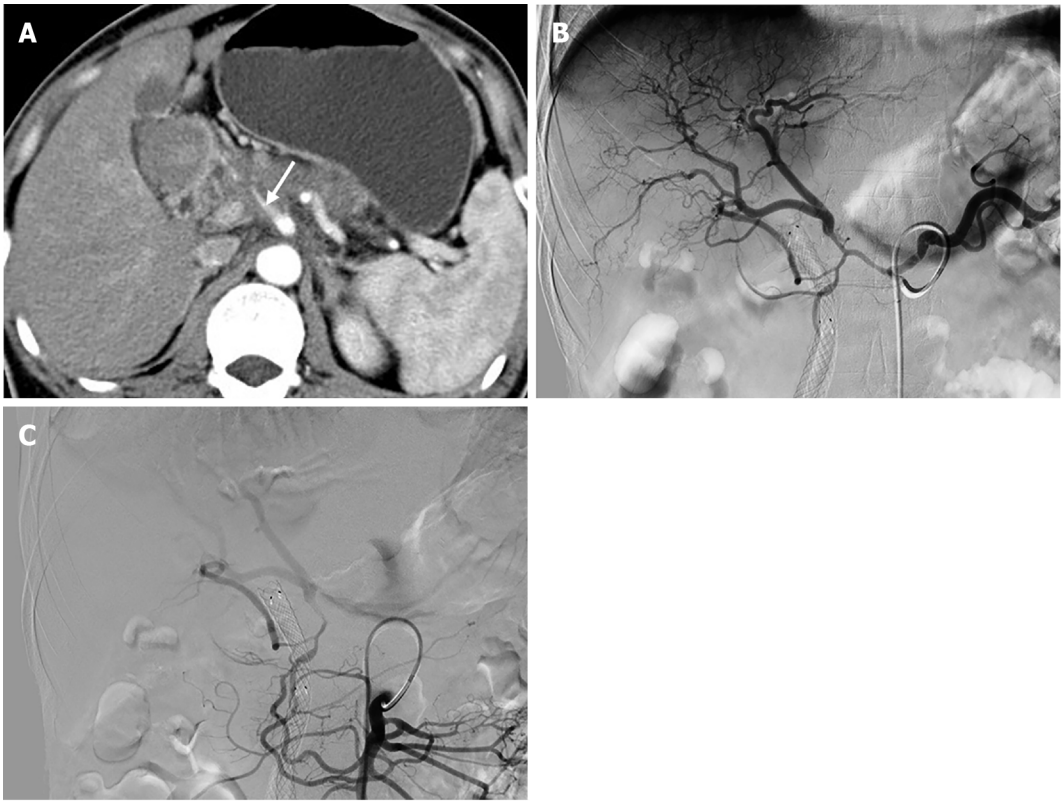
minimally invasive PD (MIPD) have reported negative outcomes (Table 2)[3-5,7,17,25,26,30,31,33,34,53]. Although duration of surgery can be prolonged[3,17,26], the AHA does not jeopardize surgical outcomes of PD[5,7,31,33]. Nevertheless, the presence of AHA may predispose patients to intraoperative injury, increasing the risk of hepatic hypoperfusion and ultimately leading to necrosis, liver abscess, and even liver failure. Nearly 10% of patients undergoing PD have a vascular injury, with the incidence of hepatic artery injury ranging from 0.5% to 1.7%[54-56]. Although the PV supply, extrahepatic

Table 2 Surgical outcomes of pancreaticoduodenectomy in patients with and without aberrant hepatic artery (> 50 cases)

Ref.	Total, *n*	AHA, *n*	Morbidity, *n* (%)		POPF, *n* (%)		PPH, *n* (%)		DGE, *n* (%)		Reoperation, *n* (%)		Mortality, *n* (%)	
			AHA	n-AHA	AHA	n-AHA	AHA	n-AHA	AHA	n-AHA	AHA	n-AHA	AHA	n-AHA
OPD														
Rammohan *et al*[17]	225	43	26 (60.5)	111 (61.0)	2 (4.7)	9 (4.9)	1 (2.3)	4 (2.1)	23 (53.4)	98 (53.8)	NA	NA	1 (2.3)	3 (1.7)
Kim *et al*[26]	249	37[1]	9[2] (24.3)	88[2] (41.5)	1 (2.7)	12 (5.6)	1 (2.7)	16 (7.6)	4 (10.8)	16 (7.6)	NA	NA	0	1 (0.5)
Sulpice[3] *et al*[30]	84	29[1]	14 (48.3)	32 (58.2)	3 (10.3)	9 (16.4)	4 (13.8)	9 (16.4)	10 (34.5)	24 (43.6)	NA	NA	3 (10.3)	3 (5.5)
Eshuis *et al*[53]	758	143	80 (55.9)	303 (49.3)	18 (12.6)	87 (14.1)	11 (7.7)	44 (7.2)	48 (33.6)	193 (31.4)	10 (7.0)	68 (11.0)	2 (1.4)	13 (2.1)
Mansour[3] *et al*[5]	82	41	22 (53.7)	27 (65.9)	8 (19.5)	12 (29.3)	4 (9.8)	3 (7.3)	6 (14.6)	7 (17.1)	0	0	1 (2.4)	0
Crocetti *et al*[34]	297	44[1]	32 (72.7)	185 (73.1)	5 (11.3)	27 (10.7)	2 (4.5)	12 (4.7)	5 (11.4)	37 (14.6)	3 (6.8)	28 (11.7)	7 (15.9)	33 (13.0)
Alexakis[3] *et al*[4]	105	35	4 (11.4)	19 (27.1)	2 (5.7)	9 (12.9)	0	2 (2.9)	1 (2.9)	1 (1.4)	1 (2.9)	5 (7.1)	2 (5.7)	4 (5.7)
LPD														
Wang *et al*[7]	576	127	NA	NA	21 (16.5)	68 (15.1)	11 (9.0)	37 (8.2)	3 (2.5)	9 (2.0)	4 (3.1)	24 (5.3)	4 (3.1)	12 (2.7)
Giani *et al*[25]	72	14[1]	5 (35.7)	34 (58.6)	2 (14.3)	10 (17.2)	2 (14.3)	10 (17.2)	2 (14.3)	14 (24.1)	NA	NA	0	4 (6.9)
Zhang *et al*[3]	218	54	22 (40.7)	70 (42.7)	5 (2.3)	21 (9.6)	5 (2.3)	15 (6.9)	NA	NA	NA	NA	3 (3.7)	7 (4.3)
RPD														
Nguyen *et al*[31]	142	30	19 (63.3)	74 (66.0)	4 (13.3)	9 (8.1)	NA	NA	3 (10.0)	26 (23.2)	NA	NA	2 (6.7)	3 (2.7)
Kim *et al*[33]	73	15[1]	5 (33.3)	29 (50.0)	2 (13.3)	5 (8.6)	1 (6.7)	5 (8.6)	NA	NA	2 (13.3)	4 (6.9)	0	2 (3.4)

[1]AHA in these studies included only right hepatic artery variants.
[2]The *P* value for this comparison was 0.04, while all others were > 0.05.
[3]These studies provided matched analysis.
AHA: Aberrant hepatic artery; DGE: Delayed gastric emptying; LPD: Laparoscopic pancreaticoduodenectomy; n-AHA: Non-aberrant hepatic artery; NA: Not available; OPD: Open pancreaticoduodenectomy; POPF: Postoperative pancreatic fistula; PPH: Post-pancreatectomy hemorrhage; RPD: Robotic pancreaticoduodenectomy.

collaterals, and interlobular communicating arteries may compensate to some extent for hepatic hypoperfusion, the incidence of catastrophic complications in the postoperative period is approximately 20%[34,57,58]. Liver ischemia after pancreatic resection is classified into four types: Hypoperfusion without major hepatic vessel occlusion, arterial occlusion, PV occlusion, and PV plus arterial occlusion [59]. This classification helps surgeons identify the degree of liver ischemia and escalate treatment appropriately. In addition to the liver, the biliary tree may be involved in an AHA injury. The extrahepatic biliary system receives its blood supply from the retroduodenal artery, RHA, and GDA[26, 60]. After ligation of the GDA in PD, the remaining bile duct relies mainly on the RHA for its blood



DOI: 10.3748/wjg.v28.i19.2057 **Copyright** ©The Author(s) 2022.

Figure 5 Retrograde flow from the superior mesenteric artery due to tumor involvement of the hepatic artery. A: Computed tomography scan showed a low-density mass in the pancreatic head with common hepatic artery involvement (arrow); B: Selective celiacography showed involvement of the hepatic artery from the origin of the celiac artery to the bifurcation of the left and right hepatic arteries, as well as involvement of the gastroduodenal artery. Additionally, an accessory right hepatic artery was seen originating from the gastroduodenal artery; C: Superior mesenteric angiography showed retrograde flow to the liver from the superior mesenteric artery *via* the pancreaticoduodenal arcade.

supply. Therefore, bile leakage may occur because of possible ischemia of the bilioenteric anastomosis [6].

Ischemic complications of PD can occur in patients with hepatic artery injury or CAS. Even in the absence of arterial stenosis or intraoperative arterial trauma, calcified plaques or atherosclerosis in the CHA can cause fatal complications[37]. Compression by a CHA pseudoaneurysm due to postoperative pancreatic fistula may cause ischemia of the abdominal organs, sepsis, and multiorgan dysfunction syndrome, which can be life threatening[61].

Most studies reported no significant differences in R0 resection rates between patients with and without AHA. Furthermore, the median overall survival and number of lymph nodes harvested did not differ significantly between the two groups. Based on these results, the presence of AHA does not seem to affect the radical outcome of pancreatic cancer surgery. The effects of AHA on oncological outcomes in pancreatic cancer, such as R0 resection, median overall survival, and number of lymph nodes harvested, are listed in Table 3[3,4,7,17,25,26,28-31,34,62].

PREVENTION AND MANAGEMENT OF INTRAOPERATIVE AHA INJURY

Among the types of AHA, aberrant RHA or CHA from the SMA may increase the difficulty of PD; therefore, these should be of greater concern during surgery (Figure 7). Even when using radiological techniques with high sensitivity, an AHA may still be missed preoperatively. Hence, the anatomy of the hepatic artery should be determined by performing extended kocherization before dissection. There are various approaches to manage anomalous vessels. Of these, traction away from the ongoing surgical site and revascularization are of paramount importance[17]. Artery-first approaches, such as the posterior and inferior infracolic "SMA first" approach, can be used to identify AHAs[63]. The direct tactile feedback of arterial pulsation is a unique advantage of OPD. For example, normal PHA pulsation can be felt intraoperatively at the left margin of the hepatoduodenal ligament. If an anomaly in this normal condition is detected, surgeons should assess whether an AHA is present. Arterial pulsation behind the pancreatic head or PV may be an aberrant RHA or CHA[64]. The AHA originating from the LGA is vulnerable to injury during partial gastrectomy and may be palpated at the gastrohepatic ligament[18].

Table 3 Oncological outcomes of pancreaticoduodenectomy in patients with and without aberrant hepatic artery (> 50 cases)

Author	Total, *n*	AHA, *n*	R0 resection, *n* (%)		Median OS (mo)		Median HLN, *n*	
			AHA	n-AHA	AHA	n-AHA	AHA	n-AHA
OPD								
Crocetti *et al*[34]	297	44[1]	42 (95.5)	220 (87.0)	30	25	NA	NA
Alexakis[2] *et al*[4]	105	35	29 (82.9)	56 (80.0)	NA	NA	NA	NA
Rubio-Manzanares-Dorado *et al*[62]	151	11	11 (100.0)	116 (82.9)	NA	NA	10	12
Rammohan *et al*[17]	225	43	40 (93.1)	169 (92.9)	NA	NA	12	12
Kim *et al*[26]	249	37[1]	33 (89.2)	178 (84.0)	17	23	17	17
Sulpice[2] *et al*[30]	84	29[1]	25 (86.2)	49 (89.1)	21.8	23.6	16	26
Turrini *et al*[29]	62	31	25 (80.7)	26 (83.9)	23	17	11	13
Lee *et al*[28]	103	15[1]	12 (80.0)	66 (75.0)	29.8	28.7	NA	NA
LPD								
Wang *et al*[7]	576	127	NA	NA	28	32	15	14
Giani *et al*[25]	72	14[1]	11 (84.6)	50 (86.2)	NA	NA	22[3]	17[3]
Zhang *et al*[3]	218	54	54 (100.0)	163 (99.4)	NA	NA	18.59	18.26
RPD								
Nguyen *et al*[31]	115	27	25 (92.6)	77 (87.5)	NA	NA	22.3	17.5

[1]AHA in these studies included only right hepatic artery variants.

[2]These studies provided matched analysis.

[3]The *P* value for this comparison was 0.032, while all others were > 0.05.

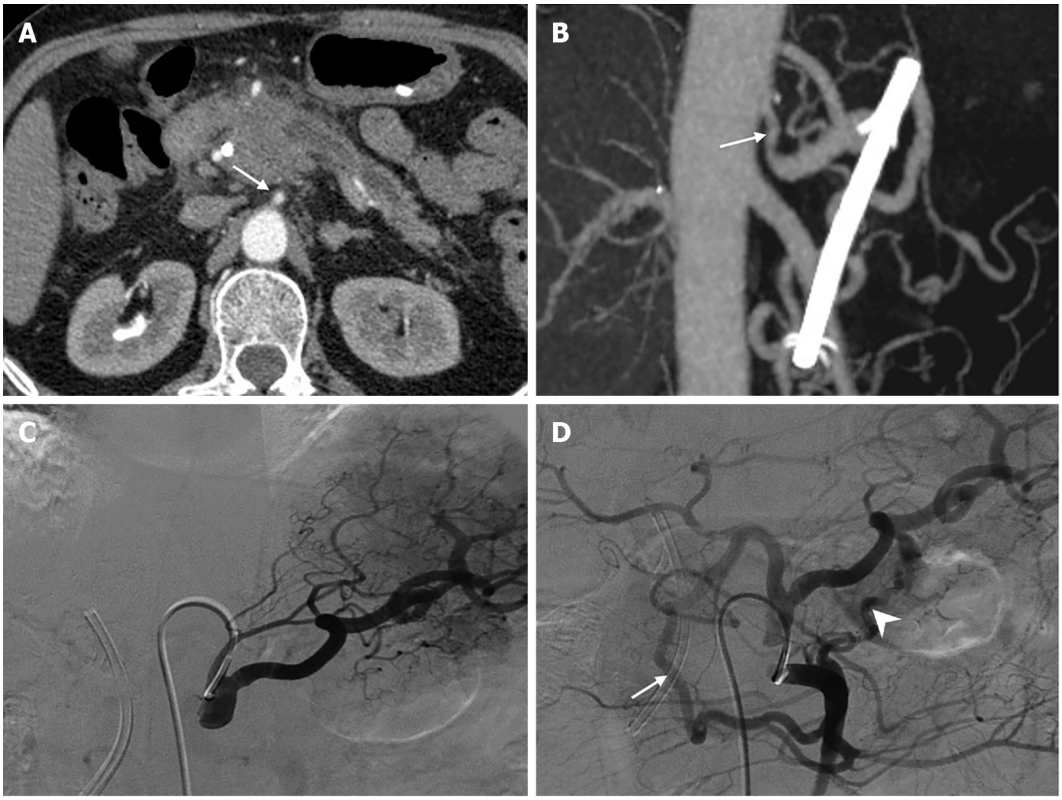
AHA: Aberrant hepatic artery; HLN: Number of harvested lymph nodes; LPD: Laparoscopic pancreaticoduodenectomy; n-AHA: Non-aberrant hepatic artery; NA: Not available; OPD: Open pancreaticoduodenectomy; OS: Overall survival; RPD: Robotic pancreaticoduodenectomy.

Therefore, during distal gastrectomy in PD, the LGA branch should be ligated away from the origin of the aberrant artery or close to the gastric wall[65].

In addition, some specific AHAs may have embarrassing pitfalls. One such AHA is the aberrant RHA arising from the GDA, which has been reported in 3.5% of patients undergoing PD[66]. This variant sets an obstacle to achieving R0 resection because its origin is close to the pancreatic head. It can be accidentally ligated if the GDA is divided close to the CHA. In this case, a clamping test should be performed before transection of the GDA, followed by palpation of the hepatic artery[18]. Another pitfall is the aberrant retropancreatic RHA originating from the SMA. To avoid intraoperative injury to this artery, dissection of the hepatoduodenal ligament above the pancreas is essential after detecting the aberrant RHA by palpation or intraoperative ultrasonography. Skeletonization of the common bile duct may prevent it from being mistakenly ligated[67]. Rarely, an rRHA from the SMA can give rise to GDA after coursing to the right in front of the superior mesenteric vein (Figure 8). This type of aberrant RHA is of real concern because it is vulnerable to pancreatic neck dissection. It can be protected during OPD by accurate preoperative identification, intraoperative tactile feedback of arterial pulsation, and Doppler ultrasonography.

In recent years, with the rapid development of surgical techniques, MIPD has been shown to be as safe as OPD[68]. However, the absence of tactile feedback from arterial pulsation during MIPD complicates the entire procedure, particularly in response to AHA[31]. Can *et al*[69] provided a series of tips to avoid AHA injury during laparoscopic PD (LPD), including the use of the hepatoduodenal ligament as a reliable marker to detect AHA during the dissection of the uncinate process, moderate retraction, and skillful differentiation of the AHA from arterial-like lymphatics and elongated lymph nodes. In terms of the surgical approach, the posterior approach is most often used for LPD[3,65]. This approach can be applied to all patients, regardless of the presence of AHA, because it adheres to the principle of "artery first"[3,65].

Although the feasibility and safety of robotic PD (RPD) have been confirmed[70], a major limitation is the lack of tactile feedback. It has been suggested that aberrant RHA should be suspected when the tissue thickness on the right side of the PV increases or the CHA becomes thin[33]. In such cases, careful dissection is required to prevent vascular injury. During RPD, artery injury can be avoided by strict adherence to the no-touch technique[31]. An additional robotic arm provides sufficient tension to the surrounding tissue to ensure safe dissection. Combining a low-energy robotic hook with a bipolar



DOI: 10.3748/wjg.v28.i19.2057 **Copyright** ©The Author(s) 2022.

Figure 6 Collateral pathways due to celiac axis stenosis. A: Computed tomography scan showed a mass in the pancreatic head with dilated biliary-pancreatic duct, and celiac axis stenosis (CAS, arrow); B: Sagittal maximum intensity projection image demonstrated CAS (arrow); C: Selective celiac angiographic examination revealed the left gastric artery and splenic artery, with no hepatic arteries depicted, which is compatible with occlusion of the common hepatic artery; D: Superior mesenteric arteriogram demonstrated retrograde filling of the celiac branches *via* the pancreaticoduodenal arcades (arrow) by way of the gastroduodenal artery and anomalous blood vessels traversing the pancreas (arrowhead).

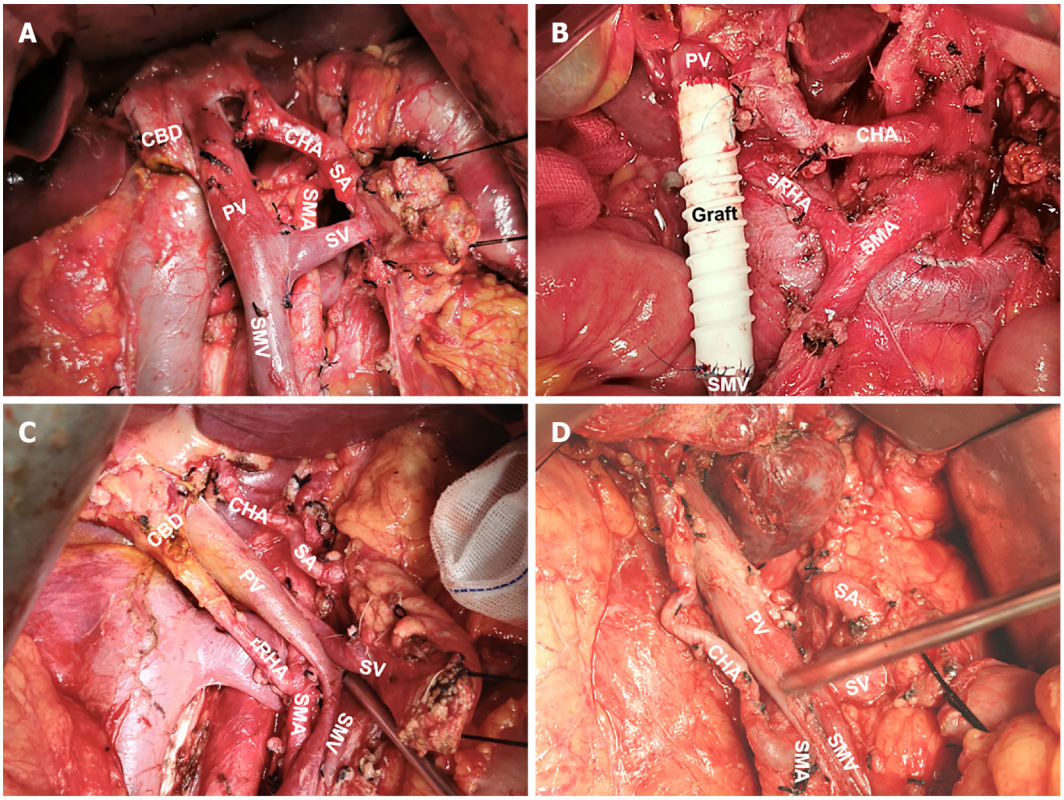
grabber promises effective handling of tiny branches of the uncinate process with minimal heat dissipation to anomalous vessels[31].

Although many studies have analyzed the clinical outcomes of AHA in pancreatic resection, few studies have reported the management of unexpected intraoperative AHA injuries. The early detection of accidental artery injuries is crucial. Remedial reconstruction of a damaged hepatic artery is considered a reliable option[54]. No significant difference in surgical outcomes has been reported between intentional and unintentional revascularization[55]. Ligation of inadvertently injured hepatic arteries may be attempted in view of the presence of collaterals, such as the subcostal arteries and the right inferior phrenic artery. This is like a planned resection of tumor-involved AHA without revascularization[55]. In brief, timely identification and proper management of an inadvertently damaged AHA are important to prevent hepatic hypoperfusion.

MANAGEMENT OF TUMOR INVOLVEMENT OF THE AHA

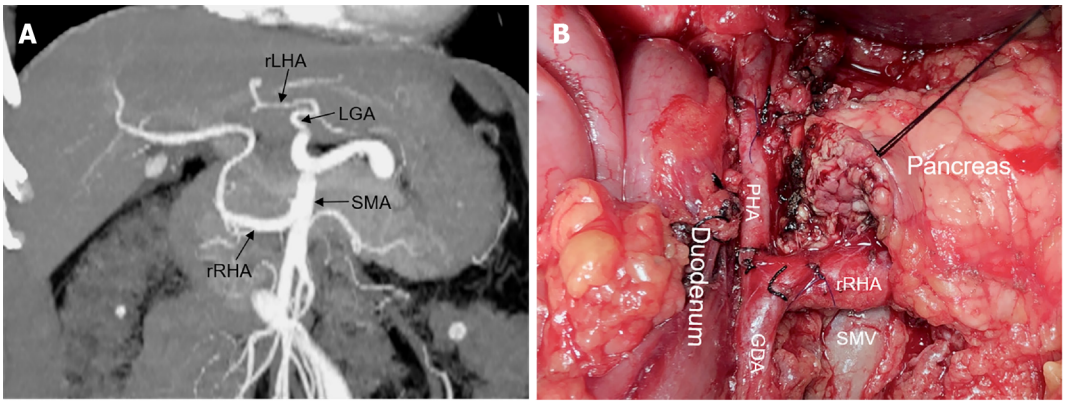
Intraoperative preservation of the AHA is an ideal surgical option, provided that radical surgical treatment is guaranteed[18]. Vascular invasion is common in patients with pancreatic cancer. In cases where tumor involvement of the AHA is suspected preoperatively, neoadjuvant therapy is recommended to allow translational surgery[71-73]. Unfortunately, even with neoadjuvant chemoradiation, it is sometimes still difficult to preserve the AHA involved in R0 resection[74,75]. However, despite the potential risks, planned artery resection has become acceptable in carefully selected patients [76,77]. If the cancer is located less than 1 cm from the origin of the AHA or if the AHA penetrates through the tumor, it should be resected to achieve R0 resection[7]. After clamping the AHA, intraoperative Doppler ultrasound can be used to assess the hepatic blood supply and determine the requirement for arterial reconstruction[7,78]. Revascularization may not be mandatory in some cases; for example, when an accessory hepatic artery is present, the diameter of the involved branch is thin, and adequate hepatic blood supply is confirmed after dissection[26,55,77].

However, hepatic artery reconstruction is sometimes necessary to prevent postoperative liver ischemia[79]. If the two stumps of the artery are less than 1-2 cm apart, most of them are amenable to



DOI: 10.3748/wjg.v28.i19.2057 **Copyright** ©The Author(s) 2022.

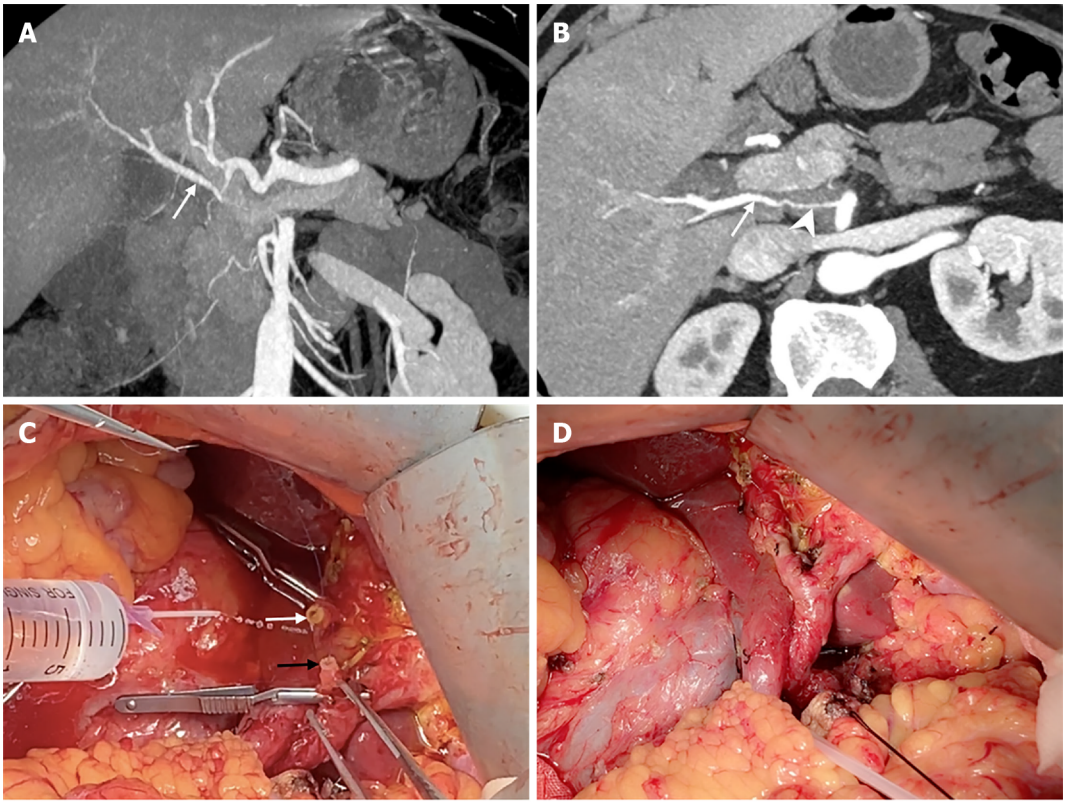
Figure 7 Significant hepatic artery variants during open pancreaticoduodenectomy. A: Normal anatomy of hepatic artery; B: Accessory right hepatic artery from the superior mesenteric artery (SMA); C: Replaced right hepatic artery from the SMA; D: Common hepatic artery from the SMA. CBD: Common bile duct; PV: Portal vein; SA: Splenic artery; SV: Splenic vein; SMV: Superior mesenteric vein.



DOI: 10.3748/wjg.v28.i19.2057 **Copyright** ©The Author(s) 2022.

Figure 8 A rare replaced right hepatic artery from the superior mesenteric artery susceptible to injury during pancreaticoduodenectomy. A: Coronal maximum intensity projection image showed Michels type IV hepatic artery variant; B. Intraoperative image showed that replaced right hepatic artery (rRHA) originated from the superior mesenteric artery and traveled to the right behind the inferior margin of the pancreatic neck *via* the superior mesenteric vein anteriorly and gave rise to the gastroduodenal artery and proper hepatic artery. LGA: Left gastric artery; rLHA: Replaced left hepatic artery; SMA: Superior mesenteric artery; GDA: Gastroduodenal artery; SMV: Superior mesenteric vein; PHA: Proper hepatic artery; rRHA: Replaced right hepatic artery.

primary end-to-end anastomosis[18,72,80]. Tension-free anastomosis is necessary because of the potential risk of pseudoaneurysms[18]. If the distance between the stumps is too long to achieve primary anastomosis, transposition or graft interposition may be an option[18,81]. When compared, transposition may be more effective (Figure 9). In addition, the middle colonic, splenic, and dorsal pancreatic arteries are alternative options for anastomosis[81-83]. However, graft interposition is sometimes unavoidable and can be achieved using a saphenous vein or prosthetic graft[80]. In summary, various methods of hepatic artery reconstruction have been reliably performed, as illustrated by Figure 10[71,72,80-83].



DOI: 10.3748/wjg.v28.i19.2057 **Copyright** ©The Author(s) 2022.

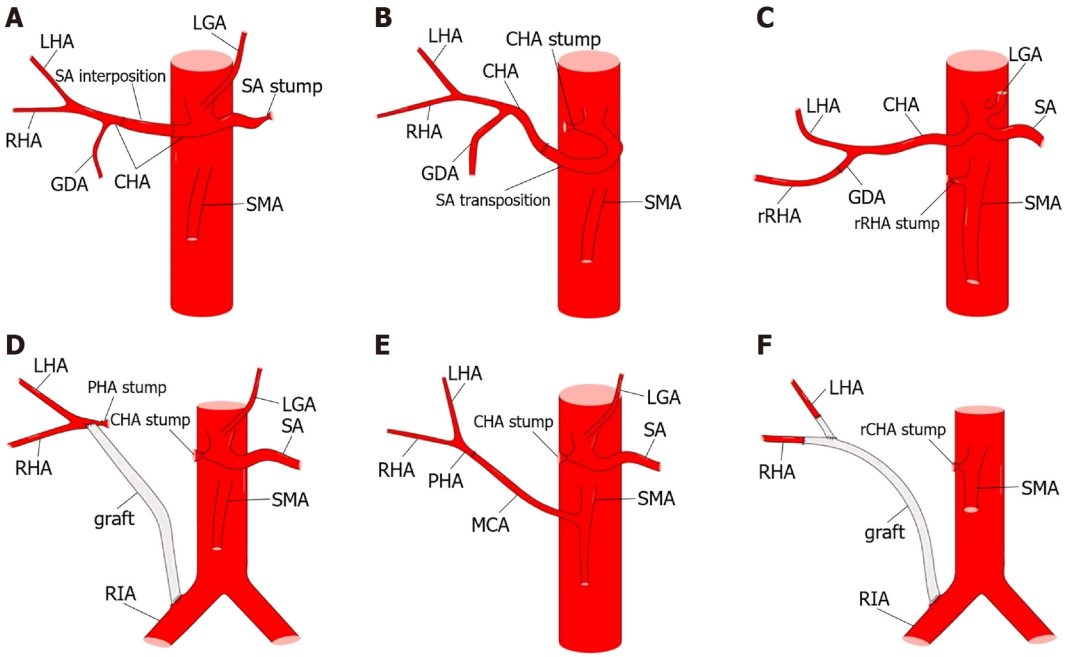
Figure 9 The replaced right hepatic artery reconstruction with gastroduodenal artery remnant during pancreaticoduodenectomy. A and B: Coronal and axial maximum intensity projection images showed the replaced right hepatic artery (rRHA, arrow) originated from the superior mesenteric artery and penetrated through the pancreatic head with tumor invasion resulting in significant stenosis (arrowhead); C: Intraoperative image showed a long length of the gastroduodenal artery (GDA) remnant (black arrow) was available for direct end-to-end anastomosis with the rRHA (white arrow); D: The rRHA-GDA anastomosis is complete.

Preoperative arterial embolization is an alternative approach to the prevention of liver ischemia after AHA resection[18,84,85]. Theoretically, preoperative coil embolization may lead to insufficient perfusion of the CHA, causing hepatic artery thrombosis. Migration of embolic material leading to liver ischemia, necrosis, and the risk of bleeding are other possible complications[86]. However, preoperative embolization can improve blood supply to the hepatobiliary system and stomach while providing valuable information to decide whether a partial hepatectomy is required[87]. In short, despite the invasiveness of this approach, it can lead to the prevention of postoperative liver ischemia without causing major complications[18,85].

AHA IN PANCREATECTOMY WITH CELIAC AXIS RESECTION

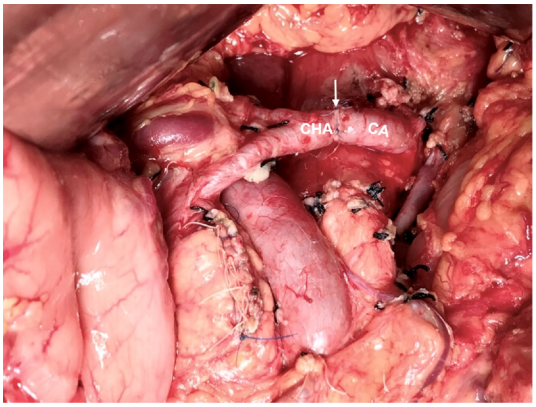
With the increased use of neoadjuvant chemoradiation, pancreatectomy with en bloc celiac axis resection (CAR) has become more commonly used to treat locally advanced pancreatic cancer[46,88]. Distal pancreatectomy with CAR (DP-CAR), also known as the modified Appleby procedure, is widely used due to its acceptable surgical and oncological outcomes[89-91]. Nevertheless, maintenance of visceral blood supply following DP-CAR, especially in the liver and stomach, remains a hot topic. Preoperative embolization has been recommended because it may reduce the incidence of ischemic complications by promoting associated collaterals[87,91,92]. Nevertheless, this may be avoided when the rRHA or CHA originates from the SMA. However, its application has several limitations, including failure to reduce the incidence of postoperative ischemic complications[84,93], coil migration and secondary ischemia[46,90,94], and complicating revascularization[95].

Hepatic artery reconstruction is an option to prevent postoperative ischemic complications and can be performed by anastomosis with the CA stump[71,86,96], splenic artery interposition[88], abdominal aorta[94,97], middle colonic artery[45], and iliac artery[79,98], as shown in Figures 11 and 12. However, the need for hepatic artery reconstruction remains a controversial issue. Liver perfusion can be intraoperatively assessed by palpation, Doppler ultrasonography, and indocyanine green fluorescence angiography[46,84,90,91,94,99]. Mittal *et al*[86] proposed a novel method to objectively assess liver blood supply by measuring CHA blood pressure. If CHA blood pressure decreases by more than 25% or 18



DOI: 10.3748/wjg.v28.i19.2057 **Copyright** ©The Author(s) 2022.

Figure 10 Methods of hepatic artery reconstruction during pancreaticoduodenectomy. A: Splenic artery (SA) interposition between two ends of the common hepatic artery (CHA); B: SA transposition to be anastomosed with the CHA; C: Direct end-to-end anastomosis between replaced right hepatic artery (rRHA) and gastroduodenal artery (GDA); D: Graft interposition between proper hepatic artery (PHA) and right iliac artery (RIA); E: Direct end-to-end anastomosis between PHA and middle colic artery; F: Graft interposition between RHA and RIA, and end-to-side anastomosis between left hepatic artery and graft. CA: Celiac artery; LGA: Left gastric artery; rCHA: Replaced common hepatic artery; SMA: Superior mesenteric artery; rRHA: Replaced right hepatic artery; CHA: Common hepatic artery; GDA: Gastroduodenal artery; LHA: Left hepatic artery; MCA: Middle colic artery; SA: Splenic artery.

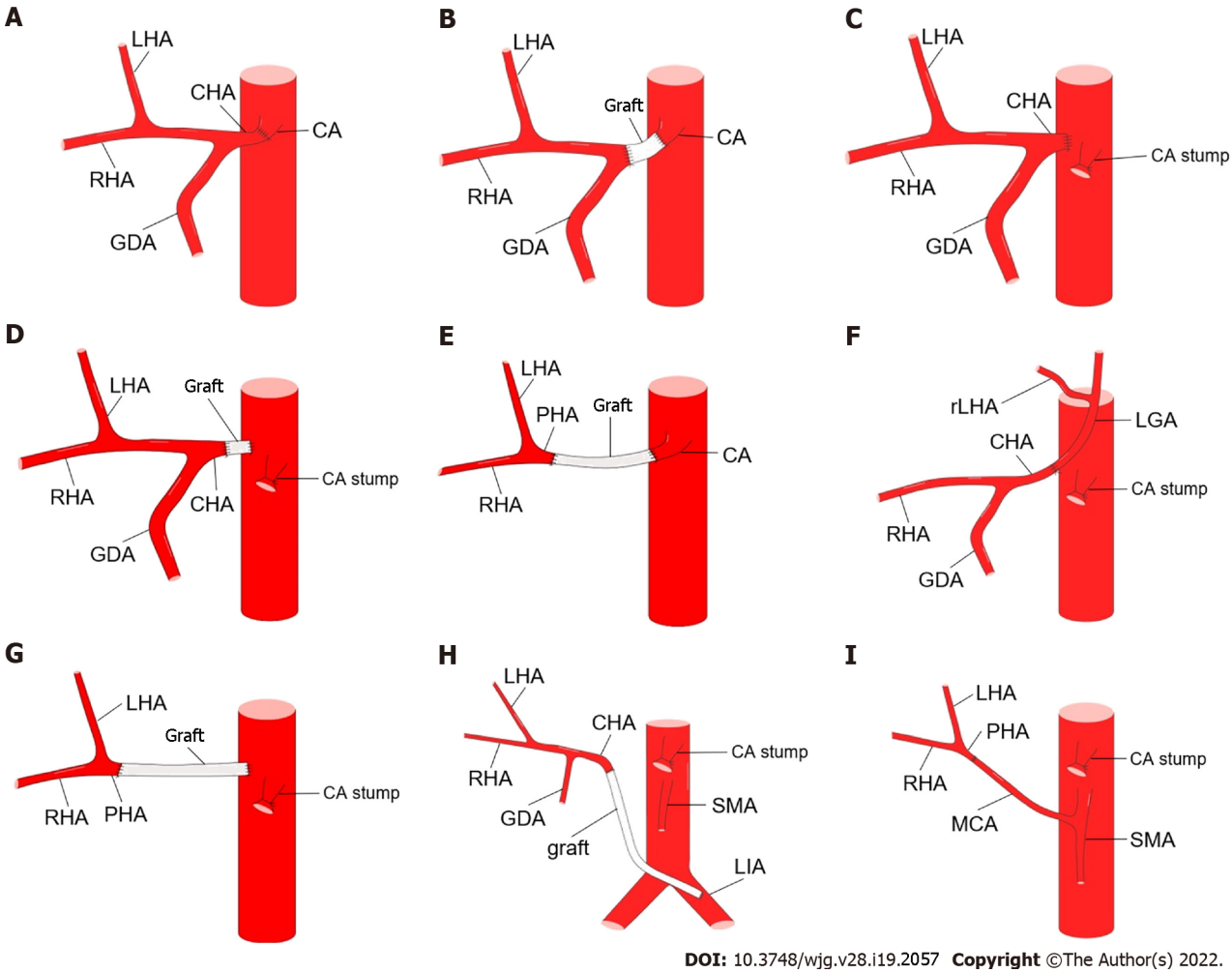


DOI: 10.3748/wjg.v28.i19.2057 **Copyright** ©The Author(s) 2022.

Figure 11 The common hepatic artery-celiac artery anastomosis during the modified Appleby procedure. Intraoperative image showed direct end-to-end anastomosis between common hepatic artery and celiac artery following distal pancreatectomy with celiac axis resection. The white arrow marks the anastomosis. CHA: Common hepatic artery; CA: Celiac artery.

mmHg, hepatic artery reconstruction should be performed. Although current opinions are not unanimous[79,97], arterial reconstruction may not be required in most cases when liver perfusion is confirmed to be adequate[87,92,94,100].

Unfortunately, despite the increasing detection rate of AHAs, few studies have described the effect of AHA on DP-CAR. In contrast to PD, which requires attention to aberrant RHA or CHA from the SMA, DP-CAR requires caution for aberrant LHA originating from the LGA[18]. This variant may result in left hepatic ischemia when the LGA is transected[101]. Therefore, to prevent aberrant LHA damage and preserve the intact hepatic blood supply, surgeons may preserve the tumor-free LGA or perform anastomosis between the LGA and CHA[84,90,96]. The complexity of the procedure may be mitigated by the presence of an aberrant RHA or CHA from the SMA. For example, the presence of Michels type IV may help avoid arterial reconstruction in TP with en bloc CAR (TP-CAR)[102]. Nevertheless, in the absence of this variant (Michels type IV), TP-CAR should be revascularized[88].



DOI: 10.3748/wjg.v28.i19.2057 **Copyright** ©The Author(s) 2022.

Figure 12 Methods of hepatic artery reconstruction during pancreatectomy with en bloc celiac axis resection. A: Direct end-to-end anastomosis between common hepatic artery (CHA) and celiac artery (CA); B: Graft interposition between CHA and CA; C: Direct end-to-end anastomosis between CHA and abdominal aorta (AA); D: Graft interposition between CHA and AA; E: Graft interposition between proper hepatic artery (PHA) and CA; F: Direct end-to-end anastomosis between CHA and left gastric artery [LGA, with replaced left hepatic artery (rLHA) from it]; G: Graft interposition between PHA and AA; H: Graft interposition between CHA and left iliac artery; I: Direct end-to-end anastomosis between PHA and middle colic artery. GDA: Gastroduodenal artery; LHA: Left hepatic artery; RHA: Right hepatic artery; SMA: Superior mesenteric artery.

CONCLUSION

In conclusion, AHA is not rare in patients undergoing pancreatic resection, and its clinical significance sometimes resembles a double-edged sword. The presence of AHA does not worsen surgical and oncological outcomes, if it is accurately identified preoperatively and appropriately managed intraoperatively. Given the potential risk of hepatic hypoperfusion caused by AHA injury or resection, hepatic artery reconstruction is sometimes necessary.

FOOTNOTES

Author contributions: Xu YC contributed to data acquisition, drafting the article, and final approval of the version to be published; Yang F contributed to the conception and design of this paper, data acquisition, drafting and revising the article, and final approval of the version to be published; Fu DL contributed to the conception and design of this paper, and final approval of it.

Supported by National Key R&D Program of China (Dr Yang), No. 2017YFC1308604.

Conflict-of-interest statement: We declare no conflicts of interest.

Open-Access: This article is an open-access article that was selected by an in-house editor and fully peer-reviewed by external reviewers. It is distributed in accordance with the Creative Commons Attribution NonCommercial (CC BY-NC 4.0) license, which permits others to distribute, remix, adapt, build upon this work non-commercially, and license

their derivative works on different terms, provided the original work is properly cited and the use is non-commercial. See: https://creativecommons.org/Licenses/by-nc/4.0/

Country/Territory of origin: China

ORCID number: Ye-Cheng Xu 0000-0001-8678-4843; Feng Yang 0000-0001-8790-6072; De-Liang Fu 0000-0003-4060-8101.

S-Editor: Fan JR
L-Editor: A
P-Editor: Fan JR

REFERENCES

1 **Yang F**, Jin C, Warshaw AL, You L, Mao Y, Fu D. Total pancreatectomy for pancreatic malignancy with preservation of the spleen. *J Surg Oncol* 2019; **119**: 784-793 [PMID: 30636049 DOI: 10.1002/jso.25377]
2 **Yang F**, Jin C, Li J, Di Y, Zhang J, Fu D. Clinical significance of drain fluid culture after pancreaticoduodenectomy. *J Hepatobiliary Pancreat Sci* 2018; **25**: 508-517 [PMID: 30328297 DOI: 10.1002/jhbp.589]
3 **Zhang W**, Wang K, Liu S, Wang Y, Liu K, Meng L, Chen Q, Jia B, Liu Y. A single-center clinical study of hepatic artery variations in laparoscopic pancreaticoduodenectomy: A retrospective analysis of data from 218 cases. *Medicine (Baltimore)* 2020; **99**: e20403 [PMID: 32481341 DOI: 10.1097/MD.0000000000020403]
4 **Alexakis N**, Bramis K, Toutouzas K, Zografos G, Konstadoulakis M. Variant hepatic arterial anatomy encountered during pancreatoduodenectomy does not influence postoperative outcomes or resection margin status: A matched pair analysis of 105 patients. *J Surg Oncol* 2019; **119**: 1122-1127 [PMID: 30919967 DOI: 10.1002/jso.25461]
5 **Mansour S**, Damouny M, Obeid M, Farah A, Halloun K, Marjiyeh R, Ghalia J, Kluger Y, Khuri S. Impact of Vascular Anomalies on Pancreatoduodenectomy Procedure. *J Clin Med Res* 2021; **13**: 158-163 [PMID: 33854655 DOI: 10.14740/jocmr4455]
6 **Khan MR**, Begum S, Khan DB, Inam Pal KM. Surgical and oncological implications of aberrant arterial anatomy in patients undergoing pancreatoduodenectomy. *J Pak Med Assoc* 2020; **70**: 930-934 [PMID: 32400757 DOI: 10.5455/JPMA.4875]
7 **Wang S**, Chen Q, Liu S, Zhang W, Ji B, Liu Y. The Impact of Aberrant Hepatic Artery on Resection Margin and Outcomes of Laparoscopic Pancreatoduodenectomy: A Single-Center Report. *World J Surg* 2021; **45**: 3183-3190 [PMID: 34258649 DOI: 10.1007/s00268-021-06231-z]
8 **Yang F**, Long J, Fu DL, Jin C, Yu XJ, Xu J, Ni QX. Aberrant hepatic artery in patients undergoing pancreaticoduodenectomy. *Pancreatology* 2008; **8**: 50-54 [PMID: 18230918 DOI: 10.1159/000114867]
9 **Balzan SMP**, Gava VG, Pedrotti S, Magalhães MA, Schwengber A, Dotto ML, Krebs CR. Prevalence of hepatic arterial variations with implications in pancreatoduodenectomy. *Arq Bras Cir Dig* 2019; **32**: e1455 [PMID: 31644675 DOI: 10.1590/0102-672020190001e1455]
10 **Kikuya K**, Einama T, Miyata Y, Iwasaki T, Yamagishi Y, Takihata Y, Morimura F, Edo H, Otsuka Y, Mori S, Tsunenari T, Fujinuma I, Hirose Y, Tsujimoto H, Ueno H, Kishi Y. Destruction of a wandering accessory right hepatic artery in a patient with pancreatic body cancer: a case report. *Clin J Gastroenterol* 2021; **14**: 560-565 [PMID: 33394330 DOI: 10.1007/s12328-020-01304-3]
11 **Mrowiec S**, Król R, Jabłońska B. Absence of the celiac trunk and anomalous very low origin of the common hepatic artery arising independently from the abdominal aorta just above aortic bifurcation in patient undergoing radical pancreaticoduodenectomy. *Surg Radiol Anat* 2021; **43**: 585-588 [PMID: 33449141 DOI: 10.1007/s00276-020-02666-6]
12 **Losanoff JE**, Millis JM, Harland RC, Testa G. Hepato-spleno-mesenteric trunk. *J Am Coll Surg* 2007; **204**: 511 [PMID: 17324790 DOI: 10.1016/j.jamcollsurg.2006.07.045]
13 **Namba Y**, Oishi K, Okimoto S, Moriuchi T, Bekki T, Mukai S, Saito Y, Fujisaki S, Takahashi M, Fukuda T, Ohdan H. Imaging diagnosis of aberrant proper hepatic and gastroduodenal arteries prior to pancreaticoduodenectomy: A case report. *Radiol Case Rep* 2021; **16**: 1650-1654 [PMID: 34007377 DOI: 10.1016/j.radcr.2021.03.062]
14 **Wang Y**, Cheng C, Wang L, Li R, Chen JH, Gong SG. Anatomical variations in the origins of the celiac axis and the superior mesenteric artery: MDCT angiographic findings and their probable embryological mechanisms. *Eur Radiol* 2014; **24**: 1777-1784 [PMID: 24859597 DOI: 10.1007/s00330-014-3215-9]
15 **Marín-Gómez LM**, Gómez-Bravo MA, Bernal-Bellido C, Alamo-Martínez JM, Suárez-Artacho G, Serrano-Díez-Canedo J. Variability of the extrahepatic arterial anatomy in 500 hepatic grafts. *Transplant Proc* 2010; **42**: 3159-3161 [PMID: 20970635 DOI: 10.1016/j.transproceed.2010.05.078]
16 **Nakata K**, Higuchi R, Ikenaga N, Sakuma L, Ban D, Nagakawa Y, Ohtsuka T, Asbun HJ, Boggi U, Tang CN, Wolfgang CL, Nishino H, Endo I, Tsuchida A, Nakamura M; Study Group of Precision Anatomy for Minimally Invasive Hepato-Biliary-Pancreatic surgery (PAM-HBP Surgery. Precision anatomy for safe approach to pancreatoduodenectomy for both open and minimally invasive procedure: A systematic review. *J Hepatobiliary Pancreat Sci* 2022; **29**: 99-113 [PMID: 33533158 DOI: 10.1002/jhbp.901]
17 **Rammohan A**, Palaniappan R, Pitchaimuthu A, Rajendran K, Perumal SK, Balaraman K, Ramasamy R, Sathyanesan J, Govindan M. Implications of the presence of an aberrant right hepatic artery in patients undergoing pancreaticoduodenectomy. *World J Gastrointest Surg* 2014; **6**: 9-13 [PMID: 24627736 DOI: 10.4240/wjgs.v6.i1.9]
18 **Swami A**, Yadav T, Varshney VK, Sreesanth KS, Dixit SG. Hepatic Arterial Variations and Its Implication During Pancreatic Cancer Surgeries. *J Gastrointest Cancer* 2021; **52**: 462-470 [PMID: 33616844 DOI: 10.1007/s12029-021-00598-x]

19 **Hiatt JR**, Gabbay J, Busuttil RW. Surgical anatomy of the hepatic arteries in 1000 cases. *Ann Surg* 1994; **220**: 50-52 [PMID: 8024358 DOI: 10.1097/00000658-199407000-00008]

20 **Michels NA**. Newer anatomy of the liver and its variant blood supply and collateral circulation. *Am J Surg* 1966; **112**: 337-347 [PMID: 5917302 DOI: 10.1016/0002-9610(66)90201-7]

21 **Garg S**, Sahni D, Kumar H, Yadav TD, Aggarwal A, Gupta T. The segmental branching of the hepatic arteries in the liver: a cadaveric study. *Anat Sci Int* 2019; **94**: 216-223 [PMID: 30617459 DOI: 10.1007/s12565-018-00475-x]

22 **Katagiri H**, Sakamoto T, Okumura K, Lefor AK, Kubota T. Aberrant right hepatic artery arising from the celiac trunk: A potential pitfall during laparoscopic cholecystectomy. *Asian J Endosc Surg* 2016; **9**: 72-74 [PMID: 26781532 DOI: 10.1111/ases.12247]

23 **Bolintineanu LA**, Costea AN, Iacob N, Pusztai AM, Pleş H, Matusz P. Hepato-spleno-mesenteric trunk, in association with an accessory left hepatic artery, and common trunk of right and left inferior phrenic arteries, independently arising from left gastric artery: case report using MDCT angiography. *Rom J Morphol Embryol* 2019; **60**: 1323-1331 [PMID: 32239112]

24 **Matusz P**, Loukas M, Iacob N, Ples H. Common stem origin of left gastric, right and left inferior phrenic arteries, in association with a hepatosplenomesenteric trunk, independently arising from the abdominal aorta: case report using MDCT angiography. *Clin Anat* 2013; **26**: 980-983 [PMID: 23255305 DOI: 10.1002/ca.22204]

25 **Giani A**, Mazzola M, Morini L, Zironda A, Bertoglio CL, De Martini P, Magistro C, Ferrari G. Hepatic vascular anomalies during totally laparoscopic pancreaticoduodenectomy: challenging the challenge. *Updates Surg* 2022; **74**: 583-590 [PMID: 34406616 DOI: 10.1007/s13304-021-01152-x]

26 **Kim PT**, Temple S, Atenafu EG, Cleary SP, Moulton CA, McGilvray ID, Gallinger S, Greig PD, Wei AC. Aberrant right hepatic artery in pancreaticoduodenectomy for adenocarcinoma: impact on resectability and postoperative outcomes. *HPB (Oxford)* 2014; **16**: 204-211 [PMID: 23782313 DOI: 10.1111/hpb.12120]

27 **Ishigami K**, Nishie A, Asayama Y, Ushijima Y, Takayama Y, Okamoto D, Fujita N, Yoshizumi T, Harimoto N, Ohtsuka T, Nakata K, Honda H. The prevalence of transpancreatic common hepatic artery and coexisting variant anatomy. *Clin Anat* 2018; **31**: 598-604 [PMID: 28726321 DOI: 10.1002/ca.22957]

28 **Lee JM**, Lee YJ, Kim CW, Moon KM, Kim MW. Clinical implications of an aberrant right hepatic artery in patients undergoing pancreaticoduodenectomy. *World J Surg* 2009; **33**: 1727-1732 [PMID: 19459000 DOI: 10.1007/s00268-009-0063-x]

29 **Turrini O**, Wiebke EA, Delpero JR, Viret F, Lillemoe KD, Schmidt CM. Preservation of replaced or accessory right hepatic artery during pancreaticoduodenectomy for adenocarcinoma: impact on margin status and survival. *J Gastrointest Surg* 2010; **14**: 1813-1819 [PMID: 20697832 DOI: 10.1007/s11605-010-1272-1]

30 **Sulpice L**, Rayar M, Paquet C, Bergeat D, Merdrignac A, Cunin D, Meunier B, Boudjema K. Does an aberrant right hepatic artery really influence the short- and long-term results of a pancreaticoduodenectomy for malignant disease? *J Surg Res* 2013; **185**: 620-625 [PMID: 24011920 DOI: 10.1016/j.jss.2013.07.015]

31 **Nguyen TK**, Zenati MS, Boone BA, Steve J, Hogg ME, Bartlett DL, Zeh HJ 3rd, Zureikat AH. Robotic pancreaticoduodenectomy in the presence of aberrant or anomalous hepatic arterial anatomy: safety and oncologic outcomes. *HPB (Oxford)* 2015; **17**: 594-599 [PMID: 25913696 DOI: 10.1111/hpb.12414]

32 **Yang F**, Di Y, Li J, Wang XY, Yao L, Hao SJ, Jiang YJ, Jin C, Fu DL. Accuracy of routine multidetector computed tomography to identify arterial variants in patients scheduled for pancreaticoduodenectomy. *World J Gastroenterol* 2015; **21**: 969-976 [PMID: 25624732 DOI: 10.3748/wjg.v21.i3.969]

33 **Kim JH**, Gonzalez-Heredia R, Daskalaki D, Rashdan M, Masrur M, Giulianotti PC. Totally replaced right hepatic artery in pancreaticoduodenectomy: is this anatomical condition a contraindication to minimally invasive surgery? *HPB (Oxford)* 2016; **18**: 580-585 [PMID: 27346138 DOI: 10.1016/j.hpb.2016.04.009]

34 **Crocetti D**, Sapienza P, Ossola P, Tarallo M, Cavallaro G, Serra R, Grande R, Mingoli A, Fiori E, DE Toma G. Does Aberrant Right Hepatic Artery Influence the Surgical Short- and Long-term Outcome of Pancreatoduodenectomy? *In Vivo* 2019; **33**: 1285-1292 [PMID: 31280220 DOI: 10.21873/invivo.11601]

35 **McCracken E**, Turley R, Cox M, Suhocki P, Blazer DG 3rd. Leveraging Aberrant Vasculature in Celiac Artery Stenosis: The Arc of Buhler in Pancreaticoduodenectomy. *J Pancreat Cancer* 2018; **4**: 4-6 [PMID: 30631850 DOI: 10.1089/pancan.2017.0020]

36 **Pallisera A**, Morales R, Ramia JM. Tricks and tips in pancreatoduodenectomy. *World J Gastrointest Oncol* 2014; **6**: 344-350 [PMID: 25232459 DOI: 10.4251/wjgo.v6.i9.344]

37 **Gaujoux S**, Sauvanet A, Vullierme MP, Cortes A, Dokmak S, Sibert A, Vilgrain V, Belghiti J. Ischemic complications after pancreaticoduodenectomy: incidence, prevention, and management. *Ann Surg* 2009; **249**: 111-117 [PMID: 19106685 DOI: 10.1097/SLA.0b013e3181930249]

38 **Zwolak RM**. Can duplex ultrasound replace arteriography in screening for mesenteric ischemia? *Semin Vasc Surg* 1999; **12**: 252-260 [PMID: 10651454]

39 **Zwolak RM**, Fillinger MF, Walsh DB, LaBombard FE, Musson A, Darling CE, Cronenwett JL. Mesenteric and celiac duplex scanning: a validation study. *J Vasc Surg* 1998; **27**: 1078-87; discussion 1088 [PMID: 9652470 DOI: 10.1016/s0741-5214(98)60010-0]

40 **Sakorafas GH**, Sarr MG, Peros G. Celiac artery stenosis: an underappreciated and unpleasant surprise in patients undergoing pancreaticoduodenectomy. *J Am Coll Surg* 2008; **206**: 349-356 [PMID: 18222391 DOI: 10.1016/j.jamcollsurg.2007.09.002]

41 **Kurosaki I**, Hatakeyama K, Nihei KE, Oyamatsu M. Celiac axis stenosis in pancreaticoduodenectomy. *J Hepatobiliary Pancreat Surg* 2004; **11**: 119-124 [PMID: 15127275 DOI: 10.1007/s00534-003-0871-6]

42 **Koops A**, Wojciechowski B, Broering DC, Adam G, Krupski-Berdien G. Anatomic variations of the hepatic arteries in 604 selective celiac and superior mesenteric angiographies. *Surg Radiol Anat* 2004; **26**: 239-244 [PMID: 14968265 DOI: 10.1007/s00276-004-0229-z]

43 **Song SY**, Chung JW, Kwon JW, Joh JH, Shin SJ, Kim HB, Park JH. Collateral pathways in patients with celiac axis stenosis: angiographic-spiral CT correlation. *Radiographics* 2002; **22**: 881-893 [PMID: 12110717 DOI:

10.1148/radiographics.22.4.g02jl13881]
44 **Yang F**, Jin C, Fu D. Celiac axis compression syndrome and pancreatic head cancer. *Pancreatology* 2014; **14**: 310-311 [PMID: 25207337 DOI: 10.1016/j.pan.2014.05.795]
45 **Suzuki H**, Hosouchi Y, Sasaki S, Araki K, Kubo N, Watanabe A, Kuwano H. Reconstruction of the hepatic artery with the middle colic artery is feasible in distal pancreatectomy with celiac axis resection: A case report. *World J Gastrointest Surg* 2013; **5**: 224-228 [PMID: 23894691 DOI: 10.4240/wjgs.v5.i7.224]
46 **Truty MJ**, Colglazier JJ, Mendes BC, Nagorney DM, Bower TC, Smoot RL, DeMartino RR, Cleary SP, Oderich GS, Kendrick ML. En Bloc Celiac Axis Resection for Pancreatic Cancer: Classification of Anatomical Variants Based on Tumor Extent. *J Am Coll Surg* 2020; **231**: 8-29 [PMID: 32422348 DOI: 10.1016/j.jamcollsurg.2020.05.005]
47 **Puippe GD**, Alkadhi H, Hunziker R, Nanz D, Pfammatter T, Baumueller S. Performance of unenhanced respiratory-gated 3D SSFP MRA to depict hepatic and visceral artery anatomy and variants. *Eur J Radiol* 2012; **81**: e823-e829 [PMID: 22578837 DOI: 10.1016/j.ejrad.2012.02.016]
48 **Costea AN**, Iacob N, Pusztai AM, Pleş H, Matusz P. Replaced right hepatic artery arising from inferior pancreaticoduodenal artery, in association with left multiple renal arteries: a case report using MDCT angiography. *Rom J Morphol Embryol* 2019; **60**: 971-977 [PMID: 31912111]
49 **Gündoğdu E**, Kebapçı M. Two novel hepatic arterial variations in a living liver donor detected by multidetector computed tomography angiography. *Surg Radiol Anat* 2021; **43**: 1385-1389 [PMID: 33682016 DOI: 10.1007/s00276-021-02730-9]
50 **Takahashi S**, Murakami T, Takamura M, Kim T, Hori M, Narumi Y, Nakamura H, Kudo M. Multi-detector row helical CT angiography of hepatic vessels: depiction with dual-arterial phase acquisition during single breath hold. *Radiology* 2002; **222**: 81-88 [PMID: 11756709 DOI: 10.1148/radiol.2221010326]
51 **Subbiah Nagaraj S**, Kaman L, Dahiya D, Ramavath K, Kalra N, Behera A. Correlation of Multi-Detector Computed Tomography and Intraoperative Variations of the Celiac Trunk and Hepatic Artery in Resectable Hepatobiliary Pancreatic Cancers. *Cureus* 2020; **12**: e12106 [PMID: 33489523 DOI: 10.7759/cureus.12106]
52 **Matoba M**, Tonami H, Kuginuki M, Yokota H, Takashima S, Yamamoto I. Comparison of high-resolution contrast-enhanced 3D MRA with digital subtraction angiography in the evaluation of hepatic arterial anatomy. *Clin Radiol* 2003; **58**: 463-468 [PMID: 12788315 DOI: 10.1016/s0009-9260(03)00085-0]
53 **Eshuis WJ**, Olde Loohuis KM, Busch OR, van Gulik TM, Gouma DJ. Influence of aberrant right hepatic artery on perioperative course and longterm survival after pancreatoduodenectomy. *HPB (Oxford)* 2011; **13**: 161-167 [DOI: 10.1111/j.1477-2574.2010.00258.x]
54 **Kim AW**, McCarthy WJ 3rd, Maxhimer JB, Quiros RM, Hollinger EF, Doolas A, Millikan KW, Deziel DJ, Godellas CV, Prinz RA. Vascular complications associated with pancreaticoduodenectomy adversely affect clinical outcome. *Surgery* 2002; **132**: 738-44; discussion 744 [PMID: 12407360 DOI: 10.1067/msy.2002.127688]
55 **Asano T**, Nakamura T, Noji T, Okamura K, Tsuchikawa T, Nakanishi Y, Tanaka K, Murakami S, Ebihara Y, Kurashima Y, Shichinohe T, Hirano S. Outcome of concomitant resection of the replaced right hepatic artery in pancreaticoduodenectomy without reconstruction. *Langenbecks Arch Surg* 2018; **403**: 195-202 [PMID: 29362881 DOI: 10.1007/s00423-018-1650-9]
56 **Bacalbasa N**, Balescu I, Vilcu M, Croitoru A, Dima S, Brasoveanu V, Brezean I, Popescu I. Pancreatoduodenectomy After Neoadjuvant Chemotherapy for Locally Advanced Pancreatic Cancer in the Presence of an Aberrant Right Hepatic Artery. *In Vivo* 2020; **34**: 401-406 [PMID: 31882506 DOI: 10.21873/invivo.11788]
57 **Majno PE**, Prêtre R, Mentha G, Morel P. Operative injury to the hepatic artery. Consequences of a biliary-enteric anastomosis and principles for rational management. *Arch Surg* 1996; **131**: 211-215 [PMID: 8611081 DOI: 10.1001/archsurg.1996.01430140101025]
58 **Yamamoto M**, Zaima M, Yamamoto H, Harada H, Kawamura J, Yamada M, Yazawa T, Kawasoe J. Liver necrosis shortly after pancreaticoduodenectomy with resection of the replaced left hepatic artery. *World J Surg Oncol* 2017; **15**: 77 [PMID: 28399882 DOI: 10.1186/s12957-017-1151-2]
59 **Hackert T**, Stampfl U, Schulz H, Strobel O, Büchler MW, Werner J. Clinical significance of liver ischaemia after pancreatic resection. *Br J Surg* 2011; **98**: 1760-1765 [PMID: 22021030 DOI: 10.1002/bjs.7675]
60 **Northover JM**, Terblanche J. A new look at the arterial supply of the bile duct in man and its surgical implications. *Br J Surg* 1979; **66**: 379-384 [PMID: 466017 DOI: 10.1002/bjs.1800660603]
61 **Asai K**, Watanabe M, Kusachi S, Matsukiyo H, Saito T, Kodama H, Enomoto T, Nakamura Y, Okamoto Y, Saida Y, Iijima R, Nagao J. Successful treatment of a common hepatic artery pseudoaneurysm using a coronary covered stent following pancreatoduodenectomy: report of a case. *Surg Today* 2014; **44**: 160-165 [PMID: 22932840 DOI: 10.1007/s00595-012-0314-6]
62 **Rubio-Manzanares-Dorado M**, Marín-Gómez LM, Aparicio-Sánchez D, Suárez-Artacho G, Bellido C, Álamo JM, Serrano-Díaz-Canedo J, Padillo-Ruiz FJ, Gómez-Bravo MÁ. Implication of the presence of a variant hepatic artery during the Whipple procedure. *Rev Esp Enferm Dig* 2015; **107**: 417-422 [PMID: 26140634 DOI: 10.17235/reed.2015.3701/2015]
63 **Sanjay P**, Takaori K, Govil S, Shrikhande SV, Windsor JA. 'Artery-first' approaches to pancreatoduodenectomy. *Br J Surg* 2012; **99**: 1027-1035 [PMID: 22569924 DOI: 10.1002/bjs.8763]
64 **Shukla PJ**, Barreto SG, Kulkarni A, Nagarajan G, Fingerhut A. Vascular anomalies encountered during pancreatoduodenectomy: do they influence outcomes? *Ann Surg Oncol* 2010; **17**: 186-193 [PMID: 19838756 DOI: 10.1245/s10434-009-0757-1]
65 **Ogiso S**, Conrad C, Araki K, Basso V, Gayet B. Posterior approach for laparoscopic pancreaticoduodenectomy to prevent replaced hepatic artery injury. *Ann Surg Oncol* 2013; **20**: 3120 [PMID: 23793363 DOI: 10.1245/s10434-013-3058-7]
66 **Yamaguchi T**, Hasegawa K, Sauvain MO, Passoni S, Kazami Y, Kokudo T, Cristaudi A, Melloul E, Uldry E, Kobayashi K, Akamatsu N, Kaneko J, Arita J, Sakamoto Y, Demartines N, Kokudo N, Halkic N. An aberrant right hepatic artery arising from the gastroduodenal artery: a pitfall encountered during pancreaticoduodenectomy. *Surg Today* 2021; **51**: 1577-1582 [PMID: 33575949 DOI: 10.1007/s00595-021-02242-4]
67 **Jah A**, Jamieson N, Huguet E, Praseedom R. The implications of the presence of an aberrant right hepatic artery in

patients undergoing a pancreaticoduodenectomy. *Surg Today* 2009; **39**: 669-674 [PMID: 19639433 DOI: 10.1007/s00595-009-3947-3]

68 **Wang M**, Li D, Chen R, Huang X, Li J, Liu Y, Liu J, Cheng W, Chen X, Zhao W, Tan Z, Huang H, Zhu F, Qin T, Ma J, Yu G, Zhou B, Zheng S, Tang Y, Han W, Meng L, Ke J, Feng F, Chen B, Yin X, Chen W, Ma H, Xu J, Lin R, Dong Y, Yu Y, Zhang H, Qin R; Minimally Invasive Treatment Group in the Pancreatic Disease Branch of China's International Exchange and Promotion Association for Medicine and Healthcare (MITG-P-CPAM). Laparoscopic versus open pancreatoduodenectomy for pancreatic or periampullary tumours: a multicentre, open-label, randomised controlled trial. *Lancet Gastroenterol Hepatol* 2021; **6**: 438-447 [PMID: 33915091 DOI: 10.1016/S2468-1253(21)00054-6]

69 **Can MF**, Kerem M, Dikmen K. Prevention of inadvertent injury to aberrant hepatic artery arising from superior mesenteric artery during laparoscopic pancreaticoduodenectomy. *Turk J Surg* 2018; 1-2 [PMID: 30216174 DOI: 10.5152/turkjsurg.2018.3853]

70 **Rice MK**, Hodges JC, Bellon J, Borrebach J, Al Abbas AI, Hamad A, Knab LM, Moser AJ, Zureikat AH, Zeh HJ, Hogg ME. Association of Mentorship and a Formal Robotic Proficiency Skills Curriculum With Subsequent Generations' Learning Curve and Safety for Robotic Pancreaticoduodenectomy. *JAMA Surg* 2020; **155**: 607-615 [PMID: 32432666 DOI: 10.1001/jamasurg.2020.1040]

71 **Christians KK**, Pilgrim CH, Tsai S, Ritch P, George B, Erickson B, Tolat P, Evans DB. Arterial resection at the time of pancreatectomy for cancer. *Surgery* 2014; **155**: 919-926 [PMID: 24787115 DOI: 10.1016/j.surg.2014.01.003]

72 **Zhang Q**, Wu J, Tian Y, Duan J, Shao Y, Yan S, Wang W. Arterial resection and reconstruction in pancreatectomy: surgical technique and outcomes. *BMC Surg* 2019; **19**: 141 [PMID: 31601220 DOI: 10.1186/s12893-019-0560-2]

73 **Kuribara T**, Ichikawa T, Osa K, Inoue T, Ono S, Asanuma K, Kaneko S, Sano T, Shigeyoshi I, Matsubara K, Irie N, Iai A, Shinobi T, Ishizu H, Miura K. Combined resection of the hepatic artery without reconstruction in pancreaticoduodenectomy: a case report of pancreatic cancer with an aberrant hepatic artery. *Surg Case Rep* 2020; **6**: 228 [PMID: 32990830 DOI: 10.1186/s40792-020-00997-5]

74 **Noussios G**, Dimitriou I, Chatzis I, Katsourakis A. The Main Anatomic Variations of the Hepatic Artery and Their Importance in Surgical Practice: Review of the Literature. *J Clin Med Res* 2017; **9**: 248-252 [PMID: 28270883 DOI: 10.14740/jocmr2902w]

75 **Landen S**, Ursaru D, Delugeau V, Landen C. How to deal with hepatic artery injury during pancreaticoduodenectomy. A systematic review. *J Visc Surg* 2017; **154**: 261-268 [PMID: 28668523 DOI: 10.1016/j.jviscsurg.2017.05.013]

76 **Bachellier P**, Addeo P, Faitot F, Nappo G, Dufour P. Pancreatectomy With Arterial Resection for Pancreatic Adenocarcinoma: How Can It Be Done Safely and With Which Outcomes? *Ann Surg* 2020; **271**: 932-940 [PMID: 30188399 DOI: 10.1097/SLA.0000000000003010]

77 **Yang F**, Wang X, Jin C, He H, Fu D. Pancreatectomy with Hepatic Artery Resection for Pancreatic Head Cancer. *World J Surg* 2019; **43**: 2909-2919 [PMID: 31396672 DOI: 10.1007/s00268-019-05106-8]

78 **Ramanadham S**, Toomay SM, Yopp AC, Balch GC, Sharma R, Schwarz RE, Mansour JC. Rare hepatic arterial anatomic variants in patients requiring pancreatoduodenectomy and review of the literature. *Case Rep Surg* 2012; **2012**: 953195 [PMID: 22900221 DOI: 10.1155/2012/953195]

79 **Özsoy M**, Şahin E, Yavuz M, Özsoy Z, Okur N, Şahin S, Yılmaz S, Arıkan Y. Alternative hepatic arterial reconstruction technique in a case of total pancreaticoduodenectomy after celiac artery resection in pancreas cancer: Iliac-hepatic bypass. *Turk J Surg* 2019; **35**: 146-150 [PMID: 32550321 DOI: 10.5578/turkjsurg.3983]

80 **Kimura Y**, Imamura M, Kuroda Y, Nagayama M, Itoh T, Oota S, Murakami T, Yamaguchi H, Nobuoka T, Kawaharada N, Takemasa I. Clinical usefulness of saphenous vein graft in major arterial reconstruction during extended pancreatectomy. *Langenbecks Arch Surg* 2020; **405**: 1051-1059 [PMID: 32737589 DOI: 10.1007/s00423-020-01947-3]

81 **Hackert T**, Weitz J, Büchler MW. Splenic artery use for arterial reconstruction in pancreatic surgery. *Langenbecks Arch Surg* 2014; **399**: 667-671 [PMID: 24789810 DOI: 10.1007/s00423-014-1200-z]

82 **Tinelli G**, Montanari F, Sica S, Razionale F, Ardito F, Minelli F, De Nigris F, Tshomba Y, Giuliante F. Splenic artery transposition for hepatic arterial reconstruction in a locally advanced pancreatic cancer: a case report and literature review. *Eur Rev Med Pharmacol Sci* 2021; **25**: 3679-3683 [PMID: 34109577 DOI: 10.26355/eurrev_202105_25934]

83 **Yoshida R**, Yagi T, Yasui K, Umeda Y, Yoshida K, Fuji T, Takagi K, Kumano K, Yoshimoto M, Fujiwara T. Usefulness of Middle Colic Artery Transposition Technique for Hepatic Arterial Reconstruction in Conversion Surgery for an Initially Unresectable, Locally Advanced Pancreatic Cancer. *Acta Med Okayama* 2021; **75**: 543-548 [PMID: 34511625 DOI: 10.18926/AMO/62410]

84 **Addeo P**, Guerra M, Bachellier P. Distal pancreatectomy with en bloc celiac axis resection (DP-CAR) and arterial reconstruction: Techniques and outcomes. *J Surg Oncol* 2021; **123**: 1592-1598 [PMID: 33684225 DOI: 10.1002/jso.26424]

85 **El Amrani M**, Pruvot FR, Truant S. Management of the right hepatic artery in pancreaticoduodenectomy: a systematic review. *J Gastrointest Oncol* 2016; **7**: 298-305 [PMID: 27034799 DOI: 10.3978/j.issn.2078-6891.2015.093]

86 **Mittal A**, de Reuver PR, Shanbhag S, Staerkle RF, Neale M, Thoo C, Hugh TJ, Gill AJ, Samra JS. Distal pancreatectomy, splenectomy, and celiac axis resection (DPS-CAR): common hepatic arterial stump pressure should determine the need for arterial reconstruction. *Surgery* 2015; **157**: 811-817 [PMID: 25532436 DOI: 10.1016/j.surg.2014.10.006]

87 **Cesaretti M**, Abdel-Rehim M, Barbier L, Dokmak S, Hammel P, Sauvanet A. Modified Appleby procedure for borderline resectable/locally advanced distal pancreatic adenocarcinoma: A major procedure for selected patients. *J Visc Surg* 2016; **153**: 173-181 [PMID: 26775202 DOI: 10.1016/j.jviscsurg.2015.11.014]

88 **Aosasa S**, Nishikawa M, Noro T, Yamamoto J. Total Pancreatectomy with Celiac Axis Resection and Hepatic Artery Restoration Using Splenic Artery Autograft Interposition. *J Gastrointest Surg* 2016; **20**: 644-647 [PMID: 26487332 DOI: 10.1007/s11605-015-2991-0]

89 **Nigri G**, Petrucciani N, Belloni E, Lucarini A, Aurello P, D'Angelo F, di Saverio S, Fancellu A, Ramacciato G. Distal Pancreatectomy with Celiac Axis Resection: Systematic Review and Meta-Analysis. *Cancers (Basel)* 2021; **13** [PMID: 33921838 DOI: 10.3390/cancers13081967]

90 **Inoue Y**, Oba A, Ono Y, Sato T, Ito H, Takahashi Y. Radical Resection for Locally Advanced Pancreatic Cancers in the

Era of New Neoadjuvant Therapy-Arterial Resection, Arterial Divestment and Total Pancreatectomy. *Cancers (Basel)* 2021; **13** [PMID: 33920314 DOI: 10.3390/cancers13081818]

91 **Colombo PE**, Quenet F, Alric P, Mourregot A, Neron M, Portales F, Rouanet P, Carrier G. Distal Pancreatectomy with Celiac Axis Resection (Modified Appleby Procedure) and Arterial Reconstruction for Locally Advanced Pancreatic Adenocarcinoma After FOLFIRINOX Chemotherapy and Chemoradiation Therapy. *Ann Surg Oncol* 2021; **28**: 1106-1108 [PMID: 32588265 DOI: 10.1245/s10434-020-08740-y]

92 **Toguchi M**, Tsurusaki M, Numoto I, Hidaka S, Yamakawa M, Asato N, Im S, Yagyu Y, Matsuki M, Takeyama Y, Murakami T. Utility of Amplatzer Vascular Plug with Preoperative Common Hepatic Artery Embolization for Distal Pancreatectomy with En Bloc Celiac Axis Resection. *Cardiovasc Intervent Radiol* 2017; **40**: 445-449 [PMID: 27858118 DOI: 10.1007/s00270-016-1509-9]

93 **Gong H**, Ma R, Gong J, Cai C, Song Z, Xu B. Distal Pancreatectomy With En Bloc Celiac Axis Resection for Locally Advanced Pancreatic Cancer: A Systematic Review and Meta-Analysis. *Medicine (Baltimore)* 2016; **95**: e3061 [PMID: 26962836 DOI: 10.1097/MD.0000000000003061]

94 **Baumgartner JM**, Krasinskas A, Daouadi M, Zureikat A, Marsh W, Lee K, Bartlett D, Moser AJ, Zeh HJ 3rd. Distal pancreatectomy with en bloc celiac axis resection for locally advanced pancreatic adenocarcinoma following neoadjuvant therapy. *J Gastrointest Surg* 2012; **16**: 1152-1159 [PMID: 22399269 DOI: 10.1007/s11605-012-1839-0]

95 **Ueda A**, Sakai N, Yoshitomi H, Furukawa K, Takayashiki T, Kuboki S, Takano S, Suzuki D, Kagawa S, Mishima T, Nakadai E, Miyazaki M, Ohtsuka M. Is hepatic artery coil embolization useful in distal pancreatectomy with en bloc celiac axis resection for locally advanced pancreatic cancer? *World J Surg Oncol* 2019; **17**: 124 [PMID: 31315628 DOI: 10.1186/s12957-019-1667-8]

96 **Deal S**, Nathan D, Rocha FG. Modified Appleby procedure for locally advanced pancreatic cancer. *Am J Surg* 2018; **215**: 853-855 [PMID: 29397891 DOI: 10.1016/j.amjsurg.2018.01.004]

97 **Ielpo B**, Ferri V, Caruso R, Duran H, Diaz E, Fabra I, Oliva C, Olivares S, Quijano Y, Vicente E. Alternative arterial reconstruction after extended pancreatectomy. Case report and some considerations of locally advanced pancreatic cancer. *JOP* 2013; **14**: 432-437 [PMID: 23846942 DOI: 10.6092/1590-8577/1468]

98 **Machado MA**, Surjan RC, Nishinari K, Makdissi FF, Machado MC. Iliac-hepatic arterial bypass for compromised collateral flow during modified Appleby operation for advanced pancreatic cancer. *Eur J Surg Oncol* 2009; **35**: 1124-1127 [PMID: 19410414 DOI: 10.1016/j.ejso.2009.04.005]

99 **Delpero JR**, Sauvanet A. Vascular Resection for Pancreatic Cancer: 2019 French Recommendations Based on a Literature Review From 2008 to 6-2019. *Front Oncol* 2020; **10**: 40 [PMID: 32117714 DOI: 10.3389/fonc.2020.00040]

100 **Morris M**, Price T, Callahan Z, Yeo CJ. Celiac Axis Resection with Distal Pancreatectomy (Modified Appleby Procedure) Allows for R0 Resection of Pancreatic Body and Tail Mass Following Neoadjuvant Therapy: Case Report and Literature Review. *Case Rep Pancreat Cancer* 2016; **2**: 53-57 [PMID: 30631817 DOI: 10.1089/crpc.2016.0011]

101 **Cannella R**, Borhani AA, Zureikat AH, Tublin ME. Appleby Procedure (Distal Pancreatectomy With Celiac Artery Resection) for Locally Advanced Pancreatic Carcinoma: Indications, Outcomes, and Imaging. *AJR Am J Roentgenol* 2019; **213**: 35-44 [PMID: 30917026 DOI: 10.2214/AJR.18.20887]

102 **Nara S**, Oguro S, Hata S, Kishi Y, Esaki M, Shimada K, Kosuge T. Total pancreatectomy with en bloc celiac axis resection for a pancreatic adenocarcinoma involving both the gastroduodenal artery and the celiac artery. *Hepatogastroenterology* 2012; **59**: 1635-1637 [PMID: 22155851 DOI: 10.5754/hge11687]

World Journal of Gastroenterology

Submit a Manuscript: https://www.f6publishing.com

World J Gastroenterol 2022 May 21; 28(19): 2076-2087

DOI: 10.3748/wjg.v28.i19.2076

ISSN 1007-9327 (print) ISSN 2219-2840 (online)

MINIREVIEWS

Mixed neuroendocrine-non-neuroendocrine neoplasms of the digestive system: A mini-review

Deepak Toor, Jonathan M Loree, Zu-Hua Gao, Gang Wang, Chen Zhou

Specialty type: Gastroenterology and hepatology

Provenance and peer review: Invited article; Externally peer reviewed.

Peer-review model: Single blind

Peer-review report's scientific quality classification

Grade A (Excellent): 0
Grade B (Very good): B
Grade C (Good): C
Grade D (Fair): 0
Grade E (Poor): 0

P-Reviewer: Jesinghaus M, Germany; Yang Y, China

Received: November 9, 2021
Peer-review started: November 9, 2021
First decision: March 11, 2022
Revised: March 25, 2022
Accepted: April 28, 2022
Article in press: April 28, 2022
Published online: May 21, 2022

Deepak Toor, Zu-Hua Gao, Gang Wang, Chen Zhou, Department of Pathology and Laboratory Medicine, BC Cancer, Vancouver V5Z 1H5, Canada

Deepak Toor, Zu-Hua Gao, Gang Wang, Chen Zhou, Department of Pathology and Laboratory Medicine, University of British Columbia, Vancouver V5Z 1H5, Canada

Jonathan M Loree, Department of Medicine, BC Cancer, Vancouver V5Z 4E6, Canada

Corresponding author: Chen Zhou, MD, PhD, Associate Professor, Department of Pathology and Laboratory Medicine, BC Cancer, 600 West 10th Avenue, Vancouver V5Z 1H5, Canada. czhou@bccancer.bc.ca

Abstract

Mixed neuroendocrine-non-neuroendocrine neoplasms (MiNENs) are rare mixed tumors containing both neuroendocrine (NE) and non-NE components. Each component must occupy at least 30% of the tumor volume by definition. Recent molecular evidence suggests MiNENs are clonal neoplasms and potentially harbor targetable mutations similar to conventional carcinomas. There have been multiple changes in the nomenclature and classification of MiNENs which has created some confusion among pathologists on how to integrate the contributions of each component in a MiNEN, an issue which in turn has resulted in confusion in communication with front-line treating oncologists. This mini review summarizes our current understanding of MiNENs and outline diagnosis, prognosis, and management of these neoplasms. The authors emphasize the importance of treating the most aggressive component of the tumor regardless of its percentage volume.

Key Words: Mixed neuroendocrine non-neuroendocrine neoplasms; Mixed adenoneuorendocrine carcinoma; Mixed neuroendocrine neoplasms; Neuroendocrine; Non-neuroendocrine

©The Author(s) 2022. Published by Baishideng Publishing Group Inc. All rights reserved.

Core Tip: Mixed neuroendocrine neoplasms have been referred to by a long list of names. The latest term, mixed neuroendocrine-non-neuroendocrine neoplasm (MiNEN), captures a wider spectrum of neoplasms than did previous nomenclature. This mini review summarizes the development of the term MiNEN and reviews current knowledge about the molecular pathogenesis, diagnosis, prognosis, and management of these neoplasms. MiNENs are viewed as clonal neoplasms and their clinical behaviour and management are ultimately determined by the most aggressive component present.

Citation: Toor D, Loree JM, Gao ZH, Wang G, Zhou C. Mixed neuroendocrine-non-neuroendocrine neoplasms of the digestive system: A mini-review. *World J Gastroenterol* 2022; 28(19): 2076-2087
URL: https://www.wjgnet.com/1007-9327/full/v28/i19/2076.htm
DOI: https://dx.doi.org/10.3748/wjg.v28.i19.2076

INTRODUCTION

Mixed neuroendocrine-non-neuroendocrine neoplasms (MiNENs) are tumors containing two or more histologically distinct components with one component showing neuroendocrine (NE) differentiation [1]. The non-NE component consists of an adenocarcinoma in over 90% of cases, but it can consist of any other epithelial neoplasm, including squamous cell carcinoma or hepatocellular carcinoma[1,2]. By definition each component must individually comprise > 30% of the total tumor volume in order for the tumor to qualify as a MiNEN[3].

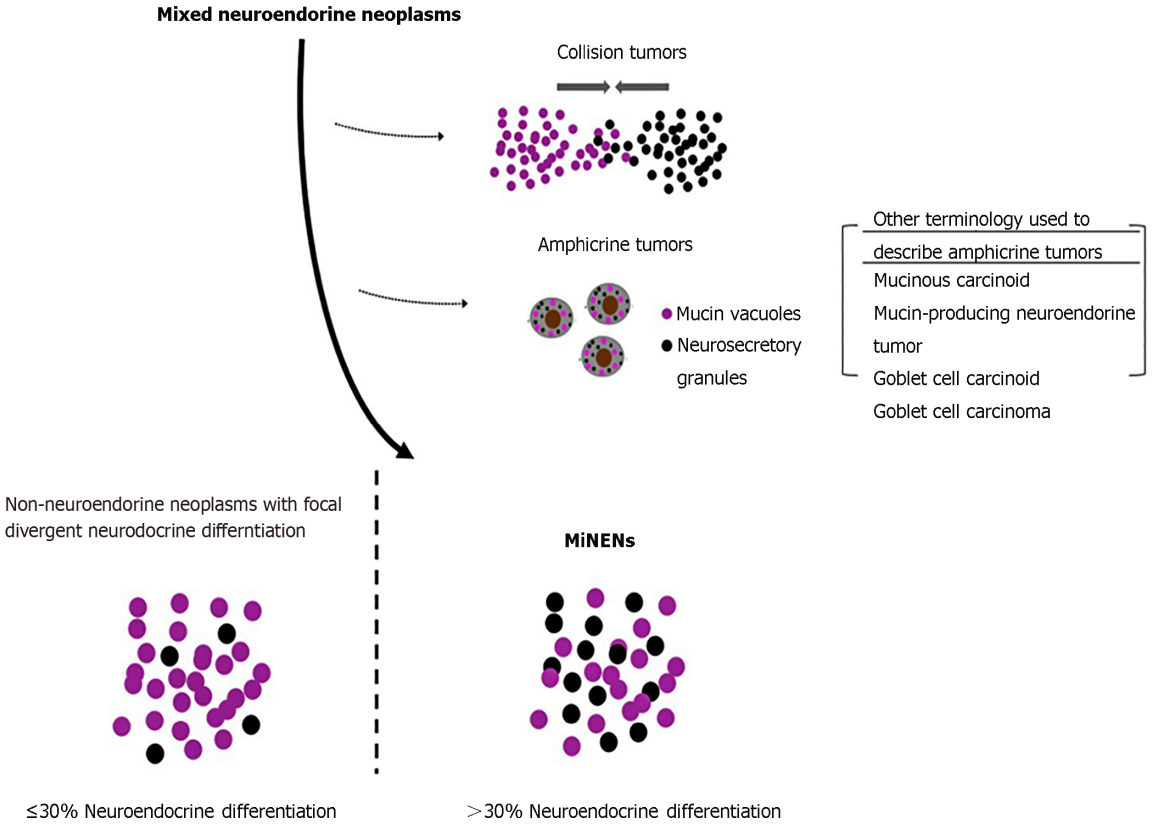
MiNENs are a specific subtype of mixed NE neoplasms (Figure 1)[4]. Traditionally, mixed NE neoplasms include composite tumor, collision tumors, amphicrine tumors and non-NE neoplasms with focal neuroendocrine differentiation (NNE-NEDs). Strictly speaking, in MiNENs the distinct NE and non-NE components are intimately intermingled and both are derived from a common single precursor cell, morphologically expressing usually as composite tumors. Collision tumors consist of two independent primary neoplasms which have grown into the same space by chance. Each neoplasm is derived from a separate precursor cell which has independently undergone its own molecular evolution [5]. Amphicrine neoplasms consist of a single cell type in which each cell displays both NE and non-NE phenotypes simultaneously. For example, electron microscopy may demonstrate both mucous vacuoles and neurosecretory granules in the same cell. These tumors are extremely rare, with approximately only 4 reported in the stomach[6] but are slightly more common in the pancreas. Despite that collision tumors might not come from a common single precursor cell; they have still been referred to as MiNENs by authors based on the traditional practice.

NNE-NEDs are non-NE neoplasms which show NE differentiation but not enough to meet the criteria to be considered MiNENs. The exact percentage threshold of NED required to be considered a MiNEN is artificial and will likely continue to evolve in the future as we learn more about these neoplasms. The current 30% threshold was originally defined arbitrarily in 1987 to recognize and create a new diagnostic entity for truly mixed NE tumors with substantial amounts of both non-NE and NE components, and to exclude non-NE tumors with scattered NE cells of uncertain clinical significance[4,7]. Although it has served a valuable role in the establishment of MiNENs as distinct diagnostic entities, this cut-off does not have a basis in clinical or scientific evidence[1]. Recent studies suggest a lower threshold may be more appropriate, with even 10% NED significantly affecting prognosis, thus raising the possibility the formally defined threshold may change in the future[8,9]. Indeed, poorly differentiated NE or even non-NE components, even when < 5% of the tumor volume, may determine patient outcome. Regardless of what the threshold is, it is important to note neoplasms may show a spectrum of divergent NED, and that only a subset of these neoplasms should be classified as MiNENs.

Other entities which may be confused with MiNENs include usual adenocarcinomas displaying aberrant expression of NE markers (*i.e.*, synaptophysin and chromogranin) but no histologically recognizable NE morphology[7]. These features do not qualify a neoplasm as a MiNEN, and aberrant synaptophysin expression in conventional adenocarcinomas does not affect prognosis[10]. Neoplasms which overgrow and entrap physiologic NE structures, for example acinar adenocarcinoma in the pancreas which can entrap normal physiologic islets of Langerhans, should also not be mistaken for MiNENs despite the pitfall of positive staining for NE markers[7].

NOMENCLATURE

The individual components of MiNENs are common entities which pathologists and oncologists encounter routinely. The major challenge in understanding MiNENs is simply an issue of nomenclature. Unfortunately, the nomenclature has undergone numerous rapid and successive changes over the past 20 years. This has been complicated by substantial changes in the nomenclature for simple pure NE



DOI: 10.3748/wjg.v28.i19.2076 **Copyright** ©The Author(s) 2022.

Figure 1 Classification of mixed neuroendocrine neoplasms. Mixed neuroendocrine-non-neuroendocrine neoplasms are specific mixed neuroendocrine tumors, which show an intimate mixture of neuroendocrine and non-neuroendocrine cells and are both derived from a common precursor cell. MiNEN: Mixed neuroendocrine-non-neuroendocrine neoplasms.

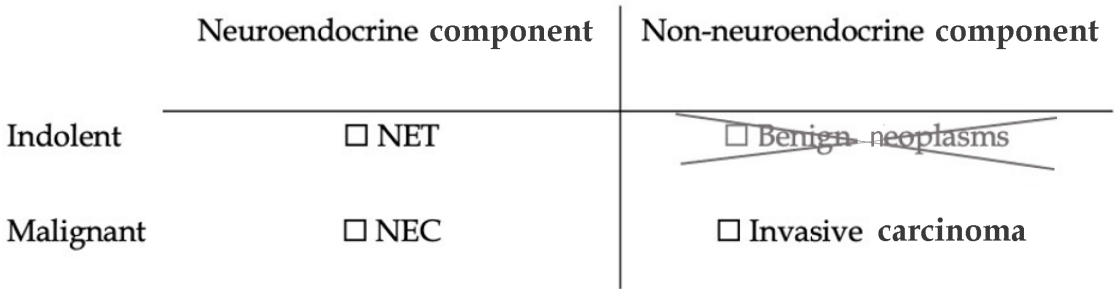
neoplasms themselves which have occurred over the same timeframe. The potential clinical confusion which may occur because of these rapid changes is not insignificant. An illustrative example of such potential confusion comes from appendiceal goblet cell neoplasms which have similarly undergone numerous changes in nomenclature. Two cases diagnosed as "goblet cell adenocarcinoma" and "adenocarcinoma ex goblet cell carcinoid" were misinterpreted by oncologists as NE tumors and then considered for inappropriate adjuvant chemotherapy[11].

A conceptual framework for understanding MiNENs is shown in Figure 2. In order to constitute a MiNEN a tumor must show at least two lines of differentiation, one of which is NE and the other of which is epithelial but non-NE. In the digestive system only, there is an additional stipulation that each component of the neoplasm is required to be malignant in order for it to qualify as a MiNEN[3]. Low-grade NE tumors, formerly known as carcinoids, satisfy this "malignant" requirement because of their potential for metastasis, despite their usually indolent behavior[1,3]. However indolent non-NE epithelial tumors, such as adenomas or papillomas, do not metastasize and so would not constitute MiNENs in the digestive system[3]. For example, mixed adenomas well-differentiated NE tumors, or "MANETs", consisting of a composite tubular adenoma-carcinoid tumor, are no longer considered MiNENs with these updated criteria[12]. Similarly, in-situ lesions such as intraductal papillary mucinous neoplasms of the pancreas were formerly included as potential non-NE components of digestive system MiNENs, but now have been excluded by the latest WHO classification[1,3]. The non-NE component is required to be an invasive carcinoma.

Although perhaps daunting, becoming familiar with the host of names that has been used to refer to MiNENs in the past may help reduce confusion in clinical practice. We will attempt to briefly summarize the history of the nomenclature of MiNENs towards this end. We begin by describing the changes in nomenclature of pure NE neoplasms, before moving on to the broader category of MiNENs.

NE neoplasms

The nomenclature of NE neoplasms in the digestive system has undergone a series of changes in the last 20 years. After being first recognized in 1907, NE neoplasms were designated "carcinoid tumors" and referred to as such for almost a century thereafter[8,13]. By 1994 poorly differentiated NE neoplasms were noted to have a drastically worse prognosis than their well-differentiated counterparts[8,14]. The



DOI: 10.3748/wjg.v28.i19.2076 **Copyright** ©The Author(s) 2022.

Figure 2 Conceptual framework for mixed neuroendocrine-non-neuroendocrine neoplasm of the digestive system. The tumor must include one neuroendocrine component and one non-neuroendocrine component. In the digestive system both components must have metastatic potential, excluding benign non-neuroendocrine neoplasms such as adenomas or squamous papillomas. NET: Neuroendocrine tumors; NEC: Neuroendocrine carcinomas.

poorly differentiated neoplasms were designated "small cell carcinomas". The term carcinoid continued to refer to well-differentiated NE neoplasms.

Increasing use of Ki-67 immunohistochemistry revealed a wide spectrum of proliferative rates within carcinoid tumors and small cell carcinomas. A grading system based on Ki-67 index was proposed in 2006 and formally adopted by the WHO classification in 2010[15,16]. NE tumors with low Ki-67 indices (≤ 20%; grades 1 or 2) were called neuroendocrine tumors (NETs) while tumors with high Ki-67 index (> 20%; grade 3) were called neuroendocrine carcinomas (NECs).

Grade 3 tumors were recently recognized to consist of two types of tumors, although both have increased Ki-67 indices. One type of tumors shows well-differentiated morphology while another type shows poorly differentiated morphology[8]. Further studies have revealed tumors showing poorly differentiated morphology have half the survival of their well-differentiated counterparts[8]. Genetic studies further show the two tumor populations actually develop *via* entirely separate and independent molecular pathways[8,17]. These findings have led to any poorly differentiated tumor being referred to as a NEC, regardless of Ki-67 index. Well-differentiated tumors which are designated NETs and further graded according to their proliferation rate[3].

Any NE neoplasm, either a NET or a NEC, can constitute the NE component of a MiNEN.

Non-NE component

Mixed NE neoplasms were first recognized in 1924, only shortly after pure NE neoplasms themselves were first recognized[7,18]. In 1987 Lewin[4] formally proposed a classification system for mixed NE neoplasms in which he termed what we now call MiNENs as "composite glandular-endocrine cell carcinomas"[4]. His classification system distinguished these tumors from collision tumors and amphicrine tumors, as well as from usual adenocarcinomas with < 30% NED.

In 2000 these neoplasms were adopted into the *WHO Classification of Tumors of the Digestive System* as "mixed exocrine-endocrine carcinomas" (MEECs)[7,19]. This terminology was short-lived and changed to "mixed adenoneuroendocrine carcinoma" (MANEC) in the subsequent 2010 edition of the classification[16].

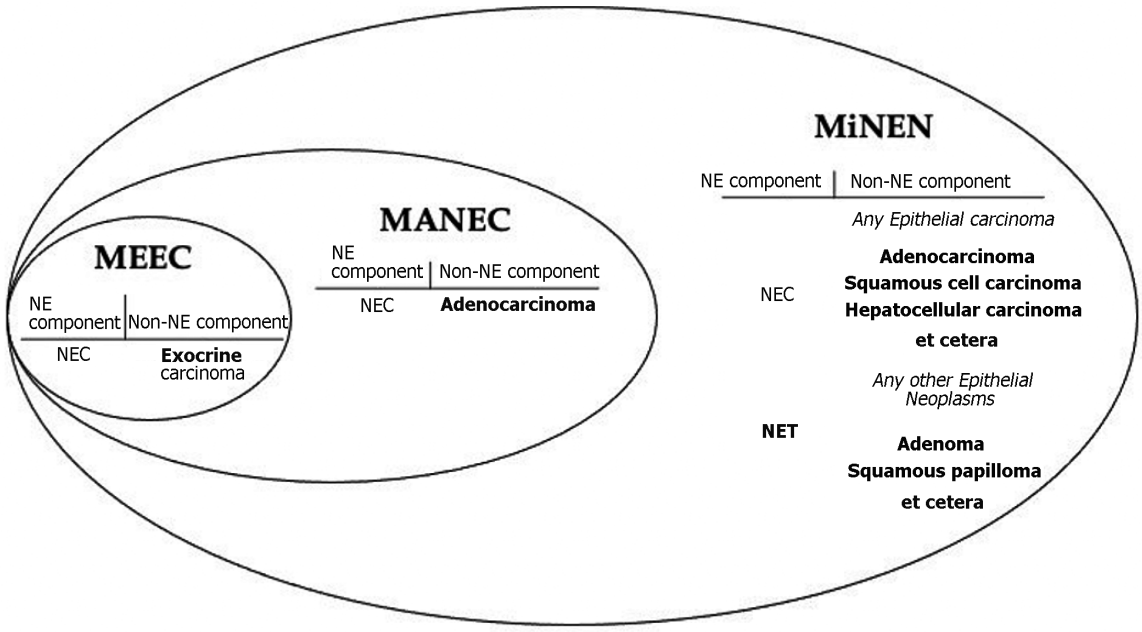
It soon became apparent adenocarcinomas were not the only non-NE neoplasms observed in mixed NE tumors. Other epithelial neoplasms, such as squamous cell carcinomas and hepatocellular carcinomas, were also observed in mixed NE neoplasms[1,7]. This prompted "mixed adenoneuroendocrine carcinomas" (MANECs) to instead be viewed as "mixed neuroendocrine-non-neuroendocrine carcinomas" (Figure 3).

MiNENs

In 2016, La Rosa *et al*[1] proposed the term "mixed neuroendocrine-non-neuroendocrine neoplasms" (MiNENs)[1]. The intention was to create an umbrella term for mixed NE neoplasms broad enough to encompass all the changes we have discussed so far, while also being generalizable to any mixed NE tumor occurring in any organ in the body. The latter task is difficult considering the heterogeneity in nomenclature for NE neoplasms in different sites such as the lung. It is even more difficult if one anticipates the nomenclature for pure NE neoplasms continuing to evolve in other organs such as it has in the digestive system.

MiNENs are 'neoplasms' instead of 'carcinomas' because benign non-NE components such as adenomas or papillomas can still be a part of MiNENs in sites outside of the digestive system[1]. This had been the case in the digestive system as well until only recently when the latest WHO classification was published in 2019.

The current prevailing view is that MiNENs are clonal neoplasms derived from a single pluripotent stem cell[8]. Multiple studies have compared the mutational landscape in the NE and non-NE



DOI: 10.3748/wjg.v28.i19.2076 **Copyright** ©The Author(s) 2022.

Figure 3 Evolution of the terminology of mixed neuroendocrine-non-neuroendocrine neoplasm. The terminology has been broadened to include other non-neuroendocrine epithelial components beyond adenocarcinoma as well as including indolent or benign tumors such as neuroendocrine tumors. NE: Neuroendocrine; NEC: Neuroendocrine carcinoma; NET: Neuroendocrine tumor; MEEC: Mixed exocrine-endocrine carcinoma; MANEC: Mixed adenoneuroendocrine carcinoma; MiNEN: Mixed neuroendocrine-non-neuroendocrine neoplasm.

components and have demonstrated a common trunk of mutations shared between them, beyond which are further mutations specific to each component[20-22]. Interestingly these shared mutations are very similar to the mutations found in standard pure adenocarcinomas from the same anatomic site[22]. For example, in the colon, MiNENs can show *BRAF*, *KRAS*, and *APC* mutations in both components[22]. The mutated genes are expressed at similar levels in both components, and expression is significantly altered in comparison to normal background tissue[20,21].

Some authors have theorized MiNENs may begin as non-NE tumors and then at some point trans-differentiate to form an aggressive NEC component[2,23-26]. Several reports suggest *c-Myc* and *SMARCA* mutations may play a role in trans-differentiation, with one study even finding only a single additional *SMARCA* mutation in the NE component of a MiNEN[23-25]. Other studies have shown increased chromosomal aberrations and allelic imbalances in the NE component[26].

CHALLENGES IN DIAGNOSIS

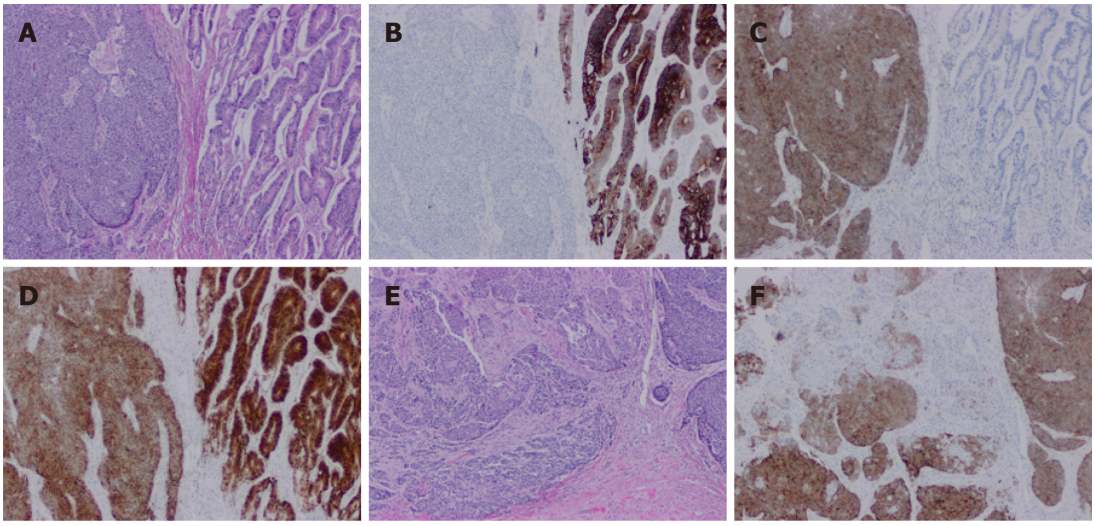
Definitive diagnosis of a MiNEN usually follows after surgical resection. The presurgical biopsy diagnoses are roughly evenly split between 1/3 adenocarcinoma, 1/3 NEC, and 1/3 suspicious for MiNEN[2]. The NE component tends to lie deeper in the tumor which can influence the diagnosis on biopsy depending on the depth of tumor sampled[27,28].

Identifying the components

Diagnosing a MiNEN is equivalent to individually diagnosing the constituent components with a few additional steps. Neither the NE nor non-NE components differ from their pure counterparts, including their immunohistochemical profiles.

Figure 4 illustrates a typical MiNEN of colon origin. Both morphologic and immunohistochemical evidence of NED is required to diagnose a NE component in a MiNEN[3,7]. Morphologic evidence is required avoid the pitfall of focal aberrant NE marker expression on immunohistochemistry in otherwise standard non-NE tumors, a commonly recognized phenomenon with no current known clinical significance[10,29]. Common markers of NED that are used include synaptophysin, chromogranin, INSM1, CD56, and neuron-specific enolase. Synaptophysin is traditionally be regarded as the most sensitive and chromogranin as the most specific[30].

The NE component may be either a NEC or a NET[3,7]. Ki-67 proliferative index (or equivalently mitotic rate) should be reported for all NE neoplasms, including the NE component present in MiNENs. NETs are graded as usual by Ki-67 index: Grade 1 tumors are < 3%; grade 2 between 3%-20%; and grade 3 > 20%[3]. Grade 3 NETs usually have a Ki-67 index less than 60%, while the indices for NECs are



DOI: 10.3748/wjg.v28.i19.2076 **Copyright** ©The Author(s) 2022.

Figure 4 Histopathology of a mixed neuroendocrine-non-neuroendocrine neoplasm of colon. A: Hematoxylin and eosin (H&E) stain of mixed neuroendocrine-non-neuroendocrine neoplasm. On the right side is a well-differentiated invasive adenocarcinoma. On the left side is a poorly differentiated neuroendocrine carcinoma (20 ×, H&E); B: The adenocarcinoma component is positive for cytokeratin 20, but the neuroendocrine component is negative (20 ×); C: Positive synaptophysin staining in the neuroendocrine component but negative staining in the adenocarcinoma component (20 ×); D: Positive CDX2 staining in both adenocarcinoma and neuroendocrine carcinoma components (20 ×); E: Merging area of adenocarcinoma and neuroendocrine carcinoma components (20 ×); F: Positive synaptophysin staining of neuroendocrine cells in the merged area (20 ×).

higher, typically more than 50%-60%[8].

Well-differentiated NETs are usually organized in nested, solid, trabecular, ribbon, or insular patterns. Rosette-like formations can be present. Tumors are cohesive without isolated single cells. Granular eosinophilic cytoplasm may be appreciated. Lymphovascular or perineural invasion is allowed in NETs and does not necessitate a diagnosis of NEC. NETs retain immunohistochemical markers from the primary site of origin[8].

The majority of MiNENs do not contain NETs but rather contain poorly differentiated NECs. Tumor cells in NECs show nuclear crowding and pleomorphism. Nuclei are hyperchromatic with increased nuclear membrane irregularity. Single cells are common, and mitoses are obvious. Necrosis can be present, and nuclei display smearing or crush artifact. NE markers remain sensitive, however immunohistochemical markers for the primary site of origin are lost[8,30]. Aberrant expression of TTF-1 and CDX-2 is common, making these markers unreliable and a potential pitfall for mistaking the site of origin[8]. The average Ki-67 proliferative index of NECs in MiNENs is 70%[30].

Morphologically NECs can show either small or large cell patterns. Small cell morphology is similar to traditional small cell carcinoma elsewhere with small uniform round to oval nuclei and evenly distributed finely granular ("salt and pepper") chromatin. Cytoplasm is scant. Cells are crowded with nuclear moulding and indistinct cell membranes. In contrast, large cell NECs (LCNECs) have a larger cell size than small cell carcinoma and a vesicular nucleus with prominent nucleolus. They can have appreciable eosinophilic cytoplasm. Distinguishing LCNECs from small cell carcinoma can sometimes be a difficult task. Ki-67 index can potentially be helpful as the index of LCNECs ranges from 40%-80% while small cell carcinoma averages 80%[31]. In MiNENs the NEC component is more commonly a LCNECs than a small cell carcinoma[32,33].

The non-NE component of MiNENs is adenocarcinoma 92% of the time[2]. Squamous cell carcinoma, hepatocellular carcinoma, and mixed adenosquamous carcinoma make up the majority of remaining non-NE components in reported cases thus far[2].

Extent of NE differentiation

The exact threshold of NED required to define a tumor as a MiNEN *vs* an NNE-NED is an area of current controversy in the literature. As mentioned, the 30% threshold which persists today was originally chosen arbitrarily. A commonly cited and relatively recent study by Park *et al*[9] provides evidence arguing in favor of lowering the threshold to 10%[9]. The authors examined 88 gastric carcinomas with varying degrees of NED and compared overall survival to 650 gastric carcinomas with no NED. NED of just under 10% was associated with worse survival: Overall 5-year survival in cases with < 10% NED was 85.6% compared to only 53.3% survival in cases with ≥ 10% NED.

Another similar study found 20% NED to be associated with significantly worse prognosis in adenocarcinomas, again suggesting the 30% threshold may be too high[34]. The current formal threshold for diagnosing a MiNEN remains 30% but this is likely to be lowered in the future. In the interim while this does preclude a diagnosis of MiNEN in cases with 10%-30% NED, we recommend

always quantifying the percentage of NED in non-NE tumors and informing the oncologist of the possible prognostic impact, for example by making a diagnostic comment citing the studies above. Regardless of how the report is handled, the possible prognostic impact of 10%–30% is an important topic to be raised in multidisciplinary meetings discussing diagnosis and management of these rare tumors.

The significance of divergent differentiation in NECs is a less well explored topic. This may be because even small degrees of NED, beginning at as little as 10% as mentioned above, quickly approach the same dismal prognosis as NECs regardless of the size of the non-NE component (Table 1).

Grading

There is currently no widely accepted system for grading MiNENs. This is somewhat unfortunate because MiNEN is an umbrella term for a wide range of neoplasms whose behaviour can range from indolent (*i.e.*, a MiNEN in which a NET is the most biologically aggressive component) to aggressively malignant, paralleling the prognosis of NECs. Simply designating a tumor as a MiNEN is insufficient and does not convey much useful information. Therefore, it is incumbent upon the pathologist to clearly communicate the nature and aggressiveness of each component present in the tumor to ensure appropriate management.

The original publication by La Rosa *et al*[1] in which the term MiNEN was coined also proposed a grading scheme in which MiNENs were divided into low-grade, intermediate grade, and high grade categories[1]. Tumors with a NEC component, which constitute the vast majority of MiNENs, would be designated high grade neoplasms. Tumors in which the non-NE component was the most aggressive, such as adenocarcinomas with a NET component, would be intermediate grade. Indolent tumors in which a NET was the most aggressive component would be low-grade. This scheme succinctly classifies MiNENs according to their most aggressive component. It is also clinically useful because the most aggressive component usually drives prognosis and management. While the scheme may not be widely used, it still serves as a useful guide as to how to portray grade in MiNENs.

Staging

The fact that MiNENs are considered single clonal neoplasms greatly simplifies staging. The two components do not need to be staged separately as they would in a collision tumor. Standard TNM staging applies as *per* AJCC guidelines, using the same protocols as for other carcinomas from the same body site. For the rare MiNENs in which a NET is the most aggressive component the protocol for NETs from the same body site is used. There does not appear to be literature yet to consider alternative methods for staging MiNENs.

Lymph nodes

While lymph node staging proceeds as *per* staging of the rest of the MiNEN as described above, the composition of lymph node metastases in MiNENs is an interesting issue because of the many different possible scenarios: Only one component may have metastasized, or both may have; the components may metastasize together to the same lymph node, or separately to different lymph nodes. Further it is interesting to consider whether the metastatic component of a MiNEN is a better marker of the biologic behavior of the tumor than the de facto assumption that behaviour is dictated by the worst component found in the primary tumor.

The pattern of metastasis in MiNENs was investigated in a study of 80 patients[35]. In approximately 70% of patients only one component metastasized; this was usually the more aggressive NEC component. In 20% of patients both components metastasized, but none were found together in the same lymph node. In 10% of patients there was lymph node metastasis present containing both components within the same node.

In terms of the components present in metastases, they reflected the composition of the primary tumor; in a tumor composed of 60% NEC and 40% adenocarcinoma, roughly 60% of metastases would be NEC and 40% would be adenocarcinoma[35].

Included in the study were 3 cases of NNE-NEDs. In all 3 of these cases the metastases were composed solely of the NEC component. Notably, by current criteria these tumors would not have qualified as MiNENs, providing further evidence that < 30% NED can be biologically significant.

The question of whether the biologic behaviour of MiNENs is better reflected by the metastatic component or the most aggressive component in the primary tumor is moot since these data show the composition of the metastases simply reflect the composition of the primary tumor; in other words, it is unlikely further useful information will be gained by determining the pattern of lymph node metastasis once the composition of the primary tumor is known. The grading scheme proposed by La Rosa appears to be the most useful gauge of the potential biological behavior of the tumor.

Reporting

'MiNEN' is not a diagnosis but rather an umbrella term for mixed NE neoplasms[1]. The term in and of itself does not convey useful information to the oncologist. The useful information is knowing the components which make up the tumor, and pathologists must ensure these are communicated clearly to

Table 1 Prognostic impact of neuroendocrine differentiation (summarized from Park *et al*[9])

Classification					
Neuroendocrine differentiation (%)	0	< 10	10-30	30-70	> 70
Current classification	Non-NE	Non-NE	NNE-NED	MiNEN	NEC
5-yr overall survival	85	89	17[1]	54	59

[1]The 8 cases of non-NE tumors with NED in this study presented at a higher stage than the other tumors.
NE: Neuroendocrine; NED: Neuroendocrine differentiation; NNE: Non-neuroendocrine; MiNEN: Mixed neuroendocrine-non-neuroendocrine neoplasm; NEC: Neuroendocrine carcinoma.

allow oncologists to stratify risk and plan management accordingly.

Figure 5 shows the example of the pathology report of a MiNEN. The first line of the report should identify that the tumor is a MiNEN. Because there is currently no widely accepted grading system, grade must be conveyed within the next few lines. The most aggressive or high-grade component should be listed first, and the system by La Rosa *et al*[1] serves a useful guide here[1]. A NEC component is the highest possible grade neoplasm found in MiNENs and should always be listed first. Next in the hierarchy of grade usually comes a non-NE carcinoma component, usually an adenocarcinoma, which is then followed by a NET component, and then lastly followed by the lowest grade component possible, a benign epithelial neoplasm such as an adenoma or papilloma. Accordingly, La Rosa's scheme describes tumors driven by a NEC component as high-grade, tumors driven by a carcinoma component intermediate grade, and tumors driven by a NET component low-grade or indolent. For each component listed the histologic subtype and grade should be described the same way they would be as if the component were a pure neoplasm. The percentage of total tumor volume occupied by each component should also be listed.

We recommend designating non-NE tumors with 10%-30% NED (NNE-NEDs) as 'mixed neoplasms' and then reporting them in the same manner as a MiNEN. A diagnostic comment citing the Park *et al*[9] and Jiang *et al*[34] studies mentioning the possible prognostic impact of NE components occupying < 30% of the tumor volume may help provide important background information for these rare tumors[9,34].

Because of their genetic similarity to adenocarcinomas, we recommend performing the same molecular studies on MiNENs as one would perform for an adenocarcinoma from the same anatomic site. Alterations involving MMR, BRAF V600E, and Her-2 have been demonstrated to exist in both components of MiNENs, inviting the exciting possibility of using the same targeted therapies during treatment[22,25,36]. Although ideally both components in a MiNEN would be tested individually to allow for better prediction of how the entire tumor will respond to a targeted therapy, in practice this may be very difficult or impossible to achieve with the closely intermingled components.

PROGNOSIS AND MANAGEMENT

The rarity of MiNENs, combined with their changing terminology over the years, has made it difficult to examine outcomes data. Controversy exists as to whether MiNENs behave better than pure NECs, but ultimately the prognosis appears to be similar[2,30,37,38]. A recently reported survival comparison of 503 NECs, 401 MiNENs, and 2785 adenocarcinomas of the stomach showed that the 5-year disease-free survival (DFS) was 47.5%, 51.1%, and 57.8% respectively[37]. The shorter DFS of NECs and MiNENs compared to adenocarcinoma was statistically significant while the difference between NECs and MiNENs was not.

In the digestive system in general, 82% of MiNENs present with localized disease and 18% present with distant metastases[2]. Patients with localized disease generally proceed to surgical resection. Select patients with advanced disease may undergo palliative resection[38]. The median overall survival for localized MiNENs, including regional lymph node metastases (Stages I-III), is 39 mo. For advanced disease with distant metastasis (Stage IV) median overall survival is 11 mo[38].

MiNENs may be missed in patients with an accessible metastasis that is used for the initial diagnostic biopsy. These cases may be diagnosed as pure NECs or pure adenocarcinomas, if resection is not indicated and further tissue is not sampled, thus may result in under recognition of MiNENs[30]. This leads to bias in outcome data as lower stage tumors are more likely to undergo surgical resection and be diagnosed as MiNENs whereas higher stage tumors are more likely to be missed and labeled pure NECs or pure adenocarcinomas. Thus, MiNENs may appear to have improved prognosis, when in reality they are just more likely to be diagnosed at a lower stage.

Management for these rare tumors is usually discussed at multidisciplinary rounds with the expertise of pathologists and oncologists who have special interest in NE neoplasms. Treatment is tailored

Left colon, hemicolectomy with lymph node dissection:
Mixed neuroendocrine-non-neuroendocrine neoplasms
Component 1: Neuroendocrine carcinoma
(1) Comprises 60% of total tumor volume; (2) Histologic subtype: Small cell carcinoma; and (3) Ki-67 proliferative index: 87%.
Component 2: Intestinal adenocarcinoma
(1) Comprises 40% of total tumor volume; and (2) Tumor grade: Grade 2 (moderately differentiated)
Tumor size: 4.3 cm
Tumor invades serosa and pericolonic tissue (stage pT4a)
Lymphovascular invasion present
Perineural invasion present
No tumor deposits identified
Margins: (1) Proximal margin: Negative; (2) Distal margin: POSITIVE for invasive carcinoma; and (3) Radial margin: Negative.
Total lymph nodes present: 15
Sixlymph nodes POSITIVE for metastatic carcinoma (6/15; stage pN2a): (1) Five lymph nodes are positive for metastatic neuroendocrine carcinoma only; and (2) One lymph node positive for both metastatic neuroendocrine carcinoma and adenocarcinoma.
Ancillary tests: (1) BRAF: POSITIVE for V600E mutation (immunohistochemistry)-Mutation present in both the neuroendocrine carcinoma and adenocarcinoma components; (2) MMR proficient/wild-type (immunohistochemistry); and (3) KRAS, NRAS negative (sanger sequencing)
Final stage: pT4a pN2a MX

DOI: 10.3748/wjg.v28.i19.2076 **Copyright** ©The Author(s) 2022.

Figure 5 Sample pathology report. MiNEN: Mixed neuroendocrine-non-neuroendocrine neoplasm.

towards the most aggressive component of the tumor, which is usually a NEC. MiNENs in which the most aggressive component is an adenocarcinoma (*i.e.*, tumors composed of adenocarcinomas with a NET component) are much rarer, but in these cases treatment is tailored towards the adenocarcinoma component.

No guidelines exist currently for adjuvant or neoadjuvant chemotherapy. NEC driven tumors are usually treated with etoposide and cisplatin-based regimens[2,27,39]. Adenocarcinoma driven cancers are commonly treated with 5-FU based backbones, however treatment options vary based on the site of the primary, with chemotherapies for MiNENs arising from a particular organ mirroring the systemic therapy for adenocarcinomas at that site. The oncologist may attempt a tailored combination of therapy in which the agents employed display efficacy against both components[30]. Radiation therapy has been suggested in tumors from the esophagus, stomach, rectum, and anus[40].

The genetic similarity of MiNENs to adenocarcinomas and reports of *KRAS, BRAF V600E, APC, MMR* , and *HER-2* amplifications occurring in both components of MiNENs invites the possibility of targeted therapies in these tumors[2,22,40,41]. One series of 44 cases found MMR deficiency in 39% of these tumors[40]. While this did not appear to have prognostic impact, it is an exciting finding raising the possibility for potential response to programmed death 1 blockade.

CONCLUSION

Mixed NE neoplasms have a complex history particularly in regard to nomenclature which has evolved alongside our increasing recognition of these tumors. The term 'MiNEN' was created to encompass a broader range of non-NE epithelial components beyond just adenocarcinomas. The term also incorporates updates in terminology used for NE neoplasms. MiNEN can be used to refer to tumors outside of the digestive system as well, although the digestive system has been the leading-edge area for these tumors. Diagnosis is in fact very familiar to both pathologists and oncologists alike, with no significant differences compared to diagnosis of each individual neoplasms. Staging is simplified because MiNENs are considered single clonal neoplasms. Prognosis and management are based on, and in general equivalent to, that of the most aggressive component.

FOOTNOTES

Author contributions: Toor D performed the majority of the writing; Wang G provided input in writing the paper and contributed histology images; Loree JM provided input and opinions on the clinical management portion of the writing; Gao ZH defined the concepts and ensured the overall quality of the writing; Zhou C designed the outline and coordinated the writing of the paper.

Conflict-of-interest statement: JL has received consulting fees from Taiho, Ipsen, Novartis, Amgen, Eisai, and Bayer;

research funding from Ipsen Biopharmaceuticals, Amgen, and Foundation Medicine.

Open-Access: This article is an open-access article that was selected by an in-house editor and fully peer-reviewed by external reviewers. It is distributed in accordance with the Creative Commons Attribution NonCommercial (CC BY-NC 4.0) license, which permits others to distribute, remix, adapt, build upon this work non-commercially, and license their derivative works on different terms, provided the original work is properly cited and the use is non-commercial. See: https://creativecommons.org/Licenses/by-nc/4.0/

Country/Territory of origin: Canada

ORCID number: Deepak Toor 0000-0002-1859-1246; Jonathan M Loree 0000-0001-8189-2132; Zu-Hua Gao 0000-0001-7232-0933; Gang Wang 0000-0002-0225-4173; Chen Zhou 0000-0002-7898-4201.

S-Editor: Fan JR
L-Editor: A
P-Editor: Fan JR

REFERENCES

1 **La Rosa S**, Sessa F, Uccella S. Mixed Neuroendocrine-Nonneuroendocrine Neoplasms (MiNENs): Unifying the Concept of a Heterogeneous Group of Neoplasms. *Endocr Pathol* 2016; **27**: 284-311 [PMID: 27169712 DOI: 10.1007/s12022-016-9432-9]
2 **Frizziero M**, Chakrabarty B, Nagy B, Lamarca A, Hubner RA, Valle JW, McNamara MG. Mixed Neuroendocrine Non-Neuroendocrine Neoplasms: A Systematic Review of a Controversial and Underestimated Diagnosis. *J Clin Med* 2020; **9** [PMID: 31963850 DOI: 10.3390/jcm9010273]
3 **Lokuhetty D**, White VA, Watanabe R, Cree IA, World Health O, International Agency for Research on C. Digestive system tumours. Fifth ed. Lyon: International Agency for Research on Cancer, 2019
4 **Lewin K**. Carcinoid tumors and the mixed (composite) glandular-endocrine cell carcinomas. *Am J Surg Pathol* 1987; **11** Suppl 1: 71-86 [PMID: 3544888 DOI: 10.1097/00000478-198700111-00007]
5 **Furlan D**, Cerutti R, Genasetti A, Pelosi G, Uccella S, La Rosa S, Capella C. Microallelotyping defines the monoclonal or the polyclonal origin of mixed and collision endocrine-exocrine tumors of the gut. *Lab Invest* 2003; **83**: 963-971 [PMID: 12861036 DOI: 10.1097/01.lab.0000079006.91414.be]
6 **La Rosa S**, Marando A, Sessa F, Capella C. Mixed Adenoneuroendocrine Carcinomas (MANECs) of the Gastrointestinal Tract: An Update. *Cancers (Basel)* 2012; **4**: 11-30 [PMID: 24213223 DOI: 10.3390/cancers4010011]
7 **Uccella S**, La Rosa S. Looking into digestive mixed neuroendocrine - nonneuroendocrine neoplasms: subtypes, prognosis, and predictive factors. *Histopathology* 2020; **77**: 700-717 [PMID: 32538468 DOI: 10.1111/his.14178]
8 **La Rosa S**. Challenges in High-grade Neuroendocrine Neoplasms and Mixed Neuroendocrine/Non-neuroendocrine Neoplasms. *Endocr Pathol* 2021; **32**: 245-257 [PMID: 33786701 DOI: 10.1007/s12022-021-09676-z]
9 **Park JY**, Ryu MH, Park YS, Park HJ, Ryoo BY, Kim MG, Yook JH, Kim BS, Kang YK. Prognostic significance of neuroendocrine components in gastric carcinomas. *Eur J Cancer* 2014; **50**: 2802-2809 [PMID: 25201164 DOI: 10.1016/j.ejca.2014.08.004]
10 **Konukiewitz B**, Kasajima A, Schmitt M, Schwamborn K, Groll T, Schicktanz F, Delbridge C, Schütze LM, Wilhelm D, Lang C, Lange S, Foersch S, Jank P, Steiger K, Werder AV, Denkert C, Weichert W, Klöppel G, Jesinghaus M. Neuroendocrine Differentiation in Conventional Colorectal Adenocarcinomas: Incidental Finding or Prognostic Biomarker? *Cancers (Basel)* 2021; **13** [PMID: 34680258 DOI: 10.3390/cancers13205111]
11 **Zhang K**, Meyerson C, Kassardjian A, Westbrook LM, Zheng W, Wang HL. Goblet Cell Carcinoid/Carcinoma: An Update. *Adv Anat Pathol* 2019; **26**: 75-83 [PMID: 30601149 DOI: 10.1097/PAP.0000000000000222]
12 **La Rosa S**, Uccella S, Molinari F, Savio A, Mete O, Vanoli A, Maragliano R, Frattini M, Mazzucchelli L, Sessa F, Bongiovanni M. Mixed Adenoma Well-differentiated Neuroendocrine Tumor (MANET) of the Digestive System: An Indolent Subtype of Mixed Neuroendocrine-NonNeuroendocrine Neoplasm (MiNEN). *Am J Surg Pathol* 2018; **42**: 1503-1512 [PMID: 30001239 DOI: 10.1097/PAS.0000000000001123]
13 **Oberndorfer S**. Uber die kleinen dunndarmcarcinome. *Verh Dtsch Ges Pathol* 1907; **11**: 113-116
14 **Capella C**, Heitz PU, Höfler H, Solcia E, Klöppel G. Revised classification of neuroendocrine tumors of the lung, pancreas and gut. *Digestion* 1994; **55** Suppl 3: 11-23 [PMID: 7698533 DOI: 10.1159/000201197]
15 **Rindi G**, Klöppel G, Alhman H, Caplin M, Couvelard A, de Herder WW, Erikssson B, Falchetti A, Falconi M, Komminoth P, Körner M, Lopes JM, McNicol AM, Nilsson O, Perren A, Scarpa A, Scoazec JY, Wiedenmann B; all other Frascati Consensus Conference participants; European Neuroendocrine Tumor Society (ENETS). TNM staging of foregut (neuro)endocrine tumors: a consensus proposal including a grading system. *Virchows Arch* 2006; **449**: 395-401 [PMID: 16967267 DOI: 10.1007/s00428-006-0250-1]
16 **Bosman FT**, Carneiro F, Hruban RH, Theise ND. WHO classification of tumours of the digestive system: World Health Organization, 2010
17 **Rindi G**, Klimstra DS, Abedi-Ardekani B, Asa SL, Bosman FT, Brambilla E, Busam KJ, de Krijger RR, Dietel M, El-Naggar AK, Fernandez-Cuesta L, Klöppel G, McCluggage WG, Moch H, Ohgaki H, Rakha EA, Reed NS, Rous BA, Sasano H, Scarpa A, Scoazec JY, Travis WD, Tallini G, Trouillas J, van Krieken JH, Cree IA. A common classification framework for neuroendocrine neoplasms: an International Agency for Research on Cancer (IARC) and World Health

Organization (WHO) expert consensus proposal. *Mod Pathol* 2018; **31**: 1770-1786 [PMID: 30140036 DOI: 10.1038/s41379-018-0110-y]
18 **Cordier R**. Les cellules argentaffines dans les tumeurs intestinales. *Arch Int Med Exp* 1924; **1**
19 **Hamilton SR**, Aaltonen LA. Pathology and genetics of tumours of the digestive system: IARC press Lyon: 2000
20 **Sun L**, Zhang J, Wang C, Zhao S, Shao B, Guo Y, Liu Y, Sun Y. Chromosomal and molecular pathway alterations in the neuroendocrine carcinoma and adenocarcinoma components of gastric mixed neuroendocrine-nonneuroendocrine neoplasm. *Mod Pathol* 2020; **33**: 2602-2613 [PMID: 32461621 DOI: 10.1038/s41379-020-0579-z]
21 **Yuan W**, Liu Z, Lei W, Sun L, Yang H, Wang Y, Ramdas S, Dong X, Xu R, Cai H, Li JZ, Ke Y. Mutation landscape and intra-tumor heterogeneity of two MANECs of the esophagus revealed by multi-region sequencing. *Oncotarget* 2017; **8**: 69610-69621 [PMID: 29050228 DOI: 10.18632/oncotarget.18678]
22 **Jesinghaus M**, Konukiewitz B, Keller G, Kloor M, Steiger K, Reiche M, Penzel R, Endris V, Arsenic R, Hermann G, Stenzinger A, Weichert W, Pfarr N, Klöppel G. Colorectal mixed adenoneuroendocrine carcinomas and neuroendocrine carcinomas are genetically closely related to colorectal adenocarcinomas. *Mod Pathol* 2017; **30**: 610-619 [PMID: 28059096 DOI: 10.1038/modpathol.2016.220]
23 **Sinha N**, Gaston D, Manders D, Goudie M, Matsuoka M, Xie T, Huang WY. Characterization of genome-wide copy number aberrations in colonic mixed adenoneuroendocrine carcinoma and neuroendocrine carcinoma reveals recurrent amplification of PTGER4 and MYC genes. *Hum Pathol* 2018; **73**: 16-25 [PMID: 28899736 DOI: 10.1016/j.humpath.2017.08.036]
24 **La Rosa S**, Bernasconi B, Vanoli A, Sciarra A, Notohara K, Albarello L, Casnedi S, Billo P, Zhang L, Tibiletti MG, Sessa F. c-MYC amplification and c-myc protein expression in pancreatic acinar cell carcinomas. New insights into the molecular signature of these rare cancers. *Virchows Archiv* 2018; **473**: 435-441 [DOI: 10.1007/s00428-018-2366-5]
25 **Vanacker L**, Smeets D, Hoorens A, Teugels E, Algaba R, Dehou Mf, De Becker A, Lambrechts D, De Greve J. Mixed Adenoneuroendocrine Carcinoma of the Colon: Molecular Pathogenesis and Treatment. *Anticancer Res* 2014; **34**: 5517-5521 [PMID: 25275049]
26 **Fujita Y**, Uesugi N, Sugimoto R, Eizuka M, Matsumoto T, Sugai T. Gastric mixed neuroendocrine-non-neuroendocrine neoplasm (MiNEN) with pancreatic acinar differentiation: a case report. *Diagn Pathol* 2019; **14**: 38 [PMID: 31077220 DOI: 10.1186/s13000-019-0815-3]
27 **Desai GS**, Pande P, Shah RC, Jagannath P. Dilemmas in Diagnosis and Management of Gastroenteropancreatic Mixed Neuroendocrine Non-neuroendocrine Neoplasms: First Single-Centre Report from India. *J Gastrointest Cancer* 2020; **51**: 102-108 [PMID: 30784017 DOI: 10.1007/s12029-019-00213-0]
28 **Moritz AW**, Schlumbrecht MP, Nadji M, Pinto A. Expression of neuroendocrine markers in non-neuroendocrine endometrial carcinomas. *Pathology* 2019; **51**: 369-374 [PMID: 31040050 DOI: 10.1016/j.pathol.2019.02.003]
29 **Duan K**, Mete O. Algorithmic approach to neuroendocrine tumors in targeted biopsies: Practical applications of immunohistochemical markers. *Cancer Cytopathol* 2016; **124**: 871-884 [PMID: 27529763 DOI: 10.1002/cncy.21765]
30 **Frizziero M**, Wang X, Chakrabarty B, Childs A, Luong TV, Walter T, Khan MS, Morgan M, Christian A, Elshafie M, Shah T, Minicozzi A, Mansoor W, Meyer T, Lamarca A, Hubner RA, Valle JW, McNamara MG. Retrospective study on mixed neuroendocrine non-neuroendocrine neoplasms from five European centres. *World J Gastroenterol* 2019; **25**: 5991-6005 [PMID: 31660035 DOI: 10.3748/wjg.v25.i39.5991]
31 World Health Organization. WHO Classification of Tumours Editorial Board. Thoracic tumours. 5th ed. Lyon: IARC Press, 2021
32 **Olevian DC**, Nikiforova MN, Chiosea S, Sun W, Bahary N, Kuan SF, Pai RK. Colorectal poorly differentiated neuroendocrine carcinomas frequently exhibit BRAF mutations and are associated with poor overall survival. *Hum Pathol* 2016; **49**: 124-134 [PMID: 26826419 DOI: 10.1016/j.humpath.2015.11.004]
33 **Watanabe J**, Suwa Y, Ota M, Ishibe A, Masui H, Nagahori K, Tsuura Y, Endo I. Clinicopathological and Prognostic Evaluations of Mixed Adenoneuroendocrine Carcinoma of the Colon and Rectum: A Case-Matched Study. *Dis Colon Rectum* 2016; **59**: 1160-1167 [PMID: 27824701 DOI: 10.1097/DCR.0000000000000702]
34 **Jiang SX**, Mikami T, Umezawa A, Saegusa M, Kameya T, Okayasu I. Gastric large cell neuroendocrine carcinomas: a distinct clinicopathologic entity. *Am J Surg Pathol* 2006; **30**: 945-953 [PMID: 16861964 DOI: 10.1097/00000478-200608000-00003]
35 **Zhang P**, Li Z, Li J, Zhang X, Lu Z, Sun Y, Li Y, Zhou J, Wang X, Peng Z, Shen L, Lu M. Clinicopathological features and lymph node and distant metastasis patterns in patients with gastroenteropancreatic mixed neuroendocrine-non-neuroendocrine neoplasm. *Cancer Med* 2021; **10**: 4855-4863 [PMID: 34109756 DOI: 10.1002/cam4.4031]
36 **Girardi DM**, Silva ACB, Rêgo JFM, Coudry RA, Riechelmann RP. Unraveling molecular pathways of poorly differentiated neuroendocrine carcinomas of the gastroenteropancreatic system: A systematic review. *Cancer Treat Rev* 2017; **56**: 28-35 [PMID: 28456055 DOI: 10.1016/j.ctrv.2017.04.002]
37 **Lin J**, Zhao Y, Zhou Y, Tian Y, He Q, Lin J, Hao H, Zou B, Jiang L, Zhao G, Lin W, Xu Y, Li Z, Xue F, Li S, Fu W, Li Y, Xu Z, Chen J, Zhou X, Zhu Z, Cai L, Li E, Li H, Zheng C, Li P, Huang C, Xie J. Comparison of Survival and Patterns of Recurrence in Gastric Neuroendocrine Carcinoma, Mixed Adenoneuroendocrine Carcinoma, and Adenocarcinoma. *JAMA Netw Open* 2021; **4**: e2114180 [PMID: 34313744 DOI: 10.1001/jamanetworkopen.2021.14180]
38 **Pommergaard HC**, Nielsen K, Sorbye H, Federspiel B, Tabaksblat EM, Vestermark LW, Janson ET, Hansen CP, Ladekarl M, Garresori H, Hjortland GO, Sundlöv A, Galleberg R, Knigge P, Kjaer A, Langer SW, Knigge U. Surgery of the primary tumour in 201 patients with high-grade gastroenteropancreatic neuroendocrine and mixed neuroendocrine-non-neuroendocrine neoplasms. *J Neuroendocrinol* 2021; **33**: e12967 [PMID: 33769624 DOI: 10.1111/jne.12967]
39 **de Mestier L**, Cros J, Neuzillet C, Hentic O, Egal A, Muller N, Bouché O, Cadiot G, Ruszniewski P, Couvelard A, Hammel P. Digestive System Mixed Neuroendocrine-Non-Neuroendocrine Neoplasms. *Neuroendocrinology* 2017; **105**: 412-425 [PMID: 28803232 DOI: 10.1159/000475527]
40 **Lou L**, Lv F, Wu X, Li Y, Zhang X. Clinical implications of mismatch repair deficiency screening in patients with mixed neuroendocrine non-neuroendocrine neoplasms (MiNEN). *Eur J Surg Oncol* 2021; **47**: 323-330 [PMID: 32907775 DOI: 10.1016/j.ejso.2020.08.022]

41 **Golombek T**, Henker R, Rehak M, Quäschling U, Lordick F, Knödler M. A Rare Case of Mixed Adenoneuroendocrine Carcinoma (MANEC) of the Gastroesophageal Junction with HER2/neu Overexpression and Distinct Orbital and Optic Nerve Toxicity after Intravenous Administration of Cisplatin. *Oncol Res Treat* 2019; **42**: 123-127 [PMID: 30799422 DOI: 10.1159/000495218]

World Journal of Gastroenterology

Submit a Manuscript: https://www.f6publishing.com

World J Gastroenterol 2022 May 21; 28(19): 2088-2099

DOI: 10.3748/wjg.v28.i19.2088

ISSN 1007-9327 (print) ISSN 2219-2840 (online)

MINIREVIEWS

Mechanisms of ductular reaction in non-alcoholic steatohepatitis

Yue Chen, Wen-Kang Gao, Yan-Yun Shu, Jin Ye

Specialty type: Medicine, research and experimental

Provenance and peer review: Invited article; Externally peer reviewed.

Peer-review model: Single blind

Peer-review report's scientific quality classification

Grade A (Excellent): A
Grade B (Very good): 0
Grade C (Good): C
Grade D (Fair): 0
Grade E (Poor): 0

P-Reviewer: Kotlyarov S, Russia; Moldovan C, Romania

Received: January 17, 2022
Peer-review started: January 17, 2022
First decision: February 7, 2022
Revised: February 18, 2022
Accepted: April 3, 2022
Article in press: April 3, 2022
Published online: May 21, 2022

Yue Chen, Wen-Kang Gao, Yan-Yun Shu, Jin Ye, Division of Gastroenterology, Union Hospital, Tongji Medical College, Huazhong University of Science and Technology, Wuhan 430022, Hubei Province, China

Corresponding author: Jin Ye, MD, PhD, Chief Doctor, Professor, Division of Gastroenterology, Union Hospital, Tongji Medical College, Huazhong University of Science and Technology, No. 1277 Jiefang Avenue, Wuhan 430022, Hubei Province, China. yejin8688@sina.com

Abstract

Non-alcoholic fatty liver disease (NAFLD) is a disease spectrum caused in part by insulin resistance and genetic predisposition. This disease is primarily characterized by excessive lipid accumulation in hepatocytes in the absence of alcohol abuse and other causes of liver damage. Histologically, NAFLD is divided into several periods: simple steatosis, non-alcoholic steatohepatitis (NASH), hepatic fibrosis, cirrhosis, and hepatocellular carcinoma. With the increasing prevalence of obesity and hyperlipidemia, NAFLD has become the main cause of chronic liver disease worldwide. As a result, the pathogenesis of this disease is drawing increasing attention. Ductular reaction (DR) is a reactive bile duct hyperplasia caused by liver injury that involves hepatocytes, cholangiocytes, and hepatic progenitor cells. Recently, DR is shown to play a pivotal role in simple steatosis progression to NASH or liver fibrosis, providing new research and treatment options. This study reviews several DR signaling pathways, including Notch, Hippo/YAP-TAZ, Wnt/β-catenin, Hedgehog, HGF/c-Met, and TWEAK/Fn14, and their role in the occurrence and development of NASH.

Key Words: Non-alcoholic fatty liver disease; Non-alcoholic steatohepatitis; Ductular reaction; Mechanisms; Signaling pathways

©The Author(s) 2022. Published by Baishideng Publishing Group Inc. All rights reserved.

Core Tip: With the increasing prevalence of obesity and hyperlipidemia, Non-alcoholic fatty liver disease (NAFLD) has become the primary cause of chronic liver disease worldwide. Thus, the pathogenesis of non-alcoholic steatohepatitis (NASH) is drawing increasing attention. Ductular reaction (DR) is a reactive bile duct hyperplasia involving hepatocytes, cholangiocytes, and hepatic progenitor cells, that plays an important role in NAFLD pathogenesis and promotes the occurrence and development of NASH and liver fibrosis. This minireview describes the characteristics of DR and summarizes its pivotal mechanisms. A role for DR during NASH is described that supplements current knowledge about the pathogenesis of this disease and informs potential prevention and treatment strategies.

Citation: Chen Y, Gao WK, Shu YY, Ye J. Mechanisms of ductular reaction in non-alcoholic steatohepatitis. *World J Gastroenterol* 2022; 28(19): 2088-2099
URL: https://www.wjgnet.com/1007-9327/full/v28/i19/2088.htm
DOI: https://dx.doi.org/10.3748/wjg.v28.i19.2088

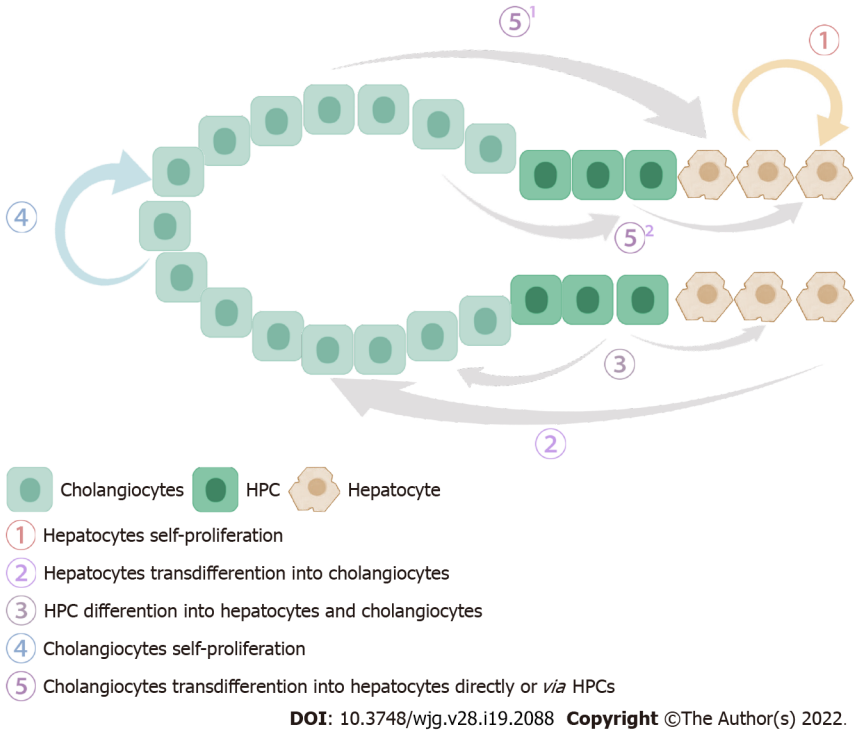
INTRODUCTION

Non-alcoholic fatty liver disease (NAFLD) is defined as the presence of > 5% hepatic steatosis in the absence of significant alcohol consumption or other liver disease-induced steatosis. This is one of the most important causes of liver disease worldwide and will likely emerge as the leading cause of end-stage liver disease in the coming decades. The epidemiology and demographic characteristics of NAFLD vary from country to country, correlating with the prevalence of obesity and risk factors for metabolic comorbidities. The global prevalence of NAFLD is currently estimated to be 29.1%, with more than 240 million individuals in China. NAFLD and its complications inflict a heavy financial burden on the global health system, patients, and their families. Thus, it is critical to conduct more research on NAFLD pathogenesis to inform the development of new prevention or treatment strategies[1,2].

As a result of fat accumulation, insulin resistance, and oxidative stress, a subgroup (approximately 20%-30%) of NAFLD, a relatively benign condition, can develop into non-alcoholic steatohepatitis (NASH) within three years. This is defined as the presence of hepatic steatosis with evidence of hepatocyte damage accompanied by inflammation and regeneration, that can progress into liver fibrosis, cirrhosis, and hepatocellular carcinoma[3,4]. Chronic hepatocyte death often occurs during NASH, and liver regeneration is a common way to restore normal liver structure characterized by phenotypic fidelity of hepatocytes and/or cholangiocytes. There are two primary mechanisms of liver regeneration. Under physiological conditions, liver parenchymal cells are repaired by the division of adjacent resting hepatocytes. During chronic liver diseases, such as NASH, liver regeneration capacity is impaired, activating the alternate regenerative pathway and resulting in ductular reaction (DR). Under these circumstances, macrophages, hepatic stellate cells (HSCs), and the extracellular matrix (ECM) act together to form the inflammatory micro-environment, releasing inflammatory and pro-fibrotic factors and promoting type I collagen deposition. When this occurs, hepatocytes, cholangiocytes, and hepatic progenitor cells (HPCs) in the Hering duct around the portal vein become activated, resulting in DR and eventually leading to liver fibrosis. HPC expansion is shown to occur in NAFLD patients and is strongly correlated with DR[5,6]. This is a common phenomenon during NASH, affecting the stage of fibrosis and disease progression and prognosis[7,8]. In this study, the signaling pathways and the roles of DR during NASH are explored to better understand the pathogenesis of this disease and provide potential treatment strategies to improve NASH outcomes.

DEFINITION OF DR

In 1957, Popper *et al*[9] first characterized DR as a ductular reaction involved in both acute and chronic liver diseases and found that it was associated with recovery from liver homeostasis. Cells involved in DR include pre-existing cholangiocytes, HPCs, and hepatocytes, together known as ductular reaction cells (DRCs) (Figure 1)[10]. However, DR does not just manifest as bile duct hyperplasia but also as liver injury and cell microenvironment-dependent liver regeneration. In diseases involving cholangiocyte damage, biliary cell number and function can be compensated by cholangiocyte and/or HPC proliferation and the transdifferentiation of hepatocytes into biliary-like cells. During hepatocyte injury and other related diseases, cholangiocytes can transdifferentiate into hepatocytes *via* HPCs[10,11]. DRCs exist in a niche with myofibroblasts and macrophages, and can actively promote liver inflammation and fibrosis. In human diseases such as primary sclerosing cholangitis, alcoholic or non-alcoholic steatohepatitis, and viral hepatitis, the number of DRCs in the liver directly correlates with fibrosis severity. In a mouse model, targeted apoptosis of DRCs alleviates fibrosis, while inhibition of DRC apoptosis aggravates liver fibrosis, suggesting that DR correlates with poor prognosis of liver diseases such as



DOI: 10.3748/wjg.v28.i19.2088 **Copyright** ©The Author(s) 2022.

Figure 1 The different compartments of the ductular reaction, including hepatocyte self-proliferation and transdifferentiation, hepatic progenitor cell differentiation, and cholangiocyte proliferation and transdifferention. HPC: Hepatic progenitor cell.

fibrosis and even cirrhosis[12-14]. Thus, research on the mechanism and intervention of DR is of great significance to liver disease treatment. EpCAM and NCAM/SOX9 have been proposed as HPC markers, CK7 and CK19 are used to identify cholangiocytes, and albumin and HNF 4α are regarded as hepatocyte markers (Table 1)[11,15-17]. CK7 immunohistochemistry is positive in HPCs and both initial and late intermediate hepatobiliary cell stages during DR[18]. By calculating the ratio of CK-positive cells in damaged liver tissue using immunostaining, DR can be divided into five grades, and liver injury severity can be predicted. Morphologically DR is divided into three types: (1) Regular bile duct structure commonly seen in biliary obstruction; (2) Incomplete bile duct structure observed in chronic active hepatitis; and (3) Small bile ducts reorganized by bile duct epithelial cells and hepatocytes, seen after submassive liver necrosis[19]. This allows the disease type and degree to be defined through the pathological manifestation of DR and informs disease treatment.

DR AND LIVER FIBROSIS IN NASH

Liver fibrosis is a major complication of almost all types of chronic liver damage including NASH. NAFLD includes three patterns of liver fibrosis according to histological characteristics, portal fibrosis, centrilobular fibrosis, and septal fibrosis[20]. In human liver diseases, fibrosis in the portal area is associated with poor prognosis even when the primary site of injury is lobular hepatocytes. Initially, NASH presents as active lobular necroinflammatory and typical centrilobular fibrosis, characterized by pericentral monocyte infiltration, myofibroblast activation, and localized collagen deposition, that can progress to portal fibrosis, septal fibrosis, and eventually lead to liver cirrhosis[7,21]. The DR correlates closely with fibrosis severity during NASH[6]. A rat model of liver fibrosis induced by chronic 2-acetylaminofluorene showed that HPC expansion aggravated liver fibrosis by driving myofibroblastic transformation of fibroblasts and/or HSCs in the injured liver[22]. However, whether fibrosis aids the regeneration mediated by HPC or DR exacerbates fibrosis remain unclear[7,23].

Periportal DR in NASH

Periportal fibrosis is closely related to NASH progression. Periportal DR is a typical injury response caused by portal inflammatory infiltration that leads to periportal fibrosis[6,24]. Lobular injury activates macrophages to release pro-inflammatory factors such as TNF and IL-1β and promotes formation of the portal inflammatory infiltration microenvironment that is dominated by CD68+ macrophages, CD8+ lymphocytes, collagen I, and laminin, contributing to cell fate. As cell damage increases during NASH, HPC proliferation induces DR around the portal vein. DR activates HSCs and induces HPC differentiation by releasing inflammatory mediators and pro-fibrogenic factors, eventually resulting in

Table 1 Identifying markers of cholangiocytes, hepatic progenitor cells, and hepatocytes

Cell types	Markers	Ref.
Cholangiocytes	CK7/CK19/EpCAM/SOX9/TFF/*etc.*	[15-17]
Hepatic progenitor cells	EpCAM/NCAM/SOX9/MCAM/Foxl1/Lgr5/A6/OV6/NGA2/CXCR4/*etc.*	
	TROP2/CD24/CD133/CLDN3/FGFR2/CK7/CK19/SPP1/*etc.* (biliary progenitors)	
	ALB/AFP/DLK1/APOE/TF/HNF4α/*etc.* (hepatic progenitors)	
Hepatocytes	ALB/HNF4α/RBP4/PCNA/Ki67/Hep Par-1/ASGPR1/*etc.*	

periportal fibrosis that resembles biliary fibrosis[25]. Except for hepatic parenchymal and nonparenchymal cells, current studies have confirmed that mixed infiltration of lymphocytes, neutrophils, monocytes, and a small number of eosinophils participate in DR, but the relative number of different cells and their relationship to disease progression is not fully understood[26].

Studies have shown that DR and portal inflammation are closely related during NASH and are independently related to fibrosis. In the portal vein area, inflammatory cells and their mediators affect HPC differentiation and this process affects the balance between liver regeneration and fibrogenesis. In a rat model using a 3,5-methoxycarbonyl-1,4-dihydrocollidine (DDC)-enriched diet, DRCs proliferated at the capillary bile duct and migrated radially from the portal area to the hepatic parenchymal region [27]. This suggests that the portal DR may interact with the centrilobular DR, leading to progressive fibrosis and even septal fibrosis.

Centrilobular DR in NASH

DR has primarily been described in the periportal compartment. However, a recent study demonstrated that the DR also occurs in the centrilobular regions, suggesting that hepatocytes mount a metaplastic response to chronic injury and/or chronic ischemia, and promote transformation into a more ductular phenotype rather than a progenitor cell reaction[28]. Studies have shown that centrilobular DR is common in NASH and correlates well with lobular inflammation, hepatocellular ballooning degeneration, Mallory-Denk bodies, and necroinflammation. A cross-sectional analysis supported these findings, showing that centrilobular DR is highly correlated with the stage of fibrosis during adult NASH. Moreover, there was a distinct difference in centrilobular DR frequency between patients with progressive and non-progressive fibrosis, suggesting that centrilobular DR can serve as a histologic marker of fibrosis progression[22].

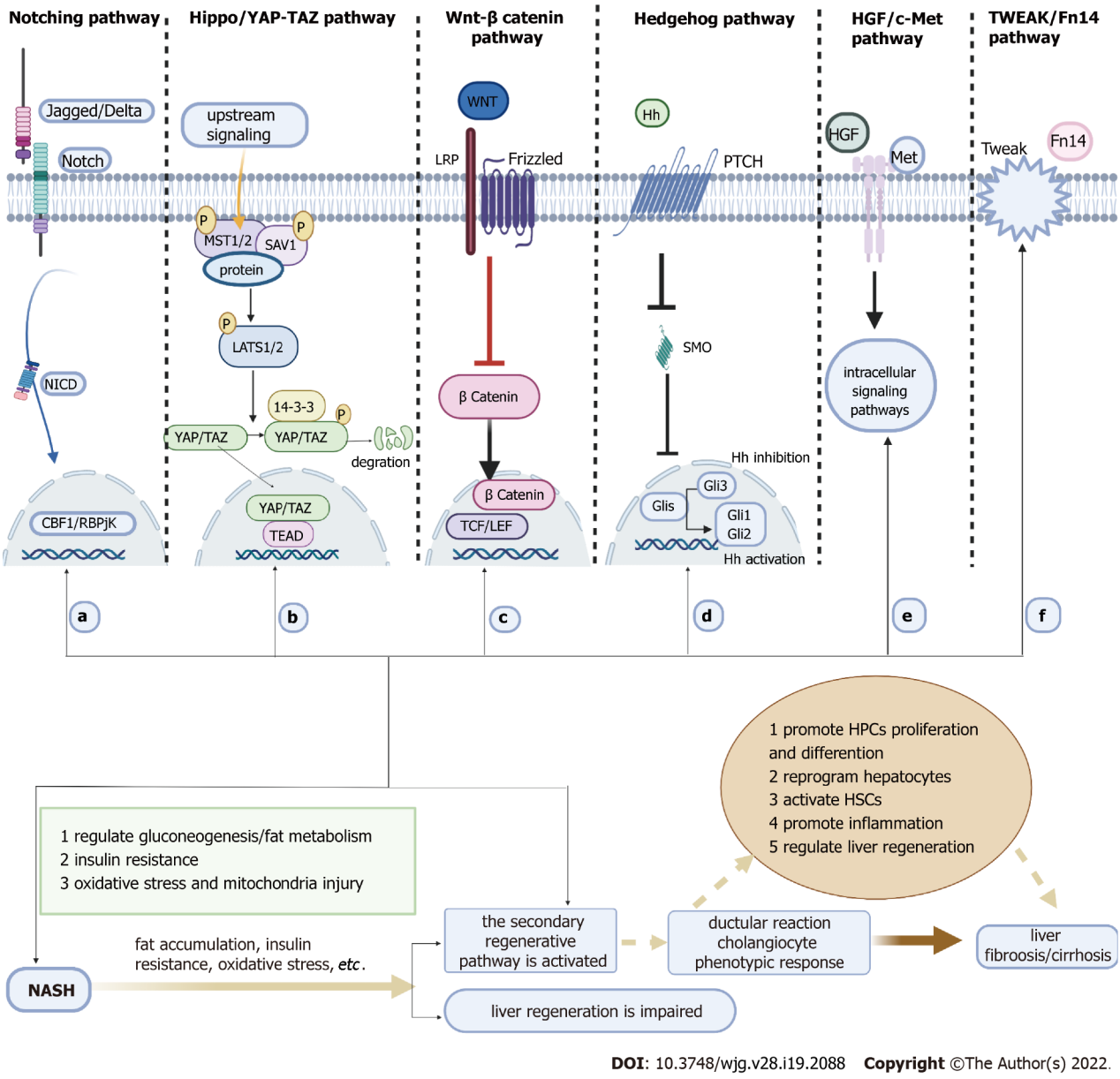
NASH begins with the accumulation of fatty acids and reactive oxygen species in the central area of the lobules, resulting in hepatocyte mitochondrial injury and activation of nearby macrophages and HSCs. Macrophages can release cytokines like TNF-α that promote insulin resistance and inflammation and result in hepatocyte damage. This can promote the transdifferentiation of hepatocytes into DRCs, the expression of inflammatory mediators and pro-fibrotic cytokines, and the activation of nearby HSCs to secrete type I collagen, eventually resulting in peripheral and subsinus fibrosis in the central area of the lobules[20]. Thus, DR in the central area is associated with liver regeneration and repairment of NASH. Centrilobular DR may be an important driver of fibrosis, in which case the degree of centrilobular DR could serve as a histological marker of fibrosis development[22,29].

DR MECHANISMS DURING NASH

During chronic liver diseases such as NASH, an alternative pathway for HPC proliferation is activated when hepatic self-renewal becomes impaired. Persistent HPC activation accompanies the recruitment of pro-inflammatory factors and the production of pro-fibrotic factors and results in DR, aiding pathological repair of the liver. HPCs can proliferate and differentiate into hepatocytes or cholangiocytes, and hepatocytes can further transdifferentiate into cholangiocytes (Figure 1). DR promotes liver and biliary fibrosis using similar mechanisms. A series of highly conservative signaling pathways, including Notch, Hippo/YAP-TAZ, Wnt/β-catenin, Hedgehog (Hh), HGF/c-Met, and TWEAK/Fn14, in the DR play an important role in driving HPC activation and/or HSC activation in chronic liver injury (Figure 2).

Notch signaling during NASH

The Notch ligands, Jagged (Jagged1, 2) and Delta-like (Delta-like, Dll1, 3, and 4), activate Notch receptors (Notch-1, -4) through cell-cell contact, determining cleavage of the Notch intracellular domain (NICD). NICD binds with CBF1/RBPjK in the nucleus and promotes transcription of several genes including the Hes and Hey-related family of transcription factors and SOX9. During embryonic development, Notch signaling can promote HPC differentiation into cells in the biliary lineage and



DOI: 10.3748/wjg.v28.i19.2088 **Copyright** ©The Author(s) 2022.

Figure 2 A series of highly conserved signaling pathways in the ductular reaction which promotes the occurrence of non-alcoholic fatty liver disease and aggravates the prognosis of non-alcoholic steatohepatitis (Created with BioRender.com). A: The Notch signaling pathway regulates expression of genes, such as the Hes and Hey-related family, to determine cell differentiation and function, maintain liver homeostasis, repair liver damage, and regulate liver metabolism, inflammation, and cancer; B: The Hippo/YAP-TAZ signaling pathway can regulate liver size, metabolism, cell proliferation, cell migration, the epithelial-mesenchymal transition, and formation of the extracellular matrix and cytoskeleton formation, *etc*; C: The Wnt/β-catenin signaling pathway affects liver development and physiological functions of all liver disease stages, from initial injury and inflammation to fibrosis, cirrhosis and tumor occurrence; D: The hedgehog signaling pathway affects cell proliferation, migration, and differentiation; E: The HGF/c-Met signaling pathway activates multiple intracellular signaling pathways and affect cell proliferation, migration, and differentiation; F: The TWEAK/Fn14 signaling pathway regulates tissue inflammation and damage repair in addition to cell survival and death. HPC: Hepatic progenitor cell; NASH: Non-alcoholic steatohepatitis.

induce morphogenesis and maturation of the intrahepatic biliary tree. In the DR that occurs during adult liver injury, Notch signaling can determine HPC differentiation into cells in the biliary (Notch activation) or hepatocyte lineage (Notch inhibition). In addition, Notch signaling reprograms hepatocytes into biliary epithelial cells to repair the biliary tract[30,31].

During NASH, inflammatory cells express Notch ligands and promote Notch signaling, increasing FoxO1-induced insulin resistance to regulate glucose production by hepatocytes[32]. The Notch signaling pathway can interact with the mTOR pathway to increase intracellular triglyceride synthesis and lipogenesis by regulating SREBP-1c expression[33]. Thus, it is believed that Notch signaling regulates adipogenesis, steatosis, and insulin resistance, and promotes NAFLD occurrence and progression.

Notch signaling is downregulated following liver cell differentiation in healthy individuals but is upregulated in NASH patients and mice. In Notch-2- and RPB-jK-deficient mice with DDC diet-induced

biliary damage, HPC activation is severely impaired, suggesting that Notch signaling plays an essential role in HPC driven biliary repair and biliary tubule formation[34]. One study indicated that continuous Notch signaling during lipid accumulation could induce liver steatosis and promote fibrogenesis, while suppression of Notch signaling could ameliorate liver fibrosis. Notch signaling also correlates strongly with the NAFLD activity score and alanine aminotransferase level, indicating that its activity is related to NAFLD progression to NASH. Notch signaling can directly promote liver fibrosis by activating HSCs through osteopontin and sinusoidal endothelial cells and can indirectly affect liver fibrosis through inflammation and DR[35,36]. In NASH mice induced using a methionine-choline deficient diet, high Notch ligand levels were found in activated HSCs and HPC activation was linked to inflammation and fibrosis. Liver fibrosis is improved by inhibiting Notch signaling, which reduces HPCs/DR expansion and hepatocyte transdifferentiation. Meanwhile, immunohistochemistry showed that about 2% of CK19+ cells were derived from Notch-1 induced Sox9+ hepatocytes reprogramming[37]. Lineage tracing showed that hepatocytes undergo extensive reprogramming to biliary epithelial cells (BECs) in the DR following chronic injury[38]. In summary, liver cell reprogramming into HPCs during the DR is Notch-dependent, and inhibition of Notch signaling improves fibrosis, providing a potential target for NASH treatment.

Hippo/YAP-TAZ signaling during NASH

In the canonical mammalian Hippo pathway kinase cascade, the tumor suppressor genes, MST1/2 and LATS1/2, are phosphorylated by the upstream kinase tumor suppressor, Hippo, resulting in YAP and TAZ phosphorylation and inactivation. SAV1 and MOB1A/B can act as adaptor proteins to enhance MST1/2 and LATS1/2 phosphorylation and inactivation, respectively. YAP/TAZ interacts with the DNA-binding transcription factors, TEAD (1-4), to regulate target gene expression, and this can be antagonized by TEAD family corepressors such as VGLL4[39].

Hippo-YAP/TAZ signaling participates in various metabolic processes such as liver glycolysis, gluconeogenesis, fatty acid accumulation, and amino acid metabolism. In mice with an MST1 deletion, fasting and high-fat diet aggravated liver metabolic damage. MST1 overexpression is induced by fasting, which decreases SREBP-1c and improves antioxidant genes expression[40]. A previous study demonstrated that AKT overexpression leads to the development of NAFLD by promoting maturation of the transcription factor, SREBP-1c[41]. Studies have shown a positive feedback loop between the Hippo and AKT signaling pathways to promote the development of NAFLD[42]. Thus, regulation of lipid metabolism by Hippo/YAP-TAZ can induce NAFLD. As a result, researchers have turned to the Hippo pathway as a potential therapeutic mechanism for preventing this disease.

Hippo-YAP signaling is related to DR and regulates regeneration of chronic liver disease by determining cellular fates. One study found that YAP levels were increased in NAFLD patients and mice and were primarily localized in the nucleus of DRCs that expressed progenitor markers, correlating with the degree of fibrosis. This suggests that Hippo/YAP signaling is associated with DR and promotes liver fibrosis rather than effective liver regeneration during NASH[43]. In DDC-injured livers, YAP activation occurs in the process of hepatocyte degeneration, and loss of YAP in hepatocytes results in a significant decrease in DR post-DDC injury. In addition, lineage traced hepatocytes in mice showed that YAP was necessary for hepatocytes to form duct-like structures after DDC injury[44]. In several DR mice models, YAP signaling occurred in CK19+ BEC (facultative liver stem cells) and periportal hepatocytes around the portal vein were activated, confirming that YAP was important for BEC expansion and organoid formation and growth. In mice lacking YAP, Sox9 expression in hepatocytes around the portal vein did not increase significantly, and BEC proliferation was significantly reduced. This indicates that YAP mediates the transdifferentiation of Sox9+ hepatocytes and promotes BEC expansion[45]. Another study showed that Hippo signaling could reprogram hepatocytes into ductal cells with characteristics of hepatic progenitors, supporting the idea that YAP could dedifferentiate hepatocytes and reprogram them into cholangiocytes *via* HPCs[46]. Taken together, these findings indicate that the YAP-driven transcriptional program is critical for liver regeneration and hepatocyte reprogramming towards a progenitor, biliary-like fate following liver injury.

In addition, TAZ levels are elevated in NASH patients and mice. When TAZ is silenced, liver inflammation, fibrosis, and cell death are suppressed in NASH mouse models. In contrast, TAZ expression in hepatocytes induces the Indian Hedgehog (Ihh) pathway in mice, promoting pro-fibrotic gene expression in HSCs and mediating the DR process. Both *in vitro* and *in vivo* data indicate that TAZ promotes NASH progression in hepatocytes largely by inducing the Ihh pathway, while silencing TAZ reverses liver inflammation and fibrosis, with the exception of steatosis[47]. In summary, the Hippo-YAP/TAZ signaling pathway provides a potential therapeutic target to prevent the progression of NAFLD to NASH or improve liver fibrosis when NASH is already occurring.

Wnt-β catenin signaling in NASH

Wnt was first discovered in Drosophila, and the canonical Wnt signaling pathway was defined as the Wnt-β-catenin mediated transcription pathway. Wnt ligand binds to Frizzled and co-receptor LRPs and blocks β-catenin degradation, causing the transcription of target genes in a T-cell factor/lymphoid enhancer factor dependent manner[48]. Wnt/β-catenin signaling is important for HPC and hepatoblast

proliferation and final differentiation into mature hepatocytes and for maintaining bile duct homeostasis. In the adult liver, Wnt signaling is only activated in hepatocytes around the central vein, and maintains a static state in other areas of the liver. When hepatocytes are impaired, Wnt-β catenin signaling is activated[49,50]. The β-catenin-T cell factor complex regulates cyclin expression and induces the cell-cycle G1/S transition, promoting liver regeneration[51].

β-catenin induces insulin resistance by interacting with FoxO1 during gluconeogenesis, promoting NASH. Inhibiting Wnt signaling reduces body lipid content, inhibits liver gluconeogenesis, and increases hepatic insulin sensitivity in NASH mice. These findings suggest that Wnt/β-catenin signaling is related to NASH pathogenesis[52]. Wnt/β-catenin signaling may induce DRC differentiation into hepatocytes, and inhibiting this pathway may improve liver cirrhosis. Wnt levels are higher in the area around the portal vein following continuous damage, suggesting that Wnt/β-catenin signaling regulates hepatobiliary repair[53]. Studies indicate that CK19+ DRCs are regulated by Notch signaling and finally differentiate into cells in the biliary system. Wnt/β-catenin signaling may change the fate of biliary-derived DRCs and instead induce their differentiation into hepatocytes, aiding liver regeneration. However, some studies suggest that DRCs make little contribution to liver regeneration, and Wnt/β-catenin signaling cannot alter DRC differentiation[54]. The differentiation of quiescent HSCs into active myofibroblasts is similar to the dedifferentiation of adipocytes into preadipocytes (loss of adipogenic properties), requiring Wnt/β-catenin signaling. In turn, inhibition of Wnt/β-catenin signaling can block liver fibrosis[52]. The effect of Wnt/β-catenin signaling on the repair of liver damage through DRC proliferation provides a new potential research target for hepatobiliary diseases. However, a more comprehensive understanding of the mechanism by which DRCs and Wnt/β-catenin signaling contribute to hepatobiliary regeneration and repair remains unclear, and more studies are needed to determine whether Wnt/β-catenin signaling regulates DRC differentiation[27].

Hh signaling in NASH

Hh was first discovered in drosophila and shown to be critical for promoting tissue development and maintaining homeostasis. There are three Hh ligands, sonic hedgehog (Shh), Ihh, and desert Hh. In the canonical Hh signaling pathway, Hh ligand binding to the transmembrane receptor relieves its inhibitory effect on smoothed, activating the transcriptional mediator glioma-associated oncogene homologues, Glis (Gli1, Gli2, and Gli3). Gli1 is a signal amplifier of Gli2-mediated transcriptional responses, Gli2 is the primary activator of Hh signaling, and Gli3 is responsible for inhibits Hh signaling. Gli1/2 or Gli3 bind to DNA in the nucleus and regulate the transcription of target genes. The Hh pathway plays an important role in hepatic injury repair and fibrogenesis by regulating HPC and mesenchymal cell proliferation and/or differentiation[55,56].

There are multiple mesenchymal cell types that exist in the liver, of which HSCs play a major role in liver fibrosis. In healthy adult liver, liver resident cells produce few Hh ligands and resting HSCs produce Hh inhibitors. As a result, the Hh signaling pathway is relatively quiescent[57,58]. Hh signaling induces HSCs and Gli1+ peribiliary mesenchymal cell proliferation and acquisition of a myofibroblast phenotype responsible for ECM deposition, thus contributing to fibrosis during chronic liver disease[57,59]. Hh signaling recruits bone marrow-derived monocytes to the liver and promotes their transformation into fibrocytes and induces the epithelial-mesenchymal transition in DRCs in response to chronic liver injury[60]. Hepatocytes are the main source of Shh ligands and in the carbon tetrachloride-induced DR model, Shh and Hippo-YAP1 activity are upregulated and correlate with the regulation of DRC fate for liver regeneration. Shh downstream molecular inhibitor, Gant61, can reduce Shh and Yap signaling thereby inhibiting DR and improving liver injury[61]. Thus, Hh signaling is important for the development of antifibrotic therapies because of its potential to regulate the fibrotic process and interact with the Hippo-YAP signaling pathway.

HGF/c-Met signaling in NASH

HGF is a pleiotropic growth factor derived from non-parenchymal cells. HGF combines with the c-Met to activate multiple intracellular signaling pathways that impact cell proliferation, migration, and differentiation. HGF acts as an essential cell mitogen, motogen, and morphogen and plays an important role in mesenchymal-epithelial transformation. C-Met is a receptor tyrosine kinase that activates cell growth and morphogenesis, and HGF/c-Met signaling is strongly associated with epithelial, mesenchymal, and hematological malignancy[62].

HGF expression is upregulated in mice with partial liver excision, promoting liver cell division and maturation. Animal studies have shown that knocking out c-Met during embryonic development hinders liver development and can even result in death. The absence of c-Met and epidermal growth factor receptors arrests liver regeneration and can cause mice to die following partial hepatectomy. These findings highlight the importance of HGF/c-Met signaling in liver regeneration and protection [63,64]. Experiments indicate that HPCs can express c-Met. Inhibiting c-Met phosphorylation inhibits HPC proliferation and the transdifferentiation of hepatocytes into cholangiocytes[65]. HGF also enhances collagenase activity. When the liver is severely damaged, HGF expression is up-regulated, increasing the degradation of collagen fibers and the inhibiting liver fibrosis[66]. HGF induces hepatic progenitor marker gene expression and promotes hepatocyte proliferation and HPC conversion into hepatocytes[67]. These findings suggest that HGF/c-Met signaling can promote regeneration and

improve fibrosis during chronic liver injury.

TWEAK/Fn14 signaling in NASH

TWEAK is a member of the tumor necrosis factor ligand superfamily. Once bound to its receptor, Fn14 participates in many pivotal cellular activities like tissue inflammation, damage repair, cell survival, and death. TWEAK is produced by many myeloid and immune cells and Fn14 is upregulated by fibroblast-like growth factor and other factors associated with injury and inflammation. While the physiological role of the TWEAK/Fn14 axis is to protect against tissue injury, excessive production of TWEAK or Fn14 can drive and orchestrate inflammation, fibrosis, and tissue remodeling[68]. Previous studies show that TWEAK can promote collagen production and pro-inflammatory cytokine secretion and regulate HSC senescence and migration[69].

TWEAK is widely expressed in adult tissue including activated monocytes, natural killer cells, and macrophages in the liver. TWEAK is a direct mitogen to HPCs, and TWEAK/Fn14 signaling can activate NF-κB and STAT3 signaling to increase pro-inflammatory cytokine secretion during liver disease[70]. Fn14 expression is relatively low in resting HSCs, but during chronic liver injury, Fn14 is highly expressed in HPCs and activated HSCs[71]. TWEAK promotes HSC migration through activation of the EGFR/Src and PI3K/AKT pathways, which are important for liver fibrogenesis[69]. One study demonstrated that Fn14-deficient mice treated with a choline-deficient, ethionine-supplemented diet had diminished HPC proliferation, inflammation, collagen deposition, and profibrotic cytokine production that resulted in considerably more mild liver fibrosis[72,73]. Given its effect on pathological remodeling, HSC migration, and pro-inflammatory cytokine expression, TWEAK/Fn14 signaling may serve as a potential strategy of antifibrotic treatment strategy for NASH by regulating HPC proliferation and fibrogenesis.

Signaling pathway crosstalk

Recent studies have supported the view that there is an interactive network between different signaling pathways to regulate DR during NASH. Signaling pathways such as the Hippo/YAP, Wnt/β-catenin, Shh pathway can interact with Notch signaling directly or indirectly to regulate cellular gene expression. Wnt/β-catenin promotes DRCs to differentiate into hepatocytes and inhibits Notch signaling[74]. Both *in vitro* and *in vivo* data indicate that hepatocyte TAZ promotes NASH progression in large part by inducing Ihh signaling, playing an important role in fibrogenesis[47]. Notch signaling is one important downstream YAP target in liver cells[46]. Hippo/YAP-TAZ can upregulate Notch ligands or cooperate with Notch signaling to manipulate target genes in DR[75]. These signaling pathways have distinct roles in DR, including regulating proliferation and transdifferentiation of hepatocytes, cholangiocytes, and HPCs, activating HSCs and fibrogenesis. These pathways can enhance or weaken each other's effects through complicated signaling networks which will require more in-depth understanding and research.

CONCLUSION

In summary, the DR is a response to the bile duct phenotype during liver injury, which aims to restore liver homeostasis and promote regeneration during chronic liver injury by regulating HPC, cholangiocyte, and hepatocyte proliferation and differentiation. The DR plays an important role in NAFLD pathogenesis and promotes the occurrence and development of NASH and liver fibrosis. It is shown that Notch, Hippo/YAP, Wnt/β-catenin, Hh, HGF/c-Met, TWEAK/Fn14, and other intracellular signaling pathways interact with each other to form a crosstalk network, which is related to the DR. In chronic liver disease, these signaling pathways can affect liver inflammation, regeneration, HSC activation, and collagen deposition by regulating corresponding target gene expression. Several molecular inhibitors and modulators are being considered for anti-fibrotic treatment during NASH. While the specific mechanisms for these signaling pathways require more exploration, NASH treatment looks promising in near future.

ACKNOWLEDGEMENTS

Figures were created using BioRender (www.bioreder.com).

FOOTNOTES

Author contributions: Chen Y searched the literature and drafted the manuscript; Gao WK checked the manuscript and provided assistance regarding illustrations; Shu YY assisted in designing and polishing the manuscript; Ye J revised the important intellectual content in this manuscript; all authors have read and approved the final

manuscript.

Supported by the National Natural Science Foundation of China, No. 81770582; and the Graduates' Innovation Fund, Huazhong University of Science and Technology, No. 2021yjsCXCY106.

Conflict-of-interest statement: The authors declare no conflict of interest for this article.

Open-Access: This article is an open-access article that was selected by an in-house editor and fully peer-reviewed by external reviewers. It is distributed in accordance with the Creative Commons Attribution NonCommercial (CC BY-NC 4.0) license, which permits others to distribute, remix, adapt, build upon this work non-commercially, and license their derivative works on different terms, provided the original work is properly cited and the use is non-commercial. See: https://creativecommons.org/Licenses/by-nc/4.0/

Country/Territory of origin: China

ORCID number: Yue Chen 0000-0002-3024-2778; Wen-Kang Gao 0000-0003-0187-5573; Yan-Yun Shu 0000-0002-0833-6436; Jin Ye 0000-0002-1521-1746.

S-Editor: Zhang H
L-Editor: A
P-Editor: Zhang H

REFERENCES

1 **Younossi ZM**, Koenig AB, Abdelatif D, Fazel Y, Henry L, Wymer M. Global epidemiology of nonalcoholic fatty liver disease-Meta-analytic assessment of prevalence, incidence, and outcomes. *Hepatology* 2016; **64**: 73-84 [PMID: 26707365 DOI: 10.1002/hep.28431]
2 **Li J**, Zou B, Yeo YH, Feng Y, Xie X, Lee DH, Fujii H, Wu Y, Kam LY, Ji F, Li X, Chien N, Wei M, Ogawa E, Zhao C, Wu X, Stave CD, Henry L, Barnett S, Takahashi H, Furusyo N, Eguchi Y, Hsu YC, Lee TY, Ren W, Qin C, Jun DW, Toyoda H, Wong VW, Cheung R, Zhu Q, Nguyen MH. Prevalence, incidence, and outcome of non-alcoholic fatty liver disease in Asia, 1999-2019: a systematic review and meta-analysis. *Lancet Gastroenterol Hepatol* 2019; **4**: 389-398 [PMID: 30902670 DOI: 10.1016/S2468-1253(19)30039-1]
3 **Calzadilla Bertot L**, Adams LA. The Natural Course of Non-Alcoholic Fatty Liver Disease. *Int J Mol Sci* 2016; **17** [PMID: 27213358 DOI: 10.3390/ijms17050774]
4 **Rinella ME**. Nonalcoholic fatty liver disease: a systematic review. *JAMA* 2015; **313**: 2263-2273 [PMID: 26057287 DOI: 10.1001/jama.2015.5370]
5 **Dezső K**, Nagy P, Paku S. Human liver regeneration following massive hepatic necrosis: Two distinct patterns. *J Gastroenterol Hepatol* 2020; **35**: 124-134 [PMID: 31090096 DOI: 10.1111/jgh.14721]
6 **Richardson MM**, Jonsson JR, Powell EE, Brunt EM, Neuschwander-Tetri BA, Bhathal PS, Dixon JB, Weltman MD, Tilg H, Moschen AR, Purdie DM, Demetris AJ, Clouston AD. Progressive fibrosis in nonalcoholic steatohepatitis: association with altered regeneration and a ductular reaction. *Gastroenterology* 2007; **133**: 80-90 [PMID: 17631134 DOI: 10.1053/j.gastro.2007.05.012]
7 **Clouston AD**, Jonsson JR, Powell EE. Hepatic progenitor cell-mediated regeneration and fibrosis: chicken or egg? *Hepatology* 2009; **49**: 1424-1426 [PMID: 19399908 DOI: 10.1002/hep.22893]
8 **Peverill W**, Powell LW, Skoien R. Evolving concepts in the pathogenesis of NASH: beyond steatosis and inflammation. *Int J Mol Sci* 2014; **15**: 8591-8638 [PMID: 24830559 DOI: 10.3390/ijms15058591]
9 **Popper H**, Kent G, Stein R. Ductular cell reaction in the liver in hepatic injury. *J Mt Sinai Hosp N Y* 1957; **24**: 551-556 [PMID: 13476145]
10 **Roskams TA**, Theise ND, Balabaud C, Bhagat G, Bhathal PS, Bioulac-Sage P, Brunt EM, Crawford JM, Crosby HA, Desmet V, Finegold MJ, Geller SA, Gouw AS, Hytiroglou P, Knisely AS, Kojiro M, Lefkowitch JH, Nakanuma Y, Olynyk JK, Park YN, Portmann B, Saxena R, Scheuer PJ, Strain AJ, Thung SN, Wanless IR, West AB. Nomenclature of the finer branches of the biliary tree: canals, ductules, and ductular reactions in human livers. *Hepatology* 2004; **39**: 1739-1745 [PMID: 15185318 DOI: 10.1002/hep.20130]
11 **Sato K**, Marzioni M, Meng F, Francis H, Glaser S, Alpini G. Ductular Reaction in Liver Diseases: Pathological Mechanisms and Translational Significances. *Hepatology* 2019; **69**: 420-430 [PMID: 30070383 DOI: 10.1002/hep.30150]
12 **Krishnan A**, Katsumi T, Guicciardi ME, Azad AI, Ozturk NB, Trussoni CE, Gores GJ. Tumor Necrosis Factor-Related Apoptosis-Inducing Ligand Receptor Deficiency Promotes the Ductular Reaction, Macrophage Accumulation, and Hepatic Fibrosis in the Abcb4$^{-/-}$ Mouse. *Am J Pathol* 2020; **190**: 1284-1297 [PMID: 32240619 DOI: 10.1016/j.ajpath.2020.02.013]
13 **Bird TG**, Lu WY, Boulter L, Gordon-Keylock S, Ridgway RA, Williams MJ, Taube J, Thomas JA, Wojtacha D, Gambardella A, Sansom OJ, Iredale JP, Forbes SJ. Bone marrow injection stimulates hepatic ductular reactions in the absence of injury *via* macrophage-mediated TWEAK signaling. *Proc Natl Acad Sci U S A* 2013; **110**: 6542-6547 [PMID: 23576749 DOI: 10.1073/pnas.1302168110]
14 **Azad AI**, Krishnan A, Troop L, Li Y, Katsumi T, Pavelko K, Kostallari E, Guicciardi ME, Gores GJ. Targeted Apoptosis of Ductular Reactive Cells Reduces Hepatic Fibrosis in a Mouse Model of Cholestasis. *Hepatology* 2020; **72**: 1013-1028 [PMID: 32128842 DOI: 10.1002/hep.31211]
15 **Segal JM**, Kent D, Wesche DJ, Ng SS, Serra M, Oulès B, Kar G, Emerton G, Blackford SJI, Darmanis S, Miquel R, Luong

TV, Yamamoto R, Bonham A, Jassem W, Heaton N, Vigilante A, King A, Sancho R, Teichmann S, Quake SR, Nakauchi H, Rashid ST. Single cell analysis of human foetal liver captures the transcriptional profile of hepatobiliary hybrid progenitors. *Nat Commun* 2019; **10**: 3350 [PMID: 31350390 DOI: 10.1038/s41467-019-11266-x]

16 **Schmelzer E**, Pietrosi G, Gridelli B, Gerlach J. Characterization of CD326-positive human hepatic stem cells. *Clin Exp Hepatol* 2021; **7**: 101-110 [PMID: 34027122 DOI: 10.5114/ceh.2021.104459]

17 **Abou Monsef Y**, Kutsal O. Immunohistochemical evaluation of hepatic progenitor cells in different types of feline liver diseases. *J Vet Med Sci* 2021; **83**: 613-621 [PMID: 33583913 DOI: 10.1292/jvms.20-0435]

18 **Misra S**, Majumdar K, Sakhuja P, Jain P, Singh L, Kumar P, Dubey AP. Differentiating Biliary Atresia From Idiopathic Neonatal Hepatitis: A Novel Keratin 7 Based Mathematical Approach on Liver Biopsies. *Pediatr Dev Pathol* 2021; **24**: 103-115 [PMID: 33439108 DOI: 10.1177/1093526620983730]

19 **Zheng YJ**. Bile duct reaction related to clinical hepatobiliary diseases and its significance. *Zhonghua Ganzang Bing Zazhi* 2018; **26**: 637-640

20 **Skoien R**, Richardson MM, Jonsson JR, Powell EE, Brunt EM, Neuschwander-Tetri BA, Bhathal PS, Dixon JB, O'Brien PE, Tilg H, Moschen AR, Baumann U, Brown RM, Couper RT, Manton ND, Ee LC, Weltman M, Clouston AD. Heterogeneity of fibrosis patterns in non-alcoholic fatty liver disease supports the presence of multiple fibrogenic pathways. *Liver Int* 2013; **33**: 624-632 [PMID: 23356584 DOI: 10.1111/liv.12100]

21 **Melino M**, Gadd VL, Alexander KA, Beattie L, Lineburg KE, Martinez M, Teal B, Le Texier L, Irvine KM, Miller GC, Boyle GM, Hill GR, Clouston AD, Powell EE, MacDonald KP. Spatiotemporal Characterization of the Cellular and Molecular Contributors to Liver Fibrosis in a Murine Hepatotoxic-Injury Model. *Am J Pathol* 2016; **186**: 524-538 [PMID: 26762581 DOI: 10.1016/j.ajpath.2015.10.029]

22 **Zhao L**, Westerhoff M, Pai RK, Choi WT, Gao ZH, Hart J. Centrilobular ductular reaction correlates with fibrosis stage and fibrosis progression in non-alcoholic steatohepatitis. *Mod Pathol* 2018; **31**: 150-159 [PMID: 28862262 DOI: 10.1038/modpathol.2017.115]

23 **Williams MJ**, Clouston AD, Forbes SJ. Links between hepatic fibrosis, ductular reaction, and progenitor cell expansion. *Gastroenterology* 2014; **146**: 349-356 [PMID: 24315991 DOI: 10.1053/j.gastro.2013.11.034]

24 **Gouw AS**, Clouston AD, Theise ND. Ductular reactions in human liver: diversity at the interface. *Hepatology* 2011; **54**: 1853-1863 [PMID: 21983984 DOI: 10.1002/hep.24613]

25 **Gadd VL**, Skoien R, Powell EE, Fagan KJ, Winterford C, Horsfall L, Irvine K, Clouston AD. The portal inflammatory infiltrate and ductular reaction in human nonalcoholic fatty liver disease. *Hepatology* 2014; **59**: 1393-1405 [PMID: 24254368 DOI: 10.1002/hep.26937]

26 **Brunt EM**, Kleiner DE, Wilson LA, Unalp A, Behling CE, Lavine JE, Neuschwander-Tetri BA; NASH Clinical Research NetworkA list of members of the Nonalcoholic Steatohepatitis Clinical Research Network can be found in the Appendix. Portal chronic inflammation in nonalcoholic fatty liver disease (NAFLD): a histologic marker of advanced NAFLD-Clinicopathologic correlations from the nonalcoholic steatohepatitis clinical research network. *Hepatology* 2009; **49**: 809-820 [PMID: 19142989 DOI: 10.1002/hep.22724]

27 **Wang N**, Kong R, Han W, Lu J. Wnt/β-catenin signalling controls bile duct regeneration by regulating differentiation of ductular reaction cells. *J Cell Mol Med* 2020; **24**: 14050-14058 [PMID: 33124779 DOI: 10.1111/jcmm.16017]

28 **Gill RM**, Belt P, Wilson L, Bass NM, Ferrell LD. Centrizonal arteries and microvessels in nonalcoholic steatohepatitis. *Am J Surg Pathol* 2011; **35**: 1400-1404 [PMID: 21836480 DOI: 10.1097/PAS.0b013e3182254283]

29 **Nagahama Y**, Sone M, Chen X, Okada Y, Yamamoto M, Xin B, Matsuo Y, Komatsu M, Suzuki A, Enomoto K, Nishikawa Y. Contributions of hepatocytes and bile ductular cells in ductular reactions and remodeling of the biliary system after chronic liver injury. *Am J Pathol* 2014; **184**: 3001-3012 [PMID: 25193593 DOI: 10.1016/j.ajpath.2014.07.005]

30 **Bray SJ**. Notch signalling in context. *Nat Rev Mol Cell Biol* 2016; **17**: 722-735 [PMID: 27507209 DOI: 10.1038/nrm.2016.94]

31 **Geisler F**, Strazzabosco M. Emerging roles of Notch signaling in liver disease. *Hepatology* 2015; **61**: 382-392 [PMID: 24930574 DOI: 10.1002/hep.27268]

32 **Pajvani UB**, Shawber CJ, Samuel VT, Birkenfeld AL, Shulman GI, Kitajewski J, Accili D. Inhibition of Notch signaling ameliorates insulin resistance in a FoxO1-dependent manner. *Nat Med* 2011; **17**: 961-967 [PMID: 21804540 DOI: 10.1038/nm.2378]

33 **Bi P**, Kuang S. Notch signaling as a novel regulator of metabolism. *Trends Endocrinol Metab* 2015; **26**: 248-255 [PMID: 25805408 DOI: 10.1016/j.tem.2015.02.006]

34 **Fiorotto R**, Raizner A, Morell CM, Torsello B, Scirpo R, Fabris L, Spirli C, Strazzabosco M. Notch signaling regulates tubular morphogenesis during repair from biliary damage in mice. *J Hepatol* 2013; **59**: 124-130 [PMID: 23500150 DOI: 10.1016/j.jhep.2013.02.025]

35 **Valenti L**, Mendoza RM, Rametta R, Maggioni M, Kitajewski C, Shawber CJ, Pajvani UB. Hepatic notch signaling correlates with insulin resistance and nonalcoholic fatty liver disease. *Diabetes* 2013; **62**: 4052-4062 [PMID: 23990360 DOI: 10.2337/db13-0769]

36 **Zhu C**, Kim K, Wang X, Bartolome A, Salomao M, Dongiovanni P, Meroni M, Graham MJ, Yates KP, Diehl AM, Schwabe RF, Tabas I, Valenti L, Lavine JE, Pajvani UB. Hepatocyte Notch activation induces liver fibrosis in nonalcoholic steatohepatitis. *Sci Transl Med* 2018; **10** [PMID: 30463916 DOI: 10.1126/scitranslmed.aat0344]

37 **Morell CM**, Fiorotto R, Meroni M, Raizner A, Torsello B, Cadamuro M, Spagnuolo G, Kaffe E, Sutti S, Albano E, Strazzabosco M. Notch signaling and progenitor/ductular reaction in steatohepatitis. *PLoS One* 2017; **12**: e0187384 [PMID: 29140985 DOI: 10.1371/journal.pone.0187384]

38 **Yanger K**, Zong Y, Maggs LR, Shapira SN, Maddipati R, Aiello NM, Thung SN, Wells RG, Greenbaum LE, Stanger BZ. Robust cellular reprogramming occurs spontaneously during liver regeneration. *Genes Dev* 2013; **27**: 719-724 [PMID: 23520387 DOI: 10.1101/gad.207803.112]

39 **Driskill JH**, Pan D. The Hippo Pathway in Liver Homeostasis and Pathophysiology. *Annu Rev Pathol* 2021; **16**: 299-322 [PMID: 33234023 DOI: 10.1146/annurev-pathol-030420-105050]

40 **Geng C**, Zhang Y, Gao Y, Tao W, Zhang H, Liu X, Fang F, Chang Y. Mst1 regulates hepatic lipid metabolism by

inhibiting Sirt1 ubiquitination in mice. *Biochem Biophys Res Commun* 2016; **471**: 444-449 [PMID: 26903296 DOI: 10.1016/j.bbrc.2016.02.059]

41 **Krycer JR**, Sharpe LJ, Luu W, Brown AJ. The Akt-SREBP nexus: cell signaling meets lipid metabolism. *Trends Endocrinol Metab* 2010; **21**: 268-276 [PMID: 20117946 DOI: 10.1016/j.tem.2010.01.001]

42 **Jeong SH**, Kim HB, Kim MC, Lee JM, Lee JH, Kim JH, Kim JW, Park WY, Kim SY, Kim JB, Kim H, Kim JM, Choi HS, Lim DS. Hippo-mediated suppression of IRS2/AKT signaling prevents hepatic steatosis and liver cancer. *J Clin Invest* 2018; **128**: 1010-1025 [PMID: 29400692 DOI: 10.1172/JCI95802]

43 **Machado MV**, Michelotti GA, Pereira TA, Xie G, Premont R, Cortez-Pinto H, Diehl AM. Accumulation of duct cells with activated YAP parallels fibrosis progression in non-alcoholic fatty liver disease. *J Hepatol* 2015; **63**: 962-970 [PMID: 26070409 DOI: 10.1016/j.jhep.2015.05.031]

44 **Pepe-Mooney BJ**, Dill MT, Alemany A, Ordovas-Montanes J, Matsushita Y, Rao A, Sen A, Miyazaki M, Anakk S, Dawson PA, Ono N, Shalek AK, van Oudenaarden A, Camargo FD. Single-Cell Analysis of the Liver Epithelium Reveals Dynamic Heterogeneity and an Essential Role for YAP in Homeostasis and Regeneration. *Cell Stem Cell* 2019; **25**: 23-38.e8 [PMID: 31080134 DOI: 10.1016/j.stem.2019.04.004]

45 **Planas-Paz L**, Sun T, Pikiolek M, Cochran NR, Bergling S, Orsini V, Yang Z, Sigoillot F, Jetzer J, Syed M, Neri M, Schuierer S, Morelli L, Hoppe PS, Schwarzer W, Cobos CM, Alford JL, Zhang L, Cuttat R, Waldt A, Carballido-Perrig N, Nigsch F, Kinzel B, Nicholson TB, Yang Y, Mao X, Terracciano LM, Russ C, Reece-Hoyes JS, Gubser Keller C, Sailer AW, Bouwmeester T, Greenbaum LE, Lugus JJ, Cong F, McAllister G, Hoffman GR, Roma G, Tchorz JS. YAP, but Not RSPO-LGR4/5, Signaling in Biliary Epithelial Cells Promotes a Ductular Reaction in Response to Liver Injury. *Cell Stem Cell* 2019; **25**: 39-53.e10 [PMID: 31080135 DOI: 10.1016/j.stem.2019.04.005]

46 **Yimlamai D**, Christodoulou C, Galli GG, Yanger K, Pepe-Mooney B, Gurung B, Shrestha K, Cahan P, Stanger BZ, Camargo FD. Hippo pathway activity influences liver cell fate. *Cell* 2014; **157**: 1324-1338 [PMID: 24906150 DOI: 10.1016/j.cell.2014.03.060]

47 **Wang X**, Zheng Z, Caviglia JM, Corey KE, Herfel TM, Cai B, Masia R, Chung RT, Lefkowitch JH, Schwabe RF, Tabas I. Hepatocyte TAZ/WWTR1 Promotes Inflammation and Fibrosis in Nonalcoholic Steatohepatitis. *Cell Metab* 2016; **24**: 848-862 [PMID: 28068223 DOI: 10.1016/j.cmet.2016.09.016]

48 **Tortelote GG**, Reis RR, de Almeida Mendes F, Abreu JG. Complexity of the Wnt/βcatenin pathway: Searching for an activation model. *Cell Signal* 2017; **40**: 30-43 [PMID: 28844868 DOI: 10.1016/j.cellsig.2017.08.008]

49 **Benhamouche S**, Decaens T, Godard C, Chambrey R, Rickman DS, Moinard C, Vasseur-Cognet M, Kuo CJ, Kahn A, Perret C, Colnot S. Apc tumor suppressor gene is the "zonation-keeper" of mouse liver. *Dev Cell* 2006; **10**: 759-770 [PMID: 16740478 DOI: 10.1016/j.devcel.2006.03.015]

50 **Hu M**, Kurobe M, Jeong YJ, Fuerer C, Ghole S, Nusse R, Sylvester KG. Wnt/beta-catenin signaling in murine hepatic transit amplifying progenitor cells. *Gastroenterology* 2007; **133**: 1579-1591 [PMID: 17983805 DOI: 10.1053/j.gastro.2007.08.036]

51 **Monga SP**. Role and regulation of β-catenin signaling during physiological liver growth. *Gene Expr* 2014; **16**: 51-62 [PMID: 24801166 DOI: 10.3727/105221614X13919976902138]

52 **Monga SP**. β-Catenin Signaling and Roles in Liver Homeostasis, Injury, and Tumorigenesis. *Gastroenterology* 2015; **148**: 1294-1310 [PMID: 25747274 DOI: 10.1053/j.gastro.2015.02.056]

53 **Okabe H**, Yang J, Sylakowski K, Yovchev M, Miyagawa Y, Nagarajan S, Chikina M, Thompson M, Oertel M, Baba H, Monga SP, Nejak-Bowen KN. Wnt signaling regulates hepatobiliary repair following cholestatic liver injury in mice. *Hepatology* 2016; **64**: 1652-1666 [PMID: 27533619 DOI: 10.1002/hep.28774]

54 **Jörs S**, Jeliazkova P, Ringelhan M, Thalhammer J, Dürl S, Ferrer J, Sander M, Heikenwalder M, Schmid RM, Siveke JT, Geisler F. Lineage fate of ductular reactions in liver injury and carcinogenesis. *J Clin Invest* 2015; **125**: 2445-2457 [PMID: 25915586 DOI: 10.1172/JCI78585]

55 **Kopinke D**, Norris AM, Mukhopadhyay S. Developmental and regenerative paradigms of cilia regulated hedgehog signaling. *Semin Cell Dev Biol* 2021; **110**: 89-103 [PMID: 32540122 DOI: 10.1016/j.semcdb.2020.05.029]

56 **Briscoe J**, Thérond PP. The mechanisms of Hedgehog signalling and its roles in development and disease. *Nat Rev Mol Cell Biol* 2013; **14**: 416-429 [PMID: 23719536 DOI: 10.1038/nrm3598]

57 **Omenetti A**, Choi S, Michelotti G, Diehl AM. Hedgehog signaling in the liver. *J Hepatol* 2011; **54**: 366-373 [PMID: 21093090 DOI: 10.1016/j.jhep.2010.10.003]

58 **Sicklick JK**, Li YX, Melhem A, Schmelzer E, Zdanowicz M, Huang J, Caballero M, Fair JH, Ludlow JW, McClelland RE, Reid LM, Diehl AM. Hedgehog signaling maintains resident hepatic progenitors throughout life. *Am J Physiol Gastrointest Liver Physiol* 2006; **290**: G859-G870 [PMID: 16322088 DOI: 10.1152/ajpgi.00456.2005]

59 **Gupta V**, Gupta I, Park J, Bram Y, Schwartz RE. Hedgehog Signaling Demarcates a Niche of Fibrogenic Peribiliary Mesenchymal Cells. *Gastroenterology* 2020; **159**: 624-638.e9 [PMID: 32289375 DOI: 10.1053/j.gastro.2020.03.075]

60 **Shen X**, Peng Y, Li H. The Injury-Related Activation of Hedgehog Signaling Pathway Modulates the Repair-Associated Inflammation in Liver Fibrosis. *Front Immunol* 2017; **8**: 1450 [PMID: 29163520 DOI: 10.3389/fimmu.2017.01450]

61 **Jin L**, Huang H, Ni J, Shen J, Liu Z, Li L, Fu S, Yan J, Hu B. Shh-Yap signaling controls hepatic ductular reactions in CCl_4-induced liver injury. *Environ Toxicol* 2021; **36**: 194-203 [PMID: 32996673 DOI: 10.1002/tox.23025]

62 **Ma Y**, Yu X, Li YX, Wang YL. HGF/c-Met signaling regulates early differentiation of placental trophoblast cells. *J Reprod Dev* 2021; **67**: 89-97 [PMID: 33455972 DOI: 10.1262/jrd.2020-107]

63 **Jeon HM**, Lee J. MET: roles in epithelial-mesenchymal transition and cancer stemness. *Ann Transl Med* 2017; **5**: 5 [PMID: 28164090 DOI: 10.21037/atm.2016.12.67]

64 **Paranjpe S**, Bowen WC, Mars WM, Orr A, Haynes MM, DeFrances MC, Liu S, Tseng GC, Tsagianni A, Michalopoulos GK. Combined systemic elimination of MET and epidermal growth factor receptor signaling completely abolishes liver regeneration and leads to liver decompensation. *Hepatology* 2016; **64**: 1711-1724 [PMID: 27397846 DOI: 10.1002/hep.28721]

65 **Zang JF**, Yuan Y, Gao JY, Qian HX. The role of HGF/c-Met related signal pathways in the proliferation of rat liver progenitor cells. *Zhongguo Laonian Xue Zazhi* 2014; **34**: 2800-2803

66 **Wu ZH**, Meng X, Hu JW, Ding YF, Peng YR. Research progress on the correlation between TLR4-MyD88-NF-kB signaling pathway and hepatitis-hepatic fibrosis-hepatocellular carcinoma axis. *J Int Pharm Res* 2017; **44**: 396-401 [DOI: 10.13220/j.cnki.jipr.2017.05.003]

67 **Huang Y**, Miyamoto D, Li PL, Sakai Y, Hara T, Adachi T, Soyama A, Hidaka M, Kanetaka K, Gu WL, Eguchi S. Chemical conversion of aged hepatocytes into bipotent liver progenitor cells. *Hepatol Res* 2021; **51**: 323-335 [PMID: 33378128 DOI: 10.1111/hepr.13609]

68 **Croft M**, Siegel RM. Beyond TNF: TNF superfamily cytokines as targets for the treatment of rheumatic diseases. *Nat Rev Rheumatol* 2017; **13**: 217-233 [PMID: 28275260 DOI: 10.1038/nrrheum.2017.22]

69 **Zhang F**, Xu M, Yin X, Guo H, Zhang B, Wang Y, Xiao J, Zou X, Zhang M, Zhuge Y. TWEAK promotes hepatic stellate cell migration through activating EGFR/Src and PI3K/AKT pathways. *Cell Biol Int* 2019 [PMID: 31498529 DOI: 10.1002/cbin.11230]

70 **Wang A**, Zhang F, Xu H, Xu M, Cao Y, Wang C, Xu Y, Su M, Zhang M, Zhuge Y. TWEAK/Fn14 promotes pro-inflammatory cytokine secretion in hepatic stellate cells *via* NF-κB/STAT3 pathways. *Mol Immunol* 2017; **87**: 67-75 [PMID: 28411440 DOI: 10.1016/j.molimm.2017.04.003]

71 **Zhang Y**, Zeng W, Xia Y. TWEAK/Fn14 axis is an important player in fibrosis. *J Cell Physiol* 2021; **236**: 3304-3316 [PMID: 33000480 DOI: 10.1002/jcp.30089]

72 **Tirnitz-Parker JE**, Viebahn CS, Jakubowski A, Klopcic BR, Olynyk JK, Yeoh GC, Knight B. Tumor necrosis factor-like weak inducer of apoptosis is a mitogen for liver progenitor cells. *Hepatology* 2010; **52**: 291-302 [PMID: 20578156 DOI: 10.1002/hep.23663]

73 **Tirnitz-Parker JE**, Olynyk JK, Ramm GA. Role of TWEAK in coregulating liver progenitor cell and fibrogenic responses. *Hepatology* 2014; **59**: 1198-1201 [PMID: 24038142 DOI: 10.1002/hep.26701]

74 **Zhu C**, Tabas I, Schwabe RF, Pajvani UB. Maladaptive regeneration - the reawakening of developmental pathways in NASH and fibrosis. *Nat Rev Gastroenterol Hepatol* 2021; **18**: 131-142 [PMID: 33051603 DOI: 10.1038/s41575-020-00365-6]

75 **Schwabe RF**, Tabas I, Pajvani UB. Mechanisms of Fibrosis Development in Nonalcoholic Steatohepatitis. *Gastroenterology* 2020; **158**: 1913-1928 [PMID: 32044315 DOI: 10.1053/j.gastro.2019.11.311]

World Journal of Gastroenterology

Submit a Manuscript: https://www.f6publishing.com

World J Gastroenterol 2022 May 21; 28(19): 2100-2111

DOI: 10.3748/wjg.v28.i19.2100

ISSN 1007-9327 (print) ISSN 2219-2840 (online)

ORIGINAL ARTICLE

Basic Study

Ultrastructural changes in porcine liver sinusoidal endothelial cells of machine perfused liver donated after cardiac death

Hiroki Bochimoto, Yo Ishihara, Nur Khatijah Mohd Zin, Hiroyoshi Iwata, Daisuke Kondoh, Hiromichi Obara, Naoto Matsuno

Specialty type: Transplantation

Provenance and peer review: Invited article; Externally peer reviewed.

Peer-review model: Single blind

Peer-review report's scientific quality classification

Grade A (Excellent): 0
Grade B (Very good): B, B
Grade C (Good): 0
Grade D (Fair): 0
Grade E (Poor): 0

P-Reviewer: De Carlis R, Italy; Zhu C, China

Received: May 19, 2021
Peer-review started: May 19, 2021
First decision: June 12, 2021
Revised: July 17, 2021
Accepted: April 3, 2022
Article in press: April 3, 2022
Published online: May 21, 2022

Hiroki Bochimoto, Nur Khatijah Mohd Zin, Department of Cell Physiology, The Jikei University School of Medicine, Minato-ku 105-8461, Tokyo, Japan

Hiroki Bochimoto, Yo Ishihara, Hiromichi Obara, Naoto Matsuno, Department of Transplantation Technology and Therapeutic Development, Asahikawa Medical University, Asahikawa 078-8510, Hokkaido, Japan

Hiroyoshi Iwata, Naoto Matsuno, Department of Surgery, Asahikawa Medical University, Asahikawa 078-8510, Hokkaido, Japan

Daisuke Kondoh, Laboratory of Veterinary Anatomy, Obihiro University of Agriculture and Veterinary Medicine, Obihiro 080-8555, Hokkaido, Japan

Hiromichi Obara, Department of Mechanical Engineering, Tokyo Metropolitan University, Hachioji 192-0397, Tokyo, Japan

Corresponding author: Hiroki Bochimoto, MD, PhD, Assistant Professor, Department of Cell Physiology, The Jikei University School of Medicine, 3-25-8 Nishishimbashi, Minato-ku 105-8461, Tokyo, Japan. botimoto@jikei.ac.jp

Abstract

BACKGROUND

The machine perfusion (MP) preservation including hypothermic MP (HMP) and midthermic MP (MMP) has been considered as a promising strategy to preserve the functions of liver donated after cardiac death. The importance of understanding liver sinusoidal endothelial cells (LSEC) damage in regulating liver injury during MP has been emphasized. However, the ultrastructural changes in the LSEC and sinusoids around them after MP are unclear.

AIM

To investigate the ultrastructural changes in the LSEC and sinusoids around them after MP.

METHODS

Porcine liver grafts undergo a warm ischemia time of 60 minutes perfused for 4 h with modified University of Wisconsin gluconate solution. Group A grafts were preserved with HMP at 8 °C constantly for 4 h. Group B grafts were preserved

with a rewarming solution at 22 °C by MMP for 4 h. Then the ultrastructural changes in the LSEC and sinusoids in Group A and B were comparatively analyzed by using osmium-maceration scanning electron microscopy with complementary transmission electron microscopy methods.

RESULTS

An analysis of the LSEC after warm ischemia revealed that mitochondria with condensed-shaped cristae, abnormal vesicles, reduction of ribosomes and the endoplasmic reticulum (ER) surround the mitochondria appeared. The MP subsequent after warm ischemia alleviate the abnormal vesicles and reduction of ribosomes in LSEC, which indicated the reduction of the ER damage. However, MMP could restore the tubular mitochondrial cristae, while after HMP the condensed and narrow mitochondrial cristae remained. In addition, the volume of the sinusoidal space in the liver grafts after MMP were restored, which indicated a lower risk of pressure injury than HMP.

CONCLUSION

MMP alleviates the ER damage of LSEC by warm ischemia, additionally restore the metabolism of LSEC *via* the normalization of mitochondria and prevent the share stress damage of liver grafts.

Key Words: Liver; Sinusoidal endothelial cells; Warm ischemia; Machine perfusion preservation; Transplantation; Ultrastructure

©The Author(s) 2022. Published by Baishideng Publishing Group Inc. All rights reserved.

Core Tip: The importance of understanding liver sinusoidal endothelial cells (LSEC) damage in regulating liver injury during machine perfusion (MP) preservation has been emphasized. Here, we comparatively analyzed the ultrastructural changes in the LSEC and sinusoids around them at four hours after hypothermic MP (HMP) or midthermic MP (MMP). MP alleviated the ER damage of LSEC caused by warm ischemia. Moreover, MMP temperature conditions restore the metabolism of LSEC *via* the normalization of cristae of mitochondria and prevent the damage of the liver graft by share stress.

Citation: Bochimoto H, Ishihara Y, Mohd Zin NK, Iwata H, Kondoh D, Obara H, Matsuno N. Ultrastructural changes in porcine liver sinusoidal endothelial cells of machine perfused liver donated after cardiac death. *World J Gastroenterol* 2022; 28(19): 2100-2111

URL: https://www.wjgnet.com/1007-9327/full/v28/i19/2100.htm

DOI: https://dx.doi.org/10.3748/wjg.v28.i19.2100

INTRODUCTION

The shortage of brain-dead donors for liver grafts is a serious problem worldwide[1]. One way to expand the donor organ liver pool is by using grafts with extended criteria including liver donated after cardiac death (DCD)[2-4]. However, there is a high risk of acute and chronic liver injury of primary nonfunction caused by ischemia-reperfusion injury after transplantation of DCD liver grafts[5]. Thus, the development of the preservation methods of the liver grafts after cardiac death is required to overcome these problems[1].

The superiority of machine perfusion (MP) preservation to simple cold storage was reported in clinical kidney preservation[6]. Similarly, strategies as MP with oxygen and nutrition-containing solution have also been reported to have numerous advantages to liver transplantation[7,8]. On the other hand, the MP of the DCD grafts has been discussed about the optimal conditions including perfusion temperature, oxygenation, flow rate and pressure, steady or pulsatile flow. Recently, hypothermic machine perfusion (HMP) has been established to preserve the functions of liver grafts, and its application in clinical practice has begun[9].

In addition, the warm MP including midthermic MP (MMP) has also been reported as a promising strategy to maintain the liver graft function to avoid cold ischemic injury and possibly repair the metabolic activity compared to HMP[10,11]. Our previous study also indicated the utilization of MMP reduces the hepatocellular enzyme release to perfusate[12]. We further confirmed that hepatocytes and bile canaliculi of DCD liver grafts after MMP retain a functional ultrastructure compared to HMP, by using scanning electron microscopy after osmium-maceration (OM-SEM) with complementary transmission electron microscopy (TEM)[9,13]. These results showed the practicality of OM-SEM with complementary TEM not only for determining 3D detailed ultrastructure in porcine hepatocytes but in evaluating the function of the transplanted liver which is reflected by ultrastructural characteristics of hepatocytes.

In addition to hepatocyte and bile canaliculi, the importance of liver sinusoidal endothelial cells (LSEC) damage in regulating liver injury during MP has been affirmed[14]. The inferior outcomes following extended criteria donor liver transplantation are thought to be endothelial dysfunction-related, however, it ultimately culminates in early graft dysfunction[14]. Thus, in this study, we comparatively analyzed the ultrastructural changes in the LSEC and sinusoids around them at four hours after HMP or MMP by using OM-SEM with complementary TEM methods. As a consequence, the LSEC that regressed one hour after warm ischemia showed a tendency to recover after MP, especially in MMP, suggesting the preventative effects of HMP and MMP on LSEC-related functions in liver grafts.

MATERIALS AND METHODS

Antibody

Rabbit anti-ERG monoclonal antibody was purchased from Nichirei Bioscience Corporation (Tokyo, Japan; clone EP111) for chromogenic visualization of viable LSEC in liver grafts and observation by bright field microscopy.

Animals

Domestic female porcine (cross-bred Large White, Landrace, and Duroc pigs; age, 2-3 mo; body weight, approximately 25 kg) from Taisetsusanroku-sya Co., Ltd. (Asahikawa, Japan). The animals were kept in a well-ventilated and temperature/humidity controlled room (in which a light on 12-h cycle), and ad libitum access to food and water. All animal work was performed according to the Guide for the Care and Use of Laboratory Animals at Asahikawa Medical University. All animal studies and procedures were approved by the Institutional Animal Ethics Committee of the Clinical Research Center, Asahikawa Medical University (permit No. 14172).

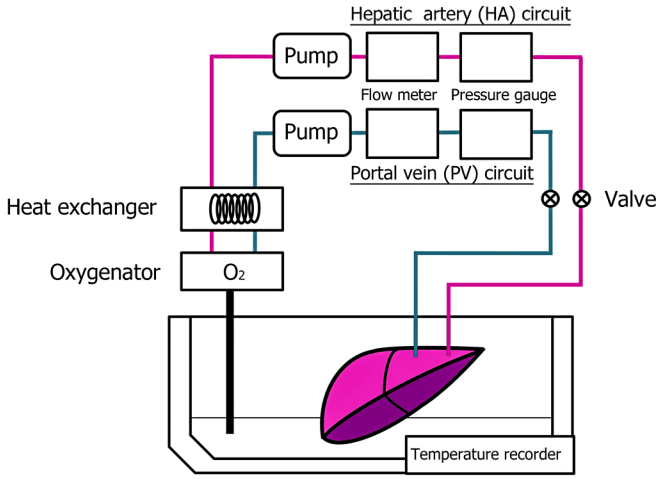
MP

The harvested porcine liver was perfused with MP systems (Figure 1), as described previously[9,13]. This system consists of 2 separate circulating perfusion circuits for the hepatic artery (HA) and portal vein (PV), where each has a roller pump, a pressure sensor, and a flow meter connected to a separate circulation system *via* plastic connectors, allowing pulsatile and non-pulsatile flow, respectively. A gas blender attached to the oxygenator mixes air with oxygen is installed to the PV and HA circuit. Both circuits were connected to the hepatic vessels *via* plastic connectors and oxygen concentration was perfused and maintained at PO2 200-300 mmHg, where they are monitored by using dissolved oxygen meter installed. Waterproof thermocouples were installed in the perfusion systems to measure the solution temperature, and the heat exchanger was installed in the systems where ice-cold water controls the temperature in the organ chamber. As described previously, the flow rate was controlled as 0.22 mL/min/g for the PV and 0.06 mL/min/g for the HA[9,13].

Preparation and preservation of the liver donated after cardiac death

Pigs weighing approximately 25 kg were used as liver graft donors. In this study, the animals were intubated and ventilated under inhalation anesthesia with isoflurane (Forane; Abbott, Japan), and laparotomized. Immediately after laparotomy, the tissue samples were biopsied from the liver surface as a control. Then the animals were injected with potassium chloride intravenously to induce cardiac arrest followed by the removal of ventilation, as described previously[9,13]. The time of the induction of cardiac arrest was set as the point of 0 min of warm ischemia. During warm ischemia, the HA and PV were isolated from the surrounded tissues to connect with organ flush lines. After 60 min of warm ischemia, the tissue samples of the liver were biopsied from distinct regions of the liver surface. Immediately after tissue sampling, the liver grafts that were procured were initially flushed with a Euro-Collins solution that is less viscous *via* the HA and PV routes at 8 °C as a back table operation. After the operation, the organ flush lines were connected to the perfusion preservation machine systems, and the liver was continuously perfused for 4 h with a modified University of Wisconsin gluconate solution, described previously[9]. The liver grafts were conserved as two groups, A and B. The grafts in group A were perfused at a constant temperature of 8 °C as HMP (n = 3), on the other hand, the grafts in group B were gradually warmed from 8 °C to 22 °C during perfusion as MMP (n = 3), as described previously[13]. After 4 h of MP, liver tissue samples in each group were collected from the well-perfused area of the surface of liver grafts. All the blocks of liver samples were immediately fixed with appropriate fixative for the analysis as described below.

The viability of LSEC in liver grafts preserved for 4 h was evaluated by hyaluronic acid (HyA) levels in perfusate collected from the suprahepatic vena cava as described previously[15]. These results in the text and figures are expressed by the means ± SEM. Comparisons of the significance of differences between each MP group A and B were performed by using unpaired two-tailed *t*-tests.



DOI: 10.3748/wjg.v28.i19.2100 **Copyright** ©The Author(s) 2022.

Figure 1 Schematic representation of the continuous machine perfusion preservation system.

Immunohistochemistry

The tissue samples biopsied from the liver of porcine were immediately immersed into 10% buffered formalin subsequently embedded in paraffin. The paraffin-embedded samples were sectioned into 4 μm slices and mounted on microscope glass slides. After the paraffin was removed by xylene, these tissue slices were rehydrated with series of graded ethanol, subsequently transferred into EDTA (pH 9.0) for antigen retrieval. After washing with PBS, the tissue slices were incubated in 0.3% hydrogen peroxide in methanol for 15 min, subsequently transferred into SuperBlock Blocking Buffer for 20 min as blocking. After these treatments, the tissue slices were incubated in a dilution (1:10) of primary antibody for 1 h at room temperature. Then the tissue slices were visualized by the Envision system (DAKO; Glostrup, Denmark), counterstained by using the hematoxylin. After the dehydration with a series of graded ethanol and xylene, the tissue slices were mounted with Malinol. The sections were observed by light microscopy.

TEM

The biopsied tissue samples from the liver of porcine were cut into small pieces and immersed in the fixative mixture of 2% glutaraldehyde (GA)/2% paraformaldehyde (PFA) in 0.1 M phosphate buffer (PB, pH 7.4) for 2 h at 4 °C. After washing with 0.1 M PB containing 7.5% sucrose, the samples were post-fixed with 1% osmium tetroxide (OsO4) in 0.1 M PB for 2 h at 4 °C. After washing with 0.1 M PB containing 7.5% sucrose, the samples were dehydrated in a series of graded ethanol solutions (starting with 50% and increasing to 100% ethanol). Then the samples were embedded in epoxy resin (Epon 812). Ultrathin sections (80 nm thick) from the embedded samples in Epoxy resin were cut using a diamond knife. The sections were observed by using TEM (HT7700; Hitachi High Technologies Inc., Tokyo, Japan) without staining by uranyl acetate and lead citrate.

OM-SEM

The osmium maceration method was described previously[9,13]. In brief, the biopsied liver tissue samples of porcine were incised into small pieces and fixed with a fixative mixture of 0.5% GA/0.5% PFA in 0.1 M PB (pH 7.4), for 30 min at 4 °C. Then the tissue samples were fixed with 1% OsO4 in 0.1 M PB for 6 h at 4 °C. After washing thoroughly with 0.1 M PB, the samples were immersed into 25% dimethyl sulfoxide (DMSO) for 30 min and subsequently 50% DMSO for 30 min as cryoprotection. Cryoprotected samples were frozen on a precooled aluminum plate chilled with liquid nitrogen. The frozen tissue samples were fractured into two pieces by using a 2.0 mm flathead screwdriver and a hammer. After freeze-fracture, the samples were transferred into 50% DMSO again for thawing, washed with 0.1 M PB, and then immersed into 0.1% OsO4 in 0.1 M PB solution for 96 h at 20 °C under the light for osmium maceration. After osmium maceration, the tissue samples were further fixed with 1% OsO4 in 0.1 M PB for 1 h at 4 °C. The samples were then washed thoroughly with 0.1 M PB before being conductive stained with 1% tannic acid in 0.1 M PB and subsequently with 1% OsO4 in 0.1 M PB. Then the samples were dehydrated in a series of graded ethanol solutions (starting 70% and increasing to 100% ethanol) and immersed in t-butyl alcohol and dried in a freeze dryer (ES2030; Hitachi High Technologies Inc., Tokyo, Japan). The dried specimens were then mounted onto an aluminum plate with silver paste and received the surface coating with platinum-palladium in an ion sputter coating equipment (E1010; Hitachi High Technologies Inc., Tokyo, Japan). After all the processes said were completed, the specimens were evaluated by using a field emission scanning electron microscopy (FE-

SEM, S4100; Hitachi High Technologies Inc., Tokyo, Japan).

RESULTS

Localization and ultrastructural characteristics of liver sinusoidal endothelial cells in the porcine liver

In the porcine liver, the interspersed ERG positive sinusoidal endothelial cells were observed (Figure 2A). Observation of the intercellular ultrastructure of the sinusoidal endothelial cells by TEM showed that the rough endoplasmic reticulum formed narrow networks of lumens (Figure 2B, arrow), and cytoplasmic vesicles or caveolae occasionally open to the plasma membrane. LSEC had abundant free-ribosome in their cytoplasm and the small sausage-shaped mitochondria (Figure 2B, green) localized around the nucleus (Figure 2B, blue). Observation utilized by SEM revealed more detailed ultrastructural characteristics of LSEC. Low magnified observation showed the flat-shaped LSEC lined the sinusoids (Figure 2C). Also, the space of Disse presented the normal appearance in which apical microvilli of the hepatocytes protruded. In high magnification by SEM, LSEC had the network of rough endoplasmic reticulum and vesicles correspond to TEM observation. In LSEC, mitochondria (Figure 2D, green) had tubular or plate-formed cristae sparsely arranged identified around the nucleus (Figure 2D, blue).

Changes of intracellular ultrastructure in LSEC after warm ischemia

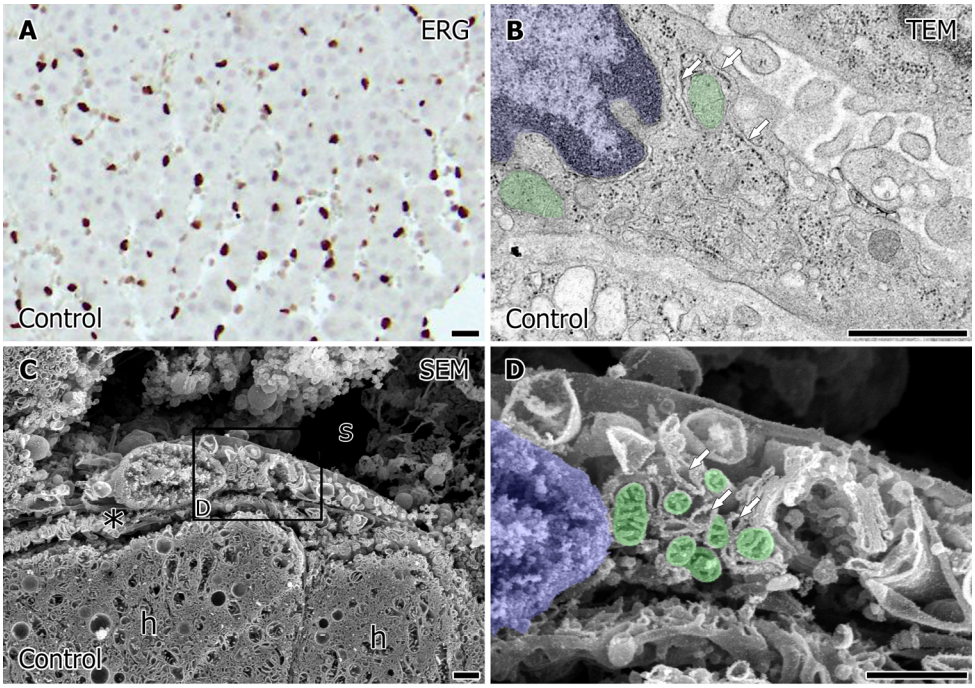
Even after warm ischemia, ERG-positive viable LSEC was detected in liver grafts similar to the samples before warm ischemia (Figure 3A). However, the ultrastructural characteristics of LSEC were substantially changed after warm ischemia. TEM observation revealed that LSEC had a slightly expanded rER, lysosome-like structure, and numerous vesicles. Furthermore, it appears to have a decrease of free ribosomes from the cytoplasm of LSEC (Figure 3B) and membranous structure (Figure 3B, arrowhead) surrounding mitochondria (Figure 3B, green) at the peripheral region from the nucleus (Figure 3B, blue). Low magnified SEM observation showed the LSEC-covered sinusoid in liver grafts after warm ischemia; however, its lumen was reduced reflecting the loss of blood flow (Figure 3C). Additionally, the space of Disse between LSEC and hepatocytes (Figure 3C) was reduced and microvilli were regressed. High magnified SEM observation revealed that a slightly expanded network of rER (Figure 3D, arrow) and numerous vesicles in LSEC. Around the nucleus (Figure 3D, blue), small mitochondria with densely distributed tubular cristae (Figure 3D, green) were surrounded by rER (Figure 3D and D′, arrowhead).

Comparison of ultrastructural changes in LSEC after HMP or MMP

An immunohistochemical study for ERG showed similarly viable LSEC in liver grafts after 4 h for both HMP and MMP (Figures 4A and 5A). The value of HyA in the perfusate did not indicate a significant difference between HMP and MMP. However, there was a trend of improvement in MMP (Supplementary Figure 1, 38.33 ± 8.88 HMP_4h *vs* 26.00 ± 3.46 ng/mL MMP_4h, $P = 0.27$). Furthermore, the ultrastructural characteristics of LSEC after each MP also showed a difference (Figures 4 and 5). TEM observation of LSEC after 4 h of HMP showed that small globular mitochondria and the slightly expanded network formation of rER localized in the cytoplasm (Figure 4B, arrow). Besides, intracellular vesicles and free ribosomes in LSEC after HMP were decreased from the point of warm ischemia 1 h. Low magnified SEM observation showed that the lumen of the sinusoids (Figure 4C) were lined by LSEC, although there were scarcely spaced cavities of Disse between the LSEC and hepatocytes (Figure 4C). At higher magnification, intracellular expanded rER networks were observed in LSEC. Besides, the spherical mitochondria (Figure 4D, green) had densely but shrinking tubular cristae and remained localized around the nucleus (Figure 4D, blue). On the other hand, after 4 h of MMP, expanded rER (Figure 5B, arrow) and the network of endomembranous structures that had a smooth surface and expanded lumen with high electron density simultaneously appeared in LSEC by TEM observation (Figure 5B, red). Moreover, LSEC had the relatively abundant interspersed free-ribosomes in their cytoplasm and mitochondria with sausage-like formation neighboring to the nucleus (Figure 5B). Observation by SEM revealed more detailed intrahepatic ultrastructure containing LSEC. In low magnification, sinusoids of liver grafts after 4 h of MMP tend to enlarge and form the cavity of Disse than that of HMP (Figure 5C). High-magnified SEM observation revealed that LSEC had the expanded rER attached to the surface-smoothed vacuolar structure in the cytoplasm (Figure 5D). Furthermore, the mitochondria with regularly arranged cristae localized around the nucleus in LSEC take a form of sausage-like structure again (Figure 5D, green).

DISCUSSION

In this present study, we confirmed the usefulness of the OM-SEM with complementary TEM for the description of the ultrastructure of organelles in LSEC. Based on this, we revealed the intracellular



DOI: 10.3748/wjg.v28.i19.2100 **Copyright** ©The Author(s) 2022.

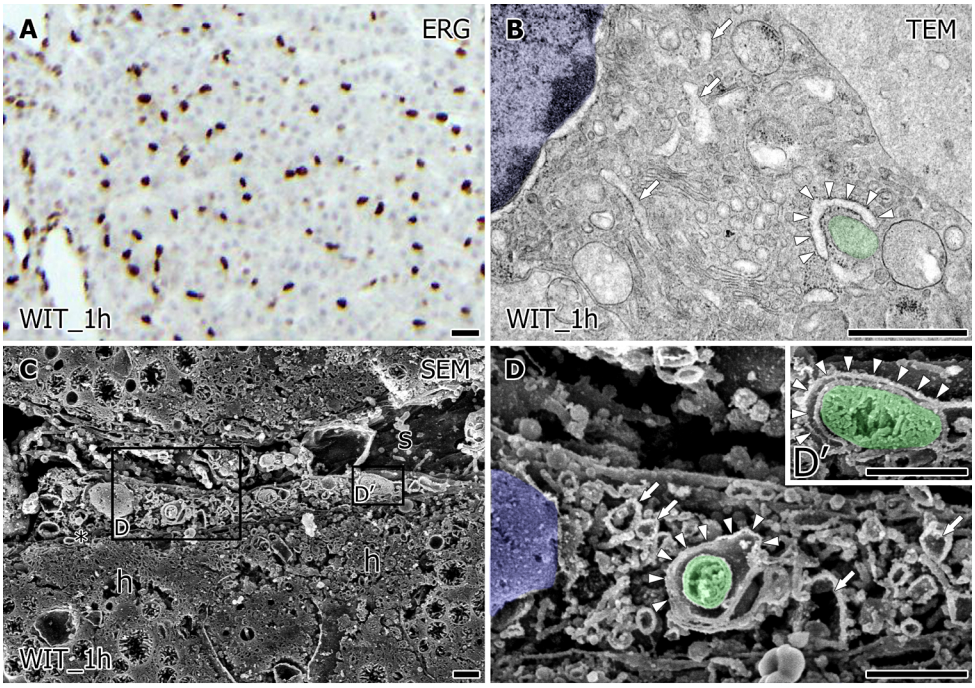
Figure 2 The distribution and ultrastructural characteristics in porcine liver sinusoidal endothelial cells of the control liver. A: The representative image of the distribution of liver sinusoidal endothelial cells (LSEC) in the porcine liver indicated by the immunohistochemical staining with antibody to ERG. Bar = 10 μm; B: Typical LSEC were identified in the ultrathin sections (90 nm) of the Epon 812-embedded control liver tissue. Bars = 1 μm; C and D: LSEC was observed by scanning electron microscopy in osmium-macerated control porcine liver. s: sinusoid. h: Hepatocyte. The space of Disse was indicated by an asterisk. The partial area indicated in C was further observed in high magnification D. Bars = 1 μm. Mitochondria is represented in green and the nucleus is represented in blue. Arrows indicate the rough endoplasmic reticulum (rER). TEM: Transmission electron microscopy; SEM: Scanning electron microscopy.

ultrastructural characteristics of porcine LSEC post warm ischemia after HMP and MMP preservation by utilizing osmium maceration for SEM and complementary TEM methods.

OM-SEM observation could demonstrate the 3-dimensional architecture of mitochondria cristae in porcine LSEC (Figure 1D). Previous studies using OM-SEM analyzed the intracellular ultrastructure of hepatocytes including bile canaliculi but did not describe the porcine LSEC[9,13,16]. Our data revealed for the first time that the mitochondria in porcine LSEC have tubular cristae with a relative expansion of matrix. The orthodox-shaped mitochondrial cristae are thought to reflect the state of Low ADP[17].

The distribution of anti-ERG antibody-positive cells which indicate viable LSEC in the liver after 60 min of warm ischemia does not differ from normal, which is consistent with our previous report[18]. Nevertheless, the intracellular ultrastructural characteristics of LSEC were altered after warm ischemia. Our data revealed that mitochondria with condensed-shaped cristae, vesicles, and the ER surround the mitochondria appeared in the LSEC after warm ischemia (Figure 3D and D′). It is known that LSECs are specifically sensitive to energy deficiency[19]. The condensed-shaped cristae of mitochondria reflect an energy substrate deficiency[17]. During warm ischemia, the lack of energetic substrate interferes with active transmembrane transport in LSEC[20]. ER injury of LSEC also precedes mitochondrial disintegration in the setting of warm ischemia[4]. Damaged ER may cause the appearance of vesicles and vacuoles in LSEC after warm ischemia[21,22]. These suggest that warm ischemia impaired the membrane transport between the ER and mitochondria consequently caused morphological distortion of ER including vesiculation and membranes surrounding mitochondria.

The MP after warm ischemia alleviates the abnormal vesicles and promotes the reduction of ribosomes in LSEC (Figures 4 and 5). In previous studies, it was indicated that LSEC injury reduces liver viability, and MP protects against and alleviates the effects of endothelial injury at the ultrastructural level[23-25]. One of the potential protective factors of our machine perfusion systems is the early hypothermic period. The lowest degree of damage on LSEC using electron microscopy was seen at the 4 and 25 °C of machine perfusion groups[26]. Hypothermic state of machine perfusion rescue DCD livers subjected to prolonged warm ischemia *via* downregulation of LSEC activation[27]. The flow of machine perfusion is also another potential protective factor. The flow stasis leads to acute endothelial dysfunction and apoptosis *via* rapid loss of shear-stress-dependent KLF2 in LSEC[28]. Machine perfusion which triggers protection of LSEC *via* upregulation of shear stress-sensitive protective genes [29], consequently may alleviate the ultrastructural abnormalities shown by the present study. Furthermore, the high oxygen availability during machine perfusion also maintains the structural integrity of LSEC[30]. Short-term oxygenated perfusion potentially reduces the risk of a possible release



DOI: 10.3748/wjg.v28.i19.2100 **Copyright** ©The Author(s) 2022.

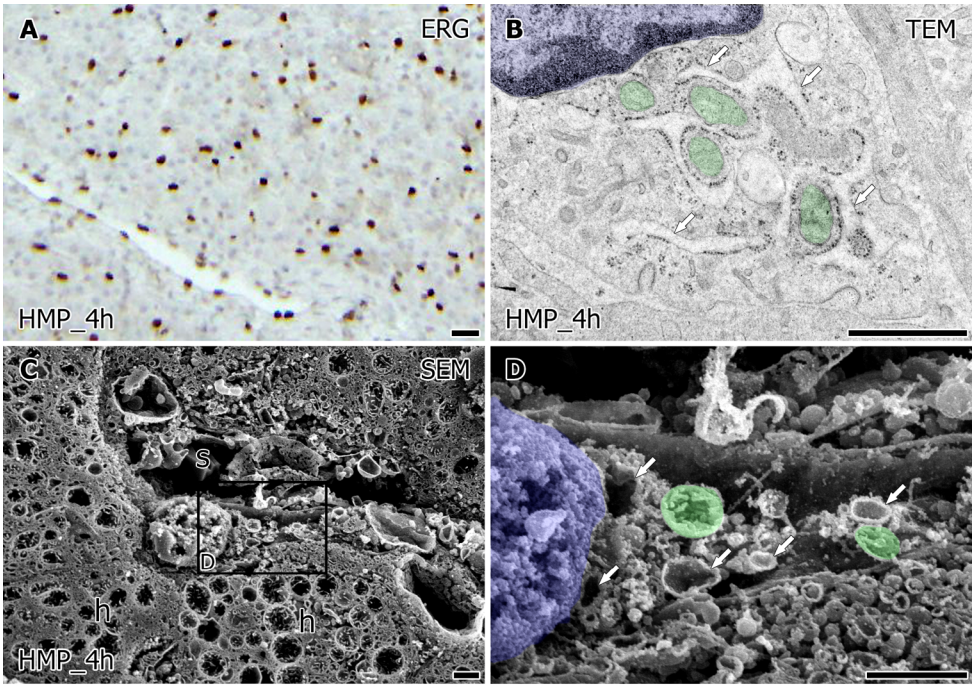
Figure 3 Changes in the intracellular ultrastructure of the porcine liver sinusoidal endothelial cells after warm ischemia. A: The distribution of viable liver sinusoidal endothelial cells (LSEC) indicated by ERG-positive cells in the porcine liver after warm ischemia for 60 min. Bar = 10 μm; B: Transmission electron microscopy image of the LSEC after warm ischemia. Bars = 1 μm; C and D: LSEC after warm ischemia was observed by SEM in the osmium-macerated porcine liver. s: sinusoid. h: Hepatocyte. The space of Disse was indicated by an asterisk. The partial area indicated in C was further observed in high magnification D. Bars = 1 μm. Mitochondria is represented in green and the nucleus is represented in blue. Arrows indicate the rER. The rER surround the mitochondria were indicated by arrowheads. TEM: Transmission electron microscopy; SEM: Scanning electron microscopy.

of reactive oxygen species and endothelial shear stress[4]. Consistent with these studies, our present study showed that MP alleviates the ultrastructural abnormalities that appeared in LSEC after warm ischemia.

After warm ischemia, MMP restores the tubular mitochondrial cristae, while after HMP the condensed and narrow mitochondrial cristae remained (Figures 4 and 5). This is consistent with the finding of the previous study that the hepatocyte preserved by HMP has strongly swollen mitochondria, in contrast, MMP could preserve the functional appearance of mitochondria in hepatocytes[13]. These differences of findings rely on the temperature condition during MP. The ultrastructural feature of mitochondria with narrow cristae which appeared after HMP is similar to mitochondria observed in LSEC after cold incubation in UW solution *in vitro*[31]. During hypothermia, LSEC undergoes a cold-induced decrease in mitochondrial membrane potential and finally loses viability and induces apoptosis [31-33]. Similarly, *in vivo*, the HMP compromises liver grafts by prompting cold-induced damage to LSEC[34]. HMP led to a significant slowdown of mitochondrial respiration rate[33], therefore, interrupting the balance of oxygen supply/demand of LSEC. Furthermore, the reduction of membrane fluidity induced by continuous cool perfusion temperatures of HMP was examined in a previous study [35]. Extended times of HMP may also be subject to disadvantages and limitations concerning endoplasmic stress and alteration of LSEC[16].

On the other hand, the controlled oxygenated rewarming, similar to MMP, was reported to significantly increase gene expression and protein levels of the autophagy-related beclin-1 in liver grafts [11]. Electron-dense endomembranous structure that appears in LSEC after MMP resembles autophagolysosome which suggests that the LSEC is protected by autophagy[36]. The restored tubular orthodox-shaped mitochondrial cristae in LSEC after MMP (Figures 5B and D), could supply more appropriate energy to match the demand of intracellular function of LSEC. MMP perfusate tends to have lower HyA levels compared to HMP (Supplementary Figure 1) supports the justification of LSEC has more functional integrity after MMP[15].

In addition to hypothermia, fluid shear stress can further aggravate the damage in LSEC after HMP[7, 37]. It was observed that the reduction of the space of Disse in the liver grafts after HMP may be the cause of the pressure injury (Figures 4 and 5). Liver sinusoids are also known to be very sensitive to endothelial shear stress because LSEC is easily damaged by high pressure[38,39]. Endothelial injury by shear stress is the main risk of HMP[4,24,37,40]. Vascular perfusion of the liver at 4 °C induces vasoconstriction of the hepatic vasculature[41] and alters LSEC, which is vulnerable to hypothermia[31]. Morphological changes in LSEC structures and increased vascular resistance in the liver graft occurred



DOI: 10.3748/wjg.v28.i19.2100 **Copyright** ©The Author(s) 2022.

Figure 4 The ultrastructural alteration in porcine liver sinusoidal endothelial cells preserved by hypothermic machine perfusion. A: The distribution of viable liver sinusoidal endothelial cells (LSEC) which is indicated with ERG-positive cells in the porcine liver preserved by hypothermic machine perfusion (HMP) for 4 h after 60 min of warm ischemia. Bar = 10 μm; B: transmission electron microscopy image of the LSEC in porcine liver preserved by HMP for 4 h after 60 min of warm ischemia. Bars = 1 μm; C and D: LSEC was observed by scanning electron microscopy in osmium-macerated porcine liver preserved by HMP for 4 h after 60 min of warm ischemia. s: Sinusoid. h: Hepatocyte. The partial area indicated in C was further observed in high magnification D. Bars = 1 μm. Mitochondria are labeled in green and the nucleus is labeled in blue. Arrows indicate the rER. TEM: Transmission electron microscopy; SEM: Scanning electron microscopy.

during HMP, which obstruct the sinusoidal flow[37]. In the present study, the LSEC after HMP was observed as flat-shaped, which consistent with the findings reported by Chai *et al*[42].

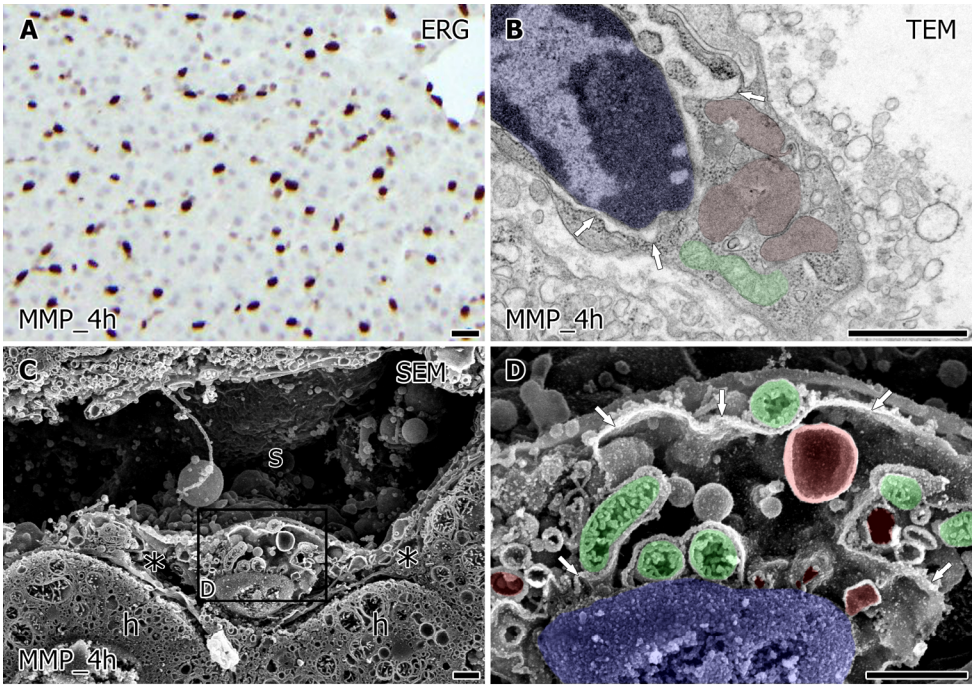
In contrast to the HMP, our previous study showed that the pressure transitions of the HA decrease in the initial stage of MMP[12], which suggests the lower risk of shear stress in LSEC after MMP. In the present study, we showed that the volume of the sinusoidal space in the liver grafts after MMP was restored as control liver, which suggests that the decreased vascular resistance *via* sinusoidal space enlargement led to reducing the risk of pressure injury in MMP.

This present study has several limitations. First, the condition of MP including temperature during perfusion should be more refined for clinical application. Similar to the previous study of allogenic transplantation of porcine liver grafts under similar conditions as this study[18], the present MMP condition is not suitable for clinical transplantation. Our previous studies suggested that the liver grafts preserved by MMP suffered damage to some extent[13]. The MP with rewarming gave a more promising alternative, as many results preferring these temperature settings were reported in previous studies[43]. Furthermore, previous studies suggest that oxidative stress and endothelial shear stress can be reduced by modulating the perfusion temperature and oxygenation[44]. However, the rewarming velocity of liver grafts, the critical temperature, and the appropriate period of warm temperature needed to adjust metabolic parameters are yet to be sufficiently defined[43]. Therefore, the ultrastructural characteristics of the LSEC preserved by a better-modified MP method should be analyzed in future studies.

However, this study did not evaluate the ultrastructural characteristics of the LSEC in the liver monitored after MP for evaluation of the ischemic reperfusion injury. The most marked destructive changes of ultrastructure in LSEC are seen during reperfusion[45]. Thus, the results of the present study should be further investigated by future studies utilized normothermic reperfusion ex-situ.

CONCLUSION

In conclusion, MP preservation alleviated the ER damage of LSEC caused by warm ischemia. Moreover, MMP temperature conditions restore the metabolism of LSEC *via* the normalization of cristae of mitochondria and prevent the damage of the liver graft by share stress. In the future, more appropriate MP conditions clinically to preserve the LSEC functions of the liver grafts should be established by



DOI: 10.3748/wjg.28i19.2100 **Copyright** ©The Author(s) 2022.

Figure 5 The ultrastructural characteristics in porcine liver sinusoidal endothelial cells preserved by midthermic machine perfusion. A: The distribution of ERG-positive liver sinusoidal endothelial cells (LSEC) in the porcine liver preserved by midthermic machine perfusion (MMP) for 4 h after 60 min of warm ischemia. Bar = 10 μm; B: Transmission electron microscopy image of the LSEC in porcine liver preserved by MMP for 4 hr after 60 min of warm ischemia. Bars = 1 μm; C and D: LSEC was observed by scanning electron microscopy in osmium-macerated porcine liver preserved by MMP for 4 hr after 60 min of warm ischemia. s: Sinusoid. h: Hepatocyte. The space of Disse was indicated by an asterisk. The partial area indicated in C was further observed in high magnification D. Bars = 1 μm. Arrows indicate the rER. Mitochondria are labeled in green; the nucleus is labeled in blue, expanded rER is labeled in red. TEM: Transmission electron microscopy; SEM: Scanning electron microscopy.

using normothermic reperfusion machine systems. Further analysis of detailed mechanisms of the ultrastructural changes in LSEC under various conditions, including different levels of oxygenation and different temperatures, during perfusion storage, is required for the application of MP to clinical transplantation.

ARTICLE HIGHLIGHTS

Research background

Using liver grafts donated after cardiac death (DCD) is one way to solve the shortage of donors for liver transplantation. Machine perfusion (MP) preservation has been considered as a promising, and the optimal conditions of perfusion temperature of MP of the DCD grafts, including hypothermic MP (HMP) and midthermic MP (MMP) has been discussed.

Research motivation

Recent research showed the practicality of scanning electron microscopy after osmium-maceration (OM-SEM) with complementary transmission electron microscopy (TEM) in evaluating the function of the liver grafts which is reflected by ultrastructural characteristics of hepatocytes. This has prompted the application of this novel strategy for the evaluation of liver sinusoidal endothelial cells (LSEC) damage in regulating liver injury during MP.

Research objectives

The present study aimed to establish the usefulness of the OM-SEM with complementary TEM for the evaluation of LSEC damage, and comparatively investigate the ultrastructural changes associated with LSEC at 4 h after HMP or MMP.

Research methods

Female pigs were intubated and ventilated under anesthesia, and their liver tissues were biopsied immediately after laparotomy, as control, and 60 min of warm ischemia. The liver grafts which had warm ischemia of 60 min were perfused for 4 h with modified University of Wisconsin gluconate

solution by HMP at 8 °C constantly or MMP rewarming up to 22 °C and biopsied at the endpoint of MP. the LSEC in all biopsied liver samples were analyzed by immunohistochemistry and OM-SEM with complementary TEM. The viability of LSEC in liver grafts preserved for 4 h was evaluated by hyaluronic acid levels in the perfusate.

Research results

Immunohistochemistry showed the interspersed viable ERG positive sinusoidal endothelial cells in all biopsied liver samples. After warm ischemia, the LSEC showed the mitochondria with condensed-shaped cristae, abnormal vesicles, reduction of ribosomes and the ER surrounding the mitochondria. Both the HMP and MMP after warm ischemia alleviate the ER damage in LSEC indicated by the abnormal vesicles and reduction of ribosomes. The value of HyA in the perfusate did not indicate a significant difference between HMP and MMP, although there was a trend of improvement in MMP, moreover, only MMP, not HMP, could restore the tubular cristae of mitochondria.

Research conclusions

This research confirmed the usefulness of the OM-SEM with complementary TEM for the evaluation of LSEC damage reflected on the ultrastructure of organelles. MP alleviate the ultrastructural abnormalities indicating ER damage of LSEC caused by warm ischemia. Moreover, MMP temperature conditions restore the metabolism of LSEC *via* the normalization of ultrastructural characteristics of cristae of mitochondria and prevent the damage of the liver graft by share stress.

Research perspectives

The OM-SEM with complementary TEM is applicable for the detailed evaluation of LSEC damage reflected on the ultrastructure of the MP of various conditions, including different temperatures during perfusion storage, for clinically application of the MP for liver transplantation.

ACKNOWLEDGEMENTS

We thank all of the lab members and colleagues for their helpful suggestions and assistance in the experiments. We are extremely grateful to Dr. Hiroyuki Kanazawa for assistance with immunohistochemistry and Mr. Yoshiyasu Satake for assistance with carrying out all of the research.

FOOTNOTES

Author contributions: Bochimoto H and Ishihara Y contributed equally to this work; Bochimoto H, Obara H and Matsuno N designed and coordinated the study; Bochimoto H, Ishihara Y, Kondoh D, Obara H and Matsuno N performed the experiments, acquired and analyzed data; Bochimoto H, Ishihara Y, Mohd Zin NK, Iwata H, Kondoh D, Obara H and Matsuno N interpreted the data; Bochimoto H wrote the manuscript; all authors approved the final version of the article.

Supported by JSPS KAKENHI Grant, No. JP17K10503 (to Matsuno N) and JP20K11539 (to Bochimoto H).

Institutional review board statement: The study was reviewed and approved by the Institutional Animal Ethics Committee of the Clinical Research Center, Asahikawa Medical University.

Institutional animal care and use committee statement: All animal experiments conformed to the internationally accepted principles for the care and use of laboratory animals (permit No. 14172, The Institutional Animal Ethics Committee of the Clinical Research Center, Asahikawa Medical University, Asahikawa, Japan).

Conflict-of-interest statement: All of the authors have nothing to disclose.

Data sharing statement: No additional data are available.

ARRIVE guidelines statement: The authors have read the ARRIVE guidelines, and the manuscript was prepared and revised according to the ARRIVE guidelines.

Open-Access: This article is an open-access article that was selected by an in-house editor and fully peer-reviewed by external reviewers. It is distributed in accordance with the Creative Commons Attribution NonCommercial (CC BY-NC 4.0) license, which permits others to distribute, remix, adapt, build upon this work non-commercially, and license their derivative works on different terms, provided the original work is properly cited and the use is non-commercial. See: https://creativecommons.org/Licenses/by-nc/4.0/

Country/Territory of origin: Japan

ORCID number: Hiroki Bochimoto 0000-0002-1708-0348; Yo Ishihara 0000-0002-5675-4026; Nur Khatijah Mohd Zin 0000-0002-5584-3019; Hiroyoshi Iwata 0000-0002-3970-0827; Daisuke Kondoh 0000-0002-3015-5156; Hiromichi Obara 0000-0003-0662-6138; Naoto Matsuno 0000-0001-5186-7331.

S-Editor: Chang KL
L-Editor: A
P-Editor: Chang KL

REFERENCES

1 **Dutkowski P**, Linecker M, DeOliveira ML, Müllhaupt B, Clavien PA. Challenges to liver transplantation and strategies to improve outcomes. *Gastroenterology* 2015; **148**: 307-323 [PMID: 25224524 DOI: 10.1053/j.gastro.2014.08.045]
2 **Okamura Y**, Hata K, Tanaka H, Hirao H, Kubota T, Inamoto O, Kageyama S, Tamaki I, Yermek N, Yoshikawa J, Uemoto S. Impact of Subnormothermic Machine Perfusion Preservation in Severely Steatotic Rat Livers: A Detailed Assessment in an Isolated Setting. *Am J Transplant* 2017; **17**: 1204-1215 [PMID: 27860296 DOI: 10.1111/ajt.14110]
3 **Goldaracena N**, Barbas AS, Selzner M. Normothermic and subnormothermic ex-vivo liver perfusion in liver transplantation. *Curr Opin Organ Transplant* 2016; **21**: 315-321 [PMID: 27093224 DOI: 10.1097/MOT.0000000000000305]
4 **Dutkowski P**, de Rougemont O, Clavien PA. Machine perfusion for 'marginal' liver grafts. *Am J Transplant* 2008; **8**: 917-924 [PMID: 18416733 DOI: 10.1111/j.1600-6143.2008.02165.x]
5 **Mourad MM**, Algarni A, Liossis C, Bramhall SR. Aetiology and risk factors of ischaemic cholangiopathy after liver transplantation. *World J Gastroenterol* 2014; **20**: 6159-6169 [PMID: 24876737 DOI: 10.3748/wjg.v20.i20.6159]
6 **Moers C**, Pirenne J, Paul A, Ploeg RJ; Machine Preservation Trial Study Group. Machine perfusion or cold storage in deceased-donor kidney transplantation. *N Engl J Med* 2012; **366**: 770-771 [PMID: 22356343 DOI: 10.1056/NEJMc1111038]
7 **Burra P**, Zanetto A, Russo FP, Germani G. Organ Preservation in Liver Transplantation. *Semin Liver Dis* 2018; **38**: 260-269 [PMID: 30041278 DOI: 10.1055/s-0038-1666840]
8 **Westerkamp AC**, Mahboub P, Meyer SL, Hottenrott M, Ottens PJ, Wiersema-Buist J, Gouw AS, Lisman T, Leuvenink HG, Porte RJ. End-ischemic machine perfusion reduces bile duct injury in donation after circulatory death rat donor livers independent of the machine perfusion temperature. *Liver Transpl* 2015; **21**: 1300-1311 [PMID: 26097213 DOI: 10.1002/lt.24200]
9 **Ishihara Y**, Bochimoto H, Kondoh D, Obara H, Matsuno N. The ultrastructural characteristics of bile canaliculus in porcine liver donated after cardiac death and machine perfusion preservation. *PLoS One* 2020; **15**: e0233917 [PMID: 32470051 DOI: 10.1371/journal.pone.0233917]
10 **Hoyer DP**, Mathé Z, Gallinat A, Canbay AC, Treckmann JW, Rauen U, Paul A, Minor T. Controlled Oxygenated Rewarming of Cold Stored Livers Prior to Transplantation: First Clinical Application of a New Concept. *Transplantation* 2016; **100**: 147-152 [PMID: 26479280 DOI: 10.1097/TP.0000000000000915]
11 **Minor T**, Efferz P, Fox M, Wohlschlaeger J, Lüer B. Controlled oxygenated rewarming of cold stored liver grafts by thermally graduated machine perfusion prior to reperfusion. *Am J Transplant* 2013; **13**: 1450-1460 [PMID: 23617781 DOI: 10.1111/ajt.12235]
12 **Obara H**, Matsuno N, Shigeta T, Hirano T, Enosawa S, Mizunuma H. Temperature controlled machine perfusion system for liver. *Transplant Proc* 2013; **45**: 1690-1692 [PMID: 23769025 DOI: 10.1016/j.transproceed.2013.01.087]
13 **Bochimoto H**, Matsuno N, Ishihara Y, Shonaka T, Koga D, Hira Y, Nishikawa Y, Furukawa H, Watanabe T. The ultrastructural characteristics of porcine hepatocytes donated after cardiac death and preserved with warm machine perfusion preservation. *PLoS One* 2017; **12**: e0186352 [PMID: 29023512 DOI: 10.1371/journal.pone.0186352]
14 **Bhogal RH**, Mergental H, Mirza DF, Afford SC. The Emerging Importance of Liver Sinusoidal Endothelial Cells in Regulating Injury during Machine Perfusion of Deceased Liver Donors. *Semin Liver Dis* 2018; **38**: 252-259 [PMID: 30041277 DOI: 10.1055/s-0038-1661371]
15 **Tamaki I**, Hata K, Okamura Y, Nigmet Y, Hirao H, Kubota T, Inamoto O, Kusakabe J, Goto T, Tajima T, Yoshikawa J, Tanaka H, Tsuruyama T, Tolba RH, Uemoto S. Hydrogen Flush After Cold Storage as a New End-Ischemic Ex Vivo Treatment for Liver Grafts Against Ischemia/Reperfusion Injury. *Liver Transpl* 2018; **24**: 1589-1602 [PMID: 30120877 DOI: 10.1002/lt.25326]
16 **Okouchi Y**, Sasaki K, Tamaki T. Ultrastructural changes in hepatocytes, sinusoidal endothelial cells and macrophages in hypothermic preservation of the rat liver with University of Wisconsin solution. *Virchows Arch* 1994; **424**: 477-484 [PMID: 8032528 DOI: 10.1007/BF00191432]
17 **Mannella CA**. Structure and dynamics of the mitochondrial inner membrane cristae. *Biochim Biophys Acta* 2006; **1763**: 542-548 [PMID: 16730811 DOI: 10.1016/j.bbamcr.2006.04.006]
18 **Kanazawa H**, Obara H, Yoshikawa R, Meng L, Hirano T, Okada Y, Nishikawa Y, Matsuno N. Impact of Machine Perfusion on Sinusoid Microcirculation of Liver Graft Donated After Cardiac Death. *J Surg Res* 2020; **245**: 410-419 [PMID: 31437648 DOI: 10.1016/j.jss.2019.07.058]
19 **Minor T**, Hachenberg A, Tolba R, Pauleit D, Akbar S. Fibrinolytic preflush upon liver retrieval from non-heart beating donors to enhance postpreservation viability and energetic recovery upon reperfusion. *Transplantation* 2001; **71**: 1792-1796 [PMID: 11455260 DOI: 10.1097/00007890-200106270-00015]
20 **Vollmar B**, Glasz J, Leiderer R, Post S, Menger MD. Hepatic microcirculatory perfusion failure is a determinant of liver dysfunction in warm ischemia-reperfusion. *Am J Pathol* 1994; **145**: 1421-1431 [PMID: 7992845]
21 **Li X**, Elwell MR, Ryan AM, Ochoa R. Morphogenesis of postmortem hepatocyte vacuolation and liver weight increases in

Sprague-Dawley rats. *Toxicol Pathol* 2003; **31**: 682-688 [PMID: 14585737 DOI: 10.1080/01926230390241981]

22 **Jurado F**, Buján J, Mora NP, Jiménez M, Arahuetes R, Bellón JM. A histopathological study of anoxic-resuscitated liver allografts. *Histol Histopathol* 1997; **12**: 123-133 [PMID: 9046050]

23 **de Vries RJ**, Pendexter CA, Cronin SEJ, Marques B, Hafiz EOA, Muzikansky A, van Gulik TM, Markmann JF, Stott SL, Yeh H, Toner M, Uygun K, Tessier SN. Cell release during perfusion reflects cold ischemic injury in rat livers. *Sci Rep* 2020; **10**: 1102 [PMID: 31980677 DOI: 10.1038/s41598-020-57589-4]

24 **Schlegel A**, Dutkowski P. Role of hypothermic machine perfusion in liver transplantation. *Transpl Int* 2015; **28**: 677-689 [PMID: 24852621 DOI: 10.1111/tri.12354]

25 **van der Plaats A**, Maathuis MH, 'T Hart NA, Bellekom AA, Hofker HS, van der Houwen EB, Verkerke GJ, Leuvenink HG, Verdonck P, Ploeg RJ, Rakhorst G. The Groningen hypothermic liver perfusion pump: functional evaluation of a new machine perfusion system. *Ann Biomed Eng* 2006; **34**: 1924-1934 [PMID: 17066322 DOI: 10.1007/s10439-006-9207-4]

26 **Nostedt JJ**, Churchill T, Ghosh S, Thiesen A, Hopkins J, Lees MC, Adam B, Freed DH, Shapiro AMJ, Bigam DL. Avoiding initial hypothermia does not improve liver graft quality in a porcine donation after circulatory death (DCD) model of normothermic perfusion. *PLoS One* 2019; **14**: e0220786 [PMID: 31386697 DOI: 10.1371/journal.pone.0220786]

27 **Schlegel A**, Kron P, Graf R, Dutkowski P, Clavien PA. Warm vs. cold perfusion techniques to rescue rodent liver grafts. *J Hepatol* 2014; **61**: 1267-1275 [PMID: 25086285 DOI: 10.1016/j.jhep.2014.07.023]

28 **Selten J**, Schlegel A, de Jonge J, Dutkowski P. Hypo- and normothermic perfusion of the liver: Which way to go? *Best Pract Res Clin Gastroenterol* 2017; **31**: 171-179 [PMID: 28624105 DOI: 10.1016/j.bpg.2017.04.001]

29 **Russo L**, Gracia-Sancho J, García-Calderó H, Marrone G, García-Pagán JC, García-Cardeña G, Bosch J. Addition of simvastatin to cold storage solution prevents endothelial dysfunction in explanted rat livers. *Hepatology* 2012; **55**: 921-930 [PMID: 22031447 DOI: 10.1002/hep.24755]

30 **Minor T**, Akbar S, Tolba R, Dombrowski F. Cold preservation of fatty liver grafts: prevention of functional and ultrastructural impairments by venous oxygen persufflation. *J Hepatol* 2000; **32**: 105-111 [PMID: 10673074 DOI: 10.1016/s0168-8278(00)80196-8]

31 **Kerkweg U**, Jacob M, De Groot H, Mannherz HG, Rauen U. Cold-induced apoptosis of rat liver endothelial cells: contribution of mitochondrial alterations. *Transplantation* 2003; **76**: 501-508 [PMID: 12923435 DOI: 10.1097/01.TP.0000069830.78758.1C]

32 **Rauen U**, Polzar B, Stephan H, Mannherz HG, de Groot H. Cold-induced apoptosis in cultured hepatocytes and liver endothelial cells: mediation by reactive oxygen species. *FASEB J* 1999; **13**: 155-168 [PMID: 9872940 DOI: 10.1096/fasebj.13.1.155]

33 **Schlegel A**, de Rougemont O, Graf R, Clavien PA, Dutkowski P. Protective mechanisms of end-ischemic cold machine perfusion in DCD liver grafts. *J Hepatol* 2013; **58**: 278-286 [PMID: 23063573 DOI: 10.1016/j.jhep.2012.10.004]

34 **Olthof PB**, Reiniers MJ, Dirkes MC, Gulik TMV, Golen RFV. Protective Mechanisms of Hypothermia in Liver Surgery and Transplantation. *Mol Med* 2016; **21**: 833-846 [PMID: 26552060 DOI: 10.2119/molmed.2015.00158]

35 **Czigany Z**, Lurje I, Schmelzle M, Schöning W, Öllinger R, Raschzok N, Sauer IM, Tacke F, Strnad P, Trautwein C, Neumann UP, Fronek J, Mehrabi A, Pratschke J, Schlegel A, Lurje G. Ischemia-Reperfusion Injury in Marginal Liver Grafts and the Role of Hypothermic Machine Perfusion: Molecular Mechanisms and Clinical Implications. *J Clin Med* 2020; **9** [PMID: 32244972 DOI: 10.3390/jcm9030846]

36 **Boteon YL**, Laing R, Mergental H, Reynolds GM, Mirza DF, Afford SC, Bhogal RH. Mechanisms of autophagy activation in endothelial cell and their targeting during normothermic machine liver perfusion. *World J Gastroenterol* 2017; **23**: 8443-8451 [PMID: 29358854 DOI: 10.3748/wjg.v23.i48.8443]

37 **Jain S**, Xu H, Duncan H, Jones JW Jr, Zhang JX, Clemens MG, Lee CY. Ex-vivo study of flow dynamics and endothelial cell structure during extended hypothermic machine perfusion preservation of livers. *Cryobiology* 2004; **48**: 322-332 [PMID: 15157780 DOI: 10.1016/j.cryobiol.2004.01.010]

38 **Schlegel A**, Kron P, Dutkowski P. Hypothermic Oxygenated Liver Perfusion: Basic Mechanisms and Clinical Application. *Curr Transplant Rep* 2015; **2**: 52-62 [PMID: 26097802 DOI: 10.1007/s40472-014-0046-1]

39 **Jomaa A**, Gurusamy K, Siriwardana PN, Claworthy I, Collier S, de Muylder P, Fuller B, Davidson B. Does hypothermic machine perfusion of human donor livers affect risks of sinusoidal endothelial injury and microbial infection? *Transplant Proc* 2013; **45**: 1677-1683 [PMID: 23769023 DOI: 10.1016/j.transproceed.2013.01.011]

40 **Schlegel A**, Kron P, Dutkowski P. Hypothermic machine perfusion in liver transplantation. *Curr Opin Organ Transplant* 2016; **21**: 308-314 [PMID: 26918882 DOI: 10.1097/MOT.0000000000000303]

41 **van der Plaats A**, 't Hart NA, Verkerke GJ, Leuvenink HG, Ploeg RJ, Rakhorst G. Hypothermic machine preservation in liver transplantation revisited: concepts and criteria in the new millennium. *Ann Biomed Eng* 2004; **32**: 623-631 [PMID: 15117035 DOI: 10.1023/B:ABME.0000019181.18194.51]

42 **Chai YC**, Dang GX, He HQ, Shi JH, Zhang HK, Zhang RT, Wang B, Hu LS, Lv Y. Hypothermic machine perfusion with metformin-University of Wisconsin solution for *ex vivo* preservation of standard and marginal liver grafts in a rat model. *World J Gastroenterol* 2017; **23**: 7221-7231 [PMID: 29142469 DOI: 10.3748/wjg.v23.i40.7221]

43 **Marecki H**, Bozorgzadeh A, Porte RJ, Leuvenink HG, Uygun K, Martins PN. Liver ex situ machine perfusion preservation: A review of the methodology and results of large animal studies and clinical trials. *Liver Transpl* 2017; **23**: 679-695 [PMID: 28240817 DOI: 10.1002/lt.24751]

44 **Ishii D**, Matsuno N, Gochi M, Otani M, Shonaka T, Takahashi H, Nishikawa Y, Yoshikawa R, Obara H, Miyamoto K, Furukawa H. Applicability of Hypothermic Oxygenate Machine Perfusion Preservation for Split-Liver Transplantation in a Porcine Model: An Experimental Study. *Ann Transplant* 2020; **25**: e919920 [PMID: 31932575 DOI: 10.12659/AOT.919920]

45 **Perri RE**, Shah V. Hepatic Sinusoidal Endothelial Cells [Internet]. In: Signaling Pathways in Liver Diseases. Berlin/Heidelberg: Springer-Verlag 1996: 53-62. Available from: http://Link.springer.com/10.1007/3-540-27194-5_5

World Journal of Gastroenterology

Submit a Manuscript: https://www.f6publishing.com

World J Gastroenterol 2022 May 21; 28(19): 2112-2122

DOI: 10.3748/wjg.v28.i19.2112

ISSN 1007-9327 (print) ISSN 2219-2840 (online)

ORIGINAL ARTICLE

Basic Study

Snare-assisted flexible endoscope in trans-gastric endoscopic gallbladder-preserving surgery: A pilot animal study

Xian-Wen Guo, Yun-Xiao Liang, Peng-Yu Huang, Lie-Xin Liang, Yi-Qing Zeng, Zhen Ding

Specialty type: Gastroenterology and hepatology

Provenance and peer review: Unsolicited article; Externally peer reviewed.

Peer-review model: Single blind

Peer-review report's scientific quality classification

Grade A (Excellent): 0
Grade B (Very good): B, B
Grade C (Good): 0
Grade D (Fair): 0
Grade E (Poor): 0

P-Reviewer: Badessi G, Italy; Wang S, China

Received: December 19, 2021
Peer-review started: December 19, 2021
First decision: March 10, 2022
Revised: March 23, 2022
Accepted: April 15, 2022
Article in press: April 15, 2022
Published online: May 21, 2022

Xian-Wen Guo, Zhen Ding, Department of Gastroenterology, Union Hospital, Tongji Medical College, Huazhong University of Science and Technology, Wuhan 430022, Hubei Province, China

Xian-Wen Guo, Yun-Xiao Liang, Peng-Yu Huang, Lie-Xin Liang, Yi-Qing Zeng, Department of Gastroenterology, The People's Hospital of Guangxi Zhuang Autonomous Region, Nanning 530021, Guangxi Zhuang Autonomous Region, China

Corresponding author: Zhen Ding, PhD, Chief Doctor, Department of Gastroenterology, Union Hospital, Tongji Medical College, Huazhong University of Science and Technology, No. 1277 Jiefang Avenue, Wuhan 430022, Hubei Province, China. docd720@126.com

Abstract

BACKGROUND

Natural orifice transluminal endoscopic surgery (NOTES) gallbladder-preserving surgery by flexible endoscopy is an emerging technology. However, the gallbladder fails to obtain traction and positioning functions during the operation.

AIM

To evaluate the feasibility and safety of a new surgical method, "snare-assisted pure NOTES gallbladder-preserving surgery".

METHODS

Eight miniature pigs were randomly divided into the experimental group [NOTES gallbladder-preserving surgery using the snare device, snare assisted (SA)] and the control group (NOTES gallbladder-preserving surgery without using the snare device, NC), with four cases in each group. The differences between the two groups of animals in operating time, operating workload, complications, adverse events, white blood cells, and liver function were determined.

RESULTS

No differences were found in the surgical success rate, gallbladder incision closure, white blood cell count, or liver function between the two groups. The total operating time, gallbladder incision blood loss, gallbladder disorientation time, gallbladder incision closure time, and workload scores on the National Aeronautics and Space Administration-Task Load Index were significantly reduced in the SA group ($P < 0.05$).

CONCLUSION
These results indicated that snare-assisted pure NOTES gallbladder-preservation surgery using standard endoscopic instruments reduced the difficulty of operation, shortened operation time, and did not increase complications in pigs. A new method for pure NOTES gallbladder-preservation surgery was provided.

Key Words: Snare; Flexible endoscope; Endoscopic gallbladder-preserving surgery; Natural orifice transluminal endoscopic surgery; Transgastric; Minimally invasive

©The Author(s) 2022. Published by Baishideng Publishing Group Inc. All rights reserved.

Core Tip: This study aimed to evaluate the feasibility and safety of a new surgical method, "snare-assisted pure natural orifice transluminal endoscopic surgery (NOTES) gallbladder-preserving surgery". Eight miniature pigs were randomly divided into an experimental group [snare assisted (SA)] and a control group. The total operating time, gallbladder incision blood loss, gallbladder disorientation time, gallbladder incision closure time, and workload scores on the National Aeronautics and Space Administration-Task Load Index were significantly reduced in the SA group. These results indicated that snare-assisted pure NOTES gallbladder-preservation surgery reduced the difficulty of the operation, shortened the operation time, and did not increase complications.

Citation: Guo XW, Liang YX, Huang PY, Liang LX, Zeng YQ, Ding Z. Snare-assisted flexible endoscope in transgastric endoscopic gallbladder-preserving surgery: A pilot animal study. *World J Gastroenterol* 2022; 28(19): 2112-2122
URL: https://www.wjgnet.com/1007-9327/full/v28/i19/2112.htm
DOI: https://dx.doi.org/10.3748/wjg.v28.i19.2112

INTRODUCTION

The incidence of benign gallbladder diseases, such as gallbladder stones and gallbladder polyps, has been increasing yearly[1], and the total prevalence of gallbladder stones in adults worldwide has reached 10%–20%[2]. Currently, cholecystectomy is still the main method used for the treatment of gallbladder stones and polyps. However, many complications occur after the patient loses the gallbladder[3,4]; moreover, gallbladder loss leads to an increased incidence of colorectal, pancreatic, esophageal, and liver cancers[5-8]. With the development of medicine, some doctors have realized that gallbladder removal may not be suitable for all patients with benign gallbladder diseases. The operation and concept of preserving the gallbladder and curing benign gallbladder diseases are now widely supported. In addition, some patients refuse open or laparoscopic cholecystectomy because it can cause surgical scars on the abdominal wall. They believe that these scars have a negative impact on their physical and mental health[9]. As an emerging technology, gallbladder-preservation surgery *via* natural orifice transluminal endoscopic surgery (NOTES) has obvious advantages in the complete resection of gallbladder polyps, removal of gallbladder stones, and preservation of gallbladder function. It is minimally invasive, painless, and scar-free. However, there are some technical obstacles to the clinical application of this operation. For example, the gallbladder bed is close to the liver, is obscured by fatty tissue, and has a poor field of vision; therefore, it can be difficult to locate the gallbladder[10]. In addition, the gallbladder collapses and shrinks quickly after incision, and the instruments used for gallbladder operation lose their focus, thereby making the operation very difficult[11]. The single-channel flexible endoscope for gallbladder-preservation surgery *via* NOTES requires additional navigation and traction.

Our inspiration came from the use of snares to assist in traction and exposure of lesions during endoscopic submucosal dissection. We tried a similar surgical method, which involved using a snare to assist in the traction and positioning of the gallbladder. The aim of this study was to evaluate the feasibility and safety of a newly proposed operative method, "a snare-assisted pure NOTES gallbladder-preserving surgery by a single-channel flexible endoscope".

MATERIALS AND METHODS

Animals

Eight Bama mini pigs weighing 15–20 kg that were in good health (with qualified certification) were chosen. The eight animals were randomly divided into two groups: The experimental group [NOTES gallbladder-preserving surgery using the snare device, snare assisted (SA)] and the control group (NOTES gallbladder-preserving surgery without using the snare device, NC). Each group had four animals. This study was conducted in the Experimental Center of the People's Hospital of Guangxi Zhuang Autonomous Region. The study was reviewed and approved by the Ethics Committee of the People's Hospital of Guangxi Zhuang Autonomous Region and the Ethics Committee of the Tongji Medical College, No. KY-LW-2019-4, [2020]-S322.

Equipment

A single-channel flexible endoscope (GIF-Q260J, Olympus, Tokyo, Japan) and an electrosurgical generator (Endocut ICC200; Erbe, Tubingen, Germany) were used. Other equipment included a snare (Boston Scientific, Ref; M00562650), a transparent cap (Olympus), an insulated IT-knife (model KD-610L, Olympus), a hook knife (model KD-620LR, Olympus), an injection needle (model 19G, Olympus), hemostatic clips and a release device (Olympus), and hot hemostatic forceps (KD610, Olympus). All endoscopes and accessories were sterilized prior to use.

Medications

The medications used in the study included xylazine hydrochloride injection, propofol injection, diazepam, 2% pentobarbital sodium, atropine, cimetidine, and ceftiofur sodium for injection (Chengdu Zhongmu Biological Pharmaceutical Co., Ltd.).

Anesthesia

The pigs fasted for 48–72 h. They were given 200 mL of milk and 500 mL of 50% glucose for their daily drink. Preoperative intramuscular injection of xylazine hydrochloride (2 mL) was completed, after which blood was immediately collected from the anterior vena cava of the neck. Then, an intravenous injection needle was placed in the dorsal ear vein, and intravenous infusion of propofol injection (4 mg/kg/h) was completed to maintain anesthesia. Endotracheal intubation was not performed. The ECG oxygen saturation meter was connected to monitor vital signs, and electrode pads were pasted on the abdominal skin after shaving. Preoperative intramuscular injection of ceftiofur sodium (5 mg/kg) was performed to prevent infection.

Description of technology (pure NOTES gallbladder-preserving surgery)

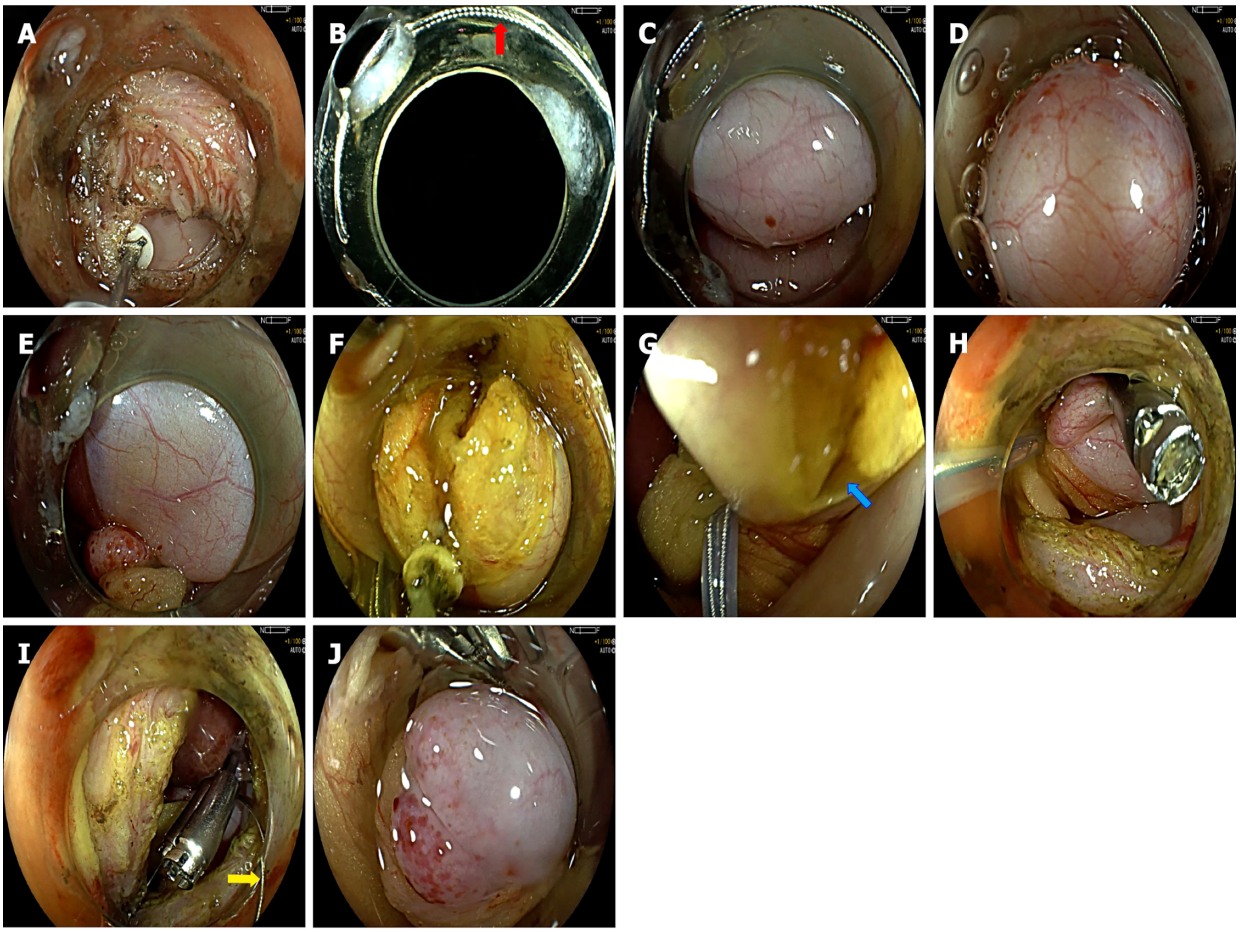
SA group: Each generally anesthetized pig was placed on its left side on the operating table. Each one wore a sterile mouth ring and was covered with sterile towels. An ordinary gastroscope was preinserted into the stomach. The stomach, esophagus, and duodenum were flushed with normal saline (> 1000 mL). A transparent cap was placed on the front end of the sterile gastroscope, and the anterior wall of the gastric antrum was incised using a hook knife and IT knife (Figure 1A). The snare was placed on the transparent cap and inserted into the abdominal cavity along with the endoscope (Figure 1B). The liver and gallbladder were examined (Figure 1C). The transparent cap clung to the gallbladder wall, and the gallbladder wall was sucked in it. The snare was released, and the gallbladder wall was ligated (Figure 1D). Under this ligation state (Figure 1E), a hook knife and IT knife were used to make an incision of approximately 13 mm in the gallbladder wall (Figure 1F and G). The endoscope entered the gallbladder and was used to observe and flush the gallbladder mucosa. Metal clips were employed to close the gallbladder incision (Figure 1H). The snare was loosened (Figure 1I and J). The abdominal cavity was flushed with normal saline (> 2000 mL). Further observation was performed to ensure that there was no bleeding or bile leakage at the gallbladder incision. Then, the gastric wall incision was closed with clips.

NC group: Except for the fact that the snare was not used, the operating procedures performed for this group were the same as those mentioned above.

During the operation, the intra-abdominal pressure was not measured. The anesthesiologist monitored the abdominal wall pressure and the oxygenation index of the ear skin, which prompted the endoscopist to suck the gas from the abdominal cavity with an endoscope in time to reduce the intra-abdominal pressure.

Video description

The video came from a single surgical procedure in the SA group. A pig model was used to demonstrate snare-assisted pure NOTES gallbladder-preserving surgery by a single-channel flexible endoscope (Videos 1 and 2).



DOI: 10.3748/wjg.v28.i19.2112 Copyright ©The Author(s) 2022.

Figure 1 Snare-assisted flexible endoscope in transgastric endoscopic gallbladder-preserving surgery. A: The anterior wall of the gastric antrum was incised; B: The snare was placed on the transparent cap (red arrow); C: The endoscope was inserted into the abdominal cavity. The gallbladder was located; D: The transparent cap clung to the gallbladder wall, and the gallbladder wall was sucked in it. The snare was released, and the gallbladder wall was ligated; E: This ligation state was maintained; F: The gallbladder wall was incised with the assistance of the snare; G: With the navigation of the snare, the endoscopist quickly found the gallbladder and gallbladder incision again (blue arrow); H: With the help of the snare, clips were used to close the gallbladder wall incision; I: The snare was loosened (yellow array); J: The gallbladder wall returned to normal.

Postoperative follow-up

All pigs were given liquid food after fasting for 24 h. All animals received ceftiofur sodium *via* injection (5 mg/kg, qd, 3 d) to prevent infection. An experienced physician conducted extensive monitoring of these animals daily to observe whether complications or adverse events occurred. Blood was collected at 24 h and 28 d after the operation. Gastroscopy was performed 28 d after the operation.

Animal care and use statement

The animal protocol was designed to minimize pain or discomfort to the animals. All animals were killed by barbiturate overdose (intravenous injection, 150 mg/kg pentobarbital sodium) for autopsy.

Outcome parameters

Changes in the number of white blood cells, blood amylase, and liver function were observed before and after the operation. The operation success rate, operation time, intraoperative and postoperative complications, and animal survival rate were recorded. The National Aeronautics and Space Administration-Task Load Index (NASA-TLX)[12] was used to assess the difficulty of the operation. The conditions of the abdominal cavity, stomach wall, and gallbladder were observed by autopsy.

Statistical analysis

Quantitative data are expressed as the mean ± SD. The results were analyzed by *SPSS* 23.0 statistical software. The significance of the data was determined by Student's *t*-test. P value < 0.05 was considered statistically significant.

RESULTS

Short-term operation outcomes

The operation was completed on all animals, and a success rate of 100% was achieved. It took 10.9 ± 4.3 min to cut the stomach wall, and the bleeding volume was 12.4 ± 6.6 mL. Although entry into the abdominal cavity occurred through the anterior wall of the gastric antrum, which was close to the gallbladder, the mirror body had no bending and showed good mobility. The operation space and visual field were small, and it took 11.0 ± 3.6 min to locate the gallbladder. Fortunately, under the assisted traction and navigation positioning of the snare, blood loss during gallbladder incision was reduced ($P < 0.05$). The total operating time, gallbladder disorientation time during the operation, and gallbladder incision closure time were significantly reduced in the SA group ($P < 0.05$) (Table 1). No differences were found between the two groups in the time involved in gallbladder incision and the number of clips required to close the gallbladder incision ($P > 0.05$), as shown in Table 1. However, removal of the clip was needed in 50% (2/4) of the animals in the NC group due to the incorrect placement of the clip; this situation did not occur in the SA group. The inside of the gallbladder of all animals was fully explored and flushed. None of the animals had bile leakage from the gallbladder incision.

Using the NASA-TLX to evaluate the difficulty of operation, the results showed that under the auxiliary traction and positioning of the snare, the mental demand, physical burden, temporal demand, effort, and frustration of the endoscopist were significantly reduced ($P < 0.05$), as shown in Table 1 and Figure 2.

Operation safety

During the operation, 75% (3/4) of the animals in the NC group showed a significant decrease in the "blood oxygen index" of the ear skin, which returned to normal after the gas in the abdominal cavity was sucked through an endoscope. However, the animals in the SA group did not show these adverse events. In addition, 100% (4/4) of the animals in the NC group had electric burn scars on their livers (Figure 3), whereas only 25% (1/4) of the animals in the SA group showed a similar condition.

All animals survived, and their body weight increased appropriately (an increase of 1.88 ± 0.69 kg) until euthanasia on Day 28. The follow-up found that the animals in the SA group were normal after the operation, and no complications occurred. In addition, no significant differences were found between the groups in the number of white blood cells and neutrophils, liver function, or the amount of amylase in the blood at 24 h and 28 d after surgery ($P > 0.05$) (Table 2).

Gastroscope review and necropsy

The gastric wall incisions of all animals healed without ulcers and incision fistulas (Figure 4A). A small number of omental adhesions existed on the gastric serosal surface of all animals. After the adhesions were released, the gastric wall incisions healed well. The gallbladder incisions of all animals were closed well, and no biliary fistulas, peritoneal effusions, abdominal hematomas, or abdominal abscesses were found. However, there were some adhesions around the gallbladder incisions, and the metal clip was wrapped in it (Figure 4B-D). The gallbladder was opened, and the gallbladder mucosa was smooth, with no formation of stones or polyps. The mucosa at the original incision healed well (Figure 4E), and the local mucosa was slightly edematous (Figure 4F), with an average thickness of 4.2 ± 0.7 mm. However, there was no difference in the thickness of the gallbladder mucosa between the two groups ($P > 0.05$).

DISCUSSION

At present, cholecystectomy is still the gold standard for the treatment of gallbladder stones and polyps. However, the gallbladder has an irreplaceable role in the digestion process of the human body. Many complications and adverse reactions can occur after gallbladder resection[5-8]. Therefore, both physicians and patients expect to find a better treatment that will preserve the gallbladder and cure gallbladder stones and polyps. This paper reports the successful application of flexible endoscopy *via* NOTES gallbladder-preservation surgery. This seems to be a promising new surgery for patients who wish to preserve the gallbladder without scarring of the abdominal wall.

In previous single-channel flexible endoscopy *via* NOTES gallbladder-preservation surgery, the gallbladder was not effectively tracted and navigated, and the gallbladder and gallbladder incision were often lost during the operation, thereby significantly prolonging the operation time and increasing the damage to the surrounding organs[13]. These disadvantages make it extremely difficult to promote this kind of surgery. If the gallbladder and gallbladder incision can be positioned quickly and accurately during the operation and the gallbladder can be pulled safely and effectively, then the difficulty and risk of the operation will be greatly reduced, and the operation time will be shortened. Both physicians and the patients will benefit.

Table 1 Differences in surgical indicators between the two groups of animals

Content	NC group	SA group	*t* value	*P* value
Time required for gallbladder incision (min)	18.5 ± 7.0	10.0 ± 1.8	2.335	0.058
Bleeding volume of gallbladder incision (mL)	7.5 ± 2.9	2.0 ± 2.2	3.051	0.022
Number of gallbladder disorientations	2.0 ± 0.8	1.3 ± 0.5	1.567	0.168
Longest time of gallbladder disorientation (min)	11.5 ± 4.7	2.0 ± 0.8	4.020	0.007
Time involved in closing the gallbladder (min)	18.3 ± 1.7	12.5 ± 2.1	4.271	0.005
Number of clamps used to close the gallbladder (pieces)	6.3 ± 0.5	6.5 ± 1.0	-0.447	0.670
Total operation time (min)	142.3 ± 10.2	102.5 ± 5.5	6.853	0.000
NASA-TLX mental demand	18.5 ± 2.1	11.5 ± 1.9	4.950	0.003
NASA-TLX physical	18.0 ± 1.6	11.0 ± 1.4	6.481	0.001
NASA-TLX temporal demand	18.8 ± 1.0	11.3 ± 2.6	5.359	0.002
NASA-TLX effort	18.5 ± 1.3	11.5 ± 2.4	5.170	0.004
NASA-TLX frustration	15.0 ± 2.9	7.5 ± 1.3	4.666	0.003

NASA-TLX: National Aeronautics and Space Administration-Task Load Index; NC: Control; SA: Snare assisted.

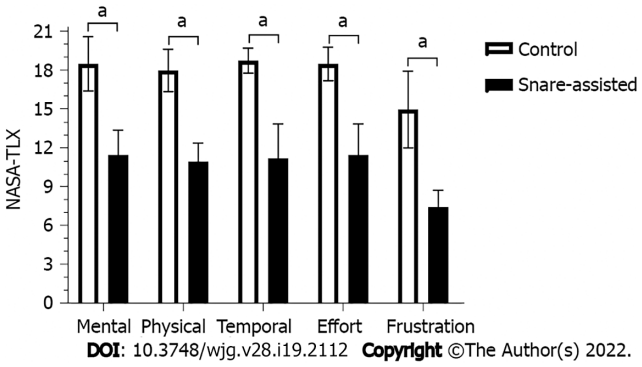
Table 2 Comparison of blood indices of the two groups of animals at 24 h and 28 d after operation

Blood	24 h after operation				28 d after operation			
	NC group	SA group	*t* value	*P* value	NC group	SA group	*t* value	*P* value
Number of white blood cells ($\times 10^9$/L)	28.83 ± 3.43	30.10 ± 3.47	-0.521	0.621	26.16 ± 3.64	25.59 ± 4.40	0.201	0.847
Number of neutrophils ($\times 10^9$/L)	18.39 ± 1.67	19.76 ± 3.65	-0.682	0.521	16.03 ± 1.31	16.67 ± 2.39	-0.472	0.654
Number of lymphocytes ($\times 10^9$/L)	8.63 ± 3.71	9.35 ± 1.30	-0.368	0.732	8.79 ± 2.68	7.95 ± 2.34	0.472	0.654
Number of red blood cells ($\times 10^{12}$/L)	7.12 ± 0.92	6.23 ± 0.41	1.763	0.128	6.27 ± 0.26	5.79 ± 0.43	1.909	0.105
Hemoglobin (g/L)	129.3 ± 8.5	115.8 ± 6.9	2.466	0.049	120.50 ± 3.42	111.50 ± 5.69	2.714	0.035
Total bilirubin (μmol/L)	1.85 ± 0.98	2.73 ± 0.74	-1.426	0.204	2.30 ± 0.96	2.73 ± 0.62	-0.743	0.486
Direct bilirubin (μmol/L)	1.28 ± 0.99	2.15 ± 0.66	-1.469	0.192	1.58 ± 0.87	2.05 ± 0.59	-0.901	0.402
ALT (U/L)	58.3 ± 22.9	41.5 ± 3.7	1.446	0.198	49.75 ± 11.32	40.50 ± 2.08	1.607	0.201
AST (U/L)	78.3 ± 66.3	50.8 ± 12.7	0.815	0.446	61.25 ± 19.36	49.75 ± 8.26	1.093	0.317
Alkaline phosphatase (U/L)	183.5 ± 35.9	189.8 ± 57.3	-0.185	0.859	178.75 ± 36.29	176.00 ± 38.40	0.104	0.920
γ-GT (U/L)	73.8 ± 32.9	77.8 ± 20.3	-0.207	0.843	72.50 ± 16.76	64.25 ± 12.31	0.793	0.458
Amylase (U/L)	2684.8 ± 465.9	2829.5 ± 170.6	-0.584	0.581	2583.25 ± 130.31	2770.00 ± 102.56	-2.252	0.065

ALT: Alanine aminotransferase; AST: Aspartate aminotransferase; γ-GT: Gamma-glutamyl transpeptidase; NC: Control; SA: Snare assisted.

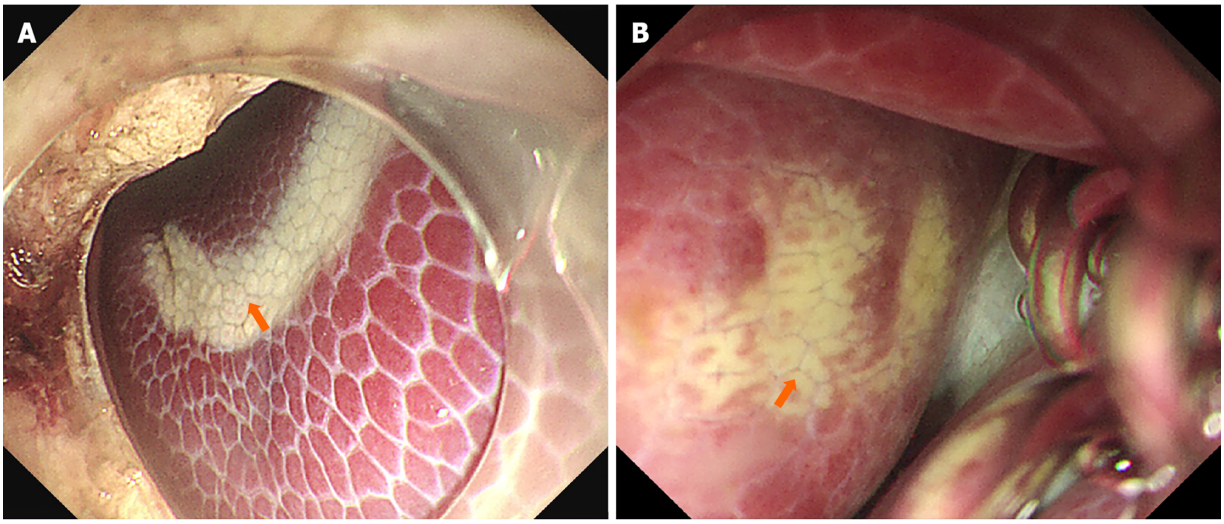
In recent years, snares have been used in endoscopic submucosal dissection to assist in traction and exposure of lesions[14]. Inspired by this use, we applied the snare device to gallbladder-preserving surgery, which is called "snare-assisted pure NOTES gallbladder-preserving surgery by flexible endoscope". Compared with the non-snare group, the use of the snare significantly reduced the duration and difficulty of the operation. Moreover, the NASA-TLX workload score was significantly reduced, and no adverse reactions or complications occurred.

Although the endoscope enters the abdominal cavity through the stomach, the organs and structures in the four quadrants of the abdominal cavity can be clearly observed[15]. However, this study found that the gallbladder of pigs is deeply buried in the liver lobe and is mostly covered by the surrounding omentum. This affected the surgical vision and caused the disorientation of the gallbladder during the operation. This increased the difficulty of locating the gallbladder and gallbladder incision again and significantly prolonged the operation time. Given the navigation guidance of the snare during the operation, the endoscopist quickly found the gallbladder and gallbladder incision again. Thus, the



DOI: 10.3748/wjg.v28.i19.2112 Copyright ©The Author(s) 2022.

Figure 2 Overall multivariate analysis of all subjects in the control group *vs* the snare-assisted group. The workload for each subscale was significantly less when using snare-assisted compared with control group ($^aP < 0.05$). Lower performance workload subscores corresponded to an improvement in perceived performance. NASA-TLX: National Aeronautics and Space Administration-Task Load Index.



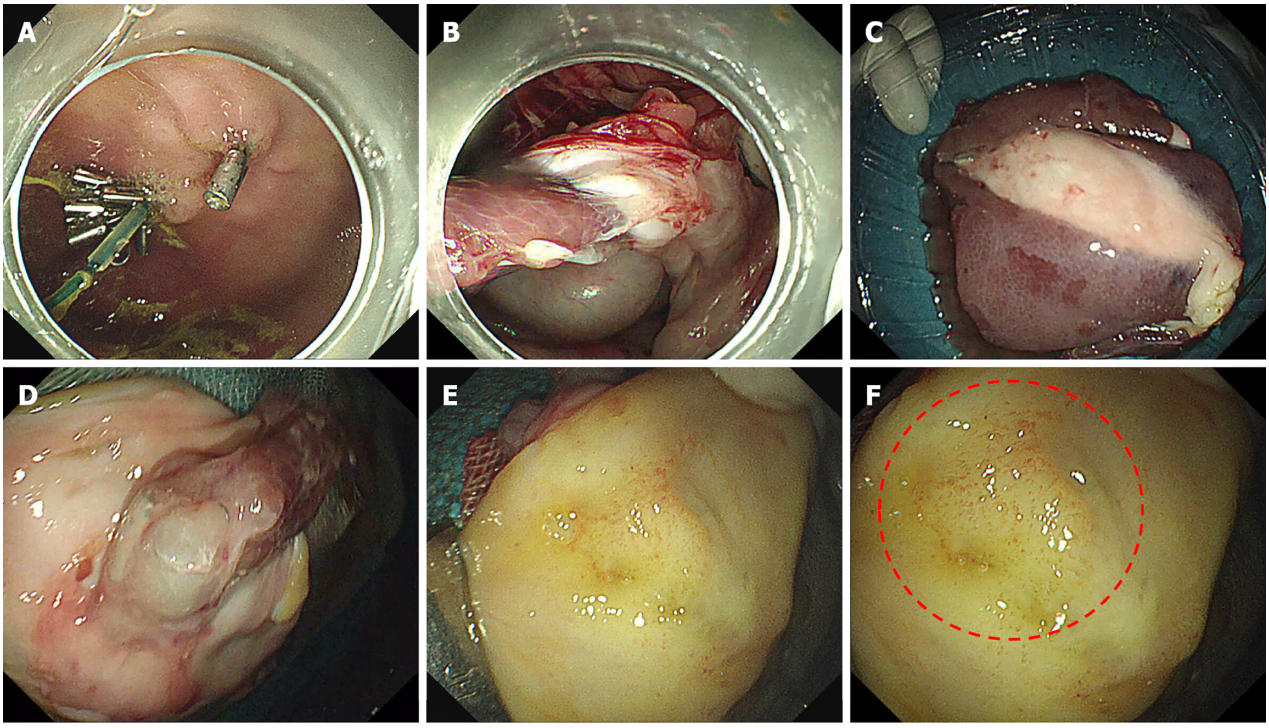
DOI: 10.3748/wjg.v28.i19.2112 Copyright ©The Author(s) 2022.

Figure 3 The livers of animals in the control group had electric burn scars (arrow). A: The electric burn scars were farther from the gallbladder; B: The electric burn scars were near the gallbladder.

duration of gallbladder disorientation during the operation and the total operation time were significantly shortened.

This study found that after the incision of the gallbladder, the bile flowed out, the gallbladder collapsed and shrank, and the surgical instruments lost their focus, thereby increasing the difficulty of the operation. The use of a snare to pull or drag the gallbladder can significantly reduce the difficulty of operation, shorten the time of gallbladder exploration, and reduce electrical coagulation damage to the nearby liver. Particularly in the case of massive hemorrhage from the gallbladder incision, blood obstructs the vision of the endoscope. The gallbladder is raised or pulled into the stomach by the snare, which can better expose the bleeding point. This is conducive to the electrocoagulation and hemostasis of the hot hemostatic forceps. This study showed that the blood loss from the gallbladder incision in the SA group was smaller than that in the NC group. Another issue is the poor closure of the gallbladder incision, which can lead to a bile fistula[10]. Although metal clips were used in this study to close the gallbladder incision, no complications, such as biliary fistula or peritonitis, occurred after the operation. However, the time involved in closing the gallbladder incision in the SA group was significantly shortened, and there were no adverse events that required the removal of the metal clip due to its incorrect placement.

This study found that 75% of the animals in the NC group experienced a significant drop in the blood oxygen index of the ears during the operation. The abdominal gas was sucked through the endoscope, and the operation was suspended to return to normal. It is possible that the abdominal pressure was too high, which inhibited the animals' breathing and heartbeats[16]. However, the blood oxygen index of the ear skin of the animals in the SA group remained normal. Given the traction and positioning of the snare, it can assist the surgical operation and expose the surgical field without blowing excess air into the abdominal cavity.



DOI: 10.3748/wjg.v28.i19.2112 Copyright ©The Author(s) 2022.

Figure 4 Gastroscopic review and necropsy were performed 28 d after the operation. A: The gastric wall incision healed well, with some clips remaining; B-D: A small number of adhesions appeared around the gallbladder incision, and the metal clip was wrapped in it; E: The gallbladder mucosa at the original incision healed well; F: The local mucosa surface was slightly edematous (red circle).

Although there are many microorganisms in the digestive tract, the strong acidity of gastric juice makes it difficult for most microorganisms to survive. Therefore, transgastric NOTES gallbladder-preserving surgery might not increase the risk of infection. A study showed that there was no significant difference in C-reactive protein and tumor necrosis factor-α levels after open surgery, laparoscopic surgery, and pure NOTES[17]. The present study found that although the leukocytes and neutrophils in the blood of all animals increased 24 h after the operation, they quickly returned to normal, and no difference was found between the two groups of animals at 24 h and 28 d after surgery. Therefore, using the snare did not increase the risk of infection during surgery.

The gallbladders of all animals were opened, and their gallbladder mucosae were smooth without the formation of stones and polyps. The mucosal surface at the original incision healed well, and no difference was found in the thickness of the gallbladder healing area between the two groups. The snare did not affect the healing of gallbladder mucosa or gallbladder incision. Moreover, some adhesions appeared around the gallbladder incision in all animals, and the metal clip was wrapped in it. This finding may be due to the body's response to abdominal organ damage and foreign bodies[10]. However, the snare did not aggravate this reaction.

To the best of our knowledge, this is the first experimental study of snare-assisted pure NOTES gallbladder-preserving surgery. However, several limitations of this study bear consideration. First, we only applied snare assistance for endoscopic trans-gastric gallbladder-preserving surgery. Thus, we cannot generalize the efficacy of snare assistance with other surgical paths, such as endoscopic transrectal gallbladder-preserving surgery and endoscopic transvaginal gallbladder-preserving surgery. Studies with other surgery paths are necessary in the future for a complete evaluation of the efficacy and safety of snare-assisted pure NOTES gallbladder-preserving surgery. Second, the number of animals used was small, and more studies with larger sample sizes are needed to confirm these findings. Third, it was undertaken on animals; thus, clinical trials are needed to demonstrate the effectiveness of snare-assisted pure NOTES gallbladder-preserving surgery in humans.

CONCLUSION

In summary, we successfully performed a flexible endoscopic gallbladder-preserving operation on pigs through pure NOTES. The use of a snare to assist the operation can reduce the difficulty of the operation and shorten the operation time; it does not increase the risk of the operation. Translating this new technology to human subjects seems straightforward and has great practical value in the clinic. However, further studies with large sample sizes are needed to confirm its clinical benefits, especially in

humans.

ARTICLE HIGHLIGHTS

Research background

With the development of medicine, the operation and concept of preserving the gallbladder and curing benign gallbladder diseases are now widely supported. As an emerging technology, gallbladder-preservation surgery *via* natural orifice transluminal endoscopic surgery (NOTES) has obvious advantages in the complete resection of gallbladder polyps, removal of gallbladder stones, improvement of gallbladder inflammation, and preservation of gallbladder function. However, there are some technical obstacles to the clinical application of this operation. For example, the gallbladder bed is close to the liver, is obscured by fatty tissue, and has a poor field of vision, indicating that it can be difficult to locate the gallbladder. In addition, the gallbladder collapses and shrinks quickly after incision, and the instruments used for gallbladder operation lose their focus, thereby making the operation very difficult.

Research motivation

The single-channel flexible endoscope for gallbladder-preservation surgery *via* NOTES requires additional navigation and traction. We proposed a new operative method that involved using a snare to assist in the traction and positioning of the gallbladder.

Research objectives

This study aimed to evaluate the feasibility and safety of a new surgical method, "snare-assisted pure NOTES gallbladder-preserving surgery".

Research methods

Eight miniature pigs were randomly divided into the experimental group [NOTES gallbladder-preserving surgery using the snare device, snare assisted (SA)] and the control group (NOTES gallbladder-preserving surgery without using the snare device, NC), with four cases in each group. The differences between the two groups of animals in operating time, operating workload, complications, adverse events, white blood cells, and liver function were determined.

Research results

No differences were found in the surgical success rate, gallbladder incision closure, white blood cell count, or liver function between the two groups. The total operating time, gallbladder incision blood loss, gallbladder disorientation time, gallbladder incision closure time, and workload scores of the National Aeronautics and Space Administration-Task Load Index were significantly reduced in the SA group ($P < 0.05$).

Research conclusions

These results indicated that snare-assisted pure NOTES gallbladder-preservation surgery using standard endoscopic instruments reduced the difficulty of the operation, shortened operation time, and did not increase complications in pigs.

Research perspectives

A new method for pure NOTES gallbladder-preservation surgery was provided. Translating this new technology to human subjects seems straightforward and has great practical value in the clinic.

ACKNOWLEDGEMENTS

The authors thank Dr Jiao Lan, Dr Fei Liu and Rui-Ping Xiao from Scientific Research Center of the People's Hospital of Guangxi Zhuang Autonomous Region for their valuable technological assistance on our projects.

FOOTNOTES

Author contributions: Guo XW and Ding Z contributed equally to this work; Guo XW and Ding Z were responsible for the study concept and design, including endoscopic procedures; all authors conducted the endoscopic operations together; Guo XW drafted the manuscript; Ding Z revised and finalized the manuscript.

Supported by National Natural Science Foundation of China, No. 82060104; and Construction of Guangxi Clinical

Medical Research Center for Digestive Diseases, No. AD17129027.

Institutional review board statement: The study was reviewed and approved by the Ethics Committee of the People's Hospital of Guangxi Zhuang Autonomous Region and the Ethics Committee of the Tongji Medical College, No. KY-LW-2019-4, [2020]-S322.

Institutional animal care and use committee statement: All procedures involving animals were reviewed and approved by the Institutional Animal Care and Use Committee of People's Hospital of Guangxi Zhuang Autonomous Region (No. KY-LW-2019-4) and the Institutional Animal Care and Committee at Huazhong University of Science and Technology Tongji Medical College (No. 2625).

Conflict-of-interest statement: To the best of our knowledge, no conflict of interest exists.

Data sharing statement: No additional data are available.

ARRIVE guidelines statement: The authors have read the ARRIVE guidelines, and the manuscript was prepared and revised according to the ARRIVE guidelines.

Open-Access: This article is an open-access article that was selected by an in-house editor and fully peer-reviewed by external reviewers. It is distributed in accordance with the Creative Commons Attribution NonCommercial (CC BY-NC 4.0) license, which permits others to distribute, remix, adapt, build upon this work non-commercially, and license their derivative works on different terms, provided the original work is properly cited and the use is non-commercial. See: https://creativecommons.org/Licenses/by-nc/4.0/

Country/Territory of origin: China

ORCID number: Xian-Wen Guo 0000-0003-3989-7460; Yun-Xiao Liang 0000-0002-6049-9216; Peng-Yu Huang 0000-0002-3593-0991; Lie-Xin Liang 0000-0002-2029-5059; Yi-Qing Zeng 0000-0003-1505-0142; Zhen Ding 0000-0001-8575-5282.

S-Editor: Fan JR
L-Editor: A
P-Editor: Fan JR

REFERENCES

1 **Jian W**, Song YZ, Xiang QF, Tian HY, Xie ZZ, Yang JB, Zhang YM, Zhang RK, Liu JL. Application of Transparent Cap-assisted Choledochoscopy in Endoscopic Gallbladder-preserving Surgery. *Surg Laparosc Endosc Percutan Tech* 2020; **30**: 317-321 [PMID: 32287110 DOI: 10.1097/SLE.0000000000000786]
2 **Lammert F**, Gurusamy K, Ko CW, Miquel JF, Méndez-Sánchez N, Portincasa P, van Erpecum KJ, van Laarhoven CJ, Wang DQ. Gallstones. *Nat Rev Dis Primers* 2016; **2**: 16024 [PMID: 27121416 DOI: 10.1038/nrdp.2016.24]
3 **Stewart L**. Iatrogenic biliary injuries: identification, classification, and management. *Surg Clin North Am* 2014; **94**: 297-310 [PMID: 24679422 DOI: 10.1016/j.suc.2014.01.008]
4 **Saxena P**, Khashab MA. New NOTES Clinical Training and Program Development. *Gastrointest Endosc Clin N Am* 2016; **26**: 385-400 [PMID: 27036904 DOI: 10.1016/j.giec.2015.12.009]
5 **Shao T**, Yang YX. Cholecystectomy and the risk of colorectal cancer. *Am J Gastroenterol* 2005; **100**: 1813-1820 [PMID: 16086719 DOI: 10.1111/j.1572-0241.2005.41610.x]
6 **Fan Y**, Hu J, Feng B, Wang W, Yao G, Zhai J, Li X. Increased Risk of Pancreatic Cancer Related to Gallstones and Cholecystectomy: A Systematic Review and Meta-Analysis. *Pancreas* 2016; **45**: 503-509 [PMID: 26684857 DOI: 10.1097/MPA.0000000000000502]
7 **Lagergren J**, Mattsson F. Cholecystectomy as a risk factor for oesophageal adenocarcinoma. *Br J Surg* 2011; **98**: 1133-1137 [PMID: 21590760 DOI: 10.1002/bjs.7504]
8 **Lagergren J**, Mattsson F, El-Serag H, Nordenstedt H. Increased risk of hepatocellular carcinoma after cholecystectomy. *Br J Cancer* 2011; **105**: 154-156 [PMID: 21610710 DOI: 10.1038/bjc.2011.181]
9 **Yasuda K**, Shiroshita H, Inomata M, Kitano S. [Natural orifice translumenal endoscopic surgery: historical and future perspectives]. *Nihon Geka Gakkai Zasshi* 2013; **114**: 298-302 [PMID: 24358724]
10 **Liu BR**, Kong LJ, Song JT, Liu W, Yu H, Dou QF. Feasibility and safety of functional cholecystectomy by pure NOTES: a pilot animal study. *J Laparoendosc Adv Surg Tech A* 2012; **22**: 740-745 [PMID: 22970657 DOI: 10.1089/lap.2012.0154]
11 **Liu BR**, Ullah S, Li DL, Liu D, Zhao LX, Yang W, Kong LJ, Zhang JY. A snare-assisted pure NOTES retrograde cholecystectomy using a single channel flexible endoscope: a pilot experiment in a porcine model. *Surg Endosc* 2020; **34**: 3706-3710 [PMID: 32300939 DOI: 10.1007/s00464-020-07561-0]
12 **Lowndes BR**, Forsyth KL, Blocker RC, Dean PG, Truty MJ, Heller SF, Blackmon S, Hallbeck MS, Nelson H. NASA-TLX Assessment of Surgeon Workload Variation Across Specialties. *Ann Surg* 2020; **271**: 686-692 [PMID: 30247331 DOI: 10.1097/SLA.0000000000003058]
13 **Soltes M**, Radoňak J. A risk score to predict the difficulty of elective laparoscopic cholecystectomy. *Wideochir Inne Tech Maloinwazyjne* 2014; **9**: 608-612 [PMID: 25562000 DOI: 10.5114/wiitm.2014.47642]

14 **Zhang Q**, Cai JQ, Wang Z, Xiao B, Bai Y. Snare combined with endoscopic clips in endoscopic resection of gastric submucosal tumor: a method of tumor traction. *Endosc Int Open* 2019; **7**: E1150-E1162 [PMID: 31475234 DOI: 10.1055/a-0849-9625]

15 **Li Y**, Han S. Transgastric endoscopic gallbladder polypectomy and cholecystolithiasis: A case report. *Exp Ther Med* 2020; **19**: 95-98 [PMID: 31853277 DOI: 10.3892/etm.2019.8195]

16 **Adelsdorfer C**, Taura P, Ibarzabal A, Vendrell M, Delitala A, Deulofeu R, Adelsdorfer W, Delgado S, Lacy AM. Effect of transgastric natural orifice transluminal endoscopic surgery peritoneoscopy on abdominal organ microcirculation: an experimental controlled study. *Gastrointest Endosc* 2016; **83**: 427-433 [PMID: 26272856 DOI: 10.1016/j.gie.2015.06.055]

17 **Arroyo Vázquez J**, Bergström M, Dot J, Abu-Suboh-Abadia M, Fonseca C, Esteves M, Azadani A, Armengol J, Masachs M, Armengol-Miró JR, Park PO. Surgical Trauma Caused by Different Abdominal Access Routes-Comparison of Open Surgical, Laparoscopic, and NOTES Transgastric Techniques in a Porcine Model. *J Laparoendosc Adv Surg Tech A* 2016; **26**: 511-516 [PMID: 27163486 DOI: 10.1089/lap.2016.0034]

World Journal of Gastroenterology

Submit a Manuscript: https://www.f6publishing.com

World J Gastroenterol 2022 May 21; 28(19): 2123-2136

DOI: 10.3748/wjg.v28.i19.2123

ISSN 1007-9327 (print) ISSN 2219-2840 (online)

ORIGINAL ARTICLE

Retrospective Cohort Study

Development and external validation of models to predict acute respiratory distress syndrome related to severe acute pancreatitis

Yun-Long Li, Ding-Ding Zhang, Yang-Yang Xiong, Rui-Feng Wang, Xiao-Mao Gao, Hui Gong, Shi-Cheng Zheng, Dong Wu

Specialty type: Gastroenterology and hepatology

Provenance and peer review: Invited article; Externally peer reviewed.

Peer-review model: Single blind

Peer-review report's scientific quality classification

Grade A (Excellent): 0
Grade B (Very good): B
Grade C (Good): C
Grade D (Fair): 0
Grade E (Poor): 0

P-Reviewer: de Oliveira I, Brazil; Kitamura K, Japan

Received: December 4, 2021
Peer-review started: December 4, 2021
First decision: January 27, 2022
Revised: February 9, 2022
Accepted: April 3, 2022
Article in press: April 3, 2022
Published online: May 21, 2022

Yun-Long Li, Yang-Yang Xiong, Dong Wu, Department of Gastroenterology, Peking Union Medical College Hospital, Beijing 100730, China

Ding-Ding Zhang, Medical Research Center, Peking Union Medical College Hospital, Beijing 100730, China

Ding-Ding Zhang, Dong Wu, Clinical Epidemiology Unit, International Clinical Epidemiology Network, Beijing 100730, China

Yang-Yang Xiong, Department of Gastroenterology, The First Affiliated Hospital, Zhejiang University School of Medicine, Hangzhou 310003, Zhejiang Province, China

Rui-Feng Wang, Department of Gastroenterology, The Fourth Affiliated Hospital of Harbin Medical University, Harbin 150001, Heilongjiang Province, China

Xiao-Mao Gao, Department of Gastroenterology, The Sixth Hospital of Beijing, Beijing 100191, China

Hui Gong, Shi-Cheng Zheng, Department of Gastroenterology, West China Longquan Hospital Sichuan University, Chengdu 610100, Sichuan Province, China

Corresponding author: Dong Wu, MD, Professor, Department of Gastroenterology, Peking Union Medical College Hospital, No. 1 Shuaifuyuan Wangfujing, Dongcheng District, Beijing 100730, China. wudong061002@aliyun.com

Abstract

BACKGROUND

Acute respiratory distress syndrome (ARDS) is a major cause of death in patients with severe acute pancreatitis (SAP). Although a series of prediction models have been developed for early identification of such patients, the majority are complicated or lack validation. A simpler and more credible model is required for clinical practice.

AIM

To develop and validate a predictive model for SAP related ARDS.

METHODS

Patients diagnosed with AP from four hospitals located at different regions of

China were retrospectively grouped into derivation and validation cohorts. Statistically significant variables were identified using the least absolute shrinkage and selection operator regression method. Predictive models with nomograms were further built using multiple logistic regression analysis with these picked predictors. The discriminatory power of new models was compared with some common models. The performance of calibration ability and clinical utility of the predictive models were evaluated.

RESULTS

Out of 597 patients with AP, 139 were diagnosed with SAP (80 in derivation cohort and 59 in validation cohort) and 99 with ARDS (62 in derivation cohort and 37 in validation cohort). Four identical variables were identified as independent risk factors for both SAP and ARDS: heart rate [odds ratio (OR) = 1.05; 95%CI: 1.04-1.07; $P < 0.001$; OR = 1.05, 95%CI: 1.03-1.07, $P < 0.001$], respiratory rate (OR = 1.08, 95%CI: 1.0-1.17, $P = 0.047$; OR = 1.10, 95%CI: 1.02-1.19, $P = 0.014$), serum calcium concentration (OR = 0.26, 95%CI: 0.09-0.73, $P = 0.011$; OR = 0.17, 95%CI: 0.06-0.48, $P = 0.001$) and blood urea nitrogen (OR = 1.15, 95%CI: 1.09-1.23, $P < 0.001$; OR = 1.12, 95%CI: 1.05-1.19, $P < 0.001$). The area under receiver operating characteristic curve was 0.879 (95%CI: 0.830-0.928) and 0.898 (95%CI: 0.848-0.949) for SAP prediction in derivation and validation cohorts, respectively. This value was 0.892 (95%CI: 0.843-0.941) and 0.833 (95%CI: 0.754-0.912) for ARDS prediction, respectively. The discriminatory power of our models was improved compared with that of other widely used models and the calibration ability and clinical utility of the prediction models performed adequately.

CONCLUSION

The present study constructed and validated a simple and accurate predictive model for SAP-related ARDS in patients with AP.

Key Words: Acute pancreatitis; Acute respiratory distress syndrome; Nomogram; Calibration; Early identification; Predictive model

©The Author(s) 2022. Published by Baishideng Publishing Group Inc. All rights reserved.

Core Tip: Severe acute pancreatitis (SAP)-related acute respiratory distress syndrome (ARDS) affect the mortality of patients with AP. Early identification of patients at high risk for SAP and ARDS can aid clinicians to adopt interventions to stop disease progression. However, current predictive models are either too complicated due to various parameters or unreliable due to lack of validation. This study developed new models to predict SAP and ARDS using only four routine clinical items within 24 h of admission. New models were externally validated and performed as well as or with a higher efficiency than other models.

Citation: Li YL, Zhang DD, Xiong YY, Wang RF, Gao XM, Gong H, Zheng SC, Wu D. Development and external validation of models to predict acute respiratory distress syndrome related to severe acute pancreatitis. *World J Gastroenterol* 2022; 28(19): 2123-2136

URL: https://www.wjgnet.com/1007-9327/full/v28/i19/2123.htm

DOI: https://dx.doi.org/10.3748/wjg.v28.i19.2123

INTRODUCTION

Acute pancreatitis (AP) is a common event incurring pain, socioeconomic loss, and even death. The majority of the patients who present with mild organ injury and self-limited course are diagnosed with mild acute pancreatitis (MAP) or moderately severe acute pancreatitis (MSAP)[1,2]. However, it is estimated that approximately 20% of patients are critically ill and develop SAP, leading to consistent organ failure and significant mortality[2,3]. Our previous studies indicated that the lung are the most commonly affected organs in SAP[4,5], and acute respiratory distress syndrome (ARDS) is recognized as an important cause of respiratory failure, with a high mortality rate[6-8]. It is reported that 4%-15% of AP patients are complicated with ARDS[9], while this proportion might be as high as one third in SAP [10]. However, to date, the therapeutic options for SAP and ARDS are limited. Therefore, it is necessary to identify patients at risk and adopt interventions to prevent MAP or MSAP from progressing to SAP and ARDS. The protective effect of early intervention for patients with predicted SAP or patients at risk of ARDS has been confirmed by numerous clinical trials and meta-analyses, although the inclusion

criteria for patients have varied according to different studies[11-15].

A plethora of models have been published to predict the risk of SAP in AP patients, including acute physiology and chronic health evaluation II (APACHE-II) score, Ranson criteria, computed tomography severity index (CTSI), and bedside index for severity in acute pancreatitis (BISAP)[16,17]. Lung injury prediction score (LIPS) and other models have also been used to evaluate the risk of ARDS in patients with non-AP[18-20]. However, to date the models used to predict ARDS in AP are scarce. Furthermore, the majority of the SAP predictive models are hard to use in practice due to various parameters, complicated calculation and dependence on radiological assessment. The majority of the models also lack internal or external validation, which reduces their reliability in other cohorts[16]. Therefore, a new concise model may be more practical in the emergency department in order to identify SAP and ARDS in the early course of AP. This model should involve limited available clinical data and should not rely on radiological examinations.

The objective of the present study was to develop and validate models to predict SAP and ARDS in patients with AP based on multicenter retrospective cohorts. The comparison of novel models with quick sequential organ failure assessment (qSOFA), systemic inflammatory response syndrome (SIRS) and BISAP is essential to display the power of different models with a low number of variables. These models usually contain three, four and five items, respectively[21,22].

MATERIALS AND METHODS

Study design and participants

This was a multicenter retrospective study. Sample size was calculated with PASS 11.0. The proportion of SAP was set to 20%, and the incidence of ARDS in SAP and non-SAP patients was set to 1/3 and 4%, respectively. Considering that the dropout rate was low in hospitals, we set it to 5%. In the end, with α = 0.01 and β = 0.10, a total of 211 participants were needed. Patients diagnosed with AP between 1 January 2017 and 31 December 2019 were recruited from different regions of China (Peking Union Medical College Hospital and The Sixth Hospital of Beijing at Northern China, The Fourth Affiliated Hospital of Harbin Medical University at Northeastern China, West China Longquan Hospital Sichuan University at Southwestern China). The patients were categorized into the derivation cohort in order to develop a clinical predictive model. The independent external validation cohort consisted of patients diagnosed with AP between 1 January 2020 and 31 May 2021 at the Peking Union Medical College Hospital. AP was diagnosed if at least two of the three following criteria were met: (1) abdominal pain consistent with AP; (2) serum lipase or amylase levels that were more than three times the upper limit of the normal range; and (3) characteristic radiological findings of AP on computed tomography (CT) and magnetic resonance imaging or ultrasonography[23]. SAP was identified by the presence of persistent organ failure for > 48 h[23]. ARDS was diagnosed based on Berlin definition[24]. Patients aged < 18 years who lacked the necessary information provided by the Atlanta Classification or relevant etiology information were excluded.

Clinical variables

The following demographic and laboratory data were collected from the electronic medical record system within 24 h of admission: age, sex, temperature, heart rate (HR), respiratory rate (RR), systolic blood pressure, Glasgow coma score (GCS), white blood counts, hematocrit, platelet, serum electrolyte concentration (K, Na and Ca), creatine, blood urea nitrogen (BUN) and glucose. Other clinical information, such as, admission date, local complication, length of hospital stay, length of intensive care unit stay, mortality and ventilator use, was also collected. Weekend admission corresponded to admission on Saturday or Sunday and local complication included acute peripancreatitc fluid collection, acute necrosis collection, pseudocyst and walled-off necrosis. The ventilator included invasive or noninvasive mechanical ventilation. qSOFA, SIRS and BISAP scores were calculated based on the aforementioned data. All data were collected and checked by two or more authors independently. Missing items were added following review of the clinical records. The data that could not be completed were removed and the complete-case dataset was finally analyzed.

Statistical analysis

Categorical variables were expressed as frequencies and percentages and compared using χ^2 or Fisher's exact tests. Normally distributed continuous variables were described as the mean ± SD and compared using a two-sided Student's *t* test. Non-normally distributed continuous variables were expressed as the median with the interquartile range and compared using the Mann-Whitney *U* test. Continuous variables were analyzed in their original forms to preserve information[25]. The least absolute shrinkage and selection operator (LASSO) regression method was used to select predictors in the derivation cohort. The predictive models were further built using multiple logistic regression analysis. The nomogram was formulated based on multivariate logistic regression analysis. Receiver operating characteristic (ROC) curve and the area under ROC curve (AUC) were used to evaluate the discriminative power of the predictive model, which referred to the ability of the model to differentiate between

the subjects that did or did not experience the outcome event[25]. The calibration curves were plotted to measure the predictive accuracy of the model, which reflected the agreement between predictions from the model and observed outcomes. A well-calibrated model indicated that the prediction was lying on or around the 45° line of the calibration plot[25]. Hosmer-Lemeshow (H-L) goodness of fit test was used to quantify the calibration curve. The *P* value was determined by the H-L test. $P > 0.05$ suggested an optimal consistency between model prediction and the criteria required for standard diagnosis. Decision curve analysis (DCA) was used to assess the clinical utility of the model, which indicated he relationship between a model-predicted probability threshold and the relative value of net benefit[25].

Statistical analysis was performed using R 4.0.3[26] and MedCalc 15.8 software. A two-side $P < 0.05$ was considered to indicate a statistically significant difference. The nomogram and calibration curve were plotted using rms package and DCA was plotted using rmda package. ROC was plotted with MedCalc 15.8.

RESULTS

Baseline characteristics

Between January 1 2017 and May 31 2021, 628 patients with AP were recruited from four hospitals and reviewed. The exclusion criteria included the following: age < 18 years (2 patients), lack of Atlanta Classification or etiology (26 patients) and incomplete data (3 patients). Following screening, 407 and 190 patients were involved in the derivation and validation cohorts, respectively. The number of participants in each cohort met the requirement of sample size. The detailed demographic and clinical information were described in Tables 1 and 2.

Predictors and model construction

Four variables (HR, RR, Ca and BUN) were extracted as the predictors of SAP through LASSO regression. Supplementary Figure 1 and Supplementary Table 1 show this process in more detail. Multivariable logistic regression revealed that all four variables were independent predictors (Table 3). The probability (PA) of SAP could be calculated according to the following formula: PA = 1/{1 + exp [-(-6.42 + 0.05 × HR + 0.08 × RR - 1.30 × Ca + 0.14 × BUN)]}. Analysis of ARDS obtained similar results (Table 3). The following formula was used for ARDS: PA = 1/{1 + exp [- (-5.46 + 0.05 × HR + 0.10 × RR - 1.78 × Ca + 0.11 × BUN)]}. Two nomogram plots were displayed using prediction models (Figure 1).

Model performance

The new model indicated a great power of discrimination for SAP. Following 1000 interactions of bootstrapping to minimize the risk of overfitting to the original models, the AUC in the derivation cohort was estimated to 0.879 (95%CI: 0.830-0.928), which was significantly superior to that of SIRS (AUC = 0.808, 95%CI: 0.757-0.859, $P = 0.002$) and qSOFA (AUC = 0.730, 95%CI: 0.672-0.789, $P < 0.001$) and not inferior to that of the BISAP score (AUC = 0.888, 95%CI: 0.847-0.929, $P = 0.6629$) (Figure 2A, Table 4). In addition, the model indicated an optimal behavior in the validation cohort (AUC = 0.898, 95%CI: 0.848-0.949) (Figure 2B). The AUC of the new model in derivation was 0.892 (95%CI: 0.843-0.941) for ARDS prediction, which was superior to SIRS (AUC = 0.815, 95%CI: 0.766-0.864, $P = 0.001$) and qSOFA (AUC = 0.742, 95%CI: 0.678-0.807, $P < 0.001$) and not inferior to BISAP (AUC = 0.871, 95%CI: 0.827-0.916, $P = 0.344$) (Figure 2C, Table 4). Despite the assessment of the model in the validation cohort, its performance was moderate (AUC = 0.833. 95%CI: 0.754-0.912) (Figure 2D). When the cut-off value was set as PA > 25% for SAP prediction, the novel model suggested an optimal performance in the combined dataset (sensitivity 0.78, specificity 0.88) (Table 4). The best cut-off value was PA > 18% for ARDS prediction, with a sensitivity of 0.78 and a specificity of 0.85 (Table 4).

Graphical assessment indicated a strong agreement between prediction and observation in both new models (Figure 3). The H-L test indicated that the difference between prediction and observation was not significant both in the derivation ($\chi^2 = 12.675$, $P = 0.124$) and validation cohorts ($\chi^2 = 5.852$, $P = 0.664$) with regard to SAP prediction. The model for ARDS prediction revealed improved performance with regard to the calibration in the derivation ($\chi^2 = 3.753$, $P = 0.879$) and validation cohorts ($\chi^2 = 2.933$, $P = 0.939$).

DCA indicated that if the threshold PA was < 80%, using the new model to recognize and manage SAP had a positive net benefit compared with either the treat-all or treat-none (Figure 4A). In case the threshold probability was set to < 70%, the prediction and intervention for ARDS also produced net benefit (Figure 4B).

DISCUSSION

In the current study, novel prediction models were established for SAP and ARDS in patients with AP. The models were also externally validated and exhibited remarkable discriminative power and high

Table 1 Characteristics of non-severe acute pancreatitis and severe acute pancreatitis patients in derivation and validation cohort

Characteristic	Derivation cohort		*P* value	Validation cohort		*P* value
	non-SAP (*n* = 327)	SAP (*n* = 80)		non-SAP (*n* = 131)	SAP (*n* = 59)	
Age (yr)	49.0 (36.0; 63.5)	46.0 (34.8; 62.2)	0.424	40.0 (32.0; 58.5)	44.0 (38.0; 53.0)	0.371
Female (%)	131 (40.1)	27 (33.8)	0.363	63 (48.1)	14 (23.7)	0.003
Weekend admission (%)	65 (19.9)	26 (32.5)	0.023	37 (28.2)	13 (22.0)	0.471
Etiology (%)			0.021			0.003
Biliary	113 (34.6)	31 (38.8)		54 (41.2)	11 (18.6)	
Hypertriglyceridemia	113 (34.6)	36 (45.0)		44 (33.6)	21 (35.6)	
Alcoholic	27 (8.26)	7 (8.75)		5 (3.82)	8 (13.6)	
Others	74 (22.6)	6 (7.50)		28 (21.4)	19 (32.2)	
Peritoneal irritation (%)	74 (22.6)	31 (38.8)	0.005	27 (20.6)	32 (54.2)	< 0.001
GCS < 15 (%)	2 (0.61)	5 (6.25)	0.004	3 (2.29)	7 (11.9)	0.011
Tem (℃)	36.6 (36.4; 37.0)	37.2 (36.5; 38.2)	< 0.001	37.0 (36.8; 37.4)	38.0 (37.5; 38.4)	< 0.001
SBP (KPa)	17.2 (15.9; 18.7)	16.4 (14.9; 18.8)	0.119	16.3 (15.2; 18.4)	16.8 (14.7; 19.5)	0.949
HR (bpm)	82.0 (76.0; 94.5)	118 (99.5; 132)	< 0.001	89.0 (79.0; 102)	110 (100; 130)	< 0.001
RR (bpm)	20.0 (18.0; 20.0)	22.0 (20.0; 28.2)	< 0.001	20.0 (18.0; 21.0)	23.0 (20.5; 29.5)	< 0.001
WBC ($\times 10^9$/L)	11.6 (8.74; 15.2)	14.2 (10.2; 18.7)	0.001	12.4 (8.70; 15.6)	16.4 (12.2; 21.1)	< 0.001
HCT (%)	40.8 (37.5; 44.8)	43.6 (36.9; 48.4)	0.022	41.3 (37.8; 45.0)	42.9 (36.5; 49.0)	0.218
PLT ($\times 10^9$/L)	221 (178; 276)	192 (156; 274)	0.03	232 (196; 278)	202 (166; 264)	0.025
K (mmol/L)	3.90 (3.60; 4.25)	3.90 (3.50; 4.30)	0.817	3.90 (3.50; 4.10)	4.00 (3.50; 4.55)	0.074
Na (mmol/L)	137 (134; 140)	137 (132; 140)	0.909	137 (133; 140)	137 (133; 140)	0.664
Ca (mmol/L)	2.26 (2.13; 2.34)	1.96 (1.74; 2.16)	< 0.001	2.22 (2.08; 2.32)	1.93 (1.77; 2.10)	< 0.001
Cr (μmol/L)	67.0 (55.0; 80.0)	90.0 (70.8; 142)	< 0.001	61.0 (52.0; 77.0)	90.0 (62.5; 227)	< 0.001
BUN (mmol/L)	5.00 (3.88; 6.34)	7.06 (5.26; 10.4)	< 0.001	4.66 (3.32; 5.84)	6.67 (4.91; 14.2)	< 0.001
Glu (mmol/L)	8.00 (6.50; 12.9)	11.0 (7.45; 16.3)	< 0.001	8.70 (6.80; 11.8)	11.3 (8.05; 17.2)	0.004
Local complication (%)	104 (31.8)	73 (91.2)	< 0.001	66 (50.4)	55 (93.2)	< 0.001
ICU admission (%)	12 (3.67)	37 (46.2)	< 0.001	12 (9.16)	38 (64.4)	< 0.001
ICU stays (d)	0.00 (0.00; 0.00)	0.00 (0.00; 10.0)	< 0.001	0.00 (0.00; 0.00)	5.00 (0.00; 9.00)	< 0.001
Hospital stays (d)	10.0 (7.00; 14.0)	17.5 (8.75; 25.0)	< 0.001	9.00 (4.00; 15.0)	23.0 (15.0; 30.0)	< 0.001
Mortality (%)	0 (0.00)	3 (3.75)	0.007	1 (0.76)	4 (6.78)	0.033
qSOFA	0.00 (0.00; 0.00)	1.00 (0.00; 1.00)	< 0.001	0.00 (0.00; 1.00)	1.00 (0.00; 1.00)	< 0.001
SIRS	1.00 (0.00; 2.00)	3.00 (2.00; 3.00)	< 0.001	1.00 (0.00; 2.00)	3.00 (2.00; 3.00)	< 0.001
BISAP	1.00 (0.00; 1.00)	2.00 (2.00; 3.00)	< 0.001	1.00 (0.00; 2.00)	2.00 (2.00; 3.00)	< 0.001

SAP: Severe acute pancreatitis; GCS: Glasgow coma score; Tem: Temperature; SBP: Systolic blood pressure; HR: Heart rate; RR: Respiratory rate; WBC: White blood cell; HCT: Hematocrit; PLT: Platelet; Cr: Creatine; BUN: Blood urea nitrogen; Glu: Glucose; ICU: Intensive care unit; qSOFA: Quick sequential organ failure assessment; SIRS: Systemic inflammatory response syndrome; BISAP: Bedside index for severity in acute pancreatitis.

degree of consistency with the observation both in the derivation and external validation cohorts. These models suggested that patients with AP who manifested a higher heart rate, respiratory rate, blood urea nitrogen concentrations and lower serum calcium concentrations at admission exhibited a higher risk of developing SAP and ARDS.

AP is a major cause of acute abdomen. Patients with AP usually present with multiple organ dysfunction syndrome (MODS). Although organ dysfunction is mild and transient (< 48 h), approximately 20% of patients will proceed to consistent organ failure (> 48 h), leading to SAP and a high risk

Table 2 Characteristics of non-acute respiratory distress syndrome and acute respiratory distress syndrome patients in derivation and validation cohorts

Characteristic	Derivation cohort		*P* value	Validation cohort		*P* value
	non-ARDS (*n* = 345)	ARDS (*n* = 62)		non-ARDS (*n* = 153)	ARDS (*n* = 37)	
Age (yr)	49.0 (36.0; 64.0)	42.0 (33.2; 59.5)	0.062	40.0 (33.0; 57.0)	48.0 (41.0; 57.0)	0.082
Female (%)	138 (40.0)	20 (32.3)	0.312	67 (43.8)	10 (27.0)	0.093
Weekend admission (%)	73 (21.2)	18 (29.0)	0.228	39 (25.5)	11 (29.7)	0.751
Etiology (%)			0.024			0.187
Biliary	122 (35.4)	22 (35.5)		56 (36.6)	9 (24.3)	
Hypertriglyceridemia	119 (34.5)	30 (48.4)		53 (34.6)	12 (32.4)	
Alcoholic	28 (8.12)	6 (9.68)		8 (5.23)	5 (13.5)	
Others	76 (22.0)	4 (6.45)		36 (23.5)	11 (29.7)	
Peritoneal irritation (%)	80 (23.2)	25 (40.3)	0.007	39 (25.5)	20 (54.1)	0.002
GCS < 15 (%)	4 (1.16)	3 (4.84)	0.075	4 (2.61)	6 (16.2)	0.004
Tem (°C)	36.6 (36.4; 37.0)	37.5 (36.5; 38.2)	< 0.001	37.0 (36.8; 37.5)	38.0 (37.8; 38.5)	< 0.001
SBP (mmHg)	129 (119; 140)	123 (110; 141)	0.113	123 (116; 140)	119 (106; 147)	0.192
HR (bpm)	82.0 (76.0; 96.0)	120 (103; 134)	< 0.001	90.0 (80.0; 110)	115 (100; 140)	< 0.001
RR (bpm)	20.0 (18.0; 20.0)	23.0 (20.0; 30.0)	< 0.001	20.0 (18.0; 22.0)	24.0 (20.0; 29.0)	< 0.001
WBC ($\times 10^9$/L)	11.9 (8.76; 15.3)	13.9 (9.91; 19.5)	0.006	12.5 (9.07; 16.3)	17.6 (13.6; 22.8)	< 0.001
HCT (%)	40.8 (37.5; 44.8)	45.2 (38.3; 48.7)	0.002	41.3 (37.4; 45.2)	43.9 (38.0; 49.4)	0.094
PLT ($\times 10^9$/L)	218 (176; 275)	207 (167; 274)	0.26	228 (192; 278)	208 (168; 261)	0.112
K (mmol/L)	3.90 (3.60; 4.30)	3.90 (3.50; 4.20)	0.441	3.90 (3.50; 4.20)	3.90 (3.50; 4.40)	0.429
Na (mmol/L)	137 (134; 140)	137 (132; 140)	0.95	137 (133; 140)	139 (132; 144)	0.038
Ca (mmol/L)	2.25 (2.12; 2.34)	1.88 (1.65; 2.12)	< 0.001	2.16 (2.01; 2.29)	1.96 (1.77; 2.22)	0.002
Cr (μmol/L)	67.0 (55.0; 81.0)	86.5 (72.0; 134)	< 0.001	62.0 (53.0; 79.0)	96.0 (65.0; 230)	< 0.001
BUN (mmol/L)	5.03 (3.90; 6.44)	7.28 (5.25; 10.3)	< 0.001	4.80 (3.37; 6.48)	6.97 (5.37; 14.4)	< 0.001
Glu (mmol/L)	8.10 (6.50; 13.1)	11.0 (7.67; 16.1)	< 0.001	8.80 (6.90; 13.6)	11.3 (8.10; 16.8)	0.032
Local complication (%)	115 (33.3)	62 (100)	< 0.001	88 (57.5)	33 (89.2)	0.001
Ventilator (%)	3 (0.87)	4 (6.45)	0.012	0 (0.00)	23 (62.2)	< 0.001
ICU admission (%)	16 (4.64)	33 (53.2)	< 0.001	21 (13.7)	29 (78.4)	< 0.001
ICU stays (d)	0.00 (0.00; 0.00)	2.50 (0.00; 11.8)	< 0.001	0.00 (0.00; 0.00)	7.00 (1.00; 11.0)	< 0.001
Hospital stays (d)	10.0 (7.00; 15.0)	19.0 (11.0; 25.0)	< 0.001	10.0 (4.00; 19.0)	23.0 (15.0; 30.0)	< 0.001
Mortality (%)	1 (0.29)	2 (3.23)	0.062	1 (0.65)	4 (10.8)	0.005

ARDS: Acute respiratory distress syndrome; GCS: Glasgow coma score; Tem: Temperature; SBP: Systolic blood pressure; HR: Heart rate; RR: Respiratory rate; WBC: White blood cell; HCT: Hematocrit; PLT: Platelet; Cr: Creatine; BUN: Blood urea nitrogen; Glu: Glucose; ICU: Intensive care unit; qSOFA: Quick sequential organ failure assessment; SIRS: Systemic inflammatory response syndrome; BISAP: Bedside index for severity in acute pancreatitis.

of mortality[27]. AP primarily affects the respiratory system and to a lesser extent the renal and cardiovascular systems[23]. ARDS is the critical event, which is noted during lung injury in AP[28]. Cyclooxygenase-2 inhibitors and enteral nutrition have been shown to prevent SAP, shorten the length of hospital stay and reduce infectious complications and mortality in patients with predicted SAP[11,12,29]. Administration of antiplatelet therapy, withdrawal of prehospital amiodarone treatment and administration of nebulized heparin may decrease the incidence of ARDS, inhibit the progression of lung injury and accelerate the recovery of patients at risk of developing ARDS[13-15,30]. Therefore, early identification of patients at risk of developing SAP and ARDS is clinically significant for improving the prognosis of AP.

Table 3 Multivariable logistic regression analysis for severe acute pancreatitis and acute respiratory distress syndrome prediction in derivation cohort

Variable	SAP			ARDS		
	β	OR (95% CI)	*P* value	β	OR (95% CI)	*P* value
Intercept	-6.42	0.00 (0.00-0.05)	< 0.001	-5.46	0.00 (0.00-0.13)	0.002
HR	0.05	1.05 (1.04-1.07)	< 0.001	0.05	1.05 (1.03-1.07)	< 0.001
RR	0.08	1.08 (1.00-1.17)	0.047	0.10	1.10 (1.02-1.19)	0.014
Ca	-1.30	0.26 (0.09-0.73)	0.011	-1.78	0.17 (0.06-0.48)	0.001
BUN	0.14	1.15 (1.09-1.23)	< 0.001	0.11	1.12 (1.05-1.19)	< 0.001

SAP: Severe acute pancreatitis; ARDS: Acute respiratory distress syndrome; OR: Odds ratio; HR: Heart rate; RR: Respiratory rate; Ca: Serum calcium concentration; BUN: Blood urea nitrogen.

Table 4 Sensitivity, specificity, positive predictive value, negative predictive value for of the predictive models in combined cohort

SAP						ARDS					
PA	SE	SP	Youden index	PPV	NPV	PA	SE	SP	Youden index	PPV	NPV
> 10%	0.91	0.63	0.54	0.43	0.96	> 5%	0.94	0.48	0.42	0.26	0.98
> 20%	0.82	0.83	0.65	0.59	0.94	> 10%	0.85	0.71	0.56	0.37	0.96
> 25%	0.78	0.88	0.66	0.66	0.93	> 18%	0.78	0.85	0.63	0.51	0.95
> 40%	0.71	0.93	0.64	0.75	0.91	> 30%	0.67	0.93	0.59	0.65	0.93
> 60%	0.51	0.97	0.48	0.84	0.87	> 50%	0.46	0.96	0.43	0.71	0.90
> 80%	0.32	0.99	0.30	0.88	0.83	> 70%	0.29	0.98	0.27	0.71	0.87
> 95%	0.14	1.00	0.14	0.91	0.79	> 85%	0.12	1.00	0.12	0.86	0.85

PA: Probability; SE: Sensitivity; SP: Specificity; PPV: Positive predictive value; NPV: Negative predictive value.

Various models have been developed to predict SAP and organ dysfunction for AP management[16]. Although the majority of the models were deficient due to some limitations, such as small sample size, single center studies and lack of internal or external validation, several SAP models have been widely used and validated in different cohorts. These validations were performed using APACHE-II score, Ranson criteria, CTSI and BISAP[31-34]. BISAP contains only five variables and is simpler than APACHE-II score (18 items) and the Ranson criteria (11 items). However, their predictive power is equal [35]. In addition, ultrasound is preferred to CT as an efficient and nonradioactive examination used in the emergency department to initially evaluate potential development of AP. Therefore, pleural effusion and CT presentation could not be evaluated in this case to gain the BISAP and CTSI scores. Although LIPS is a popular model to predict ARDS for patients at risk, its calculation is considerably complicated [18]. In addition, its original developing cohort involved only a small part of patients with AP. LIPS had not been previously validated in patients with AP.

Therefore, a simple model with a low number of parameters and without radiology findings would be more practical. The novel predictive model reported in the current study involved only four parameters for both SAP and ARDS prediction and all these variables were routinely tested. The discriminatory power of the novel model was not inferior to that of BISAP. To the best of our knowledge, the prediction of SAP or ARDS for patients with AP has not been previously assessed by models that were as simple and accurate as this reported in the current study.

Using LASSO regression, calcium was identified as a predictor for both SAP and ARDS. Multiple logistic regression analysis indicated that serum calcium concentration was also the independent predictor. The models of the present study were easier to use than the APACHE-II, Ranson, CTSI and BISAP models and demonstrated improved efficacy than the other two simple models, suggesting their potential clinical significance. ARDS was a non-negligible manifestation of MODS in patients with AP. The majority of the models have mainly focused on the severity classification or mortality prediction of ARDS, whereas the identification of ARDS at an early stage is still challenging. Although LIPS was widely used to predict ARDS, the calculation of the LIPS score was complicated for patients admitted to the emergency department, since certain parameters may be unavailable[18]. The pathogenesis of ARDS

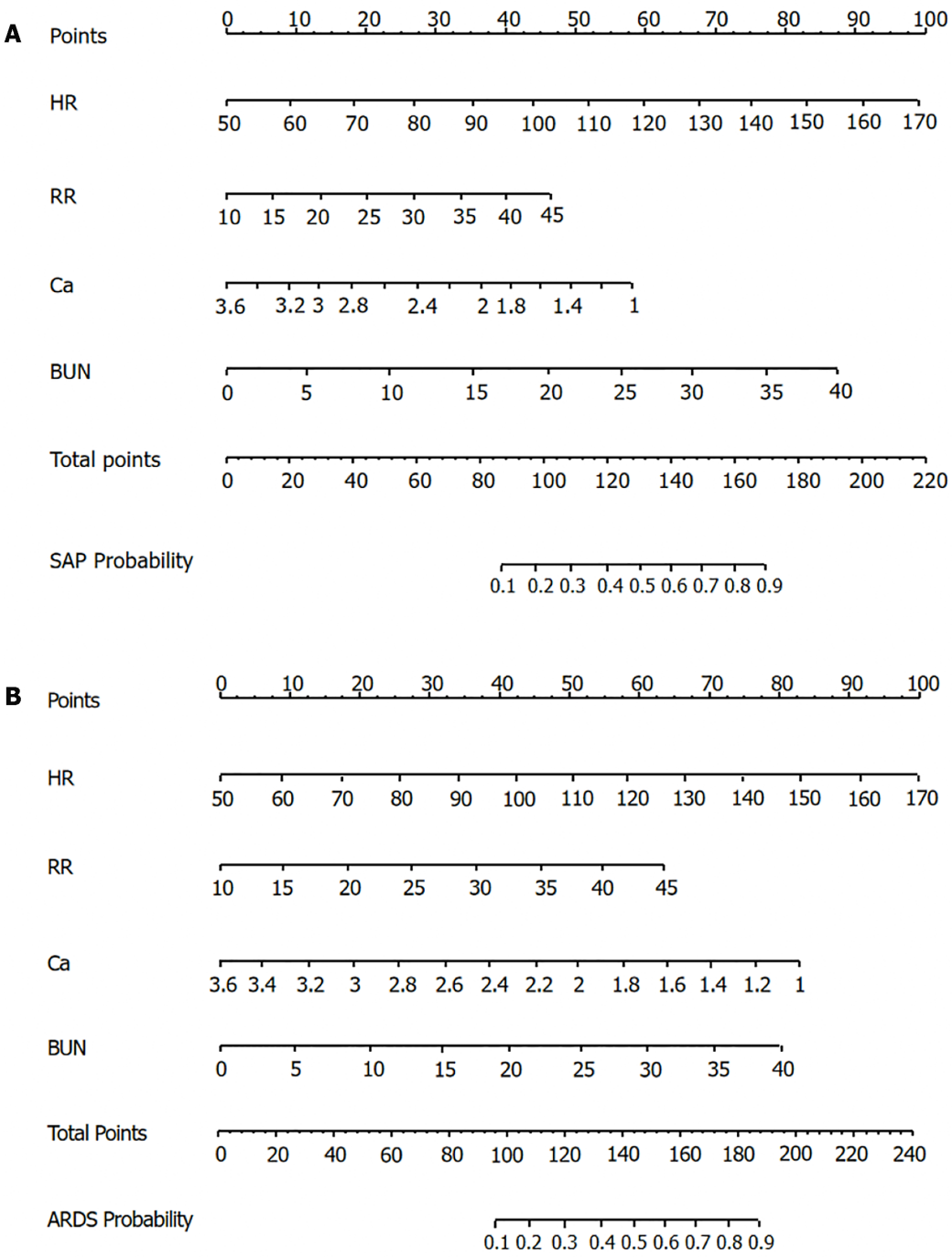


Figure 1 Nomograms of new predictive models. A: Nomogram of severe acute pancreatitis predictive model; B: Nomogram of acute respiratory distress syndrome prediction model. SAP: Severe acute pancreatitis; ARDS: Acute respiratory distress syndrome; HR: Heart rate; RR: Respiratory rate; Ca: Serum calcium concentration; BUN: Blood urea nitrogen.

involves the activation of signaling pathways, which include various cytokines and inflammatory mediators. Certain molecules, such as interleukin (IL)-6, IL-8, protein C, angiopoietin-2 and miRNAs and specific imaging examinations (X-ray and lung ultrasound) were also identified as predictors of ARDS in single or combined forms[8,36-38]. The data indicated that these new predictors seemed promising. However, the molecules and the examinations identified were not part of the routine clinical practice, which limited their clinical utility. Fei *et al*[10] used an artificial neural network algorithm to predict ARDS following SAP. The model by Fei *et al*[10] indicated high accuracy. However, the variable pancreatic necrosis rate was hard to assess when CT was not used and was not evident in the early course of AP.

The pathogenesis of SAP and ARDS involves a series of acute inflammatory reactions[2,39]. SIRS is widely adopted to assess the severity of diseases associated with acute inflammation. Both HR and RR are used in the SIRS model. Therefore, it is reasonable that both HR and RR were identified as predictors of SAP and ARDS. BUN has been shown to reflect volume depletion, renal function, the quality of

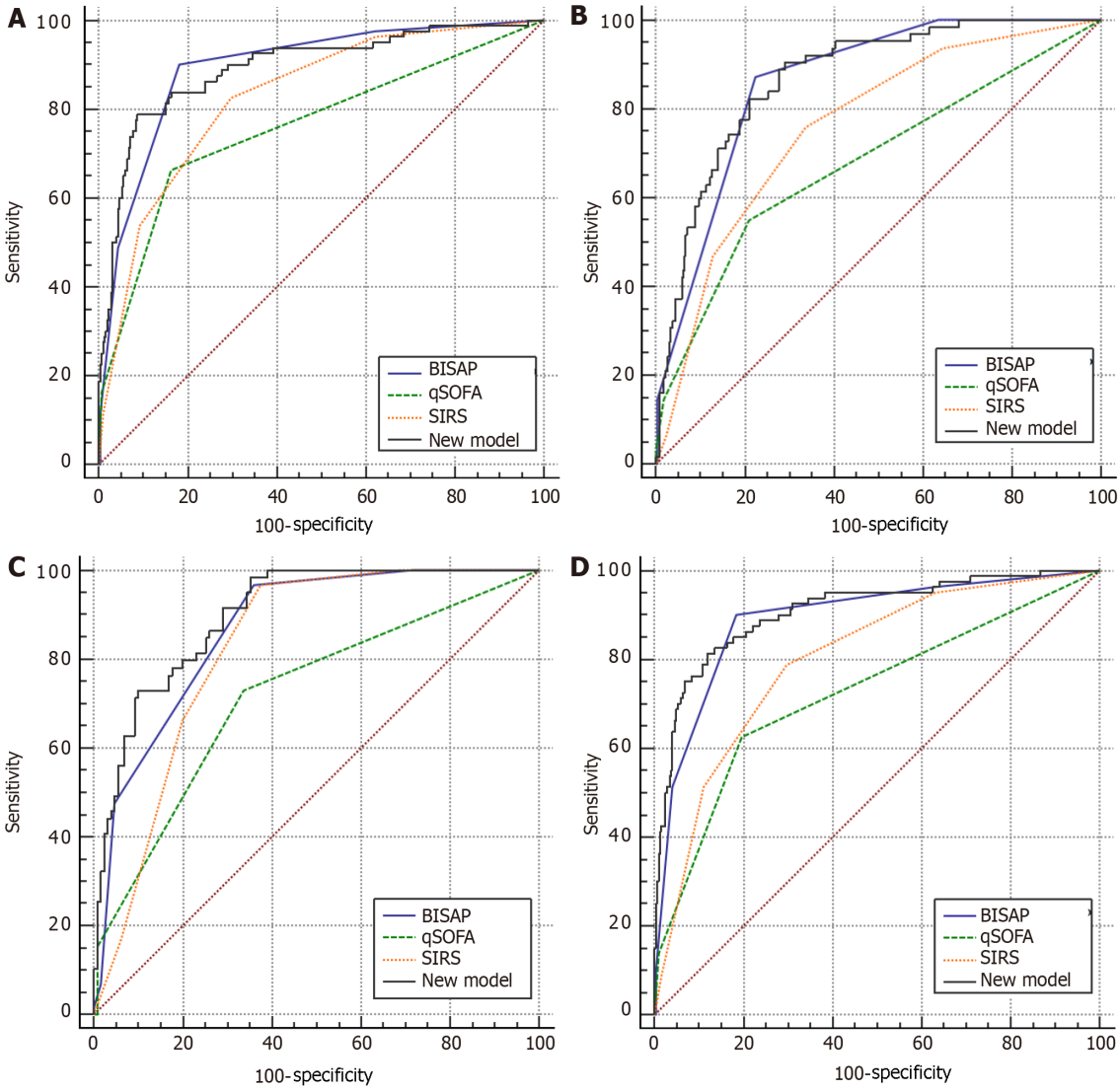


Figure 2 Receiver operating characteristic curves of different predictive models in derivation and validation cohort. A: Receiver operating characteristic (ROC) curves of severe acute pancreatitis (SAP) predictive models in derivation cohort; B: ROC curves of SAP predictive models in validation cohort; C: ROC curves of acute respiratory distress syndrome (ARDS) predictive models in derivation cohort; D: ROC curves of ARDS predictive models in validation cohort. BISAP: Bedside index for severity in acute pancreatitis; qSOFA: Quick sequential organ failure assessment; SIRS: Systemic inflammatory response syndrome.

resuscitates and even the ischemic injury of the pancreas during AP[40]. It has been reported that BUN can independently predict both SAP and the mortality of SAP[40-44]. Therefore, BUN was also involved in other predictive models of SAP, such as GCS, Ranson criteria and BISAP, in addition to our new model. The levels of BUN have not been used as a direct predictor of ARDS. However, this marker can be used as a predictor of pathogenesis in association with other risk factors, such as pancreatitis[39]. Calcium concentration has been closely associated with AP[45]. Hypocalcemia was common in the cohort of the present study and in other AP cohorts; notably in critically ill patients[46]. Elevated cytosolic calcium of pancreatic acinar cells causes premature trypsinogen activation, vacuolization and acinar cell death, which play critical roles in the pathogenesis of AP[47]. However, during the development of certain models for the prediction of SAP, serum calcium was excluded for a variety of factors[48]. Calcium is also involved in the pathogenesis of ARDS as a signaling molecule, leading to paracellular hyperpermeability through endothelial junction-cytoskeleton dissociation[49]. The current model suggested that calcium was an independent predictor of SAP and ARDS in AP, indicating the potential of developing novel drugs for the treatment of AP[50]. To the best of our knowledge, the model of the present study was the simplest used to predict SAP and ARDS within 24 h of AP admission. It is also the first model that involved serum calcium concentration to predict ARDS in AP.

The present study had several limitations. Firstly, organ dysfunction occurred mainly in the first week of AP, whereas accurate onset time was not available in the present study. Therefore, certain patients with SAP or ARDS may have been missed. Moreover, the exact onset time of ARDS was not recorded, so the new model only predicted the risk of ARDS during the whole admission (7-15 d) using the scores gained within 24 h of admission. It might not be appropriate, and the new model could not

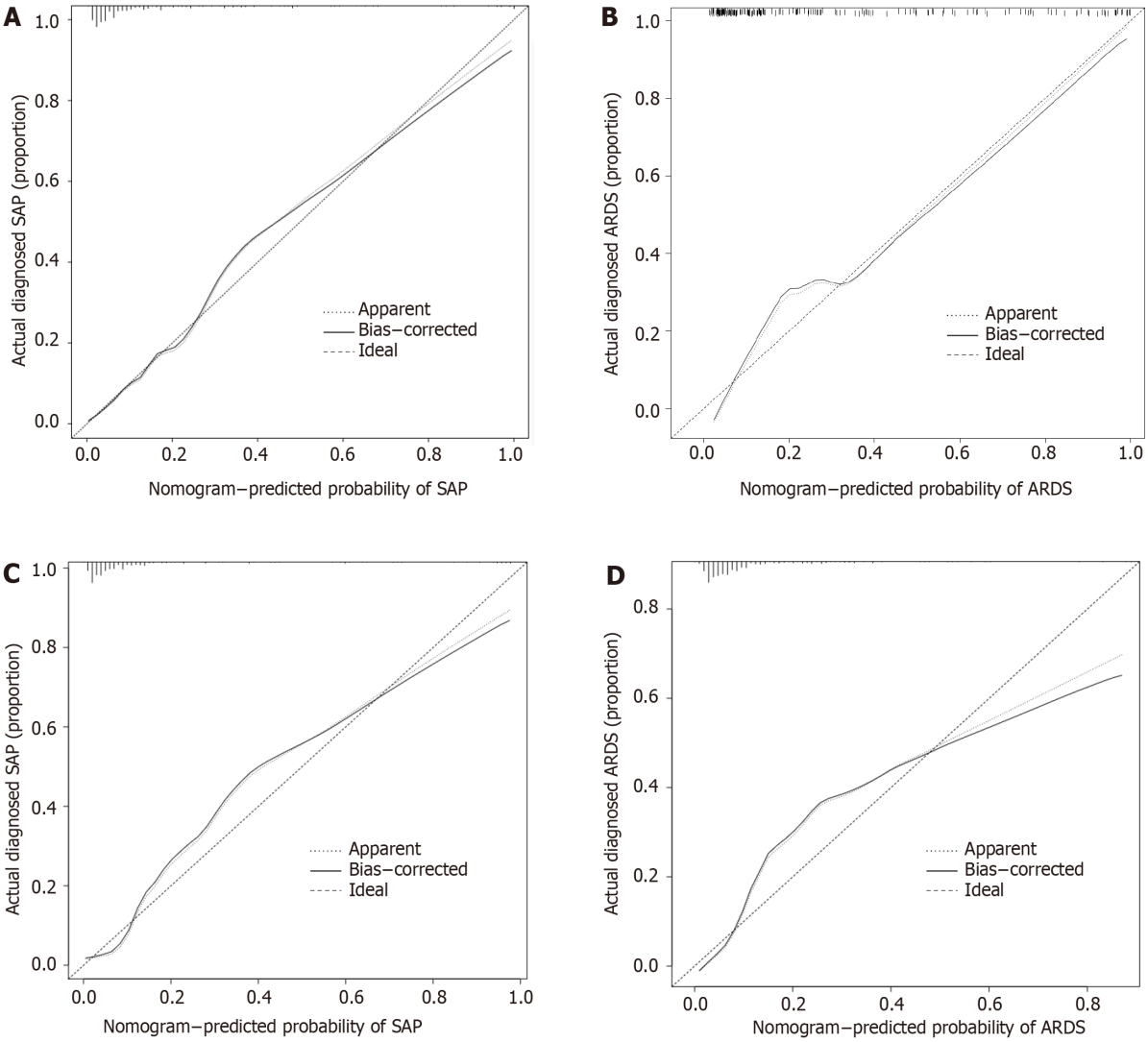


Figure 3 Calibration curves of new predictive models. A: Calibration plot of severe acute pancreatitis (SAP) predictive model in derivation cohort; B: Calibration plot of SAP predictive model in validation cohort; C: Calibration plot of acute respiratory distress syndrome (ARDS) predictive model in derivation cohort; D: Calibration plot of ARDS predictive model in validation cohort.

tell the clinicians when they should prepare for the possible onset of ARDS. Further studies are needed to verify the value of new models on a dynamic timescale. Secondly, the derivation cohort comprised tertiary and secondary hospitals from different regions of China. However, model validation was performed in a tertiary teaching hospital. Although the result of validation was also encouraging, it is hard to ignore that the incidence of SAP and ARDS in the validation cohort was considerably higher than that of the derivation cohort, which could reduce the generalizability in primary or secondary class hospitals, where MAP and MSAP exhibited high proportions. Moreover, certain laboratory examination technologies were different among four hospitals, which increased the systemic error of the data. It must be mentioned that mechanical ventilation will attenuate systemic inflammation of ARDS and the effect varies with patterns[51]. It is unavoidable that new scores to predict ARDS will also be affected. Unfortunately, detailed information of mechanical ventilation was not collected in this study, and further research is needed to investigate the influence of different ventilatory patterns on new models. Thirdly, selection bias was inevitable in a retrospective study. Furthermore, any missing value was deleted to obtain a complete-case dataset for analysis rather than imputating missing data with statistical methods (*e.g.*, multi-imputation), which were not recommended. However, in the present study, only three individuals were removed due to missing data, accounting for a tiny part of the cohort. It was considered that complete data analysis would not affect the overall conclusion. Finally, other common predictive models, such as APACHE-II score, Ranson criteria, CTSI and LIPS were not evaluated due to lack of essential parameters. Therefore, direct comparison among different models was unavailable.

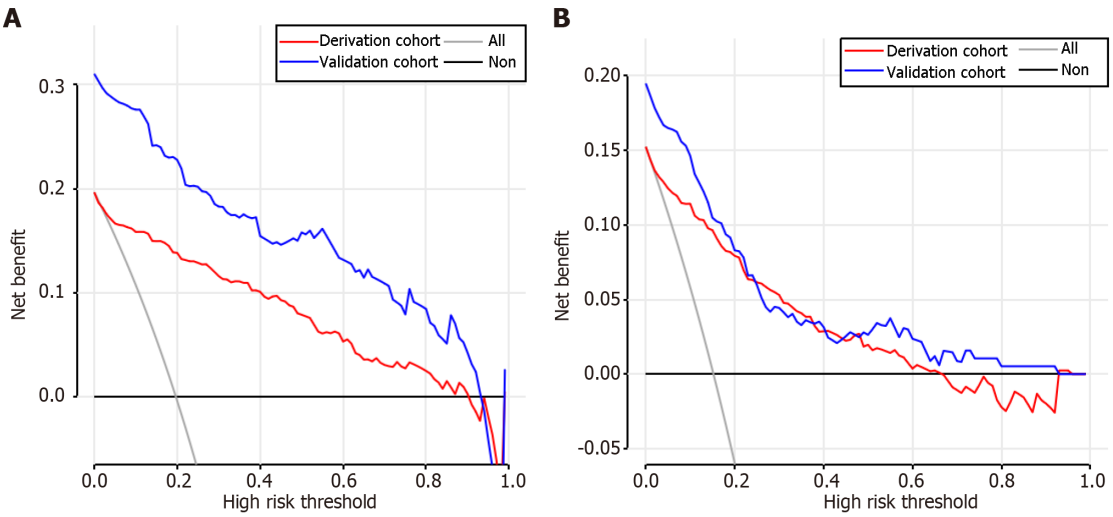


Figure 4 Decision curve analysis of new predictive models. A: Decision curve analysis of severe acute pancreatitis predictive model in derivation and validation cohort; B: Decision curve analysis of acute respiratory distress syndrome predictive model in derivation and validation cohort.

CONCLUSION

Novel models were developed containing only four items to predict SAP and ARDS in patients with AP, which were as accurate as BISAP but simpler. Serum calcium was identified as an important predictor, indicating a potential new strategy for management of AP. Further prospective studies are required to reveal whether early intervention based on novel prediction models could reduce the incidence of SAP and ARDS and finally improve the outcome of patients with AP.

ARTICLE HIGHLIGHTS

Research background

Acute respiratory distress syndrome (ARDS) is a major cause of death in patients with severe acute pancreatitis (SAP), but simple and credible predictive models are absent.

Research motivation

Use of models to predict and identify early patients with SAP and SAP-related ARDS, so that clinicians can manage these patients early to decrease mortality during admission.

Research objectives

To develop and verify new models to predict SAP and SAP-related ARDS.

Research methods

Clinical data from four centers were retrospectively collected. Items selected with least absolute shrinkage and selection operator regression method were involved in multiple logistic regression to develop the final model in development cohort. New models were than verified in validation cohort and assessed with C-index, calibration curve and decision-curve analysis.

Research results

New models could predict SAP and SAP-related ARDS with four easily available items, and performed well.

Research conclusions

We developed and verified simple and reliable models to predict SAP and SAP-related ARDS.

Research perspectives

To verify new models in a larger size of sample, and to investigate the questions raised by reviewer.

FOOTNOTES

Author contributions: Li YL, Zhang DD, and Xiong YY contributed equally to this work; Li YL, Zhang DD, Xiong YY and Wu D designed the research study; Li YL, Xiong YY, Wang RF, Gao XM, Gong H, Zheng SC, and Wu D performed the study and collected the data; Li YL, Zhang DD, and Xiong YY analyzed the data and wrote the manuscript; All authors have read and approved the final manuscript.

Supported by the Chinese Natural Science Foundation, No. 32170788.

Institutional review board statement: This study was approved by the Ethics Committee of Peking Union Medical College Hospital (Approval No. S-K1772).

Conflict-of-interest statement: All authors have no conflict of interest to disclose.

Data sharing statement: No additional data are available.

STROBE statement: The authors have read the STROBE statement, and the manuscript was prepared and revised according to the STROBE statement.

Open-Access: This article is an open-access article that was selected by an in-house editor and fully peer-reviewed by external reviewers. It is distributed in accordance with the Creative Commons Attribution NonCommercial (CC BY-NC 4.0) license, which permits others to distribute, remix, adapt, build upon this work non-commercially, and license their derivative works on different terms, provided the original work is properly cited and the use is non-commercial. See: https://creativecommons.org/Licenses/by-nc/4.0/

Country/Territory of origin: China

ORCID number: Yun-Long Li 0000-0002-7367-0772; Ding-Ding Zhang 0000-0002-5234-752X; Yang-Yang Xiong 0000-0002-0266-7592; Rui-Feng Wang 0000-0002-8614-8481; Xiao-Mao Gao 0000-0001-5913-2735; Hui Gong 0000-0001-6398-384X; Shi-Cheng Zheng 0000-0003-1548-4282; Dong Wu 0000-0001-9430-9874.

S-Editor: Zhang H
L-Editor: Kerr C
P-Editor: Zhang H

REFERENCES

1 **Xiao AY**, Tan ML, Wu LM, Asrani VM, Windsor JA, Yadav D, Petrov MS. Global incidence and mortality of pancreatic diseases: a systematic review, meta-analysis, and meta-regression of population-based cohort studies. *Lancet Gastroenterol Hepatol* 2016; **1**: 45-55 [PMID: 28404111 DOI: 10.1016/S2468-1253(16)30004-8]
2 **Boxhoorn L**, Voermans RP, Bouwense SA, Bruno MJ, Verdonk RC, Boermeester MA, van Santvoort HC, Besselink MG. Acute pancreatitis. *Lancet* 2020; **396**: 726-734 [PMID: 32891214 DOI: 10.1016/S0140-6736(20)31310-6]
3 **Matta B**, Gougol A, Gao X, Reddy N, Talukdar R, Kochhar R, Goenka MK, Gulla A, Gonzalez JA, Singh VK, Ferreira M, Stevens T, Barbu ST, Nawaz H, Gutierrez SC, Zarnescu NO, Capurso G, Easler J, Triantafyllou K, Pelaez-Luna M, Thakkar S, Ocampo C, de-Madaria E, Cote GA, Wu BU, Paragomi P, Pothoulakis I, Tang G, Papachristou GI. Worldwide Variations in Demographics, Management, and Outcomes of Acute Pancreatitis. *Clin Gastroenterol Hepatol* 2020; **18**: 1567-1575.e2 [PMID: 31712075 DOI: 10.1016/j.cgh.2019.11.017]
4 **Wu D**, Lu B, Yang H, Li J, Qian J. [The three-category classification of severe acute pancreatitis: a single-center pilot study]. *Zhonghua Nei Ke Za Zhi* 2014; **53**: 937-940 [PMID: 25623558]
5 **Wu D**, Lu B, Xue HD, Yang H, Qian JM, Lee P, Windsor JA. Validation of Modified Determinant-Based Classification of severity for acute pancreatitis in a tertiary teaching hospital. *Pancreatology* 2019; **19**: 217-223 [PMID: 30642724 DOI: 10.1016/j.pan.2019.01.003]
6 **Elder AS**, Saccone GT, Dixon DL. Lung injury in acute pancreatitis: mechanisms underlying augmented secondary injury. *Pancreatology* 2012; **12**: 49-56 [PMID: 22487475 DOI: 10.1016/j.pan.2011.12.012]
7 **Andersson B**, Ansari D, Andersson E, Persson S, Andersson R. Fatal acute pancreatitis occurring outside of the hospital: clinical and social characteristics. *World J Surg* 2010; **34**: 2286-2291 [PMID: 20574639 DOI: 10.1007/s00268-010-0693-z]
8 **Shah J**, Rana SS. Acute respiratory distress syndrome in acute pancreatitis. *Indian J Gastroenterol* 2020; **39**: 123-132 [PMID: 32285399 DOI: 10.1007/s12664-020-01016-z]
9 **Bryner BS**, Smith C, Cooley E, Bartlett RH, Mychaliska GB. Extracorporeal life support for pancreatitis-induced acute respiratory distress syndrome. *Ann Surg* 2012; **256**: 1073-1077 [PMID: 22824856 DOI: 10.1097/SLA.0b013e31825d33c1]
10 **Fei Y**, Gao K, Li WQ. Prediction and evaluation of the severity of acute respiratory distress syndrome following severe acute pancreatitis using an artificial neural network algorithm model. *HPB (Oxford)* 2019; **21**: 891-897 [PMID: 30591306 DOI: 10.1016/j.hpb.2018.11.009]
11 **Huang Z**, Ma X, Jia X, Wang R, Liu L, Zhang M, Wan X, Tang C, Huang L. Prevention of Severe Acute Pancreatitis With Cyclooxygenase-2 Inhibitors: A Randomized Controlled Clinical Trial. *Am J Gastroenterol* 2020; **115**: 473-480 [PMID: 32142484 DOI: 10.14309/ajg.0000000000000529]

12 **Vaughn VM**, Shuster D, Rogers MAM, Mann J, Conte ML, Saint S, Chopra V. Early Versus Delayed Feeding in Patients With Acute Pancreatitis: A Systematic Review. *Ann Intern Med* 2017; **166**: 883-892 [PMID: 28505667 DOI: 10.7326/M16-2533]

13 **Jin W**, Chuang CC, Jin H, Ye J, Kandaswamy E, Wang L, Zuo L. Effects of Pre-Hospital Antiplatelet Therapy on the Incidence of ARDS. *Respir Care* 2020; **65**: 1039-1045 [PMID: 32047121 DOI: 10.4187/respcare.07177]

14 **Dixon B**, Smith RJ, Campbell DJ, Moran JL, Doig GS, Rechnitzer T, MacIsaac CM, Simpson N, van Haren FMP, Ghosh AN, Gupta S, Broadfield EJC, Crozier TME, French C, Santamaria JD; CHARLI Study Group. Nebulised heparin for patients with or at risk of acute respiratory distress syndrome: a multicentre, randomised, double-blind, placebo-controlled phase 3 trial. *Lancet Respir Med* 2021; **9**: 360-372 [PMID: 33493448 DOI: 10.1016/S2213-2600(20)30470-7]

15 **Wang Y**, Zhong M, Wang Z, Song J, Wu W, Zhu D. The preventive effect of antiplatelet therapy in acute respiratory distress syndrome: a meta-analysis. *Crit Care* 2018; **22**: 60 [PMID: 29519254 DOI: 10.1186/s13054-018-1988-y]

16 **Di MY**, Liu H, Yang ZY, Bonis PA, Tang JL, Lau J. Prediction Models of Mortality in Acute Pancreatitis in Adults: A Systematic Review. *Ann Intern Med* 2016; **165**: 482-490 [PMID: 27454310 DOI: 10.7326/M16-0650]

17 **Mofidi R**, Patil PV, Suttie SA, Parks RW. Risk assessment in acute pancreatitis. *Br J Surg* 2009; **96**: 137-150 [PMID: 19125435 DOI: 10.1002/bjs.6431]

18 **Gajic O**, Dabbagh O, Park PK, Adesanya A, Chang SY, Hou P, Anderson H 3rd, Hoth JJ, Mikkelsen ME, Gentile NT, Gong MN, Talmor D, Bajwa E, Watkins TR, Festic E, Yilmaz M, Iscimen R, Kaufman DA, Esper AM, Sadikot R, Douglas I, Sevransky J, Malinchoc M; U. S. Critical Illness and Injury Trials Group: Lung Injury Prevention Study Investigators (USCIITG-LIPS). Early identification of patients at risk of acute lung injury: evaluation of lung injury prediction score in a multicenter cohort study. *Am J Respir Crit Care Med* 2011; **183**: 462-470 [PMID: 20802164 DOI: 10.1164/rccm.201004-0549OC]

19 **Liang M**, He M, Tang J, He X, Liu Z, Feng S, Chen P, Li H, Xue Y, Bai T, Ma Y, Zhang J. Novel risk scoring system for predicting acute respiratory distress syndrome among hospitalized patients with coronavirus disease 2019 in Wuhan, China. *BMC Infect Dis* 2020; **20**: 960 [PMID: 33334314 DOI: 10.1186/s12879-020-05561-y]

20 **Anan K**, Ichikado K, Ishihara T, Shintani A, Kawamura K, Suga M, Sakagami T. A Scoring System with High-Resolution Computed Tomography to Predict Drug-Associated Acute Respiratory Distress Syndrome: Development and Internal Validation. *Sci Rep* 2019; **9**: 8601 [PMID: 31197186 DOI: 10.1038/s41598-019-45063-9]

21 **Seymour CW**, Liu VX, Iwashyna TJ, Brunkhorst FM, Rea TD, Scherag A, Rubenfeld G, Kahn JM, Shankar-Hari M, Singer M, Deutschman CS, Escobar GJ, Angus DC. Assessment of Clinical Criteria for Sepsis: For the Third International Consensus Definitions for Sepsis and Septic Shock (Sepsis-3). *JAMA* 2016; **315**: 762-774 [PMID: 26903335 DOI: 10.1001/jama.2016.0288]

22 **Bone RC**, Balk RA, Cerra FB, Dellinger RP, Fein AM, Knaus WA, Schein RM, Sibbald WJ. Definitions for sepsis and organ failure and guidelines for the use of innovative therapies in sepsis. The ACCP/SCCM Consensus Conference Committee. American College of Chest Physicians/Society of Critical Care Medicine. *Chest* 1992; **101**: 1644-1655 [PMID: 1303622 DOI: 10.1378/chest.101.6.1644]

23 **Banks PA**, Bollen TL, Dervenis C, Gooszen HG, Johnson CD, Sarr MG, Tsiotos GG, Vege SS; Acute Pancreatitis Classification Working Group. Classification of acute pancreatitis--2012: revision of the Atlanta classification and definitions by international consensus. *Gut* 2013; **62**: 102-111 [PMID: 23100216 DOI: 10.1136/gutjnl-2012-302779]

24 **ARDS Definition Task Force**, Ranieri VM, Rubenfeld GD, Thompson BT, Ferguson ND, Caldwell E, Fan E, Camporota L, Slutsky AS. Acute respiratory distress syndrome: the Berlin Definition. *JAMA* 2012; **307**: 2526-2533 [PMID: 22797452 DOI: 10.1001/jama.2012.5669]

25 **Moons KG**, Altman DG, Reitsma JB, Ioannidis JP, Macaskill P, Steyerberg EW, Vickers AJ, Ransohoff DF, Collins GS. Transparent Reporting of a multivariable prediction model for Individual Prognosis or Diagnosis (TRIPOD): explanation and elaboration. *Ann Intern Med* 2015; **162**: W1-73 [PMID: 25560730 DOI: 10.7326/M14-0698]

26 **Prise KM**, O'Sullivan JM. Radiation-induced bystander signalling in cancer therapy. *Nat Rev Cancer* 2009; **9**: 351-360 [PMID: 19377507 DOI: 10.1038/nrc2603]

27 **Garg PK**, Singh VP. Organ Failure Due to Systemic Injury in Acute Pancreatitis. *Gastroenterology* 2019; **156**: 2008-2023 [PMID: 30768987 DOI: 10.1053/j.gastro.2018.12.041]

28 **Shi N**, Liu T, de la Iglesia-Garcia D, Deng L, Jin T, Lan L, Zhu P, Hu W, Zhou Z, Singh V, Dominguez-Munoz JE, Windsor J, Huang W, Xia Q, Sutton R. Duration of organ failure impacts mortality in acute pancreatitis. *Gut* 2020; **69**: 604-605 [PMID: 31233394 DOI: 10.1136/gutjnl-2019-318241]

29 **Petrov MS**, van Santvoort HC, Besselink MG, van der Heijden GJ, Windsor JA, Gooszen HG. Enteral nutrition and the risk of mortality and infectious complications in patients with severe acute pancreatitis: a meta-analysis of randomized trials. *Arch Surg* 2008; **143**: 1111-1117 [PMID: 19015471 DOI: 10.1001/archsurg.143.11.1111]

30 **Karnatovskaia LV**, Festic E, Gajic O, Carter RE, Lee AS; US Critical Illness and Injury Trials Group: Lung Injury Prevention Study Investigators (USCIITG-LIPS). Prehospital amiodarone may increase the incidence of acute respiratory distress syndrome among patients at risk. *J Crit Care* 2012; **27**: 447-453 [PMID: 22226422 DOI: 10.1016/j.jcrc.2011.10.009]

31 **Larvin M**, McMahon MJ. APACHE-II score for assessment and monitoring of acute pancreatitis. *Lancet* 1989; **2**: 201-205 [PMID: 2568529 DOI: 10.1016/s0140-6736(89)90381-4]

32 **Ranson JH**, Rifkind KM, Roses DF, Fink SD, Eng K, Localio SA. Objective early identification of severe acute pancreatitis. *Am J Gastroenterol* 1974; **61**: 443-451 [PMID: 4835417]

33 **Balthazar EJ**, Robinson DL, Megibow AJ, Ranson JH. Acute pancreatitis: value of CT in establishing prognosis. *Radiology* 1990; **174**: 331-336 [PMID: 2296641 DOI: 10.1148/radiology.174.2.2296641]

34 **Singh VK**, Wu BU, Bollen TL, Repas K, Maurer R, Johannes RS, Mortele KJ, Conwell DL, Banks PA. A prospective evaluation of the bedside index for severity in acute pancreatitis score in assessing mortality and intermediate markers of severity in acute pancreatitis. *Am J Gastroenterol* 2009; **104**: 966-971 [PMID: 19293787 DOI: 10.1038/ajg.2009.28]

35 **Papachristou GI**, Muddana V, Yadav D, O'Connell M, Sanders MK, Slivka A, Whitcomb DC. Comparison of BISAP, Ranson's, APACHE-II, and CTSI scores in predicting organ failure, complications, and mortality in acute pancreatitis. *Am J*

Gastroenterol 2010; **105**: 435-41; quiz 442 [PMID: 19861954 DOI: 10.1038/ajg.2009.622]

36 **Sinha P**, Delucchi KL, McAuley DF, O'Kane CM, Matthay MA, Calfee CS. Development and validation of parsimonious algorithms to classify acute respiratory distress syndrome phenotypes: a secondary analysis of randomised controlled trials. *Lancet Respir Med* 2020; **8**: 247-257 [PMID: 31948926 DOI: 10.1016/S2213-2600(19)30369-8]

37 **Reilly JP**, Wang F, Jones TK, Palakshappa JA, Anderson BJ, Shashaty MGS, Dunn TG, Johansson ED, Riley TR, Lim B, Abbott J, Ittner CAG, Cantu E, Lin X, Mikacenic C, Wurfel MM, Christiani DC, Calfee CS, Matthay MA, Christie JD, Feng R, Meyer NJ. Plasma angiopoietin-2 as a potential causal marker in sepsis-associated ARDS development: evidence from Mendelian randomization and mediation analysis. *Intensive Care Med* 2018; **44**: 1849-1858 [PMID: 30343317 DOI: 10.1007/s00134-018-5328-0]

38 **Xu Z**, Wu GM, Li Q, Ji FY, Shi Z, Guo H, Yin JB, Zhou J, Gong L, Mei CX, Wang GS. Predictive Value of Combined LIPS and ANG-2 Level in Critically Ill Patients with ARDS Risk Factors. *Mediators Inflamm* 2018; **2018**: 1739615 [PMID: 30008611 DOI: 10.1155/2018/1739615]

39 **Thompson BT**, Chambers RC, Liu KD. Acute Respiratory Distress Syndrome. *N Engl J Med* 2017; **377**: 562-572 [PMID: 28792873 DOI: 10.1056/NEJMra1608077]

40 **Lin S**, Hong W, Basharat Z, Wang Q, Pan J, Zhou M. Blood Urea Nitrogen as a Predictor of Severe Acute Pancreatitis Based on the Revised Atlanta Criteria: Timing of Measurement and Cutoff Points. *Can J Gastroenterol Hepatol* 2017; **2017**: 9592831 [PMID: 28487848 DOI: 10.1155/2017/9592831]

41 **Wu BU**, Johannes RS, Sun X, Conwell DL, Banks PA. Early changes in blood urea nitrogen predict mortality in acute pancreatitis. *Gastroenterology* 2009; **137**: 129-135 [PMID: 19344722 DOI: 10.1053/j.gastro.2009.03.056]

42 **Pando E**, Alberti P, Mata R, Gomez MJ, Vidal L, Cirera A, Dopazo C, Blanco L, Gomez C, Caralt M, Balsells J, Charco R. Early Changes in Blood Urea Nitrogen (BUN) Can Predict Mortality in Acute Pancreatitis: Comparative Study between BISAP Score, APACHE-II, and Other Laboratory Markers-A Prospective Observational Study. *Can J Gastroenterol Hepatol* 2021; **2021**: 6643595 [PMID: 33824864 DOI: 10.1155/2021/6643595]

43 **Koutroumpakis E**, Wu BU, Bakker OJ, Dudekula A, Singh VK, Besselink MG, Yadav D, Mounzer R, van Santvoort HC, Whitcomb DC, Gooszen HG, Banks PA, Papachristou GI. Admission Hematocrit and Rise in Blood Urea Nitrogen at 24 h Outperform other Laboratory Markers in Predicting Persistent Organ Failure and Pancreatic Necrosis in Acute Pancreatitis: A Post Hoc Analysis of Three Large Prospective Databases. *Am J Gastroenterol* 2015; **110**: 1707-1716 [PMID: 26553208 DOI: 10.1038/ajg.2015.370]

44 **Hong W**, Lin S, Zippi M, Geng W, Stock S, Zimmer V, Xu C, Zhou M. High-Density Lipoprotein Cholesterol, Blood Urea Nitrogen, and Serum Creatinine Can Predict Severe Acute Pancreatitis. *Biomed Res Int* 2017; **2017**: 1648385 [PMID: 28904946 DOI: 10.1155/2017/1648385]

45 **Gerasimenko JV**, Peng S, Tsugorka T, Gerasimenko OV. Ca^{2+} signalling underlying pancreatitis. *Cell Calcium* 2018; **70**: 95-101 [PMID: 28552244 DOI: 10.1016/j.ceca.2017.05.010]

46 **Ahmed A**, Azim A, Gurjar M, Baronia AK. Hypocalcemia in acute pancreatitis revisited. *Indian J Crit Care Med* 2016; **20**: 173-177 [PMID: 27076730 DOI: 10.4103/0972-5229.178182]

47 **Pallagi P**, Madácsy T, Varga Á, Maléth J. Intracellular Ca^{2+} Signalling in the Pathogenesis of Acute Pancreatitis: Recent Advances and Translational Perspectives. *Int J Mol Sci* 2020; **21** [PMID: 32503336 DOI: 10.3390/ijms21114005]

48 **Wu BU**, Johannes RS, Sun X, Tabak Y, Conwell DL, Banks PA. The early prediction of mortality in acute pancreatitis: a large population-based study. *Gut* 2008; **57**: 1698-1703 [PMID: 18519429 DOI: 10.1136/gut.2008.152702]

49 **Kumar P**, Shen Q, Pivetti CD, Lee ES, Wu MH, Yuan SY. Molecular mechanisms of endothelial hyperpermeability: implications in inflammation. *Expert Rev Mol Med* 2009; **11**: e19 [PMID: 19563700 DOI: 10.1017/S1462399409001112]

50 **Serafini M**, Cordero-Sanchez C, Di Paola R, Bhela IP, Aprile S, Purghè B, Fusco R, Cuzzocrea S, Genazzani AA, Riva B, Pirali T. Store-Operated Calcium Entry as a Therapeutic Target in Acute Pancreatitis: Discovery and Development of Drug-Like SOCE Inhibitors. *J Med Chem* 2020; **63**: 14761-14779 [PMID: 33253576 DOI: 10.1021/acs.jmedchem.0c01305]

51 **Matthay MA**, Zemans RL, Zimmerman GA, Arabi YM, Beitler JR, Mercat A, Herridge M, Randolph AG, Calfee CS. Acute respiratory distress syndrome. *Nat Rev Dis Primers* 2019; **5**: 18 [PMID: 30872586 DOI: 10.1038/s41572-019-0069-0]

World Journal of Gastroenterology

Submit a Manuscript: https://www.f6publishing.com

World J Gastroenterol 2022 May 21; 28(19): 2137-2147

DOI: 10.3748/wjg.v28.i19.2137

ISSN 1007-9327 (print) ISSN 2219-2840 (online)

ORIGINAL ARTICLE

Prospective Study

Non-optical polyp-based resect and discard strategy: A prospective clinical study

Mahsa Taghiakbari, Celia Hammar, Mira Frenn, Roupen Djinbachian, Heiko Pohl, Erik Deslandres, Simon Bouchard, Mickael Bouin, Daniel von Renteln

Specialty type: Gastroenterology and hepatology

Provenance and peer review: Invited article; Externally peer reviewed.

Peer-review model: Single blind

Peer-review report's scientific quality classification
Grade A (Excellent): 0
Grade B (Very good): B
Grade C (Good): C
Grade D (Fair): 0
Grade E (Poor): 0

P-Reviewer: Pausawasdi N, Thailand; Yeniova A, Turkey

Received: January 2, 2022
Peer-review started: January 2, 2022
First decision: March 10, 2022
Revised: March 21, 2022
Accepted: April 9, 2022
Article in press: April 9, 2022
Published online: May 21, 2022

Mahsa Taghiakbari, Celia Hammar, Mira Frenn, Roupen Djinbachian, Erik Deslandres, Simon Bouchard, Mickael Bouin, Daniel von Renteln, Department of Gastroenterology, Montreal University Hospital Research Center (CRCHUM), Montréal H2X 0A9, Quebec, Canada

Celia Hammar, Mira Frenn, Department of Gastroenterology, University of Montreal, Faculty of Medicine, Montreal H2X 0A9, Quebce, Canada

Roupen Djinbachian, Department of Internal Medicine, University of Montreal Hospital Center (CHUM), Montreal H2X 0A9, Quebec, Canada

Heiko Pohl, Department of Medicine, Veterans Affairs Medical Center, White River Junction, VT 05009, United States

Heiko Pohl, Department of Gastroenterology, Dartmouth Geisel School of Medicine and The Dartmouth Institute, Hanover, NH 03755, United States

Corresponding author: Mahsa Taghiakbari, MD, Research Scientist, Department of Gastroenterology, Montreal University Hospital Research Center (CRCHUM), 900 Rue Saint-Denis, Montréal H2X 0A9, Quebec, Canada. mahtakbar@gmail.com

Abstract

BACKGROUND

Post-polypectomy surveillance intervals are currently determined based on pathology results.

AIM

To evaluate a polyp-based resect and discard model that assigns surveillance intervals based solely on polyp number and size.

METHODS

Patients undergoing elective colonoscopies at the Montreal University Medical Center were enrolled prospectively. The polyp-based strategy was used to assign the next surveillance interval using polyp size and number. Surveillance intervals were also assigned using optical diagnosis for small polyps (< 10 mm). The primary outcome was surveillance interval agreement between the polyp-based model, optical diagnosis, and the pathology-based reference standard using the 2020 United States Multi-Society Task Force guidelines. Secondary outcomes

included the proportion of reduction in required histopathology evaluations and proportion of immediate post-colonoscopy recommendations provided to patients.

RESULTS

Of 944 patients (mean age 62.6 years, 49.3% male, 933 polyps) were enrolled. The surveillance interval agreement for the polyp-based strategy was 98.0% [95% confidence interval (CI): 0.97–0.99] compared with pathology-based assignment. Optical diagnosis-based intervals achieved 95.8% (95%CI: 0.94–0.97) agreement with pathology. When using the polyp-based strategy and optical diagnosis, the need for pathology assessment was reduced by 87.8% and 70.6%, respectively. The polyp-based strategy provided 93.7% of patients with immediate surveillance interval recommendations *vs* 76.1% for optical diagnosis.

CONCLUSION

The polyp-based strategy achieved almost perfect surveillance interval agreement compared with pathology-based assignments, significantly reduced the number of required pathology evaluations, and provided most patients with immediate surveillance interval recommendations.

Key Words: Colonoscopy; Colorectal pathology; Colorectal adenomas; Endoscopy; Surveillance; Optical diagnosis

©The Author(s) 2022. Published by Baishideng Publishing Group Inc. All rights reserved.

Core Tip: Background current post-polypectomy surveillance intervals are based on pathology outcomes. Our aim was to test a novel polyp-based resect and discard model that assigns surveillance interval based on number and size of polyps. Findings Surveillance interval based on a polyp-based strategy achieved 98.0% (95% confidence interval: 0.97–0.99) agreement with pathology-based intervals when applied according to the current surveillance guideline. Implications for patient care the polyp-based strategy can easily be implemented without any requirement for specialist devices and training. The majority of patients can be provided with immediate surveillance interval recommendations, without having to wait for results of pathology analysis.

Citation: Taghiakbari M, Hammar C, Frenn M, Djinbachian R, Pohl H, Deslandres E, Bouchard S, Bouin M, von Renteln D. Non-optical polyp-based resect and discard strategy: A prospective clinical study. *World J Gastroenterol* 2022; 28(19): 2137-2147

URL: https://www.wjgnet.com/1007-9327/full/v28/i19/2137.htm

DOI: https://dx.doi.org/10.3748/wjg.v28.i19.2137

INTRODUCTION

Screening colonoscopy and removal of detected polyps has been utilized to reduce colorectal cancer (CRC) morbidity and mortality[1]. The majority (90%) of polyps found during colonoscopies are less than 10 mm in size, with diminutive polyps (< 5 mm) accounting for about 70%–80%[2]. Most of these small polyps have been shown to be at very low risk for progression towards CRC. Advanced histology is found in only 0.5% of diminutive polyps and 1.5% of small polyps[2]. Histopathologic evaluation of small polyps can incur significant costs, therefore alternative modalities have been proposed, such as image-enhanced endoscopy-assisted optical polyp diagnosis (the "resect and discard" strategy)[3-5].

While optical diagnosis has achieved high level of accuracy in academic settings[6,7], reports from general clinical practice have not been able to reproduce these results, with accuracies ranging between 75% and 85%, and surveillance interval assignment agreement with pathology of only 81%[8,9]. In a recent survey study, 59.9% of endoscopists reported that optical diagnosis was not feasible for clinical implementation, and 84.2% were not using the strategy in their current clinical practice[10]. Limitations of the resect and discard strategy included fear of making an incorrect optical diagnosis, assigning incorrect surveillance intervals, and training requirements[10]. Therefore, we aimed to develop a resect and discard model that did not require optical diagnosis to assign colonoscopy surveillance intervals. A retrospective study using this model, named the polyp-based resect and discard (PBRD) strategy, showed an 89.3% agreement with pathology-based surveillance recommendations[11]. This current study aimed to evaluate the PBRD model in a prospective clinical study comparing the strategy with optical polyp diagnosis using pathology-based surveillance interval recommendations as the reference standard.

MATERIALS AND METHODS

Methods

Patients (aged 45–80 years) undergoing elective screening, surveillance, or diagnostic colonoscopies between May 2017 and December 2018 at the Centre Hospitalier de l'Université de Montréal (CHUM) were included. Exclusion criteria were known inflammatory bowel disease, active colitis, coagulopathy, familial polyposis syndromes, American Society of Anesthesiologists classification score of > 3, emergency colonoscopies, personal history of CRC, hospitalized patients, and presence of CRC during colonoscopy. The study was planned and conducted as a sub-study in patients enrolled in two prospective clinical studies (NCT04032912 and NCT03515343, respectively). The study protocol and data collection were approved by the local institutional research board as an amendment to the two prospective clinical studies (17.135 and 16.367, respectively).

Colonoscopy procedures

Colonoscopy procedures were performed as *per* the standard of care. Adequate bowel preparation was determined by a Boston Bowel Preparation Score (BBPS) of ≥ 6. Location, size, and morphology according to the Paris classification were documented for each polyp. All polyps were removed and sent for histopathology evaluation. Polyps 1–10 mm were optically diagnosed using either i-Scan or Optivista image-enhanced endoscopy (Pentax, Montvale, NJ, United States) and classified using the Narrow-band imaging international colorectal endoscopic (NICE) classification system[4,12]. Endoscopist level of confidence (low or high) in optical histology prediction was documented. Endoscopists then used the PBRD strategy to assign the next surveillance interval immediately after colonoscopy (real-time application). Then, a research assistant (MT) used the PBRD strategy (post hoc) to determine whether endoscopists had deviated from the intended PBRD strategy and assessed the PBRD model results when used without deviations.

The PBRD model

The PBRD strategy was developed by the research group and previously tested in a pilot study[11]. There was no overlap between the cohort enrolled in the pilot study and the cohort presented herein. The PBRD uses number and size of polyps, and first-degree family history of CRC to predict the next surveillance interval. At the time of the study, the 2012 United States Multi-Society Task Force (USMSTF) guidelines[13] were the most current guidelines used to develop the PBRD strategy (Table 1). With the publication of the updated 2020 USMSTF guidelines[14] during the course of the study, we adapted the PBRD model to reflect those changes through consensus between two researchers (RD and DvR), and tested its performance post hoc (Table 1). Since the 2020 guidelines are the most contemporaneous, the 2020-based analysis was used as the primary outcome of the study. Pathology-based surveillance intervals were therefore determined using 2012 or 2020 USMSTF guidelines as appropriate [13,14]. In cases of multiple recommended intervals (for example, 7–10 years), the longest interval was chosen to compare the strategies.

Study outcomes

The primary outcome was the agreement between PBRD-based surveillance intervals and pathology-based surveillance intervals and agreement between updated PBRD-based surveillance intervals and pathology-based surveillance intervals. Secondary endpoints were: Agreement between optical diagnosis-based surveillance intervals and pathology-based intervals; agreement between real-time endoscopist allocation of intervals based on PBRD compared with pathology-based intervals; proportion of immediate post-colonoscopy surveillance recommendations provided to patients based on both PBRD (real-time and post hoc) and optical diagnosis; proportion of required histopathology evaluations when using PBRD and optical diagnosis. Other secondary outcomes included the proportion of patients with findings that could have been provided with immediate surveillance interval recommendations: no polyps detected; inadequate bowel preparation; polyps sized 1–10 mm that were all optically diagnosed with high confidence (for the optical diagnosis strategy); patients fitting scenarios 1, 2, 3, and 6 (for the PBRD strategy) (Table 1). Polyps undergoing low-confidence optical diagnosis, polyps > 10 mm in size, and all polyps in patients fitting scenarios 4 and 5 (for the PBRD strategy) required histopathology evaluation.

Statistical analysis

Patient, procedure, and polyp characteristics were presented as crude numbers and frequency for categorical variables, and mean ± SD or median (range) for continuous variables. Agreements between the PBRD model, optical diagnosis, and pathology-based surveillance recommendations were presented as proportions with two-tailed 95% confidence interval (CI). For secondary outcomes, proportional estimates with two-tailed 95%CI were presented. A chi-squared test or a two-tailed Fisher's exact test was used to compare proportions. SPSS version 26.0 (IBM Corp., Armonk, New York, United States) and MedCalc version 19.4 (MedCalc Software bv, Ostend, Belgium; https://www.medcalc.org) were used for analyses.

Table 1 The polyp-based resect and discard strategy

Scenario	Rule		If family history of CRC (first-degree relative)
		Surveillance interval recommendation based on 2012 guidelines, yr	
1	No polyp	10	5
2	1–2 diminutive polyps (largest polyp max 5 mm)	10	5
3	1–3 small polyps (all polyps 1–9 mm and the largest polyp max < 10 mm)	5	5
4	≥ 4 polyps, any size	Follow-up pathology results	-
5	At least 1 polyp ≥ 10 mm	Follow-up pathology results	-
6	Insufficient or inadequate bowel preparation	1	-
7	Unclear	-	-
		Surveillance interval recommendation based on 2020 guidelines, yr	
1	No polyp	10	5
2	1–3 diminutive polyps; or 2 diminutive polyps and 1 small polyp	10	5
3	1–2 small polyps exclusively	10	5
4	> 3 polyps, any size, or > 2 polyps 6–9 mm	Follow-up pathology results	–
5	≥ 1 polyp ≥ 10 mm	Follow-up pathology results	–
6	Insufficient or inadequate bowel preparation	1	1

CRC: Colorectal cancer.

RESULTS

Patient and polyp characteristics

A total of 1157 patients were screened, and 944 patients with 933 polyps were included in the final analysis (mean ± SD age 62.6 ± 8.6 years; 49.3% male) (Supplementary Figure 1). Most colonoscopies were performed for screening and surveillance. Among all detected polyps, 819 (87.8%) were either diminutive or small (1–9 mm). Table 2 shows the details of patient, procedure, and polyp characteristics.

PBRD strategy surveillance intervals

The PBRD strategy based on the 2020 guidelines reached 98.0% (95%CI: 0.97–0.99) agreement with pathology-based surveillance intervals (Figure 1). Based on the 2012 guidelines, surveillance interval agreement between real-time PBRD strategy and pathology was 76.4% (95%CI: 0.74–0.79). Endoscopists using the PBRD strategy assigned shorter and longer surveillance intervals in 15.4% and 8.3% of patients, respectively. When applied post hoc, the PBRD strategy based on the 2012 guidelines reached 90.7% (95%CI: 0.89–0.92) agreement with pathology-based recommendations, with shorter and longer intervals assigned in 5.8% and 3.5% of patients, respectively. The proportion of endoscopist assigned surveillance intervals that adhered to pathology-based intervals was significantly lower than those assigned post-hoc using the same strategy ($P < 0.0001$) (Table 3). None of the patients that should have received shorter surveillance intervals through the post-hoc PBRD model had a polyp with advanced histology. Only 3/145 patients that should have been assigned to shorter surveillance intervals by endoscopists had polyps with advanced histology. Deviations from the strategy decreased as the study progressed (Figure 2).

Optical diagnosis-based surveillance intervals

A total of 842 (90.2%) polyps ≤ 10 mm were optically diagnosed using NICE; of those, 648 (69.5%) were classified with high confidence (Table 2). The agreement between surveillance intervals assigned by optical diagnosis and pathology-based intervals using 2012 guidelines was 95.8% (95%CI: 0.94–0.97) (Figure 1). The agreement with pathology for surveillance intervals assigned by optical diagnosis was significantly higher than that for both the PBRD strategy used by endoscopists ($P < 0.0001$) and the PBRD strategy calculated post-hoc based on 2012 ($P < 0.0001$). Supplementary Table 1 shows allocation of surveillance intervals between optical diagnosis and pathology.

Table 2 Patient, procedure, and polyp characteristics[1] (mean ± SD)

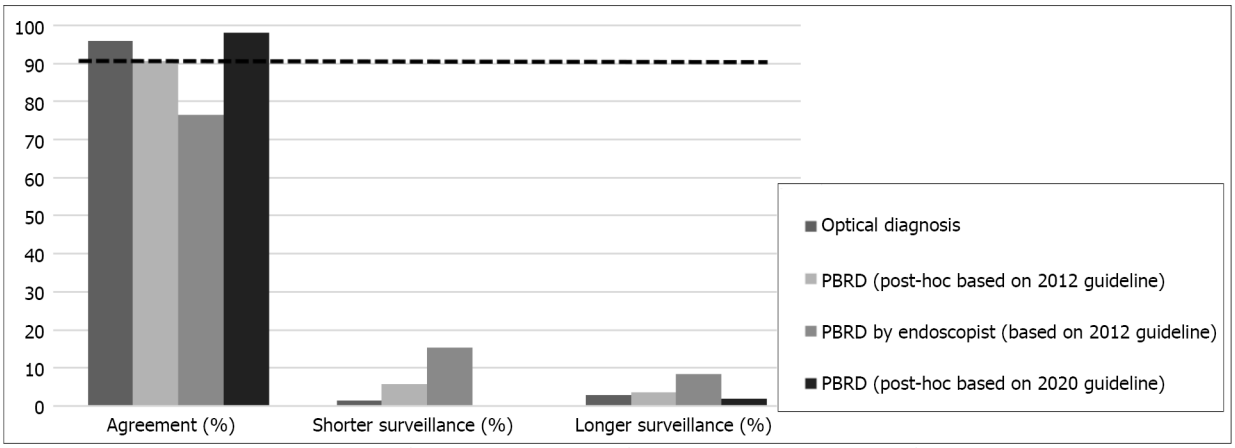
Characteristics	
Patients, *n*	**944**
Age, yr	62.6 (8.6)
Male sex, *n* (%)	465 (49.3)
Family history of CRC[2], *n* (%)	
No	682 (72.2)
Yes	259 (27.4)
Colonoscopy indication, *n* (%)	
Screening	299 (31.7)
FIT+	39 (4.1)
Adenoma surveillance	206 (21.8)
Anemia/bleeding	158 (16.7)
Diarrhea	28 (3.0)
Other	214 (22.7)
Procedures	
Bowel preparation quality, *n* (%)	
Adequate	851 (90.1)
Inadequate[3]	93 (9.9)
Cecal intubation rate, *n* (%)	902 (95.6)
Polyp detection rate[4], %	53.7%
Adenoma detection rate[4], %	36.4%
Polyps, *n*	**933**
Polyp size, mm	5.8 (8.3)
Polyp size, *n* (%)	
≤ 5 mm	689 (73.8)
6–9 mm	130 (13.9)
≥ 10 mm	114 (12.2)
Histopathology, *n* (%)	
Hyperplastic polyp	274 (29.4)
Tubular adenoma	468 (50.2)
Villous adenoma	36 (3.9)
Traditional serrated adenoma	1 (0.1)
Sessile serrated adenoma/polyp	38 (4.1)
Other	103 (11.0)
High-grade dysplasia	13 (1.4)
Tubular adenoma with HGD	3/13 (23.1)
Villous adenoma with HGD	10/13 (76.9)
Optical histology prediction based on NICE classification	842/933 (90.2)[5]
Non-neoplastic	345 (41.0)
Neoplastic	497 (59.0)
High-confidence optical diagnosis	648 (69.5)

[1]Patients with at least 1 ≤ 10 mm polyp.
[2]Unknown family history of CRC = 3 (0.3%).
[3]Defined as Boston bowel preparation score < 6.
[4]Defined as percentage of patients where at least 1 polyp/adenoma was found.
[5]All polyps were ≤ 10 mm.
CRC: Colorectal cancer; FIT: Fecal immunochemical test; HGD: High-grade dysplasia; NICE: Narrow-band imaging international colorectal endoscopic.

Table 3 Concordance between endoscopist polyp-based resect and discard strategy and post-hoc polyp-based resect and discard surveillance interval assignment compared with histopathology[1]

Endoscopist PBRD	Post-hoc PBRD			*P* value
	Shorter	Correct	Longer	
Shorter	54	89	3	< 0.0001[a]
Correct	1	714	3	
Longer	0	51	28	

[1]Surveillance intervals based on the 2012 guideline.
[a]$P < 0.05$.
PBRD: Polyp-based resect and discard.



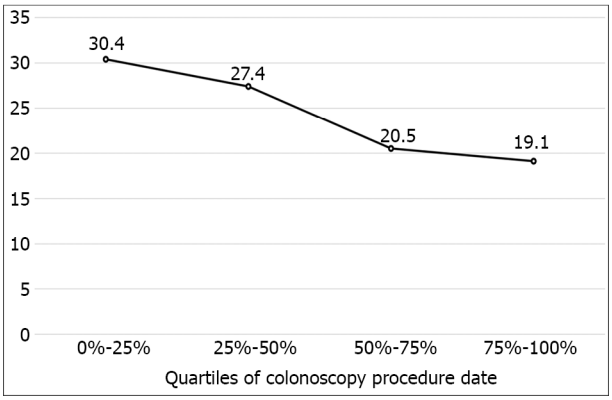
Strategy	Agreement, % (95%CI)	Shorter surveillance, % (95%CI)	Longer surveillance, % (95%CI)
Optical diagnosis (*vs* reference standard based on 2012 guideline)	95.8 (0.94–0.97)	1.4 (0.007–0.02)	2.8 (0.02–0.04)
PBRD (post-hoc *vs* reference standard based on 2012 guideline)	90.7 (0.89–0.92)	5.8 (0.04–0.07)	3.5 (0.02–0.05)
PBRD (by endoscopist *vs* reference standard based on 2012 guideline)	76.4 (0.74–0.79)	15.4 (0.13–0.18)	8.3 (0.07–0.10)
PBRD (post-hoc *vs* reference standard based on 2020 guideline)	98.0 (0.97–0.99)	0.1 (0–0.006)	1.9 (0.01–0.03)

DOI: 10.3748/wjg.v28.i19.2137 **Copyright** ©The Author(s) 2022.

Figure 1 Surveillance agreement of optical diagnosis and polyp-based resect and discard strategy compared with histopathology. The dashed black line represents the 90% agreement of surveillance interval. PBRD: Polyp-based resect and discard.

Histopathology evaluations and immediate surveillance recommendations

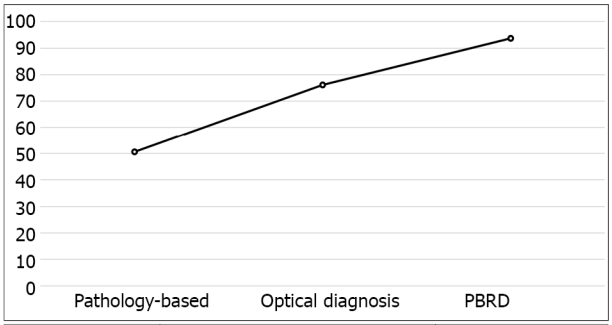
When using the standard clinical approach, 50.6% of patients could have been given an immediate surveillance recommendation post-colonoscopy. The PBRD strategy (based on 2020 guidelines) and optical diagnosis would have allowed for immediate surveillance interval recommendation in 93.7% (95%CI: 0.92–0.95, and 76.1% (95%CI: 0.73-0.79) of patients, respectively (Figure 3A). The PBRD strategy reduced 87.8% of histopathology evaluations compared with 70.6% for optical diagnosis (Figure 3B).



DOI: 10.3748/wjg.v28.i19.2137 **Copyright** ©The Author(s) 2022.

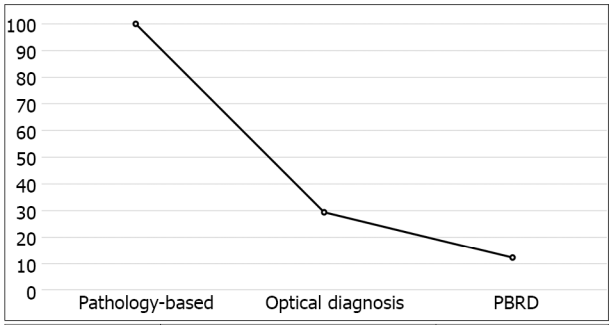
Figure 2 Proportion of the deviation from the polyp-based resect and discard strategy by endoscopists during the study by quartiles of procedure date.

A



Strategy	Immediate surveillance interval recommendations, %	95%CI
Pathology based	50.6	0.47–0.54
Optical diagnosis	76.1	0.73–0.79
PBRD	93.7	0.92–0.95

B



Strategy	Pathology examinations required, %	95%CI
Pathology based	Ref.	Ref.
Optical diagnosis	29.4	0.26–0.32
PBRD	12.2	0.10–0.15

DOI: 10.3748/wjg.v28.i19.2137 **Copyright** ©The Author(s) 2022.

Figure 3 Pathology-based outcomes, polyp-based resect and discard strategy, and optical diagnosis. A: Proportion of immediate surveillance interval recommendations provided to patients; B: Proportion of pathology examinations, the black bars represent the 95%CI. PBRD: Polyp-based resect and discard.

DISCUSSION

Our study found that surveillance interval assignment using the PBRD strategy based on the 2020 USMSTF guidelines reached 98.0% agreement with pathology. This agreement was significantly higher compared to optical diagnosis-based strategies. In contrast to optical diagnosis, the use of the PBRD strategy is independent of operator skill, leading to increased reproducibility in routine endoscopic practice.

Interestingly, we found that when the PBRD strategy was used in real-time by endoscopists, adherence to guideline recommendations was lower; endoscopists chose a different surveillance interval than the PBRD strategy in 20% of patients, possibly due to clinical information not reflected in the strategy, such as second-degree relatives with CRC or other individual factors. Our findings also reflect previously described practice patterns where endoscopists often assigned shorter surveillance intervals for low-risk lesions and normal colonoscopies, with highly variable but often low (< 50%) adherence to guidelines. Reasons for non-adherence stated in the literature included disagreement with guidelines, inadequate or suboptimal bowel preparation, and concern for missed polyps[15,16]. These factors potentially played a role in endoscopist deviations from the PBRD strategy in our study. Another explanation to these deviations could be the learning curve for PBRD implementation. We found that as the study progressed, the percentage of deviations from the PBRD strategy decreased (Figure 2).

Agreement between pathology-based and post-hoc allocation of surveillance intervals using the PBRD strategy based on 2020 USMSTF guidelines was significantly higher than the agreement between pathology-based and optical-based allocation of surveillance intervals [98.0% (95%CI: 0.97–0.99) *vs*

95.8% (95%CI: 0.94–0.97); P = 0.005]. Additionally, the agreement between optical diagnosis-based surveillance intervals and pathology surpassed the American Society for Gastrointestinal Endoscopy Preservation and Incorporation of Valuable endoscopic Innovations 90% benchmark[3]. However, agreement between surveillance interval assignments using real-time application of PBRD by endoscopists, and pathology was significantly lower than for optical diagnosis. In our study, 70% of polyps were optically classified with high confidence, similar to the rates reported by other studies[17]. Increasing the rate of high-confidence optical diagnosis would contribute to the acceptance of this technique in routine endoscopic practice, particularly for non-academic endoscopists. However, endoscopists are often reluctant to use optical diagnosis due to concerns of incorrect diagnosis, inappropriate surveillance interval assignment, and fear of potential medicolegal repercussions[10]. As our adaptation of the PBRD strategy to reflect the updated 2020 USMSTF guideline resulted in a significantly higher agreement compared with the 2012-based PBRD model [98.0% (95%CI: 0.97–0.99) *vs* 90.7% (95%CI: 0.89–0.92); P < 0.0001], we believe that the PBRD strategy may be a safe alternative that can be easily applied by endoscopists pending further research confirming efficacy in real-time endoscopic practice, and gastroenterology society endorsements. The PBRD strategy and optical diagnosis resulted in significant reductions in required histopathology evaluations, and increased the percentage of patients with same-day surveillance interval assignment. A significant proportion of post-colonoscopy colorectal cancers (PCCRCs) are due to administrative or decision-making errors[18]. Fail-safe mechanisms are therefore needed to ensure the assignment of an appropriate surveillance interval during the index session for follow-up examination. For instance, histopathology might not be followed up adequately, or patients might fail to receive their surveillance interval after pathology results are available. This would exacerbate loss to follow-up and increase the chance of PCCRC. The PBRD strategy could offer a simple solution for endoscopists to communicate the appropriate time for the next surveillance colonoscopy without requiring histopathology evaluation.

Another advantage of the PBRD strategy is that very high agreement with pathology-based surveillance intervals can be achieved without any specialized training, skill, or dedicated equipment. The PBRD strategy might be easier to implement and may address fears cited by endoscopists. As the fear of discarding polyps with advanced histology remains a significant concern and could limit the widespread adoption of resect and discard strategies, revised versions of PBRD could exclude polyps with morphology of potentially advanced lesions (*e.g.*, Paris IIc or III). Furthermore, it might be beneficial to limit the use of the PBRD strategy to diminutive polyps only, which would reduce the risk of assigning polyps with high-grade dysplasia or serrated adenomas to longer surveillance intervals, as advanced pathology occurs more frequently in polyps of 6–9 mm. Notably, the post hoc application of the PBRD strategy did not result in discarding any polyp with advanced histology in our study. Limiting this strategy to 1–3 mm polyps could also be feasible, especially when optical diagnosis is not possible and pathology examination to determine the histology of these polyps not reliable. Approaches to replace pathology for these polyps are likely safe as a recent study showed that advanced histologic features in diminutive polyps did not contribute towards metachronous CRC[19].

The emergence of new modalities such as artificial intelligence (AI)-assisted classification could provide an alternative to the proposed approach in the future. However, the accuracy of AI-based optical diagnosis in broader clinical practice with different endoscopists, platforms, and settings remains to be evaluated, with widespread clinical implementation far from reality. Furthermore, it is unlikely that every endoscopy unit could implement this cutting-edge technology immediately or at all once available. Therefore, the PRBD strategy could be used as a bridge or complementary system to AI. The current strategy of resection and histopathologic analysis of all polyps is associated with high costs. Previous studies estimated that the annual cost saving in the United States population following the adoption of a resect and discard policy for diminutive polyps ranges from United States $33 million to $1 billion annually[20]. By reducing such costs, healthcare systems could increase efficiency and reallocate savings to other resources in CRC prevention, such as screening in younger age groups.

Several limitations should be discussed. Patient recruitment was at a single academic center, limiting the generalizability of our results. Future research should assess PBRD in multicentered studies and community-based practices. The PBRD strategy could be improved by considering other important clinical factors, such as in-depth family and personal history of CRC and/or polyps, suboptimal bowel preparation score (*e.g.*, BBPS of 5 or 6), or offering more granular choices to clinicians. Furthermore, results of this study may have been improved if PBRD was limited to diminutive or 1–3 mm polyps only, due to the low prevalence of advanced histology in such polyps at the expense of lower proportion of patients with same day surveillance interval assignment and higher proportion of required pathology examinations[2].

CONCLUSION

In conclusion, the PBRD strategy reached 98.0% agreement with surveillance intervals assigned through pathology using the 2020 USMSTF guidelines. Performance with the 2012 guidelines was lower when implemented correctly but still surpassed the 90% benchmark. Optical diagnosis also performed above

the 90% benchmark in our study. Therefore, the PBRD strategy may be a feasible alternative to resect and discard that can be used without specialized equipment, training, or optical diagnosis skills.

ARTICLE HIGHLIGHTS

Research background

The majority (90%) of polyps found during colonoscopies are less than 10 mm in size, with diminutive polyps (< 5 mm) accounting for about 70%–80%. Advanced histology is found in only 1.7% of diminutive polyps and 10.1% of small polyps. Current post-polypectomy surveillance intervals are based on pathology outcomes. However, histopathologic evaluation of small polyps can incur significant costs.

Research motivation

Alternative modalities have been proposed, such as image-enhanced endoscopy-assisted optical polyp diagnosis. Limitations of the optical diagnosis included fear of making an incorrect optical diagnosis, assigning incorrect surveillance intervals, and training requirements.

Research objectives

We aimed to develop a novel resect and discard model that did not require optical diagnosis to assign colonoscopy surveillance intervals, and assigned surveillance interval based on number and size of polyps, so-called the polyp-based resect and discard (PBRD) strategy.

Research methods

In a clinical prospective study, all patients undergoing elective colonoscopies were enrolled. The polyp-based strategy was used to assign the next surveillance interval using polyp size and number. Surveillance intervals were also assigned using optical diagnosis for small polyps (< 10 mm). The primary outcome was surveillance interval agreement between the polyp-based model and the pathology-based reference standard using the 2020 United States Multi-Society Task Force guidelines.

Research results

Surveillance interval based on a polyp-based strategy achieved 98.0% (95% confidence interval: 0.97–0.99) agreement with pathology-based intervals when applied according to the current surveillance guideline.

Research conclusions

The polyp-based strategy can easily be implemented without any requirement for specialist devices and training. The majority of patients can be provided with immediate surveillance interval recommendations, without having to wait for results of pathology analysis.

Research perspectives

Future research should assess PBRD in multicentered studies and community-based practices.

FOOTNOTES

Author contributions: Taghiakbari M contributed to analysis and interpretation of data, drafting the manuscript under the supervision of von Renteln D; Hammar C and Frenn M performed the acquisition of data; Hammar C, Frenn M and von Renteln D contributed to analysis and interpretation of data, drafting of the manuscript; Frenn M, Djinbachian R, Pohl H and von Renteln D contributed to the study concept and design, critical revision of the manuscript for important intellectual content; Deslandres E, Bouchard S and Bouin M contributed to the critical revision of the manuscript for important intellectual content.

Institutional review board statement: The study protocol and data collection were approved by the local institutional research board as an amendment to the two prospective clinical studies (17.135 and 16.367, respectively).

Clinical trial registration statement: This study is registered at the Protocol Registration and Results System.

Conflict-of-interest statement: Mahsa Taghiakbari, Celia Hammar, Mira Frenn, Roupen Djinbachian, Heiko Pohl, Erik Deslandres, Simon Bouchard, and Mickael Bouin have no conflicts of interest relevant to this paper to disclose. Daniel von Renteln is supported by the "Fonds de Recherche du Québec Santé" career development award and has received research funding from ERBE, Ventage, Pendopharm and Pentax and is a consultant for Boston Scientific and Pendopharm. The findings, statements, and views expressed are those of the authors and do not represent the views of the Department of Veterans Affairs or the United States Government.

Data sharing statement: Technical appendix, statistical code, and dataset available from the corresponding author at mahsa.taghiakbari@umontreal.ca. Participants gave informed consent for data sharing. No additional data are available.

CONSORT 2010 statement: The authors have read the CONSORT 2010 Statement, and the manuscript was prepared and revised according to the CONSORT 2010 Statement.

Open-Access: This article is an open-access article that was selected by an in-house editor and fully peer-reviewed by external reviewers. It is distributed in accordance with the Creative Commons Attribution NonCommercial (CC BY-NC 4.0) license, which permits others to distribute, remix, adapt, build upon this work non-commercially, and license their derivative works on different terms, provided the original work is properly cited and the use is non-commercial. See: https://creativecommons.org/Licenses/by-nc/4.0/

Country/Territory of origin: Canada

ORCID number: Mahsa Taghiakbari 0000-0001-6011-3400; Celia Hammar 0000-0002-4371-9512; Mira Frenn 0000-0002-0336-2766; Roupen Djinbachian 0000-0002-0649-0691; Heiko Pohl 0000-0002-2778-6790; Erik Deslandres 0000-0003-0225-7347; Simon Bouchard 0000-0002-9079-4494; Mickael Bouin 0000-0003-4272-6793; Daniel von Renteln 0000-0002-6125-0068.

S-Editor: Fan JR
L-Editor: A
P-Editor: Fan JR

REFERENCES

1 **Zhang R**, Zheng Y, Mak TW, Yu R, Wong SH, Lau JY, Poon CC. Automatic Detection and Classification of Colorectal Polyps by Transferring Low-Level CNN Features From Nonmedical Domain. *IEEE J Biomed Health Inform* 2017; **21**: 41-47 [PMID: 28114040 DOI: 10.1109/JBHI.2016.2635662]
2 **Gupta N**, Bansal A, Rao D, Early DS, Jonnalagadda S, Wani SB, Edmundowicz SA, Sharma P, Rastogi A. Prevalence of advanced histological features in diminutive and small colon polyps. *Gastrointest Endosc* 2012; **75**: 1022-1030 [PMID: 22405698 DOI: 10.1016/j.gie.2012.01.020]
3 **Rex DK**, Kahi C, O'Brien M, Levin TR, Pohl H, Rastogi A, Burgart L, Imperiale T, Ladabaum U, Cohen J, Lieberman DA. The American Society for Gastrointestinal Endoscopy PIVI (Preservation and Incorporation of Valuable Endoscopic Innovations) on real-time endoscopic assessment of the histology of diminutive colorectal polyps. *Gastrointest Endosc* 2011; **73**: 419-422 [PMID: 21353837 DOI: 10.1016/j.gie.2011.01.023]
4 **ASGE Technology Committee**, Abu Dayyeh BK, Thosani N, Konda V, Wallace MB, Rex DK, Chauhan SS, Hwang JH, Komanduri S, Manfredi M, Maple JT, Murad FM, Siddiqui UD, Banerjee S. ASGE Technology Committee systematic review and meta-analysis assessing the ASGE PIVI thresholds for adopting real-time endoscopic assessment of the histology of diminutive colorectal polyps. *Gastrointest Endosc* 2015; **81**: 502.e1-502.e16 [PMID: 25597420 DOI: 10.1016/j.gie.2014.12.022]
5 **Schachschal G**, Mayr M, Treszl A, Balzer K, Wegscheider K, Aschenbeck J, Aminalai A, Drossel R, Schröder A, Scheel M, Bothe CH, Bruhn JP, Burmeister W, Stange G, Bähr C, Kießlich R, Rösch T. Endoscopic *vs* histological characterisation of polyps during screening colonoscopy. *Gut* 2014; **63**: 458-465 [PMID: 23812324 DOI: 10.1136/gutjnl-2013-304562]
6 **Kaltenbach T**, Rex DK, Wilson A, Hewett DG, Sanduleanu S, Rastogi A, Wallace M, Soetikno R. Implementation of optical diagnosis for colorectal polyps: standardization of studies is needed. *Clin Gastroenterol Hepatol* 2015; **13**: 6-10.e1 [PMID: 25511846 DOI: 10.1016/j.cgh.2014.10.009]
7 **Glover B**, Patel N, Ashrafian H, Teare J. Diagnostic accuracy of i-scan image enhancement for real-time endoscopic diagnosis of small colorectal polyps: a meta-analysis. *Therap Adv Gastroenterol* 2018; **11**: 1756284818814948 [PMID: 30574190 DOI: 10.1177/1756284818814948]
8 **van den Broek FJ**, van Soest EJ, Naber AH, van Oijen AH, Mallant-Hent RCh, Böhmer CJ, Scholten P, Stokkers PC, Marsman WA, Mathus-Vliegen EM, Curvers WL, Bergman JJ, van Eeden S, Hardwick JC, Fockens P, Reitsma JB, Dekker E. Combining autofluorescence imaging and narrow-band imaging for the differentiation of adenomas from non-neoplastic colonic polyps among experienced and non-experienced endoscopists. *Am J Gastroenterol* 2009; **104**: 1498-1507 [PMID: 19491863 DOI: 10.1038/ajg.2009.161]
9 **Kuiper T**, Marsman WA, Jansen JM, van Soest EJ, Haan YC, Bakker GJ, Fockens P, Dekker E. Accuracy for optical diagnosis of small colorectal polyps in nonacademic settings. *Clin Gastroenterol Hepatol* 2012; **10**: 1016-20; quiz e79 [PMID: 22609999 DOI: 10.1016/j.cgh.2012.05.004]
10 **Willems P**, Djinbachian R, Ditisheim S, Orkut S, Pohl H, Barkun A, Bouin M, Faulques B, von Renteln D. Uptake and barriers for implementation of the resect and discard strategy: an international survey. *Endosc Int Open* 2020; **8**: E684-E692 [PMID: 32355888 DOI: 10.1055/a-1132-5371]
11 **Duong A**, Bouin M, Leduc R, Deslandres E, Deshêtres A, Weber A, Pohl H, Barkun AN, von Renteln D. A7 the polyp-based resect-and-discard strategy. *J Can Assoc Gastroenterol* 2019; **2** (Suppl 2): 15-16 [DOI: 10.1093/jcag/gwz006.006]
12 **Patrun J**, Okreša L, Iveković H, Rustemović N. Diagnostic Accuracy of NICE Classification System for Optical

Recognition of Predictive Morphology of Colorectal Polyps. *Gastroenterol Res Pract* 2018; **2018**: 7531368 [PMID: 29725349 DOI: 10.1155/2018/7531368]

13 **Lieberman DA**, Rex DK, Winawer SJ, Giardiello FM, Johnson DA, Levin TR. Guidelines for colonoscopy surveillance after screening and polypectomy: a consensus update by the US Multi-Society Task Force on Colorectal Cancer. *Gastroenterology* 2012; **143**: 844-857 [PMID: 22763141 DOI: 10.1053/j.gastro.2012.06.001]

14 **Gupta S**, Lieberman D, Anderson JC, Burke CA, Dominitz JA, Kaltenbach T, Robertson DJ, Shaukat A, Syngal S, Rex DK. Recommendations for follow-up after colonoscopy and polypectomy: A consensus update by the us multi-society task force on colorectal cancer. *Gastroenterology* 2020; **158**: 1131-1153.e5 [PMID: 32044092 DOI: 10.1053/j.gastro.2019.10.026]

15 **Goodwin JS**, Singh A, Reddy N, Riall TS, Kuo YF. Overuse of screening colonoscopy in the Medicare population. *Arch Intern Med* 2011; **171**: 1335-1343 [PMID: 21555653 DOI: 10.1001/archinternmed.2011.212]

16 **van Heijningen EM**, Lansdorp-Vogelaar I, Steyerberg EW, Goede SL, Dekker E, Lesterhuis W, ter Borg F, Vecht J, Spoelstra P, Engels L, Bolwerk CJ, Timmer R, Kleibeuker JH, Koornstra JJ, de Koning HJ, Kuipers EJ, van Ballegooijen M. Adherence to surveillance guidelines after removal of colorectal adenomas: a large, community-based study. *Gut* 2015; **64**: 1584-1592 [PMID: 25586057 DOI: 10.1136/gutjnl-2013-306453]

17 **Iwatate M**, Sano Y, Hattori S, Sano W, Hasuike N, Ikumoto T, Kotaka M, Murakami Y, Hewett DG, Soetikno R, Kaltenbach T, Fujimori T. The addition of high magnifying endoscopy improves rates of high confidence optical diagnosis of colorectal polyps. *Endosc Int Open* 2015; **3**: E140-E145 [PMID: 26135657 DOI: 10.1055/s-0034-1391362]

18 **Kaminski MF**. Avoiding a plane crash with colonoscopy. *Endoscopy* 2022; **54**: 278-280 [PMID: 35100654 DOI: 10.1055/a-1722-2999]

19 **Tang Y**, Anandasabapathy S, Richards-Kortum R. Advances in optical gastrointestinal endoscopy: a technical review. *Mol Oncol* 2021; **15**: 2580-2599 [PMID: 32915503 DOI: 10.1002/1878-0261.12792]

20 **Kandel P**, Wallace MB. Should We Resect and Discard Low Risk Diminutive Colon Polyps. *Clin Endosc* 2019; **52**: 239-246 [PMID: 30661337 DOI: 10.5946/ce.2018.136]

World Journal of Gastroenterology

Submit a Manuscript: https://www.f6publishing.com

World J Gastroenterol 2022 May 21; 28(19): 2148-2151

DOI: 10.3748/wjg.v28.i19.2148

ISSN 1007-9327 (print) ISSN 2219-2840 (online)

LETTER TO THE EDITOR

Effects of diabetes type 2 and metformin treatment in Swedish patients with colorectal cancer

Jan Dimberg, Levar Shamoun, Kalle Landerholm, Dick Wågsäter

Specialty type: Gastroenterology and hepatology

Provenance and peer review: Unsolicited article; Externally peer reviewed.

Peer-review model: Single blind

Peer-review report's scientific quality classification

Grade A (Excellent): 0
Grade B (Very good): B, B
Grade C (Good): 0
Grade D (Fair): 0
Grade E (Poor): E

P-Reviewer: Liu J, China; Wang QY, China; Wu QN, China

Received: December 16, 2021
Peer-review started: December 16, 2021
First decision: January 27, 2022
Revised: February 1, 2022
Accepted: April 9, 2022
Article in press: April 9, 2022
Published online: May 21, 2022

Jan Dimberg, Department of Natural Science and Biomedicine, School of Health and Welfare, Jönköping University, Jönköping 551 11, Sweden

Levar Shamoun, Department of Laboratory Medicine and Pathology, Region Jönköping County, Jönköping 553 05, Sweden

Levar Shamoun, Dick Wågsäter, Department of Medical Cell Biology, Uppsala University, Uppsala 751 23, Sweden

Kalle Landerholm, Department of Surgery, Region Jönköping County, Jönköping 553 05, Sweden

Kalle Landerholm, Department of Biomedical and Clinical Sciences, Linköping University, Linköping 581 85, Sweden

Corresponding author: Dick Wågsäter, PhD, Professor, Department of Medical Cell Biology, Uppsala University, D1:3, Husargatan 3, Uppsala 751 23, Sweden. dick.wagsater@mcb.uu.se

Abstract

The association between type 2 diabetes mellitus (DM) and colorectal cancer (CRC) has been thoroughly investigated and reports have demonstrated that the risk of CRC is increased in DM patients. The association between DM and the survival of patients with CRC is controversial. Evidence suggests that metformin with its anti-inflammatory effects is a protective factor against the development of CRC among DM patients and that metformin therapy is associated with a better prognosis in patients with DM. In our cohort, we did not find any associations between the presence of DM or metformin and cancer specific survival or any relation to plasma levels of a panel of 40 inflammatory factors and irisin. On the other hand, we identified that the insulin-like growth factor binding protein 7 single nucleotide polymorphism rs2041437 was associated with DM in CRC patients. The dominance of the T bearing genotypes in patients with DM was statistically significant (P = 0.038), with an odds ratio of 1.66 (95% confidence interval: 1.03-2.69).

Key Words: Diabetes; Metformin; Cytokines; Survival; Colorectal cancer; Polymorphism

©The Author(s) 2022. Published by Baishideng Publishing Group Inc. All rights reserved.

Core Tip: Type 2 diabetes mellitus (DM) or metformin treatment does not influence mortality in colorectal cancer (CRC). Type 2 DM or metformin does not influence the levels of inflammatory factors in plasma in patients with CRC. Single nucleotide polymorphisms of insulin-like growth factor binding protein 7 are associated with type 2 DM in patients with CRC.

Citation: Dimberg J, Shamoun L, Landerholm K, Wågsäter D. Effects of diabetes type 2 and metformin treatment in Swedish patients with colorectal cancer. *World J Gastroenterol* 2022; 28(19): 2148-2151
URL: https://www.wjgnet.com/1007-9327/full/v28/i19/2148.htm
DOI: https://dx.doi.org/10.3748/wjg.v28.i19.2148

TO THE EDITOR

Having read the article "How far along are we in revealing the connection between metformin and colorectal cancer?" by Cigrovski Berkovic *et al*[1] in *World Journal of Gastroenterology* 2021, we want to contribute with some aspects and data on this matter.

Colorectal cancer (CRC) is one of the most common cancer types worldwide and several genetic pathways affecting CRC initiation and progression have been described[2]. The association between type 2 diabetes mellitus (DM) and CRC has been thoroughly investigated and reports have demonstrated that the risk of CRC is higher in DM patients[3]. However, the association between DM and the survival of patients with CRC is controversial[4,5].

Metformin is an oral glucose-lowering agent used to treat DM. It has also been reported to possess properties that inhibit the proliferation and growth of certain types of cancer[6]. Moreover, recent studies show that metformin has anti-inflammatory effects, a property that can be beneficial in conditions other than DM, such as cardiovascular disease and cancer[7].

Overall, evidence suggests that metformin could protect against the development of CRC among DM patients and that metformin therapy is associated with a better prognosis in patients with DM[1,6,8]. However, this protective role of metformin in CRC remains controversial[1,8]. In light of the above and with special reference to a report by Cigrovski Berkovic *et al*[1], we here add our observations of CRC patients (n = 408) without DM (n = 310) or with DM (n = 98), treated with metformin (n = 63) or not (n = 35), and any associations of these factors with cancer-specific survival, inflammatory factors, or single nucleotide polymorphisms (SNPs).

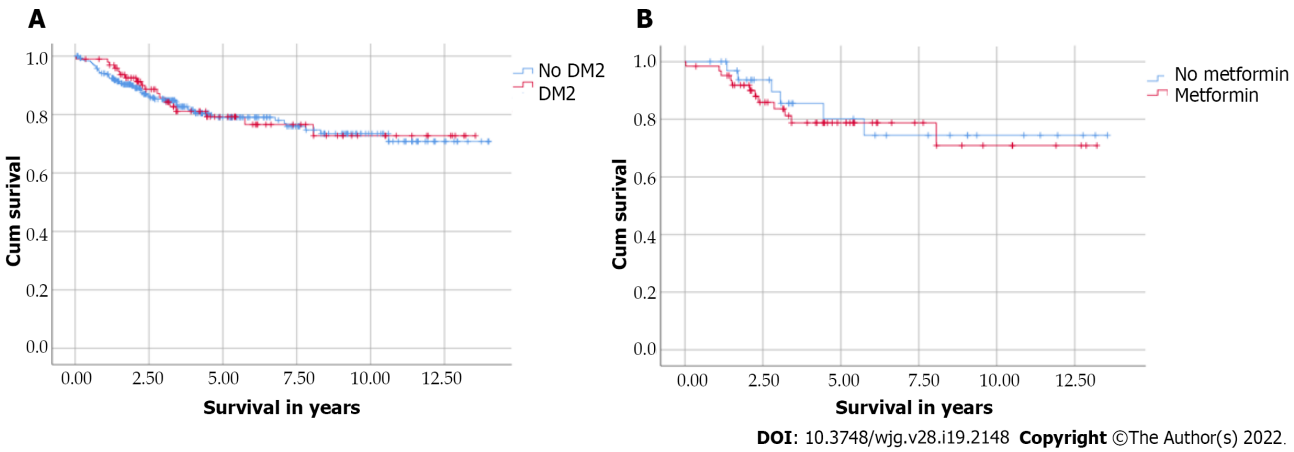
Blood samples were obtained from all consecutive CRC patients who underwent surgical resection for primary colorectal adenocarcinomas between 2006 and 2019 at the Department of Surgery, Ryhov County Hospital, Jönköping, Sweden. Follow-up for the estimation of cancer-specific survival ended on the date of death or on February 23, 2021. The patient data have been prospectively recorded in a database, comprising 236 males and 172 females with a mean age of 71 years. The study included 172 patients with rectal cancer and 236 patients with colon cancer, based on the primary tumor site. The tumors were classified as stage I in 63 patients, stage II in 148, stage III in 148, and stage IV in 49. The study was approved by the Regional Ethical Review Board in Linköping, Sweden, and informed consent was obtained from each participant.

We did not find any relationships between the presence of DM or metformin and cancer-specific survival in patients with CRC in our cohort, as demonstrated by Kaplan-Maier curves (Figure 1). Receiver operating characteristic curve analysis confirmed this result (data not shown).

Against the background that inflammation has a driving force in carcinogenesis of CRC[2] and that metformin has anti-inflammatory effects, we have applied data that we have previously published in *World J Gastroenterology*[9] regarding a panel of 40 circulating inflammatory factors in a cohort of 174 CRC patients, of whom 44 had DM and 17 were treated with metformin. We found that plasma levels of these factors did not differ between CRC patients with or without DM, whether treated with metformin or not (data not shown). This was also the case when similar analyses were performed regarding carcinoembryonic antigen (CEA) levels, which were available for 332 of the patients.

Irisin is a relatively recently discovered hormone (myokine) that is involved in the regulation of metabolic processes such as stimulation of glycogenesis and inhibition of glycogenolysis and has been suggested to play an important role in DM[10]. However, studies have reported both decreased and increased irisin levels in DM patients[10]. In a clinical study, Zhu *et al*[11] showed reduced serum levels of irisin in CRC patients and suggested that irisin might be used as a serum diagnostic marker. In our analysis, we found no general difference in cancer-specific survival depending on the levels of irisin. Nor were differences in cancer-specific survival observed in those with or without DM and with or without metformin treatment.

Insulin-like growth factor-binding protein 7 (IGFBP 7) binds strongly to insulin and has been found, by us[12] and others[13], to be increased in CRC tissue. Moreover, we have investigated the IGFBP 7 SNP rs2041437 (C > T) in relation to CRC development[12]. When adding further CRC patients (n = 340)



DOI: 10.3748/wjg.v28.i19.2148 **Copyright** ©The Author(s) 2022.

Figure 1 Kaplan-Meier curves. A: Kaplan-Meier curves for colorectal cancer patients with and without type 2 diabetes, revealing no statistically significant differences; B: Kaplan-Meier curves for patients with colorectal cancer and type 2 diabetes using or not using metformin, revealing no statistically significant differences.DM: Diabetes mellitus.

to the earlier study, we found that the rate of the CC genotype was 45.4% and that of CT/TT was 54.6% among patients without DM, while they were 33.3% and 66.7%, respectively, in patients with DM. The dominance of the T-bearing genotypes in patients with DM was statistically significant (P = 0.038), with an odds ratio of 1.66 (95% confidence interval: 1.03-2.69).

In summary, our data do not support the hypothesis that DM increases mortality in CRC or that metformin prevents death from CRC, at least in patients in Swedish healthcare. We could not see any association between circulatory inflammatory factors, irisin, or CEA levels and DM or metformin among CRC patients. On the other hand, we identified that the IGFBP 7 SNP rs2041437 was associated with DM in CRC patients. It should be pointed out that patients with metformin treatment were relatively few, rendering interpretation of data regarding this group uncertain.

FOOTNOTES

Author contributions: Dimberg J and Wågsäter D designed and coordinated the study; Shamoun L performed the experiments, and acquired and analysed the data; Dimberg J, Shamoun L, Landerholm K, and Wågsäter D interpreted the data; Landerholm K recruited the patients; Dimberg J, Landerholm K, and Wågsäter D wrote the manuscript; all authors made critical revisions to the manuscript and approved the final version of the article.

Supported by the Medical Research Council of Southeast Sweden, No. FORSS-931897; and the Division of Medical Diagnostics of Region Jönköping County, No. Futurum-970572.

Conflict-of-interest statement: The study was supported by grants from Medical Research Council of Southeast Sweden (FORSS-931897) and Division of Medical Diagnostics (Futurum-970572), Region Jönköping County, Sweden. The funding organizations had no role in the design, management, analysis, interpretation of the data, preparation, review, or approval of the manuscript.

Open-Access: This article is an open-access article that was selected by an in-house editor and fully peer-reviewed by external reviewers. It is distributed in accordance with the Creative Commons Attribution NonCommercial (CC BY-NC 4.0) license, which permits others to distribute, remix, adapt, build upon this work non-commercially, and license their derivative works on different terms, provided the original work is properly cited and the use is non-commercial. See: https://creativecommons.org/Licenses/by-nc/4.0/

Country/Territory of origin: Sweden

ORCID number: Jan Dimberg 0000-0003-2328-7334; Levar Shamoun 0000-0003-3519-7491; Kalle Landerholm 0000-0001-6808-371X; Dick Wågsäter 0000-0002-3655-2419.

S-Editor: Chen YL
L-Editor: Wang TQ
P-Editor: Chen YL

REFERENCES

1 **Berkovic MC**, Mikulic D, Bilic-Curcic I, Mrzljak A. How far along are we in revealing the connection between metformin and colorectal cancer? *World J Gastroenterol* 2021; **27**: 1362-1368 [PMID: 33911461 DOI: 10.3748/wjg.v27.i14.1362]

2 **Ahmad R**, Singh JK, Wunnava A, Al-Obeed O, Abdulla M, Srivastava SK. Emerging trends in colorectal cancer: Dysregulated signaling pathways (Review). *Int J Mol Med* 2021; **47** [PMID: 33655327 DOI: 10.3892/ijmm.2021.4847]

3 **Larsson SC**, Orsini N, Wolk A. Diabetes mellitus and risk of colorectal cancer: a meta-analysis. *J Natl Cancer Inst* 2005; **97**: 1679-1687 [PMID: 16288121 DOI: 10.1093/jnci/dji375]

4 **Noh GY**, Hwang DY, Choi YH, Lee YY. Effect of diabetes mellitus on outcomes of colorectal cancer. *J Korean Soc Coloproctol* 2010; **26**: 424-428 [PMID: 21221244 DOI: 10.3393/jksc.2010.26.6.424]

5 **Mills KT**, Bellows CF, Hoffman AE, Kelly TN, Gagliardi G. Diabetes mellitus and colorectal cancer prognosis: a meta-analysis. *Dis Colon Rectum* 2013; **56**: 1304-1319 [PMID: 24105007 DOI: 10.1097/DCR.0b013e3182a479f9]

6 **Yu H**, Zhong X, Gao P, Shi J, Wu Z, Guo Z, Wang Z, Song Y. The Potential Effect of Metformin on Cancer: An Umbrella Review. *Front Endocrinol (Lausanne)* 2019; **10**: 617 [PMID: 31620081 DOI: 10.3389/fendo.2019.00617]

7 **Bai B**, Chen H. Metformin: A Novel Weapon Against Inflammation. *Front Pharmacol* 2021; **12**: 622262 [PMID: 33584319 DOI: 10.3389/fphar.2021.622262]

8 **Wang Q**, Shi M. Effect of metformin use on the risk and prognosis of colorectal cancer in diabetes mellitus: a meta-analysis. *Anticancer Drugs* 2022; **33**: 191-199 [PMID: 34620743 DOI: 10.1097/CAD.0000000000001254]

9 **Olsen RS**, Nijm J, Andersson RE, Dimberg J, Wågsäter D. Circulating inflammatory factors associated with worse long-term prognosis in colorectal cancer. *World J Gastroenterol* 2017; **23**: 6212-6219 [PMID: 28974887 DOI: 10.3748/wjg.v23.i34.6212]

10 **Mahgoub MO**, D'Souza C, Al Darmaki RSMH, Baniyas MMYH, Adeghate E. An update on the role of irisin in the regulation of endocrine and metabolic functions. *Peptides* 2018; **104**: 15-23 [PMID: 29608940 DOI: 10.1016/j.peptides.2018.03.018]

11 **Zhu H**, Liu M, Zhang N, Pan H, Lin G, Li N, Wang L, Yang H, Yan K, Gong F. Serum and Adipose Tissue mRNA Levels of ATF3 and FNDC5/Irisin in Colorectal Cancer Patients With or Without Obesity. *Front Physiol* 2018; **9**: 1125 [PMID: 30246803 DOI: 10.3389/fphys.2018.01125]

12 **Mälarstig A**, Wågsäter D, Löfgren S, Hugander A, Zar N, Dimberg J. Tumour-derived adhesion factor in colorectal cancer. *Mol Med Rep* 2009; **2**: 971-976 [PMID: 21475929 DOI: 10.3892/mmr_00000200]

13 **Jin L**, Shen F, Weinfeld M, Sergi C. Insulin Growth Factor Binding Protein 7 (IGFBP7)-Related Cancer and IGFBP3 and IGFBP7 Crosstalk. *Front Oncol* 2020; **10**: 727 [PMID: 32500027 DOI: 10.3389/fonc.2020.00727]



Published by **Baishideng Publishing Group Inc**
7041 Koll Center Parkway, Suite 160, Pleasanton, CA 94566, USA
Telephone: +1-925-3991568
E-mail: bpgoffice@wjgnet.com
Help Desk: https://www.f6publishing.com/helpdesk
https://www.wjgnet.com



© 2022 Baishideng Publishing Group Inc. All rights reserved.

ISSN 1007-9327 (print)
ISSN 2219-2840 (online)

World Journal of *Gastroenterology*

World J Gastroenterol 2022 May 28; 28(20): 2152-2250



Published by Baishideng Publishing Group Inc

World Journal of Gastroenterology

Contents

Weekly Volume 28 Number 20 May 28, 2022

MINIREVIEWS

2152 Artificial intelligence: Emerging player in the diagnosis and treatment of digestive disease

Chen HY, Ge P, Liu JY, Qu JL, Bao F, Xu CM, Chen HL, Shang D, Zhang GX

2163 Advances in medical treatment for pancreatic neuroendocrine neoplasms

Li YL, Cheng ZX, Yu FH, Tian C, Tan HY

2176 Radiomics for the detection of microvascular invasion in hepatocellular carcinoma

Lv K, Cao X, Du P, Fu JY, Geng DY, Zhang J

ORIGINAL ARTICLE

Basic Study

2184 Long noncoding RNA TNFRSF10A-AS1 promotes colorectal cancer through upregulation of HuR

Wang DD, Sun DL, Yang SP, Song J, Wu MY, Niu WW, Song M, Zhang XL

Retrospective Cohort Study

2201 Digital single-operator video cholangioscopy improves endoscopic management in patients with primary sclerosing cholangitis-a retrospective observational study

Bokemeyer A, Lenze F, Stoica V, Sensoy TS, Kabar I, Schmidt H, Ullerich H

Retrospective Study

2214 Gadolinium-ethoxybenzyl-diethylenetriamine penta-acetic acid-enhanced magnetic resonance imaging for evaluating fibrosis regression in chronic hepatitis C patients after direct-acting antiviral

Li XH, Huang R, Yang M, Wang J, Gao YH, Jin Q, Ma DL, Wei L, Rao HY

Observational Study

2227 First prospective European study for the feasibility and safety of magnetically controlled capsule endoscopy in gastric mucosal abnormalities

Szalai M, Helle K, Lovász BD, Finta Á, Rosztóczy A, Oczella L, Madácsy L

CASE REPORT

2243 Endoscopic management of intramural spontaneous duodenal hematoma: A case report

Valerii G, Ormando VM, Cellini C, Sacco L, Barbera C

LETTER TO THE EDITOR

2248 Future prospect of "Gut microbiome composition can predict the response to nivolumab in advanced hepatocellular carcinoma patients"

Kang YB, Cai Y

ABOUT COVER

Editorial Board Member of *World Journal of Gastroenterology*, Donatella Barisani, MD, MSc, Associate Professor, School of Medicine and Surgery, University of Milano Bicocca, Via Cadore 48, Monza 20900, Italy. donatella.barisani@unimib.it

AIMS AND SCOPE

The primary aim of *World Journal of Gastroenterology* (*WJG*, *World J Gastroenterol*) is to provide scholars and readers from various fields of gastroenterology and hepatology with a platform to publish high-quality basic and clinical research articles and communicate their research findings online. *WJG* mainly publishes articles reporting research results and findings obtained in the field of gastroenterology and hepatology and covering a wide range of topics including gastroenterology, hepatology, gastrointestinal endoscopy, gastrointestinal surgery, gastrointestinal oncology, and pediatric gastroenterology.

INDEXING/ABSTRACTING

The *WJG* is now indexed in Current Contents®/Clinical Medicine, Science Citation Index Expanded (also known as SciSearch®), Journal Citation Reports®, Index Medicus, MEDLINE, PubMed, PubMed Central, and Scopus. The 2021 edition of Journal Citation Report® cites the 2020 impact factor (IF) for *WJG* as 5.742; Journal Citation Indicator: 0.79; IF without journal self cites: 5.590; 5-year IF: 5.044; Ranking: 28 among 92 journals in gastroenterology and hepatology; and Quartile category: Q2. The *WJG*'s CiteScore for 2020 is 6.9 and Scopus CiteScore rank 2020: Gastroenterology is 19/136.

RESPONSIBLE EDITORS FOR THIS ISSUE

Production Editor: *Yu-Xi Chen*; **Production Department Director:** *Xu Guo*; **Editorial Office Director:** *Ze-Mao Gong*.

NAME OF JOURNAL
World Journal of Gastroenterology

ISSN
ISSN 1007-9327 (print) ISSN 2219-2840 (online)

LAUNCH DATE
October 1, 1995

FREQUENCY
Weekly

EDITORS-IN-CHIEF
Andrzej S Tarnawski

EDITORIAL BOARD MEMBERS
http://www.wjgnet.com/1007-9327/editorialboard.htm

PUBLICATION DATE
May 28, 2022

COPYRIGHT
© 2022 Baishideng Publishing Group Inc

INSTRUCTIONS TO AUTHORS
https://www.wjgnet.com/bpg/gerinfo/204

GUIDELINES FOR ETHICS DOCUMENTS
https://www.wjgnet.com/bpg/GerInfo/287

GUIDELINES FOR NON-NATIVE SPEAKERS OF ENGLISH
https://www.wjgnet.com/bpg/gerinfo/240

PUBLICATION ETHICS
https://www.wjgnet.com/bpg/GerInfo/288

PUBLICATION MISCONDUCT
https://www.wjgnet.com/bpg/gerinfo/208

ARTICLE PROCESSING CHARGE
https://www.wjgnet.com/bpg/gerinfo/242

STEPS FOR SUBMITTING MANUSCRIPTS
https://www.wjgnet.com/bpg/GerInfo/239

ONLINE SUBMISSION
https://www.f6publishing.com

© 2022 Baishideng Publishing Group Inc. All rights reserved. 7041 Koll Center Parkway, Suite 160, Pleasanton, CA 94566, USA
E-mail: bpgoffice@wjgnet.com https://www.wjgnet.com

World Journal of Gastroenterology

Submit a Manuscript: https://www.f6publishing.com

World J Gastroenterol 2022 May 28; 28(20): 2152-2162

DOI: 10.3748/wjg.v28.i20.2152

ISSN 1007-9327 (print) ISSN 2219-2840 (online)

MINIREVIEWS

Artificial intelligence: Emerging player in the diagnosis and treatment of digestive disease

Hai-Yang Chen, Peng Ge, Jia-Yue Liu, Jia-Lin Qu, Fang Bao, Cai-Ming Xu, Hai-Long Chen, Dong Shang, Gui-Xin Zhang

Specialty type: Gastroenterology and hepatology

Provenance and peer review: Invited article; Externally peer reviewed.

Peer-review model: Single blind

Peer-review report's scientific quality classification

Grade A (Excellent): A
Grade B (Very good): B
Grade C (Good): 0
Grade D (Fair): 0
Grade E (Poor): 0

P-Reviewer: Salvi M, Italy; Shafqat S, Pakistan

Received: September 24, 2021
Peer-review started: September 24, 2021
First decision: November 16, 2021
Revised: November 24, 2021
Accepted: April 24, 2022
Article in press: April 24, 2022
Published online: May 28, 2022

Hai-Yang Chen, Peng Ge, Jia-Yue Liu, Jia-Lin Qu, Fang Bao, Cai-Ming Xu, Hai-Long Chen, Dong Shang, Gui-Xin Zhang, Laboratory of Integrative Medicine, The First Affiliated Hospital of Dalian Medical University, Dalian 116011, Liaoning Province, China

Hai-Yang Chen, Peng Ge, Jia-Yue Liu, Fang Bao, Cai-Ming Xu, Hai-Long Chen, Dong Shang, Gui-Xin Zhang, Department of General Surgery, Pancreatic-Biliary Center, The First Affiliated Hospital of Dalian Medical University, Dalian 116011, Liaoning Province, China

Jia-Lin Qu, Cai-Ming Xu, Hai-Long Chen, Dong Shang, Gui-Xin Zhang, Institute (College) of Integrative Medicine, Dalian Medical University, Dalian 116044, Liaoning Province, China

Corresponding author: Gui-Xin Zhang, PhD, Professor, Director, Department of General Surgery, Pancreatic-Biliary Center, The First Affiliated Hospital of Dalian Medical University, No. 222 Zhongshan Road, Dalian 116011, Liaoning Province, China. zgx0109@126.com

Abstract

Given the breakthroughs in key technologies, such as image recognition, deep learning and neural networks, artificial intelligence (AI) continues to be increasingly developed, leading to closer and deeper integration with an increasingly data-, knowledge- and brain labor-intensive medical industry. As society continues to advance and individuals become more aware of their health needs, the problems associated with the aging of the population are receiving increasing attention, and there is an urgent demand for improving medical technology, prolonging human life and enhancing health. Digestive system diseases are the most common clinical diseases and are characterized by complex clinical manifestations and a general lack of obvious symptoms in the early stage. Such diseases are very difficult to diagnose and treat. In recent years, the incidence of diseases of the digestive system has increased. As AI applications in the field of health care continue to be developed, AI has begun playing an important role in the diagnosis and treatment of diseases of the digestive system. In this paper, the application of AI in assisted diagnosis and the application and prospects of AI in malignant and benign digestive system diseases are reviewed.

Key Words: Artificial intelligence; Digestive disease; Convolutional neural network; Deep learning; Review

©The Author(s) 2022. Published by Baishideng Publishing Group Inc. All rights reserved.

Core Tip: With the continuous development of artificial intelligence, its integration in the field of medical and health care has received increasing attention, allowing the development and application of medical expert systems and artificial neural networks in the medical field. The development of artificial intelligence has resulted in not only more accurate diagnoses of digestive system diseases but also new treatments. Further research on the progress of artificial intelligence in digestive system diseases is needed to better serve patients.

Citation: Chen HY, Ge P, Liu JY, Qu JL, Bao F, Xu CM, Chen HL, Shang D, Zhang GX. Artificial intelligence: Emerging player in the diagnosis and treatment of digestive disease. *World J Gastroenterol* 2022; 28(20): 2152-2162
URL: https://www.wjgnet.com/1007-9327/full/v28/i20/2152.htm
DOI: https://dx.doi.org/10.3748/wjg.v28.i20.2152

INTRODUCTION

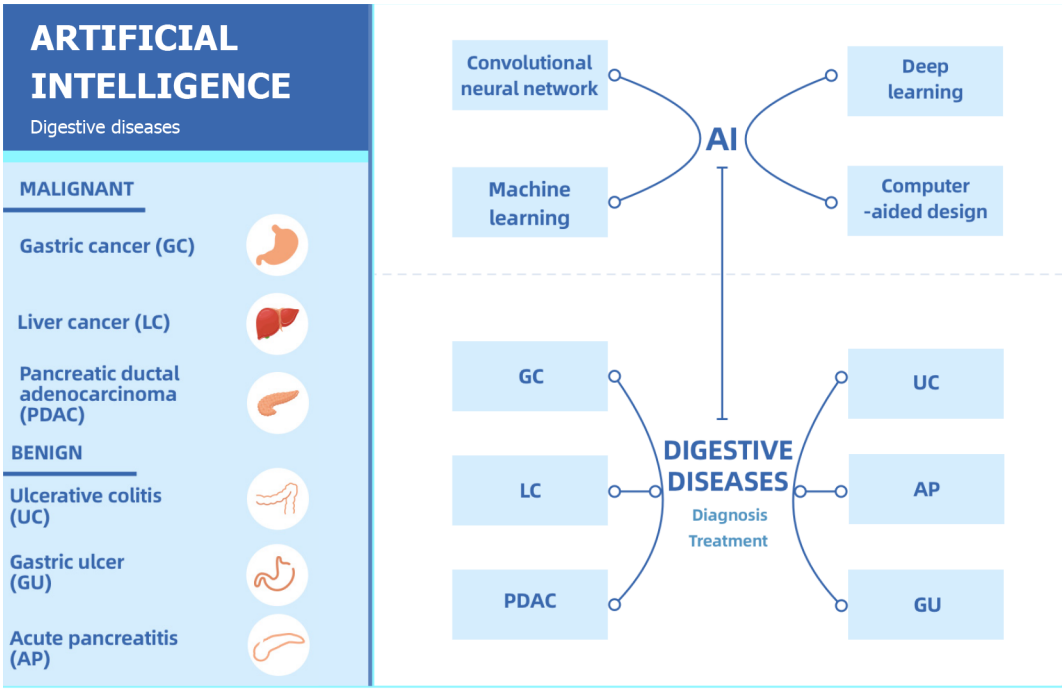
Artificial intelligence (AI) is a branch of computer science[1] inspired by human intelligence that operates in a different way. AI can be considered a set of computing techniques that allow machines to sense, learn, reason, act, *etc.* AI was first used at the Dartmouth AI Conference in the summer of 1956, which is considered the official birth of AI. In the 1990s, as technology continued to improve, hardware became more affordable, performance became more reliable, computing power, storage capacity and the ability to process data were greatly improved, and AI returned to life. In recent years, the application of AI in the medical field has reached an unprecedented height and scale. To date, great progress has been achieve in the use of AI in medicine and health, including speech recognition, medical imaging, wearable devices, risk management, pathology, *etc*[2].

The digestive system contains the largest number of organs in the human body and can be divided into the digestive tract and digestive glands. The digestive tract includes the oral cavity, pharynx, esophagus, stomach, duodenum, small intestine, large intestine, colon, *etc*. The digestive glands comprise the salivary glands, liver, pancreas, *etc.* The digestive system digests food, takes up nutrients and eliminates waste. The coordination of gastrointestinal physiological activities depends on the completion of the normal physiological function of the digestive system. Digestive system diseases, which are the most common clinical diseases, have complicated clinical manifestations, are interrelated with each other, and form a hot spot in the medical field[3]. The incidence of digestive system diseases is high, and often, there are no obvious symptoms in the early stage. Consequently, most digestive diseases are first noted in the middle and late stages; at this point, the prognosis is poor. As AI technology has continued to be developed, its strong computing power and learning ability have been gradually applied to solve complex medical problems. In the field of digestive diseases, such as gastric, liver, and pancreatic cancer and ulcerative colitis, AI can help improve the accuracy and sensitivity of the diagnosis and provide treatment options (Figure 1). AI not only improves the diagnostic accuracy of the disease but also provides a plan for clinical treatment.

In this review, we discuss AI and related technologies, their applications in digestive diseases and their future developments. We used PubMed and Google to search for relevant articles by using the keywords “digestive system diseases”, “artificial intelligence”, “machine learning”, “deep learning”, “computer-aided diagnosis”, “convolutional neural network”, and “endoscopy and endoscope images” for this review.

AI AUXILIARY DIAGNOSIS

In China, the development of AI has received considerable attention, particularly in the application of AI in the medical field. The development of AI has laid a solid foundation for precision medicine. In 2017, the China State Council announced that AI application should be promoted in the health care system. Subsequently, hundreds of new companies dedicated to the application of medical AI have emerged in China, promoting the development of AI in the medical field[4]. AI effectively improves the uneven allocation of medical resources, reduces medical costs and enhances medical efficiency. AI algorithms improve the ease of medical work and lead to not only technological innovations but also a transformation of the medical service mode. AI is applied in all fields of medicine and health, especially in the auxiliary diagnosis of diseases, and includes the following three aspects: intelligent guidance, electronic health records and risk monitoring of diagnosis and treatment.



DOI: 10.3748/wjg.v28.i20.2152 **Copyright** © The Author(s) 2022.

Figure 1 Artificial intelligence and digestive diseases. AI: Artificial intelligence; GC: Gastric cancer; LC: Liver cancer; PDAC: Pancreatic ductal adenocarcinoma; UC: Ulcerative colitis; AP: Acute pancreatitis; GU: Gastric ulcer.

Intelligent guidance

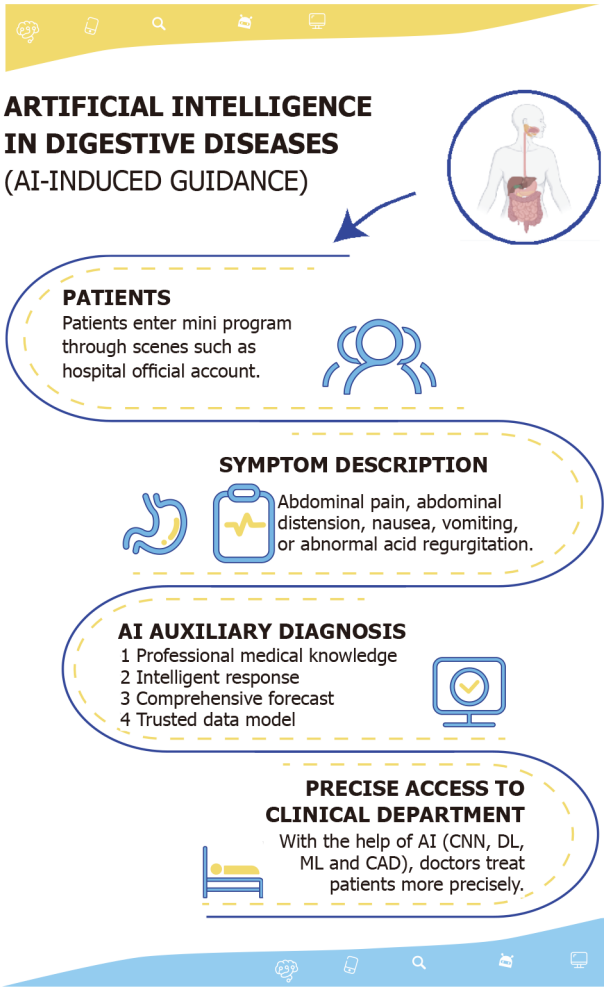
Outpatient triage has gradually transitioned from a traditional manual system to an internet- and intelligence-based system. Most admitted patients lack an understanding of their disease and the hospital. To improve the efficiency and experience of the patients, intelligent guidance systems have been developed. Patients enter the Mini Program through screens on official hospital accounts to describe symptoms or diseases, and guidance assistants intelligently follow up and guide the patients to provide symptoms to accurately match departments, recommend doctors with the most consistent professional direction, and perform online guidance registration in one step. The research and development leading to intelligent guidance systems has led to a reduction in not only the workload of outpatient staff but also the human resource needs and costs of hospitals. These systems can guide patients to seek medical treatment quickly and accurately, improve the accuracy of patient registration and the efficiency of the physician response, increase efficiency at all steps of the patient stay, and effectively provide accurate medical treatment (Figure 2).

Electronic health record

Traditional health records are typically kept on paper, which tend to be scattered in hospital archives, limiting their value. The widespread use of the internet has facilitated the creation of electronic health records (EHRs), which are currently widely used worldwide[5]. EHRs can improve management processes, overcome problems with paper documentation, and ensure the quality of treatment. Both theoretically and practically, EHRs have guiding and economic value, while their applicative value continues to improve. In addition, EHRs can improve clinical decision-making, collaboration between health care teams, and medical efficiency.

Risk monitoring of diagnosis and treatment

Diagnostic risk monitoring systems can improve the diagnostic accuracy and greatly reduce the risk of misdiagnosis, and in this regard, AI has significant advantages over clinical experience. Compared with the United States, domestic equipment is used much more frequently under the same resource allocation[6]. This is the main point of medical care in China. Additionally, the large associated workload and high repeatability result in a cumbersome manual analysis and diagnosis. An accurate diagnosis rate is important for ensuring that radiologists can provide high-quality care to patients. A report in 1999 showed that 98000 people die of misdiagnosis each year, and diagnostic errors by radiologists are a key contributor[7]. Under a heavy workload, the diagnosis results can only be judged and analyzed by subjective individual experience, leading to high misdiagnosis and missed diagnosis rates. The large market demand for pathologists and diagnostic efficiency have also led to new challenges in the medical service industry. However, digestive system diseases increasingly depend on auxiliary diagnoses based on medical images while continuing to demonstrate a yearly increase in



DOI: 10.3748/wjg.v28.i20.2152 **Copyright** © The Author(s) 2022.

Figure 2 Artificial intelligence and Intelligent guidance. CNN: Convolutional neural network; DL: Deep learning; ML: machine learning; CAD: Computer-aided design.

incidence.

The emergence of AI has led to its gradual use in digestive diseases. Machine learning (ML) is a branch of AI that aims to predict results by analyzing existing data and performing calculations based on an understanding of these data. Deep learning (DL) is a relatively new branch of ML that imitates learning through machine algorithms and provides a set of possible and reasonable solutions[8,9]. In esophageal cancer, van der Sommen *et al*[10] developed an automatic algorithm to distinguish early neoplastic lesions. Huang *et al*[11] used 84 images from 30 patients to train an AI-based neural network model to predict Helicobacter pylori infection. DL can be used to share more comprehensive medical diagnosis and treatment information with doctors with lightweight methods. At a higher level, we can comprehensively manage and guide the overall diagnosis and treatment level of the physician team to build a more scientific, accurate and friendly diagnosis and treatment risk monitoring system.

MALIGNANT DIGESTIVE DISEASES

The digestive system is a common site for malignant tumors, particularly gastric cancer, liver cancer, colorectal cancer and pancreatic cancer. Given the changes in lifestyle, diet and disease spectrum of the population, the incidence of malignant tumors of the digestive system continues to rise[12]. The early diagnosis of malignant tumors is critical for treatment, but patients with malignant tumors often have no obvious symptoms at the early stage, leading to difficulties in early diagnosis. This section summarizes the application of AI in the following three types of malignant tumors with high morbidity and mortality: gastric, liver and pancreatic cancer. The latest clinical studies concerning AI, gastric cancer, liver cancer, and pancreatic ductal adenocarcinoma are summarized in Table 1.

Table 1 Recent researches on artificial intelligence in malignant digestive system diseases

Ref.	Study design	Study population	Year	Disease	Country/Region	Number of cases	Methods	Results
Tang *et al*[48]	Retrospective	Hospital	2020	GC	China	45240 Images	DCNN	Accuracy: 85.1%-91.2%; Sensitivity: 85.9%-95.5%; Specificity: 81.7%-90.3%; AUC: 0.887-0.940
Zhang *et al*[49]	Retrospective	Hospital	2020	GC	China	21,217 Images	CNN	Accuracy: 78.7%
Nagao *et al*[50]	Retrospective	Hospital	2020	GC	Japan	16557 images	CNN	Accuracy: WLI (94.5%); Accuracy: NBI (94.3%); Accuracy: Indigo (95.5%)
Song *et al*[51]	Retrospective	Hospital	2020	GC	China	3212 Images	DL	Accuracy: 0.873; Sensitivity: 0.996; Specificity: 0.843; AUC: 0.986
Ma *et al*[52]	Retrospective	Hospital	2020	GC	China	763 Images	CNN	Accuracy: 98.4%; Specificity: 98.9%; Sensitivity: 98.0%;
Zhen *et al*[17]	Retrospective	Hospital	2020	LC	China	31608 Images	CNN	AUC: 0.946
Giordano *et al*[53]	Retrospective	Hospital	2020	LC	Italy	167 Cases	SVM, RF	Accuracy: Exceeded 94%
Jeong *et al*[54]	Retrospective	Cancer Institute	2020	LC	China	1421 Cases	DL	AUC: 0.84
Appelbaum *et al*[31]	Retrospective	Hospital	2020	PDAC	America	594 Cases	LR	AUC: 0.71
Marya *et al*[44]	Retrospective	Hospital	2020	PDAC	America	1174461 EUS Images	EUS-CNN	Sensitivity: 99%; Specificity: 98%
Tonozuka *et al*[55]	Retrospective	Hospital	2020	PDAC	Japan	920 Cases	EUS-CAD	AUC: 0.94

GC: Gastric cancer; LC: Liver cancer; PDAC: Pancreatic ductal adenocarcinoma; DCNN: Deep convolutional neural network; CNN: Convolutional neural network; DL: Deep learning; SVM: Support vector machine; RF: Random forest; LR: Logistic regression; EUS-CNN: Endoscopic ultrasound convolutional neural network; EUS-CAD: Computer-assisted diagnosis system using deep learning analysis of EUS images; AUC: area under the curve; WLI: White-light imaging; NBI: Nonmagnifying narrow-band imaging.

AI and gastric cancer

Gastric cancer (GC) is the fifth most common cancer and ranks third in cancer mortality worldwide, with more than 1 million new cases and 780000 deaths each year[13]. The stage at which GC is diagnosed can greatly affect the prognosis, with a poor prognosis typical in the late stage and a 5-year survival rate of early GC (EGC) exceeding 90%[14]. There are two difficulties in the early diagnosis of GC. First, EGC is difficult to detect, often presenting with slight reddish bulges or depressions under endoscopy that are not easily distinguished from inflammatory lesions. The second difficulty lies in judging the depth of the invasion of GC. In general, intramucosal GC or GC invading the superficial submucosal layer should be resected endoscopically, while GC invading the deep submucosal layer should be resected with open surgery; otherwise, there could be a risk of lymph node and distant metastasis. However, it is difficult to distinguish among these three forms of GC. The rapid development of DL and ML has led to great progress in AI, whose image recognition has transcended that of humans. By reviewing the published literature, this section discusses the diagnosis, treatment and prognosis of GC with AI.

Hirasawa *et al*[15] constructed a diagnostic system based on a convolutional neural network (CNN). The authors used 13584 endoscopic images to train the web-based learning model and 2296 GC images from 69 patients to evaluate its performance. The model took 47 s to analyze 2296 images and correctly diagnosed 77 GC lesions with a total sensitivity of 92%. This web-based learning model for the detection of EGC processes a large number of stored endoscopic images with clinical-related diagnostic capabilities in a very short time and may play a role in real-time gastroscopy[15].

Kubota *et al*[16] used a back propagation neural network algorithm to analyze the depth of gastric wall infiltration in endoscopic images of 344 GC patients and developed a computer-aided design (CAD) system. The cross-validation results revealed that the diagnostic accuracy of T1, T2, T3 and T4 GC was 77%, 49%, 51% and 55%, respectively. The accuracy in detecting intramucosal carcinoma (T1a) and submucosal invasive carcinoma (T1b) is 69%[16]. This study may be used to screen for EGC in the near future.

AI and liver cancer

Liver cancer (LC) is the second leading cause of death worldwide, and its incidence continues to increase[17]. In recent years, AI has been used in various aspects of LC diagnosis and treatment, especially in the field of imaging. However, individual differences in liver morphology and the internal anatomy and the highly heterogeneous molecular and pathological features of LC lead to great challenges in the implementation of AI, ML and DL for the diagnosis and treatment of this disease[18].

The following two modes of AI application are commonly used in the diagnosis of LC: DL and radiomics. Imaging plays a key role in the identification and diagnosis of hepatobiliary diseases and the establishment of surgical treatment plans. Radiologists and surgeons demarcate organs and diagnose diseases based on their experience and judgment, which can be subjective, time consuming and unreproducible; AI can address these limitations. DL is mainly used for the diagnosis of LC *via* traditional machine learning (TML) and CNNs. In TML, a well-developed anatomical model must be established in advance and manually corrected in the later stages[19], while the application of CNNs allows images to be directly used in the learning process, allowing the extraction and utilization of all information contained in the image for DL[20]. Shaw Hospital of Zhejiang University developed a DL system for liver tumor diagnosis through a CNN. In addition to learning more than 30000 magnetic resonance (MR) images, the system incorporates patient clinical data (medical records, examination results, etc.) and demonstrates excellent diagnostic performance with a coincidence rate with a final pathological result of 92%[17].

The application of AI in the treatment of LC has led to new opportunities and challenges, promoting the standardization and intelligence of LC management. Hu *et al*[21] used 3D visualization to evaluate the spatial relationship between tumors and surrounding blood vessels before hepatectomy, which serves as a suitable guide for surgical resection. In the treatment of LC by radiofrequency ablation, fusion imaging can integrate enhanced computed tomography (CT)/MR images with real-time ultrasound imaging by electromagnetic tracking to accurately locate the target lesions[22-24]. AI has been applied to all aspects of LC treatment and auxiliary diagnosis, but further prospective research is needed.

AI and pancreatic ductal adenocarcinoma

Pancreatic ductal adenocarcinoma (PDAC) is a rapidly progressive and highly malignant tumor of the digestive tract[25]. Although many methods have been developed for the diagnosis and treatment of PDAC in recent years, the effective rate of treatment and prognosis remain poor (the 5-year survival rate is only 9%[26]). The early detection and accurate treatment of PDAC are important directions requiring urgent solutions.

Recently, rapid developments have been achieved in the AI-based screening and diagnosis of PDAC, leading to acceptable effects. Ansari *et al*[27] applied artificial neural networks (ANNs) to a long-term survival prediction of patients after radical surgery for PDAC for the first time and achieved a consistency index of 0.79, indicating that their ANN could predict the survival rate of PDAC patients after radical surgery. Fine needle aspiration (FNA) biopsy is an elaborate approach used to diagnose solid masses of the pancreas. Due to the small number of cases, its development is limited. Momeni-Boroujeni *et al*[28] used a multilayer-perceptron neural network (MNN) to evaluate 277 cell mass images from 75 pancreatic FNA patients and achieved an accuracy of 100% in the classification of benign and malignant tumors. In particular, the sensitivity and specificity of MNN in identifying atypical cases were 80% and 75%, respectively. Intraductal papillary mucinous neoplasm (IPMN), a papillary mucinous tumor with many subtypes, has particular malignant potential. Endoscopic ultrasonography (EUS) can reveal the structure of the pancreas and the dilation of the pancreatic duct and can be used to evaluate the degree of malignancy of IPMN. Indeed, Kuwahara *et al*[29] used AI to build a system to perform this function. The authors uploaded 3970 EUS images of 50 patients to the system for DL analysis. The endpoint of their system was the accuracy in diagnosing the malignancy degree of IPMNs by AI. The results showed that the AI system had significantly better value in diagnosing malignant IPMNs than benign IPMNs, with an area under the receiver operating characteristic curve of 0.91 in diagnosing malignant IPMNs. In addition, a three-dimensional depth supervised segmentation network has been developed to classify CT images from PDAC patients and control groups. Chu *et al*[30] standardized the number of cases, the sizes of the segmented images, and the selection of organs and then segmented the boundaries of the abdominal organs and pancreatic tumors in 575 control subjects and 750 patients with PDAC. The results showed that the sensitivity and specificity of the algorithm in detecting PDAC in patients were 94.1% and 98.5%, respectively. The early diagnosis of PDAC is a problem that many physicians find difficult. Appelbaum *et al*[31] developed a risk model for the prediction of PDAC based on patient EHRs that could identify high-risk groups one year in advance,

suggesting that their risk scores could also be used as an initial filter for PDAC.

BENIGN DIGESTIVE DISEASES

In addition to gastric cancer, liver cancer and other malignant tumors, other digestive system diseases include ulcerative colitis, pancreatitis, gastric ulcer, gastritis, intestinal polyp and other benign digestive system diseases. We summarize the application of AI for the benign digestive system diseases discussed below. The latest applications of AI in ulcerative colitis, severe acute pancreatitis, gastric ulcers, gastritis and intestinal polyps are summarized in Table 2.

AI and ulcerative colitis

Ulcerative colitis (UC) is a common chronic intestinal disease; however, there is no single gold standard for the diagnosis of this disease. Combining clinical, laboratory, imaging, endoscopic and histopathological findings, the diagnosis is made by excluding infectious and other noninfectious forms of colitis [32]. Endoscopy is essential, but the accuracy and precision of the diagnosis are limited by doctors' subjectivity. Yao *et al*[33] established a fully automatic endoscopic disease grading video analysis system through AI. These authors used a CNN to train models to predict the amount of information in still images and, thus, determine the severity of the disease. Then, the authors examined 51 and 264 videos from developed high-resolution and multicenter clinical trial test sets, respectively. The results showed that the static image information classification system had good performance, with a sensitivity of 0.902 and specificity of 0.870. For the high-resolution videos, the fully automated methods correctly predicted the Mayo endoscopic score (MES) in 78%. The automated MES grading of the clinical trial videos (often low resolution) correctly distinguished remitted *vs* active disease in 83.7%. To analyze endoscopic images of UC more accurately, Takenaka *et al*[34] developed a deep neural network system and tested 40758 colonoscopy images and 6885 biopsy results from 2012 UC patients. The results identified endoscopic remission with 90.1% accuracy and histologic remission with 92.9% accuracy. In addition, Maeda *et al*[35] developed a CAD system to predict persistent histologic inflammation using endocytoscopy and evaluated its accuracy using 12900 endocytoscopy images. The results showed that the CAD system provided a diagnostic sensitivity, specificity, and accuracy of 74%, 97% and 91%, respectively. In recent years, great progress has been achieved in the treatment of UC, but surgery remains important [36]. These results show that AI has great potential in the diagnosis and treatment of UC.

AI and pancreatitis

Acute pancreatitis (AP) is a common clinical acute abdomen disease with a complex and variable presentation. Severe AP (SAP) is often life threatening, with multiple organ dysfunction induced by SAP being a particularly difficult clinical problem[37]. Qiu *et al*[38] developed three ML algorithms to predict the risk of organ failure in moderate SAP (MSAP) and SAP. These authors inputted 16 parameters from 263 patients with MSAP and SAP into a support vector machine (SVM), logical regression analysis (LRA) and ANN models. The results showed that the SVM, LRA and ANN models could effectively predict the risk of multiorgan failure in MSAP and SAP. Respiratory failure is the main cause of early death in SAP. The early prediction of acute lung injury (ALI) is beneficial for reducing mortality from SAP. The ANN model established by Fei *et al*[39] can effectively predict the occurrence of ALI induced by SAP, with the accuracy of predicting severe acute respiratory distress syndrome reaching 82.8%. Abdominal infection is an important risk factor for organ failure induced by SAP. Compared with logistic regression analyses, the ANN model developed by Qiu *et al*[40] can more accurately predict abdominal infection in MSAP and SAP, with a sensitivity and specificity of 80.99% and 89.44%, respectively. Fei *et al*[41] constructed and verified an ANN model based on clinical and laboratory data from 72 patients with AP. Notably, the sensitivity, specificity, positive predictive value and negative predictive value of the ANN model for portosplenomesenteric venous thrombosis (PSMVT) were 80%, 85.7%, 77.6% and 90.7%, respectively. Thus, this model provides a good reference for the clinical prediction of the occurrence of PSMVT. The recurrence rate after the first attack of AP is approximately 22%, but few indicators can predict this recurrence. Chen *et al*[42] developed a quantitative radiology model based on contrast-enhanced CT. The results of the verification analysis showed that the model can predict the recurrence of AP well in the main and verification populations, with accuracies of 87.1% and 89.0%, respectively. This finding suggests that their model may be a good quantitative method for the prediction of recurrence in patients with AP. Chronic pancreatitis (CP), which is another common clinical digestive system disease, is an important factor in inducing pancreatic cancer. Although traditional pancreaticoduodenectomy, distal pancreatectomy, and the Frey and Beger procedures have achieved considerable success in relieving CP pain, the approaches are often accompanied by serious complications. Therefore, minimally invasive surgery and robot platforms are gradually being applied in the surgical treatment of CP. A retrospective study based on 812 cases of robotic pancreatectomy and reconstruction showed that the robotic platform is safe and feasible in performing complex pancreatectomy to alleviate the sequelae of CP[43]. Autoimmune pancreatitis (AIP) is a rare and special type of chronic pancreatitis, and its diagnosis is clinically challenging. Marya *et al*

Table 2 Recent researches on artificial intelligence in benign digestive system diseases

Ref.	Study design	Study population	Year	Disease	Country/Region	Number of cases	Methods	Results
Maeda *et al*[35]	Retrospective	Hospital	2019	UC	Japan	12900 Images	CAD	Sensitivity: 74%; Specificity: 97%; Accuracy: 91%
Popa *et al*[56]	Retrospective	Hospital	2020	UC	Romania	55 Cases	ML	Accuracy: 90%; AUC: 0.92
Tong *et al*[57]	Retrospective	Hospital	2020	UC	China	6399 Cases	RF, CNN	Sensitivity: RF (0.89); Sensitivity: CNN (0.90)
Qiu *et al*[38]	Retrospective	Hospital	2019	SAP	China	263 Cases	ANN	Sensitivity: 80.99%; Specificity: 89.44%
Chen *et al*[42]	Retrospective	Hospital	2019	SAP	China	389 Cases	LR	Accuracy: 87.1%
Namikawa *et al*[45]	Retrospective	Hospital	2020	Gastric ulcer	Japan	720 Images	A-CNN	Sensitivity: 93.3%; Specificity: 99.0%; PPV: 99.1%
Steinbuss *et al*[46]	Retrospective	Hospital	2020	Gastritis	Germany	1230 Images	CNN	Accuracy: 84%; Sensitivity: 100%; Specificity: 93%
Ozawa *et al*[47]	Retrospective	Hospital	2020	Colorectal polyps	Japan	16418 Images	CNN	Sensitivity: 92%; PPV: 86%

UC: Ulcerative colitis; SAP: Severe acute pancreatitis; CAD: Computer-aided diagnosis; ML: Machine learning; RF: Random forest; CNN: Convolutional neural network; ANN: Artificial neural networks; LR: Logistic regression; A-CNN: Advanced convolutional neural network; AUC: Area under the curve; PPV: Positive predictive value.

[44] developed and validated a CNN model based on a database containing 174461 EUS images and videos from 583 patients. After training, the model could accurately distinguish AIP from PDAC and other benign pancreatic diseases with a sensitivity and specificity of 90% and 85%, respectively.

AI and other diseases

AI has been used in numerous applications for other diseases, such as gastric ulcers, gastritis and colorectal polyps. Namikawa *et al*[45] developed an advanced CNN (A-CNN) based on the original convolutional neural network and evaluated its applicability in the classification of gastric ulcers. These authors used 720 images from 120 patients with gastric ulcers to evaluate the diagnostic performance of the A-CNN. The results showed that the sensitivity, specificity, and positive predictive value of the A-CNN in classifying gastric ulcers were 93.3%, 99.0%, and 99.1%, respectively. There are several subtypes of gastritis, including autoimmune, bacterial, and chemical. Steinbuss *et al*[46] evaluated the ability of a CNN to classify the common gastritis subtypes using a small data set of 1230 gastric antrum and corpus biopsy images. The results showed that the overall accuracy in the test set was 84%, and the sensitivity and specificity for bacterial gastritis were 100% and 93%, respectively. Ozawa *et al*[47] constructed a deep CNN architecture and trained the CNN using 16418 images from 4752 colorectal polyps and 4013 normal colorectal images. Then, the performance of the trained CNN was verified with 7077 additional colonoscopy images. The results showed that the sensitivity of the CNN was 92%, and the positive predictive value was 86%, proving that it has excellent potential as a colonoscopy CP-diagnosis support system based on AI.

CONCLUSION

With the steady development of AI and its heavy integration in the medical industry, AI has received increasing attention in the fields of medicine and health. Digestive system AI technology differs from other AI technologies because of the nonstandard nature of most digestive endoscopic images and the large number of influencing factors, resulting in difficulty in developing such technology. Currently, AI plays an important role in digestive system diseases, particularly in its gradual application in diagnosis and treatment in the clinic. AI has broad prospects in the field of medicine and health, but the cooperation of medical workers and computer experts is needed to develop more intelligent applications and higher-quality services for patients. In summary, as an emerging player, AI will continue to play an increasingly important role in future development. The close combination of AI and medicine can address problems, such as the insufficient supply and uneven distribution of medical resources and

low degree of medical efficiency. More in-depth research should be performed to investigate the application of AI in digestive system diseases from various perspectives to obtain additional diagnosis and treatment measures, promote diagnosis, optimize treatment, improve patient prognosis, and gradually achieve intelligent and accurate medical treatment.

FOOTNOTES

Author contributions: Chen HY, Ge P, Liu JY contributed equally to the manuscript; Chen HY conceived this review and drafted the manuscript; Ge P, Liu JY, Bao F and Qu JL are responsible for the figure drawing and literature collation; Xu CM, Chen HL and Shang D edited and finalized the manuscript for submission; Zhang GX reviewed and approved the submitted manuscript.

Supported by Key Discipline of Liaoning Traditional Chinese Medicine Clinical Ability Promote Construction Project, No. LNZYXZY201903; and Development Guidance Plan Projects in Liaoning Province, No. 2019JH-8/10300028.

Conflict-of-interest statement: There is no conflict of interest associated with any of the senior author or other coauthors contributed their efforts in this manuscript.

Open-Access: This article is an open-access article that was selected by an in-house editor and fully peer-reviewed by external reviewers. It is distributed in accordance with the Creative Commons Attribution NonCommercial (CC BY-NC 4.0) license, which permits others to distribute, remix, adapt, build upon this work non-commercially, and license their derivative works on different terms, provided the original work is properly cited and the use is non-commercial. See: https://creativecommons.org/Licenses/by-nc/4.0/

Country/Territory of origin: China

ORCID number: Hai-Yang Chen 0000-0002-6705-2249; Peng Ge 0000-0002-2647-2474; Jia-Yue Liu 0000-0001-9294-7493; Jia-Lin Qu 0000-0003-2020-4783; Fang Bao 0000-0002-1609-2953; Cai-Ming Xu 0000-0001-7794-2301; Hai-Long Chen 0000-0001-5247-7343; Dong Shang 0000-0002-4300-359X; Gui-Xin Zhang 0000-0002-6171-394X.

S-Editor: Wang JL
L-Editor: A
P-Editor: Wang JL

REFERENCES

1 **Parasher G**, Wong M, Rawat M. Evolving role of artificial intelligence in gastrointestinal endoscopy. *World J Gastroenterol* 2020; **26**: 7287-7298 [PMID: 33362384 DOI: 10.3748/wjg.v26.i46.7287]
2 **Sensakovic WF**, Mahesh M. Role of the Medical Physicist in the Health Care Artificial Intelligence Revolution. *J Am Coll Radiol* 2019; **16**: 393-394 [PMID: 30446397 DOI: 10.1016/j.jacr.2018.09.022]
3 **Togashi K**. Applications of artificial intelligence to endoscopy practice: The view from Japan Digestive Disease Week 2018. *Dig Endosc* 2019; **31**: 270-272 [PMID: 30681203 DOI: 10.1111/den.13354]
4 **He J**, Baxter SL, Xu J, Zhou X, Zhang K. The practical implementation of artificial intelligence technologies in medicine. *Nat Med* 2019; **25**: 30-36 [PMID: 30617336 DOI: 10.1038/s41591-018-0307-0]
5 **Rudin RS**, Friedberg MW, Shekelle P, Shah N, Bates DW. Getting Value From Electronic Health Records: Research Needed to Improve Practice. *Ann Intern Med* 2020; **172**: S130-S136 [PMID: 32479182 DOI: 10.7326/M19-0878]
6 **Hershberger AG**. Review of 'Delivering Health Care in America: A Systems Approach, 3rd edition'. 2005
7 **Kohn LT**, Corrigan JM, Donaldson MS; Institute of Medicine (US) Committee on Quality of Health Care in America. To err is human: building a safer health system. Washington: National Academies Press (US), 2000: 245-246 [PMID: 25077248 DOI: 10.17226/9728]
8 **Schmidhuber J**. Deep learning in neural networks: an overview. *Neural Netw* 2015; **61**: 85-117 [PMID: 25462637 DOI: 10.1016/j.neunet.2014.09.003]
9 **Deo RC**. Machine Learning in Medicine. *Circulation* 2015; **132**: 1920-1930 [PMID: 26572668 DOI: 10.1161/CIRCULATIONAHA.115.001593]
10 **van der Sommen F**, Zinger S, Curvers WL, Bisschops R, Pech O, Weusten BL, Bergman JJ, de With PH, Schoon EJ. Computer-aided detection of early neoplastic lesions in Barrett's esophagus. *Endoscopy* 2016; **48**: 617-624 [PMID: 27100718 DOI: 10.1055/s-0042-105284]
11 **Huang CR**, Sheu BS, Chung PC, Yang HB. Computerized diagnosis of Helicobacter pylori infection and associated gastric inflammation from endoscopic images by refined feature selection using a neural network. *Endoscopy* 2004; **36**: 601-608 [PMID: 15243882 DOI: 10.1055/s-2004-814519]
12 **Bray F**, Ferlay J, Soerjomataram I, Siegel RL, Torre LA, Jemal A. Global cancer statistics 2018: GLOBOCAN estimates of incidence and mortality worldwide for 36 cancers in 185 countries. *CA Cancer J Clin* 2018; **68**: 394-424 [PMID: 30207593 DOI: 10.3322/caac.21492]
13 **Hirasawa T**, Ikenoyama Y, Ishioka M, Namikawa K, Horiuchi Y, Nakashima H, Fujisaki J. Current status and future

perspective of artificial intelligence applications in endoscopic diagnosis and management of gastric cancer. *Dig Endosc* 2021; **33**: 263-272 [PMID: 33159692 DOI: 10.1111/den.13890]

14 **Sano T**, Coit DG, Kim HH, Roviello F, Kassab P, Wittekind C, Yamamoto Y, Ohashi Y. Proposal of a new stage grouping of gastric cancer for TNM classification: International Gastric Cancer Association staging project. *Gastric Cancer* 2017; **20**: 217-225 [PMID: 26897166 DOI: 10.1007/s10120-016-0601-9]

15 **Hirasawa T**, Aoyama K, Tanimoto T, Ishihara S, Shichijo S, Ozawa T, Ohnishi T, Fujishiro M, Matsuo K, Fujisaki J, Tada T. Application of artificial intelligence using a convolutional neural network for detecting gastric cancer in endoscopic images. *Gastric Cancer* 2018; **21**: 653-660 [PMID: 29335825 DOI: 10.1007/s10120-018-0793-2]

16 **Kubota K**, Kuroda J, Yoshida M, Ohta K, Kitajima M. Medical image analysis: computer-aided diagnosis of gastric cancer invasion on endoscopic images. *Surg Endosc* 2012; **26**: 1485-1489 [PMID: 22083334 DOI: 10.1007/s00464-011-2036-z]

17 **Zhen SH**, Cheng M, Tao YB, Wang YF, Juengpanich S, Jiang ZY, Jiang YK, Yan YY, Lu W, Lue JM, Qian JH, Wu ZY, Sun JH, Lin H, Cai XJ. Deep Learning for Accurate Diagnosis of Liver Tumor Based on Magnetic Resonance Imaging and Clinical Data. *Front Oncol* 2020; **10**: 680 [PMID: 32547939 DOI: 10.3389/fonc.2020.00680]

18 **Calderaro J**, Ziol M, Paradis V, Zucman-Rossi J. Molecular and histological correlations in liver cancer. *J Hepatol* 2019; **71**: 616-630 [PMID: 31195064 DOI: 10.1016/j.jhep.2019.06.001]

19 **Wang CJ**, Hamm CA, Savic LJ, Ferrante M, Schobert I, Schlachter T, Lin M, Weinreb JC, Duncan JS, Chapiro J, Letzen B. Deep learning for liver tumor diagnosis part II: convolutional neural network interpretation using radiologic imaging features. *Eur Radiol* 2019; **29**: 3348-3357 [PMID: 31093705 DOI: 10.1007/s00330-019-06214-8]

20 **Hamm CA**, Wang CJ, Savic LJ, Ferrante M, Schobert I, Schlachter T, Lin M, Duncan JS, Weinreb JC, Chapiro J, Letzen B. Deep learning for liver tumor diagnosis part I: development of a convolutional neural network classifier for multi-phasic MRI. *Eur Radiol* 2019; **29**: 3338-3347 [PMID: 31016442 DOI: 10.1007/s00330-019-06205-9]

21 **Hu M**, Hu H, Cai W, Mo Z, Xiang N, Yang J, Fang C. The Safety and Feasibility of Three-Dimensional Visualization Technology Assisted Right Posterior Lobe Allied with Part of V and VIII Sectionectomy for Right Hepatic Malignancy Therapy. *J Laparoendosc Adv Surg Tech A* 2018; **28**: 586-594 [PMID: 29172950 DOI: 10.1089/lap.2017.0479]

22 **Citone M**, Fanelli F, Falcone G, Mondaini F, Cozzi D, Miele V. A closer look to the new frontier of artificial intelligence in the percutaneous treatment of primary lesions of the liver. *Med Oncol* 2020; **37**: 55 [PMID: 32424627 DOI: 10.1007/s12032-020-01380-y]

23 **Ahn SJ**, Lee JM, Lee DH, Lee SM, Yoon JH, Kim YJ, Lee JH, Yu SJ, Han JK. Real-time US-CT/MR fusion imaging for percutaneous radiofrequency ablation of hepatocellular carcinoma. *J Hepatol* 2017; **66**: 347-354 [PMID: 27650284 DOI: 10.1016/j.jhep.2016.09.003]

24 **Huang Q**, Zeng Q, Long Y, Tan L, Zheng R, Xu E, Li K. Fusion imaging techniques and contrast-enhanced ultrasound for thermal ablation of hepatocellular carcinoma - A prospective randomized controlled trial. *Int J Hyperthermia* 2019; **36**: 1207-1215 [PMID: 31813295 DOI: 10.1080/02656736.2019.1687945]

25 **Iovanna J**. Implementing biological markers as a tool to guide clinical care of patients with pancreatic cancer. *Transl Oncol* 2021; **14**: 100965 [PMID: 33248412 DOI: 10.1016/j.tranon.2020.100965]

26 **Siegel RL**, Miller KD, Jemal A. Cancer statistics, 2020. *CA Cancer J Clin* 2020; **70**: 7-30 [PMID: 31912902 DOI: 10.3322/caac.21590]

27 **Ansari D**, Nilsson J, Andersson R, Regnér S, Tingstedt B, Andersson B. Artificial neural networks predict survival from pancreatic cancer after radical surgery. *Am J Surg* 2013; **205**: 1-7 [PMID: 23245432 DOI: 10.1016/j.amjsurg.2012.05.032]

28 **Momeni-Boroujeni A**, Yousefi E, Somma J. Computer-assisted cytologic diagnosis in pancreatic FNA: An application of neural networks to image analysis. *Cancer Cytopathol* 2017; **125**: 926-933 [PMID: 28885766 DOI: 10.1002/cncy.21915]

29 **Kuwahara T**, Hara K, Mizuno N, Okuno N, Matsumoto S, Obata M, Kurita Y, Koda H, Toriyama K, Onishi S, Ishihara M, Tanaka T, Tajika M, Niwa Y. Usefulness of Deep Learning Analysis for the Diagnosis of Malignancy in Intraductal Papillary Mucinous Neoplasms of the Pancreas. *Clin Transl Gastroenterol* 2019; **10**: 1-8 [PMID: 31117111 DOI: 10.14309/ctg.0000000000000045]

30 **Chu LC**, Park S, Kawamoto S, Wang Y, Zhou Y, Shen W, Zhu Z, Xia Y, Xie L, Liu F, Yu Q, Fouladi DF, Shayesteh S, Zinreich E, Graves JS, Horton KM, Yuille AL, Hruban RH, Kinzler KW, Vogelstein B, Fishman EK. Application of Deep Learning to Pancreatic Cancer Detection: Lessons Learned From Our Initial Experience. *J Am Coll Radiol* 2019; **16**: 1338-1342 [PMID: 31492412 DOI: 10.1016/j.jacr.2019.05.034]

31 **Appelbaum L**, Cambronero JP, Stevens JP, Horng S, Pollick K, Silva G, Haneuse S, Piatkowski G, Benhaga N, Duey S, Stevenson MA, Mamon H, Kaplan ID, Rinard MC. Development and validation of a pancreatic cancer risk model for the general population using electronic health records: An observational study. *Eur J Cancer* 2021; **143**: 19-30 [PMID: 33278770 DOI: 10.1016/j.ejca.2020.10.019]

32 **Ooi CJ**, Fock KM, Makharia GK, Goh KL, Ling KL, Hilmi I, Lim WC, Kelvin T, Gibson PR, Gearry RB, Ouyang Q, Sollano J, Manatsathit S, Rerknimitr R, Wei SC, Leung WK, de Silva HJ, Leong RW; Asia Pacific Association of Gastroenterology Working Group on Inflammatory Bowel Disease. The Asia-Pacific consensus on ulcerative colitis. *J Gastroenterol Hepatol* 2010; **25**: 453-468 [PMID: 20370724 DOI: 10.1111/j.1440-1746.2010.06241.x]

33 **Yao H**, Najarian K, Gryak J, Bishu S, Rice MD, Waljee AK, Wilkins HJ, Stidham RW. Fully automated endoscopic disease activity assessment in ulcerative colitis. *Gastrointest Endosc* 2021; **93**: 728-736.e1 [PMID: 32810479 DOI: 10.1016/j.gie.2020.08.011]

34 **Takenaka K**, Ohtsuka K, Fujii T, Negi M, Suzuki K, Shimizu H, Oshima S, Akiyama S, Motobayashi M, Nagahori M, Saito E, Matsuoka K, Watanabe M. Development and Validation of a Deep Neural Network for Accurate Evaluation of Endoscopic Images From Patients With Ulcerative Colitis. *Gastroenterology* 2020; **158**: 2150-2157 [PMID: 32060000 DOI: 10.1053/j.gastro.2020.02.012]

35 **Maeda Y**, Kudo SE, Mori Y, Misawa M, Ogata N, Sasanuma S, Wakamura K, Oda M, Mori K, Ohtsuka K. Fully automated diagnostic system with artificial intelligence using endocytoscopy to identify the presence of histologic inflammation associated with ulcerative colitis (with video). *Gastrointest Endosc* 2019; **89**: 408-415 [PMID: 30268542 DOI: 10.1016/j.gie.2018.09.024]

36 **Crippa J**, Carvello M, Kotze PG, Spinelli A. Robotic Surgery in Inflammatory Bowel Disease. *Curr Drug Targets* 2021;

22: 112-116 [PMID: 33109059 DOI: 10.2174/1389450121999200820125918]
37 **Ge P**, Luo Y, Okoye CS, Chen H, Liu J, Zhang G, Xu C. Intestinal barrier damage, systemic inflammatory response syndrome, and acute lung injury: A troublesome trio for acute pancreatitis. *Biomed Pharmacother* 2020; **132**: 110770 [PMID: 33011613 DOI: 10.1016/j.biopha.2020.110770]
38 **Qiu Q**, Nian YJ, Guo Y, Tang L, Lu N, Wen LZ, Wang B, Chen DF, Liu KJ. Development and validation of three machine-learning models for predicting multiple organ failure in moderately severe and severe acute pancreatitis. *BMC Gastroenterol* 2019; **19**: 118 [PMID: 31272385 DOI: 10.1186/s12876-019-1016-y]
39 **Fei Y**, Gao K, Li WQ. Artificial neural network algorithm model as powerful tool to predict acute lung injury following to severe acute pancreatitis. *Pancreatology* 2018; **18**: 892-899 [PMID: 30268673 DOI: 10.1016/j.pan.2018.09.007]
40 **Qiu Q**, Nian YJ, Tang L, Guo Y, Wen LZ, Wang B, Chen DF, Liu KJ. Artificial neural networks accurately predict intra-abdominal infection in moderately severe and severe acute pancreatitis. *J Dig Dis* 2019; **20**: 486-494 [PMID: 31328389 DOI: 10.1111/1751-2980.12796]
41 **Fei Y**, Hu J, Li WQ, Wang W, Zong GQ. Artificial neural networks predict the incidence of portosplenomesenteric venous thrombosis in patients with acute pancreatitis. *J Thromb Haemost* 2017; **15**: 439-445 [PMID: 27960048 DOI: 10.1111/jth.13588]
42 **Chen Y**, Chen TW, Wu CQ, Lin Q, Hu R, Xie CL, Zuo HD, Wu JL, Mu QW, Fu QS, Yang GQ, Zhang XM. Radiomics model of contrast-enhanced computed tomography for predicting the recurrence of acute pancreatitis. *Eur Radiol* 2019; **29**: 4408-4417 [PMID: 30413966 DOI: 10.1007/s00330-018-5824-1]
43 **Hamad A**, Zenati MS, Nguyen TK, Hogg ME, Zeh HJ 3rd, Zureikat AH. Safety and feasibility of the robotic platform in the management of surgical sequelae of chronic pancreatitis. *Surg Endosc* 2018; **32**: 1056-1065 [PMID: 29273874 DOI: 10.1007/s00464-017-6010-2]
44 **Marya NB**, Powers PD, Chari ST, Gleeson FC, Leggett CL, Abu Dayyeh BK, Chandrasekhara V, Iyer PG, Majumder S, Pearson RK, Petersen BT, Rajan E, Sawas T, Storm AC, Vege SS, Chen S, Long Z, Hough DM, Mara K, Levy MJ. Utilisation of artificial intelligence for the development of an EUS-convolutional neural network model trained to enhance the diagnosis of autoimmune pancreatitis. *Gut* 2021; **70**: 1335-1344 [PMID: 33028668 DOI: 10.1136/gutjnl-2020-322821]
45 **Namikawa K**, Hirasawa T, Nakano K, Ikenoyama Y, Ishioka M, Shiroma S, Tokai Y, Yoshimizu S, Horiuchi Y, Ishiyama A, Yoshio T, Tsuchida T, Fujisaki J, Tada T. Artificial intelligence-based diagnostic system classifying gastric cancers and ulcers: comparison between the original and newly developed systems. *Endoscopy* 2020; **52**: 1077-1083 [PMID: 32503056 DOI: 10.1055/a-1194-8771]
46 **Steinbuss G**, Kriegsmann K, Kriegsmann M. Identification of Gastritis Subtypes by Convolutional Neuronal Networks on Histological Images of Antrum and Corpus Biopsies. *Int J Mol Sci* 2020; **21** [PMID: 32932860 DOI: 10.3390/ijms21186652]
47 **Ozawa T**, Ishihara S, Fujishiro M, Kumagai Y, Shichijo S, Tada T. Automated endoscopic detection and classification of colorectal polyps using convolutional neural networks. *Therap Adv Gastroenterol* 2020; **13**: 1756284820910659 [PMID: 32231710 DOI: 10.1177/1756284820910659]
48 **Tang D**, Wang L, Ling T, Lv Y, Ni M, Zhan Q, Fu Y, Zhuang D, Guo H, Dou X, Zhang W, Xu G, Zou X. Development and validation of a real-time artificial intelligence-assisted system for detecting early gastric cancer: A multicentre retrospective diagnostic study. *EBioMedicine* 2020; **62**: 103146 [PMID: 33254026 DOI: 10.1016/j.ebiom.2020.103146]
49 **Zhang L**, Zhang Y, Wang L, Wang J, Liu Y. Diagnosis of gastric lesions through a deep convolutional neural network. *Dig Endosc* 2021; **33**: 788-796 [PMID: 32961597 DOI: 10.1111/den.13844]
50 **Nagao S**, Tsuji Y, Sakaguchi Y, Takahashi Y, Minatsuki C, Niimi K, Yamashita H, Yamamichi N, Seto Y, Tada T, Koike K. Highly accurate artificial intelligence systems to predict the invasion depth of gastric cancer: efficacy of conventional white-light imaging, nonmagnifying narrow-band imaging, and indigo-carmine dye contrast imaging. *Gastrointest Endosc* 2020; **92**: 866-873.e1 [PMID: 32592776 DOI: 10.1016/j.gie.2020.06.047]
51 **Song Z**, Zou S, Zhou W, Huang Y, Shao L, Yuan J, Gou X, Jin W, Wang Z, Chen X, Ding X, Liu J, Yu C, Ku C, Liu C, Sun Z, Xu G, Wang Y, Zhang X, Wang D, Wang S, Xu W, Davis RC, Shi H. Clinically applicable histopathological diagnosis system for gastric cancer detection using deep learning. *Nat Commun* 2020; **11**: 4294 [PMID: 32855423 DOI: 10.1038/s41467-020-18147-8]
52 **Ma B**, Guo Y, Hu W, Yuan F, Zhu Z, Yu Y, Zou H. Artificial Intelligence-Based Multiclass Classification of Benign or Malignant Mucosal Lesions of the Stomach. *Front Pharmacol* 2020; **11**: 572372 [PMID: 33132910 DOI: 10.3389/fphar.2020.572372]
53 **Giordano S**, Takeda S, Donadon M, Saiki H, Brunelli L, Pastorelli R, Cimino M, Soldani C, Franceschini B, Di Tommaso L, Lleo A, Yoshimura K, Nakajima H, Torzilli G, Davoli E. Rapid automated diagnosis of primary hepatic tumour by mass spectrometry and artificial intelligence. *Liver Int* 2020; **40**: 3117-3124 [PMID: 32662575 DOI: 10.1111/liv.14604]
54 **Jeong S**, Ge Y, Chen J, Gao Q, Luo G, Zheng B, Sha M, Shen F, Cheng Q, Sui C, Liu J, Wang H, Xia Q, Chen L. Latent Risk Intrahepatic Cholangiocarcinoma Susceptible to Adjuvant Treatment After Resection: A Clinical Deep Learning Approach. *Front Oncol* 2020; **10**: 143 [PMID: 32140448 DOI: 10.3389/fonc.2020.00143]
55 **Tonozuka R**, Itoi T, Nagata N, Kojima H, Sofuni A, Tsuchiya T, Ishii K, Tanaka R, Nagakawa Y, Mukai S. Deep learning analysis for the detection of pancreatic cancer on endosonographic images: a pilot study. *J Hepatobiliary Pancreat Sci* 2021; **28**: 95-104 [PMID: 32910528 DOI: 10.1002/jhbp.825]
56 **Popa IV**, Burlacu A, Mihai C, Prelipcean CC. A Machine Learning Model Accurately Predicts Ulcerative Colitis Activity at One Year in Patients Treated with Anti-Tumour Necrosis Factor α Agents. *Medicina (Kaunas)* 2020; **56** [PMID: 33233514 DOI: 10.3390/medicina56110628]
57 **Tong Y**, Lu K, Yang Y, Li J, Lin Y, Wu D, Yang A, Li Y, Yu S, Qian J. Can natural language processing help differentiate inflammatory intestinal diseases in China? *BMC Med Inform Decis Mak* 2020; **20**: 248 [PMID: 32993636 DOI: 10.1186/s12911-020-01277-w]

World Journal of Gastroenterology

Submit a Manuscript: https://www.f6publishing.com

World J Gastroenterol 2022 May 28; 28(20): 2163-2175

DOI: 10.3748/wjg.v28.i20.2163

ISSN 1007-9327 (print) ISSN 2219-2840 (online)

MINIREVIEWS

Advances in medical treatment for pancreatic neuroendocrine neoplasms

Yuan-Liang Li, Zi-Xuan Cheng, Fu-Huan Yu, Chao Tian, Huang-Ying Tan

Specialty type: Oncology

Provenance and peer review: Invited article; Externally peer reviewed.

Peer-review model: Single blind

Peer-review report's scientific quality classification

Grade A (Excellent): A
Grade B (Very good): 0
Grade C (Good): C
Grade D (Fair): 0
Grade E (Poor): 0

P-Reviewer: Fujimori N, Japan; Maurea S, Italy

Received: October 27, 2021
Peer-review started: October 27, 2021
First decision: December 27, 2021
Revised: December 31, 2021
Accepted: April 15, 2022
Article in press: April 15, 2022
Published online: May 28, 2022

Yuan-Liang Li, Zi-Xuan Cheng, Fu-Huan Yu, Chao Tian, Huang-Ying Tan, Department of Integrative Oncology, China-Japan Friendship Hospital, Beijing 100029, China

Yuan-Liang Li, Zi-Xuan Cheng, Fu-Huan Yu, Chao Tian, Graduate School, Beijing University of Chinese Medicine, Beijing 100029, China

Corresponding author: Huang-Ying Tan, MD, PhD, Professor, Department of Integrative Oncology, China-Japan Friendship Hospital, No. 2 Yinghuayuan East Street, Chaoyang District, Beijing 100029, China. tanhuangying@263.net

Abstract

Pancreatic neuroendocrine neoplasms (PanNENs) are rare neoplasms with strong heterogeneity that have experienced an increasing incidence rate in recent years. For patients with locally advanced or distant metastatic PanNENs, systemic treatment options vary due to the different differentiations, grades and stages. The available options for systemic therapy include somatostatin analogs, molecularly targeted agents, cytotoxic chemotherapeutic agents, immune checkpoint inhibitors, and peptide receptor radionuclide therapy. In addition, the development of novel molecularly targeted agents is currently in progress. The sequence of selection between different chemotherapy regimens has been of great interest, and resistance to chemotherapeutic agents is the major limitation in their clinical application. Novel agents and high-level clinical evidence continue to emerge in the field of antiangiogenic agents. Peptide receptor radionuclide therapy is increasingly employed for the treatment of advanced neuroendocrine tumors, and greater therapeutic efficacy may be achieved by emerging radiolabeled peptides. Since immune checkpoint inhibitor monotherapies for PanNENs appear to have limited antitumor activity, dual immune checkpoint inhibitor therapies or combinations of antiangiogenic therapies and immune checkpoint inhibitors have been applied in the clinic to improve clinical efficacy. Combining the use of a variety of agents with different mechanisms of action provides new possibilities for clinical treatments. In the future, the study of systemic therapies will continue to focus on the screening of the optimal benefit population and the selection of the best treatment sequence strategy with the aim of truly achieving individualized precise treatment of PanNENs.

Key Words: Pancreatic neuroendocrine neoplasms; Advanced neuroendocrine tumors; Medical treatment; Peptide receptor radionuclide therapy; Advances

©The Author(s) 2022. Published by Baishideng Publishing Group Inc. All rights reserved.

Core Tip: Pancreatic neuroendocrine neoplasms (PanNENs) are rare neoplasms with strong heterogeneity. The systemic treatment options of advanced PanNENs vary due to the different differentiations, grades and stages and include somatostatin analogs, molecularly targeted agents, cytotoxic chemotherapeutic agents, immune checkpoint inhibitors, and peptide receptor radionuclide therapy. Despite the multiple systemic therapeutic options for PanNENs, problems such as drug resistance, adverse side effects and limited scope of application still exist. Thus, we review the clinical development of medical treatment options, focusing on ongoing clinical studies and the development of novel targeted drugs, to provide a reference for clinicians and researchers.

Citation: Li YL, Cheng ZX, Yu FH, Tian C, Tan HY. Advances in medical treatment for pancreatic neuroendocrine neoplasms. *World J Gastroenterol* 2022; 28(20): 2163-2175
URL: https://www.wjgnet.com/1007-9327/full/v28/i20/2163.htm
DOI: https://dx.doi.org/10.3748/wjg.v28.i20.2163

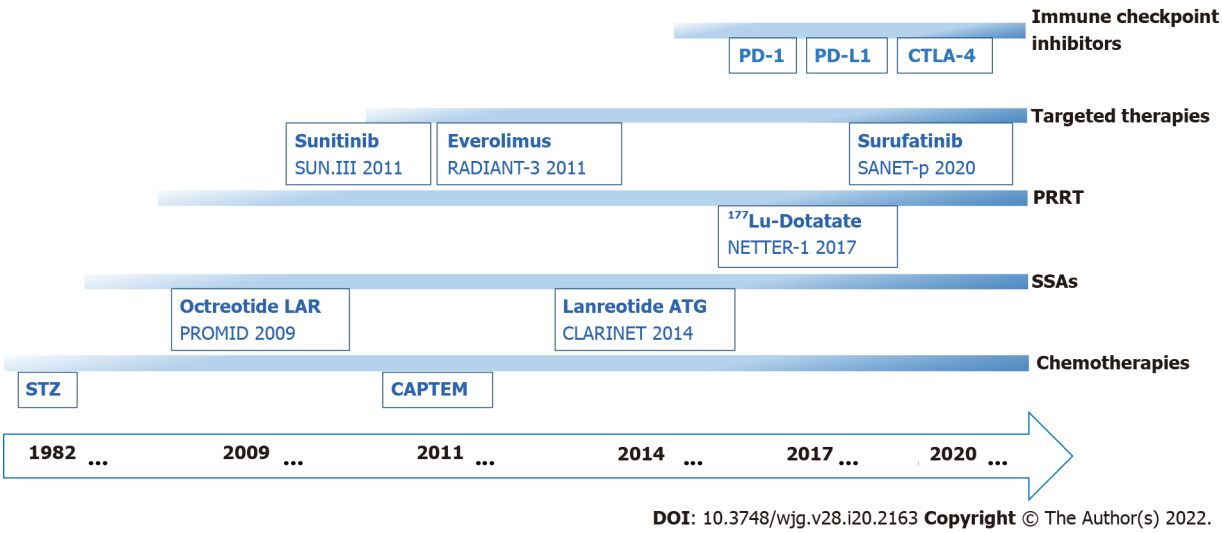
INTRODUCTION

Neuroendocrine neoplasms (NENs) are a group of rare neoplasms originating from neuroendocrine cells. However, with the development of diagnostic techniques and improvements in the clinical understanding of these tumors, the incidence is increasing yearly. Based on the United States Surveillance, Epidemiology, and End Results database, the age-adjusted incidence of NENs has increased nearly 6.4-fold from 1.09 per 100000 persons in 1973 to 6.98 per 100000 in 2012. The pancreas (0.84 per 100000 persons) is one of the most common primary sites of NENs, ranked after the lung, small intestine, and rectum[1]. In countries such as China and India, pancreatic NENs (PanNETs) are the most common gastroenteropancreatic neuroendocrine tumors (GEP-NETs) and have the highest morbidity [2].

PanNENs are highly heterogeneous neoplasms that appear as various clinical manifestations and biological behaviors. PanNENs can be classified as nonfunctional PanNENs (60%-90%) or functional PanNETs based on the absence or presence of symptoms associated with the overproduction of specific hormones, respectively[3]. The most common functional PanNETs are gastrinomas and insulinomas; less frequent are glucagonomas, somatostatinomas, vasoactive intestinal polypeptide-secreting tumors, and adrenocorticotropic hormone-secreting tumors[4-7]. The majority of PanNETs are sporadic, although PanNETs can occur as part of hereditary multiple tumor syndromes, such as multiple endocrine neoplasia type 1 and von Hippel-Lindau (VHL) disease[8]. PanNENs are classified into three main histological categories according to the 2019 World Health Organization Classification of Tumors of the Digestive System (5th edition): well-differentiated neuroendocrine tumors (NETs), poorly differentiated neuroendocrine carcinomas (NECs), and mixed neuroendocrine-non-neuroendocrine neoplasms. NETs are further classified into three grades (G1, G2, and G3) according to their mitotic rate (mitoses/2 mm^2) and Ki-67 proliferation index[9]. PanNENs clinical staging is currently based on the eighth edition of the American Joint Committee on Cancer tumor node metastasis (TNM) staging system. Well-differentiated PanNETs are staged by PanNENs TNMs, whereas poorly differentiated PanNECs are staged according to the TNM staging of pancreatic cancer[10].

Therapeutic strategies vary due to the different grades and stages of PanNENs. Radical surgery is the primary treatment option for patients with locally resectable PanNENs; however, 40%-50% of NENs present with distant metastases at the time of initial diagnosis, limiting the opportunity for surgical resection. Moreover, many patients with resected PanNENs will develop recurrence with distant metastases[11,12]. Systemic therapeutic options for patients with locally advanced or distant metastatic PanNENs involve somatostatin analogs (SSAs), molecularly targeted agents, cytotoxic chemotherapeutic agents, immune checkpoint inhibitors, and peptide receptor radionuclide therapy (PRRT) (Figure 1).

The therapeutic goals for patients with locally unresectable and metastatic PanNENs include both hormone control and anti-tumor therapy. The scope of this article does not include medical treatments for the control of functional PanNENs hormone-related symptoms, but rather focuses on anti-tumor therapy. Despite the multiple systemic therapeutic options for PanNENs, problems such as drug resistance, adverse side effects and limited scope of application still exist, and clinical needs have not been met. Thus, conquering drug resistance, expanding the scope of application and developing new clinical drugs have been the main focus of researchers in recent decades. This article reviews the clinical development of existing drugs, focusing on ongoing clinical studies and the development of novel targeted drugs, to provide a reference for addressing the current clinical treatment dilemma and the future direction of PanNENs drug research.



DOI: 10.3748/wjg.v28.i20.2163 **Copyright** © The Author(s) 2022.

Figure 1 History and key events in the development of pancreatic neuroendocrine neoplasms systemic therapy. PRRT: Peptide receptor radionuclide therapy; SSAs: Somatostatin analogs; PD-L1: Programmed cell death-ligand 1 inhibitor; PD-1: Programmed cell death-1 inhibitor; CTLA-4: Cytotoxic T-lymphocyte antigen 4 inhibitor; STZ: Streptozotocin; CAPTEM: Capecitabine and temozolomide regimen; PROMID[13], NCT00171873; CLARINET[14], NCT00353496; SUN.III[15], NCT00428597; RADIANT-3[16], NCT00510068; SANET-P[17], NCT02589821; NETTER-1[18], NCT01578239.

ADVANCES IN CHEMOTHERAPY

Systemic treatment with chemotherapy is one of the main therapies for advanced PanNENs. Appropriate chemotherapy regimens are delivered according to pathological classification and grades, mainly including temozolomide-based combination regimens and platinum-based regimens. Among them, temozolomide-based combination chemotherapy (CAPTEM and STEM) regimens can be used for the first-line treatment of patients with advanced PanNETs G2/G3[19-21] and for the second-line treatment of patients with PanNECs[22,23]. The synergistic effect of capecitabine in combination with temozolomide chemotherapy may be due to its ability to deplete O6-methylguanine DNA methyltransferase (MGMT) levels in tumor cells, thereby enhancing the alkylating effect of temozolomide[24]. The association between MGMT expression status and temozolomide efficacy has been demonstrated in other tumor types, and several studies in NENs have suggested that MGMT promoter methylation or low protein expression correlates better with a favorable therapeutic response to temozolomide and that MGMT status can be used as a biological indicator of the response to alkylating agent treatment in NENs[25,26]. However, because most of the current studies on the relationship between MGMT status and temozolomide efficacy are small-sample, retrospective studies, there is some controversy. A prospective study (NCT03217097) of the relationship between MGMT status and temozolomide efficacy in NETs is underway in which patients with advanced NETs have been divided into two groups according to whether they have MGMT methylation and are receiving temozolomide or oxaliplatin-based chemotherapy at a 1:1 (unmethylated group) and 2:1 (methylated group) ratio, respectively. ORR was used as the primary outcome indicator[27]. Additional prospective studies (NCT02698410, NCT01824875, NCT01525082) have evaluated MGMT status as a secondary outcome.

In clinical practice, drug resistance is one of the major obstacles to the effective treatment of temozolomide-based chemotherapy in PanNENs. Current studies on temozolomide resistance mechanisms are mainly conducted in the field of glioma. In addition to the overexpression of MGMT, the overexpression of the base excision repair (BER) pathway, alteration of autophagy, and activation of the phosphoinositide 3-kinase/protein kinase B/mammalian target of rapamycin (PI3K/AKT/mTOR) pathway contribute to acquired temozolomide resistance[28]. Wu *et al*[29] found enhanced temozolomide sensitivity in a preclinical study of glioblastoma multiforme (GBM) that poly (ADP-ribose) polymerase (PARP) inhibitors, particularly in MGMT-unmethylated GBM, and this effect may be mediated by inhibition of MGMT-mediated repair by abolishing MGMT function and inhibition of BER-mediated repair (Figure 2). Therefore, the combination of PARP inhibitors and temozolomide may be one solution for overcoming temozolomide resistance, and clinical trials applying this combination regimen in patients with small-cell lung cancer have yielded good clinical results[30]. A phase II clinical trial (NCT04394858) is currently evaluating the efficacy of single-agent temozolomide *vs* the combination of temozolomide and olaparib in patients with advanced pheochromocytoma and paraganglioma; however, no clinical trials of temozolomide in combination with PARP inhibitors for PanNENs have been conducted. Temozolomide resistance has also been observed to be associated with activation of the PI3K/AKT/mTOR pathway, and inhibition of the PI3K/AKT/mTOR pathway sensitizes tumor cells to apoptosis upon temozolomide treatment[31]. In a prospective phase II clinical trial, temozolomide in combination with everolimus as second-line therapy for advanced PanNETs resulted in an ORR of 40%

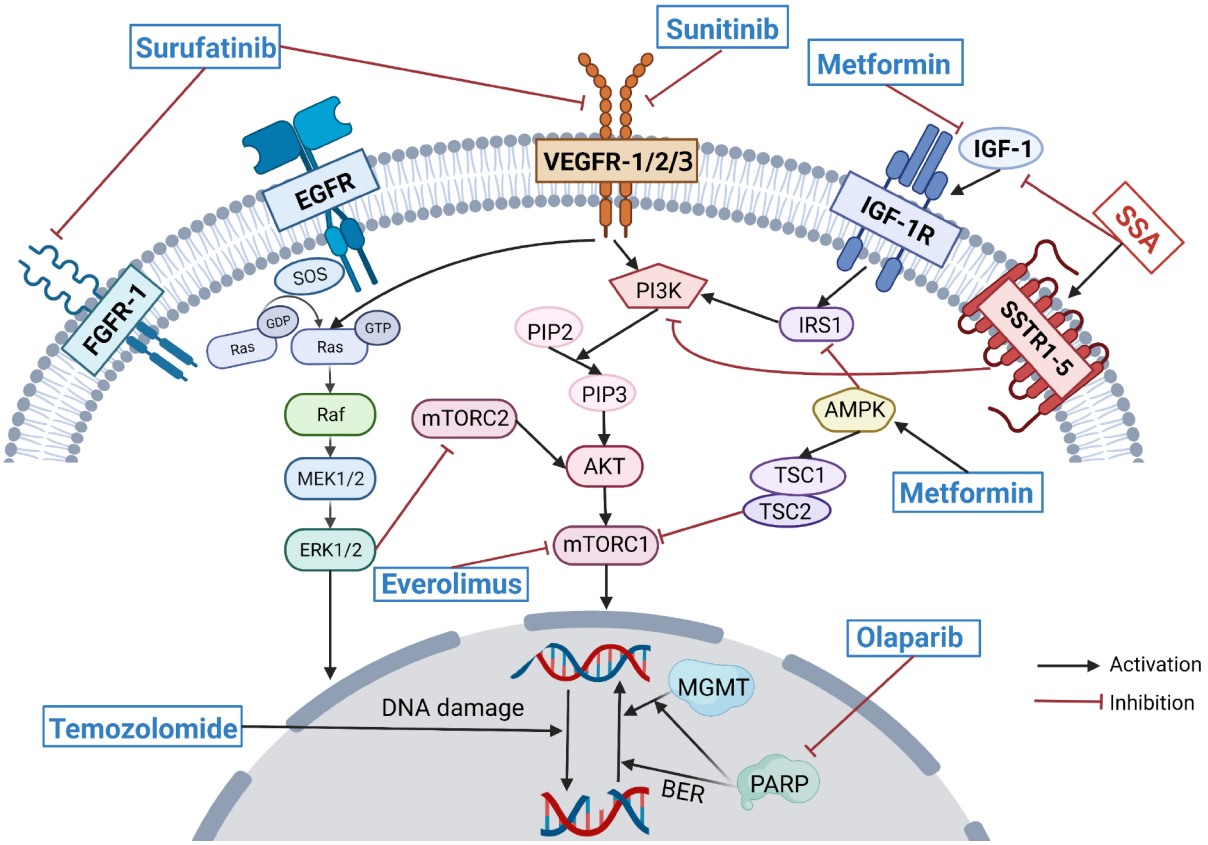


Figure 2 Molecular mechanisms of the action of somatostatin analog, antiangiogenic agents, everolimus, temozolomide, olaparib, and metformin on pancreatic neuroendocrine neoplasms and interactions. FGFR: Fibroblast growth factor receptor; EGFR: Epidermal growth factor receptor; VEGFR: Vascular endothelial growth factor receptor; IGF-1: Type 1 insulin-like growth factor; IGF-1R: Type 1 insulin-like growth factor receptor; SSTR: Somatostatin receptor; PI3K: Phosphoinositide 3-kinase; PIP2: Phosphatidylinositol-4,5-bisphosphate; PIP3: Phosphatidylinositol-3,4,5-triphosphate; AKT: Protein kinase B; mTORC1: Mechanistic target of rapamycin complex 1; mTORC2: Mechanistic target of rapamycin complex 2; IRS1: Insulin receptor substrate 1; AMPK: Adenosine 5'-monophosphate-activated protein kinase; TSC1: Tuberous sclerosis complex 1; TSC2: Tuberous sclerosis complex 2; SOS: Son of sevenless; RAS: Rat sarcoma virus; RAF: Rapidly accelerated fibrosarcoma; MEK: Methyl ethyl ketone; ERK: Extracellular signal-regulated kinase; BER: Base-excision repair; MGMT: O6-methylguanine DNA methyltransferase; PARP: Poly (ADP-ribose) polymerase. Citation: Created with BioRender.com.

and a median PFS of 15.4 mo, with no synergistic toxicity observed[32].

The most frequent chemotherapy schemes in advanced PanNECs are platinum-based (EP, EC) regimens for first-line therapy and FOLFOX, FOLFIRI, or CAPTEM regimens for second-line therapy [19,33,34]. For other options of first-line treatment regimens for PanNECs, a prospective study (NCT04325425) is evaluating the mFOLFIRINOX regimen *vs* the EP/EC regimen for advanced gastroenteropancreatic neuroendocrine carcinomas (GEP-NECs) as first-line therapy. Another study (NCT03387592) is evaluating the efficiency of the CAPTEM regimen *vs* the FOLFIRI regimen as second-line therapy for advanced NECs. These prospective clinical studies provide additional treatment options for patients with advanced PanNECs and high-level evidence for clinical decision-making.

ADVANCES IN SOMATOSTATIN ANALOGS

SSAs, with their antisecretory and antiproliferative effects, are some of the most common first-line treatments for patients with advanced PanNENs and can be used to control hormonal symptoms in patients with functional PanNETs[35] and for patients with advanced nonfunctional PanNENs to play an antiproliferative role. SSAs are primary treatment options for patients with PanNETs-G1/G2, Ki-67 < 10%, SSTR-positive, and slow-growing tumors[11-14,19,36]. The most widely used clinical SSAs include octreotide LAR and lanreotide autogel, both of which bind primarily to SSTR2 and SSTR5.

Several investigators have also evaluated the efficacy of SSAs in exerting antitumor effects in PanNENs with Ki-67 ≥ 10%. A multicenter retrospective study included advanced, well-differentiated PanNETs with Ki-67 of 10%-35% receiving first-line, long-acting SSAs and observed that SSAs still exert antiproliferative activity against PanNETs with Ki-67 ≥ 10% but have limited effect in PanNETs with high grade (G3) and hepatic tumor load > 25%[37].

In clinical practice, using SSAs at nonconventional high doses (increased administered dose or reduced administration interval) is a common empirical option in patients with progression PanNETs on a standard SSA first-line treatment[38]. A multicenter retrospective study of nonconventional doses of SSAs for GEP-NETs showed that in well-differentiated G1/G2 GEP-NETs, the overall median PFS was 31 mo with high-dose SSA (HD-SSA) therapy after progression on a standard SSA therapy, suggesting that HD-SSAs are active and safe treatment options in patients with progressive well-differentiated GEP-NETs[39]. A prospective single-arm phase II study (NCT02651987) assessed the efficacy of increasing the dose frequency of 120 mg lanreotide autogel (LAN) in 48 patients with progressive G1/G2 PanNETs and showed that 120 mg LAN every 14 d in PanNETs (progressive on standard 120 mg LAN every 28 d) produced promising PFS and DCR, especially in patients with Ki-67 ≤ 10%[40].

In addition, SSAs in combination with other agents (chemotherapy agents, antiangiogenic therapies, everolimus, immune checkpoint inhibitors, *etc.*) are also frequent second-line treatment options in real-world studies[41]. SSA combination therapy may have better efficacy in well-differentiated PanNETs with Ki-67 > 10% or high tumor burden, and a prospective multicenter phase II clinical study (NCT02231762) evaluating the efficacy of the combination of LAN and temozolomide in patients with advanced GEP-NETs is being conducted.

The efficacy of SSAs is correlated with the expression of somatostatin receptors on the tumor cell surface[38]. DNA methyltransferase inhibitors and histone deacetylase inhibitors were observed to upregulate SSTR2 expression in NET cell lines in some preclinical studies and could potentially be an option for overcoming SSA resistance, but the lack of progress in clinical studies requires further validation[42,43]. In clinical management, it is essential to identify the population favorable for SSA therapy, and SSAs in combination with other agents are expected to be synergistic in patients with higher grade, higher tumor load, and SSTR-positive PanNETs.

ADVANCES IN TARGETED THERAPIES

The targeted therapies currently used in PanNETs mainly include mammalian target of rapamycin (mTOR) inhibitors and antiangiogenic agents. FDA-approved target agents for the treatment of PanNENs include everolimus (mTOR inhibitor) and sunitinib (tyrosine kinase inhibitor)[12,19], and the recommendation of surufatinib (tyrosine kinase inhibitor) has been added to the Chinese guidelines for the diagnosis and treatment of pancreatic neuroendocrine neoplasms (2020)[36].

Everolimus, a mTOR inhibitor, has been shown to inhibit tumor cell growth through suppression of the PI3K/AKT/mTOR pathway. The primary results of the RADIANT-3 trial reported that patients with advanced PanNETs in the everolimus group had a median PFS of 11 mo, with a 6.4-mo increase *vs* the placebo group, and the safety profile of everolimus was good[16]. Everolimus resistance is thought to be related to its ability to inhibit only partial mTORC1 but not mTORC2, thus causing over-activation of upstream signaling, including PI3K/AKT[44]. Thus, both the dual PI3K/mTOR inhibitor BEZ235 and the dual inhibitor of mTORC1 and mTORC2, CC-223, are thought to have the potential to overcome everolimus resistance, but the phase II clinical trial of BEZ235 failed due to severe adverse effects[45]. The results of a phase II clinical trial of CC-233 in nonpancreatic NETs patients who failed first-line therapy suggested a DCR of 90% (95%CI: 76.9-97.3%) and a median PFS of 19.5 mo (95%CI: 10.4-28.5 mo), with a safety profile comparable with that of everolimus, but its use in PanNET patients still needs to be prospectively explored[46].

Several preclinical studies suggest that SSAs can inhibit insulin-like growth factor-1 (IGF-1), an upstream signal of the PI3K/AKT/mTOR pathway (Figure 2), and LAN was observed to reduce the survival rate of everolimus-resistant cell lines. SSAs may be able to overcome resistance to everolimus [38,47]. Unfortunately, in the COOPERATE-2 study of everolimus in combination with pasireotide LAR *vs* everolimus monotherapy in patients with advanced PanNETs, no prolongation of PFS was observed in the combination group *vs* the monotherapy group[48]. However, the trial extension results of the LUNA study of everolimus in combination with pasireotide LAR for advanced pulmonary and thymic NETs suggested that the everolimus combined with pasireotide group had a significantly longer median PFS than the pasireotide monotherapy group and the everolimus monotherapy group (8.51 mo *vs* 12.48 mo *vs* 16.53 mo)[49]. The Japan Clinical Oncology Group is also conducting a multicenter, randomized, controlled, phase III trial (jRCT1031200023) to confirm the superiority of combined everolimus plus lanreotide therapy over everolimus monotherapy for advanced GEP-NETs[50].

Resistance to everolimus may also be overcome by combined metformin therapy. Pusceddu *et al*[51] conducted a retrospective analysis of 445 patients with advanced PanNETs treated with everolimus and/or SSAs in 24 medical centers in Italy and observed that the median PFS of 44.2 mo was significantly longer in patients treated with metformin glucose-lowering therapy than in nondiabetic patients (15.1 mo) and longer than that in diabetic patients receiving other glucose-lowering treatments (20.8 mo). Metformin is associated with increased PFS in patients treated with SSA and in patients treated with everolimus (with or without SSAs). A preclinical study showed that metformin may induce more effective mTOR blockade through its effects on IGF-1 and adenosine 5'-monophosphate-activated protein kinase and may counteract the resistance mechanism triggered by everolimus (Figure 2)[52].

Because both metformin and SSA were observed to have the potential to overcome everolimus resistance in preclinical studies, a prospective study evaluating the efficacy of the triple-drug combination of everolimus, octreotide, and metformin for the treatment of advanced PanNENs (NCT02294006) is underway.

Antiangiogenic agents include tyrosine kinase inhibitors (TKIs) and non-TKI agents such as bevacizumab [anti-vascular endothelial growth factor (VEGF) monoclonal antibody]. PanNETs are highly vascularized with overexpression of proangiogenic factors such as VEGF, so antitumor angiogenesis is an effective therapeutic approach[53]. Antiangiogenic agents have evolved rapidly in the field of PanNET therapy in recent years, with new agents and high-grade clinical evidence emerging. Sunitinib, a polytyrosine kinase inhibitor, became the first antiangiogenic agent approved by the FDA for the treatment of patients with advanced PanNETs based on favorable results from a randomized double-blind phase III clinical trial[15]. Surufatinib is a new multitargeted TKI that blocks tumor angiogenesis by inhibiting both vascular endothelial growth factor receptor-1/2/3 (VEGFR-1/2/3) and fibroblast growth factor receptor-1 (FGFR-1) (Figure 2) and regulates tumor-associated macrophages to promote the immune response of the body to tumor cells by inhibiting colony-stimulating factor-1 receptor[54]. The SANET-p study, a phase III clinical trial of surufatinib in patients with advanced PanNETs, suggested a significant prolongation of median PFS (10.9 mo *vs* 3.7 mo) and improvement of ORR (19% *vs* 2%) in the surufatinib group compared with the placebo group[17]. The results from the PanNET cohort of the phase II cohort study (NCT01466036) of cabozantinib, a multitargeted tyrosine kinase inhibitor targeting VEGFR2 and cellular-mesenchymal epithelial transition factor, suggested a median PFS of 21.8 mo (95%CI: 8.5-32.0 mo) and an ORR of 15% (95%CI: 5%-36%)[55]. This result has raised expectations for the publication of the results of the ongoing randomized, double-blind phase III clinical trial of cabozantinib (NCT03375320). The TALENT study (GETNE1509) is a phase II clinical study of the VEGFR1-3 and FGFR1-4 inhibitors lenvatinib in which good clinical efficacy was observed in the PanNET cohort with a tolerable safety profile[56]. In addition, the TALENT study quantified a series of proangiogenic factors, such as VEGF-A, angiopoietin-2 (Ang2), and VEGFR-2. The results suggested that high Ang2 Levels and low FGF2 Levels were significantly associated with ORR, and Ang2 and VEGFR-2 Levels in patients treated with sunitinib could predict the efficacy of lenvatinib, confirming that biomarkers can not only predict drug efficacy but also provide a reference for patient sequential therapy selection[57]. Axitinib[58] and pazopanib[59] have also demonstrated efficacy in phase II clinical trials for the treatment of NETs. Clinical advances in antiangiogenic agents have brought more new options for the treatment of advanced PanNETs.

ADVANCES IN IMMUNOTHERAPY

With the advent of the immunotherapy era, phase I/II clinical trials of various immune checkpoint inhibitors such as programmed cell death-ligand 1 (PD-L1) inhibitors, programmed cell death-1 (PD-1) inhibitors and cytotoxic T-lymphocyte antigen 4 inhibitors have been widely conducted and rapidly developed in the PanNEN field. The results of a phase Ib study of toripalimab as a second-line regimen for the treatment of patients with advanced NENs suggested an ORR of 22.2% and a DCR of 55.5% in the PanNEN subgroup and observed that patients with positive PD-L1 expression, TMB-H (top 10%) and/or MSI-H positivity may preferentially benefit from the treatment[60]. The results of some current clinical trials have shown no significant benefit observed in patients with NENs treated with immune checkpoint inhibitors alone[61,62], and dual immunotherapy with PD-L1/PD-1 inhibitors in combination with CLTA-4 inhibitors is starting to gain interest. The DUNE study (GETNE 1601) is a phase II multicohort clinical study assessing the efficacy of durvalumab in combination with tremelimumab for the treatment of advanced GEP-NENs and pulmonary NETs, with recent results suggesting an ORR of 6.3% for the G1/G2 grade PanNET cohort, 9.1% for the G3 grade GEP-NEN cohort, and 7.4% and 0% for the pulmonary NET and giNET cohorts respectively[63]. A multicohort phase II clinical trial (NCT02923934) assessed the efficacy of ipilimumab in combination with nivolumab in NETs, with the latest results suggesting an ORR of 25% for the NET cohort (20 pts), and the study is still ongoing[64]. Clinical trials of immune checkpoint inhibitors in combination with other agents (antiangiogenic agents, chemotherapy, PRRT, and SSAs) continue to emerge, and some current clinical studies of immunotherapy in combination with antiangiogenic agents suggest better efficacy. An ORR of 20% and a median PFS of 3.94 mo were observed in a phase II clinical trial of toripalimab in combination with surufatinib in patients with advanced NECs after the failure of first-line chemotherapy. Surufatinib in combination with toripalimab has been suggested as a second-line treatment option for patients with advanced NECs[65], and a phase III clinical trial (NCT05015621) is evaluating the efficacy of the combination of surufatinib and toripalimab versus FOLFIRI regimen as a second-line treatment option for patients with advanced NECs. Clinical trials of immunotherapy in combination with other therapies being conducted in patients with NENs are shown in Table 1.

Table 1 Ongoing clinical trials of immune checkpoint inhibitors in combination with other therapies for the treatment of neuroendocrine neoplasms

Drugs	Population	*n*	Phase	Primary outcomes	NCT number
Surufatinib + toripalimab *vs* FOLFIRI	NEC	194	III	OS	NCT05015621
Penpulimab + anlotinib	NET	150	II	ORR	NCT04207463
Pembrolizumab + liver-directed/PRRT	NET	32		ORR	NCT03457948
Nivolumab + chemotherapy	NEN G3	38	II	OS	NCT03980925
Toripalimab + FOLFSIM *vs* EP/EC	Advanced NEC	336	II/III	OS	NCT03992911
Nivolumab + ipilimumab + cabozantinib	PD-NET	30	II	ORR	NCT04079712
Pembrolizumab + lanreotide depot	GEP-NET	22	Ib/II	ORR	NCT03043664

FOLFIRI: Folinic acid, fluorouracil and irinotecan regimen; FOLFSIM: Simmtecan and 5-FU/LV regimen; EP: Etoposide and cisplatin regimen; EC: Etoposide and carboplatin regimen; PD-NET: Poorly differentiated neuroendocrine tumor; ORR: Objective response rate; OS: Overall survival.

ADVANCES IN PEPTIDE RECEPTOR RADIONUCLIDE THERAPY

PRRT has been widely used in the treatment of NETs in Europe, the USA and Asia[66]. ^{177}Lu-DOTATATE has been used for more than a decade, but clinical studies of PRRT are still dominated by phase I/II clinical trials, and there is a lack of phase III clinical trials with large samples for NETs. The NETTER-1 study, a pivotal phase III clinical study of PRRT, treated two groups of midgut NETs with ^{177}Lu-DOTATATE combined with long-acting octreotide (30 mg every 28 d) and high-dose long-acting octreotide (60 mg every 28 d) and observed that ^{177}Lu-DOTATATE significantly increased the ORR (18% *vs* 3%) and prolonged the median OS of patients (48 *vs* 36.3 mo)[18,67]. Unfortunately, the NETTER-1 study, while suggesting good efficacy of PRRT, did not involve PanNETs, and the subsequent NETTER-2 study (NCT03972488), which is still ongoing enrolled SSTR+ G2/G3 GEP-NETs to evaluate the efficacy of ^{177}Lu-DOTATATE in combination with long-acting octreotide (30 mg every 28 days) compared with a high dose of long-acting octreotide (60 mg every 28 d). Prior to the results of the NETTER-2 study, the results of the multicenter retrospective NETTER-R study, which provided evidence for the use of PRRT in PanNETs, suggested that ^{177}Lu-DOTATATE had a median PFS of 24.8 (95%CI: 17.5-34.5) months and an ORR of 40.3% (95%CI: 28.1-53.6) in patients with advanced SSTR-positive PanNETs[68]. ^{177}Lu-DOTA-JR11 is a novel radiolabeled SSTR2 antagonist, and its application in SSTR-positive NETs in phase I/II clinical trials resulted in a DCR (12 mo) of 90% and an acceptable safety profile, suggesting that ^{177}Lu-DOTA-JR11 has good research potential[69]. Among emerging α-emitters, ^{225}Ac-DOTATATE, ^{213}Bi-DOTATOC and ^{212}Pb-DOTAMTATE have also shown good results in small samples of NETs, and clinical trials are underway[70].

NEW TARGETED AGENTS

In addition to common targets such as SSTR2, mTOR, and VEGFR, researchers are actively exploring new targeted agents for clinical application in the field of PanNENs. Cyclin-dependent kinases (CDKs), which regulate cell cycle progression, have been considered promising new targets for tumor therapy. Palbociclib, a small molecule compound that specifically inhibits CDK4 and CDK6, induced G1 phase blockade in Rb-positive CDK4-overexpressing PanNET cell lines in an *in vitro* assay, blocking and inhibiting the growth of PanNET cell lines[71,72]. However, the results of a phase II clinical trial of palbociclib for G1/G2 grade PanNETs suggested a median PFS of only 2.6 mo (95%CI: 0-14.4)[71]. ONC201, an agent with specific targeting of the dopamine-like DRD2 receptor and the mitochondrial protease ClpP, inhibits the growth of PanNET cell lines by TRAIL/DR5 upregulation, dual AKT/ERK pathway inhibition and promotion of a comprehensive stress response to exerting anticancer effects. The phase II study of ONC201 for NETs (NCT03034200) included 10 patients with metastatic PC-PGs (Group A) and 12 patients with other neuroendocrine tumors (Group B), and the latest results of this study suggested 5 PRs and 2 SDs in Group A and 1 PR and 2 SDs in Group B. A full outcome report is still pending[73]. Antibody-coupled drugs developed against SSTR targets have received much attention. PEN-221, an antibody-drug conjugate (ADC) targeting SSTR2, connects the cytotoxic microtubule protein inhibitor DM1 to Tyr3-octreotate and can rapidly internalize DM1 into SSTR2-expressing cells and exert cytotoxic effects after binding to SSTR2[74]. A phase II clinical study of PEN221 in SSTR2-positive gastrointestinal NETs is ongoing, and the latest results suggested that 23

Table 2 Ongoing clinical trials of new targeted agents

Drugs	Targets	Population	*n*	Phase	Primary outcomes	NCT number
Ribociclib + Everolimus	CDK4/6 Inhibitor	Advanced NET	21	II	PFS	NCT03070301
Abemaciclib	CDK4/6 Inhibitor	Advanced GEP-NET	37	II	ORR	NCT03891784
BAY 1895344	ATR Kinase Inhibitor	SCLC/PD-NEC/PDA	87	I	MTD, AEs	NCT04514497
Lurbinectedin, berzosertib	ATR Kinase Inhibitor	SCLC/HGNEC	75	I/II	MTD, ORR	NCT04802174
BI 764532	DLL3 Inhibitor	SCLC/NEN Expressing DLL3	110	I	MTD	NCT04429087
Entinostat	HDAC Inhibitor	Abdominal NET	40	II	ORR	NCT03211988
Niraparib + dostarlimab	PARP Inhibitor	SCLC/HGNEC	48		PFS, ORR	NCT04701307

SCLC: Small-cell lung carcinoma; PD-NEC: Poorly differentiated neuroendocrine carcinoma; PDA: Pancreatic adenocarcinoma; HGNEC: High-grade neuroendocrine cancer; CDK: Cyclin-dependent kinase; ATR kinase: Ataxia telangiectasia and RAD3-related kinase; DLL3: Delta-like protein 3; HDAC: Histone deacetylase; PARP: Poly (ADP-ribose) polymerase; PFS: Progression-free survival; MTD: Maximum tolerated dose; ORR: Objective response rate; AEs: Adverse events.

(88.5%) of 26 evaluable patients were assessed as SD, with a median PFS of 9 mo[75]. Belzutifan is a second-generation small-molecule hypoxia-inducible factor (HIF)-2α inhibitor, which is recommended in the latest NCCN guidelines for advanced PanNET patients with germline VHL alteration[19]. In a phase II, open-label, single-group trial of belzutifan in patients with renal cell carcinoma associated with VHL disease, 22 patients with PanNETs were included, among them 20 patients (91%) had a confirmed response (including 3 patients (14%) who had a complete response)[76]. Phase I/II clinical trials of new targeted agents such as ATR inhibitors, DLL3 inhibitors, HDAC inhibitors, and PARP inhibitors applied to NETs are currently underway (Table 2), but there is still a long way to go before clinical application.

CONCLUSION

Although there are various treatments for PanNENs, choosing appropriate therapeutic schemes for different patients in terms of pathological classification, grades and stages is still difficult. The selection of a cytotoxic chemotherapy regimen is a concern of researchers, and the results of prospective studies may help to address it. First, the problem of drug resistance facing CAPTEM regimen, the most widely used plan, will probably be solved by the combination of PARP inhibitors and mTOR inhibitors, although more evidence is needed. Due to the limited effect of SSAs on inhibiting cancer cell proliferation, progress has mainly been made in the selection of appropriate patients and the synergistic effect of combination therapy. Many new antiangiogenic agents and high-level clinical evidence have emerged, and the reversal of drug resistance to everolimus has also advanced. The use of PRRT in the treatment of NETs is increasingly common, and new radiolabeled peptides appear to be more effective. Immunotherapy faces challenges, and the better curative effect of dual immune checkpoint inhibitor therapies and the combinations of immune checkpoint inhibitors plus other agents need further investigation. Although there are limited choices in the treatment of PanNENs, the combination of common medicines such as SSAs, cytotoxic chemotherapy, everolimus, sunitinib and immune checkpoint inhibitors can have synergistic effects or alleviate drug resistance, thus bringing new vitality to the treatment of PanNENs. The development of biomarkers in clinical research provides a reference for the prediction of curative effects and the selection of sequential therapy, and biomarker-directed therapy helps in choosing appropriate medicines for different people. Advances in the search for new targets and the use of new medicines on common targets will provide more choices for the treatment of PanNENs, but applying them in clinical practice will still take time. Further investigation of PRRT and immunotherapy and the development of new targeted agents will be the focus of future research, and the progress made in the reversal of drug resistance will help clinical practice. In addition, the selection of appropriate therapeutic schemes for different patients and the execution of individualized and precise therapy will be a continuous concern for researchers.

FOOTNOTES

Author contributions: Li YL and Cheng ZX made equal contributions to this paper and should be regarded as a co-

first author; Li YL and Cheng ZX searched the literature and wrote the manuscript; Yu FH and Tian C translated the manuscript; Tan HY revised the manuscript.

Supported by National Key R&D Program of China, No. 2019YFB1309704.

Conflict-of-interest statement: Authors declare no conflict of interests for this article.

Open-Access: This article is an open-access article that was selected by an in-house editor and fully peer-reviewed by external reviewers. It is distributed in accordance with the Creative Commons Attribution NonCommercial (CC BY-NC 4.0) license, which permits others to distribute, remix, adapt, build upon this work non-commercially, and license their derivative works on different terms, provided the original work is properly cited and the use is non-commercial. See: https://creativecommons.org/Licenses/by-nc/4.0/

Country/Territory of origin: China

ORCID number: Yuan-Liang Li 0000-0003-0774-614X; Zi-Xuan Cheng 0000-0002-5183-3198; Fu-Huan Yu 0000-0003-2634-3530; Chao Tian 0000-0002-6635-1079; Huang-Ying Tan 0000-0002-6165-5196.

S-Editor: Wang JL
L-Editor: A
P-Editor: Wang JL

REFERENCES

1 **Dasari A**, Shen C, Halperin D, Zhao B, Zhou S, Xu Y, Shih T, Yao JC. Trends in the Incidence, Prevalence, and Survival Outcomes in Patients With Neuroendocrine Tumors in the United States. *JAMA Oncol* 2017; **3**: 1335-1342 [PMID: 28448665 DOI: 10.1001/jamaoncol.2017.0589]
2 **Das S**, Dasari A. Epidemiology, Incidence, and Prevalence of Neuroendocrine Neoplasms: Are There Global Differences? *Curr Oncol Rep* 2021; **23**: 43 [PMID: 33719003 DOI: 10.1007/s11912-021-01029-7]
3 **Falconi M**, Eriksson B, Kaltsas G, Bartsch DK, Capdevila J, Caplin M, Kos-Kudla B, Kwekkeboom D, Rindi G, Klöppel G, Reed N, Kianmanesh R, Jensen RT; Vienna Consensus Conference participants. ENETS Consensus Guidelines Update for the Management of Patients with Functional Pancreatic Neuroendocrine Tumors and Non-Functional Pancreatic Neuroendocrine Tumors. *Neuroendocrinology* 2016; **103**: 153-171 [PMID: 26742109 DOI: 10.1159/000443171]
4 **Wu W**, Jin G, Li H, Miao Y, Wang C, Liang T, Ou J, Zhao Y, Yuan C, Li Y, Lou W, Wu Z, Qin R, Wang H, Hao J, Yu X, Huang H, Tan G, Liu X, Xu K, Wang L, Yang Y, Hao C, Wang W, Guo K, Wei J, Wang Y, Peng C, Wang X, Cai S, Jiang J, Wu X, Li F, Pancreatic SSGO. The current surgical treatment of pancreatic neuroendocrine neoplasms in China: a national wide cross-sectional study. *J Pancreatol* 2019; **2**: 35-42 [DOI: 10.1097/JP9.0000000000000019]
5 **Ito T**, Igarashi H, Nakamura K, Sasano H, Okusaka T, Takano K, Komoto I, Tanaka M, Imamura M, Jensen RT, Takayanagi R, Shimatsu A. Epidemiological trends of pancreatic and gastrointestinal neuroendocrine tumors in Japan: a nationwide survey analysis. *J Gastroenterol* 2015; **50**: 58-64 [PMID: 24499825 DOI: 10.1007/s00535-014-0934-2]
6 **Halfdanarson TR**, Rabe KG, Rubin J, Petersen GM. Pancreatic neuroendocrine tumors (PNETs): incidence, prognosis and recent trend toward improved survival. *Ann Oncol* 2008; **19**: 1727-1733 [PMID: 18515795 DOI: 10.1093/annonc/mdn351]
7 **Garcia-Carbonero R**, Capdevila J, Crespo-Herrero G, Díaz-Pérez JA, Martínez Del Prado MP, Alonso Orduña V, Sevilla-García I, Villabona-Artero C, Beguiristain-Gómez A, Llanos-Muñoz M, Marazuela M, Alvarez-Escola C, Castellano D, Vilar E, Jiménez-Fonseca P, Teulé A, Sastre-Valera J, Benavent-Viñuelas M, Monleon A, Salazar R. Incidence, patterns of care and prognostic factors for outcome of gastroenteropancreatic neuroendocrine tumors (GEP-NETs): results from the National Cancer Registry of Spain (RGETNE). *Ann Oncol* 2010; **21**: 1794-1803 [PMID: 20139156 DOI: 10.1093/annonc/mdq022]
8 **Jensen RT**, Berna MJ, Bingham DB, Norton JA. Inherited pancreatic endocrine tumor syndromes: advances in molecular pathogenesis, diagnosis, management, and controversies. *Cancer* 2008; **113**: 1807-1843 [PMID: 18798544 DOI: 10.1002/cncr.23648]
9 **Nagtegaal ID**, Odze RD, Klimstra D, Paradis V, Rugge M, Schirmacher P, Washington KM, Carneiro F, Cree IA; WHO Classification of Tumours Editorial Board. The 2019 WHO classification of tumours of the digestive system. *Histopathology* 2020; **76**: 182-188 [PMID: 31433515 DOI: 10.1111/his.13975]
10 **Doescher J**, Veit JA, Hoffmann TK. [The 8th edition of the AJCC Cancer Staging Manual: Updates in otorhinolaryngology, head and neck surgery]. *HNO* 2017; **65**: 956-961 [PMID: 28717958 DOI: 10.1007/s00106-017-0391-3]
11 **Halfdanarson TR**, Strosberg JR, Tang L, Bellizzi AM, Bergsland EK, O'Dorisio TM, Halperin DM, Fishbein L, Eads J, Hope TA, Singh S, Salem R, Metz DC, Naraev BG, Reidy-Lagunes DL, Howe JR, Pommier RF, Menda Y, Chan JA. The North American Neuroendocrine Tumor Society Consensus Guidelines for Surveillance and Medical Management of Pancreatic Neuroendocrine Tumors. *Pancreas* 2020; **49**: 863-881 [PMID: 32675783 DOI: 10.1097/MPA.0000000000001597]
12 **Pavel M**, O'Toole D, Costa F, Capdevila J, Gross D, Kianmanesh R, Krenning E, Knigge U, Salazar R, Pape UF, Öberg K; Vienna Consensus Conference participants. ENETS Consensus Guidelines Update for the Management of Distant Metastatic Disease of Intestinal, Pancreatic, Bronchial Neuroendocrine Neoplasms (NEN) and NEN of Unknown Primary Site. *Neuroendocrinology* 2016; **103**: 172-185 [PMID: 26731013 DOI: 10.1159/000443167]
13 **Rinke A**, Müller HH, Schade-Brittinger C, Klose KJ, Barth P, Wied M, Mayer C, Aminossadati B, Pape UF, Bläker M,

Harder J, Arnold C, Gress T, Arnold R; PROMID Study Group. Placebo-controlled, double-blind, prospective, randomized study on the effect of octreotide LAR in the control of tumor growth in patients with metastatic neuroendocrine midgut tumors: a report from the PROMID Study Group. *J Clin Oncol* 2009; **27**: 4656-4663 [PMID: 19704057 DOI: 10.1200/JCO.2009.22.8510]

14 **Caplin ME**, Pavel M, Ćwikła JB, Phan AT, Raderer M, Sedláčková E, Cadiot G, Wolin EM, Capdevila J, Wall L, Rindi G, Langley A, Martinez S, Blumberg J, Ruszniewski P; CLARINET Investigators. Lanreotide in metastatic enteropancreatic neuroendocrine tumors. *N Engl J Med* 2014; **371**: 224-233 [PMID: 25014687 DOI: 10.1056/NEJMoa1316158]

15 **Raymond E**, Dahan L, Raoul JL, Bang YJ, Borbath I, Lombard-Bohas C, Valle J, Metrakos P, Smith D, Vinik A, Chen JS, Hörsch D, Hammel P, Wiedenmann B, Van Cutsem E, Patyna S, Lu DR, Blanckmeister C, Chao R, Ruszniewski P. Sunitinib malate for the treatment of pancreatic neuroendocrine tumors. *N Engl J Med* 2011; **364**: 501-513 [PMID: 21306237 DOI: 10.1056/NEJMoa1003825]

16 **Yao JC**, Shah MH, Ito T, Bohas CL, Wolin EM, Van Cutsem E, Hobday TJ, Okusaka T, Capdevila J, de Vries EG, Tomassetti P, Pavel ME, Hoosen S, Haas T, Lincy J, Lebwohl D, Öberg K; RAD001 in Advanced Neuroendocrine Tumors, Third Trial (RADIANT-3) Study Group. Everolimus for advanced pancreatic neuroendocrine tumors. *N Engl J Med* 2011; **364**: 514-523 [PMID: 21306238 DOI: 10.1056/NEJMoa1009290]

17 **Xu J**, Shen L, Bai C, Wang W, Li J, Yu X, Li Z, Li E, Yuan X, Chi Y, Yin Y, Lou W, Xu N, Bai Y, Zhang T, Xiu D, Wang X, Yuan Y, Chen J, Qin S, Jia R, Lu M, Cheng Y, Zhou Z, He J, Su W. Surufatinib in advanced pancreatic neuroendocrine tumours (SANET-p): a randomised, double-blind, placebo-controlled, phase 3 study. *Lancet Oncol* 2020; **21**: 1489-1499 [PMID: 32966810 DOI: 10.1016/S1470-2045(20)30493-9]

18 **Strosberg J**, El-Haddad G, Wolin E, Hendifar A, Yao J, Chasen B, Mittra E, Kunz PL, Kulke MH, Jacene H, Bushnell D, O'Dorisio TM, Baum RP, Kulkarni HR, Caplin M, Lebtahi R, Hobday T, Delpassand E, Van Cutsem E, Benson A, Srirajaskanthan R, Pavel M, Mora J, Berlin J, Grande E, Reed N, Seregni E, Öberg K, Lopera Sierra M, Santoro P, Thevenet T, Erion JL, Ruszniewski P, Kwekkeboom D, Krenning E; NETTER-1 Trial Investigators. Phase 3 Trial of ^{177}Lu-Dotatate for Midgut Neuroendocrine Tumors. *N Engl J Med* 2017; **376**: 125-135 [PMID: 28076709 DOI: 10.1056/NEJMoa1607427]

19 **Shah MH**, Goldner WS, Benson AB, Bergsland E, Blaszkowsky LS, Brock P, Chan J, Das S, Dickson PV, Fanta P, Giordano T, Halfdanarson TR, Halperin D, He J, Heaney A, Heslin M J, Kandeel F, Kardan A, Khan SA, Kuvshinoff BW, Lieu C, Miller K, Pillarisetty VG, Reidy D, Salgado SA, Shaheen S, Soares HP, Soulen MC, Strosberg JR, Sussman CR, Trikalinos NA, Uboha NA, Vijayvergia N, Wong T, Lynn B, Hochstetler C. National Comprehensive Cancer Network Clinical Practice Guidelines in Oncology: Neuroendocrine and Adrenal Tumors Version 4; 2021. Available from: https://www.nccn.org/Login?ReturnURL=https://www.nccn.org/professionals/physician_gls/pdf/neuroendocrine.pdf

20 **Zhao J**, Zhao H, Chi Y. Safety and Efficacy of the S-1/Temozolomide Regimen in Patients with Metastatic Neuroendocrine Tumors. *Neuroendocrinology* 2018; **106**: 318-323 [PMID: 28817826 DOI: 10.1159/000480402]

21 **Strosberg JR**, Fine RL, Choi J, Nasir A, Coppola D, Chen DT, Helm J, Kvols L. First-line chemotherapy with capecitabine and temozolomide in patients with metastatic pancreatic endocrine carcinomas. *Cancer* 2011; **117**: 268-275 [PMID: 20824724 DOI: 10.1002/cncr.25425]

22 **Pavel M**, Öberg K, Falconi M, Krenning EP, Sundin A, Perren A, Berruti A; ESMO Guidelines Committee. Electronic address: clinicalguidelines@esmo.org. Gastroenteropancreatic neuroendocrine neoplasms: ESMO Clinical Practice Guidelines for diagnosis, treatment and follow-up. *Ann Oncol* 2020; **31**: 844-860 [PMID: 32272208 DOI: 10.1016/j.annonc.2020.03.304]

23 **Rogowski W**, Wachuła E, Gorzelak A, Lebiedzińska A, Sulżyc-Bielicka V, Iżycka-Świeszewska E, Żołnierek J, Kos-Kudła B. Capecitabine and temozolomide combination for treatment of high-grade, well-differentiated neuroendocrine tumour and poorly-differentiated neuroendocrine carcinoma - retrospective analysis. *Endokrynol Pol* 2019; **70**: 313-317 [PMID: 30843182 DOI: 10.5603/EP.a2019.0010]

24 **Chatzellis E**, Angelousi A, Daskalakis K, Tsoli M, Alexandraki KI, Wachuła E, Meirovitz A, Maimon O, Grozinsky-Glasberg S, Gross D, Kos-Kudła B, Koumarianou A, Kaltsas G. Activity and Safety of Standard and Prolonged Capecitabine/Temozolomide Administration in Patients with Advanced Neuroendocrine Neoplasms. *Neuroendocrinology* 2019; **109**: 333-345 [PMID: 31167197 DOI: 10.1159/000500135]

25 **Trillo Aliaga P**, Spada F, Peveri G, Bagnardi V, Fumagalli C, Laffi A, Rubino M, Gervaso L, Guerini Rocco E, Pisa E, Curigliano G, Fazio N. Should temozolomide be used on the basis of O^6-methylguanine DNA methyltransferase status in patients with advanced neuroendocrine tumors? *Cancer Treat Rev* 2021; **99**: 102261 [PMID: 34332293 DOI: 10.1016/j.ctrv.2021.102261]

26 **Qi Z**, Tan H. Association between MGMT status and response to alkylating agents in patients with neuroendocrine neoplasms: a systematic review and meta-analysis. *Biosci Rep* 2020; **40** [PMID: 32141507 DOI: 10.1042/BSR20194127]

27 **Lemelin A**, Barritault M, Hervieu V, Payen L, Péron J, Couvelard A, Cros J, Scoazec JY, Bin S, Villeneuve L, Lombard-Bohas C, Walter T; MGMT-NET investigators. O6-methylguanine-DNA methyltransferase (MGMT) status in neuroendocrine tumors: a randomized phase II study (MGMT-NET). *Dig Liver Dis* 2019; **51**: 595-599 [PMID: 30824408 DOI: 10.1016/j.dld.2019.02.001]

28 **Yan Y**, Xu Z, Dai S, Qian L, Sun L, Gong Z. Targeting autophagy to sensitive glioma to temozolomide treatment. *J Exp Clin Cancer Res* 2016; **35**: 23 [PMID: 26830677 DOI: 10.1186/s13046-016-0303-5]

29 **Wu S**, Li X, Gao F, de Groot JF, Koul D, Yung WKA. PARP-mediated PARylation of MGMT is critical to promote repair of temozolomide-induced O6-methylguanine DNA damage in glioblastoma. *Neuro Oncol* 2021; **23**: 920-931 [PMID: 33433610 DOI: 10.1093/neuonc/noab003]

30 **Farago AF**, Yeap BY, Stanzione M, Hung YP, Heist RS, Marcoux JP, Zhong J, Rangachari D, Barbie DA, Phat S, Myers DT, Morris R, Kem M, Dubash TD, Kennedy EA, Digumarthy SR, Sequist LV, Hata AN, Maheswaran S, Haber DA, Lawrence MS, Shaw AT, Mino-Kenudson M, Dyson NJ, Drapkin BJ. Combination Olaparib and Temozolomide in Relapsed Small-Cell Lung Cancer. *Cancer Discov* 2019; **9**: 1372-1387 [PMID: 31416802 DOI: 10.1158/2159-8290.CD-19-0582]

31 **Zając A**, Sumorek-Wiadro J, Langner E, Wertel I, Maciejczyk A, Pawlikowska-Pawlęga B, Pawelec J, Wasiak M, Hułas-

Stasiak M, Bądziul D, Rzeski W, Reichert M, Jakubowicz-Gil J. Involvement of PI3K Pathway in Glioma Cell Resistance to Temozolomide Treatment. *Int J Mol Sci* 2021; **22** [PMID: 34068110 DOI: 10.3390/ijms22105155]

32 **Chan JA**, Blaszkowsky L, Stuart K, Zhu AX, Allen J, Wadlow R, Ryan DP, Meyerhardt J, Gonzalez M, Regan E, Zheng H, Kulke MH. A prospective, phase 1/2 study of everolimus and temozolomide in patients with advanced pancreatic neuroendocrine tumor. *Cancer* 2013; **119**: 3212-3218 [PMID: 23733618 DOI: 10.1002/cncr.28142]

33 **Bardasi C**, Spallanzani A, Benatti S, Spada F, Laffi A, Antonuzzo L, Lavacchi D, Marconcini R, Ferrari M, Rimini M, Caputo F, Santini C, Cerma K, Casadei-Gardini A, Andrikou K, Salati M, Bertolini F, Fontana A, Dominici M, Luppi G, Gelsomino F. Irinotecan-based chemotherapy in extrapulmonary neuroendocrine carcinomas: survival and safety data from a multicentric Italian experience. *Endocrine* 2021; **74**: 707-713 [PMID: 34231124 DOI: 10.1007/s12020-021-02813-y]

34 **Hadoux J**, Malka D, Planchard D, Scoazec JY, Caramella C, Guigay J, Boige V, Leboulleux S, Burtin P, Berdelou A, Loriot Y, Duvillard P, Chougnet CN, Déandréis D, Schlumberger M, Borget I, Ducreux M, Baudin E. Post-first-line FOLFOX chemotherapy for grade 3 neuroendocrine carcinoma. *Endocr Relat Cancer* 2015; **22**: 289-298 [PMID: 25770151 DOI: 10.1530/ERC-15-0075]

35 **Stueven AK**, Kayser A, Wetz C, Amthauer H, Wree A, Tacke F, Wiedenmann B, Roderburg C, Jann H. Somatostatin Analogues in the Treatment of Neuroendocrine Tumors: Past, Present and Future. *Int J Mol Sci* 2019; **20** [PMID: 31234481 DOI: 10.3390/ijms20123049]

36 **Wu WM**, Chen J, Bai CM, Chi Y, Du YQ, Feng ST, Huo L, Jiang YX, Li JN, Lou WH, Luo J, Shao CH, Shen L, Wang F, Wang LW, Wang O, Wang Y, Wu HW, Xing XP, Xu JM, Xue HD, Xue L, Yang Y, Yu XJ, Yuan CH, Zhao H, Zhu XZ, Zhao YP; Chinese Pancreatic Surgery Association, Chinese Society of Surgery, Chinese Medical Association. [The Chinese guidelines for the diagnosis and treatment of pancreatic neuroendocrine neoplasms (2020)]. *Zhonghua Wai Ke Za Zhi* 2021; **59**: 401-421 [PMID: 34102722 DOI: 10.3760/cma.j.cn112139-20210319-00135]

37 **Merola E**, Alonso Gordoa T, Zhang P, Al-Toubah T, Pellè E, Kolasińska-Ćwikła A, Zandee W, Laskaratos F, de Mestier L, Lamarca A, Hernando J, Cwikla J, Strosberg J, de Herder W, Caplin M, Cives M, van Leeuwaarde R. Somatostatin Analogs for Pancreatic Neuroendocrine Tumors: Any Benefit When Ki-67 Is ≥10%? *Oncologist* 2021; **26**: 294-301 [PMID: 33301235 DOI: 10.1002/onco.13633]

38 **Carmona-Bayonas A**, Jiménez-Fonseca P, Custodio A, Grande E, Capdevila J, López C, Teule A, Garcia-Carbonero R; Spanish Neuroendocrine Tumor Group (GETNE). Optimizing Somatostatin Analog Use in Well or Moderately Differentiated Gastroenteropancreatic Neuroendocrine Tumors. *Curr Oncol Rep* 2017; **19**: 72 [PMID: 28920153 DOI: 10.1007/s11912-017-0633-2]

39 **Lamberti G**, Faggiano A, Brighi N, Tafuto S, Ibrahim T, Brizzi MP, Pusceddu S, Albertelli M, Massironi S, Panzuto F, Badalamenti G, Riccardi F, Butturini G, Gelsomino F, De Divitiis C, Modica R, Bongiovanni A, La Salvia A, Torchio M, Colao A, Ferone D, Campana D. Nonconventional Doses of Somatostatin Analogs in Patients With Progressing Well-Differentiated Neuroendocrine Tumor. *J Clin Endocrinol Metab* 2020; **105** [PMID: 31545377 DOI: 10.1210/clinem/dgz035]

40 **Pavel M**, Ćwikła JB, Lombard-Bohas C, Borbath I, Shah T, Pape UF, Capdevila J, Panzuto F, Truong Thanh XM, Houchard A, Ruszniewski P. Efficacy and safety of high-dose lanreotide autogel in patients with progressive pancreatic or midgut neuroendocrine tumours: CLARINET FORTE phase 2 study results. *Eur J Cancer* 2021; **157**: 403-414 [PMID: 34597974 DOI: 10.1016/j.ejca.2021.06.056]

41 **Jalbert JJ**, Casciano R, Meng J, Brais LK, Pulgar SJ, Berthon A, Dinet J, Kulke MH. Treatment Patterns and Health Resource Use Among Patients with Metastatic Gastroenteropancreatic Neuroendocrine Tumors Treated at a Tertiary Referral Center. *Oncologist* 2020; **25**: e644-e650 [PMID: 31999024 DOI: 10.1634/theoncologist.2019-0691]

42 **Guenter RE**, Aweda T, Carmona Matos DM, Whitt J, Chang AW, Cheng EY, Liu XM, Chen H, Lapi SE, Jaskula-Sztul R. Pulmonary Carcinoid Surface Receptor Modulation Using Histone Deacetylase Inhibitors. *Cancers (Basel)* 2019; **11** [PMID: 31163616 DOI: 10.3390/cancers11060767]

43 **Jin XF**, Auernhammer CJ, Ilhan H, Lindner S, Nölting S, Maurer J, Spöttl G, Orth M. Combination of 5-Fluorouracil with Epigenetic Modifiers Induces Radiosensitization, Somatostatin Receptor 2 Expression, and Radioligand Binding in Neuroendocrine Tumor Cells In Vitro. *J Nucl Med* 2019; **60**: 1240-1246 [PMID: 30796167 DOI: 10.2967/jnumed.118.224048]

44 **Lee L**, Ito T, Jensen RT. Everolimus in the treatment of neuroendocrine tumors: efficacy, side-effects, resistance, and factors affecting its place in the treatment sequence. *Expert Opin Pharmacother* 2018; **19**: 909-928 [PMID: 29757017 DOI: 10.1080/14656566.2018.1476492]

45 **Fazio N**, Buzzoni R, Baudin E, Antonuzzo L, Hubner RA, Lahner H, DE Herder WW, Raderer M, Teulé A, Capdevila J, Libutti SK, Kulke MH, Shah M, Dey D, Turri S, Aimone P, Massacesi C, Verslype C. A Phase II Study of BEZ235 in Patients with Everolimus-resistant, Advanced Pancreatic Neuroendocrine Tumours. *Anticancer Res* 2016; **36**: 713-719 [PMID: 26851029]

46 **Wolin E**, Mita A, Mahipal A, Meyer T, Bendell J, Nemunaitis J, Munster PN, Paz-Ares L, Filvaroff EH, Li S, Hege K, de Haan H, Mita M. A phase 2 study of an oral mTORC1/mTORC2 kinase inhibitor (CC-223) for non-pancreatic neuroendocrine tumors with or without carcinoid symptoms. *PLoS One* 2019; **14**: e0221994 [PMID: 31527867 DOI: 10.1371/journal.pone.0221994]

47 **Sciammarella C**, Luce A, Riccardi F, Mocerino C, Modica R, Berretta M, Misso G, Cossu AM, Colao A, Vitale G, Necas A, Fedacko J, Galdiero M, Correale P, Faggiano A, Caraglia M, Capasso A, Grimaldi A. Lanreotide Induces Cytokine Modulation in Intestinal Neuroendocrine Tumors and Overcomes Resistance to Everolimus. *Front Oncol* 2020; **10**: 1047 [PMID: 32766136 DOI: 10.3389/fonc.2020.01047]

48 **Kulke MH**, Ruszniewski P, Van Cutsem E, Lombard-Bohas C, Valle JW, De Herder WW, Pavel M, Degtyarev E, Brase JC, Bubuteishvili-Pacaud L, Voi M, Salazar R, Borbath I, Fazio N, Smith D, Capdevila J, Riechelmann RP, Yao JC. A randomized, open-label, phase 2 study of everolimus in combination with pasireotide LAR or everolimus alone in advanced, well-differentiated, progressive pancreatic neuroendocrine tumors: COOPERATE-2 trial. *Ann Oncol* 2019; **30**: 1846 [PMID: 31407000 DOI: 10.1093/annonc/mdz219]

49 **Baudin E**, Berruti A, Giuliano M, Mansoor W, Bobirca C, Houtsma E, Fagan N, Oberg K E, Ferolla P. First long-term

results on efficacy and safety of long-acting pasireotide in combination with everolimus in patients with advanced carcinoids (NET) of the lung/thymus: Phase II LUNA trial. *J Clin Oncol* 2021; **39**: 8574-8574 [DOI: 10.1200/JCO.2021.39.15_suppl.8574]

50 **Hijioka S**, Morizane C, Ikeda M, Ishii H, Okusaka T, Furuse J. Current status of medical treatment for gastroenteropancreatic neuroendocrine neoplasms and future perspectives. *Jpn J Clin Oncol* 2021; **51**: 1185-1196 [PMID: 34038547 DOI: 10.1093/jjco/hyab076]

51 **Pusceddu S**, Vernieri C, Di Maio M, Marconcini R, Spada F, Massironi S, Ibrahim T, Brizzi MP, Campana D, Faggiano A, Giuffrida D, Rinzivillo M, Cingarlini S, Aroldi F, Antonuzzo L, Berardi R, Catena L, De Divitiis C, Ermacora P, Perfetti V, Fontana A, Razzore P, Carnaghi C, Davì MV, Cauchi C, Duro M, Ricci S, Fazio N, Cavalcoli F, Bongiovanni A, La Salvia A, Brighi N, Colao A, Puliafito I, Panzuto F, Ortolani S, Zaniboni A, Di Costanzo F, Torniai M, Bajetta E, Tafuto S, Garattini SK, Femia D, Prinzi N, Concas L, Lo Russo G, Milione M, Giacomelli L, Buzzoni R, Delle Fave G, Mazzaferro V, de Braud F. Metformin Use Is Associated With Longer Progression-Free Survival of Patients With Diabetes and Pancreatic Neuroendocrine Tumors Receiving Everolimus and/or Somatostatin Analogues. *Gastroenterology* 2018; **155**: 479-489.e7 [PMID: 29655834 DOI: 10.1053/j.gastro.2018.04.010]

52 **Vitali E**, Boemi I, Tarantola G, Piccini S, Zerbi A, Veronesi G, Baldelli R, Mazziotti G, Smiroldo V, Lavezzi E, Spada A, Mantovani G, Lania AG. Metformin and Everolimus: A Promising Combination for Neuroendocrine Tumors Treatment. *Cancers (Basel)* 2020; **12** [PMID: 32748870 DOI: 10.3390/cancers12082143]

53 **Couvelard A**, O'Toole D, Turley H, Leek R, Sauvanet A, Degott C, Ruszniewski P, Belghiti J, Harris AL, Gatter K, Pezzella F. Microvascular density and hypoxia-inducible factor pathway in pancreatic endocrine tumours: negative correlation of microvascular density and VEGF expression with tumour progression. *Br J Cancer* 2005; **92**: 94-101 [PMID: 15558070 DOI: 10.1038/sj.bjc.6602245]

54 **Xu JM**, Wang Y, Chen YL, Jia R, Li J, Gong JF, Qi C, Hua Y, Tan CR, Wang J, Li K, Sai Y, Zhou F, Ren YX, Qing WG, Jia H, Su WG, Shen L. Sulfatinib, a novel kinase inhibitor, in patients with advanced solid tumors: results from a phase I study. *Oncotarget* 2017; **8**: 42076-42086 [PMID: 28159938 DOI: 10.18632/oncotarget.14942]

55 **Chan JA**, Faris JE, Murphy JE, Blaszkowsky LS, Kwak EL, McCleary NJ, Fuchs CS, Meyerhardt JA, Ng K, Zhu AX, Abrams TA, Wolpin BM, Zhang S, Reardon A, Fitzpatrick B, Kulke MH, Ryan DP. Phase II trial of cabozantinib in patients with carcinoid and pancreatic neuroendocrine tumors (pNET). *J Clin Oncol* 2017; **35**: 228-228 [DOI: 10.1200/JCO.2017.35.4_suppl.228]

56 **Capdevila J**, Fazio N, Lopez Lopez C, Teule A, Valle J W, Tafuto S, Custodio A B, Reed N, Raderer M, Grande E, Garcia-Carbonero R, Jiménez-Fonseca P, Alonso V, Antonuzzo L, Spallanzani A, Berruti A, Sevilla I, La Casta Munoa A, Hernando-Cubero J, Ibrahim T. Final results of the TALENT trial (GETNE1509): a prospective multicohort phase II study of lenvatinib in patients (pts) with G1/G2 advanced pancreatic (panNETs) and gastrointestinal (giNETs) neuroendocrine tumors (NETs). *J Clin Oncol* 2019; **37**: 4106-4106 [DOI: 10.1200/JCO.2019.37.15_suppl.4106]

57 **Capdevila J**, Jimenez-Valerio G, Martinez A, Hernando J, Ibrahim T, Fazio N, Lopez C, Teule A, Valle W, Tafuto S, Custodio B, Reed NS, Raderer M, Grande E, Garcia-Carbonero R, Jiménez-Fonseca P, Alonso V, Casanovas O. Plasma biomarker study of lenvatinib in gastroenteropancreatic neuroendocrine tumors reveals Ang2 and FGF2 as predictors of treatment response: Results from the international phase II TALENT trial (GETNE 1509). *J Clin Oncol* 2021; **39**: 4113-4113 [DOI: 10.1200/JCO.2021.39.15_suppl.4113]

58 **Strosberg JR**, Cives M, Hwang J, Weber T, Nickerson M, Atreya CE, Venook A, Kelley RK, Valone T, Morse B, Coppola D, Bergsland EK. A phase II study of axitinib in advanced neuroendocrine tumors. *Endocr Relat Cancer* 2016; **23**: 411-418 [PMID: 27080472 DOI: 10.1530/ERC-16-0008]

59 **Grande E**, Capdevila J, Castellano D, Teulé A, Durán I, Fuster J, Sevilla I, Escudero P, Sastre J, García-Donas J, Casanovas O, Earl J, Ortega L, Apellaniz-Ruiz M, Rodriguez-Antona C, Alonso-Gordoa T, Díez JJ, Carrato A, García-Carbonero R. Pazopanib in pretreated advanced neuroendocrine tumors: a phase II, open-label trial of the Spanish Task Force Group for Neuroendocrine Tumors (GETNE). *Ann Oncol* 2015; **26**: 1987-1993 [PMID: 26063633 DOI: 10.1093/annonc/mdv252]

60 **Lu M**, Zhang P, Zhang Y, Li Z, Gong J, Li J, Li Y, Zhang X, Lu Z, Wang X, Zhou J, Peng Z, Wang W, Feng H, Wu H, Yao S, Shen L. Efficacy, Safety, and Biomarkers of Toripalimab in Patients with Recurrent or Metastatic Neuroendocrine Neoplasms: A Multiple-Center Phase Ib Trial. *Clin Cancer Res* 2020; **26**: 2337-2345 [PMID: 32086343 DOI: 10.1158/1078-0432.CCR-19-4000]

61 **Strosberg J**, Mizuno N, Doi T, Grande E, Delord JP, Shapira-Frommer R, Bergsland E, Shah M, Fakih M, Takahashi S, Piha-Paul SA, O'Neil B, Thomas S, Lolkema MP, Chen M, Ibrahim N, Norwood K, Hadoux J. Efficacy and Safety of Pembrolizumab in Previously Treated Advanced Neuroendocrine Tumors: Results From the Phase II KEYNOTE-158 Study. *Clin Cancer Res* 2020; **26**: 2124-2130 [PMID: 31980466 DOI: 10.1158/1078-0432.CCR-19-3014]

62 **Mulvey C**, Raj NP, Chan JA, Aggarwal RR, Cinar P, Hope T A, Kolli K, Zhang L, Calabrese S, Grabowsky JA, Modarresi L, Kelly V, Stonely D, Munster PN, Reidy DL, Fong L, Bergsland EK. Phase II study of pembrolizumab-based therapy in previously treated extrapulmonary poorly differentiated neuroendocrine carcinomas: Results of Part A (pembrolizumab alone). *J Clin Oncol* 2019; **37**: 363-363 [DOI: 10.1200/JCO.2019.37.4_suppl.363]

63 **Matos Garcia I**, Grande E, Garcia-Carbonero R, Lopez C, Teule A, Capdevila J. A multicohort phase II study of durvalumab plus tremelimumab for the treatment of patients (PTS) with advanced neuroendocrine neoplasms (NENs) of gastroenteropancreatic (GEP) or lung origin (the DUNE trial-GETNE1601-). *J Clin Oncol* 2017; **35**: TPS4146-TPS4146 [DOI: 10.1200/JCO.2017.35.15_suppl.TPS4146]

64 **Klein O**, Kee D, Markman B, Chang Lee R, Michael M, Mileshkin LR, Scott CL, Linklater R, Menon S, Tebbutt NC, Palmer J, Behren A, Cebon JS. A phase II clinical trial of ipilimumab/nivolumab combination immunotherapy in patients with rare upper gastrointestinal, neuroendocrine, and gynecological malignancies. *J Clin Oncol* 2019; **37**: 2570-2570 [DOI: 10.1200/JCO.2019.37.15_suppl.2570]

65 **Shen L**, Yu X, Lu M, Zhang X, Cheng Y, Zhang Y, Li Z, Xu J, Weng D, Wu C, Ma Y, Cheng K, WANG W, Gao H, Li Y, Zhou J, Shi H, Tan P, Su W. Surufatinib in combination with toripalimab in patients with advanced neuroendocrine carcinoma: Results from a multicenter, open-label, single-arm, phase II trial. *J Clin Oncol* 2021; **39**: e16199-e16199 [DOI:

10.1200/JCO.2021.39.15_suppl.e16199]

66 **Ito T**, Masui T, Komoto I, Doi R, Osamura RY, Sakurai A, Ikeda M, Takano K, Igarashi H, Shimatsu A, Nakamura K, Nakamoto Y, Hijioka S, Morita K, Ishikawa Y, Ohike N, Kasajima A, Kushima R, Kojima M, Sasano H, Hirano S, Mizuno N, Aoki T, Ohtsuka T, Okumura T, Kimura Y, Kudo A, Konishi T, Matsumoto I, Kobayashi N, Fujimori N, Honma Y, Morizane C, Uchino S, Horiuchi K, Yamasaki M, Matsubayashi J, Sato Y, Sekiguchi M, Abe S, Okusaka T, Kida M, Kimura W, Tanaka M, Majima Y, Jensen RT, Hirata K, Imamura M, Uemoto S. JNETS clinical practice guidelines for gastroenteropancreatic neuroendocrine neoplasms: diagnosis, treatment, and follow-up: a synopsis. *J Gastroenterol* 2021; **56**: 1033-1044 [PMID: 34586495 DOI: 10.1007/s00535-021-01827-7]

67 **Strosberg JR**, Caplin ME, Kunz PL, Ruszniewski PB, Bodei L, Hendifar AE, Mittra E, Wolin E M, Yao JC, Pavel ME, Grande E, Van Cutsem E, Seregni E, Duarte H, Gericke G, Bartalotta A, Demange A, Mutevelic S, Krenning E. Final overall survival in the phase 3 NETTER-1 study of lutetium-177-DOTATATE in patients with midgut neuroendocrine tumors. *J Clin Oncol* 2021; **39**: 4112-4112 [DOI: 10.1200/JCO.2021.39.15_suppl.4112]

68 **Clement D**, Navalkissoor S, Srirajaskanthan R, Courbon F, Dierickx L, Eccles A, Lewington V, Mitjavila M, Percovich J C, Lequoy B, He B, Folitar I, Ramage J. Efficacy and safety of 177Lu-DOTATATE in patients (pts) with advanced pancreatic neuroendocrine tumors (PanNETs): Data from the NETTER-R international, retrospective registry. *J Clin Oncol* 2021; **39**: 4116-4116 [DOI: 10.1200/JCO.2021.39.15_suppl.4116]

69 **Nicolas GP**, Ansquer C, Lenzo NP, Grønbæk H, Haug A, Navalkissoor S, Beauregard J, Germann N, McEwan S, Wild D, Hicks RJ. An international open-label study on safety and efficacy of 177Lu-satoreotide tetraxetan in somatostatin receptor positive neuroendocrine tumours (NETs): An interim analysis. *Ann Oncol* 2020; **31**: S711-S724 [DOI: 10.1016/j.annonc.2020.08.1373]

70 **Cives M**, Pelle' E, Strosberg J. Emerging Treatment Options for Gastroenteropancreatic Neuroendocrine Tumors. *J Clin Med* 2020; **9** [PMID: 33202931 DOI: 10.3390/jcm9113655]

71 **Grande E**, Teulé A, Alonso-Gordoa T, Jiménez-Fonseca P, Benavent M, Capdevila J, Custodio A, Vera R, Munarriz J, La Casta A, Díez JJ, Gajate P, Molina-Cerrillo J, Matos I, Cristóbal EM, Ruffinelli JC, Palacios J, García-Carbonero R. The PALBONET Trial: A Phase II Study of Palbociclib in Metastatic Grade 1 and 2 Pancreatic Neuroendocrine Tumors (GETNE-1407). *Oncologist* 2020; **25**: 745-e1265 [PMID: 32045050 DOI: 10.1634/theoncologist.2020-0033]

72 **Tang LH**, Contractor T, Clausen R, Klimstra DS, Du YC, Allen PJ, Brennan MF, Levine AJ, Harris CR. Attenuation of the retinoblastoma pathway in pancreatic neuroendocrine tumors due to increased cdk4/cdk6. *Clin Cancer Res* 2012; **18**: 4612-4620 [PMID: 22761470 DOI: 10.1158/1078-0432.CCR-11-3264]

73 **Anderson PM**, Gortz J. Phase 2 study of DRD2 antagonist/ClpP agonist ONC201 in neuroendocrine tumors. *J Clin Oncol* 2021; **39**: 3002-3002 [DOI: 10.1200/JCO.2021.39.15_suppl.3002]

74 **White BH**, Whalen K, Kriksciukaite K, Alargova R, Au Yeung T, Bazinet P, Brockman A, DuPont M, Oller H, Lemelin CA, Lim Soo P, Moreau B, Perino S, Quinn JM, Sharma G, Shinde R, Sweryda-Krawiec B, Wooster R, Bilodeau MT. Discovery of an SSTR2-Targeting Maytansinoid Conjugate (PEN-221) with Potent Activity in Vitro and in Vivo. *J Med Chem* 2019; **62**: 2708-2719 [PMID: 30735385 DOI: 10.1021/acs.jmedchem.8b02036]

75 **Halperin DM**, Johnson ML, Chan JA, Hart LL, Cook N, Patel VM, Schlechter BL, Cave J, Dowlati A, Blaszkowsky LS, Meyer T, Eads JR, Culp D, Kriksciukaite K, Mei L, Bilodeau M, Bloss J, Kulke MH. The safety and efficacy of PEN-221 somatostatin analog (SSA)-DM1 conjugate in patients (PTS) with advanced GI mid-gut neuroendocrine tumor (NET): Phase 2 results. *J Clin Oncol* 2021; **39**: 4110-4110 [DOI: 10.1200/JCO.2021.39.15_suppl.4110]

76 **Jonasch E**, Donskov F, Iliopoulos O, Rathmell WK, Narayan VK, Maughan BL, Oudard S, Else T, Maranchie JK, Welsh SJ, Thamake S, Park EK, Perini RF, Linehan WM, Srinivasan R; MK-6482-004 Investigators. Belzutifan for Renal Cell Carcinoma in von Hippel-Lindau Disease. *N Engl J Med* 2021; **385**: 2036-2046 [PMID: 34818478 DOI: 10.1056/NEJMoa2103425]

World Journal of Gastroenterology

Submit a Manuscript: https://www.f6publishing.com

World J Gastroenterol 2022 May 28; 28(20): 2176-2183

DOI: 10.3748/wjg.v28.i20.2176

ISSN 1007-9327 (print) ISSN 2219-2840 (online)

MINIREVIEWS

Radiomics for the detection of microvascular invasion in hepatocellular carcinoma

Kun Lv, Xin Cao, Peng Du, Jun-Yan Fu, Dao-Ying Geng, Jun Zhang

Specialty type: Gastroenterology and hepatology

Provenance and peer review: Invited article; Externally peer reviewed.

Peer-review model: Single blind

Peer-review report's scientific quality classification

Grade A (Excellent): A
Grade B (Very good): B
Grade C (Good): 0
Grade D (Fair): 0
Grade E (Poor): 0

P-Reviewer: Granito A, Italy; Zhou X, China

Received: November 16, 2021
Peer-review started: November 16, 2021
First decision: December 26, 2021
Revised: January 9, 2022
Accepted: April 22, 2022
Article in press: April 22, 2022
Published online: May 28, 2022

Kun Lv, Xin Cao, Peng Du, Jun-Yan Fu, Dao-Ying Geng, Jun Zhang, Department of Radiology, Huashan Hospital, Fudan University, Shanghai 200040, China

Xin Cao, Dao-Ying Geng, Jun Zhang, Institute of Functional and Molecular Medical Imaging, Fudan University, Shanghai 200040, China

Xin Cao, Dao-Ying Geng, Jun Zhang, Center for Shanghai Intelligent Imaging for Critical Brain Diseases Engineering and Technology Research, Science and Technology Commission of Shanghai Municipality, Shanghai 200040, China

Xin Cao, Dao-Ying Geng, Jun Zhang, Institute of Intelligent Imaging Phenomics, International Human Phenome Institutes (Shanghai), Shanghai 200040, China

Corresponding author: Dao-Ying Geng, MD, PhD, Dean, Doctor, Department of Radiology, Huashan Hospital, Fudan University, No. 12 Wulumuqi Road (Middle), Shanghai 200040, China. gdy_2019@163.com

Abstract

Hepatocellular carcinoma (HCC) is the most common primary liver cancer, accounting for about 90% of liver cancer cases. It is currently the fifth most common cancer in the world and the third leading cause of cancer-related mortality. Moreover, recurrence of HCC is common. Microvascular invasion (MVI) is a major factor associated with recurrence in postoperative HCC. It is difficult to evaluate MVI using traditional imaging modalities. Currently, MVI is assessed primarily through pathological and immunohistochemical analyses of postoperative tissue samples. Needle biopsy is the primary method used to confirm MVI diagnosis before surgery. As the puncture specimens represent just a small part of the tumor, and given the heterogeneity of HCC, biopsy samples may yield false-negative results. Radiomics, an emerging, powerful, and non-invasive tool based on various imaging modalities, such as computed tomography, magnetic resonance imaging, ultrasound, and positron emission tomography, can predict the HCC-MVI status preoperatively by delineating the tumor and/or the regions at a certain distance from the surface of the tumor to extract the image features. Although positive results have been reported for radiomics, its drawbacks have limited its clinical translation. This article reviews the application of radiomics, based on various imaging modalities, in preoperative evaluation of HCC-MVI and explores future research directions that facilitate its clinical translation.

Key Words: Microvascular invasion; Hepatocellular carcinoma; Radiomics; Texture analysis; Diagnostic imaging; Liver

©The Author(s) 2022. Published by Baishideng Publishing Group Inc. All rights reserved.

Core Tip: Hepatocellular carcinoma-microvascular invasion (HCC-MVI) is closely related to the prognosis of patients, so accurate and individualized prediction of MVI status before treatment is very important. Radiomics is a non-invasive method for predicting HCC-MVI status preoperatively. The standardization of relevant implementation processes of radiomics, such as the delineation of the region of interest, the improvement of algorithms, and the combination of liver imaging reporting and data system, will all contribute to the accurate prediction of MVI. In addition, the introduction of the biological significance of the disease can make up for the shortcomings of the clinical transformation of radiomics to a certain extent.

Citation: Lv K, Cao X, Du P, Fu JY, Geng DY, Zhang J. Radiomics for the detection of microvascular invasion in hepatocellular carcinoma. *World J Gastroenterol* 2022; 28(20): 2176-2183
URL: https://www.wjgnet.com/1007-9327/full/v28/i20/2176.htm
DOI: https://dx.doi.org/10.3748/wjg.v28.i20.2176

INTRODUCTION

Hepatocellular carcinoma (HCC) is the most common primary liver cancer, accounting for about 90% of liver cancers cases[1]. According to the World Health Organization, HCC is currently the fifth most common cancer in the world and the third leading cause of cancer-related mortality[2]. The rate of HCC occurrence varies with geographic regions. It is more commonly observed in the underdeveloped regions of the world; for example, its annual incidence rate in East Asia and Sub-Saharan Africa is higher, exceeding 15 per 100000 individuals. Nonetheless, the incidence of HCC is rising rapidly in Europe and the United States, and is expected to continue to rise over the next 10 years[3-5]. Although various treatment modalities are available for different stages of HCC, recurrence is common in the following types of HCC patients: patients with single masses with preserved liver function, no portal hypertension, and treated with resection; patients with multiple intrahepatic tumors or poor liver function, no major comorbidities, and listed for transplantation; patients with up to three tumors (each 4 cm or smaller), not eligible for transplantation, and treated with ablation; patients not eligible for ablation and receiving embolization; and some patients subjected to systemic and radiation treatments [6-8]. According to a previous study, about 70% of HCC patients relapse within 5 years after surgical resection and 35% relapse within 5 years after liver transplantation[9]. Microvascular invasion (MVI) is defined as the invasion of tumor cells into the vascular endothelial cell space, including microvessels of the portal vein, hepatic artery, and lymphatic vessels[10]. Previous studies[11,12] demonstrated that MVI is the strongest independent predictor of early HCC recurrence. It is primarily detected through immunohistochemical and pathological analyses of postoperative tissue specimens[13]. The inability to identify MVI preoperatively leads to incomplete surgical resection and increases the risk of postoperative recurrence. This limits the effectiveness of treatment and affects the long-term survival of liver cancer patients. Although conventional imaging examinations, such as computed tomography (CT)-based quantitative image analysis and dynamic contrast enhanced ultrasound (CEUS)[14,15] can predict MVI preoperatively, routine analyses of these images provide insufficient information, such as two-dimensional analysis of lesion morphology, size, *etc* based on conventional images.

Radiomics is an emerging, powerful, and non-invasive tool that uses a series of data mining algorithms and statistical analysis tools for the high-throughput analysis of image features. It can detect delicate features from conventional radiological images that are invisible to the naked eye and has been increasingly adopted to predict MVI. This enables extraction of many features at the whole lesion level. These features may provide information regarding heterogeneity and invasiveness of the disease that can be of predictive or prognostic value, thus leading to the selection of the best possible treatment[16]. HCC shows a large amount of intra- and inter-tumor heterogeneity at the biological level[17-20]. Biopsy, which is the main method for diagnosing HCC, usually involves removal of only a small part of the tumor, thus excluding the possibility of assessing intratumoral heterogeneity. Hence, in recent years, research pertaining to HCC using radiomics has attracted increasing attention[21]. Quantitative radiomics data, along with models or nomograms based on multiple imaging modalities including CT, magnetic resonance imaging (MRI), ultrasound (US), and positron emission tomography (PET), demonstrate high accuracy in predicting HCC-MVI preoperatively. In this review, we discuss the

applications of radiomics based on various imaging modalities in the preoperative detection of HCC-MVI (Table 1). In addition, future research directions are explored.

CT-BASED RADIOMICS

Liver cirrhosis or hepatitis B-related HCC can be diagnosed highly accurately through non-invasive approaches based on multi-phase CT/MRI imaging features, such as hyperenhancement in the arterial phase (AP) and hypoenhancement in the portal venous phase (PVP)[22]. For example, Peng *et al*[23] constructed a radiomics model based on hepatic AP and PVP images to delineate tumor regions and extract radiomic features to predict the preoperative MVI status of HCC related to hepatitis B. They found that radiomics signature, the alpha-fetoprotein (AFP) level, hypoattenuating halo, internal arteries, and non-smooth tumor margins are independent predictors of MVI. This model showed good correction and discrimination capabilities in the training and validation cohorts. The C indices for the training and validation cohorts were 0.846 and 0.844, respectively, and the area under the curve (AUC) of the radiomics nomogram in the MVI risk analysis was 0.845. In a similar study, Ma *et al*[24] found that the radiomics features of PVP were better than those of the AP and delayed phase (DP); the C index and AUC values of the model, combined with radiomic features and clinical factors, were close to those reported by Peng *et al*[23]. In a recent study based on AP and PVP images, Xu *et al*[9] marked the tumor regions and regions 5 mm away from the tumor surface, as regions of interest (ROI) to extract radiomic features to predict the HCC-MVI status and long-term clinical outcomes of patients with HCC. It was found that aspartate aminotransferase (AST) and AFP levels, tumor margin, growth pattern, capsule, peritumoral enhancement, radio-genomic venous invasion (RVI), and the radiomic score (R-score) were all predictors of MVI. The AUC of this model was 0.909, and the progression-free survival and overall survival of the MVI group were significantly lower than those of the non-MVI group. This showed that combining large-scale clinical radiology and radiomics analyses could reliably predict MVI and clinical outcomes.

MRI-BASED RADIOMICS

Although both conventional multi-phase contrast enhanced CT and MRI can be used to obtain the unique image features of HCC, MRI provides many additional imaging sequences that are helpful in diagnosing HCC without radiation damage; the additional sequences include T2-weighted imaging (T2WI), diffusion weighted imaging (DWI), and enhanced scanning by combined use of some extracellular and hepatocyte contrast agents, such as gadoxetic acid, that have the ability to distinguish relatively small and subtle lesions through the hypointensity received in the hepatobiliary phase (HBP)[25]. Moreover, a combination of MRI parameters can facilitate early diagnosis of small HCC. For example, double hypointensity in the portal/venous phase and HBP can be considered an MRI pattern that is highly suggestive of hypovascular HCC[26]. Thus, MRI-based radiomics provides more possibilities for HCC-MVI assessment. Feng *et al*[27], based on a gadolinium-ethoxybenzyl-diethylenetriamine (Gd-EOB-DTPA) MRI HBP image, delineated the tumor and designated a 1-cm area around it as the ROI. The combined intratumoral and peritumoral radiomics model presented in that study predicted the AUC value of MVI to be 0.85. In another study, Yang *et al*[28] used gadoxetic acid-enhanced MRI to delineate the tumor, which was then used as the ROI. They found that the AFP level, non-smooth tumor margins, arterial peritumoral enhancement, and radiomics signatures of HBP T1WI and HBP T1 maps could all be used as predictors of MVI. The prediction model that combined clinical radiation factors and fusion radiomic features from HBP images predicted the AUC of MVI to be 0.943, which was higher than that reported by Feng *et al*[27]. Meanwhile, the C indices of the generated nomograms in the training and validation groups were 0.936 and 0.864, respectively. This may stem from the varied delineation of the ROIs and the construction of models based on different sequences. Recently, Nebbia *et al*[29] devised a method based on radiomics through multi-sequence and traditional Gd-DTPA MRI for preoperative detection of MVI. It was found that the T2 and PVP sequences were superior to other MRI sequences in single-sequence models (*i.e.* T1, DWI, and late AP). The combination of these two sequences obtained the highest AUC value of 0.867 in predicting MVI, indicating that preoperative liver MRI scans are promising for predicting MVI and that the information obtained from a multi-parameter MRI sequence is crucial in identifying MVI.

US-BASED RADIOMICS

Compared with CT/MR, US is radiation-free, easy to implement, and simple to use for liver examinations. If potential predictors can be identified, US/CEUS may become an alternative technique to provide additional information for the detection of MVI. Hu *et al*[30], based on US images, outlined the

Table 1 Based on various imaging modalities radiomics in the application of microvascular invasion

Ref.	Modality/images/patients/ROI	Software	Predictors of MVI
Peng *et al*[23]	CT/AP and PVP CT images/304/tumor	IBEX software package	Radiomics signature, AFP level, hypoattenuating halo, internal arteries, and nonsmooth tumor margin
Ma *et al*[24]	CT/AP, PVP and DP CT images/157/tumor	ITK-Snap	Age, MTD, AFP, Radiomics signature, hepatitis B
Xu *et al*[9]	CT/AP and PVP CT images/495/VOI^{entire}, $VOI^{50\%}$, and $VOI^{penumbra}$	In-house software written in Python 3.6.1	AST, AFP, tumor margin, growth pattern, capsule, peritumoral enhance, RVI, R-score of VOI^{entire} on PP
Feng *et al*[27]	MRI/HBP of Gd-EOB-DTPA/160/tumoural and peritumoural (1cm) regions	ITK-Snap	NA
Yang *et al*[28]	MRI/T1, T2, DWI, Gd-EOB-DTPA MRI AP, PVP, DP, and HBP/208/tumor	ITK-Snap	AFP, nonsmooth tumor margin, arterial peritumoral enhancement, radiomics signatures of HBP T1WI and HBP T1 maps
Nebbia *et al*[29]	MRI/T1, T2, DWI, Gd-DTPA MRI AP and PVP/99/tumoural and peritumoural (1 cm) regions	NA	NA
Hu *et al*[30]	US/Grayscale US/482/tumor	A.K. software	radiomics score, AFP, and tumor size
Dong *et al*[31]	US/Grayscale US/322/tumor and peri-tumor (half of the tumor radius)	MITK	NA
Li *et al*[35]	PET-CT/[^{18}F]FDG PET-CT/80/areas with abnormal uptake	Lifex software	SUV_{max}, TLR, Rad-score

AFP: Alpha-fetoprotein; A.K. software: Artificial Intelligence Kit, version 1.1, GE Healthcare; AP: Artery phase; AST: Aspartate aminotransferase; CT: Computed tomography; DP: Delay phase; DWI: Diffusion weighted imaging; [^{18}F]FDG PET: 18-fluorodeoxyglucose positron emission tomography; Gd-DTPA: Gadopentetic acid; Gd-EOB-DTPA: Gadolinium-ethoxybenzyl-diethylenetriamine; HBP: Hepatobiliary phase; MITK: Medical Imaging Interaction Toolkit; MRI: Magnetic resonance imaging; MTD: Maximum tumour diameter; MVI: Microvascular invasion; NA: Not available; PP: Portal-venous phase imaging; PVP: Portal venous phase; ROI: Region of interest; R-score: Radiomic score; RVI: Radiogenomic venous invasion; SUV_{max}: Maximum standard uptake value; TLR: Maximum SUV of the tumor/mean SUV of the normal liver; US: Ultrasound; VOI^{entire}: Entire-volumetric interest; $VOI^{50\%}$: 50% of the entire tumor volume; $VOI^{penumbra}$: A region with 5 mm distance to tumor surface.

tumor region as the ROI to extract radiomic features and constructed a US-based radiomics score for preoperative prediction of HCC-MVI. The study showed that an AFP level > 400 ng/mL and tumor size > 5 cm were significantly related to MVI. The AFP level, gray-scale US-based tumor size, and radiomics score were identified to be independent predictors of MVI. The radiomics-based nomogram (AUC: 0.731) showed better performance in MVI detection than the clinical nomogram (AUC: 0.634). However, there was no significant difference between the MVI-positive and -negative groups in terms of other clinical and pathological features, as well as CEUS features. Similarly, Dong *et al*[31] envisaged that radiomic algorithms based on US images might have potential predictive value in the detection of MVI in patients with HCC. Unlike Hu *et al*[30], Dong *et al*[31] delineated the gross-tumor region (GTR) and the peri-tumoral region (PTR, the uniform dilated half of the tumor radius) and showed that the AUC of the radiomic nomogram, combined with the AFP level, characteristics of the tumor, and the area around the tumor, was 0.744, which was slightly higher than that reported by Hu *et al*[30]. This also supports the idea that the peritumoral area is an onset area of MVI. It is thought to be the main blood transmission route of portal vein thrombosis and the main route for intra- and extra-hepatic metastases [32]. This signifies that, when evaluating HCC-MVI based on radiomics, the area around the tumor also needs to be evaluated.

PET-BASED RADIOMICS

High glucose consumption by the tumor cell microenvironment, including that in HCC, can be reflected in 18-fluorodeoxyglucose PET (^{18}FDG-PET). Although the tumor detection efficiency is affected by liver cirrhosis and a high background signal, studies have confirmed that the maximum standard uptake value (SUVmax) of ^{18}FDG-PET is related to the recurrence rate of HCC and patient survival, and that the combination of MRI and ^{18}FDG-PET can improve the accuracy of HCC histopathological grading[33,34]. In a recent study[35], the PET/CT model, after integrating the radiomic features composed of five PET- and six CT-derived texture features, showed an AUC of 0.891 in the training cohort. The prediction of disease-free survival (DFS) was also more accurate (C index of 0.831). This study indicated that the newly developed [^{18}F]FDG PET/CT radiomics feature is an independent biomarker for evaluating MVI

and DFS in patients with ultra-early and early HCC.

LIMITATIONS

Although radiomics has achieved some exciting results in evaluating the HCC-MVI status, many limitations still exist. The current lack of standardization in image acquisition schemes, segmentation methods, and radiomics tools used for analysis may lead to differences in the measurement of radiomic features that do not stem from biological differences[16]. Existing studies[36] have shown varied reproducibility in extracting quantitative imaging features from tumor regions segmented by different methods. Fortunately, the radiomics quality score (RQS) has been proposed to assess whether radiomics research meets best practices[37]. In addition, there are huge challenges in interpreting the correlation between radiomics features and their biological significance, especially that of the texture features obtained from high-level analysis. This leads to restrictions on the use of radiomics in clinical applications[38].

FUTURE DIRECTIONS

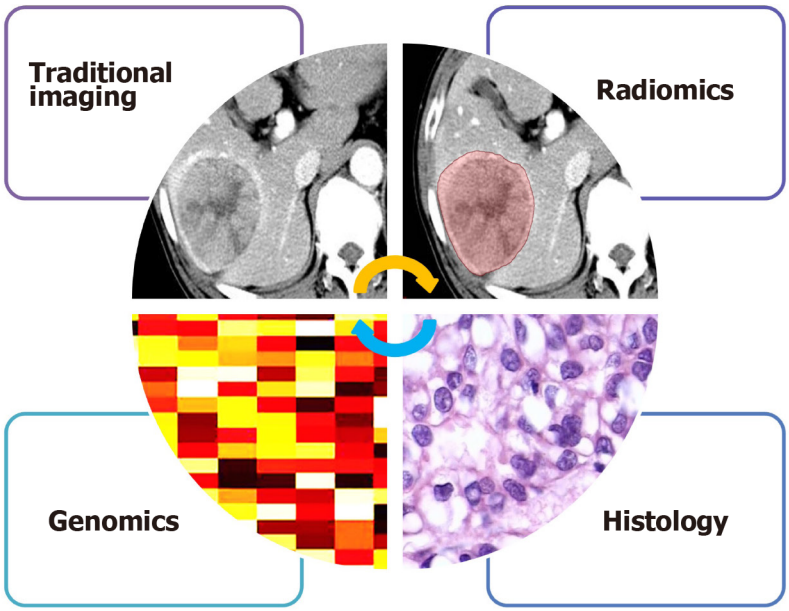
Every step involved in radiomics-based analyses needs to be optimized and standardized, including the adjustment of imaging schemes and parameters, development of (semi-) automated segmentation methods, and refinement of algorithms and high-throughput analysis modeling methods. In addition, in the process of establishing a radiomics model, potential independent variables should be included in the multivariate analysis (such as protein induced by vitamin K absence or antagonist-II), which will help improve the sensitivity, specificity, and predictive ability of the model[39]. In addition, the imaging characteristics of certain liver nodules in patients with chronic liver disease are complex and diverse. For example, the imaging manifestations of primary and recurrent cirrhosis nodules are different[40], and tuberculosis nodules are easily misdiagnosed as HCC[41]. Through targeted collection of a large number of these different liver nodules, corresponding predictions can also be made using radiomics. Furthermore, due to the complexity and similarity in imaging characteristics of certain hepatic nodules in high-risk HCC, the American College of Radiology (ACR) has issued a diagnostic program, namely the liver imaging reporting and data system (LI-RADS, https://www.acr.org). Several studies[42-44] have indicated that ACR CT/MRI LI-RADS and CEUS LI-RADS possess high application value in identifying primary hepatic nodules in patients with high-risk HCC, and especially display high diagnostic performance with LR-5 and LR-M nodules. In a recent study, Zhou *et al*[45] observed that the model incorporating CEUS LR-M and clinical features was able to predict the MVI status of HCC. Therefore, undoubtedly, LI-RADS combined with radiomics using various imaging modalities shows promise in the prediction of HCC-MVI.

Although radiomics can predict MVI and determine related predictors, there are differences between groups. With the exponential growth of interest in the development of artificial intelligence (AI)-based applications, there is now an opportunity to apply AI in radiomics analyses. Deep learning, especially convolutional neural networks (CNNs), can capture texture information in the initial convolution layer. CNNs may replace several current radiomics-based analysis methods[46]. Recently, a new concept of "deep radiomics" was proposed. This technique combines radiomics and deep learning analysis by creating feature images based on texture features and then using them as input for CNNs to classify the images. Therefore, along with the prediction of MVI, the use of AI-based technology is also expected to identify individual MVI.

Data-driven radiomics is inherently unable to provide insights into the biological basis of the observed relationship. It is important to note that HCC shows large intra- and inter-tumor heterogeneity at the biological level. With the rapid development and popularization of machine learning, researchers are paying increasing attention to the improvement of prediction ability; however, they are far from understanding the biological significance of the observed research results. This disconnect between the predictive models and their biological significance inherently limits their widespread clinical translation. Therefore, it is necessary to introduce biological significance into the radiomics field through various available biological methods, such as genome association, immunohistochemical analyses, local microscopic pathological image texture analyses, and evaluation of macroscopic histopathological marker expression (Figure 1)[47].

CONCLUSION

Radiomics based on multiple imaging modalities has performed remarkably well in predicting the HCC-MVI status. In future, researchers need to focus on standardizing image segmentation and radiomics processing processes and the optimization of algorithms to further improve the accuracy of



DOI: 10.3748/wjg.v28.i20.2176 **Copyright** © The Author(s) 2022.

Figure 1 Histology and genomic analysis can provide specific small-scale insights and help validate radiomic results.

individualized prediction. Importantly, it may be possible to provide some new insights through combining deep learning and LI-RADS with radiomics and introducing biological significance.

FOOTNOTES

Author contributions: All authors contributed to this paper; Geng DY and Zhang J designed the outline for the review; Lv K wrote the review; Cao X, Du P, and Fu JY offered assistance for correct the syntax errors of the paper; Zhang J and Lv K revised and edited the final version.

Supported by the Shanghai Municipal Commission of Science and Technology, No. 19411951200; Clinical Research Plan of SHDC, No. SHDC2020CR3020A; and the Research Startup Fund of Huashan Hospital Fudan University, No. 2021QD035.

Conflict-of-interest statement: There is no conflict of interest associated with any of the senior author or other coauthors contributed their efforts in this manuscript.

Open-Access: This article is an open-access article that was selected by an in-house editor and fully peer-reviewed by external reviewers. It is distributed in accordance with the Creative Commons Attribution NonCommercial (CC BY-NC 4.0) license, which permits others to distribute, remix, adapt, build upon this work non-commercially, and license their derivative works on different terms, provided the original work is properly cited and the use is non-commercial. See: https://creativecommons.org/Licenses/by-nc/4.0/

Country/Territory of origin: China

ORCID number: Kun Lv 0000-0003-4967-3727; Xin Cao 0000-0003-3839-3076; Peng Du 0000-0002-6970-1329; Jun-Yan Fu 0000-0002-1000-2507; Dao-Ying Geng 0000-0002-3585-6883; Jun Zhang 0000-0003-1849-9199.

S-Editor: Yan JP
L-Editor: Filipodia
P-Editor: Yan JP

REFERENCES

1 **Omata M**, Cheng AL, Kokudo N, Kudo M, Lee JM, Jia J, Tateishi R, Han KH, Chawla YK, Shiina S, Jafri W, Payawal DA, Ohki T, Ogasawara S, Chen PJ, Lesmana CRA, Lesmana LA, Gani RA, Obi S, Dokmeci AK, Sarin SK. Asia-Pacific clinical practice guidelines on the management of hepatocellular carcinoma: a 2017 update. *Hepatol Int* 2017; **11**: 317-370 [PMID: 28620797 DOI: 10.1007/s12072-017-9799-9]

2 **Marrero JA**, Kulik LM, Sirlin CB, Zhu AX, Finn RS, Abecassis MM, Roberts LR, Heimbach JK. Diagnosis, Staging, and Management of Hepatocellular Carcinoma: 2018 Practice Guidance by the American Association for the Study of Liver Diseases. *Hepatology* 2018; **68**: 723-750 [PMID: 29624699 DOI: 10.1002/hep.29913]

3 **European Association for the Study of the Liver**. EASL Clinical Practice Guidelines: Management of hepatocellular carcinoma. *J Hepatol* 2018; **69**: 182-236 [PMID: 29628281 DOI: 10.1016/j.jhep.2018.03.019]

4 **Petrick JL**, Braunlin M, Laversanne M, Valery PC, Bray F, McGlynn KA. International trends in liver cancer incidence, overall and by histologic subtype, 1978-2007. *Int J Cancer* 2016; **139**: 1534-1545 [PMID: 27244487 DOI: 10.1002/ijc.30211]

5 **Petrick JL**, Kelly SP, Altekruse SF, McGlynn KA, Rosenberg PS. Future of Hepatocellular Carcinoma Incidence in the United States Forecast Through 2030. *J Clin Oncol* 2016; **34**: 1787-1794 [PMID: 27044939 DOI: 10.1200/JCO.2015.64.7412]

6 **Tabrizian P**, Jibara G, Shrager B, Schwartz M, Roayaie S. Recurrence of hepatocellular cancer after resection: patterns, treatments, and prognosis. *Ann Surg* 2015; **261**: 947-955 [PMID: 25010665 DOI: 10.1097/SLA.0000000000000710]

7 **Grandhi MS**, Kim AK, Ronnekleiv-Kelly SM, Kamel IR, Ghasebeh MA, Pawlik TM. Hepatocellular carcinoma: From diagnosis to treatment. *Surg Oncol* 2016; **25**: 74-85 [PMID: 27312032 DOI: 10.1016/j.suronc.2016.03.002]

8 **Witt JS**, Rosenberg SA, Bassetti MF. MRI-guided adaptive radiotherapy for liver tumours: visualising the future. *Lancet Oncol* 2020; **21**: e74-e82 [PMID: 32007208 DOI: 10.1016/S1470-2045(20)30034-6]

9 **Xu X**, Zhang HL, Liu QP, Sun SW, Zhang J, Zhu FP, Yang G, Yan X, Zhang YD, Liu XS. Radiomic analysis of contrast-enhanced CT predicts microvascular invasion and outcome in hepatocellular carcinoma. *J Hepatol* 2019; **70**: 1133-1144 [PMID: 30876945 DOI: 10.1016/j.jhep.2019.02.023]

10 **Gouw AS**, Balabaud C, Kusano H, Todo S, Ichida T, Kojiro M. Markers for microvascular invasion in hepatocellular carcinoma: where do we stand? *Liver Transpl* 2011; **17** Suppl 2: S72-S80 [PMID: 21714066 DOI: 10.1002/lt.22368]

11 **Roayaie S**, Blume IN, Thung SN, Guido M, Fiel MI, Hiotis S, Labow DM, Llovet JM, Schwartz ME. A system of classifying microvascular invasion to predict outcome after resection in patients with hepatocellular carcinoma. *Gastroenterology* 2009; **137**: 850-855 [PMID: 19524573 DOI: 10.1053/j.gastro.2009.06.003]

12 **Lim KC**, Chow PK, Allen JC, Chia GS, Lim M, Cheow PC, Chung AY, Ooi LL, Tan SB. Microvascular invasion is a better predictor of tumor recurrence and overall survival following surgical resection for hepatocellular carcinoma compared to the Milan criteria. *Ann Surg* 2011; **254**: 108-113 [PMID: 21527845 DOI: 10.1097/SLA.0b013e31821ad884]

13 **Rodríguez-Perálvarez M**, Luong TV, Andreana L, Meyer T, Dhillon AP, Burroughs AK. A systematic review of microvascular invasion in hepatocellular carcinoma: diagnostic and prognostic variability. *Ann Surg Oncol* 2013; **20**: 325-339 [PMID: 23149850 DOI: 10.1245/s10434-012-2513-1]

14 **Zheng J**, Chakraborty J, Chapman WC, Gerst S, Gonen M, Pak LM, Jarnagin WR, DeMatteo RP, Do RKG, Simpson AL; Hepatopancreatobiliary Service in the Department of Surgery of the Memorial Sloan Kettering Cancer Center; Research Staff in the Department of Surgery at Washington University School of Medicine. Preoperative Prediction of Microvascular Invasion in Hepatocellular Carcinoma Using Quantitative Image Analysis. *J Am Coll Surg* 2017; **225**: 778-788.e1 [PMID: 28941728 DOI: 10.1016/j.jamcollsurg.2017.09.003]

15 **Dong Y**, Qiu Y, Yang D, Yu L, Zuo D, Zhang Q, Tian X, Wang WP, Jung EM. Potential application of dynamic contrast enhanced ultrasound in predicting microvascular invasion of hepatocellular carcinoma. *Clin Hemorheol Microcirc* 2021; **77**: 461-469 [PMID: 33459703 DOI: 10.3233/CH-201085]

16 **Gillies RJ**, Kinahan PE, Hricak H. Radiomics: Images Are More than Pictures, They Are Data. *Radiology* 2016; **278**: 563-577 [PMID: 26579733 DOI: 10.1148/radiol.2015151169]

17 **Fransvea E**, Paradiso A, Antonaci S, Giannelli G. HCC heterogeneity: molecular pathogenesis and clinical implications. *Cell Oncol* 2009; **31**: 227-233 [PMID: 19478390 DOI: 10.3233/CLO-2009-0473]

18 **Friemel J**, Rechsteiner M, Frick L, Böhm F, Struckmann K, Egger M, Moch H, Heikenwalder M, Weber A. Intratumor heterogeneity in hepatocellular carcinoma. *Clin Cancer Res* 2015; **21**: 1951-1961 [PMID: 25248380 DOI: 10.1158/1078-0432.CCR-14-0122]

19 **Lin DC**, Mayakonda A, Dinh HQ, Huang P, Lin L, Liu X, Ding LW, Wang J, Berman BP, Song EW, Yin D, Koeffler HP. Genomic and Epigenomic Heterogeneity of Hepatocellular Carcinoma. *Cancer Res* 2017; **77**: 2255-2265 [PMID: 28302680 DOI: 10.1158/0008-5472.CAN-16-2822]

20 **Zhu S**, Hoshida Y. Molecular heterogeneity in hepatocellular carcinoma. *Hepat Oncol* 2018; **5**: HEP10 [PMID: 30302198 DOI: 10.2217/hep-2018-0005]

21 **Yip SS**, Aerts HJ. Applications and limitations of radiomics. *Phys Med Biol* 2016; **61**: R150-R166 [PMID: 27269645 DOI: 10.1088/0031-9155/61/13/R150]

22 **Heimbach JK**, Kulik LM, Finn RS, Sirlin CB, Abecassis MM, Roberts LR, Zhu AX, Murad MH, Marrero JA. AASLD guidelines for the treatment of hepatocellular carcinoma. *Hepatology* 2018; **67**: 358-380 [PMID: 28130846 DOI: 10.1002/hep.29086]

23 **Peng J**, Zhang J, Zhang Q, Xu Y, Zhou J, Liu L. A radiomics nomogram for preoperative prediction of microvascular invasion risk in hepatitis B virus-related hepatocellular carcinoma. *Diagn Interv Radiol* 2018; **24**: 121-127 [PMID: 29770763 DOI: 10.5152/dir.2018.17467]

24 **Ma X**, Wei J, Gu D, Zhu Y, Feng B, Liang M, Wang S, Zhao X, Tian J. Preoperative radiomics nomogram for microvascular invasion prediction in hepatocellular carcinoma using contrast-enhanced CT. *Eur Radiol* 2019; **29**: 3595-3605 [PMID: 30770969 DOI: 10.1007/s00330-018-5985-y]

25 **Roberts LR**, Sirlin CB, Zaiem F, Almasri J, Prokop LJ, Heimbach JK, Murad MH, Mohammed K. Imaging for the diagnosis of hepatocellular carcinoma: A systematic review and meta-analysis. *Hepatology* 2018; **67**: 401-421 [PMID: 28859233 DOI: 10.1002/hep.29487]

26 **Granito A**, Galassi M, Piscaglia F, Romanini L, Lucidi V, Renzulli M, Borghi A, Grazioli L, Golfieri R, Bolondi L. Impact of gadoxetic acid (Gd-EOB-DTPA)-enhanced magnetic resonance on the non-invasive diagnosis of small hepatocellular carcinoma: a prospective study. *Aliment Pharmacol Ther* 2013; **37**: 355-363 [PMID: 23199022 DOI: 10.1111/apt.12166]

27 **Feng ST**, Jia Y, Liao B, Huang B, Zhou Q, Li X, Wei K, Chen L, Li B, Wang W, Chen S, He X, Wang H, Peng S, Chen

ZB, Tang M, Chen Z, Hou Y, Peng Z, Kuang M. Preoperative prediction of microvascular invasion in hepatocellular cancer: a radiomics model using Gd-EOB-DTPA-enhanced MRI. *Eur Radiol* 2019; **29**: 4648-4659 [PMID: 30689032 DOI: 10.1007/s00330-018-5935-8]

28 **Yang L**, Gu D, Wei J, Yang C, Rao S, Wang W, Chen C, Ding Y, Tian J, Zeng M. A Radiomics Nomogram for Preoperative Prediction of Microvascular Invasion in Hepatocellular Carcinoma. *Liver Cancer* 2019; **8**: 373-386 [PMID: 31768346 DOI: 10.1159/000494099]

29 **Nebbia G**, Zhang Q, Arefan D, Zhao X, Wu S. Pre-operative Microvascular Invasion Prediction Using Multi-parametric Liver MRI Radiomics. *J Digit Imaging* 2020; **33**: 1376-1386 [PMID: 32495126 DOI: 10.1007/s10278-020-00353-x]

30 **Hu HT**, Wang Z, Huang XW, Chen SL, Zheng X, Ruan SM, Xie XY, Lu MD, Yu J, Tian J, Liang P, Wang W, Kuang M. Ultrasound-based radiomics score: a potential biomarker for the prediction of microvascular invasion in hepatocellular carcinoma. *Eur Radiol* 2019; **29**: 2890-2901 [PMID: 30421015 DOI: 10.1007/s00330-018-5797-0]

31 **Dong Y**, Zhou L, Xia W, Zhao XY, Zhang Q, Jian JM, Gao X, Wang WP. Preoperative Prediction of Microvascular Invasion in Hepatocellular Carcinoma: Initial Application of a Radiomic Algorithm Based on Grayscale Ultrasound Images. *Front Oncol* 2020; **10**: 353 [PMID: 32266138 DOI: 10.3389/fonc.2020.00353]

32 **Hu HT**, Shen SL, Wang Z, Shan QY, Huang XW, Zheng Q, Xie XY, Lu MD, Wang W, Kuang M. Peritumoral tissue on preoperative imaging reveals microvascular invasion in hepatocellular carcinoma: a systematic review and meta-analysis. *Abdom Radiol (NY)* 2018; **43**: 3324-3330 [PMID: 29845312 DOI: 10.1007/s00261-018-1646-5]

33 **Cho KJ**, Choi NK, Shin MH, Chong AR. Clinical usefulness of FDG-PET in patients with hepatocellular carcinoma undergoing surgical resection. *Ann Hepatobiliary Pancreat Surg* 2017; **21**: 194-198 [PMID: 29264581 DOI: 10.14701/ahbps.2017.21.4.194]

34 **Kaissis GA**, Lohöfer FK, Hörl M, Heid I, Steiger K, Munoz-Alvarez KA, Schwaiger M, Rummeny EJ, Weichert W, Paprottka P, Braren R. Combined DCE-MRI- and FDG-PET enable histopathological grading prediction in a rat model of hepatocellular carcinoma. *Eur J Radiol* 2020; **124**: 108848 [PMID: 32006931 DOI: 10.1016/j.ejrad.2020.108848]

35 **Li Y**, Zhang Y, Fang Q, Zhang X, Hou P, Wu H, Wang X. Radiomics analysis of [^{18}F]FDG PET/CT for microvascular invasion and prognosis prediction in very-early- and early-stage hepatocellular carcinoma. *Eur J Nucl Med Mol Imaging* 2021; **48**: 2599-2614 [PMID: 33416951 DOI: 10.1007/s00259-020-05119-9]

36 **Qiu Q**, Duan J, Duan Z, Meng X, Ma C, Zhu J, Lu J, Liu T, Yin Y. Reproducibility and non-redundancy of radiomic features extracted from arterial phase CT scans in hepatocellular carcinoma patients: impact of tumor segmentation variability. *Quant Imaging Med Surg* 2019; **9**: 453-464 [PMID: 31032192 DOI: 10.21037/qims.2019.03.02]

37 **Lambin P**, Leijenaar RTH, Deist TM, Peerlings J, de Jong EEC, van Timmeren J, Sanduleanu S, Larue RTHM, Even AJG, Jochems A, van Wijk Y, Woodruff H, van Soest J, Lustberg T, Roelofs E, van Elmpt W, Dekker A, Mottaghy FM, Wildberger JE, Walsh S. Radiomics: the bridge between medical imaging and personalized medicine. *Nat Rev Clin Oncol* 2017; **14**: 749-762 [PMID: 28975929 DOI: 10.1038/nrclinonc.2017.141]

38 **Lewis S**, Hectors S, Taouli B. Radiomics of hepatocellular carcinoma. *Abdom Radiol (NY)* 2021; **46**: 111-123 [PMID: 31925492 DOI: 10.1007/s00261-019-02378-5]

39 **Xu XF**, Yu JJ, Xing H, Shen F, Yang T. How to better predict microvascular invasion and recurrence of hepatocellular carcinoma. *J Hepatol* 2017; **67**: 1119-1120 [PMID: 28736140 DOI: 10.1016/j.jhep.2017.06.034]

40 **Leoni S**, Piscaglia F, Granito A, Borghi A, Galassi M, Marinelli S, Terzi E, Bolondi L. Characterization of primary and recurrent nodules in liver cirrhosis using contrast-enhanced ultrasound: which vascular criteria should be adopted? *Ultraschall Med* 2013; **34**: 280-287 [PMID: 23616066 DOI: 10.1055/s-0033-1335024]

41 **Yang C**, Liu X, Ling W, Song B, Liu F. Primary isolated hepatic tuberculosis mimicking small hepatocellular carcinoma: A case report. *Medicine (Baltimore)* 2020; **99**: e22580 [PMID: 33031307 DOI: 10.1097/MD.0000000000022580]

42 **Lee SM**, Lee JM, Ahn SJ, Kang HJ, Yang HK, Yoon JH. LI-RADS Version 2017 *vs* Version 2018: Diagnosis of Hepatocellular Carcinoma on Gadoxetate Disodium-enhanced MRI. *Radiology* 2019; **292**: 655-663 [PMID: 31310175 DOI: 10.1148/radiol.2019182867]

43 **Lv K**, Cao X, Dong Y, Geng D, Zhang J. CT/MRI LI-RADS version 2018 *vs* CEUS LI-RADS version 2017 in the diagnosis of primary hepatic nodules in patients with high-risk hepatocellular carcinoma. *Ann Transl Med* 2021; **9**: 1076 [PMID: 34422988 DOI: 10.21037/atm-21-1035]

44 **Zhang T**, Huang ZX, Wei Y, Jiang HY, Chen J, Liu XJ, Cao LK, Duan T, He XP, Xia CC, Song B. Hepatocellular carcinoma: Can LI-RADS v2017 with gadoxetic-acid enhancement magnetic resonance and diffusion-weighted imaging improve diagnostic accuracy? *World J Gastroenterol* 2019; **25**: 622-631 [PMID: 30774276 DOI: 10.3748/wjg.v25.i5.622]

45 **Zhou H**, Sun J, Jiang T, Wu J, Li Q, Zhang C, Zhang Y, Cao J, Sun Y, Jiang Y, Liu Y, Zhou X, Huang P. A Nomogram Based on Combining Clinical Features and Contrast Enhanced Ultrasound LI-RADS Improves Prediction of Microvascular Invasion in Hepatocellular Carcinoma. *Front Oncol* 2021; **11**: 699290 [PMID: 34307168 DOI: 10.3389/fonc.2021.699290]

46 **Parekh VS**, Jacobs MA. Deep learning and radiomics in precision medicine. *Expert Rev Precis Med Drug Dev* 2019; **4**: 59-72 [PMID: 31080889 DOI: 10.1080/23808993.2019.1585805]

47 **Tomaszewski MR**, Gillies RJ. The Biological Meaning of Radiomic Features. *Radiology* 2021; **298**: 505-516 [PMID: 33399513 DOI: 10.1148/radiol.2021202553]

World Journal of Gastroenterology

Submit a Manuscript: https://www.f6publishing.com

World J Gastroenterol 2022 May 28; 28(20): 2184-2200

DOI: 10.3748/wjg.v28.i20.2184

ISSN 1007-9327 (print) ISSN 2219-2840 (online)

ORIGINAL ARTICLE

Basic Study

Long noncoding RNA TNFRSF10A-AS1 promotes colorectal cancer through upregulation of HuR

Dan-Dan Wang, Dong-Lei Sun, Shao-Peng Yang, Jia Song, Meng-Yao Wu, Wei-Wei Niu, Mei Song, Xiao-Lan Zhang

Specialty type: Gastroenterology and hepatology

Provenance and peer review: Unsolicited article; Externally peer reviewed.

Peer-review model: Single blind

Peer-review report's scientific quality classification

Grade A (Excellent): 0
Grade B (Very good): B, B
Grade C (Good): 0
Grade D (Fair): 0
Grade E (Poor): 0

P-Reviewer: Kołat D, Poland; Yoshimatsu K, Japan

Received: October 26, 2021
Peer-review started: October 26, 2021
First decision: December 27, 2021
Revised: January 10, 2022
Accepted: April 20, 2022
Article in press: April 20, 2022
Published online: May 28, 2022

Dan-Dan Wang, Dong-Lei Sun, Shao-Peng Yang, Jia Song, Meng-Yao Wu, Wei-Wei Niu, Mei Song, Xiao-Lan Zhang, Department of Gastroenterology, The Second Hospital of Hebei Medical University, Shijiazhuang 050000, Hebei Province, China

Corresponding author: Xiao-Lan Zhang, MD, PhD, Chief Physician, Department of Gastroenterology, The Second Hospital of Hebei Medical University, No. 215 Heping West Road, Shijiazhuang 050000, Hebei Province, China. xiaolanzh@126.com

Abstract

BACKGROUND

Recent studies have emphasized the emerging importance of long noncoding RNAs (lncRNAs) in colorectal cancer (CRC). However, the functions and regulatory mechanisms of numerous lncRNAs in CRC have not been fully elucidated.

AIM

To explore the functional role and underlying molecular mechanisms of lncRNA TNFRSF10A-AS1 in CRC.

METHODS

TNFRSF10A-AS1 expression was measured by quantitative real-time polymerase chain reaction in CRC, and the relationship between TNFRSF10A-AS1 levels and the clinicopathological features of CRC patients was analyzed. The effect of TNFRSF10A-AS1 expression on CRC proliferation and metastasis was examined *in vitro* and *in vivo*. Mechanistically, we investigated how TNFRSF10A-AS1 is involved in CRC as a competitive endogenous RNA.

RESULTS

TNFRSF10A-AS1 was expressed at a high level in CRC and the upregulation of TNFRSF10A-AS1 was associated with advanced T grade and tumor size in CRC patients. A functional investigation revealed that TNFRSF10A-AS1 enhanced the proliferation, migration ability and invasion ability of colon cancer cells *in vitro* and *in vivo*. A mechanistic analysis demonstrated that TNFRSF10A-AS1 acted as a miR-3121-3p molecular sponge to regulate HuR expression, ultimately promoting colorectal tumorigenesis and progression.

CONCLUSION

TNFRSF10A-AS1 exerts a tumor-promoting function through the miR-3121-3p/HuR axis in CRC, indicating that it may be a novel target for CRC therapy.

Key Words: Colorectal cancer; Long noncoding RNA; TNFRSF10A-AS1; miR-3121-3p; HuR

©The Author(s) 2022. Published by Baishideng Publishing Group Inc. All rights reserved.

Core Tip: TNFRSF10A-AS1 was upregulated in colorectal cancer (CRC) tumor tissues and cell lines, and it was positively correlated with tumor grade and size in patients with CRC. In addition, TNFRSF10A-AS1 facilitated CRC growth and metastasis. Mechanistically, TNFRSF10A-AS1 was predominantly found in the cytoplasm of CRC cell lines and upregulated the level of the downstream target, HuR, by sponging miR-3121-3p, thereby further promoting colorectal tumorigenesis and progression.

Citation: Wang DD, Sun DL, Yang SP, Song J, Wu MY, Niu WW, Song M, Zhang XL. Long noncoding RNA TNFRSF10A-AS1 promotes colorectal cancer through upregulation of HuR. *World J Gastroenterol* 2022; 28(20): 2184-2200
URL: https://www.wjgnet.com/1007-9327/full/v28/i20/2184.htm
DOI: https://dx.doi.org/10.3748/wjg.v28.i20.2184

INTRODUCTION

Colorectal cancer (CRC) is one of the most commonly diagnosed cancers and the third leading cause of cancer-related deaths around the world[1]. Despite marked advances in CRC diagnosis and therapy in recent years, the prognosis remains poor for many patients due to a lack of timely diagnosis and individualized disease management measures. The 5-year survival rate for CRC patients with distant metastases is approximately 14%[2]. Notably, CRC incidence and mortality rates are rising rapidly in developing countries[3]. In addition, epidemiological studies have shown an increasing incidence in adolescents and adults less than 50 years of age[4]. Genetic factors and poor lifestyle habits are the main predisposing factors for CRC, but the exact pathogenesis is unknown. Therefore, in-depth studies of the pathogenesis of CRC are of great clinical importance.

Recent evidence from studies of CRC-related pathogenesis has suggested that tumor-specific long noncoding RNAs (lncRNAs) may contribute to early diagnosis and prognostic assessment as well as improve disease treatment outcomes. LncRNAs are long (over 200 nucleotides) RNAs[5] that can interact with DNA, RNA and proteins. The function of lncRNAs mainly depends on their subcellular localization. Nuclear lncRNAs tend to bind DNA and proteins to regulate chromatin interactions, transcription and RNA processing, while cytoplasmic lncRNAs modulate mRNA stability or translation to influence cellular signaling cascades and can also act as competing endogenous RNAs (ceRNAs). CeRNAs competitively bind microRNA response elements (MREs) to regulate downstream gene expression[6,7]. In cells, ceRNAs containing the same MREs can competitively bind to the same microRNA (miRNA) and play posttranscriptional regulatory roles. Recent studies have shown that lncRNA/miRNA/mRNA mechanisms are involved in several aspects of CRC, including tumorigenesis, epithelial-mesenchymal transition (EMT), inflammatory processes and chemo-/radio-resistance[8]. For example, lncRNA SNHG6 serves as a ceRNA of miR-26a/b and miR-214, thereby regulating their common target, EZH2, to promote CRC growth and metastasis[9]. However, the functions and mechanisms of a vast majority of CRC-associated lncRNAs remain unclear.

LncRNA TNFRSF10A-AS1 is a novel lncRNA that has been demonstrated to be associated with the mechanism of autophagy in CRC, and Kaplan-Meier survival analysis has indicated that patients with high expression of TNFRSF10A-AS1 have a better prognosis. However, TNFRSF10A-AS1 expression in CRC cell lines is relatively high, which is inconsistent with the above findings[10]. Another study has identified five lncRNAs, including TNFRSF10A-AS1, by the expression of genome-wide lncRNAs in high-throughput RNA sequencing data, which may be useful to predict gastric cancer prognosis[11]. The current evidence on TNFRSF10A-AS1 is all based on The Cancer Genome Atlas (TCGA) data analysis, and the role of TNFRSF10A-AS1 in tumors is inconsistent. Moreover, the exact mechanism of TNFRSF10A-AS1 is unclear. Therefore, clinical and biological studies are needed to validate these findings. Our work is aimed to study the expression, functional roles and exact mechanisms of TNFRSF10A-AS1 in CRC. In the present study, our findings suggested that TNFRSF10A-AS1 was a novel oncogenic lncRNA that promoted CRC progression and might provide new ideas for CRC therapy.

MATERIALS AND METHODS

Database search

The expression of lncRNA TNFRSF10A-AS1 in colon adenocarcinoma (COAD) and rectum adenocarcinoma (READ) was analyzed using Gene Expression Profiling Interactive Analysis (GEPIA). GEPIA is an online analysis tool that is available to provide fast and customizable analysis based on TCGA data. We compared the expression of TNFRSF10A-AS1 between CRC tumor and nontumor tissues by box plots, which used $\log_2$(TPM + 1) for log-scale ($P < 0.05$ compared to control).

Patient tissue samples

We collected 40 pairs of surgically resected CRC tumor tissues and matched adjacent non-tumor tissue samples. These samples were obtained from patients with pathologically diagnosed CRC at the Second Hospital of Hebei Medical University. Patients were required to be free of radiotherapy, chemotherapy and other antitumor treatments prior to surgery, as well as free of any other malignant disease other than CRC. After isolation, some specimens were immediately placed in liquid nitrogen and stored at -80 °C for RNA and protein analysis, and other specimens were fixed in 4% paraformaldehyde for histological examination. All patients who met the above criteria signed informed consent forms. The study was approved by the Ethics Committee of the Second Hospital of Hebei Medical University (2021-R241).

Cell lines

Six human colon cancer cell lines (Caco-2, DLD1, HCT116, HCT15, HT29 and SW480) and one normal colonic epithelial cell line (FHC) were obtained from American Type Culture Collection (ATCC; Manassas, VA, United States). All cell lines were routinely cultured in Dulbecco's modified Eagle's medium (DMEM; Gibco BRL, Grand Island, NY, United States), containing 10% fetal bovine serum (FBS; Gibco BRL).

We conducted cell transfection using Lipofectamine 2000 (Invitrogen, Carlsbad, CA, United States), including small interfering RNA (siRNA), miRNA mimics, miRNA inhibitor and negative control oligonucleotides (Shanghai GenePharma Co., Ltd., Shanghai, China). The stable TNFRSF10A-AS1 overexpression lentiviral vector, TNFRSF10A-AS1 knockdown vector and empty vector were designed and synthesized by GenePharma. And finally, cell lines were screened according to the resistance carried by the lentivirus.

RNA extraction and quantitative real-time polymerase chain reaction

Total RNA was isolated from CRC tissue and cell samples, and then reverse transcribed into complementary DNA (cDNA), and finally quantitative real-time polymerase chain reaction (qRT-PCR) was conducted with cDNA and specific primers. Gene expression was calculated using GAPDH or U6 as internal reference genes. Table 1 lists all the qRT-PCR primer sequences involved in the study.

Cell counting kit-8 proliferation assay

Seeded colon cancer cells into 96-well cell culture plates at 1000 cells/100 μL per well according to the experimental grouping. At 24, 48, 72, 96 and 120 h, 10 μL of Cell Counting Kit-8 (CCK-8) reagent (Shanghai Share-bio Biotechnology Co., Shanghai, China) was added directly to each well. After incubation for 2 h at 37 °C, the optical density (OD) value (450 nm) was estimated.

Colony formation assay

Colon cancer cells were plated in 6-well cell culture plates at 1000 cells per well according to the experimental grouping and routinely cultured in a cell incubator. Cell culture was terminated once colonies were visible. Cells were then washed, fixed, stained, photographed and counted.

Cell cycle and apoptosis assays

Cell cycle analysis was performed using a Cell Cycle and Apoptosis Analysis Kit (Beyotime Biotechnology Co., Shanghai, China) following the manufacturer's protocol. Cells were fixed with ethanol, washed and stained with PI staining solution. Cell apoptosis was assayed using an Annexin V-FITC Apoptosis Detection Kit (Beyotime Biotechnology Co.), in which early and late apoptotic/dead cells were labeled using Annexin-V and PI, respectively.

Transwell assay

The upper chamber of Transwells (Corning, Kennebunk, ME, United States) was seeded with cells in 200 μL of culture medium without serum. The bottom chamber of Transwells was filled with medium supplemented with 10% FBS. The invasion and migration characteristics assay were distinguished by the presence or absence of Matrigel in the upper chamber. Cells in the bottom chambers of Transwells were fixed, stained and photographed following twenty-four hours of routine culture.

Table 1 Primers for real-time polymerase chain reaction

Primer name	Forward (5'-3')	Reverse (5'-3')
TNFRSF10A-AS1	TCTCAGATCACGTGACCTTGA	GTGGGCAGCTCTCATCCTAA
U2 snRNA	CATCGCTTCTCGGCCTTTTG	TGGAGGTACTGCAATACCAGG
S14	GGCAGACCGAGATGAATCCTC	CAGGTCCAGGGGTCTTGGTCC
GAPDH	CAGGGGGGAGCCAAAAGGGTCA	TGGGTGGCAGTGATGGCATGGA
HuR	CCAAAUCUUUGCAUAGGUATT	UACCUAUGCAAAGAUUUGGTTA
miR-3121-3p	TAAATAGAGTAGGCAAAGGACA	
miR-663a	AGGCGGGGCGCCGCGGGACCGC	
miR-4529-3p	ATTGGACTGCTGATGGCCCGT	
miR-505-3p	CGTCAACACTTGCTGGTTTCCT	
miR-5002-5p	AATTTGGTTTCTGAGGCACTTAGT	
miR-934	TGTCTACTACTGGAGACACTGG	
miR-1263	ATGGTACCCTGGCATTACTGAGT	
miR-5009-5p	TTGGACTTTTTCAGATTTGGGGAT	
miR-2115-5p	AGCTTCCATGACTCCTGATGGA	
miR-377-3p	ATCACACAAAGGCAACTTTTGT	
miR-3144-3p	ATATACCTGTTCGGTCTCTTTA	
miR-548av-5p	AAAAGTACTTGCGGATTT	
miR-4426	GAAGATGGACGTACTTT	
miR-224-5p	CAAGTCACTAGTGGTTCCGTT	
miR-548k	AAAAGTACTTGCGGATTTTGCT	
U6	TCGTCCCGTAGACAAAATGG	

Western blot assay

Total protein from tissue and cell samples was extracted and the protein concentrations were tested. Different concentrations of polyacrylamide gels were prepared according to the molecular weight of the protein to be detected. Proteins were then electrophoresed and transferred to polyvinylidene fluoride (PVDF) membranes. Finally, the membranes were first incubated with primary antibodies against cyclin D1, proliferating cell nuclear antigen (PCNA), cleaved caspase-3, cleaved PARP, HuR as well as GAPDH (Cell Signaling Technology, Danvers, MA, United States) at 4 °C overnight and then the proteins were incubated with secondary antibodies (Cell Signaling Technology) for 1 h.

Immunohistochemistry

Tissue samples were fixed in paraformaldehyde, dehydrated in alcohol, embedded in paraffin as well as sectioned. In addition, immunohistochemical staining of tissue sections was carried out according to the experimental steps. Finally, staining of the sections was observed under a microscope.

Luciferase reporter assay

TNFRSF10A-AS1 containing wild-type (WT) or mutant (MUT) miR-3121-3p-binding sequences was designed, synthesized and sub-cloned into the pmiRGLO vector (Shanghai GenePharma Co., Ltd.). DLD1 cells were cotransfected with reporter plasmid, miR-3121-3p mimics or mimics NC. After cotransfection under routine culture conditions for 48 h, the Dual-Luciferase Reporter Assay System (Promega, Madison, WI, United States) was used to evaluate the luciferase activity of all the above reporter vectors.

Subcutaneous xenograft models

We performed animal experiments for *in vivo* validation. BALB/c nude mice at four- to six-week-old were subcutaneously injected with DLD1 cells stably transfected with sh-TNFRSF10A-AS1 (sh-lnc) or sh-negative control vector (sh-NC) (1×10^7, 200 μL) and HCT116 cells stably overexpressing TNFRSF10A-AS1 (oe-lnc) or empty vector (control) (1×10^7, 200 μL) into the right and left dorsal flanks of the nude mice, respectively. After implantation, the tumor volume was observed and measured every 2 d. The tumor volume was calculated using the measured length and width of the tumor according to

Table 2 Associations between TNFRSF10A-AS1 levels and clinicopathological features in colorectal cancer patients

Characteristics	Case	TNFRSF10A-AS1 expression		*P* value
		Low	High	
Age (yr)				0.751
< 60	18	10	8	
≥ 60	22	10	12	
Gender				0.751
Male	22	12	10	
Female	18	8	10	
Tumor location				1.000
Colon	19	9	10	
Rectum	21	11	10	
Tumor size (cm)				0.001[a]
≥ 5	21	5	16	
< 5	19	15	4	
T grade				0.014[a]
T1 + T2	12	10	2	
T3 + T4	28	10	18	
TNM stage				1.000
I-II	30	15	15	
III-IV	10	5	5	
Histological grade				0.661
Low	6	2	4	
Middle-High	34	18	16	

[a]$P < 0.05$.

the formula: Tumor volume = (length × width^2)/2. At the end of the animal study, subcutaneous tumors were removed and used to assess tumor volume and weight as well as to perform qRT-PCR, Western blot and histological analyses.

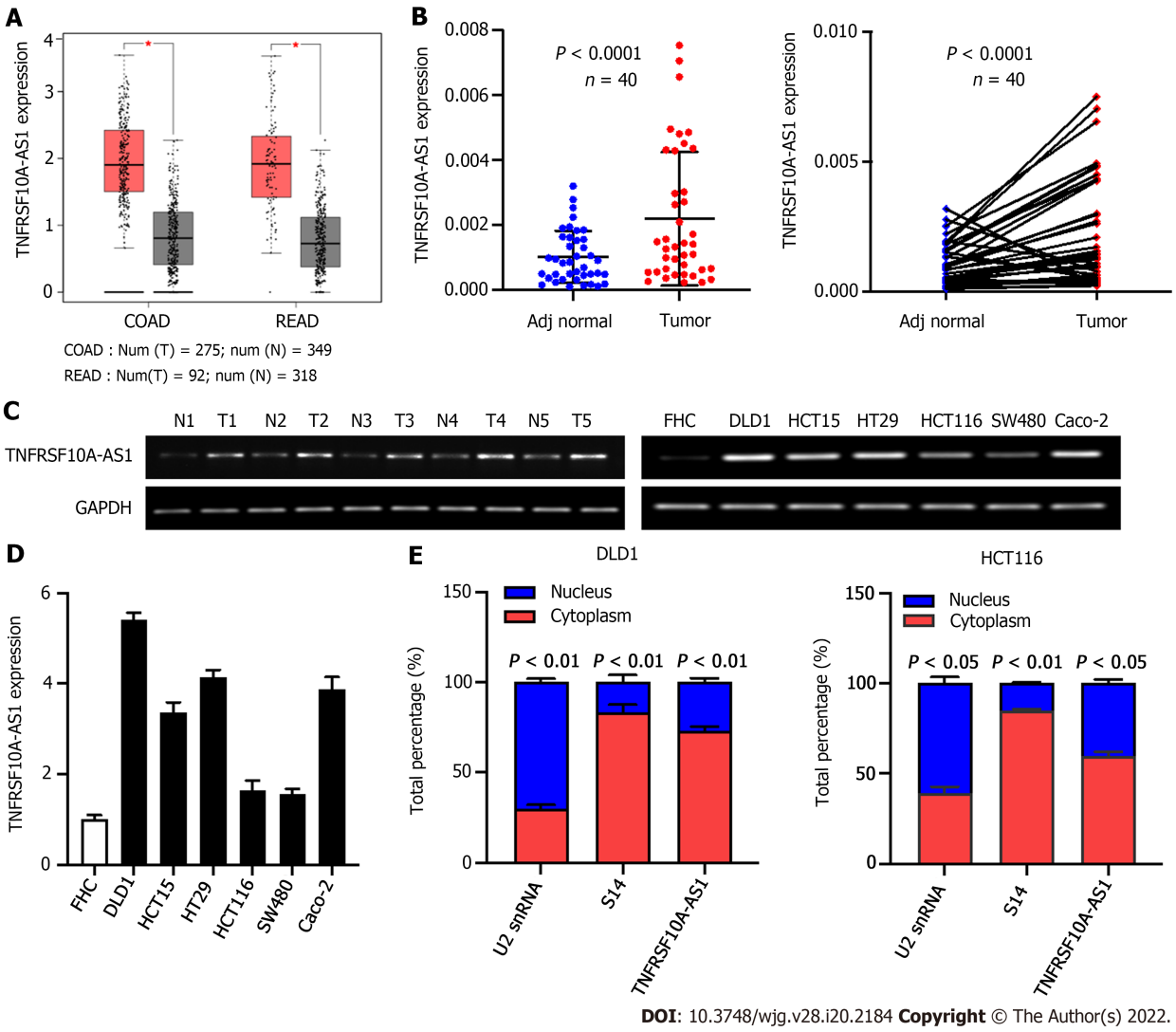
Statistical analysis

Statistical analyses were performed using GraphPad Prism 9 software or SPSS 22.0 software. Data were presented as the mean ± SD. TNFRSF10A-AS1 and miR-3121-3p expression levels in CRC patients were compared using the paired-sample *t* test. Statistical significance between groups was analyzed using the χ^2 test, Fisher's exact probability, Student's *t* test or one-way Analysis of Variance (ANOVA). $P < 0.05$ was considered statistically significant.

RESULTS

TNFRSF10A-AS1 is upregulated in CRC

To identify whether lncRNA TNFRSF10A-AS1 is differentially expressed in CRC, we first analyzed TNFRSF10A-AS1 expression in TCGA database. We used the GEPIA online database to analyze TNFRSF10A-AS1 expression of CRC tissues, and results showed that TNFRSF10A-AS1 was expressed higher in both colon and rectal carcinoma tissues than that of corresponding adjacent normal tissues (Figure 1A). We then examined TNFRSF10A-AS1 expression in 40 pairs of CRC tissue samples. TNFRSF10A-AS1 expression was significantly increased in 34 of 40 (75%) tumor samples compared to the adjacent normal mucosa tissues (Figure 1B). Next, TNFRSF10A-AS1 expression was verified in multiple colon cancer cell lines, namely, DLD1, HCT15, HT29, HCT116, SW480 and Caco-2, and human colon mucosal epithelial FHC cells. TNFRSF10A-AS1 was significantly upregulated in the colon cancer



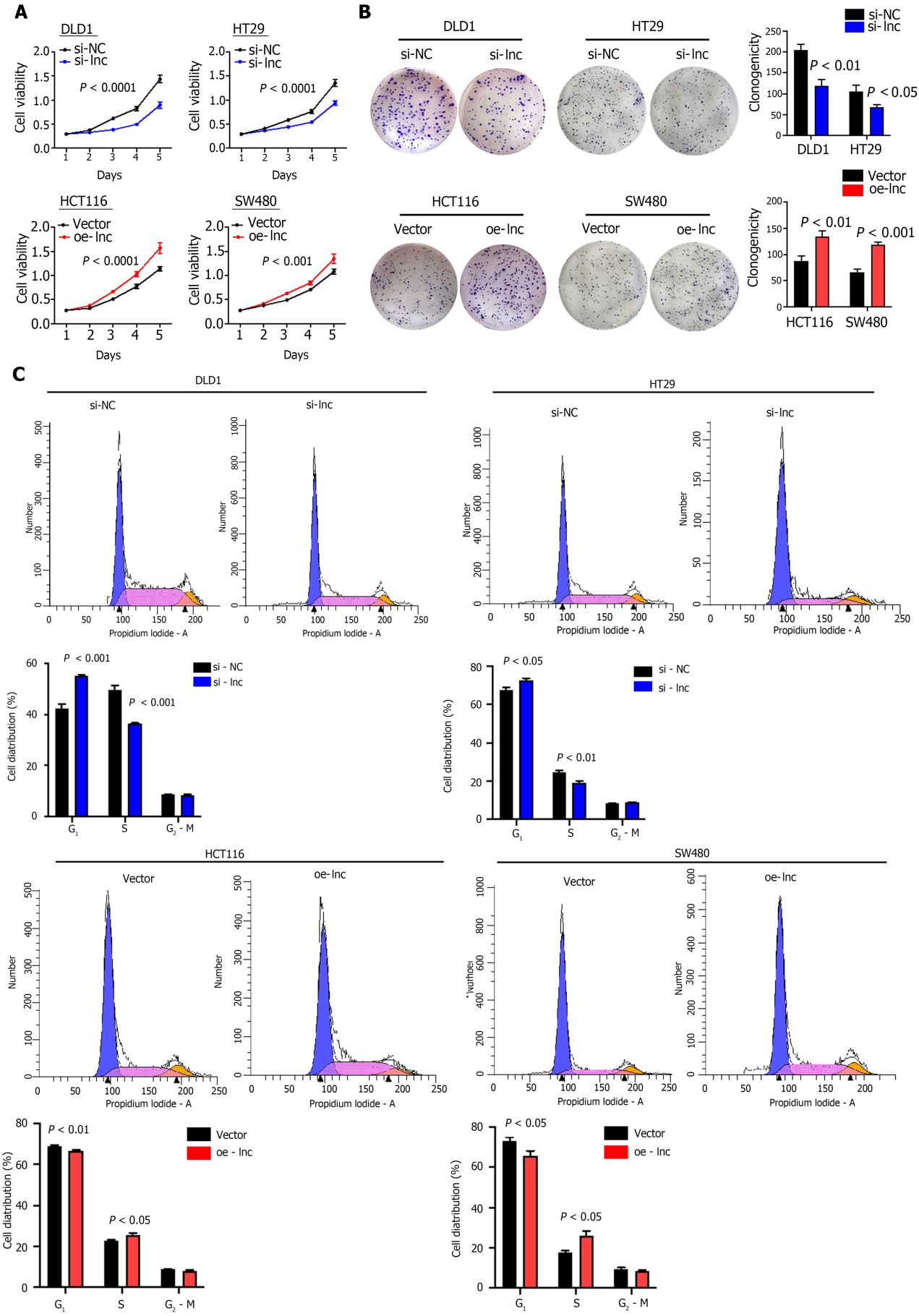
DOI: 10.3748/wjg.v28.i20.2184 **Copyright** © The Author(s) 2022.

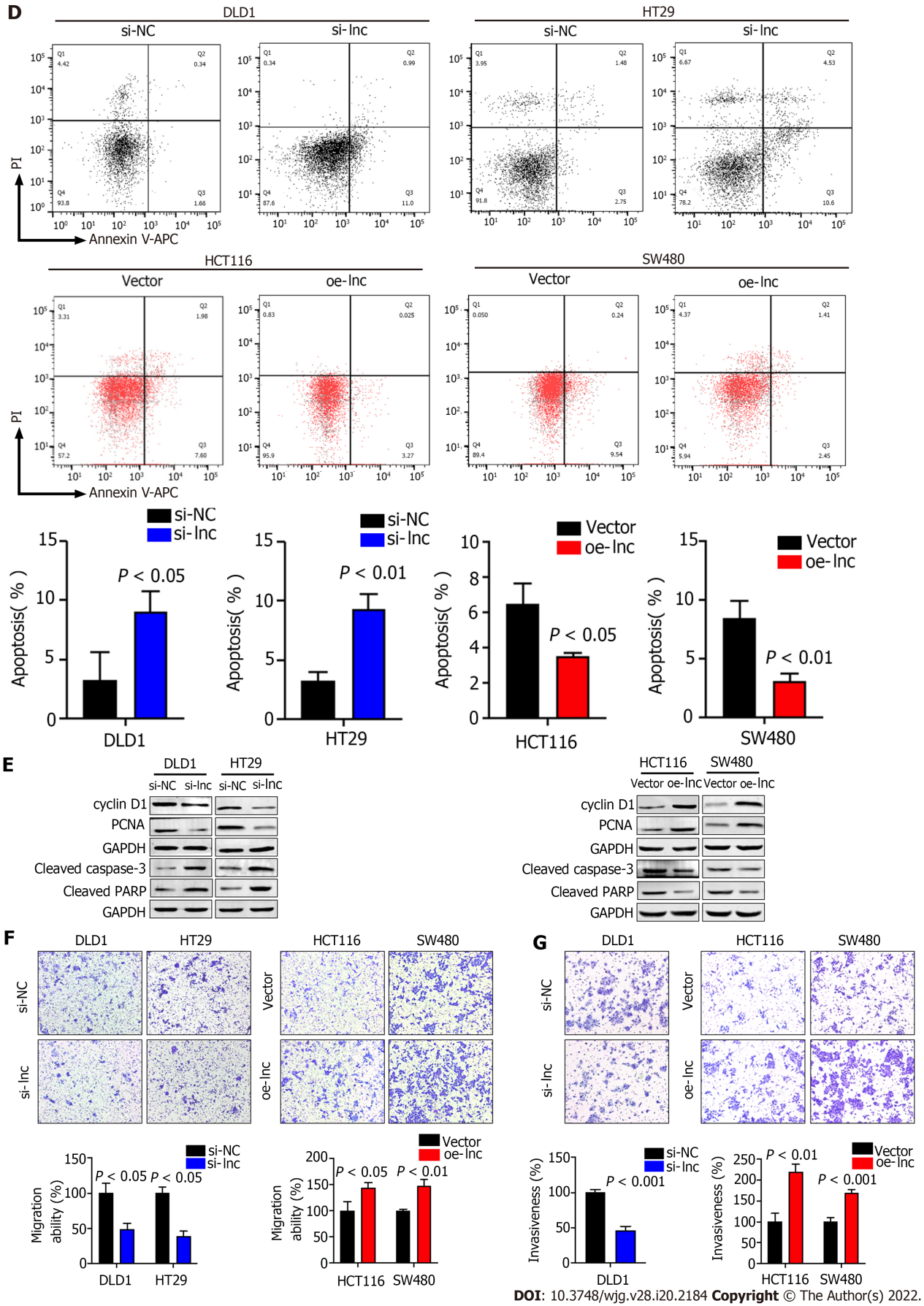
Figure 1 TNFRSF10A-AS1 is upregulated in colorectal cancer. A: TNFRSF10A-AS1 was upregulated in tumor tissues compared to normal tissues in TCGA colorectal cancer (CRC) database; B: TNFRSF10A-AS1 was overexpressed in CRC tumor tissues compared to matched adjacent nontumor tissues (n = 40); C: Levels of TNFRSF10A-AS1 in CRC were measured by reverse transcription-polymerase chain reaction (RT-PCR); D: TNFRSF10A-AS1 was higher in colon cancer cell lines than in colon mucosal epithelial FHC cells; E: The expression levels of TNFRSF10A-AS1 in the cytoplasm and nucleus of DLD1 and HCT116 cells were detected by quantitative real-time polymerase chain reaction (qRT-PCR). U2 snRNA was used as the internal reference for genes expressed in the nucleus, and S14 was used as the internal reference for genes expressed in the cytoplasm. COAD: Colon adenocarcinoma; READ: Rectum adenocarcinoma.

cell lines compared to FHC cells (Figure 1D). RT-PCR also confirmed that TNFRSF10A-AS1 was upregulated in CRC tissues and cells (Figure 1C). We further explored the cellular localization of TNFRSF10A-AS1 in DLD1 and HCT116 cells. qRT-PCR results showed that TNFRSF10A-AS1 was predominantly found in the cytoplasm (Figure 1E), which indicated that TNFRSF10A-AS1 might function in the cytoplasm. In addition, we analyzed associations between TNFRSF10A-AS1 and clinicopathological features of CRC patients and found that the upregulation of TNFRSF10A-AS1 was associated with advanced T grade and tumor size (Table 2). Collectively, the above findings indicated that TNFRSF10A-AS1 was increased in CRC and might be involved in colorectal carcinogenesis as an oncogene.

TNFRSF10A-AS1 promotes colon cancer cell proliferation, migration and invasion as well as inhibits cell apoptosis

To explore the biological function of TNFRSF10A-AS1 in colon cancer cells, we first designed a siRNA against TNFRSF10A-AS1, a short hairpin RNA (shRNA) against TNFRSF10A-AS1 and a lentiviral overexpression vector for TNFRSF10A-AS1. Silencing TNFRSF10A-AS1 in DLD1 and HT29 cells significantly inhibited cell viability and clonogenicity, whereas ectopic expression of TNFRSF10A-AS1 in HCT116 and SW480 cells significantly promoted cell viability and clonogenicity (Figure 2A and B). We also conducted flow cytometry to clarify the role of TNFRSF10A-AS1 in cell cycle distribution. Knockdown of TNFRSF10A-AS1 led to a significant increase in G1 phase cells and a decrease in S-phase cells in both DLD1 and HT29 cells. In contrast, the opposite results were exhibited in both HCT116 and


A
DLD1
HT29
HCT116
SW480
si-NC
si-lnc
Vector
oe-lnc
Cell viability
Days
P < 0.0001
P < 0.001
B
DLD1
HT29
HCT116
SW480
si-NC
si-lnc
Vector
oe-lnc
Clonogenicity
P < 0.01
P < 0.05
P < 0.001
C
Number
Propidium Iodide - A
Cell diatribution (%)
si - NC
si - lnc
Vector
oe - lnc
P < 0.001
P < 0.05
P < 0.01
G1
S
G2 - M



DOI: 10.3748/wjg.v28.i20.2184 **Copyright** © The Author(s) 2022.

Figure 2 TNFRSF10A-AS1 promotes colon cancer cell proliferation, migration and invasion as well as inhibits cell apoptosis *in vitro*. A and B: Downregulation of TNFRSF10A-AS1 decreased cell viability and clonogenicity in DLD1 and HT29 cells, whereas upregulation of TNFRSF10A-AS1 greatly

increased cell viability and clonogenicity in HCT116 and SW480 cells; C: Silencing TNFRSF10A-AS1 arrested cells at the G1/S transition, whereas overexpressing TNFRSF10A-AS1 facilitated this transition; D: Downregulation of TNFRSF10A-AS1 enhanced cell apoptosis, whereas upregulation of TNFRSF10A-AS1 inhibited cell apoptosis; E: Western blot analysis showed that TNFRSF10A-AS1 knockdown decreased the expression of cyclin D1 and PCNA but increased the activation of caspase-3 and PARP, whereas TNFRSF10A-AS1 overexpression had the opposite effect; F and G: Silencing TNFRSF10A-AS1 suppressed DLD1 and HT29 cell migration and invasion abilities, whereas these abilities were significantly enhanced by overexpressing TNFRSF10A-AS1 in HCT116 and SW480 cells.

SW480 cells with overexpression of TNFRSF10A-AS1 (Figure 2C). Moreover, Western blot analysis revealed that downregulation of TNFRSF10A-AS1 decreased cyclin D1 and PCNA expression, while the upregulation of TNFRSF10A-AS1 increased cyclin D1 and PCNA expression (Figure 2E). In general, genes that promote proliferation can suppress cell apoptosis. Therefore, we conducted Annexin V-APC/PI staining and Western blot analysis to test the impact of TNFRSF10A-AS1 on the apoptosis of colon cancer cells. The results showed that downregulation of TNFRSF10A-AS1 increased the apoptosis rate and the expression of the cleaved forms of caspase-3 and PARP, which are markers of cell apoptosis, whereas upregulation of TNFRSF10A-AS1 led to the opposite effects (Figure 2D and E).

In addition to malignant proliferation, tumor cells also exhibit migration and invasion abilities. Therefore, we performed Transwell assays with or without Matrigel to explore the impact of TNFRSF10A-AS1 on the migration and invasion properties of colon cancer cells. Downregulation of TNFRSF10A-AS1 markedly suppressed the migration and invasion abilities of DLD1 and HT29 cells, whereas overexpressing TNFRSF10A-AS1 significantly enhanced the abilities of HCT116 and SW480 cells (Figure 2F and G). Therefore, these findings demonstrated that TNFRSF10A-AS1 exerted a cancer-promoting role in CRC, prompting further investigations of its potential regulatory mechanisms.

miR-3121-3p is downregulated in CRC

The above findings suggested that TNFRSF10A-AS1 might play a tumor-promoting role in the cytoplasm. Thus, we explored the potential molecular mechanism of TNFRSF10A-AS1 based on the ceRNA mechanism. We first predicted potential target miRNAs of TNFRSF10A-AS1 by using miRNA target prediction tools, including miRDB, DIANA and LncRNAMAP. The prediction results of the three databases yielded 15 candidate miRNAs (Figure 3A). Among them, miR-3121-3p expression was upregulated in TNFRSF10A-AS1-deficient cells and downregulated in TNFRSF10A-AS1-overexpressing cells, consistent with the ceRNA mechanism theory (Figure 3B). Subsequently, we performed qRT-PCR to evaluate miR-3121-3p expression in CRC tissues, which indicated significant downregulation of miR-3121-3p in colorectal tumor tissues compared to matched nontumor tissues (Figure 3C). We further confirmed the interaction between TNFRSF10A-AS1 and miR-3121-3p using a dual-luciferase reporter assay (Figure 3E). Luciferase activity was reduced in cells cotransfected with TNFRSF10A-AS1-WT and the miR-3121-3p mimics, whereas there was no difference between cells cotransfected with TNFRSF10A-AS1-MUT and the miR-3121-3p mimics and cells cotransfected with TNFRSF10A-AS1-MUT and mimics NC (Figure 3F). Finally, we analyzed the correlation between miR-3121-3p levels and the clinicopathological features of CRC patients and discovered that downregulation of miR-3121-3p was associated with large tumor size (Table 3). These results suggested that miR-3121-3p might be a tumor suppressor and exert an inhibitory effect on CRC.

miR-3121-3p inhibits the proliferation, migration and invasion of colon cancer cells by silencing HuR

Because there are few studies related to miR-3121-3p and no relevant studies in CRC, we set out to investigate the function and mechanism of miR-3121-3p in CRC. We first predicted the downstream proteins of miR-3121-3p using four online databases, *i.e.*, miRDB, TargetScan, miRTarBase and RNA22, and then obtained 3 candidate genes (ELAVL1, PLEKHA6 and ATL3) after taking the intersection (Figure 4A). Of the three candidate genes, ELAVL1 (HuR) has been demonstrated to be involved in CRC progression and may act as an oncogene in CRC. qRT-PCR showed that the expression of miR-3121-3p was relatively lower in DLD1 cells and higher in HCT116 cells (Figure 3D). Thus, we selected DLD1 cells and HCT116 cells for transfection with miR-3121-3p mimics and inhibitor, respectively, to further identify the effects of miR-3121-3p on the malignant phenotype of CRC. Experimental results at both the mRNA and protein levels indicated that upregulation of miR-3121-3p decreased HuR expression, whereas downregulation of miR-3121-3p increased HuR expression (Figure 4B), suggesting that HuR might be a downstream target protein of miR-3121-3p.

We next studied the impacts of miR-3121-3p on the biological function of colon cancer cells. Growth curves based on the CCK-8 assay displayed that upregulation of miR-3121-3p suppressed the proliferation and viability of DLD1 cells, whereas downregulation of miR-3121-3p enhanced the proliferation and viability of HCT116 cells (Figure 4C). The colony number of DLD1 cells transfected with the miR-3121-3p mimics was significantly lower than that of the control group, whereas the colony number of HCT116 cells transfected with the miR-3121-3p inhibitor was significantly higher than the control group (Figure 4D). In addition, Transwell assays indicated that upregulation of miR-3121-3p in DLD1 cells significantly impaired the migration and invasion abilities, whereas downregulation of miR-3121-3p in HCT116 cells significantly enhanced these abilities (Figure 4E). In summary, the above results confirmed

Table 3 Associations between miR-3121-3p levels and clinicopathological features in colorectal cancer patients

Characteristics	Case	miR-3121-3p expression		*P* value
		Low	High	
Age (yr)				0.751
< 60	18	10	8	
≥ 60	22	10	12	
Gender				0.751
Male	22	12	10	
Female	18	8	10	
Tumor location				1.000
Colon	19	10	9	
Rectum	21	10	11	
Tumor size (cm)				0.010[a]
≥ 5	21	15	6	
< 5	19	5	14	
T grade				0.082
T1 + T2	12	9	3	
T3 + T4	28	11	17	
TNM stage				0.716
I-II	30	14	16	
III-IV	10	6	4	
Histological grade				1.000
Low	6	3	3	
Middle-High	34	17	17	

[a]$P < 0.05$.

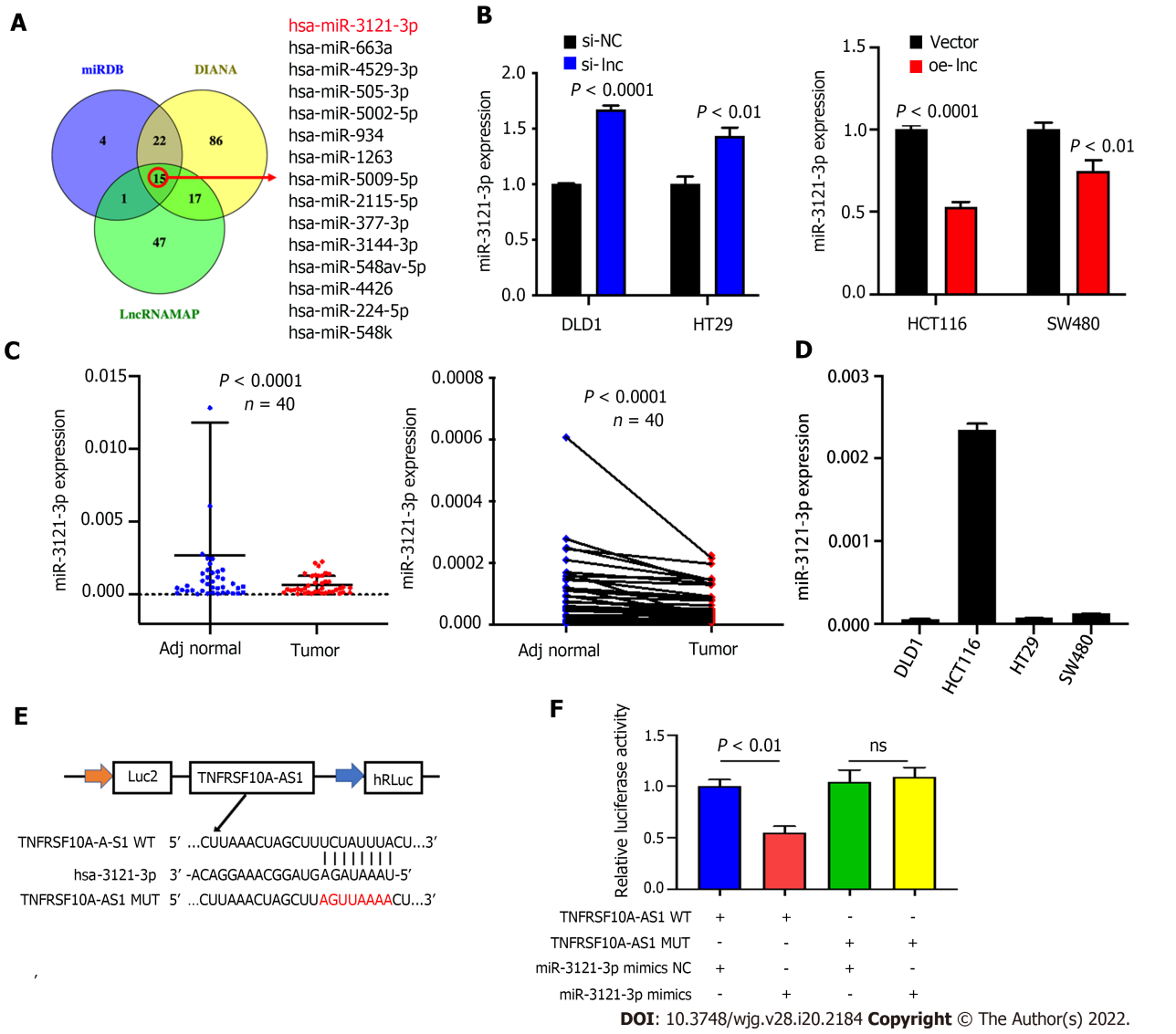
that miR-3121-3p played a suppressive effect in the malignant phenotype of CRC, including aberrant proliferation and metastasis.

TNFRSF10A-AS1 accelerates the proliferation, migration and invasion of colon cancer cells via the miR-3121-3p/HuR axis

We performed rescue experiments using miR-3121-3p mimics and inhibitor with the aim of verifying whether TNFRSF10A-AS1 exerts a tumor-promoting effect through the miR-3121-3p/HuR axis. We first examined HuR expression at the mRNA and protein levels. Silencing TNFRSF10A-AS1 decreased the mRNA and protein levels of HuR in DLD1 cells, whereas overexpressing TNFRSF10A-AS1 in HCT116 cells enhanced HuR expression. In addition, the miR-3121-3p inhibitor and mimics reversed the regulatory effects on HuR expression caused by TNFRSF10A-AS1 silencing and overexpression, respectively (Figure 5A). Furthermore, we sought to clarify whether the miR-3121-3p mimics and inhibitor reverse the impacts of TNFRSF10A-AS1 on CRC biological functions. All the experiments results, including CCK-8, colony formation as well as Transwell assays, indicated that the suppressive impacts on DLD1 cells caused by TNFRSF10A-AS1 knockdown could be balanced by miR-3121-3p inhibitor, while miR-3121-3p mimics could counteract the promoting effect of TNFRSF10A-AS1 overexpression on HCT116 cells (Figure 5B-E). The above results indicated that the miR-3121-3p/HuR regulatory axis might be one of the mechanisms by which TNFRSF10A-AS1 promoted CRC proliferation, migration and invasion.

TNFRSF10A-AS1 promotes CRC growth in vivo

Given that the above *in vitro* experimental results suggested that TNFRSF10A-AS1 had a tumor-promoting effect on colon cancer cells, we selected TNFRSF10A-AS1-deficient DLD1 cells and TNFRSF10A-AS1-overexpressing HCT116 cells for tumor xenograft experiments to verify the effect of TNFRSF10A-AS1 *in vivo*. Consistent with the results of *in vitro* experiments, we found that the downreg-



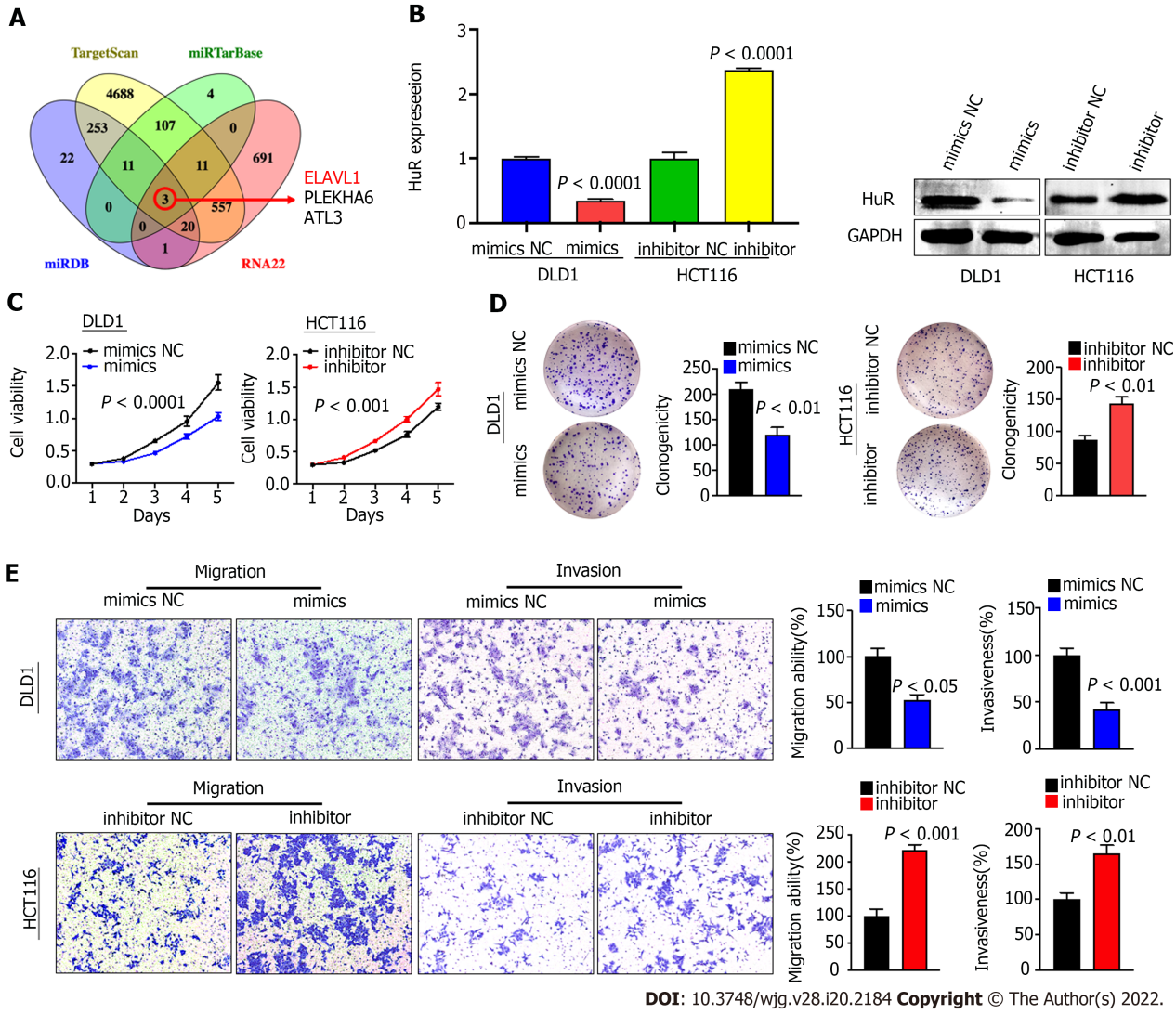
DOI: 10.3748/wjg.v28.i20.2184 **Copyright** © The Author(s) 2022.

Figure 3 miR-3121-3p is downregulated in colorectal cancer. A: We used three websites (miRDB, DIANA and LncRNAMAP) to predict 15 microRNAs with binding sites for TNFRSF10A-AS1; B: miR-3121-3p expression was increased in cells transfected with si-lnc and decreased in cells transfected with oe-lnc; C: miR-3121-3p was downregulated in colorectal cancer tumor tissues compared to matched nontumor tissues (n = 40); D: Levels of miR-3121-3p in colon cancer cell lines were detected by quantitative real-time polymerase chain reaction; E: Schematic illustration of the predicted binding sites of miR-3121-3p in the TNFRSF10A-AS1 sequence; F: Relative luciferase activities after cotransfection with TNFRSF10A-AS1-WT, TNFRSF10A-AS1-MUT, miR-3121-3p mimics or NC in DLD1 cells. WT: Wild-type; MUT: Mutant.

ulation of TNFRSF10A-AS1 significantly reduced the tumor size and weight of DLD1 xenografts (Figure 6A), whereas upregulation of TNFRSF10A-AS1 markedly promoted HCT116 xenograft growth (Figure 6B). Moreover, IHC assays demonstrated that downregulation of TNFRSF10A-AS1 reduced the expression of the Ki-67 proliferation marker in xenograft tumor tissues, whereas upregulation of TNFRSF10A-AS1 produced the opposite effect (Figure 6C). qRT-PCR, Western blot and IHC analyses all revealed that HuR expression was downregulated in TNFRSF10A-AS1-deficient xenograft tumor tissues but upregulated in TNFRSF10A-AS1-overexpressing xenograft tumor tissues (Figure 6C-E). Western blot analysis of tissue samples from CRC patients also showed that HuR was increased in tumor tissues compared to paired nontumor tissues (Figure 6F). Therefore, these *in vivo* results further supported the tumor-promoting role of TNFRSF10A-AS1 in CRC, which functioned at least in part as a molecular sponge of miR-3121-3p to upregulate HuR expression.

DISCUSSION

In this study, we first uncovered TNFRSF10A-AS1 as an oncogene that participated in colorectal carcinogenesis and progression. Although the available findings have demonstrated that TNFRSF10A-AS1 is involved in the autophagic mechanism of CRC as well as gastric cancer prognosis, the current

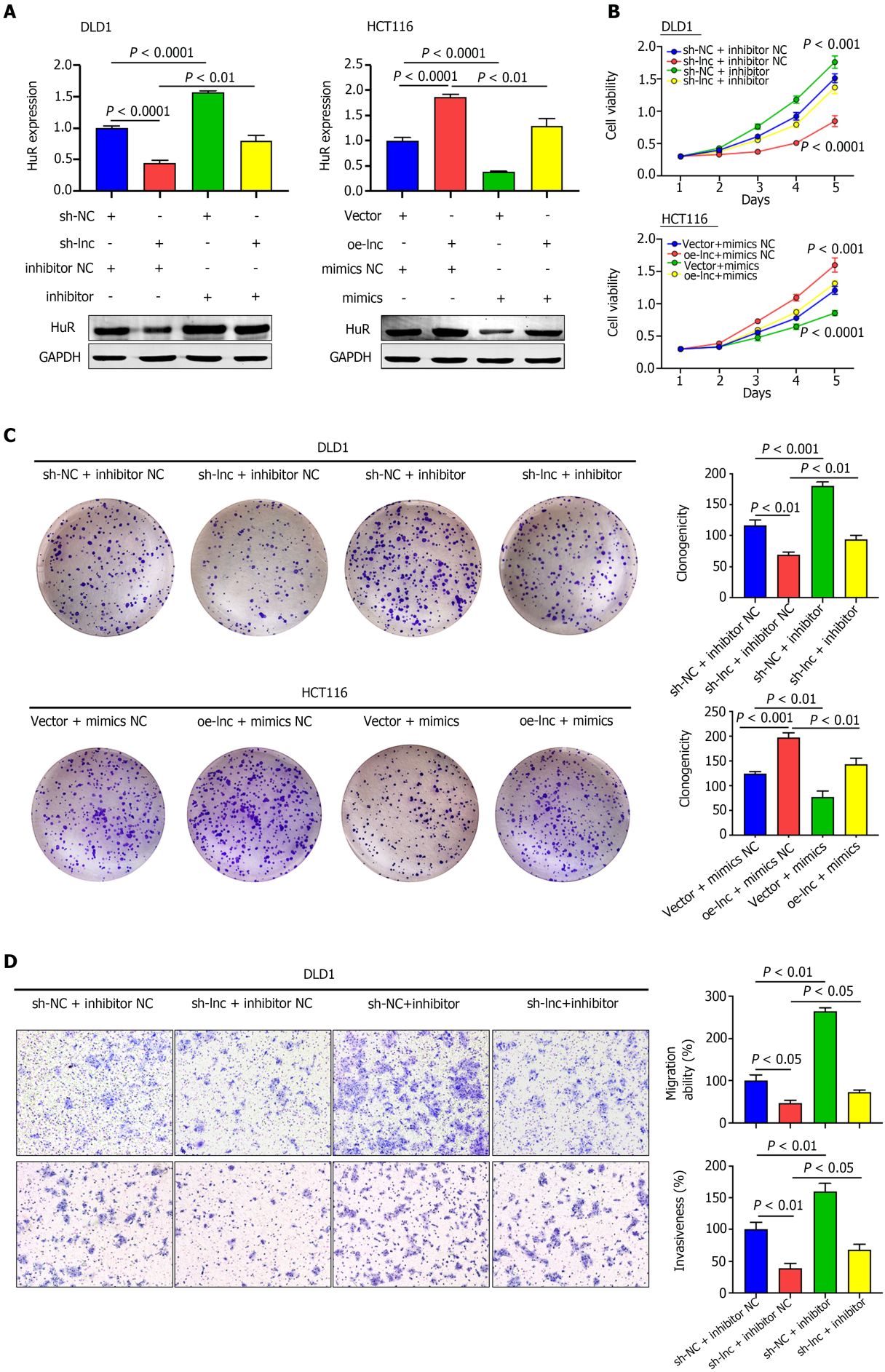


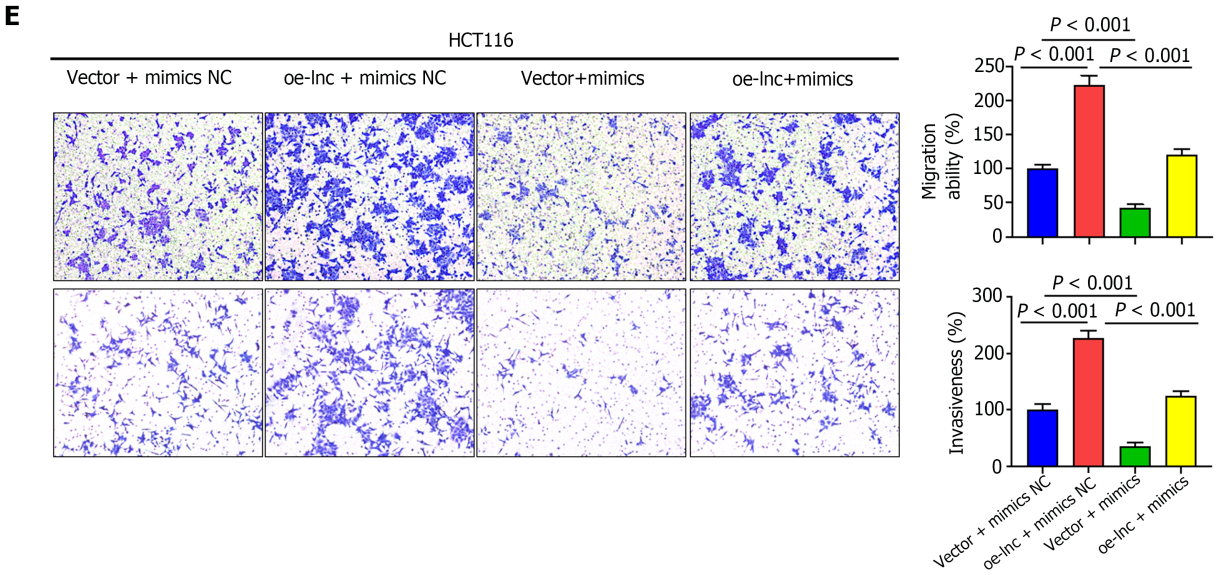
DOI: 10.3748/wjg.v28.i20.2184 **Copyright** © The Author(s) 2022.

Figure 4 miR-3121-3p suppresses colon cancer cell proliferation, migration and invasion *in vitro*. A: Four websites (miRDB, TargetScan, miRTarBase and RNA22) were used to predict 3 downstream target mRNAs with binding sites for miR-3121-3p; B: HuR expression was assessed in DLD1 and HCT116 cells transfected with miR-3121-3p mimics, miR-3121-3p inhibitor or NC using quantitative real-time polymerase chain reaction and Western blot assays; C and D: miR-3121-3p mimics inhibited cell viability and clonogenicity, but miR-3121-3p inhibitor enhanced cell viability and clonogenicity; E: Upregulation of miR-3121-3p inhibited cell migration and invasion capabilities, whereas downregulation of miR-3121-3p enhanced these capabilities.

evidence is all based on the analysis of TCGA data, and its functional roles and detailed mechanisms in CRC cannot be determined. Our study showed that TNFRSF10A-AS1 was upregulated in CRC and the upregulation of TNFRSF10A-AS1 was associated with advanced tumor size and T grade. In functional experiments both *in vitro* and *in vivo*, we found that TNFRSF10A-AS1 enhanced the malignant phenotype of colon cancer cells. Regarding the molecular mechanism of TNFRSF10A-AS1, we identified miR-3121-3p by bioinformatics analyses and verified the direct interaction between TNFRSF10A-AS1 and miR-3121-3p by dual-luciferase reporter assays. In contrast to TNFRSF10A-AS1, miR-3121-3p was downregulated in CRC, negatively associated with the tumor size as well as exerted inhibitory effects on the malignant phenotype of colon cancer cells, which is consistent with ceRNA mechanism theory. Mechanistically, one of the ways in which TNFRSF10A-AS1 exerted its pro-cancer effects was through sponging miR-3121-3p. By binding to miR-3121-3p, TNFRSF10A-AS1 attenuated the silencing effect of miR-3121-3p on its downstream target gene, HuR. Taken together, our findings provide evidence for an important role of TNFRSF10A-AS1 and the TNFRSF10A-AS1/miR-3121-3p/HuR axis in CRC progression, thereby providing a theoretical basis for the diagnosis and treatment of CRC.

ceRNA is an important regulatory mode of cytoplasmic lncRNA. Here, after confirming that TNFRSF10A-AS1 was more abundant in the cytoplasm of CRC cell lines, we used online tools to predict potential target miRNAs of TNFRSF10A-AS1. We further validated the expression relationship between TNFRSF10A-AS1 and candidate miRNAs, and we discovered that miR-3121-3p might be a downstream target miRNA of TNFRSF10A-AS1. And the dual-luciferase reporter assay further confirmed that TNFRSF10A-AS1 might function as the molecular sponge of miR-3121-3p. In the lncRNA-miRNA-mRNA network, miRNAs, as intermediate mediators, exert biological effects by modulating


A
DLD1
HCT116
HuR expression
P < 0.0001
P < 0.01
sh-NC
sh-lnc
inhibitor NC
inhibitor
Vector
oe-lnc
mimics NC
mimics
HuR
GAPDH
B
DLD1
HCT116
Cell viability
Days
sh-NC + inhibitor NC
sh-lnc + inhibitor NC
sh-NC + inhibitor
sh-lnc + inhibitor
Vector+mimics NC
oe-lnc+mimics NC
Vector+mimics
oe-lnc+mimics
C
DLD1
HCT116
Clonogenicity
sh-NC + inhibitor NC
sh-lnc + inhibitor NC
sh-NC + inhibitor
sh-lnc + inhibitor
Vector + mimics NC
oe-lnc + mimics NC
Vector + mimics
oe-lnc + mimics
D
DLD1
sh-NC+inhibitor
sh-lnc+inhibitor
Migration ability (%)
Invasiveness (%)



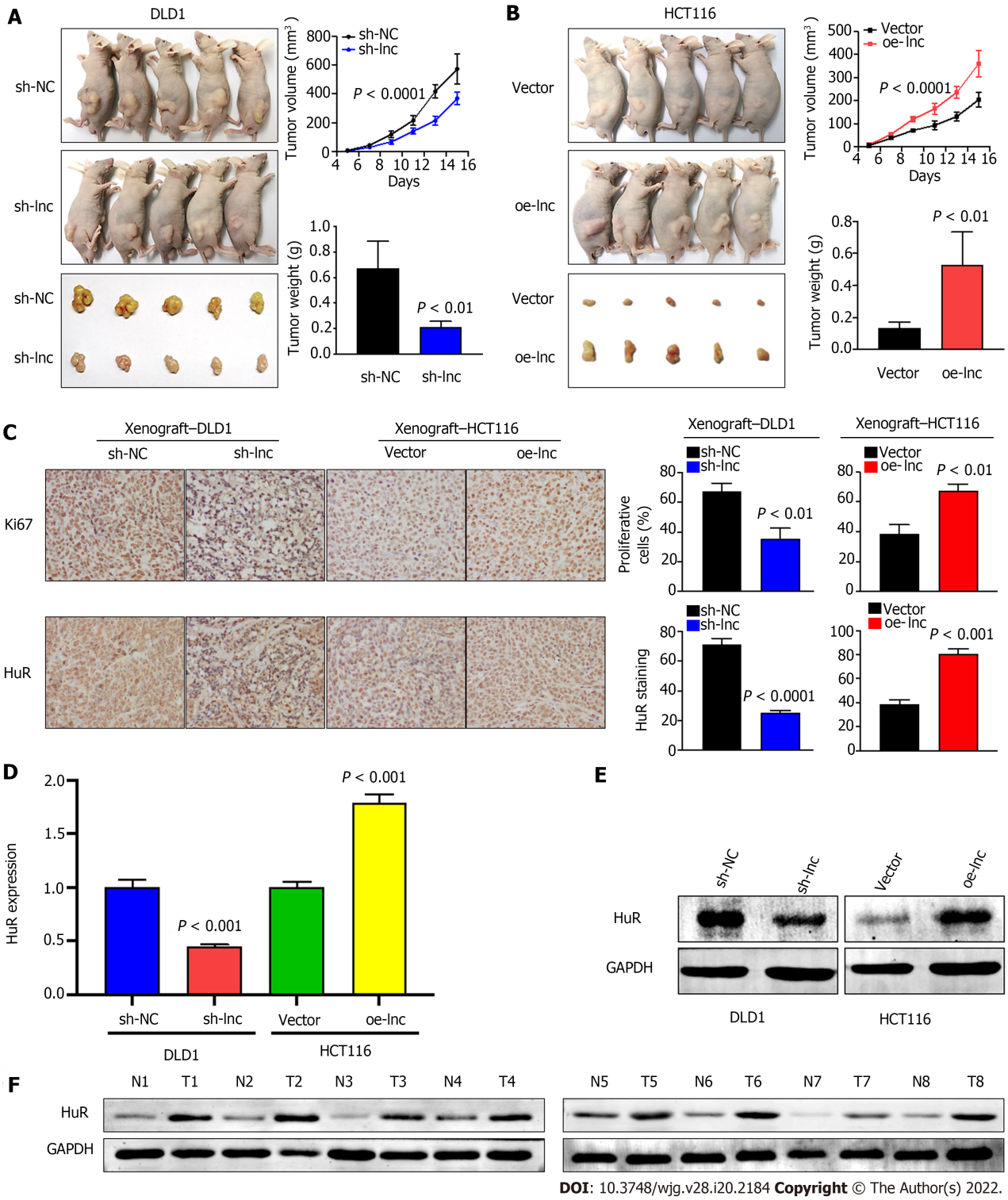
DOI: 10.3748/wjg.v28.i20.2184 **Copyright** © The Author(s) 2022.

Figure 5 TNFRSF10A-AS1 promotes colon cancer cell proliferation, migration and invasion *via* the miR-3121-3p/HuR axis. A: HuR was evaluated in DLD1 and HCT116 cells transfected with miR-3121-3p mimics, miR-3121-3p inhibitor, NC, sh-lnc or oe-lnc; B and C: Cell proliferation abilities were estimated using Counting Kit-8 and colony formation assays in DLD1 and HCT116 cells transfected with miR-3121-3p mimics, miR-3121-3p inhibitor, NC, sh-lnc or oe-lnc; D and E: Transwell assays were performed to analyze cell migration and invasion abilities in DLD1 and HCT116 cells transfected with miR-3121-3p mimics, miR-3121-3p inhibitor, NC, sh-lnc or oe-lnc.

downstream target proteins. After experimental evidence established that TNFRSF10A-AS1 could sponge miR-3121-3p, we explored its effector genes. Among candidate target genes predicted by target prediction software, only HuR has been shown previously to regulate CRC progression, and our results also verified that miR-3121-3p exerted a negative regulatory effect on HuR expression. Rescue experiments also confirmed that miR-3121-3p mimics and inhibitor counteracted the regulatory effects of TNFRSF10A-AS1 overexpression and knockdown, respectively, on HuR expression, cell proliferation, migration ability and invasion ability. Thus, one of the mechanisms by which TNFRSF10A-AS1 acts may be as a molecular sponge for miR-3121-3p, which upregulates HuR expression and ultimately promotes colorectal carcinogenesis and progression.

HuR, a cancer-associated RNA-binding protein (RBP), is a member of the embryonic lethal abnormal vision (ELAV) family, and it increases mRNA stability by binding to conserved AU-rich elements (AREs) within 3′ untranslated regions (UTRs), thereby preventing gene degradation[12]. HuR expression is upregulated in different tumors, including breast cancer, CRC, gastric cancer and prostate cancer, and it is correlated with advanced clinicopathological parameters, expression of tumor-associated proteins, a low survival rate and poor prognosis[13-16]. CRC-related studies show that HuR is upregulated and promotes colon cancer growth by targeting RNA in the cytoplasm[17]. In addition, increased HuR protein in the cytoplasm is correlated with T stage, and importantly, HuR overexpression increases the growth of colon cancer cells in nude mouse models[18]. A recent study has revealed that miR-22, as a tumor suppressive miRNA, directly binds to HuR and downregulates its expression to inhibit proliferation and migration abilities of CRC, as well as xenogeneic tumor growth [19]. Through our experimental research, we found that the upstream lncRNA TNFRSF10A-AS1 sponged an important tumor suppressive miRNA in CRC, miR-3121-3p, which negatively regulated HuR expression. Consistent with previous studies, HuR was highly expressed in CRC. Our study results further suggested that the expression of HuR might be positively regulated by the upstream molecular TNFRSF10A-AS1, which might be one of the mechanisms by which TNFRSF10A-AS1 exerted a pro-cancer effect in CRC.

Based on the results of comprehensive analyses, including bioinformatics analyses, cell functional experiments and clinical research tools, we have sufficient evidence that TNFRSF10A-AS1 is a novel oncogene that promotes tumor malignancy in CRC. Mechanistically, TNFRSF10A-AS1 regulates the expression of the downstream target, HuR, by sponging miR-3121-3p, which further promotes CRC progression. Targeting the TNFRSF10A-AS1/miR-3121-3p/HuR axis may have potential therapeutic implications for CRC.



DOI: 10.3748/wjg.v28.i20.2184 **Copyright** © The Author(s) 2022.

Figure 6 TNFRSF10A-AS1 promotes the growth of colorectal cancer *in vivo*. A and B: Tumor volume and weight were significantly decreased in the TNFRSF10A-AS1 knockdown group but markedly increased in the TNFRSF10A-AS1 overexpression group; C-E: TNFRSF10A-AS1 enhanced cell proliferation (as assessed by Ki67 staining) and increased HuR expression (as assessed by HuR staining, quantitative real-time polymerase chain reaction and Western blot) in xenograft tumor tissues; F: HuR was upregulated in colorectal cancer patient tumor tissues compared to matched nontumor tissues by Western blot analysis.

CONCLUSION

TNFRSF10A-AS1 as a ceRNA promotes tumor malignancy of CRC through the miR-3121-3p/HuR axis. TNFRSF10A-AS1/miR-3121-3p/HuR axis may provide more effective targets for CRC therapy.

ARTICLE HIGHLIGHTS

Research background

The critical importance of long noncoding RNAs (lncRNAs) to the onset and exacerbation of colorectal cancer (CRC) has been validated in an increasing number of studies. However, numerous lncRNAs associated with CRC remain unidentified and the detailed mechanisms remain poorly understood. TNFRSF10A-AS1 is a new lncRNA, the function in CRC and gastric cancer is inconsistent and the exact mechanism is unclear.

Research motivation

The present study will clarify the oncogenic pathogenesis of TNFRSF10A-AS1 in CRC progression, leading to new ideas for CRC therapy.

Research objectives

To detect TNFRSF10A-AS1 expression in CRC and investigate the functions and potential mechanisms of TNFRSF10A-AS1 in CRC onset and exacerbation.

Research methods

In this study, the authors detected TNFRSF10A-AS1 expression in CRC and clarified the relationship between TNFRSF10A-AS1 levels and clinicopathological features of CRC patients. Furthermore, a series of functional experiments both *in vitro* and *in vivo* were performed to explore the role of TNFRSF10A-AS1. The mechanism of TNFRSF10A-AS1 mainly focused on its role as a miRNA molecular sponge.

Research results

TNFRSF10A-AS1 expression was increased in CRC and positively associated with advanced tumor size and T grade of CRC patients. TNFRSF10A-AS1 enhanced the malignant phenotype of colon cancer cells by promoting CRC proliferation and metastasis. Mechanistically, TNFRSF10A-AS1 was more abundant in the cytoplasm and upregulated the downstream target, HuR, by sponging miR-3121-3p, ultimately promoting CRC progression.

Research conclusions

TNFRSF10A-AS1 upregulates HuR expression by sponging miR-3121-3p, ultimately promoting colorectal tumorigenesis and progression. Therefore, TNFRSF10A-AS1 and the TNFRSF10A-AS1/miR-3121-3p/HuR axis may play an important role in CRC onset and exacerbation.

Research perspectives

Targeting TNFRSF10A-AS1 and the TNFRSF10A-AS1/miR-3121-3p/HuR axis may have potential novel therapeutic implications for CRC.

ACKNOWLEDGEMENTS

The authors acknowledge the support of Dr. Jun Yu (The Chinese University of Hong Kong) for supervising this study and revising the manuscript.

FOOTNOTES

Author contributions: Wang DD, Sun DL and Zhang XL conceived, designed the study; Wang DD, Sun DL, Yang SP and Song J performed most experiments, analyzed the data, wrote the manuscript and edited the paper; Sun DL and Zhang XL helped to supervise the study; Wu MY, Niu WW and Song M helped to perform the experiments and analyzed the data; Sun DL and Zhang XL helped to edit the paper.

Institutional review board statement: The study was reviewed and approved by the Ethics Committee of the Second Hospital of Hebei Medical University (No. 2021-R241).

Institutional animal care and use committee statement: All procedures involving animals were reviewed and approved by the Ethics Committee of the Second Hospital of Hebei Medical University (No. 2021-AE011).

Conflict-of-interest statement: There are no conflicts of interest to report.

Data sharing statement: No additional data are available.

ARRIVE guidelines statement: The authors have read the ARRIVE Guidelines, and the manuscript was prepared and

revised according to the ARRIVE Guidelines.

Open-Access: This article is an open-access article that was selected by an in-house editor and fully peer-reviewed by external reviewers. It is distributed in accordance with the Creative Commons Attribution NonCommercial (CC BY-NC 4.0) license, which permits others to distribute, remix, adapt, build upon this work non-commercially, and license their derivative works on different terms, provided the original work is properly cited and the use is non-commercial. See: https://creativecommons.org/Licenses/by-nc/4.0/

Country/Territory of origin: China

ORCID number: Dan-Dan Wang 0000-0001-7809-7429; Dong-Lei Sun 0000-0002-7930-7544; Shao-Peng Yang 0000-0002-1322-1609; Jia Song 0000-0003-4291-6837; Meng-Yao Wu 0000-0003-0510-8654; Wei-Wei Niu 0000-0002-9243-3625; Mei Song 0000-0002-2504-2480; Xiao-Lan Zhang 0000-0003-4951-0952.

S-Editor: Chen YL
L-Editor: A
P-Editor: Cai YX

REFERENCES

1 **Siegel RL**, Miller KD, Jemal A. Cancer statistics, 2020. *CA Cancer J Clin* 2020; **70**: 7-30 [PMID: 31912902 DOI: 10.3322/caac.21590]
2 **Yang KM**, Park IJ, Lee JL, Kim CW, Yoon YS, Lim SB, Yu CS, Kim JC. Benefits of repeated resections for liver and lung metastases from colorectal cancer. *Asian J Surg* 2020; **43**: 102-109 [PMID: 30910376 DOI: 10.1016/j.asjsur.2019.03.002]
3 **Zhou LL**, Zou MD, Li WM. Recent advances in colorectal cancer-specific nucleic acid aptamers for diagnostic and therapeutic applications. *Sci Adv Mater* 2020; **12**: 38-43 [DOI: 10.1166/sam.2020.3727]
4 **The Lancet Oncology**. Colorectal cancer: a disease of the young? *Lancet Oncol* 2017; **18**: 413 [PMID: 28368245 DOI: 10.1016/S1470-2045(17)30202-4]
5 **Fang Y**, Fullwood MJ. Roles, Functions, and Mechanisms of Long Non-coding RNAs in Cancer. *Genomics Proteomics Bioinformatics* 2016; **14**: 42-54 [PMID: 26883671 DOI: 10.1016/j.gpb.2015.09.006]
6 **Schmitt AM**, Chang HY. Long Noncoding RNAs in Cancer Pathways. *Cancer Cell* 2016; **29**: 452-463 [PMID: 27070700 DOI: 10.1016/j.ccell.2016.03.010]
7 **Tsagakis I**, Douka K, Birds I, Aspden JL. Long non-coding RNAs in development and disease: conservation to mechanisms. *J Pathol* 2020; **250**: 480-495 [PMID: 32100288 DOI: 10.1002/path.5405]
8 **Wang L**, Cho KB, Li Y, Tao G, Xie Z, Guo B. Long Noncoding RNA (lncRNA)-Mediated Competing Endogenous RNA Networks Provide Novel Potential Biomarkers and Therapeutic Targets for Colorectal Cancer. *Int J Mol Sci* 2019; **20** [PMID: 31744051 DOI: 10.3390/ijms20225758]
9 **Xu M**, Chen X, Lin K, Zeng K, Liu X, Xu X, Pan B, Xu T, Sun L, He B, Pan Y, Sun H, Wang S. lncRNA SNHG6 regulates EZH2 expression by sponging miR-26a/b and miR-214 in colorectal cancer. *J Hematol Oncol* 2019; **12**: 3 [PMID: 30626446 DOI: 10.1186/s13045-018-0690-5]
10 **Wei J**, Ge X, Tang Y, Qian Y, Lu W, Jiang K, Fang Y, Hwang M, Fu D, Xiao Q, Ding K. An Autophagy-Related Long Noncoding RNA Signature Contributes to Poor Prognosis in Colorectal Cancer. *J Oncol* 2020; **2020**: 4728947 [PMID: 33149738 DOI: 10.1155/2020/4728947]
11 **Ren W**, Zhang J, Li W, Li Z, Hu S, Suo J, Ying X. A Tumor-Specific Prognostic Long Non-Coding RNA Signature in Gastric Cancer. *Med Sci Monit* 2016; **22**: 3647-3657 [PMID: 27727196 DOI: 10.12659/msm.901190]
12 **Brennan CM**, Steitz JA. HuR and mRNA stability. *Cell Mol Life Sci* 2001; **58**: 266-277 [PMID: 11289308 DOI: 10.1007/PL00000854]
13 **Kotta-Loizou I**, Giaginis C, Theocharis S. Clinical significance of HuR expression in human malignancy. *Med Oncol* 2014; **31**: 161 [PMID: 25112469 DOI: 10.1007/s12032-014-0161-y]
14 **Heinonen M**, Bono P, Narko K, Chang SH, Lundin J, Joensuu H, Furneaux H, Hla T, Haglund C, Ristimäki A. Cytoplasmic HuR expression is a prognostic factor in invasive ductal breast carcinoma. *Cancer Res* 2005; **65**: 2157-2161 [PMID: 15781626 DOI: 10.1158/0008-5472.CAN-04-3765]
15 **Denkert C**, Koch I, von Keyserlingk N, Noske A, Niesporek S, Dietel M, Weichert W. Expression of the ELAV-like protein HuR in human colon cancer: association with tumor stage and cyclooxygenase-2. *Mod Pathol* 2006; **19**: 1261-1269 [PMID: 16799479 DOI: 10.1038/modpathol.3800645]
16 **Mrena J**, Wiksten JP, Thiel A, Kokkola A, Pohjola L, Lundin J, Nordling S, Ristimäki A, Haglund C. Cyclooxygenase-2 is an independent prognostic factor in gastric cancer and its expression is regulated by the messenger RNA stability factor HuR. *Clin Cancer Res* 2005; **11**: 7362-7368 [PMID: 16243808 DOI: 10.1158/1078-0432.CCR-05-0764]
17 **Al-Haidari A**, Algaber A, Madhi R, Syk I, Thorlacius H. MiR-155-5p controls colon cancer cell migration *via* post-transcriptional regulation of Human Antigen R (HuR). *Cancer Lett* 2018; **421**: 145-151 [PMID: 29471005 DOI: 10.1016/j.canlet.2018.02.026]
18 **López de Silanes I**, Fan J, Yang X, Zonderman AB, Potapova O, Pizer ES, Gorospe M. Role of the RNA-binding protein HuR in colon carcinogenesis. *Oncogene* 2003; **22**: 7146-7154 [PMID: 14562043 DOI: 10.1038/sj.onc.1206862]
19 **Liu Y**, Chen X, Cheng R, Yang F, Yu M, Wang C, Cui S, Hong Y, Liang H, Liu M, Zhao C, Ding M, Sun W, Liu Z, Sun F, Zhang C, Zhou Z, Jiang X. The Jun/miR-22/HuR regulatory axis contributes to tumourigenesis in colorectal cancer. *Mol Cancer* 2018; **17**: 11 [PMID: 29351796 DOI: 10.1186/s12943-017-0751-3]

World Journal of Gastroenterology

Submit a Manuscript: https://www.f6publishing.com

World J Gastroenterol 2022 May 28; 28(20): 2201-2213

DOI: 10.3748/wjg.v28.i20.2201

ISSN 1007-9327 (print) ISSN 2219-2840 (online)

ORIGINAL ARTICLE

Retrospective Cohort Study

Digital single-operator video cholangioscopy improves endoscopic management in patients with primary sclerosing cholangitis-a retrospective observational study

Arne Bokemeyer, Frank Lenze, Viorelia Stoica, Timur Selcuk Sensoy, Iyad Kabar, Hartmut Schmidt, Hansjoerg Ullerich

Specialty type: Gastroenterology and hepatology

Provenance and peer review: Invited article; Externally peer reviewed.

Peer-review model: Single blind

Peer-review report's scientific quality classification

Grade A (Excellent): 0
Grade B (Very good): B
Grade C (Good): C, C
Grade D (Fair): D
Grade E (Poor): 0

P-Reviewer: Fujimori N, Japan; Gerussi A, Italy; Kitamura K, Japan

Received: January 2, 2022
Peer-review started: January 2, 2022
First decision: March 10, 2022
Revised: March 18, 2022
Accepted: April 20, 2022
Article in press: April 20, 2022
Published online: May 28, 2022

Arne Bokemeyer, Frank Lenze, Viorelia Stoica, Iyad Kabar, Hansjoerg Ullerich, Department of Medicine B (Gastroenterology, Hepatology, Endocrinology, Clinical Infectiology), University Hospital Muenster, Muenster 48149, Germany

Arne Bokemeyer, Timur Selcuk Sensoy, Hartmut Schmidt, Department of Gastroenterology, Hepatology and Transplant Medicine, University Hospital Essen, Essen 45147, Germany

Corresponding author: Arne Bokemeyer, MD, Academic Research, Doctor, Postdoc, Research Scientist, Department of Gastroenterology, Hepatology and Transplant Medicine, University Hospital Essen, Hufelandstraße 55, Essen 45147, Germany. arne.bokemeyer@googlemail.com

Abstract

BACKGROUND

Patients with primary sclerosing cholangitis (PSC) are at a high risk of developing cholestatic liver disease and biliary cancer, and endoscopy is crucial for the complex management of these patients.

AIM

To clarify the utility of recently introduced digital single-operator video cholangioscopy (SOVC) for the endoscopic management of PSC patients.

METHODS

In this observational study, all patients with a history of PSC and in whom digital SOVC (using the SpyGlass DS System) was performed between 2015 and 2019 were included and retrospectively analysed. Examinations were performed at a tertiary referral centre in Germany. In total, 46 SOVCs performed in 38 patients with a history of PSC were identified. The primary endpoint was the evaluation of dominant biliary strictures using digital SOVC, and the secondary endpoints were the performance of selective guidewire passage across biliary strictures and the diagnosis and treatment of biliary stone disease in PSC patients.

RESULTS

The 22 of 38 patients had a dominant biliary stricture (57.9%). In 4 of these 22 patients, a cholangiocellular carcinoma was diagnosed within the stricture (18.2%). Diagnostic evaluation of dominant biliary strictures using optical signs

showed a sensitivity of 75% and a specificity of 94.4% to detect malignant strictures, whereas SOVC-guided biopsies to gain tissue for histopathological analysis showed a sensitivity of 50% and a specificity of 100%. In 13% of examinations, SOVC was helpful for guidewire passage across biliary strictures that could not be passed by conventional methods (technical success rate 100%). Biliary stone disease was observed in 17.4% of examinations; of these, in 37.5% of examinations, biliary stones could only be visualized by SOVC and not by standard fluoroscopy. Biliary stone treatment was successful in all cases (100%); 25% required SOVC-assisted electrohydraulic lithotripsy. Complications, such as postinterventional cholangitis and pancreatitis, occurred in 13% of examinations; however, no procedure-associated mortality occurred.

CONCLUSION

Digital SOVC is effective and safe for the endoscopic management of PSC patients and may be regularly considered an additive tool for the complex endoscopic management of these patients.

Key Words: Cholangitis; Sclerosing; Biliary tract diseases; Biliary strictures; Endoscopy; Gastrointestinal; Cholangioscopy; Digital single-operator video cholangioscopy

©The Author(s) 2022. Published by Baishideng Publishing Group Inc. All rights reserved.

Core Tip: Endoscopic management of patients with primary sclerosing cholangitis (PSC) is complex; our study is the first to evaluate the utility of single-operator video cholangioscopy (SOVC) with digital imaging quality in these patients. Our data indicate that the use of digital SOVC in PSC patients substantially improves the evaluation of biliary strictures and that SOVC effectively supports interventions, such as stricture dilation and biliary stone treatment, in PSC patients; mild to moderate complications occurred in a minority of cases. Concluding digital SOVC may be effective and safe as an additive tool for the complex endoscopic management of PSC patients.

Citation: Bokemeyer A, Lenze F, Stoica V, Sensoy TS, Kabar I, Schmidt H, Ullerich H. Digital single-operator video cholangioscopy improves endoscopic management in patients with primary sclerosing cholangitis-a retrospective observational study. *World J Gastroenterol* 2022; 28(20): 2201-2213
URL: https://www.wjgnet.com/1007-9327/full/v28/i20/2201.htm
DOI: https://dx.doi.org/10.3748/wjg.v28.i20.2201

INTRODUCTION

Primary sclerosing cholangitis (PSC) is an immune-mediated chronic liver disease characterized by inflammatory, fibrotic, and destructive changes of the bile ducts, leading to cholestasis, biliary stricture development and hepatic fibrosis. Because of the chronic disease course, PSC patients are at a high risk of developing liver cirrhosis and cholangiocellular carcinoma (CCC)[1,2]. Although PSC patients do not regularly show clinical symptoms in early disease, those with advanced disease often develop typical clinical symptoms including right upper quadrant pain (20%), pruritus (10%), jaundice (6%) and fatigue (6%)[1]. Endoscopy is crucial for the diagnostic and therapeutic management of PSC patients, as documented by recent guidelines[2,3]. Standard endoscopic management of PSC patients includes endoscopic retrograde cholangiography (ERC) and is often challenging. In particular, standard endoscopic management is required in patients with biliary strictures: Diagnostic assessment of strictures may become necessary to exclude malignancy, and therapeutic interventions, including stricture dilation to improve cholestatic disease, may be needed[2,3]. Despite endoscopic treatment, PSC patients may develop advanced liver cirrhosis requiring organ transplantation[4], revealing the unmet need for additional therapeutic options.

Cholangioscopic techniques have progressed in recent years. In 2015, the first digital single-operator video cholangioscope (SpyGlass™ DS System, Boston Scientific, Marlborough, MA, United States) was released[5]. Compared with the previous fibre-optic system, this digital single-operator video cholangioscopy (SOVC) instrument is armed with digital imaging, enabling up to four-times higher resolution, a 60% wider field of view, improved manoeuvrability, and irrigation capacities to clean the field of view [5-9]. Furthermore, forceps biopsies are available, allowing SOVC-guided tissue sampling[5,6,8,9], guidewires can be selectively passed across biliary strictures to allow subsequent interventions[8], and SOVC-assisted lithotripsy devices are ready to treat biliary stone disease[10]. Recently, digital SOVC was technically updated, leading to further advances in lighting and image resolution (SpyGlassDS 2.0; Boston Scientific, Marlborough, MA, United States).

The latest guidelines state that intraductal cholangioscopy can help to diagnose indeterminate biliary strictures in PSC patients and that cholangioscopy may be useful for tissue sampling[2,3]. However, the data are rare, and no study thus far has reported the use of newly introduced digital SOVC in PSC patients. Considering the superior imaging quality and manoeuvrability of digital SOVC instruments, further research is required to address the question of whether digital SOVC may offer an effective additive endoscopic treatment in these patients.

Therefore, this study aimed to evaluate the efficacy and safety of digital SOVC for the diagnostic and interventional endoscopic management of patients with PSC.

MATERIALS AND METHODS

Study design and inclusion criteria

This retrospective, monocentre study was performed at the Department of Medicine B for Gastroenterology, Hepatology, Endocrinology and Clinical Infectiology of the University Hospital Muenster, Germany. The data from all patients ≥ 18 years of age and with a previously diagnosed PSC who had undergone digital SOVC using the SpyGlass DS System (Boston Scientific, Marlborough, MA, United States) between December 2015 and November 2019 were retrieved from the clinical data systems. PSC diagnosis was previously known and not initially established during performed SOVC examinations. Biliary tract cancer was not previously diagnosed in these patients; likewise, IgG4-related sclerosing cholangitis was not known in our patient cohort. The study conformed to the ethical guidelines of the 1975 Declaration of Helsinki and was approved by the Ethics Board of the Westphalian Wilhelms-University of Muenster and Medical Council of Westphalia-Lippe, Germany. To minimize known sources of bias, this trial was reported according to the STROBE statement, wherever appropriate and applicable[11].

Technical aspects of digital single-operator video cholangioscopy

Cholangioscopies were performed by highly experienced endoscopists according to the generally accepted guidelines using an ERC case volume exceeding 200/year and performing ERC procedures for at least five years[12]. Before examination, all the patients received prophylactic antibiotic treatment; nonsteroidal anti-inflammatory drugs (NSAIDs; *e.g.*, indomethacin) were not regularly administered before the procedure. CO_2 insufflation was used during all examinations. Before cholangioscopy, an endoscopic papillotomy was performed, or one had been previously performed. The cholangioscope (digital SOVC; Boston Scientific, Marlborough, MA, United States) was inserted into the biliary duct in a guidewire-assisted method; targeted biopsies were acquired using SpyBite forceps (Boston Scientific, Marlborough, MA, United States). For biliary stone treatment, electrohydraulic lithotripsy (EHL) was performed using a bipolar lithotripsy 2.4 F catheter probe (Walz Elektrotechnik GmbH, Rohrdorf, Germany) with saline solution irrigation (SSI) controlled over a dedicated irrigation pump. The probe produces high-frequency hydraulic pressure waves, resulting in the fragmentation of biliary stones[10,13].

The primary endpoint of this study was to evaluate the efficacy and safety of digital SOVC to detect malignancy in dominant biliary strictures in patients with PSC, depending on the visual inspection and histological evaluation of SOVC-acquired biopsies. According to the European guidelines, strictures were defined as dominant if they had a diameter smaller than 1.5 mm in the common bile duct and smaller than 1 mm in the right and left hepatic ducts[14]. Visual signs suggesting malignancy were documented if the performing endoscopists classified visual findings as suspicious for malignancy in the presence of irregular vessels, easy bleeding, irregular surfaces and elevated masses protruding into the duct lumen[15,16]. Acquired biopsy material was analysed by an experienced pathologist and classified as suspicious for malignancy if cancer cells or high-grade cell dysplasia were detected. The final diagnosis (reference standard) of biliary stricture dignity was based on a detailed evaluation of all the available data, including clinical information, cross-sectional imaging reports and histopathological analyses, which could be found in the electronic patient chart. The median follow-up time was 12 mo [interquartile range (IQR) 7-27 mo]; during this time, the patients were followed up by repeated checks of the available electronic medical records.

For secondary endpoint analysis, the use of digital SOVC for the diagnosis and treatment of biliary stone disease in PSC patients was documented. Furthermore, the use of digital SOVC for selective guidewire insertion across biliary strictures in cases that were solely performed because of a previous failure of conventional endoscopic methods to treat a biliary stricture *via* selective guidewire placement was evaluated.

Safety analysis

Adverse events following examination were documented as follows: (1) Postinterventional pancreatitis was defined if patients developed abdominal pain and a threefold increase in the serum lipase levels within 48 h of the examination[17]; (2) Postinterventional cholangitis was documented as the presence of new fever (> 38.0 °C) and newly or significantly higher cholestatic and inflammatory markers

requiring antibiotics within three days of the examination[17]; and (3) Severe bleeding was diagnosed if bleeding was observed during intervention that required immediate endoscopic therapy or if haemoglobin level decreased by two points or more[17]. Adverse events were graded as mild, moderate, or severe, depending on the length of additional hospital stay (mild = 1-3 d, moderate = 4-10 d, severe = > 10 d)[17].

Statistical analysis

The data were analysed using IBM SPSS Statistics 27.0 (IBM Corp., Armonk, United States). Additionally, contingency table-derived data were determined using StatPages[18]. Frequencies and percentages were recorded for categorical variables; means and standard errors (SEs) were reported for continuous variables. Missing data are indicated and reported in the text and tables. The statistical methods of this study were reviewed by Arne Bokemeyer.

RESULTS

Study population

During the study period, 151 ERCs were performed in 72 patients with PSC, and in 30.5% of these ERCs, digital SOVC was additionally carried out (46/151). These 46 cholangioscopies, conducted in 38 PSC patients, were included in the final dataset (Figures 1 and 2). The main indication for SOVC use was the assessment of biliary strictures (80.4%), followed by selective guidewire placement across biliary strictures (13%) and treatment of biliary stone disease (4.3%). A total of 68.4% of the patients were male, whereas 31.6% of the patients were female. The mean age was 44.8 years (SE: ± 2.1 years). Considering all patients, the mean period from the initial ERC performed for PSC diagnosis to the performance of the first SOVC was 99.9 mo (SE ± 16.6). A total of 52.6% of the patients had liver cirrhosis, and 29% were enrolled for liver transplantation. In 10.5% of patients, a final diagnosis of a malignant biliary tumour was established (Table 1). In these patients, the mean time from initial ERC performed for PSC diagnosis to the digital SOVC, which was sufficient to establish bile duct cancer diagnosis, was 71.3 mo (standard error: ± 16.6) with a range of at least 11 mo up to 150 mo.

Of the cholangioscopies, 38 examinations were initial, and 8 were repeated examinations (Table 2). All the examinations were ERC-based (100%). The median total examination time was 73 min (± 5.2 min; missing data in 6/46 examinations). In one case, the digital SOVC system technically failed during examination and could not be relaunched (2.2%; Table 2).

During SOVC, the main procedures were selective SOVC-assisted guidewire insertions to support diagnostic assessment and therapeutic interventions of the biliary tract in 84.7% of examinations, SOVC-assisted forceps biopsy acquisition in 54.3% of examinations, and the performance of SOVC-assisted EHL for refractory biliary stone disease in 4.3% of examinations. Biliary strictures were dilated in 76.1% of examinations, and endoprostheses were placed in 10.9% of examinations (Table 2).

Diagnostic efficacy of stricture assessment in PSC using SOVC

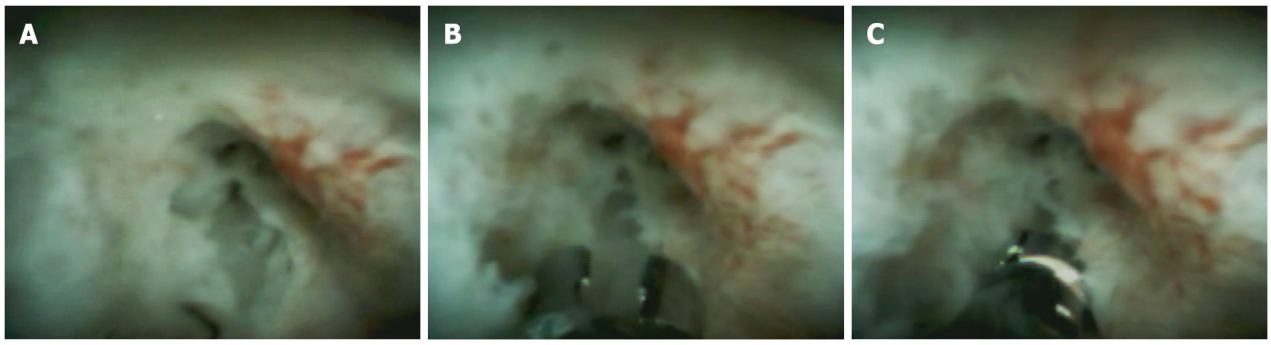
Dominant biliary strictures were present in 22 of 38 patients (57.9%; Table 3). Dominant strictures were mainly localized intrahepatically (59.1%), followed by strictures at the intra- and extrahepatic passages (27.3%) and extrahepatic strictures (13.6%). In 4 of 22 patients, dominant strictures were of a malignant entity (18.2%). The malignant strictures were localized at the intra- and extrahepatic crossing in three patients, and in one patient the stricture was localized intrahepatically at the left hepatic duct. Using SOVC, visual signs of malignancy could be observed in 18.2% of patients. In 13 of 22 patients, SOVC-assisted forceps biopsies were obtained (59.1%; Figure 1). In 2 of 13 biopsies, histopathological analysis revealed signs of malignancy (carcinoma or high-grade dysplasia; 15.4%). In 1 of 13 patients, insufficient tissue was obtained using forceps biopsies, making an accurate histopathological analysis impossible (7.7%; Table 3). The visual examination of dominant strictures had an accuracy of 90.9% (CI: 72.8%-99.2%), a sensitivity of 75% (CI: 25.2%-97.8%), a specificity of 94.4% (83.4%-99.5%), a positive predictive value of 75% (25.2%-97.8%), and a negative predictive value of 94.4% (83.4%-99.5%; Table 4). Histopathological analysis of SOVC-assisted biopsy acquisition had an accuracy of 83.3% (CI: 57.2%-83.3%), a sensitivity of 50% (10.8%-50%), a specificity of 100% (80.4%-100%), a positive predictive value of 100% (21.7%-100%), and a negative predictive value of 80% (64.3%-80%) (Table 4).

Use of SOVC for biliary stone treatment in patients with PSC

In 8 of 46 examinations (17.3%), biliary stones were found (Table 5). Stones were localized intrahepatically (37.5%), extrahepatically (37.5%) and both intra- and extrahepatically (25%). The stone size ranged between 3 and 20 mm, and the number of stones ranged between 1 and 5 *per* examination. In 3 of 8 cases (37.5%), biliary stones were only visualized using SOVC, and standard fluoroscopy failed to detect biliary stones. In all 8 examinations, biliary stone treatment was finally successful; however, in 2 of 8 examinations (25%), biliary stone disease was refractory to standard ERC methods, including stone extraction with baskets and/or balloon catheters, which was why EHL was applied for stone

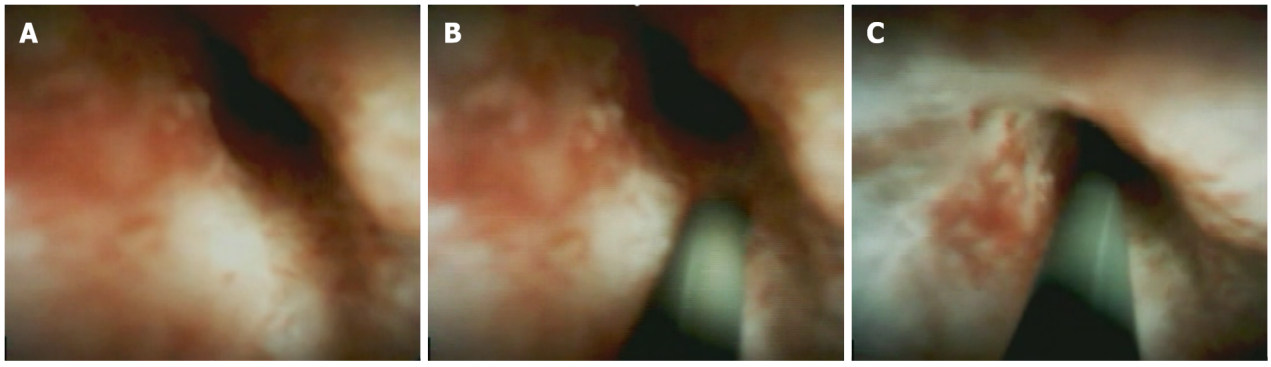
Table 1 Characteristics of patients with primary sclerosing cholangitis undergoing digital single-operator video cholangioscopy

Variable	Patients (*n* = 38)
Primary sclerosing cholangitis, *n* (%)	38 (100)
Age (in years)	44.8 (± 2.1)
Male, *n* (%)	26 (68.4)
Female, *n* (%)	12 (31.6)
Liver cirrhosis, *n* (%)	20 (52.6)
Enlisted for liver transplantation, *n* (%)	11 (28.9)
Diagnosis of a cholangiocellular carcinoma, *n* (%)	4 (10.5)



DOI: 10.3748/wjg.v28.i20.2201 **Copyright** © The Author(s) 2022.

Figure 1 Digital single-operator video cholangioscopy-assisted biliary stricture evaluation in a patient with primary sclerosing cholangitis. A: Using digital single-operator video cholangioscopy (SOVC) enabled the direct visualization of a biliary stricture showing typical signs of chronic inflammation in a patient with primary sclerosing cholangitis; B and C: To rule out malignancy, multiple SOVC-guided forceps biopsies of the biliary stricture were obtained.



DOI: 10.3748/wjg.v28.i20.2201 **Copyright** © The Author(s) 2022.

Figure 2 Selective guidewire placement across a biliary stricture in a patient with primary sclerosing cholangitis using digital single-operator video cholangioscopy. A: Multiple attempts to pass a biliary stricture in a patient with primary sclerosing cholangitis using conventional selective guidewire insertion failed, which is why digital single-operator video cholangioscopy (SOVC) was used and helped visualize the stricture; B and C: Under SOVC-assisted guidance, a guidewire was successfully placed across the biliary stricture, enabling subsequent endoscopic therapy.

fragmentation. In both cases, EHL successfully led to complete stone fragmentation (100%; Table 5).

SOVC-assisted selective guidewire passage across PSC-associated strictures

The 6 of 46 examinations were solely performed because of a previous failure of conventional endoscopic methods to treat a biliary stricture *via* selective guidewire placement (13%; Figure 2). Of these, 5 were initial SOVC procedures, and one was a repeated procedure. The technical success rate of SOVC-assisted guidewire insertions across biliary strictures was 100%, enabling subsequent dilation of the stricture (Table 5).

Table 2 Basic analysis of digital single-operator video cholangioscopies performed in patients with primary sclerosing cholangitis

Variable	Digital SOVC (*n* = 46)
Type of digital SOVC	
Initial examinations, *n* (%)	38 (82.6)
Repeated examinations, *n* (%)	8 (17.4)
Main indication for using SOVC	
Stricture assessment, *n* (%)	37 (80.4)
Selective guidewire placement, *n* (%)	6 (13)
Cholangiolithiasis, *n* (%)	2 (4.3)
Others, *n* (%)	1 (2.2)
Clinical patient data before SOVC (multiple items permitted)	
Prior papillotomy, *n* (%)	41 (89.1)
Elevated serum bilirubin level (> 1.2 mg/dl), *n* (%)	30 (65.2)
Prior post-ERC-pancreatitis, *n* (%)	10 (21.7)
Type of digital SOVC	
ERC-based digital SOVC, *n* (%)	46 (100)
Total examination time (ERC + digital SOVC; min)	73 (± 5.2); *n* = 40/46
Dysfunction of the SOVC-system, *n* (%)	1 (2.2)
Procedures during SOVC-examination (multiple items permitted)	
SOVC-assisted guidewire insertion, *n* (%)	39 (84.7)
SOVC-assisted forceps biopsies, *n* (%)	25 (54.3)
SOVC-assisted EHL, *n* (%)	2 (4.3)
Additive procedures during ERC-examination (multiple items permitted)	
Balloon dilation of the biliary tract, *n* (%)	35 (76.1)
New papillotomy, *n* (%)	7 (15.2)
Conventional transpapillary biopsy, *n* (%)	6 (13.0)
Endoprosthesis placement, *n* (%)	5 (10.9)
Periinterventional application of drugs to prevent AE	
Antibiotics, *n* (%)	46 (100)
NSAID (Diclofenac/Indomethacin), *n* (%)	6 (13)

SOVC: Single-operator video cholangioscopy; EHL: Electrohydraulic lithotripsy; AE: Adverse event; ERC: Endoscopic retrograde cholangiography; NSAID: Nonsteroidal anti-inflammatory drug.

Adverse events

In 13% of the procedures, adverse events were documented (Table 6). More specifically, postinterventional pancreatitis was observed in 6.5% of cases, of which 67% had a moderate and 33% a severe disease course. Postinterventional cholangitis occurred in 6.5% of cases, of which all had a moderate disease course (100%). Other procedure-related adverse events, including severe bleeding or organ perforations, did not occur. All procedure-related complications could be successfully managed by conservative therapeutic approaches. No mortality due to procedure-related adverse events occurred. Because of side effects, patients needed to stay in the hospital for 6.5 more days (SE ± 1.5 d) (Table 6).

DISCUSSION

Although a few previous reports evaluated the utility of cholangioscopy in PSC patients in general[19, 20], our study is the first to evaluate the efficacy and safety of SOVC with digital imaging quality in patients with PSC. Digital SOVC is effective and safe as an additive tool for the complex endoscopic

Table 3 Evaluation of dominant biliary strictures in patients with primary sclerosing cholangitis using digital single-operator video cholangioscopy (*n* = 22)

Variable	Dominant strictures (*n* = 22)
Entity of dominant stricture, *n* (%)	
Benign	18 (81.8)
Malignant	4 (18.2)
Localization of dominant stricture, *n* (%)	
Intrahepatic	13 (59.1)
Extrahepatic	3 (13.6)
Intra- and extrahepatic crossing	6 (27.3)
Visual evaluation of stricture by endoscopists, *n* (%)	
Suspicious for malignancy	4 (18.2)
Suspicious for benignancy	18 (81.8)
SOVC-guided forceps biopsies, *n* (%)	
Carcinoma/high-grade dysplasia	2 (9.1)
Benign findings	10 (45.5)
Inadequate material	1 (4.5)

SOVC: Single-operator video cholangioscopy.

Table 4 Diagnostic efficacy of digital single-operator video cholangioscopy for diagnosing malignancy in dominant biliary strictures in patients with primary sclerosing cholangitis (*n* = 22; cholangioscopic-assisted visual evaluation, *n* = 22 and cholangioscopic-guided biopsies, *n* = 12)

Variable	Accuracy (%)	Sensitivity (%)	Specificity (%)	Pos. pred. value (%)	Neg. pred. value (%)
Visual evaluation (95%CI)	90.9 (72.8-99.2)	75 (25.2-97.8)	94.4 (83.4-99.5)	75 (25.2-97.8)	94.4 (83.4-99.5)
Histological evaluation (95%CI)	83.3 (57.2-83.3)	50 (10.8-50.0)	100 (80.4-100)	100 (21.7-100)	80 (64.3-80)

95%CI: 95% confidence interval; pos.: Positive; neg.: Negative; pred.: Predictive.

management of these patients. In addition to evaluating biliary strictures, digital SOVC facilitates interventions to the biliary tract because of selective guidewire placements across biliary strictures and helps to diagnose and treat biliary stone disease.

Stricture assessment of biliary strictures in PSC patients is critical to excluding malignancy: PSC patients have a lifetime risk of developing CCC of up to 20%[2]. Clinical judgement, laboratory markers, and cross-sectional imaging are insufficient to exclude malignancy, explaining why endoscopic evaluation, including tissue sampling, becomes necessary[2,3,21]. If a standard work-up including ERC with transpapillary tissue sampling fails to determine stricture aetiology, the performance of peroral cholangioscopy is suggested[21]. Visual interpretation of biliary strictures using cholangioscopy may help diagnose indeterminate biliary strictures: A recent meta-analysis including 283 procedures with digital SOVC in unselected patients found a sensitivity of 94% and a specificity of 95% in detecting malignancy in biliary strictures[22]. In addition to optical evaluation, cholangioscopic-guided biopsies can be obtained: Another recent meta-analysis in unselected patients found a sensitivity of 72% and a specificity of 99% in diagnosing biliary malignancy using cholangioscopy-guided biopsies[23]. Despite these promising results in unselected patients, the results in selected PSC patients might be different: A prospective trial using legacy fibreoptic SOVC in 47 patients with PSC evaluated the use of SOVC-assisted forceps biopsies and found a sensitivity of only 33% and a specificity of 100% in detecting malignant biliary strictures[20]. In our study, visual evaluation of indeterminate biliary strictures identified malignancy with a sensitivity of 75% and a specificity of 94% and histopathological analysis of SOVC-guided biopsies showed a sensitivity of 50% and specificity of 100%. In comparison, our study showed a lower sensitivity and specificity of visual and bioptical stricture assessment than those in

Table 5 Diagnosis and treatment of biliary stone disease and performance of selective guidewire placements across biliary strictures (with a previous failure of conventional endoscopic methods to pass a guidewire) using digital single-operator video cholangioscopy in patients with primary sclerosing cholangitis

Variable	Examinations (*n* = 46)
Cholangiolithiasis, *n* (%)	**8/46 (17.3)**
Localization	
Extrahepatic, *n* (%)	3/8 (37.5)
Intrahepatic, *n* (%)	3/8 (37.5)
Intra- and extrahepatic, *n* (%)	2/8 (25)
Stone size (range)	3-20 mm
Stone number (range)	1-5
Treatment	
Complete success (conventional ± EHL), *n* (%)	8/8 (100)
Success only *via* use of EHL, *n* (%)	2/8 (25)
Stone identification only *via* SOVC, *n* (%)	3/8 (37.5)
Selective guidewire insertion across biliary strictures, *n* (%)	**6/46 (13)**
Kind of procedures	
Initial examinations, *n* (%)	5/6 (83.3)
Repeated examinations, *n* (%)	1/6 (16.7)
Technical success, *n* (%)	6/6 (100)

EHL: Electrohydraulic lithotripsy; SOVC: Single-operator video cholangioscopy.

Table 6 Safety data of digital single-operator video cholangioscopies in patients with primary sclerosing cholangitis

Variable	Digital SOVCs (*n* = 46)
Overall complications, *n* (%)	**6 (13)**
Pancreatitis, *n* (%)	3 (6.5)
Grade 1	0 (0)
Grade 2	2 (4.3)
Grade 3	1 (2.2)
Cholangitis, *n* (%)	3 (6.5)
Grade 1	0 (0)
Grade 2	3 (6.5)
Grade 3	0 (0)
Others (bleeding/perforation), *n* (%)	0 (0)
Procedure-related mortality, *n* (%)	0 (0)
Suspected prolonged hospital stay due to complications (in days)	6.5 (± 1.5)

SOVC: Single-operator video cholangioscopy.

previous studies in unselected patients using SOVC. However, comparing our results to previous studies with fibreoptic SOVC including only selected PSC patients, our sensitivity and specificity rates for the diagnostic evaluation of biliary strictures might be improved. As a limitation, digital SOVCs might only be advanced with difficulties to all intrahepatic strictures due to the decreasing lumen of the proximal bile ducts making proximal intrahepatic ducts partially inaccessible for cholangioscopic assessment. To guide cholangioscopy intrahepatically, the use of guidewires can help to advance the

cholangioscope to more proximal localized strictures.

In conclusion, this study shows that using SOVC with digital imaging quality may significantly improve the diagnostic evaluation of indeterminate strictures in PSC patients. However, validated criteria for optical evaluation of strictures are missing and may be particularly needed in stricture evaluation of PSC patients because inflammatory tissue alterations of the bile ducts hinder easy evaluation of biliary stricture aetiology. Furthermore, no consensus exists concerning the number of biopsies that should be obtained to ensure adequate biopsy material[24]. Speculatively, the sensitivity rates of histopathological evaluation may be improved by a higher number of SOVC-guided biopsies [25]; furthermore, larger forceps biopsies for digital SOVC were recently introduced, promising to further improve cholangioscopic diagnostics in the future. Histopathological analysis is essential for excluding differential diagnoses including Ig4-related sclerosing cholangitis, which may mimic a PSC-like disease. In addition to radiologic and serological assessment, tissue acquisition for histopathological analysis is important for diagnostic assessment[26], and SOVCs might help to gain sufficient histopathological material for correct assessment.

Endoscopic interventions, including stricture dilation, can be performed to improve cholestatic disease in PSC patients and are part of current guideline recommendations[2,3]. Technically, biliary dilation should be preferred to inserting biliary stents[2,3]: Notably, in our cohort, stricture dilation was regularly performed in most patients (76%), whereas only a few received biliary stenting (10.9%). To facilitate biliary dilation or stenting, a guidewire must be placed across the biliary stricture[8,27,28]; however, this selective guidewire placement might fail using standard ERC techniques. A previous trial using fiberoptic SOVCs in 15 patients after liver transplantation showed a technical success rate of 60% of placing a guidewire across a stricture[28]. Another study, which was published by our group, using digital SOVC for selective guidewire insertion in 23 unselected patients showed an overall technical success rate of 70%; notably, the technical success rate was significantly higher in benign strictures than in malignant strictures (88% *vs* 46%; $P = 0.02$)[8]. In the current study, in 6 examinations, conventional ERC techniques failed to pass a guidewire across a biliary stricture, and digital SOVC helped in all cases to perform selective guidewire placement, enabling subsequent stricture dilation (technical success rate: 100%). In conclusion, digital SOVC with improved imaging quality is highly successful in facilitating selective guidewire placement across biliary strictures, even in PSC patients in whom previous attempts to pass a stricture with a guidewire failed using standard ERC techniques.

Patients with PSC may have a high incidence of biliary stone disease[29,30]. In two previous studies, PSC patients had an incidence of biliary stone disease of up to 50%[29,30]. In our cohort, we found a slightly lower incidence of biliary stone disease; however, stones were still frequently found in 17.3% of examinations. A previous trial with 41 PSC patients undergoing fibreoptic cholangioscopy using the mother-baby-technique suggested that 30% of biliary stones were missed by standard fluoroscopy and could only be visualized using cholangioscopy[29]. In our cohort, nearly 40% of biliary stones were missed on fluoroscopy and could only be detected using digital SOVC likely confirming that digital SOVC with improved imaging quality substantially helps detect biliary stones in PSC patients. Although the utility of cholangioscopy for stone detection in PSC patients might be superior using digital SOVC, it might be less likely that a routine use of digital SOVCs for stone detection in PSC patients is cost-effective, which might especially be true for MRCP-negative cases. Sometimes the extraction of biliary stones proximal to biliary strictures might be challenging. Dilation of the distal biliary stricture might substantially help extract stones. Furthermore, EHL might be used for stone fragmentation. In 25% of our cases, SOVC-assisted EHL was used for refractory biliary stone disease and showed complete treatment success (100%). This high technical success rate of biliary stone treatment was similar to that in previous trials, varying from 86% to 100%[9,10,15,16,31] supporting the role of digital SOVC as an effective treatment for refractory biliary stone disease, even in PSC patients.

Additionally, we evaluated the safety of using digital SOVC in PSC patients. In ERC, adverse events occurred in approximately 7% of examinations[32]. Concerning digital SOVC, earlier studies observed complication rates ranging from 0 to 16.4%[9,10,15,16,31], and a recent meta-analysis applying digital SOVC to evaluate biliary strictures found a complication rate of 7%[33]. We found a complication rate of 13%, which is in the upper range of previous trials, although only fully trained endoscopists performed procedures in our cohort. Our cholangitis rate (6.5%) was slightly higher than that of unselected patients (4%), likely because of the complexity of our cases: Only PSC patients were included in our cohort; among these, more than 50% had cirrhotic liver disease, and nearly 30% were enlisted for liver transplantation. The risk of cholangioscopy in PSC patients is controversial: Considering that the stricturing disease course hampers adequate biliary drainage post contrast injection, PSC patients may be at special risk of developing post-ERC cholangitis[34]. Furthermore, our pancreatitis rate (6.5%) was slightly higher than the post-ERC pancreatitis rates observed in unselected patients (2%-4%)[32,35]. Fortunately, all cases of pancreatitis could be managed conservatively, and no surgical management was necessary. In our cohort, rectal NSAIDs were not routinely applied at the start of the study; however, considering our results, rectal NSAIDs should be regularly dispensed in all patients with PSC undergoing digital SOVC, which is the current standard of care in our department and part of recent guideline recommendations[17]. In summary, considering this moderate rate of complications, digital SOVC should be performed in selected cases and by experienced endoscopists at tertiary referral centres.

Our study has several limitations. First, our study was retrospective and is limited by a small sample size comprising only 46 procedures; however, it is the first to exclusively evaluate digital SOVC use in PSC patients; furthermore, PSC is a rare disease, making our number of procedures noteworthy. Second, we included cases at only one hospital in our analysis; however, our centre is a large tertiary referral centre offering special endoscopic experience to perform cholangioscopic procedures, and we could ensure that all endoscopists were fully trained, improving the reliability of our results. Nevertheless, our study results are limited by a lack of validation, making future prospective multicentre studies necessary. Third, our endoscopists were not blinded to patient history, likely biasing their visual impression to determine the biliary stricture dignity; however, digital SOVC was performed because strictures were still indeterminate despite previously performed diagnostics. Fourth, in all our patients, a previous traditional cholangiography was performed before the use of digital SOVC, which might have confounded the rate of cholangitis described in our study. However, this setting was our routine clinical practice. Initially, endoscopists performed traditional cholangiography, which revealed findings making further cholangioscopic assessment instantly necessary.

CONCLUSION

In summary, our data indicate that using digital SOVC in patients with PSC is efficient and safe. In addition to evaluating biliary strictures, which may be substantially improved because of superior image quality, SOVC supports interventions due to selective guidewire placements across biliary strictures and helps diagnose and treat biliary stone disease, explaining why digital SOVC might be frequently used as an additive tool for the complex endoscopic management of PSC patients.

ARTICLE HIGHLIGHTS

Research background

Patients with primary sclerosing cholangitis (PSC) have a high risk of developing cholestatic liver disease, biliary strictures, and biliary cancer, which frequently require endoscopy for diagnostic and therapeutic management.

Research motivation

Recently, digital single-operator video cholangioscopy (SOVC) was introduced, offering superior image quality and manoeuvrability. However, no study thus far has reported the use of newly introduced digital SOVC in PSC patients.

Research objectives

To clarify the efficacy and safety of the recently introduced SOVC for the endoscopic management of patients with PSC.

Research methods

This observational study retrospectively included all patients with a known PSC and in whom digital SOVC (with the SpyGlass DS System) was performed between 2015 and 2019 at a tertiary referral centre. In total, 46 SOVCs performed in 38 patients with PSC were identified. The primary endpoint was the evaluation of dominant biliary strictures using digital SOVC.

Research results

The 22 of 38 patients had a dominant biliary stricture (57.9%), and in 18.2% of these cases, a cholangiocellular carcinoma was diagnosed within the stricture. Diagnostic evaluation of dominant biliary strictures using optical signs showed a sensitivity of 75% and a specificity of 94.4% in detecting malignant strictures, whereas SOVC-guided biopsies to obtain tissue for histopathological analysis showed a sensitivity of 50% and a specificity of 100%. In 13% of examinations, SOVC was helpful for guidewire passage across biliary strictures that could not be passed by conventional methods (technical success rate 100%) and furthermore, in 8 examinations, SOVC helped visualize and treat biliary stone disease (100% success rate). Mild to moderate complications occurred in 13% of examinations.

Research conclusions

Digital SOVC is effective and safe for the complex endoscopic management of PSC patients.

Research perspectives

In the future, digital SOVC might be regularly considered as an additive tool for the endoscopic management of patients with PSC.

FOOTNOTES

Author contributions: Bokemeyer A and Ullerich H conceived and designed the study and performed the data analysis, literature review, and manuscript writing; Lenze F, Stoica V, Sensoy T, Kabar I and Schmidt H performed the data collection, data analysis, manuscript writing, and literature review; All the authors have read and approve the final manuscript.

Institutional review board statement: The study was approved by the Ethics Board of the Westphalian Wilhelms-University of Muenster and Medical Council of Westphalia-Lippe, Germany, No. 2017-490-f-S.

Informed consent statement: As approved by the Ethics Board, informed patient consent was not required for this study because of its retrospective design.

Conflict-of-interest statement: The authors declare no potential conflict of interests related to this study.

Data sharing statement: No additional data are available.

STROBE statement: The authors have read the STROBE Statement—checklist of items, and the manuscript was prepared and revised according to the STROBE Statement—checklist of items.

Open-Access: This article is an open-access article that was selected by an in-house editor and fully peer-reviewed by external reviewers. It is distributed in accordance with the Creative Commons Attribution NonCommercial (CC BY-NC 4.0) license, which permits others to distribute, remix, adapt, build upon this work non-commercially, and license their derivative works on different terms, provided the original work is properly cited and the use is non-commercial. See: https://creativecommons.org/Licenses/by-nc/4.0/

Country/Territory of origin: Germany

ORCID number: Arne Bokemeyer 0000-0002-4238-751X; Frank Lenze 0000-0002-5645-4138; Viorelia Stoica 0000-0001-9736-9573; Timur Selcuk Sensoy 0000-0002-4316-3649; Iyad Kabar 0000-0001-5132-3166; Hartmut Schmidt 0000-0002-2402-7764; Hansjoerg Ullerich 0000-0003-2447-3323.

S-Editor: Fan JR
L-Editor: A
P-Editor: Fan JR

REFERENCES

1 **Lazaridis KN**, LaRusso NF. Primary Sclerosing Cholangitis. *N Engl J Med* 2016; **375**: 2501-2502 [PMID: 28002707 DOI: 10.1056/NEJMc1613273]
2 **Chapman MH**, Thorburn D, Hirschfield GM, Webster GGJ, Rushbrook SM, Alexander G, Collier J, Dyson JK, Jones DE, Patanwala I, Thain C, Walmsley M, Pereira SP. British Society of Gastroenterology and UK-PSC guidelines for the diagnosis and management of primary sclerosing cholangitis. *Gut* 2019; **68**: 1356-1378 [PMID: 31154395 DOI: 10.1136/gutjnl-2018-317993]
3 **Aabakken L**, Karlsen TH, Albert J, Arvanitakis M, Chazouilleres O, Dumonceau JM, Färkkilä M, Fickert P, Hirschfield GM, Laghi A, Marzioni M, Fernandez M, Pereira SP, Pohl J, Poley JW, Ponsioen CY, Schramm C, Swahn F, Tringali A, Hassan C. Role of endoscopy in primary sclerosing cholangitis: European Society of Gastrointestinal Endoscopy (ESGE) and European Association for the Study of the Liver (EASL) Clinical Guideline. *Endoscopy* 2017; **49**: 588-608 [PMID: 28420030 DOI: 10.1055/s-0043-107029]
4 **Bjøro K**, Brandsaeter B, Foss A, Schrumpf E. Liver transplantation in primary sclerosing cholangitis. *Semin Liver Dis* 2006; **26**: 69-79 [PMID: 16496235 DOI: 10.1055/s-2006-933565]
5 **SpyGlass-DS-System-ebrochure**. SpyGlass™ DS II Direct Visualization System. [cited 10 January 2022]. Available from: http://www.bostonscientific.com/content/dam/bostonscientific/endo/portfolio-group/SpyGlass%20DS/SpyGlass-DS-System-ebrochure.pdf
6 **Pereira P**, Peixoto A, Andrade P, Macedo G. Peroral cholangiopancreatoscopy with the SpyGlass® system: what do we know 10 years later. *J Gastrointestin Liver Dis* 2017; **26**: 165-170 [PMID: 28617887 DOI: 10.15403/jgld.2014.1121.262.cho]
7 **Shah RJ**, Neuhaus H, Parsi M, Reddy DN, Pleskow DK. Randomized study of digital single-operator cholangioscope compared to fiberoptic single-operator cholangioscope in a novel cholangioscopy bench model. *Endosc Int Open* 2018; **6**: E851-E856 [PMID: 29978005 DOI: 10.1055/a-0584-6458]
8 **Bokemeyer A**, Gross D, Brückner M, Nowacki T, Bettenworth D, Schmidt H, Heinzow H, Kabar I, Ullerich H, Lenze F. Digital single-operator cholangioscopy: a useful tool for selective guidewire placements across complex biliary strictures. *Surg Endosc* 2019; **33**: 731-737 [PMID: 30006839 DOI: 10.1007/s00464-018-6334-6]
9 **Lenze F**, Bokemeyer A, Gross D, Nowacki T, Bettenworth D, Ullerich H. Safety, diagnostic accuracy and therapeutic efficacy of digital single-operator cholangioscopy. *United European Gastroenterol J* 2018; **6**: 902-909 [PMID: 30023068 DOI: 10.1177/2050640618764943]
10 **Brewer Gutierrez OI**, Bekkali NLH, Raijman I, Sturgess R, Sejpal DV, Aridi HD, Sherman S, Shah RJ, Kwon RS,

Buxbaum JL, Zulli C, Wassef W, Adler DG, Kushnir V, Wang AY, Krishnan K, Kaul V, Tzimas D, DiMaio CJ, Ho S, Petersen B, Moon JH, Elmunzer BJ, Webster GJM, Chen YI, Dwyer LK, Inamdar S, Patrick VB, Attwell A, Hosmer A, Ko C, Maurano A, Sarkar A, Taylor LJ, Gregory MH, Strand DS, Raza A, Kothari S, Harris JP, Kumta NA, Manvar A, Topazian MD, Lee YN, Spiceland CM, Trindade AJ, Bukhari MA, Sanaei O, Ngamruengphong S, Khashab MA. Efficacy and Safety of Digital Single-Operator Cholangioscopy for Difficult Biliary Stones. *Clin Gastroenterol Hepatol* 2018; **16**: 918-926.e1 [PMID: 29074446 DOI: 10.1016/j.cgh.2017.10.017]

11 **STROBE**. What is STROBE? [cited 10 January 2022]. Available from: https://www.strobe-statement.org/

12 **Baron TH**, Petersen BT, Mergener K, Chak A, Cohen J, Deal SE, Hoffinan B, Jacobson BC, Petrini JL, Safdi MA, Faigel DO, Pike IM; ASGE/ACG Taskforce on Quality in Endoscopy. Quality indicators for endoscopic retrograde cholangiopancreatography. *Am J Gastroenterol* 2006; **101**: 892-897 [PMID: 16635233 DOI: 10.1111/j.1572-0241.2006.00675.x]

13 **ASGE Technology Committee**, Watson RR, Parsi MA, Aslanian HR, Goodman AJ, Lichtenstein DR, Melson J, Navaneethan U, Pannala R, Sethi A, Sullivan SA, Thosani NC, Trikudanathan G, Trindade AJ, Maple JT. Biliary and pancreatic lithotripsy devices. *VideoGIE* 2018; **3**: 329-338 [PMID: 30402576 DOI: 10.1016/j.vgie.2018.07.010]

14 **European Society of Gastrointestinal Endoscopy**; European Association for the Study of the Liver. Role of endoscopy in primary sclerosing cholangitis: European Society of Gastrointestinal Endoscopy (ESGE) and European Association for the Study of the Liver (EASL) Clinical Guideline. *J Hepatol* 2017; **66**: 1265-1281 [DOI: 10.1016/j.jhep.2017.02.013]

15 **Navaneethan U**, Hasan MK, Kommaraju K, Zhu X, Hebert-Magee S, Hawes RH, Vargo JJ, Varadarajulu S, Parsi MA. Digital, single-operator cholangiopancreatoscopy in the diagnosis and management of pancreatobiliary disorders: a multicenter clinical experience (with video). *Gastrointest Endosc* 2016; **84**: 649-655 [PMID: 26995690 DOI: 10.1016/j.gie.2016.03.789]

16 **Ogura T**, Imanishi M, Kurisu Y, Onda S, Sano T, Takagi W, Okuda A, Miyano A, Amano M, Nishioka N, Yamada T, Masuda D, Takenaka M, Kitano M, Higuchi K. Prospective evaluation of digital single-operator cholangioscope for diagnostic and therapeutic procedures (with videos). *Dig Endosc* 2017; **29**: 782-789 [PMID: 28349613 DOI: 10.1111/den.12878]

17 **ASGE Standards of Practice Committee**, Chandrasekhara V, Khashab MA, Muthusamy VR, Acosta RD, Agrawal D, Bruining DH, Eloubeidi MA, Fanelli RD, Faulx AL, Gurudu SR, Kothari S, Lightdale JR, Qumseya BJ, Shaukat A, Wang A, Wani SB, Yang J, DeWitt JM. Adverse events associated with ERCP. *Gastrointest Endosc* 2017; **85**: 32-47 [PMID: 27546389 DOI: 10.1016/j.gie.2016.06.051]

18 **2-way Contingency**. 2-way Contingency Table Analysis. 2018. [cited 10 January 2022]. Available from: http://statpages.info/ctab2x2.html

19 **Siiki A**, Rinta-Kiikka I, Koivisto T, Vasama K, Sand J, Laukkarinen J. Spyglass single-operator peroral cholangioscopy seems promising in the evaluation of primary sclerosing cholangitis-related biliary strictures. *Scand J Gastroenterol* 2014; **49**: 1385-1390 [PMID: 25259419 DOI: 10.3109/00365521.2014.940376]

20 **Arnelo U**, von Seth E, Bergquist A. Prospective evaluation of the clinical utility of single-operator peroral cholangioscopy in patients with primary sclerosing cholangitis. *Endoscopy* 2015; **47**: 696-702 [PMID: 25826274 DOI: 10.1055/s-0034-1391845]

21 **Pouw RE**, Barret M, Biermann K, Bisschops R, Czakó L, Gecse KB, de Hertogh G, Hucl T, Iacucci M, Jansen M, Rutter M, Savarino E, Spaander MCW, Schmidt PT, Vieth M, Dinis-Ribeiro M, van Hooft JE. Endoscopic tissue sampling - Part 1: Upper gastrointestinal and hepatopancreatobiliary tracts. European Society of Gastrointestinal Endoscopy (ESGE) Guideline. *Endoscopy* 2021; **53**: 1174-1188 [PMID: 34535035 DOI: 10.1055/a-1611-5091]

22 **de Oliveira PVAG**, de Moura DTH, Ribeiro IB, Bazarbashi AN, Franzini TAP, Dos Santos MEL, Bernardo WM, de Moura EGH. Efficacy of digital single-operator cholangioscopy in the visual interpretation of indeterminate biliary strictures: a systematic review and meta-analysis. *Surg Endosc* 2020; **34**: 3321-3329 [PMID: 32342216 DOI: 10.1007/s00464-020-07583-8]

23 **Badshah MB**, Vanar V, Kandula M, Kalva N, Badshah MB, Revenur V, Bechtold ML, Forcione DG, Donthireddy K, Puli SR. Peroral cholangioscopy with cholangioscopy-directed biopsies in the diagnosis of biliary malignancies: a systemic review and meta-analysis. *Eur J Gastroenterol Hepatol* 2019; **31**: 935-940 [PMID: 30896553 DOI: 10.1097/MEG.0000000000001402]

24 **Martinez NS**, Trindade AJ, Sejpal DV. Determining the Indeterminate Biliary Stricture: Cholangioscopy and Beyond. *Curr Gastroenterol Rep* 2020; **22**: 58 [PMID: 33141356 DOI: 10.1007/s11894-020-00797-9]

25 **Kawashima H**, Itoh A, Ohno E, Goto H, Hirooka Y. Transpapillary biliary forceps biopsy to distinguish benign biliary stricture from malignancy: how many tissue samples should be obtained? *Dig Endosc* 2012; **24** Suppl 1: 22-27 [PMID: 22533747 DOI: 10.1111/j.1443-1661.2012.01253.x]

26 **Kamisawa T**, Nakazawa T, Tazuma S, Zen Y, Tanaka A, Ohara H, Muraki T, Inui K, Inoue D, Nishino T, Naitoh I, Itoi T, Notohara K, Kanno A, Kubota K, Hirano K, Isayama H, Shimizu K, Tsuyuguchi T, Shimosegawa T, Kawa S, Chiba T, Okazaki K, Takikawa H, Kimura W, Unno M, Yoshida M. Clinical practice guidelines for IgG4-related sclerosing cholangitis. *J Hepatobiliary Pancreat Sci* 2019; **26**: 9-42 [PMID: 30575336 DOI: 10.1002/jhbp.596]

27 **Lee YY**, Gwak GY, Lee KH, Lee JK, Lee KT, Kwon CH, Joh JW, Lee SK. Predictors of the feasibility of primary endoscopic management of biliary strictures after adult living donor liver transplantation. *Liver Transpl* 2011; **17**: 1467-1473 [PMID: 21898773 DOI: 10.1002/lt.22432]

28 **Woo YS**, Lee JK, Noh DH, Park JK, Lee KH, Lee KT. SpyGlass cholangioscopy-assisted guidewire placement for post-LDLT biliary strictures: a case series. *Surg Endosc* 2016; **30**: 3897-3903 [PMID: 26684207 DOI: 10.1007/s00464-015-4695-7]

29 **Awadallah NS**, Chen YK, Piraka C, Antillon MR, Shah RJ. Is there a role for cholangioscopy in patients with primary sclerosing cholangitis? *Am J Gastroenterol* 2006; **101**: 284-291 [PMID: 16454832 DOI: 10.1111/j.1572-0241.2006.00383.x]

30 **Gluck M**, Cantone NR, Brandabur JJ, Patterson DJ, Bredfeldt JE, Kozarek RA. A twenty-year experience with endoscopic therapy for symptomatic primary sclerosing cholangitis. *J Clin Gastroenterol* 2008; **42**: 1032-1039 [PMID: 18580600 DOI:

10.1097/MCG.0b013e3181646713]
31 **Imanishi M**, Ogura T, Kurisu Y, Onda S, Takagi W, Okuda A, Miyano A, Amano M, Nishioka N, Masuda D, Higuchi K. A feasibility study of digital single-operator cholangioscopy for diagnostic and therapeutic procedure (with videos). *Medicine (Baltimore)* 2017; **96**: e6619 [PMID: 28403110 DOI: 10.1097/MD.0000000000006619]
32 **Andriulli A**, Loperfido S, Napolitano G, Niro G, Valvano MR, Spirito F, Pilotto A, Forlano R. Incidence rates of post-ERCP complications: a systematic survey of prospective studies. *Am J Gastroenterol* 2007; **102**: 1781-1788 [PMID: 17509029 DOI: 10.1111/j.1572-0241.2007.01279.x]
33 **Wen LJ**, Chen JH, Xu HJ, Yu Q, Liu K. Efficacy and Safety of Digital Single-Operator Cholangioscopy in the Diagnosis of Indeterminate Biliary Strictures by Targeted Biopsies: A Systematic Review and Meta-Analysis. *Diagnostics (Basel)* 2020; **10** [PMID: 32887436 DOI: 10.3390/diagnostics10090666]
34 **Navaneethan U**, Jegadeesan R, Nayak S, Lourdusamy V, Sanaka MR, Vargo JJ, Parsi MA. ERCP-related adverse events in patients with primary sclerosing cholangitis. *Gastrointest Endosc* 2015; **81**: 410-419 [PMID: 25085336 DOI: 10.1016/j.gie.2014.06.030]
35 **Korrapati P**, Ciolino J, Wani S, Shah J, Watson R, Muthusamy VR, Klapman J, Komanduri S. The efficacy of peroral cholangioscopy for difficult bile duct stones and indeterminate strictures: a systematic review and meta-analysis. *Endosc Int Open* 2016; **4**: E263-E275 [PMID: 27004242 DOI: 10.1055/s-0042-100194]

World Journal of Gastroenterology

Submit a Manuscript: https://www.f6publishing.com

World J Gastroenterol 2022 May 28; 28(20): 2214-2226

DOI: 10.3748/wjg.v28.i20.2214

ISSN 1007-9327 (print) ISSN 2219-2840 (online)

ORIGINAL ARTICLE

Retrospective Study

Gadolinium-ethoxybenzyl-diethylenetriamine penta-acetic acid-enhanced magnetic resonance imaging for evaluating fibrosis regression in chronic hepatitis C patients after direct-acting antiviral

Xiao-He Li, Rui Huang, Ming Yang, Jian Wang, Ying-Hui Gao, Qian Jin, Dan-Li Ma, Lai Wei, Hui-Ying Rao

Specialty type: Gastroenterology and hepatology

Provenance and peer review: Unsolicited article; Externally peer reviewed.

Peer-review model: Single blind

Peer-review report's scientific quality classification

Grade A (Excellent): 0
Grade B (Very good): B
Grade C (Good): 0
Grade D (Fair): 0
Grade E (Poor): 0

P-Reviewer: Mogahed EA, Egypt

Received: September 30, 2021
Peer-review started: September 30, 2021
First decision: March 11, 2022
Revised: March 25, 2022
Accepted: April 21, 2022
Article in press: April 21, 2022
Published online: May 28, 2022

Xiao-He Li, Rui Huang, Ming Yang, Jian Wang, Ying-Hui Gao, Qian Jin, Dan-Li Ma, Lai Wei, Hui-Ying Rao, Peking University Hepatology Institute, Beijing Key Laboratory of Hepatitis C and Immunotherapy for Liver Diseases, Beijing International Cooperation Base for Science and Technology on NAFLD Diagnosis, Peking University People's Hospital, Beijing 100044, China

Ming Yang, Lai Wei, Hepatopancreatobiliary Center, Beijing Tsinghua Changgung Hospital, Tsinghua University, Beijing 100044, China

Corresponding author: Hui-Ying Rao, MD, Chief Doctor, Professor, Peking University Hepatology Institute, Beijing Key Laboratory of Hepatitis C and Immunotherapy for Liver Diseases, Beijing International Cooperation Base for Science and Technology on NAFLD Diagnosis, Peking University People's Hospital, No.11 Xizhimen South Street, Xicheng District, Beijing 100044, China. rao.huiying@163.com

Abstract

BACKGROUND

Direct acting antiviral (DAA) therapy has enabled hepatitis C virus infection to become curable, while histological changes remain uncontained. Few valid non-invasive methods can be confirmed for use in surveillance. Gadolinium-ethoxy-benzyl-diethylenetriamine penta-acetic acid (Gd-EOB-DTPA) is a liver-specific magnetic resonance imaging (MRI) contrast, related to liver function in the hepatobiliary phase (HBP). Whether Gd-EOB-DTPA-enhanced MRI can be used in the diagnosis and follow up of hepatic fibrosis in patients with chronic hepatitis C (CHC) has not been investigated.

AIM

To investigate the diagnostic and follow-up values of Gd-EOB-DTPA-enhanced MRI for hepatic histology in patients with CHC.

METHODS

Patients with CHC were invited to undergo Gd-EOB-DTPA-enhanced MRI and liver biopsy before treatment, and those with paired qualified MRI and liver biopsy specimens were included. Transient elastography (TE) and blood tests were also arranged. Patients treated with DAAs who achieved 24-wk sustained

virological response (SVR) underwent Gd-EOB-DTPA-enhanced MRI and liver biopsy again. The signal intensity (SI) of the liver and muscle were measured in the unenhanced phase (UEP) ($SI_{UEP\text{-}liver}$, $SI_{UEP\text{-}muscle}$) and HBP ($SI_{HBP\text{-}liver}$, $SI_{HBP\text{-}muscle}$) *via* MRI. The contrast enhancement index (CEI) was calculated as $[(SI_{HBP\text{-}liver}/SI_{HBP\text{-}muscle})]/[(SI_{UEP\text{-}liver}/SI_{UEP\text{-}muscle})]$. Liver stiffness measurement (LSM) was confirmed with TE. Serologic markers, aspartate aminotransferase-to-platelet ratio index (APRI) and Fibrosis-4 (FIB-4), were also calculated according to blood tests. The grade of inflammation and stage of fibrosis were evaluated with the modified histology activity index (mHAI) and Ishak fibrosis score, respectively. Fibrosis regression was defined as a ≥ 1-point decrease in the Ishak fibrosis score. The correlation between the CEI and liver pathology was evaluated. The diagnostic and follow-up values of the CEI, LSM, and serologic markers were compared.

RESULTS

Thirty-nine patients with CHC were enrolled [average age, 42.3 ± 14.4 years; 20/39 (51.3%) male]. Twenty-one enrolled patients had eligible paired Gd-EOB-DTPA-enhanced MRI and liver tissues after achieving SVR. The mHAI median significantly decreased after SVR [baseline 6.0 (4.5-13.5) *vs* SVR 2.0 (1.5-5.5), $Z = 3.322$, $P = 0.017$], but the median stage of fibrosis did not notably change ($P > 0.05$). Sixty pairs of qualified MRI and liver tissue samples were available for use to analyze the relationship between the CEI and hepatic pathology. The CEI was negatively correlated with the mHAI ($r = -0.56$, $P < 0.001$) and Ishak score ($r = -0.69$, $P < 0.001$). Further stratified analysis showed that the value of the CEI decreased with the progression of the stage of fibrosis rather than with the grade of necroinflammation. For patients with Ishak score ≥ 5, the areas under receiver operating characteristics curve of the CEI, LSM, APRI, and FIB-4 were approximately at baseline, 0.87–0.93, and after achieving SVR, 0.83–0.91. The CEI cut-off value was stable (baseline 1.58 and SVR 1.59), but those of the APRI (from 1.05 to 0.24), FIB-4 (from 1.78 to 1.28), and LSM (from 10.8 kpa to 7.1 kpa) decreased dramatically. The APRI and FIB-4 cannot be used as diagnostic means for SVR in patients with Ishak score ≥ 3 ($P > 0.05$). Seven patients achieved fibrosis regression after achieving SVR. In these patients, the CEI median increased (from 1.71 to 1.83, $Z = -1.981$, $P = 0.048$) and those of the APRI (from 1.71 to 1.83, $Z = -2.878$, $P = 0.004$) and LSM (from 6.6 to 4.8, $Z = -2.366$, $P = 0.018$) decreased. However, in patients without fibrosis regression, the medians of the APRI, FIB-4, and LSM also changed significantly ($P < 0.05$).

CONCLUSION

Gd-EOB-DTPA-enhanced MRI has good diagnostic value for staging fibrosis in patients with CHC. It can be used for fibrotic-change monitoring post SVR in patients with CHC treated with DAAs.

Key Words: Gadolinium-ethoxybenzyl-diethylenetriamine penta-acetic acid-enhanced magnetic resonance imaging; Contrast enhancement index; Hepatitis C virus; Direct acting antiviral; Sustained virological response; Fibrosis regression

©The Author(s) 2022. Published by Baishideng Publishing Group Inc. All rights reserved.

Core Tip: In this prospective, comparative study, the correlation between the contrast enhancement index (CEI) in the hepatobiliary phase of gadolinium-ethoxybenzyl-diethylenetriamine penta-acetic acid enhanced magnetic resonance imaging and liver pathology measures was analyzed in patients with chronic hepatitis C. It was determined that the CEI has good diagnostic performance and is more useful than serological markers and transient elastography for hepatic-fibrosis monitoring in patients achieving sustained virological response.

Citation: Li XH, Huang R, Yang M, Wang J, Gao YH, Jin Q, Ma DL, Wei L, Rao HY. Gadolinium-ethoxybenzyl-diethylenetriamine penta-acetic acid-enhanced magnetic resonance imaging for evaluating fibrosis regression in chronic hepatitis C patients after direct-acting antiviral. *World J Gastroenterol* 2022; 28(20): 2214-2226
URL: https://www.wjgnet.com/1007-9327/full/v28/i20/2214.htm
DOI: https://dx.doi.org/10.3748/wjg.v28.i20.2214

INTRODUCTION

Chronic hepatitis C (CHC) remains one of the major etiologies of chronic liver disease, causing

substantial morbidity and mortality globally[1,2]. Remarkably well-tolerated, effective, and short-time direct acting antiviral (DAA) regimens have revolutionized therapy for hepatitis C virus (HCV) infection, achieving a high rate of sustained virological response (SVR). However, it has also been reported that despite achieving SVR, patients may still experience disease progression[3,4]. It is critical to follow up pathological changes in the liver after DAA therapy. A growing number of studies have focused on the use of non-invasive tests to substitute liver biopsy[5-7]. However, there are few validated thresholds for longitudinal assessment that correspond to histologic changes in fibrosis, and there is no definite non-invasive method for diagnosing the stage changes in fibrosis after SVR.

Gadolinium-ethoxybenzyl-diethylenetriamine penta-acetic acid (Gd-EOB-DTPA; Promovist® in Europe and Eovist® in the United States, Bayer Healthcare, Berlin, Germany) is a liver-specific magnetic resonance imaging (MRI) contrast agent[8]. The hepatocyte uptake and biliary excretion of Gd-EOB-DTPA mainly take place *via* organic anion transporting polypeptides OATP1B1/3 on the sinusoidal membrane and multidrug resistance-associated proteins MRP2 on the canalicular membrane. Therefore, after intravenous injection, Gd-EOB-DTPA shows extracellular distribution in the dynamic phase and hepatocyte-specific transportation in the hepatobiliary phase (HBP). Decrease in the number of normal hepatocytes and impaired hepatocyte function may reduce the hepatic enhancement of the HBP[9]. It has been reported using Gd-EOB-DTPA-enhanced MRI to identify hepatocellular carcinoma[10], evaluate liver function[11,12], stage liver fibrosis[13,14], and predict liver failure after hepatectomy[15].

To the best of our knowledge, no studies have used Gd-EOB-DTPA-enhanced MRI to evaluate changes in fibrosis after SVR with paired liver biopsy. The primary aim of our study was to evaluate the diagnostic performance of Gd-EOB-DTPA-enhanced MRI in staging liver fibrosis. The secondary aim was to confirm whether this diagnostic test can be used for longitudinal assessment of liver fibrosis in patients with CHC after achieving SVR treated by DAA regimens.

MATERIALS AND METHODS

Study design

Patients with chronic HCV infection treated with DAAs in our hepatology center between January 2014 and December 2016 were prospectively invited to undergo Gd-EOB-DTPA-enhanced MRI and liver biopsy. Patients with qualified Gd-EOB-DTPA-enhanced MRI data and liver biopsy samples were enrolled. The selection of DAA regimens was based on the genotype and state of liver disease. The patients who achieved SVR after DAA therapy underwent the examinations a second time. Exclusion criterias were: (1) Non-HCV etiology-related chronic liver disease (such as chronic hepatitis B, drug-or alcohol-related liver disease, non-alcoholic steatohepatitis, *etc.*); (2) Clinical hepatic decompensation; (3) Solid organ transplantation; (4) Malignancy; (5) Combined with other systemic disease (immune system disease, blood system disease, *etc.*) and (6) Contraindications for MRI and liver biopsy. SVR was defined as undetectable HCV RNA 24 wk after the end of treatment.

Liver biopsy was performed within 1 mo before treatment and 3 mo after SVR. MRI was performed prior to liver biopsy within 1 mo. MRI with marked motion artifacts and specimens of liver tissue with lengths < 10 mm or < six portal areas under the microscope were regarded as inappropriate[16]. Demographic information, virologic data, and laboratory findings were collected.

MRI protocol

All liver MRI examinations were performed with a Discover 750 3.0 T MR scanner (GE Healthcare, Milwaukee, WI, United States) using a 32-channel torso array coil. Patients were in the supine position during horizontal axis scanning and had received prior training on how to breathe. Gd-EOB-DTPA (Promovist®, Bayer Healthcare) was injected intravenously as a contrast agent at a dose of 0.1 mL/kg body weight with a flow rate of 2 mL/s, followed by a 20-mL 0.09% NaCl flush. Three-dimensional T1-weighted contrast-enhanced MRI was conducted in the unenhanced phase (UEP), arterial phase (AP, 25 s), portal phase (60 s), and HBP (20 min).

Image analysis

The signal intensities (SIs) of the liver parenchyma and paraspinal muscle in the UEP ($SI_{UEP\text{-}liver}$ and $SI_{UEP\text{-}muscle}$) and HBP ($SI_{HBP\text{-}liver}$ and $SI_{HBP\text{-}muscle}$) were independently measured by two professional radiologists with nearly 4 and 6 years of experience in interpreting abdominal MRIs, using regions of interests (ROIs). The radiologists were blinded to the patients' clinical data and pathological changes.

Four ROIs were manually circled (size: 100–150 mm^2) in the posterior and anterior segments of the right hepatic lobe and inner and lateral segments of the left hepatic lobe at the hepatic hilar level. The location of the ROIs had to be at the center of each segment, far from the abdominal wall, and avoiding visible blood vessels, bile ducts, and lesions. The ROI of the paraspinal muscle was mainly circled on the left side.

The contrast enhancement index (CEI) was calculated using the following formula[17]:

$CEI = (SI_{HBP\text{-}liver}/SI_{HBP\text{-}muscle})/(SI_{UEP\text{-}liver}/SI_{UEP\text{-}muscle})$

The change rate in the CEI (Δ CEI%) between pre-treatment (CEI_{pre}) and post-SVR (CEI_{post}) was calculated as ($CEI_{post}/CEI_{pre} \times 100\%$).

Histopathological analysis

Specimens were fixed in formalin immediately after liver biopsy and embedded in paraffin; 4-μm-thick sections were cut and stained with hematoxylin and eosin and Masson's trichrome. Two professional hepato-pathologists, both with nearly 30 years of working experience, assessed the degree and stage of necroinflammation and fibrosis of the specimens using the Ishak scoring system [modified histological activity index (mHAI) and Ishak score][18]. The pathologists were blinded to the imaging results and patient clinical data. The stages of liver fibrosis were divided into three groups according to the Ishak score, 0-2, 3-4, and 5-6, respectively. Necro-inflammatory severity was graded according to the mHAI score as 0-4, 5-8, 9-12, and 13-18[19]. Fibrosis regression was defined as a decrease of at least one point in the Ishak score after SVR[20].

Non-invasive fibrosis measurements

Experienced technicians conducted liver stiffness measurements (LSMs) with FibroScan (Echosens, Paris, France). An effective result should have a successful rate > 60% and interquartile range/median ratio ≤ 30%.

With respect to serologic biomarkers of fibrosis, the aspartate aminotransferase (AST)-to-platelet ratio (APRI) and Fibrosis-4 (FIB-4) were calculated as following:

APRI = [(AST/ULN)/platelet count ($\times 10^9$/L)] × 100[21]; FIB-4 = (age × AST)/[(platelet count) ($\times 10^9$/L) × ALT1/2][22]

The change rates in APRI, FIB-4, and LSM between pre-SVR ($value_{pre}$) and post-SVR ($value_{post}$) were calculated similarly with the CEI calculation.

Statistical analyses

Descriptive analyses were performed for sociodemographic characteristics (age, sex), clinical data [alanine aminotransferase (ALT), AST, total bilirubin (TB), albumin (Alb), platelet (PLT) count, HCV RNA, genotype, FIB-4, APRI, LSM, and CEI], histological grading, and staging.

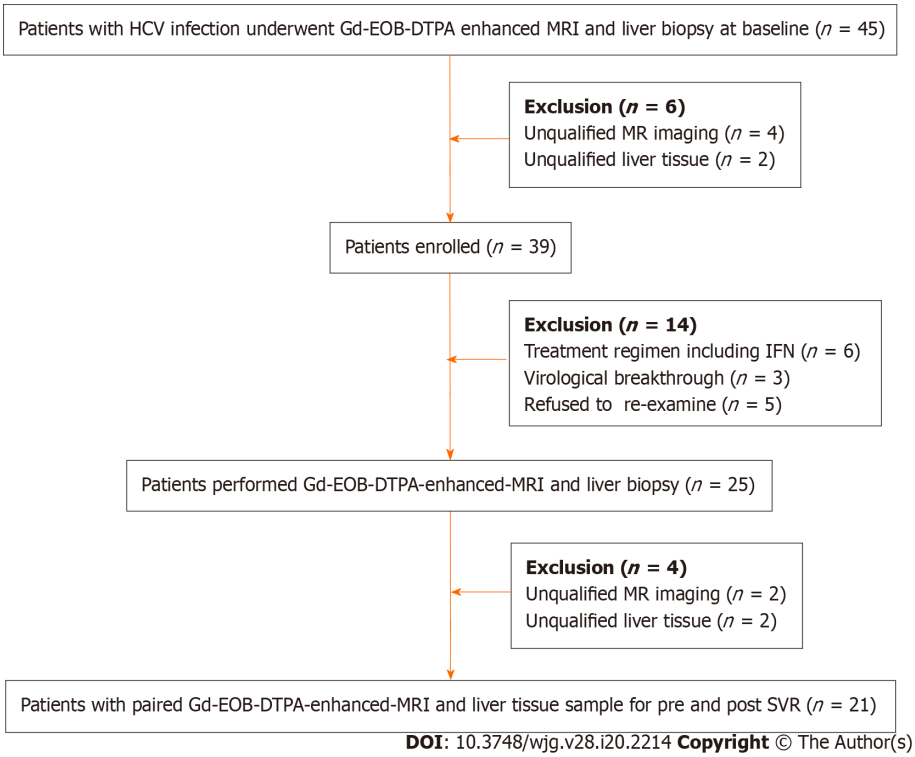
Descriptive analyses were performed for sociodemographic characteristics, clinical data, histological characteristics, and the CEI. The value of HCV RNA was logarithmically transformed with 10 as the base. Continuous variables are expressed as median (interquartile range) (ALT, AST, TB, PLT, APRI, FIB-4, and LSM) or mean ± SD [age, Alb, international normalized ratio (INR), HCV RNA, mHAI, and CEI]. Categorical variables (sex, numbers of patients in the different mHAI and Ishak score groups) are presented as counts and percentages. The absolute values of the interclass correlation coefficients (ICC) were measured for SIs to confirm the interobserver reliability between reviewers. Student's t-test (age, Alb, INR, HCV RNA, mHAI, and CEI) and Mann-Whitney U test (ALT, AST, TB, and PLT) were used to compare continuous variables, and the chi-square test was used for classified variables (sex, HCV genotype). The comparison between pre-and post-SVR was performed with the Wilcoxon sign rank test (ALT, AST, TB, PLT, FIB-4, APRI, and LSM) and paired sample t-test (Alb, INR, and CEI). Spearman's correlation coefficient was calculated for the CEI, mHAI, and Ishak score. The predictive value of the CEI, APRI, FIB-4, and LSM for liver fibrosis was assessed using the area under the receiver operating characteristic curve (AUROC). Sensitivity, specificity, positive predictive value, and negative predictive value were also calculated. An optimal cut-off value was chosen to maximize the Youden index, which is defined as (sensitivity + specificity-1). P values < 0.05 were considered statistically significant. Statistical analyses were performed using IBM SPSS version 26.0 (IBM Corp., Armonk, NY, United States).

RESULTS

Forty-five patients underwent Gd-EOB-DTPA-enhanced MRI and liver biopsy at baseline and six with unqualified samples were excluded. Among the enrolled patients (n = 39), six were recommended to receive treatment with DAA plus Peg-IFN, and three had virological breakthrough. Twenty-five patients underwent MRI and liver biopsy again after achieving SVR, and 21 pairs of data were eligible. Therefore, there were 60 qualified and pairable MRI images and liver tissue samples available for analyzing correlation between CEI and liver pathology. The study flow chart is shown in Figure 1.

Intraclass correlation coefficients

Two radiologists interpreted the Gd-EOB-DTPA-enhanced MRI images. The ICC for the measured SI values were excellent (greater than 0.9) for before and after achieving SVR. The ICC of the CEI was 0.729 (0.481, 0.858) and 0.886 (0.744, 0.952) pre and post SVR, respectively. Details of the inter-observer agreements of the ROI measurements and CEI are presented in Supplementary Table 1.



DOI: 10.3748/wjg.v28.i20.2214 **Copyright** © The Author(s) 2022.

Figure 1 The study flow chart. HCV: Hepatitis C virus; Gd-EOD-DTPA: Gadolinium ethoxybenzyl diethylenetriamine penta-acetic acid; MRI: Magnetic resonance imaging; IFN: Interferon; SVR: Sustained virological response.

Patient characteristics

The 39 patients enrolled had a mean age of (42.3 ± 14.4) years, mean HCV RNA of (6.4 ± 0.7) $\log_{10}$ IU/mL, and 20 (51.3%) were male. The distribution of HCV genotypes (GT) was 1, 2, 3, and 6 in 19 (48.7%), 4 (10.3%), 13 (33.3%), and 3 (7.7%) patients, respectively. Patients with Ishak score of 5-6 were elder, had higher ALT and lower PLT levels than those with Ishak scores of 0–2 ($P < 0.05$) (Table 1).

Of the 21 patients who achieved SVR and had paired MRI and liver tissue samples, 13 (62%) received sofosbuvir/ribavirin therapy, and the other eight (38%) received daclatasvir/asunaprevir regimens. As expected, the values of ALT, AST ($P < 0.001$), and necroinflammation grade ($P = 0.023$) significantly decreased post SVR (Table 2). No significant change in fibrosis stage was observed. Among the noninvasive measurements, the median of LSM, FIB-4, and APRI decreased significantly, the mean of the CEI increased slightly without statistically significant ($P = 0.29$) (Table 2). After achieving SVR, 7 (33%) patients achieved fibrosis regression. No patient with Ishak 5-6 ($n = 7$) achieved fibrosis regression.

The CEI decreased with the progression of liver fibrosis

In patients with CHC, the CEI was negatively correlated with the grade of inflammation ($r = -0.56$, $P < 0.001$) and stage of fibrosis ($r = -0.69$, $P < 0.001$). The CEI decreased significantly among patients with Ishak scores 0–2, 3–4, and 5–6 (1.78 ± 0.11, 1.64 ± 0.11, and 1.50 ± 0.09, respectively, $P < 0.001$) (Figure 2A). To further analyze the relationship between the CEI and liver pathology, we stratified the patients according to the mHAI (0–4, 5–8, 9–12, and 13–18) and Ishak score (0–2, 3–4, and 5–6; the numbers of patients in each subgroup are shown in Table 3).

In patients with a mHAI of 0–4, the CEI in Group 2 ($n = 11$) was significantly lower than that in Group 1 ($n = 14$) [(1.67 ± 0.11) *vs* (1.79 ± 0.11), $P = 0.021$] and the CEI of the only patient in Group 3 was 1.52 (Figure 2B). When the mHAI was 5–8, the CEI decreased in the order of fibrosis Group 1 ($n = 3$), 2 ($n = 13$), and 3 ($n = 9$) at 1.75 ± 0.06, 1.62 ± 0.11, and 1.49 ± 0.12, respectively ($P = 0.032$) (Figure 2C). All patients with an mHAI of 13–18 had liver cirrhosis ($n = 9$), and they were not grouped. In contrast, after subgrouping the patients based on the fibrosis grade, there were no significant differences in the CEI among the inflammation groups (all $P > 0.05$) (Figure 2D–F). Therefore, we believe that decrease in the CEI is mainly associated with the progression of fibrosis.

The CEI is more useful for liver fibrosis diagnosis than the LSM, APRI, and FIB-4

Table 4 shows a comparison of the predictive values between the CEI and other non-invasive methods. According to the AUROCs and cut-off values, we found that the diagnostic efficacy of the CEI, LSM, APRI, and FIB-4 before and after DAA treatment was similar for liver cirrhosis (Ishak score ≥ 5), while

Table 1 Comparison of demographic and clinical data of patients

Parameters	Ishak 0-2 (*n* = 9)	Ishak 3-4 (*n* = 18)	Ishak 5-6 (*n* = 12)
Age (yr)	36.3 ± 15.5	37.9 ± 12.4	53.1 ± 11.0[b]
Male, *n* (%)	2 (22.2)	11 (61.1)	7 (58.3)
ALT (U/L)	44 (22.5)	52.5 (35.5)	75.5 (98.7)[a]
TB (μmol/L)	11 (7.5)	14 (3.5)	12.5 (7.5)
Alb (g/L)	46.78 ± 3.77	45.72 ± 3.75	44.17 ± 3.35
INR	0.99 ± 0.07	1.00 ± 0.09	1.09 ± 0.16
PLT (× 10^9/L)	171 (62.5)	177.5 (64.7)	114 (67.5)[b]
HCV RNA (log_{10} IU/mL)	6.43 ± 0.96	6.50 ± 0.71	6.33 ± 0.64
mHAI score	3.4 ± 1.7	5.3 ± 1.6[a]	11.3 ± 4.0[c]

[a]$P < 0.05$ compared with patients with Ishak 0-2.
[b]$P < 0.01$ compared with patients with Ishak 0-2.
[c]$P < 0.001$ compared with patients with Ishak 0-2.
ALT: Alanine aminotransferase; TB: Total bilirubin; INR: International normalized ratio; HCV: Hepatitis C virus; mHAI: Modified histology activity index.

Table 2 Clinical characteristics of patients for pre and post sustained virological response

	Pre SVR	Post SVR	*Z/t* value	*P* value
ALT (U/L)	55 (29.5)	17 (11)	-4.015	< 0.001
AST (U/L)	40 (29.5)	20 (10.5)	-4.016	< 0.001
TB (μmol/L)	14 (6.5)	15.5 (11.3)	-0.541	0.588
Alb (g/L)	44.90 ± 3.40	47.43 ± 3.06	-3.919	0.001
Platelet (× 10^9/L)	165 (87)	199 (130)	-2.576	0.01
INR	1.04 ± 0.14	1.02 ± 0.07	0.425	0.675
mHAI score, *n* (%)			-2.362	0.023
0-4	5 (24)	15 (71)		
5-8	10 (48)	4 (9)		
13-18	6 (28)	2 (10)		
Ishak score, *n* (%)			-0.370	0.713
0-2	5 (24)	7 (33)		
3-4	9 (43)	7 (33)		
5-6	7 (33)	7 (33)		
APRI	0.58 (1.32)	0.25 (0.40)	-4.015	< 0.001
FIB-4	1.34 (3.61)	0.99 (1.81)	-3.007	0.003
LSM (kpa)	6.6 (7.5)	5.8 (4.0)	-2.746	0.006
CEI	1.65 ± 0.11	1.68 ± 0.16	-1.087	0.29

ALT: Alanine aminotransferase; AST: Aspartate aminotransferase; APRI: AST-to platelet ratio index; CEI: Contrast enhancement index; HCV: Hepatitis C virus; INR: International normalized ratio; mHAI: Modified histology activity index; LSM: Liver stiffness measurement; SVR: Sustained virological response; TB: Total bilirubin.

the cut-off values of serological markers such as the APRI and FIB-4 significantly decreased post SVR. The cut-off value of the LSM also showed a similar trend. For significant fibrosis (Ishak score ≥ 3), post SVR, the diagnostic efficacy of the LSM decreased, and the APRI and FIB-4 showed no diagnostic value.

Table 3 Distribution of patients in stratified analysis

Stratified analysis	Group 1	Group 2	Group 3
mHAI score	**Ishak score**		
	0-2	3-4	5-6
0-4	14	11	1
5-8	3	13	9
13-18	0	0	9
Ishak score	**mHAI score**		
	0-4	5-8	13-18
0-4	14	2	0
3-4	10	15	0
5-6	1	9	9

mHAI: Modified histology activity index.

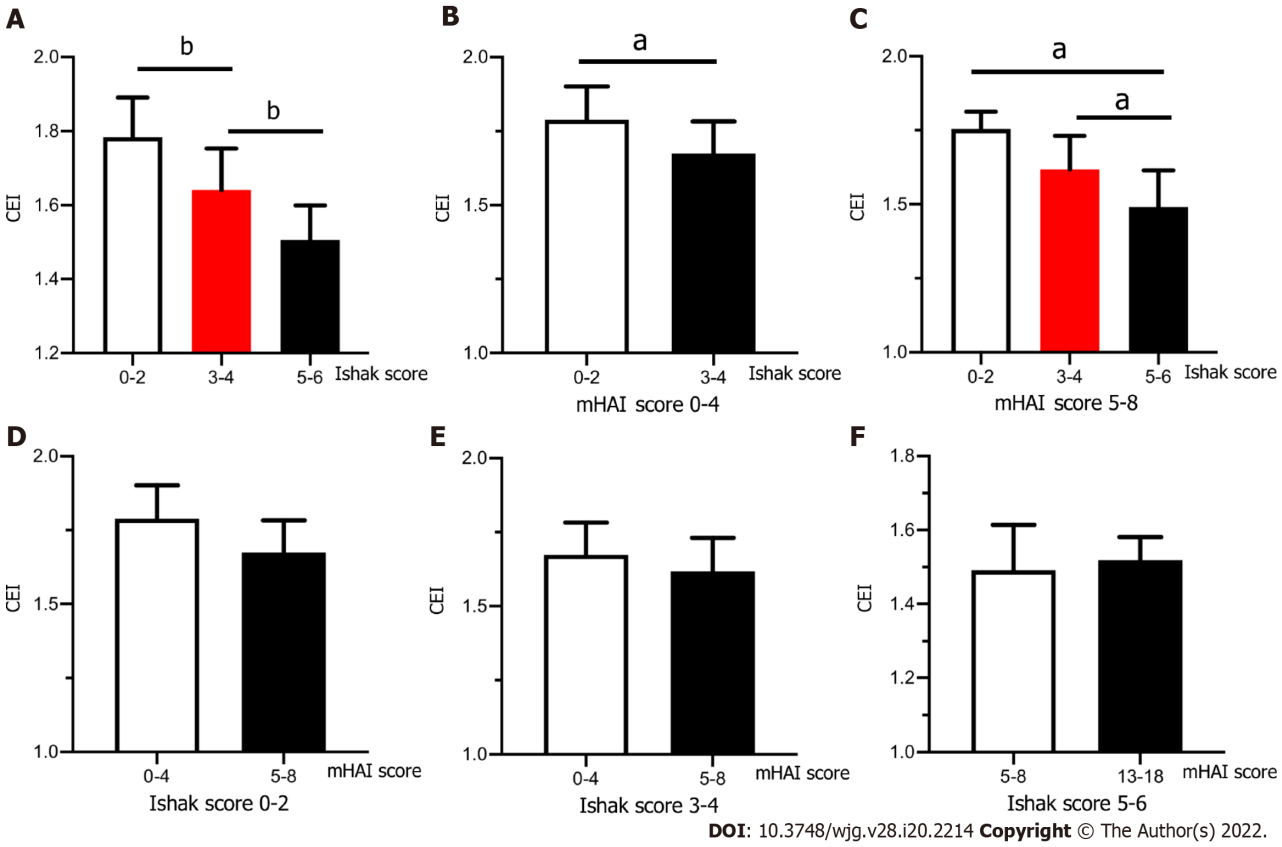
Table 4 The area under receiver operating curve and cut-off value for liver cirrhosis and significant liver fibrosis at pre-sustained virological response and post-sustained virological response with contrast enhancement index, aspartate aminotransferase-to-platelet ratio index, Fibrosis-4 and liver stiffness measurement

	Ishak score ≥ 5		Ishak score ≥ 3	
	Pre SVR	Post SVR	Pre SVR	Post SVR
CEI				
AUROC (95%CI)	0.93 (0.74, 0.97)	0.87 (0.65, 0.97)	0.88 (0.79, 1.00)	0.87 (0.71, 1.00)
Cut-off value	1.58	1.59	1.71	1.68
LSM				
AUROC (95%CI)	0.87(0.71, 1.00)	0.87(0.79, 1.00)	0.91(0.78, 1.00)	0.80(0.60,0.98)
Cut-off value	10.8	7.1	6.2	5.95
APRI				
AUROC (95%CI)	0.89(0.72, 1.00)	0.89(0.74, 1.00)	0.83(0.64, 1.00)	N[2]
Cut-off value	1.05	0.24[1]	0.39	N[2]
FIB-4				
AUROC (95%CI)	0.92(0.80, 1.00)	0.92(0.79, 1.00)	0.80(0.58, 1.00)	N[2]
Cut-off value	1.78	1.28[1]	0.87	N[2]

[1]The cutoff values of aspartate aminotransferase-to-platelet ratio index (APRI) and Fibrosis-4 (FIB-4) or the diagnosis of liver cirrhosis decreased dramatically after sustained virological response (SVR).
[2]N: No diagnosis value of APRI or FIB-4 in patients with significant fibrosis after achieving SVR.
APRI: Aspartate aminotransferase-to-platelet ratio index; AUROC: Area under receiver operating curve; CEI: Contrast enhancement index; CI: Confidence interval; FIB-4: Fibrosis-4; LSM: Liver stiffness measurement; SVR: Sustained virological response.

Only dynamic change in the CEI can be used to evaluate fibrosis regression after achieving SVR

Figure 3 shows the change of the CEI and other non-invasive methods in patients with (red column) and without (black column) fibrosis regression. Among the patients with fibrosis regression (n = 7), the CEI increased significantly (from 1.68 ± 0.09 to 1.83 ± 0.18, P = 0.043) after DAA treatment; similarly, the LSM [from 6.6 (2.6) to 4.8 (1.2), P = 0.018] and APRI [from 0.37 (0.22) to 0.20 (0.08), P = 0.018] values decreased significantly. For patients who did not achieve fibrosis regression (n = 14), only the CEI remained stable (P > 0.05), while the LSM, APRI, and FIB-4 decreased significantly (P < 0.05). It is suggested that the decrease in the latter three noninvasive measurements after treatment may not be related to fibrosis regression. By comparing the change ratios of the four noninvasive indexes before and after treatment, only CEI% changed significantly, and CEI% was moderately positively correlated with



DOI: 10.3748/wjg.v28.i20.2214 **Copyright** © The Author(s) 2022.

Figure 2 Contrast enhancement index decreased with the progression of liver fibrosis. A: Contrast enhancement index (CEI) decreased with the progression of fibrosis, and there was significant difference between patients with Ishak score 0-2, 3-4 and 5-6; B: In patients with modified histology activity index (mHAI) score of 0-4, CEI was lower in patients with Ishak score of 3-4 compared with 0-2; C: In patients with mHAI score of 5-8, CEI decreased with the progression of fibrosis stage; D-F: When the Ishak scores was fixed as 0-2, 3-4 and 5-6 respectively, the value of CEI was not related to the progression of inflammation. $^{a}P < 0.05$; $^{b}P < 0.001$. CEI: Contrast enhancement index; mHAI: Modified histology activity index.

fibrosis regression ($r = 0.50$, $P = 0.021$) (Table 5).

DISCUSSION

In this study, paired liver biopsy and Gd-EOB-DTPA-enhanced MRI data of patients with CHC before and after SVR were reported for the first time. This study concluded that the CEI of Gd-EOB-DTPA-enhanced MRI in the HBP decreased with the progression of liver fibrosis. For patients with CHC, the CEI can be used to distinguish among the different stages of liver fibrosis at baseline and after achieving SVR more effectively than the APRI, FIB-4, and LSM. The change in the CEI between pre and post SVR was related to fibrosis regression. This result increased the options for dynamic assessment of liver fibrosis after achieving SVR.

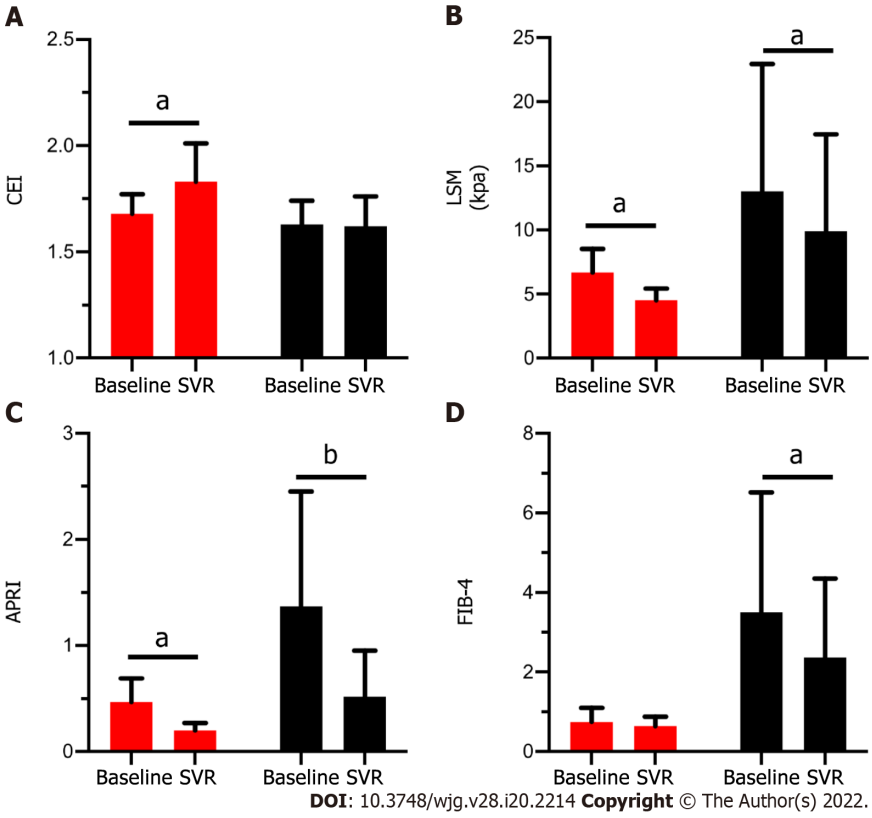
In our study, patients treated with DAA plus interferon were excluded. Although the combination therapy may have no effect on the evaluation of liver pathology, based on the current situation of CHC treatment, majority of patients can be cured by simple DAAs. So, we pay more attention on correlation between CEI and pathology changes in patients cured by simple DAAs. It is worth mentioning that, HCV RNA was both detected at 12- and 24-wk after the end of treatment. The value of HCV RNA at 12-wk were also undetectable in patients achieving SVR24. Since patients were enrolled between 2014-2016, SVR12 and SVR24 both could be used at that time, while the 24-wk SVR last longer, it was used in our article. We specially agree that the current definition of SVR as an undetectable HCV RNA at 12 wk after the end of treatment.

In the correlation analysis, we found that the CEI was mild negative related to both grade of inflammation and stage of fibrosis. Further hierarchical analysis showed that the CEI mainly decreased with the progression of liver fibrosis, which was consistent with the results of a previous multiple regression analysis[23]. As mentioned above, after achieving SVR, the overall liver fibrosis status was not notably improved, and the CEI also did not change significantly. Therefore, we combined 60 pairs of CEI and liver pathology data before and after treatment for analysis. It should be mentioned that the overall mHAI decreased after treatment, which may have affected the results. However, in our pre-analysis, we

Table 5 Relationship between the changes of contrast enhancement index, aminotransferase-to-platelet ratio index, Fibrosis-4, liver stiffness measurement and fibrosis regression

	Fibrosis regression		*P* value
	Yes (*n* = 7)	No (*n* = 14)	
CEI%[1]	107.36 ± 6.33	99.23 ± 7.14	0.020
LSM%	72.06 ± 20.32	81.31 ± 27.44	0.441
APRI%	45.40 ± 13.16	42.51 ± 16.41	0.702
FIB-4%	90.39 ± 24.09	75.69 ± 23.66	0.936

[1]Value% = $Value_{post}/Value_{pre}$ × 100%.
CEI: Contrast enhancement index; SVR: Sustained virological response; LSM: Liver stiffness measurement; APRI: Aspartate aminotransferase-to-platelet ratio index; FIB-4: Fibrosis-4.



DOI: 10.3748/wjg.v28.i20.2214 **Copyright** © The Author(s) 2022.

Figure 3 Comparison of four noninvasive methods before and after sustained virological response between patients with fibrosis regression or not. A: Value of contrast enhancement index; B: Value of liver stiffness measurement; C: Value of aspartate aminotransferase-to-platelet ratio index; D: Value or Fibrosis-4 in patients with (Red column) and without (Black column) fibrosis regression at baseline and after achieving sustained virological response (SVR). Red column: Patients had fibrosis regression after achieving SVR (*n* = 7). Black column: Patients didn't have fibrosis regression after achieving SVR (*n* = 14). $^{a}P < 0.05$; $^{b}P < 0.001$. CEI: Contrast enhancement index; SVR: Sustained virological response; LSM: Liver stiffness measurement; APRI: Aspartate aminotransferase-to-platelet ratio index; FIB-4: Fibrosis-4.

found that in the 21 paired MRI and liver biopsy samples after treatment, the correlation between the mHAI and Ishak score ($r = 0.74$, $P < 0.001$) remained significant. This may be because the patients with a mHAI > 13 at baseline had liver cirrhosis. After achieving SVR, there was no significant improvement in fibrosis or in the inflammation status. It was also shown that the correlation between the CEI and fibrosis stage remained relatively stable and was not related to the treatment state.

In patients with liver cirrhosis (Ishak score 5-6), the diagnostic values of the CEI and of the other non-invasive methods were similar, which was also partly previously reported by a cross-sectional comparative analysis[23]. As the inflammatory status improved with antiviral treatment, the cut-off values of the APRI (from 1.05 to 0.24) and FIB-4 (from 1.78 to 1.28) both substantially decreased for the same fibrosis status. The serological biomarkers had no diagnostic value for significant fibrosis after HCV eradication, mainly because with the rapid regression of liver necroinflammation, the ALT and

AST levels returned to normal, reducing the diagnostic accuracy of serological biomarkers. Although accessible and common, the APRI and FIB-4 may not be suitable for the surveillance of patients with CHC post SVR[21,24].

Other than the serological biomarkers, the LSM obtained with TE is currently considered useful for fibrosis monitoring[25-27]. However, several studies have reported a rapid decrease in the LSM mainly related to inflammation regression, and its cut-off values are influenced by liver morphometry. Hence, the decrease in the LSM may be misinterpreted as change in the liver fibrosis stage[6,28]. A longitudinal study of 2 years showed that following SVR attainment, the improvements in the LSM were overstated compared to histologic staging[28]. Therefore, the follow-up value of liver fibrosis regression in patients with HCV SVR needs to be further verified. Our findings strengthened this notion in a relative short follow-up time (median of 6.2 mo). The cut-off value of the LSM decreased slightly in patients with liver cirrhosis (from 10.8 kPa to 7.1 kPa), wherein an LSM value of 7.1 kPa obtained with TE was defined as the threshold for absence of or minimal fibrosis in patients with CHC[29]. The comparative analysis also showed significant decrease in the LSM value in patients without fibrosis regression.

Apart from the CEI, several studies have reported multiple hepatobiliary liver enhancement indexes of Gd-EOB-DTPA-enhanced MRI, including RE (calculated as $[SI_{HBP}-SI_{UEP}]/SI_{UEP}$ of the liver parenchyma), liver-to-portal vein contrast ratio (calculated by dividing the liver parenchyma SI by the portal vein SI on HBP images), and liver-to-spleen contrast ratio (calculated by dividing the liver parenchyma SI by the spleen SI on HBP images)[30-32]. In previous reports, the signals of the portal vein and spleen were integrated with plasma or extracellular extravascular space exposure to the contrast agent, thus showing that the liver-to-portal vein contrast ratio and liver-to-spleen contrast ratio were more strongly related to liver function than to liver fibrosis[12,33]. Adjustment of the signal of the paraspinal muscle for SI_{liver} on the same slice was performed to normalize the shimming influences and correct for technical bias. Compared with other organs, SI_{muscle} was more stable and less influenced by age and liver function. Jang *et al*[23] also validated this view. A few articles have shown similar diagnostic accuracies for RE and the CEI. In our study, RE was mildly negatively associated with liver inflammation (r = -0.57, P = 0.007) and fibrosis (r = -0.44, P = 0.043) (unreported), possibly because the SI of the liver after injecting Gd-EOB-DTPA changes, as the window level and width differ in the images [34].

There were several limitations in our study. First, limited by the inclusion criteria, the sample size was small, and the CEI% of patients with fibrosis regression was close to 1. We will explore further by expanding the sample size. Second, we did not use MR elastography (MRE) or T1-mapping to predict liver fibrosis, which have a superior diagnostic value in predicting liver fibrosis than Gd-EOB-DTPA-enhanced MRI[35,36]. However, except for the influence of body mass index and ascites on TE, the sequencing method in MRE is not unified, and the threshold value changes across different methods [26]. In recent years, MR relaxometry in the form of T1 mapping has been considered promising as a non-invasive method for characterizing hepatic fibrosis using the look-locker technique for measurement. Our patients were enrolled between 2014 and 2016, when T1 mapping was not in use. Third, although histology is a gold standard procedure, the tissues used in our study were all from liver biopsies rather than from hepatectomy, and there may have been misjudgment regarding the histological changes. Fourth, the mean follow-up duration after achieving SVR was only 6.2 mo, and a longer follow-up period is warranted.

CONCLUSION

In conclusion, the CEI of Gd-EOB-DTPA-enhanced MRI can be used to diagnose liver fibrosis in patients with CHC. The change of the CEI can be used to monitor fibrosis regression post SVR by DAA therapy.

ARTICLE HIGHLIGHTS

Research background

The histological change and non-invasive method surveillance after hepatitis C virus (HCV) eradication by direct acting antiviral (DAA) therapy have not been elucidated. As using a liver-specific magnetic resonance imaging (MRI) contrast, whether Gadolinium-ethoxybenzyl-diethylenetriamine penta-acetic acid (Gd-EOB-DTPA) enhanced MRI can be used to diagnose and follow-up the liver fibrosis in patients with chronic hepatitis C (CHC) has not been investigated.

Research motivation

The key issues are whether Gd-EOB-DTPA enhanced MRI can be used in diagnosing and following-up in patients with CHC. The result will provide important information on non-invasive method selection for dynamic assessment of liver fibrosis in patients with CHC and histology change after achieving SVR treated by DAAs.

Research objectives

To investigated the diagnostic and follow-up values of Gd-EOB-DTPA-enhanced MRI for hepatic histology in patients with CHC. We further explore the value of Gd-EOB-DTPA enhanced MRI in evaluating fibrosis regression in patients with CHC after achieving sustained virological response (SVR) treated by DAAs.

Research methods

Chronic HCV infected patients with paired liver biopsy and Gd-EOB-DTPA enhanced MRI before and after DAA treated was included. Contrast enhancement index (CEI) was calculated according with signal intensity *via* MRI, and the correlation between CEI and histology change was evaluated. Fibrosis regression was defined as a ≥ 1-point decrease in the Ishak fibrosis score. The diagnostic and follow-up values of the CEI, liver stiffness measurements (LSM), aminotransferase (AST)-to-platelet ratio (APRI) and Fibrosis-4 (FIB-4) were compared.

Research results

Thirty-nine patients with CHC were enrolled, with average age of 42.3 ± 14.4 years and 20/39 (51.3%) were male. Twenty-one enrolled patients had eligible paired Gd-EOB-DTPA-enhanced MRI and liver tissues after achieving SVR. According to correlation and the hierarchical analysis, the CEI mainly decreased with the progression of liver fibrosis. Compared with LSM, APRI and FIB-4, the CEI is more useful for liver fibrosis diagnosis, the correlation between the CEI and fibrosis stage was relatively stable and was not related to the treatment state. In paired analysis using liver pathology and CEI before and after treatment, only the dynamic change in the CEI can be used to evaluate fibrosis regression after achieving SVR.

Research conclusions

The CEI of Gd-EOB-DTPA-enhanced MRI can be used as a non-invasive method to diagnose liver fibrosis in patients with CHC. The dynamic change of the CEI can be used to monitor fibrosis regression post SVR in patients with CHC after DAA therapy.

Research perspectives

Larger and longer-term prospective studies in patients with CHC should be performed in future studies.

ACKNOWLEDGEMENTS

We are sincerely grateful to the radiologists Dr. Xiao-Xuan Jia and Dr. Xin-Yu Zhang for their involvement in the MRI analysis. We also thank Prof. Aileen Wee and Guang-De Zhou for their involvement in the liver pathology confirmation. We also thank Hui-Xin Liu, MD, for help with the statistical review.

FOOTNOTES

Author contributions: Li XH, Rao HY and Wei L designed the protocol of this study; Li XH, Huang R, Yang M, Wang J, Gao YH, Jin Q and Ma DL collected the data; Li XH analyzed and interpreted the patient data and was major contributors in writing the manuscript; Wei L and Rao HY give advice in study design, statistical analysis and writing the manuscript; All authors read and approved the final manuscript.

Supported by National Natural Science Foundation of China, No. 81870406; and Nature Science Foundation of Beijing Municipality, No. 7182174.

Institutional review board statement: This study was reviewed and approved by the Institutional Review Board of Peking University People's Hospital (2020PHB039-01), and the requirement for patient informed consent was waived.

Informed consent statement: Patients were not required to provide informed consent for this study, as the analysis used anonymous clinical data. The Institutional Review Board of Peking University People's Hospital approved waiving the requirement for patient informed consent.

Conflict-of-interest statement: Prof. Rao reports grants from National Natural Science Foundation of China (NSFC), No. 81870406, and Beijing Natural Science Foundation, No. 7182174 during the conduct of the study.

Data sharing statement: No additional data are available.

Open-Access: This article is an open-access article that was selected by an in-house editor and fully peer-reviewed by external reviewers. It is distributed in accordance with the Creative Commons Attribution NonCommercial (CC BY-NC 4.0) license, which permits others to distribute, remix, adapt, build upon this work non-commercially, and license their derivative works on different terms, provided the original work is properly cited and the use is non-commercial. See: https://creativecommons.org/Licenses/by-nc/4.0/

Country/Territory of origin: China

ORCID number: Xiao-He Li 0000-0001-6600-6067; Rui Huang 0000-0001-5561-8746; Ming Yang 0000-0001-5765-3844; Jian Wang 0000-0002-9578-8288; Ying-Hui Gao 0000-0003-4532-3412; Qian Jin 0000-0002-5213-8680; Dan-Li Ma 0000-0002-0936-6792; Lai Wei 0000-0003-2326-1257; Hui-Ying Rao 0000-0003-2431-3872.

S-Editor: Fan JR
L-Editor: A
P-Editor: Chen YX

REFERENCES

1 **WHO**. Global hepatitis report, 2017. Geneva: World Health Organization, 2017. [cited 10 October 2021]. Available from: https://www.who.int/
2 **Global Burden of Disease Study 2013 Collaborators**. Global, regional, and national incidence, prevalence, and years lived with disability for 301 acute and chronic diseases and injuries in 188 countries, 1990-2013: a systematic analysis for the Global Burden of Disease Study 2013. *Lancet* 2015; **386**: 743-800 [PMID: 26063472 DOI: 10.1016/S0140-6736(15)60692-4]
3 **Lohmann V**, Bartenschlager R. Indelibly Stamped by Hepatitis C Virus Infection: Persistent Epigenetic Signatures Increasing Liver Cancer Risk. *Gastroenterology* 2019; **156**: 2130-2133 [PMID: 31034828 DOI: 10.1053/j.gastro.2019.04.033]
4 **Ahumada A**, Rayón L, Usón C, Bañares R, Alonso Lopez S. Hepatocellular carcinoma risk after viral response in hepatitis C virus-advanced fibrosis: Who to screen and for how long? *World J Gastroenterol* 2021; **27**: 6737-6749 [PMID: 34790004 DOI: 10.3748/wjg.v27.i40.6737]
5 **Knop V**, Hoppe D, Welzel T, Vermehren J, Herrmann E, Vermehren A, Friedrich-Rust M, Sarrazin C, Zeuzem S, Welker MW. Regression of fibrosis and portal hypertension in HCV-associated cirrhosis and sustained virologic response after interferon-free antiviral therapy. *J Viral Hepat* 2016; **23**: 994-1002 [PMID: 27500382 DOI: 10.1111/jvh.12578]
6 **Laursen TL**, Siggaard CB, Kazankov K, Sandahl TD, Møller HJ, Tarp B, Kristensen LH, Laursen AL, Leutscher P, Grønbaek H. Time-dependent improvement of liver inflammation, fibrosis and metabolic liver function after successful direct-acting antiviral therapy of chronic hepatitis C. *J Viral Hepat* 2020; **27**: 28-35 [PMID: 31502741 DOI: 10.1111/jvh.13204]
7 **Jayaswal ANA**, Levick C, Collier J, Tunnicliffe EM, Kelly MD, Neubauer S, Barnes E, Pavlides M. Liver cT_1 decreases following direct-acting antiviral therapy in patients with chronic hepatitis C virus. *Abdom Radiol (NY)* 2021; **46**: 1947-1957 [PMID: 33247768 DOI: 10.1007/s00261-020-02860-5]
8 **Bluemke DA**, Sahani D, Amendola M, Balzer T, Breuer J, Brown JJ, Casalino DD, Davis PL, Francis IR, Krinsky G, Lee FT Jr, Lu D, Paulson EK, Schwartz LH, Siegelman ES, Small WC, Weber TM, Welber A, Shamsi K. Efficacy and safety of MR imaging with liver-specific contrast agent: U.S. multicenter phase III study. *Radiology* 2005; **237**: 89-98 [PMID: 16126918 DOI: 10.1148/radiol.2371031842]
9 **Kim T**, Murakami T, Hasuike Y, Gotoh M, Kato N, Takahashi M, Miyazawa T, Narumi Y, Monden M, Nakamura H. Experimental hepatic dysfunction: evaluation by MRI with Gd-EOB-DTPA. *J Magn Reson Imaging* 1997; **7**: 683-688 [PMID: 9243389 DOI: 10.1002/jmri.1880070413]
10 **Kitao A**, Matsui O, Yoneda N, Kozaka K, Kobayashi S, Koda W, Inoue D, Ogi T, Yoshida K, Gabata T. Gadoxetic acid-enhanced MR imaging for hepatocellular carcinoma: molecular and genetic background. *Eur Radiol* 2020; **30**: 3438-3447 [PMID: 32064560 DOI: 10.1007/s00330-020-06687-y]
11 **Schulze J**, Lenzen H, Hinrichs JB, Ringe B, Manns MP, Wacker F, Ringe KI. An Imaging Biomarker for Assessing Hepatic Function in Patients With Primary Sclerosing Cholangitis. *Clin Gastroenterol Hepatol* 2019; **17**: 192-199.e3 [PMID: 29775791 DOI: 10.1016/j.cgh.2018.05.011]
12 **Yang M**, Zhang Y, Zhao W, Cheng W, Wang H, Guo S. Evaluation of liver function using liver parenchyma, spleen and portal vein signal intensities during the hepatobiliary phase in Gd-EOB-D TPA-enhanced MRI. *BMC Med Imaging* 2020; **20**: 119 [PMID: 33081713 DOI: 10.1186/s12880-020-00519-7]
13 **Kim SW**, Kim YR, Choi KH, Cho EY, Song JS, Kim JE, Kim TH, Lee YH, Yoon KH. Staging of Liver Fibrosis by Means of Semiautomatic Measurement of Liver Surface Nodularity in MRI. *AJR Am J Roentgenol* 2020; **215**: 624-630 [PMID: 32755157 DOI: 10.2214/AJR.19.22041]
14 **Verloh N**, Probst U, Utpatel K, Zeman F, Brennfleck F, Werner JM, Fellner C, Stroszczynski C, Evert M, Wiggermann P, Haimerl M. Influence of hepatic fibrosis and inflammation: Correlation between histopathological changes and Gd-EOB-DTPA-enhanced MR imaging. *PLoS One* 2019; **14**: e0215752 [PMID: 31083680 DOI: 10.1371/journal.pone.0215752]
15 **Chuang YH**, Ou HY, Lazo MZ, Chen CL, Chen MH, Weng CC, Cheng YF. Predicting post-hepatectomy liver failure by combined volumetric, functional MR image and laboratory analysis. *Liver Int* 2018; **38**: 868-874 [PMID: 28987012 DOI: 10.1111/liv.13608]
16 **Mauro E**, Crespo G, Montironi C, Londoño MC, Hernández-Gea V, Ruiz P, Sastre L, Lombardo J, Mariño Z, Díaz A,

Colmenero J, Rimola A, Garcia-Pagán JC, Brunet M, Forns X, Navasa M. Portal pressure and liver stiffness measurements in the prediction of fibrosis regression after sustained virological response in recurrent hepatitis C. *Hepatology* 2018; **67**: 1683-1694 [PMID: 28960366 DOI: 10.1002/hep.29557]

17 **Choi YR**, Lee JM, Yoon JH, Han JK, Choi BI. Comparison of magnetic resonance elastography and gadoxetate disodium-enhanced magnetic resonance imaging for the evaluation of hepatic fibrosis. *Invest Radiol* 2013; **48**: 607-613 [PMID: 23538889 DOI: 10.1097/RLI.0b013e318289ff8f]

18 **Goodman ZD**. Grading and staging systems for inflammation and fibrosis in chronic liver diseases. *J Hepatol* 2007; **47**: 598-607 [PMID: 17692984 DOI: 10.1016/j.jhep.2007.07.006]

19 **Rozario R**, Ramakrishna B. Histopathological study of chronic hepatitis B and C: a comparison of two scoring systems. *J Hepatol* 2003; **38**: 223-229 [PMID: 12547412 DOI: 10.1016/s0168-8278(02)00357-4]

20 **Huang R**, Rao H, Yang M, Gao Y, Wang J, Jin Q, Ma D, Wei L. Noninvasive Measurements Predict Liver Fibrosis Well in Hepatitis C Virus Patients After Direct-Acting Antiviral Therapy. *Dig Dis Sci* 2020; **65**: 1491-1500 [PMID: 31654313 DOI: 10.1007/s10620-019-05886-y]

21 **Wai CT**, Greenson JK, Fontana RJ, Kalbfleisch JD, Marrero JA, Conjeevaram HS, Lok AS. A simple noninvasive index can predict both significant fibrosis and cirrhosis in patients with chronic hepatitis C. *Hepatology* 2003; **38**: 518-526 [PMID: 12883497 DOI: 10.1053/jhep.2003.50346]

22 **Sterling RK**, Lissen E, Clumeck N, Sola R, Correa MC, Montaner J, S Sulkowski M, Torriani FJ, Dieterich DT, Thomas DL, Messinger D, Nelson M; APRICOT Clinical Investigators. Development of a simple noninvasive index to predict significant fibrosis in patients with HIV/HCV coinfection. *Hepatology* 2006; **43**: 1317-1325 [PMID: 16729309 DOI: 10.1002/hep.21178]

23 **Jang HJ**, Min JH, Lee JE, Shin KS, Kim KH, Choi SY. Assessment of liver fibrosis with gadoxetic acid-enhanced MRI: comparisons with transient elastography, ElastPQ, and serologic fibrosis markers. *Abdom Radiol (NY)* 2019; **44**: 2769-2780 [PMID: 31041497 DOI: 10.1007/s00261-019-02041-z]

24 **Hsu WF**, Lai HC, Su WP, Lin CH, Chuang PH, Chen SH, Chen HY, Wang HW, Huang GT, Peng CY. Rapid decline of noninvasive fibrosis index values in patients with hepatitis C receiving treatment with direct-acting antiviral agents. *BMC Gastroenterol* 2019; **19**: 63 [PMID: 31029101 DOI: 10.1186/s12876-019-0973-5]

25 **Ioannou GN**, Feld JJ. What Are the Benefits of a Sustained Virologic Response to Direct-Acting Antiviral Therapy for Hepatitis C Virus Infection? *Gastroenterology* 2019; **156**: 446-460.e2 [PMID: 30367836 DOI: 10.1053/j.gastro.2018.10.033]

26 **Patel K**, Sebastiani G. Limitations of non-invasive tests for assessment of liver fibrosis. *JHEP Rep* 2020; **2**: 100067 [PMID: 32118201 DOI: 10.1016/j.jhepr.2020.100067]

27 **Loomba R**, Adams LA. Advances in non-invasive assessment of hepatic fibrosis. *Gut* 2020; **69**: 1343-1352 [PMID: 32066623 DOI: 10.1136/gutjnl-2018-317593]

28 **Pan JJ**, Bao F, Du E, Skillin C, Frenette CT, Waalen J, Alaparthi L, Goodman ZD, Pockros PJ. Morphometry Confirms Fibrosis Regression From Sustained Virologic Response to Direct-Acting Antivirals for Hepatitis C. *Hepatol Commun* 2018; **2**: 1320-1330 [PMID: 30411079 DOI: 10.1002/hep4.1228]

29 **Poynard T**, Munteanu M, Colombo M, Bruix J, Schiff E, Terg R, Flamm S, Moreno-Otero R, Carrilho F, Schmidt W, Berg T, McGarrity T, Heathcote EJ, Gonçales F, Diago M, Craxi A, Silva M, Boparai N, Griffel L, Burroughs M, Brass C, Albrecht J. FibroTest is an independent predictor of virologic response in chronic hepatitis C patients retreated with pegylated interferon alfa-2b and ribavirin in the EPIC^3 program. *J Hepatol* 2011; **54**: 227-235 [PMID: 21056496 DOI: 10.1016/j.jhep.2010.06.038]

30 **Watanabe H**, Kanematsu M, Goshima S, Kondo H, Onozuka M, Moriyama N, Bae KT. Staging hepatic fibrosis: comparison of gadoxetate disodium-enhanced and diffusion-weighted MR imaging--preliminary observations. *Radiology* 2011; **259**: 142-150 [PMID: 21248234 DOI: 10.1148/radiol.10100621]

31 **Verloh N**, Utpatel K, Haimerl M, Zeman F, Fellner C, Fichtner-Feigl S, Teufel A, Stroszczynski C, Evert M, Wiggermann P. Liver fibrosis and Gd-EOB-DTPA-enhanced MRI: A histopathologic correlation. *Sci Rep* 2015; **5**: 15408 [PMID: 26478097 DOI: 10.1038/srep15408]

32 **Hako R**, Kristian P, Jarčuška P, Haková I, Hockicková I, Schréter I, Janičko M. Noninvasive Assessment of Liver Fibrosis in Patients with Chronic Hepatitis B or C by Contrast-Enhanced Magnetic Resonance Imaging. *Can J Gastroenterol Hepatol* 2019; **2019**: 3024630 [PMID: 31058108 DOI: 10.1155/2019/3024630]

33 **Dahlqvist Leinhard O**, Dahlström N, Kihlberg J, Sandström P, Brismar TB, Smedby O, Lundberg P. Quantifying differences in hepatic uptake of the liver specific contrast agents Gd-EOB-DTPA and Gd-BOPTA: a pilot study. *Eur Radiol* 2012; **22**: 642-653 [PMID: 21984449 DOI: 10.1007/s00330-011-2302-4]

34 **Katsube T**, Okada M, Kumano S, Imaoka I, Kagawa Y, Hori M, Ishii K, Tanigawa N, Imai Y, Kudo M, Murakami T. Estimation of liver function using T2* mapping on gadolinium ethoxybenzyl diethylenetriamine pentaacetic acid enhanced magnetic resonance imaging. *Eur J Radiol* 2012; **81**: 1460-1464 [PMID: 21514080 DOI: 10.1016/j.ejrad.2011.03.073]

35 **Wu WP**, Hoi CI, Chen RC, Lin CP, Chou CT. Comparison of the efficacy of Gd-EOB-DTPA-enhanced magnetic resonance imaging and magnetic resonance elastography in the detection and staging of hepatic fibrosis. *Medicine (Baltimore)* 2017; **96**: e8339 [PMID: 29049250 DOI: 10.1097/MD.0000000000008339]

36 **Obmann VC**, Berzigotti A, Catucci D, Ebner L, Gräni C, Heverhagen JT, Christe A, Huber AT. T1 mapping of the liver and the spleen in patients with liver fibrosis-does normalization to the blood pool increase the predictive value? *Eur Radiol* 2021; **31**: 4308-4318 [PMID: 33313965 DOI: 10.1007/s00330-020-07447-8]

World Journal of Gastroenterology

Submit a Manuscript: https://www.f6publishing.com

World J Gastroenterol 2022 May 28; 28(20): 2227-2242

DOI: 10.3748/wjg.v28.i20.2227

ISSN 1007-9327 (print) ISSN 2219-2840 (online)

ORIGINAL ARTICLE

Observational Study

First prospective European study for the feasibility and safety of magnetically controlled capsule endoscopy in gastric mucosal abnormalities

Milán Szalai, Krisztina Helle, Barbara Dorottya Lovász, Ádám Finta, András Rosztóczy, László Oczella, László Madácsy

Specialty type: Gastroenterology and hepatology

Provenance and peer review: Unsolicited article; Externally peer reviewed.

Peer-review model: Single blind

Peer-review report's scientific quality classification

Grade A (Excellent): 0
Grade B (Very good): 0
Grade C (Good): C, C, C
Grade D (Fair): D
Grade E (Poor): 0

P-Reviewer: Kawano S, Japan; Nam SJ, South Korea; Nishida T, Japan

Received: January 3, 2022
Peer-review started: January 3, 2022
First decision: January 27, 2022
Revised: February 14, 2022
Accepted: April 27, 2022
Article in press: April 27, 2022
Published online: May 28, 2022

Milán Szalai, Ádám Finta, László Oczella, László Madácsy, Department of Gastroenterology, Endo-Kapszula Health Centre and Endoscopy Unit, Székesfehérvár 8000, Hungary

Krisztina Helle, András Rosztóczy, Department of Internal Medicine, University of Szeged, Szeged 6725, Hungary

Corresponding author: László Madácsy, MD, PhD, Professor, Department of Gastroenterology, Endo-Kapszula Health Centre and Endoscopy Unit, No. 316 Budai Road, Székesfehérvár 8000, Hungary. endomabt1@gmail.com

Abstract

BACKGROUND

While capsule endoscopy (CE) is the gold standard diagnostic method of detecting small bowel (SB) diseases and disorders, a novel magnetically controlled capsule endoscopy (MCCE) system provides non-invasive evaluation of the gastric mucosal surface, which can be performed without sedation or discomfort. During standard SBCE, passive movement of the CE may cause areas of the complex anatomy of the gastric mucosa to remain unexplored, whereas the precision of MCCE capsule movements inside the stomach promises better visualization of the entire mucosa.

AIM

To evaluate the Ankon MCCE system's feasibility, safety, and diagnostic yield in patients with gastric or SB disorders.

METHODS

Of outpatients who were referred for SBCE, 284 (male/female: 149/135) were prospectively enrolled and evaluated by MCCE. The stomach was examined in the supine, left, and right lateral decubitus positions without sedation. Next, all patients underwent a complete SBCE study protocol. The gastric mucosa was explored with the Ankon MCCE system with active magnetic control of the capsule endoscope in the stomach, applying three standardized pre-programmed computerized algorithms in combination with manual control of the magnetic movements.

RESULTS

The urea breath test revealed *Helicobacter pylori* positivity in 32.7% of patients. The mean gastric and SB transit times with MCCE were 0 h 47 min 40 s and 3 h 46 min 22 s, respectively. The average total time of upper gastrointestinal MCCE examination was 5 h 48 min 35 s. Active magnetic movement of the Ankon capsule through the pylorus was successful in 41.9% of patients. Overall diagnostic yield for detecting abnormalities in the stomach and SB was 81.9% (68.6% minor; 13.3% major pathologies); 25.8% of abnormalities were in the SB; 74.2% were in the stomach. The diagnostic yield for stomach/SB was 55.9%/12.7% for minor and 4.9%/8.4% for major pathologies.

CONCLUSION

MCCE is a feasible, safe diagnostic method for evaluating gastric mucosal lesions and is a promising non-invasive screening tool to decrease morbidity and mortality in upper gastrointestinal diseases.

Key Words: Bowel diseases; Capsule endoscopy; Diagnostic techniques; Gastrointestinal diseases; Gastric mucosa; *Helicobacter pylori*

©The Author(s) 2022. Published by Baishideng Publishing Group Inc. All rights reserved.

Core Tip: We evaluate the feasibility, safety, and diagnostic yield of magnetically controlled capsule endoscopy (CE) system developed by Ankon and AnX robotics that provides non-invasive evaluation of the gastric mucosal surface, which can be performed without sedation or patient discomfort. During gold-standard small bowel CE, passive movement may cause areas of the complex gastric mucosa to remain unexplored, whereas the precision of magnetically controlled capsule endoscopy (MCCE) capsule movements inside the gastrointestinal tract achieves better visualization of the entire mucosa, including the stomach. The Ankon MCCE system is a promising, non-invasive screening tool that achieved ~90% diagnostic yield of mucosal abnormalities in this study.

Citation: Szalai M, Helle K, Lovász BD, Finta Á, Rosztóczy A, Oczella L, Madácsy L. First prospective European study for the feasibility and safety of magnetically controlled capsule endoscopy in gastric mucosal abnormalities. *World J Gastroenterol* 2022; 28(20): 2227-2242

URL: https://www.wjgnet.com/1007-9327/full/v28/i20/2227.htm

DOI: https://dx.doi.org/10.3748/wjg.v28.i20.2227

INTRODUCTION

Capsule endoscopy (CE) is a non-invasive, painless, patient-friendly, and safe diagnostic method. It is currently the gold standard examination for small bowel (SB) diseases, including inflammatory bowel disease, suspected polyposis syndromes, unexplained abdominal pain, celiac disease, and obscure gastrointestinal bleeding (OGIB). Small bowel capsule endoscopy (SBCE) provides excellent diagnostic yield, which has been proven in many clinical trials since its introduction in the late 1990s. Currently, it has a fundamental role in gastrointestinal (GI) endoscopy, especially in patients with suspected SB diseases[1]. Attempts to expand the diagnostic role of CE to areas that are traditionally explored with standard endoscopic procedures (gastroscopy and colonoscopy), *e.g.*, the esophagus, stomach, and colon. These aims have been challenged by significant drawbacks in the past due to a lack of optimal preparation, standardized procedural design, and ability to visualize the entire mucosal surface[2]. A common perception is that the anatomical structures of the stomach and colon are too complex for adequate visualization with a passive capsule endoscope[3-5].

Although the SB seems to be a simple pipe, the more complex gastric anatomy with passive movements may cause unexplored areas of the gastric mucosa when utilizing standard CE. Magnetically controlled capsule endoscopy (MCCE) systems were developed over the past ten years to precisely control capsule movements inside the GI tract and to achieve better visualization of the entire mucosa, especially in the stomach. Different approaches have been developed and studied over time, which have enabled manual steering or active movement of the capsule systems. The external magnetic field seems to be the most adequate and energetically effective method for steering and holding the capsule within the stomach[6,7].

According to recent, prospective studies that were mainly conducted in China, a methodology developed by Ankon and AnX robotics could be an optimal method for non-invasive screening and

early diagnosis of gastric diseases such as gastric cancer and intramucosal high-grade dysplasia. It has the potential to become a valuable and accepted screening method in a population with high gastric cancer risk[8].

The aim of this study was to evaluate the feasibility, safety, and diagnostic yield of the Ankon MCCE system in patients with gastric and SB disorders who were referred to our endoscopy unit for SBCE examination between September 2017 and December 2020. Our secondary aim was to evaluate the overall gastric examinations, SB transit times (TTs) and efficacy of MCCE to achieve complete gastric and SBCE investigation by utilizing the same upper GI capsule.

MATERIALS AND METHODS

Study design

Our present study prospectively enrolled outpatients who were seen at the Endo-Kapszula Endoscopy Unit, Székesfehérvár, Hungary, between September 2017 and December 2020. A combined investigation of the stomach and SB of patients referred to for SBCE was performed with a robotically MCCE system (NaviCam, Ankon Technologies Co, Ltd, Shanghai, China).

The primary endpoint of the recent study was to investigate the diagnostic yield of MCCE in the evaluation of gastric and SB abnormalities. The secondary endpoints were to evaluate the feasibility of performing complete gastric and SB investigation by utilizing the same diagnostic procedure; to address safety parameters, including adverse and severe adverse events, and to calculate the capsule TTs, such as esophageal, gastric, and SB TTs, and the overall procedure time.

Patients

All patients who were referred to our endoscopy unit for SBCE and who agreed to our gastric study protocol were included in the current study. During the study period, we enrolled 284 consecutive, eligible patients, of which there were 149 males (52.5%) and 135 females (47.5 %), with a mean age of 44 years. Detailed patient characteristics are shown in Table 1. The indications of MCCE were iron deficiency anemia, OGIB, suspected/established SB Crohn's disease, suspected/confirmed celiac disease, suspected SB neoplastic disease, carcinoid syndrome, and SB polyposis syndromes.

This study was approved by the Ethical Committee of the University of Szeged (Registry No. 5/17.04.26) and registered in the ClinicalTrials.gov trial registry (Identifier: NCT03234725). The present study was conducted according to the World Medical Association's Declaration of Helsinki provisions in 1995. Patients agreed to undergo capsule endoscopies and *Helicobacter pylori* (*H. pylori*) urea breath tests (UBTs) by written informed consent.

Patient preparation for MCCE

According to the SBCE guidelines, we applied the following patient preparation and study protocol: Patients followed a liquid diet and consumed 2 L of water with two sacks of polyethylene glycol (PEG) the day before the study. First, *H. pylori* C^{13} UBT was performed on the morning of the study, while the patient was in a fasting condition. The UBT requires an average of 30 min, during which time the patient should not consume any fluids or food. During that visit, the patient's medical history was recorded, and a physical examination was performed. After the UBT, the patient ingested 2 dL water with simethicone suspension (80 mg) to reduce mucus in the stomach. Then, to distend the stomach properly, approximately 8-10 dL of clean water consumed by all patients within 10 min. Water ingestion may be repeated as needed to enhance gastric distension during examination. After complete visualization of the total gastric mucosal surface, active pyloric propulsion of the capsule was attempted in all patients with the external magnetic field. If it was unsuccessful, 10 mg intravenous metoclopramide was applied 60 min after the capsule was swallowed.

Contraindications of MCCE were the same as of those of SBCE and magnetic resonance imaging (MRI) examination. In our study, absolute contraindications were the patients with previous abdominal surgery and/or a previous capsule retention; with implanted MRI-incompatible electronic devices (*e.g.*, implantable cardioverter-defibrillator and pacemakers), or magnetic, metal foreign bodies; and who were not competent or refused the informed consent form; who were under age 18 or above age 70; and those who were pregnant. A patency capsule test was initially performed in all patients to determine those with relative contraindications, including known or suspected GI obstruction due to SB Crohn's disease, neoplasia, or SB surgery.

Technical methods of MCCE

Our system involves a special static magnet with robotic and manual guidance, computer workstation with ESNavi software (Ankon Technologies Co, Ltd) (Figure 1), magnetic capsule endoscope, capsule locator, and data recorder. The capsule endoscope sizes 26.8 × 11.6 mm, weighs 4.8 g, and has a permanent spherical magnet inside (Figure 2). The operator can adjust the frequency of captured pictures from 0.5 to 6 frames per second (fps). Capsule functioning can be stopped temporarily and

Table 1 Indications of small bowel capsule endoscopy (grouped by gender)

	All cases	Male	Female
Patient characteristics			
n	284	149	135
Age (mean ± SD)	44.0 ± 13.3	44.0 ± 13.3	44.0 ± 13.3
BMI	26.5	27.1	25.5
Indications			
OGiV	61 (21.5%)	30 (20.1%)	31 (22.9%)
Celiac disease	80 (28.2%)	40 (26.8%)	40 (29.7%)
Crohn's or susp. Crohn's	47 (16.5%)	31 (20.9%)	16 (11.9%)
Unexplained abdominal pain	92 (32.4%)	47 (31.5%)	45 (33.3%)
Susp. SB tumor	4 (1.4%)	1 (0.7%)	3 (2.2%)
13C urea breath test			
No. of performed tests	110(38.7%)	56 (50.1%)	54 (49.1%)
Positive	36 (32.7%)	16 (44.4%)	20 (55.6%)
Negative	74 (67.3%)	40 (54%)	34 (46%)

BMI: Body mass index; SB: Small bowel.



DOI: 10.3748/wjg.v28.i20.2227 **Copyright** © The Author(s) 2022.

Figure 1 Robotic C-arm, investigation table, and computer workstation for magnetically controlled capsule endoscopy.

restarted by the operator remotely from the workstation. The picture resolution is 480 × 480 pixels, and the field of view is 140°. The illumination can be automatically adjusted by an automatic picture focusing mechanism, which enables the view depth to shift from 0 mm to 60 mm. Depending on the fps, the battery life can be over 10 h, which allows combined gastric and SB capsule investigations with the same capsule.

The magnetic robotic C-arm generates an adjustable magnetic field outside of the body with a maximum strength of 0.2 T, which allows precise controlled movements in three spatial directions. During the process, the physician guides the magnetic capsule by two joysticks in any chosen, spatial direction or along its axis, and therefore, he can rotate or tilt it. Moreover, the capsule can advance forward 360° by a rotational automatism in the direction of the capsule visual axis, which is helpful for transposition of the capsule from the long axis of the stomach.

The capsule locator is a unique device that activates the capsule by infrared light prior to the patient swallowing it. The presence of the capsule can be detected in the case of suspected capsule retention (Figure 3).

The system is capable of real-time digital transmission of images to the operating system. At the same time, it is continuously obtaining information about the gyroscope, which is built into the capsule



DOI: 10.3748/wjg.v28.i20.2227 **Copyright** © The Author(s) 2022.

Figure 2 Magnetic capsule endoscope (NaviCam).



DOI: 10.3748/wjg.v28.i20.2227 **Copyright** © The Author(s) 2022.

Figure 3 Capsule locator device.

[three-dimensional (3D) motion detector]. It also receives data from the actual spatial location of the camera and localizes the capsule inside the body at any time. The data recorder (Figure 4) may receive all motion information and high-quality pictures *via* wireless transmission from the capsule endoscope. In contrast, the connection between the data recorder and the workstation *via* a USB wire makes visible the real-time pictures and gyroscope information.

Magnetic CE can be transferred along five different axes with the controlling magnet: two rotational and three 3D spaces. To achieve this, there are two joysticks on the workstation desktop: the left one controls the capsule in two rotational axes (horizontal and vertical directions) and the right joystick directs it in the three translational axes (forward/backwards, up/down, left/right). Precise magnetic control is achieved by positioning the examining table, modifying the position of the spherical magnet axis along the 3D space, and dynamically adjusting the strength and direction of the vectorial magnetic fields perpendicular to each other. The above-mentioned robotic systems can also automatically run the magnetic field vector and position it by robotically controlled computer-based software (scripts) in default mode, which can achieve a standardized mucosal scanning during the MCCE procedure without the direct intervention of a physician.

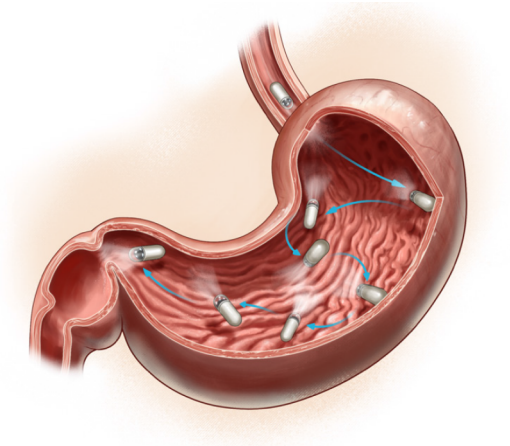
MCCE study protocol and gastric stations

To achieve optimal gastric mucosal visualization and standardization of the MCCE protocol in the stomach, we defined eight different stations with different patient positions to visualize the entire inner gastric surface as during upper GI endoscopy. Changing the patient position from the left lateral decubitus to the supine and right lateral position is necessary to combine gravity and magnetic force, which improve capsule maneuvering (Figure 5). The capsule swallowed by the patients in the left lateral decubitus position (Figure 6).



DOI: 10.3748/wjg.v28.i20.2227 **Copyright** © The Author(s) 2022.

Figure 4 Data recorder.



DOI: 10.3748/wjg.v28.i20.2227 **Copyright** © The Author(s) 2022.

Figure 5 Different magnetically controlled capsule endoscopy stations and capsule camera orientations defined to achieve a complete gastric mucosal surface visualization and mapping (created by Zoltán Tóbiás, MD).

Stations at the left lateral decubitus position: Station I. Visualization of the gastric fundus and subcardial region with the cardia (posterior J type retroflexion).

After entering the stomach, the capsule was lowered into the large curvature at the body of the stomach. The magnetic ball was held high up at the level of the patient's right shoulder. The capsule camera was maintained in an obliquely upward orientation of 45° and then horizontally rotated to observe the gastric fundus and the cardia (Figure 7A-C).

Station II. Moving closer to the cardia and the fundus (anterior J type retroflexion).

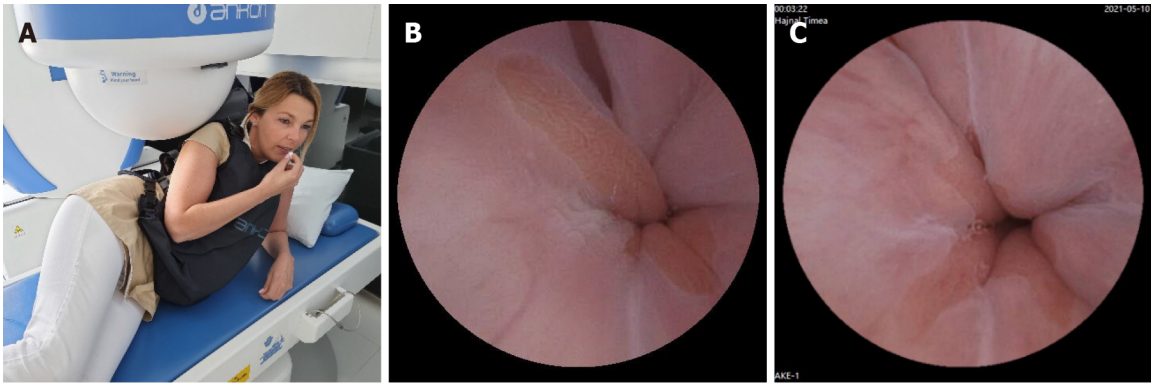
While using the right joystick, the ball magnet was lowered and fitted closely to the patient's right arm. Due to the proximity of the magnetic field, the capsule rose to the anterior wall and small curvature of the stomach. The capsule was then rotated with the camera oriented vertically upward to observe the cardia up close, with the fundus at a distance (Figure 7D-F).

Station III. Visualization of the gastric body from the fundus.

With the ball magnet in the same position, using the left joystick, the capsule camera was rotated and tilted downwards, enabling visualization of the proximal body of the stomach (corpus) and the gastric folds at the large curvature with a longitudinal view (Figure 7G-I).

Stations in the supine position: Station IV. Visualization of the angular incisure.

Patients were asked to lie on their back, in a supine position. The capsule was moved and located to the distal body into the angular region due to a change of gravity and stepwise magnetic movements. The magnetic ball was moved to the left upper abdomen (hypochondrium) and then lowered, close to the patient abdomen. In this case, the capsule was raised to the anterior wall of the stomach; therefore, the small curvature and the angular incisure were examined as well (Figure 8A-C).



DOI: 10.3748/wjg.v28.i20.2227 **Copyright** © The Author(s) 2022.

Figure 6 The capsule swallowed by the patients in the left lateral decubitus position. A: Patients and ball magnet position; B and C: Pictures of the Z-line by CE from our database.

Station V. Visualization of the larger curvature of the distal body from the angular incisure (U type of retroversion).

The magnetic ball was moved to the epigastric area, close to the abdomen. Then the capsule camera was oriented upward to observe the anterior wall of the gastric body. In this position, the capsule can be turned and rotated (*e.g.*, towards the cardia), enabling visualization of the distal body of the stomach longitudinally, as in the endoscopic view of U-type retroversion (Figure 8D-F).

Stations at the right lateral decubitus patient position: Station VI. Visualization of the antral canal.

In the next phase, patients were asked to turn to the right lateral decubitus position. Due to the gravity force, the capsule sank and moved spontaneously into the antral region. Then, the ball magnet was positioned over the left kidney. The capsule was brought closer to the large curvature with the camera oriented obliquely downward at 45°, which enabled observation of the antrum. Then, the antral canal could be examined with the pylorus, and the angular incisure became visible from the antrum (Figure 9A-C).

Stations in the supine position: Station VII. Prepyloric view and visualization of the pylorus.

After that, each patients were asked to lie on his or her back in the supine position. The ball magnet was positioned close to the body on the right upper abdomen (hypochondrium). The capsule camera was oriented horizontally and laterally toward the pylorus for closer observation. The magnet position ensured that the capsule remained in the antrum. Using both the right and left joysticks, we moved the capsule closer to the pylorus (Figure 10A-C).

Station VIII: Magnetically controlled transpyloric passage of the capsule.

The magnetic ball was placed at the patient's right side at the level of the duodenal bulb. The capsule was then rotated until the camera faced the pylorus. The capsule was dragged close to the pylorus under the guidance of the magnet robot. As the pylorus was opened, peristalsis assisted the capsule into the duodenum. After transpyloric passage, first we depicted the duodenal bulb, then from the descending and inferior horizontal part of the duodenum, we visualized the ampulla of the Vater by tilting the capsule camera upwards to facilitate the retrograde view (Figure 10D-G).

Examining the small intestine

If the capsule entered *via* the small intestine, patients were asked to drink 1 L of PEG solution, and from then on, they were requested to drink clear fluids (*i.e.*, water). The movement of the capsule in the small intestine was then monitored hourly in real-time visualization mode. The examination ended when the capsule arrives at the colon or stops functioning due to the low battery.

RESULTS

An UBT test revealed *H. pylori* positivity in 32.7% of cases. (Table 2). No significant association with HP status and the type (proximal or distal), distribution (diffuse or focal) and severity (minimal or active, erosive) of the gastritis described on MCCE results were depicted.

The mean gastric, SB, and colon TT with MCCE was: 47 h 40 min (M/F: 44 h 15 min/51 h 14 min), 3 h 46 min 22 s (3 h 52 min 44 s/3 h 38 min 21 s) and 1 h 4 min 34 s (1 h 1 min 16 s/1 h 8 min 53 s), respectively. Average total time of MCCE examination: 5 h 48 min 35 s (5 h 46 min 37 s/5 h 50 min 18 s) (Table 3).

Table 2 The results of *Helicobacter pylori* C13 urea breath tests

	n	*H. pylori* positive	%	*H. pylori* negative	%	χ^2	*P* value	
Normal	30	7	23%	23	77%	0.9775	0.3228	NS
Minor proximalgastritis	19	9	47%	10	53%	1.529	0.2163	NS
Minor antralgastritis	19	4	21%	15	79%	1.0322	0.3096	NS
Active, erosive antralgastritis	15	6	40%	9	60%	0.3129	0.5759	NS
Proximal erosivegastritis	22	7	32%	15	68%	0.0069	0.9338	NS
Pangastritis (proximal and antral)	4	3	75%	1	25%	0.5	0.4795	NS
Total HP tested patients	110	36	33%	74	67%	-	-	-

H. pylori: *Helicobacter pylori*.

Table 3 Mean gastric, small bowel, and overall transit times of magnetically controlled capsule endoscopy

Transit time	All cases	SD	Male	Female
Stomach	0 h 47 min 40 s	0 h 43 min 29 s	0 h 44 min 15 s	0 h 51 min 14 s
Small bowel	3 h 46 min 22 s	2 h 1 min 24 s	3 h 52 min 46 s	3 h 38 min 21 s
Total	5 h 48 min 35 s	1 h 50 min 49 s	5 h 46 min 37 s	5 h 50 min 18 s

The diagnostic yields for detecting any abnormalities in the stomach and SB with MCCE were 81.9%: 68.6% for minor pathologies and 13.3% for major pathologies. 25.8% of the abnormalities were found in the SB, and 74.2% were in the stomach. The diagnostic yield for stomach/SB was 4.9%/8.4% for major pathologies and 55.9%/12.7% for minor pathologies (Table 4). In the stomach, ulcers and polyps were considered major, while signs of gastritis were minor pathologies. In the SB signs of Crohn's and celiac disease were the major and non-specific inflammation, diverticula and angiodysplasia the minor pathologies. Based on findings from MCCE examinations, the distribution of pathologies is depicted in Table 5.

The capsule's active magnetic movement through the pylorus was successful using the magnet in 41.9% of all patients (automatized protocol in 56 patients and active manually controlled magnetic activity in 63 patients) (Table 6).

In 18 (M/F: 6/12) patients (6.3%), SB visualization with MCCE was incomplete. There were 13 occurrences of incomplete examinations as a result of capsule depletion. In 3 of these 13 cases, the capsule was depleted within 5 h of operation, indicating a manufacturing flaw. The average total study time in the remaining 10 cases was 9 h 12 min 9 s. From the pylorus to the last image, the average transit time was 8 h 26 min 4 s. The examination was discontinued sooner than planned in 3 cases due to the patient's request. In 2 cases, there was capsule retention due to Crohn's-like ulceration, accompanied by a narrow bowel lumen (Table 6). These problems were resolved spontaneously without surgery, but with medical treatment. There were no serious adverse events or capsule retention during the study period.

DISCUSSION

There are two main directions in developing capsule endoscopes with active movements: internally and externally guided techniques. Internal guidance means that the locomotive system is integrated into the capsule, but these systems require longer-lasting batteries for full functionality. Its main advantage is a more precise navigation with the help of the internalized locomotive system. External guidance refers to outwardly conducted capsule movements, *e.g.*, with a magnetic control unit or device/moving arm generating the magnetic field. The exceptional advantage of this method is that the magnetic field (and its adjustment) built by the external unit controls the locomotive mechanism, thus making this an energy-saving solution. However, a disadvantage of this technique is that it is limited to more passive, less flexible locomotion. The examining physician controls the capsule outside the body with an external control unit, which decreases the accuracy of the spatial and temporal movements. Locomotion of the capsule endoscope would result in numerous long-term advantages in the diagnostics and therapy of GI diseases (focused biopsies, treatment options, *e.g.*, laser tumor ablation, local targeted release of certain medications, and endoscopic ultrasound applications)[1].

Table 4 Diagnostic yield of magnetically controlled capsule endoscopy

Diagnostic yield	Major	Minor	Total
Total	38 (13.3%)	195 (68.6%)	233 (81.9%)
Gastric	14 (4.9%)	159 (55.9%)	173 (60.8%)
SB	24 (8.4%)	36 (12.7%)	60 (21.1%)

SB: Small bowel.

Table 5 Distribution of pathologies detected by magnetically controlled capsule endoscopy

	Polyp ventriculi	Ulcus ventriculi	Coeliakia	Crohn	Gastritis	Small intestinal diverticula	Angiodysplasia	Aspecific infalmmation in small bowel
Major pathologies	5	9	1	23	159	1	26	9

Table 6 Distribution of different types of transpyloric transit in complete and incomplete small bowel studies

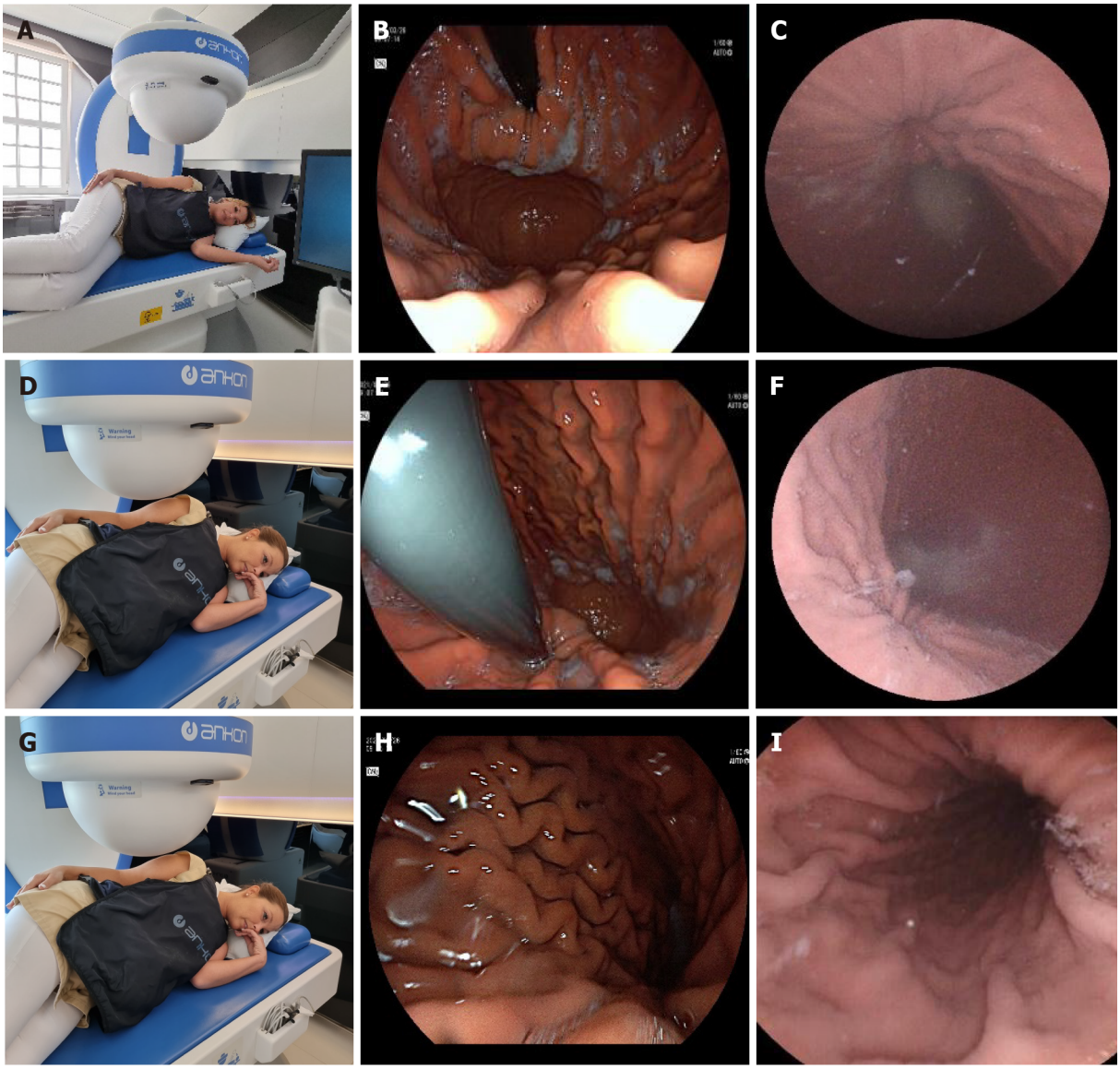
	Cases (*n*)	Mean total transit time	Mean gastric transit time	Mean SB transit time	Transpyloric transit		
					With magnet by automatic protocol	With magnet manually	Without magnet
Total study population	284	5 h 48 min 35 s	0 h 47 min 40 s	3 h 46 min 22 s	56 (19.7%)	63 (22.2%)	165 (58.1%)
Incomplete studies	18 (6.3%)	7 h 13 min 41 s	0 h 52 min 35 s	6 h 19 min 51 s	2	5	11
The capsule depleted (> 5 h)	10 (3.5%)	9 h 12 min 9 s	0 h 46 min 5 s	8 h 26 min 4 s	0	3	7
The capsule depleted (< 5 h)	3 (1%)	2 h 23 min 25 s	0 h 24 min 9 s	1 h 51 min 22 s	1	0	2
The patient requested to terminate	3 (1%)	4 h 45 min 9 s	0 h 50 min 3 s	3 h 55 min 6 s	1	1	1
The capsule stopped because of a disease	2 (0.7%)	8 h 19 min 36 s	2 h 11 min 33 s	6 h 8 min 33 s	0	1	1

SB: Small bowel.

Magnetic assisted capsule endoscopy (MACE) systems have been developed over the past 5-10 years, primarily for research goals. Experiences drawn from previously conducted *in vitro* studies showed that locomotion and precision of the capsule are significantly influenced by the physical characteristics of the generated magnetic field created by the external magnetic unit while travelling in the human body[1].

In 2011, Olympus was the first to introduce a modified MRI machine prototype that moved a MACE system which allowed the operator to successfully guide the capsule in a chosen spatial direction inside the stomach after drinking water. However, the adoption of this diagnostic procedure did not spread worldwide and get medical acceptance[6].

In 2014, IntroMedic developed a navigation (NAVI) magnetic capsule system that could be moved externally with a small, hammer-shaped, external static magnet device. The technology involving a magnet that assisted the physician in manually moving the capsule endoscope appeared viable and valuable in many experimental settings. However, it did not achieve any breakthroughs, as it only allowed sudden and harsh position changes of the capsule. In clinical trials studying the application of the NAVI capsule system using a small cohort, 65%-86% of the mucosal layer of the stomach was visualized accurately using external magnetically controlled locomotion after the ingestion of water. Its diagnostic accuracy was similar to that of traditional gastroscopy[9]. Using a similar type of NAVI capsule system, CE was performed on the large intestines, where magnetic locomotion directed the capsule from the cecum to the sigmoid colon. At the same time, a colonoscopy probe was inserted to monitor capsule movements to provide dilatation[10]. In iron deficiency anemia, after routine colonoscopy of 49 patients, the performance of a MACE system was compared with the IntroMedic Navi system in providing a diagnostic examination of the stomach and small intestine in one sitting.



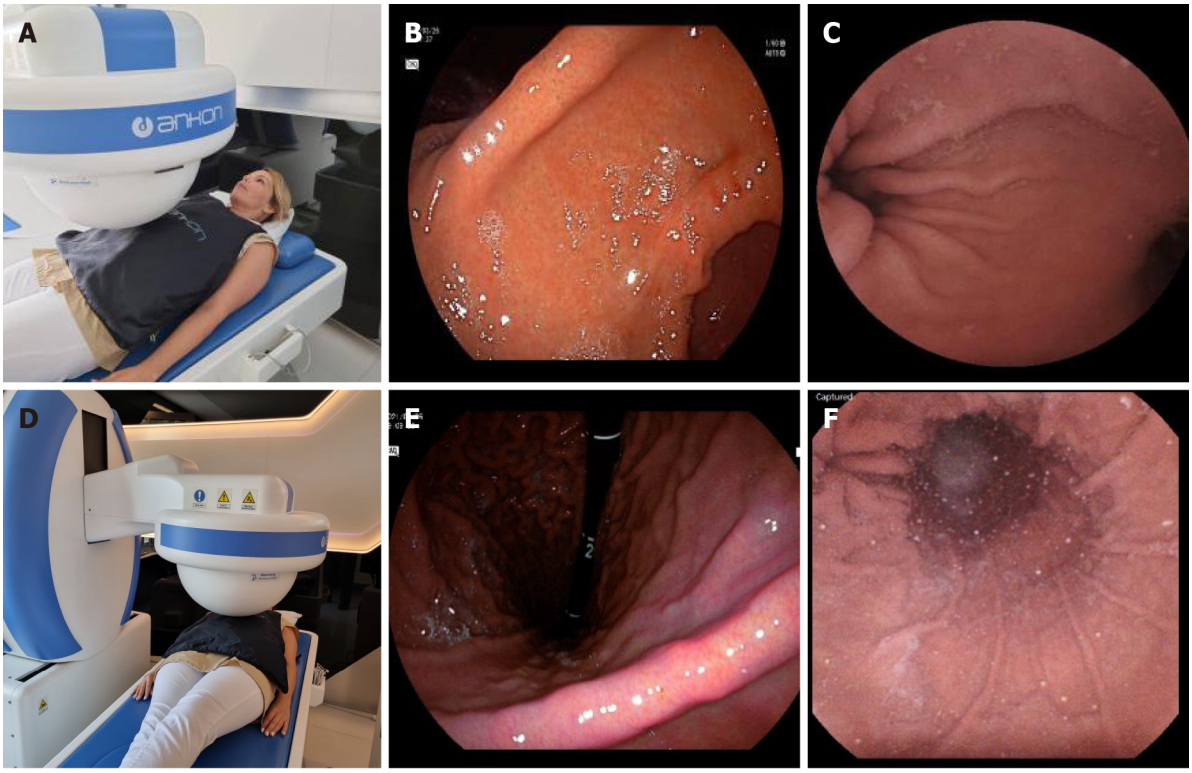
DOI: 10.3748/wjg.v28.i20.2227 **Copyright** © The Author(s) 2022.

Figure 7 Stations I-III at the left lateral decubitus position. A: Patients' position (Station I); B: Cardia by a gastroscope (Station I); C: Cardia by CE (Station I); D: Patients' position (Station II); E: Cardia by a gastroscope (Station II); F: Cardia by CE (Station II); G: Patients' position (Station III); H: Corpus by a gastroscope (Station III); I: Corpus by a capsule (Station III).

According to the results, MACE detected more pathologies than by gastroscopy alone, and no significant difference in diagnostic sensitivity was found between the methods when examining the upper GI tract[11].

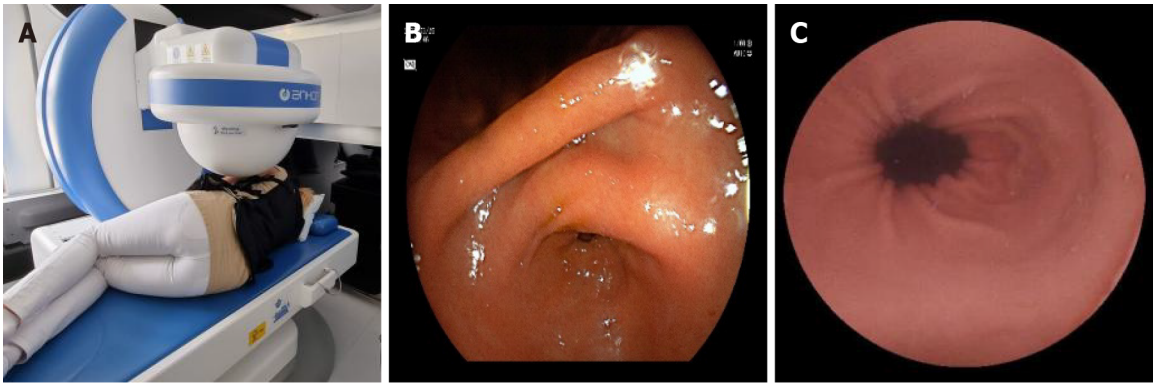
Precise locomotion of the magnetic capsule inside the GI tract by manual control is not possible due to the variable density of tissues and variable distance of the capsule, *e.g.*, in the stomach from the external magnet. Moreover, exact spatial location of the capsule, its relation to the surrounding organs, or the ante-/retrograde orientation cannot be judged accurately. Therefore, a control mechanism is needed alongside the magnetic capsule, which is based on external robotics that enable the physician's input to be executed (*i.e.*, joystick: in forward, backward, upward, downward, and sideways directions). By pre-programming instruction sequences (script) in the computing control unit to examine the stomach from the fundus to the antrum, we created a reproducible examination of the complete inner mucosal lining of the stomach, which lowered the variability among investigations. If the examining physician notices significant pathology, he/she can intervene and move the examination to manual control and revisit the alteration; doing so increases the number of images taken of the lesion and optimizes the diagnostic accuracy of the study.

NaviCam was the first magnetically controlled capsule system that enables bidirectional data transmission and robotic control. The capsule functions at 1-6 fps and its spatial orientation with continuous monitoring of energy levels are transmitted *via* the recording vest to control the data and screen of the computing unit. At the console, we can control the precise locomotion of the capsule, image capturing speed, and brightness, as well as turn it on or off.



DOI: 10.3748/wjg.v28.i20.2227 **Copyright** © The Author(s) 2022.

Figure 8 Stations IV and V in the supine position. A: Patients' position (Station IV); B: Angular incisure by a gastroscope (Station IV); C: Angular incisure by CE (Station IV); A: Patients' position (Station V); B: Angular incisure by a gastroscope (Station V); C: Angular incisure by CE (Station V).

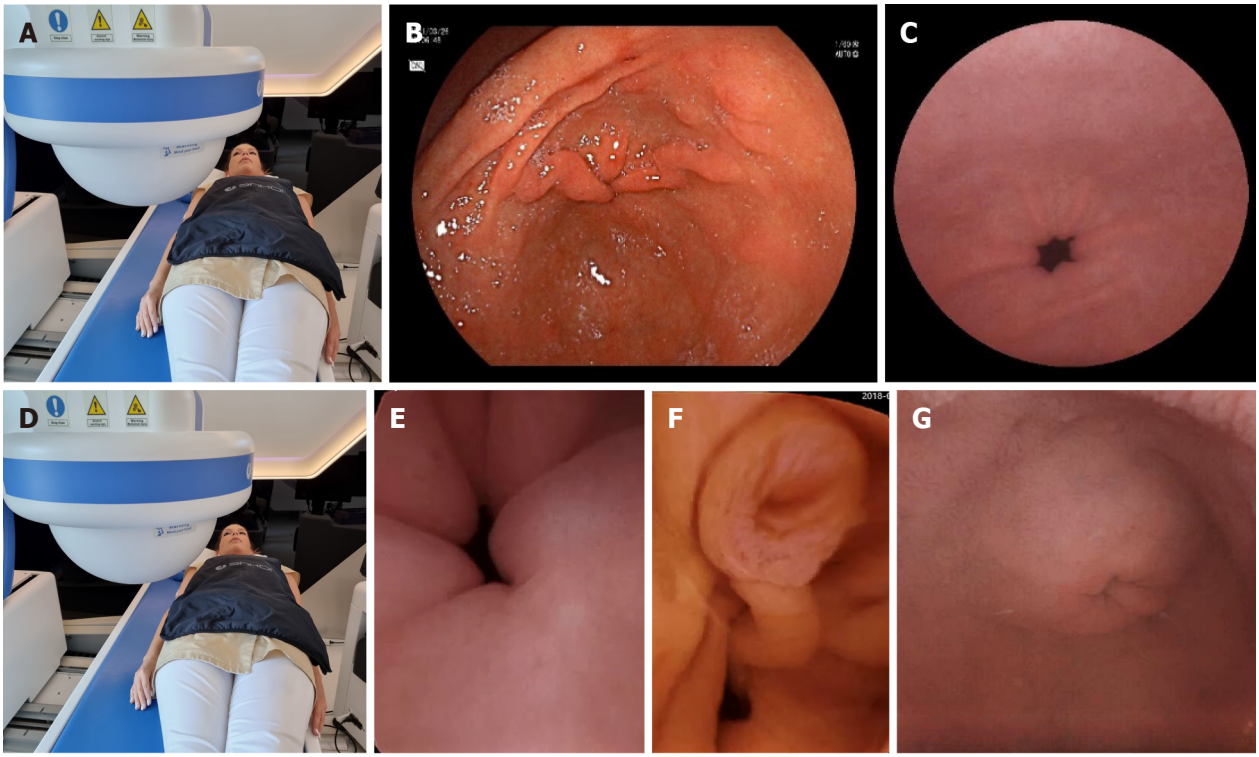


DOI: 10.3748/wjg.v28.i20.2227 **Copyright** © The Author(s) 2022.

Figure 9 Station at the right lateral decubitus patient position. A: Patients' position (Station VI); B: Antrum canal of stomach by gastroscope (Station VI); C: Antrum canal of stomach by CE (Station VI).

We combined manual and automatic, robotic capsule control to optimize the gastric procedure. As we previously published in an *in vitro* setting, complete 100% visualization of the inner surface of a plastic stomach model with the medium and large stomach autoscan program module and with the freehand controlling method could be successfully achieved in all cases. With the small and medium stomach mode, we could observe only 97.5% of the inner surface, because of the incomplete visualization of the prepyloric region. With freehand method, we needed nearly twice as much average time (749 s) to make a complete examination, compared to the robotic maneuvering with autoscan program (390 s). In an everyday praxis, in each patient position, the following stations and capsule positioning were performed after running the 3 different autoscan programs[12,13].

CE is a potentially patient-friendly and noncontact/infection-free diagnostic modality of screening for gastric diseases, which may result in complete and excellent examinations of the stomach. During the coronavirus disease 2019 pandemic, direct contact with the patients in the practice is a potential risk factor for infections. Non-contact medicine is a possibility for further examinations, such as remote control of CE[14]. The prevalence of focal gastric lesions (polyps, gastric ulcers, submucosal tumors, *etc*.)



DOI: 10.3748/wjg.v28.i20.2227 **Copyright** © The Author(s) 2022.

Figure 10 Stations VII and VIII in the supine position. A: Patient's position (Station VII); B: Antrum canal of stomach by gastroscope (Station VII); C: Antrum canal of stomach by CE (Station VII); D: Patient's position (Station VIII); E: Pyloric ring (Station VIII); F: Ampulla of Vater (Station VIII); G: Pylorus from the duodenal bulb with a capsule (Station VIII).

increases with age, and they may be detected with MCCE as effectively as with gastroscopy[8]. The sensitivity is between 90% and 92%, and the specificity is between 94% and 96.7%[15]. Several studies proved that, altogether, reliable preparation (gastric cleanliness), careful examination, and MCCE are pivotal for adequate gastric visualization and, therefore, for the detection of superficial gastric neoplasms[16]. In a large multicenter gastric cancer screening trial conducted in China seven asymptomatic patients out of 3182 were diagnosed with advanced cancer by MCCE. Cancer prevalence was highest in the gastric body (3 cases), followed by 2 cases in the cardia and 2 in the antrum, while 1-1 cases were detected in the region of the angulus, in the fundus and in the esophagus. All were confirmed to be adenocarcinoma pathologically. These results indicate that screening with MCCE may be useful in high family risk populations or people aged over 50 years old as a gastric cancer screening modality[8].

Magnetic steering may also impact TTs, as delayed gastric transit of the CE (especially in patients with gastroparesis) may lead to an incomplete SB exam. This method may increase the papilla detection rate as well. In addition to magnetic steering, there are several other independent factors, such as male gender and higher BMI, which increase gastric TTs and decrease SB TTs, thus impacting the time required for CE completion[10]. Despite the fact that delayed gastric TT may cause incomplete SBCE, we should avoid esophago-gastro-duodenoscopy to resolve temporary gastric capsule retention and instead use MCCE[17].

The visual diagnosis of the presence of *H. pylori* with standard white light endoscopy (WLI) has a relatively low accuracy, especially in population with a low pretest probability. Moreover, WLI endoscopy correlates poorly with histopathological findings of *H. pylori* induced gastritis too. Recently, low quality retrospective studies proposed the theory, that with the application of a special electronic chromoendoscopy, linked color imaging, diffuse reddish appearance of the mucosa in the gastric body and fundic glands correlates with the presence of HP[18].

In our study we found no correlation between the HP status and the activity and type of gastritis observed on MCCE as follows, but not included this into the Table 2, since it would be relevant in another publication, focusing HP status and gastritis on MCCE.

MCCE is an excellent method to visualize the entire gastric mucosal surface up to 100% precision in healthy volunteers[5]. In a previous study of 75 consecutive patients, we demonstrated that with our combined method with automatic and manual control, a complete visualization of the cardia, fundus, corpus, angulus, antrum, and duodenal bulb was 95.4%, 100%, 100%, 100%, 100% and 100%, respectively. The ampulla of Vater was detected and observed in 20 patients (26%). Moreover, the visualization of the distal esophagus and the Z-line was possible in 67/75 patients (89%), which was

assessed as complete in 23, and partially complete in 44 patients. The mean stationary time for MCCE in the distal esophagus was 1 min and 32 s[19].

The use of MCCE needs to be considered in western and eastern countries, as there are two different scenarios, depending on the different levels of prevalence of UGI diseases and gastric cancer in each country. Nowadays, MCCE is mostly used for the detection of malignant and premalignant gastric lesions, which are more prevalent in eastern countries. However, the present technology opens the door to further, new technologies; subsequent developments would allow MCCE technology to be extended to other regions of the GI tract, *e.g.*, the esophagus, which may facilitate the detection of more relevant lesions, such as Barrett metaplasia in western countries as well. With second-generation MCCE, visualization of the esophagus, Z-line, and duodenal papilla would be improved, according to a study by Jiang *et al*[20] Furthermore, the gastric TT could shorten by one-third, which was nearly achieved by conventional endoscopy with an examination of approximately 10 min.

It is known that the current gold standard gastroscopy has some clear disadvantages, as it is commonly uncomfortable for patients, and therefore it is mostly performed under sedation, which carries definite procedure related risks. MCCE, as a patient-friendly, non-invasive test, might be an alternative for patients who refuse to undergo gastroscopy and increase patients' adherence for screening. Furthermore, MCCE of the stomach was recently approved by the Chinese Food and Drug Association for the following diagnostic indications: (1) As an alternative diagnostic tool for patients who refuse to undergo gastroscopy; (2) Screening of gastric diseases as a part of physical examination; (3) Screening for gastric cancer; (4) To diagnose various causes of GI inflammation; (5) To perform follow-up for diseases like gastric varices, gastric ulcer, atrophic gastritis, and polyps after surgical or endoscopic removal[21].

There is no similar study in the literature, as we performed a complete upper GI capsule examination, including the stomach and the SB with the same capsule endoscope during MCCE. Denzer *et al*[22] published a blinded, prospective trial from two French centers with the Intromedic manually controlled MCCE. A total of 189 patients were enrolled into this multicenter study. Lesions were defined as major (requiring biopsy or removal) or minor ones. The final gold-standard was unblinded conventional gastroscopy with biopsy, under sedation with propofol. Twenty-three major lesions were found in 21 patients and in this population, the capsule accuracy was 90.5% as compared to gastroscopy. Of the remaining 168 patients, 94% had minor and mostly multiple lesions; the capsule accuracy was 88.1%. All patients preferred MCCE over gastroscopy[22].

One of the risk factors of incomplete SB capsule endoscopy is a prolonged gastric transit time, which could be considered as a limitation of our combined gastric and SB study protocol. In our patient population, the average gastric transit time with magnetic transpyloric, manual control was 26 min. In contrast, in those cases where the magnetic transpyloric control failed, after examining the stomach, we left the capsule to propel through the pylorus by spontaneous peristaltic activity. In these patient groups, the average gastric transit time took 1 h and 9 min. In 10 cases out of 18 incomplete SB studies caused by battery low energy, this event occurred in 3 patients with manual magnetic passage and in 7 patients with spontaneous transpyloric passage[23].

Visibility and identification of landmarks are important factors to consider in accurate examination of stomach using MCCE. Gastric landmarks and typical stations described in the methods were always forced to achieve during combined automatic and manual maneuvering. For improving the learning curve of our gastroenterologist, we started to train the examinations in a plastic stomach model. In our previously published abstract, we described the improvement of the learning curves with manual magnetic controls both in experts and in trainees[1]. In this study, we find significant differences in the examination time of the complete inner surface mapping between trainees and experts, and moreover automatic protocols were faster and equally accurate as experts to achieve a complete inner surface mapping.

The problem how to minimalize bubbles and mucoid secretions is an existing problem in real life studies. To improve visibility, we established a unique preparation process with a combination of bicarbonate, Pronase B, and simethicone combined with a patient body rotation technique[2]. Moreover, in our described stations, we rotate our patients from left lateral to supine, then from supine top right lateral, and finally from right lateral to supine position during MCCE study. During this protocol, the gastric mucoid secretions also moving into different parts of the stomach due to the gravity making visible all the landmarks and the majority of the mucosal abnormalities. Application of prokinetics or motilin agonist erythromycin might also be an option in future studies to improve the visibility and reduce gastric lake content[24,25].

An inherent limitation of our present study that we performed gastroscopy only in a few patients with major gastric pathologies to accomplish final diagnosis and biopsy; and therefore, we could not assess the accuracy of MCCE in all patients compared to gastroscopy. However, several previous studies demonstrated excellent diagnostic value and high accuracy. In a recent meta-analysis of Zhang *et al*[26] four studies with 612 patients were included, in which the results of blinded MCCE and gastroscopy were compared. MCCE demonstrated a pooled sensitivity and specificity of 91% (95%CI: 0.87-0.93) and 90% (95%CI: 0.75-0.96), respectively. The diagnostic accuracy of MCCE was 91% (95%CI: 0.88-0.94) for assessing gastric diseases.

CONCLUSION

MCCE is an effective and safe diagnostic method for evaluating gastric and SB mucosal lesions while being utilized as a single upper GI capsule endoscope in patients referred for SBCE evaluation. MCCE using the novel Ankon capsule endoscopic technique is a proper diagnostic method for evaluating the gastric mucosa. It is a promising non-invasive screening tool that may be applied in future monitoring of patients with high gastric cancer family risk to decrease morbidity and mortality of benign and malignant upper GI disorders.

ARTICLE HIGHLIGHTS

Research background

While capsule endoscopy (CE) is the gold standard diagnostic method of detecting small bowel diseases and disorders, a novel magnetically controlled capsule endoscopy (MCCE) system provides non-invasive evaluation of the gastric mucosal surface, which can be performed without sedation or discomfort.

Research motivation

During standard small bowel capsule endoscopy (SBCE), passive movement of the CE may cause areas of the complex anatomy of the gastric mucosa to remain unexplored, whereas the precision of MCCE capsule movements inside the stomach promises better visualization of the entire mucosa.

Research objectives

To evaluate the Ankon MCCE system's feasibility, safety and diagnostic yield in patients with gastric or small bowel disorders.

Research methods

Of outpatients who were referred for SBCE, 284 (male/female: 149/135) were prospectively enrolled and evaluated by MCCE. The stomach was examined in the supine, left, and right lateral decubitus positions without sedation. Next, all patients underwent a complete small bowel CE study protocol. The gastric mucosa was explored with the Ankon MCCE system with active magnetic control of the capsule endoscope in the stomach, applying three standardized pre-programmed computerized algorithms in combination with manual control of the magnetic movements.

Research results

The urea breath test revealed *Helicobacter pylori* positivity in 32.7% of patients. The mean gastric and small bowel transit times with MCCE were 47 min 40 s and 3 h 46 min 22 s, respectively. The average total time of upper GI MCCE examination was 5 h 48 min 35 s min. Active magnetic movement of the Ankon capsule through the pylorus was successful in 41.9% of patients. Overall diagnostic yield for detecting abnormalities in the stomach and small bowel was 81.9% (68.6% minor; 13.3% major pathologies); 25.8% of abnormalities were in the small bowel; 74.2% were in the stomach. The diagnostic yield for stomach/small bowel was 55.9%/12.7% for minor and 4.9%/8.4% for major pathologies.

Research conclusions

MCCE is a feasible, safe diagnostic method for evaluating gastric mucosal lesions and is a promising non-invasive screening tool to decrease morbidity and mortality in upper gastrointestinal diseases.

Research perspectives

MCCE is promising as a non-invasive screening tool that may be applied in future monitoring of patients for evaluating gastric mucosal lesions and decreasing morbidity and mortality of benign and malignant upper GI disorders.

ACKNOWLEDGEMENTS

Acknowledgements: special thanks for Zoltán Tóbiás MD for the graphical work and visual explanations of different gastric stations and Kata Tőgl our nurse manager for assistance and modelling the patients positioning during magnetically controlled capsule endoscopy.

FOOTNOTES

Author contributions: Szalai M, Madácsy L and Finta Á performed the capsule endoscopy examinations; Szalai M, Helle K, Finta Á, Oczella L and Madácsy L performed the data collection; Szalai M, Helle K, Lovász BD, Finta Á, Rosztóczy A, Oczella L and Madácsy L drafted the manuscript; Oczella L enrolled participants; Szalai M and Madá csy L reviewed capsule endoscopy images as expert endoscopists with high experience in capsule endoscope; Rosztó czy A and Madácsy L planned the study concept, consulted with the authors, performed manuscript database validation, supervised the manuscript preparation and writing, and acted as the submission's guarantor; All authors finally read and approved the manuscript.

Institutional review board statement: This study was approved by the Ethical Committee of the University of Szeged (registry No. 5/17.04.26) and registered in the trial registry: ClinicalTrials.gov (Identifier: NCT03234725). The present study was conducted according to the World Medical Association's Declaration of Helsinki provisions in 1995.

Informed consent statement: All involved participants gave their informed consent (in written form) prior to study inclusion. Patients agreed to participate in the present study, undergo capsule endoscopy and Helicobacter pylori breaths tests by written informed consent. All details that might disclose the identity of the subjects under study are anonymized. The institutional review board of University of Szeged waived the requirement to obtain informed consents from patients.

Conflict-of-interest statement: No conflict-of-interest.

Data sharing statement: Data (deidentified participant data) are available upon reasonable request. Contact details: endomabt1@gmail.com; László Madácsy (0000-0002-7589-6193). No additional information or data is available.

STROBE statement: The authors have read the STROBE Statement-checklist of items, and the manuscript was prepared and revised according to the STROBE Statement-checklist of items.

Open-Access: This article is an open-access article that was selected by an in-house editor and fully peer-reviewed by external reviewers. It is distributed in accordance with the Creative Commons Attribution NonCommercial (CC BY-NC 4.0) license, which permits others to distribute, remix, adapt, build upon this work non-commercially, and license their derivative works on different terms, provided the original work is properly cited and the use is non-commercial. See: https://creativecommons.org/Licenses/by-nc/4.0/

Country/Territory of origin: Hungary

ORCID number: Milán Szalai 0000-0002-5314-7693; Krisztina Helle 0000-0002-5477-2618; Barbara Dorottya Lovasz 0000-0003-0894-5669; Ádám Finta 0000-0002-2455-1056; András Rosztóczy 0000-0002-8597-8934; László Oczella 0000-0003-1454-4917; Laszlo Madacsy 0000-0002-7589-6193.

Corresponding Author's Membership in Professional Societies: Hungarian Society of Gastroenterology, 45326.

S-Editor: Zhang H
L-Editor: A
P-Editor: Zhang H

REFERENCES

1 **Adler SN**. The history of time for capsule endoscopy. *Ann Transl Med* 2017; **5**: 194 [PMID: 28567374 DOI: 10.21037/atm.2017.03.90]
2 **Eliakim R**, Yassin K, Shlomi I, Suissa A, Eisen GM. A novel diagnostic tool for detecting oesophageal pathology: the PillCam oesophageal video capsule. *Aliment Pharmacol Ther* 2004; **20**: 1083-1089 [PMID: 15569110 DOI: 10.1111/j.1365-2036.2004.02206.x]
3 **Iddan G**, Meron G, Glukhovsky A, Swain P. Wireless capsule endoscopy. *Nature* 2000; **405**: 417 [PMID: 10839527 DOI: 10.1038/35013140]
4 **Keller J**, Fibbe C, Volke F, Gerber J, Mosse AC, Reimann-Zawadzki M, Rabinovitz E, Layer P, Schmitt D, Andresen V, Rosien U, Swain P. Inspection of the human stomach using remote-controlled capsule endoscopy: a feasibility study in healthy volunteers (with videos). *Gastrointest Endosc* 2011; **73**: 22-28 [PMID: 21067740 DOI: 10.1016/j.gie.2010.08.053]
5 **Liao Z**, Duan XD, Xin L, Bo LM, Wang XH, Xiao GH, Hu LH, Zhuang SL, Li ZS. Feasibility and safety of magnetic-controlled capsule endoscopy system in examination of human stomach: a pilot study in healthy volunteers. *J Interv Gastroenterol* 2012; **2**: 155-160 [PMID: 23687601 DOI: 10.4161/jig.23751]
6 **Rey JF**, Ogata H, Hosoe N, Ohtsuka K, Ogata N, Ikeda K, Aihara H, Pangtay I, Hibi T, Kudo S, Tajiri H. Feasibility of stomach exploration with a guided capsule endoscope. *Endoscopy* 2010; **42**: 541-545 [PMID: 20593331 DOI: 10.1055/s-0030-1255521]
7 **Rey JF**, Ogata H, Hosoe N, Ohtsuka K, Ogata N, Ikeda K, Aihara H, Pangtay I, Hibi T, Kudo SE, Tajiri H. Blinded nonrandomized comparative study of gastric examination with a magnetically guided capsule endoscope and standard videoendoscope. *Gastrointest Endosc* 2012; **75**: 373-381 [PMID: 22154417 DOI: 10.1016/j.gie.2011.09.030]

8 **Zhao AJ**, Qian YY, Sun H, Hou X, Pan J, Liu X, Zhou W, Chen YZ, Jiang X, Li ZS, Liao Z. Screening for gastric cancer with magnetically controlled capsule gastroscopy in asymptomatic individuals. *Gastrointest Endosc* 2018; **88**: 466-474.e1 [PMID: 29753039 DOI: 10.1016/j.gie.2018.05.003]

9 **Nam SJ**, Lee HS, Lim YJ. Evaluation of Gastric Disease with Capsule Endoscopy. *Clin Endosc* 2018; **51**: 323-328 [PMID: 30078305 DOI: 10.5946/ce.2018.092]

10 **Gu H**, Zheng H, Cui X, Huang Y, Jiang B. Maneuverability and safety of a magnetic-controlled capsule endoscopy system to examine the human colon under real-time monitoring by colonoscopy: a pilot study (with video). *Gastrointest Endosc* 2017; **85**: 438-443 [PMID: 27480288 DOI: 10.1016/j.gie.2016.07.053]

11 **Ching HL**, Hale MF, Kurien M, Campbell JA, Chetcuti Zammit S, Healy A, Thurston V, Hebden JM, Sidhu R, McAlindon ME. Diagnostic yield of magnetically assisted capsule endoscopy versus gastroscopy in recurrent and refractory iron deficiency anemia. *Endoscopy* 2019; **51**: 409-418 [PMID: 30360012 DOI: 10.1055/a-0750-5682]

12 **Szalai M**, Oczella L, Lovasz BD, Madacsy L. Surface mapping in plasctic gastric model assisted by a robotic autoscan program with new magnetically controlled gastroc capsule endoscopy system compared to manual controlling. *United European Gastroenterol J* 2018; 865

13 **Jiang X**, Qian YY, Liu X, Pan J, Zou WB, Zhou W, Luo YY, Chen YZ, Li ZS, Liao Z. Impact of magnetic steering on gastric transit time of a capsule endoscopy (with video). *Gastrointest Endosc* 2018; **88**: 746-754 [PMID: 30005825 DOI: 10.1016/j.gie.2018.06.031]

14 **Pan J**, Li Z, Liao Z. Noncontact endoscopy for infection-free gastric examination during the COVID-19 pandemic. *VideoGIE* 2020; **5**: 402-403.e1 [PMID: 32391446 DOI: 10.1016/j.vgie.2020.04.026]

15 **Liao Z**, Hou X, Lin-Hu EQ, Sheng JQ, Ge ZZ, Jiang B, Hou XH, Liu JY, Li Z, Huang QY, Zhao XJ, Li N, Gao YJ, Zhang Y, Zhou JQ, Wang XY, Liu J, Xie XP, Yang CM, Liu HL, Sun XT, Zou WB, Li ZS. Accuracy of Magnetically Controlled Capsule Endoscopy, Compared With Conventional Gastroscopy, in Detection of Gastric Diseases. *Clin Gastroenterol Hepatol* 2016; **14**: 1266-1273.e1 [PMID: 27211503 DOI: 10.1016/j.cgh.2016.05.013]

16 **Qian YY**, Zhu SG, Hou X, Zhou W, An W, Su XJ, McAlindon ME, Li ZS, Liao Z. Preliminary study of magnetically controlled capsule gastroscopy for diagnosing superficial gastric neoplasia. *Dig Liver Dis* 2018; **50**: 1041-1046 [PMID: 29779696 DOI: 10.1016/j.dld.2018.04.013]

17 **Luo YY**, Pan J, Chen YZ, Jiang X, Zou WB, Qian YY, Zhou W, Liu X, Li ZS, Liao Z. Magnetic Steering of Capsule Endoscopy Improves Small Bowel Capsule Endoscopy Completion Rate. *Dig Dis Sci* 2019; **64**: 1908-1915 [PMID: 30725289 DOI: 10.1007/s10620-019-5479-z]

18 **Madacsy L**, Lovasz BD, Zsobrak K, Szalai M, Oczella L. Feasibility and safety of robotocally controlled magnetic capsule endoscopy in the visualization of the upper gastrointestinal tract. *United European Gastroenterol J* 2018; 1484

19 **Dohi O**, Yagi N, Onozawa Y, Kimura-Tsuchiya R, Majima A, Kitaichi T, Horii Y, Suzuki K, Tomie A, Okayama T, Yoshida N, Kamada K, Katada K, Uchiyama K, Ishikawa T, Takagi T, Handa O, Konishi H, Naito Y, Itoh Y. Linked color imaging improves endoscopic diagnosis of active Helicobacter pylori infection. *Endosc Int Open* 2016; **4**: E800-E805 [PMID: 27556101 DOI: 10.1055/s-0042-109049]

20 **Jiang B**, Qian YY, Pan J, Jiang X, Wang YC, Zhu JH, Zou WB, Zhou W, Li ZS, Liao Z. Second-generation magnetically controlled capsule gastroscopy with improved image resolution and frame rate: a randomized controlled clinical trial (with video). *Gastrointest Endosc* 2020; **91**: 1379-1387 [PMID: 31981648 DOI: 10.1016/j.gie.2020.01.027]

21 **Chinese Digestive Endoscopist Committee**, Chinese Endoscopist Association, the Health Management and Physical Examination Committee of Digestive Endoscopy; Capsule Endoscopy Collaboration Group of Chinese Society of Digestive Endoscopy; Chinese Anti-Cancer Association, the Society of Oncological Endoscopy; Chinese Society of Health Management. [The China expert consensus of clinical practice for magnetically controlled capsule gastroscopy(2017, Shanghai)]. *Zhonghua Nei Ke Za Zhi* 2017; **56**: 876-884 [PMID: 29136725 DOI: 10.3760/cma.j.issn.0578-1426.2017.11.023]

22 **Denzer UW**, Rösch T, Hoytat B, Abdel-Hamid M, Hebuterne X, Vanbiervielt G, Filippi J, Ogata H, Hosoe N, Ohtsuka K, Ogata N, Ikeda K, Aihara H, Kudo SE, Tajiri H, Treszl A, Wegscheider K, Greff M, Rey JF. Magnetically guided capsule versus conventional gastroscopy for upper abdominal complaints: a prospective blinded study. *J Clin Gastroenterol* 2015; **49**: 101-107 [PMID: 24618504 DOI: 10.1097/MCG.0000000000000110]

23 **Westerhof J**, Weersma RK, Koornstra JJ. Risk factors for incomplete small-bowel capsule endoscopy. *Gastrointest Endosc* 2009; **69**: 74-80 [PMID: 18691709 DOI: 10.1016/j.gie.2008.04.034]

24 **Szalai M**, Oczella L, Lovasz BD, Madacsy L. Surface mapping in plastic gastric model assisted by a robotic autoscan program with a new magnetically controlled gastric capsule endoscopy system compared to manual controlling. *United European Gastroenterol J* 2018; 415-A415

25 **Schmiedt P**, Szalai M, Oczella L, Zsobrak K, Lovasz BD, Dubravcsik Z, Madacsy L. A new preparation method for improving gastric mucosal visibility and cleanliness during magnetically assisted capsule endoscopy: A prospective study. *Endoscopy* 2019; **51**: S7

26 **Zhang H**, Chen J, Li J, Huang C, Li M, Wu W, Jiang J. Use of magnetically controlled capsule endoscopy for the diagnosis of gastric diseases in adults: a systematic review and meta-analysis. Dig Med Res 2020; 3: 42 [DOI: 10.21037/dmr-20-141]

World Journal of Gastroenterology

Submit a Manuscript: https://www.f6publishing.com

World J Gastroenterol 2022 May 28; 28(20): 2243-2247

DOI: 10.3748/wjg.v28.i20.2243

ISSN 1007-9327 (print) ISSN 2219-2840 (online)

CASE REPORT

Endoscopic management of intramural spontaneous duodenal hematoma: A case report

Giorgio Valerii, Vittorio Maria Ormando, Carlo Cellini, Luca Sacco, Carmelo Barbera

Specialty type: Gastroenterology and hepatology

Provenance and peer review: Unsolicited article; Externally peer reviewed.

Peer-review model: Single blind

Peer-review report's scientific quality classification

Grade A (Excellent): 0
Grade B (Very good): B
Grade C (Good): C
Grade D (Fair): 0
Grade E (Poor): 0

P-Reviewer: Kumar R, India; Tanpowpong P, Thailand

Received: November 28, 2021
Peer-review started: November 28, 2021
First decision: January 8, 2022
Revised: January 12, 2022
Accepted: April 21, 2022
Article in press: April 21, 2022
Published online: May 28, 2022

Giorgio Valerii, Carlo Cellini, Carmelo Barbera, Gastroenterology and Endoscopy Unit, Ospedale G. Mazzini, Teramo 64100, Italy

Vittorio Maria Ormando, Gastroenterology and Endoscopy Unit, AORN San Giuseppe Moscati, Avellino 83100, Italy

Luca Sacco, Surgery Unit, Ospedale G. Mazzini, Teramo 64100, Italy

Corresponding author: Giorgio Valerii, MD, PhD, Doctor, Gastroenterology and Endoscopy Unit, Ospedale G. Mazzini, Piazza Italia, 1, Teramo 64100, Italy. gioval83@hotmail.it

Abstract

BACKGROUND

Intramural duodenal hematoma is a rare condition described for the first time in 1838. This condition is usually associated with blunt abdominal trauma in children. Other non-traumatic risk factors for spontaneous duodenal haematoma include several pancreatic diseases, coagulation disorders, malignancy, collagenosis, peptic ulcers, vasculitis and upper endoscopy procedures. In adults the most common risk factor reported is anticoagulation therapy. The clinical presentation may vary from mild abdominal pain to acute abdomen and intestinal obstruction or gastrointestinal bleeding.

CASE SUMMARY

The aim of this case summary is to show a case of intramural spontaneous hematoma with symptoms of intestinal obstruction that was properly drained endoscopically by an innovative system lumen-apposing metal stent Hot AXIOS™ stent (Boston Scientific Corp., Marlborough, MA, United States).

CONCLUSION

Endoscopic lumen-apposing metal stent Hot AXIOS™ stent is a safe and feasible treatment of duodenal intramural hematoma in our case.

Key Words: Duodenal hematoma; Several pancreatic diseases; Endoscopy complication; AXIOS™ stent; Case report

©The Author(s) 2022. Published by Baishideng Publishing Group Inc. All rights reserved.

Core Tip: The present case explored the feasibility, safety and efficacy of endoscopic ultrasound-guided drainage of spontaneous duodenal hematoma. The new lumen-apposing self-expandable metallic stent Hot AXIOS™ could be considered a valid alternative to conventional endoscopic incision of the hematoma by using a needle-knife, a biopsy forceps or surgical drainage and percutaneous drainage to relieve pain and a persistent duodenal ulcer.

Citation: Valerii G, Ormando VM, Cellini C, Sacco L, Barbera C. Endoscopic management of intramural spontaneous duodenal hematoma: A case report. *World J Gastroenterol* 2022; 28(20): 2243-2247
URL: https://www.wjgnet.com/1007-9327/full/v28/i20/2243.htm
DOI: https://dx.doi.org/10.3748/wjg.v28.i20.2243

INTRODUCTION

Intramural duodenal hematoma (IDH) is a rare intestinal condition described for the first time at autopsy in 1838[1], and the first source in the PubMed database accessing the MEDLINE database (http://www.ncbi.nlm.nih.gov/pubmed/) dates from 1952[2].

This condition is usually associated with blunt abdominal trauma in children[3] and upper endoscopy procedures (duodenal biopsy or injection therapy for bleeding peptic ulcers) or various non-traumatic conditions in adults (> 70% of cases). These include several pancreatic diseases even if the association remains unclear, such as certain coagulation disorders (anticoagulant therapy, haemophilia, Von Willebrand disease, Henoch-Schönlein purpura), malignancy, collagenosis, peptic ulcers and vasculitis[4-7].

Clinical symptoms for IDH may vary from vague abdominal pain to acute abdomen, intestinal obstruction or gastrointestinal bleeding[3,8], and diagnosis is subsequently confirmed by magnetic resonance imaging or computed tomography (CT) and upper gastrointestinal endoscopy (UGIE).

Most IDH cases resolve spontaneously or with correction of abnormal coagulation. Percutaneous drainage or surgery may be needed in some refractory IDH cases, malignancy, perforation and intestinal tract obstruction.

Here we present the use of the innovative lumen apposing metal stent catheter (LAMS) Hot AXIOS™ (Boston Scientific Corp., Marlborough, MA, United States) in the case of spontaneous IDH with intestinal substenosis, which was non-responsive to conservative management, in a patient without risk factors. This innovative device, with a lumen apposing self-expandable metal stent fitted onto an electrocautery-enhanced tip catheter, is safe and feasible in gallbladder drainage, choledochoduodenostomy and drainage of pancreatic fluid collections. In recent years, Hot AXIOS™ has also been used for off-label indications including gastrojejunostomy, gastro-gastrostomy and drainage of postsurgical collections. Herein we report the use of Hot AXIOS™ in the rare digestive disorder spontaneous IDH.

CASE PRESENTATION

Chief complaints

A 51-year-old man was admitted to the hospital with abdominal pain, bloating and vomiting.

History of present illness

The clinical data suggested a diagnosis of intestinal obstruction.

History of past illness

The patient did not report comorbidities or recent abdominal trauma without relevant previous medical history and in particular without having taken anti-platelet medication.

Personal and family history

He did not have relevant family history.

Physical examination

Physical examination on admission revealed slight tenderness over the epigastric region and right flank.

Laboratory examinations

Initial biochemical analysis indicated neutrophilic leukocytosis (13.07 × 10^9/L) and an increased level of C-reactive protein without alterations of serum haemoglobin, D-dimer, platelet function and

coagulation parameters.

Imaging examinations

A contrast-enhanced abdominal CT scan revealed an IDH (Figure 1A). On admission UGIE and then endoscopic ultrasound (EUS) confirmed submucosal swelling of the second part of the duodenum that measured approximately 90 mm along the long axis with substenosis of the duodenal lumen (Figure 1B).

MULTIDISCIPLINARY EXPERT CONSULTATION

A conservative approach was attempted with clinical observation and empirical antibiotic therapy. The patient was discharged in good clinical condition after 8 d of intravenous antibiotic therapy.

FINAL DIAGNOSIS

Intramural spontaneous duodenal hematoma.

TREATMENT

After 48 h the patient was readmitted to the hospital due to clinical relapse. Biochemical analysis indicated a significant increase of both leukocytosis and C-reactive protein, and the radiological evaluation confirmed the previous diagnosis. After 10 d a multidisciplinary evaluation was performed, and minimally invasive endoscopic treatment was proposed.

EUS-guided drainage was performed with the Hot AXIOS™ system. A direct LAMS 15 mm × 10 mm was inserted into the submucosa lumen with an electrocautery-enhanced tip catheter and released under complete EUS control after the second flange was deployed in the duodenal lumen (Figure 2A). UGIE control confirmed the correct LAMS placement, and hematinic material associated with slightly purulent drainage was observed (Figure 2B).

OUTCOME AND FOLLOW-UP

A control CT scan demonstrated the presence of LAMS and the complete drainage of the intramural collection (Figure 2C). The patient was discharged in good clinical condition after 7 d. After an additional 2 wk he repeated UGIE, which revealed a complete resolution of the duodenal bulging, and the LAMS was contextually removed with complete closure of the mucosal defect with a clip. At the 30-d follow-up the patient was completely asymptomatic.

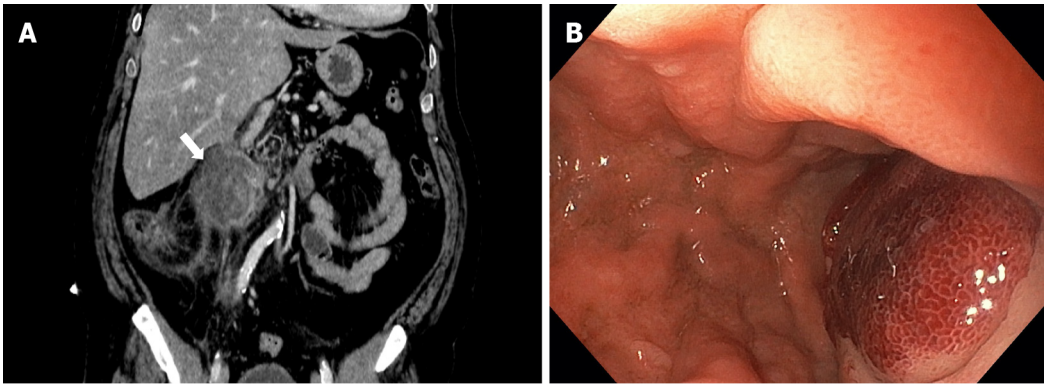
DISCUSSION

IDH is a rare condition usually caused by trauma, anticoagulant therapy, rupture of a duodenal aneurysm or biopsy[4-7,9]. Rare cases of IDH have also been described as a consequence of acute pancreatitis[3] or after endoscopic retrograde cholangiopancreatography procedures[10].

CT and magnetic resonance imaging represent the most sensitive diagnostic exams for IDH. Radiological exams have a role both for diagnosis as well as follow-up of small bowel hematoma within 2 wk[11,12]. Once IDH is confirmed, conservative management with fasting and total parenteral nutrition should be given[13]. Traditionally, in the case of persistent IDH, surgical drainage[14,15] and percutaneous drainage were performed[16], both causing great trauma for the patient. The indications for surgical intervention are not well clarified, certainly in the case of occlusive symptoms over 7-10 d or where there is evidence of perforation with a generalized peritonitis[17].

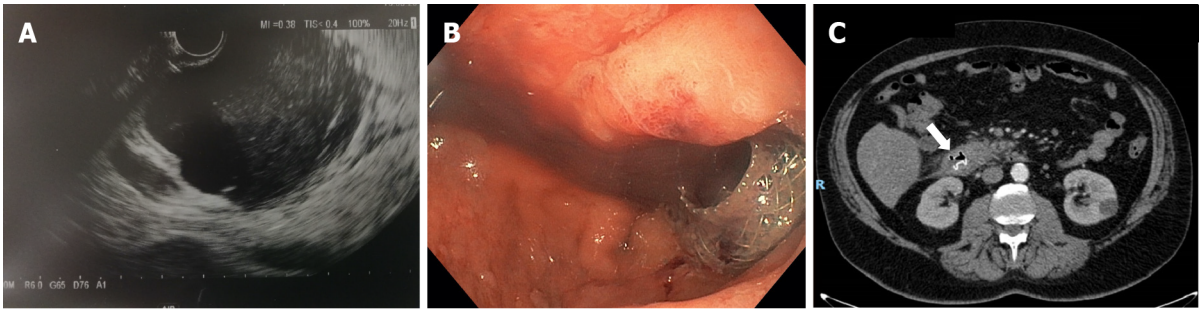
To date there are few described cases of endoscopic drainage of duodenal hematoma. This consists of endoscopic incision of the hematoma using a needle-knife or a biopsy forceps in order to obtain rapid submucosal decompression[18,19] with improvement of abnormal laboratory findings and abdominal pain in up to 1 wk. The persistence of duodenal ulcer at the site of endoscopic incision has also been described with a complete resolution only after 1 mo[18].

In our case we had a patient with an unremarkable previous medical history, with no risk factors for IDH who presented with intestinal pseudo-obstruction symptoms and leukocytosis without evidence of pancreatitis. We first attempted a conservative approach according to the existing data, but after recurrence of symptoms an endoscopic approach was proposed.



DOI: 10.3748/wjg.v28.i20.2243 **Copyright** © The Author(s) 2022.

Figure 1 Intramural duodenal hematoma. A: Contrast-enhanced abdominal computed tomography in coronal section; B: Endoscopic visualization with substenosis of duodenal lumen.



DOI: 10.3748/wjg.v28.i20.2243 **Copyright** © The Author(s) 2022.

Figure 2 Intramural duodenal hematoma after endoscopic treatment. A: Endoscopic ultrasonography (EUS) image showed deployment of the distal flange of a cautery-tipped lumen apposing metal stent (LAMS) in the intramural duodenal hematoma under EUS guidance; B: Endoscopic views showed the proximal flange of the LAMS; C: Control abdominal computed tomography confirmed the correct position of the LAMS.

The Hot AXIOS™ lumen-apposing stent is a novel double-flanged covered, self-expanding metal stent, safe and effective in gallbladder drainage, choledochoduodenostomy and drainage of pancreatic fluid collections. In the recent years, Hot AXIOS™ stents have also been used for off-label indications including gastrojejunostomy, gastro-gastrostomy and drainage of postsurgical collections.

Here we present the use of Hot AXIOS™ in a rare but possible digestive disorder with a rapid and complete resolution of this insidious clinical entity, as confirmed by CT scan and with only 7 d length of stay without abnormal laboratory findings and abdominal pain after the procedure.

CONCLUSION

In our experience Hot AXIOS™ is a safe and effective endoscopic procedure for the treatment of IDH, reserved for patients who are not responsive to conservative management. However, it should be performed by expert endoscopists trained in EUS and radiological procedures. To reduce the rate of postoperative complications and improve clinical outcome a previous careful clinical evaluation focusing on coagulopathies is mandatory.

FOOTNOTES

Author contributions: All authors contributed to writing this case report.

Informed consent statement: Informed written consent was obtained from the patient for publication of this report and any accompanying images.

Conflict-of-interest statement: All authors declare no conflict of interest for this case report.

CARE Checklist (2016) statement: The authors have read the CARE Checklist (2016), and the manuscript was

prepared and revised according to the CARE Checklist (2016).

Open-Access: This article is an open-access article that was selected by an in-house editor and fully peer-reviewed by external reviewers. It is distributed in accordance with the Creative Commons Attribution NonCommercial (CC BY-NC 4.0) license, which permits others to distribute, remix, adapt, build upon this work non-commercially, and license their derivative works on different terms, provided the original work is properly cited and the use is non-commercial. See: https://creativecommons.org/Licenses/by-nc/4.0/

Country/Territory of origin: Italy

ORCID number: Giorgio Valerii 0000-0001-8268-2022; Vittorio Maria Ormando 0000-0003-4481-755X; Carlo Cellini 0000-0001-7210-0439; Luca Sacco 0000-0003-1007-9894; Carmelo Barbera 0000-0002-4051-4976.

S-Editor: Yan JP
L-Editor: Filipodia
P-Editor: Yan JP

REFERENCES

1 **McLauchlan J**. False aneurysmaltumouroccupyingnearly the whole of the duodenum. *Lancet* 1838; 2243-2247 [DOI: 10.1016/S0140-6736(02)95675-8]
2 **Dey DL**. Acute duodenal obstruction due to an intramural haematoma. *Med J Aust* 1952; **1**: 708 [PMID: 14940187 DOI: 10.5694/j.1326-5377.1952.tb84095.x]
3 **Kumar R**, Athwal PSS, Kumar M, Devi K, Kahlon S. Spontaneous Intramural Duodenal Hematoma: A Rare Complication of Pancreatitis. *Cureus* 2020; **12**: e8491 [PMID: 32656009 DOI: 10.7759/cureus.8491]
4 **Chang CM**, Huang HH, How CK. Acute pancreatitis with an intramural duodenal hematoma. *Intern Med* 2015; **54**: 755-757 [PMID: 25832937 DOI: 10.2169/internalmedicine.54.3147]
5 **Eichele DD**, Ross M, Tang P, Hutchins GF, Mailliard M. Spontaneous intramural duodenal hematoma in type 2B von Willebrand disease. *World J Gastroenterol* 2013; **19**: 7205-7208 [PMID: 24222967 DOI: 10.3748/wjg.v19.i41.7205]
6 **Frostick SP**, Collin J, Daar AS, Kettlewell M, Nolan DJ. Non-traumatic intramural haematoma: an unusual cause of duodenal obstruction. *Br J Surg* 1984; **71**: 313-314 [PMID: 6608393 DOI: 10.1002/bjs.1800710421]
7 **Tseng CY**, Fan JS, Yang SC, Huang HH, Chen JD, Yen DH, Huang CI. Anticoagulant-induced intramural intestinal hemorrhage. *Am J Emerg Med* 2010; **28**: 937-940 [PMID: 20887911 DOI: 10.1016/j.ajem.2009.08.002]
8 **Kang EA**, Han SJ, Chun J, Lee HJ, Chung H, Im JP, Kim SG, Kim JS, Yoon H, Shin CM, Park YS, Kim N, Lee DH, Jung HC. Clinical features and outcomes in spontaneous intramural small bowel hematoma: Cohort study and literature review. *Intest Res* 2019; **17**: 135-143 [PMID: 30301344 DOI: 10.5217/ir.2018.00085]
9 **Iuchtman M**, Steiner T, Faierman T, Breitgand A, Bartal G. Post-traumatic intramural duodenal hematoma in children. *Isr Med Assoc J* 2006; **8**: 95-97 [PMID: 16544730]
10 **Pan YM**, Wang TT, Wu J, Hu B. Endoscopic drainage for duodenal hematoma following endoscopic retrograde cholangiopancreatography: a case report. *World J Gastroenterol* 2013; **19**: 2118-2121 [PMID: 23599635 DOI: 10.3748/wjg.v19.i13.2118]
11 **Abbas MA**, Collins JM, Olden KW, Kelly KA. Spontaneous intramural small-bowel hematoma: clinical presentation and long-term outcome. *Arch Surg* 2002; **137**: 306-310 [PMID: 11888455 DOI: 10.1001/archsurg.137.3.306]
12 **Zhou H**, Ma X, Sheng M, Lai C, Fu J. Evolution of intramural duodenal hematomas on magnetic resonance imaging. *Pediatr Radiol* 2018; **48**: 1593-1599 [PMID: 30109380 DOI: 10.1007/s00247-018-4178-9]
13 **Eurboonyanun C**, Somsap K, Ruangwannasak S, Sripanaskul A. Spontaneous Intramural Duodenal Hematoma: Pancreatitis, Obstructive Jaundice, and Upper Intestinal Obstruction. *Case Rep Surg* 2016; **2016**: 5321081 [PMID: 27891286 DOI: 10.1155/2016/5321081]
14 **Banieghbal B**, Vermaak C, Beale P. Laparoscopic drainage of a post-traumatic intramural duodenal hematoma in a child. *J Laparoendosc Adv Surg Tech A* 2008; **18**: 469-472 [PMID: 18503387 DOI: 10.1089/lap.2007.0147]
15 **Chirkov RN**, Abakumov MM, Blokhin VN. [Diagnostics and surgical treatment of traumatic intramural duodenal haematomes]. *Khirurgiia (Mosk)* 2008; 33-36 [PMID: 18577968]
16 **Kwon CI**, Choi KH, Ko EH, Lee JH, Song YJ, Ko KH, Hong SP, Park PW. [A case of duodenal intramural hematoma treated by percutaneous external drainage]. *Korean J Gastroenterol* 2007; **49**: 45-49 [PMID: 18167434]
17 **Jewett TC Jr**, Caldarola V, Karp MP, Allen JE, Cooney DR. Intramural hematoma of the duodenum. *Arch Surg* 1988; **123**: 54-58 [PMID: 3257385 DOI: 10.1001/archsurg.1988.01400250064011]
18 **Kwon CI**, Ko KH, Kim HY, Hong SP, Hwang SG, Park PW, Rim KS. Bowel obstruction caused by an intramural duodenal hematoma: a case report of endoscopic incision and drainage. *J Korean Med Sci* 2009; **24**: 179-183 [PMID: 19270837 DOI: 10.3346/jkms.2009.24.1.179]
19 **Lee JY**, Chung JS, Kim TH. Successful endoscopic decompression for intramural duodenal hematoma with gastric outlet obstruction complicating acute pancreatitis. *Clin Endosc* 2012; **45**: 202-204 [PMID: 22977802 DOI: 10.5946/ce.2012.45.3.202]

World Journal of Gastroenterology

Submit a Manuscript: https://www.f6publishing.com

World J Gastroenterol 2022 May 28; 28(20): 2248-2250

DOI: 10.3748/wjg.v28.i20.2248

ISSN 1007-9327 (print) ISSN 2219-2840 (online)

LETTER TO THE EDITOR

Future prospect of "Gut microbiome composition can predict the response to nivolumab in advanced hepatocellular carcinoma patients"

Yong-Bo Kang, Yue Cai

Specialty type: Gastroenterology and hepatology

Provenance and peer review: Unsolicited article; Externally peer reviewed.

Peer-review model: Single blind

Peer-review report's scientific quality classification

Grade A (Excellent): A
Grade B (Very good): B
Grade C (Good): 0
Grade D (Fair): 0
Grade E (Poor): 0

P-Reviewer: Gorrell MD, Australia; Yu L, Singapore

Received: December 10, 2021
Peer-review started: December 10, 2021
First decision: January 8, 2022
Revised: January 14, 2021
Accepted: April 24, 2022
Article in press: April 24, 2022
Published online: May 28, 2022

Yong-Bo Kang, Yue Cai, Department of Microbiology and Immunology, School of Basic Medical Sciences, Shanxi Medical University, Jinzhong 030600, Shanxi Province, China

Corresponding author: Yong-Bo Kang, PhD, Associate Professor, Department of Microbiology and Immunology, School of Basic Medical Sciences, Shanxi Medical University, Wenhua Street, Jinzhong 030600, Shanxi Province, China. 657151276@qq.com

Abstract

Recently, we read the article "Gut microbiome composition can predict the response to nivolumab in advanced hepatocellular carcinoma patients" with interest, and it is preliminary suggested that gut microbiota is closely related to therapeutic effect of nivolumab. Based on the meaningful results of this article, several valuable research directions are proposed to enhance the therapeutic effect of immune checkpoint inhibitors on advanced hepatocellular carcinoma.

Key Words: Gut microbiome; Immunotherapy; Immune checkpoint inhibitor resistance; Probiotics; Faecal microbiota transplantation; Hepatocellular carcinoma; Prognosis

©The Author(s) 2022. Published by Baishideng Publishing Group Inc. All rights reserved.

Core Tip: We read the article "Gut microbiome composition can predict the response to nivolumab in advanced hepatocellular carcinoma patients" with interest, and it is preliminary suggested that the gut microbiota is closely related to therapeutic effect of nivolumab. Future research should pay attention to the relationship between the gut microbiota and therapeutic effect of immune checkpoint inhibitors (ICIs) on advanced hepatocellular carcinoma and the way of regulating the gut microbiota to improve the therapeutic effect of ICIs.

Citation: Kang YB, Cai Y. Future prospect of "Gut microbiome composition can predict the response to nivolumab in advanced hepatocellular carcinoma patients". *World J Gastroenterol* 2022; 28(20): 2248-2250
URL: https://www.wjgnet.com/1007-9327/full/v28/i20/2248.htm
DOI: https://dx.doi.org/10.3748/wjg.v28.i20.2248

TO THE EDITOR

We read with interest the article "Gut microbiome composition can predict the response to nivolumab in advanced hepatocellular carcinoma patients"[1], in which the authors analyzed and summarized the correlation between gut bacterial composition and the prognosis of nivolumab therapy in hepatocellular carcinoma (HCC) patients. The highlight of this article was that gut microbiota composition and diversity of responders differed significantly from those of non-responders following nivolumab therapy. Several intestinal bacterial species such as *Citrobacter freundii, Azospirillum species*, and *Enterococcus durans* were specific to the responders. Moreover, a higher *Prevotella/Bacteroides* ratio and the presence of *Akkermansia species* can serve as predictive markers of response. Altogether, the study not only demonstrated that the therapeutic effect of nivolumab has something to do with the composition of the gut microbiota in advanced HCC patients, but also provided some inspiration for future research direction.

In our opinion, it is of importance to underline that the relationship between the therapeutic effect of various immune checkpoint inhibitors (ICIs) such as pembrolizumab, nivolumab atezolizumab, durvalumab, and avelumab on HCC and the gut microbiota. At present, the response rates to ICIs are very low in advanced HCC. To be specific, the response rate to ICI monotherapy is merely 15%-23%, which is increased to approximately 30% after combination treatment[2]. How to improve the effectiveness of ICI treatment is essential and has been extensively investigated. While the human gut microbiota has been shown to be associated with clinical responses to ICIs in HCC[3], the available data in this field remain limited and the relevant scientific work is only in the initial stage. Thus, more research is required in the future. First, clinical studies with large sample sizes are needed to further clarify the relationship between the gut microbiota and the therapeutic effect of various ICIs. At the same time, which types of gut microbiota are suitable for which ICIs should also be figured out. Furthermore, construction based on the gut microbiota can function as a prognostic marker for the response to various ICI therapies. These results will provide clinicians with a valuable reference for rational use of ICIs and personalized precision therapy. Second, the mechanism by which the gut microbiota promotes the therapeutic effect of various ICIs needs to be further studied, with the focus on key pathways such as intestinal mucosal barrier function, bacterial metabolites, and microorganism-related molecular patterns, thus being conducive to discovering how to enhance the therapeutic effect of various ICIs by targeting the gut microbiota. Third, probiotics, prebiotics, synbiotics, and antibiotics may represent innovative, safe, and low-cost strategies for promoting the therapeutic effect of various ICIs[4]. In this respect, it is of necessity to determine which beneficial bacteria and harmful bacteria are bound up with the therapeutic effects of which ICIs. Meanwhile, it will also be significant to confirm how probiotics, prebiotics, synbiotics, and antibiotics alter the composition of the gut microbiota and how relevant it is to the therapeutic effect of various ICIs. In other words, these results will contribute to the identification of probiotics, prebiotics, synbiotics, and antibiotics that may increase the efficacy of ICIs when being used in combination. Last but not least, faecal microbiota transplantation (FMT) may be a direct and superior approach to enhancing the therapeutic effect of various ICIs through modulating the gut microbiota in human beings. Considering that, it is extremely valuable to explore the therapeutic method of FMT in combination with ICIs. Besides, the optimal gut microbiota composition for enhancing the therapeutic effect of various ICIs should be recognized. On this basis, it is of great importance to choose the right donors[5].

In summary, based on the meaningful research results of this article, it is expected that readers can pay attention to the relationship between the gut microbiota and therapeutic effect of ICIs on advanced HCC and the method of regulating the gut microbiota to improve the therapeutic effect of ICIs.

FOOTNOTES

Author contributions: Kang YB and Cai Y wrote the letter and conceived the manuscript; Kang YB supervised the manuscript drafting and reviewed the literature data; and all authors contributed important intellectual content during manuscript drafting or revision.

Conflict-of-interest statement: There is no conflict to declare.

Open-Access: This article is an open-access article that was selected by an in-house editor and fully peer-reviewed by external reviewers. It is distributed in accordance with the Creative Commons Attribution NonCommercial (CC BY-NC 4.0) license, which permits others to distribute, remix, adapt, build upon this work non-commercially, and license their derivative works on different terms, provided the original work is properly cited and the use is non-commercial. See: https://creativecommons.org/Licenses/by-nc/4.0/

Country/Territory of origin: China

ORCID number: Yong-Bo Kang 0000-0002-1584-5546; Yue Cai 0000-0001-6314-0463.

S-Editor: Wang JJ
L-Editor: Wang TQ
P-Editor: Wang JJ

REFERENCES

1 **Chung MW**, Kim MJ, Won EJ, Lee YJ, Yun YW, Cho SB, Joo YE, Hwang JE, Bae WK, Chung IJ, Shin MG, Shin JH. Gut microbiome composition can predict the response to nivolumab in advanced hepatocellular carcinoma patients. *World J Gastroenterol* 2021; **27**: 7340-7349 [PMID: 34876793 DOI: 10.3748/wjg.v27.i42.7340]
2 **Pinter M**, Jain RK, Duda DG. The Current Landscape of Immune Checkpoint Blockade in Hepatocellular Carcinoma: A Review. *JAMA Oncol* 2021; **7**: 113-123 [PMID: 33090190 DOI: 10.1001/jamaoncol.2020.3381]
3 **Li L**, Ye J. Characterization of gut microbiota in patients with primary hepatocellular carcinoma received immune checkpoint inhibitors: A Chinese population-based study. *Medicine (Baltimore)* 2020; **99**: e21788 [PMID: 32925716 DOI: 10.1097/MD.0000000000021788]
4 **Kang Y**, Cai Y, Yang Y. The gut microbiome and hepatocellular carcinoma: Implications for early diagnostic biomarkers and novel therapies. *Liver Cancer* 2021 [DOI: 10.1159/000521358]
5 **Kang YB**, Cai Y. Faecal microbiota transplantation enhances efficacy of immune checkpoint inhibitors therapy against cancer. *World J Gastroenterol* 2021; **27**: 5362-5375 [PMID: 34539138 DOI: 10.3748/wjg.v27.i32.5362]



Published by **Baishideng Publishing Group Inc**
7041 Koll Center Parkway, Suite 160, Pleasanton, CA 94566, USA
Telephone: +1-925-3991568
E-mail: bpgoffice@wjgnet.com
Help Desk: https://www.f6publishing.com/helpdesk
https://www.wjgnet.com



© 2022 Baishideng Publishing Group Inc. All rights reserved.

ISSN 1007-9327 (print)
ISSN 2219-2840 (online)

World Journal of *Gastroenterology*

World J Gastroenterol 2022 June 7; 28(21): 2251-2402



Published by Baishideng Publishing Group Inc

World Journal of Gastroenterology

Contents

Weekly Volume 28 Number 21 June 7, 2022

REVIEW

2251 Viral hepatitis and hepatocellular carcinoma: From molecular pathways to the role of clinical surveillance and antiviral treatment

Stella L, Santopaolo F, Gasbarrini A, Pompili M, Ponziani FR

MINIREVIEWS

2282 Updates in therapeutic drug monitoring in inflammatory bowel disease

Lodhia N, Rao S

2291 Serological biomarkers for management of primary sclerosing cholangitis

Tornai D, Ven PL, Lakatos PL, Papp M

ORIGINAL ARTICLE

Basic Study

2302 Impact of radiotherapy on the immune landscape in oesophageal adenocarcinoma

Donlon NE, Davern M, O'Connell F, Sheppard A, Heeran A, Bhardwaj A, Butler C, Narayanasamy R, Donohoe C, Phelan JJ, Lynam-Lennon N, Dunne MR, Maher S, O'Sullivan J, Reynolds JV, Lysaght J

Case Control Study

2320 Intermittent hypoxia is involved in gut microbial dysbiosis in type 2 diabetes mellitus and obstructive sleep apnea-hypopnea syndrome

Tang SS, Liang CH, Liu YL, Wei W, Deng XR, Shi XY, Wang LM, Zhang LJ, Yuan HJ

Retrospective Study

2334 Serotonin type 3 receptor subunit gene polymorphisms associated with psychosomatic symptoms in irritable bowel syndrome: A multicenter retrospective study

Berens S, Dong Y, Fritz N, Walstab J, D'Amato M, Zheng T, Wahl V, Boekstegers F, Bermejo JL, Martinez C, Schmitteckert S, Clevers E, Engel F, Gauss A, Herzog W, Spiller R, Goebel-Stengel M, Mönnikes H, Andresen V, Thomas F, Keller J, Pehl C, Stein-Thöringer C, Clarke G, Dinan TG, Quigley EM, Sayuk G, Simrén M, Tesarz J, Rappold G, van Oudenhove L, Schaefert R, Niesler B

2350 Differentiating malignant and benign focal liver lesions in children using CEUS LI-RADS combined with serum alpha-fetoprotein

Jiang ZP, Zeng KY, Huang JY, Yang J, Yang R, Li JW, Qiu TT, Luo Y, Lu Q

Observational Study

2361 Socioeconomics and attributable etiology of primary liver cancer, 1990-2019

Xing QQ, Li JM, Dong X, Zeng DY, Chen ZJ, Lin XY, Pan JS

World Journal of Gastroenterology

Weekly Volume 28 Number 21 June 7, 2022

Contents

SYSTEMATIC REVIEWS

2383 Endoscopic ultrasound-guided injectable therapy for pancreatic cancer: A systematic review

Kaur J, Jaruvongvanich V, Chandrasekhara V

LETTER TO THE EDITOR

2396 Peripancreatic paraganglioma: Lesson from a round table

Petrelli F, Fratini G, Sbrozzi-Vanni A, Giusti A, Manta R, Vignali C, Nesi G, Amorosi A, Cavazzana A, Arganini M, Ambrosio MR

World Journal of Gastroenterology

Weekly Volume 28 Number 21 June 7, 2022

Contents

ABOUT COVER

Editorial Board Member of *World Journal of Gastroenterology*, Somashekar G Krishna, MD, MPH, AGAF, FASGE, FACG, Professor of Medicine, Director of Clinical Research, Division of Gastroenterology, Hepatology and Nutrition, The Ohio State University Wexner Medical Center, 395 West 12th Avenue, Room 226, Columbus, OH 43210, United States. somashekar.krishna@osumc.edu

AIMS AND SCOPE

The primary aim of *World Journal of Gastroenterology* (*WJG*, *World J Gastroenterol*) is to provide scholars and readers from various fields of gastroenterology and hepatology with a platform to publish high-quality basic and clinical research articles and communicate their research findings online. *WJG* mainly publishes articles reporting research results and findings obtained in the field of gastroenterology and hepatology and covering a wide range of topics including gastroenterology, hepatology, gastrointestinal endoscopy, gastrointestinal surgery, gastrointestinal oncology, and pediatric gastroenterology.

INDEXING/ABSTRACTING

The *WJG* is now indexed in Current Contents®/Clinical Medicine, Science Citation Index Expanded (also known as SciSearch®), Journal Citation Reports®, Index Medicus, MEDLINE, PubMed, PubMed Central, and Scopus. The 2021 edition of Journal Citation Report® cites the 2020 impact factor (IF) for *WJG* as 5.742; Journal Citation Indicator: 0.79; IF without journal self cites: 5.590; 5-year IF: 5.044; Ranking: 28 among 92 journals in gastroenterology and hepatology; and Quartile category: Q2. The *WJG*'s CiteScore for 2020 is 6.9 and Scopus CiteScore rank 2020: Gastroenterology is 19/136.

RESPONSIBLE EDITORS FOR THIS ISSUE

Production Editor: *Ying-Yi Yuan*; **Production Department Director:** *Xiang Li*; **Editorial Office Director:** *Ze-Mao Gong*.

NAME OF JOURNAL
World Journal of Gastroenterology

ISSN
ISSN 1007-9327 (print) ISSN 2219-2840 (online)

LAUNCH DATE
October 1, 1995

FREQUENCY
Weekly

EDITORS-IN-CHIEF
Andrzej S Tarnawski

EDITORIAL BOARD MEMBERS
http://www.wjgnet.com/1007-9327/editorialboard.htm

PUBLICATION DATE
June 7, 2022

COPYRIGHT
© 2022 Baishideng Publishing Group Inc

INSTRUCTIONS TO AUTHORS
https://www.wjgnet.com/bpg/gerinfo/204

GUIDELINES FOR ETHICS DOCUMENTS
https://www.wjgnet.com/bpg/GerInfo/287

GUIDELINES FOR NON-NATIVE SPEAKERS OF ENGLISH
https://www.wjgnet.com/bpg/gerinfo/240

PUBLICATION ETHICS
https://www.wjgnet.com/bpg/GerInfo/288

PUBLICATION MISCONDUCT
https://www.wjgnet.com/bpg/gerinfo/208

ARTICLE PROCESSING CHARGE
https://www.wjgnet.com/bpg/gerinfo/242

STEPS FOR SUBMITTING MANUSCRIPTS
https://www.wjgnet.com/bpg/GerInfo/239

ONLINE SUBMISSION
https://www.f6publishing.com

© 2022 Baishideng Publishing Group Inc. All rights reserved. 7041 Koll Center Parkway, Suite 160, Pleasanton, CA 94566, USA
E-mail: bpgoffice@wjgnet.com https://www.wjgnet.com

World Journal of Gastroenterology

Submit a Manuscript: https://www.f6publishing.com

World J Gastroenterol 2022 June 7; 28(21): 2251-2281

DOI: 10.3748/wjg.v28.i21.2251

ISSN 1007-9327 (print) ISSN 2219-2840 (online)

REVIEW

Viral hepatitis and hepatocellular carcinoma: From molecular pathways to the role of clinical surveillance and antiviral treatment

Leonardo Stella, Francesco Santopaolo, Antonio Gasbarrini, Maurizio Pompili, Francesca Romana Ponziani

Specialty type: Gastroenterology and hepatology

Provenance and peer review: Invited article; Externally peer reviewed.

Peer-review model: Single blind

Peer-review report's scientific quality classification

Grade A (Excellent): A
Grade B (Very good): B
Grade C (Good): C, C
Grade D (Fair): D
Grade E (Poor): 0

P-Reviewer: El-Shabrawi MH, Egypt; Liu LJ, China; Tanwandee T, Thailand; Wang X, China; Zhang J, China

Received: September 13, 2021
Peer-review started: September 13, 2021
First decision: November 16, 2021
Revised: December 8, 2021
Accepted: April 26, 2022
Article in press: April 26, 2022
Published online: June 7, 2022

Leonardo Stella, Francesco Santopaolo, Antonio Gasbarrini, Maurizio Pompili, Francesca Romana Ponziani, Internal Medicine and Gastroenterology, Hepatology Unit, Fondazione Policlinico Universitario Agostino Gemelli IRCCS, Rome 00168, Italy

Corresponding author: Francesca Romana Ponziani, MD, PhD, Research Assistant, Internal Medicine and Gastroenterology, Hepatology Unit, Fondazione Policlinico Universitario Agostino Gemelli IRCCS, Largo Agostino Gemelli 8, Rome 00168, Italy.
francesca.ponziani@gmail.com

Abstract

Hepatocellular carcinoma (HCC) is a global health challenge. Due to the high prevalence in low-income countries, hepatitis B virus (HBV) and hepatitis C virus infections remain the main risk factors for HCC occurrence, despite the increasing frequencies of non-viral etiologies. In addition, hepatitis D virus coinfection increases the oncogenic risk in patients with HBV infection. The molecular processes underlying HCC development are complex and various, either independent from liver disease etiology or etiology-related. The reciprocal interlinkage among non-viral and viral risk factors, the damaged cellular microenvironment, the dysregulation of the immune system and the alteration of gut-liver-axis are known to participate in liver cancer induction and progression. Oncogenic mechanisms and pathways change throughout the natural history of viral hepatitis with the worsening of liver fibrosis. The high risk of cancer incidence in chronic viral hepatitis infected patients compared to other liver disease etiologies makes it necessary to implement a proper surveillance, both through clinical-biochemical scores and periodic ultrasound assessment. This review aims to outline viral and microenvironmental factors contributing to HCC occurrence in patients with chronic viral hepatitis and to point out the importance of surveillance programs recommended by international guidelines to promote early diagnosis of HCC.

Key Words: Hepatitis C virus; Hepatitis B virus; Hepatitis D virus; Hepatocellular carcinoma; Cirrhosis; Liver

©The Author(s) 2022. Published by Baishideng Publishing Group Inc. All rights reserved.

Core Tip: Chronic hepatitis B virus (HBV), hepatitis C virus (HCV) and hepatitis D virus (HDV) infection represents a global health burden leading to liver fibrosis, cirrhosis and hepatocellular carcinoma (HCC). Among these complications, HCC accounts for 3.5% of all deaths worldwide. Thus, the understanding of the role of chronic hepatitis virus infection in HCC development is necessary in order to clarify the mechanisms underlying oncogenesis and design future treatments for this cancer. This review outlines pathophysiological and molecular pathways that contribute to carcinogenesis in HBV, HCV and HDV chronic infection focusing on the impact of clinical surveillance and antiviral treatment on the risk of HCC development.

Citation: Stella L, Santopaolo F, Gasbarrini A, Pompili M, Ponziani FR. Viral hepatitis and hepatocellular carcinoma: From molecular pathways to the role of clinical surveillance and antiviral treatment. *World J Gastroenterol* 2022; 28(21): 2251-2281
URL: https://www.wjgnet.com/1007-9327/full/v28/i21/2251.htm
DOI: https://dx.doi.org/10.3748/wjg.v28.i21.2251

INTRODUCTION

Primary liver cancer is the sixth most common cancer worldwide accounting for 800000 new cases per year and one of the major causes of cancer-related death in men with 745000 deaths per year. It has been estimated that there will be an increased incidence after the year 2025 with more than 1 million cases per year[1]. Hepatocellular carcinoma (HCC) represents the most common histologic type among liver cancers (70%-90%)[2]. According to recent epidemiologic studies, the mortality rate from HCC is increasing in some of the European and North American countries. Indeed, HCC has been recognized as the cause of death in 54%-70% of patients with compensated cirrhosis of different etiologies[3]. Nevertheless, HCC is one of the most prevalent cancers in less developed world regions. About 60%-70% of HCCs have been linked with chronic hepatitis B virus (HBV) or hepatitis C virus (HCV) infection, with a total incidence of 16/100000 cases globally (Table 1)[4], while the linkage with hepatitis D virus (HDV) is less clear[5].

HCC is associated with many risk factors (Table 2) with the highest odds ratio (OR) for viral ones. Cirrhosis precedes most cases of HCC and may exert a promoting effect *via* hepatocyte regeneration and chronic inflammation[4]. There are other environmental and genetic risk factors involved in the pathogenesis of HCC such as excessive alcohol consumption, aflatoxin intake, diabetes, obesity and hereditary hemochromatosis[6]. This review outlines the pathophysiology and molecular pathways that contribute to carcinogenesis in HBV, HCV and HBV/HDV chronic infection and investigates the impact of surveillance programs and antiviral treatments on the risk of HCC occurrence.

HBV INFECTION AND HCC DEVELOPMENT

Epidemiology

HBV infection is the most widespread chronic viral infection in the world. Currently, 2 billion people have been infected and more than 350 million are chronic carriers of the virus[7]. Worldwide HBV surface antigen (HBsAg) seroprevalence is 3.6% with the highest prevalence in Africa (8.83%) and in Western Pacific Asia (5.26%)[8]. In contrast, the prevalence of chronic HBV infection is low in most of European countries and it is estimated to be around 0.5%-0.7%[9]. Underdiagnosis and undertreatment are still unresolved issues and public awareness is largely suboptimal with less than 25% of infected Europeans aware of HBV transmission risk at the moment of their diagnosis[9]. Thus, chronic HBV infection is the tenth leading cause of global deaths accounting for 3.5% of all deaths worldwide (786000 deaths per year). Half of the total liver cancer mortality in 2010 has been attributed to HBV infection[10].

Molecular pathways and HCC development in chronic hepatitis B

Chronic HBV infection is the most important cause of HCC worldwide. Prospective cohort studies show a 5-100-fold increase in the risk of developing HCC among patients with untreated chronic HBV infection[2]. A systematic review estimates a yearly HCC incidence rate of 0.2% in HBV inactive carriers, of 0.6% in those with chronic infection without cirrhosis and of 3.7% in those with compensated cirrhosis[11]. Meta-analyses show a 15-20 times greater relative risk for HCC occurrence in HBsAg positive individuals than in HBsAg negative individuals[2].

Most of HBV-infected individuals (70%-90%) develop HCC related to the onset of cirrhosis and secondary to chronic inflammation[2]. However, in up to one-third of patients, HCC occurs in the absence of cirrhosis[12]. Oncogenesis in HBV infected patients is a complex phenomenon involving

Table 1 Hepatocellular carcinoma incidence and risk factors

Location	Chronic HBV infection		Chronic HCV infection		Alcoholic liver disease		Non-alcoholic steatohepatitis	
	NC	CC	NC	CC	NC	CC	NC	CC
Europe	0.12	2.2	0-1.8	3.7	0.1	1.8	0.5	1.1
East Asia	0.8	4.3	F0/1 0.4; F2 1.5; F3 5.1	7.1	0.1	1.7	a	a

HBV: Hepatitis B virus; HCV: Hepatitis C virus; NC: Non cirrhotic; CC: Compensated cirrhosis; a: Lack of proper data in the selected area.

most of the cell cycle regulation molecular pathways (Table 3 and Figure 1). As a noncytopathic virus, the pathogenesis of HBV tissue damage is mainly mediated by cell-mediated immune response to HBV epitopes surface proteins. Persistent HBV replication triggers immune response against the virus leading to genetic damage and perpetrating oxidative stress. In addition to chronic inflammation, other viral mechanisms contribute to HBV carcinogenesis involving the HBs and HBx proteins, the insertional mutagenesis caused by HBV DNA integration into the host genome, which induces chromosomal instability and alters the expression of endogenous genes, the epigenetic modifications through DNA methylation and the regulation of microRNA (miRNA) expression[13].

There are other factors increasing HCC risk among HBV carriers that can be divided into: Viral factors (high rates of HBV replication, long term infection, coinfection with HCV/human immunodeficiency virus/HDV, high risk genotype) and host-related factors, such as genetic or demographic (older ages, male sex, Asian or African origin, family history of HCC), clinical (presence of cirrhosis) and environmental (diabetes, overweight, alcohol abuse, aflatoxin exposure)[14].

VIRAL FACTORS

Role of HBV DNA level

The risk of developing HCC strictly correlates with HBV viraemia. Multiple integrations have been detected in liver tissues and integrated HBV sequences have been observed in almost 90% of HBV-related HCCs[13]. The reveal-HBV study shows increased HCC-related mortality in subjects with baseline HBV DNA higher than 10^6 copies/mL compared to those with baseline DNA lower than 300 copies/mL. A multivariate cyclooxygenase (COX) regression analysis identifies an increase in HBV DNA levels as the strongest independent predictor of death from HCC, after adjusting for age, sex, smoking, alcohol consumption and hepatitis B e antigen (HBeAg) serostatus[15]. Nevertheless, patients previously defined as "inactive carriers" (HBeAg negative, HBV DNA < 10000 copies/mL and normal liver function tests) have a 5-fold higher risk of developing HCC compared to HBsAg negative controls [16].

The integration of HBV DNA into the host genome represents a major pathogenetic pathway. The plasmid-like covalently closed circular DNA (cccDNA), derived from the conversion of HBV DNA soon after the entry into the hepatocyte, is recognized in the nucleus as a damaged product triggering DNA repair pathways such as the activation of cell cycle checkpoints and histone degradation, which enhances DNA recombination rates[17-19]. The integration of HBV DNA can also contribute to hepatocarcinogenesis by altering several cancer-relevant genes[20]. Viral promoter-driven human transcripts have also been identified adjacent to repetitive non-coding sequences, in particular long interspersed nuclear elements or short interspersed nuclear elements[20]. Evidence for fusion proteins have been collected for retinoic acid receptor-β and human cyclin A gene resulting in tumor-specific chimeric proteins endowed with pro-carcinogenic functions[21].

Despite this evidence, HBV integration is random and hardly ever leads to direct oncogene activation or tumor suppressor genes inactivation. However, it is widely accepted that integration contributes to hepatocytes genetic instability leading to clonal proliferation[22]; this can occur in HBV infected patients even before liver tissue damage is clinically evident[23].

Role of HBsAg

A study shows that the presence of HBV-DNA integration increases more than 100 times the risk for HCC occurrence among HBsAg carriers compared with HBsAg negative individuals[13]. HBsAg seems to have effects on the mitochondrial function, as it reduces the lipid b-oxidative activity of enoyl-coenzyme A hydratase short chain 1. On one hand, this interaction induces cell apoptosis by decreasing the mitochondrial membrane potential and reduces the phosphorylation of a serine/threonine protein kinase (Akt). On the other hand, it leads to an increased reactive oxygen species (ROS) production and promotes UDP-glucose ceramide glycosyltransferase which contributes to the alteration of ceramide metabolism[24]. Furthermore, HBsAg can inhibit jumping translocation breakpoints leading to increased cell motility and decreased apoptosis[13].

Table 2 Risk factors for hepatocellular carcinoma development[6,181-183]

Risk factors in hepatocellular carcinoma (other than liver cirrhosis)		OR (95%CI)
Strong risk factors (OR > 10)	**Europe**	
	Untreated chronic HBV/HCV hepatitis	191.0
	Untreated chronic HCV hepatitis	31.2
	Untreated chronic HBV hepatitis	18.8
	East Asia and Africa	
	Untreated chronic HBV/HCV hepatitis	75.6
	Untreated chronic HBV hepatitis	20.8
	Untreated chronic HCV hepatitis	11.5
Moderate risk factors (OR = 2-10)	Aflatoxin B1 exposure	5.9
	Untreated chronic HDV infection	3.9
	Diabetes	3.2
	Asian race	3.2
	Male gender	2.8
	Alcohol intake	2.3
	Severe iron overload	2.1
Weak risk factors (OR < 2)	Obesity (BMI > 30 kg/m^2)	1.9
	Mild iron overload	1.6
	Current smoking	1.6
	HCV genotype 1b	1.6
	PNPLA3 rs738409 single nucleotide polymorphism	1.4

HBV: Hepatitis B virus; HCV: Hepatitis C virus; HDV: Hepatitis D virus; OR: Odds ratio; CI: Confidence interval; BMI: Body mass index.

Role of HBeAg

The association between HBeAg and HCC has been well established by epidemiological studies although the pathophysiological mechanisms of HBeAg-mediated oncogenesis remain unknown. A large study investigates the effect of HBV replication on HCC development risk among 11893 Taiwanese men followed up for a mean of 8.5 years: The incidence rate of HCC is 1169 per 100000 person-years among HBsAg/HBeAg positive men, 324 per 100000 person-years for HBsAg positive HBeAg negative men and 39 per 100000 person-years among HBsAg negative men[25]. HBeAg enhances cell proliferation by means of promotion by a G1/S transition. Data suggests that miR-106b upregulation mediated by HBeAg is involved in the pathogenesis of HBV-related HCC by downregulating retinoblastoma (RB) gene[26].

Role of HBV preS/S proteins, oxidative stress and interaction with endoplasmic reticulum

The preS/S open reading frame encodes three envelope proteins (S or HBsAg, M, and L proteins)[27]. Various specific mutations in the preS/S gene may imbalance surface proteins' synthesis and their consequent retention within hepatocytes' endoplasmic reticulum (ER)[13,28]. This process occurs mainly in the presence of HBsAg or pre-S2 mutants: The viral proteins amassed in the ER can lead to oxidative stress, stimulate cell growth and survival signaling pathways and cause mutation through the generation of free radicals. The induced ER stress upregulates the cytoplasmic cyclin A pathway promoting chromosome instability through centrosome over-duplication[29]. Moreover, pre-S2 mutant protein in hepatocytes can directly interact with the c-Jun activation domain-binding protein 1 inducing hyperphosphorylation of the RB tumor-suppressor and its inactivation[13,30].

Role of HBx protein

HBx is a 154 aminoacids long protein which is essential for the HBV viral life cycle. HBx is usually expressed at low levels during the first stages of infection but with the rise of HBV DNA integration frequency during infection, relative HBx expression can increase[31]. HBx is involved in multiple and complex molecular pathways linked to mitogen and apoptotic signaling cascades, resulting in one of the most relevant oncogenic proteins in HBV proteome. It does not interact directly with DNA, but rather it

Table 3 Molecular pathways of hepatocellular carcinoma carcinogenesis in hepatitis B virus infected patients

HBx related pathways
DNA repair impairment and DNA instability
HBx - binds to DDB1 - instability of Scm5/6 - impairment in DNA replication and repair
HBx - interacts with TFIIH - impairment in DNA replication and repair
HBx - blocks BER pathway - impairment in DNA repair
HBx - binds to CRM1 and sequestering it in cytoplasm - aberrant centrosome duplication and chromatin's segregation - chromosome instability
DNA replication increase
HBx - upregulates RLF and CDT1 and downregulates geminin - DNA replication
HBx - binds to cccDNA - recruiting PCAF - histone H3 acetylation - inhibition of chromatin's methylation - DNA replication
Cell cycle deregulation *via* signal pathways
HBx - binds to p53 - impaired function of p53 - cell cycle dysregulation
HBx - induces AFP expression - activation of PTEN and PI3K/mTOR pathway - cell cycle deregulation
HBx - activates Notch1 and Notch4 receptor - cell cycle progression
HBx - upregulates NF-kB, AP-1, AP-2, c-EBP, RNA-polymerase, ATF - altered oncogenes expression and cell cycle deregulation
HBx - upregulates NF-kB - upregulation of EGR1 - upregulation of miR-3928v - downregulation of $VDAC_3$ - tumor suppressor inhibition
HBx - downregulates SFRP1 and SFRP5 - DNMT1 recruitment - inhibition of WNT/β-catenin pathway - epithelial mesenchymal transition
Epigenetic modification impairment
HBx - interacts with MBD2 and CBP - P3 and P4 promoters' activation through hypomethylation - recruitment of IGF2 - oncogenesis
HBx - stimulates deacetylation of IGFBP3 gene - upregulation of IGF1 - mitogenic and anti-apoptotic effects
HBx - upregulates DNMT1 - hypermethylation of RASSF1A - tumor suppressor inhibition
HBx - downregulates DNMT3a/DNMT3L and recruits HDAC1 - hypomethylation of oncogenes promoters including JAK/STAT3 - impairment in cell differentiation
HBx - downregulates CD82, MTA1, PCDH10 through hypermethylation - tumor progression
HBx - inhibits CDH1 through deacetylation - E-cadherin upregulation - metastasis promotion
Apoptosis impairment
HBx - upregulates Bcl2 and Mcl1, inhibits Bax - apoptosis inhibition
HBx - upregulates Foxo4 - increased resistance to ROS damage, avoiding cell death and apoptosis
HBx - upregulates NF-kB - increase of DR5 - TRAIL induced apoptosis
HBx - inhibits caspase-8 inhibitor A 20 - TRAIL induced apoptosis
mi/lnc RNA related pathways
HBx - impairs miRNA regulation and synthesis - cell cycle deregulation
HBx - impairs lncRNA regulation and synthesis - cell cycle deregulation
Oxidative stress
HBx - downregulates NQO1 - mitochondrial injury - ROS production
C-terminal truncated HBx - mitochondrial DNA damage - ROS production
Neoangiogenesis
HBx - upregulates VEGF, HIF1 and ANG2 - neoangiogenesis
Unknown mechanism
HBx - binds to HSP60 and HSP70 - unknown function but involved in HCC carcinogenesis
Pre-S/S related pathways
pre-S2 - retention of HBV proteins in ER - ROS increase - cell DNA damages
pre-S2 - retention of HBV proteins in ER - upregulation of CCNA - chromosome instability and centrosome overduplication

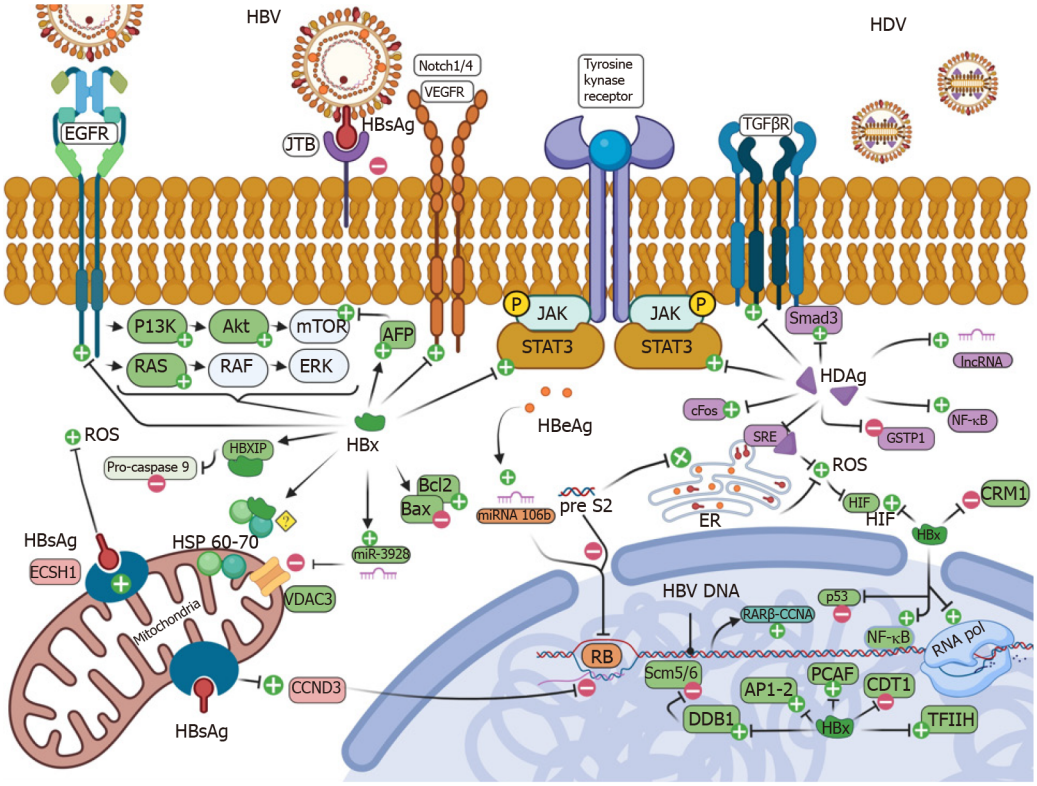
pre-S2 - interacts with JAB1 - RB tumor suppressor inhibition
HBsAg related pathways
HBsAg - binds to ECHS1 - ROS increase - cell DNA damages
HBsAg - binds to JTB - decreased apoptosis and increased cell mobility
HBeAg related pathways
HBeAg - stimulates upregulation of miR-106b - RB tumor suppressor inhibition
HBV DNA related pathways
cccDNA - triggers DNA repair pathways - histone degradation and cell cycle checkpoints activation - enhanced DNA recombination rate
HBV DNA - genome integration - oncogene activation or tumor suppressor inhibition with evidence of fusion proteins
HBV DNA - genome integration - genetic instability - clonal proliferation
Inflammatory pathways
Increased cytokines production (TGF-β, IL-4, IL-10, IL-12, IL-13) - JAK/STAT3 activation - cell proliferation
CD4+ T follicular helper decrease - loss of growth inhibition and death control of cancer cells
CD8+ cell dysfunction - impaired growth inhibition and death control of cancer cells
Functional exhausted CD8+TIM-3+ T cells - increased viral replication - increased viral factors in HCC development
NK cells - increase in IL-4 and IL-13 - activation of HSCs - increased cytokines production - cell cycle deregulation
NK cells - miR-146a increase - reduced cytotoxicity and decreased IFN-γ production - reduction in immunosurveillance
Tregs - PD1 and CTLA4 overexpression - C
Gut microbiota-related pathways
HBV related dysbiosis - circulating LPS - TLR4 activation - cytokines production - JAK/STAT3 activation - cell proliferation

DDB: Damage specific DNA binding protein; Scm5/6: Structural maintenance of chromosomes 5/6; TFIIH: Transcription factor II H; BER: Base excision repair; RLF: Rearranged L-Myc fusion gene protein; cccDNA: Covalently closed circular DNA; PCAF: P300/CBP-associated factor; AFP: Alpha fetoprotein; PTEN: Phosphatase and tensin homolog; PI3K: Phosphatidylinositol 3-Kinase; mTOR: Mechanistic target of rapamycin kinase; NF-kB: Nuclear factor-kappa B; AP-1: Activator protein 1; ATF: Activating transcription factor; EGR1: Early growth response protein 1; VDAC: Voltage dependent anion channel; SFRP: Secreted frizzled-related protein; DNMT: DNA methyltransferase; WNT: Wingless-related integration site; MBD: Methyl-CpG binding domain protein; CBP: CREB binding protein; IGF: Insulin like growth factor; IGFBP: Insulin like growth factor binding protein; MTA: Metastasis associated; Bcl2: B-cell lymphoma 2; Mcl1: Myeloid cell leukemia-1; PCDH: Protocadherins; miRNA: Micro-RNA; lncRNA: Long non coding RNA ; ROS: Reactive oxygen species; HIF: Hypoxia-inducible factor; ANG: Angiogenin; VEGF: Vascular endothelial growth factor; HSP: Heat shock protein; HCC: Hepatocellular carcinoma; ER: Endoplasmic reticulum; CCNA: Cytoplasmatic Cyclin A; RB: Retinoblastoma; ECHS: Enoyl-CoA hydratase short chain; JTB: Jumping translocation breakpoint; HBeAg: Hepatitis B e antigen; HBV: Hepatitis B Virus; TGF: Transforming growth factor; IL: Interleukin; NK: Natural killer; HSC: Hematopoietic stem cells; IFN: Interferon; PD1: Programmed cell death 1; CTLA4: Cytotoxic T-lymphocyte antigen 4; LPS: Lipopolysaccharides; TLR4: Toll-like receptor 4.

acts on cellular promoters, impairs DNA repair pathways, enhances DNA replication, alters epigenetic processing and inhibits apoptosis mechanisms. HBx effects are proven to contribute to HCC progression as well, by means of angiogenesis upregulation and stimulation of cell motility.

Some preclinical studies show that HBx interacts with cell cycle regulatory pathways activating a plethora of genes involved in mitogen signaling cascades and their downstream transcription factors, including, nuclear factor-κB (NF-κB), phosphatidylinositol 3-kinase (PI3K) and phosphatase and tensin homolog through upregulation of alpha-fetoprotein (AFP), Notch1 and Notch4, wingless-related integration site (WNT)/β-catenin signaling, activator protein 1 (AP-1), AP-2, CCAAT-enhancer-binding protein, RNA polymerase and nuclear factor of activated T cells. The activation of these pathways leads to altered expression of growth-control genes[32]. Other significant targets of HBx are the p53 family genes; The viral protein directly binds to p53 and impairs its function (p53-mediated apoptosis, p53-mediated transactivation properties and cell cycle regulation)[33].

In vitro studies have provided mechanistic insights towards the understanding of the role of HBx in HBV-mediated carcinogenesis showing an interesting effect on DNA replication. Indeed, HBx expressing cells exhibit increased DNA replication licensing factor, chromatin licensing and DNA replication factor 1, as well as reduced expression of geminin. The impairment in these molecules homeostatic balance leads to an increase in DNA replication[34]. Furthermore, HBx impairs DNA repair enzymes, interacting with transcription factor IIH, and deregulating all other proteins involved in the base excision repair pathway[32]. HBx is also involved in HBV transcription from cccDNA in the beginning and maintaining phase of viral replication. This leads to chromatin modulation and chromosomal instability because the HBx bond with cccDNA induces the recruitment of acetyltrans-



DOI: 10.3748/wjg.v28.i21.2251 **Copyright** ©The Author(s) 2022.

Figure 1 Molecular pathways in hepatitis B virus and hepatitis D virus carcinogenesis. Created with BioRender.com. HBV: Hepatitis B virus; HDV: Hepatitis D virus; EGFR: Epidermal growth factor receptor; JTB: Jumping translocation breakpoint; HBsAg: Hepatitis B virus surface antigen; VEGFR: Vascular endothelial growth factor receptor; TGF: Transforming growth factor; PI3K: Phosphatidylinositol 3-kinase; Akt: AKT serine/threonine kinase; RAS: Rat sarcoma virus gene; RAF: Rapidly accelerated fibrosarcoma; mTOR: Mechanistic target of rapamycin kinase; JAK: Janus kinase; STAT3: Signal transducer and activator of transcription 3; Smad3: Mothers against decapentaplegic homolog 3; lncRNA: Long non coding RNA; NF-kB: Nuclear factor-kappa B; ROS: Reactive oxygen species; HSP: Heat shock protein; ECSH1: Enoyl-CoA hydratase short chain 1; VDAC: Voltage dependent anion channel; CCND3: Cytoplasmatic Cyclin D3; RB: Retinoblastoma; Bcl2: B-cell lymphoma 2; Bax: Bcl2 associated X; ER: Endoplasmic reticulum; HIF: Hypoxia-inducible factor; AP: Activator protein; DDB: Damage specific DNA binding protein; Scm5/6: Structural maintenance of chromosomes 5/6; PCAF: P300/CBP-associated factor; TFIIH: Transcription factor II H.

ferases P300/CREB-binding protein (CBP)-associated factor and acetylation of histone H3, inhibiting chromatin's methylation[35]. HBx seems to induce multipolar spindle formation, chromosome segregation defects and aberrant centrosome duplication, probably by sequestrating the nuclear transport receptor Chromosomal Maintenance 1 in the cytoplasm[36]. HBx binds to the HBx interacting protein regulating the centrosome duplication or to the UV-damaged DNA binding protein 1 that influences the stability of proteins such as the structural maintenance of chromosome proteins 5 and 6 complex which plays a role in nuclear DNA replication and repair[37,38].

In mitochondria, HBx binds heat shock proteins 60 and 70 (HSP60 and HSP70) and increased levels of the resulting complex have been found in HCC cells, even if the underlying carcinogenetic mechanism has not been understood yet[39]. HBx, through miR-3928v upregulation, downregulates voltage dependent anion channel 3 (VDAC3) expression in mitochondria leading to the loss of its tumor suppression activity[40].

The role of HBx on apoptosis has been controversial. On one hand, HBx upregulates B-cell lymphoma 2 (Bcl-2) and myeloid cell leukemia-1 that exert an anti-apoptotic role and downregulates Bcl-2-associated X protein, a cytosolic protein inducing apoptosis by its interaction with VDAC3 channels on the mitochondrial membrane. On the other hand, HBx stimulates apoptosis by increasing the cell surface concentration of death receptor 5 and inhibits caspase-8 inhibitor A20 that have central roles in tumor necrosis factor (TNF) α-related apoptosis-inducing ligand mediated apoptosis. Moreover, HBx increases resistance to apoptosis through the forkhead box protein 4 avoiding cell death primed by oxidative stress damage[32]. In addition, HBx controls hepatic angiogenesis, upregulating vascular endothelial growth factor (VEGF), hypoxia inducible factor 1 (HIF-1) and proangiogenic growth factor angiopoietin 2 (ANG2)[41].

HBx effects on DNA methylation and acetylation

DNA methylation and acetylation are two of the most studied epigenetic modifications and usually occur in the early stage of HCC development. The genomic hypomethylation/hypoacetylation increases chromosome instability while localized hypermethylation/hyperacetylation decreases the expression of

Table 4 Hepatocellular carcinoma surveillance in hepatitis B virus infected patients

HCC surveillance in HBV-infected patients		
Western medical societies		
EASL, 2017	High-risk-patients: (1) HBV cirrhotic patients; (2) HBV and F3 fibrosis; and (3) HBsAg-positive patient on NA treatment with a PAGE-B of ≥ 18 at the onset of therapy. Medium risk-patients: HBsAg-positive patient on NA treatment with a PAGE-B of 10 - 17 at the onset of therapy	Screening with US examination with or without AFP every 6 mo for medium and high-risk patients. No specific HCC screening needed for low-risk patients
AASLD, 2018	High-risk patients: (1) HBV cirrhotic patients; (2) Special population of HBsAg-positive adults: Asian or African men (> 40 yr) and Asian women (> 50 yr), first-degree family member with a history of HCC, HDV coinfected; and (3) HBsAg-positive children/adolescents with advanced F3 or cirrhosis and first-degree family member with HCC	Screening with US examination with or without AFP every 6 mo; if in areas where US is not readily available, screening with AFP every 6 mo
Eastern medical societies		
JSH, 2014-2021	Extremely-high-risk patients: HBV cirrhotic patients. High-risk patients: Special population of HBsAg positive patients: age ≥ 40, male, alcohol consumption, high HBV load, family history of HCC, HCV/HDV/HIV coinfection, F3 fibrosis, low platelet count associated with advanced fibrosis, genotype C, and core promoter mutation	Screening with US and tumor marker measurements (AFP, protein induced by vitamin K absence or antagonist-II and AFP-lectin fraction 3) every 3-4 mo in the super-high-risk population. A 6-12 mo dynamic CT scan or dynamic MRI should be performed. Screening every 6 mo in high-risk populations
APASL, 2016	High-risk patients: All patients with HBV-related cirrhosis. HBsAg-positive without cirrhosis, based on the economic situation of each country and on the available risk scores	Surveillance by US and AFP should be performed every 6 mo and preferably every 3-4 mo in cirrhotic patients and those at high risk of HCC
KLCSG, 2014-18	High-risk patients: HBV cirrhotic patients; chronic hepatitis B patients	Screening with US examination with or without AFP every 6 mo. If liver US cannot be performed properly, liver dynamic CT or dynamic contrast-enhanced MRI can be performed

HCC: Hepatocellular carcinoma; HBV: Hepatitis B virus; HCV: Hepatitis C virus; HDV: Hepatitis D virus; HIV: Human immunodeficiency virus; EASL: European Association for the Study of the Liver; AASLD: American Association for the Study of Liver Diseases; JSH: Japan Society of Hepatology; APASL: The Asian Pacific Association for the Study of the Liver; KLCSG: Korean Liver Cancer Study Group; US: Ultrasound; AFP: Alpha-fetoprotein; F3: Fibrosis; HBsAg: Hepatitis B virus surface antigen; CT: Computed tomography; MRI: Magnetic resonance imaging.

tumor suppressor genes[13]. DNA hypermethylation in the promoter region of specific oncosuppressor genes has been found in HBV-related HCC mainly due to HBx effect.

HBx upregulates DNA methyltransferases 1 (DNMT1) causing a hypermethylation of rat sarcoma (RAS) association domain family member 1 (RASSF1A), involved in cell cycle maintenance, altering its expression from the very early stages of HCC development[42]. On the contrary, the downregulation of DNA methyltransferases (DNMT) 3A and DNMT 3L and the recruitment of histone deacetylase 1 causes the hypomethylation of intragenic CpG islands resulting in dedifferentiation of liver cells[43]. The upregulation of methyl-CpG binding domain protein 2 and CBP triggers a molecular pathway leading to hypomethylation of promoters 3 (P3) and 4 (P4) of insulin-like growth factor 2 gene that stimulates cell duplication pathways as well as G1/S transition[44]. Hypomethylation has been found in the promoter region of Telomerase Reverse Transcriptase (TERT), increasing the proliferative potential of the cell, and in the promoter region of COX-2, leading to a proinflammatory condition[45]. Hypermethylation has also been found in a cluster of differentiation 82, a metastasis suppressor protein involved in the p53 pathway, metastasis-associated protein 1 and protocadherin 10. Deacetylation of Cadherin-1 promoter leads to E-cadherin upregulation and a progression to metastatic disease[32].

A growing number of studies identify and investigate the role of specific miRNA, small non-coding RNA molecules (up to 25 nucleotides in length) that regulate gene expression at transcriptional and post-transcriptional levels as mediators in the hepatocarcinogenic process. Recent publications, summarized by Sartorius *et al*[46] in a meta-analysis, have found miRNAs that are involved in HBV-related HCC leading to more aggressive cancer phenotypes by means of both tumor suppressor genes inactivation and oncogenes activation.

Role of occult HBV infection

Studies with highly sensitive polymerase chain reaction assays show that HBV DNA may persist in the liver of people who have serologic recovery from acute HBV infection, as an occult HBV infection. A systematic review identifies a modest association between occult HBV infection and the risk of HCC occurrence [risk ratio (RR) = 2.83][47]. Another case-control study performed in Hong Kong shows an increased prevalence of occult HBV infection in cryptogenic HCC[48]. None of these studies is population based and most of them have a small sample size. Thus, the association between HBV occult infection and HCC lacks convincing evidence.

Role of HBV genotypes

HCC is more common in patients with HBV genotype C, D and F than in those with genotype A[49].

The majority of retrospective and case-control studies indicate that patients with genotype C HBV have a more severe course of liver disease and a higher risk of HCC occurrence has been reported. A community-based Taiwanese cohort study shows that genotype C is associated with an increased risk of HCC in HBV carriers [hazard ratio (HR) = 2.35, 95% confidence interval (CI): 1.68-3.30, $P < 0.001$] as well [50]. The Eradicate-B study, by analyzing HBsAg positive patients without evidence of cirrhosis and a mean follow-up of 14.7 years, points out a higher annual incidence rate of HCC in genotype C than genotype B patients[51].

HBV genotype also influences the features of HCC. In genotype B patients, solitary HCC nodules are more frequent than in genotype C (94% *vs* 86%), but are more often associated with satellite nodules (22% *vs* 12%)[52]. Indeed, several reports show that HBV genotype type B is associated with a higher risk of HCC development in youth, whereas genotype C is associated with HCC development in the elderly[53]. Genotype D has been noticed to be prevalent in HCC patients younger than 40 years of age, as compared to other genotypes (63% *vs* 44%; $P = 0.06$). Furthermore, a study carried out among Alaska native HBV infected patients shows that the HCC is more prevalent in genotype F than other genotypes (OR= 7.73, 95%CI: 3.69-16.4, $P < 0.001$)[54]. Data about genotype E, endemic in Africa, are lacking and further studies are needed to outline the carcinogenic role of this genotype. Differently from HBV genotypes, the clinical significance of HBV subtypes is still unclear[55].

Role of HBV variants

Several mutations in the X gene of the HBV genome are frequently found in HBV mutants of individuals with HCC. Some studies show that 3′-end X gene is commonly deleted in HCC cells leading to a C-terminal truncated HBx protein that may have a key role in the carcinogenetic process[56]. In a Taiwanese cohort, genotype C shows a higher prevalence of BCP A1762T/G1764A variant than genotype B. Patients with BCP A1762T/G1764A variant have a higher risk of developing HCC and a long-term follow up study reveals BCP A1762T/G1764A variant as an independent predictor for progression to HCC[57]. Mutations in enhancer II (C1653T) and elsewhere in the basal core promoter (T1753V) have also been found to be associated with HCC development[57].

ENVIRONMENTAL FACTORS

Role of chronic inflammation

Chronic tissue inflammation plays a central part in oncogenesis through various complex mechanisms. In the liver, continuous inflammation and regeneration increases the risk of hepatocarcinogenesis. Cytokines production and inflammation-mediated alteration of key signaling pathways, such as signal transducer and activator of transcription 3 (STAT3) and NF-κB pathways, play an important role as well [13,58]. The most common immune alterations found during HBV infection are: Cytokines production [such as tumor growth factor (TGF-β), interleukin (IL)-4, IL-10, IL-12, IL-13], decreased CD4+ and CD8+ cells function, Treg cells dysfunction and innate immune response suppression[59].

CD4+ Th1 and CD8+ cells play an important role in cell cycle regulation and death control of cancer cells; thus, T cells dysfunction can lead to a higher risk of HCC development[60]. The impairment of HBV-specific CD8+ T cell functions in patients with chronic hepatitis B is mainly shown by the high expression levels of inhibitory receptors such as cytotoxic T-lymphocyte antigen 4, programmed cell death protein (PD) 1 and T cell immunoglobulin and mucin-domain containing (TIM) 3. CD8+TIM-3+ T cells are functionally exhausted because of the continuous immune activation and are unable to effectively produce cytokines and exert anti-viral activity[60]. Additionally, non-specific CD8+ T cells with memory phenotypes secrete interferon (IFN)-γ, recruiting hepatic macrophages which promote HCC through the secretion of TNF-α, IL-6 and Monocyte Chemoattractant Protein 1[61]. The frequency of circulating CD4+ T follicular helper cells decreases and their function results are impaired during disease progression in patients with HBV-related HCC; CD4+ cells infiltrate seems to be significantly reduced in HCC tumor regions compared to non-tumor regions[62].

Natural killer (NK) cells from HCC patients show significant increase in the expression of miR-146a which downregulates NK cell's function and leads to a decreased IFN-γ and TNF-α production. Activation of non-virus-specific cells may result in widespread inflammation promoting HCC development. NK cells promote hepatic stellate cells (HSCs) activation in liver fibrogenesis through the production of the inflammatory cytokines IL-4 and IL-13[63]. HSCs enhance the recruitment of regulatory T cells (Tregs) in the liver increasing the fibrotic processes and therefore hepatocarcinogenesis. Indeed, Tregs show enhanced suppressive function by PD-1 over-expression leading to a more immunosuppressive and exhausted cellular microenvironment in HBV-related HCC compared to non-virus-related HCC[64]. Thus, HBV-induced immune imbalance is a major risk factor in the pathway of HCC development.

Role of the gut microbiota

The link between the gut-liver axis and HCC has been studied in animal models as well as small cohorts of patients and is based on the theories that inflammation related to chronic liver disease causes

dysbiosis and intestinal barrier dysfunction. Translocation of bacterial products in portal and systemic circulation can trigger molecular pathways leading to inflammation, in particular lipopolysaccharide (LPS) from Gram-negative bacteria wall activates the Toll-like receptor (TLR) 4 causing an increase in inflammatory cytokines production. In turn, cytokines are linked to the activation of signaling pathways of cell proliferation, such as Janus kinase (JAK)/STAT3[65]. A well characterized pattern of inflammatory cytokines and chemokines has been associated with cirrhosis and HCC, characterized by increased plasmatic levels of IL-8, IL-13, C-C motif chemokine ligand (CCL) 3, CCL4 and CCL5[66]. This correlates alteration in gut microbiota with replication and immortalization of HCC cells. Indeed, several studies suggest that the gut microbiota might play a key role in the process. The inflammatory role of LPS is in fact mediated by TLR4; TLR4 knock-out mice show a much lower incidence of HCC [67]. Some other studies demonstrate that diethylnitrosamine (DEN)-exposed mice have an increased abundance of Gram-negative bacteria and therefore, of LPS (*Escherichia coli*, *Atopobium*, *Collinsella*, *Eggerthella* and *Coriobacterium)*[68]. High-dose probiotics administration in these animals is able not only to reverse dysbiosis but can reduce the number and size of cancer nodules as well.

There are limited studies comparing the gut microbiota of HBV-related HCC and non-HBV non-HCV-related HCC. A small Asian study enrolled 90 patients, divided in three groups: HBV-related HCC (B-HCC), non-HBV non-HCV-related HCC (NBNC-HCC) and healthy controls. The gut microbiota of B-HCC patients is more heterogeneous with higher bacterial alpha diversity indices, whereas, those of healthy controls and NBNC-HCC patients exhibits similar features. However, butyrate-producing bacteria (genus *Ruminococcus*, *Feacalibacterium*, *Clostridium*) present heterogeneity in B-HCC and NBNC-HCC in the study[69]. In addition, a set of *Bifidobacterium* species is found to mark predominant dysbiosis in HBV cirrhosis patients[70]. More studies are needed to clarify the possible oncogenic role of the gut microbiota related to HBV infection in the pathogenesis of HCC.

HCC surveillance in patients with chronic hepatitis B

Eastern and western hepatological societies have the difficult task of identifying patient populations at high risk for HCC occurrence, in whom clinical and radiological surveillance is mandatory (risk above threshold, usually cumulative incidence > 1.5% yearly) and other populations where there is no certain benefit in carrying out the surveillance programs (risk unknown or below threshold)[71]. Based on these considerations, surveillance must include patients affected by cirrhosis of all causes and a subset of non-cirrhotic HBV carriers (Table 4). HCC screening and surveillance is recommended by the American Association for the Study of Liver Diseases (AASLD) guidelines in patients with cirrhosis of any cause and non-cirrhotic HBV carriers at higher risk (*i.e.,* Asian men older than 40-years-old, Asian women older than 50-years-old, patients with a family history of HCC and African or North American Blacks of any age)[72,73]. The European Association for the Study of the Liver (EASL) guidelines also include non-cirrhotic patients with high or medium risk calculated with the PAGE-B score[74,75]. The Japan Society of Hepatology (JSH) differentiates ''extremely-high-risk patients'' (hepatitis B cirrhosis) in whom surveillance is recommended every 3-4 mo and ''high-risk patients'', in whom surveillance is recommended every 6 mo and ''risk factors other than hepatitis virus infection or liver cirrhosis'' in whom the benefits of surveillance are uncertain[76,77].

Risk scores

As individual HCC risk factors cannot adequately classify patients with chronic hepatitis B according to their HCC risk, several risk scores have been developed for those undergoing viral treatment with nucleotide analogues: CU-HCC, CAG-HCC, REACH-B, PAGE-B, modified PAGE-B (mPAGE-B)[78].

CU-HCC, GAG-HCC and REACH-B have been validated in a cohort of Asian patients with chronic hepatitis B, 22% of whom with cirrhosis, treated with entecavir (ETV): The 5-year HCC cumulative incidence rates were 12.9% in cirrhotic patients and 2.1% in non-cirrhotic ones while the accuracy of CU-HCC, GAG-HCC and REACH-B scores for HCC prediction at baseline was 0.8, 0.76 and 0.71, respectively[79]. Other studies confirmed an analogue predicting value of the REACH-B score in patients treated with tenofovir[80-82].

However, CU-HCC, GAG-HCC and REACH-B predictability is proven to be poor in Caucasian subjects with chronic hepatitis B. A large study including patients treated with ETV or tenofovir showed an accuracy of 0.66, 0.74 and 0.54, respectively[83]. Subsequently, Papatheodoridis *et al*[84] validated the PAGE-B score on 1815 Caucasians treated with ETV or tenofovir for at least 12 mo. The PAGE-B score had the advantage of including simple variables (platelets, age and gender) and was able to stratify the risk of HCC development within 5 years in: Low (0%), for PAGE-B score < 10; medium (4%), for PAGE-B score 10-17; or high (about 16%), for PAGE-B score > 17. Kim *et al*[85] developed the mPAGE-B score, adding serum albumin to the PAGE-B parameters, and validating the score on Asian populations. The mPAGE-B differentiated the 5-years HCC risk in low (< 8) or high (> 13). Therefore, the PAGE B score seems to perform with an adequate accuracy both in Caucasian and Asian chronic hepatitis B patients under the current oral antiviral drugs.

Novel biomarkers

Recently, the usefulness of two novel biomarkers, hepatitis B core-related antigen (HBcrAg) and

Table 5 Molecular pathways of hepatocellular carcinoma carcinogenesis in hepatitis D virus infected patients

Cell cycle deregulation *via* signal pathways
L-HDAg - Smad 3 activation - TGFβ upregulation - cells growth and dedifferentiation
L-HDAg - antagonizes c-Jun inhibitory effect over TGFβ - TGFβ upregulation - cells growth and epithelial-mesenchymal transition
L-HDAg - TNF-α stimulation - NF-κB activation - inflammation and proliferation
L-HDAg - activates STAT3 downstream protein - JAK/STAT pathway activation - cell growth
L-HDAg - stimulates c-Fos activation - cells growth and dedifferentiation
L-HDAg - downregulates GSTP1 - tumor oncosuppressor inhibition
Oxidative stress
L-HDAg - NF-κB and STAT3 activation - ROS production - DNA damage
L-HDAg - activates promoters of GRP78 and GRP94 - ROS production - DNA damage
L-HDAg - activates TGFβ1 - Nox4 activity - ROS production - DNA damage
S-HDAg and L-HDAg - increase in TRAF2 - inflammation and ROS production
S-HDAg and L-HDAg - bind to SRE - targeting proinflammatory genes - inflammation and ROS production
Epigenetic mechanisms
S-HDAg and L-HDAg - increased activity of histone acetyltransferases and CBP - histone H3 acetylation of clusterin promoter - increased clusterin expression - prolonged cell survival
S-HDAg - stimulates Histone H1e acetylation - clusterin promoter activation - prolonged cell survival
HDV - DNMT1 and 3b increased activity - tumor suppressor inhibition
S-HDAg and L-HDAg - hypermethylation of E2F1 promoter - cell cycle dysregulation

HDAg: Hepatitis D virus antigen; Smad3: Small mother against decapentaplegic 3; TGF: Transforming growth factor; TNF: Tumor necrosis factor; NF-kB: Nuclear factor-kappa B; GSTP: Glutathione S-transferase Pi; ROS: Reactive oxygen species; GRP: Gastrin releasing peptide; HDV: Hepatitis D virus; STAT3: Signal transducer and activator of transcription 3; SRE: Stress response element; Nox4: NADPH oxidase; TRAF: Tumor necrosis factor-receptor associated factor; CBP: CREB-binding protein; DNMT1: DNA methyltransferases 1; JAK: Janus kinase.

Wisteria floribunda agglutinin-positive Mac-2 binding protein (M2BPGi), has been evaluated for the prediction of HCC occurrence. HBcrAg is a novel biomarker of HCC occurrence and consists of three products of the precore/core gene: HBeAg, hepatitis B core antigen and p22cr, a 22kDa protein present in DNA-negative Dane-like particles. It is used in Japan to support HCC screening in patients with chronic hepatitis B. Serum HBcr levels correlate with HBV replication, serum HBV DNA, intrahepatic cccDNA levels and transcriptional activity. In a large cohort study, HBcrAg is proven to be superior to HBV DNA in predicting HCC development in treatment-naïve patients with chronic hepatitis B. Tseng *et al*[51] showed that HBcrAg level is an independent risk factor of HCC in individuals with chronic hepatitis B and intermediate viral load. Another cohort study suggests a correlation between M2BPGi, a serum glycoprotein-based biomarker (glycobiomarker), fibrosis (FIB) stage and HCC. In patients with cirrhosis M2BPGi serum levels > 1.8 cut-off index are associated with a higher risk of HCC development ($P < 0.001$). Although the area under the receiver operating characteristic curves for M2BPGi and AFP are similar in cirrhotic patients of all etiologies (0.77 *vs* 0.72; $P = 0.15$), M2BPGi outperforms AFP in chronic hepatitis B patients (0.84 *vs* 0.75; $P = 0.02$)[86]. Furthermore, M2BPGi serum level before receiving NA and 48 wk after the beginning of treatment is predictive of HCC occurrence.

The impact of therapies for chronic hepatitis B infection on HCC occurrence

Nowadays, only a few classes of drugs have been licensed and therefore approved for hepatitis B treatment: Nucleos(t)ide reverse transcriptase inhibitors (NRTIs) and IFN-α.

Lamivudine

Lamivudine (LAM) has been the first nucleoside analogue used for the treatment of chronic HBV infection. In an Asian study, the cumulative incidence of HCC is 3.9% in the LAM arm *vs* 7.4% in the placebo arm ($P = 0.047$), yet the clinical benefits on disease progression and HCC occurrence are lost when patients developed resistance (11% *vs* 5% placebo)[87]. A meta-analysis of 5 studies including 1267 patients treated with LAM compared with 1022 untreated patients demonstrates that HCC incidence is reduced by 78% (2.5% *vs* 11.7%, RR = 0.22; $P < 0.001$)[87,88]. Therefore, LAM treatment seems to reduce but not to eliminate the risk of HCC.

ETV and tenofovir

Second-generation NRTIs, ETV and tenofovir [tenofovir disoproxil fumarate (TDF) or tenofovir alafenamide), have a potent suppressive effect on the DNA synthesis mechanism during HBV replication, although they have poor effect on the intracellular concentration and activity of cccDNA, which persist for years in the infected liver due to the long half-life and the resistant molecular structure. In an Asian study, ETV treated patients have a 63% reduction in the incidence of HCC at 5 years compared to those not treated (3.7% *vs* 13.7%; $P < 0.001$)[89]. A Greek study followed 321 patients with chronic hepatitis B under ETV for 30 mo comparing them with 818 patients on LAM treatment; the cumulative HCC incidence in the ETV group is 4.8% *vs* 5.6% ($P = 0.096$)[49]. In another European multicenter cohort study after a median follow-up of 39 mo, HCC developed in 71 (4.3%) out of 1666 patients with chronic hepatitis B treated with ETV or TDF; the cumulative probability of HCC results 1.3% at the first year, 3.4% at the third year and 8.7% at the fifth year after the initiation of treatment [90]. ETV and tenofovir seem to improve liver FIB to prevent cirrhosis complications and to reduce, though not eliminate, the risk of HCC.

IFN-α

Patients with a clinical response to conventional IFN-α therapy schemes show a lower incidence of cirrhosis decompensation and a decrease in HCC occurrence with a better overall survival compared with non-responders. A recent meta-analysis of 14 trials suggests that pegylated-IFN facilitates HBsAg clearance or seroconversion in chronic hepatitis B patients[15,91]. In another study evaluating long-term outcomes of IFN-α therapy in HBeAg seropositive patients by comparing 233 patients undergoing IFN-based treatment with 233 matched controls, the cumulative HCC incidence at the end of 15 years of follow-up is 2.7% *vs* 12.5% ($P = 0.01$)[92]. Finally, a meta-analysis on 2742 subjects pooled from 12 studies also shows that IFN-α treatment reduces the risk of HCC occurrence by 34% (RR = 0.66, 95%CI: 0.48-0.89)[93].

HBV vaccines

HBV vaccination prevents children from becoming HBV carriers and reduces the incidence of HCC in vaccinated populations. In Taiwan, after a vaccination campaign, the average incidence of HCC in children (6 years to 14 years) fell from 0.70 per 100000 children in 1981-1986 to 0.57 in 1986-1990 and further to 0.36 in 1990-1994 ($P < 0.01$). Moreover, after the universal HBV immunization program in the 1990s, HCC incidence reduced from 0.293-0.117 per 100000 person-years[94]. Similar findings result from South Eastern Asian and Alaskan studies[95-97]. More than 70%-80% of HCC in all developing countries are linked to chronic hepatitis B infection so widespread vaccination is the most important step to prevent more than 500000 HCC cases per year worldwide[98].

HDV INFECTION AND HCC DEVELOPMENT

Epidemiology

Recent studies estimate that between 20 and 72 million people are infected with HDV[99]. Indeed, the precise global prevalence of HDV infection has remained unestablished due to the non-standardized screening programs in different nations and the inaccessibility to testing in most highly endemic areas [100,101]. In Western Europe, the prevalence of the infection has decreased in the last 20 years as a consequence of ameliorated socioeconomic conditions and national vaccination campaigns against HBV [102,103].

Chronic hepatitis D is considered the most severe form of chronic viral hepatitis leading to a rapid progression towards liver cirrhosis and a higher mortality rate compared to other types of viral hepatitis. More than 10% of chronically HDV infected patients develop liver cirrhosis within 5 years from infection and in 30 years, more than 80% of patients suffer from cirrhosis decompensation[104].

Molecular pathways and HCC development in chronic hepatitis D infection

Recent cohort studies have found a risk as much as nine times higher in HDV-infected patients compared to HBV monoinfected ones despite the common belief that HDV doesn't represent a certain major risk factor for HCC development[105,106]. Furthermore, persistent HDV replication has been proven to be a risk factor for liver disease progression to liver cirrhosis and HCC[107]. A study by the European Concerted Action on Viral Hepatitis demonstrates an increase of HCC occurrence by a factor of 3.2 in anti-HDV positive cirrhotic patients compared to negative ones[105]. Other recent studies show an increased risk of HCC for HDV/HBV coinfected patients than in HBV monoinfected ones (adjusted HR = 9.30)[108]. One large study estimates a risk of HCC occurrence significantly higher among patients with chronic HDV infection (RR = 3.9) than among those with HBV monoinfection[109]. On the contrary, an English retrospective study reports that despite the increasing prevalence of HDV infected patients in South London, liver cancer occurrence is only slightly increased between HBV monoinfected and HBV/HDV coinfected patients (OR = 1.34)[110].

In conclusion, recent findings identify HDV infection as a risk factor for HCC even if a direct oncogenic mechanism is unlikely. So, it is uncertain whether HDV adds oncogenic effects beyond those carried by chronic inflammation, FIB and cirrhosis. The genomic signature of HDV-related HCC has been poorly understood but several studies have pointed out some potential oncogenic mechanisms involving: Interference of HDV antigen (HDAg) in the cell cycle through STAT3 and cyclophilin, alteration of protein synthesis, oxidative stress as a result of severe inflammation, aberrant silencing of tumor suppressor genes by DNA methyltransferases and a possible epigenetic control on HBV transcription[5]. These mechanisms are summarized in Table 5 and Figure 1.

VIRAL FACTORS

Role of HDV replication levels

Even if HDV replicative activity has been related to a poor prognosis, it is still uncertain whether levels of HDV DNA increase the risk of HCC development. Some studies find no correlation between viral load and HCC occurrence in HDV infected patients while some others show an increased risk of cirrhosis complications in patients with a higher HDV viraemia[104]. Further investigations are needed to point out the role of HDV replication as a risk factor in liver oncogenesis.

Role of HDAg

HDAg expression alone does not appear to have oncogenic potential. Moreover, since high levels of antigen and viral RNA can lead to a cell cycle arrest in G1 phase, this mechanism can promote DNA damage and oncogenes mutation. L-HDAg plays a key role in HDV-related oncogenesis. It can stimulate inflammatory and cell growth pathways by enhancing TNF-α production and NF-kB upregulation triggering STAT3 downstream proteins in the JAK/STAT molecular signaling and recruiting small mothers against decapentaplegic (Smad) 3 protein, involved in TGF-β activation[104]. In a similar way, L-HDAg downregulates glutathione S-transferase pi 1 (GSTP1), a tumor suppressor, and antagonizes c-Jun, by neutralizing its inhibitory effect on TGF-β cascade[111]. HBx and L-HDAg can act synergistically on NF-kB and JAK/STAT regulation increasing each other's effect.

Oxidative stress

The severe inflammation occurring in HDV infection can by itself produce free radicals through NF-kB and STAT3 pathways. In addition, L-HDAg-induced TGF-β1 can activate NADPH oxidase (Nox) 4, resulting in a further ROS levels increase[111]. Either L-HDAg and S-HDAg bind to ER stress response element and stimulate an increase in TNF receptor-associated factor 2 targeting proinflammatory genes in the generation of oxygen-derived reactive products[112]. Furthermore, HDAg can stimulate the promoters of immunoglobulin protein gastrin releasing peptide (GRP)78 and GRP94 targeting inflammatory genes and upregulating ROS production[111]. Even if the damage carried to the host genome by HDV through oxidative stress is indirect, it represents one of the most important oncogenic effects of the virus. Novel therapies such as bulevirtide can stop this process by inhibiting viral replication and consequently virus-related inflammation and oxidative stress.

Epigenetic regulation and DNA methylation/acetylation

Both HBV and HDV-related HCC enhance oncogenes and inhibit tumor suppressor genes by epigenetic regulation mostly through DNMT1 and DNMT3b proteins involved in the maintenance of methylation patterns in the human genome. The molecular mechanism of DNMT1 deregulation in HDV infected patients has not been established yet, even if some studies identify STAT3 regulation over DNMTs protein as the culprit of DNA methylation impairment in HDV-related HCC[111].

Moreover, S and L-HDAg can increase E2F transcription factor 1 promoter leading to cell cycle deregulation (G2/M switch) and Nox4 activation[111]. HDAgs impair the DNA acetylation as well, mainly by the recruitment of histone acetyltransferases and P300/CBP[104]. Histone acetyltransferases increase clusterin expression and prolongs cellular survival through its antiapoptotic effect[43].

Potential role on HBV replication

An epigenetic control of HDV over HBV transcription and regulation has been postulated. There are some evidences that long-lasting active proliferation of both viruses can lead to more severe disease until HCC development[5,113].

ENVIRONMENTAL FACTORS

Potential role of inflammation

The histological examination of liver tissue of chronically HDV-infected patients shows an increase in

HDAg specific T CD4+ lymphocytes that rises gradually along the course of the infection. Recent findings suggest that hepatitis D is an immune-mediated disease and chronic immune activation may promote hepatocarcinogenesis[5].

PATHWAYS NEEDING FURTHER INVESTIGATION

Potential role of small and long non-coding RNAs

There is increasing interest in the study of non-coding RNAs including small non-coding RNA and long non-coding RNAs (lncRNAs). According to a recent study Y3 lncRNA results significantly downregulated in HDV-related HCC suggesting a possible role in the pathogenesis of HDV-related HCC[114].

Impact of therapies for chronic hepatitis D infection on HCC occurrence

Recent long-term studies point out that pegylated (PEG)-IFN treatment is independently associated with a better clinical outcome and a longer survival. A retrospective study shows a reduced rate of liver decompensation in PEG-IFNα treated patients without any difference in terms of HCC development. In addition, complete loss of HDV RNA reached with IFN-α therapy does not seem to reduce the HCC occurrence rate[5,115]. Whether PEG-IFN treatment can reduce the risk of HCC development in HDV infected patients is unknown and more studies are needed to clarify this point. Given the recent approval of bulevirtide, data on its effect on HCC occurrence is still lacking.

HCV INFECTION AND HCC DEVELOPMENT

Epidemiology

Global prevalence of HCV, based on detectability of anti-HCV antibodies, has been estimated to be 1.6% which corresponds to almost 115 million individuals[116]. The prevalence of viremic individuals is estimated at 1% or 71 million[117]. HCV seroprevalence varies across geographical regions and is highest in Central Asia, East Asia, North-Africa and the Middle East where more than 3.5% of the total population is affected[118]. Russia, Egypt, Nigeria, India, Pakistan and China account for more than 50% of the total viremic HCV infection[116,118] whereas Western countries contribute only a small percentage (seroprevalence < 1%)[119]. The number of HCV-related deaths due to liver cirrhosis decompensation or HCC has been increased from almost 900000 deaths in the 1990s to almost 1500000 deaths in the 2010s as the result of the high prevalence and the lack of therapies[120].

Molecular pathways and HCC development in chronic hepatitis C

HCV infection has been identified as one of the major risk factors for HCC development worldwide. Prospective studies show a 15-30-fold increased risk of HCC occurrence among chronically HCV infected patients compared with HCV negative ones. HCV genetic material doesn't integrate into the host genome; therefore, HCV needs continuous replication to maintain chronic infection. Despite this, HCV exerts indirect and direct effects on hepatocarcinogenesis. On one hand, the indirect effect is related to FIB and cirrhosis. The probability of HCC development rises with the stage of FIB and most of HCV-related HCCs occur in patients with advanced FIB or cirrhosis (annual rate up to 8%, average 1%-4%)[121]. On the other hand, viral factors such as HCV core protein, non-structural proteins, structural proteins and HCV genotypes and subtypes have a direct effect on the risk of HCC development through the modulation of hepatocytes gene expression. The multifaceted HCV infection effects on cells molecular pathways and microenvironment are summarized in Table 6 and Figure 2.

VIRAL FACTORS

Role of HCV core protein

HCV core protein presents a broad intracellular distribution in host cells suggesting a role in the modulation of multiple metabolic and replicative processes. Host proto-oncogenes and tumor-suppressors are direct targets of the HCV core protein which interact with tumor-suppressor proteins such as p53, p73 and RB, downregulating their functions. Interaction between p73 and the HCV core protein leads to inhibition of cell growth arrest mechanisms[122].

Moreover, increased TERT gene activity, typical of cells undergoing malignant transformation, is observed in primary human hepatocytes transfected with HCV core protein. TERT expression seems to be one of the earliest neoplastic events in HCC conferring an immortalized phenotype to transformed hepatocytes[123]. The HCV core protein inhibits the expression of the cyclin-dependent kinase inhibitor p21/WAF that has a role in the regulation of the cell cycle and in the induction of apoptosis. In a similar way, HCV core protein activates the rapidly accelerated fibrosarcoma 1/mitogen-activated protein

Table 6 Molecular pathways of hepatocellular carcinoma carcinogenesis in hepatitis C virus infected patients

HCV core protein-related pathways
Signaling pathways
HCV core protein - binds p53, p73 and RB - tumor suppressors inactivation
HCV core protein - increased TERT gene activity – oncogenesis
HCV core protein - induces expression of cyclin E/CDK2 - G1/S transition
HCV core protein - inhibits CKI1 - cell cycle deregulation
HCV core protein - induces RAF/MAPK pathway – oncogenesis
HCV core protein - inhibits E-cadherin expression and SFRP1 *via* histone modification - activation of WNT/β-catenin signaling - epithelial mesenchymal transition
HCV core protein - interacts with TBR1 - inhibit TGFβ signaling and prevent translocation of Smad - cell spreading, cell growth regulation
Oxidative stress and mitochondrial impairment
HCV core protein - impairs lipid β-oxidation - reduces mitochondrial electron transport chain - ROS production
HCV core protein - impairs mitophagy - mitochondrial damage - ROS production
HCV core protein -interacts with HSP60 - ROS production and inhibition of TNFα induced apoptosis
Angiogenesis
HCV core protein - stimulate an increasing in HIF1α and AP-1 - upregulation of VEGF expression - angiogenesis
HCV core protein - activates PI3K/Akt and JAK/STAT - AR activation - angiogenesis
HCV core protein - activates COX2, MMP-2 and MMP-9 – angiogenesis
Inflammation
HCV core protein - suppresses of NF-kB pathways - impaired immune response
HCV core protein - upregulates cytokines and deregulates HSCs activity - impaired immune response
E2 protein-related pathways
E2 protein - interacts with CD81 - impaired host immune system
E2 protein - activates MAPK/ERK pathway - promoting cell proliferation
E2 protein - inhibits PKR - inhibition of protein synthesis
NS2 protein-related pathways
NS2 - activates cyclinD/CDK4 - induces expression of cyclin E/CDK2 - G1/S transition
NS2 - binds p53 - tumor suppressors inactivation
NS3-related pathways
NS3 - inhibits p53 - tumor suppressor inactivation
NS3 - inhibits ATM - tumor suppressor inactivation
NS3 - suppresses of NF-kB pathways - impaired immune response
NS3 - blocks TLR3 and RIG-I - impaired immune response
NS5A-related pathways: Signaling pathways
NS5A - inhibits p53 - tumor suppression inactivation
NS5A - interacts with TGFBR1 - inhibit TGFβ signaling and prevent translocation of Smad 3/4 - cell spreading, cell growth regulation
NS5A - increases phosphorylation of GSK3β - activates β-catenin - upregulates c-Myc - cell growth
NS5A - activates Akt pathway – oncogenesis
NS5A - interacts with PI3K p85 subunit - upregulates cell survival cascade
NS5A - activates Twist 2 - epithelial mesenchymal transition
NS5A - activates RAS - enhance tumor cell invasiveness
NS5A - inhibits JAK/STAT pathway - blockage of IFN signaling

NS5A - inhibits PKR - inhibition of protein synthesis
NS5A - activates TLR4 - amplified NANOG - Twist 1 induction - oncogenesis and epithelial mesenchymal transition
NS5A-related pathways: Apoptosis
NS5A - inhibits TNFα mediated apoptosis - cell immortalization
NS5A - inactivates caspase 3 - inhibition of apoptosis
NS5A - inhibits proteolytic cleavage of death substrates (PARPs pathway) - impaired DNA repair and apoptosis
NS5A-related pathways: Oxidative stress
NS5A - induces of WNT/β-catenin signaling - upregulation of c-Myc - ROS production
NS5A - increases calcium release from ER - mitochondrial calcium uptake - ROS production
Epigenetic modifications
HCV - alters histone mark H3K27ac - TNFα and IL2 pathways - cell growth deregulation and epithelial mesenchymal transition
HCV - upregulates DNMT1 and SMYD3 - increased methylation of CDKN2A, GSTP1, APC, SOCS1, RASSF1A - tumor suppressors inhibition
HCV - increases miR-141 - inhibition of DLC1 - tumor suppressor inhibition
Inflammatory pathways
HCV - activates CCL20-CCR6 - endothelial cell invasion and angiogenesis
Switch from Th1 to Th2 - increasing in IL4-5-8-10 - loss of death control on cancer cells
Switch from Th1 to Th2 - decreasing in IL1-2-12-15 - loss of death control on cancer cells
Gut microbiota-related pathways
HCV-related dysbiosis - circulating LPS - TLR4 activation - cytokines production - JAK/STAT3 activation - cell proliferation

HCV: Hepatitis C virus; RB: Retinoblastoma; TERT: Telomerase reverse transcriptase; MAPK: Mitogen-activated protein kinase; SFRP: Secreted frizzled-related protein; WNT: Wingless-related integration site; TBR1: T-Box brain transcription factor 1; TGF: Transforming growth factor; Smad: Small mother against decapentaplegic; ROS: Reactive oxygen species; HSP60: Heat shock protein 60; TNF: Tumor necrosis factor; HIF: Hypoxia-inducible factor; AP-1: Activator protein 1; VEGF: Vascular-endothelial growth factor; PI3K: Phosphatidylinositol 3-kinase; MMP: Matrix metalloproteinase; NF-kB: Nuclear factor-kappa B; HSC: Hematopoietic stem cells; ATM: Ataxia telangiectasia mutated; TLR: Toll-like Receptor; RIG: Retinoic acid-inducible gene; TGFBR: Transforming growth factor beta receptor; GSK: Glycogen synthase kinase; RAS: Rat sarcoma virus gene; PKR: Protein kinase R; PARP: PolyADP-Ribose polymerase; IL: Interleukin; GSTP: Glutathione S-transferase Pi; DNMT1: DNA methyltransferase 1; SMYD: SET and MYND domain-containing proteins; APC: Adenomatous polyposis coli; SOCS1: Suppressor of cytokine signaling 1; RASSF1A: RAS Association Domain Family Protein 1A; DLC1: Deleted in liver cancer 1; LPS: Lipopolysaccharides; JAK: Janus kinase; STAT3: Signal transducer and activator of transcription 3; CCL: C-C motif chemokine ligand; PARPs: Poly(ADP-ribose) polymerases; CDK4: Cyclin-dependent kinase 4; COX2: Cyclooxygenase 2; RAF: Rapidly accelerated fibrosarcoma; ANG2: Angiopoietin 2; CCR: Chemokine receptor type.

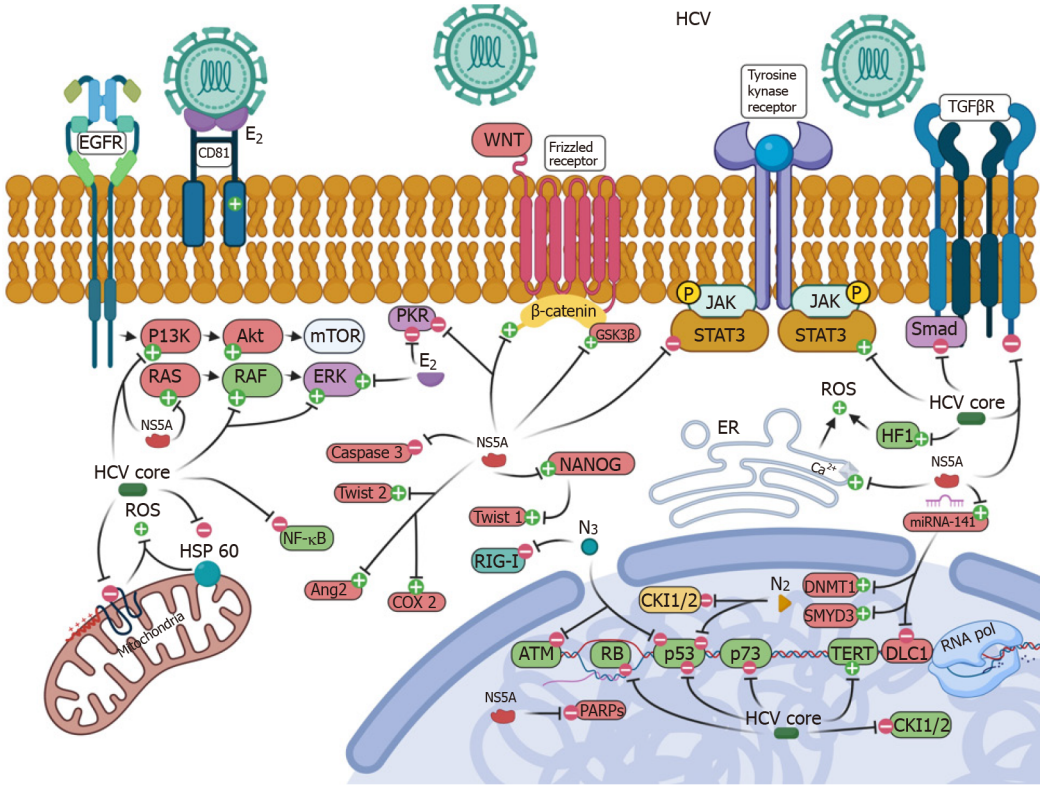
kinase (MAPK) proto-oncogene pathway and nonspecific hepatitis-induced cell proliferation[124].

Furthermore, overexpression of the HCV core protein seems to be important for the regulation of epithelial mesenchymal transition (EMT) driving the activation of HSCs. The induction of EMT is mediated by the inhibition of E-cadherin expression and the induction of secreted frizzled-related protein 1 *via* DNA methylation and histone modifications. This pathway leads to activation of WNT/β-catenin signaling[123]. Finally, the HCV core protein can suppress NF-κB, impairing downstream immune response.

Indirect HCV core protein mediated damage is carried by oxidative stress through an impairment of lipid β-oxidation and alteration of intracellular lipid metabolism which is associated with a reduction of mitochondrial electron transport chain's function. This process induces further ROS production and regulates apoptosis through inhibition of the HSP60 leading to a TNF-α-mediated apoptosis. Recently, the HCV core protein has also been proven to impair mitophagy contributing to mitochondrial damage; the resulting oxidative stress has been identified as a key trigger of the hepatocarcinogenetic process [122]. Dysregulation in angiogenetic processes and upregulation of inflammatory pathways represent other targets of indirect damage mediated by the HCV core protein.

Role of other viral proteins

HCV-encoded proteins have been directly involved in the oncogenic process through interaction with several signaling pathways mainly in experimental animal models. The HCV E2 glycoprotein interacts with CD81, a cell surface marker of NK cells. This process leads to the alteration of cytokines production and dysregulation of cytotoxic granules release which impairs the host immune system[14]. In addition, E2 protein leads to MAPK/extracellular signal-regulated kinases pathway activation promoting cell proliferation and maintaining cell survival[125]. The NS2 protein can activate cyclin D/cyclin-dependent kinase 4 (CDK4) inducing cyclin E expression and stimulating cell cycle progression from G1



DOI: 10.3748/wjg.v28.i21.2251 **Copyright** ©The Author(s) 2022.

Figure 2 Molecular pathways in hepatitis C virus carcinogenesis. Created with BioRender.com. HCV: Hepatitis C virus; EGFR: Epidermal growth factor receptor; WNT: Wingless-related integration site; TGF: Transforming growth factor; PI3K: Phosphatidylinositol 3-kinase; Akt: AKT serine/threonine kinase; RAS: Rat sarcoma virus gene; RAF: Rapidly accelerated fibrosarcoma; mTOR: Mechanistic target of rapamycin kinase; JAK: Janus kinase; STAT3: Signal transducer and activator of transcription 3; Smad3: Mothers against decapentaplegic homolog 3; NS5A: Non-structural protein 5A; NF-kB: Nuclear factor-kappa B; ROS: Reactive oxygen species; RIG1: Retinoic acid-inducible gene 1; ERK: Extracellular signal-regulated kinases; NANOG: Nanog homeobox; ATM: Ataxia telangiectasia mutated; RB: Retinoblastoma; ER: Endoplasmic reticulum; DNMT1: DNA methyltransferase 1; TERT: Telomerase reverse transcriptase; DLC: Deleted in liver cancer; CK1/2: Casein kinase 1/2; GSK: Glycogen synthase kinase.

phase to S phase. NS2 protein is involved in HCC carcinogenesis through tumor suppressor inactivation of p53 and consequent transcriptional activation[126]. The NS3 protein is involved in tumor cell transformation, by loss of contact inhibition and growth anchorage, evasion of innate immunity, interaction with mitochondrial signaling protein, tumor suppressors inactivation (p53 and ataxia telangiectasia mutated kinase or ATM) and alteration of immunoregulatory pathways such as TLR3, retinoic acid-inducible gene I (RIG-I) and NF-κB pathways[127].

Similarly, the NS5A protein plays a role in cell cycle dysregulation through signaling pathways, immune escape, impairment of cell apoptosis and ROS production. NS5A is involved in proliferative pathways by the inactivation of p53, blockade of IFN signaling through JAK-STAT cascade and inhibition of host protein synthesis through protein kinase R (PKR)[126]. In addition, NS5A protein, like HCV core protein, can inhibit TGF-β signaling through interaction with T-box brain transcription factor 1 or direct binding to TGF-β receptor 1 and through prevention of translocation of Smad proteins[128]. On the other hand, NS5A interacts with the PI3K p85 regulatory subunit that regulates apoptotic activity of PI3K and upregulates cell survival cascade, activating Akt and Twist family BHLH transcription factor 2 pathways favoring EMT, and interacts with RAS oncogene to enhance tumor cell invasiveness[129]. NS5A stimulates TLR4 activation and its signaling through homeobox protein NANOG and consequent Twist 1 activation leading to hepatocytes dedifferentiation[126].

NS5A affects apoptosis trough downregulatory effect on TNFα-mediated apoptosis. It deactivates caspase-3 and inhibits proteolytic cleavage of death substrates known as polyADP-ribose polymerases, impairing PD cascade[126]. Moreover, HCV seems to enhance ROS formation and aberrant cell-cycle arrest due to DNA damage through dysregulation of ER-mediated calcium uptake and induction of glycogen synthase kinase 3β phosphorylation with consequent beta-catenin-dependent upregulation of c-Myc *via* NS5A[122]. Non-structural viral proteins, together with HCV core protein, play a key role in HCV mediated oncogenesis. Their multifaceted interaction with basic hepatocytes signaling pathways favors deep dysregulation of cells homeostasis and accumulation of DNA damage until malignant transformation.

Viral effect on angiogenesis

A higher vascular density has been reported in nodules of HCV-related HCC in relation to HCC nodules in patients affected by other liver diseases. Studies show upregulation of VEGF expression in patients with HCV-related HCC compared to the control group. HCV core protein can increase cellular VEGF expression through HIF-1α transcription factors and AP-1. Similarly, core protein can induce overexpression and stabilization of HIF-1α and ANG2 which upregulate VEGF expression[130]. Moreover, HCV core protein binds androgen receptor (AR), impairing transcriptional activity by activating several signaling pathways such as PI3K/Akt and JAK/STAT3. Since AR targets the VEGF gene in the liver tissue, HCV core protein upregulates VEGF expression through enhanced activity of the AR pathway[123].

Other mechanisms of HCV core-protein promoted angiogenesis and rely on upregulation of COX-2 and metalloproteinases 2 and 9 (MMP-2 and MMP-9)[126]. CCL20/C-C chemokine receptor type (CCR) 6 axis is directly involved in stimulating angiogenesis in the microenvironment of HCV-related HCC. *In vitro* experiments pointed out CCL20 as a direct promotor of angiogenesis inducing endothelial cells invasion and sprouting and migration of CCR6-positive leukocytes. A study demonstrates that HCV-induced CCL20 protein expression and secretion in hepatoma cells can be diminished and even abolished by means of antiviral treatment proving CCL20 expression to be dependent on HCV replication[131].

Role of epigenetic modifications

Epigenetic modifications in patients' liver tissue can derive both from infected hepatocytes and from virus-induced inflammatory or fibrotic responses in the cells' microenvironment. HCV-induced histone modifications and fibrogenesis are interdependent during the course of liver disease; epigenetic changes orchestrate fibrogenesis through the activation of HSCs. Specific epigenetic modifications have been identified in patients' liver tissue and humanized mouse's liver tissue where no necrotic nor inflammatory response are present, therefore, it is probable that part of the changes observed can be a direct consequence of HCV-hepatocyte interaction.

HCV upregulates methyltransferase DNMT1 that hypomethylates tumor suppressor genes such as Cyclin Dependent Kinase Inhibitor 2A, GSTP1, RUNX family transcription factor 3, suppressor of cytokine signaling 1 and RASSF1A[126]. In a similar way, an upregulation of "suppressor of variegation, enhancer of Zeste, trithorax" and myeloid nervy deaf 1 domain-containing protein 3, also named SMYD3, leads to a specific hypermethylation of histone marks H3K4 and H4K5 in tumor suppressor genes, such as RASSF1A[126].

A recent study shows that chronic HCV infection induces changes in histone mark H3K27ac which are associated with HCC risk and seem to persist after HCV cure[132]. H3K27ac is involved in pathways related to TNF-α, inflammatory response, IL-2 and activator of transcription 5 signaling. Furthermore, lower levels of H3K27ac can alter pathways associated with metabolism and coagulative cascade, such as oxidative phosphorylation, impaired fatty acid regulation or adipogenesis. Several alterations in these pathways (*e.g.*, epigenetic alteration in TNF-α signaling, G2M-checkpoint, epithelial-mesenchymal transition, PI3K, Akt and mTOR) persist even after direct-acting antiviral agents (DAAs) therapy[132].

Recently, several studies outlined the role of miRNAs-mediated epigenetic alterations in HCV-related carcinogenetic processes. One study examines the expression profiles of miRNA in more than 50 HCV-related HCCs by quantitative real-time polymerase chain reaction. Five miRNAs are examined: MiR-122, miR-100, and miR-10a seem to be upregulated, while miR-198 and miR-145 are downregulated up to 5-fold in tumors than in normal liver tissue[133]. MiR-122 is highly expressed in the liver of HCV-infected individuals due to its essential role in the stability and replication of HCV RNA[134]. Another study develops an *in vitro* model of HCV infection in primary human hepatocytes to evaluate the role of miRNAs; miR-141, which targets the tumor-suppressor gene Deleted in Liver Cancer (DLC)-1, is upregulated in HCV genotypes 1a-, 1b-, and 2a-infected cells. The rise in miR-141 levels in HCV-infected cells correlates with an inhibitory effect on DLC-1 protein and a subsequent increase in HCC development risk[122].

Role of HCV genotypes

HCV genotype 1b is associated with at least a doubled risk of HCC compared to other HCV genotypes [135,136]. HCV genotype 3 is considered a major risk factor for hepatic carcinogenesis. A multicenter Asian cohort study shows a 4.3-fold in the risk of HCC development in patients with chronic HCV genotype 3 infection compared to other genotypes[137]. Another Asian study shows a 5-year occurrence rate of HCC of 34% in genotype 3 and of 17% in non-genotype 3 groups, respectively (P = 0.002); in a multivariate analysis, HCV genotype 3 infection is independently associated with a rise of HCC occurrence rates (HR = 3.54), even after adjustment for confounding factors[138]. A further study finds an approximately doubled risk of all-cause mortality and HCC in patients with HCV genotype 3 infection, related to individuals infected with other genotypes[139]. However, the exact role of HCV genotypes in hepatocarcinogenesis processes and in the worsening of liver disease still needs to be established.

ENVIRONMENTAL FACTORS

Role of chronic inflammation and FIB

Most of HCV-related HCCs occur in cirrhotic livers following decades of chronic inflammation underscoring the key role of the virus-induced inflammatory response in the hepatic carcinogenetic processes. Generally, the inflammatory response is beneficial to the host, but in HCV patients innate and adaptive immunity result ineffective. This cycle can be primed by HCV proteins but host immune response tends to self-maintenance.

HCV interferes with various defense mechanisms; TLR3 and RIG-I gene downstream pathogen-recognition signaling pathways are blocked by the HCV protease NS3/4A; HCV proteins NS5A and core proteins can block IFN signaling interfering with JAK–STAT pathway; HCV proteins E2 and NS5A inhibit PKR, an antiviral effector that impairs protein synthesis of infected cells; HCV core protein stimulates the release of cytokines that can lead to a direct decrease in plasmacytoid dendritic cells levels among HCV-infected patients[140,141].

The persistence of chronic inflammatory response leads to the release of free radicals such as ROS and nitric oxide (NO)[142]. NO contributes to viral persistence leading to antiapoptotic effects in hepatocytes and may induce viral mutations and promote suppression of Th1 cells[143]. Also, it directly influences liver cell survival by preventing apoptosis through the activation of the NF-κB pathway. ROS induce modifications in structure and function of cancer-related proteins and genes including those fundamental for cell-cycle control, apoptosis, and DNA repair[144]. There is evidence that HCV-mediated inflammation is responsible for the promotion of hepatic carcinogenesis through oxidative DNA damage[145].

In patients affected by HCC, Th1 dominance is progressively lost due to an increase of Th2 cells[146]. Some studies typify the microenvironment of HCC metastatic phenotype as composed by a Th2-like cytokine profile, consisting in higher levels of IL-4, IL-8, IL-10 and IL-5, and lower levels of Th1-like cytokines as IL-1α, IL-1β, IL-2, IL-12p35, IL-12p40, IL-15, TNF-α and IFN-γ[147]. Moreover, the peripheral blood and the tumor tissue of HCC patients show an increased number of Tregs (with a positive direct correlation with HCV RNA levels). IL-10 seems to be highly expressed in HCC patients and its presence correlates with disease progression[148].

In conclusion, inadequate immune response is a necessary factor for hepatic cells transformation but not a sufficient one. It builds a favorable microenvironment in which all factors (etiology, genetic, epigenetic, humoral and cellular inflammation, chronic liver injury) contribute to the development of FIB and liver cells proliferation. These oncogenic factors promote DNA abnormalities that ultimately transform the hepatocytes into malignant cells.

Role of the gut microbiota

HCV-related cirrhosis is characterized by a disruption of the gut microbiota composition leading to an increased intestinal permeability and bacterial translocation. Compared to healthy individuals, bacterial alpha diversity seems to be lower in patients affected by chronic HCV infection with a reduction in bacteria of the order *Clostridiales* and an expansion in *Streptococcus species*. Gut dysbiosis begins to occur in the very early stages of the infection with the transient increase in *Bacteroidaceae* and *Enterobacteriaceae*. A decrease in the abundance of *Bifidobacteriaceae* and *Lactobacillaceae* with an increase of *Bacteroidaceae* and *Enterobacteriaceae* has been reported in the gut microbiota of patients with HCV-related HCC[149, 150]. Predicted metagenomics of microbial communities show an upregulation of urease gene, mainly encoded by *Streptococcus viridans* during chronic hepatic disease course, consistent with a significantly higher faecal pH than in healthy individuals[151]. A small study shows an increase in *Streptococcus salivarius* (*S. salivarius*) in oral and gut microbiota of patients with HCV-related HCC suggesting a possible role in oncogenesis. It has been noticed that *S. salivarius* impairs and deregulates the innate immune response of epithelial cells with a possible contribution in HCC progression[152].

DAAs treatment has proven to modulate the composition of the gut microbiota contributing to a decrease in inflammatory markers and liver stiffness but without effect on the gut barrier and its permeability. The eradication of the infection cannot resolve the intestinal dysfunction caused by liver cirrhosis but can improve the pre-existing dysbiosis[153]. Therefore, alterations of the gut microbiota may be focused as a predisposing factor for liver disease progression but further studies are necessary to establish its possible pathogenetic role in HCC development.

Role of host genetic factors

The genetic background of the host has a growing role in hepatic carcinogenesis. A systematic review found 16 genes associated with HCV-related HCC[154]. The polymorphisms identified in patients with HCV-related HCC involve genes encoding for: TGF-β1, TNF-α, mitochondrial aldehyde dehydrogenase enzyme 2, catalase, EGF, glutathione S-transferase mu 1 protein, glutathione S-transferase theta 1, HLA-Bw4, HLA-B1814 and HLA-DR11, HSPA1B, leptin receptor, IL-1b, a regulator of the p53 tumor suppressor named mouse double minute 2 homolog, UDP glucuronosyltransferase 1 family-polypeptide A7, manganese-dependent superoxide dismutase mitochondrial protein, IFN lambda 3 and lambda 4 cytokine, patatin-like phospholipase domain–containing protein 3 (PNPLA3) and MHC class I

polypeptide-related sequence A (MICA/HCP5)[154-156]. Nowadays, the genetic risk score, designed using the combination of four high risk variants in the PNPLA3, TM6SF2, MBOAT7, and Glucokinase Regulator GCKR genes, estimates the inherited predisposition to accumulate liver fat (Genetic Risk Score) and is reported as an independent risk factor for *de novo* occurrence of HCC after DAAs treatment [157].

HCC surveillance in patients with chronic hepatitis C

As already discussed, HCC surveillance in HCV-infected patients must include patients affected by cirrhosis of all causes and patients with chronic HCV infection with advanced liver FIB (Table 7). The AASLD and EASL practice guidelines recommend HCC screening and surveillance in patients with cirrhosis or with stage 3 FIB[73,75,158]. JSH still differentiates ''super-high-risk patients'' (hepatitis C cirrhosis) in whom surveillance is recommended every 3-4 mo and ''high-risk patients'', in whom surveillance is recommended every 6 mo[124].

The impact of chronic hepatitis C treatment on HCC occurrence

The utmost importance of viral clearance in the reduction of HCC occurrence among chronically HCV-infected patients has been largely established. Since the first studies on IFN-based therapy, HCC incidence shows a significant difference between patients with sustained virological response (SVR) and non-SVR patients (5.1% and 21.8%)[159]. A large meta-analysis including 31528 HCV-infected patients shows that SVR is a key factor in reducing the incidence of HCC (1.5% in SVR patients *vs* 6.2% in non-SVR patients at 3-8 years of follow up)[139,160].

PEG-IFNα

IFN-α was approved to treat HCV infection in the 1980s but its efficacy was limited (SVR rates 54%-56%). A meta-analysis of 8 long-term studies on 2649 patients with chronic hepatitis C demonstrates that HCC occurrence is significantly reduced in patients with SVR after IFN-based therapy compared to non-responder (4.2% *vs* 17.8%, HR = 0.23)[161]. The majority of the studies report that older ages, male gender, advanced liver FIB, fatty liver disease and a high post-treatment serum AFP level are the main risk factors for HCC development even after SVR[162].

DAAs

The perspective of HCV therapy has changed over the years after the introduction of DAAs therapy, which has increased the SVR rate up to 90%, with excellent tolerance compared to IFN-based regimens. Even if the therapies demonstrated high efficacy, two retrospective studies, published in 2016 and conducted respectively in Spain and Italy, supposed the existence of a higher risk of HCC occurrence and recurrence following DAAs treatment course, raising the debate about the safety profile of DAAs and, in particular, the relation between SVR with and HCC occurrence and recurrence[163]. The Spanish study registered a high recurrence rate of HCC (27.6%) among 58 patients with previous history of HCC who received DAAs[164]. In the Italian study, HCC was detected in 7.6% of patients following DAAs treatment, 28.81% of patients with and 3.16% of patients without previous HCC[165]. Furthermore, an unpredictable increase in the amount of advanced stage HCC was noticed by the same authors.

Later debates arose owing some possible biases in these studies (the small size of the cohorts, lack of untreated controls and short follow-up periods). Subsequently, further data from large real-world retrospective cohort studies with extended follow-up periods after DAAs treatment have been released. On the heels of the studies listed so far, in 2017 another meta-analysis conducted by Waziry *et al*[166] reported lack of a statistically significant increase in HCC recurrence or occurrences in either patients having undergone DAAs or IFN treatment after achieving SVR. Subsequently in 2017, a systematic review from Ioannou *et al*[167] including 62354 patients treated with DAAs, IFN or a combination of both showed no significant difference in HCC occurrence or recurrence between the three treatment regimens. In fact, SVR was associated with a 71% decrease in HCC occurrence risk with no particular differences between DAAs and IFNs. Nahon *et al*[168] enrolled 1270 HCV-infected patients with compensated cirrhosis in France, demonstrating that there wasn't any statistically significant increase in the risk of HCC occurrence following DAAs treatment (HR = 0.89), after adjustment for age, diabetes and reduced liver function. In 2018, another American study from Singer *et al*[169] showed that DAAs therapy was associated with a lower risk of HCC as compared to untreated patients (HR = 0.84) and to IFN based treatment (HR = 0.69). During the same year, an Italian study found that SVR after DAAs treatment led to a lower incidence rate of HCC in patients with HCV-related cirrhosis over a follow up of 14 mo[170]. At the end of 2018, another Italian review from Guarino *et al*[171] outlined that the alarmist data on HCC recurrence after DAAs treatment and more aggressive pattern of disease have not been confirmed by subsequent studies.

Recently, a French prospective cohort study on 9895 HCV-infected patients with a long term follow-up (mean 33.4 mo) reported that after adjusting for several variables (including non-modifiable risk factor as age, sex, geographical origin, HCV genotype and modifiable ones as FIB score, alcohol consumption, diabetes, arterial hypertension, and model for end-stage liver disease score in patients with cirrhosis), DAAs exposure decreased all-cause mortality (adjusted HR = 0.48) and the risk of HCC

Table 7 Hepatocellular carcinoma surveillance in hepatitis C virus infected patients

HCC surveillance in HCV infected patients		
Western medical societies		
EASL, 2018	High-risk patients: HCV-related cirrhosis. Chronic hepatitis C and stage	Screening with US examination with or without AFP every 6 mo for high-risk patients (incidence > 1.5%/yr)
AASLD, 2018	High-risk patients: HCV-related cirrhosis. Chronic hepatitis C and stage 3 fibrosis	Screening with US examination with or without AFP every 6 mo for high-risk group (incidence > 1.5%/yr)
Eastern medical societies		
JSH, 2017-2021	Extremely-high-risk patients: All patients with HCV-related cirrhosis. High-risk patients: Patients with chronic hepatitis C	Screening with US and tumor marker measurements (AFP, PIVKA-II and AFP-L3) every 3-4 mo in the super-high-risk population. A 6-12 mo dynamic CT scan, dynamic MRI should be performed or Sonazoid CEUS. Screening every 6 mo in high-risk populations
APASL, 2017	High-risk patients: All patients with HCV-related cirrhosis. SVR patients with chronic hepatitis C with advanced liver fibrosis, independently of the histologic response to therapy. SVR patients with chronic hepatitis C with any histologic stage of HCV with comorbidities, such as alcohol abuse and DM	Surveillance by US and AFP should be performed every 6 mo and preferably every 3-4 mo in cirrhotic patients and those at high risk of HCC
KLCSG, 2014-2018	High-risk patients: All patients with HCV-related cirrhosis. Patients with chronic hepatitis C and advanced fibrosis	Screening with US examination with or without AFP every 6 mo. If liver US cannot be performed properly, liver dynamic CT or dynamic contrast-enhanced MRI can be performed as an alternative

HCC: Hepatocellular carcinoma; HCV: Hepatitis C virus; US: Ultrasound; AFP: Alpha-fetoprotein; SVR: Sustained virological response; PIVKA-II: Protein induced vitamin K absence or antagonist-II; CEUS: Contrast enhanced ultrasound; CT: Computed tomography; MRI: Magnetic resonance imaging; EASL: European Association for the Study of the Liver; AASLD: American Association for the Study of Liver Diseases; JSH: Japan Society of Hepatology; APASL: The Asian Pacific Association for the Study of the Liver; KLCSG: Korean Liver Cancer Study Group.

development (adjusted HR = 0.66)[172]. Another large American retrospective cohort study concluded that DAAs treatment and SVR resulted in a significant benefit in overall mortality[173].

Watanabe *et al*[174] recognized FIB-4 index ≥ 4.0 and albumin ≤ 3.8 g/dL before DAAs therapy and a FIB-4 index ≥ 4.0 and AFP ≥ 6.0 after the end of DAAs therapy as independent predictors for HCC occurrence. Another study confirmed a linkage between the risk of HCC and persistently high FIB-4/[aminotransferase/platelet ratio index (APRI)], either with or without cirrhosis. HCC development risk shows a significative reduction in cirrhotic patients who showed a decrease of FIB-4/APRI scores after DAAs therapy[175].

In 2020, an Egyptian study designed with three large independent cohorts, enrolled 4400 patients with chronic hepatitis C and advanced FIB, and identified predictors of HCC development after DAAs treatment developing and validating a simple risk score (GES risk score). GES identifies three groups of patients with a different risk of HCC occurrence along the follow-up by means of simple and readily available predictors: Age, male gender, low albumin, high AFP levels and presence of cirrhosis at baseline. The cumulative incidence of HCC for GES low-risk group at 2 years was 1.2% in the derivation cohort and 0.22% in validation cohorts, while GES high-risk group showed a 6 to 30 folds higher risk, with a cumulative incidence of 7.1% and 6.1% in the derivation and validation cohorts, respectively. The study enrolled mostly genotype 4-infected patients thus further studies are needed to assess the utility of this score in clinical practice[176].

These data underline that the rise in HCC incidence suggested by the first studies in patients with HCV-related cirrhosis treated with DAAs who achieve SVR compared to those treated with IFN-based therapy may be due to confounders as patients features (age, diabetes, reduced liver function) and/or lower screening frequency. Therefore, DAAs treatment should not be withheld for the potential risk of HCC occurrence or recurrence. According to long-term post-SVR observational studies, HCC development risk remains high in patients with cirrhosis who eliminate HCV, although it is significantly reduced compared to untreated patients or patients not achieving SVR (10-year cumulative incidence rate 21.8% *vs* 5.1%)[139].

CLINICAL PRESENTATION OF HBV AND HCV-RELATED HCC: A COMPARISON

Several studies assessed the difference in clinical manifestation in HCC patients between different etiologies. Different HCC surveillance strategies need to be set according to the viral etiologies in relation to HCC age of presentation and clinical features. Two Italian studies noticed that HBV-infected patients are younger at HCC diagnosis, with a higher staging, increased probability of vascular invasion

and a worse prognosis[177]. An Asian study showed a peak incidence of HBV-related HCC in the 50-59 years old group whereas the peak annual incidence in HCV patients is over 70 years. In an HBV high endemic area, the outcome analysis of the study showed a reduced survival in HBV-related HCC compared to HCV-related HCC (1.34 years *vs* 2.17 years, adjusted for confounders). There was also a slight increase in frequency of large tumors (> 5 cm) and portal vein invasion at diagnosis in HBV-related HCC group, while multiple tumors occurred more frequently in HCV patients[178]. A cross sectional observational study from Pakistan, an HCV high endemic country, confirmed that HBV-related HCC patients were younger at presentation, but HCV-related HCC was larger, with higher AFP serum levels and more frequent vascular invasion at diagnosis[179]. Similar results were obtained in a large cohort including Asian and European patients[180-183]. These differences can be explained by the high prevalence of perinatal infections in high endemic areas and to the specific oncogenic potential of HBV. However, there was no difference in post-operative or post-treatment outcomes in the studies listed above between HBV and HCV-related HCC groups.

CONCLUSION

Chronic HBV- and HCV-related hepatitis are still pandemic, with an increased spread in low and middle-income continents, such as Asia and Africa. HBV- and HCV-infected patients have a higher oncogenic risk compared to other liver disease aetiology, mostly because of the interactions between viral proteome and transcriptome and host cells molecular pathways involving inflammation and cells replication. New data about gut-liver axis and systemic inflammation are pointing out their key role as a cofactor in hepatocarcinogenesis. Therefore, viral hepatitis B and C still represent a major public health problem worldwide although health organizations have made substantial efforts to contain their spread in recent years through the global HBV vaccination campaign and the widespread accessibility of DAAs for HCV. The broad availability of generic antivirals would allow low- and middle-income countries to strengthen their contribution to the HCV eradication program. In the meantime, one of the most important challenges is to adapt the timing of HCC surveillance in these patients with the aim of ensuring early diagnosis and rapid management to improve prognosis. In the era of coronavirus disease 2019, well-organized and accessible HCC surveillance becomes even more important due to the limited healthcare resources allocated to secondary prevention and the reluctance of patients to access healthcare facilities. In the future, new biomarkers and risk stratification systems may help clinicians to identify patients for closer follow-up leading to a more personalized approach to HCC surveillance.

FOOTNOTES

Author contributions: Stella L, Santopaolo F, Gasbarrini A, Pompili M, Ponziani FR were responsible for the manuscript concept and design, revision of data, interpretation of data, critical revision of the manuscript for important intellectual content; Stella L, Santopaolo F, Ponziani FR drafted the manuscript; and all authors were involved in the final approval of the final version of the manuscript.

Conflict-of-interest statement: The authors declare no conflict of interest.

Open-Access: This article is an open-access article that was selected by an in-house editor and fully peer-reviewed by external reviewers. It is distributed in accordance with the Creative Commons Attribution NonCommercial (CC BY-NC 4.0) license, which permits others to distribute, remix, adapt, build upon this work non-commercially, and license their derivative works on different terms, provided the original work is properly cited and the use is non-commercial. See: https://creativecommons.org/Licenses/by-nc/4.0/

Country/Territory of origin: Italy

ORCID number: Leonardo Stella 0000-0002-3431-0803; Francesco Santopaolo 0000-0002-1773-1171; Antonio Gasbarrini 0000-0003-4863-6924; Maurizio Pompili 0000-0001-6699-7980; Francesca Romana Ponziani 0000-0002-5924-6238.

S-Editor: Wang JJ
L-Editor: Filipodia
P-Editor: Wang JJ

REFERENCES

1 **Llovet JM**, Kelley RK, Villanueva A, Singal AG, Pikarsky E, Roayaie S, Lencioni R, Koike K, Zucman-Rossi J, Finn RS. Hepatocellular carcinoma. *Nat Rev Dis Primers* 2021; **7**: 6 [PMID: 33479224 DOI: 10.1038/s41572-020-00240-3]
2 **El-Serag HB**. Epidemiology of viral hepatitis and hepatocellular carcinoma. *Gastroenterology* 2012; **142**: 1264-1273.e1

[PMID: 22537432 DOI: 10.1053/j.gastro.2011.12.061]
3 **Anthony PP**. Hepatocellular carcinoma: an overview. *Histopathology* 2001; **39**: 109-118 [PMID: 11493326 DOI: 10.1046/j.1365-2559.2001.01188.x]
4 **Ferlay J**, Soerjomataram I, Dikshit R, Eser S, Mathers C, Rebelo M, Parkin DM, Forman D, Bray F. Cancer incidence and mortality worldwide: sources, methods and major patterns in GLOBOCAN 2012. *Int J Cancer* 2015; **136**: E359-E386 [PMID: 25220842 DOI: 10.1002/ijc.29210]
5 **Romeo R**, Petruzziello A, Pecheur EI, Facchetti F, Perbellini R, Galmozzi E, Khan NU, Di Capua L, Sabatino R, Botti G, Loquercio G. Hepatitis delta virus and hepatocellular carcinoma: an update. *Epidemiol Infect* 2018; **146**: 1612-1618 [PMID: 29991359 DOI: 10.1017/S0950268818001942]
6 **Gomaa AI**, Khan SA, Toledano MB, Waked I, Taylor-Robinson SD. Hepatocellular carcinoma: epidemiology, risk factors and pathogenesis. *World J Gastroenterol* 2008; **14**: 4300-4308 [PMID: 18666317 DOI: 10.3748/wjg.14.4300]
7 **Trépo C**, Chan HL, Lok A. Hepatitis B virus infection. *Lancet* 2014; **384**: 2053-2063 [PMID: 24954675 DOI: 10.1016/S0140-6736(14)60220-8]
8 **Chang MS**, Nguyen MH. Epidemiology of hepatitis B and the role of vaccination. *Best Pract Res Clin Gastroenterol* 2017; **31**: 239-247 [PMID: 28774405 DOI: 10.1016/j.bpg.2017.05.008]
9 **Blachier M**, Leleu H, Peck-Radosavljevic M, Valla DC, Roudot-Thoraval F. The burden of liver disease in Europe: a review of available epidemiological data. *J Hepatol* 2013; **58**: 593-608 [PMID: 23419824 DOI: 10.1016/j.jhep.2012.12.005]
10 **Lozano R**, Naghavi M, Foreman K, Lim S, Shibuya K, Aboyans V, Abraham J, Adair T, Aggarwal R, Ahn SY, Alvarado M, Anderson HR, Anderson LM, Andrews KG, Atkinson C, Baddour LM, Barker-Collo S, Bartels DH, Bell ML, Benjamin EJ, Bennett D, Bhalla K, Bikbov B, Bin Abdulhak A, Birbeck G, Blyth F, Bolliger I, Boufous S, Bucello C, Burch M, Burney P, Carapetis J, Chen H, Chou D, Chugh SS, Coffeng LE, Colan SD, Colquhoun S, Colson KE, Condon J, Connor MD, Cooper LT, Corriere M, Cortinovis M, de Vaccaro KC, Couser W, Cowie BC, Criqui MH, Cross M, Dabhadkar KC, Dahodwala N, De Leo D, Degenhardt L, Delossantos A, Denenberg J, Des Jarlais DC, Dharmaratne SD, Dorsey ER, Driscoll T, Duber H, Ebel B, Erwin PJ, Espindola P, Ezzati M, Feigin V, Flaxman AD, Forouzanfar MH, Fowkes FG, Franklin R, Fransen M, Freeman MK, Gabriel SE, Gakidou E, Gaspari F, Gillum RF, Gonzalez-Medina D, Halasa YA, Haring D, Harrison JE, Havmoeller R, Hay RJ, Hoen B, Hotez PJ, Hoy D, Jacobsen KH, James SL, Jasrasaria R, Jayaraman S, Johns N, Karthikeyan G, Kassebaum N, Keren A, Khoo JP, Knowlton LM, Kobusingye O, Koranteng A, Krishnamurthi R, Lipnick M, Lipshultz SE, Ohno SL, Mabweijano J, MacIntyre MF, Mallinger L, March L, Marks GB, Marks R, Matsumori A, Matzopoulos R, Mayosi BM, McAnulty JH, McDermott MM, McGrath J, Mensah GA, Merriman TR, Michaud C, Miller M, Miller TR, Mock C, Mocumbi AO, Mokdad AA, Moran A, Mulholland K, Nair MN, Naldi L, Narayan KM, Nasseri K, Norman P, O'Donnell M, Omer SB, Ortblad K, Osborne R, Ozgediz D, Pahari B, Pandian JD, Rivero AP, Padilla RP, Perez-Ruiz F, Perico N, Phillips D, Pierce K, Pope CA 3rd, Porrini E, Pourmalek F, Raju M, Ranganathan D, Rehm JT, Rein DB, Remuzzi G, Rivara FP, Roberts T, De León FR, Rosenfeld LC, Rushton L, Sacco RL, Salomon JA, Sampson U, Sanman E, Schwebel DC, Segui-Gomez M, Shepard DS, Singh D, Singleton J, Sliwa K, Smith E, Steer A, Taylor JA, Thomas B, Tleyjeh IM, Towbin JA, Truelsen T, Undurraga EA, Venketasubramanian N, Vijayakumar L, Vos T, Wagner GR, Wang M, Wang W, Watt K, Weinstock MA, Weintraub R, Wilkinson JD, Woolf AD, Wulf S, Yeh PH, Yip P, Zabetian A, Zheng ZJ, Lopez AD, Murray CJ, AlMazroa MA, Memish ZA. Global and regional mortality from 235 causes of death for 20 age groups in 1990 and 2010: a systematic analysis for the Global Burden of Disease Study 2010. *Lancet* 2012; **380**: 2095-2128 [PMID: 23245604 DOI: 10.1016/S0140-6736(12)61728-0]
11 **Fattovich G**, Bortolotti F, Donato F. Natural history of chronic hepatitis B: special emphasis on disease progression and prognostic factors. *J Hepatol* 2008; **48**: 335-352 [PMID: 18096267 DOI: 10.1016/j.jhep.2007.11.011]
12 **Zamor PJ**, deLemos AS, Russo MW. Viral hepatitis and hepatocellular carcinoma: etiology and management. *J Gastrointest Oncol* 2017; **8**: 229-242 [PMID: 28480063 DOI: 10.21037/jgo.2017.03.14]
13 **Tarocchi M**, Polvani S, Marroncini G, Galli A. Molecular mechanism of hepatitis B virus-induced hepatocarcinogenesis. *World J Gastroenterol* 2014; **20**: 11630-11640 [PMID: 25206269 DOI: 10.3748/wjg.v20.i33.11630]
14 **Lin CL**, Kao JH. Hepatitis B virus genotypes and variants. *Cold Spring Harb Perspect Med* 2015; **5**: a021436 [PMID: 25934462 DOI: 10.1101/cshperspect.a021436]
15 **Chen CJ**, Iloeje UH, Yang HI. Long-term outcomes in hepatitis B: the REVEAL-HBV study. *Clin Liver Dis* 2007; **11**: 797-816, viii [PMID: 17981229 DOI: 10.1016/j.cld.2007.08.005]
16 **Chen JD**, Yang HI, Iloeje UH, You SL, Lu SN, Wang LY, Su J, Sun CA, Liaw YF, Chen CJ; Risk Evaluation of Viral Load Elevation and Associated Liver Disease/Cancer in HBV (REVEAL-HBV) Study Group. Carriers of inactive hepatitis B virus are still at risk for hepatocellular carcinoma and liver-related death. *Gastroenterology* 2010; **138**: 1747-1754 [PMID: 20114048 DOI: 10.1053/j.gastro.2010.01.042]
17 **Nassal M**. HBV cccDNA: viral persistence reservoir and key obstacle for a cure of chronic hepatitis B. *Gut* 2015; **64**: 1972-1984 [PMID: 26048673 DOI: 10.1136/gutjnl-2015-309809]
18 **Galli A**, Svegliati-Baroni G, Ceni E, Milani S, Ridolfi F, Salzano R, Tarocchi M, Grappone C, Pellegrini G, Benedetti A, Surrenti C, Casini A. Oxidative stress stimulates proliferation and invasiveness of hepatic stellate cells *via* a MMP2-mediated mechanism. *Hepatology* 2005; **41**: 1074-1084 [PMID: 15841469 DOI: 10.1002/hep.20683]
19 **Wang Y**, Jiang L, Ji X, Yang B, Zhang Y, Fu XD. Hepatitis B viral RNA directly mediates down-regulation of the tumor suppressor microRNA miR-15a/miR-16-1 in hepatocytes. *J Biol Chem* 2013; **288**: 18484-18493 [PMID: 23649629 DOI: 10.1074/jbc.M113.458158]
20 **Lau CC**, Sun T, Ching AK, He M, Li JW, Wong AM, Co NN, Chan AW, Li PS, Lung RW, Tong JH, Lai PB, Chan HL, To KF, Chan TF, Wong N. Viral-human chimeric transcript predisposes risk to liver cancer development and progression. *Cancer Cell* 2014; **25**: 335-349 [PMID: 24582836 DOI: 10.1016/j.ccr.2014.01.030]
21 **Guerrieri F**, Belloni L, Pediconi N, Levrero M. Molecular mechanisms of HBV-associated hepatocarcinogenesis. *Semin Liver Dis* 2013; **33**: 147-156 [PMID: 23749671 DOI: 10.1055/s-0033-1345721]
22 **Ringelhan M**, O'Connor T, Protzer U, Heikenwalder M. The direct and indirect roles of HBV in liver cancer: prospective markers for HCC screening and potential therapeutic targets. *J Pathol* 2015; **235**: 355-367 [PMID: 25196558 DOI:

10.1002/path.4434]
23 **Mason WS**, Gill US, Litwin S, Zhou Y, Peri S, Pop O, Hong ML, Naik S, Quaglia A, Bertoletti A, Kennedy PT. HBV DNA Integration and Clonal Hepatocyte Expansion in Chronic Hepatitis B Patients Considered Immune Tolerant. *Gastroenterology* 2016; **151**: 986-998.e4 [PMID: 27453547 DOI: 10.1053/j.gastro.2016.07.012]
24 **Li R**, Hao Y, Wang Q, Meng Y, Wu K, Liu C, Xu L, Liu Z, Zhao L. ECHS1, an interacting protein of LASP1, induces sphingolipid-metabolism imbalance to promote colorectal cancer progression by regulating ceramide glycosylation. *Cell Death Dis* 2021; **12**: 911 [PMID: 34615856 DOI: 10.1038/s41419-021-04213-6]
25 **Yang HI**, Lu SN, Liaw YF, You SL, Sun CA, Wang LY, Hsiao CK, Chen PJ, Chen DS, Chen CJ; Taiwan Community-Based Cancer Screening Project Group. Hepatitis B e antigen and the risk of hepatocellular carcinoma. *N Engl J Med* 2002; **347**: 168-174 [PMID: 12124405 DOI: 10.1056/NEJMoa013215]
26 **Samal J**, Kandpal M, Vivekanandan P. HBeAg-induced miR-106b promotes cell growth by targeting the retinoblastoma gene. *Sci Rep* 2017; **7**: 14371 [PMID: 29085029 DOI: 10.1038/s41598-017-14652-x]
27 **Pollicino T**, Cacciola I, Saffioti F, Raimondo G. Hepatitis B virus PreS/S gene variants: pathobiology and clinical implications. *J Hepatol* 2014; **61**: 408-417 [PMID: 24801416 DOI: 10.1016/j.jhep.2014.04.041]
28 **Mani SKK**, Andrisani O. Hepatitis B Virus-Associated Hepatocellular Carcinoma and Hepatic Cancer Stem Cells. *Genes (Basel)* 2018; **9** [PMID: 29498629 DOI: 10.3390/genes9030137]
29 **Wang LH**, Huang W, Lai MD, Su IJ. Aberrant cyclin A expression and centrosome overduplication induced by hepatitis B virus pre-S2 mutants and its implication in hepatocarcinogenesis. *Carcinogenesis* 2012; **33**: 466-472 [PMID: 22159224 DOI: 10.1093/carcin/bgr296]
30 **Hsieh YH**, Su IJ, Yen CJ, Tsai TF, Tsai HW, Tsai HN, Huang YJ, Chen YY, Ai YL, Kao LY, Hsieh WC, Wu HC, Huang W. Histone deacetylase inhibitor suberoylanilide hydroxamic acid suppresses the pro-oncogenic effects induced by hepatitis B virus pre-S2 mutant oncoprotein and represents a potential chemopreventive agent in high-risk chronic HBV patients. *Carcinogenesis* 2013; **34**: 475-485 [PMID: 23172669 DOI: 10.1093/carcin/bgs365]
31 **Tropberger P**, Mercier A, Robinson M, Zhong W, Ganem DE, Holdorf M. Mapping of histone modifications in episomal HBV cccDNA uncovers an unusual chromatin organization amenable to epigenetic manipulation. *Proc Natl Acad Sci U S A* 2015; **112**: E5715-E5724 [PMID: 26438841 DOI: 10.1073/pnas.1518090112]
32 **Liu S**, Koh SS, Lee CG. Hepatitis B Virus X Protein and Hepatocarcinogenesis. *Int J Mol Sci* 2016; **17** [PMID: 27314335 DOI: 10.3390/ijms17060940]
33 **Knoll S**, Fürst K, Thomas S, Villanueva Baselga S, Stoll A, Schaefer S, Pützer BM. Dissection of cell context-dependent interactions between HBx and p53 family members in regulation of apoptosis: a role for HBV-induced HCC. *Cell Cycle* 2011; **10**: 3554-3565 [PMID: 22030623 DOI: 10.4161/cc.10.20.17856]
34 **Rakotomalala L**, Studach L, Wang WH, Gregori G, Hullinger RL, Andrisani O. Hepatitis B virus X protein increases the Cdt1-to-geminin ratio inducing DNA re-replication and polyploidy. *J Biol Chem* 2008; **283**: 28729-28740 [PMID: 18693245 DOI: 10.1074/jbc.M802751200]
35 **Belloni L**, Pollicino T, De Nicola F, Guerrieri F, Raffa G, Fanciulli M, Raimondo G, Levrero M. Nuclear HBx binds the HBV minichromosome and modifies the epigenetic regulation of cccDNA function. *Proc Natl Acad Sci U S A* 2009; **106**: 19975-19979 [PMID: 19906987 DOI: 10.1073/pnas.0908365106]
36 **Forgues M**, Difilippantonio MJ, Linke SP, Ried T, Nagashima K, Feden J, Valerie K, Fukasawa K, Wang XW. Involvement of Crm1 in hepatitis B virus X protein-induced aberrant centriole replication and abnormal mitotic spindles. *Mol Cell Biol* 2003; **23**: 5282-5292 [PMID: 12861014 DOI: 10.1128/mcb.23.15.5282-5292.2003]
37 **Decorsière A**, Mueller H, van Breugel PC, Abdul F, Gerossier L, Beran RK, Livingston CM, Niu C, Fletcher SP, Hantz O, Strubin M. Hepatitis B virus X protein identifies the Smc5/6 complex as a host restriction factor. *Nature* 2016; **531**: 386-389 [PMID: 26983541 DOI: 10.1038/nature17170]
38 **Menolfi D**, Delamarre A, Lengronne A, Pasero P, Branzei D. Essential Roles of the Smc5/6 Complex in Replication through Natural Pausing Sites and Endogenous DNA Damage Tolerance. *Mol Cell* 2015; **60**: 835-846 [PMID: 26698660 DOI: 10.1016/j.molcel.2015.10.023]
39 **Hoter A**, Rizk S, Naim HY. Heat Shock Protein 60 in Hepatocellular Carcinoma: Insights and Perspectives. *Front Mol Biosci* 2020; **7**: 60 [PMID: 32351972 DOI: 10.3389/fmolb.2020.00060]
40 **Zhang Q**, Song G, Yao L, Liu Y, Liu M, Li S, Tang H. miR-3928v is induced by HBx *via* NF-κB/EGR1 and contributes to hepatocellular carcinoma malignancy by down-regulating VDAC3. *J Exp Clin Cancer Res* 2018; **37**: 14 [PMID: 29378599 DOI: 10.1186/s13046-018-0681-y]
41 **Lee JO**, Kwun HJ, Jung JK, Choi KH, Min DS, Jang KL. Hepatitis B virus X protein represses E-cadherin expression *via* activation of DNA methyltransferase 1. *Oncogene* 2005; **24**: 6617-6625 [PMID: 16007161 DOI: 10.1038/sj.onc.1208827]
42 **Qiu X**, Zhang L, Lu S, Song Y, Lao Y, Hu J, Fan H. Upregulation of DNMT1 mediated by HBx suppresses RASSF1A expression independent of DNA methylation. *Oncol Rep* 2014; **31**: 202-208 [PMID: 24247422 DOI: 10.3892/or.2013.2848]
43 **Freese K**, Seitz T, Dietrich P, Lee SML, Thasler WE, Bosserhoff A, Hellerbrand C. Histone Deacetylase Expressions in Hepatocellular Carcinoma and Functional Effects of Histone Deacetylase Inhibitors on Liver Cancer Cells In Vitro. *Cancers (Basel)* 2019; **11** [PMID: 31635225 DOI: 10.3390/cancers11101587]
44 **Martinez-Quetglas I**, Pinyol R, Dauch D, Torrecilla S, Tovar V, Moeini A, Alsinet C, Portela A, Rodriguez-Carunchio L, Solé M, Lujambio A, Villanueva A, Thung S, Esteller M, Zender L, Llovet JM. IGF2 Is Up-regulated by Epigenetic Mechanisms in Hepatocellular Carcinomas and Is an Actionable Oncogene Product in Experimental Models. *Gastroenterology* 2016; **151**: 1192-1205 [PMID: 27614046 DOI: 10.1053/j.gastro.2016.09.001]
45 **Calvisi DF**, Ladu S, Gorden A, Farina M, Lee JS, Conner EA, Schroeder I, Factor VM, Thorgeirsson SS. Mechanistic and prognostic significance of aberrant methylation in the molecular pathogenesis of human hepatocellular carcinoma. *J Clin Invest* 2007; **117**: 2713-2722 [PMID: 17717605 DOI: 10.1172/JCI31457]
46 **Sartorius K**, Makarova J, Sartorius B, An P, Winkler C, Chuturgoon A, Kramvis A. The Regulatory Role of MicroRNA in Hepatitis-B Virus-Associated Hepatocellular Carcinoma (HBV-HCC) Pathogenesis. *Cells* 2019; **8** [PMID: 31771261

DOI: 10.3390/cells8121504]
47 **Shi Y**, Wu YH, Wu W, Zhang WJ, Yang J, Chen Z. Association between occult hepatitis B infection and the risk of hepatocellular carcinoma: a meta-analysis. *Liver Int* 2012; **32**: 231-240 [PMID: 21745272 DOI: 10.1111/j.1478-3231.2011.02481.x]
48 **Wong DK**, Huang FY, Lai CL, Poon RT, Seto WK, Fung J, Hung IF, Yuen MF. Occult hepatitis B infection and HBV replicative activity in patients with cryptogenic cause of hepatocellular carcinoma. *Hepatology* 2011; **54**: 829-836 [PMID: 21809355 DOI: 10.1002/hep.24551]
49 **Papatheodoridis GV**, Manolakopoulos S, Touloumi G, Nikolopoulou G, Raptopoulou-Gigi M, Gogos C, Vafiadis-Zouboulis I, Karamanolis D, Chouta A, Ilias A, Drakoulis C, Mimidis K, Ketikoglou I, Manesis E, Mela M, Hatzis G, Dalekos GN; HepNet. Greece Study Group. Hepatocellular carcinoma risk in HBeAg-negative chronic hepatitis B patients with or without cirrhosis treated with entecavir: HepNet.Greece cohort. *J Viral Hepat* 2015; **22**: 120-127 [PMID: 25040685 DOI: 10.1111/jvh.12283]
50 **Yang HI**, Yeh SH, Chen PJ, Iloeje UH, Jen CL, Su J, Wang LY, Lu SN, You SL, Chen DS, Liaw YF, Chen CJ; REVEAL-HBV Study Group. Associations between hepatitis B virus genotype and mutants and the risk of hepatocellular carcinoma. *J Natl Cancer Inst* 2008; **100**: 1134-1143 [PMID: 18695135 DOI: 10.1093/jnci/djn243]
51 **Tseng TC**, Liu CJ, Yang HC, Su TH, Wang CC, Chen CL, Kuo SF, Liu CH, Chen PJ, Chen DS, Kao JH. High levels of hepatitis B surface antigen increase risk of hepatocellular carcinoma in patients with low HBV load. *Gastroenterology* 2012; **142**: 1140-1149.e3; quiz e13 [PMID: 22333950 DOI: 10.1053/j.gastro.2012.02.007]
52 **Chen BF**, Chen PJ, Jow GM, Sablon E, Liu CJ, Chen DS, Kao JH. High prevalence of mixed genotype infections in hepatitis B virus infected intravenous drug users. *J Med Virol* 2004; **74**: 536-542 [PMID: 15484267 DOI: 10.1002/jmv.20211]
53 **Ni YH**, Chang MH, Wang KJ, Hsu HY, Chen HL, Kao JH, Yeh SH, Jeng YM, Tsai KS, Chen DS. Clinical relevance of hepatitis B virus genotype in children with chronic infection and hepatocellular carcinoma. *Gastroenterology* 2004; **127**: 1733-1738 [PMID: 15578511 DOI: 10.1053/j.gastro.2004.09.048]
54 **Livingston SE**, Simonetti JP, McMahon BJ, Bulkow LR, Hurlburt KJ, Homan CE, Snowball MM, Cagle HH, Williams JL, Chulanov VP. Hepatitis B virus genotypes in Alaska Native people with hepatocellular carcinoma: preponderance of genotype F. *J Infect Dis* 2007; **195**: 5-11 [PMID: 17152003 DOI: 10.1086/509894]
55 **Orito E**, Sugauchi F, Tanaka Y, Ichida T, Sata M, Tanaka E, Okanoue T, Sakugawa H, Watanabe H, Miyakawa H, Nishiguchi S, Kumada H, Ueda R, Mizokami M. Differences of hepatocellular carcinoma patients with hepatitis B virus genotypes of Ba, Bj or C in Japan. *Intervirology* 2005; **48**: 239-245 [PMID: 15920348 DOI: 10.1159/000084601]
56 **Song C**, Lv J, Liu Y, Chen JG, Ge Z, Zhu J, Dai J, Du LB, Yu C, Guo Y, Bian Z, Yang L, Chen Y, Chen Z, Liu J, Jiang J, Zhu L, Zhai X, Jiang Y, Ma H, Jin G, Shen H, Li L, Hu Z; China Kadoorie Biobank Collaborative Group. Associations Between Hepatitis B Virus Infection and Risk of All Cancer Types. *JAMA Netw Open* 2019; **2**: e195718 [PMID: 31199446 DOI: 10.1001/jamanetworkopen.2019.5718]
57 **Yuen MF**, Wong DK, Fung J, Ip P, But D, Hung I, Lau K, Yuen JC, Lai CL. HBsAg Seroclearance in chronic hepatitis B in Asian patients: replicative level and risk of hepatocellular carcinoma. *Gastroenterology* 2008; **135**: 1192-1199 [PMID: 18722377 DOI: 10.1053/j.gastro.2008.07.008]
58 **Fan Y**, Mao R, Yang J. NF-κB and STAT3 signaling pathways collaboratively link inflammation to cancer. *Protein Cell* 2013; **4**: 176-185 [PMID: 23483479 DOI: 10.1007/s13238-013-2084-3]
59 **Chen Y**, Tian Z. HBV-Induced Immune Imbalance in the Development of HCC. *Front Immunol* 2019; **10**: 2048 [PMID: 31507621 DOI: 10.3389/fimmu.2019.02048]
60 **Fisicaro P**, Barili V, Rossi M, Montali I, Vecchi A, Acerbi G, Laccabue D, Zecca A, Penna A, Missale G, Ferrari C, Boni C. Pathogenetic Mechanisms of T Cell Dysfunction in Chronic HBV Infection and Related Therapeutic Approaches. *Front Immunol* 2020; **11**: 849 [PMID: 32477347 DOI: 10.3389/fimmu.2020.00849]
61 **Park JJ**, Wong DK, Wahed AS, Lee WM, Feld JJ, Terrault N, Khalili M, Sterling RK, Kowdley KV, Bzowej N, Lau DT, Kim WR, Smith C, Carithers RL, Torrey KW, Keith JW, Levine DL, Traum D, Ho S, Valiga ME, Johnson GS, Doo E, Lok AS, Chang KM; Hepatitis B Research Network. Hepatitis B Virus--Specific and Global T-Cell Dysfunction in Chronic Hepatitis B. *Gastroenterology* 2016; **150**: 684-695.e5 [PMID: 26684441 DOI: 10.1053/j.gastro.2015.11.050]
62 **Jia Y**, Zeng Z, Li Y, Li Z, Jin L, Zhang Z, Wang L, Wang FS. Impaired function of CD4+ T follicular helper (Tfh) cells associated with hepatocellular carcinoma progression. *PLoS One* 2015; **10**: e0117458 [PMID: 25689070 DOI: 10.1371/journal.pone.0117458]
63 **Xu D**, Han Q, Hou Z, Zhang C, Zhang J. miR-146a negatively regulates NK cell functions *via* STAT1 signaling. *Cell Mol Immunol* 2017; **14**: 712-720 [PMID: 26996068 DOI: 10.1038/cmi.2015.113]
64 **Li X**, Su Y, Hua X, Xie C, Liu J, Huang Y, Zhou L, Zhang M, Li X, Gao Z. Levels of hepatic Th17 cells and regulatory T cells upregulated by hepatic stellate cells in advanced HBV-related liver fibrosis. *J Transl Med* 2017; **15**: 75 [PMID: 28399886 DOI: 10.1186/s12967-017-1167-y]
65 **Ponziani FR**, Nicoletti A, Gasbarrini A, Pompili M. Diagnostic and therapeutic potential of the gut microbiota in patients with early hepatocellular carcinoma. *Ther Adv Med Oncol* 2019; **11**: 1758835919848184 [PMID: 31205505 DOI: 10.1177/1758835919848184]
66 **Ponziani FR**, Bhoori S, Castelli C, Putignani L, Rivoltini L, Del Chierico F, Sanguinetti M, Morelli D, Paroni Sterbini F, Petito V, Reddel S, Calvani R, Camisaschi C, Picca A, Tuccitto A, Gasbarrini A, Pompili M, Mazzaferro V. Hepatocellular Carcinoma Is Associated With Gut Microbiota Profile and Inflammation in Nonalcoholic Fatty Liver Disease. *Hepatology* 2019; **69**: 107-120 [PMID: 29665135 DOI: 10.1002/hep.30036]
67 **Yu LX**, Yan HX, Liu Q, Yang W, Wu HP, Dong W, Tang L, Lin Y, He YQ, Zou SS, Wang C, Zhang HL, Cao GW, Wu MC, Wang HY. Endotoxin accumulation prevents carcinogen-induced apoptosis and promotes liver tumorigenesis in rodents. *Hepatology* 2010; **52**: 1322-1333 [PMID: 20803560 DOI: 10.1002/hep.23845]
68 **Rattan P**, Minacapelli CD, Rustgi V. The Microbiome and Hepatocellular Carcinoma. *Liver Transpl* 2020; **26**: 1316-1327 [PMID: 32564483 DOI: 10.1002/lt.25828]
69 **Liu Q**, Li F, Zhuang Y, Xu J, Wang J, Mao X, Zhang Y, Liu X. Alteration in gut microbiota associated with hepatitis B

and non-hepatitis virus related hepatocellular carcinoma. *Gut Pathog* 2019; **11**: 1 [PMID: 30675188 DOI: 10.1186/s13099-018-0281-6]

70 **Gupta H**, Youn GS, Shin MJ, Suk KT. Role of Gut Microbiota in Hepatocarcinogenesis. *Microorganisms* 2019; **7** [PMID: 31060311 DOI: 10.3390/microorganisms7050121]

71 **Tang A**, Hallouch O, Chernyak V, Kamaya A, Sirlin CB. Epidemiology of hepatocellular carcinoma: target population for surveillance and diagnosis. *Abdom Radiol (NY)* 2018; **43**: 13-25 [PMID: 28647765 DOI: 10.1007/s00261-017-1209-1]

72 **Terrault NA**, Bzowej NH, Chang KM, Hwang JP, Jonas MM, Murad MH; American Association for the Study of Liver Diseases. AASLD guidelines for treatment of chronic hepatitis B. *Hepatology* 2016; **63**: 261-283 [PMID: 26566064 DOI: 10.1002/hep.28156]

73 **AASLD-IDSA HCV Guidance Panel**. Hepatitis C Guidance 2018 Update: AASLD-IDSA Recommendations for Testing, Managing, and Treating Hepatitis C Virus Infection. *Clin Infect Dis* 2018; **67**: 1477-1492 [PMID: 30215672 DOI: 10.1093/cid/ciy585]

74 **European Association for the Study of the Liver**. EASL 2017 Clinical Practice Guidelines on the management of hepatitis B virus infection. *J Hepatol* 2017; **67**: 370-398 [PMID: 28427875 DOI: 10.1016/j.jhep.2017.03.021]

75 **European Association for the Study of the Liver**. EASL Recommendations on Treatment of Hepatitis C 2018. *J Hepatol* 2018; **69**: 461-511 [PMID: 29650333 DOI: 10.1016/j.jhep.2018.03.026]

76 **Kudo M**, Kawamura Y, Hasegawa K, Tateishi R, Kariyama K, Shiina S, Toyoda H, Imai Y, Hiraoka A, Ikeda M, Izumi N, Moriguchi M, Ogasawara S, Minami Y, Ueshima K, Murakami T, Miyayama S, Nakashima O, Yano H, Sakamoto M, Hatano E, Shimada M, Kokudo N, Mochida S, Takehara T. Management of Hepatocellular Carcinoma in Japan: JSH Consensus Statements and Recommendations 2021 Update. *Liver Cancer* 2021; **10**: 181-223 [PMID: 34239808 DOI: 10.1159/000514174]

77 **Drafting Committee for Hepatitis Management Guidelines and the Japan Society of Hepatology**. JSH Guidelines for the Management of Hepatitis B Virus Infection. *Hepatol Res* 2014; **44** Suppl S1: 1-58 [PMID: 24397839 DOI: 10.1111/hepr.12269]

78 **Varbobitis I**, Papatheodoridis GV. The assessment of hepatocellular carcinoma risk in patients with chronic hepatitis B under antiviral therapy. *Clin Mol Hepatol* 2016; **22**: 319-326 [PMID: 27729632 DOI: 10.3350/cmh.2016.0045]

79 **Wong GL**, Chan HL, Chan HY, Tse PC, Tse YK, Mak CW, Lee SK, Ip ZM, Lam AT, Iu HW, Leung JM, Wong VW. Accuracy of risk scores for patients with chronic hepatitis B receiving entecavir treatment. *Gastroenterology* 2013; **144**: 933-944 [PMID: 23415803 DOI: 10.1053/j.gastro.2013.02.002]

80 **Coffin CS**, Rezaeeaval M, Pang JX, Alcantara L, Klein P, Burak KW, Myers RP. The incidence of hepatocellular carcinoma is reduced in patients with chronic hepatitis B on long-term nucleos(t)ide analogue therapy. *Aliment Pharmacol Ther* 2014; **40**: 1262-1269 [PMID: 25312649 DOI: 10.1111/apt.12990]

81 **Ahn J**, Lim JK, Lee HM, Lok AS, Nguyen M, Pan CQ, Mannalithara A, Te H, Reddy KR, Trinh H, Chu D, Tran T, Lau D, Leduc TS, Min A, Trong Le L, Bae H, Van Tran S, Do S, Hann HW, Wong C, Han S, Pillai A, Park JS, Tong M, Scaglione S, Woog J, Kim WR. Lower Observed Hepatocellular Carcinoma Incidence in Chronic Hepatitis B Patients Treated With Entecavir: Results of the ENUMERATE Study. *Am J Gastroenterol* 2016; **111**: 1297-1304 [PMID: 27325221 DOI: 10.1038/ajg.2016.257]

82 **Kim WR**, Loomba R, Berg T, Aguilar Schall RE, Yee LJ, Dinh PV, Flaherty JF, Martins EB, Therneau TM, Jacobson I, Fung S, Gurel S, Buti M, Marcellin P. Impact of long-term tenofovir disoproxil fumarate on incidence of hepatocellular carcinoma in patients with chronic hepatitis B. *Cancer* 2015; **121**: 3631-3638 [PMID: 26177866 DOI: 10.1002/cncr.29537]

83 **Arends P**, Sonneveld MJ, Zoutendijk R, Carey I, Brown A, Fasano M, Mutimer D, Deterding K, Reijnders JG, Oo Y, Petersen J, van Bömmel F, de Knegt RJ, Santantonio T, Berg T, Welzel TM, Wedemeyer H, Buti M, Pradat P, Zoulim F, Hansen B, Janssen HL; VIRGIL Surveillance Study Group. Entecavir treatment does not eliminate the risk of hepatocellular carcinoma in chronic hepatitis B: limited role for risk scores in Caucasians. *Gut* 2015; **64**: 1289-1295 [PMID: 25011935 DOI: 10.1136/gutjnl-2014-307023]

84 **Papatheodoridis G**, Dalekos G, Sypsa V, Yurdaydin C, Buti M, Goulis J, Calleja JL, Chi H, Manolakopoulos S, Mangia G, Gatselis N, Keskin O, Savvidou S, de la Revilla J, Hansen BE, Vlachogiannakos I, Galanis K, Idilman R, Colombo M, Esteban R, Janssen HL, Lampertico P. PAGE-B predicts the risk of developing hepatocellular carcinoma in Caucasians with chronic hepatitis B on 5-year antiviral therapy. *J Hepatol* 2016; **64**: 800-806 [PMID: 26678008 DOI: 10.1016/j.jhep.2015.11.035]

85 **Kim JH**, Kim YD, Lee M, Jun BG, Kim TS, Suk KT, Kang SH, Kim MY, Cheon GJ, Kim DJ, Baik SK, Choi DH. Modified PAGE-B score predicts the risk of hepatocellular carcinoma in Asians with chronic hepatitis B on antiviral therapy. *J Hepatol* 2018; **69**: 1066-1073 [PMID: 30075230 DOI: 10.1016/j.jhep.2018.07.018]

86 **Baudi I**, Inoue T, Tanaka Y. Novel Biomarkers of Hepatitis B and Hepatocellular Carcinoma: Clinical Significance of HBcrAg and M2BPGi. *Int J Mol Sci* 2020; **21** [PMID: 32023902 DOI: 10.3390/ijms21030949]

87 **Rapti I**, Hadziyannis S. Risk for hepatocellular carcinoma in the course of chronic hepatitis B virus infection and the protective effect of therapy with nucleos(t)ide analogues. *World J Hepatol* 2015; **7**: 1064-1073 [PMID: 26052395 DOI: 10.4254/wjh.v7.i8.1064]

88 **Sung JJ**, Tsoi KK, Wong VW, Li KC, Chan HL. Meta-analysis: Treatment of hepatitis B infection reduces risk of hepatocellular carcinoma. *Aliment Pharmacol Ther* 2008; **28**: 1067-1077 [PMID: 18657133 DOI: 10.1111/j.1365-2036.2008.03816.x]

89 **Hosaka T**, Suzuki F, Kobayashi M, Seko Y, Kawamura Y, Sezaki H, Akuta N, Suzuki Y, Saitoh S, Arase Y, Ikeda K, Kumada H. Long-term entecavir treatment reduces hepatocellular carcinoma incidence in patients with hepatitis B virus infection. *Hepatology* 2013; **58**: 98-107 [PMID: 23213040 DOI: 10.1002/hep.26180]

90 **Papatheodoridis GV**, Dalekos GN, Yurdaydin C, Buti M, Goulis J, Arends P, Sypsa V, Manolakopoulos S, Mangia G, Gatselis N, Keskın O, Savvidou S, Hansen BE, Papaioannou C, Galanis K, Idilman R, Colombo M, Esteban R, Janssen HL, Lampertico P. Incidence and predictors of hepatocellular carcinoma in Caucasian chronic hepatitis B patients receiving entecavir or tenofovir. *J Hepatol* 2015; **62**: 363-370 [PMID: 25195548 DOI: 10.1016/j.jhep.2014.08.045]

91 **Chen LP**, Zhao J, Du Y, Han YF, Su T, Zhang HW, Cao GW. Antiviral treatment to prevent chronic hepatitis B or C-related hepatocellular carcinoma. *World J Virol* 2012; **1**: 174-183 [PMID: 24175223 DOI: 10.5501/wjv.v1.i6.174]

92 **Lin SM**, Yu ML, Lee CM, Chien RN, Sheen IS, Chu CM, Liaw YF. Interferon therapy in HBeAg positive chronic hepatitis reduces progression to cirrhosis and hepatocellular carcinoma. *J Hepatol* 2007; **46**: 45-52 [PMID: 17107734 DOI: 10.1016/j.jhep.2006.08.021]

93 **Fontana RJ**, Hann HW, Perrillo RP, Vierling JM, Wright T, Rakela J, Anschuetz G, Davis R, Gardner SD, Brown NA. Determinants of early mortality in patients with decompensated chronic hepatitis B treated with antiviral therapy. *Gastroenterology* 2002; **123**: 719-727 [PMID: 12198698 DOI: 10.1053/gast.2002.35352]

94 **Chang MH**, Chen CJ, Lai MS, Hsu HM, Wu TC, Kong MS, Liang DC, Shau WY, Chen DS. Universal hepatitis B vaccination in Taiwan and the incidence of hepatocellular carcinoma in children. Taiwan Childhood Hepatoma Study Group. *N Engl J Med* 1997; **336**: 1855-1859 [PMID: 9197213 DOI: 10.1056/NEJM199706263362602]

95 **Qu C**, Chen T, Fan C, Zhan Q, Wang Y, Lu J, Lu LL, Ni Z, Huang F, Yao H, Zhu J, Fan J, Zhu Y, Wu Z, Liu G, Gao W, Zang M, Wang D, Dai M, Hsia CC, Zhang Y, Sun Z. Efficacy of neonatal HBV vaccination on liver cancer and other liver diseases over 30-year follow-up of the Qidong hepatitis B intervention study: a cluster randomized controlled trial. *PLoS Med* 2014; **11**: e1001774 [PMID: 25549238 DOI: 10.1371/journal.pmed.1001774]

96 **Wiangnon S**, Kamsa-ard S, Suwanrungruang K, Promthet S, Mahaweerawat S, Khuntikeo N. Trends in incidence of hepatocellular carcinoma, 1990-2009, Khon Kaen, Thailand. *Asian Pac J Cancer Prev* 2012; **13**: 1065-1068 [PMID: 22631639 DOI: 10.7314/apjcp.2012.13.3.1065]

97 **McMahon BJ**, Bulkow LR, Singleton RJ, Williams J, Snowball M, Homan C, Parkinson AJ. Elimination of hepatocellular carcinoma and acute hepatitis B in children 25 years after a hepatitis B newborn and catch-up immunization program. *Hepatology* 2011; **54**: 801-807 [PMID: 21618565 DOI: 10.1002/hep.24442]

98 **Kao JH**. Hepatitis B vaccination and prevention of hepatocellular carcinoma. *Best Pract Res Clin Gastroenterol* 2015; **29**: 907-917 [PMID: 26651252 DOI: 10.1016/j.bpg.2015.09.011]

99 **Mentha N**, Clément S, Negro F, Alfaiate D. A review on hepatitis D: From virology to new therapies. *J Adv Res* 2019; **17**: 3-15 [PMID: 31193285 DOI: 10.1016/j.jare.2019.03.009]

100 **Stockdale AJ**, Kreuels B, Henrion MRY, Giorgi E, Kyomuhangi I, Geretti AM. Hepatitis D prevalence: problems with extrapolation to global population estimates. *Gut* 2020; **69**: 396-397 [PMID: 30567743 DOI: 10.1136/gutjnl-2018-317874]

101 **Chen HY**, Shen DT, Ji DZ, Han PC, Zhang WM, Ma JF, Chen WS, Goyal H, Pan S, Xu HG. Prevalence and burden of hepatitis D virus infection in the global population: a systematic review and meta-analysis. *Gut* 2019; **68**: 512-521 [PMID: 30228220 DOI: 10.1136/gutjnl-2018-316601]

102 **Sagnelli E**, Sagnelli C, Pisaturo M, Macera M, Coppola N. Epidemiology of acute and chronic hepatitis B and delta over the last 5 decades in Italy. *World J Gastroenterol* 2014; **20**: 7635-7643 [PMID: 24976701 DOI: 10.3748/wjg.v20.i24.7635]

103 **Stroffolini T**, Sagnelli E, Sagnelli C, Russello M, De Luca M, Rosina F, Cacopardo B, Brancaccio G, Furlan C, Gaeta GB, Licata A, Almasio PL; behalf of EPACRON study group. Hepatitis delta infection in Italian patients: towards the end of the story? *Infection* 2017; **45**: 277-281 [PMID: 27817147 DOI: 10.1007/s15010-016-0956-1]

104 **Farci P**, Niro GA, Zamboni F, Diaz G. Hepatitis D Virus and Hepatocellular Carcinoma. *Viruses* 2021; **13** [PMID: 34064419 DOI: 10.3390/v13050830]

105 **Fattovich G**, Giustina G, Christensen E, Pantalena M, Zagni I, Realdi G, Schalm SW. Influence of hepatitis delta virus infection on morbidity and mortality in compensated cirrhosis type B. The European Concerted Action on Viral Hepatitis (Eurohep). *Gut* 2000; **46**: 420-426 [PMID: 10673308 DOI: 10.1136/gut.46.3.420]

106 **Ji J**, Sundquist K, Sundquist J. A population-based study of hepatitis D virus as potential risk factor for hepatocellular carcinoma. *J Natl Cancer Inst* 2012; **104**: 790-792 [PMID: 22423008 DOI: 10.1093/jnci/djs168]

107 **Romeo R**, Foglieni B, Casazza G, Spreafico M, Colombo M, Prati D. High serum levels of HDV RNA are predictors of cirrhosis and liver cancer in patients with chronic hepatitis delta. *PLoS One* 2014; **9**: e92062 [PMID: 24658127 DOI: 10.1371/journal.pone.0092062]

108 **Amougou MA**, Noah DN, Moundipa PF, Pineau P, Njouom R. A prominent role of Hepatitis D Virus in liver cancers documented in Central Africa. *BMC Infect Dis* 2016; **16**: 647 [PMID: 27821080 DOI: 10.1186/s12879-016-1992-2]

109 **Ioannou GN**, Beste LA, Green PK, Singal AG, Tapper EB, Waljee AK, Sterling RK, Feld JJ, Kaplan DE, Taddei TH, Berry K. Increased Risk for Hepatocellular Carcinoma Persists Up to 10 Years After HCV Eradication in Patients With Baseline Cirrhosis or High FIB-4 Scores. *Gastroenterology* 2019; **157**: 1264-1278.e4 [PMID: 31356807 DOI: 10.1053/j.gastro.2019.07.033]

110 **Cross TJ**, Rizzi P, Horner M, Jolly A, Hussain MJ, Smith HM, Vergani D, Harrison PM. The increasing prevalence of hepatitis delta virus (HDV) infection in South London. *J Med Virol* 2008; **80**: 277-282 [PMID: 18098143 DOI: 10.1002/jmv.21078]

111 **Abbas Z**, Abbas M, Abbas S, Shazi L. Hepatitis D and hepatocellular carcinoma. *World J Hepatol* 2015; **7**: 777-786 [PMID: 25914778 DOI: 10.4254/wjh.v7.i5.777]

112 **Puigvehí M**, Moctezuma-Velázquez C, Villanueva A, Llovet JM. The oncogenic role of hepatitis delta virus in hepatocellular carcinoma. *JHEP Rep* 2019; **1**: 120-130 [PMID: 32039360 DOI: 10.1016/j.jhepr.2019.05.001]

113 **Benegiamo G**, Vinciguerra M, Guarnieri V, Niro GA, Andriulli A, Pazienza V. Hepatitis delta virus induces specific DNA methylation processes in Huh-7 liver cancer cells. *FEBS Lett* 2013; **587**: 1424-1428 [PMID: 23523924 DOI: 10.1016/j.febslet.2013.03.021]

114 **Zhang Q**, Matsuura K, Kleiner DE, Zamboni F, Alter HJ, Farci P. Analysis of long noncoding RNA expression in hepatocellular carcinoma of different viral etiology. *J Transl Med* 2016; **14**: 328 [PMID: 27894309 DOI: 10.1186/s12967-016-1085-4]

115 **Wedemeyer H**, Yurdaydin C, Hardtke S, Caruntu FA, Curescu MG, Yalcin K, Akarca US, Gürel S, Zeuzem S, Erhardt A, Lüth S, Papatheodoridis GV, Keskin O, Port K, Radu M, Celen MK, Idilman R, Weber K, Stift J, Wittkop U, Heidrich B, Mederacke I, von der Leyen H, Dienes HP, Cornberg M, Koch A, Manns MP; HIDIT-II study team. Peginterferon alfa-2a plus tenofovir disoproxil fumarate for hepatitis D (HIDIT-II): a randomised, placebo controlled, phase 2 trial. *Lancet*

Infect Dis 2019; **19**: 275-286 [PMID: 30833068 DOI: 10.1016/S1473-3099(18)30663-7]

116 **Gower E**, Estes C, Blach S, Razavi-Shearer K, Razavi H. Global epidemiology and genotype distribution of the hepatitis C virus infection. *J Hepatol* 2014; **61**: S45-S57 [PMID: 25086286 DOI: 10.1016/j.jhep.2014.07.027]

117 **Polaris Observatory HCV Collaborators**. Global prevalence and genotype distribution of hepatitis C virus infection in 2015: a modelling study. *Lancet Gastroenterol Hepatol* 2017; **2**: 161-176 [PMID: 28404132 DOI: 10.1016/S2468-1253(16)30181-9]

118 **Davis GL**, Albright JE, Cook SF, Rosenberg DM. Projecting future complications of chronic hepatitis C in the United States. *Liver Transpl* 2003; **9**: 331-338 [PMID: 12682882 DOI: 10.1053/jlts.2003.50073]

119 **Lok AS**, McMahon BJ. Chronic hepatitis B: update 2009. *Hepatology* 2009; **50**: 661-662 [PMID: 19714720 DOI: 10.1002/hep.23190]

120 **Alfaleh FZ**, Nugrahini N, Matičič M, Tolmane I, Alzaabi M, Hajarizadeh B, Valantinas J, Kim DY, Hunyady B, Abaalkhail F, Abbas Z, Abdou A, Abourached A, Al Braiki F, Al Hosani F, Al Jaberi K, Al Khatry M, Al Mulla MA, Al Quraishi H, Al Rifai A, Al Serkal Y, Alam A, Alashgar HI, Alavian SM, Alawadhi S, Al-Dabal L, Aldins P, Alghamdi AS, Al-Hakeem R, Aljumah AA, Almessabi A, Alqutub AN, Alswat KA, Altraif I, Andrea N, Assiri AM, Babatin MA, Baqir A, Barakat MT, Bergmann OM, Bizri AR, Chaudhry A, Choi MS, Diab T, Djauzi S, El Hassan ES, El Khoury S, Estes C, Fakhry S, Farooqi JI, Fridjonsdottir H, Gani RA, Ghafoor Khan A, Gheorghe L, Goldis A, Gottfredsson M, Gregorcic S, Gunter J, Hamid S, Han KH, Hasan I, Hashim A, Horvath G, Husni R, Jafri W, Jeruma A, Jonasson JG, Karlsdottir B, Kim YS, Koutoubi Z, Lesmana LA, Liakina V, Lim YS, Löve A, Maimets M, Makara M, Malekzadeh R, Memon MS, Merat S, Mokhbat JE, Mourad FH, Muljono DH, Nawaz A, Olafsson S, Priohutomo S, Qureshi H, Rassam P, Razavi H, Razavi-Shearer D, Razavi-Shearer K, Rozentale B, Sadik M, Saeed K, Salamat A, Salupere R, Sanai FM, Sanityoso Sulaiman A, Sayegh RA, Schmelzer JD, Sharara AI, Sibley A, Siddiq M, Siddiqui AM, Sigmundsdottir G, Sigurdardottir B, Speiciene D, Sulaiman A, Sultan MA, Taha M, Tanaka J, Tarifi H, Tayyab G, Ud Din M, Umar M, Videčnik-Zorman J, Yaghi C, Yunihastuti E, Yusuf MA, Zuberi BF, Blach S. Strategies to manage hepatitis C virus infection disease burden - volume 3. *J Viral Hepat* 2015; **22** Suppl 4: 42-65 [PMID: 26513447 DOI: 10.1111/jvh.12474]

121 **Freeman AJ**, Dore GJ, Law MG, Thorpe M, Von Overbeck J, Lloyd AR, Marinos G, Kaldor JM. Estimating progression to cirrhosis in chronic hepatitis C virus infection. *Hepatology* 2001; **34**: 809-816 [PMID: 11584380 DOI: 10.1053/jhep.2001.27831]

122 **Lin MV**, King LY, Chung RT. Hepatitis C virus-associated cancer. *Annu Rev Pathol* 2015; **10**: 345-370 [PMID: 25387053 DOI: 10.1146/annurev-pathol-012414-040323]

123 **Mahmoudvand S**, Shokri S, Taherkhani R, Farshadpour F. Hepatitis C virus core protein modulates several signaling pathways involved in hepatocellular carcinoma. *World J Gastroenterol* 2019; **25**: 42-58 [PMID: 30643357 DOI: 10.3748/wjg.v25.i1.42]

124 **Alisi A**, Giambartolomei S, Cupelli F, Merlo P, Fontemaggi G, Spaziani A, Balsano C. Physical and functional interaction between HCV core protein and the different p73 isoforms. *Oncogene* 2003; **22**: 2573-2580 [PMID: 12730672 DOI: 10.1038/sj.onc.1206333]

125 **Zhao LJ**, Wang L, Ren H, Cao J, Li L, Ke JS, Qi ZT. Hepatitis C virus E2 protein promotes human hepatoma cell proliferation through the MAPK/ERK signaling pathway *via* cellular receptors. *Exp Cell Res* 2005; **305**: 23-32 [PMID: 15777784 DOI: 10.1016/j.yexcr.2004.12.024]

126 **Vescovo T**, Refolo G, Vitagliano G, Fimia GM, Piacentini M. Molecular mechanisms of hepatitis C virus-induced hepatocellular carcinoma. *Clin Microbiol Infect* 2016; **22**: 853-861 [PMID: 27476823 DOI: 10.1016/j.cmi.2016.07.019]

127 **Deng L**, Nagano-Fujii M, Tanaka M, Nomura-Takigawa Y, Ikeda M, Kato N, Sada K, Hotta H. NS3 protein of Hepatitis C virus associates with the tumour suppressor p53 and inhibits its function in an NS3 sequence-dependent manner. *J Gen Virol* 2006; **87**: 1703-1713 [PMID: 16690937 DOI: 10.1099/vir.0.81735-0]

128 **Yoshida K**, Murata M, Yamaguchi T, Matsuzaki K. TGF-β/Smad signaling during hepatic fibro-carcinogenesis (review). *Int J Oncol* 2014; **45**: 1363-1371 [PMID: 25050845 DOI: 10.3892/ijo.2014.2552]

129 **Street A**, Macdonald A, Crowder K, Harris M. The Hepatitis C virus NS5A protein activates a phosphoinositide 3-kinase-dependent survival signaling cascade. *J Biol Chem* 2004; **279**: 12232-12241 [PMID: 14709551 DOI: 10.1074/jbc.M312245200]

130 **Zhu C**, Liu X, Wang S, Yan X, Tang Z, Wu K, Li Y, Liu F. Hepatitis C virus core protein induces hypoxia-inducible factor 1α-mediated vascular endothelial growth factor expression in Huh7.5.1 cells. *Mol Med Rep* 2014; **9**: 2010-2014 [PMID: 24626461 DOI: 10.3892/mmr.2014.2039]

131 **Benkheil M**, Van Haele M, Roskams T, Laporte M, Noppen S, Abbasi K, Delang L, Neyts J, Liekens S. CCL20, a direct-acting pro-angiogenic chemokine induced by hepatitis C virus (HCV): Potential role in HCV-related liver cancer. *Exp Cell Res* 2018; **372**: 168-177 [PMID: 30287142 DOI: 10.1016/j.yexcr.2018.09.023]

132 **Hamdane N**, Jühling F, Crouchet E, El Saghire H, Thumann C, Oudot MA, Bandiera S, Saviano A, Ponsolles C, Roca Suarez AA, Li S, Fujiwara N, Ono A, Davidson I, Bardeesy N, Schmidl C, Bock C, Schuster C, Lupberger J, Habersetzer F, Doffoël M, Piardi T, Sommacale D, Imamura M, Uchida T, Ohdan H, Aikata H, Chayama K, Boldanova T, Pessaux P, Fuchs BC, Hoshida Y, Zeisel MB, Duong FHT, Baumert TF. HCV-Induced Epigenetic Changes Associated With Liver Cancer Risk Persist After Sustained Virologic Response. *Gastroenterology* 2019; **156**: 2313-2329.e7 [PMID: 30836093 DOI: 10.1053/j.gastro.2019.02.038]

133 **Varnholt H**, Drebber U, Schulze F, Wedemeyer I, Schirmacher P, Dienes HP, Odenthal M. MicroRNA gene expression profile of hepatitis C virus-associated hepatocellular carcinoma. *Hepatology* 2008; **47**: 1223-1232 [PMID: 18307259 DOI: 10.1002/hep.22158]

134 **Jopling CL**, Yi M, Lancaster AM, Lemon SM, Sarnow P. Modulation of hepatitis C virus RNA abundance by a liver-specific MicroRNA. *Science* 2005; **309**: 1577-1581 [PMID: 16141076 DOI: 10.1126/science.1113329]

135 **Bruno S**, Crosignani A, Maisonneuve P, Rossi S, Silini E, Mondelli MU. Hepatitis C virus genotype 1b as a major risk factor associated with hepatocellular carcinoma in patients with cirrhosis: a seventeen-year prospective cohort study. *Hepatology* 2007; **46**: 1350-1356 [PMID: 17680653 DOI: 10.1002/hep.21826]

136 **Raimondi S**, Bruno S, Mondelli MU, Maisonneuve P. Hepatitis C virus genotype 1b as a risk factor for hepatocellular

carcinoma development: a meta-analysis. *J Hepatol* 2009; **50**: 1142-1154 [PMID: 19395111 DOI: 10.1016/j.jhep.2009.01.019]

137 **Lee SS**, Kim CY, Kim BR, Cha RR, Kim WS, Kim JJ, Lee JM, Kim HJ, Ha CY, Kim TH, Jung WT, Lee OJ. Hepatitis C virus genotype 3 was associated with the development of hepatocellular carcinoma in Korea. *J Viral Hepat* 2019; **26**: 459-465 [PMID: 30516858 DOI: 10.1111/jvh.13047]

138 **Nkontchou G**, Ziol M, Aout M, Lhabadie M, Baazia Y, Mahmoudi A, Roulot D, Ganne-Carrie N, Grando-Lemaire V, Trinchet JC, Gordien E, Vicaut E, Baghad I, Beaugrand M. HCV genotype 3 is associated with a higher hepatocellular carcinoma incidence in patients with ongoing viral C cirrhosis. *J Viral Hepat* 2011; **18**: e516-e522 [PMID: 21914071 DOI: 10.1111/j.1365-2893.2011.01441.x]

139 **van der Meer AJ**, Veldt BJ, Feld JJ, Wedemeyer H, Dufour JF, Lammert F, Duarte-Rojo A, Heathcote EJ, Manns MP, Kuske L, Zeuzem S, Hofmann WP, de Knegt RJ, Hansen BE, Janssen HL. Association between sustained virological response and all-cause mortality among patients with chronic hepatitis C and advanced hepatic fibrosis. *JAMA* 2012; **308**: 2584-2593 [PMID: 23268517 DOI: 10.1001/jama.2012.144878]

140 **Castello G**, Scala S, Palmieri G, Curley SA, Izzo F. HCV-related hepatocellular carcinoma: From chronic inflammation to cancer. *Clin Immunol* 2010; **134**: 237-250 [PMID: 19910258 DOI: 10.1016/j.clim.2009.10.007]

141 **Waggoner SN**, Hall CH, Hahn YS. HCV core protein interaction with gC1q receptor inhibits Th1 differentiation of CD4+ T cells *via* suppression of dendritic cell IL-12 production. *J Leukoc Biol* 2007; **82**: 1407-1419 [PMID: 17881511 DOI: 10.1189/jlb.0507268]

142 **Hussain SP**, Hofseth LJ, Harris CC. Radical causes of cancer. *Nat Rev Cancer* 2003; **3**: 276-285 [PMID: 12671666 DOI: 10.1038/nrc1046]

143 **Majano PL**, Garcia-Monzon C. Does nitric oxide play a pathogenic role in hepatitis C virus infection? *Cell Death Differ* 2003; **10** Suppl 1: S13-S15 [PMID: 12655339 DOI: 10.1038/sj.cdd.4401115]

144 **Kato N**, Yoshida H, Ono-Nita SK, Kato J, Goto T, Otsuka M, Lan K, Matsushima K, Shiratori Y, Omata M. Activation of intracellular signaling by hepatitis B and C viruses: C-viral core is the most potent signal inducer. *Hepatology* 2000; **32**: 405-412 [PMID: 10915750 DOI: 10.1053/jhep.2000.9198]

145 **Maki A**, Kono H, Gupta M, Asakawa M, Suzuki T, Matsuda M, Fujii H, Rusyn I. Predictive power of biomarkers of oxidative stress and inflammation in patients with hepatitis C virus-associated hepatocellular carcinoma. *Ann Surg Oncol* 2007; **14**: 1182-1190 [PMID: 17195915 DOI: 10.1245/s10434-006-9049-1]

146 **Matsui T**, Nagai H, Sumino Y, Miki K. Relationship of peripheral blood CD4-positive T cells to carcinogenesis in patients with HCV-related chronic hepatitis and liver cirrhosis. *Cancer Chemother Pharmacol* 2008; **62**: 401-406 [PMID: 17932673 DOI: 10.1007/s00280-007-0618-1]

147 **Budhu A**, Wang XW. The role of cytokines in hepatocellular carcinoma. *J Leukoc Biol* 2006; **80**: 1197-1213 [PMID: 16946019 DOI: 10.1189/jlb.0506297]

148 **Cabrera R**, Tu Z, Xu Y, Firpi RJ, Rosen HR, Liu C, Nelson DR. An immunomodulatory role for CD4(+)CD25(+) regulatory T lymphocytes in hepatitis C virus infection. *Hepatology* 2004; **40**: 1062-1071 [PMID: 15486925 DOI: 10.1002/hep.20454]

149 **Li L**, Ye J. Characterization of gut microbiota in patients with primary hepatocellular carcinoma received immune checkpoint inhibitors: A Chinese population-based study. *Medicine (Baltimore)* 2020; **99**: e21788 [PMID: 32925716 DOI: 10.1097/MD.0000000000021788]

150 **Wang L**, Wan YY. The role of gut microbiota in liver disease development and treatment. *Liver Res* 2019; **3**: 3-18 [PMID: 32461811 DOI: 10.1016/j.livres.2019.02.001]

151 **Inoue T**, Nakayama J, Moriya K, Kawaratani H, Momoda R, Ito K, Iio E, Nojiri S, Fujiwara K, Yoneda M, Yoshiji H, Tanaka Y. Gut Dysbiosis Associated With Hepatitis C Virus Infection. *Clin Infect Dis* 2018; **67**: 869-877 [PMID: 29718124 DOI: 10.1093/cid/ciy205]

152 **Cosseau C**, Devine DA, Dullaghan E, Gardy JL, Chikatamarla A, Gellatly S, Yu LL, Pistolic J, Falsafi R, Tagg J, Hancock RE. The commensal Streptococcus salivarius K12 downregulates the innate immune responses of human epithelial cells and promotes host-microbe homeostasis. *Infect Immun* 2008; **76**: 4163-4175 [PMID: 18625732 DOI: 10.1128/IAI.00188-08]

153 **Ponziani FR**, Putignani L, Paroni Sterbini F, Petito V, Picca A, Del Chierico F, Reddel S, Calvani R, Marzetti E, Sanguinetti M, Gasbarrini A, Pompili M. Influence of hepatitis C virus eradication with direct-acting antivirals on the gut microbiota in patients with cirrhosis. *Aliment Pharmacol Ther* 2018; **48**: 1301-1311 [PMID: 30345704 DOI: 10.1111/apt.15004]

154 **Walker AJ**, Peacock CJ, Pedergnana V; STOP-HCV Consortium, Irving WL. Host genetic factors associated with hepatocellular carcinoma in patients with hepatitis C virus infection: A systematic review. *J Viral Hepat* 2018; **25**: 442-456 [PMID: 29397014 DOI: 10.1111/jvh.12871]

155 **Thrift AP**, El-Serag HB, Kanwal F. Global epidemiology and burden of HCV infection and HCV-related disease. *Nat Rev Gastroenterol Hepatol* 2017; **14**: 122-132 [PMID: 27924080 DOI: 10.1038/nrgastro.2016.176]

156 **Bandiera S**, Billie Bian C, Hoshida Y, Baumert TF, Zeisel MB. Chronic hepatitis C virus infection and pathogenesis of hepatocellular carcinoma. *Curr Opin Virol* 2016; **20**: 99-105 [PMID: 27741441 DOI: 10.1016/j.coviro.2016.09.010]

157 **Degasperi E**, Galmozzi E, Pelusi S, D'Ambrosio R, Soffredini R, Borghi M, Perbellini R, Facchetti F, Iavarone M, Sangiovanni A, Valenti L, Lampertico P. Hepatic Fat-Genetic Risk Score Predicts Hepatocellular Carcinoma in Patients With Cirrhotic HCV Treated With DAAs. *Hepatology* 2020; **72**: 1912-1923 [PMID: 32762045 DOI: 10.1002/hep.31500]

158 **Marrero JA**, Kulik LM, Sirlin CB, Zhu AX, Finn RS, Abecassis MM, Roberts LR, Heimbach JK. Diagnosis, Staging, and Management of Hepatocellular Carcinoma: 2018 Practice Guidance by the American Association for the Study of Liver Diseases. *Hepatology* 2018; **68**: 723-750 [PMID: 29624699 DOI: 10.1002/hep.29913]

159 **Kudo M**, Matsui O, Izumi N, Iijima H, Kadoya M, Imai Y, Okusaka T, Miyayama S, Tsuchiya K, Ueshima K, Hiraoka A, Ikeda M, Ogasawara S, Yamashita T, Minami T, Yamakado K; Liver Cancer Study Group of Japan. JSH Consensus-Based Clinical Practice Guidelines for the Management of Hepatocellular Carcinoma: 2014 Update by the Liver Cancer Study Group of Japan. *Liver Cancer* 2014; **3**: 458-468 [PMID: 26280007 DOI: 10.1159/000343875]

160 **Ponziani FR**, Mangiola F, Binda C, Zocco MA, Siciliano M, Grieco A, Rapaccini GL, Pompili M, Gasbarrini A. Future of liver disease in the era of direct acting antivirals for the treatment of hepatitis C. *World J Hepatol* 2017; **9**: 352-367 [PMID: 28321272 DOI: 10.4254/wjh.v9.i7.352]

161 **Morgan RL**, Baack B, Smith BD, Yartel A, Pitasi M, Falck-Ytter Y. Eradication of hepatitis C virus infection and the development of hepatocellular carcinoma: a meta-analysis of observational studies. *Ann Intern Med* 2013; **158**: 329-337 [PMID: 23460056 DOI: 10.7326/0003-4819-158-5-201303050-00005]

162 **Quartuccio L**, Benucci M, De Vita S. Answer to Vieira *et al*. "Cytokine profile as a prognostic tool in coronavirus disease 2019". *Joint Bone Spine* 2021; **88**: 105076 [PMID: 32950703 DOI: 10.1016/j.jbspin.2020.09.008]

163 **Pascut D**, Pratama MY, Tiribelli C. HCC occurrence after DAA treatments: molecular tools to assess the post-treatment risk and surveillance. *Hepat Oncol* 2020; **7**: HEP21 [PMID: 32647566 DOI: 10.2217/hep-2020-0010]

164 **Reig M**, Mariño Z, Perelló C, Iñarrairaegui M, Ribeiro A, Lens S, Díaz A, Vilana R, Darnell A, Varela M, Sangro B, Calleja JL, Forns X, Bruix J. Unexpected high rate of early tumor recurrence in patients with HCV-related HCC undergoing interferon-free therapy. *J Hepatol* 2016; **65**: 719-726 [PMID: 27084592 DOI: 10.1016/j.jhep.2016.04.008]

165 **Conti F**, Buonfiglioli F, Scuteri A, Crespi C, Bolondi L, Caraceni P, Foschi FG, Lenzi M, Mazzella G, Verucchi G, Andreone P, Brillanti S. Early occurrence and recurrence of hepatocellular carcinoma in HCV-related cirrhosis treated with direct-acting antivirals. *J Hepatol* 2016; **65**: 727-733 [PMID: 27349488 DOI: 10.1016/j.jhep.2016.06.015]

166 **Waziry R**, Hajarizadeh B, Grebely J, Amin J, Law M, Danta M, George J, Dore GJ. Hepatocellular carcinoma risk following direct-acting antiviral HCV therapy: A systematic review, meta-analyses, and meta-regression. *J Hepatol* 2017; **67**: 1204-1212 [PMID: 28802876 DOI: 10.1016/j.jhep.2017.07.025]

167 **Ioannou GN**, Green PK, Berry K. HCV eradication induced by direct-acting antiviral agents reduces the risk of hepatocellular carcinoma. *J Hepatol* 2017 [PMID: 28887168 DOI: 10.1016/j.jhep.2017.08.030]

168 **Nahon P**, Layese R, Bourcier V, Cagnot C, Marcellin P, Guyader D, Pol S, Larrey D, De Lédinghen V, Ouzan D, Zoulim F, Roulot D, Tran A, Bronowicki JP, Zarski JP, Riachi G, Calès P, Péron JM, Alric L, Bourlière M, Mathurin P, Blanc JF, Abergel A, Serfaty L, Mallat A, Grangé JD, Attali P, Bacq Y, Wartelle C, Dao T, Thabut D, Pilette C, Silvain C, Christidis C, Nguyen-Khac E, Bernard-Chabert B, Zucman D, Di Martino V, Sutton A, Roudot-Thoraval F, Audureau E; ANRS CO12 CirVir Group. Incidence of Hepatocellular Carcinoma After Direct Antiviral Therapy for HCV in Patients With Cirrhosis Included in Surveillance Programs. *Gastroenterology* 2018; **155**: 1436-1450.e6 [PMID: 30031138 DOI: 10.1053/j.gastro.2018.07.015]

169 **Singer AW**, Reddy KR, Telep LE, Osinusi AO, Brainard DM, Buti M, Chokkalingam AP. Direct-acting antiviral treatment for hepatitis C virus infection and risk of incident liver cancer: a retrospective cohort study. *Aliment Pharmacol Ther* 2018; **47**: 1278-1287 [PMID: 29516535 DOI: 10.1111/apt.14593]

170 **Calvaruso V**, Cabibbo G, Cacciola I, Petta S, Madonia S, Bellia A, Tinè F, Distefano M, Licata A, Giannitrapani L, Prestileo T, Mazzola G, Di Rosolini MA, Larocca L, Bertino G, Digiacomo A, Benanti F, Guarneri L, Averna A, Iacobello C, Magro A, Scalisi I, Cartabellotta F, Savalli F, Barbara M, Davì A, Russello M, Scifo G, Squadrito G, Cammà C, Raimondo G, Craxì A, Di Marco V; Rete Sicilia Selezione Terapia–HCV (RESIST-HCV). Incidence of Hepatocellular Carcinoma in Patients With HCV-Associated Cirrhosis Treated With Direct-Acting Antiviral Agents. *Gastroenterology* 2018; **155**: 411-421.e4 [PMID: 29655836 DOI: 10.1053/j.gastro.2018.04.008]

171 **Guarino M**, Viganò L, Ponziani FR, Giannini EG, Lai Q, Morisco F; Special Interest Group on Hepatocellular carcinoma and new anti-HCV therapies" of the Italian Association for the Study of the Liver. Recurrence of hepatocellular carcinoma after direct acting antiviral treatment for hepatitis C virus infection: Literature review and risk analysis. *Dig Liver Dis* 2018; **50**: 1105-1114 [PMID: 30170908 DOI: 10.1016/j.dld.2018.08.001]

172 **Carrat F**, Fontaine H, Dorival C, Simony M, Diallo A, Hezode C, De Ledinghen V, Larrey D, Haour G, Bronowicki JP, Zoulim F, Asselah T, Marcellin P, Thabut D, Leroy V, Tran A, Habersetzer F, Samuel D, Guyader D, Chazouilleres O, Mathurin P, Metivier S, Alric L, Riachi G, Gournay J, Abergel A, Cales P, Ganne N, Loustaud-Ratti V, D'Alteroche L, Causse X, Geist C, Minello A, Rosa I, Gelu-Simeon M, Portal I, Raffi F, Bourliere M, Pol S; French ANRS CO22 Hepather cohort. Clinical outcomes in patients with chronic hepatitis C after direct-acting antiviral treatment: a prospective cohort study. *Lancet* 2019; **393**: 1453-1464 [PMID: 30765123 DOI: 10.1016/S0140-6736(18)32111-1]

173 **Butt AA**, Yan P, Simon TG, Abou-Samra AB. Effect of Paritaprevir/Ritonavir/Ombitasvir/Dasabuvir and Ledipasvir/Sofosbuvir Regimens on Survival Compared With Untreated Hepatitis C Virus-Infected Persons: Results From ERCHIVES. *Clin Infect Dis* 2017; **65**: 1006-1011 [PMID: 28903508 DOI: 10.1093/cid/cix364]

174 **Watanabe T**, Tokumoto Y, Joko K, Michitaka K, Horiike N, Tanaka Y, Tada F, Kisaka Y, Nakanishi S, Yamauchi K, Yukimoto A, Hirooka M, Abe M, Hiasa Y. Predictors of hepatocellular carcinoma occurrence after direct-acting antiviral therapy in patients with hepatitis C virus infection. *Hepatol Res* 2019; **49**: 136-146 [PMID: 30335208 DOI: 10.1111/hepr.13278]

175 **Kanwal F**, Kramer JR, Asch SM, Cao Y, Li L, El-Serag HB. Long-Term Risk of Hepatocellular Carcinoma in HCV Patients Treated With Direct Acting Antiviral Agents. *Hepatology* 2020; **71**: 44-55 [PMID: 31222774 DOI: 10.1002/hep.30823]

176 **Shiha G**, Waked I, Soliman R, Elbasiony M, Gomaa A, Mikhail NNH, Eslam M. GES: A validated simple score to predict the risk of HCC in patients with HCV-GT4-associated advanced liver fibrosis after oral antivirals. *Liver Int* 2020; **40**: 2828-2833 [PMID: 32946647 DOI: 10.1111/liv.14666]

177 **Xue X**, Liao W, Xing Y. Comparison of clinical features and outcomes between HBV-related and non-B non-C hepatocellular carcinoma. *Infect Agent Cancer* 2020; **15**: 11 [PMID: 32082414 DOI: 10.1186/s13027-020-0273-2]

178 **Sinn DH**, Gwak GY, Cho J, Paik SW, Yoo BC. Comparison of clinical manifestations and outcomes between hepatitis B virus- and hepatitis C virus-related hepatocellular carcinoma: analysis of a nationwide cohort. *PLoS One* 2014; **9**: e112184 [PMID: 25372403 DOI: 10.1371/journal.pone.0112184]

179 **Munaf A**, Memon MS, Kumar P, Ahmed S, Kumar MB. Comparison of viral hepatitis-associated hepatocellular carcinoma due to HBV and HCV - cohort from liver clinics in Pakistan. *Asian Pac J Cancer Prev* 2014; **15**: 7563-7567 [PMID: 25292029 DOI: 10.7314/apjcp.2014.15.18.7563]

180 **Carr BI**, Guerra V, Steel JL, Lu SN. A comparison of patients with hepatitis B- or hepatitis C-based advanced-stage

hepatocellular carcinoma. *Semin Oncol* 2015; **42**: 309-315 [PMID: 25843735 DOI: 10.1053/j.seminoncol.2014.12.019]

181 **Chuang SC**, La Vecchia C, Boffetta P. Liver cancer: descriptive epidemiology and risk factors other than HBV and HCV infection. *Cancer Lett* 2009; **286**: 9-14 [PMID: 19091458 DOI: 10.1016/j.canlet.2008.10.040]

182 **Polesel J**, Zucchetto A, Montella M, Dal Maso L, Crispo A, La Vecchia C, Serraino D, Franceschi S, Talamini R. The impact of obesity and diabetes mellitus on the risk of hepatocellular carcinoma. *Ann Oncol* 2009; **20**: 353-357 [PMID: 18723550 DOI: 10.1093/annonc/mdn565]

183 **Liu Y**, Chang CC, Marsh GM, Wu F. Population attributable risk of aflatoxin-related liver cancer: systematic review and meta-analysis. *Eur J Cancer* 2012; **48**: 2125-2136 [PMID: 22405700 DOI: 10.1016/j.ejca.2012.02.009]

World Journal of Gastroenterology

Submit a Manuscript: https://www.f6publishing.com

World J Gastroenterol 2022 June 7; 28(21): 2282-2290

DOI: 10.3748/wjg.v28.i21.2282

ISSN 1007-9327 (print) ISSN 2219-2840 (online)

MINIREVIEWS

Updates in therapeutic drug monitoring in inflammatory bowel disease

Nilesh Lodhia, Shanti Rao

Specialty type: Gastroenterology and hepatology

Provenance and peer review: Unsolicited article; Externally peer reviewed.

Peer-review model: Single blind

Peer-review report's scientific quality classification

Grade A (Excellent): 0
Grade B (Very good): 0
Grade C (Good): C, C
Grade D (Fair): 0
Grade E (Poor): 0

P-Reviewer: Gazouli M, Greece; Tulumović E, Bosnia and Herzegovina

Received: November 22, 2021
Peer-review started: November 22, 2021
First decision: December 27, 2021
Revised: January 9, 2021
Accepted: April 21, 2022
Article in press: April 21, 2022
Published online: June 7, 2022

Nilesh Lodhia, Shanti Rao, Department of Gastroenterology and Hepatology, Atrium Health, Charlotte, NC 28203, United States

Corresponding author: Nilesh Lodhia, MD, Associate Professor, Department of Gastroenterology and Hepatology, Atrium Health, CHS Digestive Health 1025 Morehead Medical Drive, Suite 300, Charlotte, NC 28203, United States. nilesh.lodhia@atriumhealth.org

Abstract

Biologics and immunomodulators (IMM) are generally considered the most effective therapies for the treatment of ulcerative colitis and Crohn's disease. However, despite the efficacy of these therapies, many patients either have a primary lack of response or a secondary loss of response to these medications. Therapeutic drug monitoring (TDM) is a systematic approach to managing such patients. In this review, we summarize the latest data on TDM, including reactive and proactive TDM, in patients with inflammatory bowel disease on biologics and/or IMM.

Key Words: Inflammatory bowel disease; Therapeutic drug monitoring; Crohn's disease; Ulcerative colitis

©The Author(s) 2022. Published by Baishideng Publishing Group Inc. All rights reserved.

Core Tip: Inflammatory bowel disease (IBD), such as ulcerative colitis and Crohn's disease, are best treated with immunomodulators (IMM) or biologics. The rate of response clinically and endoscopically varies between the medications and within patient populations. Therapeutic drug monitoring (TDM) is a useful technique to assess drug and metabolite levels as well as anti-drug levels in patients on biologics or IMM in order to improve clinical outcome and prevent a multitude of complications. Here we discuss the role of TDM in patients with IBD with a focus on reactive *vs* proactive TDM.

Citation: Lodhia N, Rao S. Updates in therapeutic drug monitoring in inflammatory bowel disease. *World J Gastroenterol* 2022; 28(21): 2282-2290
URL: https://www.wjgnet.com/1007-9327/full/v28/i21/2282.htm
DOI: https://dx.doi.org/10.3748/wjg.v28.i21.2282

INTRODUCTION

Since the approval of the first biologic for inflammatory bowel disease (IBD) in the 1990s, treatment for IBD has evolved tremendously. In addition to tumor necrosis factor (TNF) inhibitors, thiopurines, natalizumab, vedolizumab, ustekinumab, and tofacitinib have all been approved for the treatment of IBD. Previously, patients were treated based on symptoms, but we have now discovered that utilizing more objective parameters such as clinical and endoscopic remission reduces complications and leads to better outcomes[1].

Despite having effective treatments for ulcerative colitis (UC) and Crohn's disease (CD), one-third of patients (primary non-responders) will not respond to induction therapy after a biologic. Risk factors for primary non-response include long duration of disease, smoking, extensive small bowel disease, a normal C-reactive protein (CRP) at the start of therapy, and previous exposure to a biologic agent[2].

Secondary loss of response occurs when a patient initially had response to therapy but lost that benefit over time. This can occur in up to 50% of patients and can lead to the need for either dose intensification, or the use of an alternate agent. The formation of anti-drug antibodies (ADA) and inadequate drug exposure are the main factors contributing to secondary loss of response in patients on biologic therapies[1].

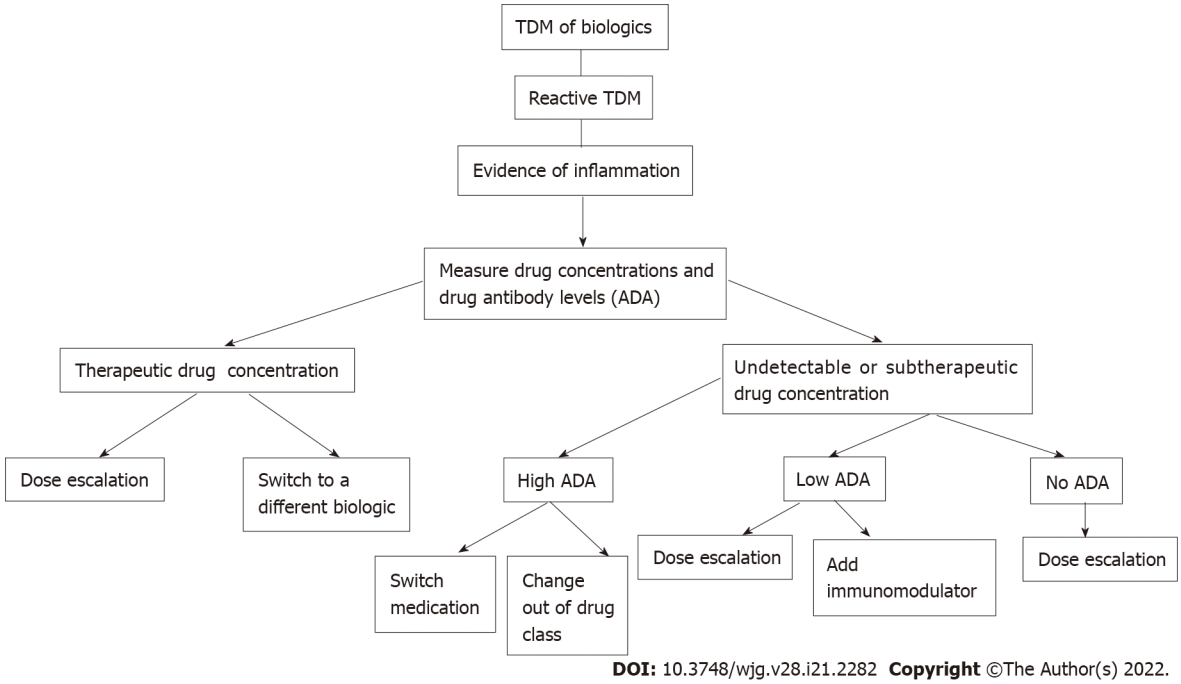
Therapeutic drug monitoring (TDM) is a way to optimize the dose of biologics and immunomodulators (IMM) to optimize treatment outcomes. The levels or metabolites, as well as the development of antibodies, are used to help guide drug dosing in order to enhance drug efficacy and reduce disease complications[3]. Current AGA guidelines published in 2017 recommend reactive TDM for patients with active IBD. Reactive TDM occurs when dosing of a therapy is changed following either primary non-response or secondary loss of response. Proactive TDM involves routine monitoring of drug levels and antibodies at set intervals with dose adjustments based on drug levels. Many studies have shown that there is a correlation between positive clinical outcomes and therapeutic ranges of serum drug concentrations for each agent available to treat IBD[4]. This review aims to discuss TDM for biologics and thiopurines in treatment of active IBD.

TNF INHIBITORS

TNF inhibitors available for treating active IBD include infliximab, adalimumab, certolizumab, and golimumab. Studies have confirmed that there is a correlation between clinical response and drug concentrations of anti-TNF agents measured *via* serologic work-up.

Infliximab is a chimeric monoclonal anti-TNF agent approved for patients with active UC or CD. Studies have shown that higher infliximab concentrations lead to improved outcomes in patients with IBD. TAXIT, a prospective trial on patients with CD on infliximab, demonstrated a significant improvement in remission and lower rates of ADA with dose escalation[5]. The TAILORIX trial was a second prospective trial for patients with CD on infliximab that tried to assess whether increasing the dose of infliximab based upon a combination of symptoms, biomarkers, and serum drug concentrations leads to improved outcomes compared to dose intensification based purely upon symptoms. This trial did not reach its primary endpoint of sustained corticosteroid-free clinical remission from weeks 22 through 54[6]. However, a post-hoc analysis of the TAILORIX trial demonstrated that infliximab drug concentrations were higher in patients that achieved endoscopic remission by week 12 compared to patients who did not achieve remission, which supports TDM is beneficial for patients on infliximab[7]. Furthermore, the TAILORIX utilized an infliximab drug concentration of 3 μg/mL as a target, which is widely considered low based upon the results of several recent studies[8-11]. The low target infliximab level could have limited the efficacy analysis of TDM in the trial. Patients with UC on infliximab maintenance therapy were examined in a retrospective study that utilized TDM and endoscopic evaluation. This study was able to demonstrate that patients with endoscopic and histologic remission had significantly higher serum drug levels[12]. A cost-analysis performed on TDM for infliximab suggested that proactive TDM led to fewer flares than the reactive method, and that more patients remained on therapy with proactive TDM. Fewer flares paired with a reduction in the cost of infliximab over time suggests that proactive TDM may be more suitable for patients with IBD on biologic agents [13].

Adalimumab is a human monoclonal immunoglobulin G (IgG0 anti-TNF agent used for the treatment of active CD and UC. Numerous studies have demonstrated improved outcomes in patients with higher drug concentrations of adalimumab. Park *et al*[14] observed that higher serum drug levels of adalimumab were associated with more quiescent disease and normal CRP. The patients in this study also had higher rates of endoscopic and radiologic remission with higher serum concentrations of adalimumab. The POETIC study was a prospective study on patients with CD on adalimumab designed to evaluate the evolution of ADA over time, and its correlation with clinical outcomes. Many patients developed ADA as early as week 2, and the early development of antibodies correlated with primary non-response[15].



DOI: 10.3748/wjg.v28.i21.2282 **Copyright** ©The Author(s) 2022.

Figure 1 In-depth algorithm for reactive therapeutic drug monitoring. TDM: Therapeutic drug monitoring; ADA: Anti-drug antibodies.

Golimumab is a human IgG1 kappa monoclonal anti-TNF therapy for patients with UC, which was approved based on the results from the PURSUIT trial. In the PURSUIT trial, serum golimumab concentrations and ADA were measured during induction as well as through maintenance therapy. An exposure-response relationship was noted; patients receiving the lowest dose of the drug had a higher incidence of ADA, as well as a higher fecal calprotectin and serum CRP[16]. Another study was able to demonstrate a positive correlation between golimumab concentrations and clinical and endoscopic outcomes[17].

Certolizumab pegol is a PEGylated Fab' fragment of a humanized monoclonal antibody that binds to TNF. It is unique in that it lacks the Fc component that other TNF inhibitors have, making it incapable of fixing complement or binding Fc receptors[18]. Current studies show that higher certolizumab plasma concentrations lead to increased remission as well as decreased levels of CRP[19]. Patients with higher concentrations of certolizumab as early as week 2 had clinical remission by week 6 of induction, as well as continued positive outcomes during maintenance therapy[20].

VEDOLIZUMAB

Vedolizumab is a monoclonal antibody that binds $\alpha_4\beta_7$ integrin for the treatment of moderate-to-severe UC and CD. A post hoc analyses of the GEMINI data confirmed the relationship between higher vedolizumab exposure and clinical remission in patents with IBD. Both patients with UC and CD showed higher rates of remission at week 6 with higher drug concentrations, which correlated with clinical response and mucosal healing, thus confirming an exposure-efficacy relationship[21-23]. The LOVE-CD trial was a prospective trial in patients with active CD receiving vedolizumab that showed higher serum levels of vedolizumab correlated with higher rates of endoscopic and histologic remission at weeks 26 and 52[24]. One single-center, cross-sectional, retrospective study showed higher serum levels of vedolizumab correlated with lower CRP levels. However, this study failed to demonstrate a correlation between vedolizumab concentrations and mucosal healing[25]. Notably, the rate of ADA to vedolizumab seems to be relatively low[25,26].

USTEKINUMAB

Ustekinumab is a human monoclonal antibody that binds to the p40 subunit of interleukin (IL)-12 and IL-23, thus preventing the interaction with the cell surface IL-12RB1 receptor. This prevents IL-12 and IL-23 mediated cell signaling[27]. The efficacy of ustekinumab for the treatment of moderate to severe CD was demonstrated in the UNITI-1 and UNITI-2 studies[28]. An analysis of data from phase 3 studies of patients with active CD on ustekinumab demonstrated a dose response. Drug serum concentrations

were positively associated with clinical remission and endoscopic improvement at week 44; there was also an inverse association with the CRP level. IMM were not found to have a significant effect on the serum concentration of ustekinumab[29,30]. The available data also suggest an extremely low rate of antibody formation in ustekinumab[28,29].

THIOPURINES

IMM, including azathioprine (AZA) and 6-mercaptopurine (6-MP) have been used for the treatment of IBD for many years. AZA is converted to 6-MP using a non-enzymatic pathway. 6-MP is broken down in three different ways: Into 6-thiouric acid by xanthine oxidase, activated to 6-methyl-mercaptopurine (6-MMP) by thiopurine methyltransferase (TPMT), or to 6-thioguanine dehydrogenase (6-TGN) by three different enzymes. TPMT has variants that can lead to a reduction in activity, therefore patients should have their TPMT phenotype checked prior to use. Once a thiopurine has been added to a regimen, thiopurine metabolites should be assessed, as patients have better outcomes with higher 6-TGN levels and lower 6-MMP levels[31]. Thiopurines play a role in reducing the risk of antibody formation, particularly to TNF inhibitors A study on patients with multiple different autoimmune diseases showed a reduction in ADA with the use of supplemental immunosuppressants[32].

The SONIC study is a landmark prospective trial that showed a combination therapy of AZA and infliximab for CD was more effective than infliximab monotherapy in induction and maintenance of steroid-free clinical remission at 26 and 52 wk. Combination therapy also led to lower rates of antibodies to infliximab and higher serum drug concentrations[33].

THE TRANSIENT NATURE OF SOME ADA

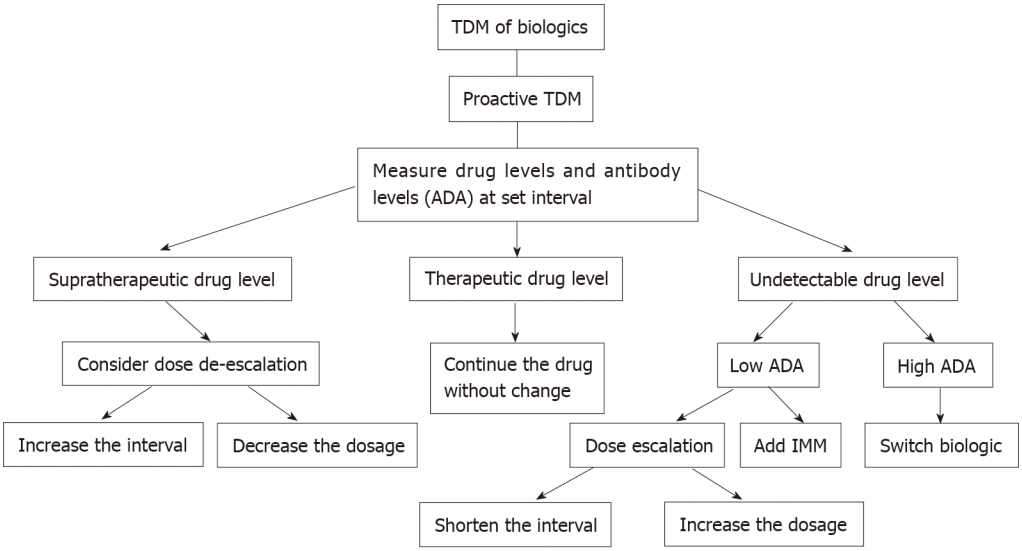
Although the formation of ADA can correlate to poor clinical outcomes, ADA levels may sometimes be transient[34,35]. Low levels of ADA may be overcome with higher serum drug concentrations and the addition of immunomodulators. However, if patients have sustained elevated levels of ADA, permanent loss of response is more likely to occur[36]. A small retrospective analysis of 5 patients investigated the addition of immunomodulators (thiopurines and methotrexate) to patients after the development of ADA to infliximab. All five patients had restoration of clinical response, and ADA levels gradually diminished over time[37]. It will be important for the future of IBD therapy to understand the role ADA formation plays in loss of response in patients on biologics, and the benefit of immunomodulators to recapturing response.

REACTIVE TDM

Reactive TDM is the current standard of care when treating IBD patients who have a loss of response to biologic therapy[4]. This approach can identify the subset of patients that would benefit from dose escalation of their current agent *vs* transitioning to a different therapy. Once a patient has a flare of their symptoms, drug concentrations and ADA levels are measured, and further management is based upon these results (Figure 1). A retrospective study of patients with suspected loss of response was performed that determined that the measurement of trough levels of anti-TNF agents or ADAs during a suspected loss of response led to improved interventions. Patients with high ADA levels benefited more from switching agents than from dose escalation, whereas patients with no or low ADA levels did benefit from dose intensification. This study also demonstrated that patients with adequate levels of infliximab or adalimumab with inadequate response would benefit from an agent that is out of the anti-TNF class [38]. A retrospective analysis of patients receiving infliximab who underwent dose escalation was examined, and clinical decisions with or without the use of TDM were compared. Patients for whom decisions were based upon TDM had improved endoscopic outcomes, higher rates of clinical remission, fewer hospitalizations, and less steroid use[39]. Reactive TDM has the benefit of cost savings, as less drug can be utilized, as well as the ability to try to optimize drug levels and increase the chance of recapturing response in order to prevent treatment failure[7].

PROACTIVE TDM

Proactive TDM differs from reactive TDM in that it aims to optimize drug concentrations by measuring serum drug concentrations and ADA levels at set intervals in order to prevent loss of response (Figure 2). Since the best therapeutic effect is obtained with the first biologic agent received, proponents of this approach consider it imperative to optimize the dose of the agent early in the treatment course



DOI: 10.3748/wjg.v28.i21.2282 **Copyright** ©The Author(s) 2022.

Figure 2 In-depth algorithm for proactive therapeutic drug monitoring. TDM: Therapeutic drug monitoring; IMM: Immunomodulators; ADA: Anti-drug antibodies.

[40].

Fernandes *et al*[41] demonstrated in a prospective study on patients on infliximab therapy with CD and UC that proactive TDM had better outcomes than management without the use of TDM. Patients on infliximab underwent trough and ADA level measurements before the fourth infusion and at every 2 infusions, and dose-adjustment was made in order to keep a goal trough level between 3 and 7 μg/mL for CD and 5 and 10 μg/mL for UC. Compared to a retrospective cohort treated with infliximab without the use of TDM, the TDM group showed improved mucosal healing, fewer surgeries and hospitalizations, and less treatment discontinuation. A randomized, controlled trial of children with CD, the PAILOT trial, investigated proactive TDM *vs* reactive TDM. The primary endpoint was corticosteroid-free remission on adalimumab therapy. The results showed significantly higher rates of steroid-free remission in patients receiving proactive TDM than reactive TDM, as 31 children (82%) in the proactive group reached the primary endpoint, meanwhile 19 children (48%) reached the endpoint using reactive TDM[42]. Papamichael *et al*[43] performed a multicenter, retrospective study on patients receiving infliximab therapy for IBD. Proactive TDM had better clinical outcomes when compared to reactive TDM, including fewer surgeries, hospitalizations, lower ADA levels, longer time to treatment failure[44-46]. Much of the current data for TDM seems to demonstrate that proactive TDM leads to better clinical outcomes compared to reactive TDM. However, a universal analysis on cost-effectiveness is much more difficult given varying degrees of coverage on biologics and TDM assays[47,48].

IMMUNOASSAY METHODS FOR THE DETECTION OF ANTIBODIES

Although it is well known that patients with inflammatory bowel disease are at risk of developing antibodies to biologics, more attention should be paid toward the optimal methodology used to detect these antibodies. The various immunoassay methods for detection of drug antibodies are suspected to yield varying results when assessing immunogenicity of biologics due to the presence of drug and the potential underestimation of ADA[49]. Drug interference limits the detection of ADA due to the formation of ADA-drug complexes in the assay. Drug tolerant assays were developed that can detect free ADA and ADA bound in a complex. This assay can dissociate the ADA from the drug to estimate the quantity of ADA more accurately in a sample. Drug-sensitive antibody detection methods such as the antibody binding test (ABT) and bridging enzyme-linked immunosorbent assay (ELISA) preceded the drug-tolerant assays[50].

A study by Ruwaard *et al*[49] compared the efficacy of three different immunoassays to detect ADA, including ABT, ELISA, and drug-tolerant assays in 86 patients on adalimumab. There was a significant difference in the ability to detect ADA between the assays, with drug-tolerant assays detecting ADA in 69% of patients, compared to 30% in the ABT, and 2% using the ELISA. This suggests that drug-tolerant assays should be the standard when detecting ADA in patients on adalimumab. A study by Wang *et al* [50] compared ELISA to a drug tolerant assay, the homogenous mobility shift assay (HMSA), in patients treated with infliximab. This study illustrated that the HMSA was significantly more sensitive in detecting ADA, especially in the presence of high serum drug concentrations. HMSA can overcome artifacts encountered using drug-sensitive assays, as it can dissociate the ADA from the drug. These

studies suggest that future studies should consider using drug-tolerant assays as their method of detecting ADA to standardize the methodology and prevent inconsistent results between different studies.

It is still well-known that ADA formation leads to lower drug concentrations and worse outcomes in patients with IBD on biologics. The data suggest that drug-tolerant assays are ideal for detection of ADA in patients on adalimumab and infliximab. Standardization in detection of ADA would improve the variability amongst studies, thus improving clinicians' ability to use and perform TDM. Unfortunately, the available data focus on TNF inhibitors, and the applicability to non-TNF inhibitor biologics is limited. Further studies with inclusion of all biologics could help lead to implementation of international standards and improve our understanding on the impact of ADA on clinical outcomes[51].

CONCLUSION

TDM plays an important role in treatment outcomes for patients with IBD on biologic agents. TDM is useful for predicting loss of response and preventing treatment failure. Higher serum drug concentrations lead to improved outcomes, with fewer hospitalizations, surgeries, and treatment failures. Lower serum drug concentrations and the development of ADA lead to worse outcomes and loss of response. The addition of immunomodulators has not been standardized, but studies have shown that the addition of an immunomodulator to TNF inhibitors can lead to a reduction in the development of ADA as well as higher serum drug concentrations, thus eliminating the potential for failure of an agent.

Despite a multitude of studies, there are still limitations regarding the use of TDM in IBD patients. There is likely a fair amount of inter-individual variation regarding the appropriate serum concentration of various biologics, and the optimal target levels have therefore not been fully elucidated. Similarly, further research needs to be done regarding the significance of different levels of ADA. Different serum concentration and ADA assays can also complicate our interpretation of these values. Finally, analyses regarding cost-effectiveness of reactive *vs* proactive TDM in the setting of a variety of different health care settings are difficult to conduct.

FOOTNOTES

Author contributions: Rao S reviewed prior publications and composed the paper; Lodhia N revised the paper.

Conflict-of-interest statement: No potential conflicts of interest.

Open-Access: This article is an open-access article that was selected by an in-house editor and fully peer-reviewed by external reviewers. It is distributed in accordance with the Creative Commons Attribution NonCommercial (CC BY-NC 4.0) license, which permits others to distribute, remix, adapt, build upon this work non-commercially, and license their derivative works on different terms, provided the original work is properly cited and the use is non-commercial. See: https://creativecommons.org/Licenses/by-nc/4.0/

Country/Territory of origin: United States

ORCID number: Nilesh Lodhia 0000-0003-4177-7548; Shanti Rao 0000-0001-9798-711X.

S-Editor: Wang JJ
L-Editor: A
P-Editor: Wang JJ

REFERENCES

1 **Papamichael K**, Cheifetz AS, Melmed GY, Irving PM, Vande Casteele N, Kozuch PL, Raffals LE, Baidoo L, Bressler B, Devlin SM, Jones J, Kaplan GG, Sparrow MP, Velayos FS, Ullman T, Siegel CA. Appropriate Therapeutic Drug Monitoring of Biologic Agents for Patients With Inflammatory Bowel Diseases. *Clin Gastroenterol Hepatol* 2019; **17**: 1655-1668.e3 [PMID: 30928454 DOI: 10.1016/j.cgh.2019.03.037]

2 **Sparrow MP**, Papamichael K, Ward MG, Riviere P, Laharie D, Paul S, Roblin X. Therapeutic Drug Monitoring of Biologics During Induction to Prevent Primary Non-Response. *J Crohns Colitis* 2020; **14**: 542-556 [PMID: 31549158 DOI: 10.1093/ecco-jcc/jjz162]

3 **Colombel JF**, Feagan BG, Sandborn WJ, Van Assche G, Robinson AM. Therapeutic drug monitoring of biologics for inflammatory bowel disease. *Inflamm Bowel Dis* 2012; **18**: 349-358 [PMID: 22021134 DOI: 10.1002/ibd.21831]

4 **Feuerstein JD**, Nguyen GC, Kupfer SS, Falck-Ytter Y, Singh S; American Gastroenterological Association Institute Clinical Guidelines Committee. American Gastroenterological Association Institute Guideline on Therapeutic Drug Monitoring in Inflammatory Bowel Disease. *Gastroenterology* 2017; **153**: 827-834 [PMID: 28780013 DOI:

10.1053/j.gastro.2017.07.032]
5 **Vande Casteele N**, Ferrante M, Van Assche G, Ballet V, Compernolle G, Van Steen K, Simoens S, Rutgeerts P, Gils A, Vermeire S. Trough concentrations of infliximab guide dosing for patients with inflammatory bowel disease. *Gastroenterology* 2015; **148**: 1320-9.e3 [PMID: 25724455 DOI: 10.1053/j.gastro.2015.02.031]
6 **D'Haens G**, Vermeire S, Lambrecht G, Baert F, Bossuyt P, Pariente B, Buisson A, Bouhnik Y, Filippi J, Vander Woude J, Van Hootegem P, Moreau J, Louis E, Franchimont D, De Vos M, Mana F, Peyrin-Biroulet L, Brixi H, Allez M, Caenepeel P, Aubourg A, Oldenburg B, Pierik M, Gils A, Chevret S, Laharie D; GETAID. Increasing Infliximab Dose Based on Symptoms, Biomarkers, and Serum Drug Concentrations Does Not Increase Clinical, Endoscopic, and Corticosteroid-Free Remission in Patients With Active Luminal Crohn's Disease. *Gastroenterology* 2018; **154**: 1343-1351.e1 [PMID: 29317275 DOI: 10.1053/j.gastro.2018.01.004]
7 **Dreesen E**, D'Haens G, Baert F, Pariente B, Bouhnik Y, vander Woude J, Moreau J, Laharie D, Vermeire S, Gils A. DOP047 Infliximab exposure predicts superior endoscopic outcomes in patients with active Crohn's disease: pharmacokinetic–pharmacodynamic analysis of TAILORIX. *J Crohns Colitis* 2018; **12**: S063-S064 [DOI: 10.1093/ecco-jcc/jjx180.084]
8 **Yarur AJ**, Kanagala V, Stein DJ, Czul F, Quintero MA, Agrawal D, Patel A, Best K, Fox C, Idstein K, Abreu MT. Higher infliximab trough levels are associated with perianal fistula healing in patients with Crohn's disease. *Aliment Pharmacol Ther* 2017; **45**: 933-940 [PMID: 28211593 DOI: 10.1111/apt.13970]
9 **Valdés Delgado T**, Guerra Veloz MF, Castro Laria L, Maldonado Pérez B, Perea Amarillo R, Merino Bohórquez V, Sáez A, Caunedo Álvarez Á, Argüelles Arias F. Cut-off ranges of infliximab serum levels in Crohn's disease in the clinical practice. *Rev Esp Enferm Dig* 2020; **112**: 756-761 [PMID: 32954770 DOI: 10.17235/reed.2020.6539/2019]
10 **Ward MG**, Warner B, Unsworth N, Chuah SW, Brownclarke C, Shieh S, Parkes M, Sanderson JD, Arkir Z, Reynolds J, Gibson PR, Irving PM. Infliximab and adalimumab drug levels in Crohn's disease: contrasting associations with disease activity and influencing factors. *Aliment Pharmacol Ther* 2017; **46**: 150-161 [PMID: 28481014 DOI: 10.1111/apt.14124]
11 **van Hoeve K**, Dreesen E, Hoffman I, Van Assche G, Ferrante M, Gils A, Vermeire S. Higher Infliximab Trough Levels Are Associated With Better Outcome in Paediatric Patients With Inflammatory Bowel Disease. *J Crohns Colitis* 2018; **12**: 1316-1325 [PMID: 30239644 DOI: 10.1093/ecco-jcc/jjy111]
12 **Papamichael K**, Rakowsky S, Rivera C, Cheifetz AS, Osterman MT. Infliximab trough concentrations during maintenance therapy are associated with endoscopic and histologic healing in ulcerative colitis. *Aliment Pharmacol Ther* 2018; **47**: 478-484 [PMID: 29210094 DOI: 10.1111/apt.14458]
13 **Negoescu DM**, Enns EA, Swanhorst B, Baumgartner B, Campbell JP, Osterman MT, Papamichael K, Cheifetz AS, Vaughn BP. Proactive Vs Reactive Therapeutic Drug Monitoring of Infliximab in Crohn's Disease: A Cost-Effectiveness Analysis in a Simulated Cohort. *Inflamm Bowel Dis* 2020; **26**: 103-111 [PMID: 31184366 DOI: 10.1093/ibd/izz113]
14 **Park SH**, Al-Bawardy B, Aniwan S, Kane SV, Coelho-Prabhu N, Papadakis KA, Kisiel JB, Bruining DH, Faubion WA, Raffals LE, Pardi DS, Tremaine WJ, Stephens MC, Tung J, Khanna S, Willrich MAV, Loftus EV. Distinct Cutoff Values of Adalimumab Trough Levels Are Associated With Different Therapeutic Outcomes in Patients With Inflammatory Bowel Disease. *Crohn Colitis 360* 2019; **1**: otz047 [DOI: 10.1093/crocol/otz047]
15 **Ungar B**, Engel T, Yablecovitch D, Lahat A, Lang A, Avidan B, Har-Noy O, Carter D, Levhar N, Selinger L, Neuman S, Natour OH, Yavzori M, Fudim E, Picard O, Kopylov U, Chowers Y, Naftali T, Broide E, Shachar E, Eliakim R, Ben-Horin S. Prospective Observational Evaluation of Time-Dependency of Adalimumab Immunogenicity and Drug Concentrations: The POETIC Study. *Am J Gastroenterol* 2018; **113**: 890-898 [PMID: 29867175 DOI: 10.1038/s41395-018-0073-0]
16 **Adedokun OJ**, Xu Z, Marano CW, Strauss R, Zhang H, Johanns J, Zhou H, Davis HM, Reinisch W, Feagan BG, Rutgeerts P, Sandborn WJ. Pharmacokinetics and Exposure-response Relationship of Golimumab in Patients with Moderately-to-Severely Active Ulcerative Colitis: Results from Phase 2/3 PURSUIT Induction and Maintenance Studies. *J Crohns Colitis* 2017; **11**: 35-46 [PMID: 27440869 DOI: 10.1093/ecco-jcc/jjw133]
17 **Detrez I**, Dreesen E, Van Stappen T, de Vries A, Brouwers E, Van Assche G, Vermeire S, Ferrante M, Gils A. Variability in Golimumab Exposure: A 'Real-Life' Observational Study in Active Ulcerative Colitis. *J Crohns Colitis* 2016; **10**: 575-581 [PMID: 26738756 DOI: 10.1093/ecco-jcc/jjv241]
18 **Nesbitt A**, Fossati G, Bergin M, Stephens P, Stephens S, Foulkes R, Brown D, Robinson M, Bourne T. Mechanism of action of certolizumab pegol (CDP870): in vitro comparison with other anti-tumor necrosis factor alpha agents. *Inflamm Bowel Dis* 2007; **13**: 1323-1332 [PMID: 17636564 DOI: 10.1002/ibd.20225]
19 **Colombel JF**, Sandborn WJ, Allez M, Dupas JL, Dewit O, D'Haens G, Bouhnik Y, Parker G, Pierre-Louis B, Hébuterne X. Association between plasma concentrations of certolizumab pegol and endoscopic outcomes of patients with Crohn's disease. *Clin Gastroenterol Hepatol* 2014; **12**: 423-31.e1 [PMID: 24184736 DOI: 10.1016/j.cgh.2013.10.025]
20 **Vande Casteele N**, Feagan BG, Vermeire S, Yassine M, Coarse J, Kosutic G, Sandborn WJ. Exposure-response relationship of certolizumab pegol induction and maintenance therapy in patients with Crohn's disease. *Aliment Pharmacol Ther* 2018; **47**: 229-237 [PMID: 29159893 DOI: 10.1111/apt.14421]
21 **Feagan BG**, Rutgeerts P, Sands BE, Hanauer S, Colombel JF, Sandborn WJ, Van Assche G, Axler J, Kim HJ, Danese S, Fox I, Milch C, Sankoh S, Wyant T, Xu J, Parikh A; GEMINI 1 Study Group. Vedolizumab as induction and maintenance therapy for ulcerative colitis. *N Engl J Med* 2013; **369**: 699-710 [PMID: 23964932 DOI: 10.1056/NEJMoa1215734]
22 **Sandborn WJ**, Feagan BG, Rutgeerts P, Hanauer S, Colombel JF, Sands BE, Lukas M, Fedorak RN, Lee S, Bressler B, Fox I, Rosario M, Sankoh S, Xu J, Stephens K, Milch C, Parikh A; GEMINI 2 Study Group. Vedolizumab as induction and maintenance therapy for Crohn's disease. *N Engl J Med* 2013; **369**: 711-721 [PMID: 23964933 DOI: 10.1056/NEJMoa1215739]
23 **Rosario M**, French JL, Dirks NL, Sankoh S, Parikh A, Yang H, Danese S, Colombel JF, Smyth M, Sandborn WJ, Feagan BG, Reinisch W, Sands BE, Sans M, Fox I. Exposure-efficacy Relationships for Vedolizumab Induction Therapy in Patients with Ulcerative Colitis or Crohn's Disease. *J Crohns Colitis* 2017; **11**: 921-929 [PMID: 28333288 DOI: 10.1093/ecco-jcc/jjx021]
24 **Löwenberg M**, Vermeire S, Mostafavi N, Hoentjen F, Franchimont D, Bossuyt P, Hindryckx P, Rispens T, de Vries A, van der Woude CJ, Berends S, Ambarus CA, Mathot R, Clasquin E, Baert F, D'Haens G. Vedolizumab Induces Endoscopic and

Histologic Remission in Patients With Crohn's Disease. *Gastroenterology* 2019; **157**: 997-1006.e6 [PMID: 31175865 DOI: 10.1053/j.gastro.2019.05.067]

25 **Al-Bawardy B**, Ramos GP, Willrich MAV, Jenkins SM, Park SH, Aniwan S, Schoenoff SA, Bruining DH, Papadakis KA, Raffals L, Tremaine WJ, Loftus EV. Vedolizumab Drug Level Correlation With Clinical Remission, Biomarker Normalization, and Mucosal Healing in Inflammatory Bowel Disease. *Inflamm Bowel Dis* 2019; **25**: 580-586 [PMID: 30165638 DOI: 10.1093/ibd/izy272]

26 **Restellini S**, Khanna R, Afif W. Therapeutic Drug Monitoring With Ustekinumab and Vedolizumab in Inflammatory Bowel Disease. *Inflamm Bowel Dis* 2018; **24**: 2165-2172 [PMID: 29788272 DOI: 10.1093/ibd/izy134]

27 **Benson JM**, Peritt D, Scallon BJ, Heavner GA, Shealy DJ, Giles-Komar JM, Mascelli MA. Discovery and mechanism of ustekinumab: a human monoclonal antibody targeting interleukin-12 and interleukin-23 for treatment of immune-mediated disorders. *MAbs* 2011; **3**: 535-545 [PMID: 22123062 DOI: 10.4161/mabs.3.6.17815]

28 **Feagan BG**, Sandborn WJ, Gasink C, Jacobstein D, Lang Y, Friedman JR, Blank MA, Johanns J, Gao LL, Miao Y, Adedokun OJ, Sands BE, Hanauer SB, Vermeire S, Targan S, Ghosh S, de Villiers WJ, Colombel JF, Tulassay Z, Seidler U, Salzberg BA, Desreumaux P, Lee SD, Loftus EV Jr, Dieleman LA, Katz S, Rutgeerts P; UNITI–IM-UNITI Study Group. Ustekinumab as Induction and Maintenance Therapy for Crohn's Disease. *N Engl J Med* 2016; **375**: 1946-1960 [PMID: 27959607 DOI: 10.1056/NEJMoa1602773]

29 **Adedokun OJ**, Xu Z, Gasink C, Jacobstein D, Szapary P, Johanns J, Gao LL, Davis HM, Hanauer SB, Feagan BG, Ghosh S, Sandborn WJ. Pharmacokinetics and Exposure Response Relationships of Ustekinumab in Patients With Crohn's Disease. *Gastroenterology* 2018; **154**: 1660-1671 [PMID: 29409871 DOI: 10.1053/j.gastro.2018.01.043]

30 **Battat R**, Kopylov U, Bessissow T, Bitton A, Cohen A, Jain A, Martel M, Seidman E, Afif W. Association Between Ustekinumab Trough Concentrations and Clinical, Biomarker, and Endoscopic Outcomes in Patients With Crohn's Disease. *Clin Gastroenterol Hepatol* 2017; **15**: 1427-1434.e2 [PMID: 28365485 DOI: 10.1016/j.cgh.2017.03.032]

31 **Kopylov U**, Ben-Horin S, Seidman E. Therapeutic drug monitoring in inflammatory bowel disease. *Ann Gastroenterol* 2014; **27**: 304-312 [PMID: 25331715]

32 **Thomas SS**, Borazan N, Barroso N, Duan L, Taroumian S, Kretzmann B, Bardales R, Elashoff D, Vangala S, Furst DE. Comparative Immunogenicity of TNF Inhibitors: Impact on Clinical Efficacy and Tolerability in the Management of Autoimmune Diseases. A Systematic Review and Meta-Analysis. *BioDrugs* 2015; **29**: 241-258 [PMID: 26280210 DOI: 10.1007/s40259-015-0134-5]

33 **Colombel JF**, Sandborn WJ, Reinisch W, Mantzaris GJ, Kornbluth A, Rachmilewitz D, Lichtiger S, D'Haens G, Diamond RH, Broussard DL, Tang KL, van der Woude CJ, Rutgeerts P; SONIC Study Group. Infliximab, azathioprine, or combination therapy for Crohn's disease. *N Engl J Med* 2010; **362**: 1383-1395 [PMID: 20393175 DOI: 10.1056/NEJMoa0904492]

34 **Vande Casteele N**, Gils A, Singh S, Ohrmund L, Hauenstein S, Rutgeerts P, Vermeire S. Antibody response to infliximab and its impact on pharmacokinetics can be transient. *Am J Gastroenterol* 2013; **108**: 962-971 [PMID: 23419382 DOI: 10.1038/ajg.2013.12]

35 **Hindryckx P**, Novak G, Vande Casteele N, Khanna R, Laukens D, Jairath V, Feagan BG. Incidence, Prevention and Management of Anti-Drug Antibodies Against Therapeutic Antibodies in Inflammatory Bowel Disease: A Practical Overview. *Drugs* 2017; **77**: 363-377 [PMID: 28233275 DOI: 10.1007/s40265-017-0693-5]

36 **Cohen RZ**, Schoen BT, Kugathasan S, Sauer CG. Management of Anti-drug Antibodies to Biologic Medications in Children With Inflammatory Bowel Disease. *J Pediatr Gastroenterol Nutr* 2019; **69**: 551-556 [PMID: 31335833 DOI: 10.1097/MPG.0000000000002440]

37 **Ben-Horin S**, Waterman M, Kopylov U, Yavzori M, Picard O, Fudim E, Awadie H, Weiss B, Chowers Y. Addition of an immunomodulator to infliximab therapy eliminates antidrug antibodies in serum and restores clinical response of patients with inflammatory bowel disease. *Clin Gastroenterol Hepatol* 2013; **11**: 444-447 [PMID: 23103905 DOI: 10.1016/j.cgh.2012.10.020]

38 **Yanai H**, Lichtenstein L, Assa A, Mazor Y, Weiss B, Levine A, Ron Y, Kopylov U, Bujanover Y, Rosenbach Y, Ungar B, Eliakim R, Chowers Y, Shamir R, Fraser G, Dotan I, Ben-Horin S. Levels of drug and antidrug antibodies are associated with outcome of interventions after loss of response to infliximab or adalimumab. *Clin Gastroenterol Hepatol* 2015; **13**: 522-530.e2 [PMID: 25066837 DOI: 10.1016/j.cgh.2014.07.029]

39 **Kelly OB**, Donnell SO, Stempak JM, Steinhart AH, Silverberg MS. Therapeutic Drug Monitoring to Guide Infliximab Dose Adjustment is Associated with Better Endoscopic Outcomes than Clinical Decision Making Alone in Active Inflammatory Bowel Disease. *Inflamm Bowel Dis* 2017; **23**: 1202-1209 [PMID: 28498155 DOI: 10.1097/MIB.0000000000001126]

40 **Charabaty A**. Are We Ready for Proactive Therapeutic Drug Monitoring of Anti-TNF to Optimize Care of Patients With Inflammatory Bowel Disease? *Crohn Colitis 360* 2020; **2**: otz056 [DOI: 10.1093/crocol/otz056]

41 **Fernandes SR**, Bernardo S, Simões C, Gonçalves AR, Valente A, Baldaia C, Moura Santos P, Correia LA, Tato Marinho R. Proactive Infliximab Drug Monitoring Is Superior to Conventional Management in Inflammatory Bowel Disease. *Inflamm Bowel Dis* 2020; **26**: 263-270 [PMID: 31247074 DOI: 10.1093/ibd/izz131]

42 **Assa A**, Matar M, Turner D, Broide E, Weiss B, Ledder O, Guz-Mark A, Rinawi F, Cohen S, Topf-Olivestone C, Shaoul R, Yerushalmi B, Shamir R. Proactive Monitoring of Adalimumab Trough Concentration Associated With Increased Clinical Remission in Children With Crohn's Disease Compared With Reactive Monitoring. *Gastroenterology* 2019; **157**: 985-996.e2 [PMID: 31194979 DOI: 10.1053/j.gastro.2019.06.003]

43 **Papamichael K**, Chachu KA, Vajravelu RK, Vaughn BP, Ni J, Osterman MT, Cheifetz AS. Improved Long-term Outcomes of Patients With Inflammatory Bowel Disease Receiving Proactive Compared With Reactive Monitoring of Serum Concentrations of Infliximab. *Clin Gastroenterol Hepatol* 2017; **15**: 1580-1588.e3 [PMID: 28365486 DOI: 10.1016/j.cgh.2017.03.031]

44 **Argollo M**, Kotze PG, Kakkadasam P, D'Haens G. Optimizing biologic therapy in IBD: how essential is therapeutic drug monitoring? *Nat Rev Gastroenterol Hepatol* 2020; **17**: 702-710 [PMID: 32879465 DOI: 10.1038/s41575-020-0352-2]

45 **Strik AS**, Berends SE, Löwenberg M. Therapeutic drug monitoring-based dosing of TNF inhibitors in inflammatory bowel

disease: the way forward? *Expert Rev Clin Pharmacol* 2019; **12**: 885-891 [PMID: 31305158 DOI: 10.1080/17512433.2019.1642745]

46 **Roblin X**, Rinaudo M, Del Tedesco E, Phelip JM, Genin C, Peyrin-Biroulet L, Paul S. Development of an algorithm incorporating pharmacokinetics of adalimumab in inflammatory bowel diseases. *Am J Gastroenterol* 2014; **109**: 1250-1256 [PMID: 24913041 DOI: 10.1038/ajg.2014.146]

47 **Ungar B**, Levy I, Yavne Y, Yavzori M, Picard O, Fudim E, Loebstein R, Chowers Y, Eliakim R, Kopylov U, Ben-Horin S. Optimizing Anti-TNF-α Therapy: Serum Levels of Infliximab and Adalimumab Are Associated With Mucosal Healing in Patients With Inflammatory Bowel Diseases. *Clin Gastroenterol Hepatol* 2016; **14**: 550-557.e2 [PMID: 26538204 DOI: 10.1016/j.cgh.2015.10.025]

48 **Bodini G**, Giannini EG, Savarino V, Del Nero L, Pellegatta G, De Maria C, Baldissarro I, Savarino E. Adalimumab trough serum levels and anti-adalimumab antibodies in the long-term clinical outcome of patients with Crohn's disease. *Scand J Gastroenterol* 2016; **51**: 1081-1086 [PMID: 27207330 DOI: 10.3109/00365521.2016.1157894]

49 **Ruwaard J**, Marsman AF, Nurmohamed MT, van der Horst-Bruinsma IE, Te Velthuis H, Bloem K, de Vries A, Rispens T, Wolbink G. Antidrug antibody detection for adalimumab depends on the type of assay used: an experimental approach to help clinicians interpret diagnostic data. *Clin Exp Rheumatol* 2019; **37**: 756-761 [PMID: 30943139]

50 **Wang SL**, Ohrmund L, Hauenstein S, Salbato J, Reddy R, Monk P, Lockton S, Ling N, Singh S. Development and validation of a homogeneous mobility shift assay for the measurement of infliximab and antibodies-to-infliximab levels in patient serum. *J Immunol Methods* 2012; **382**: 177-188 [PMID: 22691619 DOI: 10.1016/j.jim.2012.06.002]

51 **Gorovits B**, Baltrukonis DJ, Bhattacharya I, Birchler MA, Finco D, Sikkema D, Vincent MS, Lula S, Marshall L, Hickling TP. Immunoassay methods used in clinical studies for the detection of anti-drug antibodies to adalimumab and infliximab. *Clin Exp Immunol* 2018; **192**: 348-365 [PMID: 29431871 DOI: 10.1111/cei.13112]

World Journal of Gastroenterology

Submit a Manuscript: https://www.f6publishing.com

World J Gastroenterol 2022 June 7; 28(21): 2291-2301

DOI: 10.3748/wjg.v28.i21.2291

ISSN 1007-9327 (print) ISSN 2219-2840 (online)

MINIREVIEWS

Serological biomarkers for management of primary sclerosing cholangitis

David Tornai, Peter Laszlo Ven, Peter Laszlo Lakatos, Maria Papp

Specialty type: Gastroenterology and hepatology

Provenance and peer review: Invited Conference articles; Externally peer reviewed.

Peer-review model: Single blind

Peer-review report's scientific quality classification

Grade A (Excellent): 0
Grade B (Very good): B
Grade C (Good): C
Grade D (Fair): 0
Grade E (Poor): 0

P-Reviewer: Losurdo G, Italy; Wen XL, China

Received: December 13, 2021
Peer-review started: December 13, 2021
First decision: January 23, 2022
Revised: February 1, 2022
Accepted: April 25, 2022
Article in press: April 25, 2022
Published online: June 7, 2022

David Tornai, Maria Papp, Division of Gastroenterology, Department of Internal Medicine, Faculty of Medicine, University of Debrecen, Debrecen H-4032, Hajdu-Bihar, Hungary

David Tornai, Maria Papp, European Reference Network on Hepatological Diseases, ERN RARE-LIVER, Debrecen H-4032, Hajdu-Bihar, Hungary

Peter Laszlo Ven, The First Department of Medicine, Division of Gastroenterology, University of Pécs, Pécs H-7624, Baranya, Hungary

Peter Laszlo Ven, Kálmán Laki Doctoral School of Biomedical and Clinical Sciences, Faculty of Medicine, University of Debrecen, Debrecen H-4032, Hajdu-Bihar, Hungary

Peter Laszlo Lakatos, Division of Gastroenterology, McGill University Health Centre, Montreal QC H4A 3J1, Quebec, Canada

Peter Laszlo Lakatos, The First Department of Medicine, Semmelweis University, Budapest H-1083, Pest, Hungary

Corresponding author: Maria Papp, DSc, FEBG, MD, PhD, Full Professor, Division of Gastroenterology, Department of Internal Medicine, Faculty of Medicine, University of Debrecen, 98 Nagyerdei krt, Debrecen H-4032, Hajdu-Bihar, Hungary.
papp.maria@med.unideb.hu

Abstract

Clinical manifestations and progression of primary sclerosing cholangitis (PSC) are heterogeneous, and its pathogenesis is poorly understood. The importance of gut-liver interactions in the pathogenesis has been clinically confirmed and highlighted in different theories. Recent advances regarding biomarkers of biliary-gut crosstalk may help to identify clinically relevant PSC subgroups assisting everyday clinical work-up (*e.g.*, diagnosis, disease stratification, or surveillance) and the exploration of potential therapeutic targets. Alkaline phosphatase produced by the biliary epithelium is consistently associated with prognosis. However, its level shows natural fluctuation limiting its use in individual patients. Inflammatory, cell activation, and tissue remodeling markers have been reported to predict clinical outcome. Elevated immunoglobulin (Ig) G4 level is associated with a shorter transplantation-free survival. IgG type atypical perinuclear anti-neutrophil cytoplasmic antibodies (P-ANCAs) are non-specific markers of various autoimmune liver diseases and may reflect an abnormal B-cell response to gut microbial antigens. IgG type atypical P-ANCA identifies PSC

patients with particular clinical and genetic (for human leukocyte antigens) characteristics. The presence of IgA type anti-F-actin antibody (AAA) may predict a progressive disease course, and it is associated with enhanced mucosal immune response to various microbial antigens and enterocyte damage. IgA type anti-glycoprotein 2 (GP2) antibodies identify patients with a severe disease phenotype and poor survival due to enhanced fibrogenesis or development of cholangiocarcinoma. Elevated soluble vascular adhesion protein-1 (sVAP-1) level is associated with adverse disease outcomes in PSC. High sVAP-1 levels correlate with mucosal addressin cell adhesion molecule-1 (MAdCAM-1) expression in the liver that contributes to gut activated T-cell homing to the hepatobiliary tract. In the present paper, we review the evidence on these possible serological markers that could potentially help address the unmet clinical needs in PSC.

Key Words: Primary sclerosing cholangitis; Hepatobiliary; Serological biomarker; Immunoglobulin; Inflammatory; Tissue remodeling

©The Author(s) 2022. Published by Baishideng Publishing Group Inc. All rights reserved.

Core Tip: Recent advances in biomarker research may help clinicians identify relevant subgroups of primary sclerosing cholangitis (PSC) and assist everyday clinical work-up. However, a diagnostic biomarker is still an unmet need. On the other hand, several biomarkers have been reported to predict outcome in PSC; however, most of them have not been validated by subsequent studies. The IgA type anti-glycoprotein 2 antibody is the first one to be supported by a satisfactory number of clinical studies and could be incorporated into clinical practice. These discoveries also reveal different aspects of PSC providing with potential therapeutic targets.

Citation: Tornai D, Ven PL, Lakatos PL, Papp M. Serological biomarkers for management of primary sclerosing cholangitis. *World J Gastroenterol* 2022; 28(21): 2291-2301
URL: https://www.wjgnet.com/1007-9327/full/v28/i21/2291.htm
DOI: https://dx.doi.org/10.3748/wjg.v28.i21.2291

INTRODUCTION

Primary sclerosing cholangitis (PSC) is a chronic and progressive inflammatory disease of the bile ducts, leading to the formation of intermitting bile duct strictures and dilatations, with periductal fibrosis that in most cases progresses to cirrhosis and decompensated disease stage. Moreover, PSC is associated with the development of cholangiocarcinoma (CCA) and colorectal cancer[1]. The etiology of PSC is poorly understood. However, the gut-liver interaction seems to be a driving factor in its development. It has been hypothesized that the interaction of the gut microbiome and certain genetically determined factors [such as certain human leukocyte antigens (HLA)] leads to the development of disrupted immunological pathways, as a result of an autoimmune reaction to yet unknown antigen(s). Most abnormalities discovered by genetic studies support a disruption of T cell functions. Gut-derived antigens significantly induce antigen presentation by major histocompatibility complexes (MHCs) on the surface of antigen-presenting cells to T cells, which, following clonal expansion, can be delivered to both the intestinal tract and the liver[2]. Abnormal T cell activation results in increased release of various cytokines [such as transforming growth factor-β (TGF-β)] involved in the development of fibrosis. Activation of B cells is indicated by the frequent appearance of bacterial translocation (BT) related serological antibodies [*e.g.*, anti-neutrophil cytoplasmic antibodies (ANCAs)].

The diagnosis of PSC is difficult, and no biomarker specific to the disease has been identified so far. In the presence of chronic cholestasis, the diagnosis is based on magnetic resonance cholangiography (MRCP) or, much less frequently today, endoscopic retrograde cholangiopancreatography (ERCP) with confirmation of biliary lesions and strictures. Careful exclusion of known causes of secondary sclerosing cholangitis (SSC) is also necessary. Immunoglobulin (Ig) G elevation and the presence of atypical perinuclear ANCA (P-ANCA) in serum are common but are not disease-specific serological alterations [3]. Routine liver biopsy is no longer routinely performed in the diagnosis of PSC and is only necessary in suspected cases of small duct PSC, when the cholangiogram is normal, or to confirm overlap syndrome with autoimmune hepatitis.

The disease course of PSC is variable. There are a few promising biomarkers to predict disease activity and progression, yet almost none has been validated in subsequent studies. A recently discovered serological biomarker [IgA type antibodies against pancreatic glycoprotein 2 (anti-GP2 IgA)] [4,5] is the first that has predictive value in PSC confirmed in multiple studies[6,7]. However, it has not

been integrated into clinical practice. Consequently, the question of accurate risk assessment, disease stratification, and follow-up strategy for patients with PSC is still unresolved[8].

Studying biomarkers characterizing the dialogue between the biliary tract and the intestine in PSC may not only identify clinically relevant subgroups for disease stratification, but can also unravel new pathogenesis-relevant correlations. This could in turn lead to the discovery of new therapeutic targets.

While biomarkers from other body fluids (*e.g.*, bile) can reveal important aspects of the pathogenesis, blood is more readily available for clinicians and can be obtained in a highly controlled fashion (in contrast to, *e.g.*, stool). This makes serological biomarkers the most appropriate for everyday clinical use, therefore these are the markers that we focus on in this review.

ROUTINE LABORATORY TESTS AND COMPOSITE SCORES

Alkaline phosphatase

Various clinical studies have consistently reported a correlation between alkaline phosphatase (ALP) levels and disease progression, but its individual application is difficult. In PSC, the fluctuation pattern of ALP is different from that observed in primary biliary cholangitis, and the degree of elevation is influenced by the development of various biliary complications (cholangitis, gallstones, or the appearance of a dominant stricture). Thus, it is not surprising that the ALP thresholds or values of change associated with disease outcomes in certain studies were not confirmed by other studies[9]. However, certain studies highlighted the importance of ALP fluctuation in CCA development free survival. The risk of developing CCA was significantly higher in patients with constantly high ALP levels without reduction[10-13]. Thus, further studies are needed to determine the significance of ALP level variation also in transplant free survival (due to progression of fibrosis) and treatment response.

Mayo risk score

In the absence of individual predictive markers, researchers tried to develop predictive models incorporating multiple markers. These scoring systems, however, also contain clinical parameters besides serological markers. The first and still the most widely used clinical prognostic model is the Mayo risk score (MRS), which, as modified in 2000, no longer includes invasive or subjective parameters [14]. Abnormal value of the factors included in the MRS [serum bilirubin, albumin, and aspartate aminotransferase (AST) levels, and esophageal variceal bleeding], with the exception of age, represents advanced liver disease. Thus, the discriminatory potential of this scoring system is inadequate in the early stages of PSC. In addition, the predictable time period for disease progression is only around 4 years. The model was also not able to predict the adverse disease outcome associated to high-dose ursodeoxycholic acid treatment (28-30 mg/kg/d) either[15].

Amsterdam-Oxford model

The Amsterdam-Oxford model (AOM) is another prognostic scoring system for PSC[16], which includes seven objective parameters (PSC subtype, age at diagnosis, platelet count, serum albumin, ALP, AST, and bilirubin levels). This scoring system was developed to overcome the limitations of MRS in the prediction of transplant-free survival. It can be used to estimate a longer-term prognosis of PSC (15 years) and can be recalculated at a later timepoint. However, the discriminative power of the model was only moderate (C-statistic: 0.68). In contrast, it has the advantage of being much more widely applicable (the reliability of the model was consistent in the two populations and at different timepoints) as it was developed using population-based data rather than data from transplant centers.

UK-PSC scores

The UK-PSC scores were also developed to predict transplant-free survival[17]. Two models were created for 2-year and for 10-year prediction, derived from a cohort of 1001 PSC patients and validated in two independent cohorts adding up to 451 patients. The incorporated variables were serum bilirubin, ALP, albumin, platelets, presence of extrahepatic biliary disease, and variceal hemorrhage. "Both short- and long-term UK-PSC risk scores had better performance than MRS and AST-to-platelet ratio index when predicting outcomes [C-statistics for 2-year survival (short-term) were 0.81 *vs* 0.75 and 0.81 *vs* 0.63, respectively; for 10-year survival (long-term) were 0.80 *vs* 0.79 and 0.80 *vs* 0.59, respectively]."

PSC risk estimate tool

PSC risk estimate tool (PREsTo) was developed to predict the advent of hepatic decompensation (ascites, variceal hemorrhage, or encephalopathy). The model was derived from data of a multicenter North American cohort and validated in an international multicenter cohort including 509 and 278 subjects, respectively. Individuals with advanced PSC or CCA at baseline were excluded. PREsTo incorporates nine variables: Bilirubin, albumin, serum ALP times the upper limit of normal, platelets, AST, hemoglobin, sodium, patient age, and number of years since the diagnosis of PSC. In predicting hepatic decompensation, PREsTo performed better than model of end stage of liver disease (MELD)

score and MRS (C-statistics: 0.90 *vs* 0.72 and 0.90 *vs* 0.85, respectively)[18]. The equation is not provided, and only an online calculator is available.

Enhanced liver fibrosis test

The enhanced liver fibrosis (ELF) test (Siemens ADVIA Centaur) is based on purely serological measurements summarizing three direct components of fibrogenesis (hyaluronic acid, tissue inhibitor of metalloproteinase 1, and type III procollagen amino-terminal propeptide). It has been reported to be a strong predictor of prognosis (mortality and liver transplantation) in PSC independently of MRS. Validation of this result was successful in multiple studies (C-statistic: 0.79-0.81)[19,20]. In a recent study, the ELF score slightly increased in PSC patients over a 5-year follow-up period and showed low intrapersonal variability supporting the consistency of this score[21].

IMMUNOGLOBULINS

IgG4

About 10% of patients have elevated serum IgG4 levels without IgG4-associated disease. Recently, IgG4 determination is recommended at least once in all patients with PSC[22]. Elevated serum IgG4 levels (> 140 mg/dL) in PSC patients were associated with higher values of liver function tests, higher MRS, and shorter time to liver transplantation, which clearly indicates a more severe disease course in this subgroup of patients[23]. It is unknown whether the addition of a systemic glucocorticoid to treatment in the high IgG4 subtype of PSC may be beneficial in curbing disease progression[24].

ANCAs

Various other serum autoantibodies have been described in PSC patients; however, they are considered unspecific, since they may be present also in other diseases. The most frequently observed antibodies in PSC are ANCAs, but antinuclear antibodies and anti-smooth muscle antibodies were also reported to be frequently associated with PSC[25].

The occurrence of IgG isotype atypical P-ANCAs in PSC are common (up to 80% of cases). The putative role of intestinal bacteria in ANCA formation (homology between human beta-tubulin isotype 5 and bacterial FtsZ protein, molecular mimicry) has been described[26]. Early, small scale, case-control clinical studies[27] found no correlation between ANCA formation and clinical or genetic features of PSC. Hov *et al*[28], however, in a large comprehensive case-control study, demonstrated that risk genes with a strong association to PSC formation (HLA-B*08 and DRB1*03) were also associated with ANCA formation. Interestingly, association between the presence of PSC related HLA alleles (B*08, C*07, and DRB1*03) and increased risk of acute rejection syndrome in liver transplant recipients has also been reported (while DRB1*04 was found to be a protecting factor)[29].

The antibody against serine proteinase-3 (PR3) is a type of cytoplasmic ANCA (C-ANCAs). PR3-ANCA is typically observed in small vessel vasculitis[30] but recently has been reported in ulcerative colitis (UC)[31], which prompted researchers to investigate this antibody in PSC as well. Interestingly, in the setting of PSC, PR3-ANCA seems to be associated with worse liver biochemistry rather than with a co-diagnosis of UC[32]. In a recent study by Wunsch *et al*[7], besides worse liver function tests and MELD score, PR3-ANCA has been shown to be associated with CCA development [hazard ratio (HR) = 9.8, 95% confidence interval (CI) = 1.3-74.5; P = 0.03] and risk of shorter transplant free survival (HR = 1.8; 95%CI = 1.3-2.8; P = 0.01). However, the predictive capacity of PR3-ANCA was not confirmed in the validation cohort where the frequency of PR3-ANCA was found to be surprisingly low (5% in contrast to 54% in the discovery cohort) and CCA development was also less prevalent[7].

IgA type autoantibodies

IgA is the most important immunoglobulin isotype involved in mucosal immunity[33]. Since the gut-liver interaction plays a central role in the pathogenesis of PSC, the formation of IgA type autoreactive antibodies is a characteristic feature of the disease. Under physiological conditions, monomeric IgA in serum inhibits immunological processes (so-called immunosuppressive effect). However, in pathological conditions, immune complexes formed by aggregation of monomeric IgA molecules can activate immunological processes by binding to myeloid cells[34]. IgA, produced by plasma cells lining the gut and biliary epithelium, is a highly abundant immunoglobulin in bile and plays a central role in the defense against intestinal pathogens. Biliary epithelial cells (that are the cellular targets of injury in PSC) and intestinal epithelial cells transport the IgA molecules into the biliary and intestinal lumens, respectively (→secretory IgA)[35-37]. However, in the past, most studies on serological antibodies in autoimmune liver diseases, like in the case of ANCA, have focused mainly on IgG isotype antibodies, and the IgA isotype is only recently gaining attention[38].

The work of Berglin *et al*[39] is an example, which highlighted the described importance of IgA isotype antibody related pathogenetic pathways in PSC. They demonstrated that in the presence of IgA isotype autoantibodies against biliary epithelial cells, disease progression was faster than in their

absence. No similar correlation was observed for IgG isotype antibodies.

In 2015, our group reported the association between PSC and the presence of anti- GP2 IgA antibodies in inflammatory bowel disease (IBD) patients[40]. Subsequently, anti-GP2 IgA positivity was demonstrated to be able to predict a progressive disease course in PSC by our and another group[4,5]. These results were confirmed later by further studies[6,7]. In total, 1111 PSC patients have been evaluated for the presence of anti-GP2 IgA and the prevalence was found between 30.8% and 52.2%[8]. Anti-GP2 IgA was consistently reported to be associated with a more severe PSC phenotype with a 2- to 5-fold higher risk to develop end stage liver disease with a need for liver transplantation (Figure 1). Consequently, anti-GP2 IgA may soon be integrated into clinical practice for risk assessment in PSC. Moreover, anti-GP2 IgA can also identify a subset of PSC patients with existing biliary tract cancer or with an increased risk of developing it during the disease course. This association between anti-GP2 IgA and CCA was reported by Jendrek *et al*[4] and confirmed by Wunsch *et al*[7] both evaluating two cohorts each, providing strong evidence that incorporation of anti-GP2 IgA into CCA surveillance protocols could be beneficial (Figure 1).

IgA autoantibody against F-actin has been also reported to be associated with enhanced mucosal immune response to various microbial antigens and enterocyte damage in PSC, and to identify PSC patients with progressive disease (HR = 4.54; 95%CI = 1.14-18.18; P = 0.032)[41]. Cytoskeletal F-actin initiates an extracellular damage-associated molecular pattern signaling pathway through DNGR-1/CLEC9A and Syk-SFK that results in antigen cross-presentation to $CD8^+$ T cells[42-45]. $CD8^+$ T cells, after activation in the gut, can be recruited to the liver and induce immune-mediated cholangitis in mice [46].

OTHER SEROLOGICAL BIOMARKERS

Interleukin-8

As a result of increased lipopolysaccharide (LPS) exposure, biliary epithelial cells produce interleukin-8 (IL-8), which has a proliferation-promoting effect and enhances fibrogenesis related gene expression. In the study by Vesterhus *et al*[47], using modern antibody array technology, elevated serum IL-8 showed the strongest association with poor transplant-free survival among pro-inflammatory markers. However, the predictive value of MRS and ELF test for clinical outcomes was found to be higher than that of IL-8.

Macrophage activation markers

Bossen *et al*[48] found that macrophage activation markers, soluble CD163 (sCD163) and mannose receptor (sMR), were increased according to disease severity in two independent PSC cohorts of 138 and 159 patients. In both cohorts, sCD163 and sMR levels rose in parallel with increasing liver enzymes, MRS, and ELF test. Patients with high baseline levels of sCD163 (> 3.86 mg/L) had decreased transplant-free survival during the 8-year follow-up in both cohorts (35.2% *vs* 83.0% in the combined cohort). sMR showed similar association only in one of the cohorts with more severe disease features. In Cox regression, sCD163 also performed better in the more severe cohort (HR = 3.15 and 2.89) but it lost significance in the multivariate model against ELF test and AOM score.

BT markers

In a study investigating serum markers of BT, serum levels of zonulin, intestinal fatty acid binding protein, soluble CD14 (sCD14), LPS, and LPS-binding protein (LBP) were measured in 166 PSC patients and 100 healthy controls[49]. LBP and sCD14 levels were higher, whilst zonulin levels were lower in PSC patients compared to controls. This latter difference disappeared with the exclusion of PSC patients with elevated prothrombin time (indicating advanced liver disease). In patients with CCA, sCD14 levels were higher compared to patients without it. High sCD14 and LBP values (> 1638 ng/mL and > 13942 ng/mL, respectively) were associated with reduced transplantation-free survival independently of MRS (HR = 2.26; 95%CI = 1.15-4.43; P = 0.018 and HR = 2.00; 95%CI = 1.17-3.43; P = 0.011, respectively). Further studies are needed to validate these findings.

Extracellular remodeling markers

In a cohort of 138 large-duct PSC patients (74% with IBD) using 52 UC patients as controls, Nielsen *et al* [50] investigated the predictive potential of four extracellular remodeling markers related to collagen formation (PRO-C3 and PRO-C5) and collagen degradation (C3M and C4M). All markers were elevated in PSC compared to UC patients, with PRO-C3 showing the most robust difference. High serum levels of three markers (with the exception of C3M) were associated with a shorter transplant-free survival during a 4-year follow-up period. In the univariate Cox regression model (using tertiles of the markers), PRO-C3 had the highest HR (HR = 3.02; 95%CI = 1.96-4.67, P < 0.001) but it failed to predict survival in the multivariate model including ELF test, while PRO-C5 remained an independent predictor (multivariate HR = 1.92; 95%CI = 1.28-2.88; P = 0.002). The combination of PRO-C3 and PRO-C5 resulted in a significantly improved odds ratio (OR = 47.3; P < 0.001) compared to the individual markers and

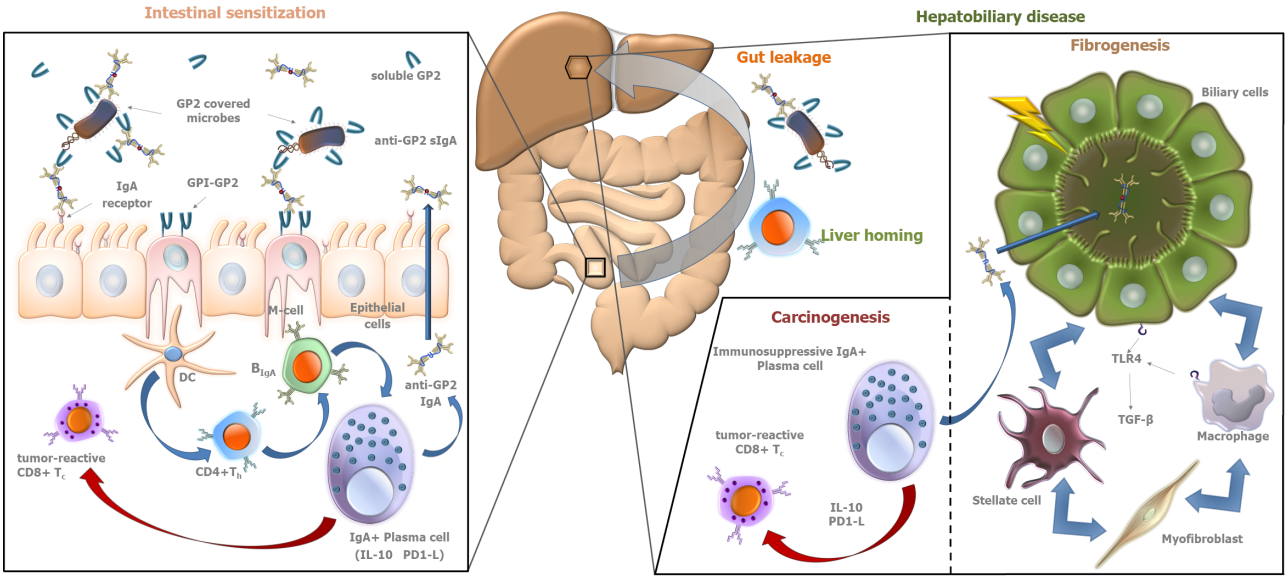


Figure 1 Autoimmunity-driven putative role of pancreatic glycoprotein 2 in fibro- and tumorigenesis in primary sclerosing cholangitis. Along with digestive enzymes, glycoprotein 2 (GP2) is secreted from pancreatic acinar cells into the intestinal lumen. In addition, GP2 is also expressed on the luminal surface of microfold cells [M-cells in Peyer's patches anchored by glycosylphosphatidylinositol (GPI)]. Both forms of the molecule interact with FimH+ bacteria and opsonize them. The anchored form may be involved in the transcytosis of bound ligands (FimH+ microbes) through M cells, which pass them to antigen-presenting cells like dendritic cells (DC) located in the mucosa-associated immune system. Microbe-bound GP2 epitopes are presented to CD4-positive T helper cells ($CD4^+ T_h$) along with bacterial antigens that lead to loss of tolerance to GP2. After clonal expansion, these sensitized cells can "home" to both the gut and the liver where they trigger (blue arrows) the differentiation of IgA^+ B cells into IgA^+ plasma cells. The produced anti-GP2 IgA is actively transported by epithelial cells to the intestinal and biliary lumens as secretory IgA (sIgA), where it binds to GP2. Epithelial cells express IgA receptors on their luminal surface that are involved in active retrograde transport of sIgA molecules (typically coupled by antigens). This process may contribute to bacterial overload of the gut mucosa, elevating the levels of bacterial components in the circulation. In the hepato-biliary tract, bacterial components trigger the Toll-like receptor 4 (TLR4)-transforming growth factor-β (TGF-β) pathway, facilitating fibrosis and cirrhosis. Meanwhile, as a response to the continuous inflammation, a line of IgA^+ plasma cells develops an immunosuppressor phenotype expressing interleukin-10 (IL-10) and programmed cell-death 1 Ligand (PD1-L). These molecules inhibit (red arrow) tumor-suppressing cytotoxic $CD8^+$ T cells ($CD8^+$ Tc), contributing to tumor development in the hepatobiliary and intestinal tract. Citation: Tornai D, Papp M. Editorial: serologic antibodies in primary sclerosing cholangitis a tell-tale sign of compromised gut-liver immunity? *Aliment Pharmacol Ther* 2021; 53: 350-351[8]. Copyright ©The Authors 2021. Published by John Wiley and Sons. (Supplementary material).

ELF test. However, in this latter test, the authors compared the outcomes associated with the first (lowest) tertile of the markers to those associated with the third (highest) tertile. Further studies are needed to confirm the importance of these findings as well.

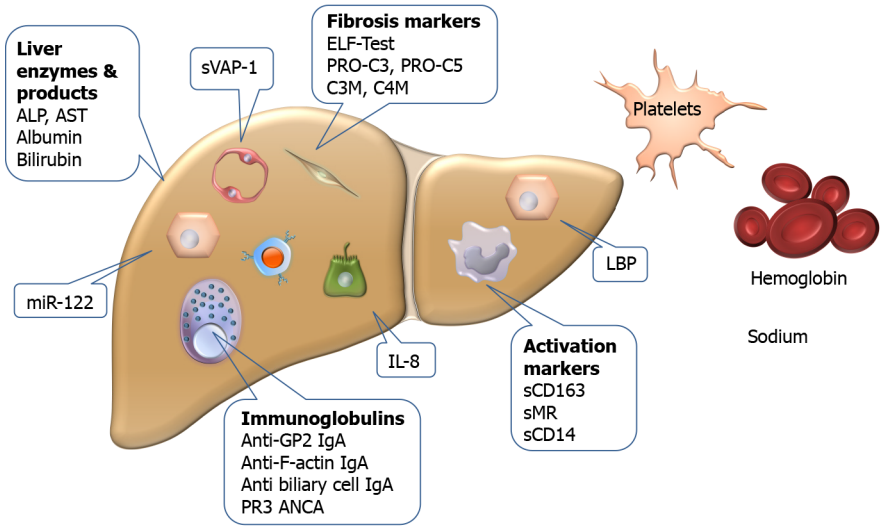
MicroRNA-122

MicroRNA-122 (miR-122) is the most abundant microRNA in the liver, orchestrating molecular pathways in hepatocytes and regulating liver functions including lipid and cholesterol homeostasis. MiR-122 deficiency leads to inflammation, cholestasis, and ultimately fibrosis of the liver[51]. Friedrich *et al*[52] investigated the predictive potential of miR-122 in 114 PSC patients with a prospective follow-up of 10 years. They divided the population to patients with low and high miR-122 levels based on the median value of the marker (CT-value of 28.5). Low miR-122 levels were associated with a higher risk of death or need for liver transplantation (HR = 1.27; 95%CI = 1.04-1.39; P = 0.009) even in the multivariate Cox regression model including MRS, presence of dominant stricture, and IBD (HR = 1.19; 95%CI = 1.00-1.43; P = 0.045).

Soluble vascular adhesion protein 1

Expression of vascular adhesion protein 1 (VAP-1) and amine oxidase enzyme activity in the liver endothelium are increased in PSC. The former results in an elevation of its soluble form (sVAP-1) in patients' sera. Elevated levels of sVAP-1 (> 529 ng/mL) in PSC are associated with an adverse disease outcome, independent of the presence of cirrhosis (HR = 3.85; 95%CI = 1.57 to 9.34; P = 0.003)[53].

Increased VAP-1 activity results in the expression of mucosal addressin cell adhesion molecule (MAdCAM-1) in liver tissue, which is otherwise expressed only in the intestinal endothelium. MAdCAM-1 binds to α4β7 integrin receptors on effector T lymphocytes, which is required for lymphocyte homing. Thus, abnormally expressed MAdCAM-1 in the liver results in the entry of gut activated effector T lymphocytes into liver tissue[53]. The increased expression and intrahepatic activity of VAP-1 may be attributed to the altered intestinal flora and the increased amine influx into the portal tract due to the inflamed, permeable bowel. The pathological amine substrate of VAP-1 is cysteamine [53], which causes colitis and colorectal carcinoma in mice. The *Escherichia* genus, which is able to



DOI: 10.3748/wjg.v28.i21.2291 **Copyright** ©The Author(s) 2022.

Figure 2 Biomarkers with potential to predict the clinical course of primary sclerosing cholangitis. The markers have various cellular origins, and some (LPS-binding protein, interleukin-8, and enzymes) have multiple sources that limit their specificity. ALP: Alkaline phosphatase; AST: Aspartate aminotransferase; GP2: Pancreatic glycoprotein 2; IL: Interleukin; LBP: Lipopolysaccharide binding protein; miR: Micro-ribonucleic acid; sMR: Soluble mannose receptor; sVAP: Soluble vascular adhesion protein.

produce cysteamine *in vitro*, is upregulated in the mucosa-associated microbiota population in PSC. However, the intestinal epithelium itself is capable of cysteamine production *via* the ectoenzyme vanin-1. The observation that cysteamine enhances colonic inflammation and carcinogenesis is consistent with the increased colon carcinoma formation observed in PSC. The aldehyde derivative formed during the metabolism of cysteamine causes abnormal collagen cross-binding, which could theoretically contribute to increased fibrogenesis. Increased VAP-1 activity in liver and colonic tissue is most likely an attempt to counteract the increased amine load resulting from colitis.

The newly discovered VAP-1 pathway is one explanation of how colitis and increased amine production lead to damage of liver tissue. VAP-1 may be a potential therapeutic target in the future due to its effect in promoting α4β7/MAdCAM-1 interaction. A VAP-1 antagonist may also be able to regulate the migration of effector T lymphocytes from the inflamed intestine to the liver and thereby inhibit fibrogenesis[53].

The biomarkers used individually or as parts of score systems are summarized in Figure 2.

SEROLOGICAL BIOMARKERS FOR DETECTING CHOLANGIOCARCINOMA IN PSC

Carbohydrate antigen 19-9 (CA19-9) is the most commonly used serological marker for screening CCA, but its application is limited in PSC by the lack of comprehensive studies comparing PSC patients with and without CCA. Most studies were too small and ultimately provided inconsistent cut-off values[54]. A recent development in this field is the discovery of the role of fucosyltransferase (FUT) 2 and 3 in influencing the serum levels of CA19-9 in patients with PSC. These enzymes catalyze the final steps of CA19-9 biosynthesis. The study identified FUT genotypes with low, intermediate, and high CA19-9 synthesis capacity displaying distinct CA19-9 serum levels[55]. According to these data, CA19-9 is not an appropriate marker for CCA screening in patients with a low CA19-9 biosynthesis genotype since they do not synthetize CA19-9. This group can be identified by a Lewis-negative blood group which is also determined by these enzymes. In contrast, the high CA19-9 biosynthesis genotype might be a reason for false positive results[55]. In addition, bacterial cholangitis can be another explanation for increased CA19-9 level in PSC patients without CCA[56].

Finally, a study demonstrated a significant influence of FUT2 genotype also on CEA serum levels. The most prominent effect was observed in the subgroup incapable of CA19-9 biosynthesis[57]. Studies with other serological biomarkers, like angiopoetin-2[58] or cytokeratin fraction 21-1[59], have not reached satisfactory results in terms of identifying individuals with CCA among PSC patients.

CONCLUSION

Several promising discoveries have been made on biomarkers for PSC. The first validated prognostic biomarker (anti-GP2 IgA) is finally ready to be incorporated into clinical practice, and the investigations

highlighted important pathophysiological mechanisms for future research that might open new avenues for medical therapy. However, we still lack specific serological markers that could support the diagnosis of PSC. Additionally, a serological marker with satisfactory discriminative power to aid the recognition of CCA in PSC patients is another unmet need.

FOOTNOTES

Author contributions: Tornai D and Ven PL performed the literature review; Tornai D wrote the manuscript; Papp M and Lakatos PL supervised the work and provided expert insights; all authors have read and approved the final manuscript.

Supported by the Ministry of Innovation and Technology of Hungary from the National Research, Development and Innovation Fund, No. 138041; and the EFOP projects co-financed by the European Union and the European Social Fund, No. EFOP-3.6.1-16-2016-00022.

Conflict-of-interest statement: There are no conflicts of interest to report.

Open-Access: This article is an open-access article that was selected by an in-house editor and fully peer-reviewed by external reviewers. It is distributed in accordance with the Creative Commons Attribution NonCommercial (CC BY-NC 4.0) license, which permits others to distribute, remix, adapt, build upon this work non-commercially, and license their derivative works on different terms, provided the original work is properly cited and the use is non-commercial. See: https://creativecommons.org/Licenses/by-nc/4.0/

Country/Territory of origin: Hungary

ORCID number: David Tornai 0000-0002-1335-5498; Peter Laszlo Ven 0000-0001-8990-7757; Peter Laszlo Lakatos 0000-0002-3948-6488; Maria Papp 0000-0003-3662-4010.

S-Editor: Chen YL
L-Editor: Wang TQ
P-Editor: Chen YL

REFERENCES

1 **Eaton JE**, Talwalkar JA, Lazaridis KN, Gores GJ, Lindor KD. Pathogenesis of primary sclerosing cholangitis and advances in diagnosis and management. *Gastroenterology* 2013; **145**: 521-536 [PMID: 23827861 DOI: 10.1053/j.gastro.2013.06.052]
2 **Trivedi PJ**, Adams DH. Mucosal immunity in liver autoimmunity: a comprehensive review. *J Autoimmun* 2013; **46**: 97-111 [PMID: 23891169 DOI: 10.1016/j.jaut.2013.06.013]
3 **Dyson JK**, Beuers U, Jones DEJ, Lohse AW, Hudson M. Primary sclerosing cholangitis. *Lancet* 2018; **391**: 2547-2559 [PMID: 29452711 DOI: 10.1016/S0140-6736(18)30300-3]
4 **Jendrek ST**, Gotthardt D, Nitzsche T, Widmann L, Korf T, Michaels MA, Weiss KH, Liaskou E, Vesterhus M, Karlsen TH, Mindorf S, Schemmer P, Bär F, Teegen B, Schröder T, Ehlers M, Hammers CM, Komorowski L, Lehnert H, Fellermann K, Derer S, Hov JR, Sina C. Anti-GP2 IgA autoantibodies are associated with poor survival and cholangiocarcinoma in primary sclerosing cholangitis. *Gut* 2017; **66**: 137-144 [PMID: 27406039 DOI: 10.1136/gutjnl-2016-311739]
5 **Tornai T**, Tornai D, Sipeki N, Tornai I, Alsulaimani R, Fechner K, Roggenbuck D, Norman GL, Veres G, Par G, Par A, Szalay F, Lakatos PL, Antal-Szalmas P, Papp M. Loss of tolerance to gut immunity protein, glycoprotein 2 (GP2) is associated with progressive disease course in primary sclerosing cholangitis. *Sci Rep* 2018; **8**: 399 [PMID: 29321484 DOI: 10.1038/s41598-017-18622-1]
6 **Sowa M**, Kolenda R, Baumgart DC, Pratschke J, Papp M, Tornai T, Suchanski J, Bogdanos DP, Mytilinaiou MG, Hammermann J, Laass MW, Conrad K, Schramm C, Franke A, Roggenbuck D, Schierack P. Mucosal Autoimmunity to Cell-Bound GP2 Isoforms Is a Sensitive Marker in PSC and Associated With the Clinical Phenotype. *Front Immunol* 2018; **9**: 1959 [PMID: 30233574 DOI: 10.3389/fimmu.2018.01959]
7 **Wunsch E**, Norman GL, Milkiewicz M, Krawczyk M, Bentow C, Shums Z, Mahler M, Lopens S, Reinhold D, Franke A, Schramm C, Roggenbuck D, Milkiewicz P. Anti-glycoprotein 2 (anti-GP2) IgA and anti-neutrophil cytoplasmic antibodies to serine proteinase 3 (PR3-ANCA): antibodies to predict severe disease, poor survival and cholangiocarcinoma in primary sclerosing cholangitis. *Aliment Pharmacol Ther* 2021; **53**: 302-313 [PMID: 33159471 DOI: 10.1111/apt.16153]
8 **Tornai D**, Papp M. Editorial: serologic antibodies in primary sclerosing cholangitis - a tell-tale sign of compromised gut-liver immunity? *Aliment Pharmacol Ther* 2021; **53**: 350-351 [PMID: 33368511 DOI: 10.1111/apt.16201]
9 **Karlsen TH**, Folseraas T, Thorburn D, Vesterhus M. Primary sclerosing cholangitis - a comprehensive review. *J Hepatol* 2017; **67**: 1298-1323 [PMID: 28802875 DOI: 10.1016/j.jhep.2017.07.022]
10 **Al Mamari S**, Djordjevic J, Halliday JS, Chapman RW. Improvement of serum alkaline phosphatase to <1.5 upper limit of normal predicts better outcome and reduced risk of cholangiocarcinoma in primary sclerosing cholangitis. *J Hepatol* 2013; **58**: 329-334 [PMID: 23085647 DOI: 10.1016/j.jhep.2012.10.013]

11 **Hilscher M**, Enders FB, Carey EJ, Lindor KD, Tabibian JH. Alkaline phosphatase normalization is a biomarker of improved survival in primary sclerosing cholangitis. *Ann Hepatol* 2016; **15**: 246-253 [PMID: 26845602 DOI: 10.5604/16652681.1193721]

12 **Lindström L**, Hultcrantz R, Boberg KM, Friis-Liby I, Bergquist A. Association between reduced levels of alkaline phosphatase and survival times of patients with primary sclerosing cholangitis. *Clin Gastroenterol Hepatol* 2013; **11**: 841-846 [PMID: 23353641 DOI: 10.1016/j.cgh.2012.12.032]

13 **Stanich PP**, Björnsson E, Gossard AA, Enders F, Jorgensen R, Lindor KD. Alkaline phosphatase normalization is associated with better prognosis in primary sclerosing cholangitis. *Dig Liver Dis* 2011; **43**: 309-313 [PMID: 21251891 DOI: 10.1016/j.dld.2010.12.008]

14 **Kim WR**, Therneau TM, Wiesner RH, Poterucha JJ, Benson JT, Malinchoc M, LaRusso NF, Lindor KD, Dickson ER. A revised natural history model for primary sclerosing cholangitis. *Mayo Clin Proc* 2000; **75**: 688-694 [PMID: 10907383 DOI: 10.4065/75.7.688]

15 **Thorburn D**. Prognostic scores and non-invasive markers in primary sclerosing cholangitis: good for patients or for papers? *Lancet Gastroenterol Hepatol* 2017; **2**: 774-776 [PMID: 29017709 DOI: 10.1016/S2468-1253(17)30296-0]

16 **de Vries EM**, Wang J, Williamson KD, Leeflang MM, Boonstra K, Weersma RK, Beuers U, Chapman RW, Geskus RB, Ponsioen CY. A novel prognostic model for transplant-free survival in primary sclerosing cholangitis. *Gut* 2018; **67**: 1864-1869 [PMID: 28739581 DOI: 10.1136/gutjnl-2016-313681]

17 **Goode EC**, Clark AB, Mells GF, Srivastava B, Spiess K, Gelson WTH, Trivedi PJ, Lynch KD, Castren E, Vesterhus MN, Karlsen TH, Ji SG, Anderson CA, Thorburn D, Hudson M, Heneghan MA, Aldersley MA, Bathgate A, Sandford RN, Alexander GJ, Chapman RW, Walmsley M; UK-PSC Consortium, Hirschfield GM, Rushbrook SM. Factors Associated With Outcomes of Patients With Primary Sclerosing Cholangitis and Development and Validation of a Risk Scoring System. *Hepatology* 2019; **69**: 2120-2135 [PMID: 30566748 DOI: 10.1002/hep.30479]

18 **Eaton JE**, Vesterhus M, McCauley BM, Atkinson EJ, Schlicht EM, Juran BD, Gossard AA, LaRusso NF, Gores GJ, Karlsen TH, Lazaridis KN. Primary Sclerosing Cholangitis Risk Estimate Tool (PREsTo) Predicts Outcomes of the Disease: A Derivation and Validation Study Using Machine Learning. *Hepatology* 2020; **71**: 214-224 [PMID: 29742811 DOI: 10.1002/hep.30085]

19 **de Vries EMG**, Färkkilä M, Milkiewicz P, Hov JR, Eksteen B, Thorburn D, Chazouillères O, Pares A, Nygård S, Gilja OH, Wunsch E, Invernizzi P, Carbone M, Bernuzzi F, Boberg KM, Røsjø H, Rosenberg W, Beuers UH, Ponsioen CY, Karlsen TH, Vesterhus M. Enhanced liver fibrosis test predicts transplant-free survival in primary sclerosing cholangitis, a multi-centre study. *Liver Int* 2017; **37**: 1554-1561 [PMID: 28267887 DOI: 10.1111/Liv.13402]

20 **Vesterhus M**, Hov JR, Holm A, Schrumpf E, Nygård S, Godang K, Andersen IM, Naess S, Thorburn D, Saffioti F, Vatn M, Gilja OH, Lund-Johansen F, Syversveen T, Brabrand K, Parés A, Ponsioen CY, Pinzani M, Färkkilä M, Moum B, Ueland T, Røsjø H, Rosenberg W, Boberg KM, Karlsen TH. Enhanced liver fibrosis score predicts transplant-free survival in primary sclerosing cholangitis. *Hepatology* 2015; **62**: 188-197 [PMID: 25833813 DOI: 10.1002/hep.27825]

21 **Fossdal G**, Mjelle AB, Wiencke K, Bjørk I, Gilja OH, Folseraas T, Karlsen TH, Rosenberg W, Giil LM, Vesterhus M. Fluctuating biomarkers in primary sclerosing cholangitis: A longitudinal comparison of alkaline phosphatase, liver stiffness, and ELF. *JHEP Rep* 2021; **3**: 100328 [PMID: 34485881 DOI: 10.1016/j.jhepr.2021.100328]

22 **Lindor KD**, Kowdley KV, Harrison ME; American College of Gastroenterology. ACG Clinical Guideline: Primary Sclerosing Cholangitis. *Am J Gastroenterol* 2015; **110**: 646-59; quiz 660 [PMID: 25869391 DOI: 10.1038/ajg.2015.112]

23 **Mendes FD**, Jorgensen R, Keach J, Katzmann JA, Smyrk T, Donlinger J, Chari S, Lindor KD. Elevated serum IgG4 concentration in patients with primary sclerosing cholangitis. *Am J Gastroenterol* 2006; **101**: 2070-2075 [PMID: 16879434 DOI: 10.1111/j.1572-0241.2006.00772.x]

24 **Björnsson E**, Chari S, Silveira M, Gossard A, Takahashi N, Smyrk T, Lindor K. Primary sclerosing cholangitis associated with elevated immunoglobulin G4: clinical characteristics and response to therapy. *Am J Ther* 2011; **18**: 198-205 [PMID: 20228674 DOI: 10.1097/MJT.0b013e3181c9dac6]

25 **Sebode M**, Weiler-Normann C, Liwinski T, Schramm C. Autoantibodies in Autoimmune Liver Disease-Clinical and Diagnostic Relevance. *Front Immunol* 2018; **9**: 609 [PMID: 29636752 DOI: 10.3389/fimmu.2018.00609]

26 **Terjung B**, Spengler U. Atypical p-ANCA in PSC and AIH: a hint toward a "leaky gut"? *Clin Rev Allergy Immunol* 2009; **36**: 40-51 [PMID: 18626795 DOI: 10.1007/s12016-008-8088-8]

27 **Hov JR**, Boberg KM, Karlsen TH. Autoantibodies in primary sclerosing cholangitis. *World J Gastroenterol* 2008; **14**: 3781-3791 [PMID: 18609700 DOI: 10.3748/wjg.14.3781]

28 **Hov JR**, Boberg KM, Taraldsrud E, Vesterhus M, Boyadzhieva M, Solberg IC, Schrumpf E, Vatn MH, Lie BA, Molberg Ø, Karlsen TH. Antineutrophil antibodies define clinical and genetic subgroups in primary sclerosing cholangitis. *Liver Int* 2017; **37**: 458-465 [PMID: 27558072 DOI: 10.1111/Liv.13238]

29 **Fosby B**, Næss S, Hov JR, Traherne J, Boberg KM, Trowsdale J, Foss A, Line PD, Franke A, Melum E, Scott H, Karlsen TH. HLA variants related to primary sclerosing cholangitis influence rejection after liver transplantation. *World J Gastroenterol* 2014; **20**: 3986-4000 [PMID: 24744588 DOI: 10.3748/wjg.v20.i14.3986]

30 **Savige J**, Gillis D, Benson E, Davies D, Esnault V, Falk RJ, Hagen EC, Jayne D, Jennette JC, Paspaliaris B, Pollock W, Pusey C, Savage CO, Silvestrini R, van der Woude F, Wieslander J, Wiik A. International Consensus Statement on Testing and Reporting of Antineutrophil Cytoplasmic Antibodies (ANCA). *Am J Clin Pathol* 1999; **111**: 507-513 [PMID: 10191771 DOI: 10.1093/ajcp/111.4.507]

31 **Mahler M**, Bogdanos DP, Pavlidis P, Fritzler MJ, Csernok E, Damoiseaux J, Bentow C, Shums Z, Forbes A, Norman GL. PR3-ANCA: a promising biomarker for ulcerative colitis with extensive disease. *Clin Chim Acta* 2013; **424**: 267-273 [PMID: 23806819 DOI: 10.1016/j.cca.2013.06.005]

32 **Stinton LM**, Bentow C, Mahler M, Norman GL, Eksteen B, Mason AL, Kaplan GG, Lindkvist B, Hirschfield GM, Milkiewicz P, Cheung A, Janssen HL, Fritzler MJ. PR3-ANCA: a promising biomarker in primary sclerosing cholangitis (PSC). *PLoS One* 2014; **9**: e112877 [PMID: 25397578 DOI: 10.1371/journal.pone.0112877]

33 **Woof JM**, Russell MW. Structure and function relationships in IgA. *Mucosal Immunol* 2011; **4**: 590-597 [PMID:

21937984 DOI: 10.1038/mi.2011.39]
34 **Monteiro RC**. Role of IgA and IgA fc receptors in inflammation. *J Clin Immunol* 2010; **30**: 1-9 [PMID: 19834792 DOI: 10.1007/s10875-009-9338-0]
35 **Chen XM**, O'Hara SP, LaRusso NF. The immunobiology of cholangiocytes. *Immunol Cell Biol* 2008; **86**: 497-505 [PMID: 18504452 DOI: 10.1038/icb.2008.37]
36 **Mantis NJ**, Rol N, Corthésy B. Secretory IgA's complex roles in immunity and mucosal homeostasis in the gut. *Mucosal Immunol* 2011; **4**: 603-611 [PMID: 21975936 DOI: 10.1038/mi.2011.41]
37 **Woof JM**, Kerr MA. The function of immunoglobulin A in immunity. *J Pathol* 2006; **208**: 270-282 [PMID: 16362985 DOI: 10.1002/path.1877]
38 **Schwarze C**, Terjung B, Lilienweiss P, Beuers U, Herzog V, Sauerbruch T, Spengler U. IgA class antineutrophil cytoplasmic antibodies in primary sclerosing cholangitis and autoimmune hepatitis. *Clin Exp Immunol* 2003; **133**: 283-289 [PMID: 12869036 DOI: 10.1046/j.1365-2249.2003.02195.x]
39 **Berglin L**, Björkström NK, Bergquist A. Primary sclerosing cholangitis is associated with autoreactive IgA antibodies against biliary epithelial cells. *Scand J Gastroenterol* 2013; **48**: 719-728 [PMID: 23713804 DOI: 10.3109/00365521.2013.786131]
40 **Papp M**, Sipeki N, Tornai T, Altorjay I, Norman GL, Shums Z, Roggenbuck D, Fechner K, Stöcker W, Antal-Szalmas P, Veres G, Lakatos PL. Rediscovery of the Anti-Pancreatic Antibodies and Evaluation of their Prognostic Value in a Prospective Clinical Cohort of Crohn's Patients: The Importance of Specific Target Antigens [GP2 and CUZD1]. *J Crohns Colitis* 2015; **9**: 659-668 [PMID: 25968583 DOI: 10.1093/ecco-jcc/jjv087]
41 **Tornai T**, Palyu E, Vitalis Z, Tornai I, Tornai D, Antal-Szalmas P, Norman GL, Shums Z, Veres G, Dezsofi A, Par G, Par A, Orosz P, Szalay F, Lakatos PL, Papp M. Gut barrier failure biomarkers are associated with poor disease outcome in patients with primary sclerosing cholangitis. *World J Gastroenterol* 2017; **23**: 5412-5421 [PMID: 28839442 DOI: 10.3748/wjg.v23.i29.5412]
42 **Sancho D**, Joffre OP, Keller AM, Rogers NC, Martínez D, Hernanz-Falcón P, Rosewell I, Reis e Sousa C. Identification of a dendritic cell receptor that couples sensing of necrosis to immunity. *Nature* 2009; **458**: 899-903 [PMID: 19219027 DOI: 10.1038/nature07750]
43 **Brown GD**. Immunology: Actin' dangerously. *Nature* 2012; **485**: 589-590 [PMID: 22660316 DOI: 10.1038/485589a]
44 **Ahrens S**, Zelenay S, Sancho D, Hanč P, Kjær S, Feest C, Fletcher G, Durkin C, Postigo A, Skehel M, Batista F, Thompson B, Way M, Reis e Sousa C, Schulz O. F-actin is an evolutionarily conserved damage-associated molecular pattern recognized by DNGR-1, a receptor for dead cells. *Immunity* 2012; **36**: 635-645 [PMID: 22483800 DOI: 10.1016/j.immuni.2012.03.008]
45 **Hanč P**, Fujii T, Iborra S, Yamada Y, Huotari J, Schulz O, Ahrens S, Kjær S, Way M, Sancho D, Namba K, Reis e Sousa C. Structure of the Complex of F-Actin and DNGR-1, a C-Type Lectin Receptor Involved in Dendritic Cell Cross-Presentation of Dead Cell-Associated Antigens. *Immunity* 2015; **42**: 839-849 [PMID: 25979418 DOI: 10.1016/j.immuni.2015.04.009]
46 **Mathies F**, Steffens N, Kleinschmidt D, Stuhlmann F, Huber FJ, Roy U, Meyer T, Luetgehetmann M, von Petersdorff M, Seiz O, Herkel J, Schramm C, Flavell RA, Gagliani N, Krebs C, Panzer U, Abdullah Z, Strowig T, Bedke T, Huber S. Colitis Promotes a Pathological Condition of the Liver in the Absence of Foxp3^{+} Regulatory T Cells. *J Immunol* 2018; **201**: 3558-3568 [PMID: 30446566 DOI: 10.4049/jimmunol.1800711]
47 **Vesterhus M**, Holm A, Hov JR, Nygård S, Schrumpf E, Melum E, Thorbjørnsen LW, Paulsen V, Lundin K, Dale I, Gilja OH, Zweers SJLB, Vatn M, Schaap FG, Jansen PLM, Ueland T, Røsjø H, Moum B, Ponsioen CY, Boberg KM, Färkkilä M, Karlsen TH, Lund-Johansen F. Novel serum and bile protein markers predict primary sclerosing cholangitis disease severity and prognosis. *J Hepatol* 2017; **66**: 1214-1222 [PMID: 28161472 DOI: 10.1016/j.jhep.2017.01.019]
48 **Bossen L**, Vesterhus M, Hov JR, Färkkilä M, Rosenberg WM, Møller HJ, Boberg KM, Karlsen TH, Grønbæk H. Circulating Macrophage Activation Markers Predict Transplant-Free Survival in Patients With Primary Sclerosing Cholangitis. *Clin Transl Gastroenterol* 2021; **12**: e00315 [PMID: 33646203 DOI: 10.14309/ctg.0000000000000315]
49 **Dhillon AK**, Kummen M, Trøseid M, Åkra S, Liaskou E, Moum B, Vesterhus M, Karlsen TH, Seljeflot I, Hov JR. Circulating markers of gut barrier function associated with disease severity in primary sclerosing cholangitis. *Liver Int* 2019; **39**: 371-381 [PMID: 30269440 DOI: 10.1111/Liv.13979]
50 **Nielsen MJ**, Thorburn D, Leeming DJ, Hov JR, Nygård S, Moum B, Saffioti F, Gilja OH, Boberg KM, Mazza G, Røsjø H, Pinzani M, Karlsen TH, Karsdal MA, Vesterhus M. Serological markers of extracellular matrix remodeling predict transplant-free survival in primary sclerosing cholangitis. *Aliment Pharmacol Ther* 2018; **48**: 179-189 [PMID: 29851098 DOI: 10.1111/apt.14806]
51 **Hu J**, Xu Y, Hao J, Wang S, Li C, Meng S. MiR-122 in hepatic function and liver diseases. *Protein Cell* 2012; **3**: 364-371 [PMID: 22610888 DOI: 10.1007/s13238-012-2036-3]
52 **Friedrich K**, Baumann C, Wannhoff A, Rupp C, Mehrabi A, Weiss KH, Gotthardt DN. Serum miRNA-122 is an independent biomarker of survival in patients with primary sclerosing cholangitis. *J Gastrointestin Liver Dis* 2018; **27**: 145-150 [PMID: 29922759 DOI: 10.15403/jgld.2014.1121.272.cho]
53 **Trivedi PJ**, Tickle J, Vesterhus MN, Eddowes PJ, Bruns T, Vainio J, Parker R, Smith D, Liaskou E, Thorbjørnsen LW, Hirschfield GM, Auvinen K, Hubscher SG, Salmi M, Adams DH, Weston CJ. Vascular adhesion protein-1 is elevated in primary sclerosing cholangitis, is predictive of clinical outcome and facilitates recruitment of gut-tropic lymphocytes to liver in a substrate-dependent manner. *Gut* 2018; **67**: 1135-1145 [PMID: 28428344 DOI: 10.1136/gutjnl-2016-312354]
54 **Wannhoff A**, Gotthardt DN. Recent developments in the research on biomarkers of cholangiocarcinoma in primary sclerosing cholangitis. *Clin Res Hepatol Gastroenterol* 2019; **43**: 236-243 [PMID: 30266579 DOI: 10.1016/j.clinre.2018.08.013]
55 **Rizvi S**, Eaton JE, Gores GJ. Primary Sclerosing Cholangitis as a Premalignant Biliary Tract Disease: Surveillance and Management. *Clin Gastroenterol Hepatol* 2015; **13**: 2152-2165 [PMID: 26051390 DOI: 10.1016/j.cgh.2015.05.035]
56 **Sinakos E**, Saenger AK, Keach J, Kim WR, Lindor KD. Many patients with primary sclerosing cholangitis and increased serum levels of carbohydrate antigen 19-9 do not have cholangiocarcinoma. *Clin Gastroenterol Hepatol* 2011; **9**: 434-9.e1

[PMID: 21334457 DOI: 10.1016/j.cgh.2011.02.007]

57 **Wannhoff A**, Folseraas T, Brune M, Rupp C, Friedrich K, Knierim J, Weiss KH, Sauer P, Flechtenmacher C, Schirmacher P, Stremmel W, Hov JR, Gotthardt DN. A common genetic variant of fucosyltransferase 2 correlates with serum carcinoembryonic antigen levels and affects cancer screening in patients with primary sclerosing cholangitis. *United European Gastroenterol J* 2016; **4**: 84-91 [PMID: 26966527 DOI: 10.1177/2050640615581577]

58 **Voigtländer T**, David S, Thamm K, Schlué J, Metzger J, Manns MP, Lankisch TO. Angiopoietin-2 and biliary diseases: elevated serum, but not bile levels are associated with cholangiocarcinoma. *PLoS One* 2014; **9**: e97046 [PMID: 24823366 DOI: 10.1371/journal.pone.0097046]

59 **Chapman MH**, Sandanayake NS, Andreola F, Dhar DK, Webster GJ, Dooley JS, Pereira SP. Circulating CYFRA 21-1 is a Specific Diagnostic and Prognostic Biomarker in Biliary Tract Cancer. *J Clin Exp Hepatol* 2011; **1**: 6-12 [PMID: 22228935 DOI: 10.1016/S0973-6883(11)60110-2]

World Journal of Gastroenterology

Submit a Manuscript: https://www.f6publishing.com

World J Gastroenterol 2022 June 7; 28(21): 2302-2319

DOI: 10.3748/wjg.v28.i21.2302

ISSN 1007-9327 (print) ISSN 2219-2840 (online)

ORIGINAL ARTICLE

Basic Study

Impact of radiotherapy on the immune landscape in oesophageal adenocarcinoma

Noel E Donlon, Maria Davern, Fiona O'Connell, Andrew Sheppard, Aisling Heeran, Anshul Bhardwaj, Christine Butler, Ravi Narayanasamy, Claire Donohoe, James J Phelan, Niamh Lynam-Lennon, Margaret R Dunne, Stephen Maher, Jacintha O'Sullivan, John V Reynolds, Joanne Lysaght

Specialty type: Surgery

Provenance and peer review: Invited article; Externally peer reviewed.

Peer-review model: Single blind

Peer-review report's scientific quality classification

Grade A (Excellent): 0
Grade B (Very good): B
Grade C (Good): C
Grade D (Fair): 0
Grade E (Poor): 0

P-Reviewer: Casà C, Italy; Kim S, South Korea

Received: December 3, 2021
Peer-review started: December 3, 2021
First decision: January 27, 2022
Revised: February 19, 2022
Accepted: April 26, 2022
Article in press: April 26, 2022
Published online: June 7, 2022

Noel E Donlon, Maria Davern, Fiona O'Connell, Andrew Sheppard, Aisling Heeran, Anshul Bhardwaj, Christine Butler, Ravi Narayanasamy, Claire Donohoe, James J Phelan, Niamh Lynam-Lennon, Margaret R Dunne, Stephen Maher, Jacintha O'Sullivan, John V Reynolds, Joanne Lysaght, Department of Surgery, Trinity Translational Medicine Institute, St James Hospital, Dublin D08, Ireland

Corresponding author: Noel E Donlon, MD, Assistant Professor, Department of Surgery, Trinity Translational Medicine Institute, St James Hospital, James's Street, Dublin D08, Ireland. donlonn@tcd.ie

Abstract

BACKGROUND

In the contemporary era of cancer immunotherapy, an abundance of clinical and translational studies have reported radiotherapy (RT) and immunotherapies as a viable option for immunomodulation of many cancer subtypes, with many related clinical trials ongoing. In locally advanced disease, chemotherapy or chemoradiotherapy followed by surgical excision of the tumour remain the principal treatment strategy in oesophageal adenocarcinoma (OAC), however, the use of the host immune system to improve anti-tumour immunity is rapidly garnering increased support in the curative setting.

AIM

To immunophenotype OAC patients' immune checkpoint (IC) expression with and without radiation and evaluate the effects of checkpoint blockade on cell viability.

METHODS

In the contemporary era of cancer immunotherapy, an abundance of studies have demonstrated that combination RT and IC inhibitors (ICIs) are effective in the immunomodulation of many cancer subtypes, with many related clinical trials ongoing. Although surgical excision and elimination of tumour cells by chemotherapy or chemoradiotherapy remains the gold standard approach in OAC, the propagation of anti-tumour immune responses is rapidly garnering increased support in the curative setting. The aim of this body of work was to immunophenotype OAC patients' IC expression with and without radiation and

to establish the impact of checkpoint blockade on cell viability. This study was a hybrid combination of *in vitro* and *ex vivo* models. Quantification of serum immune proteins was performed by enzyme-linked immunosorbent assay. Flow cytometry staining was performed to evaluate IC expression for *in vitro* OAC cell lines and *ex vivo* OAC biopsies. Cell viability in the presence of radiation with and without IC blockade was assessed by a cell counting kit-8 assay.

RESULTS

We identified that conventional dosing and hypofractionated approaches resulted in increased IC expression (PD-1, PD-L1, TIM3, TIGIT) *in vitro* and *ex vivo* in OAC. There were two distinct subcohorts with one demonstrating significant upregulation of ICs and the contrary in the other cohort. Increasing IC expression post RT was associated with a more aggressive tumour phenotype and adverse features of tumour biology. The use of anti-PD-1 and anti-PD-L1 immunotherapies in combination with radiation resulted in a significant and synergistic reduction in viability of both radiosensitive and radioresistant OAC cells *in vitro.* Interleukin-21 (IL-21) and IL-31 significantly increased, with a concomitant reduction in IL-23 as a consequence of 4 Gray radiation. Similarly, radiation induced an anti-angiogenic tumour milieu with reduced expression of vascular endothelial growth factor-A, basic fibroblast growth factor, Flt-1 and placental growth factor.

CONCLUSION

The findings of the current study demonstrate synergistic potential for the use of ICIs and ionising radiation to potentiate established anti-tumour responses in the neoadjuvant setting and is of particular interest in those with advanced disease, adverse features of tumour biology and poor treatment responses to conventional therapies.

Key Words: Oesophageal Cancer; Radiotherapy; Immunotherapy; Immunology; Surgery; Oncology

©The Author(s) 2022. Published by Baishideng Publishing Group Inc. All rights reserved.

Core Tip: This body of work evaluates the impact of radiotherapy on the immune profile in oesophageal adenocarcinoma with an added caveat of immunotherapy effects on tumour cell killing.

Citation: Donlon NE, Davern M, O'Connell F, Sheppard A, Heeran A, Bhardwaj A, Butler C, Narayanasamy R, Donohoe C, Phelan JJ, Lynam-Lennon N, Dunne MR, Maher S, O'Sullivan J, Reynolds JV, Lysaght J. Impact of radiotherapy on the immune landscape in oesophageal adenocarcinoma. *World J Gastroenterol* 2022; 28(21): 2302-2319

URL: https://www.wjgnet.com/1007-9327/full/v28/i21/2302.htm

DOI: https://dx.doi.org/10.3748/wjg.v28.i21.2302

INTRODUCTION

Oesophageal adenocarcinoma (OAC) is rapidly increasing in incidence in the western world, and five year survival rates rarely exceed 40%[1]. Multimodal therapy alongside surgical resection has become standard of care for locally advanced cancer of the oesophagus or the oesophagogastric junction[2]. One option is the CROSS regimen, which includes preoperative administration of carboplatin and paclitaxel with concomitant radiotherapy (RT)[3]. In Europe, radiation is delivered in 23 fractions of 1.8 Gray (Gy), giving a total dose of 41.4 Gy but this varies worldwide, with North American centres delivering up to 50.0-51.4 Gy[4], while Asian regimens can feature cumulative doses of 60 Gy[5].

Hypofractionated RT is where radiation is delivered in fewer fractions of 2.4 Gy to 5.0 Gy, but often the same cumulative dose[6]. This has the potential to reduce costs, increase patient comfort, and could be more effective compared to conventional treatment[7]. Randomised trials in breast and prostate cancer have found that both high- (≥ 5 Gy per fraction) and moderately (2.4-3.4 Gy per fraction) hypofractionated RT is non-inferior to traditional regimens[7-10]. As RT is a mainstay of treatment, and oesophageal malignancies are associated with considerable morbidity, there is interest in evaluating whether this paradigm can be applied in the upper gastrointestinal context.

Disappointingly, a pathologic complete response to treatment is observed in less than 30% of patients with oesophageal cancer undergoing chemoradiotherapy[11], and it is this small subgroup that benefits most in terms of survival[12]. More effective strategies are therefore required. One emerging approach is combining chemoradiotherapy with immune checkpoint blockade (ICB). The most widely used ICB

involves blocking the interaction of PD-1 expressed on T cells and it's ligand, PD-L1 expressed on tumour cells[13], and seeks to re-invigorate anti-tumour cytotoxic T cells[14]. Phase III trials of single agent ICB have delivered mixed results in chemorefractory advanced oesophagogastric cancer[15], but some recent encouraging results have been reported in earlier stage disease[16,17].

Radiation can sensitise tumours to immunotherapy through three main mechanisms[18]. First, radiation can increase neoantigen expression and induce immunogenic cell death, whereby release of damage associated molecular patterns (DAMPs) results in more efficient tumour antigen presentation and immune stimulation[19]. Second, radiation induced DNA damage can activate the GMP-AMP stimulator of interferon genes (cGAS-STING) cytosolic DNA sensor, resulting in type I interferon production[20,21]. Finally, RT can result in remodeling of the tumour microenvironment (TME), promoting infiltration of immune cells[22]. The latter effect is particularly affected by radiation dosage and some limited preclinical evidence suggests that hypofractionated RT can have more immunostimulatory effects than conventional fractionation[18]. However, the majority of studies in the literature to date have focused on more inherently immunogenic tumour models like melanoma or non-small cell lung cancer, or common malignancies like breast or colon cancer. There are a number of clinical studies evaluating hypofractionation in the context of squamous cell cancer of the oesophagus, however, data is lacking for OAC. In addition, there are no translational studies characterising immune response in OAC in the context of immunotherapy and thus was the premise for this study.

This study assessed the effects of hypofractionated RT on IC expression in oesophageal cancer cells *in vitro* and *ex vivo* and correlated this with clinical outcomes. We also assessed the synergistic effects of ICB and radiation on OAC cell lines. Through this, we aimed to enhance our understanding of the interplay between immunotherapy, radiation and the TME in oesophageal cancer, with the goal of identifying the most effective radiation dosing strategy to combine with immunotherapy.

MATERIALS AND METHODS

Ethics statement

We secured ethical approval for this study from the Tallaght/St James's Hospital Ethics Committee. All patients provided formal written consent for all sample and variable data collection. During the course of all steps of sample and data collection good clinical practice was maintained and ethical standards upheld. We also pseudonymised patient data to protect privacy.

Specimen collection

We secured tissue from those patients who consented to participate from 2018-2021. Tumour biopsies were obtained from patients with OAC prior to treatment at the National Centre for Oesophageal and Gastric Cancer at St James's Hospital, Dublin. A total of 17 biopsies were used for analysis with all patient samples being treatment naïve prior to having neoadjuvant therapies to ensure clinical relevance of the study population. A total of 12 men and 5 women with a mean age of 64.23 years (SD11.5) in the study. All patients had locally advanced disease and were $T3N_{any.}$

Generation of tumour conditioned media

Tumour treatment naïve tissue samples were added to L-15 (Leibovitz) Lonza™ BioWhittaker™ X-vivo media for in a 12 well plate and subsequently cultured for a period of 24 h at 37 °C, 5% CO_2. After the 24 h period expired, the tissue conditioned media was collected for storage at -80 °C.

Quantification of serum immune proteins

Tumour conditioned media (TCM) was collected based on a standard operating procedure designed as per MSD United States instructions (Meso Scale Diagnostics, United States). To assess markers of angiogenesis, vascular injury, pro-inflammatory, cytokines, chemokine as well as soluble checkpoints from TCM, a 54-plex enzyme-linked immunosorbent assay (ELISA) kit was used (Meso Scale Diagnostics, United States). The ELISA was utilized to determine the level of secretions of the following markers: C-reactive protein (CRP), Eotaxin, Eotaxin-3, FGF (basic), Flt-1, GM-CSF, ICAM-1, IFN-γ, interleukin-10 (IL-10), IL-12/IL-23p40, IL-12p70, IL-13, IL-15, IL-16, IL-17A, IL-17A/F, IL-7, IL-8, MCP-1, MCP-4, MDC, MIP-1α, MIP-1β, MIP-3α, PlGF, SAA, TARC, Tie-2, TNF-α, TNF-β, TSLP, VCAM-1, vascular endothelial growth factor (VEGF)-A, VEGF-C and VEGF-D and ICs TIM-3, TIGIT, PD-1, PD-L1, CD276 and CD80 from TCM. These assays were processed according to a standard operating procedure following consultation of the manufacturer's guidelines. The derived data with respect to all markers were normalised to protein content as determined using a Pierce bicinchoninic acid assay.

Neoplastic tissue sample digestion

In preparation for flow cytometry, the tissue samples were digested to enable phenotyping of the cancer cells. The tissue was resected using a surgical blade and added to collagenase solution (2 mg/mL of collagenase type IV (Sigma) in Hanks Balanced Salt Solution (GE healthcare) supplemented with 4%

(v/v) foetal bovine serum) at 37 °C and 1500 rpm on an orbital shaker. The cancer cells were stained with flow cytometry antibodies for subsequent analysis.

Cell culture of OAC cell lines

Human OAC cell lines OE33 were purchased from The European Collection of Authenticated Cell Cultures (ECACC), established from a poorly differentiated stage IIA adenocarcinoma of the lower oesophagus of a 73-year old female patient. An in-house isogenic radioresistant model was generated [23].

Cell viability cholecystokinin octapeptide assay

A cell counting kit-8 (CCK-8) viability assay was used to determine the impact of ionising radiation on the viability of OE33P and passage matched OE33R cells. The impact of anti-PD-1, and anti PD-L1 therapies in isolation, and dual ICB with and without radiation, at both hypofractionation and bolus dosing of clinically relevant doses on the viability of OE33P and R cells was also assessed using a CCK-8 assay. OAC cells (5×10^3) were adhered in a 96 well plate at 37 °C, 5% CO2 overnight. Cells were treated with bolus dosing or three consecutive fractionated doses of radiation with an interval of 24 h using the X-Strahl RS225 irradiator. In addition to this, the cancer cells were treated with and without radiation in the absence or presence of pembrolizumab (10 μg/mL), atezolizumab (10 μg/mL), nivolumab (10 μg/mL) or combination atezolizumab (10 μg/mL) and nivolumab (10 μg/mL), or dual atezolizumab (10 μg/mL) and pembrolizumab (10 μg/mL). All of the data were analysed from three independent experiments (Supplementary material).

Flow cytometry staining for in vitro OAC cell lines and ex vivo OAC biopsies

OE33 cells were trypsinised and stained with zombie aqua viability (Biolegend, United States) dye. Antibodies used for OAC cell lines included: PD-L1-FITC, PD-L2-PE, TIGIT-PE/Cy7, PD-1-APC/Cy7 (Biolegend, United States), OE33P and OE33R cells were fixed with 1% paraformaldehyde solution and acquired using BD FACs CANTO II (BD Biosciences) using Diva software and analysed using FlowJo v10 software (TreeStar Inc.). Tumour tissue biopsies were stained with zombie aqua viability dye (Biolegend, United States) as per manufacturer's recommendations.

Statistical analysis

GraphPad Prism 9 was utilized to analyze the results. In order to determine statistical differences between treatments in cell lines, a paired parametric statistical *t*-test was utilized. In order to determine the differences between the OE33P and OE33R cell lines an unpaired parametric *t*-test was performed. To evaluate any differences between paired treatments of patient samples, Wilcoxon signed rank test was performed. Statistical significance was pre-determined as $P \leq 0.05$.

RESULTS

IC expression by an isogenic model of radioresistance following bolus and hypofractionated RT dosing

In order to ascertain if different expression levels of IC proteins were detectable on a radiosensitive (OE33P) and a radioresistant (OE33R) OAC cell line at baseline and following variable fractions of radiation, cells were stained with antibodies for a range of IC proteins and assessed by flow cytometry 24 h after the last dose. The administration of fractionated dosing resulted in significantly higher expression of PD-1, PD-L1, PD-L2 and TIGIT ($P < 0.05$) in both parental and resistant cell lines when compared to bolus dosing (Figure 1). There was a significantly higher expression of checkpoints and their ligands in the parental cell line compared to the passage matched radioresistant cell line. There was also a significantly higher expression of PD-1 and its ligands PD-L1 and PD-L2 with bolus dosing 10 Gy and 20 Gy in OE33P cell lines compared to the radioresistant passage matched cell line ($P < 0.05$). Globally there was a higher expression of PD-1, PD-L1 and PD-L2 on the parental cell line with fractionated dosing regimens of 3X1 Gy, 3X2 Gy and 3X8 Gy compared to the radioresistant cell line ($P < 0.05$). In the case of TIGIT, there was a significantly higher upregulation in the OE33P cell line compared to the radioresistant cell line following fractionated dosing of 3X4 Gy and 3X8 Gy ($P < 0.05$) (Figure 1).

Cell viability in the context of radiation and IC blockade

IC blockade alone reduced the viability of both OE33P and OE33R cell lines, for both anti-PD-1 and anti-PD-L1 therapies. Multimodal use of both anti-PD-1 and anti-PD-L1 therapies with ionising radiation resulted in a synergistic reduction in viability in both cell lines (Figure 2).

In the OE33P cell line, 2 Gy radiation alone reduced viability to 78.49% (± 2.05, $P < 0.01$) and 4 Gy to 35.48% (± 2.08, $P < 0.01$) compared with unirradiated cells and there was a significant reduction in viability when comparing 2 Gy to 4 Gy ($P < 0.05$). In the OE33R cell line, 4 Gy reduced viability to

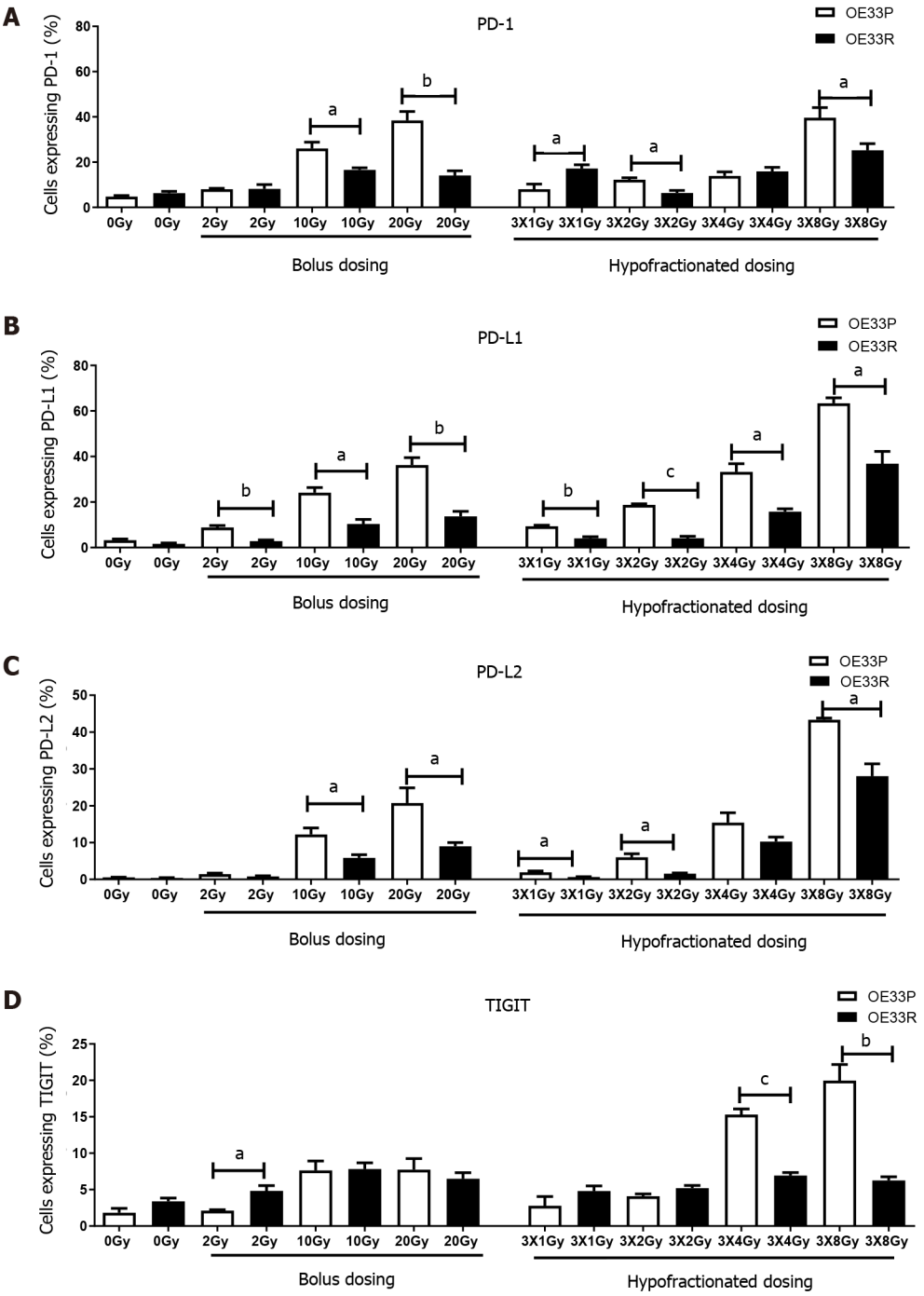


Figure 1 OE33P and R cell lines were screened for the surface expression of immune checkpoints by flow cytometry. Inhibitory immune checkpoints are expressed at a higher level on parental cell lines than the passage matched radioresistant cell line (n = 3). A: PD-1; B: PD-L1; C: PD-L2; D: TIGIT. Graph shows % expression (± SE). [a]P < 0.05; [b]P < 0.01; [c]P < 0.001 by unpaired parametric t-test.

63.33% (± 2.67, P < 0.05). Both 2 Gy and 4 Gy radiation resulted in a significantly greater reduction in viability in the OE33P cell line compared to the OE33R (P < 0.05) (Figure 2).

Compared with untreated cells, when the OE33P cells were treated with Atezolizumab alone, viability was reduced to 91.3% (± 0.30, P < 0.01) and with the addition of 2 Gy radiation viability reduced to 66.57% (± 2.40, P < 0.01) and to 48.92% (± 5.76, P < 0.01) with 4 Gy radiation. Compared with untreated OE33R cells, viability of OE33R cells treated with Atezolizumab alone was reduced to 88% (± 2.65,P < 0.05), with the addition of 2 Gy radiation viability was reduced to 75.67% (± 2.33, P < 0.01) and 38% (± 3.06, P < 0.01) with 4 Gy radiation (Figure 2B).

In the OE33P cells, Pembrolizumab treatment alone non-significantly reduced viability to 91.54% (± 2.67) compared with the untreated cells, however with the addition of 2 Gy radiation viability reduced to 65.36% (± 2.81, P < 0.01) and 48.18% (± 3.20, P < 0.01) with 4 Gy radiation when compared to untreated OE33P cells. When the OE33R cells were treated with Pembrolizumab, viability was non-significantly reduced to 92% (± 2.52), but the addition of 2 Gy radiation reduced viability to 75.33% (±

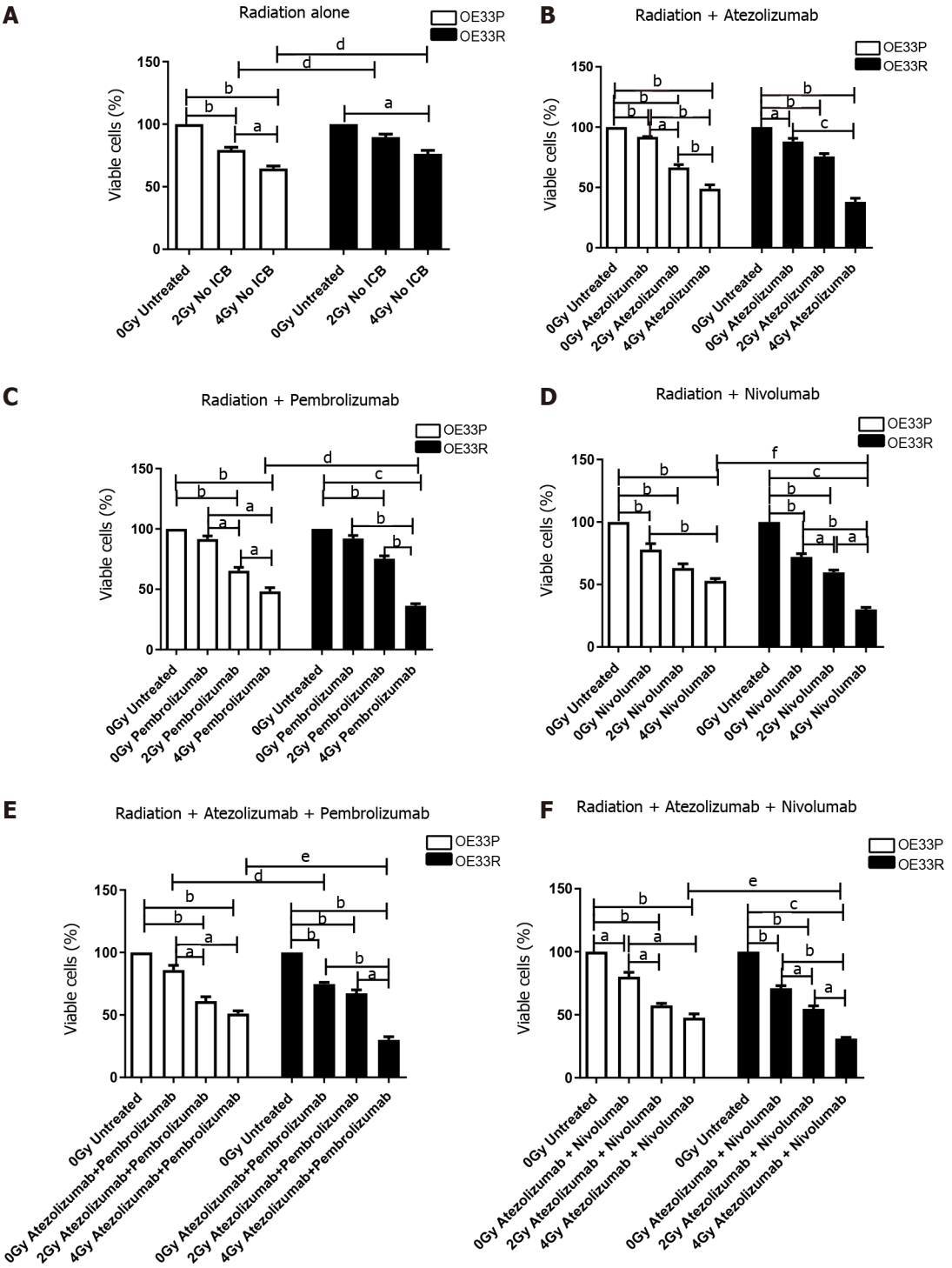


Figure 2 Viability (± SE) of OE33P and OE33R cells were assessed using a cell counting kit-8 assay with or without radiation (*n* = 3). Ionising radiation with immune checkpoint blockade results in a greater reduction in cell viability when compared to either modality alone. Graph shows % expression (± SE). A: Treatment with radiation dosing only; B: Treatment with radiation and single agent immunotherapy Atezolizumab; C: Treatment with radiation and single agent immunotherapy Pembrolizumab; D: Treatment with radiation and single agent immunotherapy Nivolumab; E: Treatment with radiation and dual immunotherapy agents Atezolizumab & Pembrolizumab; F: Treatment with radiation and dual immunotherapy agents Atezolizumab & Nivolumab. $^{a}P < 0.05$, $^{b}P < 0.01$, $^{c}P < 0.001$ paired *t*-test; $^{d}P < 0.05$, $^{e}P < 0.01$, $^{f}P < 0.001$ unpaired *t*-test.

2.33, $P < 0.01$) and 36.33% (± 1.67, $P < 0.001$) with 4 Gy radiation. Four Gy radiation with Pembrolizumab resulted in a significantly greater reduction in viability in the radioresistant OE33R cell line compared to the radiosensitive OE33P cell line ($P < 0.05$) (Figure 2C).

In the OE33P cells Nivolumab reduced viability to 77.94% (± 4.79, $P < 0.05$) and with the addition of 2 Gy radiation viability reduced to 63.21% (± 3.41, $P < 0.01$) and 52.98% (± 1.82, $P < 0.01$) with 4 Gy radiation compared with untreated OE33P cells. When the OE33R cells were treated with Nivolumab, viability was reduced to 72% (± 2.62, $P < 0.01$) and with the addition of 2 Gy radiation viability reduced to 59.67% (± 1.86, $P < 0.01$) and 30% (± 1.73, $P < 0.001$) with 4 Gy radiation compared with untreated

OE33R cells. Treatment with 4 Gy radiation and Nivolumab resulted in a significantly greater reduction in viability in the OE33R cell line compared to the radiosensitive cell line ($P < 0.001$) (Figure 2D).

In the OE33P cells, combination Atezolizumab and Pembrolizumab non-significantly reduced viability to 85.94% (± 3.79) but the addition of 2 Gy radiation significantly reduced viability to 61.10% (± 3.44, $P < 0.01$) and 51.07% (± 2.27, $P < 0.01$) with 4 Gy radiation compared with untreated OE33P cells. When the OE33R cells were treated with combination Atezolizumab and Pembrolizumab, viability was significantly reduced to 74.67% (± 1.33, $P < 0.01$), and with the addition of 2 Gy radiation viability was reduced to 67.33% (± 2.73, $P < 0.01$) and 30% (± 2.52, $P < 0.01$) with 4 Gy radiation. Four Gy radiation with combination Atezolizumab and Pembrolizumab resulted in a significantly greater reduction in viability in the OE33R cell line compared to the radiosensitive cell line ($P < 0.01$) (Figure 2E).

In the OE33P cells combination Atezolizumab and Nivolumab reduced viability to 80.18% (± 3.48, $P < 0.05$) and with the addition of 2 Gy radiation reduced viability further to 57.48% (± 1.64, $P < 0.01$) and 47.63% (± 3.11, $P < 0.01$) with 4 Gy radiation, compared with untreated OE33P cells. When the OE33R cells were treated with combination Atezolizumab and Nivolumab, viability was reduced to 71% (± 2.08, $P < 0.01$) and with the addition of 2 Gy radiation viability reduced to 54.67% (± 2.40, $P < 0.01$) and 31% (± 1.03, $P < 0.001$) with 4 Gy radiation compared with untreated OE33R cells. Treatment with 4 Gy radiation and combination Atezolizumab and Nivolumab resulted in a significantly greater reduction in viability in the OE33R cell line compared to the OE33P cell line ($P < 0.01$) (Figure 2F).

Profiling IC expression in fresh patient tissue samples

The *in vitro* data revealed an increase in IC expression on OAC cells post irradiation. To determine if this held true in *ex vivo* OAC tumour tissue, we profiled IC expression post irradiation with 2 Gy and 4 Gy. Subcohorts of patients demonstrated an upregulation and others a downregulation in checkpoint expression upon exposure to conventional radiation doses and hypofractionation for $CD3^+$, $CD3^+CD4^+$, $CD3^+CD8^+$ tumour-infiltrating T cells. There was a significant increase in the frequency of $CD3^+PD\text{-}1^+$ and $CD3^+CD8^+PD\text{-}1^+$ T cells in tumour tissue when irradiated with 2 Gy (26.76 ± 8.80 *vs* 16.62 ± 5.40 at 0 Gy, and 14.8 ± 4.1 *vs* 7.70 ± 2.01 at 0 Gy, respectively, $P < 0.05$). There was a significant increase in the frequency of $CD3^+CD4^+$ $PD\text{-}L1^+$ cells with 4 Gy radiation (19.4 ± 2.9 *vs* 6.27 ± 1.02 at 0 Gy, $P < 0.05$). There was an significant increase in $CD3^+TIGIT^+$ and $CD3^+CD4^+TIGIT^+$ expression with both 2 Gy (55.6 ± 8.6 *vs* 40.12 ± 5.40, and 61.29 ± 8.20 *vs* 52.17 ± 7.70, respectively, $P < 0.05$) and 4 Gy radiation dosing regimens (48.06 ± 3.10 *vs* 40.12 ± 5.40, and 65.16 ± 6.90 *vs* 52.17 ± 7.90, respectively, $P < 0.05$) when compared with unirradiated cells, and an increase in $CD3^+CD8^+$ $TIGIT^+$ expression following 4 Gy irradiation (49.55 ± 4.90 *vs* 31.07 ± 7.70, $P < 0.05$). Of interest, this population was significantly associated with advanced disease at initial presentation, poorer treatment responses, and adverse features of tumour biology, notably, lymphovascular invasion and perineural invasion.

In the cohort of patients which displayed a reduction in IC protein expression following radiation, there was a significant decrease in expression of PD-1 by $CD3^+$, $CD3^+CD4^+$ and $CD3^+CD8^+$ cells in tumour tissue when irradiated with 2 Gy *vs* 0 Gy (18.44 ± 5.90 *vs* 26.48 ± 7.50, $P < 0.05$; 10.33 ± 3.40 *vs* 14.46 ± 3.90, $P < 0.01$; 12.96 ± 5.10 *vs* 17.77 ± 8.20, $P < 0.05$; respectively) and PD-1 expression by $CD3^+$ and $CD3^+CD4^+$ when irradiated with 4 Gy *vs* 0 Gy (21.06 ± 6.90 *vs* 26.48 ± 7.50, and 10.04 ± 4.20 *vs* 14.46 ± 3.90, respectively, $P < 0.05$). There was also a significant decrease $CD3^+$, $CD3^+CD4^+$ and $CD3^+CD8^+$ cells expressing PD-L1 (15.6 ± 4.2 *vs* 20.6 ± 5.5, $P < 0.01$; 18.73 ± 11.50 *vs* 25.1 ± 13.1, $P < 0.05$; and 4.13 ± 0.90 *vs* 11.17 ± 2.80, $P < 0.05$; respectively) , TIGIT (48.61 ± 5.60 *vs* 60.13 ± 6.20, 59.88 ± 4.50 *vs* 69.57 ± 4.10, and 21.67 ± 6.40 *vs* 30.76 ± 4.50, respectively, $P < 0.05$) and TIM-3 (3.24 ± 0.90 *vs* 6.86 ± 2.50, 4.07 ± 1.30 *vs* 10.91 ± 3.30, and 3.37 ± 119.00 *vs* 9.13 ± 3.10, respectively, $P < 0.01$) with 2 Gy radiation. Similar findings were identified with 4 Gy irradiation compared to basal expression by $CD3^+CD8^+$ for PD-L1 (3.51 ± 0.60 *vs* 11.17 ± 2.80, $P < 0.05$) and TIM-3 (2.93 ± 0.70 *vs* 9.13 ± 3.10, $P < 0.05$) (Figure 3).

Clinical correlations

In order to understand potential clinical implications of these cohorts with increased and decreased IC expression post radiation, clinicopathological correlations were made based on patient tumour stage, adverse features of tumour biology, radiation and IC positivity (Table 1). There was a positive correlation basally with $PD\text{-}1^+CD3^+$ cells and lymphovascular invasion ($P = 0.04$). In terms of tumour staging, clinically there was a positive association of increasing tumour stage and $PD\text{-}L1^+CD3^+$ ($P = 0.02$) basally, $PD\text{-}L1^+CD3^+$, $TIM\text{-}3^+CD3^+$ and $TIM\text{-}3^+CD4^+$ at 2 Gy, and $TIM3^+CD8^+$ at 4 Gy ($P < 0.05$). There was a negative association between $PD\text{-}1^+CD8^+$ at 2 Gy ($P = 0.01$). In terms of clinical nodal status, there was a positive association with nodal positivity and $PD\text{-}L1^+CD4^+$ basally ($P < 0.001$) and $PD\text{-}1^+CD4^+$, $TIM\text{-}3^+CD4^+$, $TIM\text{-}3^+CD8^+$ at 4 Gy ($P < 0.05$). Pathologically, advancing tumour stage was negatively associated with $TIGIT^+CD3^+$ at 2 and 4 Gy ($P < 0.01$). Pathological nodal positivity was associated with $PD\text{-}L1^+CD4^+$ basally at 0 Gy, and $TIGIT^+CD3^+$ at 4 Gy ($P < 0.05$). It was negatively associated with $PD\text{-}L1^+CD8^+$ cells and $TIGIT^+CD3^+$ cells at 2 Gy ($P < 0.05$).

Release of angiogenic markers, cytokines, co-stimulatory molecules and soluble checkpoints post irradiation

Given the complex interplay in the tumour microenvironment between immunosuppressive factors and

Table 1 Clinicopathological characteristics of the study population illustrating the correlation for the percentage of $CD3^+$, $CD3^+CD4^+$ and $CD3^+CD8^+$ cells expressing immune checkpoints present in oesophageal adenocarcinoma tumour tissue

Clinical factor	IC expression	Radiation dose	Spearman *r*	*P* value (two-tailed)
Lymphovascular invasion	PD-1 $CD3^+$	0 Gy	0.6396022	0.046435
Clinical T stage	PD-L1 $CD3^+$	0 Gy	0.6411189	0.024659
	PD-1 $CD8^+$	2 Gy	-0.7000000	0.016471
	PD-L1 $CD3^+$	2 Gy	0.7768986	0.004908
	TIM-3 $CD3^+$	2 Gy	0.7171372	0.012993
	TIM-3 $CD4^+$	2 Gy	0.7171372	0.012993
	TIM-3 $CD8^+$	4 Gy	0.6963106	0.025293
Clinical N stage	PD-L1 $CD4^+$	0 Gy	0.8568931	0.000370
	PD-1 $CD4^+$	4 Gy	0.7311262	0.016282
	TIM-3 $CD4^+$	4 Gy	0.6614951	0.037241
	TIM-3 $CD8^+$	4 Gy	0.6614951	0.037241
Pathological T stage	TIGIT $CD3^+$	2 Gy	-0.7395740	0.014492
	TIGIT $CD3^+$	4 Gy	-0.8964215	0.006267
Pathological N stage	PD-L1 $CD4^+$	0 Gy	0.6510135	0.041473
	PD-L1 $CD8^+$	2 Gy	-0.6443043	0.044345
	TIGIT $CD3^+$	2 Gy	-0.7471188	0.013014
	TIGIT $CD4^+$	4 Gy	0.8981774	0.006011

Positive values indicate positive correlation, negative values indicate negative correlation. Spearman correlation. Only significant data shown. Spearman *r* = 0.40-0.59 moderate, 0.60-0.79 strong and 0.80-1.00 very strong. IC: Immune checkpoint.

anti-tumour immunity, we investigated the expression of cytokines, ICs, co-stimulatory molecules, markers of angiogenesis and vascular injury with and without radiation. The administration of 4 Gy radiation was effective in significantly reducing angiogenic markers over that of untreated 0 Gy tissue; basic fibroblast growth factor (bFGF, 57.7 ± 24.5 *vs* 197.5 ± 76.2, $P < 0.05$), Flt-1 (113.5 ± 47.7 *vs* 364.7 ± 145.8, $P < 0.05$), placental growth factor (PIGF, 18.7 ± 12.1 *vs* 32.8 ± 17.8, $P < 0.05$). Whereas, a significant reduction was observed in VEGF-A following 4 Gy radiation over that of 2 Gy (522.8 ± 144.2 *vs* 583.7 ± 86.2, $P < 0.05$) (Figure 4).

There was a significant increase in the level of IL-21 (1.98 ± 0.30 *vs* 1.3 ± 0.3, $P < 0.01$) and IL-31 (0.24 ± 0.04 *vs* 0.18 ± 0.02, $P < 0.01$) with the administration of 4 Gy radiation compared to 0 Gy with a significant decrease in IL-23 (3.53 ± 1.40 *vs* 5.24 ± 1.90, $P < 0.05$) following 4 Gy radiation compared with 2 Gy. CRP, a marker of vascular injury increased significantly with 2 Gy radiation dosing compared to untreated 0 Gy tissue (7568 ± 5750 *vs* 5425 ± 2925, $P < 0.05$) but was reduced with 4 Gy compared to non-irradiated tissue (Figure 5).

In terms of IC receptor and ligand expression, there was a significant reduction in levels of soluble PD-1 (6.44 ± 2.40 *vs* 15.72 ± 6.20, $P < 0.05$), PD-L1 (3.76 ± 0.70 *vs* 8.12 ± 1.70, $P < 0.05$), TIM-3 (24.11 ± 6.20 *vs* 76.02 ± 23.50, $P < 0.05$), TIGIT (4.26 ± 1.50 *vs* 39.0 ± 3.6, $P < 0.05$) and CD276 (58.81 ± 12.80 *vs* 164.30 ± 61.02, $P < 0.05$) in the TCM following 4 Gy radiation compared with 0 Gy. In addition, 4 Gy radiation also induced a significant decrease in the release of the soluble co-stimulatory molecules CD28 (82.18 ± 27.70 *vs* 163.2 ± 56.3, $P < 0.05$), glucocorticoid-induced TNF receptor (GITR, 5.27 ± 4.10 *vs* 5.7 ± 3.8, $P < 0.05$) and OX-40 (6.7 ± 2.1 *vs* 11.9 ± 2.9, $P < 0.05$) compared to untreated tissue 0 Gy (Figure 6).

DISCUSSION

The visceral appeal of modulating the host immune system is one of simplicity in an effort to harness a profound anti-tumour response and is a principle that has existed since the development of the field of cellular immunology as an entity. Quintessentially, skewing the hosts innate immune system to boost anti-tumour immunity consists of two processes compliant to exploitation: These being the stimulant as well as the reaction. The most logical way to perturb the tumour and its microenvironment is through promoting tumouricidal effects, through systemic chemotherapy or the radiation therapy delivered.

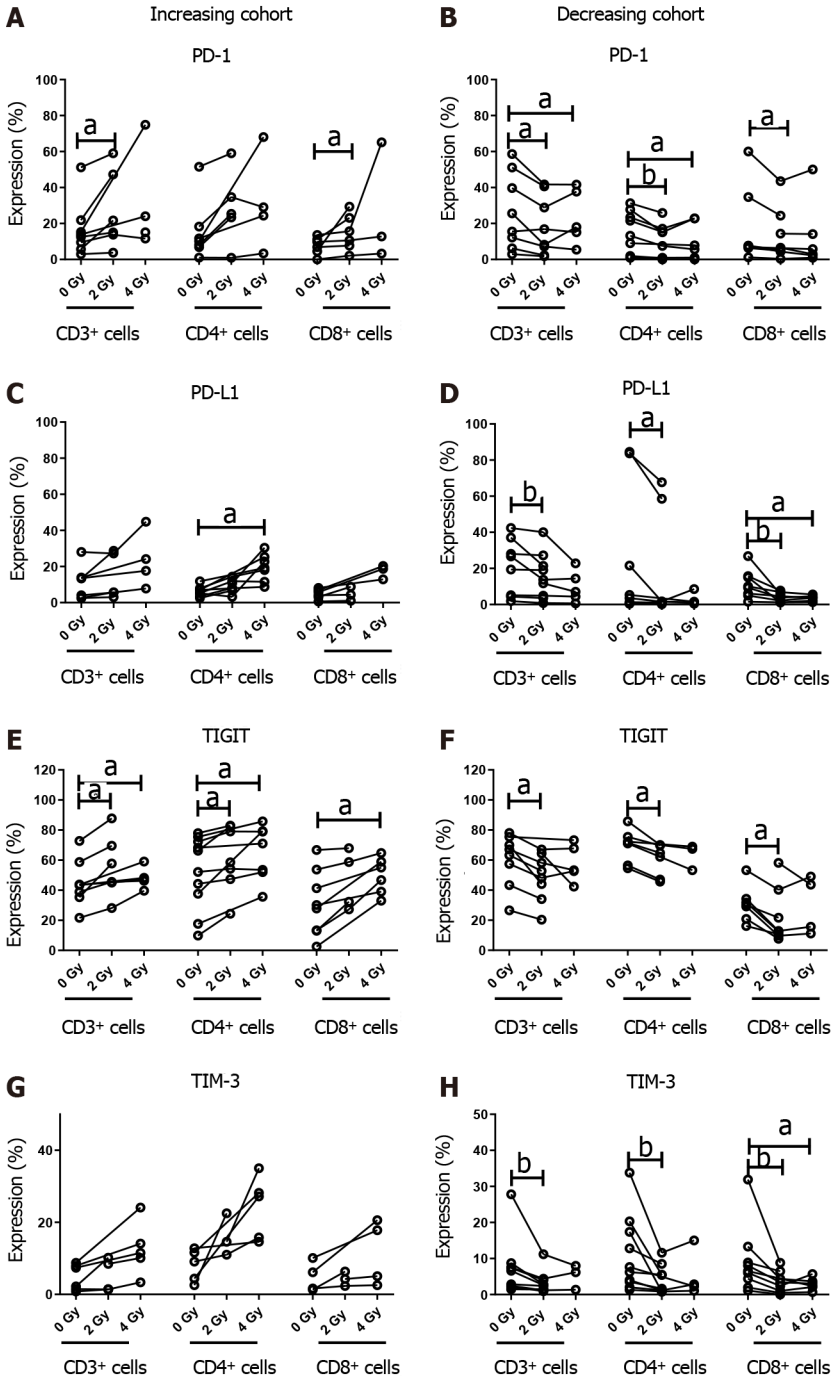


Figure 3 Oesophageal adenocarcinoma patients were screened for the surface expression of immune checkpoints *ex vivo* by flow cytometric analysis. Subcohorts where ionising radiation induced upregulation and downregulation of immune checkpoints (ICs). Inhibitory ICs are expressed at a higher level with conventional and hypofractionated dosing regimens in one cohort (n = 8). Inhibitory ICs are expressed at a lower level with conventional and hypofractionated dosing regimens in a separate cohort (n = 9). A and B: Increasing and decreasing cohort of PD-1; C and D: Increasing and decreasing cohort of PD-L1; E and F: Increasing and decreasing cohort of TIGIT; G and H: Increasing and decreasing cohort of TIM-3. [a]$P < 0.05$; [b]$P < 0.01$ by Wilcoxon signed rank test.

Increasing and propagating the anti-tumour responses thereby facilitating immune activation with optimal kinetics may achieve a synergistic anti-tumour response, producing a more profoundly durable effect on the immune system than chemo (radio) therapy alone. In this context, the landmark Checkmate-577 trial has demonstrated significantly improved disease free survival in the adjuvant setting of resectable gastroesophageal cancer[16]. The findings of increased IC expression *in vitro* and *ex vivo* through the use of radiation in the current body of work provides promising translational therapeutic rationale for their use in the multimodal paradigm. RT propagates the priming and effector phases of the anti-tumour immune response rendering it an appropriate combination with IC inhibitors (ICIs)[24]. However, inherently radioresistant tumours may pose a particular therapeutic dilemma, as they may not have a similar synergism with ICB as radiosensitive tumours. Ionising radiation is currently under investigation in metastatic oesophageal cancer with pembrolizumab (NCT02642809)

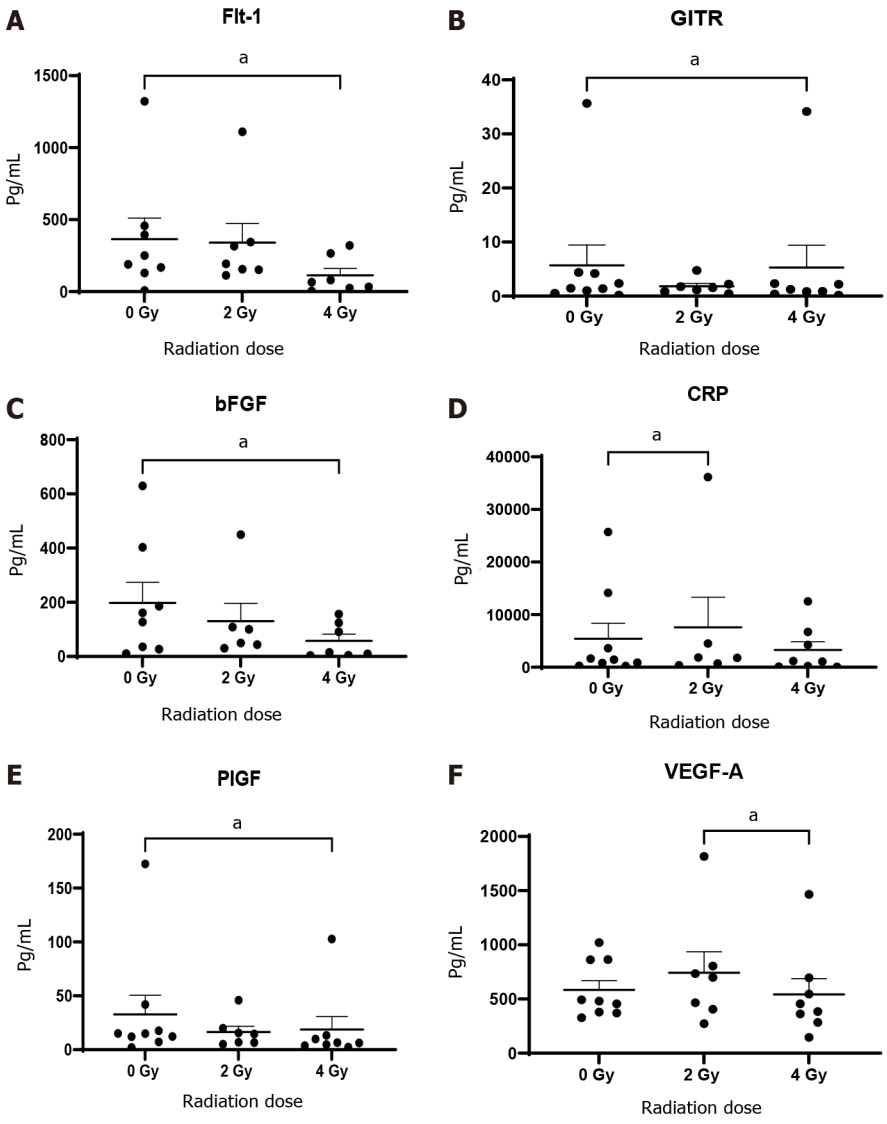


Figure 4 Conditioned media generated using oesophageal adenocarcinoma patient tumour was screened for markers by multiplex immunosorbent assay kit. Angiogenic markers Flt-1, basic fibroblast growth factor (bFGF), placental growth factor (PlGF) and vascular endothelial growth factor (VEGF)-A and vascular injury marker C-reactive protein (CRP) decrease significantly with 4 Gy radiation (n = 9). A: Flt-1; B: GITH; C: bFGF; D: CRP; E: PlGF; F: VEGF-A. $^{a}P < 0.05$ by Wilcoxon signed rank test.

and is currently under investigation in the curative setting with neoadjuvant trimodal therapy of Pembrolizumab and chemoradiotherapy in oesophageal squamous cell carcinoma (NCT03792347), with a similar trial investigating durvalumab and chemoradiotherapy in squamous cell carcinoma (SCC) and OAC (NCT02735239). The SKY-SKRAPER-07 trial is currently evaluating anti-PD-L1 Atezolizumab with anti-TIGIT therapy following chemoradiotherapy in advanced oesophageal cancer (NCT04543617). Of note, in a study by Zhao *et al*[25], they reported that with PD-1 positivity correlated with TIM-3 expression, and CD8^{+} tumour infiltrating lymphocyte density as a risk factor for recurrence free and overall survival (OS) in oesophageal SCC. The increasing expression in OAC cells and a cohort of patients following RT in this study represents promising therapeutic targets in OAC.

The clinically important observation in this study that half of the patients assessed displayed a reduction in IC expression post RT is an interesting caveat, one which suggests very different susceptibility to ICB in combination with RT and therefore, the stratification of patients into potential responders and non-responders should be addressed. In the same vein, the activation of cGAS-STING signaling, which has been recognized to potentiate systemic anti-tumour immunity and subsequent tumour rejection by dual RT and checkpoint blockade administration is promising even in those with checkpoint downregulation. A study by Vanpouille-Box *et al*[26], highlighting the importance of the cGAS-STING pathway in response to combination RT and immunotherapy, reported the knockdown of cGAS in murine cancer cells abrogated the priming of CD8^{+} T cells in tumour-draining lymph nodes and spleen, and prevented the infiltration of abscopal tumours by CD8^{+} T cells. Importantly, the synergistic and significant reduction in viability of radioresistant OAC cancer cells which we observed in this study following the dual administration of ICIs and ionising radiation is very promising.

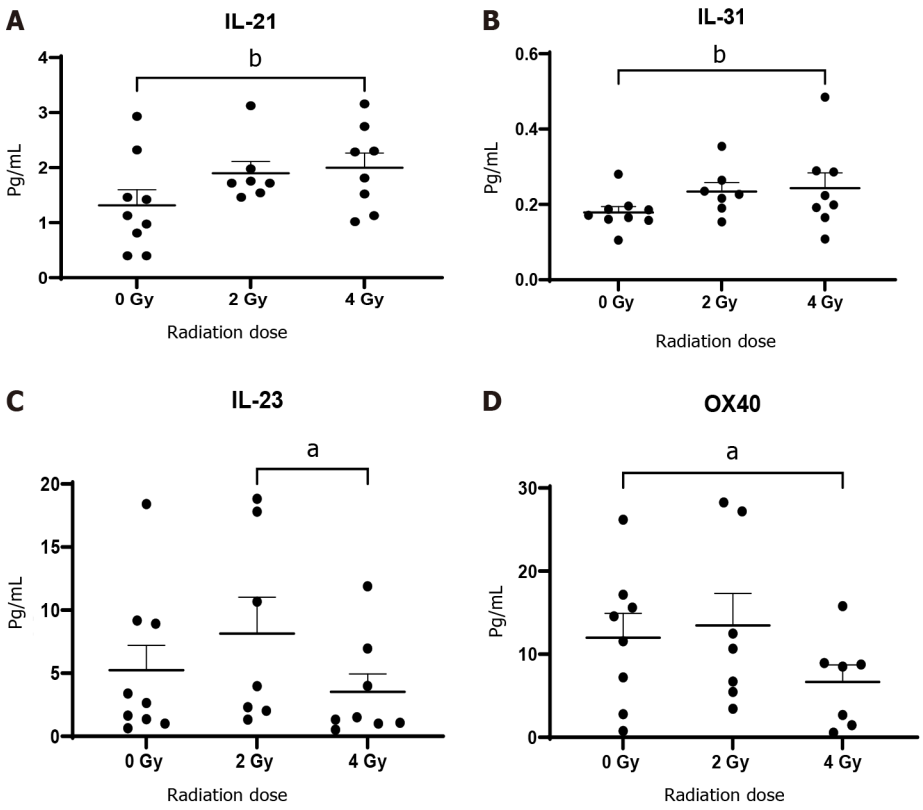


Figure 5 Oesophageal adenocarcinoma patients tumour conditioned media were screened by multiplex immunosorbent assay kit (*n* = 9). The cytokines interleukin (IL)-21 and IL-31 increase with ionising radiation while IL-23 and OX-40 decrease. A: IL-21; B: IL-31; C: IL-23; D: OX-40. [a]*P* < 0.05; [b]*P* < 0.01. Wilcoxon signed rank test to compare expression between basal levels and dosing regimens.

With respect to the use of hypofractionation in the curative setting for oesophageal cancer, there is an increasing volume of evidence demonstrating the safety and efficacy of this approach[27]. There are studies demonstrating a survival benefit of this approach particularly in the context of metastatic nodal disease. In one such study, hypofractionated radiotherapy (HFR) administered with taxane based chemotherapy in the management of post-surgery tracheoesophageal groove lymph node (TGLN) metastasis demonstrated improved OS in the HFR group compared with that of the conventional dosing treatment arm [24.1 mo (95%CI, 16.2-32.1 mo) *vs* 11.9 mo (95%CI, 9.2-14.4 mo), P = 0.024)[28]. Importantly, the study did not find a significant difference in pulmonary complications such as radiation pneumonitis (grades 3-4, 16.0% *vs* 7.1%; P = 0.314)[28].

Radiation induced lymphopenia is a frequent complication of multimodal cancer therapy and poorer outcomes are directly linked to the severity of lymphopenia[29]. Furthermore, it has been demonstrated that circulating lymphocyte count during neoadjuvant chemoradiation (CRT) in oesophageal cancer patients can predict pathological complete response (pCR) rates and low absolute circulating lymphocytes are associated with poorer outcomes[30]. The widespread adoption of immunotherapy has garnered new support and focus on the preservation of a pool of lymphocytes that are functional in enhancing immune function in the circulation and a study in pancreatic adenocarcinoma demonstrated hypofractionated CRT of 10 Gy in 3 doses over one week resulted in a decrease in the loss of T cells systemically compared to 28 daily doses of 1.8 Gy equating to 50.4 Gy[31,32].

The literature to date is concentrated primarily on evaluation of adverse events and of RT or immunotherapy in isolation. With improvements in targeted radiation delivery modalities, and technological advances, hypofractionated RT is now utilised without evidence of increased toxicities in a number of malignancies[33,34]. The Hypofractionated RT used in this instance was safe, well tolerated and provided robust survival results in those who could not receive chemoradiotherapy[35]. Furthermore, there is data in lung that conventional radiation dosing and immunotherapy is safe and feasible with no increases in adverse events[36-38].

The ATTRACTION 3 trial demonstrated a 50% reduction in serious adverse events in those treated with nivolumab *vs* conventional chemotherapy in Esophageal Squamous cell carcinoma[39]. In a study evaluating and immunotherapy in renal cell cancer, melanoma and lung, fatigue and pneumonitis were the most common adverse event. They found that toxicity did not correlate with hypofractionation or tumour type. Hypofractionated RT of pulmonary lesions was found to induce a complete response more consistently than in other sites. This study found that combining body Hypofractionated RT with immunotherapy is safe and viable, however, level I evidence is needed[40].

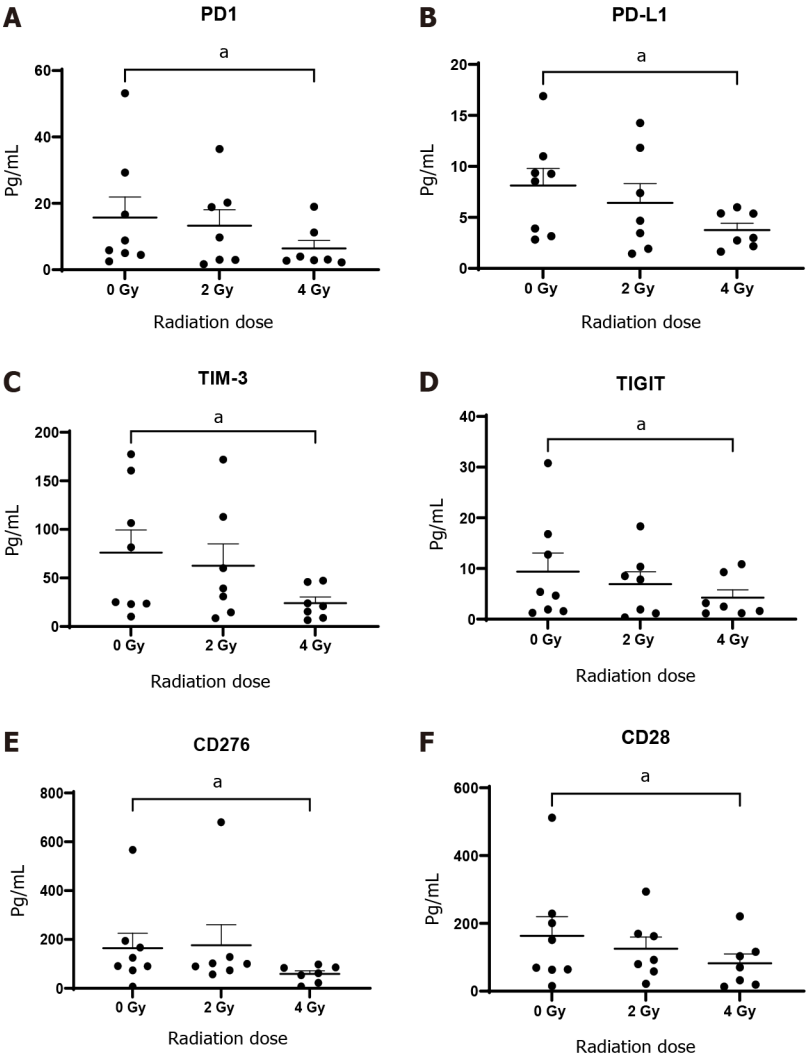


Figure 6 Oesophageal adenocarcinoma patient's tumour conditioned media were screened by multiplex immunosorbent assay kit. The inhibitory checkpoints PD-1 and its ligand PD-L1, TIGT, TIM3, immunosuppressive molecule and checkpoint CD276 (B7-H3) and costimulatory molecule CD28 significantly decrease with fractionated radiotherapy (n = 8). A: PD-1; B: PD-L1; C: TIM-3; D: TIGIT; E: CD276; F: CD28. $^{a}P < 0.05$ by Wilcoxon signed rank test.

VEGF is a mitogen essential for angiogenesis and Ramucirumab is approved for use in advanced gastroesophageal cancer patients. The use of anti-VEGF agents have shown promise in promoting improved survival when used in combination with chemoradiotherapy in colon cancer, however treatment resistance is a common problem[41]. This can be due compensatory mechanisms resulting in resistance, namely hypoxia- induced increases of other angiogenic promoters such as PIGF[42]. VEGF, bFGF and PIGF are crucial angiogenic promoters linked with tumourigenesis and Flt-1, is involved in tumour growth and metastatic dissemination, most likely *via* stimulation of macrophage-lineage cells [43]. PIGF/Flt-1 signaling can contribute to colorectal cancer progression through increasing the phosphorylation of p38 mitogen-activated protein kinase (MAPK), thereby upregulating MMP9 expression; resulting in increasing cellular migration/invasion. Therefore inhibition of PIGF/Flt-1 signalling will have therapeutic potential in lower gastrointestinal cancers[44]. In the current study radiation therapy was demonstrated to reduce the expression of these promoters of angiogenesis, which is crucial in the mitigating the risk of metastatic disease for upper gastrointestinal cancers.

The subset of cytokines expressed post radiation and immunotherapy treatment play a key role in determining the subsequent immune response elicited. In this study the OAC tumour tissue released significantly more anti-tumour IL-21 and IL-31 in response to radiation. IL-21 is produced by numerous T helper cells, such as Th1 and Th17 cells, activated Natural Killer T cells[45]. It promotes B cell differentiation into plasma cells, regulates immunoglobulin production, reshaping the tumour microenvironment and influencing the proliferation and/or effector function of both $CD4^+$ and $CD8^+$ T cells, while limiting the differentiation of Tregs[46]. IL-21 has distinct anti-tumour properties as a consequence of its ability to increase the availability of $CD8^+$ T cells through the induction of an early differentiation phenotype and Natural Killer cells[33]. IL-31 has immunoregulatory properties, with a study demonstrating that mice infused with IL-31 had tumour growth disruption and a decreased metastatic burden, supporting the use of IL-31 to offset the risk for metastatic disease development[47]. Similarly,

in a breast cancer murine model, the tumouricidal effects of T cells are increased, and myeloid derived suppressor cells and tumour-associated macrophages are reduced in tumours with high expression of IL-31, with an immunophenotype supporting antitumour immunity[48]. While both IL-21 and IL-31 were significantly increased in the TCM, the expression of IL-23, which has been documented to promote tumour metastases was decreased. IL-23 has metastases promoting properties *via* suppressing the anti-tumour properties of T cells and the anti-metastatic function of NK cells[49]. In addition to this, IL-23 was found to be overexpressed in many human cancers including colorectal and gastric cancer, and was found to be a negative prognostic indicator[50]. Of note CRP, an acute phase protein and marker of vascular injury was found to increase with 2 Gy radiation in our study. There have been epidemiologic studies to suggest that elevated CRP levels in circulation are linked with poorer outcomes in those with solid cancers, whereas elevated levels in apparently healthy subjects, is a potential independent risk factor for future risk of developing cancer of any type including lung, colorectal and gastric cancers due to chronic low inflammatory states, which is of particular relevance in OAC[51]. Therefore, the exact role of CRP in response to RT and immunotherapy requires further study.

Co-stimulatory and IC molecules can have both immunostimulatory and immunosuppressive effects. In this study a range of soluble ICIs and ligands were significantly downregulated following 4 Gy radiation treatment of OAC tumour explants. The role of soluble receptors however, and its effects on immune function remain yet to be elucidated and therefore its potential use as an oncological treatment remain unclear. Through this body of work, we observed a significant down regulation of PD-1, PD-L1, TIM-3 and TIGIT and this was paralleled by a concomitant increase in OAC cell line surface expression and a cohort of OAC tumour explants, which may go some way to explain the decrease in the soluble forms of these IC proteins post irradiation. B7-H3 (also known as CD276) is an IC molecule, with many cancers exhibiting aberrant overexpression and such upregulation is associated with aggressiveness and a poor clinical prognosis[52]. Furthermore, there are studies demonstrating a vital role for B7-H3 in promoting tumourigenesis and metastatic dissemination, proliferation, invasion and migration[52-54]. CD276 promotes tumour proliferation and invasion[55]. In addition, soluble CD276 was found to stimulate the invasion and metastatic dissemination of pancreatic adenocarcinoma cells *via* the Toll like Receptor 4/nuclear factor kappa-light-chain-enhancer of activated B cells pathway (50). Overall, additional studies are required in gastroesophageal cancers to determine the true function of soluble IC proteins and how they pertain to treatment response and immune regulation.

CD28 which is a co-stimulatory molecule is essential in the augmentation of T cell activation and metabolism, driving tumour-infiltrating T cell glycolysis. It is antagonized by CTLA-4 and PD-1[56]. In the current study, soluble CD28 is reduced with radiation, which may be immunosuppressive. Soluble CD80-Fc has been found to maintain IFN-γ release by PD-1$^+$ specific activated T cells even with PD-L1$^+$ tumour cells[57]. Soluble GITR, which was reduced in this study, represents a potential immunotherapeutic target and is found to be expressed at high levels on Tregs[58,59]. A number of phase 1 trials have identified anti-GITR antibodies to have safe pharmacological profiles, with phase II trials ongoing evaluating its combination with RT and anti-PD-1 therapy (NCT04225039). New promising approaches are focusing on the activation of co-stimulatory pathways to enhance antitumour immune responses. GITR activation can result in the inhibition of T-cell (Treg) function and promote effector T-cell function [58], and may also provide theoretical basis for the clinical application of combinations with monoclonal antibody therapy such as bFGF in molecular targeted therapies[60].

Lastly, OX40 has been demonstrated to have a crucial part to play in maintaining the immune responses in the immediate term and ongoing responses through enhancing T cell expansion, differentiation, and survival[61]. OX40 activation can have a significant impact T cell receptor (TCR) signaling through the PI3-K/PKB pathway, influencing T cell division, survival and cytokine production. This can directly increase calcium influx, and lead to IL-2, IL-4, IL-5, and IFN-γ secretion[62]. OX40 triggering regressed Treg cells, thus this allows Dendritic cells to reach the lymph nodes draining the tumour and in doing so prime the tumour-specific CD8 lymphocytes response [63]. However, in the current study radiation induces a downregulation of OX40 in TCM which may indeed be an immunosuppressive consequence of radiation therapy and one which requires further investigation. Again, more robust studies will be helpful to determine the functions of soluble co-stimulatory molecules as they may have alternate functions compared with their cell membrane bound counterparts in the tumour microenvironment.

CONCLUSION

The introduction of ICIs has resulted in enhanced survival in melanoma and non-small cell lung cancer treatment and has evolved to involve the spectrum of solid gastrointestinal malignancies with positive results of the landmark Checkmate 577 trial in the adjuvant setting most notable to date. However, there remains many issues to be interrogated including an appropriate RT regimen in conjunction with immunotherapies. There is considerable translational, preclinical and clinical data in favour of fractionated RT, and timing of RT delivery and target delineation, there remains disparity and no universal approach applicable to the clinical setting. In the current study, IC blockade in combination

with radiation synergistically reduces viability in radioresistant cells and Nivolumab appears most efficacious. There remains a need to delineate the effects of RT on host anti-tumour immunity. Additionally, lymphopenia induced by RT delivery may negate the effects of immunotherapy on offsetting T cell exhaustion, thus protocols that can minimize lymphopenia need careful design for maximal therapeutic potential. Finally, more concentrated and robust studies to determine and validate potential biomarkers to predict those who will be suitable for these treatment modalities are urgently required with profiling next-generation sequencing of tumour mutation burden based profiling, immune signatures, gene profiling signatures and the repertoire of T-cell receptors potential avenues to elucidate this.

ARTICLE HIGHLIGHTS

Research background

Oesophageal cancer is represents a difficult treatment dilemma with poor 5 year overall survival due to presentation at advanced stages due to its indolent nature as well as poor treatment responses to conventional therapies.

Research motivation

The advent of immunotherapy represents a shift in the multimodal treatment paradigm for esophageal cancer and has had mixed results in many solid tumours to date. The Checkmate 577 trial is a landmark study and is sure to revolutionize immune checkpoint blockade as the treatment modality of choice in the adjuvant setting.

Research objectives

To determine the impact of radiotherapy (RT) on immune checkpoint expression, and to determine the prevailing immune milieu in terms of markers of angiogenesis, cytokines and metastatic markers.

Research methods

This hybrid *in vitro* and *ex vivo* study is a mixture of flow cytometry, enzyme-linked immunosorbent assay kit work and cell viability by a cell counting kit-8 assay.

Research results

Radiation results in a decrease in angiogenic and metastatic markers with an increase in anti-tumour cytokines. There were two distinct subpopulations, with one cohort of patients demonstrating increased checkpoint expression as a consequence of radiation and a separate cohort demonstrating the opposite effects. The cohort with increased checkpoint expression had poorer treatment responses and were associated with adverse tumour biology.

Research conclusions

Oesophageal cancer represents an immune active tumour and is a viable target in both the neoadjuvant and adjuvant setting and should be combined with RT to exert maximum synergistic effects.

Research perspectives

This seminal study is the first of its kind and is a truly clinical and translational evaluation of the immune landscape of esophageal cancer.

FOOTNOTES

Author contributions: Donlon NE and Davern M contributed equally to this work; Donlon NE and Davern M contributed to experimental design and execution, and manuscript drafting and revision; O'Connell F and Sheppard A contributed to experiments; Heeran A, Bhardwaj A, and Butler C contributed to sample acquisition; Narayanasamy R, Donohoe C, Phelan JJ, Lynam-Lennon N, Dunne MR, and Maher S contributed to concept design; Phelan JJ contributed to statistical analysis; O'Sullivan J, Reynolds JV, and Lysaght J contributed to paper revision and supervision of the project.

Institutional review board statement: The study was reviewed and approved by the Tallaght/St James's Hospital Ethics Committee.

Conflict-of-interest statement: There are no conflicts of interest to report.

Data sharing statement: Data generated in this study will be available upon specific request from the corresponding author.

Open-Access: This article is an open-access article that was selected by an in-house editor and fully peer-reviewed by external reviewers. It is distributed in accordance with the Creative Commons Attribution NonCommercial (CC BY-NC 4.0) license, which permits others to distribute, remix, adapt, build upon this work non-commercially, and license their derivative works on different terms, provided the original work is properly cited and the use is non-commercial. See: https://creativecommons.org/Licenses/by-nc/4.0/

Country/Territory of origin: Ireland

ORCID number: Noel E Donlon 0000-0002-4073-3896; Maria Davern 0000-0003-2278-5497; Fiona O'Connell 0000-0002-3641-4374; Andrew Sheppard 0000-0002-5973-7192; Aisling Heeran 0000-0002-7209-155; Anshul Bhardwaj 0000-0003-4421-8987; Christine Butler 0000-0002-1597-5551; Ravi Narayanasamy 0000-0001-9794-622; Claire Donohoe 0000-0001-9373-2662; James J Phelan 0000-0001-9431-2002; Niamh Lynam-Lennon 0000-0001-8659-4943; Margaret R Dunne 0000-0002-2816-5064; Stephen Maher 0000-0003-0126-7906; Jacintha O'Sullivan 0000-0001-8622-9858; John V Reynolds 0000-0002-5501-9521; Joanne Lysaght 0000-0003-3363-3763.

S-Editor: Chen YL
L-Editor: A
P-Editor: Yuan YY

REFERENCES

1 **Smyth EC**, Lagergren J, Fitzgerald RC, Lordick F, Shah MA, Lagergren P, Cunningham D. Oesophageal cancer. *Nat Rev Dis Primers* 2017; **3**: 17048 [PMID: 28748917 DOI: 10.1038/nrdp.2017.48]
2 **Lagergren J**, Smyth E, Cunningham D, Lagergren P. Oesophageal cancer. *Lancet* 2017; **390**: 2383-2396 [PMID: 28648400 DOI: 10.1016/S0140-6736(17)31462-9]
3 **van Hagen P**, Hulshof MC, van Lanschot JJ, Steyerberg EW, van Berge Henegouwen MI, Wijnhoven BP, Richel DJ, Nieuwenhuijzen GA, Hospers GA, Bonenkamp JJ, Cuesta MA, Blaisse RJ, Busch OR, ten Kate FJ, Creemers GJ, Punt CJ, Plukker JT, Verheul HM, Spillenaar Bilgen EJ, van Dekken H, van der Sangen MJ, Rozema T, Biermann K, Beukema JC, Piet AH, van Rij CM, Reinders JG, Tilanus HW, van der Gaast A; CROSS Group. Preoperative chemoradiotherapy for esophageal or junctional cancer. *N Engl J Med* 2012; **366**: 2074-2084 [PMID: 22646630 DOI: 10.1056/NEJMoa1112088]
4 **Minsky BD**, Pajak TF, Ginsberg RJ, Pisansky TM, Martenson J, Komaki R, Okawara G, Rosenthal SA, Kelsen DP. INT 0123 (Radiation Therapy Oncology Group 94-05) phase III trial of combined-modality therapy for esophageal cancer: high-dose versus standard-dose radiation therapy. *J Clin Oncol* 2002; **20**: 1167-1174 [PMID: 11870157 DOI: 10.1200/JCO.2002.20.5.1167]
5 **Nemoto K**, Kawashiro S, Toh Y, Numasaki H, Tachimori Y, Uno T, Jingu K, Matsubara H. Comparison of the effects of radiotherapy doses of 50.4 Gy and 60 Gy on outcomes of chemoradiotherapy for thoracic esophageal cancer: subgroup analysis based on the Comprehensive Registry of Esophageal Cancer in Japan from 2009 to 2011 by the Japan Esophageal Society. *Esophagus* 2020; **17**: 122-126 [PMID: 31912332 DOI: 10.1007/s10388-019-00711-x]
6 **Liu L**, Yang Y, Guo Q, Ren B, Peng Q, Zou L, Zhu Y, Tian Y. Comparing hypofractionated to conventional fractionated radiotherapy in postmastectomy breast cancer: a meta-analysis and systematic review. *Radiat Oncol* 2020; **15**: 17 [PMID: 31952507 DOI: 10.1186/s13014-020-1463-1]
7 **Whelan TJ**, Pignol JP, Levine MN, Julian JA, MacKenzie R, Parpia S, Shelley W, Grimard L, Bowen J, Lukka H, Perera F, Fyles A, Schneider K, Gulavita S, Freeman C. Long-term results of hypofractionated radiation therapy for breast cancer. *N Engl J Med* 2010; **362**: 513-520 [PMID: 20147717 DOI: 10.1056/NEJMoa0906260]
8 **Murray Brunt A**, Haviland JS, Wheatley DA, Sydenham MA, Alhasso A, Bloomfield DJ, Chan C, Churn M, Cleator S, Coles CE, Goodman A, Harnett A, Hopwood P, Kirby AM, Kirwan CC, Morris C, Nabi Z, Sawyer E, Somaiah N, Stones L, Syndikus I, Bliss JM, Yarnold JR; FAST-Forward Trial Management Group. Hypofractionated breast radiotherapy for 1 week versus 3 weeks (FAST-Forward): 5-year efficacy and late normal tissue effects results from a multicentre, non-inferiority, randomised, phase 3 trial. *Lancet* 2020; **395**: 1613-1626 [PMID: 32580883 DOI: 10.1016/S0140-6736(20)30932-6]
9 **Widmark A**, Gunnlaugsson A, Beckman L, Thellenberg-Karlsson C, Hoyer M, Lagerlund M, Kindblom J, Ginman C, Johansson B, Björnlinger K, Seke M, Agrup M, Fransson P, Tavelin B, Norman D, Zackrisson B, Anderson H, Kjellén E, Franzén L, Nilsson P. Ultra-hypofractionated versus conventionally fractionated radiotherapy for prostate cancer: 5-year outcomes of the HYPO-RT-PC randomised, non-inferiority, phase 3 trial. *Lancet* 2019; **394**: 385-395 [PMID: 31227373 DOI: 10.1016/S0140-6736(19)31131-6]
10 **Dearnaley D**, Syndikus I, Sumo G, Bidmead M, Bloomfield D, Clark C, Gao A, Hassan S, Horwich A, Huddart R, Khoo V, Kirkbride P, Mayles H, Mayles P, Naismith O, Parker C, Patterson H, Russell M, Scrase C, South C, Staffurth J, Hall E. Conventional versus hypofractionated high-dose intensity-modulated radiotherapy for prostate cancer: preliminary safety results from the CHHiP randomised controlled trial. *Lancet Oncol* 2012; **13**: 43-54 [PMID: 22169269 DOI: 10.1016/S1470-2045(11)70293-5]
11 **Donohoe CL**, O'Farrell NJ, Grant T, King S, Clarke L, Muldoon C, Reynolds JV. Classification of pathologic response to neoadjuvant therapy in esophageal and junctional cancer: assessment of existing measures and proposal of a novel 3-point standard. *Ann Surg* 2013; **258**: 784-92; discussion 792 [PMID: 24045450 DOI: 10.1097/SLA.0b013e3182a66588]
12 **Noble F**, Lloyd MA, Turkington R, Griffiths E, O'Donovan M, O'Neill JR, Mercer S, Parsons SL, Fitzgerald RC, Underwood TJ; OCCAMS consortium. Multicentre cohort study to define and validate pathological assessment of response to neoadjuvant therapy in oesophagogastric adenocarcinoma. *Br J Surg* 2017; **104**: 1816-1828 [PMID: 28944954 DOI:

10.1002/bjs.10627]
13 **Iwai Y**, Ishida M, Tanaka Y, Okazaki T, Honjo T, Minato N. Involvement of PD-L1 on tumour cells in the escape from host immune system and tumour immunotherapy by PD-L1 blockade. *Proc Natl Acad Sci U S A* 2002; **99**: 12293-12297 [PMID: 12218188 DOI: 10.1073/pnas.192461099]
14 **Chen DS**, Mellman I. Elements of cancer immunity and the cancer-immune set point. *Nature* 2017; **541**: 321-330 [PMID: 28102259 DOI: 10.1038/nature21349]
15 **Power R**, Lowery MA, Reynolds JV, Dunne MR. The Cancer-Immune Set Point in Oesophageal Cancer. *Front Oncol* 2020; **10**: 891 [PMID: 32582553 DOI: 10.3389/fonc.2020.00891]
16 **Kelly RJ**, Ajani JA, Kuzdzal J, Zander T, Van Cutsem E, Piessen G, Mendez G, Feliciano J, Motoyama S, Lièvre A, Uronis H, Elimova E, Grootscholten C, Geboes K, Zafar S, Snow S, Ko AH, Feeney K, Schenker M, Kocon P, Zhang J, Zhu L, Lei M, Singh P, Kondo K, Cleary JM, Moehler M; CheckMate 577 Investigators. Adjuvant Nivolumab in Resected Esophageal or Gastroesophageal Junction Cancer. *N Engl J Med* 2021; **384**: 1191-1203 [PMID: 33789008 DOI: 10.1056/NEJMoa2032125]
17 **Smyth EC**, Cervantes A. Addition of nivolumab to chemotherapy in patients with advanced gastric cancer: a relevant step ahead, but still many questions to answer. *ESMO Open* 2020; **5**: e001107 [PMID: 33208490 DOI: 10.1136/esmoopen-2020-001107]
18 **Donlon NE**, Power R, Hayes C, Reynolds JV, Lysaght J. Radiotherapy, immunotherapy, and the tumour microenvironment: Turning an immunosuppressive milieu into a therapeutic opportunity. *Cancer Lett* 2021; **502**: 84-96 [PMID: 33450360 DOI: 10.1016/j.canlet.2020.12.045]
19 **Golden EB**, Frances D, Pellicciotta I, Demaria S, Helen Barcellos-Hoff M, Formenti SC. Radiation fosters dose-dependent and chemotherapy-induced immunogenic cell death. *Oncoimmunology* 2014; **3**: e28518 [PMID: 25071979 DOI: 10.4161/onci.28518]
20 **Deng L**, Liang H, Xu M, Yang X, Burnette B, Arina A, Li XD, Mauceri H, Beckett M, Darga T, Huang X, Gajewski TF, Chen ZJ, Fu YX, Weichselbaum RR. STING-Dependent Cytosolic DNA Sensing Promotes Radiation-Induced Type I Interferon-Dependent Antitumour Immunity in Immunogenic Tumours. *Immunity* 2014; **41**: 843-852 [PMID: 25517616 DOI: 10.1016/j.immuni.2014.10.019]
21 **Hou Y**, Liang H, Rao E, Zheng W, Huang X, Deng L, Zhang Y, Yu X, Xu M, Mauceri H, Arina A, Weichselbaum RR, Fu YX. Non-canonical NF-κB Antagonizes STING Sensor-Mediated DNA Sensing in Radiotherapy. *Immunity* 2018; **49**: 490-503.e4 [PMID: 30170810 DOI: 10.1016/j.immuni.2018.07.008]
22 **McLaughlin M**, Patin EC, Pedersen M, Wilkins A, Dillon MT, Melcher AA, Harrington KJ. Inflammatory microenvironment remodelling by tumour cells after radiotherapy. *Nat Rev Cancer* 2020; **20**: 203-217 [PMID: 32161398 DOI: 10.1038/s41568-020-0246-1]
23 **Lynam-Lennon N**, Reynolds JV, Pidgeon GP, Lysaght J, Marignol L, Maher SG. Alterations in DNA repair efficiency are involved in the radioresistance of esophageal adenocarcinoma. *Radiat Res* 2010; **174**: 703-711 [PMID: 21128793 DOI: 10.1667/RR2295.1]
24 **Gong J**, Le TQ, Massarelli E, Hendifar AE, Tuli R. Radiation therapy and PD-1/PD-L1 blockade: the clinical development of an evolving anticancer combination. *J Immunother Cancer* 2018; **6**: 46 [PMID: 29866197 DOI: 10.1186/s40425-018-0361-7]
25 **Zhao Y**, Chen D, Wang W, Zhao T, Wen J, Zhang F, Duan S, Chen C, Sang Y, Zhang Y, Chen Y. Significance of TIM-3 Expression in Resected Esophageal Squamous Cell Carcinoma. *Ann Thorac Surg* 2020; **109**: 1551-1557 [PMID: 31987829 DOI: 10.1016/j.athoracsur.2019.12.017]
26 **Vanpouille-Box C**, Alard A, Aryankalayil MJ, Sarfraz Y, Diamond JM, Schneider RJ, Inghirami G, Coleman CN, Formenti SC, Demaria S. DNA exonuclease Trex1 regulates radiotherapy-induced tumour immunogenicity. *Nat Commun* 2017; **8**: 15618 [PMID: 28598415 DOI: 10.1038/ncomms15618]
27 **Lyu J**, Liu T, Li T, Li F, Wang Q, Wang J, Han Y, Zhang J, Peng L, Lang J. Comparison of efficacy, safety, and costs between neoadjuvant hypofractionated radiotherapy and conventionally fractionated radiotherapy for esophageal carcinoma. *Cancer Med* 2019; **8**: 3710-3718 [PMID: 31119872 DOI: 10.1002/cam4.2250]
28 **Wang J**, Yu J, Jiang Y, Pei D, Zhu H, Wang J. Hypofractionated Radiotherapy in Combination With Chemotherapy Improves Outcome of Patients With Esophageal Carcinoma Tracheoesophageal Groove Lymph Node Metastasis. *Front Oncol* 2020; **10**: 1540 [PMID: 32984011 DOI: 10.3389/fonc.2020.01540]
29 **Xie X**, Lin SH, Welsh JW, Wei X, Jin H, Mohan R, Liao Z, Xu T. Radiation-induced lymphopenia during chemoradiation therapy for non-small cell lung cancer is linked with age, lung V5, and XRCC1 rs25487 genotypes in lymphocytes. *Radiother Oncol* 2021; **154**: 187-193 [PMID: 32916236 DOI: 10.1016/j.radonc.2020.09.002]
30 **Wu Y**, Chen J, Zhao L, Li Q, Zhu J, Yang H, Guo S, Xi M. Prediction of Pathologic Response to Neoadjuvant Chemoradiotherapy in Patients with Esophageal Squamous Cell Carcinoma Incorporating Hematological Biomarkers. *Cancer Res Treat* 2021; **53**: 172-183 [PMID: 32898941 DOI: 10.4143/crt.2020.594]
31 **Wang X**, Wang P, Zhao Z, Mao Q, Yu J, Li M. A review of radiation-induced lymphopenia in patients with esophageal cancer: an immunological perspective for radiotherapy. *Ther Adv Med Oncol* 2020; **12**: 1758835920926822 [PMID: 32518598 DOI: 10.1177/1758835920926822]
32 **Crocenzi T**, Cottam B, Newell P, Wolf RF, Hansen PD, Hammill C, Solhjem MC, To YY, Greathouse A, Tormoen G, Jutric Z, Young K, Bahjat KS, Gough MJ, Crittenden MR. A hypofractionated radiation regimen avoids the lymphopenia associated with neoadjuvant chemoradiation therapy of borderline resectable and locally advanced pancreatic adenocarcinoma. *J Immunother Cancer* 2016; **4**: 45 [PMID: 27532020 DOI: 10.1186/s40425-016-0149-6]
33 **Rodin D**, Tawk B, Mohamad O, Grover S, Moraes FY, Yap ML, Zubizarreta E, Lievens Y. Hypofractionated radiotherapy in the real-world setting: An international ESTRO-GIRO survey. *Radiother Oncol* 2021; **157**: 32-39 [PMID: 33453312 DOI: 10.1016/j.radonc.2021.01.003]
34 **Vapiwala N**, Wong JK, Handorf E, Paly J, Grewal A, Tendulkar R, Godfrey D, Carpenter D, Mendenhall NP, Henderson RH, Stish BJ, Vargas C, Salama JK, Davis BJ, Horwitz EM. A Pooled Toxicity Analysis of Moderately Hypofractionated Proton Beam Therapy and Intensity Modulated Radiation Therapy in Early-Stage Prostate Cancer Patients. *Int J Radiat*

Oncol Biol Phys 2021; **110**: 1082-1089 [PMID: 33539968 DOI: 10.1016/j.ijrobp.2021.01.043]
35 **Jones CM**, Spencer K, Hitchen C, Pelly T, Wood B, Hatfield P, Crellin A, Sebag-Montefiore D, Goody R, Crosby T, Radhakrishna G. Hypofractionated Radiotherapy in Oesophageal Cancer for Patients Unfit for Systemic Therapy: A Retrospective Single-Centre Analysis. *Clin Oncol (R Coll Radiol)* 2019; **31**: 356-364 [PMID: 30737068 DOI: 10.1016/j.clon.2019.01.010]
36 **Spaas M**, Lievens Y. Is the Combination of Immunotherapy and Radiotherapy in Non-small Cell Lung Cancer a Feasible and Effective Approach? *Front Med (Lausanne)* 2019; **6**: 244 [PMID: 31788476 DOI: 10.3389/fmed.2019.00244]
37 **Meng L**, Xu J, Ye Y, Wang Y, Luo S, Gong X. The Combination of Radiotherapy With Immunotherapy and Potential Predictive Biomarkers for Treatment of Non-Small Cell Lung Cancer Patients. *Front Immunol* 2021; **12**: 723609 [PMID: 34621270 DOI: 10.3389/fimmu.2021.723609]
38 **Chicas-Sett R**, Zafra-Martin J, Morales-Orue I, Castilla-Martinez J, Berenguer-Frances MA, Gonzalez-Rodriguez E, Rodriguez-Abreu D, Couñago F. Immunoradiotherapy as An Effective Therapeutic Strategy in Lung Cancer: From Palliative Care to Curative Intent. *Cancers (Basel)* 2020; **12** [PMID: 32764371 DOI: 10.3390/cancers12082178]
39 **Kato K**, Cho BC, Takahashi M, Okada M, Lin CY, Chin K, Kadowaki S, Ahn MJ, Hamamoto Y, Doki Y, Yen CC, Kubota Y, Kim SB, Hsu CH, Holtved E, Xynos I, Kodani M, Kitagawa Y. Nivolumab versus chemotherapy in patients with advanced oesophageal squamous cell carcinoma refractory or intolerant to previous chemotherapy (ATTRACTION-3): a multicentre, randomised, open-label, phase 3 trial. *Lancet Oncol* 2019; **20**: 1506-1517 [PMID: 31582355 DOI: 10.1016/S1470-2045(19)30626-6]
40 **Mohamad O**, Diaz de Leon A, Schroeder S, Leiker A, Christie A, Zhang-Velten E, Trivedi L, Khan S, Desai NB, Laine A, Albuquerque K, Iyengar P, Arriaga Y, Courtney K, Gerber DE, Hammers H, Choy H, Timmerman R, Brugarolas J, Hannan R. Safety and efficacy of concurrent immune checkpoint inhibitors and hypofractionated body radiotherapy. *Oncoimmunology* 2018; **7**: e1440168 [PMID: 29900043 DOI: 10.1080/2162402X.2018.1440168]
41 **Haibe Y**, Kreidieh M, El Hajj H, Khalifeh I, Mukherji D, Temraz S, Shamseddine A. Resistance Mechanisms to Anti-angiogenic Therapies in Cancer. *Front Oncol* 2020; **10**: 221 [PMID: 32175278 DOI: 10.3389/fonc.2020.00221]
42 **Macarulla T**, Montagut C, Sánchez-Martin FJ, Granja M, Verdaguer H, Sastre J, Tabernero J. The role of PIGF blockade in the treatment of colorectal cancer: overcoming the pitfalls. *Expert Opin Biol Ther* 2020; **20**: 15-22 [PMID: 31608707 DOI: 10.1080/14712598.2020.1677603]
43 **Qian BZ**, Zhang H, Li J, He T, Yeo EJ, Soong DY, Carragher NO, Munro A, Chang A, Bresnick AR, Lang RA, Pollard JW. FLT1 signaling in metastasis-associated macrophages activates an inflammatory signature that promotes breast cancer metastasis. *J Exp Med* 2015; **212**: 1433-1448 [PMID: 26261265 DOI: 10.1084/jem.20141555]
44 **Wei SC**, Tsao PN, Weng MT, Cao Z, Wong JM. Flt-1 in colorectal cancer cells is required for the tumour invasive effect of placental growth factor through a p38-MMP9 pathway. *J Biomed Sci* 2013; **20**: 39 [PMID: 23799978 DOI: 10.1186/1423-0127-20-39]
45 **Tian Y**, Zajac AJ. IL-21 and T Cell Differentiation: Consider the Context. *Trends Immunol* 2016; **37**: 557-568 [PMID: 27389961 DOI: 10.1016/j.it.2016.06.001]
46 **Deng S**, Sun Z, Qiao J, Liang Y, Liu L, Dong C, Shen A, Wang Y, Tang H, Fu YX, Peng H. Targeting tumours with IL-21 reshapes the tumour microenvironment by proliferating PD-1intTim-3-CD8+ T cells. *JCI Insight* 2020; **5** [PMID: 32271164 DOI: 10.1172/jci.insight.132000]
47 **Davidi S**, Fremder E, Kan T, Raviv Z, Timaner M, Karin N, Hershkovitz D, Arohneim A, Shaked Y. The antiangiogenic role of the pro-inflammatory cytokine interleukin-31. *Oncotarget* 2017; **8**: 16430-16444 [PMID: 28147314 DOI: 10.18632/oncotarget.14857]
48 **Kan T**, Feldman E, Timaner M, Raviv Z, Shen-Orr S, Aronheim A, Shaked Y. IL-31 induces antitumour immunity in breast carcinoma. *J Immunother Cancer* 2020; **8** [PMID: 32843492 DOI: 10.1136/jitc-2020-001010]
49 **Teng MW**, Andrews DM, McLaughlin N, von Scheidt B, Ngiow SF, Möller A, Hill GR, Iwakura Y, Oft M, Smyth MJ. IL-23 suppresses innate immune response independently of IL-17A during carcinogenesis and metastasis. *Proc Natl Acad Sci U S A* 2010; **107**: 8328-8333 [PMID: 20404142 DOI: 10.1073/pnas.1003251107]
50 **Yan J**, Smyth MJ, Teng MWL. Interleukin (IL)-12 and IL-23 and Their Conflicting Roles in Cancer. *Cold Spring Harb Perspect Biol* 2018; **10** [PMID: 28716888 DOI: 10.1101/cshperspect.a028530]
51 **Allin KH**, Nordestgaard BG. Elevated C-reactive protein in the diagnosis, prognosis, and cause of cancer. *Crit Rev Clin Lab Sci* 2011; **48**: 155-170 [PMID: 22035340 DOI: 10.3109/10408363.2011.599831]
52 **Liu S**, Liang J, Liu Z, Zhang C, Wang Y, Watson AH, Zhou C, Zhang F, Wu K, Lu Y, Wang X. The Role of CD276 in Cancers. *Front Oncol* 2021; **11**: 654684 [PMID: 33842369 DOI: 10.3389/fonc.2021.654684]
53 **Dong P**, Xiong Y, Yue J, Hanley SJB, Watari H. B7H3 As a Promoter of Metastasis and Promising Therapeutic Target. *Front Oncol* 2018; **8**: 264 [PMID: 30035102 DOI: 10.3389/fonc.2018.00264]
54 **Xie C**, Liu D, Chen Q, Yang C, Wang B, Wu H. Soluble B7-H3 promotes the invasion and metastasis of pancreatic carcinoma cells through the TLR4/NF-κB pathway. *Sci Rep* 2016; **6**: 27528 [PMID: 27273624 DOI: 10.1038/srep27528]
55 **Dai W**, Shen G, Qiu J, Zhao X, Gao Q. Aberrant expression of B7-H3 in gastric adenocarcinoma promotes cancer cell metastasis. *Oncol Rep* 2014; **32**: 2086-2092 [PMID: 25120098 DOI: 10.3892/or.2014.3405]
56 **Beckermann KE**, Hongo R, Ye X, Young K, Carbonell K, Healey DCC, Siska PJ, Barone S, Roe CE, Smith CC, Vincent BG, Mason FM, Irish JM, Rathmell WK, Rathmell JC. CD28 costimulation drives tumour-infiltrating T cell glycolysis to promote inflammation. *JCI Insight* 2020; **5** [PMID: 32814710 DOI: 10.1172/jci.insight.138729]
57 **Haile ST**, Dalal SP, Clements V, Tamada K, Ostrand-Rosenberg S. Soluble CD80 restores T cell activation and overcomes tumour cell programmed death ligand 1-mediated immune suppression. *J Immunol* 2013; **191**: 2829-2836 [PMID: 23918985 DOI: 10.4049/jimmunol.1202777]
58 **Zhu MMT**, Burugu S, Gao D, Yu J, Kos Z, Leung S, Horst BA, Nielsen TO. Evaluation of glucocorticoid-induced TNF receptor (GITR) expression in breast cancer and across multiple tumour types. *Mod Pathol* 2020; **33**: 1753-1763 [PMID: 32350416 DOI: 10.1038/s41379-020-0550-z]
59 **van Beek AA**, Zhou G, Doukas M, Boor PPC, Noordam L, Mancham S, Campos Carrascosa L, van der Heide-Mulder M, Polak WG, Ijzermans JNM, Pan Q, Heirman C, Mahne A, Bucktrout SL, Bruno MJ, Sprengers D, Kwekkeboom J. GITR

ligation enhances functionality of tumour-infiltrating T cells in hepatocellular carcinoma. *Int J Cancer* 2019; **145**: 1111-1124 [PMID: 30719701 DOI: 10.1002/ijc.32181]

60 **Liu M**, Xing LQ. Basic fibroblast growth factor as a potential biomarker for diagnosing malignant tumour metastasis in women. *Oncol Lett* 2017; **14**: 1561-1567 [PMID: 28789380 DOI: 10.3892/ol.2017.6335]

61 **Redmond WL**, Ruby CE, Weinberg AD. The role of OX40-mediated co-stimulation in T-cell activation and survival. *Crit Rev Immunol* 2009; **29**: 187-201 [PMID: 19538134 DOI: 10.1615/critrevimmunol.v29.i3.10]

62 **Willoughby J**, Griffiths J, Tews I, Cragg MS. OX40: Structure and function - What questions remain? *Mol Immunol* 2017; **83**: 13-22 [PMID: 28092803 DOI: 10.1016/j.molimm.2017.01.006]

63 **Weixler B**, Cremonesi E, Sorge R, Muraro MG, Delko T, Nebiker CA, Däster S, Governa V, Amicarella F, Soysal SD, Kettelhack C, von Holzen UW, Eppenberger-Castori S, Spagnoli GC, Oertli D, Iezzi G, Terracciano L, Tornillo L, Sconocchia G, Droeser RA. OX40 expression enhances the prognostic significance of CD8 positive lymphocyte infiltration in colorectal cancer. *Oncotarget* 2015; **6**: 37588-37599 [PMID: 26439988 DOI: 10.18632/oncotarget.5940]

World Journal of Gastroenterology

Submit a Manuscript: https://www.f6publishing.com

World J Gastroenterol 2022 June 7; 28(21): 2320-2333

DOI: 10.3748/wjg.v28.i21.2320

ISSN 1007-9327 (print) ISSN 2219-2840 (online)

ORIGINAL ARTICLE

Case Control Study

Intermittent hypoxia is involved in gut microbial dysbiosis in type 2 diabetes mellitus and obstructive sleep apnea-hypopnea syndrome

Sha-Sha Tang, Cheng-Hong Liang, Ya-Lei Liu, Wei Wei, Xin-Ru Deng, Xiao-Yang Shi, Li-Min Wang, Li-Jun Zhang, Hui-Juan Yuan

Specialty type: Gastroenterology and hepatology

Provenance and peer review: Unsolicited article; Externally peer reviewed.

Peer-review model: Single blind

Peer-review report's scientific quality classification

Grade A (Excellent): 0
Grade B (Very good): B
Grade C (Good): C
Grade D (Fair): 0
Grade E (Poor): 0

P-Reviewer: Papazafiropoulou A, Greece; Trujillo X, Mexico

Received: January 8, 2022
Peer-review started: January 8, 2022
First decision: March 9, 2022
Revised: March 19, 2022
Accepted: April 22, 2022
Article in press: April 22, 2022
Published online: June 7, 2022

Sha-Sha Tang, Cheng-Hong Liang, Ya-Lei Liu, Wei Wei, Xin-Ru Deng, Xiao-Yang Shi, Li-Min Wang, Li-Jun Zhang, Hui-Juan Yuan, Department of Endocrinology, Henan Provincial Key Medicine Laboratory of Intestinal Microecology and Diabetes, Henan Provincial People's Hospital, People's Hospital of Zhengzhou University, Zhengzhou 450003, Henan Province, China

Corresponding author: Hui-Juan Yuan, PhD, Chief Doctor, Department of Endocrinology, Henan Provincial Key Medicine Laboratory of Intestinal Microecology and Diabetes, Henan Provincial People's Hospital, People's Hospital of Zhengzhou University, No. 7 Weiwu Road, Zhengzhou 450003, Henan Province, China. hjyuan@zzu.edu.cn

Abstract

BACKGROUND

Obstructive sleep apnea (OSA)-hypopnea syndrome (OSAHS) has been recognized as a comorbidity of type 2 diabetes mellitus (T2DM); more than half of T2DM patients suffer from OSAHS. Intermittent hypoxia (IH) plays an important role in metabolic diseases, such as obesity and OSAHS, through various mechanisms, including altering the gut microecological composition and function. Therefore, it is important to study the role of gut microbiota in T2DM patients with OSAHS, which has a high incidence and is prone to several complications.

AIM

To assess whether IH is involved in altering the fecal microbiome in T2DM patients with OSAHS.

METHODS

Seventy-eight participants were enrolled from Henan Province People's Hospital and divided into healthy control (HC, n = 26), T2DM (n = 25), and T2DM + OSA (n = 27) groups based on their conditions. The fecal bacterial DNA of the research participants was extracted and subjected to 16S ribosomal RNA sequencing. The clinical indices, such as insulin resistance index, homocysteine (HCY) concentration, and the concentrations of inflammatory factors in the peripheral blood, were assessed and recorded.

RESULTS

Group T2DM + OSA had the highest apnea-hypopnea index (AHI) (2.3 *vs* 3.7 *vs* 13.7), oxygen desaturation index (0.65 *vs* 2.2 *vs* 9.1), HCY concentration (9.6

μmol/L *vs* 10.3 μmol/L *vs* 13.81 μmol/L) and C-reactive protein (CRP) concentrations (0.3 mg/L *vs* 1.43 mg/L *vs* 2.11 mg/L), and lowest mean oxygen saturation (97.05% *vs* 96.6% *vs* 94.7%) among the three groups. Twelve and fifteen key differences in amplicon sequence variants were identified when comparing group T2DM + OSA with groups T2DM and HC, respectively. We found progressively decreased levels of *Faecalibacterium*, *Eubacterium,* and *Lachnospiraceae,* and an increase in the level of *Actinomyces,* which strongly correlated with the HCY, CRP, fasting plasma glucose, and hemoglobin A1c concentrations, AHI, mean oxygen saturation, and insulin resistance index in group T2DM + OSA ($P < 0.05$).

CONCLUSION

For T2DM patients with OSAHS, IH may be involved in selective alterations of the gut microbiota, which may affect the pathophysiological development of T2DM and DM-related complications.

Key Words: Gut microbiota; Obstructive sleep apnea-hypopnea syndrome; Type 2 diabetes mellitus; Intermittent hypoxia; Obstructive sleep apnea

©The Author(s) 2022. Published by Baishideng Publishing Group Inc. All rights reserved.

Core Tip: Clinically, type 2 diabetes mellitus (T2DM) patients have a significantly higher prevalence of obstructive sleep apnea-hypopnea syndrome (OSAHS) than non-T2DM patients and are more prone to diabetes-related complications and metabolic syndrome, including obesity and hypertension. In recent years, the imbalance of gut microbiota has been found to be associated with various metabolic disorders. This study revealed that intermittent hypoxia was associated with changes in the gut microbiota in patients with T2DM complicated by OSAHS. These changes may be involved in the progression of metabolic disorders through increased proinflammatory factors and impaired intestinal barrier function.

Citation: Tang SS, Liang CH, Liu YL, Wei W, Deng XR, Shi XY, Wang LM, Zhang LJ, Yuan HJ. Intermittent hypoxia is involved in gut microbial dysbiosis in type 2 diabetes mellitus and obstructive sleep apnea-hypopnea syndrome. *World J Gastroenterol* 2022; 28(21): 2320-2333
URL: https://www.wjgnet.com/1007-9327/full/v28/i21/2320.htm
DOI: https://dx.doi.org/10.3748/wjg.v28.i21.2320

INTRODUCTION

Obstructive sleep apnea (OSA)-hypopnea syndrome (OSAHS) is characterized by recurrent partial or complete pharyngeal obstruction during sleep[1], resulting in intermittent hypoxia (IH); cyclical adverse changes in heart rate, blood pressure (BP), and sympathetic activity; and disruption of sleep architecture [2]. Epidemiological studies have shown that OSAHS is a globally prevalent chronic sleep disorder, especially in adults with type 2 diabetes mellitus (T2DM), with rates varying from 23% to 87%[3,4]. Moderate to severe OSAHS has been found to be associated with an increase in the incidence of T2DM, and the incidence of OSAHS in patients with T2DM was > 50% higher than that in those without diabetes, independent of traditional risk factors, such as obesity and other confounders. IH, a hallmark of OSAHS, plays an important role not only in the pathogenesis of OSAHS but also in reducing glycemic control and insulin resistance in patients with T2DM and diabetes-related complications[5-7], probably by activating several systematic inflammatory mediators and enhancing the oxidative stress cascade and hypothalamic-pituitary-adrenal function, among others[8].

Commensal bacteria, termed microbiota, cover every surface of our body exposed to the external environment, with 70% of these residing in the gastrointestinal tract[9]. The microbiome is a vast and complex polymicrobial ecosystem that coexists with the human organism and has been identified as playing important roles in the development of host immunological phenotypes. Gut microbiota dysbiosis has been linked to a series of metabolic disorders, such as diabetes and hypertension[10]. In a study of IH mimicking OSAHS, in an *Ldlr*$^{-/-}$ mice fed a high-fat diet, the imbalance of gut microbiota was found to be associated with adverse cardiovascular events and metabolic disorders[11,12]. Similarly, sleep fragmentation induced by OSAHS alters feeding behavior and promotes obesity and metabolic abnormalities, while the host gut microbiome changes, leading to increased intestinal permeability and chronic inflammation of adipose tissues[11,12]. For T2DM patients with OSAHS, only a few studies have focused on the relationship between severe metabolic disorders caused by IH and gut microbial dysbiosis, independent of conventional risk factors, such as obesity and hypertension. Hence, our study aimed to investigate the gut microbiota changes in T2DM patients with OSAHS.

Clinical indices, such as inflammatory factors and homocysteine (HCY), were compared for the groups as well.

MATERIALS AND METHODS

Participants

In total, 78 participants, including 25 hospitalized patients with T2DM (Group T2DM), 27 hospitalized patients with T2DM complicated by OSAHS (Group T2DM + OSA), and 26 healthy controls (HC) who were examined with a type IV portable monitor (PM, Sleep Fairy-A7, China) overnight (from 10 p.m. to 7 a.m.), were recruited from July 2019 to July 2020. Most of the sleep recording took place in a quiet and comfortable hospital ward at Henan Provincial People's Hospital; the remainder was performed by participants sleeping at home after being systematically trained in using the PM. The patient-reported periods before sleep onset and after awakening in the morning were excluded before manual scoring [13]. We collected fasting blood and fecal samples the next morning. General questionnaires were used to collect information on demographic characteristics and health status.

OSAHS assessment

Pulse oximetry was used to assess oxyhemoglobin saturation, and respiratory effort was measured with a pneumatic sensor attached to an effort belt. Nasal airflow was recorded using a nasal cannula connected to a pressure transducer. The final data were automatically generated by the software system. The scoring rules were based on the 2007 American Academy of Sleep Medicine manual. The apnea-hypopnea index (AHI) was calculated as the total number of episodes of apnea (continuous cessation of airflow for at least 10 s) and hypopnea (reduction in airflow for ≥ 10 s with oxygen desaturation of ≥ 4%) divided by the total duration of sleep events, and OSAHS was defined as an AHI of 5 events/h.

Inclusion and exclusion criteria

The inclusion criteria were as follows: (1) Age of 18-70 years; (2) Treatment-naïve type 2 diabetes based on the 1999 World Health Organization Criteria[14]; (3) 6.5% ≤ glycated hemoglobin A1c (HbA1c) ≤ 11%; (4) No antibiotic use within the 12 wk before enrollment and no probiotics and/or prebiotics; and (5) No glucose-lowering drugs other than insulin during the 12 wk before enrollment in patients with diabetes.

The exclusion criteria were as follows: (1) Body mass index (BMI) of > 28 kg/m^2; (2) Diagnoses of chronic respiratory disease, central system sleep apnea syndrome, severe heart failure, BP of ≥ 140/90 mmHg, and severe organic diseases such as cancer, myocardial infarction, and stroke; (3) Diagnoses of other types of diabetes, for example, type 1 diabetes; (4) Diagnoses of inflammatory bowel disease, coagulation disorders, connective tissue diseases, or gastrointestinal surgery, except for appendicitis and hernia surgery; (5) Participation in other programs during the previous 3 mo; (6) Alcoholism (drinking more than five times in 1 wk: > 100 g of spirits, 250 g of rice wine, or 5 bottles of beer); (7) Pregnancy; and (8) Taking drugs that may affect respiratory function, for example, anxiolytics, hypnotics, or mood stabilizers.

Sample collection

Biological samples and anthropometric data were obtained without medical treatment. Blood samples were collected after overnight fasting and centrifuged using centrifuge (Multifuge X3R, Thermo Fisher Scientific, United States) at 3000 rpm for 20 min after standing at 24 °C for 30 min to obtain serum. Fresh fecal samples, morning urine, and serum samples were immediately frozen on dry ice after collection and stored at -80 °C until further analysis.

Clinical indices

Fasting plasma glucose (FPG) concentrations were measured with the Automatic Biochemical Analyzer (TBA-120 FR, Toshiba, Japan). Fasting insulin concentrations were measured using immunochemiluminometric assays (ADVIA Centaur, Siemens A.G., German). Plasma HbAlc concentrations were measured by high-performance liquid chromatography (Bio-Rad D-10, Bio-Rad Laboratories Co., Ltd., Germany). Routine blood tests were performed using the Swelab Alfa Cell analyzer (Boule Diagnostics AB, Sweden). The Homeostatic Model Assessment for Insulin Resistance (HOMA-IR) was calculated using the following formula: FPG*FIN/22.5, where FIN is fasting insulin.

Inflammatory factors and HCY

C-reactive protein (CRP) and HCY concentrations were measured with the Automatic Biochemical Analyzer. The determination of the plasma concentrations of the lipopolysaccharide-binding protein (LBP), interleukin (IL)-6, IL-17, and transforming growth factor (TGF)-β1 was performed using human ELISA kits according to the manufacturer's instructions. The ELISA kits for the assessment of the concentrations of human LBP, tumor necrosis factor (TNF)-α, IL-17, and TGF-β1 were all from Cusabio

Biotech, Wuhan, China. The kits for high sensitivity IL-6 were purchased from Multi-Science, Hangzhou, China.

16S rRNA gene amplification sequencing

The DNA of the participants was extracted using the E.Z.N.A.® Stool DNA Kit (Omega Bio-tek, Inc., Norcross, GA, Unite States). The isolated DNA was used as the template for polymerase chain reaction (PCR) amplification of the V3-V4 region of 16S rRNA genes. The forward primer (341F) was 5'-CCTACGGGNGGCWGCAG-3', and the reverse primer (805R) was 5'-GACTACHVGGGTATC-TAATCC-3.' PCR was performed with an EasyCycler 96 PCR system (Analytik Jena Corp., AG), and the products from different samples were indexed and mixed at equal ratios for sequencing by Shanghai Mobio Biomedical Technology Co. Ltd. using the Miseq platform (Illumina Inc., San Diego, CA, Unite States) according to the manufacturer's instructions.

Sequencing data analysis

Amplicon sequence variants (ASVs) were identified with the DADA2 algorithm. The representative sequences for each ASV were annotated using the SILVA reference database (SSU138). The alpha diversity metrics (Shannon–Wiener diversity index and Simpson diversity index) were assessed by using Mothur v1.42.1. The non-parametric Mann–Whitney U test was used to test for significant differences between the two groups. The comparison of multiple groups was performed using a nonparametric Kruskal–Wallis test. Principal coordinates analysis (PCoA) based on Bray–Curtis and unweighted UniFrac distance was conducted using the R program (version 3.6.0, http://www.R-project.org/) to display microbiome space between samples. The key ASVs associated with T2DM and OSA were identified by random forest models, and those significantly associated with BMI selected by MaAsLin2 (https://github.com/biobakery/Maaslin2) were removed. A heatmap plot was drawn to indicate the distributions of the rest of the key ASVs. The linear discriminant analysis effect size (LEfSe) method (lefse 1.1, https://github.com/SegataLab/Lefse) was used to detect taxa with differential abundance. PICRUSt2 v2.4.1 (https://github.com/picrust/picrust2/wiki) was used to predict functional abundance based on 16S rRNA gene sequences.

Statistical analyses

Continuous variables are expressed as means ± SD or medians with interquartile ranges for normal distribution data or non-normal distribution data, respectively. Categorical variables are expressed as percentages. All the statistical analyses, including one-way analysis of variance, Kruskal–Wallis test, Mann-Whitney U test, and least significant difference *t*-test, were performed using SPSS version 26.0, with a two-sided P value of < 0.05 denoting statistical significance. Significant differences were adjusted by Bonferroni correction. The correlation coefficients for the concentrations of the gut microbiota, inflammatory factors, and HCY were evaluated using Spearman correlation.

RESULTS

Clinical parameters and inflammatory levels among three groups

Applying the strict inclusion and exclusion criteria described above, a total of 78 fecal samples were collected for analysis after PM assessment. We characterized the clinical indices and gut microbiomes of patients in groups HC, T2DM, and T2DM + OSA (Figure 1). There were no significant differences in sex and age among the three groups ($P > 0.05$). Compared with group T2DM, there were no significant differences in the insulin resistance index (HOMA-IR), BMI, waist-to-hip ratio, neck circumference, FPG, HbA1c, systolic BP, and diastolic BP in group T2DM + OSA; however, they were significantly increased compared with those in group HC ($P < 0.05$).

The HCY level was the highest in group T2DM + OSA compared with the other two groups. Our PM data revealed that the AHI and oxygen desaturation index (ODI) increased significantly, accompanied by a decrease in the mean oxygen saturation (SpO_2); group T2DM + OSA had lower SpO_2 than group HC. Further details on the clinical parameters of the participants with diverse severities are shown in Table 1.

The concentration of CRP increased gradually from the HC group to the T2DM group and even more in the T2DM + OSA group. In addition, the levels of TNF-α, IL-17, IL-6, and LBP increased and the levels of TGF-β1 decreased in group T2DM + OSA compared with those in group HC, while the level of TNF-α increased compared with that in group T2DM ($P < 0.05$) (Figure 2 and Supplementary Table 1).

IH is related to differences in the gut microbiota of T2DM + OSA patients

The resulting rarefaction curves showed that the microbial richness of the sampled guts was near saturation at the applied sequencing depth (Supplementary Figure 1), which was sufficient to identify most of the bacterial community members for each microbiome. The alpha diversity of the gut microbiota expressed by the Shannon estimator, ACE estimator, and Simpson index (Figure 3A-C and

Table 1 Participant characteristics and clinical parameters

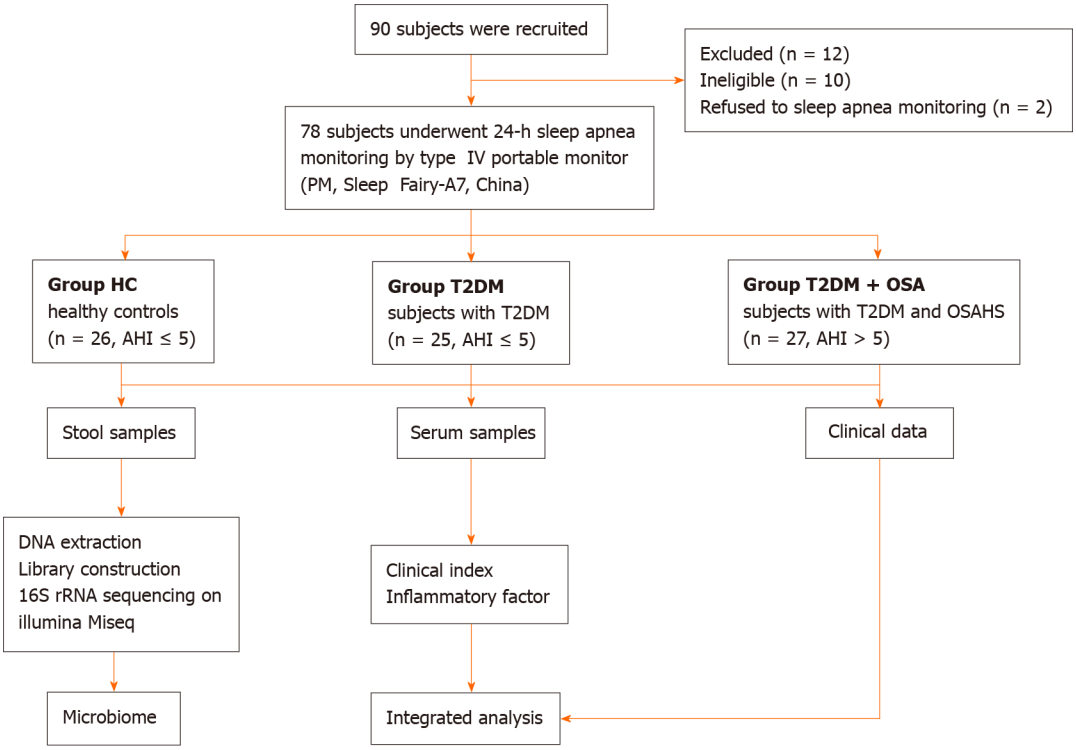
	HC (*n* = 26)	T2DM (*n* = 25)	T2DM + OSA (*n* =27)	*P* value
Sex, male/female	17/9	17/8	21/6	0.584
Age, yr	45.58 ± 8.81	45.92 ± 13.89	47.59 ± 5.18	0.728
BMI, kg/m^2	24.63 ± 2.61	25.84 ± 3.45	27.03 ± 2.11[b]	0.009
WHR, cm	0.85 ± 0.06	0.95 ± 0.07	0.98 ± 0.05[b]	< 0.001
NC, cm	32.88 ± 3.70	36.25 ± 4.75	38.37 ± 2.31[b]	< 0.001
FPG, mmol/L	5.30 (4.70, 5.43)	6.90 (6.30, 8.05)	8.00 (6.40, 9.25)[b]	< 0.001
HOMA-IR	1.50 (1.09, 2.03)	2.10 (1.02, 3.53)	2.38 (1.37, 3.22)[a]	0.099
HbA1c, %	5.30 (5.10, 5.60)	9.70 (7.30, 10.80)	8.70 (7.70, 9.70)[b]	< 0.001
SBP, mmHg	117.50 (112.00, 123.25)	130.00 (117.00, 143.00)	131.00 (128.00, 144.00)[b]	< 0.001
DBP, mmHg	71.96 ± 5.44	81.13 ± 11.33	82.26 ± 8.58[b]	< 0.001
HCY, μmol/L	9.60 (8.30, 12.53)	10.30 (8.05, 12.03)	13.81 (10.73, 20.54)[b,c]	< 0.001
AHI	2.30 (1.48, 3.05)	3.70 (2.00, 4.15)	13.70 (9.80, 20.10)[b,c]	< 0.001
Mean SpO_2, %	97.05 (96.50, 97.53)	96.60 (96.05, 96.95)	94.70 (93.80, 95.20)[b,c]	< 0.001
Lowest SpO_2, %	85.50 (82.00, 90.25)	85.00 (76.00, 87.50)	81.00 (73.00, 84.00)[b]	0.002
ODI	0.65 (0.40, 1.23)	2.20 (1.10, 5.45)	9.10 (5.90, 15.30)[b,c]	< 0.001

[a]*P* < 0.05 *vs* HC.
[b]*P* < 0.01 *vs* HC.
[c]*P* < 0.01 *vs* T2DM.
P value: Comparison of three groups. Data are presented as the mean ± SD or median with interquartile range. The *P* value was based on Kruskal–Wallis test or one-way ANOVA. Mann–Whitney U test or least significant difference *t*-test was used to compare two groups. Significant differences were adjusted by Bonferroni correction. WHR: Waist-hip ratio; NC: Neck circumstance; FPG: Fasting plasma glucose; HOMA-IR: Insulin resistance index; HbA1c: Hemoglobin A1c; SBP: Systolic pressure; DBP: Diastolic pressure; HCY: Homocysteine; AHI: Apnea–hypopnea indices; ODI: Oxygen desaturation index; HC: Healthy control; T2DM: Type 2 diabetes mellitus; OSA: Obstructive sleep apnea.

Supplementary Table 2) showed that there were no significant differences in groups HC, T2DM, and T2DM + OSA ($P > 0.05$). The overall structures of the gut microbiota in the three groups showed a minimal difference as revealed by the PCoA plot (Figure 3D); however, the difference was not significant (Adonis, $P > 0.05$).

We further analyzed the taxonomic composition and alterations of the gut microbiome. The composition and abundance of the bacterial community in each sample at the phylum and genus levels are shown in Supplementary Figure 2. At the phylum level, *Firmicutes* and *Proteobacteria* were the dominant bacteria in groups HC, T2DM, and T2DM + OSA (Figure 4A). At the genus level, we found no significant differences in the relative abundance of *Escherichia−Shigella,* which had the highest abundance among the three groups ($P > 0.05$) (Figure 4B). The relative abundance of the following genera significantly differed among groups: *Faecalibacterium* ($P = 0.0434$), *Streptococcus* ($P = 0.0393$), *Haemophilus* ($P = 0.0286$), *Phascolarctobacterium* ($P = 0.0242$), and *Oscillibacter* ($P = 0.0274$) (Figure 4C). Among the above genera, the levels of *Phascolarctobacterium* decreased and the levels of *Oscillibacter* increased in group T2DM + OSA compared with group T2DM, and the levels of *Faecalibacterium* significantly decreased in group T2DM + OSA compared with group HC. A gradually decreasing trend of *Faecalibacterium* abundance from group HC to groups T2DM and T2DM + OSA was observed (Figure 4C). Through LEfSe, we also found a significant decrease in the level of *Faecalibacterium* in group T2DM + OSA (Figure 4D).

We found 12 ASVs associated with gut microbial dysbiosis in group T2DM + OSA compared with group T2DM, including ASV632 (*Streptococcus*), ASV450 (*Clostridiaceae_Clostridium_sensu_stricto*), ASV352 (*Faecalibacterium*), ASV511 (*Roseburia*), ASV307 (*[Eubacterium]_hallii_group*), ASV1000 (*[Eubacterium]_eligens_group*), ASV995 (*Blautia*), ASV584 (*Eggerthella*), ASV535 (*Erysipelotrichaceae*_UCG-003), ASV87 (*Phascolarctobacterium*), ASV1112 (*Prevotella*), and ASV548 (*Oscillibacter*). On comparing groups HC and T2DM + OSA, 15 ASVs were different: ASV450 (*Clostridiaceae_Clostridium_sensu_stricto*), ASV511 (*Roseburia*), ASV1000 (*[Eubacterium]_eligens_group*), ASV266 (*Lachnospiraceae_unclassified*), ASV763 (*Lachnospiraceae_unclassified*), ASV367 (*Faecalibacterium*), ASV779 (*Actinomyces*), ASV986 (*Haemophilus*), ASV352 (*Faecalibacterium*), ASV436 (*Faecalibacterium*), ASV265 (*Streptococcus*), ASV535 (*Erysipelotrichaceae_UCG-003*), ASV68 (*Blautia*), ASV347 (*Saccharimonadales*), and ASV1022 (*Acinetobacter*) (Figure 5A). Therein, the relative abundance of ASV1022 (*Acinetobacter*), ASV367 (*Faecalibacterium*),



DOI: 10.3748/wjg.v28.i21.2320 **Copyright** ©The Author(s) 2022.

Figure 1 Flowchart of the study.

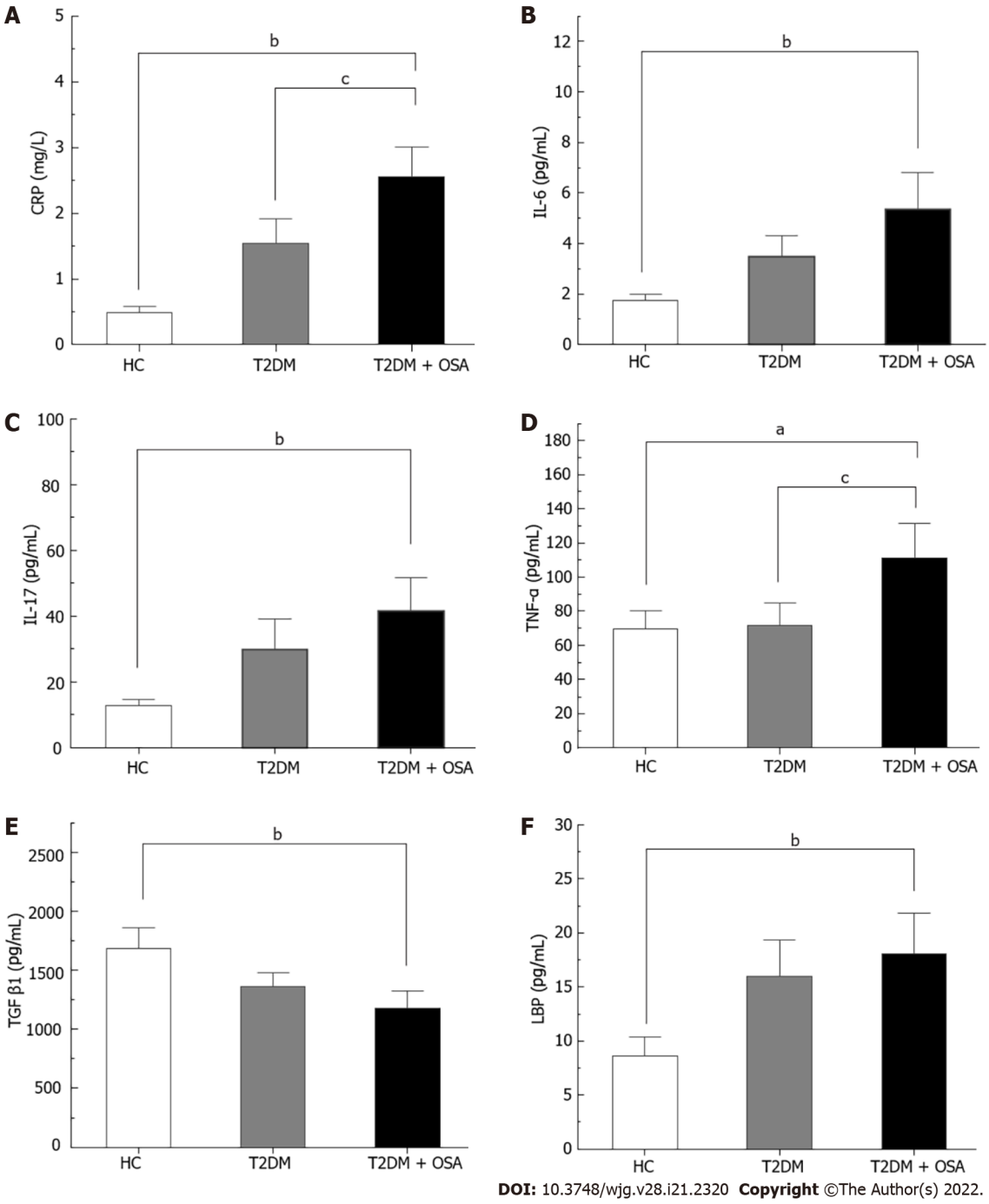
ASV436 (*Faecalibacterium*), ASV763 (*Lachnospiraceae_unclassified*), and ASV266 (*Lachnospiraceae_unclassified*) were progressively decreased, and the abundance of ASV779 (*Actinomyces*) increased from group HC to group T2DM and to group T2DM + OSA (Figure 5B).

IH-related gut microbiota dysbiosis was associated with abnormal metabolic and inflammatory indicators of T2DM + OSA patients

We further studied the correlations among metabolic indicators, inflammatory factors, and the above six key ASVs with ascending or decreasing trends. Spearman correlation analysis revealed that the decreased abundance of ASVs showed a significant negative correlation with indicators related to IH or respiratory disorders, such as the ODI and AHI; glucose metabolism indicators, such as HbA1c, FPG, and HOMA-IR; cardiovascular disease-related metabolic indicators, such as HCY; and inflammatory factors, such as CRP, TNF-α, and LBP. The ASV436 (*Faecalibacterium*) was negatively correlated with the AHI, ODI, FPG, HbA1c, CRP concentrations, and HOMA-IR, while the ASV763 (*Lachnospiraceae_unclassified*) was negatively correlated with the AHI and FPG, HbA1c, CRP, and LBP concentrations ($P < 0.05$). Furthermore, the ASV436 (*Faecalibacterium*), ASV1000 (*[Eubacterium]_eligens_group*), and ASV367 (*Faecalibacterium*) were positively correlated with the mean SpO_2, another IH-related indicator. Among the three groups, the gradually increasing abundance of ASV779 (*Actinomyces*) showed an opposite relationship; it was significantly positively correlated with the AHI, ODI, and TNF-α concentration and negatively correlated with the mean SpO_2 ($P < 0.05$) (Figure 6 and Supplementary Table 3).

DISCUSSION

T2DM has been linked to gut dysbiosis and chronic inflammation in several clinical and animal experiments[15-17], which may be a consequence of the loss of or deficiency in a beneficial function, such as short-chain fatty acid (SCFA)-producing bacteria production from carbohydrate fermentation, in the gut ecosystem[16]. Diseases previously partially attributed to lifestyle, such as obesity and OSAHS, are now considered microbiota-related as well[12,18]. Although much epidemiological and clinical evidence has suggested that OSAHS is an independent risk factor for the development of T2DM[19], the underlying pathogenesis of altered glucose metabolism in T2DM patients with OSAHS remains to be elucidated. Meanwhile, a longitudinal cohort study over a period of 6 years found that the insulin resistance index (HOMA-IR) was a predictor of incident "witnessed apnea", independent of obesity [20]. This showed that dysglycemia and insulin resistance may lead to the development of OSAHS. Together with the findings of the above-mentioned studies, this strongly suggests that the relationship

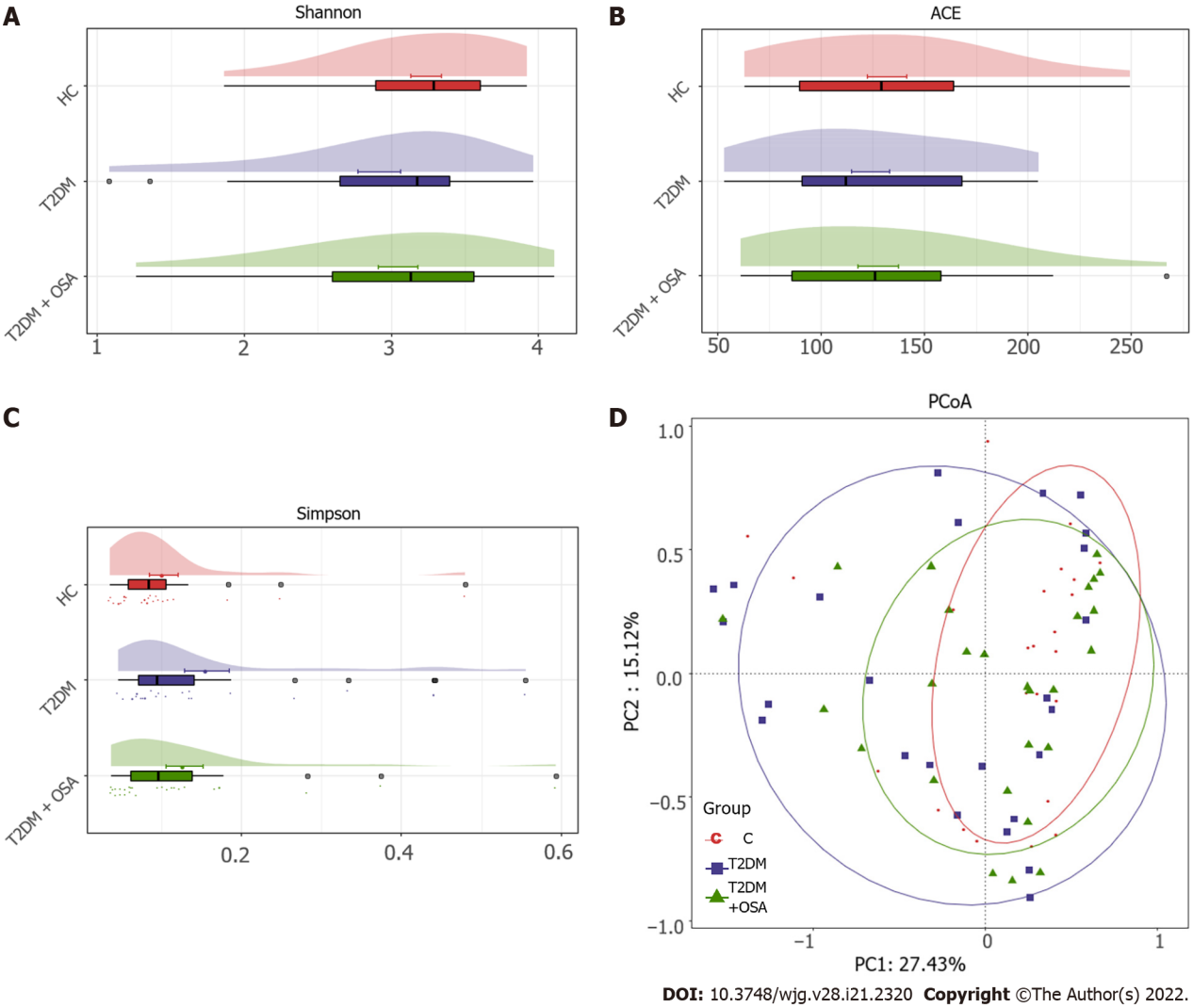


DOI: 10.3748/wjg.v28.i21.2320 **Copyright** ©The Author(s) 2022.

Figure 2 The concentrations of inflammatory factors in groups healthy control, type 2 diabetes mellitus, and type 2 diabetes mellitus plus obstructive sleep apnea. A: CRP; B: IL-6; C: IL-17; D: TNF-α; E: TGF-β1; F: LBP. Bar charts show the means ± SE of the mean. [a]*P* < 0.05 *vs* healthy control (HC); [b]*P* < 0.01 *vs* HC; [c]*P* < 0.05 *vs* type 2 diabetes mellitus. The *P* value was based on Kruskal–Wallis test or one-way ANOVA. A significant difference was shown by the least significant difference *t*-test or Mann–Whitney U test. Significant differences were adjusted by Bonferroni correction. CRP: C-reaction protein; IL-6: Interleukin-6; IL-17: Interleukin-17; TNF-α: Tumor necrosis factor-α; TGF-β1: Transforming growth factor beta 1; LBP: Lipopolysaccharide-binding protein; HC: Healthy control; T2DM: Type 2 diabetes mellitus; OSA: Obstructive sleep apnea.

between T2DM and OSAHS may be bidirectional[2]. Therefore, it is necessary to investigate whether the imbalance of the intestinal microbiota plays a key role in the pathophysiology underlying metabolic dysfunction of patients with T2DM complicated by OSAHS.

In our study, the sequencing analysis of the 16S rRNA gene-tags applied to fecal samples from T2DM patients complicated by OSAHS showed differences in the relative abundances of the predominant taxa of the genera levels. We found that the concentrations of various IH-related gut bacteria, including SCFA-producing bacteria such as *Faecalibacterium* and *Lachnospiraceae,* were significantly correlated with the concentrations of FPG HbA1c and HOMA-IR, as well as the concentration of HCY, a risk predictor of hypertension and arteriosclerosis[21,22]. IH can result in hypoxia/re-oxygenation cycling events within the gut microbiome and, as a result, the biological diversity of gut microorganisms may be

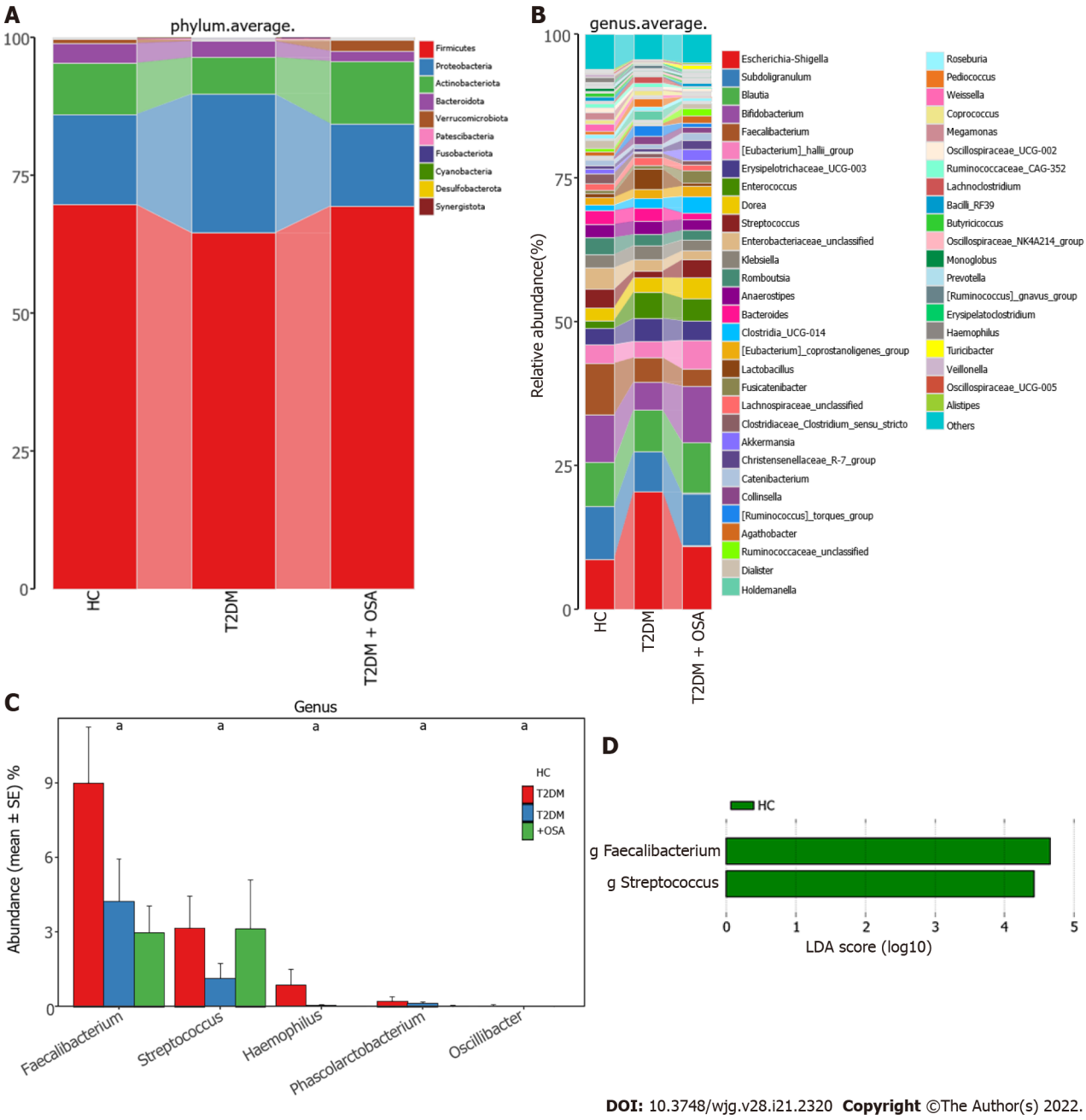


DOI: 10.3748/wjg.v28.i21.2320 **Copyright** ©The Author(s) 2022.

Figure 3 The gut microbial diversity and structures of the gut microbiota in groups healthy control, type 2 diabetes mellitus, and type 2 diabetes mellitus plus obstructive sleep apnea. A: Shannon index; B: ACE estimator; C: Simpson index; D: Principal coordinates analysis plot of the gut microbiota among groups healthy control, type 2 diabetes mellitus, and type 2 diabetes mellitus plus obstructive sleep apnea. HC: Healthy control; T2DM: Type 2 diabetes mellitus; OSA: Obstructive sleep apnea.

modified[16]. Although the intestinal epithelium is significantly resistant to hypoxia, regulating the absorption and barrier function of the intestinal epithelium is sensitive to the oxygen level in the intestine[23]. Hypoxia/re-oxygenation can directly impair cellular function *via* an increase in permeability and bacterial translocation and a decrease in tight junction integrity[16]. In addition, studies have shown that after prolonged normoxic recovery after IH exposure, the gut microbiota and circulating endotoxemia remain negatively affected[8]. Our results do not show significant differences in α-diversity and β−diversity. However, the gradual decrease in the relative abundance of SCFA-producing bacteria (such as the ASVs of *Faecalibacterium*, *Eubacterium*, and *Lachnospiraceae*) associated with abnormal indicators of oxygen metabolism, as well as elevated levels of inflammatory indicators (including CRP, IL-17, and TNF-α), which are critically involved in the development of insulin resistance and pathogenesis of T2DM, was observed in T2DM + OSA patients[24]. Emerging evidence shows that SCFAs can modulate glycemic control, exhibit anti-inflammatory and antitumorigenic activity, and decrease oxidative stress[25-28]. Short chain fatty acids contribute to mucin synthesis, decrease bacterial translocation, maintain gut integrity, and mitigate inflammation in the intestine[29, 30]. Thus, we speculated that SCFAs may be regarded as potential targets for recognizing metabolic comorbidities in patients with T2DM complicated by OSAHS.

There are several potential mechanisms by which IH mediates its effect on metabolic dysfunction. It induces macrophages to polarize toward the pro-inflammatory subtype of M1, leading to the production of more pro-inflammatory mediators in visceral adipose tissue, such as TNF-α, IL-6, and IL-8, resulting in subsequent impairment of insulin signaling pathways and insulin resistance[7]. Here, we found that the concentration of *Lachnospiraceae* was negatively correlated with that of LBP, which is one of the reference indicators of intestinal barrier disruption, suggesting that the induction of inflammatory

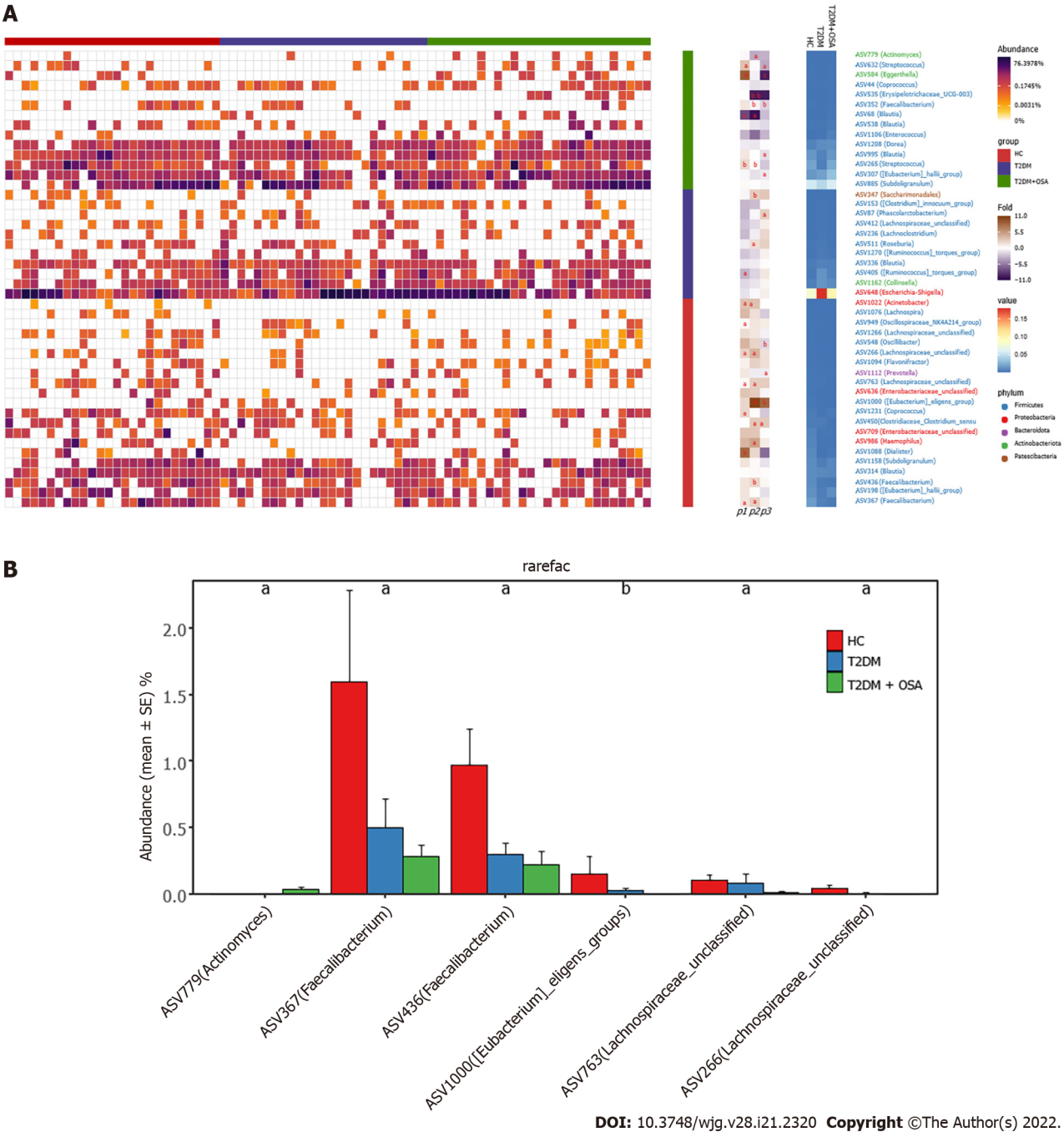


DOI: 10.3748/wjg.v28.i21.2320 **Copyright** ©The Author(s) 2022.

Figure 4 Average compositions and relative abundance of the bacterial community among three groups at different levels. A: Average relative abundance histogram of dominant species composition stratified by group at the phylum levels; B: Average relative abundance histogram of dominant species composition stratified by group at the genus levels; C: Histograms for genera with significant differences. Bar chart showing the mean ± SE of each group; D: Linear discriminant analysis analysis column diagram. LDA: Linear discriminant analysis. $^{a}P < 0.05$. Significant difference shown by the Kruskal–Wallis rank-sum test.

processes may be due to the leakage of microbial metabolites into the circulation induced by IH. We found certain changes in the gut microbiota among the three groups over time; however, there were no significant differences between patients with T2DM with and without OSAHS. Nonetheless, the concentrations of inflammatory indicators, such as CRP, TNF-α, and IL-17, were significantly increased in T2DM patients with OSAHS, which indicates that the changes in gut microbiota may have been delayed relative to the chronic inflammatory changes in T2DM patients with OSAHS. On the other hand, some patients with relatively mild disease were included to prevent confounding by factors, including hyperglycemia and obesity, which affect the composition of intestinal microbiota[31]; as a result, the intestinal flora appeared not to have changed remarkably.

Various respiratory diseases have been associated with dysbiosis not only in the airway microbiota but also in the intestinal microbiota[32,33]. This evidence reinforced the existence of a gut-lung axis and the close relationship between intestinal and respiratory compartments; changes at one of the two sites could impact the other[34]. As a minor constituent of the airway microbiota, *Actinomyces* is related to anaerobic enzymes through GLUT1-dependent glucose elevation and MCT4-dependent lactate transport[35,36]. In our study, we observed that the increase in the relative abundance of *Actinomyces*

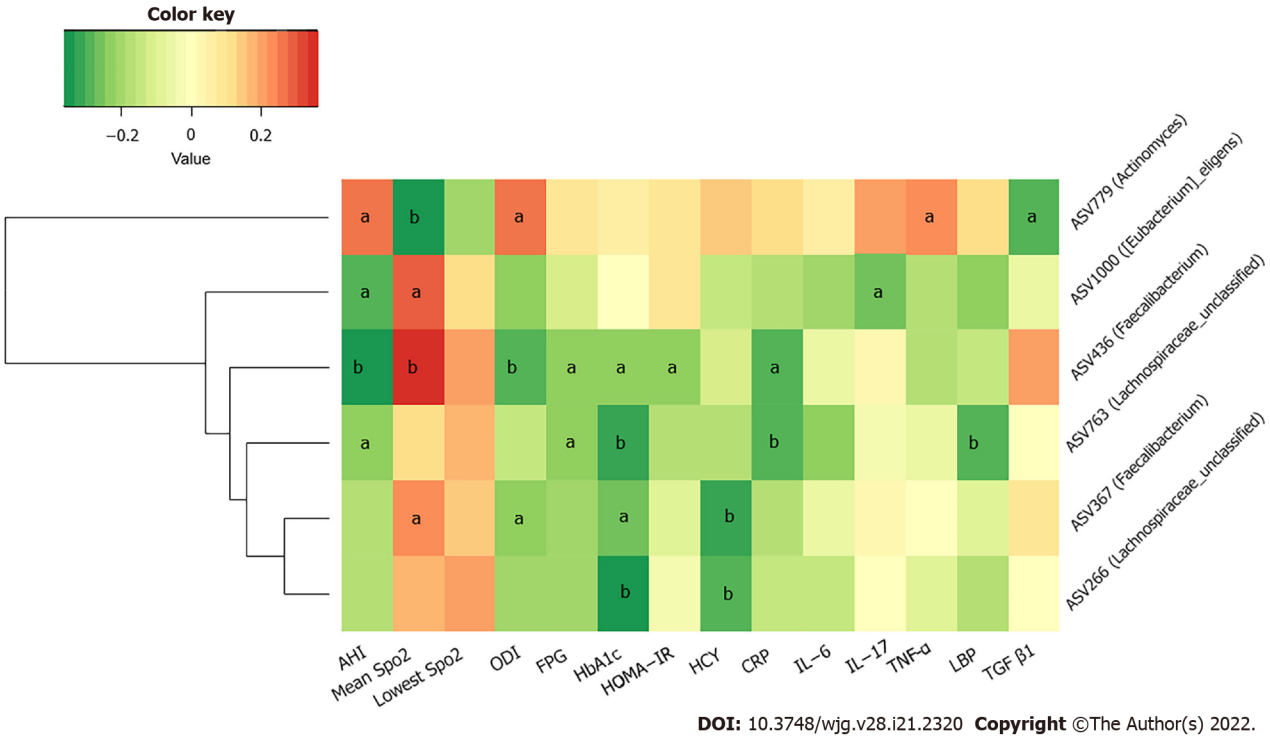


DOI: 10.3748/wjg.v28.i21.2320 **Copyright** ©The Author(s) 2022.

Figure 5 Amplicon sequence variants contributing to the changes in the gut microbiota in groups healthy control, type 2 diabetes mellitus, and type 2 diabetes mellitus plus obstructive sleep apnea. A: The heatmap shows the relative abundance of the 46 amplicon sequence variants (ASVs) significantly different in the three groups. The fold ratio (log2-transformed) indicated the relative abundance of the 46 ASVs between the two different groups [*P*1: Type 2 diabetes mellitus (T2DM) + obstructive sleep apnea (OSA) *vs* T2DM; *P*2: T2DM + OSA *vs* healthy control (HC); *P*3: HC *vs* T2DM]. $^{a}P < 0.05$, $^{b}P < 0.01$, $^{c}P < 0.001$. Significant difference shown by the Mann–Whitney U test; B: With the increase in disease components, six key ASVs showed increasing or decreasing trends. $^{a}P < 0.05$, $^{b}P < 0.01$.

was positively correlated with OSAHS severity indices and the concentration of TNF-α. We did not test for lung microbes; however, we speculate that they may be related to the gut-lung axis. Further experimental approaches to exploring causal links may be needed.

There are some limitations to our study. First, the sample size was relatively small. Second, the causal relationship between T2DM complicated by OSAHS and the gut microbiota was unclear. Large-scale clinical trials and gnotobiotic mice model validation may be required in the future.



DOI: 10.3748/wjg.v28.i21.2320 **Copyright** ©The Author(s) 2022.

Figure 6 Heatmap of correlation among key amplicon sequence variants of gut microbiota and metabolic and inflammatory indicators. The color of the cells represents the Spearman's correlation coefficient between each amplicon sequence variant and clinical parameter. [a]*P* < 0.05; [b]*P* < 0.01.

CONCLUSION

T2DM patients with OSAHS may have a higher prevalence of gut microbial dysbiosis. IH may be involved in selective alterations of gut microbiota, which may be related to increased gut permeability and concurrent systemic inflammatory changes in patients with T2DM complicated by OSAHS. These findings provide foundations for further studies on the mechanisms and interventional approaches aimed at restoration of the gut microbiota to prevent or to palliate the adverse effects of T2DM patients with OSAHS.

ARTICLE HIGHLIGHTS

Research background

Obstructive sleep apnea (OSA)-hypopnea syndrome (OSAHS), as a chronic and treatable sleep disorder, has a high prevalence in type 2 diabetes mellitus (T2DM) patients. As a landmark feature of OSAHS, intermittent hypoxia (IH) plays an important role in the occurrence and development of related complications in T2DM patients. However, the pathological mechanisms are varied and unknown. Therefore, it is important to study the role of gut microbiota, a meaningful new target, in T2DM patients with OSAHS.

Research motivation

In recent years, it has been found that gut microbiota imbalance is related to metabolic diseases. However, most studies have not discussed the relationship between gut microbiota changes and T2DM patients with OSAHS.

Research objectives

In this study we focused on IH that might be involved in altering the gut dysbiosis in T2DM patients with OSAHS. Meanwhile, we further assessed the changes of clinical indicators and inflammatory factors related to dysbiosis, aiming to provide new targets and perspectives for the pathogenesis and prevention strategies of T2DM patients complicated with OSAHS.

Research methods

A case-control study was conducted to select subjects who were divided into T2DM + OSA group, T2DM group, and healthy control group. They were examined with a type IV portable monitor

overnight. The clinical indexes, respiratory parameters, inflammatory indexes, and gut microbial community of the three groups were measured.

Research results

Among the three groups, T2DM + OSA group showed the most severe changes in sleep apnea parameters and increased systemic inflammatory factors. We found the decreased levels of short-chain fatty acid-related *Faecalibacterium, Eubacterium,* and *Lachnospiraceae* and the increased levels of *Actinomyces* at the amplicon sequence variant level. The changes in these gut microbiotas were closely related to clinical indicators as well.

Research conclusions

IH may be involved in the selective changes of intestinal microbiota, which may be related to the increased intestinal permeability and systemic inflammation response in T2DM patients with OSAHS.

Research perspectives

This study shows that IH may change the state of gut microbiota and systemic inflammation, which participate in the occurrence and development of T2MD complicated with OSAHS. In the future, large-scale clinical randomized controlled prospective trials and animal trials may be needed to further explore the corresponding causality.

ACKNOWLEDGEMENTS

We would like to thank the participants involved in this study.

FOOTNOTES

Author contributions: Tang SS designed the research and conducted microbiome analysis; Liu YL conducted the research except the microbiome analysis; Tang SS and Liang CH analyzed the microbiome data and wrote the paper; all other data were analyzed by Shi XY and Deng XR with oversight by Wei W; Zhang LJ and Wang LM were responsible for the data acquisition and input and proofreading of the manuscript; Tang SS and Yuan HJ had primary responsibility for the final content; all authors have read and approved the final manuscript.

Supported by National Natural Science Foundation of China, No. 81970705; and Central Plains Thousand Talents Plan, No. 204200510026.

Institutional review board statement: This study was reviewed and approved by the Ethics Committee of Henan Provincial People's Hospital (IRB No. 2019-62).

Informed consent statement: All study participants provided informed written consent before the study enrollment.

Conflict-of-interest statement: All authors declare no conflicts of interest.

Data sharing statement: Raw sequencing data and associated metadata were deposited in the NCBI short-read archive with BioProject accession number PRJNA788301.

STROBE statement: The authors have read the STROBE Statement—checklist of items, and the manuscript was prepared and revised according to the STROBE Statement—checklist of items.

Open-Access: This article is an open-access article that was selected by an in-house editor and fully peer-reviewed by external reviewers. It is distributed in accordance with the Creative Commons Attribution NonCommercial (CC BY-NC 4.0) license, which permits others to distribute, remix, adapt, build upon this work non-commercially, and license their derivative works on different terms, provided the original work is properly cited and the use is non-commercial. See: https://creativecommons.org/Licenses/by-nc/4.0/

Country/Territory of origin: China

ORCID number: Sha-Sha Tang 0000-0002-1307-3124; Cheng-Hong Liang 0000-0003-0661-9472; Ya-Lei Liu 0000-0003-0946-4605; Wei Wei 0000-0003-1045-1449; Xin-Ru Deng 0000-0003-3747-9310; Xiao-Yang Shi 0000-0001-7917-2048; Li-Min Wang 0000-0002-6396-390X; Li-Jun Zhang 0000-0003-1401-5775; Hui-Juan Yuan 0000-0002-0486-0994.

S-Editor: Fan JR
L-Editor: A
P-Editor: Yu HG

REFERENCES

1 **Xu H**, Wang H, Guan J, Yi H, Qian Y, Zou J, Xia Y, Fu Y, Li X, Jiao X, Huang H, Dong P, Yu Z, Yang J, Xiang M, Li J, Chen Y, Wang P, Sun Y, Li Y, Zheng X, Jia W, Yin S. Effects of continuous positive airway pressure on neurocognitive architecture and function in patients with obstructive sleep apnoea: Study protocol for a multicentre randomised controlled trial. *BMJ Open* 2017; **7**: e014932 [PMID: 28550021 DOI: 10.1136/bmjopen-2016-014932]

2 **Subramanian A**, Adderley NJ, Tracy A, Taverner T, Hanif W, Toulis KA, Thomas GN, Tahrani AA, Nirantharakumar K. Risk of Incident Obstructive Sleep Apnea Among Patients With Type 2 Diabetes. *Diabetes Care* 2019; **42**: 954-963 [PMID: 30862657 DOI: 10.2337/dc18-2004]

3 **Foster GD**, Sanders MH, Millman R, Zammit G, Borradaile KE, Newman AB, Wadden TA, Kelley D, Wing RR, Sunyer FX, Darcey V, Kuna ST; Sleep AHEAD Research Group. Obstructive sleep apnea among obese patients with type 2 diabetes. *Diabetes Care* 2009; **32**: 1017-1019 [PMID: 19279303 DOI: 10.2337/dc08-1776]

4 **West SD**, Prudon B, Hughes J, Gupta R, Mohammed SB, Gerry S, Stradling JR; ROSA trial investigators. Continuous positive airway pressure effect on visual acuity in patients with type 2 diabetes and obstructive sleep apnoea: a multicentre randomised controlled trial. *Eur Respir J* 2018; **52** [PMID: 30166323 DOI: 10.1183/13993003.01177-2018]

5 **Tahrani AA**. Obstructive sleep apnoea in diabetes: Does it matter? *Diab Vasc Dis Res* 2017; **14**: 454-462 [PMID: 28610436 DOI: 10.1177/1479164117714397]

6 **Leong WB**, Jadhakhan F, Taheri S, Chen YF, Adab P, Thomas GN. Effect of obstructive sleep apnoea on diabetic retinopathy and maculopathy: a systematic review and meta-analysis. *Diabet Med* 2016; **33**: 158-168 [PMID: 26031931 DOI: 10.1111/dme.12817]

7 **Ryan S**. Adipose tissue inflammation by intermittent hypoxia: mechanistic link between obstructive sleep apnoea and metabolic dysfunction. *J Physiol* 2017; **595**: 2423-2430 [PMID: 27901270 DOI: 10.1113/JP273312]

8 **Moreno-Indias I**, Torres M, Sanchez-Alcoholado L, Cardona F, Almendros I, Gozal D, Montserrat JM, Queipo-Ortuño MI, Farré R. Normoxic Recovery Mimicking Treatment of Sleep Apnea Does Not Reverse Intermittent Hypoxia-Induced Bacterial Dysbiosis and Low-Grade Endotoxemia in Mice. *Sleep* 2016; **39**: 1891-1897 [PMID: 27397563 DOI: 10.5665/sleep.6176]

9 **Schippa S**, Conte MP. Dysbiotic events in gut microbiota: impact on human health. *Nutrients* 2014; **6**: 5786-5805 [PMID: 25514560 DOI: 10.3390/nu6125786]

10 **Okubo H**, Nakatsu Y, Kushiyama A, Yamamotoya T, Matsunaga Y, Inoue MK, Fujishiro M, Sakoda H, Ohno H, Yoneda M, Ono H, Asano T. Gut Microbiota as a Therapeutic Target for Metabolic Disorders. *Curr Med Chem* 2018; **25**: 984-1001 [PMID: 28990516 DOI: 10.2174/0929867324666171009121702]

11 **Tripathi A**, Melnik AV, Xue J, Poulsen O, Meehan MJ, Humphrey G, Jiang L, Ackermann G, McDonald D, Zhou D, Knight R, Dorrestein PC, Haddad GG. Intermittent Hypoxia and Hypercapnia, a Hallmark of Obstructive Sleep Apnea, Alters the Gut Microbiome and Metabolome. *mSystems* 2018; **3** [PMID: 29896566 DOI: 10.1128/mSystems.00020-18]

12 **Ko CY**, Liu QQ, Su HZ, Zhang HP, Fan JM, Yang JH, Hu AK, Liu YQ, Chou D, Zeng YM. Gut microbiota in obstructive sleep apnea-hypopnea syndrome: disease-related dysbiosis and metabolic comorbidities. *Clin Sci (Lond)* 2019; **133**: 905-917 [PMID: 30957778 DOI: 10.1042/CS20180891]

13 **Bjorvatn B**, Lehmann S, Gulati S, Aurlien H, Pallesen S, Saxvig IW. Prevalence of excessive sleepiness is higher whereas insomnia is lower with greater severity of obstructive sleep apnea. *Sleep Breath* 2015; **19**: 1387-1393 [PMID: 25855469 DOI: 10.1007/s11325-015-1155-5]

14 **Zhang X**, Fang Z, Zhang C, Xia H, Jie Z, Han X, Chen Y, Ji L. Effects of Acarbose on the Gut Microbiota of Prediabetic Patients: A Randomized, Double-blind, Controlled Crossover Trial. *Diabetes Ther* 2017; **8**: 293-307 [PMID: 28130771 DOI: 10.1007/s13300-017-0226-y]

15 **Canfora EE**, Meex RCR, Venema K, Blaak EE. Gut microbial metabolites in obesity, NAFLD and T2DM. *Nat Rev Endocrinol* 2019; **15**: 261-273 [PMID: 30670819 DOI: 10.1038/s41574-019-0156-z]

16 **Zhao L**, Zhang F, Ding X, Wu G, Lam YY, Wang X, Fu H, Xue X, Lu C, Ma J, Yu L, Xu C, Ren Z, Xu Y, Xu S, Shen H, Zhu X, Shi Y, Shen Q, Dong W, Liu R, Ling Y, Zeng Y, Zhang Q, Wang J, Wang L, Wu Y, Zeng B, Wei H, Zhang M, Peng Y, Zhang C. Gut bacteria selectively promoted by dietary fibers alleviate type 2 diabetes. *Science* 2018; **359**: 1151-1156 [PMID: 29590046 DOI: 10.1126/science.aao5774]

17 **Cani PD**, Osto M, Geurts L, Everard A. Involvement of gut microbiota in the development of low-grade inflammation and type 2 diabetes associated with obesity. *Gut Microbes* 2012; **3**: 279-288 [PMID: 22572877 DOI: 10.4161/gmic.19625]

18 **Labarca G**, Reyes T, Jorquera J, Dreyse J, Drake L. CPAP in patients with obstructive sleep apnea and type 2 diabetes mellitus: Systematic review and meta-analysis. *Clin Respir J* 2018; **12**: 2361-2368 [PMID: 30073792 DOI: 10.1111/crj.12915]

19 **Wang X**, Bi Y, Zhang Q, Pan F. Obstructive sleep apnoea and the risk of type 2 diabetes: a meta-analysis of prospective cohort studies. *Respirology* 2013; **18**: 140-146 [PMID: 22988888 DOI: 10.1111/j.1440-1843.2012.02267.x]

20 **Balkau B**, Vol S, Loko S, Andriamboavonjy T, Lantieri O, Gusto G, Meslier N, Racineux JL, Tichet J; Epidemiologic Study on the Insulin Resistance Syndrome Study Group. High baseline insulin levels associated with 6-year incident observed sleep apnea. *Diabetes Care* 2010; **33**: 1044-1049 [PMID: 20185739 DOI: 10.2337/dc09-1901]

21 **Monneret D**, Tamisier R, Ducros V, Garrel C, Levy P, Baguet JP, Faure P, Pépin JL. The impact of obstructive sleep apnea on homocysteine and carotid remodeling in metabolic syndrome. *Respir Physiol Neurobiol* 2012; **180**: 298-304 [PMID: 22210465 DOI: 10.1016/j.resp.2011.12.009]

22 **Hu Y**, Xu Y, Wang G. Homocysteine Levels are Associated with Endothelial Function in Newly Diagnosed Type 2 Diabetes Mellitus Patients. *Metab Syndr Relat Disord* 2019; **17**: 323-327 [PMID: 31045466 DOI: 10.1089/met.2019.0011]

23 **Eltzschig HK**, Carmeliet P. Hypoxia and inflammation. *N Engl J Med* 2011; **364**: 656-665 [PMID: 21323543 DOI: 10.1056/NEJMra0910283]

24 **Abdel-Moneim A**, Bakery HH, Allam G. The potential pathogenic role of IL-17/Th17 cells in both type 1 and type 2 diabetes mellitus. *Biomed Pharmacother* 2018; **101**: 287-292 [PMID: 29499402 DOI: 10.1016/j.biopha.2018.02.103]

25 **Kasahara K**, Krautkramer KA, Org E, Romano KA, Kerby RL, Vivas EI, Mehrabian M, Denu JM, Bäckhed F, Lusis AJ, Rey FE. Interactions between Roseburia intestinalis and diet modulate atherogenesis in a murine model. *Nat Microbiol* 2018; **3**: 1461-1471 [PMID: 30397344 DOI: 10.1038/s41564-018-0272-x]

26 **Xu J**, Liang R, Zhang W, Tian K, Li J, Chen X, Yu T, Chen Q. Faecalibacterium prausnitzii-derived microbial anti-inflammatory molecule regulates intestinal integrity in diabetes mellitus mice *via* modulating tight junction protein expression. *J Diabetes* 2020; **12**: 224-236 [PMID: 31503404 DOI: 10.1111/1753-0407.12986]

27 **Kang JD**, Myers CJ, Harris SC, Kakiyama G, Lee IK, Yun BS, Matsuzaki K, Furukawa M, Min HK, Bajaj JS, Zhou H, Hylemon PB. Bile Acid 7α-Dehydroxylating Gut Bacteria Secrete Antibiotics that Inhibit Clostridium difficile: Role of Secondary Bile Acids. *Cell Chem Biol* 2019; **26**: 27-34.e4 [PMID: 30482679 DOI: 10.1016/j.chembiol.2018.10.003]

28 **Boesmans L**, Valles-Colomer M, Wang J, Eeckhaut V, Falony G, Ducatelle R, Van Immerseel F, Raes J, Verbeke K. Butyrate Producers as Potential Next-Generation Probiotics: Safety Assessment of the Administration of *Butyricicoccus pullicaecorum* to Healthy Volunteers. *mSystems* 2018; **3** [PMID: 30417112 DOI: 10.1128/mSystems.00094-18]

29 **Cox AJ**, West NP, Cripps AW. Obesity, inflammation, and the gut microbiota. *Lancet Diabetes Endocrinol* 2015; **3**: 207-215 [PMID: 25066177 DOI: 10.1016/S2213-8587(14)70134-2]

30 **Moustafa A**, Li W, Anderson EL, Wong EHM, Dulai PS, Sandborn WJ, Biggs W, Yooseph S, Jones MB, Venter JC, Nelson KE, Chang JT, Telenti A, Boland BS. Genetic risk, dysbiosis, and treatment stratification using host genome and gut microbiome in inflammatory bowel disease. *Clin Transl Gastroenterol* 2018; **9**: e132 [PMID: 29345635 DOI: 10.1038/ctg.2017.58]

31 **He FF**, Li YM. Role of gut microbiota in the development of insulin resistance and the mechanism underlying polycystic ovary syndrome: a review. *J Ovarian Res* 2020; **13**: 73 [PMID: 32552864 DOI: 10.1186/s13048-020-00670-3]

32 **Bruzzese E**, Callegari ML, Raia V, Viscovo S, Scotto R, Ferrari S, Morelli L, Buccigrossi V, Lo Vecchio A, Ruberto E, Guarino A. Disrupted intestinal microbiota and intestinal inflammation in children with cystic fibrosis and its restoration with Lactobacillus GG: a randomised clinical trial. *PLoS One* 2014; **9**: e87796 [PMID: 24586292 DOI: 10.1371/journal.pone.0087796]

33 **Enaud R**, Prevel R, Ciarlo E, Beaufils F, Wieërs G, Guery B, Delhaes L. The Gut-Lung Axis in Health and Respiratory Diseases: A Place for Inter-Organ and Inter-Kingdom Crosstalks. *Front Cell Infect Microbiol* 2020; **10**: 9 [PMID: 32140452 DOI: 10.3389/fcimb.2020.00009]

34 **Marsland BJ**, Trompette A, Gollwitzer ES. The Gut-Lung Axis in Respiratory Disease. *Ann Am Thorac Soc* 2015; **12** Suppl 2: S150-S156 [PMID: 26595731 DOI: 10.1513/AnnalsATS.201503-133AW]

35 **Huang D**, Su X, Yuan M, Zhang S, He J, Deng Q, Qiu W, Dong H, Cai S. The characterization of lung microbiome in lung cancer patients with different clinicopathology. *Am J Cancer Res* 2019; **9**: 2047-2063 [PMID: 31598405]

36 **Coburn B**, Wang PW, Diaz Caballero J, Clark ST, Brahma V, Donaldson S, Zhang Y, Surendra A, Gong Y, Elizabeth Tullis D, Yau YC, Waters VJ, Hwang DM, Guttman DS. Lung microbiota across age and disease stage in cystic fibrosis. *Sci Rep* 2015; **5**: 10241 [PMID: 25974282 DOI: 10.1038/srep10241]

World Journal of Gastroenterology

Submit a Manuscript: https://www.f6publishing.com

World J Gastroenterol 2022 June 7; 28(21): 2334-2349

DOI: 10.3748/wjg.v28.i21.2334

ISSN 1007-9327 (print) ISSN 2219-2840 (online)

ORIGINAL ARTICLE

Retrospective Study

Serotonin type 3 receptor subunit gene polymorphisms associated with psychosomatic symptoms in irritable bowel syndrome: A multicenter retrospective study

Sabrina Berens, Yuanjun Dong, Nikola Fritz, Jutta Walstab, Mauro D'Amato, Tenghao Zheng, Verena Wahl, Felix Boekstegers, Justo Lorenzo Bermejo, Cristina Martinez, Stefanie Schmitteckert, Egbert Clevers, Felicitas Engel, Annika Gauss, Wolfgang Herzog, Robin Spiller, Miriam Goebel-Stengel, Hubert Mönnikes, Viola Andresen, Frieling Thomas, Jutta Keller, Christian Pehl, Christoph Stein-Thöringer, Gerard Clarke, Timothy G Dinan, Eamonn M Quigley, Gregory Sayuk, Magnus Simrén, Jonas Tesarz, Gudrun Rappold, Lukas van Oudenhove, Rainer Schaefert, Beate Niesler

Specialty type: Gastroenterology and hepatology

Provenance and peer review: Unsolicited article; Externally peer reviewed.

Peer-review model: Single blind

Peer-review report's scientific quality classification

Grade A (Excellent): A
Grade B (Very good): 0
Grade C (Good): 0
Grade D (Fair): 0
Grade E (Poor): 0

P-Reviewer: Yin ZT, China

Received: July 19, 2021
Peer-review started: July 19, 2021
First decision: August 9, 2021
Revised: August 21, 2021
Accepted: April 22, 2022
Article in press: April 22, 2022
Published online: June 7, 2022

Sabrina Berens, Department of General Internal Medicine and Psychosomatics, University Hospital Heidelberg, Heidelberg 69120, Germany

Yuanjun Dong, Nikola Fritz, Verena Wahl, Cristina Martinez, Stefanie Schmitteckert, Gudrun Rappold, Department of Human Molecular Genetics, Institute of Human Genetics, University of Heidelberg, Heidelberg 69120, Germany

Yuanjun Dong, Felicitas Engel, Jonas Tesarz, Rainer Schaefert, Department of General Internal Medicine and Psychosomatics, Internal Medicine II, University Hospital Heidelberg, Heidelberg 69120, Germany

Jutta Walstab, Department of Human Molecular Genetics, University of Heidelberg, Heidelberg 69120, Germany

Mauro D'Amato, Gastrointestinal Genetics Lab, CIC bioGUNE - BRTA, Derio 48160, Spain

Mauro D'Amato, IKERBASQUE, Basque Foundation for Science, Bilbao 48001, Spain

Mauro D'Amato, Tenghao Zheng, Unit of Clinical Epidemiology, Department of Medicine Solna, Karolinska Institutet, Stockholm 17177, Sweden

Felix Boekstegers, Justo Lorenzo Bermejo, Institute of Medical Biometry and Informatics, Heidelberg University, Heidelberg 69120, Germany

Cristina Martinez, Lleida Institute for Biomedical Research Dr. Pifarré Foundation (IRBLleida), Av. Alcalde Rovira Roure, Lleida 25198, Spain

Egbert Clevers, Department of Clinical and Experimental Medicine, Translational Research Center for Gastrointestinal Disorders, KU Leuven, Leuven 3000, Belgium

Annika Gauss, Department of Gastroenterology, Infectious Diseases and Intoxications, University of Heidelberg, Heidelberg 69120, Germany

Wolfgang Herzog, Department of General Internal Medicine and Psychosomatics, Heidelberg University, Heidelberg 69120, Germany

Robin Spiller, Nottingham Digestive Diseases Centre, University of Nottingham, Nottingham NG7 2QL, United Kingdom

Miriam Goebel-Stengel, Helios Klinikum Rottweil, Rottweil 78628, Germany

Hubert Mönnikes, Department of Medicine, Institute of Neurogastroenterology (H.M.), Martin-Luther-Hospital, Belin 14193, Germany

Viola Andresen, Israelitisches Krankenhaus in Hamburg, Hamburg 22297, Germany

Frieling Thomas, Internal Medicine II, Helios Klinikum Krefeld, Krefeld 47805, Germany

Jutta Keller, Israelitisches Krankenhaus Hamburg, Hamburg 22297, Ghana

Christian Pehl, Krankenhaus Vilsbiburg, Vilsbiburg 84137, Germany

Christoph Stein-Thöringer, Division of Microbiome and Cancer, German Cancer Research Center (DKFZ), Heidelberg 69120, Germany

Gerard Clarke, Timothy G Dinan, Department of Psychiatry and Neurobehavioral Science, University College Cork, Cork T23, Ireland

Eamonn M Quigley, Medicine in Digestive Disorders, Department of Medicine, Lynda K. and David M. Underwood Center for Digestive Disorders, Houston Methodist, Houston, TX 77030, United States

Gregory Sayuk, Division of Gastroenterology, Washington University School of Medicine, Department of Psychiatry, School of Medicine, John Cochran Veteran Affairs Medical Center, St. Louis, MO 63110, United States

Magnus Simrén, Department of Internal Medicine, Section of Gastroenterology and Hepatology, Sahlgrenska University Hospital, Gothenburg SE-41685, Sweden

Gudrun Rappold, Beate Niesler, Interdisciplinary Center for Neurosciences (IZN), University of Heidelberg, Heidelberg 69120, Germany

Lukas van Oudenhove, Cognitive and Affective Neuroscience Lab, Department of Psychological and Brain Sciences, Dartmouth College, Hanover, NH 03748, United States

Lukas van Oudenhove, Laboratory for Brain-Gut Axis Studies, Translational Research Center for Gastrointestinal Disorders, Department of Chronic Diseases, Metabolism, and Ageing, KU Leuven, Leuven 3000, Belgium

Rainer Schaefert, Department of Psychosomatic Medicine, Division of Internal Medicine, University Hospital Basel, Basel CH-4031, Switzerland

Beate Niesler, Department of Human Molecular Genetics, Heidelberg University, Heidelberg 69120, Germany

Corresponding author: Beate Niesler, PhD, Academic Fellow, Full Professor, Senior Scientist, Department of Human Molecular Genetics, Heidelberg University, Neuenheimer Feld 366, Heidelberg 69120, Germany.
beate.niesler@med.uni-heidelberg.de

Abstract

BACKGROUND

Single-nucleotide polymorphisms (SNPs) of the serotonin type 3 receptor subunit (*HTR3*) genes have been associated with psychosomatic symptoms, but it is not clear whether these associations exist in irritable bowel syndrome (IBS).

AIM

To assess the association of *HTR3* polymorphisms with depressive, anxiety, and somatization symptoms in individuals with IBS.

METHODS

In this retrospective study, 623 participants with IBS were recruited from five specialty centers in Germany, Sweden, the United States, the United Kingdom, and Ireland. Depressive, anxiety, and

somatization symptoms and sociodemographic characteristics were collected. Four functional SNPs — *HTR3A* c.-42C>T, *HTR3B* c.386A>C, *HTR3C* c.489C>A, and *HTR3E* c.*76G>A — were genotyped and analyzed using the dominant and recessive models. We also performed separate analyses for sex and IBS subtypes. SNP scores were calculated as the number of minor alleles of the SNPs above. The impact of *HTR3C* c.489C>A was tested by radioligand-binding and calcium influx assays.

RESULTS

Depressive and anxiety symptoms significantly worsened with increasing numbers of minor *HTR3C* c.489C>A alleles in the dominant model ($F_{depressive}$ = 7.475, $P_{depressive}$ = 0.006; $F_{anxiety}$ = 6.535, $P_{anxiety}$ = 0.011). A higher SNP score (range 0-6) was linked to a worsened depressive symptoms score (F = 7.710, *P-linear trend* = 0.006) in IBS. The potential relevance of the *HTR3C* SNP was corroborated, showing changes in the expression level of 5-HT$_3$AC variant receptors.

CONCLUSION

We have provided the first evidence that *HTR3C* c.489C>A is involved in depressive and anxiety symptoms in individuals with IBS. The SNP score indicated that an increasing number of minor alleles is linked to the worsening of depressive symptoms in IBS.

Key Words: Irritable bowel syndrome; 5-HT$_3$ receptor subunit gene polymorphisms; Single-nucleotide polymorphism score; Depression; Anxiety; Somatization

©The Author(s) 2022. Published by Baishideng Publishing Group Inc. All rights reserved.

Core Tip: Bringing together high quality data as well as methodological expertise, our results show that: In the dominant model, *HTR3C* c.489C>A was correlated with depressive and anxiety symptoms in irritable bowel syndrome (IBS); a higher number of minor alleles, which was computed by combining the individual SNP status of *HTR3A* c.-42C>T, *HTR3B* c.386A>C, *HTR3C* c.489C>A, and *HTR3E* c.*76G>A, was linked to more severe depressive symptoms in IBS; and the potential relevance of the *HTR3C* SNP was corroborated in functional assays showing changes in the expression level of 5-HT$_3$AC variant receptors. These results will contribute towards standardization and harmonization of genetic research strategies in IBS.

Citation: Berens S, Dong Y, Fritz N, Walstab J, D'Amato M, Zheng T, Wahl V, Boekstegers F, Bermejo JL, Martinez C, Schmitteckert S, Clevers E, Engel F, Gauss A, Herzog W, Spiller R, Goebel-Stengel M, Mönnikes H, Andresen V, Thomas F, Keller J, Pehl C, Stein-Thöringer C, Clarke G, Dinan TG, Quigley EM, Sayuk G, Simrén M, Tesarz J, Rappold G, van Oudenhove L, Schaefert R, Niesler B. Serotonin type 3 receptor subunit gene polymorphisms associated with psychosomatic symptoms in irritable bowel syndrome: A multicenter retrospective study. *World J Gastroenterol* 2022; 28(21): 2334-2349

URL: https://www.wjgnet.com/1007-9327/full/v28/i21/2334.htm

DOI: https://dx.doi.org/10.3748/wjg.v28.i21.2334

INTRODUCTION

Irritable bowel syndrome (IBS) is a chronic functional gastrointestinal (GI) disorder characterized by abdominal pain and altered bowel habits[1-4]. The pathophysiology of IBS has not entirely been resolved, but is understood to be biopsychosocial and affected by an impaired function of the central and enteric nervous systems and their crosstalk *via* the brain-gut axis[5,6]. IBS patients often present with increased comorbid depressive and anxiety symptoms[7-11], highlighting the complex relationship between visceral sensitivity and subjective psychological perceptions[12,13]. Nevertheless, about 50% of IBS patients report GI symptoms but show no comorbid affective symptoms[14].

There is evidence that disturbances of the serotonergic system are important in GI disorders such as IBS and in mental disorders, both of which interact *via* the brain-gut axis[15,16]. The serotonin type 3 receptors (5-HT$_3$R) modulate key functions in the GI tract[17,18]. In line with such functions, 5-HT$_3$R antagonists are beneficial in the treatment of diarrhea-predominant IBS (IBS-D)[19-22]. 5-HT$_3$Rs are also involved in emotional processing, mood regulation, and visceral perception and have been associated with depressive and anxiety symptoms that represent comorbid phenotypes in IBS[23]. Single-nucleotide polymorphisms (SNPs) in the 5-HT$_3$R subunit genes (*HTR3*), namely *HTR3A* c.-42C>T (rs1062613), *HTR3B* c.386A>C (rs1176744), *HTR3C* c.489C>A (rs6766410), and *HTR3E* c.*76G>A

(rs56109847), are associated with IBS according to studies investigating the effects of sex or IBS subtypes [12,24-30]. However, whether *HTR3* polymorphisms are associated with IBS and comorbid depressive and anxiety symptoms has not been determined because existing studies have missing phenotypic data on comorbidities and small sample sizes. These studies had case-control designs and investigated associations between these polymorphisms in individuals with IBS phenotypes or mental behavioral conditions and controls rather than combining genetic data with specific psychosocial characteristics of IBS patients.

This multicenter observational study focused on a large IBS patient cohort comprising 768 participants from centers in Germany, Sweden, the United States, the United Kingdom, and Ireland with the aim of meeting three objectives: (1) To explore the associations between functional *HTR3* polymorphisms and psychosomatic burden (*i.e.*, depressive, anxiety, and somatization symptoms) within an IBS population; (2) To investigate the impact of the *HTR3* SNP score (computed as the number of minor alleles) on psychosomatic burden, based on our hypothesis that the observed number of minor alleles was associated with specific mental characteristics in IBS patients; and (3) To perform a functional analysis of variant 5-HT$_3$AC receptors.

MATERIALS AND METHODS

Subjects

The study population was pooled from five different tertiary care expert centers. German participants were recruited from the Specialty Clinic for Functional GI Disorders at the Department of General Internal Medicine and Psychosomatics of Heidelberg University Hospital[31] and from our clinical partners in the IBS-Net in Hamburg, Krefeld, Berlin, Vilsbiburg, and Munich (www.ibs.uni-hd.de). Swedish participants were recruited at the specialized unit for patients with functional GI disorders at Sahlgrenska University Hospital in Gothenburg. United States participants were recruited at Washington University, Barnes-Jewish Hospital in St. Louis, Missouri. United Kingdom participants were recruited at the Nottingham Digestive Diseases Center and participants from Ireland from a specialty clinic at Cork University Hospital. Participant recruitment is shown in Figure 1.

Written informed consent was obtained from all participants and the experiments were in accordance with the principles of the WMA Declaration of Helsinki and the Department of Health and Human Services Belmont Report. All studies were approved by the following local Ethics Committees: Heidelberg, Germany: Ethical Committee, Medical Faculty of the Heidelberg University Hospital (S067/2010); Cork, Ireland: Clinical Research Ethics Committee (APC024); Gothenburg, Sweden: Regional Ethical Review Board in Gothenburg (S489-02 and 731-09); Nottingham, United Kingdom: registered at clinical trial clinicaltrials.gov (identifier NCT00745004) and approved by Nottingham Research Ethics Committee 2 (REC reference number 08/H0408/134)[21]; and St-Louis, United States: Washington University St. Louis, Human Research Protection Office (IRB ID #: 201103220).

Inclusion/exclusion criteria

Only patients diagnosed with IBS according to the ROME III criteria were included in the analysis. All participants were of Caucasian ancestry and had comparable population stratification. Patients under 18 years of age or without SNP test results were excluded.

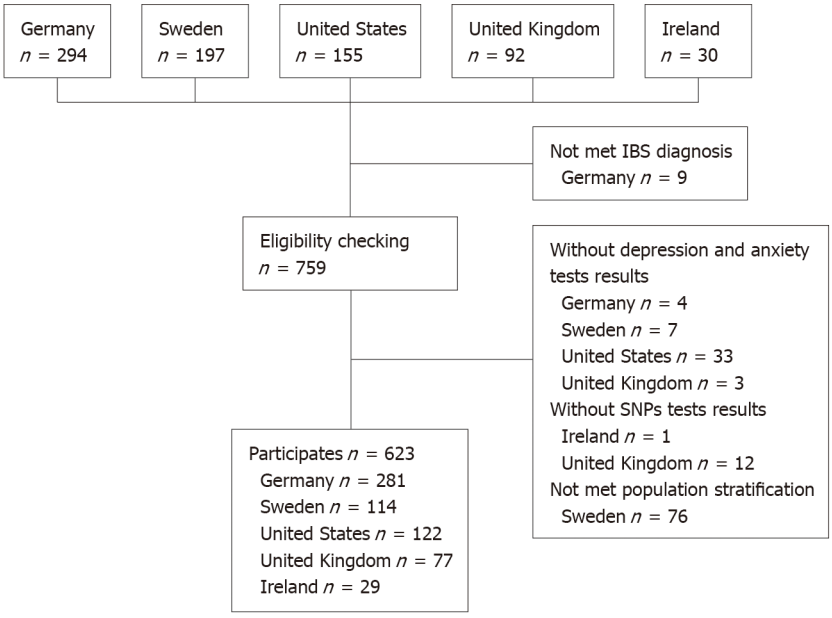
Genotyping

Genomic DNA was isolated from IBS patient blood samples using ethylenediaminetetraacetic acid according to standard protocols[32]. Four polymorphic *HTR3* loci, namely *HTR3A* c.-42C>T (rs1062613), *HTR3B* c.386A>C (rs1176744), *HTR3C* c.489C>A (rs6766410), and *HTR3E* c.*76G>A (rs56109847) were selected as target SNPs for this study. The corresponding primers were designed and synthesized using AssayDesigner 3.1 software. Genotyping was performed at the Department of Human Molecular Genetics at Heidelberg University Hospital using the KASPar® SNP Genotyping System (KBiosciences, Ltd, Hoddesdon, United Kingdom). To analyze *HTR3* SNPs, the fluorescence plate reader of the 7500 Fast Real-Time PCR System (Applied Biosystems, Foster City, California, United States) was used as recommended. About 10% of the samples were repeat tested to ensure genotyping accuracy.

Data collection

In addition to sociodemographic characteristics and IBS diagnosis, we also collected data on depressive, anxiety, and somatization symptoms[33] and genetic markers of the serotonergic system.

IBS diagnosis: The diagnostic classification of IBS was based on the Scoring Algorithm for Rome III Diagnostic Questionnaire for Adult Functional GI Disorders (SA for Rome III-DQ)[34,35] in all five centers. Percentages of the different IBS subtypes, *i.e.*, constipation-predominant IBS, IBS-D, IBS with mixed bowel habits, and unclassified IBS, were also calculated.



DOI: 10.3748/wjg.v28.i21.2334 **Copyright** ©The Author(s) 2022.

Figure 1 Recruitment strategy. IBS: Irritable bowel syndrome.

Depressive symptoms: The nine-item depression module from the Patient Health Questionnaire (PHQ-9)[36,37] was used to measure depressive symptoms in the German cohort. The Hospital Anxiety and Depression Scale depression subscale[38] was used to identify depressive symptoms in participants from Sweden, the United Kingdom, and Ireland and the Beck Depression Inventory[39] was used to measure the severity of depressive symptoms in United States participants.

Anxiety symptoms: In the German cohort, symptoms of generalized anxiety were assessed using the brief measurement for generalized anxiety disorder (GAD-7)[40]. In the cohorts from Sweden, the United Kingdom, and Ireland, the HADS anxiety subscale was used to identify anxiety symptoms. The Beck Anxiety Inventory[41] was used to assess anxiety in the United States cohort.

Somatization symptoms: In the cohorts from Germany, Sweden, and the United States, the 15-item somatization module from the PHQ-15[42] was used to identify somatization symptoms.

Genetic markers of the serotonergic system: The four functional SNPs *HTR3A* c.-42C>T (rs1062613), *HTR3B* c.386A>C (rs1176744), *HTR3C* c.489C>A (rs6766410), and *HTR3E* c.*76G>A (rs56109847) were selected for validation based on previous reports as outlined above[25].

Ligand binding and calcium influx assays

These procedures are described in the Supplementary material.

Statistical analysis

All statistical procedures were carried out using IBM SPSS Statistics 22.0 for Windows. Variables with a skewed distribution were log-transformed prior to further analysis. If different measurements had been collected in the five centers, *z* values were calculated to enable pooling. The Hardy-Weinberg equilibrium (HWE) of genotype frequency distribution was tested using SHEsis[43]. Genome-wide SNP data were generated by the Bellygenes team of D'Amato M using the Illumina Global Screening array and platform[44,45]. We used the multidimensional scaling approach to correct for population stratification in PLINK[46]. Following the guidance provided at https://github.com/MareesAT/GWA_tutorial/, our data were anchored by data of the 1000 Genomes project (http://www.1000genomes.org/). The 10 main components were used as covariates in the association tests to correct for population stratification[46] and exclude outliers. Polymorphisms were analyzed separately using the dominant and the recessive models. Also, stratified analyses based on sex and IBS subtypes were carried out. ANOVA was used to analyze group differences and to check for linear trends in depressive, anxiety, and somatization symptoms. For the independent variable, a SNP score was computed based on the number of minor alleles (*i.e.*, continuous from 0 to 8 for the four SNPs). Based on the first human *HTR3* locus-specific variant database (www.htr3.uni-hd.de)[25], scoring criteria were as follows: major allele homozygous variant gene = 0; heterozygous variant gene = 1; and minor allele homozygous variant gene = 2 (for details see Table 1). Statistical comparisons were made between the two groups using the χ^2 test or Fisher's exact test for frequencies and *t* tests or Mann-Whitney *U* tests for metric

Table 1 Strategy for computing the single-nucleotide polymorphism score

	Major allele homozygous genotype	Heterozygous variant genotype	Minor allele homozygous genotype
HTR3A c.-42C>T (rs1062613)	CC	CT	TT
HTR3B c.386A>C (rs1176744)	AA	AC	CC
HTR3C c.489C>A (rs6766410)	CC	CA	AA
HTR3E c.*76G>A (rs56109847)	GG	GA	AA

variables. Normal distribution and variance homogeneity were checked as conditions. Statistical tests were two-sided based on an alpha error of 0.05%. All analyses were explorative and not confirmatory. False discovery rates (FDRs) were calculated based on overall *P* values using the Benjamini-Hochberg method[47]. Significant values that were no longer significant after FDR multiple testing correction were named "nominally significant".

RESULTS

Sociodemographic and symptomatic characteristics

In total, 623 participants from five independent expert centers were included in this study (45.1% from Germany, 18.3% from Sweden, 19.6% from the United States, 12.4% from the United Kingdom, and 4.7% from Ireland). We excluded 76 Swedish participants who did not meet the population stratification criteria (Supplementary Figure 1). Participants from the United Kingdom and Ireland were excluded from the main analysis because the sample size was small. Table 2 presents the sociodemographic characteristics, IBS subtypes, and psychosomatic symptoms of the included participants. Participants had a mean ± SD age of 41.7 ± 16.1 years and 69.5% were female. Overall, IBS patients showed minimal to mild levels of depressive and anxiety symptoms, moderate levels of IBS symptoms, and moderate levels of somatization symptoms.

HTR3 SNP genotypes and allele frequencies

Genotype and allele frequencies of the functional *HTR3A* c.-42C>T, *HTR3B* c.386A>, *HTR3C* c.489C>A, and *HTR3E* c.*76G>A polymorphisms were calculated. No significant differences in genotype frequency were observed between sexes or IBS subtypes. For *HTR3A* c.-42C>T, the frequency of the minor *T* allele was 21.5%; for *HTR3B* c.386A>C, the frequency of the minor *C* allele was 29.6%; for *HTR3C* c.489C>A, the frequency of the minor *A* allele was 41.6%; and for *HTR3E* c.*76G>A, the frequency of minor *A* allele was 6.1%. The genotypic distribution of the four polymorphic loci of rs1062613, rs1176744, rs6766410, and rs56109847 were in accordance with HWE (all $P > 0.05$). The results are shown in Supplementary Tables 1-3.

HTR3 SNP analysis using the dominant and the recessive model

HTR3 SNPs were separately analyzed using the dominant model and the recessive model stratified for sex and IBS subtypes. Depressive and anxiety symptoms worsened significantly with increasing numbers of minor alleles of *HTR3C* c.489C>A in the dominant model ($F_{depressive} = 7.475$, $P_{depressive} = 0.006$; $F_{anxiety} = 6.535$, $P_{anxiety} = 0.011$). This seemed to be driven by female sex ($F_{depressive} = 7.040$, $P_{depressive} = 0.008$; $F_{anxiety} = 7.550$, $P_{anxiety} = 0.006$) and IBS-D ($F_{depressive} = 5.670$, $P_{depressive} = 0.018$; $F_{anxiety} = 13.444$, $P_{anxiety} < 0.001$). The same trend was also found for *HTR3A* c.-42C>T in male participants with depressive symptoms in the dominant model ($F_{depressive} = 4.149$, $P_{depressive} = 0.043$). For the recessive model, depressive and somatization symptoms worsened with increasing numbers of minor alleles of *HTR3C c.489C>A* ($F_{depressive} = 6.190$, $P_{depressive} = 0.014$) and *HTR3B c.386A>C* ($F_{depressive} = 6.482$, $P_{depressive} = 0.011$), respectively in IBS-D participants. *F* values from the ANOVA are shown in Table 3. As mentioned above, the analyses of participants from the United Kingdom and Ireland are presented separately in the Supplementary Table 4.

Effect of SNP score on psychosomatic symptoms

SNP scores ranged from 0 to 6; 37.1% had one or zero minor alleles of the analyzed *HTR3* SNPs and 30.8% had three or more minor alleles of the analyzed *HTR3* SNPs. No significant differences in SNP scores were observed between sexes ($F = 3.550$, $P = 0.060$) or IBS subtypes ($F = 1.485$, $P = 0.227$). ANOVAs were conducted and linear trends were checked to analyze the effect of SNP scores on depressive, anxiety, and somatization symptoms. Overall, an increasing number of minor alleles was linked to worsening depressive symptoms ($F = 7.710$, *P-linear trend* = 0.006). However, material trends did not reveal a link between more minor alleles and worsening anxiety or somatization symptoms. By stratifying analyses for sex, an increasing number of minor alleles was linked to worsened depressive

Table 2 Sociodemographic and symptomatic characteristics of the study participants

	Total	Centers				
		Germany	Sweden	United States	United Kingdom	Ireland
n	100.0 (623)	45.1 (281)	18.3 (114)	19.6 (122)	12.4 (77)	4.7 (29)
Age	41.7 ± 16.1 (18, 91)	40.7 ± 16.4 (18, 88)	33.7 ± 11.8 (18, 60)	54.9 ± 14.6 (25, 91)	40.8 ± 11.6 (18, 70)	30.3 ± 8.6 (19, 51)
Sex						
Female	69.5 (433)	63.3 (178)	69.3 (79)	77.9 (95)	72.7 (56)	86.2 (25)
IBS subtypes						
IBS-C	14.1 (87)	8.9 (25)	12.3 (14)	36.7 (44)	0	13.8 (4)
IBS-D	41.7 (258)	43.4 (122)	19.6 (22)	28.3 (34)	100.0 (77)	10.3 (3)
IBS-M	42.5 (263)	45.6 (128)	67.0 (75)	31.7 (38)	0	75.9 (22)
IBS-U[1]	1.8 (11)	2.1 (6)	0.9 (1)	3.3 (4)	0	0
Depressive symptoms	-	9.4 ± 5.9[2]	5.2 ± 3.5[4]	13.2 ± 9.6[5]	5.9 ± 4.0[4]	4.3 ± 3.2[4]
Anxiety symptoms	-	7.7 ± 4.8[3]	8.3 ± 4.5[4]	14.6 ± 9.7[6]	9.6 ± 4.6[4]	7.8 ± 4.5[4]
Symptom severity	-	280.3 ± 90.7[7]	297.3 ± 100.5[7]	43.2 ± 16.2[8]	-	-
Somatization symptoms[9]	14.8±6.3	16.2 ± 7.3	13.3 ± 4.7	13.8 ± 5.0	-	-

Sample size, sex, IBS subtypes, and severity of depressive and anxiety symptoms are presented as % (*n*). Age is presented as mean ± SD (range). Scores of depressive and anxiety symptoms are presented as mean ± SD.

[1]Was not included in the later analysis because of the small sample size.

[2]Evaluated by the nine-item depression module from the Patient Health Questionnaire.

[3]Evaluated by the brief measurement for generalized anxiety disorder.

[4]Evaluated by Hospital Anxiety and Depression Scale.

[5]Evaluated by Beck Depression Inventory.

[6]Evaluated by Beck Anxiety Inventory.

[7]Evaluated by irritable bowel syndrome (IBS) symptom severity scale.

[8]Evaluated by the gastrointestinal symptom rating scale for IBS.

[9]Evaluated by the somatization module for the Patient Health Questionnaire.

IBS: Irritable bowel syndrome; IBS-C: Constipation-predominant IBS; IBS-D: Diarrhea-predominant IBS; IBS-M: IBS with mixed bowel habits; IBS-U: Unclassified IBS.

symptoms in female participants (F = 5.770, *P-linear trend* = 0.017). There was no significant association between SNP score and depressive, anxiety, or somatization symptoms when looking at IBS subtypes separately (Table 4). As mentioned above, the analyses of participants from the United Kingdom and Ireland are presented separately in the Supplementary Table 5.

Functional analysis of variant 5-HT$_3$AC receptors

The *HTR3C* SNP encodes the amino acid exchange p.Asn163Lys (p.N163K), and recombinantly expressed 5-HT$_3$AC receptors harboring variant 5-HT$_3$C subunits that mimic the homozygous minor allele and the heterozygous state presented with increased cell surface expression and enhanced 5-HT maximum response. Radioligand-binding assays revealed higher B_{max} values of 117.1% ± 4.38% and 111.9% ± 1.79%. Calcium influx assays showed increased 5-HT-induced maximum effects of 137.2% ± 9.0% and 151.9% ± 17.3% for the minor allele 5-HT$_3$AC 163K or combined 5-HT$_3$AC 163N/5-HT$_3$AC 163K receptors compared with the major allele representing 5-HT$_3$AC 163N receptors, respectively. The affinity of the specific 5-HT$_3$ receptor antagonist [^{3}H]GR65630, as reflected by the Kd values, and the potency of 5-HT, as reflected by the EC_{50} values, did not differ between the receptor variants (Figure 2).

DISCUSSION

Main findings

The 5-HT$_3$ receptors modulate essential functions in the GI tract such as GI motility as well as mood and emotions[19], and *HTR3* SNPs have been associated with depression, anxiety, and IBS[25]. In this study, we showed that: (1) In the dominant model, *HTR3C c.489C>A* was correlated with depressive and anxiety symptoms in IBS; (2) A higher number of minor alleles (*i.e.*, a higher SNP score, which was computed by combining the individual SNP status of *HTR3A c.-42C>T, HTR3B c.386A>C, HTR3C*

Table 3 Differences between single-nucleotide polymorphisms in depressive and anxiety symptoms, separately analyzed with ANOVA using the dominant model and the recessive model

Models	Mental symptoms	SNPs	Total	Sex		IBS subtypes		
				Male	Female	IBS-C	IBS-D	IBS-M
Dominant model	Depressive symptoms	*HTR3A* c.-42C>T (rs1062613)	2.541	**4.149** ↑	0286	0.998	0.376	0.694
		HTR3B c.386A>C (rs1176744)	0.067	0.005	0.198	0.282	0.124	0.232
		HTR3C c.489C>A (rs6766410)	**7.475** ↑	0.672	**7.040** ↑	0.261	**5.670** ↑	2.328
		HTR3E c.*76G>A (rs62625044)	0.054	0.013	0.180	0.208	0.461	0.010
	Anxiety symptoms	*HTR3A* c.-42C>T (rs1062613)	0.511	0.210	0.280	0.604	0.672	0.162
		HTR3B c.386A>C (rs1176744)	0.926	0.406	0.801	0.468	1.369	0.770
		HTR3C c.489C>A (rs6766410)	**6.535** ↑	0.158	**7.550** ↑	0.186	**13.444** ↑	0.045
		HTR3E c.*76G>A (rs62625044)	1.055	0.429	0.853	0.000	0.495	1.109
	Somatization symptoms	*HTR3A* c.-42C>T (rs1062613)	0.016	0.141	0.106	0.086	0.017	0.203
		HTR3B c.386A>C (rs1176744)	0.217	0.332	0.326	0.407	0.415	2.125
		HTR3C c.489C>A (rs6766410)	0.784	0.035	1.085	0.269	0.000	1.962
		HTR3E c.*76G>A (rs62625044)	0.002	1.554	0.263	0.128	0.729	0.354
Recessive model	Depressive symptoms	*HTR3A* c.-42C>T (rs1062613)	0.002	0.421	0.132	0.093	1.320	1.064
		HTR3B c.386A>C (rs1176744)	1.118	2.027	0.107	1.741	0.197	0.744
		HTR3C c.489C>A (rs6766410)	0.047	0.821	0.401	2.306	**6.190** ↑	0.676
		HTR3E c.*76G>A (rs62625044)	0.677	-	0.574	0.541	-	-
	Anxiety symptoms	*HTR3A* c.-42C>T (rs1062613)	0.479	0.027	0.549	0.057	0.315	0.350
		HTR3B c.386A>C (rs1176744)	0.872	0.081	1.691	0.476	0.361	1.923
		HTR3C c.489C>A (rs6766410)	0.028	2.562	0.344	0.570	3.509	2.093
		HTR3E c.*76G>A (rs62625044)	0.216	-	0.179	0.242	-	-
	Somatization symptoms	*HTR3A* c.-42C>T (rs1062613)	0.217	0.018	0.257	0.138	0.092	0.431
		HTR3B c.386A>C (rs1176744)	**6.482** ↑	2.245	3.575	0.142	**14.033** ↑	0.341
		HTR3C c.489C>A (rs6766410)	0.468	1.813	0.128	**4.715** ↓	0.002	0.113
		HTR3E c.*76G>A (rs62625044)	0.001	-	0.011	0.000	-	-

F values are shown in the table. Arrows represent the direction of the associations. ↑ dependent variable increases from major to minor alleles; ↓ dependent variable decreases from major to minor alleles. The underlined values were significant. Values in bold were "nominally significant" (*i.e.*, lacking

significance after false discovery rate multiple testing correction). IBS: Irritable bowel syndrome; IBS-C: Constipation-predominant IBS; IBS-D: Diarrhea-predominant IBS; IBS-M: IBS with mixed bowel habits; SNPs: Single-nucleotide polymorphisms.

Table 4 Association of depressive, anxiety, and somatization symptoms with the single-nucleotide polymorphism score of the four tested polymorphisms

	Total	Sex		IBS subtypes		
		Male	Female	IBS-C	IBS-D	IBS-M
Depressive symptoms						
F value	**7.710**	1.336	**5.770**	1.551	2.159	0.196
P-linear trend value	**0.006**	0.250	**0.017**	0.184	0.144	0.659
Anxiety symptoms						
F value	2.150	0.028	2.514	1.372	2.400	1.412
P-linear trend value	0.143	0.866	0.114	0.245	0.123	0.236
Somatization symptoms						
F value	1.15	0.354	1.028	0.716	2.718	0.628
P-linear trend value	0.283	0.553	0.311	0.614	0.102	0.429

Values in bold were "nominally significant" (*i.e.*, lacking significance after false discovery rate multiple testing correction). IBS: Irritable bowel syndrome; IBS-C: Constipation-predominant IBS; IBS-D: Diarrhea-predominant IBS; IBS-M: IBS with mixed bowel habits.

c.489C>A, and *HTR3E c.*76G>A*) was linked to more severe depressive symptoms in IBS; and (3) The potential relevance of the *HTR3C* SNP was corroborated in functional assays showing changes in the expression level of 5-HT_3AC variant receptors. These findings are discussed in more detail below.

Sample characteristics

Participants with IBS were more frequently female than male, in line with previous findings[48,49] that IBS is more prevalent in young and middle-aged females. Most participants with IBS were only mildly affected by depression and anxiety symptoms. Of note, German participants only visited the Specialty Clinic for Functional GI Disorders at Heidelberg University Hospital after a long history of dealing with IBS[31]; therefore, these participants reported more severe depressive symptoms. However, causal relationships between IBS symptoms, depression, and anxiety are still controversial.

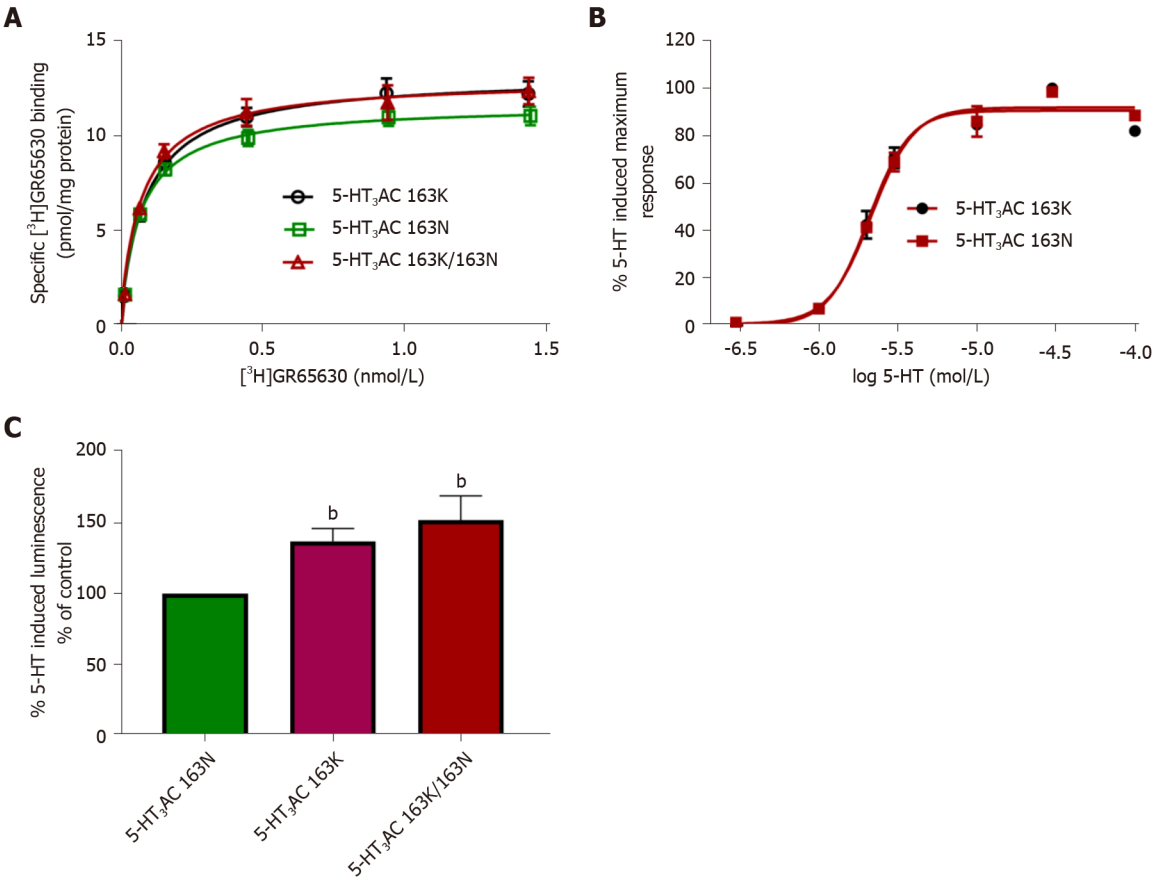
The investigated SNPs rs1062613, rs1176744, rs6766410, and rs56109847 were in accordance with HWE. There was no population stratification, and the sample was representative and excluded genotyping errors. Although participants were recruited from various centers in different countries, there were no obvious selective differences.

Connections between HTR3 SNPs and mental symptoms

***HTR3A* c.-42C>T (rs1062613):** Depressive symptoms were "nominally significantly" more severe with increasing numbers of minor *HTR3A* c.-42C>T alleles in male participants according to the dominant model. This SNP has been associated with bipolar affective disorder[50], IBS symptom severity, amygdaloid activity[29,51], early life trauma[52], altered emotional networks in the human brain, and the onset of depression[53]. However, these studies only included single sex participants and did not include subgroup analyses.

***HTR3B* c.386A>C (rs1176744):** Somatization symptoms worsened significantly with increasing numbers of minor *HTR3B c.386A>C* alleles in the dominant model. The *HTR3B* variant p.Tyr129Ser (rs1176744) has been associated with bipolar affective disorder in males and with major depression in females as well as with pain catastrophizing, a coping style characterized by excessively negative thoughts and emotions related to pain[30,54-56]. This discrepancy may be due to an enhancement or weakening of this association by polymorphic interactions in the serotonin pathways[56].

***HTR3C* c.489C>A (rs6766410):** Depressive and anxiety symptoms worsened significantly with increasing numbers of minor *HTR3C* c.489C>A alleles in the dominant model. This effect seemed to be driven by female sex and IBS-D. *HTR3C* c.489C>A was previously associated with IBS-D in female patients[57], but the proportion of male patients was small in this study, which may limit the applicability of these findings. In the recessive model, depressive and anxiety symptoms "nominally



DOI: 10.3748/wjg.v28.i21.2334 **Copyright** ©The Author(s) 2022.

Figure 2 Comparative analysis of 5-HT$_3$AC 163N (major allele homozygous), 5-HT$_3$AC 163K (minor allele homozygous), and 5-HT$_3$AC 163K/163N (heterozygous) receptors. A: Radioligand-binding studies Saturation experiments were performed in membranes of HEK293 cells transiently expressing different 5-HT$_3$ subunit combinations in triplicate with six increasing concentrations of [3H]GR65630 (0.02-1.5 nmol/L); Kd values were 0.07 ± 0.01 for 5-HT$_3$AC 163N; 0.08 ± 0.01 for 5-HT$_3$AC 163K, and 0.07 ± 0.01 for 5-HT$_3$AC 163K/163N. *n* = 6 experiments; B: Concentration response curves were assessed in a calcium influx assay (aequorin assay) in HEK293 cells transiently transfected with different 5-HT$_3$ subunit combinations in quadruplicate with seven increasing concentrations of 5-HT. pEC50 values were as follows: 68 ± 0.03 for 5-HT$_3$AC 163N 5 and 5.66 ± 0.02 for 5-HT$_3$AC 163K; C: Respective maximal calcium influx values (E_{max}) evoked by 5-HT (10 μmol/L). Data are expressed as percentages of the E_{max} of the heteromeric 5-HT$_3$AC 163N receptor (% of control), *n* = 8 experiments. Bars represent mean ± SE. $^bP < 0.01$ from ANOVA followed by Dunnett's post-test or unpaired Student's test for comparison of only two groups.

significantly" worsened with increasing numbers of minor alleles of *HTR3C* c.489C>A in Irish participants. However, these results should be interpreted with caution because the Irish sample size was low. As far as we are aware, *HTR3C* c.489C>A has not been analyzed in individuals with affective disorders before.

***HTR3E* c.*76G>A (rs56109847):** *HTR3E* is restrictedly and robustly expressed in the GI tract[58,59], suggesting that it plays a special role in 5-HT$_3$ receptor function in the gut. In this study, we did not find a relationship between functional polymorphisms of *HTR3E* and depressive and anxiety symptoms in IBS patients. This may be attributed to a floor effect because depressive and anxiety symptoms were minimal to mild in our sample[60].

The SNP score and its impact on depressive symptoms

A single gene variant is not sufficient to explain all symptoms shaping the clinical phenotype of a complex disorder like IBS[61]. By computing SNP scores based on the number of minor alleles of rs1062613, rs1176744, rs6766410, and rs56109847, our study revealed that an increasing number of minor alleles is linked to increasing severity of depressive symptoms. However, there was no obvious association between an increasing number of minor alleles and the severity of anxiety or somatization symptoms. Stratification for sex revealed a correlation between increasing numbers of minor alleles and worsening depressive symptoms in female participants.

Functional properties of variant 5-HT$_3$AC receptors

HTR3 genes encode different 5-HT$_3$ subunits to make up heteromeric receptors. The 5-HT$_3$A subunits play a major role in these receptors because they can form functional receptors on their own. The other

subunits can only form functional receptors with 5-HT$_3$A and seem to modulate the function and properties of the receptors[62]. How these native receptors might contribute to the pathogenesis of IBS, particularly regarding co-expression patterns of *HTR3*, has not been established yet. The *HTR3A* and *HTR3E* variants reside within untranslated regions and the respective SNPs correlate with increased expression levels, whereas the *HTR3B* variant changes the channel properties[25]. To gain insight into the pathophysiological relevance of the associated *HTR3C* variant c.489C>A (rs6766410), we characterized the pharmacological and functional properties of those 5-HT$_3$AC receptors that altered the 5-HT-mediated maximum response and expression of variant 5-HT$_3$AC receptors. However, how structural modifications in these receptors affect their function *in vivo* and how they modulate the serotonergic system to influence mood, emotional processing, and the manifestation of IBS and comorbid conditions remains to be determined.

Limitations and strengths

Our study has some limitations. First, different instruments were used by different centers to assess phenotypic features. To correct for this, scale scores were converted into *z* standard scores. However, given that the participants reported no severe psychosomatic symptoms, the discovery chances might be limited. Second, there is no sufficient evidence to show the relationship between risk alleles and respective major/minor alleles as patients and healthy controls were not compared in this study. Similarly, the relative strength of the cumulative effect represented by the SNP score was also affected to a certain extent. Third, our participants were all Caucasian, so the results may not apply to other ethnic groups.

Despite these limitations, our study has some strengths. First, this was a multicenter study so had a large sample size. Large, well-characterized samples like ours are necessary to identify molecular causes of IBS and comorbid conditions[12]. Second, this study investigated the association between polymorphisms in *HTR3* genes and comorbid psychosomatic symptoms for the first time. We conducted population stratification tests to ensure that the included populations were comparable. We also performed stratified analyses of sex and IBS subtypes and a more stringent multiple testing correction by FDR. Third, SNP scores have higher power and are better suited to testing multiple instead of single variants. This is useful because the pathogenesis of IBS is complex with multiple factors contributing to the manifestation of various subtypes. Also, individual genes may only play a minor role[12].

Clinical implications and further research

IBS is a complex condition. The continuous improvement of the allelic variation database for *HTR3*[25] and deep phenotyping combined with gene information (also in other datasets) may help to identify disease subgroups accurately and consistently, thereby facilitating future treatment[33,63]. This will be an important step towards standardization and unification of IBS genetic research strategies.

CONCLUSION

Our results provide the first evidence that the accumulation of *HTR3* SNPs (reflected by the SNP score computed by *HTR3A* c.-42C>T, *HTR3B* c.386A>C, *HTR3C* c.489C>A, and *HTR3E* c.*76G>A) may play a role in the pathophysiology of depressive and anxiety symptoms in IBS. This study has revealed that depressive and anxiety symptoms significantly worsened from the major to the minor allele of *HTR3C* c.489C>A in the dominant model and an increasing number of minor alleles are linked to more severe depressive symptoms in IBS.

ARTICLE HIGHLIGHTS

Research background

Over the past decades, genetic evidence on the key players within the serotonergic system including the serotonin type 3 (5-HT$_3$) receptor subunit genes (*HTR3*) accumulated showing association with irritable bowel syndrome (IBS) as well as mental illnesses. However, it has never been explored whether associations of the single-nucleotide polymorphisms (SNPs) of *HTR3* genes to depressive and anxiety symptoms can be replicated within IBS.

Research motivation

In order to address this knowledge gap, This multicenter observational study focused on a large IBS patient cohort comprising 768 participants from centers in Germany, Sweden, the United States, the United Kingdom, and Ireland.

Research objectives

The objectives are: (1) To explore the associations between functional *HTR3* polymorphisms and psychosomatic burden within an IBS population; (2) To investigate the impact of the *HTR3* SNP score on psychosomatic burden, based on our hypothesis that the observed number of minor alleles was associated with specific mental characteristics in IBS patients; and (3) To perform a functional analysis of variant 5-HT$_3$AC receptors.

Research methods

In this retrospective study, 623 participants with IBS were recruited from five specialty centers in Germany, Sweden, the United States, the United Kingdom, and Ireland. Depressive, anxiety, and somatization symptoms and sociodemographic characteristics were collected. Four functional SNPs — *HTR3A* c.-42C>T, *HTR3B* c.386A>C, *HTR3C* c.489C>A, and *HTR3E* c.*76G>A — were genotyped and analyzed using the dominant and recessive models. We also performed separate analyses for sex and IBS subtypes. SNP scores were calculated as the number of minor alleles of the SNPs above. The impact of *HTR3C* c.489C>A was tested by radioligand-binding and calcium influx assays.

Research results

Bringing together high quality data as well as methodological expertise, our results show that: (1) In the dominant model, *HTR3C c.489C>A* was correlated with depressive and anxiety symptoms in IBS; (2) A higher number of minor alleles (*i.e.*, the higher the SNP score, which was computed by combining the individual SNP status of *HTR3A c.-42C>T, HTR3B c.386A>C, HTR3C c.489C>A*, and *HTR3E c.*76G>A*) was linked to more severe depressive symptoms in IBS; and (3) The potential relevance of the *HTR3C* SNP was corroborated in functional assays showing changes in the expression level of 5-HT$_3$AC variant receptors.

Research conclusions

Our results provide the first evidence that the accumulation of *HTR3* SNPs (reflected by the SNP score computed by *HTR3A* c.-42C>T, *HTR3B* c.386A>C, *HTR3C* c.489C>A, and *HTR3E* c.*76G>A) may play a role in the pathophysiology of depressive and anxiety symptoms in IBS.

Research perspectives

We are confident that these results are of interest to your readership, as they contribute substantially to update current knowledge regarding the role of accumulation of *HTR3* SNPs in depressive and anxiety symptoms in IBS patients. In turn, our data will contribute towards standardization and harmonization of genetic research strategies in IBS.

ACKNOWLEDGEMENTS

We would like to thank all patients for their participation in this study and the supporting staff at each site. We acknowledge the kind support of Bartram CR and Hinderhofer K. We would also thank Startt B for proofreading and Bacon C for editing the manuscript. This manuscript results in part from collaboration and network activities promoted under the frame of the international network GENIEUR (Genes in Irritable Bowel Syndrome Research Network Europe), which has been funded by the COST program (BM1106, www.GENIEUR.eu) and is currently supported by the European Society of Neurogastroenterology and Motility (ESNM, www.ESNM.eu).

FOOTNOTES

Author contributions: Mönnikes H, Keller J, Walstab J and Wahl V performed the experiments; Dong Y, Berens S, Schaefert R, Clevers E and Walstab J carried out data analyses; Berens S, Engel F, Gauss A, Herzog W, Spiller R, Clarke G, Dinan TG, Quigley EM, Sayuk G, Simrén M, Tesarz J, Sayuk G and IBS-Net Germany characterized and enrolled the patients; Dong Y, Berens S, and Schaefert R drafted the manuscript; all authors contributed to discussing and editing of the manuscript; Niesler B, Schaefert R and van Oudenhove L designed and supervised the study and revised and finalized the manuscript; Berens S and Dong Y equally contributed to the paper; Schaefert R and Niesler B shared last authorship.

Institutional review board statement: The study was reviewed and approved by the Ethical Committee, Medical Faculty of the Heidelberg University Hospital (approval No. S067/2010).

Informed consent statement: All study participants, or their legal guardian, provided informed written consent prior to study enrollment.

Conflict-of-interest statement: APC Microbiome Ireland has conducted studies in collaboration with several

companies, including GSK, Pfizer, Cremo, Suntory, Wyeth, Mead Johnson, Nutricia, 4D Pharma, and DuPont. Dinan TG has been an invited speaker at meetings organized by Servier, Lundbeck, Janssen, and AstraZeneca and has received research funding from Mead Johnson, Cremo, Suntory Wellness, Nutricia, and 4D Pharma. Clarke G has been an invited speaker at meetings organized by Janssen and is receipt of research funding from Pharmavite. The authors are not aware of any affiliations, memberships, funding, or financial holdings that might be perceived as affecting the objectivity of this report.

Data sharing statement: No additional data are available.

Open-Access: This article is an open-access article that was selected by an in-house editor and fully peer-reviewed by external reviewers. It is distributed in accordance with the Creative Commons Attribution NonCommercial (CC BY-NC 4.0) license, which permits others to distribute, remix, adapt, build upon this work non-commercially, and license their derivative works on different terms, provided the original work is properly cited and the use is non-commercial. See: https://creativecommons.org/Licenses/by-nc/4.0/

Country/Territory of origin: Germany

ORCID number: Sabrina Berens 0000-0001-8585-5304; Yuanjun Dong 0000-0002-7817-767X; Nikola Fritz 0000-0003-2662-4340; Jutta Walstab 0000-0001-9546-2205; Mauro D'Amato 0000-0003-2743-5197; Tenghao Zheng 0000-0003-1587-7481; Verena Wahl 0000-0001-9887-5873; Felix Boekstegers 0000-0002-0587-7624; Justo Lorenzo Bermejo 0000-0002-6568-5333; Cristina Martinez 0000-0002-9368-1356; Stefanie Schmitteckert 0000-0001-9555-2614; Egbert Clevers 0000-0003-1931-4926; Felicitas Engel 0000-0002-9300-5681; Annika Gauss 0000-0001-8661-449X; Wolfgang Herzog 0000-0003-2778-4135; Robin Spiller 0000-0001-6371-4500; Miriam Goebel-Stengel 0000-0003-0995-3062; Hubert Mönnikes 0000-0002-7447-6373; Viola Andresen 0000-0002-3695-3327; Frieling Thomas 0000-0001-8270-1975; Jutta Keller 0000-0002-5884-1115; Christian Pehl 0000-0002-0205-3582; Christoph Stein-Thöringer 0000-0002-8020-6986; Gerard Clarke 0000-0001-9771-3979; Timothy G Dinan 0000-0002-2316-7220; Eamonn M Quigley 0000-0003-4151-7180; Gregory Sayuk 0000-0003-1586-199X; Magnus Simrén 0000-0002-1155-1313; Jonas Tesarz 0000-0003-3268-7778; Gudrun Rappold 0000-0002-3126-1508; Lukas van Oudenhove 0000-0002-6540-3113; Rainer Schaefert 0000-0002-3077-7289; Beate Niesler 0000-0001-7881-6112.

S-Editor: Gao CC
L-Editor: A
P-Editor: Gao CC

REFERENCES

1 **Layer P**, Andresen V, Pehl C, Allescher H, Bischoff SC, Classen M, Enck P, Frieling T, Haag S, Holtmann G, Karaus M, Kathemann S, Keller J, Kuhlbusch-Zicklam R, Kruis W, Langhorst J, Matthes H, Mönnikes H, Müller-Lissner S, Musial F, Otto B, Rosenberger C, Schemann M, van der Voort I, Dathe K, Preiss JC; Deutschen Gesellschaft für Verdauungs- und Stoffwechselkrankheiten; Deutschen Gesellschaft für Neurogastroenterologie und Motilität. [Irritable bowel syndrome: German consensus guidelines on definition, pathophysiology and management]. *Z Gastroenterol* 2011; **49**: 237-293 [PMID: 21287438 DOI: 10.1055/s-0029-1245976]

2 **Dong Y**, Baumeister D, Berens S, Eich W, Tesarz J. Stressful Life Events Moderate the Relationship Between Changes in Symptom Severity and Health-related Quality of Life in Patients With Irritable Bowel Syndrome. *J Clin Gastroenterol* 2020; **54**: 445-451 [PMID: 31503051 DOI: 10.1097/MCG.0000000000001261]

3 **Palsson OS**, Whitehead W, Törnblom H, Sperber AD, Simren M. Prevalence of Rome IV Functional Bowel Disorders Among Adults in the United States, Canada, and the United Kingdom. *Gastroenterology* 2020; **158**: 1262-1273.e3 [PMID: 31917991 DOI: 10.1053/j.gastro.2019.12.021]

4 **Black CJ**, Yiannakou Y, Houghton LA, Ford AC. Epidemiological, Clinical, and Psychological Characteristics of Individuals with Self-reported Irritable Bowel Syndrome Based on the Rome IV *vs* Rome III Criteria. *Clin Gastroenterol Hepatol* 2020; **18**: 392-398.e2 [PMID: 31154027 DOI: 10.1016/j.cgh.2019.05.037]

5 **Mearin F**, Lacy BE, Chang L, Chey WD, Lembo AJ, Simren M, Spiller R. Bowel Disorders. *Gastroenterology* 2016 [PMID: 27144627 DOI: 10.1053/j.gastro.2016.02.031]

6 **Stasi C**, Caserta A, Nisita C, Cortopassi S, Fani B, Salvadori S, Pancetti A, Bertani L, Gambaccini D, de Bortoli N, Dell'Osso L, Blandizzi C, Marchi S, Bellini M. The complex interplay between gastrointestinal and psychiatric symptoms in irritable bowel syndrome: A longitudinal assessment. *J Gastroenterol Hepatol* 2019; **34**: 713-719 [PMID: 29971822 DOI: 10.1111/jgh.14375]

7 **Melchior C**, Desprez C, Riachi G, Leroi AM, Déchelotte P, Achamrah N, Ducrotté P, Tavolacci MP, Gourcerol G. Anxiety and Depression Profile Is Associated With Eating Disorders in Patients With Irritable Bowel Syndrome. *Front Psychiatry* 2019; **10**: 928 [PMID: 31969841 DOI: 10.3389/fpsyt.2019.00928]

8 **Weinberg DS**, Smalley W, Heidelbaugh JJ, Sultan S; Amercian Gastroenterological Association. American Gastroenterological Association Institute Guideline on the pharmacological management of irritable bowel syndrome. *Gastroenterology* 2014; **147**: 1146-1148 [PMID: 25224526 DOI: 10.1053/j.gastro.2014.09.001]

9 **Simpson CA**, Mu A, Haslam N, Schwartz OS, Simmons JG. Feeling down? *J Affect Disord* 2020; **266**: 429-446 [PMID: 32056910 DOI: 10.1016/j.jad.2020.01.124]

10 **Gros DF**, Antony MM, McCabe RE, Swinson RP. Frequency and severity of the symptoms of irritable bowel syndrome

across the anxiety disorders and depression. *J Anxiety Disord* 2009; **23**: 290-296 [PMID: 18819774 DOI: 10.1016/j.janxdis.2008.08.004]

11 **Black CJ**, Yiannakou Y, Houghton LA, Shuweihdi F, West R, Guthrie E, Ford AC. Anxiety-related factors associated with symptom severity in irritable bowel syndrome. *Neurogastroenterol Motil* 2020; **32**: e13872 [PMID: 32396247 DOI: 10.1111/nmo.13872]

12 **Gazouli M**, Wouters MM, Kapur-Pojskić L, Bengtson MB, Friedman E, Nikčević G, Demetriou CA, Mulak A, Santos J, Niesler B. Lessons learned--resolving the enigma of genetic factors in IBS. *Nat Rev Gastroenterol Hepatol* 2016; **13**: 77-87 [PMID: 26726033 DOI: 10.1038/nrgastro.2015.206]

13 **Zhang WX**, Zhang Y, Qin G, Li KM, Wei W, Li SY, Yao SK. Altered profiles of fecal metabolites correlate with visceral hypersensitivity and may contribute to symptom severity of diarrhea-predominant irritable bowel syndrome. *World J Gastroenterol* 2019; **25**: 6416-6429 [PMID: 31798278 DOI: 10.3748/wjg.v25.i43.6416]

14 **Hausteiner-Wiehle C**, Henningsen P. Irritable bowel syndrome: relations with functional, mental, and somatoform disorders. *World J Gastroenterol* 2014; **20**: 6024-6030 [PMID: 24876725 DOI: 10.3748/wjg.v20.i20.6024]

15 **Enck P**, Aziz Q, Barbara G, Farmer AD, Fukudo S, Mayer EA, Niesler B, Quigley EM, Rajilić-Stojanović M, Schemann M, Schwille-Kiuntke J, Simren M, Zipfel S, Spiller RC. Irritable bowel syndrome. *Nat Rev Dis Primers* 2016; **2**: 16014 [PMID: 27159638 DOI: 10.1038/nrdp.2016.14]

16 **Whitaker-Azmitia PM**. Serotonin and brain development: role in human developmental diseases. *Brain Res Bull* 2001; **56**: 479-485 [PMID: 11750793 DOI: 10.1016/s0361-9230(01)00615-3]

17 **Painsipp E**, Shahbazian A, Holzer P. Alosetron, cilansetron and tegaserod modify mesenteric but not colonic blood flow in rats. *Br J Pharmacol* 2009; **158**: 1210-1226 [PMID: 19785647 DOI: 10.1111/j.1476-5381.2009.00392.x]

18 **Trump D**. Commentary on: "Ipilimumab *vs* placebo after radiotherapy in patients with metastatic castration-resistant prostate cancer that had progressed after docetaxel chemotherapy (CA184-043): A multicentre, randomised, double-blind, phase 3 trial." Kwon ED, Drake CG, Scher HI, Fizazi K, Bossi A, van den Eertwegh AJ, Krainer M, Houede N, Santos R, Mahammedi H, Ng S, Maio M, Franke FA, Sundar S, Agarwal N, Bergman AM, Ciuleanu TE, Korbenfeld E, Sengeløv L, Hansen S, Logothetis C, Beer TM, McHenry MB, Gagnier P, Liu D, Gerritsen WR, CA184-043 Investigators. Departments of Urology and Immunology and Mayo Clinic Comprehensive Cancer Center, Mayo Clinic, Rochester, MN, USA, Electronic address: kwon.eugene@mayo.edu; Johns Hopkins Sidney Kimmel Comprehensive Cancer Center and Brady Urological Institute, Baltimore, MD, USA; Memorial Sloan Kettering Cancer Center and Weill Cornell Medical College, New York, NY, USA; Institut Gustave Roussy, University of Paris-Sud, Villejuif, France; Institut Gustave Roussy, Villejuif, France; VU University Medical Centre, Amsterdam, Netherlands; Vienna General Hospital, Medical University Vienna, Vienna, Austria; Institut Bergonié, Bordeaux, France; CHU Caremeau, Nimes, France; Centro Médico Austral, Buenos Aires, Argentina; Centre Jean Perrin, Clermont-Ferrand, France; St John of God Hospital, Subiaco, WA, Australia; University Hospital of Siena, Istituto Toscano Tumori, Siena, Italy; Hospital de Caridade de Ijuí, Ijuí, Brazil; Nottingham University Hospital, Nottingham, UK; Huntsman Cancer Institute, University of Utah, Salt Lake City, UT, USA; Netherlands Cancer Institute and Antoni van Leeuwenhoek Hospital, Amsterdam, Netherlands; Institute of Oncology Ion Chiricuta and University of Medicine and Pharmacy Iuliu Hatieganu, Cluj-Napoca, Romania; Hospital Británico de Buenos Aires, Buenos Aires, Argentina; Herlev Hospital, Herlev, Denmark; Odense University Hospital, Odense, Denmark; University of Texas MD Anderson Cancer Center, Houston,. *Urol Oncol* 2016; **34**: 249-250 [PMID: 25907621 DOI: 10.1016/j.urolonc.2015.03.013]

19 **Walstab J**, Rappold G, Niesler B. 5-HT(3) receptors: role in disease and target of drugs. *Pharmacol Ther* 2010; **128**: 146-169 [PMID: 20621123 DOI: 10.1016/j.pharmthera.2010.07.001]

20 **Fukudo S**, Ida M, Akiho H, Nakashima Y, Matsueda K. Effect of ramosetron on stool consistency in male patients with irritable bowel syndrome with diarrhea. *Clin Gastroenterol Hepatol* 2014; **12**: 953-9.e4 [PMID: 24315882 DOI: 10.1016/j.cgh.2013.11.024]

21 **Garsed K**, Chernova J, Hastings M, Lam C, Marciani L, Singh G, Henry A, Hall I, Whorwell P, Spiller R. A randomised trial of ondansetron for the treatment of irritable bowel syndrome with diarrhoea. *Gut* 2014; **63**: 1617-1625 [PMID: 24334242 DOI: 10.1136/gutjnl-2013-305989]

22 **Spiller RC**. Targeting the 5-HT(3) receptor in the treatment of irritable bowel syndrome. *Curr Opin Pharmacol* 2011; **11**: 68-74 [PMID: 21398180 DOI: 10.1016/j.coph.2011.02.005]

23 **Grzesiak M**, Beszłej JA, Waszczuk E, Szechiński M, Szewczuk-Bogusławska M, Frydecka D, Dobosz T, Jonkisz A, Lebioda A, Małodobra M, Mulak A. Serotonin-Related Gene Variants in Patients with Irritable Bowel Syndrome and Depressive or Anxiety Disorders. *Gastroenterol Res Pract* 2017; **2017**: 4290430 [PMID: 28951738 DOI: 10.1155/2017/4290430]

24 **Niesler B**, Walstab J, Combrink S, Möller D, Kapeller J, Rietdorf J, Bönisch H, Göthert M, Rappold G, Brüss M. Characterization of the novel human serotonin receptor subunits 5-HT3C,5-HT3D, and 5-HT3E. *Mol Pharmacol* 2007; **72**: 8-17 [PMID: 17392525 DOI: 10.1124/mol.106.032144]

25 **Celli J**, Rappold G, Niesler B. The Human Serotonin Type 3 Receptor Gene (HTR3A-E) Allelic Variant Database. *Hum Mutat* 2017; **38**: 137-147 [PMID: 27763704 DOI: 10.1002/humu.23136]

26 **Guan T**, Li T, Cai W, Huang D, Ouyang P, Wang Y, Chen H, Wu K, Ma X. HTR3A and HTR3E gene polymorphisms and diarrhea predominant irritable bowel syndrome risk: evidence from a meta-analysis. *Oncotarget* 2017; **8**: 100459-100468 [PMID: 29245992 DOI: 10.18632/oncotarget.19682]

27 **Melke J**, Westberg L, Nilsson S, Landen M, Soderstrom H, Baghaei F, Rosmond R, Holm G, Björntorp P, Nilsson LG, Adolfsson R, Eriksson E. A polymorphism in the serotonin receptor 3A (HTR3A) gene and its association with harm avoidance in women. *Arch Gen Psychiatry* 2003; **60**: 1017-1023 [PMID: 14557147 DOI: 10.1001/archpsyc.60.10.1017]

28 **Niesler B**, Weiss B, Fischer C, Nöthen MM, Propping P, Bondy B, Rietschel M, Maier W, Albus M, Franzek E, Rappold GA. Serotonin receptor gene HTR3A variants in schizophrenic and bipolar affective patients. *Pharmacogenetics* 2001; **11**: 21-27 [PMID: 11207027 DOI: 10.1097/00008571-200102000-00003]

29 **Kilpatrick LA**, Labus JS, Coveleskie K, Hammer C, Rappold G, Tillisch K, Bueller JA, Suyenobu B, Jarcho JM, McRoberts JA, Niesler B, Mayer EA. The HTR3A polymorphism c. -42C>T is associated with amygdala responsiveness in

patients with irritable bowel syndrome. *Gastroenterology* 2011; **140**: 1943-1951 [PMID: 21420406 DOI: 10.1053/j.gastro.2011.03.011]

30 **Yamada K**, Hattori E, Iwayama Y, Ohnishi T, Ohba H, Toyota T, Takao H, Minabe Y, Nakatani N, Higuchi T, Detera-Wadleigh SD, Yoshikawa T. Distinguishable haplotype blocks in the HTR3A and HTR3B region in the Japanese reveal evidence of association of HTR3B with female major depression. *Biol Psychiatry* 2006; **60**: 192-201 [PMID: 16487942 DOI: 10.1016/j.biopsych.2005.11.008]

31 **Berens S**, Kraus F, Gauss A, Tesarz J, Herzog W, Niesler B, Stroe-Kunold E, Schaefert R. A Specialty Clinic for Functional Gastrointestinal Disorders in Tertiary Care: Concept and Patient Population. *Clin Gastroenterol Hepatol* 2017; **15**: 1127-1129 [PMID: 28300691 DOI: 10.1016/j.cgh.2017.02.039]

32 **Kapeller J**, Houghton LA, Mönnikes H, Walstab J, Möller D, Bönisch H, Burwinkel B, Autschbach F, Funke B, Lasitschka F, Gassler N, Fischer C, Whorwell PJ, Atkinson W, Fell C, Büchner KJ, Schmidtmann M, van der Voort I, Wisser AS, Berg T, Rappold G, Niesler B. First evidence for an association of a functional variant in the microRNA-510 target site of the serotonin receptor-type 3E gene with diarrhea predominant irritable bowel syndrome. *Hum Mol Genet* 2008; **17**: 2967-2977 [PMID: 18614545 DOI: 10.1093/hmg/ddn195]

33 **Boeckxstaens GE**, Drug V, Dumitrascu D, Farmer AD, Hammer J, Hausken T, Niesler B, Pohl D, Pojskic L, Polster A, Simren M, Goebel-Stengel M, Van Oudenhove L, Vassallo M, Wensaas KA, Aziz Q, Houghton LA; COST Action BM1106 GENIEUR members. Phenotyping of subjects for large scale studies on patients with IBS. *Neurogastroenterol Motil* 2016; **28**: 1134-1147 [PMID: 27319981 DOI: 10.1111/nmo.12886]

34 **Dong Y**, Baumeister D, Berens S, Eich W, Tesarz J. High Rates of Non-Response Across Treatment Attempts in Chronic Irritable Bowel Syndrome: Results From a Follow-Up Study in Tertiary Care. *Front Psychiatry* 2019; **10**: 714 [PMID: 31681031 DOI: 10.3389/fpsyt.2019.00714]

35 **Drossman DA**. The functional gastrointestinal disorders and the Rome III process. *Gastroenterology* 2006; **130**: 1377-1390 [PMID: 16678553 DOI: 10.1053/j.gastro.2006.03.008]

36 **Kroenke K**, Spitzer RL. The PHQ-9: A new depression diagnostic and severity measure. *Psychiatr Ann* 2002; **32**: 509-515 [DOI: 10.3928/0048-5713-20020901-06]

37 **Berens S**, Schaefert R, Baumeister D, Gauss A, Eich W, Tesarz J. Does symptom activity explain psychological differences in patients with irritable bowel syndrome and inflammatory bowel disease? *J Psychosom Res* 2019; **126**: 109836 [PMID: 31627144 DOI: 10.1016/j.jpsychores.2019.109836]

38 **Montazeri A**, Vahdaninia M, Ebrahimi M, Jarvandi S. The Hospital Anxiety and Depression Scale (HADS): translation and validation study of the Iranian version. *Health Qual Life Outcomes* 2003; **1**: 14 [PMID: 12816545 DOI: 10.1186/1477-7525-1-14]

39 **Wong KM**, Mak ADP, Yuen SY, Leung ONW, Ma DY, Chan Y, Cheong PK, Lui R, Wong SH, Wu JC. Nature and specificity of altered cognitive functioning in IBS. *Neurogastroenterol Motil* 2019; **31**: e13696 [PMID: 31389109 DOI: 10.1111/nmo.13696]

40 **Spitzer RL**, Kroenke K, Williams JB, Löwe B. A brief measure for assessing generalized anxiety disorder: the GAD-7. *Arch Intern Med* 2006; **166**: 1092-1097 [PMID: 16717171 DOI: 10.1001/archinte.166.10.1092]

41 **Julian LJ**. Measures of anxiety: State-Trait Anxiety Inventory (STAI), Beck Anxiety Inventory (BAI), and Hospital Anxiety and Depression Scale-Anxiety (HADS-A). *Arthritis Care Res (Hoboken)* 2011; **63** Suppl 11: S467-S472 [PMID: 22588767 DOI: 10.1002/acr.20561]

42 **Kroenke K**, Spitzer RL, Williams JB. The PHQ-15: validity of a new measure for evaluating the severity of somatic symptoms. *Psychosom Med* 2002; **64**: 258-266 [PMID: 11914441 DOI: 10.1097/00006842-200203000-00008]

43 **Shi YY**, He L. SHEsis, a powerful software platform for analyses of linkage disequilibrium, haplotype construction, and genetic association at polymorphism loci. *Cell Res* 2005; **15**: 97-98 [PMID: 15740637 DOI: 10.1038/sj.cr.7290272]

44 **Nelson SC**, Romm JM, Doheny KF, Pugh EW, Laurie CC. Imputation-based genomic coverage assessments of current genotyping arrays: Illumina HumanCore, OmniExpress, Multi-Ethnic global array and sub-arrays, Global Screening Array, Omni2. 5M, Omni5M, and Affymetrix UK Biobank. 2017 Preprint. Available from: bioRxiv:150219 [DOI: 10.1101/150219]

45 **Bonfiglio F**, Henström M, Nag A, Hadizadeh F, Zheng T, Cenit MC, Tigchelaar E, Williams F, Reznichenko A, Ek WE, Rivera NV, Homuth G, Aghdassi AA, Kacprowski T, Männikkö M, Karhunen V, Bujanda L, Rafter J, Wijmenga C, Ronkainen J, Hysi P, Zhernakova A, D'Amato M. A GWAS meta-analysis from 5 population-based cohorts implicates ion channel genes in the pathogenesis of irritable bowel syndrome. *Neurogastroenterol Motil* 2018; **30**: e13358 [PMID: 29673008 DOI: 10.1111/nmo.13358]

46 **Marees AT**, de Kluiver H, Stringer S, Vorspan F, Curis E, Marie-Claire C, Derks EM. A tutorial on conducting genome-wide association studies: Quality control and statistical analysis. *Int J Methods Psychiatr Res* 2018; **27**: e1608 [PMID: 29484742 DOI: 10.1002/mpr.1608]

47 **Benjamini Y**, Hochberg Y. Controlling the False Discovery Rate - a Practical and Powerful Approach to Multiple Testing. *J R Stat Soc Series B Stat Methodol* 1995; **57**: 289-300 [DOI: 10.1111/j.2517-6161.1995.tb02031.x]

48 **Zhu L**, Huang D, Shi L, Liang L, Xu T, Chang M, Chen W, Wu D, Zhang F, Fang X. Intestinal symptoms and psychological factors jointly affect quality of life of patients with irritable bowel syndrome with diarrhea. *Health Qual Life Outcomes* 2015; **13**: 49 [PMID: 25925746 DOI: 10.1186/s12955-015-0243-3]

49 **Simrén M**, Ringström G, Björnsson ES, Abrahamsson H. Treatment with hypnotherapy reduces the sensory and motor component of the gastrocolonic response in irritable bowel syndrome. *Psychosom Med* 2004; **66**: 233-238 [PMID: 15039508 DOI: 10.1097/01.psy.0000116964.76529.6e]

50 **Niesler B**, Flohr T, Nöthen MM, Fischer C, Rietschel M, Franzek E, Albus M, Propping P, Rappold GA. Association between the 5' UTR variant C178T of the serotonin receptor gene HTR3A and bipolar affective disorder. *Pharmacogenetics* 2001; **11**: 471-475 [PMID: 11505217 DOI: 10.1097/00008571-200108000-00002]

51 **Iidaka T**, Ozaki N, Matsumoto A, Nogawa J, Kinoshita Y, Suzuki T, Iwata N, Yamamoto Y, Okada T, Sadato N. A variant C178T in the regulatory region of the serotonin receptor gene HTR3A modulates neural activation in the human amygdala. *J Neurosci* 2005; **25**: 6460-6466 [PMID: 16000636 DOI: 10.1523/JNEUROSCI.5261-04.2005]

52 **Gatt JM**, Williams LM, Schofield PR, Dobson-Stone C, Paul RH, Grieve SM, Clark CR, Gordon E, Nemeroff CB. Impact of the HTR3A gene with early life trauma on emotional brain networks and depressed mood. *Depress Anxiety* 2010; **27**: 752-759 [PMID: 20694966 DOI: 10.1002/da.20726]

53 **Gatt JM**, Nemeroff CB, Schofield PR, Paul RH, Clark CR, Gordon E, Williams LM. Early life stress combined with serotonin 3A receptor and brain-derived neurotrophic factor valine 66 to methionine genotypes impacts emotional brain and arousal correlates of risk for depression. *Biol Psychiatry* 2010; **68**: 818-824 [PMID: 20728877 DOI: 10.1016/j.biopsych.2010.06.025]

54 **Hammer C**, Cichon S, Mühleisen TW, Haenisch B, Degenhardt F, Mattheisen M, Breuer R, Witt SH, Strohmaier J, Oruc L, Rivas F, Babadjanova G, Grigoroiu-Serbanescu M, Hauser J, Röth R, Rappold G, Rietschel M, Nöthen MM, Niesler B. Replication of functional serotonin receptor type 3A and B variants in bipolar affective disorder: a European multicenter study. *Transl Psychiatry* 2012; **2**: e103 [PMID: 22832903 DOI: 10.1038/tp.2012.30]

55 **Frank B**, Niesler B, Nöthen MM, Neidt H, Propping P, Bondy B, Rietschel M, Maier W, Albus M, Rappold G. Investigation of the human serotonin receptor gene HTR3B in bipolar affective and schizophrenic patients. *Am J Med Genet B Neuropsychiatr Genet* 2004; **131B**: 1-5 [PMID: 15389765 DOI: 10.1002/ajmg.b.30070]

56 **Horjales-Araujo E**, Demontis D, Lund EK, Finnerup NB, Børglum AD, Jensen TS, Svensson P, Vase L. Polymorphism in serotonin receptor 3B is associated with pain catastrophizing. *PLoS One* 2013; **8**: e78889 [PMID: 24244382 DOI: 10.1371/journal.pone.0078889]

57 **Kapeller J**, Houghton LA, Walstab J, Boenisch H, Rappold G, Niesler B. 1003 A Coding Variant in the Serotonin Receptor 3C Subunit Is Associated with Diarrhea-Predominant Irritable Bowel Syndrome. *Gastroenterology* 2009; **136**: A-155 [DOI: 10.1016/s0016-5085(09)60701-0]

58 **Niesler B**, Frank B, Kapeller J, Rappold GA. Cloning, physical mapping and expression analysis of the human 5-HT3 serotonin receptor-like genes HTR3C, HTR3D and HTR3E. *Gene* 2003; **310**: 101-111 [PMID: 12801637 DOI: 10.1016/s0378-1119(03)00503-1]

59 **Karnovsky AM**, Gotow LF, McKinley DD, Piechan JL, Ruble CL, Mills CJ, Schellin KA, Slightom JL, Fitzgerald LR, Benjamin CW, Roberds SL. A cluster of novel serotonin receptor 3-like genes on human chromosome 3. *Gene* 2003; **319**: 137-148 [PMID: 14597179 DOI: 10.1016/s0378-1119(03)00803-5]

60 **Maxwell SE**, Delaney HD. Measurement and Statistics - an Examination of Construct-Validity. *Psychol Bull* 1985; **97**: 85-93 [DOI: 10.1037/0033-2909.97.1.85]

61 **Mayer EA**, Labus JS, Tillisch K, Cole SW, Baldi P. Towards a systems view of IBS. *Nat Rev Gastroenterol Hepatol* 2015; **12**: 592-605 [PMID: 26303675 DOI: 10.1038/nrgastro.2015.121]

62 **Yaakob NS**, Nguyen DT, Exintaris B, Irving HR. The C and E subunits of the serotonin 5-HT$_3$ receptor subtly modulate electrical properties of the receptor. *Biomed Pharmacother* 2018; **97**: 1701-1709 [PMID: 29793334 DOI: 10.1016/j.biopha.2017.12.010]

63 **Katsnelson A**. Diagnostics: Filling in the missing pieces. *Nature* 2016; **533**: S110-S111 [PMID: 27191489 DOI: 10.1038/533S110a]

World Journal of Gastroenterology

Submit a Manuscript: https://www.f6publishing.com

World J Gastroenterol 2022 June 7; 28(21): 2350-2360

DOI: 10.3748/wjg.v28.i21.2350

ISSN 1007-9327 (print) ISSN 2219-2840 (online)

ORIGINAL ARTICLE

Retrospective Study

Differentiating malignant and benign focal liver lesions in children using CEUS LI-RADS combined with serum alpha-fetoprotein

Zhen-Peng Jiang, Ke-Yu Zeng, Jia-Yan Huang, Jie Yang, Rui Yang, Jia-Wu Li, Ting-Ting Qiu, Yan Luo, Qiang Lu

Specialty type: Radiology, nuclear medicine and medical imaging

Provenance and peer review: Unsolicited article; Externally peer reviewed.

Peer-review model: Single blind

Peer-review report's scientific quality classification

Grade A (Excellent): A
Grade B (Very good): 0
Grade C (Good): C
Grade D (Fair): 0
Grade E (Poor): 0

P-Reviewer: Bianchi F, Spain; Boscarelli A, Italy

Received: December 10, 2021
Peer-review started: December 10, 2021
First decision: January 27, 2022
Revised: February 8, 2022
Accepted: April 21, 2022
Article in press: April 21, 2022
Published online: June 7, 2022

Zhen-Peng Jiang, Ke-Yu Zeng, Jia-Yan Huang, Jie Yang, Rui Yang, Jia-Wu Li, Ting-Ting Qiu, Yan Luo, Qiang Lu, Department of Medical Ultrasound, West China Hospital of Sichuan University, Chengdu 610041, Sichuan Province, China

Corresponding author: Qiang Lu, MD, Professor, Department of Medical Ultrasound, West China Hospital of Sichuan University, No. 37 Guoxue Xiang, Chengdu 610041, Sichuan Province, China. luqiang@scu.edu.cn

Abstract

BACKGROUND

Contrast-enhanced ultrasound (CEUS) can be used to diagnose focal liver lesions (FLLs) in children. The America College of Radiology developed the CEUS liver imaging reporting and data system (LI-RADS) for standardizing CEUS diagnosis of FLLs in adult patients. Until now, no similar consensus or guidelines have existed for pediatric patients to improve imaging interpretation as adults.

AIM

To evaluate the performance of CEUS LI-RADS combined with alpha-fetoprotein (AFP) in differentiating benign and malignant FLLs in pediatric patients.

METHODS

Between January 2011 and January 2021, patients ≤ 18 years old who underwent CEUS for FLLs were retrospectively evaluated. The following criteria for diagnosing malignancy were proposed: Criterion I considered LR-4, LR-5, or LR-M lesions as malignancies; criterion II regarded LR-4, LR-5 or LR-M lesions with simultaneously elevated AFP (≥ 20 ng/mL) as malignancies; criterion III took LR-4 Lesions with elevated AFP or LR-5 or LR-M lesions as malignancies. The sensitivity, specificity, accuracy and area under the receiver operating characteristic curve (AUC) were calculated to determine the diagnostic value of the aforementioned criteria.

RESULTS

The study included 63 nodules in 60 patients (mean age, 11.0 ± 5.2 years; 26 male). There were no statistically significant differences between the specificity, accuracy, or AUC of criterion II and criterion III (95.1% *vs* 80.5%, 84.1% *vs* 87.3%, and 0.794 *vs* 0.902; all $P > 0.017$). Notably, criterion III showed a higher diagnostic

sensitivity than criterion II (100% *vs* 63.6%; $P < 0.017$). However, both the specificity and accuracy of criterion I was inferior to those of criterion II and criterion III (all $P < 0.017$). For pediatric patients more than 5 years old, the performance of the three criteria was overall similar when patients were subcategorized by age when compared to all patients in aggregate.

CONCLUSION
CEUS LI-RADS combined with AFP may be a powerful diagnostic tool in pediatric patients. LR-4 with elevated AFP, LR-5 or LR-M lesions is highly suggestive of malignant tumors.

Key Words: Pediatric; Contrast-enhanced ultrasound; Liver imaging reporting and data system; Diagnosis; Focal liver lesions; Alpha-fetoprotein

©The Author(s) 2022. Published by Baishideng Publishing Group Inc. All rights reserved.

Core Tip: Contrast-enhanced ultrasound liver imaging reporting and data system (CEUS LI-RADS) is used for the diagnosis of focal liver lesions (FLLs) in adult patients at high risk of hepatocellular carcinoma. CEUS has recently been approved to be used in characterization of FLLs in children. Our study investigated the diagnostic value of CEUS LI-RADS in association with serum alpha-fetoprotein (AFP) in differentiating malignant from benign FLLs in pediatric patients. Our study demonstrated that CEUS LI-RADS combined with AFP may be a powerful diagnostic tool for pediatric patients. LR-4 with elevated AFP, LR-5 or LR-M lesions are highly indicative of malignant tumors.

Citation: Jiang ZP, Zeng KY, Huang JY, Yang J, Yang R, Li JW, Qiu TT, Luo Y, Lu Q. Differentiating malignant and benign focal liver lesions in children using CEUS LI-RADS combined with serum alpha-fetoprotein. *World J Gastroenterol* 2022; 28(21): 2350-2360
URL: https://www.wjgnet.com/1007-9327/full/v28/i21/2350.htm
DOI: https://dx.doi.org/10.3748/wjg.v28.i21.2350

INTRODUCTION

Pediatric patients have different treatment strategies regarding benign and malignant focal liver lesions (FLLs)[1]. Hepatoblastoma (HB) constitutes the most common malignant tumor, accounting for 67% of all pediatric malignant FLLs, followed by hepatocellular carcinoma (HCC), at 28%[2-4]. Thanks to the development of surgical techniques and chemotherapy, the overall 5-year survival rates of HB exceed 80% with timely treatment, and those of nonmetastatic HCC patients who can be treated surgically are 70%-80%[5]. In comparison, the survival rate of children with inoperable hepatic malignancies was less than 20%[6].

Although computed tomography (CT) and magnetic resonance imaging (MRI) are usually recommended for the differential diagnosis of pediatric FLLs[7], both have some limitations. CT increases children's radiation exposure, while MRI requires a long imaging time and high cost[8-10]. Furthermore, children are exposed to the risk of contrast-induced nephrotoxicity and potential use of sedation[11]. Serum alpha-fetoprotein (AFP) is the most widely used tumor biomarker for the screening of HCC and HB in high-risk pediatric populations[12]. However, AFP levels remained in the normal range in 30%-40% of HCC patients and 10% of HB patients. Moreover, the positive predictive value of AFP is poor, making the value of AFP alone as a diagnostic tool very limited[13,14]. Therefore, developing a potent diagnostic method for differentiating benign from malignant FLLs in children is urgently needed.

The American College of Radiology developed the Liver Imaging Reporting and Data System (LI-RADS) to standardize the diagnosis of HCC and assist in the diagnosis of other hepatic malignant tumors[7]. In addition, CEUS can overcome the shortcomings of the aforementioned imaging modalities [15]. Moreover, CEUS has been approved for use in the diagnosis of FLL in the pediatric population [16]. Therefore, this study aimed to evaluate the diagnostic performance of the combination of CEUS LI-RADS and AFP in differentiating benign and malignant FLLs in a pediatric population.

MATERIALS AND METHODS

This retrospective study was approved by the institutional review board of our hospital, and informed consent was waived.

Patient selection

From January 2011 to January 2021, hepatic CEUS examinations performed in a tertiary academic medical center were retrospectively collected.

The inclusion criteria were: (1) Age ≤ 18 years at the time of examination; (2) visible liver nodules at baseline US; and (3) sufficient images of the arterial phase, portal phase, and parenchymal phase.

The exclusion criteria were: (1) Lesions previously treated; (2) known or strongly suspected active extrahepatic primary malignancy; (3) poor image quality; and (4) no accepted reference standard (see more detail in a later section).

Ultrasound examination

Conventional and contrast-enhanced US examinations were performed using a Philips IU22 system (Philips Medical Solutions; Mountain View, CA, United States) with a C5-1 convex or an L9-3 Linear probe. After routine ultrasound examinations, all pediatric patients underwent CEUS examinations using the pulse inversion harmonic imaging technique with a mechanical index less than 0.1. A bolus injection of 1.2 mL of ultrasound contrast agent (SonoVue; Bracco, Milan, Italy) was administered through a vascular catheter needle placed in the anterior cubital vein. The imaging timer was started immediately upon completion of the contrast agent injection. A 5 mL flush of 0.9% sodium chloride solution followed the ultrasound contrast agent injection. The target area was continuously scanned in the first 60 s, followed by intermittent scans and records until the examiner confidently observed washout or faded liver parenchymal enhancement, typically 5 min or longer. CEUS imaging was digitally stored for further evaluation.

Reference standards

Pathological diagnosis from surgical resection or percutaneous biopsy was taken as the reference standard. In addition, lesions without pathological diagnosis were considered benign if their size increased less than 50% at the 12-mo imaging follow-up. Meanwhile, serum AFP ≥ 20 ng/mL was regarded as elevated[13].

Diagnostic criteria for differentiating benign and malignant fills

In a previous study, lesions with categories of LR-1, LR-2 or LR-3 were considered benign, while LR-4, LR-5 or LR-M was defined as malignancy[16]. Moreover, the meta–analysis conducted by Christian *et al* [17], including 17 studies (2760 patients, 3556 lesions), showed that 80% of LR-4, 97% of LR-5, and 93% of LR-M lesions were malignant. Therefore, we proposed the following criteria for the diagnosis of malignancy in the pediatric population: Criterion I considered LR-4, LR-5, or LR-M lesions as malignancies; criterion II regarded LR-4, LR-5 or LR-M lesions with simultaneously elevated AFP (≥ 20 ng/mL) as malignancies; and criterion III took LR-4 lesions with elevated AFP or LR-5 or LR-M lesions as malignancies.

Imaging analysis

Two certified radiologists (Qiu TT and LI JW, with more than 3 years and 5 years of experience in hepatic CEUS, respectively) who were blinded to the reference standard and other clinical data reviewed the CEUS examinations of all cases independently and assigned a category according to the CEUS LI-RADS (2017 version). When there was an inconformity, arbitration from a blinded expert radiologist (Lu Q, with 17 years of experience) was performed. Briefly, the main diagnostic criteria of CEUS LI-RADS are nodule size, enhancement degree and pattern in the arterial phase, timing and degree of washout. Moreover, the ancillary features for category adjustment are nodule-in-nodule architecture and mosaic architecture.

Statistical analysis

Qualitative data are presented as the numbers and percentages. Quantitative data are presented as a combination of the mean values and standard deviations. The comparison of numeric variables was performed using t tests. Differences in categorical variables were analyzed using χ^2 tests or Fisher's exact tests. The unit of analysis is each FLL rather than each patient. The accuracy, sensitivity, specificity, area under the curve (AUC) and 95% confidence intervals (CI) were calculated to evaluate the diagnostic power of CEUS LI-RADS in association with AFP in distinguishing benign and malignant FLLs. The performance of the diagnostic criteria was further assessed by the fourfold table and compared by using the McNemar test. A P value less than 0.05 was considered statistically significant. The P values were corrected for multiple comparisons through the Bonferroni method (Bonferroni-adjusted P values < 0.017). Given that HCC more commonly occurs in children over 5 years old among pediatric patients[18], subgroup analysis was also conducted. Based on the value of κ, the strength of agreement is defined as follows: κ < 0.20 suggests poor agreement, 0.21-0.40 suggests fair agreement, 0.41-0.60 suggests moderate agreement, 0.61-0.80 suggests good agreement, and 0.80-1.00 suggests almost perfect agreement. Statistical analyses were performed using statistical software (MedCalc10.4.7.0; MedCalc Software, Ostend, Belgium).

RESULTS

Patients and liver nodule characteristics

According to the inclusion and exclusion criteria, 63 lesions from 60 patients were enrolled in this study (Figure 1), among which 3 patients had 2 FLLs. The main clinical characteristics of the patients, including age, sex, serum AFP, tumor size, and high-risk factors for HCC, are shown in Table 1. The average size of the 63 lesions was 68 ± 39 mm, ranging from 11 to 163 mm. Males accounted for 43.3% of the included patients, and AFP levels exceeding 20 ng/mL were present in 14 patients. The AFP level of malignant lesions (Figure 2) was higher than that of benign lesions [63.6% (14/22) *vs* 4.9% (2/41), $P < 0.0001$]. In our study, 14 patients had high-risk factors for HCC, including 8 chronic hepatitis B and 6 cirrhosis.

Histopathological results and follow-up results of the lesions are summarized in Table 2. Histopathological results of 52 (82.5%) lesions were obtained by surgical resections or US-guided core needle biopsies. The 11 (17.5%) lesions were regarded as benign through the one-year follow-up.

The distribution of FLLs in CEUS LI-RADS categories and lesions with elevated AFP levels are displayed in Table 3. In this study, 2 benign lesions were classified as LR-M, including one granulomatous inflammation and one abscess. Furthermore, 4 benign lesions in LR-5 included one adenomatoid hyperplasia, one abscess, and 2 focal nodular hyperplasia (FNH). Among the lesions defined as LR-4, there were only two lesions with elevated AFP. Postoperative pathology confirmed them as a regenerative nodule and an infantile hemangioendothelioma (Figure 3). The CEUS characteristics of various FLLs are presented in Table 4.

Interobserver agreement in CEUS LI-RADS classification

The rating of liver nodules according to CEUS LI-RADS of the two readers indicated good agreement, with a κ value of 0.76 (95%CI: 0.62-0.90).

The diagnostic performance of CEUS LI-RADS combined with AFP

Table 5 summarizes the diagnostic performances of different diagnostic criteria in differentiating benign and malignant FLLs in children. Table 6 shows a comparison of different criteria on indicators of diagnostic performance. Notably, there was no statistically significant difference between the specificity, accuracy, or AUC of criterion II and criterion III (95.1% *vs* 80.5%, 84.1% *vs* 87.3%, and 0.794 *vs* 0.902; all $P > 0.017$). Notably, criterion III showed a higher diagnostic sensitivity than criterion II (100% *vs* 63.6%; $P < 0.017$). However, both the specificity and accuracy of criterion I was inferior to those of criterion II and criterion III (all P values < 0.017).

Diagnostic performance of CEUS LI-RADS combined with AFP in pediatric patients > 5 years of age

In total, 53 FLLs were included in this subgroup analysis. The diagnostic performance of CEUS LI-RADS in association with AFP for predicting overall hepatic malignancy and HCC among patients older than 5 years is shown in Supplementary Table 1. Moreover, a comparison of indicators for diagnostic power among the three criteria is shown in Supplementary Table 2. The performance of the three criteria was similar overall when patients were subcategorized by age when compared to all patients in aggregate. In short, there was no statistically significant difference between the specificity, accuracy, or AUC of criterion II and criterion III (97.2% *vs* 86.1%, 83.3% *vs* 87.0%, and 0.780 *vs* 0.931; all $P > 0.017$). Notably, criterion III showed a higher diagnostic sensitivity than criterion II (100% *vs*58.8%; $P < 0.017$). However, both the specificity and accuracy of criterion I was inferior to those of criterion II and criterion III (all $P < 0.017$). Interestingly, if LR-5 lesions with elevated AFP were regarded as HCC in this subgroup, the sensitivity, specificity, accuracy, and AUC of diagnosing HCC were 80.0% (95%CI: 44.4%-97.5%), 95.4% (95%CI: 84.2%-99.4%), 94.4% (95%CI: 84.6%-98.8%) and 0.877 (95%CI: 0.757-0.951), respectively.

DISCUSSION

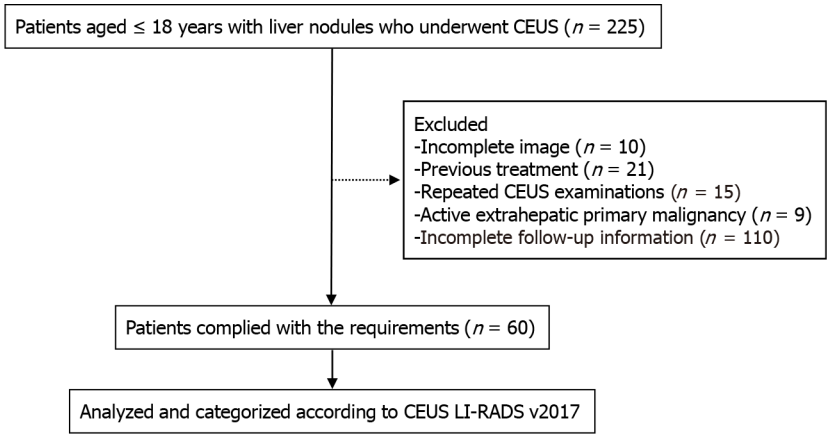
Proper differentiation between benign and malignant FLLs is essential in the treatment of pediatric liver disease. We found that CEUS LI-RADS in association with AFP presented an effective way to differentiate benign tumors from malignancies in pediatric patients. The sensitivity and specificity of criterion III (LR-4 with elevated AFP or LR-5 or LR-M lesions) reached 100.0% and 80.5%, respectively.

The specificity (29.3%) of diagnostic criterion I (LR-4, LR-5, or LR-M lesions) was significantly reduced compared to criteria II and III. This may be because there were a considerable number of benign lesions in LR-4. Notably, differentiation between benign and malignant FLLs in pediatric patients by CEUS LI-RADS alone had an accuracy of 54.0% and specificity of 29.3%, suggesting that CEUS LI-RADS alone is not suitable for this scenario. CEUS LI-RADS was mainly used as a diagnostic tool for HCC in adults at high risk. This study explored the possibility of expanding the application of this diagnostic algorithm in pediatric patients. However, only a few pediatric patients have high-risk

Table 1 The clinical characteristics of enrolled 60 patients

Characteristics	All Patients (*n* = 60)	Patients with malignant lesions (*n* = 20)	Patients with benign lesions (*n* = 40)	*P* value[2]
Age, yr; mean ± SD, (range)	11.0 ± 5.2 (0-18)	9.7 ± 5.4 (0-18)	11.7 ± 5.1 (0-18)	0.98
Gender, *n* (%)				0.54
Male	26 (43.3)	10 (50.0)	16 (40.0)	
Female	34 (56.7)	10 (50.0)	24 (60.0)	
AFP level (ng/mL), *n* (%)				< 0.05
AFP > 20	14 (23.3)	12 (60.0)	2 (5.0)	
AFP < 20	46 (76.7)	8 (40.0)	38 (95.0)	
High-risk factors[1]				0.24
High risk for HCC[1]	14 (23.3)	7 (35.0)	7 (17.5)	
No high risk for HCC[1]	46 (76.7)	13 (75.0)	33 (82.5)	

[1]High risk for hepatocellular carcinoma (HCC) in focal liver lesions in contrast-enhanced ultrasound liver imaging reporting and data system included cirrhosis, chronic hepatitis B viral infection, and current or prior HCC.
[2]*P* values showed whether there were significant differences in age, gender, alpha-fetoprotein level or high-risk factors between the benign and malignant groups.
Note-data are numbers of patients with percentages in parentheses. AFP: Alpha-fetoprotein; HCC: Hepatocellular carcinoma.



DOI: 10.3748/wjg.v28.i21.2350 **Copyright** ©The Author(s) 2022.

Figure 1 Flow diagram for the study population. CEUS: Contrast-enhanced ultrasound; LI-RADS: Liver imaging reporting and data system.

factors for HCC, and the disease spectrum of FLLs between adults and children is different. HB and HCC account for a majority of pediatric hepatic malignancies, while hemangioma and FNH account for a majority of pediatric hepatic benign lesions. Because a significant difference in AFP was found between benign and malignant FLLs[19], CEUS LI-RADS combined with serum AFP is proposed for better characterization of FLLs in pediatric patients.

Compared with criterion III, the sensitivity (63.6%) of criterion II decreased significantly. A possible explanation was that 2 HCC patients and 6 patients with other hepatic malignancies presented normal serum AFP values (< 20 ng/mL), resulting in false negatives of the aforementioned lesions according to criterion II.

In this study, 13 FNHs were assigned to LR-4, and 2 FNHs were assigned to LR-5. A retrospective study by Kong *et al*[20] found that 42.9% of FNHs displayed global homogeneous hyperenhancement, and 42.9% of FNHs showed centrifugal enhancement in the arterial phase. Centrifugal arterial enhancement was often present in FNH < 3 cm. This is probably because the blood supply of larger lesions is more abundant[21]. Moreover, atypical FNHs could demonstrate washout in the portal and late phases[22]. Due to the above reasons, FNHs could be classified as LR-4 or LR-5 Lesions. However, AFP in patients with FNH is generally within the normal range[23]. Therefore, the combination of CEUS LI-RADS and AFP may potentially avoid diagnosing FNH as a malignancy.

Table 2 Number of included fills with each diagnosis, stratified by reference standard

Diagnosis	All fills (*n* = 63)	FIls from Patients > 5 yr (*n* = 53)
Pathologic analysis	2	42
Malignant liver lesions	22	17
HCC	10	10
HB	6	2
Undifferentiated sarcoma	2	1
Non-Hodgkin's lymphoma	1	1
Neuroendocrine carcinoma	1	1
Desmoplastic small round cell tumor	1	1
Perivascular epithelioid cell tumor	1	1
Benign liver lesions	30	25
FNH	14	12
RN/DN	3	3
Area of granulomatous inflammation	3	3
Adenomatoid hyperplasia	3	3
Infantile hemangioendothelioma	2	0
Liver abscess	1	0
Other benign tumors	3	3
Follow-up < 50% size increase in 12 mo	11	11
Hemangioma	3	3
FNH	3	1
RN/DN	2	2
Other benign tumors	3	3

FLLs: Focal liver lesions; HCC: Hepatocellular carcinoma; HB: Hepatoblastoma; FNH: Focal nodular hyperplasia; DN: Dysplastic nodule; RN: Regenerative nodule.

Table 3 All focal liver lesions in contrast-enhanced ultrasound liver imaging reporting and data system categorization and distribution of elevated alpha-fetoprotein

CEUS LI-RADS	No. of nodules (*n* = 63)	No. of malignant lesions (*n* = 22)	No. of benign lesions (*n* = 41)	AFP > 20 ng/mL (*n* = 16)
LR-1	4	0	4	0
LR-2	0	0	0	0
LR-3	8	0	8	0
LR-4	23	0	23	2
LR-5	22	18	4	13
LR-M	6	4	2	1

FLLs: Focal liver lesions; CEUS LI-RADS: Focal liver lesions in contrast-enhanced ultrasound liver imaging reporting and data system; AFP: Alpha-fetoprotein.

We also performed subgroup analysis by the age of 5 to explore whether those patients could use CEUS LI-RADS combined with AFP to identify malignant FLLs or even HCC. For differentiating malignant from benign FLLs, the results of subgroup analysis were similar to the overall analysis. LR-5 in adult patients had a high diagnostic specificity for HCC. In this study, LR-5 Lesions with elevated AFP for diagnosing HCC presented high specificity (95.4%) in pediatric patients over 5 years old.

Table 4 Imaging characteristics of different types of focal liver lesions

Image features	Malignant lesions			Benign lesions		
	HCC (*n* = 10)	HB (*n* = 6)	Other malignant lesions (*n* = 6)	FNH (*n* = 17)	RN/DN (*n* = 5)	Other benign tumors (*n* = 18)
Gray-scale echogenicity						
Hyperechoic	3	4	5	4	2	9
Hypoechoic	7	2	1	13	3	9
Arterial phase, hyperenhancement						
Homogeneous	4	2		9	1	4
Inhomogenous	6	4	5	8		5
Rim			1			2
Peripheral nodular						3
Isoenhancement					2	2
Hypoenhancement					2	2
Late phase						
Hyperenhancement				10		5
Isoenhancement				5	5	8
Hypoenhancement	10	6	6	2		5
Washout						
< 60 s		1	3			1
Marked, ≤ 120 s			1			

Data are numbers of nodules. FLLs: Focal liver lesions; HCC: Hepatocellular carcinoma; HB: Hepatoblastoma; FNH: Focal nodular hyperplasia; DN: Dysplastic nodule; RN: Regenerative nodule.

Table 5 Performance of various diagnostic criteria for differentiating benign and malignant focal liver lesions

Diagnostic criteria	Sensitivity (%)	Specificity (%)	Accuracy (%)	AUC
Criterion I	100.0 (84.6-100.0)	29.3 (16.1-45.5)	54.0 (40.9-66.6)	0.646 (0.516-0.763)
Criterion II	63.6 (40.7-82.8)	95.1 (83.5-99.4)	84.1 (72.7-92.1)	0.794 (0.673-0.885)
Criterion III	100.0 (84.6-100.0)	80.5 (65.1-91.2)	87.3 (76.5-94.4)	0.902 (0.801-0.963)

Criterion I considered LR-4, LR-5, or LR-M lesions as malignancies; criterion II regarded LR-4, LR-5 or LR-M lesions with simultaneously elevated alpha-fetoprotein (AFP, ≥ 20 ng/mL) as malignancies; criterion III took LR-4 lesions with elevated AFP or LR-5 or LR-M lesions as malignancies. AUC: Area under the curve.

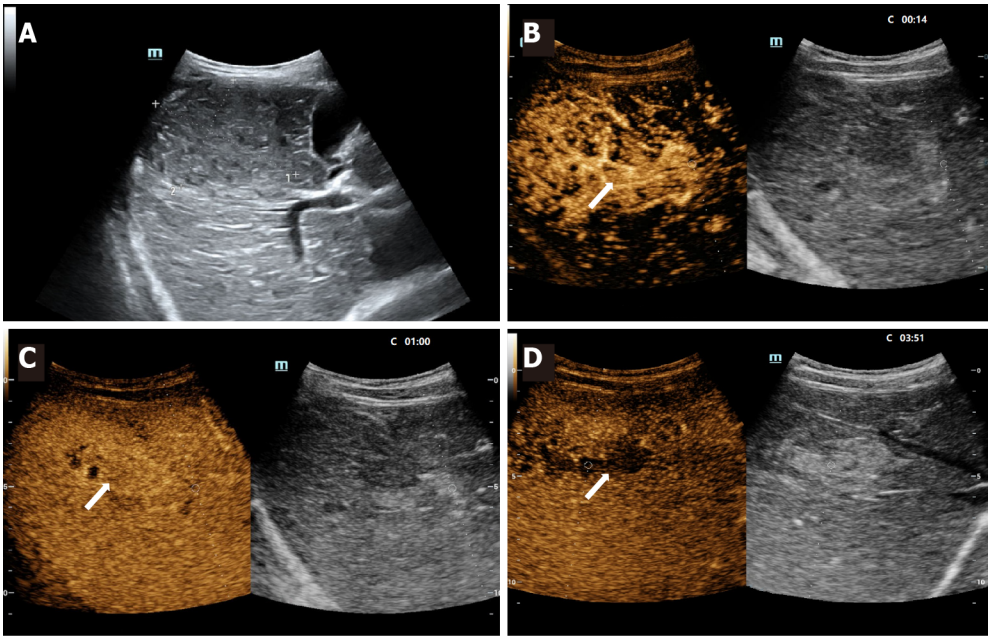
Consequently, we speculate that CEUS LI-RADS combined with AFP has the potential to diagnose HCC in children older than 5 years. Nevertheless, the number (*n* = 10) of pediatric HCC patients included in this study was too small. Further study with a larger sample is needed to validate this hypothesis.

In this study, a 19-hour-old newborn patient with infantile hemangioendothelioma presented a significant increase in AFP levels (AFP > 1210 ng/mL). Regarding the features of CEUS, the patient showed inhomogeneous hyperenhancement in the arterial phase and isoenhancement in the portal and delayed phases, and there were areas of nonenhancement within the lesion. The aforementioned feature indicated that the lesion was likely a benign lesion. However, because the lesion was diagnosed as malignant by contrast-enhanced CT, the patient underwent surgical resection of the hepatic mass. Postoperative pathology confirmed that the lesion was an infantile hemangioendothelioma. Within 60 ± 24 h after birth, the serum AFP of newborns can range from 9700 to 11190 ng/mL and drop rapidly to a level close to the normal level of adults within one year[24]. Therefore, we should be meticulous with elevated AFP in differentiating FLLs of newborns. In addition, infantile hemangioendothelioma is a common benign tumor in newborns, most of which do not require surgical treatment[25]. Therefore, the diagnosis of benign and malignant FLLs in newborns should be made with caution, and the diagnostic

Table 6 Comparison of different criteria on indicators of diagnostic performance

P value	Sensitivity	Specificity	Accuracy	AUC
Criterion I *vs* criterion II	< 0.017	< 0.0001	< 0.017	> 0.017
Criterion I *vs* criterion III	-	< 0.0001	< 0.0001	< 0.0001
Criterion II *vs* criterion III	< 0.017	> 0.017	> 0.05	> 0.05

Criterion I considered LR-4, LR-5, or LR-M lesions as malignancies; criterion II regarded LR-4, LR-5 or LR-M lesions with simultaneously elevated alpha-fetoprotein (AFP, ≥ 20 ng/mL) as malignancies; criterion III took LR-4 lesions with elevated AFP or LR-5 or LR-M lesions as malignancies. AUC: Area under the curve.



DOI: 10.3748/wjg.v28.i21.2350 **Copyright** ©The Author(s) 2022.

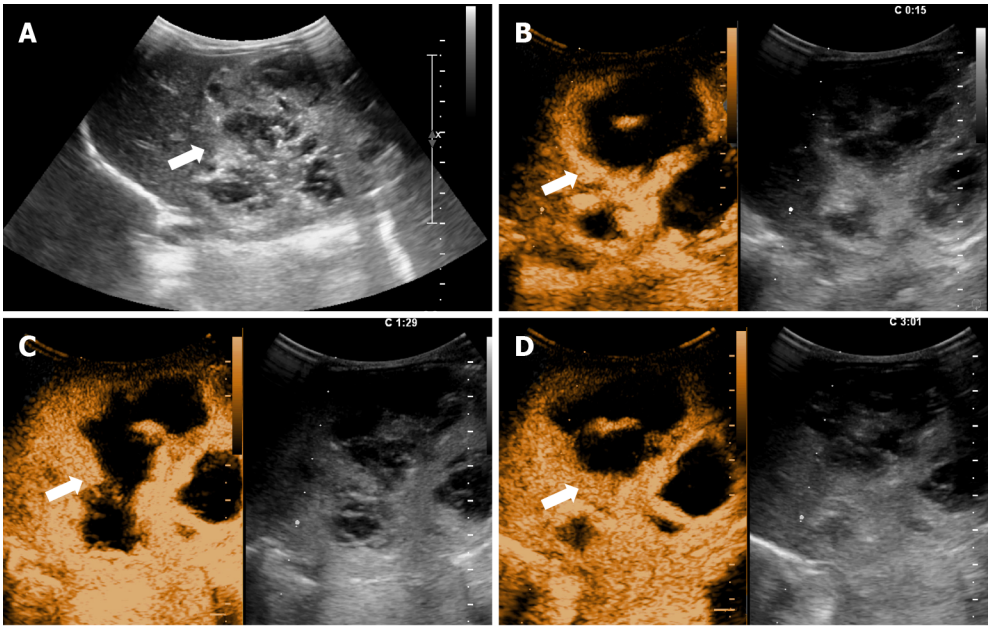
Figure 2 LR-5 nodule in a 10-year-old boy. A: A hypoechoic nodule (arrow) measuring 7.3 cm in the right lobe of the liver was shown at conventional gray-scale US; B: The lesion was inhomogeneously hyperenhanced (arrow) in the arterial phase (14 s) at contrast-enhanced US; C: The lesion was seen iso-enhanced in the portal phase (60 s); D: Mild washout in the late phase (231 s) was shown. There were small areas of nonenhancement within the lesion during the whole process. The patient had a chronic hepatitis B viral infection. The serum AFP level was greater than 1210 ng/mL. This lesion was assigned to LR-5 and was confirmed as hepatocellular carcinoma by histopathologic analysis.

method needs to be further explored.

This study had several limitations. First, this was a retrospective study with a relatively small sample size, which may inevitably lead to selection bias. Second, CEUS LI-RADS was mainly used for patients at risk of HCC, while only 14 patients in this study met the prerequisites for risk factors. Moreover, the risk factors for HCC in children do not exactly correspond to those in adults. Lastly, there were a considerable number of benign lesions confirmed by histopathology results, which might have led to the selection of benign lesions with atypical imaging findings. Thus, the specificity of the diagnostic criteria may have been underestimated.

CONCLUSION

We propose a novel method that might be a powerful diagnostic tool to differentiate malignant from benign FLLs in pediatric patients. LR-4 with elevated AFP, LR-5 or LR-M lesions could effectively differentiate benign and malignant tumors in pediatric patients.



DOI: 10.3748/wjg.v28.i21.2350 **Copyright** ©The Author(s) 2022.

Figure 3 LR-4 nodule in a 19-hour-old newborn. A: An inhomogeneous hyperechoic nodule measuring 7.2-cm (arrow) in the left lobe of the liver was shown at conventional gray-scale US; B: The lesion was inhomogeneously hyperenhanced (arrow) with large area of unenhancement in the arterial phase (15 s) at contrast-enhanced US; C: The enhanced area of the lesion was seen slightly hyperenhanced (arrow) in the portal phase (89 s); D: The enhanced area of the lesion was seen iso-enhanced (arrow) in the late phase (181 s). There were patchy areas of nonenhancement within the lesion during the whole process. The serum AFP level was greater than 1210 ng/mL. Infantile hemangioendothelioma was confirmed at histopathologic analysis.

ARTICLE HIGHLIGHTS

Research background

Contrast-enhanced ultrasound (CEUS) has recently been approved to be used in characterization of focal liver lesions (FLLs) in children. The America College of Radiology developed the CEUS liver imaging reporting and data system (LI-RADS) for standardizing CEUS diagnosis of FLLs in adult patients. However, it is not suitable for pediatric patients.

Research motivation

To explore a method for differentiating benign and malignant FLLs in pediatric patients.

Research objectives

To evaluate the performance of CEUS LI-RADS combined with alpha-fetoprotein (AFP) in differentiating benign and malignant FLLs in pediatric patients.

Research methods

The following criteria for diagnosing malignancy were proposed: Criterion I considered LR-4, LR-5, or LR-M lesions as malignancies; criterion II regarded LR-4, LR-5 or LR-M lesions with simultaneously elevated AFP (≥ 20 ng/mL) as malignancies; criterion III took LR-4 Lesions with elevated AFP or LR-5 or LR-M lesions as malignancies. The sensitivity, specificity, accuracy and area under the receiver operating characteristic curve (AUC) were calculated to determine the diagnostic value of the aforementioned criteria.

Research results

There were no statistically significant differences between the specificity, accuracy, or AUC of criterion II and criterion III. Notably, criterion III showed a higher diagnostic sensitivity than criterion II. However, both the specificity and accuracy of criterion I was inferior to those of criterion II and criterion III. For pediatric patients more than 5 years old, the performance of the three criteria was overall similar when patients were subcategorized by age when compared to all patients in aggregate.

Research conclusions

We propose a novel method that might be a powerful diagnostic tool to differentiate malignant from benign FLLs in pediatric patients. LR-4 with elevated AFP, LR-5 or LR-M lesions could effectively differentiate benign and malignant tumors in pediatric patients.

Research perspectives

CEUS LI-RADS combined with AFP might be a powerful diagnostic tool to differentiate malignant from benign FLLs in pediatric patients.

ACKNOWLEDGEMENTS

We thank all medical staff and technicians who agreed to participate in this study.

FOOTNOTES

Author contributions: Jiang ZP and Lu Q designed the research; Jiang ZP, Li JW, Qiu TT, Luo Y and Lu Q performed the research; Jiang ZP, Zeng KY, Huang JY, Yang J and Yang R collected the data; Jiang ZP and Lu Q drafted the manuscript and review the literatures; Luo Y and Lu Q revised the manuscript; all authors contributed to approval of final version of submitted manuscript and agree to ensure that any questions related to the work are appropriately resolved.

Supported by the National Natural Science Foundation of China, No. 81571697; and the Science and Technology Department of Sichuan Province, No.2017SZ003 and No. 2018FZ0044.

Institutional review board statement: The study was reviewed and approved by the West China Hospital of Sichuan University Institutional Review Board.

Conflict-of-interest statement: There are no conflicts of interest to report.

Data sharing statement: Technical appendix, statistical code, and dataset available from the corresponding author at luqiang@scu.edu.cn.

Open-Access: This article is an open-access article that was selected by an in-house editor and fully peer-reviewed by external reviewers. It is distributed in accordance with the Creative Commons Attribution NonCommercial (CC BY-NC 4.0) license, which permits others to distribute, remix, adapt, build upon this work non-commercially, and license their derivative works on different terms, provided the original work is properly cited and the use is non-commercial. See: https://creativecommons.org/Licenses/by-nc/4.0/

Country/Territory of origin: China

ORCID number: Zhen-Peng Jiang 0000-0002-2812-0536; Ke-Yu Zeng 0000-0002-0836-3186; Jia-Yan Huang 0000-0002-1918-2874; Jie Yang 0000-0002-6819-146X; Rui Yang 0000-0002-7733-0636; Jia-Wu Li 0000-0003-0844-5883; Ting-Ting Qiu 0000-0002-1510-9960; Yan Luo 0000-0003-2985-1768; Qiang Lu 0000-0002-4057-1997.

S-Editor: Chen YL
L-Editor: A
P-Editor: Chen YL

REFERENCES

1 **Kelgeri C**, Renz D, McGuirk S, Schmid I, Sharif K, Baumann U. Liver Tumours in Children: The Hepatologist's View. *J Pediatr Gastroenterol Nutr* 2021; **72**: 487-493 [PMID: 33264187 DOI: 10.1097/MPG.0000000000003006]
2 **Ranganathan S**, Lopez-Terrada D, Alaggio R. Hepatoblastoma and Pediatric Hepatocellular Carcinoma: An Update. *Pediatr Dev Pathol* 2020; **23**: 79-95 [PMID: 31554479 DOI: 10.1177/1093526619875228]
3 **Varol Fİ**. Pediatric Hepatocellular Carcinoma. *J Gastrointest Cancer* 2020; **51**: 1169-1175 [PMID: 32856229 DOI: 10.1007/s12029-020-00494-w]
4 **Chavhan GB**, Siddiqui I, Ingley KM, Gupta AA. Rare malignant liver tumors in children. *Pediatr Radiol* 2019; **49**: 1404-1421 [PMID: 31620842 DOI: 10.1007/s00247-019-04402-8]
5 **Di Giuseppe G**, Youlden DR, Aitken JF, Pole JD. Pediatric hepatic cancer incidence and survival: 30-year trends in Ontario, Canada; the United States; and Australia. *Cancer* 2021; **127**: 769-776 [PMID: 33197043 DOI: 10.1002/cncr.33319]
6 **Angelico R**, Grimaldi C, Saffioti MC, Castellano A, Spada M. Hepatocellular carcinoma in children: hepatic resection and liver transplantation. *Transl Gastroenterol Hepatol* 2018; **3**: 59 [PMID: 30363724 DOI: 10.21037/tgh.2018.09.05]
7 **Schooler GR**, Squires JH, Alazraki A, Chavhan GB, Chernyak V, Davis JT, Khanna G, Krishnamurthy R, Lungren MP, Masand PM, Podberesky DJ, Sirlin CB, Towbin AJ. Pediatric Hepatoblastoma, Hepatocellular Carcinoma, and Other Hepatic Neoplasms: Consensus Imaging Recommendations from American College of Radiology Pediatric Liver Reporting and Data System (LI-RADS) Working Group. *Radiology* 2020; **296**: 493-497 [PMID: 32602829 DOI: 10.1148/radiol.2020200751]

8 **Li S**, Zhou L, Chen R, Chen Y, Niu Z, Qian L, Fang Y, Xu L, Xu H, Zhang L. Diagnostic efficacy of contrast-enhanced ultrasound versus MRI Liver Imaging Reporting and Data System (LI-RADS) for categorising hepatic observations in patients at risk of hepatocellular carcinoma. *Clin Radiol* 2021; **76**: 161.e1-161.e10 [PMID: 33198943 DOI: 10.1016/j.crad.2020.10.009]

9 **Ma L**, Liang WZ, Zhu YP, Zhu YQ, Zhang DZ. Differences in CEUS and CE-MRI appearance of HCC: a case report. *AUDT* 2019; **3** (4): 197-199 [DOI: 10.37015/audt.2019.191208]

10 **He MN**, Xu L, Jiang TA. Time-intensity curve analysis of hepatocellular carcinoma using two contrast-enhanced ultrasound methods: contrast pulse sequencing and contrast harmonic imaging. *AUDT* 2020; **4** (3): 217-222 [DOI: 10.37015/audt.2020.200007]

11 **Schreiber-Dietrich DG**, Cui XW, Piscaglia F, Gilja OH, Dietrich CF. Contrast enhanced ultrasound in pediatric patients: a real challenge. *Z Gastroenterol* 2014; **52**: 1178-1184 [PMID: 25313631 DOI: 10.1055/s-0034-1366766]

12 **Ferraro S**, Panzeri A, Braga F, Panteghini M. Serum α-fetoprotein in pediatric oncology: not a children's tale. *Clin Chem Lab Med* 2019; **57**: 783-797 [PMID: 30367785 DOI: 10.1515/cclm-2018-0803]

13 **Galle PR**, Foerster F, Kudo M, Chan SL, Llovet JM, Qin S, Schelman WR, Chintharlapalli S, Abada PB, Sherman M, Zhu AX. Biology and significance of alpha-fetoprotein in hepatocellular carcinoma. *Liver Int* 2019; **39**: 2214-2229 [PMID: 31436873 DOI: 10.1111/liv.14223]

14 **Rojas Y**, Guillerman RP, Zhang W, Vasudevan SA, Nuchtern JG, Thompson PA. Relapse surveillance in AFP-positive hepatoblastoma: re-evaluating the role of imaging. *Pediatr Radiol* 2014; **44**: 1275-1280 [PMID: 24839140 DOI: 10.1007/s00247-014-3000-6]

15 **El-Ali AM**, Davis JC, Cickelli JM, Squires JH. Contrast-enhanced ultrasound of liver lesions in children. *Pediatr Radiol* 2019; **49**: 1422-1432 [PMID: 31620843 DOI: 10.1007/s00247-019-04361-0]

16 **Khanna G**, Chavhan GB, Schooler GR, Fraum TJ, Alazraki AL, Squires JH, Salter A, Podberesky DJ, Towbin AJ. Diagnostic Performance of LI-RADS Version 2018 for Evaluation of Pediatric Hepatocellular Carcinoma. *Radiology* 2021; **299**: 190-199 [PMID: 33620289 DOI: 10.1148/radiol.2021203559]

17 **van der Pol CB**, Lim CS, Sirlin CB, McGrath TA, Salameh JP, Bashir MR, Tang A, Singal AG, Costa AF, Fowler K, McInnes MDF. Accuracy of the Liver Imaging Reporting and Data System in Computed Tomography and Magnetic Resonance Image Analysis of Hepatocellular Carcinoma or Overall Malignancy-A Systematic Review. *Gastroenterology* 2019; **156**: 976-986 [PMID: 30445016 DOI: 10.1053/j.gastro.2018.11.020]

18 **Ludwig DR**, Romberg EK, Fraum TJ, Rohe E, Fowler KJ, Khanna G. Diagnostic performance of Liver Imaging Reporting and Data System (LI-RADS) v2017 in predicting malignant liver lesions in pediatric patients: a preliminary study. *Pediatr Radiol* 2019; **49**: 746-758 [PMID: 31069473 DOI: 10.1007/s00247-019-04358-9]

19 **Rozell JM**, Catanzano T, Polansky SM, Rakita D, Fox L. Primary liver tumors in pediatric patients: proper imaging technique for diagnosis and staging. *Semin Ultrasound CT MR* 2014; **35**: 382-393 [PMID: 25129215 DOI: 10.1053/j.sult.2014.05.006]

20 **Kong WT**, Wang WP, Huang BJ, Ding H, Mao F, Si Q. Contrast-enhanced ultrasound in combination with color Doppler ultrasound can improve the diagnostic performance of focal nodular hyperplasia and hepatocellular adenoma. *Ultrasound Med Biol* 2015; **41**: 944-951 [PMID: 25701530 DOI: 10.1016/j.ultrasmedbio.2014.11.012]

21 **Wang W**, Chen LD, Lu MD, Liu GJ, Shen SL, Xu ZF, Xie XY, Wang Y, Zhou LY. Contrast-enhanced ultrasound features of histologically proven focal nodular hyperplasia: diagnostic performance compared with contrast-enhanced CT. *Eur Radiol* 2013; **23**: 2546-2554 [PMID: 23624595 DOI: 10.1007/s00330-013-2849-3]

22 **Zarzour JG**, Porter KK, Tchelepi H, Robbin ML. Contrast-enhanced ultrasound of benign liver lesions. *Abdom Radiol (NY)* 2018; **43**: 848-860 [PMID: 29167944 DOI: 10.1007/s00261-017-1402-2]

23 **Mneimneh W**, Farges O, Bedossa P, Belghiti J, Paradis V. High serum level of alpha-fetoprotein in focal nodular hyperplasia of the liver. *Pathol Int* 2011; **61**: 491-494 [PMID: 21790865 DOI: 10.1111/j.1440-1827.2011.02691.x]

24 **Koklu E**, Gunes T, Akcakus M, Ozturk MA, Kurtoglu S. Alpha-fetoprotein levels in the neonatal period. *Eur J Pediatr* 2008; **167**: 961-2; author reply 963 [PMID: 17952463 DOI: 10.1007/s00431-007-0621-x]

25 **Kupeli S**. Evolving strategy in treatment of infantile hemangiomas: from steroids to propranolol. *Cukurova Med J* 2016; **41** (2): 354-359 [DOI: 10.17826/cutf.201781]

World Journal of Gastroenterology

Submit a Manuscript: https://www.f6publishing.com

World J Gastroenterol 2022 June 7; 28(21): 2361-2382

DOI: 10.3748/wjg.v28.i21.2361

ISSN 1007-9327 (print) ISSN 2219-2840 (online)

ORIGINAL ARTICLE

Observational Study

Socioeconomics and attributable etiology of primary liver cancer, 1990-2019

Qing-Qing Xing, Jing-Mao Li, Xuan Dong, Dan-Yi Zeng, Zhi-Jian Chen, Xiao-Yun Lin, Jin-Shui Pan

Specialty type: Gastroenterology and hepatology

Provenance and peer review: Invited article; Externally peer reviewed.

Peer-review model: Single blind

Peer-review report's scientific quality classification

Grade A (Excellent): 0
Grade B (Very good): B, B
Grade C (Good): C, C
Grade D (Fair): 0
Grade E (Poor): 0

P-Reviewer: Karatza AA, Greece; Muhammad Irham L, Indonesia; Naseri M, Iran; Salama II, Egypt

Received: October 18, 2021
Peer-review started: October 18, 2021
First decision: December 27, 2021
Revised: January 7, 2022
Accepted: April 24, 2022
Article in press: April 24, 2022
Published online: June 7, 2022

Qing-Qing Xing, Xuan Dong, Dan-Yi Zeng, Zhi-Jian Chen, Xiao-Yun Lin, Jin-Shui Pan, Department of Hepatology, The First Affiliated Hospital of Fujian Medical University, Fuzhou 350005, Fujian Province, China

Qing-Qing Xing, Xuan Dong, Dan-Yi Zeng, Zhi-Jian Chen, Xiao-Yun Lin, Jin-Shui Pan, Hepatology Research Institute, Fujian Medical University, Fuzhou 350005, Fujian Province, China

Jing-Mao Li, Department of Statistics, Xiamen University, Xiamen 361000, Fujian Province, China

Xuan Dong, Dan-Yi Zeng, School of Medicine, Xiamen University, Xiamen 361000, Fujian Province, China

Corresponding author: Jin-Shui Pan, MD, PhD, Chief Doctor, Professor, Department of Hepatology, The First Affiliated Hospital of Fujian Medical University, No. 20 Chazhong Road, Fuzhou 350005, Fujian Province, China. j.s.pan76@fjmu.edu.cn

Abstract

BACKGROUND

Primary liver cancer (PLC) is a major contributor to cancer-related deaths. Data on global and country-specific levels and trends of PLC are essential for understanding the effects of this disease and helping policymakers to allocate resources.

AIM

To investigate the association between the burden of PLC and socioeconomic development status.

METHODS

Cancer mortality and incidence rates were obtained from the Global Burden of Disease (GBD) 2019, and the data were stratified by country and territory, sex, and the Socio-demographic Index (SDI) level. The association between the attributable etiology of PLC and socioeconomic development status, represented using the SDI, was described. The attributable etiology of PLC included hepatitis B, hepatitis C, alcohol use, and nonalcoholic steatohepatitis. The association between the attributable etiology of PLC and SDI was further stratified by sex and geographical location. A confidence analysis was also performed based on bootstrap draw.

RESULTS

The age-standardized incidence rate of PLC was 6.5 [95% confidence intervals (CI): 5.9-7.2] per 100000 person-years, which decreased by -27.5% (-37.0 to -16.6) from 1990 to 2019. Several countries located in East Asia, South Asia, West Africa, and North Africa shouldered the heaviest burden of PLC in 2019. In terms of incidence rates, the first leading underlying cause of PLC identified was hepatitis B, followed by hepatitis C, alcohol use, and nonalcoholic steatohepatitis. Regarding stratification using the SDI, the incidence rate of PLC was the highest for high and middle SDI locations. Further, the leading attributable etiologies of PLC were hepatitis B for the middle and high middle SDI locations while hepatitis C and nonalcoholic steatohepatitis for the high SDI locations.

CONCLUSION

The pronounced association between socioeconomic development status and PLC burden indicates socioeconomic development status affects attributable etiologies for PLC. GBD 2019 data are valuable for policymakers implementing PLC cost-effective interventions.

Key Words: Epidemiology; Public health; Socioeconomics; Primary liver cancer; Hepatitis; Alcohol

©The Author(s) 2022. Published by Baishideng Publishing Group Inc. All rights reserved.

Core Tip: Primary liver cancer (PLC) is a common cancer with high morbidity and mortality rates. PLC usually occurs as a preventable disease. An association was identified between socioeconomic development status and PLC burden. The leading attributable etiologies of PLC were hepatitis B for the middle and high middle Socio-demographic Index (SDI) locations, and hepatitis C and nonalcoholic steatohepatitis for the high SDI locations. Our findings are valuable to implement tailored prevention strategies for PLC.

Citation: Xing QQ, Li JM, Dong X, Zeng DY, Chen ZJ, Lin XY, Pan JS. Socioeconomics and attributable etiology of primary liver cancer, 1990-2019. *World J Gastroenterol* 2022; 28(21): 2361-2382
URL: https://www.wjgnet.com/1007-9327/full/v28/i21/2361.htm
DOI: https://dx.doi.org/10.3748/wjg.v28.i21.2361

INTRODUCTION

Primary liver cancer (PLC) was the third leading cause of cancer deaths in 2020 following lung and colorectal cancer[1]. In terms of cancer-related mortality, PLC was the third leading cause in China[2] and the fifth leading cause in the United States[3]. The burden of PLC varies significantly in terms of sex and geographic region due to different risk-factor exposure. The major risk factors include chronic viral infections [hepatitis B virus (HBV), hepatitis C virus (HCV)], alcohol use, and nonalcoholic steatohepatitis (NASH), and they have been widely studied in recent years[4]. PLC is caused by chronic hepatitis B (CHB) (60%) in Africa and East Asia, whereas chronic hepatitis C (CHC) appears to be the major risk factor in the Western world[5]. Thus, it is expected that the appropriate handling of risk factors can significantly contribute to the overall reduction of PLC-related deaths in the near future.

The Global Burden of Disease (GBD) database has been constructed to improve health systems and eliminate disparities; this database comprises a comprehensive catalog of censuses, vital statistics, surveys, and other health-related data. Policymakers can benefit from the GBD database as it enables them to understand the true nature of the health challenges of a country and the shifting challenges over time. In recent years, the prevention of PLC has been eclipsed by substantial improvements in PLC treatment. Given the marked lag between risk factor exposure and the development of PLC, even the well-proven prevention approaches would take decades to reduce of the PLC burden. Although several prior studies have focused on the global prevalence of PLC[4,6], few studies focus on the tailored prevention of PLC. In this study, we focused on identifying the effect of socioeconomic development status on the attributable etiologies of PLC from a global perspective. We hope our findings will be helpful contributions for developing specialized prevention strategies for PLC. Considering the heavy burden of PLC, characterizing this association will help health workers to design tailored prevention strategies and policymakers to allocate research and clinical resources for implementing cost-effective interventions for PLC.

MATERIALS AND METHODS

Data sources

For this study, the incidence and death rates of PLC were acquired from the GBD 2019 (http://ghdx.healthdata.org/gbd-2019) that covered 204 countries and territories[7]. The incidence and death rates were age-standardized according to the GBD 2019 world population recorded per 100000 person-years. The International Classification of Diseases, Tenth Revision (ICD-10) was adopted. The ICD-10 codes for PLC are C22-C22.4, C22.7-C22.8, and Z85.05 (Supplementary material, page 17). Mortality and non-fatal estimates have been described in detail in previous studies[8,9]. Additional information is provided in the Supplementary material.

Confidence analysis

We assumed that the incidence or death rates in each year followed a log-normal distribution and that the rates in different years were independent of each other. Based on these assumptions, in each bootstrap draw, we measured the increase rates and 95%CIs based on the 25th and 975th ranked values across all 1000 draws. The 2.5% and 97.5% quantiles from the 1000 draws of the posterior distribution were used to generate 95%CIs.

Socio-demographic Index

The Socio-demographic Index (SDI) incorporates the mean education level for individuals aged 15 years and older, the total fertility rate in women under the age of 25 years, and lag-distributed income per person. The method of generating the SDI is described in the report by the GBD 2016 Mortality Collaborators[10]. Further, the SDI was used to evaluate the effect of the development levels of a country or region on the burden of PLC based on data obtained from the GBD 2019 (Supplementary material, pages 1-15). The values of the SDI range from 0 to 1, which correspond to the development level of a country or region from the worst to the best. The SDI was categorized based on the references bound as low SDI, low middle SDI, middle SDI, high middle SDI, and high SDI, as shown in the Supplementary material, page 16.

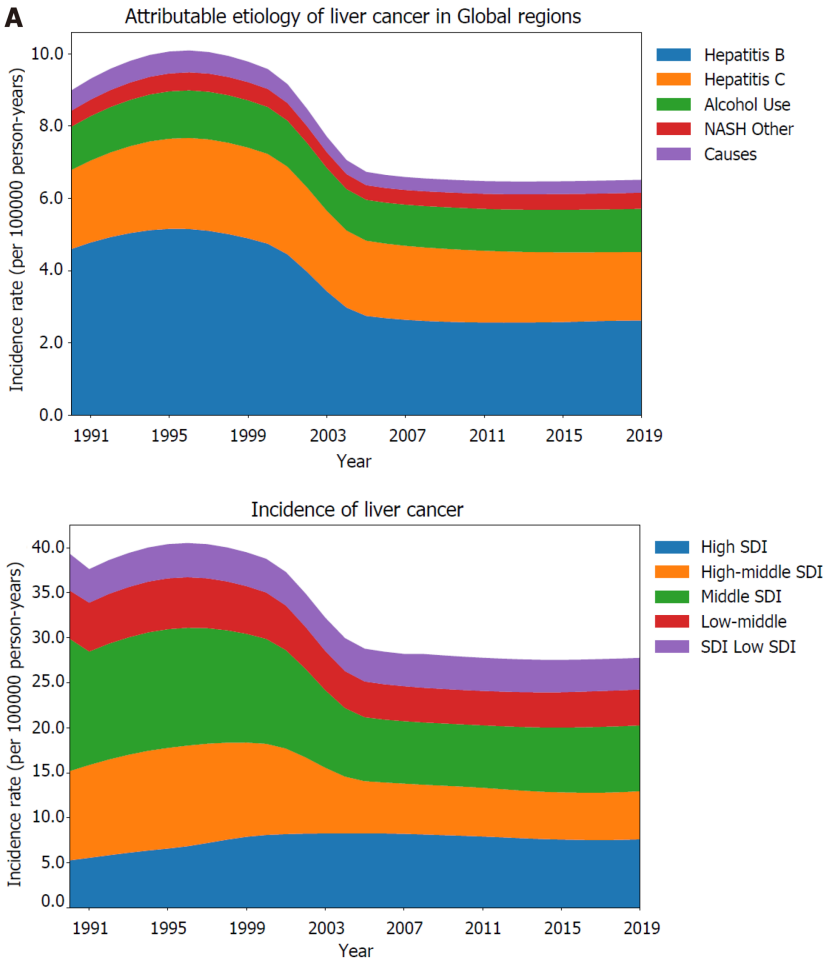
Ethic statement

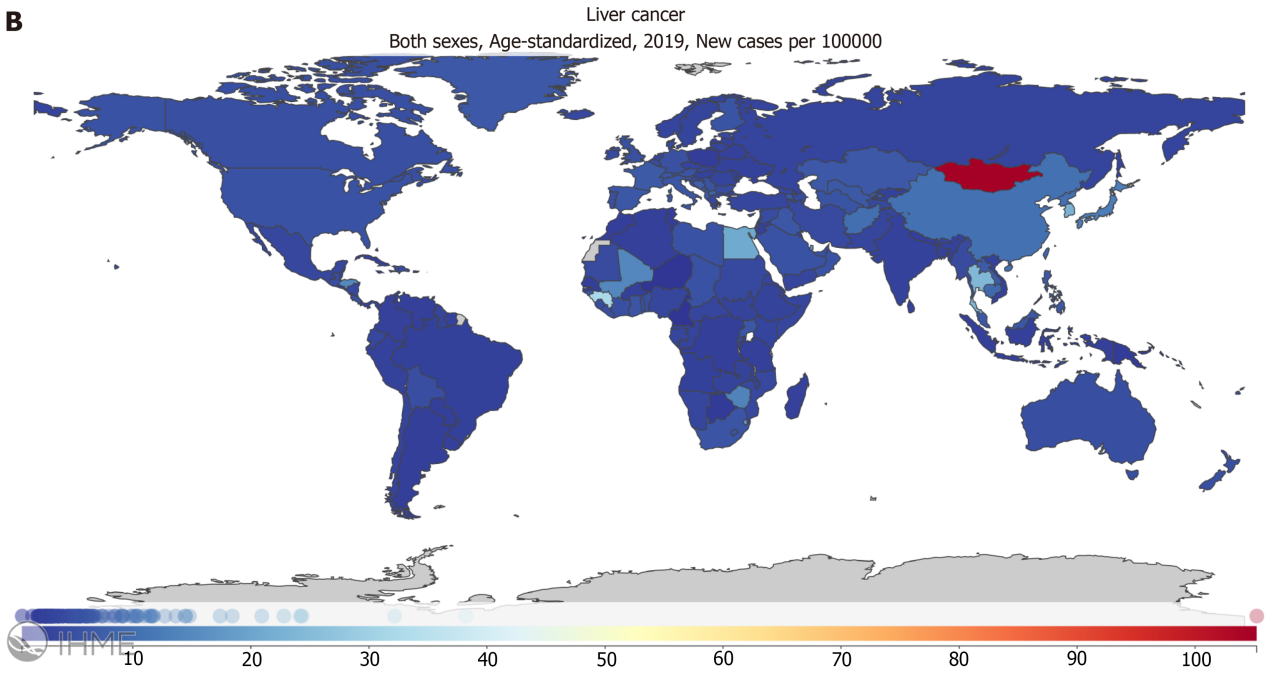
The study was reviewed and approved by the Ethics Committee of First Affiliated Hospital of Fujian Medical University (MTCA, ECFAH of FMU[2015]084-1).

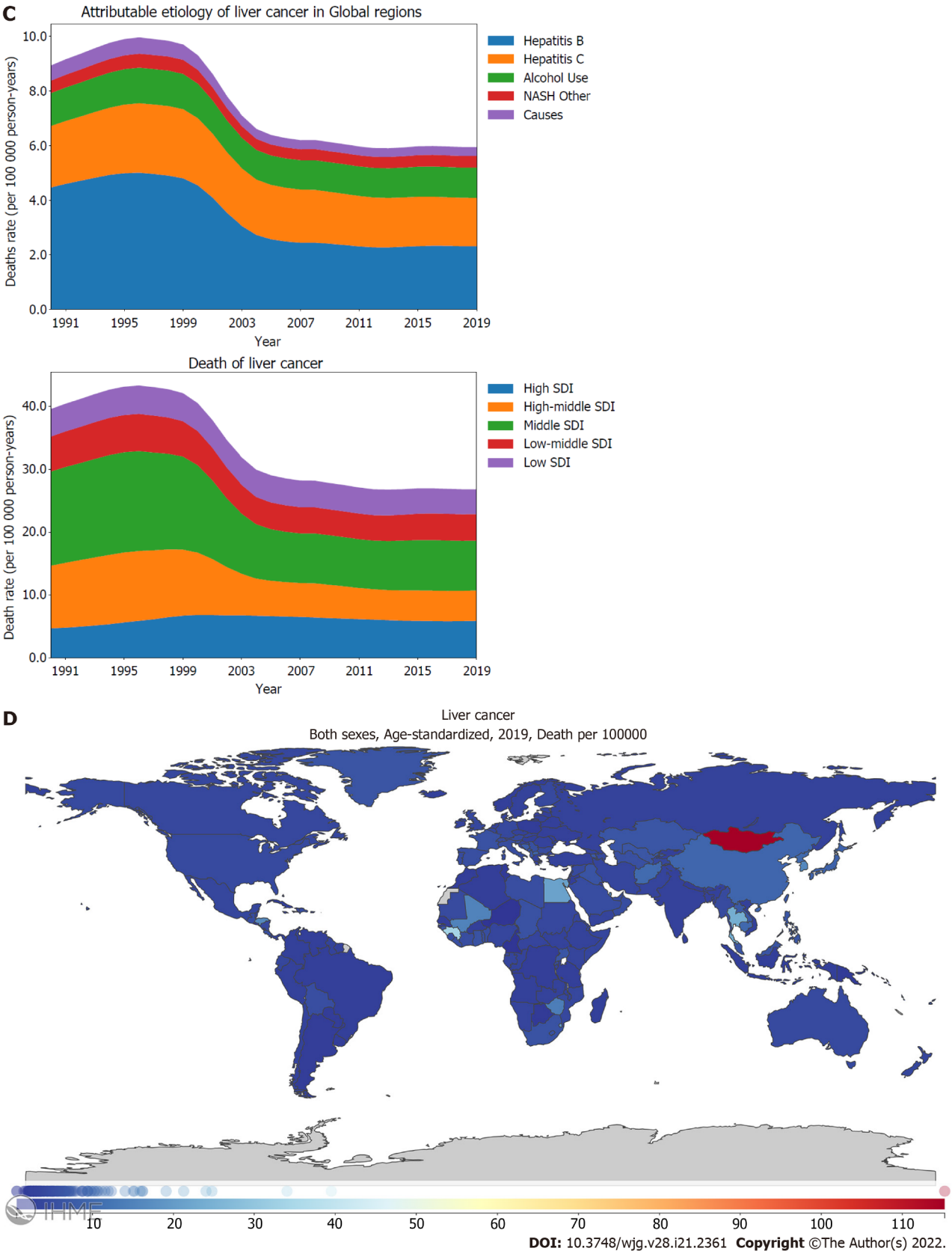
RESULTS

Burden of liver cancer

Liver cancer is one the most common cancers. In 2019, the global age-standardized incidence rate of PLC was 6.5 (95%CI: 5.9-7.2) per 100000 person-years (Supplementary material, page 25). Fortunately, the incidence rate of PLC has declined significantly by -27.5% (-37.0 to -16.6) from 1990 to 2019 (Figure 1A; Supplementary material, page 18). The main contributor for this drop was the decreasing burden of PLC caused by hepatitis B and the declining burden of PLC in the middle SDI locations. Between 1990 and 2019, the global incidence rate of PLC peaked in 1995-1996, and then, it decreased gradually. However, the incidence rate of PLC has not declined further since 2010 (Figure 1A; Supplementary material, pages 23-25). Before 2004, the incidence rate of PLC for middle SDI locations surpassed that for high SDI locations whereas high SDI locations exceeded middle SDI locations in terms of the burden of PLC after 2004 (Figure 1A; Supplementary Figure 1B; Supplementary material, pages 29-32). In terms of the incidence rates, the leading underlying cause of PLC was HBV, followed by HCV, alcohol use, and NASH (Figure 1A). Hepatitis B manifested the most drastic decline between 1990 and 2019 as the underlying causes of PLC [57.0% (45.3-71.4)] (Figure 1A; Supplementary material, pages 19-20). Stratified using the SDI, the age-standardized incidence rate of PLC was found to be the highest for high and middle SDI locations compared to those for high middle, low middle, and low SDI locations (Figure 1A; Supplementary Figure 1B; Supplementary material, pages 29-32). Further, a declining pattern was observed for the age-standardized incidence rate of PLC in the high middle [53.8% (45.1-64.5)] and middle SDI locations [49.7% (41.1-59.9)] compared with the increasing trend in the high SDI locations [144.5% (130.3-159.6)] (Figure 1A; Supplementary Figure 1B; Supplementary material, page 18). Between 1990 and 2019, PLC caused by hepatitis B and hepatitis C showed a decreasing trend in the death rate (Figure 1C; Supplementary material, pages 21-22). Stratified using the SDI, the high middle, middle, and low middle SDI locations showed decreasing trends in the age-standardized death rate of PLC. In contrast, the high SDI location showed an increasing trend in the age-standardized death rate of PLC (Figure 1C; Supplementary material, page 18). Several countries located in East Asia, South Asia, West Africa, and North Africa shouldered the heaviest burden of the PLC incidence and death rates. For the age-standardized incidence rate of PLC, Mongolia demonstrated the highest burden [105.2 (82.6-131.5)] per 100000 person-years), followed by Gambia and Guinea (Figure 1B; Supplementary material,


A
Attributable etiology of liver cancer in Global regions
Incidence rate (per 100000 person-years)
Year
Hepatitis B
Hepatitis C
Alcohol Use
NASH Other
Causes
Incidence of liver cancer
Incidence rate (per 100000 person-years)
Year
High SDI
High-middle SDI
Middle SDI
Low-middle
SDI Low SDI


B
Liver cancer
Both sexes, Age-standardized, 2019, New cases per 100000
10
20
30
40
50
60
70
80
90
100



DOI: 10.3748/wjg.v28.i21.2361 **Copyright** ©The Author(s) 2022.

Figure 1 Burden of liver cancer for 204 countries and territories. A and C: Age-standardized incidence (A) and death (C) rates per 100000 population for liver cancer from 1990 through 2019, stratified by the attributable etiology of liver cancer or the Socio-demographic Index; B and D: Age-standardized incidence (B) and death (D) rate of liver cancer per 100000 person-years by country and territory, in 2019. The maps in (B) and (D) are generated using the Global Burden of Disease 2019 tool. SDI: Socio-demographic Index; NASH: Nonalcoholic steatohepatitis.

pages 33-35). Countries that possessed the highest burden PLC incidence rate also had the highest burden PLC death rate (Figure 1D; Supplementary material, pages 46-48).

Burden of liver cancer caused by hepatitis B

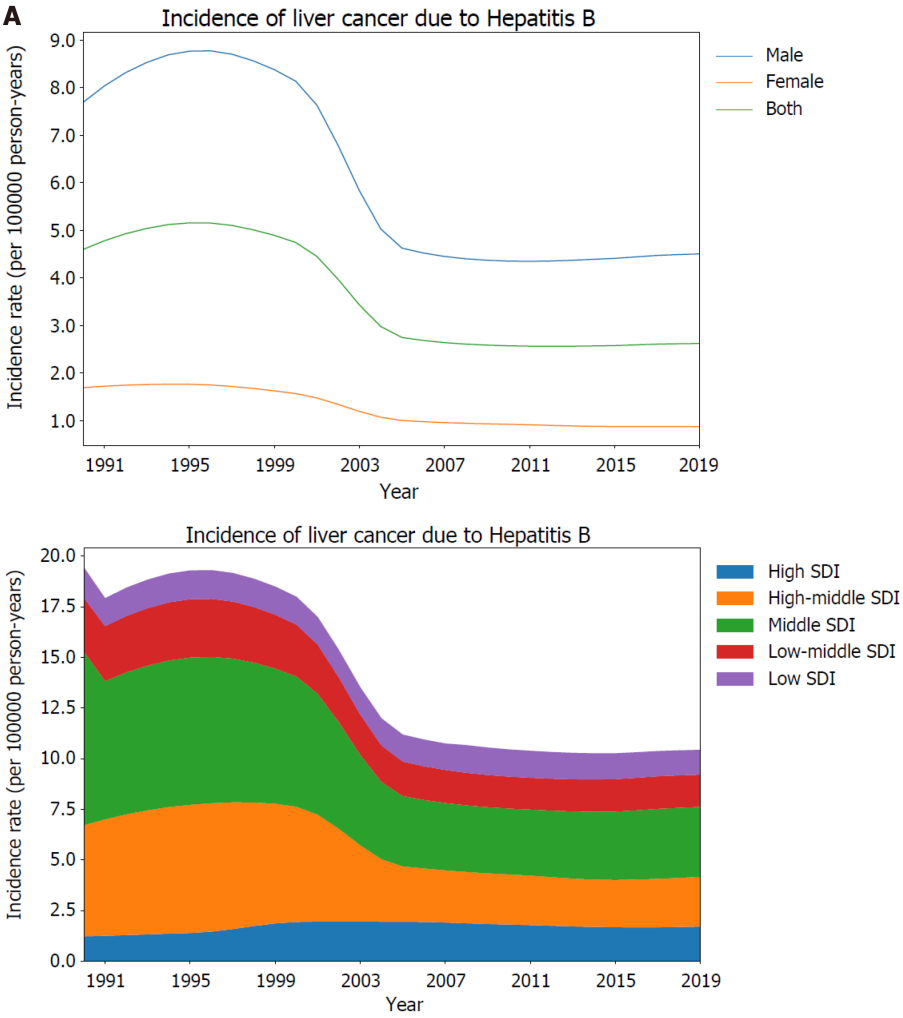
The global age-standardized incidence rate of PLC caused by hepatitis B reached its peak in 1995-1996, and then decreased gradually. However, the burden of the incidence rate has remained stable and has not declined further since 2005. By stratification using sex, the age-standardized incidence rate of PLC caused by hepatitis B was found to be four times higher in males than that in females (Figure 2A; Supplementary material, pages 49-50). Moreover, the age-standardized incidence rate of PLC caused by hepatitis B was found to be higher for middle and high middle SDI locations than for high, low middle, and low SDI locations (Figure 2A; Supplementary Figure 2A; Supplementary material, pages 51-57). Between 1990 and 2019, the decreasing trend in the age-standardized incidence rate of PLC caused by hepatitis B differed significantly based on SDI regions, with the highest declines in the middle [40.3% (31.1-51.8)] and high middle SDI locations [44.8% (34.2-58.8)]. In contrast, high SDI locations showed an increasing trend [139.3% (112.1-173.3)] (Figure 2A; Supplementary Figure 2A; Supplementary material, pages 19-20). In 2019, the incidence rate of PLC caused by hepatitis B differed dramatically between countries or regions. In particular, the highest age-standardized incidence rate was recorded in Mongolia with 27.3 (18.0-39.1) per 100000 person-years, followed by Gambia and Guinea (Figure 2B; Supplementary material, pages 58-61). Similar to the age-standardized incidence rate of PLC caused by hepatitis B, the burden of the PLC death rate caused by hepatitis B was higher for males than that for females (Figure 2C; Supplementary material, pages 62-63). Between 1990 and 2019, the age-standardized death rate of PLC caused by hepatitis B decreased significantly in the high middle [39.0% (30.2-50.6)] and middle SDI locations [44.7% (34.7-57.4)]. However, the high SDI locations showed an increasing trend [113.4% (90.6-141.6)] (Figure 2C; Supplementary Figure 2B; Supplementary material, pages 21-22). In 2019, Mongolia had the highest age-standardized death rate with 28.2 (18.9-40.8) per 100000 person-years, followed by Gambia and Guinea (Figure 2D; Supplementary material, pages 67-70).

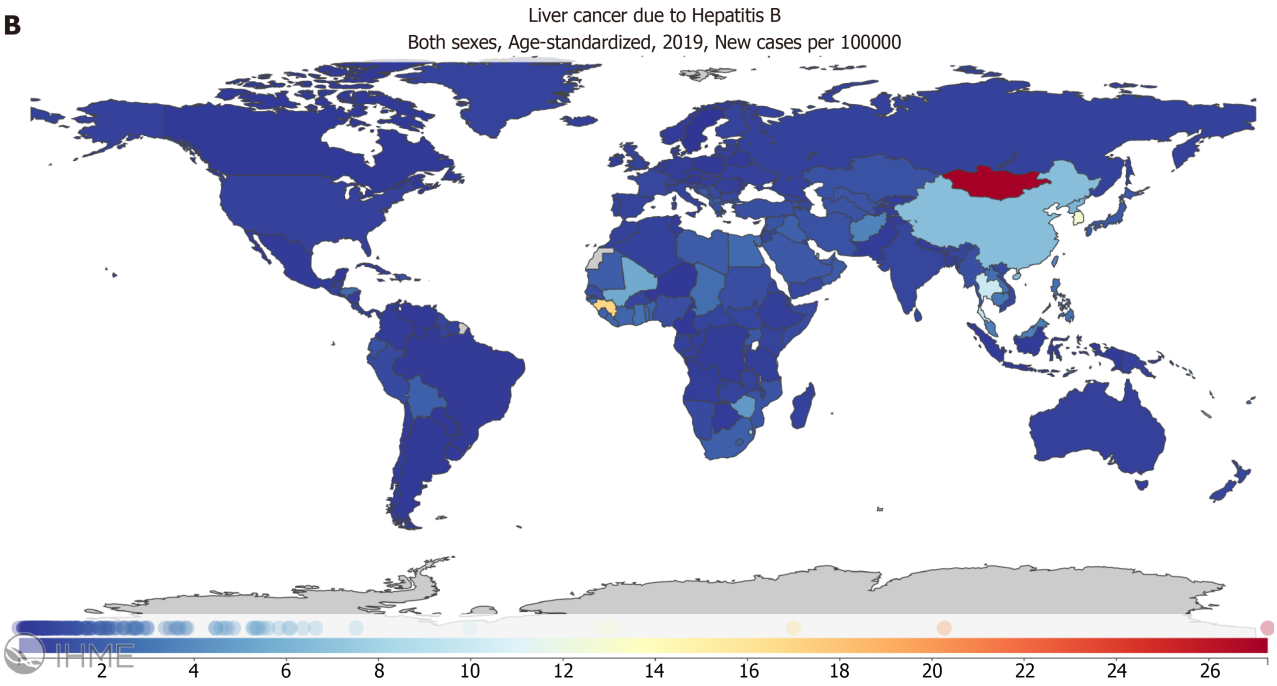
Burden of liver cancer caused by hepatitis C

Hepatitis C is the second leading cause of PLC. By stratification using sex, the age-standardized incidence rate and mortality rate of PLC caused by hepatitis C in males was found to be higher than those in females (Figure 3A and C; Supplementary material, pages 71-72 and 80-81). Further, the age-standardized incidence rate of PLC caused by hepatitis C was higher for high and middle SDI locations than for high middle, low middle, and low SDI locations (Figure 3A; Supplementary Figure 3A; Supplementary material, pages 73-75). From 1990 through 2019, the age-standardized incidence rate of PLC caused by hepatitis C differed significantly between the SDI regions, with the middle [59.5% (46.5-76.3)] and high middle SDI locations [63.3% (51.3-78.0)] exhibiting declining trends whereas the high SDI location [133.4% (112.5-158.2)] showed increasing trends (Figure 3A; Supplementary Figure 3A; Supplementary material, pages 19-20). In 2019, the incidence rate of PLC caused by hepatitis C manifested a substantial variance between countries or regions. The highest age-standardized incidence rate was recorded in Mongolia with 35.0 (24.7-46.8) per 100000 person-years, followed by Egypt and Japan (Figure 3B; Supplementary material, pages 76-79). Between 1990 and 2019, the age-standardized death rate of PLC caused by hepatitis C decreased significantly in high middle [57.9% (47.5-71.1)] and middle SDI locations [58.7% (46.2-74.4)]. However, the high SDI locations showed an increasing trend [119.5% (101.8-139.8)] (Figure 3C; Supplementary Figure 3B; Supplementary material, pages 21-22). In 2019, Mongolia had the highest age-standardized death rate with 40.3 (28.6-53.3) per 100000 person-years, followed by Egypt (Figure 3D; Supplementary material, pages 85-88).

Burden of liver cancer caused by alcohol use

For PLC caused by alcohol use, the age-standardized incidence rate in males was four times higher than that in females (Figure 4A; Supplementary material, pages 89-90). Similar to PLC caused by hepatitis C, the age-standardized incidence rate of PLC caused by alcohol use was found to be higher for high SDI locations than other SDI locations when stratified using the SDI (Figure 4A; Supplementary Figure 4A; Supplementary material, pages 91-93). From 1990 through 2019, there was a notable difference in the trends for age-standardized incidence rates of PLC caused by alcohol use between SDI regions; high middle SDI locations [72.7% (54.3-96.4)] showed a significant decline. In contrast, high SDI locations showed a significant increase [163.5% (126.4-209.8)] (Figure 4A; Supplementary Figure 4A; Supplementary material, pages 19-20). In 2019, the highest incidence rate of PLC caused by alcohol use was recorded in Mongolia with 31.8 (21.3-44.7) per 100000 person-years, followed by Gambia and Thailand (Figure 4B; Supplementary material, pages 94-97). Males showed a higher burden of death rate of PLC caused by alcohol use than females, which corresponds with the higher incidence rate of PLC caused by alcohol use in males (Figure 4C; Supplementary material, pages 98-99). Between 1990 and 2019, the age-standardized death rate of PLC caused by alcohol use decreased significantly in high middle SDI locations [67.6% (50.9-88.9)]. However, high SDI locations showed an increasing trend [141.2% (111.0-179.2)] (Figure 4C; Supplementary Figure 4B; Supplementary material, pages 21-22). In 2019, Mongolia had the highest age-standardized death rate with 34.2 (23.1-47.8) per 100000 person-years, followed by


A
Incidence of liver cancer due to Hepatitis B
Incidence rate (per 100000 person-years)
9.0
8.0
7.0
6.0
5.0
4.0
3.0
2.0
1.0
1991
1995
1999
2003
2007
2011
2015
2019
Year
Male
Female
Both
Incidence of liver cancer due to Hepatitis B
Incidence rate (per 100000 person-years)
20.0
17.5
15.0
12.5
10.0
7.5
5.0
2.5
0.0
Year
High SDI
High-middle SDI
Middle SDI
Low-middle SDI
Low SDI


B
Liver cancer due to Hepatitis B
Both sexes, Age-standardized, 2019, New cases per 100000
IHME
2
4
6
8
10
12
14
16
18
20
22
24
26

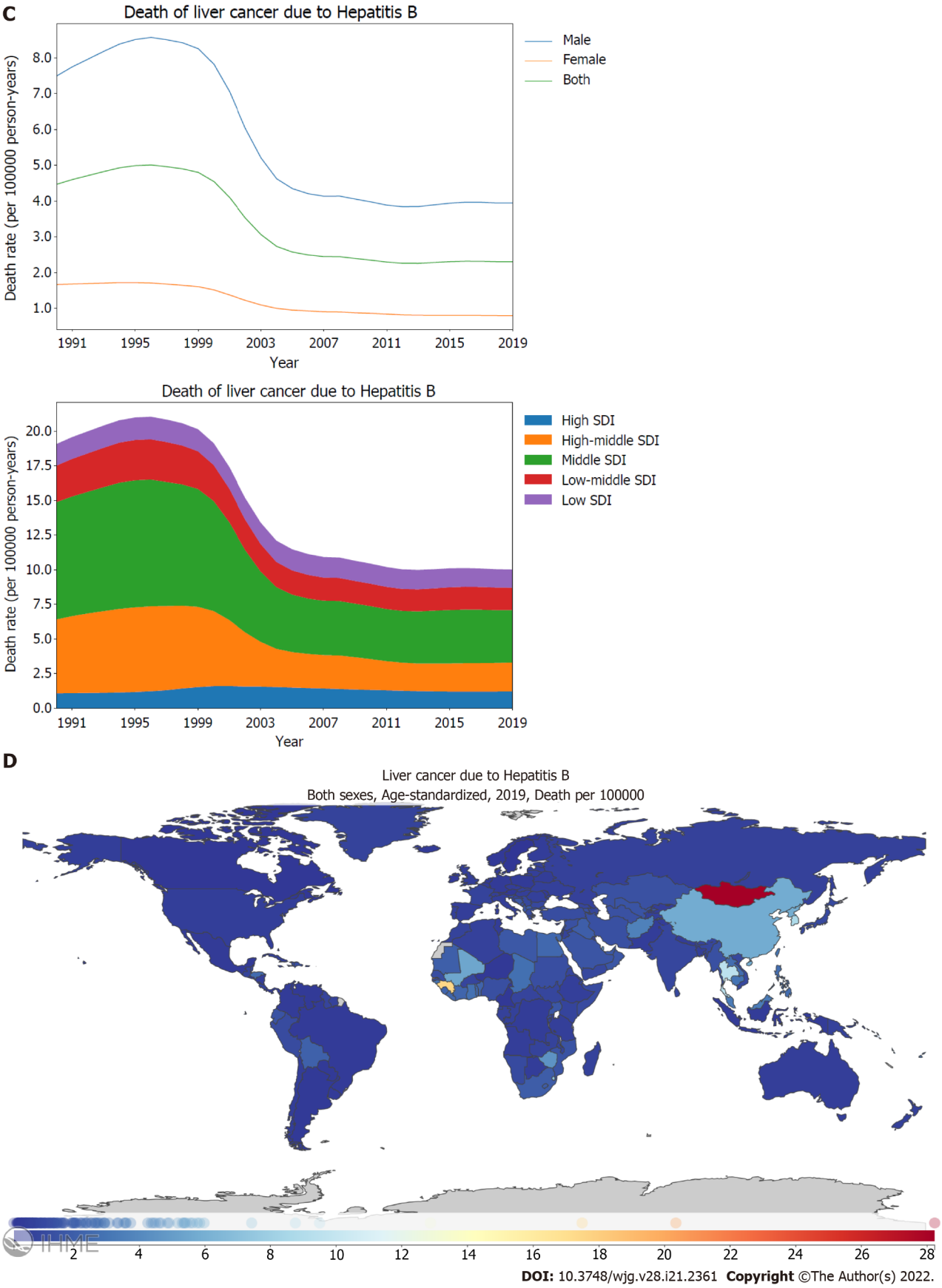
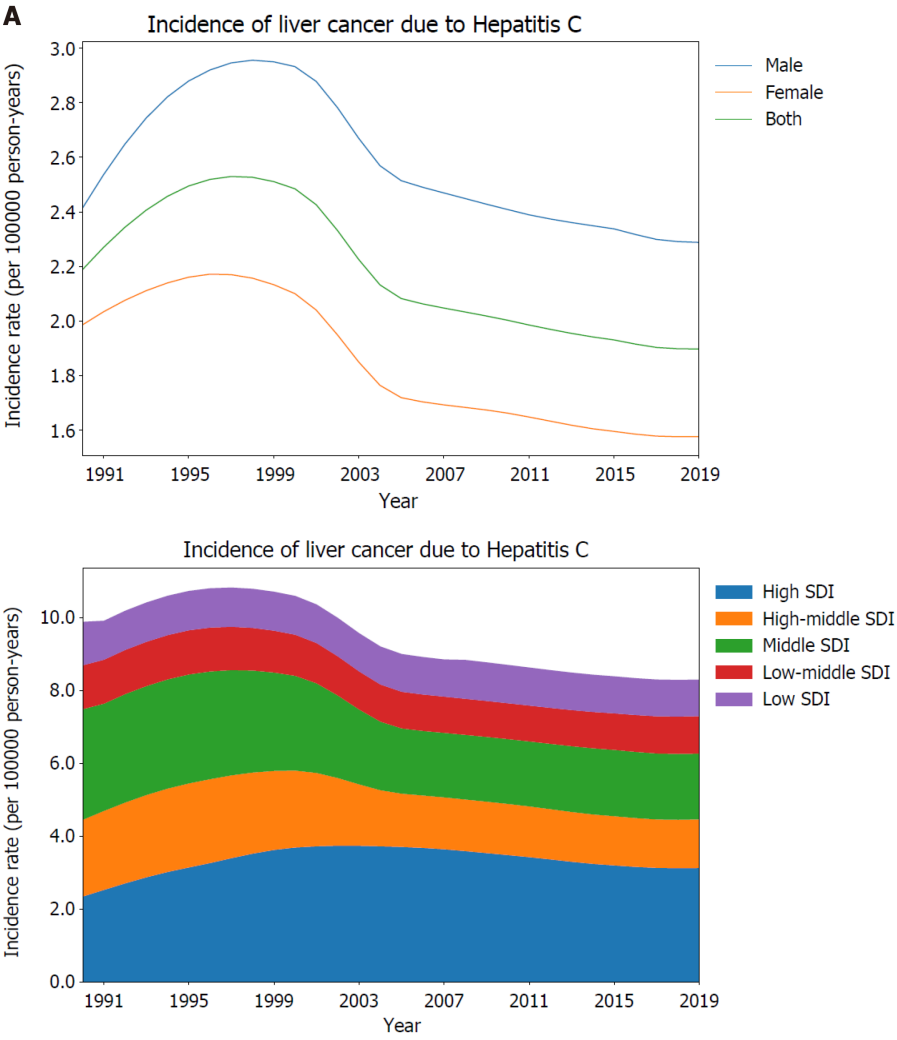
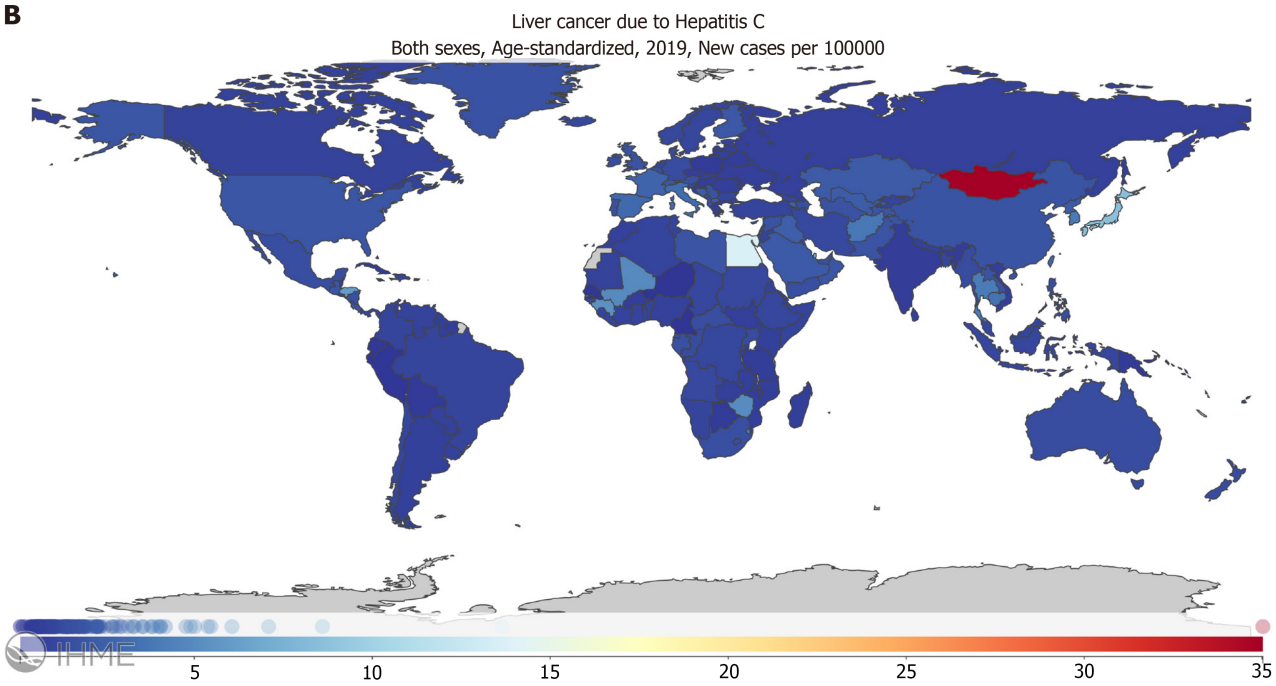
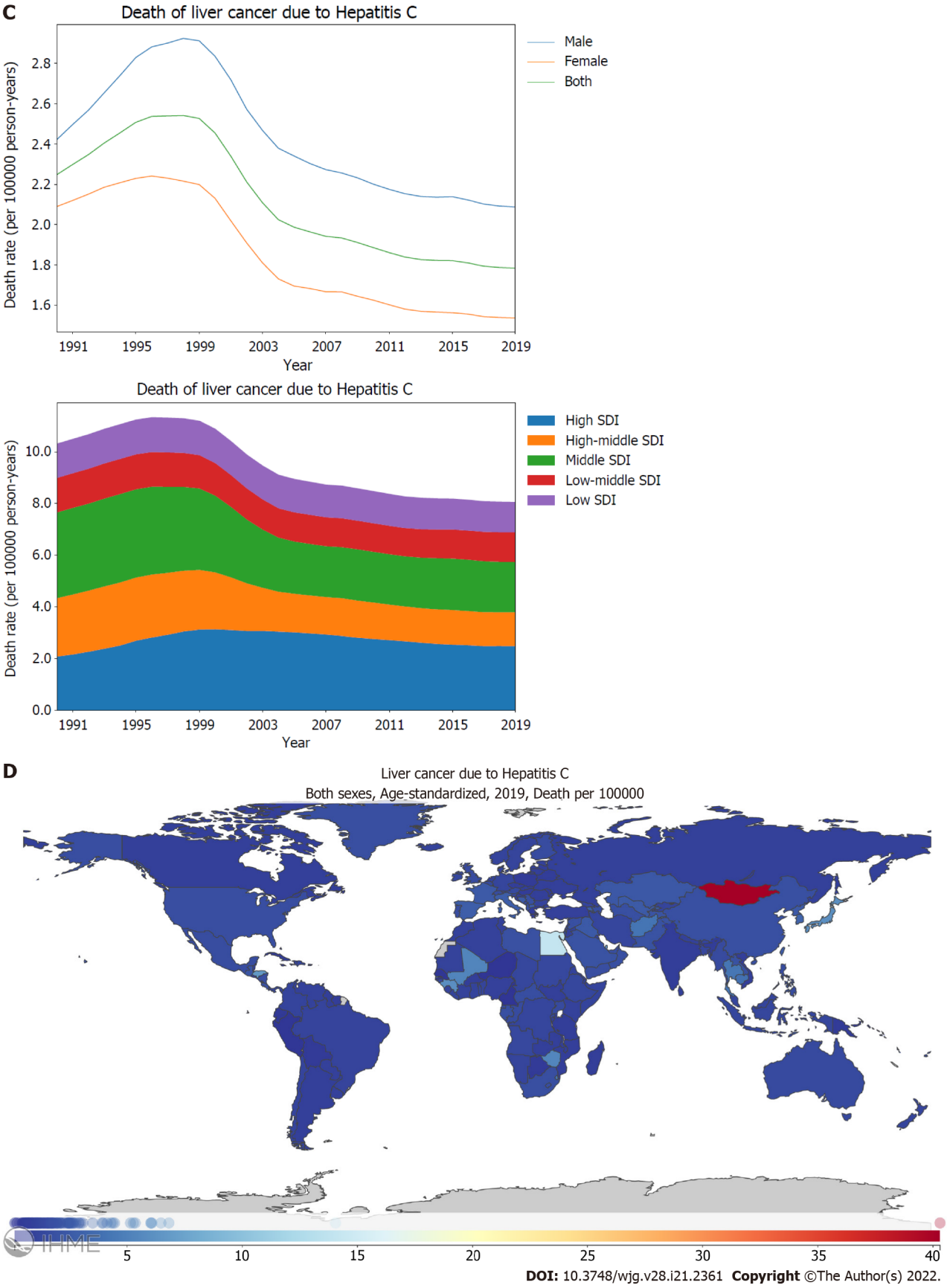


Figure 2 Burden of liver cancer caused by hepatitis B for 204 countries and territories. A and C: Age-standardized incidence (A) and death (C) rates per 100000 population of liver cancer caused by hepatitis B from 1990 through 2019, stratified by sex or the Socio-demographic Index; B and D: Age-standardized incidence (B) and death (D) rate of liver cancer caused by hepatitis B per 100000 person-years by country and territory, in 2019. The maps in (B) and (D) are generated using the Global Burden of Disease 2019 tool. SDI: Socio-demographic Index.


A
Incidence of liver cancer due to Hepatitis C
Incidence rate (per 100000 person-years)
3.0
2.8
2.6
2.4
2.2
2.0
1.8
1.6
1991
1995
1999
2003
2007
2011
2015
2019
Year
Male
Female
Both
Incidence of liver cancer due to Hepatitis C
Incidence rate (per 100000 person-years)
10.0
8.0
6.0
4.0
2.0
0.0
Year
High SDI
High-middle SDI
Middle SDI
Low-middle SDI
Low SDI


B
Liver cancer due to Hepatitis C
Both sexes, Age-standardized, 2019, New cases per 100000
IHME
5
10
15
20
25
30
35



DOI: 10.3748/wjg.v28.i21.2361 **Copyright** ©The Author(s) 2022.

Figure 3 Burden of liver cancer caused by hepatitis C for 204 countries and territories. A and C: Age-standardized incidence (A) and death (C) rate per 100000 population of liver cancer caused by hepatitis C from 1990 through 2019, stratified by sex or the Socio-demographic Index; B and D: Age-standardized incidence (B) and death (D) rate of liver cancer caused by hepatitis C per 100000 person-years by country and territory, in 2019. The maps in (B) and (D) are generated using the Global Burden of Disease 2019 tool. SDI: Socio-demographic Index.

Gambia and Thailand (Figure 4D; Supplementary material, pages 103-106).

Burden of liver cancer caused by NASH

By stratification using sex, the age-standardized incidence and mortality rates of PLC attributed to NASH in males was found to be higher than in females (Figure 5A and C; Supplementary material, pages 107-108 and 116-117). Similar to the geographical variance observed in PLC caused by alcohol use, the highest age-standardized incidence and death rates of PLC attributed to NASH were reported in the high and middle SDI locations (Figure 5A and C). Between 1990 and 2019, a remarkable difference was observed in the trends of age-standardized incidence rates of PLC attributed to NASH between SDI regions, with the high middle SDI locations [72.9% (55.1-96.0)] showing a declining trend and the high SDI locations showing an increasing trend [182.9% (135.4-248.6)] (Figure 5A; Supplementary Figure 5A; Supplementary material, pages 19-20). The changing pattern for the age-standardized death rate across SDI locations was comparable to that observed in the incidence rate of the same period. In 2019, Mongolia [7.6 (4.9-11.4)] depicted the highest age-standardized incidence rate, followed by Gambia and Qatar (Figure 5B; Supplementary material, pages 112-115). Similar to the order of age-standardized incidence rate, Mongolia [8.7 (5.6-12.9)], Gambia, and Guinea had the highest age-standardized death rate (Figure 5D; Supplementary material, pages 121-124).

Burden of liver cancer attributed to other causes

In terms of sex variance, the age-standardized incidence and mortality rates of PLC attributed to other causes were found to be higher in males (Figure 6A and C). When stratified using the SDI, higher incidence and mortality rates of PLC attributed to other causes were observed for high and middle SDI locations than for low middle and low SDI locations (Figure 6A and C). Between 1990 and 2019, there were remarkable geographical differences in the changing trend of age-standardized incidence rates of PLC attributed to other causes across the SDI regions; the high middle, middle, and low middle SDI locations showed a declining trend, whereas the high SDI locations showed an increasing trend [144.8% (112.8-186.3)] (Figure 6A; Supplementary Figure 6A; Supplementary material, pages 19-20). The geographical differences observed in the age-standardized death rate of PLC attributed to other causes across the SDI regions were comparable to the incidence rate (Figure 6C; Supplementary Figure 6B; Supplementary material, pages 21-22). The highest incidence and death rates of PLC attributed to other causes were observed for Mongolia, Gambia, and Guinea (Figure 6B and D; Supplementary material, pages 130-133 and 139-142).

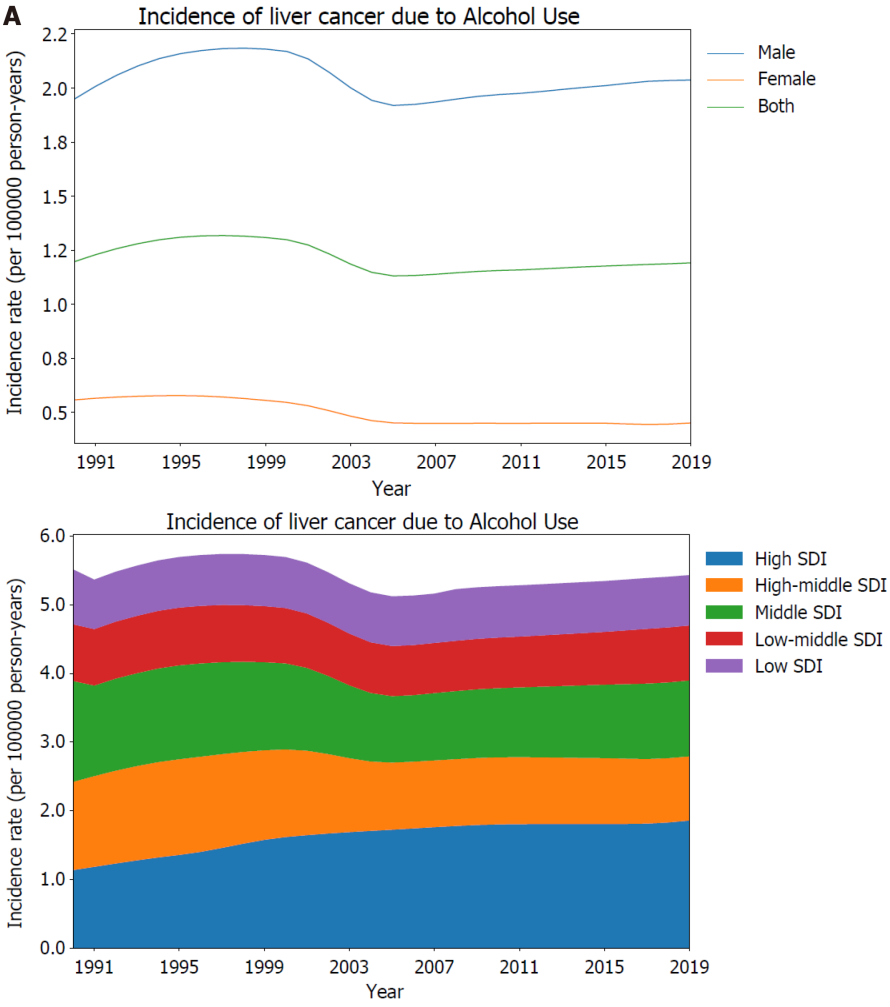
DISCUSSION

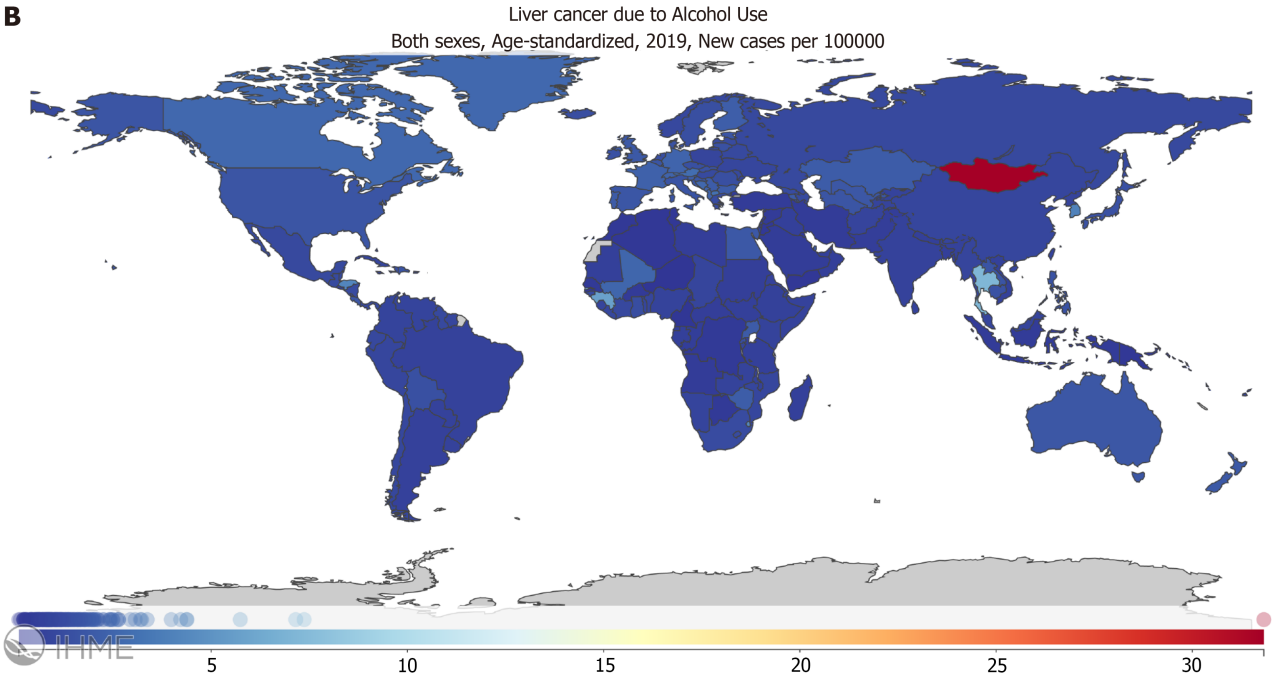
Main findings

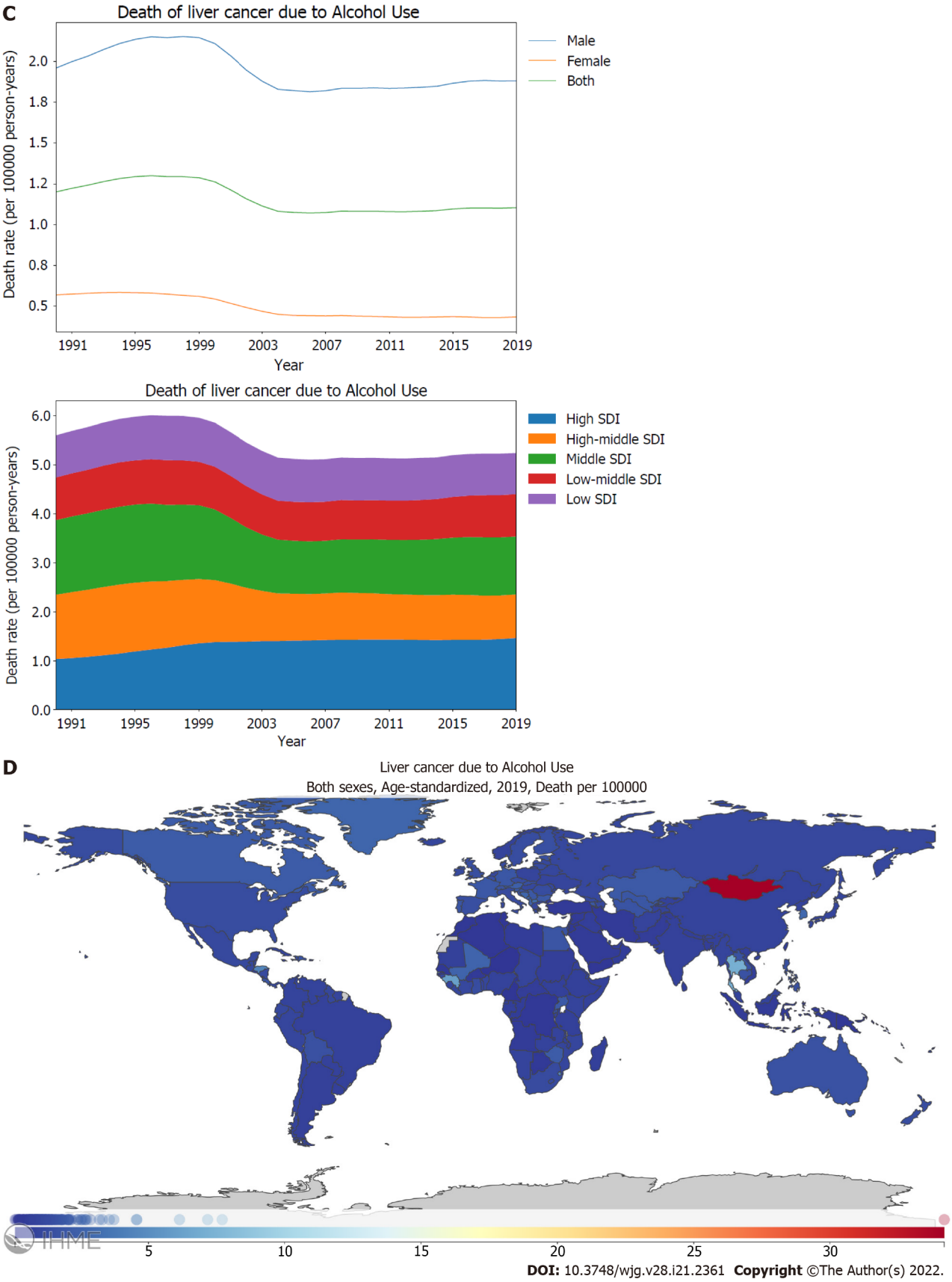
Based on the data from the GBD 2019, we explored the global burden of PLC and focused on the relationship between socioeconomics and the attributable etiologies of PLC. Our main findings are listed below: (1) Global incidence and mortality rates of PLC declined between 1990 and 2019. The decreasing burden of PLC caused by hepatitis B and the declining PLC burden in middle SDI locations was considered the main driver for this favorable trend; (2) PLC had higher prevalence in males; (3) The highest attributable etiology of PLC was hepatitis B, followed by hepatitis C, and alcohol use; (4) The leading attributable etiology of PLC in the middle SDI locations was hepatitis B; and hepatitis C and alcohol use in the high SDI locations; (5) Before 2004, the middle SDI locations surpassed high SDI locations in terms of PLC burden. However, the high SDI locations exceeded the middle SDI locations in terms of PLC burden after 2004; (6) Between 1990 and 2019, the incidence rate of PLC decreased for the high middle SDI locations; it increased for the high SDI locations, according to the stratified causes of PLC including hepatitis B, hepatitis C, alcohol use, and NASH; and (7) In 2019, several countries located in East Asia, South Asia, West Africa, and North Africa shouldered the heaviest burden for incidence and death rates of PLC.

Liver cancer

The risk factors for liver cancer include HBV, HCV, alcohol consumption, metabolic syndrome, diabetes [11]. Although there are substantial variations between countries in the underlying etiologies; globally, HBV accounts for 33%; alcohol, 30%; HCV, 21%, and other causes, 16% of liver cancer deaths[4]. Similar to these findings, we found that the leading attributable etiology of PLC was hepatitis B, followed by hepatitis C, alcohol use, NASH, and other causes, based on the GBD 2019. CHB and CHC cause sustained or repeated inflammatory damage, followed by liver fibrosis and cirrhosis. After liver cirrhosis is established, the risk of hepatocellular carcinoma (HCC) increases substantially. Further, liver cirrhosis caused by NASH substantially increases the risk for HCC[12]. A superimposed condition can enhance the possibility of PLC. For example, alcohol use can contribute to the occurrence of PLC in the setting of CHC.

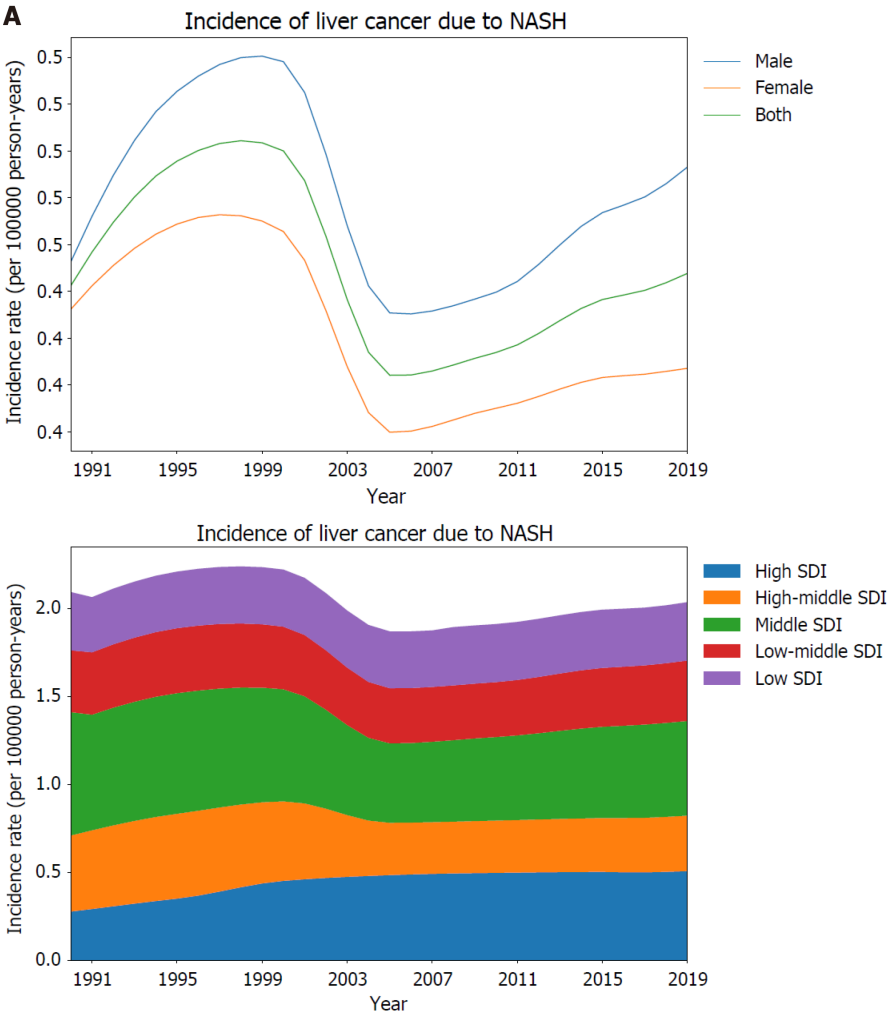

A
Incidence of liver cancer due to Alcohol Use
Incidence rate (per 100000 person-years)
Year
Male
Female
Both
Incidence of liver cancer due to Alcohol Use
Incidence rate (per 100000 person-years)
Year
High SDI
High-middle SDI
Middle SDI
Low-middle SDI
Low SDI

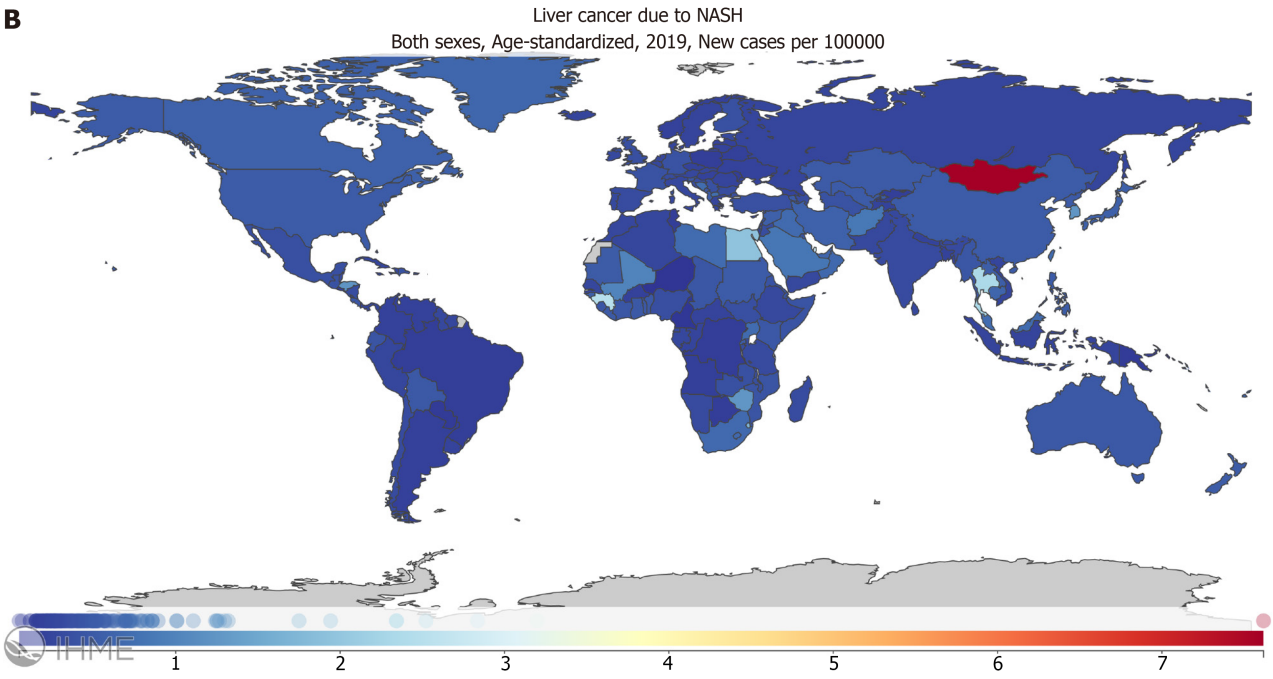

B
Liver cancer due to Alcohol Use
Both sexes, Age-standardized, 2019, New cases per 100000
IHME
5
10
15
20
25
30

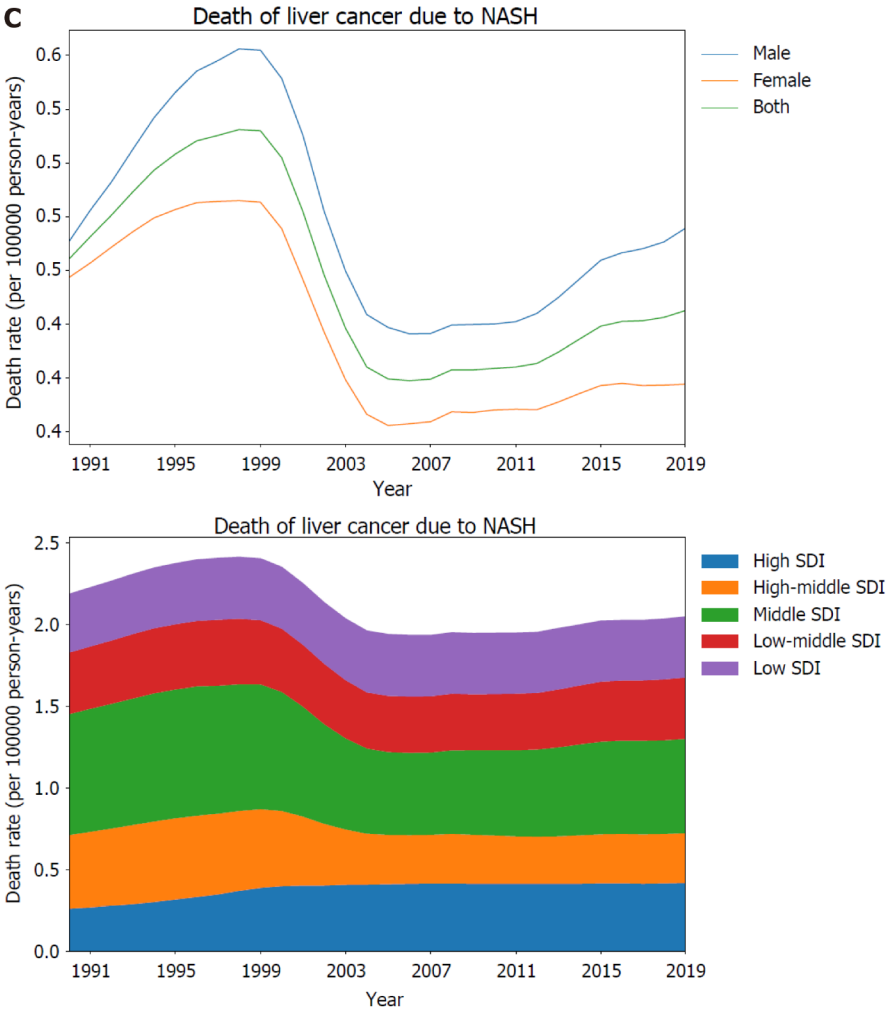


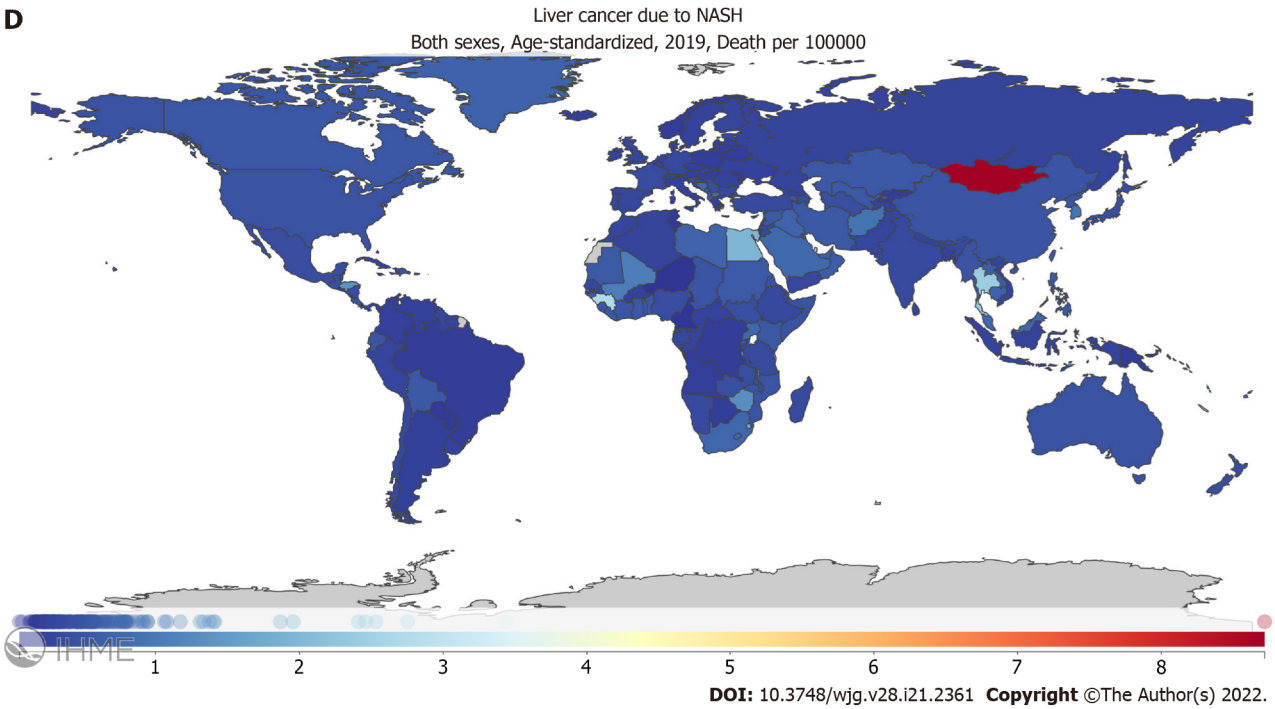
DOI: 10.3748/wjg.v28.i21.2361 **Copyright** ©The Author(s) 2022.

Figure 4 Burden of liver cancer attributed to alcohol use for 204 countries and territories. A and C: Age-standardized incidence (A) and death (C) rate per 100000 population of liver cancer attributed to alcohol use from 1990 through 2019, stratified by sex or the Socio-demographic Index; B and D: Age-standardized incidence (B) and death (D) rate of liver cancer attributed to alcohol use per 100000 person-years by country and territory, in 2019. The maps in (B) and (D) are generated using the Global Burden of Disease 2019 tool. SDI: Socio-demographic Index.


A
Incidence of liver cancer due to NASH
Incidence rate (per 100000 person-years)
0.5
0.5
0.5
0.5
0.5
0.4
0.4
0.4
0.4
1991
1995
1999
2003
2007
2011
2015
2019
Year
Male
Female
Both
Incidence of liver cancer due to NASH
Incidence rate (per 100000 person-years)
2.0
1.5
1.0
0.5
0.0
1991
1995
1999
2003
2007
2011
2015
2019
Year
High SDI
High-middle SDI
Middle SDI
Low-middle SDI
Low SDI


B
Liver cancer due to NASH
Both sexes, Age-standardized, 2019, New cases per 100000
IHME
1
2
3
4
5
6
7





DOI: 10.3748/wjg.v28.i21.2361 **Copyright** ©The Author(s) 2022.

Figure 5 Burden of liver cancer attributed to nonalcoholic steatohepatitis for 204 countries and territories. A and C: Age-standardized incidence (A) and death (C) rate per 100000 population of liver cancer attributed to nonalcoholic steatohepatitis (NASH) from 1990 through 2019, stratified by sex or the Socio-demographic Index; B and D: Age-standardized incidence (B) and death (D) rate of liver cancer attributed to NASH per 100000 person-years by country and territory, in 2019. The maps in (B) and (D) are generated using the Global Burden of Disease 2019 tool. SDI: Socio-demographic Index.

We observed an impressive association between socioeconomic status and the attributable etiologies of PLC. For high middle and middle SDI regions, hepatitis B was the main etiology of PLC whereas hepatitis C was the main etiology of PLC for high SDI regions; this was in accordance with another similar study[6]. In addition to the heavier burden of PLC caused by hepatitis C, the high SDI locations had a higher prevalence of PLC attributed to alcohol use. Given that the prevalence of drinking is greatest for high SDI locations and the least in low middle SDI locations[13], this finding was expected. Although viral hepatitis including CHB and CHC remains the most common cause of liver deaths, nonalcoholic fatty liver disease (NAFLD) is a rapidly growing contributor to liver mortality and morbidity. A similar phenomenon has been observed in China. In 2016, NAFLD cases requiring inpatient care in China outnumbered their counterparts for chronic viral hepatitis[14]. In the United States, the attributable population factors for HCC were greatest for metabolic disorders[15]. Interestingly, the global age-standardized incidence rate of PLC due to hepatitis B reached its peak in 1995-1996, then decreased gradually, as was shown in the GBD 2019. Wide HBV vaccine coverage may have been the potential cause of this beneficial phenomenon. A genetically engineered hepatitis B vaccine was available in 1986. In China, vaccination against HBV began in 1985 using a plasma-derived hepatitis B vaccine. In 1992, a genetically engineered hepatitis B vaccine was licensed in China and managed nationally. The integration of the HBV vaccination into the Expanded Program on Immunization in China has reduced chronic HBV infection by 90% among children < 15 years of age [16]. One of our studies found that the global incidence of acute hepatitis B has decreased gradually since 1990[17]. Usually, a declining trend for HBV incidence precedes a decreasing trend of PLC incidence due to hepatitis B by 10 to 20 years. Similarly, wide HBV vaccine coverage may have contributed to the declining PLC burden in high middle SDI locations since hepatitis B was the most important attributable etiology of PLC in these regions.

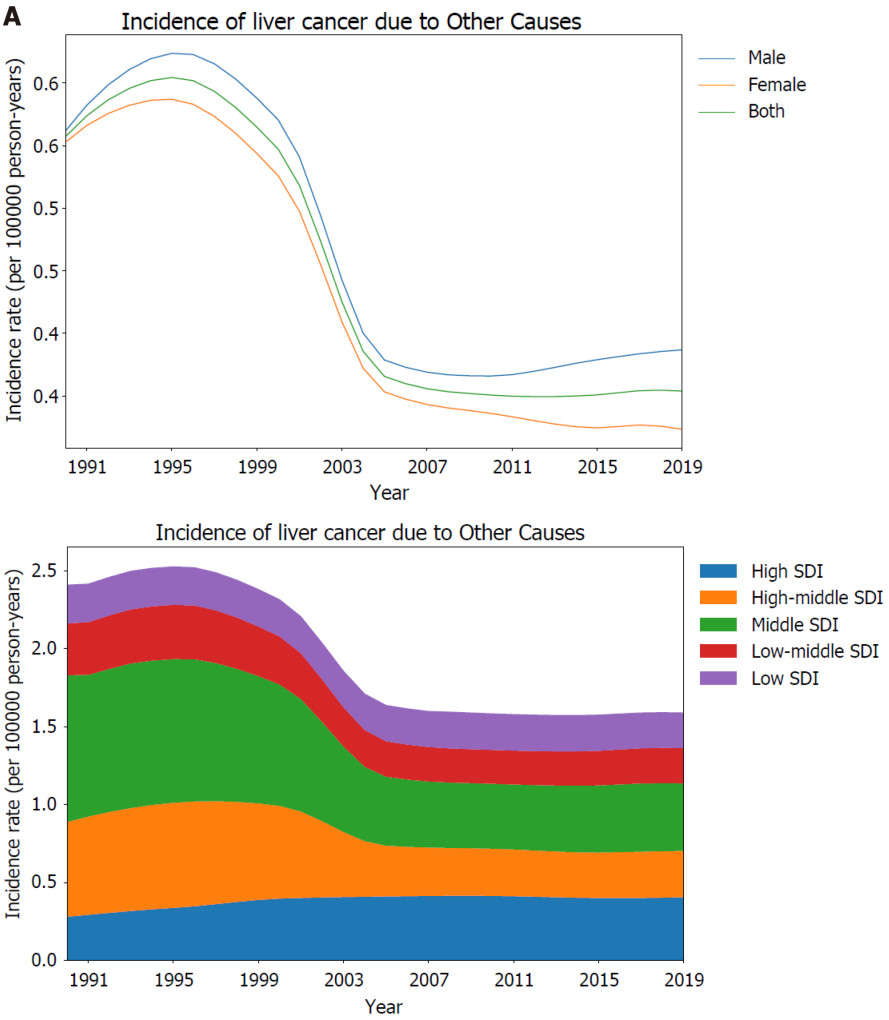
According to the GBD 2019 data, PLC is more prevalent in males. In fact, this is in line with several other observations[4,11]. MyD88-dependent IL-6 production, Foxa1, and Foxa2 play a role in the gender disparity in PLC[18,19]. Furthermore, according to the GBD 2019, there were 534000 (487000-589000) incident cases, and 485000 (444000-526000) deaths attributed to liver cancer globally in 2019; these were significantly lower than those reported in the GBD 2017 and GLOBOCAN 2020[1,6]. In the GBD 2019, the mapping of ICD-10 C22.9 was changed to a garbage code because this would have included both primary and secondary or metastatic cancers (see also https://www.thelancet.com/pb-assets/Lancet/gbd/summaries/diseases/Liver-cancer.pdf). In clinical practice, liver metastasis originating from colorectal cancer or stomach cancer is rather common. Therefore, fewer deaths were mapped for liver cancer in the GBD 2019 than in the GBD 2017. That is, the data of PLC from the databases of the GBD 2016 and GBD 2017 may have unintentionally included cases of metastatic liver cancer.

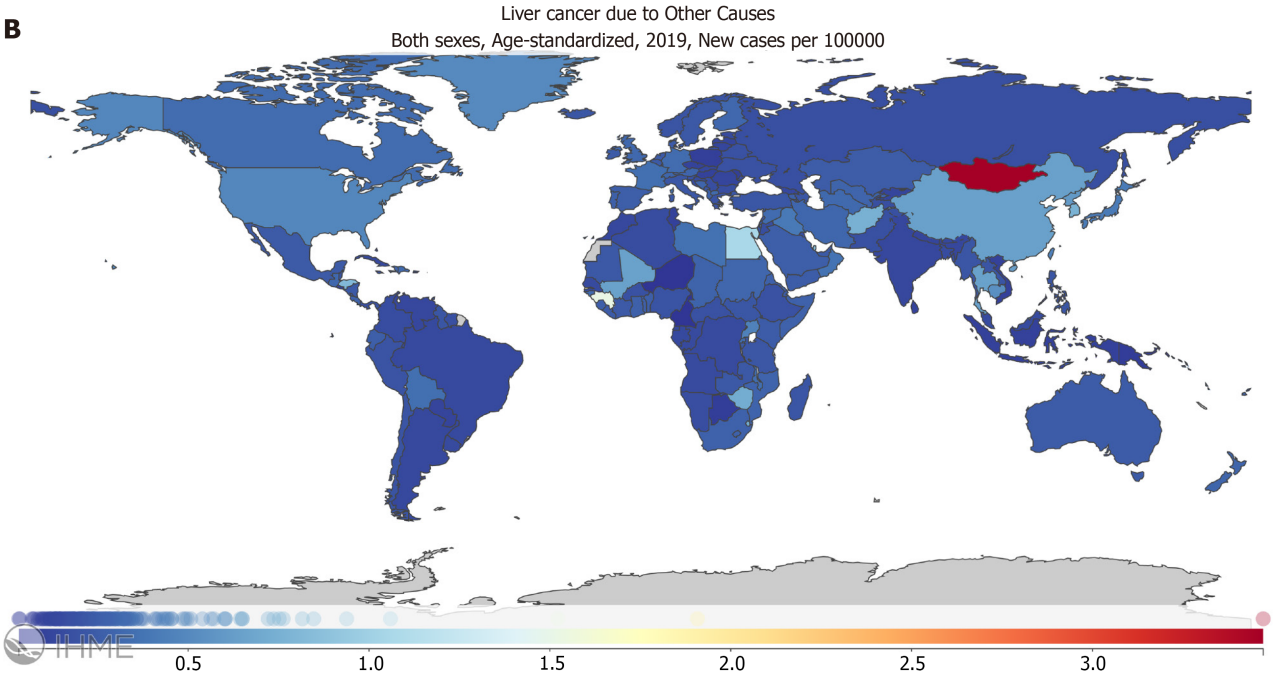
Prospects

In recent years, incidence and mortality rates of PLC have declined in middle SDI locations, such as China and other Eastern and Southeastern Asian countries[20-22]. In line with these findings, the PLC burden has been declining in the high middle and middle SDI locations from 1990 to 2019 according to the GBD 2019; this decline has benefited from the decreasing trend of viral hepatitis, such as CHB. However, the incidence and mortality rates of PLC increased in high SDI locations during the same period, which is in line with several other studies[4,23,24]. After 2004, the PLC burden in high SDI locations surpassed that in middle SDI locations. Several factors contributed to this reversal. First, hepatitis B was the leading attributable etiology of PLC in middle SDI locations. However, vaccination coverage for hepatitis B contributed to the declining trend of PLC in the middle SDI locations. Second, the increasing trend of PLC burden in high SDI locations was attributed to the increasing prevalence of alcohol use and metabolic risk factors for HCC, including metabolic syndrome, obesity, type II diabetes, and NASH[11,13]. As shown in Figures 4A, 4C, 5A and 5C, the gradually increasing burdens of alcohol use and NASH aggravated the burden of PLC in high SDI locations. The epidemiology of HCC has been shifting away from a disease predominated by viral hepatitis to NASH. A similar phenomenon was observed in the United States[25]. Thus, maintaining adequate surveillance of alcohol abuse and NASH is vital to develop strategies against the burden of PLC caused by these conditions.

Prevention

Although PLC causes a heavy burden of cancer incidence and mortality, it (to be precise, HCC) can be prevented by avoiding the risk factors. Compared with the cohort without vaccination, universal HBV vaccination reduced the relative prevalence of HBsAg to 0.24 (0.16-0.35)[26]. Similarly, escalating vaccination policy in China has significantly reduced the prevalence of HBsAg in the recent three decades[16]. Given the heavy burden of PLC caused by hepatitis B in middle and high middle SDI locations, universal HBV vaccination in these areas is considered a practical and principal strategy to minimize the liver cancer burden. Data have indicated that universal HBV vaccination has contributed to a dramatic decline in the PLC burden in several countries and regions[27,28]. For CHB or HBV-related liver cirrhosis, effective antiviral treatment should be provided based on the relative guidelines [29]. Treatment with > 5 years of oral antiviral therapy effectively decreases the HCC incidence regardless of whether patients have baseline cirrhosis[30]. The early diagnosis of CHB and CHC before liver cirrhosis is important considering that liver cirrhosis substantially contributes to the risk of PLC. In


A
Incidence of liver cancer due to Other Causes
Incidence rate (per 100000 person-years)
0.6
0.6
0.5
0.5
0.4
0.4
1991
1995
1999
2003
2007
2011
2015
2019
Year
Male
Female
Both
Incidence of liver cancer due to Other Causes
Incidence rate (per 100000 person-years)
2.5
2.0
1.5
1.0
0.5
0.0
1991
1995
1999
2003
2007
2011
2015
2019
Year
High SDI
High-middle SDI
Middle SDI
Low-middle SDI
Low SDI


B
Liver cancer due to Other Causes
Both sexes, Age-standardized, 2019, New cases per 100000
IHME
0.5
1.0
1.5
2.0
2.5
3.0

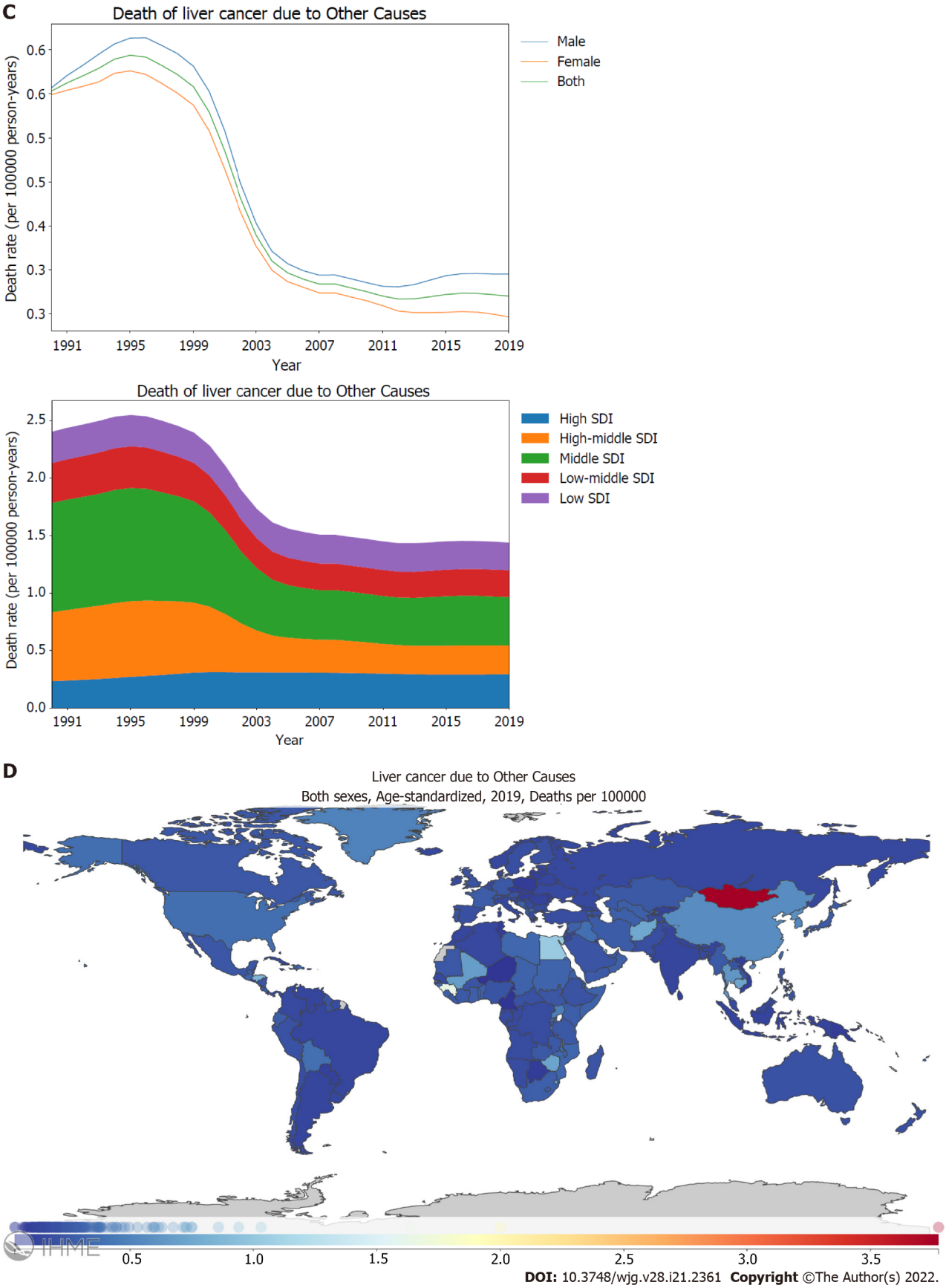


Figure 6 Burden of liver cancer attributed to other causes for 204 countries and territories. A and C: Age-standardized incidence (A) and death (C) rate per 100000 population of liver cancer attributed to other cause from 1990 through 2019, stratified by sex or the Socio-demographic Index; B and D: Age-standardized incidence (B) and death (D) rate of liver cancer attributed to other causes per 100000 person-years by country and territory, in 2019. The maps in (B) and (D) are generated using the Global Burden of Disease 2019 tool. SDI: Socio-demographic Index.

areas where conditions permit, performing non-invasive examinations, such as liver stiffness measure, for individuals with high risk may be potentially beneficial. Unfortunately, there is no effective vaccine for HCV available now; however, DAA have made the eradication of HCV a reality. The achievement of an HCV cure before HCC diagnosis is associated with improved survival[31].

Globally, alcohol use was the seventh leading risk factor for deaths in 2016[13]. As shown in the GBD 2019, alcohol use is a major cause of PLC, especially in high SDI locations. This highlights the need for developing strategies to decrease alcohol use. NAFLD is the third-most common cause of cancer-related deaths worldwide and the seventh most common cause in the United States[32]. Considering the increasing trend of PLC due to NASH, especially in high SDI and middle SDI locations, the control or even reversal of NASH is of critical importance, and this can be attained with lifestyle changes comprising diet, exercise, and weight loss.

Limitations

There are several limitations to this study: (1) There is a possibility of the underestimation of the PLC burden in low middle and low SDI locations because of inadequate cancer screening. However, underestimation of the PLC burden is an inevitable problem, especially in low middle and low SDI locations owing to inadequate cancer screening and lack of registration. Similar limitations have been reported in cervical cancer screenings in low- and middle-income countries[33]. Additionally, in one of our previous studies, the underestimation of acute hepatitis in low-income countries was evident[17]; (2) Insufficient disclosure of geographical variances in large countries such as China and the United States. The GBD reports cancer burden by country or region; however, a large country has significant geographical variances in cancer burden for the urban or rural regions; (3) The lack of finer data for complex cancer, as PLC can be further divided into HCC and cholangiocarcinoma. These subgroups of cancer tend to have different etiologies and exhibit different features in terms of incidence and mortality rates; and (4) The inclusion of undefined etiologies in "other causes" can be leading causes in certain locations.

Despite these limitations, the GBD 2019 data are valuable for policymakers to implement cost-effective interventions, address modifiable risk factors, and prevent PLC efficiently.

CONCLUSION

The pronounced association between socioeconomic development status and PLC burden indicates socioeconomic development status affects attributable etiologies for PLC. GBD 2019 data are valuable for policymakers implementing PLC cost-effective interventions.

ARTICLE HIGHLIGHTS

Research background

Primary liver cancer (PLC) is a common cancer with high morbidity and mortality rates. PLC usually occurs as a preventable disease. Data on global and country-specific levels and trends of PLC are essential for understanding the effects of this disease and helping policymakers to allocate resources.

Research motivation

The association between socioeconomic development status and attributable etiologies for PLC is still unclear.

Research objectives

To investigate the association between the burden of PLC and socioeconomic development status.

Research methods

Cancer mortality and incidence rates of PLC were obtained from the Global Burden of Disease (GBD) 2019, and the data were stratified by the Socio-demographic Index (SDI) level. The association between the attributable etiology of PLC and SDI was described.

Research results

Several countries located in East Asia, South Asia, West Africa, and North Africa shouldered the heaviest burden of PLC in 2019. In terms of incidence rates, the first leading underlying cause of PLC identified was hepatitis B. The incidence rate of PLC was the highest for high and middle SDI locations. The leading attributable etiologies of PLC were hepatitis B for the middle and high middle SDI locations and hepatitis C and nonalcoholic steatohepatitis for the high SDI locations.

Research conclusions

Socioeconomic development status significantly affects attributable etiologies for PLC.

Research perspectives

Our findings are valuable to implement tailored prevention strategies for PLC.

FOOTNOTES

Author contributions: Pan JS had full access to all the data in the study and takes responsibility for the integrity of the data and the accuracy of the data analysis; Pan JS was responsible for its conception and design; Xing QQ, Li JM, Dong X, Zeng DY, Chen ZJ, and Lin XY were responsible for the acquisition, analysis, or interpretation of data; Pan JS drafted the manuscript; Li JM and Dong X made critical revision of the manuscript for important intellectual content; Li JM and Pan JS conducted the data analysis; Xing QQ, Li JM, and Dong X contributed equally to the study.

Supported by the National Natural Science Foundation of China, No. 81871645 (to Pan JS).

Institutional review board statement: The study was reviewed and approved by the Ethics Committee of First Affiliated Hospital of Fujian Medical University (MTCA, ECFAH of FMU[2015]084-1).

Informed consent statement: Not required.

Conflict-of-interest statement: All authors report no conflicts interests.

Data sharing statement: All data are available in the Supplementary material.

STROBE statement: The authors have read the STROBE Statement—checklist of items, and the manuscript was prepared and revised according to the STROBE Statement—checklist of items.

Open-Access: This article is an open-access article that was selected by an in-house editor and fully peer-reviewed by external reviewers. It is distributed in accordance with the Creative Commons Attribution NonCommercial (CC BY-NC 4.0) license, which permits others to distribute, remix, adapt, build upon this work non-commercially, and license their derivative works on different terms, provided the original work is properly cited and the use is non-commercial. See: https://creativecommons.org/Licenses/by-nc/4.0/

Country/Territory of origin: China

ORCID number: Qing-Qing Xing 0000-0002-7578-014X; Jing-Mao Li 0000-0001-5473-5107; Xuan Dong 0000-0002-5853-2136; Dan-Yi Zeng 0000-0002-7233-884X; Zhi-Jian Chen 0000-0003-0478-2188; Xiao-Yun Lin 0000-0002-2724-0333; Jin-Shui Pan 0000-0002-9586-7760.

S-Editor: Yan JP
L-Editor: A
P-Editor: Guo X

REFERENCES

1 **Sung H**, Ferlay J, Siegel RL, Laversanne M, Soerjomataram I, Jemal A, Bray F. Global Cancer Statistics 2020: GLOBOCAN Estimates of Incidence and Mortality Worldwide for 36 Cancers in 185 Countries. *CA Cancer J Clin* 2021; **71**: 209-249 [PMID: 33538338 DOI: 10.3322/caac.21660]
2 **Chen W**, Zheng R, Baade PD, Zhang S, Zeng H, Bray F, Jemal A, Yu XQ, He J. Cancer statistics in China, 2015. *CA Cancer J Clin* 2016; **66**: 115-132 [PMID: 26808342 DOI: 10.3322/caac.21338]
3 **Siegel RL**, Miller KD, Fuchs HE, Jemal A. Cancer Statistics, 2021. *CA Cancer J Clin* 2021; **71**: 7-33 [PMID: 33433946 DOI: 10.3322/caac.21654]
4 **Global Burden of Disease Liver Cancer Collaboration**, Akinyemiju T, Abera S, Ahmed M, Alam N, Alemayohu MA, Allen C, Al-Raddadi R, Alvis-Guzman N, Amoako Y, Artaman A, Ayele TA, Barac A, Bensenor I, Berhane A, Bhutta Z, Castillo-Rivas J, Chitheer A, Choi JY, Cowie B, Dandona L, Dandona R, Dey S, Dicker D, Phuc H, Ekwueme DU, Zaki MS, Fischer F, Fürst T, Hancock J, Hay SI, Hotez P, Jee SH, Kasaeian A, Khader Y, Khang YH, Kumar A, Kutz M, Larson H, Lopez A, Lunevicius R, Malekzadeh R, McAlinden C, Meier T, Mendoza W, Mokdad A, Moradi-Lakeh M, Nagel G, Nguyen Q, Nguyen G, Ogbo F, Patton G, Pereira DM, Pourmalek F, Qorbani M, Radfar A, Roshandel G, Salomon JA, Sanabria J, Sartorius B, Satpathy M, Sawhney M, Sepanlou S, Shackelford K, Shore H, Sun J, Mengistu DT, Topór-Mądry R, Tran B, Ukwaja KN, Vlassov V, Vollset SE, Vos T, Wakayo T, Weiderpass E, Werdecker A, Yonemoto N, Younis M, Yu C, Zaidi Z, Zhu L, Murray CJL, Naghavi M, Fitzmaurice C. The Burden of Primary Liver Cancer and Underlying Etiologies From 1990 to 2015 at the Global, Regional, and National Level: Results From the Global Burden of Disease Study 2015. *JAMA Oncol* 2017; **3**: 1683-1691 [PMID: 28983565 DOI: 10.1001/jamaoncol.2017.3055]

5 **European Association for the Study of the Liver**. EASL Clinical Practice Guidelines: Management of hepatocellular carcinoma. *J Hepatol* 2018; **69**: 182-236 [PMID: 29628281 DOI: 10.1016/j.jhep.2018.03.019]

6 **Lin L**, Yan L, Liu Y, Qu C, Ni J, Li H. The Burden and Trends of Primary Liver Cancer Caused by Specific Etiologies from 1990 to 2017 at the Global, Regional, National, Age, and Sex Level Results from the Global Burden of Disease Study 2017. *Liver Cancer* 2020; **9**: 563-582 [PMID: 33083281 DOI: 10.1159/000508568]

7 **GBD 2019 Diseases and Injuries Collaborators**. Global burden of 369 diseases and injuries in 204 countries and territories, 1990-2019: a systematic analysis for the Global Burden of Disease Study 2019. *Lancet* 2020; **396**: 1204-1222 [PMID: 33069326 DOI: 10.1016/S0140-6736(20)30925-9]

8 **GBD 2017 Colorectal Cancer Collaborators**. The global, regional, and national burden of colorectal cancer and its attributable risk factors in 195 countries and territories, 1990-2017: a systematic analysis for the Global Burden of Disease Study 2017. *Lancet Gastroenterol Hepatol* 2019; **4**: 913-933 [PMID: 31648977 DOI: 10.1016/S2468-1253(19)30345-0]

9 **GBD 2017 Stomach Cancer Collaborators**. The global, regional, and national burden of stomach cancer in 195 countries, 1990-2017: a systematic analysis for the Global Burden of Disease study 2017. *Lancet Gastroenterol Hepatol* 2020; **5**: 42-54 [PMID: 31648970 DOI: 10.1016/S2468-1253(19)30328-0]

10 **GBD 2016 Mortality Collaborators**. Global, regional, and national under-5 mortality, adult mortality, age-specific mortality, and life expectancy, 1970-2016: a systematic analysis for the Global Burden of Disease Study 2016. *Lancet* 2017; **390**: 1084-1150 [PMID: 28919115 DOI: 10.1016/S0140-6736(17)31833-0]

11 **McGlynn KA**, Petrick JL, El-Serag HB. Epidemiology of Hepatocellular Carcinoma. *Hepatology* 2021; **73** Suppl 1: 4-13 [PMID: 32319693 DOI: 10.1002/hep.31288]

12 **Kanwal F**, Kramer JR, Mapakshi S, Natarajan Y, Chayanupatkul M, Richardson PA, Li L, Desiderio R, Thrift AP, Asch SM, Chu J, El-Serag HB. Risk of Hepatocellular Cancer in Patients With Non-Alcoholic Fatty Liver Disease. *Gastroenterology* 2018; **155**: 1828-1837.e2 [PMID: 30144434 DOI: 10.1053/j.gastro.2018.08.024]

13 **GBD 2016 Alcohol Collaborators**. Alcohol use and burden for 195 countries and territories, 1990-2016: a systematic analysis for the Global Burden of Disease Study 2016. *Lancet* 2018; **392**: 1015-1035 [PMID: 30146330 DOI: 10.1016/S0140-6736(18)31310-2]

14 **Xiao J**, Wang F, Wong NK, He J, Zhang R, Sun R, Xu Y, Liu Y, Li W, Koike K, He W, You H, Miao Y, Liu X, Meng M, Gao B, Wang H, Li C. Global liver disease burdens and research trends: Analysis from a Chinese perspective. *J Hepatol* 2019; **71**: 212-221 [PMID: 30871980 DOI: 10.1016/j.jhep.2019.03.004]

15 **Makarova-Rusher OV**, Altekruse SF, McNeel TS, Ulahannan S, Duffy AG, Graubard BI, Greten TF, McGlynn KA. Population attributable fractions of risk factors for hepatocellular carcinoma in the United States. *Cancer* 2016; **122**: 1757-1765 [PMID: 26998818 DOI: 10.1002/cncr.29971]

16 **Cui F**, Shen L, Li L, Wang H, Wang F, Bi S, Liu J, Zhang G, Zheng H, Sun X, Miao N, Yin Z, Feng Z, Liang X, Wang Y. Prevention of Chronic Hepatitis B after 3 Decades of Escalating Vaccination Policy, China. *Emerg Infect Dis* 2017; **23**: 765-772 [PMID: 28418296 DOI: 10.3201/eid2305.161477]

17 **Zeng DY**, Li JM, Lin S, Dong X, You J, Xing QQ, Ren YD, Chen WM, Cai YY, Fang K, Hong MZ, Zhu Y, Pan JS. Global burden of acute viral hepatitis and its association with socioeconomic development status, 1990-2019. *J Hepatol* 2021; **75**: 547-556 [PMID: 33961940 DOI: 10.1016/j.jhep.2021.04.035]

18 **Naugler WE**, Sakurai T, Kim S, Maeda S, Kim K, Elsharkawy AM, Karin M. Gender disparity in liver cancer due to sex differences in MyD88-dependent IL-6 production. *Science* 2007; **317**: 121-124 [PMID: 17615358 DOI: 10.1126/science.1140485]

19 **Li Z**, Tuteja G, Schug J, Kaestner KH. Foxa1 and Foxa2 are essential for sexual dimorphism in liver cancer. *Cell* 2012; **148**: 72-83 [PMID: 22265403 DOI: 10.1016/j.cell.2011.11.026]

20 **Zheng R**, Qu C, Zhang S, Zeng H, Sun K, Gu X, Xia C, Yang Z, Li H, Wei W, Chen W, He J. Liver cancer incidence and mortality in China: Temporal trends and projections to 2030. *Chin J Cancer Res* 2018; **30**: 571-579 [PMID: 30700925 DOI: 10.21147/j.issn.1000-9604.2018.06.01]

21 **Bai L**, Liu Z, Fang Q, Yan Q, Shi O, Bao P, Mu L, Chen X, Zhang T. The trends and projections in the incidence and mortality of liver cancer in urban Shanghai: a population-based study from 1973 to 2020. *Clin Epidemiol* 2018; **10**: 277-288 [PMID: 29563840 DOI: 10.2147/CLEP.S153951]

22 **Wu J**, Yang S, Xu K, Ding C, Zhou Y, Fu X, Li Y, Deng M, Wang C, Liu X, Li L. Patterns and Trends of Liver Cancer Incidence Rates in Eastern and Southeastern Asian Countries (1983-2007) and Predictions to 2030. *Gastroenterology* 2018; **154**: 1719-1728.e5 [PMID: 29549041 DOI: 10.1053/j.gastro.2018.01.033]

23 **Pinheiro PS**, Callahan KE, Jones PD, Morris C, Ransdell JM, Kwon D, Brown CP, Kobetz EN. Liver cancer: A leading cause of cancer death in the United States and the role of the 1945-1965 birth cohort by ethnicity. *JHEP Rep* 2019; **1**: 162-169 [PMID: 32039366 DOI: 10.1016/j.jhepr.2019.05.008]

24 **White DL**, Thrift AP, Kanwal F, Davila J, El-Serag HB. Incidence of Hepatocellular Carcinoma in All 50 United States, From 2000 Through 2012. *Gastroenterology* 2017; **152**: 812-820.e5 [PMID: 27889576 DOI: 10.1053/j.gastro.2016.11.020]

25 **Moon AM**, Singal AG, Tapper EB. Contemporary Epidemiology of Chronic Liver Disease and Cirrhosis. *Clin Gastroenterol Hepatol* 2020; **18**: 2650-2666 [PMID: 31401364 DOI: 10.1016/j.cgh.2019.07.060]

26 **Whitford K**, Liu B, Micallef J, Yin JK, Macartney K, Van Damme P, Kaldor JM. Long-term impact of infant immunization on hepatitis B prevalence: a systematic review and meta-analysis. *Bull World Health Organ* 2018; **96**: 484-497 [PMID: 29962551 DOI: 10.2471/BLT.17.205153]

27 **Chiang CJ**, Yang YW, You SL, Lai MS, Chen CJ. Thirty-year outcomes of the national hepatitis B immunization program in Taiwan. *JAMA* 2013; **310**: 974-976 [PMID: 24002285 DOI: 10.1001/jama.2013.276701]

28 **McGlynn KA**, Petrick JL, London WT. Global epidemiology of hepatocellular carcinoma: an emphasis on demographic and regional variability. *Clin Liver Dis* 2015; **19**: 223-238 [PMID: 25921660 DOI: 10.1016/j.cld.2015.01.001]

29 **Sarin SK**, Kumar M, Lau GK, Abbas Z, Chan HL, Chen CJ, Chen DS, Chen HL, Chen PJ, Chien RN, Dokmeci AK, Gane E, Hou JL, Jafri W, Jia J, Kim JH, Lai CL, Lee HC, Lim SG, Liu CJ, Locarnini S, Al Mahtab M, Mohamed R, Omata M, Park J, Piratvisuth T, Sharma BC, Sollano J, Wang FS, Wei L, Yuen MF, Zheng SS, Kao JH. Asian-Pacific clinical practice guidelines on the management of hepatitis B: a 2015 update. *Hepatol Int* 2016; **10**: 1-98 [PMID: 26563120 DOI:

10.1007/s12072-015-9675-4]

30 **Papatheodoridis GV**, Idilman R, Dalekos GN, Buti M, Chi H, van Boemmel F, Calleja JL, Sypsa V, Goulis J, Manolakopoulos S, Loglio A, Siakavellas S, Keskın O, Gatselis N, Hansen BE, Lehretz M, de la Revilla J, Savvidou S, Kourikou A, Vlachogiannakos I, Galanis K, Yurdaydin C, Berg T, Colombo M, Esteban R, Janssen HLA, Lampertico P. The risk of hepatocellular carcinoma decreases after the first 5 years of entecavir or tenofovir in Caucasians with chronic hepatitis B. *Hepatology* 2017; **66**: 1444-1453 [PMID: 28622419 DOI: 10.1002/hep.29320]

31 **Lockart I**, Hajarizadeh B, Alavi M, Davison S, Prakoso E, Levy MT, George J, Dore GJ, Danta M. Hepatitis C virus cure before hepatocellular carcinoma diagnosis is associated with improved survival. *J Viral Hepat* 2021; **28**: 710-718 [PMID: 33481322 DOI: 10.1111/jvh.13475]

32 **Younossi Z**, Tacke F, Arrese M, Chander Sharma B, Mostafa I, Bugianesi E, Wai-Sun Wong V, Yilmaz Y, George J, Fan J, Vos MB. Global Perspectives on Nonalcoholic Fatty Liver Disease and Nonalcoholic Steatohepatitis. *Hepatology* 2019; **69**: 2672-2682 [PMID: 30179269 DOI: 10.1002/hep.30251]

33 **Lemp JM**, De Neve JW, Bussmann H, Chen S, Manne-Goehler J, Theilmann M, Marcus ME, Ebert C, Probst C, Tsabedze-Sibanyoni L, Sturua L, Kibachio JM, Moghaddam SS, Martins JS, Houinato D, Houehanou C, Gurung MS, Gathecha G, Farzadfar F, Dryden-Peterson S, Davies JI, Atun R, Vollmer S, Bärnighausen T, Geldsetzer P. Lifetime Prevalence of Cervical Cancer Screening in 55 Low- and Middle-Income Countries. *JAMA* 2020; **324**: 1532-1542 [PMID: 33079153 DOI: 10.1001/jama.2020.16244]

World Journal of Gastroenterology

Submit a Manuscript: https://www.f6publishing.com

World J Gastroenterol 2022 June 7; 28(21): 2383-2395

DOI: 10.3748/wjg.v28.i21.2383

ISSN 1007-9327 (print) ISSN 2219-2840 (online)

SYSTEMATIC REVIEWS

Endoscopic ultrasound-guided injectable therapy for pancreatic cancer: A systematic review

Jyotroop Kaur, Veeravich Jaruvongvanich, Vinay Chandrasekhara

Specialty type: Gastroenterology and hepatology

Provenance and peer review: Invited article; Externally peer reviewed.

Peer-review model: Single blind

Peer-review report's scientific quality classification

Grade A (Excellent): A
Grade B (Very good): B
Grade C (Good): 0
Grade D (Fair): 0
Grade E (Poor): 0

P-Reviewer: Chen YH, China; Wang YF, China

Received: December 10, 2021
Peer-review started: December 10, 2021
First decision: January 8, 2022
Revised: January 18, 2022
Accepted: April 22, 2022
Article in press: April 22, 2022
Published online: June 7, 2022

Jyotroop Kaur, Veeravich Jaruvongvanich, Vinay Chandrasekhara, Department of Gastroenterology and Hepatology, Mayo Clinic, Rochester, MN 55905, United States

Corresponding author: Vinay Chandrasekhara, FASGE, MD, Associate Professor, Attending Doctor, Department of Gastroenterology and Hepatology, Mayo Clinic, 200 First St. SW, Rochester, MN 55905, United States. chandrasekhara.vinay@mayo.edu

Abstract

BACKGROUND

Given the low survival rate in pancreatic cancer, new therapeutic techniques have been explored, especially for unresectable or borderline resectable disease. Endoscopic ultrasound (EUS) provides real-time imaging and minimally invasive access for local and targeted injection of anti-tumor agents directly into the pancreatic tumor. Limited studies have been reported using this technique for the treatment of pancreatic ductal adenocarcinoma (PDAC).

AIM

To evaluate the progress made with EUS-guided injectable therapies in the treatment of PDAC.

METHODS

All original articles published in English until July 15, 2021, were retrieved *via* a library-assisted literature search from Ovid Evidence-Based Medicine Reviews and Scopus databases. Reference lists were reviewed to identify additional relevant articles. Prospective clinical studies evaluating the use of EUS-guided injectable therapies in PDAC were included. Studies primarily directed at non-EUS injectable therapies and other malignancies were excluded. Retrieved manuscripts were reviewed descriptively with on critical appraisal of published studies based on their methods and outcome measures such as safety, feasibility, and effectiveness in terms of tumor response and survival. Heterogeneity in data outcomes and therapeutic techniques limited the ability to perform comparative statistical analysis.

RESULTS

A total of thirteen articles (503 patients) were found eligible for inclusion. The EUS-injectable therapies used were heterogeneous among the studies consisting of immunotherapy (n = 5) in 59 patients, chemotherapy (n = 1) in 36 patients, and viral and other biological therapies (n = 7) in 408 patients. Eleven of the studies reviewed were single armed while two were double armed with one randomized

trial and one non-randomized comparative study. Overall, the included studies demonstrated EUS-guided injectable therapies to be safe and feasible with different agents as monotherapy or in conjunction with other modalities. Promising results were also observed regarding their efficacy and survival parameters in patients with PDAC.

CONCLUSION
EUS-guided injectable therapies, including immunotherapy, chemotherapy, and viral or other biological therapies have shown minimal adverse events and potential efficacy in the treatment of PDAC. Comparative studies, including controlled trials, are required to confirm these results in order to offer novel EUS-based treatment options for patients with PDAC.

Key Words: Pancreatic ductal adenocarcinoma; Endoscopic ultrasound-guided fine-needle injection; Local injectable therapy; Immunotherapy; Chemotherapy; Oncolytic viral therapy

©The Author(s) 2022. Published by Baishideng Publishing Group Inc. All rights reserved.

Core Tip: Pancreatic ductal adenocarcinoma (PDAC) is a highly lethal malignancy. Resistance to systemic therapies may be attributable to the dense stromal matrix in the pancreatic tumor mass. Endoscopic ultrasound-guided fine-needle injection (EUS-FNI) is a novel technique to deliver various anti-tumor agents locally in real-time and may overcome this limitation. This review examines the EUS-FNI therapies used to treat PDAC.

Citation: Kaur J, Jaruvongvanich V, Chandrasekhara V. Endoscopic ultrasound-guided injectable therapy for pancreatic cancer: A systematic review. *World J Gastroenterol* 2022; 28(21): 2383-2395
URL: https://www.wjgnet.com/1007-9327/full/v28/i21/2383.htm
DOI: https://dx.doi.org/10.3748/wjg.v28.i21.2383

INTRODUCTION

Pancreatic cancer is associated with a 5-year survival rate of approximately 10% at diagnosis and is the seventh leading cause of cancer-related deaths worldwide[1]. Pancreatic ductal adenocarcinoma (PDAC) accounts for more than 90% of cases of pancreatic cancer. The very low survival rate is partly due to the lack of early diagnosis and limited response to systemic therapies[2]. Only 15%-20% of patients present with surgically resectable disease and less than 10% undergo complete resection, which is the only curative intervention[3,4]. The majority of patients who present with unresectable locally advanced pancreatic cancer (LAPC) or metastatic disease are managed with systemic chemotherapy and/or radiotherapy with a very limited prognosis. The introduction of newer chemotherapy combinations and regimens have shown some promising results but still the overall survival (OS) remains dismal[5,6]. One of the many reasons for failure of systemic chemotherapy has been hypothesized as poor delivery of these agents due to abundant stromal matrix and deficient vasculature[7]. This justifies the rationale to explore the use of direct intratumoral injection for targeted delivery of an anti-tumor agent into the tumor mass while minimizing systemic complications. Percutaneous injection of direct intratumoral agents under ultrasound or computed tomography (CT) guidance has been demonstrated to be safe and feasible in phase I trials but this is technically cumbersome and difficult for administering multiple doses[8,9]. Endoscopic ultrasound (EUS) provides the opportunity for real-time visualization of the pancreatic mass and allows minimally invasive access for injectable therapies. This systematic review focuses on the methodology and outcomes of previously published clinical studies on EUS-guided fine needle injection (EUS-FNI) of anti-tumor agents in patients with PDAC.

MATERIALS AND METHODS

Literature search

An expert librarian conducted searches of the Ovid Evidence-Based Medicine Reviews (Embase, MEDLINE, Cochrane Central Register of Controlled Trials, Cochrane Database of Systematic Reviews) and Scopus databases to identify studies published between database inception until July 15, 2021, using the search strategy in Supplementary Table 1. The search was limited to full reports and articles published in English. The titles and abstracts were screened by two independent reviewers (JK and VC) and were assessed for eligibility based on the evaluation of the full manuscript. Disagreements between

the two reviewers were resolved by discussion. Additional studies were identified from searching through references and were screened similarly.

Inclusion criteria

The review is restricted to published prospective studies reporting the effects of injectable interventions primarily using the EUS-FNI technique in patients with PDAC, irrespective of the stage. Therapeutic interventions may include any form of immunotherapy, chemotherapy, or biological agents. Studies that utilized co-interventions and other modes of therapy delivery along with EUS-FNI were included. Studies were eligible if they assessed at least one of the outcomes of interest: Safety, feasibility, and efficacy in terms of tumor response and/or survival.

Exclusion criteria

Benchtop and animal models were excluded as were studies using non-EUS directed therapies. Studies investigating other pancreatic tumors and multiple gastrointestinal cancers where data for the PDAC group was not separately reported were also excluded. Studies were not considered eligible for inclusion if they did not focus on the treatment of PDAC and rather explored the effects of the interventions on palliation and symptom control.

Data extraction

Data was extracted on studies' characteristics of interest- participants, study design, interventions (*e.g.*, therapeutic agent, dosage, and EUS-FNI technique), prior therapies and co-interventions, outcome measures, and results. Relevant data from the included articles were recorded in itemized tables using Microsoft Excel for Microsoft 365 (MSO 16.0.13801.21002) 64 bit.

Outcomes

Outcome parameters of toxicity and clinical efficacy (tumor response and/or survival parameters) were reported as defined by the individual studies. Grade 3-4 AEs included those with severe or life-threatening toxicity.

Statistical analysis

Heterogeneity in data outcomes and therapeutic techniques limited the ability to perform comparative statistical analysis.

Quality assessment

The risk of bias in the included studies was assessed by two independent reviewers (JK, VJ) using the NIH Study Quality Assessment tools for controlled intervention studies and the before-after (pre-post) studies with no control group[10]. These guidelines help to rate the studies as good, fair, or poor based on a set of quality criteria questions. The tools were adapted keeping in mind the nature of the study being reviewed by identifying and reporting some questions as non-applicable as deemed by the reviewers. The results were compared, and any differences were resolved by discussion.

RESULTS

The literature search yielded 101 publications. Title and abstract screening further yielded 30 potentially eligible publications. A full review of manuscripts identified 9 eligible reports along with 4 eligible reports found after backward reference searching leading to a total of 13 full-text articles with 503 patients that were included in the systematic review. The baseline characteristics of these studies are included in Table 1. All were single arm studies except 2, one of which was a randomized controlled trial (RCT) while the other was a non-randomized study. The EUS-injectable therapy administered was heterogeneous among the studies and consisted of immunotherapy (n = 5) in 59 patients, chemotherapy (n = 1) in 36 patients, and viral and other biological therapies (n = 7) in 408 patients.

The quality assessment process identified 11 studies as good and 2 as fair, the details of which are attached in Supplementary Tables 2 and 3.

EUS-guided fine needle injection

Linear array echoendoscopes have facilitated the simultaneous visualization of a target lesion and advancement of a needle from the distal tip of the echoendoscope under precise control to aspirate, inject, or gain access to the organ[11]. This has expanded the role of EUS into the realm of therapeutic interventions with a wide range of applications. EUS-FNI has demonstrated safety and feasibility in applications such as celiac plexus block/neurolysis for the management of pancreas-related pain or pancreatic cyst ablation[12,13]. More recently, its use has been explored for the injection of anti-tumor agents in patients with pancreatic cancer as an attractive method of delivery of such agents considering its minimal invasiveness and low rate of adverse events (AEs)[14].

Table 1 Characteristics of published clinical studies using endoscopic ultrasound-guided fine-needle injection for pancreatic ductal adenocarcinoma

Ref.	Disease	Country	No. of subjects, No. of groups	Study type	EUS-FNI injectable agent	Type of therapy	Aes	Tumor response	Median survival
Chang *et al* [17], 2000	Unresectable PDAC	United States	8, single arm	Phase I	Allogeneic mixed lymphocyte culture	Immunotherapy	DLT-0	Partial remission 25%, minor response 12.5%	13.2 mo (OS)
Irisawa *et al* [21], 2007	Unresectable PDAC refractory to gemcitabine	Japan	7, single arm	Pilot clinical study	Dcs	Immunotherapy	Aes-0	Mixed response 28.6%, stable disease 28.6%	9.9 mo (OS)
Hirooka *et al* [22], 2009	LAPC	Japan	5, single arm	Phase I	OK-432-pulsed dcs	Immunotherapy	Grade 3 or 4 aes-0	Effective response 60% (partial remission 20%, stable disease 40%)	15.9 mo (OS)
Endo *et al*[24], 2012	Resectable PDAC	Japan	24, two arms	Phase I	Idcs and OK-432	Immunotherapy	Grade 3 aes-1	NA	No difference
Hirooka *et al* [25], 2017	LAPC	Japan	15, single arm	Phase I/II	Zoledronate-pulsed dcs	Immunotherapy	DLT-0 (grade 3 aes-4)	Stable disease 46.7%	11.5 mo (OS)
Levy *et al*[27], 2017	Unresectable PDAC	United States	36, single arm	Prospective non-randomized	Gemcitabine	Chemotherapy	Aes-0	Partial response 25%, stable disease 57%	10.4 mo (OS)
Hecht *et al*[31], 2003	Unresectable PDAC without liver metastasis	United States	21, single arm	Phase I/II	ONYX-015	Viral therapy	Aes-8 (four related to the virus and four to the injection technique)	Partial response 10%, stable disease 38%	7.5 mo (OS)
Hecht *et al*[9], 2012	LAPC	United States	50, single arm	Phase I/II	Tnferade Biologic	Viral therapy	DLT-3	Complete response 2%, partial response 6%, minor response 8%, stable disease 24%	297 d (OS)
Herman *et al* [33], 2013	LAPC	United States	304, two arms	Randomized phase III	Tnferade Biologic	Viral therapy	No difference in grade 3 to 4 aes	No difference	10.0 mo (OS) for both arms
Hirooka *et al* [35], 2018	LAPC	Japan	12, single arm	Phase I	HF-10	Viral therapy	DLT-0, Serious aes-2, Grade 3 aes-5	Effective response 78%	5.5 mo (OS)
Lee *et al*[36], 2020	LAPC	South Korea	9, single arm	Phase I	Ad5-DS	Viral therapy	DLT-0	Overall response 11%, disease control rate 100%	11.4 mo (PFS)
Nishimura *et al* [40], 2018	Unresectable PDAC	Japan	6, single arm	Prospective non-randomized	STNM01	RNA oligonuc-leotide	Aes-0	NA	5.8 mo (OS)
Hanna *et al* [42], 2012	Unresectable PDAC	United States, Israel	6, single arm	Phase I/IIA	BC-819	DNA plasmid	DLT-1	Overall response 33.3% and 66.7% in the two dose cohorts respectively	100% and 66.7% (six-month survival) in the two dose cohorts

AEs: Adverse events; NA: Not available; PDAC: Pancreatic ductal adenocarcinoma; LAPC: Locally advanced pancreatic cancer; iDC: Immature dendritic cell; DLT: Dose-limiting toxicity; OS: Overall survival; PFS: Progression-free survival.

Immunotherapy

Cancer immunotherapy aims to harness the inherent ability of the host immune system to mount an effective anti-tumor response against cancer cells through multiple strategies. Therapeutic cancer vaccines stimulate the activation of cytotoxic T lymphocytes (CTLs) against unique immunogenic tumor antigens by enhancing the delivery of these antigens[15].Targeting immune checkpoint inhibitor molecules aids in disrupting the immune suppressive mechanisms developed by cancer cells to evade immunosurveillance while the adoptive transfer of engineered lymphocytes expressing tumor epitopes or chimeric receptors aims to mediate anti-tumor response[16]. After mixed results with studies employing systemic immunotherapy in PDAC, direct administration with EUS-FNI has been used.

Allogeneic mixed lymphocyte culture: The first reported clinical study that used the novel delivery technique of EUS-FNI as local injectable therapy for PDAC was reported in 2000[17]. It was also the first attempt at administering biological response modifier or cellular-based immune therapy for the treatment of PDAC. The authors used allogeneic mixed lymphocyte culture prepared by coincubation of peripheral blood mononuclear cells from the patient and an allogeneic blood donor to generate a mixed lymphocyte reaction (MLR). It was based on the hypothesis that the MLR results in a high concentration of cytokines within the tumor which upregulates host anti-tumor effector mechanisms to aid in tumor regression. Patients with unresectable PDAC underwent a single session EUS-FNI procedure using 3, 6, and 9 billion cells in a dose-escalation manner. The median OS was documented to be 13.2 mo although there were only 2 partial responses and 1 minor response on either CT or EUS. Dose-limiting toxicity (DLT) was not reached and there were no procedure-related AEs were reported. Low-grade fever was the most common AE but was not associated with leukocytosis and was treated with acetaminophen. There were three grade 3 gastrointestinal toxicities and three grade 3 elevations in bilirubin which were transient and resolved after replacing the preexisting biliary stents in the patients. The encouraging results led to a multicenter RCT comparing EUS-guided injection of the allogeneic mixed lymphocyte culture to conventional IV gemcitabine therapy, but it was not completed as interim results suggested better survival and tumor response in the gemcitabine arm.

Dendritic cells as cancer vaccine: Dendritic cells (DCs) act as potent antigen-presenting cells (APCs) to generate anti-cancer immunity through stimulation of host primary T cell response. Immature or unloaded DCs (iDCs) acquire specific tumor-derived antigens, process them in situ, and migrate to lymphoid organs for presentation to CTLs[18]. Although vaccine strategies for delivering immunogenic tumor antigens themselves as synthetic peptides have been developed for different tumors, these require identification of specific antigens and evidence of their immunogenicity in the tumor microenvironment (TME). Despite autologous tumor cell lysates being used to provide specific tumor antigens in the clinical studies involving cancers with poorly defined antigens, there is evidence to support APCs as potent vaccines to more effectively cross-prime the CTLs with apoptotic tumor cells and apoptotic bodies[19,20]. Considering the difficulty in attaining sufficient quantities of tumor cells for *ex vivo* loading of DCs, it is reasonable to inject iDCs that can get exposed to tumor antigens *in vivo* after administration of apoptosis-inducing therapy like radiotherapy or chemotherapy.

The first report of the use of iDC injection for pancreatic cancer was a pilot clinical study in patients with unsuccessfully treated (gemcitabine resistant) unresectable PDAC[21]. Seven patients underwent cycles of EUS-FNI of unpulsed iDCs in the dose of 10 million cells or more at 2 to 3 sites within the pancreatic mass. iDCs were injected on days 1, 8, and 15 with cycles repeated every 28 d. Five patients received prior radiation therapy to induce apoptosis and facilitate tumor antigen cross-presentation. No procedural AEs were noted, and all DC injections were tolerated without clinical toxicity. Two patients demonstrated a mixed response and two others had stable disease for more than 6 mo. Median patient survival was 9.9 mo despite resistance to gemcitabine.

Hirooka *et al*[22] explored DC-based vaccination as first-line therapy for unresectable LAPC and combined it with gemcitabine based on its known apoptosis-inducing effects. It was postulated to release tumor antigens slowly over time for processing and presentation by DCs. The study used DCs pulsed with OK-432, penicillin killed and lyophilized preparation of a low-virulence strain of Streptococcus pyogenes, which acts as an immunopotentiating agent reported to stimulate DC maturation and T cell activation[23,24]. Conventional lymphokine-activated killer cells stimulated with anti-CD3 monoclonal antibody (CD3-LAKs) were also administrated systemically to induce additional anti-cancer activity. The results showed the combined therapy to be safe and synergistically effective with a median survival of 15.9 mo. Effective radiological tumor response was evidenced in three patients with 1 partial response and 2 long stable diseases for more than 6 mo. Interestingly, the patient with partial remission and the longest survival of 25.4 mo also exhibited significant immunological response with respect to the number of interferon gamma producing cells in peripheral blood lymphocytes (PBLs) and tumor-antigen specific CTL activity.

Based on this study, the authors reported a recent clinical study assessing the safety and efficacy of comprehensive immunotherapy combined with IV gemcitabine as first-line therapy for patients with LAPC[25]. Twelve cycles of EUS-FNI were performed using zoledronate-pulsed DCs rather than the previously used OK-432 pulsed DCs along with systemic administration of adoptive activated T lymphocytes (αβT) and gemcitabine every 14 d. DLT was reported. Grade 3 toxicity was recorded in

four patients, including the two patients that were attributed to gemcitabine. Seven of the 15 patients showed a stable disease tumor response with most showing long-term clinical responses. Patients receiving this therapy were noted to have a higher quality of life assessments as well as the immunological response which was evaluated by the ratio of the number of $CD8^+$ T cells to that of regulatory T cells ($CD8^+$/Treg ratio) was found to be significantly higher in patients with stable disease. The median OS and progression-free-survival (PFS) of 15 patients were 12.0 mo and 5.5 mo, respectively. Patients with pre-treatment neutrophil/lymphocyte ratio (NLR) lower than 5.0 demonstrated significantly longer survival. In an analysis limited to patients with an NLR lower than 5.0, the patients whose $CD8^+$/Treg ratio increased more than twofold survived longer. This suggests that using precise biomarkers such as NLR and $CD8^+$/Treg ratio can make comprehensive immunotherapy more beneficial for subgroups of patients with PDAC.

Another study compared 9 patients who received EUS-FNI of iDCs and OK-432 prior to the pancreatectomy surgery to 15 patients who did not receive this therapy[24]. The intervention group patients also received intra-operative radiotherapy to the retroperitoneal space. There were no severe toxicities following the pre-operative iDC injection except for one transient grade 3 fever. The incidence of postoperative complications was similar in both DC and non-DC groups. Although there was no statistically significant difference in OS times of both groups, the authors reported that 2 patients from the DC group, one of which was stage IV with distant lymph node metastasis, survived more than 5 years without requiring adjuvant therapy. Immunohistochemical examination of the surgically dissected lymph nodes revealed significantly higher $CD83^+$ cells in the regional lymph nodes and higher accumulated $Foxp3^+$ cells in both regional and distant lymph nodes in the DC group. This study not only demonstrated the safety and feasibility of preoperative EUS-FNI but also illustrated the potential of inducing an effective immune response against PDAC.

Chemotherapy

Although systemic chemotherapy forms the basis of standard of care (SOC) treatment for unresectable PDAC primarily LAPC, only one clinical study has so far reported the use of a chemotherapeutic agent being injected locally *via* the EUS-FNI technique.

Gemcitabine

Gemcitabine has been standard therapy for surgically unresectable PDAC since 1997 with an established record of use, safety, and relative benefit when administered intravenously[26]. Given its safety profile, it was selected to be administered in a prospective study conducted at our institution[27]. Patients with locally advanced (n = 20) and metastatic (n = 13) PDAC in whom surgical resection was not performed were included to undergo a single session of EUS-FNI using gemcitabine in the concentration of 38 mg/mL injected *via* a 22-gauge needle. The needle tip was placed 0.5-1.0 cm from the distal tumor edge with injection as the needle retracted proximally to inject approximately 50% of the dose uniformly along the perimeter of the tumor at sites of local infiltration (*e.g.*, blood vessels) and 50% within the remainder of the tumor. Multiple needle passes were performed (median 3, range 1-4) until the injectate was not limited within the tumor but instead began to infiltrate along needle tract or peritumoral sites, leading to varied injection volumes. The median volume of injectate per patient was 2.5 mL (range, 0.7-7.0 mL) corresponding to an intratumoral gemcitabine dose of 95 mg (range, 27-266 mg). Patients underwent subsequent conventional multimodality therapy: Chemoradiotherapy (n = 22), chemotherapy alone (n = 10), no therapy (n = 1), or indeterminate therapy (n = 3). There were no AEs attributable to the EUS-FNI procedure. OS at 6 mo, 12 mo, and 5 years were 78%, 44%, and 3%, respectively. The median OS was 10.4 mo [95% confidence interval (CI): 2.7-68.0]. From the 20 patients with stage III unresectable disease, 4 (20.0%) were downstaged and underwent an R0 resection. Patients who had a more complete therapy based on a visual score showed the greatest increase in median survival (P < 0.0001) with a consistent trend of increasing survival as completeness increased. Although completeness of therapy corresponded to prolonged survival, the significance of this finding is potentially limited by the subjective nature of its assessment.

Oncolytic viral therapy

Oncolytic viruses (OVs) are increasingly being explored as a therapeutic option because of their ability to be engineered for tumor selectivity and express genes of interest within the tumor cells to cause cytotoxic effects and cell death[28,29]. Unlike gene therapy, OVs are replication-competent and propagate within tumor cells, generating infectious progeny that further spreads to surrounding cells after tumor cell lysis. Therefore, in theory, OVs have the potential for efficient oncolysis in solid tumor masses[30].

Onyx-015: ONYX-015 is the first replication selective virus used in clinical trials. It is a chimeric human group C adenovirus with a deletion in the E1B-55kD gene inhibiting p53 function which is already lost in most cancer cells making them susceptible to this agent[31]. In a clinical study of 21 patients with unresectable PDAC, eight sessions of EUS-FNI with ONYX-015 were administered over 8 wk along with systemic gemcitabine therapy. The viral agent was administered in the dosage of 2×10^{10} particles/session (n = 3) and 2×10^{11} particles/session (n = 3) in phase I, and 2×10^{11} particles/session (n = 15) in

phase II of the same study which was the MTD (maximum tolerated dose). EUS-FNI was performed using a transgastric or transduodenal approach with a 22-gauge needle in a fanning pattern during the withdrawal of the needle. Two cases of duodenal perforation that were observed were attributed to the stiff tip of the echoendoscope and thus the protocol was modified only allowing for transgastric FNI. Subsequently, no luminal perforations were noted. Additionally, two cases of sepsis were noted, which may have been related to the injection technique. Thus, the protocol was again modified such that the needles were not fully retracted into the lumen during repositioning and repassage of the needle. Furthermore, the study authors instituted prophylactic administration of oral ciprofloxacin. ONYX-015 itself was well tolerated. Asymptomatic grade 3 and 4 increases in amylase and lipase were detected in 10% of patients, but no clinical pancreatitis was observed. After the combination therapy, objective partial regression of > 50% was seen in 2 out of 21 patients (10%) treated. Two patients demonstrated minor radiographic response to treatment, 6 had stable disease, and the remaining 11 had progressive disease or had to go off study because of treatment toxicity. This study established that EUS guided transgastric injection of ONYX-015 adenovirus into PDAC was both feasible and safe and that such an approach may be extended to other novel biological agents.

TNFerade: TNFerade™ Biologic (also called "AdGVEGR.TNF.11D" or "TNFerade"), is a replication-deficient adenoviral vector for selective delivery of tumor necrosis factor-α (TNF-α) into tumor cells. It consists of Egr-1 promoter gene located upstream to the cDNA which is radiation inducible, hence providing spatial and temporal control of the cytotoxicity by TNF-α[9]. TNF- α may also act as a radiosensitizer and enhance the effect of subsequent radiation therapy[32]. In a multicenter study investigating the safety and feasibility of intratumoral gene therapy with TNFerade Biologic along with standard chemoradiotherapy as first-line treatment for LAPC, subjects were administered either EUS-FNI or percutaneous injection under ultrasound or CT guidance[9]. Twenty-seven patients underwent EUS-FNI and 23 received a percutaneous injection of TNFerade once a week for 5 wk in a dose-escalation manner. A total volume of 2 mL was administered per session of EUS-FNI and injected as four 0.5 mL injections into different areas of the tumor. The maximum tolerated dose was calculated as 4×10^{11} PU after the appearance of DLT of pancreatitis and cholangitis in 3 patients at the highest dose. Overall grade 3 and 4 toxicities included GI bleeding, deep vein thrombosis (DVT), pulmonary emboli, pancreatitis, and cholangitis which had an unclear attributability to the treatment which was therefore concluded to be well tolerated. There occurred 1 complete response (2%), 3 partial responses (6%), 4 minor response (8%) and 12 had stable disease (24%). Seven patients subsequently had an operative resection, 6 of which had clear margins, and 3 had a survival of more than 24 mo. Furthermore, the overall outcome was not influenced by the mode of delivery of TNFerade Biologic (either by EUS or percutaneous injection).

Based on these results, a multicenter RCT was conducted in patients with LAPC who were assigned to receive either TNFerade along with SOC chemoradiotherapy or SOC alone[33]. TNFerade intratumoral injection was delivered in the dose of 4×10^{11} PU using a CT or ultrasound-guided percutaneous transabdominal approach (PTA) or EUS-guided transgastric or transduodenal approach before the first fraction of radiotherapy each week for 5 wk. The mode of delivery was based on the discretion of the individual study sites. SOC consisted of continuous infusion 5-fluorouracil and radiotherapy, followed by gemcitabine or gemcitabine plus erlotinib maintenance therapy. The trial was discontinued based on futility after planned interim analysis. Median OS of TNFerade plus SOC *vs* SOC alone (10.0 mo *vs* 10.0 mo; HR: 0.90; 95%CI: 0.66-1.22; $P = 0.26$) and median PFS (6.8 mo *vs* 7.0 mo, respectively; HR: 0.96; 95%CI: 0.69-1.32; $P = 0.51$) were similar in both groups. Multivariate analyses showed that the EUS-FNI approach rather than the percutaneous transabdominal approach was a risk factor for lower PFS (HR: 2.08; 95%CI: 1.06-4.06; $P = 0.032$). Higher rates of definite or probable grade 1 and 2 fever and chills were observed in TNFerade plus SOC *vs* SOC arm alone. Significantly more grade 2 to 4 toxicities were present in the TNFerade plus SOC arm, but this was not dose-limiting suggesting that conditional expression of TNF-α through Egr-1 promoter limits systemic toxicity. TNFerade administration in this study did not prove effective in prolonging survival in patients with LAPC.

HF-10: HF-10 is a spontaneously mutated oncolytic herpes simplex virus-1 reported to have high tumor selectivity and reduced neuro invasiveness[34]. A phase 1 trial published in 2018 evaluated the safety and anti-tumor effectiveness of a triple combination therapy consisting of EUS-guided intratumoral injection of HF-10 along with systemic gemcitabine and erlotinib therapy for unresectable LAPC[35]. Patients underwent twice-weekly HF10 injections to a total of four injections unless DLT appeared. Three cohorts were designed in a dose escalation of 1×10^6, 3×10^6, and 1×10^7 pfu/d. Five patients developed grade III myelosuppression due to chemotherapy and two had serious AEs (perforation of duodenum and grade IV hepatic dysfunction) which were concluded to be unrelated to HF-10. Out of the nine subjects who completed the treatment, the tumor response was three partial responses and four stable diseases. Although the median PFS was relatively short as 6.3 mo, the median OS was 15.5 mo and two patients achieved long-term survival over 3 years. Infiltration of $CD4^+$or $CD8^+$cells was well documented in surgical specimens of two patients who ultimately downstaged and underwent surgery, highlighting the idea that oncolytic viruses might not only aid in tumor destruction but may also trigger host anti-tumor response.

Ad5-DS: Ad5-DS is a second-generation, replication-competent oncolytic adenovirus containing double suicide genes that convert prodrugs, 5-fluorocytosine, and valganciclovir, to active cytotoxic metabolites. In a recent Phase I study, nine patients with newly diagnosed LAPC received EUS-guided injection of Ad5-DS with concomitant oral 5- fluorocytosine and valganciclovir along with standard-dose intravenous gemcitabine[36]. The dose cohorts were 1×10^{11}, 3×10^{11}, and 1×10^{12} viral particles (viral particles)/mL. The therapy was reported to be well tolerated no DLT occurred. Tumor response from nine patients who underwent this therapy showed that one patient had a partial response while the other eight had stable disease at 12 wk. The overall response rate was 11%, and the disease control rate was 100%. Disease progression was noted in two patients at 6.5 mo (median PFS of 11.4 mo). Adenoviral DNA was detected in the peripheral blood of 4 patients at 8 wk. Although the trends in tumor size and carbohydrate antigen 19-9 levels seemed more favorable in patients who received higher doses of Ad5-DS, no dose-response relationship was established statistically[37].

Other gene transfer therapies

STNM01: Carbohydrate sulfotransferase 15 (CHST15) is a specific enzyme that has been shown to initiate pancreatic cell mobilization and invasion through its product chondroitin sulphate-E which cleaves CD44 and releases the sCD44 variant into the extracellular space. STNM01 is a synthetic double-stranded RNA oligonucleotide that selectively represses CHST15 expression[38,39]. Six patients with unresectable pancreatic cancer were administered STNM01 *via* a single EUS-FNI procedure with 16 mL (250 nM) injectate using a conventional 22-gauge needle in an open-labeled trial[40]. The agent was injected into 16 different sites within the tumor (1 mL each). Additional STNM01 injections were delivered after 4 wk of observation for AEs and were continued until disease progression occurred. All patients tolerated the procedure well and no AEs were observed. Median tumor size changed from 31 mm to 29 mm along with a significant decrease in median serum soluble CD44 variant, 6 which may reflect CHST15 inhibition and decreased cleavage of CD44, although this finding is limited by the lack of a reference range for sCD44v6 in healthy individuals. Histological evidence of high baseline expression of CHST15 positive cancer cells was noted which showed a large reduction in 2 patients after 4 wk of treatment. Interestingly, these patients also demonstrated tumor necrosis and longest OS (15.5 mo and 18 mo, respectively) indicating that STNM01 acts on CHST15 positive cells to reverse invasion and induce local tumor necrosis although this needs further confirmatory data in future studies.

BC-819: BC-819 is a double-stranded DNA plasmid that carries the cytotoxic gene for diphtheria toxin. Its expression is controlled by the presence of the H19 promoter sequence, which is overexpressed in some tumors like PDAC, leading to selective tumor cell destruction[41]. In a clinical study involving nine patients with unresectable locally advanced PDAC (positive for H19 expression), 2 wk of twice-weekly intratumoral injection of BC-819 under either CT (n = 3) or EUS (n = 6) guidance was administered[42]. The mode of delivery was determined by the principal investigator depending on tumor size, location, and ease of injection. Injection volumes of 1 mL (4 mg of BC-819) and 2 mL (8 mg of BC-819) were delivered in a dose-escalation manner in the two cohorts using a 21- to a 22-gauge needle in a clockwise alternating injection site scheme for maximum distribution. The treatment was safe and well-tolerated. Asymptomatic elevation of lipase in one patient was considered as DLT but MTD was not reached. Partial response was observed in 3 of the 6 patients treated with the higher dose (8 mg) at three-month follow-up. Resectability assessment showed that two individuals who received chemotherapy or chemoradiation therapy after experimental treatment were down staged to resectable PDAC at three months with one patient subsequently undergoing surgery with negative margins. This indicates that BC-819 may provide additional therapeutic benefits for advanced PDAC along with systemic chemotherapy.

DISCUSSION

Pancreatic cancer remains a highly lethal malignancy. One of the challenges hypothesized with systemic administration of therapeutic agents is their lack of penetration into the pancreatic tumor bed owing to surrounding desmoplasia. Direct injection therapies are an attractive option as they can lead to greater intratumoral concentration of the drug or biologic agent while minimizing systemic side effects. EUS-FNI has emerged as an attractive delivery option as this modality can visualize the tumor and surrounding structures in real-time. This allows for precise intratumoral delivery of biological agents while minimizing the risk for AEs such as avoiding vascular or surrounding structures. Multiple candidate agents for local therapy have been identified.

Successful local delivery of chemotherapeutics is a logical option given their proven safety profile with systemic therapy. Some of these agents have been delivered into normal pancreatic tissue in animal studies using EUS-FNI with no significant AEs[43,44] Results of the clinical study using EUS-guided gemcitabine injections are encouraging although additional data is required to confirm these findings with regulated delivery of standard multimodality therapy and controlled trials assessing the effect of multiple sessions and escalating doses towards significant clinical advantage. In theory, immuno-

therapy is an attractive option, but various challenges with PDAC include the immune-suppressive TME including stromal cellular and molecular components, and other multiple immunological barriers making PDAC a "cold" tumor. Direct delivery of these iDCs into the tumor mass makes tumor antigen loading theoretically more effective for inciting T-cell response mechanisms and has provided a renaissance in the exploration of immunotherapy for PDAC. Although the mentioned limited clinical reports have established safety, feasibility, and some immunological response in their studies, there appears to be a need for increased understanding of the complex immunotherapeutic pathways in PDAC for determining the most efficacious DC activating agent and most suited combination therapy for improving outcomes. Further studies are required to confirm survival benefits, explore synergism with immune checkpoint inhibitors, and select the most appropriate patient population to benefit from these immunotherapies based on precise biomarkers like neutrophil to lymphocyte ratio (NLR) and $CD8^+$/Treg ratio[25] Novel molecular markers may also help in identifying patients with predominantly locoregional complications from PDAC that would benefit from localized therapies.

Oncolytic viral therapy is among the most promising agents for local delivery in pancreatic tumors. Although different strains of adenovirus, herpes virus, measles virus, and other viruses have shown positive results in cancer cell lines and preclinical models, limited clinical studies have performed intratumoral injection of these agents using EUS-FNI[45,46]. As PDAC mass consists of islands of neoplastic cells interspersed with dense stroma which can hinder the spread of injectable agents, OVs can overcome this problem to some extent through their replicative potential and hence increased dissemination within the tumor. Other future areas of research can include viruses targeted towards extracellular matrix disruption and combination with anti-stromal agents to allow better penetration of viral therapy.

EUS-FNI technique can further enhance tumor penetration regardless of tumor cell distribution and composition of the surrounding stroma. Injection into multiple sites in the pancreatic mass using EUS-FNI may assist with even distribution of the agent throughout the tumor. Furthermore, EUS can be used to assess response, and allow for subsequent FNI therapy. EUS, however, is associated with the need for sedation, which may add additional cost and risks associated with sedation. Further studies are needed to compare and firmly establish the most effective EUS-FNI delivery technique including the use of multiple injection sites within the tumor, multiple passes, or use of newer designed needle devices for enhanced dispersion of the agents within the desmoplastic pancreatic stroma[47].

EUS-FNI is an emerging modality for enhanced local intratumoral drug delivery[48]. Current data demonstrate that EUS-guided injectable therapies are safe for the treatment of PDAC. Larger studies, including RCTs should consider using EUS-FNI and these data are needed to establish efficacy and survival data, identify the most suitable anti-tumor agents, including combination therapy, and determine the best patient populations that may benefit from local drug delivery. Regenerative therapies, including the use of immunotherapy, DCs, and oncolytic viruses offer new hope in the management of PDAC. These advances towards novel EUS-FNI therapies should more actively involve endoscopists as part of the multidisciplinary treatment team as we hope to improve survival of our patients with PDAC.

CONCLUSION

EUS-guided injectable therapies, including immunotherapy, chemotherapy, and viral or other biological therapies have shown minimal AEs and potential efficacy in the treatment of PDAC. Comparative studies, including controlled trials, are required to confirm improved survival and establish the most effective therapeutic options. Further research is needed to offer novel EUS-based therapies as a promising treatment for patients with PDAC in the future.

ARTICLE HIGHLIGHTS

Research background

Many new treatment options for pancreatic cancer are being explored owing to its poor prognosis. Advent of therapeutic Endoscopic ultrasound (EUS) guided therapies in recent years paved the way to explore the local delivery of injectable agents. In the last 22 years, very few studies have explored the use of EUS-guided fine-needle injection (EUS-FNI) to treat pancreatic ductal adenocarcinoma (PDAC). These are mostly phase I/II clinical studies using different agents and varied methodologies with mixed results.

Research motivation

EUS-FNI has the theoretical advantage of targeted delivery of anti-tumor agents under real-time visualization and minimal invasiveness. It can also overcome the limitations of systemic therapy mainly the low penetration of these agents into the desmoplastic tumor mass of PDAC. Limited literature and

heterogeneity in methodologies and outcomes necessitated a systematic review of the present literature to understand and guide future research in this promising field.

Research objectives

To evaluate the current status of research in the novel area of EUS-guided injectable treatment for PDAC. This has helped to understand the progress made so far and draw meaningful conclusions based on the limitations and gaps found in the literature. This has also enabled the development of focused future directives for research on this topic which can potentially advance the treatment of PDAC.

Research methods

A systematic and comprehensive review of clinical studies which used EUS-guided injectable therapy for the treatment of PDAC was done. Expert librarian assisted in the electronic search of various databases. Screening of papers for eligibility was done by two study members independently. Data were collected in a standardized manner with regard to the methodologies and outcomes of these studies. A critical appraisal of the present literature on this topic was performed.

Research results

Our study demonstrates that immunotherapy, chemotherapy, oncolytic viral, and other biological therapies have been used *via* EUS-guided injection technique in different ways to study the safety and efficacy of such treatment in PDAC patients. The review of the present literature indicates that these therapies are well tolerated and feasible overall. Mixed results are demonstrated in terms of clinical efficacy.

Research conclusions

This study concludes that EUS-FNI based treatment may be administered to patients with advanced PDAC without significant toxicity. Clinical efficacy with respect to the standard of care (SOC) is not yet established. Further research should be undertaken to find out the most effective therapeutic agent, dose, and techniques that may be employed to the appropriate population of PDAC patients who would benefit the most from these.

Research perspectives

The direction of future research should be to design controlled studies and phase III trials using the data from present literature to establish efficacy in terms of tumor response and survival with respect to the SOC. Anti-tumor agents may be administered at higher doses and multiple EUS-FNI sessions to maintain the appropriate concentration in the tumor bed. Studies using appropriate combination therapies (using chemotherapy and/or radiotherapy) and different EUS-FNI techniques, for example, multiple needle passes should be encouraged as they may help in overcoming hostile tumor microenvironment of pancreatic cancer.

FOOTNOTES

Author contributions: Kaur J and Chandrasekhara V conceived and designed the study and critically reviewed the manuscript; Kaur J and Chandrasekhara V conducted the literature search, screened for eligibility, and drafted the manuscript; Kaur J and Jaruvongvanich V collected, analyzed, and interpreted the data; all authors reviewed the literature and revised the manuscript, read and approved the final manuscript.

Conflict-of-interest statement: There are no conflicts of interest to report.

PRISMA 2009 Checklist statement: The authors have read the PRISMA 2009 Checklist, and the manuscript was prepared and revised according to the PRISMA 2009 Checklist.

Open-Access: This article is an open-access article that was selected by an in-house editor and fully peer-reviewed by external reviewers. It is distributed in accordance with the Creative Commons Attribution NonCommercial (CC BY-NC 4.0) license, which permits others to distribute, remix, adapt, build upon this work non-commercially, and license their derivative works on different terms, provided the original work is properly cited and the use is non-commercial. See: https://creativecommons.org/Licenses/by-nc/4.0/

Country/Territory of origin: United States

ORCID number: Jyotroop Kaur 0000-0002-5085-9265; Veeravich Jaruvongvanich 0000-0002-3419-2296; Vinay Chandrasekhara 0000-0001-6209-9905.

S-Editor: Chen YL

L-Editor: A

P-Editor: Chen YL

REFERENCES

1 **Khalaf N**, El-Serag HB, Abrams HR, Thrift AP. Burden of Pancreatic Cancer: From Epidemiology to Practice. *Clin Gastroenterol Hepatol* 2021; **19**: 876-884 [PMID: 32147593 DOI: 10.1016/j.cgh.2020.02.054]

2 **Siegel RL**, Miller KD, Fuchs HE, Jemal A. Cancer Statistics, 2021. *CA Cancer J Clin* 2021; **71**: 7-33 [PMID: 33433946 DOI: 10.3322/caac.21654]

3 **Ujiki MB**, Talamonti MS. Guidelines for the surgical management of pancreatic adenocarcinoma. *Semin Oncol* 2007; **34**: 311-320 [PMID: 17674959 DOI: 10.1053/j.seminoncol.2007.05.004]

4 **Sener SF**, Fremgen A, Menck HR, Winchester DP. Pancreatic cancer: a report of treatment and survival trends for 100,313 patients diagnosed from 1985-1995, using the National Cancer Database. *J Am Coll Surg* 1999; **189**: 1-7 [PMID: 10401733 DOI: 10.1016/s1072-7515(99)00075-7]

5 **Barcellini A**, Peloso A, Pugliese L, Vitolo V, Cobianchi L. Locally Advanced Pancreatic Ductal Adenocarcinoma: Challenges and Progress. *Onco Targets Ther* 2020; **13**: 12705-12720 [PMID: 33335406 DOI: 10.2147/OTT.S220971]

6 **Seufferlein T**, Hammel P, Delpero JR, Macarulla T, Pfeiffer P, Prager GW, Reni M, Falconi M, Philip PA, Van Cutsem E. Optimizing the management of locally advanced pancreatic cancer with a focus on induction chemotherapy: Expert opinion based on a review of current evidence. *Cancer Treat Rev* 2019; **77**: 1-10 [PMID: 31163334 DOI: 10.1016/j.ctrv.2019.05.007]

7 **Neesse A**, Michl P, Frese KK, Feig C, Cook N, Jacobetz MA, Lolkema MP, Buchholz M, Olive KP, Gress TM, Tuveson DA. Stromal biology and therapy in pancreatic cancer. *Gut* 2011; **60**: 861-868 [PMID: 20966025 DOI: 10.1136/gut.2010.226092]

8 **Mulvihill S**, Warren R, Venook A, Adler A, Randlev B, Heise C, Kirn D. Safety and feasibility of injection with an E1B-55 kDa gene-deleted, replication-selective adenovirus (ONYX-015) into primary carcinomas of the pancreas: a phase I trial. *Gene Ther* 2001; **8**: 308-315 [PMID: 11313805 DOI: 10.1038/sj.gt.3301398]

9 **Hecht JR**, Farrell JJ, Senzer N, Nemunaitis J, Rosemurgy A, Chung T, Hanna N, Chang KJ, Javle M, Posner M, Waxman I, Reid A, Erickson R, Canto M, Chak A, Blatner G, Kovacevic M, Thornton M. EUS or percutaneously guided intratumoral TNFerade biologic with 5-fluorouracil and radiotherapy for first-line treatment of locally advanced pancreatic cancer: a phase I/II study. *Gastrointest Endosc* 2012; **75**: 332-338 [PMID: 22248601 DOI: 10.1016/j.gie.2011.10.007]

10 **National Heart L**, Blood Institute. Study Quality Assessment Tools. n.d [DOI: 10.1111/jcpe.12388]

11 **Yamao K**, Bhatia V, Mizuno N, Sawaki A, Shimizu Y, Irisawa A. Interventional endoscopic ultrasonography. *J Gastroenterol Hepatol* 2009; **24**: 509-519 [PMID: 19220671 DOI: 10.1111/j.1440-1746.2009.05783.x]

12 **Moyer MT**, Maranki JL, DeWitt JM. EUS-Guided Pancreatic Cyst Ablation: a Clinical and Technical Review. *Curr Gastroenterol Rep* 2019; **21**: 19 [PMID: 31016391 DOI: 10.1007/s11894-019-0686-5]

13 **Levy MJ**, Topazian MD, Wiersema MJ, Clain JE, Rajan E, Wang KK, de la Mora JG, Gleeson FC, Pearson RK, Pelaez MC, Petersen BT, Vege SS, Chari ST. Initial evaluation of the efficacy and safety of endoscopic ultrasound-guided direct Ganglia neurolysis and block. *Am J Gastroenterol* 2008; **103**: 98-103 [PMID: 17970834 DOI: 10.1111/j.1572-0241.2007.01607.x]

14 **Klapman JB**, Chang KJ. Endoscopic ultrasound-guided fine-needle injection. *Gastrointest Endosc Clin N Am* 2005; **15**: 169-177 [PMID: 15555959 DOI: 10.1016/j.giec.2004.07.009]

15 **Mellman I**, Coukos G, Dranoff G. Cancer immunotherapy comes of age. *Nature* 2011; **480**: 480-489 [PMID: 22193102 DOI: 10.1038/nature10673]

16 **Jiang J**, Zhou H, Ni C, Hu X, Mou Y, Huang D, Yang L. Immunotherapy in pancreatic cancer: New hope or mission impossible? *Cancer Lett* 2019; **445**: 57-64 [PMID: 30641107 DOI: 10.1016/j.canlet.2018.10.045]

17 **Chang KJ**, Nguyen PT, Thompson JA, Kurosaki TT, Casey LR, Leung EC, Granger GA. Phase I clinical trial of allogeneic mixed lymphocyte culture (cytoimplant) delivered by endoscopic ultrasound-guided fine-needle injection in patients with advanced pancreatic carcinoma. *Cancer* 2000; **88**: 1325-1335 [PMID: 10717613 DOI: 10.1002/(sici)1097-0142(20000315)88:6<1325::aid-cncr8>3.0.co;2-t]

18 **Sabado RL**, Balan S, Bhardwaj N. Dendritic cell-based immunotherapy. *Cell Res* 2017; **27**: 74-95 [PMID: 28025976 DOI: 10.1038/cr.2016.157]

19 **Yu JS**, Liu G, Ying H, Yong WH, Black KL, Wheeler CJ. Vaccination with tumor lysate-pulsed dendritic cells elicits antigen-specific, cytotoxic T-cells in patients with malignant glioma. *Cancer Res* 2004; **64**: 4973-4979 [PMID: 15256471 DOI: 10.1158/0008-5472.CAN-03-3505]

20 **Henry F**, Boisteau O, Bretaudeau L, Lieubeau B, Meflah K, Grégoire M. Antigen-presenting cells that phagocytose apoptotic tumor-derived cells are potent tumor vaccines. *Cancer Res* 1999; **59**: 3329-3332 [PMID: 10416588]

21 **Irisawa A**, Takagi T, Kanazawa M, Ogata T, Sato Y, Takenoshita S, Ohto H, Ohira H. Endoscopic ultrasound-guided fine-needle injection of immature dendritic cells into advanced pancreatic cancer refractory to gemcitabine: a pilot study. *Pancreas* 2007; **35**: 189-190 [PMID: 17632329 DOI: 10.1097/01.mpa.0000250141.25639.e9]

22 **Hirooka Y**, Itoh A, Kawashima H, Hara K, Nonogaki K, Kasugai T, Ohno E, Ishikawa T, Matsubara H, Ishigami M, Katano Y, Ohmiya N, Niwa Y, Yamamoto K, Kaneko T, Nieda M, Yokokawa K, Goto H. A combination therapy of gemcitabine with immunotherapy for patients with inoperable locally advanced pancreatic cancer. *Pancreas* 2009; **38**: e69-e74 [PMID: 19276867 DOI: 10.1097/MPA.0b013e318197a9e3]

23 **Nakahara S**, Tsunoda T, Baba T, Asabe S, Tahara H. Dendritic cells stimulated with a bacterial product, OK-432, efficiently induce cytotoxic T lymphocytes specific to tumor rejection peptide. *Cancer Res* 2003; **63**: 4112-4118 [PMID: 12874015]

24 **Endo H**, Saito T, Kenjo A, Hoshino M, Terashima M, Sato T, Anazawa T, Kimura T, Tsuchiya T, Irisawa A, Ohira H,

Hikichi T, Takagi T, Gotoh M. Phase I trial of preoperative intratumoral injection of immature dendritic cells and OK-432 for resectable pancreatic cancer patients. *J Hepatobiliary Pancreat Sci* 2012; **19**: 465-475 [PMID: 21983893 DOI: 10.1007/s00534-011-0457-7]

25 **Hirooka Y**, Kawashima H, Ohno E, Ishikawa T, Kamigaki T, Goto S, Takahara M, Goto H. Comprehensive immunotherapy combined with intratumoral injection of zoledronate-pulsed dendritic cells, intravenous adoptive activated T lymphocyte and gemcitabine in unresectable locally advanced pancreatic carcinoma: a phase I/II trial. *Oncotarget* 2018; **9**: 2838-2847 [PMID: 29416816 DOI: 10.18632/oncotarget.22974]

26 **Burris HA 3rd**, Moore MJ, Andersen J, Green MR, Rothenberg ML, Modiano MR, Cripps MC, Portenoy RK, Storniolo AM, Tarassoff P, Nelson R, Dorr FA, Stephens CD, Von Hoff DD. Improvements in survival and clinical benefit with gemcitabine as first-line therapy for patients with advanced pancreas cancer: a randomized trial. *J Clin Oncol* 1997; **15**: 2403-2413 [PMID: 9196156 DOI: 10.1200/JCO.1997.15.6.2403]

27 **Levy MJ**, Alberts SR, Bamlet WR, Burch PA, Farnell MB, Gleeson FC, Haddock MG, Kendrick ML, Oberg AL, Petersen GM, Takahashi N, Chari ST. EUS-guided fine-needle injection of gemcitabine for locally advanced and metastatic pancreatic cancer. *Gastrointest Endosc* 2017; **86**: 161-169 [PMID: 27889543 DOI: 10.1016/j.gie.2016.11.014]

28 **Freytag SO**, Movsas B, Aref I, Stricker H, Peabody J, Pegg J, Zhang Y, Barton KN, Brown SL, Lu M, Savera A, Kim JH. Phase I trial of replication-competent adenovirus-mediated suicide gene therapy combined with IMRT for prostate cancer. *Mol Ther* 2007; **15**: 1016-1023 [PMID: 17375076 DOI: 10.1038/mt.sj.6300120]

29 **Vacchelli E**, Eggermont A, Sautès-Fridman C, Galon J, Zitvogel L, Kroemer G, Galluzzi L. Trial watch: Oncolytic viruses for cancer therapy. *Oncoimmunology* 2013; **2**: e24612 [PMID: 23894720 DOI: 10.4161/onci.24612]

30 **Zeyaullah M**, Patro M, Ahmad I, Ibraheem K, Sultan P, Nehal M, Ali A. Oncolytic viruses in the treatment of cancer: a review of current strategies. *Pathol Oncol Res* 2012; **18**: 771-781 [PMID: 22714538 DOI: 10.1007/s12253-012-9548-2]

31 **Hecht JR**, Bedford R, Abbruzzese JL, Lahoti S, Reid TR, Soetikno RM, Kirn DH, Freeman SM. A phase I/II trial of intratumoral endoscopic ultrasound injection of ONYX-015 with intravenous gemcitabine in unresectable pancreatic carcinoma. *Clin Cancer Res* 2003; **9**: 555-561 [PMID: 12576418]

32 **Hallahan DE**, Vokes EE, Rubin SJ, O'Brien S, Samuels B, Vijaykumar S, Kufe DW, Phillips R, Weichselbaum RR. Phase I dose-escalation study of tumor necrosis factor-alpha and concomitant radiation therapy. *Cancer J Sci Am* 1995; **1**: 204-209 [PMID: 9166477]

33 **Herman JM**, Wild AT, Wang H, Tran PT, Chang KJ, Taylor GE, Donehower RC, Pawlik TM, Ziegler MA, Cai H, Savage DT, Canto MI, Klapman J, Reid T, Shah RJ, Hoffe SE, Rosemurgy A, Wolfgang CL, Laheru DA. Randomized phase III multi-institutional study of TNFerade biologic with fluorouracil and radiotherapy for locally advanced pancreatic cancer: final results. *J Clin Oncol* 2013; **31**: 886-894 [PMID: 23341531 DOI: 10.1200/JCO.2012.44.7516]

34 **Koshizuka T**, Goshima F, Takakuwa H, Nozawa N, Daikoku T, Koiwai O, Nishiyama Y. Identification and characterization of the UL56 gene product of herpes simplex virus type 2. *J Virol* 2002; **76**: 6718-6728 [PMID: 12050385 DOI: 10.1128/jvi.76.13.6718-6728.2002]

35 **Hirooka Y**, Kasuya H, Ishikawa T, Kawashima H, Ohno E, Villalobos IB, Naoe Y, Ichinose T, Koyama N, Tanaka M, Kodera Y, Goto H. A Phase I clinical trial of EUS-guided intratumoral injection of the oncolytic virus, HF10 for unresectable locally advanced pancreatic cancer. *BMC Cancer* 2018; **18**: 596 [PMID: 29801474 DOI: 10.1186/s12885-018-4453-z]

36 **Lee JC**, Shin DW, Park H, Kim J, Youn Y, Kim JH, Hwang JH. Tolerability and safety of EUS-injected adenovirus-mediated double-suicide gene therapy with chemotherapy in locally advanced pancreatic cancer: a phase 1 trial. *Gastrointest Endosc* 2020; **92**: 1044-1052.e1 [PMID: 32084409 DOI: 10.1016/j.gie.2020.02.012]

37 **Bouvet M**, Bold RJ, Lee J, Evans DB, Abbruzzese JL, Chiao PJ, McConkey DJ, Chandra J, Chada S, Fang B, Roth JA. Adenovirus-mediated wild-type p53 tumor suppressor gene therapy induces apoptosis and suppresses growth of human pancreatic cancer [seecomments]. *Ann Surg Oncol* 1998; **5**: 681-688 [PMID: 9869513 DOI: 10.1007/BF02303477]

38 **Suzuki K**, Yokoyama J, Kawauchi Y, Honda Y, Sato H, Aoyagi Y, Terai S, Okazaki K, Suzuki Y, Sameshima Y, Fukushima T, Sugahara K, Atreya R, Neurath MF, Watanabe K, Yoneyama H, Asakura H. Phase 1 Clinical Study of siRNA Targeting Carbohydrate Sulphotransferase 15 in Crohn's Disease Patients with Active Mucosal Lesions. *J Crohns Colitis* 2017; **11**: 221-228 [PMID: 27484097 DOI: 10.1093/ecco-jcc/jjw143]

39 **Takakura K**, Shibazaki Y, Yoneyama H, Fujii M, Hashiguchi T, Ito Z, Kajihara M, Misawa T, Homma S, Ohkusa T, Koido S. Inhibition of Cell Proliferation and Growth of Pancreatic Cancer by Silencing of Carbohydrate Sulfotransferase 15 In Vitro and in a Xenograft Model. *PLoS One* 2015; **10**: e0142981 [PMID: 26642349 DOI: 10.1371/journal.pone.0142981]

40 **Nishimura M**, Matsukawa M, Fujii Y, Matsuda Y, Arai T, Ochiai Y, Itoi T, Yahagi N. Effects of EUS-guided intratumoral injection of oligonucleotide STNM01 on tumor growth, histology, and overall survival in patients with unresectable pancreatic cancer. *Gastrointest Endosc* 2018; **87**: 1126-1131 [PMID: 29122598 DOI: 10.1016/j.gie.2017.10.030]

41 **Scaiewicz V**, Sorin V, Fellig Y, Birman T, Mizrahi A, Galula J, Abu-Lail R, Shneider T, Ohana P, Buscail L, Hochberg A, Czerniak A. Use of H19 Gene Regulatory Sequences in DNA-Based Therapy for Pancreatic Cancer. *J Oncol* 2010; **2010**: 178174 [PMID: 21052499 DOI: 10.1155/2010/178174]

42 **Hanna N**, Ohana P, Konikoff FM, Leichtmann G, Hubert A, Appelbaum L, Kopelman Y, Czerniak A, Hochberg A. Phase 1/2a, dose-escalation, safety, pharmacokinetic and preliminary efficacy study of intratumoral administration of BC-819 in patients with unresectable pancreatic cancer. *Cancer Gene Ther* 2012; **19**: 374-381 [PMID: 22498722 DOI: 10.1038/cgt.2012.10]

43 **Sun S**, Wang S, Ge N, Lei T, Lu Q, Zhou Z, Yang A, Wang Z, Sun M. Endoscopic ultrasound-guided interstitial chemotherapy in the pancreas: results in a canine model. *Endoscopy* 2007; **39**: 530-534 [PMID: 17554649 DOI: 10.1055/s-2007-966353]

44 **Caceres J**, Munoz-Sagastibelza M, Hossian AKMN, Paredes J, Barrera K, Mattheolabakis G, Martello LA, Vignesh S. Evaluation of the feasibility of intrapancreatic delivery of drug-loaded microparticles *via* EUS-guided fine needle injection using a swine model. *Endosc Int Open* 2019; **7**: E1008-E1017 [PMID: 31404394 DOI: 10.1055/a-0953-2070]

45 **Sangro B**, Mazzolini G, Ruiz J, Herraiz M, Quiroga J, Herrero I, Benito A, Larrache J, Pueyo J, Subtil JC, Olagüe C, Sola J, Sádaba B, Lacasa C, Melero I, Qian C, Prieto J. Phase I trial of intratumoral injection of an adenovirus encoding

interleukin-12 for advanced digestive tumors. *J Clin Oncol* 2004; **22**: 1389-1397 [PMID: 15084613 DOI: 10.1200/JCO.2004.04.059]

46 **Ady JW**, Heffner J, Klein E, Fong Y. Oncolytic viral therapy for pancreatic cancer: current research and future directions. *Oncolytic Virother* 2014; **3**: 35-46 [PMID: 27512661 DOI: 10.2147/OV.S53858]

47 **Ohara K**, Kohno M, Horibe T, Kawakami K. Local drug delivery to a human pancreatic tumor *via* a newly designed multiple injectable needle. *Mol Clin Oncol* 2013; **1**: 231-234 [PMID: 24649152 DOI: 10.3892/mco.2012.47]

48 **Hwang JS**, Joo HD, Song TJ. Endoscopic Ultrasound-Guided Local Therapy for Pancreatic Neoplasms. *Clin Endosc* 2020; **53**: 535-540 [PMID: 33027583 DOI: 10.5946/ce.2020.181]

World Journal of Gastroenterology

Submit a Manuscript: https://www.f6publishing.com

World J Gastroenterol 2022 June 7; 28(21): 2396-2402

DOI: 10.3748/wjg.v28.i21.2396

ISSN 1007-9327 (print) ISSN 2219-2840 (online)

LETTER TO THE EDITOR

Peripancreatic paraganglioma: Lesson from a round table

Federica Petrelli, Geri Fratini, Andrea Sbrozzi-Vanni, Andrea Giusti, Raffele Manta, Claudio Vignali, Gabriella Nesi, Andrea Amorosi, Andrea Cavazzana, Marco Arganini, Maria Raffaella Ambrosio

Specialty type: Gastroenterology and hepatology

Provenance and peer review: Unsolicited article; Externally peer reviewed.

Peer-review model: Single blind

Peer-review report's scientific quality classification
Grade A (Excellent): 0
Grade B (Very good): B
Grade C (Good): C
Grade D (Fair): 0
Grade E (Poor): 0

P-Reviewer: de Souza HSP, Brazil; Zhang CZ, China
A-Editor: Nakaji K

Received: December 7, 2021
Peer-review started: December 7, 2021
First decision: January 8, 2022
Revised: January 18, 2022
Accepted: May 14, 2022
Article in press: May 14, 2022
Published online: June 7, 2022

Federica Petrelli, Andrea Giusti, Andrea Cavazzana, Maria Raffaella Ambrosio, Pathology Unit, Azienda Sanitaria Toscana Nord Ovest, Pisa 56121, Italy

Geri Fratini, Marco Arganini, Surgery Unit, Azienda Sanitaria Toscana Nord Ovest, Pisa 56121, Italy

Andrea Sbrozzi-Vanni, Endoscopic Unit, Azienda Sanitaria Toscana Nord Ovest, Pisa 56121, Italy

Raffele Manta, Endoscopic Unit, Santa Maria Misericordia Hospital, Perugia 06122, Italy

Claudio Vignali, Interventional Radiology Unit, Azienda Sanitaria Toscana Nord Ovest, Pisa 56121, Italy

Gabriella Nesi, Department of Health Sciences, University of Florence, Florence 50139, Italy

Andrea Amorosi, Pathology Unit, Università Magna Graecia, Catanzaro 88100, Italy

Corresponding author: Maria Raffaella Ambrosio, PhD, Academic Research, Chief Doctor, Pathology Unit, Azienda Sanitaria Toscana Nord Ovest, Via Cocchi, Pisa 56121, Italy.
mariaraffaella.ambrosio@uslnordovest.toscana.it

Abstract

We described the case of a peripancreatic paraganglioma (PGL) misdiagnosed as pancreatic lesion. Surgical exploration revealed an unremarkable pancreas and a large well-defined cystic mass originating at the mesocolon root. Radical enucleation of the mass was performed, preserving the pancreatic tail. Histologically, a diagnosis of PGL was rendered. Interestingly, two previously unreported mutations, one affecting the *KDR* gene in exon 7 and another on the *JAK3* gene in exon 4 were detected. Both mutations are known to be pathogenetic. Imaging and cytologic findings were blindly reviewed by an expert panel of clinicians, radiologists, and pathologists to identify possible causes of the misdiagnosis. The major issue was lack of evidence of a cleavage plane from the pancreas at imaging, which prompted radiologists to establish an intraparenchymal origin. The blinded revision shifted the diagnosis towards an extrapancreatic lesion, as the pancreatic parenchyma showed no structural alterations and no dislocation of the Wirsung duct. *Ex post*, the identified biases were the emergency setting of the radiologic examination and the very thin mesocolon sheet, which hindered clear definition of the lesion borders. Original endoscopic ultrasonography diagnosis was confirmed, emphasizing the intrinsic limit of this

technique in detecting large masses. Finally, pathologic review favored a diagnosis of PGL due to the morphological features and immonohistochemical profile. Eighteen months after tumor excision, the patient is asymptomatic with no disease relapse evident by either radiology or laboratory tests. Our report strongly highlights the difficulties in rendering an accurate pre-operative diagnosis of PGL.

Key Words: Peripancreatic paraganglioma; Pancreatic neuroendocrine tumor; Solid pseudopapillary neoplasm; S100; Succinate dehydrogenase subunit B gene and expression; Fine needle biopsy

©The Author(s) 2022. Published by Baishideng Publishing Group Inc. All rights reserved.

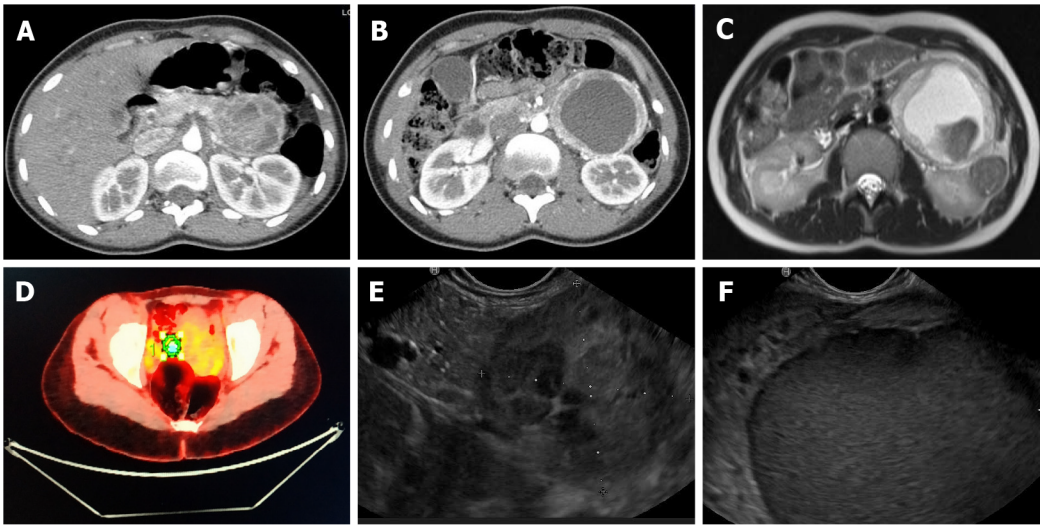
Core Tip: Our report strongly supports that paraganglioma should be included in the differential diagnosis of peripancreatic/pancreatic masses, highlighting the difficulties in establishing the accurate preoperative diagnosis, even after a second-round evaluation. In fact, due to the deep localization and the lack of specific clinical manifestations and imaging data, early diagnosis often relies solely on a level of suspicion, thus making it more probable to have a missed diagnosis or misdiagnosis. Moreover, the limited time spent with a patient in an emergency setting might impair the accuracy of the diagnosis, lowering quality and outcomes of healthcare delivery. A multidisciplinary team approach, involving skilled radiologists, endoscopists, pathologists, and surgeons, is of foremost importance for proper diagnosis and management, preventing undue surgical resections.

Citation: Petrelli F, Fratini G, Sbrozzi-Vanni A, Giusti A, Manta R, Vignali C, Nesi G, Amorosi A, Cavazzana A, Arganini M, Ambrosio MR. Peripancreatic paraganglioma: Lesson from a round table. *World J Gastroenterol* 2022; 28(21): 2396-2402
URL: https://www.wjgnet.com/1007-9327/full/v28/i21/2396.htm
DOI: https://dx.doi.org/10.3748/wjg.v28.i21.2396

TO THE EDITOR

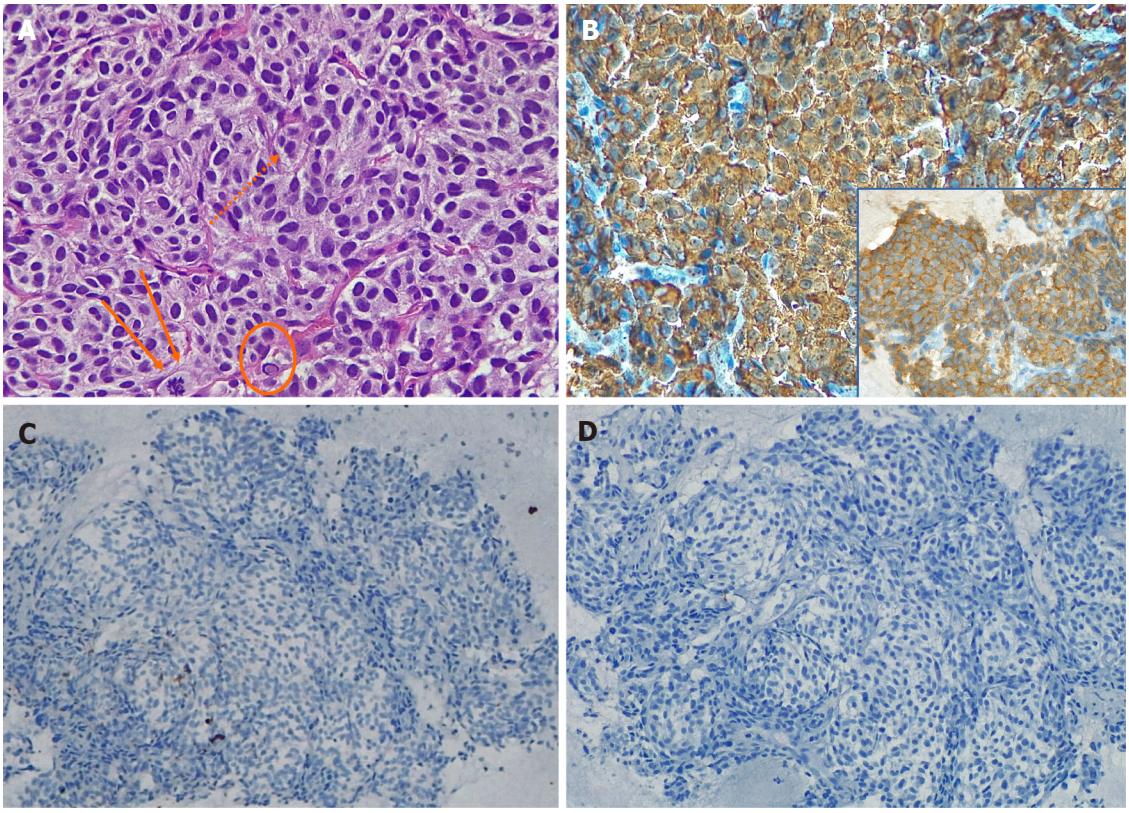
We read with interest the paper authored by Lanke *et al*[1] on a peripancreatic paraganglioma (PPGL) successfully diagnosed pre-operatively by endoscopic ultrasonography (EUS)-fine needle aspiration. After a careful review of the literature, the report highlights the enduring difficulties in achieving an accurate diagnosis of this rare entity prior to surgery. Among the 47 pancreatic/peripancreatic PGL reported so far, only 8 (17%) were correctly identified pre-operatively; the majority (n = 29, 62%) were misdiagnosed as pancreatic neuroendocine tumors or pancreatic neoplasms/cysts. In almost all cases (80%), the treatment of choice was surgery, demonstrating the uncertainty of classification for such lesion and its unpredictable behavior[1].

In November 2020, a 23-year-old woman complaining of left hypocondrial pain, diarrhea, and sweating lasting for 4 d, was referred to the Emergency Unit of Ospedale Unico della Versilia. The physical examination was unremarkable, but the abdominal US showed a large cystic, liquid-filled mass close to the pancreatic tail. Whole-body computed tomography (CT) scan confirmed the presence of a 95-mm cystic lesion with thickened, contrast-enhanced walls and a marked inhomogeneous boundary with the pancreatic tail. The mass seemed to be adherent to the left renal artery, left kidney hilum, and homolateral ureter (Figures 1A and 1B). Imaging work-up was completed with abdominal nuclear magnetic resonance (NMR) revealing T1 signal hyperintensity (Figure 1C) and positron emission tomography disclosing abnormal hyperactivity of the mass (standard uptake value 4.7%) (Figure 1D). The suspicion of a solid-pseudopapillary neoplasm (SPN) *vs* a cystic pancreatic tumor was posed. Blood tests, including vasoactive intestinal peptide, C-peptide, pancreatic polypeptide, serotonin, carcinoembryonic antigen (CEA), Ca-125, and Ca-19.9, were within normal range; whereas chromogranin A (CgA) serum levels exceeded 1800 ng/mL (reference range: 0-108 ng/mL). EUS-fine needle biopsy (FNB) was scheduled. EUS examination showed a 10-cm lesion of the pancreatic tail. The lesion was hypoechoic with well-defined borders and a cystic component (Figures 1E and 1F). Two FNB passes were made using a 20 Gauge needle with Rapid On-Site Evaluation to ensure adequate sampling[2]. Intracystic fluid was aspirated and analyzed with the following results: Glucose, 45 mg/dL; pancreatic amylase, 5 U/L; CEA, 1.0 ng/mL; Ca-19.9, 9 U/mL. Cell block examination disclosed nests of small to medium-sized epithelioid cells exhibiting moderate amount of amphophilic granular cytoplasm and oval to round nuclei with smooth contours and dense chromatin (Figure 2A). Occasionally, small nucleoli (Figure 2A dots), sparse mitotic figures (Figure 2A arrows), and intra-cytoplasmic hyaline globules (Figure 2A encircled) were noted, as well as vague rosette-like formations and branching hyalinized



DOI: 10.3748/wjg.v28.i21.2396 **Copyright** ©The Author(s) 2022.

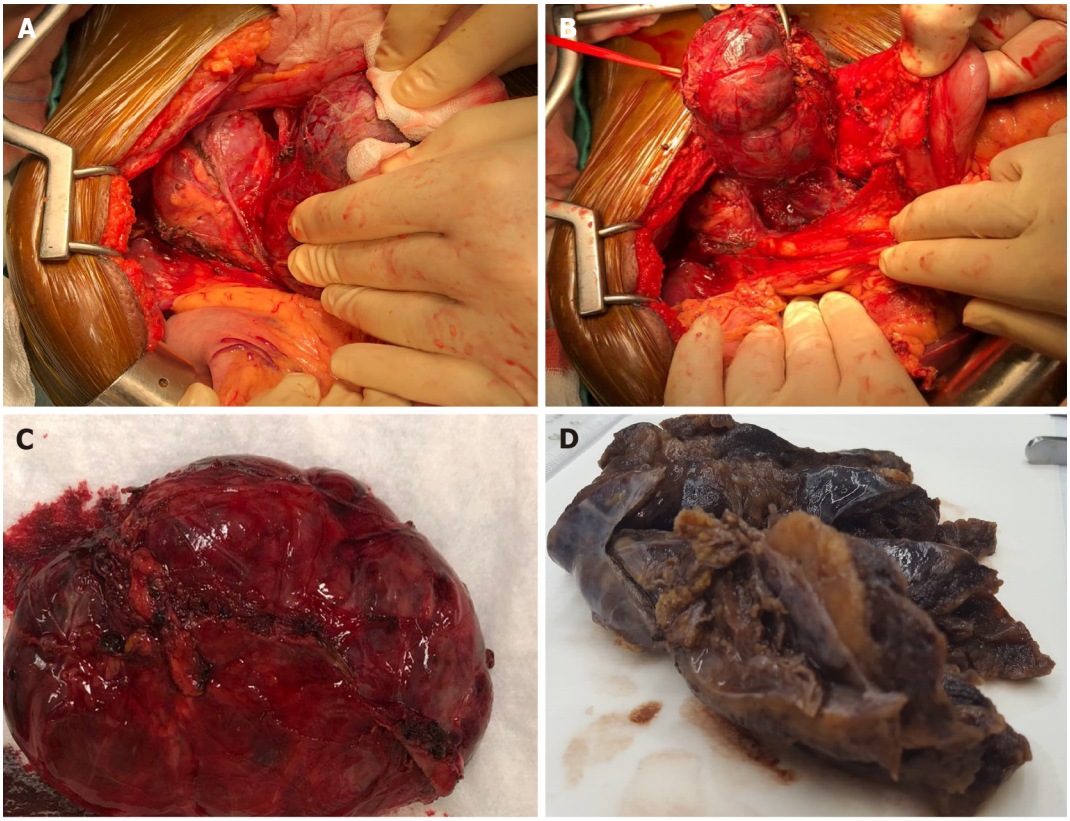
Figure 1 Radiologic findings. A and B: Computed tomography-scan showed a 95-mm cystic lesion with no cleavage plane from the pancreas; C: Nuclear magnetic resonance evidenced that the lesion was hyper-intense in T1; D: Positron emission tomography demonstrated a 4.7% standard uptake value; E and F: Endoscopic ultrasonography identified a hypoechoic mass close to the pancreatic tail.



DOI: 10.3748/wjg.v28.i21.2396 **Copyright** ©The Author(s) 2022.

Figure 2 Fine needle biopsy findings. A: Proliferation of small to medium-sized cells arranged in a nest pattern was evident, the cells occasionally showed small nucleoli (dots), mitotic figures (arrows), and intra-cytoplasmic hyaline globules (encircled), hematoxylin and eosin original magnification (O.M) × 40; B: Chromogranin A (CgA) positivity of neoplastic cells; inset: Synaptophysin positivity of neoplastic cells, CgA stain, O.M. × 20; B inset, synaptophysin stain, O.M. × 20; C: AE1/AE3 cytokeratins expression in scattered cells, cytokeratin AE1/AE3 stain, O.M. × 20; D: S100 negativity, S100 stain, O.M. × 20).

fibrovascular cores lined by neoplastic cells. Tumor cells diffusely expressed CgA (Figure 2B), synaptophysin (Figure 2B, inset), and GATA-3. Scattered cells were dot-like positive for AE1/AE3 cytokeratins (Figure 2C). Epithelial membrane antigen (EMA), PAX-8, and S100 protein (Figure 2D) were negative. A provisional diagnosis of neoplasm with neuroendocrine differentiation (either PGL or PanNET) *vs* SNP was made.



DOI: 10.3748/wjg.v28.i21.2396 **Copyright** ©The Author(s) 2022.

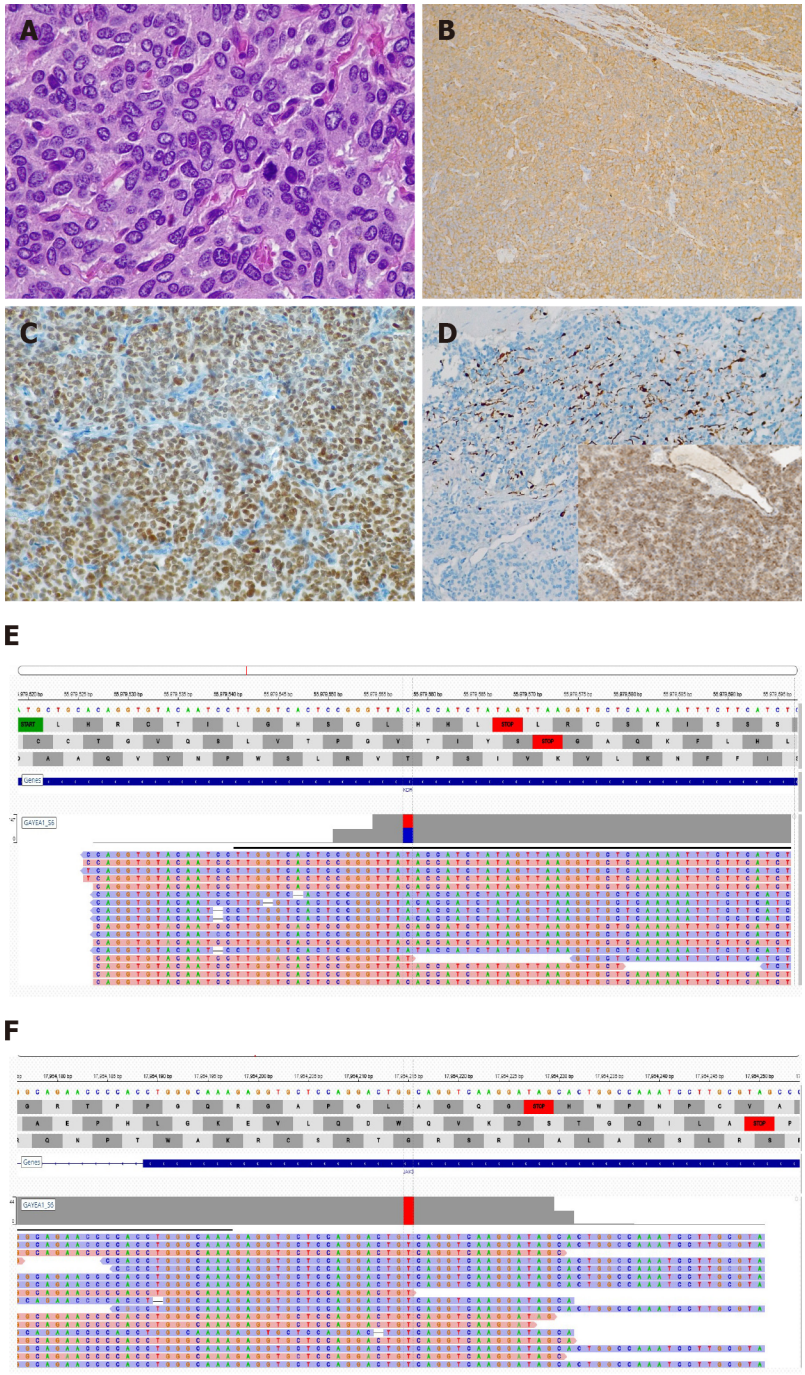
Figure 3 Macroscopic findings. A and B: At surgical exploration a large well-defined cystic mass located underneath the mesocolon plane was found; C: Radical enucleation of the lesion; D: Grossly, the cystic lesion showed a thick fibrous wall with a solid component and a yellowish, lobulated appearance on cut surface.

Surgical exploration revealed an unremarkable pancreas and a large well-defined cystic mass underneath the mesocolon plane, originating at the mesocolon root (Figures 3A and 3B). The lesion extended to the inferior margin of the pancreas and was strictly adherent but did not involve the organ parenchyma. As the capsule could be easily detached from the mesocolon sheets and vessels, radical enucleation was performed, preserving the pancreatic tail (Figure 3C).

The surgical specimen consisted of a 12-cm hemorrhagic cystic lesion, surrounded by a thick fibrous wall, with a solid component showing a yellowish, lobulated appearance on cut surface (Figure 3D). Microscopically, the tumor was composed of polygonal cells with abundant finely granular eosinophilic to amphophilic cytoplasm, mostly arranged in nests and anastomosing cords (Figure 4A). Areas with a diffuse growth pattern were also noted. Nuclei were regular, round to oval, with granular fine chromatin, small nucleoli, and occasional pseudoinclusions. The stroma was richly vascular. In the more cellular areas, pleomorphic cells with prominent nucleoli and occasional mitotic figures (2/high power field) were observed. There was evidence of focal capsular disruption. Cells were confirmed to be positive for CgA (Figure 4B), synaptophysin, GATA-3 (Figure 4C), and substantially negative for AE1/AE3 cytokeratins, EMA, and PAX-8. S100 and GFAP stained scanty cells encircling cell nests (Figure 4D). A final pathologic diagnosis of PGL, Grading System for Adrenal Phaeochromocytoma and Paraganglioma score 6 (intermediate risk), was rendered[3,4].

Given the young age of the patient and the rarity of the tumor, succinate dehydrogenase subunit B (SDHB) protein expression was evaluated, and next generation sequencing (NGS) analysis, using the commercial kit "Miriapod NGS-IL" (Diatech) on MiSeq Illumina Platform, was carried out to identify mutations affecting genes associated with syndromic and/or familial conditions (*i.e.*, *SDHB*, *VHL*, *NF1*, *RET*). *SDHB* expression was preserved (Figure 4D, inset) and none of the above-mentioned genes were found to be mutated, thus ruling out a hereditary condition[5]. Interestingly, we detected two previously unreported mutations, one affecting the *KDR* gene in exon 7 (c.889G>A missense variant)[6], and another on the *JAK3* gene (c.394C>A missense variant) in exon 4[7,8] (Figures 4E and 4F). Both mutations are known to be pathogenetic in olfactory neuroblastoma[6], some forms of leukemia, and solid tumors, such as neuroendocrine tumors[7,8].

Imaging and cytologic findings were blindly reviewed by an expert panel of clinicians, radiologists, and pathologists to identify possible causes of misdiagnosis. The major issue was lack of evidence of a cleavage plane from the pancreas at US, CT, and NMR, which prompted radiologists to establish an intra-parenchymal origin. The blinded revision shifted the diagnosis towards an extra-pancreatic lesion



DOI: 10.3748/wjg.v28.i21.2396 **Copyright** ©The Author(s) 2022.

Figure 4 Histologic and molecular findings. A: The lesion was composed of nests and cords of polygonal cells with abundant granular cytoplasm, and occasional mitotic figures in the more cellular areas, hematoxylin and eosin original magnification (O.M) × 60; B: Chromogranin A (CgA) positivity in neoplastic cells; inset: Synaptophysin positivity in neoplastic cells, CgA stain, O.M × 10; C: GATA-3 positivity in neoplastic cells, GATA-3 stain, O.M. × 10; D: S100-positive cells were scattered; inset: Succinate dehydrogenase subunit B (SDHB) expression was preserved, S100 stain, O.M. × 10; inset, SDHB stain, O.M. × 10; E: *KDR* mutation; F: *JAK3* mutation.

as the pancreatic parenchyma showed no structural alterations and no dislocation of the Wirsung duct. *Ex post*, the identified biases were the emergency regimen of radiologic examination, which impaired a precise assessment, and the very thin mesocolon sheet, probably on account of the patient's leanness, which hindered clear definition of the lesion borders, also masked by the extensive hemorrhagic component. Original EUS diagnosis was confirmed, emphasizing the intrinsic limit of the bi-dimensional image of trans-abdominal US in detecting a large mass in the same examination field. Finally, pathologic review of the FNB findings favored a diagnosis of PGL due to substantial negativity for cytokeratins and PAX-8, usually positive in PanNet[9,10], and absence of folded nuclei with longitudinal grooves, cholesterol crystals, and foamy macrophages, usually found in SPN[9]. Furthermore, diffuse cytoplasmic CgA reactivity is typically not seen in SPN[9]. The detection of S100-positive

sustentacular cells and zellballen pattern, considering the hallmarks of PGL, has limited value in the diagnosis of PGL, since they may not be present in small samples or in sympathetic PGLs, as in our case [2,11]. Eighteen months after tumor excision, the patient is asymptomatic with no disease relapse evident with CT or NMR imaging; CgA levels are within the reference range.

In conclusion, our report strongly supports the suggestion by Lanke *et al*[1] that PGL should be included in the differential diagnosis of peripancreatic/pancreatic masses, and highlights the difficulties in establishing an accurate preoperative diagnosis even after a second round evaluation. Indeed, due to the deep localization and lack of specific clinical manifestations and imaging data, early diagnosis of PGL often relies solely on the level of suspicion, thus easily resulting in misdiagnosis or missed diagnosis[12,13]. A multidisciplinary team approach, involving skilled radiologists, endoscopists, pathologists, and surgeons, is of foremost importance for proper PGL diagnosis and management in order to prevent undue surgical resections[14]. In the present case, the first radiologic mistake affected all the diagnostic work-up, even after second round evaluation, and only the long-lasting experience of the surgeon avoided over-treatment (*i.e.*, distal splenopancreasectomy, as reported in most of the cases described so far)[1]. Since there are no definite criteria for malignancy, a close follow-up after surgery is mandatory[14,15]. Pathologists play a key role in providing clues that may disclose genetic profile and predict malignant potential of the tumor[1,3,4,14,15].

FOOTNOTES

Author contributions: Ambrosio MR, Amorosi A, and Arganini M contributed to the conception and design; Fratini G and Sbrozzi-Vanni A acquired the data; Cavazzana A, Giusti A, and Nesi G analyzed and interpreted of the data; Ambrosio MR, Fratini G, and Petrelli F drafted the article; Amorosi A, Arganini M, Manta R, Nesi G, and Vignali C contributed to the critical revision of the article for important intellectual content; and all authors approved the final manuscript to be published.

Conflict-of-interest statement: The authors have no conflicts of interest to declare.

Open-Access: This article is an open-access article that was selected by an in-house editor and fully peer-reviewed by external reviewers. It is distributed in accordance with the Creative Commons Attribution NonCommercial (CC BY-NC 4.0) license, which permits others to distribute, remix, adapt, build upon this work non-commercially, and license their derivative works on different terms, provided the original work is properly cited and the use is non-commercial. See: https://creativecommons.org/Licenses/by-nc/4.0/

Country/Territory of origin: Italy

ORCID number: Federica Petrelli 0000-0002-7352-6770; Geri Fratini 0000-0002-7355-6770; Andrea Sbrozzi-Vanni 0000-0002-7352-6760; Andrea Giusti 0000-0002-7342-6770; Raffele Manta 0000-0002-2168-8372; Claudio Vignali 0000-0003-7355-6770; Gabriella Nesi 0000-0002-2614-944X; Andrea Amorosi 0000-0001-5576-494; Andrea Cavazzana 0000-0001-5576-594; Marco Arganini 0000-0002-0972-1672; Maria Raffaella Ambrosio 0000-0002-1172-6902.

S-Editor: Wang JJ
L-Editor: Filipodia
P-Editor: Wang JJ

REFERENCES

1 **Lanke G**, Stewart JM, Lee JH. Pancreatic paraganglioma diagnosed by endoscopic ultrasound-guided fine needle aspiration: A case report and review of literature. *World J Gastroenterol* 2021; **27**: 6322-6331 [PMID: 34712035 DOI: 10.3748/wjg.v27.i37.6322]
2 **Zeng J**, Simsir A, Oweity T, Hajdu C, Cohen S, Shi Y. Peripancreatic paraganglioma mimics pancreatic/gastrointestinal neuroendocrine tumor on fine needle aspiration: Report of two cases and review of the literature. *Diagn Cytopathol* 2017; **45**: 947-952 [PMID: 28560856 DOI: 10.1002/dc.23761]
3 **Kimura N**, Takayanagi R, Takizawa N, Itagaki E, Katabami T, Kakoi N, Rakugi H, Ikeda Y, Tanabe A, Nigawara T, Ito S, Kimura I, Naruse M; Phaeochromocytoma Study Group in Japan. Pathological grading for predicting metastasis in phaeochromocytoma and paraganglioma. *Endocr Relat Cancer* 2014; **21**: 405-414 [PMID: 24521857 DOI: 10.1530/ERC-13-0494]
4 **Wang Y**, Li M, Deng H, Pang Y, Liu L, Guan X. The systems of metastatic potential prediction in pheochromocytoma and paraganglioma. *Am J Cancer Res* 2020; **10**: 769-780 [PMID: 32266090]
5 **Lam AK**. Update on Paragangliomas and Pheochromocytomas. *Turk Patoloji Derg* 2015; **31** Suppl 1: 105-112 [PMID: 26177321 DOI: 10.5146/tjpath.2015.01318]
6 **Wang L**, Ding Y, Wei L, Zhao D, Wang R, Zhang Y, Gu X, Wang Z. Recurrent Olfactory Neuroblastoma Treated With Cetuximab and Sunitinib: A Case Report. *Medicine (Baltimore)* 2016; **95**: e3536 [PMID: 27149458 DOI: 10.1097/MD.0000000000003536]

7 **Quintás-Cardama A**, Manshouri T, Estrov Z, Harris D, Zhang Y, Gaikwad A, Kantarjian HM, Verstovsek S. Preclinical characterization of atiprimod, a novel JAK2 AND JAK3 inhibitor. *Invest New Drugs* 2011; **29**: 818-826 [PMID: 20372971 DOI: 10.1007/s10637-010-9429-z]

8 **MacConaill LE**, Garcia E, Shivdasani P, Ducar M, Adusumilli R, Breneiser M, Byrne M, Chung L, Conneely J, Crosby L, Garraway LA, Gong X, Hahn WC, Hatton C, Kantoff PW, Kluk M, Kuo F, Jia Y, Joshi R, Longtine J, Manning A, Palescandolo E, Sharaf N, Sholl L, van Hummelen P, Wade J, Wollinson BM, Zepf D, Rollins BJ, Lindeman NI. Prospective enterprise-level molecular genotyping of a cohort of cancer patients. *J Mol Diagn* 2014; **16**: 660-672 [PMID: 25157968 DOI: 10.1016/j.jmoldx.2014.06.004]

9 **Ohara Y**, Oda T, Hashimoto S, Akashi Y, Miyamoto R, Enomoto T, Satomi K, Morishita Y, Ohkohchi N. Pancreatic neuroendocrine tumor and solid-pseudopapillary neoplasm: Key immunohistochemical profiles for differential diagnosis. *World J Gastroenterol* 2016; **22**: 8596-8604 [PMID: 27784972 DOI: 10.3748/wjg.v22.i38.8596]

10 **Abbasi A**, Wakeman KM, Pillarisetty VG. Pancreatic paraganglioma mimicking pancreatic neuroendocrine tumor. *Rare Tumors* 2020; **12**: 2036361320982799 [PMID: 33425308 DOI: 10.1177/2036361320982799]

11 **Singhi AD**, Hruban RH, Fabre M, Imura J, Schulick R, Wolfgang C, Ali SZ. Peripancreatic paraganglioma: a potential diagnostic challenge in cytopathology and surgical pathology. *Am J Surg Pathol* 2011; **35**: 1498-1504 [PMID: 21921779 DOI: 10.1097/PAS.0b013e3182281767]

12 **Zhang Z**, Tu Z, Lv Z, Luo Y, Yuan J. Case Report: Totally Laparoscopic Resection of Retroperitoneal Paraganglioma Masquerading as a Duodenal Gastrointestinal Stromal Tumor. *Front Surg* 2021; **8**: 586503 [PMID: 33768109 DOI: 10.3389/fsurg.2021.586503]

13 **Lin S**, Peng L, Huang S, Li Y, Xiao W. Primary pancreatic paraganglioma: a case report and literature review. *World J Surg Oncol* 2016; **14**: 19 [PMID: 26801079 DOI: 10.1186/s12957-016-0771-2]

14 **Tischler AS**. Pheochromocytoma and extra-adrenal paraganglioma: updates. *Arch Pathol Lab Med* 2008; **132**: 1272-1284 [PMID: 18684026 DOI: 10.5858/2008-132-1272-PAEPU]

15 **Kimura N**, Takekoshi K, Naruse M. Risk Stratification on Pheochromocytoma and Paraganglioma from Laboratory and Clinical Medicine. *J Clin Med* 2018; **7** [PMID: 30150569 DOI: 10.3390/jcm7090242]



Published by **Baishideng Publishing Group Inc**
7041 Koll Center Parkway, Suite 160, Pleasanton, CA 94566, USA
Telephone: +1-925-3991568
E-mail: bpgoffice@wjgnet.com
Help Desk: https://www.f6publishing.com/helpdesk
https://www.wjgnet.com



© 2022 Baishideng Publishing Group Inc. All rights reserved.

ISSN 1007-9327 (print)
ISSN 2219-2840 (online)

World Journal of *Gastroenterology*

World J Gastroenterol 2022 June 14; 28(22): 2403-2526



Published by Baishideng Publishing Group Inc

World Journal of Gastroenterology

Contents

Weekly Volume 28 Number 22 June 14, 2022

REVIEW

2403 Prehabilitation prior to intestinal resection in Crohn's disease patients: An opinion review

Bak MTJ, Ruiterkamp MFE, van Ruler O, Campmans-Kuijpers MJE, Bongers BC, van Meeteren NLU, van der Woude CJ, Stassen LPS, de Vries AC

2417 Hepatocellular carcinoma, hepatitis C virus infection and miRNA involvement: Perspectives for new therapeutic approaches

Badami E, Busà R, Douradinha B, Russelli G, Miceli V, Gallo A, Zito G, Conaldi PG, Iannolo G

MINIREVIEWS

2429 Metabolic aspects of hepatitis C virus

El-Kassas M, Awad A

ORIGINAL ARTICLE

Basic Study

2437 18β-glycyrrhetinic acid regulates mitochondrial ribosomal protein L35-associated apoptosis signaling pathways to inhibit proliferation of gastric carcinoma cells

Yuan L, Yang Y, Li X, Zhou X, Du YH, Liu WJ, Zhang L, Yu L, Ma TT, Li JX, Chen Y, Nan Y

Retrospective Study

2457 Application of endoscopic ultrasonography for detecting esophageal lesions based on convolutional neural network

Liu GS, Huang PY, Wen ML, Zhuang SS, Hua J, He XP

2468 Prognostic value of preoperative enhanced computed tomography as a quantitative imaging biomarker in pancreatic cancer

Gao JF, Pan Y, Lin XC, Lu FC, Qiu DS, Liu JJ, Huang HG

2482 Endoscopic classification and pathological features of primary intestinal lymphangiectasia

Meng MM, Liu KL, Xue XY, Hao K, Dong J, Yu CK, Liu H, Wang CH, Su H, Lin W, Jiang GJ, Wei N, Wang RG, Shen WB, Wu J

Observational Study

2494 Accurate and generalizable quantitative scoring of liver steatosis from ultrasound images *via* scalable deep learning

Li B, Tai DI, Yan K, Chen YC, Chen CJ, Huang SF, Hsu TH, Yu WT, Xiao J, Le L, Harrison AP

Randomized Controlled Trial

2509 *Saccharomyces cerevisiae* I-3856 in irritable bowel syndrome with predominant constipation

Mourey F, Decherf A, Jeanne JF, Clément-Ziza M, Grisoni ML, Machuron F, Legrain-Raspaud S, Bourreille A, Desreumaux P

LETTER TO THE EDITOR

2523 Future therapies for pancreatic carcinoma: Insights into cancer precision medicine

Jiang QY, Chen ZX, Zhang S, Xue RY

World Journal of Gastroenterology

Weekly Volume 28 Number 22 June 14, 2022

Contents

ABOUT COVER

Editorial Board of *World Journal of Gastroenterology*, Conrado M Fernandez-Rodriguez, MD, PhD, Associate Professor, Unit of Gastroenterology, Hospital Universitario Fundacion Alcorcon, Av. Budapest-1, Alcorcón, Madrid 28922, Spain. cfernandez@fhalcorcon.es

AIMS AND SCOPE

The primary aim of *World Journal of Gastroenterology* (*WJG*, *World J Gastroenterol*) is to provide scholars and readers from various fields of gastroenterology and hepatology with a platform to publish high-quality basic and clinical research articles and communicate their research findings online. *WJG* mainly publishes articles reporting research results and findings obtained in the field of gastroenterology and hepatology and covering a wide range of topics including gastroenterology, hepatology, gastrointestinal endoscopy, gastrointestinal surgery, gastrointestinal oncology, and pediatric gastroenterology.

INDEXING/ABSTRACTING

The *WJG* is now indexed in Current Contents®/Clinical Medicine, Science Citation Index Expanded (also known as SciSearch®), Journal Citation Reports®, Index Medicus, MEDLINE, PubMed, PubMed Central, and Scopus. The 2021 edition of Journal Citation Report® cites the 2020 impact factor (IF) for *WJG* as 5.742; Journal Citation Indicator: 0.79; IF without journal self cites: 5.590; 5-year IF: 5.044; Ranking: 28 among 92 journals in gastroenterology and hepatology; and Quartile category: Q2. The *WJG*'s CiteScore for 2020 is 6.9 and Scopus CiteScore rank 2020: Gastroenterology is 19/136.

RESPONSIBLE EDITORS FOR THIS ISSUE

Production Editor: *Hua-Ge Yu*; **Production Department Director:** *Xu Guo*; **Editorial Office Director:** *Ze-Mao Gong*.

NAME OF JOURNAL

World Journal of Gastroenterology

ISSN

ISSN 1007-9327 (print) ISSN 2219-2840 (online)

LAUNCH DATE

October 1, 1995

FREQUENCY

Weekly

EDITORS-IN-CHIEF

Andrzej S Tarnawski

EDITORIAL BOARD MEMBERS

http://www.wjgnet.com/1007-9327/editorialboard.htm

PUBLICATION DATE

June 14, 2022

COPYRIGHT

© 2022 Baishideng Publishing Group Inc

INSTRUCTIONS TO AUTHORS

https://www.wjgnet.com/bpg/gerinfo/204

GUIDELINES FOR ETHICS DOCUMENTS

https://www.wjgnet.com/bpg/GerInfo/287

GUIDELINES FOR NON-NATIVE SPEAKERS OF ENGLISH

https://www.wjgnet.com/bpg/gerinfo/240

PUBLICATION ETHICS

https://www.wjgnet.com/bpg/GerInfo/288

PUBLICATION MISCONDUCT

https://www.wjgnet.com/bpg/gerinfo/208

ARTICLE PROCESSING CHARGE

https://www.wjgnet.com/bpg/gerinfo/242

STEPS FOR SUBMITTING MANUSCRIPTS

https://www.wjgnet.com/bpg/GerInfo/239

ONLINE SUBMISSION

https://www.f6publishing.com

© 2022 Baishideng Publishing Group Inc. All rights reserved. 7041 Koll Center Parkway, Suite 160, Pleasanton, CA 94566, USA

E-mail: bpgoffice@wjgnet.com https://www.wjgnet.com

World Journal of Gastroenterology

Submit a Manuscript: https://www.f6publishing.com

World J Gastroenterol 2022 June 14; 28(22): 2403-2416

DOI: 10.3748/wjg.v28.i22.2403

ISSN 1007-9327 (print) ISSN 2219-2840 (online)

REVIEW

Prehabilitation prior to intestinal resection in Crohn's disease patients: An opinion review

Michiel T J Bak, Marit F E Ruiterkamp, Oddeke van Ruler, Marjo J E Campmans-Kuijpers, Bart C Bongers, Nico L U van Meeteren, C Janneke van der Woude, Laurents P S Stassen, Annemarie C de Vries

Specialty type: Gastroenterology and hepatology

Provenance and peer review: Invited article; Externally peer reviewed.

Peer-review model: Single blind

Peer-review report's scientific quality classification

Grade A (Excellent): 0
Grade B (Very good): 0
Grade C (Good): C, C
Grade D (Fair): 0
Grade E (Poor): 0

P-Reviewer: Gangl A, Austria; Garg P, India
A-Editor: De Nardi P, Italy

Received: January 10, 2022
Peer-review started: January 10, 2022
First decision: March 8, 2022
Revised: March 21, 2022
Accepted: May 22, 2022
Article in press: May 22, 2022
Published online: June 14, 2022

Michiel T J Bak, Marit F E Ruiterkamp, C Janneke van der Woude, Annemarie C de Vries, Department of Gastroenterology and Hepatology, Erasmus University Medical Center Rotterdam, Rotterdam 3015 GD, Netherlands

Oddeke van Ruler, Department of Surgery, IJsselland Hospital, Capelle aan den IJssel 2906 ZC, Netherlands

Oddeke van Ruler, Department of Surgery, Erasmus University Medical Center Rotterdam, Rotterdam 3015 GD, Netherlands

Marjo J E Campmans-Kuijpers, Department of Gastroenterology and Hepatology, University Medical Center Groningen and University of Groningen, Groningen 9713 GZ, Netherlands

Bart C Bongers, Department of Nutrition and Movement Sciences, School of Nutrition and Translational Research in Metabolism, Maastricht University, Maastricht 6200 MD, Netherlands

Bart C Bongers, Department of Epidemiology, Care and Public Health Research Institute, Maastricht University, Maastricht 6200 MD, Netherlands

Nico L U van Meeteren, Department of Anaesthesiology, Erasmus MC University Medical Center Rotterdam, Rotterdam 3015 GD, Netherlands

Laurents P S Stassen, Department of Surgery, Maastricht University Medical Center, Maastricht 6229 HX, Netherlands

Corresponding author: Annemarie C de Vries, MD, PhD, Doctor, Staff Physician, Department of Gastroenterology and Hepatology, Erasmus University Medical Center Rotterdam, Doctor Molewaterplein 40, Rotterdam 3015 GD, Netherlands. a.c.devries@erasmusmc.nl

Abstract

Patients with Crohn's disease (CD) are at a considerable risk for intestinal surgery. Approximately 25% of patients with CD will undergo an intestinal resection within 10 years of diagnosis. Postoperative complications after CD surgery have been reported in 20%-47% of the patients. Both general and CD-related risk factors are associated with postoperative complications, and comprise non-modifiable (*e.g.*, age) and potentially modifiable risk factors (*e.g.*, malnutrition). Prehabilitation focuses on the preoperative period with strategies designed to optimize

modifiable risk factors concerning the physical and mental condition of the individual patient. The aim of prehabilitation is to enhance postoperative recovery and return to or even improve preoperative functional capacity. Preoperative improvement of nutritional status, physical fitness, cessation of smoking, psychological support, and critical revision of preoperative use of CD medication are important strategies. Studies of the effect on postoperative outcome in CD patients are scarce, and guidelines lack recommendations on tailored management. In this opinion review, we review the current evidence on the impact of screening and management of nutritional status, physical fitness, CD medication and laboratory values on the postoperative course following an intestinal resection in CD patients. In addition, we aim to provide guidance for individualized multimodal prehabilitation in clinical practice concerning these modifiable factors.

Key Words: Crohn's disease; Prehabilitation strategies; Nutrition; Physical fitness; Medication; Laboratory values

©The Author(s) 2022. Published by Baishideng Publishing Group Inc. All rights reserved.

Core Tip: Nutritional status, medication, and laboratory values are modifiable factors that influence the postoperative course of patients with Crohn's disease. In addition, physical fitness is impaired in the perioperative course and therefore preoperative screening is warranted. Individualized multimodal prehabilitation programs aim to improve these modifiable risk factors before surgery, including smoking cessation and psychological screening and support, and should be integrated in the preoperative preparation period in order to reduce both postoperative complications and undesirable outcomes.

Citation: Bak MTJ, Ruiterkamp MFE, van Ruler O, Campmans-Kuijpers MJE, Bongers BC, van Meeteren NLU, van der Woude CJ, Stassen LPS, de Vries AC. Prehabilitation prior to intestinal resection in Crohn's disease patients: An opinion review. *World J Gastroenterol* 2022; 28(22): 2403-2416
URL: https://www.wjgnet.com/1007-9327/full/v28/i22/2403.htm
DOI: https://dx.doi.org/10.3748/wjg.v28.i22.2403

INTRODUCTION

Crohn's disease (CD) is a chronic inflammatory bowel disease (IBD) characterized by segmental, transmural inflammation, which most commonly affects the ileum and/or colon[1]. Although the risk of intestinal resection and re-resection has declined considerably over the past decades, approximately 25% of patients will undergo an intestinal resection within 10 years of CD diagnosis[2,3].

An intestinal resection is potentially perceived as a major life event and has a significant psychological impact on CD patients, which can result in anxiety and depressive symptoms in the pre- and postoperative setting[4]. Despite the immediate relief of symptoms and a potential increase of quality of life after CD surgery[5], important concerns are the risk of potential (severe) complications and recurrence of CD[6]. Reports on the frequency of postoperative complications, following intestinal resection in CD patients, range from 20%-47%[7-12]. Several general and CD-specific risk factors for postoperative complications have been identified. Both non-modifiable risk factors (*i.e.*, comorbidity, older age) and modifiable risk factors (*i.e.*, malnutrition, preoperative medication use, abnormal preoperative laboratory values and smoking) have been associated with postoperative complications[8-10,12,13]. In addition, preoperative physical fitness, specifically aerobic fitness, seems impaired in patients with CD[14], which may increase the risk for adverse postoperative outcomes as has been observed in colorectal cancer (CRC) surgery[15,16].

Prehabilitation focuses on the preoperative period by suggesting strategies designed to optimize modifiable risk factors concerning the physical and mental condition of the individual patient. As such, prehabilitation aims to improve the postoperative course and promotes an earlier postoperative recovery and return to functional capacity[6]. A four-pillar multimodal prehabilitation program tailored to the individual patient involves improving: (1) Physical; (2) Nutritional; (3) Psychological status; and (4) Cessation of smoking, resulted in a significant earlier recovery to the baseline functional capacity in patients with CRC[17]. In addition, preoperative physical exercise training to improve aerobic fitness significantly reduced postoperative complications in high-risk patients, both in general[18] and those with CRC[19], undergoing abdominal surgery as compared to usual care. These programs may also benefit patients in other settings of abdominal surgery, including CD[20]. However, literature on prehabilitation in CD patients scheduled for intestinal resection is scarce and guidelines lack recommendations on tailored management[21,22].

Table 1 Recommendations on screening for prehabilitation prior to intestinal surgery in Crohn's disease

Screening	
Nutritional status	Screening in all patients: Body mass index, evaluation of unintentional weight loss and assessment of dietary intake with nutritional or immunological screening tools (*e.g.*, GLIM and OPNI). Preferably assess the muscle mass (*e.g.*, with handgrip strength or consider available imaging techniques) to complement the measures of nutritional status
Physical fitness	Screening in all patients to estimate aerobic fitness with validated self-reporting questionnaire (*e.g.*, Duke activity status index, veterans-specific activity questionnaire). Consider referral of patients at risk for impaired physical fitness for comprehensive objective assessment by an exercise specialist
CD medication	Critically revise all current CD medication on a case-by-case basis
Laboratory assessment	Preoperative assessment of full blood count, CRP, and serum albumin. Assessment of vitamins and other trace elements may only be indicative in patients with biochemical remission
Smoking psychological status	Screen all patients on active smoking Discussion of expectations and potential fears for the perioperative course by treating physicians IBD team members

CD: Crohn's disease; CRP: C-reactive protein; GLIM: Global Leadership Initiative on Malnutrition; IBD: Inflammatory bowel disease; OPNI: Onodera's prognostic nutritional index.

Table 2 Recommendations for prehabilitation interventions prior to intestinal surgery in Crohn's disease

Intervention	
Nutritional	Nutritional support may be considered in case of impaired nutritional status and/or inadequate intake with regard to proteins and calories. Minimum duration of nutritional support is 1-2 wk and may be extended to 6-8 wk to fully benefit from the dietary intervention. EEN may be considered as nutritional support for immunomodulatory effect and reduction of postoperative complications. TPN seems a valid option only when enteral nutrition is contraindicated, not effective or tolerated
Physical fitness	Physical exercise aerobic activity and muscular resistance training may be considered to improve physical fitness in the preoperative course. High-intensity physical exercise should be avoided due to risk of exacerbation of inflammation and symptoms
CD medication	Wean off corticosteroids to a minimal dose (preferably < 20 mg) 6 wk prior to surgery. Consider cessation of anti-TNF-α agents (especially in case of therapy-refractory disease). If considered, a time-interval of 4 wk (ADA) or 6-8 wk (IFX) seems appropriate
Laboratory assessment	Preoperative intravenous iron therapy is recommended in case of iron deficiency anemia in the preoperative course. In case of hypoalbuminemia and an impaired nutritional status, nutritional support is advised (see nutritional and physical status)
Smoking	Preoperative cessation is recommended (*e.g.*, within smoking cessation program)
Psychological status	Provide individualized psychosocial support or refer to psychologist

CD: Crohn's disease; ADA: Adalimumab; EEN: Exclusive enteral nutrition; IFX: Infliximab; TNF-α: Tumor necrosis factor-alpha; TPN: Total parenteral nutrition.

In this opinion review, the available literature on the effect of potentially modifiable preoperative factors on the postoperative course following an intestinal resection in CD is critically appraised, with a focus on nutritional status, physical fitness, CD medication, and laboratory values. In addition, we aim to provide guidance for screening and specific interventions on these items during the preoperative course of patients with CD (Tables 1 and 2). Although psychological screening and support, as well as smoking cessation are considered essential during preoperative optimization in CD, these topics will not be addressed in this review. For these topics, management in accordance with general guidelines and integration into a multimodal prehabilitation program is recommended.

METHODS

A literature search of the EMBASE, Medline, Web of Science, Google Scholar and Cochrane Library databases was conducted, in collaboration with the Medical School Library of the Erasmus University Rotterdam. High-quality articles were cited in Reference Citation Analysis (*RCA*) (https://www.referencecitationanalysis.com). The following keywords, synonyms and their Medical Subject Headings terms were used for this search: 'Crohn's disease', 'intestinal surgery', and 'risk factors' (Supplementary material).

Studies published in the English language up to July 2021 were considered according to their topical relevance for the impact of screening and management of nutritional status, physical fitness, CD medication and laboratory values in the preoperative period related to the postoperative course

following an intestinal resection in CD patients. In the case that no relevant studies were present virtually for any of these topical contents, the literature was re-assessed in other settings of abdominal surgery (*e.g.*, patients with CRC). Only randomized controlled trials, meta-analyses, systematic reviews, observational studies (case-control study and patient series without control) were selected. Study selection was independently performed by both two reviewers (Bak MTJ and Ruiterkamp MFE) based on title and abstract. The snowball method was then applied to all of the final selected studies.

HOW TO SCREEN AND OPTIMIZE THE NUTRITIONAL STATUS AND PHYSICAL FITNESS OF PATIENTS WITH CD PRIOR TO INTESTINAL RESECTION?

Preoperative screening of nutritional status

Malnutrition is an important risk factor for a dismal postoperative course after intestinal resection in CD [23]. Malnutrition encompasses undernutrition and overnutrition. CD patients are prone to undernutrition due to inadequate nutritional intake attributable to several causes (*e.g.*, anorexia, strictures), malabsorption (*e.g.*, active inflammation or after prior resection) and chronic inflammation. However, obesity in the CD population has increased over the years[24]. Recognition of nutritional status as the key issue in preoperative optimization for patients with CD is gaining ground, since a significant benefit from dietary intervention may not only be expected after optimization of the nutritional status but also from its potential immunomodulatory effect on CD.

A first screening for malnutrition is readily available to all caregivers treating patients with CD and is recommended in all preoperative CD patients according to current guidelines[21-23]. Since a survey among 146 gastroenterologists in 2016 revealed that one-third of respondents did not routinely screen for malnutrition, exploration of the reasons for non-adherence is required[25]. The initial nutritional assessment during preoperative screening requires a combination of: (1) Body mass index (BMI); (2) Evaluation of unintentional weight loss; and (3) Assessment of dietary intake. Assessment of muscle mass preferably complements these measures. Laboratory assessment of albumin and micronutrients is not a reliable marker of malnutrition, and will be addressed in a later paragraph[23].

BMI is a commonly used indicator for body fat and thus a proxy of nutritional status. Preoperative BMI value and the rate of postoperative complications are only moderately correlated, according to abundant reports[26-30]. Nevertheless, clearly underweight patients, defined with varying cut-off values in the literature (from BMI < 16.2 kg/m^2 to BMI < 18.5 kg/m^2), are at an increased risk of a dismal postoperative course after intestinal resection, including creation of an ileostomy[9], readmission[31], intra-abdominal septic complications (IASCs)[32], and overall postoperative complications[33,34]. Similarly, clearly overweight patients suffering from obesity, defined as a BMI cut-off > 30 kg/m^2, also face an elevated risk of complications[9,28,34-36]. In addition, another study reported an increasing BMI by 1 unit (U) associated with an increased risk [odds ratio (OR) = 1.04; 95% confidence interval (CI): 1.0-1.1; P = 0.008] of postoperative complications[35].

Unintentional preoperative weight loss may occur in all CD patients independent of their baseline weight. Various studies assessing the effect of preoperative weight loss have confirmed the association with postoperative complications in CD patients. Unintentional weight loss of > 10%, as compared to baseline over the last 6 mo prior to surgery, is a commonly described cut-off[9,10,36-38]. This cut-off of significant weight loss has been observed in 23%-54% of CD patients scheduled for intestinal resection [23]. Various studies have reported a clear negative association between recent unintentional weight loss and postoperative complications in CD patients[9,10,36-38].

In addition, other measures of body composition may warrant evaluation during the preoperative assessment. The most important is sarcopenia, which is defined as low lean muscle mass in combination with either low muscle strength or low physical performance[39]. Sarcopenia can be present in both under- and overweight individuals[40]. Moreover, sarcopenia is common in CD patients, with a reported overall incidence of 52%, as determined by radiologic assessment of body mass composition (*e.g.*, skeletal mass index, total psoas index and/or Hounsfield U average calculations at the level of the third lumbar vertebral body)[40,41]. A recent meta-analysis identified sarcopenia as an independent predictor for both postoperative complications and/or undesirable outcomes (*i.e.*, poor quality of life, inadequate response to therapy) in the IBD population[42]. Especially in patients younger than 40 years, sarcopenia was a strong and independent risk factor for postoperative complications, and patients with a low or normal BMI were affected more often[43]. Handgrip strength is an accessible and reliable diagnostic method for sarcopenia applied in routine practice. When sarcopenia in CD patients is detected in the preoperative setting, a combined intervention to optimize the closely related nutritional status and improved physical fitness may enhance postoperative prognosis[44]. However, data on these specific interventions are lacking.

To date, several nutritional screening tools are available to assess the nutritional status in the IBD population. These tools combine such clinical features as BMI, weight loss, and symptoms (for instance diarrhea). Amongst these tools are the following: Nutrition Risk Screening (NRS-2002)[45]; Malnutrition Universal Screening Tool (MUST)[46]; Global Leadership Initiative on Malnutrition (GLIM) criteria[47]; and more IBD-specific tools, such as the Malnutrition Inflammatory Risk Tool (MIRT)[48] and Saskat-

chewan IBD Nutrition Risk Tool[49]. The GLIM has a higher rate of malnutrition detection in preoperative IBD patients as compared to several other screening tools (namely NRS-2002, MUST, MIRT, and Saskatchewan IBD Nutrition Risk Tool)[50]. Moreover, chronic inflammation is used as an indicator in this nutritional screening tool[47]. The Onodera's prognostic nutritional index (OPNI) is a simple and useful index to merely reflect the preoperative immunological status using serum albumin level and total lymphocyte counts. OPNI predicts the risk of postoperative complications in various types of cancer[51]. Limited data of the prognostic value of the OPNI in CD suggests that OPNI < 40 is a predictor of infectious complications or postoperative abdominal bleeding[52-54]. Overall, more data on the association between malnutrition detected by these screening tools and the postoperative course are required to support their routine use.

Future nutritional screening methods

An altered body composition is a known risk factor for postoperative complications[23]. Current available imaging techniques provide the opportunity to screen the body composition and develop new nutritional predictors for postoperative outcome. Although cross-sectional imaging with the sole purpose of evaluating body composition is not indicated, and available scans may be used for objective evaluation. Visceral fat promotes both local and systemic inflammation, resulting in a chronic inflammatory status[55,56]. Increased[57] and decreased[58] subcutaneous fat as well as increased visceral fat [59] are associated with increased risk of early postoperative complications in CD patients. Moreover, an expanded visceral/subcutaneous fat ratio (VSR) was identified as a better predictor of the postoperative outcome compared to BMI[58]. However, another study reported no association between VSR and postoperative complications[60]. In addition, there seems to be different cut-off points of total subcutaneous fat for CD patients, compared to other patients[57]. Therefore, these promising markers warrant further investigation.

Preoperative screening of physical fitness

To date, there is no routine screening for physical fitness in patients with CD in the preoperative course. In general, the physical fitness of CD patients is impaired[14,61]. Two cross-sectional studies concluded that physical fitness, specifically aerobic fitness, is impaired in the perioperative course of patients with CD as compared to the general population or other subgroups undergoing abdominal surgery[14,62]. This impairment is attributed to a lack of physical activity due to illness behavior and/or impaired nutritional status affecting muscle function[14,61,63,64]. More objective insights into the level of physical fitness in patients with CD are required, as well as into the association between physical fitness and patient-, disease-, and treatment-related outcomes. The specific subgroups of patients with impaired aerobic fitness may benefit most from a targeted and personalized physical exercise intervention. A validated self-reporting questionnaire (*e.g.*, Duke activity status index, veterans-specific activity questionnaire) may serve as a simple screening tool to identify patients with impaired aerobic fitness[65,66]. These patients may receive a comprehensive objective assessment by an exercise specialist (*e.g.*, physical therapist, clinical exercise physiologist) to evaluate the specific exercise intolerance and propose a personalized prescription for physical exercise training.

A cardiopulmonary exercise test is considered the gold standard for assessing aerobic fitness and also provides valuable information to determine physical exercise training safety (*e.g.*, contraindications) by assessing the body's integrated physiological response to progressive exercise[67]. Moreover, cardiopulmonary exercise test results can be used to optimize and personalize training intensity. When performance of a cardiopulmonary exercise test is not possible, a more practical performance-based field test to evaluate a patient's aerobic fitness can be used. The steep-ramp test is a short time maximal exercise test on a cycle ergometer, of which its primary outcome parameter (the achieved peak work rate) is highly correlated with aerobic fitness indicators obtained at the cardiopulmonary exercise test [68].

Low- to moderate-intensity physical exercise training interventions are feasible and safe in IBD patients in the non-perioperative setting, and have been associated with improved physical fitness as well as with a significant reduction of (severe) fatigue and stress, and a significant improvement of quality of life[69-71]. To date, no preoperative physical exercise training studies have been conducted in patients with CD. As aerobic and resistance training have been found to be effective for the reduction of postoperative complications and accelerates recovery of functional capacity in unfit patients undergoing abdominal surgery[18,19], patients with CD may benefit from these interventions as well in the preoperative course[72]. It seems that high-intensity physical exercise training should be avoided, as it may lead to an acute exacerbation of inflammation and CD symptoms[73]. Overall, future research for the effect of physical interventions on the preoperative course of CD patients is warranted.

Preoperative optimization of nutritional status

To reverse the negative impact of malnutrition on the postoperative course in CD patients, preoperative optimization of the nutritional status is indicated. The European Society of Clinical Nutrition and Metabolism (ESPEN) states that the preoperative optimization of the nutritional status by enteral nutrition (EN) for 7-10 d, in the case of mildly malnourished patients, or 7-14 d in the case of a severe nutritional risk, is appropriate[74]. Nutritional support is administered enterally, and only parenteral in

case EN has failed or is contraindicated (*e.g.*, due to an intestinal obstruction)[74].

A Cochrane review on preoperative nutritional support in patients scheduled for gastrointestinal surgery reported a significant reduction of anastomotic leakage and need for a temporary diverting stoma [overall risk ratio (RR) = 0.67; 95%CI: 0.53-0.85][75]. In line with these findings, a meta-analysis showed that preoperative nutritional therapy significantly reduces postoperative complications in patients with CD (OR = 0.26; 95%CI: 0.07-0.99)[76]. In particular, EN was superior to usual care (defined as no nutritional support) (OR = 0.09; 95%CI: 0.06-0.013)[76,77]. A trend towards superiority of total parenteral nutrition (TPN) as compared to standard care was observed, but statistical significance was not reached[76].

Exclusive EN (EEN) consists of complete liquid diet of various compositions and has been widely used as induction therapy in pediatric CD patients with a duration of 6 wk to 8 wk[78,79]. EEN is effective as preoperative therapy by inducing both clinical and histological remission in adult CD patients[80,81]. The anti-inflammatory effect of EEN can be attributed to the reduction of mucosal cytokines and composite alterations of the gut microbiome[81,82]. Cohort studies, which investigated the effect of EEN in the preoperative setting in the CD population, demonstrated a significant reduction in overall postoperative complications[83-85], IASCs[86,87], and postoperative abscesses and anastomotic leakage[80,86,88]. Moreover, EEN has proven to be beneficial in the reduction of C-reactive protein (CRP)[80,83-85] and the increase of albumin, OPNI, and hemoglobin level[83,84].

In case EN fails or is contraindicated, PN is suggested. PN can be divided into partial PN (PPN) and TPN. PN is administered into the venous system *via* a catheter into the superior vena cava or a peripherally-inserted central catheter. Patients treated with TPN only receive a completely intravenous (IV) nutritional liquid diet, while patients with PPN may receive nutrients from other sources alongside PN. The literature on the effect of PN on postoperative complications following intestinal resection in CD is scarce. Available studies reported a significant decrease in overall postoperative complications [89], non-infectious complications[90], anastomotic leakage[88], and the length of the resection specimen [91]. Benefits of TPN were observed in patients who were treated with TPN for ≥ 60 d[90] or for the duration of 18-90 d[89]. However, the benefit of PN as nutritional support needs to be weighed against the possible risk of catheter-related infections[92].

Reviewers' opinion

In summary, since extremes in BMI (< 18.5 kg/m^2 or > 30 kg/m^2) and recent unintentional weight loss (> 10% within 6 mo prior to surgery) have been associated with a dismal postoperative course in CD patients, we recommend the assessment of both in the preoperative setting. The detection of significant unintentional weight loss is a red flag and postponement of the intestinal resection until after restoration of the catabolic status should be considered. Moreover, assessment of handgrip strength may be used to detect sarcopenia. We consider GLIM as an appropriate screening tool for malnutrition in CD patients as chronic inflammation is included as one of the indicators. Moreover, the GLIM had a higher detection rate of malnutrition as compared to other screening tools in preoperative IBD patients. In addition, the OPNI can be used as an immunological screening tool. However, the prognostic value of these tools on the postoperative course requires further research. In our opinion, nutritional support during preoperative optimization may be considered for all patients with either an impaired nutritional status and/or inadequate intake with regard to proteins and calories. After a diagnosis of malnutrition, an individualized window to surgery needs to be decided to optimize nutritional status. As physical fitness is impaired in CD and therefore may influence the postoperative course, preoperative screening is warranted with use of self-reporting questionnaires. In addition, patients at risk may benefit from an objective assessment to evaluate specific exercise intolerance and a personalized prescription for physical exercise training. When pre- and postoperative physical fitness is impaired in patients with CD, aerobic and resistance training are recommended. The optimization period as suggested by the ESPEN (7-14 d) may be considered a minimum and, after careful evaluation per individual case, be extended up to 6-8 wk in most cases to fully benefit from the dietary intervention. EEN seems a promising preoperative nutritional intervention to improve prognosis due to its immunomodulatory effect, especially in patients with penetrating CD complications. Nutritional support is administered enterally (oral or *via* a nasogastric tube) (*i.e.*, EN), and only in exceptional situations parenterally (when enteral nutritional support fails). TPN seems a valid option only when EN is contraindicated, not effective, more tolerable.

WHAT IS THE OPTIMAL TIMING TO DISCONTINUE CD MEDICATION PREOPERATIVELY?

CD-related medication has an immunomodulatory effect and may increase the risk of infections. This may also result in postoperative surgical site infections (SSIs) and/or IASCs. The European Crohn & Colitis Organization (ECCO) guideline recommends to wean off corticosteroids 6 wk before surgery [21], while the guideline of the British Society for Gastroenterology (BSG) recommends to stop corticosteroids or minimize the dose, without specifying a window to surgery[22]. Moreover, the BSG recommends cessation of infliximab and adalimumab 6-8 wk and 4 wk prior to surgery, respectively

[22], whereas the ECCO guideline states that cessation of anti-tumor necrosis factor-alpha (TNF)-α therapy prior to surgery is not mandatory[21].

A recent Cochrane review studied the potential impact of perioperative IBD medication on the risk of postoperative (infectious) complications within 30 d in IBD patients[93]. The pooled data of this meta-analysis reported a significant association of corticosteroids with the risk of overall infectious postoperative complications (OR = 1.70; 95%CI: 1.38-2.09) and intra-abdominal infections (OR = 5.95; 95%CI: 1.04-34.1) in CD patients[93]. Furthermore, a significant increased risk of overall infectious complications (OR = 1.60; 95%CI: 1.20-2.13) was observed in patients treated with an anti-TNF-α agent [93]. No significant association was reported for patients who received the last dose of anti-TNF-α more than 8 wk before surgery[93]. However, these results should be interpreted with caution since the evidence for all outcomes was of low or very low quality, mostly due to the observational design, heterogeneity, and risk of bias of the included studies[93].

Pooled data of that meta-analysis demonstrated no significantly increased risk of overall postoperative infectious complications in CD patients treated with immunomodulatory, anti-interleukin and anti-integrin therapy[93]. Nevertheless, two retrospective studies have found a significant association of thiopurines, in combination with anti-TNF-α or corticosteroids, with IASC and overall infectious complications in the postoperative course[94,95]. The relation between vedolizumab, an anti-integrin agent, and postoperative complications has been studied in nine observational cohort studies including a total number of 799 patients and predominantly evaluating patients who underwent abdominal surgery with overall postoperative (infectious) complications as the primary endpoint[29,96-102]. Two studies found a significant increased risk of SSIs in patients treated with vedolizumab in the preoperative course[29,96]. Another study reported a significant decreased risk of postoperative ileus in CD patients with detectable vedolizumab levels as compared to non-detectable vedolizumab levels[99]. Four observational studies found the outcomes of preoperative ustekinumab use on postoperative complications and infectious complications, and found no significantly increased risk[96-98,103].

Reviewers' opinion

In accordance to the current literature and guidelines, we would recommend to wean off corticosteroids to a minimal dose, preferably < 20 mg, 6 wk prior to surgery. Moreover, cessation of anti-TNF-α agents may be considered, especially in non-responders and/or therapy refractory CD. When cessation is considered, a time interval of 4-8 wk (depending on type of anti-TNF-α agent) prior to surgery seems appropriate. Although the evidence on an association with increased risk of infections is unclear for other CD-medication, critical revision of the benefit of continuation until the date of surgery is indicated in all patients on an individual basis. In addition, since the biologic effect may last longer and vary per agent from 1 mo (prednisolone < 10 mg) to 3 mo (immunomodulators, anti-TNF-α) or longer (vedolizumab and ustekinumab), data on the effect of intervention are required to prove the beneficial effect of timely cessation[104].

WHICH LABORATORY VALUES ARE ASSOCIATED WITH THE POSTOPERATIVE COURSE AND NEED TO BE ASSESSED PRIOR TO INTESTINAL RESECTION IN PATIENTS WITH CD?

Specific recommendations concerning the preoperative assessment of laboratory values in CD patients are lacking in the BSG and ECCO guidelines[21,22]. Nevertheless, abnormal laboratory values in the preoperative setting have been associated with a dismal postoperative course in CD. Hypoalbuminemia (defined as serum albumin < 30 g/L) is one of the criteria for the diagnosis of (severe) malnutrition in general[74]. However, albumin is an acute-phase reactant protein and serum levels may decrease due to active inflammation[23]. Probably due to the chronic inflammatory state, serum albumin levels are lower in CD patients, as compared to the general population, and are reversely correlated to the disease activity[105]. Therefore, serum albumin is not a reliable marker for malnutrition in CD. Nevertheless, low serum albumin (ranging from < 29 g/L to 35 g/L) is associated with an increased risk of postoperative complications in CD patients[10,102,106-108]. These complications comprised overall early post-operative complications (< 30 d)[60,102,109-111], IASCs[10,106,112,113], SSIs[107,114], anastomotic leakage[88], and infectious complications[33,108,115].

Assessment of a full blood count, including hemoglobin and leucocyte and platelet counts, is advised in patients undergoing elective abdominal surgery[116]. The most important test seems to be that for hemoglobin, as anemia is present in up to 78% of patients requiring a surgical intervention[117]. Both a preoperative anemia (defined as < 10 g/dL)[9,37,106,108,118] and a lowered hemoglobin level (defined as lower than the reference value)[27,38,102,119] are associated with postoperative complications in CD patients. Iron deficiency anemia is the most common cause of anemia in the preoperative setting of CD. Preoperative IV iron therapy is highly effective to rapidly increase hemoglobin levels, and should be considered the first choice. Blood transfusion is a common practice to treat anemia when treatment for the underlying cause has been unsuccessful. Both intra- and perioperative blood transfusions have been

associated with infectious- and/or non-infectious postoperative complications in CD patients, whereas a preoperative blood transfusion was not associated with postoperative complications[120-123].

Elevated levels of the inflammatory markers (*i.e.*, leucocyte count) are risk factors for postoperative complications[30,120,121,124]. Furthermore, a preoperative elevated CRP level has been associated significantly with overall postoperative complications[52,125-127], infectious complications[33,57,125-127], and SSIs[57]. It is known that the malabsorption of vitamins and other trace elements is prevalent in CD patients. Plasma concentrations are influenced by active disease or result from earlier intestinal resections. These micronutrient deficiencies comprise several vitamins (most often B6, B12, D, and K), iron, folic acid, selenium, and zinc. Micronutrient deficiencies are associated with a complicated course of disease[128]. For reliable assessment of body micronutrient status, the patient needs to be in biochemical remission. However, in cases of high suspicion due to deficiency-related complaints or malnutrition, assessment of these values is indicated[23,128].

Reviewers' opinion

Although preoperative anemia, hypoalbuminemia, elevated CRP and elevated leucocyte count are associated with postoperative complications, CD-specific recommendations concerning the preoperative assessment of laboratory values and subsequent management cannot be derived from the current literature. Laboratory findings for vitamins and other trace elements are often disturbed in CD and may not reflect the actual nutritional status. These assessments only reflect the patient's nutritional status when a patient is in remission. We recommend to assess full blood count, CRP and serum albumin preoperatively as predictive markers of a complicated postoperative course and to preoperatively correct iron deficiency anemia, in accordance with the ECCO guideline[21].

CONCLUSION

Nutritional status, medication and laboratory values are modifiable factors that influence the postoperative course of patients with CD. In addition, physical fitness is impaired in CD patients and may impact postoperative outcomes. As a lower preoperative physical fitness is associated with a higher risk for postoperative complications in other populations undergoing intestinal resection, further research into interventions in CD patients is warranted. Individualized multimodal prehabilitation programs aim to improve these modifiable risk factors before surgery, including smoking cessation and psychological screening and support, and should be integrated in the preoperative preparation period in order to reduce both postoperative complications and undesirable outcomes.

ACKNOWLEDGEMENTS

The authors would like to acknowledge the contribution of Wichor Bramer, biomedical information specialist of the Erasmus University Medical Center, for performing the systematic literature search.

FOOTNOTES

Author contributions: Bak MTJ reviewed and summarized the literature, and drafted the article; Ruiterkamp MFE reviewed the literature; de Vries AC supervised the study; and all authors contributed substantially to the concept and design of the study, critically revised the article, and approved the final version.

Conflict-of-interest statement: van der Woude CJ received grants and or fee for advisory boards and presentations from Pfizer, Abbvie, Celltrion, Falk Benelux, Takeda, Janssen, and Ferring outside the submitted work; de Vries AC has served on advisory boards for Takeda, Janssen, Bristol Myers Squibb, Abbvie, Pfizer, and Galapagos and has received unrestricted research grants from Takeda, Janssen, and Pfizer outside the submitted work; and all other authors declare that they have no conflict of interest.

Open-Access: This article is an open-access article that was selected by an in-house editor and fully peer-reviewed by external reviewers. It is distributed in accordance with the Creative Commons Attribution NonCommercial (CC BY-NC 4.0) license, which permits others to distribute, remix, adapt, build upon this work non-commercially, and license their derivative works on different terms, provided the original work is properly cited and the use is non-commercial. See: https://creativecommons.org/Licenses/by-nc/4.0/

Country/Territory of origin: Netherlands

ORCID number: Michiel T J Bak 0000-0001-8515-425X; Marit F E Ruiterkamp 0000-0001-6165-0582; Oddeke van Ruler 0000-0003-1620-1854; Marjo J E Campmans-Kuijpers 0000-0002-8111-6026; Bart C Bongers 0000-0002-1948-9788; Nico L U

van Meeteren 0000-0002-3067-4167; C Janneke van der Woude 0000-0003-3875-6957; Laurents P S Stassen 0000-0002-3383-9035; Annemarie C de Vries 0000-0002-3988-9201.

S-Editor: Wang JJ
L-Editor: A
P-Editor: Wang JJ

REFERENCES

1 **Abraham C**, Cho JH. Inflammatory bowel disease. *N Engl J Med* 2009; **361**: 2066-2078 [PMID: 19923578 DOI: 10.1056/NEJMra0804647]
2 **Tsai L**, Ma C, Dulai PS, Prokop LJ, Eisenstein S, Ramamoorthy SL, Feagan BG, Jairath V, Sandborn WJ, Singh S. Contemporary Risk of Surgery in Patients With Ulcerative Colitis and Crohn's Disease: A Meta-Analysis of Population-Based Cohorts. *Clin Gastroenterol Hepatol* 2021; **19**: 2031-2045.e11 [PMID: 33127595 DOI: 10.1016/j.cgh.2020.10.039]
3 **Beelen EMJ**, van der Woude CJ, Pierik MJ, Hoentjen F, de Boer NK, Oldenburg B, van der Meulen AE, Ponsioen CIJ, Dijkstra G, Bruggink AH, Erler NS, Schouten WR, de Vries AC; Dutch Initiative on Crohn's and Colitis (ICC). Decreasing Trends in Intestinal Resection and Re-Resection in Crohn's Disease: A Nationwide Cohort Study. *Ann Surg* 2021; **273**: 557-563 [PMID: 31188225 DOI: 10.1097/SLA.0000000000003395]
4 **Menichetti J**, Fiorino G, Vegni E. Personalizing Psychological Treatment Along the IBD Journey: From Diagnosis to Surgery. *Curr Drug Targets* 2018; **19**: 722-728 [PMID: 28464774 DOI: 10.2174/1389450118666170502142939]
5 **de Groof EJ**, Stevens TW, Eshuis EJ, Gardenbroek TJ, Bosmans JE, van Dongen JM, Mol B, Buskens CJ, Stokkers PCF, Hart A, D'Haens GR, Bemelman WA, Ponsioen CY; LIR!C study group. Cost-effectiveness of laparoscopic ileocaecal resection versus infliximab treatment of terminal ileitis in Crohn's disease: the LIR! *Gut* 2019; **68**: 1774-1780 [PMID: 31233395 DOI: 10.1136/gutjnl-2018-317539]
6 **Zangenberg MS**, Horesh N, Kopylov U, El-Hussuna A. Preoperative optimization of patients with inflammatory bowel disease undergoing gastrointestinal surgery: a systematic review. *Int J Colorectal Dis* 2017; **32**: 1663-1676 [PMID: 29051981 DOI: 10.1007/s00384-017-2915-4]
7 **SICCR Current status of Crohn's disease surgery collaborative**. Surgical treatment of colonic Crohn's disease: a national snapshot study. *Langenbecks Arch Surg* 2021; **406**: 1165-1172 [PMID: 33263140 DOI: 10.1007/s00423-020-02038-z]
8 **Galata C**, Hodapp J, Weiß C, Karampinis I, Vassilev G, Reißfelder C, Otto M. Skeletal Muscle Mass Index Predicts Postoperative Complications in Intestinal Surgery for Crohn's Disease. *JPEN J Parenter Enteral Nutr* 2020; **44**: 714-721 [PMID: 31444789 DOI: 10.1002/jpen.1696]
9 **Brouquet A**, Maggiori L, Zerbib P, Lefevre JH, Denost Q, Germain A, Cotte E, Beyer-Berjot L, Munoz-Bongrand N, Desfourneaux V, Rahili A, Duffas JP, Pautrat K, Denet C, Bridoux V, Meurette G, Faucheron JL, Loriau J, Guillon F, Vicaut E, Benoist S, Panis Y; GETAID chirurgie group. Anti-TNF Therapy Is Associated With an Increased Risk of Postoperative Morbidity After Surgery for Ileocolonic Crohn Disease: Results of a Prospective Nationwide Cohort. *Ann Surg* 2018; **267**: 221-228 [PMID: 29300710 DOI: 10.1097/SLA.0000000000002017]
10 **Alves A**, Panis Y, Bouhnik Y, Pocard M, Vicaut E, Valleur P. Risk factors for intra-abdominal septic complications after a first ileocecal resection for Crohn's disease: a multivariate analysis in 161 consecutive patients. *Dis Colon Rectum* 2007; **50**: 331-336 [PMID: 17252288 DOI: 10.1007/s10350-006-0782-0]
11 **Yamamoto T**, Spinelli A, Suzuki Y, Saad-Hossne R, Teixeira FV, de Albuquerque IC, da Silva RN, de Barcelos IF, Takeuchi K, Yamada A, Shimoyama T, da Silva Kotze LM, Sacchi M, Danese S, Kotze PG. Risk factors for complications after ileocolonic resection for Crohn's disease with a major focus on the impact of preoperative immunosuppressive and biologic therapy: A retrospective international multicentre study. *United European Gastroenterol J* 2016; **4**: 784-793 [PMID: 28408996 DOI: 10.1177/2050640615600116]
12 **Fumery M**, Seksik P, Auzolle C, Munoz-Bongrand N, Gornet JM, Boschetti G, Cotte E, Buisson A, Dubois A, Pariente B, Zerbib P, Chafai N, Stefanescu C, Panis Y, Marteau P, Pautrat K, Sabbagh C, Filippi J, Chevrier M, Houze P, Jouven X, Treton X, Allez M; REMIND study group investigators. Postoperative Complications after Ileocecal Resection in Crohn's Disease: A Prospective Study From the REMIND Group. *Am J Gastroenterol* 2017; **112**: 337-345 [PMID: 27958285 DOI: 10.1038/ajg.2016.541]
13 **Spinelli A**, Allocca M, Jovani M, Danese S. Review article: optimal preparation for surgery in Crohn's disease. *Aliment Pharmacol Ther* 2014; **40**: 1009-1022 [PMID: 25209947 DOI: 10.1111/apt.12947]
14 **Otto JM**, O'Doherty AF, Hennis PJ, Mitchell K, Pate JS, Cooper JA, Grocott MP, Montgomery HE. Preoperative exercise capacity in adult inflammatory bowel disease sufferers, determined by cardiopulmonary exercise testing. *Int J Colorectal Dis* 2012; **27**: 1485-1491 [PMID: 22842663 DOI: 10.1007/s00384-012-1533-4]
15 **West MA**, Asher R, Browning M, Minto G, Swart M, Richardson K, McGarrity L, Jack S, Grocott MP; Perioperative Exercise Testing and Training Society. Validation of preoperative cardiopulmonary exercise testing-derived variables to predict in-hospital morbidity after major colorectal surgery. *Br J Surg* 2016; **103**: 744-752 [PMID: 26914526 DOI: 10.1002/bjs.10112]
16 **Cuijpers ACM**, Heldens AFJM, Bours MJL, van Meeteren NLU, Stassen LPS, Lubbers T, Bongers BC. Relation between preoperative aerobic fitness estimated by steep ramp test performance and postoperative morbidity in colorectal cancer surgery: prospective observational study. *Br J Surg* 2022; **109**: 155-159 [PMID: 34536001 DOI: 10.1093/bjs/znab292]
17 **van Rooijen SJ**, Molenaar CJL, Schep G, van Lieshout RHMA, Beijer S, Dubbers R, Rademakers N, Papen-Botterhuis NE, van Kempen S, Carli F, Roumen RMH, Slooter GD. Making Patients Fit for Surgery: Introducing a Four Pillar

Multimodal Prehabilitation Program in Colorectal Cancer. *Am J Phys Med Rehabil* 2019; **98**: 888-896 [PMID: 31090551 DOI: 10.1097/PHM.0000000000001221]

18 **Barberan-Garcia A**, Ubré M, Roca J, Lacy AM, Burgos F, Risco R, Momblán D, Balust J, Blanco I, Martínez-Pallí G. Personalised Prehabilitation in High-risk Patients Undergoing Elective Major Abdominal Surgery: A Randomized Blinded Controlled Trial. *Ann Surg* 2018; **267**: 50-56 [PMID: 28489682 DOI: 10.1097/SLA.0000000000002293]

19 **Berkel AEM**, Bongers BC, Kotte H, Weltevreden P, de Jongh FHC, Eijsvogel MMM, Wymenga M, Bigirwamungu-Bargeman M, van der Palen J, van Det MJ, van Meeteren NLU, Klaase JM. Effects of Community-based Exercise Prehabilitation for Patients Scheduled for Colorectal Surgery With High Risk for Postoperative Complications: Results of a Randomized Clinical Trial. *Ann Surg* 2022; **275**: e299-e306 [PMID: 33443905 DOI: 10.1097/SLA.0000000000004702]

20 **Bongers BC**, Dejong CHC, den Dulk M. Enhanced recovery after surgery programmes in older patients undergoing hepatopancreatobiliary surgery: what benefits might prehabilitation have? *Eur J Surg Oncol* 2021; **47**: 551-559 [PMID: 32253075 DOI: 10.1016/j.ejso.2020.03.211]

21 **Adamina M**, Bonovas S, Raine T, Spinelli A, Warusavitarne J, Armuzzi A, Bachmann O, Bager P, Biancone L, Bokemeyer B, Bossuyt P, Burisch J, Collins P, Doherty G, El-Hussuna A, Ellul P, Fiorino G, Frei-Lanter C, Furfaro F, Gingert C, Gionchetti P, Gisbert JP, Gomollon F, González Lorenzo M, Gordon H, Hlavaty T, Juillerat P, Katsanos K, Kopylov U, Krustins E, Kucharzik T, Lytras T, Maaser C, Magro F, Marshall JK, Myrelid P, Pellino G, Rosa I, Sabino J, Savarino E, Stassen L, Torres J, Uzzan M, Vavricka S, Verstockt B, Zmora O. ECCO Guidelines on Therapeutics in Crohn's Disease: Surgical Treatment. *J Crohns Colitis* 2020; **14**: 155-168 [PMID: 31742338 DOI: 10.1093/ecco-jcc/jjz187]

22 **Lamb CA**, Kennedy NA, Raine T, Hendy PA, Smith PJ, Limdi JK, Hayee B, Lomer MCE, Parkes GC, Selinger C, Barrett KJ, Davies RJ, Bennett C, Gittens S, Dunlop MG, Faiz O, Fraser A, Garrick V, Johnston PD, Parkes M, Sanderson J, Terry H; IBD guidelines eDelphi consensus group, Gaya DR, Iqbal TH, Taylor SA, Smith M, Brookes M, Hansen R, Hawthorne AB. British Society of Gastroenterology consensus guidelines on the management of inflammatory bowel disease in adults. *Gut* 2019; **68**: s1-s106 [PMID: 31562236 DOI: 10.1136/gutjnl-2019-318484]

23 **Adamina M**, Gerasimidis K, Sigall-Boneh R, Zmora O, de Buck van Overstraeten A, Campmans-Kuijpers M, Ellul P, Katsanos K, Kotze PG, Noor N, Schäfli-Thurnherr J, Vavricka S, Wall C, Wierdsma N, Yassin N, Lomer M. Perioperative Dietary Therapy in Inflammatory Bowel Disease. *J Crohns Colitis* 2020; **14**: 431-444 [PMID: 31550347 DOI: 10.1093/ecco-jcc/jjz160]

24 **Steed H**, Walsh S, Reynolds N. A brief report of the epidemiology of obesity in the inflammatory bowel disease population of Tayside, Scotland. *Obes Facts* 2009; **2**: 370-372 [PMID: 20090388 DOI: 10.1159/000262276]

25 **Tinsley A**, Ehrlich OG, Hwang C, Issokson K, Zapala S, Weaver A, Siegel CA, Melmed GY. Knowledge, Attitudes, and Beliefs Regarding the Role of Nutrition in IBD Among Patients and Providers. *Inflamm Bowel Dis* 2016; **22**: 2474-2481 [PMID: 27598738 DOI: 10.1097/MIB.0000000000000901]

26 **Grass F**, Ansell J, Petersen M, Mathis KL, Lightner AL. Risk factors for 90-day readmission and return to the operating room following abdominal operations for Crohn's disease. *Surgery* 2019; **166**: 1068-1075 [PMID: 31548096 DOI: 10.1016/j.surg.2019.08.006]

27 **Uchino M**, Ikeuchi H, Bando T, Chohno T, Sasaki H, Horio Y, Nakajima K, Takesue Y. Efficacy of Preoperative Oral Antibiotic Prophylaxis for the Prevention of Surgical Site Infections in Patients With Crohn Disease: A Randomized Controlled Trial. *Ann Surg* 2019; **269**: 420-426 [PMID: 29064884 DOI: 10.1097/SLA.0000000000002567]

28 **Krane MK**, Allaix ME, Zoccali M, Umanskiy K, Rubin MA, Villa A, Hurst RD, Fichera A. Does morbid obesity change outcomes after laparoscopic surgery for inflammatory bowel disease? *J Am Coll Surg* 2013; **216**: 986-996 [PMID: 23523148 DOI: 10.1016/j.jamcollsurg.2013.01.053]

29 **Lightner AL**, Raffals LE, Mathis KL, Cima RR, Tse CS, Pemberton JH, Dozois EJ, Loftus EV. Postoperative Outcomes in Vedolizumab-Treated Patients Undergoing Abdominal Operations for Inflammatory Bowel Disease. *J Crohns Colitis* 2017; **11**: 185-190 [PMID: 27543504 DOI: 10.1093/ecco-jcc/jjw147]

30 **O'Brien SJ**, Chen RC, Stephen VT, Jorden J, Farmer R, Manek S, Schmidt M, Pan J, Rai SN, Galandiuk S. Preoperative Opioid Prescription Is Associated With Major Complications in Patients With Crohn's Disease Undergoing Elective Ileocolic Resection. *Dis Colon Rectum* 2020; **63**: 1090-1101 [PMID: 32015287 DOI: 10.1097/DCR.0000000000001571]

31 **Kulaylat AN**, Hollenbeak CS, Sangster W, Stewart DB Sr. Impact of smoking on the surgical outcome of Crohn's disease: a propensity-score matched National Surgical Quality Improvement Program analysis. *Colorectal Dis* 2015; **17**: 891-902 [PMID: 25808234 DOI: 10.1111/codi.12958]

32 **Zhang M**, Gao X, Chen Y, Zhi M, Chen H, Tang J, Su M, Yao J, Yang Q, Chen J, Hu P, Liu H, Min L. Body Mass Index Is a Marker of Nutrition Preparation Sufficiency Before Surgery for Crohn's Disease From the Perspective of Intra-Abdominal Septic Complications: A Retrospective Cohort Study. *Medicine (Baltimore)* 2015; **94**: 1 [PMID: 26334908 DOI: 10.1097/MD.0000000000001455]

33 **Zhu Y**, Zhou W, Qi W, Liu W, Chen M, Zhu H, Xiang J, Xie Q, Chen P. Body mass index is a practical preoperative nutritional index for postoperative infectious complications after intestinal resection in patients with Crohn's disease. *Medicine (Baltimore)* 2017; **96**: e7113 [PMID: 28591060 DOI: 10.1097/MD.0000000000007113]

34 **Hossne RS**, Sassaki LY, Baima JP, Meira Júnior JD, Campos LM. ANALYSIS OF RISK FACTORS AND POSTOPERATIVE COMPLICATIONS IN PATIENTS WITH CROHN'S DISEASE. *Arq Gastroenterol* 2018; **55**: 252-257 [PMID: 30540087 DOI: 10.1590/S0004-2803.201800000-63]

35 **Nguyen GC**, Elnahas A, Jackson TD. The impact of preoperative steroid use on short-term outcomes following surgery for inflammatory bowel disease. *J Crohns Colitis* 2014; **8**: 1661-1667 [PMID: 25107847 DOI: 10.1016/j.crohns.2014.07.007]

36 **Alavi K**, Sturrock PR, Sweeney WB, Maykel JA, Cervera-Servin JA, Tseng J, Cook EF. A simple risk score for predicting surgical site infections in inflammatory bowel disease. *Dis Colon Rectum* 2010; **53**: 1480-1486 [PMID: 20940595 DOI: 10.1007/DCR.0b013e3181f1f0fd]

37 **Aydinli HH**, Aytac E, Remzi FH, Bernstein M, Grucela AL. Factors Associated with Short-Term Morbidity in Patients Undergoing Colon Resection for Crohn's Disease. *J Gastrointest Surg* 2018; **22**: 1434-1441 [PMID: 29663305 DOI:

10.1007/s11605-018-3763-4]
38 **Iesalnieks I**, Hoene M, Bittermann T, Schlitt HJ, Hackl C. Mechanical Bowel Preparation (MBP) Prior to Elective Colorectal Resections in Crohn's Disease Patients. *Inflamm Bowel Dis* 2018; **24**: 908-915 [PMID: 29529206 DOI: 10.1093/ibd/izx088]
39 **Cruz-Jentoft AJ**, Baeyens JP, Bauer JM, Boirie Y, Cederholm T, Landi F, Martin FC, Michel JP, Rolland Y, Schneider SM, Topinková E, Vandewoude M, Zamboni M; European Working Group on Sarcopenia in Older People. Sarcopenia: European consensus on definition and diagnosis: Report of the European Working Group on Sarcopenia in Older People. *Age Ageing* 2010; **39**: 412-423 [PMID: 20392703 DOI: 10.1093/ageing/afq034]
40 **Adams DW**, Gurwara S, Silver HJ, Horst SN, Beaulieu DB, Schwartz DA, Seidner DL. Sarcopenia Is Common in Overweight Patients with Inflammatory Bowel Disease and May Predict Need for Surgery. *Inflamm Bowel Dis* 2017; **23**: 1182-1186 [PMID: 28410342 DOI: 10.1097/MIB.0000000000001128]
41 **Ryan E**, McNicholas D, Creavin B, Kelly ME, Walsh T, Beddy D. Sarcopenia and Inflammatory Bowel Disease: A Systematic Review. *Inflamm Bowel Dis* 2019; **25**: 67-73 [PMID: 29889230 DOI: 10.1093/ibd/izy212]
42 **Erős A**, Soós A, Hegyi P, Szakács Z, Benke M, Szűcs Á, Hartmann P, Erőss B, Sarlós P. Sarcopenia as an independent predictor of the surgical outcomes of patients with inflammatory bowel disease: a meta-analysis. *Surg Today* 2020; **50**: 1138-1150 [PMID: 31617016 DOI: 10.1007/s00595-019-01893-8]
43 **Pedersen M**, Cromwell J, Nau P. Sarcopenia is a Predictor of Surgical Morbidity in Inflammatory Bowel Disease. *Inflamm Bowel Dis* 2017; **23**: 1867-1872 [PMID: 28604415 DOI: 10.1097/MIB.0000000000001166]
44 **Sayer AA**, Robinson SM, Patel HP, Shavlakadze T, Cooper C, Grounds MD. New horizons in the pathogenesis, diagnosis and management of sarcopenia. *Age Ageing* 2013; **42**: 145-150 [PMID: 23315797 DOI: 10.1093/ageing/afs191]
45 **Kondrup J**, Allison SP, Elia M, Vellas B, Plauth M; Educational and Clinical Practice Committee, European Society of Parenteral and Enteral Nutrition (ESPEN). ESPEN guidelines for nutrition screening 2002. *Clin Nutr* 2003; **22**: 415-421 [PMID: 12880610 DOI: 10.1016/s0261-5614(03)00098-0]
46 **Elia M**. Screening for malnutrition: A multidisciplinary responsibility. Development and Use of the Malnutrition Universal Screening Tool (MUST) for Adults. Redditch: BAPEN, 2003
47 **Jensen GL**, Cederholm T, Correia MITD, Gonzalez MC, Fukushima R, Higashiguchi T, de Baptista GA, Barazzoni R, Blaauw R, Coats AJS, Crivelli A, Evans DC, Gramlich L, Fuchs-Tarlovsky V, Keller H, Llido L, Malone A, Mogensen KM, Morley JE, Muscaritoli M, Nyulasi I, Pirlich M, Pisprasert V, de van der Schueren M, Siltharm S, Singer P, Tappenden KA, Velasco N, Waitzberg DL, Yamwong P, Yu J, Compher C, Van Gossum A. GLIM Criteria for the Diagnosis of Malnutrition: A Consensus Report From the Global Clinical Nutrition Community. *JPEN J Parenter Enteral Nutr* 2019; **43**: 32-40 [PMID: 30175461 DOI: 10.1002/jpen.1440]
48 **Jansen I**, Prager M, Valentini L, Büning C. Inflammation-driven malnutrition: a new screening tool predicts outcome in Crohn's disease. *Br J Nutr* 2016; **116**: 1061-1067 [PMID: 27546478 DOI: 10.1017/S0007114516003044]
49 **Haskey N**, Peña-Sánchez JN, Jones JL, Fowler SA. Development of a screening tool to detect nutrition risk in patients with inflammatory bowel disease. *Asia Pac J Clin Nutr* 2018; **27**: 756-762 [PMID: 30045418 DOI: 10.6133/apjcn.112017.01]
50 **Fiorindi C**, Luceri C, Dragoni G, Piemonte G, Scaringi S, Staderini F, Nannoni A, Ficari F, Giudici F. GLIM Criteria for Malnutrition in Surgical IBD Patients: A Pilot Study. *Nutrients* 2020; **12** [PMID: 32722435 DOI: 10.3390/nu12082222]
51 **Jian-Hui C**, Iskandar EA, Cai ShI, Chen CQ, Wu H, Xu JB, He YL. Significance of Onodera's prognostic nutritional index in patients with colorectal cancer: a large cohort study in a single Chinese institution. *Tumour Biol* 2016; **37**: 3277-3283 [PMID: 26438061 DOI: 10.1007/s13277-015-4008-8]
52 **Zhou W**, Cao Q, Qi W, Xu Y, Liu W, Xiang J, Xia B. Prognostic Nutritional Index Predicts Short-Term Postoperative Outcomes After Bowel Resection for Crohn's Disease. *Nutr Clin Pract* 2017; **32**: 92-97 [PMID: 27566600 DOI: 10.1177/0884533616661844]
53 **Maeda K**, Nagahara H, Shibutani M, Otani H, Sakurai K, Toyokawa T, Tanaka H, Kubo N, Muguruma K, Kamata N, Yamagami H, Hirakawa K. A preoperative low nutritional prognostic index correlates with the incidence of incisional surgical site infections after bowel resection in patients with Crohn's disease. *Surg Today* 2015; **45**: 1366-1372 [PMID: 25319215 DOI: 10.1007/s00595-014-1044-8]
54 **Kang WM**, Zhu CZ, Yang XX, Yu JC, Ma ZQ, Ye X, Li K, Liu D. Application of the Onodera prognostic nutrition index and neutrophil-to-lymphocyte ratio in risk evaluation of postoperative complications in Crohn's disease. *Sci Rep* 2017; **7**: 8481 [PMID: 28814767 DOI: 10.1038/s41598-017-09265-3]
55 **Bertin B**, Desreumaux P, Dubuquoy L. Obesity, visceral fat and Crohn's disease. *Curr Opin Clin Nutr Metab Care* 2010; **13**: 574-580 [PMID: 20625283 DOI: 10.1097/MCO.0b013e32833cf0f4]
56 **Erhayiem B**, Dhingsa R, Hawkey CJ, Subramanian V. Ratio of visceral to subcutaneous fat area is a biomarker of complicated Crohn's disease. *Clin Gastroenterol Hepatol* 2011; **9**: 684-687.e1 [PMID: 21642015 DOI: 10.1016/j.cgh.2011.05.005]
57 **Cai X**, Shen W, Guo Z, Li Y, Cao L, Gong J, Zhu W. Thickness of Subcutaneous Fat Is a Predictive Factor of Incisional Surgical Site Infection in Crohn's Disease Surgery: A Retrospective Study. *Gastroenterol Res Pract* 2018; **2018**: 1546075 [PMID: 30140279 DOI: 10.1155/2018/1546075]
58 **Connelly TM**, Juza RM, Sangster W, Sehgal R, Tappouni RF, Messaris E. Volumetric fat ratio and not body mass index is predictive of ileocolectomy outcomes in Crohn's disease patients. *Dig Surg* 2014; **31**: 219-224 [PMID: 25277149 DOI: 10.1159/000365359]
59 **Ding Z**, Wu XR, Remer EM, Lian L, Stocchi L, Li Y, McCullough A, Remzi FH, Shen B. Association between high visceral fat area and postoperative complications in patients with Crohn's disease following primary surgery. *Colorectal Dis* 2016; **18**: 163-172 [PMID: 26391914 DOI: 10.1111/codi.13128]
60 **Zhang T**, Cao L, Cao T, Yang J, Gong J, Zhu W, Li N, Li J. Prevalence of Sarcopenia and Its Impact on Postoperative Outcome in Patients With Crohn's Disease Undergoing Bowel Resection. *JPEN J Parenter Enteral Nutr* 2017; **41**: 592-600 [PMID: 26471990 DOI: 10.1177/0148607115612054]
61 **Wiroth JB**, Filippi J, Schneider SM, Al-Jaouni R, Horvais N, Gavarry O, Bermon S, Hébuterne X. Muscle performance in

patients with Crohn's disease in clinical remission. *Inflamm Bowel Dis* 2005; **11**: 296-303 [PMID: 15735436 DOI: 10.1097/01.mib.0000160810.76729.9c]

62 **Brevinge H**, Berglund B, Bosaeus I, Tölli J, Nordgren S, Lundholm K. Exercise capacity in patients undergoing proctocolectomy and small bowel resection for Crohn's disease. *Br J Surg* 1995; **82**: 1040-1045 [PMID: 7648147 DOI: 10.1002/bjs.1800820813]

63 **van Langenberg DR**, Papandony MC, Gibson PR. Sleep and physical activity measured by accelerometry in Crohn's disease. *Aliment Pharmacol Ther* 2015; **41**: 991-1004 [PMID: 25783784 DOI: 10.1111/apt.13160]

64 **Mack DE**, Wilson PM, Gilmore JC, Gunnell KE. Leisure-time physical activity in Canadians living with Crohn disease and ulcerative colitis: population-based estimates. *Gastroenterol Nurs* 2011; **34**: 288-294 [PMID: 21814062 DOI: 10.1097/SGA.0b013e3182248732]

65 **Hlatky MA**, Boineau RE, Higginbotham MB, Lee KL, Mark DB, Califf RM, Cobb FR, Pryor DB. A brief self-administered questionnaire to determine functional capacity (the Duke Activity Status Index). *Am J Cardiol* 1989; **64**: 651-654 [PMID: 2782256 DOI: 10.1016/0002-9149(89)90496-7]

66 **McAuley P**, Myers J, Abella J, Froelicher V. Evaluation of a specific activity questionnaire to predict mortality in men referred for exercise testing. *Am Heart J* 2006; **151**: 890.e1-890.e7 [PMID: 16569555 DOI: 10.1016/j.ahj.2005.09.017]

67 **Tran D**. Cardiopulmonary Exercise Testing. *Methods Mol Biol* 2018; **1735**: 285-295 [PMID: 29380321 DOI: 10.1007/978-1-4939-7614-0_18]

68 **Weemaes ATR**, Beelen M, Bongers BC, Weijenberg MP, Lenssen AF. Criterion Validity and Responsiveness of the Steep Ramp Test to Evaluate Aerobic Capacity in Survivors of Cancer Participating in a Supervised Exercise Rehabilitation Program. *Arch Phys Med Rehabil* 2021; **102**: 2150-2156 [PMID: 34023324 DOI: 10.1016/j.apmr.2021.04.016]

69 **van Erp LW**, Roosenboom B, Komdeur P, Dijkstra-Heida W, Wisse J, Horjus Talabur Horje CS, Liem CS, van Cingel REH, Wahab PJ, Groenen MJM. Improvement of Fatigue and Quality of Life in Patients with Quiescent Inflammatory Bowel Disease Following a Personalized Exercise Program. *Dig Dis Sci* 2021; **66**: 597-604 [PMID: 32239380 DOI: 10.1007/s10620-020-06222-5]

70 **Ng V**, Millard W, Lebrun C, Howard J. Low-intensity exercise improves quality of life in patients with Crohn's disease. *Clin J Sport Med* 2007; **17**: 384-388 [PMID: 17873551 DOI: 10.1097/JSM.0b013e31802b4fda]

71 **Loudon CP**, Corroll V, Butcher J, Rawsthorne P, Bernstein CN. The effects of physical exercise on patients with Crohn's disease. *Am J Gastroenterol* 1999; **94**: 697-703 [PMID: 10086654 DOI: 10.1111/j.1572-0241.1999.00939.x]

72 **Pérez CA**. Prescription of physical exercise in Crohn's disease. *J Crohns Colitis* 2009; **3**: 225-231 [PMID: 21172280 DOI: 10.1016/j.crohns.2009.08.006]

73 **Bilski J**, Brzozowski B, Mazur-Bialy A, Sliwowski Z, Brzozowski T. The role of physical exercise in inflammatory bowel disease. *Biomed Res Int* 2014; **2014**: 429031 [PMID: 24877092 DOI: 10.1155/2014/429031]

74 **Weimann A**, Braga M, Carli F, Higashiguchi T, Hübner M, Klek S, Laviano A, Ljungqvist O, Lobo DN, Martindale R, Waitzberg DL, Bischoff SC, Singer P. ESPEN guideline: Clinical nutrition in surgery. *Clin Nutr* 2017; **36**: 623-650 [PMID: 28385477 DOI: 10.1016/j.clnu.2017.02.013]

75 **Burden S**, Todd C, Hill J, Lal S. Pre-operative nutrition support in patients undergoing gastrointestinal surgery. *Cochrane Database Syst Rev* 2012; **11**: CD008879 [PMID: 23152265 DOI: 10.1002/14651858.CD008879.pub2]

76 **Brennan GT**, Ha I, Hogan C, Nguyen E, Jamal MM, Bechtold ML, Nguyen DL. Does preoperative enteral or parenteral nutrition reduce postoperative complications in Crohn's disease patients: a meta-analysis. *Eur J Gastroenterol Hepatol* 2018; **30**: 997-1002 [PMID: 29738326 DOI: 10.1097/MEG.0000000000001162]

77 **Grass F**, Pache B, Martin D, Hahnloser D, Demartines N, Hübner M. Preoperative Nutritional Conditioning of Crohn's Patients-Systematic Review of Current Evidence and Practice. *Nutrients* 2017; **9** [PMID: 28587182 DOI: 10.3390/nu9060562]

78 **Ruemmele FM**, Veres G, Kolho KL, Griffiths A, Levine A, Escher JC, Amil Dias J, Barabino A, Braegger CP, Bronsky J, Buderus S, Martín-de-Carpi J, De Ridder L, Fagerberg UL, Hugot JP, Kierkus J, Kolacek S, Koletzko S, Lionetti P, Miele E, Navas López VM, Paerregaard A, Russell RK, Serban DE, Shaoul R, Van Rheenen P, Veereman G, Weiss B, Wilson D, Dignass A, Eliakim A, Winter H, Turner D; European Crohn's and Colitis Organisation; European Society of Pediatric Gastroenterology, Hepatology and Nutrition. Consensus guidelines of ECCO/ESPGHAN on the medical management of pediatric Crohn's disease. *J Crohns Colitis* 2014; **8**: 1179-1207 [PMID: 24909831 DOI: 10.1016/j.crohns.2014.04.005]

79 **Logan M**, Gkikas K, Svolos V, Nichols B, Milling S, Gaya DR, Seenan JP, Macdonald J, Hansen R, Ijaz UZ, Russell RK, Gerasimidis K. Analysis of 61 exclusive enteral nutrition formulas used in the management of active Crohn's disease-new insights into dietary disease triggers. *Aliment Pharmacol Ther* 2020; **51**: 935-947 [PMID: 32249975 DOI: 10.1111/apt.15695]

80 **Heerasing N**, Thompson B, Hendy P, Heap GA, Walker G, Bethune R, Mansfield S, Calvert C, Kennedy NA, Ahmad T, Goodhand JR. Exclusive enteral nutrition provides an effective bridge to safer interval elective surgery for adults with Crohn's disease. *Aliment Pharmacol Ther* 2017; **45**: 660-669 [PMID: 28105752 DOI: 10.1111/apt.13934]

81 **Yamamoto T**, Nakahigashi M, Umegae S, Kitagawa T, Matsumoto K. Impact of elemental diet on mucosal inflammation in patients with active Crohn's disease: cytokine production and endoscopic and histological findings. *Inflamm Bowel Dis* 2005; **11**: 580-588 [PMID: 15905706 DOI: 10.1097/01.mib.0000161307.58327.96]

82 **Horwat P**, Kopeć S, Garczyk A, Kaliciak I, Staręga Z, Drogowski K, Mardas M, Stelmach-Mardas M. Influence of Enteral Nutrition on Gut Microbiota Composition in Patients with Crohn's Disease: A Systematic Review. *Nutrients* 2020; **12** [PMID: 32842543 DOI: 10.3390/nu12092551]

83 **Ge X**, Tang S, Yang X, Liu W, Ye L, Yu W, Xu H, Cao Q, Zhou W, Cai X. The role of exclusive enteral nutrition in the preoperative optimization of laparoscopic surgery for patients with Crohn's disease: A cohort study. *Int J Surg* 2019; **65**: 39-44 [PMID: 30905758 DOI: 10.1016/j.ijsu.2019.03.012]

84 **Li Y**, Zuo L, Zhu W, Gong J, Zhang W, Gu L, Guo Z, Cao L, Li N, Li J. Role of exclusive enteral nutrition in the preoperative optimization of patients with Crohn's disease following immunosuppressive therapy. *Medicine (Baltimore)*

2015; **94**: e478 [PMID: 25654387 DOI: 10.1097/MD.0000000000000478]
85 **Wang H**, Zuo L, Zhao J, Dong J, Li Y, Gu L, Gong J, Liu Q, Zhu W. Impact of Preoperative Exclusive Enteral Nutrition on Postoperative Complications and Recurrence After Bowel Resection in Patients with Active Crohn's Disease. *World J Surg* 2016; **40**: 1993-2000 [PMID: 26940580 DOI: 10.1007/s00268-016-3488-z]
86 **Li G**, Ren J, Wang G, Hu D, Gu G, Liu S, Ren H, Wu X, Li J. Preoperative exclusive enteral nutrition reduces the postoperative septic complications of fistulizing Crohn's disease. *Eur J Clin Nutr* 2014; **68**: 441-446 [PMID: 24549026 DOI: 10.1038/ejcn.2014.16]
87 **Zhu F**, Li Y, Guo Z, Cao L, Feng D, Zhang T, Zhu W, Gong J. Nomogram to Predict Postoperative Intra-abdominal Septic Complications After Bowel Resection and Primary Anastomosis for Crohn's Disease. *Dis Colon Rectum* 2020; **63**: 629-638 [PMID: 32032204 DOI: 10.1097/DCR.0000000000001602]
88 **Guo Z**, Guo D, Gong J, Zhu W, Zuo L, Sun J, Li N, Li J. Preoperative Nutritional Therapy Reduces the Risk of Anastomotic Leakage in Patients with Crohn's Disease Requiring Resections. *Gastroenterol Res Pract* 2016; **2016**: 5017856 [PMID: 26858749 DOI: 10.1155/2016/5017856]
89 **Jacobson S**. Early postoperative complications in patients with Crohn's disease given and not given preoperative total parenteral nutrition. *Scand J Gastroenterol* 2012; **47**: 170-177 [PMID: 22242614 DOI: 10.3109/00365521.2011.648954]
90 **Ayoub F**, Kamel AY, Ouni A, Chaudhry N, Ader Y, Tan S, Iqbal A, Zimmermann EM, Glover SC. Pre-operative total parenteral nutrition improves post-operative outcomes in a subset of Crohn's disease patients undergoing major abdominal surgery. *Gastroenterol Rep (Oxf)* 2019; **7**: 107-114 [PMID: 30976423 DOI: 10.1093/gastro/goy033]
91 **Lashner BA**, Evans AA, Hanauer SB. Preoperative total parenteral nutrition for bowel resection in Crohn's disease. *Dig Dis Sci* 1989; **34**: 741-746 [PMID: 2496960 DOI: 10.1007/BF01540346]
92 **Attar A**, Messing B. Evidence-based prevention of catheter infection during parenteral nutrition. *Curr Opin Clin Nutr Metab Care* 2001; **4**: 211-218 [PMID: 11517355 DOI: 10.1097/00075197-200105000-00008]
93 **Law CC**, Bell C, Koh D, Bao Y, Jairath V, Narula N. Risk of postoperative infectious complications from medical therapies in inflammatory bowel disease. *Cochrane Database Syst Rev* 2020; **10**: CD013256 [PMID: 33098570 DOI: 10.1002/14651858.CD013256.pub2]
94 **Myrelid P**, Olaison G, Sjödahl R, Nyström PO, Almer S, Andersson P. Thiopurine therapy is associated with postoperative intra-abdominal septic complications in abdominal surgery for Crohn's disease. *Dis Colon Rectum* 2009; **52**: 1387-1394 [PMID: 19617749 DOI: 10.1007/DCR.0b013e3181a7ba96]
95 **Yu CS**, Jung SW, Lee JL, Lim SB, Park IJ, Yoon YS, Kim CW, Yang SK, Ye BD, Park SH, Han M, Kim JC. The Influence of Preoperative Medications on Postoperative Complications in Patients After Intestinal Surgery for Crohn's Disease. *Inflamm Bowel Dis* 2019; **25**: 1559-1568 [PMID: 30753560 DOI: 10.1093/ibd/izz010]
96 **Lightner AL**, Mathis KL, Tse CS, Pemberton JH, Shen B, Kochhar G, Singh A, Dulai PS, Eisenstein S, Sandborn WJ, Parry L, Stringfield S, Hudesman D, Remzi F, Loftus EV Jr. Postoperative Outcomes in Vedolizumab-Treated Patients Undergoing Major Abdominal Operations for Inflammatory Bowel Disease: Retrospective Multicenter Cohort Study. *Inflamm Bowel Dis* 2018; **24**: 871-876 [PMID: 29509927 DOI: 10.1093/ibd/izx076]
97 **Lightner AL**, McKenna NP, Alsughayer A, Harmsen WS, Taparra K, Parker ME, Raffals LE, Loftus EV Jr. Biologics and 30-Day Postoperative Complications After Abdominal Operations for Crohn's Disease: Are There Differences in the Safety Profiles? *Dis Colon Rectum* 2019; **62**: 1352-1362 [PMID: 31567927 DOI: 10.1097/DCR.0000000000001482]
98 **Novello M**, Stocchi L, Holubar S, Shawki S, Lipman J, Gorgun E, Hull T, Steele SR. Surgical outcomes of patients treated with ustekinumab vs. vedolizumab in inflammatory bowel disease: a matched case analysis. *Int J Colorectal Dis* 2019; **34**: 451-457 [PMID: 30535559 DOI: 10.1007/s00384-018-3212-6]
99 **Parrish AB**, Lopez NE, Truong A, Zaghiyan K, Melmed GY, McGovern DPB, Ha C, Syal G, Bonthala N, Jain A, Landers CJ, Targan SR, Fleshner P. Preoperative Serum Vedolizumab Levels Do Not Impact Postoperative Outcomes in Inflammatory Bowel Disease. *Dis Colon Rectum* 2021; **64**: 1259-1266 [PMID: 34516445 DOI: 10.1097/DCR.0000000000001920]
100 **Kotze PG**, Ma C, Mckenna N, Almutairdi A, Kaplan GG, Raffals LE, Loftus EV Jr, Panaccione R, Lightner AL. Vedolizumab and early postoperative complications in nonintestinal surgery: a case-matched analysis. *Therap Adv Gastroenterol* 2018; **11**: 1756284818783614 [PMID: 29977340 DOI: 10.1177/1756284818783614]
101 **Park KT**, Sceats L, Dehghan M, Trickey AW, Wren A, Wong JJ, Bensen R, Limketkai BN, Keyashian K, Kin C. Risk of post-operative surgical site infections after vedolizumab vs anti-tumour necrosis factor therapy: a propensity score matching analysis in inflammatory bowel disease. *Aliment Pharmacol Ther* 2018; **48**: 340-346 [PMID: 29876995 DOI: 10.1111/apt.14842]
102 **Yamada A**, Komaki Y, Patel N, Komaki F, Aelvoet AS, Tran AL, Pekow J, Dalal S, Cohen RD, Cannon L, Umanskiy K, Smith R, Hurst R, Hyman N, Rubin DT, Sakuraba A. Risk of Postoperative Complications Among Inflammatory Bowel Disease Patients Treated Preoperatively With Vedolizumab. *Am J Gastroenterol* 2017; **112**: 1423-1429 [PMID: 28719595 DOI: 10.1038/ajg.2017.201]
103 **Shim HH**, Ma C, Kotze PG, Seow CH, Al-Farhan H, Al-Darmaki AK, Pang JXQ, Fedorak RN, Devlin SM, Dieleman LA, Kaplan GG, Novak KL, Kroeker KI, Halloran BP, Panaccione R. Preoperative Ustekinumab Treatment Is Not Associated With Increased Postoperative Complications in Crohn's Disease: A Canadian Multi-Centre Observational Cohort Study. *J Can Assoc Gastroenterol* 2018; **1**: 115-123 [PMID: 31294352 DOI: 10.1093/jcag/gwy013]
104 **Rijksinstituut voor Volksgezondheid en Milieu**. Vaccinatie bij chronisch inflammatoire aandoeningen. [cited 11 December 2021]. Available from: https://lci.rivm.nl/richtlijnen/vaccinatie-bij-chronisch-inflammatoire-aandoeningen
105 **Su Q**, Li X, Mo W, Yang Z. Low serum bilirubin, albumin, and uric acid levels in patients with Crohn's disease. *Medicine (Baltimore)* 2019; **98**: e15664 [PMID: 31083269 DOI: 10.1097/MD.0000000000015664]
106 **Morar PS**, Hodgkinson JD, Thalayasingam S, Koysombat K, Purcell M, Hart AL, Warusavitarne J, Faiz O. Determining Predictors for Intra-abdominal Septic Complications Following Ileocolonic Resection for Crohn's Disease-Considerations in Pre-operative and Peri-operative Optimisation Techniques to Improve Outcome. *J Crohns Colitis* 2015; **9**: 483-491 [PMID: 25796553 DOI: 10.1093/ecco-jcc/jjv051]
107 **Uchino M**, Ikeuchi H, Matsuoka H, Bando T, Ichiki K, Nakajima K, Tomita N, Takesue Y. Risk factors for surgical site

infection and association with infliximab administration during surgery for Crohn's disease. *Dis Colon Rectum* 2013; **56**: 1156-1165 [PMID: 24022533 DOI: 10.1097/DCR.0b013e31829f682c]

108 **Nguyen GC**, Du L, Chong RY, Jackson TD. Hypoalbuminaemia and Postoperative Outcomes in Inflammatory Bowel Disease: the NSQIP Surgical Cohort. *J Crohns Colitis* 2019; **13**: 1433-1438 [PMID: 31253985 DOI: 10.1093/ecco-jcc/jjz083]

109 **Ge X**, Liu H, Tang S, Wu Y, Pan Y, Liu W, Qi W, Ye L, Cao Q, Zhou W. Preoperative hypoalbuminemia is an independent risk factor for postoperative complications in Crohn's disease patients with normal BMI: A cohort study. *Int J Surg* 2020; **79**: 294-299 [PMID: 32505647 DOI: 10.1016/j.ijsu.2020.05.064]

110 **Galata C**, Kienle P, Weiss C, Seyfried S, Reißfelder C, Hardt J. Risk factors for early postoperative complications in patients with Crohn's disease after colorectal surgery other than ileocecal resection or right hemicolectomy. *Int J Colorectal Dis* 2019; **34**: 293-300 [PMID: 30460473 DOI: 10.1007/s00384-018-3196-2]

111 **Li Y**, Zuo L, Zhu W, Gong J, Zhang W, Gu L, Guo Z, Li N, Li J. The impact of bacterial DNA translocation on early postoperative outcomes in Crohn's patients undergoing abdominal surgery. *J Crohns Colitis* 2015; **9**: 259-265 [PMID: 25555386 DOI: 10.1093/ecco-jcc/jju029]

112 **Liu X**, Wu X, Zhou C, Hu T, Ke J, Chen Y, He X, Zheng X, Hu J, Zhi M, Gao X, Hu P, Lan P. Preoperative hypoalbuminemia is associated with an increased risk for intra-abdominal septic complications after primary anastomosis for Crohn's disease. *Gastroenterol Rep (Oxf)* 2017; **5**: 298-304 [PMID: 29230300 DOI: 10.1093/gastro/gox002]

113 **Kotze PG**, Saab MP, Saab B, da Silva Kotze LM, Olandoski M, Pinheiro LV, Martinez CA, Ayrizono ML, Magro DO, Coy CS. Tumor Necrosis Factor Alpha Inhibitors Did Not Influence Postoperative Morbidity After Elective Surgical Resections in Crohn's Disease. *Dig Dis Sci* 2017; **62**: 456-464 [PMID: 27933472 DOI: 10.1007/s10620-016-4400-2]

114 **Liu S**, Miao J, Wang G, Wang M, Wu X, Guo K, Feng M, Guan W, Ren J. Risk factors for postoperative surgical site infections in patients with Crohn's disease receiving definitive bowel resection. *Sci Rep* 2017; **7**: 9828 [PMID: 28852175 DOI: 10.1038/s41598-017-10603-8]

115 **Higgens C**, Allan RN, Keighley MR, Arabi Y, Alexander-Williams J. Sepsis following operation for inflammatory intestinal disease. *Dis Colon Rectum* 1980; **23**: 102-105 [PMID: 7379654 DOI: 10.1007/BF02587605]

116 Routine preoperative tests for elective surgery: © NICE (2016) Routine preoperative tests for elective surgery. *BJU Int* 2018; **121**: 12-16 [PMID: 29314537 DOI: 10.1111/bju.14079]

117 **Hans GA**, Jones N. Preoperative anaemia. *BJA Education* 2013; **13**: 71-74 [DOI: 10.1093/bjaceaccp/mks064]

118 **Novello M**, Stocchi L, Steele SR, Holubar SD, Duraes LC, Kessler H, Shawki S, Hull LT. Case-matched Comparison of Postoperative Outcomes Following Surgery for Inflammatory Bowel Disease After Exposure to Vedolizumab vs Other Biologics. *J Crohns Colitis* 2020; **14**: 185-191 [PMID: 31328222 DOI: 10.1093/ecco-jcc/jjz129]

119 **Michailidou M**, Nfonsam VN. Preoperative anemia and outcomes in patients undergoing surgery for inflammatory bowel disease. *Am J Surg* 2018; **215**: 78-81 [PMID: 28359559 DOI: 10.1016/j.amjsurg.2017.02.016]

120 **Rahal MA**, Karaoui WR, Mailhac A, Tamim H, Shaib Y. Surgical outcomes among inflammatory bowel disease patients undergoing colectomy : results from a national database. *Acta Gastroenterol Belg* 2018; **81**: 387-392 [PMID: 30350526 DOI: 10.1016/S0016-5085(17)31469-5]

121 **Li Y**, Stocchi L, Rui Y, Liu G, Gorgun E, Remzi FH, Shen B. Perioperative Blood Transfusion and Postoperative Outcome in Patients with Crohn's Disease Undergoing Primary Ileocolonic Resection in the "Biological Era". *J Gastrointest Surg* 2015; **19**: 1842-1851 [PMID: 26286365 DOI: 10.1007/s11605-015-2893-1]

122 **Moon T**, Smith A, Pak T, Park BH, Beutler SS, Brown T, Kaye AD, Urman RD. Preoperative Anemia Treatment with Intravenous Iron Therapy in Patients Undergoing Abdominal Surgery: A Systematic Review. *Adv Ther* 2021; **38**: 1447-1469 [PMID: 33580485 DOI: 10.1007/s12325-021-01628-7]

123 **Miller JL**. Iron deficiency anemia: a common and curable disease. *Cold Spring Harb Perspect Med* 2013; **3** [PMID: 23613366 DOI: 10.1101/cshperspect.a011866]

124 **Galata C**, Weiss C, Hardt J, Seyfried S, Post S, Kienle P, Horisberger K. Risk factors for early postoperative complications and length of hospital stay in ileocecal resection and right hemicolectomy for Crohn's disease: a single-center experience. *Int J Colorectal Dis* 2018; **33**: 937-945 [PMID: 29736773 DOI: 10.1007/s00384-018-3072-0]

125 **Riss S**, Bittermann C, Schwameis K, Kristo I, Mittlböck M, Herbst F, Stift A. Determinants for postoperative complications after laparoscopic intestinal resection for Crohn's disease. *Surg Endosc* 2012; **26**: 933-938 [PMID: 22002203 DOI: 10.1007/s00464-011-1970-0]

126 **Zhang W**, Zhu W, Ren J, Zuo L, Wu X, Li J. Skeletal muscle percentage: a protective factor for postoperative morbidity in Crohn's disease patients with severe malnutrition. *J Gastrointest Surg* 2015; **19**: 715-721 [PMID: 25666099 DOI: 10.1007/s11605-015-2763-x]

127 **Tang S**, Dong X, Liu W, Qi W, Ye L, Yang X, Cao Q, Ge X, Zhou W. Compare risk factors associated with postoperative infectious complication in Crohn's disease with and without preoperative infliximab therapy: a cohort study. *Int J Colorectal Dis* 2020; **35**: 727-737 [PMID: 32060607 DOI: 10.1007/s00384-019-03481-1]

128 **Weisshof R**, Chermesh I. Micronutrient deficiencies in inflammatory bowel disease. *Curr Opin Clin Nutr Metab Care* 2015; **18**: 576-581 [PMID: 26418823 DOI: 10.1097/MCO.0000000000000226]

World Journal of Gastroenterology

Submit a Manuscript: https://www.f6publishing.com

World J Gastroenterol 2022 June 14; 28(22): 2417-2428

DOI: 10.3748/wjg.v28.i22.2417

ISSN 1007-9327 (print) ISSN 2219-2840 (online)

REVIEW

Hepatocellular carcinoma, hepatitis C virus infection and miRNA involvement: Perspectives for new therapeutic approaches

Ester Badami, Rosalia Busà, Bruno Douradinha, Giovanna Russelli, Vitale Miceli, Alessia Gallo, Giovanni Zito, Pier Giulio Conaldi, Gioacchin Iannolo

Specialty type: Gastroenterology and hepatology

Provenance and peer review: Invited article; Externally peer reviewed.

Peer-review model: Single blind

Peer-review report's scientific quality classification

Grade A (Excellent): 0
Grade B (Very good): B
Grade C (Good): C
Grade D (Fair): 0
Grade E (Poor): 0

P-Reviewer: Kumar R, India; Zhang C, China

Received: February 16, 2022
Peer-review started: February 16, 2022
First decision: March 9, 2022
Revised: March 22, 2022
Accepted: April 15, 2022
Article in press: April 15, 2022
Published online: June 14, 2022

Ester Badami, Bruno Douradinha, Regenerative Medicine and Immunotherapy Area, Fondazione Ri.MED, Palermo 90127, Italy

Rosalia Busà, Giovanna Russelli, Vitale Miceli, Alessia Gallo, Giovanni Zito, Pier Giulio Conaldi, Gioacchin Iannolo, Department of Research, Mediterranean Institute for Transplantation and Advanced Specialized Therapies (IRCCS-ISMETT), Palermo 90127, Italy

Corresponding author: Gioacchin Iannolo, BSc, PhD, Research Scientist, Department of Research, Mediterranean Institute for Transplantation and Advanced Specialized Therapies (IRCCS-ISMETT), Via E. Tricomi 5, Palermo 90127, Italy. giannolo@ismett.edu

Abstract

Chronic hepatitis C virus (HCV) infection is the principal etiology of cirrhosis and, ultimately, hepatocellular carcinoma (HCC). At present, approximately 71 million people are chronically infected with HCV, and 10%–20% of these are expected to develop severe liver complications throughout their lifetime. Scientific evidence has clearly shown the causal association between miRNAs, HCV infection and HCC. Although it is not completely clear whether miRNA dysregulation in HCC is the cause or the consequence of its development, variations in miRNA patterns have been described in different liver diseases, including HCC. Many studies have analyzed the importance of circulating miRNAs and their effect on cell proliferation and apoptosis. In this Review, we aim to summarize current knowledge on the association between miRNA, HCV and HCC from a diagnostic point of view, and also the potential implications for therapeutic approaches.

Key Words: Hepatocellular carcinoma; miRNA; Liver; Hepatitis C virus; miRNAs; Direct-acting antivirals; Extracellular vesicles; Transplantation

©The Author(s) 2022. Published by Baishideng Publishing Group Inc. All rights reserved.

Core tip: Hepatocellular carcinoma (HCC) is one of the most life-threatening cancers worldwide. Among other factors, HCC is frequently caused by chronic hepatitis C virus infection. Currently, the mechanisms responsible for its neoplastic transformation are not completely understood. Regardless of the recent discovery and therapeutic use of latest-generation direct-acting antivirals, HCC remains an unresolved problem, even after viral eradication. In this scenario, miRNAs can become both a diagnostic tool and, hopefully, a novel therapeutic approach.

Citation: Badami E, Busà R, Douradinha B, Russelli G, Miceli V, Gallo A, Zito G, Conaldi PG, Iannolo G. Hepatocellular carcinoma, hepatitis C virus infection and miRNA involvement: Perspectives for new therapeutic approaches. *World J Gastroenterol* 2022; 28(22): 2417-2428
URL: https://www.wjgnet.com/1007-9327/full/v28/i22/2417.htm
DOI: https://dx.doi.org/10.3748/wjg.v28.i22.2417

INTRODUCTION

Chronic hepatitis C virus (HCV) infection is a well-known risk factor for hepatocellular carcinoma (HCC)[1,2]. The virus belongs to the Flaviviridae family, and is the only member of the hepacivirus genus[3-6], and is presently classified in seven main genotypes, although 11 genotypes and at least 67 confirmed subtypes are known[7-10].

HCV is a single-stranded positive-sense RNA virus consisting of an icosahedral symmetrical nucleocapsid, surrounded by a double-layer lipid envelope in which the envelope glycoproteins E1 and E2 are inserted[6]. Its genome of 9.6 kb harbors an open reading frame encoding a polyprotein precursor of about 3000 amino acids, which is processed through proteolytic cleavage by viral and host proteases into smaller molecules, including structural (core, E1 and E2), p7, and nonstructural proteins (NS2, NS3, NS4A, NS4B, NS5A and NS5B)[11].

The total global prevalence of chronic HCV infection is estimated at 71 million people by the World Health Organization (WHO)[12], and varies according to health conditions, sociodemographic characteristics, and the presence of risk factors for transmission that can alter the efficiency of the transmission routes[9,13]. HCV is transmitted primarily parenterally, through large or repeated direct percutaneous exposures to infected blood[9,13-15]. Major high-risk populations include people who inject drugs (PWIDs), men who have sex with men, and prisoners[16].

The outcome of HCV infection depends strictly on the strength and breadth of the host response during the acute phase. Around 30% of HCV-infected people spontaneously clear the virus within 6 mo of infection, although the remaining 60%–80% of people, despite developing an efficient antiviral immune response, are unable to clear the virus, resulting in persistent infection[17,18]. Activation of the immune response against HCV contributes importantly to the establishment of long-lasting inflammation and consequent liver damage. The deregulation of cytotoxic cells and the continued activation of an apoptosis pathway results in scarring and progression to cirrhosis that, in 25% of HCV infected patients, can result in HCC over a period of 20–30 years post-infection[2,19,20].

Until the last decade, interferon (IFN) and ribavirin (RBV) were the only available therapies against chronic HCV infection, although they were accompanied by significant side effects. Moreover, IFN-based therapies had only limited efficacy, as the response was genotype dependent[21-24]. The recent introduction of direct-acting antivirals (DAAs) has resulted in remarkable therapeutic improvements. These are currently the standard therapeutic choice, and a sustained virology response (SVR) > 90% is attained after 12 wk of treatment. However, some patients show relapse of HCV infection, even after DAA treatment, and achieving SVR does not completely rule out the risk of developing HCC[25]. Also, following DAA treatment and subsequent viral clearance, HCV reinfections remain a problem among individuals with high-risk behaviors, *e.g.*, PWIDs[26,27].

Moreover, access to DAA therapy is not simple for all patients, and only the 62% of HCV-diagnosed patients have been treated with DAAs (WHO) (https://www.who.int/news-room/fact-sheets/detail/hepatitis-c).

Although the pathogenesis of HCV infection has not been fully elucidated, interactions between structural and nonstructural viral proteins and host cell components, such as miRNAs, have been reported by many groups. It has been shown that host miRNAs are involved in many steps of the biological cycle of HCV, such as infection and replication. Likewise, HCV infection regulates the expression of many cellular miRNAs involved, for example in liver fibrosis, hepatocarcinogenesis and HCC progression[28-31]. Due to such mutual interactions, miRNAs can be used for risk assessment and prognosis of HCV-related HCC, and could be considered for diagnostic approaches and new therapeutic strategies.

HCC

HCC is the main type of liver cancer, and the most life-threatening cancer worldwide. HCC onset consists of several processes involving multiple risk factors, but most often it presents in people with chronic liver diseases and cirrhosis[32].

The most common etiological factors that lead to liver cirrhosis, therefore predisposing to HCC transformation, are chronic infection with hepatitis B virus (HBV), HCV, or hepatitis D virus, alcoholic liver disease, and nonalcoholic steatohepatitis/nonalcoholic fatty liver disease (NAFLD). The less common causes are hereditary hemochromatosis, 1 antitrypsin deficiency, autoimmune hepatitis, porphyria, disorders of steroid hormones, Wilson's disease, and dietary aflatoxins[33-36].

Approximately 50% of all liver cancers are related to chronic viral hepatitis, which can develop into cirrhosis and HCC[37]. In particular, HCV causes chronic infections in 70%–80% of cases, while HBV leads to chronicity in only 10% of infected people[38]. Among HCV chronically infected patients, about 20% develop liver cirrhosis within 20–30 years and, once cirrhosis is established, the rate of HCC development increases by 1%–4% per year. Moreover, chronic HCV infection is associated with a 20–30-fold increased risk of developing into HCC compared to healthy individuals[39]. HCV-related HCC is mediated both by virus-related factors and host-induced immunological responses. In addition, HCV damage is a gradual and continual process, characterized by recurrent infection that induces the immune system to attack liver cells, provoking repeated damage to the genomic material that can lead to mistakes during proofreading repair[38]. Recent studies suggest that HCV core protein can promote initial development of HCC, acting on cell signaling pathways. Indeed, HCV core protein may directly inhibit the tumor suppressor genes and the cell cycle checkpoints, inducing the activation of signaling pathways that upregulate growth and cell division[40]. The specific tumor suppressor genes inhibited by HCV core protein include retinoblastoma protein and p53 tumor suppressor, which, if synergistically lost, lead to a higher degree of carcinogenesis[41]. Repeated cell cycles are associated with the accumulation of mutations that may transform hepatocytes into cancer cells. Among the genes most mutated are telomerase reverse transcriptase, tumor protein 53, and β-catenin. These mutations not only threaten telomere maintenance, but also lead to increased oxidative stress on hepatocytes, inducing chronic inflammation secondary to HCV, thus promoting HCC progression[42].

Over the last few years, in an attempt to identify new therapies and more accurate biomarkers for early diagnosis and treatment of HCC, the pivotal role played by miRNAs in the development and progression of cancer has emerged[43].

Recently, progress has been made in the study of miRNAs in HCC, with the discovery that some of them are upregulated or downregulated in HCC. Aberrant expression of miRNAs has been linked to HCC proliferation, apoptosis and invasion, but also metastasis formation, epithelial–mesenchymal transition, angiogenesis, drug resistance, and autophagy. In addition, some miRNAs can also be potential diagnostic and prediction markers for HCC[44].

HCV THERAPY

The principal goal of anti-HCV therapy is to eradicate HCV infection, thus resolving the liver disease. In the past, the standard of care for eradication of chronic HCV treatment was IFN-based therapy; most commonly in combination with RBV. However, this combination therapy had an outcome that depended on the viral genotype, was poorly tolerated, and also associated with severe side effects such as depression, flu-like symptoms, fatigue, diarrhea, and hematological toxicity[45]. These unwanted adverse effects were the main reason for patients abandoning therapy. With the introduction of the first NS5B polymerase inhibitor, sofosbuvir, in 2014, IFN-free treatment became available[46]. Hence, DAAs were introduced in clinical practice to treat HCV^+ patients, obtaining SVR rates above 90%[47,48], where SVR corresponds to a cure of the HCV infection, as late relapse occurs in less than 0.2% of cases beyond 6 mo of follow-up[49]. While patients with cirrhosis are often not treatable with IFN-based treatment, DAAs, including NS5B and NS5A inhibitors, are effective for patients with any stage of liver fibrosis, including those with advanced liver disease and decompensated cirrhosis, which predispose to developing HCC at a higher degree. This has allowed a significant increase in the number of treatable patients, with excellent safety profiles[50].

Clinically, SVR leads to stabilization and improvement of the liver function, and is thus associated with a lower risk of hepatic dysfunction, a reduced need for liver transplantation, and lower overall mortality. It has been demonstrated that DAA therapy attains much higher SVR rates than IFN-based treatment by reducing the inflammatory cargo in the liver, fibrosis, and neoplastic formation[51].

With more successful SVR obtained using DAAs in the clinic, there were higher expectations in terms of a significant reduction in the incidence of HCC. However, such expectations were not always met. In fact, despite the documented positive impact on HCV infection clearance, the effect of DAA treatment on the development and/or recurrence of HCC in patients treated for liver cirrhosis remains hard to define[52].

In a meta-analysis, Frazzoni *et al*[53] compared different trials based either on the use of DAAs or IFN [53]. The aim of this study was to define the long-term incidence and occurrence of HCC after the achievement of SVR using either IFN-free or IFN-based therapies. This investigation showed the higher safety profile of DAA therapy, accompanied by a lower risk of HCC recurrence[53]. A controversial subject is the effect of DAA-based SVR on the recurrence of HCC following curative treatment of early HCC. It has also been found that about 30% of patients with a history of curative treatment for HCC undergoing DAA therapy for HCV infection develop HCC recurrence, raising many surgical and clinical questions[54].

Some studies initially suggested that DAA treatment might increase the recurrence rate for HCC, with consequent doubts on the use of this therapy for patients with previous HCC[55]. However, these studies were not confirmed by further trials, and new guidelines were provided recommending the use of DAAs for patients with a history of HCC[56]. At present, patients with HCV-related cirrhosis who have undergone resection or ablation for HCC should not be dissuaded from receiving DAA therapy to prevent the progression of the liver disease.

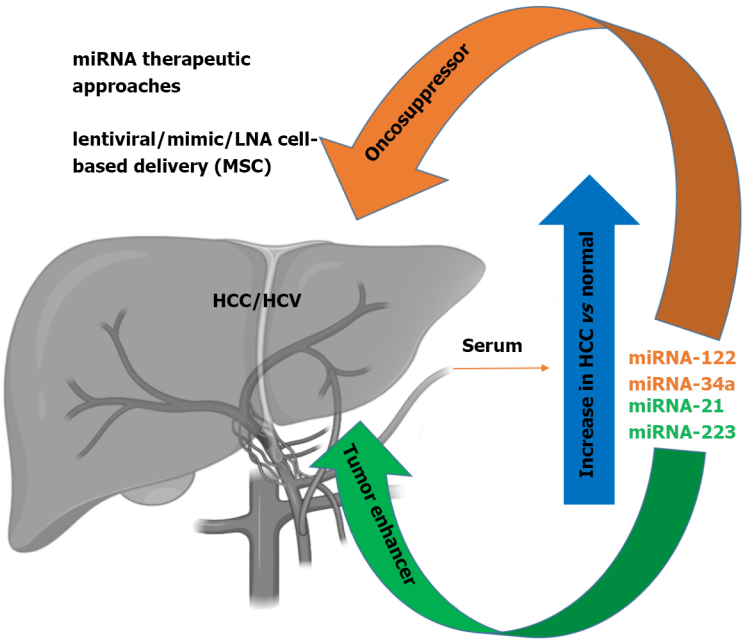
The putative correlation between DAA treatment and *de novo* HCC occurrence is still a matter of debate. Some studies have shown how HCV^+ patients diagnosed as negative for HCC develop aggressive and fatal forms of liver cancer after DAA treatment[57-61]. These studies highlighted the importance of the surveillance of patients before and during DAA treatment, pointing to a possible correlation between the stage of fibrosis and the pre-existence of decompensated cirrhosis, with increased susceptibility to the development of *de novo* HCC[58,61,62].To conclude, patients failing to respond to antiviral treatment are at high risk and often need to be monitored during therapy[63]. In light of these observations, it appears clear how the use of biomarkers such as HCV/HCC/liver-related miRNA are important for early HCC diagnosis before and during DAA treatment.

HCV INFECTION AND miRNAs

As discussed above, miRNAs are active players in tumor initiation and progression for their involvement in the regulation of expression for proteins implicated in the pathophysiological mechanisms of cancer development, including cell growth, apoptosis, and metastasis[64-66]. In the liver, it has been shown that liver-enriched transcription factors such as HNF1A, HNF3A and HNF3B regulate miR-122 expression, which can function as a tumor suppressor factor by inhibiting angiogenesis, HCC growth/invasion, and high levels of HCC apoptosis and cell cycle arrest[67,68]. This miRNA represents 70% of the total miRNAs in hepatocytes[69,70], and has been therefore nicknamed hepatic miRNA. It has been found that HCV RNA possesses two tandem miR-122 complementary sites at the 5′ end of the viral genome[71], responsible for viral RNA accumulation[72]. The miR-122 binding with the HCV RNA has been described at multiple levels: miR-122 affects folding of the viral internal ribosomal entry site (IRES)[73], required for viral translation, and modulates viral replication and polyprotein translation [74]. In addition, it has been found that the stability of HCV RNA is mediated by RNA-induced silencing-like complex (RISC-like), suggesting the coordination of Ago2 and miR-122 in stabilizing and protecting the viral genome from 5′ exonuclease activity[75]. Furthermore, HCV RNA acts as a sponge for miR-122, leading to de-repression of host mRNAs normally targeted by miR-122, thus providing a fertile environment for the long-term oncogenic potential of HCV[76]. The serum levels of miR-122 are clearly higher in HCV-infected patients with HCC[77-79]. During the course of HCV infection, miR-122 is coupled with miR-34a[80] (Figure 1). While several studies have reported a downregulation of miR-34a in neoplastic transformation in various tissues[81], miR-34a was found increased in HCC[82]. Moreover, we recently reported an increase of miR-34a in HCC cells after HCV infection, the effect of which can be modulated by p53 induction[31]. It has recently been proposed that flaviviruses can upregulate expression of miRNAs that inhibit viral replication in target cells[31], demonstrating that miR34 overexpression induces the IFN-mediated response in dengue virus, West Nile virus and Japanese encephalitis virus infection[83]. In HCC cells, miR-34a induces cell cycle arrest and apoptosis. Concomitantly, other groups have also demonstrated that miR-34 inhibits fibrosis in stellate cells by regulating the TGF-β1/Smad3 pathway[84].

Expression of miR-21 increases in patients with HCV-related HCC[85], while miR-223 expression is increased in patients with advanced fibrosis compared to moderate/minimal fibrosis[86]. In contrast, during HCV-related chronic hepatitis, miR-21 and miR-223 display a pro-fibrotic/tumorigenic effect[85] (Figure 1).

Depending on the role played in viral infection, some miRNAs have been classified as pro- or antiviral. For example, miR-135a has been described as proviral miRNA because of its ability to enhance HCV RNA replication in hepatocytes. In addition, miR-135a inhibits the expression of host restriction factors, such as CXCL2, MyD88 and IRPK2, which are involved in antiviral immunity[87]. Likewise, miR-146a-5p enhances HCV infection by playing an immunoregulatory role through the downregulation of the inflammatory signaling, and by turning off the immune response in hepatocytes. Moreover, miR-146a-5p promotes the late steps of the HCV replication cycle, likely by modulating HCV assembly [88]. Another example is represented by miR-21-5p, which triggers HCC growth and metastasis by



DOI: 10.3748/wjg.v28.i22.2417 **Copyright** ©The Author(s) 2022.

Figure 1 Schematic representation of some major miRNAs upregulated in serum after hepatocellular carcinoma occurrence. Noteworthy, some of them (mir-122 and mi-R34a) display a tumor suppressor effect and represent not only a diagnostic target, but have been proposed in novel therapeutic approaches (Figure was created using BioRender.com). HCC: Hepatocellular carcinoma; HCV: Hepatitis C virus; LNA: Locked nucleic acid; MSC: Mesenchymal stem cell.

modulating a PTEN-dependent pathway[89].

Conversely, let-7 family miRNAs have demonstrated strong anti-HCV activity, thus being classified as antiviral miRNA[90]. It has been found that let-7b potentially reduces HCV replication through the targeting of IGF2BP1 required for HCV replication[90], and increases the cell apoptosis rate[91]. Similar to other antiviral miRNAs, mir-199a* is a HCV RNA binder in IRES, targeting the HCV 5′-UTR[64,92].

HCV-RELATED HCC miRNA-BASED APPROACHES

The mechanisms that drive liver injury during HCV infection have not been fully elucidated. Several studies have attempted to understand the interactions between viral proteins and the cellular host machinery[93]. An important effort has been made to address and understand the complex interconnections between HCV infection and miRNAs, aimed at finding new therapeutic and diagnostic tools.

It has recently been shown that the expression of specific patterns of miRNAs in HCC patients may be used for diagnostic purposes, with a sufficient level of reliability, thus highlighting a potential role of miRNAs as biomarkers[94]. Specific circulating miRNA profiles are associated with several diseases, including HCV infection. These miRNAs have been proposed as biomarkers of HCV-related HCC pathophysiology and prognosis. Many studies have focused on setting miRNA panels to be tested in HCV-related HCC patients, and used to discriminate healthy individuals from ill patients; above all, during the early phases of disease. For example, Ali *et al*[95] described and validated a panel of nine liver-associated miRNAs (miR-21, miR-30c, miR-93, miR-122, miR-125b, miR-126, miR-130a, miR-193b and miR-222)[95], while Zekri *et al*[96] identified miR-122, miR-885-5p and miR-29b as associated with fluctuations in the levels of the diagnostic liver-specific biomarker -fetoprotein (AFP)[96]. Wahb *et al*[97] suggested the use of circulating miR-9-3p and endocan as novel biomarkers for risk assessment in the early diagnosis of HCV-related HCC[97]. It has been shown that circulating extracellular vesicles (EVs) containing specific patterns of noncoding RNAs are highly related to disease progression of HCV-associated HCC[98]. Recent reports have highlighted the importance of serum miR-34a and miR-122 as biomarkers of HCV-related HCC[80]. We recently showed that HCV infection induces an increase in miR-34a expression in the HCC cell line HuH7.5, and acts as a tumor suppressor[31]. We also found that HCV infection induces the release of EVs containing miR-34a, and these EVs can exert a growth inhibition effect and induce apoptosis[31]. We were able to demonstrate that miR-34 action is not limited only to the infected cells, as EV release has a paracrine effect on neighboring hepatocytes, thus underscoring the potential use of this miRNA for therapeutic purposes[31] (Figure 1). A newly generated polymer-based nanosystem redox-sensitive, oligopeptide-guided, self-assembling, and efficiency-enhanced (ROSE) loaded with miR-34a inhibits HCC proliferation *in vitro* and *in vivo*,

reducing the epithelial mesenchymal transition[99].

Conversely, it has been demonstrated that miR-21 can act as an oncogene by stimulating HCC growth, invasion, and migration[89,100]. Indeed, it has been shown that the inhibition of miR-21 suppresses HCC growth both *in vitro* and *in vivo*[100].

It is worth mentioning that miR-122 is known to potentiate HCV replication by inhibiting the degradation of the viral genome[70]. Several clinical trials are testing the ability of reducing HCV replication using locked nucleic acid inhibition of miR-122[101-103], perhaps evidence for the efficacy of this treatment, which is devoid of adverse effects[64]. For example, miR-122 antagonists can be used as a therapeutic approach in synergistic association with DAA therapy to obtain an enhancement of the clinical outcome. These results point out the potential therapeutic interest of miR-122, in particular, for patients who do not respond to antiviral agents[104]. Recently, the use of EVs to treat HCC has become an interesting topic, but one that requires further studies. Lou *et al*[105] revealed that the injection of EVs derived from miR-122-modified mesenchymal stem cells (MSCs) can significantly improve chemotherapeutic sensitivity of HCC, and increase the efficacy of sorafenib treatment[105] (Figure 1). Wei *et al*[106] found that there are different miRNA expression patterns between HCC cells and their EVs, suggesting a self-modulating mechanism whereby HCC-cell-derived EVs were able to shuttle miRNAs to recipient cells, promote cell growth, and migration and invasion of HCC cells[106]. EVs contain both oncogenic and tumor suppressor miRNAs, and their deregulated expression in HCC tissues can promote HCC development. Therefore, EV-mediated miRNA transfer might represent a crucial mechanism, exploitable on the one hand as a diagnostic tool by identifying circulating EV-derived miRNA, and, on the other, EV-derived miRNAs could be a useful target to inhibit HCC growth. In agreement, Zhang *et al*[107] generated virus-like vectors containing both miRNA-21-sponge and pre-miRNA-122, and demonstrated that virus-like particles were able to correct HCC miRNA dysregulation, and to decrease proliferation, migration, and invasion of HCC[107].

Currently, 20 clinical trials (Table 1) are investigating both tissue-specific and circulating miRNAs as a diagnostic/prognostic tool for HCC or for monitoring HCC during a specific treatment (clinicaltrial.gov). Future clinical trials will be needed to provide appropriate analysis of the performance of miRNAs as biomarkers, and to discover new miRNA-related HCC targets for implementation of new treatments.

PERSPECTIVES FOR TUMOUR DETECTION AND INTERVENTION

As described above, there is a strong correlation between miRNA expression and HCC. However, some of the regulated miRNAs are not only related to HCV infection, but also with other pathological liver conditions. In particular, alterations in some miRNAs have been also found in NAFLD[108-110]. Among the identified miRNAs, a significant upregulation of miR-122 in the serum of NAFLD patients was noted. This variation is comparable to the upregulation of the same miRNA observed in the serum of HCC/HCV patients. Another group reported a significant increase of miR-34a expression in the serum of NAFLD patients[110], in agreement with our observations in HCV HCC cells infections[31]. These results indicate that these miRNAs could be considered potential markers of pathological liver conditions induced by inflammation or transformation (Figure 1). The most direct implication of this finding is the possibility of having new, noninvasive, and reliable biomarkers for early HCC detection that could be applied in the near future. In particular, a specific circulating miRNA expression, in association with conventional tumor markers such as AFP, protein induced by vitamin K absence/antagonist II (PIVKA-II), and classical clinical parameters has been observed[111,112]. The definition of an miRNA expression signature (88 miRNAs) provides a substantial increase of accuracy in the detection of HCC (up to 99.5%), associated with a strong sensitivity (100%), while AFP evaluation as a tumor biomarker has an accuracy and a sensitivity of 76.5% and 63.8%, respectively[111]. The strength of these results refers mostly to the detection of small HCC tumors (< 3 cm). This analysis also revealed that an miRNA expression signature shows specific variations for HCC compared to other pathological liver conditions, where cirrhotic patients or chronic hepatitis B infection can be distinguished by a characteristic alteration of expression pattern[110]. These results strengthen the possibility of using miRNAs as a new approach for early tumor detection and subsequent early intervention, particularly considering that, after HCV DAA treatment, there is still the need to monitor HCC occurrence after viral eradication, as also suggested elsewhere[31,113,114].

CONCLUSION

The introduction of DAA therapy signals a milestone in the history of HCV treatment, with achievement of SVR at high rates. However, whether the development of HCC is related to pre-existing HCV infections after DAA treatment is disputed. Not all HCV patients are eligible for DAA treatment, and HCV reinfection in high-risk populations frequently occurs. In light of this, understanding the molecular mechanisms of HCV viral infection that lead to development of liver cancer in the host is

Table 1 List of registered trials that use miRNAs as diagnostic and/or prognostic tool for hepatocellular carcinoma

Study title	Phase	Status	NCT number
MicroRNAs as diagnostic biomarkers in hepatocellular carcinoma among Somali patients	NA	Unknown	NCT03227510
Prospective cohort study of changes in circulatory microRNA of resected hepatocellular carcinoma	NA	Recruiting	NCT05148572
Clinical significance of hepatic and circulating microRNAs miR-221 and miR-222 in hepatocellular carcinoma	NA	Unknown	NCT02928627
Study of microRNAs as a diagnostic tool for HCV-related hepatocellular carcinoma	NA	Unknown	NCT03429530
Impact of IL-28B rs12979860 and rs4803217 gene polymorphisms associated with miRNAs deregulation on HCV-related hepatocellular carcinoma	NA	Unknown	NCT02507882
MiRNA as a diagnostic and prognostic biomarker of hepatocellular carcinoma	NA	Not yet recruiting	NCT02448056
Early Detection of Hepatocellular Carcinoma in a High-risk Prospective Cohort (ELEGANCE)	NA	Recruiting	NCT04965259
Blood sample collection for experimental blood test to track liver cancer	NA	Recruiting	NCT04720430
Different genetic features associated with hepatic carcinogenesis	NA	Unknown	NCT01247506
Genetic profiling of liver cancer in patients undergoing liver transplantation	NA	Active, not recruiting	NCT02412579
A study of individualized radiotherapy based on a prediction model of lymph node metastasis in hepatocellular carcinoma	NA	Unknown	NCT03416803
Fingerprint characterization of sorafenib treated HCC	NA	Unknown	NCT03958669
Risk of HCC in cirrhotic patients post DAAs treatment	NA	Unknown	NCT03414554
Risk of hepatocellular carcinoma in patient with liver cirrhosis	NA	Unknown	NCT03083002
Axitinib for the treatment of advanced hepatocellular carcinoma	2	Completed	NCT01210495
The phase III study of icaritin versus sorafenib in PD-L1 positive advanced hepatocellular carcinoma subjects	3	Recruiting	NCT03236649
The phase III study of icaritin versus HUACHANSU PIAN in hepatocellular carcinoma subjects	3	Recruiting	NCT03236636
A study of rSIFN-co in subjects with advanced solid tumors	1	Completed	NCT02387307
Stereotactic body radiation therapy and transarterial chemoembolization in treating patients with liver cancer that cannot be removed by surgery	1	Completed	NCT02507765
Nal-IRI with 5-fluorouracil (5-FU) and leucovorin or gemcitabine plus cisplatin in advanced biliary-tract cancer	2	Active, not recruiting	NCT03044587

NA: Not applicable.

fundamental.

It has been reported that cellular miRNAs may contribute to HCV pathogenesis, either by direct or indirect interactions with the viral genome or proteins. Several miRNAs and their targets have been shown to be associated with HCV and HCC progression, and might represent a diagnostic biomarker for the early prognosis of HCC. Early HCC prognosis acquires relevance during DAA treatment to minimize the risks of HCC development in HCV^+ patients. Likewise, many miRNAs could be used also for therapeutic purposes. However, further studies are needed to elucidate the molecular interplay between miRNA and HCC, and the development of novel therapeutic strategies for the treatment of HCC is a major critical goal to be achieved.

FOOTNOTES

Author contributions: Badami E, Busà R, Douradinha B, Russelli G, Miceli V, Gallo A, Zito G, Conaldi PG and Iannolo G carried out the research for the manuscript and edited all drafts of the paper; Badami E, Busà R and Douradinha B equally contributed to the manuscript.

Conflict-of-interest statement: The authors declare that they have no conflict of interest.

Open-Access: This article is an open-access article that was selected by an in-house editor and fully peer-reviewed by external reviewers. It is distributed in accordance with the Creative Commons Attribution NonCommercial (CC BY-NC 4.0) license, which permits others to distribute, remix, adapt, build upon this work non-commercially, and license their derivative works on different terms, provided the original work is properly cited and the use is non-

commercial. See: https://creativecommons.org/Licenses/by-nc/4.0/

Country/Territory of origin: Italy

ORCID number: Ester Badami 0000-0002-0154-6270; Rosalia Busà 0000-0002-7546-7209; Bruno Douradinha 0000-0002-9980-4505; Giovanna Russelli 0000-0002-1920-0892; Vitale Miceli 0000-0001-8922-9909; Alessia Gallo 0000-0001-6737-9770; Giovanni Zito 0000-0002-0482-6729; Pier Giulio Conaldi 0000-0003-1994-8005; Gioacchin Iannolo 0000-0002-7710-4735.

S-Editor: Fan JR
L-Editor: Kerr C
P-Editor: Fan JR

REFERENCES

1 **IARC Working Group on the Evaluation of Carcinogenic Risks to Humans**. Biological agents. Volume 100 B. A review of human carcinogens. *IARC Monogr Eval Carcinog Risks Hum* 2012; **100**: 1-441 [PMID: 23189750]
2 **McGlynn KA**, Petrick JL, El-Serag HB. Epidemiology of Hepatocellular Carcinoma. *Hepatology* 2021; **73** Suppl 1: 4-13 [PMID: 32319693 DOI: 10.1002/hep.31288]
3 **Bartenschlager R**, Lohmann V. Replication of hepatitis C virus. *J Gen Virol* 2000; **81**: 1631-1648 [PMID: 10859368 DOI: 10.1099/0022-1317-81-7-1631]
4 **Bartenschlager R**, Lohmann V. Novel cell culture systems for the hepatitis C virus. *Antiviral Res* 2001; **52**: 1-17 [PMID: 11530183 DOI: 10.1016/s0166-3542(01)00164-4]
5 **Goutagny N**, Fatmi A, De Ledinghen V, Penin F, Couzigou P, Inchauspé G, Bain C. Evidence of viral replication in circulating dendritic cells during hepatitis C virus infection. *J Infect Dis* 2003; **187**: 1951-1958 [PMID: 12792872 DOI: 10.1086/375350]
6 **Moradpour D**, Penin F, Rice CM. Replication of hepatitis C virus. *Nat Rev Microbiol* 2007; **5**: 453-463 [PMID: 17487147 DOI: 10.1038/nrmicro1645]
7 **Horner SM**. Activation and evasion of antiviral innate immunity by hepatitis C virus. *J Mol Biol* 2014; **426**: 1198-1209 [PMID: 24184198 DOI: 10.1016/j.jmb.2013.10.032]
8 **Jackowiak P**, Kuls K, Budzko L, Mania A, Figlerowicz M. Phylogeny and molecular evolution of the hepatitis C virus. *Infect Genet Evol* 2014; **21**: 67-82 [PMID: 24200590 DOI: 10.1016/j.meegid.2013.10.021]
9 **Preciado MV**, Valva P, Escobar-Gutierrez A, Rahal P, Ruiz-Tovar K, Yamasaki L, Vazquez-Chacon C, Martinez-Guarneros A, Carpio-Pedroza JC, Fonseca-Coronado S, Cruz-Rivera M. Hepatitis C virus molecular evolution: transmission, disease progression and antiviral therapy. *World J Gastroenterol* 2014; **20**: 15992-16013 [PMID: 25473152 DOI: 10.3748/wjg.v20.i43.15992]
10 **Sharma SD**. Hepatitis C virus: molecular biology & current therapeutic options. *Indian J Med Res* 2010; **131**: 17-34 [PMID: 20167971]
11 **Paul D**, Madan V, Bartenschlager R. Hepatitis C virus RNA replication and assembly: living on the fat of the land. *Cell Host Microbe* 2014; **16**: 569-579 [PMID: 25525790 DOI: 10.1016/j.chom.2014.10.008]
12 **Rabaan AA**, Al-Ahmed SH, Bazzi AM, Alfouzan WA, Alsuliman SA, Aldrazi FA, Haque S. Overview of hepatitis C infection, molecular biology, and new treatment. *J Infect Public Health* 2020; **13**: 773-783 [PMID: 31870632 DOI: 10.1016/j.jiph.2019.11.015]
13 **Papatheodoridis G**, Hatzakis A. Public health issues of hepatitis C virus infection. *Best Pract Res Clin Gastroenterol* 2012; **26**: 371-380 [PMID: 23199497 DOI: 10.1016/j.bpg.2012.09.012]
14 **Lemoine M**, Thursz M. Hepatitis C, a global issue: access to care and new therapeutic and preventive approaches in resource-constrained areas. *Semin Liver Dis* 2014; **34**: 89-97 [PMID: 24782262 DOI: 10.1055/s-0034-1371082]
15 **Liang TJ**. Current progress in development of hepatitis C virus vaccines. *Nat Med* 2013; **19**: 869-878 [PMID: 23836237 DOI: 10.1038/nm.3183]
16 **Averhoff FM**, Glass N, Holtzman D. Global burden of hepatitis C: considerations for healthcare providers in the United States. *Clin Infect Dis* 2012; **55** Suppl 1: S10-S15 [PMID: 22715208 DOI: 10.1093/cid/cis361]
17 **Seeff LB**. The history of the "natural history" of hepatitis C (1968-2009). *Liver Int* 2009; **29** Suppl 1: 89-99 [PMID: 19207971 DOI: 10.1111/j.1478-3231.2008.01927.x]
18 **Zeisel MB**, Fafi-Kremer S, Fofana I, Barth H, Stoll-Keller F, Doffoel M, Baumert TF. Neutralizing antibodies in hepatitis C virus infection. *World J Gastroenterol* 2007; **13**: 4824-4830 [PMID: 17828813 DOI: 10.3748/wjg.v13.i36.4824]
19 **Spengler U**, Nattermann J. Immunopathogenesis in hepatitis C virus cirrhosis. *Clin Sci (Lond)* 2007; **112**: 141-155 [PMID: 17199558 DOI: 10.1042/CS20060171]
20 **Zeisel MB**, Fafi-Kremer S, Robinet E, Habersetzer F, Baumert TF, Stoll-Keller F. Adaptive immunity to hepatitis C virus. *Viruses* 2009; **1**: 276-297 [PMID: 21994550 DOI: 10.3390/v1020276]
21 **Boyer N**, Marcellin P. Pathogenesis, diagnosis and management of hepatitis C. *J Hepatol* 2000; **32**: 98-112 [PMID: 10728798 DOI: 10.1016/s0168-8278(00)80419-5]
22 **Farci P**, Strazzera R, Alter HJ, Farci S, Degioannis D, Coiana A, Peddis G, Usai F, Serra G, Chessa L, Diaz G, Balestrieri A, Purcell RH. Early changes in hepatitis C viral quasispecies during interferon therapy predict the therapeutic outcome. *Proc Natl Acad Sci U S A* 2002; **99**: 3081-3086 [PMID: 11880647 DOI: 10.1073/pnas.052712599]
23 **Feeney ER**, Chung RT. Antiviral treatment of hepatitis C. *BMJ* 2014; **348**: g3308 [PMID: 25002352 DOI: 10.1136/bmj.g3308]

24 **McHutchison JG**, Gordon SC, Schiff ER, Shiffman ML, Lee WM, Rustgi VK, Goodman ZD, Ling MH, Cort S, Albrecht JK. Interferon alfa-2b alone or in combination with ribavirin as initial treatment for chronic hepatitis C. Hepatitis Interventional Therapy Group. *N Engl J Med* 1998; **339**: 1485-1492 [PMID: 9819446 DOI: 10.1056/NEJM199811193392101]

25 **Aleman S**, Rahbin N, Weiland O, Davidsdottir L, Hedenstierna M, Rose N, Verbaan H, Stål P, Carlsson T, Norrgren H, Ekbom A, Granath F, Hultcrantz R. A risk for hepatocellular carcinoma persists long-term after sustained virologic response in patients with hepatitis C-associated liver cirrhosis. *Clin Infect Dis* 2013; **57**: 230-236 [PMID: 23616492 DOI: 10.1093/cid/cit234]

26 **Shoukry NH**. Hepatitis C Vaccines, Antibodies, and T Cells. *Front Immunol* 2018; **9**: 1480 [PMID: 30002657 DOI: 10.3389/fimmu.2018.01480]

27 **Heo YA**, Deeks ED. Sofosbuvir/Velpatasvir/Voxilaprevir: A Review in Chronic Hepatitis C. *Drugs* 2018; **78**: 577-587 [PMID: 29546556 DOI: 10.1007/s40265-018-0895-5]

28 **Lee CH**, Kim JH, Lee SW. The role of microRNAs in hepatitis C virus replication and related liver diseases. *J Microbiol* 2014; **52**: 445-451 [PMID: 24871972 DOI: 10.1007/s12275-014-4267-x]

29 **Tamori A**, Murakami Y, Kubo S, Itami S, Uchida-Kobayashi S, Morikawa H, Enomoto M, Takemura S, Tanahashi T, Taguchi YH, Kawada N. MicroRNA expression in hepatocellular carcinoma after the eradication of chronic hepatitis virus C infection using interferon therapy. *Hepatol Res* 2016; **46**: E26-E35 [PMID: 25788219 DOI: 10.1111/hepr.12518]

30 **Xu G**, Zhang Y, Wei J, Jia W, Ge Z, Zhang Z, Liu X. MicroRNA-21 promotes hepatocellular carcinoma HepG2 cell proliferation through repression of mitogen-activated protein kinase-kinase 3. *BMC Cancer* 2013; **13**: 469 [PMID: 24112539 DOI: 10.1186/1471-2407-13-469]

31 **Badami E**, Carcione C, Chinnici CM, Tinnirello R, Conaldi PG, Iannolo G. HCV Interplay With Mir34a: Implications in Hepatocellular Carcinoma. *Front Oncol* 2021; **11**: 803278 [PMID: 35127513 DOI: 10.3389/fonc.2021.803278]

32 **Ghouri YA**, Mian I, Rowe JH. Review of hepatocellular carcinoma: Epidemiology, etiology, and carcinogenesis. *J Carcinog* 2017; **16**: 1 [PMID: 28694740 DOI: 10.4103/jcar.JCar_9_16]

33 **El-Serag HB**. Hepatocellular carcinoma. *N Engl J Med* 2011; **365**: 1118-1127 [PMID: 21992124 DOI: 10.1056/NEJMra1001683]

34 **Sukocheva OA**. Estrogen, estrogen receptors, and hepatocellular carcinoma: Are we there yet? *World J Gastroenterol* 2018; **24**: 1-4 [PMID: 29358876 DOI: 10.3748/wjg.v24.i1.1]

35 **Miceli V**, Cervello M, Azzolina A, Montalto G, Calabrò M, Carruba G. Aromatase and amphiregulin are correspondingly expressed in human liver cancer cells. *Ann N Y Acad Sci* 2009; **1155**: 252-256 [PMID: 19250212 DOI: 10.1111/j.1749-6632.2009.03695.x]

36 **Granata OM**, Cocciadiferro L, Miceli V, Polito LM, Campisi I, Carruba G. Metabolic profiles of androgens in malignant human liver cell lines. *Ann N Y Acad Sci* 2006; **1089**: 262-267 [PMID: 17261773 DOI: 10.1196/annals.1386.028]

37 **Bruix J**, Sherman M; American Association for the Study of Liver Diseases. Management of hepatocellular carcinoma: an update. *Hepatology* 2011; **53**: 1020-1022 [PMID: 21374666 DOI: 10.1002/hep.24199]

38 **Rehermann B**, Nascimbeni M. Immunology of hepatitis B virus and hepatitis C virus infection. *Nat Rev Immunol* 2005; **5**: 215-229 [PMID: 15738952 DOI: 10.1038/nri1573]

39 **El-Serag HB**. Epidemiology of viral hepatitis and hepatocellular carcinoma. *Gastroenterology* 2012; **142**: 1264-1273.e1 [PMID: 22537432 DOI: 10.1053/j.gastro.2011.12.061]

40 **Okuda M**, Li K, Beard MR, Showalter LA, Scholle F, Lemon SM, Weinman SA. Mitochondrial injury, oxidative stress, and antioxidant gene expression are induced by hepatitis C virus core protein. *Gastroenterology* 2002; **122**: 366-375 [PMID: 11832451 DOI: 10.1053/gast.2002.30983]

41 **Lemon SM**, McGivern DR. Is hepatitis C virus carcinogenic? *Gastroenterology* 2012; **142**: 1274-1278 [PMID: 22537433 DOI: 10.1053/j.gastro.2012.01.045]

42 **Axley P**, Ahmed Z, Ravi S, Singal AK. Hepatitis C Virus and Hepatocellular Carcinoma: A Narrative Review. *J Clin Transl Hepatol* 2018; **6**: 79-84 [PMID: 29607308 DOI: 10.14218/JCTH.2017.00067]

43 **O'Brien J**, Hayder H, Zayed Y, Peng C. Overview of MicroRNA Biogenesis, Mechanisms of Actions, and Circulation. *Front Endocrinol (Lausanne)* 2018; **9**: 402 [PMID: 30123182 DOI: 10.3389/fendo.2018.00402]

44 **Xu X**, Tao Y, Shan L, Chen R, Jiang H, Qian Z, Cai F, Ma L, Yu Y. The Role of MicroRNAs in Hepatocellular Carcinoma. *J Cancer* 2018; **9**: 3557-3569 [PMID: 30310513 DOI: 10.7150/jca.26350]

45 **Younossi ZM**, Stepanova M, Nader F, Lam B, Hunt S. The patient's journey with chronic hepatitis C from interferon plus ribavirin to interferon- and ribavirin-free regimens: a study of health-related quality of life. *Aliment Pharmacol Ther* 2015; **42**: 286-295 [PMID: 26059536 DOI: 10.1111/apt.13269]

46 **Lawitz E**, Poordad FF, Pang PS, Hyland RH, Ding X, Mo H, Symonds WT, McHutchison JG, Membreno FE. Sofosbuvir and ledipasvir fixed-dose combination with and without ribavirin in treatment-naive and previously treated patients with genotype 1 hepatitis C virus infection (LONESTAR): an open-label, randomised, phase 2 trial. *Lancet* 2014; **383**: 515-523 [PMID: 24209977 DOI: 10.1016/S0140-6736(13)62121-2]

47 **Bourlière M**, Gordon SC, Flamm SL, Cooper CL, Ramji A, Tong M, Ravendhran N, Vierling JM, Tran TT, Pianko S, Bansal MB, de Lédinghen V, Hyland RH, Stamm LM, Dvory-Sobol H, Svarovskaia E, Zhang J, Huang KC, Subramanian GM, Brainard DM, McHutchison JG, Verna EC, Buggisch P, Landis CS, Younes ZH, Curry MP, Strasser SI, Schiff ER, Reddy KR, Manns MP, Kowdley KV, Zeuzem S; POLARIS-1 and POLARIS-4 Investigators. Sofosbuvir, Velpatasvir, and Voxilaprevir for Previously Treated HCV Infection. *N Engl J Med* 2017; **376**: 2134-2146 [PMID: 28564569 DOI: 10.1056/NEJMoa1613512]

48 **Poordad F**, Hezode C, Trinh R, Kowdley KV, Zeuzem S, Agarwal K, Shiffman ML, Wedemeyer H, Berg T, Yoshida EM, Forns X, Lovell SS, Da Silva-Tillmann B, Collins CA, Campbell AL, Podsadecki T, Bernstein B. ABT-450/r-ombitasvir and dasabuvir with ribavirin for hepatitis C with cirrhosis. *N Engl J Med* 2014; **370**: 1973-1982 [PMID: 24725237 DOI: 10.1056/NEJMoa1402869]

49 **Sarrazin C**, Isakov V, Svarovskaia ES, Hedskog C, Martin R, Chodavarapu K, Brainard DM, Miller MD, Mo H, Molina JM, Sulkowski MS. Late Relapse Versus Hepatitis C Virus Reinfection in Patients With Sustained Virologic Response

After Sofosbuvir-Based Therapies. *Clin Infect Dis* 2017; **64**: 44-52 [PMID: 27737953 DOI: 10.1093/cid/ciw676]

50 **Guarino M**, Morisco F, Valvano MR, Ippolito AM, Librandi M, Andriulli N, Greco M, Amoruso A, Iacobellis A, Niro G, Caporaso N, Andriulli A. Systematic review: interferon-free regimens for patients with HCV-related Child C cirrhosis. *Aliment Pharmacol Ther* 2017; **45**: 1193-1200 [PMID: 28261822 DOI: 10.1111/apt.14017]

51 **Probst A**, Dang T, Bochud M, Egger M, Negro F, Bochud PY. Role of hepatitis C virus genotype 3 in liver fibrosis progression--a systematic review and meta-analysis. *J Viral Hepat* 2011; **18**: 745-759 [PMID: 21992794 DOI: 10.1111/j.1365-2893.2011.01481.x]

52 **Roche B**, Coilly A, Duclos-Vallee JC, Samuel D. The impact of treatment of hepatitis C with DAAs on the occurrence of HCC. *Liver Int* 2018; **38** Suppl 1: 139-145 [PMID: 29427487 DOI: 10.1111/liv.13659]

53 **Frazzoni L**, Sikandar U, Metelli F, Sadalla S, Mazzella G, Bazzoli F, Fuccio L, Azzaroli F. Hepatocellular Carcinoma Recurrence after Hepatitis C Virus Therapy with Direct-Acting Antivirals. A Systematic Review and Meta-Analysis. *J Clin Med* 2021; **10** [PMID: 33920785 DOI: 10.3390/jcm10081694]

54 **Miyasaka A**, Yoshida Y, Suzuki A, Sawara K, Takikawa Y. A Novel Standard for Hepatocellular Carcinoma Screening Intensity After Hepatitis C Elimination. *Int J Gen Med* 2021; **14**: 8935-8943 [PMID: 34866934 DOI: 10.2147/IJGM.S344492]

55 **Conti F**, Buonfiglioli F, Scuteri A, Crespi C, Bolondi L, Caraceni P, Foschi FG, Lenzi M, Mazzella G, Verucchi G, Andreone P, Brillanti S. Early occurrence and recurrence of hepatocellular carcinoma in HCV-related cirrhosis treated with direct-acting antivirals. *J Hepatol* 2016; **65**: 727-733 [PMID: 27349488 DOI: 10.1016/j.jhep.2016.06.015]

56 **European Association for the Study of the Liver**; Clinical Practice Guidelines Panel: Chair; EASL Governing Board representative; Panel members. EASL recommendations on treatment of hepatitis C: Final update of the series☆. *J Hepatol* 2020; **73**: 1170-1218 [PMID: 32956768 DOI: 10.1016/j.jhep.2020.08.018]

57 **Abdelaziz AO**, Nabil MM, Abdelmaksoud AH, Shousha HI, Cordie AA, Hassan EM, Omran DA, Leithy R, Elbaz TM. De-novo versus recurrent hepatocellular carcinoma following direct-acting antiviral therapy for hepatitis C virus. *Eur J Gastroenterol Hepatol* 2018; **30**: 39-43 [PMID: 29064851 DOI: 10.1097/MEG.0000000000001004]

58 **Kuftinec G**, Loehfelm T, Corwin M, Durbin-Johnson B, Candido M, Hluhanich R, Sarkar S. *De novo* hepatocellular carcinoma occurrence in hepatitis C cirrhotics treated with direct-acting antiviral agents. *Hepat Oncol* 2018; **5**: HEP06 [PMID: 30302197 DOI: 10.2217/hep-2018-0003]

59 **Nishijima N**, Nasu A, Kimura T, Osaki Y. Two Cases of Hepatocellular Carcinoma Occurring Immediately after Direct-acting Antiviral Agents against Hepatitis C Virus. *Intern Med* 2019; **58**: 225-231 [PMID: 30146562 DOI: 10.2169/internalmedicine.0712-17]

60 **Tapia-Sosa R**, Hernández-Cabral F, Gabutti A, Páez-Zayas VM, García-Juárez I. Hepatocellular carcinoma associated with direct-acting antiviral therapy for hepatitis C virus: A report of two cases. *Rev Gastroenterol Mex (Engl Ed)* 2021; **86**: 197-199 [PMID: 33187768 DOI: 10.1016/j.rgmx.2020.04.008]

61 **Tayyab GUN**, Rasool S, Nasir B, Rubi G, Abou-Samra AB, Butt AA. Hepatocellular carcinoma occurs frequently and early after treatment in HCV genotype 3 infected persons treated with DAA regimens. *BMC Gastroenterol* 2020; **20**: 93 [PMID: 32252635 DOI: 10.1186/s12876-020-01249-4]

62 **Flisiak R**, Zarębska-Michaluk D, Janczewska E, Łapiński T, Rogalska M, Karpińska E, Mikuła T, Bolewska B, Białkowska J, Flejscher-Stępniewska K, Tomasiewicz K, Karwowska K, Pazgan-Simon M, Piekarska A, Berak H, Tronina O, Garlicki A, Jaroszewicz J. Five-Year Follow-Up of Cured HCV Patients under Real-World Interferon-Free Therapy. *Cancers (Basel)* 2021; **13** [PMID: 34359594 DOI: 10.3390/cancers13153694]

63 **Finkelmeier F**, Dultz G, Peiffer KH, Kronenberger B, Krauss F, Zeuzem S, Sarrazin C, Vermehren J, Waidmann O. Risk of de novo Hepatocellular Carcinoma after HCV Treatment with Direct-Acting Antivirals. *Liver Cancer* 2018; **7**: 190-204 [PMID: 29888208 DOI: 10.1159/000486812]

64 **Gallo A**, Miceli V, Bulati M, Iannolo G, Contino F, Conaldi PG. Viral miRNAs as Active Players and Participants in Tumorigenesis. *Cancers (Basel)* 2020; **12** [PMID: 32033193 DOI: 10.3390/cancers12020358]

65 **Peng Y**, Croce CM. The role of MicroRNAs in human cancer. *Signal Transduct Target Ther* 2016; **1**: 15004 [PMID: 29263891 DOI: 10.1038/sigtrans.2015.4]

66 **Sartorius K**, Makarova J, Sartorius B, An P, Winkler C, Chuturgoon A, Kramvis A. The Regulatory Role of MicroRNA in Hepatitis-B Virus-Associated Hepatocellular Carcinoma (HBV-HCC) Pathogenesis. *Cells* 2019; **8** [PMID: 31771261 DOI: 10.3390/cells8121504]

67 **Bandiera S**, Pfeffer S, Baumert TF, Zeisel MB. miR-122--a key factor and therapeutic target in liver disease. *J Hepatol* 2015; **62**: 448-457 [PMID: 25308172 DOI: 10.1016/j.jhep.2014.10.004]

68 **Coulouarn C**, Factor VM, Andersen JB, Durkin ME, Thorgeirsson SS. Loss of miR-122 expression in liver cancer correlates with suppression of the hepatic phenotype and gain of metastatic properties. *Oncogene* 2009; **28**: 3526-3536 [PMID: 19617899 DOI: 10.1038/onc.2009.211]

69 **Chang J**, Nicolas E, Marks D, Sander C, Lerro A, Buendia MA, Xu C, Mason WS, Moloshok T, Bort R, Zaret KS, Taylor JM. miR-122, a mammalian liver-specific microRNA, is processed from hcr mRNA and may downregulate the high affinity cationic amino acid transporter CAT-1. *RNA Biol* 2004; **1**: 106-113 [PMID: 17179747 DOI: 10.4161/rna.1.2.1066]

70 **Jopling CL**, Yi M, Lancaster AM, Lemon SM, Sarnow P. Modulation of hepatitis C virus RNA abundance by a liver-specific MicroRNA. *Science* 2005; **309**: 1577-1581 [PMID: 16141076 DOI: 10.1126/science.1113329]

71 **Jopling CL**, Schütz S, Sarnow P. Position-dependent function for a tandem microRNA miR-122-binding site located in the hepatitis C virus RNA genome. *Cell Host Microbe* 2008; **4**: 77-85 [PMID: 18621012 DOI: 10.1016/j.chom.2008.05.013]

72 **Jopling CL**. Regulation of hepatitis C virus by microRNA-122. *Biochem Soc Trans* 2008; **36**: 1220-1223 [PMID: 19021529 DOI: 10.1042/BST0361220]

73 **Schult P**, Roth H, Adams RL, Mas C, Imbert L, Orlik C, Ruggieri A, Pyle AM, Lohmann V. microRNA-122 amplifies hepatitis C virus translation by shaping the structure of the internal ribosomal entry site. *Nat Commun* 2018; **9**: 2613 [PMID: 29973597 DOI: 10.1038/s41467-018-05053-3]

74 **Masaki T**, Arend KC, Li Y, Yamane D, McGivern DR, Kato T, Wakita T, Moorman NJ, Lemon SM. miR-122 stimulates

hepatitis C virus RNA synthesis by altering the balance of viral RNAs engaged in replication versus translation. *Cell Host Microbe* 2015; **17**: 217-228 [PMID: 25662750 DOI: 10.1016/j.chom.2014.12.014]

75 **Shimakami T**, Yamane D, Jangra RK, Kempf BJ, Spaniel C, Barton DJ, Lemon SM. Stabilization of hepatitis C virus RNA by an Ago2-miR-122 complex. *Proc Natl Acad Sci U S A* 2012; **109**: 941-946 [PMID: 22215596 DOI: 10.1073/pnas.1112263109]

76 **Luna JM**, Scheel TK, Danino T, Shaw KS, Mele A, Fak JJ, Nishiuchi E, Takacs CN, Catanese MT, de Jong YP, Jacobson IM, Rice CM, Darnell RB. Hepatitis C virus RNA functionally sequesters miR-122. *Cell* 2015; **160**: 1099-1110 [PMID: 25768906 DOI: 10.1016/j.cell.2015.02.025]

77 **Amr KS**, Elmawgoud Atia HA, Elazeem Elbnhawy RA, Ezzat WM. Early diagnostic evaluation of miR-122 and miR-224 as biomarkers for hepatocellular carcinoma. *Genes Dis* 2017; **4**: 215-221 [PMID: 30258925 DOI: 10.1016/j.gendis.2017.10.003]

78 **Li G**, Shen Q, Li C, Li D, Chen J, He M. Identification of circulating MicroRNAs as novel potential biomarkers for hepatocellular carcinoma detection: a systematic review and meta-analysis. *Clin Transl Oncol* 2015; **17**: 684-693 [PMID: 25956842 DOI: 10.1007/s12094-015-1294-y]

79 **Li J**, Jin B, Wang T, Li W, Wang Z, Zhang H, Song Y, Li N. Serum microRNA expression profiling identifies serum biomarkers for HCV-related hepatocellular carcinoma. *Cancer Biomark* 2019; **26**: 501-512 [PMID: 31658041 DOI: 10.3233/CBM-181970]

80 **Cermelli S**, Ruggieri A, Marrero JA, Ioannou GN, Beretta L. Circulating microRNAs in patients with chronic hepatitis C and non-alcoholic fatty liver disease. *PLoS One* 2011; **6**: e23937 [PMID: 21886843 DOI: 10.1371/journal.pone.0023937]

81 **Hermeking H**. p53 enters the microRNA world. *Cancer Cell* 2007; **12**: 414-418 [PMID: 17996645 DOI: 10.1016/j.ccr.2007.10.028]

82 **Mizuguchi Y**, Mishima T, Yokomuro S, Arima Y, Kawahigashi Y, Shigehara K, Kanda T, Yoshida H, Uchida E, Tajiri T, Takizawa T. Sequencing and bioinformatics-based analyses of the microRNA transcriptome in hepatitis B-related hepatocellular carcinoma. *PLoS One* 2011; **6**: e15304 [PMID: 21283620 DOI: 10.1371/journal.pone.0015304]

83 **Smith JL**, Jeng S, McWeeney SK, Hirsch AJ. A MicroRNA Screen Identifies the Wnt Signaling Pathway as a Regulator of the Interferon Response during Flavivirus Infection. *J Virol* 2017; **91** [PMID: 28148804 DOI: 10.1128/JVI.02388-16]

84 **Feili X**, Wu S, Ye W, Tu J, Lou L. MicroRNA-34a-5p inhibits liver fibrosis by regulating TGF-β1/Smad3 pathway in hepatic stellate cells. *Cell Biol Int* 2018; **42**: 1370-1376 [PMID: 29957876 DOI: 10.1002/cbin.11022]

85 **Bihrer V**, Waidmann O, Friedrich-Rust M, Forestier N, Susser S, Haupenthal J, Welker M, Shi Y, Peveling-Oberhag J, Polta A, von Wagner M, Radeke HH, Sarrazin C, Trojan J, Zeuzem S, Kronenberger B, Piiper A. Serum microRNA-21 as marker for necroinflammation in hepatitis C patients with and without hepatocellular carcinoma. *PLoS One* 2011; **6**: e26971 [PMID: 22066022 DOI: 10.1371/journal.pone.0026971]

86 **Shaker OG**, Senousy MA. Serum microRNAs as predictors for liver fibrosis staging in hepatitis C virus-associated chronic liver disease patients. *J Viral Hepat* 2017; **24**: 636-644 [PMID: 28211229 DOI: 10.1111/jvh.12696]

87 **Sodroski C**, Lowey B, Hertz L, Jake Liang T, Li Q. MicroRNA-135a Modulates Hepatitis C Virus Genome Replication through Downregulation of Host Antiviral Factors. *Virol Sin* 2019; **34**: 197-210 [PMID: 30456659 DOI: 10.1007/s12250-018-0055-9]

88 **Bandiera S**, Pernot S, El Saghire H, Durand SC, Thumann C, Crouchet E, Ye T, Fofana I, Oudot MA, Barths J, Schuster C, Pessaux P, Heim MH, Baumert TF, Zeisel MB. Hepatitis C Virus-Induced Upregulation of MicroRNA miR-146a-5p in Hepatocytes Promotes Viral Infection and Deregulates Metabolic Pathways Associated with Liver Disease Pathogenesis. *J Virol* 2016; **90**: 6387-6400 [PMID: 27147737 DOI: 10.1128/JVI.00619-16]

89 **Meng F**, Henson R, Wehbe-Janek H, Ghoshal K, Jacob ST, Patel T. MicroRNA-21 regulates expression of the PTEN tumor suppressor gene in human hepatocellular cancer. *Gastroenterology* 2007; **133**: 647-658 [PMID: 17681183 DOI: 10.1053/j.gastro.2007.05.022]

90 **Cheng M**, Si Y, Niu Y, Liu X, Li X, Zhao J, Jin Q, Yang W. High-throughput profiling of alpha interferon- and interleukin-28B-regulated microRNAs and identification of let-7s with anti-hepatitis C virus activity by targeting IGF2BP1. *J Virol* 2013; **87**: 9707-9718 [PMID: 23824794 DOI: 10.1128/JVI.00802-13]

91 **Jamalidoust M**, Shafaati M, Kalani M, Zare M, Ziyeayan M. MicroRNA let-7b inhibits hepatitis C virus and induces apoptosis in human hepatoma cells. *Mol Biol Rep* 2022; **49**: 1273-1280 [PMID: 34807376 DOI: 10.1007/s11033-021-06955-0]

92 **Murakami Y**, Aly HH, Tajima A, Inoue I, Shimotohno K. Regulation of the hepatitis C virus genome replication by miR-199a. *J Hepatol* 2009; **50**: 453-460 [PMID: 19144437 DOI: 10.1016/j.jhep.2008.06.010]

93 **Pascut D**, Hoang M, Nguyen NNQ, Pratama MY, Tiribelli C. HCV Proteins Modulate the Host Cell miRNA Expression Contributing to Hepatitis C Pathogenesis and Hepatocellular Carcinoma Development. *Cancers (Basel)* 2021; **13** [PMID: 34069740 DOI: 10.3390/cancers13102485]

94 **Xu J**, An P, Winkler CA, Yu Y. Dysregulated microRNAs in Hepatitis B Virus-Related Hepatocellular Carcinoma: Potential as Biomarkers and Therapeutic Targets. *Front Oncol* 2020; **10**: 1271 [PMID: 32850386 DOI: 10.3389/fonc.2020.01271]

95 **Ali HEA**, Abdel Hameed R, Effat H, Ahmed EK, Atef AA, Sharawi SK, Ali M, Abd Elmageed ZY, Abdel Wahab AH. Circulating microRNAs panel as a diagnostic tool for discrimination of HCV-associated hepatocellular carcinoma. *Clin Res Hepatol Gastroenterol* 2017; **41**: e51-e62 [PMID: 28750770 DOI: 10.1016/j.clinre.2017.06.004]

96 **Zekri AN**, Youssef AS, El-Desouky ED, Ahmed OS, Lotfy MM, Nassar AA, Bahnassey AA. Serum microRNA panels as potential biomarkers for early detection of hepatocellular carcinoma on top of HCV infection. *Tumour Biol* 2016; **37**: 12273-12286 [PMID: 27271989 DOI: 10.1007/s13277-016-5097-8]

97 **Wahb AMSE**, El Kassas M, Khamis AK, Elhelbawy M, Elhelbawy N, Habieb MSE. Circulating microRNA 9-3p and serum endocan as potential biomarkers for hepatitis C virus-related hepatocellular carcinoma. *World J Hepatol* 2021; **13**: 1753-1765 [PMID: 34904043 DOI: 10.4254/wjh.v13.i11.1753]

98 **Wang SC**, Li CY, Chang WT, Cheng WC, Yen CH, Tu WY, Lin ZY, Lin CC, Yeh ML, Huang CF, Huang JF, Dai CY, Chuang WL, Chen YL, Yu ML. Exosome-derived differentiation antagonizing non-protein coding RNA with risk of

hepatitis C virus-related hepatocellular carcinoma recurrence. *Liver Int* 2021; **41**: 956-968 [PMID: 33346937 DOI: 10.1111/liv.14772]

99 **Hu Q**, Wang K, Sun X, Li Y, Fu Q, Liang T, Tang G. A redox-sensitive, oligopeptide-guided, self-assembling, and efficiency-enhanced (ROSE) system for functional delivery of microRNA therapeutics for treatment of hepatocellular carcinoma. *Biomaterials* 2016; **104**: 192-200 [PMID: 27459325 DOI: 10.1016/j.biomaterials.2016.07.016]

100 **Wagenaar TR**, Zabludoff S, Ahn SM, Allerson C, Arlt H, Baffa R, Cao H, Davis S, Garcia-Echeverria C, Gaur R, Huang SM, Jiang L, Kim D, Metz-Weidmann C, Pavlicek A, Pollard J, Reeves J, Rocnik JL, Scheidler S, Shi C, Sun F, Tolstykh T, Weber W, Winter C, Yu E, Yu Q, Zheng G, Wiederschain D. Anti-miR-21 Suppresses Hepatocellular Carcinoma Growth *via* Broad Transcriptional Network Deregulation. *Mol Cancer Res* 2015; **13**: 1009-1021 [PMID: 25758165 DOI: 10.1158/1541-7786.MCR-14-0703]

101 **Janssen HL**, Reesink HW, Lawitz EJ, Zeuzem S, Rodriguez-Torres M, Patel K, van der Meer AJ, Patick AK, Chen A, Zhou Y, Persson R, King BD, Kauppinen S, Levin AA, Hodges MR. Treatment of HCV infection by targeting microRNA. *N Engl J Med* 2013; **368**: 1685-1694 [PMID: 23534542 DOI: 10.1056/NEJMoa1209026]

102 **Ottosen S**, Parsley TB, Yang L, Zeh K, van Doorn LJ, van der Veer E, Raney AK, Hodges MR, Patick AK. In vitro antiviral activity and preclinical and clinical resistance profile of miravirsen, a novel anti-hepatitis C virus therapeutic targeting the human factor miR-122. *Antimicrob Agents Chemother* 2015; **59**: 599-608 [PMID: 25385103 DOI: 10.1128/AAC.04220-14]

103 **van der Ree MH**, de Vree JM, Stelma F, Willemse S, van der Valk M, Rietdijk S, Molenkamp R, Schinkel J, van Nuenen AC, Beuers U, Hadi S, Harbers M, van der Veer E, Liu K, Grundy J, Patick AK, Pavlicek A, Blem J, Huang M, Grint P, Neben S, Gibson NW, Kootstra NA, Reesink HW. Safety, tolerability, and antiviral effect of RG-101 in patients with chronic hepatitis C: a phase 1B, double-blind, randomised controlled trial. *Lancet* 2017; **389**: 709-717 [PMID: 28087069 DOI: 10.1016/S0140-6736(16)31715-9]

104 **Liu F**, Shimakami T, Murai K, Shirasaki T, Funaki M, Honda M, Murakami S, Yi M, Tang H, Kaneko S. Efficient Suppression of Hepatitis C Virus Replication by Combination Treatment with miR-122 Antagonism and Direct-acting Antivirals in Cell Culture Systems. *Sci Rep* 2016; **6**: 30939 [PMID: 27484655 DOI: 10.1038/srep30939]

105 **Lou G**, Song X, Yang F, Wu S, Wang J, Chen Z, Liu Y. Exosomes derived from miR-122-modified adipose tissue-derived MSCs increase chemosensitivity of hepatocellular carcinoma. *J Hematol Oncol* 2015; **8**: 122 [PMID: 26514126 DOI: 10.1186/s13045-015-0220-7]

106 **Wei JX**, Lv LH, Wan YL, Cao Y, Li GL, Lin HM, Zhou R, Shang CZ, Cao J, He H, Han QF, Liu PQ, Zhou G, Min J. Vps4A functions as a tumor suppressor by regulating the secretion and uptake of exosomal microRNAs in human hepatoma cells. *Hepatology* 2015; **61**: 1284-1294 [PMID: 25503676 DOI: 10.1002/hep.27660]

107 **Zhang J**, Li D, Zhang R, Peng R, Li J. Delivery of microRNA-21-sponge and pre-microRNA-122 by MS2 virus-like particles to therapeutically target hepatocellular carcinoma cells. *Exp Biol Med (Maywood)* 2021; **246**: 2463-2472 [PMID: 34644206 DOI: 10.1177/15353702211035689]

108 **Gim JA**, Bang SM, Lee YS, Lee Y, Yim SY, Jung YK, Kim H, Kim BH, Kim JH, Seo YS, Yim HJ, Yeon JE, Um SH, Byun KS. Evaluation of the severity of nonalcoholic fatty liver disease through analysis of serum exosomal miRNA expression. *PLoS One* 2021; **16**: e0255822 [PMID: 34358264 DOI: 10.1371/journal.pone.0255822]

109 **Zhang JW**, Pan HT. microRNA profiles of serum exosomes derived from children with nonalcoholic fatty liver. *Genes Genomics* 2021 [PMID: 34390467 DOI: 10.1007/s13258-021-01150-8]

110 **Liu CH**, Ampuero J, Gil-Gómez A, Montero-Vallejo R, Rojas Á, Muñoz-Hernández R, Gallego-Durán R, Romero-Gómez M. miRNAs in patients with non-alcoholic fatty liver disease: A systematic review and meta-analysis. *J Hepatol* 2018; **69**: 1335-1348 [PMID: 30142428 DOI: 10.1016/j.jhep.2018.08.008]

111 **Long XR**, Zhang YJ, Zhang MY, Chen K, Zheng XFS, Wang HY. Identification of an 88-microRNA signature in whole blood for diagnosis of hepatocellular carcinoma and other chronic liver diseases. *Aging (Albany NY)* 2017; **9**: 1565-1584 [PMID: 28657540 DOI: 10.18632/aging.101253]

112 **Caviglia GP**, Abate ML, Gaia S, Petrini E, Bosco C, Olivero A, Rosso C, Ciancio A, Pellicano R, Saracco GM, Rizzetto M, Smedile A. Risk of hepatocellular carcinoma in HBV cirrhotic patients assessed by the combination of miR-122, AFP and PIVKA-II. *Panminerva Med* 2017; **59**: 283-289 [PMID: 28650134 DOI: 10.23736/S0031-0808.17.03353-5]

113 **Sapena V**, Enea M, Torres F, Celsa C, Rios J, Rizzo GEM, Nahon P, Mariño Z, Tateishi R, Minami T, Sangiovanni A, Forns X, Toyoda H, Brillanti S, Conti F, Degasperi E, Yu ML, Tsai PC, Jean K, El Kassas M, Shousha HI, Omar A, Zavaglia C, Nagata H, Nakagawa M, Asahina Y, Singal AG, Murphy C, Kohla M, Masetti C, Dufour JF, Merchante N, Cavalletto L, Chemello LL, Pol S, Crespo J, Calleja JL, Villani R, Serviddio G, Zanetto A, Shalaby S, Russo FP, Bielen R, Trevisani F, Cammà C, Bruix J, Cabibbo G, Reig M. Hepatocellular carcinoma recurrence after direct-acting antiviral therapy: an individual patient data meta-analysis. *Gut* 2022; **71**: 593-604 [PMID: 33741640 DOI: 10.1136/gutjnl-2020-323663]

114 **Ahumada A**, Rayón L, Usón C, Bañares R, Alonso Lopez S. Hepatocellular carcinoma risk after viral response in hepatitis C virus-advanced fibrosis: Who to screen and for how long? *World J Gastroenterol* 2021; **27**: 6737-6749 [PMID: 34790004 DOI: 10.3748/wjg.v27.i40.6737]

World Journal of Gastroenterology

Submit a Manuscript: https://www.f6publishing.com

World J Gastroenterol 2022 June 14; 28(22): 2429-2436

DOI: 10.3748/wjg.v28.i22.2429

ISSN 1007-9327 (print) ISSN 2219-2840 (online)

MINIREVIEWS

Metabolic aspects of hepatitis C virus

Mohamed El-Kassas, Abeer Awad

Specialty type: Gastroenterology and hepatology

Provenance and peer review: Invited article; Externally peer reviewed.

Peer-review model: Single blind

Peer-review report's scientific quality classification

Grade A (Excellent): 0
Grade B (Very good): B, B
Grade C (Good): C
Grade D (Fair): 0
Grade E (Poor): 0

P-Reviewer: Muhammad Irham L, Indonesia; Sahin TT, Turkey; Sirli RLD, Romania

Received: January 6, 2022
Peer-review started: January 6, 2022
First decision: March 9, 2022
Revised: March 18, 2022
Accepted: April 22, 2022
Article in press: April 22, 2022
Published online: June 14, 2022

Mohamed El-Kassas, Department of Endemic Medicine, Faculty of Medicine, Helwan University, Cairo 11795, Egypt

Abeer Awad, Department of Internal Medicine, Faculty of Medicine, Cairo University, Cairo 11566, Egypt

Corresponding author: Mohamed El-Kassas, MD, Full Professor, Department of Endemic Medicine, Faculty of Medicine, Helwan University, Helwan, Cairo 11795, Egypt.
m_elkassas@yahoo.com

Abstract

Many metabolic factors are associated with chronic hepatitis C virus (HCV) infection and can influence the course of the illness and impact the progression of liver and non-liver-related diseases through complex interactions. Several of these factors impact the course of chronic HCV (CHC) and result in the conceptual translation of CHC from a localized to systemic disease. Besides the traditional liver manifestations associated with CHC infection, such as cirrhosis and hepatocellular carcinoma, various extrahepatic disorders are associated with HCV infection, including atherosclerosis, glucose and lipid metabolic disturbances, alterations in the iron metabolic pathways, and lymphoproliferative diseases. The coexistence of metabolic disorders and CHC is known to influence the chronicity and virulence of HCV and accelerates the progression to liver fibrosis and hepatocellular carcinoma. Insulin resistance is one of the key factors that have a tremendous metabolic impact on CHC. Therefore, there is a great need to properly evaluate patients with CHC infection and correct the modifiable metabolic risk factors. Furthermore, patients with HCV who achieved a sustained virological response showed an overall improvement in glucose metabolism, but the exact evidence still requires further studies with long-term follow-up. This review delineates the most recent evidence on the main metabolic factors associated with CHC and the possible influence of chronic HCV infection on metabolic features.

Key Words: Hepatitis C virus; Metabolic factors; Steatosis; Insulin resistance

©The Author(s) 2022. Published by Baishideng Publishing Group Inc. All rights reserved.

Core Tip: Hepatitis C virus (HCV) infection has several metabolic aspects that are largely well understood; as such, HCV is nowadays considered a systemic disease rather than a local disease with different metabolic consequences. Moreover, these metabolic factors may affect the natural history of chronic liver disease and of diseases not related to the liver, which constitute a significant burden on the overall health of the human body, with an increased economic burden to patients, healthcare systems, and society if not adequately addressed and appropriately managed. More studies are needed to evaluate metabolic aspects associated with HCV infection and delineate their effects and the long-term outcome of antiviral therapies.

Citation: El-Kassas M, Awad A. Metabolic aspects of hepatitis C virus. *World J Gastroenterol* 2022; 28(22): 2429-2436
URL: https://www.wjgnet.com/1007-9327/full/v28/i22/2429.htm
DOI: https://dx.doi.org/10.3748/wjg.v28.i22.2429

INTRODUCTION

Hepatitis C virus (HCV) infection is considered one of the most notable causes of chronic liver disease worldwide[1]. Not only does HCV infection confer the risk of developing chronic hepatitis, cirrhosis, and hepatocellular carcinoma (HCC), it also has many extrahepatic manifestations, such as disorders of glucose and lipid metabolism, polyarthritis resembling rheumatoid arthritis, vascular atheromatous disease, mixed cryoglobulinemia, lymphoproliferative diseases, renal disorders, insulin resistance (IR), type 2 diabetes (T2DM), sicca syndrome, and autoimmune disorders[2-4]. Different metabolic aspects of HCV are demonstrated in Figure 1. There are several studies on the effect of metabolic factors on the natural history of patients with chronic HCV (CHC)[5]. The deleterious effects of metabolic complications resulting from HCV infection are mainly related to glucose and lipid metabolism impairments[6].

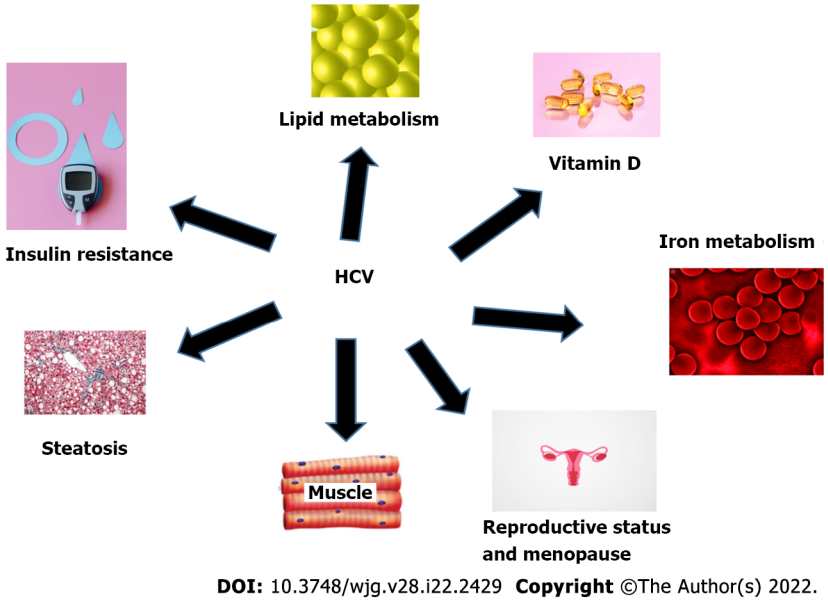
Given that it is a systemic disease, CHC infection could influence the metabolic homeostasis of the host through several complex interactions, even in light of pre-existent metabolic status and genetic background[5]. Several factors can accelerate the disease course from CHC infection to cirrhosis and may impact the likelihood of achieving a sustained virological response (SVR) after receiving antiviral therapy. Among the reported factors are metabolic factors that may change the course of illness in CHC patients and impact the results of antiviral treatments[7], despite the apparent improvement in HCV management results after the introduction of direct-acting antivirals compared with the previous standard of care interferon-based therapy[8,9]. Interestingly, this is not a "one-way street," as CHC infection can have metabolic effects due to its influence on glucose and lipid metabolism, which impacts the host's metabolic homeostasis and may result in its extrahepatic sequelae[10]. The extrahepatic burden of HCV infection exceeds its effect on the liver as it is a significant burden on the overall health of the human body, causing increased economic burden to patients and healthcare systems[11,12].

We have discussed the most recent evidence on the main metabolic factors related to CHC, along with the proposed pathophysiological machineries essential to the correlation between HCV infection and metabolic disorders and the possible influence of CHC infection on metabolic features.

IR

IR is considered a keystone of metabolic syndrome (MS) with increasing incidence worldwide, representing a major cause of morbidity and mortality[13]. As reported in the literature, HCV infection is associated with IR in up to 80% of cases; consequently, the risk of developing T2DM is found to be twice as high as in subjects without HCV[14,15]. There is a high chance of coexistence between MS and CHC owing to many related host factors, such as the presence of visceral obesity; moreover, HCV infection itself is reported to affect glucosidic homeostasis, leading to hepatic and extrahepatic IR[1]. Moreover, CHC is found to increase the risk of developing metabolic diseases with these complications[16]. IR in patients with CHC significantly impacts the severity and progression of chronic liver disease *via* direct and indirect effects by inducing steatosis[17]. Meanwhile, steatosis activates stellate cells *via* collagenous deposition and the generation of lipid peroxides[18], which, in turn, promotes fibrogenesis *via* the direct activation of hepatic stellate cells, tumor necrosis factor-α and connective growth factor production, and ductular reactions induction[19]. In this context, a high prevalence of cirrhosis and non-SVR was observed among patients with diabetes and CHC with an observed lower rate of SVR in patients with IR, not only in interferon-based treatment[7].

Moreover, there is a reported association between IR and the presence of esophageal varices in patients with HCV-related compensated cirrhosis[20]. The potential of insulin to control dynamic components of portal hypertension, such as endothelial nitric oxide and endothelin production, might explain this[21,22]. Not only are IR and DM are more prevalent in the course of HCV infection, but they



DOI: 10.3748/wjg.v28.i22.2429 **Copyright** ©The Author(s) 2022.

Figure 1 Metabolic aspects of hepatitis C virus. HCV: Hepatitis C virus.

also occur post-liver transplantation in patients with CHC infection[23-25]. It's not surprising, then, that T2D is linked to a three-fold increased risk of HCC, with a higher risk seen in patients who have both HCV and T2D; this could be due to the possible molecular mechanisms and intermediaries involved in hepatic carcinogenesis, such as IR and hyperinsulinemia, oxidative stress, and reported cytokine imbalances between proinflammatory and anti-inflammatory cytokines[26]. Several studies have reported the impact of IR and steatosis and both rapid virological response and SVR in patients with CHC treated with antiviral therapy; the plausible explanations that IR and steatosis may affect the response to antiviral therapy and the reasons for the disparities in results might be due to pre-existing variances in metabolic dysfunctions and genetic diversities among the tested groups[27]. other studies reported the efficiency of proper glucose control in HCV infected patients that improve early after antiviral treatment, with benefits that are not restricted to the diabetic patient only furthermore, achievement of SVR by direct-acting antivirals (DAAs) to eliminate HCV improves their glycemic control with a possible reduction on the faster progression of hepatic fibrosis[28,29].

Also, treatment of HCV with DAAs found to improve steatosis, hepatic inflammation, and the nutritional status in most of the studied patients[30-32].

This explains how profound and widespread effects of the impairment of insulin pathways exerted by HCV infection and vice versa.

Consequently, further evidence from long-term follow-up studies is still required to determine if successful eradication of HCV can help to ameliorate IR and improve glycemic control and clinical outcomes in patients with established DM2[33,34].

STEATOSIS

In individuals with CHC, hepatic steatosis is a frequent histological finding, with a frequency of up to 80%, which is higher than that in noninfected individuals; thus, it is considered as a distinct entity in the setting of HCV viral infection with specific clinical and prognostic implications[35,36]. Not only viral factors are responsible for steatosis in patients with CHC, but there are also different common risk factors for steatosis, such as obesity, T2D, alcohol, and dyslipidemia, which are common in the examined cohorts[5]. Specific genotypes of HCV, especially the HCV genotype 3, are more correlated with hepatic steatosis; moreover, HCV has the ability to promote the intracytoplasmic deposition of fat in the liver by enhancing hepatic fatty acid production and decreasing lipid release and breakdown processes, both directly and indirectly[37]. Interestingly, steatosis has also been related to HCV viral load and was found to decrease after SVR was achieved[35]. Many studies reported that steatosis could be a predictor of liver fibrosis in patients with CHC; additionally, in untreated CHC patients, worsening of steatosis may be an independent factor related with the advancement of liver fibrosis. This could be explained by "viral" and "metabolic" steatosis, in which elevated insulin levels and inflammatory mediators on liver stellate cells promote the advancement of fibrosis and liver disease[10,38]. Steatosis may improve and even vanish following effective antiviral treatment with interferon and ribavirin, according to some reports; however, evidence for a similar effect of direct-acting antivirals is currently limited[39,40].

In contrast, cross-sectional and longitudinal studies have shown that despite achieving SVR during CHC treatment, some patients have been found with clinically significant steatosis and fibrosis[41,42]. In this clinical setting, many studies reported the association between steatosis in fatty liver and HCC development in patients with CHC[43].

VISCERAL OBESITY

In the context of steatosis and IR, visceral obesity has been associated with liver fat accumulation in healthy subjects[44,45] and is also related to viral load. Several studies have discussed the association between HCV RNA status and obesity[46].

Plausible explanations include the feasibility of adipose tissue to promote fatty substrates and a proinflammatory status that accelerate HCV replication; moreover, the ability of HCV to interfere with adipocyte function through indirect methods, and increase the inflammatory status or *via* a direct mechanism that helps to increase the colonizing adipocytes and immune cells infiltrating adipose tissue [47]. Further studies are needed to delineate the potential role of obesity in affecting SVR rates after treatment with antiviral agents.

LIPID METABOLISM

HCV infection is involved in disrupted lipoprotein homeostasis *via* impairment of the very low-density lipoprotein levels (LDLs)-releasing pathway, which is one of the main causes of hepatic fat deposition [48]. Several studies have discussed the relationship between lipoproteins and HCV cell cycle[49] and found that patients with CHC have lower serum LDL[50], which are inversely associated with the severity of liver fibrosis[51]; however, this is still a controversial issue. As reported by Nevola *et al*[15], the average LDL levels increased significantly after viral eradication, although there were no effects on triglycerides and high-density lipoprotein[15]. However, it is still debatable whether infections with HCV are linked to an increased risk of cardiovascular events such as carotid atherosclerosis, myocardial infarction, and heart attacks[52]. Notably, studies reported that patients with CHC had more atherosclerosis, as measured by carotid artery plaques and/or intima-media thickness (IMT), than healthy controls; likewise, the frequency of asymptomatic carotid atherosclerosis was higher in patients with CHC than in matched controls[7].

HCV infection could be an independent risk factor for increased carotid IMT[53] and cerebrovascular deaths[54], as reported in many types of study; this may be explained by the proinflammatory mechanisms that underlie liver fibrogenesis and could be systemically activated, leading to the promotion of atherosclerosis[7]. In contrast, several published studies have failed to show the association between atherosclerosis and HCV infection, even with an increased prevalence of IR in patients with HCV infection[55]. Therefore, further studies are needed to validate those data.

THE ROLE OF VITAMIN D

Of 25-Hydroxyvitamin D deficiency has been discovered in patients with CHC, even in those with minimal liver damage[56]; however, some studies reported no association between vitamin D status and fibrosis stage[57]. The role of vitamin D status in treatment regimens for HCV infection is still not well understood, although it is interesting that vitamin D3 supplement augments the response to antiviral therapy in infections with HCV genotypes 1-4, as reported in some randomized clinical trials[58-60].

IRON METABOLISM

It is debatable whether iron promotes or suppresses HCV viral replication, but it is considered a central component for HCV virus replication and translation[10]. In patients with CHC, elevated serum ferritin and the associated increased iron load in liver were more evident and were considered a significant predictor for hepatic fibrosis progression[61,62]. Hepcidin is a peptide hormone with an essential role in regulating iron levels under homeostatic states. Accordingly, iron metabolism alterations in CHC are related to the decreased hepcidin concentrations, although the exact underlying mechanisms remain unclear[10,63].

Still, there is an urgent need for a better understanding of how HCV impacts iron metabolism and if it could be implemented to control disease advancement[10].

SKELETAL MUSCLE

It is well known that sarcopenia, increased intramyocellular lipid accumulation, myosteatosis, and reduced muscle mass are all connected with CHC infection, especially in the advanced stages[64,65]. A high incidence rate of sarcopenia was reported, up to 70%, in patients with cirrhosis. Because of anabolic resistance, current nutritional supplementation methods have not been successful in reversing sarcopenia[66,67]. The association between CHC infection of the liver and muscle loss is well documented[68,69]. High body mass index, IR, diabetes, hepatic steatosis, increased inflammation, increased oxidative stress, lipotoxicity, and multiple factors involved in muscle depletion all are considered as independent risk factors that predispose patients with CHC to skeletal muscle disorders [70-73].

REPRODUCTIVE STATUS AND MENOPAUSE

Several studies performed on pregnant women with HCV infection reported reduced necro-inflammatory activity, and the rate of fibrosis advancement in CHC is nearly twice as fast in males compared to females[74,75]. Another report stated that long-term hormonal replacement therapy could prevent accelerated liver fibrosis in menopausal women with CHC[76]. Noteworthy improvement in sexual dysfunction was reported in males and females after HCV treatment with direct-acting antivirals[77].

CONCLUSION

The eradication of HCV remains an essential target for preventing the progression of liver disease and improving or preventing HCV-related metabolic extrahepatic manifestations that have an essential role in morbidity and mortality, affecting the patient's health-related quality of life.

FOOTNOTES

Author contributions: El-Kassas M conceptualized the idea, revised and edited the final manuscript; Awad A drafted the manuscript; all authors have read and approved the final manuscript.

Conflict-of-interest statement: The authors declare that they have no conflict of interest.

Open-Access: This article is an open-access article that was selected by an in-house editor and fully peer-reviewed by external reviewers. It is distributed in accordance with the Creative Commons Attribution NonCommercial (CC BY-NC 4.0) license, which permits others to distribute, remix, adapt, build upon this work non-commercially, and license their derivative works on different terms, provided the original work is properly cited and the use is non-commercial. See: https://creativecommons.org/Licenses/by-nc/4.0/

Country/Territory of origin: Egypt

ORCID number: Mohamed El-Kassas 0000-0002-3396-6894; Abeer Awad 0000-0001-9945-9767.

Corresponding Author's Membership in Professional Societies: Egyptian Association for Research and Training in Hepatogastroenterology, No. 01.

S-Editor: Fan JR
L-Editor: A
P-Editor: Fan JR

REFERENCES

1 **Lavanchy D**. The global burden of hepatitis C. *Liver Int* 2009; **29** Suppl 1: 74-81 [PMID: 19207969 DOI: 10.1111/j.1478-3231.2008.01934.x]
2 **Qasim SF**, Jami A, Imran P, Mushtaque R, Khan RN. Frequency of Metabolic Syndrome in Chronic Hepatitis C Patients: Findings From a Lower Middle Income Country. *Cureus* 2020; **12**: e11975 [PMID: 33425547 DOI: 10.7759/cureus.11975]
3 **Fabrizi F**, Donato FM, Messa P. Hepatitis C and Its Metabolic Complications in Kidney Disease. *Ann Hepatol* 2017; **16**: 851-861 [PMID: 29055921 DOI: 10.5604/01.3001.0010.5275]
4 **Younossi Z**, Park H, Henry L, Adeyemi A, Stepanova M. Extrahepatic Manifestations of Hepatitis C: A Meta-analysis of Prevalence, Quality of Life, and Economic Burden. *Gastroenterology* 2016; **150**: 1599-1608 [PMID: 26924097 DOI: 10.1053/j.gastro.2016.02.039]

5 **Macaluso FS**, Maida M, Minissale MG, Li Vigni T, Attardo S, Orlando E, Petta S. Metabolic factors and chronic hepatitis C: a complex interplay. *Biomed Res Int* 2013; **2013**: 564645 [PMID: 23956991 DOI: 10.1155/2013/564645]

6 **Chang ML**. Metabolic alterations and hepatitis C: From bench to bedside. *World J Gastroenterol* 2016; **22**: 1461-1476 [PMID: 26819514 DOI: 10.3748/wjg.v22.i4.1461]

7 **Petta S**. Insulin resistance and diabetes mellitus in patients with chronic hepatitis C: spectators or actors? *Dig Liver Dis* 2012; **44**: 359-360 [PMID: 22418268 DOI: 10.1016/j.dld.2012.02.001]

8 **Esmat G**, El Kassas M, Hassany M, Gamil M, El Raziky M. Optimizing treatment for HCV genotype 4: PEG-IFN alfa 2a vs. PEG-IFN alfa 2b; the debate continues. *Liver Int* 2014; **34** Suppl 1: 24-28 [PMID: 24373075 DOI: 10.1111/liv.12397]

9 **El Kassas M**, Elbaz T, Hafez E, Esmat G. Safety of direct antiviral agents in the management of hepatitis C. *Expert Opin Drug Saf* 2016; **15**: 1643-1652 [PMID: 27661100 DOI: 10.1080/14740338.2017.1240781]

10 **Bugianesi E**, Salamone F, Negro F. The interaction of metabolic factors with HCV infection: does it matter? *J Hepatol* 2012; **56** Suppl 1: S56-S65 [PMID: 22300466 DOI: 10.1016/S0168-8278(12)60007-5]

11 **Deltenre P**, Louvet A, Lemoine M, Mourad A, Fartoux L, Moreno C, Henrion J, Mathurin P, Serfaty L. Impact of insulin resistance on sustained response in HCV patients treated with pegylated interferon and ribavirin: a meta-analysis. *J Hepatol* 2011; **55**: 1187-1194 [PMID: 21703195 DOI: 10.1016/j.jhep.2011.03.010]

12 **Chaudhari R**, Fouda S, Sainu A, Pappachan JM. Metabolic complications of hepatitis C virus infection. *World J Gastroenterol* 2021; **27**: 1267-1282 [PMID: 33833481 DOI: 10.3748/wjg.v27.i13.1267]

13 **Ziolkowska S**, Binienda A, Jabłkowski M, Szemraj J, Czarny P. The Interplay between Insulin Resistance, Inflammation, Oxidative Stress, Base Excision Repair and Metabolic Syndrome in Nonalcoholic Fatty Liver Disease. *Int J Mol Sci* 2021; **22** [PMID: 34681787 DOI: 10.3390/ijms222011128]

14 **Adinolfi LE**, Jacobson I, Bondin M, Cacoub P. Expert opinion on managing chronic HCV infection in patients with type 2 diabetes mellitus. *Antivir Ther* 2018; **23**: 11-21 [PMID: 30451154 DOI: 10.3851/IMP3255]

15 **Nevola R**, Rinaldi L, Zeni L, Sasso FC, Pafundi PC, Guerrera B, Marrone A, Giordano M, Adinolfi LE. Metabolic and renal changes in patients with chronic hepatitis C infection after hepatitis C virus clearance by direct-acting antivirals. *JGH Open* 2020; **4**: 713-721 [PMID: 32782961 DOI: 10.1002/jgh3.12324]

16 **Kierepa A**, Witkowska A, Kaczmarek M, Książek K, Mikuła-Pietrasik J, Żeromski J, Kowala-Piaskowska A, Mozer-Lisewska I. Impact of chronic HCV treatment on quality of life of patients with metabolic disorders in context of immunological disturbances. *Sci Rep* 2020; **10**: 10388 [PMID: 32587314 DOI: 10.1038/s41598-020-67296-9]

17 **Stepanova M**, Rafiq N, Younossi ZM. Components of metabolic syndrome are independent predictors of mortality in patients with chronic liver disease: a population-based study. *Gut* 2010; **59**: 1410-1415 [PMID: 20660697 DOI: 10.1136/gut.2010.213553]

18 **Browning JD**, Horton JD. Molecular mediators of hepatic steatosis and liver injury. *J Clin Invest* 2004; **114**: 147-152 [PMID: 15254578 DOI: 10.1172/JCI22422]

19 **Bridle KR**, Li L, O'Neill R, Britton RS, Bacon BR. Coordinate activation of intracellular signaling pathways by insulin-like growth factor-1 and platelet-derived growth factor in rat hepatic stellate cells. *J Lab Clin Med* 2006; **147**: 234-241 [PMID: 16697771 DOI: 10.1016/j.lab.2005.12.009]

20 **Wang XX**, Song ZZ. Insulin resistance is a risk factor for esophageal varices in hepatitis C virus cirrhosis. *Hepatology* 2009; **49**: 1775; author reply 1776 [PMID: 19402107 DOI: 10.1002/hep.22892]

21 **Vincent MA**, Montagnani M, Quon MJ. Molecular and physiologic actions of insulin related to production of nitric oxide in vascular endothelium. *Curr Diab Rep* 2003; **3**: 279-288 [PMID: 12866989 DOI: 10.1007/s11892-003-0018-9]

22 **Iwakiri Y**, Groszmann RJ. Vascular endothelial dysfunction in cirrhosis. *J Hepatol* 2007; **46**: 927-934 [PMID: 17391799 DOI: 10.1016/j.jhep.2007.02.006]

23 **Zimmet P**. The burden of type 2 diabetes: are we doing enough? *Diabetes Metab* 2003; **29**: 6S9-618 [PMID: 14502096 DOI: 10.1016/s1262-3636(03)72783-9]

24 **Wang CS**, Wang ST, Yao WJ, Chang TT, Chou P. Hepatitis C virus infection and the development of type 2 diabetes in a community-based longitudinal study. *Am J Epidemiol* 2007; **166**: 196-203 [PMID: 17496314 DOI: 10.1093/aje/kwm061]

25 **Algarem N**, Sholkamy A, Alshazly M, Daoud A. New-onset diabetes and hypertension as complications of liver transplantation. *Transplant Proc* 2014; **46**: 870-872 [PMID: 24767368 DOI: 10.1016/j.transproceed.2013.12.007]

26 **Petta S**, Craxì A. Hepatocellular carcinoma and non-alcoholic fatty liver disease: from a clinical to a molecular association. *Curr Pharm Des* 2010; **16**: 741-752 [PMID: 20388084 DOI: 10.2174/138161210790883787]

27 **Petta S**, Rosso C, Leung R, Abate ML, Booth D, Salomone F, Gambino R, Rizzetto M, Caviglia P, Smedile A, Grimaudo S, Cammà C, Craxì A, George J, Bugianesi E. Effects of IL28B rs12979860 CC genotype on metabolic profile and sustained virologic response in patients with genotype 1 chronic hepatitis C. *Clin Gastroenterol Hepatol* 2013; **11**: 311-7.e1 [PMID: 23220171 DOI: 10.1016/j.cgh.2012.11.022]

28 **Adinolfi LE**, Rinaldi L, Marrone A, Giordano M. The effect of sustained virological response by direct-acting antivirals on insulin resistance and diabetes mellitus in patients with chronic hepatitis C. *Expert Rev Anti Infect Ther* 2018; **16**: 595-597 [PMID: 30047799 DOI: 10.1080/14787210.2018.1505500]

29 **Gualerzi A**, Bellan M, Smirne C, Tran Minh M, Rigamonti C, Burlone ME, Bonometti R, Bianco S, Re A, Favretto S, Bellomo G, Minisini R, Carnevale Schianca GP, Pirisi M. Improvement of insulin sensitivity in diabetic and non diabetic patients with chronic hepatitis C treated with direct antiviral agents. *PLoS One* 2018; **13**: e0209216 [PMID: 30571711 DOI: 10.1371/journal.pone.0209216]

30 **Saldarriaga OA**, Dye B, Pham J, Wanninger TG, Millian D, Kueht M, Freiberg B, Utay N, Stevenson HL. Comparison of liver biopsies before and after direct-acting antiviral therapy for hepatitis C and correlation with clinical outcome. *Sci Rep* 2021; **11**: 14506 [PMID: 34267267 DOI: 10.1038/s41598-021-93881-7]

31 **Shimada M**, Iwase H, Hirashima N, Ryuge N, Urata N. Nutritional status and liver steatosis after direct-acting antiviral treatment for chronic hepatitis C virus infection. *J Transl Sci* 2017; 3 [DOI: 10.15761/jts.1000194]

32 **Kawagishi N**, Suda G, Nakamura A, Kimura M, Maehara O, Suzuki K, Ohara M, Izumi T, Umemura M, Nakai M, Sho T, Natsuizaka M, Morikawa K, Ogawa K, Kudo Y, Nishida M, Miyoshi H, Sakamoto N. Liver steatosis and dyslipidemia after

HCV eradication by direct acting antiviral agents are synergistic risks of atherosclerosis. *PLoS One* 2018; **13**: e0209615 [PMID: 30576386 DOI: 10.1371/journal.pone.0209615]

33 **Ciancio A**, Bosio R, Bo S, Pellegrini M, Sacco M, Vogliotti E, Fassio G, Bianco Mauthe Degerfeld AGF, Gallo M, Giordanino C, Terzi di Bergamo L, Ribaldone D, Bugianesi E, Smedile A, Rizzetto M, Saracco GM. Significant improvement of glycemic control in diabetic patients with HCV infection responding to direct-acting antiviral agents. *J Med Virol* 2018; **90**: 320-327 [PMID: 28960353 DOI: 10.1002/jmv.24954]

34 **Estefan S**, Brandão-Melo CE, Dos Santos Silva CM, Gomes DCK, Cardoso P, Costa MHS. Metabolic Evaluation in Patients With Hepatitis C Treated With Direct Antiviral Agents. *Front Med (Lausanne)* 2021; **8**: 631600 [PMID: 34136497 DOI: 10.3389/fmed.2021.631600]

35 **Adinolfi LE**, Gambardella M, Andreana A, Tripodi MF, Utili R, Ruggiero G. Steatosis accelerates the progression of liver damage of chronic hepatitis C patients and correlates with specific HCV genotype and visceral obesity. *Hepatology* 2001; **33**: 1358-1364 [PMID: 11391523 DOI: 10.1053/jhep.2001.24432]

36 **Lonardo A**, Loria P, Adinolfi LE, Carulli N, Ruggiero G. Hepatitis C and steatosis: a reappraisal. *J Viral Hepat* 2006; **13**: 73-80 [PMID: 16436124 DOI: 10.1111/j.1365-2893.2005.00669.x]

37 **Negro F**. Mechanisms and significance of liver steatosis in hepatitis C virus infection. *World J Gastroenterol* 2006; **12**: 6756-6765 [PMID: 17106922 DOI: 10.3748/wjg.v12.i42.6756]

38 **Castéra L**, Hézode C, Roudot-Thoraval F, Bastie A, Zafrani ES, Pawlotsky JM, Dhumeaux D. Worsening of steatosis is an independent factor of fibrosis progression in untreated patients with chronic hepatitis C and paired liver biopsies. *Gut* 2003; **52**: 288-292 [PMID: 12524415 DOI: 10.1136/gut.52.2.288]

39 **Mihm S**. Hepatitis C virus, diabetes and steatosis: clinical evidence in favor of a linkage and role of genotypes. *Dig Dis* 2010; **28**: 280-284 [PMID: 20460924 DOI: 10.1159/000282103]

40 **Esmat G**, El Akel W, Metwally M, Soliman A, Doss W, Hamid MA, Kamal M, Zalata K, Khattab H, El-Kassas M, Esmat M, Hasan A, El-Raziky M. Improvement of steatosis after interferon therapy in HCV genotype 4 is related to weight loss. *Indian J Gastroenterol* 2009; **28**: 45-48 [PMID: 19696987 DOI: 10.1007/s12664-009-0016-1]

41 **Persico M**, Iolascon A. Steatosis as a co-factor in chronic liver diseases. *World J Gastroenterol* 2010; **16**: 1171-1176 [PMID: 20222159 DOI: 10.3748/wjg.v16.i10.1171]

42 **Younossi ZM**, Stepanova M, Nader F, Younossi Z, Elsheikh E. Associations of chronic hepatitis C with metabolic and cardiac outcomes. *Aliment Pharmacol Ther* 2013; **37**: 647-652 [PMID: 23384408 DOI: 10.1111/apt.12234]

43 **Pekow JR**, Bhan AK, Zheng H, Chung RT. Hepatic steatosis is associated with increased frequency of hepatocellular carcinoma in patients with hepatitis C-related cirrhosis. *Cancer* 2007; **109**: 2490-2496 [PMID: 17487861 DOI: 10.1002/cncr.22701]

44 **González-Reimers E**, Castellano-Higuera A, Alemán-Valls R, Alvarez-Argüelles H, de la Vega-Prieto MJ, Abreu-González P, López-Prieto J, Santolaria-Fernández F, Valladares-Parrilla F. Relation between body fat and liver fat accumulation and cytokine pattern in non-alcoholic patients with chronic HCV infection. *Ann Nutr Metab* 2009; **55**: 351-357 [PMID: 19851063 DOI: 10.1159/000252351]

45 **Leandro G**, Mangia A, Hui J, Fabris P, Rubbia-Brandt L, Colloredo G, Adinolfi LE, Asselah T, Jonsson JR, Smedile A, Terrault N, Pazienza V, Giordani MT, Giostra E, Sonzogni A, Ruggiero G, Marcellin P, Powell EE, George J, Negro F; HCV Meta-Analysis (on) Individual Patients' Data Study Group. Relationship between steatosis, inflammation, and fibrosis in chronic hepatitis C: a meta-analysis of individual patient data. *Gastroenterology* 2006; **130**: 1636-1642 [PMID: 16697727 DOI: 10.1053/j.gastro.2006.03.014]

46 **Chen W**, Wong T, Tomlinson G, Krahn M, Heathcote EJ. Prevalence and predictors of obesity among individuals with positive hepatitis C antibody in a tertiary referral clinic. *J Hepatol* 2008; **49**: 711-717 [PMID: 18619698 DOI: 10.1016/j.jhep.2008.05.013]

47 **Everhart JE**, Lok AS, Kim HY, Morgan TR, Lindsay KL, Chung RT, Bonkovsky HL, Ghany MG; HALT-C Trial Group. Weight-related effects on disease progression in the hepatitis C antiviral long-term treatment against cirrhosis trial. *Gastroenterology* 2009; **137**: 549-557 [PMID: 19445938 DOI: 10.1053/j.gastro.2009.05.007]

48 **Yoshimura T**, Oppenheim JJ. Chemerin reveals its chimeric nature. *J Exp Med* 2008; **205**: 2187-2190 [PMID: 18809717 DOI: 10.1084/jem.20081736]

49 **André P**, Perlemuter G, Budkowska A, Bréchot C, Lotteau V. Hepatitis C virus particles and lipoprotein metabolism. *Semin Liver Dis* 2005; **25**: 93-104 [PMID: 15732001 DOI: 10.1055/s-2005-864785]

50 **Kanda T**, Moriyama M. Direct-acting antiviral agents against hepatitis C virus and lipid metabolism. *World J Gastroenterol* 2017; **23**: 5645-5649 [PMID: 28883690 DOI: 10.3748/wjg.v23.i31.5645]

51 **Lange CM**, von Wagner M, Bojunga J, Berg T, Farnik H, Hassler A, Sarrazin C, Herrmann E, Zeuzem S. Serum lipids in European chronic HCV genotype 1 patients during and after treatment with pegylated interferon-α-2a and ribavirin. *Eur J Gastroenterol Hepatol* 2010; **22**: 1303-1307 [PMID: 20729742 DOI: 10.1097/MEG.0b013e32833de92c]

52 **Butt AA**, Xiaoqiang W, Budoff M, Leaf D, Kuller LH, Justice AC. Hepatitis C virus infection and the risk of coronary disease. *Clin Infect Dis* 2009; **49**: 225-232 [PMID: 19508169 DOI: 10.1086/599371]

53 **Marzouk D**, Sass J, Bakr I, El Hosseiny M, Abdel-Hamid M, Rekacewicz C, Chaturvedi N, Mohamed MK, Fontanet A. Metabolic and cardiovascular risk profiles and hepatitis C virus infection in rural Egypt. *Gut* 2007; **56**: 1105-1110 [PMID: 16956918 DOI: 10.1136/gut.2006.091983]

54 **Lee MH**, Yang HI, Wang CH, Jen CL, Yeh SH, Liu CJ, You SL, Chen WJ, Chen CJ. Hepatitis C virus infection and increased risk of cerebrovascular disease. *Stroke* 2010; **41**: 2894-2900 [PMID: 20966408 DOI: 10.1161/STROKEAHA.110.598136]

55 **Miyajima I**, Kawaguchi T, Fukami A, Nagao Y, Adachi H, Sasaki S, Imaizumi T, Sata M. Chronic HCV infection was associated with severe insulin resistance and mild atherosclerosis: a population-based study in an HCV hyperendemic area. *J Gastroenterol* 2013; **48**: 93-100 [PMID: 22678465 DOI: 10.1007/s00535-012-0610-3]

56 **Petta S**, Grimaudo S, Marco VD, Scazzone C, Macaluso FS, Cammà C, Cabibi D, Pipitone R, Craxì A. Association of vitamin D serum levels and its common genetic determinants, with severity of liver fibrosis in genotype 1 chronic hepatitis C patients. *J Viral Hepat* 2013; **20**: 486-493 [PMID: 23730842 DOI: 10.1111/jvh.12072]

57 **Esmat G**, El Raziky M, Elsharkawy A, Sabry D, Hassany M, Ahmed A, Assem N, El Kassas M, Doss W. Impact of vitamin D supplementation on sustained virological response in chronic hepatitis C genotype 4 patients treated by pegylated interferon/ribavirin. *J Interferon Cytokine Res* 2015; **35**: 49-54 [PMID: 25061714 DOI: 10.1089/jir.2014.0060]

58 **Kitson MT**, Dore GJ, George J, Button P, McCaughan GW, Crawford DH, Sievert W, Weltman MD, Cheng WS, Roberts SK. Vitamin D status does not predict sustained virologic response or fibrosis stage in chronic hepatitis C genotype 1 infection. *J Hepatol* 2013; **58**: 467-472 [DOI: 10.1016/j.jhep.2012.11.017]

59 **Abu-Mouch S**, Fireman Z, Jarchovsky J, Zeina AR, Assy N. Vitamin D supplementation improves sustained virologic response in chronic hepatitis C (genotype 1)-naïve patients. *World J Gastroenterol* 2011; **17**: 5184-5190 [PMID: 22215943 DOI: 10.3748/wjg.v17.i47.5184]

60 **Nimer A**, Mouch A. Vitamin D improves viral response in hepatitis C genotype 2-3 naïve patients. *World J Gastroenterol* 2012; **18**: 800-805 [PMID: 22371640 DOI: 10.3748/wjg.v18.i8.800]

61 **Chang ML**, Hu JH, Yen CH, Chen KH, Kuo CJ, Lin MS, Lee CH, Chen SC, Chien RN. Evolution of ferritin levels in hepatitis C patients treated with antivirals. *Sci Rep* 2020; **10**: 19744 [PMID: 33184464 DOI: 10.1038/s41598-020-76871-z]

62 **Zou DM**, Sun WL. Relationship between Hepatitis C Virus Infection and Iron Overload. *Chin Med J (Engl)* 2017; **130**: 866-871 [PMID: 28345552 DOI: 10.4103/0366-6999.202737]

63 **Fujita N**, Sugimoto R, Takeo M, Urawa N, Mifuji R, Tanaka H, Kobayashi Y, Iwasa M, Watanabe S, Adachi Y, Kaito M. Hepcidin expression in the liver: relatively low level in patients with chronic hepatitis C. *Mol Med* 2007; **13**: 97-104 [PMID: 17515961 DOI: 10.2119/2006-00057.Fujita]

64 **Petta S**, Ciminnisi S, Di Marco V, Cabibi D, Cammà C, Licata A, Marchesini G, Craxì A. Sarcopenia is associated with severe liver fibrosis in patients with non-alcoholic fatty liver disease. *Aliment Pharmacol Ther* 2017; **45**: 510-518 [PMID: 28028821 DOI: 10.1111/apt.13889]

65 **Gowda C**, Compher C, Amorosa VK, Lo Re V 3rd. Association between chronic hepatitis C virus infection and low muscle mass in US adults. *J Viral Hepat* 2014; **21**: 938-943 [PMID: 24989435 DOI: 10.1111/jvh.12273]

66 **Dasarathy S**. Cause and management of muscle wasting in chronic liver disease. *Curr Opin Gastroenterol* 2016; **32**: 159-165 [PMID: 26974417 DOI: 10.1097/MOG.0000000000000261]

67 **Gumucio JP**, Qasawa AH, Ferrara PJ, Malik AN, Funai K, McDonagh B, Mendias CL. Reduced mitochondrial lipid oxidation leads to fat accumulation in myosteatosis. *FASEB J* 2019; **33**: 7863-7881 [PMID: 30939247 DOI: 10.1096/fj.201802457RR]

68 **Fernández-Mincone T**, Contreras-Briceño F, Espinosa-Ramírez M, García-Valdés P, López-Fuenzalida A, Riquelme A, Arab JP, Cabrera D, Arrese M, Barrera F. Nonalcoholic fatty liver disease and sarcopenia: pathophysiological connections and therapeutic implications. *Expert Rev Gastroenterol Hepatol* 2020; **14**: 1141-1157 [PMID: 32811209 DOI: 10.1080/17474124.2020.1810563]

69 **Cruz-Jentoft AJ**, Sayer AA. Sarcopenia. *Lancet* 2019; **393**: 2636-2646 [PMID: 31171417 DOI: 10.1016/S0140-6736(19)31138-9]

70 **Zhai Y**, Xiao Q. The Common Mechanisms of Sarcopenia and NAFLD. *Biomed Res Int* 2017; **2017**: 6297651 [PMID: 29387723 DOI: 10.1155/2017/6297651]

71 **Hsu CS**, Kao JH. Sarcopenia and chronic liver diseases. *Expert Rev Gastroenterol Hepatol* 2018; **12**: 1229-1244 [PMID: 30791794 DOI: 10.1080/17474124.2018.1534586]

72 **Hiraoka A**, Michitaka K, Ueki H, Kaneto M, Aibiki T, Okudaira T, Kawakami T, Yamago H, Suga Y, Tomida H, Miyamoto Y, Azemoto N, Mori K, Miyata H, Tsubouchi E, Ninomiya T, Hirooka M, Abe M, Matsuura B, Hiasa Y. Sarcopenia and two types of presarcopenia in Japanese patients with chronic liver disease. *Eur J Gastroenterol Hepatol* 2016; **28**: 940-947 [PMID: 27232361 DOI: 10.1097/MEG.0000000000000661]

73 **Kalafateli M**, Konstantakis C, Thomopoulos K, Triantos C. Impact of muscle wasting on survival in patients with liver cirrhosis. *World J Gastroenterol* 2015; **21**: 7357-7361 [PMID: 26139982 DOI: 10.3748/wjg.v21.i24.7357]

74 **Poynard T**, Bedossa P, Opolon P. Natural history of liver fibrosis progression in patients with chronic hepatitis C. The OBSVIRC, METAVIR, CLINIVIR, and DOSVIRC groups. *Lancet* 1997; **349**: 825-832 [PMID: 9121257 DOI: 10.1016/s0140-6736(96)07642-8]

75 **Deuffic-Burban S**, Poynard T, Valleron AJ. Quantification of fibrosis progression in patients with chronic hepatitis C using a Markov model. *J Viral Hepat* 2002; **9**: 114-122 [DOI: 10.1046/j.1365-2893.2002.00340.x]

76 **Di Martino V**, Lebray P, Myers RP, Pannier E, Paradis V, Charlotte F, Moussalli J, Thabut D, Buffet C, Poynard T. Progression of liver fibrosis in women infected with hepatitis C: long-term benefit of estrogen exposure. *Hepatology* 2004; **40**: 1426-1433 [PMID: 15565616 DOI: 10.1002/hep.20463]

77 **El Kassas M**, Salah E, Gad A, Hosny A. Improvement of sexual dysfunction in patients after treatment of hepatitis C virus using directly acting antivirals. *Curr Med Res Opin* 2021; **37**: 967-972 [PMID: 33688780 DOI: 10.1080/03007995.2021.1901677]

World Journal of Gastroenterology

Submit a Manuscript: https://www.f6publishing.com

World J Gastroenterol 2022 June 14; 28(22): 2437-2456

DOI: 10.3748/wjg.v28.i22.2437

ISSN 1007-9327 (print) ISSN 2219-2840 (online)

ORIGINAL ARTICLE

Basic Study

18β-glycyrrhetinic acid regulates mitochondrial ribosomal protein L35-associated apoptosis signaling pathways to inhibit proliferation of gastric carcinoma cells

Ling Yuan, Yi Yang, Xia Li, Xin Zhou, Yu-Hua Du, Wen-Jing Liu, Lei Zhang, Lei Yu, Ting-Ting Ma, Jia-Xin Li, Yan Chen, Yi Nan

Specialty type: Gastroenterology and hepatology

Provenance and peer review: Unsolicited article; Externally peer reviewed.

Peer-review model: Single blind

Peer-review report's scientific quality classification

Grade A (Excellent): 0
Grade B (Very good): B, B
Grade C (Good): C
Grade D (Fair): 0
Grade E (Poor): 0

P-Reviewer: Matsuoka T, Japan; Nakajima N, Japan; Vorobjova T, Estonia

Received: December 8, 2021
Peer-review started: December 8, 2021
First decision: March 11, 2022
Revised: March 24, 2022
Accepted: April 27, 2022
Article in press: April 27, 2022
Published online: June 14, 2022

Ling Yuan, Yi Yang, Xia Li, Yu-Hua Du, Ting-Ting Ma, Jia-Xin Li, College of Pharmacy, Ningxia Medical University, Yinchuan 750004, Ningxia Hui Autonomous Region, China

Xin Zhou, Yan Chen, Yi Nan, Traditional Chinese Medicine College, Ningxia Medical University, Yinchuan 750004, Ningxia Hui Autonomous Region, China

Wen-Jing Liu, Lei Zhang, Yan Chen, Yi Nan, Key Laboratory of Hui Ethnic Medicine Modernization of Ministry of Education, Ningxia Medical University, Yinchuan 750004, Ningxia Hui Autonomous Region, China

Lei Yu, Department of Infectious Diseases, The Fourth Hospital of Harbin Medical University, Harbin 150001, Heilongjiang Province, China

Corresponding author: Yi Nan, MD, PhD, Professor, Key Laboratory of Hui Ethnic Medicine Modernization of Ministry of Education, Ningxia Medical University, No. 1160 Shengli Street, Yinchuan 750004, Ningxia Hui Autonomous Region, China. 20080011@nxmu.edu.cn

Abstract

BACKGROUND

Gastric carcinoma (GC) is a common gastrointestinal malignancy worldwide. Based on the cancer-related mortality, the current prevention and treatment strategies for GC still show poor clinical results. Therefore, it is important to find effective drug treatment targets.

AIM

To explore the mechanism by which 18β-glycyrrhetinic acid (18β-GRA) regulates mitochondrial ribosomal protein L35 (MRPL35) related signal proteins to inhibit the proliferation of GC cells.

METHODS

Cell counting kit-8 assay was used to detect the effects of 18β-GRA on the survival rate of human normal gastric mucosal cell line GES-1 and the proliferation of GC cell lines MGC80-3 and BGC-823. The apoptosis and cell cycle were assessed by flow cytometry. Cell invasion and migration were evaluated by Transwell assay, and cell scratch test was used to detect cell migration. Furthermore, a tumor

model was established by hypodermic injection of 2.5 × 10^6 BGC-823 cells at the selected positions of BALB/c nude mice to determine the effect of 18β-GRA on GC cell proliferation, and quantitative reverse transcription-polymerase chain reaction (qRT-PCR) was used to detect *MRPL35* expression in the engrafted tumors in mice. We used the term tandem mass tag (TMT) labeling combined with liquid chromatography–tandem mass spectrometry to screen for differentially expressed proteins (DEPs) extracted from GC cells and control cells after 18β-GRA intervention. A detailed bioinformatics analysis of these DEPs was performed, including Gene Ontology annotation and enrichment analysis, Kyoto Encyclopedia of Genes and Genomes pathway enrichment analysis, and so on. Moreover, STRING database (https://string-db.org/) was used to predict protein-protein interaction (PPI) relationships and Western blot was used to detect the expression of proteins of interest in GC cells.

RESULTS

The results indicated that 18β-GRA could inhibit the proliferation of GC cells in a dose- and time-dependent manner. It could induce GC cell apoptosis and arrest the cell cycle at G0/G1 phase. The proportion of cells arrested at S phase decreased with the increase of 18-GRA dose, and the migration and invasiveness of GC cells were inhibited. The results of animal experiments showed that 18β-GRA could inhibit tumor formation in BALB/c nude mice, and qRT-PCR results showed that *MRPL35* expression level was significantly reduced in the engrafted tumors in mice. Using TMT technology, 609 DEPs, among which 335 were up-regulated and 274 were down-regulated, were identified in 18β-GRA intervention compared with control. We found that the intervention of 18β-GRA in GC cells involved many important biological processes and signaling pathways, such as cellular processes, biological regulation, and TP53 signaling pathway. Notably, after the drug intervention, MRPL35 expression was significantly down-regulated (P = 0.000247), TP53 expression was up-regulated (P = 0.02676), and BCL2L1 was down-regulated (P = 0.01699). Combined with the Retrieval of Interacting Genes/Proteins database, we analyzed the relationship between MRPL35, TP53, and BCL2L1 signaling proteins, and we found that COPS5, BAX, and BAD proteins can form a PPI network with MRPL35, TP53, and BCL2L1. Western blot analysis confirmed the intervention effect of 18β-GRA on GC cells, MRPL35, TP53, and BCL2L1 showed dose-dependent up/down-regulation, and the expression of COPS5, BAX, and BAD also increased/decreased with the change of 18β-GRA concentration.

CONCLUSION

18β-GRA can inhibit the proliferation of GC cells by regulating MRPL35, COPS5, TP53, BCL2L1, BAX, and BAD.

Key Words: Gastric carcinoma; 18β-glycyrrhetinic acid; Mitochondrial ribosomal protein L35; Proliferation; Invasion; Apoptosis

©The Author(s) 2022. Published by Baishideng Publishing Group Inc. All rights reserved.

Core Tip: 18β-glycyrrhetinic acid (18β-GRA) is a pentacyclic triterpene derivative extracted from the natural medicine licorice. Our results showed that 18β-GRA could inhibit gastric carcinoma (GC) cell proliferation, migration, invasion, and tumor formation, induce GC cell apoptosis, and arrest the cell cycle. Tandem mass tag analysis revealed that the expression of mitochondrial ribosomal protein L35 (MRPL35) was significantly decreased after 18β-GRA intervention in GC cells, which was confirmed by Western blot results. These data indicate that 18β-GRA inhibits the proliferation/migration and promotes apoptosis of GC cells by down-regulating MRPL35 expression, suggesting that MRPL35 is a therapeutic target for GC.

Citation: Yuan L, Yang Y, Li X, Zhou X, Du YH, Liu WJ, Zhang L, Yu L, Ma TT, Li JX, Chen Y, Nan Y. 18β-glycyrrhetinic acid regulates mitochondrial ribosomal protein L35-associated apoptosis signaling pathways to inhibit proliferation of gastric carcinoma cells. *World J Gastroenterol* 2022; 28(22): 2437-2456
URL: https://www.wjgnet.com/1007-9327/full/v28/i22/2437.htm
DOI: https://dx.doi.org/10.3748/wjg.v28.i22.2437

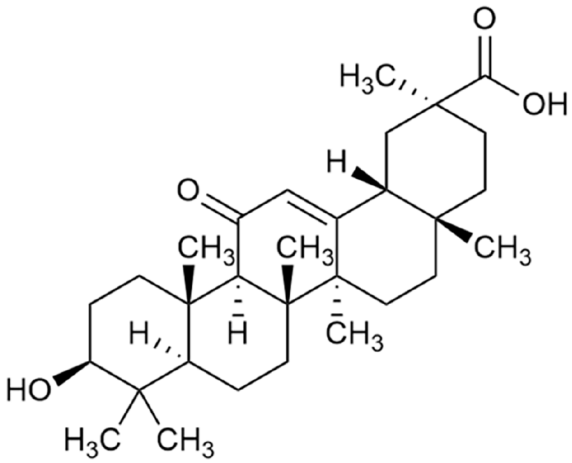
INTRODUCTION

Gastric carcinoma (GC) is among the most common cancers as well as one of the most common causes of cancer-related mortality worldwide. Based on the Global Cancer Observatory (GLOBOCAN) database, GC ranks fifth in the incidence and fourth in the mortality among various types of cancers worldwide, after lung cancer, colorectal cancer, and liver cancer, and there would be more than one million new cases per year since 2020 by the World Health Organization predicting[1]. The current treatment of GC is mainly based on surgery, chemotherapy, and radiotherapy[2]. Most patients with early and advanced GC can be treated by surgery, but the treatment effect is very poor for patients with advanced GC and metastasis[3]. Although chemotherapy and radiotherapy are effective, they have severe side effects, such as hair loss and gastrointestinal reactions, leading to low compliance. Therefore, it is critical to find an effective therapeutic target for GC.

18β-glycyrrhetinic acid (18β-GRA) is a pentacyclic triterpene derivative extracted from the natural medicine licorice (Figure 1). It has significant anti-inflammatory[4], anti-oxidant, anti-bacterial, and anti-proliferative effects[5]. Recent studies have shown that 18β-GRA has reliable anticancer effects on human malignant tumors, such as lung cancer[6], breast cancer[7], colon cancer, and GC. Huang *et al*[6] found that 18β-GRA inhibited the extracellular signal-regulated kinase (ERK)/cyclic adenosine monophosphate response element binding protein (CREB) pathway by inhibiting thromboxane synthase (TxAS), thereby reducing the cell proliferation of non-small cell lung cancer (NSCLC) cells[6]. 18β-GRA showed potent inhibitory effects on human breast carcinoma MCF-7 cell proliferation in a concentration- and time-dependent manner, without affecting immortalized normal mammary epithelial cell line. 18β-GRA induced apoptosis in MCF-7 cells *via* caspase activation and modulation of the protein kinase B (Akt)/phosphorylated forkhead box O3 (FOXO3a) pathway[7]. *In vivo* and *in vitro*, 18β-GRA inhibited the proliferation, invasion, and migration of colorectal cancer cells, and had no obvious inhibitory effect on normal cells. It prolonged the survival of tumor-bearing mice by promoting apoptosis of colorectal cancer cells. Moreover, 18β-GRA inhibited the initiation and progression of gastric tumors by ameliorating the inflammatory microenvironment through down-regulation of cyclooxygenase-2 (COX-2) expression and by inhibiting Wnt-1 expression through the up-regulation of tumor suppressor miR-149-3p[8]. 18β-GRA inhibited the migration and invasion of SGC-7901 cells *via* the reactive oxygen species (ROS)/protein kinase C-α/ERK signaling pathway, and suppressed MMP-2 and 9 activities in SGC-7901 cells in a dose-dependent manner[9]. Toll-like receptor 2 (TLR2) mRNA and protein expression levels were elevated in the GC cell lines and human GC tissues. Overexpression of TLR2 was correlated with high histological grade. However, the expression of TLR2 was found to be down-regulated by 18β-GRA through a dynamic process of DNA methylation regulation. GRA pretreatment inhibited TLR2-activated GC cell proliferation, energy metabolism, and carcinogenesis [10]. In general, 18β-GRA showed an excellent inhibitory effect on GC, and its pharmacological mechanism is still worth exploring.

The human mitochondrial ribosomal protein (*MRP*) gene family consists of 30 members encoding small mitochondrial ribosomal subunits and 50 members encoding large subunits. All MRPs encoded by nuclear genes are important for the mitochondrial function and protein synthesis, which are involved in ribosomal protein transcription and translation, and mitochondrial oxidative phosphorylation. MRPs can regulate cellular functions outside mitochondria, such as cell proliferation, apoptosis, protein biosynthesis, and signal transduction. In NSCLC, overexpression of MRPL15 was associated with a poor prognosis[11]. MRPL15 plays a role in ovarian cancer through cell cycle, DNA repair, and the mTOR1 signaling pathway, suggesting that MRPL15 may be a prognostic indicator and therapeutic target for ovarian cancer[12]. Hao *et al*[13] found that MRPL42 expression was tested to be up-regulated in glioma tissues compared with normal tissues. The proliferation of glioma cells was largely blunted by silencing MRPL42. The results suggested that MRPL42 silencing resulted in increased distribution of cell cycle at G and G/M phases, while the S-phase cells decreased. Taken together, *MRPL42* is a novel oncogene in glioma[13]. In conclusion, these findings suggest that MRPs should play a crucial role in regulating the development of various malignant tumors.

Mitochondrial ribosomal protein L35 (MRPL35) is a 25 ku protein encoded by the *MRPL35* gene located on chromosome 2p11.2, which is a mitotic component of the central protuberance of the mitochondria. It is a member of the large subunit family of MRPs[14] and plays an important role in the assembly of cytochrome C oxidase complex (COX) as the specific component of mitochondrial ribosomes[15]. The expression of MRPL35 rises in the tissues of colorectal carcinoma (CRC), compared with the matched cancer-adjacent tissues. *In vitro*, down-regulation of MRPL35 resulted in increased production of ROS along with DNA damage, reduction of cell proliferation, G/M arrest, apoptosis, and autophagy induction[16]. Silencing MRPL35 suppresses the proliferation of esophageal cancer TE-1 cells, down-regulates MMP-2, and promotes cell apoptosis, after transfection of human esophageal cancer cells with lentivirus[17]. Our previous study found that the expression of MRPL35 was significantly up-regulated in GC, and the survival analysis showed that the up-regulated MRPL35 was associated with a poor survival rate in GC. Knockdown of MRPL35 was showed to inhibit proliferation of GC cells by regulating BCL-XL, PICK1, and AGR2 which are apoptosis-related proteins[18].



DOI: 10.3748/wjg.v28.i22.2437 **Copyright** ©The Author(s) 2022.

Figure 1 Structure of 18β-glycyrrhetinic acid. The molecular formula for 18β-glycyrrhetinic acid is C30H46O4, and the molecular weight is 470.68.

In order to more significantly explore the mechanism of 18β-GRA, we detected the expression abundance of MRPL35 in AGS, SGC-7901, MGC80-3, and BGC-823 cell lines by quantitative reverse transcription-polymerase chain reaction (qRT-PCR), and the results showed that MRPL35 expression levels in MGC80-3 and BGC-823 cell lines were similar, so we did experiment on these two cell lines (Supplementary Figure 1).

In this study, we focused on examining the effects of 18β-GRA intervention on GC cell function *in vitro* and tumor formation in nude mice *in vivo*. Tandem mass tag (TMT) analysis and STRING database prediction were used to investigate the molecular mechanism, and Western blot was used to verify the expression changes of related proteins. An important conclusion is that 18β-GRA inhibits GC cell proliferation/migration and promotes apoptosis by interfering with the expression of MRPL35-related signaling proteins, which may contribute to the development of effective therapies. These results suggest that MRPL35 may be a potential therapeutic target for the inhibition of GC by 18β-GRA.

MATERIALS AND METHODS

Cell culture and animals

Human gastric mucosal epithelial cells GES-1 (Cat. No. BNCC353464, BNCC, China) were cultured in DMEM (Cat. No. C11995500BT, Gibco, United States) containing 100 mL/L fetal bovine serum (FBS; Cat. No. SH30256.01, Gibco) and penicillin and streptomycin (Cat. No. p1400-100, Gibco). GC cell lines BGC-823 (Cat. No. GCC-ST0008CS, GeneChem, China) and MGC80-3 (Cat. No. GCC-ST0004CS, GeneChem) were cultured in RPMI-1640 (Cat. No. C11875500BT, Gibco) containing 100 mL/L FBS and penicillin and streptomycin. The culture flasks were placed in an incubator at a constant temperature of 37 ℃, with 50 mL/L CO_2 and saturated humidity. BALB/c nude mice (male, weighing 18-22 g) of specific pathogen-free (SPF) grade were purchased from the Animal Experiment Center of Ningxia Medical University. All animals were fed standard laboratory feed and water in 12 h light/dark cycle environment. The animal protocols (IACUC-NYLAC-2019-083) were approved by the Institutional Animal Care and Use Committee of Ningxia Medical University.

Cell proliferation assessed by cell counting kit-8 assay

Normal gastric mucosal epithelial GSE-1 cells were cultured in an incubator at 37 ℃ and 50 mL/L CO_2, collected, and inoculated in a 96-well plate at a density of 4 × 10^4 cells/mL. On the next day, the cells were treated with different concentrations of 18β-GRA (purity > 97%; Cat. No. G10105-10G, Sigma, United States) for 24 h, 48 h, and 72 h. Thereafter, 10 μL of cell counting kit-8 (CCK-8) (Cat. No. KGA317, KeyGEN, China) was added to each well and incubated for 2 h. Optical density (OD) was detected at 450 nm. All experiments were repeated three times.

MGC80-3 and BGC-823 cells were cultured in an incubator at 37 ℃ and 50 mL/L CO_2. Cells in the logarithmic growth phase were inoculated in 96-well plates at an adjusted concentration of 4 × 10^4 cells/mL. After 24 h, cells were treated with different concentrations of 18β-GRA for 24 h, 48 h, and 72 h. Thereafter, 10 μL of CCK-8 was added to each well and incubated for 2 h. OD was detected at 450 nm. All experiments were independently repeated at least three times.

Cell cycle and apoptosis detection via flow cytometry analysis

MGC80-3 and BGC-823 cells were inoculated in 6-well plates. The cells were treated with 18-GRA for 48

h on the second day. Then the cells were collected and centrifuged at 3000 r/min for 5 min. Annexin V-FITC apoptosis detection kit (Cat. No. KGA107, KeyGEN) was used for staining and apoptosis was detected by flow cytometry after 15 min at room temperature in dark. Cells from each group were collected, washed with pre-cooled PBS, and fixed overnight in 750 mL/L ethanol. The cells were stained with cell cycle kit and incubated at room temperature for 30-60 min in the dark. The cell cycle was detected by flow cytometry. All experiments were repeated three times.

Transwell assay

First, 8 μmol/L pore size Transwell (Cat. No. Costar.3422, Corning, United States) with and without Matrigel were placed into a 24-well plate. MGC80-3 and BGC-823 cells were inoculated into the upper chambers at 2 × 10^5 cells/mL. After adding 750 μL complete medium in the lower chambers and culturing at 37 ℃ for 24 h, the medium was replaced with medium containing different concentrations of 18β-GRA and cultured for 48 h. The cells were gently wiped off with cotton swabs and fixed with 4% paraformaldehyde for 5 min, stained with crystal violet for 5 min, and washed with PBS. Thereafter, the cells were observed with an inverted microscope and photographed to count and compare the differences in the cell invasion between groups. The number of migrated cells was counted, and the average value was used for statistical analysis. All experiments were repeated three times.

Wound scratch assay

GC cells MGC80-3 and BGC-823 were inoculated on 6-well plates. After the cells were attached, a scratch was made with a 200 μL pipette tip. The cells were washed with PBS. Then medium containing 18-GRA was added, and the cells were cultured in a 50 mL/L CO_2 incubator at 37 ℃ for 0 h and 48 h, and photographed with a microscope to calculate the cell migration rate of each group. All experiments were repeated three times.

Tumor formation experiment in BALB/c nude mice

Four-week-old male BALB/c nude mice (18-22 g) of SPF grade were purchased from the Animal Experiment Center of Ningxia Medical University. All animals were housed in polypropylene cages at a temperature of 22 ± 1 ℃ and 50 ± 5% humidity, in a 12:12 h light/dark cycle, and provided free access to standard laboratory chow and water. There were six BALB/c nude mice in each group. A microsyringe was used to extract 200 μL of BGC-823 cell suspension in logarithmic growth phase at a concentration of 2.5 × 10^6 cells/mL, which was subcutaneously injected into the right back of each nude mouse. The 18β-GRA group was intragastrically administered with 18β-GRA at 50 mg/kg[10,19] every other day, and the control group was similarly administered with equal volume of normal saline. Intragastric gavage administration was carried out in conscious animals. The tumor volume was measured daily using the formula $V = \frac{w^2 \times L}{2}$ (V, volume; W, width; L, length). All animals were euthanized by exposure to 1000 mL/L CO_2 for 5 min for tissue collection. The animal protocols were approved by the Institutional Animal Care and Use Committee of Ningxia Medical University.

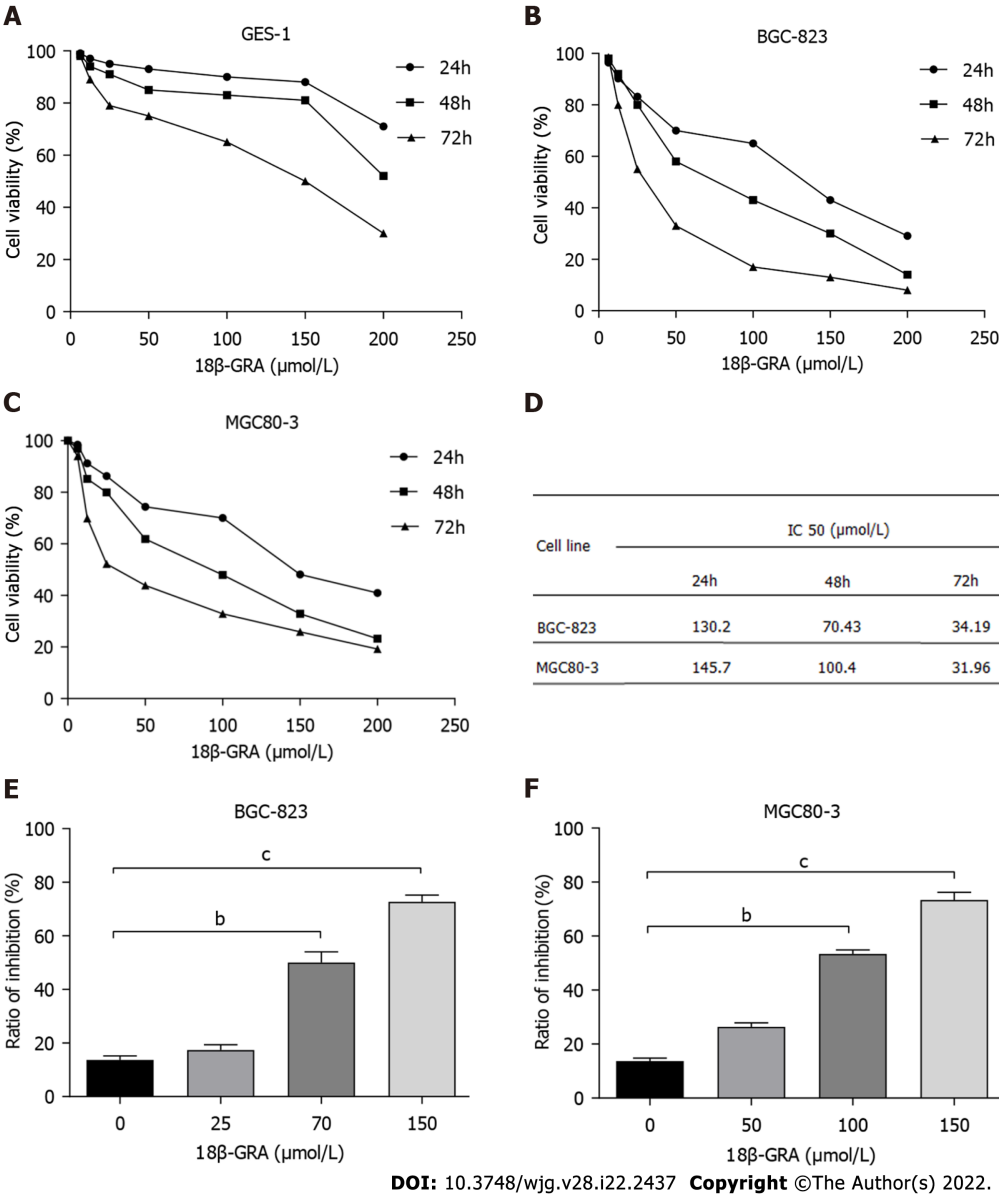
qRT-PCR

Total RNA of the transplanted tumor tissue from mice was extracted using Trizol reagent (Cat. No. DP424, Tiagen Biochemical Technology, China), and PrimeScript RT reagent Kit with gDNA Eraser was used to synthesize first-strand cDNA from total RNA. qRT-PCR was used to detect by using BlazeTaq SYBR Green qPCR Mix 2.0 (Cat. No. QP031-S, GeneCopoeia, United States) according to the manufacturer's instructions. The primers used are as follows: *MRPL35*: Forward, 5′-TTGGCATCTTCAACCTACCGC-3′ and reverse, 5′-GGAGGAAACAACTGGTGTCTGA-3′; *GAPDH*: Forward, 5′-TGACTTCAACAGCGACACCCA-3′ and reverse, 5′-CACCCTGTTGCTGTAGCCAAA-3′. All experiments were repeated three times.

Protein extraction, trypsin digestion, and TMT proteomic labeling

SDT buffer was added into the control and 18β-GRA-treated GC cells. After being boiled for 15 min, the protein content was quantified with the BCA Protein Assay Kit (Cat. No. P0012, Beyotime, China), 20 μg proteins were taken, and 6 × loading buffer (Cat. No. P0015F, Beyotime) was added. After being boiled for 5 min, the proteins were separated by 12.5% sodium dodecyl sulfate-polyacrylamide gel electrophoresis (SDS-PAGE) and protein bands were visualized by Coomassie Blue R-250 staining.

The method of filter-aided sample preparation digestion was performed by adding dithiothreitol (DTT; Cat. No. 43819-5G, Sigma) to a 200 μg protein solution to a final concentration of 100 mmol/L, boiling reduced protein lysate for 5 min, and alkylation with 100 μL iodoacetamide buffer (IAA) for 15 min at room temperature protected from light. Then, 100 μL of 0.1 M tetraethyl ammonium bromide (TEAB; Cat. No. SE252676/90114, Thermo Fisher, United States) solution was added, and the mixture was centrifuged for 15 min. After 40 μL of trypsin buffer (4 μg trypsin in 40 μL of 0.1 M TEAB solution) was added, the filtrate was collected overnight at 37 ℃ to obtain peptide segments. One hundred microliters of peptide mixture was then labeled using TMT 6plex Isobaric Mass Tag Labeling kit



DOI: 10.3748/wjg.v28.i22.2437 **Copyright** ©The Author(s) 2022.

Figure 2 Effect of 18β-glycyrrhetinic acid on survival rate of GES-1 cells and proliferation of MGC80-3 and BGC-823 cells detected by CCK-8 method. A: GES-1 cells; B: BGC-823 cells; C: MGC80-3 cells; D: IC_{50} values of 18β-glycyrrhetinic acid (18β-GRA) for BGC-823 cells and MGC80-3 cells after 24 h, 48 h, and 72 h; E and F: Inhibition rate of 18β-GRA acid at different concentrations on BGC-823 and MGC80-3 cell proliferation. All analyses were repeated three times. The data is represented as the mean ± SD. $^{a}P < 0.05$; $^{b}P < 0.01$; $^{c}P < 0.001$. 18β-GRA: 18β-glycyrrhetinic acid.

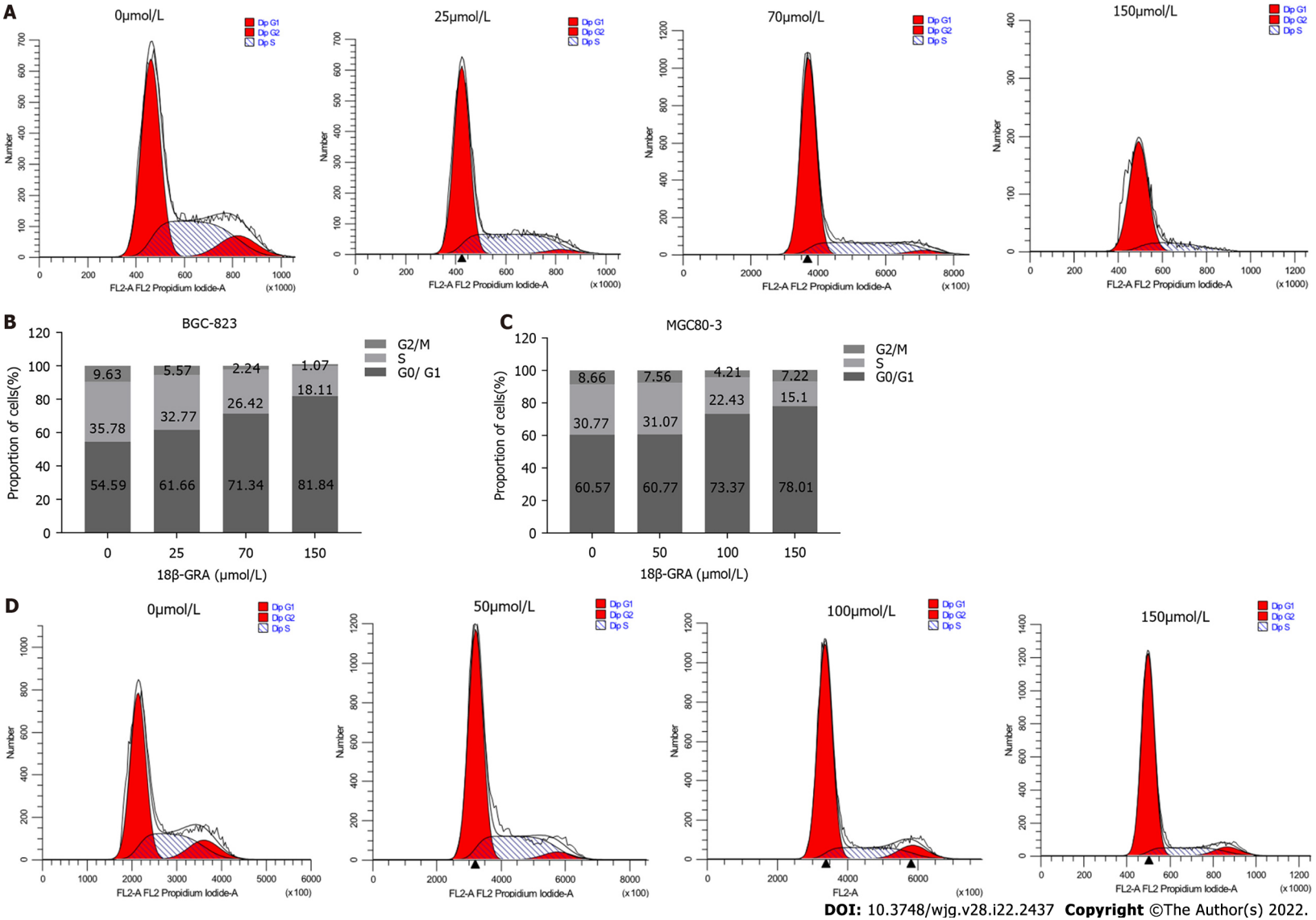
(Thermo Fisher, United States) according to the manufacturer's instructions.

HPLC fractionation, liquid chromatography–tandem mass spectrometry analysis, and data analysis

The labeled peptides of the two groups were fractionated with Agilent 1260 Infinity HPLC system. The peptide mixture was diluted with buffer A (10 mmol/L HCOONH4, 5%/85% ACN, pH 10.0). Liquid chromatography–tandem mass spectrometry (LC-MS/MS) analysis was performed on a Q Exactive Plus mass spectrometer (Thermo Fisher, United States), and peptides were detected on MS at a resolution of 70000 with a scan range of 350-1800 m/z and with automatic gain control of 5e4. All the original data files obtained were processed with Proteome Discoverer 2.2 (Thermo Fisher, United States) software. Proteins that met the expression fold change > 1.2 and *P* value (Student's *t* test) < 0.05 were considered to be differentially expressed proteins (DEPs).

Bioinformatics analysis

Blast2GO and InterProScan software are used to analyze the cellular processes of DEPs, the biological processes involved, and the corresponding molecular functions. The Fisher's exact test was employed to test Gene Ontology (GO) annotation/Kyoto Encyclopedia of Genes and Genomes (KEGG) pathway/InterPro domain enrichment analysis. Fisher's exact test was used to test enrichment pathways; InterPro was used to determine enrichment domains. We used WoLFPSOR to locate and



DOI: 10.3748/wjg.v28.i22.2437 **Copyright** ©The Author(s) 2022.

Figure 3 Effects of different concentrations of 18β-glycyrrhetinic acid on gastric carcinoma cell cycle. A and B: Cell cycle and statistical graph of BGC-823 cells; C and D: Cell cycle and statistical graph of MGC80-3 cells. All analyses were repeated three times. The data is represented as the mean ± SD. $^{a}P < 0.05$; $^{b}P < 0.01$; $^{c}P < 0.001$. 18β-GRA: 18β-glycyrrhetinic acid.

predict DEPs. Matplotlib was used to classify samples and protein expression levels at the same time to form hierarchical cluster heat maps. A protein-protein interaction (PPI) network incorporating identified target proteins was prepared with the STRING database, using a score > 0.4 as the significance threshold for identified interactions.

Western blot analysis

The cells were collected after drug intervention. Whole cell lysates were obtained by gentle lysis (Cat. No. KGP250, KeyGEN). Protein quantitation was performed by the BCA method (Cat. No. KGPBCA, KeyGEN). The protein was separated by SDS-PAGE, and the protein was transferred to PVDF membranes by wet-transfer method. Thereafter, the membrane was incubated with 50 mL/L skim milk powder at room temperature for 1 h. Later on, the membranes were incubated with the primary antibodies, including anti-MRPL35 (Cat. No. YT5669, Immunoway; 1:2000), anti-TP53 (Cat. No. YM3052, Immunoway; 1:2000), anti-BCL2L1 (Cat. No. YT0477, Immunoway; 1:2000), anti-BAX (Cat. No. YM3619, Immunoway; 1:500), anti-COPS5 (Cat. No. ab124720, Abcam; 1:2000), anti-BAD (Cat. No. 9292, Cell Signaling Technology; 1:1000), and anti-β-tubulin (Cat. No. YM3030, Immunoway; 1:10000). Then, the membranes were washed with TBST and incubated with anti-mouse/rabbit IgG antibody (Cat. No. S001 S004, TDYBio; 1:10000) at 37 ℃ for 1 h. After washing, the proteins were detected with an ECL detection system. ImageJ software was used to measure the band intensity.

Statistical analysis

The statistical methods of this study were reviewed by Li-Qun Wang from Department of Epidemiology, Department of Medical Statistics, Institute of Public Health and Management, Ningxia Medical University. All analyses were performed using GraphPad Prism 7.0. All the data are expressed as the mean ± SE. Statistical significance was analyzed using one-way ANOVA. $P < 0.05$ was considered statistically significant.

RESULTS

18β-GRA inhibits GC cell proliferation

CCK-8 assay was used to evaluate the effect of 18-GRA on the survival rate of normal gastric mucosal GES-1 cells. The results showed that 12.5-150 μmol/L of 18β-GRA had little effect on the survival rate of GES-1 cells at 24 h and 48 h. However, when the concentration of 18β-GRA was greater than 150 μmol/L, the survival rate of GES-1 cells was significantly decreased (Figure 2A).

CCK-8 results showed that 6.25-200 μmol/L of 18β-GRA inhibited the proliferation of BGC-823 and MGC80-3 cells in a time- and dose-dependent manner (Figure 2B and C). After the intervention of 18-GRA in BGC-823 and MGC80-3 cells for 24 h, 48 h, and 72 h, the 50% inhibitory concentration (IC50) of cells was calculated and is shown in Figure 2D. Based on the above results, 25 μmol/L (low), 70 μmol/L (medium), and 150 μmol/L (high) were determined for BGC-823 cells, and 50 μmol/L (low), 100 μmol/L (medium), and 150 μmol/L (high) were determined for MGC80-3 cells. Compared with the 0 μmol/L (control), the different concentrations of 18-GRA inhibited the proliferation of BGC-823 and MGC80-3 cells ($P < 0.01$) (Figure 2E and F).

18β-GRA arrests GC cell cycle

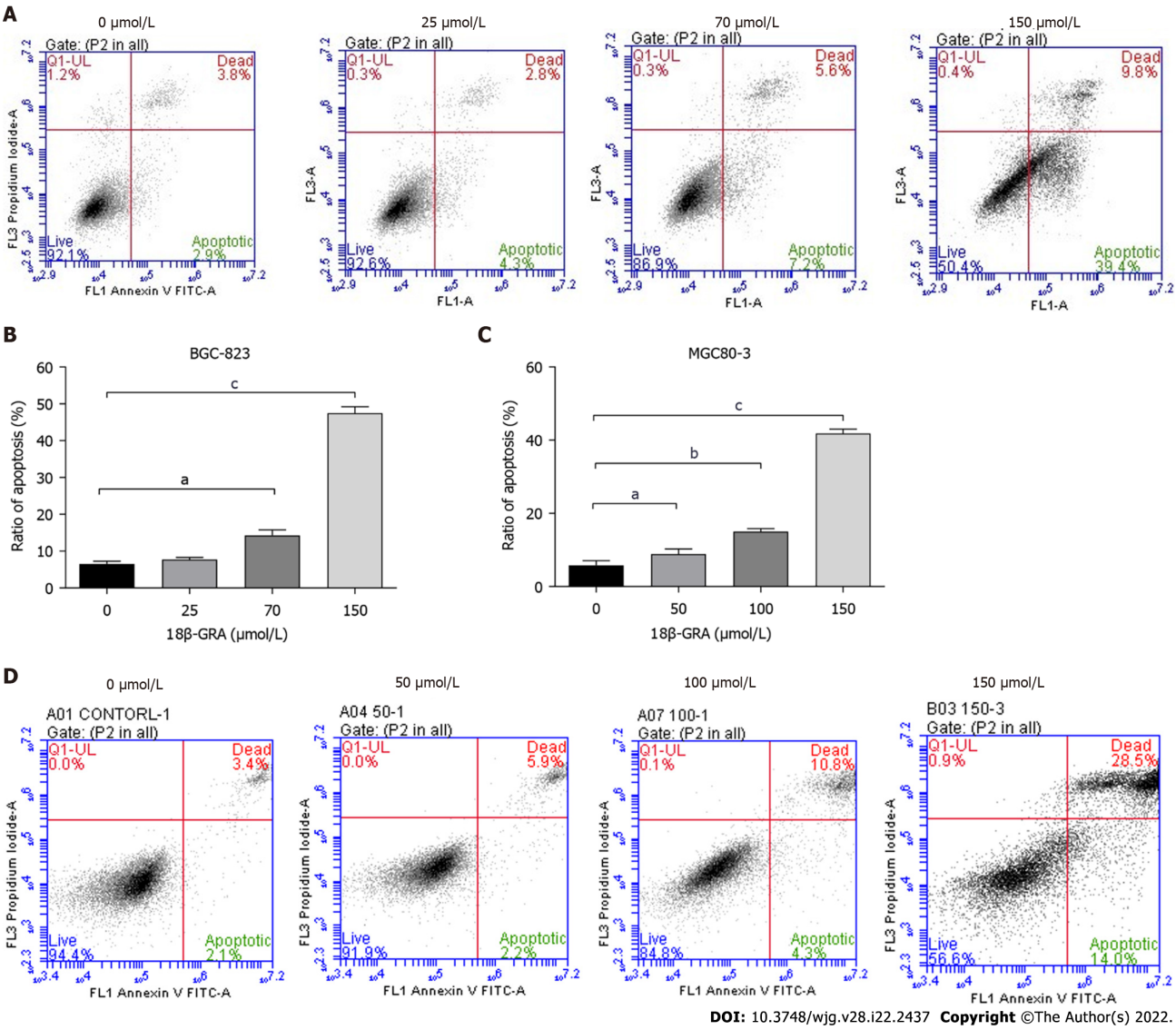
In order to study the effect of 18β-GRA on GC cell cycle, BGC-823 and MGC80-3 cells were treated with different concentrations of 18β-GRA, and the cell cycle of BGC-823 was arrested at G0/G1 phase; the proportions of cells at G0/G1 phase were 81.84% (150 μmol/L), 71.34% (70 μmol/L), and 61.66% (25 μmol/L) (Figure 3A and B). The cell cycle of MGC80-3 cells was arrested at G0/G1 phase; the proportions of cells at G0/G1 phase were 78.01% (150 μmol/L) and 73.37% (100 μmol/L) and higher than 60.57% (control). And with the increase of 18-GRA concentration, the proportion of cells in S-phase decreased (Figure 3C and D).

18β-GRA promotes GC cell apoptosis

Flow cytometry was used to detect the effects of different concentrations of 18β-GRA on GC cell apoptosis. After intervention with different concentrations of 18β-GRA in BGC-823 and MGC80-3 cells for 48 h, the apoptosis rates of BGC-823 cells were 14.27% (70 μmol/L) and 47.47% (150 μmol/L), which were higher than 6.53% (control) (Figure 4A and B). The apoptosis rates of MGC80-3 cells were 8.87% (50 μmol/L), 15.03% (100 μmol/L), and 41.8% (150 μmol/L), which were all higher than 5.8% (control) (Figure 4C and D).

18β-GRA inhibits GC cell invasion ability

BGC-823 and MGC80-3 cells were treated with different concentrations of 18β-GRA for 48 h, and the cell invasion ability was detected. The results of Transwell assay are shown in Figure 5. Compared with control, the different concentrations of 18β-GRA inhibited the invasion of BGC-823 and MGC80-3 cells (



DOI: 10.3748/wjg.v28.i22.2437 **Copyright** ©The Author(s) 2022.

Figure 4 Effects of different concentrations of 18β-glycyrrhetinic acid on gastric carcinoma cell apoptosis. A and B: Cell apoptosis and statistics graph of BGC-823 cells; C and D: Cell apoptosis and statistics graph of MGC80-3 cells. All analyses were repeated three times. The data is represented as the mean ± SD. [a]*P* < 0.05; [b]*P* < 0.01; [c]*P* < 0.001. 18β-GRA: 18β-glycyrrhetinic acid.

P < 0.05).

18β-GRA inhibits the migration ability of GC cells

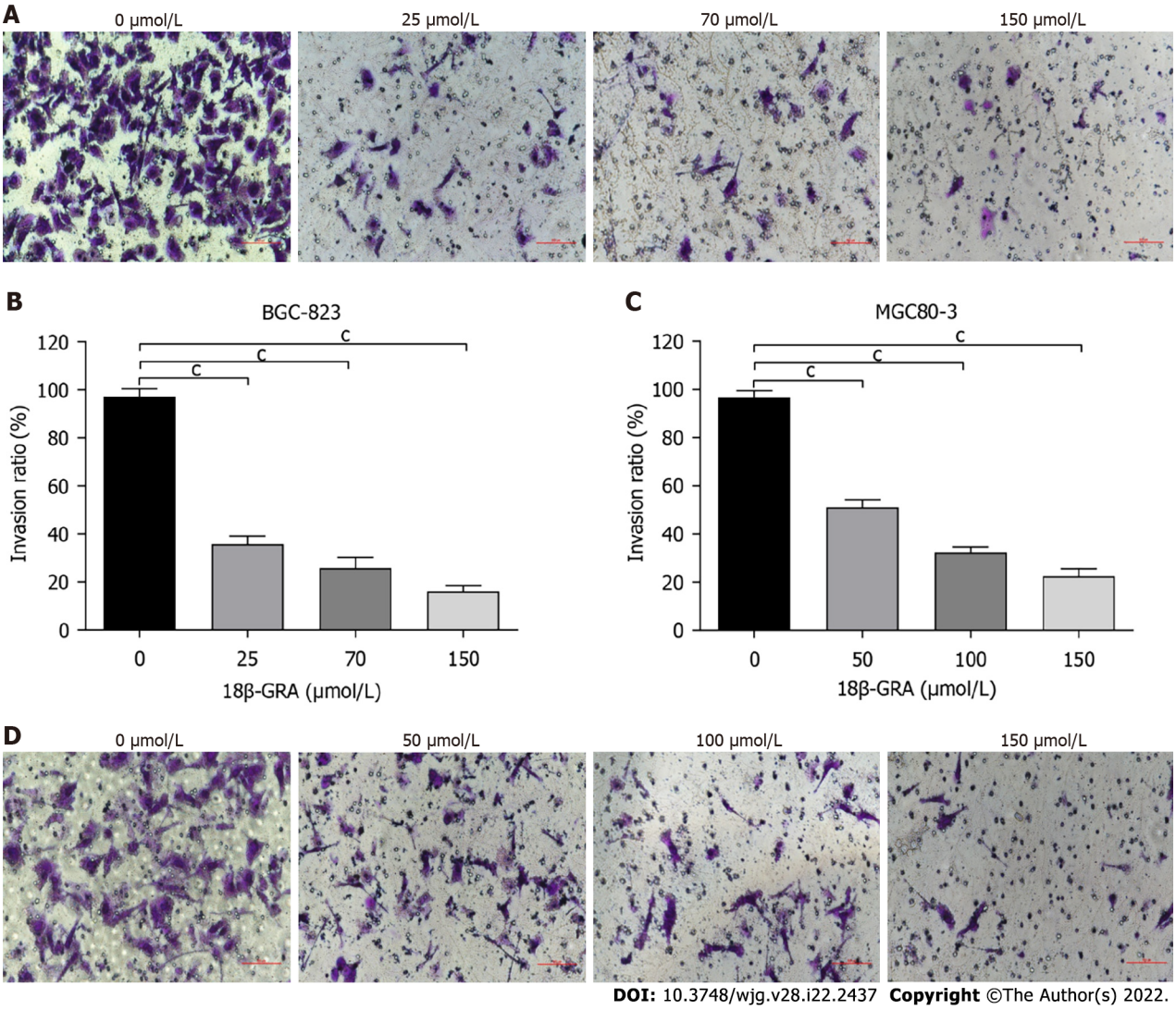
The effect of 18β-GRA on GC cell migration was evaluated in Transwell chambers without matrigel. The migration of BGC-823 and MGC80-3 cells was inhibited after 48 h of treatment with different concentrations of 18-GRA (Figure 6).

We also evaluated the effect of 18β-GRA on GC cell migration by wound scratch assays. The migration of MGC80-3 and BGC-823 cells was inhibited by different concentrations of 18β-GRA for 48 h (Figure 7). With the increase of 18β-GRA concentration, the inhibitory effect was gradually enhanced (*P* < 0.05).

18β-GRA inhibits tumor formation in nude mice

The results of tumor formation experiments in nude mice showed that after 2 wk of continuous intragastric administration, the tumor volume in the 18β-GRA group was significantly smaller than that in the control (Figure 8A and B). The tumor volume was recorded within 2 wk, and the tumor growth curve was drawn (Figure 8C). The tumor growth rate of the 18β-GRA group was lower than that of the control (*P* < 0.01).

qRT-PCR was used to detect the expression level of *MRPL35* in the transplanted tumor tissues of mice. The results showed that the expression level of *MRPL35* in the transplanted tumor tissues of mice in the 18β-GRA group was significantly lower than that in the control (*P* < 0.001) (Figure 8D).



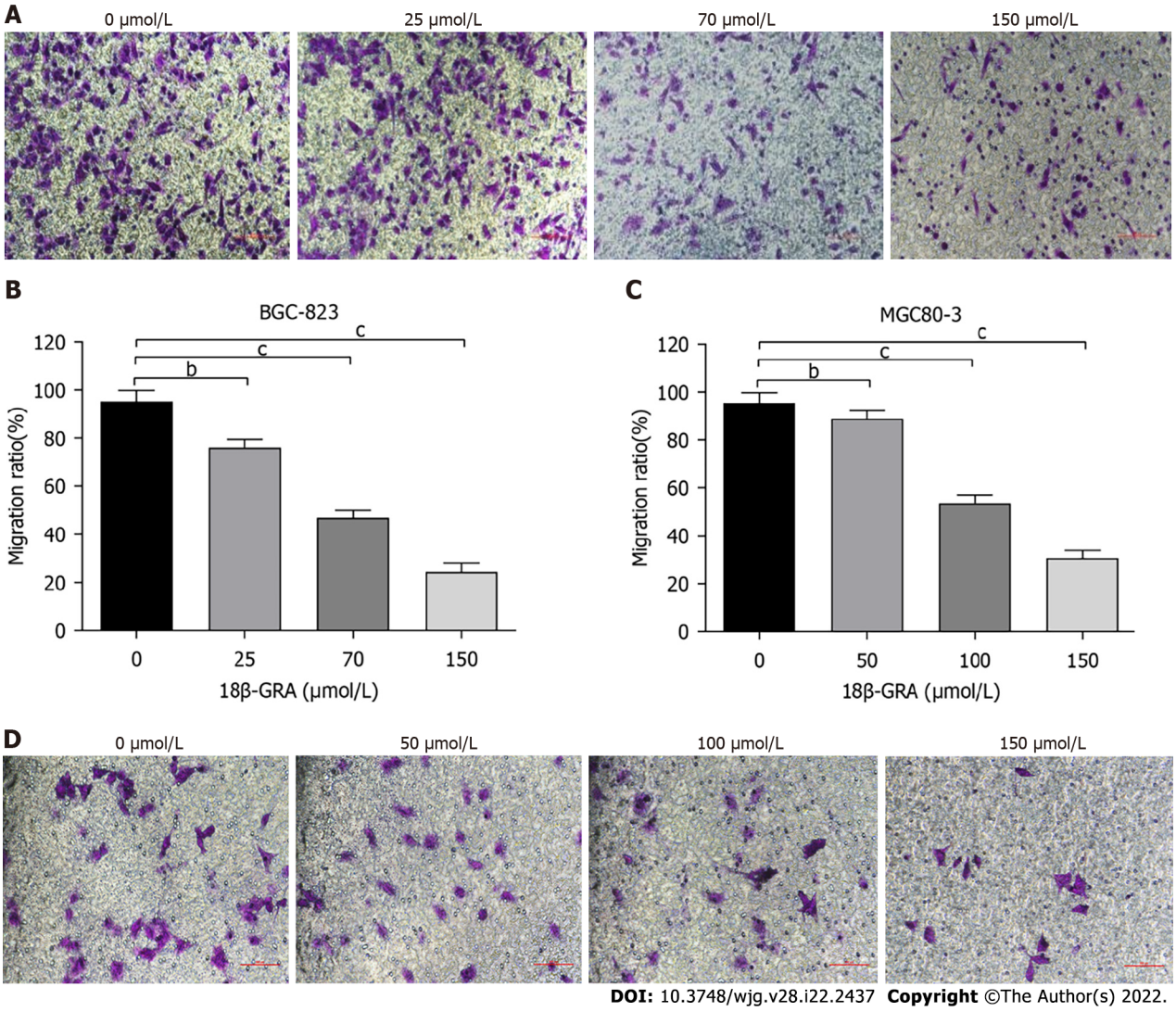
DOI: 10.3748/wjg.v28.i22.2437 **Copyright** ©The Author(s) 2022.

Figure 5 Effects of different concentrations of 18β-glycyrrhetinic acid on invasion of human gastric carcinoma cells. A and B: Invasion ability of BGC-823 cells measured by Transwell of Matrigel matrix gel and the statistical graph; C and D: Invasion ability of MGC80-3 cells and statistical graph. All analyses were repeated three times. The data is represented as the mean ± SD. $^{a}P < 0.05$; $^{b}P < 0.01$; $^{c}P < 0.001$. 18β-GRA: 18β-glycyrrhetinic acid.

During the experiment, we also monitored the influence on body weight, food, and water intake in mice, and found that there was little toxic effect of 18β-GRA on them (Supplementary Figures 2-4).

18β-GRA inhibits GC cell proliferation by regulating MRPL35-related apoptosis signaling pathways

Proteomic analysis based on TMT labeling-based was performed on control and GC cells treated with 18 β-GRA. A total of 6275 proteins were identified by proteomic analysis, and 609 DEPs were screened using the expression difference ratio > 1.2 and $P < 0.05$ as the standard, among which 335 were up-regulated and 274 were down-regulated. To better visualize the DEPs, we drew the volcano plot. The red dots indicate significantly up-regulated proteins and blue dots indicate significantly down-regulated proteins (Figure 9A). Notably, after 18β-GRA intervention, MRPL35 expression was significantly down-regulated ($P = 0.000247$), TP53 expression was up-regulated ($P = 0.02676$), and BCL2L1 was down-regulated ($P = 0.01699$). The GO annotation and enrichment analysis was used to analyze the DEPs and to determine their biological processes (BP), molecular functions (MF), and cellular components (CC) (Figure 9B and C). In the BP analysis, DEPs were mainly involved in cellular processes, biological regulation, and molecular metabolism. It is mainly enriched in complement activation, alternative pathway and classical pathway, and mitochondrial translational termination. With respect to MF, the DEPs are involved in the binding, catalytic activity, molecular function regular, and so on. It is mainly enriched in the binding of collagen and fibronectin, and serine-type endopeptidase inhibitor activity. In the CC analysis, we found that the DEPs were highly localized in the cell, organelle, and protein-containing complex part. Those DEPs are mainly enriched in extracellular space, collagen-containing extracellular matrix, membrane attack complex, and mitochondrial large ribosomal subunit. The DEPs were classified by KEGG pathway enrichment analysis (Figure 9D). KEGG pathway enrichment analyses revealed these DEPs to be enriched in



DOI: 10.3748/wjg.v28.i22.2437 **Copyright** ©The Author(s) 2022.

Figure 6 Effects of different concentrations of 18β-glycyrrhetinic acid on migration of human gastric carcinoma cells. A and B: Migration ability of BGC-823 cells determined by Transwell assay without Matrigel matrix gel and statistical graph; C and D: Migration ability of MGC80-3 cells and statistical graph. All analyses were repeated three times. The data is represented as the mean ± SD. $^{a}P < 0.05$; $^{b}P < 0.01$; $^{c}P < 0.001$. 18β-GRA: 18β-glycyrrhetinic acid.

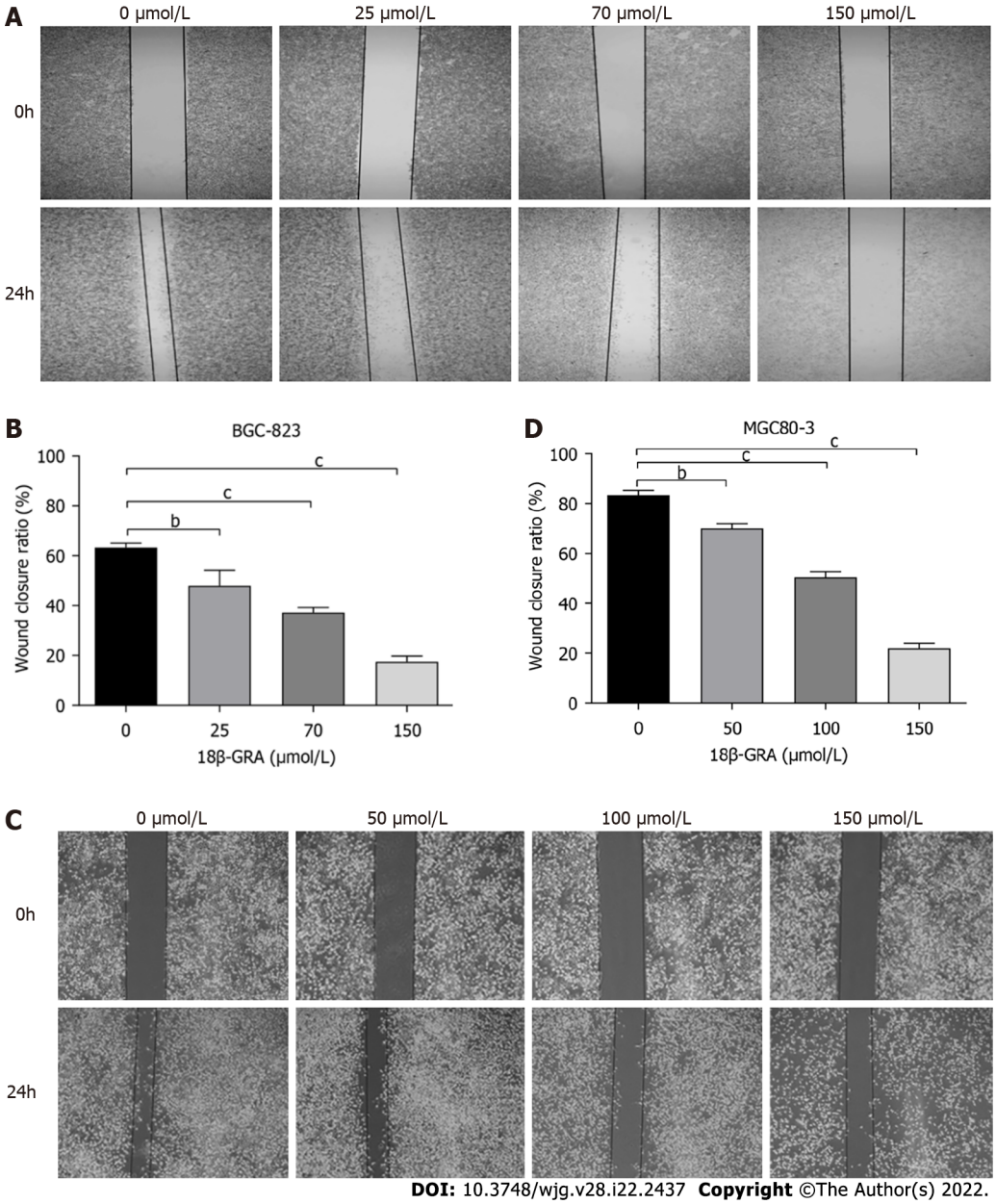
complement and coagulation cascades, ECM-receptor interaction, and cell adhesion molecules. It is worth noting that these DEPs are also involved in the TP53 signaling pathway.

Wolfpsort was used to predict the subcellular localization of these DEPs, which were primarily localized to the nucleus (28.1%), cytosol (23.2%), extracellular space (18.4%), mitochondria (13.6%), and so on (Figure 10A). Further protein domain enrichment analysis showed that DEPs were significantly enriched in the immunoglobulin-like fold domain, thrombospondin type-1 (TSP1) repeat and superfamily, and fibronectin type III and superfamily protein domain (Figure 10B). Cluster analysis was performed on DEPs and drawn as a heat map (Figure 10C). Each row in the figure represents a DEP, red represents up-regulated DEP expression and green for down-regulated DEP expression; the darker the color is, the more significant the difference is.

Finally, in order to further explore the function of MRPL35, TP53, and BCL2L1, the STRING database was used to construct a PPI network, and the results are shown in Figure 10D. And we found that COPS5 is the protein connecting MRPL35 and TP53. In addition, we also found that TP53 and BCL2L1 are closely related to the pro-apoptotic proteins BAX and BAD.

Effect of 18β-GRA on the expression of MRPL35-related apoptosis proteins

Western blot was used to detect the effect of 18β-GRA on the expression of MRPL35 related proteins in gastric cancer cells. The results showed that with the increase of 18β-GRA concentration, the expression levels of MRPL35 and BCL2L1 proteins were gradually down-regulated, while the expression of TP53 protein was up-regulated. The expression of COPS5, the protein linking MRPL35 and TP53, was down-regulated, and the expression levels of pro-apoptotic proteins BAX and BAD were up-regulated. These results confirm the results of our proteomics and bioinformatics analysis above (Figure 11).

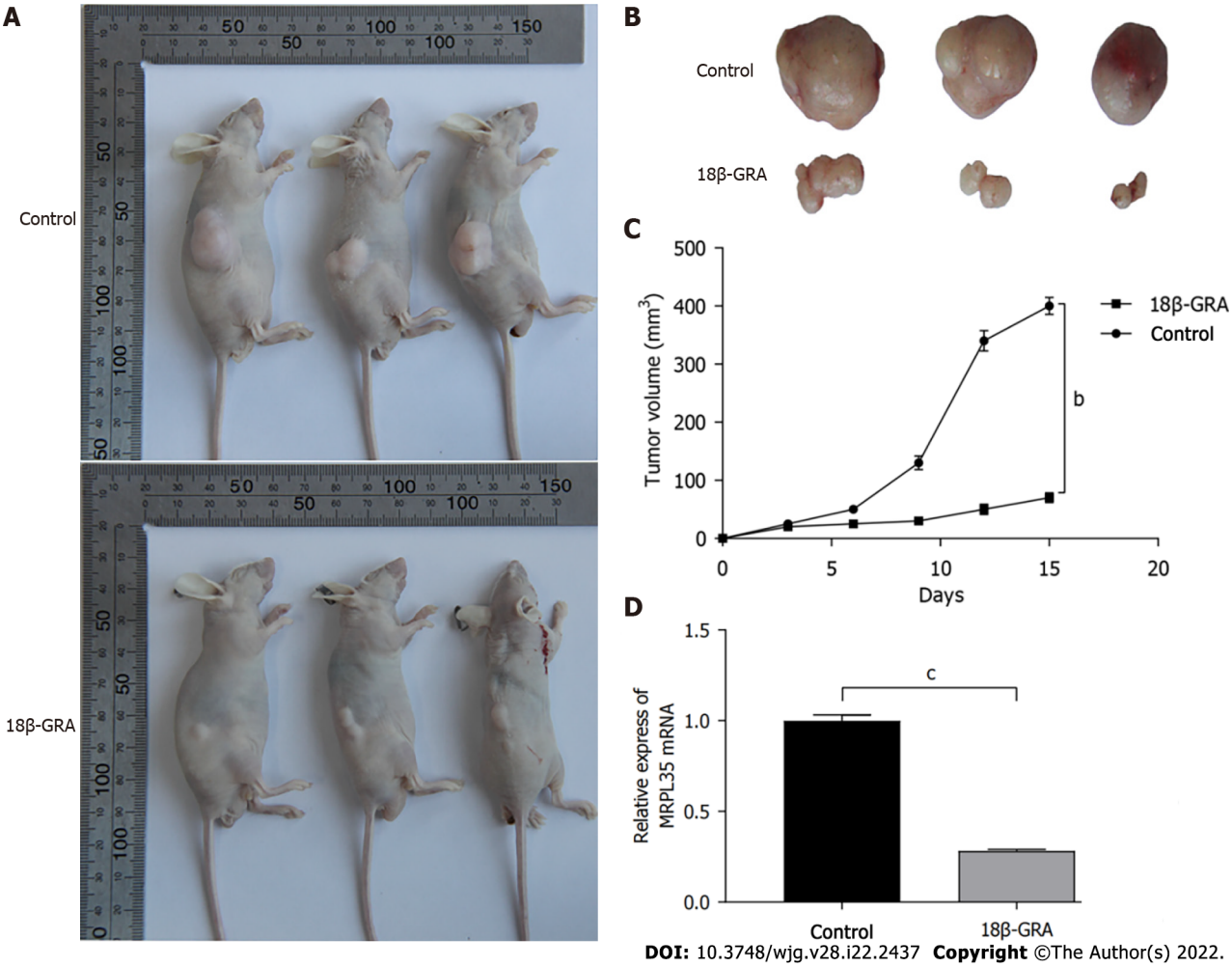


DOI: 10.3748/wjg.v28.i22.2437 **Copyright** ©The Author(s) 2022.

Figure 7 Effects of different concentrations of 18β-glycyrrhetinic acid on migration of human gastric carcinoma cells. A and B: Effect of 18β-glycyrrhetinic acid (18β-GRA) on migration of BGC-823 cells evaluated by Wound-scratch assay and statistical graph; C and D: Effect of 18β-GRA on the migration of MGC80-3 cells and statistical graph. All analyses were repeated three times. The data is represented as the mean ± SD. $^{a}P < 0.05$; $^{b}P < 0.01$; $^{c}P < 0.001$. 18β-GRA: 18β-glycyrrhetinic acid.

DISCUSSION

In this study, the functional changes of GC cells after 18β-GRA intervention were tested by *in vitro* experiments, and the results showed that 18β-GRA had little effect on the survival rate of normal gastric epithelial GES-1 cells, and significantly inhibited the proliferation of BGC-823 and MGC80-3 cells. Next, we detected the cell cycle and found that 18β-GRA could arrest the GC cell cycle at G0/G1 phase. After drug intervention in GC cells, the cells can either exit the cell cycle reversibly, by initiating quiescence, or irreversibly, by senescence or apoptosis. The decision to exit the cell cycle solely depends on the DNA damage checkpoint[20]. In response to irreparable DNA damage, DNA damage checkpoints can initiate quiescence, senescence, or programmed cell death, primarily through TP53-dependent pathways[21, 22]. Moreover, TP53 mutations are the most common mutations in cancer. However, even if cancer-related mutations prevent cell cycle exit, continuous proliferation of cells can still be prevented by blocking the entry of G1 cell cycle prior to replication, which relies on the activation of E2F-dependent transcription[23,24]. We investigated the effect of 18β-GRA on the apoptosis of two types of GC cells, and confirmed the results of cell cycle arrest. It was found that the cells chose to undergo apoptosis and exit the cell cycle, and TP53 played a crucial role in this process.

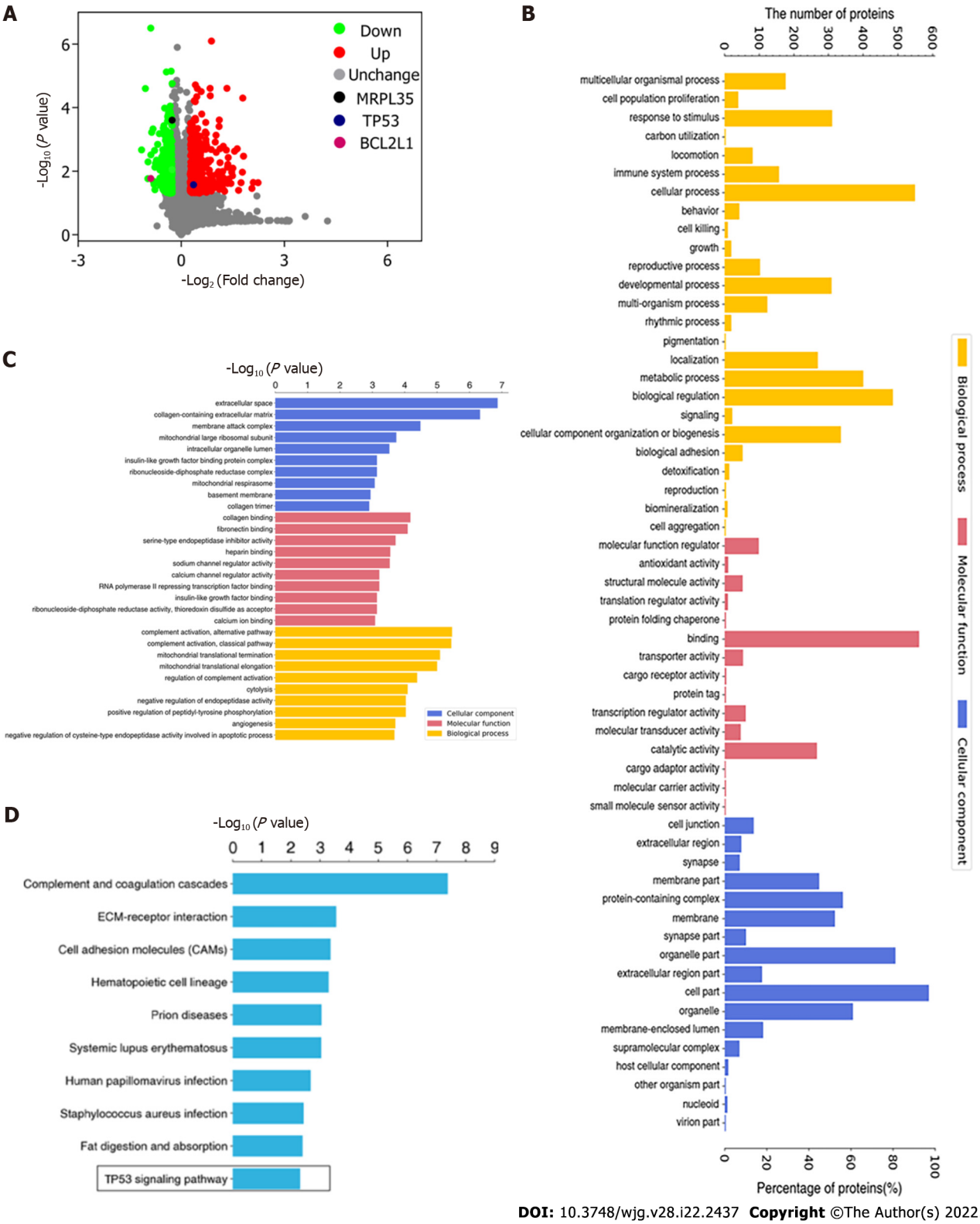


DOI: 10.3748/wjg.v28.i22.2437 **Copyright** ©The Author(s) 2022.

Figure 8 Effect of 18β-glycyrrhetinic acid on tumor size in nude mice. A: Nude mouse gastric carcinoma xenograft model; B: Subcutaneously transplanted tumor in nude mice. *n* = 6; C: Tumor growth curve of transplanted tumor model; D: Quantitative reverse transcription-polymerase chain reaction was used to detect the expression level of *MRPL35* in the transplanted tumor tissues of mice. $^{a}P < 0.05$; $^{b}P < 0.01$; $^{c}P < 0.001$. 18β-GRA: 18β-glycyrrhetinic acid.

The cell invasion and migration experiments showed that cell invasion and migration were significantly suppressed after 18β-GRA intervention in GC cells. Epithelial-to-mesenchymal transition (EMT) plays an important role in the occurrence of metastasis and invasion of malignant tumors[25]. The loss of epithelial characteristics and the acquisition of mesenchymal features reduce cell adhesion and increase cell mobility. In addition, our previous experiments also showed that LINC00514 was up-regulated in GC specimens compared with non-tumor specimens, and overexpression of LINC00514 induced GC cell growth and EMT progression[26]. We used immunodeficient nude mice for tumor-forming experiments *in vivo*. It was found that subcutaneous tumor volume was significantly inhibited in nude mice after 2 wk of intragastric administration of 18β-GRA compared with the control group, and the expression level of *MRPL35* in the transplanted tumor tissues of the 18β-GRA group was significantly decreased, which also confirmed the results of cell function *in vivo*.

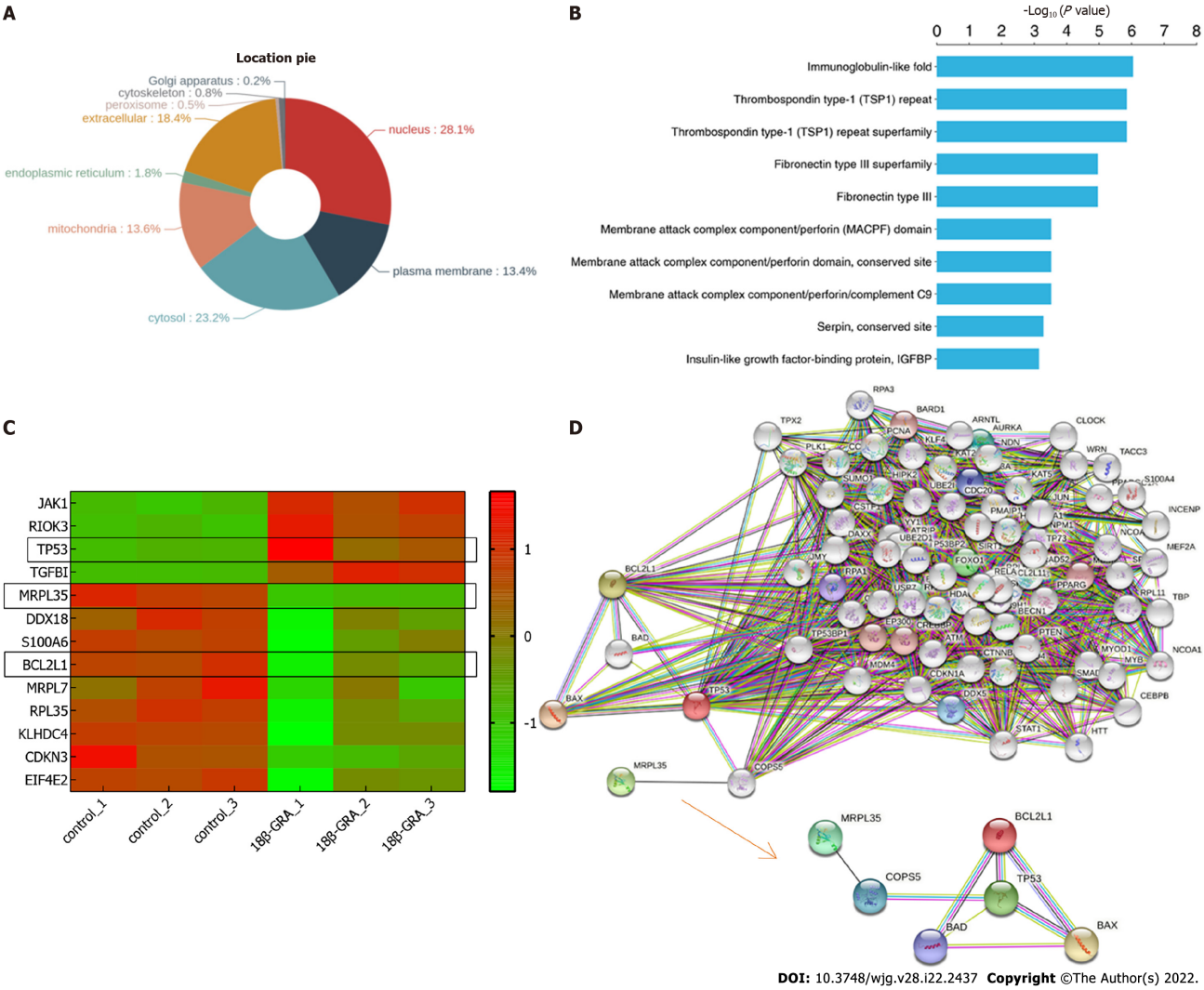
Based on the above results, we further investigated the mechanism of 18β-GRA in inhibiting GC cell proliferation, and promoting cell apoptosis. TMT analysis showed that there were 609 DEPs in GC cells treated with 18β-GRA, among which the expression of MRPL35, TP53, and BCL2L1 was significantly altered. GO analysis found that all these DEPs were mainly involved in cellular processes, biological regulation, and molecular metabolism, and were enriched in membrane attack complexes and mitochondrial large ribosomal subunits. In addition, subcellular localization analysis of DEPs showed that these DEPs were mainly distributed in the nucleus, cytoplasm, extracellular space, and mitochondria. Our previous study showed that the high expression of MRPL35, a member of the large subunit family of MRPs, was correlated with the poor survival rate in GC, and knocking down MRPL35 could inhibit GC cell proliferation. Interestingly, KEGG results showed that these DEPs were enriched in the TP53 signaling pathway, which was ranked tenth in the analysis. TP53 is an important protein involved in the process of cell apoptosis. As a transcription factor, TP53 is mutated in most human cancers[27]. To inhibit cancer, TP53 protein regulates the transcription of many different genes, including *BAX*, *NOXA1*, and *GADD45A*, in response to multiple stress signals, such as DNA repair, cell cycle arrest, senescence, and apoptosis, while tumor mutations can make them resistant to apoptosis



DOI: 10.3748/wjg.v28.i22.2437 **Copyright** ©The Author(s) 2022.

Figure 9 Volcano plot of differentially expressed proteins and Gene Ontology annotation analysis. A: Volcano plot of differentially expressed proteins (DEPs). The horizontal axis is the relative quantitative value of protein after log2 conversion, and the vertical axis is the *P* value of difference significance test after -log10 conversion; B: Gene Ontology (GO) annotation analysis of DEPs. The number of DEPs categorized as biological processes, molecular functions, and cellular components; C: GO enrichment analysis of DEPs. The Y axis denotes the GO functional classification enriched by the DEPs, and the X axis denotes the −log10 of the *P* value of Fisher's exact test of the significance of the enrichment; D: KEGG pathway enrichment analysis. The Y axis denotes the categories of KEGG pathways. The X axis is the −log10 of the *P* value of Fisher's exact test of the significance of enrichment.

induced by the TP53 pathway. Combined with the expression changes of BCL2L1, we speculated that 18 β-GRA might play a role in inhibiting the proliferation of GC by regulating TP53 apoptosis-related signaling pathways through MRPL35. Enrichment analysis of DEP domains showed that they were significantly enriched in immunoglobulin-like folding domain, TSP1 repeats and superfamily, and



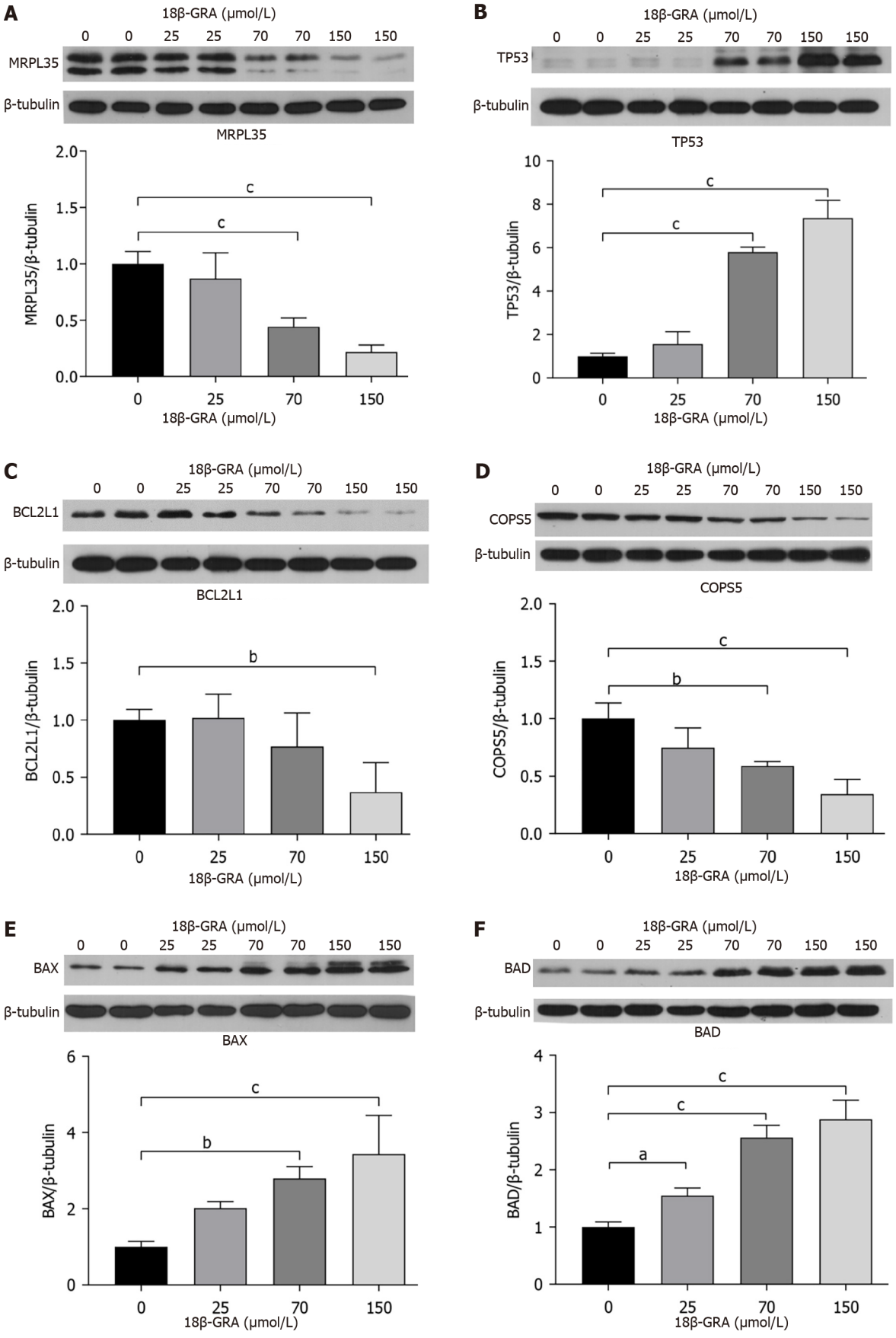
DOI: 10.3748/wjg.v28.i22.2437 **Copyright** ©The Author(s) 2022.

Figure 10 Differentially expressed proteins. A: Subcellular localization chart of differentially expressed proteins (DEPs); B: Protein domain enrichment analysis. The Y axis denotes the categories of the protein domain. The X axis denotes the enrichment score [−log(*P* value)]; C: Heatmap of the MRPL35, TP53, BCL2L1, and so on. The X-coordinate stands for the DEPs, while Y-coordinate stands for different groups; D: Network analysis of MRPL35, TP53, and BCL2L1. The connection was illustrated using the web-based tool STRING.

fibronectin type III and superfamily protein domain. Hence, we speculate that 18β-GRA might regulate the expression of MRPL35, induce the changes of apoptosis-related proteins TP53 and BCL2L1, and play a role in inhibiting the proliferation of GC cells.

Finally, we analyzed the input STRING database of these three signaling proteins, and found that COPS5 is the protein connecting MRPL35 and TP53. Therefore, we believe that MRPL35 is likely to play a pro-apoptotic role by regulating COPS5. In addition, we also found that TP53 and BCL2L1 are closely related to BAX and BAD. As a major regulator of mitochondrial involvement in the intrinsic apoptosis pathway, BAX controls a cell's commitment to the pathway by changing the physiology of resident mitochondria. BAX undergoes a series of ordered events that lead to the formation of pores in the outer membrane of mitochondria, facilitating the release of signaling molecules such as cytochrome C[28]. This event is commonly considered as the "point of no return" in cell death[29]. BAD, a ligand of the pro-survival protein 14-3-3, is an on-off protein in the mitochondria-induced apoptotic pathway[30]. When separated from 14-3-3, BAD may interact with BCL-2/BCL2L1 and release BAX, revealing its apoptotic activity. Binding of BAD to BCL2/BCL2L1 has also been reported to release the activator BH3-only molecules, such as Bim, Bid, and Puma, to directly activate BAX[31,32].

Based on the above mentioned proteomics and STRING analyses, we concluded that 18β-GRA is likely to inhibit the proliferation of GC cells by regulating the expression of MRPL35, thereby affecting the expression of TP53, BCL2L1, COPS5, BAX, and BAD proteins. Consistent with the above hypothesis, the expression of MRPL35, COPS5, apoptosis-related protein TP53, pro-apoptotic proteins BAX and BAD, and anti-apoptotic protein BCL2L1 was down-regulated after 18β-GRA intervention. The anti-tumor activity of GRA and its derivatives are associated with the mitochondrial apoptotic pathway of mitochondrial membrane potential depolarization, which leads to the activation of caspase-9 and caspase-3, and the production of ROS. Cancer cells can avoid apoptosis by destroying the balance



DOI: 10.3748/wjg.v28.i22.2437 **Copyright** ©The Author(s) 2022.

Figure 11 Validation of proteomics results using Western blot analysis of MRPL35, TP53, BCL2L1, COPS5, BAX, and BAD in cells treated with different concentrations of 18β-glycyrrhetinic acid for 48 h. β-tubulin was used as the loading control. A: MRPL35; B: TP53; C: BCL2L1; D: COPS5; E: BAX; F: BAD $n = 4$, $^{a}P < 0.05$; $^{b}P < 0.01$; $^{c}P < 0.001$. 18β-GRA: 18β-glycyrrhetinic acid; MRPL35: Mitochondrial Ribosomal Protein L35.

between pro-apoptosis and pro-survival, so that the apoptotic signal of mitochondria is insensitive to cell death. Studies have shown that 18β-GRA may potentiate the heat shock protein 90 inhibition-induced apoptosis in ovarian carcinoma cell lines *via* the activation of the apoptosis-related proteins and the mitochondria-mediated cell death pathway, leading to activation of caspases[33].

MRPs play a critical role in protein synthesis and mitochondrial function, and also participate in the regulation of cell apoptosis, protein biosynthesis, and signal transduction. MRPL35 and its partner MRP7 play a key role in coordinating the synthesis of the COX1 subunit with its assembly into the COX enzyme[15]. The expression of MRPL35 was found to be higher in CRC tissues than in matched cancer-adjacent tissues. *In vitro*, down-regulation of MRPL35 led to increased production of ROS along with DNA damage, decrease in mitochondrial membrane potential, and autophagy induction, thereby inhibiting the progression of CRC[16]. Oncomine showed that the expression of MRPL35 in GC tissues was significantly higher than that in adjacent tissues. Our previous results also showed that the expression of MRPL35 was significantly up-regulated in GC, which was associated with a poor survival rate of GC patients. Moreover, the knockdown of MRPL35 could inhibit the proliferation and colony formation of GC cells and induce apoptosis[18].

This study demonstrated that 18-GRA inhibited the proliferation and promoted apoptosis of GC cells by down-regulating the expression of MRPL35, which regulated TP53 and BCL2L1 proteins, both *in vivo* and *in vitro*. Our proposed research in the future will be divided into three stages: In the first stage, the signaling pathways of MRPL35, TP53, and BCL2L1 proteins will be explored, possibly through methylation, ubiquitination, acetylation, and phosphorylation. The second stage will be to evaluate the interaction mechanism between MRPL35 and COPS5 proteins. Two modes of action will be considered: Direct action and through tool protein action. Co-immunoprecipitation (Co-IP) or yeast two-hybrid system may be used. In the third stage, MRPL35 and COPS5 protein interaction sites will be explored. After silencing the MRPL35 and COPS5 domains, GST pull-down and Co-IP will be used to verify whether the two proteins interact. The present study aimed to provide a scientific basis for the treatment of GC and identify an effective drug target for the early prevention of GC.

CONCLUSION

18β-GRA can down-regulate the expression of MRPL35 protein, suppress the expression of anti-apoptotic protein BCL2L1, and promote the pro-apoptotic proteins TP53, BAX, and BAD through COPS5, thus inhibiting the proliferation of gastric cancer cells.

ARTICLE HIGHLIGHTS

Research background

Gastric cancer (GC) is a common malignant tumor of the digestive tract in the world, with more than 1 million new cases to be expected each year since 2020. Mitochondrial ribosomal protein L35 (MRPL35) is a member of the large subunit family of mitochondrial ribosomal proteins, which plays an important role in the development of cancer.

Research motivation

At present, the treatment of gastric cancer is based mainly on surgery, chemotherapy, and radiotherapy, and the first-line treatment drugs are mainly harmful due to side effects.

Research objectives

The purpose of this study was to investigate the correlation between MRPL35 apoptosis related signaling pathway and GC.

Research methods

Cell functional indexes were determined by cell counting kit-8, flow cytometry, Transwell assay, and cell scratch assay. The effect of 18β-glycyrrhetinic acid (18β-GRA) on proliferation of gastric cancer cells was observed by BALB/C tumor-forming experiments in nude mice. Tandem mass tag labeling combined with liquid chromatography–tandem mass spectrometry were used to screen for differentially expressed proteins extracted from GC cells and control cells after 18β-GRA intervention. Moreover, STRING database was used to predict protein-protein interaction (PPI) relationships and Western blot was used to detect the expression of proteins of interest in GC cells.

Research results

18β-GRA can inhibit the proliferation of gastric cancer cells, induce apoptosis, arrest the cell cycle at G0/G1 phase, and inhibit the migration and invasion of gastric cancer cells. 18β-GRA can inhibit tumor

formation in BALB/c nude mice. Compared with the control group, MRPL35 and BCL2L1 expression was significantly down-regulated and TP53 expression was up-regulated after 18β-GRA intervention. STRING analysis showed that COPS5, BAX, and BAD proteins could form PPI network with MRPL35, TP53, and BCL2L1 proteins. After 18β-GRA intervention, MRPL35, TP53, and BCL2L1 were up-regulated/down-regulated in a dose-dependent manner, as were COPS5, BAX, and BAD.

Research conclusions

18β-GRA can inhibit the proliferation of GC cells by regulating MRPL35, COPS5, TP53, BCL2L1, BAX, and BAD.

Research perspectives

MRPL35 can be used for targeted therapy of GC, and can also be used as a new biomarker for GC.

ACKNOWLEDGEMENTS

The authors would like to acknowledge Li-Qun Wang for statistical analysis assistance, as well as Joanna Japhet Tibenda for polishing the language.

FOOTNOTES

Author contributions: Yuan L carried out most of the *in vivo* studies, analyzed the data, and wrote the manuscript; Yang Y carried out most of the *in vitro* experiments, wrote the manuscript, and carried out the chart-making work; Li X, Zhou X, Du YH, and Li JX were responsible for the proteomic analysis and PPI network; Ma TT performed parts of the *in vivo* and *in vitro* experiments, and conducted statistical analysis of the data; Yu L supervised the process of research and provided clinical guidance; Liu WJ and Zhang L conducted molecular biological experiments; all authors have read and approved the manuscript; Nan Y provided the conceptual and technical guidance as well as revised the manuscript critically for important intellectual content; Chen Y designed the study and revised the manuscript.

Supported by Ningxia Natural Science Foundation, No. 2020AAC03130; and Ningxia Medical University Project, No. XM2020005.

Institutional review board statement: The study was reviewed and approved by the Institutional Review Board of Ningxia Medical University (No. 2020-071 and No. 2021-018).

Institutional animal care and use committee statement: All procedures involving animals were reviewed and approved by the Institutional Animal Care and Use Committee of the Ningxia Medical University (IACUC protocol number: 2019-083).

Conflict-of-interest statement: All authors declare no financial or commercial conflict of interest for this article.

Data sharing statement: All data generated or analyzed during this study are included in this paper, and further inquiries can be directed to the corresponding author (E-mail: 20080011@nxmu.edu.cn).

ARRIVE guidelines statement: The authors have read the ARRIVE guidelines, and the manuscript was prepared and revised according to the ARRIVE guidelines.

Open-Access: This article is an open-access article that was selected by an in-house editor and fully peer-reviewed by external reviewers. It is distributed in accordance with the Creative Commons Attribution NonCommercial (CC BY-NC 4.0) license, which permits others to distribute, remix, adapt, build upon this work non-commercially, and license their derivative works on different terms, provided the original work is properly cited and the use is non-commercial. See: https://creativecommons.org/Licenses/by-nc/4.0/

Country/Territory of origin: China

ORCID number: Ling Yuan 0000-0003-2838-0976; Yi Yang 0000-0002-8466-5717; Xia Li 0000-0002-4981-9768; Xin Zhou 0000-0001-8517-2212; Yu-Hua Du 0000-0002-9669-8065; Wen-Jing Liu 0000-0002-2934-6182; Lei Zhang 0000-0002-3553-2547; Lei Yu 0000-0002-8837-2022; Ting-Ting Ma 0000-0002-2415-2354; Jia-Xin Li 0000-0002-6413-2542; Yan Chen 0000-0002-8673-398X; Yi Nan 0000-0002-5511-9266.

S-Editor: Fan JR
L-Editor: Wang TQ
P-Editor: Yu HG

REFERENCES

1 **Sung H**, Ferlay J, Siegel RL, Laversanne M, Soerjomataram I, Jemal A, Bray F. Global Cancer Statistics 2020: GLOBOCAN Estimates of Incidence and Mortality Worldwide for 36 Cancers in 185 Countries. *CA Cancer J Clin* 2021; **71**: 209-249 [PMID: 33538338 DOI: 10.3322/caac.21660]

2 **Duan R**, Li X, Zeng D, Chen X, Shen B, Zhu D, Zhu L, Yu Y, Wang D. Tumor Microenvironment Status Predicts the Efficacy of Postoperative Chemotherapy or Radiochemotherapy in Resected Gastric Cancer. *Front Immunol* 2020; **11**: 609337 [PMID: 33569057 DOI: 10.3389/fimmu.2020.609337]

3 **Sun W**, Jiang C, Ji Y, Xiao C, Song H. Long Noncoding RNAs: New Regulators of Resistance to Systemic Therapies for Gastric Cancer. *Biomed Res Int* 2021; **2021**: 8853269 [PMID: 33506041 DOI: 10.1155/2021/8853269]

4 **Wang CY**, Kao TC, Lo WH, Yen GC. Glycyrrhizic acid and 18β-glycyrrhetinic acid modulate lipopolysaccharide-induced inflammatory response by suppression of NF-κB through PI3K p110δ and p110γ inhibitions. *J Agric Food Chem* 2011; **59**: 7726-7733 [PMID: 21644799 DOI: 10.1021/jf2013265]

5 **Huang M**, Gong P, Wang Y, Xie X, Ma Z, Xu Q, Liu D, Jing Y, Zhao L. Synthesis and antitumor effects of novel 18β-glycyrrhetinic acid derivatives featuring an exocyclic α,β-unsaturated carbonyl moiety in ring A. *Bioorg Chem* 2020; **103**: 104187 [PMID: 32890994 DOI: 10.1016/j.bioorg.2020.104187]

6 **Huang RY**, Chu YL, Huang QC, Chen XM, Jiang ZB, Zhang X, Zeng X. 18β-Glycyrrhetinic acid suppresses cell proliferation through inhibiting thromboxane synthase in non-small cell lung cancer. *PLoS One* 2014; **9**: e93690 [PMID: 24695790 DOI: 10.1371/journal.pone.0093690]

7 **Sharma G**, Kar S, Palit S, Das PK. 18β-glycyrrhetinic acid induces apoptosis through modulation of Akt/FOXO3a/Bim pathway in human breast cancer MCF-7 cells. *J Cell Physiol* 2012; **227**: 1923-1931 [PMID: 21732363 DOI: 10.1002/jcp.22920]

8 **Cao D**, Jia Z, You L, Wu Y, Hou Z, Suo Y, Zhang H, Wen S, Tsukamoto T, Oshima M, Jiang J, Cao X. 18β-glycyrrhetinic acid suppresses gastric cancer by activation of miR-149-3p-Wnt-1 signaling. *Oncotarget* 2016; **7**: 71960-71973 [PMID: 27713126 DOI: 10.18632/oncotarget.12443]

9 **Cai H**, Chen X, Zhang J, Wang J. 18β-glycyrrhetinic acid inhibits migration and invasion of human gastric cancer cells *via* the ROS/PKC-α/ERK pathway. *J Nat Med* 2018; **72**: 252-259 [PMID: 29098529 DOI: 10.1007/s11418-017-1145-y]

10 **Cao D**, Wu Y, Jia Z, Zhao D, Zhang Y, Zhou T, Wu M, Zhang H, Tsukamoto T, Oshima M, Jiang J, Cao X. 18β-glycyrrhetinic acid inhibited mitochondrial energy metabolism and gastric carcinogenesis through methylation-regulated TLR2 signaling pathway. *Carcinogenesis* 2019; **40**: 234-245 [PMID: 30364936 DOI: 10.1093/carcin/bgy150]

11 **Zeng Y**, Shi Y, Xu L, Zeng Y, Cui X, Wang Y, Yang N, Zhou F, Zhou Y. Prognostic Value and Related Regulatory Networks of MRPL15 in Non-Small-Cell Lung Cancer. *Front Oncol* 2021; **11**: 656172 [PMID: 34026630 DOI: 10.3389/fonc.2021.656172]

12 **Xu H**, Zou R, Li F, Liu J, Luan N, Wang S, Zhu L. MRPL15 is a novel prognostic biomarker and therapeutic target for epithelial ovarian cancer. *Cancer Med* 2021; **10**: 3655-3673 [PMID: 33934540 DOI: 10.1002/cam4.3907]

13 **Hao C**, Duan H, Li H, Wang H, Liu Y, Fan Y, Zhang C. Knockdown of MRPL42 suppresses glioma cell proliferation by inducing cell cycle arrest and apoptosis. *Biosci Rep* 2018; **38** [PMID: 29531015 DOI: 10.1042/BSR20171456]

14 **Brown A**, Amunts A, Bai XC, Sugimoto Y, Edwards PC, Murshudov G, Scheres SHW, Ramakrishnan V. Structure of the large ribosomal subunit from human mitochondria. *Science* 2014; **346**: 718-722 [PMID: 25278503 DOI: 10.1126/science.1258026]

15 **Box JM**, Kaur J, Stuart RA. MrpL35, a mitospecific component of mitoribosomes, plays a key role in cytochrome *c* oxidase assembly. *Mol Biol Cell* 2017; **28**: 3489-3499 [PMID: 28931599 DOI: 10.1091/mbc.E17-04-0239]

16 **Zhang L**, Lu P, Yan L, Yang L, Wang Y, Chen J, Dai J, Li Y, Kang Z, Bai T, Xi Y, Xu J, Sun G, Yang T. MRPL35 Is Up-Regulated in Colorectal Cancer and Regulates Colorectal Cancer Cell Growth and Apoptosis. *Am J Pathol* 2019; **189**: 1105-1120 [PMID: 30862482 DOI: 10.1016/j.ajpath.2019.02.003]

17 **Wang AF**, Zhang Q, Zhang DM, Xiu YT, Ding YM, Liu LL. The effect of silencing mitochondrial ribosomal protein L35 gene on the growth of human esophageal cancer TE-1 cells. *J Jilin University* 2019; **45**: 28-32+217

18 **Yuan L**, Li JX, Yang Y, Chen Y, Ma TT, Liang S, Bu Y, Yu L, Nan Y. Depletion of MRPL35 inhibits gastric carcinoma cell proliferation by regulating downstream signaling proteins. *World J Gastroenterol* 2021; **27**: 1785-1804 [PMID: 33967557 DOI: 10.3748/wjg.v27.i16.1785]

19 **Lin D**, Zhong W, Li J, Zhang B, Song G, Hu T. Involvement of BID translocation in glycyrrhetinic acid and 11-deoxy glycyrrhetinic acid-induced attenuation of gastric cancer growth. *Nutr Cancer* 2014; **66**: 463-473 [PMID: 24547973 DOI: 10.1080/01635581.2013.877498]

20 **Matthews HK**, Bertoli C, de Bruin RAM. Cell cycle control in cancer. *Nat Rev Mol Cell Biol* 2022; **23**: 74-88 [PMID: 34508254 DOI: 10.1038/s41580-021-00404-3]

21 **Zilfou JT**, Lowe SW. Tumor suppressive functions of p53. *Cold Spring Harb Perspect Biol* 2009; **1**: a001883 [PMID: 20066118 DOI: 10.1101/cshperspect.a001883]

22 **Chen J**. The Cell-Cycle Arrest and Apoptotic Functions of p53 in Tumor Initiation and Progression. *Cold Spring Harb Perspect Med* 2016; **6**: a026104 [PMID: 26931810 DOI: 10.1101/cshperspect.a026104]

23 **Bertoli C**, Skotheim JM, de Bruin RA. Control of cell cycle transcription during G1 and S phases. *Nat Rev Mol Cell Biol* 2013; **14**: 518-528 [PMID: 23877564 DOI: 10.1038/nrm3629]

24 **Bertoli C**, Herlihy AE, Pennycook BR, Kriston-Vizi J, de Bruin RAM. Sustained E2F-Dependent Transcription Is a Key Mechanism to Prevent Replication-Stress-Induced DNA Damage. *Cell Rep* 2016; **15**: 1412-1422 [PMID: 27160911 DOI: 10.1016/j.celrep.2016.04.036]

25 **Yeung KT**, Yang J. Epithelial-mesenchymal transition in tumor metastasis. *Mol Oncol* 2017; **11**: 28-39 [PMID: 28085222 DOI: 10.1002/1878-0261.12017]

26 **Yuan L**, Li J, Yang Y, Chen Y, Bu Y, Ye M, Mao X, Ma T, Yu L, Nan Y. LINC00514 promotes gastric cancer cell growth and EMT progression *via* miR-204-3p/KRAS. *Aging (Albany NY)* 2021; **13**: 12007-12015 [PMID: 33888645 DOI: 10.18632/aging.202905]

27 **Hafner A**, Bulyk ML, Jambhekar A, Lahav G. The multiple mechanisms that regulate p53 activity and cell fate. *Nat Rev Mol Cell Biol* 2019; **20**: 199-210 [PMID: 30824861 DOI: 10.1038/s41580-019-0110-x]

28 **Maes ME**, Schlamp CL, Nickells RW. BAX to basics: How the BCL2 gene family controls the death of retinal ganglion cells. *Prog Retin Eye Res* 2017; **57**: 1-25 [PMID: 28064040 DOI: 10.1016/j.preteyeres.2017.01.002]

29 **Chang LK**, Putcha GV, Deshmukh M, Johnson EM Jr. Mitochondrial involvement in the point of no return in neuronal apoptosis. *Biochimie* 2002; **84**: 223-231 [PMID: 12022953 DOI: 10.1016/s0300-9084(02)01372-x]

30 **Chang CY**, Shen CC, Su HL, Chen CJ. Gefitinib induces apoptosis in human glioma cells by targeting Bad phosphorylation. *J Neurooncol* 2011; **105**: 507-522 [PMID: 21744078 DOI: 10.1007/s11060-011-0632-3]

31 **Kroemer G**, Galluzzi L, Brenner C. Mitochondrial membrane permeabilization in cell death. *Physiol Rev* 2007; **87**: 99-163 [PMID: 17237344 DOI: 10.1152/physrev.00013.2006]

32 **Zha J**, Harada H, Yang E, Jockel J, Korsmeyer SJ. Serine phosphorylation of death agonist BAD in response to survival factor results in binding to 14-3-3 not BCL-X(L). *Cell* 1996; **87**: 619-628 [PMID: 8929531 DOI: 10.1016/s0092-8674(00)81382-3]

33 **Yang JC**, Myung SC, Kim W, Lee CS. 18β-glycyrrhetinic acid potentiates Hsp90 inhibition-induced apoptosis in human epithelial ovarian carcinoma cells *via* activation of death receptor and mitochondrial pathway. *Mol Cell Biochem* 2012; **370**: 209-219 [PMID: 22865487 DOI: 10.1007/s11010-012-1412-x]

World Journal of Gastroenterology

Submit a Manuscript: https://www.f6publishing.com

World J Gastroenterol 2022 June 14; 28(22): 2457-2467

DOI: 10.3748/wjg.v28.i22.2457

ISSN 1007-9327 (print) ISSN 2219-2840 (online)

ORIGINAL ARTICLE

Retrospective Study

Application of endoscopic ultrasonography for detecting esophageal lesions based on convolutional neural network

Gao-Shuang Liu, Pei-Yun Huang, Min-Li Wen, Shuai-Shuai Zhuang, Jie Hua, Xiao-Pu He

Specialty type: Gastroenterology and hepatology

Provenance and peer review: Invited article; Externally peer reviewed.

Peer-review model: Single blind

Peer-review report's scientific quality classification

Grade A (Excellent): 0
Grade B (Very good): B, B
Grade C (Good): 0
Grade D (Fair): 0
Grade E (Poor): 0

P-Reviewer: Popovic DD, Serbia; Zaghloul MS, Egypt

Received: April 27, 2021
Peer-review started: April 28, 2021
First decision: June 13, 2021
Revised: June 27, 2021
Accepted: April 29, 2022
Article in press: April 29, 2022
Published online: June 14, 2022

Gao-Shuang Liu, Department of Gastroenterology, Nanjing BenQ Medical Center, The Affiliated BenQ Hospital of Nanjing Medical University, Nanjing 210000, Jiangsu Province, China

Pei-Yun Huang, Shuai-Shuai Zhuang, Xiao-Pu He, Department of Geriatric Gastroenterology, The First Affiliated Hospital of Nanjing Medical University, Nanjing 210000, Jiangsu Province, China

Min-Li Wen, School of Computer Science and Engineering, Southeast University, Nanjing 211102, Jiangsu Province, China

Jie Hua, Department of Gastroenterology, The First Affiliated Hospital of Nanjing Medical University, Nanjing 210000, Jiangsu Province, China

Corresponding author: Jie Hua, MD, Chief Physician, Doctor, Department of Gastroenterology, The First Affiliated Hospital of Nanjing Medical University, No. 300 Guangzhou Road, Nanjing 210000, Jiangsu Province, China. huajie@njmu.edu.cn

Abstract

BACKGROUND

A convolutional neural network (CNN) is a deep learning algorithm based on the principle of human brain visual cortex processing and image recognition.

AIM

To automatically identify the invasion depth and origin of esophageal lesions based on a CNN.

METHODS

A total of 1670 white-light images were used to train and validate the CNN system. The method proposed in this paper included the following two parts: (1) Location module, an object detection network, locating the classified main image feature regions of the image for subsequent classification tasks; and (2) Classification module, a traditional classification CNN, classifying the images cut out by the object detection network.

RESULTS

The CNN system proposed in this study achieved an overall accuracy of 82.49%, sensitivity of 80.23%, and specificity of 90.56%. In this study, after follow-up

pathology, 726 patients were compared for endoscopic pathology. The misdiagnosis rate of endoscopic diagnosis in the lesion invasion range was approximately 9.5%; 41 patients showed no lesion invasion to the muscularis propria, but 36 of them pathologically showed invasion to the superficial muscularis propria. The patients with invasion of the tunica adventitia were all treated by surgery with an accuracy rate of 100%. For the examination of submucosal lesions, the accuracy of endoscopic ultrasonography (EUS) was approximately 99.3%. Results of this study showed that EUS had a high accuracy rate for the origin of submucosal lesions, whereas the misdiagnosis rate was slightly high in the evaluation of the invasion scope of lesions. Misdiagnosis could be due to different operating and diagnostic levels of endoscopists, unclear ultrasound probes, and unclear lesions.

CONCLUSION

This study is the first to recognize esophageal EUS images through deep learning, which can automatically identify the invasion depth and lesion origin of submucosal tumors and classify such tumors, thereby achieving good accuracy. In future studies, this method can provide guidance and help to clinical endoscopists.

Key Words: Endoscopic ultrasonography; Convolutional neural network; Esophageal lesion; Automatically; Classify; Identify

©The Author(s) 2022. Published by Baishideng Publishing Group Inc. All rights reserved.

Core Tip: Convolutional neural networks with self-learning abilities are an effective method in medical image classification, segmentation, and detection. Endoscopic ultrasonography plays an important role in the diagnosis and treatment of esophageal lesions. However, its operation and lesion identification are more difficult than ordinary endoscopy. Automatic identification technology is of great significance to its development.

Citation: Liu GS, Huang PY, Wen ML, Zhuang SS, Hua J, He XP. Application of endoscopic ultrasonography for detecting esophageal lesions based on convolutional neural network. *World J Gastroenterol* 2022; 28(22): 2457-2467

URL: https://www.wjgnet.com/1007-9327/full/v28/i22/2457.htm

DOI: https://dx.doi.org/10.3748/wjg.v28.i22.2457

INTRODUCTION

Endoscopic ultrasonography (EUS) is a mature and widely used invasive examination technology. It is a combination of ultrasound and endoscopy, and the micro high-frequency ultrasound probe is placed on the top of the endoscope to directly observe gastrointestinal mucosal lesions when the endoscope enters the body. It can be used for preoperative staging of digestive tract tumors[1], estimating the invasion depth and range[2], assessing the nature of submucosal lesions of the digestive tract wall[3-4], and diagnosing bilio-pancreatic system tumors[5-6]. The esophagus is the narrowest part of the digestive tract, and its diameter is not uniform. EUS can be used for high-precision evaluation of the esophagus. At present, common lesions of the esophagus include submucosal tumors (including leiomyoma, stromal tumor, and lipoma), precancerous lesions, and esophageal cancer.

China has a high incidence of esophageal cancer, and the current 5-year survival rate of esophageal cancer is 15%-25%[7-10]. A 13.5-year follow-up study has shown that 74% of patients with high-grade intraepithelial neoplasia (HGIN) have developed esophageal cancer[11]. Surgical and endoscopic resection (ER) has been approved as the standard treatment for esophageal HGIN, and endoscopic therapy has become a widely used method because of its safety, efficiency, and low risk of complications[12-13]. Compared with surgical treatment, endoscopic therapy can reduce complications and preserve esophageal function[9]. EUS plays an important role in the evaluation of esophageal lesions and in the determination of the need for surgery.

With the popularization of endoscopic ultrasonography in clinic, several endoscopic physicians are needed. However, endoscopic ultrasonography is different from other ultrasound techniques in that ultrasonic examination is performed on the basis of digestive endoscopy; therefore, the examiners should be professional endoscopic physicians with ultrasonic training. In addition, with the increase of chronic diseases, ageing populations, and dwindling resources, we need to shift to models that can intelligently extract, analyze, interpret, and understand increasingly complex data. The rapidly evolving

field of machine learning is a key to this paradigm shift. Artificial intelligence (AI) is a mathematical predictive technology that automatically learns and recognizes data patterns. Deep learning is an AI algorithm and an advanced machine learning method using neural networks[14]. This method aims to build a neural network that mimics brain's mechanisms for interpreting data, such as images, sounds, and text. Deep learning combines low-level features to form abstract high-level representation attribute categories or features and discover distributed feature representation of data. It is often used in AI algorithms, and it has been applied to medical diagnosis[15-18]. At present, relevant studies on deep learning in ultrasound have been found, including the classification of thyroid nodules[19-20], the diagnosis of liver diseases[21], the identification of benign and malignant breast masses[22], the imaging interpretation of carotid artery intima media thickness (FEATURED by its length)[23], and the prediction of the pancreatic ductal papillary mucinous tumor[5]. However, the research on the identification and classification of esophageal lesions by endoscopic ultrasonography has not yet been found.

This study aimed to construct a framework of deep learning network and study the application of deep learning in esophageal EUS in identifying the origin of submucosal lesions and defining the scope of esophageal lesions.

MATERIALS AND METHODS

The method proposed in this paper included the following two parts: (1) Location module, an object detection network, locating the main image feature regions of the image for subsequent classification tasks; and (2) Classification module, a traditional classification convolution neural network, classifying the images cut out by the object detection network. In the evaluation phase, all the metrics were calculated based on the ten-fold cross-validation results. The dataset was divided into the training (80%), testing (10%) and validating (10%) datasets, respectively. The detailed data statistics distribution from the esophageal lesion database is shown in Tables 1 and 2.

Location module

For gastric ultrasound images, identifying the classification of the whole image was not necessary because the introduction of background information can cause irrelevant features and affect the determination of the model. Therefore, the core area of the image was located, which can classify the image [24]. In this study, RetinaNet object detection network was used. RetinaNet network is a one-stage object detection method. It uses the focal loss cost function in the classification branch, which addresses the imbalance between positive and negative samples in one-stage object detection method.

Resnet50 network was used in the feature extraction part of RetinaNet network, and the FPN structure was added, that is, a top-down structure and lateral connection were adopted to detect the object of different scales. Finally, the features obtained were used to predict the classification branch and regression branch. The classification branch was retained; thus, the multitask training can improve the accuracy of the model, and it can be used to compare the experiment with the classification network (Figure 1).

For object detection anchor setting, this study adopted the default anchor setting methods, with anchor sizes of 32, 64, 128, 256, and 512 and aspect ratios of 1:2, 2:1, and 1:1.

Classification module

The object detection module cut out the core image block of the image and resize it to 224 × 224. Image augmentation artificially created training images through different ways of processing or combination of multiple processing, such as random rotation, shifts, shear, and flips, to address over-fitting and improve the generalization of the network (Table 3).

The classification convolution neural network used the VGGNet network. Compared with the previous network, the VGGNet network used small convolution and deeper network layers, which achieved better classification accuracy (ACC). The classification network was pre-trained on the ImageNet dataset. The last three fully connected layers of network were removed, and then two fully connected layers were added. The number of neurons was 256 and 5 (5 is the classification number of the dataset used in this paper; Figure 2).

Experiment

During the experiment, GPU configuration was a NVIDIA Geforce GTX1070ti. All the codes were written in Python 3.6, and keras was used as the deep learning library.

In the object detection experiment, smooth L1 cost function was used for regression, and focal loss cost function was used for classification. Adam was used as the optimizer, and the learning rate, momentum, and weight decay were set to 1e-5, 0.9, and 0.0005, respectively. The short side of the input image was rescaled to 800, and the long side was rescaled in equal proportion, with the maximum of 1333.

Table 1 Statistics distribution from esophageal lesion database

	Lesions invading the submucosa and muscularis mucosae	Lesions invading the muscularis propria	Lesions invading the serosal layer
Train	473	376	74
Validation	59	47	9
Test	59	47	9
Total	591	470	92

Table 2 Statistics distribution from esophageal submucosal lesion database

	Lesions from the muscularis propria	Lesions from the muscularis mucosae
Train	119	294
Validation	15	37
Test	15	37
Total	149	368

Table 3 Data augmentation parameter

Transformation type	Description
Rotation	Degree range for random rotations: -90°- 90°
Shift	Shift fraction of total height and total width: 0.1
Zoom	Range for random zoom: 0.9-1.1
Flip	Randomly flip image horizontally and vertically.
Shear	Shear intensity: 0.2 (shear angle in counter-clockwise direction in degrees)

In the classification experiment, the cross-entropy loss function was used. The optimizer used SGD and set the initial learning rate to 1e-3. When the loss did not decrease, the learning rate was multiplied by a factor of 0.5 until it reached 1e-6. The batch size was set to 16.

The quantitative and qualitative results of the proposed method were provided. A confusion matrix is a table that is often used to describe the performance of a classification model. Each row of the confusion matrix represents the instances of an actual class, and each column represents the instances of a predicted class. The diagonal values represent the number of correct classifications for each class, and the others represent the confusion number between every two classes. As shown in Figure 3, the ACC of using the classification network is improved compared with the classification branch of the object detection network, which is directly used for classification prediction. The classification ACC in the muscularis propria and muscularis mucosae increased significantly.

The classification performance was measured using sensitivity (SENS), specificity (SPEC), and ACC to clarify the evaluation metrics. Sensitivity measures how much a classifier can recognize positive examples. Specificity measures how much a classifier can recognize negative examples. ACC is the ratio of correct decisions made by a classifier. The sensitivity, specificity, and ACC were defined by equations (1)-(3):

$$SENS = TP / (TP + FN) \quad (1)$$

$$SPEC = TN / (FP + TN) \quad (2)$$

$$ACC = (TP + TN) / (TP + TN + FP + FN) \quad (3)$$

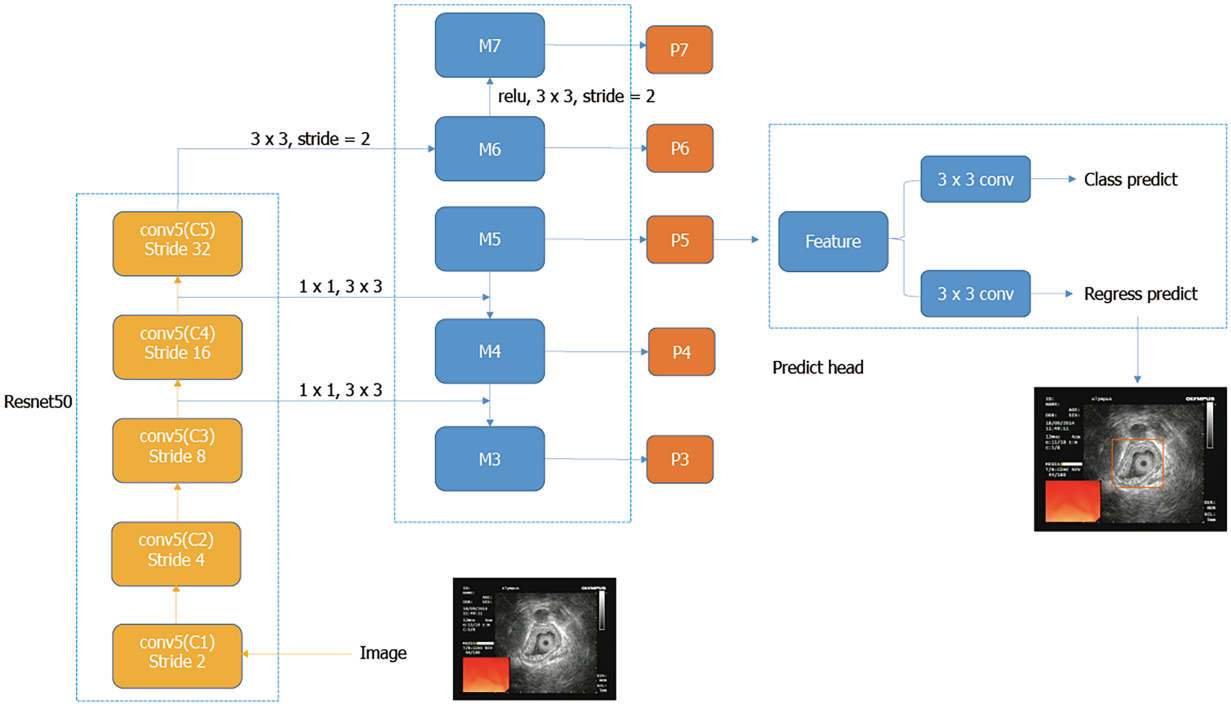
Where TP is the amount of positive elements predicted as positive; TN is the amount of negative elements predicted as negative; FP is the amount of negative elements predicted as positive; FN is the amount of positive elements predicted as negative.

As shown in Table 4, the classification network outperforms the classification branch of the object detection network in SENS, SPEC, and ACC. Class activation maps (CAM) can be used to obtain the discriminative image regions using a convolutional neural network and identify a specific class in the image. Therefore, a CAM can identify the regions in the image that were relevant to this class. The results of CAM are shown in Figure 4.

Table 4 Comparative sensitivity, specificity, and accuracy results of classification branch of object detection network and classification network alone

	SENS	SPEC	ACC
Object detection classify	0.5839	0.8404	0.7861
Classification network alone	0.7400	0.9070	0.8733

SENS: Sensitivity; SPEC: Specificity; ACC: Accuracy.



DOI: 10.3748/wjg.v28.i22.2457 **Copyright** ©The Author(s) 2022.

Figure 1 Structure of object detection network.

RESULTS

A total of 1115 patients were included in this analysis, including 694 males and 421 females. The age ranged from 24 to 88 years, with the majority of patients aged over 45 years. In this study, patients who underwent surgery or endoscopic treatment were followed for pathology, and 726 of them were compared for ultrasound diagnosis and endoscopic pathology. In the diagnosis of endoscopic ultrasonography, lesions invading the muscularis propria were not detected in 41 patients, and the misdiagnosis rate was approximately 9.5%. In addition, 36 patients showed pathologic invasion of the superficial muscularis propria. All patients with serosal invasion were treated by surgery, and the ACC rate was 100%. For the detection of submucosal lesions by EUS, the ACC was approximately 99.3% (Table 5).

Table 6 shows the ACC, SENS, and SPEC of each category in this study. The ACC of invasion of the serosa was 98.9%, and that of invasion of the muscularis propria and muscularis mucosa and submucosa was 73.4% and 77.11%, respectively. In submucosal lesions, the correct identification rate was 78.64% and 84.4%, respectively. The images of lesions originating from the muscularis mucosa were easily confused with the images of lesions invading the muscularis mucosa and submucosa.

DISCUSSION

Traditionally, the treatment for benign and malignant esophageal lesions is mostly surgery or chemoradiotherapy, but the surgical trauma and sequelae are relatively large. With the development of gastrointestinal endoscopy in recent years, some lesions can be treated by endoscopy, such as ER, particularly submucosal dissection, which has become the standard treatment for esophageal mucosal cancer [25-27]. In Japan, ER of esophageal cancer refers to the tumor located in the mucosal epithelium (T1A-EP

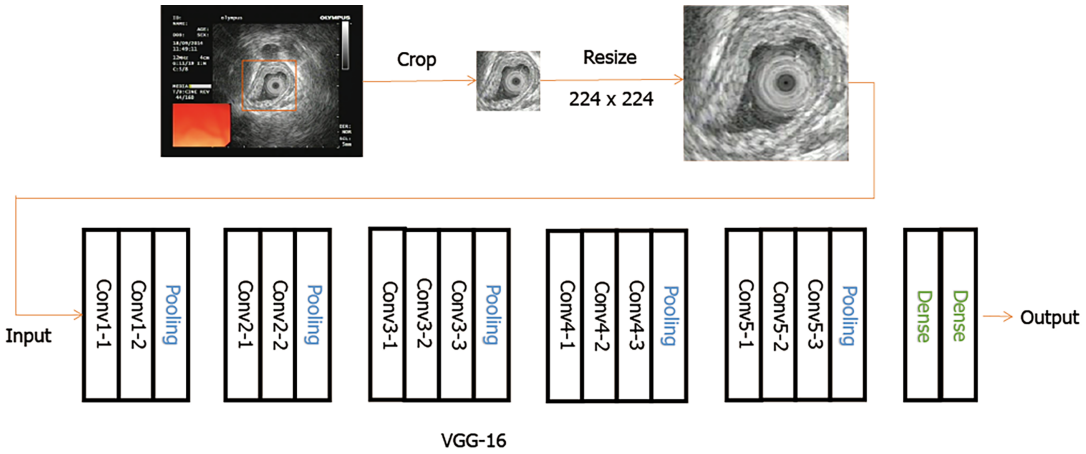
Table 5 Comparison of preoperative enhanced ultrasound diagnosis and postoperative pathological diagnosis in patients

Characteristic (n = 726)		
Gender, male/female	411/315	
Age (yr), medina (range)	54.5 (26-85)	
Invasion depth of esophageal lesion (n)	EUS diagnosis	Pathological diagnosis
Muscularis mucosa/submucosa	188	147
Muscularis propria	197	238
Serosa	45	45
Origin of esophageal lesions (n)		
Muscularis mucosa	148	150
Muscularis propria	148	146

Table 6 Results of proposed network in esophageal lesion database, %

	ACC	SENS	SPEC
Lesions invading the submucosa and muscularis mucosae	77.11	84.5	93.6
Lesions invading the muscularis propria	73.4	86.69	78.52
Lesions invading the serosa	98.9	72	99.14
Lesions from the muscularis mucosa	78.64	76.32	90.62
Lesions from the muscularis propria	84.4	81.64	90.92
Average	82.49	80.23	90.56

SENS: Sensitivity; SPEC: Specificity; ACC: Accuracy.

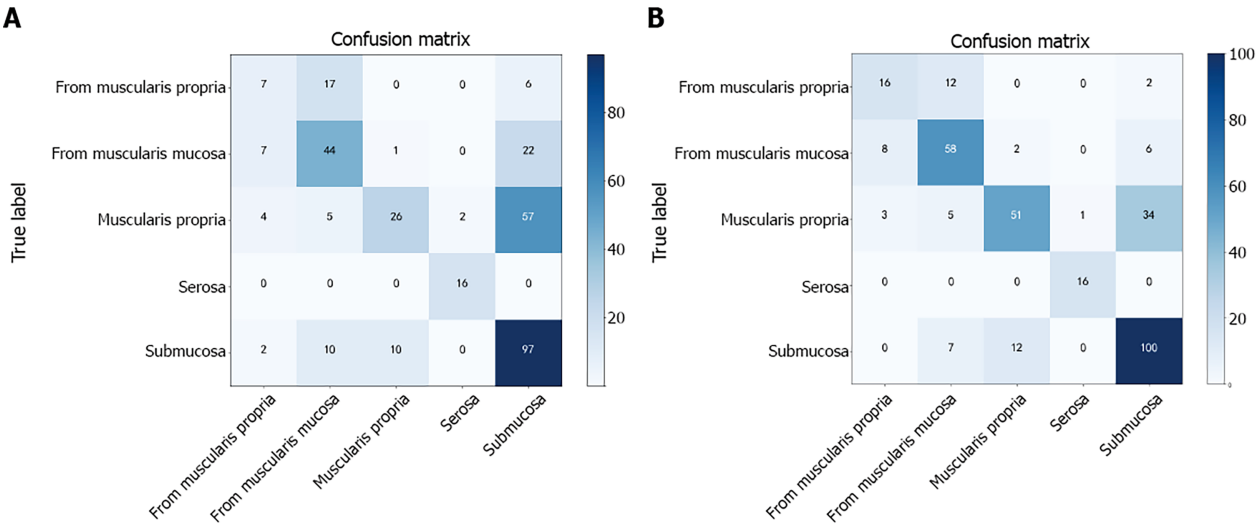


DOI: 10.3748/wjg.v28.i22.2457 **Copyright** ©The Author(s) 2022.

Figure 2 Structure of classification network.

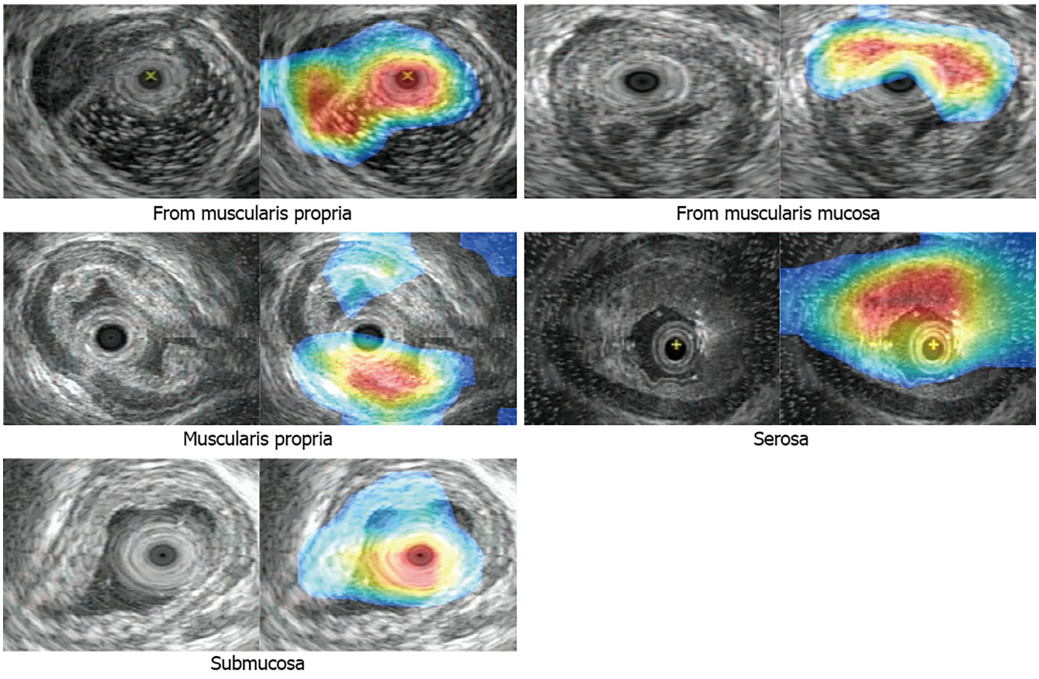
is equal to Tis *in situ* in the TNM stage[28]) or the proper mucosa (T1A-LPM) because the incidence of lymph node metastasis is low (≤ 5%)[29]. The recommended diagnostic methods are endoscopic ultrasonography[30], extended endoscopy, and narrow-band imaging (ME-NBI)[31].

Endoscopic ultrasonography plays an important role in the diagnosis and treatment of benign and malignant esophageal lesions. Xu *et al*[3] compared postoperative histological diagnosis with preoperative EUS diagnosis in patients with esophageal leiomyoma, and the diagnostic ACC of EUS was 88.6%. No treatment-related complications occurred in patients undergoing ER, and no recurrence was found in follow-up examination. In addition, Rana *et al*[32] found that small-probe EUS could predict the response to endoscopic dilation by describing the involvement degree of esophageal benign



DOI: 10.3748/wjg.v28.i22.2457 **Copyright** ©The Author(s) 2022.

Figure 3 Confusion matrix results of object detection methods (A) and classify methods (B).



DOI: 10.3748/wjg.v28.i22.2457 **Copyright** ©The Author(s) 2022.

Figure 4 Class activation map results.

stenosis and measuring the thickness of the wall. Therefore, EUS plays an important role in the diagnosis of digestive tract diseases. In this study, after follow-up pathology, 726 of the patients were compared with endoscopic pathology. The misdiagnosis rate of endoscopic diagnosis in the lesion invasion range was approximately 9.5%; 41 patients did not show lesion invasion to the muscularis propria, but 36 of them pathologically showed invasion to the superficial muscularis propria. The patients with invasion of the tunica adventitia were all treated by surgery with an ACC rate of 100%. For the examination of submucosal lesions, the ACC of EUS was approximately 99.3%. The results of this study showed that endoscopic ultrasonography had a high ACC rate for the origin of submucosal lesions, and the misdiagnosis rate was slightly higher in the evaluation of the invasion scope of lesions. Misdiagnosis might be due to the different operating and diagnostic levels of endoscopists, unclear ultrasound probes, and unclear lesions. However, when we underestimated the depth of infiltration, the disadvantage became smaller because ER combined with additional chemoradiotherapy and surgical treatment could achieve good therapeutic effects[33-34]. However, the use of EUS is difficult for non-specialist endoscopist. Therefore, a more advanced measurement method is necessary to help non-

specialists achieve diagnostic quality comparable to that of specialists without special techniques.

Deep learning is a new technique to evaluate image information objectively. In recent years, with the application of deep learning in various medical fields, remarkable progress has been made. AI is also becoming popular in ultrasonic examination. Kuwahara *et al*[5] predicted benign and malignant IPMNs by studying endoscopic ultrasonography of intraductal papillary mucinous tumors of the pancreas (IPMNs). The results showed that the SENS, SPEC, and ACC of AI for diagnosing malignant probability were 95.7%, 92.6%, and 94.0%, respectively, which were higher than those of human diagnosis. Although few studies have been conducted on AI in endoscopic ultrasonography, the diagnosis based on deep learning has shown its advantages. In this study, we found that deep learning algorithm could be used to clear the invasion scope and origin of lesions in endoscopic ultrasound images. In addition, VGGNet was used to perform classification tasks, and multiple superimposed filters were used to increase the nonlinearity of the whole function and reduce the number of parameters. The overall ACC, SENS, and SPEC were 82.49%, 80.23%, and 90.56%, respectively. However, in this study, the images of lesions invading the mucosal musculus and submucosa were easily confused with the images of lesions from the mucosal musculus, which may be caused by the lack of evident stratification due to tube wall compression or by the excessive noise in the ultrasound images caused by small lesions. No study has been conducted on the application of deep learning-based endoscopic ultrasonography in the esophagus or gastrointestinal tract, and the network framework applicable to endoscopic ultrasonography needs further screening and testing.

This study has some limitations. First, different probes or operators in endoscopic ultrasound images lead to uneven image quality levels, which may explain the low ACC in this study. Second, in this study, although the endoscopic ultrasonography probe could see seven layers of tube wall, 1-3 layers were classified into one category because the resolution of 1-3 layers was not clear in most images. Finally, the number of endoscopic ultrasound images was small, and all images were obtained from one center. Therefore, in the following study, we will obtain multi-center samples to increase the sample size and improve the image quality.

CONCLUSION

This study is the first to recognize esophageal endoscopic ultrasonography images through deep learning, which can automatically identify the lesion invasion depth and lesion source of submucosal tumors and classify such tumors, thereby achieving good ACC. In future studies, this method can provide guidance and help to clinical endoscopists.

ARTICLE HIGHLIGHTS

Research background

The esophagus is the narrowest part of the digestive tract and its diameter is not uniform. Endoscopic ultrasonography (EUS) can be used for high-precision evaluation of the esophagus. With the popularization of endoscopic ultrasonography in clinic, more and more endoscopic physicians are needed. The rapidly evolving field of machine learning is key to this paradigm shift.

Research motivation

Endoscopic ultrasonography is different from other ultrasound modalities in that ultrasonic examination is performed on the basis of digestive endoscopy, so the examiners should be professional endoscopic physicians with ultrasonic training. And as we face the interplay of increasing chronic diseases, ageing populations, and dwindling resources, we need to shift to models that can intelligently extract, analyze, interpret, and understand increasingly complex data. However, the research on the identification and classification of esophageal lesions by endoscopic ultrasonography has not yet been found.

Research objectives

The purpose of this study was to construct a framework of deep learning network to study the application of deep learning in esophageal EUS in identifying the origin of submucosal lesions and defining the scope of esophageal lesions.

Research methods

A total of 1670 white-light images were used to train and validate the convolutional neural network (CNN) system. In the study, VGGNet was used to perform classification tasks, and multiple superimposed filters were used to increase the nonlinearity of the whole function and reduce the number of parameters.

Research results

A total of 1115 patients were included in this analysis, including 694 males and 421 females. The overall accuracy, sensitivity, and specificity were 82.49%, 80.23%, and 90.56% respectively. The images of lesions originating from the muscularis mucosa were easily confused with the images of lesions invading the muscularis mucosa and submucosa.

Research conclusions

This study constructed a CNN system which can automatically identify the lesion invasion depth and the lesion source of submucosal tumors, and classify them, achieving good accuracy.

Research perspectives

In the future of medicine, artificial intelligence will reduce the workload of medical staff and make targeted tests more accurate, and in future studies, it can provide guidance and help to clinical endoscopists.

FOOTNOTES

Author contributions: Liu GS and He XP proposed the conception and design; He XP and Hua J were responsible for administrative support; Hua J and Huang PY provided the study materials or patients; Liu GS, He XP, Huang PY, and Zhuang SS collected and compiled the data; Wen ML did the data analysis and interpretation; all authors participated in manuscript writing and approved the final version of manuscript.

Supported by the Natural Science Foundation of Jiangsu, No. BK20171508.

Institutional review board statement: The study was approved by the Ethics Committee of the First Affiliated Hospital of Nanjing Medical University (No. 2019-SR-448).

Informed consent statement: Informed consent for upper gastrointestinal endoscopy (UGE) was obtained from all cases.

Conflict-of-interest statement: The authors have no conflicts of interest to disclose.

Data sharing statement: No additional data are available.

Open-Access: This article is an open-access article that was selected by an in-house editor and fully peer-reviewed by external reviewers. It is distributed in accordance with the Creative Commons Attribution NonCommercial (CC BY-NC 4.0) license, which permits others to distribute, remix, adapt, build upon this work non-commercially, and license their derivative works on different terms, provided the original work is properly cited and the use is non-commercial. See: http://creativecommons.org/Licenses/by-nc/4.0/

Country/Territory of origin: China

ORCID number: Gao-Shuang Liu 0000-0001-8450-7308; Pei-Yun Huang 0000-0003-1070-0724; Min-Li Wen 0000-0002-7945-9302; Shuai-Shuai Zhuang 0000-0003-3382-0008; Jie Hua 0000-0003-1243-0596; Xiao-Pu He 0000-0002-9915-5584.

S-Editor: Wu YXJ
L-Editor: Wang TQ
P-Editor: Wu YXJ

REFERENCES

1 **Mortensen MB**. Combined pretherapeutic endoscopic and laparoscopic ultrasonography may predict survival of patients with upper gastrointestinal tract cancer. *Surg Endosc* 2012; **26**: 891-892 [PMID: 22011950 DOI: 10.1007/s00464-011-1974-9]

2 **Rana SS**, Sharma R, Gupta R. High-frequency miniprobe endoscopic ultrasonography for evaluation of indeterminate esophageal strictures. *Ann Gastroenterol* 2018; **31**: 680-684 [PMID: 30386117 DOI: 10.20524/aog.2018.0307]

3 **Xu GQ**, Qian JJ, Chen MH, Ren GP, Chen HT. Endoscopic ultrasonography for the diagnosis and selecting treatment of esophageal leiomyoma. *J Gastroenterol Hepatol* 2012; **27**: 521-525 [PMID: 21916996 DOI: 10.1111/j.1440-1746.2011.06929.x]

4 **Sun LJ**, Chen X, Dai YN, Xu CF, Ji F, Chen LH, Chen HT, Chen CX. Endoscopic Ultrasonography in the Diagnosis and Treatment Strategy Choice of Esophageal Leiomyoma. *Clinics (Sao Paulo)* 2017; **72**: 197-201 [DOI: 10.6061/clinics/2017(04)01]

5 **Kuwahara T**, Hara K, Mizuno N, Okuno N, Matsumoto S, Obata M, Kurita Y, Koda H, Toriyama K, Onishi S, Ishihara M, Tanaka T, Tajika M, Niwa Y. Usefulness of Deep Learning Analysis for the Diagnosis of Malignancy in Intraductal

Papillary Mucinous Neoplasms of the Pancreas. *Clin Transl Gastroenterol* 2019; **10**: 1-8 [PMID: 31117111 DOI: 10.14309/ctg.0000000000000045]

6 **Sahakian AB**, Aslanian HR, Mehra M, Rossi F, Laine L, Sanchez M, Ciarleglio MM, Adimoolam V, Siddiqui UD. The utility of esophagogastroduodenoscopy before endoscopic ultrasonography in patients undergoing endoscopic ultrasonography for pancreatico-biliary and mediastinal indications. *J Clin Gastroenterol* 2013; **47**: 857-860 [PMID: 23632349 DOI: 10.1097/MCG.0b013e31828ba28c]

7 **Domper Arnal MJ**, Ferrández Arenas Á, Lanas Arbeloa Á. Esophageal cancer: Risk factors, screening and endoscopic treatment in Western and Eastern countries. *World J Gastroenterol* 2015; **21**: 7933-7943 [PMID: 26185366 DOI: 10.3748/wjg.v21.i26.7933]

8 **Zhang Y**. Epidemiology of esophageal cancer. *World J Gastroenterol* 2013; **19**: 5598-5606 [PMID: 24039351 DOI: 10.3748/wjg.v19.i34.5598]

9 **Lin Y**, Totsuka Y, He Y, Kikuchi S, Qiao Y, Ueda J, Wei W, Inoue M, Tanaka H. Epidemiology of esophageal cancer in Japan and China. *J Epidemiol* 2013; **23**: 233-242 [PMID: 23629646 DOI: 10.2188/jea.je20120162]

10 **Pennathur A**, Gibson MK, Jobe BA, Luketich JD. Oesophageal carcinoma. *Lancet* 2013; **381**: 400-412 [DOI: 10.1016/s0140-6736(12)60643-6]

11 **Wang GQ**, Abnet CC, Shen Q, Lewin KJ, Sun XD, Roth MJ, Qiao YL, Mark SD, Dong ZW, Taylor PR, Dawsey SM. Histological precursors of oesophageal squamous cell carcinoma: results from a 13 year prospective follow up study in a high risk population. *Gut* 2005; **54**: 187-192 [PMID: 15647178 DOI: 10.1136/gut.2004.046631]

12 **Pech O**, Bollschweiler E, Manner H, Leers J, Ell C, Hölscher AH. Comparison between endoscopic and surgical resection of mucosal esophageal adenocarcinoma in Barrett's esophagus at two high-volume centers. *Ann Surg* 2011; **254**: 67-72 [PMID: 21532466 DOI: 10.1097/SLA.0b013e31821d4bf6]

13 **Das A**, Singh V, Fleischer DE, Sharma VK. A comparison of endoscopic treatment and surgery in early esophageal cancer: an analysis of surveillance epidemiology and end results data. *Am J Gastroenterol* 2008; **103**: 1340-1345 [PMID: 18510606 DOI: 10.1111/j.1572-0241.2008.01889.x]

14 **LeCun Y**, Bengio Y, Hinton G. Deep learning. *Nature* 2015; **521**: 436-444 [PMID: 26017442 DOI: 10.1038/nature14539]

15 **Ting DSW**, Cheung CY, Lim G, Tan GSW, Quang ND, Gan A, Hamzah H, Garcia-Franco R, San Yeo IY, Lee SY, Wong EYM, Sabanayagam C, Baskaran M, Ibrahim F, Tan NC, Finkelstein EA, Lamoureux EL, Wong IY, Bressler NM, Sivaprasad S, Varma R, Jonas JB, He MG, Cheng CY, Cheung GCM, Aung T, Hsu W, Lee ML, Wong TY. Development and Validation of a Deep Learning System for Diabetic Retinopathy and Related Eye Diseases Using Retinal Images From Multiethnic Populations With Diabetes. *JAMA* 2017; **318**: 2211-2223 [PMID: 29234807 DOI: 10.1001/jama.2017.18152]

16 **Gulshan V**, Peng L, Coram M, Stumpe MC, Wu D, Narayanaswamy A, Venugopalan S, Widner K, Madams T, Cuadros J, Kim R, Raman R, Nelson PC, Mega JL, Webster DR. Development and Validation of a Deep Learning Algorithm for Detection of Diabetic Retinopathy in Retinal Fundus Photographs. *JAMA* 2016; **316**: 2402-2410 [PMID: 27898976 DOI: 10.1001/jama.2016.17216]

17 **Ehteshami Bejnordi B**, Veta M, Johannes van Diest P, van Ginneken B, Karssemeijer N, Litjens G, van der Laak JAWM; the CAMELYON16 Consortium, Hermsen M, Manson QF, Balkenhol M, Geessink O, Stathonikos N, van Dijk MC, Bult P, Beca F, Beck AH, Wang D, Khosla A, Gargeya R, Irshad H, Zhong A, Dou Q, Li Q, Chen H, Lin HJ, Heng PA, Haß C, Bruni E, Wong Q, Halici U, Öner MÜ, Cetin-Atalay R, Berseth M, Khvatkov V, Vylegzhanin A, Kraus O, Shaban M, Rajpoot N, Awan R, Sirinukunwattana K, Qaiser T, Tsang YW, Tellez D, Annuscheit J, Hufnagl P, Valkonen M, Kartasalo K, Latonen L, Ruusuvuori P, Liimatainen K, Albarqouni S, Mungal B, George A, Demirci S, Navab N, Watanabe S, Seno S, Takenaka Y, Matsuda H, Ahmady Phoulady H, Kovalev V, Kalinovsky A, Liauchuk V, Bueno G, Fernandez-Carrobles MM, Serrano I, Deniz O, Racoceanu D, Venâncio R. Diagnostic Assessment of Deep Learning Algorithms for Detection of Lymph Node Metastases in Women With Breast Cancer. *JAMA* 2017; **318**: 2199-2210 [PMID: 29234806 DOI: 10.1001/jama.2017.14585]

18 **Esteva A**, Kuprel B, Novoa RA, Ko J, Swetter SM, Blau HM, Thrun S. Dermatologist-level classification of skin cancer with deep neural networks. *Nature* 2017; **542**: 115-118 [PMID: 28117445 DOI: 10.1038/nature21056]

19 **Chi J**, Walia E, Babyn P, Wang J, Groot G, Eramian M. Thyroid Nodule Classification in Ultrasound Images by Fine-Tuning Deep Convolutional Neural Network. *J Digit Imaging* 2017; **30**: 477-486 [PMID: 28695342 DOI: 10.1007/s10278-017-9997-y]

20 **Seo JK**, Kim YJ, Kim KG, Shin I, Shin JH, Kwak JY. Differentiation of the Follicular Neoplasm on the Gray-Scale US by Image Selection Subsampling along with the Marginal Outline Using Convolutional Neural Network. *Biomed Res Int* 2017; **2017**: 3098293 [PMID: 29527533 DOI: 10.1155/2017/3098293]

21 **Nishida N**, Yamakawa M, Shiina T, Kudo M. Current status and perspectives for computer-aided ultrasonic diagnosis of liver lesions using deep learning technology. *Hepatol Int* 2019; **13**: 416-421 [PMID: 30790230 DOI: 10.1007/s12072-019-09937-4]

22 **Choi JS**, Han BK, Ko ES, Bae JM, Ko EY, Song SH, Kwon MR, Shin JH, Hahn SY. Effect of a Deep Learning Framework-Based Computer-Aided Diagnosis System on the Diagnostic Performance of Radiologists in Differentiating between Malignant and Benign Masses on Breast Ultrasonography. *Korean J Radiol* 2019; **20**: 749-758 [PMID: 30993926 DOI: 10.3348/kjr.2018.0530]

23 **Zhou Z**, Shin J, Feng R, Hurst RT, Kendall CB, Liang J. Integrating Active Learning and Transfer Learning for Carotid Intima-Media Thickness Video Interpretation. *J Digit Imaging* 2019; **32**: 290-299 [PMID: 30402668 DOI: 10.1007/s10278-018-0143-2]

24 **Al Jassim RA**, Andrews FM. The bacterial community of the horse gastrointestinal tract and its relation to fermentative acidosis, laminitis, colic, and stomach ulcers. *Vet Clin North Am Equine Pract* 2009; **25**: 199-215 [PMID: 19580934 DOI: 10.1016/j.cveq.2009.04.005]

25 **Takahashi H**, Arimura Y, Masao H, Okahara S, Tanuma T, Kodaira J, Kagaya H, Shimizu Y, Hokari K, Tsukagoshi H, Shinomura Y, Fujita M. Endoscopic submucosal dissection is superior to conventional endoscopic resection as a curative treatment for early squamous cell carcinoma of the esophagus (with video). *Gastrointest Endosc* 2010; **72**: 255-264, 264.e1 [PMID: 20541198 DOI: 10.1016/j.gie.2010.02.040]

26 **Repici A**, Hassan C, Carlino A, Pagano N, Zullo A, Rando G, Strangio G, Romeo F, Nicita R, Rosati R, Malesci A. Endoscopic submucosal dissection in patients with early esophageal squamous cell carcinoma: results from a prospective Western series. *Gastrointest Endosc* 2010; **71**: 715-721 [PMID: 20363414 DOI: 10.1016/j.gie.2009.11.020]

27 **Ishihara R**, Iishi H, Uedo N, Takeuchi Y, Yamamoto S, Yamada T, Masuda E, Higashino K, Kato M, Narahara H, Tatsuta M. Comparison of EMR and endoscopic submucosal dissection for en bloc resection of early esophageal cancers in Japan. *Gastrointest Endosc* 2008; **68**: 1066-1072 [PMID: 18620345 DOI: 10.1016/j.gie.2008.03.1114]

28 **Amin MB**, Greene FL, Edge SB, Compton CC, Gershenwald JE, Brookland RK, Meyer L, Gress DM, Byrd DR, Winchester DP. The Eighth Edition AJCC Cancer Staging Manual: Continuing to build a bridge from a population-based to a more "personalized" approach to cancer staging. *CA Cancer J Clin* 2017; **67**: 93-99 [PMID: 28094848 DOI: 10.3322/caac.21388]

29 **Kuwano H**, Nishimura Y, Oyama T, Kato H, Kitagawa Y, Kusano M, Shimada H, Takiuchi H, Toh Y, Doki Y, Naomoto Y, Matsubara H, Miyazaki T, Muto M, Yanagisawa A. Guidelines for Diagnosis and Treatment of Carcinoma of the Esophagus April 2012 edited by the Japan Esophageal Society. *Esophagus* 2015; **12**: 1-30 [PMID: 25620903 DOI: 10.1007/s10388-014-0465-1]

30 **Oyama T**, Inoue H, Arima M, Momma K, Omori T, Ishihara R, Hirasawa D, Takeuchi M, Tomori A, Goda K. Prediction of the invasion depth of superficial squamous cell carcinoma based on microvessel morphology: magnifying endoscopic classification of the Japan Esophageal Society. *Esophagus* 2017; **14**: 105-112 [PMID: 28386209 DOI: 10.1007/s10388-016-0527-7]

31 **Esaki M**, Matsumoto T, Moriyama T, Hizawa K, Ohji Y, Nakamura S, Hirakawa K, Hirahashi M, Yao T, Iida M. Probe EUS for the diagnosis of invasion depth in superficial esophageal cancer: a comparison between a jelly-filled method and a water-filled balloon method. *Gastrointest Endosc* 2006; **63**: 389-395 [PMID: 16500385 DOI: 10.1016/j.gie.2005.10.027]

32 **Rana SS**, Sharma R, Kishore K, Gupta R. High-frequency miniprobe endoscopic ultrasonography in the management of benign esophageal strictures. *Ann Gastroenterol* 2020; **33**: 25-29 [DOI: 10.20524/aog.2019.0436]

33 **Shimizu Y**, Kato M, Yamamoto J, Nakagawa S, Tsukagoshi H, Fujita M, Hosokawa M, Asaka M. EMR combined with chemoradiotherapy: a novel treatment for superficial esophageal squamous-cell carcinoma. *Gastrointest Endosc* 2004; **59**: 199-204 [DOI: 10.1016/s0016-5107(03)02688-9]

34 **Saeki H**, Watanabe M, Mine S, Shigaki H, Oya S, Ishiyama A, Tsuchida T, Fujisaki J, Baba H, Maehara Y, Sano T. Esophagectomy for superficial esophageal cancer after non-curative endoscopic resection. *J Gastroenterol* 2015; **50**: 406-413 [PMID: 25084980 DOI: 10.1007/s00535-014-0983-6]

World Journal of Gastroenterology

Submit a Manuscript: https://www.f6publishing.com

World J Gastroenterol 2022 June 14; 28(22): 2468-2481

DOI: 10.3748/wjg.v28.i22.2468

ISSN 1007-9327 (print) ISSN 2219-2840 (online)

ORIGINAL ARTICLE

Retrospective Study

Prognostic value of preoperative enhanced computed tomography as a quantitative imaging biomarker in pancreatic cancer

Jian-Feng Gao, Yu Pan, Xian-Chao Lin, Feng-Chun Lu, Ding-Shen Qiu, Jun-Jun Liu, He-Guang Huang

Specialty type: Gastroenterology and hepatology

Provenance and peer review: Unsolicited article; Externally peer reviewed.

Peer-review model: Single blind

Peer-review report's scientific quality classification

Grade A (Excellent): 0
Grade B (Very good): B, B
Grade C (Good): C
Grade D (Fair): D
Grade E (Poor): 0

P-Reviewer: Casà C, Italy; Lee Y, South Korea; Singh I, United States

Received: August 3, 2021
Peer-review started: August 3, 2021
First decision: October 2, 2021
Revised: October 31, 2021
Accepted: May 16, 2022
Article in press: May 16, 2022
Published online: June 14, 2022

Jian-Feng Gao, Yu Pan, Xian-Chao Lin, Feng-Chun Lu, He-Guang Huang, Department of General Surgery, Fujian Medical University Union Hospital, Fuzhou 350001, Fujian Province, China

Ding-Shen Qiu, Jun-Jun Liu, Department of Radiology, The Hospital of Changle, Fuzhou 350200, Fujian Province, China

Corresponding author: He-Guang Huang, MD, Chief Physician, Department of General Surgery, Fujian Medical University Union Hospital, No. 29 Xinquan Road, Fuzhou 350001, Fujian Province, China. Heguanghuang22@163.com

Abstract

BACKGROUND

Pancreatic ductal adenocarcinoma (PDAC) is one of the most lethal malignancies with high mortality and short survival time. Computed tomography (CT) plays an important role in the diagnosis, staging and treatment of pancreatic tumour. Pancreatic cancer generally shows a low enhancement pattern compared with normal pancreatic tissue.

AIM

To analyse whether preoperative enhanced CT could be used to predict postoperative overall survival in patients with PDAC.

METHODS

Sixty-seven patients with PDAC undergoing pancreatic resection were enrolled retrospectively. All patients underwent preoperative unenhanced and enhanced CT examination, the CT values of which were measured. The ratio of the preoperative CT value increase from the nonenhancement phase to the portal venous phase between pancreatic tumour and normal pancreatic tissue was calculated. The cut-off value of ratios was obtained by the receiver operating characteristic (ROC) curve of the tumour relative enhancement ratio (TRER), according to which patients were divided into low- and high-enhancement groups. Univariate and multivariate analyses were performed using Cox regression based on TRER grouping. Finally, the correlation between TRER and clinicopathological characteristics was analysed.

RESULTS

The area under the curve of the ROC curve was 0.768 ($P < 0.05$), and the cut-off value of the ROC curve was calculated as 0.7. TRER ≤ 0.7 was defined as the low-

enhancement group, and TRER > 0.7 was defined as the high-enhancement group. According to the TRER grouping, the Kaplan-Meier survival curve analysis results showed that the median survival (10.0 mo) with TRER ≤ 0.7 was significantly shorter than that (22.0 mo) with TRER > 0.7 (P < 0.05). In the univariate and multivariate analyses, the prognosis of patients with TRER ≤ 0.7 was significantly worse than that of patients with TRER > 0.7 (P < 0.05). Our results demonstrated that patients in the low TRER group were more likely to have higher American Joint Committee on Cancer stage, tumour stage and lymph node stage (all P < 0.05), and TRER was significantly negatively correlated with tumour size (P < 0.05).

CONCLUSION

TRER ≤ 0.7 in patients with PDAC may represent a tumour with higher clinical stage and result in a shorter overall survival.

Key Words: Pancreatic cancer; Computed tomography; Diagnostic imaging; Kaplan-Meier curve; Prognosis; Survival analysis

©The Author(s) 2022. Published by Baishideng Publishing Group Inc. All rights reserved.

Core Tip: Computed tomography (CT) plays an important role in the diagnosis, staging and treatment of pancreatic tumours. Pancreatic cancer generally shows a low enhancement pattern compared with normal pancreatic tissue. In our analysis, the prognosis of patients with the tumour relative enhancement ratio (TRER) less than or equal to 0.7 was significantly worse than that of patients with TRER greater than 0.7. TRER was significantly correlated with American Joint Committee on Cancer stage, tumour stage, and lymph node stage. Preoperative enhanced CT provides a simple and effective prediction of postoperative overall survival in pancreatic ductal adenocarcinoma.

Citation: Gao JF, Pan Y, Lin XC, Lu FC, Qiu DS, Liu JJ, Huang HG. Prognostic value of preoperative enhanced computed tomography as a quantitative imaging biomarker in pancreatic cancer. *World J Gastroenterol* 2022; 28(22): 2468-2481

URL: https://www.wjgnet.com/1007-9327/full/v28/i22/2468.htm

DOI: https://dx.doi.org/10.3748/wjg.v28.i22.2468

INTRODUCTION

Pancreatic adenocarcinoma is a highly malignant tumour with an estimated 56770 new cases and 45750 deaths in the United States in 2019, according to the American Cancer Society[1]. Very few patients with pancreatic adenocarcinoma have the opportunity for surgical treatment due to the low early diagnosis rate[2]. Surgery is the only potential curative treatment for resectable pancreatic cancer, and adjuvant chemotherapy, mainly gemcitabine-based regimen, is often used to improve outcome[3,4]. In recent years, neoadjuvant chemoradiotherapy has shown efficacy in improving the prognosis of patients with pancreatic cancer[5]. However, the overall prognosis is still unsatisfactory, with a 5-year survival rate as low as 8%[6]. Considering the extremely poor prognosis of pancreatic cancer, it is important to identify indicators of poor prognosis preoperatively or postoperatively. Currently, multiple diagnostic techniques are used to evaluate the aggressiveness or malignancy of pancreatic cancer to formulate the best treatment plan.

A previous study on endoscopic ultrasonography showed that the strain rate of the tumour was positively correlated with the stromal ratio of pancreatic cancer. The stroma of the tumour contributes to tumour growth and progression and plays an important role in chemotherapy resistance. Patients with a high strain rate had a poor prognosis postsurgery, but the survival of locally advanced pancreatic cancer patients receiving nab-paclitaxel and gemcitabine regimen chemotherapy had been improved[7]. Another study showed that tumour size, tumour-lymph node-metastasis (TNM) stage and distant metastasis were significantly correlated with overall survival (OS) in pancreatic cancer[8]. Computed tomography (CT) imaging has been widely used in the diagnosis, staging and treatment planning of pancreatic cancer[9]. Pancreatic cancer tumours generally show a low enhancement pattern compared with normal pancreatic tissue[10]. CT texture analysis is also used to evaluate the prognosis of pancreatic cancer[11,12]. Low vascular distribution and high metabolism in pancreatic cancer are important factors in evaluating invasiveness[13].

The purpose of this study was to evaluate the prognostic value of preoperative enhanced CT as a quantitative imaging biomarker in patients with pancreatic cancer based on the imaging characteristics

of poor blood supply and CT examination.

MATERIALS AND METHODS

Patient population

The Ethics Committee of Fujian Medical University Union Hospital, Fuzhou, China, approved this retrospective study and waived the requirement for informed consent (No. 2020KY0141).

From March 2011 to May 2018, a total of 138 consecutive patients diagnosed with pancreatic adenocarcinoma who underwent surgical resection in our department were reviewed. The last follow-up time was February 2020. The inclusion criteria were as follows: (1) Age over 18 years; (2) no neoadjuvant chemoradiotherapy and no previous history of gastrointestinal and pancreatic surgery; (3) nonenhanced and enhanced CT performed within 30 days before surgery; and (4) pancreatic adenocarcinoma confirmed by postoperative pathology. The exclusion criteria were as follows: (1) Stage IV pancreatic cancer; (2) severe complications or multiple primary cancers; (3) obvious pancreatic parenchymal atrophy, large cystic changes of the tumour and calcareous deposition; and (4) loss to follow-up. Patient sex, age, preoperative CT images, preoperative serum carbohydrate antigen 19-9 (CA19-9), tumour site, tumour size, American Joint Committee on Cancer (AJCC) (2017) TNM staging, lymph node metastasis, postoperative pathology and differentiation grade, postoperative OS and other data were collected for analysis.

CT image acquisition

CT examination was performed on a 16-row CT scanner (Bright Speed Elite, GE Health care, United States) or a 64-row CT scanner (Discovery CT750 HD, GE Health care, United States). The CT scanning parameters for all phases were as follows: Gantry rotation speed, 0.5 s; tube voltage, 120 kVp; effective amperage, 210 mAs-260 mAs; matrix, 512 × 512; field of view, 350 mm-512 mm; and slice thickness, 5-10 mm. After a nonenhanced scan, 1.5 mL/kg of nonionic contrast agent (ioversol injection, 320 mg of iodine per millilitre, Jiangsu Hengrui Medicine Co., LTD, Jiangsu Province, China) was injected with an automatic syringe at 3.0 mL/s. Using the bolus-tracking technique, a pancreatic parenchymal (PP) phase scan was performed 7 s after the enhanced value of the descending aorta at the aortic hiatus reached 150 HU, and a portal venous (PV) phase scan was performed 25 s after the PP phase scan. CT imaging data were uploaded to the Picture Archiving and Communication System (PACS) (Guangzhou YLZ Ruitu Information Technology Co., LTD, Guangzhou, Guangdong Province, China). In the process of collecting and reviewing the CT imaging results of the patient's imaging data, we tried our best to make the quality of each patient's tumour image meet our requirements.

The CT images and tumour relative enhanceement ratio (TRER) were analysed by two experienced radiologists using PACS. The region of the overall tumour (ROT) was delineated along the tumour edge at the largest and most visible level. Four regions of interest (ROIs) with diameters of 0.2-0.3 cm were randomly selected from the normal pancreatic tissue that were more than 1.0 cm away from ROT while avoiding obvious blood vessels, pancreatic ducts, pancreatic fissures and sites susceptible to intestinal gas interference. The average CT values of these 4 ROIs were used as CT values of pancreatic tissue outside the tumour (PTOT).

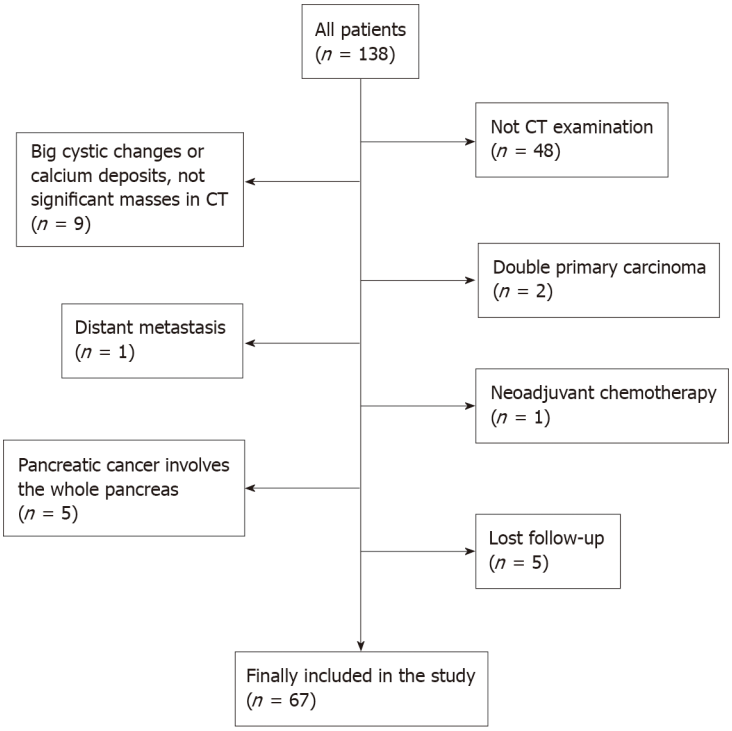
Tumour enhancement amplitude (TEA) = ROT value of the PV phase – ROT value of the nonenhancement phase.

Pancreas enhancement amplitude outside tumour (PEA) = PTOT value of the PV phase – PTOT value of the nonenhancement phase.

TRER = TEA/PEA.

Statistical analysis

SPSS 25.0 for Windows software from IBM was used to establish a database for statistical analysis. Among the patients' baseline data, those with a normal distribution of measurement data were represented by the mean ± SD, and an independent sample *t* test was used for comparisons between groups. The data with a nonnormal distribution were represented by the median and interquartile spacing, and comparisons between groups were tested by the nonparametric Mann-Whitney *U* test. Enumeration data were expressed in terms of frequency, and comparisons between groups were performed by the chi-squared test or Fisher's exact test. In the analysis of the relationship between TRER and OS, a receiver operating characteristic (ROC) curve was drawn. When the ROC curve was obtained, the "Coordinates of the Curve" and the corresponding "Sensitivity" and "1-Specificity" could be obtained, and their corresponding Youden indices could be calculated. The TRER corresponding to the maximum value of all Youden indices was the cut-off value of the ROC curve. The patients were divided into two groups according to the cut-off value. The corresponding survival curve was estimated by the Kaplan-Meier method (log-rank test). Cox regression was performed for the univariate (enter model) and multivariate analyses (forward LR model). In the case of correlation analysis between TRER and clinicopathological characteristics, when the clinicopathological features were grouped as unordered categorical variables, the chi-squared test was used for analysis and the Cramer's V



DOI: 10.3748/wjg.v28.i22.2468 **Copyright** ©The Author(s) 2022.

Figure 1 The study flowchart for patient selection. CT: Computed tomography.

correlation coefficient was calculated; When the clinicopathological features were grouped as ordinal categorical variables, Spearman rank correlation was used for analysis and the Spearman's correlation coefficient was calculated. The results were considered statistically significant below the bilateral 5% significance level.

RESULTS

Patient characteristics

Of 138 patients, a total of 71 were excluded from the study (a flowchart of patient selection is shown in Figure 1). Ultimately, 67 patients were enrolled in the study. The clinical characteristics of the 67 patients in our study are summarized in Table 1. The mean age of 67 patients was 60.2 ± 10.0 (range, 35-80) years old, with 42 males (62.7%). The tumour was located in the head or uncinate of the pancreas in 44 patients (65.7%) and other sites in 23 patients (34.3%). The median postoperative OS of all patients was 12.3 mo (range, 1.7-42.8 mo).

CT value, TRER and CT enhancement situation

The CT values of the nonenhancement and PV phases in tumour and extratumoural regions are shown in Table 2. The median TRER was 0.57 (interquartile range, 0.41-0.78).

In the analysis of CT images, we also found that the CT values of ROT and PTOT gradually increased from the nonenhancement phase to the PV phase, but not all CT values of the PV phase were higher than those of the PP phase (Table 3).

Survival analysis

The ROC curve was drawn according to TRER, as shown in Figure 2A. The area under the curve of the ROC curve was 0.768 (P = 0.007). The cut-off value of the ROC curve was calculated to be 0.7, and the patients were classified according to the cut-off value. TRER ≤ 0.7 was defined as the low-enhancement group, TRER > 0.7 was defined as the high-enhancement group, and the Kaplan-Meier survival curve analysis results showed that the median survival (10.0 mo) with TRER ≤ 0.7 was significantly worse than that (22.0 mo) with TRER > 0.7 (P < 0.05) (Figure 2B). Typical CT images of the low- and high-enhancement groups are shown in Figures 3 and 4, respectively.

There was no significant difference in age, sex, tumour location, CA19-9, tumour differentiation, vascular invasion, surgical margin or adjuvant chemotherapy distribution between the low-and high-enhancement groups except the AJCC stage (P = 0.015) (Table 4).

Table 1 Patient characteristics, *n* (%)

Patient characteristics	*n* = 67
Age (yr)	
≤ 60	31 (46.3)
> 60	36 (53.7)
Sex	
Male	42 (62.7)
Female	25 (37.3)
Tumour location	
Head/uncinate	44 (65.7)
Body/tail	23 (34.3)
CA19-9	
< 37 ng/mL	20 (29.9)
≥ 37 ng/mL	47 (70.1)
AJCC stage (2017)	
I	11 (16.4)
II	27 (40.3)
III	29 (43.3)
Tumour differentiation	
Highly/moderately	49 (73.1)
Poorly/undifferentiated	18 (26.9)
Surgical margin	
Negative	57 (85.1)
Positive	10 (14.9)
Vascular invasion	
No	51 (76.1)
Yes	16 (23.9)
Adjuvant chemotherapy	
No	33 (49.3)
Yes	34 (50.7)

CA19-9: Carbohydrate antigen 19-9; AJCC: American Joint Committee on Cancer.

Univariate and multivariate analyses

Univariate and multivariate analyses of Cox regression were performed for clinical data and TRER (Tables 5 and 6). In the univariate analysis, AJCC stage (P = 0.005), preoperative CA19-9 (P = 0.033), postoperative adjuvant chemotherapy (P = 0.000) and TRER (P = 0.001) were significantly correlated with postoperative OS, while other factors had no significant influence on postoperative OS. In the multivariate analysis, preoperative CA19-9 (P = 0.015), tumour differentiation (P = 0.001), surgical margin (P = 0.008), postoperative adjuvant chemotherapy (P = 0.000) and TRER (P = 0.009) were significantly correlated with postoperative OS.

Correlation between TRER and clinicopathological characteristics

A correlation analysis was conducted between TRER and clinicopathological characteristics (Table 7). The results showed that TRER was not significantly correlated with tumour location, preoperative serum CA19-9, lymph node metastasis, vascular invasion, or tumour differentiation (all P > 0.05). However, TRER was significantly correlated with AJCC stage (P = 0.003, Spearman correlation coefficient = -0.353), T stage (P = 0.005, Cramer's V correlation coefficient = 0.343), and N stage (P = 0.046, Spearman correlation coefficient = -0.245). The analysis of the relationship between TRER and

Table 2 Computed tomography attenuation values and tumour relative enhancement ratio

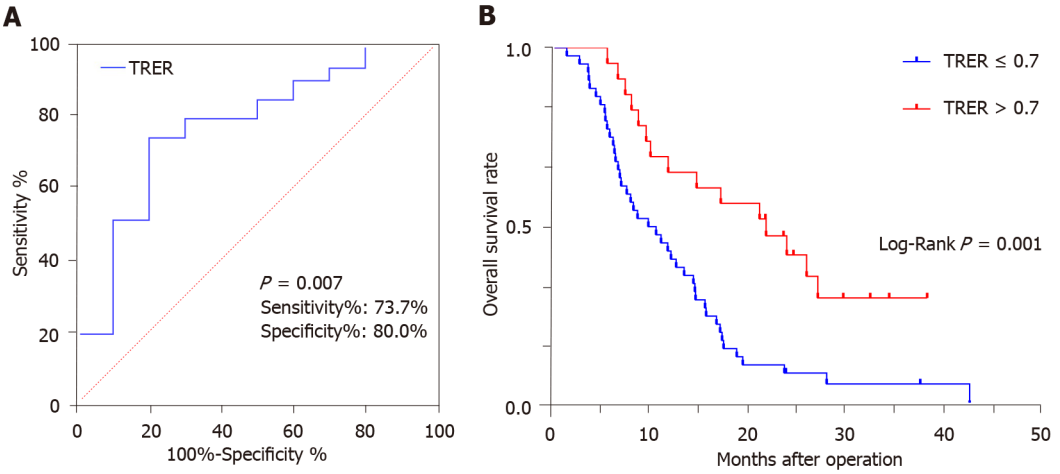
Location, phase and TRER	Value
ROT	
Nonenhancement phase (HU)	36.1 (31.0-39.2)
PV phase (HU)	58.0 (50.3-70.0)
PTOT	
Nonenhancement phase (HU)	43.5 (36.8-48.1)
PV phase (HU)	82.7 (71.8-98.4)
TRER	0.57 (0.41-0.78)

TRER: Tumour relative enhancement ratio; ROT: Region of the overall tumour; PTOT: Pancreatic tissue outside the tumour; PP: Pancreatic parenchymal; PV: Portal venous.

Table 3 Computed tomography enhancement situation comparing the portal venous phase to the pancreatic parenchymal phase

CT enhancement situation (PV phase and PP phase)	No. of patients (*n*)	
	PV phase > PP phase	PV phase < PP phase
ROT	64	3
PTOT	50	17

ROT: Region of the overall tumour; PTOT: Pancreatic tissue outside the tumour; PP: Pancreatic parenchymal; PV: Portal venous.



DOI: 10.3748/wjg.v28.i22.2468 **Copyright** ©The Author(s) 2022.

Figure 2 The receiver operating characteristic curve and Kaplan-Meier survival curve analysis. A: The receiver operating characteristic curve of tumour relative enhancement ratio (TRER) for patients with pancreatic ductal adenocarcinoma. The area under the curve was 0.768 (P = 0.007). The cut-off value was 0.7; B: Kaplan-Meier survival curve of postoperative overall survival for low-TRER patients and high-TRER patients. TRER: Tumour relative enhancement ratio.

tumour size showed that TRER was negatively correlated with tumour size (P = 0.001) (Figure 5).

DISCUSSION

Pancreatic cancer is a tumour with a very poor prognosis. CT plays important roles in the diagnosis of pancreatic cancer and the evaluation of the relationship between tumours and peripheral blood vessels. Our study found the clinical value of enhanced CT as a quantitative image in predicting the prognosis of pancreatic cancer.

Table 4 Baseline characteristics of the low-and high-enhancement groups

Variable	TRER ≤ 0.7, No. of patients, *n* (%)	TRER > 0.7, No. of patients, *n* (%)	*P* value
Age (yr)			0.397
≤ 60	22 (50.0)	9 (39.1)	
> 60	22 (50.0)	14 (60.9)	
Sex			0.170
Male	25 (56.8)	17 (73.9)	
Female	19 (43.2)	6 (26.1)	
Tumour location			0.117
Head/uncinate	26 (59.1)	18 (78.3)	
Body/tail	18 (40.9)	5 (21.7)	
CA19-9			0.230
< 37 ng/mL	11 (25.0)	9 (39.1)	
≥ 37 ng/mL	33 (75.0)	14 (60.9)	
AJCC stage (2017)			0.015
I	4 (9.1)	7 (30.4)	
II	16 (36.4)	11 (47.8)	
III	24 (54.5)	5 (21.7)	
Tumour differentiation			0.634
Highly/moderately	33 (75.0)	16 (69.6)	
Poorly/undifferentiated	11 (25.0)	7 (30.4)	
Vascular invasion			0.071
No	30 (68.2)	21 (91.3)	
Yes	14 (31.8)	2 (8.7)	
Surgical margin			0.501
Negative	36 (81.8)	21 (91.3)	
Positive	8 (18.2)	2 (8.7)	
Adjuvant chemotherapy			0.087
No	25 (56.8)	8 (34.8)	
Yes	19 (43.2)	15 (65.2)	

CA19-9: Carbohydrate antigen 19-9; AJCC: American Joint Committee on Cancer; TRER: Tumour relative enhancement ratio.

For patients with pancreatic cancer, TNM staging, tumour size, lymph node positive rate, log odds of positive lymph nodes, R0 resection and other factors are related to patient recurrence-free survival and OS[14-16]. Our analysis results showed that patients in the low TRER group were more likely to have higher TNM stage, T stage and N stage, and TRER was significantly negatively correlated with tumour size, demonstrating that TRER could be used to predict the postoperative OS of pancreatic cancer. However, in our study, the tumour stage (AJCC) was significant in the univariate analysis but not in the multivariate analysis. This difference might be due to the relatively small sample size. Many imaging techniques combining qualitative and quantitative information with pathological findings of the tumour have been used to analyse the aggressiveness of the tumour to determine the prognosis of the patient from preoperative imaging information. Dynamic contrast-enhanced CT (DCE-CT) also shows potential value in predicting tumour response to treatment and outcome[17,18].

Currently, the qualitative analysis of CT images has gained increasing attention for the prognostic analysis of pancreatic cancer. Pancreatic adenocarcinoma, unlike other solid tumours, is known as a cold tumour with insufficient blood supply. The pathological type of 90% pancreatic cancer is invasive ductal adenocarcinoma, which is one of the most stromal malignant tumours[19,20]. The pancreas is a retroperitoneal organ, very close to the common hepatic artery, celiac artery, portal vein, superior

Table 5 Univariate analysis using Cox regression for postoperative overall survival in all patients

Variable	No. of patients, *n* (%)	No. of events	Median OS (mo) (95%CI)	*P* value
Age (yr)				0.699
≤ 60	31 (46.3)	27	14.6 (9.1-20.0)	
> 60	36 (53.7)	30	10.2 (5.7-14.7)	
Sex				0.651
Male	42 (62.7)	34	10.2 (4.3-16.1)	
Female	25 (37.3)	23	13.6 (9.2-18.1)	
Tumour location				0.836
Head/uncinate	44 (65.7)	36	12.0 (7.7-16.3)	
Body/tail	23 (34.3)	21	12.8 (4.1-21.6)	
AJCC stage (2017)				0.005
I	11 (16.4)	6	27.3 (14.9-39.6)	
II	27 (40.3)	23	12.0 (10.2-13.8)	
III	29 (43.3)	28	8.9 (5.0-12.7)	
CA19-9				0.033
< 37 ng/mL	20 (29.9)	14	15.8 (10.4-21.2)	
≥ 37 ng/mL	47 (70.1)	43	11.3 (7.2-15.3)	
Tumour differentiation				0.255
Highly/moderately	49 (73.1)	42	14.7 (11.9-17.6)	
Poorly/undifferentiated	18 (26.9)	15	8.2 (5.7-10.7)	
Surgical margin				0.141
Negative	57 (85.1)	47	12.3 (7.5-17.1)	
Positive	10 (14.9)	10	12.0 (2.9-21.1)	
Vascular invasion				0.435
No	51 (76.1)	41	12.3 (7.7-16.9)	
Yes	16 (23.9)	16	12.0 (4.8-19.2)	
Adjuvant chemotherapy				0.000
No	33 (49.3)	32	8.2 (6.6-9.7)	
Yes	34 (50.7)	25	17.7 (14.4-20.9)	
TRER				0.001
≤ 0.7	44 (65.7)	42	10.0 (5.9-14.1)	
> 0.7	23 (34.3)	15	22.0 (12.4-31.6)	

CI: Confidence interval; CA19-9: Carbohydrate antigen 19-9; AJCC: American Joint Committee on Cancer; TRER: Tumour relative enhancement ratio; OS: Overall survival.

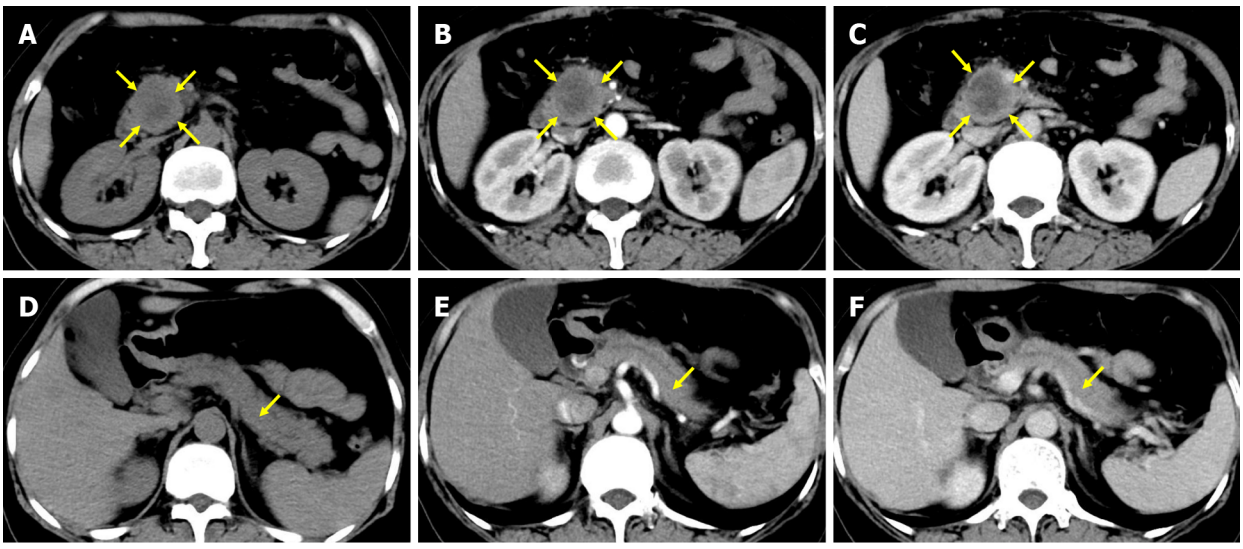
mesenteric vessels, and splenic vessels. As pancreatic cancer progresses, it has early infiltration or perivascular desmoplastic reactions, which can influence its direct blood supply. The correlation analysis in our study showed that the vascular invasion rate in the low TRER group was higher (31.8%) than that in the high TRER group (8.7%), but $P = 0.071$, which might be due to the relatively small sample size.

In our study, we did not find any relationship between TRER and pathological differentiation of pancreatic cancer. However, a previous study on DCE-CT showed that pancreatic tumour CT enhancement was negatively correlated with pathological grade and the degree of malignancy[21,22]. In pancreatic cancer, fibroblast hyperplasia and vascular reduction are caused by a high fibrinolysis response, which results in a low-enhancement CT pattern compared with PTOT[23]. Some studies have shown that there is no significant difference in the perfusion values of the pancreatic head, body and tail

Table 6 Multivariate analysis using Cox regression for postoperative overall survival in all patients

Variable	Hazard ratio	95%CI	*P* value
CA19-9 (ng/mL)	2.279	1.174-4.422	0.015
Tumour differentiation	3.057	1.585-5.898	0.001
Surgical margin	2.860	1.315-6.222	0.008
Adjuvant chemotherapy	0.200	0.106-0.380	0.000
TRER	0.432	0.229-0.812	0.009

CI: Confidence interval; CA19-9: Carbohydrate antigen 19-9; TRER: Tumour relative enhancement ratio.



DOI: 10.3748/wjg.v28.i22.2468 **Copyright** ©The Author(s) 2022.

Figure 3 A 61-year-old woman with a mass in the head of the pancreas. A-C: The nonenhancement phase (A), pancreatic parenchymal (PP) phase (B) and portal venous (PV) phase (C) of region of the overall tumour, respectively; D-F: The nonenhancement phase (D), PP phase (E) and PV phase (F) of pancreatic tissue outside the tumour, respectively. Tumour relative enhancement ratio ≤ 0.7, and the postoperative overall survival was 5.5 mo.

in normal pancreatic tissues, while the perfusion values and blood flow in the tumour centre of pancreatic cancer patients are lower than those of PTOT[24,25]. Some researchers have reported that necrosis within pancreatic adenocarcinoma influences tumour enhancement on CT[26,27]. Tumour necrosis is the final result of hypoxia, which can accelerate the progression of malignant tumours[28,29]. It is well known that larger tumours are more prone to necrosis. The indirect relationship between large tumours and weakened CT enhancement was confirmed in our research. The TRER also indirectly reflects the necrosis of the tumour. A previous study showed that patients with low CT values in pancreatic tumours at the parenchymal stage, portal venous stage, and delayed stage had shorter postoperative survival times in the univariate analysis, whereas the CT values at the pancreatic tumour parenchymal stage were positively correlated with prognosis in the multivariate analysis[30]. When Cassinotto *et al*[31] measured the average attenuation value of the overall tumour and the lowest attenuation value in the tumour centre at the PV phase, they found that lower attenuation values at the PV phase reflected higher degree of malignancy, more likely lymph node invasion, and shorter disease-free survival. The lowest attenuation in the tumour centre also reflected the degree of necrosis within the tumour tissue. However, if only the changes in pancreatic tumours after CT enhancement were analysed, it would be easy to ignore the changes in PTOT. Due to the lack of control, the difference in enhancement amplitude between ROT and PTOT could not be analysed, which would lead to the inability to analyse whether the change was caused by the tumour itself or by the blood supply of the pancreatic organs as a whole. Visually isoattenuating pancreatic cancer is defined as when the attenuation of the tumour, compared with the pancreatic parenchyma, is not visually observed to increase or decrease at both arterial and portal venous phases. In this type of tumour, the number of cancer cells is lower, the degree of tumour necrosis is lower, the prognosis is better, and an increase in serum CA19-9 is rare[27]. In our study, although the scanning period selected was the nonenhancement and PV phases, which were different from the study of visually isoattenuating pancreatic cancer, they essentially reflected the increase in tumour CT value after enhanced CT examination, and the results

Table 7 Correlation between tumour relative enhancement ratio and clinicopathological characteristics

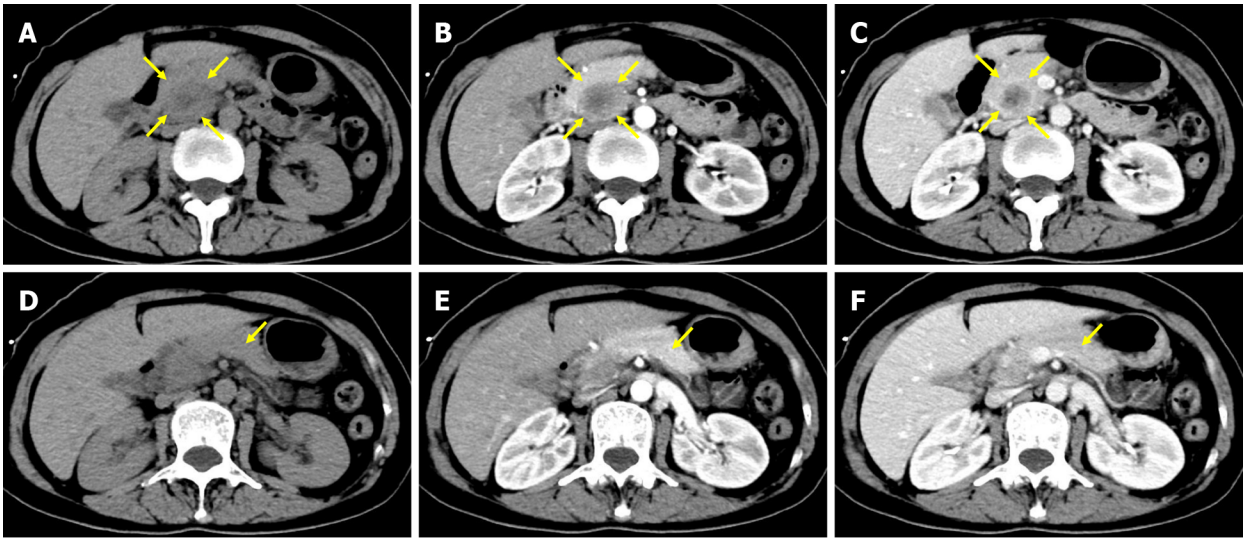
Variable	TRER ≤ 0.7, No. of patients, *n* (%)	TRER > 0.7, No. of patients, *n* (%)	*P* value	Coefficient of correlation
Tumour location			0.117	0.192
Head/uncinate	26 (59.1)	18 (78.3)		
Body/tail	18 (40.9)	5 (21.7)		
CA19-9			0.230	0.147
< 37 ng/mL	11 (25.0)	9 (39.1)		
≥ 37 ng/mL	33 (75.0)	14 (60.9)		
AJCC stage (2017)[1]			0.003	-0.353
I	4 (9.1)	7 (30.4)		
II	16 (36.4)	11 (47.8)		
III	24 (54.5)	5 (21.7)		
T stage			0.005	0.343
T1/2	13 (29.5)	15 (65.2)		
T3/4	31 (70.5)	8 (34.8)		
N stage[1]			0.046	-0.245
N0	12 (27.3)	11 (47.8)		
N1	15 (34.1)	8 (34.8)		
N2	17 (38.6)	4 (17.4)		
Lymph node metastasis			0.138	0.181
Negative	13 (29.5)	11 (47.8)		
Positive	31 (70.5)	12 (52.2)		
Vascular invasion			0.071	0.258
No	30 (68.2)	21 (91.3)		
Yes	14 (31.8)	2 (8.7)		
Tumour differentiation			0.634	0.058
Highly/moderately	33 (75.0)	16 (69.6)		
Poorly/undifferentiated	11 (25.0)	7 (30.4)		

[1]Spearman rank correlation was used, and Spearman correlation coefficient was calculated. The other variables were tested by chi-square test, and Cramer's V correlation coefficient was calculated.

CA19-9: Carbohydrate antigen 19-9; AJCC: American Joint Committee on Cancer; TRER: Tumour relative enhancement ratio.

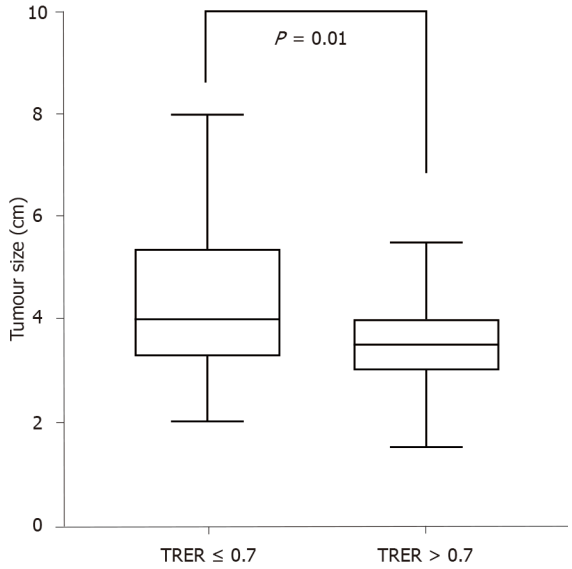
were similar; that is, patients with lower tumour CT enhancement amplitude had shorter OS. At the same time, we found no correlation between TRER and the increase in CA19-9. In Zhu *et al*'s study, the relative enhancement change (REC) was defined as the proportion of enhancement change between the tumour and pancreatic parenchyma during the PP and PV phases, showing that the postoperative OS of patients with REC < 0.9 was worse than those with REC ≥ 0.9[32]. Pancreatic cancer tissues are rich in fibrous tissue and show a pattern of delayed enhancement. However, our data showed that not all CT values of the PV phase were higher than those of the PP phase, regardless of ROT or PTOT. The CT value of the PV phase minus that of the PP phase may be negative. Therefore, when we designed the study, CT values of the PV and nonenhancement phases were selected for comparison. The final results showed that patients with a smaller TRER had worse a prognosis.

Although TRER is associated with AJCC stage, T stage, and N stage, it is not a substitute for lymph node status, tumour size, or stage. Pancreatic cancer is a kind of cold tumour with abundant stroma, and the stroma contributes to tumour growth and progression and plays an important role in the chemoresistance. This pathological feature of pancreatic cancer is similar to the pathological differentiation of tumours. It represents the characteristics of the pathology and growth of pancreatic cancer itself and will not disappear because the tumour is removed. The low-enhancement mode of CT in pancreatic



DOI: 10.3748/wjg.v28.i22.2468 **Copyright** ©The Author(s) 2022.

Figure 4 A 54-year-old woman with a mass in the head of the pancreas. A-C: The nonenhancement phase (A), pancreatic parenchymal (PP) phase (B) and portal venous (PV) phase (C) of region of the overall tumour, respectively; D-F: The nonenhancement phase (D), PP phase (E) and PV phase (F) of pancreatic tissue outside the tumour, respectively. Tumour relative enhancement ratio > 0.7, and the postoperative overall survival was 27.3 mo.



DOI: 10.3748/wjg.v28.i22.2468 **Copyright** ©The Author(s) 2022.

Figure 5 Correlation analysis between tumour size and tumour relative enhancement ratio. TRER: Tumour relative enhancement ratio.

cancer is partly due to the high stromal ratio of pancreatic cancer. Based on this, TRER is used as a quantitative reflection of the low-enhancement mode of CT in pancreatic cancer and the richness of pancreatic cancer stroma, which is used to predict postoperative OS. Moreover, because the postoperative prognosis of patients with low TRER is poor, such patients can consider whether to receive neoadjuvant chemotherapy.

Because tumour heterogeneity is affected by tumour blood supply, the ratio of tumour cells to stromal cells and tumour necrosis will lead to different CT values in different parts of the tumour. Although whole-volume quantitative analysis of tumour CTs is currently available, it has not been analysed in our study for the following reasons: (1) At the largest and most visible level of the tumour in CT images, the change of the tumour relative to surrounding tissue is relatively obvious, and it is easy to identify the boundary of the tumour. Moreover, it is simple to obtain the average CT value of ROT; and (2) compared with the largest level of the tumour, the CT value of the whole volume may be more easily affected by the obvious blood vessels and dilated pancreatic duct in the tumour.

There are several limitations in our study: (1) This was a retrospective study with a relatively small sample size at a single institution; (2) patients with metastasis were not studied; and (3) patients

received a variety of postoperative treatments, making it difficult to further accurately classify and perform a survival analysis, which might lead to a degree of bias.

CONCLUSION

In conclusion, TRER is a quantitative index of CT enhancement. This study showed that when the TRER of pancreatic adenocarcinoma patients was not more than 0.7, the prognosis was significantly worse, demonstrating the prognostic value of preoperative enhanced CT as a quantitative imaging biomarker in patients with pancreatic cancer.

ARTICLE HIGHLIGHTS

Research background

Computed tomography (CT) is widely used in the diagnosis, staging and treatment of pancreatic tumours. Because being rich in stroma, pancreatic cancer generally shows a low enhancement pattern compared with normal pancreatic tissue.

Research motivation

We want to use preoperative enhanced CT as a quantitative imaging biomarker to accurately predict the prognosis of patients with pancreatic cancer.

Research objectives

To analyse prognostic value of preoperative enhanced CT in pancreatic cancer.

Research methods

Sixty-seven patients with pancreatic ductal adenocarcinoma undergoing pancreatic resection were enrolled retrospectively. All patients underwent preoperative unenhanced and enhanced CT examination, the CT values of which were measured. The ratio of the preoperative CT value increase from the nonenhancement phase to the portal venous phase between pancreatic tumour and normal pancreatic tissue was calculated. The cut-off value of ratios was obtained by the receiver operating characteristic curve of the tumour relative enhancement ratio (TRER), according to which patients were divided into low- and high-enhancement groups. Cox regression was performed for the univariate (enter model) and multivariate analyses (forward LR model). Finally, Spearman rank correlation or chi-square test was used to analyse the correlation between TRER and clinicopathological characteristics.

Research results

TRER is a quantitative index of enhancement CT. This study showed that the prognosis of patients with the TRER ≤ 0.7 was significantly worse. TRER is a simple and effective parameter. Our results demonstrated that patients in the low TRER group were more likely to have higher American Joint Committee on Cancer stage, tumour stage, lymph node stage, and TRER was significantly negatively correlated with tumour size.

Research conclusions

TRER is a quantitative indicator of enhanced CT and can be used to predict postoperative overall survival in pancreatic cancer.

Research perspectives

In the future, we will further study the value of preoperative enhanced CT in predicting the efficacy of chemotherapy.

FOOTNOTES

Author contributions: All authors contributed to this paper; Gao JF, Pan Y, Lin XC, Lu FC, Qiu DS, Liu JJ, and Huang HG substantially contributed to conception and design of the study, acquisition of data, or analysis and interpretation of data; Gao JF, Lu FC, and Huang HG contributed to drafting the article or making critical revisions related to important intellectual content of the manuscript; Gao JF, Pan Y, Lin XC, Lu FC, Qiu DS, Liu JJ, and Huang HG finally approved the version of the article to be published.

Supported by the Medical Centre of Minimally Invasive Technology of Fujian Province, No. 2017[171], and No. 2017[4]; Joint Funds for the Innovation of Science and Technology, Fujian Province, No. 2017Y9059; and the United

Fujian Provincial Health and Education Project for Tackling the Key Research, No. 2019-WJ-07.

Institutional review board statement: The Ethics Committee of Fujian Medical University Union Hospital approved this retrospective study (No. 2020KY0141).

Informed consent statement: Because of the retrospective and anonymous character of this study, the institutional review committee waived the requirement for informed consent.

Conflict-of-interest statement: The authors declare no conflicts of interest.

Data sharing statement: No additional data are available.

Open-Access: This article is an open-access article that was selected by an in-house editor and fully peer-reviewed by external reviewers. It is distributed in accordance with the Creative Commons Attribution NonCommercial (CC BY-NC 4.0) license, which permits others to distribute, remix, adapt, build upon this work non-commercially, and license their derivative works on different terms, provided the original work is properly cited and the use is non-commercial. See: http://creativecommons.org/Licenses/by-nc/4.0/

Country/Territory of origin: China

ORCID number: Jian-Feng Gao 0000-0002-2058-9348; Yu Pan 0000-0002-7417-4551; Xian-Chao Lin 0000-0003-4165-8792; Feng-Chun Lu 0000-0002-0783-0547; Ding-Shen Qiu 0000-0003-2874-5496; Jun-Jun Liu 0000-0001-9338-4063; He-Guang Huang 0000-0003-1459-5546.

S-Editor: Yan JP
L-Editor: A
P-Editor: Yan JP

REFERENCES

1 **Siegel RL**, Miller KD, Jemal A. Cancer statistics, 2019. *CA Cancer J Clin* 2019; **69**: 7-34 [PMID: 30620402 DOI: 10.3322/caac.21551]
2 **Vincent A**, Herman J, Schulick R, Hruban RH, Goggins M. Pancreatic cancer. *Lancet* 2011; **378**: 607-620 [PMID: 21620466 DOI: 10.1016/S0140-6736(10)62307-0]
3 **Oettle H**, Post S, Neuhaus P, Gellert K, Langrehr J, Ridwelski K, Schramm H, Fahlke J, Zuelke C, Burkart C, Gutberlet K, Kettner E, Schmalenberg H, Weigang-Koehler K, Bechstein WO, Niedergethmann M, Schmidt-Wolf I, Roll L, Doerken B, Riess H. Adjuvant chemotherapy with gemcitabine *vs* observation in patients undergoing curative-intent resection of pancreatic cancer: a randomized controlled trial. *JAMA* 2007; **297**: 267-277 [PMID: 17227978 DOI: 10.1001/jama.297.3.267]
4 **Yoshitomi H**, Togawa A, Kimura F, Ito H, Shimizu H, Yoshidome H, Otsuka M, Kato A, Nozawa S, Furukawa K, Miyazaki M; Pancreatic Cancer Chemotherapy Program of the Chiba University Department of General Surgery Affiliated Hospital Group. A randomized phase II trial of adjuvant chemotherapy with uracil/tegafur and gemcitabine *vs* gemcitabine alone in patients with resected pancreatic cancer. *Cancer* 2008; **113**: 2448-2456 [PMID: 18823024 DOI: 10.1002/cncr.23863]
5 **Mokdad AA**, Minter RM, Zhu H, Augustine MM, Porembka MR, Wang SC, Yopp AC, Mansour JC, Choti MA, Polanco PM. Neoadjuvant Therapy Followed by Resection Versus Upfront Resection for Resectable Pancreatic Cancer: A Propensity Score Matched Analysis. *J Clin Oncol* 2017; **35**: 515-522 [PMID: 27621388 DOI: 10.1200/JCO.2016.68.5081]
6 **Henriksen A**, Dyhl-Polk A, Chen I, Nielsen D. Checkpoint inhibitors in pancreatic cancer. *Cancer Treat Rev* 2019; **78**: 17-30 [PMID: 31325788 DOI: 10.1016/j.ctrv.2019.06.005]
7 **Shi S**, Liang C, Xu J, Meng Q, Hua J, Yang X, Ni Q, Yu X. The Strain Ratio as Obtained by Endoscopic Ultrasonography Elastography Correlates With the Stroma Proportion and the Prognosis of Local Pancreatic Cancer. *Ann Surg* 2020; **271**: 559-565 [PMID: 30080738 DOI: 10.1097/SLA.0000000000002998]
8 **Bakkevold KE**, Kambestad B. Staging of carcinoma of the pancreas and ampulla of Vater. Tumor (T), lymph node (N), and distant metastasis (M) as prognostic factors. *Int J Pancreatol* 1995; **17**: 249-259 [PMID: 7642973 DOI: 10.1007/BF02785822]
9 **Hong SB**, Lee SS, Kim JH, Kim HJ, Byun JH, Hong SM, Song KB, Kim SC. Pancreatic Cancer CT: Prediction of Resectability according to NCCN Criteria. *Radiology* 2018; **289**: 710-718 [PMID: 30251929 DOI: 10.1148/radiol.2018180628]
10 **Hattori Y**, Gabata T, Zen Y, Mochizuki K, Kitagawa H, Matsui O. Poorly enhanced areas of pancreatic adenocarcinomas on late-phase dynamic computed tomography: comparison with pathological findings. *Pancreas* 2010; **39**: 1263-1270 [PMID: 20467344 DOI: 10.1097/MPA.0b013e3181dbc583]
11 **Sandrasegaran K**, Lin Y, Asare-Sawiri M, Taiyini T, Tann M. CT texture analysis of pancreatic cancer. *Eur Radiol* 2019; **29**: 1067-1073 [PMID: 30116961 DOI: 10.1007/s00330-018-5662-1]
12 **Kim HS**, Kim YJ, Kim KG, Park JS. Preoperative CT texture features predict prognosis after curative resection in pancreatic cancer. *Sci Rep* 2019; **9**: 17389 [PMID: 31757989 DOI: 10.1038/s41598-019-53831-w]
13 **Komar G**, Kauhanen S, Liukko K, Seppänen M, Kajander S, Ovaska J, Nuutila P, Minn H. Decreased blood flow with

increased metabolic activity: a novel sign of pancreatic tumor aggressiveness. *Clin Cancer Res* 2009; **15**: 5511-5517 [PMID: 19706808 DOI: 10.1158/1078-0432.CCR-09-0414]

14 **van Roessel S**, Kasumova GG, Verheij J, Najarian RM, Maggino L, de Pastena M, Malleo G, Marchegiani G, Salvia R, Ng SC, de Geus SW, Lof S, Giovinazzo F, van Dam JL, Kent TS, Busch OR, van Eijck CH, Koerkamp BG, Abu Hilal M, Bassi C, Tseng JF, Besselink MG. International Validation of the Eighth Edition of the American Joint Committee on Cancer (AJCC) TNM Staging System in Patients With Resected Pancreatic Cancer. *JAMA Surg* 2018; **153**: e183617 [PMID: 30285076 DOI: 10.1001/jamasurg.2018.3617]

15 **You MS**, Lee SH, Choi YH, Shin BS, Paik WH, Ryu JK, Kim YT, Jang DK, Lee JK, Kwon W, Jang JY, Kim SW. Lymph node ratio as valuable predictor in pancreatic cancer treated with R0 resection and adjuvant treatment. *BMC Cancer* 2019; **19**: 952 [PMID: 31615457 DOI: 10.1186/s12885-019-6193-0]

16 **Demir IE**, Jäger C, Schlitter AM, Konukiewitz B, Stecher L, Schorn S, Tieftrunk E, Scheufele F, Calavrezos L, Schirren R, Esposito I, Weichert W, Friess H, Ceyhan GO. R0 Versus R1 Resection Matters after Pancreaticoduodenectomy, and Less after Distal or Total Pancreatectomy for Pancreatic Cancer. *Ann Surg* 2018; **268**: 1058-1068 [PMID: 28692477 DOI: 10.1097/SLA.0000000000002345]

17 **Miles KA**, Lee TY, Goh V, Klotz E, Cuenod C, Bisdas S, Groves AM, Hayball MP, Alonzi R, Brunner T; Experimental Cancer Medicine Centre Imaging Network Group. Current status and guidelines for the assessment of tumour vascular support with dynamic contrast-enhanced computed tomography. *Eur Radiol* 2012; **22**: 1430-1441 [PMID: 22367468 DOI: 10.1007/s00330-012-2379-4]

18 **García-Figueiras R**, Goh VJ, Padhani AR, Baleato-González S, Garrido M, León L, Gómez-Caamaño A. CT perfusion in oncologic imaging: a useful tool? *AJR Am J Roentgenol* 2013; **200**: 8-19 [PMID: 23255736 DOI: 10.2214/AJR.11.8476]

19 **Cascinu S**, Falconi M, Valentini V, Jelic S; ESMO Guidelines Working Group. Pancreatic cancer: ESMO Clinical Practice Guidelines for diagnosis, treatment and follow-up. *Ann Oncol* 2010; **21** Suppl 5: v55-v58 [PMID: 20555103 DOI: 10.1093/annonc/mdq165]

20 **Feig C**, Gopinathan A, Neesse A, Chan DS, Cook N, Tuveson DA. The pancreas cancer microenvironment. *Clin Cancer Res* 2012; **18**: 4266-4276 [PMID: 22896693 DOI: 10.1158/1078-0432.CCR-11-3114]

21 **Wang SH**, Sun YF, Liu Y, Zhou Y. CT contrast enhancement correlates with pathological grade and microvessel density of pancreatic cancer tissues. *Int J Clin Exp Pathol* 2015; **8**: 5443-5449 [PMID: 26191248]

22 **Seo W**, Kim YC, Min SJ, Lee SM. Enhancement parameters of contrast-enhanced computed tomography for pancreatic ductal adenocarcinoma: Correlation with pathologic grading. *World J Gastroenterol* 2020; **26**: 4151-4158 [PMID: 32821076 DOI: 10.3748/wjg.v26.i28.4151]

23 **Cho HW**, Choi JY, Kim MJ, Park MS, Lim JS, Chung YE, Kim KW. Pancreatic tumors: emphasis on CT findings and pathologic classification. *Korean J Radiol* 2011; **12**: 731-739 [PMID: 22043156 DOI: 10.3348/kjr.2011.12.6.731]

24 **Delrue L**, Blanckaert P, Mertens D, Cesmeli E, Ceelen WP, Duyck P. Assessment of tumor vascularization in pancreatic adenocarcinoma using 128-slice perfusion computed tomography imaging. *J Comput Assist Tomogr* 2011; **35**: 434-438 [PMID: 21765297 DOI: 10.1097/RCT.0b013e318223f0c5]

25 **Klauss M**, Stiller W, Fritz F, Kieser M, Werner J, Kauczor HU, Grenacher L. Computed tomography perfusion analysis of pancreatic carcinoma. *J Comput Assist Tomogr* 2012; **36**: 237-242 [PMID: 22446366 DOI: 10.1097/RCT.0b013e31824a099e]

26 **Demachi H**, Matsui O, Kobayashi S, Akakura Y, Konishi K, Tsuji M, Miwa A, Miyata S. Histological influence on contrast-enhanced CT of pancreatic ductal adenocarcinoma. *J Comput Assist Tomogr* 1997; **21**: 980-985 [PMID: 9386294 DOI: 10.1097/00004728-199711000-00024]

27 **Kim JH**, Park SH, Yu ES, Kim MH, Kim J, Byun JH, Lee SS, Hwang HJ, Hwang JY, Lee MG. Visually isoattenuating pancreatic adenocarcinoma at dynamic-enhanced CT: frequency, clinical and pathologic characteristics, and diagnosis at imaging examinations. *Radiology* 2010; **257**: 87-96 [PMID: 20697118 DOI: 10.1148/radiol.10100015]

28 **Büchler P**, Reber HA, Lavey RS, Tomlinson J, Büchler MW, Friess H, Hines OJ. Tumor hypoxia correlates with metastatic tumor growth of pancreatic cancer in an orthotopic murine model. *J Surg Res* 2004; **120**: 295-303 [PMID: 15234226 DOI: 10.1016/j.jss.2004.02.014]

29 **Guillaumond F**, Leca J, Olivares O, Lavaut MN, Vidal N, Berthezène P, Dusetti NJ, Loncle C, Calvo E, Turrini O, Iovanna JL, Tomasini R, Vasseur S. Strengthened glycolysis under hypoxia supports tumor symbiosis and hexosamine biosynthesis in pancreatic adenocarcinoma. *Proc Natl Acad Sci U S A* 2013; **110**: 3919-3924 [PMID: 23407165 DOI: 10.1073/pnas.1219555110]

30 **Fukukura Y**, Takumi K, Higashi M, Shinchi H, Kamimura K, Yoneyama T, Tateyama A. Contrast-enhanced CT and diffusion-weighted MR imaging: performance as a prognostic factor in patients with pancreatic ductal adenocarcinoma. *Eur J Radiol* 2014; **83**: 612-619 [PMID: 24418286 DOI: 10.1016/j.ejrad.2013.12.016]

31 **Cassinotto C**, Chong J, Zogopoulos G, Reinhold C, Chiche L, Lafourcade JP, Cuggia A, Terrebonne E, Dohan A, Gallix B. Resectable pancreatic adenocarcinoma: Role of CT quantitative imaging biomarkers for predicting pathology and patient outcomes. *Eur J Radiol* 2017; **90**: 152-158 [PMID: 28583627 DOI: 10.1016/j.ejrad.2017.02.033]

32 **Zhu L**, Shi X, Xue H, Wu H, Chen G, Sun H, He Y, Jin Z, Liang Z, Zhang Z. CT Imaging Biomarkers Predict Clinical Outcomes After Pancreatic Cancer Surgery. *Medicine (Baltimore)* 2016; **95**: e2664 [PMID: 26844495 DOI: 10.1097/MD.0000000000002664]

World Journal of Gastroenterology

Submit a Manuscript: https://www.f6publishing.com

World J Gastroenterol 2022 June 14; 28(22): 2482-2493

DOI: 10.3748/wjg.v28.i22.2482

ISSN 1007-9327 (print) ISSN 2219-2840 (online)

ORIGINAL ARTICLE

Retrospective Study

Endoscopic classification and pathological features of primary intestinal lymphangiectasia

Ming-Ming Meng, Kui-Liang Liu, Xin-Ying Xue, Kun Hao, Jian Dong, Chun-Kai Yu, Hong Liu, Cang-Hai Wang, Hui Su, Wu Lin, Guo-Jun Jiang, Nan Wei, Ren-Gui Wang, Wen-Bin Shen, Jing Wu

Specialty type: Gastroenterology and hepatology

Provenance and peer review: Unsolicited article; Externally peer reviewed.

Peer-review model: Single blind

Peer-review report's scientific quality classification

Grade A (Excellent): 0
Grade B (Very good): B, B
Grade C (Good): C, C
Grade D (Fair): 0
Grade E (Poor): 0

P-Reviewer: Balakrishnan DS, India; Khayat AA, Saudi Arabia; Kotelevets SM, Russia

Received: November 2, 2021
Peer-review started: November 2, 2021
First decision: December 3, 2021
Revised: December 9, 2021
Accepted: April 28, 2022
Article in press: April 28, 2022
Published online: June 14, 2022

Ming-Ming Meng, Kui-Liang Liu, Hong Liu, Cang-Hai Wang, Hui Su, Wu Lin, Guo-Jun Jiang, Nan Wei, Jing Wu, Department of Gastroenterology, Beijing Shijitan Hospital, Capital Medical University, Beijing 100038, China

Xin-Ying Xue, Department of Respiratory and Critical Care Medicine, Beijing Shijitan Hospital, Capital Medical University, Beijing 100038, China

Kun Hao, Wen-Bin Shen, Departments of Lymphatic Surgery, Beijing Shijitan Hospital, Capital Medical University, Beijing 100038, China

Jian Dong, Ren-Gui Wang, Departments of Radiology, Beijing Shijitan Hospital, Capital Medical University, Beijing 100038, China

Chun-Kai Yu, Departments of Pathology, Beijing Shijitan Hospital, Capital Medical University, Beijing 100038, China

Corresponding author: Jing Wu, MD, PhD, Chief Doctor, Professor, Department of Gastroenterology, Beijing Shijitan Hospital, Capital Medical University, No. 10 Tieyi Street, Haidian District, Beijing 100038, China. wujing36@163.com

Abstract

BACKGROUND

The appearance of the intestinal mucosa during endoscopy varies among patients with primary intestinal lymphangiectasia (PIL).

AIM

To classify the endoscopic features of the intestinal mucosa in PIL under endoscopy, combine the patients' imaging and pathological characteristics of the patients, and explain their causes.

METHODS

We retrospectively analyzed the endoscopic images of 123 patients with PIL who were treated at the hospital between January 1, 2007 and December 31, 2018. We compared and analyzed all endoscopic images, classified them into four types according to the endoscopic features of the intestinal mucosa, and analyzed the post-lymphographic computed tomography (PLCT) and pathological characteristics of each type.

RESULTS

According to the endoscopic features of PIL in 123 patients observed during endoscopy, they were classified into four types: nodular-type, granular-type, vesicular-type, and edematous-type. PLCT showed diffuse thickening of the small intestinal wall, and no contrast agent was seen in the small intestinal wall and mesentery in the patients with nodular and granular types. Contrast agent was scattered in the small intestinal wall and mesentery in the patients with vesicular and edematous types. Analysis of the small intestinal mucosal pathology revealed that nodular-type and granular-type lymphangiectasia involved the small intestine mucosa in four layers, whereas ectasia of the vesicular- and edematous-type lymphatic vessels largely involved the lamina propria mucosae, submucosae, and muscular layers.

CONCLUSION

Endoscopic classification, combined with the patients' clinical manifestations and pathological examination results, is significant and very useful to clinicians when scoping patients with suspected PIL.

Key Words: Primary intestinal lymphangiectasia; Endoscopic features; Post-lymphangiographic computed tomography; Pathology

©The Author(s) 2022. Published by Baishideng Publishing Group Inc. All rights reserved.

Core Tip: Primary intestinal lymphangiectasia (PIL) is a rare disorder that typically presents as protein-losing enteropathy, diarrhea, and limb edema. Here we analyzed the endoscopic presentation, post-lymphographic computed tomography findings, and pathological features of 123 patients with PIL. We classified PIL into four categories - nodular, granular, vesicle, and edema types, proposed the theory of nodular and vesicle types domestically through observation, and made breakthroughs in overcoming the issue of inaccurate diagnosis based on a few independent early-stage case reports.

Citation: Meng MM, Liu KL, Xue XY, Hao K, Dong J, Yu CK, Liu H, Wang CH, Su H, Lin W, Jiang GJ, Wei N, Wang RG, Shen WB, Wu J. Endoscopic classification and pathological features of primary intestinal lymphangiectasia. *World J Gastroenterol* 2022; 28(22): 2482-2493
URL: https://www.wjgnet.com/1007-9327/full/v28/i22/2482.htm
DOI: https://dx.doi.org/10.3748/wjg.v28.i22.2482

INTRODUCTION

Primary intestinal lymphangiectasia (PIL), also known as Waldmann disease, is a type of abnormal intestinal lymphatic drainage that may be caused by congenital dysplasia of the lymphatic system[1]. Infants, children, and adolescents account for a large proportion of PIL patients, with occasional reports of cases in middle-aged and elderly patients[2]. PIL can cause leakage of lymphatic fluid into the gastrointestinal tract, eventually leading to protein-losing enteropathy (PLE). The main symptoms include diarrhea with limb edema, hypoalbuminemia, lymphopenia, and hypogammaglobulinemia[3, 4]. Prasad *et al*[5] concluded that the interval between symptom onset and a definitive diagnosis of PIL was as long as 54.8 mo due to the lack of knowledge of PIL by most clinicians, and their diagnosis relied on specialized examinations, such as endoscopy and histological diagnosis. At present, the diagnostic basis of such diseases includes visible typical endoscopic features, such as swelling and whitening of the intestinal villi, visible lymphangiectasis seen in the mucosa and submucosa through histopathological intestinal mucosal biopsy, and the characteristics of immunohistochemistry D2-40+[6].

As a rare disease, PIL is rarely reported domestically or internationally, and most reports have involved individual cases. Endoscopic images of individual cases revealed that patients had different mucosal manifestations, such as pinpoint white dots, diffuse villi thickening and whitening, and white spots[7-9]. A retrospective analysis of endoscopic images of patients diagnosed with PIL during a 12-year period at our research center summarized and classified them into four distinct endoscopic features and further explored the differences in radiologic and pathologic features of the different endoscopic features.

MATERIALS AND METHODS

Patient characteristics

We retrospectively analyzed 685 cases of PLE at Beijing Shijitan Hospital, Capital Medical University between January 1, 2007, and December 31, 2018. After strict screening, 123 patients were included in this study. The direct indicators of diagnosis were manifestations of intestinal lymphangiectasia obtained through endoscopy, visible lymphangiectasis found in the mucosa and submucosa through histopathological intestinal mucosal biopsy or surgical specimen pathology, and a positive D2-40 on immunohistochemistry. In contrast, indirect indicators were typical clinical manifestations (*e.g.*, diarrhea, edema, and abdominal pain), hypoproteinemia (albumin concentration < 30 g/L) with positive imaging of technetium-99m human serum albumin, and secondary factors[4,10]. We summarized the patients' clinical data, including age, sex, family history, clinical symptoms, laboratory inspection results, endoscopic images, imaging examination results, and pathological examination results. The imaging data were obtained from the host computer imaging system of Beijing Shijitan Hospital. This study was reviewed and approved by the Ethics Committee of Beijing Shijitan Hospital, Capital Medical University, and all patients signed a consent form.

Endoscopic imaging

All patients included in the study underwent electronic gastroscopy (GIF-H260; Olympus, Tokyo, Japan); of them, those with no significant abnormal manifestations were examined using electronic colonoscopy (CF-H260AI; Olympus, Tokyo, Japan). In addition, patients who underwent surgery underwent colonoscopy during the operation. All patients underwent endoscopic biopsy, the specimens from which were preserved after surgery. We obtained the first endoscopic images of the patients at admission for observation and invited three experienced endoscopists (deputy chief doctors or chief doctors with at least 10 years of experience in gastroscopy and enteroscopy) to interpret the endoscopic images. In cases of disagreement regarding the classification, it was determined by the endoscopists through discussion.

Computed tomography imaging and analysis

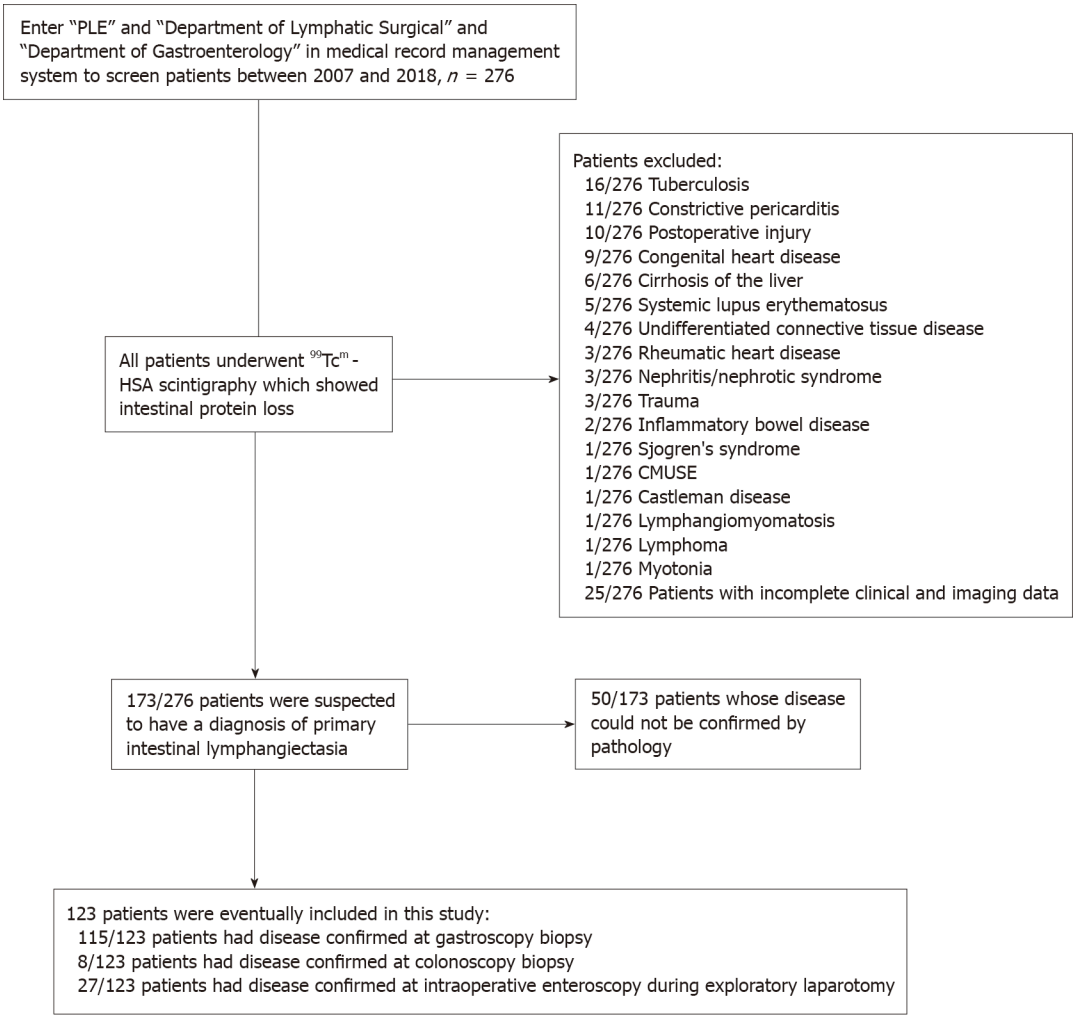
All the patients underwent direct lymphangiography. The contrast agent injection spot was located between the 1st and 2nd toes on certain sides. The lymphatic vessel was penetrated and the contrast agent iodinated oil (10 mL/ampule; Guerbet, France) was injected at a flow rate of 4-6 mL/h. Digital subtraction angiography images were dynamically collected at different intervals to observe the development of the lymphatic system. Two hours after surgery, computed tomography (CT) examination of the chest, abdomen, and pelvis was performed using the following scanning parameters: tube voltage, 80-120 kVp; tube current, 100-120 mAs; thickness of recombination layer, 2.0 mm; and interval, 1.8 mm. Post-lymphographic CT (PLCT) images were analyzed using the following evaluation items: (1) Intestinal wall thickening, when small intestinal wall thickness was ≥ 3 mm[10]; (2) edema manifestations: hydrops in the abdominal cavity, retina, and mesentery; and (3) lymphangiectasis of the small intestinal wall and mesentery, with manifestations of irregular distribution of contrast agent in multiple dots, lines, and clusters in the small intestinal wall and/or mesentery. All CT images were evaluated by two radiologists with > 10 years of experience in abdominal imaging diagnosis. In case of any differences in the evaluation results, consensus was reached through discussion and the results were recorded.

Histopathological examination

We collected the pathological data of 123 specimens from patients with PIL, of which 27 specimens were obtained through surgical resection. Hematoxylin and eosin (H&E) and immunohistochemical staining (D2-40 and CD34) were conducted on the specimens postoperatively. Visible dilated lymphatic vessels were distributed in the lamina propria of the intestinal mucosa, submucosa, muscular layer, and the serosal layer. All pathological sections were evaluated by two physicians with 5 and 10 years of experience in pathological diagnosis.

Statistical analysis

The statistical analysis was performed using the SPSS software for Windows (version 20.0; IBM Statistics, Armonk, NY, United States). Data are presented as medians with ranges and proportions. To determine the differences between the four groups, the chi-square test (with Fisher's exact test whenever applicable) was used to compare categorical variables, while the *t*-test was used to compare continuous variables. Statistical significance was set at $P < 0.05$.



DOI: 10.3748/wjg.v28.i22.2482 **Copyright** ©The Author(s) 2022.

Figure 1 Patient inclusion flowchart showing the number of patients, radionuclide imaging, digestive endoscopy evaluation, and pathologic analysis. CMUSE: Cryptogenic multifocal ulcerous stenosing enteritis; PLE: Protein-losing enteropathy.

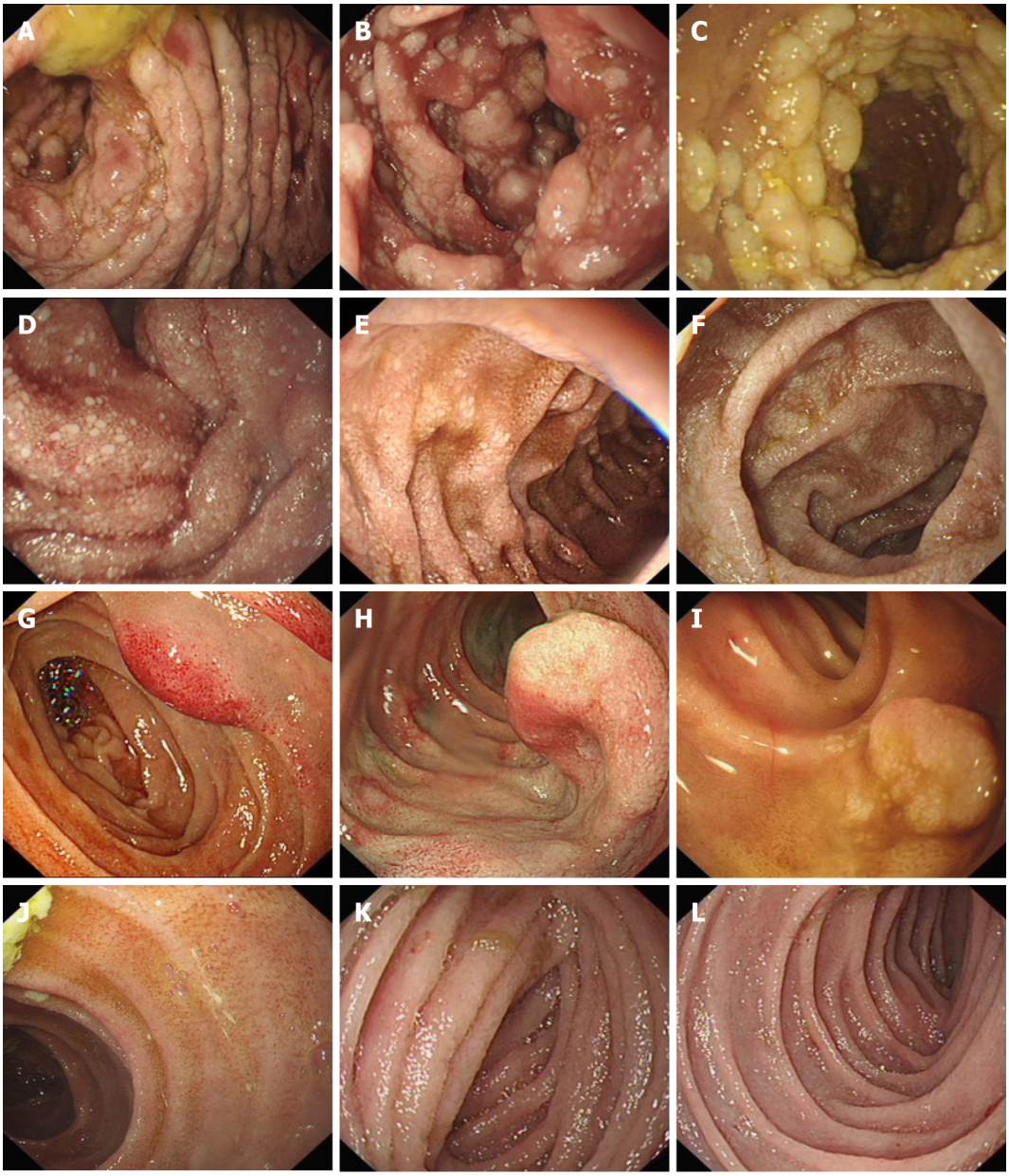
RESULTS

Endoscopic classification of PIL

Figure 1 shows a flowchart of the patient selection process. A total of 123 patients were included in this study. Gastroscopy and biopsy results were used for 115 of 123 patients with PIL, while colonoscopy and biopsy results were used for the other 8 patients with PIL. Additionally, small intestinal endoscopy was used for 27 of 123 patients with PIL, and further confirmation was made when the pathological specimens were obtained postoperatively (Figure 1). Through unanimous judgment, PIL was classified into four types according to the different morphologies of the intestinal mucosa under endoscopy: (1) Nodular type [n = 17 (13.8%); Figure 2A-C], which had a snowflake or cream yellow nodular-shaped protrusion at the surface of the mucosa, and for patients with serious symptoms, the white flakes were ring-coelom shaped, the mucosa was swollen and hypertrophic, and intestinal stenosis was present; (2) granular type [n = 74 (60.2%); Figure 2D-F], which showed white granules with disseminated changes at the surface of the mucosa, swollen villi, and lesions that were distributed regionally or in a whole section; (3) vesicular type [n = 5 (4.1%); Figure 2G-I], which showed a vesicle-shaped structure protruding from the mucosa, that part of the surface of the mucosa was hyperemic, and the lesion was isolated; and (4) edematous type [n = 27 (21.9%); Figure 2J-L], in which the villi of the small intestine were swollen and blisters were small and round, villus color was normal, and no change in the characteristic white villus was noted (Figure 2).

Clinical characteristics

Among 123 patients, 61 (49.6%) were men and 62 (50.4%) were women. The average age at onset was 17.0 ± 17.4 years (range, 0-68 years), while that at diagnosis was 22.8 ± 19.2 years. Based on the clinical manifestations, 58.5% (72/123) of the patients, including four with celiac stools, had five or more episodes of diarrhea per day. Additionally, 78.0% (96/123) of the patients had edema of the lower limbs,



DOI: 10.3748/wjg.v28.i22.2482 **Copyright** ©The Author(s) 2022.

Figure 2 Endoscopic images of patients with primary intestinal lymphangiectasia. The images show white mucosal plaques and spots in the small intestine, divided into four types. A-C: Nodular type; D-F: Granular type; G-I: Vesicular type; J-L: Edematous type.

eyelids, and face, 17.7% (17/96) had anasarca, 17.7% (17/96) had unilateral limb edema, and the rest had bilateral edema. Furthermore, 1.6% (2/123) of patients had concurrent cryptococcal or streptococcal infections. Other symptoms included abdominal distention [28 patients (22.8%)], abdominal pain [10 patients (8.1%)], nausea and vomiting [8 patients (6.5%)], and alimentary tract hemorrhage [4 patients (3.3%)]. There were no obvious differences in clinical symptoms among the four patient types. However, the laboratory results of the four types of PIL patients showed a significant decline in peripheral blood lymphocyte counts and IgG concentrations (Table 1).

CT characteristics

We summarized and analyzed the corresponding PLCT images of the four types of patients with PIL observed during endoscopy. The specific characteristics were as follows: (1) Nodular type: the images showed signs of intestinal wall thickening, increased mesenteric density, and no contrast distribution in the mesentery or intestinal wall (Figure 3A-C); (2) granular type: the images showed annular thickening of the small intestinal wall, increased mesenteric density, and no contrast distribution in the mesentery and intestinal wall (Figure 3D-F); (3) vesicular type: the images revealed an increased mesenteric density and distribution of contrast agents in the intestinal wall, mesentery, peripancreatic area, gallbladder fossa, hepatic hilum, and retroperitoneum (Figure 3G-I); and (4) edematous type: the images showed distribution of contrast agents in the intestinal wall, mesentery, peripancreatic area, hepatic hilum, and

Table 1 Demography, clinical profile and laboratory examination of patients with primary intestinal lymphangiectasia

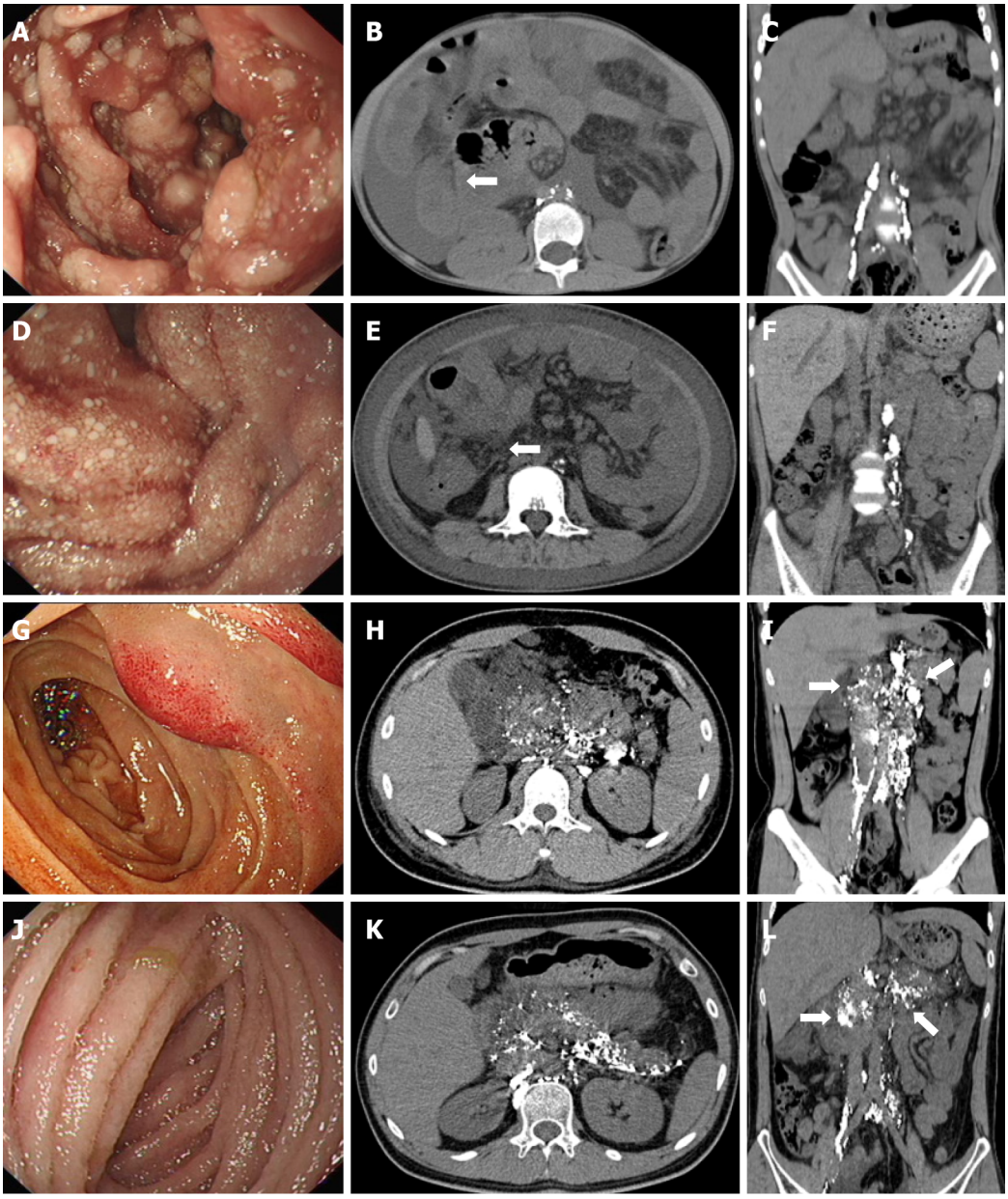
Clinical features	Total (*n* = 123)	Type				*P* value
		Nodular type (*n* = 17)	Granular type (*n* = 74)	Vesicular type (*n* = 5)	Edematous type (*n* = 27)	
Demographic characteristics, mean ± SD (age range)/*n* (%)						
Age of diagnosis (yr)	22.8 ± 19.2	10.2 ± 7.6	23.7 ± 20.6	25.2 ± 15.7	27.7 ± 18.3	< 0.001
Age of onset (yr)	17.0 ± 17.4 (0, 68)	3.7 ± 6.9 (0, 22)	17.9 ± 18.0 (0, 68)	22.2 ± 15.1 (3, 44)	21.7 ± 17.4 (0, 66)	< 0.001
Male	61 (49.6)	7 (41.2)	35 (47.3)	2 (40.0)	17 (63.0)	0.408
Clinical characteristics, *n* (%)						
Diarrhea	72 (58.5)	12 (70.6)	47 (63.5)	3 (60.0)	10 (37.0)	0.074
Edema	96 (78.0)	13 (76.5)	59 (79.7)	2 (40.0)	22 (81.5)	0.238
Abdominal distension	28 (22.8)	6 (35.3)	15 (20.3)	1 (20.0)	6 (22.2)	0.567
Abdominal pain	10 (8.1)	0 (0)	7 (9.5)	0 (0)	3 (11.1)	0.603
Nausea and vomiting	8 (6.5)	0 (0)	8 (10.8)	0 (0)	0 (0)	0.145
Gastrointestinal bleeding	4 (3.3)	0 (0)	2 (2.7)	0 (0)	2 (7.4)	0.423
Fever	2 (1.6)	0 (0)	1 (1.4)	0 (0)	1 (3.7)	0.640
Laboratory examination, mean ± SD						
LY	1.2 ± 0.9	1.0 ± 0.5	1.2 ± 1.1	0.3 ± 0.1	1.4 ± 0.9	< 0.001
HGB (g/L) (110-150)	129.9 ± 23.5	137.4±17.9	127.9 ± 24.5	116.4 ± 13.3	133.1 ± 24.3	0.221
TP (g/L) (60-80)	41.2 ± 9.0	39.9 ± 6.7	40.4 ± 8.7	39.9 ± 7.1	44.4 ± 10.8	0.218
Alb (g/L) (35-55)	25.4 ± 7.2	24.3 ± 5.9	25.5 ± 6.7	26.5 ± 5.7	25.6 ± 9.4	0.911
Glb (g/L) (20-30)	15.8 ± 4.3	15.3 ± 4.4	15.0 ± 3.2	13.4 ± 3.0	18.8 ± 5.5	0.024
IgG (g/L) (7-16)	3.91 ± 2.30	3.35 ± 1.48	3.73 ± 2.12	2.26 ± 0.43	5.01 ± 2.90	< 0.001
Ca (mmol/l) (2.1-2.75)	1.93 ± 0.28	1.90 ± 0.18	1.91 ± 0.31	1.86 ± 0.09	1.99 ± 0.26	0.556

Alb: Albumin; Ca: Calcium; Glb: Globulin; HGB: Hemoglobin; IgG: Immunoglobulin G; LY: Lymphocyte count; TP: Total protein.

retroperitoneum (Figure 3J-L).

Pathologic basis

Pathological data of 123 specimens from PIL patients were collected, and lymphatic dilation was observed in different layers of the intestinal mucosa. The specific characteristics were as follows: (1) Nodular type: Enteroscopic findings showed a white-flake nodular-type protrusion (Figure 4A). H&E staining revealed that the lamina propria and submucosa lymphatic vessels were clearly dilated. The pink liquid in the dilated lumen was lymphatic fluid, which was consistent with the manifestation observed on endoscopy (Figure 4B). Additionally, lymphangiectasia was observed in the muscular and serosal layers, and immunohistochemical staining with D2-40 (+) more clearly showed the lymphatic vessels (Figure 4C and D); (2) granular type: Enteroscopic findings showed scattered white granules (Figure 4E), and the pathological features showed that the lymphatic vessels in the mucosal lamina propria and submucosa were significantly dilated (Figure 4F). Scattered lymphangiectasia was also seen in the muscular layer and serosal layers, and the distribution of tiny blood vessels was observed around the lymphatic vessels (Figure 4G and H); (3) vesicular type: Enteroscopic findings revealed raised submucosal lesions (Figure 4I). Pathological features showed thick lymphatic vessels in the raised lesions and no obvious lymphatic dilatation in the mucosa (Figure 4J and K). A distribution of tiny blood vessels was observed around the lymphatic vessels (Figure 4L); and (4) edematous type: Enteroscopic findings revealed swollen villi and small round blisters (Figure 4M). Pathological features showed lymphatic dilatation in the submucosa and no obvious lymphatic dilatation in the lamina propria (Figure 4N and O). Tiny blood vessels were observed around the lymphatic vessels (Figure 4P).

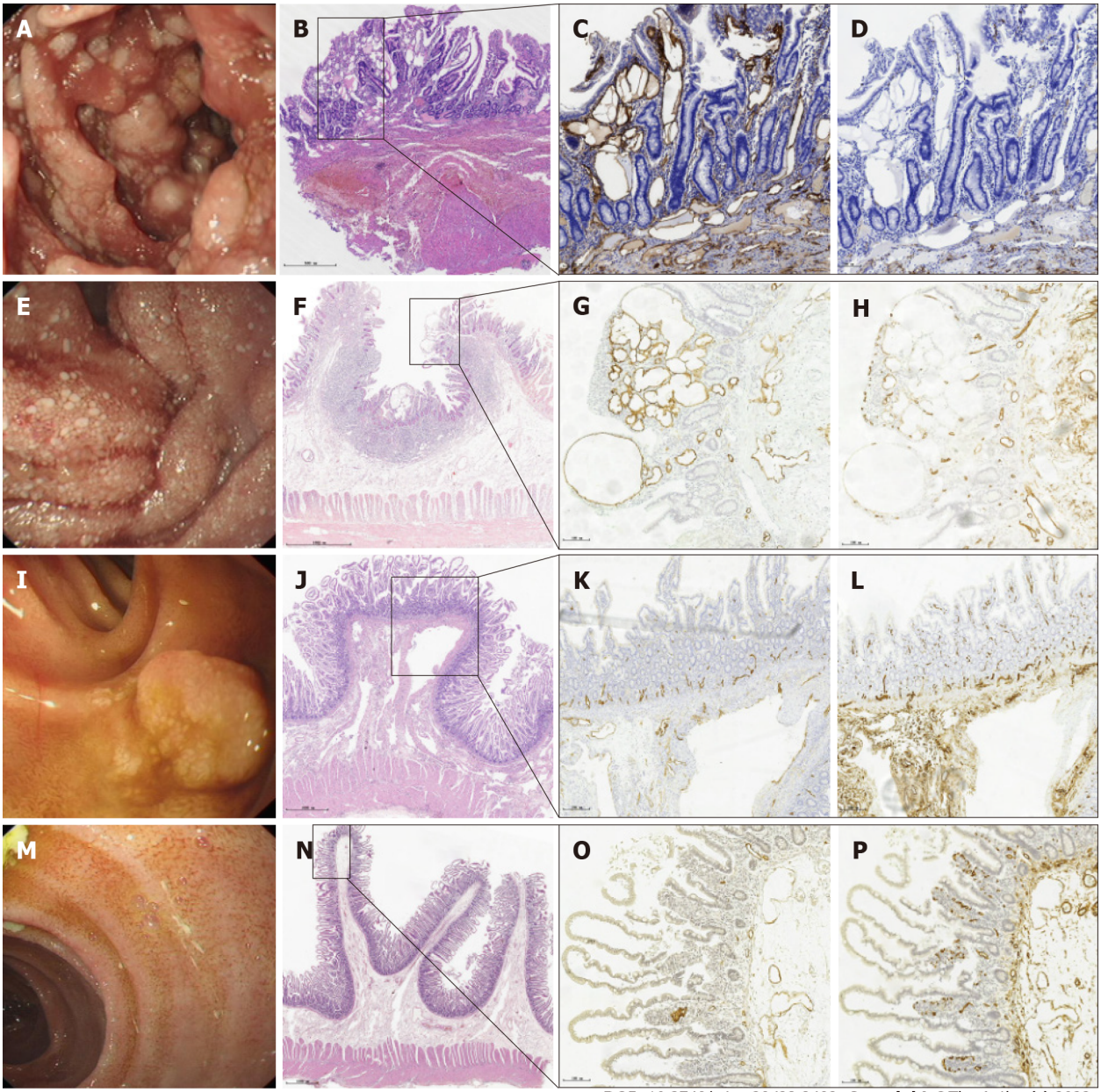


DOI: 10.3748/wjg.v28.i22.2482 **Copyright** ©The Author(s) 2022.

Figure 3 Post-lymphographic computed tomography images corresponding to the four types of primary intestinal lymphangiectasia under endoscopy. A-C: Nodular type: The post-lymphographic computed tomography (PLCT) corresponding to nodular type indicates the intestinal wall thickening of the small intestine (white arrows), increased mesenteric density, and no contrast agent distribution in the mesentery and intestinal wall; D-F: Granular type: The PLCT corresponding to granular type indicates that the intestinal wall annular thickening of the small intestine, increased mesenteric density (white arrows), and no contrast agent distribution in the mesentery and intestinal wall; G-I: Vesicular type: The PLCT corresponding to vesicular type indicates the distribution of contrast agents in the intestinal wall, mesentery, peripancreas, hilar area of the liver, and retroperitoneum (white arrows), suggesting lymphatic dilation and abnormal distribution in the above areas; J-L: Edematous type: The PLCT corresponding to edematous type indicates the distribution of contrast agents in the intestinal wall, mesentery, peripancreas, gallbladder fossa, hilar area of the liver, and retroperitoneum (white arrows).

DISCUSSION

To date, there have been few studies on PIL in the English literature, most of which were reports of single cases and reviews of small cases. At present, the diagnosis of PIL is based on small intestinal endoscopy or capsule endoscopy to identify the typical characteristics of the intestinal mucosa and is confirmed through histopathological examination of the biopsy specimen of the intestinal mucosa; intestinal lymphangiectasia due to secondary causes is excluded[9,11]. The classification of intestinal lymphangiectasis using endoscopy is limited. Ohmiya *et al*[12] divided 14 patients with intestinal lymphangiectasis into white and non-white villi. However, these few cases included patients with secondary lymphangiectasias. We evaluated the endoscopic characteristics of 123 patients with PIL and found significant differences in the intestinal mucosal findings under endoscopy in different patients. Based on their endoscopic appearance, they were divided into four types: nodular, granular, vesicular,

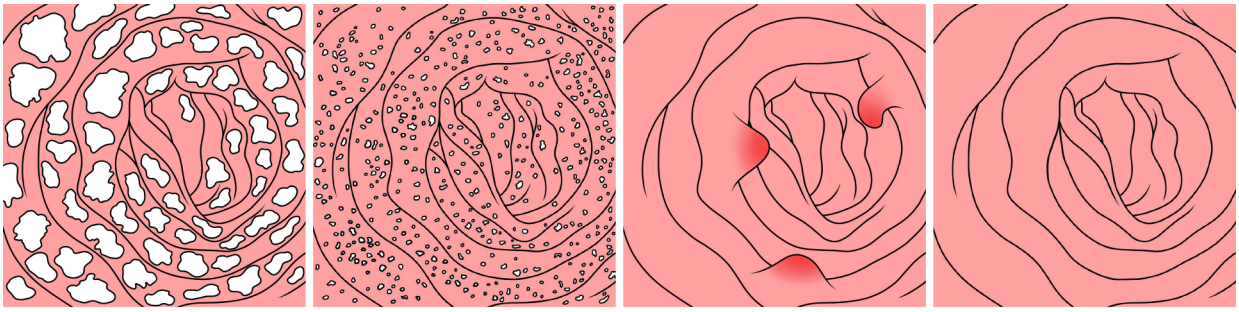


DOI: 10.3748/wjg.v28.i22.2482 **Copyright** ©The Author(s) 2022.

Figure 4 Endoscopic images and corresponding histological findings of primary intestinal lymphangiectasia. A, E, I, and M: Four types of endoscopic images in patients with primary intestinal lymphangiectasia; B, F, J, and N: Hematoxylin and eosin stain showing the full mucosa of the small intestine; C, G, K, and O: Immunohistochemical stain shows that D2-40 positive cells are located in the cytoplasm and envelope of lymphatic epithelial cells and are brownish yellow (magnification: × 10), indicating dilated lymphatics; D, H, L, and P: CD34 stain showing normal vascular endothelial cells (magnification: × 10).

and edematous. The corresponding imaging and histopathological findings of each type were comprehensively analyzed. In this study, the endoscopic mucosal signs of patients with PIL were mainly white granule-like changes, a finding that was consistent with the endoscopic images reported in most studies. The nodular and vesicular types proposed in this study have not been reported previously.

PIL often develops in childhood or youth, and most cases are diagnosed before the age of 3 years. In recent years, an increasing number of cases have been reported in adults[2,13-17]. In this study, we found that the age at onset differed among the four types of endoscopy. Among them, the age at onset in patients with nodular-type PIL was the youngest (3.7 ± 6.9 years), and the earlier the age at onset, the more severe the intestinal mucosal findings. We also found clinical differences in peripheral blood lymphocyte counts and IgG levels among the four types in the laboratory examinations. Among the four types, the values of these two indicators were the lowest in patients with vesicular-type PIL, while the corresponding hemoglobin values were the lowest. By analyzing the clinical features of five patients with vesicular-type PIL, we found that four were diagnosed with gastrointestinal bleeding. The simultaneous loss of lymphatic fluid and blood from the intestinal tract can lead to a decrease in hemoglobin, lymphocyte, and immunoglobulin levels.



DOI: 10.3748/wjg.v28.i22.2482 **Copyright** ©The Author(s) 2022.

Figure 5 Four patterns of mucosal findings under endoscopy. Type I: Nodular type; Type II: Granular type; Type III: Vesicular type; Type IV: Edematous type.

In recent years, PLCT has been of great value in the diagnosis of PIL. Our previous studies suggested that the specific signs of PIL include diffuse nodular thickening and edema of the intestinal wall as well as the presence of a "halo sign" on the intestinal wall[14]. The abnormal distribution of contrast agents in the small intestine and mesentery of the affected segment suggests the local presence of abnormally dilated lymphatic vessels and abnormal lymphatic circulation. In this study, the PLCT signs in nodular- and granular-type patients showed intestinal wall thickening and increased mesenteric density, consistent with the mucosal findings on endoscopy. In contrast, no significant intestinal wall thickening was found in vesicular- and edematous-type patients. By observing the contrast agent distribution, we found that the PLCT images of vesicular- and edematous-type patients showed contrast agent distribution in the intestinal wall, mesentery, peripancreatic, gallbladder fossa, hepatic hilum, and retroperitoneum, indicating lymphatic dilation and an abnormal distribution in these areas. However, there was no contrast agent distribution in the small intestine or mesentery in the PLCT images of nodular- and granular-type patients, which was inconsistent with the segmental and/or diffuse lymphatic dilation of the intestinal mucosa shown by the endoscopy results. Combined with the pathological results, we speculated that the lymphatic fluid in the intestinal mucosa and submucosal lymphatic vessels of nodular- and granular-type patients are subject to retention, which increases the pressure in the lymphatic vessels. In addition, there were many submucosal muscle fiber tissues that were not conducive to the counterflow of the contrast agent into the small intestine. In the nodular type, among the five children with contrast agent negativity, the lymphatic contrast agent was sparsely distributed throughout the body, which may be related to lymphatic dysplasia.

Previous reports[10,12,15] and histopathology of PIL biopsies showed that the mucosal and submucosal lymphatic vessels were significantly dilated and the lymphatic vessels were filled with protein-rich fluid and scattered lymphocytes. There are no reports on whether lymphatic dilation exists in the muscular and serosal layers. Macdonald *et al*[16] reported a strong correlation between small intestinal vascular hypoplasia and lymphatic dilation, but there was a lack of pathological examination supporting their argument. In this study, pathological examination of nodular- and granular-type PIL showed that the villi were enlarged and clubbed or cystic, with some tips ruptured. The lamina propria, submucosa, muscular layer, and serosa of the diffuse or localized mucosa showed significant dilation of the lymphatic vessels, with the most obvious lymphatic vessel dilation in the lamina propria of the intestinal mucosa, consistent with the endoscopy findings. Among them, nodular pathology has shown a large amount of muscle fiber tissue in the submucosa, which may be related to the long course of disease and chronic inflammation. Pathological examination of vesicular-type patients showed a large number of thin-walled and irregularly dilated lymphatic vessels in the submucosa; lymphatic fluid, lymphocytes, and red blood cells in the lumen; and the accumulation of lymphocytes in the stroma, which can form lymphoid follicles. This was consistent with the prominent polyp-like morphology observed on endoscopy, and a large number of small blood vessels were observed around the lymphatic vessels, further verifying that the third type of lymphatic dilation reported by Macdonald *et al*[16] was consistent with the vesicular type in our study. Therefore, our study findings complement the histopathological findings. Pathological examination of edematous-type patients showed that the lymphatic vessels in the submucosa were significantly dilated, and the lymphatic vessels in the lamina propria were not significantly dilated, which was consistent with the endoscopy findings. The histopathological results showed that the distribution of lymphatic dilation in the intestinal mucosa and the degree of lumen dilation differed; therefore, the signs of intestinal mucosa on endoscopy varied in patients with PIL.

This study analyzed the endoscopic images of 123 patients with PIL and found that the intestinal mucosa had different endoscopic features such as diffuse white nodules, white granules, polypoid protrusion, and mucosal edema, the basis of the division into four types of endoscopic features (Figure 5). However, the four distinctive phenotypic appearances may simply be endoscopic variations

at different stages of the same disease, similar to the different endoscopic findings of eosinophilic esophagitis. The classification of PIL also requires support in animal models and molecular or genotypic bases to confirm the presence of distinct phenotypes. This study is preliminary because of its small sample size and retrospective design, and requires further validation in a multicenter prospective study.

CONCLUSION

In conclusion, PIL is a rare disorder that typically presents as PLE, diarrhea, and limb edema. Unspecific symptoms and a wide range of clinical manifestations can significantly hamper the establishment of a definitive diagnosis. PIL demonstrates four characteristics of digestive endoscopy. The identification of intestinal mucosal chorionic abnormalities in this rare disorder might be helpful for ensuring an early diagnosis and optimal treatment.

ARTICLE HIGHLIGHTS

Research background

Primary intestinal lymphangiectasia (PIL) is a rare disorder that typically presents as PLE, diarrhea, and limb edema.

Research motivation

Unspecific symptoms and a wide range of clinical manifestations can significantly hamper the establishment of a definitive diagnosis.

Research objectives

This study aimed to classify the endoscopic features of the intestinal mucosa in PIL under endoscopy, combine post-lymphographic computed tomography findings and the patients' pathological characteristics of the patients, and explain their causes.

Research methods

This retrospective analysis of endoscopic images of patients diagnosed with PIL during a 12-year period at our research center summarized and classified types into four distinct endoscopic features and further explored the differences in radiologic and pathologic features of the different endoscopic features.

Research results

The endoscopic symptoms of 123 patients with PIL can be divided into four types: Nodular (13.8%), granular (60.2%), vesicular (4.1%), and edematous (21.9%).

Research conclusions

We proposed the theory of nodular and vesicle types domestically through observation, and made breakthroughs in overcoming the issue of inaccurate diagnosis based on a few independent early-stage case reports.

Research perspectives

According to the different partings under endoscopy, the clinical symptoms, therapeutic efficacy, and prognosis of patients with PIL were observed.

FOOTNOTES

Author contributions: Meng MM, Liu KL, Xue XY, Hao K, Dong J and Yu CK contributed equally to this work; Wu J, Meng MM and Liu KL were the gastroenterologists; Shen WB and Hao K were the lymphologist; Wang RG and Dong J performed the radiological diagnosis; Yu CK performed the pathological diagnosis; Meng MM and Xue XY designed the research study; Liu KL, Liu H, Wang CH, Su H, Lin W, Jiang GJ and Wei N performed the primary literature and data extraction; Meng MM, Xue XY analyzed the data and wrote the manuscript; Wu J, Shen WB and Wang RG were responsible for revising the manuscript for important intellectual content; and all authors read and approved the final version.

Supported by National Natural Science Foundation of China, No. 61876216; and Beijing Shijitan Hospital Foundation of Capital Medical University, No. 2019-LB12.

Institutional review board statement: The study was reviewed and approved by the Beijing Shijitan Hospital, Capital Medical University Institutional Review Board [Approval No. Sjtkyll-lx-2021(90)].

Informed consent statement: All study participants or their legal guardian provided informed written consent about personal and medical data collection prior to study enrolment.

Conflict-of-interest statement: The authors declare no conflicts of interest for this article.

Data sharing statement: Technical appendix, statistical code, and dataset available from the corresponding author at wujing36@163.com. Participants gave informed consent for data sharing.

Open-Access: This article is an open-access article that was selected by an in-house editor and fully peer-reviewed by external reviewers. It is distributed in accordance with the Creative Commons Attribution NonCommercial (CC BY-NC 4.0) license, which permits others to distribute, remix, adapt, build upon this work non-commercially, and license their derivative works on different terms, provided the original work is properly cited and the use is non-commercial. See: https://creativecommons.org/Licenses/by-nc/4.0/

Country/Territory of origin: China

ORCID number: Ming-Ming Meng 0000-0003-3560-1052; Kui-Liang Liu 0000-0001-8163-0394; Xin-Ying Xue 0000-0002-7847-8034; Kun Hao 0000-0003-0366-9415; Jian Dong 0000-0002-2643-0370; Chun-Kai Yu 0000-0002-5138-8100; Hong Liu 0000-0003-2443-7808; Cang-Hai Wang 0000-0001-9422-0765; Hui Su 0000-0002-0517-9981; Wu Lin 0000-0001-6279-5388; Guo-Jun Jiang 0000-0002-0500-3273; Nan Wei 0000-0003-3609-2229; Ren-Gui Wang 0000-0001-8848-1811; Wen-Bin Shen 0000-0002-1732-4939; Jing Wu 0000-0003-3009-4434.

S-Editor: Yan JP
L-Editor: A
P-Editor: Yan JP

REFERENCES

1 **Waldmann TA**, Steinfeld JL, Dutcher TF, Davidson JD, Gordon RS Jr. The role of the gastrointestinal system in "idiopathic hypoproteinemia". *Gastroenterology* 1961; **41**: 197-207 [PMID: 13782654]
2 **Freeman HJ**, Nimmo M. Intestinal lymphangiectasia in adults. *World J Gastrointest Oncol* 2011; **3**: 19-23 [PMID: 21364842 DOI: 10.4251/wjgo.v3.i2.19]
3 **Takenaka H**, Ohmiya N, Hirooka Y, Nakamura M, Ohno E, Miyahara R, Kawashima H, Itoh A, Watanabe O, Ando T, Goto H. Endoscopic and imaging findings in protein-losing enteropathy. *J Clin Gastroenterol* 2012; **46**: 575-580 [PMID: 22138845 DOI: 10.1097/MCG.0b013e31823832ac]
4 **Ingle SB**, Hinge Ingle CR. Primary intestinal lymphangiectasia: Minireview. *World J Clin Cases* 2014; **2**: 528-533 [PMID: 25325063 DOI: 10.12998/wjcc.v2.i10.528]
5 **Prasad D**, Srivastava A, Tambe A, Yachha SK, Sarma MS, Poddar U. Clinical Profile, Response to Therapy, and Outcome of Children with Primary Intestinal Lymphangiectasia. *Dig Dis* 2019; **37**: 458-466 [PMID: 31030202 DOI: 10.1159/000499450]
6 **Asakura H**, Miura S, Morishita T, Aiso S, Tanaka T, Kitahora T, Tsuchiya M, Enomoto Y, Watanabe Y. Endoscopic and histopathological study on primary and secondary intestinal lymphangiectasia. *Dig Dis Sci* 1981; **26**: 312-320 [PMID: 7238258 DOI: 10.1007/BF01308371]
7 **Cammarota G**, Cianci R, Gasbarrini G. High-resolution magnifying video endoscopy in primary intestinal lymphangiectasia: a new role for endoscopy? *Endoscopy* 2005; **37**: 607 [PMID: 15933946 DOI: 10.1055/s-2005-861338]
8 **Hirano A**, Matsumoto T, Esaki M, Fujita K, Iida M. Intestinal lymphangiectasia presenting with duodeno-jejunal polyposis: enteroscopic findings. *Endoscopy* 2010; **42** Suppl 2: E281-E282 [PMID: 21086252 DOI: 10.1055/s-0029-1244225]
9 **Oh TG**, Chung JW, Kim HM, Han SJ, Lee JS, Park JY, Song SY. Primary intestinal lymphangiectasia diagnosed by capsule endoscopy and double balloon enteroscopy. *World J Gastrointest Endosc* 2011; **3**: 235-240 [PMID: 22110841 DOI: 10.4253/wjge.v3.i11.235]
10 **Vignes S**, Bellanger J. Primary intestinal lymphangiectasia (Waldmann's disease). *Orphanet J Rare Dis* 2008; **3**: 5 [PMID: 18294365 DOI: 10.1186/1750-1172-3-5]
11 **Lai Y**, Yu T, Qiao XY, Zhao LN, Chen QK. Primary intestinal lymphangiectasia diagnosed by double-balloon enteroscopy and treated by medium-chain triglycerides: a case report. *J Med Case Rep* 2013; **7**: 19 [PMID: 23316917 DOI: 10.1186/1752-1947-7-19]
12 **Ohmiya N**, Nakamura M, Yamamura T, Yamada K, Nagura A, Yoshimura T, Hirooka Y, Hirata I, Goto H. Classification of intestinal lymphangiectasia with protein-losing enteropathy: white villi type and non-white villi type. *Digestion* 2014; **90**: 155-166 [PMID: 25278259 DOI: 10.1159/000365987]
13 **Wen J**, Tang Q, Wu J, Wang Y, Cai W. Primary intestinal lymphangiectasia: four case reports and a review of the literature. *Dig Dis Sci* 2010; **55**: 3466-3472 [PMID: 20198428 DOI: 10.1007/s10620-010-1161-1]
14 **Dong J**, Xin J, Shen W, Wen T, Chen X, Sun Y, Wang R. CT Lymphangiography (CTL) in Primary Intestinal

Lymphangiectasia (PIL): A Comparative Study with Intraoperative Enteroscopy (IOE). *Acad Radiol* 2019; **26**: 275-281 [PMID: 29885759 DOI: 10.1016/j.acra.2018.04.023]

15 **Huber T**, Paschold M, Eckardt AJ, Lang H, Kneist W. Surgical therapy of primary intestinal lymphangiectasia in adults. *J Surg Case Rep* 2015; **2015** [PMID: 26169531 DOI: 10.1093/jscr/rjv081]

16 **Macdonald J**, Porter V, Scott NW, McNamara D. Small bowel lymphangiectasia and angiodysplasia: a positive association; novel clinical marker or shared pathophysiology? *J Clin Gastroenterol* 2010; **44**: 610-614 [PMID: 20535025 DOI: 10.1097/MCG.0b013e3181dd9c3f]

17 **Huber R**, Semmler G, Mayr A, Offner F, Datz C. Primary intestinal lymphangiectasia in an adult patient: A case report and review of literature. *World J Gastroenterol* 2020; **26**: 7707-7718 [PMID: 33505146 DOI: 10.3748/wjg.v26.i48.7707]

World Journal of Gastroenterology

Submit a Manuscript: https://www.f6publishing.com

World J Gastroenterol 2022 June 14; 28(22): 2494-2508

DOI: 10.3748/wjg.v28.i22.2494

ISSN 1007-9327 (print) ISSN 2219-2840 (online)

ORIGINAL ARTICLE

Observational Study

Accurate and generalizable quantitative scoring of liver steatosis from ultrasound images *via* scalable deep learning

Bowen Li, Dar-In Tai, Ke Yan, Yi-Cheng Chen, Cheng-Jen Chen, Shiu-Feng Huang, Tse-Hwa Hsu, Wan-Ting Yu, Jing Xiao, Lu Le, Adam P Harrison

Specialty type: Radiology, nuclear medicine and medical imaging

Provenance and peer review: Invited article; Externally peer reviewed.

Peer-review model: Single blind

Peer-review report's scientific quality classification

Grade A (Excellent): 0
Grade B (Very good): B, B, B, B, B
Grade C (Good): 0
Grade D (Fair): 0
Grade E (Poor): 0

P-Reviewer: Cheng W, China; Rathnaswami A, India; Sagsoz ME, Turkey; Salvi M, Italy; Watanabe A, Japan

Received: December 18, 2021
Peer-review started: December 18, 2021
First decision: January 23, 2022
Revised: February 3, 2022
Accepted: April 22, 2022
Article in press: April 22, 2022
Published online: June 14, 2022

Bowen Li, Ke Yan, Lu Le, Adam P Harrison, Research and Development, PAII Inc., Bethesda, MD 20817, United States

Dar-In Tai, Yi-Cheng Chen, Cheng-Jen Chen, Tse-Hwa Hsu, Wan-Ting Yu, Department of Gastroenterology and Hepatology, Chang Gung Memorial Hospital, Linkou Medical Center, Taoyuan 33305, Taiwan

Shiu-Feng Huang, Division of Molecular and Genomic Medicine, National Health Research Institute, Taoyuan 33305, Taiwan

Jing Xiao, Research and Development, Ping An Insurance Group, Shenzhen 518001, Guangdong, China

Corresponding author: Dar-In Tai, MD, PhD, Professor, Department of Gastroenterology and Hepatology, Chang Gung Memorial Hospital, Linkou Medical Center, No. 5 Fuxing Street, Guishan Dist, Taoyuan 33305, Taiwan. tai48978@cgmh.org.tw

Abstract

BACKGROUND

Hepatic steatosis is a major cause of chronic liver disease. Two-dimensional (2D) ultrasound is the most widely used non-invasive tool for screening and monitoring, but associated diagnoses are highly subjective.

AIM

To develop a scalable deep learning (DL) algorithm for quantitative scoring of liver steatosis from 2D ultrasound images.

METHODS

Using multi-view ultrasound data from 3310 patients, 19513 studies, and 228075 images from a retrospective cohort of patients received elastography, we trained a DL algorithm to diagnose steatosis stages (healthy, mild, moderate, or severe) from clinical ultrasound diagnoses. Performance was validated on two multi-scanner unblinded and blinded (initially to DL developer) histology-proven cohorts (147 and 112 patients) with histopathology fatty cell percentage diagnoses and a subset with FibroScan diagnoses. We also quantified reliability across scanners and viewpoints. Results were evaluated using Bland-Altman and receiver operating characteristic (ROC) analysis.

RESULTS

The DL algorithm demonstrated repeatable measurements with a moderate number of images (three for each viewpoint) and high agreement across three premium ultrasound scanners. High diagnostic performance was observed across all viewpoints: Areas under the curve of the ROC to classify mild, moderate, and severe steatosis grades were 0.85, 0.91, and 0.93, respectively. The DL algorithm outperformed or performed at least comparably to FibroScan control attenuation parameter (CAP) with statistically significant improvements for all levels on the unblinded histology-proven cohort and for "= severe" steatosis on the blinded histology-proven cohort.

CONCLUSION

The DL algorithm provides a reliable quantitative steatosis assessment across view and scanners on two multi-scanner cohorts. Diagnostic performance was high with comparable or better performance than the CAP.

Key Words: Ultrasound; Liver steatosis; Deep learning; Screening; Computer-aided diagnosis

©The Author(s) 2022. Published by Baishideng Publishing Group Inc. All rights reserved.

Core Tip: Ultrasound is widely used to evaluate liver steatosis, but it is subjective. We developed a deep learning algorithm for quantitative steatosis scoring from ultrasound. The algorithm was trained on > 200000 images and composed of different scanners and viewpoints from both hepatic lobes. High diagnostic performance was measured across all viewpoints in separate histology proven groups, which was comparable to or better than the control attenuation parameter. We demonstrated high agreement across scanners and viewpoints. Thus, our deep learning algorithm provides a quantitative assessment with high performance and reliability.

Citation: Li B, Tai DI, Yan K, Chen YC, Chen CJ, Huang SF, Hsu TH, Yu WT, Xiao J, Le L, Harrison AP. Accurate and generalizable quantitative scoring of liver steatosis from ultrasound images *via* scalable deep learning. *World J Gastroenterol* 2022; 28(22): 2494-2508
URL: https://www.wjgnet.com/1007-9327/full/v28/i22/2494.htm
DOI: https://dx.doi.org/10.3748/wjg.v28.i22.2494

INTRODUCTION

Liver steatosis, or fatty liver disease, is a major cause of chronic liver disease worldwide. It is estimated that nonalcoholic fatty liver disease (NAFLD) affects 20%-30% of the global population[1-3] and is associated with increased risks of cardiovascular disease, type 2 diabetes, and metabolic risk factors[4]. Unfortunately, it is an undertreated and underdiagnosed disease[5]. For those patients with more aggressive nonalcoholic steatohepatitis, the risks of liver cirrhosis, liver failure, and hepatocellular carcinoma are higher[6-8]. Liver steatosis is also associated with chronic viral hepatitis. For instance, hepatitis C can impair glucose metabolism, resulting in the accumulation of fat droplets in the liver and increasing hepatocarcinogenesis[9]. There have been reports on the interaction between liver steatosis and hepatitis B. Previous reports have also suggested that liver steatosis is associated with delayed hepatitis B surface antigen seroclearance[10]. Therefore, assessing liver steatosis is also important for chronic viral hepatitis.

Liver needle biopsy is the gold standard diagnosis at present. However, even with machine learning-based interpretation[11,12], the invasiveness of the biopsy severely limits its clinical applicability as a screening and assessment tool, and at the same time it is prone to sampling error. Thus, with the growing prevalence of NAFLD and nonalcoholic steatohepatitis, accurate, reliable, and accessible non-invasive screening tools are increasingly important to quantify liver steatosis and provide follow-up monitoring[4].

Such tools include magnetic resonance imaging with derived proton density fat fraction (MRI-PDFF), quantitative ultrasound (US), and two-dimensional (2D) US diagnoses[13]. MRI-PDFF is the best non-invasive test and can be used as a gold standard in clinical trials, but it is costly for routine clinical care [5,14]. As for quantitative US, its most popular variant is FibroScan with its control attenuation parameter (CAP) scores[15]. CAP is more available than MRI-PDFF but still requires dedicated equipment. Finally, 2D US exams have been widely used for the diagnosis of liver disease for 5 decades [13], which is partly driven by the prevalence of US equipment and its low cost. In clinical practice, 2D US is also the first-line screening modality for the detection of liver cancer[16]. Therefore, steatosis can

also be assessed from studies with a primary aim of liver tumor screening. Given these considerations, it is not surprising that 2D US is the most common tool for assessing liver steatosis[4].

A recent NAFLD epidemiology meta-analysis revealed that 90.6% of 392 studies in China used 2D US as the diagnostic modality of choice[3]. Unfortunately, US steatosis scores are considered a subjective diagnosis. A meta-analysis in 2011 reported that the kappa statistics for inter- and intra-observer reliability showed poor numbers[4]. A 2014 analysis[17], focusing on US steatosis assessment derived from routine clinical care, concluded that intra- and inter-observer agreement of binary assessment was only 51%-68% and 39%-40%, respectively, and it also noted that there was a lack of reported reliability measurements of categorical assessments. Both studies attributed the low reliability to different image acquisition practices across institutions and the subjective and variable nature of US image interpretation. More recently, Hong *et al*[18] investigated the reliability of categorical US assessments of different features and reported only moderate inter-rater agreements (intra-class correlation coefficients of 0.54) for the overall steatosis impression.

A promising alternative is to apply machine learning algorithms, *e.g.*, deep learning (DL), on 2D US liver scans. The goal is to provide a quantitative measure of liver steatosis directly from 2D US images for clinical decision support. Efforts toward this end have been reported. However, limitations in the analysis, *i.e.*, small training set sizes[19,20], only binary assessments[20-24], and single-scanner data[23-27], restrict the conclusions that can be drawn. Moreover, the reliability of these assessments, either across scanners or across different US views of the liver, have not been assessed. Relatedly, the specific number of images needed for a reliable diagnosis, and of which liver viewpoints, has also not been well articulated or characterized. This is crucial for an at-large adoption of any imaging-based diagnostic tool.

To address these limitations, we developed a scalable DL algorithm to quantitatively assess liver steatosis from 2D US using a retrospectively mined big data cohort. Cross-scanner and cross-view reliability was measured in addition to diagnostic performance against gold standard histopathological diagnoses on two clinical cohorts. Direct comparisons against CAP were also performed. The DL algorithm might serve as an effective tool for liver steatosis screening and monitoring.

MATERIALS AND METHODS

Patient cohorts and image collection

Multiple patient cohorts were collected for our study, as shown in Table 1 and Figure 1. The clinicopathological makeup of each dataset can be found in Supplementary Table 1. All US images underwent the same automatic cropping and resampling preprocessing, which is described in the Supplementary material. This study was approved by the Institutional Review Board of the Chang Gung Medical Foundation (CGMH IRB No. 201801283B0).

Big data groups (big data learning group and big data validation group)

We retrospectively collected a big data dataset from the picture archiving and communication system of CGMH, a major hospital in Taiwan (over 4 million outpatient visits/year). All patients who received elastography (a quantitative US technology), specifically acoustic radiation force impulse imaging and FibroScan, between January 3, 2011 and September 28, 2018 represented the index patients. From the index patients, we extracted all 2D US studies that were acquired within the same 2011-2018 period, resulting in multiple studies per patient. Seventy percent of the patients and their corresponding US studies were randomly selected as training data (big data learning group, BD-L), totaling 2899 patients and 200654 images. We used another 10% of the patients for validating and tuning our DL algorithm (big data validation group, BD-V), totaling 411 patients and 27421 images. The remaining 20% of the patients were not used as part of this study. In addition, any patients also found in the other datasets were also moved to this excluded cohort. The collected images were generated from 13 known scanners, which are listed in Supplementary Table 2. Each US study was accompanied by a 2D US diagnosis of steatosis severity from visual assessment using established guidelines[13,28], generated through the course of routine clinical care. These labels are used to train the DL algorithm. We enrolled the maximum number of patients that fit our inclusion criteria to provide as much data as possible for the DL algorithm.

Unblinded test group (histopathology unblinded test group)

We used a collection and selection protocol reported in prior work[29-32]. Specifically, since 2011 it has been CGMH policy to obtain elastography measurements for all patients undergoing a liver biopsy, *i.e.*, acoustic radiation force impulse and FibroScan once the latter became available. The histopathology unblinded test group (HP-U) dataset (n = 147) consists of patients with FibroScan diagnoses between the dates November 27, 2014 to September 26, 2019. Identical to a prior study[29], we included patients with chronic hepatitis B virus (HBV), chronic hepatitis C virus (HCV), and non-hepatitis B/C virus (NBNC) liver diseases. We excluded those with decompensated liver disease, toxic hepatitis, alcoholism, or autoimmune liver diseases. After exclusion of these etiologies, the majority of the NBNC group were

Table 1 Overview of development and testing datasets

Stage	Name	Purpose	Labels	Patients	Studies	Images
DL learning	BD-L	Big data, to train the neural network	2D US Dx	2899	17149	200654
DL validation	BD-V	Big data, to tune model performance	2D US Dx	411	2364	27421
Testing	HP-U	Histopathology-proven group, to (a) measure the trend between DL predictions and histology (b) measure reliability across 2D US liver viewpoints	Histology	147	147	1647
	TM	Tri-machine data US Dx group, to (a) measure reliability across 2D US liver viewpoints and (b) measure reliability across scanners	-	246	733	9215
	HP-T[1]	Histology proven group to measure the trend between DL predictions and histology	Histology, CAP	112	112	1996

[1]Labels blind to deep learning researchers during course of algorithmic development.

DL: Deep learning; US: Ultrasound; BD-L: Big data learning group; BD-V: Big data validation group; HP-U: Histopathology unblinded test group; TM: Trimachine group; HP-T: Histopathology blinded test group; CAP: Control attenuation parameter; 2D: Two-dimensional; Dx: Diagnosis.

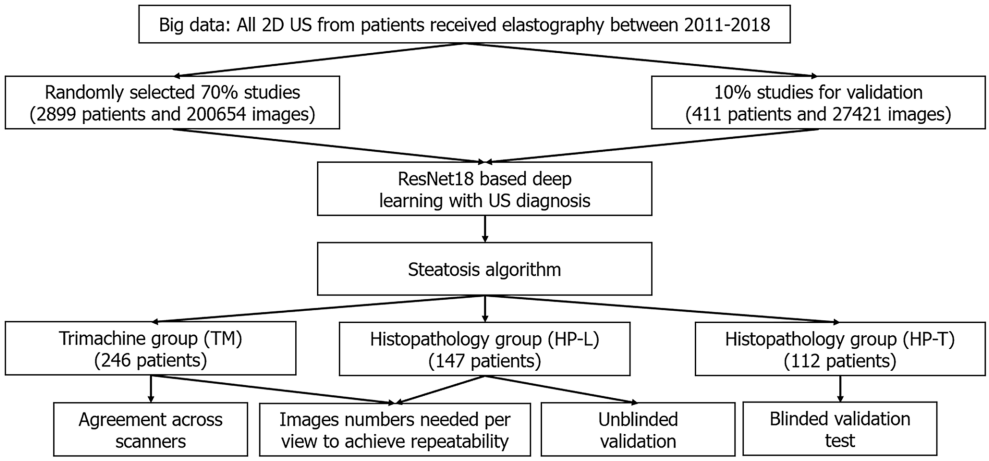


Figure 1 Flowchart. 2D-US: Two-dimensional ultrasound.

NAFLD patients (90.3% in HP-U group, Supplementary Table 1B). Histopathological analysis was performed by the same clinician (S.F.H.), and any retrospectively collected histopathological analysis not originally performed by S.F.H. was redone. Liver biopsies were collected mainly at the CGMH outpatient center and were performed to evaluate fibrosis, steatosis, or an unknown etiology[29-32]. Percutaneous liver biopsy was performed under US guidance with an 18-gauge core needle and an automatic pistol device (Magnum; Bard Peripheral Vascular, Inc, Tempe, AZ, United States). Under this standard procedure a liver specimen greater than 1.2 cm was obtained. However, a portion of the histology data was obtained from tumor resection. Following Kleiner *et al*[33], the histology diagnoses were graded into normal (5%), mild (5% and 33%), moderate (33% and 66%) and severe (66%) based on the liver fat cell fraction.

Because we were interested in US analysis, additional selection criteria were also applied. A patient must have a 2D US study that was: (1) Acquired within 3 mo of the biopsy; and (2) acquired with one of the Siemens Acuson S2000, Philips IU22, or Toshiba Aplio 300 scanners. We also excluded patients with tumors > 3 cm and with multiple cysts. Finally, US studies must have ≥ 10 images of the viewpoints depicted in Figure 1. If more than one US study qualified, we randomly selected one. All labels in HP-U were unblinded to the DL researchers of this work, but the data was treated as a test set, meaning it was only analyzed after development was complete.

Tri-machine group

We prospectively collected this cohort (n = 246) from patients that had both an US and a FibroScan study ordered and if D.I.T., Y.C.C., T.H.H., or C.J.C. conducted the image study. With the agreement of these patients, they were scanned by Siemens Acuson S2000, Philips IU22, and Toshiba Aplio 300 scanners on the same day. Studies were collected over a period from August 30, 2018 to August 27, 2019, and we only included patients diagnosed with the HBV, HCV, and NBNC criteria used in HP-U. The tri-machine (TM) cohort allowed for an assessment of agreement across scanners.

Blind testing group (histopathology blinded test group)

Finally, we included histopathology blinded test group (HP-T, n = 112), a clinical testing dataset whose labels were blind to the DL researchers involved in this project during development of the algorithm. HP-T was collected from patients that had received a liver biopsy between April 18, 2011 to May 5, 2015 and September 1, 2018 to January 29, 2021. Associated FibroScan diagnoses were only available for the later subset of patients. Also, unlike HP-U, US studies were not restricted to only the Siemens, Philips, and Toshiba scanners of TM and HP-U. In particular, 18 studies were acquired with the Aloka SSD 5500 or ATL: HDI 5000 scanners, which are not currently considered premium scanners.

Image selection

We were interested in investigating performance and reliability across viewpoints. Thus, we only included US images from the viewpoints shown in Figure 2, which can be categorized into four view groups: Left liver lobe (LLL), right liver lobe (RLL), liver/kidney contrast (LKC), and subcostal (SC). For HP-U, HP-T, and BWC, we only included studies that had ≥ 10 images of any of the studied viewpoints. BD-L and BD-V were automatically filtered with an algorithm explained in the Supplementary material.

Training steatosis assessment DL algorithm

Figure 3 illustrates the algorithmic workflow of our DL algorithm. Using the images from BD-L, we trained a multi-class deep ResNet18[34] DL classifier using the 2D US diagnoses, which were ordinal labels ranging from 0 to 3 corresponding to None; Mild; Moderate; and Severe steatosis[35]. We treated each image independently in training and followed the well-known binary decomposition approach to ordinal classification of Frank and Hall[36]. After training, a simple transformation produced a continuous score[37] for each image that ranged from 0 to 1, with higher scores corresponding to more severe steatosis. As Figure 3 indicates, during inference, we took the mean of the image-wise scores within and across each view group. The view group scores were further averaged to produce an "All View Groups" score. If one or several view groups were missing, the "All View Groups" score was calculated with what view groups were available. More details on the training strategy can be found in the Supplementary material, and a listing of hyper-parameters is given in Supplementary Table 5.

Statistical analysis

A listing of all experiments can be found in Supplementary Table 3. We evaluated the reliability and diagnostic performance of the DL algorithm. We judged P values < 0.05 as significant and corrected for multiple comparisons using the Holm-Bonferroni procedure[38].

Reliability studies

Experiment 1: We used TM and HP-U to assess how many images were needed per view group to achieve repeatability. Note, for the TM dataset we randomly selected only one US study for each patient to avoid sampling the same patient more than once. As advocated by Bland and Altman[39,40], we graphed the within-subject standard deviations across different view-group steatosis scores and measured the repeatability coefficient (RC)[40]. The difference between two repeated measurements should be within the RC value for 95% of the US studies. However, because the within-subject standard deviation was not uniform across our data (typically greater variability in repeated measurements at moderate steatosis levels), we regressed a non-uniform RC and used the worst-case RC value as a summary statistic, with 95% confidence intervals computed using percentile bootstrap (1000 bootstrap samples)[41]. More details on this calculation can be found in the Supplementary material.

Experiment 2: We also evaluated agreement across scanners using TM. We conducted a Bland-Altman analysis[39] on the difference values across view-group scores and calculated the limits of agreement (LOAs[40]), which are the limits by which 95% of the disagreements fall under[40]. Like Experiment 1, variability tended to be higher at moderate levels of severity. Therefore, we regressed non-uniform LOAs and used the maximum upper LOAs and minimum lower LOAs as summary statistics. More details can be found in the Supplementary material. We also calculated the percentage agreement, using the cutoff levels determined in Experiment 3 below.

Diagnostic testing

Experiment 3a: We validated the DL model diagnostic performance using the images and histopathological labels of HP-U. Although the HP-U labels were not blinded to the DL researchers during algorithmic development, it was treated like a test set, *i.e.* evaluation was only performed once model development was complete. Histopathological diagnoses were separated into four ordinal labels[27]. For three separations of fatty percentages, *i.e.*, grade ≥ 5%, grade ≥ 33%, and grade ≥ 66%, we used receiver operating characteristic (ROC) curve analysis and measured the area under the curve of the ROC (AUCROC). Trend tests between the DL assessment and histopathological grades were conducted using the non-parametric Jonckheere-Terpstra test[42]. The 95% confidence intervals of all AUCROCs were calculated based on DeLong's non-parametric test[43]. When needed, we determined cutoff values using the values that maximized the Youden index[44].

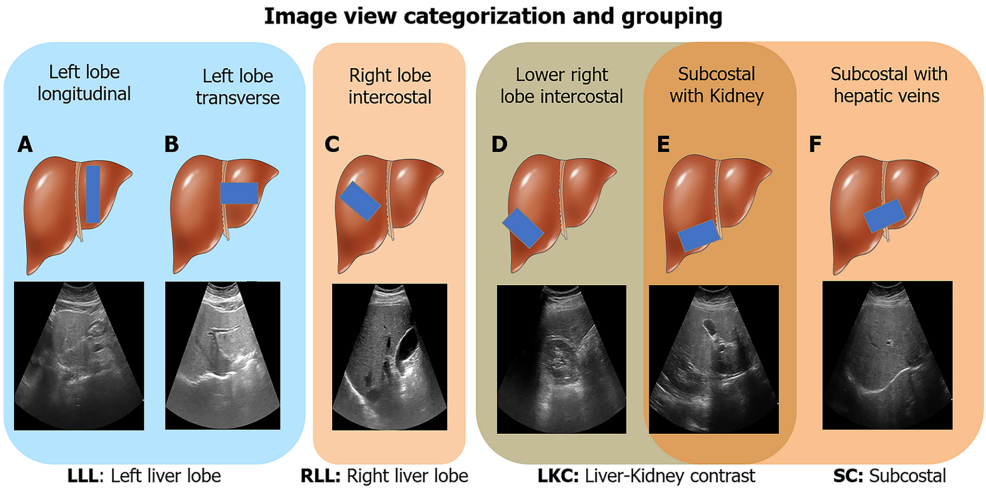


Figure 2 Image view categorization and grouping. Six ultrasound image viewpoints were used in this study. A: Left lobe longitudinal; B: Left lobe transverse; C: Right lobe intercostal; D: Lower right lobe intercostal (depicting liver/kidney contrast); E: Subcostal depicting liver/kidney contrast; F: Subcostal with hepatic veins. These views were further categorized into four groups: Left liver lobe (A and B), right liver lobe (C), liver/kidney contrast (D and E), and subcostal (E and F). LLL: Left liver lobe; RLL: Right liver lobe; LKC: Liver/kidney contrast; SC: Subcostal. Liver cartoons adapted from the DataBase Center for Life Science (https://commons.wikimedia.org/wiki/File:201405_liver.png), licensed under the Creative Commons Attribution 4.0 International[51] (Copyright permission see Supplementary material).

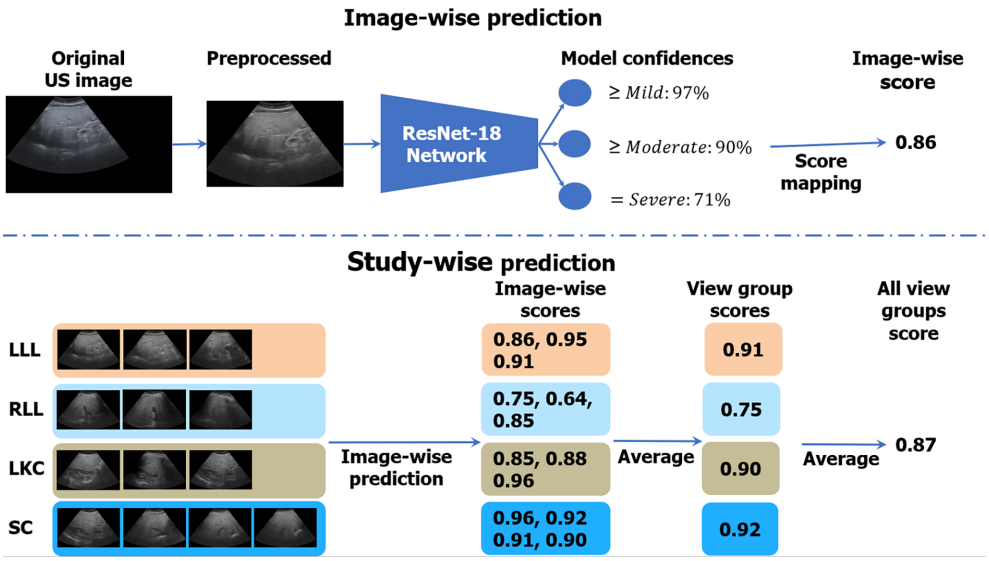


Figure 3 Algorithmic workflow. Images were first comprehensively preprocessed to remove regions outside the ultrasound beam. A deep learning neural network, called ResNet-18, was trained on individual ultrasound images in the big data learning group. The model predicted confidences in three binary cutoffs: "≥ mild", "≥ moderate", or "= severe" steatosis. The confidences were mapped to a continuous image-wise score in the range of [0, 1]. View-group scores were produced by averaging each image within the group. An "All View Groups" score was produced by averaging all available view group scores. In the figure's example, the gold standard histopathology diagnosis was a fatty cell percentage of 90%. LLL: Left liver lobe; RLL: Right liver lobe; LKC: Liver/kidney contrast; SC: Subcostal.

Experiment 3b: We compared the performance of FibroScan with that of the DL assessment, and statistical significance of any differences in AUCROCs were assessed using the StAR[45] implementation of DeLong's non-parametric test[43].

Experiment 4a: Finally, we tested our DL assessment on HP-T, whose histopathological labels were blind to the DL researchers during model development.

Experiment 4b: For patients with FibroScan diagnoses, we also compared its performance with that of the DL assessment. Experiments 4a and b used the same statistical analyses as Experiments 3a and b.

RESULTS

Repeatable measurements with a moderate number of images

We first determined how many images were needed for each view group to reach a repeatable measurement (Experiment 1 in Supplementary Table 3) using TM (one random study per patient) (n = 246) and HP-U (n = 147). The results when using three images per view group can be found in Table 2, and the complete set of results from one-to-four images can be found in Supplementary Table 6. As can be seen, depending on the view group, the max RC value was equal to or less than 30% of the DL assessment scale, which ranged from 0 to 1. In the worst case, 95% of the differences between repeated measurements should be within this max RC value. As the repeatability graph of Figure 4A demonstrates, this max RC value occurred at moderate levels of steatosis severity, which have a wide tolerance (*e.g.*, moderate fatty cell content is commonly determined as being anything between 33% and 66%). The RC values for mild and severe were much lower, suggesting that a 30% RC value was highly conservative for these ranges of severity. The repeatability graphs for all other view groups can be found in Supplementary Figure 1. Together, these data demonstrate the DL assessment can attain repeatable measurements with a moderate number of images for each view group. For the remainder of evaluations, we will only include assessments that have a minimum of three images for each view group.

Agreement across scanners was high

We used the TM dataset (n = 246) to measure agreement across measurements taken on the same day but with three different scanners (Experiment 2 in Supplementary Table 3). As the Bland-Altman plots for "All View Groups" of Figure 4B-D demonstrate, the LOAs are worse at moderate levels of severity, but they are much tighter at milder and more severe levels. This mirrors the repeatability results. Table 2 presents the Bland-Altman summary statistics for all view groups, demonstrating that the cross-scanner agreement is roughly equivalent for all view groups. For brevity we combined the results across all scanner pairs together. As can be seen, the agreement across scanners is high. The bias for "All View Groups" was close to zero, and the worst case LOAs were around 35% for every view group. The LOAs for "All View Groups" fell to 25%, suggesting that examining all view groups together can increase reliability. The percentage agreement numbers are all 92% or higher, further underscoring the high agreement across the tested scanners.

High diagnostic performance on clinical test sets

With the reliability studies completed, we validated the DL score against a histopathological gold standard for diagnosing mild-to-severe (≥ 5%), moderate-to-severe (≥ 33%), and severe (≥ 66%) fatty percentages. The results on HP-U and HP-T, Experiments 3 and 4 in Supplementary Table 3, respectively, are presented in Table 3. Focusing primarily on the HP-T results, the "Complete 4 view group study" of Table 3 only selects studies that had three or more images for every view group. This allowed an "apples-to-apples" comparison across view groups. As can be seen, the performance was comparable across view groups, suggesting that each view group provided similar diagnostic value, with all providing AUCROCs ≥ 0.84. The "Individual view group study," on the other hand, presented results when examining each view group individually, meaning only the view group in question required three or more images. This allowed for a larger sample size. In this setting "All View Groups" denoted the mean score across all view groups with three or more images, which can comprise different view groups from study to study. The ROC curves for "All View Groups" for the individual view group study can be found in Figure 5A. As can be seen in Table 3, the results for the individual view groups were broadly like those of the complete view groups study with AUCROCs ≥ 0.81. Comparing the results of HP-U to HP-T, the AUCROCs were generally similar, reinforcing the above results. However, the HP-U results were generally better, especially for diagnosing mild-to-severe steatosis. This is due to HP-T including non-premium Aloka and ATL HDI scanners in its cohort, which make it harder to accurately assess steatosis. Indeed, as Figure 5B indicates, when only selecting for the Siemens, Philips, and Toshiba premium scanners the AUCROC scores for HP-T were much improved, indicating that scanner choice does make an impact. Finally, the "FibroScan comparison study" compared the performance of FibroScan directly with the DL assessment. As can be seen, the DL assessment AUCROC values were better than FibroScan, and statistical significance was reached for all levels on the HP-U dataset and for "= severe" on the HP-T dataset (Figure 5).

DISCUSSION

Incorporating different 2D US scanner models and brands, different liver viewpoints, and prospectively and retrospectively collected images, we demonstrated that a DL-based assessment can provide quantitative and reliable hepatic steatosis scores.

Table 2 Reliability studies in different views

	Repeatability study		Cross-scanner agreement study				
View	***n***	**Max RC**	***n***	**Bias**	**Min lower LOA**	**Max upper LOA**	**Agreement**
LLL	342	0.27 (0.24, 0.29)	237	0.00 (-0.01, 0.01)	-0.37 (-0.32, -0.42)	0.37 (0.32, 0.42)	92%
RLL	370	0.21 (0.19, 0.23)	232	0.00 (-0.01, 0.01)	-0.37 (-0.33, -0.42)	0.37 (0.33, 0.42)	92%
LKC	267	0.30 (0.27, 0.34)	183	0.00 (-0.01, 0.01)	-0.35 (-0.29, -0.41)	0.35 (0.29, 0.41)	93%
SC	297	0.26 (0.24, 0.29)	182	0.00 (-0.01, 0.01)	-0.36 (-0.31, -0.42)	0.36 (0.31, 0.42)	94%
All view groups	-	-	237	0.00 (-0.01, 0.01)	-0.25 (-0.21, -0.28)	0.24 (0.21, 0.28)	94%

On the left, the max repeatability coefficient was tabulated when using three images for each view group (Histopathology unblinded test group and Trimachine group datasets). On the right, the bias, worst-case limits of agreement, and agreement (%) were tabulated across different view groups for the Trimachine dataset. The results for all scanner pairs were combined. Parentheses enclose bootstrapped 95% confidence intervals. RC: Repeatability coefficient; LOA: Limits of agreement; LLL: Left liver lobe; RLL: Right liver lobe; LKC: Liver/kidney contrast; SC: Subcostal.

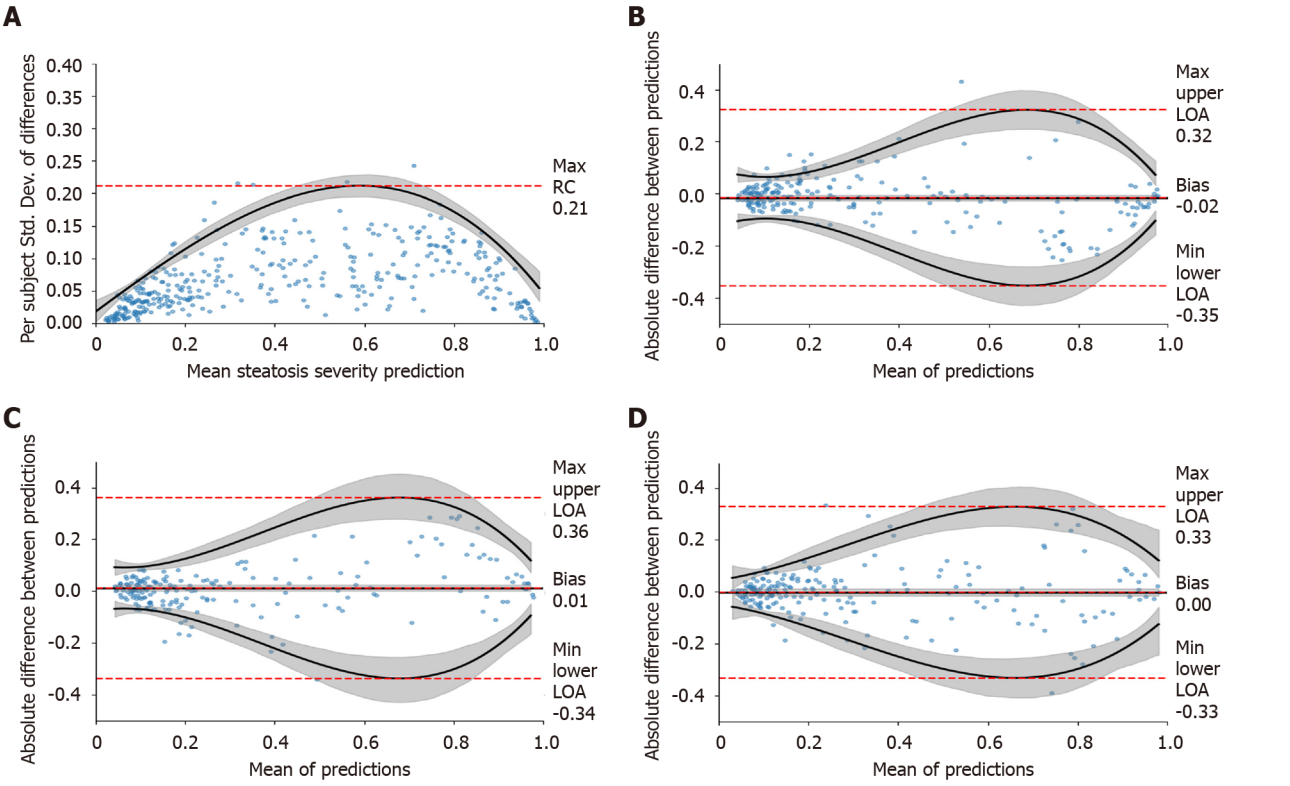


Figure 4 Repeatability study. A: A repeatability coefficient plot for right liver lobe when using three images; B-D: Cross-scanner Bland-Altman plots for Siemens-Toshiba (B), Toshiba-Philips (C), and Philips-Siemens (D), respectively. Cross-scanner plots were depicted for "All View Groups" when using ≥ three images per view group. Grey-shaded areas indicate 95% confidence intervals. RC: Repeatability coefficient; LOA: Limit of agreement.

Unlike attenuation imaging (ATI)[46], FibroScan, or some other reported DL solutions[22,25,26], our algorithm accepts images taken from both hepatic lobes rather than a selected area of interest in a specific location. We categorized 2D US images into six major viewpoints (Figure 2), which we further grouped into four view groups. We found that for each view group three images were enough to reach acceptable max RC values of 21%-30% (Table 2, Figure 4A), where the best and worst max RC values corresponded to the RLL and LKC view group, respectively. The relatively poorer repeatability of the LKC view group was likely due to the heterogenous makeup of viewpoints, as it comprises both subcostal and right lobe intercostal images. To put these repeatability ranges in context, the RC for gold standard histopathology fatty percentage assessment has been reported to be 38%[47] with poor intraclass correlation agreements of 0.57[48]. Considering our DL model's worst max RC value was 30% and that RC values tended to be much better than 30% at milder or more severe levels of steatosis (Figure 4 and Supplementary Figure 1), these repeatability measures compare well. It is also encouraging that the DL algorithm was more repeatable at milder and severe steatosis levels since such patients should indeed be less ambiguous to categorize.

Table 3 Receiver operating characteristic analysis on the histopathology unblinded test group and histopathology blinded test group cohorts for diagnosing steatosis grades

	HP-U					HP-T				
View	***n***	**AUC ≥ 5%**	**AUC ≥ 33%**	**AUC ≥ 66%**	**Acc**	***n***	**AUC ≥ 5%**	**AUC ≥ 33%**	**AUC ≥ 66%**	**Acc**
Complete 4 view group study[1]										
LLL	41	0.98 (0.93, 1.00)	0.95 (0.89, 1.00)	0.94 (0.87, 1.00)	83%	51	0.90 (0.82, 0.98)	0.92 (0.81, 1.00)	0.90 (0.82, 0.99)	88%
RLL	41	0.96 (0.90, 1.00)	0.95 (0.89, 1.00)	0.89 (0.79, 0.99)	85%	51	0.84 (0.73, 0.95)	0.93 (0.84, 1.00)	0.92 (0.85, 1.00)	96%
LKC	41	0.96 (0.90, 1.00)	0.95 (0.89, 1.00)	0.93 (0.84, 1.00)	83%	51	0.84 (0.73, 0.95)	0.95 (0.90, 1.00)	0.88 (0.79, 0.97)	90%
SC	41	0.96 (0.90, 1.00)	0.92 (0.84, 1.00)	0.89 (0.79, 0.99)	83%	51	0.88 (0.79, 0.97)	0.93 (0.86, 1.00)	0.88 (0.77, 0.99)	90%
All view groups	41	0.96 (0.90, 1.00)	0.94 (0.88, 1.00)	0.92 (0.83, 1.00)	83%	51	0.88 (0.79, 0.98)	0.95 (0.88, 1.00)	0.91 (0.83, 0.99)	94%
Individual view group study[1]										
LLL	103	0.95 (0.90, 0.99)	0.93 (0.87, 0.98)	0.91 (0.86, 0.97)	80%	96	0.84 (0.76, 0.93)	0.92 (0.85, 0.99)	0.93 (0.88, 0.98)	90%
RLL	138	0.94 (0.91, 0.98)	0.91 (0.86, 0.98)	0.85 (0.78, 0.92)	83%	109	0.82 (0.74, 0.90)	0.89 (0.83, 0.96)	0.92 (0.87, 0.97)	92%
LKC	88	0.96 (0.92, 1.00)	0.92 (0.86, 0.98)	0.84 (0.76, 0.92)	80%	71	0.81 (0.69, 0.93)	0.93 (0.87, 0.99)	0.89 (0.81, 0.96)	90%
SC	117	0.93 (0.89, 0.98)	0.91 (0.85, 0.96)	0.86 (0.79, 0.92)	79%	90	0.86 (0.77, 0.94)	0.89 (0.82, 0.96)	0.90 (0.83, 0.97)	88%
All view groups	147	0.95 (0.91, 0.98)	0.92 (0.88, 0.96)	0.87 (0.81, 0.92)	76%	112	0.85 (0.77, 0.93)	0.91 (0.85, 0.97)	0.93 (0.88, 0.98)	90%
FibroScan comparison study[1,2]										
All view groups	147	0.95[3] (0.92, 0.98)	0.95[3] (0.92, 0.98)	0.92[3] (0.88, 0.97)	77%	80	0.93 (0.87, 0.98)	0.97 (0.93, 1.00)	0.92[3] (0.86, 0.98)	91%
FibroScan	147	0.88 (0.81, 0.95)	0.88 (0.81, 0.95)	0.80 (0.73, 0.87)	62%	80	0.89 (0.82, 0.96)	0.92 (0.86, 0.98)	0.82 (0.73, 0.92)	68%

[1]Filtered with a minimum of 3 images for each view group.
[2]Selecting only studies with associated FibroScan control attenuation parameter (CAP) scores.
[3]Area under the curve of the receiver operating characteristic significantly better than FibroScan CAP scores.
"Complete 4 view groups study" only selects studies where every view group is qualifying (three or more images), whereas "Individual view group study" examines the performance of each qualifying view group individually. Numbers in parentheses are 95% confidence intervals. All trends between the deep learning/CAP score and the histopathology grades were significant ($P < 0.001$). "Acc" is the classification accuracy when the threshold values calculated by optimizing the Youden index[44] are applied. LLL: Left liver lobe; RLL: Right liver lobe; LKC: Liver/kidney contrast; SC: Subcostal; HP-U: Histopathology unblinded test group; HP-T: Histopathology blinded test group; AUC: Area under the curve.

We also demonstrated good cross-scanner agreement. Bland-Altman analysis suggested bias across scanners was near zero with acceptable LOAs (35%-37%) for individual view groups, with the LOAs falling to 25% when using "All View Groups." When using categorical labels, these numbers correspond to agreements of 90% to 96%. An encouraging sign for generalizability is that cross scanner agreement is high for the Siemens: S2000 scanner, despite it being poorly represented in BD-L.

In terms of diagnostic performance, we validated on two different histology-proven cohorts (HP-U and HP-T). The "Complete view group study" of Table 3 indicated that diagnostic performance remained stable across view groups, with comparable and high AUCROC values (≥ 0.84). These results were reinforced by the "Individual view group study," which allowed each view group to be investigated individually, with a corresponding larger sample size. Again, the DL model posted good AUCROC values (≥ 0.81) across view groups and histopathology grades. As highlighted in the results, the AUCROCs in HP-T tended to be lower than in HP-U, which was most pronounced for diagnosing > 5% fatty percentage. This is explained by the 18 earlier studies acquired by low resolution scanners in HP-T (Supplementary Table 2), which produced relatively lower quality images than the more recent premium scanners. Indeed, as Figure 4B shows, excluding the older scanners raised the HP-T AUCROC scores considerably so that they matched the HP-U group (from 0.85 to 0.90 AUCROC for ≥ 5% fatty

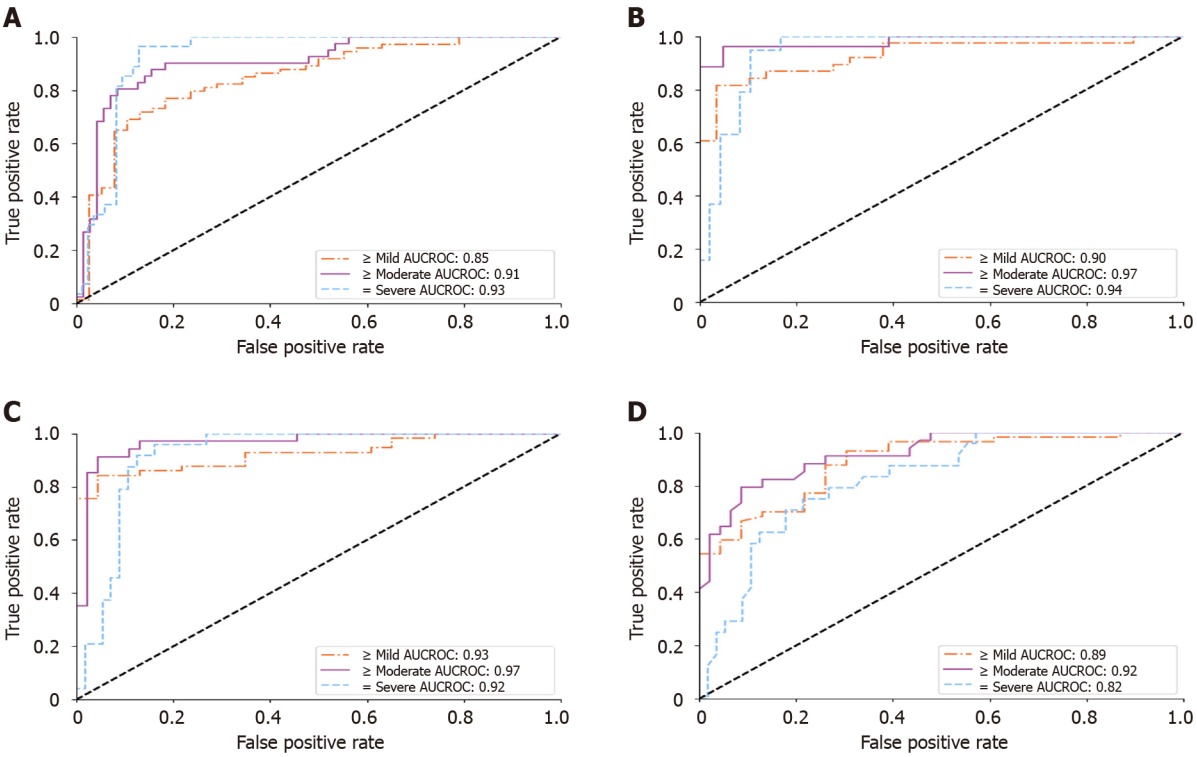


Figure 5 Receiver operating characteristic analysis on histopathology blinded test group. A and B: Receiver operating characteristic curves of the deep learning model for diagnosing hepatic steatosis grades on histopathology blinded test group (HP-T) when using all scanners and only the Siemens/Toshiba/Philips premium scanners, respectively; C and D: Only select for histopathology blinded test group studies with FibroScan diagnoses, corresponding to the performance of the deep learning algorithm and FibroScan, respectively. All receiver operating characteristic curves were measured against a histopathological gold standard. AUCROC: Area under the curve of the receiver operating characteristic.

percentage). Consequently, even though performance seemed to be stable across the tested premium scanners, the DL algorithm can be sensitive to scanner quality, which is a matter requiring further investigation.

The clinical diagnosis of our big data was generally based on the principle of Hemaguchi score, US-FLI score, and hepatorenal steatosis score[13]. Our DL algorithm demonstrated good quantitative performance despite being trained on subjective 2D US categorical labels with inter-observer variations. We speculate this is due to the exceptionally large training BD-L dataset, which included diagnoses from 63 clinicians. This allowed the DL model to "learn" and distill from a variety of clinical assessments. In addition, the DL model's continuous output allowed for a calibration against accepted gold standards. Although the distribution of etiologies between the big data training cohort and histology-proven validation cohorts were unavoidably different, validation performance remained high. Thus, these distributional differences did not seem to impede performance on a representative sample from a clinical population.

Importantly, we compared the DL algorithm's performance head-to-head with CAP of FibroScan. The DL algorithm's "All View Groups" score reported higher AUCROCs (0.92-0.97 *vs* 0.80-0.92) and accuracies (77%-91% *vs* 62%-68%) than CAP (Table 3). Statistically significant improvements were achieved for all levels on the HP-U cohort, and only for "= severe" on the HP-T cohort. This is encouraging because, unlike CAP, our DL algorithm can be applied to many different liver viewpoints and does not require additional equipment outside of an US scanner. Our DL algorithm enjoys similar advantages in flexibility over other quantitative US techniques[25,49], which examines the attenuation, brightness, or echogenicity change within a small region of interest (ROI). Such restrictions may result in missing other useful information for steatosis diagnosis (for example, liver/kidney contrast and the loss of vessel walls). Quantitative US can also not be applied to patients where the specific ROI is unable to be imaged and is often limited to a specific scanner, *e.g.*, ATI only works with Canon scanners.

The DL algorithm can be trained with large-scale retrospective datasets, which need neither costly machines nor annotation of regions of interest. Furthermore, in the inference stage, our algorithm does not require images from all hepatic views, *e.g.*, the absence of the right hepatic lobe images is acceptable, as the performance of our algorithm with left hepatic lobe images is just as good. When using "All View Groups," diagnostic AUCROCs did not improve. However, the improved cross-scanner agreement (Table 2) suggests using "All View Groups" may provide more reliability. Our algorithm could be used on different brands of scanners in different hospitals. However, each scanner or hospital may determine their cutoff values for different grades of steatosis based on their preferred gold standard (liver

histology or MRI-PDFF). Its potential applications include improved steatosis screening and longitudinal tracking in clinical settings. Our trained algorithm may be shared with researchers for non-commercial use upon reasonable requests to the clinical principal investigator (D.I.T.) and subject to IRB approval. We expect it to have good generalizability given the diversity of the BD-L dataset. Because our algorithm is trained only on retrospective US-labeled data, which are readily available in most Picture Archiving and Communication Systems, we also believe the methodology we presented here to be highly generalizable and accessible to institutions wishing to train their own algorithms.

The use of machine learning technologies for non-invasive liver steatosis assessment has received attention for a number of years[19-27]. This work represents a significant step forward. Like this work, many prior solutions were built upon recent DL techniques[22,24-27], which Supplementary Table 7 summarizes. Apart from Gummadi *et al*[22], all other works only test on a single scanner. Moreover, our evaluation includes more than one etiology: HBV, HCV, and NBNC liver diseases. In terms of training, we use so-called "big-data," which included 13 known different US scanner models and over 228000 images and 19000 US studies. This dwarfs the training set size of other works and should contribute to better model generalizability. Another important point is that most prior studies used one specific viewpoint[19,20,24] or manually defined area of interest[22,25,26], which can restrict their applicability. Like Byra *et al*[27], we investigated performance across different views. In addition, we investigated different viewpoints in both hepatic lobes. This advantage is most evident for patients with one resected hepatic lobe or a lobe whose space is occupied by a lesion. Furthermore, this study measured agreement across three different scanners and repeatability across different view groups and across different numbers of images per view group, which are analyses not found in other studies. Finally, we are the first to directly compare against a leading non-invasive alternative: CAP of FibroScan.

Our study has several limitations. First, we primarily used histology as the gold standard for assessing liver steatosis, which can suffer from sampling errors, processing variabilities, and intra- and inter-observer variability[48,50]. A histopathological gold standard also introduced patient selection bias. For example, CGMH histology is not required to initiate therapy in patients with HCV, whereas it is often required for patients with HBV or nonalcoholic steatohepatitis. In addition, we selected US studies completed within 3 mo of a liver histology study. If there were vigorous lifestyle changes within 3 mo, we may have a risk of deviation between fatty scores of US image and liver histology. Thus, investigating and validating against other non-invasive scores, both imaging and non-imaging based, remains an important task. Second, for assessing diagnostic performance we used retrospective data. To impose a degree of standardization, we required there to be at least 3 images in a view group and ≥ 10 images in the whole US study. Nonetheless, more controlled experimental settings may allow for more precise comparisons and follow-up prospective studies should implement an acquisition protocol to assess diagnostic performance in varied settings. In particular, the relatively poorer repeatability of the LKC view group should be investigated, and, if necessary, adjustments to the protocol should be made. Third, patients in HP-U and HP-T may also have co-occurring liver fibrosis, which likely has complex interactions with hepatic steatosis. The effect of this interaction on interpretations needs further study. Fourth, the scanner quality and model does seem to impact the DL model. Future work should better measure this impact, focusing on premium scanners not seen in the training data, which would better characterize generalizability. Fifth, the combined case numbers in HP-U and HP-T were more than 200, but the number with "complete view groups" was relatively small. Relatedly, the data collected in this study were all acquired from the CGMH institution, so any conclusions must be interpreted cautiously. Measuring performance across multiple centers, ideally using a prospective data collection protocol with larger evaluation cohorts, remains an important aspect of future work.

CONCLUSION

The DL algorithm provided a reliable quantitative steatosis assessment across view and scanners on two multi-scanner cohorts. Diagnostic performance was high with comparable or better performance than CAP. This algorithm could be applied to prospectively as well as retrospectively collected 2D US images.

ARTICLE HIGHLIGHTS

Research background

Two-dimensional (2D) ultrasound has been used for screening of liver steatosis for more than 5 decades. It is a cheap and non-invasive study.

Research motivation

Two-dimensional ultrasound is a subjective diagnosis that is not suitable for quantitative study.

Research objectives
To produce an objective steatosis diagnostic algorithm by deep learning from big data of 2D ultrasound images.

Research methods
Using multi-view ultrasound big data from a retrospective cohort of patients, we trained a deep learning algorithm to diagnose steatosis stages from clinical ultrasound diagnoses. Performance was validated on two multi-scanner unblinded and blinded histology-proven cohorts with histopathology diagnoses and a subset with FibroScan diagnoses. We also quantified reliability across scanners and viewpoints. Results were evaluated using Bland-Altman and receiver operating characteristic analysis.

Research results
The deep learning algorithm demonstrated repeatable measurements with a moderate number of images and high agreement across three premium ultrasound scanners. High diagnostic performance was observed across all viewpoints. Areas under the curve of the receiver operating characteristic to classify mild, moderate, and severe steatosis grades were 0.85, 0.91, and 0.93, respectively. This algorithm outperformed or performed at least comparably to FibroScan control attenuation parameter on the unblinded or blinded histology-proven cohort.

Research conclusions
This algorithm could give an objective diagnosis of steatosis from prospectively or retrospectively collected 2D ultrasound images.

Research perspectives
The cutoff values for different grades of steatosis would need future studies in different scanners and fibrosis status.

FOOTNOTES

Author contributions: Li B contributed to software, visualization, and writing original draft and investigation; Yan K contributed to formal analysis, visualization and writing review and editing; Chen YC, Chen CJ, Huang SF, Hsu TH, and Yu WT contributed to data curation; Huang SF contributed to resources; Xiao J contributed to project administration and funding acquisition, and writing review and editing; Lu L contributed to project administration, supervision, writing review and editing, and resources; Harrison AP contributed to formal analysis, supervision, software, writing review and editing, investigation, and methodology; Tai DI contributed to supervision, data curation, conceptualization, writing review and editing, validation, project administration, investigation, resources, and methodology.

Supported by the Maintenance Project of the Center for Artificial Intelligence, No. CLRPG3H0012 and No. SMRPG3I0011.

Institutional review board statement: The study was reviewed and approved by the Institutional Review Board of the Chang Gung Medical Foundation (CGMH IRB No. 201801283B0).

Informed consent statement: Patients were not required to give informed consent to the study.

Conflict-of-interest statement: All authors declare no conflict of interest.

Data sharing statement: No additional data are available.

STROBE statement: The authors have read the STROBE Statement—checklist of items, and the manuscript was prepared and revised according to the STROBE Statement—checklist of items.

Open-Access: This article is an open-access article that was selected by an in-house editor and fully peer-reviewed by external reviewers. It is distributed in accordance with the Creative Commons Attribution NonCommercial (CC BY-NC 4.0) license, which permits others to distribute, remix, adapt, build upon this work non-commercially, and license their derivative works on different terms, provided the original work is properly cited and the use is non-commercial. See: https://creativecommons.org/Licenses/by-nc/4.0/

Country/Territory of origin: Taiwan

ORCID number: Bowen Li 0000-0003-1374-5207; Dar-In Tai 0000-0003-1054-1583; Ke Yan 0000-0002-0034-9013; Yi-Cheng Chen 0000-0002-7810-7145; Cheng-Jen Chen 0000-0002-0903-0682; Shiu-Feng Huang 0000-0002-0696-5108; Tse-Hwa Hsu 0000-0002-1427-5676; Wan-Ting Yu 0000-0002-7027-1944; Jing Xiao 0000-0001-9615-4749; Lu Le 0000-0002-6799-9416; Adam P Harrison 0000-0003-3315-1772.

S-Editor: Chen YL
L-Editor: Filipodia
P-Editor: Li X

REFERENCES

1 **Younossi Z**, Anstee QM, Marietti M, Hardy T, Henry L, Eslam M, George J, Bugianesi E. Global burden of NAFLD and NASH: trends, predictions, risk factors and prevention. *Nat Rev Gastroenterol Hepatol* 2018; **15**: 11-20 [PMID: 28930295 DOI: 10.1038/nrgastro.2017.109]
2 **Dietrich P**, Hellerbrand C. Non-alcoholic fatty liver disease, obesity and the metabolic syndrome. *Best Pract Res Clin Gastroenterol* 2014; **28**: 637-653 [PMID: 25194181 DOI: 10.1016/j.bpg.2014.07.008]
3 **Zhou F**, Zhou J, Wang W, Zhang XJ, Ji YX, Zhang P, She ZG, Zhu L, Cai J, Li H. Unexpected Rapid Increase in the Burden of NAFLD in China From 2008 to 2018: A Systematic Review and Meta-Analysis. *Hepatology* 2019; **70**: 1119-1133 [PMID: 31070259 DOI: 10.1002/hep.30702]
4 **Hernaez R**, Lazo M, Bonekamp S, Kamel I, Brancati FL, Guallar E, Clark JM. Diagnostic accuracy and reliability of ultrasonography for the detection of fatty liver: a meta-analysis. *Hepatology* 2011; **54**: 1082-1090 [PMID: 21618575 DOI: 10.1002/hep.24452]
5 **Castera L**. Non-invasive tests for liver fibrosis in NAFLD: Creating pathways between primary healthcare and liver clinics. *Liver Int* 2020; **40** Suppl 1: 77-81 [PMID: 32077617 DOI: 10.1111/Liv.14347]
6 **Anstee QM**, Reeves HL, Kotsiliti E, Govaere O, Heikenwalder M. From NASH to HCC: current concepts and future challenges. *Nat Rev Gastroenterol Hepatol* 2019; **16**: 411-428 [PMID: 31028350 DOI: 10.1038/s41575-019-0145-7]
7 **Torres DM**, Harrison SA. Diagnosis and therapy of nonalcoholic steatohepatitis. *Gastroenterology* 2008; **134**: 1682-1698 [PMID: 18471547 DOI: 10.1053/j.gastro.2008.02.077]
8 **Singh S**, Allen AM, Wang Z, Prokop LJ, Murad MH, Loomba R. Fibrosis progression in nonalcoholic fatty liver vs nonalcoholic steatohepatitis: a systematic review and meta-analysis of paired-biopsy studies. *Clin Gastroenterol Hepatol* 2015; **13**: 643-54.e1 [PMID: 24768810 DOI: 10.1016/j.cgh.2014.04.014]
9 **Lupberger J**, Croonenborghs T, Roca Suarez AA, Van Renne N, Jühling F, Oudot MA, Virzì A, Bandiera S, Jamey C, Meszaros G, Brumaru D, Mukherji A, Durand SC, Heydmann L, Verrier ER, El Saghire H, Hamdane N, Bartenschlager R, Fereshetian S, Ramberger E, Sinha R, Nabian M, Everaert C, Jovanovic M, Mertins P, Carr SA, Chayama K, Dali-Youcef N, Ricci R, Bardeesy NM, Fujiwara N, Gevaert O, Zeisel MB, Hoshida Y, Pochet N, Baumert TF. Combined Analysis of Metabolomes, Proteomes, and Transcriptomes of Hepatitis C Virus-Infected Cells and Liver to Identify Pathways Associated With Disease Development. *Gastroenterology* 2019; **157**: 537-551.e9 [PMID: 30978357 DOI: 10.1053/j.gastro.2019.04.003]
10 **Tai DI**, Tsay PK, Chen WT, Chu CM, Liaw YF. Relative roles of HBsAg seroclearance and mortality in the decline of HBsAg prevalence with increasing age. *Am J Gastroenterol* 2010; **105**: 1102-1109 [PMID: 20197760 DOI: 10.1038/ajg.2009.669]
11 **Salvi M**, Molinaro L, Metovic J, Patrono D, Romagnoli R, Papotti M, Molinari F. Fully automated quantitative assessment of hepatic steatosis in liver transplants. *Comput Biol Med* 2020; **123**: 103836 [PMID: 32658781 DOI: 10.1016/j.compbiomed.2020.103836]
12 **Munsterman ID**, van Erp M, Weijers G, Bronkhorst C, de Korte CL, Drenth JPH, van der Laak JAWM, Tjwa ETTL. A Novel Automatic Digital Algorithm that Accurately Quantifies Steatosis in NAFLD on Histopathological Whole-Slide Images. *Cytometry B Clin Cytom* 2019; **96**: 521-528 [PMID: 31173462 DOI: 10.1002/cyto.b.21790]
13 **Ferraioli G**, Soares Monteiro LB. Ultrasound-based techniques for the diagnosis of liver steatosis. *World J Gastroenterol* 2019; **25**: 6053-6062 [PMID: 31686762 DOI: 10.3748/wjg.v25.i40.6053]
14 **Caussy C**, Reeder SB, Sirlin CB, Loomba R. Noninvasive, Quantitative Assessment of Liver Fat by MRI-PDFF as an Endpoint in NASH Trials. *Hepatology* 2018; **68**: 763-772 [PMID: 29356032 DOI: 10.1002/hep.29797]
15 **Castera L**, Friedrich-Rust M, Loomba R. Noninvasive Assessment of Liver Disease in Patients With Nonalcoholic Fatty Liver Disease. *Gastroenterology* 2019; **156**: 1264-1281.e4 [PMID: 30660725 DOI: 10.1053/j.gastro.2018.12.036]
16 **Liaw YF**, Tai DI, Chu CM, Lin DY, Sheen IS, Chen TJ, Pao CC. Early detection of hepatocellular carcinoma in patients with chronic type B hepatitis. A prospective study. *Gastroenterology* 1986; **90**: 263-267 [PMID: 2416625 DOI: 10.1016/0016-5085(86)90919-4]
17 **Cengiz M**, Sentürk S, Cetin B, Bayrak AH, Bilek SU. Sonographic assessment of fatty liver: intraobserver and interobserver variability. *Int J Clin Exp Med* 2014; **7**: 5453-5460 [PMID: 25664055]
18 **Hong CW**, Marsh A, Wolfson T, Paige J, Dekhordy SF, Schlein AN, Housman E, Deiranieh LH, Li CQ, Wasnik AP, Jang HJ, Dietrich CF, Piscaglia F, Casola G, O'Boyle M, Richman KM, Valasek MA, Andre M, Loomba R, Sirlin CB. Reader agreement and accuracy of ultrasound features for hepatic steatosis. *Abdom Radiol (NY)* 2019; **44**: 54-64 [PMID: 29951900 DOI: 10.1007/s00261-018-1683-0]
19 **Byra M**, Styczynski G, Szmigielski C, Kalinowski P, Michałowski Ł, Paluszkiewicz R, Ziarkiewicz-Wróblewska B, Zieniewicz K, Sobieraj P, Nowicki A. Transfer learning with deep convolutional neural network for liver steatosis assessment in ultrasound images. *Int J Comput Assist Radiol Surg* 2018; **13**: 1895-1903 [PMID: 30094778 DOI: 10.1007/s11548-018-1843-2]
20 **Biswas M**, Kuppili V, Edla DR, Suri HS, Saba L, Marinhoe RT, Sanches JM, Suri JS. Symtosis: A liver ultrasound tissue characterization and risk stratification in optimized deep learning paradigm. *Comput Methods Programs Biomed* 2018; **155**: 165-177 [PMID: 29512496 DOI: 10.1016/j.cmpb.2017.12.016]
21 **Acharya UR**, Sree SV, Ribeiro R, Krishnamurthi G, Marinho RT, Sanches J, Suri JS. Data mining framework for fatty liver disease classification in ultrasound: a hybrid feature extraction paradigm. *Med Phys* 2012; **39**: 4255-4264 [PMID:

22830759 DOI: 10.1118/1.4725759]
22 **Gummadi S**. Automated Machine Learning in the Sonographic Diagnosis of Non-alcoholic Fatty Liver Disease. AUDT 2020; 4: 176-182 [DOI: 10.37015/AUDT.2020.200008]
23 **Owjimehr M**, Danyali H, Helfroush MS, Shakibafard A. Staging of Fatty Liver Diseases Based on Hierarchical Classification and Feature Fusion for Back-Scan-Converted Ultrasound Images. *Ultrason Imaging* 2017; **39**: 79-95 [PMID: 27694278 DOI: 10.1177/0161734616649153]
24 **Han A**, Byra M, Heba E, Andre MP, Erdman JW Jr, Loomba R, Sirlin CB, O'Brien WD Jr. Noninvasive Diagnosis of Nonalcoholic Fatty Liver Disease and Quantification of Liver Fat with Radiofrequency Ultrasound Data Using One-dimensional Convolutional Neural Networks. *Radiology* 2020; **295**: 342-350 [PMID: 32096706 DOI: 10.1148/radiol.2020191160]
25 **Chen JR**, Chao YP, Tsai YW, Chan HJ, Wan YL, Tai DI, Tsui PH. Clinical Value of Information Entropy Compared with Deep Learning for Ultrasound Grading of Hepatic Steatosis. *Entropy (Basel)* 2020; **22** [PMID: 33286775 DOI: 10.3390/e22091006]
26 **Cao W**, An X, Cong L, Lyu C, Zhou Q, Guo R. Application of Deep Learning in Quantitative Analysis of 2-Dimensional Ultrasound Imaging of Nonalcoholic Fatty Liver Disease. *J Ultrasound Med* 2020; **39**: 51-59 [PMID: 31222786 DOI: 10.1002/jum.15070]
27 **Byra M**, Han A, Boehringer AS, Zhang YN, O'Brien WD Jr, Erdman JW Jr, Loomba R, Sirlin CB, Andre M. Liver Fat Assessment in Multiview Sonography Using Transfer Learning With Convolutional Neural Networks. *J Ultrasound Med* 2022; **41**: 175-184 [PMID: 33749862 DOI: 10.1002/jum.15693]
28 **Saadeh S**, Younossi ZM, Remer EM, Gramlich T, Ong JP, Hurley M, Mullen KD, Cooper JN, Sheridan MJ. The utility of radiological imaging in nonalcoholic fatty liver disease. *Gastroenterology* 2002; **123**: 745-750 [PMID: 12198701 DOI: 10.1053/gast.2002.35354]
29 **Chen CJ**, Tsay PK, Huang SF, Tsui PH, Yu WT, Hsu TH, Tai J, Tai DI. Effects of hepatic steatosis on non-invasive liver fibrosis measurements between hepatitis B and other etiologies. *APPL SCI-BASEL* 2019; **9**: 1961
30 **Lee CH**, Wan YL, Hsu TH, Huang SF, Yu MC, Lee WC, Tsui PH, Chen YC, Lin CY, Tai DI. Interpretation US Elastography in Chronic Hepatitis B with or without Anti-HBV Therapy. *APPL SCI-BASEL* 2017; **7**: 1164 [DOI: 10.3390/app7111164]
31 **Hsu TH**, Tsui PH, Yu WT, Huang SF, Tai J, Wan YL, Tai DI. Cutoff Values of Acoustic Radiation Force Impulse Two-Location Measurements in Different Etiologies of Liver Fibrosis. *J Med Ultrasound* 2019; **27**: 130-134 [PMID: 31867175 DOI: 10.4103/JMU.JMU_7_19]
32 **Tai DI**, Tsay PK, Jeng WJ, Weng CC, Huang SF, Huang CH, Lin SM, Chiu CT, Chen WT, Wan YL. Differences in liver fibrosis between patients with chronic hepatitis B and C: evaluation by acoustic radiation force impulse measurements at 2 locations. *J Ultrasound Med* 2015; **34**: 813-821 [PMID: 25911714 DOI: 10.7863/ultra.34.5.813]
33 **Kleiner DE**, Brunt EM, Van Natta M, Behling C, Contos MJ, Cummings OW, Ferrell LD, Liu YC, Torbenson MS, Unalp-Arida A, Yeh M, McCullough AJ, Sanyal AJ; Nonalcoholic Steatohepatitis Clinical Research Network. Design and validation of a histological scoring system for nonalcoholic fatty liver disease. *Hepatology* 2005; **41**: 1313-1321 [PMID: 15915461 DOI: 10.1002/hep.20701]
34 **He K**, Zhang X, Ren S, Sun J. Deep Residual Learning for Image Recognition. In: 2016 IEEE Conference on Computer Vision and Pattern Recognition (CVPR), 2016: 770-778
35 **Scatarige JC**, Scott WW, Donovan PJ, Siegelman SS, Sanders RC. Fatty infiltration of the liver: ultrasonographic and computed tomographic correlation. *J Ultrasound Med* 1984; **3**: 9-14 [PMID: 6694259 DOI: 10.7863/jum.1984.3.1.9]
36 **Frank E**, Hall M. A Simple Approach to Ordinal Classification. In: De Raedt L, Flach P, editors. Machine Learning: ECML 2001. Berlin, Heidelberg: Springer, 2001: 145-156
37 **Fürnkranz J**, Hüllermeier E, Vanderlooy S. Binary Decomposition Methods for Multipartite Ranking. In: Buntine W, Grobelnik M, Mladenić D, Shawe-Taylor J, editors. Machine Learning and Knowledge Discovery in Databases. Berlin, Heidelberg: Springer, 2009: 359-374
38 **Holm S**. A Simple Sequentially Rejective Multiple Test Procedure. *Scand Actuar J* 1979; **6**: 65-70
39 **Bland JM**, Altman DG. Statistical methods for assessing agreement between two methods of clinical measurement. *Lancet* 1986; **1**: 307-310 [PMID: 2868172 DOI: 10.1016/S0140-6736(86)90837-8]
40 **Bland JM**, Altman DG. Measuring agreement in method comparison studies. *Stat Methods Med Res* 1999; **8**: 135-160 [PMID: 10501650 DOI: 10.1177/096228029900800204]
41 **Efron B**, Tibshirani RJ. An Introduction to the Bootstrap. Boca Raton, Florida, USA: CRC Press
42 **Higgins JJ**. An Introduction to Modern Nonparametric Statistics. Pacific Grove, CA: Brooks/Cole, 2005: 101-104
43 **DeLong ER**, DeLong DM, Clarke-Pearson DL. Comparing the areas under two or more correlated receiver operating characteristic curves: a nonparametric approach. *Biometrics* 1988; **44**: 837-845 [PMID: 3203132 DOI: 10.2307/2531595]
44 **YOUDEN WJ**. Index for rating diagnostic tests. *Cancer* 1950; **3**: 32-35 [PMID: 15405679 DOI: 10.1002/1097-0142(1950)3:1<32::aid-cncr2820030106>3.0.co;2-3]
45 **Vergara IA**, Norambuena T, Ferrada E, Slater AW, Melo F. StAR: a simple tool for the statistical comparison of ROC curves. *BMC Bioinformatics* 2008; **9**: 265 [PMID: 18534022 DOI: 10.1186/1471-2105-9-265]
46 **Tada T**, Iijima H, Kobayashi N, Yoshida M, Nishimura T, Kumada T, Kondo R, Yano H, Kage M, Nakano C, Aoki T, Aizawa N, Ikeda N, Takashima T, Yuri Y, Ishii N, Hasegawa K, Takata R, Yoh K, Sakai Y, Nishikawa H, Iwata Y, Enomoto H, Hirota S, Fujimoto J, Nishiguchi S. Usefulness of Attenuation Imaging with an Ultrasound Scanner for the Evaluation of Hepatic Steatosis. *Ultrasound Med Biol* 2019; **45**: 2679-2687 [PMID: 31277922 DOI: 10.1016/j.ultrasmedbio.2019.05.033]
47 **St Pierre TG**, House MJ, Bangma SJ, Pang W, Bathgate A, Gan EK, Ayonrinde OT, Bhathal PS, Clouston A, Olynyk JK, Adams LA. Stereological Analysis of Liver Biopsy Histology Sections as a Reference Standard for Validating Non-Invasive Liver Fat Fraction Measurements by MRI. *PLoS One* 2016; **11**: e0160789 [PMID: 27501242 DOI: 10.1371/journal.pone.0160789]
48 **El-Badry AM**, Breitenstein S, Jochum W, Washington K, Paradis V, Rubbia-Brandt L, Puhan MA, Slankamenac K, Graf

R, Clavien PA. Assessment of hepatic steatosis by expert pathologists: the end of a gold standard. *Ann Surg* 2009; **250**: 691-697 [PMID: 19806055 DOI: 10.1097/SLA.0b013e3181bcd6dd]

49 **Paige JS**, Bernstein GS, Heba E, Costa EAC, Fereirra M, Wolfson T, Gamst AC, Valasek MA, Lin GY, Han A, Erdman JW Jr, O'Brien WD Jr, Andre MP, Loomba R, Sirlin CB. A Pilot Comparative Study of Quantitative Ultrasound, Conventional Ultrasound, and MRI for Predicting Histology-Determined Steatosis Grade in Adult Nonalcoholic Fatty Liver Disease. *AJR Am J Roentgenol* 2017; **208**: W168-W177 [PMID: 28267360 DOI: 10.2214/AJR.16.16726]

50 **Ratziu V**, Charlotte F, Heurtier A, Gombert S, Giral P, Bruckert E, Grimaldi A, Capron F, Poynard T; LIDO Study Group. Sampling variability of liver biopsy in nonalcoholic fatty liver disease. *Gastroenterology* 2005; **128**: 1898-1906 [PMID: 15940625 DOI: 10.1053/j.gastro.2005.03.084]

51 **DataBase Center for Life Science**. File:201405_liver.png. [cited 2 February 2022]. Available from: https://commons.wikimedia.org/wiki/File:201405_liver.png

World Journal of Gastroenterology

Submit a Manuscript: https://www.f6publishing.com

World J Gastroenterol 2022 June 14; 28(22): 2509-2522

DOI: 10.3748/wjg.v28.i22.2509

ISSN 1007-9327 (print) ISSN 2219-2840 (online)

ORIGINAL ARTICLE

Randomized Controlled Trial

Saccharomyces cerevisiae I-3856 in irritable bowel syndrome with predominant constipation

Florian Mourey, Amélie Decherf, Jean-François Jeanne, Mathieu Clément-Ziza, Marie-Lise Grisoni, François Machuron, Sophie Legrain-Raspaud, Arnaud Bourreille, Pierre Desreumaux

Specialty type: Gastroenterology and hepatology

Provenance and peer review: Unsolicited article; Externally peer reviewed.

Peer-review model: Single blind

Peer-review report's scientific quality classification

Grade A (Excellent): 0
Grade B (Very good): B, B, B
Grade C (Good): 0
Grade D (Fair): 0
Grade E (Poor): 0

P-Reviewer: Dumitrascu DL, McFarland LV

Received: December 22, 2021
Peer-review started: December 22, 2021
First decision: January 8, 2022
Revised: January 14, 2022
Accepted: April 28, 2022
Article in press: April 28, 2022
Published online: June 14, 2022

Florian Mourey, Amélie Decherf, Jean-François Jeanne, Sophie Legrain-Raspaud, Research and Applications Department, Gnosis by Lesaffre, Lesaffre Group, Marcq-en-Baroeul 59700, France

Mathieu Clément-Ziza, Marie-Lise Grisoni, François Machuron, Data Science and Bioinformatics Laboratory, Research and Development Department, Lesaffre International, Lesaffre Group, Marcq-en-Baroeul 59700, France

Arnaud Bourreille, Institut des Maladies de l'Appareil Digestif, Centre Hospitalier Universitaire de Nantes, Nantes 44093, France

Pierre Desreumaux, Institute for Translational Research in Inflammation, Centre Hospitalier Universitaire de Lille, Lille 59000, France

Corresponding author: Florian Mourey, MSc, Research Scientist, Research and Applications Department, Gnosis by Lesaffre, Lesaffre Group, 137 rue Gabriel Péri, Marcq-en-Baroeul 59700, France. f.mourey@gnosis.lesaffre.com

Abstract

BACKGROUND

Probiotics are a promising solution for managing irritable bowel syndrome (IBS). *Saccharomyces cerevisiae* (*S. cerevisiae*) I-3856 has already demonstrated beneficial effects in IBS subjects, particularly in IBS with predominant constipation (IBS-C).

AIM

To confirm the efficacy of *S. cerevisiae* I-3856 in the management of gastrointestinal symptoms in IBS-C.

METHODS

A randomized, double-blind, placebo-controlled clinical study was performed in a total of 456 subjects. After a run-in period, subjects were randomly assigned to the group receiving *S. cerevisiae* I-3856 (8×10^9 CFU daily) or the placebo for 8 wk, and they performed daily self-evaluations of gastrointestinal symptoms. The primary objective was to assess the effect of the probiotic on abdominal pain. The secondary objectives were the evaluation of other gastrointestinal symptoms, bowel movement frequency and consistency, and quality of life (QOL).

RESULTS

A significantly higher proportion of abdominal pain responders was reported in the Probiotic group (45.1% *vs* 33.9%, P = 0.017). A nonsignificant difference in the area under the curve for abdominal pain over the second month of supplementation was observed in subjects receiving probiotic *vs* placebo [P = 0.073, 95%CI: -0.59 (-1.23; 0.05)]. No statistically significant differences were reported in the evolution of bowel movement frequency and stool consistency between the groups. After 8 wk of supplementation, the overall QOL score was significantly higher in the Probiotic group than in the Placebo group [P = 0.047, 95%CI: 3.86 (0.52; 7.20)]. Furthermore, exploratory analyses showed statistically significant and clinically relevant improvements in QOL scores in abdominal pain responders *vs* nonresponders.

CONCLUSION

The results of this clinical study confirmed the abdominal pain alleviation properties of *S. cerevisiae* I-3856 in IBS-C. Abdominal pain relief was associated with improved QOL. ClinicalTrials.gov identifier: NCT03150212.

Key Words: Probiotic; Yeast; *Saccharomyces cerevisiae*; Irritable bowel syndrome; Abdominal pain; Quality of life

©The Author(s) 2022. Published by Baishideng Publishing Group Inc. All rights reserved.

Core Tip: The gut microbiota has been proposed as central in irritable bowel syndrome (IBS) pathophysiology, and microbiota-directed intervention has therefore drawn considerable interest. Probiotics have been recognized as a potential solution for acting on the multifactorial causes and clinical symptoms of IBS. Among them, *Saccharomyces cerevisiae* (*S. cerevisiae*) CNCM I-3856 is a probiotic yeast that has shown beneficial effects on gastrointestinal symptoms of individuals with IBS, especially in IBS subjects with predominant constipation. This clinical study confirmed the abdominal pain alleviation properties of *S. cerevisiae* I-3856 in IBS with predominant constipation and showed improvements in quality of life in the group receiving the probiotic.

Citation: Mourey F, Decherf A, Jeanne JF, Clément-Ziza M, Grisoni ML, Machuron F, Legrain-Raspaud S, Bourreille A, Desreumaux P. *Saccharomyces cerevisiae* I-3856 in irritable bowel syndrome with predominant constipation. *World J Gastroenterol* 2022; 28(22): 2509-2522
URL: https://www.wjgnet.com/1007-9327/full/v28/i22/2509.htm
DOI: https://dx.doi.org/10.3748/wjg.v28.i22.2509

INTRODUCTION

Irritable bowel syndrome (IBS) is a disorder of gut-brain interaction[1] that affects approximately one in ten people globally[2]. This chronic condition is characterized by recurrent abdominal pain related with altered bowel habits. In addition to the patient's suffering, it represents a significant burden from both economic and social perspectives. It has indeed been associated with important psychosocial consequences as well as considerable costs to health care systems and society[3,4]. Limitations and impairment of social and emotional daily functioning of IBS patients is demonstrated by the consistently reported profound reductions in quality of life (QOL) compared with the general population[5,6]. QOL impairments in IBS are of similar magnitude to those in more severe diseases, such as inflammatory bowel diseases or depression[5,7,8]. The high prevalence of IBS, as well as its significant morbidity, result in substantial health care utilization and loss of work productivity that represent considerable direct and indirect costs to society[4,9,10].

IBS is a complex and heterogenous condition. Although abdominal pain is the cardinal feature, IBS patients can be classified into different subtypes depending on their predominant stool pattern: IBS with predominant constipation (IBS-C), IBS with predominant diarrhoea (IBS-D), IBS with mixed bowel habits (IBS-M) and IBS unclassified. The pathogenesis of IBS has been described as multifactorial and involves a combination of factors related to motility, visceral hypersensitivity, mucosal immune dysregulation, alterations of gut microbiota, and central and enteric nervous system dysregulation[1]. However, interventions remain symptom-driven, and available pharmacological treatment options are of limited efficacy[11]. Complementary and alternative solutions to achieving satisfactory control of gastrointestinal symptoms and improve QOL in IBS patients are therefore of great interest. The gut microbiota has been proposed as central in IBS pathophysiology and has therefore drawn considerable

interest[12,13]. Among microbiota-directed interventions, probiotics have been recognized as a potential solution for acting on the multifactorial causes and clinical symptoms of IBS[14,15]. A meta-analysis of fifty-three randomized controlled trials (RCTs) involving a total of 5545 patients was recently performed. It demonstrated overall beneficial effects of probiotics on global IBS symptoms and abdominal pain with favourable safety profiles, although conclusions were drawn for probiotics in general[16]. Due to the important heterogeneity of both the tested strains and study designs, identifying which probiotics are relevant for IBS management remains a challenge[17]. However, a recently conducted meta-analysis provided further evidence to determine which probiotic strains are effective in IBS symptom management. Among the probiotics analysed, *Saccharomyces cerevisiae* (*S. cerevisiae*) CNCM I-3856 emerged as a recognized solution[18].

S. cerevisiae CNCM I-3856 provides statistically significant and clinically relevant benefits for individuals with IBS, as demonstrated in three RCTs[19-21] performed in a total of 679 subjects and an individual patient data (IPD) meta-analysis[22]. This meta-analysis confirmed previous observations linking *S. cerevisiae* CNCM I-3856 supplementation to improvement in gastrointestinal symptoms in all IBS subpopulations. Nevertheless, the strongest effects were reported in IBS with predominant constipation. Considering these results, we designed a clinical study to confirm the efficacy of *S. cerevisiae* CNCM I-3856 on gastrointestinal symptom management in an IBS population with predominant constipation.

MATERIALS AND METHODS

A large-scale, multicentric, placebo-controlled, randomized, double-blind, clinical study was conducted between March 2017 and May 2019. The study was approved by the Ethics Committee Ouest VI of Brest (France) and performed according to International Conference on Harmonization Good Clinical Practice and the ethical principles of the Declaration of Helsinki. Signed written informed consent for the study was obtained from all subjects before protocol-specific procedures were carried out.

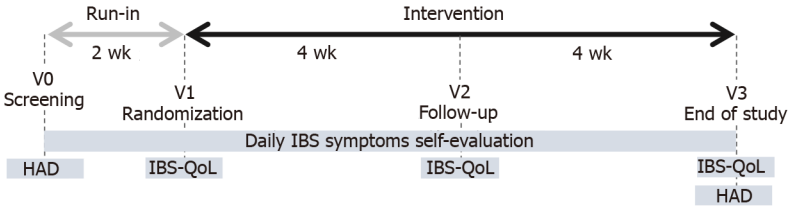
The clinical trial was registered in a clinical trials registration system at ClinicalTrials.gov with the identifier NCT03150212.

Study population

Subjects with IBS were recruited by ten French general practitioners across France and in four clinical investigation centres, including Biofortis Mérieux Nutrisciences as the principal investigational centre. Females and males aged 18-75 years were eligible to participate if they met the Rome IV criteria[23] for IBS-C with a baseline score for abdominal pain ≥ 2 and < 6 assessed on a 7-point Likert scale scored from 0 (null) to 7 (severe pain) and had an IBS history between 1 and 10 years. All volunteers agreed to maintain their lifestyle behaviours during their participation in the study. Participants were excluded if they had chronic gastrointestinal conditions other than IBS, including inflammatory bowel diseases, lactose intolerance, and celiac disease. Individuals with a metabolic disorder affecting intestinal transit function or nutrient absorption, such as diabetes or unbalanced thyroid dysfunction, were excluded. Volunteers undergoing symptomatic drug treatments acting on intestinal sensitivity or motility, such as opioids and narcotic analgesics, were not eligible. Antibiotic or antifungal therapies in progress or prescribed 4 or 2 wk before randomization, respectively, were also considered an exclusion criterion. The use of probiotics, prebiotics, symbiotics or any dietary supplement that, according to the investigator, could affect study outcomes in the four weeks preceding randomization was prohibited. However, laxatives, antibloating agents, antispasmodics, anxiolytics, antidepressants, analgesics and nonsteroidal anti-inflammatory drugs were authorized if consumed for longer than three months and maintained at a stable dosage for the entire study duration.

Study design

This study consisted of a 2-wk run-in period followed by an 8-wk treatment period. Subjects visited the clinical investigation centre or general practitioner four times: V0 (screening visit), V1 (randomization visit, 2 wk after V0), V2 (follow-up visit, 4 wk after V1) and V3 (end-of-study visit, 8 wk after V1) (Figure 1). Screening visits (V0) were planned to assess whether inclusion and exclusion criteria were met and to explain study instructions. Additionally, recommendations were given to volunteers to avoid changes in lifestyle behaviours (including dietary and physical activity habits), and volunteers were asked to perform a daily evaluation of the intensity of IBS symptoms and bowel movements. At the randomization visit (V1), investigators confirmed the eligibility (including the Rome IV diagnostic criteria for IBS-C) of the volunteers by integrating the daily evaluation of abdominal pain and bowel movement consistency. Eligible subjects were randomized to receive daily *S. cerevisiae* CNCM I-3856 (Probiotic group) or placebo (Placebo group) for 8 wk. The product allocation list was prepared using SAS® software (version 9.3, SAS Institute Inc., Cary, NJ, United States) before the study started and stored confidentially by a person not related to the clinical phase or data management. The product allocation list was generated using a dynamic randomization algorithm designed to minimize imbalance between the two supplemented groups within each investigational site. Blinding of allocation was



DOI: 10.3748/wjg.v28.i22.2509 **Copyright** ©The Author(s) 2022.

Figure 1 Study design.

maintained until the completed study database was locked.

Data collected

During the baseline and intervention periods, volunteers were asked to perform a daily evaluation of the intensity of IBS symptoms (abdominal pain, bloating, and flatulence/borborygmi) on a 7-point Likert scale rated from 0 (null) to 7 (severe). Bowel movement consistency assessed on the Bristol stool scale (BSS) was recorded daily. Volunteers completed an IBS-specific quality of life questionnaire (IBS-QOL) at randomization (V1), follow-up (V2) and the end of the intervention (V3). The IBS-QOL is a 34-item instrument that yields an overall QOL score as well as scores for eight domains (dysphoria, interference with activity, body image, health worry, food avoidance, social reaction, sexual, relationships). Final scores were normalized to a 100-point scale, with 0 indicating the worst QOL and 100 indicating the best QOL. Anxiety and depression symptoms were also assessed using the hospital anxiety and depression questionnaire at screening (V0) and end-of-study visits (V3).

Study products and compliance evaluation

The study evaluated the probiotic yeast *S. cerevisiae* CNCM I-3856. This strain is a proprietary, well-characterized strain of Lesaffre registered in the French National Collection of Cultures of Microorganisms. The *S. cerevisiae* species was characterized using phenotypic (API® ID32C, Biomerieux SAS) and genotypic referenced methods (genetic amplification and sequencing of 26S DNA)[24,25]. Moreover, strain I-3856 can be identified *via* a polymerase chain reaction interdelta typing technique[26] and complete genome sequencing. The dose tested was of 8×10^9 CFU provided daily in two capsules of 500 mg each. The probiotic dietary supplement was provided by Gnosis by Lesaffre (a business unit of Lesaffre Group, France) and comprised *S. cerevisiae* CNCM I-3856 entirely and exclusively. The comparative product was a placebo comprising inactive ingredients, *i.e.*, maize starch and magnesium stearate. All capsules were made from hydroxypropyl methylcellulose of the same size, weight, colour and taste regardless of the group and prepared according to good manufacturing practices. Every subject consumed two capsules of 500 mg per day in the morning, just before breakfast with a glass of water. Compliance was determined through the assessment of returned packaging and interviews of the subjects at each visit.

Study endpoints

The primary endpoint was the area under the curve, *i.e.*, the sum of weekly means of daily scores of abdominal pain calculated with the trapezoidal method (interpolation of scores between weeks) from week 5 to week 8 [area under the curve (AUC) (W5-W8)], and it was determined based on previously reported data on the strain[22]. Prespecified secondary endpoints were the total AUC (W0-W8) of IBS symptoms (abdominal pain, bloating, and flatulence/borborygmi) and AUC (W5-W8) of bloating and flatulence/borborygmi scores. Mean weekly scores of gastrointestinal symptoms (abdominal pain, bloating and flatulence/borborygmi) were analysed at each week of the intervention. The evolution of abdominal pain was also assessed through the analysis of the percentage of responders. Abdominal pain response was set according to recommended guidelines[27,28]. Responders were defined as subjects who experienced a reduction of at least 30% of the mean daily abdominal pain score reported at baseline (week 0) from week 5 to week 8. The global QOL score and the eight derived subscores corresponding to the different domains of QOL were assessed at V1 and V2 and at the end of the intervention. Mean stool consistency (BSS scores) and the mean daily number of bowel movements were assessed at each week of the intervention.

Safety endpoints

The safety of the intervention was assessed considering the occurrence of adverse events and the follow-up of vital signs.

Statistical analyses

Sample size: Based on previous studies performed on IBS-C subjects, considering a 5% type-one error

rate and 80% power, 205 subjects per arm would allow the detection of a 1 arbitrary unit (a.u.) difference between groups in AUC (W5-W8) of abdominal pain scores (12% difference) assuming a standard deviation of 3.6 a.u./d.wk. Enrolling a total of 456 subjects would allow for a 10% drop-out.

Efficacy analyses: Efficacy analyses were performed for the intention-to-treat (ITT) population (including all randomized subjects in the study) and for the per-protocol population (ITT population who completed the study and presented no major protocol deviations). The primary endpoint, *i.e.*, the AUC (W5-W8) for abdominal pain, and the other AUCs of IBS symptoms were analysed using an analysis of covariance (ANCOVA) model. Repeated measurements such as the mean daily number of bowel movements, the mean stool consistency and IBS-QOL questionnaire were analysed using ANOVA models. The percentage of abdominal pain responders was analysed by a Chi^2 test. IBS-QOL scores were additionally examined in exploratory analyses that focused on abdominal pain responders. These analyses were conducted through ANCOVA models for repeated measurements with the baseline (V1) as the cofactor. For all statistical tests, the 5% level of significance was used to justify a claim of a statistically significant effect and standardized mean difference (SMD) was calculated. Hochberg adjustments were used to correct for multiple testing.

Safety analyses: The safety population included all subjects who had consumed at least one dose of the products. For each term of severity and causality, the proportion of subjects showing at least an adverse event was compared between groups using a Chi^2 or Fisher's exact test. The number of events was compared between groups using a Poisson regression model.

Software: Statistical analyses were performed using SAS® software version 9.4 (SAS Institute Inc., Cary, NC, United States). Exploratory analyses were performed using R software version 4.0.3.

RESULTS

Study flowchart and baseline characteristics of the population

A total of 456 IBS subjects (392 females, 64 males) with predominant constipation matching the Rome IV criteria were included in this study and randomly assigned to the Probiotic group (n = 230) or the Placebo group (n = 226). The flowchart of subjects throughout the study is presented in Figure 2. The baseline characteristics of the subjects are presented in Table 1. The quantitative variables are described through the mean ± SD, and qualitative variables are described through the number of subjects and percentages (%).

Abdominal pain-AUC

The abdominal pain scores were similar at baseline in the Probiotic (3.97 ± 1.04 a.u.) and the Placebo (3.98 ± 1.07 a.u.) groups. Significant reductions in abdominal pain scores throughout the 8 wk of supplementation were observed in the Placebo group and in the Probiotic group, with reductions of 24.1% and 28.7%, respectively, from baseline at the end of the intervention (P < 0.001 in both groups). The abdominal pain over the 8-wk intervention period decreased similarly to previously reported results. A nonsignificant difference was observed in the AUC for abdominal pain over the second month of supplementation in subjects receiving probiotic *vs* placebo [-6.3%, P = 0.073, 95%CI: -0.59 (-1.23; 0.05)], between-group difference from ANCOVA model) (Figure 3). Similarly, no difference was reported in the AUC over the 8 wk of intervention.

Abdominal pain-percentage of responders

A significant difference between groups was found in the percentage of responders. The percentage of responders was significantly higher in the group receiving *S. cerevisiae* CNCM I-3856 (45.1%, 101 subjects among 224 subjects with available data) than in the Placebo group (33.9%, 74 subjects among 218 subjects with available data), resulting in an increase of 33% in the proportion of responders in the treated group *vs* placebo (Figure 3, Supplementary Figure 1) (P = 0.017, Chi^2 test).

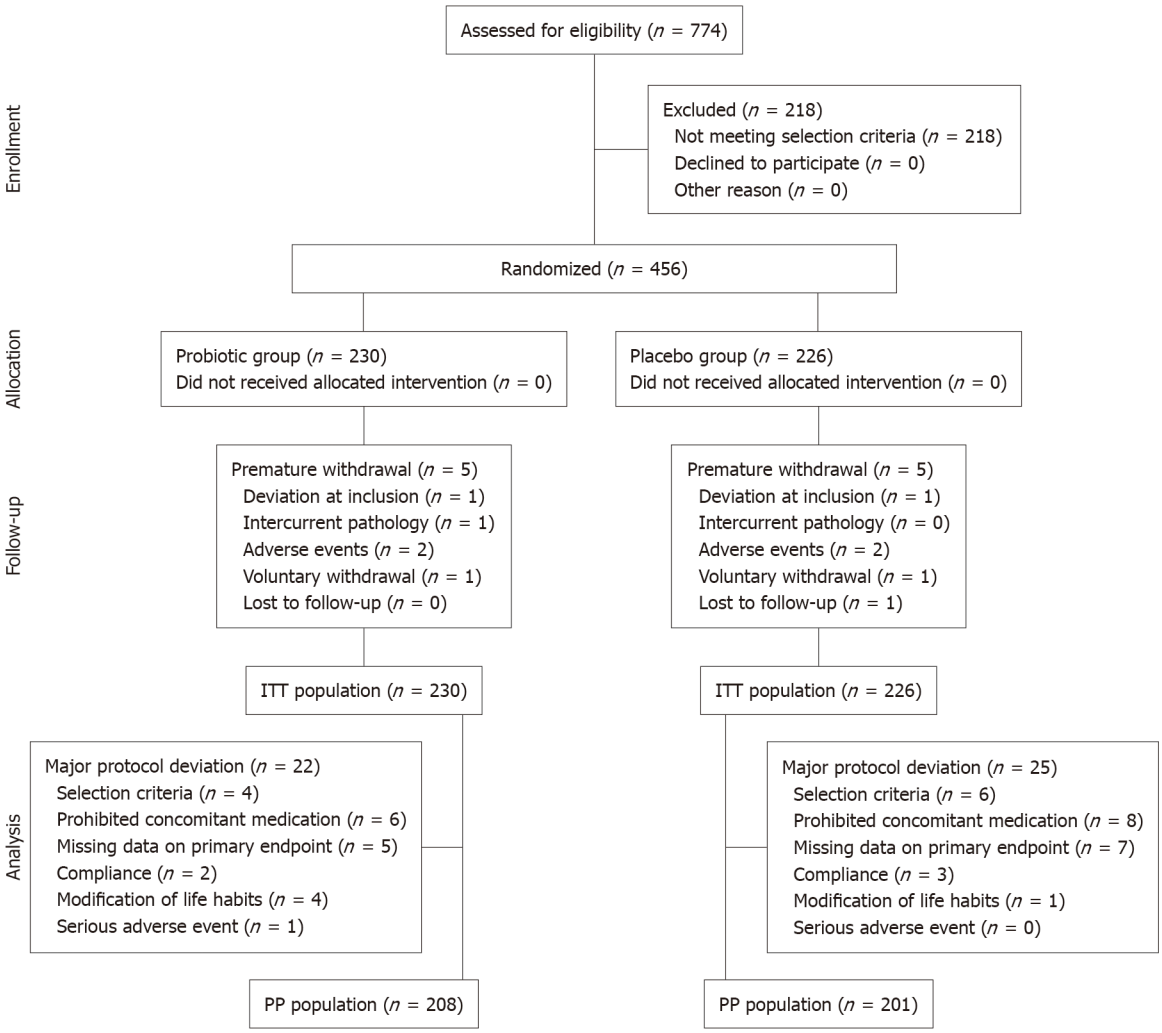
QOL (IBS-QOL)

A higher overall IBS-QOL score, indicative of better QOL, was reported at the end of the intervention in the Probiotic group (79.51 ± 2.34 a.u.) compared with the Placebo group (75.65 ± 2.39 a.u.) in the PP population [P = 0.047, 95%CI: 3.86 (0.52; 7.20), SMD = 0.18]. Improved QOL in the Probiotic group translated into a mean increase in the overall IBS-QOL score of 11.9% from baseline. The analysis of the eight domains of the IBS-QOL questionnaire showed statistically significant differences in favour of the Probiotic group for 3 domains, *i.e.*, interference with activity [P = 0.05, 95%CI: 4.30 (0.54; 8.05), SMD = 0.18)], body image [P = 0.040, 95%CI: 3.96 (0.17; 7.75), SMD = 0.17)], and food avoidance [P = 0.030, 95%CI: 5.69 (1.10; 10.28), SMD = 0.22)] (Figure 4, Supplementary Figure 2, Supplementary Table 1). Exploratory analyses of IBS-QOL scores were conducted to evaluate the evolution of the QOL among the responders during the time of supplementation with *S. cerevisiae* CNCM I-3856. The QOL was

Table 1 Baseline characteristics of the study population

	Total included subjects (*n* = 456)	Placebo group (*n* = 226)	Probiotic group (*n* = 230)
Female	392 (86)	190 (84.1)	202 (87.8)
Age (yr)	40.5 ± 14.26	39.9 ± 14.56	41.2 ± 13.96
Abdominal pain score	3.98 ± 1.05	3.98 ± 1.07	3.97 ± 1.04
Bloating score	4.01 ± 1.17	4.04 ± 1.18	3.99 ± 1.15
Flatulence/borborygmi score	3.64 ± 1.37	3.62 ± 1.46	3.66 ± 1.28
IBS-QOL global score	68.0 ± 17.02	67.2 ± 17.17	68.8 ± 16.86

Values are presented as the mean ± SD or number (%). IBS-QOL: Irritable bowel syndrome-specific quality of life.



DOI: 10.3748/wjg.v28.i22.2509 **Copyright** ©The Author(s) 2022.

Figure 2 CONSORT flow diagram.

significantly more improved in the abdominal pain responder group than in the nonresponder group; these differences in improvement following eight weeks of intervention with *S. cerevisiae* CNCM I-3856 were observed for the overall score and for the eight subscores of the IBS-QOL questionnaire. The improvements with the largest difference between responders and nonresponders were for the body image score [between-group difference from ANOVA model: $P < 0.001$, 95%CI: 11.94 (8.53; 15.35), SMD = 0.56], health worry score [$P < 0.001$, 95%CI: 10.91 (7.16; 14.66), SMD = 0.43], food avoidance score [$P < 0.001$, 95%CI: 9.90 (5.14; 14.66), SMD = 0.38] and dysphoria score [$P < 0.001$, 95%CI: 8.86 (5.79; 11.92), SMD = 0.42] (Figure 5, Supplementary Figure 3, Supplementary Table 2).

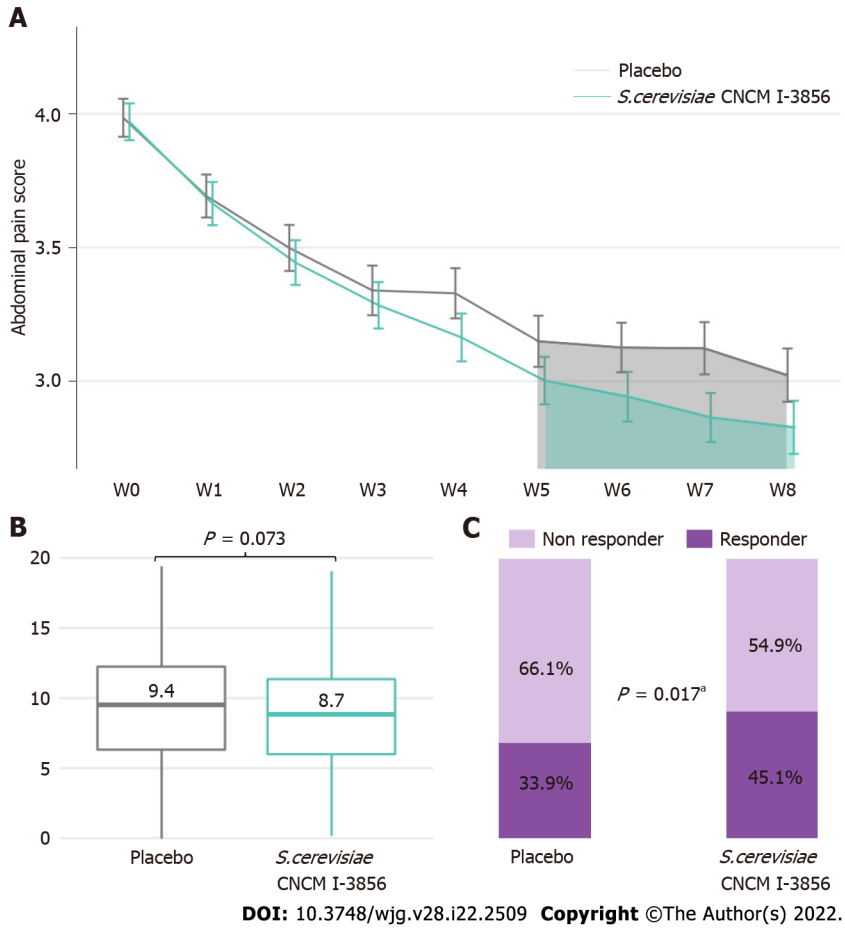


Figure 3 Abdominal pain. A: Abdominal pain score evolution; B: Area under the curve (W5-W8) of abdominal pain; C: Percentage of abdominal pain responders in the ITT population. Significant result ($^aP < 0.05$, Chi^2 test). Similar profiles were obtained for the PP population (Supplementary Figure 1).

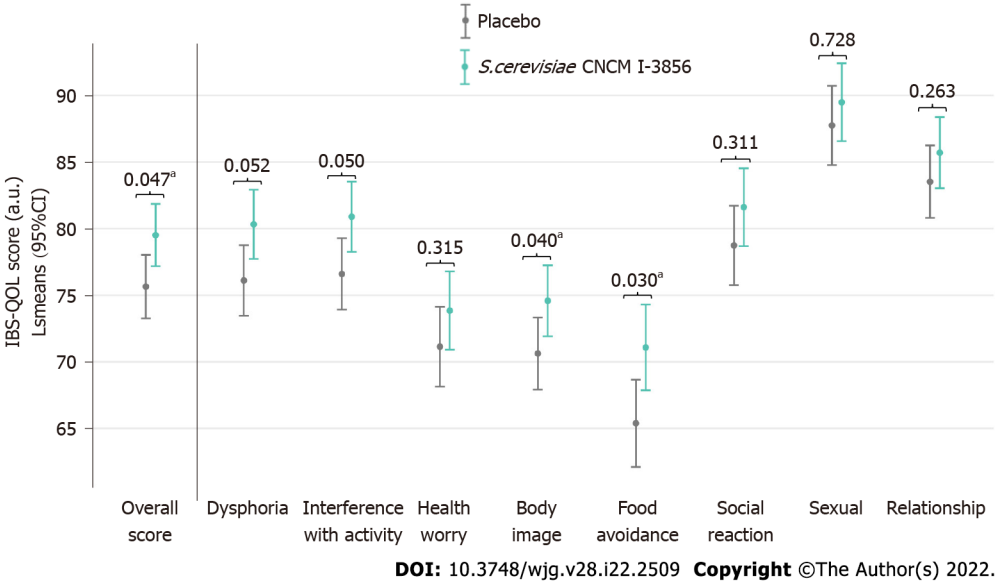
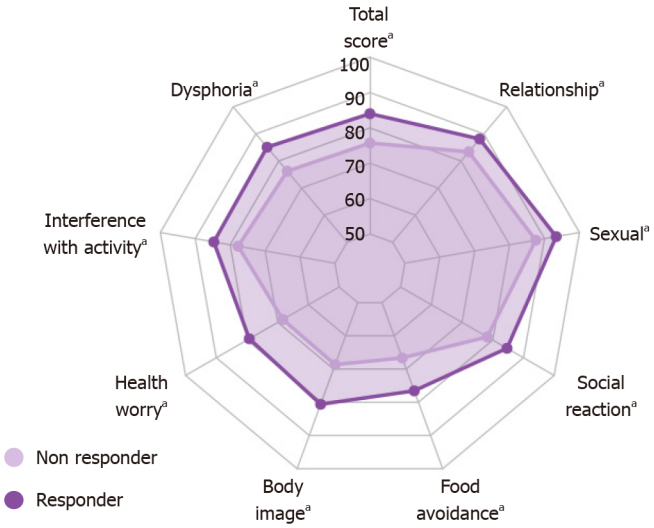


Figure 4 Irritable bowel syndrome-specific quality of life questionnaire scores at the end of the intervention (V3) in the PP population. Significant result ($^aP < 0.05$, ANOVA model).

Other gastrointestinal symptoms, bowel movement frequency and consistency

At baseline, the bloating scores were similar in both groups (3.99 ± 1.52 a.u. in the Probiotic group *vs* 4.04 ± 1.83 a.u. in the Placebo group). Kinetic profiles of the bloating score over the 8-wk supplementation period showed a statistically significant decrease in both groups corresponding to a bloating



DOI: 10.3748/wjg.v28.i22.2509 **Copyright** ©The Author(s) 2022.

Figure 5 Irritable bowel syndrome-specific quality of life questionnaire scores at the end of the intervention (V3) adjusted to baseline (V1) in ITT abdominal pain responders supplemented with *Saccharomyces cerevisiae* CNCM I-3856. PP population radar plot: Supplementary Figure 3. Significant result ([a]$P < 0.05$, ANCOVA for repeated measures). Between-group differences are shown in Supplementary Table 2.

score reduction of 28.4% (95%CI: 23.9-33.0) and 24.5% (95%CI: 19.7-29.5) in the Probiotic and Placebo groups, respectively (between W0 and W8, $P < 0.001$ in both groups, within-group differences from the ANCOVA model). A similar decrease in the flatulence/borborygmi score was observed in both the Placebo and Probiotic groups. The bowel movement frequency and BSS scores increased in Probiotic and Placebo groups between W0 and W8 ($P < 0.01$ from W1 to W8), but no statistically significant differences were found between the groups.

Safety

The number of adverse events per subject showed no statistically significant difference between the groups [$P = 0.50$, 95%CI: 1.10 (0.83; 1.46)], between-group difference from Poisson regression model). Similarly, there was no statistically significant difference between groups regarding the proportion of subjects with at least one adverse event (assessed for each term of severity and for adverse events whose causality with the study product or with the research was considered "not excluded") (Table 2). Descriptive statistics of the adverse events by body system are presented in Supplementary Table 3. Three serious adverse events occurred during the study (1 in the Probiotic group and 2 in the Placebo group). The relationship with the study product was considered "not excluded" for one serious adverse event in the placebo group (bowel obstruction).

DISCUSSION

The beneficial properties of *S. cerevisiae* CNCM I-3856 for gastrointestinal symptom management in the IBS population have been reported in three RCTs conducted in a total of 679 participants[19-21]. An individual patient data meta-analysis reported the strongest effects of the strain in IBS with predominant constipation[22]. To validate these observations, the effect of *S. cerevisiae* CNCM I-3856 was specifically investigated in this population in the present clinical study.

Effect of S. cerevisiae CNCM I-3856 on abdominal pain

The evolution of abdominal pain reported in IBS-C with moderate symptom severity in this study was consistent with previous findings. Lower abdominal pain intensity over the second month of supplementation was observed in the Probiotic group than in the Placebo group, although the difference was not significant. Abdominal pain alleviation during supplementation with *S. cerevisiae* CNCM I-3856 was confirmed by the higher proportion of abdominal pain responders in the Probiotic group than in the Placebo group. The definition of abdominal pain responder used in this study is aligned with current recommendations and corresponds to a reduction of abdominal pain intensity from baseline of at least 30%[27,28]. The higher rate of responders observed in this study during daily supplementation with *S. cerevisiae* CNCM I-3856 compared with placebo is consistent with previously reported results[19,22]. Pineton de Chambrun *et al*[19] reported a significantly higher percentage of responders in the probiotic group than in the placebo group (63% *vs* 47%, $P = 0.04$). The IPD meta-analysis conducted on *S. cerevisiae* CNCM I-3856 further confirmed this finding. Participants in the probiotic group had 1.51 higher odds of

Table 2 Descriptive statistics of the proportion of subjects with adverse events

	Placebo group (*n* = 226)	Probiotic group (*n* = 230)
Causality with the study product not excluded	13 (5.8)	15 (6.5)
Causality with the research not excluded	1 (0.4)	2 (0.9)
Serious	2 (0.9)	1 (0.4)
Severe	12 (5.3)	17 (7.4)
Moderate	55 (24.3)	74 (32.2)
Mild	39 (17.3)	46 (20.0)

Values are presented as the number of subjects with at least one adverse event, *n* (%).

being a responder than participants in the placebo group (P = 0.02)[22]. The abdominal pain responder definition used in previous studies was slightly different. Responders were defined as subjects experiencing a decrease in abdominal pain intensity greater than or equal to 1 a.u. of abdominal pain score, assessed on a 7-point Likert scale, for at least 50% of the second month of supplementation. Based on the mean level of abdominal pain intensity reported at baseline in this study, a decrease of 1 a.u. would correspond to a mean 25% decrease in abdominal pain intensity. The stricter definition of the responders used in our study likely contributes to the lower percentage of abdominal pain responders reported here. However, when using a more demanding definition, the present study confirmed the beneficial effect of *S. cerevisiae* CNCM I-3856 on abdominal pain. This result is of great clinical interest as it meets the clinically relevance threshold previously proposed[29]. Therefore, the relevance of *S. cerevisiae* CNCM I-3856 in addressing abdominal pain in IBS-C is confirmed. Effective solutions to managing abdominal pain may be even more critical in this subpopulation, as recent findings have shown that individuals with IBS-C experience more bothersome, frequent and diffuse abdominal pain [30].

Effect of S. cerevisiae CNCM I-3856 on QOL

Importantly, this clinical study also showed improvements in QOL in the probiotic group. Indeed, significant differences were found at the end of the intervention period in the overall IBS-QOL score as well as in several domains. Notwithstanding, the magnitudes of these differences were relatively low. The consequences of IBS on daily function in addition to physical symptoms were further investigated in abdominal pain responders to provide a more accurate understanding of the overall impact of diet supplementation with *S. cerevisiae* CNCM I-3856.

Specific tools have been developed to capture emotional, social and physical functions. The IBS-QOL is currently the most validated self-reported QOL measure[31-33]. Here, we showed that the abdominal pain alleviation reported in responders was accompanied by significant and clinically relevant improvements in IBS-QOL. A strong association between abdominal pain and QOL has been previously described, and a causality relation has been suggested[34]. Moreover, it has also been shown that IBS patients attributed their impairment in daily functioning directly to IBS symptoms[35].

QOL improvements appeared to be mainly driven by specific domains of QOL: dysphoria, food avoidance, health worry and body image. Improvement in the food avoidance subscale of the IBS-QOL is of interest, as perceived restrictions in lifestyle related to gastrointestinal symptoms are commonly reported in the literature and encountered in clinical practice[33,35]. A considerable proportion of IBS patients report an association between food and gastrointestinal symptoms[36]. Food-related gastrointestinal symptoms have been associated with more severe IBS symptoms and lower QOL[37]. Individuals with IBS have been reported to experience emotional dysphoria, which can also be described as feeling helpless, out of control and depressed. It may therefore not be surprising that individuals experiencing significant abdominal pain alleviation also reported improvement in the dysphoria subscale of the IBS-QOL. In addition, significant improvement was seen in the body image subscale of the IBS-QOL. This result also appears consistent with the literature, as individuals with IBS-C have been described as more likely to internalize their distress and to feel self-conscious about their body image[38].

Effect of S. cerevisiae CNCM I-3856 on gastrointestinal symptoms

In contrast with previous findings, no significant between-group differences were observed in the AUC for gastrointestinal symptoms. Although the clinical studies conducted on *S. cerevisiae* CNCM I-3856 in IBS present consistent designs, a significant change here is the use of Rome IV criteria to select the participants. A worldwide comparison of IBS prevalence by Rome IV and Rome III diagnostic criteria demonstrated that individuals diagnosed by Rome IV criteria exhibit higher IBS severity. Consistently, a higher level of abdominal pain was reported at baseline in this study than in previous clinical trials

conducted on *S. cerevisiae* CNCM I-3856. Among factors associated with response to placebo in IBS-C, higher baseline symptom severity was reported as an important predictor of placebo response[40]. Differences in the studied population could therefore have contributed to the lower between-group size effect reported in this study.

Previous studies have reported statistically significant effects of this probiotic on bowel transit in IBS-C, IBS-D and IBS-M, assessed by daily reporting of bowel movement frequency and consistency[22,21]. In contrast, we did not find between-group differences in bowel movement frequency or consistency in this study. Spiller *et al*[20] highlighted the possible role of accelerated bowel transit as central in the relief of abdominal pain and bloating in IBS-C. Instead, the absence of a significant effect on bowel transit in this study as well as the reported improvements in abdominal pain in all IBS subtypes suggest that other mechanisms of action may be involved and participate in the clinical benefits.

Regarding putative mechanisms of action of S. cerevisiae CNCM I-3856

Several putative mechanisms of action of *S. cerevisiae* CNCM I-3856 can be hypothesized. First, the anti-inflammatory effects of *S. cerevisiae* CNCM I-3856 have been reported in several preclinical models[41-45]. The immune-modulating properties of the strain may be relevant in IBS, as chronic low-grade intestinal mucosal inflammation has been implicated in IBS pathophysiology. Second, interactions with the gut microbiota might influence the multiple factors involved in IBS pathophysiology[12,46]. The results from trials conducted in a Simulator of the Human Intestinal Microbial Ecosystem (SHIME®) suggest that *S. cerevisiae* CNCM I-3856 can modulate gut microbiota activity towards an increase in short-chain fatty acids (SCFAs)[47]. This result may be of particular importance, as a recently published longitudinal multiomics study showed significantly lower levels of SCFAs in the stool samples of IBS-C patients than in those of healthy controls[48]. In addition, several lines of evidence suggest that increased levels of SCFAs, such as butyrate, may be beneficial in IBS management[49-51]. Nevertheless, these possible mechanisms of action remain speculative and would need to be addressed separately. Differences in microbiota composition and function between abdominal pain responders and nonresponders may provide a mechanistic basis for the beneficial effects of *S. cerevisiae* CNCM I-3856 in IBS management and warrant further exploration.

CONCLUSION

In conclusion, the results of this large-scale clinical study are consistent with previous findings and confirm the safety and efficacy of *S. cerevisiae* CNCM I-3856 for abdominal pain management in IBS-C. In addition, abdominal pain alleviation was associated with significant improvements in IBS-related QOL. Dietary supplementation with *S. cerevisiae* CNCM I-3856 therefore appears to be an interesting complementary or alternative solution for IBS management with positive implications for the day-to-day life of individuals with IBS-C.

ARTICLE HIGHLIGHTS

Research background

The gut microbiota has been proposed as central in irritable bowel syndrome (IBS) pathophysiology, and microbiota-directed intervention has therefore drawn considerable interest. Among them, *Saccharomyces cerevisiae* (*S. cerevisiae*) CNCM I-3856 is a probiotic yeast that has emerged as a recognized solution for managing IBS.

Research motivation

S. cerevisiae I-3856 has demonstrated beneficial effects in IBS subjects, particularly in IBS with predominant constipation.

Research objectives

To confirm the efficacy of *S. cerevisiae* CNCM I-3856 on gastrointestinal symptom management in an IBS population with predominant constipation.

Research methods

A total of 456 subjects were enrolled in a randomized, double-blind, placebo-controlled trial. After a run-in period to confirm IBS diagnosis, subjects were randomly assigned to the group receiving the probiotic or the placebo for 8 wk and performed daily self-evaluations of gastrointestinal symptoms. The primary objective was to assess the effect of the probiotic on abdominal pain. The secondary objectives were the evaluation of other gastrointestinal symptoms, bowel movement frequency and consistency, and quality of life (QOL).

Research results

Abdominal pain alleviation during supplementation with *S. cerevisiae* CNCM I-3856 was confirmed by the higher proportion of abdominal pain responders in the probiotic group than in the placebo group. Importantly, this clinical study also showed improvements in QOL in the probiotic group.

Research conclusions

The results of this large-scale clinical study are consistent with previous findings and confirm the safety and efficacy of *S. cerevisiae* CNCM I-3856 for abdominal pain management in IBS population. In addition, abdominal pain alleviation was associated with significant improvements in IBS-related QOL.

Research perspectives

Dietary supplementation with *S. cerevisiae* CNCM I-3856 appears to be an interesting complementary or alternative solution for IBS management with positive implications for the day-to-day life of individuals with IBS with predominant constipation. Differences in microbiota composition and function between abdominal pain responders and nonresponders may provide a mechanistic basis for the beneficial effects of *S. cerevisiae* CNCM I-3856 in IBS management and warrant further exploration.

ACKNOWLEDGEMENTS

The authors want to acknowledge Biofortis Merieux Nutrisciences and all the investigators for conducting the study.

FOOTNOTES

Author contributions: Decherf A designed the study; Desreumaux P and Bourreille A contributed to the design of the study; Clément-Ziza M, Grisoni ML and Machuron F supervised the statistical analysis operations; Mourey F drafted the publication manuscript; Legrain-Raspaud S gave final approval of the version to be published; All authors participated in interpretation of the results, critically reviewed the manuscript and approved the final manuscript for submission.

Institutional review board statement: The study was reviewed and approved by the Ethics Committee Ouest VI of Brest, France.

Clinical trial registration statement: This study is registered at ClinicalTrials.gov. The registration identification number is NCT03150212.

Informed consent statement: All study participants provided informed written consent prior to study enrollment.

Conflict-of-interest statement: Mourey F, Decherf A, Jeanne JF, Clément-Ziza M, Machuron F and Legrain-Raspaud S are employees of Lesaffre. Grisoni ML was an employee of Lesaffre during her main contribution to the study. Bourreille A and Desreumaux P received financial support for research from Lesaffre.

Data sharing statement: No additional data are available.

CONSORT 2010 statement: The authors have read the CONSORT 2010 statement, and the manuscript was prepared and revised according to the CONSORT 2010 statement.

Open-Access: This article is an open-access article that was selected by an in-house editor and fully peer-reviewed by external reviewers. It is distributed in accordance with the Creative Commons Attribution NonCommercial (CC BY-NC 4.0) license, which permits others to distribute, remix, adapt, build upon this work non-commercially, and license their derivative works on different terms, provided the original work is properly cited and the use is non-commercial. See: https://creativecommons.org/Licenses/by-nc/4.0/

Country/Territory of origin: France

ORCID number: Florian Mourey 0000-0002-0826-9632; Amélie Decherf 0000-0001-7721-8073; Jean-François Jeanne 0000-0002-5074-4679; Mathieu Clément-Ziza 0000-0003-2763-249X; Marie-Lise Grisoni 0000-0002-8240-6834; François Machuron 0000-0002-5709-762X; Sophie Legrain-Raspaud 0000-0001-7747-5766; Arnaud Bourreille 0000-0003-4903-3535; Pierre Desreumaux 0000-0002-6127-5281.

S-Editor: Zhang H
L-Editor: A
P-Editor: Zhang H

REFERENCES

1 **Drossman DA**. Functional Gastrointestinal Disorders: History, Pathophysiology, Clinical Features and Rome IV. *Gastroenterology* 2016 [PMID: 27144617 DOI: 10.1053/j.gastro.2016.02.032]
2 **Black CJ**, Ford AC. Global burden of irritable bowel syndrome: trends, predictions and risk factors. *Nat Rev Gastroenterol Hepatol* 2020; **17**: 473-486 [PMID: 32296140 DOI: 10.1038/s41575-020-0286-8]
3 **Hungin AP**, Whorwell PJ, Tack J, Mearin F. The prevalence, patterns and impact of irritable bowel syndrome: an international survey of 40,000 subjects. *Aliment Pharmacol Ther* 2003; **17**: 643-650 [PMID: 12641512 DOI: 10.1046/j.1365-2036.2003.01456.x]
4 **Canavan C**, West J, Card T. Review article: the economic impact of the irritable bowel syndrome. *Aliment Pharmacol Ther* 2014; **40**: 1023-1034 [PMID: 25199904 DOI: 10.1111/apt.12938]
5 **El-Serag HB**, Olden K, Bjorkman D. Health-related quality of life among persons with irritable bowel syndrome: a systematic review. *Aliment Pharmacol Ther* 2002; **16**: 1171-1185 [PMID: 12030961 DOI: 10.1046/j.1365-2036.2002.01290.x]
6 **Halder SL**, Locke GR 3rd, Talley NJ, Fett SL, Zinsmeister AR, Melton LJ 3rd. Impact of functional gastrointestinal disorders on health-related quality of life: a population-based case-control study. *Aliment Pharmacol Ther* 2004; **19**: 233-242 [PMID: 14723614 DOI: 10.1111/j.0269-2813.2004.01807.x]
7 **Simrén M**, Svedlund J, Posserud I, Björnsson ES, Abrahamsson H. Health-related quality of life in patients attending a gastroenterology outpatient clinic: functional disorders versus organic diseases. *Clin Gastroenterol Hepatol* 2006; **4**: 187-195 [PMID: 16469679 DOI: 10.1016/s1542-3565(05)00981-x]
8 **Aziz I**, Palsson OS, Törnblom H, Sperber AD, Whitehead WE, Simrén M. The Prevalence and Impact of Overlapping Rome IV-Diagnosed Functional Gastrointestinal Disorders on Somatization, Quality of Life, and Healthcare Utilization: A Cross-Sectional General Population Study in Three Countries. *Am J Gastroenterol* 2018; **113**: 86-96 [PMID: 29134969 DOI: 10.1038/ajg.2017.421]
9 **Tack J**, Stanghellini V, Mearin F, Yiannakou Y, Layer P, Coffin B, Simren M, Mackinnon J, Wiseman G, Marciniak A; IBIS-C Study group. Economic burden of moderate to severe irritable bowel syndrome with constipation in six European countries. *BMC Gastroenterol* 2019; **19**: 69 [PMID: 31064345 DOI: 10.1186/s12876-019-0985-1]
10 **Frändemark Å**, Törnblom H, Jakobsson S, Simrén M. Work Productivity and Activity Impairment in Irritable Bowel Syndrome (IBS): A Multifaceted Problem. *Am J Gastroenterol* 2018; **113**: 1540-1549 [PMID: 30254230 DOI: 10.1038/s41395-018-0262-x]
11 **Camilleri M**, Ford AC. Pharmacotherapy for Irritable Bowel Syndrome. *J Clin Med* 2017; **6** [PMID: 29077050 DOI: 10.3390/jcm6110101]
12 **Carco C**, Young W, Gearry RB, Talley NJ, McNabb WC, Roy NC. Increasing Evidence That Irritable Bowel Syndrome and Functional Gastrointestinal Disorders Have a Microbial Pathogenesis. *Front Cell Infect Microbiol* 2020; **10**: 468 [PMID: 33014892 DOI: 10.3389/fcimb.2020.00468]
13 **Bhattarai Y**, Muniz Pedrogo DA, Kashyap PC. Irritable bowel syndrome: a gut microbiota-related disorder? *Am J Physiol Gastrointest Liver Physiol* 2017; **312**: G52-G62 [PMID: 27881403 DOI: 10.1152/ajpgi.00338.2016]
14 **Simrén M**, Barbara G, Flint HJ, Spiegel BM, Spiller RC, Vanner S, Verdu EF, Whorwell PJ, Zoetendal EG; Rome Foundation Committee. Intestinal microbiota in functional bowel disorders: a Rome foundation report. *Gut* 2013; **62**: 159-176 [PMID: 22730468 DOI: 10.1136/gutjnl-2012-302167]
15 **Hungin APS**, Mitchell CR, Whorwell P, Mulligan C, Cole O, Agréus L, Fracasso P, Lionis C, Mendive J, Philippart de Foy JM, Seifert B, Wensaas KA, Winchester C, de Wit N; European Society for Primary Care Gastroenterology. Systematic review: probiotics in the management of lower gastrointestinal symptoms - an updated evidence-based international consensus. *Aliment Pharmacol Ther* 2018; **47**: 1054-1070 [PMID: 29460487 DOI: 10.1111/apt.14539]
16 **Ford AC**, Harris LA, Lacy BE, Quigley EMM, Moayyedi P. Systematic review with meta-analysis: the efficacy of prebiotics, probiotics, synbiotics and antibiotics in irritable bowel syndrome. *Aliment Pharmacol Ther* 2018; **48**: 1044-1060 [PMID: 30294792 DOI: 10.1111/apt.15001]
17 **Preidis GA**, Weizman AV, Kashyap PC, Morgan RL. AGA Technical Review on the Role of Probiotics in the Management of Gastrointestinal Disorders. *Gastroenterology* 2020; **159**: 708-738.e4 [PMID: 32531292 DOI: 10.1053/j.gastro.2020.05.060]
18 **McFarland LV**, Karakan T, Karatas A. Strain-specific and outcome-specific efficacy of probiotics for the treatment of irritable bowel syndrome: A systematic review and meta-analysis. *EClinicalMedicine* 2021; **41**: 101154 [PMID: 34712929 DOI: 10.1016/j.eclinm.2021.101154]
19 **Pineton de Chambrun G**, Neut C, Chau A, Cazaubiel M, Pelerin F, Justen P, Desreumaux P. A randomized clinical trial of Saccharomyces cerevisiae versus placebo in the irritable bowel syndrome. *Dig Liver Dis* 2015; **47**: 119-124 [PMID: 25488056 DOI: 10.1016/j.dld.2014.11.007]
20 **Spiller R**, Pélerin F, Cayzeele Decherf A, Maudet C, Housez B, Cazaubiel M, Jüsten P. Randomized double blind placebo-controlled trial of Saccharomyces cerevisiae CNCM I-3856 in irritable bowel syndrome: improvement in abdominal pain and bloating in those with predominant constipation. *United European Gastroenterol J* 2016; **4**: 353-362 [PMID: 27403301 DOI: 10.1177/2050640615602571]
21 **Gayathri R**, Aruna T, Malar S, Shilpa B, Dhanasekar KR. Efficacy of Saccharomyces cerevisiae CNCM I-3856 as an add-on therapy for irritable bowel syndrome. *Int J Colorectal Dis* 2020; **35**: 139-145 [PMID: 31807856 DOI: 10.1007/s00384-019-03462-4]
22 **Cayzeele-Decherf A**, Pélerin F, Leuillet S, Douillard B, Housez B, Cazaubiel M, Jacobson GK, Jüsten P, Desreumaux P. *Saccharomyces cerevisiae* CNCM I-3856 in irritable bowel syndrome: An individual subject meta-analysis. *World J Gastroenterol* 2017; **23**: 336-344 [PMID: 28127207 DOI: 10.3748/wjg.v23.i2.336]
23 **Mearin F**, Lacy BE, Chang L, Chey WD, Lembo AJ, Simren M, Spiller R. Bowel Disorders. *Gastroenterology* 2016 [PMID: 27144627 DOI: 10.1053/j.gastro.2016.02.031]
24 **Kurtzman CP**, Robnett CJ. Identification of clinically important ascomycetous yeasts based on nucleotide divergence in

the 5' end of the large-subunit (26S) ribosomal DNA gene. *J Clin Microbiol* 1997; **35**: 1216-1223 [PMID: 9114410 DOI: 10.1128/jcm.35.5.1216-1223.1997]

25 **Kurtzman CP**, Robnett CJ. Identification and phylogeny of ascomycetous yeasts from analysis of nuclear large subunit (26S) ribosomal DNA partial sequences. *Antonie Van Leeuwenhoek* 1998; **73**: 331-371 [PMID: 9850420 DOI: 10.1023/a:1001761008817]

26 **European Committee for Standardization**. CEN/TS 15790:2008-Animal feeding stuffs-PCR typing of probiotic strains of Saccharomyces cerevisiae (yeast). [cited 2021 Dec 12]. Available from: https://standards.iteh.ai/catalog/standards/cen/c4e77d66-4f75-4955-a168-bd50a4845cb1/cen-ts-15790-2008

27 **European Medicines Agency**. Guideline on the evaluation of medicinal products for the treatment of irritable bowel syndrome. [cited 2021 Dec 12]. Available from: https://www.ema.europa.eu/en/documents/scientific-guideline/guideline-evaluation-medicinal-products-treatment-irritable-bowel-syndrome-revision-1_en.pdf

28 **Food and Drug Administration**. Guidance for Industry on Irritable Bowel Syndrome-Clinical Evaluation of Drugs for Treatment. [cited 2021 Dec 12]. Available from: https://www.federalregister.gov/documents/2012/05/31/2012-13143/guidance-for-industry-on-irritable-bowel-syndrome-clinical-evaluation-of-drugs-for-treatment

29 **Chang L**, Lembo A, Sultan S. American Gastroenterological Association Institute Technical Review on the pharmacological management of irritable bowel syndrome. *Gastroenterology* 2014; **147**: 1149-72.e2 [PMID: 25224525 DOI: 10.1053/j.gastro.2014.09.002]

30 **Shah ED**, Almario CV, Spiegel BM, Chey WD. Presentation and Characteristics of Abdominal Pain Vary by Irritable Bowel Syndrome Subtype: Results of a Nationwide Population-Based Study. *Am J Gastroenterol* 2020; **115**: 294-301 [PMID: 31913193 DOI: 10.14309/ajg.0000000000000502]

31 **Patrick DL**, Drossman DA, Frederick IO, DiCesare J, Puder KL. Quality of life in persons with irritable bowel syndrome: development and validation of a new measure. *Dig Dis Sci* 1998; **43**: 400-411 [PMID: 9512138 DOI: 10.1023/a:1018831127942]

32 **Drossman DA**, Patrick DL, Whitehead WE, Toner BB, Diamant NE, Hu Y, Jia H, Bangdiwala SI. Further validation of the IBS-QOL: a disease-specific quality-of-life questionnaire. *Am J Gastroenterol* 2000; **95**: 999-1007 [PMID: 10763950 DOI: 10.1111/j.1572-0241.2000.01941.x]

33 **Drossman D**, Morris CB, Hu Y, Toner BB, Diamant N, Whitehead WE, Dalton CB, Leserman J, Patrick DL, Bangdiwala SI. Characterization of health related quality of life (HRQOL) for patients with functional bowel disorder (FBD) and its response to treatment. *Am J Gastroenterol* 2007; **102**: 1442-1453 [PMID: 17509027 DOI: 10.1111/j.1572-0241.2007.01283.x]

34 **Cain KC**, Headstrom P, Jarrett ME, Motzer SA, Park H, Burr RL, Surawicz CM, Heitkemper MM. Abdominal pain impacts quality of life in women with irritable bowel syndrome. *Am J Gastroenterol* 2006; **101**: 124-132 [PMID: 16405544 DOI: 10.1111/j.1572-0241.2006.00404.x]

35 **Ballou S**, Keefer L. The impact of irritable bowel syndrome on daily functioning: Characterizing and understanding daily consequences of IBS. *Neurogastroenterol Motil* 2017; **29** [PMID: 27781332 DOI: 10.1111/nmo.12982]

36 **Simrén M**, Månsson A, Langkilde AM, Svedlund J, Abrahamsson H, Bengtsson U, Björnsson ES. Food-related gastrointestinal symptoms in the irritable bowel syndrome. *Digestion* 2001; **63**: 108-115 [PMID: 11244249 DOI: 10.1159/000051878]

37 **Böhn L**, Störsrud S, Törnblom H, Bengtsson U, Simrén M. Self-reported food-related gastrointestinal symptoms in IBS are common and associated with more severe symptoms and reduced quality of life. *Am J Gastroenterol* 2013; **108**: 634-641 [PMID: 23644955 DOI: 10.1038/ajg.2013.105]

38 **Ballou S**, McMahon C, Lee HN, Katon J, Shin A, Rangan V, Singh P, Nee J, Camilleri M, Lembo A, Iturrino J. Effects of Irritable Bowel Syndrome on Daily Activities Vary Among Subtypes Based on Results From the IBS in America Survey. *Clin Gastroenterol Hepatol* 2019; **17**: 2471-2478.e3 [PMID: 31419572 DOI: 10.1016/j.cgh.2019.08.016]

39 **Ford AC**, Moayyedi P. Meta-analysis: factors affecting placebo response rate in the irritable bowel syndrome. *Aliment Pharmacol Ther* 2010; **32**: 144-158 [PMID: 20412064 DOI: 10.1111/j.1365-2036.2010.04328.x]

40 **Ballou S**, Beath A, Kaptchuk TJ, Hirsch W, Sommers T, Nee J, Iturrino J, Rangan V, Singh P, Jones M, Lembo A. Factors Associated With Response to Placebo in Patients With Irritable Bowel Syndrome and Constipation. *Clin Gastroenterol Hepatol* 2018; **16**: 1738-1744.e1 [PMID: 29654913 DOI: 10.1016/j.cgh.2018.04.009]

41 **Foligné B**, Dewulf J, Vandekerckove P, Pignède G, Pot B. Probiotic yeasts: anti-inflammatory potential of various non-pathogenic strains in experimental colitis in mice. *World J Gastroenterol* 2010; **16**: 2134-2145 [PMID: 20440854 DOI: 10.3748/wjg.v16.i17.2134]

42 **Zanello G**, Berri M, Dupont J, Sizaret PY, D'Inca R, Salmon H, Meurens F. Saccharomyces cerevisiae modulates immune gene expressions and inhibits ETEC-mediated ERK1/2 and p38 signaling pathways in intestinal epithelial cells. *PLoS One* 2011; **6**: e18573 [PMID: 21483702 DOI: 10.1371/journal.pone.0018573]

43 **Jawhara S**, Habib K, Maggiotto F, Pignede G, Vandekerckove P, Maes E, Dubuquoy L, Fontaine T, Guerardel Y, Poulain D. Modulation of intestinal inflammation by yeasts and cell wall extracts: strain dependence and unexpected anti-inflammatory role of glucan fractions. *PLoS One* 2012; **7**: e40648 [PMID: 22848391 DOI: 10.1371/journal.pone.0040648]

44 **Sivignon A**, de Vallée A, Barnich N, Denizot J, Darcha C, Pignède G, Vandekerckove P, Darfeuille-Michaud A. Saccharomyces cerevisiae CNCM I-3856 prevents colitis induced by AIEC bacteria in the transgenic mouse model mimicking Crohn's disease. *Inflamm Bowel Dis* 2015; **21**: 276-286 [PMID: 25569734 DOI: 10.1097/MIB.0000000000000280]

45 **Roussel C**, Sivignon A, de Vallée A, Garrait G, Denis S, Tsilia V, Ballet N, Vandekerckove P, Van de Wiele T, Barnich N, Blanquet-Diot S. Anti-infectious properties of the probiotic Saccharomyces cerevisiae CNCM I-3856 on enterotoxigenic E. coli (ETEC) strain H10407. *Appl Microbiol Biotechnol* 2018; **102**: 6175-6189 [PMID: 29802478 DOI: 10.1007/s00253-018-9053-y]

46 **Gu Y**, Zhou G, Qin X, Huang S, Wang B, Cao H. The Potential Role of Gut Mycobiome in Irritable Bowel Syndrome. *Front Microbiol* 2019; **10**: 1894 [PMID: 31497000 DOI: 10.3389/fmicb.2019.01894]

47 **Roussel C**, De Paepe K, Galia W, de Bodt J, Chalancon S, Denis S, Leriche F, Vandekerkove P, Ballet N, Blanquet-Diot S,

Van de Wiele T. Multi-targeted properties of the probiotic *saccharomyces cerevisiae* CNCM I-3856 against enterotoxigenic *escherichia coli* (ETEC) H10407 pathogenesis across human gut models. *Gut Microbes* 2021; **13**: 1953246 [PMID: 34432600 DOI: 10.1080/19490976.2021.1953246]

48 **Mars RAT**, Yang Y, Ward T, Houtti M, Priya S, Lekatz HR, Tang X, Sun Z, Kalari KR, Korem T, Bhattarai Y, Zheng T, Bar N, Frost G, Johnson AJ, van Treuren W, Han S, Ordog T, Grover M, Sonnenburg J, D'Amato M, Camilleri M, Elinav E, Segal E, Blekhman R, Farrugia G, Swann JR, Knights D, Kashyap PC. Longitudinal Multi-omics Reveals Subset-Specific Mechanisms Underlying Irritable Bowel Syndrome. *Cell* 2020; **182**: 1460-1473.e17 [PMID: 32916129 DOI: 10.1016/j.cell.2020.08.007]

49 **Zhang J**, Song L, Wang Y, Liu C, Zhang L, Zhu S, Liu S, Duan L. Beneficial effect of butyrate-producing Lachnospiraceae on stress-induced visceral hypersensitivity in rats. *J Gastroenterol Hepatol* 2019; **34**: 1368-1376 [PMID: 30402954 DOI: 10.1111/jgh.14536]

50 **Banasiewicz T**, Krokowicz Ł, Stojcev Z, Kaczmarek BF, Kaczmarek E, Maik J, Marciniak R, Krokowicz P, Walkowiak J, Drews M. Microencapsulated sodium butyrate reduces the frequency of abdominal pain in patients with irritable bowel syndrome. *Colorectal Dis* 2013; **15**: 204-209 [PMID: 22738315 DOI: 10.1111/j.1463-1318.2012.03152.x]

51 **El-Salhy M**, Valeur J, Hausken T, Gunnar Hatlebakk J. Changes in fecal short-chain fatty acids following fecal microbiota transplantation in patients with irritable bowel syndrome. *Neurogastroenterol Motil* 2021; **33**: e13983 [PMID: 32945066 DOI: 10.1111/nmo.13983]

World Journal of Gastroenterology

Submit a Manuscript: https://www.f6publishing.com

World J Gastroenterol 2022 June 14; 28(22): 2523-2526

DOI: 10.3748/wjg.v28.i22.2523

ISSN 1007-9327 (print) ISSN 2219-2840 (online)

LETTER TO THE EDITOR

Future therapies for pancreatic carcinoma: Insights into cancer precision medicine

Qiu-Yu Jiang, Zhi-Xue Chen, Si Zhang, Ru-Yi Xue

Specialty type: Gastroenterology and hepatology

Provenance and peer review: Invited article; Externally peer reviewed.

Peer-review model: Single blind

Peer-review report's scientific quality classification

Grade A (Excellent): 0
Grade B (Very good): B, B
Grade C (Good): C
Grade D (Fair): 0
Grade E (Poor): 0

P-Reviewer: Chisthi MM, India; Kang KM, South Korea; Pang Y, China

Received: November 4, 2021
Peer-review started: November 4, 2021
First decision: December 26, 2021
Revised: January 9, 2022
Accepted: April 28, 2022
Article in press: April 28, 2022
Published online: June 14, 2022

Qiu-Yu Jiang, Zhi-Xue Chen, Ru-Yi Xue, Department of Gastroenterology and Hepatology, Zhongshan Hospital, Shanghai Institute of Liver Disease, Fudan University, Shanghai 200032, China

Si Zhang, NHC Key Laboratory of Glycoconjugate Research, Department of Biochemistry and Molecular Biology, School of Basic Medical Sciences, Shanghai Medical College, Fudan University, Shanghai 200032, China

Corresponding author: Ru-Yi Xue, MD, PhD, Associate Chief Physician, Department of Gastroenterology and Hepatology, Zhongshan Hospital, Shanghai Institute of Liver Disease, Fudan University, No. 180 Fenglin Road, Shanghai 200032, China. xue.ruyi@zs-hospital.sh.cn

Abstract

Pancreatic carcinoma (PC) has one of the highest rates of cancer-related death worldwide. Except for surgery, adjuvant chemotherapy, chemoradiotherapy, and immunotherapy have shown various efficacies depending on the stage of the patient. We read the review "Current and emerging therapeutic strategies in pancreatic cancer: Challenges and opportunities" and offer some opinions that may improve its precision and completeness. This review presents a map of appropriate therapies for PC at different stages. Based on the clinical trial outcomes mentioned in the review, we evaluated the potential therapeutic options for PC and helped explain the contradictory efficacy between different programmed cell death protein 1/programmed cell death ligand 1 clinical trials, which may have resulted from the unique features of PC. Although R0 resection and adjuvant chemotherapy are still the gold standards for PC, new modalities, with or without clinical validation, are needed to establish more specific and precise treatments for PC.

Key Words: Pancreatic carcinoma; Immunotherapy; Chemotherapy; Radiochemotherapy; Future therapies

©The Author(s) 2022. Published by Baishideng Publishing Group Inc. All rights reserved.

Core Tip: For the treatment of pancreatic carcinoma (PC), although surgery with adjuvant chemotherapy or chemoradiotherapy remains the gold standard for most patients, attention needs to be given to immunotherapy and other research hotspots. In addition to programmed cell death protein 1/programmed cell death ligand 1, we suggest that immunotherapies such as agonistic CD40, adoptive T cell therapy, myeloid-targeted therapies, stroma-targeted therapies, multiple immunomodulatory agents, and other treatments such as small-molecule inhibitors, antibodies, or viruses targeting tumors, as well as gene editing techniques, may help improve the prognosis of patients with PC in the future.

Citation: Jiang QY, Chen ZX, Zhang S, Xue RY. Future therapies for pancreatic carcinoma: Insights into cancer precision medicine. *World J Gastroenterol* 2022; 28(22): 2523-2526
URL: https://www.wjgnet.com/1007-9327/full/v28/i22/2523.htm
DOI: https://dx.doi.org/10.3748/wjg.v28.i22.2523

TO THE EDITOR

We read with interest the review "Current and emerging therapeutic strategies in pancreatic cancer: Challenges and opportunities" by Manrai *et al*[1], who summarized the current and emerging therapeutic strategies in pancreatic cancer (PC). We agree with the main thrust of this review and want to share some ideas after a careful review and further analysis of this article.

First, we consider this topic to be of practical significance. PC is a rare cancer (3.2% in the United States in 2020[2]), but with increasing incidence and mortality (5-year overall survival: 9% in the United States[2]), it remains a burden worldwide without promising effective therapies. In this review, the authors systematically summarized the mainstream clinical trial outcomes and focused on the challenges and available treatment modalities for PC at different stages, especially the standard management of resectable, borderline resectable, locally advanced, and advanced metastatic PC. The standard management for resectable or borderline resectable PC is surgery followed by adjuvant chemotherapy. The efficacy of adjuvant or neoadjuvant chemotherapy and chemoradiotherapy has been assessed in several clinical trials. The standard treatment for locally advanced and advanced metastatic PC is gemcitabine-based chemotherapy. In addition, newer potential modalities such as immunotherapy, targeted therapy, macrophage-targeted therapy, and cancer vaccines were also mentioned, providing researchers with guidelines for present clinical applications and future research work.

Second, the efficacy of the targeted agent erlotinib in combination with gemcitabine may depend on the different stages of PC, as confirmed by various clinical trials. In contrast to the efficacy shown in patients with metastatic PC, we found that two large clinical trials that focused on different stages of PC showed little benefit. The phase III LAP07 trial in 2016 investigated the clinical value of erlotinib combined with gemcitabine in patients with locally advanced PC. Unfortunately, the median overall survival of patients who received gemcitabine alone was 13.6 mo [95% confidence interval (CI): 12.3–15.3 mo] compared with 11.9 mo (95%CI: 10.4–13.5 mo) for patients receiving gemcitabine plus erlotinib[3]. The multicenter randomized phase III CONKO-005 Trial in 2017[4] assessed this combination therapy in patients with resectable PC after R0 resection and showed median disease-free survival of 11.4 mo *vs* 11.4 mo (gemcitabine alone) and median overall survival of 24.5 mo *vs* 26.5 mo. To date, such targeted agents combined with conventional chemotherapy may not show much of an advantage. We expect to see more advances in the future.

Thirdly, in the section "Immunotherapy for pancreatic cancer," the authors stated that popular programmed cell death protein 1/programmed cell death ligand 1 (PD-1/PD-L1) suppressor pembrolizumab had limited performance in the phase II KEYNOTE-158 study, due to the rare metastatic microsatellite instability in PC. This type of poor reactivity has been explained by several unique factors in PC: The well-recognized suppressive elements in the tumor microenvironment; the functional and structural barrier imposed by stromal components; T-cell exhaustion; possible choice of the wrong immune targets; and microbial factors, including gut dysbiosis and the unexpected presence of tumor microbes[5]. We agree with this, but we want to add that the clinical feasibility of PD-1 inhibitors deserves to be recognized. Recently, several clinical trials have examined the efficacy of conventional chemotherapy in combination with PD-1 inhibitors and other antagonists that mobilize T-cell activation and have shown mild but promising success. The phase IIa COMBAT trial in 2020 utilized the CXC chemokine receptor 4 antagonist BL-8040 (motixafortide), which promoted T-cell tumor infiltration, combined with pembrolizumab and chemotherapy in metastatic pancreatic adenocarcinoma, showing that BL-8040 may increase the benefit of chemotherapy. It reveals an overall response rate of 32%, disease control rate of 77%, and median duration of response of 7.8 mo[6]. Another phase I ARC-8 trial in 2021 also preliminarily validated the feasibility of combining chemotherapy with the PD-1 inhibitor zimberelimab and AB680, which is an inhibitor of CD73, to reduce adenosine generation and thus proliferating T cells. Eleven of the 13 patients who received treatment for at least 16 wk experienced

tumor shrinkage or stabilization[7,8]. Although the outcomes were not significant, they were encouraging, and future larger controlled studies are needed, and we are hopeful of good results. We believe that the abovementioned factors will be discussed in the future.

Importantly, except for the newer modalities mentioned in the review, we found that more therapies should be included. According to previous studies, other opportunities for PC immunotherapy, such as agonistic CD40, adoptive T cell therapy, myeloid-targeted therapies, stroma-targeted therapies, and multiple immunomodulatory agents are worthy of attention, and their efficacy in various PC stages has been proven by numerous clinical trials[9].

In conclusion, this review provides a valuable clinical reference for the management of PC, helping young clinicians to learn of appropriate clinical strategies for PC. It sheds light on different strategies for dealing with PC at different stages. In addition, it summarizes both the gold standard treatments and new therapeutic strategies such as immunotherapy and targeted therapy, which can guide clinicians and researchers to find a more promising combined treatment for PC. Recently, in different types of cancer, small molecule inhibitors, antibodies, or viruses targeting tumors, as well as gene editing techniques like CRISPR-Cas9 have shown antitumor potential, based on abundant research. We should always keep in mind that although early diagnosis and R0 resection are the first and best choice for PC patients, adequate basic research is still needed aimed at new targets or mechanisms that may provide patients with more specific and precise medical care to improve their prognosis.

FOOTNOTES

Author contributions: Jiang QY and Chen ZX wrote the original draft; Xue RY conceptualized and reviewed the manuscript; Zhang S edited and revised the manuscript.

Conflict-of-interest statement: The authors declare no conflict of interest.

Open-Access: This article is an open-access article that was selected by an in-house editor and fully peer-reviewed by external reviewers. It is distributed in accordance with the Creative Commons Attribution NonCommercial (CC BY-NC 4.0) license, which permits others to distribute, remix, adapt, build upon this work non-commercially, and license their derivative works on different terms, provided the original work is properly cited and the use is non-commercial. See: https://creativecommons.org/Licenses/by-nc/4.0/

Country/Territory of origin: China

ORCID number: Qiu-Yu Jiang 0000-0003-2874-8152; Zhi-Xue Chen 0000-0002-2534-0090; Si Zhang 0000-0002-5682-4995; Ru-Yi Xue 0000-0002-5710-0091.

S-Editor: Fan JR
L-Editor: Kerr C
P-Editor: Fan JR

REFERENCES

1 **Manrai M**, Tilak TVSVGK, Dawra S, Srivastava S, Singh A. Current and emerging therapeutic strategies in pancreatic cancer: Challenges and opportunities. *World J Gastroenterol* 2021; **27**: 6572-6589 [PMID: 34754153 DOI: 10.3748/wjg.v27.i39.6572]

2 **Siegel RL**, Miller KD, Jemal A. Cancer statistics, 2020. *CA Cancer J Clin* 2020; **70**: 7-30 [PMID: 31912902 DOI: 10.3322/caac.21590]

3 **Hammel P**, Huguet F, van Laethem JL, Goldstein D, Glimelius B, Artru P, Borbath I, Bouché O, Shannon J, André T, Mineur L, Chibaudel B, Bonnetain F, Louvet C; LAP07 Trial Group. Effect of Chemoradiotherapy vs Chemotherapy on Survival in Patients With Locally Advanced Pancreatic Cancer Controlled After 4 Months of Gemcitabine With or Without Erlotinib: The LAP07 Randomized Clinical Trial. *JAMA* 2016; **315**: 1844-1853 [PMID: 27139057 DOI: 10.1001/jama.2016.4324]

4 **Sinn M**, Bahra M, Liersch T, Gellert K, Messmann H, Bechstein W, Waldschmidt D, Jacobasch L, Wilhelm M, Rau BM, Grützmann R, Weinmann A, Maschmeyer G, Pelzer U, Stieler JM, Striefler JK, Ghadimi M, Bischoff S, Dörken B, Oettle H, Riess H. CONKO-005: Adjuvant Chemotherapy With Gemcitabine Plus Erlotinib Versus Gemcitabine Alone in Patients After R0 Resection of Pancreatic Cancer: A Multicenter Randomized Phase III Trial. *J Clin Oncol* 2017; **35**: 3330-3337 [PMID: 28817370 DOI: 10.1200/JCO.2017.72.6463]

5 **Hester R**, Mazur PK, McAllister F. Immunotherapy in Pancreatic Adenocarcinoma: Beyond "Copy/Paste". *Clin Cancer Res* 2021; **27**: 6287-6297 [PMID: 34193514 DOI: 10.1158/1078-0432.CCR-18-0900]

6 **Bockorny B**, Semenisty V, Macarulla T, Borazanci E, Wolpin BM, Stemmer SM, Golan T, Geva R, Borad MJ, Pedersen KS, Park JO, Ramirez RA, Abad DG, Feliu J, Muñoz A, Ponz-Sarvise M, Peled A, Lustig TM, Bohana-Kashtan O, Shaw SM, Sorani E, Chaney M, Kadosh S, Vainstein Haras A, Von Hoff DD, Hidalgo M. BL-8040, a CXCR4 antagonist, in combination with pembrolizumab and chemotherapy for pancreatic cancer: the COMBAT trial. *Nat Med* 2020; **26**: 878-885

[PMID: 32451495 DOI: 10.1038/s41591-020-0880-x]
7 Blocking CD73 Can Shrink Pancreatic Tumors. *Cancer Discov* 2021; **11**: OF4 [PMID: 33579783 DOI: 10.1158/2159-8290.CD-NB2021-0313]
8 **Manji GA**, Wainberg ZA, Krishnan K, Giafis N, Udyavar A, Quah CS, Scott J, Berry W, DiRenzo D, Gerrick K, Jin L, Bendell JC. ARC-8: Phase I/Ib study to evaluate safety and tolerability of AB680 + chemotherapy + zimberelimab (AB122) in patients with treatment-naive metastatic pancreatic adenocarcinoma (mPDAC). *J Clin Oncol* 2021; **39**: 404 [DOI: 10.1200/JCO.2021.39.3_suppl.404]
9 **Bear AS**, Vonderheide RH, O'Hara MH. Challenges and Opportunities for Pancreatic Cancer Immunotherapy. *Cancer Cell* 2020; **38**: 788-802 [PMID: 32946773 DOI: 10.1016/j.ccell.2020.08.004]



Published by **Baishideng Publishing Group Inc**
7041 Koll Center Parkway, Suite 160, Pleasanton, CA 94566, USA
Telephone: +1-925-3991568
E-mail: bpgoffice@wjgnet.com
Help Desk: https://www.f6publishing.com/helpdesk
https://www.wjgnet.com



© 2022 Baishideng Publishing Group Inc. All rights reserved.

ISSN 1007-9327 (print)
ISSN 2219-2840 (online)

World Journal of *Gastroenterology*

World J Gastroenterol 2022 June 21; 28(23): 2527-2635



Published by Baishideng Publishing Group Inc

World Journal of Gastroenterology

Contents

Weekly Volume 28 Number 23 June 21, 2022

REVIEW

2527 Autoimmune liver diseases in systemic rheumatic diseases

Wang CR, Tsai HW

2546 Fecal microbiota transplantation in the metabolic diseases: Current status and perspectives

Zheng L, Ji YY, Wen XL, Duan SL

MINIREVIEWS

2561 Up to seven criteria in selection of systemic therapy for hepatocellular carcinoma

Silk T, Silk M, Wu J

ORIGINAL ARTICLE

Basic Study

2569 Family with sequence similarity 134 member B-mediated reticulophagy ameliorates hepatocyte apoptosis induced by dithiothreitol

Guo YX, Han B, Yang T, Chen YS, Yang Y, Li JY, Yang Q, Xie RJ

Retrospective Study

2582 Infliximab trough level combined with inflammatory biomarkers predict long-term endoscopic outcomes in Crohn's disease under infliximab therapy

Cao WT, Huang R, Liu S, Fan YH, Xu MS, Xu Y, Ni H

2597 Higher infliximab and adalimumab trough levels are associated with fistula healing in patients with fistulising perianal Crohn's disease

Gu B, Venkatesh K, Williams AJ, Ng W, Corte C, Gholamrezaei A, Ghaly S, Xuan W, Paramsothy S, Connor S

2609 Whole lesion histogram analysis of apparent diffusion coefficient predicts therapy response in locally advanced rectal cancer

Jiménez de los Santos ME, Reyes-Pérez JA, Domínguez Osorio V, Villaseñor-Navarro Y, Moreno-Astudillo L, Vela-Sarmiento I, Sollozo-Dupont I

CASE REPORT

2625 Primary gastric dedifferentiated liposarcoma resected endoscopically: A case report

Cho JH, Byeon JH, Lee SH

LETTER TO THE EDITOR

2633 Reconstructing the puzzle of the role of therapeutic endoscopy in the management of post-bariatric surgery complications

Argyriou K, Parra-Blanco A

ABOUT COVER

Editorial Board Member of *World Journal of Gastroenterology*, Osamu Toyoshima, MD, Director, Department of Gastroenterology, Toyoshima Endoscopy Clinic, 6-17-5 Seijo, Setagaya-ku, Tokyo 157-0066, Japan. t@ichou.com

AIMS AND SCOPE

The primary aim of *World Journal of Gastroenterology* (*WJG*, *World J Gastroenterol*) is to provide scholars and readers from various fields of gastroenterology and hepatology with a platform to publish high-quality basic and clinical research articles and communicate their research findings online. *WJG* mainly publishes articles reporting research results and findings obtained in the field of gastroenterology and hepatology and covering a wide range of topics including gastroenterology, hepatology, gastrointestinal endoscopy, gastrointestinal surgery, gastrointestinal oncology, and pediatric gastroenterology.

INDEXING/ABSTRACTING

The *WJG* is now indexed in Current Contents®/Clinical Medicine, Science Citation Index Expanded (also known as SciSearch®), Journal Citation Reports®, Index Medicus, MEDLINE, PubMed, PubMed Central, and Scopus. The 2021 edition of Journal Citation Report® cites the 2020 impact factor (IF) for *WJG* as 5.742; Journal Citation Indicator: 0.79; IF without journal self cites: 5.590; 5-year IF: 5.044; Ranking: 28 among 92 journals in gastroenterology and hepatology; and Quartile category: Q2. The *WJG*'s CiteScore for 2020 is 6.9 and Scopus CiteScore rank 2020: Gastroenterology is 19/136.

RESPONSIBLE EDITORS FOR THIS ISSUE

Production Editor: *Wen-Wen Qi*; **Production Department Director:** *Xiang Li*; **Editorial Office Director:** *Ze-Mao Gong*.

NAME OF JOURNAL
World Journal of Gastroenterology

ISSN
ISSN 1007-9327 (print) ISSN 2219-2840 (online)

LAUNCH DATE
October 1, 1995

FREQUENCY
Weekly

EDITORS-IN-CHIEF
Andrzej S Tarnawski

EDITORIAL BOARD MEMBERS
http://www.wjgnet.com/1007-9327/editorialboard.htm

PUBLICATION DATE
June 21, 2022

COPYRIGHT
© 2022 Baishideng Publishing Group Inc

INSTRUCTIONS TO AUTHORS
https://www.wjgnet.com/bpg/gerinfo/204

GUIDELINES FOR ETHICS DOCUMENTS
https://www.wjgnet.com/bpg/GerInfo/287

GUIDELINES FOR NON-NATIVE SPEAKERS OF ENGLISH
https://www.wjgnet.com/bpg/gerinfo/240

PUBLICATION ETHICS
https://www.wjgnet.com/bpg/GerInfo/288

PUBLICATION MISCONDUCT
https://www.wjgnet.com/bpg/gerinfo/208

ARTICLE PROCESSING CHARGE
https://www.wjgnet.com/bpg/gerinfo/242

STEPS FOR SUBMITTING MANUSCRIPTS
https://www.wjgnet.com/bpg/GerInfo/239

ONLINE SUBMISSION
https://www.f6publishing.com

© 2022 Baishideng Publishing Group Inc. All rights reserved. 7041 Koll Center Parkway, Suite 160, Pleasanton, CA 94566, USA
E-mail: bpgoffice@wjgnet.com https://www.wjgnet.com

World Journal of Gastroenterology

Submit a Manuscript: https://www.f6publishing.com

World J Gastroenterol 2022 June 21; 28(23): 2527-2545

DOI: 10.3748/wjg.v28.i23.2527

ISSN 1007-9327 (print) ISSN 2219-2840 (online)

REVIEW

Autoimmune liver diseases in systemic rheumatic diseases

Chrong-Reen Wang, Hung-Wen Tsai

Specialty type: Gastroenterology and hepatology

Provenance and peer review: Invited article; Externally peer reviewed.

Peer-review model: Single blind

Peer-review report's scientific quality classification

Grade A (Excellent): A, A
Grade B (Very good): B
Grade C (Good): 0
Grade D (Fair): 0
Grade E (Poor): 0

P-Reviewer: Fan X, China; Jagdish RK, India; Malnick SDH, Israel

Received: December 10, 2021
Peer-review started: December 10, 2021
First decision: March 11, 2022
Revised: March 11, 2022
Accepted: May 13, 2022
Article in press: May 13, 2022
Published online: June 21, 2022

Chrong-Reen Wang, Department of Internal Medicine, National Cheng Kung University Hospital, Tainan 70403, Taiwan

Hung-Wen Tsai, Department of Pathology, National Cheng Kung University Hospital, Tainan 70403, Taiwan

Corresponding author: Chrong-Reen Wang, MD, PhD, Full Professor, Department of Internal Medicine, National Cheng Kung University Hospital, No. 138 Sheng-Li Road, Tainan 70403, Taiwan. wangcr@mail.ncku.edu.tw

Abstract

Systemic rheumatic diseases (SRDs) are chronic, inflammatory, autoimmune disorders with the presence of autoantibodies that may affect any organ or system. Liver dysfunction in SRDs can be associated with prescribed drugs, viral hepatitis, alternative hepatic comorbidities and coexisting autoimmune liver diseases (AILDs), requiring an exclusion of secondary conditions before considering liver involvement. The patterns of overlap diseases depend predominantly on genetic determinants with common susceptible loci widely distributing in both disorders. In AILDs, it is important to identify the overlapping SRDs at an early stage since such a coexistence may influence the disease course and prognosis. Commonly co-occurring SRDs in AILDs are Sjögren syndrome (SS), rheumatoid arthritis (RA) or systemic lupus erythematosus (SLE) in autoimmune hepatitis (AIH), and SS, RA or systemic sclerosis in primary biliary cholangitis. Owing to different disease complications and therapies, it is imperative to differentiate between SLE liver involvement and SLE-AIH overlap disease. Therapeutic options can be personalized to control coexisting conditions of liver autoimmunity and rheumatic manifestations in AILD-SRD overlap diseases. The collaboration between hepatologists and rheumatologists can lead to significant advances in managing such a complex scenario. In this review, we provide a comprehensive overview on coexisting AILDs in different SRDs and the therapeutic approach in managing these overlap diseases.

Key Words: Autoimmune liver disease; Systemic rheumatic disease; Overlap disease; Liver function test; Drug-induced liver injury; Viral hepatitis

©The Author(s) 2022. Published by Baishideng Publishing Group Inc. All rights reserved.

Core Tip: Liver dysfunction in systemic rheumatic diseases (SRDs) can be associated with prescribed drugs, viral hepatitis, alternative hepatic comorbidities and coexisting autoimmune liver diseases (AILDs), requiring an exclusion of secondary conditions before considering liver involvement. In AILDs, it is imperative to identify the overlapping SRDs at an early stage since such a coexistence may influence the disease course and prognosis. Commonly co-occurring SRDs in AILDs are Sjögren syndrome (SS), rheumatoid arthritis (RA) or systemic lupus erythematosus in autoimmune hepatitis, and SS, RA or systemic sclerosis in primary biliary cholangitis. Therapeutic options can be personalized to control coexisting conditions of liver autoimmunity and rheumatic manifestations in AILD-SRD overlap diseases.

Citation: Wang CR, Tsai HW. Autoimmune liver diseases in systemic rheumatic diseases. *World J Gastroenterol* 2022; 28(23): 2527-2545
URL: https://www.wjgnet.com/1007-9327/full/v28/i23/2527.htm
DOI: https://dx.doi.org/10.3748/wjg.v28.i23.2527

INTRODUCTION

Systemic rheumatic diseases (SRDs) are chronic, inflammatory, autoimmune disorders with the presence of autoantibodies that may affect any organ or system; they include systemic lupus erythematosus (SLE), Sjögren syndrome (SS), systemic sclerosis (SSc), rheumatoid arthritis (RA), idiopathic inflammatory myopathies (IIM), mixed connective tissue disease (MCTD), systemic vasculitis (SV), *etc.* [1]. Although SRDs can have liver involvement, most patients only have abnormal liver enzymes without significant changes in histopathology[2,3]. Hepatic dysfunction can be a secondary phenomenon, associated with prescribed drugs, viral hepatitis (VH), alternative liver comorbidities, and coexisting autoimmune liver diseases (AILDs).

The major cause of abnormal liver function test (LFT) in patients with SRDs is associated with medications, *i.e.* drug-induced liver injury (DILI)[3]. Given that a variety of medications are used in the management of SRDs, it is frequently encountered in clinical practice. High occurrences of DILI in SRDs are due to the chronic or high-dose prescription of medications, the existence of susceptible factors that makes patients prone to hepatotoxicity, and/or the use of herbal or ayurvedic compounds[2,3]. Elevated liver enzymes with predominant cholestatic or hepatocellular damage pattern can be observed in SRDs treated with non-steroidal anti-inflammatory drugs (NSAIDs), synthetic disease modifying anti-rheumatic drugs (SDMARDs), corticosteroids (CS), immunosuppressants, biologic agents or oral small molecules[2]. Most medications only cause a mild elevation in liver enzymes, which reverses with drug cessation. On rare occasions, severely irreversible hepatic damage may occur and progress into chronic liver disease or fulminant hepatic failure. Despite the relative safety with a low-dose prescription, methotrexate, a SDMARD frequently used in SRD-related arthritis, has been reported to cause acute liver dysfunction with confounding factors like concomitant NSAIDs use, and progressive liver fibrosis and cirrhosis can occur when used chronically[4]. It usually occurs after a prolong use for no less than 2 years and with a total accumulated dose of 1.5 g[5]. Notably, there is a risk of hepatitis B virus (HBV) reactivation depending on the dose and duration of CS use and the status of hepatitis B surface antigen and hepatitis B core antibody in SRDs[6]. Furthermore, acute or progressing liver dysfunction can be related to coexisting VH, requiring screen tests for HBV and hepatitis C virus (HCV) infection to provide early antiviral treatment and avoid reactivating or worsening VH after immunosuppressive therapy[3]. Table 1 summaries the hepatic abnormalities associated with the common medications used in SRDs[2,7,8]. Although immune checkpoint inhibitors have altered the therapeutic paradigm in oncological patients, there is undesirable off-target autoimmune reaction causing adverse effects like musculoskeletal manifestations and immune hepatitis, a pan-lobular active hepatitis resembling AIH[9].

Although the liver is the largest lymphoid organ involved in the immune response against invading pathogens and in the maintenance of tolerance to self-molecules, it can also be a target of autoimmune diseases[10]. AILDs are attributed to a complex interplay of socioeconomic, environmental and genetic factors, all of which may participate in their pathogenesis[11]. Most common AILDs are autoimmune hepatitis (AIH), primary biliary cholangitis (PBC) and primary sclerosing cholangitis (PSC), which may occur individually or in combination[12]. These disorders are characterized by hepatic lymphocyte infiltration, elevated liver enzymes, generation of autoantibodies, and associated HLA loci. Coexisting extra-hepatic autoimmune diseases such as SRDs, have been well described in the literature[13]. AIH often goes into disease remission with first-line therapy, including CS alone or plus AZA[14]. PBC has a normal life expectancy if treated early with ursodeoxycholic acid (UDCA) in responsive patients, while no effective therapy has been found to alter the natural course of PSC, except liver transplantation (LT) [15,16]. Some patients with AILDs may eventually progress into end-stage liver disease requiring LT, and with an increased risk of recurrent activities and acute or chronic rejection[17,18]. Currently, AILD research has focused on obtaining a better understanding of the pathogenetic process for identification

Table 1 Hepatic abnormalities associated with common medications used in systemic rheumatic diseases

Medications	Hepatic abnormalities	[2]Likelihood score category in DILI
NSAIDs	LEE, cholestasis, acute liver failure, VBDS	A for diclofenac, ibuprofen, sulindac
Glucocorticoids	LEE, NAFLD, acute liver failure, HBV reactivation	A in high dosages
Immunosuppressive agents		
Azathioprine	LEE, cholestasis, NRH, peliosis hepatis, VOD	A
Mycophenolate mofetil	LEE	D
Cyclophosphamide	LEE, VOD	B
Cyclosporine	LEE, cholelithiasis	C
Tacrolimus	LEE	C
Conventional SDMARDs		
Hydroxychloroquine	LEE	C
Leflunomide	LEE, acute liver failure, HBV reactivation	B
Methotrexate	LEE, NAFLD, HBV reactivation, fibrosis, cirrhosis	A
Penicillamine	LEE, cholestasis	A
Sulfasalazine	LEE, cholestasis, DRESS	A
Biologic/targeted SDMARDs		
Abatacept	LEE, HBV reactivation	C
Anakinra	LEE	C
Apremilast	Unlikely liver injury	E
Belimumab	Unlikely liver injury	E
Mepolizumab	Unlikely liver injury	E
Rituximab	LEE, HBV reactivation	A
TNF blockers[1]	LEE, cholestasis, HBV reactivation, AIH	A for infliximab
Tocilizumab	LEE, HBV reactivation	C
Tofacitinib	Suspected liver injury, potential HBV reactivation	E′
Ustekinumab	Suspected liver injury, possible HBV reactivation	E′

[1]TNF blockers including adalimumab, certolizumab, etanercept, golimumab and infliximab.
[2]Categorization of Likelihood Score in drug-induced liver injury. A: Definite; B: Highly likely; C: Probable, D: Possible, E: Unlikely; E′: Suspected.
NSAIDs: Non-steroidal anti-inflammatory drugs; HBV: Hepatitis virus B; DILI: Drug-induced liver injury; DRESS: Drug rash with eosinophilia and systemic symptoms; LEE: Liver enzyme elevation; NAFLD: Nonalcoholic fatty liver disease; NRH: Nodular regenerative hyperplasia; SDMARDs: Synthetic disease-modifying antirheumatic drugs; SRDs: Systemic rheumatic disease; VBDS: Vanishing bile duct syndrome; VOD: Veno-occlusive disease.

of new therapeutic targets to reduce morbidity and improve survival[15]. Table 2 demonstrates the demographic, clinical, laboratory, pathological, therapeutic and prognostic characteristics of three common AILDs[11-20].

In AILDs, it is imperative to identify the co-occurring SRDs at an early stage by using autoantibody screening, since such a coexistence may influence their natural course and disease prognosis[21]. The patterns of overlap diseases depend predominantly on genetic determinants, with common susceptible loci widely distributing in both disorders[20]. The similar epidemiological links between AILDs and SRDs are further reflected in their shared pathogenesis, best exemplified by the concept of autoimmune epithelitis, *i.e.*, concomitant PBC and SS[22,23]. Furthermore, AILDs and SRDs have common serologic profiles with the presence of particular autoantibodies and hyper-gammaglobulinemia[21,24]. Progressive liver damage can be identified in overlap diseases despite rare complications with liver cirrhosis and hepatic failure[3]. Table 3 shows the reported prevalence of coexisting AILDs in different SRDs.

The therapeutic strategies in AILDs and SRDs are also overlapping, with CS as first-line treatment in most cases, followed by administration of immunosuppressants, and potential application of targeted therapy[21]. Nevertheless, therapeutic options can be personalized to control coexisting conditions of liver autoimmunity and rheumatic manifestations[24]. A collaboration between hepatologists and

Table 2 Demographic, clinical, laboratory, pathological, therapeutic and prognostic profiles in three common autoimmune liver diseases

Category	AIH	PBC	PSC
Demographic			
Sex	Predominant F, 4:1	Predominant F, 10:1	Predominant M, 2:1
Age	Any, median 45 yr	Common above 40 yr	Any, typical 30-50 yr
Prevalence	Rare, 4-25 per 100000	Rare, 2-40 per 100000	Rare, 4-16 per 100000
Laboratory			
Abnormal LFT	Majorly AST/ALT	Majorly ALP/GGT	Majorly ALP/GGT
Serum Ig	Elevated IgG	Elevated IgM	Elevated IgG, IgM
Autoantibody	I: ANA, ASMA; II: anti-LKM, -LC	ANA, AMA	ANCA
HLA-DR	DR3, DR4	DR8	DR52
Liver biopsy			
Interface HA	Typical finding	Occasional	Occasional
Portal infiltrate	Lymphoplasmacytic	Lymphocytic	Lymphocytic
Bile duct lesion	Occasional	Florid duct lesion	Obliterative duct
Granuloma	Rare	Typical finding	Rare
Diagnosis	AIH score for definite diagnosis	AMA, liver biopsy, Cholestatic LFT	Cholangiography, Cholestatic LFT
Coexistent SRD			
SLE	0.7%-2.8%	1.3%-3.7%	1.70%
SS	1.4%-35%	3.5%-38%	CR
SSc	0.80%	2.3%-12%	CR
RA	1.6%-5.4%	1.8%-13%	1.2%-3.4%
IIM	CR	0.6%-3.1%	CR
MCTD	CR	0.60%	NA
SV	1.60%	2.20%	CR
Sarcoidosis	0.60%	2.70%	0.80%
First-line Tx	CS or CS plus AZA	UDCA	No effective therapy
Prognosis	Generally responsive to IS, poor prognosis if untreated	Excellent prognosis if responsive to UDCA	Median survival without LT 12-16 yr after diagnosis

AIH: Autoimmune hepatitis; ALP: Alkaline phosphatase ALT: Alanine aminotransferase; AMA: Antimitochondrial autoantibody; ANA: Anti-nuclear antibody; ANCA: Perinuclear antineutrophil cytoplasmic antibody; APS: Antiphospholipid syndrome; ASMA: Anti-smooth muscle antibody; AST: Aspartate aminotransferase; AZA: Azathioprine; CR: Case report; CS: Corticosteroids; EHAID: Extra-hepatic autoimmune disease; HA: Hepatitis; Ig: Immunoglobulin; IIM: Idiopathic inflammatory myopathies; IS: Immunosuppressants; GGT: Gamma-glutamyl transferase; LC: Liver cytosol; LKM: Liver kidney microsomal; LFT: Liver function test; LT: Liver transplantation; MCTD: Mixed connective tissue disease; NA: Not available; PBC: Primary biliary cholangitis; PSC: Primary sclerosing cholangitis; RA: Rheumatoid arthritis; SLE: Systemic lupus erythematosus; SS: Sjögren syndrome; SSc: Systemic sclerosis; Tx: Treatment; UDCA: Ursodeoxycholic acid.

rheumatologists in clinical practice can lead to significant advances in managing such a complex scenario. Herein, we provide a comprehensive overview on coexisting AILDs in different SRDs and the therapeutic approach in managing these overlap diseases.

SLE

SLE is a less common SRD, occurring mostly in women of childbearing age and having heterogenous clinical manifestations affecting any organ or system as well as presenting antinuclear antibody (ANA) and a variety of autoantibodies[25]. The liver is generally not a target organ in SLE and hepatic

Table 3 Reported prevalence of concomitant autoimmune liver diseases in different systemic rheumatic diseases

Category	AIH	PBC	PSC	AIH/PBC OS
SLE	1.6%-15%	2.2%-7.5%	CR	CR
SS	0.4%-4.4%	3.4%-8.9%	CR	CR
SSc	CR	0.8%-3.3%	CR	CR
RA	1.3%	3.8%-6.3%	CR	CR
IIM	CR	0.7%	CR	CR
MCTD	1.6%	CR	NA	NA

AIH: Autoimmune hepatitis; APS: Antiphospholipid syndrome; CR: Case report; IIM: Idiopathic inflammatory myopathies; NA: Not available; OS: Overlap syndrome; PBC: Primary biliary cholangitis; PSC: Primary sclerosing cholangitis; RA: Rheumatoid arthritis; SLE: Systemic lupus erythematosus; SS: Sjögren syndrome; SSc: Systemic sclerosis.

involvement is not included in the classification or diagnostic criteria. Abnormal LFT is common in SLE, usually with subtle changes, in up to 60% of cases during the disease course, while elevated liver enzymes occur during disease flares in less than 20% of patients[3,26,27]. Hepatic dysfunction in SLE can be classified into primary form due to disease itself or secondary form including DILI, VH, vascular disorders, alternative liver comorbidities and coexisting AILDs[28]. Before considering the liver involvement in SLE, it is necessary to exclude other secondary conditions.

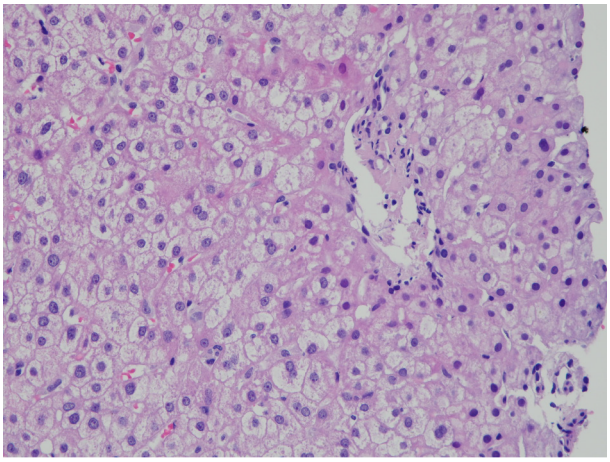
Lupus hepatitis (LH) is reactive liver damage caused by immune-complex deposition, in contrast to lupoid hepatitis, a term used in the 1950s to define what was later known as AIH[29,30]. This manifestation is usually synchronous with disease activity and affects less than 10% of patients[31-33]. It is characterized by asymptomatic transaminasemia with the presence of anti-ribosomal P antibody (commonly known as ARPA) and non-specific histopathological changes. Although CS may help to improve impaired LFT, there is a risk of flare up upon cessation of its use[34]. Figure 1 shows the liver biopsy finding from a patient with LH demonstrating non-specific histopathological changes.

The main cause of liver dysfunction in SLE was salicylate toxicity in the 1950s[35]. Later on, owing to a rare prescription, another common finding of liver biopsy was steatohepatitis, an alternative liver comorbidity. Nowadays, the known risk factors for development of non-alcoholic fatty liver disease (NAFLD) include obesity, physical inactivity and sedentary lifestyle[36], which are also shared by SLE. Furthermore, patients with SLE have been shown to have higher incidences of metabolic syndrome and insulin resistance[37], especially with the use of CS[38]. Increased frequencies of NAFLD have been found in liver biopsy specimens from patients with SLE[39].

The presence of antiphospholipid antibody (aPL) in SLE underlies an increased probability of thrombophilia, leading to antiphospholipid syndrome (APS) with vascular thrombosis[40]. APS can affect the hepatic circulation, causing hepatic arterial thrombosis, portal vein thrombosis and Budd-Chiari syndrome (BCS) as well as the rarely-observed liver infarction and hepatic veno-occlusive disease [40-42]. Notably, BCS resulting from the obstruction of hepatic venous outflow[43] can be an initial manifestation of patients with SLE-associated APS[44]. In particular, aPL has been reported to be involved in the pathogenesis of hepatic nodular regenerative hyperplasia (referred to herein as NRH), small-nodule transformation of hyperplastic hepatocytes with a later development of non-cirrhotic portal hypertension[3,45]. Although higher frequencies of aPL could be detected in AILDs, there was no definite clinical or histological correlation with their presence in such patients[3,46].

Autoimmune gastrointestinal diseases have been linked to SLE with shared pathogenic mechanisms responsible for the development of both disorders[47]. Although AIH and PBC are rare AILDs, the coexistence with either of these diseases is not uncommon among SLE patients with liver enzyme abnormalities, suggesting a causal relationship between their overlap[28,48,49]. Since SLE-PSC overlap disease rarely occurs (but has been described in case reports[28,48]), it remains to be ascertained whether they are casual associations. A review on individual AILD coexisting with SLE is depicted as follows.

AIH is a rare AILD characterized by interface hepatitis as the most specific histological change, and the presence of autoantibodies including anti-liver kidney microsomal-1 (LKM-1)/liver cytosol-1 (LC-1) in type II, a rare subgroup affecting female pediatric patients, and ANA/anti-smooth muscle antibody (ASMA) in type I[50]. Clinical manifestations vary from asymptomatic to nonspecific symptoms of varying severity, including fatigue, malaise, nausea, anorexia and abdominal pain. The criteria established by the International Autoimmune Hepatitis Group (commonly known as the IAHG) are usually used for the diagnosis of AIH[51]. Due to different disease complications and therapeutic regimens between AIH and LH, it is imperative to differentiate between two disease entities[28,34]. AIH may lead to end stage liver disease, and its immunosuppressive therapy needs to be continued for at least 2 years of hepatic biochemical remission before attempting withdrawal[50]. Liver biopsy is highly



DOI: 10.3748/wjg.v28.i23.2527 **Copyright** ©The Author(s) 2022.

Figure 1 Liver biopsied tissues from a patient with systemic lupus erythematosus liver involvement (lupus hepatitis). The portal area with minimal non-specific lymphocytic infiltration is shown. Hematoxylin and eosin staining, 400 × magnification.

recommended for their distinguishment[28,34]. LH usually demonstrates lobular infiltrates or occasionally mild periportal infiltrates, whereas AIH is characterized by portal mononuclear infiltrates invading nearby lobules to induce interface hepatitis and form hepatocyte rosettes, followed by confluent lytic necrosis and finally cirrhosis[30].

SLE-AIH overlap disease is defined by fulfilling American College of Rheumatology (commonly known as the ACR) criteria for the classification of SLE in patients who also meet IAIHG criteria for the diagnosis of AIH[34,51,52]. The prevalence of AIH in SLE ranges from 1.6% to 15%, lower in general cohorts and higher in patients with abnormal LFT[39,53-58]. Immunosuppressive treatment for AIH is also effective for SLE, and has been demonstrated to successfully apply to their overlap cases[28]. Most cases with coexisting SLE and AIH responded well to CS or plus immunosuppressants[48]. The long-term outcome for SLE-AIH overlap disease has been observed to be better than AIH alone[34]. Nevertheless, there are sporadic cases of acute liver failure or end-stage liver disease requiring LT[59, 60].

PBC is the most common AILD affecting women predominantly. It is characterized by destructive lymphocytic cholangitis involving small bile ducts, and leading to progressive ductopenia, hepatic cholestasis and biliary fibrosis[61]. Clinical manifestations vary from asymptomatic to non-specific symptoms with jaundice and pruritus. According to the guidance from American Association for the Study of Liver Diseases (commonly known as the AASLD), the diagnosis of PBC is established when two of three items are met, including biochemical cholestasis based on alkaline phosphatase (ALP) elevation, presence of antimitochondrial autoantibody (AMA), and histological evidences of nonsuppurative destructive cholangitis and interlobular bile ducts destruction[62]. The nomenclature of PBC has already shifted from cirrhosis to cholangitis, reflecting the dramatically improved prognosis upon first-line UDCA therapy without the development of cirrhosis[63,64].

SLE-PBC overlap is defined by fulfilling the diagnostic criteria for both diseases[34,52,62]. SLE usually affects younger females of childbearing age, whereas PBC is more common in middle-aged women. By genome-wide studies, both diseases have been reported to share the IRF5-TNPO3 gene-spanning haplotype loci[65]. The prevalence of PBC in SLE patients with liver dysfunction ranges from 2.2% to 7.5%, usually lower than that of AIH[39,53-55,57]. In a review of SLE overlapping with PBC, 69% were diagnosed first by PBC, 24% had coexisting SS, and 2 deaths were due to PBC-related hepatic failure[66]. For patients with concomitant SLE and PBC, regardless of the SLE treatment, UDCA is effective first-line therapy for PBC[49].

The diagnosis of PBC-AIH overlap is established with coexisting features of both diseases[67]. Two commonly used criteria for the diagnosis of PBC-AIH overlap syndrome are the IAIHG and Paris criteria[51,68]. Patients with overlapping PBC and AIH have been described to exhibit significantly higher rates of LC, portal hypertension and mortality as compared with those with AIH or PBC alone [69]. PBC with features of AIH should be considered for immunosuppressive therapy[49], while PBC-AIH overlap disease can benefit from combination treatment with UDCA and CS or plus AZA[69]. There is a rare association between SLE and PBC-AIH overlap disease[70]. In a large case series with 71 overlap patients, EHAIDs were identified in 31 (44%), while only 2 (3%) had concurrent SLE[71].

In contrast to western countries, AIH had been considered a rare etiology in the Asia-Pacific region, where VH is a major diagnosis in patients with chronic liver diseases[72]. A very low prevalence of AIH was found in Taiwan in earlier years, raising concerns about under-recognition in an area with a high prevalence of HBV infection and associated liver cirrhosis and hepatocellular carcinoma complications [73], where clinicians would have been more familiar with VH and might have tended to overlook AIH

[74]. Recent findings, however, have shown increasing annual incidences of AIH, indicating improved recognition of AIH in this region[72].

The clinical, laboratory, therapeutic and outcome profiles in 3 patients with SLE-AIH overlap disease diagnosed by ourselves are shown in Table 4. All met IAIHG diagnostic criteria for AIH[51], and case 2 also fulfilled AASLD diagnostic criteria for PBC[62]. Despite CS plus AZA therapy, case 1 progressed into advanced LC, and received LDLT with stabilized LFTs and low SLE activity. Case 2 had the initial diagnosis of AIH with transaminasemia, followed by the development of hepatic cholestasis and sicca symptoms, and finally full-blown manifestations of SLE. Under the diagnosis of coexistent AIH, PBC, SLE and SS, in addition to CS/AZA and UDCA, the patient received B-cell depleting therapy with anti-CD20 monoclonal antibody, with low-dose CS for maintenance, resulting in normalized LFT and low SLE activity. Figure 2 demonstrates histopathological findings in liver biopsy specimens from cases 1 and 2.

PSC is a rare cholestatic AILD characterized by persistent, progressive inflammation, fibrosis and stricture of the intrahepatic and extrahepatic bile ducts, leading to cirrhosis[75]. About half of the patients are asymptomatic. The diagnosis is made by cholestasis with ALP elevation and imaging of bile duct strictures, excluding secondary causes. Liver biopsy is indicated only when suspecting overlapping with other AILDs or small-duct PSC, a variant with normal cholangiogram. UDCA is the subject of debate with conflicting data to support its use in PSC[49], and end-stage liver disease requiring LT may develop in affected patients.

Although the association of SLE with PSC is considered to be extremely unusual[34,48], there are several published cases with SLE-PSC overlap disease[76-80]. Furthermore, a 1.7% occurrence of SLE was observed in a Swedish PSC cohort[81]. Whether such a coexistence indicates that both diseases might share common pathogenic pathways remains to be elucidated.

SS

SS is a common SRD affecting the exocrine glands with typical symptoms of dryness of eyes and mouth, histological evidence of focal lymphocytic sialadenitis and the presence of anti-Ro and -La antibodies [82]. The treatment of SS-related dry eyes and mouth is symptomatic with the use of artificial tear and saliva preparation. LFT abnormalities can be identified in nearly half of patients, either persistent or intermittent, and usually mild with cholestatic or hepatocellular pattern[3]. Liver involvement is considered as the most common extra-glandular feature, correlating with the disease activities of SS involving other organs[83]. In a large-scale investigation of 475 cases, after excluding DILI and alternative hepatic comorbidities, the main causes of liver dysfunction were VH in 50% and AILDs in around 20% of patients[84]. Several studies have confirmed a higher prevalence of AILDs among SS, mainly PBC (3.4% to 8.9%), followed by AIH (0.4% to 4.4%)[84-87].

The most frequently associated SRDs in PBC is SS with a prevalence ranging from 3.5% to 38%[88-94]. PBC can be considered a SS of the liver, whereas SS has been equally regarded as a PBC of the exocrine glands[21]. In addition to frequent clinical coexistence and comparable epidemiological features, SS and PBC have similar pathogenic mechanisms and genetic susceptibility backgrounds[95]. Pyruvate dehydrogenase complex E2 subunit, a PBC autoantigen, is also present on the surface of salivary epithelial cells in SS, while HLA-DR2 and -DR3 have been reported as the common susceptibility genes in both disorders[20].

Despite a higher frequency of ASMA than AMA in SS[96], the prevalence of coexisting AIH is lower than PBC[84,85,97]. Owing to a much higher prevalence of SS than SLE in the general population, the occurrence of concomitant SLE and SS in patients with AIH are 0.7% to 2.8% and 0.8% to 7.2%, respectively, lower in SLE than in SS[98-102].

There are published cases and case series describing SS-PSC overlap disease as well as a higher prevalence in small-scale PSC studies[84,103,104], implicating a causative association rather than sporadic occurrence. Notably, almost all reported patients with overlapping SS and PSC have chronic pancreatitis, demonstrating a triad syndrome complex[103]. A possibility of co-occurring IgG4-related disease (IgG4-RD) should be considered in SS-PSC overlap disease with the presentation of autoimmune pancreatitis (AIP)[104].

SSC

SSc is an uncommon SRD characterized by vasculopathy and fibrosis of the skin and internal organs, with the presence of anti-topoisomerase I and anti-centromere antibodies (ACA) in diffuse and limited cutaneous subsets, respectively[105]. It has a higher mortality rate than other SRDs. The gastrointestinal tract is affected in up to 90% of patients[106], and hepatic fibrosis has been identified at autopsy[107]. Since liver involvement is rarely observed in SSc[3], abnormal LFT should exclude other possibilities first before considering disease *per se*. There are diverse autoimmune diseases like AILDs co-occurring within SSc patients and their family members[108], suggesting common pathophysiological

Table 4 Clinical, laboratory, therapeutic and outcome data in 3 patients with systemic lupus erythematosus-autoimmune hepatitis overlap disease[1]

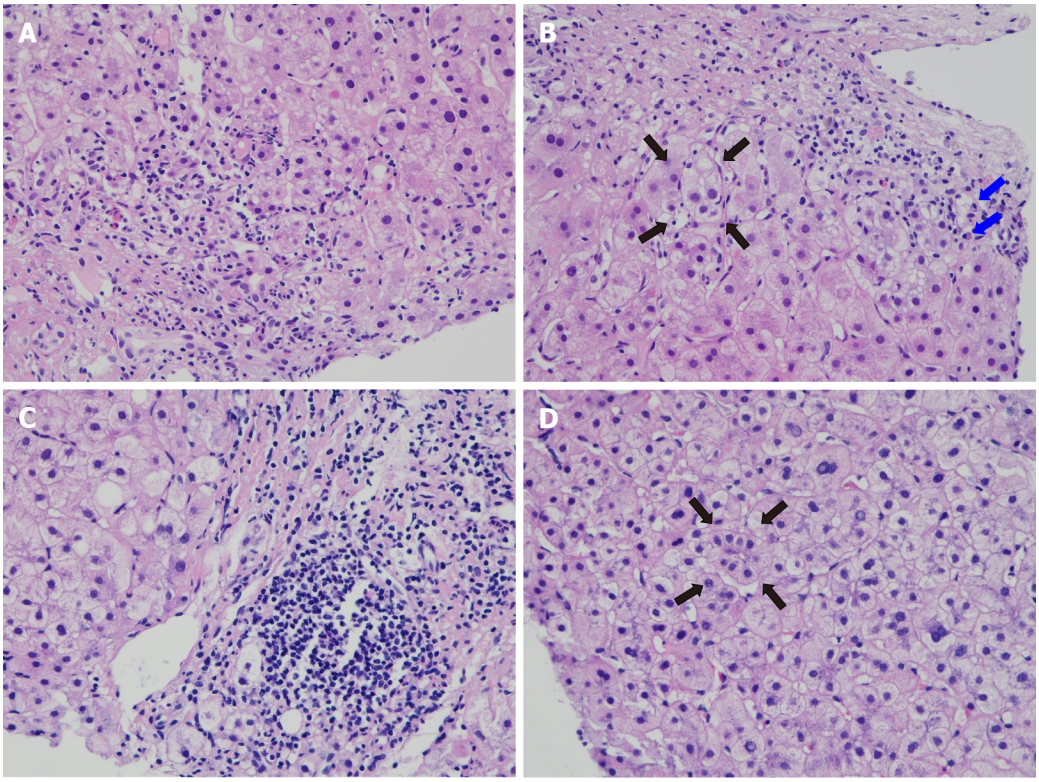
Patient number	1	2	3
Sex	Female	Female	Female
SLE Dx age	19	50	20
ACR criteria	8/11	7/11	8/11
AIH Dx age	26	37	22
IAIHG score	Definite	Definite	Definite
Clinical			
SLE	Skin, joint, renal, hematology, neurology	Skin, joint, renal, hematology, serositis	Skin, joint, renal, hematology, serositis
AILD complication	Jaundice, malaise LC with PH	Jaundice, pruritus hepatosplenomegaly	Jaundice, anorexia
Coexistent AID	Nil	PBC, SS	Nil
Laboratory			
Hemogram	HA, TP	HA, TP, leukopenia	TP, leukopenia
Proteinuria autoantibody	2 g/d	2.5 g/d	1 g/d
SLE-related	ANA, anti-dsDNA/Sm	ANA, anti-dsDNA/Sm	ANA, anti-dsDNA
AILD-related	ASMA	AMA, ASMA	ASMA
Others	ARPA, ANCA	ARPA, anti-Ro/La	ARPA
[2]IgG (mg/dL)	2130	2520	1615
[2]AST (IU/L)	1563	116	97
[2]ALT (IU/L)	1093	217	177
[2]Bil (mg/dL)	23.8	3.7	2.4
[2]ALP (IU/L)	432	621	344
HLA-DR	DR8, DR15	DR4, DR15	DR4, DR7
VH	No [3]HHV/CMV/EBV	No HHV/CMV/EBV	No HHV/CMV/EBV
Treatment	CS/AZA, LDLT and low-dose CS/FK506 after OP	CS/AZA, UDCA RTX and low-dose CS for maintenance	CS/AZA, AZA for maintenance
Outcome	Stabilized LFT and low SLEDAI	Normalized LFT and low SLEDAI	Normalized LFT and low SLEDAI

[1]Enrollment from 2018 July to 2021 June.
[2]Peak levels during autoimmune hepatitis.
[3]Human hepatitis viruses including hepatitis A virus, hepatitis B virus and hepatitis C virus.
AID: Autoimmune disease; AIH: Autoimmune hepatitis; ALP: Alkaline phosphatase ALT: Alanine aminotransferase; AMA: Antimitochondrial autoantibody; ANCA: Antineutrophil cytoplasmic antibody; ARPA: Anti-ribosomal-P antibody; ASMA: Anti-smooth muscle antibody; AST: Aspartate aminotransferase; AZA: Azathioprine; Bil: Bilirubin; CMV: Cytomegalovirus; CS: Corticosteroids; Dx: Diagnosis; EBV: Epstein-Barr virus; IAIHG: International Autoimmune Hepatitis Group; HA: Hemolytic anemia; HHV: Human hepatitis viruses; LC: Liver cirrhosis; LDLT: Living donor liver transplantation; LFT: Liver function test; OP: Operation; PBC: Primary biliary cholangitis; PH: Portal hypertension; RTX: Rituximab; SLEDAI: SLE disease activity index; SS: Sjögren syndrome; TP: Thrombocytopenia; UDCA: Ursodeoxycholic acid; VH: Viral hepatitis.

mechanisms between these disorders.

Increased prevalence of PBC has been observed in SSc, varying from 0.8% to 3.3%[108-112], and there is a 2.3% to 12.4% occurrence of SSc in PBC[90-94,111]. SSc-PBC overlap disease has the presence of both ACA and AMA[113], and tends to occur in older females with the limited cutaneous subset[114]. This overlap disorder has a slower disease progression in comparison with PBC alone; however, survival is similar due to an increase in SSc-related non-liver death. The use of UDCA has been observed to reduce skin lesions in addition to improved hepatic cholestasis in overlap patients[115].

A 0.8% prevalence of SSc has been reported from a AIH cohort[98], and patients with SSc-AIH overlap disease can be found in the literature[116,117]. In a review with 11 cases[117], all had positive ACA and a later presentation of AIH, 9 with limited cutaneous subtype and 3 with AIH-PBC overlap. Despite a risk of scleroderma renal crisis under the higher dosages of CS use, there were normalized or improved LFT without the occurrence of scleroderma renal crisis in overlap patients receiving such a



DOI: 10.3748/wjg.v28.i23.2527 **Copyright** ©The Author(s) 2022.

Figure 2 Liver biopsied tissues from 2 patients with systemic lupus erythematosus-autoimmune hepatitis overlap disease. A and B: Case 1 (A) lymphoplasmacytic infiltration with interface activity and (B) lymphoplasmacytic infiltration with interface activity. Plasma cells are indicated by blue arrows and rosette formations by black arrows; C and D: Case 2 (C) lymphoplasmacytic infiltration with interface activity, and (D) rosette formation (arrows). Hematoxylin and eosin staining, 400 × magnification.

treatment[116].

Overlap condition with large- or small-duct PSC has been observed in patients with SSc[118,119], suggesting that the extensive disturbance of connective tissues in SSc can lead to abnormal collagen deposition in the bile duct epithelium of PSC[120].

RA

RA is a common SRD primarily affecting the joints and causing cartilage and bone damage, with extra-articular presentations and the presence of rheumatoid factor (commonly referred to as RF) and anti-cyclic citrullinated peptide (commonly referred to as CCP) autoantibodies[121]. Among patients with chronic inflammatory joint diseases, liver involvement has been recognized in RA, despite not showing a significant extra-articular manifestation[122]. Elevated liver enzymes have been identified in up to 50% of patients with RA[2]. DILI is not uncommonly observed in RA, especially under the treatment of NSAIDs and SDMARDs including leflunomide, methotrexate, penicillamine and sulfasalazine, all with potential hepatotoxicity[2,7,123]. Patients are at the hazard of developing NAFLD with the risk factors of chronic inflammation and CS use[2]. Prior to the widespread use of methotrexate in RA, the hepatic histopathological findings at autopsy were most commonly mild portal tract inflammation, rarely diffuse fibrosis of advanced grades[124]. Two rare extra-articular manifestations, rheumatoid vasculitis and Felty syndrome, have been reported to cause necrotizing hepatic arteritis with liver rupture and NRH with portal hypertension, respectively[125,126].

There were no differences in the prevalence of HBV and HCV infection in RA as compared with the general population[127]. Nevertheless, immunosuppressive therapy for RA may significantly worsen underlying VH, and further affect the clinical course and disease prognosis, requiring the survey of viral markers and their antibodies before its initiation[123]. Since the use of tumor necrosis factor (TNF) blockades in RA can cause inactive HBV reactivation[7,128], HBsAg-positive individuals should receive anti-viral prophylactic treatment[129]. Although the TNF pathway is involved in perpetuation of hepatic inflammation and fibrosis progression in HCV infection[130], further studies are needed to verify the safety of anti-TNF therapy in HCV-infected patients[131]. Notably, the use of TNF antagonists has been reported to be associated with the development of AIH in RA[7,132].

The most common coexisting AILDs in RA is PBC with a prevalence of 3.8% to 6.3%[53,97,123], while the occurrence of RA in PBC has been reported to be 1.8% to 13%[90-94]. Around 50% of patients with PBC were shown to be positive for RF[133]. Since RA is usually diagnosed before PBC in patients with the overlap disease, AMA should be screened in RA with elevated cholestatic liver enzymes[134]. Genetic studies have shown that RA has HLA-DQB1, STAT4, IRF5, MMEL1 and CTLA4 genes in common with PBC, predisposing to develop PBC in RA with the overlapping genetic trait[135]. Potentially hepatotoxic drugs used in RA can be avoided in patients with RA-PBC overlap disease[123].

AIH is rarely observed in RA with a 1.3% prevalence reported from patients with liver dysfunction [97]. Furthermore, in patients with AIH, there is a 1.6% to 5.4% prevalence of RA[98,100-102]. AIH can be diagnosed during the RA progression as acute or chronic hepatitis, but rarely fulminant hepatic failure[123]. In addition, in patients with AIH-PBC overlap disease, RA is accounting for an occurrence of 4.2%[71].

High circulating levels of TNF were found in AIH, while a TNF antagonist etanercept has been demonstrated to improve the AIH histological lesions in RA[136]. Nevertheless, anti-TNF therapy can induce the production of autoantibodies, including ANA and ASMA, leading to the development of distinct autoimmune diseases[137]. Notably, anti-TNF-inhibitor-associated AIH (also known as ATIAIH), a serious idiosyncratic DILI, has been well documented in a large-scale analysis of 389 cases [138]. ATIAIH has a female predominance, a period of 3-14 mo between starting therapy and AIH occurrence, and improvement upon medication stoppage and CS use. Infliximab is the most frequently administrated medication, and RA is the most commonly reported indication.

There was a 1.2% and a 3.4% prevalence of RA in two large-scale PSC cohorts[81,139]. In patients with RA-PSC overlap disease, the presence of HLA-DR4 has been reported to have unusual progression to cirrhosis, 14-48 mo after the diagnosis of PSC[140], implicating a clinical marker at a high risk of cirrhosis development.

Psoriatic arthritis (PsA) is a less common SRD with psoriasis (PsO) and inflammatory arthritis, associating with extra-articular manifestations which have an impact on their therapeutic regimens [141]. Similar to RA, liver enzyme abnormalities in PsA and PsO can be caused by comorbid NAFLD and used medications including NSAIDs and conventional or biologic/targeted SDMARDs. Despite an increased association of AIH in PsA and PsO[142], these patients might be under anti-TNF therapy, and both diseases are commonly observed complications in ATIAIH[138].

IIM

IIM including polymyositis (PM) and dermatomyositis (DM), an uncommon group of SRDs with the presence of myositis-specific/associated antibodies, have weakness due to skeletal muscle inflammation and extra-muscular involvement[143]. Since transaminases are also muscle-derived enzymes with increased levels during IIM disease activity, an increase of aspartate aminotransferase and alanine aminotransferase more than creatine kinase or an alteration of cholestatic enzymes should consider a possibility of hepatic dysfunction[3]. During the first 3 years to 5 years after the onset of DM, the risk of cancer is increased, rarely hepatocellular carcinoma. Since DM can be associated with malignancy as a paraneoplastic syndrome[144], sporadic cases had HBV-associated hepatocellular carcinoma with a concurrent or later diagnosis of DM[145,146].

Although IIM usually occur alone, these SRDs may associate with other extra-muscular autoimmune diseases including AILDs, more frequently in patients with PM than DM[147]. Positive AMA could be identified in 2.5% of patients with IIM[148], and there were sibling cases of familial clustering with PBC-PM overlap disease[149]. PBC can be identified in IIM with a prevalence of 0.7%[148], while the occurrence of PM in PBC ranges from 0.6% to 3.1%[90,92,93]. There are sporadic cases with PM coexisting with AIH, AIH-PBC overlap disease or PSC[150-152].

MCTD

In addition to the presence of anti-U1 small nuclear ribonucleoprotein (known as snRNP) antibody in high titers, MCTD has distinct features including Raynaud's phenomenon and puffy hands as well as mixed findings from PM, SLE and SSc[153]. It is a rare SRD with a strong HLA linkage, distinctly differing from ethnically matched healthy controls and other SRDs. Hepatic dysfunction occurs in MCTD usually caused by DILI and pulmonary hypertension-related liver congestion[97,153]. Coexistent AILDs are rarely observed in patients with MCTD[153]. In addition to published case reports, a 1.6% prevalence of AIH was found in MCTD[154], while a 0.6% prevalence of MCTD could be identified in PBC[90]. There was no observed association with MCTD in two PSC case series[81,141].

SV

SV is a rare SRD characterized by inflammation of vascular walls, resulting in a broad spectrum of clinical manifestations dependent on the site, type, and size of involved vessels[155]. Although the diagnosis relies on clinical presentations confirmed by histopathological findings, large/medium and small vessel involvement can be supported by angiographical examinations and laboratory tests (*e.g.*, ANCA), respectively[155,156]. Owing to hepatic vascular involvement[2,53], polyarteritis nodosa (referred to herein as PAN), a medium-vessel SV associated with HBV infection[157], may have elevated liver enzymes. A 2.2% prevalence of SV has been reported from a large-scale PBC series with 361 cases [94], while a 1.6% occurrence of SV was identified in a 122-patient AIH series[98]. There were sporadic cases of AIH coexisting with PAN[158].

Testing for ANCA can support the diagnosis of ANCA-associated vasculitis including eosinophilic granulomatosis with polyangiitis (also referred to as EGPA), granulomatosis with polyangiitis and microscopic polyangiitis (also referred to as MPA) in spite of seropositivity in only one-third of EGPA cases[159]. Notably, ANCA has a diagnostic relevance beyond SV, justifying its occurrence in suspected type I AIH which is lacking conventional autoantibodies[160]. AILDs usually develop atypical perinuclear-ANCA not targeting the classical myeloperoxidase with the positive frequencies highest in patients with PSC[21,156]. There is no clinical nor prognostic value of ANCA testing in patients with AILDs. This atypical autoantibody, referred to as peripheral anti-nuclear neutrophil antibody, can react with beta-tubulin isotype 5 and shares structural homology with the intestinal bacterial protein FtsZ [161]. Nevertheless, it is not specific for AILDs, and it is also present in VH and alcoholic liver disease [162]. Interestingly, ANCA was detected in the bile of PSC patients and correlated with the severity of bile duct stricture[163]. Sixteen cases of ANCA-associated vasculitis-AILD overlap disease have been reported, with twelve involving women, PBC in eleven, and MPA in eight[164-166].

OTHER SRDS

Adult-onset Still's disease (AOSD) is a rare SRD usually affecting young adults, with spiking fever, polyarthritis, evanescent rash and marked hyperferritinemia as well as uncommon life-threatening macrophage activation syndrome[167]. In medical practice, hyperferritinemia is a non-specific finding related to iron overload in only 10% of cases such as hereditary hemochromatosis, while underlying causes attributing to a reactive increase in the rest 90% patients such as AOSD[168]. Hepatic dysfunction is commonly observed in AOSD, mostly due to the disease itself and without any specific histological finding[97,167]. Coexisting AILDs have rarely been observed, and there are sporadic cases of AIH-AOSD overlap disease[169].

Behçet's disease (BD) is a SRD with a variable worldwide prevalence, characterized by vasculitis affecting the small/Large venous and arterial vessels, and presenting with orogenital ulcers, ocular lesions and systemic involvement[170]. The liver is rarely involved, and the commonest hepatic complication is BCS with thrombosis of the inferior vena cava and hepatic vein[171]. Elevated ALP levels of liver origin has been reported in 10% of patients, with a correlation to disease activity[172]. Case reports of Behçet's disease concomitant with AIH or PBC can be found in the literature[173,174].

IgG4-RD is a rare SRD, characterized by elevated serum IgG4 concentrations and fibroinflammation in the affected tissues, with dense lymphoplasmacytic infiltrates rich in IgG4-positive plasma cells and storiform fibrosis[175]. Cases of type I AIP and IgG4-related sclerosing cholangitis (commonly referred to as IgG4-SC), two common forms of IgG4-RD usually occurring in combination, have painless jaundice and cholestatic LFT abnormalities due to liver involvement[176,177]. Although CS has favorable therapeutic efficacy[49], AIP and IgG4-SC are associated with significant morbidity and mortality due to extra-pancreatic organ failure and malignancy[176]. AIP has been reported to be associated with PBC and PSC[178,179]. Infiltrating IgG4-positive plasma cells can be observed in the AIH liver, suggesting involvement of IgG4 in its pathogenesis[180]. Nevertheless, the disease concept of IgG4-AIH remains to be established[181].

Sarcoidosis is an uncommon SRD, characterized by the formation of noncaseating granulomas in various organs, predominantly the lungs, lymphatic system, skin, and eyes, or a different combination of these sites[182]. Abnormal LFT has been observed in one-fourth of patients with chronic sarcoidosis; among which, 15% are suspected of having liver involvement with cholestatic pattern of injury[183]. Although hepatic sarcoidosis is mainly asymptomatic, it can progress to LC, while such cases are rare [184]. AILDs coexisting with sarcoidosis have been reported, having a prevalence of 0.6% in AIH and 0.8% in PSC[81,99]. Several case reports have described the association of sarcoidosis with PBC[88]. A 2.7% prevalence of sarcoidosis was found in a PBC cohort from Greece[185], whereas an epidemiological study with 1510 patients from the United Kingdom failed to show an association between the two disorders[186].

Relapsing polychondritis is a rare SRD, characterized by cartilaginous inflammation throughout the body, especially involving the hyaline cartilage of the ears, nose and joints, and the respiratory tract [187]. Liver involvement with cholestatic hepatic dysfunction has been observed scarcely in such

patients[188]. The association of relapsing polychondritis with AILDs has been reported with PBC or PSC overlap diseases[189,190].

CONCLUSION

SRDs are chronic, inflammatory, autoimmune disorders with the presence of autoantibodies that may affect any organ or system. Liver dysfunction in SRDs can be associated with prescribed drugs, VH, alternative hepatic comorbidities and coexisting AILDs, requiring an exclusion of secondary conditions before considering liver involvement. The patterns of overlap diseases depend predominantly on genetic determinants with common susceptible loci widely distributed in both disorders. In AILDs, it is important to identify the overlapping SRDs at an early stage, since such a coexistence may influence the disease course and prognosis. Commonly co-occurring SRDs in AILDs are SS, RA or SLE in AIH, and SS, RA or SSc in PBC. Owing to different disease complications and therapies, it is imperative to differentiate between SLE liver involvement and SLE-AIH overlap disease. Therapeutic options can be personalized to control coexisting conditions of liver autoimmunity and rheumatic manifestations in AILD-SRD overlap diseases. The collaboration between hepatologists and rheumatologists in clinical practice can lead to significant advances in managing such a complex scenario.

ACKNOWLEDGEMENTS

The authors are indebted to Dr. IC Wu (Division of Gastroenterology and Hepatology) for his valuable comments and to other doctors at the National Cheng Kung University Hospital involved in the diagnosis and management of reported patients.

FOOTNOTES

Author contributions: Wang CR designed the report; Wang CR and Tsai HW wrote the paper, collected the clinical data and analyzed the pathological specimens.

Conflict-of-interest statement: The authors declare having no real or potential conflicts of interest.

Open-Access: This article is an open-access article that was selected by an in-house editor and fully peer-reviewed by external reviewers. It is distributed in accordance with the Creative Commons Attribution NonCommercial (CC BY-NC 4.0) license, which permits others to distribute, remix, adapt, build upon this work non-commercially, and license their derivative works on different terms, provided the original work is properly cited and the use is non-commercial. See: https://creativecommons.org/Licenses/by-nc/4.0/

Country/Territory of origin: Taiwan

ORCID number: Chrong-Reen Wang 0000-0001-9881-7024; Hung-Wen Tsai 0000-0001-9223-2535.

S-Editor: Yan JP
L-Editor: A
P-Editor: Yan JP

REFERENCES

1 **Bossuyt X**, De Langhe E, Borghi MO, Meroni PL. Understanding and interpreting antinuclear antibody tests in systemic rheumatic diseases. *Nat Rev Rheumatol* 2020; **16**: 715-726 [PMID: 33154583 DOI: 10.1038/s41584-020-00522-w]
2 **Gebreselassie A**, Aduli F, Howell CD. Rheumatologic Diseases and the Liver. *Clin Liver Dis* 2019; **23**: 247-261 [PMID: 30947875 DOI: 10.1016/j.cld.2018.12.007]
3 **De Santis M**, Crotti C, Selmi C. Liver abnormalities in connective tissue diseases. *Best Pract Res Clin Gastroenterol* 2013; **27**: 543-551 [PMID: 24090941 DOI: 10.1016/j.bpg.2013.06.016]
4 **Visser K**, Katchamart W, Loza E, Martinez-Lopez JA, Salliot C, Trudeau J, Bombardier C, Carmona L, van der Heijde D, Bijlsma JW, Boumpas DT, Canhao H, Edwards CJ, Hamuryudan V, Kvien TK, Leeb BF, Martín-Mola EM, Mielants H, Müller-Ladner U, Murphy G, Østergaard M, Pereira IA, Ramos-Remus C, Valentini G, Zochling J, Dougados M. Multinational evidence-based recommendations for the use of methotrexate in rheumatic disorders with a focus on rheumatoid arthritis: integrating systematic literature research and expert opinion of a broad international panel of rheumatologists in the 3E Initiative. *Ann Rheum Dis* 2009; **68**: 1086-1093 [PMID: 19033291 DOI: 10.1136/ard.2008.094474]

5 **Conway R**, Carey JJ. Risk of liver disease in methotrexate treated patients. *World J Hepatol* 2017; **9**: 1092-1100 [PMID: 28989565 DOI: 10.4254/wjh.v9.i26.1092]
6 **Perrillo RP**, Gish R, Falck-Ytter YT. American Gastroenterological Association Institute technical review on prevention and treatment of hepatitis B virus reactivation during immunosuppressive drug therapy. *Gastroenterology* 2015; **148**: 221-244.e3 [PMID: 25447852 DOI: 10.1053/j.gastro.2014.10.038]
7 LiverTox: Clinical and Research Information on Drug-Induced Liver Injury [Internet]. Bethesda (MD): National Institute of Diabetes and Digestive and Kidney Diseases; 2012– [PMID: 31643176]
8 **Hayashi PH**. Drug-Induced Liver Injury Network Causality Assessment: Criteria and Experience in the United States. *Int J Mol Sci* 2016; **17**: 201 [PMID: 26861284 DOI: 10.3390/ijms17020201]
9 **Sanjeevaiah A**, Kerr T, Beg MS. Approach and management of checkpoint inhibitor-related immune hepatitis. *J Gastrointest Oncol* 2018; **9**: 220-224 [PMID: 29564187 DOI: 10.21037/jgo.2017.08.14]
10 **Gao B**. Basic liver immunology. *Cell Mol Immunol* 2016; **13**: 265-266 [PMID: 27041634 DOI: 10.1038/cmi.2016.09]
11 **Lee BT**, Tana MM, Kahn JA, Dara L. We Are Not Immune: Racial and Ethnic Disparities in Autoimmune Liver Diseases. *Hepatology* 2021; **74**: 2876-2887 [PMID: 34056734 DOI: 10.1002/hep.31985]
12 **Washington MK**. Autoimmune liver disease: overlap and outliers. *Mod Pathol* 2007; **20** Suppl 1: S15-S30 [PMID: 17486048 DOI: 10.1038/modpathol.3800684]
13 **Wong GW**, Heneghan MA. Association of Extrahepatic Manifestations with Autoimmune Hepatitis. *Dig Dis* 2015; **33** Suppl 2: 25-35 [PMID: 26641498 DOI: 10.1159/000440707]
14 **Terziroli Beretta-Piccoli B**, Mieli-Vergani G, Vergani D. Autoimmune hepatitis: Standard treatment and systematic review of alternative treatments. *World J Gastroenterol* 2017; **23**: 6030-6048 [PMID: 28970719 DOI: 10.3748/wjg.v23.i33.6030]
15 **Tanaka A**. Emerging novel treatments for autoimmune liver diseases. *Hepatol Res* 2019; **49**: 489-499 [PMID: 30969002 DOI: 10.1111/hepr.13347]
16 **Engel B**, Taubert R, Jaeckel E, Manns MP. The future of autoimmune liver diseases - Understanding pathogenesis and improving morbidity and mortality. *Liver Int* 2020; **40** Suppl 1: 149-153 [PMID: 32077605 DOI: 10.1111/liv.14378]
17 **Chen C**, Ke R, Yang F, Cai Q, Liu J, Huang X, Chen J, Xu F, Jiang Y. Risk factors for recurrent autoimmune liver diseases after liver transplantation: A meta-analysis. *Medicine (Baltimore)* 2020; **99**: e20205 [PMID: 32443344 DOI: 10.1097/MD.0000000000020205]
18 **Heinemann M**, Liwinski T, Adam R, Berenguer M, Mirza D, Malek-Hosseini SA, Heneghan MA, Lodge P, Pratschke J, Boudjema K, Paul A, Zieniewicz K, Fronek J, Mehrabi A, Acarli K, Tokat Y, Coker A, Yilmaz S, Karam V, Duvoux C, Lohse AW, Schramm C; all the other contributing centers (www. eltr.org) and the European Liver and Intestine Transplant Association (ELITA). Long-term outcome after living donor liver transplantation compared to donation after brain death in autoimmune liver diseases: Experience from the European Liver Transplant Registry. *Am J Transplant* 2022; **22**: 626-633 [PMID: 34605157 DOI: 10.1111/ajt.16864]
19 **Trivedi PJ**, Hirschfield GM. Recent advances in clinical practice: epidemiology of autoimmune liver diseases. *Gut* 2021; **70**: 1989-2003 [PMID: 34266966 DOI: 10.1136/gutjnl-2020-322362]
20 **Guo L**, Zhou L, Zhang N, Deng B, Wang B. Extrahepatic Autoimmune Diseases in Patients with Autoimmune Liver Diseases: A Phenomenon Neglected by Gastroenterologists. *Gastroenterol Res Pract* 2017; **2017**: 2376231 [PMID: 28191014 DOI: 10.1155/2017/2376231]
21 **Selmi C**, Generali E, Gershwin ME. Rheumatic Manifestations in Autoimmune Liver Disease. *Rheum Dis Clin North Am* 2018; **44**: 65-87 [PMID: 29149928 DOI: 10.1016/j.rdc.2017.09.008]
22 **Selmi C**, Meroni PL, Gershwin ME. Primary biliary cirrhosis and Sjögren's syndrome: autoimmune epithelitis. *J Autoimmun* 2012; **39**: 34-42 [PMID: 22178199 DOI: 10.1016/j.jaut.2011.11.005]
23 **Parisis D**, Chivasso C, Perret J, Soyfoo MS, Delporte C. Current State of Knowledge on Primary Sjögren's Syndrome, an Autoimmune Exocrinopathy. *J Clin Med* 2020; **9** [PMID: 32698400 DOI: 10.3390/jcm9072299]
24 **Sirotti S**, Generali E, Ceribelli A, Isailovic N, De Santis M, Selmi C. Personalized medicine in rheumatology: the paradigm of serum autoantibodies. *Auto Immun Highlights* 2017; **8**: 10 [PMID: 28702930 DOI: 10.1007/s13317-017-0098-1]
25 **Tsokos GC**. Systemic lupus erythematosus. *N Engl J Med* 2011; **365**: 2110-2121 [PMID: 22129255 DOI: 10.1056/NEJMra1100359]
26 **Runyon BA**, LaBrecque DR, Anuras S. The spectrum of liver disease in systemic lupus erythematosus. Report of 33 histologically-proved cases and review of the literature. *Am J Med* 1980; **69**: 187-194 [PMID: 7405944 DOI: 10.1016/0002-9343(80)90378-2]
27 **Ebert EC**, Hagspiel KD. Gastrointestinal and hepatic manifestations of systemic lupus erythematosus. *J Clin Gastroenterol* 2011; **45**: 436-441 [PMID: 21422947 DOI: 10.1097/MCG.0b013e31820f81b8]
28 **González-Regueiro JA**, Cruz-Contreras M, Merayo-Chalico J, Barrera-Vargas A, Ruiz-Margáin A, Campos-Murguía A, Espin-Nasser M, Martínez-Benítez B, Méndez-Cano VH, Macías-Rodríguez RU. Hepatic manifestations in systemic lupus erythematosus. *Lupus* 2020; **29**: 813-824 [PMID: 32390496 DOI: 10.1177/0961203320923398]
29 **Mackay IR**, Taft LI, Cowling DC. Lupoid hepatitis and the hepatic lesions of systemic lupus erythematosus. *Lancet* 1959; **1**: 65-69 [PMID: 13621639 DOI: 10.1016/s0140-6736(59)91136-5]
30 **Adiga A**, Nugent K. Lupus Hepatitis and Autoimmune Hepatitis (Lupoid Hepatitis). *Am J Med Sci* 2017; **353**: 329-335 [PMID: 28317620 DOI: 10.1016/j.amjms.2016.10.014]
31 **Piga M**, Vacca A, Porru G, Cauli A, Mathieu A. Liver involvement in systemic lupus erythematosus: incidence, clinical course and outcome of lupus hepatitis. *Clin Exp Rheumatol* 2010; **28**: 504-510 [PMID: 20609296 DOI: 10.1186/1471-2474-11-143]
32 **Zheng RH**, Wang JH, Wang SB, Chen J, Guan WM, Chen MH. Clinical and immunopathological features of patients with lupus hepatitis. *Chin Med J (Engl)* 2013; **126**: 260-266 [PMID: 23324274]
33 **Ohira H**, Takiguchi J, Rai T, Abe K, Yokokawa J, Sato Y, Takeda I, Kanno T. High frequency of anti-ribosomal P antibody in patients with systemic lupus erythematosus-associated hepatitis. *Hepatol Res* 2004; **28**: 137-139 [PMID:

15036069 DOI: 10.1016/j.hepres.2003.11.008]
34 **Afzal W**, Haghi M, Hasni SA, Newman KA. Lupus hepatitis, more than just elevated liver enzymes. *Scand J Rheumatol* 2020; **49**: 427-433 [PMID: 32942921 DOI: 10.1080/03009742.2020.1744712]
35 **Horizon AA**, Wallace DJ. Risk:benefit ratio of nonsteroidal anti-inflammatory drugs in systemic lupus erythematosus. *Expert Opin Drug Saf* 2004; **3**: 273-278 [PMID: 15268645 DOI: 10.1517/14740338.3.4.273]
36 **Tanaka N**, Kimura T, Fujimori N, Nagaya T, Komatsu M, Tanaka E. Current status, problems, and perspectives of non-alcoholic fatty liver disease research. *World J Gastroenterol* 2019; **25**: 163-177 [PMID: 30670907 DOI: 10.3748/wjg.v25.i2.163]
37 **Chung CP**, Avalos I, Oeser A, Gebretsadik T, Shintani A, Raggi P, Stein CM. High prevalence of the metabolic syndrome in patients with systemic lupus erythematosus: association with disease characteristics and cardiovascular risk factors. *Ann Rheum Dis* 2007; **66**: 208-214 [PMID: 16901956 DOI: 10.1136/ard.2006.054973]
38 **Wang CR**, Tsai HW. Anti- and non-tumor necrosis factor-α-targeted therapies effects on insulin resistance in rheumatoid arthritis, psoriatic arthritis and ankylosing spondylitis. *World J Diabetes* 2021; **12**: 238-260 [PMID: 33758645 DOI: 10.4239/wjd.v12.i3.238]
39 **Chowdhary VR**, Crowson CS, Poterucha JJ, Moder KG. Liver involvement in systemic lupus erythematosus: case review of 40 patients. *J Rheumatol* 2008; **35**: 2159-2164 [PMID: 18793002 DOI: 10.3899/jrheum.080336]
40 **Ruiz-Irastorza G**, Crowther M, Branch W, Khamashta MA. Antiphospholipid syndrome. *Lancet* 2010; **376**: 1498-1509 [PMID: 20822807 DOI: 10.1016/S0140-6736(10)60709-X]
41 **Uthman I**, Khamashta M. The abdominal manifestations of the antiphospholipid syndrome. *Rheumatology (Oxford)* 2007; **46**: 1641-1647 [PMID: 17636180 DOI: 10.1093/rheumatology/kem158]
42 **Guiu B**, Loffroy R, Cercueil JP, Sagot P, Krausé D, Tixier H. MRI diagnosis and follow-up of hepatic infarction in a patient with antiphospholipid syndrome in early pregnancy. *Arch Gynecol Obstet* 2011; **283**: 659-662 [PMID: 20411270 DOI: 10.1007/s00404-010-1467-4]
43 **Aydinli M**, Bayraktar Y. Budd-Chiari syndrome: etiology, pathogenesis and diagnosis. *World J Gastroenterol* 2007; **13**: 2693-2696 [PMID: 17569137 DOI: 10.3748/wjg.v13.i19.2693]
44 **Pandiaraja J**, Sathyaseelan A. Budd- Chiari Syndrome as an Initial Manifestation of Systemic Lupus Erythematosus. *J Clin Diagn Res* 2016; **10**: OD01-OD02 [PMID: 27190864 DOI: 10.7860/JCDR/2016/16623.7532]
45 **Hartleb M**, Gutkowski K, Milkiewicz P. Nodular regenerative hyperplasia: evolving concepts on underdiagnosed cause of portal hypertension. *World J Gastroenterol* 2011; **17**: 1400-1409 [PMID: 21472097 DOI: 10.3748/wjg.v17.i11.1400]
46 **Branger S**, Schleinitz N, Veit V, Martaresche C, Bourlière M, Roblin X, Garcia S, San Marco M, Camoin L, Durand JM, Harlé JR. [Auto-immune hepatitis and antiphospholipids]. *Rev Med Interne* 2007; **28**: 218-224 [PMID: 17331625 DOI: 10.1016/j.revmed.2006.12.005]
47 **Alves SC**, Fasano S, Isenberg DA. Autoimmune gastrointestinal complications in patients with systemic lupus erythematosus: case series and literature review. *Lupus* 2016; **25**: 1509-1519 [PMID: 27329649 DOI: 10.1177/0961203316655210]
48 **Bessone F**, Poles N, Roma MG. Challenge of liver disease in systemic lupus erythematosus: Clues for diagnosis and hints for pathogenesis. *World J Hepatol* 2014; **6**: 394-409 [PMID: 25018850 DOI: 10.4254/wjh.v6.i6.394]
49 **Ali AH**, Carey EJ, Lindor KD. The management of autoimmunity in patients with cholestatic liver diseases. *Expert Rev Gastroenterol Hepatol* 2016; **10**: 73-91 [PMID: 26523975 DOI: 10.1586/17474124.2016.1095088]
50 **Heneghan MA**, Yeoman AD, Verma S, Smith AD, Longhi MS. Autoimmune hepatitis. *Lancet* 2013; **382**: 1433-1444 [PMID: 23768844 DOI: 10.1016/S0140-6736(12)62163-1]
51 **Wiegard C**, Schramm C, Lohse AW. Scoring systems for the diagnosis of autoimmune hepatitis: past, present, and future. *Semin Liver Dis* 2009; **29**: 254-261 [PMID: 19675998 DOI: 10.1055/s-0029-1233532]
52 **Hochberg MC**. Updating the American College of Rheumatology revised criteria for the classification of systemic lupus erythematosus. *Arthritis Rheum* 1997; **40**: 1725 [PMID: 9324032 DOI: 10.1002/art.1780400928]
53 **Matsumoto T**, Kobayashi S, Shimizu H, Nakajima M, Watanabe S, Kitami N, Sato N, Abe H, Aoki Y, Hoshi T, Hashimoto H. The liver in collagen diseases: pathologic study of 160 cases with particular reference to hepatic arteritis, primary biliary cirrhosis, autoimmune hepatitis and nodular regenerative hyperplasia of the liver. *Liver* 2000; **20**: 366-373 [PMID: 11092254 DOI: 10.1034/j.1600-0676.2000.020005366.x]
54 **Efe C**, Purnak T, Ozaslan E, Ozbalkan Z, Karaaslan Y, Altiparmak E, Muratori P, Wahlin S. Autoimmune liver disease in patients with systemic lupus erythematosus: a retrospective analysis of 147 cases. *Scand J Gastroenterol* 2011; **46**: 732-737 [PMID: 21348808 DOI: 10.3109/00365521.2011.558114]
55 **Takahashi A**, Abe K, Saito R, Iwadate H, Okai K, Katsushima F, Monoe K, Kanno Y, Saito H, Kobayashi H, Watanabe H, Ohira H. Liver dysfunction in patients with systemic lupus erythematosus. *Intern Med* 2013; **52**: 1461-1465 [PMID: 23812192 DOI: 10.2169/internalmedicine.52.9458]
56 **Oka H**. The survey of autoimmune hepatitis in Japan. In: Annual Report of the Study Group on Severe Hepatitis. Tokyo: Japanese Ministry of Health and Welfare, 1988: 235-241
57 **Heijke R**, Ahmad A, Frodlund M, Wirestam L, Dahlström Ö, Dahle C, Kechagias S, Sjöwall C. Usefulness of Clinical and Laboratory Criteria for Diagnosing Autoimmune Liver Disease among Patients with Systemic Lupus Erythematosus: An Observational Study. *J Clin Med* 2021; **10** [PMID: 34501268 DOI: 10.3390/jcm10173820]
58 **Tamai Y**, Ito K, Kin F, Fukase M. American rheumatism association (ARA) preliminary criteria for the classification of systemic lupus erythematosus and autoimmune hepatitis. *Rheumachi* 1974; **14**: 88-94
59 **Barthel HR**, Wallace DJ, Klinenberg JR. Liver transplantation in patients with systemic lupus erythematosus. *Lupus* 1995; **4**: 15-17 [PMID: 7767333 DOI: 10.1177/096120339500400104]
60 **Wang CR**, Wu IC, Tsai HW. An overlap syndrome involving systemic lupus erythematosus and autoimmune hepatitis in a patient receiving a living-donor liver transplantation. *Lupus* 2020; **29**: 96-97 [PMID: 31830423 DOI: 10.1177/0961203319894381]
61 **Lleo A**, Wang GQ, Gershwin ME, Hirschfield GM. Primary biliary cholangitis. *Lancet* 2020; **396**: 1915-1926 [PMID: 33308474 DOI: 10.1016/S0140-6736(20)31607-X]

62 **Lindor KD**, Bowlus CL, Boyer J, Levy C, Mayo M. Primary Biliary Cholangitis: 2018 Practice Guidance from the American Association for the Study of Liver Diseases. *Hepatology* 2019; **69**: 394-419 [PMID: 30070375 DOI: 10.1002/hep.30145]

63 **Beuers U**, Gershwin ME, Gish RG, Invernizzi P, Jones DE, Lindor K, Ma X, Mackay IR, Parés A, Tanaka A, Vierling JM, Poupon R. Changing nomenclature for PBC: From 'cirrhosis' to 'cholangitis'. *J Hepatol* 2015; **63**: 1285-1287 [PMID: 26385765 DOI: 10.1016/j.jhep.2015.06.031]

64 **Floreani A**, Tanaka A, Bowlus C, Gershwin ME. Geoepidemiology and changing mortality in primary biliary cholangitis. *J Gastroenterol* 2017; **52**: 655-662 [PMID: 28365879 DOI: 10.1007/s00535-017-1333-2]

65 **Kottyan LC**, Zoller EE, Bene J, Lu X, Kelly JA, Rupert AM, Lessard CJ, Vaughn SE, Marion M, Weirauch MT, Namjou B, Adler A, Rasmussen A, Glenn S, Montgomery CG, Hirschfield GM, Xie G, Coltescu C, Amos C, Li H, Ice JA, Nath SK, Mariette X, Bowman S; UK Primary Sjögren's Syndrome Registry, Rischmueller M, Lester S, Brun JG, Gøransson LG, Harboe E, Omdal R, Cunninghame-Graham DS, Vyse T, Miceli-Richard C, Brennan MT, Lessard JA, Wahren-Herlenius M, Kvarnström M, Illei GG, Witte T, Jonsson R, Eriksson P, Nordmark G, Ng WF; UK Primary Sjögren's Syndrome Registry, Anaya JM, Rhodus NL, Segal BM, Merrill JT, James JA, Guthridge JM, Scofield RH, Alarcon-Riquelme M, Bae SC, Boackle SA, Criswell LA, Gilkeson G, Kamen DL, Jacob CO, Kimberly R, Brown E, Edberg J, Alarcón GS, Reveille JD, Vilá LM, Petri M, Ramsey-Goldman R, Freedman BI, Niewold T, Stevens AM, Tsao BP, Ying J, Mayes MD, Gorlova OY, Wakeland W, Radstake T, Martin E, Martin J, Siminovitch K, Moser Sivils KL, Gaffney PM, Langefeld CD, Harley JB, Kaufman KM. The IRF5-TNPO3 association with systemic lupus erythematosus has two components that other autoimmune disorders variably share. *Hum Mol Genet* 2015; **24**: 582-596 [PMID: 25205108 DOI: 10.1093/hmg/ddu455]

66 **Shizuma T**. Clinical Characteristics of Concomitant Systemic Lupus Erythematosus and Primary Biliary Cirrhosis: A Literature Review. *J Immunol Res* 2015; **2015**: 713728 [PMID: 26090497 DOI: 10.1155/2015/713728]

67 **Boberg KM**, Chapman RW, Hirschfield GM, Lohse AW, Manns MP, Schrumpf E; International Autoimmune Hepatitis Group. Overlap syndromes: the International Autoimmune Hepatitis Group (IAIHG) position statement on a controversial issue. *J Hepatol* 2011; **54**: 374-385 [PMID: 21067838 DOI: 10.1016/j.jhep.2010.09.002]

68 **Chazouillères O**, Wendum D, Serfaty L, Montembault S, Rosmorduc O, Poupon R. Primary biliary cirrhosis-autoimmune hepatitis overlap syndrome: clinical features and response to therapy. *Hepatology* 1998; **28**: 296-301 [PMID: 9695990 DOI: 10.1002/hep.510280203]

69 **To U**, Silveira M. Overlap Syndrome of Autoimmune Hepatitis and Primary Biliary Cholangitis. *Clin Liver Dis* 2018; **22**: 603-611 [PMID: 30259856 DOI: 10.1016/j.cld.2018.03.010]

70 **González LA**, Orrego M, Ramírez LA, Vásquez G. Primary biliary cirrhosis/autoimmune hepatitis overlap syndrome developing in a patient with systemic lupus erythematosus: a case report and review of the literature. *Lupus* 2011; **20**: 108-111 [PMID: 20724352 DOI: 10.1177/0961203310378673]

71 **Efe C**, Wahlin S, Ozaslan E, Berlot AH, Purnak T, Muratori L, Quarneti C, Yüksel O, Thiéfin G, Muratori P. Autoimmune hepatitis/primary biliary cirrhosis overlap syndrome and associated extrahepatic autoimmune diseases. *Eur J Gastroenterol Hepatol* 2012; **24**: 531-534 [PMID: 22465972 DOI: 10.1097/MEG.0b013e328350f95b]

72 **Tanaka A**, Ma X, Yokosuka O, Weltman M, You H, Amarapurkar DN, Kim YJ, Abbas Z, Payawal DA, Chang ML, Efe C, Ozaslan E, Abe M, Mitchell-Thain R, Zeniya M, Han KH, Vierling JM, Takikawa H. Autoimmune liver diseases in the Asia-Pacific region: Proceedings of APASL symposium on AIH and PBC 2016. *Hepatol Int* 2016; **10**: 909-915 [PMID: 27649967 DOI: 10.1007/s12072-016-9767-9]

73 **Lin CL**, Kao JH. Perspectives and control of hepatitis B virus infection in Taiwan. *J Formos Med Assoc* 2015; **114**: 901-909 [PMID: 26184565 DOI: 10.1016/j.jfma.2015.06.003]

74 **Koay LB**, Lin CY, Tsai SL, Lee C, Lin CN, Sheu MJ, Kuo HT, Sun CS. Type 1 autoimmune hepatitis in Taiwan: diagnosis using the revised criteria of the International Autoimmune Hepatitis Group. *Dig Dis Sci* 2006; **51**: 1978-1984 [PMID: 17053960 DOI: 10.1007/s10620-005-9068-y]

75 **Lazaridis KN**, LaRusso NF. Primary Sclerosing Cholangitis. *N Engl J Med* 2016; **375**: 1161-1170 [PMID: 27653566 DOI: 10.1056/NEJMra1506330]

76 **Alberti-Flor JJ**, Jeffers L, Schiff ER. Primary sclerosing cholangitis occurring in a patient with systemic lupus erythematosus and diabetes mellitus. *Am J Gastroenterol* 1984; **79**: 889-891 [PMID: 6507412]

77 **Lamy P**, Valla D, Bourgeois P, Rueff B, Benhamou JP. [Primary sclerosing cholangitis and systemic lupus erythematosus]. *Gastroenterol Clin Biol* 1988; **12**: 962-964 [PMID: 3069553]

78 **Audan A**, Bruley Des Varannes S, Georgelin T, Sagan C, Cloarec D, Serraz H, Le Bodic L. [Primary sclerosing cholangitis and systemic lupus erythematosus]. *Gastroenterol Clin Biol* 1995; **19**: 123-126 [PMID: 7720973]

79 **Kadokawa Y**, Omagari K, Matsuo I, Otsu Y, Yamamoto U, Nishino T, Ohba K, Miyazaki M, Harada T, Taguchi T, Kohno S. Primary sclerosing cholangitis associated with lupus nephritis: a rare association. *Dig Dis Sci* 2003; **48**: 911-914 [PMID: 12772788 DOI: 10.1023/A:1023095428321]

80 **Oh DC**, Ng TM, Ho J, Leong KP. Systemic lupus erythematosus with concurrent protein-losing enteropathy and primary sclerosing cholangitis: a unique association. *Lupus* 2006; **15**: 102-104 [PMID: 16539281 DOI: 10.1191/0961203306lu2251cr]

81 **Saarinen S**, Olerup O, Broomé U. Increased frequency of autoimmune diseases in patients with primary sclerosing cholangitis. *Am J Gastroenterol* 2000; **95**: 3195-3199 [PMID: 11095341 DOI: 10.1111/j.1572-0241.2000.03292.x]

82 **Mariette X**, Criswell LA. Primary Sjögren's Syndrome. *N Engl J Med* 2018; **378**: 931-939 [PMID: 29514034 DOI: 10.1056/NEJMcp1702514]

83 **Kaplan MJ**, Ike RW. The liver is a common non-exocrine target in primary Sjögren's syndrome: a retrospective review. *BMC Gastroenterol* 2002; **2**: 21 [PMID: 12230633 DOI: 10.1186/1471-230x-2-21]

84 **Ramos-Casals M**, Sánchez-Tapias JM, Parés A, Forns X, Brito-Zerón P, Nardi N, Vazquez P, Vélez D, Arias I, Bové A, Plaza J, Rodés J, Font J. Characterization and differentiation of autoimmune *vs* viral liver involvement in patients with Sjögren's syndrome. *J Rheumatol* 2006; **33**: 1593-1599 [PMID: 16881116 DOI: 10.1016/0022-4731(78)90121-8]

85 **Lindgren S**, Manthorpe R, Eriksson S. Autoimmune liver disease in patients with primary Sjögren's syndrome. *J Hepatol*

1994; **20**: 354-358 [PMID: 8014446 DOI: 10.1016/s0168-8278(94)80007-3]
86 **Hatzis GS**, Fragoulis GE, Karatzaferis A, Delladetsima I, Barbatis C, Moutsopoulos HM. Prevalence and longterm course of primary biliary cirrhosis in primary Sjögren's syndrome. *J Rheumatol* 2008; **35**: 2012-2016 [PMID: 18709690 DOI: 10.2514/6.2006-5424]
87 **Amador-Patarroyo MJ**, Arbelaez JG, Mantilla RD, Rodriguez-Rodriguez A, Cárdenas-Roldán J, Pineda-Tamayo R, Guarin MR, Kleine LL, Rojas-Villarraga A, Anaya JM. Sjögren's syndrome at the crossroad of polyautoimmunity. *J Autoimmun* 2012; **39**: 199-205 [PMID: 22749530 DOI: 10.1016/j.jaut.2012.05.008]
88 **Floreani A**, Cazzagon N. PBC and related extrahepatic diseases. *Best Pract Res Clin Gastroenterol* 2018; **34-35**: 49-54 [PMID: 30343710 DOI: 10.1016/j.bpg.2018.05.013]
89 **Tsianos EV**, Hoofnagle JH, Fox PC, Alspaugh M, Jones EA, Schafer DF, Moutsopoulos HM. Sjögren's syndrome in patients with primary biliary cirrhosis. *Hepatology* 1990; **11**: 730-734 [PMID: 2347546 DOI: 10.1002/hep.1840110504]
90 **Marasini B**, Gagetta M, Rossi V, Ferrari P. Rheumatic disorders and primary biliary cirrhosis: an appraisal of 170 Italian patients. *Ann Rheum Dis* 2001; **60**: 1046-1049 [PMID: 11602476 DOI: 10.1136/ard.60.11.1046]
91 **Watt FE**, James OF, Jones DE. Patterns of autoimmunity in primary biliary cirrhosis patients and their families: a population-based cohort study. *QJM* 2004; **97**: 397-406 [PMID: 15208427 DOI: 10.1093/qjmed/hch078]
92 **Gershwin ME**, Selmi C, Worman HJ, Gold EB, Watnik M, Utts J, Lindor KD, Kaplan MM, Vierling JM; USA PBC Epidemiology Group. Risk factors and comorbidities in primary biliary cirrhosis: a controlled interview-based study of 1032 patients. *Hepatology* 2005; **42**: 1194-1202 [PMID: 16250040 DOI: 10.1002/hep.20907]
93 **Wang L**, Zhang FC, Chen H, Zhang X, Xu D, Li YZ, Wang Q, Gao LX, Yang YJ, Kong F, Wang K. Connective tissue diseases in primary biliary cirrhosis: a population-based cohort study. *World J Gastroenterol* 2013; **19**: 5131-5137 [PMID: 23964148 DOI: 10.3748/wjg.v19.i31.5131]
94 **Floreani A**, Franceschet I, Cazzagon N, Spinazzè A, Buja A, Furlan P, Baldo V, Gershwin ME. Extrahepatic autoimmune conditions associated with primary biliary cirrhosis. *Clin Rev Allergy Immunol* 2015; **48**: 192-197 [PMID: 24809534 DOI: 10.1007/s12016-014-8427-x]
95 **Selmi C**, Gershwin ME. Chronic Autoimmune Epithelitis in Sjögren's Syndrome and Primary Biliary Cholangitis: A Comprehensive Review. *Rheumatol Ther* 2017; **4**: 263-279 [PMID: 28791611 DOI: 10.1007/s40744-017-0074-2]
96 **Bournia VK**, Vlachoyiannopoulos PG. Subgroups of Sjögren syndrome patients according to serological profiles. *J Autoimmun* 2012; **39**: 15-26 [PMID: 22575069 DOI: 10.1016/j.jaut.2012.03.001]
97 **Takahashi A**, Abe K, Yokokawa J, Iwadate H, Kobayashi H, Watanabe H, Irisawa A, Ohira H. Clinical features of liver dysfunction in collagen diseases. *Hepatol Res* 2010; **40**: 1092-1097 [PMID: 20880057 DOI: 10.1111/j.1872-034X.2010.00707.x]
98 **Czaja AJ**, Carpenter HA, Santrach PJ, Moore SB. Genetic predispositions for the immunological features of chronic active hepatitis. *Hepatology* 1993; **18**: 816-822 [PMID: 8406354 DOI: 10.1002/hep.1840180411]
99 **Werner M**, Prytz H, Ohlsson B, Almer S, Björnsson E, Bergquist A, Wallerstedt S, Sandberg-Gertzén H, Hultcrantz R, Sangfelt P, Weiland O, Danielsson A. Epidemiology and the initial presentation of autoimmune hepatitis in Sweden: a nationwide study. *Scand J Gastroenterol* 2008; **43**: 1232-1240 [PMID: 18609163 DOI: 10.1080/00365520802130183]
100 **Teufel A**, Weinmann A, Kahaly GJ, Centner C, Piendl A, Wörns M, Lohse AW, Galle PR, Kanzler S. Concurrent autoimmune diseases in patients with autoimmune hepatitis. *J Clin Gastroenterol* 2010; **44**: 208-213 [PMID: 20087196 DOI: 10.1097/MCG.0b013e3181c74e0d]
101 **Abe M**, Mashiba T, Zeniya M, Yamamoto K, Onji M, Tsubouchi H; Autoimmune Hepatitis Study Group-Subgroup of the Intractable Hepato-Biliary Disease Study Group in Japan. Present status of autoimmune hepatitis in Japan: a nationwide survey. *J Gastroenterol* 2011; **46**: 1136-1141 [PMID: 21597932 DOI: 10.1007/s00535-011-0421-y]
102 **Wong GW**, Yeong T, Lawrence D, Yeoman AD, Verma S, Heneghan MA. Concurrent extrahepatic autoimmunity in autoimmune hepatitis: implications for diagnosis, clinical course and long-term outcomes. *Liver Int* 2017; **37**: 449-457 [PMID: 27541063 DOI: 10.1111/liv.13236]
103 **Montefusco PP**, Geiss AC, Bronzo RL, Randall S, Kahn E, McKinley MJ. Sclerosing cholangitis, chronic pancreatitis, and Sjogren's syndrome: a syndrome complex. *Am J Surg* 1984; **147**: 822-826 [PMID: 6731702 DOI: 10.1016/0002-9610(84)90212-5]
104 **Zeron PB**, Retamozo S, Bové A, Kostov BA, Sisó A, Ramos-Casals M. Diagnosis of Liver Involvement in Primary Sjögren Syndrome. *J Clin Transl Hepatol* 2013; **1**: 94-102 [PMID: 26355632 DOI: 10.14218/JCTH.2013.00011]
105 **Denton CP**, Khanna D. Systemic sclerosis. *Lancet* 2017; **390**: 1685-1699 [PMID: 28413064 DOI: 10.1016/S0140-6736(17)30933-9]
106 **Forbes A**, Marie I. Gastrointestinal complications: the most frequent internal complications of systemic sclerosis. *Rheumatology (Oxford)* 2009; **48** Suppl 3: iii36-iii39 [PMID: 19487222 DOI: 10.1093/rheumatology/ken485]
107 **D'Angelo WA**, Fries JF, Masi AT, Shulman LE. Pathologic observations in systemic sclerosis (scleroderma). A study of fifty-eight autopsy cases and fifty-eight matched controls. *Am J Med* 1969; **46**: 428-440 [PMID: 5780367 DOI: 10.1016/0002-9343(69)90044-8]
108 **Hudson M**, Rojas-Villarraga A, Coral-Alvarado P, López-Guzmán S, Mantilla RD, Chalem P; Canadian Scleroderma Research Group; Colombian Scleroderma Research Group, Baron M, Anaya JM. Polyautoimmunity and familial autoimmunity in systemic sclerosis. *J Autoimmun* 2008; **31**: 156-159 [PMID: 18644698 DOI: 10.1016/j.jaut.2008.05.002]
109 **Abu-Shakra M**, Guillemin F, Lee P. Gastrointestinal manifestations of systemic sclerosis. *Semin Arthritis Rheum* 1994; **24**: 29-39 [PMID: 7985035 DOI: 10.1016/0049-0172(94)90097-3]
110 **Pope JE**, Thompson A. Antimitochondrial antibodies and their significance in diffuse and limited scleroderma. *J Clin Rheumatol* 1999; **5**: 206-209 [PMID: 19078387 DOI: 10.1097/00124743-199908000-00005]
111 **Rigamonti C**, Shand LM, Feudjo M, Bunn CC, Black CM, Denton CP, Burroughs AK. Clinical features and prognosis of primary biliary cirrhosis associated with systemic sclerosis. *Gut* 2006; **55**: 388-394 [PMID: 16150855 DOI: 10.1136/gut.2005.075002]
112 **Assassi S**, Fritzler MJ, Arnett FC, Norman GL, Shah KR, Gourh P, Manek N, Perry M, Ganesh D, Rahbar MH, Mayes MD. Primary biliary cirrhosis (PBC), PBC autoantibodies, and hepatic parameter abnormalities in a large population of

systemic sclerosis patients. *J Rheumatol* 2009; **36**: 2250-2256 [PMID: 19723904 DOI: 10.3899/jrheum.090340]
113 **Liberal R**, Grant CR, Sakkas L, Bizzaro N, Bogdanos DP. Diagnostic and clinical significance of anti-centromere antibodies in primary biliary cirrhosis. *Clin Res Hepatol Gastroenterol* 2013; **37**: 572-585 [PMID: 23876351 DOI: 10.1016/j.clinre.2013.04.005]
114 **McFarlane IM**, Bhamra MS, Kreps A, Iqbal S, Al-Ani F, Saladini-Aponte C, Grant C, Singh S, Awwal K, Koci K, Saperstein Y, Arroyo-Mercado FM, Laskar DB, Atluri P. Gastrointestinal Manifestations of Systemic Sclerosis. *Rheumatology (Sunnyvale)* 2018; **8** [PMID: 30057856 DOI: 10.4172/2161-1149.1000235]
115 **Göring HD**, Panzner M, Lakotta W, Ziemer A. [Coincidence of scleroderma and primary biliary cirrhosis. Results of a systematic study of a dermatologic patient sample]. *Hautarzt* 1998; **49**: 361-366 [PMID: 9642556 DOI: 10.1007/s001050050756]
116 **You BC**, Jeong SW, Jang JY, Goo SM, Kim SG, Kim YS, Jeon CH, Jeen YM. Liver cirrhosis due to autoimmune hepatitis combined with systemic sclerosis. *Korean J Gastroenterol* 2012; **59**: 48-52 [PMID: 22289955 DOI: 10.4166/kjg.2012.59.1.48]
117 **Assandri R**, Monari M, Montanelli A. Development of systemic sclerosis in patients with autoimmune hepatitis: an emerging overlap syndrome. *Gastroenterol Hepatol Bed Bench* 2016; **9**: 211-219 [PMID: 27458514]
118 **Fraile G**, Rodríguez-García JL, Moreno A. Primary sclerosing cholangitis associated with systemic sclerosis. *Postgrad Med J* 1991; **67**: 189-192 [PMID: 2041852 DOI: 10.1136/pgmj.67.784.189]
119 **Zampetti A**, Rinninella E, Manna R, Franceschi F. Scleroderma and liver disease: a case of an association with primary sclerosing cholangitis. *Scand J Rheumatol* 2016; **45**: 334-335 [PMID: 26690847 DOI: 10.3109/03009742.2015.1114667]
120 **Savarino E**, Furnari M, de Bortoli N, Martinucci I, Bodini G, Ghio M, Savarino V. Gastrointestinal involvement in systemic sclerosis. *Presse Med* 2014; **43**: e279-e291 [PMID: 25179275 DOI: 10.1016/j.lpm.2014.03.029]
121 **Smolen JS**, Aletaha D, McInnes IB. Rheumatoid arthritis. *Lancet* 2016; **388**: 2023-2038 [PMID: 27156434 DOI: 10.1016/S0140-6736(16)30173-8]
122 **Selmi C**, De Santis M, Gershwin ME. Liver involvement in subjects with rheumatic disease. *Arthritis Res Ther* 2011; **13**: 226 [PMID: 21722332 DOI: 10.1186/ar3319]
123 **Radovanović-Dinić B**, Tešić-Rajković S, Zivkovic V, Grgov S. Clinical connection between rheumatoid arthritis and liver damage. *Rheumatol Int* 2018; **38**: 715-724 [PMID: 29627896 DOI: 10.1007/s00296-018-4021-5]
124 **Ruderman EM**, Crawford JM, Maier A, Liu JJ, Gravallese EM, Weinblatt ME. Histologic liver abnormalities in an autopsy series of patients with rheumatoid arthritis. *Br J Rheumatol* 1997; **36**: 210-213 [PMID: 9133932 DOI: 10.1093/rheumatology/36.2.210]
125 **Hocking WG**, Lasser K, Ungerer R, Bersohn M, Palos M, Spiegel T. Spontaneous hepatic rupture in rheumatoid arthritis. *Arch Intern Med* 1981; **141**: 792-794 [PMID: 7235790 DOI: 10.1001/archinte.1981.00340060100023]
126 **Thorne C**, Urowitz MB, Wanless I, Roberts E, Blendis LM. Liver disease in Felty's syndrome. *Am J Med* 1982; **73**: 35-40 [PMID: 7091172 DOI: 10.1016/0002-9343(82)90921-4]
127 **Yılmaz N**, Karadağ Ö, Kimyon G, Yazıcı A, Yılmaz S, Kalyoncu U, Kaşifoğlu T, Temiz H, Baysal B, Tözün N. Prevalence of hepatitis B and C infections in rheumatoid arthritis and ankylosing spondylitis: A multicenter countrywide study. *Eur J Rheumatol* 2014; **1**: 51-54 [PMID: 27708874 DOI: 10.5152/eurjrheumatol.2014.018]
128 **Mori S**, Fujiyama S. Hepatitis B virus reactivation associated with antirheumatic therapy: Risk and prophylaxis recommendations. *World J Gastroenterol* 2015; **21**: 10274-10289 [PMID: 26420955 DOI: 10.3748/wjg.v21.i36.10274]
129 **Pauly MP**, Tucker LY, Szpakowski JL, Ready JB, Baer D, Hwang J, Lok AS. Incidence of Hepatitis B Virus Reactivation and Hepatotoxicity in Patients Receiving Long-term Treatment With Tumor Necrosis Factor Antagonists. *Clin Gastroenterol Hepatol* 2018; **16**: 1964-1973.e1 [PMID: 29702293 DOI: 10.1016/j.cgh.2018.04.033]
130 **Brunasso AM**, Puntoni M, Gulia A, Massone C. Safety of anti-tumour necrosis factor agents in patients with chronic hepatitis C infection: a systematic review. *Rheumatology (Oxford)* 2011; **50**: 1700-1711 [PMID: 21690185 DOI: 10.1093/rheumatology/ker190]
131 **Viganò M**, Degasperi E, Aghemo A, Lampertico P, Colombo M. Anti-TNF drugs in patients with hepatitis B or C virus infection: safety and clinical management. *Expert Opin Biol Ther* 2012; **12**: 193-207 [PMID: 22188392 DOI: 10.1517/14712598.2012.646986]
132 **Ramos-Casals M**, Brito-Zerón P, Soto MJ, Cuadrado MJ, Khamashta MA. Autoimmune diseases induced by TNF-targeted therapies. *Best Pract Res Clin Rheumatol* 2008; **22**: 847-861 [PMID: 19028367 DOI: 10.1016/j.berh.2008.09.008]
133 **Sherlock S**, Scheuer PJ. The presentation and diagnosis of 100 patients with primary biliary cirrhosis. *N Engl J Med* 1973; **289**: 674-678 [PMID: 4580473 DOI: 10.1056/NEJM197309272891306]
134 **Siegel JL**, Luthra H, Donlinger J, Angulo P, Lindor K. Association of primary biliary cirrhosis and rheumatoid arthritis. *J Clin Rheumatol* 2003; **9**: 340-343 [PMID: 17043441 DOI: 10.1097/01.rhu.0000099623.30805.2f]
135 **Smyk DS**, Bogdanos DP, Mytilinaiou MG, Burroughs AK, Rigopoulou EI. Rheumatoid arthritis and primary biliary cirrhosis: cause, consequence, or coincidence? *Arthritis* 2012; **2012**: 391567 [PMID: 23150824 DOI: 10.1155/2012/391567]
136 **Toulemonde G**, Scoazec JY, Miossec P. Treatment with etanercept of autoimmune hepatitis associated with rheumatoid arthritis: an open label proof of concept study. *Ann Rheum Dis* 2012; **71**: 1423-1424 [PMID: 22402143 DOI: 10.1136/annrheumdis-2011-200830]
137 **Perez-Alvarez R**, Pérez-de-Lis M, Ramos-Casals M; BIOGEAS study group. Biologics-induced autoimmune diseases. *Curr Opin Rheumatol* 2013; **25**: 56-64 [PMID: 23114587 DOI: 10.1097/BOR.0b013e32835b1366]
138 **Vollmer O**, Felten R, Mertz P, Lebrun-Vignes B, Salem JE, Arnaud L. Characterization of auto-immune hepatitis associated with the use of anti-TNFα agents: An analysis of 389 cases in VigiBase. *Autoimmun Rev* 2020; **19**: 102460 [PMID: 31917266 DOI: 10.1016/j.autrev.2020.102460]
139 **Lamberts LE**, Janse M, Haagsma EB, van den Berg AP, Weersma RK. Immune-mediated diseases in primary sclerosing cholangitis. *Dig Liver Dis* 2011; **43**: 802-806 [PMID: 21700515 DOI: 10.1016/j.dld.2011.05.009]
140 **Gow PJ**, Fleming KA, Chapman RW. Primary sclerosing cholangitis associated with rheumatoid arthritis and HLA DR4:

is the association a marker of patients with progressive liver disease? *J Hepatol* 2001; **34**: 631-635 [PMID: 11394667 DOI: 10.1016/s0168-8278(00)00060-x]

141 **Ogdie A**, Schwartzman S, Eder L, Maharaj AB, Zisman D, Raychaudhuri SP, Reddy SM, Husni E. Comprehensive treatment of psoriatic arthritis: managing comorbidities and extraarticular manifestations. *J Rheumatol* 2014; **41**: 2315-2322 [PMID: 25362717 DOI: 10.3899/jrheum.140882]

142 **Yousaf A**, Raiker R, Davis SM, Gayam S, Zinn Z. Association between psoriasis, psoriatic arthritis and gastrointestinal disease : An exploratory nationwide inpatient sample analysis. *Wien Klin Wochenschr* 2021; **133**: 586-593 [PMID: 32965553 DOI: 10.1007/s00508-020-01740-8]

143 **Dalakas MC**. Inflammatory muscle diseases. *N Engl J Med* 2015; **372**: 1734-1747 [PMID: 25923553 DOI: 10.1056/NEJMra1402225]

144 **Khan F**, Kleppel H, Meara A. Paraneoplastic Musculoskeletal Syndromes. *Rheum Dis Clin North Am* 2020; **46**: 577-586 [PMID: 32631605 DOI: 10.1016/j.rdc.2020.04.002]

145 **Chou JW**, Lin YL, Cheng KS, Wu PY, Reanne Ju T. Dermatomyositis Induced by Hepatitis B Virus-related Hepatocellular Carcinoma: A Case Report and Review of the Literature. *Intern Med* 2017; **56**: 1831-1837 [PMID: 28717078 DOI: 10.2169/internalmedicine.56.7595]

146 **Han J**, Wang S, Kwong TNY, Liu J. Dermatomyositis as an extrahepatic manifestation of hepatitis B virus-related hepatocellular carcinoma: A case report and literature review. *Medicine (Baltimore)* 2018; **97**: e11586 [PMID: 30113453 DOI: 10.1097/MD.0000000000011586]

147 **Dalakas MC**. Polymyositis, dermatomyositis and inclusion-body myositis. *N Engl J Med* 1991; **325**: 1487-1498 [PMID: 1658649 DOI: 10.1056/NEJM199111213252107]

148 **Zhang L**, Yang H, Lei J, Peng Q, Wang G, Lu X. Muscle pathological features and extra-muscle involvement in idiopathic inflammatory myopathies with anti-mitochondrial antibody. *Semin Arthritis Rheum* 2021; **51**: 741-748 [PMID: 34144384 DOI: 10.1016/j.semarthrit.2021.05.019]

149 **Harada N**, Dohmen K, Itoh H, Ohshima T, Yamamoto H, Nagano M, Iwata Y, Hachisuka K, Ishibashi H. Sibling cases of primary biliary cirrhosis associated with polymyositis, vasculitis and Hashimoto's thyroiditis. *Intern Med* 1992; **31**: 289-293 [PMID: 1600281 DOI: 10.2169/internalmedicine.31.289]

150 **Ko KF**, Ho T, Chan KW. Autoimmune chronic active hepatitis and polymyositis in a patient with myasthenia gravis and thymoma. *J Neurol Neurosurg Psychiatry* 1995; **59**: 558-559 [PMID: 8530953 DOI: 10.1136/jnnp.59.5.558]

151 **Kurihara Y**, Shishido T, Oku K, Takamatsu M, Ishiguro H, Suzuki A, Sekita T, Shinagawa T, Ishihara T, Nakashima R, Fujii T, Okano Y. Polymyositis associated with autoimmune hepatitis, primary biliary cirrhosis, and autoimmune thrombocytopenic purpura. *Mod Rheumatol* 2011; **21**: 325-329 [PMID: 21240621 DOI: 10.1007/s10165-010-0397-0]

152 **Seibold F**, Klein R, Jakob F. Polymyositis, alopecia universalis, and primary sclerosing cholangitis in a patient with Crohn's disease. *J Clin Gastroenterol* 1996; **23**: 121-124 [PMID: 8877639 DOI: 10.1097/00004836-199609000-00011]

153 **Gunnarsson R**, Hetlevik SO, Lilleby V, Molberg Ø. Mixed connective tissue disease. *Best Pract Res Clin Rheumatol* 2016; **30**: 95-111 [PMID: 27421219 DOI: 10.1016/j.berh.2016.03.002]

154 **Marshall JB**, Ravendhran N, Sharp GC. Liver disease in mixed connective tissue disease. *Arch Intern Med* 1983; **143**: 1817-1818 [PMID: 6615109 DOI: 10.1001/archinte.1983.00350090199039]

155 **Chung SW**. Vasculitis: From Target Molecules to Novel Therapeutic Approaches. *Biomedicines* 2021; **9** [PMID: 34209028 DOI: 10.3390/biomedicines9070757]

156 **Moiseev S**, Cohen Tervaert JW, Arimura Y, Bogdanos DP, Csernok E, Damoiseaux J, Ferrante M, Flores-Suárez LF, Fritzler MJ, Invernizzi P, Jayne D, Jennette JC, Little MA, McAdoo SP, Novikov P, Pusey CD, Radice A, Salama AD, Savige JA, Segelmark M, Shoenfeld Y, Sinico RA, Sousa MJ, Specks U, Terrier B, Tzioufas AG, Vermeire S, Zhao MH, Bossuyt X. 2020 international consensus on ANCA testing beyond systemic vasculitis. *Autoimmun Rev* 2020; **19**: 102618 [PMID: 32663621 DOI: 10.1016/j.autrev.2020.102618]

157 **Wang CR**, Tsai HW. Human hepatitis viruses-associated cutaneous and systemic vasculitis. *World J Gastroenterol* 2021; **27**: 19-36 [PMID: 33505148 DOI: 10.3748/wjg.v27.i1.19]

158 **Kennedy F**, Kapelow R, Kalyon BD, Roth NC, Rishi A, Barilla-LaBarca ML. A rare case of Polyarteritis Nodosa associated with autoimmune hepatitis: a case report. *BMC Rheumatol* 2021; **5**: 17 [PMID: 34034829 DOI: 10.1186/s41927-021-00188-1]

159 **Wang CR**, Tsai YS, Tsai HW, Lee CH. B-Cell-Depleting Therapy Improves Myocarditis in Seronegative Eosinophilic Granulomatosis with Polyangiitis. *J Clin Med* 2021; **10** [PMID: 34640595 DOI: 10.3390/jcm10194577]

160 **Terjung B**, Bogsch F, Klein R, Söhne J, Reichel C, Wasmuth JC, Beuers U, Sauerbruch T, Spengler U. Diagnostic accuracy of atypical p-ANCA in autoimmune hepatitis using ROC- and multivariate regression analysis. *Eur J Med Res* 2004; **9**: 439-448 [PMID: 15546809]

161 **Terjung B**, Söhne J, Lechtenberg B, Gottwein J, Muennich M, Herzog V, Mähler M, Sauerbruch T, Spengler U. p-ANCAs in autoimmune liver disorders recognise human beta-tubulin isotype 5 and cross-react with microbial protein FtsZ. *Gut* 2010; **59**: 808-816 [PMID: 19951907 DOI: 10.1136/gut.2008.157818]

162 **De Riva V**, Celadin M, Pittoni M, Plebani M, Angeli P. What is behind the presence of anti-neutrophil cytoplasmatic antibodies in chronic liver disease? *Liver Int* 2009; **29**: 865-870 [PMID: 19453948 DOI: 10.1111/j.1478-3231.2009.01989.x]

163 **Lenzen H**, Weismüller TJ, Negm AA, Wlecke J, Loges S, Strassburg CP, Manns MP, Lankisch TO. Antineutrophil cytoplasmic antibodies in bile are associated with disease activity in primary sclerosing cholangitis. *Scand J Gastroenterol* 2013; **48**: 1205-1212 [PMID: 23957616 DOI: 10.3109/00365521.2013.825313]

164 **Tovoli F**, Vannini A, Fusconi M, Frisoni M, Zauli D. Autoimmune liver disorders and small-vessel vasculitis: four case reports and review of the literature. *Ann Hepatol* 2013; **13**: 136-141 [PMID: 24378277 DOI: 10.1155/2014/386561]

165 **Yamashita H**, Suzuki A, Takahashi Y, Kaneko H, Kano T, Mimori A. Anti-neutrophil Cytoplasmic Antibody (ANCA)-associated Vasculitis Associated with Primary Biliary Cirrhosis: A Case Report and Literature Review. *Intern Med* 2015; **54**: 1303-1308 [PMID: 25986275 DOI: 10.2169/internalmedicine.54.3678]

166 **Lohani S**, Nazir S, Tachamo N, Pagolu P. Autoimmune hepatitis and eosinophilic granulomatosis with polyangiitis: a rare association. *BMJ Case Rep* 2017; **2017** [PMID: 28108440 DOI: 10.1136/bcr-2016-218385]

167 **Giacomelli R**, Ruscitti P, Shoenfeld Y. A comprehensive review on adult onset Still's disease. *J Autoimmun* 2018; **93**: 24-36 [PMID: 30077425 DOI: 10.1016/j.jaut.2018.07.018]

168 **Sandnes M**, Ulvik RJ, Vorland M, Reikvam H. Hyperferritinemia-A Clinical Overview. *J Clin Med* 2021; **10** [PMID: 34067164 DOI: 10.3390/jcm10092008]

169 **Fujii K**, Rokutanda R, Osugi Y, Koyama Y, Ota T. Adult-onset Still's disease complicated by autoimmune hepatitis: successful treatment with infliximab. *Intern Med* 2012; **51**: 1125-1128 [PMID: 22576401 DOI: 10.2169/internalmedicine.51.6824]

170 **Yazici Y**, Hatemi G, Bodaghi B, Cheon JH, Suzuki N, Ambrose N, Yazici H. Behçet syndrome. *Nat Rev Dis Primers* 2021; **7**: 67 [PMID: 34531393 DOI: 10.1038/s41572-021-00301-1]

171 **Bayraktar Y**, Balkanci F, Bayraktar M, Calguneri M. Budd-Chiari syndrome: a common complication of Behçet's disease. *Am J Gastroenterol* 1997; **92**: 858-862 [PMID: 9149201]

172 **Takeuchi A**, Haraoka H, Hashimoto T. Increased serum alkaline phosphatase activity in Behçet's disease. *Clin Exp Rheumatol* 1989; **7**: 619-621 [PMID: 2612081]

173 **Manna R**, Ghirlanda G, Bochicchio GB, Papa G, Annese V, Greco AV, Taranto CA, Magaro M. Chronic active hepatitis and Behçet's syndrome. *Clin Rheumatol* 1985; **4**: 93-96 [PMID: 3987204 DOI: 10.1007/BF02032326]

174 **Iwadate H**, Ohira H, Saito H, Takahashi A, Rai T, Takiguchi J, Sasajima T, Kobayashi H, Watanabe H, Sato Y. A case of primary biliary cirrhosis complicated by Behçet's disease and palmoplantar pustulosis. *World J Gastroenterol* 2006; **12**: 2136-2138 [PMID: 16610072 DOI: 10.3748/wjg.v12.i13.2136]

175 **Stone JH**, Zen Y, Deshpande V. IgG4-related disease. *N Engl J Med* 2012; **366**: 539-551 [PMID: 22316447 DOI: 10.1056/NEJMra1104650]

176 **Huggett MT**, Culver EL, Kumar M, Hurst JM, Rodriguez-Justo M, Chapman MH, Johnson GJ, Pereira SP, Chapman RW, Webster GJM, Barnes E. Type 1 autoimmune pancreatitis and IgG4-related sclerosing cholangitis is associated with extrapancreatic organ failure, malignancy, and mortality in a prospective UK cohort. *Am J Gastroenterol* 2014; **109**: 1675-1683 [PMID: 25155229 DOI: 10.1038/ajg.2014.223]

177 **Chen JH**, Deshpande V. IgG4-related Disease and the Liver. *Gastroenterol Clin North Am* 2017; **46**: 195-216 [PMID: 28506361 DOI: 10.1016/j.gtc.2017.01.001]

178 **Ichimura T**, Kondo S, Ambo Y, Hirano S, Ohmi M, Okushiba S, Morikawa T, Shimizu M, Katoh H. Primary sclerosing cholangitis associated with autoimmune pancreatitis. *Hepatogastroenterology* 2002; **49**: 1221-1224 [PMID: 12239909]

179 **Li A**, Wang Y, Deng Z. Concurrent autoimmune pancreatitis and primary biliary cirrhosis: a rare case report and literature review. *BMC Gastroenterol* 2014; **14**: 10 [PMID: 24410827 DOI: 10.1186/1471-230X-14-10]

180 **Yada N**, Kudo M, Chung H, Watanabe T. Autoimmune hepatitis and immunoglobulin G4-associated autoimmune hepatitis. *Dig Dis* 2013; **31**: 415-420 [PMID: 24281014 DOI: 10.1159/000355238]

181 **Tanaka A**, Notohara K. Immunoglobulin G4 (IgG4)-related autoimmune hepatitis and IgG4-hepatopathy: A histopathological and clinical perspective. *Hepatol Res* 2021; **51**: 850-859 [PMID: 34165225 DOI: 10.1111/hepr.13683]

182 **Valeyre D**, Prasse A, Nunes H, Uzunhan Y, Brillet PY, Müller-Quernheim J. Sarcoidosis. *Lancet* 2014; **383**: 1155-1167 [PMID: 24090799 DOI: 10.1016/S0140-6736(13)60680-7]

183 **Cremers J**, Drent M, Driessen A, Nieman F, Wijnen P, Baughman R, Koek G. Liver-test abnormalities in sarcoidosis. *Eur J Gastroenterol Hepatol* 2012; **24**: 17-24 [PMID: 22008629 DOI: 10.1097/MEG.0b013e32834c7b71]

184 **Shah N**, Mitra A. Gastrointestinal and Hepatic Sarcoidosis: A Review Article. *Clin Liver Dis (Hoboken)* 2021; **17**: 301-307 [PMID: 33968393 DOI: 10.1002/cld.1055]

185 **Mantaka A**, Koulentaki M, Chlouverakis G, Enele-Melono JM, Darivianaki A, Tzardi M, Kouroumalis EA. Primary biliary cirrhosis in a genetically homogeneous population: disease associations and familial occurrence rates. *BMC Gastroenterol* 2012; **12**: 110 [PMID: 22898439 DOI: 10.1186/1471-230X-12-110]

186 **Rajoriya N**, Wotton CJ, Yeates DG, Travis SP, Goldacre MJ. Immune-mediated and chronic inflammatory disease in people with sarcoidosis: disease associations in a large UK database. *Postgrad Med J* 2009; **85**: 233-237 [PMID: 19520873 DOI: 10.1136/pgmj.2008.067769]

187 **Lahmer T**, Treiber M, von Werder A, Foerger F, Knopf A, Heemann U, Thuermel K. Relapsing polychondritis: An autoimmune disease with many faces. *Autoimmun Rev* 2010; **9**: 540-546 [PMID: 20215048 DOI: 10.1016/j.autrev.2010.02.016]

188 **da Graça Ferronato M**, Staub LJ, Teixeira Pinto Viana RC, da Rosa L, Cacese Shiozawa MB, Narciso-Schiavon JL, Dantas-Correa EB, de Lucca Schiavon L. Cholestasis as the initial presentation of relapsing polychondritis. *Ann Hepatol* 2011; **10**: 565-567 [PMID: 21911901 DOI: 10.1016/S1665-2681(19)31528-5]

189 **Conn DL**, Dickson ER, Carpenter HA. The association of Churg-Strauss vasculitis with temporal artery involvement, primary biliary cirrhosis, and polychondritis in a single patient. *J Rheumatol* 1982; **9**: 744-748 [PMID: 7175848 DOI: 10.1007/BF02032091]

190 **Mydlak A**, Sołdacki D, Foroncewicz B, Stopa Z, Powała A, Budlewski T, Pączek L, Mucha K. Relapsing polychondritis in a liver transplant recipient: A case report. *Medicine (Baltimore)* 2017; **96**: e8360 [PMID: 29069021 DOI: 10.1097/MD.0000000000008360]

World Journal of Gastroenterology

Submit a Manuscript: https://www.f6publishing.com

World J Gastroenterol 2022 June 21; 28(23): 2546-2560

DOI: 10.3748/wjg.v28.i23.2546

ISSN 1007-9327 (print) ISSN 2219-2840 (online)

REVIEW

Fecal microbiota transplantation in the metabolic diseases: Current status and perspectives

Lie Zheng, Yong-Yi Ji, Xin-Li Wen, Sheng-Lei Duan

Specialty type: Gastroenterology and hepatology

Provenance and peer review: Unsolicited article; Externally peer reviewed.

Peer-review model: Single blind

Peer-review report's scientific quality classification

Grade A (Excellent): 0
Grade B (Very good): B, B
Grade C (Good): 0
Grade D (Fair): 0
Grade E (Poor): 0

P-Reviewer: Dhaliwal A, United States; Romano M, Italy

Received: January 4, 2022
Peer-review started: January 4, 2022
First decision: March 9, 2022
Revised: March 14, 2022
Accepted: May 7, 2022
Article in press: May 7, 2022
Published online: June 21, 2022

Lie Zheng, Xin-Li Wen, Sheng-Lei Duan, Department of Gastroenterology, Shaanxi Hospital of Traditional Chinese Medicine, Xi'an 710003, Shaanxi Province, China

Yong-Yi Ji, Department of Neurology, Xi'an Hospital of Traditional Chinese Medicine, Xi'an 710021, Shaanxi Province, China

Corresponding author: Yong-Yi Ji, MD, Department of Neurology, Xi'an Hospital of Traditional Chinese Medicine, No. 69 Fengcheng 8 Road, Xi'an 710003, Shaanxi Province, China. 925861033@qq.com

Abstract

With the development of microbiology and metabolomics, the relationship between the intestinal microbiome and intestinal diseases has been revealed. Fecal microbiota transplantation (FMT), as a new treatment method, can affect the course of many chronic diseases such as metabolic syndrome, malignant tumor, autoimmune disease and nervous system disease. Although the mechanism of action of FMT is now well understood, there is some controversy in metabolic diseases, so its clinical application may be limited. Microflora transplantation is recommended by clinical medical guidelines and consensus for the treatment of recurrent or refractory *Clostridium difficile* infection, and has been gradually promoted for the treatment of other intestinal and extraintestinal diseases. However, the initial results are varied, suggesting that the heterogeneity of the donor stools may affect the efficacy of FMT. The success of FMT depends on the microbial diversity and composition of donor feces. Therefore, clinical trials may fail due to the selection of ineffective donors, and not to faulty indication selection for FMT. A new understanding is that FMT not only improves insulin sensitivity, but may also alter the natural course of type 1 diabetes by modulating autoimmunity. In this review, we focus on the main mechanisms and deficiencies of FMT, and explore the optimal design of FMT research, especially in the field of cardiometabolic diseases.

Key Words: Fecal microbiota transplantation; Metabolic diseases; Inflammatory bowel disease; Type 1 diabetes; Metabolic syndrome

©The Author(s) 2022. Published by Baishideng Publishing Group Inc. All rights reserved.

Core Tip: The success of fecal microbiota transplantation (FMT) depends on the microbial diversity and composition of donor feces. It is newly found that FMT may not only improve insulin sensitivity, but also alter the natural course of type I diabetes by modulating autoimmunity. In this review, we focus on the main mechanisms and deficiencies of FMT, and explore the optimal design of FMT research, especially in the field of cardiometabolic diseases.

Citation: Zheng L, Ji YY, Wen XL, Duan SL. Fecal microbiota transplantation in the metabolic diseases: Current status and perspectives. *World J Gastroenterol* 2022; 28(23): 2546-2560
URL: https://www.wjgnet.com/1007-9327/full/v28/i23/2546.htm
DOI: https://dx.doi.org/10.3748/wjg.v28.i23.2546

INTRODUCTION

Most of the research on microorganisms is confined to infectious diseases and the role of microorganisms in human health is largely ignored. The average weight of these microorganisms is about 1.5 kg, equivalent to the weight of the liver. There are 10^{12}–10^{14} microorganisms, which is 10 times the number of the human body's own cells, and they are mainly parasitic in the intestinal tract[1]. These symbiotic microorganisms include bacteria, viruses, archaea, fungi and, in some cases, protists, collectively known as the microbiome. The most important advantage of fecal microbiota transplantation (FMT) is the determination of cause and effect of disease through microbiology[2] .

During the long process of human evolution, the intestinal flora has coevolved with its host, along with social development, changes in diet, lifestyle and environment. Intestinal symbiotic bacteria can regulate a variety of metabolic activities that cannot be carried out by the human body itself[3]. They can obtain energy by decomposing polysaccharides, proteins and fats in food that cannot be fully digested by the host, and produce a series of metabolites that affect the health of the host. In this process, the intestinal microecosystem is closely related to the host metabolic capacity[4].

As early as 3000 years ago, cow dung was used in India to treat gastrointestinal diseases. As early as the Eastern Jin Dynasty (317–420 AD), a treatment similar to fecal bacterial transplantation, called "Huanglong Soup", was described in Ge Hong's "Urgent Prescription for Elbow Reserve", which was used to treat food poisoning and diarrhea. In traditional Chinese medicine, it is recorded that huanglian and rhubarb, among others, have the curative effect of "quenching thirst" (ancient term for diabetes). Berberine, a monomer component from huanglian, has been recognized internationally for its effect on improving glucose and lipid metabolism earlier. During World War II, German soldiers in North Africa treated diarrhea with camel excrement[5]. At present, FMT is mainly used for the treatment of recurrent *Clostridium difficile* infection (CDI) in clinical practice, and many clinical trials have confirmed that FMT is a feasible treatment[6].

At present, with the development of fast and accurate high-throughput sequencing technology and the improvement of bioinformatics technology methods, intestinal flora is closely related to metabolic syndrome (MS), type 1 diabetes (T1D) and type 2 diabetes (T2D), various cancers, and autoimmune diseases. Currently, it is believed that the FMT donor should be carefully selected and examined for infectious diseases[7]. However, due to the large difference in metabolism and diet of FMT donors, the effect of transplantation can be different. In this review, the mechanisms and deficiencies of FMT are discussed, and the optimal design of FMT is explored to maximize scientific research and clinical application methods.

COMPOSITION AND METHOD OF FMT

The main components of FMT are the gut flora of humans and other species. Humans have evolved to come into contact with a variety of bacteria, including those produced by food fermentation. The oral cavity is an important location of intestinal microbiota, which has an important effect on human health. Studies have shown that children who grow up on farms have a lower risk of asthma; a phenomenon that may be linked to changes in their gut microbiota[8]. In addition, babies born by cesarean section are at increased risk of developing autoimmune diseases, mainly because the initial microbes passed from the vagina to the baby at birth are replaced by skin microbes from the mother and surgical team members, which alter the baby's gut microbes[9]. An infant's gut microbiome can be reshaped in breast milk by adding small amounts of bacteria from the mother's feces, creating a pattern that more closely resembles that of babies born vaginally[10].

FMT has been processed into an odorless and tasteless preparation. In clinical practice, there are three methods of bacterial flora transplantation for patients willing to accept FMT: Upper, middle and lower digestive tract. The methods of transplanting upper digestive tract microflora mainly include oral

microflora liquid and oral microflora capsule. The middle digestive tract approach includes a nasointestinal tube, endoscopic biopsy hole, percutaneous endoscopic gastrostomy and jejunal catheterization, endoscopic catheterization such as Transendoscopic enteral tubing (TET)[11]. The lower gastrointestinal pathway includes colonoscopy, colostomy, enema, and colonic pathway TET. Colonic pathway TET is not only used for microflora transplantation, but also for whole colon administration such as mesalazine, hormones and traditional Chinese medicine. As a new endoscopic technique, TET is an important supplement for interventional treatment of inflammatory bowel disease[12].

FMT focuses on flora transplantation, but other components, such as phages, should not be ignored, which may be the reason for FMT's effectiveness in the treatment of recurrent CDI. Therefore, phage research is important, and animal studies have shown that fecal virus transplantation also plays an important role. Analysis of the feces of adults on a classic British diet found that 25% of the 100 g/d excreted was made up of bacteria and 75% of fiber, protein, fat, bile acids and short-chain fatty acids (SCFAs). In most FMT, however, feces are simply mixed with salt water and filtered to remove insoluble substances[13]. Thus, the potential effects of FMT may be partly due to the combined effects of these compounds (Figure 1).

AUTOLOGOUS FMT

Most studies have focused on fecal transplants from healthy donors (known as FMT allografts). However, autologous fecal transplants have significant advantages[14], such as reducing the risk of infection and increasing the efficiency of transplantation, especially in the treatment of recurrent CDI by freezing their own feces. Autologous fecal transplants are effective in many diseases, but not in disorders caused by intestinal flora disorders, such as inflammatory bowel disease[15]. Studies have shown that disorder of intestinal flora can aggravate the disease, and intestinal inflammation can also affect the composition of intestinal flora[16]. Therefore, it is speculated that fecal biobanks may contain probiotics, which have changed the composition of intestinal flora before the relapse of the disease. This requires further confirmation of the value of probiotics in intestinal flora, but there is insufficient evidence to confirm the value of probiotics collected in clinical remission. Therefore, autologous FMT can improve clinical symptoms by regulating intestinal flora to promote metabolism[17].

In conclusion, regulating the balance of intestinal flora is the primary goal of therapy. Autologous FMT through a duodenal tube or oral capsules can reshape the composition of small intestinal flora, which play an important role in the regulation of autoimmune diseases[18], mainly because the immune system response to antigenic stimuli occurs in the small intestine. It has also been suggested that autologous FMT *via* the duodenal tube may be valuable in a new method of preserving β-cell function for T1D diagnosis that is more effective than healthy donor FMT[19].

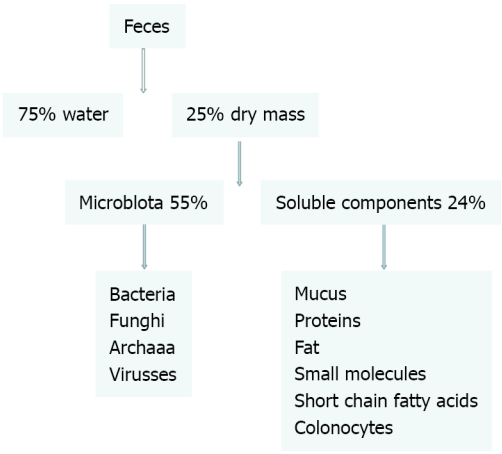
FMT AND METABOLIC DISEASES

MS

To date, the only reported study of FMT in the treatment of human MS was conducted by Witkowski *et al*[20]. This study examined the effects of FMT on glucose and lipid metabolism in men with MS in a double-blind randomized controlled trial in nine patients receiving fecal bacteria transplants from lean healthy donors (allograft group) and nine other patients[21]. They received their own fecal bacteria as a control (autologous transplantation group)[22]. After 6 wk of FMT treatment, insulin sensitivity and fecal microbial diversity were significantly increased in the allograft group, while no significant changes were observed in the autograft group. It should be noted that there were individual differences in the efficacy of FMT[23], and Gagliardi *et al*[24] suggested that the differences might have been more due to different donors than recipients, since the two subjects receiving fecal bacteria from the same donor showed similar benefits[24]. In a randomized, double-blind, controlled trial of fecal bacteria transplantation in patients with MS it was found that insulin sensitivity and butyric acid-producing intestinal flora significantly improved in patients receiving fecal donation[25]. FMT strengthened the intestinal barrier function and effectively reduced endotoxemia in a nutritionally obese rat model. It is also concluded that FMT can regulate the lipid content of obese rats and reduce hepatic steatosis[26]. There are currently four clinical trials of FMT for MS registered with clinicaltrials.gov. We believe that the results of these clinical trials can provide us with a better understanding of the role of intestinal flora in human metabolic disorders[27].

T1D

There is a close relationship between intestinal flora and diabetes mellitus. Some studies have found that the decrease of butyrate- and lactate-producing bacteria is related to the autoimmunity of β cells [28]. In addition, it has been found that the intestinal flora of children with β-cell-related autoimmune diseases lacks *Bifidobacterium*, and the bacteria producing butyrate and lactate are reduced while



DOI: 10.3748/wjg.v28.i23.2546 **Copyright** ©The Author(s) 2022.

Figure 1 Components that are transferred during fecal transplantation.

Bacteroidetes are increased[24]. Another study in Spain found similar changes in the gut flora of children with T1D, suggesting that structural changes in the gut flora may be associated with T1D[29]. A meta-genomic analysis of the intestinal flora in an included study found that, compared with the control group, patients with T1D had fewer butyrate-producing bacteria and mucin-degrading *Prevotella* and *Akkermansia*, and had more lactate-producing bacteria, and bacteria-producing SCFA other than butyrate, such as *Bacteroides* and *Riyanella*[30].All of these suggest that gut bacteria may participate in the disorder of immune function in patients with T1D[31].

Dietary fiber can be metabolized and fermented by intestinal bacteria into SCFAs, including acetic acid, propionic acid and butyric acid, which may also be involved in the pathogenesis of metabolic diseases[32]. The types and quantities of SCFAs are thought to vary with the composition of intestinal microbes. In addition to serving as an energy source for intestinal epithelial cells and liver (SCFAs are absorbed by the intestine and transported mainly through the portal vein), SCFAs are thought to have immunomodulatory effects by reducing intestinal permeability[33]. Lipopolysaccharides from intestinal translocation to the portal vein are thought to be involved in obesity-related mild inflammatory responses and insulin resistance in mice[34].

SCFAs produce a small number of microorganisms in T1D, and the incidence of T1D is significantly reduced in nonobese diabetic mice treated with *Akkermansia* or with a prebiotic diet supplemented with SCFAs[35]. It has been suggested that the restoration of intestinal flora balance through healthy donor FMT may further weaken autoimmune function and β-cell dysfunction[36]. A recent study showed that both healthy autologous and allogeneic FMT attenuates the decline of β-cell function, while donor FMT decreases at a slower rate[37]. Surprisingly, the decay rate of autologous FMT b cells was only 12 mo after three consecutive FMT treatments. Due to the significant changes in microbes from the mouth to the anus during autologous FMT[38], the immune system of the small intestine can be reshaped. Due to the lack of effective immunomodulators to treat T1D, a large number of clinical studies are needed to confirm this[39].

T2D

The association between intestinal flora and T2D was first reported by Chinese researchers led by The Shenzhen Huada Institute for Life Sciences and published in Nature in 2012[40]. This study found that the relative abundance of clostridium butyricum and its butyric acid-producing function in Chinese patients with T2D were significantly lower than those in the normal population, and lipopolysaccharide produced by conditional pathogenic Enterobacteriaceae species, hydrogen sulfide proinflammatory function and branched chain amino acid transport function levels were significantly higher than the general population[41]. These changes may be associated with impaired intestinal mucosal barrier function and increased levels of intestinal inflammation in T2D patients[42].

A randomized controlled study showed that autologous FMT can maintain normal metabolism after diet-induced weight loss[43]. It has been observed that obese donor FMT can cause rapid weight gain, so there is a link between the intestinal microbiome, obesity and insulin resistance[44]. On the contrary, non-obese donor FMT can improve insulin resistance in obese patients with MS. Another study found that donor FMT had no effect on glucose metabolism and their diets were metabolically tested. Recent studies have shown that the use of single-dose capsule FMT improves lipid metabolism and insulin resistance, mainly through continuous supplementation of low-fermenter fiber[45]. Therefore, dietary composition may affect insulin resistance of FMT, or metabolites of donor FMT may affect the enteric–brain axis[46].

NONALCOHOLIC FAATTY LIVER DISEASE

The relationship between intestinal microflora and nonalcoholic faatty liver disease (NAFLD) is increasingly close, research suggests. Intestinal flora can affect the occurrence and development of NAFLD by changing the composition of intestinal flora, increasing serum endotoxin level and intestinal permeability, producing endogenous alcohol and changing choline metabolism[47]. Animal studies have shown that FMT can improve steatohepatitis in mice induced by high-fat diet, reduce the production of lipids and proinflammatory factors in the liver, regulate the balance of intestinal flora in mice, and increase the abundance of beneficial flora[48]. After FMT treatment, the cecal butyrate concentration and intestinal tight junction protein ZO-1 increased, and the toxin release decreased, thus reducing the inflammatory response[49].

Increased intestinal permeability and metabolic endotoxin caused by changes in intestinal flora composition are involved in the progression of NAFLD in mice, and the severity of NAFLD in mice is increased when special flora are transferred to methionine- and choline-deficient diet, indicating that intestinal flora is involved in the progression of NAFLD[50]. The results of human studies also support the idea that changes in gut flora can contribute to fatty liver disease. Compared with normal subjects, NAFLD patients showed increased intestinal permeability, endotoxemia, increased numbers of g-Proteobacteria, and decreased numbers of Bacteroidetes[51].

Fatty liver often occurs in obese patients. Long-term vegans have a lower risk of NAFLD, which may be related to changes in gut flora. It is suggested that FMT treatment of long-term vegan feces can improve liver inflammation score[52]. Despite the small sample size, this study still found that the inflammatory necrotic tissue score and inflammatory gene expression were reduced after transplantation of vegan fecal flora, which may be an important indicator for predicting the progression of NAFLD to cirrhosis[53]. At the same time, an FMT study in NAFLD patients showed that healthy donor FMT reduced intestinal permeability, which is an important feature that distinguishes NAFLD from other diseases[48]. This study found that magnetic resonance imaging could not make a definitive diagnosis of hepatic adipose degeneration, which must be assessed using gold standard liver histological examination[54].

PITFALLS

Mode of delivery

Since innate and adaptive immune cell reactions occur in the small intestine, immune diseases are usually treated by oral capsules or fresh feces administered through the duodenum under strict anaerobic conditions, in order to ensure that active aerobic and anaerobic bacteria can be transplanted to the maximum extent and thus reshape the intestinal microecological balance[55]. Remodeling of the small intestinal flora is not appropriate for nonimmune diseases or diseases with distal intestinal malformations, but colonic delivery (enema or colonoscopy) may be an option[56].

Whether FMT plays an important role in other diseases besides recurrent CDI needs confirmation. Donor FMT freeze-drying capsules or frozen-solution capsules have been widely used and have gained more support due to their noninvasive administration[57], and it is also convenient for the donor and recipient to make multiple trips to the hospital for transplantation on the same day[58]. Current treatments for CDI include enemas, frozen capsules or freeze-drying formulations. However, it may not be suitable for mild intestinal microecological disorders that do not comply with GMP regulations as compared to fresh feces[59].

PREPARATION OF FMT FECAL BACTERIA LIQUID

Due to the lack of sufficient sample size and establishment of control groups in most clinical studies [55], the conclusions are not reliable, and there is controversy about the preparation of FMT fecal bacteria solution. (1) Selection of stool dilution materials[60]. It is reported that ordinary water (98.5%) has a higher disease remission rate than normal saline (86%) as a stool dilution material, but the recurrence rate of CDI with the former increased > 2 times. Other thinners, such as milk or salt water from plantain, achieved a 94% remission rate; (2) The amount of fecal bacteria liquid transplanted. When the volume of fecal bacteria liquid transplanted is > 500 mL, the remission rate of CDI is 97%, but < 200 mL, the remission rate is only 80%. However, it is difficult to compare the above conclusions because the dilution ratio of feces may vary. Currently, according to the Amsterdam protocol, 200–300 g of donor stool is dissolved in 500 mL normal saline for use (donor stool is preferably fresh within 6 h); and (3) Feasibility of frozen feces. A case report of standardized frozen stool samples used for fecal bacteria transplantation for the treatment of CDI showed that there was no statistical difference in the efficacy of standardized frozen stool compared with fresh stool. Therefore, establishment of stool donation banks and use of standardized frozen stool made fecal bacteria transplantation more feasible

in clinical practice[61]. A recent study on the treatment of CDI by oral frozen fecal bacteria capsules showed that no serious adverse reactions occurred in recurrent CDI treated by fecal bacteria transplantation *via* oral frozen fecal bacteria capsules[62]. The diarrhea relief rate of single administration was 70% (14/20), while four of six patients who did not respond to treatment achieved remission after second administration, resulting in a total remission rate of 90%. This study initially demonstrated the feasibility and safety of fecal bacteria transplantation *via* frozen fecal bacteria capsules[63].

THE PROCESSING OF FMT

Protective measures are usually taken to avoid anaerobic bacteria being killed by coming in contact with oxygen[64], but it cannot be completely avoided. Under strict anaerobic conditions, the composition of diluted or filtered microorganisms does not differ significantly before and after the entire procedure, but the activity of the preparation may have been affected[65]. Similarly, prolonged freezing at -80 °C preserved fecal components to a large extent, but whether it had an effect on fecal activity was unclear [66]. However, recent studies have shown that autologous FMT stored in glycerin at -80 °C can completely restore the intestinal lumen and mucosal microbial balance. Whether FMT regulates mild microbial disorders in these studies remains to be confirmed[67].

DIVERSITY OF THE GUT MICROBIOME

The diversity of intestinal flora increases with growth and development, and finally forms a complex and relatively stable microbial community at the age of 2–3 years, mainly including bacteria, fungi, viruses and protozoa[68]. There are > 1000 species of bacteria, most of which are obligate anaerobes, including Firmicutes, Bacteroides, Proteobacteria and Actinomycetes, among which Firmicutes and Bacteroides are dominant, accounting for > 90% of all intestinal bacteria[69].

Gut microbiome composition is temporal and spatially specific. Neonatal bacteria from the birth canal colonize the intestine within a few hours after birth. The intestinal microbial composition of early vaginally delivered babies is similar to that of the mother's vagina, while that of cesarean delivery babies is different[70]. A baby's gut microbiota can reach the level of a healthy adult at about age 1 year. Most of the microorganisms in the human intestine colonize the colon[71], and the number is 10^{12} cfu/mL. The microbial content of the jejunum, ileum and duodenum decreases successively, and there are 10^{7}, 10^{4} and 10^{3} cfu/mL, respectively. There are also differences in the types of microorganisms rich in each part. In addition, the composition of intestinal mucosa and fecal-associated microorganisms varies[72].

Individuals in the same area may have different gut microbiota. The composition and diversity of intestinal microbiota may influence the therapeutic effect of donor FMT[73], or even insulin resistance. In the past few decades, with the westernization of China's diet, intestinal microbial diversity has decreased. Preselection of donor FMT may be a feasible way to improve clinical outcomes based on the presence of a specific biological chain. Therefore, an important method to study FMT is to carefully study the baseline data of patients and the microbial composition after FMT[74]. By comparing the baseline data of the donor and the recipient and the microbial composition during a certain period of time, the number of microbes transplanted from the donor to the recipient can be calculated[75]. The most common method is fecal metagenomic sequencing, which identifies microbial species based on specific mononucleotide degeneration[76]. Sequencing techniques combined with bioinformatics analysis reveal the duration of similarity between donor and recipient strains, and how many of the transplanted microbes are likely to restore the original microbial composition[77].

DONOR-ACCEPTOR COMBINATION

FMT is thought to restore disturbed gut flora to a healthy state either by implanting a donor strain or by other donor-dependent traits, such as the amount of nonbacterial components[78]. However, not all donor gut microbiota are uniform, and comparison of gut microbiota from different donors suggests that microbial diversity and metabolites may be predictors of the success of FMT[79]. In some studies, donor microbiome and metabolomic characteristics may be associated with FMT treatment response. Therefore, the selection of appropriate donor feces is a key factor in the success of FMT[80]. However, few studies of FMT have considered the influence of the variation characteristics of the intestinal microbiome and metabolome of the donor on clinical efficacy[81].

Current studies have confirmed that after FMT treatment, the intestinal flora diversity of the recipient is significantly increased and tends to be the flora characteristics of the donor[82]. Cases that respond to FMT treatment typically show higher microbial diversity. It has been confirmed that intestinal bacterial abundance in donors that respond to FMT is significantly higher than that in donors that do not respond

[83].

To date, donor selection methods in FMT studies have included the use of a single donor or the random selection of multiple donors from a group of screened eligible donors[84]. In 2019, Zheng *et al* [85] first proposed the concept of super donors and believed that the success of FMT depends on the donor[85]. However, the definition of super donor has not been established, and the clinical efficacy of donors before FMT treatment cannot be predictedv[86]. However, the failure of randomly selected single donors may be due to the selection of ineffective donors rather than the incorrect indication selection of FMT[87]. Therefore, an alternative approach is to expose each patient to multiple donors (multidonor transplants) to reduce the risk of receiving FMT from an invalid donor[88]. However, FMT is still in the clinical research stage. Single donors can provide clearer evidence for clinical studies, while multiple donors lead to false negatives or false positives in clinical studies, thus hindering the development of the FMT field and the development of new microbiome therapies[89].

Studies have shown a surprising match between donor and recipient transplants and FMT[90]. The ability to secrete blood group antigens is associated with a reduction in gut microbial diversity, which in turn determines the likelihood of successful transplantation from nonsecreting blood group donors to secreting blood group receptors, which may also apply to human leukocyte antigens (HLAs)[91]. HLA haploidy is an important risk factor for autoimmune diseases such as T1D, and infants with HLA haploidy associated with an increased risk of T1D do form a unique microbiome[92]. What remains to be proven, however, is whether FMT can correct the high-risk microbiome associated with specific HLA haplotypes later in life[93]. In addition, it needs to be considered that intestinal immunoglobulin-secretion-binding bacteria and their components may contribute to the therapeutic effect of donor FMT [94].

CONCOMITANT MEDICATION

To facilitate colonization (also known as transplantation), the recipient's gut is usually cleaned, most commonly by enemas, laxatives, or broad-spectrum antibiotics[95]. In patients with ulcerative colitis, antibiotic administration after FMT increases the risk of transplant failure, although there is evidence that antibiotic pretreatment improves the efficacy of FMT[96]. Previous studies have shown that antibiotics, metformin, berberine and other drugs can change the intestinal flora, thus affecting the state of the body[97]. A study of Finnish children aged 2–7 years found that macrolide use was associated with subsequent long-term changes in intestinal microbiota composition and metabolism: A decrease in Actinobacteria and an increase in Bacteroidetes and Proteobacteria, decreased biliary saline hydrolyase and increased resistance to macrolides[98]. It is associated with an increased risk of asthma and weight gain. The effect of penicillin on intestinal flora was weaker than that of macrolides[99]. In addition to antibiotics, many Chinese herbal extracts can alter the intestinal flora[100]. A study in Taiwan Chang Gyeong Hospital found that ganoderma lucidum extract can reduce the body weight of high-fat-diet mice, reduce inflammatory response and insulin resistance, reduce intestinal flora Firmicutes/Bacteroidetes ratio and endotoxin levels, maintain the integrity of the intestinal barrier and reduce endotoxemia. It has been found that both berberine and metformin can reverse the changes in intestinal flora in mice induced by high-fat diet and significantly reduce the diversity of intestinal flora. Proton pump inhibitors (PPIs) are among the top 10 drugs widely used worldwide, and studies have found that PPI use is associated with intestinal infections, particularly CDI[101]. PPI users had significantly increased intestinal flora of *Enterococcus*, *Streptococcus*, *Staphylococcus* and opportunistic *Escherichia coli*[102]. In addition, cardiovascular drugs such as statins, antihypertensive drugs, antiplatelet aggregation drugs, as well as opioids and antidepressants can affect the composition of gut microbes[103]. As confounding factors such as gender and age have a great influence on these results, confounding factors should be minimized, and random number tables should be used to conduct random-grouping studies, because the reactions caused by these drugs may be caused by microbial disorders[104].

CONCOMITANT LIFESTYLE AND DIET

When a donor transplants microbes to a recipient, the difference in microbial composition between the two may be partly due to lifestyle differences between the donor and recipient[105]. If the recipient's lifestyle does not change to that of the donor after FMT, then the effect on the recipient's microbial makeup may disappear over time. People living in different continents and regions have their own unique dietary habits[106]. The diet of Europeans is rich in cheese, butter and other high-fat and high-calorie foods, while the diet of Africans is low in calories and high in dietary fiber[107]. High-throughput sequencing comparing the intestinal microbiota of European children with that of rural children from Burkina Faso, a landlocked country in Western Africa, revealed significant differences between the two[108]. *Prevotella* and Xylos bacteria, which are associated with cellulose and xylan hydrolysis, were completely absent in the intestinal flora of European children on a high-calorie and

high-fat diet, while the intestinal flora of African children on a low-calorie and high-fiber diet was rich in Bacteroidetes, especially *Prevotella* and Xylos bacteria, while Firmicutes were relatively rare[109]. In addition, African children were found to have significantly more SCFAs in their intestines than European children had, and the abundance of Enterobacteriaceae (mainly *Shigella* and *E. coli*) was found to be lower than that of European children[110]. These results suggest that the intestinal flora of African children has adapted to a diet rich in polysaccharides to ensure adequate energy intake from a fiber-rich diet and to reduce the incidence of intestinal inflammatory and infectious diseases[111]. The lack of dietary fiber in the diet of European children may be responsible for the loss of prevosiella and Xylos bacteria associated with cellulose and xylan hydrolysis[112]. Another study found that increased dietary fiber intake increased the diversity of the gut flora, as well as *Prevotella* abundance[113].

Numerous studies have shown that changes in diet determine microbial composition[114]. When autologous FMT is administered during a particular diet, the beneficial effects of the diet persist even if the diet is no longer continued[115]. Conversely, changes in an individual's microbial composition also affect diet. A large number of studies have shown that dietary response to FMT may be related to changes in microbial composition[116]. Thus, FMT transplantation using a standardized diet during clinical interventions may be more effective because an important source of microbiome variation has been eliminated, but it has been overlooked in many studies[117].

POTENTIAL MECHANISM OF ACTION

Although the causal relationship between intestinal microbiota and disease is still unclear, it is sufficient to inspire researchers to implement strategies for disease management by regulating intestinal microbiota[118]. Dietary management, antibiotics, probiotics and other interventions can directly or indirectly enable the reconstruction of intestinal flora[119]. FMT is based on microbiota treatment, in which the isolated functional bacteria are transplanted into the patient to reconstruct intestinal flora and achieve a steady state of the gut microbes so as to attain the purpose of disease treatment[120]. The specific mechanism of FMT has not been clarified yet, and its complex mechanism cannot be replaced and explained by a single strain or single signal[121]. In 2007, the "Human Microbiome Project", also known as the "Human second Genome Project", became the cornerstone of human exploration and understanding of intestinal microbes[122]. With the in-depth study of intestinal flora, the causal relationship between intestinal microbes and diseases will become more clear, and the specific action mechanism of FMT will become more clear.

FMT has made great progress in the treatment of recurrent CDI. However, due to infection and repeated use of antibiotics, the diversity of intestinal flora is low and the interactions between microorganisms are affected. Studies have shown that FMT with a healthy diversity of microbiome may increase microbial diversity levels to normal levels and enhance microbial interactions[123]. Recent studies have shown that microorganisms produced by biliary saltase may help improve the efficacy of FMT in the treatment of recurrent CDI, as the enzyme degrades taurocholic acid and effectively inhibits *C. difficile*[124]. Other studies have shown that FMT treatment can cause some subsequent problems, such as the use of antibiotics to cause bacterial dysregulation, leading to non-*C. difficile*-dependent colitis recurrence, and thus requiring new FMT corrective treatment[125].

Studies have shown that the most important source of fecal genes is prokaryotic viruses (phages)[126]. Phages are probably also the most overlooked in terms of FMT. Because diarrhea is partially relieved in patients with a small amount of microbial FMT during recurrent CDI, this suggests that phages may play an important role in maintaining host health by regulating gut microbiome composition and its phenotype[127]. Phages play an important role in gene expression of host bacteria and even determine their survival. Thus, FMT may function through donor phage regulation of the recipient flora. Currently, phage transplantation is done through aseptic filtration, which has the advantage of reducing bacterial infection. In addition, a large number of clinical studies are needed to show that phage transplantation has greater application value and potential in some diseases.

The mechanism of action of FMT therapy may be realized through multiple pathways, which may vary according to the FMT condition. However, one of the important mechanisms may be altered microbial metabolite production. This may occur during transplantation or subsequently by newly colonized microorganisms. The effect of the production of large quantities of small molecules by microorganisms on the host needs to be further clarified[128]. The most significant is SCFA butyrate, produced mainly by fibrinolytic enzyme strains, which reduces intestinal permeability and provides nutrients to intestinal cells, producing epigenetic effects[129]. In addition, fibrinolytic enzyme strains has anti-inflammatory properties and can reduce the incidence of T1D in NOD mice[130]. Therefore, FMT may modulate immune activity through autoantigens. In addition, studies have shown reduced production of butyrate strains in T1D[131]. However, when T1D patients were given high concentrations of butyrate, no significant changes were detected in immune cells, and when T1D patients were given FMT, butyrate as an active regulator of protective b cells and immune cells was not detected by metabolomics[132]. As a result, the research impact of using noninvasive biomarkers for microbial metabolism has been largely underestimated[133]. This phenomenon may partly explain some of the

differences between rodent and human studies. In addition, it should be made clear that interventional studies cannot completely exclude the potential mechanism of action of butyrate in T1D[134]. Therefore, it is a long and tortuous road to find meaningful microorganisms from clinical observational studies to improve clinical outcomes.

APPLICAATION PROSPECT OF FMT IN CLINICAL RESEARCH

FMT is a new theory and technology that has prospects in the treatment of intestinal microbiome disorders. However, the mechanism of action, ethical issues and effects of FMT are still controversial. The methodology of donor screening, the preparation and state of fecal bacteria solutions, and the approaches to transplantation are not uniform, and there are different reports on the safety and efficacy of FMT treatment[135]. In the future, more and higher-quality randomized controlled clinical trials should be carried out to address the above problems, so as to provide more adequate evidence-based medical evidence[136]. It is certain that with the deepening of scientific research, the mechanism of FMT will be gradually clarified; the intestinal microbial spectrum, microbial metabolites and their association with diseases will be more clear; and the FMT methodology will be more standardized[137]. Despite its limitations, FMT is currently one of the most important tools for studying the role of microorganisms in the pathogenesis of a range of chronic diseases. To improve the effectiveness of studies, further standardization of FMT should be carried out, such as dosage, transplantation method, and whether to use alternate pretreatment of fresh or frozen preparations[138]. In addition, accurate assessments and calculations are required to avoid type I errors in order to accurately assess efficacy. Of course, many meetings and forums are needed to reach consensus.

CONCLUSION

Donor FMT can restore intestinal microbial function and improve clinical outcomes. Therefore, the question in the future is whether the addition of specific strains of FMT to microbial-targeted therapies can help improve diet and drug therapy to improve human health. Therefore, in order to improve the clinical treatment of recurrent CDI, there is a need for more standardized FMT techniques. Rapid advances in untargeted molecules and bioinformatics have made it possible to analyze in detail the potential mechanisms of action of FMT. These results can identify important microorganisms and their metabolites, which may be used as probiotics, probiotics and epigenetic bacteria to enhance the therapeutic effect of FMT, or even replace FMT, for treatment of metabolic diseases.

FOOTNOTES

Author contributions: Zheng L, Ji YY and Duan SL reviewed the literature and prepared the manuscript, performed to the writing, revising of the manuscript; Zheng L and Wen XL contributed to design this work, and performed overall supervision; Zheng L wrote and revised the paper; all authors approved the final manuscript.

Supported by Shaanxi Province Natural Science Basic Research Program-General Project, No. 2019JM-580 and No. 2021SF-314; Project of Shaanxi Administration of Traditional Chinese Medicine, No. 2019-ZZ-JC010; and Shaanxi Provincial Hospital of Traditional Chinese Medicine, No. 2018-04 and No. 2021-07.

Conflict-of-interest statement: The authors declare that there are no conflicts of interest related to this study.

Open-Access: This article is an open-access article that was selected by an in-house editor and fully peer-reviewed by external reviewers. It is distributed in accordance with the Creative Commons Attribution NonCommercial (CC BY-NC 4.0) license, which permits others to distribute, remix, adapt, build upon this work non-commercially, and license their derivative works on different terms, provided the original work is properly cited and the use is non-commercial. See: https://creativecommons.org/Licenses/by-nc/4.0/

Country/Territory of origin: China

ORCID number: Lie Zheng 0000-0002-8243-3736; Yong-Yi Ji 0000-0003-2001-9916; Xin-Li Wen 0000-0001-5003-862X; Sheng-Lei Duan 0000-0002-4151-1718.

S-Editor: Fan JR
L-Editor: A
P-Editor: Fan JR

REFERENCES

1 **Dabke K**, Hendrick G, Devkota S. The gut microbiome and metabolic syndrome. *J Clin Invest* 2019; **129**: 4050-4057 [PMID: 31573550 DOI: 10.1172/JCI129194]
2 **Marotz CA**, Zarrinpar A. Treating Obesity and Metabolic Syndrome with Fecal Microbiota Transplantation. *Yale J Biol Med* 2016; **89**: 383-388 [PMID: 27698622]
3 **de Groot PF**, Frissen MN, de Clercq NC, Nieuwdorp M. Fecal microbiota transplantation in metabolic syndrome: History, present and future. *Gut Microbes* 2017; **8**: 253-267 [PMID: 28609252 DOI: 10.1080/19490976.2017.1293224]
4 **Paramsothy S**, Nielsen S, Kamm MA, Deshpande NP, Faith JJ, Clemente JC, Paramsothy R, Walsh AJ, van den Bogaerde J, Samuel D, Leong RWL, Connor S, Ng W, Lin E, Borody TJ, Wilkins MR, Colombel JF, Mitchell HM, Kaakoush NO. Specific Bacteria and Metabolites Associated With Response to Fecal Microbiota Transplantation in Patients With Ulcerative Colitis. *Gastroenterology* 2019; **156**: 1440-1454.e2 [PMID: 30529583 DOI: 10.1053/j.gastro.2018.12.001]
5 **Bárcena C**, Valdés-Mas R, Mayoral P, Garabaya C, Durand S, Rodríguez F, Fernández-García MT, Salazar N, Nogacka AM, Garatachea N, Bossut N, Aprahamian F, Lucia A, Kroemer G, Freije JMP, Quirós PM, López-Otín C. Healthspan and lifespan extension by fecal microbiota transplantation into progeroid mice. *Nat Med* 2019; **25**: 1234-1242 [PMID: 31332389 DOI: 10.1038/s41591-019-0504-5]
6 **Sartor RB**, Wu GD. Roles for Intestinal Bacteria, Viruses, and Fungi in Pathogenesis of Inflammatory Bowel Diseases and Therapeutic Approaches. *Gastroenterology* 2017; **152**: 327-339.e4 [PMID: 27769810 DOI: 10.1053/j.gastro.2016.10.012]
7 **Marchesi JR**, Adams DH, Fava F, Hermes GD, Hirschfield GM, Hold G, Quraishi MN, Kinross J, Smidt H, Tuohy KM, Thomas LV, Zoetendal EG, Hart A. The gut microbiota and host health: a new clinical frontier. *Gut* 2016; **65**: 330-339 [PMID: 26338727 DOI: 10.1136/gutjnl-2015-309990]
8 **Kang Y**, Cai Y. Gut microbiota and obesity: implications for fecal microbiota transplantation therapy. *Hormones (Athens)* 2017; **16**: 223-234 [PMID: 29278509 DOI: 10.14310/horm.2002.1742]
9 **Sebastián Domingo JJ**, Sánchez Sánchez C. From the intestinal flora to the microbiome. *Rev Esp Enferm Dig* 2018; **110**: 51-56 [PMID: 29271225 DOI: 10.17235/reed.2017.4947/2017]
10 **Zhang PP**, Li LL, Han X, Li QW, Zhang XH, Liu JJ, Wang Y. Fecal microbiota transplantation improves metabolism and gut microbiome composition in db/db mice. *Acta Pharmacol Sin* 2020; **41**: 678-685 [PMID: 31937933 DOI: 10.1038/s41401-019-0330-9]
11 **Song M**, Chan AT, Sun J. Influence of the Gut Microbiome, Diet, and Environment on Risk of Colorectal Cancer. *Gastroenterology* 2020; **158**: 322-340 [PMID: 31586566 DOI: 10.1053/j.gastro.2019.06.048]
12 **Pushpanathan P**, Mathew GS, Selvarajan S, Seshadri KG, Srikanth P. Gut microbiota and its mysteries. *Indian J Med Microbiol* 2019; **37**: 268-277 [PMID: 31745030 DOI: 10.4103/ijmm.IJMM_19_373]
13 **Chen X**, Devaraj S. Gut Microbiome in Obesity, Metabolic Syndrome, and Diabetes. *Curr Diab Rep* 2018; **18**: 129 [PMID: 30338410 DOI: 10.1007/s11892-018-1104-3]
14 **Muñoz-Garach A**, Diaz-Perdigones C, Tinahones FJ. Gut microbiota and type 2 diabetes mellitus. *Endocrinol Nutr* 2016; **63**: 560-568 [PMID: 27633134 DOI: 10.1016/j.endonu.2016.07.008]
15 **Smits LP**, Kootte RS, Levin E, Prodan A, Fuentes S, Zoetendal EG, Wang Z, Levison BS, Cleophas MCP, Kemper EM, Dallinga-Thie GM, Groen AK, Joosten LAB, Netea MG, Stroes ESG, de Vos WM, Hazen SL, Nieuwdorp M. Effect of Vegan Fecal Microbiota Transplantation on Carnitine- and Choline-Derived Trimethylamine-N-Oxide Production and Vascular Inflammation in Patients With Metabolic Syndrome. *J Am Heart Assoc* 2018; **7** [PMID: 29581220 DOI: 10.1161/JAHA.117.008342]
16 **Sidhu M**, van der Poorten D. The gut microbiome. *Aust Fam Physician* 2017; **46**: 206-211 [PMID: 28376573]
17 **Ballini A**, Scacco S, Boccellino M, Santacroce L, Arrigoni R. Microbiota and Obesity: Where Are We Now? *Biology (Basel)* 2020; **9** [PMID: 33255588 DOI: 10.3390/biology9120415]
18 **Ma Q**, Li Y, Li P, Wang M, Wang J, Tang Z, Wang T, Luo L, Wang C, Zhao B. Research progress in the relationship between type 2 diabetes mellitus and intestinal flora. *Biomed Pharmacother* 2019; **117**: 109138 [PMID: 31247468 DOI: 10.1016/j.biopha.2019.109138]
19 **Bonomo RR**, Cook TM, Gavini CK, White CR, Jones JR, Bovo E, Zima AV, Brown IA, Dugas LR, Zakharian E, Aubert G, Alonzo F 3rd, Calcutt NA, Mansuy-Aubert V. Fecal transplantation and butyrate improve neuropathic pain, modify immune cell profile, and gene expression in the PNS of obese mice. *Proc Natl Acad Sci U S A* 2020; **117**: 26482-26493 [PMID: 33020290 DOI: 10.1073/pnas.2006065117]
20 **Witkowski M**, Weeks TL, Hazen SL. Gut Microbiota and Cardiovascular Disease. *Circ Res* 2020; **127**: 553-570 [PMID: 32762536 DOI: 10.1161/CIRCRESAHA.120.316242]
21 **Milosevic I**, Vujovic A, Barac A, Djelic M, Korac M, Radovanovic Spurnic A, Gmizic I, Stevanovic O, Djordjevic V, Lekic N, Russo E, Amedei A. Gut-Liver Axis, Gut Microbiota, and Its Modulation in the Management of Liver Diseases: A Review of the Literature. *Int J Mol Sci* 2019; **20** [PMID: 30658519 DOI: 10.3390/ijms20020395]
22 **Sommer F**, Anderson JM, Bharti R, Raes J, Rosenstiel P. The resilience of the intestinal microbiota influences health and disease. *Nat Rev Microbiol* 2017; **15**: 630-638 [PMID: 28626231 DOI: 10.1038/nrmicro.2017.58]
23 **Proença IM**, Allegretti JR, Bernardo WM, de Moura DTH, Ponte Neto AM, Matsubayashi CO, Flor MM, Kotinda APST, de Moura EGH. Fecal microbiota transplantation improves metabolic syndrome parameters: systematic review with meta-analysis based on randomized clinical trials. *Nutr Res* 2020; **83**: 1-14 [PMID: 32987284 DOI: 10.1016/j.nutres.2020.06.018]
24 **Gagliardi A**, Totino V, Cacciotti F, Iebba V, Neroni B, Bonfiglio G, Trancassini M, Passariello C, Pantanella F, Schippa S. Rebuilding the Gut Microbiota Ecosystem. *Int J Environ Res Public Health* 2018; **15** [PMID: 30087270 DOI: 10.3390/ijerph15081679]
25 **Illiano P**, Brambilla R, Parolini C. The mutual interplay of gut microbiota, diet and human disease. *FEBS J* 2020; **287**: 833-855 [PMID: 31955527 DOI: 10.1111/febs.15217]

26 **Woting A**, Blaut M. The Intestinal Microbiota in Metabolic Disease. *Nutrients* 2016; **8**: 202 [PMID: 27058556 DOI: 10.3390/nu8040202]

27 **Cheng S**, Ma X, Geng S, Jiang X, Li Y, Hu L, Li J, Wang Y, Han X. Fecal Microbiota Transplantation Beneficially Regulates Intestinal Mucosal Autophagy and Alleviates Gut Barrier Injury. *mSystems* 2018; **3** [PMID: 30320222 DOI: 10.1128/mSystems.00137-18]

28 **Zhang F**, Cui B, He X, Nie Y, Wu K, Fan D; FMT-standardization Study Group. Microbiota transplantation: concept, methodology and strategy for its modernization. *Protein Cell* 2018; **9**: 462-473 [PMID: 29691757 DOI: 10.1007/s13238-018-0541-8]

29 **Chassaing B**, Koren O, Goodrich JK, Poole AC, Srinivasan S, Ley RE, Gewirtz AT. Dietary emulsifiers impact the mouse gut microbiota promoting colitis and metabolic syndrome. *Nature* 2015; **519**: 92-96 [PMID: 25731162 DOI: 10.1038/nature14232]

30 **Muscogiuri G**, Cantone E, Cassarano S, Tuccinardi D, Barrea L, Savastano S, Colao A; on behalf of the Obesity Programs of nutrition, Education, Research and Assessment (OPERA) group. Gut microbiota: a new path to treat obesity. *Int J Obes Suppl* 2019; **9**: 10-19 [PMID: 31391921 DOI: 10.1038/s41367-019-0011-7]

31 **Roman P**, Cardona D, Sempere L, Carvajal F. Microbiota and organophosphates. *Neurotoxicology* 2019; **75**: 200-208 [PMID: 31560873 DOI: 10.1016/j.neuro.2019.09.013]

32 **Haber SL**, Raney CRK, Larson TL, Lau JP. Fecal microbiota transplantation for recurrent Clostridioides difficile infection. *Am J Health Syst Pharm* 2019; **76**: 935-942 [PMID: 31361890 DOI: 10.1093/ajhp/zxz078]

33 **Vangoitsenhoven R**, Cresci GAM. Role of Microbiome and Antibiotics in Autoimmune Diseases. *Nutr Clin Pract* 2020; **35**: 406-416 [PMID: 32319703 DOI: 10.1002/ncp.10489]

34 **Bokoliya SC**, Dorsett Y, Panier H, Zhou Y. Procedures for Fecal Microbiota Transplantation in Murine Microbiome Studies. *Front Cell Infect Microbiol* 2021; **11**: 711055 [PMID: 34621688 DOI: 10.3389/fcimb.2021.711055]

35 **Sarin SK**, Pande A, Schnabl B. Microbiome as a therapeutic target in alcohol-related liver disease. *J Hepatol* 2019; **70**: 260-272 [PMID: 30658727 DOI: 10.1016/j.jhep.2018.10.019]

36 **Lee P**, Yacyshyn BR, Yacyshyn MB. Gut microbiota and obesity: An opportunity to alter obesity through faecal microbiota transplant (FMT). *Diabetes Obes Metab* 2019; **21**: 479-490 [PMID: 30328245 DOI: 10.1111/dom.13561]

37 **Zhang Z**, Mocanu V, Cai C, Dang J, Slater L, Deehan EC, Walter J, Madsen KL. Impact of Fecal Microbiota Transplantation on Obesity and Metabolic Syndrome-A Systematic Review. *Nutrients* 2019; **11** [PMID: 31557953 DOI: 10.3390/nu11102291]

38 **Wortelboer K**, Nieuwdorp M, Herrema H. Fecal microbiota transplantation beyond Clostridioides difficile infections. *EBioMedicine* 2019; **44**: 716-729 [PMID: 31201141 DOI: 10.1016/j.ebiom.2019.05.066]

39 **Yu EW**, Gao L, Stastka P, Cheney MC, Mahabamunuge J, Torres Soto M, Ford CB, Bryant JA, Henn MR, Hohmann EL. Fecal microbiota transplantation for the improvement of metabolism in obesity: The FMT-TRIM double-blind placebo-controlled pilot trial. *PLoS Med* 2020; **17**: e1003051 [PMID: 32150549 DOI: 10.1371/journal.pmed.1003051]

40 **Ianiro G**, Segal JP, Mullish BH, Quraishi MN, Porcari S, Fabiani G, Gasbarrini A, Cammarota G. Fecal microbiota transplantation in gastrointestinal and extraintestinal disorders. *Future Microbiol* 2020; **15**: 1173-1183 [PMID: 32954843 DOI: 10.2217/fmb-2020-0061]

41 **Brunkwall L**, Orho-Melander M. The gut microbiome as a target for prevention and treatment of hyperglycaemia in type 2 diabetes: from current human evidence to future possibilities. *Diabetologia* 2017; **60**: 943-951 [PMID: 28434033 DOI: 10.1007/s00125-017-4278-3]

42 **Mouries J**, Brescia P, Silvestri A, Spadoni I, Sorribas M, Wiest R, Mileti E, Galbiati M, Invernizzi P, Adorini L, Penna G, Rescigno M. Microbiota-driven gut vascular barrier disruption is a prerequisite for non-alcoholic steatohepatitis development. *J Hepatol* 2019; **71**: 1216-1228 [PMID: 31419514 DOI: 10.1016/j.jhep.2019.08.005]

43 **Chang CJ**, Lin CS, Lu CC, Martel J, Ko YF, Ojcius DM, Tseng SF, Wu TR, Chen YY, Young JD, Lai HC. Ganoderma lucidum reduces obesity in mice by modulating the composition of the gut microbiota. *Nat Commun* 2015; **6**: 7489 [PMID: 26102296 DOI: 10.1038/ncomms8489]

44 **Wu H**, Esteve E, Tremaroli V, Khan MT, Caesar R, Mannerås-Holm L, Ståhlman M, Olsson LM, Serino M, Planas-Fèlix M, Xifra G, Mercader JM, Torrents D, Burcelin R, Ricart W, Perkins R, Fernàndez-Real JM, Bäckhed F. Metformin alters the gut microbiome of individuals with treatment-naive type 2 diabetes, contributing to the therapeutic effects of the drug. *Nat Med* 2017; **23**: 850-858 [PMID: 28530702 DOI: 10.1038/nm.4345]

45 **De Musis C**, Granata L, Dallio M, Miranda A, Gravina AG, Romano M. Inflammatory Bowel Diseases: The Role of Gut Microbiota. *Curr Pharm Des* 2020; **26**: 2951-2961 [PMID: 32310042 DOI: 10.2174/1381612826666200420144128]

46 **Zhang X**, Tian H, Chen Q, Qin H, Li N. Fecal microbiota transplantation: standardization or diversification? *Sci China Life Sci* 2019; **62**: 1714-1716 [PMID: 31813093 DOI: 10.1007/s11427-019-1592-8]

47 **Guo XY**, Liu XJ, Hao JY. Gut microbiota in ulcerative colitis: insights on pathogenesis and treatment. *J Dig Dis* 2020; **21**: 147-159 [PMID: 32040250 DOI: 10.1111/1751-2980.12849]

48 **Burberry A**, Wells MF, Limone F, Couto A, Smith KS, Keaney J, Gillet G, van Gastel N, Wang JY, Pietilainen O, Qian M, Eggan P, Cantrell C, Mok J, Kadiu I, Scadden DT, Eggan K. C9orf72 suppresses systemic and neural inflammation induced by gut bacteria. *Nature* 2020; **582**: 89-94 [PMID: 32483373 DOI: 10.1038/s41586-020-2288-7]

49 **Schroeder BO**, Birchenough GMH, Ståhlman M, Arike L, Johansson MEV, Hansson GC, Bäckhed F. Bifidobacteria or Fiber Protects against Diet-Induced Microbiota-Mediated Colonic Mucus Deterioration. *Cell Host Microbe* 2018; **23**: 27-40.e7 [PMID: 29276171 DOI: 10.1016/j.chom.2017.11.004]

50 **Zhou L**, Foster JA. Psychobiotics and the gut-brain axis: in the pursuit of happiness. *Neuropsychiatr Dis Treat* 2015; **11**: 715-723 [PMID: 25834446 DOI: 10.2147/NDT.S61997]

51 **Bicknell B**, Liebert A, Johnstone D, Kiat H. Photobiomodulation of the microbiome: implications for metabolic and inflammatory diseases. *Lasers Med Sci* 2019; **34**: 317-327 [PMID: 30074108 DOI: 10.1007/s10103-018-2594-6]

52 **Leshem A**, Horesh N, Elinav E. Fecal Microbial Transplantation and Its Potential Application in Cardiometabolic Syndrome. *Front Immunol* 2019; **10**: 1341 [PMID: 31258528 DOI: 10.3389/fimmu.2019.01341]

53 **Cohen NA**, Maharshak N. Novel Indications for Fecal Microbial Transplantation: Update and Review of the Literature.

Dig Dis Sci 2017; **62**: 1131-1145 [PMID: 28315032 DOI: 10.1007/s10620-017-4535-9]

54 **Gong S**, Yan Z, Liu Z, Niu M, Fang H, Li N, Huang C, Li L, Chen G, Luo H, Chen X, Zhou H, Hu J, Yang W, Huang Q, Schnabl B, Chang P, Billiar TR, Jiang Y, Chen P. Intestinal Microbiota Mediates the Susceptibility to Polymicrobial Sepsis-Induced Liver Injury by Granisetron Generation in Mice. *Hepatology* 2019; **69**: 1751-1767 [PMID: 30506577 DOI: 10.1002/hep.30361]

55 **Quaranta G**, Sanguinetti M, Masucci L. Fecal Microbiota Transplantation: A Potential Tool for Treatment of Human Female Reproductive Tract Diseases. *Front Immunol* 2019; **10**: 2653 [PMID: 31827467 DOI: 10.3389/fimmu.2019.02653]

56 **Arab JP**, Martin-Mateos RM, Shah VH. Gut-liver axis, cirrhosis and portal hypertension: the chicken and the egg. *Hepatol Int* 2018; **12**: 24-33 [PMID: 28550391 DOI: 10.1007/s12072-017-9798-x]

57 **Leustean AM**, Ciocoiu M, Sava A, Costea CF, Floria M, Tarniceriu CC, Tanase DM. Implications of the Intestinal Microbiota in Diagnosing the Progression of Diabetes and the Presence of Cardiovascular Complications. *J Diabetes Res* 2018; **2018**: 5205126 [PMID: 30539026 DOI: 10.1155/2018/5205126]

58 **Nettleton JE**, Reimer RA, Shearer J. Reshaping the gut microbiota: Impact of low calorie sweeteners and the link to insulin resistance? *Physiol Behav* 2016; **164**: 488-493 [PMID: 27090230 DOI: 10.1016/j.physbeh.2016.04.029]

59 **Woodworth MH**, Carpentieri C, Sitchenko KL, Kraft CS. Challenges in fecal donor selection and screening for fecal microbiota transplantation: A review. *Gut Microbes* 2017; **8**: 225-237 [PMID: 28129018 DOI: 10.1080/19490976.2017.1286006]

60 **Reijnders D**, Goossens GH, Hermes GD, Neis EP, van der Beek CM, Most J, Holst JJ, Lenaerts K, Kootte RS, Nieuwdorp M, Groen AK, Olde Damink SW, Boekschoten MV, Smidt H, Zoetendal EG, Dejong CH, Blaak EE. Effects of Gut Microbiota Manipulation by Antibiotics on Host Metabolism in Obese Humans: A Randomized Double-Blind Placebo-Controlled Trial. *Cell Metab* 2016; **24**: 63-74 [PMID: 27411009 DOI: 10.1016/j.cmet.2016.06.016]

61 **Zhou D**, Pan Q, Shen F, Cao HX, Ding WJ, Chen YW, Fan JG. Total fecal microbiota transplantation alleviates high-fat diet-induced steatohepatitis in mice *via* beneficial regulation of gut microbiota. *Sci Rep* 2017; **7**: 1529 [PMID: 28484247 DOI: 10.1038/s41598-017-01751-y]

62 **Singh R**, Zogg H, Wei L, Bartlett A, Ghoshal UC, Rajender S, Ro S. Gut Microbial Dysbiosis in the Pathogenesis of Gastrointestinal Dysmotility and Metabolic Disorders. *J Neurogastroenterol Motil* 2021; **27**: 19-34 [PMID: 33166939 DOI: 10.5056/jnm20149]

63 **Matsuoka K**, Mizuno S, Hayashi A, Hisamatsu T, Naganuma M, Kanai T. Fecal microbiota transplantation for gastrointestinal diseases. *Keio J Med* 2014; **63**: 69-74 [PMID: 25500625 DOI: 10.2302/kjm.2014-0006-RE]

64 **van Nood E**, Speelman P, Nieuwdorp M, Keller J. Fecal microbiota transplantation: facts and controversies. *Curr Opin Gastroenterol* 2014; **30**: 34-39 [PMID: 24241245 DOI: 10.1097/MOG.0000000000000024]

65 **Thaiss CA**, Zeevi D, Levy M, Zilberman-Schapira G, Suez J, Tengeler AC, Abramson L, Katz MN, Korem T, Zmora N, Kuperman Y, Biton I, Gilad S, Harmelin A, Shapiro H, Halpern Z, Segal E, Elinav E. Transkingdom control of microbiota diurnal oscillations promotes metabolic homeostasis. *Cell* 2014; **159**: 514-529 [PMID: 25417104 DOI: 10.1016/j.cell.2014.09.048]

66 **Yu F**, Han W, Zhan G, Li S, Jiang X, Wang L, Xiang S, Zhu B, Yang L, Luo A, Hua F, Yang C. Abnormal gut microbiota composition contributes to the development of type 2 diabetes mellitus in db/db mice. *Aging (Albany NY)* 2019; **11**: 10454-10467 [PMID: 31760385 DOI: 10.18632/aging.102469]

67 **Jian X**, Zhu Y, Ouyang J, Wang Y, Lei Q, Xia J, Guan Y, Zhang J, Guo J, He Y, Wang J, Li J, Lin J, Su M, Li G, Wu M, Qiu L, Xiang J, Xie L, Jia W, Zhou W. Alterations of gut microbiome accelerate multiple myeloma progression by increasing the relative abundances of nitrogen-recycling bacteria. *Microbiome* 2020; **8**: 74 [PMID: 32466801 DOI: 10.1186/s40168-020-00854-5]

68 **Zou M**, Jie Z, Cui B, Wang H, Feng Q, Zou Y, Zhang X, Yang H, Wang J, Zhang F, Jia H. Fecal microbiota transplantation results in bacterial strain displacement in patients with inflammatory bowel diseases. *FEBS Open Bio* 2020; **10**: 41-55 [PMID: 31622538 DOI: 10.1002/2211-5463.12744]

69 **Ooijevaar RE**, Terveer EM, Verspaget HW, Kuijper EJ, Keller JJ. Clinical Application and Potential of Fecal Microbiota Transplantation. *Annu Rev Med* 2019; **70**: 335-351 [PMID: 30403550 DOI: 10.1146/annurev-med-111717-122956]

70 **Borody TJ**, Khoruts A. Fecal microbiota transplantation and emerging applications. *Nat Rev Gastroenterol Hepatol* 2011; **9**: 88-96 [PMID: 22183182 DOI: 10.1038/nrgastro.2011.244]

71 **Vezza T**, Rodríguez-Nogales A, Algieri F, Garrido-Mesa J, Romero M, Sánchez M, Toral M, Martín-García B, Gómez-Caravaca AM, Arráez-Román D, Segura-Carretero A, Micol V, García F, Utrilla MP, Duarte J, Rodríguez-Cabezas ME, Gálvez J. The metabolic and vascular protective effects of olive (Olea europaea L.) leaf extract in diet-induced obesity in mice are related to the amelioration of gut microbiota dysbiosis and to its immunomodulatory properties. *Pharmacol Res* 2019; **150**: 104487 [PMID: 31610229 DOI: 10.1016/j.phrs.2019.104487]

72 **Yiu JHC**, Chan KS, Cheung J, Li J, Liu Y, Wang Y, Fung WWL, Cai J, Cheung SWM, Dorweiler B, Wan EYF, Tso P, Xu A, Woo CW. Gut Microbiota-Associated Activation of TLR5 Induces Apolipoprotein A1 Production in the Liver. *Circ Res* 2020; **127**: 1236-1252 [PMID: 32820707 DOI: 10.1161/CIRCRESAHA.120.317362]

73 **Costello SP**, Hughes PA, Waters O, Bryant RV, Vincent AD, Blatchford P, Katsikeros R, Makanyanga J, Campaniello MA, Mavrangelos C, Rosewarne CP, Bickley C, Peters C, Schoeman MN, Conlon MA, Roberts-Thomson IC, Andrews JM. Effect of Fecal Microbiota Transplantation on 8-Week Remission in Patients With Ulcerative Colitis: A Randomized Clinical Trial. *JAMA* 2019; **321**: 156-164 [PMID: 30644982 DOI: 10.1001/jama.2018.20046]

74 **Huang Z**, Chen J, Li B, Zeng B, Chou CH, Zheng X, Xie J, Li H, Hao Y, Chen G, Pei F, Shen B, Kraus VB, Wei H, Zhou X, Cheng L. Faecal microbiota transplantation from metabolically compromised human donors accelerates osteoarthritis in mice. *Ann Rheum Dis* 2020; **79**: 646-656 [PMID: 32205337 DOI: 10.1136/annrheumdis-2019-216471]

75 **Landman C**, Quévrain E. [Gut microbiota: Description, role and pathophysiologic implications]. *Rev Med Interne* 2016; **37**: 418-423 [PMID: 26749318 DOI: 10.1016/j.revmed.2015.12.012]

76 **Soto M**, Herzog C, Pacheco JA, Fujisaka S, Bullock K, Clish CB, Kahn CR. Gut microbiota modulate neurobehavior through changes in brain insulin sensitivity and metabolism. *Mol Psychiatry* 2018; **23**: 2287-2301 [PMID: 29910467 DOI:

10.1038/s41380-018-0086-5]
77 **West CE**, Renz H, Jenmalm MC, Kozyrskyj AL, Allen KJ, Vuillermin P, Prescott SL; in-FLAME Microbiome Interest Group. The gut microbiota and inflammatory noncommunicable diseases: associations and potentials for gut microbiota therapies. *J Allergy Clin Immunol* 2015; **135**: 3-13; quiz 14 [PMID: 25567038 DOI: 10.1016/j.jaci.2014.11.012]
78 **Staley C**, Khoruts A, Sadowsky MJ. Contemporary Applications of Fecal Microbiota Transplantation to Treat Intestinal Diseases in Humans. *Arch Med Res* 2017; **48**: 766-773 [PMID: 29183720 DOI: 10.1016/j.arcmed.2017.11.006]
79 **Antushevich H**. Fecal microbiota transplantation in disease therapy. *Clin Chim Acta* 2020; **503**: 90-98 [PMID: 31968211 DOI: 10.1016/j.cca.2019.12.010]
80 **DeFilipp Z**, Bloom PP, Torres Soto M, Mansour MK, Sater MRA, Huntley MH, Turbett S, Chung RT, Chen YB, Hohmann EL. Drug-Resistant *E. coli* Bacteremia Transmitted by Fecal Microbiota Transplant. *N Engl J Med* 2019; **381**: 2043-2050 [PMID: 31665575 DOI: 10.1056/NEJMoa1910437]
81 **Zheng L**, Wen XL, Dai YC. Mechanism of Jianpi Qingchang Huashi Recipe in treating ulcerative colitis: A study based on network pharmacology and molecular docking. *World J Clin Cases* 2021; **9**: 7653-7670 [PMID: 34621817 DOI: 10.12998/wjcc.v9.i26.7653]
82 **Zhang YL**, Cai LT, Qi JY, Lin YZ, Dai YC, Jiao N, Chen YL, Zheng L, Wang BB, Zhu LX, Tang ZP, Zhu RX. Gut microbiota contributes to the distinction between two traditional Chinese medicine syndromes of ulcerative colitis. *World J Gastroenterol* 2019; **25**: 3242-3255 [PMID: 31333315 DOI: 10.3748/wjg.v25.i25.3242]
83 **Zheng L**, Zhang YL, Dai YC, Chen X, Chen DL, Dai YT, Tang ZP. Jianpi Qingchang decoction alleviates ulcerative colitis by inhibiting nuclear factor-κB activation. *World J Gastroenterol* 2017; **23**: 1180-1188 [PMID: 28275298 DOI: 10.3748/wjg.v23.i7.1180]
84 **Chen DL**, Dai YC, Zheng L, Chen YL, Zhang YL, Tang ZP. Features of the gut microbiota in ulcerative colitis patients with depression: A pilot study. *Medicine (Baltimore)* 2021; **100**: e24845 [PMID: 33607855 DOI: 10.1097/MD.0000000000024845]
85 **Zheng L**, Zhang YL, Chen X, Chen DL, Dai YC, Tang ZP. *Astragalus Polysaccharides* Protects Thapsigargin-induced Endoplasmic Reticulum Stress in HT29 Cells. *Open Life Sci* 2019; **14**: 494-501 [PMID: 33817185 DOI: 10.1515/biol-2019-0055]
86 **Gomaa EZ**. Human gut microbiota/microbiome in health and diseases: a review. *Antonie Van Leeuwenhoek* 2020; **113**: 2019-2040 [PMID: 33136284 DOI: 10.1007/s10482-020-01474-7]
87 **Aron-Wisnewsky J**, Clément K, Nieuwdorp M. Fecal Microbiota Transplantation: a Future Therapeutic Option for Obesity/Diabetes? *Curr Diab Rep* 2019; **19**: 51 [PMID: 31250122 DOI: 10.1007/s11892-019-1180-z]
88 **Bibbò S**, Ianiro G, Gasbarrini A, Cammarota G. Fecal microbiota transplantation: past, present and future perspectives. *Minerva Gastroenterol Dietol* 2017; **63**: 420-430 [PMID: 28927251 DOI: 10.23736/S1121-421X.17.02374-1]
89 **Qi X**, Yun C, Sun L, Xia J, Wu Q, Wang Y, Wang L, Zhang Y, Liang X, Gonzalez FJ, Patterson AD, Liu H, Mu L, Zhou Z, Zhao Y, Li R, Liu P, Zhong C, Pang Y, Jiang C, Qiao J. Gut microbiota-bile acid-interleukin-22 axis orchestrates polycystic ovary syndrome. *Nat Med* 2019; **25**: 1225-1233 [PMID: 31332392 DOI: 10.1038/s41591-019-0509-0]
90 **Bajaj JS**, Khoruts A. Microbiota changes and intestinal microbiota transplantation in liver diseases and cirrhosis. *J Hepatol* 2020; **72**: 1003-1027 [PMID: 32004593 DOI: 10.1016/j.jhep.2020.01.017]
91 **Green JE**, Davis JA, Berk M, Hair C, Loughman A, Castle D, Athan E, Nierenberg AA, Cryan JF, Jacka F, Marx W. Efficacy and safety of fecal microbiota transplantation for the treatment of diseases other than *Clostridium difficile* infection: a systematic review and meta-analysis. *Gut Microbes* 2020; **12**: 1-25 [PMID: 33345703 DOI: 10.1080/19490976.2020.1854640]
92 **Dagenais M**, Douglas T, Saleh M. Role of programmed necrosis and cell death in intestinal inflammation. *Curr Opin Gastroenterol* 2014; **30**: 566-575 [PMID: 25291357 DOI: 10.1097/MOG.0000000000000117]
93 **Glick LR**, Sossenheimer PH, Ollech JE, Cohen RD, Hyman NH, Hurst RD, Rubin DT. Low-Dose Metronidazole is Associated With a Decreased Rate of Endoscopic Recurrence of Crohn's Disease After Ileal Resection: A Retrospective Cohort Study. *J Crohns Colitis* 2019; **13**: 1158-1162 [PMID: 30809655 DOI: 10.1093/ecco-jcc/jjz047]
94 **Chen D**, Wu J, Jin D, Wang B, Cao H. Fecal microbiota transplantation in cancer management: Current status and perspectives. *Int J Cancer* 2019; **145**: 2021-2031 [PMID: 30458058 DOI: 10.1002/ijc.32003]
95 **Lavoie S**, Conway KL, Lassen KG, Jijon HB, Pan H, Chun E, Michaud M, Lang JK, Gallini Comeau CA, Dreyfuss JM, Glickman JN, Vlamakis H, Ananthakrishnan A, Kostic A, Garrett WS, Xavier RJ. The Crohn's disease polymorphism, *ATG16L1* T300A, alters the gut microbiota and enhances the local Th1/Th17 response. *Elife* 2019; **8** [PMID: 30666959 DOI: 10.7554/eLife.39982]
96 **Liu JZ**, van Sommeren S, Huang H, Ng SC, Alberts R, Takahashi A, Ripke S, Lee JC, Jostins L, Shah T, Abedian S, Cheon JH, Cho J, Dayani NE, Franke L, Fuyuno Y, Hart A, Juyal RC, Juyal G, Kim WH, Morris AP, Poustchi H, Newman WG, Midha V, Orchard TR, Vahedi H, Sood A, Sung JY, Malekzadeh R, Westra HJ, Yamazaki K, Yang SK; International Multiple Sclerosis Genetics Consortium; International IBD Genetics Consortium, Barrett JC, Alizadeh BZ, Parkes M, Bk T, Daly MJ, Kubo M, Anderson CA, Weersma RK. Association analyses identify 38 susceptibility loci for inflammatory bowel disease and highlight shared genetic risk across populations. *Nat Genet* 2015; **47**: 979-986 [PMID: 26192919 DOI: 10.1038/ng.3359]
97 **Ananthakrishnan AN**, Luo C, Yajnik V, Khalili H, Garber JJ, Stevens BW, Cleland T, Xavier RJ. Gut Microbiome Function Predicts Response to Anti-integrin Biologic Therapy in Inflammatory Bowel Diseases. *Cell Host Microbe* 2017; **21**: 603-610.e3 [PMID: 28494241 DOI: 10.1016/j.chom.2017.04.010]
98 **Shaw SY**, Blanchard JF, Bernstein CN. Association between early childhood otitis media and pediatric inflammatory bowel disease: an exploratory population-based analysis. *J Pediatr* 2013; **162**: 510-514 [PMID: 23084703 DOI: 10.1016/j.jpeds.2012.08.037]
99 **Ungaro R**, Bernstein CN, Gearry R, Hviid A, Kolho KL, Kronman MP, Shaw S, Van Kruiningen H, Colombel JF, Atreja A. Antibiotics associated with increased risk of new-onset Crohn's disease but not ulcerative colitis: a meta-analysis. *Am J Gastroenterol* 2014; **109**: 1728-1738 [PMID: 25223575 DOI: 10.1038/ajg.2014.246]
100 **Park S**, Chun J, Han KD, Soh H, Choi K, Kim JH, Lee J, Lee C, Im JP, Kim JS. Increased end-stage renal disease risk in

patients with inflammatory bowel disease: A nationwide population-based study. *World J Gastroenterol* 2018; **24**: 4798-4808 [PMID: 30479466 DOI: 10.3748/wjg.v24.i42.4798]

101 **Small CL**, Xing L, McPhee JB, Law HT, Coombes BK. Acute Infectious Gastroenteritis Potentiates a Crohn's Disease Pathobiont to Fuel Ongoing Inflammation in the Post-Infectious Period. *PLoS Pathog* 2016; **12**: e1005907 [PMID: 27711220 DOI: 10.1371/journal.ppat.1005907]

102 **Celiberto LS**, Graef FA, Healey GR, Bosman ES, Jacobson K, Sly LM, Vallance BA. Inflammatory bowel disease and immunonutrition: novel therapeutic approaches through modulation of diet and the gut microbiome. *Immunology* 2018; **155**: 36-52 [PMID: 29693729 DOI: 10.1111/imm.12939]

103 **Ananthakrishnan AN**, Bernstein CN, Iliopoulos D, Macpherson A, Neurath MF, Ali RAR, Vavricka SR, Fiocchi C. Environmental triggers in IBD: a review of progress and evidence. *Nat Rev Gastroenterol Hepatol* 2018; **15**: 39-49 [PMID: 29018271 DOI: 10.1038/nrgastro.2017.136]

104 **van der Sloot KWJ**, Amini M, Peters V, Dijkstra G, Alizadeh BZ. Inflammatory Bowel Diseases: Review of Known Environmental Protective and Risk Factors Involved. *Inflamm Bowel Dis* 2017; **23**: 1499-1509 [PMID: 28777099 DOI: 10.1097/MIB.0000000000001217]

105 **van der Sloot KWJ**, Weersma RK, Dijkstra G, Alizadeh BZ. Development and validation of a web-based questionnaire to identify environmental risk factors for inflammatory bowel disease: the Groningen IBD Environmental Questionnaire (GIEQ). *J Gastroenterol* 2019; **54**: 238-248 [PMID: 30109418 DOI: 10.1007/s00535-018-1501-z]

106 **Xu S**, Zou H, Zhang H, Zhu S, Zhou R, Li J. Investigation of inflammatory bowel disease risk factors in 4 families in central China. *Exp Ther Med* 2018; **15**: 1367-1375 [PMID: 29399122 DOI: 10.3892/etm.2017.5582]

107 **Allegretti J**, Eysenbach LM, El-Nachef N, Fischer M, Kelly C, Kassam Z. The Current Landscape and Lessons from Fecal Microbiota Transplantation for Inflammatory Bowel Disease: Past, Present, and Future. *Inflamm Bowel Dis* 2017; **23**: 1710-1717 [PMID: 28858073 DOI: 10.1097/MIB.0000000000001247]

108 **Miyoshi J**, Bobe AM, Miyoshi S, Huang Y, Hubert N, Delmont TO, Eren AM, Leone V, Chang EB. Peripartum Antibiotics Promote Gut Dysbiosis, Loss of Immune Tolerance, and Inflammatory Bowel Disease in Genetically Prone Offspring. *Cell Rep* 2017; **20**: 491-504 [PMID: 28700948 DOI: 10.1016/j.celrep.2017.06.060]

109 **Moossavi S**, Miliku K, Sepehri S, Khafipour E, Azad MB. The Prebiotic and Probiotic Properties of Human Milk: Implications for Infant Immune Development and Pediatric Asthma. *Front Pediatr* 2018; **6**: 197 [PMID: 30140664 DOI: 10.3389/fped.2018.00197]

110 **Li J**, Zhao F, Wang Y, Chen J, Tao J, Tian G, Wu S, Liu W, Cui Q, Geng B, Zhang W, Weldon R, Auguste K, Yang L, Liu X, Chen L, Yang X, Zhu B, Cai J. Gut microbiota dysbiosis contributes to the development of hypertension. *Microbiome* 2017; **5**: 14 [PMID: 28143587 DOI: 10.1186/s40168-016-0222-x]

111 **Huang F**, Zheng X, Ma X, Jiang R, Zhou W, Zhou S, Zhang Y, Lei S, Wang S, Kuang J, Han X, Wei M, You Y, Li M, Li Y, Liang D, Liu J, Chen T, Yan C, Wei R, Rajani C, Shen C, Xie G, Bian Z, Li H, Zhao A, Jia W. Theabrownin from Pu-erh tea attenuates hypercholesterolemia *via* modulation of gut microbiota and bile acid metabolism. *Nat Commun* 2019; **10**: 4971 [PMID: 31672964 DOI: 10.1038/s41467-019-12896-x]

112 **Peng J**, Xiao X, Hu M, Zhang X. Interaction between gut microbiome and cardiovascular disease. *Life Sci* 2018; **214**: 153-157 [PMID: 30385177 DOI: 10.1016/j.lfs.2018.10.063]

113 **Wang H**, Lu Y, Yan Y, Tian S, Zheng D, Leng D, Wang C, Jiao J, Wang Z, Bai Y. Promising Treatment for Type 2 Diabetes: Fecal Microbiota Transplantation Reverses Insulin Resistance and Impaired Islets. *Front Cell Infect Microbiol* 2019; **9**: 455 [PMID: 32010641 DOI: 10.3389/fcimb.2019.00455]

114 **Liu Y**, Wang Y, Ni Y, Cheung CKY, Lam KSL, Xia Z, Ye D, Guo J, Tse MA, Panagiotou G, Xu A. Gut Microbiome Fermentation Determines the Efficacy of Exercise for Diabetes Prevention. *Cell Metab* 2020; **31**: 77-91.e5 [PMID: 31786155 DOI: 10.1016/j.cmet.2019.11.001]

115 **Gupta A**, Khanna S. Fecal Microbiota Transplantation. *JAMA* 2017; **318**: 102 [PMID: 28672320 DOI: 10.1001/jama.2017.6466]

116 **Davidovics ZH**, Michail S, Nicholson MR, Kociolek LK, Pai N, Hansen R, Schwerd T, Maspons A, Shamir R, Szajewska H, Thapar N, de Meij T, Mosca A, Vandenplas Y, Kahn SA, Kellermayer R; FMT Special Interest Group of the North American Society of Pediatric Gastroenterology Hepatology, Nutrition, the European Society for Pediatric Gastroenterology Hepatology, Nutrition. Fecal Microbiota Transplantation for Recurrent Clostridium difficile Infection and Other Conditions in Children: A Joint Position Paper From the North American Society for Pediatric Gastroenterology, Hepatology, and Nutrition and the European Society for Pediatric Gastroenterology, Hepatology, and Nutrition. *J Pediatr Gastroenterol Nutr* 2019; **68**: 130-143 [PMID: 30540704 DOI: 10.1097/MPG.0000000000002205]

117 **Wu J**, Wei Z, Cheng P, Qian C, Xu F, Yang Y, Wang A, Chen W, Sun Z, Lu Y. Rhein modulates host purine metabolism in intestine through gut microbiota and ameliorates experimental colitis. *Theranostics* 2020; **10**: 10665-10679 [PMID: 32929373 DOI: 10.7150/thno.43528]

118 **Tanase DM**, Gosav EM, Neculae E, Costea CF, Ciocoiu M, Hurjui LL, Tarniceriu CC, Maranduca MA, Lacatusu CM, Floria M, Serban IL. Role of Gut Microbiota on Onset and Progression of Microvascular Complications of Type 2 Diabetes (T2DM). *Nutrients* 2020; **12** [PMID: 33276482 DOI: 10.3390/nu12123719]

119 **Vallianou NG**, Stratigou T, Tsagarakis S. Microbiome and diabetes: Where are we now? *Diabetes Res Clin Pract* 2018; **146**: 111-118 [PMID: 30342053 DOI: 10.1016/j.diabres.2018.10.008]

120 **Li Q**, Han Y, Dy ABC, Hagerman RJ. The Gut Microbiota and Autism Spectrum Disorders. *Front Cell Neurosci* 2017; **11**: 120 [PMID: 28503135 DOI: 10.3389/fncel.2017.00120]

121 **Lübbert C**, Salzberger B, Mössner J. Fäkaler Mikrobiomtransfer [Fecal microbiota transplantation]. *Internist (Berl)* 2017; **58**: 456-468 [PMID: 28235986 DOI: 10.1007/s00108-017-0203-6]

122 **Borsom EM**, Lee K, Cope EK. Do the Bugs in Your Gut Eat Your Memories? *Brain Sci* 2020; **10** [PMID: 33153085 DOI: 10.3390/brainsci10110814]

123 **Coman V**, Vodnar DC. Gut microbiota and old age: Modulating factors and interventions for healthy longevity. *Exp Gerontol* 2020; **141**: 111095 [PMID: 32979504 DOI: 10.1016/j.exger.2020.111095]

124 **Zeng SL**, Li SZ, Xiao PT, Cai YY, Chu C, Chen BZ, Li P, Li J, Liu EH. Citrus polymethoxyflavones attenuate metabolic

syndrome by regulating gut microbiome and amino acid metabolism. *Sci Adv* 2020; **6**: eaax6208 [PMID: 31922003 DOI: 10.1126/sciadv.aax6208]

125 **Kc D**, Sumner R, Lippmann S. Gut microbiota and health. *Postgrad Med* 2020; **132**: 274 [PMID: 31566046 DOI: 10.1080/00325481.2019.1662711]

126 **Yu F**, Jiang R, Han W, Zhan G, Xu X, Jiang X, Wang L, Xiang S, Zhou Q, Liu C, Zhu B, Hua F, Yang C. Gut microbiota transplantation from db/db mice induces diabetes-like phenotypes and alterations in Hippo signaling in pseudo germ-free mice. *Aging (Albany NY)* 2020; **12**: 24156-24167 [PMID: 33223509 DOI: 10.18632/aging.104101]

127 **Woldeamlak B**, Yirdaw K, Biadgo B. Role of Gut Microbiota in Type 2 Diabetes Mellitus and Its Complications: Novel Insights and Potential Intervention Strategies. *Korean J Gastroenterol* 2019; **74**: 314-320 [PMID: 31870137 DOI: 10.4166/kjg.2019.74.6.314]

128 **Jia Q**, Li H, Zhou H, Zhang X, Zhang A, Xie Y, Li Y, Lv S, Zhang J. Role and Effective Therapeutic Target of Gut Microbiota in Heart Failure. *Cardiovasc Ther* 2019; **2019**: 5164298 [PMID: 31819762 DOI: 10.1155/2019/5164298]

129 **Barba C**, Soulage CO, Caggiano G, Glorieux G, Fouque D, Koppe L. Effects of Fecal Microbiota Transplantation on Composition in Mice with CKD. *Toxins (Basel)* 2020; **12** [PMID: 33255454 DOI: 10.3390/toxins12120741]

130 **Gilbert B**, Schrenzel J. [Fecal microbiota transplantation : current status and prospects]. *Rev Med Suisse* 2019; **15**: 976-983 [PMID: 31066530]

131 **Bajaj JS**, Kassam Z, Fagan A, Gavis EA, Liu E, Cox IJ, Kheradman R, Heuman D, Wang J, Gurry T, Williams R, Sikaroodi M, Fuchs M, Alm E, John B, Thacker LR, Riva A, Smith M, Taylor-Robinson SD, Gillevet PM. Fecal microbiota transplant from a rational stool donor improves hepatic encephalopathy: A randomized clinical trial. *Hepatology* 2017; **66**: 1727-1738 [PMID: 28586116 DOI: 10.1002/hep.29306]

132 **Napolitano M**, Covasa M. Microbiota Transplant in the Treatment of Obesity and Diabetes: Current and Future Perspectives. *Front Microbiol* 2020; **11**: 590370 [PMID: 33304339 DOI: 10.3389/fmicb.2020.590370]

133 **Rasmussen TS**, Koefoed AK, Jakobsen RR, Deng L, Castro-Mejía JL, Brunse A, Neve H, Vogensen FK, Nielsen DS. Bacteriophage-mediated manipulation of the gut microbiome - promises and presents limitations. *FEMS Microbiol Rev* 2020; **44**: 507-521 [PMID: 32495834 DOI: 10.1093/femsre/fuaa020]

134 **Smillie CS**, Sauk J, Gevers D, Friedman J, Sung J, Youngster I, Hohmann EL, Staley C, Khoruts A, Sadowsky MJ, Allegretti JR, Smith MB, Xavier RJ, Alm EJ. Strain Tracking Reveals the Determinants of Bacterial Engraftment in the Human Gut Following Fecal Microbiota Transplantation. *Cell Host Microbe* 2018; **23**: 229-240.e5 [PMID: 29447696 DOI: 10.1016/j.chom.2018.01.003]

135 **Gurram B**, Sue PK. Fecal microbiota transplantation in children: current concepts. *Curr Opin Pediatr* 2019; **31**: 623-629 [PMID: 31169545 DOI: 10.1097/MOP.0000000000000787]

136 **Caesar R**. Pharmacologic and Nonpharmacologic Therapies for the Gut Microbiota in Type 2 Diabetes. *Can J Diabetes* 2019; **43**: 224-231 [PMID: 30929665 DOI: 10.1016/j.jcjd.2019.01.007]

137 **Schepper JD**, Collins F, Rios-Arce ND, Kang HJ, Schaefer L, Gardinier JD, Raghuvanshi R, Quinn RA, Britton R, Parameswaran N, McCabe LR. Involvement of the Gut Microbiota and Barrier Function in Glucocorticoid-Induced Osteoporosis. *J Bone Miner Res* 2020; **35**: 801-820 [PMID: 31886921 DOI: 10.1002/jbmr.3947]

138 **Fuhri Snethlage CM**, Nieuwdorp M, Hanssen NMJ. Faecal microbiota transplantation in endocrine diseases and obesity. *Best Pract Res Clin Endocrinol Metab* 2021; **35**: 101483 [PMID: 33414033 DOI: 10.1016/j.beem.2020.101483]

World Journal of Gastroenterology

Submit a Manuscript: https://www.f6publishing.com

World J Gastroenterol 2022 June 21; 28(23): 2561-2568

DOI: 10.3748/wjg.v28.i23.2561

ISSN 1007-9327 (print) ISSN 2219-2840 (online)

MINIREVIEWS

Up to seven criteria in selection of systemic therapy for hepatocellular carcinoma

Tarik Silk, Mikhail Silk, Jennifer Wu

Specialty type: Gastroenterology and hepatology

Provenance and peer review: Invited article; Externally peer reviewed.

Peer-review model: Single blind

Peer-review report's scientific quality classification

Grade A (Excellent): 0
Grade B (Very good): B
Grade C (Good): 0
Grade D (Fair): 0
Grade E (Poor): 0

P-Reviewer: Li XC, China

Received: December 29, 2021
Peer-review started: December 29, 2021
First decision: March 10, 2022
Revised: March 25, 2022
Accepted: April 30, 2022
Article in press: April 30, 2022
Published online: June 21, 2022

Tarik Silk, Department of Internal Medicine, NYU Grossman School of Medicine, New York, NY 10016, United States

Mikhail Silk, Department of Interventional Radiology, Memorial Sloan Kettering Cancer Center, New York, NY 10065, United States

Jennifer Wu, Division of Hematology and Oncology, Perlmutter Cancer Center of NYU Langone Health, NYU School of Medicine, New York, NY 10016, United States

Corresponding author: Jennifer Wu, MD, Associate Professor, Attending Doctor, Division of Hematology and Oncology, Perlmutter Cancer Center of NYU Langone Health, NYU School of Medicine, 462 First Ave, BCD556, New York, NY 10016, United States.
jennifer.wu@nyulangone.org

Abstract

Barcelona clinic liver cancer (BCLC) intermediate stage hepatocellular carcinoma is a heterogenous disease. Transarterial chemoembolization is offered as the first line therapy in this disease stage. Recent advances in systemic therapy have markedly improved outcomes even in advanced stage disease. The use of systemic therapy in BCLC intermediate stage disease may now be of therapeutic benefit in selected patients. We will focus on "the up to seven" criteria and its utility in selecting systemic therapy.

Key Words: Chemoembolization; Hepatocellular carcinoma; Immunotherapy; Drug combinations; Review; Medical oncology

©The Author(s) 2022. Published by Baishideng Publishing Group Inc. All rights reserved.

Core Tip: Barcelona clinic liver cancer intermediate stage disease that exceeds "the up to seven" criteria, especially with lesions larger than 5 cm, is less likely to respond to transarterial chemoembolization (TACE) alone and is therefore a disease that may respond better to systemic therapy. The use of "the up to seven" criteria can be a helpful guidepost for when to consider systemic therapy alone or in addition to TACE. With the recent breakthroughs in immunotherapy for advanced hepatocellular carcinoma which clearly demonstrated overall survival advantage over single agent tyrosine kinase inhibitors sorafenib, it is promising that the use of immunotherapy would likely lead to better outcome when used in intermediate disease.

Citation: Silk T, Silk M, Wu J. Up to seven criteria in selection of systemic therapy for hepatocellular carcinoma. *World J Gastroenterol* 2022; 28(23): 2561-2568
URL: https://www.wjgnet.com/1007-9327/full/v28/i23/2561.htm
DOI: https://dx.doi.org/10.3748/wjg.v28.i23.2561

INTRODUCTION

Hepatocellular carcinoma (HCC) accounts for 80% of primary liver cancers worldwide[1]. It is one of the cancers with the highest mortality rate, with a 5-year survival rate of only 20%[2]. Treatment of HCC depends on the staging according to the Barcelona clinic liver cancer (BCLC) staging system which is determined by tumor characteristics, liver function (assessed by Child-Pugh score) and patient performance status[3]. Using these criteria, patients may be categorized as early, intermediate or advanced stage disease.

"THE UP TO SEVEN" CRITERIA

Candidates for liver transplantation are most often assessed using the Milan Criteria which was published in 1996. It set strict guidelines to identify individuals who are most likely to benefit from transplantation in an effort to minimize cancer recurrence and maximize overall survival (OS)[4].

Recently the authors of the Milan Criteria have purposed an expansion of the guidelines termed "the up to seven" criteria. In a study of 1556 patients who underwent liver transplantation for HCC, the authors developed software that searched for combinations of tumor characteristics exceeding the Milan criteria, but resulted in an estimated 5-year OS of at least 70%. These found characteristics were termed "the up to seven" criteria. Seven being the sum of the size in centimeters and the number of tumors. Examples, as illustrated in the study, one tumor up to 6 cm in size 6 + 1 = 7, to multiple tumors with seven as the sum of the size plus number (*i.e.*, two tumors up to 5 cm in total size , three tumors up to 4 cm in total size, *etc.*)[5].

A recent retrospective study comparing OS among liver transplant patients based on their selection by the Milan or "the up to seven" criteria found no differences between the two groups[6].

TRANSARTERIAL CHEMOEMBOLIZATION THERAPY IN INTERMEDIATE STAGE DISEASE

Patients with intermediate stage disease, classified by multi-nodular disease, Child-Pugh A-B, with an ECOG performance status of 0, with no extra hepatic spread are candidates for transarterial chemoembolization (TACE).

TACE therapy preferentially targets HCC due to the tumor's disproportionally higher arterial vascular supply compared to normal liver parenchyma[3]. The success of TACE was demonstrated with two randomized control trials (RCTs) and a meta-analysis[7-9].

TACE therapy can be given in different forms including by conventional TACE (cTACE), by drug-eluting beads-TACE (DEB-TACE) and by bland embolization (TAE) which does not use chemotherapy [10].

In cTACE, a cytotoxic drug that has been emulsified in Lipidol is intra-arterially injected followed by the embolic agent. The efficacy of cTACE was recently reaffirmed with an estimated average median OS of 30 mo[3,11-13].

In DEB-TACE, the embolic agent is loaded with cytotoxic medications[14].

In TAE, embolization is performed without a cytotoxic drug[15].

The differences in outcomes between these techniques have been compared. In a phase III trial the Precision Italia Study Group compared DEB-TACE with cTACE and found no difference in response rates, median time to progression, or survival[16]. This finding was also supported by a meta-analysis of 4 RCTs and 8 observational studies which concluded there was a non-superiority of DEB-TACE *vs* cTACE[10]. Similarly a meta-analysis comparing TAE *vs* cTACE found no difference in OS, or objective response to therapy[15].

However despite similar outcomes TAE therapy has its critics who note TAE therapy results in less tumor necrosis compared to other forms of TACE therapy which may prevent its complete adoption[17,18].

Another criticism of TACE therapy in general is that as a therapy it is non-standardized[19]. This is especially true of TACE therapy with cytotoxic agents as there are several chemotherapeutic drugs which may be used[20]. Additionally the extent to which stasis of flow is achieve in the target vessel is also physician operator dependent[21]. This lack of standardization and dependency on the skill of the interventionist makes a more uniform approach *via* systemic therapy desirable.

THE POTENTIAL OF SYSTEMIC THERAPY IN INTERMEDIATE STAGE DISEASE

Predictive factors of whether to initiate TACE include: Tumor size, vascularity, arterial anatomy, infiltrative *vs* nodular growth, presence of splenomegaly, Alfa-fetoprotein changes, albumin and bilirubin levels[22]. Furthermore the decision to repeat TACE should depend on the response based on modified RECIST criteria to prior TACE therapy[23,24]. Of note as radiographic assessment is dependent on the reading physician it is important that this be carried out by a radiologist experienced in HCC[25]. Patients who have an initial complete response to TACE may undergo a second procedure if warranted as long as they are still candidates for therapy. For patients with a partial response or even stable disease repeat treatment at regular intervals may be offered but that decision should be weighed against liver toxicity from treatment[22,26]. Patients with no objective response to two TACE treatments are unlikely to benefit from further TACE and would likely benefit from alternative therapy[26,27]. Even if clinicians are hesitant to choose systemic therapies as initial treatments in intermediate stage HCC, survival maybe improved by switching to these therapies in TACE refractory disease[28,29]. The 2018 OPTIMIS trial followed 1650 patients with unresectable HCC who were to undergo TACE therapy. 31% of these patients became TACE ineligible during the study but only 9% received sorafenib when deemed ineligible for TACE with the remainder having systemic therapy delayed or not receiving it at all[30]. It is therefore critical to determine which patients would be unlikely to benefit from TACE early as to not delay appropriate care (Table 1).

Although current guidelines recommend TACE as first line treatment in intermediate stage HCC, this disease is characterized by high heterogeneity and its real world management may be as equally diverse [27,31].

HCC exceeding "the up to seven" criteria is less likely to respond to TACE due to higher tumor burden[32,33]. In fact, patients beyond "the up to seven" criteria who undergo TACE had higher rates of liver function deterioration post procedure[34]. This is particularly concerning considering poor liver function may preclude patient's from promising systemic therapies[35,36].

In a retrospective propensity matched study by Kudo *et al*[37], patients with BCLC intermediate stage HCC beyond "the up to seven" criteria were treated with lenvatinib systemic therapy or TACE. Whereas TACE treatment led to a decline in liver function, lenvatinib treatment did not result in such a decline. OS was significantly longer in the lenvatinib group 37.9 mo *vs* 21.3 mo; hazard ratio: 0.48, $P < 0.01$. In the study protocol, after progression on lenvatinib, second line treatment including TACE, hepatic arterial infusion chemotherapy, sorafenib, regorafenib, or investigational therapies were allowed. Of note, about 70% of the patients who received lenvatinib underwent subsequent TACE. Patients who received TACE as initial treatment where allowed to undergo repeat TACE. After becoming TACE refractory, second line treatments were identical to the ones in the levantinib group [37].

Recently results from the phase III IMbrave-150 trail have changed management of locally advanced or metastatic/unresectable HCC who are either not TACE candidates or became refractory to TACE. In this trial, the immunotherapy and vascular endothelial growth factor inhibitor combination atezolizumab + bevacizumab was compared against sorafenib, the old standard of care. Median OS was 19.2 mo with the combination therapy *vs* 13.4 mo with sorafenib [HR, 0.66 (95%CI: 0.52-0.85); $P = 0.0009$][38,39]. This combination was the first to show clinical benefit over sorafenib since 2007 and is now first line therapy in the treatment of advanced stage liver cancer[40]. Immunotherapy doublet combination treatments have also shown promise. In the Checkmate-40 trial, nivolumab plus ipilimumab in the second line setting (after sorafenib) showed median OS of 22.8 mo with an overall response rate (ORR) of 32%[41]. A similar combination in a phase II study using the anti-programmed death-ligand 1 antibody durvalumab plus tremelimumab (CTLA-4 antibody) for patients who progressed on, were intolerant to, or refused sorafenib showed a median OS of 18.7 mo and an ORR of 22.7%. A trial of this combination in the first line is being tested in the phase III HIMALAYA study[42]. A press releases from the trial stated that the combination significantly improved OS compared to sorafenib with an HR of

Table 1 Considerations in initiating systemic therapy over transarterial chemoembolization[26,44,53-55]

No.	Considerations
1	Tumor exceeds "the up to seven" criteria
2	Tumor(s) larger than 5cm
3	Contiguous multinodular tumors
4	Poorly differentiated or undifferentiated HCC
5	No objective response to 2 consecvutive TACE treatments

HCC: Hepatocellular carcinoma; TACE: Transarterial chemoembolization.

Table 2 Combination therapy trials

Trial therapies	Study name	Phase	Patient number or estimation	ORR	Median PFS	Median OS
Lenvatinib + TACE *vs* Lenvatinib[47]	LAUNCH	Phase 3	338	54.1% *vs* 25%	10.6 mo *vs* 6.4 mo	17.8 mo *vs* 11.5 mo
(cTACE or DEB-TACE) + durvalumab followed by durvalumab + placebo *vs* (DEB-TACE or cTACE) + durvalumab followed by durvalumab + bevacizumab *vs* (DEB-TACE or cTACE)[48]	EMERLD	Phase 3	600	In progress	In progress	In progress
Lenvatinib + Pembrolizumab + TACE *vs* Placebo + TACE[49]	LEAP-012	Phase 3	950	In progress	In progress	In progress
Nivolumab + Ipilimumab + TACE *vs* Nivolumab + Placebo + TACE *vs* Placebo + Placebo + TACE[50]	Checkmate-74W	Phase 3	765	In progress	In progress	In progress
Brivanib + TACE *vs* Placebo + TACE[51]	BRISK-TA	Phase 3	502	48% *vs* 42%	8.4 mo *vs* 4.9 mo[1]	26.4 mo *vs* 26.1 mo
Oranitib + TACE *vs* Placebo + TACE[52]	ORIENTAL	Phase 3	889	Not reported	2.9 mo *vs* 2.5 mo[1]	31.1 mo *vs* 32.3 mo
Tremelimumab + TACE[53]		Phase 2	11	18%	7.4 mo[1]	13.6 mo

[1]Reported as time to radiographic progression.
ORR: Overall response rate; PFS: Progression free survival; OS: Overall survival; TACE: Transarterial chemoembolization.

0.78[43,44].

In select BCLC intermediate stage disease systemic therapy should be considered in the frontline setting, especially for patients who have been refractory to TACE or in whom TACE is unlikely to be effective. Patient's unlikely to respond well to TACE include patients who exceed "the up to seven" criteria, as well as those who have tumors without a clear boundary, multifocal tumors, or poorly differentiated HCC[33,34,36,45,46].

As a heterogenous disease BCLC intermediate stage HCC maybe best treated with combination therapy. In fact, the success of combination therapy in advanced disease is now being tested in BCLC intermediate stage disease. Current investigations that combine TACE with systemic therapy include the phase III LAUNCH study in which patients with BCLC stage C disease was treated with lenvatinib + TACE *vs* lenvatinib alone. The combination group saw an improved OS from 11.5 to 17.8 mo. Additional the combination had higher ORR, 54.1% *vs* 25%, and higher disease control rate (DCR), 94.1% *vs* 73.2%, as well as a longer progression free survival, 10.6 mo *vs* 6.4 mo[47]. Other upcoming TACE and systemic therapy combination treatments include the studies EMERLD-1, LEAP-012, and Checkmate-74W. EMERLD-1 will assess efficacy and safety for durvalumab monotherapy with DEB-TACE or cTACE followed by durvalumab with or without bevacizumab therapy in patients with HCC not amenable to curative therapy. LEAP-012 will test lenvatinib plus pembrolizumab *vs* placebo in combination with TACE in patients with intermediate HCC. Checkmate-74W will analyze the combination of dual immune checkpoint blockade and TACE *vs* mono-therapy immune checkpoint blockade and TACE for patients with HCC exceeding the up to seven criteria[48-50].

Although these ongoing trials are exciting, it is worth noting that several studies which combined TACE and systemic therapy have failed to show desired efficacy. These include BRISK-TA and ORIENTAL which both compared targeted therapy and TACE to TACE alone. In both trials there was no improvement in OS compared to TACE alone[51,52]. Finally in a 2017 study by Duffy *et al*[53] the

addition of anti CTLA-4 immunotherapy in 11 patients previously treated with TACE showed a OS of 13.6 mo which is comparable to systemic therapy alone[53] (Table 2).

CONCLUSION

BCLC intermediate stage disease that exceeds "the up to seven" criteria, especially with lesions larger than 5 cm, is less likely to respond to TACE alone and is therefore a disease that may respond better to systemic therapy[32,33,37,54]. The use of "the up to seven" criteria can be a helpful guidepost for when to consider systemic therapy alone or in addition to TACE. With the recent breakthroughs in immunotherapy for advanced HCC which clearly demonstrated OS advantage over single agent tyrosine kinase inhibitors sorafenib, it is promising that the use of immunotherapy would likely lead to better outcome when used in intermediate disease. However, this conjecture requires validation from prospective phase III studies.

Improvements in the treatment of liver cancer have the ability to change the lives of the nearly 800000 patients diagnosed with liver cancer annually. The use of TACE therapy rightfully remains a cornerstone of treatment. However for patients who are unlikely to benefit from TACE therapy alone such as patients exceeding "the up to seven" criteria, alternative treatments including systemic therapies warrant consideration especially with recent advancements in the field.

FOOTNOTES

Author contributions: Silk T drafted the manuscript, coordinated all the author's efforts and provided the final revisions; Silk M edited the section related to interventional radiology and TACE; Wu J provided the concept of the manuscript, established the structure of the manuscript, offered the references and revised the drafts.

Conflict-of-interest statement: Dr. Silk has nothing to disclose.

Open-Access: This article is an open-access article that was selected by an in-house editor and fully peer-reviewed by external reviewers. It is distributed in accordance with the Creative Commons Attribution NonCommercial (CC BY-NC 4.0) license, which permits others to distribute, remix, adapt, build upon this work non-commercially, and license their derivative works on different terms, provided the original work is properly cited and the use is non-commercial. See: https://creativecommons.org/Licenses/by-nc/4.0/

Country/Territory of origin: United States

ORCID number: Tarik Silk 0000-0003-2291-2417; Mikhail Silk 0000-0002-4616-7485; Jennifer Wu 0000-0002-1714-0021.

S-Editor: Fan JR
L-Editor: A
P-Editor: Fan JR

REFERENCES

1 **McGlynn KA**, Petrick JL, London WT. Global epidemiology of hepatocellular carcinoma: an emphasis on demographic and regional variability. *Clin Liver Dis* 2015; **19**: 223-238 [PMID: 25921660 DOI: 10.1016/j.cld.2015.01.001]
2 **American Cancer Society**. Cancer Facts and Figures 2021. Atlanta, G.A.C.S. 2021. [cited 10 November 2021]. Available from: https://www.cancer.org/research/cancer-facts-statistics/all-cancer-facts-figures/cancer-facts-figures-2021.html
3 **Raoul JL**, Forner A, Bolondi L, Cheung TT, Kloeckner R, de Baere T. Updated use of TACE for hepatocellular carcinoma treatment: How and when to use it based on clinical evidence. *Cancer Treat Rev* 2019; **72**: 28-36 [PMID: 30447470 DOI: 10.1016/j.ctrv.2018.11.002]
4 **Mazzaferro V**, Regalia E, Doci R, Andreola S, Pulvirenti A, Bozzetti F, Montalto F, Ammatuna M, Morabito A, Gennari L. Liver transplantation for the treatment of small hepatocellular carcinomas in patients with cirrhosis. *N Engl J Med* 1996; **334**: 693-699 [PMID: 8594428 DOI: 10.1056/nejm199603143341104]
5 **Mazzaferro V**, Llovet JM, Miceli R, Bhoori S, Schiavo M, Mariani L, Camerini T, Roayaie S, Schwartz ME, Grazi GL, Adam R, Neuhaus P, Salizzoni M, Bruix J, Forner A, De Carlis L, Cillo U, Burroughs AK, Troisi R, Rossi M, Gerunda GE, Lerut J, Belghiti J, Boin I, Gugenheim J, Rochling F, Van Hoek B, Majno P; Metroticket Investigator Study Group. Predicting survival after liver transplantation in patients with hepatocellular carcinoma beyond the Milan criteria: a retrospective, exploratory analysis. *Lancet Oncol* 2009; **10**: 35-43 [PMID: 19058754 DOI: 10.1016/S1470-2045(08)70284-5]
6 **Martino MD**, Lai Q, Lucatelli P, Damato E, Calabrese A, Masci GM, Parisse S, Sedati P, Merli M, Mennini G, Rossi M, Corradini SG, Catalano C. Comparison of Up-to-seven criteria with Milan Criteria for liver transplantation in patients with HCC. *Trends Transplant* 2021; 14 [DOI: 10.15761/tit.1000300]

7 **Llovet JM**, Real MI, Montaña X, Planas R, Coll S, Aponte J, Ayuso C, Sala M, Muchart J, Solà R, Rodés J, Bruix J; Barcelona Liver Cancer Group. Arterial embolisation or chemoembolisation *vs* symptomatic treatment in patients with unresectable hepatocellular carcinoma: a randomised controlled trial. *Lancet* 2002; **359**: 1734-1739 [PMID: 12049862 DOI: 10.1016/S0140-6736(02)08649-X]

8 **Lo CM**, Ngan H, Tso WK, Liu CL, Lam CM, Poon RT, Fan ST, Wong J. Randomized controlled trial of transarterial lipiodol chemoembolization for unresectable hepatocellular carcinoma. *Hepatology* 2002; **35**: 1164-1171 [PMID: 11981766 DOI: 10.1053/jhep.2002.33156]

9 **Llovet JM**, Bruix J. Systematic review of randomized trials for unresectable hepatocellular carcinoma: Chemoembolization improves survival. *Hepatology* 2003; **37**: 429-442 [PMID: 12540794 DOI: 10.1053/jhep.2003.50047]

10 **Facciorusso A**, Di Maso M, Muscatiello N. Drug-eluting beads *vs* conventional chemoembolization for the treatment of unresectable hepatocellular carcinoma: A meta-analysis. *Dig Liver Dis* 2016; **48**: 571-577 [PMID: 26965785 DOI: 10.1016/j.dld.2016.02.005]

11 **Prince D**, Liu K, Xu W, Chen M, Sun JY, Lu XJ, Ji J. Management of patients with intermediate stage hepatocellular carcinoma. *Ther Adv Med Oncol* 2020; **12**: 1758835920970840 [PMID: 33224278 DOI: 10.1177/1758835920970840]

12 **Llovet JM**, De Baere T, Kulik L, Haber PK, Greten TF, Meyer T, Lencioni R. Locoregional therapies in the era of molecular and immune treatments for hepatocellular carcinoma. *Nat Rev Gastroenterol Hepatol* 2021; **18**: 293-313 [PMID: 33510460 DOI: 10.1038/s41575-020-00395-0]

13 **Llovet JM**, Kelley RK, Villanueva A, Singal AG, Pikarsky E, Roayaie S, Lencioni R, Koike K, Zucman-Rossi J, Finn RS. Hepatocellular carcinoma. *Nat Rev Dis Primers* 2021; **7**: 6 [PMID: 33479224 DOI: 10.1038/s41572-020-00240-3]

14 **Melchiorre F**, Patella F, Pescatori L, Pesapane F, Fumarola E, Biondetti P, Brambillasca P, Monaco C, Ierardi AM, Franceschelli G, Carrafiello G. DEB-TACE: a standard review. *Future Oncol* 2018; **14**: 2969-2984 [PMID: 29987957 DOI: 10.2217/fon-2018-0136]

15 **Facciorusso A**, Bellanti F, Villani R, Salvatore V, Muscatiello N, Piscaglia F, Vendemiale G, Serviddio G. Transarterial chemoembolization *vs* bland embolization in hepatocellular carcinoma: A meta-analysis of randomized trials. *United European Gastroenterol J* 2017; **5**: 511-518 [PMID: 28588882 DOI: 10.1177/2050640616673516]

16 **Golfieri R**, Giampalma E, Renzulli M, Cioni R, Bargellini I, Bartolozzi C, Breatta AD, Gandini G, Nani R, Gasparini D, Cucchetti A, Bolondi L, Trevisani F; PRECISION ITALIA STUDY GROUP. Randomised controlled trial of doxorubicin-eluting beads *vs* conventional chemoembolisation for hepatocellular carcinoma. *Br J Cancer* 2014; **111**: 255-264 [PMID: 24937669 DOI: 10.1038/bjc.2014.199]

17 **Nicolini A**, Martinetti L, Crespi S, Maggioni M, Sangiovanni A. Transarterial chemoembolization with epirubicin-eluting beads *vs* transarterial embolization before liver transplantation for hepatocellular carcinoma. *J Vasc Interv Radiol* 2010; **21**: 327-332 [PMID: 20097098 DOI: 10.1016/j.jvir.2009.10.038]

18 **Tsochatzis EA**, Fatourou E, O'Beirne J, Meyer T, Burroughs AK. Transarterial chemoembolization and bland embolization for hepatocellular carcinoma. *World J Gastroenterol* 2014; **20**: 3069-3077 [PMID: 24695579 DOI: 10.3748/wjg.v20.i12.3069]

19 **Facciorusso A**. Drug-eluting beads transarterial chemoembolization for hepatocellular carcinoma: Current state of the art. *World J Gastroenterol* 2018; **24**: 161-169 [PMID: 29375202 DOI: 10.3748/wjg.v24.i2.161]

20 **Renzulli M**, Peta G, Vasuri F, Marasco G, Caretti D, Bartalena L, Spinelli D, Giampalma E, D'Errico A, Golfieri R. Standardization of conventional chemoembolization for hepatocellular carcinoma. *Ann Hepatol* 2021; **22**: 100278 [PMID: 33129978 DOI: 10.1016/j.aohep.2020.10.006]

21 **Jin B**, Wang D, Lewandowski RJ, Riaz A, Ryu RK, Sato KT, Larson AC, Salem R, Omary RA. Chemoembolization endpoints: effect on survival among patients with hepatocellular carcinoma. *AJR Am J Roentgenol* 2011; **196**: 919-928 [PMID: 21427346 DOI: 10.2214/AJR.10.4770]

22 **Müller L**, Stoehr F, Mähringer-Kunz A, Hahn F, Weinmann A, Kloeckner R. Current Strategies to Identify Patients That Will Benefit from TACE Treatment and Future Directions a Practical Step-by-Step Guide. *J Hepatocell Carcinoma* 2021; **8**: 403-419 [PMID: 34012930 DOI: 10.2147/JHC.S285735]

23 **Lencioni R**, Llovet JM. Modified RECIST (mRECIST) assessment for hepatocellular carcinoma. *Semin Liver Dis* 2010; **30**: 52-60 [PMID: 20175033 DOI: 10.1055/s-0030-1247132]

24 **Shim JH**, Lee HC, Kim SO, Shin YM, Kim KM, Lim YS, Suh DJ. Which response criteria best help predict survival of patients with hepatocellular carcinoma following chemoembolization? *Radiology* 2012; **262**: 708-718 [PMID: 22187634 DOI: 10.1148/radiol.11110282]

25 **Tovoli F**, Renzulli M, Negrini G, Brocchi S, Ferrarini A, Andreone A, Benevento F, Golfieri R, Morselli-Labate AM, Mastroroberto M, Badea RI, Piscaglia F. Inter-operator variability and source of errors in tumour response assessment for hepatocellular carcinoma treated with sorafenib. *Eur Radiol* 2018; **28**: 3611-3620 [PMID: 29633000 DOI: 10.1007/s00330-018-5393-3]

26 **Choi J**, Lee D, Shim JH, Kim KM, Lim YS, Lee YS, Lee HC. Evaluation of transarterial chemoembolization refractoriness in patients with hepatocellular carcinoma. *PLoS One* 2020; **15**: e0229696 [PMID: 32130270 DOI: 10.1371/journal.pone.0229696]

27 **Galle PR**, Tovoli F, Foerster F, Wörns MA, Cucchetti A, Bolondi L. The treatment of intermediate stage tumours beyond TACE: From surgery to systemic therapy. *J Hepatol* 2017; **67**: 173-183 [PMID: 28323121 DOI: 10.1016/j.jhep.2017.03.007]

28 **Ogasawara S**, Chiba T, Ooka Y, Kanogawa N, Motoyama T, Suzuki E, Tawada A, Kanai F, Yoshikawa M, Yokosuka O. Efficacy of sorafenib in intermediate-stage hepatocellular carcinoma patients refractory to transarterial chemoembolization. *Oncology* 2014; **87**: 330-341 [PMID: 25227534 DOI: 10.1159/000365993]

29 **Arizumi T**, Ueshima K, Minami T, Kono M, Chishina H, Takita M, Kitai S, Inoue T, Yada N, Hagiwara S, Minami Y, Sakurai T, Nishida N, Kudo M. Effectiveness of Sorafenib in Patients with Transcatheter Arterial Chemoembolization (TACE) Refractory and Intermediate-Stage Hepatocellular Carcinoma. *Liver Cancer* 2015; **4**: 253-262 [PMID: 26734579 DOI: 10.1159/000367743]

30 **Peck-Radosavljevic M**, Kudo M, Raoul JL, Lee HC, Decaens T, Heo J, Lin S-M, Shan H, Yang Y, Bayh I, Nakajima K,

Cheng A-L. Outcomes of patients (pts) with hepatocellular carcinoma (HCC) treated with transarterial chemoembolization (TACE): Global OPTIMIS final analysis. *J Clin Oncol* 2018; **36** Suppl 15: 4018

31 **Leoni S**, Piscaglia F, Serio I, Terzi E, Pettinari I, Croci L, Marinelli S, Benevento F, Golfieri R, Bolondi L. Adherence to AASLD guidelines for the treatment of hepatocellular carcinoma in clinical practice: experience of the Bologna Liver Oncology Group. *Dig Liver Dis* 2014; **46**: 549-555 [PMID: 24630947 DOI: 10.1016/j.dld.2014.02.012]

32 **Takayasu K**, Arii S, Kudo M, Ichida T, Matsui O, Izumi N, Matsuyama Y, Sakamoto M, Nakashima O, Ku Y, Kokudo N, Makuuchi M. Superselective transarterial chemoembolization for hepatocellular carcinoma. Validation of treatment algorithm proposed by Japanese guidelines. *J Hepatol* 2012; **56**: 886-892 [PMID: 22173160 DOI: 10.1016/j.jhep.2011.10.021]

33 **Kimura H**, Ohkawa K, Miyazaki M, Sakakibara M, Imanaka K, Tamura T, Sueyoshi H, Takada R, Fukutake N, Uehara H, Ashida R, Ioka T, Nakazawa T, Nakanishi K, Katayama K. Subclassification of patients with intermediate-stage (Barcelona Clinic Liver Cancer stage-B) hepatocellular carcinoma using the up-to-seven criteria and serum tumor markers. *Hepatol Int* 2017; **11**: 105-114 [PMID: 27766479 DOI: 10.1007/s12072-016-9771-0]

34 **Eso Y**, Takai A, Takahashi K, Ueda Y, Taura K, Marusawa H, Seno H. Combination of Mac-2 Binding Protein Glycosylation Isomer and Up-To-Seven Criteria as a Useful Predictor for Child-Pugh Grade Deterioration after Transarterial Chemoembolization for Hepatocellular Carcinoma. *Cancers (Basel)* 2019; **11** [PMID: 30909405 DOI: 10.3390/cancers11030405]

35 **Memon K**, Kulik L, Lewandowski RJ, Gupta R, Ryu RK, Miller FH, Vouche M, Atassi R, Ganger D, Mulcahy MF, Salem R. Prospective evaluation of patients with early-/intermediate-stage hepatocellular carcinoma with disease progression following arterial locoregional therapy: candidacy for systemic treatment or clinical trials. *J Vasc Interv Radiol* 2013; **24**: 1189-1197.e2 [PMID: 23474327 DOI: 10.1016/j.jvir.2012.12.025]

36 **Kudo M**. A New Treatment Option for Intermediate-Stage Hepatocellular Carcinoma with High Tumor Burden: Initial Lenvatinib Therapy with Subsequent Selective TACE. *Liver Cancer* 2019; **8**: 299-311 [PMID: 31768341 DOI: 10.1159/000502905]

37 **Kudo M**, Ueshima K, Chan S, Minami T, Chishina H, Aoki T, Takita M, Hagiwara S, Minami Y, Ida H, Takenaka M, Sakurai T, Watanabe T, Morita M, Ogawa C, Wada Y, Ikeda M, Ishii H, Izumi N, Nishida N. Lenvatinib as an Initial Treatment in Patients with Intermediate-Stage Hepatocellular Carcinoma Beyond Up-To-Seven Criteria and Child-Pugh A Liver Function: A Proof-Of-Concept Study. *Cancers (Basel)* 2019; **11** [PMID: 31370183 DOI: 10.3390/cancers11081084]

38 **Finn RS**, Qin S, Ikeda M, Galle PR, Ducreux M, Kim TY, Kudo M, Breder V, Merle P, Kaseb AO, Li D, Verret W, Xu DZ, Hernandez S, Liu J, Huang C, Mulla S, Wang Y, Lim HY, Zhu AX, Cheng AL; IMbrave150 Investigators. Atezolizumab plus Bevacizumab in Unresectable Hepatocellular Carcinoma. *N Engl J Med* 2020; **382**: 1894-1905 [PMID: 32402160 DOI: 10.1056/NEJMoa1915745]

39 **Finn RS**, Qin S, Ikeda M, Galle P, Ducreux M, Kim T-Y, Lim HY, Kudo M, Breder VV, Merle P, Kaseb AO, Li D, Verret W, Shao H, Liu J, Li L, Zhu A, Cheng A-L. IMbrave150: updated overall survival (OS) data from a global, randomized, open-label phase III study of atezolizumab (atezo)+ bevacizumab (bev) *vs* sorafenib (sor) in patients (pts) with unresectable hepatocellular carcinoma (HCC). *J Clin Oncol* 2021; **39** Suppl 3: 267 [DOI: 10.1200/JCO.2021.39.3_suppl.267]

40 **Kudo M**. Recent Advances in Systemic Therapy for Hepatocellular Carcinoma in an Aging Society: 2020 Update. *Liver Cancer* 2020; **9**: 640-662 [PMID: 33442538 DOI: 10.1159/000511001]

41 **Yau T**, Kang YK, Kim TY, El-Khoueiry AB, Santoro A, Sangro B, Melero I, Kudo M, Hou MM, Matilla A, Tovoli F, Knox JJ, Ruth He A, El-Rayes BF, Acosta-Rivera M, Lim HY, Neely J, Shen Y, Wisniewski T, Anderson J, Hsu C. Efficacy and Safety of Nivolumab Plus Ipilimumab in Patients With Advanced Hepatocellular Carcinoma Previously Treated With Sorafenib: The CheckMate 040 Randomized Clinical Trial. *JAMA Oncol* 2020; **6**: e204564 [PMID: 33001135 DOI: 10.1001/jamaoncol.2020.4564]

42 **Kelley RK**, Sangro B, Harris WP, Ikeda M, Okusaka T, Kang Y-K, Qin S, Tai WMD, Lim HY, Yau T, Yong W-P, Cheng A-L, Gasbarrini A, De Braud FG, Bruix J, Borad MJ, He P, Negro A, Kudo M, Abou-Alfa GK. Efficacy, tolerability, and biologic activity of a novel regimen of tremelimumab (T) in combination with durvalumab (D) for patients (pts) with advanced hepatocellular carcinoma (aHCC). *J Clin Oncol* 2020; **38** suppl 15: 4508-4508 [DOI: 10.1200/jco.2020.38.15_suppl.4508]

43 **AstraZeneca**. Imfinzi plus tremelimumab significantly improved overall survival in HIMALAYA Phase III trial in 1st-line unresectable liver cancer. 2021. [cited 10 April 2022]. Available from: https://www.astrazeneca.com/media-centre/press-releases/2022/imfinzi-plus-tremelimumab-unprecedented-survival-1st-line-unresectable-liver-cancer.html#:~:text=Positive%20results%20from%20the%20HIMALAYA,for%20patients%20with%20unresectable%20hepatocellular

44 **AstraZeneca**. Imfinzi plus tremelimumab demonstrated unprecedented survival in 1st-line unresectable liver cancer with 31% of patients alive at three years. 2022. [cited 10 April 2022]. Available from: https://www.astrazeneca.com/media-centre/press-releases/2022/imfinzi-plus-tremelimumab-unprecedented-survival-1st-line-unresectable-liver-cancer.html

45 **Yamashita Y**, Matsukawa T, Arakawa A, Hatanaka Y, Urata J, Takahashi M. US-guided liver biopsy: predicting the effect of interventional treatment of hepatocellular carcinoma. *Radiology* 1995; **196**: 799-804 [PMID: 7644646 DOI: 10.1148/radiology.196.3.7644646]

46 **Yasui Y**, Tsuchiya K, Kurosaki M, Takeguchi T, Takeguchi Y, Okada M, Wang W, Kubota Y, Goto T, Komiyama Y, Higuchi M, Takaura K, Hayashi T, Takada H, Tamaki N, Nakanishi H, Itakura J, Takahashi Y, Asahina Y, Enomoto N, Himeno Y, Izumi N. Up-to-seven criteria as a useful predictor for tumor downstaging to within Milan criteria and Child-Pugh grade deterioration after initial conventional transarterial chemoembolization. *Hepatol Res* 2018; **48**: 442-450 [PMID: 29278654 DOI: 10.1111/hepr.13048]

47 **CancerNetwork**. Lenvatinib/TACE May Be Efficacious, Safe as First-Line Treatment for Advanced HCC. 2022. [cited 10 April 2022]. Available from: https://www.cancernetwork.com/view/

48 **Ogasawara S**, Llovet J, El-Khoueiry A, Vogel A, Madoff D, Finn R, Ren Z, Modi K, Li J, Siegel A, Dubrosky L, Kudo M. P-107 LEAP-012: A randomized, double-blind, phase 3 study of pembrolizumab plus lenvatinib in combination with transarterial chemoembolization (TACE) in patients with intermediate-stage hepatocellular carcinoma not amenable to

curative treatment. *Ann Oncol* 2020; S124-S125 [DOI: 10.1016/j.annonc.2020.04.189]

49 **Sangro B**, Kudo M, Qin S, Ren Z, Chan S, Joseph E, Arai Y, Mann H, Morgan S, Cohen, Lencioni R, P-347 A phase 3, randomized, double-blind, placebo-controlled study of transarterial chemoembolization combined with durvalumab or durvalumab plus bevacizumab therapy in patients with locoregional hepatocellular carcinoma: EMERALD-1. Ann Oncol 2020; 31: S202-S203 [DOI: 10.1016/j.annonc.2020.04.429]

50 **US National Library of Medicine**. A Study of Nivolumab and Ipilimumab and Nivolumab Alone in Combination With Trans-arterial ChemoEmbolization (TACE) in Participants With Intermediate Stage Liver Cancer (CheckMate 74W). 2020. [cited 10 April 2022]. Available from: https://clinicaltrials.gov/ct2/show/NCT04340193

51 **Kudo M**, Han G, Finn RS, Poon RT, Blanc JF, Yan L, Yang J, Lu L, Tak WY, Yu X, Lee JH, Lin SM, Wu C, Tanwandee T, Shao G, Walters IB, Dela Cruz C, Poulart V, Wang JH. Brivanib as adjuvant therapy to transarterial chemoembolization in patients with hepatocellular carcinoma: A randomized phase III trial. *Hepatology* 2014; **60**: 1697-1707 [PMID: 24996197 DOI: 10.1002/hep.27290]

52 **Kudo M**, Cheng AL, Park JW, Park JH, Liang PC, Hidaka H, Izumi N, Heo J, Lee YJ, Sheen IS, Chiu CF, Arioka H, Morita S, Arai Y. Orantinib *vs* placebo combined with transcatheter arterial chemoembolisation in patients with unresectable hepatocellular carcinoma (ORIENTAL): a randomised, double-blind, placebo-controlled, multicentre, phase 3 study. *Lancet Gastroenterol Hepatol* 2018; **3**: 37-46 [PMID: 28988687 DOI: 10.1016/S2468-1253(17)30290-X]

53 **Duffy AG**, Ulahannan SV, Makorova-Rusher O, Rahma O, Wedemeyer H, Pratt D, Davis JL, Hughes MS, Heller T, ElGindi M, Uppala A, Korangy F, Kleiner DE, Figg WD, Venzon D, Steinberg SM, Venkatesan AM, Krishnasamy V, Abi-Jaoudeh N, Levy E, Wood BJ, Greten TF. Tremelimumab in combination with ablation in patients with advanced hepatocellular carcinoma. *J Hepatol* 2017; **66**: 545-551 [PMID: 27816492 DOI: 10.1016/j.jhep.2016.10.029]

54 **Golfieri R**, Renzulli M, Mosconi C, Forlani L, Giampalma E, Piscaglia F, Trevisani F, Bolondi L; Bologna Liver Oncology Group (BLOG). Hepatocellular carcinoma responding to superselective transarterial chemoembolization: an issue of nodule dimension? *J Vasc Interv Radiol* 2013; **24**: 509-517 [PMID: 23428355 DOI: 10.1016/j.jvir.2012.12.013]

55 **Kanai T**, Hirohashi S, Upton MP, Noguchi M, Kishi K, Makuuchi M, Yamasaki S, Hasegawa H, Takayasu K, Moriyama N. Pathology of small hepatocellular carcinoma. A proposal for a new gross classification. *Cancer* 1987; **60**: 810-819 [PMID: 2439190 DOI: 10.1002/1097-0142(19870815)60:4<810::aid-cncr2820600417>3.0.co;2-1]

World Journal of Gastroenterology

Submit a Manuscript: https://www.f6publishing.com

World J Gastroenterol 2022 June 21; 28(23): 2569-2581

DOI: 10.3748/wjg.v28.i23.2569

ISSN 1007-9327 (print) ISSN 2219-2840 (online)

ORIGINAL ARTICLE

Basic Study

Family with sequence similarity 134 member B-mediated reticulophagy ameliorates hepatocyte apoptosis induced by dithiothreitol

Yi-Xin Guo, Bing Han, Ting Yang, Yu-Si Chen, Yi Yang, Jia-Yao Li, Qin Yang, Ru-Jia Xie

Specialty type: Gastroenterology and hepatology

Provenance and peer review: Unsolicited article; Externally peer reviewed.

Peer-review model: Single blind

Peer-review report's scientific quality classification

Grade A (Excellent): 0
Grade B (Very good): B, B
Grade C (Good): 0
Grade D (Fair): D
Grade E (Poor): 0

P-Reviewer: Elchaninov AV, Russia; Gassler N, Germany; Kulkeaw K, Thailand

Received: January 5, 2022
Peer-review started: January 5, 2022
First decision: March 9, 2022
Revised: March 23, 2022
Accepted: April 29, 2022
Article in press: April 29, 2022
Published online: June 21, 2022

Yi-Xin Guo, Jia-Yao Li, Department of Pathophysiology, Guizhou Provincial Key Laboratory of Pathogenesis and Drug Research on Common Chronic Diseases, Guizhou Medical University, Guiyang 550025, Guizhou Province, China

Bing Han, Ting Yang, Yu-Si Chen, Yi Yang, Qin Yang, Ru-Jia Xie, Department of Pathophysiology, College of Basic Medical Sciences, Guizhou Medical University, Guiyang 550025, Guizhou Province, China

Corresponding author: Ru-Jia Xie, MD, Academic Research, Department of Pathophysiology, College of Basic Medical Sciences, Guizhou Medical University, Dongqing Road, Guiyang 550025, Guizhou Province, China. 592153968@qq.com

Abstract

BACKGROUND

Endoplasmic reticulum (ER) stress-related hepatocyte apoptosis is responsible for multiple hepatic diseases. Previous studies have revealed that endoplasmic reticulophagy (ER-phagy) promotes the selective clearance of damaged ER fragments during ER stress, playing a crucial role in maintaining ER homeostasis and inhibiting apoptosis. Family with sequence similarity 134 member B (FAM134B) is a receptor involved in ER-phagy that can form a complex with calnexin (CNX) and microtubule-associated protein 1 light chain 3 (LC3). The complex can mediate the selective isolation of ER fragments to attenuate hepatocyte apoptosis. However, the precise regulatory mechanisms remain unclear.

AIM

To elucidate the effect of FAM134B-mediated ER-phagy on ER stress-induced apoptosis in buffalo rat liver 3A (BRL-3A) rat hepatocytes and the potential regulatory mechanisms.

METHODS

ER stress-related hepatocyte apoptosis was induced using dithiothreitol (DTT). Proteins related to ER stress and autophagy were measured with western blotting. Protein complex interactions with FAM134B were isolated by co-immunoprecipitation. ER-phagy was evaluated in immunofluorescence experiments. Cell cycle distribution and apoptosis were measured by flow cytometry. Mitochondrial Ca^{2+} levels were evaluated by the co-localization of intracellular Ca^{2+}-tracker and Mito-

tracker. The small interfering RNA against *FAM134B* was used to knockdown *FAM134B* in BRL-3A cells.

RESULTS

ER stress-related and autophagy-related proteins in BRL-3A cells were elevated by both short and long-term DTT treatment. Furthermore, co-immunoprecipitation confirmed an interaction between FAM134B, CNX, FAM134B, and LC3 in BRL-3A cells. Immunofluorescence assays revealed that autolysosomes significantly decreased following short-term DTT treatment, but increased after long-term treatment. Mitochondrial Ca^{2+} levels and apoptotic rates were dramatically elevated, and more cells were arrested in the G1 stage after short-term DTT treatment; however, these decreased 48 h later. Moreover, FAM134B downregulation accelerated mitochondrial apoptotic pathway activation and aggravated hepatocyte apoptosis under ER stress.

CONCLUSION

FAM134B-mediated ER-phagy attenuates hepatocyte apoptosis by suppressing the mitochondrial apoptotic pathway. Our findings provide new evidence highlighting the importance of FAM134B-mediated ER-phagy in attenuating hepatocyte apoptosis.

Key Words: Hepatocytes; Reticulophagy; Family with sequence similarity 134 member B; Apoptosis; Endoplasmic reticulum stress; Endoplasmic reticulum homeostasis

©The Author(s) 2022. Published by Baishideng Publishing Group Inc. All rights reserved.

Core Tip: We show that family with sequence similarity 134 member B (FAM134B)-mediated reticulophagy maintains the endoplasmic reticulum (ER) homeostasis in ER-stressed hepatocytes *via* the clearance of damaged ER fragments. Thereby FAM134B-mediated reticulophagy ameliorates dithiothreitol-induced hepatocyte apoptosis. Our findings provide emerging evidence of the prominence of ER-phagy in ER stress-related hepatocyte apoptosis. FAM134B may represent a potential therapeutic target for liver disease treatment.

Citation: Guo YX, Han B, Yang T, Chen YS, Yang Y, Li JY, Yang Q, Xie RJ. Family with sequence similarity 134 member B-mediated reticulophagy ameliorates hepatocyte apoptosis induced by dithiothreitol. *World J Gastroenterol* 2022; 28(23): 2569-2581

URL: https://www.wjgnet.com/1007-9327/full/v28/i23/2569.htm

DOI: https://dx.doi.org/10.3748/wjg.v28.i23.2569

INTRODUCTION

Endoplasmic reticulum (ER) stress-related hepatocyte apoptosis participates in multiple hepatic diseases, including viral hepatitis[1], hepatic fibrosis[2], fatty liver[3,4] and cirrhosis[5]. Therefore, the alleviation of ER stress-mediated hepatocyte apoptosis is crucial in the treatment of hepatic diseases. Recent findings have indicated that endoplasmic reticulophagy (ER-phagy) promotes degradation of damaged ER fragments during ER stress. Although ER-phagy has a vital role in maintaining ER homeostasis and inhibiting cell apoptosis[6-8], the exact regulatory mechanisms behind this are largely unknown.

Glucose-regulated protein 78 (GRP78) is a prominent ER molecular chaperone, while calnexin (CNX) is a membrane-bound lectin protein in the ER that can increase the protein folding capacity[9,10]. Even though the excessive build-up of misfolded or unfolded proteins can be alleviated *via* ER stress, previous studies reported that a selective autophagic mechanism, defined as ER-phagy, can also be activated by ER stress to restore ER homeostasis[11,12]. Family with sequence similarity 134 member B (FAM134B), an ER-resident protein, may interact with CNX in the cytosol or the ER membrane[13]. Since FAM134B is not predicted to have an ER lumenal domain, there is an indirect interaction between FAM134B and lumenal proteins through the lumen-resident segment, which has a chaperone activity attributed to CNX. CNX forms transient but relatively stable complexes with unfolded ER proteins until they either become folded or are degraded. Moreover, it has been reported that as with other cargo receptor molecules, FAM134B can interact directly with microtubule-associated protein 1 light chain 3 (LC3) when its LIR motif is exposed. The CNX-FAM134B-LC3 complex can mediate the selective isolation of ER fragments containing misfolded proteins, which are subsequently transported to lysosomes for degradation[14-16]. Thus, FAM134B-mediated ER-phagy may play an essential role in

maintaining ER homeostasis and promoting cell survival. However, it is unclear whether FAM134B-mediated ER-phagy is involved in the regulation of hepatocyte apoptosis induced by ER stress. In this study, dithiothreitol (DTT) was used to induce ER stress in buffalo rat liver 3A (BRL-3A) hepatocytes, and the expression of ER stress-related and autophagy-related proteins was assessed. In addition, small interfering RNA (siRNA) was used to knockdown the expression of *FAM134B* in hepatocytes and an apoptosis analysis followed. Our study reveals an emerging role of FAM134B-mediated ER-phagy in ER stress-mediated hepatocyte apoptosis, which may provide a novel target for the treatment of hepatic diseases.

MATERIALS AND METHODS

Antibodies and reagents

Dulbecco's modified Eagle medium (DMEM) and fetal bovine serum (FBS) were purchased from Gibco (Grand Island, NY, United States). Trypsin-EDTA solution, trypsin solution without EDTA, and penicillin-streptomycin were purchased from Biological Industries (BioInd, Israel). Bicinchoninic acid (BCA) protein assay kit, DTT, RIPA lysis buffer, and protease inhibitor were obtained from Solarbio (Beijing, China). Annexin V-FITC/PI Apoptosis Detection Kit and Cell Cycle Detection Kit were purchased from KeyGEN BioTECH (Nanjing, China). PVDF membranes were obtained from Merck Millipore. Rabbit polyclonal antibody against FAM134B was purchased from Proteintech (Wuhan, China). Rabbit polyclonal antibodies against ATG12, cytochrome c (cyt c), and cleaved caspase-3 were obtained from Cell Signaling Technology (Danvers, MA, United States). Rabbit polyclonal antibodies against β-actin, LC3, CNX, CHOP and GRP78, and the Ca^{2+} indicator (Rhod-2 AM) were purchased from Abcam (Cambridge, United Kingdom). Dynabeads protein G immunoprecipitation kit and lipofectamine 3000 reagent were purchased from Thermo Fisher Scientific, Inc. HRP-labeled Goat Anti-Rabbit IgG (H + L), Mito-Tracker Green, Lyso-Tracker Green, ER-Tracker Red, and immunofluorescence-related reagents were purchased from Beyotime Institute of Biotechnology (Nanjing, China).

Cell culture and experiment protocol

BRL-3A cells, bought from Cell Bank of the Chinese Academy of Sciences (Shanghai, China), were cultivated and maintained in DMEM culture media supplemented with 1% penicillin-streptomycin and 10% FBS. BRL-3A cells were seeded at 37 °C and 5% CO_2 in a constant temperature and humid atmosphere, pre-cultured every 3 d, and further passaged until the density reached approximately 80%. To induce the ER stress, BRL-3A cells were treated with DTT (2.0 mmol/L based on previous studies[17]) for 0, 3, 6, 12, 24, or 48 h.

Apoptosis assessment

Cells were cultured to 80% confluency and treated with 2.0 mmol/L DTT for the specified point-in-time intervals. To determine the efficacy of the different DTT treatments, a cell apoptosis analysis was evaluated with flow cytometry. Each group of cells was trypsinized without EDTA and rinsed thrice with PBS. After centrifugation at 2000 rpm for 5 min, cells were loaded with 500 μL binding buffer and labeled with 5 μL of Annexin V-FITC/PI, according to the manufacturer's instructions. Labeled cells were detected and analyzed with flow cytometry and NovoExpress® software 1.4.1. The experiments were performed in triplicate.

Cell cycle analysis

To determine the effect of DTT's 0, 3, 6, 12, 24, and 48 h incubation on the cell cycle progression of BRL-3A, the harvested cells were trypsinized without EDTA and rinsed three times with cold PBS, followed by fixation with 70% ethanol in cold storage. After 24 h incubation at 4 °C, 500 μL PI/RNase was added to each group and maintained at 37 °C for 60 min in a dark place. Stained cells were processed using flow cytometry and further measured *via* the NovoExpress® software 1.4.1. The experiments were performed in triplicate.

Western blot analysis

BRL-3A cells were grown on 10 cm diameter dishes and treated with 2.0 mmol/L DTT for different times. Cells were rinsed three times with pre-cooled PBS after experimentation and collected with cell scrapers in 100 μL RIPA buffer containing 1 mmol/L PMSF. After centrifugation at 12000 rpm for 25 min at 4 °C, the concentrations of total cellular protein extracts were determined using the BCA kit (Solarbio Science, Beijing, China), and known concentrations of BSA were used as standard. The total cellular protein extracts were denatured by boiling at 100 °C using dry bath incubator (Hangzhou Miu Instruments Co., Ltd, Zhejiang, China). Protein samples (30–40 mg) were loaded onto SDS-PAGE and transferred onto PVDF membranes for immunostaining. After blocking with 5% defatted milk for 90 min, membranes were stained overnight with primary antibodies, including β-actin (1:1000), GRP78 (1:1000), CNX (1:3000), ATG12 (1:1000), LC3 (1:1000), FAM134B (1:1000), CHOP (1:1000), cleaved

caspase-3 (1:1000), cyt c (1:1000) in cold storage, followed by incubation with secondary antibodies (1:4000). The density of protein bands on membranes was exposed and quantified *via* fluorography using Image J software. The images shown are representative of experiments carried out at least three times.

Co-immunoprecipitation analysis

BRL-3A cells, treated with DTT (2.0 mmol/L for 0 h and 24 h), were lysed in RIPA lysis buffer and the lysates were centrifuged at 12000 rpm for 15 min at 4 °C. The supernatant was resuspended in ice-cold PBS to a total volume of 500 μL, and 5 μL of the designated antibody was added overnight at 4 °C. The next day, the Ab-Ag complexes were bound to Dynabeads magnetic beads on a rotary shaker for 10 min. The magnetic bead-Ab-Ag complex was washed and eluted by adding a washing buffer and elution buffer, respectively, according to the manufacturer's protocol. Immunocomplexes were heated for 5 min at 100 °C and prepared for analysis by western blot. The images shown are representative of experiments carried out at least three times.

Calcium imaging and mitochondrial labeling

To observe the effects of DTT treatment at 2.0 mmol/L for specified time points, mitochondrial Ca^{2+} levels were determined using Rhod-2 AM, a specific detection dye for calcium. The treated cells were rinsed with HBSS three times and stained with a mixture of 5 μM Rhod-2 AM and 20 nM Mito-Tracker Green at 37 °C for 30 min in the dark. Finally, live cells were extensively rinsed thrice by adding HBSS without calcium, and images were visualized with Zeiss LSM Image Browser using a Zeiss LSM 900 confocal microscope. The images shown are representative of experiments carried out at least three times.

Live imaging of ER and lysosome

To observe the intracellular localization of the ER and lysosomes, after treatment with 2.0 mmol/L DTT for 0, 3, 6, 12, 24, and 48 h, ER and lysosomes were stained with ER-tracker and Lyso-tracker. Prior to staining, trackers were diluted appropriately in DMEM, on the basis of the manufacturer's instructions. Following dilution, cells were simultaneously incubated with the two trackers listed above, maintained for 30 min at 37 °C, and finally rinsed thrice with HBSS. Stained cells were visualized under the Zeiss LSM 900 confocal microscope. Images shown are representative of experiments carried out at least three times.

SiRNA transfections

Specific siRNA against buffalo rat *FAM134B* was designed and synthesized by OriGene. Product number and targeting sequence: SR510501A-rGrGrArArGrUrGrGrUrUrUrArUrCrArArArUr-UrCrUrGrATA; SR510501B-rArArArUrUrUrGrArCrUrUrArCrArGrUrGrGrArArArCrCAA; SR510501C-rArArGrUrGrGrUrUrUrArUrCrArArArUrUrCrUrGrArUrAGA. Cells were cultured in six-well dishes until the density of cell fusion reached 60%. Briefly, 75 pmol of *FAM134B* siRNA were added to Lipofectamine 3000 Transfection Reagent and gently mixed for 15 min, then administered to BRL-3A cells, which were resuspended in DMEM. After transfection for 6 h, cells were washed, and then supplemented with fresh medium. Finally, cells were treated with DTT (2.0 mmol/L) for a further 24 h and subjected to western blot assay and apoptosis assessment.

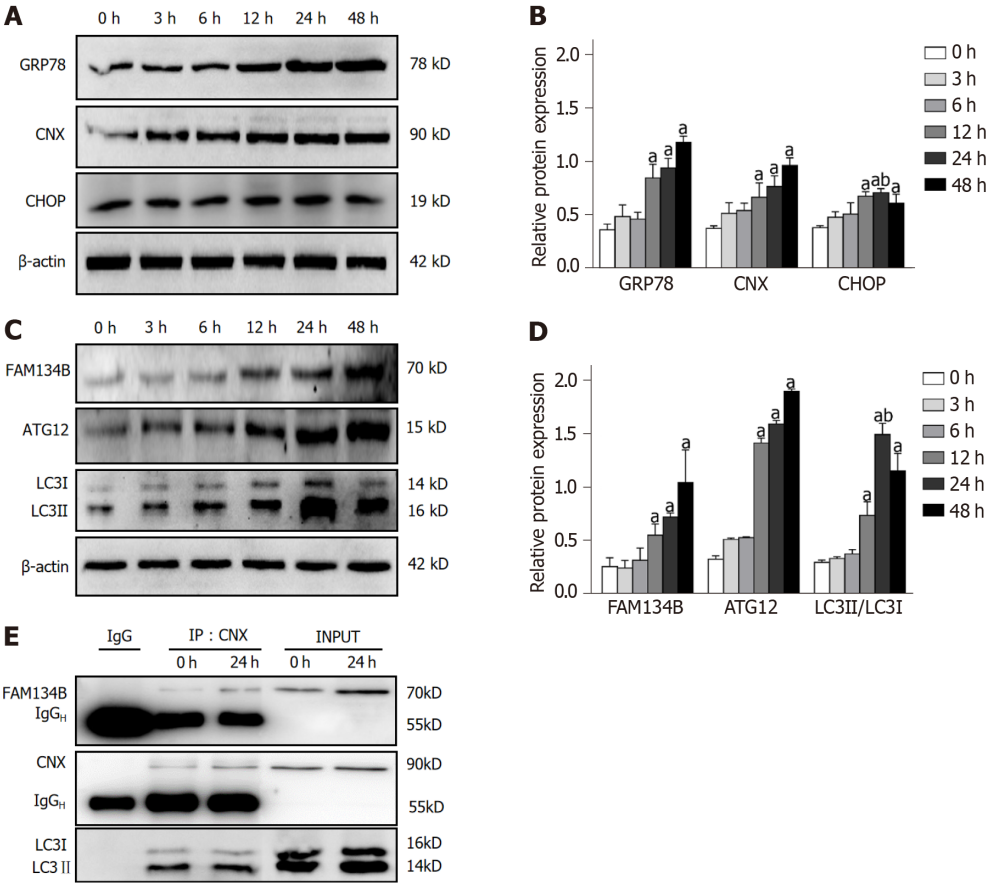
Statistical analysis

GraphPad Prism 7 software was used to perform all the statistical analyses and prepare experimental graphs. Data are expressed as the mean ± SD. Shapiro-Wilk normality test was used to test the normal distribution of the data and all the data were fit to a normal followed by Tukey's post hoc test was performed, and a significant difference was considered as $P < 0.05$.

RESULTS

DTT-mediated ER stress upregulates ER-phagy-related FAM134B in BRL-3A cells

To assess whether the drug treatments could alter the protein expression of CNX and GRP78, BRL-3A cells were subjected to short-term (3, 6, 12, 24 h) or long-term (48 h) treatment with DTT, and the protein extracts from BRL-3A cells were analyzed by western blot. We found that treatment of BRL-3A cells with 2.0 mmol/L DTT resulted in a prominent increase in CNX and GRP78 levels, both in a time-dependent manner (Figure 1A and B). Moreover, CHOP is a specific and stress-responsive transcription factor during ER stress and its protein expression was significantly increased in the 12, 24, and 48 h groups (Figure 1A and B). However, the expression of CHOP in BRL-3A cells treated with DTT for 48 h was lower than that after DTT treatment for 24 h. These alterations in CNX, GRP78, and CHOP confirm that ER stress in BRL-3A was activated.



DOI: 10.3748/wjg.v28.i23.2569 **Copyright** ©The Author(s) 2022.

Figure 1 Impact of the endoplasmic reticulum stressor, dithiothreitol, on endoplasmic reticulophagy mediated by family with sequence similarity 134 member B in buffalo rat liver 3A cells. A and B: Buffalo rat liver 3A (BRL-3A) cells were treated with 2.0 mmol/L dithiothreitol (DTT) for the time intervals (0, 3, 6, 12, 24, 48 h); Western blot showed the effect of endoplasmic reticulum (ER) stressor, DTT, on expression of the ER stress-related proteins glucose-regulated protein 78 (GRP78), calnexin (CNX), and C/EBP homologous protein (CHOP); β-actin was used as a control for normalization; C and D: Analysis of autophagy related gene 12 (ATG12), family with sequence similarity 134 member B (FAM134B), and microtubule-associated protein 1 light chain 3 (LC3) protein expression by western blot. Protein levels were normalized to β-actin; E: BRL-3A cells were treated with 2.0 mmol/L DTT for 0 and 24 h; co-immunoprecipitation analysis detected the presence of CNX-FAM134B-LC3 complex in BRL-3A cells. Values are represented as mean ± SD (n = 3), $^aP < 0.05$ *vs* 0 h group; $^bP < 0.05$ *vs* 48 h group.

To determine the effects of ER stress on FAM134B-mediated ER-phagy, alterations in FAM134B, ATG12, and LC3 expression were detected by western blot. As expected, DTT treatment for 3, 6, 12, 24, and 48 h increased the conversion ratio of LC3-I to LC3-II and the FAM134B and ATG12 expression levels compared to those in the 0 h group (Figure 1C and D). Thus, our results revealed that the expression of FAM134B is induced in response to ER stress.

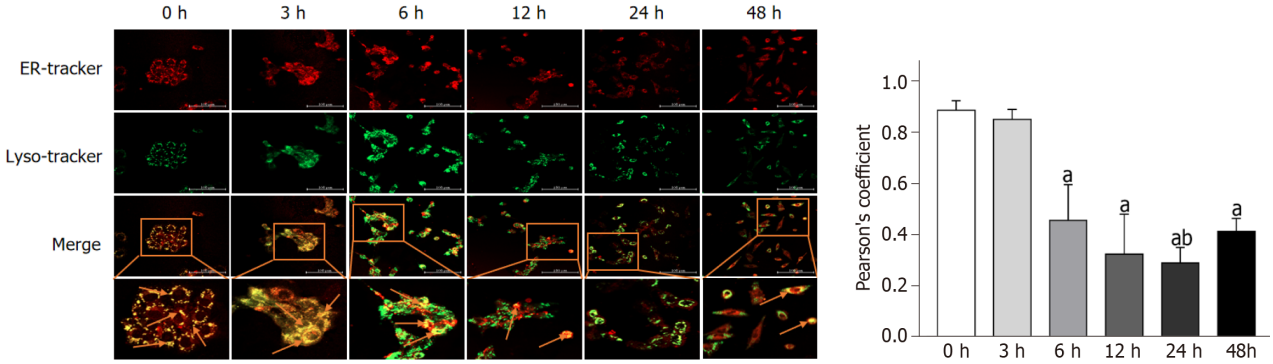
Furthermore, we used an anti-CNX antibody to immunoprecipitate the CNX-FAM134B-LC3 complex, confirming the hypothesis that FAM134B forms a complex with CNX and LC3, exerting a positive influence on ER-phagy (Figure 1E).

Long-term DTT treatment relieved the gradually blocked ER autolysosome delivery in BRL-3A cells

Typically, ER is delivered to lysosomes and finally degraded. To analyze whether ER autolysosomes are formed, we examined the subcellular location of the ER and lysosomes using cell organelle markers. As shown in Figure 2, the treatment groups of 3, 6, 12, 24, and 48 h DTT incubation significantly alleviated the co-localization of the ER with lysosomes, compared to that in the 0 h group. Notably, the colocalization of ER and lysosomes in BRL-3A cells treated with DTT for 48 h was increased compared to those treated for 24 h (Figure 2).

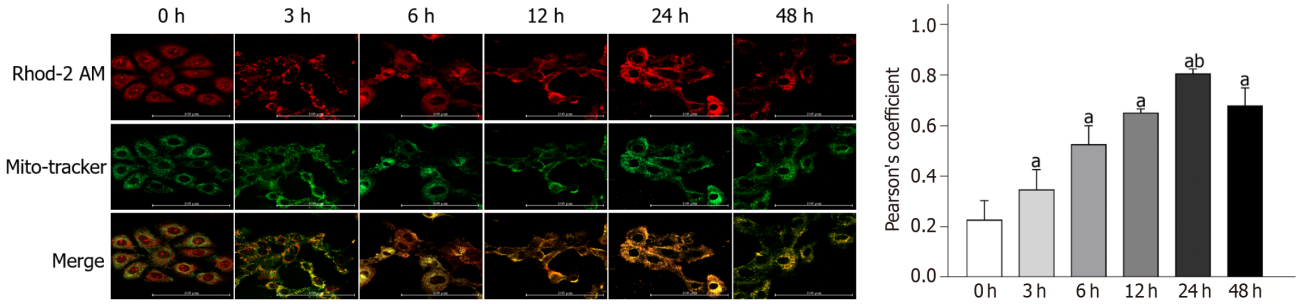
Short-term DTT treatment induces mitochondrial calcium uptake while prolonged DTT treatment reduces it

Calcium in the ER can be released and transferred to the mitochondria owing to an imbalance of ER homeostasis. To explore the altered localization of calcium, collected cells were co-loaded with Rhod-2 AM and Mito-Tracker Green. In response to DTT treatment for 3, 6, 12, 24, and 48 h, the co-localized fluorescence increased considerably (Figure 3). However, the distribution of the co-localized signal was



DOI: 10.3748/wjg.v28.i23.2569 **Copyright** ©The Author(s) 2022.

Figure 2 Impact of dithiothreitol treatment on the formation of autolysosomes in buffalo rat liver 3A cells. After dithiothreitol treatment for 0, 3, 6, 12, 24, and 48 h, the buffalo rat liver 3A cells labeled with endoplasmic reticulum (ER)-Tracker Red and Lyso-Tracker Green were observed and captured under confocal fluorescence microscopy (200 ×) in a live cell imaging experiment. Insets show the magnification of the pictures. Scale bars indicate 100 μm. Arrows head to indicate ER-localized lysosomes. Values are represented as mean ± SD (n = 3), $^{a}P < 0.05$ *vs* 0 h group; $^{b}P < 0.05$ *vs* 48 h group.



DOI: 10.3748/wjg.v28.i23.2569 **Copyright** ©The Author(s) 2022.

Figure 3 Impact of dithiothreitol treatment on mitochondrial calcium uptake in buffalo rat liver 3A cells. Buffalo rat liver 3A cells were treated for 0, 3, 6, 24, and 48 h with 2.0 mM dithiothreitol, followed by co-incubating with Mitochondria-Tracker Green and Rhod-2 AM, and visualized by confocal microscopy (400 ×). Scale bars indicate 100 μm. Values are represented as mean ± SD (n = 3), $^{a}P < 0.05$ *vs* 0 h group; $^{b}P < 0.05$ *vs* 48 h group.

weaker in the 48 h group, compared to that in the 24 h group (Figure 3). These results strongly suggest that mitochondrial calcium accumulation is related to DTT treatment.

DTT treatment induces cell cycle arrest and apoptosis in BRL-3A cells, which is relieved at 48 h

To further validate that DTT treatment leads to apoptosis in BRL-3A cells, we quantitatively measured the number of apoptotic cells using the Annexin V-FITC/PI double staining assay. As shown in Figure 4A and B, the ratio of apoptotic cells treated with DTT for 0, 3, 6, 12, and 24 h exhibited a time-dependent increase. Interestingly, the apoptotic percentage in the 48 h group was significantly lower than that in the 24 h group (Figure 4A and B). Subsequently, we sought to use flow cytometry to determine the impact of DTT treatment on the cell cycle progression, and the data suggests that the proportion of BRL-3A cells in G1 phase after DTT treatment was noticeably higher than that of the 0 h group (Figure 4C and D and Table 1). Moreover, the number of cells in G1 phase in the 48 h group was smaller than that of the 24 h group.

BRL-3A cells undergo apoptosis upon FAM134B knockdown

We further verified whether *FAM134B* knockdown could alter DTT-induced apoptosis. We first investigated the transfection efficiency of siRNA with three different siRNAs targeting *FAM134B* (siRNA 1, 2, and 3) and found that the *FAM134B* siRNA2 was the most effective (Figure 5A and B). Next, we investigated FAM134B protein levels by performing a western blot on already transfected samples, which were treated with DTT for 24 h. As shown in Figure 5C and D, FAM134B and β-actin expression levels were determined, and it was found that FAM134B protein levels were down-regulated compared with the control and control siRNA groups.

It has been reported that cyt c and cleaved caspase-3 are apoptosis-related proteins and important hallmarks of apoptosis activation involved in mitochondrial dysfunction. Consequently, siRNA-mediated silencing of *FAM134B* caused a high level of cleaved caspase-3 and cyt c in BRL-3A cells treated with DTT for 24 h (Figure 5E and F). We examined the rates of apoptotic cells using Annexin-V-FITC/PI staining assays, which revealed that the apoptotic rates also increased in the *FAM134B* siRNA

Table 1 The cell cycle distribution of buffalo rat liver 3A cells treated with dithiothreitol for different times was detected by flow cytometry

Group	G_0/G_1	S	G_2/M
0 h	17.08 ± 0.13	58.48 ± 3.82	23.05 ± 4.46
3 h	24.28 ± 2.03[a]	42.12 ± 3.98[a]	33.6 ± 4.72[a]
6 h	33.91 ± 1.39[a]	25.11 ± 0.11[a]	41.71 ± 2.45[a]
12 h	41.57 ± 1.08[a]	24.81 ± 5.45[a]	33.62 ± 4.73[a]
24 h	51.83 ± 1.14[a,b]	38.1 ± 3.00[a]	10.08 ± 3.28[a,b]
48 h	38.72 ± 1.18[a]	37.12 ± 8.06[a]	24.16 ± 8.38

[a]$P < 0.05$ *vs* 0 h group.
[b]$P < 0.05$ *vs* 48 h group.

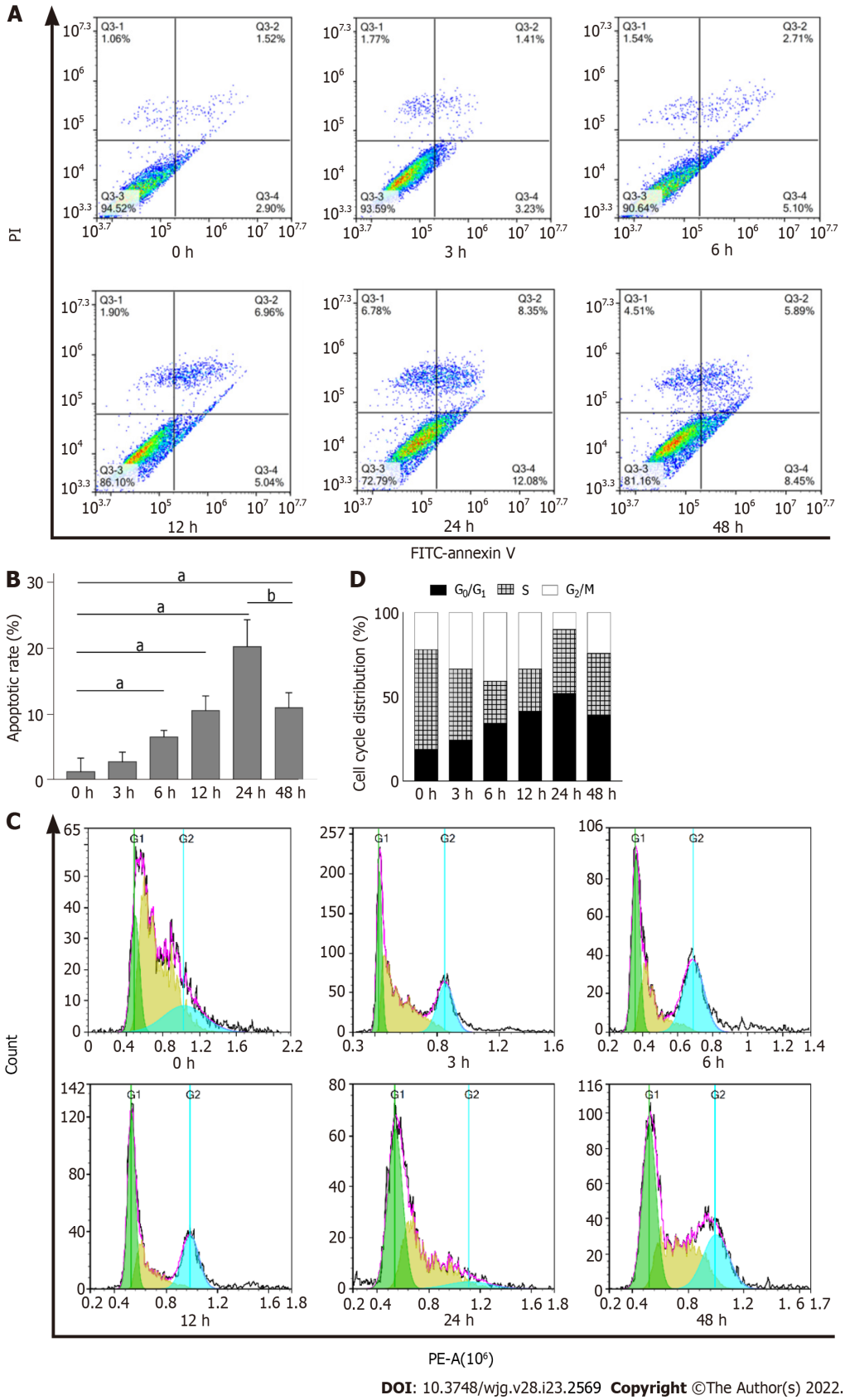
group, compared with those in the control and control siRNA groups (Figure 5G and H). These results suggest that ER-phagy mediated by FAM134B is likely to serve a cytoprotective function in response to DTT treatment in BRL-3A cells.

DISCUSSION

Hepatic injury caused by multiple harmful factors is closely associated with ER stress-induced hepatocyte apoptosis[18-20]. The ER is responsible for proper protein folding, intracellular calcium storage, and lipid biosynthesis[21,22]. Various stressors, including unfolded protein aggregation in the ER, intracellular Ca^{2+} disturbance, and pharmacological inducers, such as DTT, can disrupt ER homeostasis and lead to ER stress in hepatocytes. If the ER stress cannot be alleviated, aberrant ER stress can trigger cell apoptosis[23]. In the present study, we found that the protein levels of GRP78 and CNX, which are ER stress biomarkers, were upregulated in BRL-3A cells during ER stress. GRP78 and CNX are ER chaperone proteins and accelerate the proper folding of the accumulated unfolded proteins in the ER, which engages effector mechanisms to rebalance ER homeostasis[24,25]. A series of studies have revealed that ER-phagy is an ER selective autophagy mechanism that can promote the clearance of damaged ER lumens containing the unfolded proteins, and helps restore ER homeostasis[26-28]. ER-phagy is a critical quality control mechanism for the ER in multiple cell types. Defects in ER-phagy pathways are associated with multiple human pathologies, including infectious and neurodegenerative diseases, aging and cancer. However, whether ER-phagy is involved in the regulation of ER homeostasis in hepatocytes under ER stress remains elusive. In this study, we assessed the levels of reticulophagy-related proteins in BRL-3A cells treated with DTT. We found that the levels of FAM134B and ATG12 were markedly elevated, and the ratio of LC3II/LC3I also increased. These data indicate that DTT-induced ER stress increases the level of reticulophagy-associated proteins.

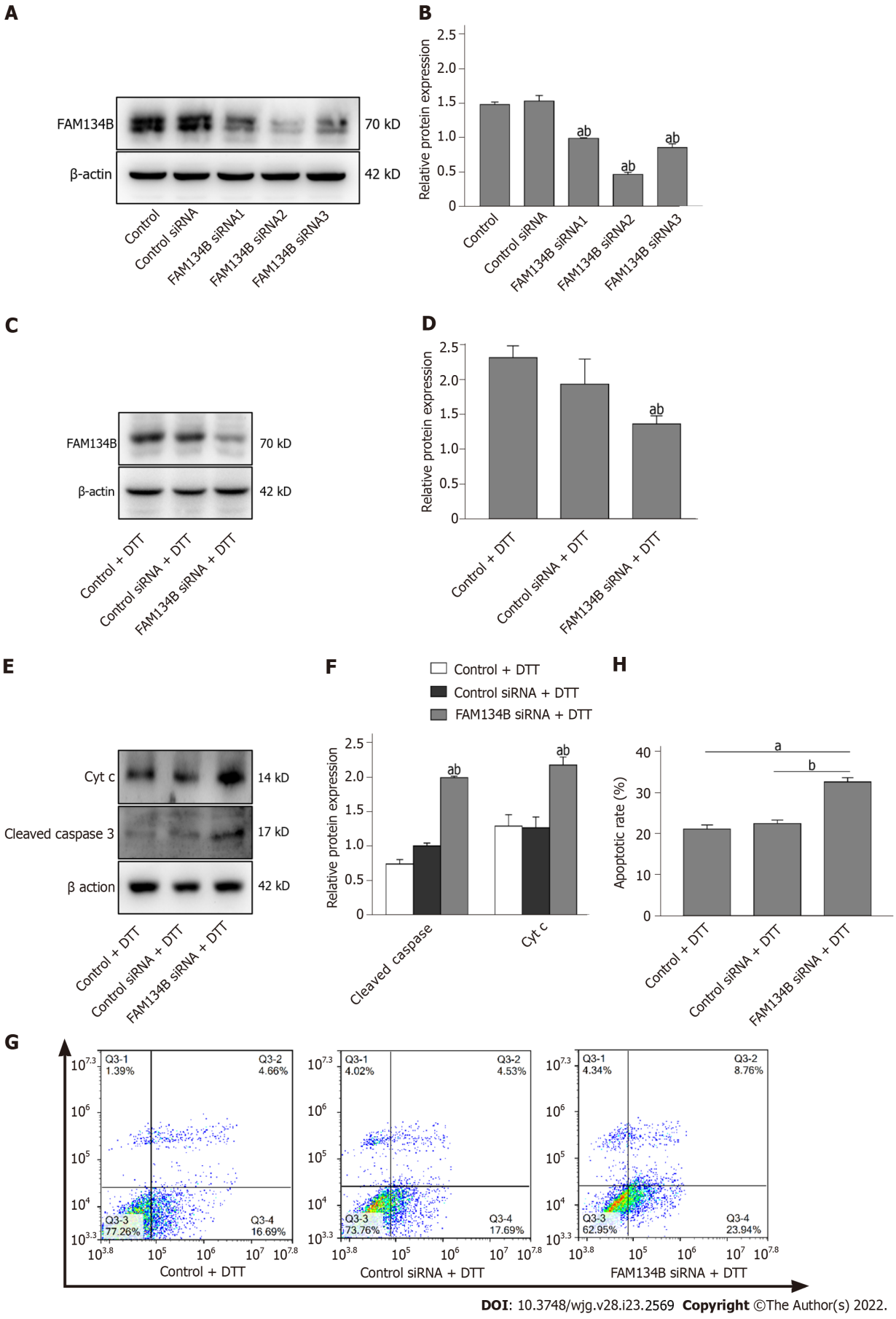
Recent findings have indicated that receptor proteins of ER-phagy play crucial roles in driving the sequestration of isolated ER fragments into autophagosomes[29]. FAM134B, an ER-anchored protein, was recently proposed as a major mammalian receptor for reticulophagy[30,31]. FAM134B contains an LC3-interacting region that can interact with LC3 protein to form autophagosomal membranes, leading to efficient ER sequestration into an autophagosomal lumen[32-34]. In a previous report, the authors found that CNX serves as a co-receptor that recognizes misfolded proteins within the ER lumen and interacts with FAM134B[35,36]. In turn, the CNX-FAM134B complex binds with LC3, the autophagosome membrane-related protein, which delivers ER lumens containing misfolded proteins to the lysosome for degradation. To investigate how FAM134B modulates ER-phagy in BRL-3A cells, immunoprecipitation was performed to detect the interaction between CNX, FAM134B, and LC3. The results confirmed that CNX interacted with FAM134B, and FAM134B interacted with LC3 after DTT treatment. Thus, the formation of the CNX-FAM134B-LC3 complex allows for the selective delivery of ER lumens containing misfolded proteins to the lysosome for eventual degradation. Complete ER-phagy indicates that autophagosomes fuse to form autolysosomes[37,38], hence, we detected the number of autolysosomes in BRL-3A cells treated with DTT. We found that the formation of autolysosomes decreased in the early stages of ER stress, whereas autolysosomes were elevated in later stages. As it has been reported that CHOP can suppress autolysosome formation[39], we speculated that decreased autolysosomes in the early stages of ER stress were associated with increased CHOP expression.

The ER is the main pool for Ca^{2+} storage, and ER dysfunction leads to Ca^{2+} efflux from the ER[40,41]. In the early stages of ER stress, the suppression of the autophagosomes' fusion with lysosomes may lead to calcium release and subsequent Ca^{2+} overload in mitochondria[42-44]. As expected, we found that



DOI: 10.3748/wjg.v28.i23.2569 **Copyright** ©The Author(s) 2022.

Figure 4 Impact of dithiothreitol treatment on cell cycle and apoptosis of buffalo rat liver 3A cells. A and B: Buffalo rat liver 3A (BRL-3A) cells were treated with 2.0 mmol/L dithiothreitol (DTT) for 0, 3, 6, 12, 24 and 48 h. The population of apoptotic cells was detected by flow cytometry. The lower right quadrant represents the early apoptotic cells, and the upper right quadrant represents the late apoptotic cells; C and D: BRL-3A cells were treated with 2.0 mmol/L DTT for 0, 3, 6, 12, 24 and 48 h. The analysis of the cell cycle was assessed by flow cytometry. $^{a}P < 0.05$ *vs* 0 h group; $^{b}P < 0.05$ *vs* 48 h group.



DOI: 10.3748/wjg.v28.i23.2569 **Copyright** ©The Author(s) 2022.

Figure 5 Impact of dithiothreitol treatment on apoptosis of buffalo rat liver 3A cells lacking *FAM134B*. A and B: Buffalo rat liver 3A (BRL-3A) cells were transfected with *FAM134B* small interfering RNAs (siRNAs) 1, 2, and 3; immunoblot was used to detect the transfection efficiency of siRNA. Protein levels were

normalized to β-actin; C and D: BRL-3A cells were transfected with *FAM134B* siRNA, followed by treatment with 2.0 mmol/L dithiothreitol (DTT) for 24 h. Immunoblot was used to detect the expression of *FAM134B* in BRL-3A cells. Protein levels were normalized to β-actin; E and F: BRL-3A cells were transfected with *FAM134B* siRNA, followed by treatment with 2.0 mmol/L DTT for 24 h. Immunoblot showed the expression of cleaved caspase-3 and cyt c. Protein levels were normalized to β-actin; G and H: BRL-3A cells were transfected with *FAM134B* siRNA, followed by treatment with 2.0 mmol/L DTT for 24 h. Representative results showed the apoptotic rate in BRL-3A cells. Untransfected cells served as controls. Cells transfected with control siRNA served as transfection controls. The lower right quadrant represents the early apoptotic cells and the upper right quadrant represents the late apoptotic cells. Values are mean ± SD (n = 3), $^{a}P < 0.05$ *vs* control group; $^{b}P < 0.05$ *vs* transfection control siRNA group.

DTT treatment dramatically elevated the levels of mitochondrial Ca^{2+}, the apoptotic rate, and G1 arrest in BRL-3A cells. Nevertheless, these trends were relieved after treatment with DTT for 48 h. Our results reveal that hepatocytes initiate adaptive mechanisms in response to DTT-induced ER stress; consequently, apoptosis in BRL-3A cells treated with DTT for 48 h was lower than that in cells treated with DTT for 24 h.

To clarify whether FAM134B is involved in the regulation of cellular homeostasis during ER stress, we used a small interference RNA technique to knockdown *FAM134B* expression in hepatocytes. We found that *FAM134B* silencing not only significantly attenuated the DTT-upregulated FAM134B expression, but also accelerated the activation of the mitochondrial apoptotic pathway and aggravated DTT-triggered hepatocyte apoptosis.

CONCLUSION

In conclusion, DTT treatment significantly upregulated the protein levels of GRP78, CNX, FAM134B, and ATG12, and also increased the ratio of LC3II/LC3I in BRL-3A cells. Moreover, FAM134B-mediated reticulophagy ameliorates DTT-induced hepatocyte apoptosis *via* selective clearance of damaged ER lumens. Accordingly, knockdown of FAM134B enhanced ER stress-mediated apoptosis in BRL-3A cells. Our data show that FAM134B-mediated reticulophagy plays a key role in rebalancing ER homeostasis in hepatocytes undergoing ER stress. Therefore, FAM134B-mediated reticulophagy may be a novel therapeutic target, and our findings may provide emerging evidence to demonstrate the prominence of ER-phagy in ER stress-related hepatocyte apoptosis. Alleviation of ER stress-mediated hepatocyte apoptosis *via* restoring ER homeostasis is critical in the treatment of liver diseases.

ARTICLE HIGHLIGHTS

Research background

Hepatocyte apoptosis induced by endoplasmic reticulum (ER) stress has a strong association with the development of fibrosis, cirrhosis, and hepatocellular carcinoma. Previous studies have revealed that endoplasmic reticulophagy (ER-phagy) promotes the selective clearance of damaged ER fragments during ER stress, playing a crucial role in maintaining ER homeostasis and inhibiting apoptosis. However, the precise regulatory mechanisms remain unclear.

Research motivation

Defects in ER-phagy pathways are associated with multiple human pathologies, including infectious and neurodegenerative diseases, aging and cancer. However, whether ER-phagy is involved in the regulation of ER homeostasis in hepatocytes under ER stress remains elusive.

Research objectives

To elucidate the effect of family with sequence similarity 134 member B (FAM134B)-mediated ER-phagy on normal buffalo rat hepatocytes apoptosis induced by dithiothreitol (DTT) and explore the potential regulatory mechanism.

Research methods

A model of ER stress was established by DTT. The levels of proteins related to ER stress and ER-phagy were determined by western blot. An interaction between FAM134B, calnexin (CNX), and microtubule-associated protein 1 light chain 3 (LC3) was investigated by co-immunoprecipitation. ER-Tracker Red probe and Lyso-Tracker Green probe were used to detect the colocalization of ER with lysosome in cells. Mito-Tracker Green and Rhod-2 AM probes were used to detect the level of mitochondrial Ca^{2+} under the confocal microscopy. Flow cytometry was conducted to analyze the effect of DTT treatment on cell cycle distribution and apoptosis. The small interfering RNA against *FAM134B* was used to knockdown *FAM134B* in buffalo rat liver 3A (BRL-3A) cells.

Research results

DTT treatment upregulated glucose-regulated protein 78 (GRP78), CNX, FAM134B, and autophagy related gene 12 (ATG12) protein levels and increased the ratio of LC3II/LC3I in BRL-3A cells. FAM134B-mediated reticulophagy maintains ER homeostasis in ER-stressed hepatocytes *via* the clearance of damaged ER fragments. FAM134B-mediated reticulophagy ameliorates DTT-induced hepatocyte apoptosis. Knockdown of *FAM134B* enhanced ER stress-mediated apoptosis in BRL-3A cells.

Research conclusions

FAM134B-mediated ER-phagy attenuates hepatocyte apoptosis by suppressing the mitochondrial apoptotic pathway.

Research perspectives

FAM134B-mediated reticulophagy may be a novel therapeutic target, and our findings provide emerging evidence demonstrating the prominence of ER-phagy in ER stress-related hepatocyte apoptosis. Alleviation of the ER stress-mediated hepatocyte apoptosis *via* restoring ER homeostasis is critical in the treatment of liver diseases.

ACKNOWLEDGEMENTS

We thank the Basic Medical Science Research Center of Guizhou Medical University for their technical advice in using the microscope.

FOOTNOTES

Author contributions: Yang Q and Xie RJ designed and coordinated the study; Guo YX, Han B and Yang T performed the experiments and acquired data; Chen YS, Yang Y and Li JY analyzed and interpreted data; Guo YX and Xie RJ drafted the manuscript; all authors approved the final version of the article.

Supported by National Natural Science Foundation of China, No. 81560105; Science and Technology Foundation of Guizhou Province, No. Qiankehe Jichu-ZK[2021]365, and No. Qiankehe Pingtai Rencai[2019]5801; and National Natural Science Foundation Cultivation Project of Guizhou Medical University, No. 20NSP016.

Institutional review board statement: This study did not involve human subjects or living animals.

Institutional animal care and use committee statement: This study did not involve human subjects or living animals.

Conflict-of-interest statement: The authors declare no conflicts of interest.

Data sharing statement: The data used to support the findings of this study are available from the corresponding author at 592153968@qq.com upon request.

Open-Access: This article is an open-access article that was selected by an in-house editor and fully peer-reviewed by external reviewers. It is distributed in accordance with the Creative Commons Attribution NonCommercial (CC BY-NC 4.0) license, which permits others to distribute, remix, adapt, build upon this work non-commercially, and license their derivative works on different terms, provided the original work is properly cited and the use is non-commercial. See: https://creativecommons.org/Licenses/by-nc/4.0/

Country/Territory of origin: China

ORCID number: Yi-Xin Guo 0000-0001-6789-8669; Bing Han 0000-0002-9577-293X; Ting Yang 0000-0001-5174-7575; Yu-Si Chen 0000-0003-2566-8878; Yi Yang 0000-0003-2756-6955; Jia-Yao Li 0000-0003-2880-4978; Qin Yang 0000-0003-1479-6700; Ru-Jia Xie 0000-0001-5991-2678.

S-Editor: Fan JR
L-Editor: A
P-Editor: Qi WW

REFERENCES

1 **Huang TJ**, Liu SH, Kuo YC, Chen CW, Chou SC. Antiviral activity of chemical compound isolated from Artemisia morrisonensis against hepatitis B virus in vitro. *Antiviral Res* 2014; **101**: 97-104 [PMID: 24269476 DOI: 10.1016/j.antiviral.2013.11.007]

2 **Tsai CC**, Chen YJ, Yu HR, Huang LT, Tain YL, Lin IC, Sheen JM, Wang PW, Tiao MM. Long term N-acetylcysteine administration rescues liver steatosis *via* endoplasmic reticulum stress with unfolded protein response in mice. *Lipids Health Dis* 2020; **19**: 105 [PMID: 32450865 DOI: 10.1186/s12944-020-01274-y]
3 **Zhang Y**, Zhang H, Zhao Z, Lv M, Jia J, Zhang L, Tian X, Chen Y, Li B, Liu M, Han D, Ji C. Enhanced expression of glucose-regulated protein 78 correlates with malondialdehyde levels during the formation of liver cirrhosis in rats. *Exp Ther Med* 2015; **10**: 2119-2125 [PMID: 26668603 DOI: 10.3892/etm.2015.2783]
4 **Schwabe RF**, Tabas I, Pajvani UB. Mechanisms of Fibrosis Development in Nonalcoholic Steatohepatitis. *Gastroenterology* 2020; **158**: 1913-1928 [PMID: 32044315 DOI: 10.1053/j.gastro.2019.11.311]
5 **Zuo L**, Zhu Y, Hu L, Liu Y, Wang Y, Hu Y, Wang H, Pan X, Li K, Du N, Huang Y. PI3-kinase/Akt pathway-regulated membrane transportation of acid-sensing ion channel 1a/Calcium ion influx/endoplasmic reticulum stress activation on PDGF-induced HSC Activation. *J Cell Mol Med* 2019; **23**: 3940-3950 [PMID: 30938088 DOI: 10.1111/jcmm.14275]
6 **Khaminets A**, Heinrich T, Mari M, Grumati P, Huebner AK, Akutsu M, Liebmann L, Stolz A, Nietzsche S, Koch N, Mauthe M, Katona I, Qualmann B, Weis J, Reggiori F, Kurth I, Hübner CA, Dikic I. Regulation of endoplasmic reticulum turnover by selective autophagy. *Nature* 2015; **522**: 354-358 [PMID: 26040720 DOI: 10.1038/nature14498]
7 **Smith MD**, Harley ME, Kemp AJ, Wills J, Lee M, Arends M, von Kriegsheim A, Behrends C, Wilkinson S. CCPG1 Is a Non-canonical Autophagy Cargo Receptor Essential for ER-Phagy and Pancreatic ER Proteostasis. *Dev Cell* 2018; **44**: 217-232.e11 [PMID: 29290589 DOI: 10.1016/j.devcel.2017.11.024]
8 **Fumagalli F**, Noack J, Bergmann TJ, Cebollero E, Pisoni GB, Fasana E, Fregno I, Galli C, Loi M, Soldà T, D'Antuono R, Raimondi A, Jung M, Melnyk A, Schorr S, Schreiber A, Simonelli L, Varani L, Wilson-Zbinden C, Zerbe O, Hofmann K, Peter M, Quadroni M, Zimmermann R, Molinari M. Translocon component Sec62 acts in endoplasmic reticulum turnover during stress recovery. *Nat Cell Biol* 2016; **18**: 1173-1184 [PMID: 27749824 DOI: 10.1038/ncb3423]
9 **Kopp MC**, Larburu N, Durairaj V, Adams CJ, Ali MMU. UPR proteins IRE1 and PERK switch BiP from chaperone to ER stress sensor. *Nat Struct Mol Biol* 2019; **26**: 1053-1062 [PMID: 31695187 DOI: 10.1038/s41594-019-0324-9]
10 **Kozlov G**, Gehring K. Calnexin cycle - structural features of the ER chaperone system. *FEBS J* 2020; **287**: 4322-4340 [PMID: 32285592 DOI: 10.1111/febs.15330]
11 **Bernales S**, McDonald KL, Walter P. Autophagy counterbalances endoplasmic reticulum expansion during the unfolded protein response. *PLoS Biol* 2006; **4**: e423 [PMID: 17132049 DOI: 10.1371/journal.pbio.0040423]
12 **Bernales S**, Schuck S, Walter P. ER-phagy: selective autophagy of the endoplasmic reticulum. *Autophagy* 2007; **3**: 285-287 [PMID: 17351330 DOI: 10.4161/auto.3930]
13 **Forrester A**, De Leonibus C, Grumati P, Fasana E, Piemontese M, Staiano L, Fregno I, Raimondi A, Marazza A, Bruno G, Iavazzo M, Intartaglia D, Seczynska M, van Anken E, Conte I, De Matteis MA, Dikic I, Molinari M, Settembre C. A selective ER-phagy exerts procollagen quality control *via* a Calnexin-FAM134B complex. *EMBO J* 2019; **38** [PMID: 30559329 DOI: 10.15252/embj.201899847]
14 **Chino H**, Mizushima N. ER-Phagy: Quality Control and Turnover of Endoplasmic Reticulum. *Trends Cell Biol* 2020; **30**: 384-398 [PMID: 32302550 DOI: 10.1016/j.tcb.2020.02.001]
15 **Wilkinson S**. ER-phagy: shaping up and destressing the endoplasmic reticulum. *FEBS J* 2019; **286**: 2645-2663 [PMID: 31116513 DOI: 10.1111/febs.14932]
16 **Molinari M**. ER-phagy: Eating the Factory. *Mol Cell* 2020; **78**: 811-813 [PMID: 32502421 DOI: 10.1016/j.molcel.2020.05.002]
17 **Chen YS**, Han B, Zheng L, Cai S, Tang L, Yang Y, Guo YX, Liang C, Zhao JY, Yang T, Yang Q. Effects of calpain-2 and autophagy-related protein 5 on hepatocyte apoptosis induced by endoplasmic reticulum stress. *Zhongguo Bingli Shengli Zazhi* 2020; **36**: 847-853
18 **Dash S**, Chava S, Aydin Y, Chandra PK, Ferraris P, Chen W, Balart LA, Wu T, Garry RF. Hepatitis C Virus Infection Induces Autophagy as a Prosurvival Mechanism to Alleviate Hepatic ER-Stress Response. *Viruses* 2016; **8** [PMID: 27223299 DOI: 10.3390/v8050150]
19 **Wang K**. Autophagy and apoptosis in liver injury. *Cell Cycle* 2015; **14**: 1631-1642 [PMID: 25927598 DOI: 10.1080/15384101.2015.1038685]
20 **Liu H**, Lai W, Liu X, Yang H, Fang Y, Tian L, Li K, Nie H, Zhang W, Shi Y, Bian L, Ding S, Yan J, Lin B, Xi Z. Exposure to copper oxide nanoparticles triggers oxidative stress and endoplasmic reticulum (ER)-stress induced toxicology and apoptosis in male rat liver and BRL-3A cell. *J Hazard Mater* 2021; **401**: 123349 [PMID: 32659578 DOI: 10.1016/j.jhazmat.2020.123349]
21 **Phillips MJ**, Voeltz GK. Structure and function of ER membrane contact sites with other organelles. *Nat Rev Mol Cell Biol* 2016; **17**: 69-82 [PMID: 26627931 DOI: 10.1038/nrm.2015.8]
22 **Kaneko M**, Imaizumi K, Saito A, Kanemoto S, Asada R, Matsuhisa K, Ohtake Y. ER Stress and Disease: Toward Prevention and Treatment. *Biol Pharm Bull* 2017; **40**: 1337-1343 [PMID: 28867719 DOI: 10.1248/bpb.b17-00342]
23 **Xie RJ**, Hu XX, Zheng L, Cai S, Chen YS, Yang Y, Yang T, Han B, Yang Q. Calpain-2 activity promotes aberrant endoplasmic reticulum stress-related apoptosis in hepatocytes. *World J Gastroenterol* 2020; **26**: 1450-1462 [PMID: 32308346 DOI: 10.3748/wjg.v26.i13.1450]
24 **Tian G**, Zhao M, Zhou J, Quan Y, Wu W, Liu X. [The potential role of calnexin in the activation of cardiac fibroblasts]. *Sheng Wu Yi Xue Gong Cheng Xue Za Zhi* 2020; **37**: 450-459 [PMID: 32597087 DOI: 10.7507/1001-5515.202001052]
25 **Zheng Z**, Shang Y, Tao J, Zhang J, Sha B. Endoplasmic Reticulum Stress Signaling Pathways: Activation and Diseases. *Curr Protein Pept Sci* 2019; **20**: 935-943 [PMID: 31223084 DOI: 10.2174/1389203720666190621103145]
26 **Fregno I**, Molinari M. Endoplasmic reticulum turnover: ER-phagy and other flavors in selective and non-selective ER clearance. *F1000Res* 2018; **7**: 454 [PMID: 29744037 DOI: 10.12688/f1000research.13968.1]
27 **Birgisdottir ÅB**, Lamark T, Johansen T. The LIR motif - crucial for selective autophagy. *J Cell Sci* 2013; **126**: 3237-3247 [PMID: 23908376 DOI: 10.1242/jcs.126128]
28 **Liang JR**, Lingeman E, Ahmed S, Corn JE. Atlastins remodel the endoplasmic reticulum for selective autophagy. *J Cell Biol* 2018; **217**: 3354-3367 [PMID: 30143524 DOI: 10.1083/jcb.201804185]

29 **Chen Q**, Xiao Y, Chai P, Zheng P, Teng J, Chen J. ATL3 Is a Tubular ER-Phagy Receptor for GABARAP-Mediated Selective Autophagy. *Curr Biol* 2019; **29**: 846-855 [PMID: 30773365 DOI: 10.1016/j.cub.2019.01.041]

30 **Schultz ML**, Krus KL, Kaushik S, Dang D, Chopra R, Qi L, Shakkottai VG, Cuervo AM, Lieberman AP. Coordinate regulation of mutant NPC1 degradation by selective ER autophagy and MARCH6-dependent ERAD. *Nat Commun* 2018; **9**: 3671 [PMID: 30202070 DOI: 10.1038/s41467-018-06115-2]

31 **Morishita H**, Mizushima N. Diverse Cellular Roles of Autophagy. *Annu Rev Cell Dev Biol* 2019; **35**: 453-475 [PMID: 31283377 DOI: 10.1146/annurev-cellbio-100818-125300]

32 **Johansen T**, Lamark T. Selective Autophagy: ATG8 Family Proteins, LIR Motifs and Cargo Receptors. *J Mol Biol* 2020; **432**: 80-103 [PMID: 31310766 DOI: 10.1016/j.jmb.2019.07.016]

33 **Jiang X**, Wang X, Ding X, Du M, Li B, Weng X, Zhang J, Li L, Tian R, Zhu Q, Chen S, Wang L, Liu W, Fang L, Neculai D, Sun Q. FAM134B oligomerization drives endoplasmic reticulum membrane scission for ER-phagy. *EMBO J* 2020; **39**: e102608 [PMID: 31930741 DOI: 10.15252/embj.2019102608]

34 **Bhaskara RM**, Grumati P, Garcia-Pardo J, Kalayil S, Covarrubias-Pinto A, Chen W, Kudryashev M, Dikic I, Hummer G. Curvature induction and membrane remodeling by FAM134B reticulon homology domain assist selective ER-phagy. *Nat Commun* 2019; **10**: 2370 [PMID: 31147549 DOI: 10.1038/s41467-019-10345-3]

35 **Fregno I**, Fasana E, Bergmann TJ, Raimondi A, Loi M, Soldà T, Galli C, D'Antuono R, Morone D, Danieli A, Paganetti P, van Anken E, Molinari M. ER-to-lysosome-associated degradation of proteasome-resistant ATZ polymers occurs *via* receptor-mediated vesicular transport. *EMBO J* 2018; **37** [PMID: 30076131 DOI: 10.15252/embj.201899259]

36 **Wilkinson S**. Emerging Principles of Selective ER Autophagy. *J Mol Biol* 2020; **432**: 185-205 [PMID: 31100386 DOI: 10.1016/j.jmb.2019.05.012]

37 **Grumati P**, Morozzi G, Hölper S, Mari M, Harwardt MI, Yan R, Müller S, Reggiori F, Heilemann M, Dikic I. Full length RTN3 regulates turnover of tubular endoplasmic reticulum *via* selective autophagy. *Elife* 2017; **6** [PMID: 28617241 DOI: 10.7554/eLife.25555]

38 **Ko SH**, Jeon JI, Myung HS, Kim YJ, Kim JM. Bacteroides fragilis Enterotoxin Induces Formation of Autophagosomes in Endothelial Cells but Interferes with Fusion with Lysosomes for Complete Autophagic Flux through a Mitogen-Activated Protein Kinase-, AP-1-, and C/EBP Homologous Protein-Dependent Pathway. *Infect Immun* 2017; **85** [PMID: 28694294 DOI: 10.1128/IAI.00420-17]

39 **Arruda AP**, Pers BM, Parlakgül G, Güney E, Inouye K, Hotamisligil GS. Chronic enrichment of hepatic endoplasmic reticulum-mitochondria contact leads to mitochondrial dysfunction in obesity. *Nat Med* 2014; **20**: 1427-1435 [PMID: 25419710 DOI: 10.1038/nm.3735]

40 **Wiel C**, Lallet-Daher H, Gitenay D, Gras B, Le Calvé B, Augert A, Ferrand M, Prevarskaya N, Simonnet H, Vindrieux D, Bernard D. Endoplasmic reticulum calcium release through ITPR2 channels leads to mitochondrial calcium accumulation and senescence. *Nat Commun* 2014; **5**: 3792 [PMID: 24797322 DOI: 10.1038/ncomms4792]

41 **Datta D**, Khatri P, Singh A, Saha DR, Verma G, Raman R, Mazumder S. *Mycobacterium fortuitum*-induced ER-Mitochondrial calcium dynamics promotes calpain/caspase-12/caspase-9 mediated apoptosis in fish macrophages. *Cell Death Discov* 2018; **4**: 30 [PMID: 29531827 DOI: 10.1038/s41420-018-0034-9]

42 **Fan Y**, Simmen T. Mechanistic Connections between Endoplasmic Reticulum (ER) Redox Control and Mitochondrial Metabolism. *Cells* 2019; **8** [PMID: 31547228 DOI: 10.3390/cells8091071]

43 **Krebs J**, Agellon LB, Michalak M. Ca(2+) homeostasis and endoplasmic reticulum (ER) stress: An integrated view of calcium signaling. *Biochem Biophys Res Commun* 2015; **460**: 114-121 [PMID: 25998740 DOI: 10.1016/j.bbrc.2015.02.004]

44 **Luciani DS**, Gwiazda KS, Yang TL, Kalynyak TB, Bychkivska Y, Frey MH, Jeffrey KD, Sampaio AV, Underhill TM, Johnson JD. Roles of IP3R and RyR Ca2+ channels in endoplasmic reticulum stress and beta-cell death. *Diabetes* 2009; **58**: 422-432 [PMID: 19033399 DOI: 10.2337/db07-1762]

World Journal of Gastroenterology

Submit a Manuscript: https://www.f6publishing.com

World J Gastroenterol 2022 June 21; 28(23): 2582-2596

DOI: 10.3748/wjg.v28.i23.2582

ISSN 1007-9327 (print) ISSN 2219-2840 (online)

ORIGINAL ARTICLE

Retrospective Study

Infliximab trough level combined with inflammatory biomarkers predict long-term endoscopic outcomes in Crohn's disease under infliximab therapy

Wan-Ting Cao, Rong Huang, Shan Liu, Yi-Hong Fan, Mao-Sheng Xu, Yi Xu, Hui Ni

Specialty type: Gastroenterology and hepatology

Provenance and peer review: Unsolicited article; Externally peer reviewed.

Peer-review model: Single blind

Peer-review report's scientific quality classification

Grade A (Excellent): 0
Grade B (Very good): 0
Grade C (Good): C, C
Grade D (Fair): 0
Grade E (Poor): 0

P-Reviewer: Leite A, Brazil; Taxonera C, Spain

Received: October 30, 2021
Peer-review started: October 30, 2021
First decision: March 11, 2022
Revised: March 25, 2022
Accepted: May 7, 2022
Article in press: May 7, 2022
Published online: June 21, 2022

Wan-Ting Cao, Rong Huang, Yi-Hong Fan, Yi Xu, Department of Gastroenterology, The First Affiliated Hospital of Zhejiang Chinese Medical University, Zhejiang Provincial Key Laboratory of Gastrointestinal Diseases Pathophysiology, Hangzhou 310006, Zhejiang Province, China

Shan Liu, Department of Clinical Evaluation Center, The First Affiliated Hospital of Zhejiang Chinese Medical University, Hangzhou 310006, Zhejiang Province, China

Mao-Sheng Xu, Department of Radiology, The First Affiliated Hospital of Zhejiang Chinese Medical University, Hangzhou 310006, Zhejiang Province, China

Hui Ni, Department of Nursing, The Second Affiliated Hospital of Zhejiang University School of Medicine, Hangzhou 310006, Zhejiang Province, China

Corresponding author: Yi-Hong Fan, MD, Associate Professor, Chief Doctor, Department of Gastroenterology, The First Affiliated Hospital of Zhejiang Chinese Medical University, Zhejiang Provincial Key Laboratory of Gastrointestinal Diseases Pathophysiology, No. 54 Youdian Road, Shangcheng District, Hangzhou 310006, Zhejiang Province, China.
yhfansjr@163.com

Abstract

BACKGROUND

Infliximab trough level (ITL) severely affects therapeutic outcomes of Crohn's disease (CD) patients under infliximab (IFX). Recently, frontier research has focused on identifying ITL based on different therapeutic targets. Although previous studies have elaborated clinical value of ITL monitoring on short-term outcomes in CD patients during therapy, studies contraposing the predictive value of ITL on long-term endoscopic outcomes in CD patients are still scarce domestically and overseas.

AIM

To explore the predictive value of ITL in combination with inflammatory biomarkers on long-term endoscopic outcomes in CD with clinical remission during IFX maintenance therapy.

METHODS

CD patients with endoscopic remission under long-term IFX maintenance therapy in the First Affiliated Hospital of Zhejiang Chinese Medicine University from January 2012 to December 2020 were collected. ITL and inflammatory biomarkers were continuously monitored during the therapy. The Step I study was conducted from weeks 14 to 54 of IFX treatment. The Step II study was conducted from weeks 54 to 108 of IFX treatment. Endoscopic outcomes were defined as endoscopic activity (Crohn's disease endoscopic index of severity score > 2 points or Rutgeerts score > i1) and endoscopic remission (Crohn's disease endoscopic index of severity score ≤ 2 points or Rutgeerts ≤ i1). Endoscopic relapse free survival was defined as endoscopic remission at the beginning of the study stage and maintaining endoscopic remission during the study stage.

RESULTS

At week 14, low ITL [odds ratio (OR) = 0.666, 95% confidence interval (CI): 0.514-0.862, $P < 0.01$] and high fecal calprotectin (FCP) level (OR = 1.002, 95%CI: 1.001-1.004, $P < 0.01$) increased the risk of endoscopic activity at week 54. At week 54, low ITL (OR = 0.466, 95%CI: 0.247-0.877, $P < 0.01$) and high C-reactive protein (CRP) level (OR = 1.590, 95%CI: 1.007-2.510, $P < 0.01$) increased the risk of endoscopic activity at week 108. At week 14, ITL ≤ 5.60 μg/mL [area under the curve (AUC) = 0.83, 95%CI: 0.73-0.90, $P < 0.001$] and FCP > 238 μg/g (AUC = 0.82, 95%CI: 0.72-0.89, $P < 0.001$) moderately predicted endoscopic activity at week 54. ITL ≤ 5.60 μg/mL in combination with FCP > 238 μg/g indicated 82.0% possibility of endoscopic activity. At week 54, ITL ≤ 2.10 μg/mL (AUC = 0.85, 95%CI: 0.72-0.93, $P < 0.001$) and CRP > 3.00 mg/L (AUC = 0.73, 95%CI: 0.60-0.84, $P = 0.012$) moderately predicted moderate endoscopic activity at week 108. ITL ≤ 2.10 μg/mL in combination with CRP > 3.00 mg/L indicated 100.0% possibility of endoscopic activity. From weeks 14 to 54 of IFX treatment, patients with ITL > 5.60 μg/mL had higher rate of endoscopic relapse free survival than those with ITL ≤ 5.60 μg/mL (95.83% *vs* 46.67%). From weeks 54 to 108 of IFX treatment, patients with ITL > 2.10 μg/mL had higher rate of endoscopic survival free relapsed rate than those with ITL ≤ 2.10 μg/mL (92.68% *vs* 30.77%).

CONCLUSION

Combination of ITL, CRP, and FCP contribute to long-term endoscopic prognosis monitoring. During IFX maintenance treatment, low ITL, high CRP level, and high FCP level were independent risk factors of CD patients with clinical remission in adverse endoscopy outcomes within 1-year follow-up.

Key Words: Infliximab trough level; C-reactive protein; Fecal calprotectin; Crohn's disease; Clinical remission; Long-term endoscopic outcomes

©The Author(s) 2022. Published by Baishideng Publishing Group Inc. All rights reserved.

Core Tip: Previous investigations, contraposing Crohn's disease patients under infliximab (IFX) maintenance therapy, have indicated that higher IFX trough levels (ITLs) were associated with sustained drug response and clinical remission in inflammatory bowel disease patients, while lower ITLs were linked to secondary unresponsiveness of IFX. Currently, endoscopic remission or mucosal healing has been considered the main goal of biological therapy. Our study manifested that Crohn's disease patients with higher levels of IFX blood concentration and lower levels of inflammatory biomarkers tended to have a better long-term endoscopic prognosis. Combining ITL, fecal calprotectin and C-reactive protein monitoring was helpful for the timely adjustment of IFX treatment strategy.

Citation: Cao WT, Huang R, Liu S, Fan YH, Xu MS, Xu Y, Ni H. Infliximab trough level combined with inflammatory biomarkers predict long-term endoscopic outcomes in Crohn's disease under infliximab therapy. *World J Gastroenterol* 2022; 28(23): 2582-2596

URL: https://www.wjgnet.com/1007-9327/full/v28/i23/2582.htm

DOI: https://dx.doi.org/10.3748/wjg.v28.i23.2582

INTRODUCTION

Crohn's disease (CD) is a persistently progressive disease with nonspecific inflammation characterized by disease scope involving the whole digestive tract and disease depth involving the whole intestinal wall. The accumulation damage of intestinal walls contributes to the occurrence of stenosis, fistula and even abscess, reducing the life quality. Therefore, recent clinical studies have consistently concluded

that therapeutic strategies and targets play key roles in controlling CD progression. Setting different therapeutic targets will have different disease outcomes. Clinical response, focusing only on the improvement of clinical symptoms, can improve the quality of daily life but not affect long-term treatment outcomes. CD patients who do not achieve deep remission may be aggravated persistently, while achieving deep remission could reduce long-term hospitalization and surgery rates. Deep remission is mainly defined in previous studies as endoscopic remission or mucosal healing. Biologics, as an important step in the therapeutic strategy of CD, can effectively control the disease progression if conducted early and completely.

In consideration of the wide use of infliximab (IFX), precisely predicting the long-term endoscopic outcomes is stressed by more and more inflammatory bowel disease (IBD) physicians. Although the IFX trough level (ITL) has been proven to be closely related to the outcome of CD, ITL alone may be biased in predicting the outcome of CD. Monitoring inflammation biomarkers is one of the important links of IFX therapy, including C-reaction protein (CRP), fecal calprotectin (FCP), *etc*. High inflammatory load affects the pharmacokinetics of IFX, inducing secondary nonresponse by decreasing blood drug concentration. Currently, it is believed that inflammatory biomarkers are good predictors of disease activity, but there is still a lack of reliable evidence for predicting disease remission. Therefore, this study intends to evaluate long-term endoscopic outcomes of CD patients receiving IFX treatment by combining the blood drug concentration and inflammatory biomarkers.

MATERIALS AND METHODS

Study subjects design

A single-center retrospective research was implemented at the First Affiliated Hospital of Zhejiang Chinese Medical University. CD patients under IFX therapy from January 2012 to December 2020 were collected. One hundred and eighty-one CD patients underwent IFX treatment. One hundred and fifty-one CD patients underwent endoscopy as well as serum concentration monitoring at week 14 after the third dose of IFX induction therapy. Inclusion criteria: (1) Endoscopic remission at week 14 [Crohn's disease endoscopic index of severity (CDEIS) score ≤ 2 points or Rutgeerts ≤ i1]; (2) Clinical remission after IFX induction therapy without corticosteroids more than 6 mo; and (3) Therapeutic strategy during maintenance stage was designed as IFX 5 mg/kg every 8 wk combined with azathioprine (AZA) 50 mg every day. Therapeutic strategic was modulated if CD patients were confronted with clinical relapse or secondary loss of response (LOR), and data analysis focused on the treatment course when patients received IFX 5 mg/kg and AZA therapy regularly. Secondary LOR was defined as a recurrence of the disease during IFX maintenance therapy. Two criteria were met to determine LOR: The recurrence of symptoms of IBD in clinical remission after induction therapy and symptoms caused by the inflammatory activity of IBD itself. Clinical relapse means Crohn's disease activity index > 150 points. Blood drug concentration monitoring and clinical, laboratory, endoscopic and imaging evaluation were implemented every 2 mo since the third dose of IFX induction therapy in all patients. The study was divided into two stages, step I study period defined as IFX maintenance therapy during week 14 to week 54 and step II study period defined as IFX maintenance therapy during week 54 to week 108.

Data collection

General data included age, sex, course, disease location, disease behavior, medication history and history of intestinal surgery. Laboratory indicators include white blood cell count, blood platelet count, CRP, erythrocyte sedimentation rate, serum albumin, FCP, ITL and anti-IFX antibody. Evaluation indicators of disease severity included Crohn's disease activity index score on clinical severity, CDEIS score on endoscopic severity in CD patients without intestinal surgery and Rutgeerts score on endoscopic severity in CD patients with intestinal surgery.

Outcome definition

Endoscopic outcomes at week 54 and week 108 after IFX initial therapy were evaluated by specialist physicians on IBD under electronic colonoscopy. Endoscopic remission was defined as CDEIS score ≤ 2 or Rutgeerts score ≤ i1, and endoscopic activity was defined as CDEIS score > 2 or Rutgeerts score > i1. Survival outcomes during IFX maintenance therapy were concentrated on endoscopic relapse-free survival, defined as sustained endoscopic remission during step I study period or step II study period.

Statistical analysis

Descriptive statistical analysis was used to describe characteristics of CD patients. Number of cases (percentage) was used to describe categorial variable. mean ± SD was used to describe continuous variable. Nonparametric Mann-Whitney test was used to compare two groups in enumeration data or measurement data without normal distribution. Two-sample t test was used to compare two groups in measurement data with normal distribution. One-way analysis of variance was used to compare multi-group if data satisfied homogeneity of variance. Nonparametric Kruskal-Wallis test was used to

compare multi-group if data not satisfied homogeneity of variance. SPSS 23.0 (Armonk, NY, United States) was used to analyze differences between groups. A P value < 0.05 was considered significant.

Receiver-operating characteristic (ROC) analysis was used to identify the best cut off level of ITL on predicting endoscopic remission as well as sensitivity, specificity, positive predictive value, negative predictive value, area under the curve and Youden Index. Univariate logistic regression analysis was used to identify the association between endoscopic activity and predictors. Log-rank test was used to identify the association between endoscopic relapse and predictors. GraphPad Prism9.0 (San Diego, CA, United States) was used to draw histograms and survival analysis curves and implement log-rank test. MedCalc19.0 was used to draw ROC curve and analyze the predictive value of indicators on endoscopic outcomes. A P value < 0.05 was considered significant.

RESULTS

Characteristics of study subjects

In total, the study cohort collected 112 CD patients achieving clinical remission after IFX induction therapy. In step I study, 19 CD patients were excluded due to data absence (n = 1, 5.26%) and endoscopic activity at week 14 (n = 18, 94.74%), while 93 CD patients with endoscopic remission at week 14 were included. In step II study, 58 CD patients were excluded due to course of therapy shorter than 2 years (n = 10, 17.24%), secondary non-response of IFX (n = 12, 20.69%), suspension of IFX therapy within 2 years for disease remission (n = 10, 17.24%) and endoscopic activity at week 54 (n = 26, 44.83%), while 54 CD patients with endoscopic remission at week 54 were included. These 12 patients did not satisfy indications of operation and received hormonotherapy as the primary choice to alleviate disease, for our center lacked other biological agents at that time. All CD patients under IFX maintenance therapy were combined with AZA (Figure 1). The dose of IFX was 5 mg/kg every 8 wk, and the dose of AZA was 50 mg every day. Characteristics of CD patients included in study are shown in Table 1.

Correlation between ITL, inflammatory biomarkers and endoscopic outcomes

In step I study, 67/93 CD patients (72.04%) sustained endoscopic remission at week 54 among. Multivariable regression analysis revealed that only ITL (OR = 0.666, 95%CI: 0.514-0.862, P = 0.002) and FCP (OR = 1.002, 95%CI: 1.001-1.004, P = 0.002) were independent risk of endoscopic activity at week 54 (Table 2). Based on incremental gain analysis, an ITL range of 5.0-7.4 μg/mL was correlated with sustained endoscopic remission rate of more than 85% (Figure 2).

In step II study, 42/54 CD patients (77.78%) sustained endoscopic remission at week 108. Multivariable regression analysis revealed that only ITL (OR = 0.466, 95%CI: 0.247-0.877, P = 0.018) and CRP (OR = 1.590, 95%CI: 1.007-2.510, P = 0.047) were independent risks of endoscopic activity at week 108 (Table 2). Based on incremental gain analysis, an ITL range of 2.0-3.9 μg/mL was correlated with sustained endoscopic remission rate of more than 85% (Figure 2).

Predictive value of ITL and inflammatory biomarkers on endoscopic outcomes

In step I study, the ROC analysis demonstrated that the best cut off level of ITL and FCP at week 14 on predicting endoscopic relapse at week 54 was 5.60 μg/ml (AUC = 0.83, 95%CI: 0.73-0.90, P < 0.001) and 238 μg/g (AUC = 0.82, 95%CI: 0.72-0.89, P < 0.001) (Table 3 and Figure 3). CD patients with ITL ≤ 5.60 μg/ml and FCP > 238 μg/g at week 14 had 82% probability of endoscopic relapse at week 54. However, CD patients with ITL > 5.60 μg/ml and FCP ≤ 238 μg/g at week 14 had 98% probability of sustained endoscopic remission at week 54.

In step II study, the ROC analysis demonstrated that the best cut off level of ITL and CRP at week 54 on predicting endoscopic relapse at week 108 was 2.10 μg/mL (AUC = 0.85, 95%CI: 0.72-0.93, P < 0.001) and 3.00 mg/L (AUC = 0.73, 95%CI: 0.60-0.84, P = 0.012) (Table 3 and Figure 3). CD patients with ITL ≤ 2.10 μg/mL and CRP > 3.00 mg/L at week 54 had 100% probability of endoscopic relapse at week 108. However, CD patients with ITL > 2.10 μg/mL and CRP ≤ 3.00 mg/L at week 54 had 97% probability of sustained endoscopic remission at week 108.

Correlation between ITL, inflammatory biomarkers and endoscopic relapse-free survival

In step I study, 26/93 (27.96%) CD patients had experienced endoscopic relapse from week 14 to week 54 of IFX maintenance therapy. The estimated endoscopic relapse-free rate was 46/48 (95.83%) in CD patients with ITL > 5.6 μg/ml and 21/45 (46.67%) in CD patients with ITL ≤ 5.6 μg/ml. The median time to endoscopic relapse of CD patients with ITL ≤ 5.6 μg/ml was 32.00 wk shorter than those with ITL > 5.6 μg/ml [hazard ratio (HR) = 16.19, 95%CI: 7.44-35.22, P < 0.0001] (Figure 4A). The estimated endoscopic relapse-free rate was 6/25 (24.00%) in CD patients with FCP > 238 μg/g and 61/68 (89.71%) in CD patients with FCP ≤ 238 μg/g. The median time to endoscopic relapse of CD patients with FCP > 238 μg/g was 21.00 wk shorter than those with FCP ≤ 238 μg/g (HR = 11.25, 95%CI: 4.26-29.73, P < 0.0001) (Figure 4B).

Table 1 Clinical characteristics of Crohn's disease patients with endoscopic remission

Variable	Week 14 (after initial IFX therapy)			Week 54 (after initial IFX therapy) *n* = 54		
	Total, *n* = 93	ER at week 54, *n* = 67	EA at week 54, *n* = 26	Total, *n* = 54	ER at week 108, *n* = 42	EA at week 108, *n* = 12
Median age in yr, mean ± SD	28.96 ± 9.37	29.03 ± 10.09	28.77 ± 7.39	27.57 ± 10.13	26.93 ± 9.87	29.83 ± 11.13
Course in yr, median (IQR)	3.0 (1.0, 6.0)	2.0 (1.0, 6.0)	3.5 (2.0, 8.3)	2.0 (1.0, 5.0)	2.0 (1.0, 5.0)	2.0 (1.3, 8.5)
Male sex, *n* (%)	55 (59.1)	43 (64.2)	12 (46.2)	35 (64.8)	28 (66.7)	7 (58.3)
Disease location, *n* (%)						
L1 (terminal ileum)	18 (19.4)	14 (20.9)	4 (15.4)	10 (18.5)	9 (21.4)	1 (8.3)
L2 (colon)	11 (11.8)	6 (9.0)	5 (19.2)	5 (9.3)	4 (9.5)	1 (8.3)
L3 (ileocolon)	64 (68.8)	47 (70.1)	17 (65.4)	39 (72.2)	29 (69.0)	10 (83.3)
L4 (upper digestive tract)	22 (23.7)	15 (22.4)	7 (26.9)	14 (25.9)	11(26.2)	3 (25.0)
Disease behavior, *n* (%)						
B1 (no)	19 (20.4)	15 (22.4)	4 (15.4)	13 (24.1)	9 (21.4)	4 (33.3)
B2 (stenosis)	11 (11.8)	9 (13.4)	2 (7.7)	6 (11.1)	5 (11.9)	1 (8.3)
B3 (penetration)	40 (43.0)	27 (40.3)	13 (50.0)	23 (42.6)	18 (42.9)	5 (41.7)
B2 (stenosis) + B3 (penetration)	23 (24.7)	16 (23.9)	7 (26.9)	12 (22.2)	10 (23.8)	2 (16.7)
Perianal diseases, *n* (%)	55 (59.1)	38 (56.7)	17 (65.4)	32 (59.3)	25 (59.5)	7 (58.3)
Previous medical therapy, *n* (%)	64 (68.8)	46 (68.7)	18 (69.2)	34 (63.0)	25 (59.5)	9 (75.0)
Previous surgical therapy, *n* (%)	15 (16.1)	11 (16.4)	4 (15.4)	8 (14.8)	8 (19.0)	0 (0.0)
Laboratory indicators, mean ± SD						
Fecal calprotectin, μg/g	399.96 ± 562.47	178.62 ± 242.38	970.35 ± 734.49	353.17 ± 557.71	178.57 ± 276.56	964.25 ± 830.56
IFX trough level, μg/ml	6.12 ± 3.72	7.23 ± 3.48	3.25 ± 2.67	3.80 ± 2.25	4.37 ± 2.02	1.80 ± 1.90
White blood count, × 10^9/L	5.32 ± 1.87	5.16 ± 1.47	5.73 ± 2.65	5.27 ± 1.41	5.27 ± 1.43	5.28 ± 1.41
Hematoglobin, g/L	128.37 ± 20.42	130.96 ± 20.03	121.69 ± 20.27	136.59 ± 16.06	136.79 ± 16.94	135.92 ± 13.13
Platelet, × 10^9/L	210.66 ± 69.77	202.36 ± 58.34	232.04 ± 90.94	205.02 ± 46.19	204.62 ± 45.82	206.42 ± 49.54
Erythrocyte sedimentation rate, mm/h	9.88 ± 12.25	6.89 ± 7.96	17.46 ± 17.28	7.31 ± 10.35	6.33 ± 6.89	10.75 ± 17.97
Albumin, g/L	42.13 ± 4.17	42.65 ± 3.93	40.77 ± 4.54	44.51 ± 3.40	44.99 ± 3.38	42.85 ± 3.02
C-reactive protein, mg/dl	2.98 ± 5.43	1.82 ± 2.77	5.96 ± 8.69	1.99 ± 3.18	1.23 ± 1.79	4.66 ± 5.19

IFX: Infliximab; IQR: Interquartile range; SD: standard deviation; EA: Experimental adhesive; ER: Endoplasmic reticulum.

In step II study, 12/54 (22.22%) CD patients had experienced endoscopic relapse from week 54 to week 108 of IFX maintenance therapy. The estimated endoscopic relapse-free rate was 38/41 (92.68%) in CD patients with ITL > 2.1 μg/mL and 4/13 (30.77%) in CD patients with ITL ≤ 2.1 μg/mL. The median time to endoscopic relapse of CD patients with ITL ≤ 2.1 μg/mL was 40.00 w, shorter than those with ITL > 2.1 μg/mL (HR = 13.14, 95%CI: 3.07-56.27, $P < 0.0001$) (Figure 4D). The estimated endoscopic relapse-free rate was 4/8 (50.00%) in CD patients with CRP > 3.00 mg/L and 40/46 (86.96%) in CD patients with CRP ≤ 3.00 mg/L. The median time to endoscopic relapse of CD patients with CRP > 3.00 mg/L was 50.00 wk shorter than those with CRP ≤ 3.00 mg/L (HR = 7.85, 95%CI: 1.31-46.85, $P < 0.0001$) (Figure 4C).

DISCUSSION

Several studies have confirmed that different ITLs brought about different outcomes of CD under IFX therapy (Table 4). Tang *et al*[1] discovered that CD patients achieving mucosal healing at week 14 of IFX

Table 2 Predictive indicators of endoscopic relapse in Crohn's disease patients with endoscopic remission

Variable	Week 14 (after initial IFX therapy), *n* = 93				Week 14 (after initial IFX therapy), *n* = 54			
	Predict endoscopic relapse at week 54				Predict endoscopic relapse at week 108			
	Univariate analysis		Multivariable analysis		Univariate analysis		Multivariable analysis	
	OR (95%CI)	*P* value	OR (95%CI)	*P* value	OR (95%CI)	*P* value	OR (95%CI)	*P* value
Median age in year, median (IQR)	0.997 (0.950-1.047)	0.904	–	–	1.028 (0.967-1.093)	0.381	–	–
Course in year, median (IQR)	1.054 (0.945-1.176)	0.346	–	–	1.065 (0.906-1.253)	0.444	–	–
Male sex, *n* (%)	0.478 (0.191-1.199)	0.116	–	–	0.700 (0.188-2.607)	0.595	–	–
Disease location, *n* (%)								
L1 (terminal ileum)	0.413 (0.114-1.495)	0.178	–	–	1.158 0.117-11.454)	0.900	–	–
L2 (colon)	1.453 (0.430-4.908)	0.548	–	–	3.000 (0.341-26.427)	0.322	–	–
L3 (ileocolon)	–	–	–	–	–	–	–	–
L4 (upper digestive tract)	1.277 (0.452-3.612)	0.645	–	–	0.939 (0.215-4.113)	0.934	–	–
Disease behavior, *n* (%)								
B1 (no)	–	–	–	–	–	–	–	–
B2 (stenosis)	0.889 (0.345-2.294)	0.808	–	–	0.600 (0.141-2.561)	0.490	–	–
B3 (penetration)	1.860 (0.658-5.264)	0.242	–	–	0.700 (0.188-2.607)	0.595	–	–
B2 (stenosis) + B3 (penetration)	–	–	–	–	–	–	–	–
Perianal diseases, *n* (%)	1.442 (0.562-3.696)	0.446	–	–	0.952 (0.259-3.502)	0.941	–	–
Previous medical therapy, *n* (%)	1.027 (0.386-2.736)	0.957			2.040 (0.481-8.650)	0.333		
Previous surgical therapy, *n* (%)	0.926 (0.266-3.218)	0.903	–	–	–	–	–	–
Laboratory indicators, median (IQR)								
Fecal calprotectin, μg/g	1.003 (1.002-1.005)	0.000	1.002 (1.001-1.004)	0.002	1.002 (1.001-1.004)	0.001	NS	NS
IFX trough level, μg/mL	0.650 (0.532-0.796)	0.000	0.666 (0.514-0.862)	0.002	0.470 (0.289-0.766)	0.002	0.466 (0.247-0.877)	0.018
White blood count, x 10^9/L	1.167 (0.921-1.478)	0.201	–	–	1.004 (0.636-1.586)	0.986	–	–
Hematoglobin, g/L	0.977 (0.954-1.000)	0.053	–	–	0.997 (0.957-1.038)	0.867	–	–
Platelet, x 10^9/L	1.006 (0.999-1.013)	0.081	–	–	1.001 (0.987-1.015)	0.904	–	–
Erythrocyte sedimentation rate, mm/h	1.073 (1.028-1.120)	0.001	NS	NS	1.035 (0.978-1.096)	0.239	–	–
Albumin, g/L	0.895 (0.800-1.002)	0.054	–	–	0.821 (0.667-1.010)	0.062	–	–
C-reactive protein, mg/dL	1.245 (1.080-1.435)	0.003	NS	NS	1.389 (1.070-1.804)	0.014	1.590 (1.007-2.510)	0.047

IFX: Infliximab; NS: Not significant; CI: Confidence interval; IQR: Interquartile range; OR: Odds ratio.

Table 3 Predictive value of indicators on endoscopic relapse

	Youden index	Sensitivity	Specificity	Positive predictive value	Negative predictive value	Area under the ROC curve	*P* value
Predictors at week 14 of Endoscopic relapse at week 54							
ITL ≤ 5.6 μg/mL	0.61 (0.41-0.72)	0.92 (0.75-0.99)	0.69 (0.56-0.79)	0.53 (0.44-0.62)	0.96 (0.86-0.99)	0.83 (0.73-0.90)	< 0.001
FCP > 238 μg/g	0.64 (0.38-0.78)	0.73 (0.52-0.88)	0.91 (0.82-0.97)	0.76 (0.59-0.88)	0.90 (0.82-0.94)	0.82 (0.72-0.89)	< 0.001
ITL ≤ 5.6 μg/mL and FCP > 238 μg/g	0.63 (0.40-0.80)	0.69 (0.48-0.86)	0.94 (0.85-0.98)	0.82 (0.63-0.92)	0.89 (0.82-0.93)	0.82 (0.72-0.89)	< 0.001
ITL ≤ 5.6 μg/mL or FCP > 238 μg/g	0.62 (0.47-0.74)	0.96 (0.80-1.00)	0.66 (0.53-0.77)	0.52 (0.44-0.60)	0.98 (0.87-1.00)	0.81 (0.71-0.88)	< 0.001
Predictors at week 54 of Endoscopic relapse at week 108							
ITL ≤ 2.1 μg/mL	0.68 (0.40-0.87)	0.75 (0.43-0.95)	0.93 (0.81-0.99)	0.75 (0.49-0.90)	0.93 (0.83-0.97)	0.85 (0.72-0.93)	< 0.001
CRP > 3.0 mg/dL	0.45 (0.20-0.68)	0.50 (0.21-0.79)	0.95 (0.84-0.99)	0.75 (0.41-0.93)	0.87 (0.79-0.92)	0.73 (0.60-0.84)	0.012
ITL ≤ 2.1 μg/mL and CRP > 3.0 mg/dL	0.33 (0.08-0.58)	0.33 (0.10-0.65)	1.00 (0.92-1.00)	1.00 (1.00-1.00)	0.84 (0.78-0.89)	0.67 (0.53-0.79)	0.019
ITL ≤ 2.1 μg/mL or CRP > 3.0 mg/dL	0.80 (0.50-0.93)	0.92 (0.62-1.00)	0.88 (0.74-0.96)	0.69 (0.49-0.84)	0.97 (0.85-1.00)	0.90 (0.79-0.96)	□0.001

ITL: Infliximab trough level; FCP: Fecal calprotectin; CRP: C-reactive protein; ROC: Receiver operating characteristic.

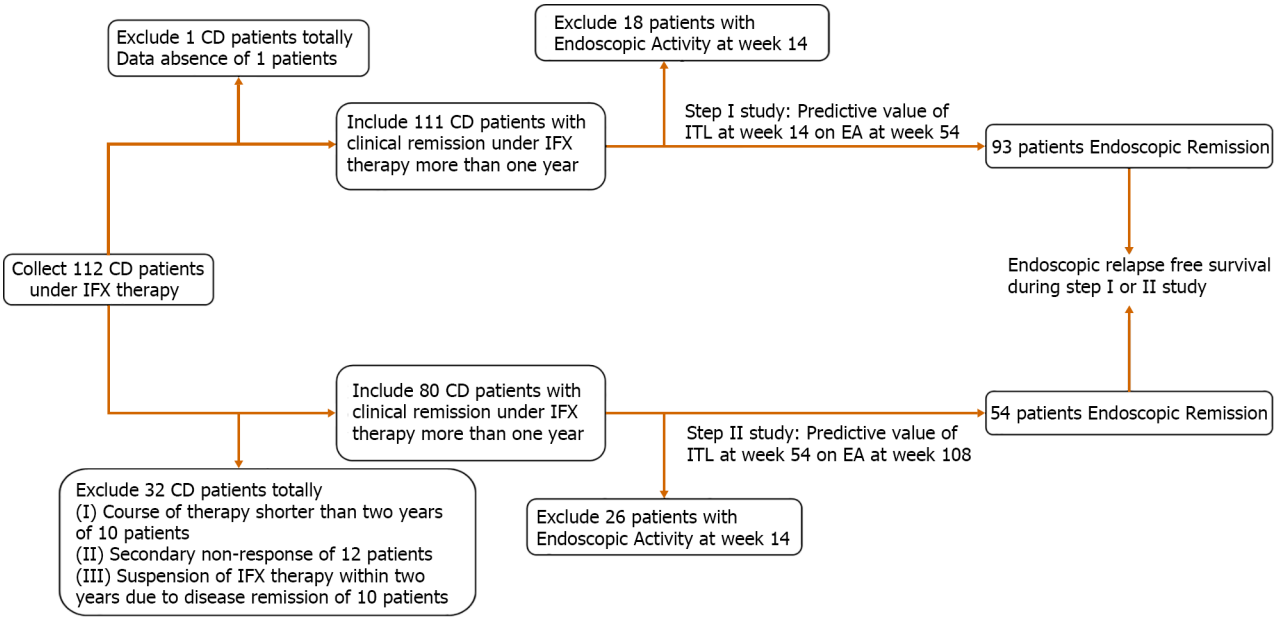


Figure 1 Patients selected and outcome of infliximab therapy. CD: Crohn's disease; EA: Endoscopic activity; IFX: Infliximab.

therapy with ITL > 2.5 μg/mL at week 14 had 71% chance of mucosal healing at week 54, while patients with ITL < 2.5 μg/mL had only 33% chance. ITL ≥ 3 μg/mL at the beginning of IFX maintenance therapy was confirmed as a predictor of sustained response to IFX in CD patients[2]. Recently a prospective study in Japan verified that CD patients with ITL ≥ 3 μg/mL at week 14 after IFX initial therapy had much better long-term clinical outcomes than patients with ITL < 3 μg/mL, of which survival analysis indicated 100% probability of clinical remission at week 108 in the former and 33.3% probability in the latter[3]. A meta-analysis determined that ITL > 2.0 μg/mL of IBD patients under IFX maintenance therapy contributes to better prognosis such as clinical remission or mucosal healing[4]. Similarly, this study found that CD patients with ITL > 5.6 μg/mL at week 14 had a large chance of

Table 4 Previous research of infliximab trough level on deep remission in inflammatory bowel disease

Study design	Optimal cut-off value	Predictive content	Yes/No, *n*	SE	SP	PPV	NPV	AUC
A retrospective observational single-center study in China	4.85 μg/mL at week 14	Mucosal healing (complete absence of any sign of ulceration)	82/59	67%	80%			0.80
	4.85 μg/mL at week 14	Mucosal healing (CDEIS of < 3)	84/57	68%	83%			0.79
	2.85 μg/mL at week 30	Mucosal healing (complete absence of any sign of ulceration)	59/50	73%	84%			0.78
	2.85 μg/mL at week 30	Mucosal healing (CDEIS of < 3)	62/47	68%	81%			0.73
A retrospective observational single-center study in China	2.50 μg/mL at week 14	Mucosal healing (SES-CD/Rutgeerts of 0 or 1) at week 52	31/42	87%	60%			0.70
	2.50 μg/mL at week 14	Sustained remission (no treatment failure, no need for surgery or intensification of IFX nor new introduction during IFX therapy) at week 52	70/38	64%	63%			0.70
A prospective multicenter study in Spanish	3.40 μg/mL	(1) SES-CD<3 for CD patients; (2) Rutgeerts score < i2 for CD patients in the postoperative setting; and (3) Mayo endoscopic score < 2 for UC patients	58/30	60%	60%	73%	42%	0.63
A multicenter, randomized, double-blind, controlled trial in Europe	23.10 mg/L at week 2	Endoscopic remission (CDEIS < 3) at week 12	54/52	56%	80%	72%	65%	0.67
	10.00 mg/L at week 6	Endoscopic remission (CDEIS < 3) at week 12	54/52	37%	89%	76%	59%	0.64
	10.60 mg/L (dose escalation to 10 mg/kg)	The absence of ulcers at week 54	85/51	94%	42%	49%	92%	0.71
A retrospective multicenter study in United States	9.70 μg/mL	Endoscopic remission (absence of any mucosal break (ulceration or erosion)/Rutgeerts score of ≤ i1)	62/34	57%	73%	80%	48%	0.65
	9.80 μg/mL	Histologic remissions (absence of active inflammation)	43/44	63%	66%	64%	64%	0.62
	2.20 μg/mL	Biochemical remission (CRP ≤ 5 mg/dL)	48/23	92%	35%	75%	67%	0.64
A retrospective observational single-center study in Japan	4.00 μg/mL	Mucosal healing (modified Rutgeerts scoring system: 0 or 1) after 30 days	20/58	71%	70%			0.63
	0.60 μg/mL	CRP normalization (≤ 0.3 mg/dL)	28/22	73%	62%			0.67
	1.00 μg/mL	Serum albumin normalization (≥ 4.0 mg/dL)	17/33	67%	71%			0.72
	1.10 μg/mL	Fecal calprotectin (≥ 300 μg/g)	13/25	72%	56%			0.63
A retrospective cross-sectional multicenter study in South Korea	4.20 μg/mL	Mucosal healing (SES-CD = 0)	51/54	65%	70%	67%	68%	0.68
	3.71 μg/mL	Partial mucosal healing (SES-CD < 3)	63/42	70%	71%	79%	61%	0.73
	3.26 μg/mL	Clinical remission (PCDAI < 10)	95/10	71%	100%	100%	73%	0.90
	2.52 μg/mL	Biochemical remission (CRP < 0.3 mg/dL)	87/18	86%	56%	90%	46%	0.71
A prospective cohort multicenter study in Canada	8.02 μg/mL	Histologic remission (an absence of active chronic inflammation)	56/48	79%	68%			0.72
	8.27 μg/mL	Sustained histologic remission (histologic remission documented at both the baseline and follow-up colonoscopies)	36/16	88%	72%			0.77
A retrospective cross-sectional study in United Kingdom	7.10 μg/mL	Fistula healing (no spontaneous discharge or no discharge on palpation in the absence of seton drainage)	18/11	78%	100%			0.93
	7.10 μg/mL	Fistula closure (the absence of an external skin opening)	13/16	64%	100%			0.97

SE: Sensitivity; SP: Specificity; PPV: Positive predictive value; NPV:Negative predictive value; AUC: Areas under the curve; CDEIS: Crohn's disease endoscopic index of severity; SES-CD: Simplified endoscopic score for Crohn's disease; CD: Crohn's disease; UC: Ulcerative colitis; CRP: C-reactive protein; PCDAI: Pediatric Crohn's disease activity index.

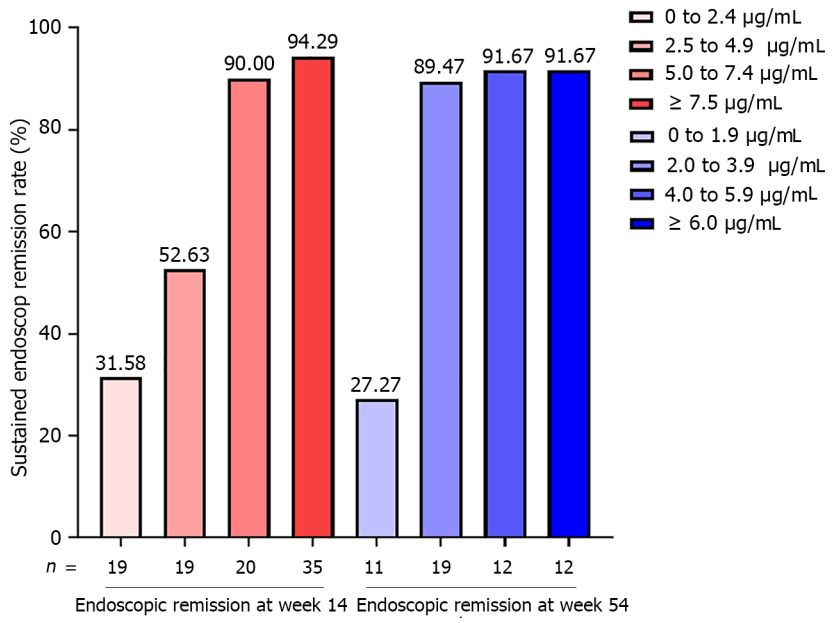


Figure 2 Incremental gain analysis of sustained endoscopic remission rate in relation to infliximab trough level at week 14 and week 54.

achieving sustained endoscopic remission during IFX maintenance therapy as well as CD patients with ITL > 2.1 μg/mL at week 54. Borren *et al*[5] implemented a multi-center retrospective study and concluded that low ITL in IBD patients during IFX maintenance therapy could not be a good predictor of clinical relapse in the next 2 years, suggesting that proactive therapeutic drug monitoring was not suitable in this group. However, this study discovered that CD patients with ITL ≤ 5.6 μg/mL at week 14 or ITL ≤ 2.1 μg/mL at week 54 were more likely to experience endoscopic relapse during the 1-year follow-up period.

According to previous studies, the challenge for IBD physicians is to frame the more suitable blood trough level of IFX to achieve better disease prognosis in clinical therapy. The elements associated with the blood trough level of IFX can be classified into three areas. Above all, the better the therapeutic goal desired by IBD physicians or patients, the higher the blood trough level of IFX is required. An observational study contraposing to CD patients with a history of intestinal surgery by Imaeda *et al*[6] verified that mucosal healing required higher ITLs as more than 4.0 μg/mL compared to those to achieve normalization of routine clinical markers. Papamichael *et al*[7] considered that ITL surpassing 9.7 μg/mL indicated 80% probability of endoscopic remission in CD patients under IFX maintenance therapy, while ITL surpassing 2.2 μg/mL was associated only with biochemical remission. Recently, a prospective study verified that ITL > 8.0 μg/mL was highly correlated with histological emission and sustained histological remission in IBD patients[8]. Perianal fistula, the most universal complications of CD patients, is another therapeutic goal. A retrospective cross-sectional study by Plevris *et al*[9] manifested that perianal fistula healing or closure is associated with higher ITLs as more than 7.1 μg/mL.

Secondly, each clinical study had different stages of IFX drug monitoring, especially during maintenance therapy. ITL continues to decrease as time passed during IFX maintenance therapy[10]. A cross-sectional study of IBD patients under IFX therapy with a fixed dose more than 6 mo found that IBD patients with ITL ≥ 3.4 μg/mL had a 73% chance of endoscopic mucosal healing[11]. Kang *et al*[12] showed that ITL ≥ 5 μg/mL during IFX maintenance therapy could identify mucosal healing in pediatric CD patients with 80% specificity. Feng *et al*[13] innovatively integrated ITL levels in different time stages to identify endoscopic mucosal healing in CD patients, indicating that patients with ITL > 4.85 μg/mL at week 14 and ITL > 2.85 μg/mL at week 30 had an 80% chance of achieving endoscopic mucosal healing. Based on incremental gain analysis in our study, sustained endoscopic remission rate at week 54 reached only 54.63% at an ITL range of 2.5 to 4.9 μg/mL at week 14 while corresponding numbers at week 108 was 89.47% at an ITL range of 2.0 to 3.9 μg/mL at week 54. Therefore, the study held the view that CD patients with endoscopic remission need higher ITL at the beginning of IFX maintenance therapy (≥ 5.6 μg/mL at week 14) than after IFX maintenance therapy over a half year (≥ 2.1 μg/mL at week 54). In addition, CD patients achieving endoscopic remission after IFX induction therapy and sustained endoscopic remission more than a half year may not need high ITL to maintain endoscopic remission.

The third element is therapeutic optimization of IFX in IBD. Adverse IFX response as high ATI level or low ITL may occur in a few CD patients during IFX maintenance therapy. Several clinical studies held the view that severe inflammatory activity of CD patients could change pharmacokinetics of anti-

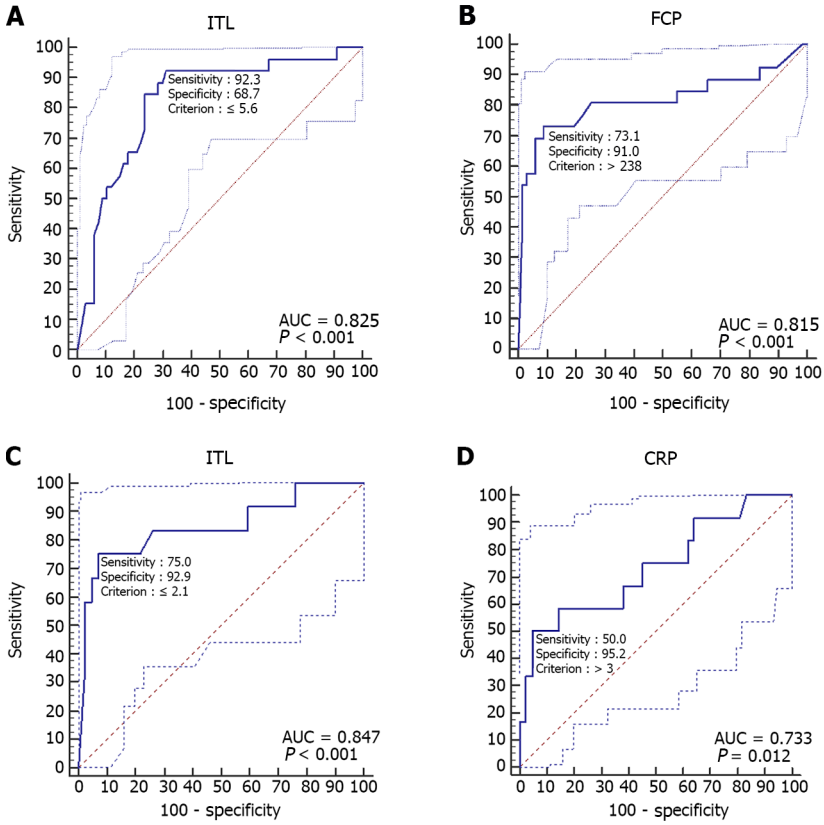


Figure 3 Receiver operator characteristic curve of infliximab trough level and inflammatory biomarkers in predicting endoscopic outcomes. A: Receiver operator characteristic (ROC) curve of infliximab trough level at week 14 in predicting endoscopic remission of Crohn's disease (CD) at week 54; B: ROC curve of fecal calprotectin at week 14 in predicting endoscopic remission of CD at week 54; C: ROC curve of infliximab trough level at week 54 in predicting endoscopic remission of CD at week 108; D: ROC of C-reactive protein at week 54 in predicting endoscopic remission of CD at week 108. ITL: Infliximab trough level; CRP: C-reactive protein; FCP: Fecal calprotectin; AUC: Area under the curve.

tumor necrosis factor α biology[14-16]. Therapeutic optimization as increasing fixed dose from 5 mg/kg to 10 mg/kg or shortening injection interval form every 8 wk to 4-6 wk contributes to increase ITL and decrease ATI level. A study from Greece demonstrated that, for the initial measurement after therapeutic adjustment, ITL increased from 1.47 μg/mL to 8.50 μg/mL in patients with therapeutic optimization while ITL decreased from 5.65 μg/mL to 3.8μg/ml in patients without therapeutic optimization[10]. A multi-center randomized clinical trial conducted by Dreesen *et al*[17] showed that CD patients under IFX maintenance therapy as 5 mg/kg had high probability of no mucosal ulcer under endoscopy at week 54 with ITL more than 7.3mg/L, and CD patients under intensified dose IFX therapy as 10 mg/kg had 94% probability of no mucosal ulcer under endoscopy with ITL rising to more than 10.6 mg/L. Therefore, intensified therapy may contribute to mucosal healing in CD patients with ulceration if IFX injection dose is less than 10 mg/kg and ITL is less than 10.6 μg/mL. However, a few CD patients will accept combination therapy of IFX and immunosuppressant to boost the efficacy, especially AZA and mercaptopurine. AZA is a precursor of mercaptopurine, and two components ultimately produce thioguanine to exert clinical effect during metabolism. A study verified that thioguanine concentration more than 125 pmol/8 × 10^8 red blood cells could enhance ITL to 8.3 μg/mL or more and decrease positive rate of ATI[18,19]. Hence, this study mainly included CD patients with sustained clinical remission more than 6 mo under fixed therapeutic strategy of IFX 5 mg/kg every 8 wk combined with AZA 50 mg every day. Retrospective records of CD patients included would suspend if therapy strategy changed, such as intensive therapy of IFX, conversion therapy of other biologics and combination therapy of surgery or other medications. The study design eliminated the influence of therapeutic adjustment on ITL.

The greatest strength of inflammatory biomarkers compared with blood trough level is that they are unaffected by time during different monitoring stages of biological therapy in IBD patients. This study showed that ITL > 5.6 μg/mL combined with FCP ≤ 238 μg/g at week 14 moderately predicted sustained endoscopic remission during the 1-year follow-up period on CD patients with positive predictive value more than 95% as well as ITL > 2.1 μg/mL combined with CRP ≤ 3.00 mg/L at week 54, superior to use ITL as the only predictor. FCP and CRP are considered as the most universal and typical biomarkers of inflammatory evaluation in IBD, also verified to be the independent risk factors of adverse endoscopic outcomes. The study confirmed that combining blood trough level with inflam-

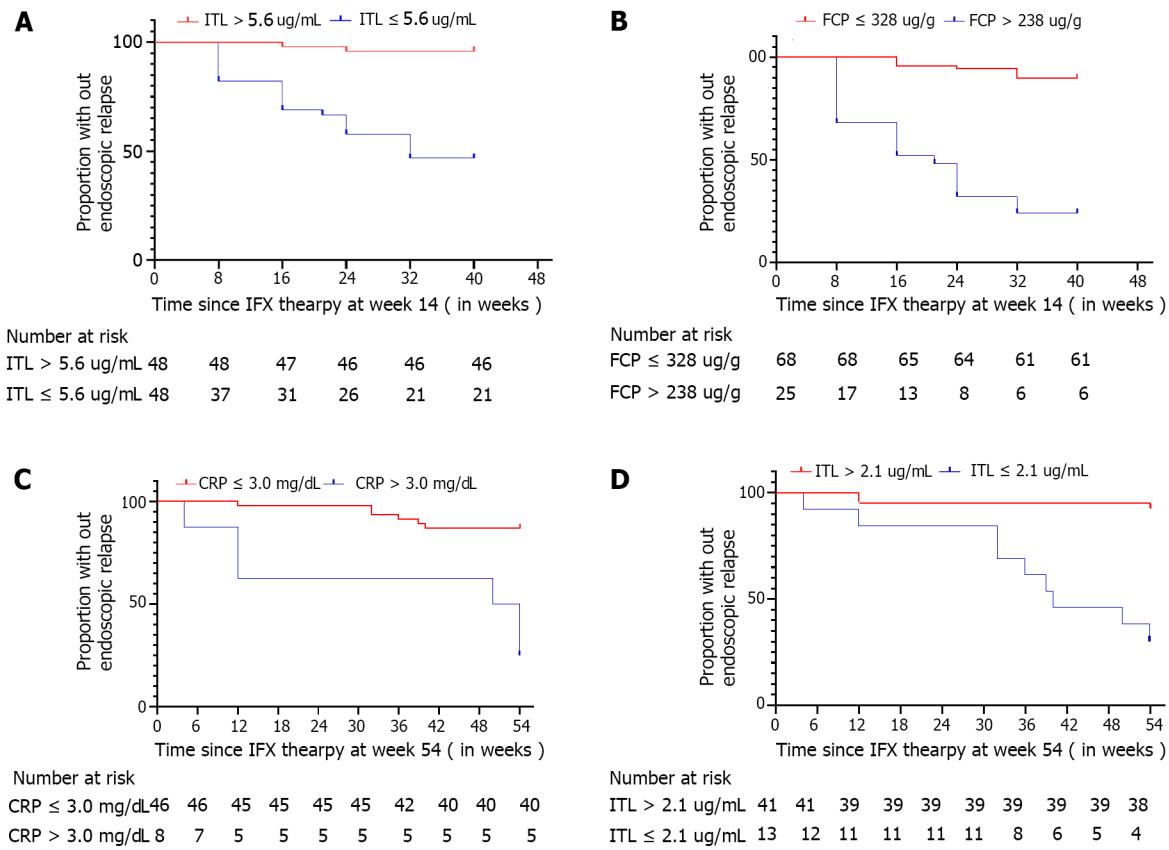


Figure 4 Proportion without endoscopic relapse. A. Time since infliximab (IFX) therapy at week 14 [IFX trough level (ITL) > 5.6 μg/mL *vs* ITL ≤ 5.6 μg/mL]; B: Time to IFX therapy at week 14 (fecal calprotectin ≤ 238 μg/g *vs* fecal calprotectin > 238 μg/g]; C: Time to IFX therapy at week 54 (C-reactive protein ≤ 3.0mg/L *vs* C-reactive protein > 3.0 mg/L); D: Time to IFX therapy at week 54 (ITL > 2.1 μg/mL *vs* ITL ≤ 2.1 μg/mL). ITL: Infliximab trough level; CRP: C-reactive protein; FCP: Fecal calprotectin; IFX: Infliximab.

matory biomarkers contributed to improving the accuracy of the prediction on endoscopic outcomes. A post hoc analysis from the CALM study manifested that CD patients with FCP < 250 μg/g mostly achieved CDEIS < 4 without deep ulceration, regardless of whether CRP < 5 mg/L. However, among patients with CRP < 5 mg/L but FCP ≥ 250 μg/g, only 16.7% achieved CDEIS < 4 without deep ulceration[20]. The result indicated that the correlation between FCP normalization and endoscopic mucosal healing in CD patients was stronger than that of CRP normalization. A previous study verified that FCP is suitable for distinguishing mild endoscopic activity from endoscopic remission, while it is difficult to distinguish partial endoscopic remission from complete endoscopic remission[21]. Similar to blood trough level, the optimal cut off value of FCP for distinguishing endoscopic activity from endoscopic remission ranges from 71 μg/g to 250 μg/g with moderate diagnostic performance[22-27]. The study identified that FCP > 276 μg/g predicted endoscopic activity at week 54 of CD patients with clinical remission at week 14 moderately with 84.6% sensitivity and 92.1% specificity. Unlike FCP, the sensitivity of CRP to mild intestinal inflammation was low and the level of CRP increased much more dramatically in CD patients with moderate to severe inflammation. Therefore, the previous study preferred to utilize CRP to distinguish moderate to severe endoscopic activity from mild to moderate endoscopic activity rather than distinguish mild endoscopic activity from endoscopic remission. A Spanish study showed that FCP > 155 μg/g in combination with CRP > 6.7 mg/L could identify endoscopic activity with 82% specificity[27].

However, the study has shortcomings in some areas. Firstly, the retrospective single-center study with small sample, inferior to prospective multi-center with greater sample, comprised some confounding factors. More real-world studies and randomized controlled trials on guidance significance of ITL to therapeutic outcomes in IBD need to be conducted. Secondly, the study primarily concentrated on mucosal inflammation located in large intestine, ignoring small intestine due to the high cost and the incomplete scoring system of small intestinal evaluation accompanied by the poor compliance of patients and the laborious operation of endoscopists. Correlation between ITL and various small intestinal examinations including endoscopy or imageology may be the focus of the future study. Last but not least, definition of deep remission on CD has been tightened. Considering transmural inflammation of CD, endoscopy is confined to mucosal inflammation and macroscopical evaluation while imageology can accurately evaluate complete volume of intestinal wall and histopathological examination, which contributes to microscopical examination. Notwithstanding endoscopic remission

considered as the main targets and histological remission considered as a novel target, the new concept of 'disease clearance', which includes clinical, endoscopic and microscopic remission, has drawn more and more attention from IBD physicians and may bring about a new upsurge of studies on IFX monitoring and new therapeutic targets[28].

CONCLUSION

In conclusion, during IFX maintenance treatment, low ITL, high CRP level and high FCP level were independent risk factors of long-term adverse endoscopy outcomes in CD patients with clinical remission. Combination of ITL, CRP and FCP contribute to long-term endoscopic prognosis monitoring. The best cut off values of ITL for predicting endoscopic activity within 1-year follow up were 5.60 μg/mL at week 14 and 2.10 μg/mL at week 54. In addition, ITL ≤ 5.60 μg/mL in combination with FCP > 238 μg/g at week 14 as well as ITL ≤ 2.10 μg/mL in combination with CRP > 3.00 mg/L at week 54 increased the precision of prediction on endoscopic outcomes at week 54 and week 108, respectively. Therapeutic optimization is still recommended in CD patients achieving endoscopic remission, provided that low ITLs or high levels of inflammatory biomarkers, such as CRP or FCP, arise to prevent endoscopic recurrence as soon as possible.

ARTICLE HIGHLIGHTS

Research background

Existing studies have confirmed that infliximab (IFX) blood concentration is closely related to remission and recurrence of Crohn's disease (CD) patients under IFX therapy. In addition, monitoring inflammatory biomarkers regularly is another important tool for prognosis assessment of CD patients. Current studies have confirmed that C-reactive protein (CRP) and fecal calprotectin (FCP) are good predictors of disease activity, but there is still a lack of reliable evidence for predicting disease remission. Therefore, in the early stage of IFX treatment, combination of IFX blood concentration and inflammatory biomarkers may contribute to predict the change of CD outcomes.

Research motivation

The best therapeutic goal of CD was initially defined as clinical remission, and then the definition was converted to endoscopic remission with precise therapy. Nowadays, some clinicians even pursue whole-wall healing with individualized therapy. However, long-term clinical prognosis rather than long-term endoscopic prognosis is still a research priority of clinical studies contrapose to CD patients under IFX therapy. Therefore, prediction on long-term endoscopic prognosis of CD patients under IFX therapy has been based solely on models because of a lack of available data.

Research objectives

To explore the predictive value of blood drug concentration on long-term endoscopic outcomes of IFX therapy for CD and establish a comprehensive outcome prediction model combining IFX blood drug concentration, CRP and FCP, so as to provide a basis for clinical decision making.

Research methods

A single-center retrospective research has been implemented in the First Affiliated Hospital of Zhejiang Chinese Medical University. CD patients under IFX therapy from January 2012 to December 2020 were collected. One hundred and eighty-one CD patients underwent IFX treatment. One hundred and fifty-three CD patients underwent endoscopy as well as serum concentration monitoring at week 14 after the third dose of IFX induction therapy. Inclusion criteria: (1) Endoscopic remission at week 14 [Crohn's disease endoscopic index of severity (CDEIS) score ≤ 2 points or Rutgeerts ≤ i1]; (2) Clinical remission after IFX induction therapy without corticosteroids more than 6 mo; and (3) Therapeutic strategy during maintenance stage was designed as IFX 5 mg/kg every 8 wk combined with azathioprine 50 mg every day. The study was divided into two stages, the Step I study was conducted from week 14 to 54 of IFX treatment, and the Step II study was conducted from week 54 to 108 of IFX treatment. Endoscopic outcomes were defined as endoscopic activity (CDEIS score > 2 points or Rutgeerts score > i1) and endoscopic remission (CDEIS score ≤ 2 points or Rutgeerts ≤ i1). Endoscopic relapse free survival was defined as endoscopic remission at the beginning of the study stage and maintaining endoscopic remission during the study stage.

Research results

In step I study, 67/93 CD patients (72.04%) sustained endoscopic remission at week 54. Multivariable regression analysis demonstrated that only ITL [odds ratio (OR) = 0.666, 95% confidence interval (CI):

0.514-0.862, P = 0.002] and FCP (OR = 1.002, 95%CI: 1.001-1.004, P = 0.002) were independent risk of endoscopic activity at week 54. The receiver-operating characteristic analysis demonstrated that the best cut off level of ITL and FCP at week 14 on predicting endoscopic relapse at week 54 was 5.60 μg/mL [area under the curve (AUC) = 0.83, 95%CI: 0.73-0.90, P < 0.001] and 238 μg/g (AUC = 0.82, 95%CI: 0.72-0.89, P < 0.001). The median time to endoscopic relapse of CD patients with ITL ≤ 5.6 μg/ml was 32.00 wk shorter than those with ITL > 5.6 μg/mL [hazard ratio (HR) = 16.19, 95%CI: 7.44-35.22, P < 0.0001]. The median time to endoscopic relapse of CD patients with FCP > 238 μg/g was 21.00 wk shorter than those with FCP ≤ 238 μg/g (HR = 11.25, 95%CI: 4.26-29.73, P < 0.0001). (II) In step II study, 42/54 CD patients (77.78%) sustained endoscopic remission at week 108. Multivariable regression analysis found that only ITL (OR = 0.466, 95%CI: 0.247-0.877, P = 0.018) and CRP (OR = 1.590, 95%CI: 1.007-2.510, P = 0.047) were independent risks of endoscopic activity at week 108. The receiver-operating characteristic analysis demonstrated that the best cut off level of ITL and CRP at week 54 on predicting endoscopic relapse at week 108 was 2.10 μg/ml (AUC = 0.85, 95%CI: 0.72-0.93, P < 0.001) and 3.00 mg/L (AUC = 0.73, 95%CI: 0.60-0.84, P = 0.012). The median time to endoscopic relapse of CD patients with ITL ≤ 2.1 μg/mL was 40.00 w shorter than those with ITL > 2.1 μg/mL (HR = 13.14, 95%CI: 3.07-56.27, P < 0.0001). The median time to endoscopic relapse of CD patients with CRP > 3.00 mg/L was 50.00 wk shorter than those with CRP ≤ 3.00 mg/L (HR = 7.85, 95%CI: 1.31-46.85, P< 0.0001).

Research conclusions

The best cut off values of ITL for predicting endoscopic activity within 1-year follow up was 5.60 μg/mL at week 14 and 2.10 μg/mL at week 54. In addition, ITL ≤ 5.60 μg/mL in combination with FCP > 238 μg/g at week 14 as well as ITL ≤ 2.10 μg/mL in combination with CRP > 3.00 mg/L at week 54 increased the precision of prediction on endoscopic outcomes at week 54 and week 108, respectively.

Research perspectives

In view of the fact that conduction of intensive monitoring for biological management plays a vital role in precise treatment for CD patients, much larger and more stringent prospective studies are warranted to provide the best predictive models as acknowledged globally in allusion to long-term endoscopic outcomes of CD patients under IFX therapy.

ACKNOWLEDGEMENTS

The authors would like to thank Dr. Bin Lv, Full Professor and Chief Physician at the First Affiliated Hospital of Zhejiang Chinese Medical University, Department of Gastroenterology, for his help in revising this paper, and Shan Liu, at the First Affiliated Hospital of Zhejiang Chinese Medical University, Clinical Evaluation Center, for help with statistical analysis.

FOOTNOTES

Author contributions: Fan YH designed the research; Cao WT performed the research; Cao WT and Liu S analyzed the data; Cao WT, Huang R, Ni H and Xu MS wrote the paper; Xu Y supervised the paper; All authors have read and approve the final manuscript.

Supported by National Natural Science Foundation of China, No. 81473506 and No. 81971600; Zhejiang TCM Science and Technology Project, No. 2019ZA056, No. 2021ZA057 and No. 2016ZA077.

Institutional review board statement: This study was reviewed and approved by the ethics committee of the First Affiliated Hospital of Zhejiang Chinese Medical University, No. 2021-KL-024-02.

Informed consent statement: All study participants, or their legal guardian, provided informed written consent prior to study enrollment.

Conflict-of-interest statement: The authors declare that they have no conflict of interest.

Data sharing statement: Some or all data, models, or code generated or used during the study are available from the corresponding author by request. People could contact the corresponding author to get the data which is not used for commercial purposes.

Open-Access: This article is an open-access article that was selected by an in-house editor and fully peer-reviewed by external reviewers. It is distributed in accordance with the Creative Commons Attribution NonCommercial (CC BY-NC 4.0) license, which permits others to distribute, remix, adapt, build upon this work non-commercially, and license their derivative works on different terms, provided the original work is properly cited and the use is non-commercial. See: https://creativecommons.org/Licenses/by-nc/4.0/

Country/Territory of origin: China

ORCID number: Wan-Ting Cao 0000-0001-7277-4492; Rong Huang 0000-0002-8360-7777; Shan Liu 0000-0001-9139-3257; Yi-Hong Fan 0000-0001-8217-9793; Mao Sheng Xu 0000-0002-2396-1600; Yi Xu 0000-0002-3265-9534; Hui Ni 0000-0001-8973-8834.

S-Editor: Ma YJ
L-Editor: Filipodia
P-Editor: Cai YX

REFERENCES

1 **Tang J**, Yang Q, Huang Z, Guo H, Chao K, Hu P, Gao X. Early serum infliximab trough level and mucosal healing could be predictors for one-year outcome after initiating therapy in Crohn's disease. *Scand J Gastroenterol* 2020; **55**: 1035-1040 [PMID: 32819192 DOI: 10.1080/00365521.2020.1800077]

2 **Bortlik M**, Duricova D, Malickova K, Machkova N, Bouzkova E, Hrdlicka L, Komarek A, Lukas M. Infliximab trough levels may predict sustained response to infliximab in patients with Crohn's disease. *J Crohns Colitis* 2013; **7**: 736-743 [PMID: 23200919 DOI: 10.1016/j.crohns.2012.10.019]

3 **Ishida N**, Miyazu T, Sugiyama T, Tamura S, Kagami T, Tani S, Yamade M, Iwaizumi M, Hamaya Y, Osawa S, Furuta T, Sugimoto K. The effect of early trough level of infliximab on subsequent disease course in patients with Crohn disease: A prospective cohort study. *Medicine (Baltimore)* 2020; **99**: e21226 [PMID: 32702894 DOI: 10.1097/MD.0000000000021226]

4 **Moore C**, Corbett G, Moss AC. Systematic Review and Meta-Analysis: Serum Infliximab Levels During Maintenance Therapy and Outcomes in Inflammatory Bowel Disease. *J Crohns Colitis* 2016; **10**: 619-625 [PMID: 26763722 DOI: 10.1093/ecco-jcc/jjw007]

5 **Borren NZ**, Paulides E, Frinack JL, Olson RN, Willrich MAV, van der Woude CJ, Ananthakrishnan AN. Infliximab Trough Levels Are Not Predictive of Relapse in Patients with IBD in Endoscopic Remission: A Multicenter Cohort Study. *Dig Dis Sci* 2021; **66**: 3548-3554 [PMID: 33037969 DOI: 10.1007/s10620-020-06645-0]

6 **Imaeda H**, Bamba S, Takahashi K, Fujimoto T, Ban H, Tsujikawa T, Sasaki M, Fujiyama Y, Andoh A. Relationship between serum infliximab trough levels and endoscopic activities in patients with Crohn's disease under scheduled maintenance treatment. *J Gastroenterol* 2014; **49**: 674-682 [PMID: 23666424 DOI: 10.1007/s00535-013-0829-7]

7 **Papamichael K**, Rakowsky S, Rivera C, Cheifetz AS, Osterman MT. Association Between Serum Infliximab Trough Concentrations During Maintenance Therapy and Biochemical, Endoscopic, and Histologic Remission in Crohn's Disease. *Inflamm Bowel Dis* 2018; **24**: 2266-2271 [PMID: 29718327 DOI: 10.1093/ibd/izy132]

8 **Wilson A**, Choi B, Sey M, Ponich T, Beaton M, Kim RB. High infliximab trough concentrations are associated with sustained histologic remission in inflammatory bowel disease: a prospective cohort study. *BMC Gastroenterol* 2021; **21**: 77 [PMID: 33602145 DOI: 10.1186/s12876-021-01650-7]

9 **Plevris N**, Jenkinson PW, Arnott ID, Jones GR, Lees CW. Higher anti-tumor necrosis factor levels are associated with perianal fistula healing and fistula closure in Crohn's disease. *Eur J Gastroenterol Hepatol* 2020; **32**: 32-37 [PMID: 31567638 DOI: 10.1097/MEG.0000000000001561]

10 **Orfanoudaki E**, Gazouli M, Foteinogiannopoulou K, Theodoraki E, Legaki E, Romanos I, Mouzas I, Koutroubakis IE. Infliximab trough levels are decreasing over time in patients with inflammatory bowel disease on maintenance treatment with infliximab. *Eur J Gastroenterol Hepatol* 2019; **31**: 187-191 [PMID: 30543573 DOI: 10.1097/MEG.0000000000001332]

11 **Chaparro M**, Barreiro-de Acosta M, Echarri A, Almendros R, Barrio J, Llao J, Gomollón F, Vera M, Cabriada JL, Guardiola J, Guerra I, Beltrán B, Roncero O, Busquets D, Taxonera C, Calvet X, Ferreiro-Iglesias R, Ollero Pena V, Bernardo D, Donday MG, Garre A, Godino A, Díaz A, Gisbert JP. Correlation Between Anti-TNF Serum Levels and Endoscopic Inflammation in Inflammatory Bowel Disease Patients. *Dig Dis Sci* 2019; **64**: 846-854 [PMID: 30426297 DOI: 10.1007/s10620-018-5362-3]

12 **Kang B**, Choi SY, Choi YO, Lee SY, Baek SY, Sohn I, Choe BH, Lee HJ, Choe YH. Infliximab Trough Levels Are Associated With Mucosal Healing During Maintenance Treatment With Infliximab in Paediatric Crohn's Disease. *J Crohns Colitis* 2019; **13**: 189-197 [PMID: 30452616 DOI: 10.1093/ecco-jcc/jjy155]

13 **Feng T**, Chen B, Ungar B, Qiu Y, Zhang S, He J, Lin S, He Y, Zeng Z, Ben-Horin S, Chen M, Mao R. Association of Infliximab Levels With Mucosal Healing Is Time-Dependent in Crohn's Disease: Higher Drug Exposure Is Required Postinduction Than During Maintenance Treatment. *Inflamm Bowel Dis* 2019; **25**: 1813-1821 [PMID: 30934050 DOI: 10.1093/ibd/izz061]

14 **Beltrán B**, Iborra M, Sáez-González E, Marqués-Miñana MR, Moret I, Cerrillo E, Tortosa L, Bastida G, Hinojosa J, Poveda-Andrés JL, Nos P. Fecal Calprotectin Pretreatment and Induction Infliximab Levels for Prediction of Primary Nonresponse to Infliximab Therapy in Crohn's Disease. *Dig Dis* 2019; **37**: 108-115 [PMID: 30149385 DOI: 10.1159/000492626]

15 **Hemperly A**, Vande Casteele N. Clinical Pharmacokinetics and Pharmacodynamics of Infliximab in the Treatment of Inflammatory Bowel Disease. *Clin Pharmacokinet* 2018; **57**: 929-942 [PMID: 29330783 DOI: 10.1007/s40262-017-0627-0]

16 **Dreesen E**, Berends S, Laharie D, D'Haens G, Vermeire S, Gils A, Mathôt R. Modelling of the relationship between infliximab exposure, faecal calprotectin and endoscopic remission in patients with Crohn's disease. *Br J Clin Pharmacol* 2021; **87**: 106-118 [PMID: 32415677 DOI: 10.1111/bcp.14364]

17 **Dreesen E**, Baert F, Laharie D, Bossuyt P, Bouhnik Y, Buisson A, Lambrecht G, Louis E, Oldenburg B, Pariente B, Pierik M, van der Woude CJ, D'Haens G, Vermeire S, Gils A. Monitoring a Combination of Calprotectin and Infliximab Identifies Patients With Mucosal Healing of Crohn's Disease. *Clin Gastroenterol Hepatol* 2020; **18**: 637-646.e11 [PMID: 31128336 DOI: 10.1016/j.cgh.2019.05.029]

18 **Yarur AJ**, Kubiliun MJ, Czul F, Sussman DA, Quintero MA, Jain A, Drake KA, Hauenstein SI, Lockton S, Deshpande AR, Barkin JS, Singh S, Abreu MT. Concentrations of 6-thioguanine nucleotide correlate with trough levels of infliximab in patients with inflammatory bowel disease on combination therapy. *Clin Gastroenterol Hepatol* 2015; **13**: 1118-24.e3 [PMID: 25562796 DOI: 10.1016/j.cgh.2014.12.026]

19 **Vermeire S**, Noman M, Van Assche G, Baert F, D'Haens G, Rutgeerts P. Effectiveness of concomitant immunosuppressive therapy in suppressing the formation of antibodies to infliximab in Crohn's disease. *Gut* 2007; **56**: 1226-1231 [PMID: 17229796 DOI: 10.1136/gut.2006.099978]

20 **Reinisch W**, Panaccione R, Bossuyt P, Baert F, Armuzzi A, Hébuterne X, Travis S, Danese S, Sandborn WJ, Schreiber S, Berg S, Zhou Q, Kligys K, Neimark E, Suleiman AA, D'Haens G, Colombel JF. Association of Biomarker Cutoffs and Endoscopic Outcomes in Crohn's Disease: A Post Hoc Analysis From the CALM Study. *Inflamm Bowel Dis* 2020; **26**: 1562-1571 [PMID: 32105310 DOI: 10.1093/ibd/izaa025]

21 **Kawashima K**, Ishihara S, Yuki T, Fukuba N, Sonoyama H, Kazumori H, Yamashita N, Tada Y, Kusunoki R, Oka A, Oshima N, Mishima Y, Moriyama I, Kinoshita Y. Fecal Calprotectin More Accurately Predicts Endoscopic Remission of Crohn's Disease than Serological Biomarkers Evaluated Using Balloon-assisted Enteroscopy. *Inflamm Bowel Dis* 2017; **23**: 2027-2034 [PMID: 28817462 DOI: 10.1097/MIB.0000000000001202]

22 **D'Haens G**, Ferrante M, Vermeire S, Baert F, Noman M, Moortgat L, Geens P, Iwens D, Aerden I, Van Assche G, Van Olmen G, Rutgeerts P. Fecal calprotectin is a surrogate marker for endoscopic lesions in inflammatory bowel disease. *Inflamm Bowel Dis* 2012; **18**: 2218-2224 [PMID: 22344983 DOI: 10.1002/ibd.22917]

23 **Kostas A**, Siakavellas SI, Kosmidis C, Takou A, Nikou J, Maropoulos G, Vlachogiannakos J, Papatheodoridis GV, Papaconstantinou I, Bamias G. Fecal calprotectin measurement is a marker of short-term clinical outcome and presence of mucosal healing in patients with inflammatory bowel disease. *World J Gastroenterol* 2017; **23**: 7387-7396 [PMID: 29151692 DOI: 10.3748/wjg.v23.i41.7387]

24 **Vázquez Morón JM**, Pallarés Manrique H, Machancoses FH, Ramos Lora M, Ruiz Frutos C. Accurate cut-offs for predicting endoscopic activity and mucosal healing in Crohn's disease with fecal calprotectin. *Rev Esp Enferm Dig* 2017; **109**: 130-136 [PMID: 28071062 DOI: 10.17235/reed.2017.4542/2016]

25 **Inokuchi T**, Kato J, Hiraoka S, Takashima S, Nakarai A, Takei D, Sugihara Y, Takahara M, Kawano S, Harada K, Okada H. Fecal Immunochemical Test Versus Fecal Calprotectin for Prediction of Mucosal Healing in Crohn's Disease. *Inflamm Bowel Dis* 2016; **22**: 1078-1085 [PMID: 26891256 DOI: 10.1097/MIB.0000000000000728]

26 **D'Arcangelo G**, Oliva S, Dilillo A, Viola F, Civitelli F, Isoldi S, Cucchiara S, Aloi M. Predictors of Long-term Clinical and Endoscopic Remission in Children With Crohn Disease Treated With Infliximab. *J Pediatr Gastroenterol Nutr* 2019; **68**: 841-846 [PMID: 30633110 DOI: 10.1097/MPG.0000000000002262]

27 **Penna FGC**, Rosa RM, Pereira FH, Cunha PFS, Sousa SCS, Ferrari TCA, Cara C, Ferrari MLA. Combined evaluation of fecal calprotectin and C-reactive protein as a therapeutic target in the management of patients with Crohn's disease. *Gastroenterol Hepatol* 2021; **44**: 87-95 [PMID: 32680729 DOI: 10.1016/j.gastrohep.2020.04.015]

28 **Dal Buono A**, Roda G, Argollo M, Zacharopoulou E, Peyrin-Biroulet L, Danese S. Treat to target or 'treat to clear' in inflammatory bowel diseases: one step further? *Expert Rev Gastroenterol Hepatol* 2020; **14**: 807-817 [PMID: 32762582 DOI: 10.1080/17474124.2020.1804361]

World Journal of Gastroenterology

Submit a Manuscript: https://www.f6publishing.com

World J Gastroenterol 2022 June 21; 28(23): 2597-2608

DOI: 10.3748/wjg.v28.i23.2597

ISSN 1007-9327 (print) ISSN 2219-2840 (online)

ORIGINAL ARTICLE

Retrospective Study

Higher infliximab and adalimumab trough levels are associated with fistula healing in patients with fistulising perianal Crohn's disease

Bonita Gu, Kavya Venkatesh, Astrid-Jane Williams, Watson Ng, Crispin Corte, Ali Gholamrezaei, Simon Ghaly, Wei Xuan, Sudarshan Paramsothy, Susan Connor

Specialty type: Gastroenterology and hepatology

Provenance and peer review: Unsolicited article; Externally peer reviewed

Peer-review model: Single blind

Peer-review report's scientific quality classification
Grade A (Excellent): A
Grade B (Very good): B, B
Grade C (Good): 0
Grade D (Fair): 0
Grade E (Poor): 0

P-Reviewer: Leal RF, Brazil; Triantafillidis J, Greece; Velikova TV, Bulgaria

Received: September 14, 2021
Peer-review started: September 14, 2021
First decision: November 7, 2021
Revised: November 21, 2021
Accepted: May 5, 2022
Article in press: May 5, 2022
Published online: June 21, 2022

Bonita Gu, Astrid-Jane Williams, Watson Ng, Wei Xuan, Susan Connor, South Western Sydney Clinical School, University of New South Wales, Sydney 2170, New South Wales, Australia

Bonita Gu, Astrid-Jane Williams, Watson Ng, Ali Gholamrezaei, Susan Connor, Department of Gastroenterology and Hepatology, Liverpool Hospital, Sydney 2170, New South Wales, Australia

Bonita Gu, Crispin Corte, AW Morrow Gastroenterology and Liver Centre, Royal Prince Alfred Hospital, Sydney 2050, New South Wales, Australia

Kavya Venkatesh, Department of Medicine, University of Newcastle, Newcastle 2308, New South Wales, Australia

Crispin Corte, Central Clinical School, University of Sydney, Sydney 2050, New South Wales, Australia

Ali Gholamrezaei, Wei Xuan, Susan Connor, Ingham Institute of Applied Medical Research, Sydney 2170, New South Wales, Australia

Simon Ghaly, Department of Gastroenterology, St Vincent's Hospital Sydney, Sydney 2010, New South Wales, Australia

Simon Ghaly, St Vincent's Clinical School, University of New South Wales, Sydney 2010, New South Wales, Australia

Sudarshan Paramsothy, Department of Gastroenterology and Hepatology, Concord Repatriation General Hospital, Sydney 2139, New South Wales, Australia

Sudarshan Paramsothy, Concord Clinical School, University of Sydney, Sydney 2139, New South Wales, Australia

Corresponding author: Bonita Gu, MD, Doctor, South Western Sydney Clinical School, University of New South Wales, Goulburn St, Liverpool, Sydney 2170, New South Wales, Australia. bonita.gu@health.nsw.gov.au

Abstract

BACKGROUND

Tumor necrosis factor-alpha inhibitors, including infliximab and adalimumab, are

effective medical treatments for perianal fistulising Crohn's disease (CD), but not all patients achieve fistula healing.

AIM

To determine the correlation between perianal fistula healing and closure with infliximab and adalimumab trough levels.

METHODS

In this multicentre retrospective study conducted across four tertiary inflammatory bowel disease centres in Australia, we identified CD patients with perianal fistulae on maintenance infliximab or adalimumab who had a trough level within twelve weeks of clinical assessment. Data collected included demographics, serum infliximab and adalimumab trough levels (mg/L) within 12 wk before or after their most recent clinical assessment and concomitant medical or surgical therapy. The primary outcome was fistula healing, defined as cessation in fistula drainage. The secondary outcome was fistula closure, defined as healing and closure of all external fistula openings. Differences between patients who did or did not achieve fistula healing were compared using the chi-square test, *t* test or Mann-Whitney *U* test.

RESULTS

One hundred and fourteen patients (66 infliximab, 48 adalimumab) were included. Forty-eight (72.7%) patients on maintenance infliximab achieved fistula healing and 18 (27.3%) achieved fistula closure. Thirty-seven (77%) patients on maintenance adalimumab achieved fistula healing and 17 (35.4%) achieved fistula closure. Patients who achieved fistula healing had significantly higher infliximab and adalimumab trough levels than patients who did not [infliximab: 6.4 (3.8-9.5) *vs* 3.0 (0.3-6.2) mg/L, $P = 0.003$; adalimumab: 9.2 (6.5-12.0) *vs* 5.4 (2.5-8.3) mg/L, $P = 0.004$]. For patients on infliximab, fistula healing was associated with lower rates of detectable anti-infliximab antibodies and younger age. For patients on adalimumab, fistula healing was associated with higher rates of combination therapy with an immunomodulator. Serum trough levels for patients with and without fistula closure were not significantly different for infliximab [6.9 (4.3-10.2) *vs* 5.5 (2.5-8.3) mg/L, $P = 0.105$] or adalimumab [10.0 (6.6-12.0) *vs* 7.8 (4.2-10.0) mg/L, $P = 0.083$].

CONCLUSION

Higher maintenance infliximab and adalimumab trough levels are associated with perianal fistula healing in CD.

Key Words: Crohn's disease; Perianal disorders; Biologics; Inflammatory bowel disease

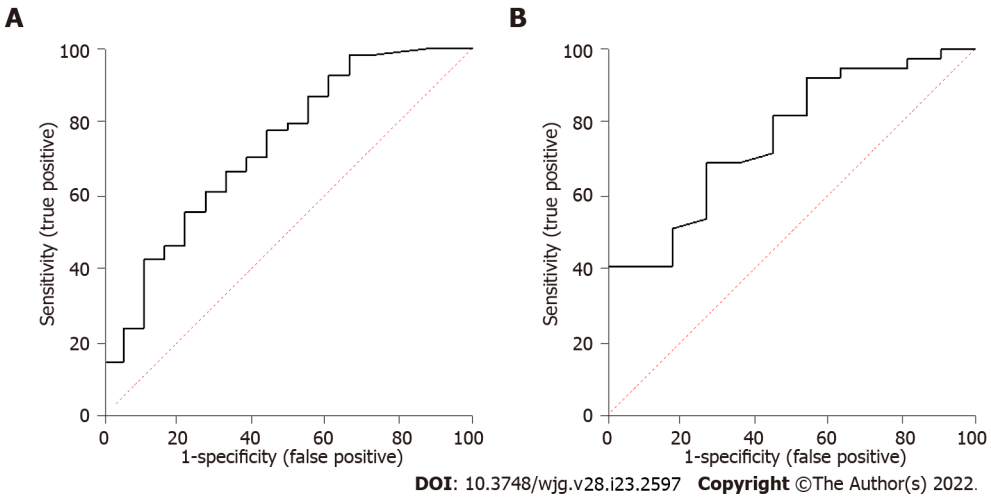
©The Author(s) 2022. Published by Baishideng Publishing Group Inc. All rights reserved.

Core Tip: This multicentre retrospective study demonstrated a significant association between both infliximab and adalimumab trough levels with fistula healing, with higher levels associated with increased healing rates. Higher tertiles of both infliximab and adalimumab levels were associated with a higher proportion of patients achieving fistula healing. Fistula healing, defined as cessation of fistula drainage, is a clinically relevant endpoint that impacts on patient quality of life. Our results support dose-escalation of both infliximab and adalimumab in non-responders, targeting higher levels to achieve fistula healing prior to changing biologic therapy. Importantly, this study is the largest study to date assessing the relationship between adalimumab trough levels and clinical fistula healing.

Citation: Gu B, Venkatesh K, Williams AJ, Ng W, Corte C, Gholamrezaei A, Ghaly S, Xuan W, Paramsothy S, Connor S. Higher infliximab and adalimumab trough levels are associated with fistula healing in patients with fistulising perianal Crohn's disease. *World J Gastroenterol* 2022; 28(23): 2597-2608
URL: https://www.wjgnet.com/1007-9327/full/v28/i23/2597.htm
DOI: https://dx.doi.org/10.3748/wjg.v28.i23.2597

INTRODUCTION

Perianal fistulising disease is a common manifestation occurring in up to 30% of patients with Crohn's disease (CD). The development of abnormal tracts between the bowel and perineum can cause perianal drainage, pain, bleeding, abscess formation, sepsis and faecal incontinence[1,2]. Perianal CD is



DOI: 10.3748/wjg.v28.i23.2597 **Copyright** ©The Author(s) 2022.

Figure 1 Correlation between serum trough level of infliximab, adalimumab and fistula healing. A: Infliximab; B: Adalimumab.

associated with significant morbidity and decreased quality of life, negatively impacting physical, emotional, sexual and social wellbeing[1-3] and is an independent predictor for decreased productivity in patients with CD[4,5]. Given that the incidence of perianal fistulising CD is highest in the third and fourth decades of life, this places significant burden on patients, society, the economy and the health care system[6].

Treatment for perianal fistulising CD requires a multidisciplinary approach involving medical management with immunosuppressants and antibiotics, as well as surgical management with sepsis control, seton insertion and sometimes diversion or resection. Anti-tumor necrosis factor (anti-TNF) alpha agents, including infliximab[7,8] and adalimumab[9,10], are the most effective medical therapies available for inducing and maintaining remission of fistulas. Unfortunately, up to 60% of patients treated with maintenance infliximab lose response within one year[7,8]. Accumulating evidence suggests that this loss of response is partly due to subtherapeutic anti-TNF trough levels. Retrospective studies and post-hoc analyses of prospective data have identified that higher infliximab trough levels are associated with fistula healing and closure compared to what is observed for mucosal healing in luminal disease, with emerging data suggesting similar results for adalimumab[11-14]. Quantitative assays for therapeutic drug monitoring (TDM) permit individualisation of infliximab and adalimumab dosing[15,16], however there are very few studies on perianal fistulising CD and the optimal target levels for perianal fistulising CD remain unclear. Our study aims to assess the association between serum trough infliximab and adalimumab levels and perianal fistula healing and closure and identify optimal target levels.

MATERIALS AND METHODS

Study design and patient population

This was a multicentre retrospective cross-sectional study of patients with perianal fistulising CD at four tertiary inflammatory bowel disease centres across Australia between January 2014 and June 2020. All patients qualified for infliximab or adalimumab under the Australian Pharmaceutical Benefits Scheme criteria[17] which constitutes the following: (1) A confirmed diagnosis of CD using clinical, radiological, histological and/or endoscopic criteria; and (2) At least one active externally draining complex perianal fistula. We included patients on maintenance infliximab or adalimumab with a documented perianal examination who had a serum infliximab or adalimumab trough level collected within 12 wk before or after their most recent clinical assessment. Infliximab and adalimumab trough levels as well as antibodies to infliximab and adalimumab were measured using a drug sensitive enzyme-linked immunosorbent assay (Grifols Promonitor for adalimumab; LISA-Tracker and Grifols Promonitor for infliximab). Infliximab and adalimumab trough levels were measured both in a proactive manner and reactive manner in patients failing treatment across the study sites. Patients who had been changed from infliximab to adalimumab or vice versa and had relevant data were included in both the infliximab and adalimumab groups.

All patients had received standard infliximab or adalimumab induction dosing (infliximab 5 mg/kg intravenously at weeks 0, 2, and 6; adalimumab subcutaneously 160 mg at week 0, 80 mg at week 2) followed by maintenance therapy. The current dose of anti-TNF therapy was recorded and patients with or without dose-escalated maintenance therapy were included. Patients who had a diversion ostomy, rectovaginal fistula or no documented perianal examination were excluded.

Demographic data

Data was retrospectively collected from a clinical database that was updated prospectively during routine clinical practice. Patient demographics collected included age, gender, weight, body mass index, smoking status and CD phenotype classified according to the Montreal Classification[18]. The location of CD was identified as ileal, ileocolonic, colonic, upper gastrointestinal involvement or no luminal disease. The presence or absence of fistulising and stricturing disease was noted, in particular the presence of anal strictures. Biochemical markers of disease activity including C-reactive protein (CRP) and albumin were also recorded.

Current management

Prior history of surgical management of perianal disease or fistula was recorded and categorised as examination under anaesthesia and curettage, examination under anaesthesia and seton insertion or fistulotomy. The duration from the last surgical procedure to the follow up visit was recorded. Concomitant medical therapy at the time of follow up was assessed, including corticosteroid use, 5-aminosalicylates and immunomodulators. The doses of infliximab and adalimumab were recorded and stratified according to dose and interval between doses. For patients on dose-escalated anti-TNF therapy, the duration between last dose escalation and follow up was recorded.

Primary and secondary outcomes

The primary outcome was fistula healing, which was defined as cessation of fistula drainage, with or without a seton *in situ*[7]. The secondary outcome was fistula closure, which was defined as healing and closure of all external fistula openings[7].

Statistical analysis

Statistical review of this study was performed by a biostatistician from the Ingham Institute for Applied Medical Research. Descriptive statistics were used to assess the baseline characteristics of both the infliximab and adalimumab cohorts. Categorical variables were expressed as percentages and compared using the chi-square test. Continuous variables were expressed using mean ± SD for normally distributed variables and median and interquartile range (IQR) for non-normally distributed variables. The means were compared using the *t* test for normally distributed variables and the mean ranks compared using the Mann-Whitney *U* test for non-normally distributed variables. A receiver operating characteristic (ROC) curve analysis was used to assess the sensitivity and specificity of infliximab and adalimumab levels at different cut-off points for predicting fistula healing. All reported *P* values were 2-sided, with $P < 0.05$ considered statistically significant. Multivariate analysis using logistic regression with forwards selection was used to analyse variables that predicted fistula healing. Variables which were statistically significant in the univariate analysis were included in the multivariate analysis model. Ethics approval was obtained from the South Western Sydney Local Health District (Human Research Ethics Committee LNR/18/LPOOL/404; Local Project Number: HE18/261).

RESULTS

Out of 454 patients screened, 114 patients (66 infliximab, 48 adalimumab) on maintenance infliximab or adalimumab for perianal CD had a trough level collected within 12 wk of clinical assessment. Five patients had been changed from infliximab to adalimumab or vice versa and were included in both the infliximab and adalimumab groups. Seventy-five (66%) patients were on combination therapy (43 azathioprine, 16 6-mercaptopurine, 16 methotrexate). Nineteen patients (28.8%) on maintenance infliximab were on dose escalated infliximab therapy (5, 7.5, 10, 15 or 20 mg/kg every 6 or 8 wk). For these patients, the median duration between last infliximab dose adjustment and follow up was 60.0 wk (IQR = 44.5-81.0). Eleven (22.9%) patients on maintenance adalimumab were on dose escalated adalimumab therapy (40 mg weekly). For these patients, the median duration between last adalimumab dose adjustment and follow up was 39.0 wk (IQR = 24.0-86.0). Fifty-nine (89.3%) patients on infliximab had prior surgical management of their fistula, with a median duration of 93.0 wk (IQR = 45.5-284.5) between their last surgical procedure and their most recent follow up visit. Thirty-seven (77.1%) patients on adalimumab had prior surgical management of their fistula, with a median duration of 83.0 wk (IQR = 28.75-223.0) between their last surgical procedure and their most recent follow up visit. Patient demographics and disease characteristics of the population are summarised in Table 1.

Association between fistula healing and closure with infliximab trough levels

Forty-eight (72.7%) patients on maintenance infliximab achieved fistula healing. Table 2 summarises the differences between patients on infliximab with and without fistula healing. Patients who achieved fistula healing had higher infliximab trough levels [6.4 (3.8-9.5) *vs* 3.0 (0.3-6.2) mg/L, $P = 0.003$], lower rates of detectable anti-infliximab antibodies (4.3% *vs* 33.3%, $P = 0.004$) and a younger age (33.0 *vs* 43.5 years old; $P = 0.003$) compared to patients who did not achieve fistula healing. The presence of

Table 1 Patient demographics and disease characteristics

	Infliximab (*n* = 66)	Adalimumab (*n* = 48)
Median age, yr (IQR)	36.0 (28.8-43.3)	34.5 (29.0-51.8)
A1, *n* (%)	2 (3.0)	7 (14.6)
A2, *n* (%)	52 (78.8)	26 (54.2)
A3, *n* (%)	9 (13.6)	13 (27.1)
Female gender, *n* (%)	28 (42.4)	14 (29.2)
Mean weight, kg (SD)	80.9 (18.7)	82.1 (21.4)
Mean BMI, kg/m^2 (SD)	28.1 (4.8)	28.5 (5.5)
Median age at diagnosis of Crohn's disease (IQR)	26.0 (21.0-34.0)	24.0 (19.0-41.3)
Current smoker, *n* (%)	12 (18.2)	5 (10.4)
Disease location		
Ileal, *n* (%)	16 (24.2)	17 (35.4)
Colonic, *n* (%)	26 (39.4)	7 (14.6)
Ileocolonic, *n* (%)	15 (22.7)	18 (37.5)
No luminal disease, *n* (%)	4 (6.1)	2 (4.2)
Upper gastrointestinal involvement, *n* (%)	4 (6.1)	2 (4.2)
Stricturing, *n* (%)	10 (15.2)	11 (22.9)
Penetrating, *n* (%)	7 (10.6)	17 (35.4)
Median duration on anti-TNF agent, wk (IQR)	144.0 (80.0-280.0)	180.0 (107.3-309.8)
Anti-TNF dosing, *n* (%)		
IFX, 5 mg/kg/8 wk	47	-
IFX, 7.5 mg/kg/8 wk	1	-
IFX, 10 mg/kg/8 wk	12	-
IFX, 15 mg/kg/8 wk	1	-
IFX, 20 mg/kg/8 wk	1	-
IFX, 5 mg/kg/6 wk	3	-
IFX, 10 mg/kg/6 wk	1	-
ADA, 40 mg fortnightly	-	37
ADA, 40 mg weekly	-	11
Concurrent steroids, *n* (%)	0 (0.0)	1 (2.1)
Concurrent aminosalicylates, *n* (%)	4 (6.1)	5 (10.4)
Combination with immunomodulator, *n* (%)	46 (69.7)	29 (60.4)
Methotrexate, *n* (%)	8 (12.1)	8 (16.7)
6-mercaptopurine, *n* (%)	9 (13.6)	7 (14.6)
Azathioprine, *n* (%)	29 (43.9)	14 (29.2)
Concurrent allopurinol, *n* (%)	10 (15.2)	4 (8.3)
Mean albumin, g/L (SD)	39.9 (4.9)	40.2 (4.7)
Median CRP, mg/L (IQR)	1.4 (0.7-5.5)	2.3 (1.2-5.2)

ADA: Adalimumab; BMI: Body mass index; CRP: C-reactive protein; IFX: Infliximab; IQR: Interquartile range; SD: Standard deviation; TNF: Tumor necrosis factor.

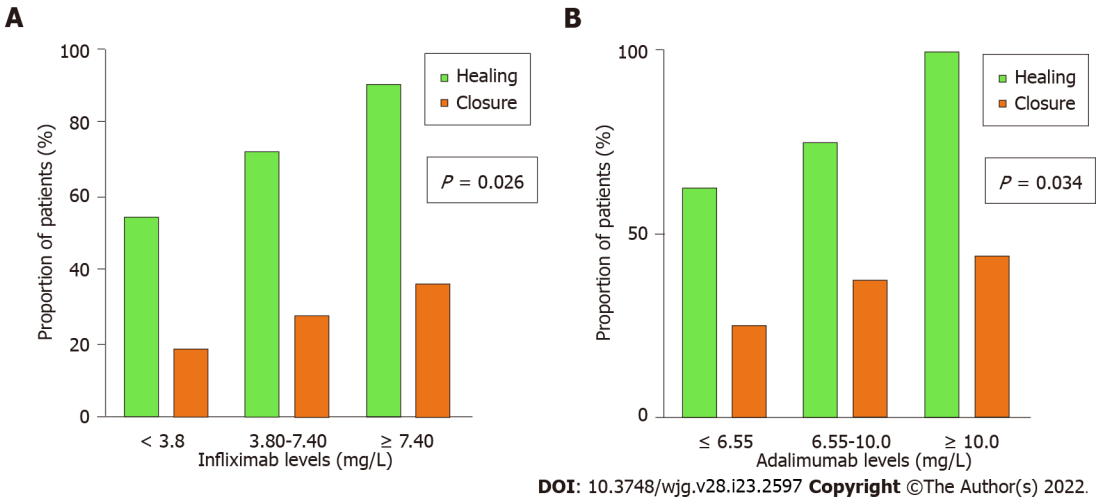
Table 2 Differences between patients on infliximab with and without fistula healing

	Patients with fistula healing (*n* = 48)	Patients without fistula healing (*n* = 18)	*P* value
Median age, yr (IQR)	33.0 (28.0-38.0)	43.5 (34.3-57.3)	0.005
Female gender, *n* (%)	20 (41.7)	8 (44.4)	0.839
Mean weight, kg (SD)	82.2 (19.4)	76.5 (15.7)	0.378
Mean BMI, kg/m^2 (SD)	28.5 (5.0)	26.7 (3.8)	0.318
Median age at diagnosis of Crohn's disease (IQR)	26.0 (20.75-30.5)	30.0 (24.0-43.0)	0.121
A1, *n* (%)	1 (2.1)	1 (5.6)	-
A2, *n* (%)	41 (85.4)	11 (61.1)	-
A3, *n* (%)	4 (8.3)	5 (27.8)	-
Current smoker, *n* (%)	8 (16.7)	4 (22.2)	0.696
Location			
Ileal, *n* (%)	14 (29.2)	2 (11.1)	-
Colonic, *n* (%)	19 (39.6)	7 (38.9)	-
Ileocolonic, *n* (%)	11 (22.9)	4 (22.2)	-
No luminal disease, *n* (%)	2 (4.2)	2 (11.1)	-
Upper gastrointestinal involvement, *n* (%)	3 (6.3)	1 (5.6)	-
Stricturing, *n* (%)	7 (14.6)	3 (16.7)	0.822
Penetrating, *n* (%)	5 (10.4)	2 (11.1)	0.927
Median duration on anti-TNF agent, wk (IQR)	153.0 (86.0-285.0)	95.5 (40.25-322.75)	0.387
Dose escalated anti-TNF therapy, *n* (%)	15 (31.3)	4 (22.2)	-
Concurrent steroids, *n* (%)	0 (0.0)	1 (5.6)	-
Concurrent aminosalicylates, *n* (%)	4 (8.3)	1 (5.6)	0.219
Combination with immunomodulator, *n* (%)	35 (72.9)	11 (61.1)	0.522
Methotrexate, *n* (%)	6 (12.5)	2 (11.1)	0.937
6-mercaptopurine, *n* (%)	6 (12.5)	3 (16.7)	0.597
Azathioprine, *n* (%)	23 (47.9)	6 (33.3)	0.368
Concurrent allopurinol, *n* (%)	9 (18.8)	1 (5.6)	0.197
Mean albumin, g/L (SD)	40.3 (4.7)	40.7 (4.6)	0.590
Median CRP, mg/L (IQR)	2.1 (1.0-4.5)	5.5 (1.1-8.7)	0.094
Median trough level, mg/L (IQR)	6.4 (3.8-9.5)	3.0 (0.3-6.2)	0.003
Detectable antibody, *n* (%)	3 (4.3)	6 (33.3)	0.004

ADA: Adalimumab; BMI: Body mass index; CRP: C-reactive protein; IFX: Infliximab; IQR: Interquartile range; SD: Standard deviation; TNF: Tumor necrosis factor.

detectable anti-infliximab antibodies was associated with lower infliximab trough levels (P = 0.02). The CRP and albumin levels were not significantly different between patients with and without fistula healing. The rates of combination therapy with an immunomodulator were not significantly different between patients who achieved fistula healing and those who did not (P = 0.522).

ROC curve analysis identified a positive correlation between infliximab trough levels and healing [area under the curve (AUC) = 0.74, 95% confidence interval (CI): 0.60-0.88, P = 0.003; Figure 1A] with an infliximab trough level of 6.10 mg/L that maximised the sensitivity and specificity of predicting fistula healing [sensitivity 58%, specificity 78%, odds ratio (OR) = 4.9, P = 0.013]. Upon tertile analysis, higher tertiles of infliximab levels were associated with a higher proportion of patients achieving fistula healing with 54.5% healing rate for tertile 1 compared to 90.1% for tertile 3 (Figure 2A; P = 0.026). Out of the patients who achieved fistula healing on infliximab, 90% and 95% of the patients who achieved fistula healing were healed with an infliximab trough level of 12.7 and 14.4 mg/L respectively. Given



DOI: 10.3748/wjg.v28.i23.2597 **Copyright** ©The Author(s) 2022.

Figure 2 Tertile analysis of infliximab and adalimumab trough levels for patients with fistula healing and fistula closure. A: Infliximab; B: Adalimumab.

that a drug-sensitive infliximab assay was used where anti-infliximab antibody titres were only performed if infliximab concentrations were < 2.0 mg/L, anti-infliximab antibodies were not included in the multivariate analysis. On multivariate logistic regression analysis, age was associated with healing ($P = 0.026$) but adequate infliximab levels ≥ 6.10 mg/L were not ($P = 0.097$). Within our cohort, 18 (27.3%) of patients on infliximab achieved fistula closure. The infliximab trough level for patients with and without fistula closure was not significantly different [6.9 (4.3-10.2) *vs* 5.5 (2.5-8.3) mg/L, $P = 0.105$].

Association between fistula healing and closure with adalimumab trough levels

Thirty-seven (77%) patients on maintenance adalimumab achieved fistula healing. Table 3 summarises the differences in patients on adalimumab with and without fistula healing. Patients who achieved fistula healing had higher adalimumab trough levels compared to those who did not [9.2 (6.5-12.0) *vs* 5.4 (2.5-8.3) mg/L, $P = 0.004$]. Patients who achieved fistula healing had higher rates of combination therapy with an immunomodulator than those who did not ($P = 0.048$). The CRP and albumin levels were not significantly different in patients with and without fistula healing. ROC curve analysis identified a positive correlation between adalimumab trough levels and healing (AUC = 0.79, 95%CI: 0.66-0.93, $P = 0.004$) with an adalimumab trough level of 7.05 mg/L that maximised the sensitivity and specificity of infliximab levels in predicting fistula healing (sensitivity 70%; specificity 73%; OR = 6.3; $P = 0.016$; Figure 1B). Upon tertile analysis, higher tertiles of adalimumab levels were associated with a higher proportion of patients achieving fistula healing, with 62.5% healing rate for tertile 1 compared to 100% for tertile 3 (Figure 2B; $P = 0.034$). Out of the patients who achieved fistula healing on adalimumab, 90% and 95% of the patients who achieved fistula healing were healed with an adalimumab trough level of 12.0 and 18.0 mg/L respectively. On multivariate logistic regression analysis, adequate adalimumab trough levels ≥ 7.05 mg/L ($P = 0.008$) and concurrent immunomodulator therapy ($P = 0.026$) both remained associated with healing. Within our cohort, 17 (35.4%) of patients on adalimumab achieved fistula closure. The adalimumab trough level for patients with and without fistula closure was not significantly different [10.0 (6.6-12.0) *vs* 7.8 (4.2-10.0) mg/L, $P = 0.083$].

DISCUSSION

Fistulising perianal CD is a highly morbid condition for which treatment outcomes remain suboptimal in many patients. While there is limited data on the role of newer biologic agents such as ustekinumab in perianal CD[19], anti-TNF agents remain the treatment of choice. Our study showed a significant association between both infliximab and adalimumab trough levels and fistula healing, with higher levels associated with increased healing rates. We demonstrated that higher tertiles of both infliximab and adalimumab levels were associated with a higher proportion of patients achieving fistula healing. Notably, when plotting the cumulative percentage of healed patients against infliximab level, we found that 50% of the patients who achieve healing will heal with a level of 6.4 mg/L, 90% of the patients who achieve healing will heal with a level of 12.7 mg/L and 95% of the patients who achieve healing will heal with a level of 14.4 mg/L. Similarly, for patients on adalimumab, 50% of the patients who achieve healing will heal with a level of 9.2 mg/L, and 90% and 95% of patients who achieved fistula healing were healed with levels of 12.0 and 18.0 mg/L respectively. Our results support dose-escalation of both infliximab and adalimumab in non-responders, targeting higher levels to achieve fistula healing prior to

Table 3 Differences in patients on adalimumab with and without fistula healing

	Patients with fistula healing (*n* = 37)	Patients without fistula healing (*n* = 11)	*P* value
Median age, yr (IQR)	33.0 (28.5-52.0)	44.9 (33.0-52.0)	0.254
Female gender, *n* (%)	10 (27.0)	4 (36.4)	0.550
Mean weight, kg (SD)	82.5 (22.3)	79.7 (16.7)	0.812
Mean BMI, kg/m^2 (SD)	29.2 (5.9)	25.5 (2.7)	0.241
Median age at diagnosis of Crohn's disease (IQR)	24.0 (18.0-42.0)	30.0 (19.0-41.0)	0.570
A1, *n* (%)	6 (16.2)	1 (9.1)	-
A2, *n* (%)	19 (51.4)	7 (63.6)	-
A3, *n* (%)	10 (27.0)	3 (27.3)	-
Current smoker, *n* (%)	5 (13.5)	0 (0.0)	0.198
Location			
Ileal, *n* (%)	12 (32.4)	5 (45.5)	-
Colonic, *n* (%)	5 (13.5)	2 (18.2)	-
Ileocolonic, *n* (%)	15 (40.5)	3 (27.3)	-
No luminal disease, *n* (%)	2 (5.4)	0 (0.0)	-
Upper gastrointestinal involvement, *n* (%)	2 (5.4)	1 (9.1)	-
Stricturing, *n* (%)	9 (24.3)	2 (18.2)	0.644
Penetrating, *n* (%)	14 (37.8)	3 (27.3)	0.481
Median duration on anti-TNF agent, wk (IQR)	194.5 (124.3-311.3)	122.5 (79.8-319.3)	0.318
Dose escalated anti-TNF therapy, *n* (%)	10 (27.0)	1 (9.1)	-
Concurrent steroids, *n* (%)	0 (0.0)	0 (0.0)	-
Concurrent aminosalicylates, *n* (%)	4 (10.8)	1 (9.1)	0.849
Combination with immunomodulator, *n* (%)	25 (67.6)	4 (36.4)	0.048
Methotrexate, *n* (%)	7 (18.9)	1 (9.1)	0.424
6-mercaptopurine, *n* (%)	6 (16.2)	1 (9.1)	0.537
Azathioprine, *n* (%)	12 (32.4)	2 (18.2)	0.336
Concurrent allopurinol, *n* (%)	4 (10.8)	0 (0.0)	0.248
Mean albumin, g/L (SD)	40.5 (4.5)	40.0 (5.7)	0.608
Median CRP, mg/L (IQR)	2.1 (1.0-4.5)	5.4 (1.7-9.3)	0.070
Median trough level (IQR)	9.2 (6.5-12.0)	5.4 (2.5-8.3)	0.004
Detectable antibody, *n* (%)	1 (2.7)	1 (9.1)	0.352

ADA: Adalimumab; BMI: Body mass index; CRP: C-reactive protein; IFX: Infliximab; IQR: Interquartile range; SD: Standard deviation; TNF: Tumor necrosis factor.

changing biologic therapy. Importantly, this study is the largest study to date assessing the relationship between adalimumab trough levels and clinical fistula healing. This data adds to the growing body of evidence that fistula healing improves with higher anti-TNF trough levels, and that higher levels may be required for perianal fistula healing than for mucosal healing in luminal CD[12-14,20].

This study did not show an association between infliximab and adalimumab trough levels and fistula closure. Not all previous studies have assessed fistula closure, but some have found that patients with fistula closure had significantly higher maintenance infliximab and adalimumab trough levels[13,14]. Our results may have been limited by inadequate power due to relatively small numbers of patients who achieved fistula closure in our cohort. We had a high fistula healing rate in this study, with 72.7% and 77% of patients on maintenance infliximab and adalimumab achieving fistula healing respectively. This finding was possibly due to high rates of combination therapy with an immunomodulator (69.7% and 60.4% in the infliximab and adalimumab groups respectively).

Randomised controlled trials have shown that infliximab is effective at both inducing and maintaining fistula healing[7,8]. Our study found that fistula healing was associated with higher infliximab trough levels. This finding is supported by a post-hoc analysis of ACCENT II which found that higher infliximab trough levels during induction were associated with a complete absence of draining fistulas at week 14[12], as well as similar findings in other studies assessing induction and maintenance infliximab therapy[11,13]. In the future, there may be a role for the infliximab biosimilar CT-P13 in order to achieve these high infliximab levels required for perianal fistula healing; with recent randomised controlled trials demonstrating higher trough levels from subcutaneous administration of CT-P13 compared to intravenous administration[21]. Interestingly, our study found that fistula healing was associated with younger age in both univariate and multivariate analyses. Whilst patient factors including albumin and body weight have previously been shown to affect infliximab trough levels[22], the influence of age is unclear. This finding may be due to the relatively younger age at diagnosis of CD for patients with fistula healing or longer duration of infliximab therapy. Five patients in this study had been changed from infliximab to adalimumab or vice versa and were included in both groups, however the anti-TNF level and anti-TNF antibody levels at the time of changing treatment were not collected. Reassuringly, previous studies have demonstrated that the presence of infliximab antibodies does not decrease future response rates to adalimumab and vice versa[23].

Adalimumab has also been shown to be effective in both inducing[9] and maintaining fistula healing [24]. Our study found that fistula healing was associated with higher adalimumab trough levels. Whilst there is limited data on the association between adalimumab trough levels and fistula healing, our findings are consistent with two smaller retrospective studies that showed that patients with fistula healing had higher adalimumab trough levels compared to those without fistula healing[14,20]. On multivariate logistic regression analysis, adalimumab trough levels ≥ 7.05 mg/L and concurrent immunomodulator therapy both remained significantly associated with healing. This reflects how concomitant immunosuppressive therapy can be used to decrease the immunogenic response and therefore improve fistula healing rates[25].

This study has several limitations. Assessment of fistula healing was based on clinical assessment, which may not be as accurate as an objective assessment such as with magnetic resonance imaging of the pelvis. A recent study has demonstrated that higher anti-TNF trough levels are associated with improved rates of radiological healing in perianal fistulising CD[26]. However, the absence of drainage remains a clinically relevant endpoint that impacts on patient quality of life. In order to provide an objective marker of response, biochemical markers of disease activity including CRP and albumin were analysed and found not to correlate with fistula healing. Data was retrospectively collected, so in order to address this we only included patients with documented perianal exams and definitions for fistula healing and closure that were in line with previous randomised controlled trials[8]. We found that fistula healing is associated with higher infliximab and adalimumab trough levels, however further randomised controlled trials are required to assess whether dose escalation to higher levels improves healing and the optimal method for dose escalation. Whilst reactive TDM with dose escalation at the time of loss of response is effective, it remains unknown whether proactive TDM with subsequent dose modification improves outcomes. Notably, all previous studies on proactive TDM have focused on luminal disease with no prospective studies evaluating proactive TDM in perianal fistulising CD.

CONCLUSION

Our study showed that higher infliximab and adalimumab trough levels are associated with perianal CD fistula healing, with higher rates of healing in higher tertiles of infliximab and adalimumab levels. However, no association with fistula closure was observed. Further prospective studies are required to confirm target infliximab and adalimumab trough levels and determine the optimal dose escalation method to achieve these target levels.

ARTICLE HIGHLIGHTS

Research background

Anti-tumor necrosis factor (anti-TNF)-alpha agents, including infliximab and adalimumab, are effective medical treatments for perianal fistulising Crohn's disease (CD), but not all patients achieve fistula healing with up to 60% of patients treated with maintenance infliximab lose response within one year.

Research motivation

Accumulating evidence suggests that this loss of response is partly due to sub-therapeutic anti-TNF trough levels. Retrospective studies and post-hoc analyses of prospective data have identified that higher infliximab trough levels are associated with fistula healing and closure compared to what is observed for mucosal healing in luminal disease, with emerging data suggesting similar results for

adalimumab. Quantitative assays for therapeutic drug monitoring permits individualisation of infliximab and adalimumab dosing, however there are very few studies on perianal fistulising CD and the optimal target levels for perianal fistulising CD remains unclear.

Research objectives
This study aims to assess the association between serum trough infliximab and adalimumab levels and perianal fistula healing and closure and identify optimal target levels.

Research methods
In this multi-centre retrospective study conducted across four tertiary inflammatory bowel disease centres in Australia, we identified CD patients with perianal fistulae on maintenance infliximab or adalimumab who had a trough level within twelve weeks of clinical assessment. The primary outcome was fistula healing, defined as cessation in fistula drainage. The secondary outcome was fistula closure, defined as healing and closure of all external fistula openings. Differences between patients who did or did not achieve fistula healing were compared using the Chi-square test, *t*-test or Mann-Whitney *U* test.

Research results
Out of a total of 114 patients (66 infliximab, 48 adalimumab), 48 (72.7%) patients and 37 (77%) patients on maintenance infliximab and adalimumab respectively achieved fistula healing. Patients who achieved fistula healing had significantly higher infliximab and adalimumab trough levels compared to patients who did not [infliximab: 6.4 (3.8-9.5) *vs* 3.0 (0.3-6.2) mg/L, $P = 0.003$; adalimumab: 9.2 (6.5-12.0) *vs* 5.4 (2.5-8.3) mg/L, $P = 0.004$]. Serum trough levels for patients with and without fistula closure were not significantly different for infliximab [6.9 (4.3-10.2) *vs* 5.5 (2.5-8.3) mg/L, $P = 0.105$] or adalimumab [10.0 (6.6-12.0) *vs* 7.8 (4.2-10.0) mg/L, $P = 0.083$].

Research conclusions
Higher maintenance infliximab and adalimumab trough levels are associated with perianal fistula healing in CD.

Research perspectives
Our study showed that higher infliximab and adalimumab trough levels are associated with perianal CD fistula healing, with higher rates of healing in higher tertiles of infliximab and adalimumab levels, but no association with fistula closure was observed. Further prospective studies are required to confirm target infliximab and adalimumab trough levels and determine the optimal dose escalation method to achieve these target levels.

FOOTNOTES

Author contributions: Gu B, Williams AJ, Ng W and Connor S conceived concept and design of study; Gu B and Venkatesh K collected the data; Gu B analysed the data; Gholamrezaei A and Xuan W provided statistical support; Gu B prepared the first draft of the manuscript; and all authors provided edits and critiqued the manuscript for intellectual content.

Institutional review board statement: Ethics approval was obtained from the South Western Sydney Local Health District (Human Research Ethics Committee LNR/18/LPOOL/404; Local Project Number: HE18/261).

Informed consent statement: According to the Ethics Board Approval for this retrospective cross-sectional study, individual patient consent was not required to obtained.

Conflict-of-interest statement: Gu B has nothing to disclose. Williams AJ has received honoraria from Takeda, Janssen and Abbvie and honoraria and grant support from Ferring. Ng W received grants from Janssen and Pfizer, during the conduct of the study; grants and personal and speaker fees from Abbvie, Takeda, Grants from Ferring and Shire. Corte C has received unrestricted educational grants from Ferring, Janssen, Shire and GESA. Corte C has received honoraria from Janssen, Ferring, Astra-Zeneca, Abbvie and Shire. Travel support and conference registration from Takeda, Shire, Janssen and Nycomed. Advisory board fees from Celgene and Gilead. Ghaly S has received educational grants from Janssen, Ferring, Pfizer and Takeda. Honoraria from Janssen, Ferring, Takeda, AbbVie, Shire. Advisory board fees from Pfizer, AbbVie, Gilead, Ferring and MSD. Paramsothy S is a consultant for Finch Therapeutics and has received speaker fees from Ferring, Janssen and Takeda. Connor S has received honoraria, speaker fees, educational support and/or grant funding from Abbvie, Aspen, BMS, Celgene, Celltrion, Chiesi, DrFalk, Ferring, Fresenius Kabi, Gilead, Janssen, MSD, Novartis, Pfizer, Takeda, Vifor, Agency for Clinical Innovation, Gastroenterological Society of Australia, Medical Research Future Fund and The Leona M and Harry B Helmsley Charitable Trust. This research project did not receive any grant funding.

Data sharing statement: According to the Ethics Board Approval for this retrospective cross-sectional study, individual patient consent was not required to obtained.

Open-Access: This article is an open-access article that was selected by an in-house editor and fully peer-reviewed by external reviewers. It is distributed in accordance with the Creative Commons Attribution NonCommercial (CC BY-NC 4.0) license, which permits others to distribute, remix, adapt, build upon this work non-commercially, and license their derivative works on different terms, provided the original work is properly cited and the use is non-commercial. See: https://creativecommons.org/Licenses/by-nc/4.0/

Country/Territory of origin: Australia

ORCID number: Bonita Gu 0000-0002-9264-1854; Kavya Venkatesh 0000-0002-6981-9116; Astrid-Jane Williams 0000-0002-1756-5329; Watson Ng 0000-0001-5424-6266; Crispin Corte 0000-0003-1286-8459; Ali Gholamrezaei 0000-0001-8674-450X; Simon Ghaly 0000-0003-2489-6430; Wei Xuan 0000-0001-7169-8299; Sudarshan Paramsothy 0000-0002-9097-6028; Susan Connor 0000-0001-5606-0270.

S-Editor: Wang JJ
L-Editor: A
P-Editor: Wang JJ

REFERENCES

1 **Schwartz DA**, Loftus EV Jr, Tremaine WJ, Panaccione R, Harmsen WS, Zinsmeister AR, Sandborn WJ. The natural history of fistulizing Crohn's disease in Olmsted County, Minnesota. *Gastroenterology* 2002; **122**: 875-880 [PMID: 11910338 DOI: 10.1053/gast.2002.32362]
2 **Makowiec F**, Jehle EC, Starlinger M. Clinical course of perianal fistulas in Crohn's disease. *Gut* 1995; **37**: 696-701 [PMID: 8549948 DOI: 10.1136/gut.37.5.696]
3 **Lockhart-Mummery HE**. Symposium. Crohn's disease: anal lesions. *Dis Colon Rectum* 1975; **18**: 200-202 [PMID: 1140047 DOI: 10.1007/BF02587272]
4 **Ramos A**, Calvet X, Sicilia B, Vergara M, Figuerola A, Motos J, Sastre A, Villoria A, Gomollón F. IBD-related work disability in the community: Prevalence, severity and predictive factors. A cross-sectional study. *United European Gastroenterol J* 2015; **3**: 335-342 [PMID: 26279841 DOI: 10.1177/2050640615577532]
5 **Vollebregt PF**, van Bodegraven AA, Markus-de Kwaadsteniet TML, van der Horst D, Felt-Bersma RJF. Impacts of perianal disease and faecal incontinence on quality of life and employment in 1092 patients with inflammatory bowel disease. *Aliment Pharmacol Ther* 2018; **47**: 1253-1260 [PMID: 29520808 DOI: 10.1111/apt.14599]
6 **Chaparro M**, Zanotti C, Burgueño P, Vera I, Bermejo F, Marín-Jiménez I, Yela C, López P, Martín MD, Taxonera C, Botella B, Pajares R, Ponferrada A, Calvo M, Algaba A, Pérez L, Casis B, Maté J, Orofino J, Lara N, García-Losa M, Badia X, Gisbert JP. Health care costs of complex perianal fistula in Crohn's disease. *Dig Dis Sci* 2013; **58**: 3400-3406 [PMID: 24026400 DOI: 10.1007/s10620-013-2830-7]
7 **Present DH**, Rutgeerts P, Targan S, Hanauer SB, Mayer L, van Hogezand RA, Podolsky DK, Sands BE, Braakman T, DeWoody KL, Schaible TF, van Deventer SJ. Infliximab for the treatment of fistulas in patients with Crohn's disease. *N Engl J Med* 1999; **340**: 1398-1405 [PMID: 10228190 DOI: 10.1056/NEJM199905063401804]
8 **Sands BE**, Anderson FH, Bernstein CN, Chey WY, Feagan BG, Fedorak RN, Kamm MA, Korzenik JR, Lashner BA, Onken JE, Rachmilewitz D, Rutgeerts P, Wild G, Wolf DC, Marsters PA, Travers SB, Blank MA, van Deventer SJ. Infliximab maintenance therapy for fistulizing Crohn's disease. *N Engl J Med* 2004; **350**: 876-885 [PMID: 14985485 DOI: 10.1056/NEJMoa030815]
9 **Colombel JF**, Sandborn WJ, Rutgeerts P, Enns R, Hanauer SB, Panaccione R, Schreiber S, Byczkowski D, Li J, Kent JD, Pollack PF. Adalimumab for maintenance of clinical response and remission in patients with Crohn's disease: the CHARM trial. *Gastroenterology* 2007; **132**: 52-65 [PMID: 17241859 DOI: 10.1053/j.gastro.2006.11.041]
10 **Colombel JF**, Schwartz DA, Sandborn WJ, Kamm MA, D'Haens G, Rutgeerts P, Enns R, Panaccione R, Schreiber S, Li J, Kent JD, Lomax KG, Pollack PF. Adalimumab for the treatment of fistulas in patients with Crohn's disease. *Gut* 2009; **58**: 940-948 [PMID: 19201775 DOI: 10.1136/gut.2008.159251]
11 **Davidov Y**, Ungar B, Bar-Yoseph H, Carter D, Haj-Natour O, Yavzori M, Chowers Y, Eliakim R, Ben-Horin S, Kopylov U. Association of Induction Infliximab Levels With Clinical Response in Perianal Crohn's Disease. *J Crohns Colitis* 2017; **11**: 549-555 [PMID: 28453755 DOI: 10.1093/ecco-jcc/jjw182]
12 **Papamichael K**, Vande Casteele N, Jeyarajah J, Osterman M, Cheifetz A. Adequate infliximab exposure during the induction phase is associated with early complete fistula response in patients with fistulizing Crohn's disease: a post-hoc analysis of the Accent-2 trial. *Gastroenterology* 2019; **156**: S-111 [DOI: 10.1016/S0016-5085(19)37070-2]
13 **Yarur AJ**, Kanagala V, Stein DJ, Czul F, Quintero MA, Agrawal D, Patel A, Best K, Fox C, Idstein K, Abreu MT. Higher infliximab trough levels are associated with perianal fistula healing in patients with Crohn's disease. *Aliment Pharmacol Ther* 2017; **45**: 933-940 [PMID: 28211593 DOI: 10.1111/apt.13970]
14 **Plevris N**, Jenkinson PW, Arnott ID, Jones GR, Lees CW. Higher anti-tumor necrosis factor levels are associated with perianal fistula healing and fistula closure in Crohn's disease. *Eur J Gastroenterol Hepatol* 2020; **32**: 32-37 [PMID: 31567638 DOI: 10.1097/MEG.0000000000001561]
15 **Baert F**, Noman M, Vermeire S, Van Assche G, D' Haens G, Carbonez A, Rutgeerts P. Influence of immunogenicity on the

long-term efficacy of infliximab in Crohn's disease. *N Engl J Med* 2003; **348**: 601-608 [PMID: 12584368 DOI: 10.1056/NEJMoa020888]

16 **Bortlik M**, Duricova D, Malickova K, Machkova N, Bouzkova E, Hrdlicka L, Komarek A, Lukas M. Infliximab trough levels may predict sustained response to infliximab in patients with Crohn's disease. *J Crohns Colitis* 2013; **7**: 736-743 [PMID: 23200919 DOI: 10.1016/j.crohns.2012.10.019]

17 **Australian Government Department of Health**. Crohn disease: infliximab, adalimumab and vedolizumab, Drug utilisation sub-committee (DUSC). [cited 14 August 2021]. Available from: https://www.pbs.gov.au/pbs/industry/listing/participants/public-release-docs/2017-06/crohn-disease-infliximab-adalimumab-vedolizumab-prd-2017-06

18 **Satsangi J**, Silverberg MS, Vermeire S, Colombel JF. The Montreal classification of inflammatory bowel disease: controversies, consensus, and implications. *Gut* 2006; **55**: 749-753 [PMID: 16698746 DOI: 10.1136/gut.2005.082909]

19 **Chapuis-Biron C**, Kirchgesner J, Pariente B, Bouhnik Y, Amiot A, Viennot S, Serrero M, Fumery M, Allez M, Siproudhis L, Buisson A, Pineton de Chambrun G, Abitbol V, Nancey S, Caillo L, Plastaras L, Savoye G, Chanteloup E, Simon M, Dib N, Rajca S, Amil M, Parmentier AL, Peyrin-Biroulet L, Vuitton L; GETAID BioLAP Study Group. Ustekinumab for Perianal Crohn's Disease: The BioLAP Multicenter Study From the GETAID. *Am J Gastroenterol* 2020; **115**: 1812-1820 [PMID: 33156100 DOI: 10.14309/ajg.0000000000000810]

20 **Strik AS**, Löwenberg M, Buskens CJ, B Gecse K, I Ponsioen C, Bemelman WA, D'Haens GR. Higher anti-TNF serum levels are associated with perianal fistula closure in Crohn's disease patients. *Scand J Gastroenterol* 2019; **54**: 453-458 [PMID: 31032686 DOI: 10.1080/00365521.2019.1600014]

21 **Westhovens R**, Yoo DH, Jaworski J, Matyska-Piekarska E, Smiyan S, Ivanova D, Zielinska A, Raussi E, Batalov A, Lee SJ, LeeSY, Suh JH. THU0191 Novel formulation of ct-p13 for subcutaneous administration in patients with rheumatoid arthritis: initial results from a phase i/iii randomised controlled trial. *Ann Rheum Dis* 2018; **77**: 315 [DOI: 10.1136/annrheumdis-2018-eular.1810]

22 **Dotan I**, Ron Y, Yanai H, Becker S, Fishman S, Yahav L, Ben Yehoyada M, Mould DR. Patient factors that increase infliximab clearance and shorten half-life in inflammatory bowel disease: a population pharmacokinetic study. *Inflamm Bowel Dis* 2014; **20**: 2247-2259 [PMID: 25358062 DOI: 10.1097/MIB.0000000000000212]

23 **Karmiris K**, Paintaud G, Noman M, Magdelaine-Beuzelin C, Ferrante M, Degenne D, Claes K, Coopman T, Van Schuerbeek N, Van Assche G, Vermeire S, Rutgeerts P. Influence of trough serum levels and immunogenicity on long-term outcome of adalimumab therapy in Crohn's disease. *Gastroenterology* 2009; **137**: 1628-1640 [PMID: 19664627 DOI: 10.1053/j.gastro.2009.07.062]

24 **Panaccione R**, Colombel JF, Sandborn WJ, D'Haens G, Zhou Q, Pollack PF, Thakkar RB, Robinson AM. Adalimumab maintains remission of Crohn's disease after up to 4 years of treatment: data from CHARM and ADHERE. *Aliment Pharmacol Ther* 2013; **38**: 1236-1247 [PMID: 24134498 DOI: 10.1111/apt.12499]

25 **Colombel JF**, Sandborn WJ, Reinisch W, Mantzaris GJ, Kornbluth A, Rachmilewitz D, Lichtiger S, D'Haens G, Diamond RH, Broussard DL, Tang KL, van der Woude CJ, Rutgeerts P; SONIC Study Group. Infliximab, azathioprine, or combination therapy for Crohn's disease. *N Engl J Med* 2010; **362**: 1383-1395 [PMID: 20393175 DOI: 10.1056/NEJMoa0904492]

26 **De Gregorio M**, Lee T, Krishnaprasad K, Amos G, An YK, Bastian-Jordan M, Begun J, Borok N, Brown DJM, Cheung W, Connor SJ, Gerstenmaier J, Gilbert LE, Gilmore R, Gu B, Kutaiba N, Lee A, Mahy G, Srinivasan A, Thin L, Thompson AJ, Welman CJ, Yong EXZ, De Cruz P, van Langenberg D, Sparrow MP, Ding NS. Higher Anti-tumor Necrosis Factor-α Levels Correlate With Improved Radiologic Outcomes in Crohn's Perianal Fistulas. *Clin Gastroenterol Hepatol* 2021 [PMID: 34389484 DOI: 10.1016/j.cgh.2021.07.053]

World Journal of Gastroenterology

Submit a Manuscript: https://www.f6publishing.com

World J Gastroenterol 2022 June 21; 28(23): 2609-2624

DOI: 10.3748/wjg.v28.i23.2609

ISSN 1007-9327 (print) ISSN 2219-2840 (online)

ORIGINAL ARTICLE

Retrospective Study

Whole lesion histogram analysis of apparent diffusion coefficient predicts therapy response in locally advanced rectal cancer

Mayra Evelia Jiménez de los Santos, Juan Armando Reyes-Pérez, Victor Domínguez Osorio, Yolanda Villaseñor-Navarro, Liliana Moreno-Astudillo, Itzel Vela-Sarmiento, Isabel Sollozo-Dupont

Specialty type: Oncology

Provenance and peer review: Unsolicited article; Externally peer reviewed.

Peer-review model: Single blind

Peer-review report's scientific quality classification

Grade A (Excellent): 0
Grade B (Very good): B
Grade C (Good): C, C
Grade D (Fair): 0
Grade E (Poor): 0

P-Reviewer: Karavaş E, Turkey; Setiawati R, Indonesia; Zhao J, China

Received: September 23, 2021
Peer-review started: September 23, 2021
First decision: November 16, 2021
Revised: November 25, 2021
Accepted: April 22, 2022
Article in press: April 22, 2022
Published online: June 21, 2022

Mayra Evelia Jiménez de los Santos, Juan Armando Reyes-Pérez, Victor Domínguez Osorio, Yolanda Villaseñor-Navarro, Liliana Moreno-Astudillo, Isabel Sollozo-Dupont, Department of Radiology, National Cancer Institute, Mexico 14080, Mexico

Itzel Vela-Sarmiento, Department of Gastrointestinal Surgery, National Cancer Institute, Mexico 14080, Mexico

Corresponding author: Isabel Sollozo-Dupont, PhD, Academic Research, Statistician, Department of Radiology, National Cancer Institute, Av. San Fernando No. 22, Col. Sección XVI Delegación Tlalpan, Mexico 14080, Mexico. sodi8507@gmail.com

Abstract

BACKGROUND

Whole-tumor apparent diffusion coefficient (ADC) histogram analysis is relevant to predicting the neoadjuvant chemoradiation therapy (nCRT) response in patients with locally advanced rectal cancer (LARC).

AIM

To evaluate the performance of ADC histogram-derived parameters for predicting the outcomes of patients with LARC.

METHODS

This is a single-center, retrospective study, which included 48 patients with LARC. All patients underwent a pre-treatment magnetic resonance imaging (MRI) scan for primary tumor staging and a second restaging MRI for response evaluation. The sample was distributed as follows: 18 responder patients (R) and 30 non-responders (non-R). Eight parameters derived from the whole-lesion histogram analysis (ADCmean, skewness, kurtosis, and ADC10th, 25th, 50th, 75th, 90th percentiles), as well as the ADCmean from the hot spot region of interest (ROI), were calculated for each patient before and after treatment. Then all data were compared between R and non-R using the Mann-Whitney U test. Two measures of diagnostic accuracy were applied: the receiver operating characteristic curve and the diagnostic odds ratio (DOR). We also reported intra- and interobserver variability by calculating the intraclass correlation coefficient (ICC).

RESULTS

Post-nCRT kurtosis, as well as post-nCRT skewness, were significantly lower in R

than in non-R (both $P < 0.001$, respectively). We also found that, after treatment, R had a larger loss of both kurtosis and skewness than non-R (Δ%kurtosis and Δskewness, $P < 0.001$). Other parameters that demonstrated changes between groups were post-nCRT ADC10th, Δ%ADC10th, Δ%ADCmean, and ROI Δ%ADCmean. However, the best diagnostic performance was achieved by Δ%kurtosis at a threshold of 11.85% (Area under the receiver operating characteristic curve [AUC] = 0.991, DOR = 376), followed by post-nCRT kurtosis = 0.78 × 10^{-3} mm^2/s (AUC = 0.985, DOR = 375.3), Δskewness = 0.16 (AUC = 0.885, DOR = 192.2) and post-nCRT skewness = 1.59 × 10^{-3} mm^2/s (AUC = 0.815, DOR = 168.6). Finally, intraclass correlation coefficient analysis showed excellent intraobserver and interobserver agreement, ensuring the implementation of histogram analysis into routine clinical practice.

CONCLUSION

Whole-tumor ADC histogram parameters, particularly kurtosis and skewness, are relevant biomarkers for predicting the nCRT response in LARC. Both parameters appear to be more reliable than ADCmean from one-slice ROI.

Key Words: Apparent diffusion coefficient; Diffusion-weighted imaging; Histogram analysis; Magnetic resonance imaging; Locally advanced rectal cancer

©The Author(s) 2022. Published by Baishideng Publishing Group Inc. All rights reserved.

Core Tip: Whole-tumor apparent diffusion coefficient (ADC) histogram analysis is an emergent imaging analysis in which every voxel is used to obtain a histogram; it thus provides statistical information about tumors. Our study revealed that ADC histogram profiling is a valuable approach that can help differentiate treatment response in locally advanced rectal cancer. When determining tailored treatments that are associated with minimal morbidities, such as the watch and wait method, an accurate treatment response prediction is critical. Given the limitations of this study, more research is needed to establish the clinical utility of our findings.

Citation: Jiménez de los Santos ME, Reyes-Pérez JA, Domínguez Osorio V, Villaseñor-Navarro Y, Moreno-Astudillo L, Vela-Sarmiento I, Sollozo-Dupont I. Whole lesion histogram analysis of apparent diffusion coefficient predicts therapy response in locally advanced rectal cancer. *World J Gastroenterol* 2022; 28(23): 2609-2624
URL: https://www.wjgnet.com/1007-9327/full/v28/i23/2609.htm
DOI: https://dx.doi.org/10.3748/wjg.v28.i23.2609

INTRODUCTION

Neoadjuvant chemoradiation therapy (nCRT) is the gold standard treatment for patients with locally advanced rectal cancer (LARC), followed by surgical resection and adjuvant chemotherapy[1,2]. After nCRT, the ability to achieve tumor reduction or even a pathological complete response (pCR) is observed in approximately 75% of treated patients, whereas the remainder exhibited no treatment response[3,4]. The ability to predict the response to nCRT is important for patients with potentially curable LARC who wish to explore personalized treatment to expand their therapeutic outcomes[5].

Functional magnetic resonance imaging (MRI) techniques, such as diffusion-weighted imaging (DWI), can provide additional physiological information about a tumor's cellular environment, offering great potential to evaluate the therapeutic response to nCRT[5]. This is because the apparent diffusion coefficient (ADC), a quantitative parameter used to assess water diffusion through tissue in DWI, shows an inverse relationship with tissue cellularity[6]. Viable tumor cells restrict the mobility of water, whereas necrotic tumor cells allow the increased diffusion of water molecules[7].

The possibility that ADC may be associated with the nCRT response has been amply investigated in LARC[8-12]; however, significant correlations have not been found in any studies to date[10]. Inconsistencies in previous findings may be due to a lack of standardized imaging and acquisition techniques[5,11], but they may also be due to the fact that the ADC measurements were performed using a manually drawn region of interest (ROI) from a single slice of the ADC map, which holds limited ability to reflect the actual whole-tumor characteristics[13-15].

In the case of whole-lesion histogram analysis of the ADC, a volumetric ROI is positioned on the entire lesion over contiguous slices and a histogram of ADC values reflecting voxel frequency is constructed, leading to the improved evaluation of heterogeneity[16]. Based on this method, first-order heterogeneity parameters can be obtained, which assess the spectrum of ADC values gained from all

voxels within a volume of interest[17]. A growing number of studies have used ADC histogram parameters, as these analyses provide additional information that can aid in the discrimination between benign and malignant regions, or they can help to better characterize the response to treatment in different tumors, such as ovarian, prostate, and breast cancer[18-21]. The application of whole-volume ADC histogram analysis in rectal tumors is increasing in frequency as well, and the role of this parameter in predicting nCRT is promising but limited[22-25].

The purpose of this study was to investigate the imaging response to nCRT using DWI in patients with LARC. We hypothesized that the ADC histogram-derived parameter might better predict treatment responses to nCRT compared with ADC from the hotspot ROI, as histogram parameters can display the heterogeneous features of tumors.

MATERIALS AND METHODS

Patients

The institutional review board approved this retrospective study, and the requirement to obtain informed consent was waived given the study's retrospective nature. The study population was selected from LARC patients at our institution between February 2015 and October 2020. According to Enkhbaatar *et al*[23], we defined the inclusion criteria as follows: (1) Proven histopathology of rectal adenocarcinoma; (2) greater than stage T2 on pre-nCRT MR imaging; with or without regional lymph node metastases and no distant metastases; (3) pre- and post-nCRT rectal MRI imaging with diffusion-weighted (DW) imaging; (4) long-course nCRT; and (5) surgical resection. Mucinous tumors were excluded from this study.

Forty-eight patients were enrolled in the study (34 men and 14 women; age range: 28–84 years). All patients were further divided into two subgroups based on the pathological response of the primary tumor: responders (R) and non-responders (non-R). Only patients with grade 0 according to the TRG-Ryan system were regarded as patients with a complete pathological response (R), while patients with TRG 1-3 were non-R.

MRI protocol

All images were obtained on a 3T MRI system (Discovery MR 750w GEM®; General Electric Healthcare, Milwaukee, WI, United States) using a phased-array body coil. Intravenous antispasmodic agents were not administered, and patients received no bowel preparation before the MRI examination. Our study groups comprised patients who underwent pre-treatment MRI for primary tumor staging, and a second restaging MRI for response evaluation 6 wk after the completion of nCRT. The scanning protocol is listed in Table 1[23]. In brief, we obtained standard T2-weighted (T2W) spin-echo sequences in axial, coronal, and sagittal directions. To improve tumor tissue visualization (including the delineation of the muscular layer), these planes were planned perpendicular to the main axis of the tumor. Moreover, a T1W spin-echo sequence in an axial direction, as well as an axial non-enhanced DWI with b = 1200 s/mm^2, were acquired. ADC maps were automatically generated using the in-line software provided by the vendor during image acquisition. Additionally, axial, sagittal, and coronal fat-suppressed contrast T1W sequences were acquired and used to suppress the signal from adipose tissue. A gadolinium-based contrast agent (Gd-DTPA, Magnevist; Bayer Schering, Berlin, Germany) was used to enhance the quality of MRI. Representative images of our MRI protocol are provided in Figure 1.

Image analysis

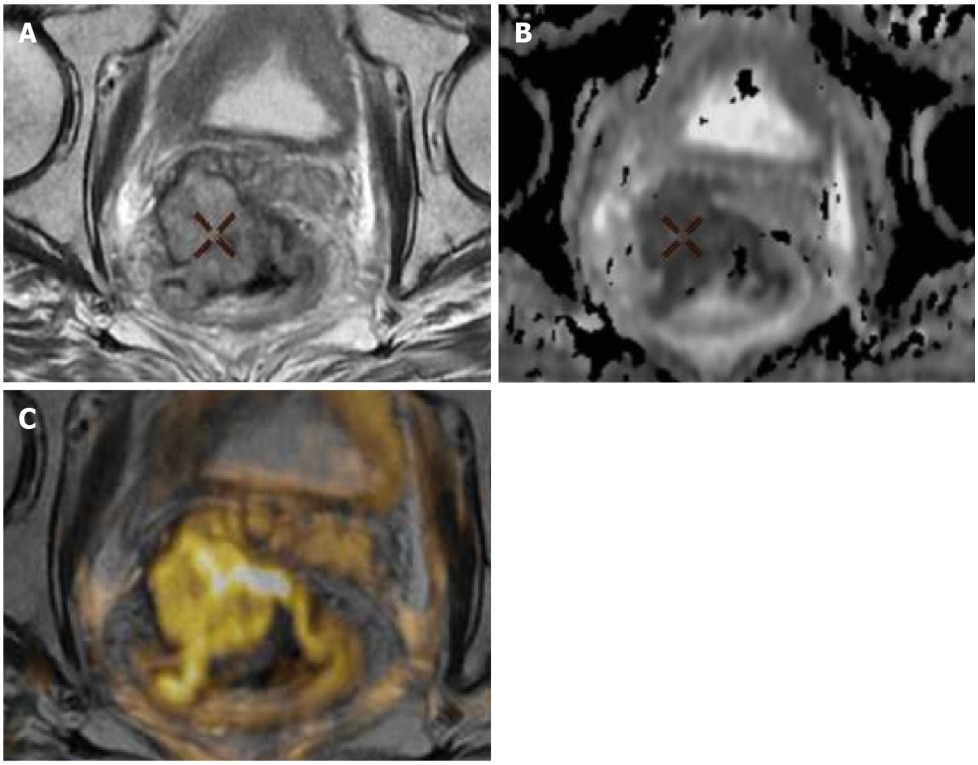
Two radiologists (JARP and MEJ, with 10 years and 5 years of experience in gastrointestinal imaging, respectively) reviewed the imaging studies and performed all tumor measurements on the pre- and post-nCRT images. At the initial review, each radiologist was blinded to the other radiologist's opinion. Also, they were blinded to the pathology results to assess interobserver and intraobserver variability. After that, the two radiologists would hold a discussion to arrive at a final decision by consensus. If a disagreement occurred, another radiologist with 25 years of experience (YVN) aided in making the final decision.

DWI analysis was performed with a workstation using the GE Advantage Workstation 4.6 software featuring the READYVIWER application (2006–2010; General Electric, Boston, MA, United States). On the pre-nCRT b1200 diffusion images, the tumor was defined as a focal mass with high signal intensity in comparison with the signal of the normal adjacent rectal wall. More precisely, the delineated ROIs covered the edge of each lesion, and the ROIs were drawn along the inner margin of the rectal walls to avoid intraluminal gas, water, and other contents. Further, necrotic areas, cysts, and vessels related to each lesion at the corresponding slice were also avoided, as identified on T2WI images. In addition, the highest and lowest slices of the DWI images were excluded given their partial volume effects[24]. After nCRT, the tumor was defined by focal areas of residual high signal, as identified on the b1200 images within the location of the primary tumor bed and/or corresponding with the residual tumor on T2WI MRI images as a reference standard. To compare and identify the tumor location, the pre-treatment images were at the readers' disposal when analyzing the post-treatment images.

Table 1 Magnetic resonance imaging sequences and data acquisition parameters

Parameter	Magnetic resonance imaging sequences							
	T2 FSE sagittal	T2 FSE axial	T2 FSE coronal	T1 FSE axial	DWI axial	T1 + GD axial	T1 + GD coronal	T1 + GD coronal
Repetition time in ms	5325	9890	7509	850	7750	435	295	265
Echo time in ms	102	102	102	Min	Min	Min	Min	Min
Slices, *n*	30	40	30	40	40	40	40	30
FOV	24	20	20	20	20	20	20	24
Slices thickness in mm	4	4	4	4	4	4	4	4
Broadband in Hz/Px	62.5	62.5	50	62.5	-	50	50	50
Phase	384	384	416	384	60	320	320	320
Acquisition time in min:s	2:35	3:08	2:45	3:53	5:18	2:31	2:16	2:02

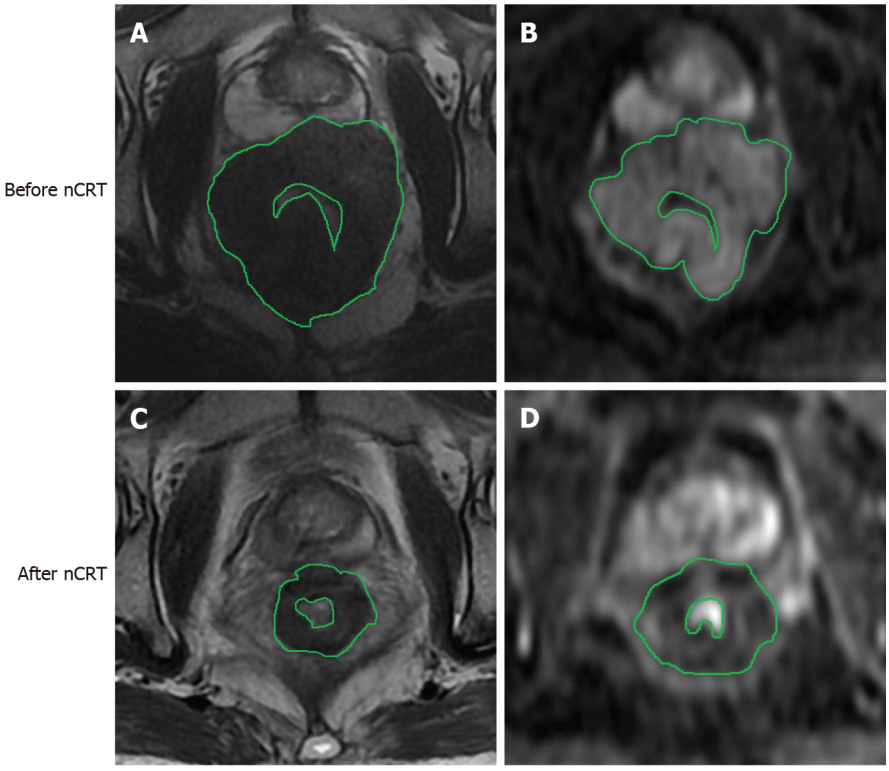
DWI: Diffusion-weighted imaging; FSE: Fast spin-echo; GD: Gadolinium; MRI: Magnetic resonance imaging.



DOI: 10.3748/wjg.v28.i23.2609 **Copyright** ©The Author(s) 2022.

Figure 1 Representative images of magnetic resonance imaging protocol. A-C: Axial T2 (A), apparent diffusion coefficient (ADC) map and T2 fusion ADC map color (B) and images of bulky tumor (C), showing tumor extending more than 5 mm into the mesorectal fat and invading the mesorectal fascia.

It should be noted that, in the first instance, one large ROI was placed to cover most of the largest axial tumor cross-section, which facilitated the calculation of the ADCmean values (ROI ADCmean). Thereafter, a volume of interest (VOI) was manually created on the ADC maps, where ROIs were drawn on all tumor slices (whole-lesion measurement). Within this VOI, the following parameters were calculated: (1) ADCmean, the average ADC value of all voxels within the VOI; (2) ADCn% (10^{th}, 25^{th}, 50^{th}, 75^{th}, and 90^{th} percentiles), the point at which the n% of the voxel values that formed the histogram were found to be at the left; (3) skewness, which measures the asymmetry of the distribution of values about the mean value; and (4) kurtosis, which is a measure of the 'peakedness' of the distribution of values in the ROI image. The corresponding frequency table for each lesion was exported, and the histogram parameters were computed by SPSS v. 26.0 (IBM Corporation, Armonk, NY, United States). Figure 2 is a schematic illustration of a representative ROI.



DOI: 10.3748/wjg.v28.i23.2609 **Copyright** ©The Author(s) 2022.

Figure 2 Images of rectal tumor before and after neoadjuvant chemoradiation therapy. A, C: T2-weighted magnetic resonance images obtained in 67-year-old man with a rectal tumor (histopathologic response Ryan 1) to evaluate tumor volume; B, D: Diffusion-weighted images (DWI) that were obtained from the same case. As we can see in the present case, regions of interest were drawn manually slice by slice on DWI images along the edge of the lesion to cover as much tumor area as possible without excluding cystic or necrotic areas. nCRT: Neoadjuvant chemoradiation therapy.

Histopathologic review

Specimens were evaluated according to an established protocol that was previously described by our research team[26]. In brief, fresh surgical specimens were evaluated to determine the quality of the mesorectal excision before being fixed in 4% formaldehyde for 48 h prior to sectioning. After fixation, the specimens were serially sectioned (in slices of 1 cm), and the mesorectal boundary was linked. When the residual tumor was visible, a minimum submission of four blocks was recommended. All mesorectal lymph nodes were histologically examined, as was the involvement of the circumferential resection margin. When no residual tumor cells were identified, each block was cut into 3 level sections, and immuhistochemistry for keratin was done. All hematoxylin and eosin slides were reviewed by an experienced pathologist (EHB, with 15 years of experience examining rectal cancer).

The pathologic response of the primary tumor was estimated using the modified Ryan's classification as follow[26,27]: TRG0, complete response with no viable cancer cells; TRG1 moderate response with single cancer cells or small groups of cancer cells; TRG2, minimal response with residual cancer outgrown by fibrosis, and TRG3, poor response with minimal or no tumor killing and extensive residual cancer.

Statistical analyses

The following formula was used to calculate changes in all metrics included in the current study: *PerC* = (Parameter post-treatment - Parameter pre-treatment) / Parameter pre−treatment × 100.

It must be noted that when pre- and post-nCRT kurtosis values were obtained, a result of +3.00 indicated the absence of kurtosis. To simplify the interpretation, we adjusted this result to 0 (*i.e.* kurtosis of –3 = 0). Thus, any reading other than 0 was referred to as an excess of kurtosis. On the other side, to negate division by 0 when calculating the percentage change in kurtosis, we added 3, *i.e.* [(Kurtosis post-treatment + 3) – (Kurtosis pre-treatment + 3) / (Kurtosis pre-treatment + 3)] × 100.

In the case of skewness, and to avoid dividing by 0, only change (not the percentage change) was used (*i.e.* skewness post treatment – skewness pre-treatment)[28]. As skewness did not have a lower bound such as kurtosis, the +/– sign was considered to calculate changes in this parameter. To compare variables among R and non-R, a Mann–Whitney *U* test (MWU) was applied, as the Kolmogorov-Smirnov test confirmed the non-normal distribution of any parameter included here. Accordingly, the data were presented as medians and interquartile ranges (IQR)[29]. When the differences in a variable were significant ($P < 0.05$) in the MWU test, the cut-off value, sensitivity, specificity, positive predictive

value, negative predictive value, area under the receiver operating characteristic (ROC) curve (AUC), and accuracy, were analyzed. The optimal cut-off values of ADCmean from the hot spot ROI and parameters derived from the histogram analysis of DWI were determined *via* the Youden index, while differences in the AUC were analyzed according to the method described by DeLong *et al*[30]. Furthermore, the diagnostic odd ratio (DOR) was designed to provide an additional measure of the performance of our potentially useful biomarkers to predict treatment response in LARC.

Finally, the intraobserver variability and interobserver variability were assessed using the intraclass correlation coefficient (ICC). For the agreement analysis, the outcomes were interpreted as follows, in accordance with Cicchetti (1994): 0.2 or less, poor agreement; 0.21–0.40, fair agreement; 0.41–0.60, moderate agreement; 0.61–0.74, good agreement; and 0.75–1.00, excellent agreement[31]. Statistical analyses were performed using SPSS v. 26. $P < 0.05$ was considered statistically significant.

RESULTS

Among the 58 patients that were originally included in this study, 10 had severe imaging artifacts. Thus, our final sample included 48 patients whose clinical and pathological characteristics are described in Table 2.

The median values and IQRs for the ROI ADCmean values and parameters derived from the histogram analysis of DWI are described in Table 3. Accordingly, post-nCRT kurtosis, as well as post-nCRT skewness, were significantly lower in R than in non-R (both $P < 0.001$, respectively). Furthermore, our results showed significant differences in the relative changes of kurtosis (Δ%kurtosis) between R and non-R ($P < 0.001$), with the largest loss of kurtosis in R. Additionally, median Δskewness displayed lower values in R than in non-R ($P < 0.001$).

We also found that patients with a favorable response (R) had higher post-nCRT ADC10th values than did non-R ($P = 0.036$). Correspondingly, the median values of Δ%ADC10th, Δ%ADCmean, and ROI Δ%ADCmean were also higher in R than in non-R, ($P = 0.020$, $P = 0.032$ and $P = 0.020$, respectively).

Receiver operating characteristics of those parameters that exhibited significant differences in the MWU test are reported in Table 4. The highest AUC values for predicting the treatment response in LARC were demonstrated by Δ%kurtosis, post-nCRT kurtosis, Δskewness and post-nCRT skewness (AUCs = 0.991, 0.985, 0.885, and 0.815, respectively). Meanwhile, the lowest diagnostic accuracy was observed in post-nCRT ADC10th (AUC = 0.681), Δ%ADCmean (AUC = 0.686), Δ%ADC10th (AUC = 0.589) and ROI Δ%ADCmean (AUC = 0.583).

The ROC curves for Δ%kurtosis, post-nCRT kurtosis, Δskewness, and post-nCRT skewness are displayed in Figure 3, while the comparison of AUC values between all of our potentially useful biomarkers for predicting the treatment response in LARC are presented in Supplementary Table 1.

It is important to mention that according to the DeLong analysis, no significant differences were found in the diagnostic accuracy of Δ%kurtosis and post-nCRT kurtosis. As well, no differences were demonstrated between Δskewness and post-nCRT skewness. However, the latter two parameters had lower accuracy than kurtosis-derivate metrics.

Finally, to verify the diagnostic accuracy of all metrics reported in Table 4, we calculated DORs. The DOR of a test is the ratio of the odds of positivity if a patient has a disease relative to the odds of positivity when a patient does not have a disease. The value of DOR ranges from 0 to infinity, with higher values indicating better discriminatory test performance[32,33]. As demonstrated in Table 5, Δ%kurtosis and post-nCRT kurtosis had the highest power of discrimination for treatment response by using DORs (approximately 376), followed by Δskewness (192.2) and post-nCRT skewness (168.6). Meanwhile, the lowest power of discrimination was observed in post-CRT ADC10th (5.48), Δ%ADCmean (4.26), Δ%ADC10th (3.65), and ROI Δ%ADCmean (3.47).

Regarding interobserver and intraobserver variability, the parameters derived from the histogram analysis of DWI, as well as the ADC values from the hotspot ROI, had an excellent agreement. The ICC measuring intraobserver variability ranges from 0.777-0.931 (Table 6), while the ICC measuring intraobserver variability ranges from 0.889-0.993 (Table 7).

DISCUSSION

Heterogeneity of malignant lesions is a feature that can be determined by characterizing changes in the histogram analysis of ADC values, which is recognized as a promising tool in cancer research when discerning between benign and malignant tumors or to better characterize the response to anti-cancer treatments[34-38].

This study focused on the ADCmean from the hot-spot ROI and a series of parameters corresponding to certain points on the ADC histogram using DWI, which have been proposed to predict treatment response in patients with rectal cancer[39,40]. As our results demonstrated, the parameters that changed significantly in response to nCRT were Δ%kurtosis, post-nCRT kurtosis, Δskewness, post-nCRT skewness, post-nCRT ADC10th, Δ%ADCmean, Δ%ADC10th, and ROI Δ%ADCmean. However, the

Table 2 Clinical and pathological characteristics of the patients' studies

Characteristics	*n* (%)
Sex	
Female	23 (48)
Male	25 (52)
RECIST 1.1	
Partial response	22 (46)
Stable disease	13 (27)
Progressive disease	13 (27)
Ryan's classification	
0	18 (38)
1	10 (21)
2	9 (19)
3	11 (22)
Treatment response	
Complete responders after nCRT	18 (38)
Non-responders' patients after nCRT	30 (62)
Tumor location	
Upper third	7 (15)
Middle third	14 (29)
Lower third	20 (41)
Diffuse	7 (15)
ypT stage	
T0	4 (8)
T1s	4 (8)
T1a	2 (4)
T2	8 (17)
T3	20 (42)
T4b	10 (21)
ypN stage	
N0	20 (42)
N1a	14 (29)
Nic	14 (29)
Degree of differentiation	
Well-differentiated adenocarcinoma	6 (13)
Moderately differentiated adenocarcinoma	35 (73)
Poorly differentiated adenocarcinoma	7 (14)
Surgical approach	
Low anterior resection	16 (33)
Intersphincteric resection	26 (54)
Abdominoperineal resection	6 (13)

nCRT: Neoadjuvant chemoradiation therapy.

Table 3 Median and interquartile range of pre- and post-neoadjuvant chemoradiation therapy parameters, as well as of changes between pre- and post-treatment values

	Responders	Non-responders	*P* value
Pre-nCRT parameters			
pre-nCRT ADCmean	0.75 (0.60-0.90)	0.85 (0.70-0.90)	0.146
10^{th} percentile	0.20 (0.17-0.23)	0.20 (0.17-0.26)	0.812
25th percentile	0.32 (0.29-0.35)	0.32 (0.23-0.41)	1.000
50^{th} percentile	0.40 (0.35-0.40)	0.40 (0.30-0.50)	0.698
75^{th} percentile	0.56 (0.47-0.58)	0.57 (0.45-0.63)	0.391
90^{th} percentile	0.71 (0.55-0.77)	0.76 (0.50-0.80)	0.556
Skewness	1.10 (0.90-1.14)	1.19 (0.88-1.37)	0.135
Kurtosis	0.89 (0.83-0.92)	0.92 (0.83-0.95)	0.296
ROI ADCmean	0.92 (0.80-1.20)	0.91 (0.83-0.93)	0.562
Post- nCRT parameters			
post- nCRT ADC_{mean}	1.20 (0.98-1.52)	1.10 (0.90-1.30)	0.065
10^{th} percentile	0.36 (0.30–0.37)	0.32 (0.31–0.34)	0.036[1]
25^{th} percentile	0.41 (0.40-0.52)	0.42 (0.41-0.50)	0.476
50^{th} percentile	0.66 (0.56-0.70)	0.65 (0.51-0.66)	0.127
75^{th} percentile	0.71 (0.67-0.80)	0.70 (0.66-0.75)	0.050
90^{th} percentile	0.89 (0.80-0.95)	0.80 (0.79-0.89)	0.105
Skewness	0.92 (0.60–1.14)	2.00 (1.15–2.67)	< 0.001[1]
Kurtosis	0.65 (0.59–0.72)	0.90 (0.80–0.90)	< 0.001[1]
ROI ADCmean	2.50 (1.50-2.70)	2.00 (1.80-2.30)	0.056
Changes between pre-treatment and post-treatment			
Δ%ADCmean	57% (14%–103%)	27% (0%–59%)	0.032[1]
Δ%$ADC10^{th}$	86% (37%–118%)	48% (11%–88%)	0.020[1]
Δ%$ADC25^{th}$	39% (19%-57%)	22% (0%-58%)	0.905
Δ%$ADC50^{th}$	70% (31%-86%)	31% (2%-65%)	0.067
Δ%$ADC75^{th}$	40% (20%-61%)	37% (0%-57%)	0.288
Δ%$ADC90^{th}$	27% (11%-58%)	9% (7%-119%)	0.061
Δskewness	–0.20 (–0.40–0.00)	0.49 (0.10–0.50)	< 0.001[1]
Δ%kurtosis	41% (18%–54%)	2.5% (1.4%–5.9%)	< 0.001[1]
ROI Δ%ADCmean	55% (48%–60%)	23% (15%–30%)	0.020[1]

[1]Statistically significant difference. ADC: Apparent diffusion coefficient; nCRT: Neoadjuvant chemoradiation therapy; ROI: Region of interest.

highest diagnostic accuracy was obtained for Δ%kurtosis, post-nCRT kurtosis, post-nCRT skewness, and Δskewness, suggesting that these metrics might be useful when selecting responders (TRG 0) for an organ preservation approach with either 'watch-and-wait' or local excision[39,40].

The results derivate from parameters with the highest diagnostic accuracy in predicting treatment response to nCRT in the current work are reviewed below.

First, we demonstrated that both post-nCRT kurtosis and post-nCRT skewness were significantly lower in R than in non-R. The overall trends from the histogram studies have shown that, following treatment, the histogram analysis of *DWI* and diffusion kurtosis imaging (DKI) shifted to the right upon decreased kurtosis and skewness in rectal cancer[39-43]. For example, in 2017, Hu *et al*[39] reported that the post-treatment mean kurtosis derived from DKI showed reduced values in R when compared with non-R patients, whereas Enkhbaatar *et al*[23] (2019) documented that the histogram of R presented negative changes in skewness following a loss of this parameter after therapy.

Table 4 Diagnostic performance of the best magnetic resonance imaging histogram derived parameters to detect responder patients

	Cutoff	Sensitivity	Specificity	PPV	NPV	Accuracy	AUC (95%CI)
Δ%kurtosis	11.85%	94.4%	96.7%	94.4%	96.7%	96.0%	0.991 (0.925-1.000)
Post-nCRT kurtosis	0.78	93.3%	99.0%	90%	99.0%	96.0%	0.985 (0.957-1.000)
Δskewness	0.16	66.7%	99.0%	64.3%	99.0%	79.2%	0.885 (0.795-0.975)
Post-nCRT skewness	1.59	63.3%	99.0%	62.0%	99.0%	77.1%	0.815 (0.795-0.634)
Post-nCRT ADC10th	0.34×10^{-3} mm^2/s	66.7%	73.3%	60.0%	79.0%	71.0%	0.681 (0.509-0.852)
Δ%ADCmean	56.00%	56.0%	77.0%	56.0%	73.3%	66.7%	0.686 (0.500-0.820
Δ%ADC10th	74.21%	61.1%	70.0%	55.0%	75.0%	66.7%	0.589 (0.483-0.815)
ROI Δ%ADCmean	55.00%	61.0%	69.0%	52.0%	72.0%	65.3%	0.583 (0.425-0.715)

ADC: Apparent diffusion coefficient; AUC: Area under the receiver operating characteristic curve; nCRT: Neoadjuvant chemoradiation therapy; NPV: Negative predictive value; PPV: Positive predictive value; ROI: Region of interest.

Table 5 Diagnostic odds ratios of magnetic resonance imaging parameters in differentiating respond and non- respond patients in locally advanced rectal cancer

	Diagnostic odds ratio	95%CI
Δ%kurtosis	376.0	228.9-842.1
Post-nCRT kurtosis	375.3	225.7-887.7
Δskewness	192.2	69.0-253.3
Post-nCRT skewness	168.6	54.0-251.7
Post-nCRT ADC10th	5.48	1.0-19.6
Δ%ADCmean	4.26	1.0-14.4
Δ%ADC10th	3.65	1.0-12.5
ROI Δ%ADCmean	3.47	1.0-11.2

ADC: Apparent diffusion coefficient; nCRT: Neoadjuvant chemoradiation therapy; ROI: Region of interest.

In the same way, kurtosis from R had greater reductions than from non-R, which indicates Gaussian or flatter distributions in patients with a complete response to the therapy. In biological tissues, it is believed that the non-Gaussian behavior (more precisely, a platykurtic curve) of water might occur because of a heterogeneous environment characterized by multiple compartments, organelles, and semipermeable membranes[44]. Thus, when an important reduction in kurtosis is noticed, a higher displacement of water molecules in DWI is assumed.

Furthermore, as mentioned above, negative changes of skewness after nCRT were seen in R, while non-R exhibited positive changes in this parameter. Negatively skewed curves show the majority of scores above the mean, and positively skewed curves are just the opposite[44]. In physiology, the association between changes in skewness and responses to antineoplastic therapy have not been fleshed out, but a curve negatively skewed suggests a loss of cellular structure[23]. Therefore, favorable treatment response is suspected.

Our MWU analysis also found differences between R and non-R across other parameters, such as ADC10th, Δ%ADCth, Δ%ADCmean and ROIΔ%ADCmean, as stated in our results section. However, both the ROC curve analysis and the DOR calculation indicated that only Δ%kurtosis, post-nCRT kurtosis, Δskewness, and post-nCRT skewness appear to predict a favorable response to the therapy, whereas the other metrics did not possess that predictive property.

Briefly, the Youden index calculation indicated that post-nCRT kurtosis, post-nCRT skewness, and Δskewness values below 0.78×10^{-3} mm^2/s, 1.59×10^{-3} mm^2/s, and 0.16, respectively, might be significant indicators of the occurrence of pCR. Meanwhile, Δ% changes above 11.85% also indicated a positive treatment effect with high accuracy. It is important to remember that, according to the DeLong analysis, the kurtosis-related parameters exhibit a better diagnostic performance than do skewness-related parameters.

Table 6 Intraobserver variability

		ICC	95%CI
Basal			
Test1 and test2, reader1	ROI ADCmean	0.850	0.742–0.800
Test1 and test2, reader2	ROI ADCmean	0.890	0.850-0.820
After treatment			
Test1 and test2, reader1	ROI ADCmean	0.800	0.750-0.819
Test1 and test2, reader2	ROI ADCmean	0.823	0.800-0.850
Basal			
Test1 and test2, reader1	ADCmean	0.850	0.756-0.920
Test1 and test2, reader2	ADCmean	0.777	0.745-0.812
After treatment			
Test1 and test2, reader1	ADCmean	0.845	0.830-0.850
Test1 and test2, reader2	ADCmean	0.823	0.800-0.833
Basal			
Test1 and test2, reader1	10^{th} percentile	0.820	0.880-0.950
Test1 and test2, reader2	10^{th} percentile	0.880	0.800-0.920
After treatment			
Test1 and test2, reader1	10^{th} percentile	0.780	0.740-0.853
Test1 and test2, reader2	10^{th} percentile	0.853	0.723-0.901
Basal			
Test1 and test2, reader1	25^{th} percentile	0.803	0.800-0.922
Test1 and test2, reader2	25^{th} percentile	0.863	0.801-0.895
After treatment			
Test1 and test2, reader1	25^{th} percentile	0.788	0.750-0.837
Test1 and test2, reader2	25^{th} percentile	0.820	0.780-0.846
Basal			
Test1 and test2, reader1	50^{th} percentile	0.850	0.840-0.920
Test1 and test2, reader2	50^{th} percentile	0.845	0.790-0.860
After treatment			
Test1 and test2, reader1	50^{th} percentile	0.821	0.800-0.913
Test1 and test2, reader2	50^{th} percentile	0.833	0.800-0.897
Basal			
Test1 and test2, reader1	75^{th} percentile	0.821	0.790-0.860
Test1 and test2, reader2	75^{th} percentile	0.859	0.820-0.920
After treatment			
Test1 and test2, reader1	75^{th} percentile	0.851	0.790-0.880
Test1 and test2, reader2	75^{th} percentile	0.837	0.791-0.856
Basal			
Test1 and test2, reader1	90^{th} percentile	0.850	0.820-0.890
Test1 and test2, reader2	90^{th} percentile	0.880	0.850-0.960
After treatment			
Test1 and test2, reader1	90^{th} percentile	0.831	0.800-0.902

Test1 and test2, reader2	90th percentile	0.901	0.850-0.975
Basal			
Test1 and test2, reader1	Skewness	0.920	0.900-0.940
Test1 and test2, reader2	Skewness	0.901	0.880-0.923
After treatment			
Test1 and test2, reader1	Skewness	0.931	0.920-0.950
Test1 and test2, reader2	Skewness	0.889	0.877-0.910
Basal			
Test1 and test2, reader1	Kurtosis	0.920	0.890-0.950
Test1 and test2, reader2	Kurtosis	0.910	0.850-0.960
After treatment			
Test1 and test2, reader1	Kurtosis	0.890	0.850-0.960
Test1 and test2, reader2	Kurtosis	0.880	0.840-0.982

ADC: Apparent diffusion coefficient; ICC: Intraclass correlation coefficient; ROI: Region of interest.

Table 7 Interobserver variability (intraclass correlation coefficient and 95% confidence intervals)

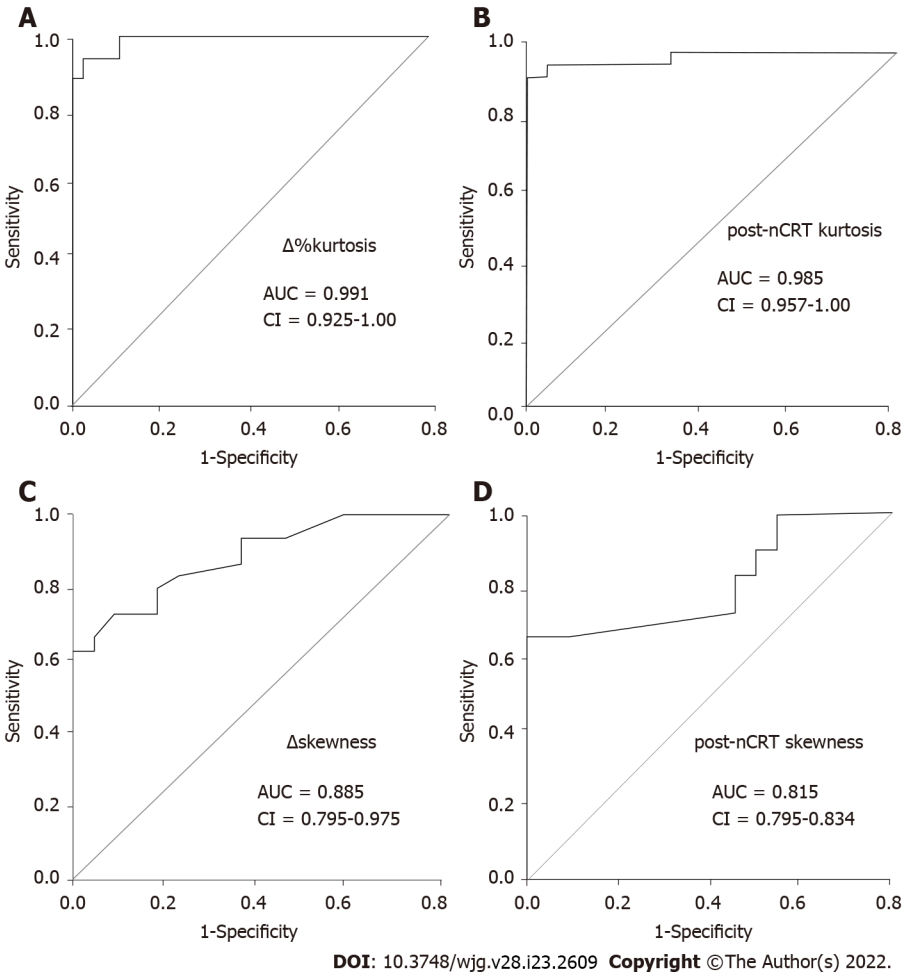
Pre-treatment	Reader one *vs* reader two	Post-treatment	Reader one *vs* reader two
ROI ADCmean	0.985 (1.900-0.999)	ROI ADCmean	0.889 (0.850-0.950)
ADCmean	0.989 (0.980–0.994)	ADCmean	0.990 (0.985-0.995)
10th percentile	0.972 (0.951–0.984)	10th percentile	0.992 (0.986–0.996)
25th percentile	0.970 (0.947–0.983)	25th percentile	0.950 (0.940-0.982)
50th percentile	0.986 (0.976–0.992)	50th percentile	0.987 (0.945-0.995)
75th percentile	0.989 (0.980–0.994)	75th percentile	0.990 (0.982–0.994)
90th percentile	0.989 (0.980–0.994)	90th percentile	0.972 (0.987–0.996)
Skewness	0.990 (0.982–0.994)	Skewness	0.993 (0.987–0.996)
Kurtosis	0.992 (0.986–0.995)	Kurtosis	0.972 (0.951–0.984)

ADC: Apparent diffusion coefficient; ROI: Region of interest.

Aligned with this finding, numerous authors have documented that kurtosis is more directly correlated to the underlying structural, physiological, molecular, and metabolic changes that occur during tumor progression than skewness[45]. This may be the reason why the kurtosis of ADC values has been used to indicate deviations from Gaussianity, even in the most challenging mathematical designs that predict the response to chemotherapy, such as radiomics analysis[46-48].

The results obtained from the ROC curved are partially supported by the estimated DORs, which were approximately 376 for both Δ%kurtosis and post-nCRT kurtosis. This means that for the cut-off points of Δ%kurtosis and post-nCRT kurtosis calculated here, the odds for positivity among subjects with a non-pCR was 376 times higher than the odds for positivity among subjects with a pCR. In the same way, Δskewness and post-nCRT skewness demonstrated respectable diagnostic performances with DOR values of 192.17 and 168.56, respectively. Although these values appear to be lower than DORs of Δ%kurtosis and post-nCRT kurtosis, the confidence intervals for these metrics clearly overlap, so we cannot conclude that the kurtosis-related parameters were statistically better than the skewness-related parameters using DOR.

Finally, this study confirm that ADC histogram analysis is a reproducible technique. Similarly, van Heeswijk *et al*[49] demonstrated that histogram-derived parameters had good interobserver agreement, with ICC values ranging from 0.80-0.98. This result supports the method's validity and suggests that it can be used in clinical practice. Furthermore, we utilized non-precise tumor delineation, which was quicker and produced comparable findings to those obtained by an expert radiologist's measurement, suggesting that this technique could be performed semiautomatically with an excellent interobserver agreement. This finding is very important when considering the implementation of histogram analysis



DOI: 10.3748/wjg.v28.i23.2609 **Copyright** ©The Author(s) 2022.

Figure 3 Receiver operating characteristic curves displaying the diagnostic performances of the four histogram parameters derived from apparent diffusion coefficient values with the highest accuracy. A: Δ%kurtosis; B: Post-neoadjuvant chemoradiation therapy (nCRT) kurtosis; C: Δskewness; D: Post-nCRT skewness. AUC: Area under the receiver operating characteristic curve.

in routine clinical practice.

Our study had important limitations. First, this was a retrospective, single-center evaluation. We believe that the present study might serve as a foundation for larger prospective studies in the future. Second, we included only a small number of patients (n = 48), while no validation group was included (both restricting the conception of a predictive model by using a multivariate logistic regression analysis). Third, the patient numbers among the different histopathologic TRGs were not well balanced. Only 18 patients (38%) achieved a histopathologic complete response, which may have introduced an element of statistical bias. However, these patients achieved a strict pCR, underlying the high degree of accuracy of our metrics. Fourth, the parameters obtained from the hotspot ROI were not conclusive enough to predict treatment response in the present study. This result is still in significant disagreement with our prior work where we demonstrated a high diagnostic accuracy of the Δ%ADCmean when distinguishing a pCR in rectal cancer by choosing a cutoff value of 55%[26]. Differences in research methods might explain this discrepancy, but we sustain that it is more reliable to use volumetric ROIs than one slice ROIs.

In summary, although further studies are needed to address the limitations of the current work, we demonstrated the benefits of considering measures other than the ROI ADCmean to evaluate the response to therapy in patients with LARC. Moreover, kurtosis and skewness have been selected by many radiomics studies of rectal cancer, emphasizing the importance of first-order statistics features for the assessment of therapy response[47,50]. Our results support the importance of these parameters, but they also helped us to standardize both the extraction and analysis of the data collected, which is a crucial step when developing and validating our own multiparametric model to predict treatment outcomes.

CONCLUSION

Based on the DWI technique, some whole-lesion histogram parameters could provide valuable information when diagnosing rectal cancer. In particular, kurtosis and skewness might be a useful indicator in the preoperative evaluation of a pCR in rectal cancer. Understanding skewness and kurtosis of the ADC parameters is the simplest way to recognize the deviation of Gaussianity, which indicates tumor heterogeneity. Moreover, we demonstrated high interobserver reliability for measurements of all of the histogram-derived parameters analyzed in the current work, addressing the challenges associated with replication that are well-known among more complex predictive models. Further long-term studies are needed to determine the ultimate clinical utility of our results.

ARTICLE HIGHLIGHTS

Research background

Studies have shown that successful treatment of many tumors can be detected using diffusion-weighted magnetic resonance imaging (MRI) as an increase in the apparent diffusion coefficient (ADC). However, findings from rectal cancer have been limited. Therefore, the criteria used for tumor staging and surveillance are largely based on anatomic criteria at this time. Broadly, whole lesion histogram analysis of ADC aims to fill this gap, extracting and analyzing the higher quantitative data with the aim of more accurate, tumor-specific evaluation and characterization.

Research motivation

ADC histogram parameters reflect the distribution and variation of all voxels within the entire lesion, which reduce the subjectivity of region of interest (ROI) placement and improves repeatability in the quantitative ADC analysis. Previous studies have applied volumetric ADC histogram analysis to predict treatment response of squamous carcinoma, breast cancers, and ovarian cancers. No ADC histogram study thus far has focused on locally advanced rectal cancer (LARC).

Research objectives

We aim to evaluate the effectiveness of whole lesion histogram analysis of ADC in the prediction to neoadjuvant chemoradiation therapy (nCRT) response in patients with LARC.

Research methods

This was a retrospective study. We collected data of 48 consecutive patients with histologically confirmed LARC. All patients underwent a pre-treatment MRI for primary tumor staging and a second restaging MRI for response evaluation. The sample was distributed as follows: responders (R), n = 18; and non-responders (non-R), n = 30. Eight parameters derived from the histogram analysis of ADC, as well as the ADCmean from the hot spot ROI, were obtained and compared between R and non-R. The diagnostic accuracy in the prediction of treatment response of all variables included in the present study was calculated as well.

Research results

Post-nCRT kurtosis, Δ%kurtosis, post-nCRT skewness an Δskewness exhibited the highest diagnostic performance in predicting a good response to nCRT.

Research conclusions

The results of our study support that histogram-parameters derived from ADC values can be used to stratify good responders into studies exploring individualized, less extensive treatment regimens, such as the omission of radiotherapy and less extensive surgery, or even deferral of surgery.

Research perspectives

We need to expand the sample size to confirm further the diagnostic accuracy of kurtosis and skewness. In addition, the long-term outcome of this analysis should be a radiomic model for predict treatment response in rectal cancer.

FOOTNOTES

Author contributions: Sollozo-Dupont I designed the study; Sollozo-Dupont I and Domínguez Osorio V analyzed the data; Domínguez Osorio V and Vela-Sarmiento I collected the data; Sollozo-Dupont I, Jiménez de los Santos ME, and Reyes-Pérez JA wrote the paper; Villaseñor-Navarro Y and Moreno-Astudillo L reviewed the study; Jiménez de los Santos ME and Reyes-Pérez JA contributed equally to this work; All authors contributed to the manuscript for

important intellectual content and approved the submission.

Institutional review board statement: The study protocol was approved by the Institutional Review Board of the National Cancer Institute from México, city, and was in accordance with the Declaration of Helsinki (Approval No. 2021/026).

Informed consent statement: Patients were not required to give informed consent to the study because the analysis used anonymous clinical data that were obtained after each patient agreed to treatment by written consent.

Conflict-of-interest statement: The authors have no conflicts of interest to declare.

Data sharing statement: The raw data supporting the conclusions of this article will be made available by the authors.

Open-Access: This article is an open-access article that was selected by an in-house editor and fully peer-reviewed by external reviewers. It is distributed in accordance with the Creative Commons Attribution NonCommercial (CC BY-NC 4.0) license, which permits others to distribute, remix, adapt, build upon this work non-commercially, and license their derivative works on different terms, provided the original work is properly cited and the use is non-commercial. See: https://creativecommons.org/Licenses/by-nc/4.0/

Country/Territory of origin: Mexico

ORCID number: Mayra Evelia Jiménez de Los Santos 0000-0003-1350-4761; Juan Armando Reyes-Pérez 0000-0002-1519-3613; Victor Domínguez Osorio 0000-0001-8660-7994; Yolanda Villaseñor-Navarro 0000-0001-5065-7922; Liliana Moreno-Astudillo 0000-0003-3125-708X; Itzel Vela-Sarmiento 0000-0002-6516-4212; Isabel Sollozo-Dupont 0000-0002-4569-3643.

S-Editor: Wang JL
L-Editor: Filipodia
P-Editor: Wang JL

REFERENCES

1 **Chen M**, Chen LZ, Xu L, Zhang JS, Song X. Neoadjuvant chemoradiation for locally advanced rectal cancer: a systematic review of the literature with network meta-analysis. *Cancer Manag Res* 2019; **11**: 741-758 [PMID: 30697067 DOI: 10.2147/CMAR.S189445]
2 **Ryan ÉJ**, Creavin B, Sheahan K. Delivery of Personalized Care for Locally Advanced Rectal Cancer: Incorporating Pathological, Molecular Genetic, and Immunological Biomarkers Into the Multimodal Paradigm. *Front Oncol* 2020; **10**: 1369 [PMID: 32923389 DOI: 10.3389/fonc.2020.01369]
3 **Curvo-Semedo L**, Lambregts DM, Maas M, Thywissen T, Mehsen RT, Lammering G, Beets GL, Caseiro-Alves F, Beets-Tan RG. Rectal cancer: assessment of complete response to preoperative combined radiation therapy with chemotherapy--conventional MR volumetry versus diffusion-weighted MR imaging. *Radiology* 2011; **260**: 734-743 [PMID: 21673229 DOI: 10.1148/radiol.11102467]
4 **Spring LM**, Fell G, Arfe A, Sharma C, Greenup R, Reynolds KL, Smith BL, Alexander B, Moy B, Isakoff SJ, Parmigiani G, Trippa L, Bardia A. Pathologic Complete Response after Neoadjuvant Chemotherapy and Impact on Breast Cancer Recurrence and Survival: A Comprehensive Meta-analysis. *Clin Cancer Res* 2020; **26**: 2838-2848 [PMID: 32046998 DOI: 10.1158/1078-0432.CCR-19-3492]
5 **Chen W**, Mao L, Li L, Wei Q, Hu S, Ye Y, Feng J, Liu B, Liu X. Predicting Treatment Response of Neoadjuvant Chemoradiotherapy in Locally Advanced Rectal Cancer Using Amide Proton Transfer MRI Combined With Diffusion-Weighted Imaging. *Front Oncol* 2021; **11**: 698427 [PMID: 34277445 DOI: 10.3389/fonc.2021.698427]
6 **Chen L**, Liu M, Bao J, Xia Y, Zhang J, Zhang L, Huang X, Wang J. The correlation between apparent diffusion coefficient and tumor cellularity in patients: a meta-analysis. *PLoS One* 2013; **8**: e79008 [PMID: 24244402 DOI: 10.1371/journal.pone.0079008]
7 **Vossen JA**, Buijs M, Geschwind JF, Liapi E, Prieto Ventura V, Lee KH, Bluemke DA, Kamel IR. Diffusion-weighted and Gd-EOB-DTPA-contrast-enhanced magnetic resonance imaging for characterization of tumor necrosis in an animal model. *J Comput Assist Tomogr* 2009; **33**: 626-630 [PMID: 19638862 DOI: 10.1097/RCT.0b013e3181953df3]
8 **Dzik-Jurasz A**, Domenig C, George M, Wolber J, Padhani A, Brown G, Doran S. Diffusion MRI for prediction of response of rectal cancer to chemoradiation. *Lancet* 2002; **360**: 307-308 [PMID: 12147376 DOI: 10.1016/S0140-6736(02)09520-X]
9 **Lambregts DM**, Vandecaveye V, Barbaro B, Bakers FC, Lambrecht M, Maas M, Haustermans K, Valentini V, Beets GL, Beets-Tan RG. Diffusion-weighted MRI for selection of complete responders after chemoradiation for locally advanced rectal cancer: a multicenter study. *Ann Surg Oncol* 2011; **18**: 2224-2231 [PMID: 21347783 DOI: 10.1245/s10434-011-1607-5]
10 **Xie H**, Sun T, Chen M, Wang H, Zhou X, Zhang Y, Zeng H, Wang J, Fu W. Effectiveness of the apparent diffusion coefficient for predicting the response to chemoradiation therapy in locally advanced rectal cancer: a systematic review and meta-analysis. *Medicine (Baltimore)* 2015; **94**: e517 [PMID: 25674749 DOI: 10.1097/MD.0000000000000517]
11 **Tarallo N**, Angeretti MG, Bracchi E, Xhepa G, Molinelli V, Tagliaferri C, Antognoni P, Novario R, Sessa F, Fugazzola C. Magnetic resonance imaging in locally advanced rectal cancer: quantitative evaluation of the complete response to neoadjuvant therapy. *Pol J Radiol* 2018; **83**: e600-e609 [PMID: 30800199 DOI: 10.5114/pjr.2018.81156]
12 **Meng X**, Huang Z, Wang R, Yu J. Prediction of response to preoperative chemoradiotherapy in patients with locally

advanced rectal cancer. *Biosci Trends* 2014; **8**: 11-23 [PMID: 24647108 DOI: 10.5582/bst.8.11]
13 **Gu J**, Khong PL, Wang S, Chan Q, Law W, Zhang J. Quantitative assessment of diffusion-weighted MR imaging in patients with primary rectal cancer: correlation with FDG-PET/CT. *Mol Imaging Biol* 2011; **13**: 1020-1028 [PMID: 20872077 DOI: 10.1007/s11307-010-0433-7]
14 **Marzi S**, Minosse S, Vidiri A, Piludu F, Giannelli M. Diffusional kurtosis imaging in head and neck cancer: On the use of trace-weighted images to estimate indices of non-Gaussian water diffusion. *Med Phys* 2018; **45**: 5411-5419 [PMID: 30317646 DOI: 10.1002/mp.13238]
15 **Guo Y**, Kong QC, Li LQ, Tang WJ, Zhang WL, Ning GY, Xue J, Zhou QW, Liang YY, Wu M, Jiang XQ. Whole Volume Apparent Diffusion Coefficient (ADC) Histogram as a Quantitative Imaging Biomarker to Differentiate Breast Lesions: Correlation with the Ki-67 Proliferation Index. *Biomed Res Int* 2021; **2021**: 4970265 [PMID: 34258262 DOI: 10.1155/2021/4970265]
16 **Tang WJ**, Jin Z, Zhang YL, Liang YS, Cheng ZX, Chen LX, Liang YY, Wei XH, Kong QC, Guo Y, Jiang XQ. Whole-Lesion Histogram Analysis of the Apparent Diffusion Coefficient as a Quantitative Imaging Biomarker for Assessing the Level of Tumor-Infiltrating Lymphocytes: Value in Molecular Subtypes of Breast Cancer. *Front Oncol* 2020; **10**: 611571 [PMID: 33489920 DOI: 10.3389/fonc.2020.611571]
17 **Ao W**, Bao X, Mao G, Yang G, Wang J, Hu J. Value of Apparent Diffusion Coefficient for Assessing Preoperative T Staging of Low Rectal Cancer and Whether This Is Correlated With Ki-67 Expression. *Can Assoc Radiol J* 2020; **71**: 5-11 [PMID: 32063001 DOI: 10.1177/0846537119885666]
18 **Donati OF**, Mazaheri Y, Afaq A, Vargas HA, Zheng J, Moskowitz CS, Hricak H, Akin O. Prostate cancer aggressiveness: assessment with whole-lesion histogram analysis of the apparent diffusion coefficient. *Radiology* 2014; **271**: 143-152 [PMID: 24475824 DOI: 10.1148/radiol.13130973]
19 **Li HM**, Zhang R, Gu WY, Zhao SH, Lu N, Zhang GF, Peng WJ, Qiang JW. Whole solid tumour volume histogram analysis of the apparent diffusion coefficient for differentiating high-grade from low-grade serous ovarian carcinoma: correlation with Ki-67 proliferation status. *Clin Radiol* 2019; **74**: 918-925 [PMID: 31471063 DOI: 10.1016/j.crad.2019.07.019]
20 **Liu HL**, Zong M, Wei H, Wang C, Lou JJ, Wang SQ, Zou QG, Jiang YN. Added value of histogram analysis of apparent diffusion coefficient maps for differentiating triple-negative breast cancer from other subtypes of breast cancer on standard MRI. *Cancer Manag Res* 2019; **11**: 8239-8247 [PMID: 31564982 DOI: 10.2147/CMAR.S210583]
21 **Lu J**, Li HM, Cai SQ, Zhao SH, Ma FH, Li YA, Ma XL, Qiang JW. Prediction of Platinum-based Chemotherapy Response in Advanced High-grade Serous Ovarian Cancer: ADC Histogram Analysis of Primary Tumors. *Acad Radiol* 2021; **28**: e77-e85 [PMID: 32061467 DOI: 10.1016/j.acra.2020.01.024]
22 **Cho SH**, Kim GC, Jang YJ, Ryeom H, Kim HJ, Shin KM, Park JS, Choi GS, Kim SH. Locally advanced rectal cancer: post-chemoradiotherapy ADC histogram analysis for predicting a complete response. *Acta Radiol* 2015; **56**: 1042-1050 [PMID: 25270374 DOI: 10.1177/0284185114550193]
23 **Enkhbaatar NE**, Inoue S, Yamamuro H, Kawada S, Miyaoka M, Nakamura N, Sadahiro S, Imai Y. MR Imaging with Apparent Diffusion Coefficient Histogram Analysis: Evaluation of Locally Advanced Rectal Cancer after Chemotherapy and Radiation Therapy. *Radiology* 2018; **288**: 129-137 [PMID: 29558294 DOI: 10.1148/radiol.2018171804]
24 **Peng Y**, Tang H, Hu X, Shen Y, Kamel I, Li Z, Hu D. Rectal Cancer Invasiveness: Whole-Lesion Diffusion-Weighted Imaging (DWI) Histogram Analysis by Comparison of Reduced Field-of-View and Conventional DWI Techniques. *Sci Rep* 2019; **9**: 18760 [PMID: 31822707 DOI: 10.1038/s41598-019-55059-0]
25 **Peng Y**, Tang H, Meng X, Shen Y, Hu D, Kamel I, Li Z. Histological grades of rectal cancer: whole-volume histogram analysis of apparent diffusion coefficient based on reduced field-of-view diffusion-weighted imaging. *Quant Imaging Med Surg* 2020; **10**: 243-256 [PMID: 31956546 DOI: 10.21037/qims.2019.11.17]
26 **Jiménez de Los Santos ME**, Reyes-Pérez JA, Sandoval-Nava RM, Villalobos-Juárez JL, Villaseñor-Navarro Y, Vela-Sarmiento I, Sollozo-Dupont I. The apparent diffusion coefficient is a useful biomarker in predicting treatment response in patients with locally advanced rectal cancer. *Acta Radiol Open* 2020; **9**: 2058460120957295 [PMID: 32974055 DOI: 10.1177/2058460120957295]
27 **Edge SB**, Compton CC. The American Joint Committee on Cancer: the 7th edition of the AJCC cancer staging manual and the future of TNM. *Ann Surg Oncol* 2010; **17**: 1471-1474 [PMID: 20180029 DOI: 10.1245/s10434-010-0985-4]
28 **Haider MA**, Vosough A, Khalvati F, Kiss A, Ganeshan B, Bjarnason GA. CT texture analysis: a potential tool for prediction of survival in patients with metastatic clear cell carcinoma treated with sunitinib. *Cancer Imaging* 2017; **17**: 4 [PMID: 28114978 DOI: 10.1186/s40644-017-0106-8]
29 **Stroup DF**, Smith CK, Truman BI. Reporting the methods used in public health research and practice. *J Public Health Emerg* 2017; **1** [PMID: 29417955 DOI: 10.21037/jphe.2017.12.01]
30 **DeLong ER**, DeLong DM, Clarke-Pearson DL. Comparing the areas under two or more correlated receiver operating characteristic curves: a nonparametric approach. *Biometrics* 1988; **44**: 837-845 [PMID: 3203132]
31 **Cicchetti DV**. Guidelines, criteria, and rules of thumb for evaluating normed and standardized assessment instruments in psychology. *Psychol Assess* 1994; **6**: 284-290 [DOI: 10.1037/1040-3590.6.4.284]
32 **Glas AS**, Lijmer JG, Prins MH, Bonsel GJ, Bossuyt PM. The diagnostic odds ratio: a single indicator of test performance. *J Clin Epidemiol* 2003; **56**: 1129-1135 [PMID: 14615004 DOI: 10.1016/s0895-4356(03)00177-x]
33 **Chang SM**, Matchar DB, Gerald W Smetana GW, Umscheid CA. Methods Guide for Medical Test Reviews. Rockville: Agency for Healthcare Research and Quality (US), 2012 [PMID: 22834019]
34 **Le Bihan D**, Iima M. Diffusion Magnetic Resonance Imaging: What Water Tells Us about Biological Tissues. *PLoS Biol* 2015; **13**: e1002203 [PMID: 26204162 DOI: 10.1371/journal.pbio.1002203]
35 **Pyatigorskaya N**, Le Bihan D, Reynaud O, Ciobanu L. Relationship between the diffusion time and the diffusion MRI signal observed at 17.2 Tesla in the healthy rat brain cortex. *Magn Reson Med* 2014; **72**: 492-500 [PMID: 24022863 DOI: 10.1002/mrm.24921]
36 **Just N**. Improving tumour heterogeneity MRI assessment with histograms. *Br J Cancer* 2014; **111**: 2205-2213 [PMID: 25268373 DOI: 10.1038/bjc.2014.512]

37 **O'Connor JP**, Rose CJ, Waterton JC, Carano RA, Parker GJ, Jackson A. Imaging intratumor heterogeneity: role in therapy response, resistance, and clinical outcome. *Clin Cancer Res* 2015; **21**: 249-257 [PMID: 25421725 DOI: 10.1158/1078-0432.CCR-14-0990]

38 **Rosenkrantz AB**. Histogram-based apparent diffusion coefficient analysis: an emerging tool for cervical cancer characterization? *AJR Am J Roentgenol* 2013; **200**: 311-313 [PMID: 23345351 DOI: 10.2214/AJR.12.9926]

39 **Hu F**, Tang W, Sun Y, Wan D, Cai S, Zhang Z, Grimm R, Yan X, Fu C, Tong T, Peng W. The value of diffusion kurtosis imaging in assessing pathological complete response to neoadjuvant chemoradiation therapy in rectal cancer: a comparison with conventional diffusion-weighted imaging. *Oncotarget* 2017; **8**: 75597-75606 [PMID: 29088894 DOI: 10.18632/oncotarget.17491]

40 **Xie H**, Wu G. Application of Diffusion Kurtosis Imaging and Histogram Analysis for Assessing Preoperative Stages of Rectal Cancer. *Gastroenterol Res Pract* 2018; **2018**: 9786932 [PMID: 29967642 DOI: 10.1155/2018/9786932]

41 **Sun YS**, Zhang XP, Tang L, Ji JF, Gu J, Cai Y, Zhang XY. Locally advanced rectal carcinoma treated with preoperative chemotherapy and radiation therapy: preliminary analysis of diffusion-weighted MR imaging for early detection of tumor histopathologic downstaging. *Radiology* 2010; **254**: 170-178 [PMID: 20019139 DOI: 10.1148/radiol.2541082230]

42 **Traverso A**, Kazmierski M, Shi Z, Kalendralis P, Welch M, Nissen HD, Jaffray D, Dekker A, Wee L. Stability of radiomic features of apparent diffusion coefficient (ADC) maps for locally advanced rectal cancer in response to image pre-processing. *Phys Med* 2019; **61**: 44-51 [PMID: 31151578 DOI: 10.1016/j.ejmp.2019.04.009]

43 **Choi MH**, Oh SN, Rha SE, Choi JI, Lee SH, Jang HS, Kim JG, Grimm R, Son Y. Diffusion-weighted imaging: Apparent diffusion coefficient histogram analysis for detecting pathologic complete response to chemoradiotherapy in locally advanced rectal cancer. *J Magn Reson Imaging* 2016; **44**: 212-220 [PMID: 26666560 DOI: 10.1002/jmri.25117]

44 **Wedeen VJ**, Hagmann P, Tseng WY, Reese TG, Weisskoff RM. Mapping complex tissue architecture with diffusion spectrum magnetic resonance imaging. *Magn Reson Med* 2005; **54**: 1377-1386 [PMID: 16247738 DOI: 10.1002/mrm.20642]

45 **De Robertis R**, Maris B, Cardobi N, Tinazzi Martini P, Gobbo S, Capelli P, Ortolani S, Cingarlini S, Paiella S, Landoni L, Butturini G, Regi P, Scarpa A, Tortora G, D'Onofrio M. Can histogram analysis of MR images predict aggressiveness in pancreatic neuroendocrine tumors? *Eur Radiol* 2018; **28**: 2582-2591 [PMID: 29352378 DOI: 10.1007/s00330-017-5236-7]

46 **Dinapoli N**, Barbaro B, Gatta R, Chiloiro G, Casà C, Masciocchi C, Damiani A, Boldrini L, Gambacorta MA, Dezio M, Mattiucci GC, Balducci M, van Soest J, Dekker A, Lambin P, Fiorino C, Sini C, De Cobelli F, Di Muzio N, Gumina C, Passoni P, Manfredi R, Valentini V. Magnetic Resonance, Vendor-independent, Intensity Histogram Analysis Predicting Pathologic Complete Response After Radiochemotherapy of Rectal Cancer. *Int J Radiat Oncol Biol Phys* 2018; **102**: 765-774 [PMID: 29891200 DOI: 10.1016/j.ijrobp.2018.04.065]

47 **Cui Y**, Yang X, Shi Z, Yang Z, Du X, Zhao Z, Cheng X. Radiomics analysis of multiparametric MRI for prediction of pathological complete response to neoadjuvant chemoradiotherapy in locally advanced rectal cancer. *Eur Radiol* 2019; **29**: 1211-1220 [PMID: 30128616 DOI: 10.1007/s00330-018-5683-9]

48 **Chen H**, Shi L, Nguyen KNB, Monjazeb AM, Matsukuma KE, Loehfelm TW, Huang H, Qiu J, Rong Y. MRI Radiomics for Prediction of Tumor Response and Downstaging in Rectal Cancer Patients after Preoperative Chemoradiation. *Adv Radiat Oncol* 2020; **5**: 1286-1295 [PMID: 33305090 DOI: 10.1016/j.adro.2020.04.016]

49 **van Heeswijk MM**, Lambregts DMJ, Maas M, Lahaye MJ, Ayas Z, Slenter JMGM, Beets GL, Bakers FCH, Beets-Tan RGH. Measuring the apparent diffusion coefficient in primary rectal tumors: is there a benefit in performing histogram analyses? *Abdom Radiol (NY)* 2017; **42**: 1627-1636 [PMID: 28160039 DOI: 10.1007/s00261-017-1062-2]

50 **Nie K**, Shi L, Chen Q, Hu X, Jabbour SK, Yue N, Niu T, Sun X. Rectal Cancer: Assessment of Neoadjuvant Chemoradiation Outcome based on Radiomics of Multiparametric MRI. *Clin Cancer Res* 2016; **22**: 5256-5264 [PMID: 27185368 DOI: 10.1158/1078-0432.CCR-15-2997]

World Journal of Gastroenterology

Submit a Manuscript: https://www.f6publishing.com

World J Gastroenterol 2022 June 21; 28(23): 2625-2632

DOI: 10.3748/wjg.v28.i23.2625

ISSN 1007-9327 (print) ISSN 2219-2840 (online)

CASE REPORT

Primary gastric dedifferentiated liposarcoma resected endoscopically: A case report

Joon Hyun Cho, Jun Hyeon Byeon, Si Hyung Lee

Specialty type: Gastroenterology and hepatology

Provenance and peer review: Unsolicited article; Externally peer reviewed.

Peer-review model: Single blind

Peer-review report's scientific quality classification

Grade A (Excellent): 0
Grade B (Very good): B, B
Grade C (Good): 0
Grade D (Fair): 0
Grade E (Poor): 0

P-Reviewer: Zhang X, United States; Zhao JW, China

Received: December 18, 2021
Peer-review started: December 18, 2021
First decision: January 23, 2022
Revised: January 29, 2022
Accepted: May 5, 2022
Article in press: May 5, 2022
Published online: June 21, 2022

Joon Hyun Cho, Jun Hyeon Byeon, Si Hyung Lee, Division of Gastroenterology and Hepatology, Department of Internal Medicine, Yeungnam University College of Medicine, Daegu 42415, South Korea

Corresponding author: Si Hyung Lee, MD, Professor, Division of Gastroenterology and Hepatology, Department of Internal Medicine, Yeungnam University College of Medicine, 170 Hyeonchung-ro, Nam-gu, Daegu 42415, South Korea. dr9696@gmail.com

Abstract

BACKGROUND

Liposarcoma is one of the most common adult mesenchymal tumors but is uncommon in the gastrointestinal tract and extremely rare in the stomach. Furthermore, the histological subtypes of liposarcoma usually reported in the stomach are well-differentiated or myxoid, and few reports have been issued on small-sized gastric liposarcomas resected endoscopically and followed up. Herein, we report a case of primary gastric dedifferentiated liposarcoma (DL) that was resected endoscopically.

CASE SUMMARY

A 67-year-old female Korean patient was referred to our institution for further evaluation of a gastric submucosal tumor (SMT) located in the lesser curvature of the gastric body by esophagogastroduodenoscopy. Endoscopic ultrasound revealed a well-circumscribed, slightly heterogeneous, isoechoic, 17 mm × 10 mm sized mass originating from the third sonographic layer. Computed tomography showed no evidence of significant lymph node enlargement or distant metastasis. Endoscopic resection was undertaken using the snare resection technique after mucosal precutting to provide a definitive histopathologic diagnosis, which proved to be consistent with DL, based on its morphology and the immunoexpressions of MDM2 and CDK4. The patient was planned for surgery because the deep resection margin was positive for malignancy. After declining any invasive procedure or adjuvant treatment, the patient was placed under close follow-up, and at one year after endoscopic resection, remained disease free.

CONCLUSION

This is the first reported case of a small primary gastric DL resected endoscopically and followed up. This report demonstrates that when diagnosis of a SMT is uncertain, the use of invasive techniques, including endoscopic resection, should be considered.

Key Words: Gastric liposarcoma; Dedifferentiated liposarcoma; Submucosal tumor; Endoscopic resection; Case report

©The Author(s) 2022. Published by Baishideng Publishing Group Inc. All rights reserved.

Core Tip: Liposarcoma is uncommon in the gastrointestinal tract and rarely encountered in the stomach. Furthermore, the dedifferentiated histologic subtype has not been previously reported in the stomach in the English literature. We experienced a case of a small (1.7 cm) primary gastric dedifferentiated liposarcoma, which was resected endoscopically. This report cautions that if a diagnosis of submucosal tumor is uncertain, the use of aggressive techniques, including endoscopic resection, should be considered.

Citation: Cho JH, Byeon JH, Lee SH. Primary gastric dedifferentiated liposarcoma resected endoscopically: A case report. *World J Gastroenterol* 2022; 28(23): 2625-2632
URL: https://www.wjgnet.com/1007-9327/full/v28/i23/2625.htm
DOI: https://dx.doi.org/10.3748/wjg.v28.i23.2625

INTRODUCTION

Liposarcoma is one of the most common adult soft tissue sarcomas and has a peak incidence between the ages 50 and 65 and a prevalence of 15%-20% among all sarcoma patients[1]. There are four histological subtypes of liposarcomas[2]. Atypical lipomatous tumor/well-differentiated liposarcoma (WDL) is the most common subtype followed by dedifferentiated liposarcoma (DL), which frequently occurs in retroperitoneum[3,4]. The myxoid and pleomorphic types usually present in the extremities [5]. Thus, liposarcoma usually arises in deep soft tissues of the proximal extremities, retroperitoneum, or trunk[6], and is encountered in the gastrointestinal tract in only 2% of cases[7].

The majority of liposarcomas of the alimentary tract arise in the esophagus[8], and liposarcomas originating at more distal sites, such as stomach, small intestine, and large intestine, are rare[9]. Less than 40 cases of primary liposarcoma of the stomach have been described in the medical literature, and the most reported histological subtypes of gastric liposarcoma are WDL and myxoid liposarcoma[10]. In fact, no report on DL of the stomach has been published in the English literature, though one case report on DL of the gastroesophageal junction was issued in 2018[11]. Here, we describe the first case of a small primary gastric DL resected endoscopically and provide a review of the literature.

CASE PRESENTATION

Chief complaints

A 67-year-old female Korean patient was referred to our institution for further evaluation and treatment of a gastric submucosal tumor (SMT) incidentally discovered by esophagogastroduodenoscopy (EGD) during a routine medical check-up.

History of present illness

The patient had experienced no abdominal pain or discomfort.

History of past illness

She had a history of breast conserving surgery due to breast cancer 6 years previously.

Personal and family history

The patient had diabetes and was being treated with oral hypoglycemic agents. She was a non-smoker and non-alcohol drinker and had no significant family history.

Physical examination

Physical examination was unremarkable, and her abdomen was soft, nontender, and nondistended with no palpable mass.

Laboratory examinations

Laboratory tests, which included common serum tumor markers such as carcinoembryonic antigen (CEA) and carbohydrate antigen 19-9 (CA 19-9), were normal.

Imaging examinations

EGD revealed a SMT-like protruding lesion of approximately 15 mm diameter located in the posterior wall of the lesser curvature of the distal part of the gastric body (Figure 1A). The lesion was covered with normally appearing mucosa except for focal mucosal erythema and depression over the lesion. Gastric endoscopic ultrasonography (EUS) examination demonstrated a well-demarcated mass, which measured 17 mm × 10 mm, located in the third layer of the gastric wall. The echo pattern of the mass was slightly heterogeneous and isoechoic (Figure 1B), but its EUS appearance was insufficient for diagnosis. The differential diagnosis included lipoma, neuroendocrine tumor, and ectopic pancreas. Initial biopsy specimens obtained at the site of the focal mucosal erythema and depression were negative for a neoplasm. Computed tomography (CT) of the abdomen showed a well-enhanced, intraluminal protruding polypoid lesion arising from the gastric body but no evidence of lymph node enlargement or distant metastasis (Figure 2).

FINAL DIAGNOSIS

After initial work-up, endoscopic resection was conducted using the snare resection technique after mucosal precutting for a definitive histopathologic result (Figure 3). At gross examination, the tumor was whitish yellow, well-shaped, and solid. Histopathologic examination showed the tumor was located submucosally and primarily composed of spindle-shaped atypical cells with pleomorphic and hyperchromatic nuclei and indistinct pale cytoplasm (Figure 4A-D). Deep resection margins were positive for tumor. Immunohistochemical staining performed for the differential diagnosis of gastrointestinal stromal tumor, schwannoma, leiomyosarcoma, malignant melanoma, and any poorly or undifferentiated sarcoma, revealed tumor cells were negative for CD117, DOG1, CD34, SMA, S-100, Desmin, HMB45, and SOX10, but positive for MDM2 and CDK4 nuclear staining (Figure 4E and F). Based on these findings, the histopathological diagnosis was consistent with DL.

TREATMENT

The patient was planned for surgery because the deep resection margin was positive for DL, but declined any invasive procedure or adjuvant treatment.

OUTCOME AND FOLLOW-UP

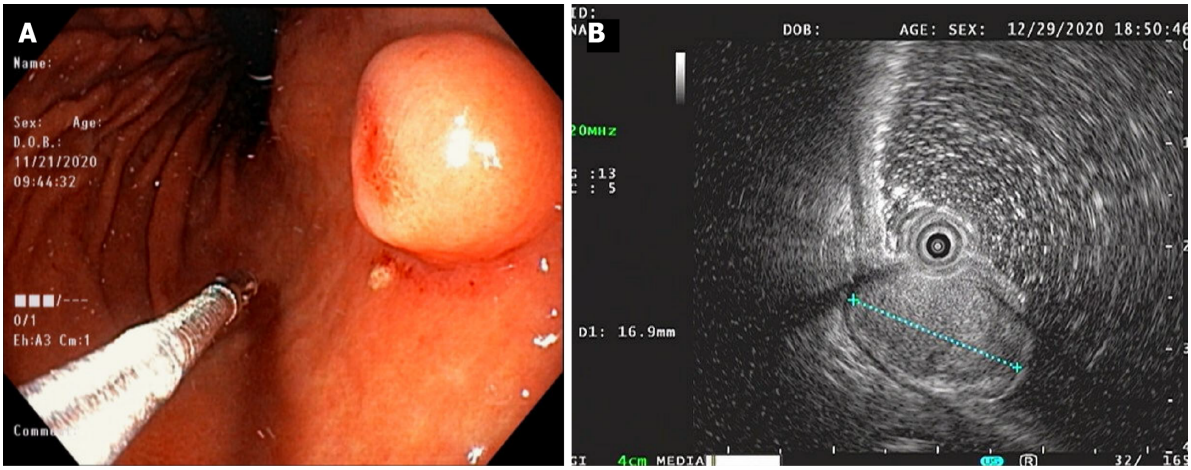
She remains under close follow-up, which includes biannual CT scanning and EGD, and at one year after endoscopic resection remained disease free.

DISCUSSION

Although they are the most common mesenchymal neoplasms, liposarcomas are rarely found in the gastrointestinal tract. Since the disease was first described by Abrams *et al*[12] in 1941, fewer than 40 cases of gastric liposarcoma have been reported in the literature worldwide[10]. The etiology of gastric liposarcoma remains uncertain, though some patients have a family history of soft tissue neoplasms, which suggests the involvement of genetic factors[13]. Gastric liposarcomas originate due to the proliferation of undifferentiated mesenchymal cells within submucosa and the tunica muscularis layer of stomach, and an exophytic growth is typical[10,14]. Most gastric liposarcomas are located in the antrum or lesser curvature.

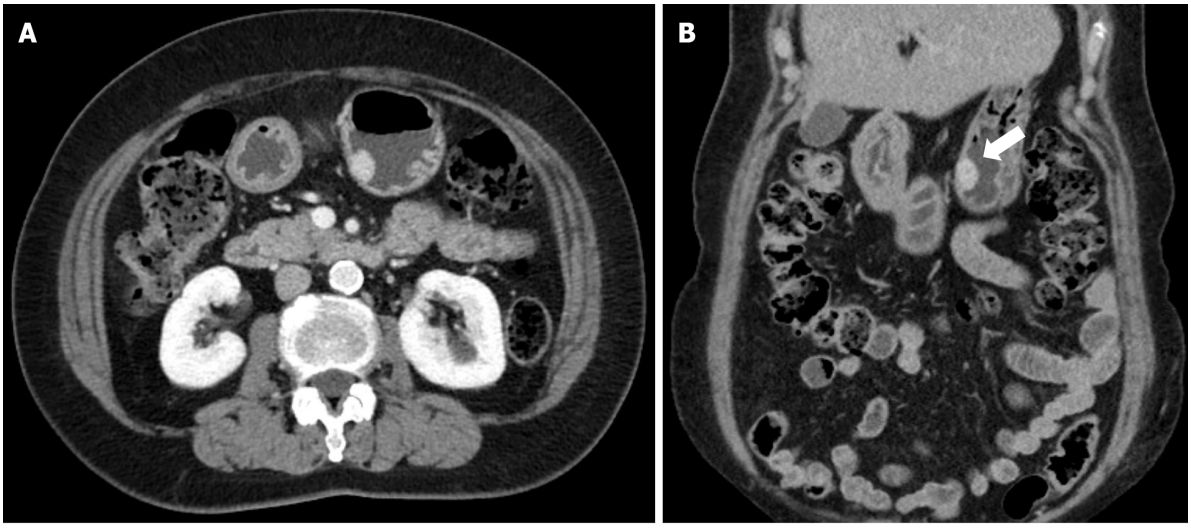
As is the case for other soft tissue sarcomas, there are no characteristic clinical findings[15], and patients may remain asymptomatic for years. Symptoms depend primarily on tumor location and size and the presence or absence of ulceration. The most common symptoms are a palpable mass, mechanical obstruction, and gastrointestinal bleeding. In general, nonspecific symptoms are the main cause of delayed diagnoses, and thus, most liposarcomas are large at diagnosis. However, our patient underwent regular biennial EGD under a national cancer screening program, and the small SMT was detected early. Furthermore, endoscopic resection performed for a definite diagnosis resulted in the diagnosis of a small, asymptomatic gastric liposarcoma.

The characteristic histological features of liposarcoma are the presence of immature fat cells and lipoblasts[14]. Liposarcomas are classified histologically as WDL, DL, myxoid/round cell liposarcoma, or pleomorphic liposarcoma[2], and considerations of histological subtype are important during the disease course. While DL, round-cell, and pleomorphic liposarcomas are high-grade aggressive tumors with the ability to metastasize, WDL and myxoid liposarcomas are low-grade tumors that progress



DOI: 10.3748/wjg.v28.i23.2625 **Copyright** ©The Author(s) 2022.

Figure 1 Endoscopy and endoscopic ultrasound images. A: Endoscopic image showing a 15-mm-sized, submucosal tumor-like, protruding lesion with focal mucosal erythema and depression of overlying mucosa; B: Endoscopic ultrasound image showing a well-circumscribed, slightly heterogeneous, 17 mm × 10 mm sized, isoechoic mass originating from the third sonographic layer.

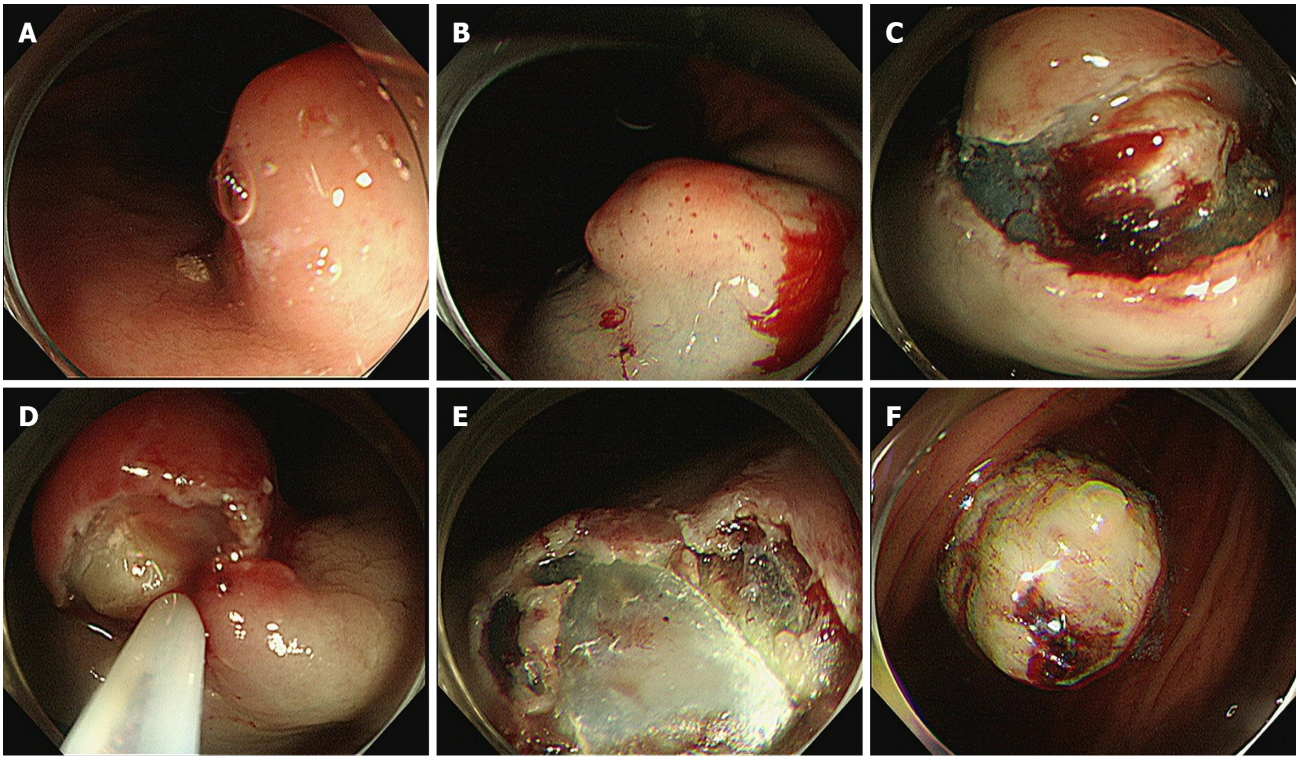


DOI: 10.3748/wjg.v28.i23.2625 **Copyright** ©The Author(s) 2022.

Figure 2 Abdominal computed tomography images. A and B: Axial and coronal computed tomography images showing a well-enhanced and protruding intraluminal mass in the gastric body.

more slowly[3,5]. Most of the gastric liposarcomas reported have been of the well-differentiated or myxoid histologic subtypes[10], and DL arising in the stomach has not been previously reported in the English literature; although a case of DL of heart and stomach was reported in 2017[16]. Notably, in this report, histopathological examination failed to determine that the primary lesion was located in the stomach. In addition, one case of primary DL of the gastroesophageal junction has been reported[11]. Thus, to the best of our knowledge, this is the first reported case of primary gastric DL.

DL is defined as a combination of WDL and high-grade sarcoma that displays evidence of non-lipogenic differentiation like undifferentiated high-grade pleomorphic sarcoma, fibrosarcoma, or myxofibrosarcoma[17,18]. DL can occur *de novo* (90% of cases) or as recurrence from a preexisting WDL (10% of cases)[19]. If DL develops from the transformation of a preexisting WDL into non-lipogenic sarcoma, dedifferentiation develops in 20% of the first and 44% of the second local recurrences and has been shown to be associated with poor progression and metastasis[5]. The histologic diagnosis of DL is generally based on the identification of WDL areas, which were scarce in our patient. In these cases, the differential diagnosis of any poorly-differentiated or undifferentiated sarcoma is important, and MDM2 and CDK4 immunohistochemical staining or FISH testing for amplification of the MDM2 and CDK4 genes is diagnostically helpful[20]. In our patient, DL was confirmed by CDK4 and MDM2 immunostaining.



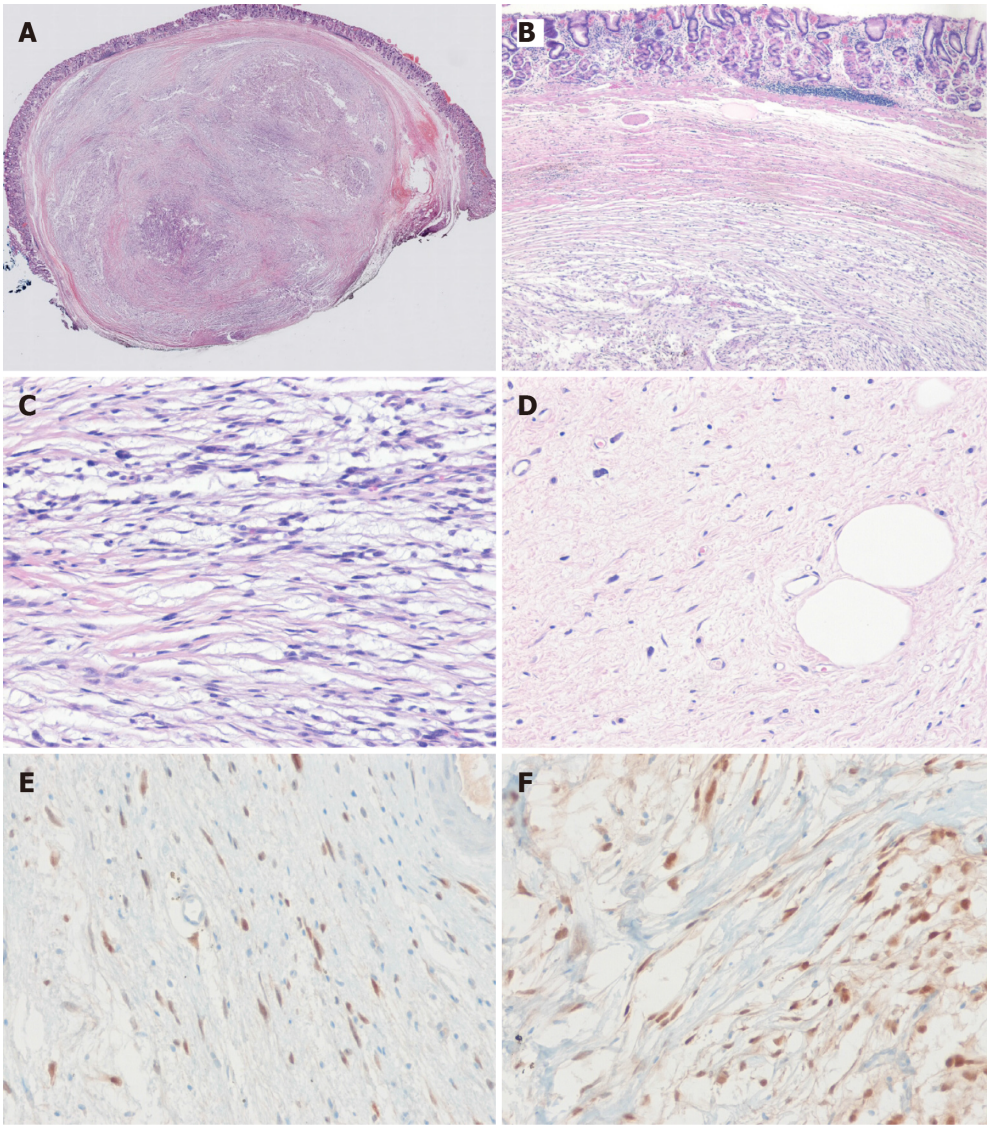
DOI: 10.3748/wjg.v28.i23.2625 **Copyright** ©The Author(s) 2022.

Figure 3 Process of the endoscopic resection. A: Marking outside the lesion; B: Injection of saline–epinephrine for submucosal lifting; C: Circumferential mucosal incision and partial submucosal dissection; D and E: Resection using a snare; F: Resected tumor.

DL often exhibits abdominal cavity involvement usually of retroperitoneum, and an intraperitoneal origin is extremely rare[3,21,22]. When DL occurs inside the abdominal cavity it presents as a space-occupying mass lesion. The pathognomonic findings of DL in CT and magnetic resonance images are a heterogeneous, non-lipogenic, encapsulated mass[23], which are sufficient for diagnosis and obviate the need for needle biopsy. In our patient, because DL arising from the gastric wall presented as a small gastric SMT, CT was not diagnostically useful. Although EUS is considered the most useful modality in terms of defining the presumptive nature of SMT, our case demonstrates the difficulty of differentiating benign and malignant SMT by EUS alone, particularly when a lesion is small. Lesion echogenicity is also worth mentioning. Unlike the hyperechogenic EUS feature of other pathologic types[10,24,25], our case showed isoechoic EUS features, which appeared to be related to a sparsity of immature lipocytes or lipoblasts as the WDL area was extremely limited in our patient. DL seems to have a better prognosis than other high-grade sarcomas, especially in terms of its metastatic potential. Yet, careful long-term follow-up is essential because approximately 40% of DLs recur locally, 17% metastasize, and 28% of patients eventually die of the disease[1]. Surgery remains the treatment of choice for DL, and it is crucial that the tumor be completely removed[4], though the efficacies of targeted chemotherapy and radiotherapy are being investigated[26].

CONCLUSION

Liposarcoma is uncommon in the gastrointestinal tract and rare in the stomach, and primary DL in the stomach is extremely rare but should be considered in the differential diagnosis of any poorly-differentiated or undifferentiated sarcoma. The reasons why this case report is valuable are: (1) It presents the first reported case of a small primary gastric DL, resected endoscopically, and followed up; and (2) it cautions that if a diagnosis of SMT is uncertain after initial examination by EGD, EUS, and/or CT, the use of aggressive techniques, including endoscopic resection, should be considered.



DOI: 10.3748/wjg.v28.i23.2625 **Copyright** ©The Author(s) 2022.

Figure 4 The histopathological diagnosis of the endoscopically resected lesion. A and B: The tumor had a smooth margin, an internal heterogeneous morphology, and was located in submucosa (H & E, original magnification × 10, × 40); the deep resection margin was positive for tumor; C: The neoplasm consists of infiltrated, atypical spindle-shaped tumor cells with nuclear hyperchromasia (H & E, original magnification × 100); D: Photomicrograph showing highly pleomorphic spindle cells with some rare lipoblasts (H&E, original magnification × 100); E and F: Immunohistochemical staining for tumor cells show diffuse positivity for MDM2 (E) and CDK4 (F).

FOOTNOTES

Author contributions: Cho JH, Byeon JH, and Lee SH were responsible for acquiring clinical data and for manuscript writing and revision.

Informed consent statement: Informed written consent was obtained from the patients for the publication of this report and any accompanying images.

Conflict-of-interest statement: The authors declare that they have no conflict of interest.

CARE Checklist (2016) statement: The authors have read the CARE Checklist (2016), and the manuscript was prepared and revised according to the CARE Checklist (2016).

Open-Access: This article is an open-access article that was selected by an in-house editor and fully peer-reviewed by external reviewers. It is distributed in accordance with the Creative Commons Attribution NonCommercial (CC BY-NC 4.0) license, which permits others to distribute, remix, adapt, build upon this work non-commercially, and license their derivative works on different terms, provided the original work is properly cited and the use is non-commercial. See: https://creativecommons.org/Licenses/by-nc/4.0/

Country/Territory of origin: South Korea

ORCID number: Joon Hyun Cho 0000-0002-3584-6300; Jun Hyeon Byeon 0000-0001-9857-1810; Si Hyung Lee 0000-0001-7221-7506.

S-Editor: Chen YL
L-Editor: A
P-Editor: Chen YL

REFERENCES

1 **Goldblum JR**, Folpe AL, Weiss SW. Enzinger and Weiss's Soft Tissue Tumors. 6th ed. Philadelphia: Elsevier, 2014 [DOI: 10.1097/pap.0000000000000020]
2 **Fletcher CDM**, Bridge JA, Hogendoom PCW. World Health Organization classification of tumours. In: Pathology and genetics of tumours of soft tissue and bone. Lyon: IARC Press, 2013: 10-238 [DOI: 10.1302/0301-620x.86b3.0860466b]
3 **Singer S**, Antonescu CR, Riedel E, Brennan MF. Histologic subtype and margin of resection predict pattern of recurrence and survival for retroperitoneal liposarcoma. *Ann Surg* 2003; **238**: 358-70; discussion 370 [PMID: 14501502 DOI: 10.1097/01.sla.0000086542.11899.38]
4 **Choi YY**, Kim YJ, Jin SY. Primary liposarcoma of the ascending colon: a rare case of mixed type presenting as hemoperitoneum combined with other type of retroperitoneal liposarcoma. *BMC Cancer* 2010; **10**: 239 [PMID: 20507577 DOI: 10.1186/1471-2407-10-239]
5 **Dalal KM**, Kattan MW, Antonescu CR, Brennan MF, Singer S. Subtype specific prognostic nomogram for patients with primary liposarcoma of the retroperitoneum, extremity, or trunk. *Ann Surg* 2006; **244**: 381-391 [PMID: 16926564 DOI: 10.1097/01.sla.0000234795.98607.00]
6 **Lahat G**, Lazar A, Lev D. Sarcoma epidemiology and etiology: potential environmental and genetic factors. *Surg Clin North Am* 2008; **88**: 451-481, v [PMID: 18514694 DOI: 10.1016/j.suc.2008.03.006]
7 **Enzinger FM**, Weiss SW. Liposarcoma. In: Soft Tissue Tumors. St Louis: Mosby Year Book, 1995: 431-466 [DOI: 10.1002/bjs.1800821050]
8 **Graham RP**, Yasir S, Fritchie KJ, Reid MD, Greipp PT, Folpe AL. Polypoid fibroadipose tumors of the esophagus: 'giant fibrovascular polyp' or liposarcoma? *Mod Pathol* 2018; **31**: 337-342 [PMID: 28984298 DOI: 10.1038/modpathol.2017.140]
9 **Gajzer DC**, Fletcher CD, Agaimy A, Brcic I, Khanlari M, Rosenberg AE. Primary gastrointestinal liposarcoma—a clinico-pathological study of 8 cases of a rare entity. *Human Pathol* 2020; **97**: 80-93 [DOI: 10.1016/j.humpath.2019.12.004]
10 **Kang WZ**, Xue LY, Wang GQ, Ma FH, Feng XL, Guo L, Li Y, Li WK, Tian YT. Liposarcoma of the stomach: Report of two cases and review of the literature. *World J Gastroenterol* 2018; **24**: 2776-2784 [PMID: 29991881 DOI: 10.3748/wjg.v24.i25.2776]
11 **Aşkan G**, Bağci P, Hameed M, Baştürk O. Dedifferentiated Liposarcoma of the Gastroesophageal Junction. *Turk Patoloji Derg* 2018; **34**: 104-107 [PMID: 25690861 DOI: 10.5146/tjpath.2014.01297]
12 **Abrams MJ**, Truberville JS. Liposarcoma of the stomach. *South Surg* 1941; **10**: 891-896
13 **Matone J**, Okazaki S, Maccapani GN, Amancio TT, Filippi RZ, Macedo AL. Giant gastric lipossarcoma: case report and review of the literature. *Einstein (Sao Paulo)* 2016; **14**: 557-560 [PMID: 28076606 DOI: 10.1590/S1679-45082016RC3770]
14 **Tepetes K**, Christodoulidis G, Spyridakis ME, Nakou M, Koukoulis G, Hatzitheofilou K. Liposarcoma of the stomach: a rare case report. *World J Gastroenterol* 2007; **13**: 4154-4155 [PMID: 17696242 DOI: 10.3748/wjg.v13.i30.4154]
15 **López-Negrete L**, Luyando L, Sala J, López C, Menéndez de Llano R, Gomez JL. Liposarcoma of the stomach. *Abdom Imaging* 1997; **22**: 373-375 [PMID: 9157853 DOI: 10.1007/s002619900213]
16 **Hisata Y**, Tasaki Y, Kozaki S, Yamada T. A case of dedifferentiated liposarcoma of the heart and stomach. *Int J Surg Case Rep* 2017; **41**: 36-38 [PMID: 29031176 DOI: 10.1016/j.ijscr.2017.10.001]
17 **Evans HL**. Liposarcoma: a study of 55 cases with a reassessment of its classification. *Am J Surg Pathol* 1979; **3**: 507-523 [PMID: 534388 DOI: 10.1097/00000478-197912000-00004]
18 **Dei Tos AP**. Liposarcoma: new entities and evolving concepts. *Ann Diagn Pathol* 2000; **4**: 252-266 [PMID: 10982304 DOI: 10.1053/adpa.2000.8133]
19 **Henricks WH**, Chu YC, Goldblum JR, Weiss SW. Dedifferentiated liposarcoma: a clinicopathological analysis of 155 cases with a proposal for an expanded definition of dedifferentiation. *Am J Surg Pathol* 1997; **21**: 271-281 [PMID: 9060596 DOI: 10.1097/00000478-199703000-00002]
20 **Binh MB**, Sastre-Garau X, Guillou L, de Pinieux G, Terrier P, Lagacé R, Aurias A, Hostein I, Coindre JM. MDM2 and CDK4 immunostainings are useful adjuncts in diagnosing well-differentiated and dedifferentiated liposarcoma subtypes: a comparative analysis of 559 soft tissue neoplasms with genetic data. *Am J Surg Pathol* 2005; **29**: 1340-1347 [PMID: 16160477 DOI: 10.1097/01.pas.0000170343.09562.39]
21 **D'Annibale M**, Cosimelli M, Covello R, Stasi E. Liposarcoma of the colon presenting as an endoluminal mass. *World J Surg Oncol* 2009; **7**: 78 [PMID: 19852822 DOI: 10.1186/1477-7819-7-78]
22 **Goel AK**, Sinha S, Kumar A, Karak AK, Chattopadhyay TK. Liposarcoma of the mesocolon--case report of a rare lesion. *Surg Today* 1994; **24**: 1003-1006 [PMID: 7772897 DOI: 10.1007/BF02215814]
23 **Murphey MD**, Arcara LK, Fanburg-Smith J. From the archives of the AFIP: imaging of musculoskeletal liposarcoma with radiologic-pathologic correlation. *Radiographics* 2005; **25**: 1371-1395 [PMID: 16160117 DOI: 10.1148/rg.255055106]
24 **Yamamoto K**, Teramae N, Uehira H, Wakabayashi N, Fukuda S, Kodama T, Kashina K, Tsuchihashi Y. Primary liposarcoma of the stomach resected endoscopically. *Endoscopy* 1995; **27**: 711 [PMID: 8903993 DOI:

10.1055/s-2007-1005798]
25 **Cure HW**, Gómez D, Pedraza M, Bulicie HC, Cabrera LF, Gil LPG, Acevedo D, Cabrera L, Moreno V, Mendoza A. Laparoscopic management of gastric liposarcoma: A case report and review of the literature. *Int J Surg Case Rep* 2020; **73**: 268-270 [PMID: 32721886 DOI: 10.1016/j.ijscr.2020.07.044]
26 **Radaelli S**, Stacchiotti S, Casali PG, Gronchi A. Emerging therapies for adult soft tissue sarcoma. *Expert Rev Anticancer Ther* 2014; **14**: 689-704 [PMID: 24555529 DOI: 10.1586/14737140.2014.885840]

World Journal of Gastroenterology

Submit a Manuscript: https://www.f6publishing.com

World J Gastroenterol 2022 June 21; 28(23): 2633-2635

DOI: 10.3748/wjg.v28.i23.2633

ISSN 1007-9327 (print) ISSN 2219-2840 (online)

LETTER TO THE EDITOR

Reconstructing the puzzle of the role of therapeutic endoscopy in the management of post-bariatric surgery complications

Konstantinos Argyriou, Adolfo Parra-Blanco

Specialty type: Gastroenterology and hepatology

Provenance and peer review: Invited article; Externally peer reviewed.

Peer-review model: Single blind

Peer-review report's scientific quality classification

Grade A (Excellent): 0
Grade B (Very good): B
Grade C (Good): C
Grade D (Fair): 0
Grade E (Poor): 0

P-Reviewer: Fusaroli P, Italy; Głuszyńska P, Poland
A-Editor: Ribeiro IB, Brazil

Received: February 3, 2022
Peer-review started: February 3, 2022
First decision: April 10, 2022
Revised: May 2, 2022
Accepted: June 3, 2022
Article in press: June 3, 2022
Published online: June 21, 2022

Konstantinos Argyriou, Department of Gastroenterology, University Hospital of Larisa, Larisa GR41110, Greece

Adolfo Parra-Blanco, Department of Gastroenterology, Nottingham University Hospitals NHS Trust, Nottingham NG5 1PB, United Kingdom

Corresponding author: Konstantinos Argyriou, MD, MSc, PhD, Academic Research, Consultant Physician-Scientist, Department of Gastroenterology, University Hospital of Larisa, P.O. box1425 Larissa Thessaly Greece, Larisa GR41110, Greece. kosnar2@yahoo.gr

Abstract

We have recently read with interest the mini-review article "Therapeutic endoscopy for the treatment of post-bariatric surgery complications". The abovementioned article is a brief overview of the different endoscopic modalities employed in the management of bariatric surgery complications and represents an important decision support tool for clinicians to improve their current practice. Although we appreciate the endeavor of Larsen and Kozarek, based on our in-depth analysis, we came across several minor issues in this article; thus, we present our comments in this letter. In case the authors contemplate these comments in their relevant research, we believe that their contribution would be considerable for future studies.

Key Words: Endoscopic treatment; Bariatric surgery; Complications; Obesity; Sleeve gastrectomy; Roux-en-Y gastric bypass

©The Author(s) 2022. Published by Baishideng Publishing Group Inc. All rights reserved.

Core Tip: Over the last decade, the incidence of bariatric surgery has substantially increased. Despite advances in surgical techniques, postoperative complications emerge and require a multidisciplinary approach. Currently, there is no standardized guideline-based algorithm for managing bariatric complications (BC); however, minimally invasive treatments are generally preferred over reoperations. Endoscopic procedures provide minimally invasive options to manage BC. However, their exact role has not been completely delineated. The article by Larsen and Kozarek successfully addressed this issue; however, we identified several limitations that require further consideration. Therefore, we would like to share our views on this interesting review.

Citation: Argyriou K, Parra-Blanco A. Reconstructing the puzzle of the role of therapeutic endoscopy in the management of post-bariatric surgery complications. *World J Gastroenterol* 2022; 28(23): 2633-2635
URL: https://www.wjgnet.com/1007-9327/full/v28/i23/2633.htm
DOI: https://dx.doi.org/10.3748/wjg.v28.i23.2633

TO THE EDITOR

We read with great interest the mini-review article "Therapeutic endoscopy for the treatment of post-bariatric surgery complications"[1]. In this article, Larsen and Kozarek[1] provided a concise overview of the role of endoscopy in the management of adverse events complicating the three most common types of the currently performed bariatric surgeries including Roux-en-Y gastric bypass, laparoscopic adjustable gastric band, and sleeve gastrectomy. From the extensive list of bariatric complications (BC), the authors confined their analysis only to those that are amenable to endoscopic treatment such as postoperative anastomotic strictures, leaks, fistulae, choledocholithiasis, weight regain, and band erosion. The salient highlights of this review were that the authors, by summarizing the relevant literature and incorporating their own clinical experience, were able to not only delineate the role of therapeutic endoscopy in the BC management but to also provide clinicians with practical tips that are expected to improve their daily practice. However, the most striking point of this article was that the authors holistically approached every referred complication from epidemiology to endoscopic treatment, highlighting areas that need to be further investigated. Therefore, we believe that this article has strong reference and practical value for future studies. Nonetheless, through our in-depth reading, we came across several limitations and anticipate a discussion with the authors.

First, by carefully analyzing the author's list of BC, we noticed that the endoscopic management of post-operative gastrointestinal bleeding (GIB) was not discussed in this review. The reason behind this exclusion was not mentioned by the authors. However, we regard this omission as a limitation of this article because the endoscopic management of GIB is challenging in bariatric patients. This occurs because the altered postoperative anatomy and the time interval of the bleeding episode from the operation impose restrictions not only on the type of the endoscopic equipment that would be used to approach the site of bleeding but also on the modality that would be used to achieve hemostasis. For example, standard endoscopes may not be able to reach sites of bleeding at the biliopancreatic limb or beyond the gastro-jejunal anastomosis in patients who underwent gastric bypass, whereas thermal ablation methods may cause unfavorable outcomes such as perforation in patients with freshly stapled anastomosis[2,3]. Considering these challenges, we believe that the endoscopic management of GIB has particular importance for the clinicians involved in the management of bariatric patients, and we suggest it to be supplemented in this mini-review.

Another limitation of this article is that the authors did not make clear to the reader the way they selected the studies included in this review. Although they successfully summarized the major findings of several reference studies, by performing our own literature search, we identified several omissions. For example, in the management of bariatric leakage and fistulae, the authors did not discuss the results of the most recent meta-analysis written by Rogalski *et al*[4] on the effectiveness of self-expandable stents, clipping, and tissue sealants. As a result, the authors did not make any reference to the use of fibrin glue as an alternative modality for fistulae closure in their review[4]. Likewise, by not including in their summary of evidence two reference studies on the effectiveness and safety of bougie dilations in the management of anastomotic stenosis, the authors did not discuss all available modalities that could be used as alternative options to balloon dilations[5,6]. We believe that the abovementioned information is important for the reader to acquire a complete overview of the pleiotropic role that endoscopy can play in the management of BC and, thus, needs to be supplemented.

The final limitation of this article refers to the different endoscopic techniques that can be used by clinicians to achieve biliopancreatic access in bariatric patients who underwent gastric bypass. Based on the included studies and their own experience, the authors referred to three techniques for performing endoscopic retrograde cholangiopancreatography (ERCP) in bariatric patients, including the overtube-assisted enteroscopy technique, the lap-assisted transgastric, and the endoscopic ultrasound-directed transgastric technique, with the first technique being their first-line option for most indications. However, considering that not all centers managing bariatric patients can perform these techniques, we performed our own literature search and came across an additional option. Specifically, we found that in bariatric patients who underwent gastric bypass, the biliopancreatic access to the excluded gastrointestinal part can be also achieved through the gastrocutaneous tract created after the removal of a gastrostomy tube without the need for reoperation or special equipment. This technique is known as gastrostomy-assisted ERCP, and it is performed in 3 steps. The first step includes the endoscopic insertion of the gastrostomy tube, which stays in situ for 5–14 d until the maturation of the tract. Then, the tube is removed, and the tract is dilated with a balloon to an extent that will allow the passage of the duodenoscope. After completion of the dilation of the tract, ERCP can be repeatedly performed[7]. Given the wide availability of gastrostomy tubes, we believe that the abovementioned technique has

particular value for the clinicians involved in the management of bariatric patients and should be supplemented in this review.

In summary, despite the abovementioned limitations, we believe that this article can be a valuable reference study, guiding clinicians in their daily practice. Thus, we offer our evidence-based considerations in this review to expand the value of the research basis that this article sets, leading to more comprehensive future studies.

FOOTNOTES

Author contributions: Argyriou K and Parra-Blanco A designed and performed the research; Argyriou K wrote this comment; Parra-Blanco A revised the manuscript.

Conflict-of-interest statement: All the authors report no relevant conflicts of interest for this article.

Open-Access: This article is an open-access article that was selected by an in-house editor and fully peer-reviewed by external reviewers. It is distributed in accordance with the Creative Commons Attribution NonCommercial (CC BY-NC 4.0) license, which permits others to distribute, remix, adapt, build upon this work non-commercially, and license their derivative works on different terms, provided the original work is properly cited and the use is non-commercial. See: https://creativecommons.org/Licenses/by-nc/4.0/

Country/Territory of origin: Greece

ORCID number: Konstantinos Argyriou 0000-0002-2026-9678; Adolfo Parra-Blanco 0000-0003-2396-0226.

Corresponding Author's Membership in Professional Societies: Hellenic Society of Gastroenterology; British Society of Gastroenterology.

S-Editor: Fan JR
L-Editor: A
P-Editor: Fan JR

REFERENCES

1 **Larsen M**, Kozarek R. Therapeutic endoscopy for the treatment of post-bariatric surgery complications. *World J Gastroenterol* 2022; **28**: 199-215 [PMID: 35110945 DOI: 10.3748/wjg.v28.i2.199]
2 **American Society for Gastrointestinal Endoscopy Standards of Practice Committee**, Evans JA, Muthusamy VR, Acosta RD, Bruining DH, Chandrasekhara V, Chathadi KV, Eloubeidi MA, Fanelli RD, Faulx AL, Fonkalsrud L, Khashab MA, Lightdale JR, Pasha SF, Saltzman JR, Shaukat A, Wang A, Stefanidis D, Richardson WS, Kothari SN, Cash BD. The role of endoscopy in the bariatric surgery patient. *Gastrointest Endosc* 2015; **81**: 1063-1072 [PMID: 25733126 DOI: 10.1016/j.gie.2014.09.044]
3 **Kumbhari V**, Cummings DE, Kalloo AN, Schauer PR. AGA Clinical Practice Update on Evaluation and Management of Early Complications After Bariatric/Metabolic Surgery: Expert Review. *Clin Gastroenterol Hepatol* 2021; **19**: 1531-1537 [PMID: 33741500 DOI: 10.1016/j.cgh.2021.03.020]
4 **Rogalski P**, Swidnicka-Siergiejko A, Wasielica-Berger J, Zienkiewicz D, Wieckowska B, Wroblewski E, Baniukiewicz A, Rogalska-Plonska M, Siergiejko G, Dabrowski A, Daniluk J. Endoscopic management of leaks and fistulas after bariatric surgery: a systematic review and meta-analysis. *Surg Endosc* 2021; **35**: 1067-1087 [PMID: 32107632 DOI: 10.1007/s00464-020-07471-1]
5 **Escalona A**, Devaud N, Boza C, Pérez G, Fernández J, Ibáñez L, Guzmán S. Gastrojejunal anastomotic stricture after Roux-en-Y gastric bypass: ambulatory management with the Savary-Gilliard dilator. *Surg Endosc* 2007; **21**: 765-768 [PMID: 17285381 DOI: 10.1007/s00464-006-9134-3]
6 **Fernández-Esparrach G**, Bordas JM, Llach J, Lacy A, Delgado S, Vidal J, Cárdenas A, Pellisé M, Ginès A, Sendino O, Zabalza M, Castells A. Endoscopic dilation with Savary-Gilliard bougies of stomal strictures after laparoscopic gastric bypass in morbidly obese patients. *Obes Surg* 2008; **18**: 155-161 [PMID: 18176830 DOI: 10.1007/s11695-007-9372-z]
7 **Papasavas P**, Docimo S Jr, Oviedo RJ, Eisenberg D; American Society for Metabolic and Bariatric Surgery Clinical Issues Committee. Biliopancreatic access following anatomy-altering bariatric surgery: a literature review. *Surg Obes Relat Dis* 2022; **18**: 21-34 [PMID: 34688572 DOI: 10.1016/j.soard.2021.09.011]



Published by **Baishideng Publishing Group Inc**
7041 Koll Center Parkway, Suite 160, Pleasanton, CA 94566, USA
Telephone: +1-925-3991568
E-mail: bpgoffice@wjgnet.com
Help Desk: https://www.f6publishing.com/helpdesk
https://www.wjgnet.com



© 2022 Baishideng Publishing Group Inc. All rights reserved.

ISSN 1007-9327 (print)
ISSN 2219-2840 (online)

World Journal of *Gastroenterology*

World J Gastroenterol 2022 June 28; 28(24): 2636-2781



Published by Baishideng Publishing Group Inc

World Journal of Gastroenterology

Contents

Weekly Volume 28 Number 24 June 28, 2022

REVIEW

2636 Patient-derived organoids for therapy personalization in inflammatory bowel diseases

Lucafò M, Muzzo A, Marcuzzi M, Giorio L, Decorti G, Stocco G

MINIREVIEWS

2654 Drug-induced autoimmune hepatitis: A minireview

Tan CK, Ho D, Wang LM, Kumar R

2667 Rebuilding trust in proton pump inhibitor therapy

Turshudzhyan A, Samuel S, Tawfik A, Tadros M

2680 Pancreatic involvement in celiac disease

Balaban DV, Enache I, Ciochina M, Popp A, Jinga M

ORIGINAL ARTICLE

Basic Study

2689 Downregulation of *TNFR2* decreases survival gene expression, promotes apoptosis and affects the cell cycle of gastric cancer cells

Rossi AFT, da Silva Manoel-Caetano F, Biselli JM, Cabral ÁS, Saiki MFC, Ribeiro ML, Silva AE

Clinical and Translational Research

2705 Novel multiplex stool-based assay for the detection of early-stage colon cancer in a Chinese population

Jiang HH, Xing SW, Tang X, Chen Y, Lin K, He LW, Lin MB, Tang EJ

Retrospective Cohort Study

2721 Utility of a deep learning model and a clinical model for predicting bleeding after endoscopic submucosal dissection in patients with early gastric cancer

Na JE, Lee YC, Kim TJ, Lee H, Won HH, Min YW, Min BH, Lee JH, Rhee PL, Kim JJ

Retrospective Study

2733 Radiomic analysis based on multi-phase magnetic resonance imaging to predict preoperatively microvascular invasion in hepatocellular carcinoma

Li YM, Zhu YM, Gao LM, Han ZW, Chen XJ, Yan C, Ye RP, Cao DR

2748 Brown slits for colorectal adenoma crypts on conventional magnifying endoscopy with narrow band imaging using the X1 system

Toyoshima O, Nishizawa T, Yoshida S, Watanabe H, Odawara N, Sakitani K, Arano T, Takiyama H, Kobayashi H, Kogure H, Fujishiro M

Observational Study

2758 Usefulness of serum C-reactive protein and calprotectin for the early detection of colorectal anastomotic leakage: A prospective observational study

Rama NJG, Lages MCC, Guarino MPS, Lourenço Ó, Motta Lima PC, Parente D, Silva CSG, Castro R, Bento A, Rocha A, Castro-Pocas F, Pimentel J

LETTER TO THE EDITOR

2775 Is long-term follow-up without surgical treatment a valid option for hepatic alveolar echinococcosis?

Maimaitinijiati Y, Meng Y, Chen X

2778 Using of artificial intelligence: Current and future applications in colorectal cancer screening

Zacharakis G, Almasoud A

ABOUT COVER

Editorial Board Member of *World Journal of Gastroenterology*, Vasiliy Ivanovich Reshetnyak, DSc, MD, Full Professor, Department of Propaedeutic of Internal Diseases and Gastroenterology, A.I. Yevdokimov Moscow State University of Medicine and Dentistry, p. 1, 20 Delegatskaya Street, Moscow 127473, Russia. vasiliy.reshetnyak@yandex.ru

AIMS AND SCOPE

The primary aim of *World Journal of Gastroenterology* (*WJG*, *World J Gastroenterol*) is to provide scholars and readers from various fields of gastroenterology and hepatology with a platform to publish high-quality basic and clinical research articles and communicate their research findings online. *WJG* mainly publishes articles reporting research results and findings obtained in the field of gastroenterology and hepatology and covering a wide range of topics including gastroenterology, hepatology, gastrointestinal endoscopy, gastrointestinal surgery, gastrointestinal oncology, and pediatric gastroenterology.

INDEXING/ABSTRACTING

The *WJG* is now indexed in Current Contents®/Clinical Medicine, Science Citation Index Expanded (also known as SciSearch®), Journal Citation Reports®, Index Medicus, MEDLINE, PubMed, PubMed Central, and Scopus. The 2021 edition of Journal Citation Report® cites the 2020 impact factor (IF) for *WJG* as 5.742; Journal Citation Indicator: 0.79; IF without journal self cites: 5.590; 5-year IF: 5.044; Ranking: 28 among 92 journals in gastroenterology and hepatology; and Quartile category: Q2. The *WJG*'s CiteScore for 2020 is 6.9 and Scopus CiteScore rank 2020: Gastroenterology is 19/136.

RESPONSIBLE EDITORS FOR THIS ISSUE

Production Editor: *Yu-Xi Chen*; **Production Department Director:** *Xu Guo*; **Editorial Office Director:** *Ze-Mao Gong*.

NAME OF JOURNAL
World Journal of Gastroenterology

ISSN
ISSN 1007-9327 (print) ISSN 2219-2840 (online)

LAUNCH DATE
October 1, 1995

FREQUENCY
Weekly

EDITORS-IN-CHIEF
Andrzej S Tarnawski

EDITORIAL BOARD MEMBERS
http://www.wjgnet.com/1007-9327/editorialboard.htm

PUBLICATION DATE
June 28, 2022

COPYRIGHT
© 2022 Baishideng Publishing Group Inc

INSTRUCTIONS TO AUTHORS
https://www.wjgnet.com/bpg/gerinfo/204

GUIDELINES FOR ETHICS DOCUMENTS
https://www.wjgnet.com/bpg/GerInfo/287

GUIDELINES FOR NON-NATIVE SPEAKERS OF ENGLISH
https://www.wjgnet.com/bpg/gerinfo/240

PUBLICATION ETHICS
https://www.wjgnet.com/bpg/GerInfo/288

PUBLICATION MISCONDUCT
https://www.wjgnet.com/bpg/gerinfo/208

ARTICLE PROCESSING CHARGE
https://www.wjgnet.com/bpg/gerinfo/242

STEPS FOR SUBMITTING MANUSCRIPTS
https://www.wjgnet.com/bpg/GerInfo/239

ONLINE SUBMISSION
https://www.f6publishing.com

© 2022 Baishideng Publishing Group Inc. All rights reserved. 7041 Koll Center Parkway, Suite 160, Pleasanton, CA 94566, USA
E-mail: bpgoffice@wjgnet.com https://www.wjgnet.com

World Journal of Gastroenterology

Submit a Manuscript: https://www.f6publishing.com

World J Gastroenterol 2022 June 28; 28(24): 2636-2653

DOI: 10.3748/wjg.v28.i24.2636

ISSN 1007-9327 (print) ISSN 2219-2840 (online)

REVIEW

Patient-derived organoids for therapy personalization in inflammatory bowel diseases

Marianna Lucafò, Antonella Muzzo, Martina Marcuzzi, Lorenzo Giorio, Giuliana Decorti, Gabriele Stocco

Specialty type: Gastroenterology and hepatology

Provenance and peer review: Invited article; Externally peer reviewed.

Peer-review model: Single blind

Peer-review report's scientific quality classification

Grade A (Excellent): A, A
Grade B (Very good): 0
Grade C (Good): 0
Grade D (Fair): 0
Grade E (Poor): 0

P-Reviewer: Liu DY, China; Zhang Y, China
A-Editor: Maslennikov R

Received: January 17, 2022
Peer-review started: January 17, 2022
First decision: March 8, 2022
Revised: March 21, 2022
Accepted: May 17, 2022
Article in press: May 17, 2022
Published online: June 28, 2022

Marianna Lucafò, Giuliana Decorti, Gabriele Stocco, Advanced Translational Diagnostics Laboratory, Institute for Maternal and Child Health-IRCCS "Burlo Garofolo", Trieste 34137, Italy

Antonella Muzzo, Giuliana Decorti, Department of Medicine, Surgery and Health Sciences, University of Trieste, Trieste 34127, Italy

Martina Marcuzzi, Lorenzo Giorio, Gabriele Stocco, Department of Life Sciences, University of Trieste, Trieste 34127, Italy

Corresponding author: Giuliana Decorti, MD, Associated Professor, Advanced Translational Diagnostics Laboratory, Institute for Maternal and Child Health-IRCCS "Burlo Garofolo", Via dell'Istria 65/1, Trieste 34137, Italy. giuliana.decorti@burlo.trieste.it

Abstract

Inflammatory bowel diseases (IBDs) are chronic inflammatory disorders of the intestinal tract that have emerged as a growing problem in industrialized countries. Knowledge of IBD pathogenesis is still incomplete, and the most widely-accepted interpretation considers genetic factors, environmental stimuli, uncontrolled immune responses and altered intestinal microbiota composition as determinants of IBD, leading to dysfunction of the intestinal epithelial functions. *In vitro* models commonly used to study the intestinal barrier do not fully reflect the proper intestinal architecture. An important innovation is represented by organoids, 3D *in vitro* cell structures derived from stem cells that can self-organize into functional organ-specific structures. Organoids may be generated from induced pluripotent stem cells or adult intestinal stem cells of IBD patients and therefore retain their genetic and transcriptomic profile. These models are powerful pharmacological tools to better understand IBD pathogenesis, to study the mechanisms of action on the epithelial barrier of drugs already used in the treatment of IBD, and to evaluate novel target-directed molecules which could improve therapeutic strategies. The aim of this review is to illustrate the potential use of organoids for therapy personalization by focusing on the most significant advances in IBD research achieved through the use of adult stem cells-derived intestinal organoids.

Key Words: Inflammatory bowel disease; Organoids; Intestinal epithelium; 3D cell cultures; Personalized medicine

©The Author(s) 2022. Published by Baishideng Publishing Group Inc. All rights reserved.

Core Tip: Intestinal organoids have helped to unveil knowledge about inflammatory bowel diseases pathogenesis, focusing on the genetic and epigenetic factors involved in the onset of these diseases, the altered intestinal epithelial cell (IEC) functions, and the interplay between IECs and other surrounding cells, including immune cells and the intestinal bacteria. Intestinal organoids are currently being evaluated in pre-clinical studies as pharmacological tools to better understand the specific mechanisms of action of already used drugs on the IECs and to identify novel pharmacological targets and approaches.

Citation: Lucafò M, Muzzo A, Marcuzzi M, Giorio L, Decorti G, Stocco G. Patient-derived organoids for therapy personalization in inflammatory bowel diseases. *World J Gastroenterol* 2022; 28(24): 2636-2653
URL: https://www.wjgnet.com/1007-9327/full/v28/i24/2636.htm
DOI: https://dx.doi.org/10.3748/wjg.v28.i24.2636

INTRODUCTION

Inflammatory bowel diseases (IBDs) are chronic inflammatory disorders of the gastrointestinal tract that have emerged as a growing problem in industrialized countries[1]. IBDs include Crohn's disease (CD) and ulcerative colitis (UC)[2], which can be distinguished by differences in genetic predisposition, clinical aspects, and risk factors[3], and by the location and nature of inflammation[4]. UC is restricted to the mucosal surface of the large intestine: It starts in the rectum and extends through the entire colon in a continuous manner[3]. The severity of symptoms depends on the intestinal areas involved in inflammation[4]: It usually occurs with bloody diarrhea with pus and mucus (often nocturnal and postprandial), fever, weight loss, abdominal pain, and signs of systemic inflammation[5]. CD is characterized by the involvement of both the small and large intestine; it most commonly affects the ileocecal region, the terminal ileum, the perianal area, and the colon, with segmental and transmural inflammation, fissuring ulcerations, non-caseating granulomas, strictures, abscesses, and fistulas[4,6,7]. The clinical presentation of CD depends on the location, extent, and severity of inflammation: Patients usually show postprandial abdominal pain, especially around the periumbilical area, bloody diarrhea, nausea, emesis, dysphagia, early satiety, and weight loss[7].

Although no curative treatment is available for these diseases, current therapeutic options aim at achieving an improvement in symptoms and can be divided in two different groups: The remission induction drugs, which are used to achieve clinical remission, and the maintenance drugs which sustain the clinical remission and prevent disease relapse[8]. Aminosalicylates are administered as first-line agents to treat mild to moderately active UC. They exert their anti-inflammatory activity by binding to the peroxisome proliferator-activated receptor[9]. Glucocorticoids are used for inducing remission; when bound to their receptor, they modulate the expression of inflammatory mediators and control inflammatory states[9,10]. The thiopurines azathioprine and mercaptopurine are efficacious for maintaining remission. Thiopurines are inactive prodrugs but their metabolites (thioguanine nucleotides) are responsible for causing immunosuppression, either by inhibiting the *de novo* purine synthesis or by incorporating into the DNA or RNA[9]. Infliximab and adalimumab, which bind the pro-inflammatory cytokine tumor necrosis factor (TNF), have been introduced both for inducing remission and for maintenance therapy[11]. Furthermore, other monoclonal antibodies such as vedolizumab, a selective α4β7 integrin inhibitor, and ustekinumab, an interleukin (IL)-12/23 p40 inhibitor, have been used as alternatives for patients who have failed or are intolerant to anti-TNF therapy[12]. Eventually, thalidomide, by selectively inhibiting TNF-α expression and suppressing TNF-α -induced nuclear factor-kappa B (NF-κB) activation, can be employed when patients do not respond to the standard therapies[9,13]. Despite the multiple therapeutic options, high interindividual variability in response to these drugs is evident, and genetic and epigenetic factors could play a key role in these differences[14,15].

IBDs are multi-etiological diseases: It is currently believed that uncontrolled immune response against intestinal microbiota, combined with environmental factors in genetically predisposed individuals, leads to bowel inflammation, perturbing the mucosal barrier and increasing intestinal epithelial cell (IEC) dysfunction[16,17]. However, even today, it is not completely understood which of these factors are the initiators of inflammation and which are contributors[18]. An altered intestinal architecture and abnormalities in the intestinal wall function have been associated with the onset of the disease[19].

The current models employed to study the intestinal barrier *in vitro* show many weaknesses: Stabilized cell lines, such as the human epithelial colorectal adenocarcinoma cells Caco2 or HT-29, do not reproduce the heterogeneous intestinal cell types[20-22] and do not represent IBD pathophysiology

[23]. Animal models are highly costly, require probands to be raised for weeks[5], and may not reflect human pathobiology, which may contribute to drug failure in clinical therapy[21,24]. Consequently, new models are necessary to better define the pathogenesis underlying IBDs and to find new clinical approaches in its treatment[25].

A major advancement in clinical research of human IECs is represented by the development of 3D organoid cultures, which re-create intestinal epithelial tissue *in vitro*[25] starting from adult stem cells (ASCs) or pluripotent stem cells (PSCs), such as embryonic stem cells or induced PSCs (iPSCs)[22]. These cells, grown under appropriate conditions and stimuli, self-organize and show the specific tissue structures, properties and functionality of the gastrointestinal tissue, forming a spheroid-like structure [26].

INTESTINAL ORGANOIDS

ASCs are located at the base of the intestinal crypts, which can be isolated from intestinal biopsies[27]. Intestinal crypts are embedded in a 3D membrane-like gel, such as matrigel, which mimics the extracellular matrix, and supplemented with an appropriate culture medium that is crucial for the development and expansion of ASCs, from which intestinal organoids can be obtained[5,28,29]. The organoids obtained *in vitro* with this method present only IECs (Paneth cells, goblet cells, enterocytes and enteroendocrine cells) derived from the crypt-based stem cells and are oriented with their apical side toward the lumen and their basolateral domain in contact with matrigel[25,28]. On the other hand, Spence *et al*[30], have demonstrated that it is possible to successfully generate intestinal organoids starting from iPSCs with a process that mimics organogenesis, and that this type of organoids may present not only epithelial cells but also mesenchymal cells, including myofibroblasts, and smooth muscle cells, thus providing a more accurate model[30,31]. This method is advantageous when it is necessary to generate organoids starting from tissues not easily accessible, reprogramming peripheral blood mononuclear cells or fibroblasts to a pluripotent state, thus obtaining iPSCs that can be differentiated to the tissue of interest by using dedicated protocols[29]. The reprogramming phase is complex and can be achieved using different methods. These methods are chosen according to efficiency, footprint (integration of viral vector sequences into reprogrammed cell genome), and type of somatic cells to be reprogrammed[32]. Subsequently, in order to obtain the different types of cells constituting the organ of interest, a microenvironment that mimics embryogenesis is required[33]. However, iPSC-derived intestinal organoids, unlike ASC-derived intestinal organoids, can acquire genetic and epigenetic variations. For example, mutations can occur during the reprogramming process or arise during the prolonged culture which can be conserved if they facilitate cell propagation[30,34,35].

After expansion, intestinal organoids can be employed in any experimental approach developed for cell lines, such as DNA-, RNA-, protein-based techniques, live imaging, drug screening and "omics" approaches (including single-cell RNA sequencing, MethylC sequencing, and mass spectrometry)[22]. For example, Yin *et al*[36] have combined genome-wide analysis of open chromatin by Omni Assay for Transposase-Accessible Chromatin-seq with the transcriptome data from RNA-seq. By correlating gene expression with open chromatin peaks, intestine-specific processes were identified. These results confirm the relevance of intestinal organoids to better define the genetic characteristics and, at the same time, to investigate crucial physiological and biochemical processes in the gut epithelium[36].

Organoid cultures are also a powerful model for genetic manipulation tools, such as transposon mutagenesis, siRNAs, and CRISPR-Cas (*e.g.*, knock-down, knock-out, knock-in, or overexpression)[29]. In particular CRISPR-Cas, along with transcription activator-like effector nuclease, and zinc finger nucleases technologies[37] allows the low frequency IBD-associated mutations to be gradually introduced into organoids derived from healthy patients, providing a better understanding of their effect on the epithelial cell functions[22,29]. In this way, intestinal organoids can be useful to explain in a more specific manner the effect of known genetic variants identified by genome-wide association studies[38] and can become crucial tools for IBD research, especially for the very early-onset IBD (VEO-IBD).

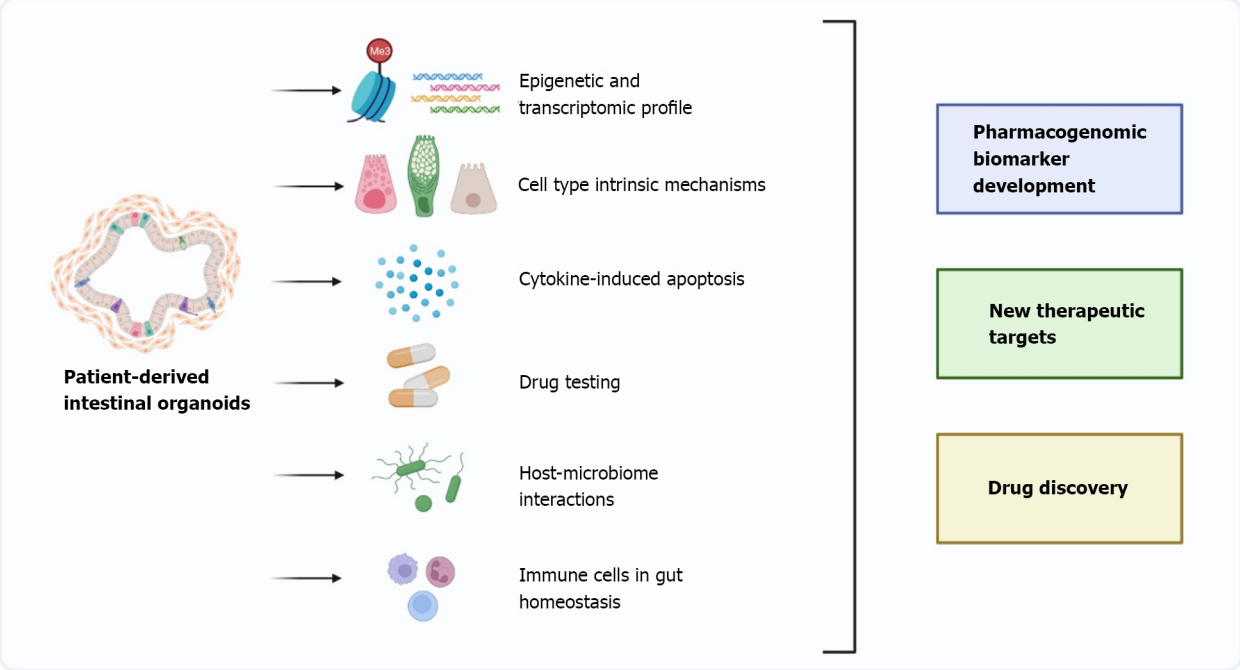
In addition, ASC-derived organoids can undergo extensive expansion in culture and maintain genome stability, which makes them suitable for biobanking[39].

In this review, we focus on the most significant advances in IBD research obtained using ASC-derived intestinal organoids (Figure 1).

Organoid models to study the genetic and epigenetic contribution on IBD epithelium

Several forms of IBD are polygenic and multiple susceptibility loci have been correlated to IBD onset [38]. Intestinal organoids retain the genetic and epigenetic signatures of the original tissue and can hence be employed for studying genetic and epigenetic-phenotypic profiles[22]. Moreover, the study of specific variants affecting the different cell types constituting the epithelium of IBD patients could identify sub-phenotypes of the disease that could help to understand their behavior and outcome[40].

Organoids also maintain the region-specific (duodenum/ileum/jejunum) gene expression of the gastrointestinal tract from which they derive[41]. Moreover, biopsies from IBD patients and derived



DOI: 10.3748/wjg.v28.i24.2636 **Copyright** ©The Author(s) 2022.

Figure 1 Intestinal organoid in inflammatory bowel disease research: The future of precision medicine. Patient-derived intestinal organoids are three-dimensional *in vitro* cell structures derived from stem cells that differentiate and self-organize into functional intestinal epithelium-specific cell types. For this reason, this model is suitable for different research approaches useful to inflammatory bowel disease (IBD) modelling and to study current and new therapeutic options. By retaining the disease-specific phenotypic defects, intestinal organoids can be employed to study epigenetic and transcriptomic profiles. In addition, the ability of intestinal organoids to differentiate into all the different cell types present in the intestinal epithelium makes this model useful to discover new cell-specific disease mechanisms. Furthermore, organoids can be used to study cytokine-induced apoptosis and to test currently used drugs to better understand their mechanisms. Co-culturing intestinal organoids with either microbiota components or immune cells helps to investigate IBD pathogenesis. Thanks to all these research approaches new pharmacogenomic biomarkers, new therapeutic targets and new drugs could be discovered, enabling the development of precision medicine for IBD patients. The image was created with https://biorender.com/.

intestinal organoids show similar expression levels of several IBD-marker genes. Dotti *et al*[42] have identified a set of genes, including *LYZ*, *CLDN18,* and *HYAL1,* upregulated both in the mucosa of patients with active UC and in the derived organoids[42]. Accordingly, the expression levels of genes encoding junctional proteins, such as *ZO-1*, also known as *tight junction protein 1*, *OCLN* and *CTNNB*, were similar in intestinal crypts from CD-patients and derived organoids.

VEO-IBDs are a subset of pediatric patients with IBD diagnosed before the age of 6 years, and up to 15% of these patients may have a rare monogenic disorder. Several defects in genes responsible for the proper intestinal epithelial barrier functions have been discovered, including *NOX1*[43] and *TTC7A*[44]. To study the impact of these mutations on IECs, Schwerd *et al*[44] generated human colonic organoids of patients affected by IBD carrying a *NOX1* p.N122H mutation[44]. These organoids show significantly less production of constitutive superoxide than organoids derived from healthy patients. This defect could favor the crypt colonization by luminal microorganisms since superoxide has an anti-adhesive or anti-invasive effect on bacteria. On the other hand, biallelic missense mutations in the *TTC7A* gene have been found in VEO-IBD patients, resulting in the activation of RhoA-dependent proteins which regulate cytoskeletal architecture by altering cell polarization and proliferation, as demonstrated in organoid cultures[45].

Among the genetic variants associated with the risk of developing IBD, polymorphisms in *NOD-2*, involved in the microbial pathogens recognition[46], and *ATG16L1*[47] genes play an important role. However, their biological functions in the intestinal epithelium of IBD patients remain unclear[47,48].

Organoids generated from *NOD2* knockout (KO) mice show increased intracellular *Escherichia coli* (*E. coli*) following metabolic stress[48], while the number of Paneth cells, known to have antimicrobial activity in the intestinal epithelium, is not affected. *Atg16L1*-deficient intestinal organoids derived from mice present a higher activation of STING-dependent type I interferon (IFN) signaling after IL-22 stimulation, leading to transient endoplasmic reticulum (ER) stress[49]. No data on patient-derived organoids with variants already associated with the increased susceptibility to IBD have been published yet.

Kelsen *et al*[50] reported transcriptomic differences from RNA sequencing between organoids derived from pediatric IBD (VEO and older onset) and non-IBD patients[50]. One of the most upregulated genes in organoids generated from pediatric IBD patients is *LYZ*, encoding for the antimicrobial protein

lysozyme, confirming previous results by Dotti *et al*[42] conducted on adult IBD patient-derived organoids[42]. In addition, an upregulation of the antigen presentation genes *HLA-DRB1* and *HLA-DRA*, necessary for T-cell activation, was demonstrated[50]. Similar results have been obtained by McDonald and Jewell[51] in mucosal epithelial cells by histological and immunohistochemical analysis on colonic biopsy specimens[51]. It is therefore possible that, since these genes are upregulated, the continuous and pathological activation of T cells may lead to the development of IBD[50]. Moreover, the same authors have found that the most downregulated gene in IBD-derived organoids was *CD177*[50], a glycosylphosphatidylinositol-anchored glycoprotein expressed in neutrophils and colon crypt cells.

Looking at the role of epigenetic modifications in IBD, a recent study showed changes in DNA methylation profiles in purified IECs from IBD, compared to non-IBD pediatric patients, that were strictly correlated to IBD pathogenesis[40]. To assess whether these alterations are also preserved in 3D models, intestinal organoids have been developed from children newly diagnosed with IBD and from healthy controls. Differences in DNA methylation and transcription profiles have been found between pediatric patient-derived organoids and controls. This suggests that IBD-associated intestinal epithelial-specific epigenetic alterations can be preserved in organoid cultures. Moreover, it has been observed that these epigenetic alterations are stable over time and therefore can contribute to chronic relapsing inflammation due to impaired IEC function[40].

These data suggest that intestinal organoids can be a promising tool to assess the molecular and functional effects on the intestinal epithelium of genetic and epigenetic variations related to IBD.

Intestinal organoids to study the epithelial barrier

The intestinal epithelium, consisting of different cell types (enterocytes, enteroendocrine cells, goblet cells, and Paneth cells), plays a fundamental role in maintaining intestinal homeostasis, acting as a physical and chemical barrier against pathogens through the production of mucus and antimicrobial peptides. A defect of these activities is evident in IBD patients, but it is still not clear whether these are primary defects or secondary effects of the inflammatory state[52].

In particular, reduced levels of trefoil factor 3 in goblet cells of IBD patients have been observed, which results in a decreased viscosity of the intestinal mucus layer and, as a consequence, the invasion of several IBD-inducing microorganisms. In IBD patients, decreased goblet cells number, diminished mucin 2 (MUC2) production, reduced mucus sulfation, and decreased mucus barrier have been detected [53-55]. Moreover, a decreased expression of constitutive defensins by Paneth cells in IBD patients has also been observed: A low expression of the constitutive human ß-defensin 1 has been demonstrated in patients with UC, while a low expression of human ß-defensin 2 and human ß-defensin 3 was demonstrated in those affected by CD, allowing bacteria to enter the intestinal mucosa[56].

Intestinal organoids can be manipulated to induce differentiation to definite lineages, allowing the study of cell-type-specific functions/dysfunctions in the context of the intestinal epithelium as described in the study conducted by Treveil *et al*[57]. Intestinal organoids can be specifically differentiated towards goblet cell or Paneth cell lineages by specific small molecules, with improved representation of these cell types within the entire organoid cell population[57]. In particular, organoids enriched in Paneth cells can be obtained with the addition of DAPT, a small molecule inhibitor of Notch signaling, whereas the differentiation towards the goblet cell lineage can be induced through the addition of DAPT and IWP-2, which inhibits Wnt signaling[58]. To characterize the effect of cell type enrichment and to predict key molecular regulators involved in Paneth cell and goblet cell specific functions, authors have used mRNA, miRNA, and lncRNA profiles[57]. Thanks to this approach, they predicted key factors involved in differentiation or maintenance of Paneth cells and goblet cells, such as Cebpa, Jun, Nr1d1, and Rxra specific to Paneth cells, Gfi1b and Myc specific for goblet cells, and Ets1, Nr3c1 and Vdr shared between them. Interestingly, several predicted regulators are associated with inflammation and IBD, indicating that their dysregulation can contribute to IBD pathogenesis[57].

Organoids derived from a mouse model of colitis were established to investigate the relationship between the differentiation state and cytokine secretion in the intestinal epithelium[59]. Undifferentiated mouse-derived intestinal organoids showed expression levels of pro-inflammatory cytokines and other inflammatory mediators higher than those differentiated into secretory or absorptive lineages. This suggests that the differentiation state of the intestinal epithelium, regardless of bacteria and immune cells, promotes the release of immunomodulatory factors and has a crucial role in maintaining intestinal homeostasis[59].

In IBD, cytokines play an important role in the pathological process. In particular, TNF-α, which is produced by immune and non-immune cells, through the activation of different pathways including NF-kB, can stimulate the production of other pro-inflammatory cytokines by macrophages and induce the death of Paneth cells, epithelial cells, and T cells[60]. TNF-α has an accepted role in the continuous immune stimulation in intestinal organoids by triggering several signaling cascades which lead to cell activation, survival, and gene expression[61]. It has also been confirmed that high expression of the TNF-α induced protein 3 gene, which encodes A20, a ubiquitin-editing enzyme and negative feedback regulator of NF-kB, promotes TNF-α dependent IEC death[62]. Intestinal organoids from A20 transgenic mice, in which A20 expression is driven by the Villin promoter, were more susceptible to TNF-dependent death. Moreover, after TNF-α addition, A20 transgenic organoids showed a strong caspase 3 and 8 expression whereas control organoids were unaffected, indicating that immune cells or gut

microbiota are not necessary for TNF-induced apoptosis of A20-expressing cells[62]. The authors demonstrated that this effect depended on receptor-interacting protein kinase 1 with its proapoptotic activity, and A20 was found to associate with the death-inducing signaling ripoptosome complex, potentiating its ability to activate caspase-8[62].

Grabinger *et al*[63] have found that both TNF-α receptors, TNFR1 and TNFR2, are involved in cell death in intestinal organoid models, although TNFR1 is the predominant mediator[63]. Indeed, the authors showed an almost complete abrogation of TNF-induced cell death in TNFR1-deficient organoids while organoids from TNFR2-deficient mice showed reduced cell death following exposure to TNF[63].

Ferrer-Picón *et al*[64] have observed that TNF-α reduces the response to butyrate of the intestinal epithelium by decreasing its uptake, oxidation, and consumption[64]. The authors have used differentiated epithelial organoids from IBD patients, which mimic the phenotype of cells residing on the luminal side of the crypt and that are directly exposed to bacteria and their metabolites, and non-IBD controls treated with butyrate and TNF-α. The expression of the butyrate transporters monocarboxylate transporter 1 (encoded by *SLC16A1*), *ABCG2,* and the butyrate receptor *GPR43* was evaluated. After TNF-α treatment, they have found a downregulation of *SLC16A1* and *ABCG2* genes, as well as an increase of *GPR43* gene expression in both IBD and non-IBD derived organoids, indicating that the response to butyrate is not intrinsically altered in IBD patients and that inflammation affected butyrate uptake and oxidation[64].

TNF-α also contributes to barrier deterioration by activating the myosin light chain kinase, which alters tight-junctions (TJ), and, therefore, intestinal permeability[63]. TJ dislocation seems to be a crucial event in IBD pathogenesis as confirmed by Hall *et al*[65]. These authors have demonstrated that the downregulation of the creatine transporter (*SLC6A8*, also known as CRT), observed in IBD patients, is associated with alterations in TJ architecture[65]. In detail, CRT-KO intestinal organoids show a leaky TJ profile, a stressed metabolic phenotype, and a diminished epithelial barrier formation. This might be caused by a decreased creatine uptake, which is required by actin and myosin to regulate TJ structure and intestinal barrier integrity[65].

The role of inflammation in the intestinal epithelial barrier function has also been investigated by the FITC-dextran 4kDa (FD4) uptake assay, using murine intestinal organoids exposed *in vitro* to dextran sodium sulfate (DSS)[66]. DSS is a sulfated polysaccharide with variable molecular weights which causes UC-like pathologies due to its toxicity to colonic epithelial cells, which results in compromised mucosal barrier function. DSS caused a decline in the absorption ability of the inflamed-organoid intestinal barrier, confirmed by FD4 altered intestinal concentration and reduced translocation to the lumen. DSS also caused increased production of TNF-α, IL-6, and other important factors involved in the epithelial barrier disruption, including matrix metallopeptidases MMP10, MMP3, the chemokine ligand CXCL1, and the proteasome-dependent protein degradation ubiquitin D (UBD)[66].

Alteration in the autophagy process within different cellular compartments could potentially lead to an inflammatory response in the gut, increasing intestinal barrier dysfunction and IBD development [67]. Autophagy is a housekeeping process that maintains cellular homeostasis, allowing the degradation and recycling of cellular components[68,69]. Autophagy is also dysregulated in intestinal organoids from patients with IBDs and in mouse intestinal organoids lacking *ATG16L1*, which show decreased Paneth cell levels and increased ER stress-induced cell death, exacerbated when cultured with TNF-α[49,68]. Additionally, recent studies have suggested a novel process by which altered autophagy is associated with IBDs: As already observed in other autophagy-deficient cellular models, such as ATG5-/- and ATG16-/- mouse embryonic fibroblast cells, Atg7−/− autophagy-deficient mouse intestinal organoids show increased levels of argonaute 2, a crucial effector of miRNAs whose upregulation in patients with IBD results in the altered expression of genes implicated in IBD pathogenesis.

Different studies have also demonstrated a crucial relationship between unresolved ER stress, failing autophagy, and pro-inflammatory mediators in IECs during active IBD. For example, IL-22 potentiates the ER stress response caused by other cytokines *via* the activation of STAT3 and induces IEC apoptosis in synergy with IL-17A[49]. Moreover, IL-22 treatment reduces the LGR5+ intestinal stem cell (ISC) levels and amplifies the number of transit-amplifying (TA) cells, an undifferentiated population in transition between stem cells and differentiated cells, by inhibiting Wnt and Notch signaling pathways [70]. All these findings show that IL-22 decreases organoid survival by limiting ISC expansion and promoting TA progenitor proliferation[71].

Intestinal organoids to study the relationship between IECs and the surrounding cells, including immune cells and microbiota

IECs are involved in complex crosstalk with other cell types, including immune and mesenchymal cells. Intestinal organoids have been used for in-depth *ex vivo* analyses of interactions between the epithelium and lamina propria cells[29] and between the epithelium and the underlying immune cells[22].

Co-culturing intestinal organoids with other specific cell types may help to investigate IBD pathogenesis. For example, Ihara *et al*[72] have established a mouse organoid–mononuclear phagocyte (MP) co-culture to study how MPs, such as dendritic cells and macrophages, accumulate in the inflamed intestine causing an imbalance between intestinal immune responses and microbiota and mediating

several interactions with other intestinal cell types[72]. The authors have revealed that excessive E-cadherin, a cell adhesion molecule crucial in the formation of adherens junctions (AJs), expressed by MPs, mediates their adhesive interactions with the epithelium, activating Notch signaling and perturbing physiological IEC differentiation and epithelial homeostasis, with the promotion of goblet cell depletion, mucus layer disruption, dysbiosis, and gut inflammation[72].

Intestinal organoids are also useful to study the interactions between IECs and luminal bacteria, involved in intestinal inflammation: Abnormal growth of a specific microorganism leads to unbalance of the gut microbiota, which may initiate intestinal inflammatory diseases, including IBD[73]. Dysregulated immune responses towards the gut microbiota induce a tissue-damaging chronic inflammatory state, leading to barrier dysfunction, infections, and intestinal inflammation[74]. Therefore, the microbiota-epithelial interaction has been investigated to understand IBD pathogenesis. Intestinal organoid models have emerged as a helpful tool to study this crucial interaction *in vitro,* showing that differences in IEC behavior can contribute to the altered composition of the gut microbiome, barrier permeability, and microbiome interaction in IBD patients[75]. This has been confirmed by Leber *et al* [74], who have used mouse intestinal organoids to study the nucleotide-binding oligomerization domain, leucine-rich repeat containing X1 (NLRX1) as a regulator of gut homeostasis, involved in the control of the immune response, microbiota composition, and metabolism[74]. Intestinal organoids derived from NLRX1-deficient mice show an altered glutamine metabolism because of increased glutamate dehydrogenase activity compared to intestinal organoids obtained from WT mice. With this abnormal host glutamine metabolism, intestinal bacteria may be less exposed to amino acids, and this may lead to increased proliferation of microorganisms capable of amino acid production[75].

In addition, it has recently been found that organoids derived from mice with highly simplified microbiota are different from those derived from mice harboring complex-conventional microbiota[76]. For example, organoids derived from mice harboring limited bacterial species have an accelerated proliferation rate, are less subjected to cell death, and respond differently to pro-inflammatory stimuli, in particular TNF-α stimulation. The effects of different concentrations of TNF-α on these two organoids have been studied: ISC growth from mice with limited bacterial species was inhibited only by the lower concentration of TNF-α tested compared to that of mice with complex bacterial species, in which growth was inhibited by all concentrations tested. Moreover, with increased concentration of the cytokine, the inhibition decreases, and, conversely, growth of organoids from mice with limited bacterial species is promoted. These results suggest that the microenvironment, such as microbial composition, of the intestinal segment from which the organoids are originated could affect ISC replication and, as a consequence, organoid growth, and could also affect the response to different concentrations of cytokines, such as TNF-α[76].

Intestinal organoids can be employed to evaluate the contribution of luminal pathogens to IBD pathogenesis. For example, the cytotoxic effect of *Clostridioides difficile* toxins on the small intestinal epithelium was studied using a jejunal-derived intestinal organoid culture developed by Engevik *et al* [77]. These organoids show high expression of the toxin A and the binary toxin *C. difficile* transferase receptors, and as a result, are more sensitive to toxin A than to toxin B, the other toxin produced by *C. difficile*, developing mucosal damage and an altered permeability[77].

In consideration of the aforementioned data, organoid models must be implemented with the intestinal microbiota to determine the specific effect of bacteria on the epithelial barrier[22]. However, organoid cultures form a spheroid with an enclosed lumen and, therefore, pathogens introduction is difficult[78]. For this reason, different techniques have been generated to better introduce microorganisms into the intestinal organoids. For example, Saxena *et al*[79] have mechanically disrupted the organoids to promote bacterial exposure; however, polarization was lost and, consequently, both the apical and basolateral domains were in contact with bacteria[79]. Leslie *et al*[80] have developed microinjection techniques to introduce bacteria into organoids but these procedures are difficult to perform and to replicate[80]. According to several studies, the culture of intestinal organoids in monolayer could overcome these limits since it preserves the major properties and factors of intestinal epithelium *in vivo*; hence, 3D organoids have been mechanically disrupted and seeded on transwell membrane gels to form a selective and permeable layer, separating the apical and basal domain which are both directly accessible[29]. This important innovation shows the ability to manipulate the model system, introducing bacteria and viruses in the culture medium on the luminal side, and represents a powerful alternative to other 2D models of primary epithelial cells by mimicking *in vivo* physiology and providing a lumen (apical side) and a lamina propria (basal domain)[29,75]. It has been demonstrated that the monolayer system successfully reflects the properties of intestinal epithelium *in vivo*, including epithelial barrier formation, polarization, and gene expression profiles[75]. The monolayer also reflects the aberrant permeability caused by pro-inflammatory cytokines, such as TNF-α and IFN-γ, which cause a mislocalization of both TJs and AJs and reduce their mRNA levels[81]. Another successful use of the organoid-derived monolayer has been demonstrated by Sayed *et al*[82]: These authors demonstrated that detection of high concentrations of the engulfment and cell motility protein 1 in the epithelium could be a diagnostic marker of dysbiosis and gut inflammation since it is a crucial intestinal bacterial sensor[82]. In addition, a co-culture of human intestinal organoid-derived monolayer and macrophages shows how epithelial and innate immune cells respond to pathogens[83]. In this model, macrophages have the capability to sense and interact with *E. coli,* when added to the apical side of IECs, by

improving their adherence properties and by promoting the generation of cell membrane projections to capture the pathogen. This system has provided an important tool to evaluate the host defense towards organisms[83].

INTESTINAL ORGANOIDS TO STUDY CURRENT THERAPIES

Intestinal organoid cultures have recently been employed to study the molecular mechanisms of action of already approved drugs (Table 1).

In IBDs, mucosal healing has emerged as a key prognostic parameter and represents the therapeutic goal in the treatment of these diseases[84]. Indeed, healing means suppression of inflammation, improvement of intestinal barrier by a dynamic interaction of cell regeneration, differentiation, and migration[19] and, consequently, sustained clinical remission, reduced rate of surgery, and lower incidence of potential long term complications such as colorectal cancer[85,86]. However, although a number of therapies have become available in recent years, IBD heterogeneity makes it difficult to obtain complete mucosal healing in order to avoid relapse, and it is not yet clear which is the optimal therapy for a specific patient. A better comprehension of the mechanisms involved in mucosal healing may contribute to ameliorating the therapeutic and clinical approaches currently used. For example, IL-10 KO mouse intestinal organoids, which spontaneously develop enterocolitis, and WT mouse intestinal organoids have been established to understand the different molecular interactions between azathioprine, 5-aminosalicylic acid, and the intestinal epithelium and the mechanistic aspects of mucosal healing[19]. In detail, the researchers have treated with TNF-α the WT and IL-10 KO organoids with and without 5-aminosalicylic acid and azathioprine and have investigated the expression levels of E-cadherin and desmoglein-2, which are closely related to the regulation of the intestinal barrier. TNF-α-treated WT organoids showed internalization and abnormal disruption of E-cadherin, while treatment with 5-aminosalicylic acid and azathioprine restored E-cadherin levels on cell membranes. On the other side, untreated IL-10 KO organoids resulted in defective E-cadherin membrane expression and increased cytoplasmatic expression, which was not further altered by TNF-α treatment. However, it was observed in both models that the effects on E-cadherin were greater with 5-aminosalicylic acid than with azathioprine treatment. Western-blot analysis confirmed that the two drugs impact only the re-distribution of proteins on the intestinal surface. Desmoglein-2 levels were reduced by TNF-α administration in WT models and restored only by 5-aminosalicylic acid whereas, in IL-10 KO organoids, desmoglein-2 expression was increased in all treatment groups by the activation of p38 mitogen-activated protein kinase pathway, a crucial factor in the maintenance of epithelial barrier[19].

Intestinal organoids have also been employed to study the effects of the thiopurine thioguanine on the replication of rotavirus, a *Reoviridae* family virus that might play a role in the pathogenesis of IBD [87]. Although thioguanine is rarely used to treat IBD due to its adverse effects, it has been proposed in the treatment or prevention of rotavirus infection *via* Rac1 inactivation. Rac1 is a member of the Rho family of small GTPases, ubiquitously expressed, which mediates several cellular signaling pathways including actin reorganization, gene transcription, apoptosis, and redox signaling. Rac1 shows two conformational states, the inactive GDP-bound structure and the active GTP-bound form which exerts the biological functions. Several viruses use Rac1 in the active conformational form to infect cells, a process impaired by a loss-of-function of Rac1 by gene knockout or knockdown. It has been demonstrated that virus replication is interrupted after thioguanine treatment at a dose of 100 ng/mL in patient-derived rotavirus isolated from human intestinal organoids. This could be due to thioguanine metabolites, deoxy-6-thioguanosine phosphate and 6-thioguanosine phosphate, that can bind to Rac1, forming a complex and inhibiting the Rac1 activity[87].

Anti-TNF agents, in particular infliximab, have been established as the reference therapy to treat refractory IBD. However, whether anti-TNF agents have any direct effect on IECs remains unknown [53]. Recently it was demonstrated that treatment of organoids from UC patients with infliximab concurrently with TNF-α did not cause a clear effect on their viability or morphology but resulted in a significant reduction of UBD mRNA expression. UBD is a ubiquitin-like modifier involved in protein degradation that is upregulated in inflamed intestinal tissue. UBD mRNA expression pattern also correlated with protein levels, as confirmed by immunoblotting of organoid lysates[88].

Glucocorticoids have beneficial effects in restoring the epithelial barrier disrupted by cytokines. Xu *et al*[89] studied the epithelial barrier function of ASCs derived intestinal organoids of CD patients and the role of glucocorticoid treatment[89]. Using confocal microscopy, they evaluated the permeation of the FD4 marker, which is used to measure macromolecular paracellular permeability from the basal to the luminal side of organoids treated with a cytokine mixture. After an increase in intraluminal FD4 concentration compared to the untreated, the authors exposed the organoids to the glucocorticoid prednisolone, which significantly reduced intraluminal FD4 permeation. In addition, prednisolone restored CLDN2 expression that was upregulated by the cytokine mixture[89]. This is crucial because CLDN2 is one of the most represented TJ components, forming cation-selective pores that make the intestinal barrier more permeable to ions and molecules and its expression is increased in CD patients biopsies[90,91]. The authors also found that the administration of mifepristone, a glucocorticoid receptor

Table 1 Molecular target identified by treatment of intestinal organoids with current therapies for inflammatory bowel disease

Molecular target	Treatment effect	Drug	Species	Ref.
E-cadherin	Re-distribution of protein on intestinal surface restored correct permeability	5-aminosalycilic acid, azathioprine	Mouse (IL-10$^{-/-}$)	[19]
Desmoglein-2	Restored physiological desmoglein-2 expression levels	5-aminosalycilic acid	Mouse (IL-10$^{-/-}$)	[19]
UBD	Restored physiological UBD expression levels	Infliximab	Human (UC patients)	[88]
CLDN-2	Restored physiological CLDN-2 expression levels	Prednisolone, tofacitinib	Human (CD and CRC patients)	[89, 92]
ZO-1	Re-distribution of protein on intestinal surface restored correct permeability	Tofacitinib	Human (CRC patients)	[92]

CD: Crohn's disease; CLDN-2: Claudin-2; CRC: Colorectal cancer; IL-10: Interleukin-10; UBD: Ubiquitin D; UC: Ulcerative colitis; ZO-1: Zonula occludens.

antagonist, reduced the beneficial effect of prednisolone, confirming that the effect is glucocorticoid receptor dependent[89].

A recent study published by Sayoc-Becerra and collaborators employed human colonic organoids to understand how tofacitinib treatment restores TJ architecture and epithelial barrier functions, achieving healing[92]. In addition to CLDNs, OCLN and tricellulin are induced by different pro-inflammatory mediators, such as IFN-γ. These proteins are highly expressed in the intestinal epithelium and control the paracellular transport of solutes, while ZO-1 regulates and assembles TJ structure. Therefore, the proper localization of these proteins is essential in the maintenance of the epithelial barrier function. Several genes are involved in regulating the epithelial barrier function, including genes that control the Janus Kinase-signal transduction and transcription pathway [Janus kinase-signal transducer and activator of transcription (JAK-STAT)]. The activation of JAK-STAT signaling induces the triggering of JAK1 and JAK2 and the phosphorylation of their downstream targets STAT1 and STAT3 which are associated with the upregulation of CLDN2, and the consequent altered permeability across the intestinal epithelium. Therefore, targeting the JAK-STAT pathway has become a new therapeutic approach in IBD, and tofacitinib has been approved as a pan-JAK inhibitor. The drug binds to the adenosine triphosphate binding site in the catalytic cleft of the kinase domain of JAK and inhibits the activation of JAK-STAT pathway. Tofacitinib has a direct effect on IECs, rescuing the permeability altered by INF-γ. After IFN-γ treatment, FD4 influx increases approximately 4-fold into the organoids, and the addition of tofacitinib restores the FD4 physiological flux. To better understand the specific mechanism of tofacitinib on IECs, ZO-1 and OCLN levels were evaluated by western blotting in intestinal organoids, but were unaltered after IFN-γ and tofacitinib treatments. These results suggest that tofacitinib is able to counter damages caused by IFN-γ on epithelial permeability by re-localization of TJ proteins rather than by increasing their expression[92].

Lloyd *et al*[93] have recently demonstrated for the first time the potential use of macrolides, in particular clarithromycin, in the treatment of IBDs[93]. Using human intestinal organoids generated from patients without evidence of IBD, these authors have demonstrated that, in addition to its antibiotic properties, clarithromycin shows anti-inflammatory effects in the intestinal epithelia, suppressing the increase in NF-kB nuclear levels induced by TNF[93].

INTESTINAL ORGANOIDS AS A RESEARCH TOOL FOR NEW POSSIBLE THERAPEUTIC APPROACHES

Recently, studies have been performed using mouse and human intestinal organoids to identify novel therapeutic targets and approaches for IBD treatment[21] (Tables 2 and 3).

The liver receptor homolog 1 (LRH-1) is a nuclear receptor that has been found in the intestinal crypts, where it promotes epithelial renewal by activating Wnt/β catenin signaling[94]. The use of human intestinal organoids has demonstrated the fundamental role of LRH-1 in intestinal epithelial homeostasis and cell survival, confirming the results derived from humanized mouse intestinal organoids in which the mouse *Lrh-1* is deleted, and the human *LRH-1* is expressed. Intestinal organoids from both CD patients and healthy controls have shown that LRH-1 overexpression abrogates TNF-α-mediated cell death and improves epithelial resistance to the effects of fluorouracil, a chemotherapeutic agent with known intestinal toxicity which has been used to mimic damaged mucosa, reducing intestinal inflammation and epithelial wounds[94]. The activation of LRH-1 is ligand-dependent and is carried out by signaling phospholipids, such as phosphatidylinositol trisphosphate, which has been demonstrated to bind with high-affinity LRH-1[95]. It has been demonstrated that modeling

Table 2 Novel potential molecular targets identified using intestinal organoids

Potential molecular targets	Effect	Species	Ref.
LRH-1	Improved resistance to pro-inflammatory mediators and induced mucosal healing	Humanized mouse (Lrh-1$^{-/-}$ LRH-1$^{+/+}$) and Human	[94]
PXR	Reduced NF-kB activity	Human (IBD patients)	[97]
IL-22-pSTAT3 SP	Restored tissue damage and intestinal homeostasis	Mouse (ATF3$^{-/-}$)	[98]
TGF-β SP	Arrested inflammatory signals	Mouse	[104]
SIRT2	Regulated Wnt/β-catenin SP	Mouse (Sirt2$^{-/-}$)	[105]

ATF3: Activating transcription factor 3; IBD: Inflammatory bowel disease; IL: Interleukin; LRH-1: Liver receptor homolog 1; NF-kB: Nuclear factor-kappa B; PXR: Pregnane X receptor; SIRT2: Human sirtuin protein 2; SP: Signaling pathway; STAT: Signal transducer and activator of transcription; TGF-β: Transforming growth factor B.

Table 3 Potential therapeutic approaches for inflammatory bowel disease treatment identified using intestinal organoids

Potential therapeutic approaches	Effect	Species	Ref.
Sex hormones	Decreased expression of ER stress markers	Human (UC female patients)	[100]
Naltrexone	Reduced ER stress levels, increased the expression of endogenous encephalins and endorphins	Human (IBD patients)	[101]
Bacillus subtilis (RZ001)	Promoted intestinal mucosa repair	Mouse	[102]
Bacterial indoleacrylic acid	Promoted anti-inflammatory cytokines secretion while inducing goblet cells differentiation	Mouse	[103]
Hyaluronan 35 kDa	Promoted epithelial wound healing	Mouse	[106]

ER: Endoplasmic reticulum; IBD: Inflammatory bowel disease; UC: Ulcerative colitis.

hydrophobic residues in the binding site of the receptor prevents ligand binding[96], resulting in a failed rescue of TNF-α-mediated cell death. This finding suggests that targeting LRH-1 could improve resistance to pro-inflammatory mediators and induce mucosal healing in IBD patients[94].

Intriguingly, pregnane X receptor (PXR), the main signal transducer in the intestinal response to xenobiotic stress, has been shown to reduce NF-kB activity, whose contribution in IBD pathogenesis is undisputed[97]. Intestinal organoids derived from patients with IBD were pretreated with TNF-α and then with the antibiotic rifampicin, a known PXR ligand. PXR inhibits the expression of several pro-inflammatory genes, especially in the IEC compartment, compared to the stromal and immunological compartments, and reduces IL-8 and IL-1β levels, which are NF-kB target genes. Therefore, the stimulation of PXR by rifampicin or other PXR ligands might be of interest as a novel therapeutic approach in IBD management, especially in patients in which hyper-activation of NF-kB pathway occurs[97].

Moreover, a novel IL-22-induced signal in IECs has been observed thanks to the use of organoids. IL-22 activates its downstream target, the activating transcription factor 3 (ATF3) which is actively involved in the IL-22-pSTAT3 signaling pathway to restore tissue damage and intestinal homeostasis [98]. Stimulation of IECs by IL-22 initiates a signal cascade leading to phosphorylation and consequent activation of STAT3 *via* the involvement of ATF3. This protein has been identified as an essential factor for IEC proliferation by directly controlling crypt regeneration and recovering and maintaining epithelial barrier functionality. To confirm these data, colon organoids from WT and ATF3$^{-/-}$ mice have been implanted into DSS-treated ATF3$^{-/-}$ mice colon through intra-rectal injection. Only mice transplanted with WT organoids showed a reduction in the inflammatory state with increased cell survival, reduced disease activity, recovered epithelial injuries, and improved colon integrity. Most importantly, inducing the IL-22 pathway can promote host defense and wound restoration and can mitigate disease progression and perpetuation[98]. However, several studies have also reported a critical role of the STAT3 signaling pathway, demonstrating that it suppresses the autophagy processes, causing bacterial invasion and intestinal inflammation[99]. Indeed, the inhibition of this pathway protects the *Salmonella*-infected-intestinal mouse-organoid model from bacterial-induced injury, reducing the pro-inflammatory cytokine levels and restoring the autophagy processes. Interestingly, persistent alteration in autophagy processes could lead to chronic intestinal inflammation, exposing the

intestinal epithelium to bacteria and pathogens[99].

In addition to IL-22, IL-28 has also emerged as a novel therapeutic approach by promoting mucosal healing and wound repair *via* the phosphorylation and activation of STAT1. This has been confirmed by using organoids derived from WT, IL28RA$^{-/-}$, and STAT1-lacking mice. IL-28 controls proliferations of intestinal crypts in WT organoids by activating IL-28RA and STAT1 signaling pathways, and induces the overexpression of several genes implicated in crucial functions, including the positive regulation of cytokine production, immune response, and wound healing. This suggests that the epithelial STAT1 phosphorylation by IL-28 balances gut homeostasis.

Of note, some pro-inflammatory cytokines have also been found to be negatively modulated by high levels of progesterone and estrogen released during pregnancy in IBD patients[100]. To clarify the effect of sex hormones, van der Giessen *et al*[100] have established intestinal organoids from UC females and mimicked the tissue inflammation with tunicamycin, which results in an increased expression of ER stress markers, including the 78 kDa glucose-regulated protein 78 (GRP78), CCAAT-enhancer-binding protein homologous protein (CHOP), and phosphorylated inositol-requiring enzyme 1 (IRE1). Specifically, GRP78 expression is decreased after progesterone addition, the stress-downstream target CHOP is reduced with estrogen alone or in combination with progesterone, and IRE1 phosphorylation is decreased upon treatment with estrogen, progesterone, or with their combination. In addition, IL-8 and IL-6, which are highly expressed in inflamed intestine, are modulated by hormones only in tunicamycin-treated organoids, thus suggesting that estrogen and progesterone decrease the stress-induced cytokine production. Moreover, sex hormones positively modulate the intestinal barrier by ameliorating TJ dynamics *via* the upregulation of CLDN1, CLDN2, and OCLN. A limitation of this study is the hormone concentration used *in vitro*, that was significantly higher than the *in vivo* hormone levels during pregnancy. However, a new possible clinical approach in IBD, applying treatment with sex hormones could be proposed[100].

ER stress has also been significantly reduced by a low dose of naltrexone, an opioid antagonist that acts on the μ-opioid receptor (MOR)[101]. This has been confirmed using intestinal organoids from patients with IBD treated with LPS, which induces the expression of GRP78, an important ER stress marker. Treatment with naltrexone reduced ER stress levels and increased the expression of encephalins and endorphins, endogenous agonists of opioid receptors. Interestingly, low doses of naltrexone induced clinical improvement in 74.5% of patients with refractory IBD and long-lasting disease remission in 25.5%. In addition, it has been reported that naltrexone is safe in pediatric IBD patients. The molecular mechanism by which naltrexone is able to reduce ER stress is not entirely clear; however, the authors hypothesize that it could be due to the antagonism on MOR[101].

Organoid cultures have also been treated with several luminal bacteria to better comprehend their positive modulation of inflammatory flares during IBD. For example, the probiotic *Bacillus subtilis* RZ001 promotes intestinal mucosa repair in organoid models by upregulating the expression of MUC2 in the mucus layer[102]. On the other hand, Wlodarska *et al*[103] have evaluated the role of bacteria that are able to use mucins as an energy source as a new possible therapeutic approach by the release of the indoleacrylic acid (IA), a beneficial bioactive tryptophan metabolite[103]. Bacterial IA treatment does not change organoid growth or size but increases the expression of genes associated with goblet cell functions, such as MUC2, which is decreased during intestinal inflammation, and the expression of target genes in the NF-E2-related factor 2-mediated antioxidant pathway, which also suppresses pro-inflammatory pathways and activates aryl hydrocarbon receptor signaling. In fact, an upregulation of the aryl hydrocarbon receptor target gene *CYP1A1* was observed. In addition, IA increases MUC2 and IL-10 levels and decreases TNF expression in LPS-treated co-cultures of bone marrow-derived macrophages and murine intestinal organoids, thus suggesting that IA can simultaneously promote anti-inflammatory cytokines secretion while inducing goblet cells differentiation[103].

Another important anti-inflammatory function has been found for transforming growth factor β (TGF-β): TGF-β signaling pathway arrests inflammatory signals in the intestinal compartment through small mother against decapentaplegic (SMAD4) activation as downstream target[104]. After the binding to its receptors, TGF-β induces the phosphorylation and activation of receptor-SMADs, which consequently bind SMAD4, translocate into the nucleus, and regulate gene transcription, thus acting as transcriptional repressors or activators of genes. The anti-inflammatory effect of TGF-β has also been demonstrated using mouse intestinal organoids: In particular, it has been observed that exposure to TNF-α induces the expression of *CCL20*, that encodes for a chemokine that is up-regulated by inflammatory signaling pathways, and that, following the addition of TGF-β, this induction is interrupted [104].

The canonical Wnt signaling pathway plays a fundamental role in maintaining intestinal epithelium homeostasis, preserving the undifferentiated ISC profile, inducing proliferation and controlling differentiation[105]. The epithelial human sirtuin protein 2 (SIRT2) is also known to be involved in cell differentiation, growth, and autophagy. To better investigate the role that these factors play in IBD, Li *et al* [105] have used WT and SIRT2 KO mouse intestinal organoids. The inhibition of SIRT2 determines the activation of the Wnt/β-catenin signaling pathway and exhibits enhanced epithelial proliferation, which coincides with what has been seen *in vivo* on the mucosa of IBD patients. Furthermore, TNF treatment of WT organoids reduces SIRT2 expression, suggesting that TNF may induce Wnt/β-catenin signaling through repression of SIRT2 expression. In this way, the critical role of Wnt pathway and the beneficial

effect of SIRT2 in the intestinal epithelium was demonstrated[105]. More studies are required to understand the effective role of Wnt signals in the intestinal epithelium.

Kim *et al*[106] have demonstrated that oral treatment with hyaluronan 35 kDa (HA35) may be an effective therapy for IBD patients, promoting epithelial wound healing *via* the activation of RhoA/Rho-associated protein kinase signaling. The use of mouse intestinal organoids has confirmed that HA35, which is specifically internalized by the layilin receptor, induces ZO-1 expression, and restores the epithelial barrier, which is disrupted during active IBD[106].

In addition to all these possible therapeutic targets, Davoudi *et al*[107] have used mouse intestinal organoids to study novel drug-delivery strategies, including nanoparticles and microparticles-based therapies, to provide drug delivery at specific areas, thus reducing the disadvantages of systemic treatments that result in non-selective distribution of drugs and side effects[107]. Authors have inserted 5-aminosalicylic acid or rhodamine B, used as a tracer dye, into polylactic-co-glycolic acid nanoparticles and have loaded them into the lumen of intestinal organoids. By confocal fluorescent microscopy, it was shown that rhodamine B was released into the lumen and digested after 3 d, demonstrating the ability of the organoid to digest nanoparticles and confirming the adsorption of nanoparticles inside the lumen with no negative consequences on organoid growth. This is a trojan horse system in which the drug is concealed from the host cells, and could represent a new therapeutic approach for delivering drugs to the specific inflamed location, reducing adverse reactions[107].

LIMITATIONS OF INTESTINAL ORGANOID TECHNOLOGY

Although the future applications and clinical contributions of intestinal organoids seem to be very encouraging, there are still several issues to overcome. One of the limitations is that several components used to culture intestinal organoids, such as the matrigel and some growth factors, are derived from cell lines. Therefore, they might contain large amounts of xenogenic factors and unknown components that could potentially cause pathogen/immunogen transmission to organoid cultures, in addition to the large variability between the different production batches used. For these reasons, growth conditions must be further optimized and standardized[21]. For example, Wnt-conditioned medium might be replaced with commercial variants[58] and matrigel might be substituted by synthetic extracellular matrices, such as collagen and hydrogel. Yin *et al*[58] have used small molecules, including valproic acid and CHIR99021, a glycogen synthase kinase 3β inhibitor, as conditioned media to maintain self-renewal of mouse $Lgr5^+$ ISCs, resulting in homogeneous cultures[58]. Moreover, the current protocols used to isolate and culture intestinal organoids must be improved because it has been shown that the intestinal crypts isolated from actively inflamed segments often do not allow for correct growth of intestinal organoids due to the loss or disruption of the epithelial layer[21]. Another limit is that intestinal organoids lack other cell and tissue types, including nervous tissue, endothelium-lined blood vessels, and immune mediators, which are crucial for drug pharmacokinetic analyses and disease modeling; in addition, they lack the physiological intestinal and blood flow, the mechanical deformations similar to those seen in the contractions of peristalsis, and the gut microbiota[21,108]. For these reasons, the intestinal organoid technology still requires standardized methods to include the intestinal microbiota and immune cells of the lamina propria, which could allow for mechanistic studies of IBDs[29]. Moreover, ASC-derived intestinal organoids miss the mesenchymal structure in contrast to those derived from iPSCs[21,22].

CONCLUSION

The intestinal epithelium plays a pivotal role in the maintenance of intestinal homeostasis by controlling the microbial composition and lamina propria factors and its study is important to increase knowledge on IBD pathogenesis. Intestinal organoids provide advantages by better reflecting the *in vivo* physiology of intestinal epithelium and are thus becoming an important tool for IBD modeling.

Intestinal organoids demonstrated that IECs play an important role in promoting the inflammatory states, by releasing several pro-inflammatory cytokines; the contribution of the interplay with surrounding cells and with bacteria-host interactions, occurring in patients with IBDs, has also been explored. Furthermore, intestinal organoids have been used to better understand the mechanisms of already-approved drugs for the management of IBD and to comprehend their effects on the intestinal epithelium. In addition, since they can be generated from a specific patient, they could be used to test different drugs to optimize and personalize treatment, reducing therapy failure and the occurrence of adverse effects.

However, it is important to underline that this recent technology still needs to be improved and currently, in the literature, the data available are few and preliminary. Therefore, more studies are required to improve this technique and to better understand how to use intestinal organoids, especially in the context of personalized therapy and drug development for IBD.

FOOTNOTES

Author contributions: Lucafò M, Decorti G, and Stocco G contributed to the conceptualization; Lucafò M, Muzzo A, Marcuzzi M, and Giorio L wrote the original draft; Lucafò M, Decorti G, and Stocco G wrote the review and edited the review; all authors have read and agree to the published version of the manuscript.

Conflict-of-interest statement: All the authors report no relevant conflicts of interest for this article.

Open-Access: This article is an open-access article that was selected by an in-house editor and fully peer-reviewed by external reviewers. It is distributed in accordance with the Creative Commons Attribution NonCommercial (CC BY-NC 4.0) license, which permits others to distribute, remix, adapt, build upon this work non-commercially, and license their derivative works on different terms, provided the original work is properly cited and the use is non-commercial. See: https://creativecommons.org/Licenses/by-nc/4.0/

Country/Territory of origin: Italy

ORCID number: Marianna Lucafò 0000-0003-1355-3782; Antonella Muzzo 0000-0002-8759-7967; Martina Marcuzzi 0000-0001-9498-5063; Lorenzo Giorio 0000-0001-8490-0150; Giuliana Decorti 0000-0002-9714-6246; Gabriele Stocco 0000-0003-0964-5879.

S-Editor: Fan JR
L-Editor: Filipodia
P-Editor: Fan JR

REFERENCES

1 **Kaplan GG**. The global burden of IBD: from 2015 to 2025. *Nat Rev Gastroenterol Hepatol* 2015; **12**: 720-727 [PMID: 26323879 DOI: 10.1038/nrgastro.2015.150]
2 **Leppkes M**, Neurath MF. Cytokines in inflammatory bowel diseases - Update 2020. *Pharmacol Res* 2020; **158**: 104835 [PMID: 32416212 DOI: 10.1016/j.phrs.2020.104835]
3 **Ordás I**, Eckmann L, Talamini M, Baumgart DC, Sandborn WJ. Ulcerative colitis. *Lancet* 2012; **380**: 1606-1619 [PMID: 22914296 DOI: 10.1016/S0140-6736(12)60150-0]
4 **Yeshi K**, Ruscher R, Hunter L, Daly NL, Loukas A, Wangchuk P. Revisiting Inflammatory Bowel Disease: Pathology, Treatments, Challenges and Emerging Therapeutics Including Drug Leads from Natural Products. *J Clin Med* 2020; **9** [PMID: 32354192 DOI: 10.3390/jcm9051273]
5 **Schulte L**, Hohwieler M, Müller M, Klaus J. Intestinal Organoids as a Novel Complementary Model to Dissect Inflammatory Bowel Disease. *Stem Cells Int* 2019; **2019**: 8010645 [PMID: 31015842 DOI: 10.1155/2019/8010645]
6 **Abraham C**, Cho JH. Inflammatory bowel disease. *N Engl J Med* 2009; **361**: 2066-2078 [PMID: 19923578 DOI: 10.1056/NEJMra0804647]
7 **Hendrickson BA**, Gokhale R, Cho JH. Clinical aspects and pathophysiology of inflammatory bowel disease. *Clin Microbiol Rev* 2002; **15**: 79-94 [PMID: 11781268 DOI: 10.1128/cmr.15.1.79-94.2002]
8 **Ham M**, Moss AC. Mesalamine in the treatment and maintenance of remission of ulcerative colitis. *Expert Rev Clin Pharmacol* 2012; **5**: 113-123 [PMID: 22390554 DOI: 10.1586/ecp.12.2]
9 **Lucafò M**, Franca R, Selvestrel D, Curci D, Pugnetti L, Decorti G, Stocco G. Pharmacogenetics of treatments for inflammatory bowel disease. *Expert Opin Drug Metab Toxicol* 2018; **14**: 1209-1223 [PMID: 30465611 DOI: 10.1080/17425255.2018.1551876]
10 **Prantera C**, Marconi S. Glucocorticosteroids in the treatment of inflammatory bowel disease and approaches to minimizing systemic activity. *Therap Adv Gastroenterol* 2013; **6**: 137-156 [PMID: 23503968 DOI: 10.1177/1756283X12473675]
11 **Travassos WJ**, Cheifetz AS. Infliximab: Use in Inflammatory Bowel Disease. *Curr Treat Options Gastroenterol* 2005; **8**: 187-196 [PMID: 15913508 DOI: 10.1007/s11938-005-0011-2]
12 **Shim HH**, Chan PW, Chuah SW, Schwender BJ, Kong SC, Ling KL. A review of vedolizumab and ustekinumab for the treatment of inflammatory bowel diseases. *JGH Open* 2018; **2**: 223-234 [PMID: 30483594 DOI: 10.1002/jgh3.12065]
13 **Bramuzzo M**, Ventura A, Martelossi S, Lazzerini M. Thalidomide for inflammatory bowel disease: Systematic review. *Medicine (Baltimore)* 2016; **95**: e4239 [PMID: 27472695 DOI: 10.1097/MD.0000000000004239]
14 **Lucafò M**, Di Silvestre A, Romano M, Avian A, Antonelli R, Martelossi S, Naviglio S, Tommasini A, Stocco G, Ventura A, Decorti G, De Iudicibus S. Role of the Long Non-Coding RNA Growth Arrest-Specific 5 in Glucocorticoid Response in Children with Inflammatory Bowel Disease. *Basic Clin Pharmacol Toxicol* 2018; **122**: 87-93 [PMID: 28722800 DOI: 10.1111/bcpt.12851]
15 **De Iudicibus S**, Lucafò M, Vitulo N, Martelossi S, Zimbello R, De Pascale F, Forcato C, Naviglio S, Di Silvestre A, Gerdol M, Stocco G, Valle G, Ventura A, Bramuzzo M, Decorti G. High-Throughput Sequencing of microRNAs in Glucocorticoid Sensitive Paediatric Inflammatory Bowel Disease Patients. *Int J Mol Sci* 2018; **19** [PMID: 29738455 DOI: 10.3390/ijms19051399]
16 **Porter RJ**, Kalla R, Ho GT. Ulcerative colitis: Recent advances in the understanding of disease pathogenesis. *F1000Res* 2020; **9** [PMID: 32399194 DOI: 10.12688/f1000research.20805.1]
17 **Caër C**, Wick MJ. Human Intestinal Mononuclear Phagocytes in Health and Inflammatory Bowel Disease. *Front Immunol* 2020; **11**: 410 [PMID: 32256490 DOI: 10.3389/fimmu.2020.00410]

18 **Holleran G**, Lopetuso L, Petito V, Graziani C, Ianiro G, McNamara D, Gasbarrini A, Scaldaferri F. The Innate and Adaptive Immune System as Targets for Biologic Therapies in Inflammatory Bowel Disease. *Int J Mol Sci* 2017; **18** [PMID: 28934123 DOI: 10.3390/ijms18102020]

19 **Khare V**, Krnjic A, Frick A, Gmainer C, Asboth M, Jimenez K, Lang M, Baumgartner M, Evstatiev R, Gasche C. Mesalamine and azathioprine modulate junctional complexes and restore epithelial barrier function in intestinal inflammation. *Sci Rep* 2019; **9**: 2842 [PMID: 30809073 DOI: 10.1038/s41598-019-39401-0]

20 **Onozato D**, Akagawa T, Kida Y, Ogawa I, Hashita T, Iwao T, Matsunaga T. Application of Human Induced Pluripotent Stem Cell-Derived Intestinal Organoids as a Model of Epithelial Damage and Fibrosis in Inflammatory Bowel Disease. *Biol Pharm Bull* 2020; **43**: 1088-1095 [PMID: 32612071 DOI: 10.1248/bpb.b20-00088]

21 **Yoo JH**, Donowitz M. Intestinal enteroids/organoids: A novel platform for drug discovery in inflammatory bowel diseases. *World J Gastroenterol* 2019; **25**: 4125-4147 [PMID: 31435168 DOI: 10.3748/wjg.v25.i30.4125]

22 **Dotti I**, Salas A. Potential Use of Human Stem Cell-Derived Intestinal Organoids to Study Inflammatory Bowel Diseases. *Inflamm Bowel Dis* 2018; **24**: 2501-2509 [PMID: 30169820 DOI: 10.1093/ibd/izy275]

23 **Rodansky ES**, Johnson LA, Huang S, Spence JR, Higgins PD. Intestinal organoids: a model of intestinal fibrosis for evaluating anti-fibrotic drugs. *Exp Mol Pathol* 2015; **98**: 346-351 [PMID: 25828392 DOI: 10.1016/j.yexmp.2015.03.033]

24 **Chandra L**, Borcherding DC, Kingsbury D, Atherly T, Ambrosini YM, Bourgois-Mochel A, Yuan W, Kimber M, Qi Y, Wang Q, Wannemuehler M, Ellinwood NM, Snella E, Martin M, Skala M, Meyerholz D, Estes M, Fernandez-Zapico ME, Jergens AE, Mochel JP, Allenspach K. Derivation of adult canine intestinal organoids for translational research in gastroenterology. *BMC Biol* 2019; **17**: 33 [PMID: 30975131 DOI: 10.1186/s12915-019-0652-6]

25 **d'Aldebert E**, Quaranta M, Sébert M, Bonnet D, Kirzin S, Portier G, Duffas JP, Chabot S, Lluel P, Allart S, Ferrand A, Alric L, Racaud-Sultan C, Mas E, Deraison C, Vergnolle N. Characterization of Human Colon Organoids From Inflammatory Bowel Disease Patients. *Front Cell Dev Biol* 2020; **8**: 363 [PMID: 32582690 DOI: 10.3389/fcell.2020.00363]

26 **Zhang M**, Liu Y, Chen YG. Generation of 3D human gastrointestinal organoids: principle and applications. *Cell Regen* 2020; **9**: 6 [PMID: 32588198 DOI: 10.1186/s13619-020-00040-w]

27 **Sato T**, Vries RG, Snippert HJ, van de Wetering M, Barker N, Stange DE, van Es JH, Abo A, Kujala P, Peters PJ, Clevers H. Single Lgr5 stem cells build crypt-villus structures in vitro without a mesenchymal niche. *Nature* 2009; **459**: 262-265 [PMID: 19329995 DOI: 10.1038/nature07935]

28 **Zachos NC**, Kovbasnjuk O, Foulke-Abel J, In J, Blutt SE, de Jonge HR, Estes MK, Donowitz M. Human Enteroids/Colonoids and Intestinal Organoids Functionally Recapitulate Normal Intestinal Physiology and Pathophysiology. *J Biol Chem* 2016; **291**: 3759-3766 [PMID: 26677228 DOI: 10.1074/jbc.R114.635995]

29 **Angus HCK**, Butt AG, Schultz M, Kemp RA. Intestinal Organoids as a Tool for Inflammatory Bowel Disease Research. *Front Med (Lausanne)* 2019; **6**: 334 [PMID: 32010704 DOI: 10.3389/fmed.2019.00334]

30 **Spence JR**, Mayhew CN, Rankin SA, Kuhar MF, Vallance JE, Tolle K, Hoskins EE, Kalinichenko VV, Wells SI, Zorn AM, Shroyer NF, Wells JM. Directed differentiation of human pluripotent stem cells into intestinal tissue in vitro. *Nature* 2011; **470**: 105-109 [PMID: 21151107 DOI: 10.1038/nature09691]

31 **Workman MJ**, Mahe MM, Trisno S, Poling HM, Watson CL, Sundaram N, Chang CF, Schiesser J, Aubert P, Stanley EG, Elefanty AG, Miyaoka Y, Mandegar MA, Conklin BR, Neunlist M, Brugmann SA, Helmrath MA, Wells JM. Engineered human pluripotent-stem-cell-derived intestinal tissues with a functional enteric nervous system. *Nat Med* 2017; **23**: 49-59 [PMID: 27869805 DOI: 10.1038/nm.4233]

32 **Malik N**, Rao MS. A review of the methods for human iPSC derivation. *Methods Mol Biol* 2013; **997**: 23-33 [PMID: 23546745 DOI: 10.1007/978-1-62703-348-0_3]

33 **Li M**, Izpisua Belmonte JC. Organoids - Preclinical Models of Human Disease. *N Engl J Med* 2019; **380**: 569-579 [PMID: 30726695 DOI: 10.1056/NEJMra1806175]

34 **Liang G**, Zhang Y. Genetic and epigenetic variations in iPSCs: potential causes and implications for application. *Cell Stem Cell* 2013; **13**: 149-159 [PMID: 23910082 DOI: 10.1016/j.stem.2013.07.001]

35 **Tsuruta S**, Uchida H, Akutsu H. Intestinal Organoids Generated from Human Pluripotent Stem Cells. *JMA J* 2020; **3**: 9-19 [PMID: 33324771 DOI: 10.31662/jmaj.2019-0027]

36 **Yin S**, Ray G, Kerschner JL, Hao S, Perez A, Drumm ML, Browne JA, Leir SH, Longworth M, Harris A. Functional genomics analysis of human colon organoids identifies key transcription factors. *Physiol Genomics* 2020; **52**: 234-244 [PMID: 32390556 DOI: 10.1152/physiolgenomics.00113.2019]

37 **Shi Y**, Inoue H, Wu JC, Yamanaka S. Induced pluripotent stem cell technology: a decade of progress. *Nat Rev Drug Discov* 2017; **16**: 115-130 [PMID: 27980341 DOI: 10.1038/nrd.2016.245]

38 **de Lange KM**, Moutsianas L, Lee JC, Lamb CA, Luo Y, Kennedy NA, Jostins L, Rice DL, Gutierrez-Achury J, Ji SG, Heap G, Nimmo ER, Edwards C, Henderson P, Mowat C, Sanderson J, Satsangi J, Simmons A, Wilson DC, Tremelling M, Hart A, Mathew CG, Newman WG, Parkes M, Lees CW, Uhlig H, Hawkey C, Prescott NJ, Ahmad T, Mansfield JC, Anderson CA, Barrett JC. Genome-wide association study implicates immune activation of multiple integrin genes in inflammatory bowel disease. *Nat Genet* 2017; **49**: 256-261 [PMID: 28067908 DOI: 10.1038/ng.3760]

39 **van de Wetering M**, Francies HE, Francis JM, Bounova G, Iorio F, Pronk A, van Houdt W, van Gorp J, Taylor-Weiner A, Kester L, McLaren-Douglas A, Blokker J, Jaksani S, Bartfeld S, Volckman R, van Sluis P, Li VS, Seepo S, Sekhar Pedamallu C, Cibulskis K, Carter SL, McKenna A, Lawrence MS, Lichtenstein L, Stewart C, Koster J, Versteeg R, van Oudenaarden A, Saez-Rodriguez J, Vries RG, Getz G, Wessels L, Stratton MR, McDermott U, Meyerson M, Garnett MJ, Clevers H. Prospective derivation of a living organoid biobank of colorectal cancer patients. *Cell* 2015; **161**: 933-945 [PMID: 25957691 DOI: 10.1016/j.cell.2015.03.053]

40 **Howell KJ**, Kraiczy J, Nayak KM, Gasparetto M, Ross A, Lee C, Mak TN, Koo BK, Kumar N, Lawley T, Sinha A, Rosenstiel P, Heuschkel R, Stegle O, Zilbauer M. DNA Methylation and Transcription Patterns in Intestinal Epithelial Cells From Pediatric Patients With Inflammatory Bowel Diseases Differentiate Disease Subtypes and Associate With Outcome. *Gastroenterology* 2018; **154**: 585-598 [PMID: 29031501 DOI: 10.1053/j.gastro.2017.10.007]

41 **Middendorp S**, Schneeberger K, Wiegerinck CL, Mokry M, Akkerman RD, van Wijngaarden S, Clevers H, Nieuwenhuis EE. Adult stem cells in the small intestine are intrinsically programmed with their location-specific function. *Stem Cells* 2014; **32**: 1083-1091 [PMID: 24496776 DOI: 10.1002/stem.1655]

42 **Dotti I**, Mora-Buch R, Ferrer-Picón E, Planell N, Jung P, Masamunt MC, Leal RF, Martín de Carpi J, Llach J, Ordás I, Batlle E, Panés J, Salas A. Alterations in the epithelial stem cell compartment could contribute to permanent changes in the mucosa of patients with ulcerative colitis. *Gut* 2017; **66**: 2069-2079 [PMID: 27803115 DOI: 10.1136/gutjnl-2016-312609]

43 **Xu P**, Becker H, Elizalde M, Masclee A, Jonkers D. Intestinal organoid culture model is a valuable system to study epithelial barrier function in IBD. *Gut* 2018; **67**: 1905-1906 [PMID: 29208677 DOI: 10.1136/gutjnl-2017-315685]

44 **Schwerd T**, Bryant RV, Pandey S, Capitani M, Meran L, Cazier JB, Jung J, Mondal K, Parkes M, Mathew CG, Fiedler K, McCarthy DJ; WGS500 Consortium; Oxford IBD cohort study investigators; COLORS in IBD group investigators; UK IBD Genetics Consortium, Sullivan PB, Rodrigues A, Travis SPL, Moore C, Sambrook J, Ouwehand WH, Roberts DJ, Danesh J; INTERVAL Study, Russell RK, Wilson DC, Kelsen JR, Cornall R, Denson LA, Kugathasan S, Knaus UG, Serra EG, Anderson CA, Duerr RH, McGovern DP, Cho J, Powrie F, Li VS, Muise AM, Uhlig HH. NOX1 loss-of-function genetic variants in patients with inflammatory bowel disease. *Mucosal Immunol* 2018; **11**: 562-574 [PMID: 29091079 DOI: 10.1038/mi.2017.74]

45 **Lemoine R**, Pachlopnik-Schmid J, Farin HF, Bigorgne A, Debré M, Sepulveda F, Héritier S, Lemale J, Talbotec C, Rieux-Laucat F, Ruemmele F, Morali A, Cathebras P, Nitschke P, Bole-Feysot C, Blanche S, Brousse N, Picard C, Clevers H, Fischer A, de Saint Basile G. Immune deficiency-related enteropathy-lymphocytopenia-alopecia syndrome results from tetratricopeptide repeat domain 7A deficiency. *J Allergy Clin Immunol* 2014; **134**: 1354-1364.e6 [PMID: 25174867 DOI: 10.1016/j.jaci.2014.07.019]

46 **Hugot JP**, Chamaillard M, Zouali H, Lesage S, Cézard JP, Belaiche J, Almer S, Tysk C, O'Morain CA, Gassull M, Binder V, Finkel Y, Cortot A, Modigliani R, Laurent-Puig P, Gower-Rousseau C, Macry J, Colombel JF, Sahbatou M, Thomas G. Association of NOD2 leucine-rich repeat variants with susceptibility to Crohn's disease. *Nature* 2001; **411**: 599-603 [PMID: 11385576 DOI: 10.1038/35079107]

47 **Rioux JD**, Xavier RJ, Taylor KD, Silverberg MS, Goyette P, Huett A, Green T, Kuballa P, Barmada MM, Datta LW, Shugart YY, Griffiths AM, Targan SR, Ippoliti AF, Bernard EJ, Mei L, Nicolae DL, Regueiro M, Schumm LP, Steinhart AH, Rotter JI, Duerr RH, Cho JH, Daly MJ, Brant SR. Genome-wide association study identifies new susceptibility loci for Crohn disease and implicates autophagy in disease pathogenesis. *Nat Genet* 2007; **39**: 596-604 [PMID: 17435756 DOI: 10.1038/ng2032]

48 **Saxena A**, Lopes F, Poon KKH, McKay DM. Absence of the NOD2 protein renders epithelia more susceptible to barrier dysfunction due to mitochondrial dysfunction. *Am J Physiol Gastrointest Liver Physiol* 2017; **313**: G26-G38 [PMID: 28450277 DOI: 10.1152/ajpgi.00070.2017]

49 **Aden K**, Tran F, Ito G, Sheibani-Tezerji R, Lipinski S, Kuiper JW, Tschurtschenthaler M, Saveljeva S, Bhattacharyya J, Häsler R, Bartsch K, Luzius A, Jentzsch M, Falk-Paulsen M, Stengel ST, Welz L, Schwarzer R, Rabe B, Barchet W, Krautwald S, Hartmann G, Pasparakis M, Blumberg RS, Schreiber S, Kaser A, Rosenstiel P. ATG16L1 orchestrates interleukin-22 signaling in the intestinal epithelium *via* cGAS-STING. *J Exp Med* 2018; **215**: 2868-2886 [PMID: 30254094 DOI: 10.1084/jem.20171029]

50 **Kelsen JR**, Dawany N, Conrad MA, Karakasheva TA, Maurer K, Wei JM, Uman S, Dent MH, Behera R, Bryant LM, Ma X, Moreira L, Chatterji P, Shraim R, Merz A, Mizuno R, Simon LA, Muir AB, Giraudo C, Behrens EM, Whelan KA, Devoto M, Russo PA, Andres SF, Sullivan KE, Hamilton KE. Colonoids From Patients With Pediatric Inflammatory Bowel Disease Exhibit Decreased Growth Associated With Inflammation Severity and Durable Upregulation of Antigen Presentation Genes. *Inflamm Bowel Dis* 2021; **27**: 256-267 [PMID: 32556182 DOI: 10.1093/ibd/izaa145]

51 **McDonald GB**, Jewell DP. Class II antigen (HLA-DR) expression by intestinal epithelial cells in inflammatory diseases of colon. *J Clin Pathol* 1987; **40**: 312-317 [PMID: 3558865 DOI: 10.1136/jcp.40.3.312]

52 **Roda G**, Sartini A, Zambon E, Calafiore A, Marocchi M, Caponi A, Belluzzi A, Roda E. Intestinal epithelial cells in inflammatory bowel diseases. *World J Gastroenterol* 2010; **16**: 4264-4271 [PMID: 20818809 DOI: 10.3748/wjg.v16.i34.4264]

53 **Tytgat KM**, van der Wal JW, Einerhand AW, Büller HA, Dekker J. Quantitative analysis of MUC2 synthesis in ulcerative colitis. *Biochem Biophys Res Commun* 1996; **224**: 397-405 [PMID: 8702401 DOI: 10.1006/bbrc.1996.1039]

54 **Okamoto R**, Watanabe M. Role of epithelial cells in the pathogenesis and treatment of inflammatory bowel disease. *J Gastroenterol* 2016; **51**: 11-21 [PMID: 26138071 DOI: 10.1007/s00535-015-1098-4]

55 **Gersemann M**, Becker S, Kübler I, Koslowski M, Wang G, Herrlinger KR, Griger J, Fritz P, Fellermann K, Schwab M, Wehkamp J, Stange EF. Differences in goblet cell differentiation between Crohn's disease and ulcerative colitis. *Differentiation* 2009; **77**: 84-94 [PMID: 19281767 DOI: 10.1016/j.diff.2008.09.008]

56 **Wehkamp J**, Schmid M, Stange EF. Defensins and other antimicrobial peptides in inflammatory bowel disease. *Curr Opin Gastroenterol* 2007; **23**: 370-378 [PMID: 17545771 DOI: 10.1097/MOG.0b013e328136c580]

57 **Treveil A**, Sudhakar P, Matthews ZJ, Wrzesiński T, Jones EJ, Brooks J, Ölbei M, Hautefort I, Hall LJ, Carding SR, Mayer U, Powell PP, Wileman T, Di Palma F, Haerty W, Korcsmáros T. Regulatory network analysis of Paneth cell and goblet cell enriched gut organoids using transcriptomics approaches. *Mol Omics* 2020; **16**: 39-58 [PMID: 31819932 DOI: 10.1039/c9mo00130a]

58 **Yin X**, Farin HF, van Es JH, Clevers H, Langer R, Karp JM. Niche-independent high-purity cultures of Lgr5+ intestinal stem cells and their progeny. *Nat Methods* 2014; **11**: 106-112 [PMID: 24292484 DOI: 10.1038/nmeth.2737]

59 **Lyons J**, Ghazi PC, Starchenko A, Tovaglieri A, Baldwin KR, Poulin EJ, Gierut JJ, Genetti C, Yajnik V, Breault DT, Lauffenburger DA, Haigis KM. The colonic epithelium plays an active role in promoting colitis by shaping the tissue cytokine profile. *PLoS Biol* 2018; **16**: e2002417 [PMID: 29596476 DOI: 10.1371/journal.pbio.2002417]

60 **Marafini I**, Sedda S, Dinallo V, Monteleone G. Inflammatory cytokines: from discoveries to therapies in IBD. *Expert Opin Biol Ther* 2019; **19**: 1207-1217 [PMID: 31373244 DOI: 10.1080/14712598.2019.1652267]

61 **Wajant H**, Pfizenmaier K, Scheurich P. Tumor necrosis factor signaling. *Cell Death Differ* 2003; **10**: 45-65 [PMID:

12655295 DOI: 10.1038/sj.cdd.4401189]

62 **Garcia-Carbonell R**, Wong J, Kim JY, Close LA, Boland BS, Wong TL, Harris PA, Ho SB, Das S, Ernst PB, Sasik R, Sandborn WJ, Bertin J, Gough PJ, Chang JT, Kelliher M, Boone D, Guma M, Karin M. Elevated A20 promotes TNF-induced and RIPK1-dependent intestinal epithelial cell death. *Proc Natl Acad Sci U S A* 2018; **115**: E9192-E9200 [PMID: 30209212 DOI: 10.1073/pnas.1810584115]

63 **Grabinger T**, Bode KJ, Demgenski J, Seitz C, Delgado ME, Kostadinova F, Reinhold C, Etemadi N, Wilhelm S, Schweinlin M, Hänggi K, Knop J, Hauck C, Walles H, Silke J, Wajant H, Nachbur U, W Wei-Lynn W, Brunner T. Inhibitor of Apoptosis Protein-1 Regulates Tumor Necrosis Factor-Mediated Destruction of Intestinal Epithelial Cells. *Gastroenterology* 2017; **152**: 867-879 [PMID: 27889570 DOI: 10.1053/j.gastro.2016.11.019]

64 **Ferrer-Picón E**, Dotti I, Corraliza AM, Mayorgas A, Esteller M, Perales JC, Ricart E, Masamunt MC, Carrasco A, Tristán E, Esteve M, Salas A. Intestinal Inflammation Modulates the Epithelial Response to Butyrate in Patients With Inflammatory Bowel Disease. *Inflamm Bowel Dis* 2020; **26**: 43-55 [PMID: 31211831 DOI: 10.1093/ibd/izz119]

65 **Hall CHT**, Lee JS, Murphy EM, Gerich ME, Dran R, Glover LE, Abdulla ZI, Skelton MR, Colgan SP. Creatine Transporter, Reduced in Colon Tissues From Patients With Inflammatory Bowel Diseases, Regulates Energy Balance in Intestinal Epithelial Cells, Epithelial Integrity, and Barrier Function. *Gastroenterology* 2020; **159**: 984-998.e1 [PMID: 32433978 DOI: 10.1053/j.gastro.2020.05.033]

66 **Rallabandi HR**, Yang H, Oh KB, Lee HC, Byun SJ, Lee BR. Evaluation of Intestinal Epithelial Barrier Function in Inflammatory Bowel Diseases Using Murine Intestinal Organoids. *Tissue Eng Regen Med* 2020; **17**: 641-650 [PMID: 32594459 DOI: 10.1007/s13770-020-00278-0]

67 **Pott J**, Kabat AM, Maloy KJ. Intestinal Epithelial Cell Autophagy Is Required to Protect against TNF-Induced Apoptosis during Chronic Colitis in Mice. *Cell Host Microbe* 2018; **23**: 191-202.e4 [PMID: 29358084 DOI: 10.1016/j.chom.2017.12.017]

68 **Matsuzawa-Ishimoto Y**, Shono Y, Gomez LE, Hubbard-Lucey VM, Cammer M, Neil J, Dewan MZ, Lieberman SR, Lazrak A, Marinis JM, Beal A, Harris PA, Bertin J, Liu C, Ding Y, van den Brink MRM, Cadwell K. Autophagy protein ATG16L1 prevents necroptosis in the intestinal epithelium. *J Exp Med* 2017; **214**: 3687-3705 [PMID: 29089374 DOI: 10.1084/jem.20170558]

69 **Salem M**, Ammitzboell M, Nys K, Seidelin JB, Nielsen OH. ATG16L1: A multifunctional susceptibility factor in Crohn disease. *Autophagy* 2015; **11**: 585-594 [PMID: 25906181 DOI: 10.1080/15548627.2015.1017187]

70 **Rees WD**, Sly LM, Steiner TS. How do immune and mesenchymal cells influence the intestinal epithelial cell compartment in inflammatory bowel disease? *J Leukoc Biol* 2020; **108**: 309-321 [PMID: 32057139 DOI: 10.1002/JLB.3MIR0120-567R]

71 **Zwarycz B**, Gracz AD, Rivera KR, Williamson IA, Samsa LA, Starmer J, Daniele MA, Salter-Cid L, Zhao Q, Magness ST. IL22 Inhibits Epithelial Stem Cell Expansion in an Ileal Organoid Model. *Cell Mol Gastroenterol Hepatol* 2019; **7**: 1-17 [PMID: 30364840 DOI: 10.1016/j.jcmgh.2018.06.008]

72 **Ihara S**, Hirata Y, Hikiba Y, Yamashita A, Tsuboi M, Hata M, Konishi M, Suzuki N, Sakitani K, Kinoshita H, Hayakawa Y, Nakagawa H, Ijichi H, Tateishi K, Koike K. Adhesive Interactions between Mononuclear Phagocytes and Intestinal Epithelium Perturb Normal Epithelial Differentiation and Serve as a Therapeutic Target in Inflammatory Bowel Disease. *J Crohns Colitis* 2018; **12**: 1219-1231 [PMID: 29917067 DOI: 10.1093/ecco-jcc/jjy088]

73 **Putignani L**, Del Chierico F, Petrucca A, Vernocchi P, Dallapiccola B. The human gut microbiota: a dynamic interplay with the host from birth to senescence settled during childhood. *Pediatr Res* 2014; **76**: 2-10 [PMID: 24732106 DOI: 10.1038/pr.2014.49]

74 **Leber A**, Hontecillas R, Tubau-Juni N, Zoccoli-Rodriguez V, Abedi V, Bassaganya-Riera J. NLRX1 Modulates Immunometabolic Mechanisms Controlling the Host-Gut Microbiota Interactions during Inflammatory Bowel Disease. *Front Immunol* 2018; **9**: 363 [PMID: 29535731 DOI: 10.3389/fimmu.2018.00363]

75 **Roodsant T**, Navis M, Aknouch I, Renes IB, van Elburg RM, Pajkrt D, Wolthers KC, Schultsz C, van der Ark KCH, Sridhar A, Muncan V. A Human 2D Primary Organoid-Derived Epithelial Monolayer Model to Study Host-Pathogen Interaction in the Small Intestine. *Front Cell Infect Microbiol* 2020; **10**: 272 [PMID: 32656095 DOI: 10.3389/fcimb.2020.00272]

76 **Sun L**, Rollins D, Qi Y, Fredericks J, Mansell TJ, Jergens A, Phillips GJ, Wannemuehler M, Wang Q. TNFα regulates intestinal organoids from mice with both defined and conventional microbiota. *Int J Biol Macromol* 2020; **164**: 548-556 [PMID: 32693143 DOI: 10.1016/j.ijbiomac.2020.07.176]

77 **Engevik MA**, Danhof HA, Chang-Graham AL, Spinler JK, Engevik KA, Herrmann B, Endres BT, Garey KW, Hyser JM, Britton RA, Versalovic J. Human intestinal enteroids as a model of *Clostridioides difficile*-induced enteritis. *Am J Physiol Gastrointest Liver Physiol* 2020; **318**: G870-G888 [PMID: 32223302 DOI: 10.1152/ajpgi.00045.2020]

78 **Hares MF**, Tiffney EA, Johnston LJ, Luu L, Stewart CJ, Flynn RJ, Coombes JL. Stem cell-derived enteroid cultures as a tool for dissecting host-parasite interactions in the small intestinal epithelium. *Parasite Immunol* 2021; **43**: e12765 [PMID: 32564379 DOI: 10.1111/pim.12765]

79 **Saxena K**, Blutt SE, Ettayebi K, Zeng XL, Broughman JR, Crawford SE, Karandikar UC, Sastri NP, Conner ME, Opekun AR, Graham DY, Qureshi W, Sherman V, Foulke-Abel J, In J, Kovbasnjuk O, Zachos NC, Donowitz M, Estes MK. Human Intestinal Enteroids: a New Model To Study Human Rotavirus Infection, Host Restriction, and Pathophysiology. *J Virol* 2016; **90**: 43-56 [PMID: 26446608 DOI: 10.1128/JVI.01930-15]

80 **Leslie JL**, Huang S, Opp JS, Nagy MS, Kobayashi M, Young VB, Spence JR. Persistence and toxin production by Clostridium difficile within human intestinal organoids result in disruption of epithelial paracellular barrier function. *Infect Immun* 2015; **83**: 138-145 [PMID: 25312952 DOI: 10.1128/IAI.02561-14]

81 **Gleeson JP**, Estrada HQ, Yamashita M, Svendsen CN, Targan SR, Barrett RJ. Development of Physiologically Responsive Human iPSC-Derived Intestinal Epithelium to Study Barrier Dysfunction in IBD. *Int J Mol Sci* 2020; **21** [PMID: 32093254 DOI: 10.3390/ijms21041438]

82 **Sayed IM**, Suarez K, Lim E, Singh S, Pereira M, Ibeawuchi SR, Katkar G, Dunkel Y, Mittal Y, Chattopadhyay R, Guma M, Boland BS, Dulai PS, Sandborn WJ, Ghosh P, Das S. Host engulfment pathway controls inflammation in inflammatory

bowel disease. *FEBS J* 2020; **287**: 3967-3988 [PMID: 32003126 DOI: 10.1111/febs.15236]
83 **Noel G**, Baetz NW, Staab JF, Donowitz M, Kovbasnjuk O, Pasetti MF, Zachos NC. A primary human macrophage-enteroid co-culture model to investigate mucosal gut physiology and host-pathogen interactions. *Sci Rep* 2017; **7**: 45270 [PMID: 28345602 DOI: 10.1038/srep45270]
84 **Neurath MF**, Travis SP. Mucosal healing in inflammatory bowel diseases: a systematic review. *Gut* 2012; **61**: 1619-1635 [PMID: 22842618 DOI: 10.1136/gutjnl-2012-302830]
85 **Pickert G**, Neufert C, Leppkes M, Zheng Y, Wittkopf N, Warntjen M, Lehr HA, Hirth S, Weigmann B, Wirtz S, Ouyang W, Neurath MF, Becker C. STAT3 links IL-22 signaling in intestinal epithelial cells to mucosal wound healing. *J Exp Med* 2009; **206**: 1465-1472 [PMID: 19564350 DOI: 10.1084/jem.20082683]
86 **Pineton de Chambrun G**, Peyrin-Biroulet L, Lémann M, Colombel JF. Clinical implications of mucosal healing for the management of IBD. *Nat Rev Gastroenterol Hepatol* 2010; **7**: 15-29 [PMID: 19949430 DOI: 10.1038/nrgastro.2009.203]
87 **Yin Y**, Chen S, Hakim MS, Wang W, Xu L, Dang W, Qu C, Verhaar AP, Su J, Fuhler GM, Peppelenbosch MP, Pan Q. 6-Thioguanine inhibits rotavirus replication through suppression of Rac1 GDP/GTP cycling. *Antiviral Res* 2018; **156**: 92-101 [PMID: 29920300 DOI: 10.1016/j.antiviral.2018.06.011]
88 **Kawamoto A**, Nagata S, Anzai S, Takahashi J, Kawai M, Hama M, Nogawa D, Yamamoto K, Kuno R, Suzuki K, Shimizu H, Hiraguri Y, Yui S, Oshima S, Tsuchiya K, Nakamura T, Ohtsuka K, Kitagawa M, Okamoto R, Watanabe M. Ubiquitin D is Upregulated by Synergy of Notch Signalling and TNF-α in the Inflamed Intestinal Epithelia of IBD Patients. *J Crohns Colitis* 2019; **13**: 495-509 [PMID: 30395194 DOI: 10.1093/ecco-jcc/jjy180]
89 **Xu P**, Elizalde M, Masclee A, Pierik M, Jonkers D. Corticosteroid enhances epithelial barrier function in intestinal organoids derived from patients with Crohn's disease. *J Mol Med (Berl)* 2021; **99**: 805-815 [PMID: 33575854 DOI: 10.1007/s00109-021-02045-7]
90 **Weber CR**, Raleigh DR, Su L, Shen L, Sullivan EA, Wang Y, Turner JR. Epithelial myosin light chain kinase activation induces mucosal interleukin-13 expression to alter tight junction ion selectivity. *J Biol Chem* 2010; **285**: 12037-12046 [PMID: 20177070 DOI: 10.1074/jbc.M109.064808]
91 **Zeissig S**, Bürgel N, Günzel D, Richter J, Mankertz J, Wahnschaffe U, Kroesen AJ, Zeitz M, Fromm M, Schulzke JD. Changes in expression and distribution of claudin 2, 5 and 8 lead to discontinuous tight junctions and barrier dysfunction in active Crohn's disease. *Gut* 2007; **56**: 61-72 [DOI: 10.1136/gut.2006.094375]
92 **Lei H**, Crawford MS, McCole DF. JAK-STAT Pathway Regulation of Intestinal Permeability: Pathogenic Roles and Therapeutic Opportunities in Inflammatory Bowel Disease. *Pharmaceuticals (Basel)* 2021; **14** [PMID: 34577540 DOI: 10.3390/ph14090840]
93 **Lloyd K**, Papoutsopoulou S, Smith E, Stegmaier P, Bergey F, Morris L, Kittner M, England H, Spiller D, White MHR, Duckworth CA, Campbell BJ, Poroikov V, Martins Dos Santos VAP, Kel A, Muller W, Pritchard DM, Probert C, Burkitt MD; SysmedIBD Consortium. Using systems medicine to identify a therapeutic agent with potential for repurposing in inflammatory bowel disease. *Dis Model Mech* 2020; **13** [PMID: 32958515 DOI: 10.1242/dmm.044040]
94 **Bayrer JR**, Wang H, Nattiv R, Suzawa M, Escusa HS, Fletterick RJ, Klein OD, Moore DD, Ingraham HA. LRH-1 mitigates intestinal inflammatory disease by maintaining epithelial homeostasis and cell survival. *Nat Commun* 2018; **9**: 4055 [PMID: 30305617 DOI: 10.1038/s41467-018-06137-w]
95 **Sablin EP**, Blind RD, Uthayaruban R, Chiu HJ, Deacon AM, Das D, Ingraham HA, Fletterick RJ. Structure of Liver Receptor Homolog-1 (NR5A2) with PIP3 hormone bound in the ligand binding pocket. *J Struct Biol* 2015; **192**: 342-348 [PMID: 26416531 DOI: 10.1016/j.jsb.2015.09.012]
96 **Sablin EP**, Krylova IN, Fletterick RJ, Ingraham HA. Structural basis for ligand-independent activation of the orphan nuclear receptor LRH-1. *Mol Cell* 2003; **11**: 1575-1585 [PMID: 12820970 DOI: 10.1016/s1097-2765(03)00236-3]
97 **Deuring JJ**, Li M, Cao W, Chen S, Wang W, de Haar C, van der Woude CJ, Peppelenbosch M. Pregnane X receptor activation constrains mucosal NF-κB activity in active inflammatory bowel disease. *PLoS One* 2019; **14**: e0221924 [PMID: 31581194 DOI: 10.1371/journal.pone.0221924]
98 **Glal D**, Sudhakar JN, Lu HH, Liu MC, Chiang HY, Liu YC, Cheng CF, Shui JW. ATF3 Sustains IL-22-Induced STAT3 Phosphorylation to Maintain Mucosal Immunity Through Inhibiting Phosphatases. *Front Immunol* 2018; **9**: 2522 [PMID: 30455690 DOI: 10.3389/fimmu.2018.02522]
99 **Zhang YG**, Zhu X, Lu R, Messer JS, Xia Y, Chang EB, Sun J. Intestinal epithelial HMGB1 inhibits bacterial infection *via* STAT3 regulation of autophagy. *Autophagy* 2019; **15**: 1935-1953 [PMID: 30894054 DOI: 10.1080/15548627.2019.1596485]
100 **van der Giessen J**, van der Woude CJ, Peppelenbosch MP, Fuhler GM. A Direct Effect of Sex Hormones on Epithelial Barrier Function in Inflammatory Bowel Disease Models. *Cells* 2019; **8** [PMID: 30893871 DOI: 10.3390/cells8030261]
101 **Lie MRKL**, van der Giessen J, Fuhler GM, de Lima A, Peppelenbosch MP, van der Ent C, van der Woude CJ. Low dose Naltrexone for induction of remission in inflammatory bowel disease patients. *J Transl Med* 2018; **16**: 55 [PMID: 29523156 DOI: 10.1186/s12967-018-1427-5]
102 **Li Y**, Zhang T, Guo C, Geng M, Gai S, Qi W, Li Z, Song Y, Luo X, Wang N. Bacillus subtilis RZ001 improves intestinal integrity and alleviates colitis by inhibiting the Notch signalling pathway and activating ATOH-1. *Pathog Dis* 2020; **78** [PMID: 32166323 DOI: 10.1093/femspd/ftaa016]
103 **Wlodarska M**, Luo C, Kolde R, d'Hennezel E, Annand JW, Heim CE, Krastel P, Schmitt EK, Omar AS, Creasey EA, Garner AL, Mohammadi S, O'Connell DJ, Abubucker S, Arthur TD, Franzosa EA, Huttenhower C, Murphy LO, Haiser HJ, Vlamakis H, Porter JA, Xavier RJ. Indoleacrylic Acid Produced by Commensal Peptostreptococcus Species Suppresses Inflammation. *Cell Host Microbe* 2017; **22**: 25-37.e6 [PMID: 28704649 DOI: 10.1016/j.chom.2017.06.007]
104 **Means AL**, Freeman TJ, Zhu J, Woodbury LG, Marincola-Smith P, Wu C, Meyer AR, Weaver CJ, Padmanabhan C, An H, Zi J, Wessinger BC, Chaturvedi R, Brown TD, Deane NG, Coffey RJ, Wilson KT, Smith JJ, Sawyers CL, Goldenring JR, Novitskiy SV, Washington MK, Shi C, Beauchamp RD. Epithelial Smad4 Deletion Up-Regulates Inflammation and Promotes Inflammation-Associated Cancer. *Cell Mol Gastroenterol Hepatol* 2018; **6**: 257-276 [PMID: 30109253 DOI: 10.1016/j.jcmgh.2018.05.006]
105 **Li C**, Zhou Y, Rychahou P, Weiss HL, Lee EY, Perry CL, Barrett TA, Wang Q, Evers BM. SIRT2 Contributes to the

Regulation of Intestinal Cell Proliferation and Differentiation. *Cell Mol Gastroenterol Hepatol* 2020; **10**: 43-57 [PMID: 31954883 DOI: 10.1016/j.jcmgh.2020.01.004]

106 **Kim Y**, West GA, Ray G, Kessler SP, Petrey AC, Fiocchi C, McDonald C, Longworth MS, Nagy LE, de la Motte CA. Layilin is critical for mediating hyaluronan 35kDa-induced intestinal epithelial tight junction protein ZO-1 in vitro and in vivo. *Matrix Biol* 2018; **66**: 93-109 [PMID: 28978412 DOI: 10.1016/j.matbio.2017.09.003]

107 **Davoudi Z**, Peroutka-Bigus N, Bellaire B, Wannemuehler M, Barrett TA, Narasimhan B, Wang Q. Intestinal organoids containing poly(lactic-co-glycolic acid) nanoparticles for the treatment of inflammatory bowel diseases. *J Biomed Mater Res A* 2018; **106**: 876-886 [PMID: 29226615 DOI: 10.1002/jbm.a.36305]

108 **Steinway SN**, Saleh J, Koo BK, Delacour D, Kim DH. Human Microphysiological Models of Intestinal Tissue and Gut Microbiome. *Front Bioeng Biotechnol* 2020; **8**: 725 [PMID: 32850690 DOI: 10.3389/fbioe.2020.00725]

World Journal of Gastroenterology

Submit a Manuscript: https://www.f6publishing.com

World J Gastroenterol 2022 June 28; 28(24): 2654-2666

DOI: 10.3748/wjg.v28.i24.2654

ISSN 1007-9327 (print) ISSN 2219-2840 (online)

MINIREVIEWS

Drug-induced autoimmune hepatitis: A minireview

Chin Kimg Tan, Danielle Ho, Lai Mun Wang, Rahul Kumar

Specialty type: Gastroenterology and hepatology

Provenance and peer review: Invited article; Externally peer reviewed.

Peer-review model: Single blind

Peer-review report's scientific quality classification

Grade A (Excellent): 0
Grade B (Very good): B, B
Grade C (Good): 0
Grade D (Fair): 0
Grade E (Poor): 0

P-Reviewer: Komori A, Japan; Malnick SDH, Israel

Received: August 5, 2021
Peer-review started: August 5, 2021
First decision: September 4, 2021
Revised: September 15, 2021
Accepted: May 14, 2022
Article in press: May 14, 2022
Published online: June 28, 2022

Chin Kimg Tan, Danielle Ho, Rahul Kumar, Gastroenterology and Hepatology, Changi General Hospital, Singapore 529889, Singapore

Chin Kimg Tan, Rahul Kumar, Medicine Academic Clinical Programme, SingHealth Duke-NUS Academic Medical Centre, Singapore 529889, Singapore

Lai Mun Wang, Section of Pathology, Department of Laboratory Medicine, Changi General Hospital, Singapore 529889, Singapore

Lai Mun Wang, Pathology Academic Clinical Programme, SingHealth Duke-NUS Academic Medical Centre, Singapore 529889, Singapore

Corresponding author: Rahul Kumar, FRCP, Assistant Professor, Gastroenterology and Hepatology, Changi General Hospital, 2 Simei Street 3, Singapore 529889, Singapore. rahul.kumar@singhealth.com.sg

Abstract

Drug-induced autoimmune hepatitis (DIAIH) is a specific phenotype of drug-induced liver injury that may lead to the devastating outcome of acute liver failure requiring liver transplantation. Drugs implicated in DIAIH include antimicrobials such as nitrofurantoin and minocycline, non-steroidal anti-inflammatory drugs, statins as well as anti-tumor necrosis agents. The clinical features of drug-induced liver injury are indistinguishable from idiopathic autoimmune hepatitis (AIH) as both may have positive AIH-related autoantibodies, elevated immunoglobulin G, as well as similar histopathological findings. In patients who show no clinical improvement, or there is progressive liver injury despite cessation of the suspected drug, a liver biopsy should be considered, whereby the presence of advance fibrosis on histology favors the diagnosis of idiopathic AIH. Empirical treatment with corticosteroids may be required in patients with non-resolving liver injury. A typical clinical scenario supportive of DIAIH includes a history of drug exposure with spontaneous resolution of liver injury after drug withdrawal and the absence of relapse after rapid steroid taper. In this article we report two cases of DIAIH secondary to Sorafenib and Atorvastatin along with a review of currently available literature. Early identification and treatment often lead to a favorable outcome in DIAIH.

Key Words: Drug-induced liver injury; Drug-induced autoimmune hepatitis; Autoimmune hepatitis; Review

©The Author(s) 2022. Published by Baishideng Publishing Group Inc. All rights reserved.

Core Tip: Drug-induced autoimmune hepatitis is uncommon in clinical practice but may have devastating consequences. It is important to distinguish drug-induced autoimmune hepatitis from idiopathic autoimmune hepatitis as the former may not require prolong course of immunosuppressant. This minireview highlights the key differences between these two closely-linked entities.

Citation: Tan CK, Ho D, Wang LM, Kumar R. Drug-induced autoimmune hepatitis: A minireview. *World J Gastroenterol* 2022; 28(24): 2654-2666
URL: https://www.wjgnet.com/1007-9327/full/v28/i24/2654.htm
DOI: https://dx.doi.org/10.3748/wjg.v28.i24.2654

INTRODUCTION

Idiosyncratic drug-induced liver injury (DILI) is rare and affects 14-19 per 100000 persons yearly[1,2]. Despite its relatively low incidence, it is a leading cause of acute liver failure in the United States[3], Europe[4,5], and Japan[6]. In patients with DILI, liver-related death and liver transplantation occur in 3.6%-10% of cases[7].

Drug-induced autoimmune hepatitis (DIAIH) is a specific phenotype of idiosyncratic DILI with features indistinguishable from idiopathic autoimmune hepatitis (AIH), as it shares serological markers and/or histological features with idiopathic AIH[8]. Various terms have been used synonymously with DIAIH, including immune-mediated DILI[9] and drug-induced AIH-like injury[10].

Due to its rare occurrence, it is difficult to estimate the frequency of DIAIH. In addition, studies use varying definitions of DIAIH and drug causality assessments, as well as having diverse patient populations with different follow-up periods (Tables 1 and 2). It is estimated that DIAIH accounts for 2%-18% of AIH cases[10-14], and 2.9%-8.8% of all DILI are due to DIAIH[15,16]. The increasing incidence of AIH has been in part attributed to prevalent use of anti-tumor necrosis factor agents[14].

DRUGS ASSOCIATED WITH DIAIH

Multiple drugs that have been associated with DIAIH are classified into those with definite association (*e.g.*, Minocycline, Nitrofurantoin, Infliximab), probable association (*e.g.*, Diclofenac, Atorvastatin, Rosuvastatin, Etanercept), and possible association, depending on the cases reported and associations as summarized in the most recent American Association Society of Liver Disease AIH Practice Guidance [10].

DIAIH is classically associated with minocycline, nitrofurantoin, methyldopa, dihydralazine, and tienilic acid[17]. DILI with autoimmune phenotype defined as DILI with presence of AIH antibodies (antibodies to nuclear antigen, smooth muscle, and soluble liver antigen) occur in 83%, 74%, 60%, and 43% of nitrofurantoin, minocycline, methyldopa, and hydralazine related DILI cases, respectively[15]. Immuno-allergic phenotype characterized by any combination of rash, fever, facial edema, lymphadenopathy, and eosinophilia is common in DILI associated with these four drugs as well, ranging from 11%-27%[15]. Another important cause of DIAIH include statins, where DIAIH or DILI with immune features occurs in about 8.5%-27.2% of all statin related DILI[18,19].

In recent years, there has been a change in the predominant culprit drugs causing DIAIH to anti-tumor necrosis factor[14], statins, and non-steroidal anti-inflammatory drugs[16,20,21] with notable contribution from complementary alternative medicines in studies from Asia[22].

PATHOGENESIS OF DIAIH

Reactive metabolites generated from hepatic metabolism of drugs bind to cellular proteins such as components of CYP450, which is then recognized as neoantigens by heightened immunological response leading to AIH[11,23,24] as a result of misdirected immune response against self[25].

In this minireview, we highlight two recent cases of DIAIH induced by Sorafenib and Atorvastatin seen at our center. We also aim to review the current literature on DIAIH and discuss distinguishing features between DIAIH and AIH.

Table 1 Studies comparing drug-induced autoimmune hepatitis and drug-induced liver injury

Ref.	a: Study population; b: Study period; c: Follow-up period	a: Definition of DIAIH; b: Causality tool assessment	No. of DIAIH cases, % of all DILI	No. of DILI cases	Key findings for DIAIH (in addition to Table 3)
Stephens *et al*[37], 2021, Spain	a: Prospective multicentre DILI database, *n* = 869; b: 1994-2018; c: Median 96-117 d in HC injury	a: Simplified AIH criteria; b: RUCAM (definite, highly probable, probable and possible)	26, 2.9%	843	Culprit drugs: Statins (31%); antimicrobials (23%)
De Boer *et al*[15], 2015, United States	a: National prospective DILI database (*n* = 1322), subgroup of DILI secondary to Nitrofurantoin, hydralazine, Minocycline and methyldopa (*n* = 88); b: 2004-2014; c: 6 mo, 12 mo or 24 mo until normalization of LFT	a: Autoimmune (AI) DILI–AI score based on seropositivity for AIH antibodies and raised IgG); b: RUCAM (definite, highly probable and probable)	47, 3.6%	Two groups: (a) 18 non-AI DILI due to 4 drugs; (b) 67 (reference cohort, DILI due to Augmentin, Isoniazid, Diclofenac)	Similar HLA-DRB1*03:01 (15%) and HLADRB1*04:01 (9%) percentage in patients with DILI compared to population controls from National Marrow Donor Program (12% and 9%, respectively)
Hisamochi *et al*[22], 2016, Japan	a: All DILI who underwent liver biopsy, *n* = 62; b: 1988-2010; c: Median 2290 d	a: Revised IAIHG criteria; b: RUCAM and JDD-W scale	23, NA	39	Culprit drugs: CAM (69.6%); NSAIDs (8.7%). IgG reduction in 87%. 50% (8/16) relapsed (4 not treated with steroids, 2 previously received steroids and 2 on tapering dose of steroid dosage). Median time to relapse 283 d (range, 47-1090 d). Rise in IgG with relapse
Licata *et al*[16], 2014, Italy	a: Single centre hospitalized patients with DILI, *n* =136 (44 with liver biopsy); b: 2000-2011; c: Mean 26 mo (12-84 mo), at least 1 yr after stopping immunosuppressants	a: Simplified AIH score ≥ 6; b: RUCAM (definite, highly probable, probable and possible)	12, 8.8%	124	Culprit drugs: NSAIDs (50%) - (Nimesulide/ketoprofen); Antimicrobials (25%) (Augmentin/Ceftriaxone); CAM (17%). 38.2% of all DILI patients had positive AIH antibodies but only 42.9% with positive antibodies have DIAIH. All DIAIH were treated with corticosteroids and all achieved remission at 15 mo. 58.3% (7/12) had addition of Azathioprine. One patient had a flare while on tapering prednisolone. In 41% (5/12), immunosuppressant was stopped after 2 yr, with no relapse

DIAIH: Drug-induced autoimmune hepatitis; DILI: Drug-induced liver injury; RUCAM: The Roussel Uclaf Causality Assessment Model; NSAIDs: Non-steroidal anti-inflammatory drugs; AIH: Autoimmune hepatitis; IAIHG: International AIH Group; IgG: Immunoglobulin G; CAM: Complementary alternative medicines.

CASE DISCUSSION

Patient A

A 61-year-old man and teetotaler presented with a 1-week history of jaundice and malaise. He was on Atorvastatin 40 mg daily for 4 years for hyperlipidemia. He had a normal liver function test (LFT) prior to admission. He was started on Sorafenib 6 wk prior to presentation with jaundice for recurrent sarcoma of the left thigh. Clinical examination was unremarkable apart from scleral icterus. The LFT showed severe hepatocellular (HC) injury [bilirubin 4.56 mg/dL, alkaline phosphatase (ALP) 190 U/L, alanine transaminase (ALT) 1004 U/L, aspartate transaminase (AST) 790 U/L, international normalized ratio (INR) of 1.53]. Viral hepatitis screen, AIH-specific antibodies, and abdominal imaging were unremarkable. Of note, serum immunoglobulin G (IgG) was elevated (18.6 g/L). The liver biopsy showed features supportive of DILI and AIH (Figure 1). The Simplified AIH score was 6. The Roussel Uclaf Causality Assessment Model (RUCAM) score was 9 for Sorafenib and 6 for Atorvastatin. Diagnosis of Sorafenib-induced AIH was made. His LFT improved spontaneously with normalization of LFT 8 wk after stopping Sorafenib (Figure 2A).

Patient B

A 65-year-old man who was on Atorvastatin 40 mg daily presented with an incidental finding of acute HC pattern of liver injury 18 mo after initiation of Atorvastatin (albumin 39 g/L, globulin 39 g/L, bilirubin 0.64 mg/dL, ALP 107 IU/L, ALT 696 U/L, AST 381 U/L). Viral hepatitis screening, AIH-specific antibodies, and abdominal imaging were unremarkable. His serum IgG was normal (14.28 g/L). Atorvastatin was stopped, and an improvement in LFT was noted within the 1 wk (albumin ALT 474 U/L, AST 195 U/L). The RUCAM score for Atorvastatin was 4. As such, he was given the diagnosis of possible Atorvastatin-induced DILI. However, despite this initial improvement in his LFT, there was subsequent deterioration 2 wk after stopping Atorvastatin (albumin 34 g/L, globulin 43 g/L, ALP 137

Table 2 Studies comparing drug-induced autoimmune hepatitis and autoimmune hepatitis

Ref.	a: Study population; b: Study period; c: Follow-up period	a: Definition of DIAIH/AIH; b: Causality tool assessment	No. of DIAIH cases, % of all AIH	No. of AIH cases	Key findings for DIAIH (in addition to Table 4)
Valgeirsson *et al* [14], 2019, Iceland	a: Population based AIH study, *n* = 71; b: 2006-2018; c: Median 4.8 yr	a: Simplified AIH score, if not fulfilled, Revised IAIHG score is used; or received corticosteroids; b: RUCAM score (highly probable, probable and possible)	13, 18% (9/13 had liver biopsy)	58	Culprit drugs: Biologics (77%) - 80% were due to infliximab; Nitrofurantoin (15%)
Martínez-Casas *et al*[34], 2018, Columbia	a: Single centre retrospective review of AIH cases, *n* = 190; b: 2010-2016; c: Mean 47.4 mo	a: Simplified AIH score; b: RUCAM	12, 6.3%	178	Culprit drugs: Nitrofurantoin (67%); NSAIDs (17%)
Wang *et al*[20], 2017, China	a: Single centre retrospective review of AIH and DILI patients; b: 2010-2014; c: NA	a: DILI with positive antibody; simplified AIH score; b: NA (DILI due to drugs/CAM within 6 mo of hospitalization)	18 (12.4% of all DILI with positive antibody)	52	Culprit drugs: CAM, NSAIDs and antibiotics (no breakdown)
Yeong *et al*[32], 2016, United Kingdom	a: Single centre retrospective AIH cases, *n* = 82; b: 2005-2013; c: Median 86.3 mo (14.6% < 18 mo)	a: Revised IAIHG criteria; b: RUCAM (highly probable, probable)	11, 13.4%	71	Culprit drugs: Nitrofurantoin (36.4%); Statins (36.4%); CAM (18%)
Weber *et al*[21], 2019, Germany	a: Single centre cohort of 288 acute liver injury patients who received corticosteroid for DILI/AIH, *n* = 44; b: 2013-2018; c: Median 19 mo in DILI; 23 mo in AIH	a: Simplified AIH score and revised IAIHG criteria; b: RUCAM	22	22	Culprit drugs: NSAIDs (27.3%); Statins (9%); Direct oral anticoagulants (9%)
Björnsson *et al* [13], 2010, United States	a: Single centre retrospective review of all AIH cases, *n* = 261; b: 1997-2007	a: Simplified AIH score	24, 9.2% (24/261)	237	Culprit drugs: Minocycline (45.8%); Nitrofurantoin (45.8%)

DIAIH: Drug-induced autoimmune hepatitis; DILI: Drug-induced liver injury; RUCAM: The Roussel Uclaf Causality Assessment Model; NSAIDs: Non-steroidal anti-inflammatory drugs; AIH: Autoimmune hepatitis; IAIHG: International AIH Group; CAM: Complementary alternative medicines.

U/L, ALT 1404 U/L, AST 676 U/L, INR 1.09). A liver biopsy was performed 3 wk after stopping Atorvastatin in view of worsening acute liver injury. This showed marked HC injury with histological features suggestive of AIH (Figure 3). Following the liver biopsy, there was again spontaneous improvement (ALT 699 U/L), but this did not persist. Two months after cessation of Atorvastatin, he had severe HC injury with jaundice (bilirubin 11.87 mg/dL, ALP 96 U/L, ALT 1095 U/L, AST 938 U/L, INR 1.33) and elevated IgG (28.35 g/L). Liver biopsy was repeated, and this again demonstrated features of AIH. He was then started on prednisolone with rapid improvement of LFT (Figure 2B). The final diagnosis was Atorvastatin-induced AIH.

WHEN TO SUSPECT DIAIH IN PATIENTS WHO PRESENTS WITH DILI

The cases described above highlight two possible presentations of DIAIH. The first patient (patient A) had DILI and histological features compatible with AIH on liver biopsy. Although Sorafenib has not been reported to be associated with DIAIH, the temporal sequence of this case presentation and subsequent spontaneous resolution after cessation of Sorafenib is in keeping with DIAIH.

DIAIH shares many similar characteristics with DILI without features of AIH. More than half of DIAIH present with acute liver injury associated with jaundice in 70%-75% of cases[16], which is similar to DILI. On top of that, rash may be present in 4.5% of DIAIH and 7.9% of DILI[26].

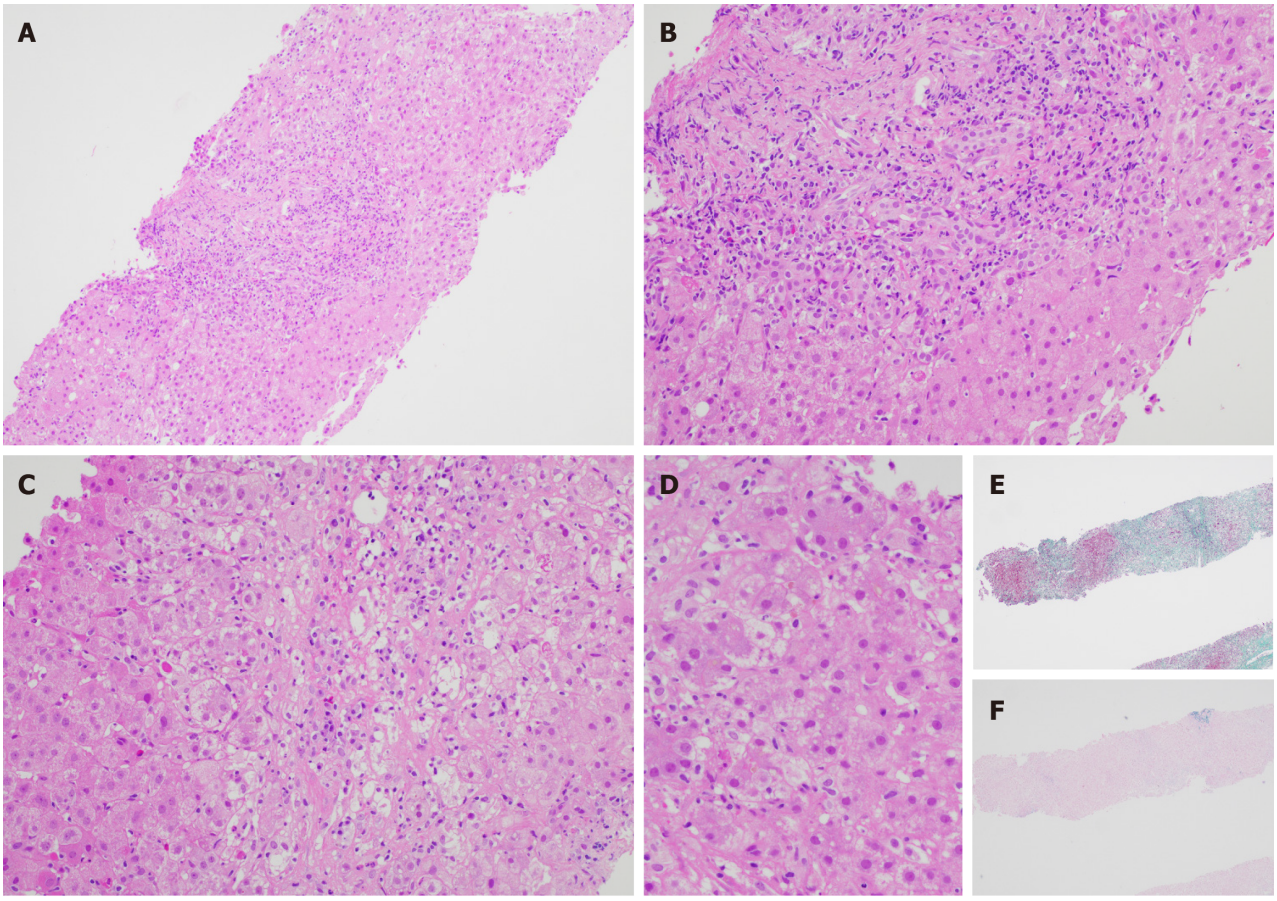
The following pointers are useful in identification of DIAIH in patients who present with DILI. The main differences between these two conditions are also summarized in Table 3: (1) DIAIH and AIH should always be considered as differentials in a patient with a hepatocellular pattern of DILI. DIAIH is rarely associated with a cholestatic/mixed picture, and it is only seen in 8% of cases[16]; (2) A detailed medication history with a focus on recent drug exposures including complementary alternative medicines is essential[10]; (3) The latency period of drug exposure in DIAIH is usually prolonged compared to other types of DILI, some with a latency period exceeding 1 year, *e.g.*, nitrofurantoin and minocycline[15]; (4) Seropositivity for AIH antibodies, *e.g.*, antinuclear antibody (ANA), anti-smooth muscle antibody, anti-liver kidney antibody, and elevated serum IgG suggest possible DIAIH. However, not all patients with DIAIH have detectable autoantibodies or elevated IgG. Similarly, a proportion of patients with DILI may have detectable AIH antibodies[15,16]; (5) In the presence of detectable AIH antibodies and elevated IgG, AIH scoring (either pre-treatment score for Revised International AIH Group criteria[27] or simplified AIH score[28]) is useful to assess for possible or

Table 3 Comparison between drug-induced autoimmune hepatitis and drug-induced liver injury

Clinical features	DIAIH	DILI
Demographics		
Female, %	62%[37]	48% (P = 0.162)[37]
Age (yr), mean ± SD	57± 17[37]; 59 ± 17[22]	54 ± 18 (P = 0.550)[37]; 47 (P = 0.002)[22]
Clinical presentation		
Jaundice, %	69%[37]; 68%[15]; 66%[16]	69% (P = 0.953)[37]; 56% (P = 0.4)[15]; 40%-47.6% (P = 0.2)[16]
Rash, %	4.5%[37]; 19%[15]	7.9% (P = 1.000)[37]; 22% (P = 0.7)[15]
Hepatocellular injury, %	92%[37]	57% (P = 0.002)[37]
Latency period (d), median (range)	65 (27-274)[37]; 277 (8-7032)[15]; 4 (1-9)[16]	27 (8-64) (P = 0.004)[37]; 100 (13-1572) (P = 0.03)[15]; 7-10 (5-50) (P = 0.7)[16]
Latency period (d), mean ± SD	143 ± 188[22]	32 ± 120 (P = 0.000)[22]
Culprit drug due to CAM, %	70%[22]	25% (P = 0.000)[22]
Biochemical results		
ALT × ULN, mean ± SD	28 ± 19[37]	19 ± 22 (P = 0.0002)[37]
AST × ULN, mean ± SD	24 ± 17[37]	15 ± 21 (P = 0.0001)[37]
Autoimmune antibodies and serology		
Detectable ANA, %	88%[37]; 72%[15]; 52%[22]	12 (P < 0.001)[37]; 22[15]; 15 (P = 0.003)[22]
Detectable ASMA, %	44%[37]; 60%[15]	8.9% (P < 0.001)[37]; 13%[15]
Detectable AMA, %	4%[37]	1.9% (P = 0.397)[37]
Detectable anti-LKM-1, %	0%[37]	1.1% (P = 1.000)[37]
Elevated IgG, %	39%[15]; (25% > 1.1 × ULN)[15]	9%[15]
Serum IgG (g/L), mean ± SD	19.5 ± 10.7[37]; 1.07 × ULN ± 0.51[22]	11.9 ± 4.6 (P < 0.001)[37]; 0.69 × ULN ± 0.28 (P = 0.000)[22]
Histopathology		
Liver biopsy[16]		
Severe portal inflammation, %	100%	56.2%-62.5%
Prominent portal plasma cells, %	58.3%	6.3%-12.5%
Rosette formation, %	66.7%	6.3%-12.5%
Severe focal necrosis, %	66%	6.3%-25%
Treatment and response to treatment		
Corticosteroid therapy, %	43%[15]	61% (P = 0.3)[15]
Immunosuppressive therapy, (corticosteroid/Azathioprine), %	58%[37]; 60.8%[22]	9.9% (P < 0.001)[37]; 10.3% (P = 0.000)[22]
Outcomes		
Mild/mod/severe DILI, %	35%/45%/7.7%[37]	31%/59%/6.2% (P = 0.784)[1][37]
Outcomes (liver transplant/death), %	3.8%/0%[37]; 6%/4%[15]	2.1%/1.5% (P = 0.784)[1][37]; 0/0 (P = 0.6 for liver transplant, P = 1.0 for death)[15]
Chronicity rate, %	17%[15]	21% (P = 0.70)[15]

[1]Combined comparisons of severity of drug-induced liver injury, mortality, and liver transplantation.

DIAIH: Drug-induced autoimmune hepatitis; DILI: Drug-induced liver injury; ALT: Alanine transaminase; AST: Aspartate transaminase; ULN: Upper limit of normal; CAM: Complementary alternative medicines; Anti-LKM: Anti-liver kidney antibody; SD: Standard deviation; IAIHG: International AIH Group.



DOI: 10.3748/wjg.v28.i24.2654 **Copyright** ©The Author(s) 2022.

Figure 1 Liver biopsy specimen for patient A. A: Low power view [hematoxylin & eosin (H&E) 100 ×] displays conspicuous portal and lobular inflammation with lobular disarray. Mild steatosis is also noted; B: Higher magnification of the portal tract (H&E 200 ×), zone 1, shows moderate chronic inflammation, lymphoplasmacytic predominantly, and rare eosinophils, with interface damage; C: At similar magnification (H&E 200 ×), the lobule including the perivenular region, *e.g.*, zones 2 and 3, exhibits lobulitis characterized by aggregates of plasma cells, swollen hepatocytes with rosetting, Councilman bodies, and hepatocyte drop-out; D: High power view (H&E 400 ×) demonstrates rosetting of hepatocytes with droplets of orange-brown bile pigment; E and F: Histochemical stains Masson trichrome (E, 40 ×) showing collapse with mild early young fibrosis and Victoria blue (F, 40 ×) revealing paucity of elastic fibers, thus in keeping with subacute injury. Overall, the appearances are supportive of subacute drug-induced liver injury in association with autoimmune hepatitis histological pattern.

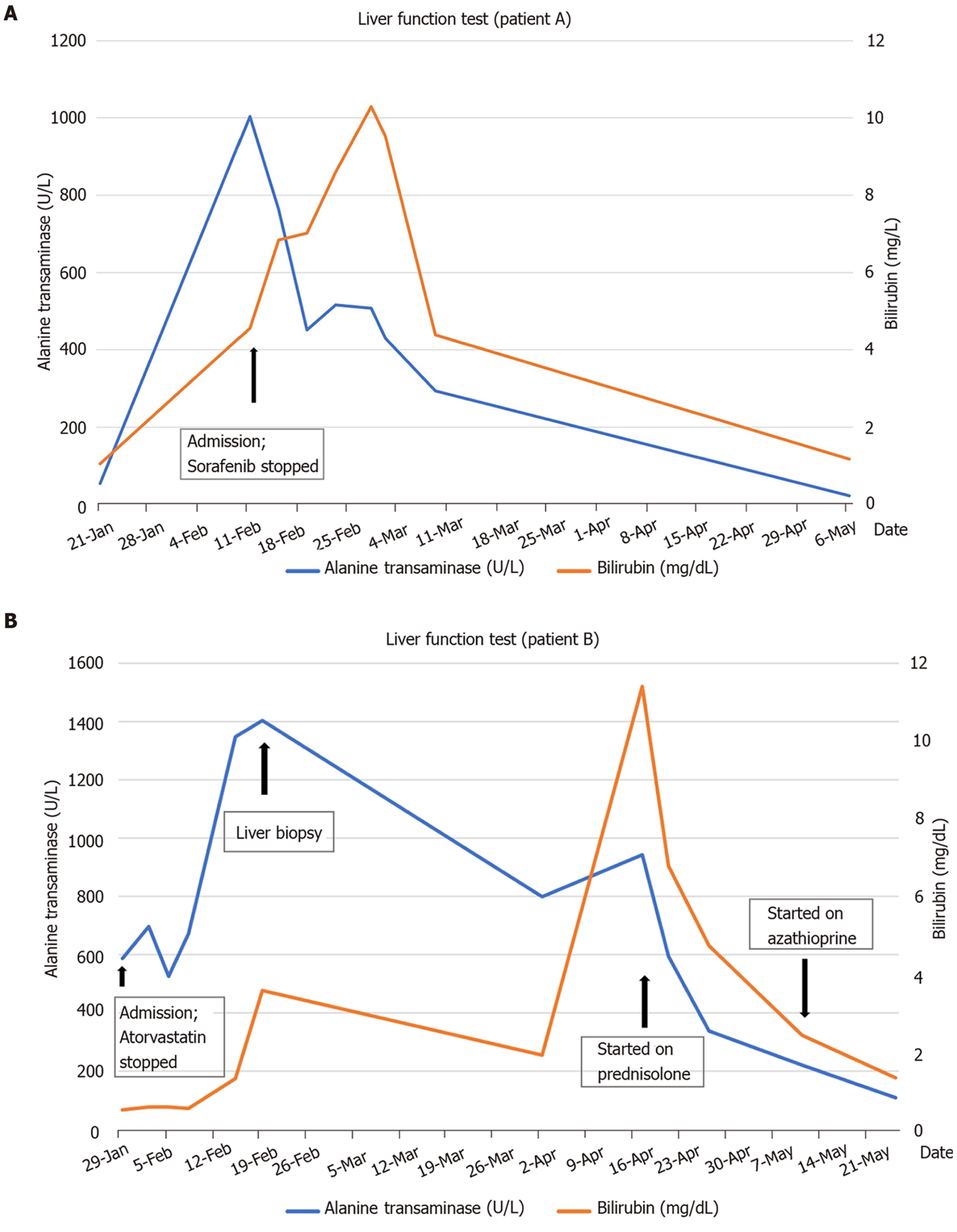
probable AIH; (6) Liver-specific causality assessment tools may be used to ascertain the strength of association between drug exposure and clinical manifestation, *e.g.*, RUCAM[29]; and (7) Liver biopsy is the cornerstone for the diagnosis of DIAIH and should be considered in the following scenarios: (a) Non resolving or worsening liver injury despite stopping possible culprit drugs; (b) Seropositivity of AIH antibodies, raised IgG, or possible AIH based on AIH scoring systems.

Known culprit drugs of DIAIH such as nitrofurantoin may be overlooked as these agents are associated with longer latency period and have a lower ALT at presentation. A higher fibrosis stage or cirrhosis may be observed as a higher proportion of these patients are unknowingly continued on Nitrofurantoin prior to the diagnosis[30]. This underscores the importance of understanding the common culprits of DIAIH, where a significant proportion of DILI presents with DIAIH[15]. LiverTox® is an up-to-date online resource that provides information on hepatotoxicity caused by medications and supplements[31].

With the increasing use of targeted tumor therapies such as kinase inhibitor and immunotherapy, there are some case reports of DIAIH associated with these medications. To our knowledge, this is the first case report of Sorafenib-induced AIH. Imatinib, another type of kinase inhibitor, has also been reported to be associated with DIAIH[14,32].

Several studies have attempted to compare the differences between DIAIH and DILI (Table 1)[15,16,22], with key features of DIAIH including significantly longer duration of drug exposure and latency; higher ALT and AST; higher proportion of patients with positive ANA and SMA, and higher level of serum IgG, as summarized in Table 3.

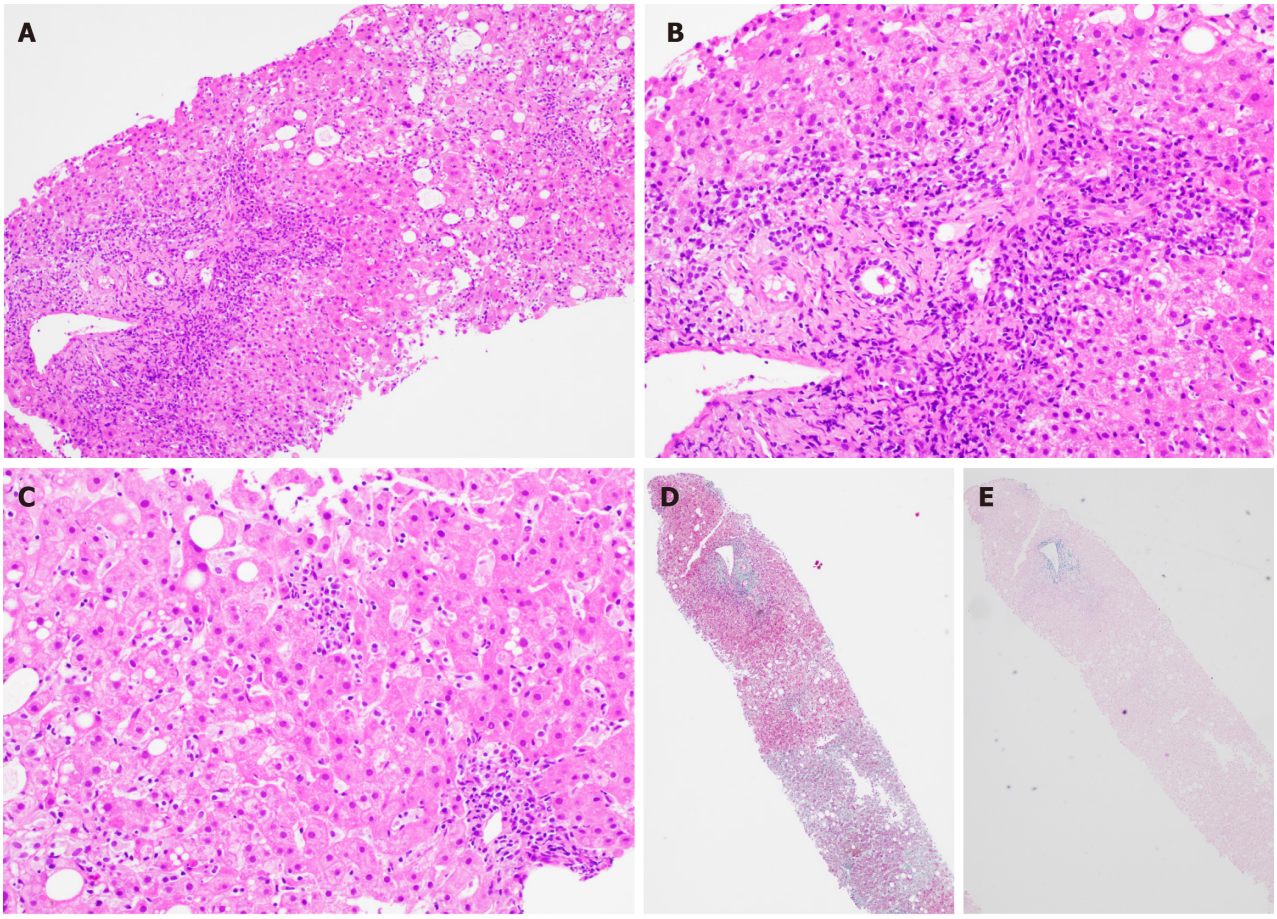
Liver biopsy is key in differentiating DIAIH from DILI without features of AIH[10,33]. In patients with DIAIH, the histopathological features are similar to that of idiopathic AIH with significantly higher proportion of patients showing severe portal inflammation, prominent portal-plasma cells, rosettes, and severe focal necrosis as compared to other types of DILI[16].



DOI: 10.3748/wjg.v28.i24.2654 **Copyright** ©The Author(s) 2022.

Figure 2 Bilirubin and alanine transaminase trend for patients A and B. A: Patient A; B: Patient B.

Though there is no significant difference in the severity and outcomes of DIAIH compared to other types of DILI, it is crucial to identify DIAIH in patients who present with DILI, as DIAIH may require treatment with immunosuppressants if liver injury does not improve with cessation of possible culprit drugs[10,31,33]. A significantly higher proportion of patients (50% to 80%) with DIAIH are treated with corticosteroids/immunosuppressants as compared to non-DIAIH DILI, and DIAIH will need longer



DOI: 10.3748/wjg.v28.i24.2654 **Copyright** ©The Author(s) 2022.

Figure 3 Liver biopsy findings for patient B. A: Low power view [hematoxylin & eosin (H&E) 100 ×] shows portal and lobular inflammation with lobular disarray and mild steatosis; B: Higher magnification of the portal tract (H&E 200 ×) demonstrates moderate plasma cell-rich chronic inflammation with continuous interface damage; C: Lobulitis with aggregates of plasma cells and rosetting of hepatocytes is present in the lobule (H&E 200 ×); D and E: Masson trichrome (D, 40 ×) and Victoria blue (E, 40 ×) display mild early young fibrosis and paucity of elastic fibers, respectively. The absence of old mature type fibrosis suggested not a chronic injury. The autoimmune hepatitis histological pattern observed was therefore interpreted to be drug related, atorvastatin-induced.

term follow up even when LFT normalizes as late relapses may occur in up to 50% of cases where immunosuppressants are stopped[22]. Majority of relapses occur within a year, but some may present late up to 3 years after the initial diagnosis, and risk factors for late disease recurrence are not clear.

DIFFERENTIATING DIAIH AND IDIOPATHIC AIH

The second case highlights the difficulty in differentiating DIAIH from idiopathic AIH. Both conditions have overlapping clinical presentations with HC pattern of liver injury and may have detectable ANA, SMA, and raised IgG in some cases[10,11]. A number of studies compared the difference between DIAIH and AIH (Table 2), with the key differences summarized in Table 4. Some useful features to distinguish between these two entities:

Clinical presentation

Majority (60%-83%) of DIAIH present with an acute presentation, whereas it is seen in less than 20%-35% of cases with idiopathic AIH[10,34]. Most studies of the two conditions do not demonstrate a significant difference in LFT levels[14,21,30,34], but ALT[13,30,34], AST[14,34], and bilirubin[14,34] tend to be higher in patients with DIAIH. Only one study[20] showed a significantly higher level of bilirubin, AST, and ALT in patients with DIAIH. There was no significant difference in the proportion of patients with detectable ANA (77-94%)[20,21] and elevated IgG (36%-59%)[14], although one study showed AIH had higher level of serum IgG compared to DIAIH; it was not, however, statistically significant[14]. Immuno-allergic presentation with skin rash, fever, lymphadenopathy, and eosinophilia favor DIAIH, as it may occur in up to 30% of DIAIH[10,11].

Table 4 Comparison between drug-induced autoimmune hepatitis and autoimmune hepatitis

Clinical features	DIAIH	AIH
Demographics		
Female, %	82%[32]; 91%[34]	80% (P = 0.635)[32]; 92% (P = 0.95)[34]
Clinical presentation		
Acute presentation	> 60%[14]; 55%[32]; 83%[34]	< 20%[14]; 47% (P = 0.618)[32]; 35% (P < 0.001)[34]
Hypersensitivity reaction (fever, rash, eosinophilia)	Up to 30%[14]	Unusual[14]
Cirrhosis at presentation, %	0%[34]	34.8% (P = 0.07)[34]
Temporal relationship with drugs	Positive	Negative
Concurrent AI disease	Unusual[14]	Present in 14%-44%[14]
Biochemical results		
ALT (U/L), mean ± SD	548 ± 335[20]	227 ± 121 (P = 0.021)[20]
AST (U/L), mean ± SD	460 ± 321[20]	202 ± 57 (P = 0.018)[20]
Serology		
IgG, mean ± SD (g/L)	13.4 g/L[14]; 21.4 ± 7.5 [34]	18.6 g/L (P value non-significant)[14]; 24.3 ± 11.2 (P = 0.422)[34]
Pre-treatment score		
RUCAM score, median (range)	6 (3-10)[21]	3.5 (0-7) (P < 0.01)[21]
Revised IAIHG score, median (range)	9.5 (4-14)[21]	13 (9-18)[21]
Simplified AIH score, median (range)	4 (2-6)[21]	5 (1-7) (P = 0.385)[21]
Histopathology		
F3-F4, %	33.3%[34]	54.4% (P = 0.15)[34]
Typical histology (portal inflammation, interface hepatitis, plasma cells infiltrates)	18.2%[20]	54%[20]
Treatment and response to treatment		
Time to biochemical remission, mean (mo)	2[34]	16.8 (P <0.001)[34]
Treatment with Azathioprine or Mycophenolic acid in addition to corticosteroids, %	57%[13]; 15%[14]; 28% [20]; 20%[21]	86% (P = 0.024)[13]; 83% (P < 0.001)[14]; 90% (P = 0.023)[20]; 85% (P < 0.01)[21]
Biochemical remission, %	95%[21]	77.3% (P = 0.08)[21]
Treatment discontinuation, %	69%[14]; 100%[20]; 85% [21]; 25%[34]	26% (P < 0.02)[14]; 25% (P = 0.013)[20]; 5% (P < 0.1)[21]; 3% (P < 0.001) [34]
Relapse rate, %	0%[14]; 15%[21]; 60% [32]; 0%[34]	43% (P = 0.022)[14]; 70% (P < 0.01)[21]; 83% (P = 0.538)[32]; 18% (P = 0.10) [34]
Time to relapse (wk), median (range)	131 (37-216)[34]	14 (1-155) (P = 0.033)[34]
Outcomes		
Liver transplant/death, %	0%/0%[32,34]	2.8%/7% (P = 0.748 for liver transplant; p = 0.65 for death)[32]; 5.6%/2.8% (P = 0.40 for liver transplant; P = 0.55 for death)[34]

DIAIH: Drug-induced autoimmune hepatitis; DILI: Drug-induced liver injury; ALT: Alanine transaminase; AST: Aspartate transaminase; RUCAM: The Roussel Uclaf Causality Assessment Model; SD: Standard deviation.

AIH scoring and causality assessment

In a cohort of 44 patients with DIAIH and AIH, the simplified AIH score was not useful in differentiating the two entities[21]. Of note, patients with AIH had significantly higher pre-treatment AIH score compared to patients with DIAIH. The sensitivity and the specificity for pre-treatment AIH score (using a cut off of ≥ 12 – probable AIH) was shown to be 59% and 82%, respectively. As for RUCAM, using a cut off of ≥ 6 (probable), the specificity reaches 91%, albeit with a low sensitivity at 32%. When these are used in combination, there is still a potential for misdiagnosis in up to 11% of patients.

Histopathology

Both DIAIH and AIH share similar histological findings (portal and periportal infiltrates of lymphocytes, lobular hepatitis, plasma cells, and eosinophils) with no clear differentiating features, except presence of advance fibrosis or cirrhosis favoring idiopathic AIH[11,34]. However, a significantly higher proportion of patients with AIH showed typical features of AIH (54%) as compared to DIAIH (18.2%)[20], specifically in terms of portal inflammation with interface hepatitis and plasma cell infiltrates. The same study also found that DIAIH tended to have more eosinophilic infiltrates, which was not noted in other studies[21].

Treatment and response to treatment

The cornerstone in the management of DIAIH is to stop the culprit drug. Spontaneous improvement of LFT may then occur, as was observed in patient A. The most consistent and significant differentiating feature between DIAIH and AIH in published case series thus far lies in the response to treatment (Table 4). In cases where liver injury does not resolve despite cessation of the culprit drug or where the degree of DILI is severe, corticosteroids are usually started as per the initial management of AIH. Most studies on DIAIH exclusively include patients who were treated with immunosuppressants[14,20,21,30]. Both DIAIH and AIH showed excellent response to corticosteroids, with remission rate exceeding 90% in most cases[21,30-34].

It should be borne in mind that there is discrepancy in literature regarding the mean time to achieve immunosuppression induced remission in DIAIH and AIH. While one study demonstrated similar 3 mo mean time to remission[21] in both conditions, another showed a significant difference, where DIAIH took a significantly shorter time than AIH to achieve remission[34] (2 mo *vs* 16.8 mo). This may be attributed to the heterogeneity of the study population. Resolution of DIAIH usually occurs after 1 mo (rarely up to 3 mo) of immunosuppression. Unlike in AIH, DIAIH rarely requires long term immunosuppression and has very low relapse rates after cessation of immunosuppressants over a long follow-up of up to 4 years[10,11,13-15,20,21,34] (Table 2). In cases where DIAIH relapses, the time to relapse is significantly longer compared to AIH[30], which implies that patients with DIAIH will require a longer period of follow-up after resolution of liver injury as compared to the usual DILI. Interestingly, despite similar time to remission in the two groups, Weber *et al*[21] showed that an early rapid response to corticosteroid treatment differentiates DIAIH from AIH with good sensitivity and specificity at 77%, respectively. The early rapid response was defined by 9% drop of ALT per day in the first week of corticosteroid therapy.

The use of steroids appears to be a promising means of differentiating DIAIH or AIH in the early course of disease with better sensitivity than RUCAM and AIH score[21]. This also has the potential benefit of avoiding long term immunosuppressive therapy in DIAIH. Also, in 30%-35% of DIAIH cases that were initially seropositive for ANA and SMA, the antibodies became undetectable at 6 mo following the initial DILI, which was independent of treatment with corticosteroids[15].

Major hepatology society guidelines recommend a similar approach in terms of corticosteroids initiation in non-resolving DIAIH and AIH[10,11]. However, there is no consensus regarding treatment duration and methods to confirm remission before discontinuation of immunosuppressants. Thus, the decision and timing to stop treatment should be assessed on case-by-case basis[10]. In fact, one study has shown success in tapering off immunosuppression within 3-17 mo without evidence of relapse[20].

Risk alleles and monocyte-derived hepatocyte like cells

Risk alleles for idiopathic AIH such as HLA DRB1 DRB1*03:01 or DRB1*04:01 are uncommon in DIAIH and, if this is detected, may favor a diagnosis of AIH[10]. The MetaHeps® test, which uses monocyte-derived hepatocyte-like cells, has been used to differentiate DIAIH from AIH with high sensitivity and specificity[21]. However, this test is not readily available, thereby limiting its utility in clinical practice. The lymphocyte toxicity assay described by Neuman *et al*[35] can sometimes be helpful in differentiating drug hypersensitivity syndromes from idiopathic AIH as well.

Outcomes

The long-term outcome of DIAIH is excellent with a survival rate between 90%-100% without liver transplantation[10]. This is in contrast with idiopathic AIH, where there is a high risk of relapse upon treatment withdrawal and risk of progression to cirrhosis, resulting in the need for liver transplantation [10,11,34]. It is also noteworthy that DIAIH can lead to chronic DILI with abnormal LFT lasting more than 6 mo in 17%-22% of cases[15,36].

CONCLUSION

In summary, it is important to differentiate between DIAIH and AIH in patients who present with DILI, as the management and outcome differ. Early recognition of DIAIH is key as the mainstay of management is cessation of culprit drug and in some cases, initiation of corticosteroids with the aim to

avoid long-term immunosuppression.

ACKNOWLEDGEMENTS

We acknowledge all our colleagues in the Department of Gastroenterology and Hepatology and Pathology at Changi General Hospital who help manage the 2 patients described in the manuscript. We would also like to thank the 2 patients described here who readily consented to be described in this manuscript.

FOOTNOTES

Author contributions: Kumar R and Tan CK conceptualized the study; Tan CK, Ho D, and Kumar R wrote the initial manuscript; Wand LM provided critical input and histo-pathological slides for the manuscript; all authors were involved in the critical revision.

Conflict-of-interest statement: All authors have no relevant conflict of interest to report.

Open-Access: This article is an open-access article that was selected by an in-house editor and fully peer-reviewed by external reviewers. It is distributed in accordance with the Creative Commons Attribution NonCommercial (CC BY-NC 4.0) license, which permits others to distribute, remix, adapt, build upon this work non-commercially, and license their derivative works on different terms, provided the original work is properly cited and the use is non-commercial. See: https://creativecommons.org/Licenses/by-nc/4.0/

Country/Territory of origin: Singapore

ORCID number: Chin Kimg Tan 0000-0002-3918-4340; Danielle Ho 0000-0003-0652-406x; Lai Mun Wang 0000-0001-7113-4215; Rahul Kumar 0000-0002-5092-4821.

S-Editor: Yan JP
L-Editor: Filipodia
P-Editor: Yan JP

REFERENCES

1 **Björnsson ES**, Bergmann OM, Björnsson HK, Kvaran RB, Olafsson S. Incidence, presentation, and outcomes in patients with drug-induced liver injury in the general population of Iceland. *Gastroenterology* 2013; **144**: 1419-1425, 1425.e1 [PMID: 23419359 DOI: 10.1053/j.gastro.2013.02.006]
2 **Shen T**, Liu Y, Shang J, Xie Q, Li J, Yan M, Xu J, Niu J, Liu J, Watkins PB, Aithal GP, Andrade RJ, Dou X, Yao L, Lv F, Wang Q, Li Y, Zhou X, Zhang Y, Zong P, Wan B, Zou Z, Yang D, Nie Y, Li D, Wang Y, Han X, Zhuang H, Mao Y, Chen C. Incidence and Etiology of Drug-Induced Liver Injury in Mainland China. *Gastroenterology* 2019; **156**: 2230-2241.e11 [PMID: 30742832 DOI: 10.1053/j.gastro.2019.02.002]
3 **Ostapowicz G**, Fontana RJ, Schiødt FV, Larson A, Davern TJ, Han SH, McCashland TM, Shakil AO, Hay JE, Hynan L, Crippin JS, Blei AT, Samuel G, Reisch J, Lee WM; U. S. Acute Liver Failure Study Group. Results of a prospective study of acute liver failure at 17 tertiary care centers in the United States. *Ann Intern Med* 2002; **137**: 947-954 [PMID: 12484709 DOI: 10.7326/0003-4819-137-12-200212170-00007]
4 **Wei G**, Bergquist A, Broomé U, Lindgren S, Wallerstedt S, Almer S, Sangfelt P, Danielsson A, Sandberg-Gertzén H, Lööf L, Prytz H, Björnsson E. Acute liver failure in Sweden: etiology and outcome. *J Intern Med* 2007; **262**: 393-401 [PMID: 17697161 DOI: 10.1111/j.1365-2796.2007.01818.x]
5 **Björnsson E**, Jerlstad P, Bergqvist A, Olsson R. Fulminant drug-induced hepatic failure leading to death or liver transplantation in Sweden. *Scand J Gastroenterol* 2005; **40**: 1095-1101 [PMID: 16165719 DOI: 10.1080/00365520510023846]
6 **Ohmori S**, Shiraki K, Inoue H, Okano H, Yamanaka T, Deguchi M, Sakai T, Takase K, Nakano T, Tameda Y. Clinical characteristics and prognostic indicators of drug-induced fulminant hepatic failure. *Hepatogastroenterology* 2003; **50**: 1531-1534 [PMID: 14571779]
7 **Chalasani N**, Bonkovsky HL, Fontana R, Lee W, Stolz A, Talwalkar J, Reddy KR, Watkins PB, Navarro V, Barnhart H, Gu J, Serrano J; United States Drug Induced Liver Injury Network. Features and Outcomes of 899 Patients With Drug-Induced Liver Injury: The DILIN Prospective Study. *Gastroenterology* 2015; **148**: 1340-52.e7 [PMID: 25754159 DOI: 10.1053/j.gastro.2015.03.006]
8 **Aithal GP**, Watkins PB, Andrade RJ, Larrey D, Molokhia M, Takikawa H, Hunt CM, Wilke RA, Avigan M, Kaplowitz N, Bjornsson E, Daly AK. Case definition and phenotype standardization in drug-induced liver injury. *Clin Pharmacol Ther* 2011; **89**: 806-815 [PMID: 21544079 DOI: 10.1038/clpt.2011.58]
9 **Weiler-Normann C**, Schramm C. Drug induced liver injury and its relationship to autoimmune hepatitis. *J Hepatol* 2011; **55**: 747-749 [PMID: 21396413 DOI: 10.1016/j.jhep.2011.02.024]

10 **Mack CL**, Adams D, Assis DN, Kerkar N, Manns MP, Mayo MJ, Vierling JM, Alsawas M, Murad MH, Czaja AJ. Diagnosis and Management of Autoimmune Hepatitis in Adults and Children: 2019 Practice Guidance and Guidelines From the American Association for the Study of Liver Diseases. *Hepatology* 2020; **72**: 671-722 [PMID: 31863477 DOI: 10.1002/hep.31065]

11 **European Association for the Study of the Liver**. EASL Clinical Practice Guidelines: Autoimmune hepatitis. *J Hepatol* 2015; **63**: 971-1004 [PMID: 26341719 DOI: 10.1016/j.jhep.2015.06.030]

12 **Gordon V**, Adhikary R, Appleby V, Das D, Day J, Delahooke T, Dixon S, Elphick D, Hardie C, Hoeroldt B, Hooper P, Hutchinson J, Jones R, Khan F, Aithal GP, McGonigle J, Nelson A, Nkhoma A, Pelitari S, Prince M, Prosser A, Sathanarayana V, Savva S, Shah N, Saksena S, Thayalasekaran S, Vani D, Yeoman A, Gleeson D; UK Multi-Centre AIH Audit Group. Diagnosis, presentation and initial severity of Autoimmune Hepatitis (AIH) in patients attending 28 hospitals in the UK. *Liver Int* 2018; **38**: 1686-1695 [PMID: 29455458 DOI: 10.1111/liv.13724]

13 **Björnsson E**, Talwalkar J, Treeprasertsuk S, Kamath PS, Takahashi N, Sanderson S, Neuhauser M, Lindor K. Drug-induced autoimmune hepatitis: clinical characteristics and prognosis. *Hepatology* 2010; **51**: 2040-2048 [PMID: 20512992 DOI: 10.1002/hep.23588]

14 **Valgeirsson KB**, Hreinsson JP, Björnsson ES. Increased incidence of autoimmune hepatitis is associated with wider use of biological drugs. *Liver Int* 2019; **39**: 2341-2349 [PMID: 31436903 DOI: 10.1111/liv.14224]

15 **de Boer YS**, Kosinski AS, Urban TJ, Zhao Z, Long N, Chalasani N, Kleiner DE, Hoofnagle JH; Drug-Induced Liver Injury Network. Features of Autoimmune Hepatitis in Patients With Drug-induced Liver Injury. *Clin Gastroenterol Hepatol* 2017; **15**: 103-112.e2 [PMID: 27311619 DOI: 10.1016/j.cgh.2016.05.043]

16 **Licata A**, Maida M, Cabibi D, Butera G, Macaluso FS, Alessi N, Caruso C, Craxì A, Almasio PL. Clinical features and outcomes of patients with drug-induced autoimmune hepatitis: a retrospective cohort study. *Dig Liver Dis* 2014; **46**: 1116-1120 [PMID: 25224696 DOI: 10.1016/j.dld.2014.08.040]

17 **Czaja AJ**. Drug-induced autoimmune-like hepatitis. *Dig Dis Sci* 2011; **56**: 958-976 [PMID: 21327704 DOI: 10.1007/s10620-011-1611-4]

18 **Russo MW**, Scobey M, Bonkovsky HL. Drug-induced liver injury associated with statins. *Semin Liver Dis* 2009; **29**: 412-422 [PMID: 19826975 DOI: 10.1055/s-0029-1240010]

19 **Perdices EV**, Medina-Cáliz I, Hernando S, Ortega A, Martín-Ocaña F, Navarro JM, Peláez G, Castiella A, Hallal H, Romero-Gómez M, González-Jiménez A, Robles-Díaz M, Lucena MI, Andrade RJ. Hepatotoxicity associated with statin use: analysis of the cases included in the Spanish Hepatotoxicity Registry. *Rev Esp Enferm Dig* 2014; **106**: 246-254 [PMID: 25075655]

20 **Wang H**, Fu J, Liu G, Wang L, Yan A, Wang G. Drug induced autoimmune hepatitis (DIAIH): Pathological and clinical study. *Biomed Res* 2017; **28**: 6028-6034

21 **Weber S**, Benesic A, Rotter I, Gerbes AL. Early ALT response to corticosteroid treatment distinguishes idiosyncratic drug-induced liver injury from autoimmune hepatitis. *Liver Int* 2019; **39**: 1906-1917 [PMID: 31319011 DOI: 10.1111/liv.14195]

22 **Hisamochi A**, Kage M, Ide T, Arinaga-Hino T, Amano K, Kuwahara R, Ogata K, Miyajima I, Kumashiro R, Sata M, Torimura T. An analysis of drug-induced liver injury, which showed histological findings similar to autoimmune hepatitis. *J Gastroenterol* 2016; **51**: 597-607 [PMID: 26519284 DOI: 10.1007/s00535-015-1131-7]

23 **Beaune P**, Dansette PM, Mansuy D, Kiffel L, Finck M, Amar C, Leroux JP, Homberg JC. Human anti-endoplasmic reticulum autoantibodies appearing in a drug-induced hepatitis are directed against a human liver cytochrome P-450 that hydroxylates the drug. *Proc Natl Acad Sci U S A* 1987; **84**: 551-555 [PMID: 3540968 DOI: 10.1073/pnas.84.2.551]

24 **Bourdi M**, Larrey D, Nataf J, Bernuau J, Pessayre D, Iwasaki M, Guengerich FP, Beaune PH. Anti-liver endoplasmic reticulum autoantibodies are directed against human cytochrome P-450IA2. A specific marker of dihydralazine-induced hepatitis. *J Clin Invest* 1990; **85**: 1967-1973 [PMID: 2347920 DOI: 10.1172/JCI114660]

25 **Czaja AJ**. Autoimmune hepatitis. Part A: pathogenesis. *Expert Rev Gastroenterol Hepatol* 2007; **1**: 113-128 [PMID: 19072440 DOI: 10.1586/17474124.1.1.113]

26 **Liu ZX**, Kaplowitz N. Immune-mediated drug-induced liver disease. *Clin Liver Dis* 2002; **6**: 755-774 [PMID: 12362579 DOI: 10.1016/s1089-3261(02)00025-9]

27 **Alvarez F**, Berg PA, Bianchi FB, Bianchi L, Burroughs AK, Cancado EL, Chapman RW, Cooksley WG, Czaja AJ, Desmet VJ, Donaldson PT, Eddleston AL, Fainboim L, Heathcote J, Homberg JC, Hoofnagle JH, Kakumu S, Krawitt EL, Mackay IR, MacSween RN, Maddrey WC, Manns MP, McFarlane IG, Meyer zum Büschenfelde KH, Zeniya M. International Autoimmune Hepatitis Group Report: review of criteria for diagnosis of autoimmune hepatitis. *J Hepatol* 1999; **31**: 929-938 [PMID: 10580593 DOI: 10.1016/s0168-8278(99)80297-9]

28 **Czaja AJ**. Performance parameters of the diagnostic scoring systems for autoimmune hepatitis. *Hepatology* 2008; **48**: 1540-1548 [PMID: 18924244 DOI: 10.1002/hep.22513]

29 **Danan G**, Benichou C. Causality assessment of adverse reactions to drugs--I. A novel method based on the conclusions of international consensus meetings: application to drug-induced liver injuries. *J Clin Epidemiol* 1993; **46**: 1323-1330 [PMID: 8229110 DOI: 10.1016/0895-4356(93)90101-6]

30 **Yeong TT**, Lim KH, Goubet S, Parnell N, Verma S. Natural history and outcomes in drug-induced autoimmune hepatitis. *Hepatol Res* 2016; **46**: E79-E88 [PMID: 25943838 DOI: 10.1111/hepr.12532]

31 LiverTox: Clinical and Research Information on Drug-Induced Liver Injury [Internet]. Bethesda (MD): National Institute of Diabetes and Digestive and Kidney Diseases; 2012– [PMID: 31643176]

32 **Aliberti S**, Grignani G, Allione P, Fizzotti M, Galatola G, Pisacane A, Aglietta M. An acute hepatitis resembling autoimmune hepatitis occurring during imatinib therapy in a gastrointestinal stromal tumor patient. *Am J Clin Oncol* 2009; **32**: 640-641 [PMID: 19955903 DOI: 10.1097/COC.0b013e31802b4ef7]

33 **Chalasani NP**, Maddur H, Russo MW, Wong RJ, Reddy KR; Practice Parameters Committee of the American College of Gastroenterology. ACG Clinical Guideline: Diagnosis and Management of Idiosyncratic Drug-Induced Liver Injury. *Am J Gastroenterol* 2021; **116**: 878-898 [PMID: 33929376 DOI: 10.14309/ajg.0000000000001259]

34 **Martínez-Casas OY**, Díaz-Ramírez GS, Marín-Zuluaga JI, Muñoz-Maya O, Santos O, Donado-Gómez JH, Restrepo-Gutiérrez JC. Differential characteristics in drug-induced autoimmune hepatitis. *JGH Open* 2018; **2**: 97-104 [PMID:

30483571 DOI: 10.1002/jgh3.12054]

35 **Neuman MG**, Malkiewicz IM, Shear NH. A novel lymphocyte toxicity assay to assess drug hypersensitivity syndromes. *Clin Biochem* 2000; **33**: 517-524 [PMID: 11124336 DOI: 10.1016/s0009-9120(00)00146-6]

36 **Castiella A**, Zapata E, Lucena MI, Andrade RJ. Drug-induced autoimmune liver disease: A diagnostic dilemma of an increasingly reported disease. *World J Hepatol* 2014; **6**: 160-168 [PMID: 24799984 DOI: 10.4254/wjh.v6.i4.160]

37 **Stephens C**, Robles-Diaz M, Medina-Caliz I, Garcia-Cortes M, Ortega-Alonso A, Sanabria-Cabrera J, Gonzalez-Jimenez A, Alvarez-Alvarez I, Slim M, Jimenez-Perez M, Gonzalez-Grande R, Fernández MC, Casado M, Soriano G, Román E, Hallal H, Romero-Gomez M, Castiella A, Conde I, Prieto M, Moreno-Planas JM, Giraldez A, Moreno-Sanfiel JM, Kaplowitz N, Lucena MI, Andrade RJ; Participating clinical centres. Comprehensive analysis and insights gained from long-term experience of the Spanish DILI Registry. *J Hepatol* 2021; **75**: 86-97 [PMID: 33539847 DOI: 10.1016/j.jhep.2021.01.029]

World Journal of Gastroenterology

Submit a Manuscript: https://www.f6publishing.com

World J Gastroenterol 2022 June 28; 28(24): 2667-2679

DOI: 10.3748/wjg.v28.i24.2667

ISSN 1007-9327 (print) ISSN 2219-2840 (online)

MINIREVIEWS

Rebuilding trust in proton pump inhibitor therapy

Alla Turshudzhyan, Sonia Samuel, Angela Tawfik, Micheal Tadros

Specialty type: Gastroenterology and hepatology

Provenance and peer review: Invited article; Externally peer reviewed.

Peer-review model: Single blind

Peer-review report's scientific quality classification

Grade A (Excellent): 0
Grade B (Very good): B, B
Grade C (Good): 0
Grade D (Fair): 0
Grade E (Poor): 0

P-Reviewer: Chen LW, Taiwan; Sano W, Japan

Received: January 10, 2022
Peer-review started: January 10, 2022
First decision: March 8, 2022
Revised: March 15, 2022
Accepted: May 8, 2022
Article in press: May 8, 2022
Published online: June 28, 2022

Alla Turshudzhyan, Department of Medicine, University of Connecticut, Farmington, CT 06030, United States

Sonia Samuel, Department of Medicine, Albany Medical College, Albany, NY 12208, United States

Angela Tawfik, Guilderland High School, Guilderland Center, Albany, NY 12085, United States

Micheal Tadros, Department of Gastroenterology and Hepatology, Albany Medical College, Albany, NY 12208, United States

Corresponding author: Micheal Tadros, FACG, MD, Associate Professor, Department of Gastroenterology and Hepatology, Albany Medical College, 49 New Scotland Ave, Albany, NY 12208, United States. tadrosm1@amc.edu

Abstract

Introduction of proton pump inhibitor (PPI) therapy into clinical practice has revolutionized treatment approach to acid-related diseases. With its clinical success came a widespread use of PPI therapy. Subsequently, several studies found that PPIs were oftentimes overprescribed in primary care and emergency setting, likely attributed to seemingly low side-effect profile and physicians having low threshold to initiate therapy. However, now there is a growing concern over PPI side-effect profile among both patients and providers. We would like to bring more awareness to the currently available guidelines on PPI use, discuss clinical indications for PPIs and the evidence behind the reported side-effects. We hope that increased awareness of proper PPI use will make the initiation or continuation of therapy a well informed and an evidence-based decision between patient and physician. We also hope that discussing evidence behind the reported side-effect profile will help clarify the growing concerns over PPI therapy.

Key Words: Proton pump inhibitor; Side-effects; Gastro-esophageal reflux disease; Therapy

©The Author(s) 2022. Published by Baishideng Publishing Group Inc. All rights reserved.

Core Tip: Proton pump inhibitor (PPI) therapy is a cornerstone therapy for acid-related diseases. Its clinical success can be attributed to anti-secretory properties superior to any prior agents and seemingly low side-effects profile. As more patients were started and continued PPI therapy long-term, some studies began reporting side-effects associated with this therapy. Concerns over risks associated with PPI use grew over the last couple of years among both patients and providers. We hope to bring awareness to the current guidelines and the evidence behind the reported side-effects as better understanding of this evidence can improve medical practice. Both patients and providers should have all the evidence at hand when discussing initiation or continuation of PPI therapy.

Citation: Turshudzhyan A, Samuel S, Tawfik A, Tadros M. Rebuilding trust in proton pump inhibitor therapy. *World J Gastroenterol* 2022; 28(24): 2667-2679
URL: https://www.wjgnet.com/1007-9327/full/v28/i24/2667.htm
DOI: https://dx.doi.org/10.3748/wjg.v28.i24.2667

INTRODUCTION

Proton pump inhibitors (PPIs) were first introduced more than two decades ago but have quickly become a cornerstone therapy for the acid-related diseases. They were regarded for their superior antisecretory properties and seemingly low side-effect profile, which ultimately contributed to low threshold for therapy initiation[1]. They became first-line treatment for esophagitis, gastro-esophageal reflux disease (GERD), peptic ulcer disease (PUD), Zollinger-Ellison syndrome (ZES), and *Helicobacter pylori* (*H. pylori*) infection[2]. Many patients started on PPI therapy continued it long-term without a clear expectation of the therapy duration. Rising number of patients on chronic PPI therapy led to growing concerns over medication side-effect profile. Especially as some reports claimed that improper long-term PPI use has risen significantly in the last decade with some data suggesting that only half of patients on PPI therapy had an appropriate indication[3,4]. Improper PPI use is multifactorial and comes from a pattern of preventable chain of events (Figure 1). This discussion is important because PPIs affect patients' quality of life, and need to be taken judiciously and according to the evidence-based guidelines.

BACKGROUND

PPIs work by suppressing gastric acid secretion by directly inhibiting gastric acid pump (H+/K+ adenosine triphosphatase (ATPase)) of the parietal cells[5]. PPIs are prodrugs that are only activated once exposed to the acidic environment of the parietal cells[6]. Once active, their half-life ranges from 0.6-1.9 h, depending on the type of PPIs used (Table 1)[7-9]. After PPIs are no longer metabolically active, they are metabolized by the hepatic P450 enzymes, primarily by CYP2C19 with minor contribution from CYP3A4 (Table 1)[6,10]. Once metabolized, they are excreted renally, with lansoprazole and dexlasoprazole also being excreted by the gut (Table 1)[11].

Not all patients metabolize PPIs at the same rate, causing variation in bioavailability. The hepatic P450 system is partially responsible for this variation. Patients of Asian ethnicity and older patients tend to have slower P450 systems and, as a result, have increased bioavailability of PPIs[6].

Currently available PPIs include esomeprazole, lansoprazole, omeprazole, dexlansoprazole, pantoprazole, and rabeprazole[12]. None of the PPIs has shown superiority in their antisecretory properties and are used interchangeably in clinical practice[13]. While there are no studies to support superiority, omeprazole is among the 10 most prescribed medications in the United States[6]. From the variety of PPIs available, esomeprazole and lansoprazole have the highest bioavailability: 89% and 80%-90%, respectively (Table 1)[11]. The lowest bioavailability is seen with rabeprazole at 52%[11]. Majority of PPIs must be taken 30 min prior to the first meal of the day. Esomeprazole requires 60 min prior to food intake administration[14]. Pharmacokinetics of dexlansoprazole, pantoprazole, and rabeprazole are unaffected by the food ingestion and can be taken at any time (Table 1)[14].

CLINICAL INDICATIONS

PPIs are used as a first line therapy for GERD, acid-related erosive esophagitis, peptic stricture, Barrett esophagus, and high risk of ulcer bleeding while on nonsteroidal anti-inflammatory drugs (NSAID) therapy[15]. It is also considered for treatment of eosinophilic esophagitis (EoE), non-erosive reflux disease (NERD), *H. pylori* infection (in combination with antibiotics), hypersecretory syndromes (*e.g.*

Table 1 Type of proton pump inhibitor available

PPI	Omeprazole	Esomeprazole	Lansoprazole	Dexlansoprazole	Pantoprazole	Rabeprazole
Half-life (T1/2) (hrs)[7-9]	0.6-1.0[7]	1.1[8]	0.9-1.6[7]	1-2[9]	0.9-1.9[7]	1[7]
Hepatic metabolism[10]	Major: CYP2C19; minor: CYP3A4	Major: CYP2C19; minor: CYP3A4	Major: CYP2C19; minor: CYP3A4	Major: CYP2C19; minor: CYP3A4	Minor: CYP3A4 CYP2C19	Non-enzymatic reduction minor: CYP2C19 and CYP3A4
Elimination[11]	Renal	Renal	Renal/fecal	Renal/fecal	Renal	Renal
Oral bioavailability (%)[11]	40-50	89	80-90	50-60	77	52
Food effect[14]	30 min before breakfast	60 min before breakfast	30 min before breakfast	Pharmacokinetics unaffected by meals	Pharmacokinetics unaffected by meals (exception oral suspension: 30 min prior to meal)	Pharmacokinetics unaffected by meals (exception capsule sprinkle: 30 min prior to meal)

PPI: Proton pump inhibitor.



DOI: 10.3748/wjg.v28.i24.2667 **Copyright** ©The Author(s) 2022.

Figure 1 Improper proton pump inhibitor use is multifactorial and comes from a pattern of preventable chain of events. PPI: Proton pump inhibitor.

ZES), prolonged mechanical ventilation, and functional dyspepsia[16]. While PPIs are considered for gastroprotection for patients on NSAID therapy, steroids are not an indication to start PPIs when used in ambulatory setting[17,18]. Some reports did suggest that there is an increased risk of PUD in patients taking steroids, but it was only statistically significant in hospitalized patients on brief courses of steroids[18]. As a result, these patients may be considered for a brief PPI therapy while inpatient. PPIs can also be used in conjunction with pancreatic enzyme replacement for refractory steatorrhea[17,19].

CURRENT GUIDELINES ON PPI USE

The current guidelines for PPIs are created for clinicians to prescribe PPIs appropriately and effectively to the patients who would benefit from the therapy. We are going to discuss guidelines proposed by multiple societies including the American College of Gastroenterology (ACG), American Gastroenterological Association (AGA), Society of American Gastrointestinal and Endoscopic Surgeons (SAGES), the Canadian Association of Gastroenterology (CAG), and the European guidelines (Table 2). All these guidelines are of moderate to high quality of evidence and are recommended strongly unless indicated

Table 2 Guidelines on proton pump inhibitor use

ACG/ACG/CAG/SAGES/European guidelines	Recommendation
GERD[19,20,22]	Trial an 8-wk duration of once daily PPI in patients with heartburn and regurgitation without reflux symptoms
	Once daily dosing-administer PPIs 30 min to 1 h before a meal; twice daily dosing-administer PPIs 30 min to 1 h before breakfast and dinner
	For patients experiencing refractory GERD, optimize PPI therapy with patient compliance, dosage and timing to achieve symptom control before further exploration
	Prescribe continuous daily PPIs over H2RAs for erosive esophagitis maintenance healing
	Continue lifelong PPIs in patients with LA Grade C or D erosive esophagitis
	If patients with normal esophageal mucosa or LA Grade A esophagitis have normal ambulatory reflux monitoring results after 2-4 wk discontinuation of PPI therapy, it is strongly recommended to stop PPI use (low level of evidence)
Dyspepsia[23]	Patients < 60 years old, tested *H. pylori* negative or symptoms persist after eradication therapy, should start empiric PPI therapy
	Functional dyspepsia patients, tested *H. pylori* negative or symptomatic after infection treatment, should be on PPIs
H. pylori infection[24]	If active or history of PUD, and tested *H. pylori* positive, start eradication treatment (10-14 d) with PPIs and antibiotics
	Dyspepsia patients found to be *H. pylori* positive on gastric biopsy, treat with eradication therapy consisting of PPIs and antibiotics for 10-14 d
	GERD patients who are found *H. pylori* positive should be offered eradication therapy for 10-14 d course
	Use levofloxacin triple regimen consisting of PPI, amoxicillin and levofloxacin as salvage therapy if first line eradication therapy fails
Barrett's esophagus[25,26]	Recommend once daily dosing PPIs primarily indicated for symptomatic relief
	Twice daily dosing can be considered in patients with esophagitis or poor symptomatic relief
EoE [28,29]	Recommend PPI therapy for clinical and histological remission of EoE
NSAIDs[31,32]	PPIs are indicated for patients at risk of GI bleeds for gastroprotection (age > 65 years, high dose NSAID use, previous history of ulcers, concomitant therapy with corticosteroids, anticoagulants and antithrombotics)
	Prescribe continuous or intermittent high dose PPI the following 3 d after GI ulcer bleed was stopped endoscopically

ACG: American College of Gastroenterology; AGA: American Gastroenterological Association; SAGES: Society of American Gastrointestinal and Endoscopic Surgeons; CAG: Canadian Association of Gastroenterology; PPI: Proton pump inhibitor; *H. pylori*: *Helicobacter pylori*; H2RA: Histamine 2 receptor antagonist; GERD: Gastro-esophageal reflux disease; PUD: Peptic ulcer disease; LA: Los Angeles; EoE: Eosinophilic esophagitis; NSAID: Nonsteroidal anti-inflammatory drug; GI: Gastrointestinal.

otherwise.

GERD treatment guidelines

An 8-wk duration of once daily PPIs is strongly recommended in patients with GERD to assess for adequate response. However, if GERD appears to be refractory, optimal PPI therapy should be confirmed first before further investigation. While there is no standardized definition of long-term PPI use, based on the ACG 2021 GERD guidelines, 8-wk therapy is the therapy duration following which patients get stratified into those who responded to therapy and those who are refractory to therapy[20]. Optimal therapy includes ensuring the patient is compliant with PPI therapy and takes medications appropriately with correct timing and dosage. Multiple studies show that a significant number of patients who optimize therapy improve symptoms[20]. In patients with known erosive esophagitis, medical therapy with daily PPIs is recommended but is given at half of the healing dose for maintenance to prevent recurrence[21]. PPIs should be prescribed over histamine 2 receptor antagonists (H2RAs) for erosive esophagitis due to their superiority in faster healing rates and better heartburn symptom control. It was found that almost all patients with Los Angeles (LA) grade C erosive esophagitis who stopped PPI therapy relapsed within 6 mo. However, recurrence of erosive esophagitis may occur as soon as 1 wk to 2 wk after PPI discontinuation. It is therefore recommended patients who have a more severe esophagitis (LA grade C or D) should be on a lifelong PPI therapy[20]. It is

important to note that PPI therapy may be ineffective in patients with large hiatal hernias. Transabdominal or transthoracic large hiatal hernia repairs should be strongly considered in patients who experience symptoms of severe gastroesophageal reflux, gastric outlet obstruction and/or strangulation. Fundoplication as a treatment option for reflux produced mixed outcomes and therefore no strong recommendation can be made[22].

In patients with an unclear GERD diagnosis, ambulatory reflux monitoring may be helpful in guiding PPI therapy in patients with refractory reflux symptoms and without severe esophagitis[23]. This diagnostic approach helps support or negate a GERD diagnosis. Patients with incomplete symptom relief after an 8-wk course of PPI therapy can discontinue PPIs for 2-4 wk. If normal results in reflux monitoring are seen after PPI cessation in patients with normal EGD findings or LA Grade A esophagitis, then other causes of symptoms should be investigated, and PPI therapy can be stopped. Although this approach is strongly recommended, more studies are necessary for high evidence support [20].

Dyspepsia treatment guidelines

Several randomized control trials (RCTs) found a statistically significant effect in use of once daily PPI dosing for symptomatic relief of dyspepsia symptoms. It is therefore strongly recommended that patients under 60 years of age who tested *H. pylori* negative or continue to experience symptoms after *H. pylori* treatment should be prescribed empiric PPI therapy. Functional dyspepsia patients are also recommended a two-to-eight-week duration of PPI course for symptomatic improvement with some RCTs suggesting a number needed to treat of 10. However, if patients do not respond after 8 wk of therapy, PPIs should be discontinued as there was no utility found in increasing the dose. Other drug therapies can therefore be considered in symptomatic management[24].

H. pylori treatment guidelines

Patients with current or history of peptic ulcer without known *H. pylori* eradication should be tested with a urea breath test, fecal antigen test or gastric mucosal biopsy. If *H. pylori* positive, treatment options should be offered. Eradication treatments include first line bismuth quadruple therapy (PPI, bismuth, tetracycline and nitroimidazole) or clarithromycin triple therapy (PPI, clarithromycin, and amoxicillin or metronidazole) for 10-14 d. If gastric biopsies are done in patients with dyspepsia and are found to be *H. pylori* positive, multiple studies demonstrated that eradication treatment improves symptoms. If patients with GERD do not experience symptoms of dyspepsia or have a history of PUD, it is unnecessary to test for *H. pylori*. However, if found to be positive, treatment options should be offered. If first line therapy for eradication treatment fails, it is recommended to use the levofloxacin triple regimen as a salvage treatment. The regimen consists of PPI, amoxicillin, and levofloxacin. A treatment duration of 14 d can be effective but supported by low quality of evidence so further studies are warranted[25].

Barrett's esophagus treatment guidelines

Patients with Barrett's esophagus are typically prescribed PPIs due to GERD symptoms and to reduce the risk of neoplastic changes. Several studies demonstrated that maintenance PPI therapy reduced risk of neoplastic changes compared to H2RA therapy or no anti-acid reflux medications. According to the AGA and ACG guidelines, once-daily PPI therapy is recommended for patients with Barrett's esophagus[26,27]. Twice daily dosing can be considered in BE patients with inadequate symptomatic control or in patients with esophagitis[26].

EoE

Previous guidelines suggested PPI use as a trial therapy to differentiate EoE from GERD[28]. However, the PPI trial should no longer be used as GERD and EoE share many similarities and are not mutually exclusive entities[29]. The 2017 United European Gastroenterology (UEG) guidelines suggested PPIs as recommended treatment for EoE which is proven to demonstrate symptomatic improvement and histological remission. Early observational studies and case reports demonstrated this phenomenon and many RCTs followed which supported the use of PPI therapy in EoE. A recent systematic review with meta-analysis showed clinical improvement and histological remission with PPI therapy[30]. Duration and dosage for treatment is however still under investigation; twice daily administration and long-term PPI therapy is recommended but has low evidence[30].

NSAID use

PPI therapy is necessary to prevent NSAID-related ulcer complications including upper gastrointestinal (GI) bleeds. Many studies reported decreased prevalence of upper GI ulcers and bleeds while on NSAID therapy if PPIs are co-administered[31]. PPI therapy is indicated in NSAID users at risk for GI bleeds which includes those on high dose NSAIDs, age greater than 65 years, prior history of ulcers, and/or concurrent use of antiplatelets, anticoagulants or corticosteroids[31,32]. Long term daily PPI therapy is not supported by high quality evidence and is a conditional recommendation. For patients who have a bleeding GI ulcer that was managed endoscopically with hemostatic therapy, high dose PPI therapy

should be given continuously or intermittently for the following 3 d for further gastroprotection[33].

RISKS ASSOCIATED WITH PPI USE

PPIs have been associated with electrolyte disturbances, increased fracture risk, gastrointestinal and lung infections, kidney disease, dementia, cardiovascular events, and gastric mucosal changes associated with potential increased risk of neoplasia. We are going to discuss the PPI-associated side-effects and the supporting data behind them (Table 3).

Electrolyte abnormalities

PPIs are thought to cause reduction in vitamins and minerals due to reduced intestinal absorption caused by decreased gastric acid secretion. While there is data on B12 and iron malabsorption associated with PPI use, some studies argue against this association. One large case control study confirmed that PPIs were associated with increased risk of iron deficiency anemia and vitamin B12 deficiency[34,35]. In contrast, a small observational study evaluated patients with ZES on chronic PPI therapy and did not find any association with iron malabsorption[36]. Another cross-sectional study found no association between long term PPI use and vitamin B12 deficiency[35].

Hypomagnesemia is another electrolyte derangement that has been attributed to PPI therapy. The first case report that linked hypomagnesemia with PPI use was in 2006, which prompted further research on this topic[37]. A 2014 meta-analysis of 9 observational studies found an association between PPI use and hypomagnesemia, but there was notable heterogeneity among the studies reported[38]. After review of 38 cases in Adverse Event Reporting System and 23 case reports, the United States Food and Drug Administration (FDA) recommends obtaining magnesium levels prior to PPI therapy initiation[39].

Hypocalcemia/fracture risk

PPIs are associated with hypocalcemia and potentially increased risk of bone fractures. Calcium salts, such as calcium carbonate, need highly acidic environment for absorption. PPIs block acid production and, as a result, prevent absorption of calcium carbonate[40]. Calcium malabsorption increases risk of osteoporosis and subsequent bone fractures. A large case control study from the United Kingdom reported that patients on chronic PPI therapy were more likely to fracture their hip with incidence rate of 4.0/1000 person years compared to non-users of 1.8/1000 person years. It is important to note that patients in the study had multiple comorbidities that could have served as confounding factors[40]. In contrast, a large-scale case control study performed among the Danish population found no dose-dependent relationship between PPI use and the risk of bone fracture[41]. In a 2018 meta-analysis, 12 of the included studies failed to show an association between PPI use and fracture incidence or decrease in bone mineral density[42]. Another meta-analysis of 18 observational studies demonstrated a modest hip, spine, and any-site fracture risk[43].

Kidney disease

In the recent studies, PPIs were noted to have an association with acute kidney injury (AKI) and subsequent development of chronic kidney disease (CKD). One of the proposed mechanisms is that PPIs lead to a cell mediated immune response causing acute intestinal nephritis (AIN). A meta-analysis of 9 observational studies supported an association relationship between PPI use with AKI and CKD[44]. Furthermore, Lazarus *et al*[45] found that PPIs were associated with a 20%-50% higher incidence rate of CKD. It was unclear from the study, however, if comorbidities served as confounding factors. Interestingly, an observational study of a veterans database consisting of mainly elderly males reported an association between PPI use and development of CKD with duration-dependent risk of end stage renal disease (ESRD)[46]. In contrast, a recent large observational study evaluating CKD patients did not confirm an association of PPI use and ESRD[47]. Although there is no clear guideline yet available, clinicians can choose to routinely monitor creatinine levels and/or obtain urinalysis testing in high-risk patients on PPI therapy to assess for kidney disease progression[48].

Dementia

PPIs are thought to increase production of β-amyloid plaques and increase affinity of tau proteins towards brain tissue. Both processes are key in pathogenesis of Alzheimer's Disease (AD)[40]. A systematic review established a 1.4-fold increased risk of dementia with PPI use. However, one of the studies demonstrated a negative correlation[49]. Additionally, a 2019 meta-analysis of 6 cohort studies found no significant association between PPI use and AD[50].

Gastrointestinal infections

PPIs are thought to alter intestinal microbiota and, as a result, may predispose patients to gastrointestinal infections[51,52]. A systemic review and a meta-analysis of 56 studies found that PPI therapy

Table 3 Proton pump inhibitor associated side effects

PPI associated adverse risks	Proposed mechanism	Evidence type	Conditional recommendations to reduce risk
Electrolyte abnormalities: Hypomagnesemia, vitamin B12, iron	Decreased acid secretion decreases intestinal absorption of minerals/vitamins	Observational studies, conflicting evidence[33,34,36,37]	Unless other risk factors present, no recommendation to increase intake of vitamins/minerals or have routine screening of levels[19]
Fracture risk/hypocalcemia	Decreased acid secretion decreases calcium carbonate absorption	Observational studies, conflicting evidence[39,40-42]	Without other risk factors for bone disease, no recommendations to increase calcium/vitamin D intake or have routine bone mineral density exam[19]
AIN/CKD/ESRD	Initiate cell mediated immune response in kidneys	Observational studies, conflicting evidence[43-46]	Without other risk factors, there is no recommendation to routinely screen for kidney function in patients on PPIs[19]
Dementia	Increase β-amyloid plaque production and increase affinity of tau proteins	Observational studies, conflicting evidence[48,49]	No recommendations on dementia prevention in patients on PPI
Gastrointestinal infections: *C. diff*, SIBO, SBP	Alter gut microbiota due to decreased acidic environment	Observational studies, conflicting evidence[34,51-55]	For patients who develop *C.diff* infection while on PPI, can consider switching to H2 blockers [55]
Community acquired Pneumonia	Increase bacterial colonization in stomach from hypochlorhydria leading to lung micro-aspiration events Alter respiratory flora	Observational studies, RCTs, conflicting evidence[57-59]	No strong recommendation can be made
Gastrointestinal malignancies	Hypergastrinemia resultant from decreased acid production increases ECL cell hyperplasia	Observational studies, RCTs, conflicting evidence[60-62,64,65]	Given conflicting data, no recommendation on prevention can be made
Adverse Cardiovascular effects- arrythmias, decreased clopidogrel bioavailability, increased digoxin toxicity	Hypomagnesemia- torsade de pointes CYP450 inhibitor- decreases drug bioavailability Interaction with ATP-dependent P-glycoprotein impair endothelial function and platelet induction	Observational studies, RCTs, conflicting evidence[59,66]	For patients with significant esophagitis (grade C or D) or with poorly controlled GERD, PPI treatment outweighs the debatable cardiovascular risks[19]

GERD: Gastro-esophageal reflux disease; PPI: Proton pump inhibitor; AIN: Acute intestinal nephritis; CKD: Chronic kidney disease; ESRD: End stage renal disease; *C. diff*: *Clostridium difficile*; SIBO: Small intestinal bacterial overgrowth; SBP: Spontaneous bacterial peritonitis; ECL: Enterochromaffin-like; RCTs: Randomized control trials.

increases the risk of *clostridium difficile (C. difficile)* infection[53]. While a nationwide cohort study in Denmark found that the risk of community acquired *C. difficile* doubles in patients on PPI, but several other studies failed to replicate these results[52,53].

A meta-analysis of 19 observational studies reported a moderate risk of small intestinal bacterial overgrowth (SIBO) for patients on long-term PPI[52]. In contrast, a retrospective case control study found no significant association between the two[54].

Another type of gastrointestinal infection that PPIs have been associated with is spontaneous bacterial peritonitis (SBP). A meta-analysis from 8 observation studies revealed a threefold higher risk of developing SBP while on PPIs in cirrhotic patients[35]. Another meta-analysis of 16 observational studies confirmed this association but only in the case control studies of the meta-analysis[55]. In contrast, one retrospective cohort study established that PPI therapy did not increase the risk of recurrent SBP in cirrhotic patient population[56].

Pneumonia risk

PPIs are thought to increase bacterial colonization in the stomach from hypochlorhydria and lead to lung micro-aspiration events or potentially alter respiratory flora leading to pulmonary infections[57,58]. A systemic review of 33 studies and a meta-analysis of 26 studies including 4 selected RCTs found a 1.5-fold increased risk of community acquired pneumonia (CAP) for patients on PPI therapy and a 1.6-fold increased hospitalization risk[58]. In contrast, another meta-analysis of RCTs found no association between PPI use and respiratory infections[59]. PPIs have been reported as possible contributors to the ventilator associated pneumonia, but the quality of evidence is low[60].

GI malignancies

There is growing number of studies reporting association of chronic PPI therapy with gastric cancer[61-63]. The decreased acid production and subsequent hypergastrinemia may cause hyperplasia of enterochromaffin-like (ECL) cells[35,64]. A meta-analysis of 7 observational studies and 1 RCT showed an increased risk of fundic gastric polyps while on PPI therapy, but the clinical significance of this finding remains undetermined[65]. It is important to note that another meta-analysis of 6 RCTs revealed that while there was ECL cell hyperplasia noted with chronic PPI use, the hyperplasia had no stigmata of dysplasia or neoplasia[66].

Adverse cardiovascular events

While PPIs do not have a direct association with cardiovascular complications, they have cardiovascular side-effects primarily thought their effects on magnesium (hypomagnesemia), drug-drug interactions, impairment of endothelial function and induction of platelets[67]. PPIs, particularly omeprazole, were thought to decrease clopidogrel efficacy from interference of its metabolism leading to increased cardiovascular events. Therefore, the FDA recommends against omeprazole and clopidogrel co-administration[67]. The COGENT study found no difference in cardiovascular events among patients on clopidogrel and omeprazole compared to patients on clopidogrel alone. Although the study was terminated early due to loss of funding[60].

The data on PPI side effect profile remains controversial. It is important to note that the evidence provided by ACG in their 2021 guidelines presented 95% confidence intervals for reported adverse events such as cardiovascular events, kidney disease, gastrointestinal complications, dementia, bone fractures, Vitamin 12 deficiency, gastric cancer, hypomagnesemia, and all-cause mortality-all of which crossed 1, making these hazard ratio and odds ratio statistically insignificant.

DRUG-DRUG INTERACTIONS

PPIs can decrease drug solubility either due to alteration in gastric pH or inhibition of the CYP450 system leading to decreased metabolism of certain drugs. The bioavailability of ketoconazole and atazanavir, for example, may be decreased by 50% or more with PPI co-administration. The metabolism of clopidogrel, simvastatin, phenytoin and many other drugs depends on the CYP450 system and coadministration of PPIs can decrease its clearance[68]. Also, PPI interaction with the ATP-dependent P-glycoprotein can inhibit digoxin efflux and increase its toxicity[69]. Another important consideration is in patients with hepatitis C who are placed on direct-acting antivirals (DAAs). There is a significant risk of failure of hepatitis C therapy in patients on concurrent PPI therapy likely because of decreased DAA bioavailability in the setting of altered gastric acidity[70]. It is important to be mindful of PPI administration especially in cases of polypharmacy in the elderly to ensure adequate efficacy of the prescribed medications.

STRATEGIES TO MINIMIZE SIDE-EFFECT PROFILE

As perception of PPI therapy is starting to change with more studies reporting consequences of long-term PPI use, strategies to minimize harm from its use become an important discussion. It is equally as important to understand the evidence behind the reported side effects and educate patients on their risks and benefits.

Strategy 1: Evidence-based initiation of therapy

The decision of starting PPI therapy should be evidence-based. There are several guidelines on disease processes that require PPI therapy, and it is important to have a good understanding of level of evidence and recommendation behind them. The 2021 ACG guidelines on GERD management have a strong recommendation supported by moderate quality evidence to start patients with heartburn and regurgitation symptoms on empiric PPI therapy for 8 wk[20]. Sometimes, further evaluation may be needed after the first empiric trial. These guidelines also have a strong recommendation supported by moderate evidence for patients who have high suspicion of GERD, but diagnosis is not definitive, to undergo reflux monitoring with BRAVO performed off PPI therapy to either confirm or rule out GERD [20]. This study may help differentiate dyspepsia from GERD. The 2017 ACG guidelines on dyspepsia and *H. pylori* had a strong recommendation supported by high quality evidence to start empiric PPI therapy on patients who were confirmed to have *H. pylori* infection, have dyspepsia but are *H. pylori* negative, have symptoms of dyspepsia persist despite *H. pylori* eradication, have functional dyspepsia [24,25]. The 2016 ACG guidelines on Barrett's esophagus provided a strong recommendation supported by moderate evidence that once-daily PPI therapy should be implemented in patients at high risk for developing Barrett's esophagus-male gender with more than 5 years of frequent (weekly or more) heartburn or regurgitation and two or more risk factors such as age greater than 50, Caucasian race,

central obesity, current or history of smoking, confirmed family history of Barrett's esophagus or esophageal adenocarcinoma[26]. While there are no official guidelines supporting this, PPIs have been successfully implemented in EoE treatment with 69.2% of patient achieving histologic remission compared to 41.7% of patients on empiric elimination diet alone[71].

Strategy 2: Need for ongoing treatment revisited at follow up

Another important strategy is to minimize risks by evaluating whether patient needs to stay on PPI therapy. Ongoing risks and benefit discussion with the patient along with weaning trials play a key role. As of 2021, ACG has a conditional recommendation supported by low evidence to have discontinuation trials of PPI therapy for patients with reflux symptoms who responded to 8-wk empiric PPI treatment attempted or for patients who have endoscopic or histologic evidence of esophageal or gastric mucosal healing[20,72]. It is important to note that weaning trials should not be attempted in patients with significant erosive esophagitis, BE, or history of esophageal adenocarcinoma[15,26].

In 2017, American Gastroenterological Association (AGA) came up with best practice advice[15]. They supported weaning off trials for patients with uncomplicated GERD. For patients who are unable to wean off therapy, BRAVO study or high-resolution manometry (HRM) are indicated to distinguish GERD from a functional syndrome[15]. HRM can be further used as a diagnostic evaluation in patients with refractory reflux symptoms prior to anti-reflux surgery[73]. HRM helps differentiate reflux from hiatal hernia and esophageal dysmotility[73]. The AGA recommended that if patients had an episode of bleeding from NSAID therapy should be started on long-term PPI therapy, especially is they must continue NSAID therapy.

Strategy 3: Dosing adjustment tailored to patient

As discussed previously, PPI metabolism relies on hepatic P450 system. Some patients are fast metabolizers, others may be slow, so it is not always easy to predict a particular patient's ability to metabolize PPIs. We know that patients of Asian descent and older patients tend to have slower P450 system and may have a higher concentration of PPIs available from the same dose[6]. This is something that is important to consider when selecting a starting dose or trying to decrease the dose later in treatment. The 2021 ACG guidelines provided conditional recommendation supported by low quality evidence that patients who require maintenance therapy with PPIs should be given the lower dose that controls their symptoms and maintains healing of tissues[20]. This was echoed in 2017 AGA guidelines as well suggesting that the lowest effective PPI dose should be used[15]. Same degree recommendation and evidence was put forward for as needed PPI therapy for patients with NERD[20]. pH testing (such as BRAVO) along with pH impedance can help facilitate titration to the minimum possible PPI dose to achieve optimal anti-secretory effects[74]. pH testing can also help tailor PPI therapy dosage and duration in Barrett's esophagus patient population[75].

Strategy 4: Looking for alternative options

While some conditions, such as erosive esophagitis, BE, prior history of esophageal adenocarcinoma, gastric ulcers, EoE require long-term acid-suppression with PPI therapy, many other conditions may be considered for an alternative therapy with H2 blockers, life-style modifications, or both[76]. One of the most common indication for PPI therapy is GERD and dyspepsia. Both conditions can be trialed with H2 blockers in attempts to come off PPI therapy. There are novel medications being developed such as potassium-competitive acid blockers (P-CABs), which bind to potassium inions thus blocking the hydrogen-potassium ATPase enzyme[77]. Similar to PPIs, P-CABs have a dose depended effects on gastric acid production[77]. Weight loss in overweight and obese patients had moderate evidence and strong recommendations for patients struggling with GERD suggested by ACG in 2021[20]. The rest of the life-style modifications, such as avoiding meals within 2-3 h of bedtime, tobacco products, trigger foods, and elevation of the head of the bed for nocturnal symptoms-all had only conditional recommendation supported by low quality evidence[20].

Surgical options need to be discussed with patients unwilling to commit to long-term PPI. Anti-reflux Surgery (LARS) is an alternative treatment to long-term pharmacologic therapy, especially in patients with large hiatal hernias or Barrett's esophagus but was noted to have higher risks of symptom recurrence, especially in obese patients[78,79]. As a result, some studies reported that the utilization of anti-reflux surgery is greater when used in conjunction with weight loss in patients with BMI over 35 [80]. Despite initial success with LARS, studies reported that as many as 48% patients who have undergone LARS resumed PPI therapy at 5-year mark[81]. Additionally, LARS requires pre-surgery work up, which includes HRM.

PATIENT'S PERCEPTION OF PPI THERAPY

Patients understanding of therapy and how it works directly contribute to patient satisfaction and treatment success. Shared decision-making regarding duration of treatment and side-effect profile is key. Patient's participation and understanding of therapy are especially important because PPI

treatment comes with limitations of short-half life and meal dependent administration.

In the setting of new concerns regarding PPI's side-effects and growing media coverage of this topic, patients are increasingly more worried about staying on PPIs long-term. Therefore, increasing awareness among primary care providers on the proper use of PPIs is crucial. Additionally, managing patient's expectations and educating on the evidence behind the reported side effects becomes important. Prior to the therapy initiation, anticipated duration of treatment should be discussed with the patient. Risks and benefit discussion needs to take place. Whether the PPI therapy is prescribed by the primary care or gastroenterology physician, the decision to start the therapy should be evidence-based and rely on most recent guidelines supported by high quality evidence. Additionally, prescribing physicians should have an ongoing discussion with their patients and re-evaluation of their need to stay on PPI therapy. Working together with the patient, setting realistic expectations from the beginning, following evidence-based guidelines, and continuing to re-evaluate of need for therapy could increase patient satisfaction with medical care, provide reassurance, and help more people to safely benefit from PPI therapy.

CONCLUSION

Since their first introduction to the medical practice, PPIs have come a long way and we now know much more about their pharmacodynamics and side-effect profile. The side-effect data remains controversial with most recent ACG guidelines arguing against significant risks associated with this therapy. While data provided by ACG is reassuring, PPI therapy should still be utilized according to evidence-based practice. We now know more about which patients are more likely to benefit from this therapy and why some patients should only be on it short term. As our understanding of this therapy deepens, our practice should change to help more patients to safely benefit from PPIs. Following evidence-based guidelines and working together with a patient managing expectations and educating on risks may be the key to successful come back of PPI therapy.

FOOTNOTES

Author contributions: Turshudzhyan A, Samuel S, and Tawfik A wrote the manuscript; Tadros M revised the manuscript.

Conflict-of-interest statement: There are no conflicts of interest to report.

Open-Access: This article is an open-access article that was selected by an in-house editor and fully peer-reviewed by external reviewers. It is distributed in accordance with the Creative Commons Attribution NonCommercial (CC BY-NC 4.0) license, which permits others to distribute, remix, adapt, build upon this work non-commercially, and license their derivative works on different terms, provided the original work is properly cited and the use is non-commercial. See: https://creativecommons.org/Licenses/by-nc/4.0/

Country/Territory of origin: United States

ORCID number: Alla Turshudzhyan 0000-0001-6867-7569; Sonia Samuel 0000-0003-3359-0222; Angela Tawfik 0000-0002-0001-8126; Micheal Tadros 0000-0003-3118-3893.

S-Editor: Chen YL
L-Editor: A
P-Editor: Chen YL

REFERENCES

1 **Chiba T**, Malfertheiner P, Satoh H. Proton Pump Inhibitors: A Balanced View. *Front Gastrointest Res* 2013; **32**: 1-17 [DOI: 10.1159/000350624]
2 **Lassen AT**. Acid-related disorders and use of antisecretory medication. *Dan Med Bull* 2007; **54**: 18-30 [PMID: 17349216]
3 **Walker MJ**, Crews NR, El-Halabi M, Fayad NF. Educational Intervention Improves Proton Pump Inhibitor Stewardship in Outpatient Gastroenterology Clinics. *Gastroenterology Res* 2019; **12**: 305-311 [PMID: 31803310 DOI: 10.14740/gr1238]
4 **Batuwitage BT**, Kingham JG, Morgan NE, Bartlett RL. Inappropriate prescribing of proton pump inhibitors in primary care. *Postgrad Med J* 2007; **83**: 66-68 [PMID: 17267683 DOI: 10.1136/pgmj.2006.051151]
5 **Robinson M**, Horn J. Clinical pharmacology of proton pump inhibitors: what the practising physician needs to know. *Drugs* 2003; **63**: 2739-2754 [PMID: 14664653 DOI: 10.2165/00003495-200363240-00004]
6 **Ahmed A**, Clarke JO. Proton Pump Inhibitors (PPI). Aug 1, 2021. [cited 10 January 2022]. Available from: https://www.ncbi.nlm.nih.gov/books/NBK557385/

7 **Stedman CA**, Barclay ML. Review article: comparison of the pharmacokinetics, acid suppression and efficacy of proton pump inhibitors. *Aliment Pharmacol Ther* 2000; **14**: 963-978 [PMID: 10930890 DOI: 10.1046/j.1365-2036.2000.00788.x]

8 **Scarpignato C**, Pelosini I. Review article: the opportunities and benefits of extended acid suppression. *Aliment Pharmacol Ther* 2006; **23** Suppl 2: 23-34 [PMID: 16700900 DOI: 10.1111/j.1365-2036.2006.02945.x]

9 **Wittbrodt ET**, Baum C, Peura DA. Delayed release dexlansoprazole in the treatment of GERD and erosive esophagitis. *Clin Exp Gastroenterol* 2009; **2**: 117-128 [PMID: 21694835 DOI: 10.2147/ceg.s5765]

10 **Ishizaki T**, Horai Y. Review article: cytochrome P450 and the metabolism of proton pump inhibitors--emphasis on rabeprazole. *Aliment Pharm Ther* 1999; **13**: 27-36 [DOI: 10.1046/j.1365-2036.1999.00022.x]

11 **Chubineh S**, Birk J. Proton pump inhibitors: the good, the bad, and the unwanted. *South Med J* 2012; **105**: 613-618 [PMID: 23128806 DOI: 10.1097/SMJ.0b013e31826efbea]

12 **Sachs G**, Shin JM, Howden CW. Review article: the clinical pharmacology of proton pump inhibitors. *Aliment Pharm Ther* 2006; **23** (2): 2-8 [DOI: 10.1111/j.1365-2036.2006.02943.x]

13 **Kaniecki T**, Abdi T, McMahan ZH. A practical approach to the evaluation and management of gastrointestinal symptoms in patients with systemic sclerosis. *Best Pract Res Clin Rheumatol* 2021; **35**: 101666 [PMID: 33676855 DOI: 10.1016/j.berh.2021.101666]

14 **Wiesner A**, Zwolińska-Wcisło M, Paśko P. Effect of Food and Dosing Regimen on Safety and Efficacy of Proton Pump Inhibitors Therapy-A Literature Review. *Int J Environ Res Public Health* 2021; **18** [PMID: 33805341 DOI: 10.3390/ijerph18073527]

15 **Freedberg DE**, Kim LS, Yang YX. The Risks and Benefits of Long-term Use of Proton Pump Inhibitors: Expert Review and Best Practice Advice From the American Gastroenterological Association. *Gastroenterology* 2017; **152**: 706-715 [PMID: 28257716 DOI: 10.1053/j.gastro.2017.01.031]

16 **Savarino V**, Dulbecco P, de Bortoli N, Ottonello A, Savarino E. The appropriate use of proton pump inhibitors (PPIs): Need for a reappraisal. *Eur J Intern Med* 2017; **37**: 19-24 [PMID: 27784575 DOI: 10.1016/j.ejim.2016.10.007]

17 **Scarpignato C**, Gatta L, Zullo A, Blandizzi C; SIF-AIGO-FIMMG Group; Italian Society of Pharmacology, the Italian Association of Hospital Gastroenterologists, and the Italian Federation of General Practitioners. Effective and safe proton pump inhibitor therapy in acid-related diseases - A position paper addressing benefits and potential harms of acid suppression. *BMC Med* 2016; **14**: 179 [PMID: 27825371 DOI: 10.1186/s12916-016-0718-z]

18 **Narum S**, Westergren T, Klemp M. Corticosteroids and risk of gastrointestinal bleeding: a systematic review and meta-analysis. *BMJ Open* 2014; **4**: e004587 [PMID: 24833682 DOI: 10.1136/bmjopen-2013-004587]

19 **He Q**, Xia B, Meng W, Fan D, Kuo ZC, Huang J, Qin X, Zou H, He Y, Zhang C, Fang S, Pan Y, Yang M, Yuan J. No Associations Between Regular Use of Proton Pump Inhibitors and Risk of All-Cause and Cause-Specific Mortality: A Population-Based Cohort of 0.44 Million Participants. *Am J Gastroenterol* 2021; **116**: 2286-2291 [PMID: 34313608 DOI: 10.14309/ajg.0000000000001377]

20 **Katz PO**, Dunbar KB, Schnoll-Sussman FH, Greer KB, Yadlapati R, Spechler SJ. ACG Clinical Guideline for the Diagnosis and Management of Gastroesophageal Reflux Disease. *Am J Gastroenterol* 2022; **117**: 27-56 [PMID: 34807007 DOI: 10.14309/ajg.0000000000001538]

21 **Kahrilas PJ**, Shaheen NJ, Vaezi MF; American Gastroenterological Association Institute; Clinical Practice and Quality Management Committee. American Gastroenterological Association Institute technical review on the management of gastroesophageal reflux disease. *Gastroenterology* 2008; **135**: 1392-1413, 1413.e1 [PMID: 18801365 DOI: 10.1053/j.gastro.2008.08.044]

22 **Kohn GP**, Price RR, DeMeester SR, Zehetner J, Muensterer OJ, Awad Z, Mittal SK, Richardson WS, Stefanidis D, Fanelli RD; SAGES Guidelines Committee. Guidelines for the management of hiatal hernia. *Surg Endosc* 2013; **27**: 4409-4428 [PMID: 24018762 DOI: 10.1007/s00464-013-3173-3]

23 **Yadlapati R**, Masihi M, Gyawali CP, Carlson DA, Kahrilas PJ, Nix BD, Jain A, Triggs JR, Vaezi MF, Kia L, Kaizer A, Pandolfino JE. Ambulatory Reflux Monitoring Guides Proton Pump Inhibitor Discontinuation in Patients With Gastroesophageal Reflux Symptoms: A Clinical Trial. *Gastroenterology* 2021; **160**: 174-182.e1 [PMID: 32949568 DOI: 10.1053/j.gastro.2020.09.013]

24 **Moayyedi P**, Lacy BE, Andrews CN, Enns RA, Howden CW, Vakil N. ACG and CAG Clinical Guideline: Management of Dyspepsia. *Am J Gastroenterol* 2017; **112**: 988-1013 [PMID: 28631728 DOI: 10.1038/ajg.2017.154]

25 **Chey WD**, Leontiadis GI, Howden CW, Moss SF. ACG Clinical Guideline: Treatment of Helicobacter pylori Infection. *Am J Gastroenterol* 2017; **112**: 212-239 [PMID: 28071659 DOI: 10.1038/ajg.2016.563]

26 **Shaheen NJ**, Falk GW, Iyer PG, Gerson LB; American College of Gastroenterology. ACG Clinical Guideline: Diagnosis and Management of Barrett's Esophagus. *Am J Gastroenterol* 2016; **111**: 30-50; quiz 51 [PMID: 26526079 DOI: 10.1038/ajg.2015.322]

27 **American Gastroenterological Association**. American Gastroenterological Association medical position statement on the management of Barrett's esophagus. *Gastroenterology* 2011; **140**: 1084-1091 [DOI: 10.1053/j.gastro.2011.01.030]

28 **Dellon ES**, Gonsalves N, Hirano I, Furuta GT, Liacouras CA, Katzka DA; American College of Gastroenterology. ACG clinical guideline: Evidenced based approach to the diagnosis and management of esophageal eosinophilia and eosinophilic esophagitis (EoE). *Am J Gastroenterol* 2013; **108**: 679-92; quiz 693 [PMID: 23567357 DOI: 10.1038/ajg.2013.71]

29 **Dellon ES**, Liacouras CA, Molina-Infante J, Furuta GT, Spergel JM, Zevit N, Spechler SJ, Attwood SE, Straumann A, Aceves SS, Alexander JA, Atkins D, Arva NC, Blanchard C, Bonis PA, Book WM, Capocelli KE, Chehade M, Cheng E, Collins MH, Davis CM, Dias JA, Di Lorenzo C, Dohil R, Dupont C, Falk GW, Ferreira CT, Fox A, Gonsalves NP, Gupta SK, Katzka DA, Kinoshita Y, Menard-Katcher C, Kodroff E, Metz DC, Miehlke S, Muir AB, Mukkada VA, Murch S, Nurko S, Ohtsuka Y, Orel R, Papadopoulou A, Peterson KA, Philpott H, Putnam PE, Richter JE, Rosen R, Rothenberg ME, Schoepfer A, Scott MM, Shah N, Sheikh J, Souza RF, Strobel MJ, Talley NJ, Vaezi MF, Vandenplas Y, Vieira MC, Walker MM, Wechsler JB, Wershil BK, Wen T, Yang GY, Hirano I, Bredenoord AJ. Updated International Consensus Diagnostic Criteria for Eosinophilic Esophagitis: Proceedings of the AGREE Conference. *Gastroenterology* 2018; **155**: 1022-1033.e10 [PMID: 30009819 DOI: 10.1053/j.gastro.2018.07.009]

30 **Lucendo AJ**, Molina-Infante J, Arias Á, von Arnim U, Bredenoord AJ, Bussmann C, Amil Dias J, Bove M, González-

Cervera J, Larsson H, Miehlke S, Papadopoulou A, Rodríguez-Sánchez J, Ravelli A, Ronkainen J, Santander C, Schoepfer AM, Storr MA, Terreehorst I, Straumann A, Attwood SE. Guidelines on eosinophilic esophagitis: evidence-based statements and recommendations for diagnosis and management in children and adults. *United European Gastroenterol J* 2017; **5**: 335-358 [PMID: 28507746 DOI: 10.1177/2050640616689525]

31 **Lanza FL**, Chan FK, Quigley EM; Practice Parameters Committee of the American College of Gastroenterology. Guidelines for prevention of NSAID-related ulcer complications. *Am J Gastroenterol* 2009; **104**: 728-738 [PMID: 19240698 DOI: 10.1038/ajg.2009.115]

32 **Laine L**, Nagar A. Long-Term PPI Use: Balancing Potential Harms and Documented Benefits. *Am J Gastroenterol* 2016; **111**: 913-915 [PMID: 27113114 DOI: 10.1038/ajg.2016.156]

33 **Laine L**, Barkun AN, Saltzman JR, Martel M, Leontiadis GI. ACG Clinical Guideline: Upper Gastrointestinal and Ulcer Bleeding. *Am J Gastroenterol* 2021; **116**: 899-917 [PMID: 33929377 DOI: 10.14309/ajg.0000000000001245]

34 **Tran-Duy A**, Connell NJ, Vanmolkot FH, Souverein PC, de Wit NJ, Stehouwer CDA, Hoes AW, de Vries F, de Boer A. Use of proton pump inhibitors and risk of iron deficiency: a population-based case-control study. *J Intern Med* 2019; **285**: 205-214 [PMID: 30141278 DOI: 10.1111/joim.12826]

35 **Eusebi LH**, Rabitti S, Artesiani ML, Gelli D, Montagnani M, Zagari RM, Bazzoli F. Proton pump inhibitors: Risks of long-term use. *J Gastroenterol Hepatol* 2017; **32**: 1295-1302 [PMID: 28092694 DOI: 10.1111/jgh.13737]

36 **Stewart CA**, Termanini B, Sutliff VE, Serrano J, Yu F, Gibril F, Jensen RT. Iron absorption in patients with Zollinger-Ellison syndrome treated with long-term gastric acid antisecretory therapy. *Aliment Pharmacol Ther* 1998; **12**: 83-98 [PMID: 9692706 DOI: 10.1046/j.1365-2036.1998.00274.x]

37 **William JH**, Danziger J. Magnesium Deficiency and Proton-Pump Inhibitor Use: A Clinical Review. *J Clin Pharmacol* 2016; **56**: 660-668 [PMID: 26582556 DOI: 10.1002/jcph.672]

38 **Park CH**, Kim EH, Roh YH, Kim HY, Lee SK. The association between the use of proton pump inhibitors and the risk of hypomagnesemia: a systematic review and meta-analysis. *PLoS One* 2014; **9**: e112558 [PMID: 25394217 DOI: 10.1371/journal.pone.0112558]

39 **U. S. Food and Drug Administration**. FDA drug safety communication: low magnesium levels can be associated with long-term use of proton pump inhibitor drugs (PPIs). [cited December 20, 2021]. Available from: http://www.fda.gov/Drugs/DrugSafety/ucm245011.htm

40 **Yang YX**, Lewis JD, Epstein S, Metz DC. Long-term proton pump inhibitor therapy and risk of hip fracture. *JAMA* 2006; **296**: 2947-2953 [PMID: 17190895 DOI: 10.1001/jama.296.24.2947]

41 **Ito T**, Jensen RT. Association of long-term proton pump inhibitor therapy with bone fractures and effects on absorption of calcium, vitamin B12, iron, and magnesium. *Curr Gastroenterol Rep* 2010; **12**: 448-457 [PMID: 20882439 DOI: 10.1007/s11894-010-0141-0]

42 **Nassar Y**, Richter S. Proton-pump Inhibitor Use and Fracture Risk: An Updated Systematic Review and Meta-analysis. *J Bone Metab* 2018; **25**: 141-151 [PMID: 30237993 DOI: 10.11005/jbm.2018.25.3.141]

43 **Zhou B**, Huang Y, Li H, Sun W, Liu J. Proton-pump inhibitors and risk of fractures: an update meta-analysis. *Osteoporos Int* 2016; **27**: 339-347 [PMID: 26462494 DOI: 10.1007/s00198-015-3365-x]

44 **Nochaiwong S**, Ruengorn C, Awiphan R, Koyratkoson K, Chaisai C, Noppakun K, Chongruksut W, Thavorn K. The association between proton pump inhibitor use and the risk of adverse kidney outcomes: a systematic review and meta-analysis. *Nephrol Dial Transplant* 2018; **33**: 331-342 [PMID: 28339835 DOI: 10.1093/ndt/gfw470]

45 **Lazarus B**, Chen Y, Wilson FP, Sang Y, Chang AR, Coresh J, Grams ME. Proton Pump Inhibitor Use and the Risk of Chronic Kidney Disease. *JAMA Intern Med* 2016; **176**: 238-246 [PMID: 26752337 DOI: 10.1001/jamainternmed.2015.7193]

46 **Xie Y**, Bowe B, Li T, Xian H, Balasubramanian S, Al-Aly Z. Proton Pump Inhibitors and Risk of Incident CKD and Progression to ESRD. *J Am Soc Nephrol* 2016; **27**: 3153-3163 [PMID: 27080976 DOI: 10.1681/ASN.2015121377]

47 **Cholin L**, Ashour T, Mehdi A, Taliercio JJ, Daou R, Arrigain S, Schold JD, Thomas G, Nally J, Nakhoul NL, Nakhoul GN. Proton-pump inhibitor vs. H2-receptor blocker use and overall risk of CKD progression. *BMC Nephrol* 2021; **22**: 264 [PMID: 34266395 DOI: 10.1186/s12882-021-02449-0]

48 **Moledina DG**, Perazella MA. Proton Pump Inhibitors and CKD. *J Am Soc Nephrol* 2016; **27**: 2926-2928 [PMID: 27080978 DOI: 10.1681/ASN.2016020192]

49 **Ortiz-Guerrero G**, Amador-Muñoz D, Calderón-Ospina CA, López-Fuentes D, Nava Mesa MO. Proton Pump Inhibitors and Dementia: Physiopathological Mechanisms and Clinical Consequences. *Neural Plast* 2018; **2018**: 5257285 [PMID: 29755512 DOI: 10.1155/2018/5257285]

50 **Li M**, Luo Z, Yu S, Tang Z. Proton pump inhibitor use and risk of dementia: Systematic review and meta-analysis. *Medicine (Baltimore)* 2019; **98**: e14422 [PMID: 30762748 DOI: 10.1097/MD.0000000000014422]

51 **Inghammar M**, Svanström H, Voldstedlund M, Melbye M, Hviid A, Mølbak K, Pasternak B. Proton-Pump Inhibitor Use and the Risk of Community-Associated Clostridium difficile Infection. *Clin Infect Dis* 2021; **72**: e1084-e1089 [PMID: 33629099 DOI: 10.1093/cid/ciaa1857]

52 **Su T**, Lai S, Lee A, He X, Chen S. Meta-analysis: proton pump inhibitors moderately increase the risk of small intestinal bacterial overgrowth. *J Gastroenterol* 2018; **53**: 27-36 [PMID: 28770351 DOI: 10.1007/s00535-017-1371-9]

53 **Trifan A**, Stanciu C, Girleanu I, Stoica OC, Singeap AM, Maxim R, Chiriac SA, Ciobica A, Boiculese L. Proton pump inhibitors therapy and risk of Clostridium difficile infection: Systematic review and meta-analysis. *World J Gastroenterol* 2017; **23**: 6500-6515 [PMID: 29085200 DOI: 10.3748/wjg.v23.i35.6500]

54 **Ratuapli SK**, Ellington TG, O'Neill MT, Umar SB, Harris LA, Foxx-Orenstein AE, Burdick GE, Dibaise JK, Lacy BE, Crowell MD. Proton pump inhibitor therapy use does not predispose to small intestinal bacterial overgrowth. *Am J Gastroenterol* 2012; **107**: 730-735 [PMID: 22334250 DOI: 10.1038/ajg.2012.4]

55 **Yu T**, Tang Y, Jiang L, Zheng Y, Xiong W, Lin L. Proton pump inhibitor therapy and its association with spontaneous bacterial peritonitis incidence and mortality: A meta-analysis. *Dig Liver Dis* 2016; **48**: 353-359 [PMID: 26795544 DOI: 10.1016/j.dld.2015.12.009]

56 **Kim JH**, Lim KS, Min YW, Lee H, Min BH, Rhee PL, Kim JJ, Koh KC, Paik SW. Proton pump inhibitors do not increase

the risk for recurrent spontaneous bacterial peritonitis in patients with cirrhosis. *J Gastroenterol Hepatol* 2017; **32**: 1064-1070 [PMID: 28449345 DOI: 10.1111/jgh.13637]

57 **Thomson AB**, Sauve MD, Kassam N, Kamitakahara H. Safety of the long-term use of proton pump inhibitors. *World J Gastroenterol* 2010; **16**: 2323-2330 [PMID: 20480516 DOI: 10.3748/wjg.v16.i19.2323]

58 **Lambert AA**, Lam JO, Paik JJ, Ugarte-Gil C, Drummond MB, Crowell TA. Risk of community-acquired pneumonia with outpatient proton-pump inhibitor therapy: a systematic review and meta-analysis. *PLoS One* 2015; **10**: e0128004 [PMID: 26042842 DOI: 10.1371/journal.pone.0128004]

59 **Sultan N**, Nazareno J, Gregor J. Association between proton pump inhibitors and respiratory infections: a systematic review and meta-analysis of clinical trials. *Can J Gastroenterol* 2008; **22**: 761-766 [PMID: 18818790 DOI: 10.1155/2008/821385]

60 **Jaynes M**, Kumar AB. The risks of long-term use of proton pump inhibitors: a critical review. *Ther Adv Drug Saf* 2019; **10**: 2042098618809927 [PMID: 31019676 DOI: 10.1177/2042098618809927]

61 **Ahn JS**, Eom CS, Jeon CY, Park SM. Acid suppressive drugs and gastric cancer: a meta-analysis of observational studies. *World J Gastroenterol* 2013; **19**: 2560-2568 [PMID: 23674860 DOI: 10.3748/wjg.v19.i16.2560]

62 **Cheung KS**, Leung WK. Long-term use of proton-pump inhibitors and risk of gastric cancer: a review of the current evidence. *Therap Adv Gastroenterol* 2019; **12**: 1756284819834511 [PMID: 30886648 DOI: 10.1177/1756284819834511]

63 **Abrahami D**, McDonald EG, Schnitzer ME, Barkun AN, Suissa S, Azoulay L. Proton pump inhibitors and risk of gastric cancer: population-based cohort study. *Gut* 2022; **71**: 16-24 [PMID: 34226290 DOI: 10.1136/gutjnl-2021-325097]

64 **Yibirin M**, De Oliveira D, Valera R, Plitt AE, Lutgen S. Adverse Effects Associated with Proton Pump Inhibitor Use. *Cureus* 2021; **13**: e12759 [PMID: 33614352 DOI: 10.7759/cureus.12759]

65 **Tran-Duy A**, Spaetgens B, Hoes AW, de Wit NJ, Stehouwer CD. Use of Proton Pump Inhibitors and Risks of Fundic Gland Polyps and Gastric Cancer: Systematic Review and Meta-analysis. *Clin Gastroenterol Hepatol* 2016; **14**: 1706-1719.e5 [PMID: 27211501 DOI: 10.1016/j.cgh.2016.05.018]

66 **Song H**, Zhu J, Lu D. Long-term proton pump inhibitor (PPI) use and the development of gastric pre-malignant lesions. *Cochrane Database Syst Rev* 2014; CD010623 [PMID: 25464111 DOI: 10.1002/14651858.CD010623.pub2]

67 **Ariel H**, Cooke JP. Cardiovascular Risk of Proton Pump Inhibitors. *Methodist Debakey Cardiovasc J* 2019; **15**: 214-219 [PMID: 31687101 DOI: 10.14797/mdcj-15-3-214]

68 **Ogawa R**, Echizen H. Drug-drug interaction profiles of proton pump inhibitors. *Clin Pharmacokinet* 2010; **49**: 509-533 [PMID: 20608754 DOI: 10.2165/11531320-000000000-00000]

69 **Blume H**, Donath F, Warnke A, Schug BS. Pharmacokinetic drug interaction profiles of proton pump inhibitors. *Drug Saf* 2006; **29**: 769-784 [PMID: 16944963 DOI: 10.2165/00002018-200629090-00002]

70 **Wijarnpreecha K**, Chesdachai S, Thongprayoon C, Jaruvongvanich V, Ungprasert P, Cheungpasitporn W. Efficacy and Safety of Direct-acting Antivirals in Hepatitis C Virus-infected Patients Taking Proton Pump Inhibitors. *J Clin Transl Hepatol* 2017; **5**: 327-334 [PMID: 29226099 DOI: 10.14218/JCTH.2017.00017]

71 **Laserna-Mendieta EJ**, Casabona S, Savarino E, Perelló A, Pérez-Martínez I, Guagnozzi D, Barrio J, Guardiola A, Asensio T, de la Riva S, Ruiz-Ponce M, Rodríguez-Oballe JA, Santander C, Arias Á, Lucendo AJ; EUREOS EoE CONNECT research group. Efficacy of Therapy for Eosinophilic Esophagitis in Real-World Practice. *Clin Gastroenterol Hepatol* 2020; **18**: 2903-2911.e4 [PMID: 31988045 DOI: 10.1016/j.cgh.2020.01.024]

72 **Pandolfino J**. Discontinuation of proton pump inhibitor therapy and the role of esophageal testing. *Gastroenterol Hepatol (N Y)* 2013; **9**: 747-764 [PMID: 24764794]

73 **Keller J**. What Is the Impact of High-Resolution Manometry in the Functional Diagnostic Workup of Gastroesophageal Reflux Disease? *Visc Med* 2018; **34**: 101-108 [PMID: 29888238 DOI: 10.1159/000486883]

74 **Graham DY**. Optimal PPI Dosing for Improving GERD Symptoms: Is Timing Everything? *Dig Dis Sci* 2019; **64**: 4-6 [PMID: 30238199 DOI: 10.1007/s10620-018-5288-9]

75 **Neumann CS**, Cooper BT. Oesophageal pH monitoring in Barrett's oesophagus. *Gut* 2003; **52**: 153; author reply 153-153; author reply 154 [PMID: 12477781 DOI: 10.1136/gut.52.1.153-a]

76 **Sollano JD**, Romano RP, Ibanez-Guzaman L, Lontok MADC, de Ocampo SQ, Policarpio AA, de Guzman Jr RN, Dulanpang CD, Galang AJG, Olympia EG, Chua MAL, Moscoso BA, Tan JA, Pangilinan JAN, Vitug AO, Naval MC, Encarnacion DA, Sy PP, Ong EG, Cabahug OT, Daez MLO, Ismael AE, Bocobo JC. Clinical Practice Guidelines on the Diagnosis and Treatment of Gastroesophageal Reflux Disease (GERD). *hilippine J of Intern Med* 2015; **53** (3): 1-17

77 **Rawla P**, Sunkara T, Ofosu A, Gaduputi V. Potassium-competitive acid blockers - are they the next generation of proton pump inhibitors? *World J Gastrointest Pharmacol Ther* 2018; **9**: 63-68 [PMID: 30595950 DOI: 10.4292/wjgpt.v9.i7.63]

78 **Abdelrahman T**, Latif A, Chan DS, Jones H, Farag M, Lewis WG, Havard T, Escofet X. Outcomes after laparoscopic anti-reflux surgery related to obesity: A systematic review and meta-analysis. *Int J Surg* 2018; **51**: 76-82 [PMID: 29367036 DOI: 10.1016/j.ijsu.2018.01.013]

79 **Simonka Z**, Paszt A, Abrahám S, Pieler J, Tajti J, Tiszlavicz L, Németh I, Izbéki F, Rosztóczy A, Wittmann T, Rárosi F, Lázár G. The effects of laparoscopic Nissen fundoplication on Barrett's esophagus: long-term results. *Scand J Gastroenterol* 2012; **47**: 13-21 [PMID: 22150083 DOI: 10.3109/00365521.2011.639081]

80 **Kaplan LM**. Treatment of gastroesophageal reflux disease in obese patients. *Gastroenterol Hepatol (N Y)* 2008; **4**: 841-843 [PMID: 21904472]

81 **Robertson AG**, Patel RN, Couper GW, de Beaux AC, Paterson-Brown S, Lamb PJ. Long-term outcomes following laparoscopic anterior and Nissen fundoplication. *ANZ J Surg* 2017; **87**: 300-304 [PMID: 26478259 DOI: 10.1111/ans.13358]

World Journal of Gastroenterology

Submit a Manuscript: https://www.f6publishing.com

World J Gastroenterol 2022 June 28; 28(24): 2680-2688

DOI: 10.3748/wjg.v28.i24.2680

ISSN 1007-9327 (print) ISSN 2219-2840 (online)

MINIREVIEWS

Pancreatic involvement in celiac disease

Daniel Vasile Balaban, Iulia Enache, Marina Ciochina, Alina Popp, Mariana Jinga

Specialty type: Gastroenterology and hepatology

Provenance and peer review: Invited article; Externally peer reviewed.

Peer-review model: Single blind

Peer-review report's scientific quality classification

Grade A (Excellent): 0
Grade B (Very good): B, B
Grade C (Good): 0
Grade D (Fair): D
Grade E (Poor): 0

P-Reviewer: Ashkar M, United States; Ghazanfar A, United Kingdom; Lee Y, South Korea
A-Editor: Yao QG, China

Received: January 15, 2022
Peer-review started: January 15, 2022
First decision: April 12, 2022
Revised: April 17, 2022
Accepted: May 27, 2022
Article in press: May 27, 2022
Published online: June 28, 2022

Daniel Vasile Balaban, Iulia Enache, Marina Ciochina, Mariana Jinga, Department of Internal Medicine and Gastroenterology, Carol Davila University of Medicine and Pharmacy, Bucharest 020021, Romania

Daniel Vasile Balaban, Iulia Enache, Marina Ciochina, Mariana Jinga, Dr. Carol Davila Central Military Emergency University Hospital, Bucharest 020021, Romania

Alina Popp, Department of Pediatrics, Carol Davila University of Medicine and Pharmacy, Bucharest 020021, Romania

Alina Popp, National Institute for Mother and Child Health, Bucharest 020021, Romania

Corresponding author: Daniel Vasile Balaban, MD, PhD, Senior Lecturer, Department of Internal Medicine and Gastroenterology, Carol Davila University of Medicine and Pharmacy, 134 Calea Plevnei, Bucharest 020021, Romania. vbalaban@yahoo.com

Abstract

Celiac disease (CD) is well recognized as a systemic, chronic autoimmune disease mainly characterized by gluten-sensitive enteropathy in genetically predisposed individuals but with various extraintestinal features. One of the affected organs in CD is the pancreas, consisting of both endocrine and exocrine alterations. Over the last decades there has been increasing interest in the pancreatic changes in CD, and this has been reflected by a great number of publications looking at this extraintestinal involvement during the course of CD. While pancreatic endocrine changes in CD, focusing on type 1 diabetes mellitus, are well documented in the literature, the relationship with the exocrine pancreas has been less studied. This review summarizes currently available evidence with regard to pancreatic exocrine alterations in CD, focusing on risk of pancreatitis in CD patients, association with autoimmune pancreatitis, prevalence and outcomes of pancreatic exocrine insufficiency in newly diagnosed and gluten-free diet treated CD patients, and the link with cystic fibrosis. In addition, we discuss mechanisms behind the associated pancreatic exocrine impairment in CD and highlight the recommendations for clinical practice.

Key Words: Pancreas; Celiac disease; Autoimmune; Pancreatitis; Cystic fibrosis; Exocrine insufficiency

©The Author(s) 2022. Published by Baishideng Publishing Group Inc. All rights reserved.

Core Tip: Celiac disease (CD) is currently regarded as a systemic, chronic, immune-mediated disease triggered by gluten ingestion in genetically susceptible individuals. In the last decade there has been an increasing number of publications on extraintestinal involvement during the course of CD, some of which have assessed the pancreatic changes associated with this disease. This review summarizes currently available data with respect to exocrine pancreatic changes in CD, focusing on practices for clinicians.

Citation: Balaban DV, Enache I, Ciochina M, Popp A, Jinga M. Pancreatic involvement in celiac disease. *World J Gastroenterol* 2022; 28(24): 2680-2688
URL: https://www.wjgnet.com/1007-9327/full/v28/i24/2680.htm
DOI: https://dx.doi.org/10.3748/wjg.v28.i24.2680

INTRODUCTION

Celiac disease (CD) is an immune-mediated enteropathy that occurs in genetically predisposed individuals upon ingestion of gluten. Initially considered a small bowel disease, now it is widely recognized as a systemic illness, which accounts for its many protean manifestations. The systemic character along with its various clinical presentations make CD a sometimes difficult to recognize clinical chameleon. The wide spectrum of presenting features, sometimes subclinical, hinders case-finding strategies and delays diagnosis, as CD is often not considered among the differential diagnoses [1,2]. Moreover, there is also the further drawback of poor awareness among different medical specialties[3].

Among the extraintestinal features of CD[4-6], pancreatic involvement has rarely been reported compared to other organ-specific manifestations such as cutaneous, hematologic, liver-related, rheumatologic, cardiovascular, or neurological impairments[7-13]. Moreover, while some of these systemic features have been incorporated into case-finding and screening strategies such as anemia, osteoporosis or chronic liver disease[14], pancreatic-associated involvement in CD is scarcely reported in currently available guidelines[15-17]. The association between the pancreas and CD covered in guidelines is limited to the need to consider pancreatic exocrine insufficiency (PEI) as an alternative diagnosis in non-responsive CD and the fact that upper gastrointestinal surgery including pancreas-related indications may unmask subclinical CD[15,16]. This has also been highlighted by previous reports on the impact of CD on exocrine and endocrine pancreas, which also set the need for further research focused on this association[18]. Contrasting the well-documented pancreatic endocrine changes in CD, referring to type 1 diabetes mellitus in particular, the relationship with the exocrine pancreas has been less covered in the literature.

On the other hand, the wide spectrum of pancreatic diseases does not include CD as a risk factor or associated condition, except counting CD as a potential cause of PEI[19]. Pancreatic involvement can occur in patients with CD, either caused by the small-bowel disease or co-existing with it. The main mechanisms for this association are believed to be the impaired cholecystokinin (CCK) and secretin release, but also the chronic duodenal inflammation that can lead to secondary modifications of papillary mucosal area[20].

Our aim was to summarize currently available evidence with regard to exocrine pancreatic involvement in CD, looking at CD as a risk factor or associated condition with pathologies of the exocrine pancreas, and testing indications regarding the bidirectional association of the two diseases.

SEARCH STRATEGY

For this purpose, we searched PubMed in January 2022 for all publications on the association between pancreas and CD, using the medical subject headings (MeSH) terms–"pancreas" (ID: D010179) and "celiac disease" (ID: D002446), with the following search syntax (("pancreas" [Mesh]) OR (pancreas [Title/Abstract])) AND (("celiac disease" [Mesh]) OR (celiac disease [Title/Abstract])). We performed additional searches with pancreas-related terms, "Pancreas, exocrine" (ID: D046790), "pancreatitis" (ID: D010195), "pancreatitis, chronic" (ID: D050500), "autoimmune pancreatitis" (ID: D000081012) and "celiac disease" (ID: D002446). The extended search yielded a total of 889 results, of which 145 were duplicates. Search results were imported into Reference Citation Analysis (Baishideng Publishing Group, Inc.), which was used for article processing and selection. We filtered the search for reviews, editorials, comments and opinion articles (n = 140). We excluded papers referring to the association of CD with diabetes or alterations of the endocrine pancreas (n = 66). The remaining titles and consecutive abstracts were screened for pertinence to the topic. We selected relevant articles on exocrine pancreatic involvement in CD for full-text analysis and summarized findings according to significant associations. References and citing articles of selected papers were also analyzed for potentially relevant articles that

might have been missed in the initial search. The process of article selection is detailed in Figure 1.

CD AND RISK OF PANCREATITIS

CD patients are at risk both for acute pancreatitis (AP) and chronic pancreatitis (CP)[21-23]. While some have described worse outcomes and increased medical burden among CD individuals[21], others have found lower morbidity and mortality among this patient group[24] (Table 1).

Several pathogenic mechanisms have been theorized to account for the elevated pancreatitis risk in CD–malnutrition, papillary stenosis, and immune phenomena[25] (Figure 2). Severe malnutrition affects pancreatic secretion and can cause pancreatic atrophy[26]. Also, chronic inflammation of the duodenal mucosa in CD patients can also involve the papillary area and lead to papillary stenosis and consequent pancreatic disease[20]. Finally, autoimmune pancreatitis (AIP) or other autoimmune phenomena such as islet-specific autoantibodies in CD-associated type 1 diabetes mellitus can contribute to the link between pancreatitis and CD[27,28].

With regard to CP, results are also discordant using similar diagnostic criteria; while some authors have reported CP features to be common in CD patients undergoing endoscopic ultrasound (EUS) assessment[29], others did not reveal significant structural alterations in the pancreatic parenchyma of CD individuals[30]. In their study using EUS criteria and elastography, Rana *et al*[30] concluded that PEI is functional and reversible after gluten-free diet (GFD). Supporting this finding, the pathognomonic pancreatic calcifications have been rarely reported in CD[31-35]. However, a biopsy-based study published as abstract has shown CD prevalence as high as 7.4% in established CP, recommending screening in this group[36].

Concerning CD screening in pancreatic diseases, there have been reports of asymptomatic hyperenzymemia, macrolipasemia, or macroamylasemia[37-42] in CD patients, but prevalence studies are missing. According to these reports, decrease or even resolution of macroamylasemia/macrolipasemia or elevated pancreatic enzyme levels can be seen on GFD. Of note, the occurrence of hyperenzymemia in CD can be a confounder for the reported elevated risk of AP associated with CD, by overdiagnosing AP in this scenario.

On the other hand, idiopathic recurrent pancreatitis and sphincter of Oddi dysfunction might be considered a testing indication for CD, given the mechanism of chronic papillitis[20,43]. Non-response to treatment in CP might warrant testing for CD, as suggested in some case reports[31].

EXOCRINE PANCREATIC INSUFFICIENCY AND CD

CD is a well-recognized less common etiology of PEI[19,44,45]. This is well reported in currently available guidelines[46]. EPI has been reported with variable frequency in CD patients, depending on the test used to diagnose it. Early studies were based on direct pancreatic function testing (pancreatic enzyme or bicarbonate secretions measurements) and found that PEI is common in classical CD, but non-severe[47]. Fecal elastase (FE) is recommended for detecting PEI in newly diagnosed CD[48]. Impairment of pancreatic exocrine function can be seen both in newly diagnosed CD, in up to 80% of cases[19], and in treated CD, where it should be considered a cause of treatment failure in patients unresponsive to GFD[49,50]. In this latter group comprising GFD-treated CD patients with continuing diarrhea, EPI has been reported in 12%-18% of cases[51,52]. While CD patients improve with pancreatic enzyme replacement therapy (PERT), probably paralleling the restoring of mucosal architecture on GFD, some authors have reported that PERT could be discontinued in some patients who experience improvement in symptoms[53]. However, in CD patients with PEI, who report good adherence to GFD but experience continued malabsorption with adequate dosing PERT, additional pathogenic mechanisms such as enteric infections (*e.g.*, *Giardia*), small intestinal bacterial overgrowth, or complications such as refractory CD and enteropathy associated T-cell lymphoma should be sought[54]. Moreover, gastroparesis in the setting of type 1 diabetes mellitus associated with CD could contribute to incomplete response to PERT. PEI should be readily recognized in slowly recovering children with CD on GFD, as it might accelerate weight increase with adequate enzyme supplementation[55].

Correlation of certain genetic polymorphisms with PEI has also been studied, but without conclusive associations in a small cohort of CD patients[56].

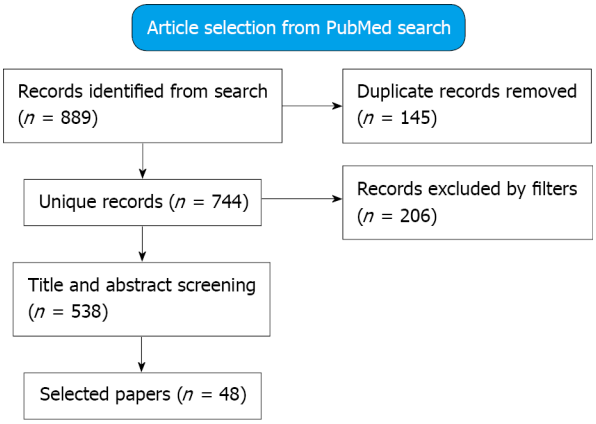
A concern with using FE is represented by the lower diagnostic accuracy compared to direct pancreatic function testing, variability among different tests and analytical processing of samples, taking into account the potential dilution due to diarrhea[57-59].

Despite the increased risk of pancreatitis in CD discussed above, changes in pancreatic enzyme secretion in these patients seen to be mainly functional, as reported by Rana *et al*[30], who found no correlation with structural parenchymal alterations, assessed by EUS. Another study, based on magnetic resonance imaging assessment, did not reveal morphological changes in CD patients with PEI[60]. This impaired function of the exocrine pancreas is also supported by the inverse correlation between mucosal damage and pancreatic enzyme levels, with reversal of PEI on GFD[19,61]. However, protein

Table 1 Summary of studies looking at acute pancreatitis and chronic pancreatitis prevalence among individuals with celiac disease

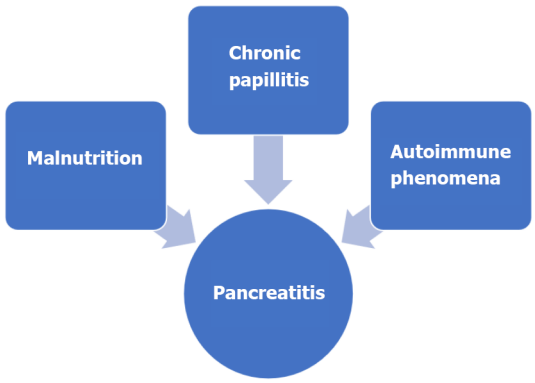
Ref.	CD, *n*	Pancreatitis prevalence	OR of AP	Outcome
Alkhayyat *et al* [21], 2021	133400	AP 1.06%; CP 0.52%	OR for AP = 2.66; OR for CP = 2.18	Worse outcomes compared to non-CD
Osagiede *et al* [24], 2020	337201	AP 2.2%	OR = 1.92	Lower morbidity and mortality, attributed to less severe forms of AP or lower baseline comorbidities
Sadr-Azodi *et al* [22], 2012	28908	Pancreatitis 1.4%	HR for gallstone-related AP = 1.59; HR for non-gallstone-related AP = 1.86; HR for CP = 3.33	Increased risk of severe AP (gallstone-related: HR = 3.18; non-gallstone related: HR = 2.00)
Ludvigsson *et al* [23], 2007	14239	Pancreatitis any type 0.66%	HR for pancreatitis of any type = 3.3; HR for CP = 19.8	Patient population was represented by hospital inpatients, leaving out those managed as outpatients

AP: Acute pancreatitis; CD: Celiac disease; CP: Chronic pancreatitis; HR: Hazard ratio; OR: Odds ratio.



DOI: 10.3748/wjg.v28.i24.2680 Copyright ©The Author(s) 2022.

Figure 1 Flow diagram of the article selection process.



DOI: 10.3748/wjg.v28.i24.2680 Copyright ©The Author(s) 2022.

Figure 2 Mechanism behind the increased pancreatitis risk in celiac disease patients.

malnutrition, also present in CD patients, has been shown to be associated with acinar cell atrophy and fibrosis[18].

The main mechanism of PEI in CD patients is disruption of mucosal release of enteric hormones, mainly CCK and secretin, which represent a potent stimulus for pancreatic function. While exocrine pancreatic function is intrinsically normal, impaired CCK and secretin release from the atrophic mucosa leads to decreased secretion of enzymes into the duodenal lumen. The functional PEI that occurs in CD is reversible upon exogenous administration of CCK-pancreozymin[62]. Others have suggested that PEI can develop independent of this reduced entero-hormone release[63]. Another theorized mechanism is deficiency of amino acids, which leads to reduced protein synthesis for pancreatic enzymes. This mechanism is also backed up by the fact that correction of deficiencies alleviates PEI in CD patients[64].

Table 2 Mechanisms of pancreatic exocrine insufficiency in celiac disease

No.	
1	Impaired secretion of cholecystokinin and secretin from the diseased small bowel mucosa
2	Reduced amino acid uptake in the small bowel, which subsequently leads to reduction in precursors for synthesis of pancreatic enzymes
3	Morphologic alterations in pancreatic parenchyma secondary to protein malnutrition

Another hypothesis, but probably of less significance, is that of structural changes in the pancreatic parenchyma (acinar atrophy, fibrosis) seen in advanced malnutrition[65]. Mechanisms behind EPI in CD are summarized in Table 2[18,47,50,66].

CYSTIC FIBROSIS AND CD

Another underrecognized, pancreas-related association for CD is cystic fibrosis (CF), an autosomal recessive disease characterized by mutations in the CF transmembrane conductance regulator gene, which encodes a chloride and bicarbonate channel expressed in epithelial cells in multiple organs[67]. While the pancreatic dysfunction in CF is well known, altered immune regulation has been described in these patients, which predisposes them to developing autoimmune phenomena. The systematic review and meta-analysis by Imrei *et al*[68] showed pooled prevalence of 1.8%-2.3% of biopsy-proven CD among CF patients, which is more than twice that of the general population[69]. Based on this observation, the authors recommend routine screening for CD in CF patients. This recommendation is supported by another group[70], who suggested performing CD screening in CF with persistent gastrointestinal symptoms or malabsorption (including improper weight and/or height gain in pediatric patients), despite adequate enzyme replacement therapy.

AIP AND CD

AIP is a chronic fibroinflammatory disease of the pancreas, with a relapsing steroid-responsive pattern. Given the common immune dysregulation background of both AIP and CD, researchers have looked whether there is an association of the two. While some isolated reports have shown a potential link between AIP and CD[71,72], a study looking at CD frequency in a cohort of AIP patients did not show an increased CD prevalence among this group (1.4%) and concluded that serologic screening for CD is not supported[73]. However, a murine model of AIP has provided insight that gliadin sensitization and challenge can induce pancreatitis and extrapancreatic inflammation in HLA-DQ8 transgenic mice[74]. On the other hand, immunoglobulin G4-positive cells, which have been searched for in duodenal/ampullary biopsies as an alternative to pancreatic biopsy for diagnosing AIP, have also been reported in 7 of 18 CD patients in the study by Cebe *et al*[75]. Given the scarce data on AIP and CD, further research is warranted to conclude if there is a link between the two beyond the plausible biologic mechanism. A recognized association is that of type 2 AIP and ulcerative colitis, and considering the also established connection between CD and inflammatory bowel diseases[76], linking the three diseases might provide some insight on the relationship between AIP and CD.

CONCLUSION

Pancreatic involvement, both endocrine and exocrine, is frequent in CD and should be searched for in the appropriate clinical setting. Conversely, certain pancreatic-related diseases should prompt looking for CD–CF with ongoing digestive symptoms, non-responsive CP, idiopathic recurrent pancreatitis. Concomitant pancreatic disease in a CD patient may contribute to aggravated malnutrition and should be readily recognized in order to improve nutritional status and prognosis. Also, there is increasing data that impaired pancreatic function in CD can improve on a GFD.

FOOTNOTES

Author contributions: Balaban DV proposed the research idea; Balaban DV, Enache I, and Ciochina M performed the literature search and article selection, and drafted the initial version of the manuscript; Popp A and Jinga M critically reviewed the manuscript and supervised the project; All authors contributed to drawing the figures and tables, and have read and approved the final version of the manuscript.

Conflict-of-interest statement: All the authors report no relevant conflicts of interest for this article.

Open-Access: This article is an open-access article that was selected by an in-house editor and fully peer-reviewed by external reviewers. It is distributed in accordance with the Creative Commons Attribution NonCommercial (CC BY-NC 4.0) license, which permits others to distribute, remix, adapt, build upon this work non-commercially, and license their derivative works on different terms, provided the original work is properly cited and the use is non-commercial. See: https://creativecommons.org/Licenses/by-nc/4.0/

Country/Territory of origin: Romania

ORCID number: Daniel Vasile Balaban 0000-0003-3436-8041; Iulia Enache 0000-0001-6905-5008; Marina Ciochina 0000-0002-1573-6358; Alina Popp 0000-0002-7809-5762; Mariana Jinga 0000-0001-5826-0815.

Corresponding Author's Membership in Professional Societies: European Society for Gastrointestinal Endoscopy, No. 45910264; Association for Pancreatic Pathology Romania; European Society for the Study of Coeliac Disease (ESsCD); Romanian Society of Gastroenterology and Hepatology; Romanian Society of Digestive Endoscopy; European Pancreatic Club; World Endoscopy Organization

S-Editor: Fan JR
L-Editor: Filipodia
P-Editor: Fan JR

REFERENCES

1 **Makharia GK**, Singh P, Catassi C, Sanders DS, Leffler D, Ali RAR, Bai JC. The global burden of coeliac disease: opportunities and challenges. *Nat Rev Gastroenterol Hepatol* 2022 [PMID: 34980921 DOI: 10.1038/s41575-021-00552-z]
2 **Pinto-Sanchez MI**, Silvester JA, Lebwohl B, Leffler DA, Anderson RP, Therrien A, Kelly CP, Verdu EF. Society for the Study of Celiac Disease position statement on gaps and opportunities in coeliac disease. *Nat Rev Gastroenterol Hepatol* 2021; **18**: 875-884 [PMID: 34526700 DOI: 10.1038/s41575-021-00511-8]
3 **Jinga M**, Popp A, Balaban DV, Dima A, Jurcut C. Physicians' attitude and perception regarding celiac disease: A questionnaire-based study. *Turk J Gastroenterol* 2018; **29**: 419-426 [PMID: 30249556 DOI: 10.5152/tjg.2018.17236]
4 **Therrien A**, Kelly CP, Silvester JA. Celiac Disease: Extraintestinal Manifestations and Associated Conditions. *J Clin Gastroenterol* 2020; **54**: 8-21 [PMID: 31513026 DOI: 10.1097/MCG.0000000000001267]
5 **Leffler DA**, Green PH, Fasano A. Extraintestinal manifestations of coeliac disease. *Nat Rev Gastroenterol Hepatol* 2015; **12**: 561-571 [PMID: 26260366 DOI: 10.1038/nrgastro.2015.131]
6 **Durazzo M**, Ferro A, Brascugli I, Mattivi S, Fagoonee S, Pellicano R. Extra-Intestinal Manifestations of Celiac Disease: What Should We Know in 2022? *J Clin Med* 2022; **11** [PMID: 35011999 DOI: 10.3390/jcm11010258]
7 **Balaban DV**, Mihai A, Dima A, Popp A, Jinga M, Jurcut C. Celiac disease and Sjögren's syndrome: A case report and review of literature. *World J Clin Cases* 2020; **8**: 4151-4161 [PMID: 33024773 DOI: 10.12998/wjcc.v8.i18.4151]
8 **Dima A**, Jurcut C, Jinga M. Rheumatologic manifestations in celiac disease: what should we remember? *Rom J Intern Med* 2019; **57**: 3-5 [PMID: 30375355 DOI: 10.2478/rjim-2018-0024]
9 **Ciaccio EJ**, Lewis SK, Biviano AB, Iyer V, Garan H, Green PH. Cardiovascular involvement in celiac disease. *World J Cardiol* 2017; **9**: 652-666 [PMID: 28932354 DOI: 10.4330/wjc.v9.i8.652]
10 **Haggård L**, Glimberg I, Lebwohl B, Sharma R, Verna EC, Green PHR, Ludvigsson JF. High prevalence of celiac disease in autoimmune hepatitis: Systematic review and meta-analysis. *Liver Int* 2021; **41**: 2693-2702 [PMID: 34219350 DOI: 10.1111/liv.15000]
11 **Mearns ES**, Taylor A, Thomas Craig KJ, Puglielli S, Leffler DA, Sanders DS, Lebwohl B, Hadjivassiliou M. Neurological Manifestations of Neuropathy and Ataxia in Celiac Disease: A Systematic Review. *Nutrients* 2019; **11** [PMID: 30759885 DOI: 10.3390/nu11020380]
12 **Rodrigo L**, Beteta-Gorriti V, Alvarez N, Gómez de Castro C, de Dios A, Palacios L, Santos-Juanes J. Cutaneous and Mucosal Manifestations Associated with Celiac Disease. *Nutrients* 2018; **10** [PMID: 29933630 DOI: 10.3390/nu10070800]
13 **Laurikka P**, Nurminen S, Kivelä L, Kurppa K. Extraintestinal Manifestations of Celiac Disease: Early Detection for Better Long-Term Outcomes. *Nutrients* 2018; **10** [PMID: 30081502 DOI: 10.3390/nu10081015]
14 **Elwenspoek MMC**, Jackson J, O'Donnell R, Sinobas A, Dawson S, Everitt H, Gillett P, Hay AD, Lane DL, Mallett S, Robins G, Watson JC, Jones HE, Whiting P. The accuracy of diagnostic indicators for coeliac disease: A systematic review and meta-analysis. *PLoS One* 2021; **16**: e0258501 [PMID: 34695139 DOI: 10.1371/journal.pone.0258501]
15 **Al-Toma A**, Volta U, Auricchio R, Castillejo G, Sanders DS, Cellier C, Mulder CJ, Lundin KEA. European Society for the Study of Coeliac Disease (ESsCD) guideline for coeliac disease and other gluten-related disorders. *United European Gastroenterol J* 2019; **7**: 583-613 [PMID: 31210940 DOI: 10.1177/2050640619844125]
16 **Rubio-Tapia A**, Hill ID, Kelly CP, Calderwood AH, Murray JA; American College of Gastroenterology. ACG clinical guidelines: diagnosis and management of celiac disease. *Am J Gastroenterol* 2013; **108**: 656-76; quiz 677 [PMID: 23609613 DOI: 10.1038/ajg.2013.79]
17 **Ludvigsson JF**, Bai JC, Biagi F, Card TR, Ciacci C, Ciclitira PJ, Green PH, Hadjivassiliou M, Holdoway A, van Heel DA, Kaukinen K, Leffler DA, Leonard JN, Lundin KE, McGough N, Davidson M, Murray JA, Swift GL, Walker MM, Zingone F, Sanders DS; BSG Coeliac Disease Guidelines Development Group; British Society of Gastroenterology. Diagnosis and

management of adult coeliac disease: guidelines from the British Society of Gastroenterology. *Gut* 2014; **63**: 1210-1228 [PMID: 24917550 DOI: 10.1136/gutjnl-2013-306578]

18 **Freeman HJ**. Pancreatic endocrine and exocrine changes in celiac disease. *World J Gastroenterol* 2007; **13**: 6344-6346 [PMID: 18081222 DOI: 10.3748/wjg.v13.i47.6344]

19 **Singh VK**, Haupt ME, Geller DE, Hall JA, Quintana Diez PM. Less common etiologies of exocrine pancreatic insufficiency. *World J Gastroenterol* 2017; **23**: 7059-7076 [PMID: 29093615 DOI: 10.3748/wjg.v23.i39.7059]

20 **Patel RS**, Johlin FC Jr, Murray JA. Celiac disease and recurrent pancreatitis. *Gastrointest Endosc* 1999; **50**: 823-827 [PMID: 10570344 DOI: 10.1016/s0016-5107(99)70166-5]

21 **Alkhayyat M**, Saleh MA, Abureesh M, Khoudari G, Qapaja T, Mansoor E, Simons-Linares CR, Vargo J, Stevens T, Rubio-Tapia A, Chahal P. The Risk of Acute and Chronic Pancreatitis in Celiac Disease. *Dig Dis Sci* 2021; **66**: 2691-2699 [PMID: 32809104 DOI: 10.1007/s10620-020-06546-2]

22 **Sadr-Azodi O**, Sanders DS, Murray JA, Ludvigsson JF. Patients with celiac disease have an increased risk for pancreatitis. *Clin Gastroenterol Hepatol* 2012; **10**: 1136-1142.e3 [PMID: 22801059 DOI: 10.1016/j.cgh.2012.06.023]

23 **Ludvigsson JF**, Montgomery SM, Ekbom A. Risk of pancreatitis in 14,000 individuals with celiac disease. *Clin Gastroenterol Hepatol* 2007; **5**: 1347-1353 [PMID: 17702659 DOI: 10.1016/j.cgh.2007.06.002]

24 **Osagiede O**, Lukens FJ, Wijarnpreecha K, Corral JE, Raimondo M, Kröner PT. Acute Pancreatitis in Celiac Disease: Has the Inpatient Prevalence Changed and Is It Associated With Worse Outcomes? *Pancreas* 2020; **49**: 1202-1206 [PMID: 32898005 DOI: 10.1097/MPA.0000000000001657]

25 **Basha J**, Appasani S, Vaiphei K, Singh K, Kochhar R. Celiac disease presenting as recurrent pancreatitis and pseudocyst. *JOP* 2012; **13**: 533-535 [PMID: 22964961 DOI: 10.6092/1590-8577/1091]

26 **Brooks SE**, Golden MH. The exocrine pancreas in kwashiorkor and marasmus. Light and electron microscopy. *West Indian Med J* 1992; **41**: 56-60 [PMID: 1523833]

27 **Leeds JS**, Sanders DS. Risk of pancreatitis in patients with celiac disease: is autoimmune pancreatitis a biologically plausible mechanism? *Clin Gastroenterol Hepatol* 2008; **6**: 951; author reply 951 [PMID: 18674737 DOI: 10.1016/j.cgh.2007.12.025]

28 **Sasamori H**, Fukui T, Hayashi T, Yamamoto T, Ohara M, Yamamoto S, Kobayashi T, Hirano T. Analysis of pancreatic volume in acute-onset, slowly-progressive and fulminant type 1 diabetes in a Japanese population. *J Diabetes Investig* 2018; **9**: 1091-1099 [PMID: 29427469 DOI: 10.1111/jdi.12816]

29 **Kumar S**, Gress F, Green PH, Lebwohl B. Chronic Pancreatitis is a Common Finding in Celiac Patients Who Undergo Endoscopic Ultrasound. *J Clin Gastroenterol* 2019; **53**: e128-e129 [PMID: 27749638 DOI: 10.1097/MCG.0000000000000726]

30 **Rana SS**, Dambalkar A, Chhabra P, Sharma R, Nada R, Sharma V, Rana S, Bhasin DK. Is pancreatic exocrine insufficiency in celiac disease related to structural alterations in pancreatic parenchyma? *Ann Gastroenterol* 2016; **29**: 363-366 [PMID: 27366039 DOI: 10.20524/aog.2016.0042]

31 **Rana SS**, Bhasin DK, Sinha SK, Singh K. Coexistence of chronic calcific pancreatitis and celiac disease. *Indian J Gastroenterol* 2007; **26**: 150; author reply 150 [PMID: 17704598]

32 **Pitchumoni CS**, Thomas E, Balthazar E, Sherling B. Chronic calcific pancreatitis in association with celiac disease. *Am J Gastroenterol* 1977; **68**: 358-361 [PMID: 605891]

33 **Fitzgerald O**, Fitzgerald P, Fennelly J, Mcmullin JP, Boland SJ. A clinical study of chronic pancreatitis. *Gut* 1963; **4**: 193-216 [PMID: 14058261 DOI: 10.1136/gut.4.3.193]

34 **Nanda R**, Anand BS. Celiac disease and tropical calcific pancreatitis. *Am J Gastroenterol* 1993; **88**: 1790-1792 [PMID: 8213729]

35 **Arya S**, Rana SS, Sinha SK, Nagi B, Bhasin DK. Celiac disease and chronic calcific pancreatitis with pancreas divisum. *Gastrointest Endosc* 2006; **63**: 1080-1081 [PMID: 16733138 DOI: 10.1016/j.gie.2006.01.001]

36 **Nett A**, Wamsterker E, DiMagno M. Should Patients With Established Chronic Pancreatitis Undergo Testing for Celiac Disease? Abstracts of Papers Submitted to the 47th Meeting of the American Pancreatic Association, October 26–29, 2016, Boston, Massachusetts. Pancreas 2016: 1494–551

37 **Rabsztyn A**, Green PH, Berti I, Fasano A, Perman JA, Horvath K. Macroamylasemia in patients with celiac disease. *Am J Gastroenterol* 2001; **96**: 1096-1100 [PMID: 11316153 DOI: 10.1111/j.1572-0241.2001.03746.x]

38 **Bonetti G**, Serricchio G, Giudici A, Bettonagli M, Vadacca GB, Bruno R, Coslovich E, Moratti R. Hyperamylasemia due to macroamylasemia in adult gluten enteropathy. *Scand J Clin Lab Invest* 1997; **57**: 271-273 [PMID: 9238763 DOI: 10.3109/00365519709060036]

39 **Bermejo JF**, Carbone J, Rodriguez JJ, Macias R, Rodriguez M, Gil J, Marin MA, Torres F, Fernandez-Cruz E. Macroamylasaemia, IgA hypergammaglobulinaemia and autoimmunity in a patient with Down syndrome and coeliac disease. *Scand J Gastroenterol* 2003; **38**: 445-447 [PMID: 12739720 DOI: 10.1080/00365520310000933]

40 **Barera G**, Bazzigaluppi E, Viscardi M, Renzetti F, Bianchi C, Chiumello G, Bosi E. Macroamylasemia attributable to gluten-related amylase autoantibodies: a case report. *Pediatrics* 2001; **107**: E93 [PMID: 11389291 DOI: 10.1542/peds.107.6.e93]

41 **La Villa G**, Pantaleo P, Tarquini R, Cirami L, Perfetto F, Mancuso F, Laffi G. Multiple immune disorders in unrecognized celiac disease: a case report. *World J Gastroenterol* 2003; **9**: 1377-1380 [PMID: 12800261 DOI: 10.3748/wjg.v9.i6.1377]

42 **Liu Z**, Wang J, Qian J, Tang F. Hyperamylasemia, reactive plasmacytosis, and immune abnormalities in a patient with celiac disease. *Dig Dis Sci* 2007; **52**: 1444-1447 [PMID: 17443408 DOI: 10.1007/s10620-006-9268-0]

43 **Rodrigo L**, Alvarez N, Riestra S, de Francisco R, González Bernardo O, García Isidro L, López Vázquez A, López Larrea C. [Relapsing acute pancreatitis associated with gluten enteropathy. Clinical, laboratory, and evolutive characteristics in thirty-four patients]. *Rev Esp Enferm Dig* 2008; **100**: 746-751 [PMID: 19222332 DOI: 10.4321/s1130-01082008001200002]

44 **Kunovský L**, Dítě P, Jabandžiev P, Eid M, Poredská K, Vaculová J, Sochorová D, Janeček P, Tesaříková P, Blaho M, Trna J, Hlavsa J, Kala Z. Causes of Exocrine Pancreatic Insufficiency Other Than Chronic Pancreatitis. *J Clin Med* 2021; **10** [PMID: 34945075 DOI: 10.3390/jcm10245779]

45 **Leeds JS**, Hopper AD, Hurlstone DP, Edwards SJ, McAlindon ME, Lobo AJ, Donnelly MT, Morley S, Sanders DS. Is exocrine pancreatic insufficiency in adult coeliac disease a cause of persisting symptoms? *Aliment Pharmacol Ther* 2007; **25**: 265-271 [PMID: 17269988 DOI: 10.1111/j.1365-2036.2006.03206.x]

46 **Gheorghe C**, Seicean A, Saftoiu A, Tantau M, Dumitru E, Jinga M, Negreanu L, Mateescu B, Gheorghe L, Ciocirlan M, Cijevschi C, Constantinescu G, Dima S, Diculescu M; Romanian Association for Pancreatic Pathology. Romanian guidelines on the diagnosis and treatment of exocrine pancreatic insufficiency. *J Gastrointestin Liver Dis* 2015; **24**: 117-123 [PMID: 25822444 DOI: 10.15403/jgld.2014.1121.app]

47 **DiMagno M**. Exocrine Pancreatic Insufficiency and Pancreatitis Associated with Celiac Disease [Internet]. [cited 10 January 2022]. Available from: https://pancreapedia.org/sites/default/files/Exocrine-Pancreatic-Insufficiency-Pancreatitis-Celiac-Disease_0.pdf

48 **Pezzilli R**. Exocrine pancreas involvement in celiac disease: a review. *Recent Pat Inflamm Allergy Drug Discov* 2014; **8**: 167-172 [PMID: 25417707 DOI: 10.2174/1872213x08666141122210738]

49 **Weizman Z**, Hamilton JR, Kopelman HR, Cleghorn G, Durie PR. Treatment failure in celiac disease due to coexistent exocrine pancreatic insufficiency. *Pediatrics* 1987; **80**: 924-926 [PMID: 3684405]

50 **Regan PT**, DiMagno EP. Exocrine pancreatic insufficiency in celiac sprue: a cause of treatment failure. *Gastroenterology* 1980; **78**: 484-487 [PMID: 7351287]

51 **Fine KD**, Meyer RL, Lee EL. The prevalence and causes of chronic diarrhea in patients with celiac sprue treated with a gluten-free diet. *Gastroenterology* 1997; **112**: 1830-1838 [PMID: 9178673 DOI: 10.1053/gast.1997.v112.pm9178673]

52 **Abdulkarim AS**, Burgart LJ, See J, Murray JA. Etiology of nonresponsive celiac disease: results of a systematic approach. *Am J Gastroenterol* 2002; **97**: 2016-2021 [PMID: 12190170 DOI: 10.1111/j.1572-0241.2002.05917.x]

53 **Evans KE**, Leeds JS, Morley S, Sanders DS. Pancreatic insufficiency in adult celiac disease: do patients require long-term enzyme supplementation? *Dig Dis Sci* 2010; **55**: 2999-3004 [PMID: 20458623 DOI: 10.1007/s10620-010-1261-y]

54 **Struyvenberg MR**, Martin CR, Freedman SD. Practical guide to exocrine pancreatic insufficiency - Breaking the myths. *BMC Med* 2017; **15**: 29 [PMID: 28183317 DOI: 10.1186/s12916-017-0783-y]

55 **Carroccio A**, Iacono G, Lerro P, Cavataio F, Malorgio E, Soresi M, Baldassarre M, Notarbartolo A, Ansaldi N, Montalto G. Role of pancreatic impairment in growth recovery during gluten-free diet in childhood celiac disease. *Gastroenterology* 1997; **112**: 1839-1844 [PMID: 9178674 DOI: 10.1053/gast.1997.v112.pm9178674]

56 **Licul V**, Cizmarević NS, Ristić S, Mikolasević I, Mijandrusić BS. CTLA-4 +49 and TNF-alpha-308 gene polymorphisms in celiac patients with exocrine pancreatic insufficiency. *Coll Antropol* 2013; **37**: 1191-1194 [PMID: 24611333]

57 **Brydon WG**, Kingstone K, Ghosh S. Limitations of faecal elastase-1 and chymotrypsin as tests of exocrine pancreatic disease in adults. *Ann Clin Biochem* 2004; **41**: 78-81 [PMID: 14713391 DOI: 10.1258/000456304322664753]

58 **Kampanis P**, Ford L, Berg J. Development and validation of an improved test for the measurement of human faecal elastase-1. *Ann Clin Biochem* 2009; **46**: 33-37 [PMID: 19008259 DOI: 10.1258/acb.2008.008123]

59 **Vanga RR**, Tansel A, Sidiq S, El-Serag HB, Othman MO. Diagnostic Performance of Measurement of Fecal Elastase-1 in Detection of Exocrine Pancreatic Insufficiency: Systematic Review and Meta-analysis. *Clin Gastroenterol Hepatol* 2018; **16**: 1220-1228.e4 [PMID: 29374614 DOI: 10.1016/j.cgh.2018.01.027]

60 **Vujasinovic M**, Tepes B, Volfand J, Rudolf S. Exocrine pancreatic insufficiency, MRI of the pancreas and serum nutritional markers in patients with coeliac disease. *Postgrad Med J* 2015; **91**: 497-500 [PMID: 26253920 DOI: 10.1136/postgradmedj-2015-133262]

61 **Nousia-Arvanitakis S**, Karagiozoglou-Lamboudes T, Aggouridaki C, Malaka-Lambrellis E, Galli-Tsinopoulou A, Xefteri M. Influence of jejunal morphology changes on exocrine pancreatic function in celiac disease. *J Pediatr Gastroenterol Nutr* 1999; **29**: 81-85 [PMID: 10400109 DOI: 10.1097/00005176-199907000-00019]

62 **DiMagno EP**, Go WL, Summerskill WH. Impaired cholecystokinin-pancreozymin secretion, intraluminal dilution, and maldigestion of fat in sprue. *Gastroenterology* 1972; **63**: 25-32 [PMID: 5055745]

63 **Carroccio A**, Iacono G, Montalto G, Cavataio F, Di Marco C, Balsamo V, Notarbartolo A. Exocrine pancreatic function in children with coeliac disease before and after a gluten free diet. *Gut* 1991; **32**: 796-799 [PMID: 1855688 DOI: 10.1136/gut.32.7.796]

64 **Tandon BN**, Banks PA, George PK, Sama SK, Ramachandran K, Gandhi PC. Recovery of exocrine pancreatic function in adult protein-calorie malnutrition. *Gastroenterology* 1970; **58**: 358-362 [PMID: 5437989]

65 **Tandon BN**, George PK, Sama SK, Ramachandran K, Gandhi PC. Exocrine pancreatic function in protein--calorie malnutrition disease of adults. *Am J Clin Nutr* 1969; **22**: 1476-1482 [PMID: 5350763 DOI: 10.1093/ajcn/22.11.1476]

66 **Buchan AM**, Grant S, Brown JC, Freeman HJ. A quantitative study of enteric endocrine cells in celiac sprue. *J Pediatr Gastroenterol Nutr* 1984; **3**: 665-671 [PMID: 6150077 DOI: 10.1097/00005176-198411000-00004]

67 **Shteinberg M**, Haq IJ, Polineni D, Davies JC. Cystic fibrosis. *Lancet* 2021; **397**: 2195-2211 [PMID: 34090606 DOI: 10.1016/S0140-6736(20)32542-3]

68 **Imrei M**, Németh D, Szakács Z, Hegyi P, Kiss S, Alizadeh H, Dembrovszky F, Pázmány P, Bajor J, Párniczky A. Increased Prevalence of Celiac Disease in Patients with Cystic Fibrosis: A Systematic Review and Meta-Analysis. *J Pers Med* 2021; **11** [PMID: 34575636 DOI: 10.3390/jpm11090859]

69 **Singh P**, Arora A, Strand TA, Leffler DA, Catassi C, Green PH, Kelly CP, Ahuja V, Makharia GK. Global Prevalence of Celiac Disease: Systematic Review and Meta-analysis. *Clin Gastroenterol Hepatol* 2018; **16**: 823-836.e2 [PMID: 29551598 DOI: 10.1016/j.cgh.2017.06.037]

70 **Emiralioglu N**, Ademhan Tural D, Hizarcioglu Gulsen H, Ergen YM, Ozsezen B, Sunman B, Saltık Temizel İ, Yalcin E, Dogru D, Ozcelik U, Kiper N. Does cystic fibrosis make susceptible to celiac disease? *Eur J Pediatr* 2021; **180**: 2807-2813 [PMID: 33765186 DOI: 10.1007/s00431-021-04011-4]

71 **Patel BJ**, Cantor M, Retrosi G, Gheorghe R, Wrogemann J, Mujawar Q. Autoimmune Pancreatitis Masquerading as Celiac Disease. *Pancreas* 2019; **48**: e53-e54 [PMID: 31206470 DOI: 10.1097/MPA.0000000000001326]

72 **Masoodi I**, Wani H, Alsayari K, Sulaiman T, Hassan NS, Nazmi Alqutub A, Al Omair A, H Al-Lehibi A. Celiac disease and autoimmune pancreatitis: an uncommon association. A case report. *Eur J Gastroenterol Hepatol* 2011; **23**: 1270-1272

[PMID: 21946127 DOI: 10.1097/MEG.0b013e32834c7bad]

73 **De Marchi G**, Zanoni G, Conti Bellocchi MC, Betti E, Brentegani M, Capelli P, Zuliani V, Frulloni L, Klersy C, Ciccocioppo R. There Is No Association between Coeliac Disease and Autoimmune Pancreatitis. *Nutrients* 2018; **10** [PMID: 30149525 DOI: 10.3390/nu10091157]

74 **Moon SH**, Kim J, Kim MY, Park do H, Song TJ, Kim SA, Lee SS, Seo DW, Lee SK, Kim MH. Sensitization to and Challenge with Gliadin Induce Pancreatitis and Extrapancreatic Inflammation in HLA-DQ8 Mice: An Animal Model of Type 1 Autoimmune Pancreatitis. *Gut Liver* 2016; **10**: 842-850 [PMID: 27114422 DOI: 10.5009/gnl15484]

75 **Cebe KM**, Swanson PE, Upton MP, Westerhoff M. Increased IgG4+ cells in duodenal biopsies are not specific for autoimmune pancreatitis. *Am J Clin Pathol* 2013; **139**: 323-329 [PMID: 23429368 DOI: 10.1309/AJCPT00NHQHXAHDS]

76 **Pinto-Sanchez MI**, Seiler CL, Santesso N, Alaedini A, Semrad C, Lee AR, Bercik P, Lebwohl B, Leffler DA, Kelly CP, Moayyedi P, Green PH, Verdu EF. Association Between Inflammatory Bowel Diseases and Celiac Disease: A Systematic Review and Meta-Analysis. *Gastroenterology* 2020; **159**: 884-903.e31 [PMID: 32416141 DOI: 10.1053/j.gastro.2020.05.016]

World Journal of Gastroenterology

Submit a Manuscript: https://www.f6publishing.com

World J Gastroenterol 2022 June 28; 28(24): 2689-2704

DOI: 10.3748/wjg.v28.i24.2689

ISSN 1007-9327 (print) ISSN 2219-2840 (online)

ORIGINAL ARTICLE

Basic Study

Downregulation of *TNFR2* decreases survival gene expression, promotes apoptosis and affects the cell cycle of gastric cancer cells

Ana Flávia Teixeira Rossi, Fernanda da Silva Manoel-Caetano, Joice Matos Biselli, Ágata Silva Cabral, Marilia de Freitas Calmon Saiki, Marcelo Lima Ribeiro, Ana Elizabete Silva

Specialty type: Gastroenterology and hepatology

Provenance and peer review: Invited article; Externally peer reviewed.

Peer-review model: Single blind

Peer-review report's scientific quality classification

Grade A (Excellent): A, A
Grade B (Very good): 0
Grade C (Good): 0
Grade D (Fair): 0
Grade E (Poor): 0

P-Reviewer: Keikha M, Iran; Tilahun M, Ethiopia

Received: January 15, 2022
Peer-review started: January 15, 2022
First decision: February 7, 2022
Revised: February 21, 2022
Accepted: May 7, 2022
Article in press: May 7, 2022
Published online: June 28, 2022

Ana Flávia Teixeira Rossi, Fernanda da Silva Manoel-Caetano, Joice Matos Biselli, Ágata Silva Cabral, Marilia de Freitas Calmon Saiki, Ana Elizabete Silva, Department of Biological Sciences, Sao Paulo State University (UNESP), São José do Rio Preto 15054-000, São Paulo, Brazil

Marcelo Lima Ribeiro, Clinical Pharmacology and Gastroenterology Unit, São Francisco University (USF), Bragança Paulista 12916-900, São Paulo, Brazil

Corresponding author: Ana Elizabete Silva, PhD, Adjunct Associate Professor, Department of Biological Sciences, Sao Paulo State University (UNESP), Rua Cristóvão Colombo 2265, São José do Rio Preto 15054-000, São Paulo, Brazil. ae.silva@unesp.br

Abstract

BACKGROUND

Chronic inflammation due to *Helicobacter pylori* (*H. pylori*) infection promotes gastric carcinogenesis. Tumour necrosis factor-α (TNF-α), a key mediator of inflammation, induces cell survival or apoptosis by binding to two receptors (TNFR1 and TNFR2). TNFR1 can induce both survival and apoptosis, while TNFR2 results only in cell survival. The dysregulation of these processes may contribute to carcinogenesis.

AIM

To evaluate the effects of TNFR1 and TNFR2 downregulation in AGS cells treated with *H. pylori* extract on the TNF-α pathway.

METHODS

AGS cell lines containing TNFR1 and TNFR2 receptors downregulated by specific shRNAs and nonsilenced AGS cells were treated with *H. pylori* extract for 6 h. Subsequently, quantitative polymerase chain reaction with TaqMan® assays was used for the relative quantification of the mRNAs (*TNFA, TNFR1, TNFR2, TRADD, TRAF2, CFLIP, NFKB1, NFKB2, CASP8, CASP3*) and miRNAs (miR-19a, miR-34a, miR-103a, miR-130a, miR-181c) related to the TNF-α signalling pathway. Flow cytometry was employed for cell cycle analysis and apoptosis assays.

RESULTS

In nonsilenced AGS cells, *H. pylori* extract treatment increased the expression of genes involved in cell survival and inhibited both apoptosis (*NFKB1, NFKB2* and *CFLIP*) and the *TNFR1* receptor. TNFR1 downregulation significantly decreased

the expression of the *TRADD* and *CFLIP* genes, although no change was observed in the cellular process or miRNA expression. In contrast, TNFR2 downregulation decreased the expression of the *TRADD* and *TRAF2* genes, which are both important downstream mediators of the TNFR1-mediated pathway, as well as that of the *NFKB1* and *CFLIP* genes, while upregulating the expression of miR-19a and miR-34a. Consequently, a reduction in the number of cells in the G0/G1 phase and an increase in the number of cells in the S phase were observed, as well as the promotion of early apoptosis.

CONCLUSION

Our findings mainly highlight the important role of TNFR2 in the TNF-α pathway in gastric cancer, indicating that silencing it can reduce the expression of survival and anti-apoptotic genes.

Key Words: Gastric cancer; *Helicobacter pylori*; Tumour necrosis factor-α signalling pathway; *TNFR1*; *TNFR2*; miRNAs

©The Author(s) 2022. Published by Baishideng Publishing Group Inc. All rights reserved.

Core Tip: This study demonstrated for the first time the effect of TNFR1 and TNFR2 downregulation on an AGS cell line treated with *Helicobacter pylori* extract. Although TNFR1 downregulation did not promote significant changes in the expression of mRNA and miRNAs of the tumour necrosis factor-α (TNF-α) signalling pathway, TNFR2 downregulation promoted important changes in the signalling mediators evaluated. We observed a reduction in the expression of cell survival and anti-apoptotic genes and an increase in the expression of miR-19a and miR-34a, which affected cell cycle kinetics and contributed to early apoptosis. Thus, our findings highlight the important role of TNFR2 in the TNF-α signalling pathway in gastric carcinogenesis.

Citation: Rossi AFT, da Silva Manoel-Caetano F, Biselli JM, Cabral ÁS, Saiki MFC, Ribeiro ML, Silva AE. Downregulation of *TNFR2* decreases survival gene expression, promotes apoptosis and affects the cell cycle of gastric cancer cells. *World J Gastroenterol* 2022; 28(24): 2689-2704

URL: https://www.wjgnet.com/1007-9327/full/v28/i24/2689.htm

DOI: https://dx.doi.org/10.3748/wjg.v28.i24.2689

INTRODUCTION

Gastric cancer (GC) has high rates of incidence and mortality worldwide, especially in Eastern Asia, Eastern Europe and Latin America[1]. In Brazil, it is the fourth most common cancer in men and the sixth most common in women[2]. *Helicobacter pylori* (*H. pylori*) is the main risk factor for the development of gastric neoplasms, since it is responsible for chronic inflammation in the gastric mucosa and for the GC progression cascade[3]. Consequently, it can trigger the host's immune response, which leads to changes in the expression of genes related to inflammation, cell kinetic regulation and miRNAs [4-6]. After infection by this bacterium, tumour necrosis factor-α (TNF-α) stands out among the mediators of inflammation and is considered to be a key mediator linking inflammation and cancer[7,8].

TNF-α is a pleiotropic proinflammatory cytokine that is important in the signalling and regulation of multiple cellular responses and processes, such as the production of other inflammatory cytokines, and cell communication, survival, proliferation and apoptosis[9]. These different functions are accomplished due to the ability of TNF-α to bind to TNFR1 (TNFRSF1A) or TNFR2 (TNFRSF1B) receptors, thus resulting in different cellular processes. Both receptors are transmembrane proteins, and although they are largely similar in terms of extracellular structure, their intracellular domains are different, and thus dictate the cellular fate for either survival or death. Though only TNFR1 has a death domain, the TNF-α signalling pathway triggered by this receptor is able to induce both cell survival and apoptosis, while TNFR2 results only in cell survival[10,11]. The signalling cascade after TNF-α/TNFR1 binding that results in cell survival starts with the recruitment of TRADD and is mediated by activation of nuclear factor-kappaB (NF-κB) and transcription of pro-survival and anti-apoptotic genes, such as cellular inhibitor of apoptosis proteins (cIAP), TRAF2 and cFLIP, and of inflammatory cytokines. However, this signal complex is transient; TNF-α rapidly dissociates from TNFR1 and binds to the Fas-associated death domain protein to form another signal complex, which coordinates downstream signalling of the caspase cascade and apoptosis. Conversely, as TNFR2 does not have a death domain, it induces long-lasting NF-kB activation by recruiting existing cytoplasmic TRAF-2/cIAP-1/cIAP-2 complexes that can inhibit pro-apoptotic factors and maintain cell survival and proliferation[9-12].

Regulation of signal transduction triggered by TNF-α requires a constant balance between the opposing functions of cell survival and cell death to maintain homeostasis. Thus, an imbalance in these processes due to changes in the expression of receptors, downstream genes, ligands and pro-/anti-apoptotic mediators may support the tumorigenic process[13]. A recent study by our research group showed dysregulation in the TNF-α signalling pathway in GC samples with an upregulation of cell survival-related genes and of TNFR2 expression, thus suggesting a prominent protumor role by TNA-α /TNFR2 binding in gastric neoplasm[14]. Furthermore, we showed through a miRNA:mRNA interaction network that this signalling pathway can be regulated by miRNAs. In addition, *H. pylori* infection was also associated with an increased expression of *TNF-α* mRNA and protein, and dysregulated miRNA expression in chronic gastritis patients. The expression pattern of these genes/miRNAs was normalized after treatment to eradicate bacteria, indicating that this pathogen influences the host's inflammatory response in part by its action on miRNAs[6].

In accordance with our previous results, we thought it was important to evaluate the effect of silencing TNFR1 and TNFR2 receptors in an AGS gastric cell line after treatment with an *H. pylori* extract on *TNF-α* mRNA expression and on downstream genes related to its signalling pathway (*TRADD, TRAF2, CFLIP, NFKB1, NFKB2, CASP8* and *CASP3)*. In addition, we also investigated the same miRNAs previously studied (miR-19a, miR-34a, miR-103a, miR-130a and miR-181c)[14], as well as the cell cycle and apoptosis. Overall, our results highlight the main role of the TNFR2 in TNF-α signalling in an AGS cell line, while treatment with *H. pylori* extract induces prosurvival gene expression mainly through TNFR1.

MATERIALS AND METHODS

Cell culture

AGS GC cells from the Cell Bank of Rio de Janeiro, Brazil (BCRJ code 0311) were incubated at 37 °C and 5% CO_2 in HAM-F10 medium (Cultilab, SP, Brazil) supplemented with 10% foetal bovine serum and 1× antibiotic/antimycotic (Gibco, Invitrogen Life Technologies, Carlsbad, CA, United States). The culture medium was replaced every two to three days. The HGC-27 GC cell line, provided by Dr Marcelo Lima Ribeiro (São Francisco University-USF, SP, Brazil), was also used in early experiments as an alternative line for follow-up experiments, and 293T cells of human embryonic kidney were provided by Dr Luisa Lina Villa (University of São Paulo–USP, SP, Brazil) for transfection experiments. The cells were maintained under the same conditions as the AGS cell line except for the culture medium, which was Dulbecco's modified Eagle medium (Gibco, Invitrogen Life Technologies, Carlsbad, CA, United States). Stable shRNA-expressing cell lines with reduced expression of TNFR1 (called shTNFR1) and TNFR2 (called shTNFR2) were kept in a similar culture medium to the nonsilenced AGS cells, and further supplemented with 0.5 μg/mL puromycin or 200 μg/mL G418, respectively.

Treatment with H. pylori extract

The previously described *H. pylori* Tox+ strain (cagA+/vacA s1m1) was grown in a selective medium (pylori-Gelose; BioMérieux, Marcy-l'Étoile, France) at 37 °C under microaerophilic conditions[15]. This strain is not resistant to any antibiotic used to treat *H. pylori*. *H. pylori* extract was prepared according to the protocol described by Li *et al*[16]. In brief, the *H. pylori* Tox+ strain was harvested and suspended in distilled water at a concentration of 2 × 10^8 CFU/mL. Next, the suspension was incubated at room temperature for 40 min and centrifuged at 20000 *g* for 20 min. The supernatant was filtered using a 0.2 mm filter and stored at -20 °C until use. The extract was tested several times (4, 6 and 24 h) using differing *H. pylori* extract volumes (50, 100, 150 and 200 μL) to verify the best experimental conditions. Then, 2 × 10^5 nonsilenced AGS cells and AGS cells with downregulation of TNFR1 (shTNFR1) and TNFR2 (shTNFR2) were seeded in 12-well plates. After 48 h, the medium was replaced with 500 μL of HAM-F10 containing 30% v/v *H. pylori* extract or the same proportion of water (control). Cells were incubated with *H. pylori* extract for 6 h in an incubator at 37 °C. For all experiments, three temporally independent events were performed.

Cell viability assay

MTT ([3-(4,5-dimethylthiazol-2-yl)-2,5-diphenyltetrazolium bromide]) assays (Sigma–Aldrich, St. Louis, MO, United States) were employed to evaluate the viability of silenced and nonsilenced AGS cells after different treatment conditions with *H. pylori* extract (times and *H. pylori* extract volumes). In summary, the culture medium was removed, and 300 μL of fresh medium containing 1 mg/mL MTT reagent was added to each well. After 30 min of incubation at 37 °C, the medium with MTT reagent was replaced by the same volume of dimethyl sulfoxide (DMSO) (Sigma–Aldrich, St. Louis, MO, United States). The absorbance at 540 nm was measured using a FLUOstar Omega spectrophotometer (BMG Labtech, Ortenberg, Germany).

Transfection with shRNA

MISSION® Lentiviral Transduction Particles (Cat. SHCLNV, Sigma–Aldrich, St. Louis, MO, United States) were used to integrate shRNA into the genome of AGS cells to knockdown TNFR1 and TNFR2 expression. Verified viral vectors were purchased from Sigma–Aldrich, and the standard manufacturer's protocol was followed to generate the cell line. Stably transfected clones were selected by growing the cells in the presence of puromycin or G418, which acted as selection pressure (for TNFR1: 1 μg/mL puromycin and for TNFR2: 400 μg/mL G418). Different plasmids containing shRNAs were used to generate clones, of which the one showing the best knockdown efficiency was used for all experiments. The sequence of the shRNA in the construct was CTTGAAGGAACTACTACTAAG for *TNFR1* and GCCGGCTCAGAGAATACTATG for *TNFR2*. TNFR1 and TNFR2 levels were assessed by quantitative polymerase chain reaction (PCR) and Western blotting to verify the knockdown. Similar transfections were carried out with an empty vector (Sigma–Aldrich, St. Louis, MO, United States), which served as the transfection control.

Western blot analysis

Protein extraction was performed by lysis of nonsilenced AGS cells and AGS cells containing a shRNA or an empty vector with CelLytic™ MT Cell Lysis Reagent (Sigma–Aldrich, St. Louis, MO, United States). The lysis reaction was centrifuged at 12000 *g* for 10 min after a 15 min incubation. The protein concentration was determined using a Pierce™ BCA Protein Assay kit (Thermo Scientific, Massachusetts, United States) according to the manufacturer's protocol. Thirty micrograms of protein was separated on an 8%-12% sodium dodecyl sulphate-polyacrylamide gel by electrophoresis (120 min) and then transferred to PVDF or nitrocellulose membranes (MilliPore Corporation, Burlington, Massachusetts, EUA) using an Electrotransfer TE70XP system (Hoefer) for 80 min. Membranes were blocked with 5% nonfat dry milk for 60 min and were then incubated overnight at 4 °C with the following primary antibodies: Anti-TNFR1 (dilution 1:500) (Cell Signalling, Massachusetts, United States), anti-TNFR2 (dilution 1:5000) (Abcam Cambridge, United Kingdom) and anti-GAPDH (dilution 1:30000) (Abcam, Cambridge, United Kingdom). After being washed, the membranes were incubated at room temperature under stirring with horseradish peroxidase-conjugated goat anti-rabbit (dilution 1:2000) secondary antibodies (Abcam, Cambridge, United Kingdom). Bands were revealed by enhanced chemiluminescence, visualized in a ChemiDoc™ Imaging System (BioRad, Hercules, California, United States) and quantified using Image Lab 6.0 Software (BioRad, Hercules, California, United States).

Quantification of mRNA and miRNA expression by RT–qPCR

After 6 h of incubation, the medium containing *H. pylori* extract or water was removed, and total RNA was extracted from AGS cells with a miRNeasy Micro Kit (Qiagen, Valencia, CA, United States) according to the manufacturer's protocol. Complementary DNA (cDNA) for mRNA and miRNA was synthesized using a High-Capacity cDNA Archive Kit (Applied Biosystems, Foster City, CA, United States) and a TaqMan® MicroRNA Reverse Transcription Kit (Applied Biosystems, Foster City, CA, United States), respectively. Quantitative PCR (qPCR) was performed with TaqMan® assays (Applied Biosystems, California, United States) for the genes *TNFA* (Hs01113624_g1), *TNFR1* (*TNFRSF1A*) (Hs01042313_m1), *TNFR2* (*TNFRSF1B*) (Hs00961749_m1), *TRADD* (Hs00182558_m1), *TRAF2* (Hs00184192_m1), *CFLIP* (*CFLAR*) (Hs00153439_m1), *NFKB1* (Hs 00765730_m1), *NFKB2* (Hs01028901_g1), *CASP8* (Hs01116281_m1) and *CASP3* (Hs00234387_m1) and for the target miRNAs hsa-miR-19a-3p (MIMAT0000073; ID 000395), hsa-miR-34a-3p (MIMAT0004557; ID 002316), hsa-miR-103a-3p (MIMAT0000101; ID 000439), hsa-miR-130a-3p (MIMAT0000425; ID 000454) and hsa-miR-181c-5p (MIMAT0000258; ID 000482) (Applied Biosystems, California, United States), as described in our previous study[14]. *ACTB* (Catalogue#: 4352935E) and *GAPDH* (Catalogue#: 4352934E) genes were used for normalization of mRNA quantification, while endogenous RNU6B (ID 001093) and RNU48 (ID 001006) levels were used for miRNAs. All reactions were performed in triplicate. Relative quantification (RQ) of mRNA and miRNA expression was calculated by the $2^{(-\Delta\Delta Ct)}$ method[17], and nonsilenced AGS without *H. pylori* extract treatment was used as a calibrator (AGS-C). RQ values are expressed as the mean ± SD of gene and miRNA expression for all experimental groups in relation to nonsilenced and untreated AGS, with RQ = 1.

Cell cycle analysis

The cell distribution at different phases of the cell cycle was estimated by measuring the cellular DNA content using flow cytometry. After incubation with *H. pylori* extract or water, nonsilenced AGS, shTNFR1 and shTNFR2 cell lines were harvested with trypsin and fixed in 70% ethanol at 4 °C for at least 24 h. Subsequently, the cells were washed, centrifuged and incubated with 200 μL of Guava® Cell Cycle Reagent (Merck Millipore, Burlington, Massachusetts, United States) for 30 min in the dark. Cell cycle distribution was measured by a Guava® EasyCyte Flow Cytometer and analysed with Guava® InCyte software (Merck Millipore, Burlington, Massachusetts, United States).

Apoptosis analysis

Apoptotic cell death was also measured by flow cytometry using a fluorescein isothiocyanate (FITC)

Annexin V Apoptosis Detection Kit (BD Pharmingen™; BD Biosciences, Franklin Lakes, NJ, United States) according to the modified manufacturer's protocol. After treatment, adherent cells were harvested with Accutase® (Sigma–Aldrich, St. Louis, MO, United States) since this solution avoids membrane damage[18]. After this step, the cells were washed with cold phosphate-buffered saline, centrifuged, resuspended in 1× binding buffer and stained with 5 μL of Annexin V-FITC and 5 μL of propidium iodide (PI, 50 μg/mL) for 15 min at room temperature in the dark. The labelling of cells was evaluated using a flow cytometer and was analysed with Guava® InCyte software. From the scatter diagram and quadrant plotting, the results are presented as follows: Living cells (FITC-/PI-) located in the lower left quadrant, early apoptotic cells (FITC+/PI-) in the lower right quadrant and late apoptotic cells (FITC+/PI+) in the upper right quadrant.

Statistical analysis

Statistical analysis of the data was performed in GraphPad Prism Software version 6.01 using two-way ANOVA with Bonferroni post hoc test. The results are expressed as the mean ± SD from three experiments conducted independently. A $P < 0.05$ was considered statistically significant.

RESULTS

The AGS cell line treated with H. pylori extract expresses TNFA, TNFR1, and TNFR2 receptors

Initially, both AGS and HGC-27 cell lines were cultured to evaluate the mRNA expression levels of *TNFA, TNFR1* and *TNFR2* receptors by qPCR. The analyses showed that both cell lines expressed *TNFA* and *TNFR1,* but *TNFR2* was expressed at lower levels in HGC-27 cells than it was in AGS cells (Supplementary Figure 1). The AGS cell line was chosen for additional experiments since it was not reasonable to use HGC-27 in the TNFR2 silencing experiments.

To standardize treatment conditions, several volumes of *H. pylori* extract (50, 100, 150 and 200 μL) were tested at different incubation times (4, 6 and 24 h) in the AGS cell line to establish the best conditions for inducing *TNFA* expression without reducing cell viability. The best results were obtained with an *H. pylori* extract concentration of 30% v/v (150 μL) at 6 h of incubation (Supplementary Figures 2 and 3). Under these conditions, there was an increase in *TNFA* expression (RQ = 3.59) without an impact on cell viability (98.9%).

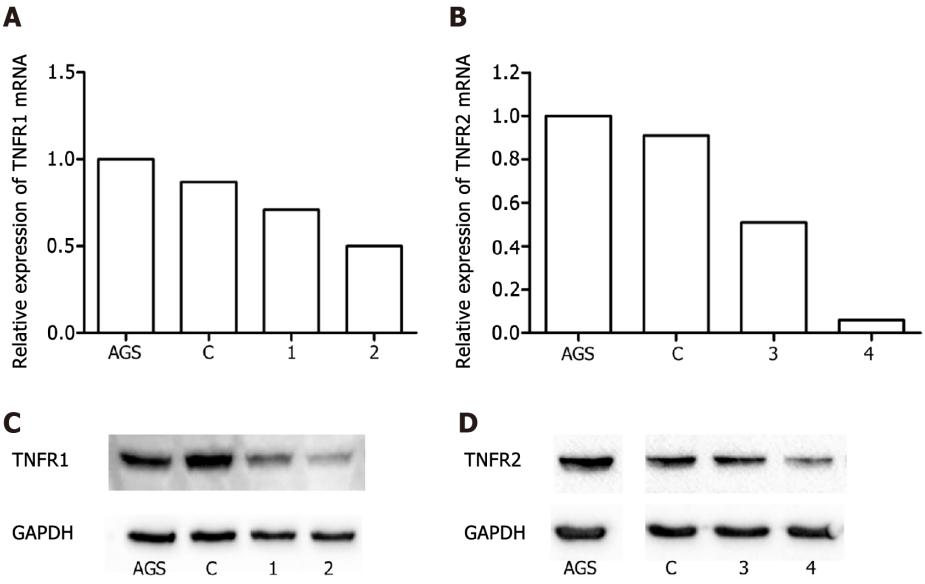
The effect of TNFR1 and TNFR2 downregulation and treatment with H. pylori extract on TNF-α signalling downstream gene expression

The effect of TNFR1 and TNFR2 downregulation on GC cells was evaluated after transfection of the AGS cell line with two specific shRNAs targeting the genes, *TNFR1* (called shTNFR1) and *TNFR2* (called shTNFR2), followed by antibiotic selection. RT–qPCR and Western blotting were used to evaluate the efficiency of silencing. Stable lines with the shRNAs exhibited a 59% reduction in TNFR1 and a 63% reduction in TNFR2 protein expression (Figure 1).

Initially, we evaluated the effect of treatment with *H. pylori* extract on the expression of genes of the TNF-α signalling pathway in nonsilenced AGS cells. After *H. pylori* extract treatment (AGS-*H. pylori* extract), nonsilenced AGS cells showed significantly upregulated mRNA expression of *TNFR1* and of anti-apoptotic and cell proliferation genes, such as *CFLIP, NFKB1* and *NFKB2* (Supplementary Figure 4A), compared to the control (AGS-C). In addition, *H. pylori* extract treatment increased the mRNA expression of *NFKB1* and *NFKB2* in a TNFR1-downregulated cell line (shTNFR1-*H. pylori* extract), whereas the expression of *TNFR2* and *TRADD* was reduced (Supplementary Figure 4B). On the other hand, the expression of the evaluated genes was not significantly changed by *H. pylori* extract treatment in the shTNFR2 cell line (Supplementary Figure 4C).

With regard to the influence of *TNFR1* and *TNFR2* downregulation on the expression of TNF-α signalling genes (Figure 2), a significantly downregulated mRNA expression of *TNFR1* (RQ = 0.83 and 1.03, respectively), *TRADD* (RQ = 0.60 and 0.41, respectively) and *CFLIP* (RQ = 1.25 and 1.36, respectively) was observed in shTNFR1-*H. pylori* extract and shTNFR2-*H. pylori* extract cells compared to that in AGS-*H. pylori* extract cells (RQ = 1.73, 0.98 and 2.09, respectively) (Figure 2B, D and F). Furthermore, *TNFR2* (RQ = 0.27, $P < 0.05$), *TRAF2* (RQ = 0.68, $P < 0.05$) and *NFKB1* (RQ = 1.67, $P < 0.05$) were reduced in shTNFR2-*H. pylori* extract cells compared to AGS-*H. pylori* extract cells (RQ = 0.86, 1.29 and 2.39, respectively) (Figure 2C, E and I). When we compared the nonsilenced and silenced AGS cell lines without *H. pylori* extract treatment (control-C), *TNFR2* mRNA expression was increased in shTNFR1-C (RQ = 1.49) compared to AGS-C (RQ = 1.00) and reduced in shTNFR2-C (RQ = 0.50) compared to shTNFR1-C and AGS-C. Likewise, *TRADD* mRNA expression was downregulated in shTNFR2-C (RQ = 0.35) compared to the other control groups (AGS-C and shTNFR1-C). There was no significant change in *TNFA, CASP3, CASP8* and *NFKB2* mRNA expression.

In general, the downregulation of TNFR1 and TNFR2 significantly influenced the mRNA expression of *TRADD* ($P < 0.001$) and *TRAF2* ($P < 0.01$), whereas the expression of *TNFR1, TNFR2* and *CFLIP* was also affected by treatment with *H. pylori* extract ($P < 0.01$ for all). In contrast, only the *H. pylori* extract



DOI: 10.3748/wjg.v28.i24.2689 **Copyright** ©The Author(s) 2022.

Figure 1 The efficiency of *TNFR1* and *TNFR2* expression silencing in AGS cells. A and B: Expression levels of *TNFR1* and *TNFR2* mRNA evaluated by real-time reverse transcription-quantitative polymerase chain reaction; C and D: Protein expression of *TNFR1* and *TNFR2* evaluated by Western blotting. Downregulation of *TNFR1* (A-C) and *TNFR2* (B-D) was confirmed by the reduction in the expression of receptors *TNFR1* and *TNFR2* following treatment with shRNAs 2 and 4, respectively. AGS: Nonsilenced cell line; C: Control transfected with empty vector; 1 and 2: Different shRNA clones for *TNFR1*; 3 and 4: Different shRNA clones for *TNFR2*.

treatment contributed to the differences observed in *NFKB1* and *NFKB2* mRNA expression ($P < 0.001$ for both).

TNFR2 downregulation upregulates miR-19a and miR-34a expression

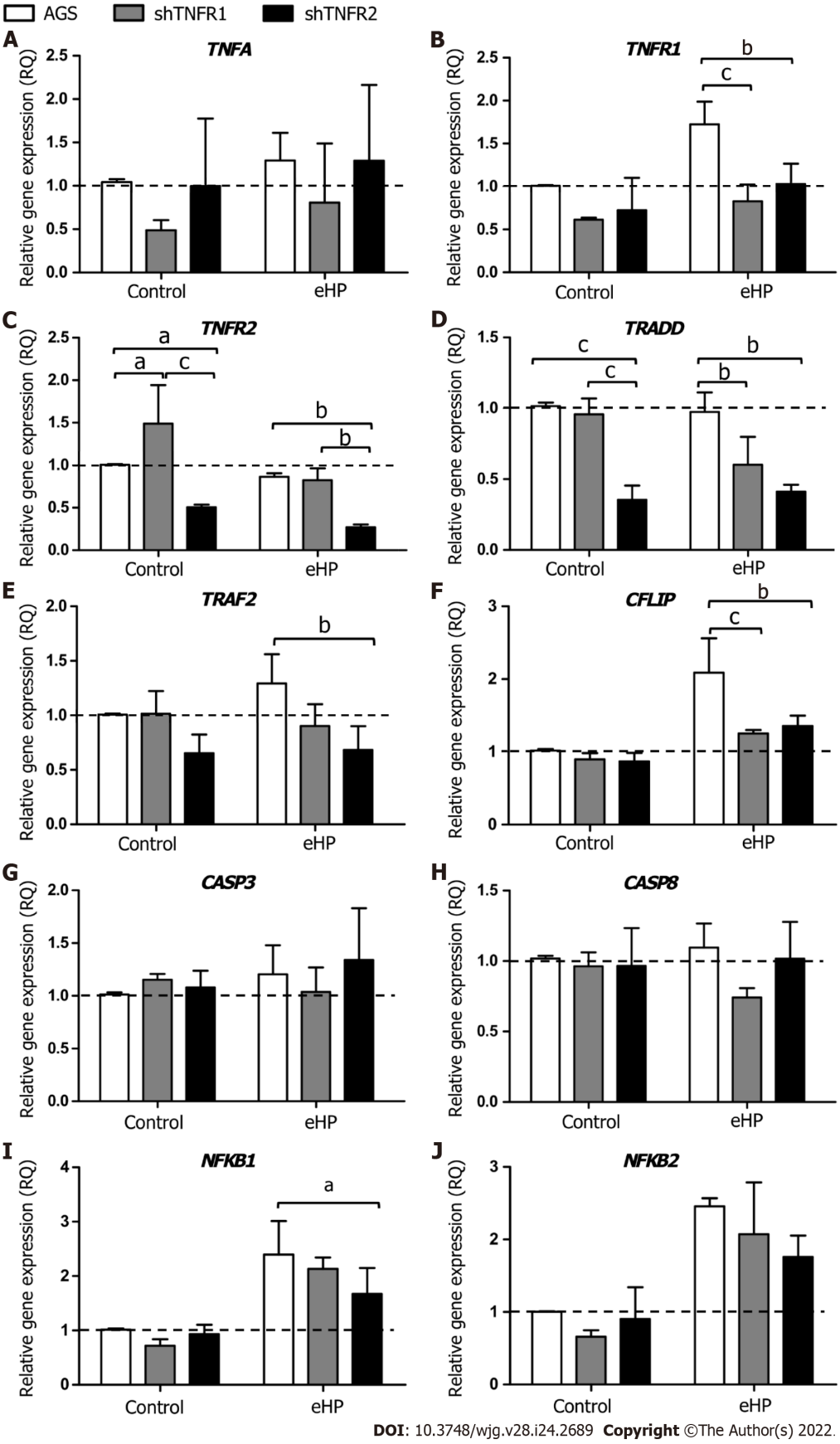
The expression of miRNAs miR-19a, miR-34a, miR-103a, miR-130a and miR-181c was evaluated in the AGS, shTNFR1 and shTNFR2 cell lines with and without *H. pylori* extract treatment (Figure 3 and Supplementary Figure 5). No significant change in the expression of these miRNAs was found in AGS and shTNFR1 cells regardless of *H. pylori* extract treatment. However, TNFR2 receptor downregulation resulted in a significant increase in the expression of miR-19a and miR-34a in shTNFR2-C cells (RQ = 3.70 and 2.64, respectively) compared with that of the AGS-C ($P < 0.01$ and $P < 0.001$, respectively) and shTNFR1-C cells ($P < 0.05$ and $P < 0.001$, respectively) cells and in shTNFR2-*H. pylori* extract cells (RQ = 3.89 and 1.69, respectively) compared to AGS-*H. pylori* extract ($P < 0.01$ and $P < 0.05$, respectively) and shTNFR1-*H. pylori* extract cells ($P < 0.01$ and $P < 0.01$, respectively) (Figure 3A and B).

TNFR2 downregulation promotes a reduction in G0/G1 phases and an increase in S phase

The effect of TNFR1 and TNFR2 downregulation after *H. pylori* extract treatment on cell cycle progression was evaluated by flow cytometry. Overall, *H. pylori* extract treatment did not affect the cellular distribution in the G0/G1, S and G2/M phases in nonsilenced AGS, shTNFR1 and shTNFR2 cells (Supplementary Figure 6). However, TNFR2 downregulation significantly reduced the number of cells in G0/G1 phase regardless of *H. pylori* extract treatment and led to an increase in the number of cells in S and G2/M phases in shTNFR2-C cells compared to that of the AGS-C cells (Figure 4).

Downregulation of TNFR2 promotes early apoptosis

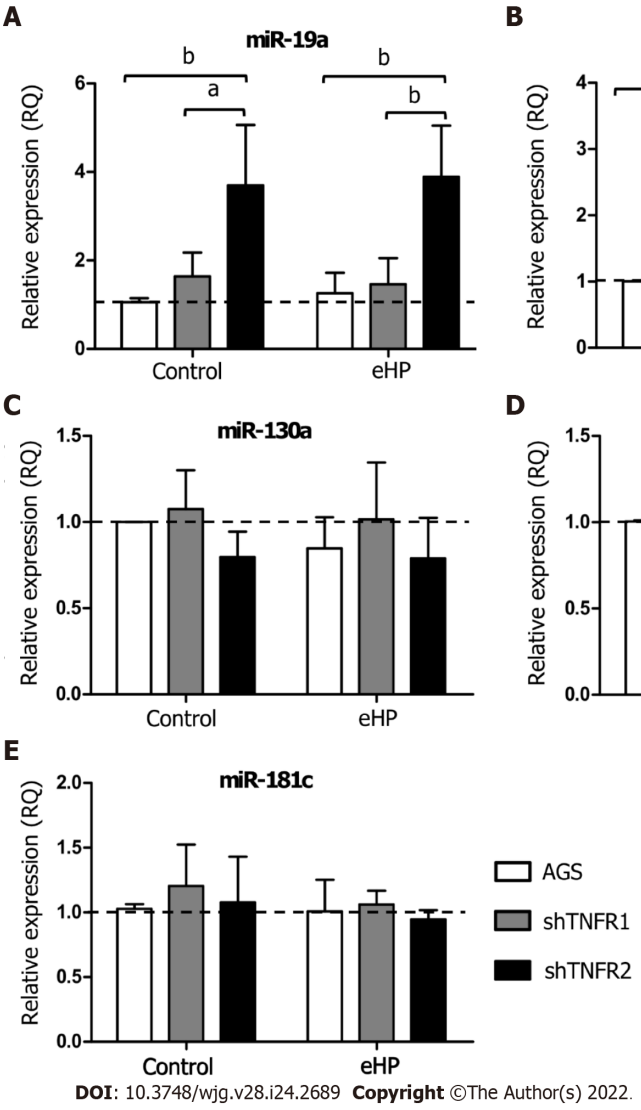
In addition, we also investigated the effect of partial TNFR1 and TNFR2 inhibition and *H. pylori* extract treatment on apoptosis, which was evaluated through Annexin-V and PI double staining by flow cytometry. Treatment with *H. pylori* extract did not induce changes in the rates of early and late apoptosis in the nonsilenced AGS and both silenced AGS cell lines compared to the respective untreated cell lines (Supplementary Figure 7). However, after *H. pylori* extract treatment, the percentage of early apoptotic cells was significantly higher in shTNFR2 cells (1.27%) than in AGS (0.56%) and shTNFR1 cells (0.52%), whereas the percentage of late apoptotic cells was significantly reduced after *H. pylori* extract treatment (Figure 5). Together with the cell cycle results, these data indicate a relationship between decreased cell quantity in the G0/G1 phase and increased early apoptosis as a result of TNFR2 downregulation.



DOI: 10.3748/wjg.v28.i24.2689 **Copyright** ©The Author(s) 2022.

Figure 2 Relative expression of tumour necrosis factor-α signalling pathway genes. Expression levels of *TNFA*, *TNFR1*, *TNFR2*, *TRADD*, *TRAF2*, *CFLIP*, *CASP8*, *CASP3*, *NFKB1* and *NFKB2* mRNA in nonsilenced AGS, AGS with TNFR1 downregulation (shTNFR1), and AGS with TNFR2 downregulation (shTNFR2) either not treated (control) or treated with a *Helicobacter pylori* extract. A: *TNFA*; B: *TNFR1*; C: *TNFR2*; D: *TRADD*; E: *TRAF2*; F: *CFLIP*; G: *CASP8*; H: *CASP3*; I: *NFKB1*; J: *NFKB2*. Bars represent the mean ± SD from three independent trials. The dotted line indicates relative quantification: RQ = 1.0. Statistically

significant difference: $^{a}P < 0.05$; $^{b}P < 0.01$; $^{c}P < 0.001$. eHP: *Helicobacter pylori* extract.



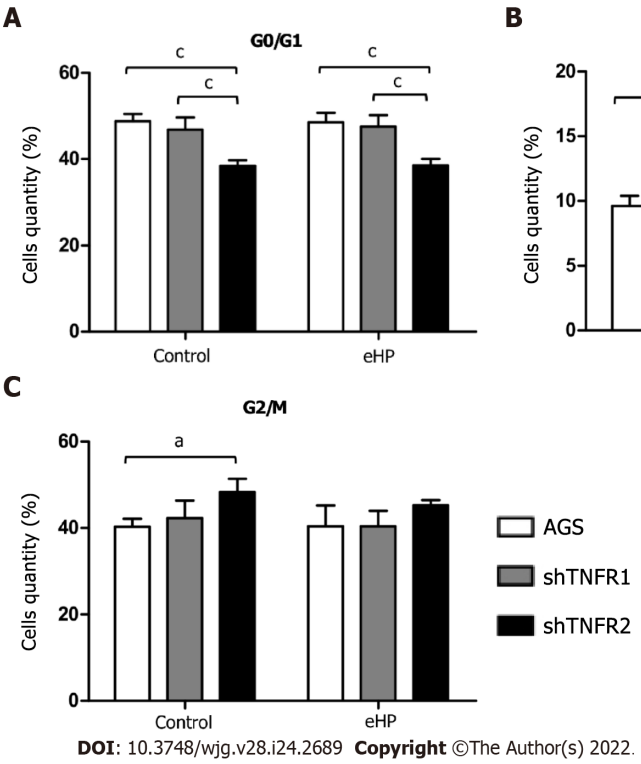
DOI: 10.3748/wjg.v28.i24.2689 **Copyright** ©The Author(s) 2022.

Figure 3 Relative expression of miRNAs related to the tumour necrosis factor-α pathway. Expression levels of miR-19a, miR-34a, miR-103a, miR-130a and miR-181c in nonsilenced AGS, AGS with TNFR1 downregulation (shTNFR1), and AGS with TNFR2 downregulation (shTNFR2) either not treated (control) or treated with the *Helicobacter pylori* extract. A: miR-19a; B: miR-34a; C: miR-103a; D: miR-130a; E: miR-181c. Bars represent the mean ± SD from three independent trials. The dotted line indicates relative quantification: RQ = 1.0. Statistically significant difference: $^{a}P < 0.05$; $^{b}P < 0.01$; $^{c}P < 0.001$. eHP: *Helicobacter pylori* extract.

DISCUSSION

TNFR1 and TNFR2 differ in their intracellular domains and cellular expression; thus, the role of each receptor in the TNF-α-triggered signalling pathway varies according to the pathological condition, activating different cellular processes, such as cell survival and apoptosis[10]. This is the first study to investigate the effect of TNFR1 and TNFR2 downregulation on AGS cells treated with *H. pylori* extract. Our results show that *H. pylori* extract treatment of nonsilenced AGS cells upregulated the mRNA expression of proliferation (*NFKB1* and *NFKB2*) and antiapoptotic genes (*CFLIP*) by activating TNFR1. TNFR1 downregulation did not promote extensive changes in the expression of genes or miRNAs involved in the TNF-α signalling pathway or in cellular processes. In contrast, TNFR2 downregulation significantly decreased *TRADD* and *TRAF2* mRNA expression, which may impair TNFR1-mediated TNF-α signalling, and increased miRNA expression, which promoted a block in the G_1/S transition and an increase in early apoptosis.

H. pylori infection can deregulate the expression of several genes and miRNAs, as previously shown by our research group[6]. Recently, increased mRNA levels of *TNFA* and other proinflammatory mediators, such as interleukin (IL)-1β and IL-8, have been reported in an AGS cell line after infection by



DOI: 10.3748/wjg.v28.i24.2689 **Copyright** ©The Author(s) 2022.

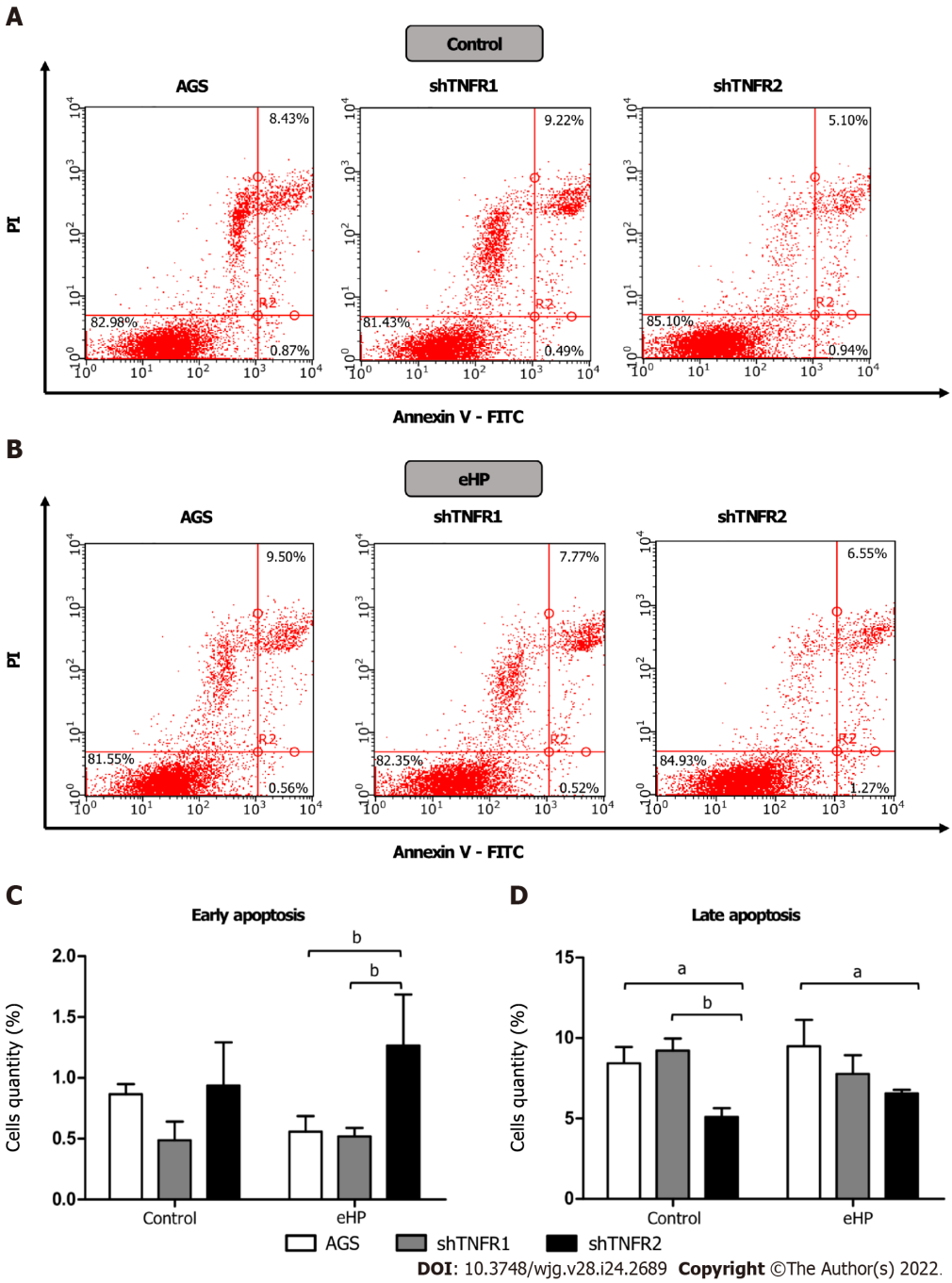
Figure 4 Cell cycle distribution analysis. Number of cells in the G0/G1, S and G2/M phases of the cell cycle in nonsilenced AGS cells, cells with TNFR1 downregulated (shTNFR1), and cells with TNFR2 downregulated (shTNFR2) without additional treatment (control) and those treated with the *Helicobacter pylori* extract. A: G0/G1; B: S; C: G2/M. Bars represent the mean ± SD from three independent trials. Statistically significant difference: $^{a}P < 0.05$; $^{b}P < 0.01$; $^{c}P < 0.001$. eHP: *Helicobacter pylori* extract.

H. pylori[19]. Our results show high *TNFR1* mRNA expression after *H. pylori* extract treatment in nonsilenced AGS cells, suggesting that *H. pylori* infection promotes activation of the TNFR1-mediated TNF-α signalling pathway in AGS cells, directing signal transduction to the cell survival pathway due to the increased expression of *NFKB1, NFKB2* and *CFLIP* (Figure 6A). In agreement with this finding, previous studies showed that *H. pylori* activates NF-κB in a manner dependent on the bacterial cell number[20] due to significant IκB-α degradation[21], resulting in the induction of anti-apoptotic gene transcription, such as *CFLIP* transcription[22]. Therefore, our results indicate that *H. pylori* extract also induces cell survival and inflammation due to TNFR1-mediated TNF-α signalling, which leads to NF-κB activation and the consequent production of antiapoptotic mediators, such as cFLIP.

TNFR1 downregulation resulted in a significant increase in *TNFR2* mRNA expression in nontreated AGS cells, while a decrease in the expression of T*RADD* and *CFLIP* mRNA was observed in cells treated with *H. pylori* extract, although no change was observed in apoptosis and cell cycle assays (Figure 6B). In oesophageal carcinoma cells treated with TNFR1-siRNA, Changhui *et al*[23] demonstrated an increase in cell proliferation and a reduction in apoptosis rate after 24 h of transfection, and the cell proliferation level was time-dependent[19]. The present study, when evaluated together with the results of *H. pylori* extract, suggests that the assays of cellular processes after 6 h of treatment may have been insufficient in shTNFR1 and nonsilenced AGS cells. Wan *et al*[24] showed that AGS cell coculture with *H. pylori* inhibited apoptosis and increased viability through upregulation of TRAF1, which was triggered by NF-κB activation. However, the peak of TRAF1 expression occurred after 12 h of infection, and its effect on cell viability started only after 24 h. Therefore, the role of TNFR1 downregulation in GC cell lines still needs to be further investigated.

Conversely, the downregulation of TNFR2 expression significantly decreased the expression of two important mediators of the TNFR1-mediated signalling pathway, TRAF2 and TRADD, in addition to *NFKB*1, *CFLIP* and *TNFR1* expression. Moreover, there was an increase in early apoptosis, with concomitant G1/S transition phase arrest (Figure 6C). These results agree with those previously reported by our group in GC patient samples, in which we found upregulation of *TNF/TNFR2* and cellular survival genes such as *TRAF2*, *CFLIP*, and *NFKB2* and downregulation of *TNFR1* and *CASP3* [14], thus emphasizing the important role of TNFR2 in gastric carcinogenesis and TNFR2 silencing as a promising strategy for anticancer therapy[25].

TRADD is an essential adaptor protein that functions in TNFR1-mediated apoptotic signalling under physiological conditions[26]. However, the dependence of this mediator seems to be cell-type specific [27], as TRADD knockout mice were resistant to TNFR1-induced toxicity in a hepatitis model[28]. However, this pathway was not completely impaired in macrophages deprived of TRADD[27].

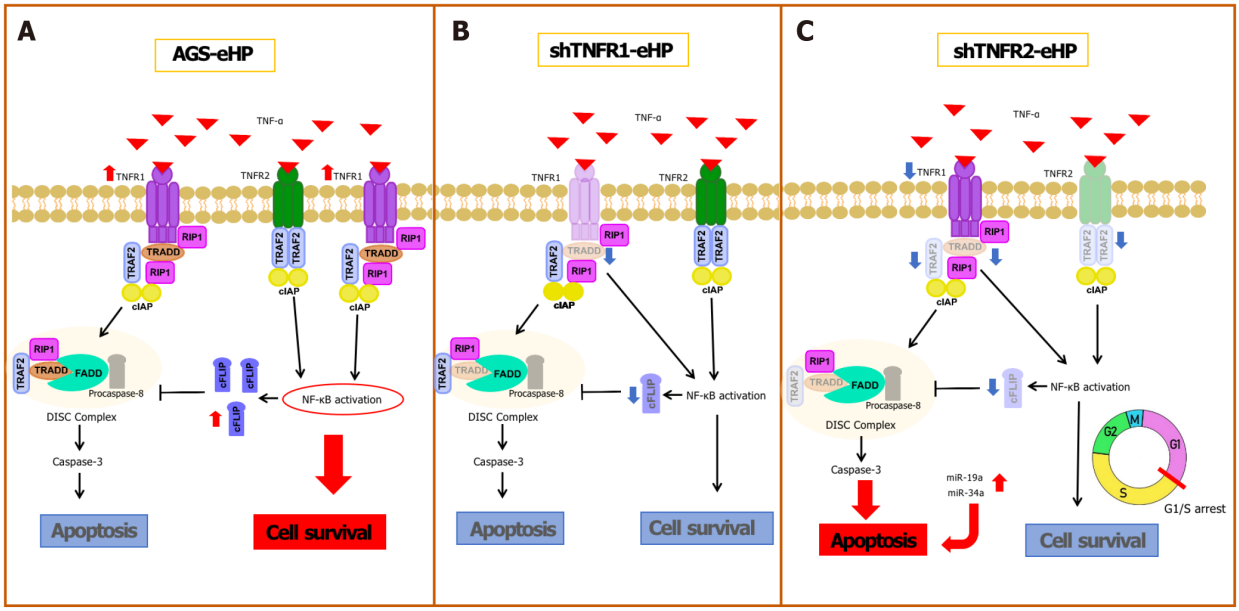


DOI: 10.3748/wjg.v28.i24.2689 **Copyright** ©The Author(s) 2022.

Figure 5 Apoptosis distribution analysis in nonsilenced AGS cells, cells with TNFR1 downregulated (shTNFR1), and cells with TNFR2 downregulated (shTNFR2). A: Cells without additional treatment (control); B: Cells treated with the *Helicobacter pylori* extract; A and B: Representative images of the cell distribution and percentage in the different quadrants indicating viable cells (Annexin V-/PI-) in the lower left, early apoptotic cells (Annexin V+/PI-) in the lower right and late apoptotic cells (Annexin V+/PI+) in the upper right; C and D: Histogram bars represent the mean ± SD from three independent trials for early (C) and late (D) apoptosis. Statistically significant difference: $^{a}P < 0.05$; $^{b}P < 0.01$. eHP: *Helicobacter pylori* extract.

Therefore, apoptosis can occur even with reduced expression of TRADD, as observed in the present study after TNFR2 downregulation. In turn, TRADD inhibition reduces NF-κB activation[12], impairing the transcription of anti-apoptotic genes, such as *TRAF2* and *CFLIP*, as observed in this study.

As mentioned, shTNFR2 cells also exhibited reduced expression of TRAF2. This protein has an essential role in signal transduction and is triggered by both TNFR1 and TNFR2, suggesting the existence of crosstalk between them[29], which influences the signalling outcome after TNF binding [30]. TRAF2 recruits cIAP1 and cIAP2 after interaction with these receptors, thereby triggering nuclear translocation of NF-κB[30]. Therefore, TRAF2 is a negative regulator of TNF-induced apoptosis[30], and the use of this protein after TNFR2 activation results in TNFR1-induced apoptosis to the detriment of proliferation[25]. Therefore, a decrease in TRAF2 expression favours TNFR1-mediated apoptosis, contributing to the increase in the percentage of early apoptotic cells after TNFR2 downregulation.



DOI: 10.3748/wjg.v28.i24.2689 **Copyright** ©The Author(s) 2022.

Figure 6 Schematic comparison of the tumour necrosis factor-α signalling pathway and cell fate in nonsilenced AGS, shTNFR1 and shTNFR2 cells with downregulation after treatment with *Helicobacter pylori* extract. After the tumour necrosis factor (TNF)-α/TNFR1 interaction, TRADD, RIP1, TRAF2 and cellular inhibitor of apoptosis proteins are recruited, which results in nuclear factor-kappaB (NF-κB) activation and transcription of prosurvival and antiapoptotic genes, such as CFLIP, that inhibit the activity of the death-inducing signalling complex, which is formed after dissociation between TRADD and TNFR1. As with TNFR1, TNFR2 stimulation leads to NF-κB activation and cell survival; A: Treatment with *Helicobacter pylori* (*H. pylori*) extract resulted in increased expression of TNFR1, NFKB1, NFKB2 and CFLIP mRNAs in nonsilenced AGS cells. Therefore, the cell survival pathway is activated due to NF-kB activation (red ellipse) through the TNFR1-TNF signalling pathway with consequent production of the antiapoptotic CFLIP; B: In shTNFR1-*H. pylori* extract cells, TNFR1 downregulation resulted in decreased expression of TRADD and CFLIP mRNAs; however, it did not change cell fate; C: In shTNFR2-*H. pylori* extract cells, TNFR2 downregulation decreased the expression of TRAF2 and TRADD, decreased NFKB1, CFLIP and TNFR1 expression, and upregulated miR-19a and miR-34a. This led to an increase in apoptosis, impairing cell survival due to arrest in the G1/S transition phase.

Moreover, we found that TNFR2 downregulation also promoted a decrease in the ratio of cells in the G0/G1 phase and an increase the ratio of cells in the S and G2/M phases, suggesting that TNFR2 inhibition may delay cell cycle progression and arrest cells at the G1/S transition[31]. These changes in the cell cycle could also be related to the DNA damage response[32], leading cells to early apoptosis, as seen in our results. Recent studies have shown increased expression of genes related to the response to DNA damage and repair, such as *APE1, H2AX* and *PARP-1,* in GC samples, thus possibly influencing the survival of tumour cells[33,34]. Yang *et al*[35] demonstrated that TNFR2 enhances DNA damage repair by regulating PARP expression in breast cancer cells. Furthermore, they showed that TNFR2 silencing led to an increase in pH2AX, which is a DNA damage marker.

Based on the function of each receptor and the existence of crosstalk between them, it is possible that the simultaneous inhibition of both TNFR1 and TNFR2 may have a greater antitumor effect on GC than the downregulation of TNFR2 alone. Furthermore, TNF-α and its receptors, in addition to being expressed by tumour cells, are also expressed by cells present in the tumour microenvironment as immune cells[36]. Oshima *et al*[8] demonstrated that the stimulation of TNFR1-mediated TNF-α signalling in cells in the tumour microenvironment promoted gastric tumorigenesis through the induction of tumour-promoting factors (*Noxo1* and *Gna14*) in tumour epithelial cells, highlighting the importance of the tumour microenvironment[37] and the need for *in vivo* studies.

Furthermore, considering the important role of miRNAs in the development of cancer, as they act as regulators of signalling pathways and are consequently involved in various cellular processes, we also evaluated the expression of miRNAs miR-19a, miR-34a, miR-103a, miR-130a and miR-181c. These miRNAs were chosen from data analysis publishedin public databases[38-42] and due to their interaction with TNF-α pathway genes, as observed in our recent study[14]. Regardless of *H. pylori* extract treatment, shTNFR1 and nonsilenced AGS cells did not dysregulate miRNA expression. However, TNFR2 downregulation caused an upregulation of miR-19a and miR-34a (Figure 3A and B).

MiR-34a is dysregulated in different types of cancer and is linked to the proliferation, differentiation, migration, invasion, treatment, and prognosis of cancer[43]. Although most studies suggest a tumour-suppressor role for miR-34a[44-46], we recently observed overexpression of this miRNA in GC samples [14], thus also indicating its oncogenic action. In contrast, in both AGS and BGC-823 cell lines, an upregulation of this miRNA inhibited proliferative and migratory abilities in sevoflurane-induced GC cells, whereas *in vivo* knockdown of miR-34a stimulated tumour growth, indicating its action as a tumour suppressor in the AGS cell line[47]. In addition, stable transfection of pre-mir-34a in KatoII cells

increased the percentage of apoptotic cells and reduced the proliferation rate, suggesting that its high expression promotes apoptosis[48]. In the present study, upregulation of this miRNA in shTNFR2 cells suggests that miR-34a expression can be modulated by TNFR2-mediated TNF-α signalling and is able to exert an anti-proliferative and pro-apoptotic effect. Similarly, miR-19a was overexpressed in the shTNFR2 cell line, indicating that miR-19a and TNFR2 are related to each other in GC. miR-19a has a known oncogenic function in various kinds of cancer[49], with *TNFA, TNFR1* and *TNFR2* being its validated targets[38,39,50]. However, miR19a may play a tumour-suppressive role, as reported in prostate cancer, by suppressing invasion and migration in bone metastasis[51], and in rectal cancer cells, by inducing apoptosis[52]. For both miRNAs, functional studies are needed to assess what targets the miRNAs are related to with respect to TNF-α signalling in GC.

The other miRNAs evaluated (miR-103a, miR-130a and miR-181c) were not dysregulated in the AGS cell line. Although different studies have shown the involvement of these miRNAs in gastric neoplasms [53-55], their pro- or antitumor roles are still controversial. This is due to the influence of several factors in the regulation of gene expression, such as the stage of tumour development and the presence or absence of infectious agents[6].

CONCLUSION

In conclusion, based on our results, shRNA-mediated downregulation of TNFR2 in AGS cells was able to reduce the expression of pro-survival and anti-apoptotic genes, in addition to affecting miRNA expression, the cell cycle, and promoter apoptosis. The blocking of TNFR2 expression may cause antitumor effects, suggesting possible targets for future studies into therapeutic strategies for treating GC. Furthermore, the *H. pylori* extract increased the expression of prosurvival genes, mainly through TNFR1-mediated TNF-α signalling, thus emphasizing the role of bacterial infection in promoting GC progression.

ARTICLE HIGHLIGHTS

Research background

The tumour necrosis factor-α (TNF-α) signalling pathway triggered by TNFR1 and TNFR2 controls several biological processes, influencing cell fate. Thus, the deregulation of this pathway to cause an imbalance between the processes of cell survival and death may contribute to the tumorigenic process. This variety of functions is exercised by the ability of TNF-α to bind to TNFR1 or TNFR2, which results in different cellular processes. Both receptors are transmembrane proteins and are largely similar in extracellular structure, but their intracellular domains are different, and dictate the cellular fate for either survival or death. Since only TNFR1 has a death domain, the TNF-α signalling pathway triggered by TNFR1 is able to induce both cell survival and apoptosis, whereas TNFR2 results only in cell survival. The TNF-α signalling pathway also modulates the immune response and inflammation, so deregulation of this pathway has been implicated in inflammatory diseases and cancer. Therefore, studies are needed to better understand the relationships of this signalling network *via* TNFR1 and TNFR2 and its protumorigenic or antitumorigenic effects.

Research motivation

We proposed the present study based on our previous studies, which showed deregulation in the expression of genes and miRNAs of the TNF-α signalling pathway and its receptors TNFR1 and TNFR2 in fresh tissues of chronic gastritis and gastric cancer (GC) patients. Therefore, we decided to evaluate the effect of silencing TNFR1 and TNFR2 on GC cell lines.

Research objectives

According to the role of TNFR1 and TNFR2 in cellular responses triggered by TNF-α, and considering that studies addressing the role of these receptors in gastric neoplasm are limited and inconclusive, we proposed to couple the silencing of TNFR1 and TNFR2 receptors in an AGS gastric cell line and the treatment with *Helicobacter pylori* (*H. pylori*) extract to determine the effects on *TNF-α* mRNA expression and on downstream genes related to its signalling pathway. Moreover, we also investigated previously studied miRNAs that target genes in the TNF-α pathway to jointly determine their influence on the cell cycle and apoptosis.

Research methods

Stable AGS GC cells containing TNFR1 and TNFR2 receptors downregulated by specific shRNAs and nonsilenced cell lines were treated with 30% v/v *H. pylori* extract [*H. pylori* Tox+ strain (cagA+/vacA s1m1)] for 6 h. After silencing, TNFR1 and TNFR2 levels were assessed by quantitative polymerase

chain reaction (qPCR) and Western blotting to confirm the knockdown effect. Subsequently, mRNA and miRNAs were quantified by qPCR using TaqMan gene and miRNA expression assays. The MTT assay was employed to evaluate the viability of silenced and nonsilenced AGS cells after different treatment conditions with *H. pylori* extract, and flow cytometry was used for cell cycle analysis and apoptosis.

Research results

Our results showed that *H. pylori* extract treatment increased the expression of genes involved in cell survival (*NFKB1* and *NFKB2*) and inhibited apoptosis (*CFLIP*) and *TNFR1* in nonsilenced AGS cells. TNFR1 downregulation significantly decreased the expression of the *TRADD* and *CFLIP* genes; however, no change in the cell cycle, apoptosis or miRNA levels was observed. In turn, TNFR2 downregulation decreased the expression of the *TRADD* and *TRAF2 genes*, which are both important downstream mediators of the TNFR1-mediated pathway, as well as the *NFKB1* and *CFLIP* genes, while upregulating the expression of miR-19a and miR-34a. Consequently, there was a decrease in the ratio of cells in the G0/G1 phase and an increase in cells in the S phase, as well as the promotion of early apoptosis.

Research conclusions

Our findings highlight that treatment with *H. pylori* extract increased the expression of pro-survival genes, mainly through TNFR1-mediated TNF-α signalling, emphasizing the role of bacterial infection in promoting GC progression. In the AGS cell line, TNFR1 and TNFR2 downregulation decreased the expression of prosurvival and antiapoptotic genes and affected miRNA expression and cellular processes, such as the cell cycle and apoptosis, emphasizing that shRNA-mediated downregulation of these receptors can have an antitumor effect.

Research perspectives

According to our results, we can mainly highlight the important role of TNFR2 in the TNF-α pathway in GC, indicating that silencing TNFR2 can reduce the expression of survival and anti-apoptotic genes. Thus, blocking this receptor may result in antitumor effects, suggesting possible targets for future *in vivo* studies into therapeutic strategies for treating GC.

ACKNOWLEDGEMENTS

We thank Dr Sonia Maria Oliani, Department of Biological Sciences, UNESP, for making the flow cytometer available, Janesly Prates for training on the flow cytometer, Dr Fernando Ferrari, Department of Computer Science and Statistics, UNESP, for the statistical support, André Brandão do Amaral for contribution to Figure 6, and Marilanda Ferreira Bellini for recording the audio core tip.

FOOTNOTES

Author contributions: Rossi AFT analysed and interpreted the results; Rossi AFT, Manoel-Caetano FS and Biselli JM performed the experiments; Rossi AFT and Silva AE outlined the study, and drafted and revised the manuscript; Cabral AS performed the Western blot assays; Saiki MFC provided technical support for the shRNA transfection experiments; Ribeiro ML provided the HGC-27 cell line and produced the *H. pylori* extract; all authors approved the final version of the manuscript.

Supported by São Paulo Research Foundation (FAPESP), No. 2015/21464-0 and No. 2015/23392-7; and National Counsel of Technological and Scientific Development (CNPq), No. 310120/2015-2.

Institutional review board statement: Not applicable. This study was performed with cell line only.

Conflict-of-interest statement: The authors declare that they have no conflict of interest.

Data sharing statement: This study was performed with cell line only. The datasets generated during the current study are available from the corresponding author on reasonable request.

Open-Access: This article is an open-access article that was selected by an in-house editor and fully peer-reviewed by external reviewers. It is distributed in accordance with the Creative Commons Attribution NonCommercial (CC BY-NC 4.0) license, which permits others to distribute, remix, adapt, build upon this work non-commercially, and license their derivative works on different terms, provided the original work is properly cited and the use is non-commercial. See: https://creativecommons.org/Licenses/by-nc/4.0/

Country/Territory of origin: Brazil

ORCID number: Ana Flávia Teixeira Rossi 0000-0002-3476-2885; Fernanda da Silva Manoel-Caetano 0000-0001-6717-5874; Joice Matos Biselli 0000-0001-5105-9537; Ágata Silva Cabral 0000-0002-7215-9331; Marilia de Freitas Calmon Saiki 0000-0001-5203-0103; Marcelo Lima Ribeiro 0000-0003-4529-7832; Ana Elizabete Silva 0000-0003-1491-8878.

S-Editor: Fan JR
L-Editor: A
P-Editor: Chen YX

REFERENCES

1 **International Agency for Research on Cancer**. Cancer Today fact Sheets, 2018. [cited 11 January 2022]. Available from http://gco.iarc.fr/today/data/factsheets/cancers/7-Stomach-fact-sheet.pdf
2 **Ministério da Saúde**, Instituto Nacional de Câncer José Alencar Gomes da Silva. Estimativa 2020-Incidência de câncer no Brasil. 2019. [cited 11 January 2022]. Available from: https://www.inca.gov.br/sites/ufu.sti.inca.local/files//media/document//estimativa-2020-incidencia-de-cancer-no-brasil.pdf
3 **Yousefi B**, Mohammadlou M, Abdollahi M, Salek Farrokhi A, Karbalaei M, Keikha M, Kokhaei P, Valizadeh S, Rezaiemanesh A, Arabkari V, Eslami M. Epigenetic changes in gastric cancer induction by Helicobacter pylori. *J Cell Physiol* 2019; **234**: 21770-21784 [PMID: 31169314 DOI: 10.1002/jcp.28925]
4 **Cadamuro AC**, Rossi AF, Maniezzo NM, Silva AE. Helicobacter pylori infection: host immune response, implications on gene expression and microRNAs. *World J Gastroenterol* 2014; **20**: 1424-1437 [PMID: 24587619 DOI: 10.3748/wjg.v20.i6.1424]
5 **Chen R**, Yang M, Huang W, Wang B. Cascades between miRNAs, lncRNAs and the NF-κB signaling pathway in gastric cancer (Review). *Exp Ther Med* 2021; **22**: 769 [PMID: 34055068 DOI: 10.3892/etm.2021.10201]
6 **Rossi AF**, Cadamuro AC, Biselli-Périco JM, Leite KR, Severino FE, Reis PP, Cordeiro JA, Silva AE. Interaction between inflammatory mediators and miRNAs in Helicobacter pylori infection. *Cell Microbiol* 2016; **18**: 1444-1458 [PMID: 26945693 DOI: 10.1111/cmi.12587]
7 **Mahdavi Sharif P**, Jabbari P, Razi S, Keshavarz-Fathi M, Rezaei N. Importance of TNF-alpha and its alterations in the development of cancers. *Cytokine* 2020; **130**: 155066 [PMID: 32208336 DOI: 10.1016/j.cyto.2020.155066]
8 **Oshima H**, Ishikawa T, Yoshida GJ, Naoi K, Maeda Y, Naka K, Ju X, Yamada Y, Minamoto T, Mukaida N, Saya H, Oshima M. TNF-α/TNFR1 signaling promotes gastric tumorigenesis through induction of Noxo1 and Gna14 in tumor cells. *Oncogene* 2014; **33**: 3820-3829 [PMID: 23975421 DOI: 10.1038/onc.2013.356]
9 **Yang S**, Wang J, Brand DD, Zheng SG. Role of TNF-TNF Receptor 2 Signal in Regulatory T Cells and Its Therapeutic Implications. *Front Immunol* 2018; **9**: 784 [PMID: 29725328 DOI: 10.3389/fimmu.2018.00784]
10 **Gough P**, Myles IA. Tumor Necrosis Factor Receptors: Pleiotropic Signaling Complexes and Their Differential Effects. *Front Immunol* 2020; **11**: 585880 [PMID: 33324405 DOI: 10.3389/fimmu.2020.585880]
11 **Josephs SF**, Ichim TE, Prince SM, Kesari S, Marincola FM, Escobedo AR, Jafri A. Unleashing endogenous TNF-alpha as a cancer immunotherapeutic. *J Transl Med* 2018; **16**: 242 [PMID: 30170620 DOI: 10.1186/s12967-018-1611-7]
12 **Li Z**, Yuan W, Lin Z. Functional roles in cell signaling of adaptor protein TRADD from a structural perspective. *Comput Struct Biotechnol J* 2020; **18**: 2867-2876 [PMID: 33163147 DOI: 10.1016/j.csbj.2020.10.008]
13 **Brenner D**, Blaser H, Mak TW. Regulation of tumour necrosis factor signalling: live or let die. *Nat Rev Immunol* 2015; **15**: 362-374 [PMID: 26008591 DOI: 10.1038/nri3834]
14 **Rossi AFT**, Contiero JC, Manoel-Caetano FDS, Severino FE, Silva AE. Up-regulation of tumor necrosis factor-α pathway survival genes and of the receptor TNFR2 in gastric cancer. *World J Gastrointest Oncol* 2019; **11**: 281-294 [PMID: 31040894 DOI: 10.4251/wjgo.v11.i4.281]
15 **Santos JC**, Gambeloni RZ, Roque AT, Oeck S, Ribeiro ML. Epigenetic Mechanisms of ATM Activation after Helicobacter pylori Infection. *Am J Pathol* 2018; **188**: 329-335 [PMID: 29128564 DOI: 10.1016/j.ajpath.2017.10.005]
16 **Li HQ**, Xu C, Li HS, Xiao ZP, Shi L, Zhu HL. Metronidazole-flavonoid derivatives as anti-Helicobacter pylori agents with potent inhibitory activity against HPE-induced interleukin-8 production by AGS cells. *ChemMedChem* 2007; **2**: 1361-1369 [PMID: 17628869 DOI: 10.1002/cmdc.200700097]
17 **Livak KJ**, Schmittgen TD. Analysis of relative gene expression data using real-time quantitative PCR and the 2(-Delta Delta C(T)) Method. *Methods* 2001; **25**: 402-408 [PMID: 11846609 DOI: 10.1006/meth.2001.1262]
18 **Riedl S**, Rinner B, Asslaber M, Schaider H, Walzer S, Novak A, Lohner K, Zweytick D. In search of a novel target - phosphatidylserine exposed by non-apoptotic tumor cells and metastases of malignancies with poor treatment efficacy. *Biochim Biophys Acta* 2011; **1808**: 2638-2645 [PMID: 21810406 DOI: 10.1016/j.bbamem.2011.07.026]
19 **Yeon MJ**, Lee MH, Kim DH, Yang JY, Woo HJ, Kwon HJ, Moon C, Kim SH, Kim JB. Anti-inflammatory effects of Kaempferol on Helicobacter pylori-induced inflammation. *Biosci Biotechnol Biochem* 2019; **83**: 166-173 [PMID: 30286691 DOI: 10.1080/09168451.2018.1528140]
20 **Maeda S**, Yoshida H, Ogura K, Mitsuno Y, Hirata Y, Yamaji Y, Akanuma M, Shiratori Y, Omata M. H. pylori activates NF-kappaB through a signaling pathway involving IkappaB kinases, NF-kappaB-inducing kinase, TRAF2, and TRAF6 in gastric cancer cells. *Gastroenterology* 2000; **119**: 97-108 [PMID: 10889159 DOI: 10.1053/gast.2000.8540]
21 **Ham B**, Fernandez MC, D'Costa Z, Brodt P. The diverse roles of the TNF axis in cancer progression and metastasis. *Trends Cancer Res* 2016; **11**: 1-27 [PMID: 27928197]
22 **Micheau O**, Lens S, Gaide O, Alevizopoulos K, Tschopp J. NF-kappaB signals induce the expression of c-FLIP. *Mol Cell Biol* 2001; **21**: 5299-5305 [PMID: 11463813 DOI: 10.1128/MCB.21.16.5299-5305.2001]
23 **Changhui M**, Tianzhong M, Zhongjing S, Ling C, Ning W, Ningxia Z, Xiancai C, Haibin C. Silencing of tumor necrosis

factor receptor 1 by siRNA in EC109 cells affects cell proliferation and apoptosis. *J Biomed Biotechnol* 2009; **2009**: 760540 [PMID: 19826638 DOI: 10.1155/2009/760540]

24 **Wan XK**, Yuan SL, Wang YC, Tao HX, Jiang W, Guan ZY, Cao C, Liu CJ. *Helicobacter pylori* inhibits the cleavage of TRAF1 *via* a CagA-dependent mechanism. *World J Gastroenterol* 2016; **22**: 10566-10574 [PMID: 28082808 DOI: 10.3748/wjg.v22.i48.10566]

25 **Moatti A**, Cohen JL. The TNF-α/TNFR2 Pathway: Targeting a Brake to Release the Anti-tumor Immune Response. *Front Cell Dev Biol* 2021; **9**: 725473 [PMID: 34712661 DOI: 10.3389/fcell.2021.725473]

26 **Pobezinskaya YL**, Liu Z. The role of TRADD in death receptor signaling. *Cell Cycle* 2012; **11**: 871-876 [PMID: 22333735 DOI: 10.4161/cc.11.5.19300]

27 **Pobezinskaya YL**, Kim YS, Choksi S, Morgan MJ, Li T, Liu C, Liu Z. The function of TRADD in signaling through tumor necrosis factor receptor 1 and TRIF-dependent Toll-like receptors. *Nat Immunol* 2008; **9**: 1047-1054 [PMID: 18641653 DOI: 10.1038/ni.1639]

28 **Ermolaeva MA**, Michallet MC, Papadopoulou N, Utermöhlen O, Kranidioti K, Kollias G, Tschopp J, Pasparakis M. Function of TRADD in tumor necrosis factor receptor 1 signaling and in TRIF-dependent inflammatory responses. *Nat Immunol* 2008; **9**: 1037-1046 [PMID: 18641654 DOI: 10.1038/ni.1638]

29 **Naudé PJ**, den Boer JA, Luiten PG, Eisel UL. Tumor necrosis factor receptor cross-talk. *FEBS J* 2011; **278**: 888-898 [PMID: 21232019 DOI: 10.1111/j.1742-4658.2011.08017.x]

30 **Borghi A**, Verstrepen L, Beyaert R. TRAF2 multitasking in TNF receptor-induced signaling to NF-κB, MAP kinases and cell death. *Biochem Pharmacol* 2016; **116**: 1-10 [PMID: 26993379 DOI: 10.1016/j.bcp.2016.03.009]

31 **Qiao F**, Gong P, Song Y, Shen X, Su X, Li Y, Wu H, Zhao Z, Fan H. Downregulated PITX1 Modulated by MiR-19a-3p Promotes Cell Malignancy and Predicts a Poor Prognosis of Gastric Cancer by Affecting Transcriptionally Activated PDCD5. *Cell Physiol Biochem* 2018; **46**: 2215-2231 [PMID: 29734189 DOI: 10.1159/000489590]

32 **DiPaola RS**. To arrest or not to G(2)-M Cell-cycle arrest : commentary re: A. K. Tyagi *et al*, Silibinin strongly synergizes human prostate carcinoma DU145 cells to doxorubicin-induced growth inhibition, G(2)-M arrest, and apoptosis. Clin. cancer res., 8: 3512-3519, 2002. *Clin Cancer Res* 2002; **8**: 3311-3314 [PMID: 12429616]

33 **Afzal H**, Yousaf S, Rahman F, Ahmed MW, Akram Z, Akhtar Kayani M, Mahjabeen I. PARP1: A potential biomarker for gastric cancer. *Pathol Res Pract* 2019; **215**: 152472 [PMID: 31174925 DOI: 10.1016/j.prp.2019.152472]

34 **Manoel-Caetano FS**, Rossi AFT, Calvet de Morais G, Severino FE, Silva AE. Upregulation of the *APE1* and *H2AX* genes and miRNAs involved in DNA damage response and repair in gastric cancer. *Genes Dis* 2019; **6**: 176-184 [PMID: 31194025 DOI: 10.1016/j.gendis.2019.03.007]

35 **Yang F**, Zhao N, Wu N. TNFR2 promotes Adriamycin resistance in breast cancer cells by repairing DNA damage. *Mol Med Rep* 2017; **16**: 2962-2968 [PMID: 28677724 DOI: 10.3892/mmr.2017.6898]

36 **Wu Y**, Zhou BP. TNF-alpha/NF-kappaB/Snail pathway in cancer cell migration and invasion. *Br J Cancer* 2010; **102**: 639-644 [PMID: 20087353 DOI: 10.1038/sj.bjc.6605530]

37 **Bubnovskaya L**, Osinsky D. Tumor microenvironment and metabolic factors: contribution to gastric cancer. *Exp Oncol* 2020; **42**: 2-10 [PMID: 32231198 DOI: 10.32471/exp-oncology.2312-8852.vol-42-no-1.14056]

38 **Vlachos IS**, Paraskevopoulou MD, Karagkouni D, Georgakilas G, Vergoulis T, Kanellos I, Anastasopoulos IL, Maniou S, Karathanou K, Kalfakakou D, Fevgas A, Dalamagas T, Hatzigeorgiou AG. DIANA-TarBase v7.0: indexing more than half a million experimentally supported miRNA:mRNA interactions. *Nucleic Acids Res* 2015; **43**: D153-D159 [PMID: 25416803 DOI: 10.1093/nar/gku1215]

39 **Dweep H**, Gretz N. miRWalk2.0: a comprehensive atlas of microRNA-target interactions. *Nat Methods* 2015; **12**: 697 [PMID: 26226356 DOI: 10.1038/nmeth.3485]

40 **Liu W**, Wang X. Prediction of functional microRNA targets by integrative modeling of microRNA binding and target expression data. *Genome Biol* 2019; **20**: 18 [PMID: 30670076 DOI: 10.1186/s13059-019-1629-z]

41 **Agarwal V**, Bell GW, Nam JW, Bartel DP. Predicting effective microRNA target sites in mammalian mRNAs. *Elife* 2015; **4** [PMID: 26267216 DOI: 10.7554/eLife.05005]

42 **Miranda KC**, Huynh T, Tay Y, Ang YS, Tam WL, Thomson AM, Lim B, Rigoutsos I. A pattern-based method for the identification of MicroRNA binding sites and their corresponding heteroduplexes. *Cell* 2006; **126**: 1203-1217 [PMID: 16990141 DOI: 10.1016/j.cell.2006.07.031]

43 **Kong J**, Wang W. A Systemic Review on the Regulatory Roles of miR-34a in Gastrointestinal Cancer. *Onco Targets Ther* 2020; **13**: 2855-2872 [PMID: 32308419 DOI: 10.2147/OTT.S234549]

44 **Deng X**, Zheng H, Li D, Xue Y, Wang Q, Yan S, Zhu Y, Deng M. MicroRNA-34a regulates proliferation and apoptosis of gastric cancer cells by targeting silent information regulator 1. *Exp Ther Med* 2018; **15**: 3705-3714 [PMID: 29581731 DOI: 10.3892/etm.2018.5920]

45 **Yu Y**, Wei SG, Weiss RM, Felder RB. TNF-α receptor 1 knockdown in the subfornical organ ameliorates sympathetic excitation and cardiac hemodynamics in heart failure rats. *Am J Physiol Heart Circ Physiol* 2017; **313**: H744-H756 [PMID: 28710070 DOI: 10.1152/ajpheart.00280.2017]

46 **Wang B**, Li D, Kovalchuk I, Apel IJ, Chinnaiyan AM, Wóycicki RK, Cantor CR, Kovalchuk O. miR-34a directly targets $tRNA_i^{Met}$ precursors and affects cellular proliferation, cell cycle, and apoptosis. *Proc Natl Acad Sci U S A* 2018; **115**: 7392-7397 [PMID: 29941603 DOI: 10.1073/pnas.1703029115]

47 **Chen H**, Zhu XM, Luo ZL, Hu YJ, Cai XC, Gu QH. Sevoflurane induction alleviates the progression of gastric cancer by upregulating the miR-34a/TGIF2 axis. *Eur Rev Med Pharmacol Sci* 2020; **24**: 11883-11890 [PMID: 33275259 DOI: 10.26355/eurrev_202011_23846]

48 **Jafari N**, Abediankenari S, Hossein-Nataj H. miR-34a mimic or pre-mir-34a, which is the better option for cancer therapy? *Cancer Cell Int* 2021; **21**: 178 [PMID: 33740991 DOI: 10.1186/s12935-021-01872-5]

49 **Cheng J**, Yang A, Cheng S, Feng L, Wu X, Lu X, Zu M, Cui J, Yu H, Zou L. Circulating miR-19a-3p and miR-483-5p as Novel Diagnostic Biomarkers for the Early Diagnosis of Gastric Cancer. *Med Sci Monit* 2020; **26**: e923444 [PMID: 32487978 DOI: 10.12659/MSM.923444]

50 **Liu M**, Wang Z, Yang S, Zhang W, He S, Hu C, Zhu H, Quan L, Bai J, Xu N. TNF-α is a novel target of miR-19a. *Int J Oncol* 2011; **38**: 1013-1022 [PMID: 21271217 DOI: 10.3892/ijo.2011.924]

51 **Wa Q**, Li L, Lin H, Peng X, Ren D, Huang Y, He P, Huang S. Downregulation of miR19a3p promotes invasion, migration and bone metastasis *via* activating TGFβ signaling in prostate cancer. *Oncol Rep* 2018; **39**: 81-90 [PMID: 29138858 DOI: 10.3892/or.2017.6096]

52 **Su YF**, Zang YF, Wang YH, Ding YL. MiR-19-3p Induces Tumor Cell Apoptosis *via* Targeting FAS in Rectal Cancer Cells. *Technol Cancer Res Treat* 2020; **19**: 1533033820917978 [PMID: 32266860 DOI: 10.1177/1533033820917978]

53 **Cui M**, Yue L, Fu Y, Yu W, Hou X, Zhang X. Association of microRNA-181c expression with the progression and prognosis of human gastric carcinoma. *Hepatogastroenterology* 2013; **60**: 961-964 [PMID: 23425811 DOI: 10.5754/hge121333]

54 **Hu X**, Miao J, Zhang M, Wang X, Wang Z, Han J, Tong D, Huang C. miRNA-103a-3p Promotes Human Gastric Cancer Cell Proliferation by Targeting and Suppressing ATF7 *in vitro*. *Mol Cells* 2018; **41**: 390-400 [PMID: 29754469 DOI: 10.14348/molcells.2018.2078]

55 **Wang S**, Han H, Hu Y, Yang W, Lv Y, Wang L, Zhang L, Ji J. MicroRNA-130a-3p suppresses cell migration and invasion by inhibition of TBL1XR1-mediated EMT in human gastric carcinoma. *Mol Carcinog* 2018; **57**: 383-392 [PMID: 29091326 DOI: 10.1002/mc.22762]

World Journal of Gastroenterology

Submit a Manuscript: https://www.f6publishing.com

World J Gastroenterol 2022 June 28; 28(24): 2705-2732

DOI: 10.3748/wjg.v28.i24.2705

ISSN 1007-9327 (print) ISSN 2219-2840 (online)

ORIGINAL ARTICLE

Clinical and Translational Research

Novel multiplex stool-based assay for the detection of early-stage colon cancer in a Chinese population

Hui-Hong Jiang, Si-Wei Xing, Xuan Tang, Ying Chen, Kang Lin, Lu-Wei He, Mou-Bin Lin, Er-Jiang Tang

Specialty type: Gastroenterology and hepatology

Provenance and peer review: Unsolicited article; Externally peer reviewed.

Peer-review model: Single blind

Peer-review report's scientific quality classification

Grade A (Excellent): 0
Grade B (Very good): B, B
Grade C (Good): 0
Grade D (Fair): 0
Grade E (Poor): 0

P-Reviewer: Jiménez Pérez M, Spain; Sharara AI, Lebanon

Received: December 4, 2021
Peer-review started: December 4, 2021
First decision: January 8, 2022
Revised: January 14, 2022
Accepted: May 13, 2022
Article in press: May 13, 2022
Published online: June 28, 2022

Hui-Hong Jiang, Xuan Tang, Kang Lin, Mou-Bin Lin, Department of General Surgery, Yangpu Hospital, Tongji University, Shanghai 200090, China

Hui-Hong Jiang, Ying Chen, Lu-Wei He, Mou-Bin Lin, Er-Jiang Tang, Institute of Gastrointestinal Surgery and Translational Medicine, Tongji University School of Medicine, Shanghai 200090, China

Si-Wei Xing, Department of Urology, Ruijin Hospital, Shanghai Jiaotong University School of Medicine, Shanghai 200025, China

Si-Wei Xing, Ying Chen, Kang Lin, Lu-Wei He, Mou-Bin Lin, Er-Jiang Tang, Center for Clinical Research and Translational Medicine, Yangpu Hospital, Tongji University, Shanghai 200090, China

Corresponding author: Er-Jiang Tang, MSc, Statistician, Center for Clinical Research and Translational Medicine, Yangpu Hospital, Tongji University, No. 450 Tengyue Road, Shanghai 200090, China. tangerjiang1988051@163.com

Abstract

BACKGROUND

Stool DNA (sDNA) methylation analysis is a promising, noninvasive approach for colorectal cancer screening; however, reliable biomarkers for detecting early-stage colon cancer (ECC) are lacking, particularly in the Chinese population.

AIM

To identify a novel stool-based assay that can improve the effectiveness of ECC screening.

METHODS

A blinded case-control study was performed using archived stool samples from 125 ECC patients, and 125 control subjects with normal colonoscopy. The cohort was randomly divided into training and test sets at a 1.5:1 ratio. Targeted bisulfite sequencing (TBSeq) was conducted on five pairs of preoperative and postoperative sDNA samples from ECC patients to identify DNA methylation biomarkers, which were validated using pyrosequencing. By logistic regression analysis, a multiplex stool-based assay was developed in the training set, and the detection performance was further assessed in the test set and combined set. The χ^2 test was used to investigate the association of detection sensitivity with clinico-

pathological features.

RESULTS

Following TBSeq, three hypermethylated cytosine-guanine sites were selected as biomarkers, including paired box 8, Ras-association domain family 1 and secreted frizzled-related protein 2, which differed between the groups and were involved in important cancer pathways. An sDNA panel containing the three biomarkers was constructed with a logistic model. Receiver operating characteristic (ROC) analysis revealed that this panel was superior to the fecal immunochemical test (FIT) or serum carcinoembryonic antigen for the detection of ECC. We further found that the combination of the sDNA panel with FIT could improve the screening effectiveness. In the combined set, the sensitivity, specificity and area under the ROC curve for this multiplex assay were 80.0%, 93.6% and 0.918, respectively, and the performance remained excellent in the subgroup analysis by tumor stage. In addition, the detection sensitivity did not differ with tumor site, tumor stage, histological differentiation, age or sex, but was significantly higher in T4 than in T1-3 stage tumors (P = 0.041).

CONCLUSION

We identified a novel multiplex stool-based assay combining sDNA methylation biomarkers and FIT, which could detect ECC with high sensitivity and specificity throughout the colon, showing a promising application perspective.

Key Words: Colon cancer; Early screening; Stool biomarker; DNA methylation; Fecal immunochemical test

©The Author(s) 2022. Published by Baishideng Publishing Group Inc. All rights reserved.

Core Tip: Stool DNA (sDNA) methylation analysis has a promising application in the early diagnosis of colorectal cancer. However, reliable biomarkers for detecting early-stage colon cancer (ECC) are lacking. In this study, by targeted bisulfite sequencing, we identified a novel multiplex stool-based assay combining three sDNA methylation biomarkers and fecal immunochemical test. Further validation in larger samples by pyrosequencing showed that it enabled the diagnosis of ECC with high sensitivity and specificity throughout the colon. To our knowledge, this is the first study to focus on ECC screening in China.

Citation: Jiang HH, Xing SW, Tang X, Chen Y, Lin K, He LW, Lin MB, Tang EJ. Novel multiplex stool-based assay for the detection of early-stage colon cancer in a Chinese population. *World J Gastroenterol* 2022; 28(24): 2705-2732

URL: https://www.wjgnet.com/1007-9327/full/v28/i24/2705.htm

DOI: https://dx.doi.org/10.3748/wjg.v28.i24.2705

INTRODUCTION

Colorectal cancer (CRC) has emerged as a major public health issue in China, with 521400 new cases and 248000 deaths occurring in 2018[1]. The incidence of colon cancer has increased significantly in the past decades, with a trend in younger patients, and most cases are in advanced stages at initial diagnosis[2]. Early screening is the key to improving survival and reducing morbidity[3]. Compared with the high positive rate of rectal palpation in rectal cancer, colonoscopy is currently the main tool and gold standard for detecting colon cancer, but is invasive, costly and poorly tolerated[4]. The fecal immunochemical test (FIT), computed tomography (CT) colonography and blood tumor markers, such as serum carcinoembryonic antigen (CEA), provide relatively noninvasive and painless methods, but their sensitivity for detecting early-stage colon cancer (ECC) is limited[5,6]. Thus, the identification of novel biomarkers that are highly specific, sensitive, and noninvasive is urgently needed for the screening of ECC.

CRC development is characterized by the progressive accumulation of genetic and epigenetic alterations that transform colonic epithelial cells into adenocarcinoma cells[7,8]. These cells are continuously shed into the colonic lumen and mixed with stool[9]. Moreover, the molecular changes caused by CRC tumorigenesis are reportedly present in the stool earlier than in the blood[10]. Hence, detecting aberrant DNA methylation in stool DNA (sDNA) has been proposed as a promising noninvasive alternative for CRC screening. To date, a number of sDNA methylation biomarkers have been reported for the detection of different stages of CRC, including secreted frizzled-related protein 2

(SFRP2), N-myc downstream-regulated gene 4 (NDRG4), ventralis intermedius, COL4A2 and GATA4 [11]. Further studies revealed that the combination of multiple biomarkers contributed to a higher diagnostic accuracy than a single biomarker[12]. For instance, a multitarget sDNA test Cologuard, combining NDRG4 and BMP3 methylation, Kirsten rat sarcoma mutations, β-actin and a hemoglobin assay, has been approved for average-risk CRC screening by the US Food and Drug Administration and is now available clinically[13]. However, the reported sensitivity and specificity of the same sDNA methylation biomarker varied greatly among studies, due to the different study populations (mainly the ethnic, geographic and dietary differences), inclusion criteria and levels of examination[14,15]. Moreover, few studies have focused on the sDNA screening test for ECC, especially in the Chinese population.

In this study, using targeted bisulfite sequencing (TBSeq), we identified a novel panel of sDNA methylation biomarkers for ECC detection, which was validated in a training and test design with pyrosequencing (PSQ). We further investigated the detection performance of the sDNA panel combining conventional screening methods, and assessed the effects of clinical covariates on test performance. To our knowledge, this is the first work to focus on ECC screening in China.

MATERIALS AND METHODS

Study design and study population

Between November 2018 and June 2020, a single-center, case-control study was performed at Yangpu Hospital Affiliated to Tongji University, using archived stool samples from 125 patients with sporadic ECC and 125 individuals with normal colonoscopy results. The diagnosis of stage I and II colon cancer was histologically confirmed after surgery. All subjects were of Han race living in Shanghai, and the inclusion of patients and controls was carried out to achieve a good match in terms of age and sex. Those who had a history of digestive cancer, inflammatory bowel disease or familial adenomatous polyposis, or an unconfirmed diagnosis were excluded. In addition, clinical information including tumor site, histological differentiation, tumor stage and preoperative serum CEA level was abstracted from medical records. These participants were randomly divided into training and test sets with a sample size ratio of 1.5:1. All subjects provided written informed consent, and this study was approved by the Ethical Committee and Institutional Review Board of our hospital (LL-2018-SCI-003). This study was registered at the Chinese Clinical Trial Registry (ChiCTR1800019552). The study design consisted of three stages: Biomarker selection, biomarker validation and model evaluation, as shown in Figure 1.

Sample collection and processing

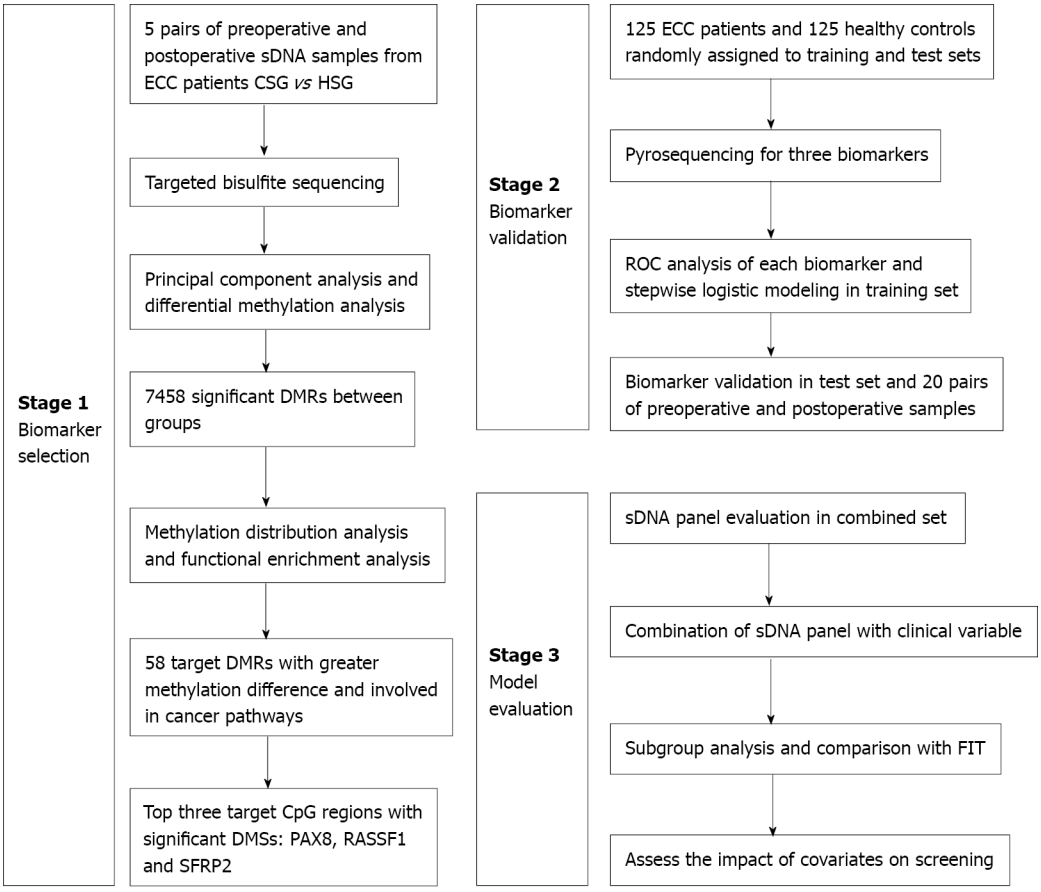
All participants were required to undergo screening colonoscopy and provide a fresh stool sample before bowel purgation. In addition, 20 randomly selected ECC patients (6 stage I and 14 stage II cases) were asked to provide stool samples at six months after radical surgery with no tumor recurrence. One part of the stool sample was used for FIT (FASURE; NewScen Coast, China), and the result was evaluated at the manufacturer's recommended positivity cut-off of 200 ng hemoglobin/mL buffer. The other part (minimum 50 g) was immediately extracted or stored at -80 °C for further use, sDNA was extracted with a QIAamp DNA Fast Stool Mini Kit (Qiagen, Germany), and the quality and concentration were determined by spectrophotometry (NanoDrop 2000; Thermo-Fisher Scientific, United States). Among the 20 pairs of preoperative and postoperative sDNA samples, five pairs (2 stage I and 3 stage II cases) were randomly selected for biomarker identification using TBSeq and named cancer sample group (CSG) and healthy sample group (HSG), respectively.

TBSeq

We used CATCH-Seq target enrichment technology (Novogene, China) to perform bisulfite sequencing, to evaluate 23441 [cytosine-guanine (CpG) islands] (CGIs) (about 83% of the 28226 CGIs in the human genome) and the promoter regions of 19369 RefSeq genes (within 2 kb before the transcription start site) [16,17]. Briefly, according to the manufacturer's protocol, genomic DNA (1 μg) was fragmented into 200-300 bp fragments using a Covaris S220 (Covarias, United States). The DNA fragments were then sheared, end-repaired and dephosphorylated. The blunt fragments were subsequently A-tailed and ligated to sequencing adaptors that were synthesized with 5′-methylcytosine instead of 5′-cytosine and index sequences. Following the liquid hybridization capture procedure, the target enriched library was bisulfite-converted (EZ DNA Methylation Kit; Zymo Research, United States) and then amplified by polymerase chain reaction (PCR). After quantification and quality control, sequencing was performed on an Illumina Hiseq 2500 platform (Illumina, United States).

Analysis of sequencing data

Preprocessing included quality control using FastQC, adapter trimming using cutadapt, and read alignment and methylation calling using Bismark with Bowtie2 (hg19/GRCh37). The coverage depth of each base and CpG site was calculated, and the results were filtered by criteria of at least 5X coverage.



DOI: 10.3748/wjg.v28.i24.2705 **Copyright** ©The Author(s) 2022.

Figure 1 Flow diagram of the study design. Candidate methylation biomarkers were selected by targeted bisulfite sequencing and then validated using pyrosequencing. At last, a diagnostic model was constructed and evaluated. CSG: Cancer sample group; HSG: Healthy sample group; DMRs: Differentially methylated regions; DMSs: Differentially methylated sites; ROC: Receiver operating characteristic; sDNA: Stool DNA; FIT: Fecal immunochemical test; PAX8: Paired box 8; RASSF1: Ras-association domain family 1; SFRP2: Secreted frizzled-related protein 2; CpG: Cytosine-guanine; ECC: Early-stage colon cancer.

The CpG sites that were located on the Y chromosome and overlapped with single nucleotide polymorphisms (SNPs) registered in the SNP database (http://www.ncbi.nlm.nih.gov/projects/SNP/) were excluded from the analysis. For the methylated sites, the methylation level was calculated using the formula: ML = mC/(mC + umC), where ML represents the methylation level, and mC and umC represent the number of methylated and unmethylated C-sites, respectively. Methylation levels of the specified functional regions including CGI, CGI shore (0-2 kb from CGI), CGI shelf (2-4 kb from CGI), promoter, 5′ untranslated regions (UTR), 3′UTR and exon, were summarized to show the distribution [18]. Methylation density was defined as the percentage of methylated CpG sites among all CpG sites within the given region.

In-house scripts were used to identify a differentially methylated site (DMS) by Fisher's exact test with false discovery rate correction. Statistical significance for DMS between the two groups was determined if the adjusted P value < 0.05 and the difference in methylation level > 0.25. A differentially methylated region (DMR) was identified by swDMR software (http://122.228.158.106/swDMR/) using the sliding-window approach, in which the window was set to 1000 bp and the step length was 100 bp. The DMR should contain at least two CpG sites (all sites are hypermethylated or hypomethylated), and the distance between the adjacent CpG sites was < 100 bp. In addition, the DMRs with an adjusted P value < 0.05 and a difference in methylation level > 0.1 were considered candidate DMRs.

Biomarker selection

By comparing the methylation status between the CSG and HSG, 7458 DMRs were obtained based on the above standards. To strengthen the robustness of the candidate biomarker, the DMRs located far from CGIs and promoter regions were filtered out. Moreover, to reduce the noise due to sample heterogeneity, it was essential to select biomarkers that had greater methylation difference between groups (P > 0.35) and that were significantly enriched in well-established cancer pathways (adjusted P < 0.05). In total, 58 target DMRs were selected, and each DMR contained at least two significant DMSs. According to the guanine-cytosine percent, primer lengths, amplicon lengths, predicted melting temperatures and the number of SNPs in the primers, the score representing the difficulty levels for all the candidate

Table 1 Primers for pyrosequencing of three DNA methylation biomarkers

Target gene	Primer	Sequence	Size (bp)	Target DMS
PAX8	Forward	5′-GGGGGTTAGGGGATTTTGATTATA-3′	166	chr2:114035984; 114035988; 114035995; 114035998; 114036006
	Reverse	Biotin-5′-ATCTCATACCCTTCTCCTAAATTTATAC-3′		
	Sequencing	5′-ATGGAGTTGTGAGGT-3′		
RASSF1	Forward	5′-TTTATTTATTGGGTGGGGTAGGA-3′	141	chr3:50378714; 50378718
	Reverse	Biotin-5′-CCTCAAAATCACCATCCAACCTCTAC-3′		
	Sequencing	5′-GGGAGATAGGTTAGTAGTTTTA-3′		
SFRP2	Forward	5′-GATTAGGGATAATTAGGTAAAAGGAGTT-3′	166	chr4:154711281; 154711305
	Reverse	Biotin-5′-ATTCATCCCCTACCTACCAAAAAACACC-3′		
	Sequencing	5′-AGTTAGAGATATTAGATTTTAGG-3′		

PAX8: Paired box 8; RASSF1: Ras-association domain family 1; SFRP2: Secreted frizzled-related protein 2; DMS: Differentially methylated site.

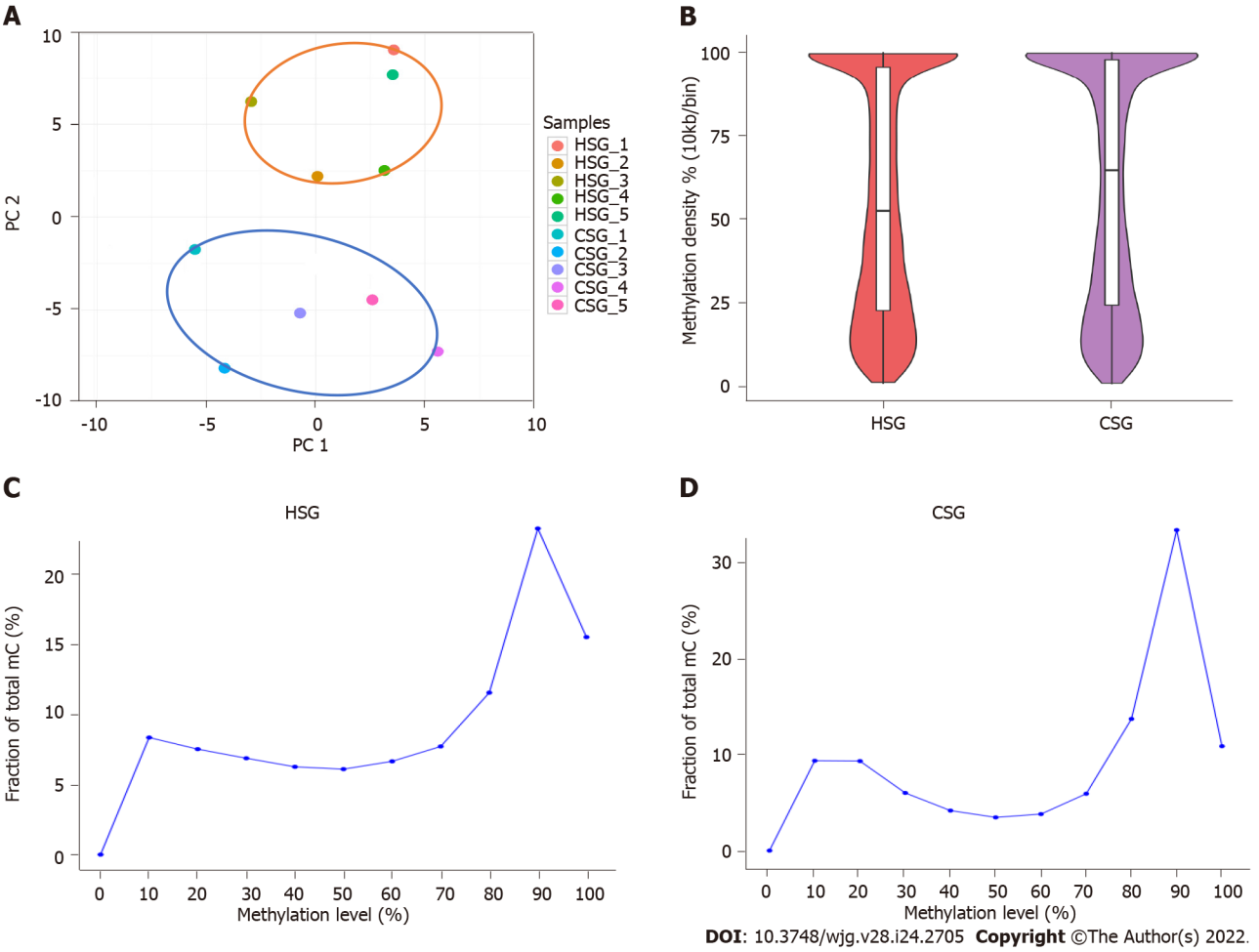


Figure 2 DNA methylation analysis by targeted bisulfite sequencing. A: Principal component analysis of the methylation profiles between cancer sample group (CSG) and healthy sample group (HSG); B: Comparison of methylation density between CSG and HSG; C: Comparison of methylation level distribution between CSG and HSG. CSG: Cancer sample group; HSG: Healthy sample group; PC: Principal component.

regions was obtained. Finally, we selected the top three target CpG regions with the best chance of being amplified and conducted in the PSQ assay, and removed the other candidate regions for further validation.

Table 2 Clinicopathological features of the early-stage colon cancer patients enrolled in this study, *n* (%)

Variable	Total (*n* = 125)	Training set (*n* = 75)	Test set (*n* = 50)
Age (yr)	69 (range, 48-94)	68 (range, 51-94)	70 (range, 48-88)
Sex			
Male	66 (52.8)	39 (52.0)	27 (54.0)
Female	59 (47.2)	36 (48.0)	23 (46.0)
Serum CEA (≥ 5 ng/mL)			
Positive	37 (29.6)	21 (28.0)	16 (32.0)
Negative	88 (70.4)	54 (72.0)	34 (68.0)
FIT (≥ 200 ng/mL)			
Positive	78 (62.4)	48 (64.0)	30 (60.0)
Negative	47 (37.6)	27 (36.0)	20 (40.0)
Tumor site			
Proximal	64 (51.2)	36 (48.0)	28 (56.0)
Distal	61 (48.8)	39 (52.0)	22 (44.0)
TNM stage			
I	47 (37.6)	30 (40.0)	17 (34.0)
II	78 (62.4)	45 (60.0)	33 (66.0)
T stage			
T1-3	71 (56.8)	44 (58.7)	27 (54.0)
T4	54 (43.2)	31 (41.3)	23 (46.0)
Histological differentiation			
Well/moderately	98 (78.4)	60 (80.0)	38 (76.0)
Poorly	27 (21.6)	15 (20.0)	12 (24.0)

CEA: Carcinoembryonic antigen; FIT: Fecal immunochemical test; TNM: Tumor-node-metastasis.

PSQ

To measure the methylation levels of the three target CpG regions in the 250 stool samples, PSQ was conducted (Oebiotech, China) without knowledge of either the clinical diagnosis or FIT result, sDNA extraction and bisulfite conversion were performed as previously described[19]. The PSQ primers were designed to amplify two to five CpG sites in target sequences using PyroMark Assay Design software (Qiagen, Germany). Primer sequences were listed in Table 1. For methylation-specific PCR (MSP), 50 ng of bisulfite modified DNA was amplified in a 25 μL reaction. The cycling conditions were recommended by the manufacturer and were as follows: A denaturing step of 15 min at 95 °C, then 45 cycles at 94 °C for 30 s, 56 °C for 30 s and 72 °C for 30 s, and a final elongation step of 10 min at 72 °C. PSQ was performed on a PSQ HS96A instrument according to the manufacturer's guidelines using PyroMark Gold Q96 Reagents (Qiagen, Germany). The methylation index of each gene in each sample was calculated as the mean percentage of mC for all examined CpGs in target regions. All experiments included a negative control without a template[19].

Diagnostic model building

Based on the PSQ results, a logistic regression model was developed to define a linear combination of variables that optimized the discrimination between ECC patients and healthy controls. The modeling strategy consisted of age, sex, FIT, preoperative CEA level and sDNA methylation biomarkers in a base model and adding quadratic and pairwise interactions of these variables using backward selection with $P < 0.05$ for retention. The formula was as follows: $Y = \beta0 + \beta1X1 + \beta2X2 + \ldots + \beta nXn$ where X represented the exploratory variable[20]. The linear discriminant score with the corresponding cut-off value was then applied to the study population. Receiver operating characteristic (ROC) analysis was applied to compare the accuracy of nested logistic models and to investigate the added value of each variable.

Table 3 Diagnostic sensitivity, specificity and area under the receiver operating characteristic curve for various indexes

Study population	Index	Sensitivity (%)	Specificity (%)	AUC (95%CI)
Training set	Serum CEA	28.0	100.0	0.640 (0.551-0.729)
(*n* = 150 subjects)	FIT	64.0	96.0	0.800 (0.726-0.874)
	PAX8_P4	76.0	77.3	0.810 (0.741-0.880)
	RASSF1_P1	50.7	93.3	0.782 (0.709-0.854)
	SFRP2_P1	50.7	86.7	0.697 (0.612-0.782)
	sDNA panel	82.7	77.3	0.866 (0.810-0.923)
	sDNA panel + FIT	86.7	86.7	0.924 (0.881-0.966)
Test set	Serum CEA	32.0	100.0	0.660 (0.552-0.768)
(*n* = 100 subjects)	FIT	60.0	98.0	0.790 (0.697-0.883)
	sDNA panel	76.0	84.0	0.864 (0.795-0.933)
	sDNA panel + FIT	82.0	96.0	0.909 (0.850-0.967)
Combined set	Serum CEA	29.6	100.0	0.648 (0.580-0.716)
(*n* = 250 subjects)	FIT	62.4	96.8	0.796 (0.738-0.854)
	sDNA panel	75.2	84.0	0.859 (0.815-0.904)
	sDNA panel + FIT	80.0	93.6	0.918 (0.884-0.952)
Subgroup for stage I	FIT	63.8	96.8	0.803 (0.716-0.891)
(*n* = 172 subjects)	sDNA panel + FIT	74.5	93.6	0.891 (0.832-0.950)
Subgroup for stage II	FIT	61.5	96.8	0.792 (0.721-0.863)
(*n* = 203 subjects)	sDNA panel + FIT	83.3	93.6	0.934 (0.899-0.970)

AUC: Area under the receiver operating characteristic curve; CI: Confidence interval; CEA: Carcinoembryonic antigen; FIT: Fecal immunochemical test; sDNA: Stool DNA.

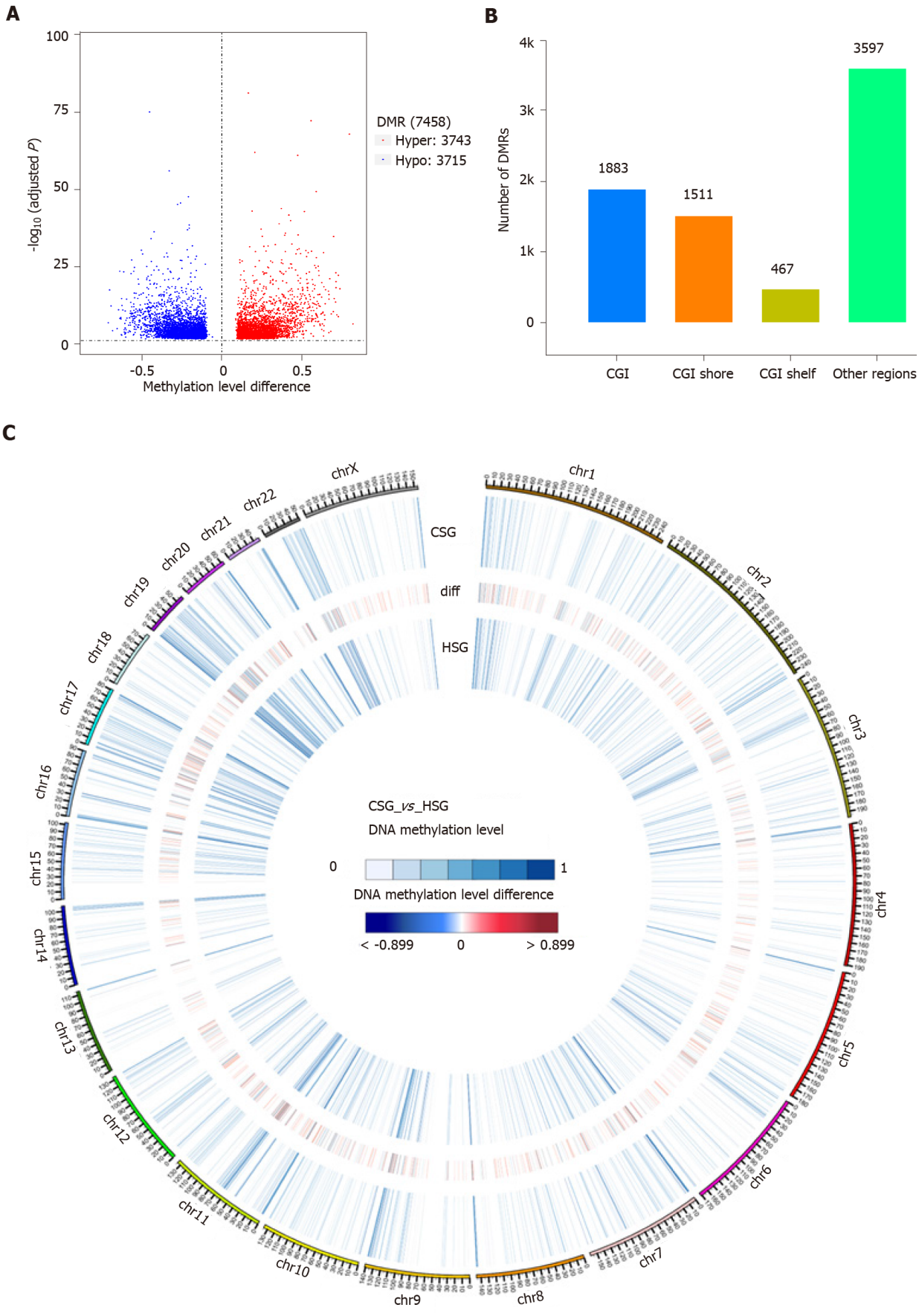
Statistical analysis

All statistical analyses were conducted using Prism 8 for Windows (GraphPad, United States) and R software v3.5.2 (R Foundation for Statistical Computing, Austria). c^2 test or Fisher's exact test was used to compare categorical variables, and Student's *t*-test or Mann-Whitney *U* test was used to compare continuous variables. Principal component analysis (PCA) was performed to visualize the degree of similarity between samples according to their DNA methylation state[21]. A volcano plot and a Circos plot were used to present the differences in DMR methylation levels between groups[22]. To determine the functions and enriched pathways of these DMR-related genes, Gene Ontology (GO) and Kyoto Encyclopedia of Genes and Genomes (KEGG) pathway analyses were performed[23]. The sensitivity, specificity, and area under the ROC curve (AUC) with corresponding 95% confidence intervals (CIs) were calculated and compared. The χ^2 test was also used to assess the association of detection sensitivity with clinicopathological covariates. For all analyses, $P < 0.05$ was considered statistically significant.

RESULTS

Clinicopathological features of the study population

Overall, this study enrolled 125 ECC patients and 125 healthy controls, with a median age of 69 (range, 48-94) and 68 (range, 42-92) years, respectively; 47.2% of patients and 49.6% of controls were females. Age and sex were well-balanced between patients and controls. With the conventional 5 ng/mL cut-off, serum CEA positivity was observed in 29.6% of patients and 0% of controls, and the difference was statistically significant ($P < 0.001$). FIT also showed a significantly higher positivity rate in the patients than in the controls (62.4% *vs* 3.2%, $P < 0.001$). Of these ECCs, 64 (51.2%) tumors were located proximal to the splenic flexure and 61 (48.8%) were distal. According to the postoperative pathological examination, there were 47 (37.6%) stage I tumors and 78 (62.4%) stage II tumors; 98 (78.4%) cases were well or moderately differentiated, and 27 (21.6%) were poorly differentiated. In addition, study participants were randomly divided into training and test sets with a 1.5:1 split. The differences in all these features between the training and test sets were not significant (all $P > 0.05$), indicating similar


A
100
75
50
25
0
-log10 (adjusted P)
-0.5
0
0.5
Methylation level difference
DMR (7458)
Hyper: 3743
Hypo: 3715
B
4k
3k
2k
1k
0
Number of DMRs
1883
1511
467
3597
CGI
CGI shore
CGI shelf
Other regions
C
chrX
chr1
chr22
chr21
chr20
chr19
chr18
chr17
chr16
chr15
chr14
chr13
chr12
chr11
chr10
chr9
chr8
chr7
chr6
chr5
chr4
chr3
chr2
CSG
diff
HSG
CSG_vs_HSG
DNA methylation level
0
1
DNA methylation level difference
< -0.899
0
> 0.899



DOI: 10.3748/wjg.v28.i24.2705 **Copyright** ©The Author(s) 2022.

Figure 3 Differentially methylated region analysis and biomarkers discovery. A: Volcano plot of differentially methylated regions (DMRs) in cancer sample group (CSG) *vs* healthy sample group (HSG); B: The distribution of the identified DMRs in the genome in relation to cytosine-guanine islands (CGIs); C:

Circos plot of 2531 candidate DMRs on each of the 22 autosomes and the X chromosome; D: Kyoto Encyclopedia of Genes and Genomes pathway analysis of 2062 DMR-related genes; E: Gene Ontology analysis of 2062 DMR-related genes; F: Venn diagram of the overlapping target DMRs among different signatures. [a]*P* < 0.05. DMRs: Differentially methylated regions; CGI: Cytosine-guanine islands.

composition and the comparability (Table 2).

DNA methylation analysis by TBSeq

A total of 11.69 G and 11.08 G raw bases were generated on average for the HSG and CSG, respectively. All samples showed a bisulfite conversion rate greater than 99%. After data filtering, approximately 2.8 million CpGs on the target sequencing region were obtained for each sample, and the depth of coverage ranged between 23.66 and 32.24 (Supplementary Table 1). A PCA was performed on the methylation profiles, and demonstrated that the groups had intragroup similarity, but also intergroup dissimilarity (Figure 2A). In addition, the mean methylation densities of the HSG and CSG were 52.8% and 65.4%, respectively (Figure 2B); compared with 50.4% of CpG sites in the HSG, 58.0% of CpG sites in the CSG had a methylation level above 80% (Figure 2C).

Candidate biomarkers discovery

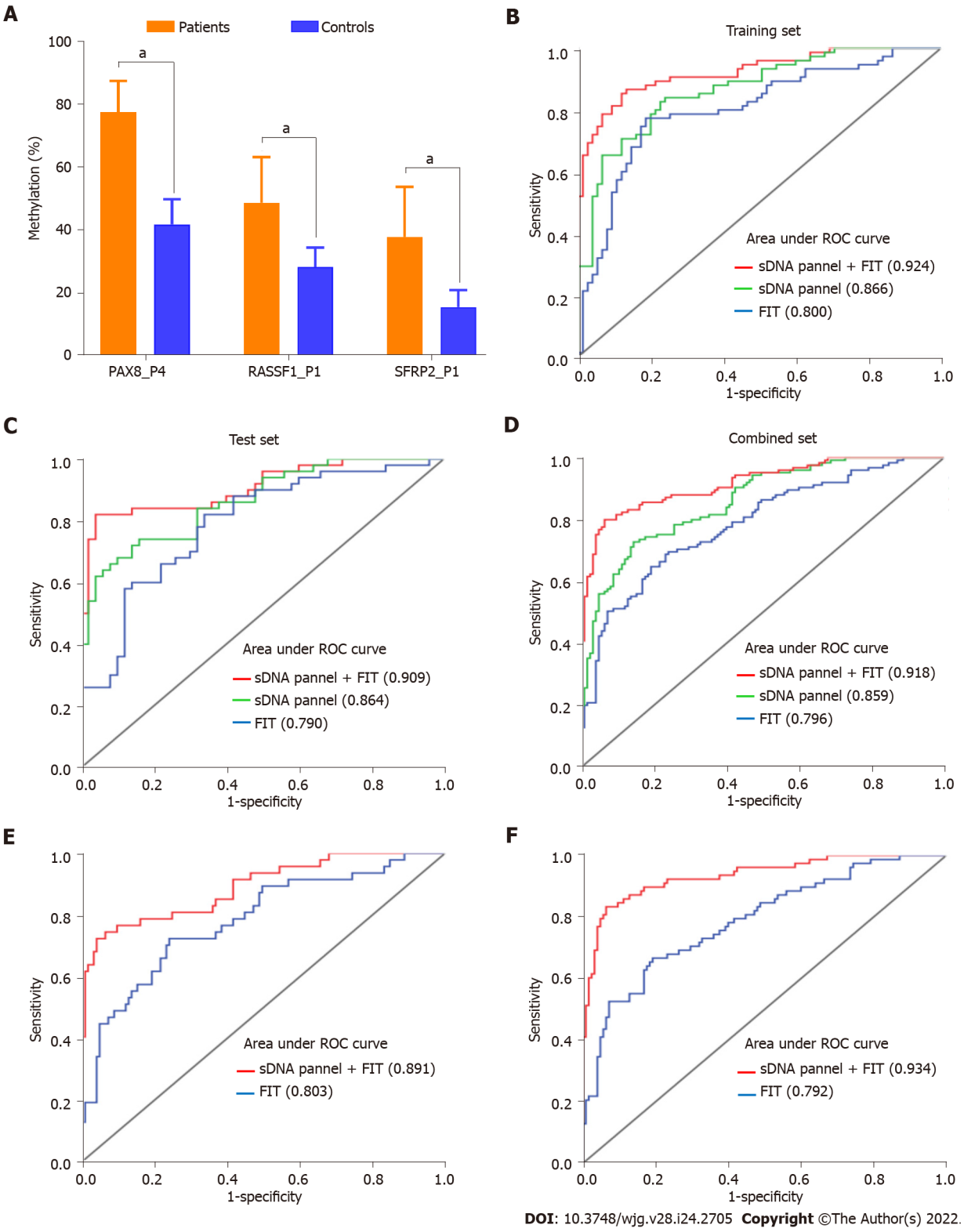
As shown in Figure 3A, in total, 7458 DMRs were identified in the CSG compared with the HSG (adjusted $P < 0.05$ and methylation level difference > 0.1), including 3743 hypermethylated and 3715 hypomethylated DMRs. Among them, 1883 DMRs (25.3%) were located in the CGIs, and 1978 (26.5%) were located in the regions flanking CGIs (CGI shore and shelf) (Figure 3B). Moreover, of the 3861 CGI-related DMRs, 2531 overlapped with the promoter regions of the 20579 genes with known functions (Figure 3C). To determine changes in the methylation status of gene functions, GO and KEGG pathway analyses were conducted and revealed that these 2062 DMR-related genes were significantly enriched in cell migration, focal adhesion, Wnt, Ras, Rap1 and MAPK signaling pathways, *etc* (Figures 3D and 3E, adjusted $P < 0.05$). To mine the data for potential early screening biomarkers, 58 DMR-related genes that differed most in methylation level between the groups and that were involved in the important cancer pathways were selected (Figure 3F). With the PSQ criteria, the top three target CpG regions within the promoters of paired box 8 (PAX8), Ras-association domain family 1 (RASSF1) and SFRP2 were finally identified, and contained five, two and two significant DMSs, respectively (Table 1).

Biomarkers validation by PSQ

To assess the screening effectiveness of these three biomarkers, PSQ was successfully performed in all sDNA samples. Using the 150 subjects in the training set, ROC analyses showed that the AUCs for the five DMSs of PAX8 ranged from 0.784 to 0.826, the AUCs for the two DMSs of RASSF1 were 0.782 and 0.763, and the AUCs for the two DMSs of SFRP2 were 0.697 and 0.641, respectively (Supplementary Figures 1A, 1B and 1C). In addition, serum CEA positivity was detected in 14.0% of the 150 subjects, with a sensitivity of 28.0% and an AUC of 0.640; FIT positivity was detected in 34.0% of the 150 subjects, with a sensitivity of 64.0% and an AUC of 0.800 (Table 3). By stepwise logistic modeling, an sDNA methylation panel including three DMSs was constructed as follows: Y = -10.937 + 0.097 × PAX8_P4 + 0.054 × RASSF1_P1 + 0.058 × SFRP2_P1. These three DMSs showed significantly increased methylation in patients compared with controls (all $P < 0.05$; Figure 4A) as well as in the comparison between the 20 pairs of preoperative and postoperative patient samples (all $P < 0.05$; Supplementary Figures 1D, 1E and 1F). The sensitivity and AUC for this sDNA panel were 82.7% and 0.866 (95%CI: 0.810-0.923), respectively, which were superior to any single index above (Figure 4B, Table 3). Subsequently, this panel was validated in an independent test set, and the AUC reached 0.864 (95%CI: 0.795-0.933), also offering an advantage over FIT (Figure 4C).

Evaluation of the diagnostic model

The diagnostic performance of the sDNA panel was also confirmed in the combined set, achieving an AUC of 0.859 (0.815-0.904) (Figure 4D). In addition, among the 168 subjects with negative FIT and the 213 subjects with negative serum CEA, the AUCs for this panel reached 0.807 (95%CI: 0.734-0.880) and 0.864 (95%CI: 0.816-0.913), respectively (Supplementary Figure 2). We further investigated whether the combination of the sDNA panel with clinical variables could improve the effectiveness of ECC screening. The results showed that the inclusion of FIT was accompanied by a relative increase in sensitivity and AUC, as compared with the sDNA panel, serum CEA or FIT alone (Table 3, Figure 5). In contrast, the contribution of age, sex or preoperative CEA level to aggregate panel discrimination was minimal (data not shown). For example, in the combined set, the sensitivity, specificity and AUC for the sDNA panel combining FIT were up to 80.0%, 93.6% and 0.918 (95%CI: 0.884-0.952), respectively (Figure 4D, Table 3). In the subgroup analysis by tumor stage, this multiplex assay showed excellent performance for both stage I and II ECCs, with an AUC of 0.891 (95%CI: 0.832-0.950) and 0.934 (95%CI: 0.899-0.970), respectively (Figures 4E and 4F).



DOI: 10.3748/wjg.v28.i24.2705 **Copyright** ©The Author(s) 2022.

Figure 4 The evaluation of diagnostic model based on pyrosequencing. A: Comparison of methylation percentage of the three target biomarkers between the patients and controls in training set; B: Receiver operating characteristic (ROC) curves comparing fecal immunochemical test (FIT), stool DNA (sDNA) panel and sDNA panel + FIT for the detection of early-stage colon cancer (ECC) in training set; C: ROC curves comparing FIT, sDNA panel and sDNA panel + FIT for the detection of ECC in test set; D: ROC curves comparing FIT, sDNA panel and sDNA panel + FIT for the detection of ECC in combined set; E: ROC curves comparing FIT and sDNA panel + FIT for the detection of stage I ECC in combined set; F: ROC curves comparing FIT and sDNA panel + FIT for the detection of stage II ECC in combined set. [a]*P* < 0.05. sDNA: Stool DNA; FIT: Fecal immunochemical test; ROC: Receiver operating characteristic; PAX8: Paired box 8; RASSF1: Ras-association domain family 1; SFRP2: Secreted frizzled-related protein 2.

Impact of covariates on screening

We also analyzed the impact of clinicopathologic covariates on assay screening. First, we found that the

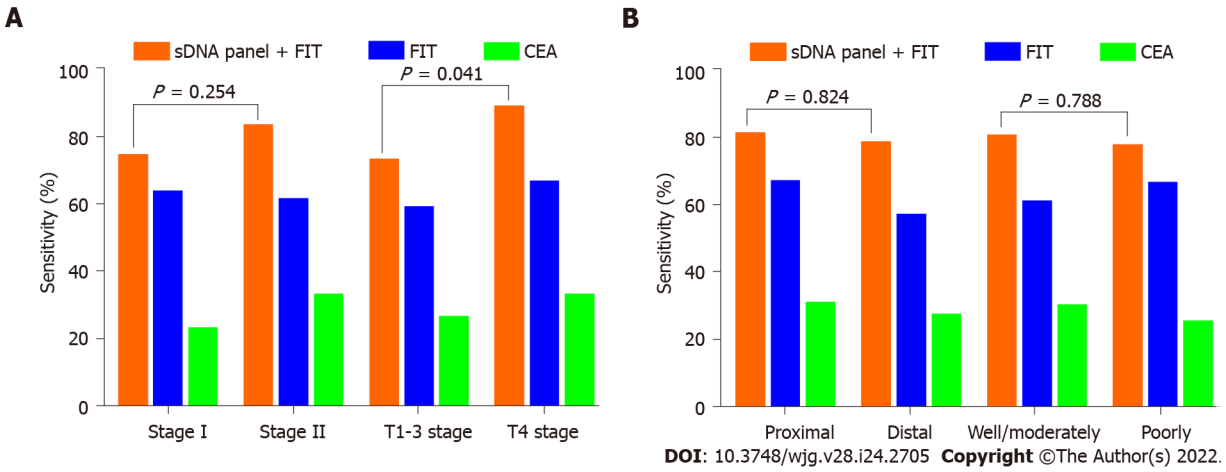


Figure 5 Impact of clinicopathologic covariates on screening. A: Sensitivities of fecal immunochemical test (FIT), serum carcinoembryonic antigen (CEA) and stool DNA (sDNA) panel + FIT for the detection of early-stage colon cancer (ECC), according to tumor-node-metastasis stage or T stage; B: Sensitivities of FIT, serum CEA and sDNA panel + FIT for the detection of ECC, according to tumor site or histological differentiation. sDNA: Stool DNA; FIT: Fecal immunochemical test; CEA: Carcinoembryonic antigen.

detection sensitivities of the sDNA panel combining FIT for stage I and II ECCs were 74.5% and 83.3%, respectively, with no statistical difference (P = 0.254; Figure 5A). However, the detection sensitivity of 88.9% for T4 stage tumors was significantly higher than the aggregate sensitivity of 73.2% for T1-3 stage tumors (P = 0.041; Figure 5A). Second, this multiplex assay detected 81.3% of proximal ECCs *vs* 78.7% of distal ECCs (P = 0.824; Figure 5B). Third, the detection rate for poorly differentiated tumors was comparable to that for well or moderately differentiated tumors (77.8% *vs* 80.6%, P = 0.788; Figure 5B). In addition, the sensitivity also did not vary significantly according to age or sex of the patients (data not shown).

DISCUSSION

CRC is the third most prevalent cancer in China, with an increasing proportion of colon cancer diagnoses over the decades[2]. Effective screening measures are highly needed to lessen this burden, especially for ECC due to its occult onset. Compared with conventional methods, the sDNA test provides a biologically rational approach based on tumor exfoliation and is noninvasive, requires no unpleasant cathartic preparation, no diet or medication restriction[24]. However, reliable biomarkers particularly for ECC detection are lacking. In the present study, we provided a novel multiplex stool-based assay that enabled the diagnosis of ECC with high sensitivity and specificity.

Aberrant DNA methylation is an early and frequent event in carcinogenesis and therefore has great potential for ECC screening[25]. To identify the candidate methylation biomarkers, we performed high throughput TBSeq with five pairs of preoperative and postoperative sDNA samples from ECC patients, where the paired design can help reduce the influence of background noise and improve the feature discriminability. Three of our candidate biomarkers were finally selected: RASSF1, SFRP2 and PAX8. The first two have been identified in various cancers including CRC[26,27], to be the commonly silenced tumor-suppressor genes by promoter hypermethylation[28]. PAX8 is a member of the paired box family of transcription factors[29], and its epigenetic silencing has also been observed in some tumor types, including colon cancer[30]. A recent study found that PAX8 hypermethylation accelerated gastrointestinal stromal tumor progression by downregulating Wnt4 expression[31]. Anglim *et al*[32] reported a panel of eight hypermethylated genes containing PAX8, which showed high sensitivity and specificity for the early detection of squamous cell lung cancer.

To date, there have been various methods for detecting abnormal DNA methylation[33,34]. MSP is a simple, rapid and inexpensive method, but is not capable of pattern recognition and identification of CpG sites outside the methylation-specific primers. Bisulfite sequencing was once considered the gold standard for DNA methylation determination. The disadvantage lies in its tedious and time-consuming procedure, and a minimum number of 10-20 clones are required to detect interindividual variabilities in DNA methylation. Methylation-sensitive high-resolution melting is a relatively new technique for methylation assessment based on post-PCR melting curve analysis. It gives a range of methylation estimates rather than a single value, being mainly suitable for large sample screening[35]. MethyLight is a sensitive, high-throughput methylation assay that was developed based on MSP, while the major disadvantage is the high cost of a TaqMan probe[36,37]. In our study, biomarker validation was performed using PSQ, which overcomes the defects of the above methods, combining the measurement

of multiple methylation biomarkers with high throughput in a single test[38]. Therefore, PSQ has been suggested as the new gold standard test for methylation detection. The results of PSQ confirmed that the three biomarkers by TBSeq were reliable and feasible.

By logistic regression analysis, a three-DMS panel was developed in this study and was proven more effective than a single biomarker for ECC screening. We further found that the combined detection of the sDNA panel and FIT was characterized by a relative increase in diagnostic performance, which was successfully validated in an independent test set, as well as in the combined dataset. Actually, many attempts at CRC early screening in the Chinese population have been made, but none have gained wide acceptance[12]. Liu *et al*[39] developed an sDNA methylation panel, including COL4A2 and TLX2, which showed a high sensitivity of 91% for advanced-stage CRC detection with 97% specificity, but the performance for early-stage CRC was significantly weakened, with a sensitivity of 52% and specificity of 86%. In the study by Zhang *et al*[40], an sDNA panel that examined SFRP2 and WIF-1 promoter methylation was identified, and the sensitivities for detecting stage I and II CRC were 55% and 80%, respectively. Recently, another novel multidimensional assay combining FIT, sDNA mutation, methylation and intestinal bacteria analysis was reported by Mo *et al*[41]. It displayed the highest sensitivity of 91.89% in stage III CRC, whereas the sensitivity for stage I-II CRC was relatively low (76.27%). Comparatively, the sensitivity, specificity and AUC of our multiplex stool-based assay for detecting ECC reached 80.0%, 93.6% and 0.918, respectively, showing a promising prospect for practical application.

The effect of covariates on test performance was also investigated. It has been suggested that the conventional screening modalities, including colonoscopy and FIT, seem less sensitive for proximal than distal colon neoplasms[42,43]. In this study, our stool multiplex assay showed comparable efficacy for the detection of both proximal and distal ECC, which was consistent with the previous finding by Imperiale *et al*[13]. Given this performance characteristic, the sDNA test has the potential to improve the screening efficiency for neoplasms throughout the colon, and would be a valuable complement to colonoscopy as an interval test. Furthermore, we found that the sensitivity of this stool multiplex assay for ECC did not vary significantly according to age, sex, histological differentiation or tumor stage, but was significantly higher at T4 stage. Further studies are needed to determine their association and causality. In addition, some studies revealed that the sDNA test sensitivity increased as the tumor size increased[13,41]. Unfortunately, this variable was not included in our study.

The major strength of our study was the training and test set design involving blinded assays in the laboratory, which provided objective data to assess the test performance. The limitations of this study should also be mentioned. First, these analyses were based on data obtained from a single institution in China, and the sample size was relatively small. Second, other factors not included in this study could not be examined for confounding effects. As a result, a large-scale, prospective multicenter study is warranted to further confirm the value of our assay.

CONCLUSION

In conclusion, we developed and validated a novel multiplex stool-based assay combining sDNA methylation biomarkers and FIT, which could detect ECC with high accuracy throughout the colon.

ARTICLE HIGHLIGHTS

Research background

Colorectal cancer (CRC) is one of the most prevalent malignancies in China with an increasing ratio of colon to rectal cancer over the decades. Early screening is the key to reducing this burden. The traditional screening methods, including colonoscopy, fecal immunochemical test (FIT) and serum carcinoembryonic antigen (CEA), have reached a bottleneck, especially for early-stage colon cancer (ECC) due to its occult onset. Thus, precision and effective non-invasive biomarkers are highly desirable.

Research motivation

Detection of aberrant methylated DNA in stool has been proven to be a promising noninvasive method for the early diagnosis of CRC. However, the reported screening efficacy of the same biomarker varied across different studies. Moreover, effective biomarkers for detecting ECC are scarce, especially in the Chinese population.

Research objectives

The objective of our study was to identify a novel assay based on stool DNA (sDNA) methylation biomarkers which could improve the effectiveness of ECC screening. We also investigated the influence of clinicopathologic covariates on test performance.

Research methods

We performed a blinded, single-center, case-control study using archived stool samples from 125 ECC patients and 125 individuals with normal colonoscopy (controls); the subjects were randomly assigned to a training or test set at a 1.5:1 ratio. Targeted bisulfite sequencing (TBSeq) was performed on five pairs of preoperative and postoperative sDNA samples from ECC patients to identify DNA methylation biomarkers. Pyrosequencing (PSQ) was used for validation of the candidate biomarkers in large samples. A stepwise logistic regression analysis was applied to the data of the training set to develop a multiplex stool-based assay. The detection performance was further evaluated in the test set and combined set. In addition, the association of detection sensitivity with clinicopathologic covariates were analyzed by χ^2 test.

Research results

Through TBSeq, the three top hypermethylated genes, paired box 8, Ras-association domain family 1 and secreted frizzled-related protein 2, that were involved in the important cancer pathways were selected as biomarkers. Based on the PSQ results, an sDNA panel containing the three biomarkers was developed by logistic regression modelling. Receiver operating characteristic (ROC) analysis showed that this panel offered an advantage over any single biomarker, FIT or serum CEA in the detection of ECC. Further analysis revealed that the inclusion of FIT could effectively improve the detection accuracy. In the combined set, the sensitivity, specificity and area under the ROC curve for the sDNA panel combining FIT reached 80.0%, 93.6% and 0.918, respectively. Moreover, this multiplex assay maintained excellent performance in the subgroup by tumor stage. Additionally, we found that the detection sensitivity of the multiplex assay was significantly higher in T4 than in T1-3 stage tumors (P = 0.041), but was not affected by tumor site, tumor stage, histological differentiation, age or sex.

Research conclusions

The present study identified a novel multiplex stool-based assay, including three sDNA methylation biomarkers and FIT, capable of detecting ECC with high sensitivity and specificity. Importantly, the detection rate by this assay was related to T stage but not tumor site, tumor stage, histological differentiation, *etc*.

Research perspectives

Our study provided a new and promising approach for improvement of ECC screening in the Chinese population. Further demonstrations on a large-scale, prospective multicenter study are needed to conclusively evaluate its value.

FOOTNOTES

Author contributions: Jiang HH, Xing SW and Lin K performed the experiments; Tang X, Chen Y, and Lin K participated to the collection of the clinical data and samples; Jiang HH, He LW, and Tang EJ analyzed and interpreted the data; Tang EJ, Lin MB and He LW conceived and managed the study; Jiang HH and Xing SW drafted the manuscript; and all authors have read and approve the final manuscript.

Supported by Shanghai Pujiang Program, No. 21PJD066; Shanghai Municipal Commission of Health and Family Planning, No. ZK2019A19; Shanghai Municipal Science and Technology Commission, No. 19411971500; and Shanghai Yangpu District Science and Technology Commission, No. YPM202101.

Institutional review board statement: This study was reviewed and approved by the Ethics Committee of Yangpu Hospital, Tongji University (LL-2018-SCI-003).

Clinical trial registration statement: This study was registered at the Chinese Clinical Trial Registry (ChiCTR1800019552).

Informed consent statement: All study participants or their legal guardian provided informed written consent about personal and medical data collection prior to study enrolment.

Conflict-of-interest statement: The authors have no conflicts of interest to declare.

Data sharing statement: No additional data are available.

Open-Access: This article is an open-access article that was selected by an in-house editor and fully peer-reviewed by external reviewers. It is distributed in accordance with the Creative Commons Attribution NonCommercial (CC BY-NC 4.0) license, which permits others to distribute, remix, adapt, build upon this work non-commercially, and license their derivative works on different terms, provided the original work is properly cited and the use is non-commercial. See: https://creativecommons.org/Licenses/by-nc/4.0/

Country/Territory of origin: China

ORCID number: Hui-Hong Jiang 0000-0002-7391-1767; Si-Wei Xing 0000-0002-7222-1043; Xuan Tang 0000-0002-5895-3467; Ying Chen 0000-0001-5084-7507; Kang Lin 0000-0002-3485-6574; Lu-Wei He 0000-0001-6564-848X; Mou-Bin Lin 0000-0002-0686-688X; Er-Jiang Tang 0000-0002-8042-5994.

S-Editor: Wang JJ
L-Editor: A
P-Editor: Wang JJ

REFERENCES

1 **Cao W**, Chen HD, Yu YW, Li N, Chen WQ. Changing profiles of cancer burden worldwide and in China: a secondary analysis of the global cancer statistics 2020. *Chin Med J (Engl)* 2021; **134**: 783-791 [PMID: 33734139 DOI: 10.1097/CM9.0000000000001474]
2 **Zhang L**, Cao F, Zhang G, Shi L, Chen S, Zhang Z, Zhi W, Ma T. Trends in and Predictions of Colorectal Cancer Incidence and Mortality in China From 1990 to 2025. *Front Oncol* 2019; **9**: 98 [PMID: 30847304 DOI: 10.3389/fonc.2019.00098]
3 **Levin TR**, Corley DA, Jensen CD, Schottinger JE, Quinn VP, Zauber AG, Lee JK, Zhao WK, Udaltsova N, Ghai NR, Lee AT, Quesenberry CP, Fireman BH, Doubeni CA. Effects of Organized Colorectal Cancer Screening on Cancer Incidence and Mortality in a Large Community-Based Population. *Gastroenterology* 2018; **155**: 1383-1391.e5 [PMID: 30031768 DOI: 10.1053/j.gastro.2018.07.017]
4 **Harrison NM**, Hjelkrem MC. Bowel cleansing before colonoscopy: Balancing efficacy, safety, cost and patient tolerance. *World J Gastrointest Endosc* 2016; **8**: 4-12 [PMID: 26788258 DOI: 10.4253/wjge.v8.i1.4]
5 **Lou S**, Shaukat A. Noninvasive strategies for colorectal cancer screening: opportunities and limitations. *Curr Opin Gastroenterol* 2021; **37**: 44-51 [PMID: 33074994 DOI: 10.1097/MOG.0000000000000688]
6 **Bailey JR**, Aggarwal A, Imperiale TF. Colorectal Cancer Screening: Stool DNA and Other Noninvasive Modalities. *Gut Liver* 2016; **10**: 204-211 [PMID: 26934885 DOI: 10.5009/gnl15420]
7 **Hong SN**. Genetic and epigenetic alterations of colorectal cancer. *Intest Res* 2018; **16**: 327-337 [PMID: 30090031 DOI: 10.5217/ir.2018.16.3.327]
8 **Ewing I**, Hurley JJ, Josephides E, Millar A. The molecular genetics of colorectal cancer. *Frontline Gastroenterol* 2014; **5**: 26-30 [PMID: 24416503 DOI: 10.1136/flgastro-2013-100329]
9 **Boynton KA**, Summerhayes IC, Ahlquist DA, Shuber AP. DNA integrity as a potential marker for stool-based detection of colorectal cancer. *Clin Chem* 2003; **49**: 1058-1065 [PMID: 12816901 DOI: 10.1373/49.7.1058]
10 **Ahlquist DA**. Molecular detection of colorectal neoplasia. *Gastroenterology* 2010; **138**: 2127-2139 [PMID: 20420950 DOI: 10.1053/j.gastro.2010.01.055]
11 **Tse JWT**, Jenkins LJ, Chionh F, Mariadason JM. Aberrant DNA Methylation in Colorectal Cancer: What Should We Target? *Trends Cancer* 2017; **3**: 698-712 [PMID: 28958388 DOI: 10.1016/j.trecan.2017.08.003]
12 **Raut JR**, Guan Z, Schrotz-King P, Brenner H. Fecal DNA methylation markers for detecting stages of colorectal cancer and its precursors: a systematic review. *Clin Epigenetics* 2020; **12**: 122 [PMID: 32778176 DOI: 10.1186/s13148-020-00904-7]
13 **Imperiale TF**, Ransohoff DF, Itzkowitz SH, Levin TR, Lavin P, Lidgard GP, Ahlquist DA, Berger BM. Multitarget stool DNA testing for colorectal-cancer screening. *N Engl J Med* 2014; **370**: 1287-1297 [PMID: 24645800 DOI: 10.1056/NEJMoa1311194]
14 **Jin H**, Wang J, Zhang C. The Value of Multi-targeted Fecal DNA Methylation Detection for Colorectal Cancer Screening in a Chinese Population. *J Cancer* 2021; **12**: 1644-1650 [PMID: 33613751 DOI: 10.7150/jca.47214]
15 **Kim MS**, Lee J, Sidransky D. DNA methylation markers in colorectal cancer. *Cancer Metastasis Rev* 2010; **29**: 181-206 [PMID: 20135198 DOI: 10.1007/s10555-010-9207-6]
16 **Lee EJ**, Luo J, Wilson JM, Shi H. Analyzing the cancer methylome through targeted bisulfite sequencing. *Cancer Lett* 2013; **340**: 171-178 [PMID: 23200671 DOI: 10.1016/j.canlet.2012.10.040]
17 **Morselli M**, Farrell C, Rubbi L, Fehling HL, Henkhaus R, Pellegrini M. Targeted bisulfite sequencing for biomarker discovery. *Methods* 2021; **187**: 13-27 [PMID: 32755621 DOI: 10.1016/j.ymeth.2020.07.006]
18 **Jones PA**. Functions of DNA methylation: islands, start sites, gene bodies and beyond. *Nat Rev Genet* 2012; **13**: 484-492 [PMID: 22641018 DOI: 10.1038/nrg3230]
19 **Delaney C**, Garg SK, Yung R. Analysis of DNA Methylation by Pyrosequencing. *Methods Mol Biol* 2015; **1343**: 249-264 [PMID: 26420722 DOI: 10.1007/978-1-4939-2963-4_19]
20 **LaValley MP**. Logistic regression. *Circulation* 2008; **117**: 2395-2399 [PMID: 18458181 DOI: 10.1161/CIRCULATIONAHA.106.682658]
21 **Jolliffe IT**, Cadima J. Principal component analysis: a review and recent developments. *Philos Trans A Math Phys Eng Sci* 2016; **374**: 20150202 [PMID: 26953178 DOI: 10.1098/rsta.2015.0202]
22 **Zhang H**, Meltzer P, Davis S. RCircos: an R package for Circos 2D track plots. *BMC Bioinformatics* 2013; **14**: 244 [PMID: 23937229 DOI: 10.1186/1471-2105-14-244]
23 **Yu G**, Wang LG, Han Y, He QY. clusterProfiler: an R package for comparing biological themes among gene clusters. *OMICS* 2012; **16**: 284-287 [PMID: 22455463 DOI: 10.1089/omi.2011.0118]
24 **Ahlquist DA**. Multi-target stool DNA test: a new high bar for noninvasive screening. *Dig Dis Sci* 2015; **60**: 623-633 [PMID: 25492503 DOI: 10.1007/s10620-014-3451-5]

25 **Verma M**, Kumar V. Epigenetic Biomarkers in Colorectal Cancer. *Mol Diagn Ther* 2017; **21**: 153-165 [PMID: 27878475 DOI: 10.1007/s40291-016-0244-x]

26 **Toyota M**, Yamamoto E. DNA methylation changes in cancer. *Prog Mol Biol Transl Sci* 2011; **101**: 447-457 [PMID: 21507361 DOI: 10.1016/B978-0-12-387685-0.00014-7]

27 **Strzelczyk JK**, Krakowczyk Ł, Owczarek AJ. Methylation status of SFRP1, SFRP2, RASSF1A, RARβ and DAPK1 genes in patients with oral squamous cell carcinoma. *Arch Oral Biol* 2019; **98**: 265-272 [PMID: 30576962 DOI: 10.1016/j.archoralbio.2018.12.001]

28 **Rasmussen SL**, Krarup HB, Sunesen KG, Pedersen IS, Madsen PH, Thorlacius-Ussing O. Hypermethylated DNA as a biomarker for colorectal cancer: a systematic review. *Colorectal Dis* 2016; **18**: 549-561 [PMID: 26998585 DOI: 10.1111/codi.13336]

29 **Laury AR**, Perets R, Piao H, Krane JF, Barletta JA, French C, Chirieac LR, Lis R, Loda M, Hornick JL, Drapkin R, Hirsch MS. A comprehensive analysis of PAX8 expression in human epithelial tumors. *Am J Surg Pathol* 2011; **35**: 816-826 [PMID: 21552115 DOI: 10.1097/PAS.0b013e318216c112]

30 **Ehrich M**, Turner J, Gibbs P, Lipton L, Giovanneti M, Cantor C, van den Boom D. Cytosine methylation profiling of cancer cell lines. *Proc Natl Acad Sci U S A* 2008; **105**: 4844-4849 [PMID: 18353987 DOI: 10.1073/pnas.0712251105]

31 **Miao Z**, Wu F, Wei H, Luo Z, Wu K, Zhang J. Enhancer of zeste homolog 2-mediated paired box 8 methylation promotes gastrointestinal stromal tumor progression through Wnt4 downregulation. *Cancer Gene Ther* 2021; **28**: 1162-1174 [PMID: 33479444 DOI: 10.1038/s41417-020-00266-5]

32 **Anglim PP**, Galler JS, Koss MN, Hagen JA, Turla S, Campan M, Weisenberger DJ, Laird PW, Siegmund KD, Laird-Offringa IA. Identification of a panel of sensitive and specific DNA methylation markers for squamous cell lung cancer. *Mol Cancer* 2008; **7**: 62 [PMID: 18616821 DOI: 10.1186/1476-4598-7-62]

33 **Hernández HG**, Tse MY, Pang SC, Arboleda H, Forero DA. Optimizing methodologies for PCR-based DNA methylation analysis. *Biotechniques* 2013; **55**: 181-197 [PMID: 24107250 DOI: 10.2144/000114087]

34 **Wani K**, Aldape KD. PCR Techniques in Characterizing DNA Methylation. *Methods Mol Biol* 2016; **1392**: 177-186 [PMID: 26843056 DOI: 10.1007/978-1-4939-3360-0_16]

35 **Akika R**, Awada Z, Mogharbil N, Zgheib NK. Region of interest methylation analysis: a comparison of MSP with MS-HRM and direct BSP. *Mol Biol Rep* 2017; **44**: 295-305 [PMID: 28676996 DOI: 10.1007/s11033-017-4110-7]

36 **Šestáková Š**, Šálek C, Remešová H. DNA Methylation Validation Methods: a Coherent Review with Practical Comparison. *Biol Proced Online* 2019; **21**: 19 [PMID: 31582911 DOI: 10.1186/s12575-019-0107-z]

37 **Umer M**, Herceg Z. Deciphering the epigenetic code: an overview of DNA methylation analysis methods. *Antioxid Redox Signal* 2013; **18**: 1972-1986 [PMID: 23121567 DOI: 10.1089/ars.2012.4923]

38 **Poulin M**, Zhou JY, Yan L, Shioda T. Pyrosequencing Methylation Analysis. *Methods Mol Biol* 2018; **1856**: 283-296 [PMID: 30178259 DOI: 10.1007/978-1-4939-8751-1_17]

39 **Liu X**, Wen J, Li C, Wang H, Wang J, Zou H. High-Yield Methylation Markers for Stool-Based Detection of Colorectal Cancer. *Dig Dis Sci* 2020; **65**: 1710-1719 [PMID: 31720923 DOI: 10.1007/s10620-019-05908-9]

40 **Zhang H**, Zhu YQ, Wu YQ, Zhang P, Qi J. Detection of promoter hypermethylation of Wnt antagonist genes in fecal samples for diagnosis of early colorectal cancer. *World J Gastroenterol* 2014; **20**: 6329-6335 [PMID: 24876755 DOI: 10.3748/wjg.v20.i20.6329]

41 **Mo S**, Wang H, Han L, Xiang W, Dai W, Zhao P, Pei F, Su Z, Ma C, Li Q, Wang Z, Cai S, Liu R, Cai G. Fecal Multidimensional Assay for Non-Invasive Detection of Colorectal Cancer: Fecal Immunochemical Test, Stool DNA Mutation, Methylation, and Intestinal Bacteria Analysis. *Front Oncol* 2021; **11**: 643136 [PMID: 33718241 DOI: 10.3389/fonc.2021.643136]

42 **Morikawa T**, Kato J, Yamaji Y, Wada R, Mitsushima T, Shiratori Y. A comparison of the immunochemical fecal occult blood test and total colonoscopy in the asymptomatic population. *Gastroenterology* 2005; **129**: 422-428 [PMID: 16083699 DOI: 10.1016/j.gastro.2005.05.056]

43 **Brenner H**, Chang-Claude J, Seiler CM, Rickert A, Hoffmeister M. Protection from colorectal cancer after colonoscopy: a population-based, case-control study. *Ann Intern Med* 2011; **154**: 22-30 [PMID: 21200035 DOI: 10.7326/0003-4819-154-1-201101040-00004]

World Journal of Gastroenterology

Submit a Manuscript: https://www.f6publishing.com

World J Gastroenterol 2022 June 28; 28(24): 2721-2732

DOI: 10.3748/wjg.v28.i24.2721

ISSN 1007-9327 (print) ISSN 2219-2840 (online)

ORIGINAL ARTICLE

Retrospective Cohort Study

Utility of a deep learning model and a clinical model for predicting bleeding after endoscopic submucosal dissection in patients with early gastric cancer

Ji Eun Na, Yeong Chan Lee, Tae Jun Kim, Hyuk Lee, Hong-Hee Won, Yang Won Min, Byung-Hoon Min, Jun Haeng Lee, Poong-Lyul Rhee, Jae J Kim

Specialty type: Gastroenterology and hepatology

Provenance and peer review: Unsolicited article; Externally peer reviewed.

Peer-review model: Single blind

Peer-review report's scientific quality classification

Grade A (Excellent): 0
Grade B (Very good): B, B
Grade C (Good): C
Grade D (Fair): 0
Grade E (Poor): 0

P-Reviewer: Pattarajierapan S, Thailand; Singh A, India; Sulbaran MN, Brazil

Received: October 30, 2021
Peer-review started: October 30, 2021
First decision: March 11, 2022
Revised: March 25, 2022
Accepted: May 8, 2022
Article in press: May 8, 2022
Published online: June 28, 2022

Ji Eun Na, Department of Internal Medicine, Inje University Haeundae Paik Hospital, Busan 48108, South Korea

Ji Eun Na, Tae Jun Kim, Hyuk Lee, Yang Won Min, Byung-Hoon Min, Jun Haeng Lee, Poong-Lyul Rhee, Jae J Kim, Department of Medicine, Samsung Medical Center, Sungkyunkwan University School of Medicine, Seoul 06351, South Korea

Yeong Chan Lee, Hong-Hee Won, Department of Digital Health, Samsung Advanced Institute for Health Science and Technology, Sungkyunkwan University, Seoul 06351, South Korea

Corresponding author: Hyuk Lee, MD, PhD, Doctor, Department of Medicine, Samsung Medical Center, Sungkyunkwan University School of Medicine, 81 Irwon-ro, Gangnam-gu, Seoul 06351, South Korea. leehyuk@skku.edu

Abstract

BACKGROUND

Bleeding is one of the major complications after endoscopic submucosal dissection (ESD) in early gastric cancer (EGC) patients. There are limited studies on estimating the bleeding risk after ESD using an artificial intelligence system.

AIM

To derivate and verify the performance of the deep learning model and the clinical model for predicting bleeding risk after ESD in EGC patients.

METHODS

Patients with EGC who underwent ESD between January 2010 and June 2020 at the Samsung Medical Center were enrolled, and post-ESD bleeding (PEB) was investigated retrospectively. We split the entire cohort into a development set (80%) and a validation set (20%). The deep learning and clinical model were built on the development set and tested in the validation set. The performance of the deep learning model and the clinical model were compared using the area under the curve and the stratification of bleeding risk after ESD.

RESULTS

A total of 5629 patients were included, and PEB occurred in 325 patients. The area

under the curve for predicting PEB was 0.71 (95% confidence interval: 0.63-0.78) in the deep learning model and 0.70 (95% confidence interval: 0.62-0.77) in the clinical model, without significant difference (P = 0.730). The patients expected to the low- (< 5%), intermediate- (≥ 5%, < 9%), and high-risk (≥ 9%) categories were observed with actual bleeding rate of 2.2%, 3.9%, and 11.6%, respectively, in the deep learning model; 4.0%, 8.8%, and 18.2%, respectively, in the clinical model.

CONCLUSION

A deep learning model can predict and stratify the bleeding risk after ESD in patients with EGC.

Key Words: Clinical model; Deep learning model; Post-endoscopic submucosal dissection bleeding; Stratification of bleeding risk

©The Author(s) 2022. Published by Baishideng Publishing Group Inc. All rights reserved.

Core Tip: Bleeding is one of the major complications after endoscopic submucosal dissection (ESD) in early gastric cancer patients and requires hospital-based intervention. We established a deep learning model to stratify the bleeding risk after ESD and demonstrated its performance compared with a clinical model. The deep learning model showed acceptable area under the curve and could stratify the post-ESD bleeding risk as low-, intermediate-, and high-risk categories, which correlated with actual bleeding rate comparatively. A deep learning model would be valuable in assessing the bleeding risk after ESD in early gastric cancer patients.

Citation: Na JE, Lee YC, Kim TJ, Lee H, Won HH, Min YW, Min BH, Lee JH, Rhee PL, Kim JJ. Utility of a deep learning model and a clinical model for predicting bleeding after endoscopic submucosal dissection in patients with early gastric cancer. *World J Gastroenterol* 2022; 28(24): 2721-2732
URL: https://www.wjgnet.com/1007-9327/full/v28/i24/2721.htm
DOI: https://dx.doi.org/10.3748/wjg.v28.i24.2721

INTRODUCTION

In South Korea, gastric cancer has a high incidence and is the second most common malignancy and the fourth most common cause of cancer-related mortality[1]. After the advent of screening programs for gastric cancer in South Korea and Japan, up to 50%–70% of cases with gastric cancers have been diagnosed at an early stage[2-4]. With the increasing rate of diagnosis at early stages, endoscopic submucosal dissection (ESD) is being actively applied for the minimally invasive treatment of early gastric cancer (EGC) without suspicion of regional lymph node metastasis[5,6].

In accordance with the current trend of active use of ESD, it is necessary to pay attention to the post-ESD complications. Bleeding is one of the significant complications, with an incidence of 3.6%–6.9%[7, 8]. Because bleeding after ESD requires hospitalization and hemostatic interventions, there is a need to predict patients at a high risk of bleeding after ESD. Therefore, there have been reports on risk factors related to bleeding after ESD[9-12]. Recently, a predictive risk-scoring model for bleeding after ESD was proposed in Japan; this tool is expected to raise awareness regarding the potential bleeding sources and thus, help physicians manage patients with EGC who are treated with ESD[13].

Currently, artificial intelligence systems are being applied in various fields of gastroenterology[14]. The machine learning models showed good performance in the triage of necessity for intervention in patients with upper gastrointestinal bleeding and predicting recurrent ulcer bleeding[15,16]. Deep learning is advantageous over the machine learning model among artificial intelligence systems; its performance is optimized by automatic learning while experiencing various cases. It can integrate and interpret multiple factors simultaneously without external intervention. Hence, the automatically trained deep learning model can generalize well. There has been no study on the efficacy of deep learning for predicting post-ESD bleeding (PEB), and no study has compared these systems with a clinical model.

This study aimed to develop and compare the performance of the deep learning and clinical model for predicting PEB in EGC patients. We chose deep learning among the artificial intelligence systems as a sophisticated algorithm.

MATERIALS AND METHODS

Patients

Patients who underwent ESD for EGC between January 2010 and June 2020 at the Samsung Medical Center, Seoul, South Korea, were screened retrospectively. We excluded cases with: Failure to complete ESD (n = 1); prior gastrectomy (n = 2); additional gastrectomy within 28 d after ESD (n = 497); no residual tumor in the ESD specimen (n = 48); multiple procedures, such as EMR for other benign lesions and ESD for EGC (n = 46); and missing values for important variables (n = 7) (Figure 1). A total of 5629 patients were included in the analysis, and they were randomly categorized into the development set (80%) and the validation set (20%). The Institutional Review Board of the Samsung Medical Center, Korea, approved this study, and the requirement for obtaining informed consent was waived owing to the study's retrospective nature.

Outcome, data sources, study variables, and definitions

The main outcome included the development of a deep learning model and a clinical model that predict the bleeding after ESD in patients with EGC and the comparison of performance between the deep learning model and the clinical model.

The variables used to build the deep learning and clinical models were collected from the medical records retrospectively based on the date of ESD. These variables included: Age; sex; comorbidities such as hypertension, diabetes mellitus, liver cirrhosis, and chronic kidney disease (estimated glomerular filtration rate < 60 mL/min per 1.73 m^2); patient management with antithrombotic agents (ATs) [aspirin, P2Y12 receptor agonist (P2Y12RA), warfarin, direct-acting oral anticoagulants (DOAC), and cilostazol], non-steroidal anti-inflammatory drugs (NSAIDs), interruption of ATs, replacement of antiplatelet agents (APA), and heparin bridging; tumor characteristics (single or multiple lesions, location, pathologic size, type of differentiation); piecemeal resection; and laboratory data (albumin level and international normalized ratio).

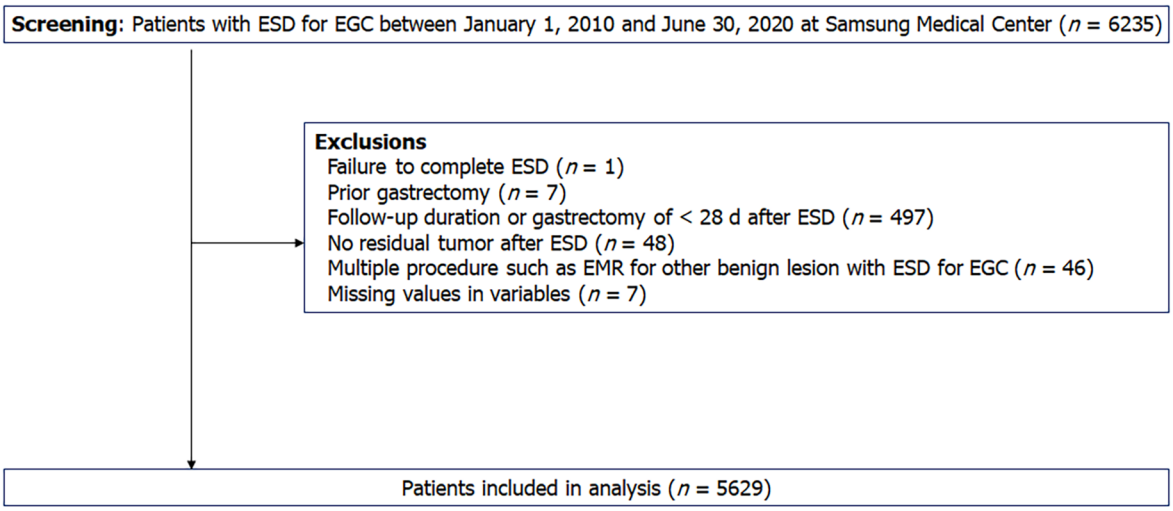
Bleeding after ESD was defined as the presence of signs of bleeding (melena, hematemesis, or a decrease in the hemoglobin level by > 2 g/dL) along with endoscopic stigmata of recent bleeding, such as Forrest class Ia, Ib, IIa, and IIb, within 28 d after ESD. Interruption of ATs was defined as the discontinuation of these medications before the procedure, according to the recommended duration. Replacement of APA was described as when the procedure was performed with aspirin or cilostazol alone in patients who were receiving multiple APAs. Heparin bridging was defined as the administration of heparin during the period between the discontinuation and resumption of anticoagulants. A hemoglobin reduction of > 2 g/dL was evaluated by calculating the differences in the hemoglobin levels between the day before and after ESD.

Development of the deep learning and clinical models

We built a deep learning model and a clinical model based on the development set, which comprised 80% of the overall cohort. Subsequently, we validated the deep learning and clinical models in the validation set, which comprised 20% of the overall cohort. The categorical variables were converted using one-hot encoding, and the continuous variables were normalized, as preprocessing. We built the deep learning model as follows: First, we augmented the development set using the borderline synthetic minority over-sampling technique to overcome the imbalance of the dataset. Synthetic data were generated from 5%–100% of the majority class. Second, we constructed the deep learning model using automated machine learning, called Keras Tuner, to tune hyperparameters automatically. The initial architecture of the model was configured similarly to a transformer based on the attention mechanism [17]. Then, we set the number of neurons as a hyperparameter variable, ranging from 12 to 24, in four dense layers. The learning rate was also set to a range from 1e-2 − to 1e-4 −. The combination of hyperparameters was determined using Bayesian optimization. Finally, we evaluated the performance in the validation set using a model tuned with the 20% of synthetic data of the majority class. The optimal units of dense layers were selected to 24. The optimal number of attention head was chosen to 16. The architecture is depicted in Supplementary Figure 1. The optimal learning rate with Adam optimizer was 1e-3.

Multivariable logistic regression analysis was performed in the development set to build the clinical model. Then, the clinical model was constructed as a formula with the sum of the beta coefficient values of significant factors with a P value of < 0.05.

The calculated value from the deep learning and clinical models was multiplied by 1000 and converted as a score. The score that indicated the risk probability was divided by the decile in the development set. We selected cutoff to discriminate the risk categories as low-, intermediate-, and high-risk at a bleeding rate of < 5% and < 9% in the development set referred to in a previous report[13]. Decile 1st to 4th was allocated to low risk, 5th to 8th to intermediate risk, and 9th to 10th to high-risk category. Link to the deep learning and clinical models: https:// github.com/YeongChanLee/Predict-PEB.



DOI: 10.3748/wjg.v28.i24.2721 **Copyright** ©The Author(s) 2022.

Figure 1 Patient flowchart. EGC: Early gastric cancer; ESD: Endoscopic submucosal dissection.

Statistical analysis

Descriptive statistics for continuous and categorical variables are presented as means (standard deviation) and frequencies (%). The deep learning model and the clinical model for prediction of bleeding after ESD were evaluated using two methods. First, sensitivity, specificity, positive predictive value (PPV), negative predictive value (NPV), and receiver operating characteristic area (ROC) curve along with the area under the curve (AUC) were analyzed. The performance with AUC was compared using the bootstrap test. Second, the risk stratification of PEB based on the development set was applied to the validation set and compared with the actual bleeding rate in the validation set. For example, if the score of calculated cases belongs to the high-risk category, we verified that the real bleeding rate was in the predicted range of 9% or higher. The predictors for PEB were identified with multivariable logistic regression analysis in the entire cohort and development set. Model development for deep learning was performed using Tensor Flow 2.4.0, and Python 3.8.5. statistical analyses were performed using the R software (version 3.5.1, Vienna, Austria).

RESULTS

Baseline characteristics

Of the 5629 patients, 325 experienced post-ESD bleeding (PEB). The non-PEB and PEB groups were comparable in age, liver cirrhosis status, albumin level, international normalized ratio level, a proportion of aspirin or cilostazol use, undifferentiated tumor type, and piecemeal resection. The PEB group had a higher proportion of males and comorbidities (hypertension, diabetes mellitus, and chronic kidney disease) than the non-PEB group. P2Y12RA and anticoagulants (warfarin or DOAC) and the proportion of patients receiving replacement therapy or heparin bridging were higher in the PEB group than in the non-PEB group. The PEB group had a higher proportion of multiple tumors and middle location of tumors and larger size of tumors than the non-PEB group (Table 1). There was no difference in the baseline characteristics between the development and validation sets (Supplementary Table 1).

Predictors for bleeding after ESD

In the overall cohort, the independent predictors were identified as follows: Age [odds ratio (OR) = 0.98; 95% confidence interval (CI): 0.96–0.99; *P* value < 0.001], male (OR = 1.65; 95%CI: 1.19–2.28; *P* value = 0.003), hypertension (OR = 1.56; 95%CI: 1.19–2.03; p value = 0.001), chronic kidney disease (OR = 1.78; 95%CI: 1.18–2.70; *P* value = 0.006), P2Y12RA (OR = 2.40; 95%CI: 1.22–4.74; *P* value = 0.011), DOAC (OR = 4.31; 95%CI: 1.26–14.78; *P* value = 0.020), middle location (OR = 1.72; 95%CI: 1.07–2.74; *P* value = 0.024), and size (OR = 1.03; 95%CI: 1.02–1.04; *P* value < 0.001) (Supplementary Table 2).

In the development set, age (OR = 0.98; 95%CI: 0.96–0.99; *P* value = 0.001), male (OR = 1.54; 95%CI: 1.09–2.19; *P* value = 0.015), hypertension (OR = 1.35; 95%CI: 1.00–1.82; *P* value = 0.049), chronic kidney disease (OR = 1.78; 95%CI: 1.12–2.84; *P* value = 0.015), P2Y12RA (OR = 2.26; 95%CI: 1.05–4.88; *P* value = 0.037), middle location (OR = 1.97; 95%CI: 1.14–3.41; *P* value = 0.015), and size (OR = 1.04; 95%CI: 1.03–1.05; *P* value < 0.001) were identified as independent predictors. The clinical model was a formula described bottom of Table 2.

Table 1 Baseline characteristics of patients in entire cohort

Variable	Non-PEB, *n* = 5304	PEB, *n* = 325	*P* value[1]
Age[2]	64 ± 10	63 ± 11	0.065
Sex			0.001
Female	1245 (23.5)	49 (15.1)	
Male	4059 (76.5)	276 (84.9)	
Hypertension	1413 (26.6)	120 (36.9)	< 0.001
Diabetes mellitus	936 (17.6)	74 (22.8)	0.024
Liver cirrhosis	93 (1.8)	4 (1.2)	0.629
Chronic kidney disease	299 (5.6)	33 (10.2)	0.001
Aspirin	515 (9.7)	42 (12.9)	0.074
P2Y12RA	181 (3.4)	23 (7.1)	0.001
Warfarin	22 (0.4)	7 (2.2)	< 0.001
DOAC	31 (0.6)	6 (1.8)	0.017
Cilostazol	47 (0.9)	3 (0.9)	1.000
NSAIDs	28 (0.5)	3 (0.9)	0.583
Preprocedure management of AT			< 0.001
No indication	4605 (86.8)	264 (81.2)	
Interruption	676 (12.7)	53 (16.3)	
Replacement or heparin bridge	23 (0.4)	8 (2.5)	
Tumor			
Multiple	284 (5.4)	28 (8.6)	0.018
Location			< 0.001
Upper	433 (8.2)	22 (6.8)	
Middle	1728 (32.6)	157 (48.3)	
Lower	3143 (59.3)	146 (44.9)	
Size[2], mm	17 ± 10	21 ± 13	< 0.001
Undifferentiated type	125 (2.4)	7 (2.2)	0.963
Piecemeal resection	64 (1.2)	4 (1.2)	1.000
Laboratory data			
Albumin[2], g/dL	4.3 ± 0.3	4.4 ± 0.4	0.345
INR[2]	1.0 ± 0.1	1.0 ± 0.1	0.106

[1]*P* value calculated using Student's *t*-test for continuous variables or Pearson's chi-square test for categorical variables for overall data.
[2]mean ± SD presented for continuous variables.
Values are expressed as *n* (%) unless otherwise specified. AT: Antithrombotic; DOAC: Direct oral anticoagulant; INR: International normalized ratio; NSAIDs: Non-steroidal anti-inflammatory drugs; PEB: Post-endoscopic submucosal dissection bleeding; P2Y12RA: P2Y12 receptor antagonist.

Performance and comparison of deep learning model and clinical model

The deep learning model was found to have a sensitivity of 64.3%, specificity of 74.0%, PPV of 11.4%, NPV of 97.5%, and AUC of 0.71 (95%CI: 0.63–0.78). The clinical model had a sensitivity of 69.6%, specificity of 71.0%, PPV of 11.1%, NPV of 97.8%, and AUC of 0.70 (95%CI: 0.62–0.77) (Table 3 and Figure 2). There were no significant differences in the AUCs between the deep learning and clinical models (Table 3).

The score multiplied by 1000 to the derived value based on the deep learning and clinical models reflects the risk probability and was divided into deciles. The maximum cutoff was 35.9 in low risk, 57.5 in intermediate risk, and over the 57.5 was assigned to a high-risk category of the deep learning model based on development set (Table 4). In the clinical model, the maximum cutoff was 12.7 in low risk, 24.6

Table 2 Logistic regression analysis for predictors of bleeding after endoscopic submucosal dissection in development set

Variables		Multivariable			
		OR	95%CI	*P* value	ß regression coefficient
Age		0.98	0.96–0.99	0.001	-0.024
Sex	Female/male	1.54	1.09–2.19	0.015	0.435
Hypertension	No/yes	1.35	1.00–1.82	0.049	0.299
Diabetes mellitus	No/yes	1.27	0.92–1.75	0.145	0.238
Liver cirrhosis	No/yes	0.59	0.18–1.95	0.385	-0.532
Chronic kidney disease	No/yes	1.78	1.12–2.84	0.015	0.578
Aspirin	No/yes	1.51	0.62–3.69	0.363	0.414
P2Y12RA	No/yes	2.26	1.05–4.88	0.037	0.818
Warfarin	No/yes	1.51	0.28–8.07	0.629	0.413
DOAC	No/yes	3.24	0.76–13.82	0.113	1.174
Cilostazol	No/yes	1.35	0.35–5.18	0.662	0.300
NSAIDs	No/yes	2.65	0.77–9.14	0.124	0.973
Preprocedure management of AT	No indication	1			
	Interruption	0.63	0.24–1.67	0.353	-0.464
	Replacement orHeparin bridge	3.32	0.47–23.60	0.231	1.199
Multiple	No/yes	1.48	0.92–2.38	0.104	0.393
Location	Upper	1			
	Middle	1.97	1.14–3.41	0.015	0.680
	Lower	1.11	0.64–1.91	0.711	0.103
Size		1.04	1.03–1.05	< 0.001	0.036
Undifferentiated type	No/yes	0.56	0.20–1.57	0.271	-0.579
Piecemeal	No/yes	0.98	0.30–3.22	0.976	-0.019
Albumin, g/dL		1.33	0.89–2.00	0.168	0.286
INR		2.04	0.37–11.08	0.410	0.711

Clinical model = 1/[1 + exp(-1 × [-0.024 × Age in years + 0.435 × Sex (0: female, 1: male) + 0.299 × Hypertension (0: no, 1: yes) + 0.578 × Chronic kidney disease (0: no, yes: 1) + 0.818 × P2Y12RA (0: no, 1: yes) + 0.680 × Middle location (0: no, 1: yes) + 0.036 × Size in mm])]. AT: Antithrombotic; DOAC: Direct oral anticoagulant; ESD: Endoscopic submucosal dissection; INR: International normalized ratio; NSAIDs, Non-steroidal anti-inflammatory drugs; P2Y12RA: P2Y12 receptor antagonist; OR: Odds ratio; CI: Confidence interval.

in intermediate risk, and over 24.6 was considered a high-risk category based on development set (Table 4). In the validated set, the deep learning model showed an actual bleeding rate in low-, intermediate-, high-risk categories, respectively, of 2.2%, 3.9%, and 11.6%; the clinical model showed an actual bleeding rate of 4.0%, 8.8%, and 18.2%, respectively, in low-, intermediate-, high-risk categories (Table 4).

DISCUSSION

The deep learning and clinical models for predicting bleeding after ESD in patients with EGC showed good performance. We demonstrated that deep learning and clinical models could stratify the PEB risk, which correlated with actual bleeding rates. Hence, we suggest that the deep learning model can aid in the prediction of bleeding after ESD, in addition to the clinical model.

This study was the first to establish a deep learning model for predicting bleeding after ESD and demonstrate its performance compared to that of a clinical model. The strengths of this study were its large sample size and the relatively recent data from a single institution. In addition, we included all essential variables and sought the advantages of the deep learning model that can deal with extensive

Table 3 Utility of deep learning model and clinical model

	Deep learning model	Clinical model	*P* value
Sensitivity (%)	64.3 (45.8–84.1)	69.6 (54.2–80.8)	
Specificity (%)	74.0 (50.6–89.2)	71.0 (68.5–79.5)	
PPV (%)	11.4 (7.4–18.1)	11.1 (8.0–15.4)	
NPV (%)	97.5 (96.4–98.7)	97.8 (96.6–98.7)	
AUC (95%CI)	0.71 (0.63–0.78)	0.70 (0.62–0.77)	0.730

One thousand times for bootstrapping were conducted to measure 95% confidence intervals. *P* value for statistical significance between area under the curves was derived from Delong's test. AUC: Area under the curve; CI: Confidence interval; NPV: Negative predictive value; PPV: Positive predictive value.

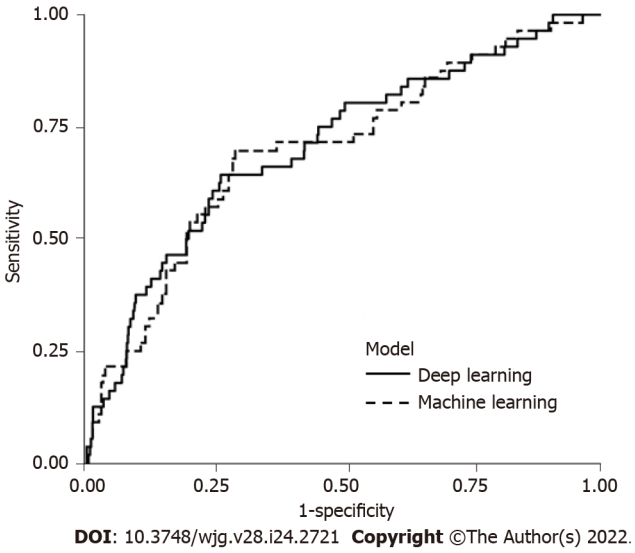
Table 4 Decile of risk probability based on deep learning model and clinical model

Decile	Risk categories	Deep learning				Clinical model			
		Score[1]	Patients	Bleeding	Rate (%)	Score[1]	Patients	Bleeding	Rate (%)
Development set									
1	Low	25.7	451	11	2.4	8.4	451	12	2.6
2		29.1	451	15	3.3	12.2	451	15	3.3
3		32.5	451	6	1.3	12.4	451	12	2.6
4		35.9	450	17	3.8	12.7	450	20	4.4
5	Intermediate	40.2	450	27	6.0	14.8	450	34	7.6
6		45.3	450	29	6.4	16.6	450	15	3.3
7		50.8	450	36	8.0	23.3	450	24	5.3
8		57.5	450	24	5.3	24.6	450	32	7.1
9	High	67.2	450	41	9.1	31.0	450	54	12.0
10		197.0	450	63	14.0	122.0	450	51	11.3
Validation set									
	Low	35.9	411	9	2.2	12.7	956	38	4.0
	Intermediate	57.5	466	18	3.9	24.5	137	12	8.8
	High	147.0	249	29	11.6	155.0	33	6	18.2

[1]The score is calculated with probability multiplied by 1000 and presented as maximum cutoff in each decile.
Decile 1st to 4th: Low-risk category. Decile 5th to 8th: Intermediate-risk category. Decile 9th to 10th: High-risk category. The Cochran–Armitage test for trend was performed.

data and complex problems and improve its performance incrementally by automated learning. We included all types of ATs separately and clarified the distinction between patients without an indication for ATs, patients who received an interruption before the procedure, and patients who received replacement or heparin bridging.

Our study identified younger age, male sex, hypertension, chronic kidney disease, P2Y12RA use, DOAC use, middle tumor location, and tumor size as the predictors of PEB. Previous studies also reported that younger age was associated with PEB[18-20]. It is unclear why younger age was associated with PEB. Several reports proposed that atrophic change along with aging might relate to decreasing the vascularity on the mucosal and submucosal layers[18,20-23]. Although aging and changes in intestinal vasculature have not been clearly elucidated, a decrease in the volume of vasculature with aging was observed in animals[24]. Aspirin did not increase the PEB risk after discontinuation about 1 wk[25]. Although some reported that maintaining aspirin did not increase the PEB risk[25-28], a meta-analysis showed that aspirin was associated with increased bleeding risk, requiring clinical caution[29]. There is still controversial due to limited evidence for P2Y12R[9,13,20,30]. In comparison, an increased bleeding risk after ESD has been reported consistently in patients receiving dual antiplatelets. In addition, there



DOI: 10.3748/wjg.v28.i24.2721 **Copyright** ©The Author(s) 2022.

Figure 2 Area under the curve for prediction of bleeding after endoscopic submucosal dissection in deep learning model and clinical model.

were reports that warfarin or DOAC are related to bleeding risk[13]; rather, some reported heparin bridging was associated with PEB risk[9,26]. The irony is that most of the patients who experience heparin bridging take warfarin or DOAC, but the results about each factor were inconsistent in previous retrospective studies. It is assumed that the duration of discontinuation and other individual factors might influence these results. In addition, it has been suggested that large size[8,19,20], CKD with hemodialysis[13,26,31], and long procedure time[20] were associated with bleeding after ESD. The upper location showed increased PEB risk[18,32]; in contrast, some others reported lower location related to increased PEB risk[18,32]; a recent meta-analysis did not prove significance according to the location[8].

Recently, a predictive risk-scoring model for PEB in Japan showed that CKD with hemodialysis, usage of aspirin, P2Y12RA, cilostazol, warfarin, DOAC, lower third tumor location, tumor size > 30 mm, and the presence of multiple tumors were the predictors of PEB, whereas interruption was a protective factor against PEB[13]. Another recent model proposed a simple algorithm including significant factors with continuous use of ATs, size ≥ 49 mm, and age < 62 years. We also found an association between P2Y12RA or DOAC usage and PEB; however, other ATs were not associated with PEB, and interruption and heparin bridging or replacement of APA were not identified as the protective factors. In our institution, ESD is classified as a high-risk procedure based on the national practice guidelines, and experts are consulted before ESD in patients receiving ATs. The expert assesses the thromboembolic risk depending on the underlying disease and recommends the possibility of interruption, duration of interruption, and the need for heparin bridging or replacement of APA[33-36]. Recently, a guideline published in South Korea also categorized ESD as an ultra-high-risk procedure and recommended interruption of ATs with heparin bridging or replacement of APA according to the thromboembolic risk [37].

The deep learning model in our study showed an AUC of 0.71, which was comparable to the AUC of 0.72 for a risk-scoring model in Japan[13] and the AUC of 0.70 for the clinical model in our study. In the validation set, predicted low-, intermediate-, and high-risk categories showed an actual bleeding rate of 2.2%, 3.9%, and 11.6%, respectively in the deep learning; 4.0%, 8.8%, and 18.2%, respectively, in the clinical model. Our study demonstrated that the deep learning and clinical models can stratify the bleeding risk after ESD. The predicted risk categories correlated with actual bleeding rate; even considering the actual bleeding rate was slightly lower than predicted range of ≥ 5% and < 9% (intermediate risk) in the deep learning and was close to upper range in the clinical model. Our findings support the clinical potential of the deep learning model for predicting PEB risk based on its comparable performance. Because bleeding after ESD requires intervention and hospitalization, physicians are concerned about the occurrence of PEB as a major complication. Based on the risk-prediction model, physicians could carefully assess the bleeding risk and perform preventive hemostasis during the procedure. Suppose additional management like the shielding method for preventing PEB in the selected high-risk group is attempted; in that case, it is anticipated that the deep learning model could support risk stratification.

Our study has several limitations. Due to its retrospective design, information such as the timing of the resumption of ATs, endoscopist's experience, defect size, and procedure duration was missing. Furthermore, our study was designed as a single-center study; hence, hospital-based validation in other hospitals was not performed, and further proof is warranted. However, the deep learning model might

be generalizable because it automatically identifies the risk or probability of bleeding without the external intervention of known relevant factors. Both the deep learning and clinical models showed a low PPV, which may be related to the low incidence of bleeding after ESD, even though bleeding is one of the major complications. In our cohort, the number of patients who received anticoagulants (warfarin or DOAC) was small; therefore, it is possible that the statistical significance of these variables was insufficient for establishing a clinical model in the development set. In this regard, despite the fact that our study focused on the development of a deep learning model and a clinical model, as well as the utility of the deep learning model, further accumulation of data and additional analysis will be required before the commencement of the clinical application of artificial intelligence systems.

CONCLUSION

In conclusion, we introduced a deep learning model to predict the risk of bleeding after ESD in patients with EGC. The model demonstrated its performance as comparable to the clinical model. The deep learning model could help physicians raise caution to the PEB and would be a desirable tool for supporting ESD application.

ARTICLE HIGHLIGHTS

Research background

With the increasing rate of diagnosis at early stages of gastric cancer, endoscopic submucosal dissection (ESD) is being actively applied as the minimally invasive treatment. Bleeding is one of the significant complications, with an incidence of 3.6%–6.9%. Because bleeding after ESD requires hospitalization and hemostatic interventions, there is a need to predict patients at a high risk of bleeding after ESD.

Research motivation

Currently, artificial intelligence systems are being applied in various fields of gastroenterology. Deep learning among artificial intelligence systems was automatically trained so that it could be generalized well. There has been no study on the efficacy of deep learning for predicting post-ESD bleeding (PEB), and no study has compared these systems with a clinical model.

Research objectives

This study aimed to develop and compare the performance of the deep learning and clinical model for predicting PEB in early gastric cancer (EGC) patients.

Research methods

Patients who underwent ESD for EGC between January 2010 and June 2020 at the Samsung Medical Center, Seoul, South Korea, were screened retrospectively. We built a deep learning model and a clinical model based on the development set, which comprised 80% of the overall cohort. Subsequently, we validated the deep learning and clinical models in the validation set, which comprised 20% of the overall cohort. The deep learning model and the clinical model for prediction of bleeding after ESD were evaluated using two methods. First, sensitivity, specificity, positive predictive value, negative predictive value, and receiver operating characteristic area curve along with the area under the curve (AUC) were analyzed. The performance with AUC was compared using the bootstrap test. Second, the risk stratification of PEB based on the development set was applied to the validation set and compared with the actual bleeding rate. The authors selected cutoff to discriminate the risk categories as low-, intermediate-, and high-risk at a bleeding rate of < 5% and < 9% in the development set referred to in a previous report.

Research results

Of the 5629 patients, 325 experienced PEB. The AUC for predicting PEB was 0.71 (95% confidence interval: 0.63-0.78) in the deep learning model and 0.70 (95% confidence interval: 0.62-0.77) in the clinical model, without significant difference (P = 0.730). In the validated set, the deep learning model showed an actual bleeding rate of 2.2%, 3.9%, and 11.6% in low-, intermediate-, high-risk categories, respectively; the clinical model showed an actual bleeding rate of 4.0%, 8.8%, and 18.2% in low-, intermediate-, high-risk categories, respectively.

Research conclusions

In conclusion, we introduced a deep learning model to predict the risk of bleeding after ESD in patients with EGC. The model demonstrated its performance as comparable to the clinical model.

Research perspectives

Based on the risk-prediction model, physicians could carefully assess the bleeding risk and perform preventive hemostasis during the procedure. Suppose additional management like the shielding method for preventing PEB in the selected high-risk group is attempted; in that case, it is anticipated that the deep learning model could support risk stratification.

FOOTNOTES

Author contributions: Na JE, Lee YC and Kim TJ contributed equally to this work as co-first authors of this paper; Na JE, Lee YC, Kim TJ, and Lee H contributed to the study concept and design, acquisition, analysis, or interpretation of data, and writing and drafting of the manuscript; Kim TJ, Lee H, Won HH, Min YW, Min BH, Lee JH, Rhee PL, and Kim JJ contributed to the critical revision of the manuscript for important intellectual content; Lee YC contributed to the statistical analysis; All authors approved the final submission.

Institutional review board statement: The Institutional review board of the Samsung Medical Center, Korea, approved this study, and the requirement for obtaining informed consent was waived owing to the study's retrospective nature.

Conflict-of-interest statement: The authors declare no conflict of interest.

Data sharing statement: Data available on request due to privacy. The data presented in this study are available on request from the corresponding author. The data are not publicly available due to privacy.

Open-Access: This article is an open-access article that was selected by an in-house editor and fully peer-reviewed by external reviewers. It is distributed in accordance with the Creative Commons Attribution NonCommercial (CC BY-NC 4.0) license, which permits others to distribute, remix, adapt, build upon this work non-commercially, and license their derivative works on different terms, provided the original work is properly cited and the use is non-commercial. See: https://creativecommons.org/Licenses/by-nc/4.0/

Country/Territory of origin: South Korea

ORCID number: Ji Eun Na 0000-0003-3092-9630; Yeong Chan Lee 0000-0002-2093-3161; Tae Jun Kim 0000-0001-8101-9034; Hyuk Lee 0000-0003-4271-7205; Hong-Hee Won 0000-0001-5719-0552; Yang Won Min 0000-0001-7471-1305; Byung-Hoon Min 0000-0001-8048-361X; Jun Haeng Lee 0000-0002-5272-1841; Poong-Lyul Rhee 0000-0003-0495-5296; Jae J. Kim 0000-0002-0226-1330.

S-Editor: Ma YJ
L-Editor: Filipodia
P-Editor: Ma YJ

REFERENCES

1 **Hong S**, Won YJ, Park YR, Jung KW, Kong HJ, Lee ES; Community of Population-Based Regional Cancer Registries. Cancer Statistics in Korea: Incidence, Mortality, Survival, and Prevalence in 2017. *Cancer Res Treat* 2020; **52**: 335-350 [PMID: 32178489 DOI: 10.4143/crt.2020.206]
2 **Kim YG**, Kong SH, Oh SY, Lee KG, Suh YS, Yang JY, Choi J, Kim SG, Kim JS, Kim WH, Lee HJ, Yang HK. Effects of screening on gastric cancer management: comparative analysis of the results in 2006 and in 2011. *J Gastric Cancer* 2014; **14**: 129-134 [PMID: 25061541 DOI: 10.5230/jgc.2014.14.2.129]
3 **Hamashima C**; Systematic Review Group and Guideline Development Group for Gastric Cancer Screening Guidelines. Update version of the Japanese Guidelines for Gastric Cancer Screening. *Jpn J Clin Oncol* 2018; **48**: 673-683 [PMID: 29889263 DOI: 10.1093/jjco/hyy077]
4 **Japanese Gastric Cancer Association Registration Committee**, Maruyama K, Kaminishi M, Hayashi K, Isobe Y, Honda I, Katai H, Arai K, Kodera Y, Nashimoto A. Gastric cancer treated in 1991 in Japan: data analysis of nationwide registry. *Gastric Cancer* 2006; **9**: 51-66 [PMID: 16767357 DOI: 10.1007/s10120-006-0370-y]
5 **Park CH**, Yang DH, Kim JW, Kim JH, Min YW, Lee SH, Bae JH, Chung H, Choi KD, Park JC, Lee H, Kwak MS, Kim B, Lee HJ, Lee HS, Choi M, Park DA, Lee JY, Byeon JS, Park CG, Cho JY, Lee ST, Chun HJ. Clinical Practice Guideline for Endoscopic Resection of Early Gastrointestinal Cancer. *Clin Endosc* 2020; **53**: 142-166 [PMID: 32252507 DOI: 10.5946/ce.2020.032]
6 **Hatta W**, Gotoda T, Koike T, Masamune A. History and future perspectives in Japanese guidelines for endoscopic resection of early gastric cancer. *Dig Endosc* 2020; **32**: 180-190 [PMID: 31529716 DOI: 10.1111/den.13531]
7 **Saito I**, Tsuji Y, Sakaguchi Y, Niimi K, Ono S, Kodashima S, Yamamichi N, Fujishiro M, Koike K. Complications related to gastric endoscopic submucosal dissection and their managements. *Clin Endosc* 2014; **47**: 398-403 [PMID: 25324997 DOI: 10.5946/ce.2014.47.5.398]
8 **Libânio D**, Costa MN, Pimentel-Nunes P, Dinis-Ribeiro M. Risk factors for bleeding after gastric endoscopic submucosal

dissection: a systematic review and meta-analysis. *Gastrointest Endosc* 2016; **84**: 572-586 [PMID: 27345132 DOI: 10.1016/j.gie.2016.06.033]

9 **Sato C**, Hirasawa K, Koh R, Ikeda R, Fukuchi T, Kobayashi R, Kaneko H, Makazu M, Maeda S. Postoperative bleeding in patients on antithrombotic therapy after gastric endoscopic submucosal dissection. *World J Gastroenterol* 2017; **23**: 5557-5566 [PMID: 28852315 DOI: 10.3748/wjg.v23.i30.5557]

10 **Yano T**, Tanabe S, Ishido K, Suzuki M, Kawanishi N, Yamane S, Watanabe A, Wada T, Azuma M, Katada C, Koizumi W. Different clinical characteristics associated with acute bleeding and delayed bleeding after endoscopic submucosal dissection in patients with early gastric cancer. *Surg Endosc* 2017; **31**: 4542-4550 [PMID: 28378078 DOI: 10.1007/s00464-017-5513-1]

11 **Hashimoto M**, Hatta W, Tsuji Y, Yoshio T, Yabuuchi Y, Hoteya S, Doyama H, Nagami Y, Hikichi T, Kobayashi M, Morita Y, Sumiyoshi T, Iguchi M, Tomida H, Inoue T, Mikami T, Hasatani K, Nishikawa J, Matsumura T, Nebiki H, Nakamatsu D, Ohnita K, Suzuki H, Ueyama H, Hayashi Y, Sugimoto M, Fujishiro M, Masamune A, Ohira H; Collaborators. Rebleeding in patients with delayed bleeding after endoscopic submucosal dissection for early gastric cancer. *Dig Endosc* 2021; **33**: 1120-1130 [PMID: 33539035 DOI: 10.1111/den.13943]

12 **Kataoka Y**, Tsuji Y, Sakaguchi Y, Minatsuki C, Asada-Hirayama I, Niimi K, Ono S, Kodashima S, Yamamichi N, Fujishiro M, Koike K. Bleeding after endoscopic submucosal dissection: Risk factors and preventive methods. *World J Gastroenterol* 2016; **22**: 5927-5935 [PMID: 27468187 DOI: 10.3748/wjg.v22.i26.5927]

13 **Hatta W**, Tsuji Y, Yoshio T, Kakushima N, Hoteya S, Doyama H, Nagami Y, Hikichi T, Kobayashi M, Morita Y, Sumiyoshi T, Iguchi M, Tomida H, Inoue T, Koike T, Mikami T, Hasatani K, Nishikawa J, Matsumura T, Nebiki H, Nakamatsu D, Ohnita K, Suzuki H, Ueyama H, Hayashi Y, Sugimoto M, Yamaguchi S, Michida T, Yada T, Asahina Y, Narasaka T, Kuribasyashi S, Kiyotoki S, Mabe K, Nakamura T, Nakaya N, Fujishiro M, Masamune A. Prediction model of bleeding after endoscopic submucosal dissection for early gastric cancer: BEST-J score. *Gut* 2021; **70**: 476-484 [PMID: 32499390 DOI: 10.1136/gutjnl-2019-319926]

14 **Glissen Brown JR**, Waljee AK, Mori Y, Sharma P, Berzin TM. Charting a path forward for clinical research in artificial intelligence and gastroenterology. *Dig Endosc* 2022; **34**: 4-12 [PMID: 33715244 DOI: 10.1111/den.13974]

15 **Shung DL**, Au B, Taylor RA, Tay JK, Laursen SB, Stanley AJ, Dalton HR, Ngu J, Schultz M, Laine L. Validation of a Machine Learning Model That Outperforms Clinical Risk Scoring Systems for Upper Gastrointestinal Bleeding. *Gastroenterology* 2020; **158**: 160-167 [PMID: 31562847 DOI: 10.1053/j.gastro.2019.09.009]

16 **Wong GL**, Ma AJ, Deng H, Ching JY, Wong VW, Tse YK, Yip TC, Lau LH, Liu HH, Leung CM, Tsang SW, Chan CW, Lau JY, Yuen PC, Chan FK. Machine learning model to predict recurrent ulcer bleeding in patients with history of idiopathic gastroduodenal ulcer bleeding. *Aliment Pharmacol Ther* 2019; **49**: 912-918 [PMID: 30761584 DOI: 10.1111/apt.15145]

17 **Vaswani A**, Shazeer N, Parmar N, Uszkoreit J, Jones L, Gomez AN, Kaiser L, Polosukhin I. Attention is all you need. 31st Conference on Neural Information Processing Systems (NIPS 2017), Long Beach, CA, USA. [cited April 1, 2021] Available from: https://arxiv.org/pdf/1706.03762.pdf

18 **Jeon SW**, Jung MK, Cho CM, Tak WY, Kweon YO, Kim SK, Choi YH. Predictors of immediate bleeding during endoscopic submucosal dissection in gastric lesions. *Surg Endosc* 2009; **23**: 1974-1979 [PMID: 18553202 DOI: 10.1007/s00464-008-9988-7]

19 **Choe YH**, Jung DH, Park JC, Kim HY, Shin SK, Lee SK, Lee YC. Prediction model for bleeding after endoscopic submucosal dissection of gastric neoplasms from a high-volume center. *J Gastroenterol Hepatol* 2021; **36**: 2217-2223 [PMID: 33646614 DOI: 10.1111/jgh.15478]

20 **Nam HS**, Choi CW, Kim SJ, Kim HW, Kang DH, Park SB, Ryu DG. Risk factors for delayed bleeding by onset time after endoscopic submucosal dissection for gastric neoplasm. *Sci Rep* 2019; **9**: 2674 [PMID: 30804386 DOI: 10.1038/s41598-019-39381-1]

21 **Kim JW**, Kim HS, Park DH, Park YS, Jee MG, Baik SK, Kwon SO, Lee DK. Risk factors for delayed postendoscopic mucosal resection hemorrhage in patients with gastric tumor. *Eur J Gastroenterol Hepatol* 2007; **19**: 409-415 [PMID: 17413293 DOI: 10.1097/MEG.0b013e32801015be]

22 **Kim N**, Park YS, Cho SI, Lee HS, Choe G, Kim IW, Won YD, Park JH, Kim JS, Jung HC, Song IS. Prevalence and risk factors of atrophic gastritis and intestinal metaplasia in a Korean population without significant gastroduodenal disease. *Helicobacter* 2008; **13**: 245-255 [PMID: 18665932 DOI: 10.1111/j.1523-5378.2008.00604.x]

23 **Joo YE**, Park HK, Myung DS, Baik GH, Shin JE, Seo GS, Kim GH, Kim HU, Kim HY, Cho SI, Kim N. Prevalence and risk factors of atrophic gastritis and intestinal metaplasia: a nationwide multicenter prospective study in Korea. *Gut Liver* 2013; **7**: 303-310 [PMID: 23710311 DOI: 10.5009/gnl.2013.7.3.303]

24 **Chen YM**, Zhang JS, Duan XL. Changes of microvascular architecture, ultrastructure and permeability of rat jejunal villi at different ages. *World J Gastroenterol* 2003; **9**: 795-799 [PMID: 12679935 DOI: 10.3748/wjg.v9.i4.795]

25 **Lim JH**, Kim SG, Kim JW, Choi YJ, Kwon J, Kim JY, Lee YB, Choi J, Im JP, Kim JS, Jung HC, Song IS. Do antiplatelets increase the risk of bleeding after endoscopic submucosal dissection of gastric neoplasms? *Gastrointest Endosc* 2012; **75**: 719-727 [PMID: 22317881 DOI: 10.1016/j.gie.2011.11.034]

26 **Matsumura T**, Arai M, Maruoka D, Okimoto K, Minemura S, Ishigami H, Saito K, Nakagawa T, Katsuno T, Yokosuka O. Risk factors for early and delayed post-operative bleeding after endoscopic submucosal dissection of gastric neoplasms, including patients with continued use of antithrombotic agents. *BMC Gastroenterol* 2014; **14**: 172 [PMID: 25280756 DOI: 10.1186/1471-230X-14-172]

27 **Harada H**, Suehiro S, Murakami D, Nakahara R, Nagasaka T, Ujihara T, Sagami R, Katsuyama Y, Hayasaka K, Amano Y. Feasibility of gastric endoscopic submucosal dissection with continuous low-dose aspirin for patients receiving dual antiplatelet therapy. *World J Gastroenterol* 2019; **25**: 457-468 [PMID: 30700942 DOI: 10.3748/wjg.v25.i4.457]

28 **Sanomura Y**, Oka S, Tanaka S, Numata N, Higashiyama M, Kanao H, Yoshida S, Ueno Y, Chayama K. Continued use of low-dose aspirin does not increase the risk of bleeding during or after endoscopic submucosal dissection for early gastric cancer. *Gastric Cancer* 2014; **17**: 489-496 [PMID: 24142107 DOI: 10.1007/s10120-013-0305-3]

29 **Wu W**, Chen J, Ding Q, Yang D, Yu H, Lin J. Continued use of low-dose aspirin may increase risk of bleeding after

gastrointestinal endoscopic submucosal dissection: A meta-analysis. *Turk J Gastroenterol* 2017; **28**: 329-336 [PMID: 28797987 DOI: 10.5152/tjg.2017.16573]

30 **Oh S**, Kim SG, Kim J, Choi JM, Lim JH, Yang HJ, Park JY, Han SJ, Kim JL, Chung H, Jung HC. Continuous Use of Thienopyridine May Be as Safe as Low-Dose Aspirin in Endoscopic Resection of Gastric Tumors. *Gut Liver* 2018; **12**: 393-401 [PMID: 29429155 DOI: 10.5009/gnl17384]

31 **Numata N**, Oka S, Tanaka S, Higashiyama M, Sanomura Y, Yoshida S, Arihiro K, Chayama K. Clinical outcomes of endoscopic submucosal dissection for early gastric cancer in patients with chronic kidney disease. *J Gastroenterol Hepatol* 2013; **28**: 1632-1637 [PMID: 23808356 DOI: 10.1111/jgh.12320]

32 **Chung IK**, Lee JH, Lee SH, Kim SJ, Cho JY, Cho WY, Hwangbo Y, Keum BR, Park JJ, Chun HJ, Kim HJ, Kim JJ, Ji SR, Seol SY. Therapeutic outcomes in 1000 cases of endoscopic submucosal dissection for early gastric neoplasms: Korean ESD Study Group multicenter study. *Gastrointest Endosc* 2009; **69**: 1228-1235 [PMID: 19249769 DOI: 10.1016/j.gie.2008.09.027]

33 **ASGE Standards of Practice Committee**, Acosta RD, Abraham NS, Chandrasekhara V, Chathadi KV, Early DS, Eloubeidi MA, Evans JA, Faulx AL, Fisher DA, Fonkalsrud L, Hwang JH, Khashab MA, Lightdale JR, Muthusamy VR, Pasha SF, Saltzman JR, Shaukat A, Shergill AK, Wang A, Cash BD, DeWitt JM. The management of antithrombotic agents for patients undergoing GI endoscopy. *Gastrointest Endosc* 2016; **83**: 3-16 [PMID: 26621548 DOI: 10.1016/j.gie.2015.09.035]

34 **Chan FKL**, Goh KL, Reddy N, Fujimoto K, Ho KY, Hokimoto S, Jeong YH, Kitazono T, Lee HS, Mahachai V, Tsoi KKF, Wu MS, Yan BP, Sugano K. Management of patients on antithrombotic agents undergoing emergency and elective endoscopy: joint Asian Pacific Association of Gastroenterology (APAGE) and Asian Pacific Society for Digestive Endoscopy (APSDE) practice guidelines. *Gut* 2018; **67**: 405-417 [PMID: 29331946 DOI: 10.1136/gutjnl-2017-315131]

35 **Fujimoto K**, Fujishiro M, Kato M, Higuchi K, Iwakiri R, Sakamoto C, Uchiyama S, Kashiwagi A, Ogawa H, Murakami K, Mine T, Yoshino J, Kinoshita Y, Ichinose M, Matsui T; Japan Gastroenterological Endoscopy Society. Guidelines for gastroenterological endoscopy in patients undergoing antithrombotic treatment. *Dig Endosc* 2014; **26**: 1-14 [PMID: 24215155 DOI: 10.1111/den.12183]

36 **Veitch AM**, Vanbiervliet G, Gershlick AH, Boustiere C, Baglin TP, Smith LA, Radaelli F, Knight E, Gralnek IM, Hassan C, Dumonceau JM. Endoscopy in patients on antiplatelet or anticoagulant therapy, including direct oral anticoagulants: British Society of Gastroenterology (BSG) and European Society of Gastrointestinal Endoscopy (ESGE) guidelines. *Gut* 2016; **65**: 374-389 [PMID: 26873868 DOI: 10.1136/gutjnl-2015-311110]

37 **Lim H**, Gong EJ, Min BH, Kang SJ, Shin CM, Byeon JS, Choi M, Park CG, Cho JY, Lee ST, Kim HG, Chun HJ. Clinical Practice Guideline for the Management of Antithrombotic Agents in Patients Undergoing Gastrointestinal Endoscopy. *Clin Endosc* 2020; **53**: 663-677 [PMID: 33242928 DOI: 10.5946/ce.2020.192]

World Journal of Gastroenterology

Submit a Manuscript: https://www.f6publishing.com

World J Gastroenterol 2022 June 28; 28(24): 2733-2747

DOI: 10.3748/wjg.v28.i24.2733

ISSN 1007-9327 (print) ISSN 2219-2840 (online)

ORIGINAL ARTICLE

Retrospective Study

Radiomic analysis based on multi-phase magnetic resonance imaging to predict preoperatively microvascular invasion in hepatocellular carcinoma

Yue-Ming Li, Yue-Min Zhu, Lan-Mei Gao, Ze-Wen Han, Xiao-Jie Chen, Chuan Yan, Rong-Ping Ye, Dai-Rong Cao

Specialty type: Gastroenterology and hepatology

Provenance and peer review: Unsolicited article; Externally peer reviewed.

Peer-review model: Single blind

Peer-review report's scientific quality classification

Grade A (Excellent): 0
Grade B (Very good): B
Grade C (Good): C, C, C
Grade D (Fair): 0
Grade E (Poor): 0

P-Reviewer: Li L, New Zealand; Shomura M, Japan; Suda T, Japan

Received: December 24, 2021
Peer-review started: December 24, 2021
First decision: March 10, 2022
Revised: March 20, 2022
Accepted: May 12, 2022
Article in press: May 12, 2022
Published online: June 28, 2022

Yue-Ming Li, Yue-Min Zhu, Lan-Mei Gao, Ze-Wen Han, Xiao-Jie Chen, Chuan Yan, Rong-Ping Ye, Dai-Rong Cao, Department of Radiology, The First Affiliated Hospital of Fujian Medical University, Fuzhou 350005, Fujian Province, China

Yue-Ming Li, Key Laboratory of Radiation Biology (Fujian Medical University), Fujian Province University, Fuzhou 350005, Fujian Province, China

Corresponding author: Dai-Rong Cao, MD, Chief Doctor, Department of Radiology, The First Affiliated Hospital of Fujian Medical University, No. 20 Chazhong Road, Fuzhou 350005, Fujian Province, China. 3502505836@qq.com

Abstract

BACKGROUND

The prognosis of hepatocellular carcinoma (HCC) remains poor and relapse occurs in more than half of patients within 2 years after hepatectomy. In terms of recent studies, microvascular invasion (MVI) is one of the potential predictors of recurrence. Accurate preoperative prediction of MVI is potentially beneficial to the optimization of treatment planning.

AIM

To develop a radiomic analysis model based on pre-operative magnetic resonance imaging (MRI) data to predict MVI in HCC.

METHODS

A total of 113 patients recruited to this study have been diagnosed as having HCC with histological confirmation, among whom 73 were found to have MVI and 40 were not. All the patients received preoperative examination by Gd-enhanced MRI and then curative hepatectomy. We manually delineated the tumor lesion on the largest cross-sectional area of the tumor and the adjacent two images on MRI, namely, the regions of interest. Quantitative analyses included most discriminant factors (MDFs) developed using linear discriminant analysis algorithm and histogram analysis with MaZda software. Independent significant variables of clinical and radiological features and MDFs for the prediction of MVI were estimated and a discriminant model was established by univariate and

multivariate logistic regression analysis. Prediction ability of the above-mentioned parameters or model was then evaluated by receiver operating characteristic (ROC) curve analysis. Five-fold cross-validation was also applied *via* R software.

RESULTS

The area under the ROC curve (AUC) of the MDF (0.77-0.85) outperformed that of histogram parameters (0.51-0.74). After multivariate analysis, MDF values of the arterial and portal venous phase, and peritumoral hypointensity in the hepatobiliary phase were identified to be independent predictors of MVI ($P < 0.05$). The AUC value of the model was 0.939 [95% confidence interval (CI): 0.893-0.984, standard error: 0.023]. The result of internal five-fold cross-validation (AUC: 0.912, 95%CI: 0.841-0.959, standard error: 0.0298) also showed favorable predictive efficacy.

CONCLUSION

Noninvasive MRI radiomic model based on MDF values and imaging biomarkers may be useful to make preoperative prediction of MVI in patients with primary HCC.

Key Words: Hepatocellular carcinoma; Microvascular invasion; Magnetic resonance imaging; Radiomic analysis; Imaging biomarkers

©The Author(s) 2022. Published by Baishideng Publishing Group Inc. All rights reserved.

Core Tip: We developed a radiomic analysis model based on pre-operative magnetic resonance imaging data to predict microvascular invasion (MVI) in hepatocellular carcinoma (HCC). Quantitative analyses included most discriminant factors (MDFs) developed using the linear discriminant analysis algorithm and histogram analysis with MaZda software. The area under the receiver operating characteristic curve value of the model and the result of internal five-fold cross-validation showed favorable predictive efficacy. Noninvasive radiomic model based on MDF values and imaging biomarkers may be useful to make preoperative prediction of MVI in patients with primary HCC.

Citation: Li YM, Zhu YM, Gao LM, Han ZW, Chen XJ, Yan C, Ye RP, Cao DR. Radiomic analysis based on multi-phase magnetic resonance imaging to predict preoperatively microvascular invasion in hepatocellular carcinoma. *World J Gastroenterol* 2022; 28(24): 2733-2747

URL: https://www.wjgnet.com/1007-9327/full/v28/i24/2733.htm

DOI: https://dx.doi.org/10.3748/wjg.v28.i24.2733

INTRODUCTION

As important therapies for hepatocellular carcinoma (HCC), liver resection and transplantation are widely applied in clinic and the techniques have great advances. However, the prognosis remains poor and relapse occurs in more than half patients within 2 years after hepatectomy[1]. In terms of recent studies, microvascular invasion (MVI) is one of the potential predictors of recurrence[2,3]. MVI, only seen under the microscope, is defined as the appearance of tumor cells in smaller vessels inside the liver which include small portal vein and small lymphatic vessels or hepatic artery[4,5]. And MVI can be classified as four subclasses varying from M0 to M3, and higher grade usually indicates higher invasiveness of HCC and poorer survival rate[6]. Nonetheless, MVI is diagnosed by post-surgery histological result at present, which is the gold standard. The accurate prediction of MVI before operation can help achieve the anatomic resection with expanding resection margin even for a small tumor[7]. Thus, accurate preoperative prediction of MVI is potentially beneficial to the optimization of treatment planning[3,8].

There have been some studies to preoperatively predict MVI in terms of serum markers, radiological features, or imaging techniques[9-11]. For example, albumin was independently associated with MVI [9]. Besides, non-smooth tumor margins had strong diagnostic power and were of great importance for MVI assessment[10]. Moreover, gadolinium ethoxybenzyl-diethylenetriaminepentaacetic acid (Gd-EOB-DTPA), a special hepatocellular parenchymal contrast agent for magnetic resonance imaging (MRI), was valuable for MVI prediction as well[11,12]. However, the levels of serum markers are instable and likely to be affected by other diseases, and the imaging characteristics are evaluated subjectively and lack of conformance between observers. Thus, a more reliable biomarker is needed for preoperative prediction of MVI.

Quantitative analysis may have advantages over subjective analysis in reflecting valuable microscopic image features. Radiomic analysis can quantify the spatial variations in gray-level patterns, image spectral properties, and pixel interrelationships, which therefore has attracted great interest[13-15]. Using automation algorithms based on big data and with the advantages of noninvasiveness, radiomics analysis provides a powerful tool for modern medicine, and it can broadly combine multiple biomarkers and then guide clinical decision-making for patients suspected with cancer[16]. Various machine-learning methods have been used for radiomic analysis for MVI prediction, such as support vector machine and random forest[17,18]. To the best of our knowledge, there is not yet radiomics study based on linear discriminant analysis (LDA) algorithm to predict MVI. Additionally, even without spatial information, histogram analysis alone can indicate a gray-level distribution and is used for MVI prediction[19,20].

Our aim was to identify the histogram parameters alone that are predictive for MVI, and determined the prediction capacity of LDA radiomic models based on multiple phases in pre-operative Gd-enhanced MRI alone or combined with the image features for detecting MVI.

MATERIALS AND METHODS

Patients

Patients who underwent Gd-enhanced MRI examination before surgery were consecutively recruited between June 2019 and November 2021. The inclusion criteria were: (1) Solitary HCC lesion which was resectable or multiple HCC lesions appearing within one liver lobe; (2) No macroscopic vascular invasion; (3) Received the examination of Gd-enhanced MRI of the liver [with or without hepatobiliary phase (HBP)] within 1 mo before surgery; (4) Received curative hepatectomy; and (5) Verification of MVI by pathological evidence. The exclusion criteria were as follows: (1) Other anti-tumor therapies had been performed before surgery; (2) Pathological or clinical information was incomplete; (3) Imaging was not enough for analysis as a result of motion artifact; and (4) MRI performed in a different 3.0T MR machine. A total of 113 patients (91 men and 22 women; age ranging from 29–88 years, median age 58 years old) were included. According to pathologic results, HCC patients were allocated into MVI-positive (MVI+) and MVI-negative (MVI-) groups. The inclusion and exclusion criteria are shown in the flow diagram (Figure 1). This single-center retrospective cohort study was approved by the Institutional Review Board (No. [2019]283), and the requirement for informed consent was waived.

MRI examination

A 3.0T MR machine (MAGNETOM Verio; Siemens, Healthcare, Erlangen, Germany) with a dedicated phased-array body coil was used for MRI. The standard abdominal MRI protocol included: (1) Axial T2-weighted fat-suppressed turbo-spin-echo: Repetition time (TR)/echo time (TE), 4700/79 msec, slice thickness, 5 mm, slice gap, 1 mm, FOV, 21 mm × 38 mm; (2) In-phase and out-of-phase axial T1-weighted imaging (T1WI): TR/TE, 133/2.5 msec (in-phase), 6.2 msec (out-phase), slice thickness, 5 mm, slice gap, 1 mm, FOV, 21 mm × 38 mm; (3) Diffusion-weighted imaging (b = 50, 800 sec/mm^2) performed using a free-breathing single-shot echo-planar technique, TR/TE, 9965/73 msec, slice thickness, 5 mm, slice gap, 1 mm, FOV, 21 mm × 38 mm. The MRI system automatically calculated the corresponding ADC maps; and (4) Contrast enhanced MRI: A 3D gradient echo sequence with volumetric interpolated breath-hold examination was performed before and after injection of gadobenate dimeglumine (MultiHance; Bracco) at a dose of 0.2 mL/kg and at a rate of 2 mL/sec followed by a 20 mL saline flush with the following parameters: TR/TE, 3.9/1.4 msec, slice thickness 3 mm, slice gap, 0.6 mm, FOV, 25 mm × 38 mm. Hepatic arterial phase (AP), portal venous phase (PVP), equilibrium phase (EP), and HBP images were obtained at 20–30 sec, 70–80 sec, 180 sec, and 90 min after contrast medium injection, respectively.

Radiomic analysis

MaZda software (version 4.6.0, available at http://www.eletel.p.lodz.pl/mazda/) was used for radiomic analysis[21], and Digital Imaging Transformation and Communications in Medicine (DICOM) format was needed for compatibility with MaZda software. Images (MVI+ and MVI-) were loaded into the MaZda software; then, regions of interest (ROIs) were segmented manually by one radiologist, on the largest cross-sectional area and adjacent two images of the tumor or largest lesion (in the case of multiple lesions), which also included cystic necrotic regions. To delineate the tumor, the reference was based on HBP or T2-weighted imaging (T2WI) (in the case of artifact) images which were first segmented. Subsequently, the ROI was overlaid onto other phase images as required. If the respiratory movement caused the change of tumor location, the ROI was finely adjusted.

Radiomic analysis was performed with the MaZda package after loading all segmented tumor T2WI and T1WI + Gd images; within each ROI, 101 features were generated. Six different statistical image descriptors including gradient features, histogram features, gray level co-occurrence matrix, gray level run-length matrix, wavelet transform, and autoregressive model were used to create these radiomic features[21,22]. In each ROI, gray-level was normalized to minimize the effect of brightness and contrast

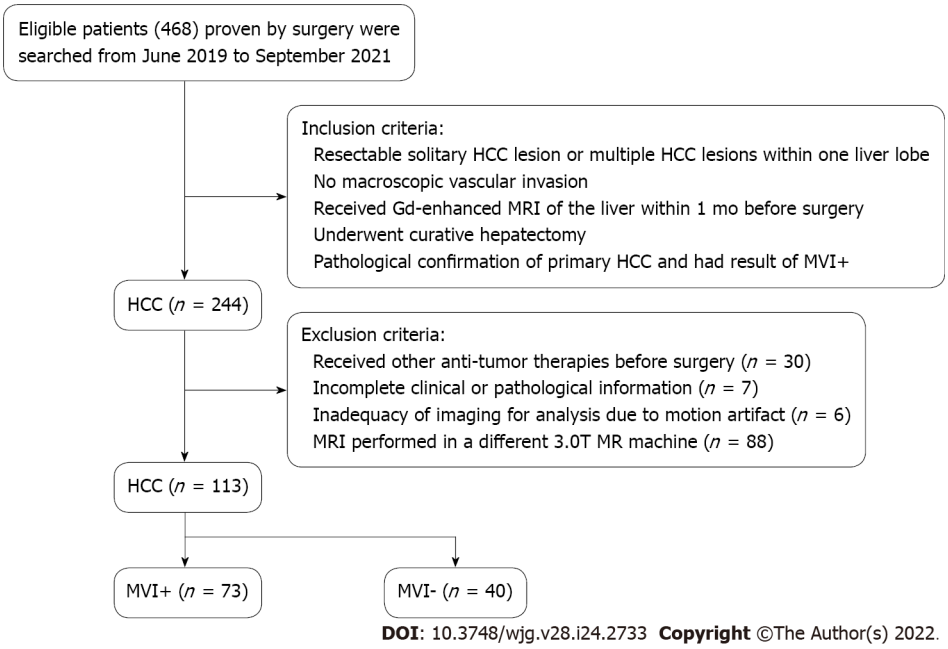


Figure 1 Flowchart of study selection process. HCC: Hepatocellular carcinoma; MVI: Microvascular invasion.

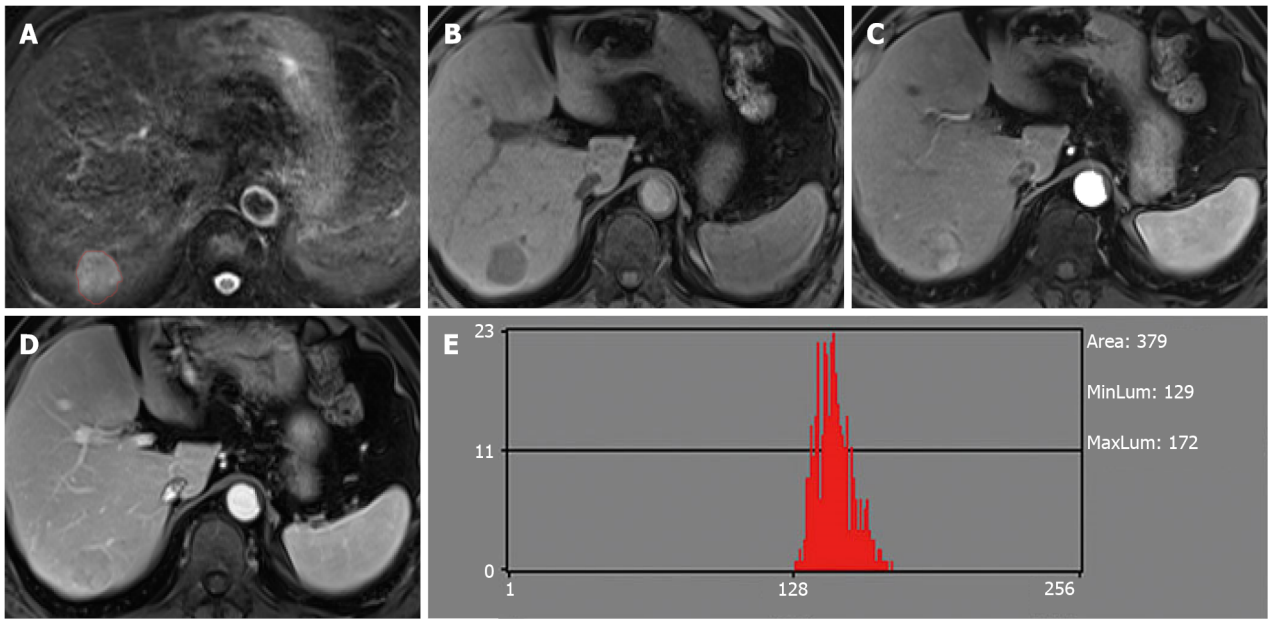
variation by image intensities in the range μ ± 3σ (μ, gray-level mean; σ, standard deviation), and the range was quantized to 6 bits/pixel[23,24].

Dimension reduction is necessary because it is impractical for clinicians to analyze all radiomic features on each patient and curse of dimensionality may happen in the case of too many features. Thus, the useful features were selected among 101 features in each sequence using algorithms, *i.e.*, mutual information (MI), Fisher coefficient (Fisher), and probability of classification error and average correlation coefficients (POE + ACC). These algorithms were used to select 30 highest discriminative power features in each sequence for further analysis. The statistical B11 radiomic analysis package (a plug-in of Mazda software) was used for analyzing these 30 features. A LDA model with the lowest misclassification rate was used to calculate the most discriminant factor (MDF)[25], which served as a comprehensive variable for discrimination and represented a linear transformation of these input 30 features that achieved the maximum separation for samples the between MVI+ and MVI- groups and the minimum separation of samples within each group. Hence, there were six MDFs, *i.e.*, MDF_{T1WI}, MDF_{T2WI}, MDF_{AP}, DMF_{PVP}, MDF_{EP}, and MDF_{HBP}.

The values of the nine histogram features (mean, variance, skewness, kurtosis, percent 1%, percent 10%, percent 50%, percent 90% and percent 99%) previously described (*i.e.*, one of six different statistical image descriptors used for radiomic analysis) were separately saved in addition for the comparison with MDF values. All characteristics of radiomic analysis were generated as presented in Figures 2 and 3.

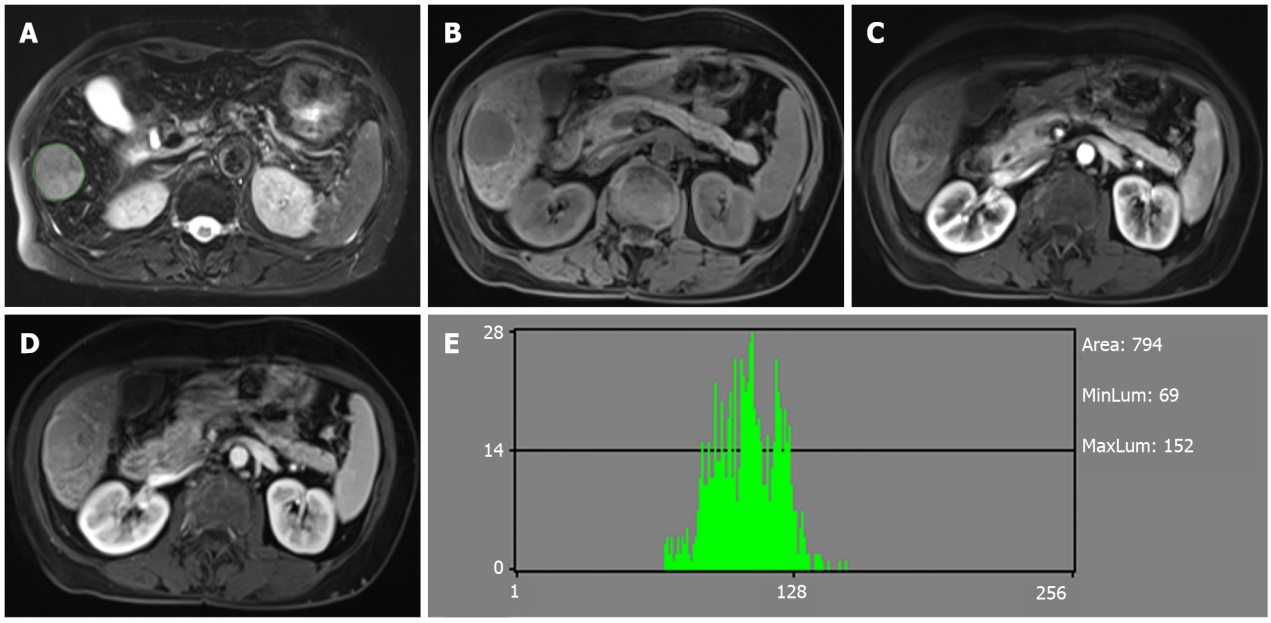
Analysis of semantic features

In each case, an optimal window setting was adjusted to evaluate the preoperative MR images in the Picture Archiving and Communication System. The imaging features for each HCC were evaluated by two abdominal radiologists independently based on the following criteria: (1) Arterial rim enhancement, defined based on the image with irregular ring-like enhancement with relatively hypovascular central areas in the AP[26,27]; (2) Arterial peritumoral enhancement, defined based on the detectable crescent or polygonal shaped enhancement outside the tumor margin, which broadly contact with the tumor border in the AP, changing to isointense with liver parenchyma background in the delayed phase [28]; (3) Tumor margin, also defined as smooth margin, with the representative image being nodular tumors with smooth contour, or non-smooth margin presenting as non-nodular tumors with irregular margin that had surrounding budding portion in the transverse and coronal HBP images[10,28]; (4) Radiological capsule, presenting as peripheral edge of smooth hyperenhancement in the portal venous or EP[28,29]; (5) Tumor hypointensity in the HBP, shown as lower SI than that of the surrounding liver [12,30]; and (6) Peritumoral hypointensity in the HBP, defined as wedge-shaped or flame-like hypointense area of hepatic parenchyma located outside of the tumor margin in the HBP[31]. Two radiologists assessed the features of the HCC images or the largest lesion (in the case of multiple lesions). The final decision was based on their consensus.



DOI: 10.3748/wjg.v28.i24.2733 **Copyright** ©The Author(s) 2022.

Figure 2 Hepatocellular carcinoma without microvascular invasion in a 60-year-old man. A: The lesion showed slightly high signal intensity on T2-weighted imaging (T2WI) and was first regions of interest segmented; B: T1WI showed hypointensity; C: Hyper-enhancement in the arterial phase; D: The lesion showed wash-out in the portal venous phase; E: Histogram map derived from the portal venous phase.

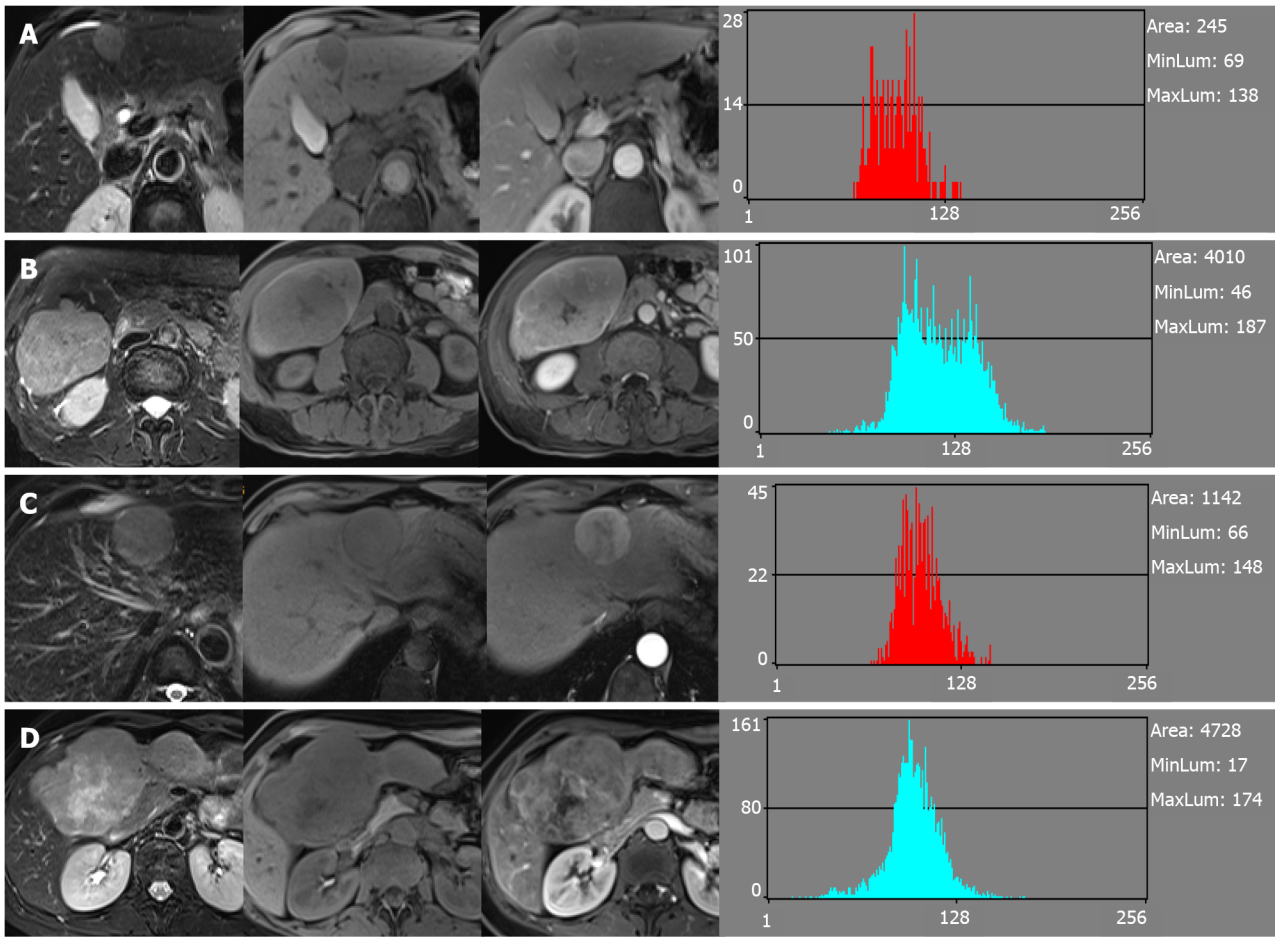


DOI: 10.3748/wjg.v28.i24.2733 **Copyright** ©The Author(s) 2022.

Figure 3 Hepatocellular carcinoma with microvascular invasion in a 68-year-old woman. A: The lesion also showed slightly high signal intensity on T2-weighted imaging (T2WI) and was segmented; B: T1WI showed hypointensity; C: Hyper-enhancement in the arterial phase; D: The lesion showed wash-out in the portal venous phase; E: Histogram map derived from the portal venous phase indicating that the parameter of histogram was significantly different between the two groups.

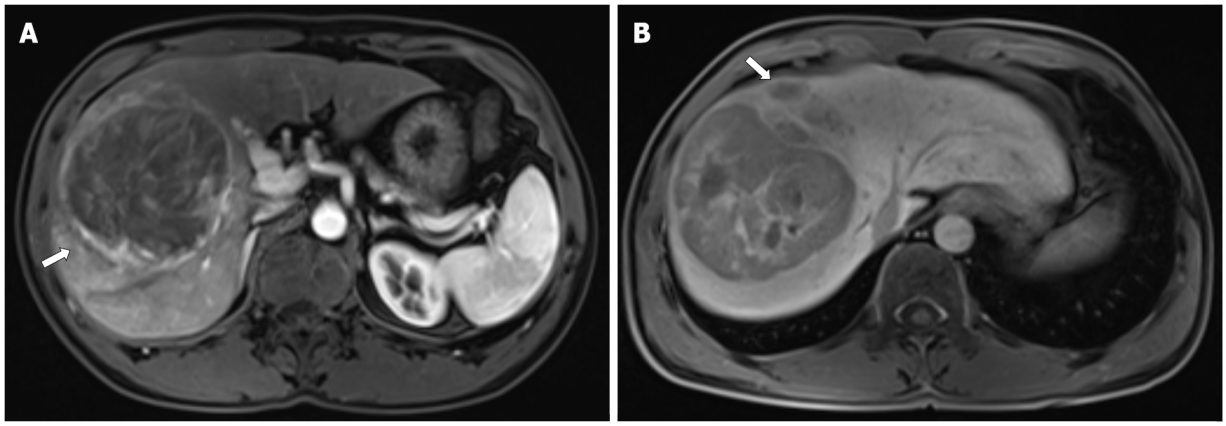
Histopathological analysis

The tumor size, number, and capsule condition were collected and analyzed. The histological type, differentiation grade, lymphocyte infiltration, satellite nodules, MVI status, and chronic liver disease were compared[32]. The definition of MVI was the presence of tumor emboli in an endothelial cells-lined vascular space. The experienced pathologists reported the histopathological results after reviewing the clinical and imaging files.



DOI: 10.3748/wjg.v28.i24.2733 **Copyright** ©The Author(s) 2022.

Figure 4 Similar histogram features but different most discriminant factors. A: Hepatocellular carcinoma without microvascular invasion and the feature derived from the portal venous phase (PVP); B: Hepatocellular carcinoma with microvascular invasion and features derived from the PVP. Case B showed similar histogram features but different most discriminant factors (MDF) compared with case A; C: Hepatocellular carcinoma without microvascular invasion and features derived from the arterial phase (AP); D: Hepatocellular carcinoma with microvascular invasion and features derived from the AP. Case D showed similar histogram features but different MDF compared with case C.



DOI: 10.3748/wjg.v28.i24.2733 **Copyright** ©The Author(s) 2022.

Figure 5 Hepatocellular carcinoma with microvascular invasion in a 47-year-old man. A: Gd-enhanced arterial phase magnetic resonance imaging showed arterial rim enhancement (arrow); B: Hepatobiliary phase image showing peritumoral hypointensity (arrow).

Statistical analysis

SPSS for Windows (version 25.0) and Medcalc (Version 15.2.2) were used to generate the receiver operating characteristic (ROC) curves and compare the diagnostic performance for identifying MVI. The

Table 1 Comparison of patient characteristics according to microvascular invasion

Characteristic	MVI+ (*n* = 73)	MVI- (*n* = 40)	*P* value
Age (yr)[1]	56.82 ± 13.38	57.50 ± 11.98	0.790
Gender, *n* (%)			0.374
Male	57 (78.1)	34 (85.0)	
Female	16 (21.9)	6 (15.0)	
Tumor number, *n* (%)			0.152
1	58 (79.5)	36 (90.0)	
≥ 2	15 (20.5)	4 (10.0)	
AFP, *n* (%)			0.023
≤ 20	23 (31.5)	23 (57.5)	
20-400	22 (30.1)	9 (22.5)	
> 400	28 (38.4)	8 (20.0)	
HBsAg, *n* (%)			0.267
Negative	13 (17.8)	4 (10.0)	
Positive	60 (82.2)	36 (90.0)	
Pathologic grade, *n* (%)			0.042
Well	0 (0.0)	1 (2.5)	
Moderate	39 (53.4)	28 (70.0)	
Poor	34 (46.6)	11 (27.5)	
Location, *n* (%)			0.891
Left lobe	21 (28.8)	13 (32.5)	
Right lobe	51 (69.9)	27 (67.5)	
Caudate lobe	1 (1.3)	0 (0.0)	

[1]Data are the mean ± SD.

AFP: Alpha-fetoprotein; HBsAg: Hepatitis B surface antigen; MVI: Microvascular invasion.

areas under the ROC curve (AUCs) were used to assess the predictive efficacy and the optimal cutoff values from the maximum Youden's index were calculated, as well as the corresponding sensitivity and specificity for discriminating between MVI+ and MVI-. Univariate and multivariate logistic regression analyses were performed to confirm the significant variables related to MVI including clinical factors, imaging features, and MDFs in different sequences, and then build a discriminant model. Multivariate logistic regression analysis was performed using forward stepwise elimination method to identify the independent predictors. The prediction ability of significant MDF and the discriminant model was evaluated by AUC. Five-fold cross-validation was performed using the "caret" package, and nomogram was used as a graphical representation using the "rms" package (R software version 4.0.2, http://www.r-project.org). Student's *t*-test or Mann-Whitney U test was used to compare the continuous variables. Fisher's exact test or Pearson's chi-squared test was used to compare the categorical variables. $P < 0.05$ indicated statistical significance.

RESULTS

Patient characteristics

The patients were divided into two groups according to the histopathological results: MVI+ group and the MVI- group. Among 113 HCCs, 73 had MVI (4 patients had no HBP images), while 40 had no MVI (4 patients had no HBP images). The patients' clinical and radiological characteristics are listed in Tables 1 and 2, respectively. There were statistically significant differences in alpha-fetoprotein (AFP), pathologic grade, maximum tumor diameter (MTD), arterial rim enhancement, tumor margin, and peritumoral hypointensity in the HBP between the MVI+ and MVI- groups ($P < 0.050$).

Table 2 Comparison of different imaging features according to microvascular invasion

MRI feature	MVI+ (*n* = 73)	MVI- (*n* = 40)	*P* value
MTD (cm)[1]	7.23 ± 4.30	3.80 ± 2.43	< 0.001
Arterial rim enhancement (%)			0.002
Absent	37 (50.7)	32 (80)	
Present	36 (49.3)	8 (20)	
Arterial peritumoral enhancement (%)			0.134
Absent	53 (72.6)	34 (85)	
Present	20 (27.4)	6 (15)	
Tumor margin (%)			0.004
Smooth	36 (49.3)	31 (77.5)	
Non-smooth	37 (50.7)	9 (22.5)	
Radiological capsule (%)			0.303
Absent	19 (26.0)	7 (17.5)	
Present	54 (74.0)	33 (82.5)	
Tumor hypointensity in the HBP (%)			0.336
Absent	2 (2.9)	3 (8.3)	
Present	67 (97.1)	33 (91.7)	
Peritumoral hypointensity in the HBP (%)			0.016
Absent	17 (24.6)	34 (94.4)	
Present	52 (75.4)	2 (5.6)	

[1]Data are the mean ± SD.

There were eight patients who had no HBP images. HBP: Hepatobiliary phase; MVI: Microvascular invasion; MTD: Maximum tumor diameter; MRI: Magnetic resonance imaging.

Radiomic analysis

For the MVI+ and MVI- patients, the values of MDFs resulting from the LDA model under B11 analysis were significantly different between the two groups ($P < 0.001$). The analysis of MDF values with ROCs generated an AUC of 0.82 [95% confidence interval (CI): 0.77-0.87] for T1WI; 0.77 (95%CI: 0.72-0.83) for T2WI; 0.84 (95%CI: 0.80-0.88) for AP; 0.85 (95%CI: 0.81-0.90) for PVP; 0.84 (95%CI: 0.79-0.88) for EP; and 0.83 (95%CI: 0.78-0.87) for HBP images. Cutoff values of -1.38×10^{-3} (T1WI), 4.73×10^{-3} (T2WI), 1.97×10^{-2} (AP), 4.17×10^{-3} (PVP), 2.25×10^{-2} (EP), and 4.30×10^{-4} (HBP) were obtained with corresponding high sensitivities and specificities (T1WI: 78% and 78%; T2WI: 59% and 80%; AP: 87% and 66%; PVP: 67% and 90%; EP: 68% and 85%; HBP: 76% and 79%, respectively). The predictive power (AUC) of MDFs derived from the radiomics analysis was better than that of all other histogram parameters (T1WI: 0.52-0.68; T2WI: 0.53-0.70; AP: 0.54-0.69; PVP: 0.50-0.74; EP: 0.51-0.74; HBP: 0.52-0.65) (Tables 3 and 4). The MRI images of four MVI+ and MVI- cases in the AP and PVP are presented, which show similar histogram features but different MDFs (Figure 4 and Supplementary Table 1).

Association of MDFs and patient characteristics with microvascular invasion

We excluded the patients who had no HBP images. MDF values were derived from the largest cross-sectional area of images for univariate analysis. Univariate analysis showed that MDF_{T1WI} greater than -1.38×10^{-3} [odds ratio (OR) = 11.2000, 95%CI: 4.346-28.861; $P < 0.001$], MDF_{T2WI} greater than 4.73×10^{-3} (OR = 6.066, 95%CI: 2.334-15.765; $P < 0.001$), MDF_{AP} greater than 1.97×10^{-2} (OR = 8.552, 95%CI: 2.967-24.650; $P < 0.001$), MDF_{PVP} less than 4.17×10^{-3} (OR = 0.050, 95%CI: 0.017-0.143; $P < 0.001$), MDF_{EP} less than 2.25×10^{-2} (OR = 0.095, 95%CI: 0.037-0.244; $P < 0.001$), and MDF_{HBP} greater than 4.30×10^{-4} (OR = 8.800, 95%CI: 3.222-24.032; $P < 0.001$) were important risk factors related to the presence of MVI. Among patient characteristics, univariate analysis showed that MTD (OR = 1.351, 95%CI: 1.146–1.593; $P < 0.001$), AFP level (OR = 3.818, 95%CI: 1.357–10.605; $P = 0.028$), arterial rim enhancement (present *vs* absent, OR = 5.683, 95%CI: 1.977–16.340; $P = 0.001$), tumor margin (non-smooth *vs* smooth, OR = 4.024, 95%CI: 1.555–10.414; $P = 0.004$), and peritumoral hypointensity in the HBP (present *vs* absent, OR = 52.000, 95%CI: 11.287–239.569; $P < 0.001$) were significant risk factors associated with the presence of MVI

Table 3 Receiver operating characteristic results of radiomic analysis based on most discriminant factors in arterial phase and histogram parameters to discriminate between microvascular invasion+ and microvascular invasion- groups

	MVI (-)	MVI (+)	AUC	Sensitivity	Specificity	*P* value	Cut-off value
MDF	(-4.80 ± 6.14) × 10^{-2}	(2.63 ± 4.74) × 10^{-2}	0.84 (0.80-0.88)	87%	66%	< 0.001	1.97 × 10^{-2}
Histogram parameters							
Mean	(1.27 ± 0.28) × 10^{2}	(1.09 ± 0.26) × 10^{2}	0.68 (0.63-0.74)	78%	52%	< 0.001	1.06 × 10^{2}
Variance	(5.28 ± 4.24) × 10^{2}	(4.57 ± 3.21) × 10^{2}	0.54 (0.48-0.61)	68%	45%	0.204	3.32 × 10^{2}
Skewness	(-9.71 ± 58.46) × 10^{-2}	(2.52 ± 5.79) × 10^{-1}	0.68 (0.62-0.74)	76%	58%	< 0.001	1.30 × 10^{-1}
Kurtosis	(-5.24 ± 91.73) × 10^{-2}	(4.06 ± 11.19) × 10^{-1}	0.60 (0.53-0.66)	90%	25%	0.004	-5.96 × 10^{-1}
Perc.01%	(0.80 ± 0.20) × 10^{2}	(0.68 ± 0.20) × 10^{2}	0.68 (0.62-0.74)	78%	50%	< 0.001	64.5
Perc.10%	(0.99 ± 0.23) × 10^{2}	(0.84 ± 0.22) × 10^{2}	0.68 (0.62-0.74)	96%	32%	< 0.001	69.5
Perc.50%	(1.28 ± 0.30) × 10^{2}	(1.08 ± 0.27) × 10^{2}	0.69 (0.63-0.74)	76%	47%	< 0.001	105.5
Perc.90%	(1.54 ± 0.34) × 10^{2}	(1.35 ± 0.31) × 10^{2}	0.65 (0.59-0.71)	57%	70%	< 0.001	148.5
Perc.99%	(1.73 ± 0.39) × 10^{2}	(1.57 ± 0.35) × 10^{2}	0.62 (0.55-0.68)	48%	74%	< 0.001	177.5

AUC: Area under the receiver operating characteristic curve; MDF: Most discriminant factor; MVI: Microvascular invasion.

Table 4 Receiver operating characteristic results of radiomic analysis based on most discriminant factors in portal venous phase and histogram parameters to discriminate between microvascular invasion+ and microvascular invasion- groups

	MVI (-)	MVI (+)	AUC	Sensitivity	Specificity	*P* value	Cut-off value
MDF	(7.84 ± 9.26) × 10^{-3}	(-4.30 ± 7.00) × 10^{-3}	0.85 (0.81-0.90)	67%	90%	< 0.001	4.17 × 10^{-3}
Histogram parameters							
Mean	(1.24 ± 0.24) × 10^{2}	(1.08 ± 0.24) × 10^{2}	0.69 (0.63-0.75)	78%	54%	< 0.001	106.6
Variance	(3.07 ± 4.11) × 10^{2}	(4.30 ± 3.59) × 10^{2}	0.67 (0.61-0.74)	80%	50%	< 0.001	165.9
Skewness	(1.93 ± 6.11) × 10^{-1}	(1.87 ± 5.85) × 10^{-1}	0.50 (0.44-0.57)	16%	88%	0.09	7.76 × 10^{-1}
Kurtosis	(0.60 ± 1.20)	(0.62 ± 1.19)	0.51 (0.44-0.57)	57%	51%	0.787	1.62 × 10^{-1}
Perc.01%	(91.84 ± 30.33)	(67.16 ± 24.85)	0.74 (0.68-0.80)	50%	90%	< 0.001	101.5
Perc.10%	(1.06 ± 0.29) × 10^{2}	(0.84 ± 0.25) × 10^{2}	0.72 (0.67-0.78)	56%	81%	< 0.001	107.5
Perc.50%	(1.25 ± 0.24) × 10^{2}	(1.07 ± 0.24) × 10^{2}	0.69 (0.64-0.75)	78%	55%	< 0.001	106.5
Perc.90%	(1.44 ± 0.27) × 10^{2}	(1.32 ± 0.27) × 10^{2}	0.62 (0.56-0.68)	63%	61%	< 0.001	137.5
Perc.99%	(1.61 ± 0.31) × 10^{2}	(1.56 ± 0.34) × 10^{2}	0.55 (0.49-0.61)	35%	77%	0.179	176.5

AUC: Area under the receiver operating characteristic curve; MDF: Most discriminant factor; MVI: Microvascular invasion.

(Table 5).

Multivariate analysis of MDF values and patient characteristics with microvascular invasion

Multivariate analysis of the above 11 significant parameters showed that only MDF_{AP} (> 1.97 × 10^{-2} *vs* ≤ 1.97 × 10^{-2}, OR = 7.654, 95%CI: 1.860-31.501; P = 0.005), MDF_{PVP} (> 4.17 × 10^{-3} *vs* ≤ 4.17 × 10^{-3}, OR = 0.182, 95%CI: 0.047-0.705; P = 0.014), and peritumoral hypointensity in the HBP (present *vs* absent, OR = 37.098, 95%CI: 6.861-200.581; P < 0.001) were independent predictors related to the presence of MVI (Figure 5).

Table 5 Univariate analysis of risk factors for most discriminant factors and patient characteristic

Variable	OR	95%CI	*P* value
MDF_{T1}	11.200	4.346-28.861	< 0.001[a]
MDF_{T2}	6.066	2.334-15.765	< 0.001[a]
MDF_{AP}	8.552	2.967-24.650	< 0.001[a]
MDF_{PVP}	0.050	0.017-0.143	< 0.001[a]
MDF_{EP}	0.095	0.037-0.244	< 0.001[a]
MDF_{HBP}	8.800	3.222-24.032	< 0.001[a]
MTD	1.351	1.146-1.593	< 0.001[a]
AFP	3.818	1.375-10.605	0.028[a]
Pathologic grade			0.105
Arterial rim enhancement	5.683	1.977-16.340	0.001[a]
Arterial peritumoral enhancement			0.215
Tumor margin	4.024	1.555-10.414	0.004[a]
Radiological capsule			0.275
Tumor hypointensity in HBP			0.215
Peritumoral hypointensity in HBP	52.000	11.287-239.569	< 0.001[a]

[a]*P* < 0.05, statistically significant results from logistic regression analysis. Variables with [a]*P* < 0.05 in univariate logistic regression analysis were applied to a multivariate logistic regression analysis.

MDF: Most discriminant factor; AFP: Alpha-fetoprotein; AP: Arterial phase; CI: Confidence interval; EP: Equilibrium phase; HBP: Hepatobiliary phase; MTD: Maximum tumor diameter; OR: Odds ratio; PVP: Portal venous phase.

The risk scores for individual patients based on the final discriminant model were calculated using the following formula: Logit (P) = −4.612 + 3.614 × peritumoral hypointensity on HBP (absent = 0, present = 1) + 2.035 × MDF_{AP} (≤ 1.97×10^{-2} *vs* > 1.97×10^{-2}, ≤ 1.97×10^{-2} = 0, > 1.97×10^{-2} = 1) - 1.876 × MDF_{PVP} (≤ 4.17×10^{-3} *vs* > 4.17×10^{-3}, ≤ 4.17×10^{-3} = 0, > 4.17×10^{-3} = 1). The probabilities of MVI were calculated by the formula [P = e Logit (P)/1 + e Logit (P)].

The AUC of the final model was 0.939 (95%CI: 0.893-0.984; standard error: 0.023) and the optimal cutoff value was 0.595881 ≈ 0.60 (specificity: 89%; sensitivity: 90%; Youden's index: 0.788) (Figure 6A). The result of internal five-fold cross-validation (AUC: 0.912; 95%CI: 0.841-0.959; standard error: 0.0298) also showed favorable predictive efficacy (Figure 6A). The independent predictive factors were integrated into a nomogram by the multivariate logistic regression analysis (Figure 6B).

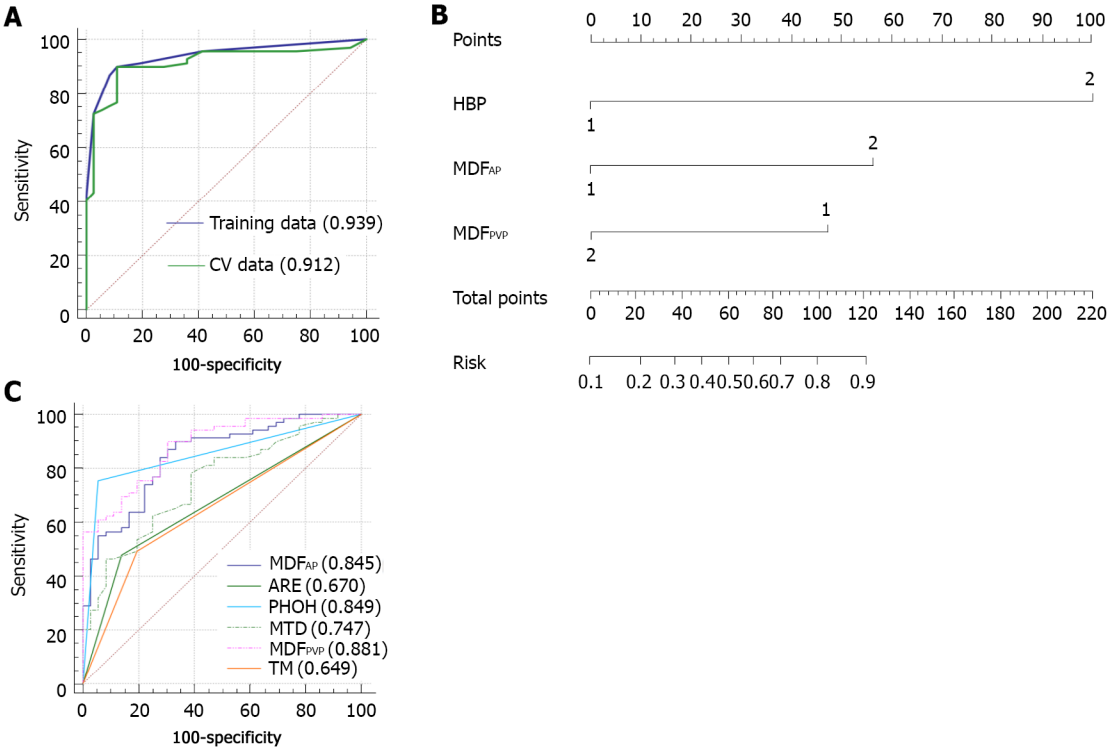
Comparison of area under the receiver operating characteristic curve values of MDF values and imaging features

We generated the ROC curves of MDF_{AP} and $MDF_{PVP,}$ respectively, which were independent predictors. The ROC curves of imaging features which were significantly different were also generated alone. The results were compared using the Delong test. The MDF_{AP} and MDF_{PVP} had significantly higher AUCs than MTDs, arterial rim enhancement, and tumor margin ($P < 0.05$; Supplementary Table 2). However, there were no differences in AUCs among MDF_{AP}, MDF_{PVP}, and peritumoral hypointensity in the HBP ($P > 0.05$; Supplementary Table 1). Comparison of ROC curves is shown in Figure 6C.

DISCUSSION

MVI indicates the invasiveness of HCC and poor prognosis[2,3]. Therefore, the pre-operative prediction of MVI is an important factor for assessing long-term patient survival and treatment optimization. The quantification of MRI images by radiomic analysis can characterize the heterogeneity of tumor and has demonstrated previous success in reflecting histological subtype[33,34]. In the present study, through the analysis of the top 30 parameters in each sequence, an overall discriminator, MDF, was generated with the LDA model, providing better prediction ability for MVI than the histogram features.

Our study showed a high sensitivity of MDF values from radiomic analysis on preoperative Gd-enhanced MRI images and/or specificity in distinguishing between MVI+ and MVI-. The AUCs of MDF values of six sequences, all of which were more than 0.75, outperformed those of all histogram



DOI: 10.3748/wjg.v28.i24.2733 **Copyright** ©The Author(s) 2022.

Figure 6 Area under the receiver operating characteristic curve of the final model. A: Receiver operating characteristic (ROC) curves of the selected model and the ROC curve of the 5-fold cross-validation; B: Nomogram of the integrated model. Hepatobiliary phase (HBP) means peritumoral hypointensity in the HBP, most discriminant factor (MDF)$_{AP}$ means the MDF of the arterial phase, and MDF$_{PVP}$ means the MDF of the portal venous phase; C: Comparison of ROC curves for prediction of microvascular invasion. The area under the ROC curve (AUC) was largest for the MDF$_{PVP}$ alone (AUC = 0.881). ARE: Arterial rim enhancement; MTD: Maximum tumor diameter; PHOH: Peritumoral hypointensity in the HBP; TM: Tumor margin.

parameters and imaging features. The MDF values of AP and PVP images had significantly higher AUCs than most of imaging features. MDF values could provide additional information useful for clinical management decisions. Moreover, MaZda software can be easily used for general clinicians without additional requirement of expertise, easily serving as a potential powerful tool in preoperative prediction of MVI.

LDA has been used in radiomics studies recently[35]. Han *et al*[35] found that LDA and support vector machine achieved optimal performance when compared with multiple machine learning methods[35]. In our study, among the LDA models based on various sequences, MDF$_{AP}$ and MDF$_{PVP}$ were significant independent factors for the prediction of MVI, and showed satisfactory predictive efficacy with an AUC greater than 0.80. Histogram parameters have been used in quantitative analysis of MVI in clinical studies[19,20]. Li *et al*[19] performed histogram analysis of intravoxel incoherent motion and the best parameter provided a sensitivity of 81% and specificity of 85%[19]. It was based on whole tumor volume, but only 41 patients were enrolled. Wang *et al*[20] used computational quantitative measures based on the maximum cross-sectional area to predict MVI of small HCC, but only in HBP images[20]; the AUC, sensitivity, and specificity were 0.91, 0.87, and 0.80, respectively. In our study, the radiomic analysis-based MDF outperformed each individual histogram parameter in predicting the presence of MVI. Therefore, we considered that MDFs on the basis of LDA model that contained more comprehensive information could evaluate the Gd-enhanced MR images and determine MVI status better than histogram analysis alone.

Multivariate analysis of the 11 risk factors identified in the univariate analysis found that only peritumoral hypointensity in HCCs in the HBP, MDF$_{PVP}$, and MDF$_{AP}$ were independent predictors of MVI. Pathologically, MVI is usually found in the small portal vein and hepatic artery[4]. It may be detected in the small liver lymphatic vessels. But it is mostly found in small branches of the portal vein. This may explain why the MDF$_{PVP}$ and MDF$_{AP}$ were independent predictors of MDF values in the model that predicted MVI. The MDF$_{PVP}$ whose OR was less than 1 may be a protective factor, which means that the higher the MDF$_{PVP}$, the less possible the presence of MVI. MVI may affect the biological functions of the canalicular transporter multidrug resistance-associated protein 2 or the organic anion transporting peptides, both of which lead to the elimination of gadoxetate disodium. That may be the reason why peritumoral hypointensity appeared in HCCs in the HBP[12]. The OR of peritumoral hypointensity in the HBP was quite high, which may result from relatively small sample size.

It has been reported that MR findings including arterial peritumoral enhancement and non-smooth tumor margin were independent predictors associated with the presence of MVI or indicated the association between the hypointensity of HCCs in HBP images and a higher frequency of MVI[12,17], which is not consistent with our study. One possible reason for the inconsistence may be the differences between study populations, as all patients enrolled in that study had a single HCC with a diameter ≤ 5 cm. The inherent and technical inconsistencies between the observers in two studies may also account for the incompatible results. Arterial rim enhancement can predict biological characters of HCCs, including MVI, rapid progression, and early recurrence[26,36]. Our study showed that rim enhancement in the AP was not an independent predictor of MVI, and the reason may be that rim enhancement in AP is uncommon in HCC but more often seen in mass-forming cholangiocarcinoma or metastasis[37].

There are some limitations in this study. First, a selection bias may exist due to the retrospective study. Second, the radiomic analysis was performed only on the largest cross-sectional area and two adjacent images of the tumor. There may be information loss compared to whole tumors. In spite of this, our results showed excellent discriminative efficacy between the MVI+ and MVI- groups. Third, different MVI grading indicates a decreasing gradient of overall survival and time to early recurrence, which was not analyzed in the MVI+ group due to the small sample size. Finally, this study was performed at only one institution, causing the sample size small relative to the number of variables. Further multicenter, prospective studies are needed to validate the results of this study.

CONCLUSION

In conclusion, radiomic analysis based on preoperative Gd-enhanced MR images may be feasible for predicting MVI of HCC. Upon the application of MRI findings and radiomic variables in our model, the diagnostic prediction of MVI showed a high specificity and sensitivity, indicating that this method is a useful tool for clinicians in treatment decision-making.

ARTICLE HIGHLIGHTS

Research background

The prognosis of hepatocellular carcinoma (HCC) remains poor and relapse occurs in more than half of the patients within 2 years after hepatectomy. Microvascular invasion (MVI) is one of the potential predictors of recurrence. MVI is defined as the appearance of tumor cells in smaller vessels inside the liver which include small portal vein, and small lymphatic vessels or hepatic arteries. Accurate preoperative prediction of MVI is potentially beneficial to the optimization of treatment planning.

Research motivation

There have been some studies to preoperatively predict MVI in terms of serum markers, radiological features, or imaging techniques. However, the levels of serum markers are instable and likely to be affected by other diseases, and the imaging characteristics are evaluated subjectively and lack of conformance between observers. Thus, a more reliable biomarker is needed for preoperative prediction of MVI.

Research objectives

The aim of this study was to develop a radiomic analysis model based on pre-operative magnetic resonance imaging (MRI) data to predict MVI in HCC.

Research methods

A total of 113 patients recruited to this study have been diagnosed as having HCC with histological confirmation, among whom, 73 were found to have MVI and 40 were not. All the patients received preoperative examination by Gd-enhanced MRI and then curative hepatectomy. We manually delineated the tumor lesion on the largest cross-sectional area of the tumor and the two adjacent images on MRI. Quantitative analyses included most discriminant factors (MDFs) developed using a linear discriminant analysis algorithm and histogram analysis *via* MaZda software. Independent significant variables of clinical and radiological features and MDFs for the prediction of MVI were estimated and a discriminant model was established by univariate and multivariate logistic regression analysis. Prediction ability of the above-mentioned parameters or model was then evaluated by receiver operating characteristic (ROC) curve analysis, and five-fold cross-validation was applied *via* R software.

Research results

The area under the ROC curve of the MDF (0.77-0.85) outperformed the histogram parameters (0.51-0.74). After multivariate analysis, MDF values of the arterial and portal venous phase, and peritumoral

hypointensity in the hepatobiliary phase were identified to be independent predictors of MVI ($P < 0.05$). The area under the ROC curve (AUC) value of the model was 0.939. The result of internal five-fold cross-validation (AUC: 0.912) also showed favorable predictive efficacy.

Research conclusions

Noninvasive MRI radiomic model based on MDF values and imaging biomarkers may be useful to make preoperative prediction of MVI in patients with primary HCC.

Research perspectives

We believe that noninvasive radiomic models based on pre-operative MRI data have potential to be widely used in clinical fields.

ACKNOWLEDGEMENTS

We thank the radiographers at the First Affiliated Hospital of Fujian Medical University for scanning the patients and data collections in this study.

FOOTNOTES

Author contributions: Li YM, Zhu YM, and Cao DR worked out the conceptualization; Li YM, Cao DR, and Zhu YM did the methodology; Zhu YM and Yan C analyzed, collected, and interpreted the data; Li YM and Cao DR contributed to study supervision; all authors edited and reviewed the manuscript, and have read and approved the final manuscript.

Supported by Joint Funds for the Innovation of Science and Technology, Fujian Province (CN), No. 2019Y9125.

Institutional review board statement: This study was reviewed and approved by the Ethics Committee of the First Affiliated Hospital of Fujian Medical University.

Informed consent statement: This study was approved by the institutional review board of our institution. The requirement for written informed consent was waived for this retrospective study.

Conflict-of-interest statement: The authors declare that the research was conducted in the absence of any commercial or financial relationships that could be construed as a potential conflict of interest.

Data sharing statement: No additional data are available.

Open-Access: This article is an open-access article that was selected by an in-house editor and fully peer-reviewed by external reviewers. It is distributed in accordance with the Creative Commons Attribution NonCommercial (CC BY-NC 4.0) license, which permits others to distribute, remix, adapt, build upon this work non-commercially, and license their derivative works on different terms, provided the original work is properly cited and the use is non-commercial. See: https://creativecommons.org/Licenses/by-nc/4.0/

Country/Territory of origin: China

ORCID number: Yue-Ming Li 0000-0002-3669-568X; Yue-Min Zhu 0000-0001-9630-0160; Lan-Mei Gao 0000-0002-6032-6884; Ze-Wen Han 0000-0002-0146-8583; Xiao-Jie Chen 0000-0003-4521-3803; Chuan Yan 0000-0003-4106-8995; Rong-Ping Ye 0000-0001-7867-9752; Dai-Rong Cao 0000-0002-0051-3143.

S-Editor: Fan JR
L-Editor: Wang TQ
P-Editor: Fan JR

REFERENCES

1 **Llovet JM**, Kelley RK, Villanueva A, Singal AG, Pikarsky E, Roayaie S, Lencioni R, Koike K, Zucman-Rossi J, Finn RS. Hepatocellular carcinoma. *Nat Rev Dis Primers* 2021; **7**: 6 [PMID: 33479224 DOI: 10.1038/s41572-020-00240-3]
2 **Zhang X**, Li J, Shen F, Lau WY. Significance of presence of microvascular invasion in specimens obtained after surgical treatment of hepatocellular carcinoma. *J Gastroenterol Hepatol* 2018; **33**: 347-354 [PMID: 28589639 DOI: 10.1111/jgh.13843]
3 **Erstad DJ**, Tanabe KK. Prognostic and Therapeutic Implications of Microvascular Invasion in Hepatocellular Carcinoma. *Ann Surg Oncol* 2019; **26**: 1474-1493 [PMID: 30788629 DOI: 10.1245/s10434-019-07227-9]

4 **Gouw AS**, Balabaud C, Kusano H, Todo S, Ichida T, Kojiro M. Markers for microvascular invasion in hepatocellular carcinoma: where do we stand? *Liver Transpl* 2011; **17** Suppl 2: S72-S80 [PMID: 21714066 DOI: 10.1002/lt.22368]

5 **European Association for the Study of the Liver**. EASL Clinical Practice Guidelines: Management of hepatocellular carcinoma. *J Hepatol* 2018; **69**: 182-236 [PMID: 29628281 DOI: 10.1016/j.jhep.2018.03.019]

6 **Feng LH**, Dong H, Lau WY, Yu H, Zhu YY, Zhao Y, Lin YX, Chen J, Wu MC, Cong WM. Novel microvascular invasion-based prognostic nomograms to predict survival outcomes in patients after R0 resection for hepatocellular carcinoma. *J Cancer Res Clin Oncol* 2017; **143**: 293-303 [PMID: 27743138 DOI: 10.1007/s00432-016-2286-1]

7 **Han J**, Li ZL, Xing H, Wu H, Zhu P, Lau WY, Zhou YH, Gu WM, Wang H, Chen TH, Zeng YY, Wu MC, Shen F, Yang T. The impact of resection margin and microvascular invasion on long-term prognosis after curative resection of hepatocellular carcinoma: a multi-institutional study. *HPB (Oxford)* 2019; **21**: 962-971 [PMID: 30718183 DOI: 10.1016/j.hpb.2018.11.005]

8 **Lei Z**, Li J, Wu D, Xia Y, Wang Q, Si A, Wang K, Wan X, Lau WY, Wu M, Shen F. Nomogram for Preoperative Estimation of Microvascular Invasion Risk in Hepatitis B Virus-Related Hepatocellular Carcinoma Within the Milan Criteria. *JAMA Surg* 2016; **151**: 356-363 [PMID: 26579636 DOI: 10.1001/jamasurg.2015.4257]

9 **Zheng J**, Seier K, Gonen M, Balachandran VP, Kingham TP, D'Angelica MI, Allen PJ, Jarnagin WR, DeMatteo RP. Utility of Serum Inflammatory Markers for Predicting Microvascular Invasion and Survival for Patients with Hepatocellular Carcinoma. *Ann Surg Oncol* 2017; **24**: 3706-3714 [PMID: 28840521 DOI: 10.1245/s10434-017-6060-7]

10 **Hu H**, Zheng Q, Huang Y, Huang XW, Lai ZC, Liu J, Xie X, Feng ST, Wang W, Lu M. A non-smooth tumor margin on preoperative imaging assesses microvascular invasion of hepatocellular carcinoma: A systematic review and meta-analysis. *Sci Rep* 2017; **7**: 15375 [PMID: 29133822 DOI: 10.1038/s41598-017-15491-6]

11 **Huang M**, Liao B, Xu P, Cai H, Huang K, Dong Z, Xu L, Peng Z, Luo Y, Zheng K, Peng B, Li ZP, Feng ST. Prediction of Microvascular Invasion in Hepatocellular Carcinoma: Preoperative Gd-EOB-DTPA-Dynamic Enhanced MRI and Histopathological Correlation. *Contrast Media Mol Imaging* 2018; **2018**: 9674565 [PMID: 29606926 DOI: 10.1155/2018/9674565]

12 **Lee S**, Kim SH, Lee JE, Sinn DH, Park CK. Preoperative gadoxetic acid-enhanced MRI for predicting microvascular invasion in patients with single hepatocellular carcinoma. *J Hepatol* 2017; **67**: 526-534 [PMID: 28483680 DOI: 10.1016/j.jhep.2017.04.024]

13 **Chamming's F**, Ueno Y, Ferré R, Kao E, Jannot AS, Chong J, Omeroglu A, Mesurolle B, Reinhold C, Gallix B. Features from Computerized Texture Analysis of Breast Cancers at Pretreatment MR Imaging Are Associated with Response to Neoadjuvant Chemotherapy. *Radiology* 2018; **286**: 412-420 [PMID: 28980886 DOI: 10.1148/radiol.2017170143]

14 **Yang L**, Gu D, Wei J, Yang C, Rao S, Wang W, Chen C, Ding Y, Tian J, Zeng M. A Radiomics Nomogram for Preoperative Prediction of Microvascular Invasion in Hepatocellular Carcinoma. *Liver Cancer* 2019; **8**: 373-386 [PMID: 31768346 DOI: 10.1159/000494099]

15 **He B**, Dong D, She Y, Zhou C, Fang M, Zhu Y, Zhang H, Huang Z, Jiang T, Tian J, Chen C. Predicting response to immunotherapy in advanced non-small-cell lung cancer using tumor mutational burden radiomic biomarker. *J Immunother Cancer* 2020; **8** [PMID: 32636239 DOI: 10.1136/jitc-2020-000550]

16 **Lambin P**, Leijenaar RTH, Deist TM, Peerlings J, de Jong EEC, van Timmeren J, Sanduleanu S, Larue RTHM, Even AJG, Jochems A, van Wijk Y, Woodruff H, van Soest J, Lustberg T, Roelofs E, van Elmpt W, Dekker A, Mottaghy FM, Wildberger JE, Walsh S. Radiomics: the bridge between medical imaging and personalized medicine. *Nat Rev Clin Oncol* 2017; **14**: 749-762 [PMID: 28975929 DOI: 10.1038/nrclinonc.2017.141]

17 **Xu X**, Zhang HL, Liu QP, Sun SW, Zhang J, Zhu FP, Yang G, Yan X, Zhang YD, Liu XS. Radiomic analysis of contrast-enhanced CT predicts microvascular invasion and outcome in hepatocellular carcinoma. *J Hepatol* 2019; **70**: 1133-1144 [PMID: 30876945 DOI: 10.1016/j.jhep.2019.02.023]

18 **Chong HH**, Yang L, Sheng RF, Yu YL, Wu DJ, Rao SX, Yang C, Zeng MS. Multi-scale and multi-parametric radiomics of gadoxetate disodium-enhanced MRI predicts microvascular invasion and outcome in patients with solitary hepatocellular carcinoma ≤ 5 cm. *Eur Radiol* 2021; **31**: 4824-4838 [PMID: 33447861 DOI: 10.1007/s00330-020-07601-2]

19 **Li H**, Zhang J, Zheng Z, Guo Y, Chen M, Xie C, Zhang Z, Mei Y, Feng Y, Xu Y. Preoperative histogram analysis of intravoxel incoherent motion (IVIM) for predicting microvascular invasion in patients with single hepatocellular carcinoma. *Eur J Radiol* 2018; **105**: 65-71 [PMID: 30017300 DOI: 10.1016/j.ejrad.2018.05.032]

20 **Wang X**, Zhang Z, Zhou X, Zhang Y, Zhou J, Tang S, Liu Y, Zhou Y. Computational quantitative measures of Gd-EOB-DTPA enhanced MRI hepatobiliary phase images can predict microvascular invasion of small HCC. *Eur J Radiol* 2020; **133**: 109361 [PMID: 33120240 DOI: 10.1016/j.ejrad.2020.109361]

21 **Szczypiński PM**, Strzelecki M, Materka A, Klepaczko A. MaZda--a software package for image texture analysis. *Comput Methods Programs Biomed* 2009; **94**: 66-76 [PMID: 18922598 DOI: 10.1016/j.cmpb.2008.08.005]

22 **Strzelecki M**, Szczypinski P, Materka A, Klepaczko A. A software tool for automatic classification and segmentation of 2D/3D medical images. *Nucl Instrum Methods Phys Res* 2013; **702**: 137-140 [DOI: 10.1016/j.nima.2012.09.006]

23 **Yan PF**, Yan L, Hu TT, Xiao DD, Zhang Z, Zhao HY, Feng J. The Potential Value of Preoperative MRI Texture and Shape Analysis in Grading Meningiomas: A Preliminary Investigation. *Transl Oncol* 2017; **10**: 570-577 [PMID: 28654820 DOI: 10.1016/j.tranon.2017.04.006]

24 **Vallières M**, Freeman CR, Skamene SR, El Naqa I. A radiomics model from joint FDG-PET and MRI texture features for the prediction of lung metastases in soft-tissue sarcomas of the extremities. *Phys Med Biol* 2015; **60**: 5471-5496 [PMID: 26119045 DOI: 10.1088/0031-9155/60/14/5471]

25 **Brown AM**, Nagala S, McLean MA, Lu Y, Scoffings D, Apte A, Gonen M, Stambuk HE, Shaha AR, Tuttle RM, Deasy JO, Priest AN, Jani P, Shukla-Dave A, Griffiths J. Multi-institutional validation of a novel textural analysis tool for preoperative stratification of suspected thyroid tumors on diffusion-weighted MRI. *Magn Reson Med* 2016; **75**: 1708-1716 [PMID: 25995019 DOI: 10.1002/mrm.25743]

26 **Rhee H**, An C, Kim HY, Yoo JE, Park YN, Kim MJ. Hepatocellular Carcinoma with Irregular Rim-Like Arterial Phase Hyperenhancement: More Aggressive Pathologic Features. *Liver Cancer* 2019; **8**: 24-40 [PMID: 30815393 DOI: 10.1159/000488540]

27 **Kawamura Y**, Ikeda K, Hirakawa M, Yatsuji H, Sezaki H, Hosaka T, Akuta N, Kobayashi M, Saitoh S, Suzuki F, Suzuki Y, Arase Y, Kumada H. New classification of dynamic computed tomography images predictive of malignant characteristics of hepatocellular carcinoma. *Hepatol Res* 2010; **40**: 1006-1014 [PMID: 20887336 DOI: 10.1111/j.1872-034X.2010.00703.x]

28 **Kim H**, Park MS, Choi JY, Park YN, Kim MJ, Kim KS, Choi JS, Han KH, Kim E, Kim KW. Can microvessel invasion of hepatocellular carcinoma be predicted by pre-operative MRI? *Eur Radiol* 2009; **19**: 1744-1751 [PMID: 19247666 DOI: 10.1007/s00330-009-1331-8]

29 **Choi JY**, Lee JM, Sirlin CB. CT and MR imaging diagnosis and staging of hepatocellular carcinoma: part II. Extracellular agents, hepatobiliary agents, and ancillary imaging features. *Radiology* 2014; **273**: 30-50 [PMID: 25247563 DOI: 10.1148/radiol.14132362]

30 **Kitao A**, Matsui O, Yoneda N, Kozaka K, Kobayashi S, Koda W, Gabata T, Yamashita T, Kaneko S, Nakanuma Y, Kita R, Arii S. Hypervascular hepatocellular carcinoma: correlation between biologic features and signal intensity on gadoxetic acid-enhanced MR images. *Radiology* 2012; **265**: 780-789 [PMID: 23175543 DOI: 10.1148/radiol.12120226]

31 **Kim KA**, Kim MJ, Jeon HM, Kim KS, Choi JS, Ahn SH, Cha SJ, Chung YE. Prediction of microvascular invasion of hepatocellular carcinoma: usefulness of peritumoral hypointensity seen on gadoxetate disodium-enhanced hepatobiliary phase images. *J Magn Reson Imaging* 2012; **35**: 629-634 [PMID: 22069244 DOI: 10.1002/jmri.22876]

32 **Roayaie S**, Blume IN, Thung SN, Guido M, Fiel MI, Hiotis S, Labow DM, Llovet JM, Schwartz ME. A system of classifying microvascular invasion to predict outcome after resection in patients with hepatocellular carcinoma. *Gastroenterology* 2009; **137**: 850-855 [PMID: 19524573 DOI: 10.1053/j.gastro.2009.06.003]

33 **Li Y**, Yan C, Weng S, Shi Z, Sun H, Chen J, Xu X, Ye R, Hong J. Texture analysis of multi-phase MRI images to detect expression of Ki67 in hepatocellular carcinoma. *Clin Radiol* 2019; **74**: 813.e19-813.e27 [PMID: 31362887 DOI: 10.1016/j.crad.2019.06.024]

34 **Zhang S**, Chiang GC, Magge RS, Fine HA, Ramakrishna R, Chang EW, Pulisetty T, Wang Y, Zhu W, Kovanlikaya I. Texture analysis on conventional MRI images accurately predicts early malignant transformation of low-grade gliomas. *Eur Radiol* 2019; **29**: 2751-2759 [PMID: 30617484 DOI: 10.1007/s00330-018-5921-1]

35 **Han Y**, Ma Y, Wu Z, Zhang F, Zheng D, Liu X, Tao L, Liang Z, Yang Z, Li X, Huang J, Guo X. Histologic subtype classification of non-small cell lung cancer using PET/CT images. *Eur J Nucl Med Mol Imaging* 2021; **48**: 350-360 [PMID: 32776232 DOI: 10.1007/s00259-020-04771-5]

36 **Kierans AS**, Leonardou P, Hayashi P, Brubaker LM, Elazzazi M, Shaikh F, Semelka RC. MRI findings of rapidly progressive hepatocellular carcinoma. *Magn Reson Imaging* 2010; **28**: 790-796 [PMID: 20427139 DOI: 10.1016/j.mri.2010.03.005]

37 **Zou X**, Luo Y, Morelli JN, Hu X, Shen Y, Hu D. Differentiation of hepatocellular carcinoma from intrahepatic cholangiocarcinoma and combined hepatocellular-cholangiocarcinoma in high-risk patients matched to MR field strength: diagnostic performance of LI-RADS version 2018. *Abdom Radiol (NY)* 2021; **46**: 3168-3178 [PMID: 33660040 DOI: 10.1007/s00261-021-02996-y]

World Journal of Gastroenterology

Submit a Manuscript: https://www.f6publishing.com

World J Gastroenterol 2022 June 28; 28(24): 2748-2757

DOI: 10.3748/wjg.v28.i24.2748

ISSN 1007-9327 (print) ISSN 2219-2840 (online)

ORIGINAL ARTICLE

Retrospective Study

Brown slits for colorectal adenoma crypts on conventional magnifying endoscopy with narrow band imaging using the X1 system

Osamu Toyoshima, Toshihiro Nishizawa, Shuntaro Yoshida, Hidenobu Watanabe, Nariaki Odawara, Kosuke Sakitani, Toru Arano, Hirotoshi Takiyama, Hideyuki Kobayashi, Hirofumi Kogure, Mitsuhiro Fujishiro

Specialty type: Gastroenterology and hepatology

Provenance and peer review: Unsolicited article; Externally peer reviewed.

Peer-review model: Single blind

Peer-review report's scientific quality classification

Grade A (Excellent): 0
Grade B (Very good): B, B
Grade C (Good): C
Grade D (Fair): 0
Grade E (Poor): 0

P-Reviewer: Duan Z, China; Shafaee Z, United States; Sharaf MM, Syria
A-Editor: Sahin TT

Received: January 16, 2022
Peer-review started: January 16, 2022
First decision: March 8, 2022
Revised: March 14, 2022
Accepted: May 14, 2022
Article in press: May 14, 2022
Published online: June 28, 2022

Osamu Toyoshima, Toshihiro Nishizawa, Shuntaro Yoshida, Nariaki Odawara, Kosuke Sakitani, Toru Arano, Department of Gastroenterology, Toyoshima Endoscopy Clinic, Tokyo 157-0066, Japan

Toshihiro Nishizawa, Department of Gastroenterology and Hepatology, International University of Health and Welfare, Narita Hospital, Chiba 286-8520, Japan

Hidenobu Watanabe, Department of Pathology, Pathology and Cytology Laboratory Japan, Tokyo 166-0003, Japan

Nariaki Odawara, Hirofumi Kogure, Mitsuhiro Fujishiro, Department of Gastroenterology, Graduate School of Medicine, The University of Tokyo, Tokyo 113-8655, Japan

Kosuke Sakitani, Department of Gastroenterology, Sakitani Endoscopy Clinic, Chiba 275-0026, Japan

Toru Arano, Department of Gastroenterology, The Fraternity Memorial Hospital, Tokyo 130-8587, Japan

Hirotoshi Takiyama, Department of Surgical Oncology, The University of Tokyo, Tokyo 113-8655, Japan

Hideyuki Kobayashi, Department of Internal Medicine, Umegaoka Ekimae Clinic, Tokyo 154-0022, Japan

Corresponding author: Toshihiro Nishizawa, MD, PhD, Professor, Department of Gastroenterology and Hepatology, International University of Health and Welfare, Narita Hospital, 852 Hatakeda, Chiba 286-8520, Japan. nisizawa@kf7.so-net.ne.jp

Abstract

BACKGROUND

Accurate diagnosis of colorectal premalignant polyps, including adenomas, is vital in clinical practice.

AIM

To investigate the diagnostic yields of novel findings of brown slits for adenomas.

METHODS
Patients who underwent colonoscopy at the Toyoshima Endoscopy Clinic were enrolled. Polyps sized ≥ 5 mm suspected of adenomas or clinically significant serrated polyps were included in the study. We defined the surface structures of colorectal polyps, which were brown curves inside and along the tubular glands identified using a combination of a new X1 system (Olympus Corporation) and a conventional magnifying colonoscope with non-staining narrow band imaging (NBI), as brown slits. The brown slits corresponded to slit-like lumens on endocytoscopy and histological crypt openings of an adenoma. We evaluated the diagnostic performance of brown slits for adenoma.

RESULTS
A total of 108 Lesions from 62 patients were eligible. The average age was 60.4 years and 41.9% were male. The mean polyp size was 7.45 ± 2.83 mm. Fifty-seven lesions were positive for brown slits. Histopathological diagnosis comprised 59 low-grade tubular adenomas, 16 sessile serrated lesions, and 33 hyperplastic polyps. Among 59 adenomas, 56 (94.9%) were positive for brown slits. Among 16 sessile serrated lesions, 0 (0%) was positive for brown slits. Among 33 hyperplastic polyps, 1 (3.0%) was positive for brown slits. The sensitivity, specificity, and accuracy of brown slits for adenoma were 94.9%, 98.0%, and 96.3%, respectively. The positive predictive value and negative predictive value of brown slits for adenoma were also excellent for 98.2%, and 94.1%, respectively.

CONCLUSION
Brown slits on conventional magnifying endoscopy with non-staining NBI using the X1 system were useful for diagnosing colorectal adenoma. The new endoscopy system could be examined using new standards.

Key Words: Adenoma; Colonoscopy; Narrow band imaging; Magnifying endoscopy; X1; Serrated polyp; Colorectal neoplasm; Endocytoscopy

©The Author(s) 2022. Published by Baishideng Publishing Group Inc. All rights reserved.

Core Tip: We defined the polyp's surface structure observed on conventional magnifying endoscopy with non-staining narrow band imaging using the X1 system as brown slits. The brown slits corresponded to slit-like lumens on endocytoscopy and histological crypt openings of an adenoma. Brown slits were useful for diagnosing colorectal adenoma.

Citation: Toyoshima O, Nishizawa T, Yoshida S, Watanabe H, Odawara N, Sakitani K, Arano T, Takiyama H, Kobayashi H, Kogure H, Fujishiro M. Brown slits for colorectal adenoma crypts on conventional magnifying endoscopy with narrow band imaging using the X1 system. *World J Gastroenterol* 2022; 28(24): 2748-2757
URL: https://www.wjgnet.com/1007-9327/full/v28/i24/2748.htm
DOI: https://dx.doi.org/10.3748/wjg.v28.i24.2748

INTRODUCTION

Colorectal adenoma is a premalignant neoplasm composed of a dysplastic epithelium. Removal of adenomas reduces the risk of colorectal adenocarcinoma[1,2]. Colorectal adenomas are found in ≥ 40% of proper colonoscopies, given that an accurate diagnosis of adenoma is crucial in routine endoscopic practice[3-6]. Colorectal serrated polyps are precursors with different molecular pathways and biological behaviors from adenomas[2,7,8]. Clinically significant serrated polyps (CSSPs), comprising all sessile serrated lesions (SSLs), all traditional serrated adenomas (TSAs), hyperplastic polyps ≥ 10 mm in size anywhere in the colorectum, and hyperplastic polyps ≥ 5 mm in size between the cecum and descending colon are recommended to be endoscopically removed[9-12]. The number, size, grade of dysplasia, and histological subtype of premalignant polyps, including both adenomas and serrated polyps, are the best determinants of the long-term risk of advanced neoplasia and inform surveillance decision-making[7,13-16].

Magnification, dye sprays, and modified light wavelengths, such as narrow band imaging (NBI) and blue laser imaging (BLI), are used to diagnose premalignant polyps better. The criteria for conventional magnifying endoscopy include pit pattern diagnosis using chromoendoscopy[17] and the Japan NBI expert team (JNET) classification using NBI and BLI[18-20]. The standards for ultra-high magnifying

endocytoscopy (EC) are as follows: EC classification, which evaluates the glandular structure and cellular atypia after double staining with methylene blue and crystal violet[21-24], and EC vascular classification, which evaluates the microvessels using NBI[25,26]. Slit-like lumens and microvessels with clear margins showing a network are good indicators of adenoma in EC, whereas narrow serrated lumens and obscure microvessels predict hyperplastic polyps. Sasajima *et al*[21] and Mori *et al*[23] have elucidated that long tubular pits (slit-like lumens) on EC are histologically equivalent to the crypt opening using the horizontal and vertical sections of specimens, respectively.

In 2020, a novel endoscopic system, which is a set of an EVIS X1 Video System Center (CV-1500) and a 4K ultra-high definition 32-inch liquid crystal display (LCD) monitor (OEV321UH), was released by Olympus Corporation, Tokyo, Japan. When using the same scope, this system has higher image quality and higher magnification than the previous generation's Olympus system, which is a set of EVIS Elite Video System Center (CV-290) and a high-definition 26-inch LCD monitor (OEV262H). For example, the magnifications of conventional magnifying endoscopes of Olympus' CF-HQ290Z and PCF-H290Z were 80 × and 110 ×, respectively, using the Elite system, while the magnifications increased to 95 × and 170 ×, respectively, using the X1 system. Given this, we hypothesized that the new X1 system allows conventional magnifying endoscopy to visualize the structures that could only be observed with EC, and to improve polyp diagnosis. Using a combination of the X1 system and the conventional magnifying endoscope with non-staining NBI, we identified the findings corresponding to the slit-like lumens, which present the crypts of adenoma. Then, we defined the findings as "brown slits" (Figure 1A and B).

To the best of our knowledge, there are no studies in which conventional magnifying endoscopy has verified the evidence accumulated by EC. Therefore, we focused on brown slits detected on conventional magnifying endoscopy using the X1 system and investigated their performance for adenoma diagnosis.

MATERIALS AND METHODS

Study design and overview

This retrospective study was conducted at the Toyoshima Endoscopy Clinic, a representative outpatient endoscopy-specialized clinic in Japan. This study was conducted in accordance with the ethical guidelines for medical studies in Japan. Written informed consent to use clinical information was obtained from the patients before colonoscopy. The study design was described in a protocol prepared by the Toyoshima Endoscopy Clinic and the Sakitani Endoscopy Clinic, and was approved by the Certified Institutional Review Board, Yoyogi Mental Clinic on July 16, 2021 (approval No. RKK227). We published this study's protocol on our institute's website (www.ichou.com) so that patients could opt out of the study if desired. All clinical investigations were performed in accordance with the ethical guidelines of the Declaration of Helsinki.

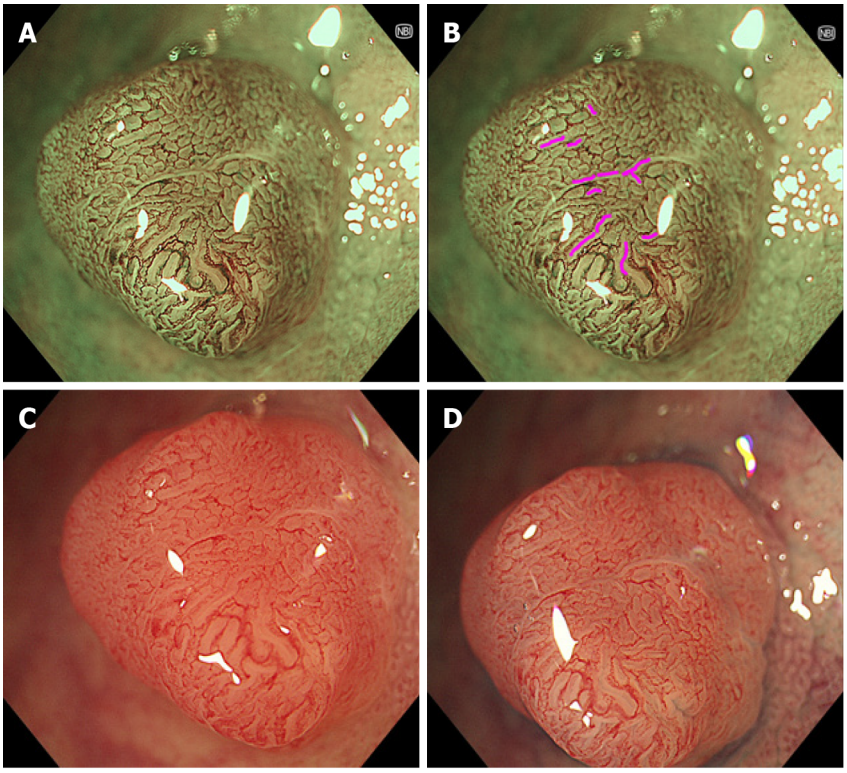
Study subjects

We enrolled patients who underwent colonoscopy at the Toyoshima Endoscopy Clinic in May and June 2021. Polyps sized ≥ 5 mm suspected of adenomas or CSSPs were included in this study[23,27,28]. The exclusion criteria were ulcerative colitis, poor bowel preparation, lesions for which endoscopic imaging could not be obtained, and lesions for which the specimen could not be collected. We also excluded histologically diagnosed adenocarcinomas, TSAs, and normal mucosa.

Brown slits for adenoma

Figure 1 shows typical images of a tubular adenoma observed using a combination of the conventional magnifying endoscope (CF-HQ290Z) and the X1 system, at full zoom magnification with NBI and WLI with or without indigo carmine spraying. Brown slits inside and along the tubular glands surrounded by microvessels were identified (pink curves in Figure 1B). We defined this brown pattern as a brown slit. The brown slit was additionally defined as having a length longer than the width of the tubular gland (approximately 100 μm). The brown slits were visible as faint and pale red slits on WLI (Figure 1C). Indigo carmine accumulated in the crypt openings that corresponded to brown slits (Figure 1A, B and D).

Figure 2 shows representative images of a tubular adenoma using a combination of the endocytoscope (CF-H290EC, Olympus Corporation) and the X1 system. To obtain a fully zoomed image with 790× magnification with a focusing depth of 35 μm, the endoscopist softly contacted the lesion with the endoscope lens[26]. On ultra-high magnifying observation with NBI, slits with a mixture of brown and white colors inside and along the tubular glands were visualized (Figure 2D, blue arrows). This tubular structure corresponded to a slit-like lumen for staining EC[22-25]. The microvessels were clearly identified surrounding the tubular gland and showed a vessel network[25]. On ultra-high magnifying observation with white light imaging (WLI), although microvessels were obscure, slits with a mixture of red and white colors were seen similar to the slits on NBI observation (Figure 2B, blue arrows). We could recognize tubular glands surrounded by the microvessels and brown and pale red slits inside and



DOI: 10.3748/wjg.v28.i24.2748 **Copyright** ©The Author(s) 2022.

Figure 1 Representative images of "brown slits" in a low-grade tubular adenoma using conventional magnifying endoscopy. A set of a conventional magnifying endoscope (CF-HQ290Z), X1 system, and 4K 32-inch monitor was used. A, B: Full-zoom (95 ×) magnification, narrow band imaging. Brown slits were observed inside and along the tubular glands surrounded by the microvessels; C: Full-zoom magnifying, white-light imaging observation without indigo carmine spraying showed faint and pale red slits inside and along the tubular glands; D: Full-zoom magnifying, white light imaging with indigo carmine spraying showed indigo carmine accumulated in the site corresponding to the brown slits.

along the tubular glands with NBI and WLI, respectively, when we observed with approximately 100 × magnification, which was similar to the full zoom of conventional magnifying endoscopy (Figure 2A and C, pink arrows).

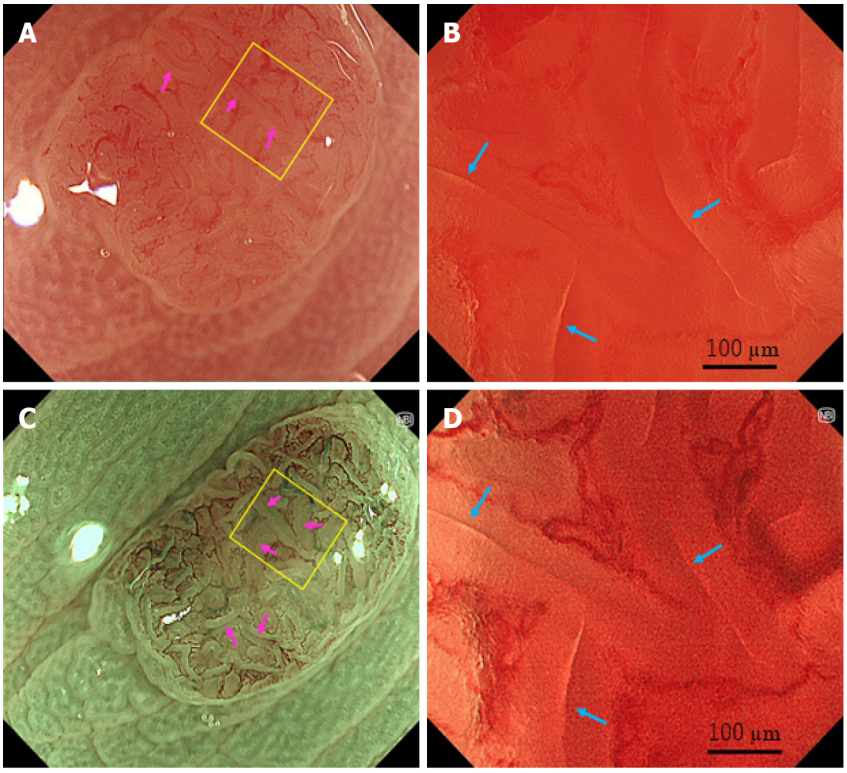
The correspondence between EC and histology is presented in Figure 3. Variably shaped tubular glands (surrounded by white and red curves in Figures 3A and B, respectively) with homogeneous widths of approximately 100 μm were observed. The crypts (blue arrows in Figure 3A and B) were detected as brown and white slits inside and along the tubular glands on EC. The microvessels (yellow arrows in Figure 3) were observed in the intervening part (black arrows in Figure 3). The size and position of the crypt, intervening part, and microvessels were consistent between EC and histology.

From the above, the brown slits on conventional magnifying endoscopy with NBI corresponded to slit-like lumens on EC and crypt openings on histology.

Colonoscopy

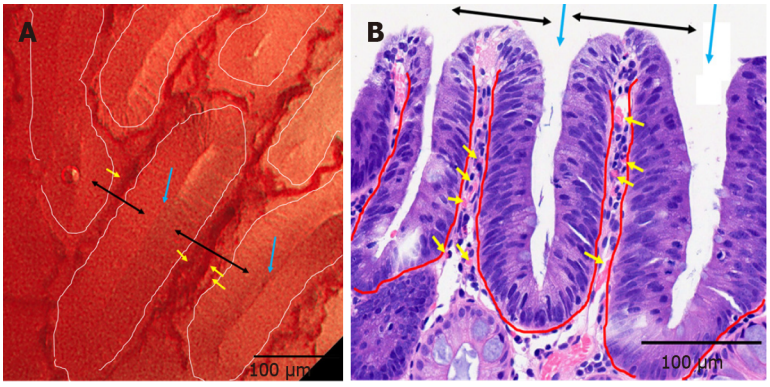
Brown slits were diagnosed in real-time during colonoscopy. Before the colonoscopy, the endoscopists discussed and obtained consensus for the brown slits while viewing the images on non-magnifying, conventional magnifying, and ultra-high magnifying observation. Two expert endoscopists conducted all colonoscopies. An endoscopic set of the X1 system and CF-HQ290Z or PCF-H290Z was used. Colonoscopes without a magnifying function and those with an autofocus function were excluded. The optical enhancement of the NBI was set in mode A8. When a lesion was detected, the surface was washed to remove mucus and dye, and a non-magnifying observation was conducted. Subsequently, the endoscopists focused on and diagnosed brown slits at almost full zoom. The polyp was observed without indigo carmine staining. Location, size, and morphology according to the Paris classification, the presence or absence of brown slits, and endoscopic polyp diagnosis were recorded. The colonoscopists classified each polyp as an adenoma, SSL, or hyperplastic polyp. The lesion size was calibrated by comparison with closed cups of biopsy forceps (approximately 2.5 mm).

Before examination, patients underwent bowel preparation with 2 L of polyethylene glycol solution or 1.8 L of isotonic magnesium citrate. If necessary, additional magnesium citrate or polyethylene glycol was provided. Patients were sedated using midazolam and pethidine hydrochloride. Scopolamine butylbromide or glucagon was intravenously administered to suppress bowel peristalsis. The polyps were resected using snear polypectomy with or without submucosal saline injection.



DOI: 10.3748/wjg.v28.i24.2748 **Copyright** ©The Author(s) 2022.

Figure 2 Representative images of "slit-like lumens" and "brown slits" in a low-grade tubular adenoma using endocytoscopy. A set of an endocytoscope (CF-H290EC), X1 system, and 4K 32-inch monitor was used. A, B: White light imaging observation; C, D: Narrow band imaging observation; A, C: Conventional (100 ×) magnifying observation. The yellow box represents the site for full-zoom observation; B, D: Full-zoom (790 ×) magnifying observation; D: Slit-like lumens were observed (blue arrows). The microvessels were clearly observed surrounding the slit-like lumen and showed a vessel network; C: A "brown slit" sign was observed (pink arrows); B: Slit-like lumens were obscurely observed (blue arrows).



DOI: 10.3748/wjg.v28.i24.2748 **Copyright** ©The Author(s) 2022.

Figure 3 Correspondence between endocytoscopy and histology in a low-grade tubular adenoma. A: A set of an endocytoscope (CF-H290EC), X1 system, and 4K 32-inch monitor was used. Full-zoom magnifying, narrow band imaging observation. Variably shaped tubular glands (surrounded by white curves) with homogeneous widths of about 100 μm. The crypts (blue arrows) are detected as brown and white slits inside and along the tubular glands. The microvessels (yellow arrows) are identified in the intervening part (black arrows); B: Vertical sections stained with hematoxylin-eosin. The tubular glands (surrounded by red curves), crypts (blue arrows), intervening parts (black arrows), and microvessels (yellow arrows) are seen in endocytoscopy.

Pathology

Fixed specimens were subjected to histological examination. The reference standard was histopathology using standard hematoxylin-eosin staining. All lesions were diagnosed according to World Health Organization criteria[2] by a gastrointestinal pathologist. The pathologist classified each polyp as a tubular adenoma, villous adenoma, adenocarcinoma, SSL, TSA, microvesicular hyperplastic polyp (MVHP), goblet cell-rich hyperplastic polyp (GCHP), or normal mucosa.

Statistical analysis

The diagnostic performance of brown slits for colorectal adenoma was calculated using BellCurve for Excel (version 3.21; Social Survey Research Information Co., Ltd., Tokyo, Japan).

RESULTS

Of the 115 Lesions in 64 patients who met the criteria, 1 adenocarcinoma in situ, 1 TSA, 4 normal mucosae, and 1 lost specimen were excluded. A total of 108 Lesions in 62 patients were enrolled. Table 1 shows the characteristics of the study participants (mean age, 60.4 years; males, 41.9%). Of the lesions, the mean polyp size was 7.45 mm (range, 5–15 mm), and 57 and 51 were positive and negative for "brown slit" signs, respectively. Histopathological diagnosis of the polyps comprised 59 low-grade tubular adenomas, 16 SSLs, 27 MVHPs, and 6 GCHPs.

Table 2 presents the number of lesions in the brown slits. The diagnostic performance of brown slits for colorectal adenomas is shown in Table 3. The sensitivity, specificity, accuracy, positive predictive value, and negative predictive value were excellent for 94.9%, 98.0%, 96.3%, 98.2%, and 94.1%, respectively.

DISCUSSION

We defined the polyp's surface structure observed on conventional magnifying endoscopy with non-staining NBI using the X1 system as brown slits. The brown slits corresponded to the slit-like lumens detected on EC and to the histological crypt opening of the tubular gland of the adenoma. This study elucidated that the brown slits were highly accurate for differentiation between colorectal adenomas and serrated polyps with a sensitivity, specificity, and accuracy of 94.6%, 98.3%, and 96.5%, respectively. Kudo *et al*[22] reported that the sensitivity, specificity, and accuracy of slit-like lumens were 82.5%, 100%, and 83.9%, respectively, when comparing colorectal adenoma and hyperplastic polyps. The strength of the brown slits is not only the high diagnostic performance, but also the convenience of identification using a conventional magnifying endoscope with non-staining NBI. Kudo *et al*[25] reported that obtaining a clear ultra-high magnification view using EC was difficult and long. Thus, brown slits are simple and meaningful in daily practice.

Compared with EC, conventional magnifying endoscopy has advantages, such as not requiring contact, thereby reducing bleeding or tissue damage; easy focusing; and high familiarity. Additionally, CF-HQ290Z (4700000 yen: $ 40941) and PCF-H290Z (4500000 yen: $ 39199) are cheaper than CF-H290EC (7900000 yen: $ 68817). In the future, it would be beneficial if the accumulating evidence with the EC could be applied with conventional magnifying endoscopy.

JNET types 1 and 2A correspond to histological classifications of hyperplastic polyp/SSL and low-grade intramucosal neoplasia, respectively. JNET classification was comprehensively judged with two scales: surface pattern and vessel pattern[18,19]. Kobayashi *et al*[19] reported that the sensitivity, specificity, and accuracy of JNET 2A for low-grade intramucosal neoplasia were 91.4%, 75.1%, and 89.1%, respectively. Because the brown slit sign is based only on the surface pattern, it may be simpler and easier than the JNET classification.

The reasons why the set of X1 system allowed the visualization of the brown slits, which accurately predicted adenomas, were considered as follows: compared to the Elite system, the X1 system has a higher magnification and image quality due to 4K resolution, additional amber color LED, and a new noise reduction system. We previously reported that the new 290 series endoscopic system had advantages in polyp detection and procedure over the previous 260 series model[29]. Improvements of the endoscopic system may increase the visibility of the polyp findings.

The present study had some limitations. The slit-like lumens and a normal pit-like structure on staining EC distinguish low-grade adenoma from advanced neoplasia and allow DISCARD strategy[13,24,30]. Fused gland formations on EC staining can predict the histological grade of differentiation and risk factors for lymph node metastasis in T1 colorectal adenocarcinoma[31]. EC with NBI can examine the diameter and caliber variation of tumor microvessels that are associated with the depth of cancer invasion[32]. EC with NBI also possibly differentiates diminutive hyperplastic polyps from adenomas based on the microvessel pattern[26]. However, the present study excluded carcinomas, TSAs, and diminutive polyps. Furthermore, there were no villous adenomas. Validation of these EC-based evidence by applying conventional magnifying endoscopy in the future is desirable. Second, this was a retrospective study that was limited to single-center expert endoscopists. Prospective analysis at multiple centers, including non-experts, is needed. Third, the NBI mode and 290 series endoscopes were used in this study. Verification using other image-enhancing modalities, such as BLI[20], linked color imaging (LCI, Fujifilm Corporation)[33], texture and color enhancement imaging (TXI, Olympus Corporation), and using new colonoscopes, such as CF-EZ1500D and CF-XZ1200 (Olympus Corporation), are warranted. Fourth, the diagnostic efficacy of brown slit sign has not been proven to be

Table 1 Characteristics of study subjects

Patient (*n*)	62
Age [mean ± SD (range), yr]	60.4 ± 12.8, (40-89)
Sex (male)	41.9%
Polyp (*n*)	108
Location (cecum/ascending/transverse/descending/sigmoid/rectum, *n*)	13/20/38/7/25/5
Morphology (0-Is/0-IIa, *n*)	13/95
Size [mean ± SD (range), mm]	7.45 (2.83, 5-15)
Brown slits (positive/negative, n)	57/51
Endoscopic diagnosis (adenoma/SSL/hyperplastic polyp, *n*)	59/30/19
Histopathological diagnosis (adenoma/SSL/MVHP/GCHP, *n*)	59[1]/16/27/6
Endoscopist (1/2, *n*)	75/33
Endoscope (CF-HQ290Z/PCF-H290Z, *n*)	60/48

[1]All adenomas were tubular, low grade.
SD: Standard deviation; SSL: Sessile serrated lesion; MVHP: Microvesicular hyperplastic polyp; GCHP: Goblet cell-rich hyperplastic polyp.

Table 2 Number of colorectal lesions for brown slits

	Adenoma[1]	SSL	MVHP	GCHP
Positive	56	0	1	0
Negative	3	16	26	6

[1]All adenomas were tubular, low grade.
SSL: Sessile serrated lesion; MVHP: Microvesicular hyperplastic polyp; GCHP: Goblet cell-rich hyperplastic polyp.

Table 3 Diagnostic performance of brown slits for colorectal adenoma

Sensitivity	**94.9 (85.9-98.9)**
Specificity	98.0 (89.1-99.9)
Accuracy	96.3 (90.8-99.0)
Positive predictive value	98.2 (90.6-100)
Negative predictive value	94.1 (83.8-98.8)

Data are presented as percentage (95% confidence interval).

equivalent to that of the JNET classification, although the brown slit sign may be simpler and easier than the JNET classification. The comparison of the diagnostic efficacy between brown slit sign and the JNET classification is future issue.

CONCLUSION

Brown slits on conventional magnifying NBI endoscopy using the X1 system were useful for diagnosing colorectal adenoma. The new endoscopy system could be examined using new standards.

ARTICLE HIGHLIGHTS

Research background

Accurate diagnosis of colorectal premalignant polyps, including adenomas, is vital in clinical practice.

Research motivation

Using a combination of the X1 system and the conventional magnifying endoscope with non-staining narrow band imaging (NBI), we identified the findings corresponding to the slit-like lumens, which present the crypts of adenoma.

Research objectives

The authors investigated the diagnostic yields of novel findings of brown slits for adenomas.

Research methods

Patients who underwent colonoscopy at the Toyoshima Endoscopy Clinic were enrolled. Polyps sized ≥ 5 mm suspected of adenomas or clinically significant serrated polyps were included in the study. We defined the surface structures of colorectal polyps, which were brown curves inside and along the tubular glands identified using a combination of a new X1 system (Olympus Corporation) and a conventional magnifying colonoscope with non-staining NBI, as brown slits. The brown slits corresponded to slit-like lumens on endocytoscopy and histological crypt openings of an adenoma. We evaluated the diagnostic performance of brown slits for adenoma.

Research results

A total of 108 Lesions from 62 patients were eligible. The average age was 60.4 years and 41.9% were male. The mean polyp size was 7.45 mm. Fifty-seven lesions were positive for brown slits. Histopathological diagnosis comprised 59 low-grade tubular adenomas, 16 sessile serrated lesions, and 33 hyperplastic polyps. The sensitivity, specificity, and accuracy of brown slits for adenoma were 94.9%, 98.0%, and 96.3%, respectively.

Research conclusions

Brown slits on conventional magnifying endoscopy with non-staining NBI using the X1 system were useful for diagnosing colorectal adenoma.

Research perspectives

The new endoscopy system could be examined using new standards.

FOOTNOTES

Author contributions: Toyoshima O contributed to the study design, endoscopic diagnosis, writing the article, statistical analysis, and final manuscript approval; Nishizawa T contributed to study design, editing of article, and final manuscript approval; Yoshida S contributed to study design, endoscopic diagnosis, critical review, and final manuscript approval; Watanabe H contributed to study design, histological diagnosis, and final manuscript approval; Odawara N, Sakitani K, Arano T, Takiyama H, Kobayashi H, Kogure H and Fujishiro M contributed to critical review and final manuscript approval.

Institutional review board statement: This study was approved by the Certificated Review Board, Yoyogi Mental Clinic on July 16, 2021 (approval No. RKK227).

Conflict-of-interest statement: All authors have no any conflicts of interest.

Data sharing statement: No additional data are available.

Open-Access: This article is an open-access article that was selected by an in-house editor and fully peer-reviewed by external reviewers. It is distributed in accordance with the Creative Commons Attribution NonCommercial (CC BY-NC 4.0) license, which permits others to distribute, remix, adapt, build upon this work non-commercially, and license their derivative works on different terms, provided the original work is properly cited and the use is non-commercial. See: https://creativecommons.org/Licenses/by-nc/4.0/

Country/Territory of origin: Japan

ORCID number: Osamu Toyoshima 0000-0002-6953-6079; Toshihiro Nishizawa 0000-0003-4876-3384; Shuntaro Yoshida 0000-0002-9437-9132; Hidenobu Watanabe 0000-0002-7871-4738; Nariaki Odawara 0000-0002-9839-4700; Kosuke Sakitani 0000-0002-4537-6023; Toru Arano 0000-0003-3205-6669; Hirotoshi Takiyama 0000-0001-9994-4666; Hideyuki Kobayashi 0000-0002-3344-6848; Hirofumi Kogure 0000-0002-2355-7309; Mitsuhiro Fujishiro 0000-0002-4074-1140.

S-Editor: Ma YJ
L-Editor: A
P-Editor: Ma YJ

REFERENCES

1 **Nishihara R**, Wu K, Lochhead P, Morikawa T, Liao X, Qian ZR, Inamura K, Kim SA, Kuchiba A, Yamauchi M, Imamura Y, Willett WC, Rosner BA, Fuchs CS, Giovannucci E, Ogino S, Chan AT. Long-term colorectal-cancer incidence and mortality after lower endoscopy. *N Engl J Med* 2013; **369**: 1095-1105 [PMID: 24047059 DOI: 10.1056/NEJMoa1301969]
2 **Nagtegaal I**, Arends MJ, Odeze RD, Lam AK. Tumours of the colon and rectum. Lyon (France), 2019
3 **Hilsden RJ**, Rose SM, Dube C, Rostom A, Bridges R, McGregor SE, Brenner DR, Heitman SJ. Defining and Applying Locally Relevant Benchmarks for the Adenoma Detection Rate. *Am J Gastroenterol* 2019; **114**: 1315-1321 [PMID: 30848731 DOI: 10.14309/ajg.0000000000000120]
4 **Kaminski MF**, Wieszczy P, Rupinski M, Wojciechowska U, Didkowska J, Kraszewska E, Kobiela J, Franczyk R, Rupinska M, Kocot B, Chaber-Ciopinska A, Pachlewski J, Polkowski M, Regula J. Increased Rate of Adenoma Detection Associates With Reduced Risk of Colorectal Cancer and Death. *Gastroenterology* 2017; **153**: 98-105 [PMID: 28428142 DOI: 10.1053/j.gastro.2017.04.006]
5 **Toyoshima O**, Nishizawa T, Yoshida S, Sekiba K, Kataoka Y, Hata K, Watanabe H, Tsuji Y, Koike K. Expert endoscopists with high adenoma detection rates frequently detect diminutive adenomas in proximal colon. *Endosc Int Open* 2020; **8**: E775-E782 [PMID: 32490163 DOI: 10.1055/a-1136-9971]
6 **Toyoshima O**, Yoshida S, Nishizawa T, Yamakawa T, Arano T, Isomura Y, Kanazawa T, Ando H, Tsuji Y, Koike K. Simple feedback of colonoscopy performance improved the number of adenomas per colonoscopy and serrated polyp detection rate. *Endosc Int Open* 2021; **9**: E1032-E1038 [PMID: 34222627 DOI: 10.1055/a-1393-5469]
7 **East JE**, Atkin WS, Bateman AC, Clark SK, Dolwani S, Ket SN, Leedham SJ, Phull PS, Rutter MD, Shepherd NA, Tomlinson I, Rees CJ. British Society of Gastroenterology position statement on serrated polyps in the colon and rectum. *Gut* 2017; **66**: 1181-1196 [PMID: 28450390 DOI: 10.1136/gutjnl-2017-314005]
8 **Nagtegaal ID**, Odze RD, Klimstra D, Paradis V, Rugge M, Schirmacher P, Washington KM, Carneiro F, Cree IA; WHO Classification of Tumours Editorial Board. The 2019 WHO classification of tumours of the digestive system. *Histopathology* 2020; **76**: 182-188 [PMID: 31433515 DOI: 10.1111/his.13975]
9 **Rex DK**, Ahnen DJ, Baron JA, Batts KP, Burke CA, Burt RW, Goldblum JR, Guillem JG, Kahi CJ, Kalady MF, O'Brien MJ, Odze RD, Ogino S, Parry S, Snover DC, Torlakovic EE, Wise PE, Young J, Church J. Serrated lesions of the colorectum: review and recommendations from an expert panel. *Am J Gastroenterol* 2012; **107**: 1315-29; quiz 1314, 1330 [PMID: 22710576 DOI: 10.1038/ajg.2012.161]
10 **Anderson JC**, Butterly LF, Weiss JE, Robinson CM. Providing data for serrated polyp detection rate benchmarks: an analysis of the New Hampshire Colonoscopy Registry. *Gastrointest Endosc* 2017; **85**: 1188-1194 [PMID: 28153571 DOI: 10.1016/j.gie.2017.01.020]
11 **Li D**, Woolfrey J, Jiang SF, Jensen CD, Zhao WK, Kakar S, Santamaria M, Rumore G, Armstrong MA, Postlethwaite D, Corley DA, Levin TR. Diagnosis and predictors of sessile serrated adenoma after educational training in a large, community-based, integrated healthcare setting. *Gastrointest Endosc* 2018; **87**: 755-765.e1 [PMID: 28843582 DOI: 10.1016/j.gie.2017.08.012]
12 **Klair JS**, Ashat M, Johnson D, Arora S, Onteddu N, Machain Palacio JG, Samuel R, Bilal M, Buddam A, Gupta A, Gunderson A, Guturu P, Soota K, Chandra S, Murali AR. Serrated polyp detection rate and advanced adenoma detection rate from a US multicenter cohort. *Endoscopy* 2020; **52**: 61-67 [PMID: 31739370 DOI: 10.1055/a-1031-5672]
13 **Rees CJ**, Rajasekhar PT, Wilson A, Close H, Rutter MD, Saunders BP, East JE, Maier R, Moorghen M, Muhammad U, Hancock H, Jayaprakash A, MacDonald C, Ramadas A, Dhar A, Mason JM. Narrow band imaging optical diagnosis of small colorectal polyps in routine clinical practice: the Detect Inspect Characterise Resect and Discard 2 (DISCARD 2) study. *Gut* 2017; **66**: 887-895 [PMID: 27196576 DOI: 10.1136/gutjnl-2015-310584]
14 **Rutter MD**, East J, Rees CJ, Cripps N, Docherty J, Dolwani S, Kaye PV, Monahan KJ, Novelli MR, Plumb A, Saunders BP, Thomas-Gibson S, Tolan DJM, Whyte S, Bonnington S, Scope A, Wong R, Hibbert B, Marsh J, Moores B, Cross A, Sharp L. British Society of Gastroenterology/Association of Coloproctology of Great Britain and Ireland/Public Health England post-polypectomy and post-colorectal cancer resection surveillance guidelines. *Gut* 2020; **69**: 201-223 [PMID: 31776230 DOI: 10.1136/gutjnl-2019-319858]
15 **Gupta S**, Lieberman D, Anderson JC, Burke CA, Dominitz JA, Kaltenbach T, Robertson DJ, Shaukat A, Syngal S, Rex DK. Recommendations for Follow-Up After Colonoscopy and Polypectomy: A Consensus Update by the US Multi-Society Task Force on Colorectal Cancer. *Gastrointest Endosc* 2020; **91**: 463-485.e5 [PMID: 32044106 DOI: 10.1016/j.gie.2020.01.014]
16 **Li D**, Liu L, Fevrier HB, Alexeeff SE, Doherty AR, Raju M, Amsden LB, Lee JK, Levin TR, Corley DA, Herrinton LJ. Increased Risk of Colorectal Cancer in Individuals With a History of Serrated Polyps. *Gastroenterology* 2020; **159**: 502-511.e2 [PMID: 32277950 DOI: 10.1053/j.gastro.2020.04.004]
17 **Kudo S**, Rubio CA, Teixeira CR, Kashida H, Kogure E. Pit pattern in colorectal neoplasia: endoscopic magnifying view. *Endoscopy* 2001; **33**: 367-373 [PMID: 11315901 DOI: 10.1055/s-2004-826104]
18 **Sano Y**, Tanaka S, Kudo SE, Saito S, Matsuda T, Wada Y, Fujii T, Ikematsu H, Uraoka T, Kobayashi N, Nakamura H, Hotta K, Horimatsu T, Sakamoto N, Fu KI, Tsuruta O, Kawano H, Kashida H, Takeuchi Y, Machida H, Kusaka T, Yoshida N, Hirata I, Terai T, Yamano HO, Kaneko K, Nakajima T, Sakamoto T, Yamaguchi Y, Tamai N, Nakano N, Hayashi N, Oka S, Iwatate M, Ishikawa H, Murakami Y, Yoshida S, Saito Y. Narrow-band imaging (NBI) magnifying endoscopic classification of colorectal tumors proposed by the Japan NBI Expert Team. *Dig Endosc* 2016; **28**: 526-533 [PMID:

26927367 DOI: 10.1111/den.12644]
19 **Kobayashi S**, Yamada M, Takamaru H, Sakamoto T, Matsuda T, Sekine S, Igarashi Y, Saito Y. Diagnostic yield of the Japan NBI Expert Team (JNET) classification for endoscopic diagnosis of superficial colorectal neoplasms in a large-scale clinical practice database. *United European Gastroenterol J* 2019; **7**: 914-923 [PMID: 31428416 DOI: 10.1177/2050640619845987]
20 **Ito R**, Ikematsu H, Murano T, Shinmura K, Kojima M, Kumahara K, Furue Y, Sunakawa H, Minamide T, Sato D, Yamamoto Y, Takashima K, Yoda Y, Hori K, Yano T. Diagnostic ability of Japan Narrow-Band Imaging Expert Team classification for colorectal lesions by magnifying endoscopy with blue laser imaging versus narrow-band imaging. *Endosc Int Open* 2021; **9**: E271-E277 [PMID: 33553592 DOI: 10.1055/a-1324-3083]
21 **Sasajima K**, Kudo SE, Inoue H, Takeuchi T, Kashida H, Hidaka E, Kawachi H, Sakashita M, Tanaka J, Shiokawa A. Real-time in vivo virtual histology of colorectal lesions when using the endocytoscopy system. *Gastrointest Endosc* 2006; **63**: 1010-1017 [PMID: 16733118 DOI: 10.1016/j.gie.2006.01.021]
22 **Kudo SE**, Wakamura K, Ikehara N, Mori Y, Inoue H, Hamatani S. Diagnosis of colorectal lesions with a novel endocytoscopic classification - a pilot study. *Endoscopy* 2011; **43**: 869-875 [PMID: 21837586 DOI: 10.1055/s-0030-1256663]
23 **Mori Y**, Kudo S, Ikehara N, Wakamura K, Wada Y, Kutsukawa M, Misawa M, Kudo T, Kobayashi Y, Miyachi H, Yamamura F, Ohtsuka K, Inoue H, Hamatani S. Comprehensive diagnostic ability of endocytoscopy compared with biopsy for colorectal neoplasms: a prospective randomized noninferiority trial. *Endoscopy* 2013; **45**: 98-105 [PMID: 23307149 DOI: 10.1055/s-0032-1325932]
24 **Kudo T**, Suzuki K, Mori Y, Misawa M, Ichimasa K, Takeda K, Nakamura H, Maeda Y, Ogawa Y, Hayashi T, Wakamura K, Ishida F, Inoue H, Kudo SE. Endocytoscopy for the differential diagnosis of colorectal low-grade adenoma: a novel possibility for the "resect and discard" strategy. *Gastrointest Endosc* 2020; **91**: 676-683 [PMID: 31785276 DOI: 10.1016/j.gie.2019.11.029]
25 **Kudo SE**, Misawa M, Wada Y, Nakamura H, Kataoka S, Maeda Y, Toyoshima N, Hayashi S, Kutsukawa M, Oikawa H, Mori Y, Ogata N, Kudo T, Hisayuki T, Hayashi T, Wakamura K, Miyachi H, Ishida F, Inoue H. Endocytoscopic microvasculature evaluation is a reliable new diagnostic method for colorectal lesions (with video). *Gastrointest Endosc* 2015; **82**: 912-923 [PMID: 26071058 DOI: 10.1016/j.gie.2015.04.039]
26 **Kataoka S**, Kudo SE, Misawa M, Nakamura H, Takeda K, Toyoshima N, Mori Y, Ogata N, Kudo T, Hisayuki T, Hayashi T, Wakamura K, Baba T, Ishida F. Endocytoscopy with NBI has the potential to correctly diagnose diminutive colorectal polyps that are difficult to diagnose using conventional NBI. *Endosc Int Open* 2020; **8**: E360-E367 [PMID: 32118108 DOI: 10.1055/a-1068-9228]
27 **Ponugoti P**, Rastogi A, Kaltenbach T, MacPhail ME, Sullivan AW, Thygesen JC, Broadley HM, Rex DK. Disagreement between high confidence endoscopic adenoma prediction and histopathological diagnosis in colonic lesions ≤ 3 mm in size. *Endoscopy* 2019; **51**: 221-226 [PMID: 30722072 DOI: 10.1055/a-0831-2348]
28 **Nishizawa T**, Yoshida S, Toyoshima A, Yamada T, Sakaguchi Y, Irako T, Ebinuma H, Kanai T, Koike K, Toyoshima O. Endoscopic diagnosis for colorectal sessile serrated lesions. *World J Gastroenterol* 2021; **27**: 1321-1329 [PMID: 33833485 DOI: 10.3748/wjg.v27.i13.1321]
29 **Toyoshima O**, Yoshida S, Nishizawa T, Yamakawa T, Sakitani K, Hata K, Takahashi Y, Fujishiro M, Watanabe H, Koike K. CF290 for pancolonic chromoendoscopy improved sessile serrated polyp detection and procedure time: a propensity score-matching study. *Endosc Int Open* 2019; **7**: E987-E993 [PMID: 31367679 DOI: 10.1055/a-0953-1909]
30 **Ignjatovic A**, East JE, Suzuki N, Vance M, Guenther T, Saunders BP. Optical diagnosis of small colorectal polyps at routine colonoscopy (Detect InSpect ChAracterise Resect and Discard; DISCARD trial): a prospective cohort study. *Lancet Oncol* 2009; **10**: 1171-1178 [PMID: 19910250 DOI: 10.1016/S1470-2045(09)70329-8]
31 **Sako T**, Kudo SE, Miyachi H, Wakamura K, Igarashi K, Misawa M, Mori Y, Kudo T, Hayashi T, Katagiri A, Ishida F, Azuma T, Inoue H, Hamatani S. A novel ability of endocytoscopy to diagnose histological grade of differentiation in T1 colorectal carcinomas. *Endoscopy* 2018; **50**: 69-74 [PMID: 28962043 DOI: 10.1055/s-0043-117403]
32 **Takeda K**, Kudo SE, Misawa M, Mori Y, Kudo T, Kodama K, Wakamura K, Miyachi H, Hidaka E, Ishida F, Inoue H. Comparison of the endocytoscopic and clinicopathologic features of colorectal neoplasms. *Endosc Int Open* 2016; **4**: E397-E402 [PMID: 27547815 DOI: 10.1055/s-0042-101753]
33 **Paggi S**, Radaelli F, Senore C, Maselli R, Amato A, Andrisani G, Di Matteo F, Cecinato P, Grillo S, Sereni G, Sassatelli R, Manfredi G, Alicante S, Buscarini E, Canova D, Milan L, Pallini P, Iwatate M, Rondonotti E, Repici A, Hassan C. Linked-color imaging versus white-light colonoscopy in an organized colorectal cancer screening program. *Gastrointest Endosc* 2020; **92**: 723-730 [PMID: 32502550 DOI: 10.1016/j.gie.2020.05.044]

World Journal of Gastroenterology

Submit a Manuscript: https://www.f6publishing.com

World J Gastroenterol 2022 June 28; 28(24): 2758-2774

DOI: 10.3748/wjg.v28.i24.2758

ISSN 1007-9327 (print) ISSN 2219-2840 (online)

ORIGINAL ARTICLE

Observational Study

Usefulness of serum C-reactive protein and calprotectin for the early detection of colorectal anastomotic leakage: A prospective observational study

Nuno J G Rama, Marlene C C Lages, Maria Pedro S Guarino, Óscar Lourenço, Patrícia C Motta Lima, Diana Parente, Cândida S G Silva, Ricardo Castro, Ana Bento, Anabela Rocha, Fernando Castro-Pocas, João Pimentel

Specialty type: Surgery

Provenance and peer review: Unsolicited article; Externally peer reviewed.

Peer-review model: Single blind

Peer-review report's scientific quality classification

Grade A (Excellent): 0
Grade B (Very good): B
Grade C (Good): C
Grade D (Fair): D
Grade E (Poor): 0

P-Reviewer: Fiori E, Italy; Kayano H, Japan; Yan T, China

Received: January 13, 2022
Peer-review started: January 13, 2022
First decision: March 8, 2022
Revised: March 22, 2022
Accepted: May 14, 2022
Article in press: May 14, 2022
Published online: June 28, 2022

Nuno J G Rama, Patrícia C Motta Lima, Diana Parente, Colorectal Surgical Division, Leiria Hospital Centre, Leiria 2410-021, Portugal

Nuno J G Rama, Anabela Rocha, Fernando Castro-Pocas, Abel Salazar Biomedical Institute (ICBAS), University of Oporto, Oporto 4099-002, Portugal

Nuno J G Rama, Marlene C C Lages, Maria Pedro S Guarino, Cândida S G Silva, Center for Innovative Care and Health Technology (ciTechCare), Polytechnic of Leiria, Leiria 2410-541, Portugal

Óscar Lourenço, Faculty of Economics, CeBER, University of Coimbra, Coimbra 3000-137, Portugal

Ricardo Castro, Ana Bento, Clinical Pathology Division, Leiria Hospital Centre, Leiria 2410-541, Portugal

Anabela Rocha, Surgical Division, Oporto Hospital Centre, Oporto 4099-001, Portugal

Fernando Castro-Pocas, Department of Gastroenterology, Santo António Hospital, Porto Hospital Center, Porto 4099-001, Portugal

Fernando Castro-Pocas, Institute of Biomedical Sciences Abel Salazar, University of Porto, Porto 4099-001, Portugal

João Pimentel, Faculty of Medicine, University of Coimbra, Coimbra 3004-531, Portugal

João Pimentel, Surgical Division, Montes Claros Hospital, Coimbra 3030-320, Portugal

Corresponding author: Nuno JG Rama, FEBS, MD, MHSc, Associate Professor, Research Assistant Professor, Surgeon, Colorectal Surgical Division, Leiria Hospital Centre, Rua das Olhalvas, Leiria 2410-021, Portugal. ramanuno@gmail.com

Abstract

BACKGROUND

Colorectal anastomotic leakage (CAL) is one of the most dreaded complications

after colorectal surgery, with an incidence that can be as high as 27%. This event is associated with increased morbidity and mortality; therefore, its early diagnosis is crucial to reduce clinical consequences and costs. Some biomarkers have been suggested as laboratory tools for the diagnosis of CAL.

AIM

To assess the usefulness of plasma C-reactive protein (CRP) and calprotectin (CLP) as early predictors of CAL.

METHODS

A prospective monocentric observational study was conducted including patients who underwent colorectal resection with anastomosis, from March 2017 to August 2019. Patients were divided into three groups: G1 – no complications; G2 – complications not related to CAL; and G3 – CAL. Five biomarkers were measured and analyzed in the first 5 postoperative days (PODs), namely white blood cell (WBC) count, eosinophil cell count (ECC), CRP, CLP, and procalcitonin (PCT). Clinical criteria, such as abdominal pain and clinical condition, were also assessed. The correlation between biomarkers and CAL was evaluated. Receiver operating characteristic (ROC) curve analysis was used to compare the accuracy of these biomarkers as predictors of CAL, and the area under the ROC curve (AUROC), specificity, sensitivity, positive predictive value, and negative predictive value (NPV) during this period were estimated.

RESULTS

In total, 25 of 396 patients developed CAL (6.3%), and the mean time for this diagnosis was 9.0 ± 6.8 d. Some operative characteristics, such as surgical approach, blood loss, intraoperative complications, and duration of the procedure, were notably related to the development of CAL. The length of hospital stay was markedly higher in the group that developed CAL compared with the group with complications other than CAL and the group with no complications (median of 21 d *vs* 13 d and 7 d respectively; $P < 0.001$). For abdominal pain, the best predictive performance was on POD4 and POD5, with the largest AUROC of 0.84 on POD4. Worsening of the clinical condition was associated with the diagnosis of CAL, presenting a higher predictive effect on POD5, with an AUROC of 0.9. WBC and ECC showed better predictive effects on POD5 (AUROC = 0.62 and 0.7, respectively). Those markers also presented a high NPV (94%-98%). PCT had the best predictive effect on POD5 (AUROC = 0.61), although it presented low accuracy. However, this biomarker revealed a high NPV on POD3, POD4, and POD5 (96%, 95%, and 96%, respectively). The mean CRP value on POD5 was significantly higher in the group that developed CAL compared with the group without complications (195.5 ± 139.9 mg/L *vs* 59.5 ± 43.4 mg/L; $P < 0.00001$). On POD5, CRP had a NPV of 98%. The mean CLP value on POD3 was significantly higher in G3 compared with G1 (5.26 ± 3.58 μg/mL *vs* 11.52 ± 6.81 μg/mL; $P < 0.00005$). On POD3, the combination of CLP and CRP values showed a high diagnostic accuracy (AUROC = 0.82), providing a 5.2 d reduction in the time to CAL diagnosis.

CONCLUSION

CRP and CLP are moderate predictors of CAL. However, the combination of these biomarkers presents an increased diagnostic accuracy, potentially decreasing the time to CAL diagnosis.

Key Words: Anastomotic leakage; Colorectal; Surgery; Biomarkers; C-reactive protein; Calprotectin

©The Author(s) 2022. Published by Baishideng Publishing Group Inc. All rights reserved.

Core Tip: Colorectal anastomotic leakage (CAL) remains a serious postoperative complication. It is associated with high morbidity rates, affecting overall costs and patients' quality of life. Clinical criteria, imaging studies, and biomarkers have been considered to increase diagnostic accuracy. Plasma C-reactive protein, calprotectin, procalcitonin, white blood cell count, and eosinophil cell count have been proposed as predictors of anastomotic leakage. The combination of C-reactive protein and calprotectin after a minimal clinical suspicion of CAL has shown good diagnostic accuracy, allowing clinicians to reduce the time to CAL detection. Regression models can facilitate building a decision model, as the score proposed for the early detection of CAL.

Citation: Rama NJG, Lages MCC, Guarino MPS, Lourenço Ó, Motta Lima PC, Parente D, Silva CSG, Castro R, Bento A, Rocha A, Castro-Pocas F, Pimentel J. Usefulness of serum C-reactive protein and calprotectin for the early detection of colorectal anastomotic leakage: A prospective observational study. *World J Gastroenterol* 2022; 28(24): 2758-2774
URL: https://www.wjgnet.com/1007-9327/full/v28/i24/2758.htm
DOI: https://dx.doi.org/10.3748/wjg.v28.i24.2758

INTRODUCTION

Colorectal anastomotic leakage (CAL) is one of the most frequent complications after colorectal surgery, representing a dreaded issue for patients and surgeons. The reported incidence ranges from 0.2% to 27.2%, depending on the study nature, level of anastomosis, or pathology[1-5]. This occurrence is associated with increased morbidity, mortality, reoperation, and health care costs[6-9]. Thus, its clinical relevance should not be underestimated. It also has a negative impact on a patient's quality of life[2,4].

Early CAL detection is key to decreasing related morbidity and mortality; therefore, a prompt and timely diagnosis is crucial[5,10,11]. Initially, it is difficult to distinguish CAL from other postoperative abdominal complications. Surgeons should be aware of subtle clinical signs, and then order additional tests including serum biomarkers, proper imaging, or even early reoperation. Unfortunately, diagnosis is often delayed, because of a misleading clinical picture, non-systematic assessment, or inconclusive investigations[11-15]. Besides clinical parameters, several biomarkers (plasma or intraperitoneal), imaging methods such as abdominal computed tomography (CT) scan or water-soluble contrast enema, and scores have been proposed to reduce the time to diagnosis and to establish an appropriate management pathway[16-19].

Plasma C-reactive protein (CRP) has been proposed as an early predictor of postoperative infectious complications[16,20-23]. This biomarker is an acute phase protein, increasing between 6 h and 48 h after surgery, and returning to baseline if inflammation ceases. After this period, a high CRP level is associated with postoperative infectious complications, especially in patients with CAL[24-26]. On the other hand, calprotectin (CLP) is a useful biomarker of inflammation and infection[18,27]. Fecal CLP has been widely used as a marker of gastrointestinal inflammation. However, some authors suggest that high levels of serum CLP could be associated with septic intra-abdominal complications, such as early-stage CAL[18,28].

The aim of this study was to evaluate the utility of plasma CRP and CLP, individually or combined, to shorten the time to CAL diagnosis.

MATERIALS AND METHODS

Study design and population

This was a prospective observational, single-center study that included adults over 18-years-old who underwent urgent or elective colorectal resection, regardless of the surgical approach (open or laparoscopic), indication (benign or malignant), and option for a protective stoma. The study was conducted in the colorectal division of a non-academic hospital accredited by Joint Commission International® and included about 500000 inhabitants. The data were collected between March 1, 2017 and August 31, 2019. The local ethics committee approved the study, and potential participants provided written informed consent before inclusion.

Definitions

CAL was defined in accordance with the following criteria[29]: (1) Clinical: Enteric discharge from abdominal drain or wound, rectovaginal fistula, or anastomotic defect found by digital examination; (2) Radiological (CT): Extravasation of endoluminally administered contrast, intra-abdominal collection around the anastomosis, presacral abscess near the anastomosis or perianastomotic air, and free intra-abdominal air; and (3) Surgical findings (reoperation): Necrosis of the anastomosis or signs of peritonitis and anastomotic defect.

Faced with clinical deterioration and/or serum biomarker increase, patients underwent further imaging with abdominopelvic CT scan (and water-soluble contrast enema if colorectal anastomosis was present). Once diagnosed, anastomotic leakage was classified into two categories: (1) Minor: Patients with CAL and Clavien-Dindo grade I or II, requiring no active intervention (radiological or surgical intervention) (Grade A of the International Study Group of Rectal Cancer definition); and (2) Major: All other patients with CAL[30,31]. Definitions of other postoperative complications, such as pneumonia, urinary tract infection, paralytic ileus, and surgical wound infection, are available in Supplementary material 1A (Definitions).

Exclusion criteria

Patients were excluded from the study if they were younger than 18-year-old, pregnant, unable to give or not providing written informed consent, R0 resection with anastomosis not having been performed, or presence of inflammatory bowel disease.

Study protocol and variables

Prospective data were collected and recorded in an electronic database according to the study protocol (Supplementary material 1B – Study protocol). Five biomarkers were measured in the first 5 postoperative days (POD), including white blood cell (WBC) count, eosinophil cell count (ECC), CRP, CLP, and procalcitonin (PCT). Clinical criteria, such as abdominal pain and clinical condition, were also assessed. Blood samples were analyzed at the Leiria Hospital Centre laboratory, according to the techniques described in Supplementary material 1C (Laboratory). The 90-d follow-up included data of all postoperative complications, the length of hospital stay, and the readmission rate. Discharge criteria are available in the Supplementary material 1B (Study protocol). All patients received prophylactic antibiotic accordingly to hospital infection control committee protocol.

Statistical analysis

Data were analyzed by using standard descriptive statistics and graphical analysis. One-way analysis of variance was performed to compare the differences in mean biomarkers' values across the three relevant groups of patients (G1 – no complications; G2 – complications not related to CAL; and G3 – CAL). Chi-squared tests were conducted to assess the association between other categorical variables and the patients. Receiver operating characteristic (ROC) curve analysis was employed to evaluate each biomarker as an appropriate classifier to detect CAL early. The area under the receiver operating characteristic curve (AUROC) was used to establish the diagnostic performance of the studied biomarker. Liu's method was used to establish the threshold value of each biomarker, and its sensitivity (SS) and specificity (SP) were defined[32]. The negative likelihood ratio (NLR) and positive likelihood ratio (PLR), and the negative predictive value (NPV) and positive predictive value (PPV) were computed by combining the observed incidence of CAL with the estimated SS and SP at the optimum cut-off value.

The added value of combining two different biomarkers, observed on POD3 or POD5, as a classifier to predict early CAL was explored. Regression models (probit, logit, and complementary log-log) were used to analyze binary dependent variables, and the observed CAL status (0/1) in a pairwise manner of all biomarkers included in our study: WBC, ECC, CRP, PCT, and CLP. Several potential classifiers of CAL were built, applying a non-linear combination of two different biomarkers. To minimize overfitting, the "leave-one-out" methodology was adopted[33]. The AUROC graph was used to select the classifier (defined by the model and the combination of two biomarkers) with the best predictive diagnostic performance. Liu's method was adopted to select the cut-off value for CAL.

The expected reduction in time to CAL diagnosis obtained by using one biomarker or a pairwise combination of biomarkers was estimated. This was the difference between the observed and the expected mean time to CAL diagnosis, if a specific classifier is used. The expected time to CAL diagnosis was computed by using the following expression: $S \times d1 + [(1 - S) \times d2]$, where S is the SS of the classifier, d1 is the POD of the classifier yielding a positive cut-off value for CAL, and d2 is the day of diagnosis if the classifier provides a false-negative result (time to CAL diagnosis estimated in the dataset). The statistical methods of this study were reviewed by Óscar Lourenço from the Faculty of Economics, CeBER, University of Coimbra, Portugal. All data management and statistical analyses were conducted with Stata Statistical software (Release 16; StataCorp, College Station, TX, United States).

RESULTS

Patients and outcomes

During the study period, we included 458 consecutive patients who underwent colorectal resection, and 62 (13.5%) were ruled out [exclusion criteria (n = 31), no consent (n = 15), no anastomosis (n = 16)] as shown in Figure 1. Patient characteristics, divided into three groups (G1, G2, and G3, as previously defined), are shown in Table 1. Age, the Charlson Comorbidity Index, and American Society of Anesthesiologists grade seem to affect CAL onset.

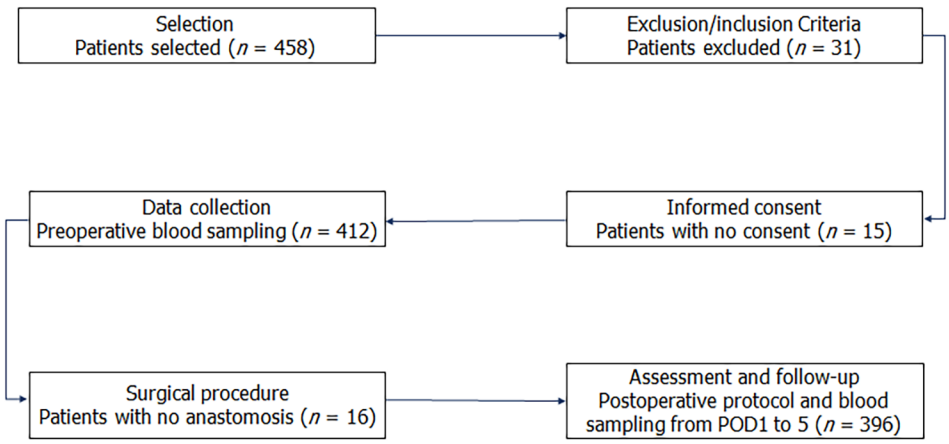
Table 2 summarizes the main operative characteristics. Eighty-two percent of patients had a laparoscopic approach, and the most common procedures performed were right colectomy (n = 196; 49.5%) and sigmoid colectomy/rectosigmoid resection (n = 74; 18.7%). The surgical approach ($P < 0.001$), the volume of blood loss ($P < 0.001$), the occurrence of intraoperative complications ($P < 0.001$), and the duration of the procedure ($P = 0.011$) were significantly related to the development of CAL.

In this study, CAL developed in 25 of 396 patients (6.3%) and was more frequent in men than women (68% *vs* 32%). Twenty-three patients with CAL (92.0%) were diagnosed during the first hospital admission. The mean ± SD and median time for CAL detection were 9.0 ± 6.8 d and 8 d (interquartile range = 7), respectively. Anastomotic leak was significantly associated with a longer hospital stay

Table 1 Patient demographic and clinical characteristics

	Group 1, *n* = 277	Group 2, *n* = 94	Group 3, *n* = 25	*P* value
Age, mean ± SD	68.8 ± 11.3	72.2 ± 14.5	73.6 ± 13.6	0.02
Sex, *n* (%)				0.505
Male	161 (58.1)	59 (62.7)	17 (68.0)	
Female	116 (41.9)	35 (37.3)	8 (32.0)	
BMI, mean ± SD	26.8 ± 3.99	26.3 ± 4.05	26.0 ± 3.97	0.33
BMI, *n* (%)				0.33
17.5 < BMI < 25	95 (35.0)	32 (34.0)	12 (48.0)	
25 ≤ BMI < 30	129 (46.0)	51 (54.0)	9 (36.0)	
BMI ≥ 30	53 (19.0)	11 (12.0)	4 (16.0)	
CCI, mean ± SD	5.12 ± 1.83	5.55 ± 2.38	6.04 ± 2.15	0.03
Prior abdominal surgery, *n* (%)	77 (27.8)	32 (34.0)	9 (36.0)	0.41
Immunosuppression, *n* (%)	10 (3.6)	5 (5.3)	0 (0)	0.45
Preoperative diagnosis malignant, *n* (%)	272 (98.2)	90 (95.7)	24 (96.0)	0.38
ASA score, *n* (%)				0.018
I–II	187 (67.5)	47 (50.0)	13 (45.8)	
III–IV	90 (32.5)	47 (50.0)	12 (54.2)	

Group 1: No complications; Group 2: Complications not related to colorectal anastomotic leakage (CAL); Group 3: CAL. BMI: Body mass index; CCI: Charlson Comorbidity Index; ASA: American Society of Anesthesiologists.



DOI: 10.3748/wjg.v28.i24.2758 **Copyright** ©The Author(s) 2022.

Figure 1 Flow diagram of patients according to the study protocol. POD1: Postoperative day 1.

(median of 21 d *vs* 7 d and 13 d, in G1 and G2 patients, respectively; $P < 0.001$), the readmission rate (20% *vs* 6.4% and 5.4%), and the reoperation rate (12% *vs* 3.2% and 1.8%). Table 3 provides a summary of 90-d morbidity and mortality rates. Based on the Clavien-Dindo classification, grades III and IV complication were significantly higher in the G3 cohort (84.0% *vs* 17.0%; $P < 0.001$) (Table 4).

Table 5 outlines the intraoperative and postoperative details of patients with CAL (G3) based on the CAL classification (minor *vs* major). Seven patients (28.0%) were managed nonoperatively and two (8.0%) underwent radiologic drainage of intraabdominal collections. The remaining 16 patients (64.0%) required surgical intervention. Of the 16 reoperated patients, 10 (56%) had an anastomosis takedown with an end stoma and 6 (44%) received a defunctioning stoma. The 90-d mortality rate was 0.8%, representing 3 patients with CAL.

Table 2 Patients' operative characteristics

	Group 1, *n* = 277	Group 2, *n* = 94	Group 3, *n* = 25	*P* value
Type of surgery, *n* (%)				0.071
Elective	238 (86.0)	72 (76.6)	19 (75.0)	
Urgent	39 (14.0)	22 (23.4)	6 (25.0)	
Surgical approach, *n* (%)				< 0.001
Open	25 (9.0)	15 (16.0)	2 (8.0)	
Laparoscopic	238 (86.0)	72 (77.0)	15 (60.0)	
Conversion	14 (5.0)	7 (7.4)	8 (32.0)	
Procedure, *n* (%)				0.739
Right colectomy[1]	138 (49.8)	47 (50.0)	11 (44.0)	
Left colectomy	17 (6.1)	7 (7.4)	1 (4.0)	
Sigmoid/RS resection	55 (19.8)	15 (15.9)	4 (16.0)	
Low anterior resection	48 (17.3)	16 (17.0)	8 (32.0)	
Other	19 (6.8)	9 (9.6)	1 (4.0)	
Level of anastomosis, *n* (%)				0.66
Ileocolic	150 (54.1)	50 (53.2)	11 (44.0)	
Colocolic	23 (8.3)	5 (5.3)	1 (4.0)	
≥ 6 cm from AV	67 (24.2)	25 (26.6)	10 (40.0)	
< 6 cm from AV	37 (13.4)	14 (14.9)	3 (12.0)	
Covering stoma, *n* (%)	23 (8.3)	8 (8.51)	2 (8.0)	0.99
Blood loss, mean ± SD, mL	51.6 ± 36.6	58.8 ± 47.7	104.0 ± 191.1	< 0.001
Intraoperative complications, *n* (%)	3 (1.1)	5 (5.3)	4 (16.0)	< 0.001
Operative time in min, mean ± SD	141.9 (48.3)	146.2 (50.0)	172.8 (57.2)	0.011

[1]Included ileocecal resection/extended right-sided colectomy.

Group 1: No complications; Group 2: Complications not related to colorectal anastomotic leakage (CAL); Group 3: CAL. RS: Rectosigmoid; AV: Anal verge.

Clinical criteria – postoperative trend and predictive effect

Abdominal pain: Abdominal pain was markedly higher and persistent from POD3 onwards in G3 patients (Figure 2A). The AUROC for abdominal pain on POD3, POD4, and POD5 was 0.77, 0.84, and 0.83, respectively, as shown in Supplementary Table E (Supplementary material 2A) and Figure 3A. The predictive effect was higher on POD4 with an estimated AUROC of 0.84.

Clinical condition: The clinical condition was worse in G3 compared with G2 patients, and it was significantly different after POD3 (P = 0.001). The overall postoperative trend was a declining clinical condition, as shown in Figure 2B. The AUROC for the clinical condition on POD3, POD4, and POD5 was 0.62, 0.81, and 0.90, respectively, as shown in Supplementary Table E (Supplementary material 2A) and Figure 3B. The prediction effect was higher on POD5 with an estimated AUROC of 0.90.

Biomarkers – postoperative trend and predictive effect

WBC count and ECC: During the first five POD, WBC in G3 patients was higher than that in patients without CAL and was significantly different on POD2, POD4, and POD5 (P = 0.01 for each day). On the other hand, ECC was lower in G3 patients and significantly different on POD1 and POD5 (P = 0.04 and P = 0.01, respectively), as presented in Supplementary Figures 1 and 2 (Supplementary material 2B). Overall, the postoperative course showed a sustained trend for both blood cell counts, except for ECC on POD5. The AUROC for WBC and ECC from POD1 to POD5 is presented in Supplementary Figures 3 and 4, respectively (Supplementary material 2B). The predictive effects of blood cell count were better on POD5. On POD5, when ECC was greater than 250 cells/μL, the AUROC, SS, and SP were 0.70, 89.0%, and 43.0%, respectively, as shown in Table 6.

CRP, PCT, and CLP: The mean values of CRP, PCT, and CLP increased promptly after surgery in all

Table 3 Ninety-day postoperative morbidity and mortality

	Patients, *n* (%)	Length of hospital stay in d, mean ± SD
With complications	119 (30.0)	16.4 ± 9.91
With no complications	277 (70)	7.4 ± 2.10
Noninfectious complications	49 (41.2)	14.2 ± 6.93
Infectious complications		
Surgical wound	36 (30.3)	14.6 ± 8.34
Respiratory tract	10 (8.4)	16.1 ± 7.22
Urinary tract	11 (9.2)	16.2 ± 6.00
Anastomotic leakage classification		
Minor	7 (28)	28.0 ± 17.00
Major	18 (72)	22.4 ± 12.88
Postoperative mortality	3 (0.8)	NA

NA: Not applicable.

Table 4 Short-term outcomes by group

	Group 1, *n* = 277	Group 2, *n* = 94	Group 3, *n* = 25	*P* value
LOHS in d				< 0.001
mean ± SD	7.4 ± 2.1	14.3 ± 7.4	24.0 ± 14.0	
Median	7	13	21	
90-d morbidity, *n* (%)				< 0.001
Clavien-Dindo I	NA	64 (68.1)	0 (0)	
Clavien-Dindo II		14 (14.9)	4 (16.0)	
Clavien-Dindo III		8 (8.5)	16 (64.0)	
Clavien-Dindo IV		8 (8.5)	5 (20.0)	
Readmission, *n* (%)	15 (5.4)	6 (6.4)	5 (20.0)	0.019
Reoperation, *n* (%)	4 (1.1)	3 (3.2)	3 (12.0)	0.005
90-d mortality, *n* (%)	0 (0)	0 (0)	3 (12.0)	< 0.001

Group 1: No complications; Group 2: Complications not related to colorectal anastomotic leakage (CAL); Group 3: CAL. LOHS: Length of hospital stay; NA: Not applicable.

groups. CRP decreased in G1 patients and remained elevated in patients with a complicated postoperative course, but was significantly higher than in G3 patients. On POD5, the mean CRP level in G3 patients was significantly higher than that in G1 patients (195.5 ± 139.9 mg/L *vs* 59.5 ± 43.4 mg/L; $P < 0.00001$) (Figure 4A). Patients with major CAL had a higher mean CRP level than those with minor CAL (251.45 mg/dL *vs* 107.64 mg/dL; $P = 0.01$) (Table 5). On POD3, POD4, and POD5, the overall diagnostic accuracy of CRP to detect CAL was expressed by an AUROC of 0.76, 0.76, and 0.81, respectively (Figure 5A). On POD5, the optimum cut-off value of 96.8 mg/L was estimated, resulting in an SS and SP of 78%, an NPV of 98%, and a PPV of 19% (Table 6).

The PCT level tended to be stable from POD3 onwards. The mean values were higher in G3 patients than in patients without CAL, but without statistical significance [on POD5, 0.23 ± 0.08 ng/mL *vs* 0.22 ± 0.07 ng/mL; Supplementary Figure 5 (Supplementary material 2C)]. The AUROC on POD3, POD4, and POD5 was 0.57, 0.50, and 0.61, respectively, as shown in Supplementary Figure 6 (Supplementary material 2C). The best predictive effect was on POD5. When PCT was greater than 0.39 ng/mL, the SS and SP were 44.0% and 79.0%, respectively (Table 6).

Table 5 Intraoperative and postoperative details of patients with colorectal anastomotic leakage (minor *vs* major)

	Minor CAL, *n* = 7	Major CAL, *n* = 18	*P* value
Type of anastomosis, *n* (%)			0.52
Intrabdominal	3 (42.8)	9 (50.0)	
Pelvic	4 (57.2)	9 (50.0)	
Covering stoma, *n* (%)	1 (14.3)	1 (5.6)	0.47
Abdominal pain			
POD3	1.86	1.94	0.08
POD4	1.57	2.13	0.04
POD5	1.86	1.92	0.03
Clinical condition			
POD3	1	1.25	0.07
POD4	1.14	1.47	0.13
POD5	1.29	1.58	0.02
CRP levels in mg/L			
POD3	178.35	221.02	0.28
POD4	146.30	226.01	0.13
POD5	107.64	251.45	0.01
CLP levels in μg/mL			
POD3	2.75	12.99	< 0.001
POD4	3.34	10.60	0.01
POD5	2.52	10.96	0.004
CAL diagnosis in d, median	8	5.5	0.07
Diagnostic method, *n* (%)			0.12
Clinical	0 (0)	7 (38.9)	
Abdominopelvic CT	7 (100)	11 (61.1)	
CAL management, *n* (%)			< 0.001
Drainage	NA	2 (11.1)	
Reoperation		16 (88.9)	
LOHS in d, mean ± SD	28.0 ± 17.0	22.4 ± 12.9	0.38

CAL: Colorectal anastomotic leakage; POD: Postoperative day; CRP: C-reactive protein; CLP: Calprotectin; CT: Computed tomography; LOHS: Length of hospital stay; NA: Not applicable.

In the first 5 POD, the mean CLP value tended to follow the pattern of CRP, although it was not as pronounced (Figure 4B). The mean CLP value was significantly higher in G3 patients from POD2 onwards. On POD3, the mean values of G1 *vs* G3 patients were 5.26 ± 3.58 μg/mL *vs* 11.52 ± 6.81 μg/mL ($P < 0.00005$). On POD3, POD4, and POD5, the CLP AUROC was 0.78, 0.67, and 0.65, respectively, as presented in Table 6 and Figure 5B. On POD3, a cut-off value of 6.57 μg/mL yielded a sensitivity of 71.0% and a specificity of 72.0% (Table 6).

Finally, when we analyzed the best predictors (CRP and CLP) for major CAL, the AUROC of CRP was 0.74 and 0.88 for POD3 and POD5, respectively. CLP was a better predictor of CAL than CRP at POD3, with an AUROC of 0.92 (Figure 5C and D).

Combination of biomarkers: Tables 7 and 8 present the AUROC of several possible classifiers of CAL, built with the Probit model, on POD3 and POD5, respectively. The combination of CRP and CLP on POD3 showed the best performance, with an AUROC of 0.82 (Table 7). Of note, on POD5, the combination of CRP and ECC also generated good predictive performance (AUROC = 0.81). However, with the aim of early CAL diagnosis, we chose the combination of CRP and CLP on POD3. Thereafter, we determined the probability of CAL, based on the computed equation P (CAL) = F [-3.0842 + (0.094 ×

Table 6 Summary of the predictive performance of the studied plasma biomarkers

	AUROC	Cut-off value	SS	SP	NPV	PPV	PLR	NLR
WBC in g/L								
POD3	0.57	9.75	0.46	0.75	0.95	0.11	1.84	0.72
POD4	0.60	8.25	0.52	0.68	0.96	0.10	1.64	0.70
POD5	0.62	7.55	0.56	0.62	0.95	0.09	1.48	0.71
ECC in cells/μL								
POD3	0.59	150	0.50	0.59	0.95	0.08	1.23	0.84
POD4	0.54	150	0.33	0.71	0.94	0.07	1.14	0.94
POD5	0.70	250	0.89	0.43	0.98	0.10	1.55	0.26
CRP in mg/L								
POD3	0.76	175.90	0.64	0.83	0.97	0.20	3.77	0.44
POD4	0.76	152.40	0.62	0.89	0.97	0.27	5.40	0.43
POD5	0.81	96.80	0.78	0.78	0.98	0.19	3.48	0.29
PCT in ng/mL								
POD3	0.57	0.19	0.68	0.47	0.96	0.08	1.28	0.68
POD4	0.50	0.31	0.38	0.76	0.95	0.10	1.56	0.82
POD5	0.61	0.39	0.44	0.79	0.96	0.12	2.10	0.71
CLP in μg/mL								
POD3	0.78	6.57	0.71	0.72	0.97	0.15	2.55	0.40
POD4	0.67	8.34	0.56	0.86	0.97	0.21	3.89	0.51
POD5	0.65	6.98	0.58	0.80	0.97	0.16	2.84	0.52

AUROC: Area under the receiver operating characteristic curve; SS: Sensitivity; SP: Specificity; NPV: Negative predictive value; PPV: Positive predictive value; PLR: Positive likelihood ratio; NLR: Negative likelihood ratio; WBC: White blood cell count; POD: Postoperative day; ECC: Eosinophil cell count; CRP: C-reactive protein; PCT: Procalcitonin; CLP: Calprotectin.

Table 7 Area under the receiver operating characteristic curve of pairwise combination of biomarkers on postoperative day 3

	CLP	PCT	CRP	ECC
PCT	0.76			
CRP	0.82	0.72		
ECC	0.77	0.52	0.72	
WBC	0.74	0.53	0.72	0.54

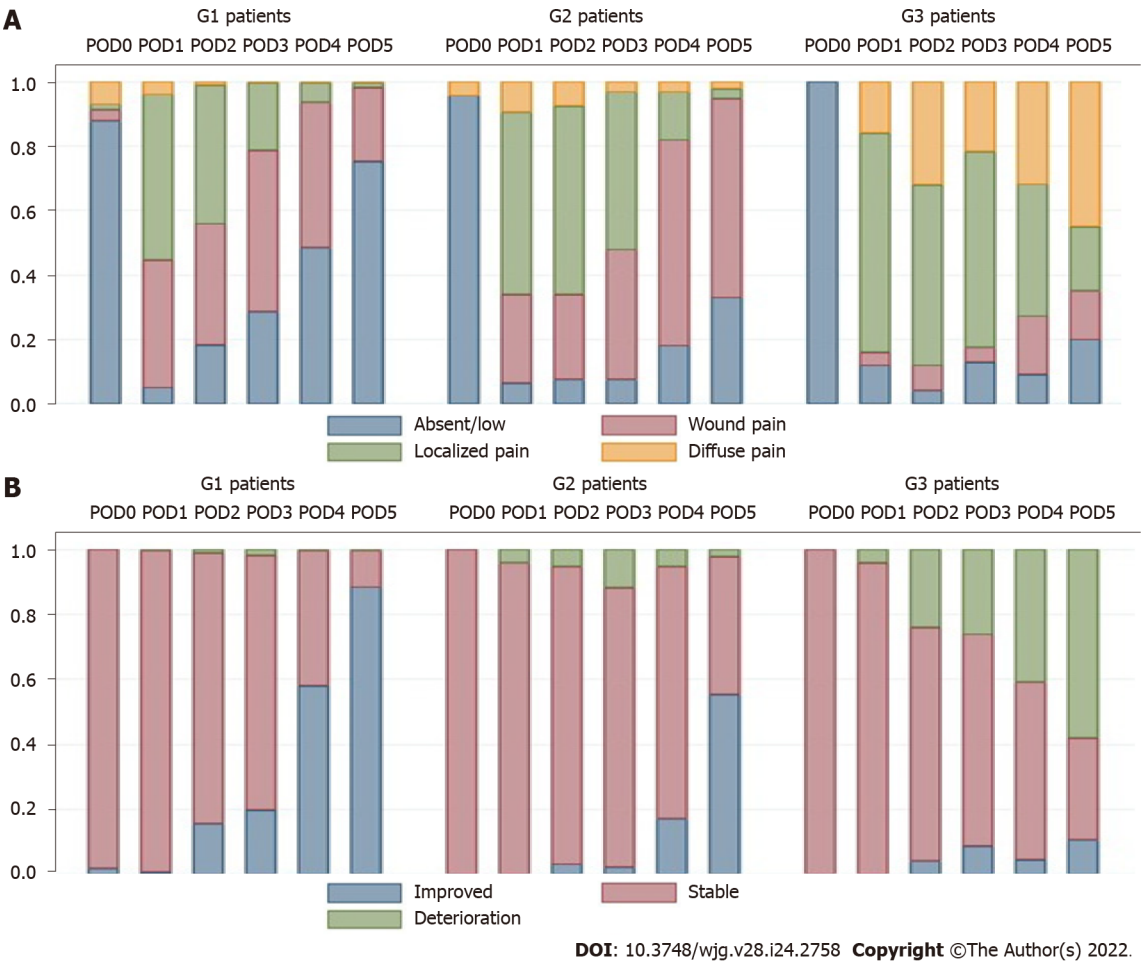
CLP: Calprotectin; PCT: Procalcitonin; CRP: C-reactive protein; ECC: Eosinophil cell count; WBC: White blood cell count.

CLP_D3) + (0.0059 × CRP_D3)], where F is the cumulative standard normal distribution. Applying Liu's method, this classifier had an optimum cut-off point of 0.055, evidencing the existence of CAL above 0.055 on POD3, with an SS and SP of 86% and 75%, respectively. For hypothetical patient X on POD3 with CRP and CLP plasma levels of 137.4 mg/L and 8.75 μg/mL, respectively, the computed probability of CAL is high (score = 0.074). By adopting this classifier, the time to CAL diagnosis is estimated as 3.8 d [(0.86 × 3) + (0.14 × 9.0)], which represents a 5.2-d reduction compared with the baseline results.

Table 8 Area under the receiver operating characteristic curve of pairwise combination of biomarkers on postoperative day 5

	CLP	PCT	CRP	ECC
PCT	0.60			
CRP	0.78	0.79		
ECC	0.61	0.63	0.81	
WBC	0.57	0.60	0.78	0.67

CLP: Calprotectin; PCT: Procalcitonin; CRP: C-reactive protein; ECC: Eosinophil cell count; WBC: White blood cell count.

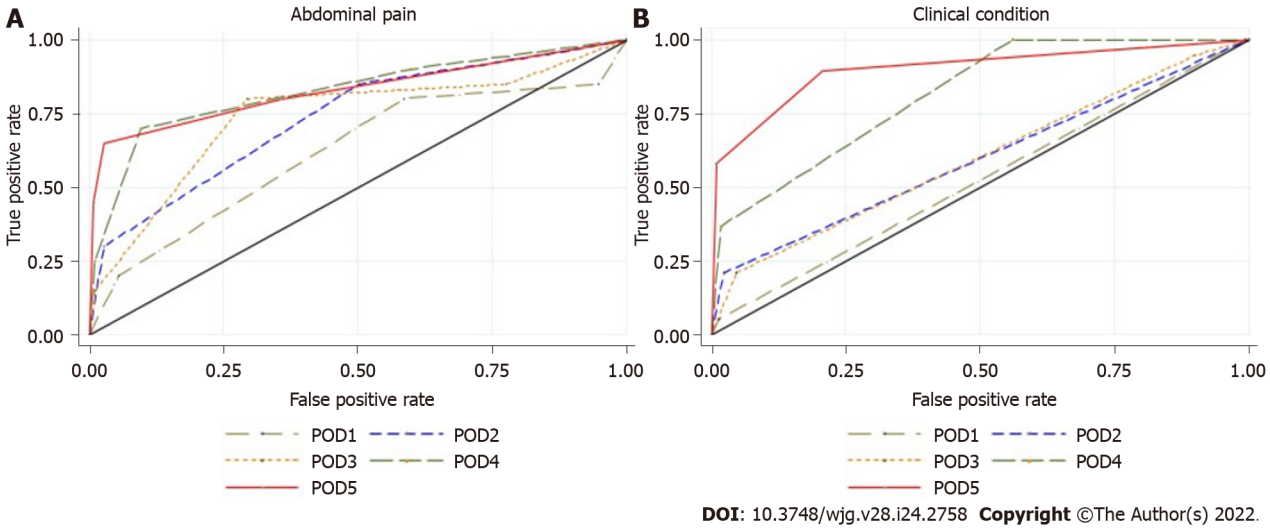


DOI: 10.3748/wjg.v28.i24.2758 **Copyright** ©The Author(s) 2022.

Figure 2 Distribution of rates of abdominal pain (A) and clinical condition (B). G1: No complications; G2: Complications not related to colorectal anastomotic leakage; G3: CAL. POD: Postoperative day.

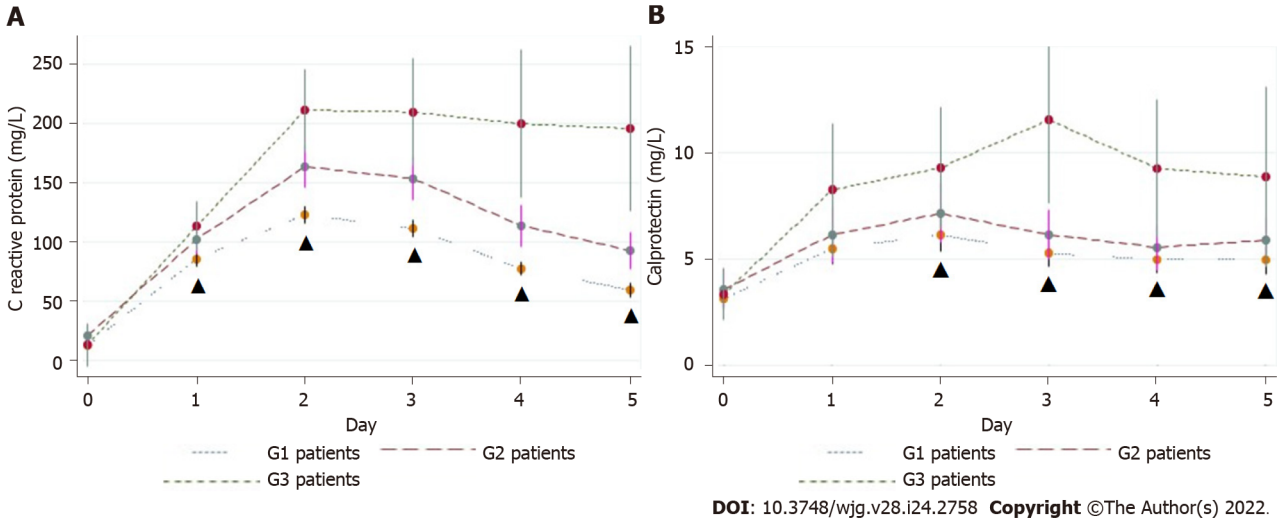
DISCUSSION

This study assessed the usefulness of biomarkers for the early detection of CAL. Clinical criteria demonstrated high diagnostic accuracy (AUROC > 0.8) on POD4 and POD5. Changes in the abdominal pain pattern and worsening of the clinical condition were associated with an increased risk of CAL diagnosis. Both clinical criteria seem to be an useful early markers for this condition, producing the best overall diagnostic accuracy of the parameters analyzed. Three large and well-conducted studies on the association between pain and postoperative complications are worth reporting. Boström *et al*[34] examined a cohort of 3084 patients and estimated that increased postoperative pain is associated with a high risk of CAL, being an independent marker and suggesting a need for further diagnostic measures. The other two studies had similar conclusions, although they were not exclusive for colorectal surgery [14,35]. A worse clinical condition and abdominal pain not localized to the wound are two of four modified Dutch leakage (DULK) score criteria, scoring 1 point each. Using a cut-off value of 1 point produced an overall SS and NPV of 97.0% and 99.5%, respectively[10]. We should bring the clinical



DOI: 10.3748/wjg.v28.i24.2758 **Copyright** ©The Author(s) 2022.

Figure 3 Area under the receiver operating characteristic curve of colorectal anastomotic leakage for clinical criteria. A: Abdominal pain from postoperative day 1 to postoperative day 5; B: Clinical condition from postoperative day 1 to postoperative day 5. POD: Postoperative day.



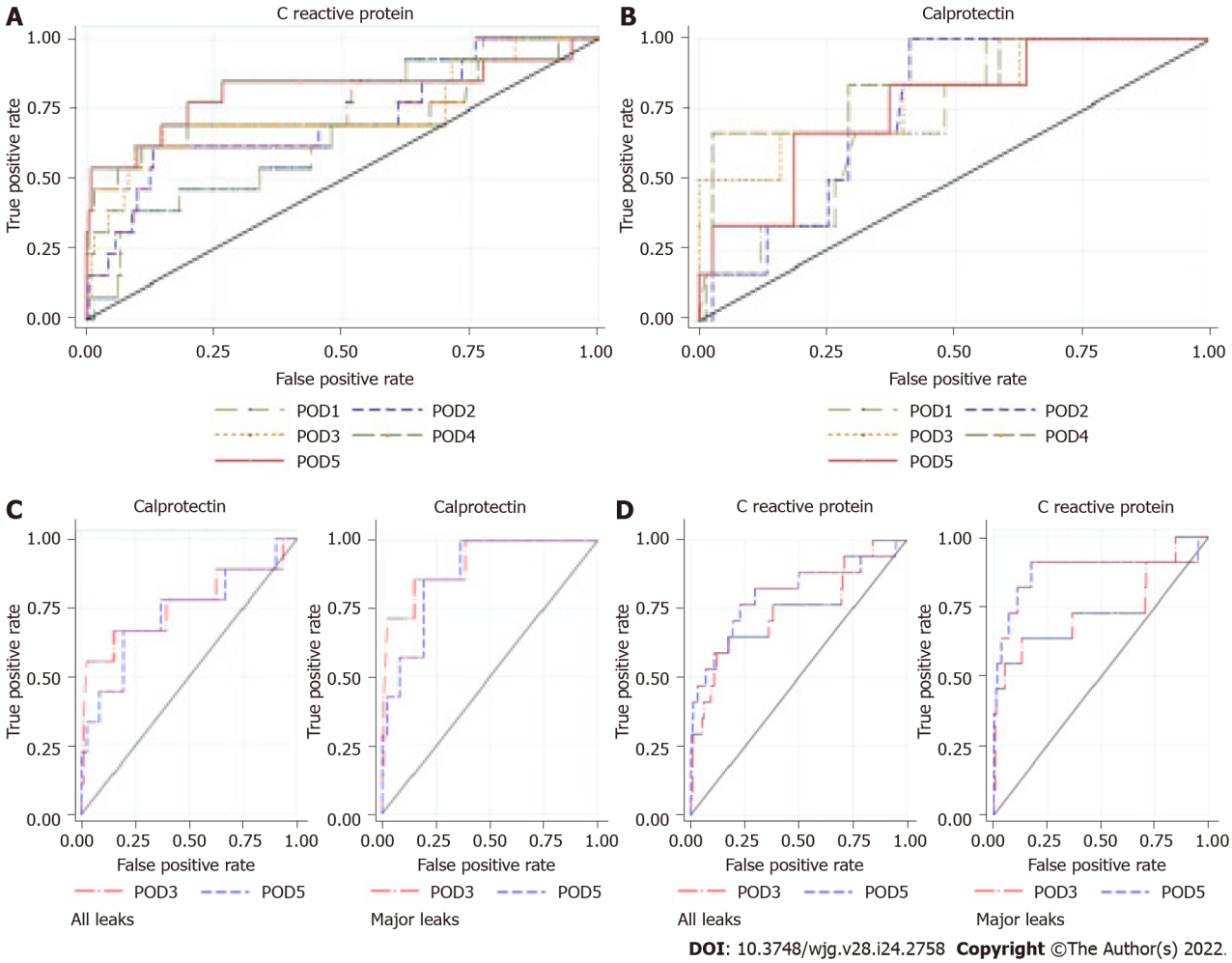
DOI: 10.3748/wjg.v28.i24.2758 **Copyright** ©The Author(s) 2022.

Figure 4 C-reactive protein (A) and calprotectin (B) levels. Values are the mean ± SE. G1: No complications; G2: Complications not related to colorectal anastomotic leakage; G3: CAL; ▲ : *P* statistically significant ($P < 0.05$).

method to the forefront, being aware of the clinical signs of CAL. They are very helpful for the early diagnosis, as "red flags" for further investigation.

In our study, particularly on POD4 and POD5, WBC and ECC showed a distinct tendency in patients with and without CAL, with a high NPV (from 94%-98%) but low accuracy (AUROC from 0.54 to 0.70). In G3 patients, WBC plateaued after the acute inflammatory response, a phenomenon that was notably different from patients without CAL. In a large retrospective study, Warschkow *et al*[16] found that the WBC level contributed little to the early detection of septic complications, with a lower diagnostic accuracy than plasma CRP. In several other studies, researchers have estimated, from POD5 to POD7, an AUROC and SS ranging from 0.63 to 0.82 and from 58% to 74%, respectively[15,16,20,24,35].

Some researchers have proposed eosinopenia as a biomarker in this scenario. They concluded that it might help to identify several sepsis-related conditions, distinguished from other causes of systemic inflammatory response syndrome. It seems to be an interesting biomarker because of its widespread availability and low cost[36]. Shaaban *et al*[37] defined an optimum cut-off value of 50 cells/μL, which produced an SS, SP, and NPV of 81%, 65% and 80%, respectively. At hospital admission, ECC < 40 cells/μL is an independent prognostic factor for mortality[38,39]. Our study is original in assessing the usefulness of ECC for the early diagnosis of CAL. The mean ECC level showed a non-significant decline after POD4 in G3 patients, and a modest diagnostic accuracy (AUROC from 0.54 to 0.70) when compared with other biomarkers. Nevertheless, ECC could still be used in CAL diagnosis as a fast, simple, convenient, and inexpensive biomarker. It should be considered in the decision-making process



DOI: 10.3748/wjg.v28.i24.2758 **Copyright** ©The Author(s) 2022.

Figure 5 Area under the receiver operating characteristic curve of colorectal anastomotic leakage. A: For C-reactive protein from postoperative day 1 to postoperative day 5; B: For calprotectin from postoperative day 1 to postoperative day 5; C: For calprotectin from postoperative day 3 to postoperative day 5; D: For C-reactive protein from postoperative day 3 to postoperative day 5. Left: All leaks; Right: Major leaks; POD: Postoperative day.

and future research[40].

The usefulness of CRP as a biomarker for early detection of CAL has been investigated by several groups[19,25,39,41,42]. In this study, the plasma CRP level exhibited a propensity to normalize from POD3 onwards in patients without CAL (G1 and G2). However, it remained steadily increased in G3 patients, with a markedly high mean value from POD1 to POD5. Yeung *et al*[43] performed the most comprehensive meta-analysis available in the literature, including nearly 7000 patients pooled from 23 studies. From POD1 to POD7, patients with CAL had a significantly higher mean CRP level compared with patients without CAL ($P < 0.001$)[43]. In this study, CRP was the best predictor for CAL on POD4 and POD5, with a maximum AUROC of 0.81 (cut-off value of 96.8 mg/L and an NPV of 98%) on POD5. Similar results have been published by other authors. Ortega-Deballon *et al*[26] estimated on POD4 an AUROC of 0.72 with a cut-off of 125 mg/L, yielding an SS and NPV of 81.8% and 95.8%, respectively. Garcia-Granero *et al*[25] reported that CRP level showed a good predictive ability for major CAL on POD5, with an AUROC of 0.85 (cut-off value of 135 mg/L and an NPV of 98%). In the Italian ColoRectal Anastomotic Leakage (iCral) multicentric prospective observational study, the CRP level was a good positive and excellent negative predictor of CAL, with an AUROC of 0.81 on POD6 (cut-off value of 81.5 mg/L), and an SS and NPV of 80.9% and 97.7%, respectively[41]. In the meta-analysis by Yeung *et al*[43], AUROC analysis established a threshold CRP level for CAL of 115 mg/L on POD5, with an SS and SP of 100%. All of these authors recommended CRP levels to predict CAL, and our group advocates a similar practice and suggests the use of this biomarker to expedite further investigation and treatment [25,26,41,43].

CLP, a sign of neutrophil activation, could be a promising early marker for excessive inflammatory response in major abdominal catastrophes, such as CAL. To date, only Reisinger *et al*[18] have studied the predictive value of CLP in CAL diagnosis. In G3 patients, the mean postoperative CLP level peaked on POD3 and was notably higher, persisting thereafter. On POD3, the AUROC (0.78) and SS (71%) were slightly higher than the CRP level, although they were lower than those obtained in the pioneering study by Reisinger *et al*[18] (0.92 and 86%, respectively). One possible explanation could be our compre-

hensive definition of CAL and the larger sample size. It remains unclear to what extent CLP level is an early predictor that is better than CRP for detecting CAL. As a neutrophil activation marker, CLP could be increased early after anastomotic failure, compared with CRP, which indicates a delayed systemic inflammatory response. Our study shows that CLP is worth evaluating for early diagnosis of CAL.

We demonstrated in the first 5 POD, the mean PCT values were marginally higher in G3 patients but with lower accuracy, SS, and SP than CRP and CLP levels. However, it had a high NPV (> 95%), making it an adequate and useful marker for early and safe discharge after colorectal surgery, considering the current enhanced recovery after surgery routine. In contrast to our study, Giaccaglia *et al*[17] estimated that on POD5, PCT had better accuracy than CRP (0.86 *vs* 0.81), as well as a high NPV (98.3%). A recent meta-analysis published by Su'a *et al*[44] determined a diagnostic accuracy of 0.88 on POD5 and an optimum cut-off value on POD3 and POD5 of 0.25 and 680 ng/mL, respectively. The NPV ranged from 95% to 100%. In agreement with these authors, we believe that PCT is a useful negative predictor for CAL; as a single test, however, it is worthless for CAL diagnosis.

We verified that, with the exception of plasma CRP on POD5 (AUROC > 0.80), each biomarker individually was a modest predictor of CAL[45]. The combination of two or more biomarkers has been considered in previous studies[17,18,41]. In this study, the combination of CRP and CLP values on POD3 increased diagnostic accuracy, shortening the mean CAL diagnosis by 5 d. This reduction would likely lead to reduced morbidity and mortality. Reisinger *et al*[18] confirmed a significant improvement in diagnostic accuracy (AUROC = 0.93) with the combination of CRP and CLP plasma levels on POD3, an SS of 100%, and an SP of 89.0%, decreasing the median time to diagnosis by 3 d. Furthermore, Giaccaglia *et al*[17] found that by adding PCT to CRP on POD5, the diagnostic accuracy markedly improved (AUROC = 0.90). Similarly, the iCral study demonstrated that the combination of CRP and PCT with a clinical score (DULK score) allowed the exclusion of CAL on POD2 (NPV = 99%)[41]. We believe that a user-friendly diagnostic tool, combining CLP and CRP levels by this mathematic model, would help the surgeon to diagnose CAL early. Consequently, this biomarkers' combination may be included in a standard postoperative surveillance program, as a warning tool for CAL. In the case of a "positive test", this protocol recommends abdominal and pelvic CT scan or early reoperation in case of imaging-dubious or -negative, to reduce the time to CAL detection and enable prompt management.

Strengths and limitations of the study

One strength of this study was its prospective design and independent data collection model, which minimized observer bias. Second, it was one of the largest monocentric sample size published to date. Based on the recent meta-analyses of Waterland *et al*[46] van Helsdingen *et al*[47], only two monocentric prospective studies have enrolled more than 400 patients. Furthermore, we analyzed five biomarkers, including plasma CLP, which was first studied by Reisinger *et al*[18]. Third, we chose a comprehensive definition of CAL, recently defined by van Helsdingen *et al*[29] to include all patients with CAL, minimizing selection bias. We did not exclude minor CAL from the cohort, which also affected the predictive effect of the analyzed biomarkers. In addition, to keep the biomarkers optimum cut-off values in AUROC analysis both standardized and reproducible, we adopted Liu's method. This method defines the optimum cut-off point as the point maximizing the product of SS and SP[48]. These reasons may explain some differences in biomarkers' diagnostic accuracy in this study. Fourth, we tried to adapt the study protocol to daily practice, making its enforcement easier in the future. Hence, we included all patients undergoing colorectal resection, even those with a diverting ostomy. In addition, clinicians were not blinded to the daily biomarkers' results and might use those data according to the study protocol. Finally, we proposed a predictive tool based on the combination of two biomarkers that improved CAL diagnostic accuracy. Adoption of this tool in daily practice might shorten the time to CAL diagnosis and management. Moreover, the data from this study provide information for the development of more complex mathematical predictive models, including machine learning methods.

This study had several limitations. First, the monocentric design may limit the external validity of the results. Second, our sample had some grade of heterogeneity, because the study population included benign and malignant disorders, elective and urgent procedures, and anastomosis within different levels of the colon and rectum. Third, we designed a phase I diagnostic study and estimated cut-off values for early CAL detection. However, we should change the direction of interpretation, running from the diagnostic test result toward the CAL diagnosis. To address this issue, we are performing a new multicentric prospective phase II diagnostic study, using the predictive tool and defined biomarkers cut-off values[49]. Fourth, plasma CLP measurement is expensive and these kits are not easily accessible in daily clinical practice. Finally, our study did not address the cost-effectiveness of biomarkers' measurement. It is crucial to estimate the economic burden of CAL, including the cost related to a delayed diagnosis, the high rate of false positives, and unjustified reoperations or frequent readmissions.

CONCLUSION

In conclusion, we found that clinical criteria have added value as a warning sign of CAL. On the other

hand, CRP and CLP levels are the best early predictors of CAL. Particularly relevant is the combination of CLP and CRP early during POD3, and its potential to markedly reduce the time to diagnosis of CAL. By reducing the time to CAL diagnosis, reduced morbidity and mortality are expected. Additional studies are needed to confirm the predictive ability of this model on early CAL detection and its utility in routine clinical care.

ARTICLE HIGHLIGHTS

Research background

Colorectal anastomotic leakage (CAL) is a major complication in abdominal surgery. Prompt diagnosis can reduce morbidity and mortality associated with this condition. Serum biomarkers have been proposed as predictors of CAL.

Research motivation

Biomarkers such as C-reactive protein (CRP) and white blood cell (WBC) count are frequently requested in the postoperative period of colorectal surgery. However, the usefulness of these and other biomarkers remains unclear.

Research objectives

To assess the role of CRP, WBC, eosinophil cell count, calprotectin (CLP), and procalcitonin in the first 5 postoperative days (PODs) after colorectal surgery, and thus, discuss in what order these biomarkers can be employed in clinical practice.

Research methods

From March 2017 to August 2019, we measured and analyzed five serum biomarkers daily in 396 patients who underwent colorectal surgery. The area under the receiver operating characteristic curve, specificity, sensitivity, positive predictive value (PPV), and negative predictive value (NPV) were used to estimate the best predictive diagnostic performance.

Research results

CRP had an NPV of 98% on POD5. The combination of CLP and CRP measurement presented a high diagnostic accuracy (AUCROC = 0.82) on POD3. We identified a reduction of 5.2 d to the diagnosis of CAL.

Research conclusions

The combination of CRP and CLP demonstrated good diagnostic accuracy. These tests can likely be used to reduce time to CAL detection.

Research perspectives

Further studies should test a warning index score built from selected predictive variables as biomarkers CRP and CLP.

FOOTNOTES

Author contributions: Rama NJM, Guarino MPS, and Lourenço Ó designed the study; Lages MCC, Castro R, Bento A, and Parente D coordinated the data collection process; Lourenço Ó and Silva CSG performed the data analyses; Rama NJM, Motta Lima PC and Guarino MPS prepared the manuscript; Rama NJM, Rocha A, Castro-Poças F, and Pimentel J revised the paper critically; All authors read and approved the final manuscript.

Supported by the Ministry of Health – Incentive Program for the Integration of Care and Valuation of Patients' Pathways in the National Health Service of Portugal.

Institutional review board statement: This study was conducted in accordance with the Declaration of Helsinki and was approved by the Local Ethical Committee of the Colorectal Referral Centre, after authorization obtained from the Portuguese Data Protection Authority. This study is registered with the number 9930/2016 and can be consulted at https://drive.google.com/file/d/1BiLxWlvcrqpX4KQrjW4F2codsOOywVF/view?usp=sharing.

Informed consent statement: Informed consent was obtained from all participants included in the study.

Conflict-of-interest statement: The authors have no conflicts of interest to declare.

Data sharing statement: For additional data, Dr. Nuno Rama can be contacted by e-mail at ramanuno@gmail.com.

STROBE statement: The authors have read the STROBE Statement – checklist of items, and the manuscript was prepared and revised according to the STROBE Statement – checklist of items.

Open-Access: This article is an open-access article that was selected by an in-house editor and fully peer-reviewed by external reviewers. It is distributed in accordance with the Creative Commons Attribution NonCommercial (CC BY-NC 4.0) license, which permits others to distribute, remix, adapt, build upon this work non-commercially, and license their derivative works on different terms, provided the original work is properly cited and the use is non-commercial. See: https://creativecommons.org/Licenses/by-nc/4.0/

Country/Territory of origin: Portugal

ORCID number: Nuno J G Rama 0000-0002-1572-2239; Marlene C C Lages 0000-0002-7389-6368; Maria Pedro S Guarino 0000-0001-6079-1105; Óscar Lourenço 0000-0002-3642-4919; Patrícia C Motta Lima 0000-0002-6427-8955; Diana Parente 0000-0003-0271-371X; Cândida S G Silva 0000-0002-7092-1169; Ricardo Castro 0000-0002-5110-0883; Ana Bento 0000-0002-3489-8774; Anabela Rocha 0000-0001-5000-5369; Fernando Castro-Pocas 0000-0002-2268-9107; João Pimentel 0000-0003-1908-8607.

S-Editor: Ma YJ
L-Editor: A
P-Editor: Ma YJ

REFERENCES

1 **Boccola MA**, Buettner PG, Rozen WM, Siu SK, Stevenson AR, Stitz R, Ho YH. Risk factors and outcomes for anastomotic leakage in colorectal surgery: a single-institution analysis of 1576 patients. *World J Surg* 2011; **35**: 186-195 [PMID: 20972678 DOI: 10.1007/s00268-010-0831-7]
2 **Trencheva K**, Morrissey KP, Wells M, Mancuso CA, Lee SW, Sonoda T, Michelassi F, Charlson ME, Milsom JW. Identifying important predictors for anastomotic leak after colon and rectal resection: prospective study on 616 patients. *Ann Surg* 2013; **257**: 108-113 [PMID: 22968068 DOI: 10.1097/SLA.0b013e318262a6cd]
3 **Pommergaard HC**, Gessler B, Burcharth J, Angenete E, Haglind E, Rosenberg J. Preoperative risk factors for anastomotic leakage after resection for colorectal cancer: a systematic review and meta-analysis. *Colorectal Dis* 2014; **16**: 662-671 [PMID: 24655784 DOI: 10.1111/codi.12618]
4 **McDermott FD**, Heeney A, Kelly ME, Steele RJ, Carlson GL, Winter DC. Systematic review of preoperative, intraoperative and postoperative risk factors for colorectal anastomotic leaks. *Br J Surg* 2015; **102**: 462-479 [PMID: 25703524 DOI: 10.1002/bjs.9697]
5 **Smith SR**, Pockney P, Holmes R, Doig F, Attia J, Holliday E, Carroll R, Draganic B. Biomarkers and anastomotic leakage in colorectal surgery: C-reactive protein trajectory is the gold standard. *ANZ J Surg* 2018; **88**: 440-444 [PMID: 28304142 DOI: 10.1111/ans.13937]
6 **Iancu C**, Mocan LC, Todea-Iancu D, Mocan T, Acalovschi I, Ionescu D, Zaharie FV, Osian G, Puia CI, Muntean V. Host-related predictive factors for anastomotic leakage following large bowel resections for colorectal cancer. *J Gastrointestin Liver Dis* 2008; **17**: 299-303 [PMID: 18836623]
7 **Cousin F**, Ortega-Deballon P, Bourredjem A, Doussot A, Giaccaglia V, Fournel I. Diagnostic Accuracy of Procalcitonin and C-reactive Protein for the Early Diagnosis of Intra-abdominal Infection After Elective Colorectal Surgery: A Meta-analysis. *Ann Surg* 2016; **264**: 252-256 [PMID: 27049766 DOI: 10.1097/SLA.0000000000001545]
8 **Watson AJ**, Krukowski ZH, Munro A. Salvage of large bowel anastomotic leaks. *Br J Surg* 1999; **86**: 499-500 [PMID: 10215823 DOI: 10.1046/j.1365-2168.1999.01096.x]
9 **Matthiessen P**, Henriksson M, Hallböök O, Grunditz E, Norén B, Arbman G. Increase of serum C-reactive protein is an early indicator of subsequent symptomatic anastomotic leakage after anterior resection. *Colorectal Dis* 2008; **10**: 75-80 [PMID: 17666099 DOI: 10.1111/j.1463-1318.2007.01300.x]
10 **den Dulk M**, Witvliet MJ, Kortram K, Neijenhuis PA, de Hingh IH, Engel AF, van de Velde CJ, de Brauw LM, Putter H, Brouwers MA, Steup WH. The DULK (Dutch leakage) and modified DULK score compared: actively seek the leak. *Colorectal Dis* 2013; **15**: e528-e533 [PMID: 24199233 DOI: 10.1111/codi.12379]
11 **Rojas-Machado SA**, Romero M, Arroyo A, Rojas-Machado A, López J, Calpena R. Anastomic leak in colorectal cancer surgery. Development of a diagnostic index (DIACOLE). *Int J Surg* 2016; **27**: 92-98 [PMID: 26827891 DOI: 10.1016/j.ijsu.2016.01.089]
12 **Doeksen A**, Tanis PJ, Vrouenraets BC, Lanschot van JJ, Tets van WF. Factors determining delay in relaparotomy for anastomotic leakage after colorectal resection. *World J Gastroenterol* 2007; **13**: 3721-3725 [PMID: 17659732 DOI: 10.3748/wjg.v13.i27.3721]
13 **Marres CCM**, van de Ven AWH, Leijssen LGJ, Verbeek PCM, Bemelman WA, Buskens CJ. Colorectal anastomotic leak: delay in reintervention after false-negative computed tomography scan is a reason for concern. *Tech Coloproctol* 2017; **21**: 709-714 [PMID: 28929306 DOI: 10.1007/s10151-017-1689-6]
14 **Regenbogen SE**, Mullard AJ, Peters N, Brooks S, Englesbe MJ, Campbell DA Jr, Hendren S. Hospital Analgesia Practices and Patient-reported Pain After Colorectal Resection. *Ann Surg* 2016; **264**: 1044-1050 [PMID: 26756749 DOI: 10.1097/sla.0000000000001541]
15 **Sutton CD**, Marshall LJ, Williams N, Berry DP, Thomas WM, Kelly MJ. Colo-rectal anastomotic leakage often

masquerades as a cardiac complication. *Colorectal Dis* 2004; **6**: 21-22 [PMID: 14692947 DOI: 10.1111/j.1463-1318.2004.00574.x]

16 **Warschkow R**, Tarantino I, Torzewski M, Näf F, Lange J, Steffen T. Diagnostic accuracy of C-reactive protein and white blood cell counts in the early detection of inflammatory complications after open resection of colorectal cancer: a retrospective study of 1,187 patients. *Int J Colorectal Dis* 2011; **26**: 1405-1413 [PMID: 21701807 DOI: 10.1007/s00384-011-1262-0]

17 **Giaccaglia V**, Salvi PF, Antonelli MS, Nigri G, Pirozzi F, Casagranda B, Giacca M, Corcione F, de Manzini N, Balducci G, Ramacciato G. Procalcitonin Reveals Early Dehiscence in Colorectal Surgery: The PREDICS Study. *Ann Surg* 2016; **263**: 967-972 [PMID: 26528879 DOI: 10.1097/SLA.0000000000001365]

18 **Reisinger KW**, Poeze M, Hulsewé KW, van Acker BA, van Bijnen AA, Hoofwijk AG, Stoot JH, Derikx JP. Accurate prediction of anastomotic leakage after colorectal surgery using plasma markers for intestinal damage and inflammation. *J Am Coll Surg* 2014; **219**: 744-751 [PMID: 25241234 DOI: 10.1016/j.jamcollsurg.2014.06.011]

19 **den Dulk M**, Noter SL, Hendriks ER, Brouwers MA, van der Vlies CH, Oostenbroek RJ, Menon AG, Steup WH, van de Velde CJ. Improved diagnosis and treatment of anastomotic leakage after colorectal surgery. *Eur J Surg Oncol* 2009; **35**: 420-426 [PMID: 18585889 DOI: 10.1016/j.ejso.2008.04.009]

20 **Welsch T**, Müller SA, Ulrich A, Kischlat A, Hinz U, Kienle P, Büchler MW, Schmidt J, Schmied BM. C-reactive protein as early predictor for infectious postoperative complications in rectal surgery. *Int J Colorectal Dis* 2007; **22**: 1499-1507 [PMID: 17639424 DOI: 10.1007/s00384-007-0354-3]

21 **Silvestre J**, Rebanda J, Lourenço C, Póvoa P. Diagnostic accuracy of C-reactive protein and procalcitonin in the early detection of infection after elective colorectal surgery - a pilot study. *BMC Infect Dis* 2014; **14**: 444 [PMID: 25132018 DOI: 10.1186/1471-2334-14-444]

22 **Kørner H**, Nielsen HJ, Søreide JA, Nedrebø BS, Søreide K, Knapp JC. Diagnostic accuracy of C-reactive protein for intraabdominal infections after colorectal resections. *J Gastrointest Surg* 2009; **13**: 1599-1606 [PMID: 19479312 DOI: 10.1007/s11605-009-0928-1]

23 **Facy O**, Paquette B, Orry D, Binquet C, Masson D, Bouvier A, Fournel I, Charles PE, Rat P, Ortega-Deballon P; IMACORS Study. Diagnostic Accuracy of Inflammatory Markers As Early Predictors of Infection After Elective Colorectal Surgery: Results From the IMACORS Study. *Ann Surg* 2016; **263**: 961-966 [PMID: 26135691 DOI: 10.1097/SLA.0000000000001303]

24 **Lagoutte N**, Facy O, Ravoire A, Chalumeau C, Jonval L, Rat P, Ortega-Deballon P. C-reactive protein and procalcitonin for the early detection of anastomotic leakage after elective colorectal surgery: pilot study in 100 patients. *J Visc Surg* 2012; **149**: e345-e349 [PMID: 23102916 DOI: 10.1016/j.jviscsurg.2012.09.003]

25 **Garcia-Granero A**, Frasson M, Flor-Lorente B, Blanco F, Puga R, Carratalá A, Garcia-Granero E. Procalcitonin and C-reactive protein as early predictors of anastomotic leak in colorectal surgery: a prospective observational study. *Dis Colon Rectum* 2013; **56**: 475-483 [PMID: 23478615 DOI: 10.1097/DCR.0b013e31826ce825]

26 **Ortega-Deballon P**, Radais F, Facy O, d'Athis P, Masson D, Charles PE, Cheynel N, Favre JP, Rat P. C-reactive protein is an early predictor of septic complications after elective colorectal surgery. *World J Surg* 2010; **34**: 808-814 [PMID: 20049435 DOI: 10.1007/s00268-009-0367-x]

27 **Cikot M**, Kones O, Gedikbası A, Kocatas A, Karabulut M, Temizgonul KB, Alis H. The marker C-reactive protein is helpful in monitoring the integrity of anastomosis: plasma calprotectin. *Am J Surg* 2016; **212**: 53-61 [PMID: 26606896 DOI: 10.1016/j.amjsurg.2015.06.018]

28 **Aadland E**, Fagerhol MK. Faecal calprotectin: a marker of inflammation throughout the intestinal tract. *Eur J Gastroenterol Hepatol* 2002; **14**: 823-825 [PMID: 12172400 DOI: 10.1097/00042737-200208000-00002]

29 **Rahbari NN**, Weitz J, Hohenberger W, Heald RJ, Moran B, Ulrich A, Holm T, Wong WD, Tiret E, Moriya Y, Laurberg S, den Dulk M, van de Velde C, Büchler MW. Definition and grading of anastomotic leakage following anterior resection of the rectum: a proposal by the International Study Group of Rectal Cancer. *Surgery* 2010; **147**: 339-351 [PMID: 20004450 DOI: 10.1016/j.surg.2009.10.012]

30 **Dindo D**, Demartines N, Clavien PA. Classification of surgical complications: a new proposal with evaluation in a cohort of 6336 patients and results of a survey. *Ann Surg* 2004; **240**: 205-213 [PMID: 15273542 DOI: 10.1097/01.sla.0000133083.54934.ae]

31 **Hand DJ**. Statistical Evaluation of Diagnostic Performance: Topics in ROC Analysis by Zou KH, Liu A, Bandos AI, Ohno-Machado L, Rockette HE. *Int Stat Rev* 2013; **81**: 335 [DOI: 10.1111/insr.12020_27]

32 **James G**, Witten D, Hastie T, Tibshira R. An introduction to statistical learning with applications in R. 1st ed. New York: Springer Science+Business Media, 2013

33 **Boström P**, Svensson J, Brorsson C, Rutegård M. Early postoperative pain as a marker of anastomotic leakage in colorectal cancer surgery. *Int J Colorectal Dis* 2021; **36**: 1955-1963 [PMID: 34272996 DOI: 10.1007/s00384-021-03984-w]

34 **van Boekel RLM**, Warlé MC, Nielen RGC, Vissers KCP, van der Sande R, Bronkhorst EM, Lerou JGC, Steegers MAH. Relationship Between Postoperative Pain and Overall 30-Day Complications in a Broad Surgical Population: An Observational Study. *Ann Surg* 2019; **269**: 856-865 [PMID: 29135493 DOI: 10.1097/SLA.0000000000002583]

35 **Garnacho-Montero J**, Huici-Moreno MJ, Gutiérrez-Pizarraya A, López I, Márquez-Vácaro JA, Macher H, Guerrero JM, Puppo-Moreno A. Prognostic and diagnostic value of eosinopenia, C-reactive protein, procalcitonin, and circulating cell-free DNA in critically ill patients admitted with suspicion of sepsis. *Crit Care* 2014; **18**: R116 [PMID: 24903083 DOI: 10.1186/cc13908]

36 **Shaaban H**, Daniel S, Sison R, Slim J, Perez G. Eosinopenia: Is it a good marker of sepsis in comparison to procalcitonin and C-reactive protein levels for patients admitted to a critical care unit in an urban hospital? *J Crit Care* 2010; **25**: 570-575 [PMID: 20435431 DOI: 10.1016/j.jcrc.2010.03.002]

37 **Abidi K**, Belayachi J, Derras Y, Khayari ME, Dendane T, Madani N, Khoudri I, Zeggwagh AA, Abouqal R. Eosinopenia, an early marker of increased mortality in critically ill medical patients. *Intensive Care Med* 2011; **37**: 1136-1142 [PMID: 21369810 DOI: 10.1007/s00134-011-2170-z]

38 **Terradas R**, Grau S, Blanch J, Riu M, Saballs P, Castells X, Horcajada JP, Knobel H. Eosinophil count and neutrophil-

lymphocyte count ratio as prognostic markers in patients with bacteremia: a retrospective cohort study. *PLoS One* 2012; **7**: e42860 [PMID: 22912753 DOI: 10.1371/journal.pone.0042860]

39 **Lin Y**, Rong J, Zhang Z. Silent existence of eosinopenia in sepsis: a systematic review and meta-analysis. *BMC Infect Dis* 2021; **21**: 471 [PMID: 34030641 DOI: 10.1186/s12879-021-06150-3]

40 **Italian ColoRectal Anastomotic Leakage (iCral) Study Group**. Anastomotic leakage after elective colorectal surgery: a prospective multicentre observational study on use of the Dutch leakage score, serum procalcitonin and serum C-reactive protein for diagnosis. *BJS Open* 2020; **4**: 499-507 [PMID: 32134216 DOI: 10.1002/bjs5.50269]

41 **Paliogiannis P**, Deidda S, Maslyankov S, Paycheva T, Farag A, Mashhour A, Misiakos E, Papakonstantinou D, Mik M, Losinska J, Scognamillo F, Sanna F, Feo CF, Porcu A, Xidas A, Zinellu A, Restivo A, Zorcolo L. C reactive protein to albumin ratio (CAR) as predictor of anastomotic leakage in colorectal surgery. *Surg Oncol* 2021; **38**: 101621 [PMID: 34126521 DOI: 10.1016/j.suronc.2021.101621]

42 **Yeung DE**, Peterknecht E, Hajibandeh S, Torrance AW. C-reactive protein can predict anastomotic leak in colorectal surgery: a systematic review and meta-analysis. *Int J Colorectal Dis* 2021; **36**: 1147-1162 [PMID: 33555423 DOI: 10.1007/s00384-021-03854-5]

43 **Su'a B**, Tutone S, MacFater W, Barazanchi A, Xia W, Zeng I, Hill AG. Diagnostic accuracy of procalcitonin for the early diagnosis of anastomotic leakage after colorectal surgery: a meta-analysis. *ANZ J Surg* 2020; **90**: 675-680 [PMID: 31230412 DOI: 10.1111/ans.15291]

44 **Mandrekar JN**. Receiver operating characteristic curve in diagnostic test assessment. *J Thorac Oncol* 2010; **5**: 1315-1316 [PMID: 20736804 DOI: 10.1097/JTO.0b013e3181ec173d]

45 **Mik M**, Dziki L, Berut M, Trzcinski R, Dziki A. Neutrophil to Lymphocyte Ratio and C-Reactive Protein as Two Predictive Tools of Anastomotic Leak in Colorectal Cancer Open Surgery. *Dig Surg* 2018; **35**: 77-84 [PMID: 28132052 DOI: 10.1159/000456081]

46 **Waterland P**, Ng J, Jones A, Broadley G, Nicol D, Patel H, Pandey S. Using CRP to predict anastomotic leakage after open and laparoscopic colorectal surgery: is there a difference? *Int J Colorectal Dis* 2016; **31**: 861-868 [PMID: 26951183 DOI: 10.1007/s00384-016-2547-0]

47 **van Helsdingen CP**, Jongen AC, de Jonge WJ, Bouvy ND, Derikx JP. Consensus on the definition of colorectal anastomotic leakage: A modified Delphi study. *World J Gastroenterol* 2020; **26**: 3293-3303 [PMID: 32684743 DOI: 10.3748/wjg.v26.i23.3293]

48 **Liu X**. Classification accuracy and cut point selection. *Stat Med* 2012; **31**: 2676-2686 [PMID: 22307964 DOI: 10.1002/sim.4509]

49 **Sackett DL**, Haynes RB. The architecture of diagnostic research. *BMJ* 2002; **324**: 539-541 [PMID: 11872558 DOI: 10.1136/bmj.324.7336.539]

World Journal of Gastroenterology

Submit a Manuscript: https://www.f6publishing.com

World J Gastroenterol 2022 June 28; 28(24): 2775-2777

DOI: 10.3748/wjg.v28.i24.2775

ISSN 1007-9327 (print) ISSN 2219-2840 (online)

LETTER TO THE EDITOR

Is long-term follow-up without surgical treatment a valid option for hepatic alveolar echinococcosis?

Yusufukadier Maimaitinijiati, Yuan Meng, Xiong Chen

Specialty type: Gastroenterology and hepatology

Provenance and peer review: Invited article; Externally peer reviewed.

Peer-review model: Single blind

Peer-review report's scientific quality classification

Grade A (Excellent): 0
Grade B (Very good): B
Grade C (Good): C
Grade D (Fair): 0
Grade E (Poor): 0

P-Reviewer: Aseni P, Italy; Augustin G, Croatia

Received: February 24, 2022
Peer-review started: February 24, 2022
First decision: April 5, 2022
Revised: April 13, 2022
Accepted: June 3, 2022
Article in press: June 3, 2022
Published online: June 28, 2022

Yusufukadier Maimaitinijiati, Yuan Meng, Xiong Chen, Department of Hepatobiliary Surgery, People's Hospital of Xinjiang Uyghur Autonomous Region, Urumqi 830001, Xinjiang Uyghur Autonomous Region, China

Yusufukadier Maimaitinijiati, School of Clinical Medicine, Medical College of Tsinghua University, Beijing 100084, China

Corresponding author: Xiong Chen, MD, Chief Doctor, Professor, Department of Hepatobiliary Surgery, People's Hospital of Xinjiang Uyghur Autonomous Region, No. 91 Tianchi Road, Tianshan District, Urumqi 830011, Xinjiang Uyghur Autonomous Region, China. 1512237458@qq.com

Abstract

We read the article titled, "Long-term follow-up of liver alveolar echinococcosis using echinococcosis multilocularis ultrasound classification," by Schuhbaur J with great interest. However, we found some worthwhile issues that we believe should be discussed with the authors, and have provided our comments in this letter. It would be valuable if the authors could provide further information about the clinical stages, follow-up time, and clinical outcomes of the patients.

Key Words: Alveolar echinococcosis; Albendazole; Surgical treatment; Ultrasound; Follow-up

©The Author(s) 2022. Published by Baishideng Publishing Group Inc. All rights reserved.

Core Tip: Although many experts suggest that radical surgery combined with albendazole treatment is the optimal option for alveolar echinococcosis patients, no clear consensus has been reached on whether long-term treatment using albendazole alone without any surgical intervention can cure or control the disease. Therefore, some professional issues need to be clarified by discussion with peers, in order to benefit as many patients as possible.

Citation: Maimaitinijiati Y, Meng Y, Chen X. Is long-term follow-up without surgical treatment a valid option for hepatic alveolar echinococcosis? *World J Gastroenterol* 2022; 28(24): 2775-2777
URL: https://www.wjgnet.com/1007-9327/full/v28/i24/2775.htm
DOI: https://dx.doi.org/10.3748/wjg.v28.i24.2775

TO THE EDITOR

We read the article titled, "Long-term follow-up of liver alveolar echinococcosis using echinococcosis multilocularis ultrasound classification," by Schuhbaur *et al*[1] with great interest. In this significant study, the authors observed changes in sonomorphology during the follow-up of hepatic lesions using a sonomorphologic classification scheme. However, after reading the article carefully, we found some worthwhile issues that we would like to discuss with the authors.

Alveolar echinococcosis (AE) is an infectious zoonotic parasitic disease, which has been a major public health problem in its epidemic area[2]. In the large majority of cases, the liver is the first organ to be infested by the larvae. Hepatic AE often invades the surrounding vessels and adjacent organs in its advanced stages. The mortality rate within 10 years after diagnosis is more than 90% if the lesion is inadequately or not treated[3]. According to the World Health Organization Informal Working Group on Echinococcosis criteria[4], radical surgery combined with albendazole treatment is the optimal option for AE patients. In this article, the authors included 59 patients from Germany's national echinococcosis database, who were "considered" to have hepatic AE, and long-term follow-up using ultrasound was performed. However, they did not mention the clinical stages, specific follow-up time, and clinical prognosis of these patients. Hepatic AE is known as "parasitic cancer," due to its tumor-like characteristics with infiltration of vessels or biliary structures and distant metastasis. To date, no clear consensus has been reached on whether long-term treatment using albendazole alone without any surgical intervention can cure or control the disease. A 5-year analysis of two distinct cohorts in Bern, Switzerland and Besancon, France demonstrated that conservative treatment was less effective than surgical therapy[5]; however, longer follow-up results have not been available. Currently, "watch and wait" is not recommended unless complete inactivity of the AE lesion can be confirmed, in order to avoid delayed treatment resulting in adverse outcomes[6].

The authors' team proposed an ultrasonographic classification scheme for hepatic AE in 2015[7], which was used to follow 59 patients. However, we noted that the authors stated that all but 1 patient received antiparasitic drugs, but they also claimed that more than half of the patients (55.9%) were defined as "probable" hepatic AE. In such a case, the use of albendazole and other drugs with hepatotoxicity may cause unnecessary harm to patients. According to a recent study with long-term observation of 117 AE patients, about 44.4% experienced adverse reactions when taking albendazole, and severe liver toxicity occurred in 7.7% patients[8]. We believe that the authors should have provided a more detailed explanation about whether the use of albendazole is indeed necessary for these patients. The high rate of inoperable disease at diagnosis underscores the need for an early, definitive diagnosis. However, in cases that cannot be confirmed by conventional examination, supplementary tests such as serology and positron emission tomography (PET)/computed tomography (CT) may be useful.

Bresson-Hadni *et al*[9] suggested that "surgical resection, if feasible, is the gold standard for treatment." We also believe that early radical resection of the lesion should be considered in patients with hepatic AE, unless it is defined as unresectable. Based on the clinical guidelines and previous reports, the objectives for the treatment of hepatic AE should include the following: Completely removing the parasitic lesion, combined with 2 years of albendazole treatment after surgery; if this is not possible, reducing the proliferating potential of echinococcosis multilocularis by continuous administration of albendazole; and lesions that are massively calcified and/or negative by CT or PET may benefit from a "watch-and-wait" approach.

In summary, we admire the efforts of the authors in using ultrasound to assess sonomorphology changes over time in hepatic AE lesions. Nevertheless, it would be valuable if the authors could provide further information about the clinical stages, follow-up time, and clinical outcomes of the patients.

FOOTNOTES

Author contributions: Maimaitinijiati Y performed the research and wrote the letter; Meng Y and Chen X revised the letter.

Conflict-of-interest statement: All authors have no conflicts of interest to declare.

Open-Access: This article is an open-access article that was selected by an in-house editor and fully peer-reviewed by external reviewers. It is distributed in accordance with the Creative Commons Attribution NonCommercial (CC BY-NC 4.0) license, which permits others to distribute, remix, adapt, build upon this work non-commercially, and license

their derivative works on different terms, provided the original work is properly cited and the use is non-commercial. See: https://creativecommons.org/Licenses/by-nc/4.0/

Country/Territory of origin: China

ORCID number: Yusufukadier Maimaitinijiati 0000-0003-2069-9202; Yuan Meng 0000-0002-2028-1175; Xiong Chen 0000-0002-2352-219X.

S-Editor: Liu X
L-Editor: A
P-Editor: Wang LL

REFERENCES

1 **Schuhbaur J**, Schweizer M, Philipp J, Schmidberger J, Schlingeloff P, Kratzer W. Long-term follow-up of liver alveolar echinococcosis using echinococcosis multilocularis ultrasound classification. *World J Gastroenterol* 2021; **27**: 6939-6950 [PMID: 34790016 DOI: 10.3748/wjg.v27.i40.6939]
2 **Torgerson PR**, Keller K, Magnotta M, Ragland N. The global burden of alveolar echinococcosis. *PLoS Negl Trop Dis* 2010; **4**: e722 [PMID: 20582310 DOI: 10.1371/journal.pntd.0000722]
3 **Vuitton DA**, Bresson-Hadni S. Alveolar echinococcosis: evaluation of therapeutic strategies. *Expert Opin Orphan D* 2014; **2**: 67-86 [DOI: 10.1517/21678707.2014.870033]
4 **Brunetti E**, Kern P, Vuitton DA; Writing Panel for the WHO-IWGE. Expert consensus for the diagnosis and treatment of cystic and alveolar echinococcosis in humans. *Acta Trop* 2010; **114**: 1-16 [PMID: 19931502 DOI: 10.1016/j.actatropica.2009.11.001]
5 **Beldi G**, Vuitton D, Lachenmayer A, Heyd B, Dufour JF, Richou C, Candinas D, Bresson-Hadni S. Is *ex vivo* liver resection and autotransplantation a valid alternative treatment for end-stage hepatic alveolar echinococcosis in Europe? *J Hepatol* 2019; **70**: 1030-1031 [PMID: 30718093 DOI: 10.1016/j.jhep.2018.12.011]
6 **Wen H**, Vuitton L, Tuxun T, Li J, Vuitton DA, Zhang W, McManus DP. Echinococcosis: Advances in the 21st Century. *Clin Microbiol Rev* 2019; **32** [PMID: 30760475 DOI: 10.1128/CMR.00075-18]
7 **Kratzer W**, Gruener B, Kaltenbach TE, Ansari-Bitzenberger S, Kern P, Fuchs M, Mason RA, Barth TF, Haenle MM, Hillenbrand A, Oeztuerk S, Graeter T. Proposal of an ultrasonographic classification for hepatic alveolar echinococcosis: Echinococcosis multilocularis Ulm classification-ultrasound. *World J Gastroenterol* 2015; **21**: 12392-12402 [PMID: 26604646 DOI: 10.3748/wjg.v21.i43.12392]
8 **Zavoikin VD**, Zelya OP, Tumolskaya NI. Clinical tolerance and efficacy of anti-parasitic treatment with albendazole in patients with alveolar echinococcosis: long-term follow-up observation in 117 patients. *Parasitol Res* 2021; **120**: 3603-3610 [PMID: 34432154 DOI: 10.1007/s00436-021-07297-3]
9 **Bresson-Hadni S**, Spahr L, Chappuis F. Hepatic Alveolar Echinococcosis. *Semin Liver Dis* 2021; **41**: 393-408 [PMID: 34161992 DOI: 10.1055/s-0041-1730925]

World Journal of Gastroenterology

Submit a Manuscript: https://www.f6publishing.com

World J Gastroenterol 2022 June 28; 28(24): 2778-2781

DOI: 10.3748/wjg.v28.i24.2778

ISSN 1007-9327 (print) ISSN 2219-2840 (online)

LETTER TO THE EDITOR

Using of artificial intelligence: Current and future applications in colorectal cancer screening

Georgios Zacharakis, Abdulaziz Almasoud

Specialty type: Gastroenterology and hepatology

Provenance and peer review: Unsolicited article; Externally peer reviewed.

Peer-review model: Single blind

Peer-review report's scientific quality classification

Grade A (Excellent): 0
Grade B (Very good): B, B
Grade C (Good): 0
Grade D (Fair): 0
Grade E (Poor): 0

P-Reviewer: Ozair A, India; Taheri S, Iran

Received: March 23, 2022
Peer-review started: March 23, 2022
First decision: April 25, 2022
Revised: April 26, 2022
Accepted: June 13, 2022
Article in press: June 13, 2022
Published online: June 28, 2022

Georgios Zacharakis, Division of Gastroenterology, Department of Internal Medicine, College of Medicine, Prince Sattam bin Abdulaziz University Hospital, Al Kharj 16277, Saudi Arabia

Abdulaziz Almasoud, Department of Gastroenterology and Hepatology, Prince Sultan Military Medical City, Riyadh 12233, Saudi Arabia

Corresponding author: Georgios Zacharakis, BSc, MSc, PhD, Professor, Division of Gastroenterology, Department of Internal Medicine, College of Medicine, Prince Sattam bin Abdulaziz University Hospital, Arrayan, Al Kharj 16277, Saudi Arabia.
g.zacharakis@psau.edu.sa

Abstract

Significant developments in colorectal cancer screening are underway and include new screening guidelines that incorporate considerations for patients aged 45 years, with unique features and new techniques at the forefront of screening. One of these new techniques is artificial intelligence which can increase adenoma detection rate and reduce the prevalence of colonic neoplasia.

Key Words: Basic concepts; Assessment of artificial intelligence in endoscopy; Current applications; Ethics; Safety challenge

©The Author(s) 2022. Published by Baishideng Publishing Group Inc. All rights reserved.

Core Tip: Artificial intelligence (AI) is an integral part of endoscopy and health care in colorectal cancer screening because it has been shown to increase adenoma detection rates and reduce the prevalence of colonic neoplasia. It will soon provide an "optical biopsy" of polyps, assisting advanced therapeutic endoscopy-resection and 'discard– no pathology present. 'Innovations in AI have changed and improved the lives of gastroenterologists by examining quality monitoring *via* a single integrated system. The only boundaries of AI are clinical research trials and reimbursement.

Citation: Zacharakis G, Almasoud A. Using of artificial intelligence: Current and future applications in colorectal cancer screening. *World J Gastroenterol* 2022; 28(24): 2778-2781
URL: https://www.wjgnet.com/1007-9327/full/v28/i24/2778.htm
DOI: https://dx.doi.org/10.3748/wjg.v28.i24.2778

TO THE EDITOR

Artificial intelligence can increase adenoma detection rate in randomized control trials

Artificial intelligence (AI) has been shown to improve the adenoma detection rate (ADR) in colorectal cancer screening. It has been evaluated in multiple randomized controlled trials, showing that the withdrawal time does not vary at any polyp size, location, or morphology[1]. It also improves detection in serrated lesions; however, its usefulness is not clear for advanced adenomas, given that data are available from only three studies. A potential weakness of these studies is that they are largely confined to China and Italy. While the ADRs in China are low, ranging from 17% to 28%, in Italy, Repici *et al*[2] reported a rate of 40% to 55%. Studies conducted in the United States will be forthcoming.

AI in gastroenterology: Potential weaknesses

In this issue of the *World Journal of Gastroenterology*, a review article by Kröner *et al*[3] is entitled "Artificial intelligence in gastroenterology: a state-of-the-art review discussing the findings and a broad spectrum of clinical applications." The authors reviewed the literature highlighting the use of AI in current and future applications, especially in the detection of lesions and identification of pre-malignant or malignant lesions. However, we would like to mention that colonic disease detection of lesions using techniques such as polyp identification and classification are limited in number; these are not available in all AI systems, and clinical trial data from the USA are particularly limited[4]. Pentax Medical, Medronic, and EndoBrain provide only colonic polyp detection, and they lack the ability to classify the features of the CAD EYE system (Fujifilm) used in Europe and Japan[4]. Although the authors outlined the study limitations because of the lack of creating "universal datasets" and the lack of validating external in clinical settings and advise on future directions for research in this field, the important boundaries of AI are around clinical research trials, assessing AI in daily clinical practice, and around reimbursement and other ethical issues and safety challenges not highlighted here[3].

We would like to mention recent studies related to these important boundaries of AI use. It is expected that AI will compensate for human errors and the limits of human capabilities in performing real-time diagnostics of colonic lesions by providing accuracy, consistency, and greater diagnostic speed. However, Byrne *et al*[5] showed that 15% of polyps can not be classified. Therefore, further clinical trials are required to assess these benefits[5]. Whether endoscopic procedures become more efficient and of a higher quality when assisted by AI is yet to be proven. However, this new technology can mimic human behavior, identify colonic lesion precursors of colorectal cancer in at-risk patients[6], and can support medical decision-making[6].

Current endoscopy practices include the real-time administration of AI with computer vision to identify and delineate colonic lesions. This was achieved using an algorithm to diagnose and classify defined lesions. By applying machine learning (ML), the algorithm was trained using a large dataset of predefined polyp-containing video frames. These images include several key characteristics such as virtual chromoendoscopy, surface pit pattern morphology, microvascular pattern, high-magnification, and endocytoscopic appearance.

However, the promising applications of AI-assisted endoscopy raise several issues. Validation and quality control, video and image limitations, and annotation burden are primary areas of concern. Additionally, the data gathered has inherent biases due to a disproportionate representation of those with certain ethnicities, geographic and cultural inequities, and small segments of the population. Even if represented proportionately, inaccuracies can result in harmful consequences. Other contributors to bias included technical differences in colonoscopy techniques, bowel preparation, and colonoscopy equipment. The algorithm is as effective as the database.

Other issues with AI/ML are ethical and can be resolved by the careful and thorough regulation of data ownership and security. Data ownership could involve the patient, doctor, and/or the healthcare system, and the involvement of the Health Insurance Portability and Accountability Act, General Data Protection Regulation, industry, and science must be addressed. Finally, the endoscopist is responsible for the patient, not the computer.

The use of AI to demonstrate and characterize colonic lesions based on real-time signalling profiles is feasible. Video camera movement and tissue pathology captures a pair of frames, identifies recognized landmarks, and matches them by computing relative frames. Tissue classification was performed for all lesion types in real-time[7]. Its accuracy is evaluated by comparing it with the dual judgments of humans; however, few health professionals and patients wish to submit tissues for histological analyses [8].

Computer-assisted endoscopy has many clinical applications, including safety alerts, no-go zones, difficult notifications, staff notifications, and auto reports. Furthermore, AI supports decision-making by endoscopists, improves advanced therapeutic endoscopy and workflow, increases safety, reduces the need for manpower, and minimizes the need for humans to perform autonomous functions. Its limitations include physician resistance, limited video availability, data ownership, regulations, liability, privacy, lack of reimbursement, and cultural perceptions.

Currently, the fees for AI services are not standardized; however, there is an implementation cost. Given that better polyp detection results in more surveillance examinations, quality-based reimbursements could result in increased compensation. On the other hand, polyp diagnosis assisted by

AI has been shown to result in cost savings for the patient, particularly when the resultant strategy is "diagnose and leave without pathology"[9]. Overall, AI did not change the withdrawal timing and reduced the time required for endoscopic procedures. However, the cost and burden of these procedures remain unproven.

Real world testing needed

Evaluation of AI in healthcare requires real-world testing, including a minimal amount of randomized control trial data and a concentration of early stage research statistics such as ex vivo data, still images, and retrospective videos. Images should be carefully selected, and study designs should meet published standards such as preservation and incorporation of valuable endoscopic innovations, resect and discard criteria, and medical device approval by the US Food and Drug Administration. Furthermore, technical performance studies such as ML accuracy, system output accuracy, and usability, in addition to workflow studies such as effectiveness, efficiency, satisfaction, ease of use, learning ability, and utilization should be conducted. Additionally, health impact studies evaluating decision impact, patient outcomes, process outcomes, cost-effectiveness, care variability, and population impact should be conducted. Therefore, examination quality metrics are necessary, such as colonoscopy quality assessment *via* AI[10].

At this time, algorithms meet the preservation and incorporation of valuable endoscopic innovation criteria; however, multi-center trials have not been started. Experience is gained primarily from single-center studies conducted by expert endoscopists. Additionally, randomized controlled trials have not been performed, and magnifying scope technology is not available in some countries such as the USA[11]. Once these requirements are met, AI can become widely used in the daily practice of endoscopy, providing examination quality, polyp detection, polyp classification, and automatic reports. There are still a lot of unanswered questions and issues to be furthered discussed. However, we believe that the AI assisted colonoscopy, all in one integrated system, quality metrics of the colonoscopy exam, detection and classification of colonic lesions will play a key role in daily endoscopy clinical settings after 4-5 years.

FOOTNOTES

Author contributions: Zacharakis G and Almasoud A designed and performed the research and analyzed the data; Zacharakis G wrote the letter; Almasoud A revised the letter.

Conflict-of-interest statement: All authors declare no competing interests.

Open-Access: This article is an open-access article that was selected by an in-house editor and fully peer-reviewed by external reviewers. It is distributed in accordance with the Creative Commons Attribution NonCommercial (CC BY-NC 4.0) license, which permits others to distribute, remix, adapt, build upon this work non-commercially, and license their derivative works on different terms, provided the original work is properly cited and the use is non-commercial. See: https://creativecommons.org/Licenses/by-nc/4.0/

Country/Territory of origin: Saudi Arabia

ORCID number: Georgios Zacharakis 0000-0002-2859-9188; Abdulaziz Almasoud 0000-0003-2731-4395.

Corresponding Author's Membership in Professional Societies: SCFHS, 15RM0044572; Athens Medical Association, No. 055597.

S-Editor: Wang LL
L-Editor: A
P-Editor: Wang LL

REFERENCES

1 **Hassan C**, Spadaccini M, Iannone A, Maselli R, Jovani M, Chandrasekar VT, Antonelli G, Yu H, Areia M, Dinis-Ribeiro M, Bhandari P, Sharma P, Rex DK, Rösch T, Wallace M, Repici A. Performance of artificial intelligence in colonoscopy for adenoma and polyp detection: a systematic review and meta-analysis. *Gastrointest Endosc* 2021; **93**: 77-85.e6 [PMID: 32598963 DOI: 10.1016/j.gie.2020.06.059]

2 **Glissen Brown JR**, Mansour NM, Wang P, Chuchuca MA, Minchenberg SB, Chandnani M, Liu L, Gross SA, Sengupta N, Berzin TM. Deep Learning Computer-aided Polyp Detection Reduces Adenoma Miss Rate: A United States Multi-center Randomized Tandem Colonoscopy Study (CADeT-CS Trial). *Clin Gastroenterol Hepatol* 2021 [DOI: 10.1016/j.cgh.2021.09.009]

3 **Kröner PT**, Engels MM, Glicksberg BS, Johnson KW, Mzaik O, van Hooft JE, Wallace MB, El-Serag HB, Krittanawong C. Artificial intelligence in gastroenterology: A state-of-the-art review. *World J Gastroenterol* 2021; **27**: 6794-6824 [PMID:

34790008 DOI: 10.3748/wjg.v27.i40.6794]
4 **Mori Y**, Neumann H, Misawa M, Kudo SE, Bretthauer M. Artificial intelligence in colonoscopy - Now on the market. What's next? *J Gastroenterol Hepatol* 2021; **36**: 7-11 [PMID: 33179322 DOI: 10.1111/jgh.15339]
5 **Byrne MF**, Chapados N, Soudan F, Oertel C, Linares Pérez M, Kelly R, Iqbal N, Chandelier F, Rex DK. Real-time differentiation of adenomatous and hyperplastic diminutive colorectal polyps during analysis of unaltered videos of standard colonoscopy using a deep learning model. *Gut* 2019; **68**: 94-100 [PMID: 29066576 DOI: 10.1136/gutjnl-2017-314547]
6 **El Hajjar A**, Rey JF. Artificial intelligence in gastrointestinal endoscopy: general overview. *Chin Med J (Engl)* 2020; **133**: 326-334 [PMID: 31929362 DOI: 10.1097/CM9.0000000000000623]
7 **Marques KF**, Marques AF, Lopes MA, Beraldo RF, Lima TB, Sassaki LY. Artificial intelligence in colorectal cancer screening in patients with inflammatory bowel disease. *Artif Intell Gastrointest Endosc* 2022; **3**: 1-8 [DOI: 10.37126/aige.v3.i1.1]
8 **Kudo SE**, Mori Y, Misawa M, Takeda K, Kudo T, Itoh H, Oda M, Mori K. Artificial intelligence and colonoscopy: Current status and future perspectives. *Dig Endosc* 2019; **31**: 363-371 [PMID: 30624835 DOI: 10.1111/den.13340]
9 **Glover B**, Teare J, Patel N. The Status of Advanced Imaging Techniques for Optical Biopsy of Colonic Polyps. *Clin Transl Gastroenterol* 2020; **11**: e00130 [PMID: 32352708 DOI: 10.14309/ctg.0000000000000130]
10 **Mori Y**, Kudo SE, East JE, Rastogi A, Bretthauer M, Misawa M, Sekiguchi M, Matsuda T, Saito Y, Ikematsu H, Hotta K, Ohtsuka K, Kudo T, Mori K. Cost savings in colonoscopy with artificial intelligence-aided polyp diagnosis: an add-on analysis of a clinical trial (with video). *Gastrointest Endosc* 2020; **92**: 905-911.e1 [PMID: 32240683 DOI: 10.1016/j.gie.2020.03.3759]
11 **Thakkr S**, Carleton NM, Rao B, Syed A. Use of artificial intelligence-based analysis from live endosocpiesto optimize the quality of the colonoscopy exam in real time: proof of concept. *Gastroenterology* 2020; **158**: 1219-1221 [DOI: 10.1053/j.gastro.2019.12.035]



Published by **Baishideng Publishing Group Inc**
7041 Koll Center Parkway, Suite 160, Pleasanton, CA 94566, USA
Telephone: +1-925-3991568
E-mail: bpgoffice@wjgnet.com
Help Desk: https://www.f6publishing.com/helpdesk
https://www.wjgnet.com



© 2022 Baishideng Publishing Group Inc. All rights reserved.